Sun. Jun 6, 2021

[J] Poster | U (Union)：Union

5:15 PM - 6:30 PM JST | 8:15 AM - 9:30 AM UTC | Ch.01_1

[U-04] Promotion of SDGs in JpGU

convener:Yukihiro Takahashi(Department of Cosmosciences, Graduate School of Science, Hokkaido University), Chiaki T. Oguchi(Institute for Environmental Science and Technology, Graduate School of Science and Engineering, Saitama University), Richard Simon Wallis(The University of Tokyo), Eiichi Tajika(Department of Earth and Planetary Science, Graduate School of Science, The University of Tokyo)

[U04-P01] SDGs and academic researches in the Solid Earth Science Section

*Michihiko Nakamura[1], Yo Fukushima[2] (1.Department of Earth Science, Graduate School of Science, Tohoku University, 2.Disaster Science Division, International Research Institute of Disaster Science, Tohoku University)

[U04-P02] **Ongoing research in Human Geosciences and its possible contributions to SDGs**

*Reiichiro Ishii[1], Makoto Taniguchi[1], Naoki Masuhara[1], Sanghyun Lee[1] (1.Research Institute for Humanity and Nature)

[U04-P03] Contribution of SDGs in Subtropical Islands

*Jun Yasumoto[1] (1.University of the Ryukyus, Faculty of Agriculuture)

[U04-P04] Education for Sustainable Development (ESD) and environmental studies promoted by Seikei Gakuen

*Hitoshi Fujiwara[1], Atsushi MIYASHITA[1], Masumi Zaiki[2], Hironobu Oda[2], Atsuko Ikegami[1] (1.Education and Research Center for Sustainable Development/Faculty of Science and Technology, Seikei University, 2.Education and Research Center for Sustainable Development/Faculty of Economics, Seikei University)

[J] Poster | U (Union)：Union

5:15 PM - 6:30 PM JST | 8:15 AM - 9:30 AM UTC | Ch.01_2

[U-09] Advancing SDGs through inclusive partnerships II: Engaging with communities

convener:Hidenroi Nakamura(Toyama Prefectural University), Vincent Tong(University College London), Mika Shimizu(Kyoto University), Fumiko Noguchi(United Nations University, Institute for the Advanced Study of Sustainability)

[U09-P01] SDGs community and social engagement in education and research: Implication for JpGU

*Hidenroi Nakamura[1] (1.Toyama Prefectural University)

[J] Oral | O (Public)：Public

3:30 PM - 5:00 PM JST | 6:30 AM - 8:00 AM UTC | Ch.01 Zoom Room 01

[O-02] Natural disasters and people -Listen to the voice of the Earth on the Japanese Geoparks-

convener:Noritaka Matsubara(Graduate School of Regional Resource Management, University of Hyogo), Kyohei Sano(Graduate School of Regional Resource Management, University of Hyogo), Suzuka Koriyama(Itoigawa city), Hikaru Yokoyama(Hokusho University), Chairperson:Kyohei Sano(Graduate School of Regional Resource Management, University of Hyogo), Suzuka Koriyama(Itoigawa city), HIROKO IMAI(Com Support Office /Wakayama University Center for Tourism Research), Hokuto Obara(Mine-Akiyoshidai Karst Plateau Geopark Promotion Council), Hikaru Yokoyama(Hokusho University)

3:30 PM - 4:00 PM JST | 6:30 AM - 7:00 AM UTC

[O02-04] Achievements and issues of online program development at Hagi Geopark

*Takaaki Shirai[1] (1.Hagi Geopark Promotion Council)

4:00 PM - 4:30 PM JST | 7:00 AM - 7:30 AM UTC

[O02-05] Our ancestors who overcame natural disasters: A case study focused on Toya-Usu UNESCO Global Geopark

★Invited Papers

*Asami Nakaya[1] (1.Toya-Usu UNESCO GLobal Geopark Council)

4:30 PM - 5:00 PM JST | 7:30 AM - 8:00 AM UTC

[O02-06] The case of One Geopark damaged by 2018 Japan floods -The 3 years for reconstruction of Seiyo City, Ehime Prefecture and the Shikoku Seiyo Geopark-

★Invited Papers

*Takumi Sakakiyama[1] (1.Seiyo City)

[J] Poster | O (Public) : Public

5:15 PM - 6:30 PM JST | 8:15 AM - 9:30 AM UTC | Ch.02_1

[O-02] Natural disasters and people -Listen to the voice of the Earth on the Japanese Geoparks-

convener:Noritaka Matsubara(Graduate School of Regional Resource Management, University of Hyogo), Kyohei Sano(Graduate School of Regional Resource Management, University of Hyogo), Suzuka Koriyama(Itoigawa city), Hikaru Yokoyama(Hokusho University)

[O02-P01] New coronavirus response in Fossa Magna Museum

*Takahiko Ogawara[1], Ko Takenouchi[1], Yousuke Ibaraki[1], Takeo Kobayashi[2], Takuma Katori[2] (1.Fossa Magna Museum, 2.Itoigawa City Hall Geopark Promotion Office)

[O02-P02] Short-Term Effects of SNS Marketing: a Case Study in Hakusan Tedorigawa Geopark

*Susan May[1] (1.Hakusan Tedorigawa Geopark Promotion Council)

[O02-P03] Activities to promote the local sustainable development - Report at the time of spread of COVID-19 infection from Mt.Kurikoma Area Geopark -

*Yui Hasegawa[1], Rie Nakagawa[1], Seiya Tanaka[1], Jun Nagao[1] (1.Mt.Kurikoma Area Geopark Promotion Committee)

[O02-P04] Geotourism in Corona (COVID-19) related crisis - Advantage of being outdoors : In case of San'in Kaigan UNESCO Global Geoprk -

*Noritaka Matsubara[1], NAGAHAMA SATOSHI[1] (1.Graduate School of Regional Resource Management, University of Hyogo)

[O02-P05] Operation of geo-tours using online delivery tools under COVID-19

*Taku Morimoto[1] (1.Unzen Volcanic Area Geopark Promotion Office)

[O02-P06] Holding of event the Lake Shikaribetsu Igloo Village under COVID-19 measures

*Kanamori Syosaku[1], Hiroki Matsumoto[1], Onishi Jun[1] (1.Tokachi-Shikaoi Geopark Promotion Council)

[O02-P07] Stay-at-home Project with Local Students in Toya-Usu UNESCO Global Geopark

*NIRE KAGAYA[1], Yoshiaki Hata[1], Akihito Kato[2], Kiyono Kuroda[2], Koki Takagi[2], Kazuma Iwamura[2], Kanako Kitada[2], Koki Tomita[2], Mina Shionoya[2] (1.Toya-Usu UNESCO Global Geopark Council, 2.Date-Midorigaoka Highschool)

[O02-P08] Developing the San’in Kaigan Geopark Trail and the promotion of geotourism during COVID-19 Pandemic

*Hiroshi Nakase[1] (1.San'in Kaigan Geopark Promotion Council)

[O02-P09] A comparative study of educational on-site and online geotours in Hamamatsu-Hamanako Aspiring Geopark, Japan

*Hiroki Nagano[1], Masato Koyama[2], Yusuke Suzuki[2], Megumi Fukuyama[2] (1.Hamamatsu Technical High School, 2.Shizuoka University)

[O02-P10] Topographic evolution after the Aso-4 pyrocrastic flow and the meaning for disaster prevention in the Oita Bungoono Geopark, Japan

*Toshikazu Yoshioka[1] (1.Oita Bungoono Geopark Promotion Council)

[O02-P11] Conservation and Utillization of Natural Disaster Monument on Tosashimizu Geopark Plan

*Moriguchi Natsuki[1], Satoru Imai[1], Aika Sakuda[1], Kouichi Saruta[1], Michiru Sakai[1] (1.Tosashimizu Geopark Promotion Council)

[O02-P12] Records and countermeasure of disasters in Shimokita Geopark

*Satoshi Ishikawa[1], Kirika Kitagawa[1] (1.Shimokita geopark promotion council)

[O02-P13] Inform of weather disasters in geoparks

*Hiroshi Sato[1,2], Shinichi Sugimoto[3], Makoto Aoi[4], Shinya Miura[4], Hinako Suzuki[4] (1.Mt.Bandai Museum, 2.Bandaisan Geopark Council, 3.Unzen Volcanic Area Global Geopark, 4.National Research Institute for Earth Science and Disaster Resilience)

[O02-P14] How to Prevent Elderly People from Natural Disasters - An Example in Unzen Volcanic Area UNESCO Global Geopark -

Shunsei OGATA[1], Hiyori KADOHATA[1], Tasuku KONDO[1], Miraku TANAKA[1], Kosei HASHIDA[1], Shinsho FUJIO[1], Mizuho IWANAGA[1], Aiko ENGUCHI[1], Seren OTA[1], Rika TANAKA[1], Toru YAMAUCHI[2], Hiroaki OSAKO[2], *Marekazu OHNO[3] (1.Glocal Course of Nagasaki Prefectural Koka High School, 2.Nagasaki Prefectural Koka High School , 3.Unzen Volcanic Area Geopark Promotion Office)

[O02-P15] Disaster and Disaster Prevention Learning in the Naeba-Sanroku Geopark

*Kouhei Nakano[1] (1.Naeba-sanroku Geopark Promotion Council)

[O02-P16] Lives of the local people on the collapsing land and the flowing land by river water -Think about geohazard program of Miyoshi geopark project-

*Azusa Tonotani[1], Katsunori Ozakai[1], Mizuki Tochitani[1], Hiroyuki Ohnishi[1], Toshiaki Matsumoto[1] (1.Geopark Promotion office in Miyoshi city)

[O02-P17] Toward restoration of Geosites damaged by natural disaster with reaching consensus in local community: a case of Suzaki Coast in Seiyo City, Japan.

*Takumi Sakakiyama[1], Kazunari Kimura[2], Yuya Kato[3], Masahito Ono[1], Tsukasa Takahashi[1] (1.Seiyo City, 2.NAIBA Co. Ltd., 3.Noyama Company)

[O02-P18] Let's investigate the earth activity from Shimonita Geopark

*Hara Hideo[1] (1.Geopark Shimonita council)

[O02-P19] **The foundations of Yuzawa Geopark: a unification and a compilation of six geological maps published by the Geological Survey of Japan and Akita Prefecture**

*Akio Sasaki[1], Kohei Yamawaki[1], Yukio Fujimoto[1], Syoichi Goi[1], Shoei Chiba[1] (1.Network of Earth Science Museum for Akita)

[O02-P20] Conservation concerns in Yuzawa Geopark: Distributions and seasonal variation in blood-sucking flies and an invasive plant species

*Haruki Takayanagi[1] (1.Yuzawa City Geopark Promotion Council)

[O02-P21] The relationship between the former plate boundary and residents, especially the signboard production process

*Kato Satomi[1] (1.Mt. Apoi Geopark Promotion Council)

[O02-P22] Fossil collecting experience to solve summer vacation indipendent study in Itoigawa UNESCO Global Geopark

*Yousuke Ibaraki[1], Yutaka Furumi, Emma Longhorn, Takahiko Ogawara[1], Ko Takenouchi[1], Takuma Katori[2], Takeo Kobayashi[2] (1.Fossa Magna Museum, 2.Itoigawa Geopark Council)

[O02-P23] Geosite Map and Card in a Fun and Interesting Way by Local Elementary School Students: a Case Study of Geosite in Nankikumano Geopark with Takaike Elementary School

*Hiroko Shibasaki[1] (1.Nanki-Kumano GeoPark Guide Club)

[O02-P24] **Examples of joint projects (or joint events) between a museum and Sado Island Geopark**

*Takeyoshi SADAKANE[1], Mituhisa AIDA[1] (1.Sado Geopark Promotion Council)

[O02-P25] A Guide program that promote Proactive learning in School trip
- Practice at Toya-Usu UNESCO Global Geopark -

*Hikaru Yokoyama[1] (1.Hokusho University)

[O02-P26] Educational Program on spring water of Aso UNESCO Global Geopark related with elcetrical conductivity (Part 2)
Cooperated Research on Minamiaso Spring Water

*Tsuneomi Kagiyama[1], Koki Nagata[2], Toshikazu Maeda[3], Yuto Takeuchi[3], Haruki Watanabe[3], Kozue Inoue[3] (1.Aso Geopark Promotion Council, 2.Aso Volcano Museum, 3.Takamori Senior High School)

[O02-P27] Looking back on 11 years of the educational activities of the Dinosaur Valley Fukui Katsuyama Geopark

*Sumiaki Machi[1] (1.Dinosaur Valley Fukui Katsuyama Geopark Promotion Council)

[J] Oral | O (Public) : Public

9:00 AM - 10:30 AM JST | 12:00 AM - 1:30 AM UTC | Ch.02 Zoom Room 02

[O-03] How to cope with meteorological disasters under rapidly changing climate

convener:Jun Matsumoto(Deaprtment of Geography, Tokyo Metropolitan University), Akira Wada(Tokyo Institute of Technology), Yukihiro Takahashi(Department of Cosmosciences, Graduate School of Science, Hokkaido University), Chairperson:Yukihiro Takahashi(Department of Cosmosciences, Graduate School of Science, Hokkaido University), Akira Wada(Tokyo Institute of Technology), Jun Matsumoto(Deaprtment of Geography, Tokyo Metropolitan University)

9:00 AM - 9:15 AM JST | 12:00 AM - 12:15 AM UTC

[O03-01] Development of typhoon hazard map and typhoon-shot project; Change the "threat" of a typhoon into a "grace" by 2050!

★Invited Papers

*Fudeyasu Hironori[1] (1.Yokohama National University)

9:15 AM - 9:30 AM JST | 12:15 AM - 12:30 AM UTC

[O03-02] Recent trends in storm and flood damage and the latest efforts on JMA’s weather warnings and information

★Invited Papers

*Takahashi Kenichi[1] (1.Japan Meteorological Agency)

9:30 AM - 9:45 AM JST | 12:30 AM - 12:45 AM UTC

[O03-03] Utilization of typhoon data before the middle 20th century

★Invited Papers

*Fumiaki Fujibe[1] (1.Department of Geography, Tokyo Metropolitan University)

9:45 AM - 10:00 AM JST | 12:45 AM - 1:00 AM UTC

[O03-04] Why was coastal damage due to T1915 concentrated in the Port of Yokohama?

★Invited Papers

*Hitoshi Tamura[1] (1.Port and Airport Research Institute)

10:00 AM - 10:15 AM JST | 1:00 AM - 1:15 AM UTC

[O03-05] Development of coastal monitoring method immediately after typhoon by remote sensing

★Invited Papers

*Yuji Sakuno[1] (1.Graduate School of Advanced Science and Engineering, Hiroshima University)

10:15 AM - 10:30 AM JST | 1:15 AM - 1:30 AM UTC

[O03-06] Proposal of Build Back Better “insurance” scheme for future wind-related disaster risk reduction

★Invited Papers

*Kazuyoshi Nishijima[1] (1.Disaster Prevention Research Institute, Kyoto University)

[J] Oral | O (Public)：Public

10:45 AM - 12:15 PM JST | 1:45 AM - 3:15 AM UTC | Ch.02 Zoom Room 02

[O-03] How to cope with meteorological disasters under rapidly changing climate

convener:Jun Matsumoto(Deaprtment of Geography, Tokyo Metropolitan University), Akira Wada(Tokyo Institute of Technology), Yukihiro Takahashi(Department of Cosmosciences, Graduate School of Science, Hokkaido University), Chairperson:Akira Wada(Tokyo Institute of Technology), Yukihiro Takahashi(Department of Cosmosciences, Graduate School of Science, Hokkaido University), Jun Matsumoto(Deaprtment of Geography, Tokyo Metropolitan University)

10:45 AM - 11:00 AM JST | 1:45 AM - 2:00 AM UTC

[O03-07] Wind-induced damage to buildings and future risk reduction

★Invited Papers

*Yukio Tamura[1] (1.Chongqing University)

11:00 AM - 11:15 AM JST | 2:00 AM - 2:15 AM UTC

[O03-08] Behaviors of infrastructures under extreme wind and future challenges

★Invited Papers

*Tomomi Yagi[1] (1.Kyoto University)

11:15 AM - 11:30 AM JST | 2:15 AM - 2:30 AM UTC

[O03-09] Simultaneous multiple accident cases and their countermeasures for electric power system against Typhoon

★Invited Papers

*Yoshiharu Shumuta[1] (1.Central Research Institute of Electric Power Industry)

11:30 AM - 11:45 AM JST | 2:30 AM - 2:45 AM UTC

[O03-10] Fires Caused by Strong Winds and Storm Surges

★Invited Papers

*U HIROI[1] (1.The University of Tokyo)

11:45 AM - 12:15 PM JST | 2:45 AM - 3:15 AM UTC

[O03-11] Discussion

[J] Oral | O (Public)：Public

9:00 AM - 10:30 AM JST | 12:00 AM - 1:30 AM UTC | Ch.01 Zoom Room 01

[O-04] Suggestion to teaching Earth science under GIGA school from online lesson

convener:Iida Kazuya(Komaba-Toho Junior and Senior High School), Iwata Makoto(Hiroshima Prefectural Ogaki High School), Satoshi Miyajima(Saitama Prefectural Kumagaya High School), Hiroaki Akimoto(Faculty of Economics,Dokkyo University), Chairperson:syo uranaka(Osaka Institute of Technology Graduate School), Hiroaki Akimoto(Faculty of Economics,Dokkyo University), Satoshi Miyajima(Saitama Prefectural Kumagaya High School), Iida Kazuya(Komaba-Toho Junior and Senior High School)

9:00 AM - 9:10 AM JST | 12:00 AM - 12:10 AM UTC

[O04-01] Introduction

9:10 AM - 9:25 AM JST | 12:10 AM - 12:25 AM UTC

[O04-02] The Potential of Online Learning to Realize "Independent and Interactive Deep Learning" in Elementary School Social Studies.

★Invited Papers

*Keiko Nakaya[1] (1.Elementary School Affiliated to the Faculty of Education chiba university)

9:25 AM - 9:40 AM JST | 12:25 AM - 12:40 AM UTC

[O04-03] Utilization of a digital globe system, Dagik Earth, in elementary schools

★Invited Papers

*Akinori Saito[1], Takuya Tsugawa[2], Miho Yamamori[3] (1.Department of Geophysics, Graduate School of Science, Kyoto University, 2.National Institute of Information and Communications Technology, 3.Tsuru University)

9:40 AM - 9:55 AM JST | 12:40 AM - 12:55 AM UTC

[O04-04] Effective use of online lesson and integrate with face to face lesson

★Invited Papers

*Hiroki Ushigome[1] (1.Otsuma nakano Junior and Senior High School)

9:55 AM - 10:10 AM JST | 12:55 AM - 1:10 AM UTC

[O04-05] Student presentations using digital devices In GIGA School Concept

★Invited Papers

*Hidenori Takemura[1] (1.Johoku Junior and Senior high school)

10:10 AM - 10:30 AM JST | 1:10 AM - 1:30 AM UTC

[O04-06] Discussion

[J] Oral | O (Public)：Public

10:45 AM - 12:15 PM JST | 1:45 AM - 3:15 AM UTC | Ch.01 Zoom Room 01

[O-04] Suggestion to teaching Earth science under GIGA school from online lesson

convener:Iida Kazuya(Komaba-Toho Junior and Senior High School), Iwata Makoto(Hiroshima Prefectural Ogaki High School), Satoshi Miyajima(Saitama Prefectural Kumagaya High School), Hiroaki Akimoto(Faculty of Economics,Dokkyo University), Chairperson:Hiroaki Akimoto(Faculty of Economics,Dokkyo University), syo uranaka(Osaka Institute of Technology Graduate School), Satoshi Miyajima(Saitama Prefectural Kumagaya High School), Iida Kazuya(Komaba-Toho Junior and Senior High School)

10:45 AM - 11:00 AM JST | 1:45 AM - 2:00 AM UTC

[O04-07] Report on the Online Teaching Experience with WebGIS in the High School Geography Classes under the COVID-19 Pandemic

★Invited Papers

*Yoshihiko Shibata[1] (1.Tokyo Metropolitan KOKUBUNJI Highschool)

11:00 AM - 11:15 AM JST | 2:00 AM - 2:15 AM UTC

[O04-08] Development of Educational Materials for the Kanagawa version of “Geological Fieldworks conducted in a Classroom" appling for High School Subject "Basic Earth Science" —Using Strata from Ikuta Ryokuchi Park—

★Invited Papers

*Yasushi Fujiwara[1], Shungo Kawagata[2] (1.Graduate School of Education, Yokohama National University, 2.College of Education, Yokohama National University)

11:15 AM - 11:30 AM JST | 2:15 AM - 2:30 AM UTC

[O04-09] Supporting school teachers with GSI’s Toolbox for geography education in the era of Society 5.0

★Invited Papers

*Yuki Kurisu[1] (1.Geospatial Information Authority of Japan)

11:30 AM - 11:45 AM JST | 2:30 AM - 2:45 AM UTC

[O04-10] The trial and error of on-line bidirectional lecture

★Invited Papers

*Yukari Kido[1] (1.Japan Agency for Marine-Earth Science and Technology)

11:45 AM - 12:15 PM JST | 2:45 AM - 3:15 AM UTC

[O04-11] General Discussion

★Invited Papers

*Iida Kazuya[1], Hiroaki Akimoto[2], Iwata Makoto[3], Satoshi Miyajima[4] (1.Komaba-Toho Junior and Senior High School, 2.Faculty of Economics, Dokkyo University, 3.Hiroshima Prefectural Ogaki High School, 4.Saitama Prefectural Kumagaya High School)

[J] Oral | O (Public)：Public

1:45 PM - 3:15 PM JST | 4:45 AM - 6:15 AM UTC | Ch.01 Zoom Room 01

[O-05] How to become a scientist? What can they do?

convener:Natsue Abe(Mantle Drilling Promotion Office, MarE3, Japan Agency for Marine-Earth Science and Technology), Rie Hori, S.(Department of Earth Science, Faculty of Science, Ehime University), Chairperson:Rie Hori(Department of Earth Science, Faculty of Science, Ehime University), Mayumi ARAI(National Museum of Emerging Science and Innovation), Natsue Abe(Mantle Drilling Promotion Office, MarE3, Japan Agency for Marine-Earth Science and Technology), Chiaki T. Oguchi(Institute for Environmental Science and Technology, Graduate School of Science and Engineering, Saitama University)

1:45 PM - 1:50 PM JST | 4:45 AM - 4:50 AM UTC

[O05-01] Introduction

1:50 PM - 2:05 PM JST | 4:50 AM - 5:05 AM UTC

[O05-02] Why do you need a PhD?

★Invited Papers

*Manabe Makoto[1] (1.National Museum of Nature and Science)

2:05 PM - 2:20 PM JST | 5:05 AM - 5:20 AM UTC

[O05-03] From Organic Chemistry, Coral Study to Ocean Policy, My Journey through Carbon

★Invited Papers

*Nobuko Nakamura[1,2] (1.The Ocean Policy Research Institute of The Sasakawa Peace Foundation, 2.Keio Univ.)

2:20 PM - 2:35 PM JST | 5:20 AM - 5:35 AM UTC

[O05-04] Living with solar sytem exploration

★Invited Papers

*Takeshi Imamura[1] (1.Graduate School of Frontier Sciences, The University of Tokyo)

2:35 PM - 2:50 PM JST | 5:35 AM - 5:50 AM UTC

[O05-05] Introduction to IODP and the works inside

★Invited Papers

*Michiko Yamamoto[1] (1.Scripps Institution of Oceanography, UCSD)

2:50 PM - 3:05 PM JST | 5:50 AM - 6:05 AM UTC

[O05-06] I’m working as a nature guide, an environmental activist, and a facilitator.

★Invited Papers

*hisashi Oiwane[1] (1.Musuhi LLC)

3:05 PM - 3:15 PM JST | 6:05 AM - 6:15 AM UTC

[O05-07] Discussion

[J] Poster | O (Public)：Public

5:15 PM - 6:30 PM JST | 8:15 AM - 9:30 AM UTC | Ch.02_2

[O-05] How to become a scientist? What can they do?

convener:Natsue Abe(Mantle Drilling Promotion Office, MarE3, Japan Agency for Marine-Earth Science and Technology), Rie Hori, S.(Department of Earth Science, Faculty of Science, Ehime University)

[O05-P01] Only Ph.D. holders can work in the research and science field?

*Natsue Abe[1,2], Rie Hori, S.[3] (1.Mantle Drilling Promotion Office, MarE3, Japan Agency for Marine-Earth Science and Technology , 2.Graduate School of Natural Science & Technology, Kanazawa University, 3.Ehime University)

[O05-P02] Skills required to work at the science museum

★Invited Papers

*Mayumi ARAI[1] (1.National Museum of Emerging Science and Innovation)

[O05-P03] Discussion

[J] Oral | O (Public)：Public

1:45 PM - 3:15 PM JST | 4:45 AM - 6:15 AM UTC | Ch.02 Zoom Room 02

[O-06] Let's talk about "the 10 years of reconstruction from the Great East Japan Earthquake"

convener:Hitoshi Nakai(Kobuchisawa Research Institute for Nature and Education), Mamoru Hayashi(University of TOYAMA), Tetsuhiko Asano(Senshu University Matsudo Junior High School High School), Chairperson:Mamoru Hayashi(University of TOYAMA), Tetsuhiko Asano(HunabashiKeimei High School), Hitoshi Nakai(Kobuchisawa Research Institute for Nature and Education)

1:45 PM - 2:15 PM JST | 4:45 AM - 5:15 AM UTC

[O06-01] Overview of reconstruction status for the 10th anniversary of the Great East Japan Earthquake

★Invited Papers

*Yoshihiro Okumura[1] (1.Kansai University)

2:15 PM - 2:45 PM JST | 5:15 AM - 5:45 AM UTC

[O06-02] Problems caused by and positive lessons to be inherited from the reconstruction of the Great East Japan Earthquake

★Invited Papers

*Hiromi ENSHU

2:45 PM - 3:15 PM JST | 5:45 AM - 6:15 AM UTC

[O06-03] One decade after the earthquake, reconstruction still not complete

★Invited Papers

*YUKIKO KIKUCHI[1] (1.general incorporated association Otsuchi Shimbun)

[J] Oral | O (Public)：Public

12:30 PM - 1:30 PM JST | 3:30 AM - 4:30 AM UTC | Ch.02 Zoom Room 02

[O-07] Poster presentations by senior high school students

Chairperson:Tatsuhiko Hara(International Institute of Seismology and Earthquake Engineering, Building Research Institute), Katsuyoshi Michibayashi(Department of Earth and Planetary Sciences, Nagoya University), Miwa Kuri(Japan Meteorological Agency), Keiko Konya(Japan Agency for Marine-Earth Science and Technology)

[J] Poster | O (Public) : Public

1:45 PM - 3:15 PM JST | 4:45 AM - 6:15 AM UTC | Ch.27

[O-07] Poster presentations by senior high school students

convener:Tatsuhiko Hara(International Institute of Seismology and Earthquake Engineering, Building Research Institute), Katsuyoshi Michibayashi(Department of Earth and Planetary Sciences, Nagoya University), Miwa Kuri(Japan Meteorological Agency), Keiko Konya(Japan Agency for Marine-Earth Science and Technology)

[O07-P01] Weather in Fukuoka Prefecture in the Edo period from the Nakamura Heizaemon diary

*Rui ANDOU[1], *Rio HAYASHIDA[1], *Hikari ARASE[1], *Mira EGUCHI[1], *Touko HAGIHARA[1] (1.Ikeda Senior High School)

[O07-P02] Discussion on Economic Effects of Muroto Deep Sea Water – How Does Deep Sea Water Industry Contribute to Revitalize the Community? –

*Kaede Yauoka[1] (1.Muroto High School)

[O07-P03] Observation of Columnar Joints and Research on its Origin

Atsushi Watanabe[1], *Iroha Kawaguchi[1], *Ryosuke Sugioka[1], *Mizuki Hukumuro[1], *Akihiro Amamiya[1], *Towa Serizawa[1] (1.Nirayama Highschool)

[O07-P04] A study of microplastics that is included in the rivers and coast of the Izu Peninsula

Atsushi Watanabe[1], *Namiki Kawai[1], *Koji Sadakane[1], *Yuichirou Takahashi[1], *Mayuko Toriikouji[1], *Daisuke Yamamoto[1], *Miori Yabuta[2], *Tubasa Ozawa[2], *Takaya Nishida[2], *Haruki Mimura[2], *Nanami Hujii[2], Ryosuke Yoshida[2] (1.Nirayama Highschool, 2.Shimoda Highschool)

[O07-P05] Consideration of method to increase artificial ruby

Atsushi Watanabe[1], *Yuichirou Nagatsu[1], *Moe Hatakeyama[1], *Koutarou Matsumoto[1], *Yudai Komiyama[1] (1.Nirayama Highschool)

[O07-P06] Earthquake prediction by Electric magnetic wave

*Masayuki Masa[1], *Nozomu Sakai[1], Michiya Sasaki[1], Souhei Kato[1], Ousuke Yagasaki[1], Mizuho Fujiwara[1], Maika Yashima[1] (1. Tokyo Metropolitan Tama High School of Science and Technology)

[O07-P07] Comparison of heated products of glucose with citric acid added

*Takumi Ohtsu[1] (1.Tokyo Metropolitan Tama High School of Science and Technology)

[O07-P08] Development of iron (II) phosphate lithium-ion battery using the adsorption power of Aso loess

*Ayumi Hoshi[1], *Sora Nozaki[1] (1.Tokyo Metropolitan Tama High School of Science and Technology)

[O07-P09] Method of Recovering Perfluorinated Compounds by coffee grounds

*Kouki Morimoto[1], *Issei Yamazeki[1], *Renon Shimizu[1] (1.Tokyo Metropolitan Tama High School of Science and Technology)

[O07-P10] Research into Moriya Formation Formed in Northen Fossa Magna

*Yusuke Morozumi[1] (1.Suwa Seiryo high school)

[O07-P11] A Consideration of a Landing Exploration on Europa

*Taichi Ito[1] (1.Seishin Gakuen High School)

[O07-P12] Relationship between five gigantic jets in the past and cloud-to-ground lightning

*Fuga Suzuki[1], *Yuya Takahashi[1], Sorachi Nishibori[1], Yuki Ito[1], Takumi Miyamoto[1] (1.Shizuoka Prefectural Iwata Minami High School)

[O07-P13] Examination of the fall position by the light emission of the Narashino meteorite fireball

*Ryunosuke Kamiya[1], *Haruka Sato[1], Kosuke Arimura[1], Saki Ozawa[1], Hana Miki[1], Yuka Ogawa[1], Honoka Tanabe[1] (1.Shizuoka Prefectural Iwata Minami High School)

[O07-P14] The Change of Microtopography of Samejima Coast Caused by the Storm Surge Brought by Hagibis

*Takeshi Totsuka[1], Yuya Takahashi[1], *Kosuke Arimura[1], Koki Suzuki[1], Shun Ichikawa[1], Rabu Kato[1] (1.Shizuoka Prefectural Iwata Minami High School)

[O07-P15] Putting legs on snake swimming robot going to be useless?Seeking truth of Tetrapodophis

*Ryoya Sato[1], *Kokoro Ikeda[1], *Ryota Ogawa[1], *Riko Tomioka[1], *Akari Hitomi[1], *Kanon Yamaguchi[1] (1.Tokyo Tech High School of Science and Technology)

[O07-P16] Consideration of snowmelt type lahar at Mt. Katta, Zao

*Haruya Shishido[1], *Reiki Syoji[1], *Ryo Hikichi[1] (1.Miyagi Prefectural Tagajo Senior High School)

[O07-P17] Geological structure of Urato Katsurashima Island and Nonoshima Island, Shiogama City

*Asahi Oyama[1], *Hikaru Sasaki[1], *Yuhi Suzuki[1], *Hayato Murakami[1], *Misaki Kuga[1] (1.Miyagi Prefectural Tagajo Senior High School)

[O07-P18] Threats and impacts of urban tsunami
-Simulate a tsunami when a Nankai Trough giant earthquake occurs using a tsunami generator-

*Misaki Suda[1], *Kenshin Okazaki[1], *Zen Sato[1], *Yusei Niinuma[1], *Kousei Matsuura[1], *Ayaka Akisawa[1] (1.Miyagi Prefectural Tagajo Senior High School)

[O07-P19] Countermeasures against Heat Island Phenomenon: Proposal for a New Building System

*Hiroaki HAYASHI[1] (1.Yokohama Science Frontier High School)

[O07-P20] An evaluation of artificial landform in Chiba prefecture called “Kawamawashi”

*Kodai SHIBUYA[1] (1.Yokohama Science Frontier High School)

[O07-P21] The relationship between sunspot number and typhoons

*Takeru TODA[1] (1.Yokohama Science Frontier High School)

[O07-P22] On the study of Fukui Earthquake Fault IX

*Kazuho Kuwajima[1], *Ryouhei Matta[1], *Youhei Morise[1], *Ayano Yashima[1] (1.Fujishima High School of Fukui prefecture)

[O07-P23] **Approach to the current situation and issues of geothermal power generation utilization based on field surveys**

*Kisho Kurosawa[1], *Tatsuki Miyamoto[1], *Nozomi Kawaharata[1], *Shoki Yashima[1], *Yusuke Oba[1] (1.FurukawaReimei High School)

[O07-P24] Study of mechanism of Light Emission by Spectroscopic Observation of Meteor

*Yui Sato[1], *Yuki Kato[1] (1.Miyagi Prefectual Furukawa Reimei Senior High School)

[O07-P25] Relationship between mineral crystallization and impurities.

*Usami Kenta[1], *Ryo Nakane[1], *Hiroyuki Sueno[1], Syotaro Kawana[1], Ryota Naito[1], Kazuhiko Hoshi[1], Mitsuhide Sai[1], Takuma Watanabe[1] (1.Johoku high school)

[O07-P26] Analysis of water quality of irrigation ponds focused on land use, irrigation systems and periodic pond draining

*Ayane INOUE[1], *Haruto TAKEYAMA[1], *Kousuke MANO[1], *Rio YAMANO[1] (1.Hyogo Prefectural Kakogawa Higashi High School)

[O07-P27] The Process of Raised-Bed River Formation and Factors that Affect It

*Natsuki KAMISASA[1], *Yuta KONDO[1], *Haruto TAKEYAMA[1], *Yasuharu TOMITA[1], *Rikushi NAGAO[1], *Naka NOHAMA[1] (1.Hyogo Prefectural Kakogawa Higashi High School)

[O07-P28] Studies of the SDGs on the Sanriku Geopark. The sea urchin spread trench in the Taneichi Formation.

*Kyougo Sakashita[1], *Asahi Sekibata[1], *Rina Nakajo[1], *Yuto Kugoi[1], *Hikaru Sasaki[1] (1.Marient Chikyu-tanken club senier)

[O07-P29] Studies of the SDGs on the Sanriku Geopark. The Aoba Lake and Shimamori Basin.

*Mizuki Kimura[1], * Naho Simodate[1], *Kahono Hinata[1], *Yuma Keicho[1], *Kouki Takahashi[1] (1.Marient Chikyu-tanken club senier)

[O07-P30] Proposal of Hachinohe Canyon to Sanriku Geopark Geosite.

*Sarina Shinohe[1], * Miyu Abe[1], * Akari Nakamura[1], *Yukihito Yasuhara[1], *Kensuke Shimomura[1] (1.Marient Chikyu-tanken club senier)

[O07-P31] Proposal of an index for estimating the distance from the source rock

*Ayaka Mitsui[1], *Reiji Iwamoto[1], *Keishi Okumi[1], *Mayu Naito[1], *Yamato Yasuhara[1], *Natsuki Yamamoto[1], *Naoko Kodama[1], *Akito Sasaki[1], *Akira Tada[1], *Takuto Nakanou[1], *Tomohiko Maeda[1], *Yuya Muromoto[1], *Ryusei Moriyama[1] (1.Hyogo Prefectural Himejihigashi Senior High School)

[O07-P32] Energy calibration of a cosmic-ray detector

*moe kimura[1] (1.Tokyo Metropolitan Hibiya High School)

[O07-P33] Floating waterdrops using a straw commutator

*Aoba Takahara[1], Yuri Yasui[1], Takaya Sato[1] (1.Niigata Prefectural Takada high school)

[O07-P34] The rotating-Water-tank that is replaced hot water tank and ice water tank

*Masamune Minou[1] (1.Niigata Prefectural Takada high School)

[O07-P35] Comparison of the surface of Mars with the previous one in the approach of Mars Spread of dust storm on November 17th

*Sayaka Mizutani[1], *Takumi Uchiyama[1], Riho Kagami[1], Aoi Takemoto[1] (1.Ichinomiya High School)

[O07-P36] Tumulus inspection project by using cosmic-ray muon

*Tomoyo Ishizawa[1], *Satoshi Ono[1], *Asahi Shiozaki[1], *Wakana Yanagimoto[1], *Kenshiro Aoki[1], *Yuna Ishii[1], *Sogo Kimura[1], *Yuki Shimada[1], *Aoi Soga[1], *Yuga Takemori[1], *Rino Tomiku[1], *Kana Hashizume[1], Miki Ohtsuka[1] (1.Waseda University Honjo Senior High School)

[O07-P37] Calculating the nebula density from the size of the emission nebula

*Yuki Shirai[1] (1.Totsuka High School)

[O07-P38] Strength evaluation of structures by making and improving quake-vibration generators

*Runaya Igari[1], *Yuto Meguro[1], *Rin Goto[1], Kenshiro Kamata[1] (1.Miyagi Rifu high school)

[O07-P39] Time dependence of ocean salinity

*Honami Hashimoto[1], Annu Ito[1] (1.Miyagi Rifu highschool)

[O07-P40] Toward "Solid-State Version Chromatography" Second Report

*Yuichiro Okuno[1], *Akihisa Wada[1], *Yudai Kozono[1], *Ryota Iwamoto[2], *Mai Fujitani[2], *Kyoya Okada[3], *Kusunori Sumi[3], *Arata Fujimoto[3] (1.Imamiya Technology Senior High School of Osaka Prefecture:The evening course, 2.Otemae Senior High School of Osaka Prefecture:The evening course, 3.Kasugaoka Senior High School of Osaka Prefecture:The evening course)

[O07-P41] How to extract bioethanol effectively by distillation.

*Ataru Kunihisa[1] (1.Wakasa high school)

[O07-P42] Confusion of the people in the northwestern area of Saitama Prefecture due to rumors after the 1923 Kanto Earthquake

*Miharu Shinoda[1] (1.Sakae Higashi High School)

[O07-P43] A quest for the best condition of a crystal radio's detection

*Motoaki Osone[1] (1.Yashiro High School)

[O07-P44] What cause columner joint changes?

*Yugo Sakurai[1], *Yuki Enomoto[1], *Kanta Hayashibe[1] (1.Yashiro High School)

[O07-P45] Preliminary analysis of HAYABUSA-2's Doppler-Shift

*Azumi Sofue[1], *Naoko Nishino[1], *Riri Iida[1], *Riri Numata[1] (1.Wakayama Shin-ai Senior High School)

[O07-P46] Estimation of a ceiling thickness using the muography technique with a small cosmic-ray detector

*Nana Kobayashi[1] (1.Kaichi High School)

[O07-P47] A proposal of an inverse analysis method for ballistic ejecta flying focusing on crater shape in phreatic eruption

*Kouki Nishino[1], Neo Suzuki[1], Natsumi Waki[1] (1.Kanagawa Prefectural Yokosuka Senior High School)

[O07-P48] The survey of Micro-Plastics included in River sediments.

*Taichi Ichikawa[1], Ryuke Kawai[1], Suzuka Fukunaga[1], Tessho Yamamoto[1], Takumi Sato[1] (1.GIZAN SENIOR HIGH SCHOOL)

[O07-P49] Relationship between sprites and the lightning charge moment

*syunsuke nakao[1], *sora wake[1] (1.Prefectural Kochi Ozu High School)

[O07-P50] Potential Small Hydropower Generation in Kamikawa Basin -Hydro Energy Map Visualizing Power Generation-

*Airi Takei[1], *Akira Tamaki[1], *Naoki Kudo[1], *Asahi Takahashi[1], *Hikaru Kawashima[1] (1.Hokkaido Asahikawa Nishi High School)

[O07-P51] Consideration of brachiopod biota change events in the Kuzu limestone layer

*Omi Kono[1], Tokio Chiba[1] (1.Kaijo senior high school)

[O07-P52] Estimation of the variation in mechanism in the amount of spring water in Otomeyama Park, Shinjuku City

*Kuya Aoyama[1], Taichi Shimokobe[1], Masamune Kanou[1] (1.Kaijo high school)

[O07-P53] Modeling the earthquake damage in adeveloped land

*Shungo Kokubun[1], *Satoru Takahashi[1], *Hiroshi Takeuchi[1], *Haruki Tamakawa[1], *Masafumi Kaneko[1], Takumi Nanbu[1] (1.Miyagi Prefecture Sendai Daisan High School)

[O07-P54] Influence of Calcium chloride on frost columns

*Manaka Oya[1], Shohei Nanri[1] (1.Ichikawa gakuen Ichikawa senior high school)

[O07-P55] Differences in fog generation conditions in the Edogawa estuary -Examples of Edogawa-ku and Ichikawa-shi-

*Kenta Torii[1], Shohei Nanri[1] (1.Ichikawa gakuen Ichikawa senior high school)

[O07-P56] Development of variable slope type underwater embankment

*Kei Omura[1], Shohei Nanri[1] (1.Ichikawa gakuen Ichikawa senior high school)

[O07-P57] Environmental impact assessment of air and soil substances using spring water of Minowa as an index

*Mari Taki[1], Shohei Nanri[1] (1.Ichikawa gakuen Ichikawa senior high school)

[O07-P58] Development of an automatic meteor shower observation and the notification system ~Web broadcast of meteor appearance~

*Koichi Sato[1], *Koshi Ri[1], *Shunsuke Isoda[1], *Honoka Ohno[1] (1.Chuo University Junior and Senior High School)

[O07-P59] Meteorological and geographical conditions of river flooding-Comparison of the past and present of the Miyata River-

*Eri Yoshida[1], *Minami Oikawa[1], *Kotomi Shibata[1], *Chihiro Terazaki[1], *Kurumi Yabe[1] (1.Ibaraki prefectural Hitachi first senior high school)

[O07-P60] Where are solar panels actually used? Research on the present situation of Kashiwa City, Chiba prefecture, Japan.

*Souri Mizukami[1] (1.SHIBYA SENIOR HIGH SCHOOL)

[O07-P61] Decline and Fall of Martian Polar Capse; Whether the Dast Storm Is Warm the Polar Cap

*Kei Inoue[1], Hibiki Aminaka[1], Yuho Takagi[1], Nanami Yasuda[1], Yuki Tanaka[1], Tomoki Ugawa[1], Rio Mogi[1], Kyouka Miyake[1], Momoha Takashima[1], Mako Misumi[1], Kaho Okada[1] (1.Kumamoto Prefectural Daiichi High School)

[O07-P62] Spacial correlation between slow earthquake and mantle- derived hot spring in Southwest Japan

*Yui Kobayashi[1] (1.Shizuoka Higashi High School)

[O07-P63] **Visualize water current using vitamin B_2**

*Mutsuki Kamata[1], *Yuuma Nakagawa[1], *Io Kato[1], *Tokito Hirose[1], *Yuuki Matsui[1], *Kosuke Mafune[1], *Akihito Yamada[1], Kazumi Igawa[1] (1.Zushi-Kaisei Senior High School)

[O07-P64] Designe of lunar crater exploration rover

*Kosuke Kameoka[1] (1.Meikei High School)

[O07-P65] Distribution of Gravel in the Sakawa River and Factors Affecting the Distribution

*Nozomi Uemachi[1], *Misaki Yamamiya[1], Yosuke Saito[1] (1.Tokyo Gakugei University Senior High School)

[O07-P66] Detection of Cherenkov light with acrylic and photodetecto

*Juri Urano[1], *Yuka Kuze[1], *Kaho Kubota[1] (1.Toshimagaoka Joshigakuen senior high school)

[O07-P67] Research the View of Mt.Fuji with a Self-Made Observation Device

*Ryoo Niigawa[1], *Rin Takezoe[1] (1.Tokyo Metropolitan Tachikawa High School)

[O07-P68] Bad visibility in the past at Tachikawa High School

*Tomoya Ushizaka[1] (1.Tokyo Metropolitan Tachikawa High School)

[O07-P69] Analysis of visibility around Tachikawa High School

*Takumi Yasuhara[1] (1.Tokyo Metropolitan Tachikawa High School)

[O07-P70] The relationship between the shape and power generation amount of the simple wind power generators

*Sora Fukui[1] (1.Tokyo Metropolitan Tachikawa High School)

[O07-P71] **Is « evacuate to rise » the Right Action?**
Research and Proposition of Major Evacuation Routes to Shelters in Shibuya

*Sakura Oona Marie Sueoka[1] (1.Tokyo Metropolitan Kokusai High School)

[O07-P72] Mechanism of how the Shirata river looks blue

*Shuhei Sugai[1], *Ryosuke Yoshida[1] (1.Shimoda high school)

[O07-P73] Determining the Properties of Seyfert Galaxies

*Kuya ABE[1], *Kuranosuke IEHATA[1], *Koki TANII[1], *Tamotsu FUJIMOTO[1] (1.Nara Prefectural Seisho High School)

[O07-P74] Observation of Radio Waves from the Moon

*Koya YAMASHITA[1], *Ichika TSUTSUMI[1], *Atsushi HIRANUMA[1], *Ikumi MATSUYOSHI[1] (1.Nara Prefectural Seisho High School)

[O07-P75] Making Snow Meter Using Neutron Cosmic Rays Observation Data Collected By Cosmic Watch

*Kei Ikushima[1], Rikako Kono[2], Kaduo Tanaka[2], Akita Yuji[1] (1.Hiroo Gakuen High School, 2.Touhoku University)

[O07-P76] Water storage capacity of the green dam – Role of forest soil -

*Nanami Aoki[1] (1.Kyoto Prefectural Sagano High School)

[O07-P77] Measurement of Radon Concentration for Earthquake Prediction in the Woods for Field Practice Owned by Sagano H. S.

*Ayaka Kawabata[1], *Takahiro Kawabata[2] (1.Kyoto Prefectural Sagano High School, 2.Graduate School of Science, Osaka University)

[J] Poster | O (Public)：Public

1:45 PM - 3:15 PM JST | 4:45 AM - 6:15 AM UTC | Ch.28

[O-07] Poster presentations by senior high school students

convener:Tatsuhiko Hara(International Institute of Seismology and Earthquake Engineering, Building Research Institute), Katsuyoshi Michibayashi(Department of Earth and Planetary Sciences, Nagoya University), Miwa Kuri(Japan Meteorological Agency), Keiko Konya(Japan Agency for Marine-Earth Science and Technology)

[E] Oral | P (Space and Planetary Sciences)：P-PS Planetary Sciences

9:00 AM - 10:30 AM JST | 12:00 AM - 1:30 AM UTC | Ch.04 Zoom Room 04

[P-PS04] Small Solar System Bodies: A New Insight from Hayabusa2, OSIRIS-REx and Other Space Missions

convener:Tatsuaki Okada(Institute of Space and Astronautical Science, Japan Aerospace Exploration Agency), Taishi Nakamoto(Tokyo Institute of Technology), Daisuke Kuroda(Kyoto University), Chairperson:Tatsuaki Okada(Institute of Space and Astronautical Science, Japan Aerospace Exploration Agency), Taishi Nakamoto(Tokyo Institute of Technology), YACHEN YANG(Center for Space and Remote Sensing Research)

9:00 AM - 9:05 AM JST | 12:00 AM - 12:05 AM UTC

[PPS04-01] Introduction

9:05 AM - 9:20 AM JST | 12:05 AM - 12:20 AM UTC

[PPS04-02] Interdisiplinary Science of Hayabusa2 Mission

*Sei-ichiro WATANABE[1], Hikaru Yabuta[2], Koji Wada[3], Naru Hirata[4], Naoyuki Hirata[5], Yuri Shimaki[7], Rina Noguchi[7], Seiji Sugita[6], Kohei Kitazato[4], Tatsuaki Okada[7], Noriyuki Namiki[8], Shogo Tachibana[6,7], Masahiko Arakawa[5], Satoshi Tanaka[7] (1.Nagoya University, 2.Hiroshima University, 3.Chiba Institute of Technology, 4.University of Aizu, 5.Kobe University, 6.University of Tokyo, 7.JAXA/ISAS, 8.National Astronomical Observatory)

9:20 AM - 9:35 AM JST | 12:20 AM - 12:35 AM UTC

[PPS04-03] Progress report of initial description of the C-type asteroid Ryugu samples returned by Hayabusa2

*Toru Yada[1], Masanao Abe[1], Aiko Nakato[1], Kasumi Yogata[1], Akiko Miyazaki[1], Kazuya Kumagai[2], Kentaro Hatakeda[2], Tatsuaki Okada[1], Masahiro Nishimura[1], Shizuho Furuya[1], Yoshitake Miwa[1], Ayako Iwamae[2], Lucie Liu[1], Lionel Lourit[3], Cedric Pilorget[3], Vincent Hamm[3], Jean-Pierre Bibring[3], Yuichiro Cho[4], Koki Yumoto[4], Yuna Yabe[4], Seiji Sugita[4], Shogo Tachibana[4], Hirotaka Sawada[1], Sakamoto Kanako[1], Tasuku Hayashi[1], Daiki Yamamoto[1], Ryota Fukai[1], Haruna Sugahara[1], Hisayoshi Yurimoto[5], Tomohiro Usui[1], Sei-ichiro WATANABE[6], Yuichi Tsuda[1] (1.Japan Aerospace Exploration Agency, 2.Marine Works Japan, 3.Institut D'Astrophysique Spatiale, 4.University of Tokyo, 5.Hokkaido University, 6.Nagoya University)

9:35 AM - 9:50 AM JST | 12:35 AM - 12:50 AM UTC

[PPS04-04] EXPERIMENTAL STUDY ON IMPACT CRATERS FORMED ON MOUNTAIN-LIKE SURFACE TOPOGRAPHY OF ASTEROIDS

*Yusaku Yokota[1], Masahiko Arakawa[1], Minami Yasui[1], Yuya Yamamoto[1], Sunao Hasegawa[2], Hatsune Okawa[1] (1.Graduate School of Science, Kobe University, 2.Japan Aerospace Exploration Agency)

9:50 AM - 10:10 AM JST | 12:50 AM - 1:10 AM UTC

[PPS04-05] The collisional history in the Main Belt

★Invited Papers

*Hiroshi Kobayashi[1] (1.Department of Physics, Nagoya University)

10:10 AM - 10:30 AM JST | 1:10 AM - 1:30 AM UTC

[PPS04-06] Internal structure of pebble-pile comets inferred from thermal and mechanical properties of dust aggregates

★Invited Papers

*Sota ARAKAWA[1] (1.National Astronomical Observatory of Japan)

[E] Oral | P (Space and Planetary Sciences)：P-PS Planetary Sciences

10:45 AM - 12:15 PM JST | 1:45 AM - 3:15 AM UTC | Ch.04 Zoom Room 04

[P-PS04] Small Solar System Bodies: A New Insight from Hayabusa2, OSIRIS-REx and Other Space Missions

convener:Tatsuaki Okada(Institute of Space and Astronautical Science, Japan Aerospace Exploration Agency), Taishi Nakamoto(Tokyo Institute of Technology), Daisuke Kuroda(Kyoto University), Chairperson:Tatsuaki Okada(Institute of Space and Astronautical Science, Japan Aerospace Exploration Agency), Taishi Nakamoto(Tokyo Institute of Technology), YACHEN YANG(Center for Space and Remote Sensing Research)

10:45 AM - 11:00 AM JST | 1:45 AM - 2:00 AM UTC

[PPS04-07] Predicted strength, microporosity, thermal conductivity and grain density of Ryugu rock samples

*Jens Biele[1], Matthias Grott[2], Patrick Michel[3], Tatsuaki Okada[4], Seiji Sugita[5], Naoya Sakatani[6], Wladimir Neumann[2,7], Shingo Kameda[6], Tatsuhiro Michikami[8], Chikatoshi Honda[9] (1.German Aerospace Center, Cologne, Germany, 2.German Aerospace Center, Berlin, Germany, 3.Université Côte d'Azur, Observatoire de la Côte d'Azur, CNRS, Laboratoire Lagrange, Nice, France , 4.Japan Aerospace Exploration Agency, ISAS, Sagamihara, Japan, 5.University of Tokyo, Tokyo, Japan, 6.Rikkyo University, Tokyo, Japan, 7.Klaus-Tschira-Labor für Kosmochemie, Institut für Geowissenschaften, Universität Heidelberg, Heidelberg, Germany, 8.Kindai University, Hiroshima, Japan, 9.University of Aizu, Aizu-Wakamatsu, Japan)

11:00 AM - 11:15 AM JST | 2:00 AM - 2:15 AM UTC

[PPS04-08] Analysis of the temperature distributions of boulders on C-type asteroid 162173 Ryugu observed in low altitude operation of the asteroid explorer Hayabusa2

*Ayumu Ohsugi[1,2], Naoya Sakatani[3], Yuri Shimaki[2], Hiroki Senshu[4], Takehiko Arai[5], Hirohide Demura[6], Toru Kouyama[7], Tomohiko Sekiguchi[8], Satoshi Tanaka[2], Tetsuya Fukuhara[3], Tatsuaki Okada[1,2] (1.Graduate School of Science, The University of Tokyo, 2.Institute of Space and Astronautical Science, Japan Aerospace Exploration Agency, 3.Department of Physics, College of Science, Rikkyo University, 4.Planetary Exploration Research Center, Chiba Institute of Technology, 5.Faculty of Engineering, Department of Innovative Engineering, Division of Systems and Information Engineering,Ashikaga University, 6.Department of Computer Science and Engineering, University of Aizu, 7.National Institute of Advanced Industrial Science and Technology, 8.Hokkaido University of Education)

11:15 AM - 11:30 AM JST | 2:15 AM - 2:30 AM UTC

[PPS04-09] Surface Age of Ryugu's Boulders Based on Small Crater Statistics

*Yudai Takai[1], Tomokatsu Morota[1], Koki Yumoto[1], Rie Honda[2], Shingo Kameda[3], Eri Tatsumi[1,4], Yuichiro Cho[1], Kazuo Yoshioka[1], Hirotaka Sawada[5], Yasuhiro Yokota[2,5], Naoya Sakatani[3], Masahiko Hayakawa[5], Moe Matsuoka[5], Manabu Yamada[6], Toru Kouyama[7], Hidehiko Suzuki[8], Chikatoshi Honda[9], Kazunori Ogawa[5,10], Seiji Sugita[1] (1.University of Tokyo, 2.Kochi University, 3.Rikkyo University, 4.Instituto de Astrofísica de Canarias, 5.JAXA, 6.Chiba Institute of Technology, 7.National Institute of Advanced Industrial Science and Technology, 8.Meiji University, 9.The University of Aizu, 10.Kobe University)

11:30 AM - 11:45 AM JST | 2:30 AM - 2:45 AM UTC

[PPS04-10] Space weathering of bright boulders inferred from the spectral comparison between SCI crater and blue regions on Ryugu

*Minami Aoki[1], Chiho Sugimoto[1], Koki Yumoto[1], Naofumi Takaki[1], ERI TATSUMI[2,1], Tomokatsu Morota[1], Yasuhiro Yokota[3], Masahiko Arakawa[4], Seiji Sugita[1] (1.Department of Earth and Planetary Science, Graduate School of Science, The University of Tokyo, 2.Instituto de Astrofísica de Canarias, 3.JAXA/ISAS, 4.Kobe University)

11:45 AM - 12:00 PM JST | 2:45 AM - 3:00 AM UTC

[PPS04-11] Estimation of space weathering timescale using the number of mottles on the boulder in Hayabusa/AMICA images

*Sunho Jin[1], Masateru Ishiguro[1] (1.Seoul National University)

12:00 PM - 12:15 PM JST | 3:00 AM - 3:15 AM UTC

[PPS04-12] The Chemical Composition of Interstellar Dust in Light of the DESTINY$^+$ Mission: A Novel Tool to Measure the Elemental Abundances and Ionization of the Local Interstellar Cloud

*Hiroshi Kimura[1], Masanori Kobayashi[1], Tomoko Arai[1], DDA Team / DESTINY+ (1.Planetary Exploration Research Center, Chiba Institute of Technology)

[E] Oral | P (Space and Planetary Sciences)：P-PS Planetary Sciences

1:45 PM - 3:15 PM JST | 4:45 AM - 6:15 AM UTC | Ch.04 Zoom Room 04

[P-PS04] Small Solar System Bodies: A New Insight from Hayabusa2, OSIRIS-REx and Other Space Missions

convener:Tatsuaki Okada(Institute of Space and Astronautical Science, Japan Aerospace Exploration Agency), Taishi Nakamoto(Tokyo Institute of Technology), Daisuke Kuroda(Kyoto University), Chairperson:Tatsuaki Okada(Institute of Space and Astronautical Science, Japan Aerospace Exploration Agency), Taishi Nakamoto(Tokyo Institute of Technology), YACHEN YANG(Center for Space and Remote Sensing Research)

1:45 PM - 2:00 PM JST | 4:45 AM - 5:00 AM UTC

[PPS04-13] Regional photometric properties on asteroid Ryugu in visible wavelength

*Yasuhiro Yokota[1], Rie Honda[2], Eri Tatsumi[3], Deborah Domingue[4], Stefanus E. Schröder[5], Moe Matsuoka[1], Lucie Riu[1], Seiji Sugita[6], Tomokatsu Morota[6], Naoya Sakatani[7], Chikatoshi Honda[8], Yuichiro Cho[6], Shingo Kameda[7], Toru Kouyama[9], Manabu Yamada[10], Masahiko Hayakawa[1], Hiroki Senshu[10], Hidehiko Suzuki[11], Kazuo Yoshioka[6], Hirotaka Sawada[1], Kazunori Ogawa[1] (1.ISAS/JAXA, Japan, 2.Kochi Univ., Japan, 3.Instituto de Astrofisica de Canarias, Univ. of La Laguna, Spain, 4.Planetary Science Institute, USA, 5.DLR, Germany, 6.Univ. of Tokyo, Japan, 7.Rikkyo Univ., Japan, 8.Univ. of Aizu, Japan, 9.AIST, Japan, 10.Chiba Inst. Tech, Japan, 11.Meiji Univ., Japan)

2:00 PM - 2:15 PM JST | 5:00 AM - 5:15 AM UTC

[PPS04-14] Spectrophotometric behavior of Ryugu's surface as inferred from the Hayabusa2/NIRS3 data

*Andrea Longobardo[1], Ernesto Palomba[1,2], Anna Galiano[1], Fabrizio Dirri[1], Angelo Zinzi[2], Mario D'Amore[3], Deborah Domingue[4], Kohei Kitazato[5], Takahiro Iwata[6], Moe Matsuoka[6], Takahiro Hiroi[7], Driss Takir[8], Tomoki Nakamura[9], Masanao Abe[5], Makiko Ohtake[5], Shuji Matsuura[10], Sei-ichiro WATANABE[6,11], Makoto Yoshikawa[6], Takanao Saiki[6], Tatsuaki Okada[6], Yukio Yamamoto[6], Yoh Takei[6], Kei Shirai[6], Naru Hirata[5], Naoyuki Hirata[12], Koji Matsumoto[13], Yuichi Tsuda[6] (1.Istituto Nazionale di Astrofisica - Istituto di Astrofisica e Planetologia Spaziali, Rome, Italy, 2.ASI-SSDC, Rome, Italy, 3.German Aerospace Center, Institute of Planetary Research, Berlin, Germany, 4.PSI, Tucson, AZ, USA, 5.University of Aizu, Aizu-Wakamatsu 965-8580, Fukushima, Japan, 6.ISAS-JAXA, Japan, 7.Department of Earth, Environmental and Planetary Sciences, Brown University, Providence, RI 02912, USA, 8.Jacobs/NASA Johnson Space Center, USA, 9.Tohoku University, Miyagi, Japan, 10.Kwansei Gakuin University, Hyogo, Japan, 11.Nagoya University, Nagoya 464-8601, Japan, 12.Kobe University, Kobe 657-8501, Japan, 13.National Astronomical Observatory of Japan, Mitaka 181-8588, Japan)

2:15 PM - 2:30 PM JST | 5:15 AM - 5:30 AM UTC

[PPS04-15] Laboratory spectral constraints on the composition and origin of Phobos: Reconciling the Vis-NIR/Mid-IR contradictions

*Matthew Izawa[1], Sandra Potin[2], Edward Cloutis[2] (1.Institute for Planetary Materials, 2.University of Winnipeg)

2:30 PM - 2:45 PM JST | 5:30 AM - 5:45 AM UTC

[PPS04-16] UNSUPERVISED LEARNING OF NIRS3 DATA: RYUGU SPECTRAL SURFACE REGIONS CLASSIFICATION

*Mario D'Amore[1], E. Palomba[2,3], A. Galiano[2], A. Zinzi[3], F. Dirri[2], A. Longobardo[2], K. Kitazato[4], T. Iwata[5], M. Matsuoka[5], T. Hiroi[6], D. Takir[7], T. Nakamura[8], M. Abe[5], M.y Ohtake[5], S. Matsuura[9], S. Watanabe[10], M. Yoshikawa[5], T. Saiki[5], S. Tanaka[5], T. Okada[5], Y. Yamamoto[5], Y. Taikei[5], K. Shirai[5], N. Hirata[11,4], K. Matsumoto[12], Y. Tsuda[5] (1.German Aerospace Center, Institute of Planetary Research, Berlin, Germany, 2.INAF-IAPS, Rome, Italy, 3.SSDC-ASI, Rome, Italy, 4.University of Aizu, Aizu-Wakamatsu 965-8580, Fukushima, Japan, 5.Institute of Space and Astronautical Science (ISAS), Japan Aerospace Exploration Agency, Sagamihara, 252-5210, Japan, 6.Department of Earth, Environmental and Planetary Sciences, Brown University, Providence, RI 02912, USA, 7.Jacobs/NASA Johnson Space Center, USA, 8.Tohoku University, Miyagi, Japan, 9.Kwansei Gakuin University, Hyogo, Japan, 10.Nagoya University, Nagoya 464-8601, 11.Kobe University, Kobe 657-8501, Japan, 12.National Astronomical Observatory of Japan, Mitaka 181-8588, Japan.)

2:45 PM - 3:00 PM JST | 5:45 AM - 6:00 AM UTC

[PPS04-17] Quantitative analysis of spectral evolution of craters, boulders, and regolith on Ryugu and Bennu

*Koki Yumoto[1], Eri Tatsumi[2,1], Tatsuki Ebihara[1], DellaGiustina Daniella[3], Naofumi Takaki[1], Tomokatsu Morota[1], Yuichiro Cho[1], Golish Dathon[3], Rie Honda[4], Shingo Kameda[5], Yasuhiro Yokota[6], Naoya Sakatani[5], Toru Kouyama[7], Sawada Hirotaka[6], Masahiko Hayakawa[6], Matsuoka Moe[6], Manabu Yamada[8], Hidehiko Suzuki[9], Chikatoshi Honda[10], Kazunori Ogawa[11,12], Kazuo Yoshioka[1], Seiji Sugita[1] (1.University of Tokyo, 2.Instituto de Astrofísica de Canarias,

3.Lunar and Planetary Laboratory, Univ. of Arizona, 4.Kochi Univ., 5.Rikkyo Univ., 6.ISAS/JAXA, 7.Inst. of Adv. Ind. Sci. and Tech., 8.Chiba Inst. of Tech., 9.Meiji Univ., 10.Univ. of Aizu, 11.JSEC/JAXA, 12.Kobe Univ.)

3:00 PM - 3:15 PM JST | 6:00 AM - 6:15 AM UTC

[PPS04-18] Bennu's Global Geologic Map Reveals the Last Epoch of Resurfacing

*Erica R Jawin[1], Timothy J McCoy[1], Kevin John Walsh[2], Harold C Connolly[3], Ronald L Ballouz[4], Andrew Joseph Ryan[4], Maurizio Pajola[5], Olivier S Barnouin[6], Hannah H kaplan[7], Vicky E Hamilton[2], Josh P Emery[8], Daniella N Dellagiustina[4], Daniel Jay Scheeres[9], Michael G Daly[10], Carina A Bennett[4], Dathon R Golish[4], Mark Perry[6], R Terik Daly[6], E Beau Bierhaus[11], Michael C Nolan[4], Heather L Enos[4], Dante S Lauretta[4] (1.Smithsonian National Museum of Natural History, 2.Southwest Research Institute, 3.Rowan University, 4.University of Arizona, 5.INAF-Astronomical Observatory of Padova, 6.Johns Hopkins University Applied Physics Laboratory, 7.Goddard Space Flight Research Center, 8.Northern Arizona University, 9.University of Colorado, Boulder, 10.York University, 11.Lockheed Martin Space)

[E] Oral | P (Space and Planetary Sciences)：P-PS Planetary Sciences

3:30 PM - 5:00 PM JST | 6:30 AM - 8:00 AM UTC | Ch.04 Zoom Room 04

[P-PS04] Small Solar System Bodies: A New Insight from Hayabusa2, OSIRIS-REx and Other Space Missions

convener:Tatsuaki Okada(Institute of Space and Astronautical Science, Japan Aerospace Exploration Agency), Taishi Nakamoto(Tokyo Institute of Technology), Daisuke Kuroda(Kyoto University), Chairperson:Tatsuaki Okada(Institute of Space and Astronautical Science, Japan Aerospace Exploration Agency), Taishi Nakamoto(Tokyo Institute of Technology), YACHEN YANG(Center for Space and Remote Sensing Research)

3:30 PM - 3:50 PM JST | 6:30 AM - 6:50 AM UTC

[PPS04-19] Impact histories inferred from exogenic boulders on asteroids Ryugu and Bennu

★Invited Papers

*ERI TATSUMI[1,2], Chiho Sugimoto[2], Seiji Sugita[2], Marcel Popescu[4], Humberto Campins[11], Julia de León[3], Amy A. Simon[5], Hannah H. Kaplan[6], Yuichiro Cho[2], Tomokatsu Morota[2], Rie Honda[7], Shingo Kameda[8], Yasuhiro Yokota[3], Koki Yumoto[2], Minami Aoki[2], Daniella N. DellaGiustina[10], Dathon R. Golish[10], Javier Licandro[1], Juan Luis Rizos[1], Takahiro Hiroi[12], Deborah Domingue[13], Michel Patrick[14], Dante S. Lauretta[10], Manabu Yamada[15], Naoya Sakatani[8], Toru Kouyama[9], Chikatoshi Honda[16], Masahiko Hayakawa[3], Moe Matsuoka[3], Hidehiko Suzuki[17], Kazunori Ogawa[3], Hirotaka Sawada[3] (1.Instituto de Astrofisica de Canarias, 2.Univ. of Tokyo, 3.ISAS/JAXA, 4.Astronomical Institute of the Romanian Academy, 5.NASA Goddard Space Flight Center, 6.Southwest Research Institute, 7.Kochi Univ., 8.Rikkyo Univ., 9.AIST, 10.Univ. of Arizona, 11.Univ. of Central Florida, 12.Brown Univ., 13.Planetary Science Institute, 14.Observatoire de la Côte d'Azur, 15.Chiba Institute of Tech., 16.Univ. of Aizu, 17.Meiji Uni.)

3:50 PM - 4:10 PM JST | 6:50 AM - 7:10 AM UTC

[PPS04-20] The ESA Hera mission: rendezvous with a binary asteroid, planetary defense and science

★Invited Papers

*Patrick Michel[1], Michael Kueppers[2], Alan Fitzsimmons[3], Simon F. Green[4], Monica Lazzarin[5], Stephan Ulamec[6], Ian Carnelli[7], Paolo Martino[7] (1.Universite Côte D'Azur, Observatoire De La Côte D'Azur, CNRS, Laboratoire Lagrange, 2.ESA-European Space Astronomy Centre, 3.Queen's University Belfast, 4.The Open University, 5.Padova University, 6.DLR RB-MUSC, 7.ESA-ESTEC)

4:10 PM - 4:25 PM JST | 7:10 AM - 7:25 AM UTC

[PPS04-21] Hayabusa2 Extended Mission to rendezvous with Asteroid 1998 KY26: Investigations of an extremely small fast rotator for planetary defense

*Masatoshi Hirabayashi[1], Y. Mimasu[2], N. Sakatani[3], S. Watanabe[4], Y. Tsuda[2], T. Saiki[2], S. Kikuchi[2], T. Kouyama[5], M. Yoshikawa[2], S. Tanaka[2], S. Nakazawa[2], Y. Takei[2], F. Terui[2], H. Takeuchi[2], A. Fujii[2], T. Iwata[2], K. Tsumura[6], S. Matsuura[7], Y. Shimaki[2], S. Urakawa[8], Y. Ishibashi[9], S. Hasegawa[2], M. Ishiguro[10], D. Kuroda[11], S. Okumura[8], S. Sugita[12], T. Okada[2], S. Kameda[3], S. Kamata[13], A. Higuchi[14], H. Senshu[15], H. Noda[16], K. Matsumoto[16], R. Suetsugu[17], T. Hirai[15], K. Kitazato[18] (1.Auburn University, 2.Japan Aerospace Exploration Agency, 3.Rikkyo University, 4.Nagoya University, 5.National Institute of Advanced Industrial Science and Technology, 6.Tokyo City University, 7.Kwansei Gakuin University, 8.Japan Spaceguard Association, 9.Hosei University, 10.Seoul National University, 11.Kyoto University, 12.University of Tokyo, 13.Hokkaido University, 14.University of Occupational and Environmental Health, 15.Chiba Institute of Technology, 16.National Astronomical Observatory of Japan, 17.National Institute of Technology, 18.University of Aizu)

4:25 PM - 4:40 PM JST | 7:25 AM - 7:40 AM UTC

[PPS04-22] **Highly Time-Resolved Photometric Observations of Tiny Near Earth Objects with the Tomo-e Gozen Camera**

*Jin Beniyama[1], Shigeyuki Sako[1], Ryou Ohsawa[1], Satoshi Takita[1], Naoto Kobayashi[1], Shin-ichiro Okumura[2], Seitaro Urakawa[2], Fumihiko Usui[3], Fumi Yoshida[4,5], Makoto Yoshikawa[3] (1.Institute of Astronomy, Graduate School of Science, The University of Tokyo, 2.Japan Spaceguard Association, 3.Institute of Space and Astronautical Science, Japan Aerospace Exploration Agency, 4.University of Occupational and Environmental Health, 5.Planetary Exploration Research Center, Chiba Institute of Technology)

4:40 PM - 4:55 PM JST | 7:40 AM - 7:55 AM UTC

[PPS04-23] Color and size distributions of main belt asteroids obtained by the Subaru/Hyper Suprime-Cam

*Natsuho Maeda[1], Tsuyoshi Terai[2], Keiji Ohtsuki[1], Fumi Yoshida[3,4], Kosuke Ishihara[1,2,5], Takuto Deyama[1,6] (1.Graduate school of science, Kobe University , 2.National Astronomical Observatory of Japan, 3.Chiba Institute of

Technology, 4.University of Occupational and Environmental Health, 5.The Graduate University for Advanced Studies, 6.NTT Data MSE Corporation)

4:55 PM - 5:00 PM JST | 7:55 AM - 8:00 AM UTC

[PPS04-24] Discussion

[E] Poster | P (Space and Planetary Sciences)：P-PS Planetary Sciences

5:15 PM - 6:30 PM JST | 8:15 AM - 9:30 AM UTC | Ch.04_1

[P-PS04] Small Solar System Bodies: A New Insight from Hayabusa2, OSIRIS-REx and Other Space Missions

convener:Tatsuaki Okada(Institute of Space and Astronautical Science, Japan Aerospace Exploration Agency), Taishi Nakamoto(Tokyo Institute of Technology), Daisuke Kuroda(Kyoto University)

[PPS04-P01] Comparison of original orbits of Oort Cloud new comets given in various catalogues II. Different solutions from different observations

*Takashi Ito[1] (1.National Astronomical Observatory of Japan, National Institutes of Natural Science)

[PPS04-P02] Characteristics of high-albedo C-complex asteroids

*Sunao Hasegawa[1], Toshihiro Kasuga[2], Fumihiko Usui[1,3], Kuroda Daisuke[4] (1.Japan Aerospace Exploration Agency, 2.National Astronomical Observatory of Japan, 3.Kobe University, 4.Kyoto University)

[PPS04-P03] Thermal Radiation Pressure as a Possible Mechanism for Losing Small Particles from Near-Sun Asteroids

*Yoonsoo P. Bach[1], Masateru Ishiguro[1] (1.Department of Physics and Astronomy, Seoul National University)

[PPS04-P04] Implications of High Polarization Degree for the Surface State of Ryugu

*Daisuke Kuroda[1], Jooyeon Geem[2], Hiroshi Akitaya[3], Sunho Jin[2], Jun Takahashi[4], Koki Takahashi[5], Hiroyuki Naito[6], Kana Makino[7], Tomohiko Sekiguchi[5], Yoonsoo P. Bach[2], Jinguk Seo[2], Shuji Sato[8], Hiroshi Sasago[9], Koji S. Kawabata[3], Aoi Kawakami[4], Miyako Tozuka[4], Makoto Watanabe[10], Seiko Takagi[11], Kiyoshi Kuramoto[11], Makoto Yoshikawa[12], Sunao Hasegawa[12], Masateru Ishiguro[2] (1.Kyoto University, 2.Seoul National University, 3.Hiroshima University, 4.University of Hyogo, 5.Hokkaido University of Education, 6.Nayoro Observatory, 7.Nayoro City University, 8.Nagoya University, 9.Sasago Co.,Ltd., 10.Okayama University of Science, 11.Hokkaido University, 12.Japan Aerospace Exploration Agency)

[PPS04-P05] Three-dimensional tracking of ejecta particle: Effects of boulder size on ejecta velocity distribution

*Hatsune Okawa[1], Mizuno Toda[2], Masahiko Arakawa[1], Minami Yasui[1], Sunao Hasegawa[3], Yusaku Yokota[1], Yuya Yamamoto[1] (1.Graduate School of Science, Kobe University, 2.Science Department, Kobe University, 3.Japan Aerospace Exploration Agency)

[PPS04-P06] Experimental study on momentum transfer in high-velocity impact on asteroid

Kazuhiro Horikawa[1], *Masahiko Arakawa[1], Minami Yasui[1], Kei Shirai[1], Sunao Hasegawa[2] (1.Graduate School of Science, Kobe Univ., 2.ISAS, JAXA)

[PPS04-P07] Reconstruction of the past rotation state of asteroid (162173) Ryugu from a crater shape analysis

*Riona Yamada[1], Sei-ichiro Watanabe[1], Tomokatsu Morota[2], Naru Hirata[3], Naoyuki Hirata[4], Yuri Shimaki[5], Rina Noguchi[5], Rie Honda[6], Shingo Kameda[7], Manabu Yamada[8], Naoya Sakatani[7], Eri Tatsumi[9], Toru Kouyama[10], Yasuhiro Yokota[5,6], Yuichiro Cho[2], Hidehiko Suzuki[11], Masahiko Hayakawa[5], Moe Matsuoka[5], Chikatoshi Honda[3], Kazuo Yoshioka[2], Hirotaka Sawada[5], Kazunori Ogawa[5], Seiji Sugita[2] (1.Nagoya University, 2.University of Tokyo, 3.University of Aizu, 4.Kobe University, 5.JAXA, 6.Kochi University, 7.Rikkyo University, 8.Chiba Institute of Technology, 9.La Laguna University, 10.AIST, 11.Meiji University)

[PPS04-P08] Thermally Controlled Crack Orientation of Boulders on Ryugu: N-S Preference and Exfoliation Structure

*Sho Sasaki[1], Shiho Kanda[1], Hiroshi Kikuchi[2], Tatsuhiro Michikami[3], Tomokatsu Morota[4], Chikatoshi Honda[5], Hideaki Miyamoto[4], Ryodo Hemmi[4], Seiji Sugita[4], ERI TATSUMI[4,6], Masanori Kanamaru[2], Sei-ichiro WATANABE[7], Noriyuki Namiki[8], Patrik Michel[9], Masatoshi Hirabayashi[10], Naru Hirata[5], Tomoki Nakamura[11], Takaaki Noguchi[12], Takahiro Hiroi[13], Koji Matsumoto[8], Hirotomo Noda[8], Naoya Sakatani[14], Shingo Kameda[14], Toru Kouyama[15], Hidehiko Suzuki[16], Manabu Yamada[17], Rie Honda[18], Yuichiro Cho[4], Kazuo Yoshioka[4], Masahiko Hayakawa[2], Moe Matsuoka[2], Rina Noguchi[2], Hirotaka Sawada[2], Yasuhiro Yokota[2,18], Makoto Yoshikawa[2] (1.Department of Earth and Space Sciences, School of Science, Osaka University, 2.ISAS/JAXA, 3.Kindai University, 4.The University of Tokyo, 5.University of Aizu, 6.Instituto de Astrofisica de Canarias, 7.Nagoya University, 8.National Astronomical Observatory of Japan, 9.Observatoire de la Cote d'Azur, 10.Auburn University, 11.Tohoku University, 12.Kyushu University,

13.Brown University, 14.Rikkyo University, 15.The National Institute of Advanced Industrial Science and Technology, 16.Meiji University, 17.PERC, Chiba Institute of Technology, 18.Kochi University)

[PPS04-P09] **Orientation of Boulders and Rerationship with Gravitational Slope on Asteroid Rryugu: Implications for Surface Evolution.**

*Tatsuki Ebihara[1], Koki Yumoto[1], Seiji Sugita[1], Rie Honda[2], Shingo Kameda[3], ERI TATSUMI[1,4], Yuichiro Cho[1], Kazuo Yoshioka[1], Hirotaka Sawada[5], Yasuhiro Yokota[2,5], Naoya Sakatani[3], Masahiko Hayakawa[5], Moe Matsuoka[5], Manabu Yamada[6], Toru Kouyama[7], Hidehiko Suzuki[8], Chikatoshi Honda[9], Kazunori Ogawa[10,11], Tatsuhiro Michikami[12], Hideaki Miyamoto[1], Tomokatsu Morota[1] (1.The University of Tokyo, 2.Kochi University, 3.Rikkyo University, 4.Instituto de Astrofisica de Canarias, 5.Japan Aerospace Exploration Agency, 6.Planetary Exploration Research Center Chiba Institute of Technology, 7.National Institute of Advanced Industrial Science and Technology, 8.Meiji University, 9.University of Aizu, 10.Japan Aerospace Exploration Agency, JAXA Space Exploration Center, 11.Kobe University, 12.Kindai University)

[PPS04-P10] Apparently Layered Boulders with Multiple Textures on Bennu's Surface

*Kana Ishimaru[1], Dante S Lauretta[1], Nick Porter, Dathon Golish[1], Manar Al Asad[2], Ronald Ballouz[1], Olivier S Barnouin[3], Keara Burke[1], Mike Daly[4], Dani DellaGiustina[1], Kevin John Walsh[5] (1.Lunar and Planetary Laboratory, University of Arizona, 2.Department of Earth Ocean and Atmospheric Sciences, University of British Columbia, 3.The Johns Hopkins University, Applied Physics Laboratory, 4.The Centre for Research in Earth and Space Science, York University, 5.Southwest Research Institute)

[PPS04-P11] High-resolution global thermal images of Ryugu acquired from the dawn side

*Yuri Shimaki[1], Hiroki Senshu[2], Naoya Sakatani[3], Tatsuaki Okada[1,4], Tetsuya Fukuhara[3], Satoshi Tanaka[1,5], Takehiko Arai[6], Hirohide Demura[7], Tomohiko Sekiguchi[8], Toru Kouyama[9], Jun Takita[10], Sunao Hasegawa[1] (1.Institute of Space and Astronautical Science, Japan Aerospace Exploration Agency, 2.Planetary Exploration Research Center, Chiba Institute of Technology, 3.Rikkyo University, 4.The University of Tokyo, 5.The Graduate University for Advanced Studies, SOKENDAI, 6.Ashikaga University, 7.The University of Aizu, 8.Hokkaido University of Education, 9.National Institute of Advanced Industrial Science and Technology (AIST), 10.Hokkaido Kitami Hokuto High School)

[PPS04-P12] High-resolved temperature map of Ryugu surface observed with Thermal Infrared Imager onboard Hayabusa2

*Takehiko Arai[1], Tatsuaki Okada[2], Satoshi Tanaka[2], Tetsuya Fukuhara[3], Hirohide Demura[4], Toru Kouyama[5], Naoya Sakatani[3], Yuri Shimaki[2], Hiroki Senshu[6], Tomohiko Sekiguchi[7], Jun Takita[8] (1.Ashikaga University, 2.JAXA, 3.Rikkyo University, 4.The University of Aizu, 5.AIST, 6.Chiba Institute of Technology, 7.Hokkaido University of Education, 8.Hokkaido Kitami Hokuto High School)

[PPS04-P13] Current status and future plan of Hayabusa2 Science Data Archive in PDS4

*Shin-ya Murakami[1], Yukio Yamamoto[2], M. Katherine Crombie[3], Carol Neese[4], Yoshiaki Ishihara[2] (1.Keio University, 2.Japan Aerospace Exploration Agency, 3.Indigo Information Services, LLC, 4.Planetary Science Institute)

[PPS04-P14] **Assessing the debris generated by the small carry-on impactor operated from the *Hayabusa2* mission**

*Motoo Ito[1], Yoshinori Takano[2], Yoko Kebukawa[3], Takuji Ohigashi[4], Moe Matsuoka[5], Kento Kiryu[3], Masayuki Uesugi[6], Tomoki Nakamura[7], Hayato Yuzawa[4], Keita Yamada[8], Hiroshi Naraoka[9], Toru Yada[5], Masanao Abe[5], Masahiko Hayakawa[5], Takanao Saiki[5], Shogo Tachibana[10] (1.Kochi Institute for Core Sample Research, JAMSTEC, 2.Biogeochemistry Research Center, JAMSTEC, 3.Yokohama National University, 4.UVSOR, IMS, 5.ISAS, JAXA, 6.JASRI/SPring-8, 7.Tohoku University, 8.Tokyo Institute of Technology, 9.Kyushu University, 10.University of Tokyo)

[PPS04-P15] X-ray nanotomography of CM and CI chondrites and their heated samples: as a rehearsal of Hayabusa2 sample analysis.

*Mingqi Sun[1], Akira Tsuchiyama[1,2], Megumi Matsumoto[3], Yuri Fujioka[3], Tomoki Nakamura[3], Junya Matsuno[2], Akira Miyake[4], Shota Okumura[4], Naotaka Tomioka[5], Motoo Ito[5], Yu Kodama[6], Stefano Rubino[7], Naoto Nakano[4], Kentaro Uesugi[8], Akihisa Takeuchi[8], Masahiro Yasutake[8] (1.CAS Key laboratory of Mineralogy and Metallogeny, Guangzhou Institute of Geochemistry, Chinese Academy of Science, Guangzhou 510640, China, 2.Research Organization of Science and Technology, Ritsumeikan University, Japan, 3.Graduate School of Science, Tohoku University, Japan, 4.Graduate School of Science, Kyoto University, Japan, 5.Kochi Institute for Core Sample Research, Japan, 6.Marine Works Japan Ltd., Japan, 7.Institut d'Astrophysique Spatiale, Université Paris-Saclay, France, 8.JASRI/SPring-8, Japan)

[PPS04-P16] **Assessing the irradiation effects by a synchrotron X-ray micro-computed tomography on the organic materials in carbonaceous chondrite: Examination at SPring-8 facility**

*Haruna Sugahara[1], Yoshinori Takano[2], Toshihiro Yoshimura[2], Nanako O Ogawa[2], Naohiko Ohkouchi[2], Masayuki Uesugi[3], Akira Tsuchiyama[4], Hayabusa2 project team (1.Institute of Space and Astronautical Science, Japan Aerospace Exploration Agency (ISAS/JAXA), 2.Japan Agency for Marine-Earth Science and Technology (JAMSTEC), 3.Japan Synchrotron Radiation Research Institute, 4.Ritsumeikan University)

[PPS04-P17] Description of return sample from C-type asteroid Ryugu using the MicrOmega hyperspectral microscope in JAXA Curation Facility

*Tatsuaki Okada[1,2], KaKasumi Yogata[1], Aiko Nakato[1], Kentaro Hatakeda[1,3], Toru Yada[1], Lucie Riu[1], Akiko Miyazaki[1], Kazuya Kumagai[1,3], Masahiro Nishimura[1], Masanao Abe[1], Tomohiro Usui[1,2], Cedric Pilorget[4], Rosario Brunetto[4], Vincent Hamm[4], Lionel Lourit[4], Jean-Pierre Bibring[4] (1.Institute of Space and Astronautical Science, Japan Aerospace Exploration Agency, 2.University of Tokyo, 3.Marine Works Japan Ltd., 4.Institue d'Astrophysique Spaciale)

[PPS04-P18] Significant role of Asteroids: One step of purified rocks and minerals and life to final water planet

*Yasunori Miura[1] (1.Visiting (Yamaguchi University, EUA-Al. Univ. Toronto, LPI-NPPf))

[PPS04-P19] Simulation of Phobos internal density structure estimation by orbit determination of MMX

*Keiko Yamamoto[1], Koji Matsumoto[1], Hitoshi Ikeda[2], Hiroki Senshu[3] (1.National Astronomical Observatory of Japan, 2.Japan Aerospace Exploration Agency, 3.Chiba Institute of Technology)

[PPS04-P20] MMX InfraRed Spectrometer (MIRS) imaging spectrometer

*Jean-Michel Reess[1], Maria Antonella Barucci, Pernelle Bernardi, Michel Le Du, Eric Sawyer, Takahiro Iwata[2], Hiromu Nakagawa[3], Tomoki Nakamura[4], Alain Doressoundiram, Sonia Fornasier (1.J.-M. Reess, LESIA, Observatoire de Paris, Université PSL, CNRS, Université de Paris, Sorbonne Université, 92190 Meudon, France, 2.T. Iwata, ISAS, JAXA, Sagamihara 252-5210, Japan, 3.H. Nakagawa, JAXA, Sagamihara 252-5210, Japan, 4.T. Nakamura, JAXA, Sagamihara 252-5210, Japan)

[PPS04-P21] Thermophysical Properties of S-type Binary Didymos by Thermal Imaging in Hera Mission

*Tatsuaki Okada[1,2], Satoshi Tanaka[1,2], Naoya Sakatani[3], Yuri Shimaki[1], Takehiko Arai[4], Hiroki Senshu[5], Hirohide Demura[6], Toru Kouyama[7], Tomohiko Sekiguchi[8] (1.Institute of Space and Astronautical Science, Japan Aerospace Exploration Agency, 2.University of Tokyo, 3.Rikkyo University, 4.Ashikaga University, 5.Chiba Institute of Technology, 6.University of Aizu, 7.National Institute of Advanced Industrial Science and Technology, 8.Hokkaido University of Education)

[PPS04-P22] Current status and science of DESTINY+

*Tomoko Arai[1], Masanori Kobayashi[1], Ko Ishibashi[1], Hiroshi Kimura[1], Takayuki Hirai[1], Peng Hong[1], Fumi Yoshida[2], Naoya Ozaki[3], Takayuki Yamamoto[3], Hiroyuki Toyota[3], Kazutaka Nishiyama[3], Hiroshi Imamura[3], Takeshi Takashima[3], DESTINY+ science team (1.Planetary Exploration Research Center, Chiba Institute of Technology, 2.University of Occupational and Environmental Health, Japan, 3.ISAS, JAXA)

[PPS04-P23] Progress report of development and ground calibration of DESTINY$^+$ Dust Analyser

*Takayuki Hirai[1], Masanori Kobayashi[1], Tomoko Arai[1], Hiroshi Kimura[1], Sho Sasaki[2], Hikaru Yabuta[3], Amano Sui[3], Sachio Kobayashi[4], Motoo Ito[4], Akira Yamaguchi[5], Hajime Yano[6], Mario Trieloff[7], Jon Hillier[8], Nozair Khawaja[8], Lisa Eckart[8], Harald Krueger[9], Jonas Simolka[10], Ralf Srama[10] (1.Chiba Institute of Technology, Planetary Exploration Research Center, 2.Osaka University, 3.Hiroshima University, 4.Japan Agency for Marine-Earth Science and Technology, 5.National Institute of Polar Research, 6.Japan Aerospace Exploration Agency, 7.Heidelberg University, 8.Free University of Berlin, 9.Max Planck Institute for Solar System Research, 10.University of Stuttgart)

[PPS04-P24] Study of asteroid tracking mirror of telescopic camera onboard DESTINY+

*Peng Hong[1], Ko Ishibashi[1], Takayuki Hosonuma[2], Ozaki Naoya[3], Shunsuke Sato[3], Hiroyuki Toyota[3], Kazutaka Nishiyama[3], Masatsugu Otsuki[3], Osamu Okudaira[1], Takeshi Takashima[3] (1.Planetary Exploration Research Center, Chiba Institute of Technology, 2.Department of Aeronautics and Astronautics, The University of Tokyo, 3.Institute of Space and Astronautical Science, Japan Aerospace Exploration Agency)

[PPS04-P25] Development status of DESTINY$^+$ onboard cameras TCAP and MCAP

*Ko Ishibashi[1], Peng Hong[1], Takaya Okamoto[2], Takahiro Ishimaru[2], Manabu Yamada[1], Naoya Ozaki[2], Takayuki Hosonuma[3], Shunsuke Sato[2], Osamu Okudaira[1], Tomoko Arai[1], Fumi Yoshida[1,4], Masato Kagitani[5], Shingo Kameda[6], Takeshi Miyabara[2], Masayuki Ohta[2], Takeshi Takashima[2] (1.Chiba Institute of Technology, 2.Japan Aerospace Exploration Agency, 3.The University of Tokyo, 4.University of Occupational and Environmental Health, 5.Tohoku University, 6.Rikkyo University)

[PPS04-P26] A Ground-based Optical Calibration Plan for DESTINY$^+$ on-board Cameras, TCAP and MCAP

*Takaya Okamoto[1], Ko Ishibashi[2], Manabu Yamada[2], Peng Hong[2], Fumi Yoshida[2,3], Tomoko Arai[2], Takahiro Ishimaru[1], Masayuki Ohta[1], Takeshi Miyabara[1], Takeshi Takashima[1] (1.Japan Aerospace Exploration Agency, Institute of Space and Astronautical Science, 2.Chiba Institute of Technology, Planetary Exploration Research Center, 3.University of Occupational and Environmental Health, School of Medicine)

[PPS04-P27] **Twinkle: a low-Earth orbit, visible and infrared observatory for exoplanet and solar system spectroscopy**

*Billy Edwards[1] (1.Blue Skies Space Ltd)

[E] Oral | P (Space and Planetary Sciences)：P-EM Solar-Terrestrial Sciences, Space Electromagnetism & Space Environment

9:00 AM - 10:30 AM JST | 12:00 AM - 1:30 AM UTC | Ch.05 Zoom Room 05

[P-EM09] Dynamics of Magnetosphere and Ionosphere

convener:Akiko Fujimoto(Kyushu Institute of Technology), Mitsunori Ozaki(Faculty of Electrical and Computer Engineering, Institute of Science and Engineering, Kanazawa University), Yuka Sato(Nippon Institute of Technology), Aoi Nakamizo(Applied Electromagnetic Research Institute, National Institute of Information and Communications Technology), Chairperson:Hiroshi Hasegawa(Institute of Space and Astronautical Science, Japan Aerospace Exploration Agency), Masaki N Nishino(Japan Aerospace Exploration Agency, Institute of Space and Astronautical Science)

9:00 AM - 9:05 AM JST | 12:00 AM - 12:05 AM UTC

[PEM09-01] Introduction

9:05 AM - 9:20 AM JST | 12:05 AM - 12:20 AM UTC

[PEM09-02] Magnetic Reconnection in a Sheared Magnetic Flux Tube: Slippage versus Tearing

*Hidetaka Kuniyoshi[1], Michael Hesse[2], Cecilia Nogren[3], Paul Tenfjord[3], Norah Kaggwa Kwagala[3] (1.The University of Tokyo, Department of Earth and Planetary Science, 2.NASA Ames Research Center, 3.University of Bergen, Space Plasma Physics Group)

9:20 AM - 9:35 AM JST | 12:20 AM - 12:35 AM UTC

[PEM09-03] Fast Magnetic-Field Annihilation in Electron-scale Current Sheet in Earth's Magnetotail

*Hiroshi Hasegawa[1], Richard E. Denton[2], Kevin J. Genestreti[3], Takuma Nakamura[4], Tai D. Phan[5], Rumi Nakamura[4], Kyoung-Joo Hwang[6], Narges Ahmadi[7], Quanqi Shi[8], Michael Hesse[9], James L. Burch[6], James M. Webster[6], Roy B. Torbert[10], Barbara L. Giles[11], Dan J. Gershman[11], Christopher T. Russell[12], Robert J. Strangeway[12], Hanying Wei[12], Per-Arne Lindqvist[13], Yuri V. Khotyaintsev[14], Robert E. Ergun[15], Yoshifumi Saito[1] (1.Institute of Space and Astronautical Science, Japan Aerospace Exploration Agency, 2.Department of Physics and Astronomy, Dartmouth College, 3.Southwest Research Institute, Durham, 4.Space Research Institute, Austrian Academy of Sciences, 5.Space Sciences Laboratory, University of California, Berkeley, 6.Southwest Research Institute, San Antonio, 7.Laboratory for Atmospheric and Space Physics, University of Colorado, 8.Shandong Provincial Key Laboratory of Optical Astronomy and Solar-Terrestrial Environment, Institute of Space Sciences, Shandong University, 9.Space Plasma Physics Group, University of Bergen, 10.Physics Department, University of New Hampshire, 11.NASA Goddard Space Flight Center, 12.Department of Earth, Planetary, and Space Sciences, University of California, Los Angeles, 13.Royal Institute of Technology, Stockholm, 14.Swedish Institute of Space Physics, 15.Department of Astrophysical and Planetary Sciences, University of Colorado)

9:35 AM - 9:50 AM JST | 12:35 AM - 12:50 AM UTC

[PEM09-04] Energy dependence of field-aligned anisotropy of electrons during dipolarization at Earth's tailside

*Kaiti Wang[1], Ching-Huei Lin[2], Zhuo-Ren Lang[3], Tohru Hada[4], Toshi Nishimura[5] (1.Tamkang Univ., 2.Chien-Hsin Univ. of Sci. & Tech., 3.National Cheng Kung Univ., 4.Kyushu Univ., 5.Boston Univ.)

9:50 AM - 10:05 AM JST | 12:50 AM - 1:05 AM UTC

[PEM09-05] On the origin of cold-dense plasmas in the dusk magnetotail plasma sheet: MMS and Geotail observations

*Masaki N Nishino[1], Yoshifumi Saito[1], Hiroshi Hasegawa[1], Naritoshi Kitamura[2], Yukinaga Miyashita[3,4], Tsugunobu Nagai[1], Shoichiro Yokota[5], Daniel J Gershman[6], Christopher T Russell[7], Barbara L Giles[6] (1.Japan Aerospace Exploration Agency, Institute of Space and Astronautical Science, 2.Graduate School of Science, The University of Tokyo, 3.Korea Astronomy and Space Science Institute, South Korea, 4.Korea University of Science and Technology, South Korea, 5.Graduate School of Science, Osaka University, 6.Goddard Space Flight Center, NASA, 7.University of California, Los Angeles)

10:05 AM - 10:20 AM JST | 1:05 AM - 1:20 AM UTC

[PEM09-06] **Substorm-like events related to magnetosheath plasma jets**

*ALEXEI DMITRIEV[1,2], ALLA SUVOROVA[2] (1.Institute of Space Science, National Central University, Jungli City, Taiwan, 2.Skobeltsyn Institute of Nuclear Physics, Lomonosov Moscow State University, Moscow, Russia)

10:20 AM - 10:30 AM JST | 1:20 AM - 1:30 AM UTC

[PEM09-07] Discussion

[E] Oral | P (Space and Planetary Sciences)：P-EM Solar-Terrestrial Sciences, Space Electromagnetism & Space Environment

10:45 AM - 12:15 PM JST | 1:45 AM - 3:15 AM UTC | Ch.05 Zoom Room 05

[P-EM09] Dynamics of Magnetosphere and Ionosphere

convener:Akiko Fujimoto(Kyushu Institute of Technology), Mitsunori Ozaki(Faculty of Electrical and Computer Engineering, Institute of Science and Engineering, Kanazawa University), Yuka Sato(Nippon Institute of Technology), Aoi Nakamizo(Applied Electromagnetic Research Institute, National Institute of Information and Communications Technology), Chairperson:Hiroshi Hasegawa(Institute of Space and Astronautical Science, Japan Aerospace Exploration Agency), Masaki N Nishino(Japan Aerospace Exploration Agency, Institute of Space and Astronautical Science)

10:45 AM - 11:10 AM JST | 1:45 AM - 2:10 AM UTC

[PEM09-08] A Case Study of Transversely Heated Low-Energy Helium Ions by EMIC Waves in the Plasmasphere

★Invited Papers

*Khan-Hyuk Kim[1] (1.School of Space Research, Kyung Hee University)

11:10 AM - 11:25 AM JST | 2:10 AM - 2:25 AM UTC

[PEM09-09] CIR- and CME-driven magnetic storm effects on ion upflows in the low-altitude polar ionosphere

*Masayoshi Takada[1], Kanako Seki[1], Yasunobu Ogawa[2], Kunihiro Keika[1] (1.Tokyo University, 2.National Institute of Polar Research)

11:25 AM - 11:40 AM JST | 2:25 AM - 2:40 AM UTC

[PEM09-10] Science Objectives of FACTORS mission

*Yoshizumi Miyoshi[1], Naritoshi Kitamura[2], Kazushi Asamura[3], Takeshi Sakanoi[4], Takanori Nishiyama[6], Hirotsugu Kojima[5], Masahito Nose[1], Yuto Katoh[4], Kunihiro Keika[2], Atsuki Shinbori[4,1], Mizuki Fukizawa[4], Kiyoka Murase[6], Miki Kawamura[4] (1.Institute for Space-Earth Environmental Research, Nagoya University, 2.University of Tokyo, 3.JAXA, 4.Tohoku University, 5.Kyoto University, 6.NIPR)

11:40 AM - 11:55 AM JST | 2:40 AM - 2:55 AM UTC

[PEM09-11] **Development of a novel method for extracting the geometrical properties of the magnetic vector fields towards the era of multi-point satellite observations**

*Akimasa Yoshikawa[1], Tsubasa Hashimoto[2], Aoi Nakamizo[4], Shinichi Ohtani[3] (1.Department of Earth and Planetary Sciences, Kyushu University, 2.Gradient school of Earth and Planetary Sciences, Kyushu University, 3.JHU/APL, 4.NICT)

11:55 AM - 12:10 PM JST | 2:55 AM - 3:10 AM UTC

[PEM09-12] Dawn-dusk asymmetry in the mesoscale field-aligned currents embedded in the diminished large-scale Region 1 current

*Yoshihiro Yokoyama[1], Satoshi Taguchi[1], Toshihiko Iyemori[2] (1.Department of Geopysics, Graduate School of Science, Kyoto University, 2.Kyoto University)

12:10 PM - 12:15 PM JST | 3:10 AM - 3:15 AM UTC

[PEM09-13] Discussion

[E] Oral | P (Space and Planetary Sciences)：P-EM Solar-Terrestrial Sciences, Space Electromagnetism & Space Environment

1:45 PM - 3:15 PM JST | 4:45 AM - 6:15 AM UTC | Ch.05 Zoom Room 05

[P-EM09] Dynamics of Magnetosphere and Ionosphere

convener:Akiko Fujimoto(Kyushu Institute of Technology), Mitsunori Ozaki(Faculty of Electrical and Computer Engineering, Institute of Science and Engineering, Kanazawa University), Yuka Sato(Nippon Institute of Technology), Aoi Nakamizo(Applied Electromagnetic Research Institute, National Institute of Information and Communications Technology), Chairperson:Yuki Obana(Department of Engineering Science, Faculty of Engineering, Osaka Electro-Communication University), Yoshihiro Yokoyama(Department of Earth and Planetary Sciences, Graduate School of Science, Kyoto University)

1:45 PM - 2:10 PM JST | 4:45 AM - 5:10 AM UTC

[PEM09-14] Current and future perspectives on 3D analysis of aurora

★Invited Papers

*Yoshimasa Tanaka[1,2,3], Yasunobu Ogawa[1,2,3], Akira Kadokura[1,2,3], Bjorn Gustavsson[4], Kirsti Kauristie[5], Enell Carl-fredrik[6], Urban Brandstrom[7], Tima Sergienko[7], Alexander Kozlovsky[8], Tero Raita[8], Mizuki Fukizawa[9], Takeshi Sakanoi[9], Keisuke Hosokawa[10] (1.National Institute of Polar Research, 2.Polar Environment Data Science Center, Joint Support-Center for Data Science Research, Research Organization of Information and Systems, 3.The Graduate University for Advanced Studies, SOKENDAI, 4.The Arctic University of Norway, 5.Finnish Meteorological Institute, 6.EISCAT Scientific Association, 7.Swedish Institute of Space Physics, 8.Sodankyla Geophysical Observatory, 9.Planetary Plasma and Atmospheric Research Center, Graduate School of Science, Tohoku University, 10.Department of Communication Engineering and Informatics, University of Electro-Communications)

2:10 PM - 2:25 PM JST | 5:10 AM - 5:25 AM UTC

[PEM09-15] Reconstruction of the three-dimensional structure and precipitating electrons of pulsating auroral patches by Aurora Computed Tomography

*Mizuki Fukizawa[1], Takeshi Sakanoi[1], Yoshimasa Tanaka[2], Yasunobu Ogawa[2], Björn Gustavsson[3], Kirsti Kauristie[4], Carl-Fredrik Enell[5], Alexander Kozlovsky[6], Tero Raita[6], Urban Brändström[7], Tima Sergienko[7] (1.Planetary Plasma and Atmospheric Research Center, Graduate School of Science, Tohoku University, 2.National Institute of Polar Research, 3.University of Tromsø - The Arctic University of Norway, 4.Finnish Meteorological Institute, 5.EISCAT Scientific Association, 6.Sodankylä Geophysical Observatory, University of Oulu, 7.Swedish Institute of Space Physics)

2:25 PM - 2:40 PM JST | 5:25 AM - 5:40 AM UTC

[PEM09-16] A generation process of “Great Wall” aurora seen from ISS

*Sota Nanjo[1], Morio Tanaka[2], Natsuo Sato[3], Yuta Hozumi[1], Keisuke Hosokawa[1], Ryuho Kataoka[3,4], Yoshizumi Miyoshi[5], Shin-ichiro Oyama[3,5,6], Mitsunori Ozaki[7], Kazuo Shiokawa[5], Satoshi Kurita[2] (1.The University of Electro-Communications, 2.Kyoto University, 3.National Institute of Polar Research, 4.SOKENDAI, the Graduate University for Advanced Studies, 5.ISEE, Nagoya University, 6.University of Oulu, 7.Kanazawa University)

2:40 PM - 2:55 PM JST | 5:40 AM - 5:55 AM UTC

[PEM09-17] Exploring the Electron Acceleration Mechanism in the Poleward Boundary Intensification

*Hayato Higuchi[1], Akimasa Yoshikawa[2] (1.Department of Earth and Planetary Sciences, Graduate School of Science, Kyushu University, 2.Department of Earth and Planetary Sciences, Faculty of Science, Kyushu University)

2:55 PM - 3:10 PM JST | 5:55 AM - 6:10 AM UTC

[PEM09-18] **Antarctic large area network observation of auroral phenomena using unmanned system: Current status of project as of early 2021**

*Akira Kadokura[1], Yasunobu Ogawa[1], Yoshimasa Tanaka[1], Hisao Yamagishi[1], Masaki Okada[1], Ryuho Kataoka[1], Herbert Akihito Uchida[4], Yuichi Otsuka[2], Tetsuo Motoba[3], Natsuo Sato[1], Henri Robert[5], Ashwini K. Sinha[6], Jean Rasson[7] (1.National Institute of Polar Research, 2.Nagoya University, 3.Johns Hopkins University, Applied Physics Laboratory, 4.SOKENDAI, 5.International Polar Foundation, 6.Indian Institute of Geomagnetism, 7.Royal Meteorological Institute of Belgium)

3:10 PM - 3:15 PM JST | 6:10 AM - 6:15 AM UTC

[PEM09-19] Discussion

[E] Oral | P (Space and Planetary Sciences)：P-EM Solar-Terrestrial Sciences, Space Electromagnetism & Space Environment

3:30 PM - 5:00 PM JST | 6:30 AM - 8:00 AM UTC | Ch.05 Zoom Room 05

[P-EM09] Dynamics of Magnetosphere and Ionosphere

convener:Akiko Fujimoto(Kyushu Institute of Technology), Mitsunori Ozaki(Faculty of Electrical and Computer Engineering, Institute of Science and Engineering, Kanazawa University), Yuka Sato(Nippon Institute of Technology), Aoi Nakamizo(Applied Electromagnetic Research Institute, National Institute of Information and Communications Technology), Chairperson:Yuki Obana(Department of Engineering Science, Faculty of Engineering, Osaka Electro-Communication University), Yoshihiro Yokoyama(Department of Earth and Planetary Sciences, Graduate School of Science, Kyoto University)

3:30 PM - 3:45 PM JST | 6:30 AM - 6:45 AM UTC

[PEM09-20] Seasonal dependence of dusk-side equatorial IHFACs polarity during solar cycle 23-24

Manjula Ranasinghe[2], *Akiko Fujimoto[1], Akimasa Yoshikawa[3], Chandana Jayaratne[2] (1.Kyushu Institute of Technology, 2.University of Colombo, 3.Kyushu University)

3:45 PM - 4:00 PM JST | 6:45 AM - 7:00 AM UTC

[PEM09-21] Development of the imaging receiver system for the SuperDARN Hokkaido East radar

*Nozomu Nishitani[1], Tomoaki Hori[1], Yoshiyuki Hamaguchi[1] (1.Institute for Space-Earth Environmental Research, Nagoya University)

4:00 PM - 4:15 PM JST | 7:00 AM - 7:15 AM UTC

[PEM09-22] Seasonal and longitudinal dependence of the Sub-Auroral Polarization Streams occurrence observed by the SuperDARN radars

Kento Oya[1], *Nozomu Nishitani[1], Tomoaki Hori[1], John Mike Ruohoniemi[2], William A. Bristow[3], Simon G. Shepherd[4], Bharat Kunduri[2] (1.Institute for Space-Earth Environmental Research, Nagoya University, 2.Virginia Tech Department of Electrical and Computer Engineering, 3.The Pennsylvania State University , 4.Thayer School of Engineering, Dartmouth College)

4:15 PM - 4:30 PM JST | 7:15 AM - 7:30 AM UTC

[PEM09-23] Investigation of the mid-latitude ionospheric response during substorm based on magnetic and electric field observations

*Moe Hayashi[1], Akimasa Yoshikawa[1], Akiko Fujimoto[2], Shinichi Ohtani[3] (1.Kyushu University, 2.Kyushu Institute of Technology , 3.The Johns Hopkins University Applied Physics Laboratory)

4:30 PM - 4:55 PM JST | 7:30 AM - 7:55 AM UTC

[PEM09-24] New results of auroral hiss observations on the ground at L=5.5 in Northern Europe

★Invited Papers

*Jyrki Manninen[1], Natalia G. Kleimenova[2,3], Yury Fedorenko[4], Olga Lebed[4], Alexander Kozlovsky[1], Alexander Nikitenko[4], Liudmila Gromova[5] (1.Sodankyla Geophysical Observatory, University of Oulu, Sodankylä, Finland, 2.Schmidt Institute of Physics of the Earth RAN, Moscow, Russia, 3.Space Research Institute RAN, Moscow, Russia, 4.Polar Geophysical Institute, Apatity, Russia, 5.Pushkov Institute of Terrestrial Magnetism, Ionosphere and Radio Wave Propagation RAN, Moscow, Russia)

4:55 PM - 5:00 PM JST | 7:55 AM - 8:00 AM UTC

[PEM09-25] Discussion

[E] Poster | P (Space and Planetary Sciences)：P-EM Solar-Terrestrial Sciences, Space Electromagnetism & Space Environment

5:15 PM - 6:30 PM JST | 8:15 AM - 9:30 AM UTC | Ch.05_1

[P-EM09] Dynamics of Magnetosphere and Ionosphere

convener:Akiko Fujimoto(Kyushu Institute of Technology), Mitsunori Ozaki(Faculty of Electrical and Computer Engineering, Institute of Science and Engineering, Kanazawa University), Yuka Sato(Nippon Institute of Technology), Aoi Nakamizo(Applied Electromagnetic Research Institute, National Institute of Information and Communications Technology)

[PEM09-P01] Development of a 3-dimensional global ionospheric electrostatic potential solver using IGRF model

*Takuya Ijuin[1], Akimasa Yoshikawa[2] (1.Department of Earth and Planetary Sciences, Graduate School of Science, Kyushu University, 2.Department of Earth and Planetary Sciences, Kyushu University)

[PEM09-P02] Study on the Solar Flare Effect (SFE*) of equatorial electrojet around local noon

*Akihiro Yasunaga[1], Akiko Fujimoto[2], Akimasa Yoshikawa[1] (1.Department of Earth and Planetary Sciences, Kyushu University, 2.Kyushu Institute of Technology)

[PEM09-P03] Consideration of the CubeSat for Observation of IHFAC at LEO

*Kentarou Kitamura[1], Taku Takada[2], Kazumasa Imai[2], Manabu Shinohara[3], Makoto Wakabayashi[4], Akiko Fujimoto[1], Mariko Teramoto[1] (1.Kyushu Institute of Technology, 2.NIT, Koti College, 3.NIT, Kagoshima College, 4.NIT, Niihama College)

[PEM09-P04] Initial results of multi-event analysis of magnetosphere-ionosphere coupling for nighttime medium-scale traveling ionospheric disturbances

*Kouki Kawai[1], Kazuo Shiokawa[1], Yuichi Otsuka[1], Shin-ichiro Oyama[1,2,3], Martin G Connors[4], Yoshiya Kasahara[5], Yasumasa Kasaba[6], Atsuki Shinbori[1], Fuminori Tsuchiya[6], Atsushi Kumamoto[6], Masahiro Kitahara[1], Masafumi Shoji[1], Satoko Nakamura[1], Ayako Matsuoka[7], Shun Imajo[1], Yoichi Kazama[8], Shiang Yu Wang[8], Sunny W. Y. Tam[9], Tzu-Fang Chang[9], B J wang[8], Kazushi Asamura[10], Satoshi Kasahara[11], Shoichiro Yokota[12], Kunihiro Keika[11], Tomoaki Hori[1], Chae-Woo Jun[1], Iku Shinohara[10], Yoshizumi Miyoshi[1] (1.Institute for Space-Earth Environmental Research, Nagoya University, Japan, 2.University of Oulu, Oulu, Finland, 3.National Institute of Polar Research, Tokyo, Japan, 4.Athabasca University, Canada, 5.Kanazawa University, Kanazawa, Japan, 6.Tohoku University, Sendai, Japan, 7. Kyoto University, Kyoto, Japan, 8.Academia Sinica, Taipei, Taiwan, 9.National Cheng Kung University, Tainan, Taiwan, 10.Institute of Space and Astronautical Science, Japan Aerospace Exploration Agency, Sagamihara, Japan, 11.Tokyo University, Tokyo, Japan, 12.Osaka University, Osaka, Japan)

[PEM09-P05] Development of a new M-I coupling algorithm in global MHD magnetosphere simulation: Alfvénic-Coupling

*Aoi Nakamizo[1], Akimasa Yoshikawa[2], Hiroyuki Nakata[3], Keiichiro Fukazawa[4], Takashi Tanaka[2] (1.Applied Electromagnetic Research Institute, National Institute of Information and Communications Technology, 2.Faculty of Science, Kyushu University, 3.Faculty of Engineering, Chiba University, 4.Academic Center for Computing and Media Studies, Kyoto University)

[PEM09-P06] Understanding the 3-dimensional current between the magnetosphere and the ionosphere

*Yuto Yano[1], Yusuke Ebihara[1] (1.Research Institute for Sustainable Humanosphere, Kyoto University)

[PEM09-P07] Magnetospheric dynamics under northward IMF conditions surveyed by concurrent observations of TPA and omega-band aurora

*Motoharu Nowada[1], Yukinaga Miyashita[2,3] (1.Shandong Key Laboratory of Optical Astronomy and Solar-Terrestrial Environment, School of Space Science and Physics, Institute of Space Sciences, Shandong University at Weihai, P. R. China, 2.Korea Astronomy and Space Science Institute, Daejeon, South Korea, 3.Korea University of Science and Technology, Daejeon, South Korea)

[PEM09-P08] The terrestrial magnetosphere for zero interplanetary magnetic field

*Tsubasa Hashimoto[1], Masakazu Watanabe[2], Ryuho Kataoka[3], Shigeru Fujita[4], Takashi Tanaka[5] (1.Department of Earth and Planetary Sciences, Graduate School of Science, Kyushu University, 2.Department of Earth and Planetary Sciences, Faculty of Science, Kyushu University, 3.National Institute of Polar Research, 4.Meteorological College, Japan Meteorological Agency/ National Institute of Polar Research, 5.International Center for Space Weather Science and Education)

[PEM09-P09] Cusp ion precipitation for stably northward IMF and its relation to the magnetosheath flow

*Haruto Koike[1], Satoshi Taguchi[1] (1.Department of Geophysics, Graduate School of Science, Kyoto University)

[PEM09-P10] Topology and geometry of interchange-type reconnection in the terrestrial magnetosphere

*Masakazu Watanabe[1], Tomoya Asano[1], Dongsheng Cai[2], Peikun Xiong[2], Shigeru Fujita[3], Takashi Tanaka[1] (1.Kyushu University, 2.University of Tsukuba, 3.Meteorological College)

[PEM09-P11] **Understanding the behavior of charged particles in plasma by vector potential**

*Shinji Karasawa[1] (1.Miyagi National College of Technology Professor emeritus)

[PEM09-P12] Properties of dispersive Alfven waves and their roles in electron acceleration process in the terrestrial magnetosphere based on Plasma Distribution Solver

*Koseki Saito[1], Yuto Katoh[1], Atsushi Kumamoto[1], Tomoki Kimura[1], Yohei Kawazura[1] (1.Department of Geophysics, Graduate School of Science, Tohoku University)

[PEM09-P13] Equatorward development of electron precipitation in a longitudinally narrow region beyond the cusp

*Satoshi Taguchi[1], Keisuke Hosokawa[2], Yasunobu Ogawa[3] (1.Department of Geophysics, Graduate School of Science, Kyoto University, 2.Department of Communication Engineering and Informatics, University of Electro-Communications, 3.National Institute of Polar Research)

[PEM09-P14] Periodic variations of the high red aurora on the nightside

*kazuki yashima[1], Satoshi Taguchi[1], Keisuke Hosokawa[2] (1. Department of Geophysics, Graduate School of Science, Kyoto University, 2.Department of Communication Engineering and Informatics, The University of Electro-Communications)

[PEM09-P15] Initial study of a substorm onset auroral arc on 28 December 2018 by a ground EMCCD camera and the Arase satellite at L~5

*Liwei Chen[1], Kazuo Shiokawa[1], Yoshizumi Miyoshi[1], Shin-ichiro Oyama[1], Yasunobu Ogawa[2], Keisuke Hosokawa[12], Ryuho Kataoka[2], Yoichi Kazama[5], Shiang-Yu Wang[3], Sunny W. Y. Tam[5], Tzu-Fang Chang[1,4], Bo-Jhou Wang[5], Kazushi Asamura[6], Satoshi Kasahara[7], Shoichiro Yokota[8], Tomoaki Hori[1], Kunihiro Keika[7], Yasumasa Kasaba[9], Masafumi Shoji[1], Yoshiya Kasahara[10], Ayako Matsuoka[11], Iku Shinohara[6] (1.Institute for Space-Earth Environmental Research, Nagoya University, 2.National Institute of Polar Research, 3.National Cheng Kung University, 4.Institute of Space and Plasma Sciences, National Cheng Kung University, 5.Institute of Astronomy and Astrophysics, Academia Sinica, 6.Institute of Space and Astronautical Science, Japan Aerospace Exploration Agency, 7.University of Tokyo, 8.Osaka University, 9.Tohoku University, 10.Kanazawa University, 11.Data Analysis Center for Geomagnetism and Space Magnetism, Graduate School of Science, Kyoto University, 12.The University of Electro-Communications)

[PEM09-P16] Ionospheric control of space weather: plasma injections arising out of dynamic ionosphere

*Osuke Saka[1] (1.Office Geophysik)

[PEM09-P17] Amplitude modulations of the flickering aurora

*Nomura Kazuki[1], Yoshizumi Miyoshi[1], Satoshi Kurita[2], Kohei Toyama[1], Ryuho Kataoka[3] (1.Institute for Space-Earth Environmental Research,Nagoya University, 2.Research Institite for Subtainable Humanosphere, 3.National Institue of Polar Research)

[PEM09-P18] Simultaneous pulsating aurora and microburst observation with ground-based fast auroral imagers and the Cubesat FIREBIRD-II

*Miki Kawamura[1], Takeshi Sakanoi[1], Mizuki Fukizawa[1], Yoshizumi Miyoshi[2], Keisuke Hosokawa[3], Fuminori Tsuchiya[1], Yuto Katoh[1], Yasunobu Ogawa[4], Kazushi Asamura[6], Harlan Spence[5] (1.Tohoku University, 2.ISEE, Nagoya University, 3.University of Electro-Communicants, 4.National Institute of Polar Research, 5.University of New Hampshire, USA, 6.JAXA/ISAS)

[PEM09-P19] Analysis of Langmuir waves caused by Chorus observed by the Arase satellite

*Towa Yoshida[1], Satoshi Kurita[2], Takahiro Zushi[1], Hirotsugu Kojima[2], Yoshiya Kasahara[3], Shoya Matsuda[4], Ayako Matsuoka[5] (1.National Institute of Technology, Nara College, 2.Research institute for sustainable humanosphere, Kyoto University, 3.Information Media Center, Kanazawa University, 4.Institute of Space and Astronautical Science/Japan Aerospace Exploration Agency, 5.Data Analysis Center for Geomagnetism and Space Magnetism, Graduate School of Science, Kyoto University)

[PEM09-P20] Mode identification of MHD waves observed by the SuperDARN radars using the Lomb-Scargle analysis

*Koki Morita[1], Nozomu Nishitani[1], Tomoaki Hori[1] (1.Institute for Space-Earth Environmental Research, Nagoya University)

[PEM09-P21] Progress in the full-automatic identification of FLR events in VLOS of multiple SuperDARN radars

*Hideaki Kawano[1,2], Akira Sessai Yukimatu[3,4], Nozomu Nishitani[5], Yoshimasa Tanaka[3,4], Satoko Saita[6], Tomoaki Hori[5] (1.Department of Earth and Planetary Sciences, Kyushu University, 2.ICSWSE, Kyushu University, 3.National Institute of Polar Research, 4.SOKENDAI, 5.ISEE, Nagoya University, 6.Kitakyushu College)

[PEM09-P22] Initial results from an induction magnetometer observation at Middlemarch (L = 2.7) in New Zealand

*Yuki Obana[1], Kaori Sakaguchi[2], Masahito Nose[3], Keisuke Hosokawa[4], Kazuo Shiokawa[3], Martin Connors[5], Akira Kadokura[6], Tsutomu Nagatsuma[2] (1.Department of Engineering Science, Faculty of Engineering, Osaka Electro-Communication University, 2.National Institute of Information and Communications Technology, 3.Institute for Space-Earth Environmental Research, Nagoya University, 4.Department of Communication Engineering and Informatics, University of Electro-Communications, 5.Centre for Science, Faculty of Science and Technology, Athabasca University, 6.National Institute of Polar Research)

[PEM09-P23] Detection of Pi2 geomagnetic pulsation by machine learning and development of real-time substorm warning system

Yusuke Sakai[1], *Masahito Nose[1], Hiroshi Ichihara[2], Genta Ueno[3], Naoto Nakano[4] (1.Institute for Space-Earth Environmental Research, Nagoya University, 2.Graduate school of environmental studies, Nagoya University, 3.Institute of Statistical Mathematics, Research Organization of Information and Systems, 4.Institute for Liberal Arts and Sciences, Kyoto University)

[PEM09-P24] Current Status of the FACTORS mission for the Space-Earth Coupling System Exploration

*Masafumi Hirahara[1], Yoshifumi Saito[2], Hirotsugu Kojima[3], Kazushi Asamura[2], Takeshi Sakanoi[4], Yoshizumi Miyoshi[1], Naritoshi Kitamura[5], Masatoshi Yamauchi[6], Yoshihide Sugimoto[7] (1.Nagoya Univ., 2.JAXA, 3.Kyoto Univ., 4.Tohoku Univ., 5.Univ. Tokyo, 6.IRF, 7.LSAS Tec Co., Ltd.)

[PEM09-P25] Future formation-flight satellite mission FACTORS: Development of far-ultra-violet imagers and simulation of Alfven wave observations

*Takeshi Sakanoi[1], Mizuki Fukizawa[1], Masafumi Hirahara[2], Yoshizumi Miyoshi[2], Kazushi Asamura[3], Yoshifumi Saito[3], Hirotsugu Kojima[4], Naritoshi Kitamura[5], Takanori Nishiyama[6], Kiyoka Murase[6], Miki Kawamura[1], Kaori Sakaguchi[7], Mamoru Ishii[7], Harald U Frey[8], Nick Schneider[9] (1.Planetary Plasma and Atmospheric Research Center, Graduate School of Science, Tohoku University, 2.ISEE, Nagoya University, 3.ISAS, JAXA, 4.RISH, Kyoto University, 5.Graduate School of Science, University of Tokyo, 6.NIPR, 7.NICT, 8.SSL, University of California, Berkeley, 9.LASP, University of Colorado Boulder)

[PEM09-P26] Future formation-flight mission FACTORS: Development of plasma particle instruments and evaluation of electric field measurements with short electric field sensors

*Kazushi Asamura[1], Hirotsugu Kojima[2], Taku Namekawa[1], Takefumi Mitani[1], Motoyuki Kikukawa[2], Ibuki Fukasawa[2], Satoshi Kurita[2], Yuki Miyake[2], Hideyuki Usui[3] (1.ISAS / JAXA, 2.RISH, Kyoto University, 3.Kobe University)

[PEM09-P27] Current status of development of multi-spectral auroral camera on the LAMP rocket experiment

*Miki Kawamura[1], Takeshi Sakanoi[1], Kazushi Asamura[2], Yoshizumi Miyoshi[3], Keisuke Hosokawa[4], Sarah Jones[5], Marc Lessard[6] (1.Tohoku University, 2.JAXA,ISAS, 3.ISEE, Nagoya University, 4.University of Electro-Communicants, 5.GSFC/NASA, USA, 6.University of New Hampshire, USA)

[PEM09-P28] Development of wideband impedance probe for measurement of the ion composition in the ionosphere and magnetosphere

*Atsushi Kumamoto[1] (1.Graduate School of Science, Tohoku University)

[PEM09-P29] Numerical design of double-shell electrostatic energy analyzer with hemispherical field of view

*Atsuya Takasu[1], Masafumi Hirahara[1], Shoichiro Yokota[2] (1.Institute of Space-Earth Environmental Research, Nagoya University, 2.Graduate School of Science, Osaka University)

[PEM09-P30] Development of SDR-based scintillation detector system and observation with magnetometer and radar

*Shuji Abe[1], Akiko Fujimoto[2], Akimasa Yoshikawa[3,1] (1.International Center for Space Weather Science and Education, Japan, 2.Kyushu Institute of Technology, 3.Department of Earth and Planetary Sciences, Kyushu University)

[PEM09-P31] Application of magneto-impedance sensor to geomagnetic field measurements for constructing Distributed Arrays of Small Instruments (DASI)

Nomura Hiroshi[1], *Masahito Nose[1], Hitoshi Aoyama[2], Takeshi Kawano[2], Hiroshi Ichihara[3], Masafumi Hirahara[1] (1.Institute for Space-Earth Environmental Research, Nagoya University, 2.Aichi Steel Corporation, 3.Graduate school of environmental studies, Nagoya University)

[PEM09-P32] Closure of the Onagawa Magnetic Field Observatory of Tohoku University

*Takahiro Obara[1], Takeshi Sakanoi[1], Yasumasa Kasaba[1], Fuminori Tsuchiya[1], Hiroaki Misawa[1], Masato Kagitani[1], Aya Otomo[1] (1.Planetary Plasma and Atmospheric Research Center,Tohoku University)

[E] Oral | P (Space and Planetary Sciences)：P-EM Solar-Terrestrial Sciences, Space Electromagnetism & Space Environment

9:00 AM - 10:30 AM JST | 12:00 AM - 1:30 AM UTC | Ch.06 Zoom Room 06

[P-EM10] Frontiers in solar physics

convener:Takaaki Yokoyama(School of Science, University of Tokyo), Shinsuke Imada(Institute for Space-Earth Environmental Research, Nagoya University), Shin Toriumi(Institute of Space and Astronautical Science, Japan Aerospace Exploration Agency), Alphonse Sterling(NASA/MSFC), Chairperson:Shin Toriumi(Institute of Space and Astronautical Science, Japan Aerospace Exploration Agency)

9:00 AM - 9:01 AM JST | 12:00 AM - 12:01 AM UTC

[PEM10-01] Introduction

9:01 AM - 9:23 AM JST | 12:01 AM - 12:23 AM UTC

[PEM10-02] Sun-to-Earth MHD Simulations of Geo-Effective CMEs

★Invited Papers

*Tibor Torok[1] (1.Predictive Science Inc.)

9:23 AM - 9:45 AM JST | 12:23 AM - 12:45 AM UTC

[PEM10-03] How To Trigger the Solar Flares?

★Invited Papers

*Yumi Bamba[1] (1.Nagoya University)

9:45 AM - 10:00 AM JST | 12:45 AM - 1:00 AM UTC

[PEM10-04] The Source Locations of Major Flares and CMEs in the Emerging Active Regions

*Liu Lijuan[1], Wang Yuming[2], Zhou Zhenjun[1] (1.School of Atmospheric Sciences, Sun Yat-sen University, Zhuhai, Guangdong, 519082, China, 2.Department of Geophysics and Planetary Sciences, University of Science and Technology of China, Hefei, Anhui, 230026, China)

10:00 AM - 10:15 AM JST | 1:00 AM - 1:15 AM UTC

[PEM10-05] Evaluation of horizontal flow velocity at the solar surface with machine learning and numerical simulation

*Hiroyuki Masaki[1], Hideyuki Hotta[2] (1.Graduate School of Science and Engineering, Chiba University, 2.Chiba University)

10:15 AM - 10:30 AM JST | 1:15 AM - 1:30 AM UTC

[PEM10-06] Satellite mission: *PhoENiX* (Physics of Energetic and Non-thermal plasmas in the X (= magnetic reconnection) region)

*Noriyuki Narukage[1], Mitsuo Oka[2], Yasushi Fukazawa[3], Keiichi Matsuzaki[4], Shin Watanabe[4], Taro Sakao[4], Kouichi Hagino[5], Ikuyuki Mitsuishi[6], Tsunefumi Mizuno[3], Iku Shinohara[4], Masumi Shimojo[1], Shinsuke Takasao[7], Tomoko Kawate[8], Takafumi Kaneko[6], Hiroshi Tanabe[9], Munetaka UENO[4], Tadayuki Takahashi[10], Takeshi Takashima[4], Masayuki Ohta[4] (1.National Astronomical Observatory of Japan, 2.University of California, Berkeley, 3.Hiroshima University, 4.Japan Aerospace Exploration Agency, 5.Tokyo University of Science, 6.Nagoya University, 7.Osaka University, 8.National Institute for Fusion Science, 9.The University of Tokyo, 10.Kavli Institute for the Physics and Mathematics of the Universe)

[E] Oral | P (Space and Planetary Sciences)：P-EM Solar-Terrestrial Sciences, Space Electromagnetism & Space Environment

10:45 AM - 12:14 PM JST | 1:45 AM - 3:14 AM UTC | Ch.06 Zoom Room 06

[P-EM10] Frontiers in solar physics

convener:Takaaki Yokoyama(School of Science, University of Tokyo), Shinsuke Imada(Institute for Space-Earth Environmental Research, Nagoya University), Shin Toriumi(Institute of Space and Astronautical Science, Japan Aerospace Exploration Agency), Alphonse Sterling(NASA/MSFC), Chairperson:Takaaki Yokoyama(School of Science, University of Tokyo)

10:45 AM - 11:07 AM JST | 1:45 AM - 2:07 AM UTC

[PEM10-07] Spectroscopic and photometric observations of superflares and filament eruption on cool stars

★Invited Papers

*Kosuke Namekata[1,2], Hiroyuki Maehara[2], Ryo Sasaki[3], Hiroki Kawai[3], Yuta Notsu[4], Adam F. Kowalski[4], Joel C. Allred[5], Wataru Iwakiri[3], Yohko Tsuboi[3], Satoshi Honda[6], Soshi Okamoto[1], Kiyoshi Ichimoto[1], Daisaku Nogami[1], Kazunari Shibata[1], Katsuhiro L. Murata[7], Masafumi Niwano[7], Kazuki Shiraishi[7], Ryo Adachi[7], Kota Iida[7], Motoki Oeda[7], Miyako Tozuka[6], Noriyuki Katoh[6], Hiroki Onozuka[6], Keizuke Isogai[1], Mariko Kimura[8], Naoto Kojiguchi[1], Yasuyuki Wakamatsu[1], Yusuke Tampo[1], Futa Ogawa[7], Jun Takahashi[6], Takako T. Ishii[1], Masaki Takayama[6], Tomohito Ohshima[6], Tomoki Saito[6] (1.Kyoto Univ., 2.NAOJ, 3.Chuo Univ., 4.Colorado Univ., 5.NASA, 6.Univ. of Hyogo, 7.Tokyo Institute of Technology, 8.RIKEN)

11:07 AM - 11:29 AM JST | 2:07 AM - 2:29 AM UTC

[PEM10-08] The Solar Orbiter mission – Exploring the Sun and heliosphere

★Invited Papers

*Daniel Mueller[1] (1.European Space Agency)

11:29 AM - 11:44 AM JST | 2:29 AM - 2:44 AM UTC

[PEM10-09] Current Status of the Solar-C_EUVST Mission

*Shinsuke Imada[1], Toshifumi Shimizu[2], Tomoko Kawate[2], Shin Toriumi[2], Yukio Katsukawa[3], Masahito Kubo[3], Hirohisa Hara[3], Yoshinori Suematsu[3], Kiyoshi Ichimoto[4], Ayumi Asai[4], Kyoko Watanabe[6], Takaaki Yokoyama[5], Akiko Tei[2], Harry Warren[7], David Long[8], Louise Harra[8], Luca Teriaca[9], Sarah Matthews[8], Vincenzo Andrette[10], Frederic Auchere[11] (1.Institute for Space-Earth Environmental Research, Nagoya University, 2.ISAS, 3.NAOJ, 4.Kyoto University, 5.University of Tokyo, 6.NDA, 7.NRL, 8.UCL, 9.MPS, 10.Istituto Nazionale di Astrofisica,, 11.IAS)

11:44 AM - 11:59 AM JST | 2:44 AM - 2:59 AM UTC

[PEM10-10] Solar-C(EUVST)/SoSpIM development status and scientific studies

*Kyoko Watanabe[1], Louise Harra[2], Shinsuke Imada[3], Tomoko Kawate[4], Hirohisa Hara[5], Toshifumi Shimizu[6], Yoshizumi Miyoshi[3], Nozomu Nishitani[3], Tomoaki Hori[3], Akimasa Ieda[3], Toshiki Kawai[3], Hidekatsu Jin[7], Chihiro Tao[7], Shohei Nishimoto[1] (1.National Defense Academy of Japan, 2.Physical Meteorological Observatory in Davos, World Radiation Center, 3.Institute for Space-Earth Environmental Research, Nagoya University, 4.National Institute for Fusion Science, National Institutes of Natural Sciences, 5.National Astronomical Observatory of Japan, National Institutes of Natural Sciences, 6.Institute of Space and Astronautical Science, Japan Aerospace Exploration Agency, 7.National Institute of Information and Communications Technology)

11:59 AM - 12:14 PM JST | 2:59 AM - 3:14 AM UTC

[PEM10-11] Cross-disciplinary study on heating, transport, and turbulence dynamics in solar/astrophysical and fusion/laboratory plasmas: SoLaBo-X

*Motoki Nakata[1], Ryohtaroh T Ishikawa[4], Yukio Katsukawa[2], Yohei Masada[5], Tatsuya Kobayashi[1], Munehito Shoda[2], Shinsuke Imada[3], Shin Toriumi[6], Kenichi Nagaoka[1], SoLaBo-X project[1,2] (1.National Institute for Fusion Science , 2.National Astronomical Observatory of Japan, 3.Institute for Space-Earth Environmental Research , 4.The Graduate University for Advanced Studies, 5.Aichi University of Education, 6.Japan Aerospace Exploration Agency Institute of Space and Astronautical Science)

[E] Poster | P (Space and Planetary Sciences)：P-EM Solar-Terrestrial Sciences, Space Electromagnetism & Space Environment

5:15 PM - 6:30 PM JST | 8:15 AM - 9:30 AM UTC | Ch.06_1

[P-EM10] Frontiers in solar physics

convener:Takaaki Yokoyama(School of Science, University of Tokyo), Shinsuke Imada(Institute for Space-Earth Environmental Research, Nagoya University), Shin Toriumi(Institute of Space and Astronautical Science, Japan Aerospace Exploration Agency), Alphonse Sterling(NASA/MSFC)

[PEM10-P01] Validation of solar flare emission spectra and their impact on the ionosphere

★Invited Papers

*Shohei Nishimoto[1], Kyoko Watanabe[1], Hidekatsu Jin[3], Toshiki Kawai[2], Shinsuke Imada[2], Tomoko Kawate[4] (1.National Defense Academy, 2.Institute for Space-Earth Environmental Research, Nagoya University, 3.National Institute of Information and Communications Technology, 4.National Institute for Fusion Science)

[PEM10-P02] Electron acceleration region in a small solar flare observed with Nobeyama Radioheliograph and MUSER

*Satoshi Masuda[1], Chengming Tan[2], Yihua Yan[2], Baolin Tan[2], Hiroaki Misawa[3] (1.Institute for Space-Earth Environmental Research, Nagoya University, 2.National Astronomical Observatories of China, 3.Graduate school of science, Tohoku University)

[PEM10-P03] Test particle simulation of high energy electrons during solar flare

*Takafumi Kaneko[1], Shinsuke Takasao[2] (1.Institute for Space-Earth Environmental Research, Nagoya University, 2.Department of Earth and Space Science, Graduate School of Science, Osaka University)

[PEM10-P04] Contribution of small-scale flares to coronal heating estimated by a spectroscopic observation of Hinode.

★Invited Papers

*Toshiki Kawai[1], Shinsuke Imada[1] (1.Institute for Space-Earth Environmental Research, Nagoya University)

[PEM10-P05] A Possible Generation Mechanism for “Switchbacks” Observed in the Solar Wind by the Parker Solar Probe (PSP)

*Alphonse Sterling[1], Ronald Moore[2,1] (1.NASA/MSFC, 2.University of Alabama Huntsville)

[PEM10-P06] MHD simulations of a coronal loop with effect of Alfven wave turbulence heating

Tatsuya Kai[1], *Takaaki Yokoyama[1], Munehito Shoda[2] (1.School of Science, University of Tokyo, 2.National Astronomical Observatory of Japan)

[PEM10-P07] Heating of the low-beta chromosphere by fast magnetic shock wave

*Yikang Wang[1], Takaaki Yokoyama[1], Haruhisa Iijima[2] (1.The University of Tokyo, 2.Nagoya University)

[PEM10-P08] Calculation of solar surface flow using a magnetic element tracking module

*Kengo Matoba[1], Shinsuke Imada[1], Haruhisa Iijima[1], Yoshizumi Miyoshi[1] (1.Institute for Space-Earth Environmental Research, Nagoya University)

[PEM10-P09] Prediction of latitude/longitude distribution of sunspot and tilt angle using machine learning

*Kento Michiwaki[1], Shinsuke Imada[1], Yoshizumi Miyoshi[1] (1.Institute for Space-Earth Environmental Research, Nagoya University)

[PEM10-P10] A numerical treatment for the unresolved transition region in the solar atmosphere

*Haruhisa Iijima[1], Shinsuke Imada[1] (1.Institute for Space-Earth Environmental Research, Nagoya University)

[PEM10-P11] EUV synthesis project for the Solar-C (EUVST) mission

*Akiko Tei[1], Takaaki Yokoyama[2], Shin Toriumi[1], Hirohisa Hara[3], Shinsuke Imada[4] (1.Institute of Space and Astronautical Science, 2.The University of Tokyo, 3.National Astronomical Observatory of Japan, 4.Nagoya University)

[PEM10-P12] Soalr-C(EUVST) coordination with and ground based and space observatories

*Shinichi Nagata[1], Ayumi Asai[2], Kiyoshi Ichimoto[2], Satoru UeNo[2], Toshifumi Shimizu[3], Shin Toriumi[3], Shinsuke Imada[4], Hirohisa Hara[5], Takaaki Yokoyama[6] (1.Hida Observatory, Astronomical Observatory, Graduate School of

Science, Kyoto University, 2.Astronomical Observatory, Graduate School of Science, Kyoto University, 3.Institute of Space and Astronautical Science, JAXA, 4. Institute for Space–Earth Environmental Research, Nagoya University, 5.National Astronomical Observatory of Japan, 6.University of Tokyo)

[PEM10-P13] Comparison of the Optical Characteristics for Japanese Space Solar Telescopes: Hinode/XRT and Yohkoh/SXT

*Junho Shin[1], Ryouhei Kano[2], Takashi Sakurai[2], Yeon-Han Kim[3], Yong-Jae Moon[1] (1.Kyung Hee Univ., 2.NAOJ, 3.KASI)

[E] Oral | P (Space and Planetary Sciences) : P-AE Astronomy & Extrasolar Bodies

1:45 PM - 3:15 PM JST | 4:45 AM - 6:15 AM UTC | Ch.06 Zoom Room 06

[P-AE16] Exoplanets

convener:Masahiro Ikoma(Division of Science, National Astronomical Observatory of Japan), Norio Narita(The University of Tokyo), Yuka Fujii(National Astronomical Observatory of Japan), Chairperson:Yuka Fujii(National Astronomical Observatory of Japan)

1:45 PM - 2:00 PM JST | 4:45 AM - 5:00 AM UTC

[PAE16-01] Exploring New Worlds: An Integrative, Probabilistic Analysis of Nearby Exoplanets and Exoplanetary Systems

★Invited Papers

*Daniel Apai[1] (1.The University of Arizona)

2:00 PM - 2:15 PM JST | 5:00 AM - 5:15 AM UTC

[PAE16-02] Global climate modeling of TRAPPIST-1e using MIROC for the model intercomparison

*Takeshi Kuroda[1], Yujie Zou[1,2], Arihiro Kamada[1], Takanori Kodama[2], Naoki Terada[1] (1.Department of Geophysics, Tohoku University, 2.Komaba Institute for Science, The University of Tokyo)

2:15 PM - 2:30 PM JST | 5:15 AM - 5:30 AM UTC

[PAE16-03] Global Mapping of the Surface Composition on an Exo-Earth using Sparse Modeling

*Atsuki Kuwata[1], Hajime Kawahara[1], Masataka Aizawa[2], Takayuki Kotani[3,4,5], Motohide Tamura[1,3,4] (1.The University of Tokyo, 2.Tsung-Dao Lee Institute, 3.Astrobiology center, 4.National Astronomical Observatory of Japan, 5.University for Advanced Studies (SOKENDAI))

2:30 PM - 2:45 PM JST | 5:30 AM - 5:45 AM UTC

[PAE16-04] Search for Extra-terrestrial Mother Planets Catalogue for influence of stellar activities on the extraplanetary system.

*Yosuke Alexandre Yamashiki[1], Hiroyuki Maehara[2], Vladimir Airapetian[3], Yuta Notsu[6], Kosuke Namekata[4], Riko Shimizu[5], Nami Kimura[1], Tatsuhiko Sato[7], Takanori Sasaki[4] (1.Earth & Planetary Water Resources Assessment Laboratory Graduate School of Advanced Integrated Studies in Human Survivability Kyoto University, 2.National Astronomical Observatory of Japan, 3.NASA's Goddard Space Flight Center, 4.Graduate School of Science, Kyoto University, 5.Faculty of Science, Kyoto University, 6.University of Colorado, 7.Japan Atomic Energy Agency)

2:45 PM - 3:00 PM JST | 5:45 AM - 6:00 AM UTC

[PAE16-05] Observational implications of atmospheric and orbital evolution of super-Earths

*Naho Fujita[1], Yasunori Hori[2,3], Takanori Sasaki[1] (1.Kyoto University, 2.Astrobiology Center, 3.National Astronomical Observatory of Japan)

3:00 PM - 3:15 PM JST | 6:00 AM - 6:15 AM UTC

[PAE16-06] Effects of H_2 pumping on hot Jupiter's atmospheric escape

*Hiroto Mitani[1], Riouhei Nakatani[2], Naoki Yoshida[1] (1.The University of Tokyo, 2.RIKEN)

[E] Oral | P (Space and Planetary Sciences)：P-AE Astronomy & Extrasolar Bodies

3:30 PM - 5:00 PM JST | 6:30 AM - 8:00 AM UTC | Ch.06 Zoom Room 06

[P-AE16] Exoplanets

convener:Masahiro Ikoma(Division of Science, National Astronomical Observatory of Japan), Norio Narita(The University of Tokyo), Yuka Fujii(National Astronomical Observatory of Japan), Chairperson:Norio Narita(The University of Tokyo)

3:30 PM - 3:45 PM JST | 6:30 AM - 6:45 AM UTC

[PAE16-07] TESS legacy: the brightest, closest transiting planets for atmospheric studies.

★Invited Papers

*Rafael Luque[1] (1.Instituto de Astrofisica de Andalucia)

3:45 PM - 4:00 PM JST | 6:45 AM - 7:00 AM UTC

[PAE16-08] Development of multiband imager MuSCAT3 and its first results on followup observations of TESS transiting planets

*Akihiko Fukui[1], Norio Narita[1,2], Masahiro Ikoma[1], Keisuke Isogai[4], Kiyoe Kawauchi[1], Takanori Kodama[1], Seiya Kurita[1], Nobuhiko Kusakabe[2], Jerome Pitogo de Leon[1], John Livingston[1], Mayuko Mori[1], Taku Nishiumi[3], Motohide Tamura[1,2], Noriharu Watanabe[3], Tomoyasu Yamamuro[5], Daniel Harbeck[6], Mark Bowman[6], Mark Elphick[6], Jon Nation[6], James Armstrong[7], Jacqueline Han[7], Matt Daily[6] (1.The University of Tokyo, 2.Astrobiology Center, 3.SOKENDAI, 4.Kyoto University, 5.OptCraft, 6.Las Cumbres Observatory Global Telescope Network, 7.University of Hawaii)

4:00 PM - 4:15 PM JST | 7:00 AM - 7:15 AM UTC

[PAE16-09] New Validated Planets in Overlapping K2 Campaigns

*Jerome Pitogo de Leon[1], John Livingston[1], Michael Endl[4], William Cochran[5,4], Teruyuki Hirano[18], Masayuki Kuzuhara[15,14], Rafael Garcia[11], Savita Mathur[6,7], Fei Dai[10,9], Alessandro Trani[2], Judith Korth[6,7], Kristine Lam[8], Enrique Diez Alonzo[17], Amadeo Castro Gonzalez[17], Malcolm Fridlund[12,13], Akihiko Fukui[3], Rafa Luque[6,7], Norio Narita[16,2,15,14], Enric Palle[6,7], Motohide Tamura[1,14,15], KESPRINT team (1.Department of Astronomy, University of Tokyo, 7-3-1 Hongo, Bunkyo-ku, Tokyo 113-0033, Japan, 2.Department of Earth Science and Astronomy, College of Arts and Sciences, The University of Tokyo, 3-8-1 Komaba, Meguro-ku, Tokyo 153-8902, Japan, 3.Department of Earth and Planetary Science, University of Tokyo, 7-3-1 Hongo, Bunkyo-ky, Tokyo 113-0033, Japan, 4.Department of Astronomy and McDonald Observatory, University of Texas at Austin, 2515 Speedway, Stop C1400, Austin, TX 78712, USA, 5.Center for Planetary Systems Habitability, The University of Texas at Austin, Austin TX USA, 6.Instituto de Astrofisica de Canarias (IAC), 38205 La Laguna, Tenerife, Spain, 7.Departamento de Astrofisica, Universidad de La Laguna, 38206 La Laguna, Tenerife, Spain, 8.Center for Astronomy and Astrophysics, Technical University Berlin, Hardenbergstr. 36, 10623 Berlin, Germany, 9.Division of Geological and Planetary Sciences, California Institute of Technology, 1200 East California Blvd, Pasadena CA 91125, 10.Department of Astrophysical Sciences, Princeton University, 4 Ivy Lane, Princeton, NJ 08544, USA, 11.AIM, CEA, CNRS, Universite Paris-Saclay, Universite Paris Diderot, Sorbonne Paris Cité, F-91191 Gif-sur-Yvette, France, 12.Leiden Observatory, Leiden University, 2333CA Leiden, The Netherlands, 13.Department of Space, Earth and Environment, Chalmers University of Technology, Onsala Space Observatory, SE-439 92 Onsala, Sweden, 14.Astrobiology Center, NINS, 2-21-1 Osawa, Mitaka, Tokyo 181-8588, Japan, 15.National Astronomical Observatory of Japan, NINS, 2-21-1 Osawa, Mitaka, Tokyo 181-8588, Japan, 16.JST, PRESTO, 3-8-1 Komaba, Meguro, Tokyo 153-8902, Japan , 17.Instituto Universitario de Ciencias y Tecnologias Espaciales de Asturias (ICTEA), C.Independencia 13, E-33004 Oviedo, Spain, 18.Department of Earth and Planetary Sciences, Tokyo Institute of Technology, 2-12-1 Ookayama, Meguro-ku, Tokyo 152-8551, Japan)

4:15 PM - 4:30 PM JST | 7:15 AM - 7:30 AM UTC

[PAE16-10] Spitzer and ground-based follow-up of the young transiting multi-planet system V1298 Tau

*John Livingston[1], Trevor David[2], Gudmundur Stefansson[3], Elisabeth Newton[4], Allyson Bieryla[5], Shreyas Vissapragada[6], Samuel Hadden[5], Erik Petigura[7], Eric Mamajek[8], Lynne Hillenbrand[6], David Ciardi[6], Charles Beichman[6], Luisa Rebull[6], John Stauffer[6], Varoujan Gorjian[6], Heather Knutson[6], Akihiko Fukui[1], Norio Narita[1], Motohide Tamura[1] (1.University of Tokyo, 2.Flatiron Institute, 3.Princeton University, 4.Dartmouth College, 5.Harvard-Smithsonian, 6.California Institute of Technology, 7.University of California, Los Angeles, 8.Jet Propulsion Laboratory)

4:30 PM - 4:45 PM JST | 7:30 AM - 7:45 AM UTC

[PAE16-11] Twinkle: a low-Earth orbit, visible and infrared observatory for exoplanet and solar system spectroscopy

*Billy Edwards[1] (1.Blue Skies Space Ltd)

4:45 PM - 5:00 PM JST | 7:45 AM - 8:00 AM UTC

[PAE16-12] Multi-planetary systems deduced from the observed ALMA disks: initial conditions and evolutionary outcomes

*Shijie Wang[1], Kazuhiro D Kanagawa[1,2], Toshinori Hayashi[1], Yasushi Suto[1] (1.University of Tokyo, 2.Ibaraki University)

[E] Poster | P (Space and Planetary Sciences)：P-AE Astronomy & Extrasolar Bodies

5:15 PM - 6:30 PM JST | 8:15 AM - 9:30 AM UTC | Ch.06_2

[P-AE16] Exoplanets

convener:Masahiro Ikoma(Division of Science, National Astronomical Observatory of Japan), Norio Narita(The University of Tokyo), Yuka Fujii(National Astronomical Observatory of Japan)

[PAE16-P01] The research on the existence of helium in the atmosphere of small planets around M-type stars with Subaru/IRD

*Kiyoe Kawauchi[1], Norio Narita[1], Masayuki Kuzuhara[2,3], Teruyuki Hirano[2,3], Hiroki Harakawa[4], Sebastien Vievard[2,4], Aoi Takahashi[2,3], Takayuki Kotani[2,3], Motohide Tamura[1,2,3] (1.The University of Tokyo, 2.Natural Institute of Natural Sciences Astrobiology Center, 3.National Astronomical Observatory of Japan, NAOJ, 4.Subaru Telescope)

[PAE16-P02] Results of TESS follow-up observations by the MuSCAT series and the Subaru IRD intensive program

*Norio Narita[1,2], Akihiko Fukui[1], Masahiro Ikoma[1,3], Teruyuki Hirano[2,3], Takayuki Kotani[2,3], Motohide Tamura[1,2,3] (1.The University of Tokyo, 2.Astrobiology Center, 3.National Astronomical Observatory of Japan)

[PAE16-P03] Development of optical diffusers and the on-sky examination

*Taku Nishiumi[1,2], Norio Narita[3,2,7,8], Akihiko Fukui[3], Noriharu Watanabe[3], Kiyoe Kawauchi[3], Hideyuki Izumiura[4], Hiroyuki Maehara[4], Nobuhiko Kusakabe[2,4], Keisuke Isogai[5], Yuka Terada[6,9], John H Livingston[3], Mayuko Mori[3] (1.SOUKENDAI, 2.Astrobiology Center, 3.The University of Tokyo, 4.National Astronomical Observatory of Japan, 5.Kyoto University, 6.Academia Sinica, 7.Instituto de Astrof\'{i}sica de Canarias (IAC), 8.Japan Science and Technology Agency, 9.National Taiwan University)

[PAE16-P04] Measurement of Spin-orbit Obliquity of WASP-33b by Doppler Tomography and Transit Photometry

*Noriharu Watanabe[1], Norio Narita[1], Marshall C. Johnson[2], Akihiko Fukui[1], Nobuhiko Kusakabe[3], Enric Palle[4], John Livingston[1], Kiyoe Kawauchi[1], Jerome Pitogo de Leon[1], Taku Nishiumi[5], Mayuko Mori[1], Hannu Parviainen[4], Felipe Murgas[4], Pilar Montañes-Rodriguez[4] (1.The University of Tokyo, 2.Las Cumbres Observatory, 3.Astrobiology Center, NINS, 4.Instituto de Astrofisica de Canarias, 5.The Graduate University for Advanced Studies, SOKENDAI)

[PAE16-P05] Observation of Stellar Activities for the Planetary Hosted Stars

*Riko Shimizu[1], Yosuke Alexandre Yamashiki[1], Nami Kimura[1], Hiroyuki Maehara[2], Kosuke Namekata[1], Mikio Kurita[1], Vladimir Airapetian[3] (1.Kyoto Univ., 2.NAOJ, 3.NASA Goddard Space Flight Center)

[PAE16-P06] Climate for exo-terrestrial planets with a 3D high resolution cloud resolved climate model: Effect of obliquity

*Takanori Kodama[1], Daisuke Takasuka[2], Takeshi Kuroda[3], Tomoki Miyakawa[4], Masaki Satoh[4] (1.Komaba Institute for Science, The University of Tokyo, 2.Department of Information Science, Ochanomizu University, 3.Department of Geophysics, Tohoku University, 4.Atmosphere and Ocean Research Institute, The University of Tokyo)

[PAE16-P07] **Possible Verifications for the Inner Void Model of Rapid Planet Formation**

*Masahiro Morikawa[1] (1.Department of Physics, Ochanomizu University)

[PAE16-P08] On the origin of metal-rich close-in gas giants: planetesimals vs pebbles

*Masahiro Ikoma[1,2], Kento Kikuchi[1], Tadahiro Kimura[1], Akifumi Nakayama[1], Sho Shibata[1] (1.Department of Earth and Planetary Science, The University of Tokyo, 2.Division of Science, National Astronomical Observatory of Japan)

[E] Oral | A (Atmospheric and Hydrospheric Sciences)：A-AS Atmospheric Sciences, Meteorology & Atmospheric Environment

9:00 AM - 10:30 AM JST | 12:00 AM - 1:30 AM UTC | Ch.07 Zoom Room 07

[A-AS02] Extreme Events: Observations and Modeling

convener:Sridhara Nayak(Disaster Prevention Research Institute, Kyoto University), Tetsuya Takemi(Disaster Prevention Research Institute, Kyoto University), Satoshi Iizuka(National Research Institute for Earth Science and Disaster Resilience), Chairperson:Satoshi Iizuka(National Research Institute for Earth Science and Disaster Resilience), Sridhara Nayak(Disaster Prevention Research Institute, Kyoto University), Tetsuya Takemi(Disaster Prevention Research Institute, Kyoto University)

9:00 AM - 9:05 AM JST | 12:00 AM - 12:05 AM UTC

[AAS02-01] Introduction

9:05 AM - 9:25 AM JST | 12:05 AM - 12:25 AM UTC

[AAS02-02] Assessing the Impacts of Extreme Weather on Local-Scale Hazards under Climate Change

★Invited Papers

*Tetsuya Takemi[1] (1.Disaster Prevention Research Institute, Kyoto University)

9:25 AM - 9:45 AM JST | 12:25 AM - 12:45 AM UTC

[AAS02-03] **Estimation of moisture sources within an explosive cyclone over the Sea of Japan using an isotopic regional spectral model**

★Invited Papers

*Xiaoyang Li[1], Ryuichi Kawamura[1], Atsuko Sugimoto[2,3], Kei Yoshimura[4,5] (1.Department of Earth and Planetary Science, Faculty of Science, Kyushu University, 2.Arctic Research Center, Hokkaido University, 3.Graduate School of Environmental Science, Hokkaido University, 4.Atmosphere and Ocean Research Institute, The University of Tokyo, 5.Institute of Industrial Science, The University of Tokyo)

9:45 AM - 10:00 AM JST | 12:45 AM - 1:00 AM UTC

[AAS02-04] Influence of Warm SST in the Oyashio Region on Rainfall Distribution of Typhoon Hagibis (2019)

*Satoshi Iizuka[1], Ryuichi Kawamura[2], Hisashi Nakamura[3], Toru Miyama[4] (1.National Research Institute for Earth Science and Disaster Resilience, 2.Department of Earth and Planetary Sciences, Kyushu University, 3.Research Center for Advanced Science and Technology, University of Tokyo, 4.Japan Agency for Marine-Earth Science and Technology,)

10:00 AM - 10:15 AM JST | 1:00 AM - 1:15 AM UTC

[AAS02-05] Simulation of typhoon-induced heavy precipitation over the Philippines using the Multi-scale Kain-Fritsch Cumulus Scheme in WRF

*Jose Angelo Hokson[1], Shinjiro Kanae[1], Rie Seto[1] (1.School of Environment and Society, Tokyo Institute of Technology)

10:15 AM - 10:30 AM JST | 1:15 AM - 1:30 AM UTC

[AAS02-06] **Attribution of atmospheric circulation variations associated with winter temperature whiplash events over Northeast China**

*Zhen Liao[1], Panmao Zhai[1], Yang Chen[1] (1.LaSW, CAMS, China)

[E] Oral | A (Atmospheric and Hydrospheric Sciences)：A-AS Atmospheric Sciences, Meteorology & Atmospheric Environment

10:45 AM - 12:15 PM JST | 1:45 AM - 3:15 AM UTC | Ch.07 Zoom Room 07

[A-AS02] Extreme Events: Observations and Modeling

convener:Sridhara Nayak(Disaster Prevention Research Institute, Kyoto University), Tetsuya Takemi(Disaster Prevention Research Institute, Kyoto University), Satoshi Iizuka(National Research Institute for Earth Science and Disaster Resilience), Chairperson:Tetsuya Takemi(Disaster Prevention Research Institute, Kyoto University), Sridhara Nayak(Disaster Prevention Research Institute, Kyoto University), Satoshi Iizuka(National Research Institute for Earth Science and Disaster Resilience)

10:45 AM - 10:50 AM JST | 1:45 AM - 1:50 AM UTC

[AAS02-07] Introduction

10:50 AM - 11:10 AM JST | 1:50 AM - 2:10 AM UTC

[AAS02-08] Observations and simulations of Typhoon Faxai over the Kanto area

★Invited Papers

*Woosub Roh[1], Masaki Satoh[1] (1.AORI, the university of Tokyo)

11:10 AM - 11:30 AM JST | 2:10 AM - 2:30 AM UTC

[AAS02-09] River discharge estimation of ungauged mountainous river basin using NIED Hi-net data

★Invited Papers

*Shakti P.C.[1], Kaoru Sawazaki[1] (1.National Research institute for Earth Science and Disaster Resilience (NIED))

11:30 AM - 11:45 AM JST | 2:30 AM - 2:45 AM UTC

[AAS02-10] **Increase in the strength of typhoons to Taiwan due to global warming**

*Ravi Shankar Pandey[1], Yuei-An Liou[1] (1.National Central University)

11:45 AM - 12:00 PM JST | 2:45 AM - 3:00 AM UTC

[AAS02-11] Investigation of Uncertainties in Regional Climate Information

*Saurabh Kelkar[1] (1.University of Tsukuba)

12:00 PM - 12:15 PM JST | 3:00 AM - 3:15 AM UTC

[AAS02-12] **Precipitation patterns in landfalling typhoons over Japan**

*Sridhara Nayak[1], Tetsuya Takemi[1] (1.Disaster Prevention Research Institute, Kyoto University)

[E] Poster | A (Atmospheric and Hydrospheric Sciences)：A-AS Atmospheric Sciences, Meteorology & Atmospheric Environment

5:15 PM - 6:30 PM JST | 8:15 AM - 9:30 AM UTC | Ch.07_1

[A-AS02] Extreme Events: Observations and Modeling

convener:Sridhara Nayak(Disaster Prevention Research Institute, Kyoto University), Tetsuya Takemi(Disaster Prevention Research Institute, Kyoto University), Satoshi Iizuka(National Research Institute for Earth Science and Disaster Resilience)

[AAS02-P01] Analysis of "Typhoon-class Strong Wind" During the Non-typhoon Period for 116 Years (1904-2019) after Weather Observation on the Korean Peninsula : Basic Analysis

*Woo-Sik JUNG[1] (1.Department of Atmospheric Environment Information Engineering, INJE University, Republic of Korea.)

[AAS02-P02] Development of the KTTI(Korean Typhoon Type Index) by Analyze the Characteristics of Typhoon Affecting the Korean Peninsula

*Woo-Sik JUNG[1], Gunwoo Kim[1] (1.Department of Atmospheric Environment Information Engineering, INJE University, Republic of Korea.)

[AAS02-P03] **High precipitation rates and floods: Relation to solar wind high-speed streams**

*Paul Prikryl[1], Vojto Rušin[2], Emil A. Prikryl[3] (1.Physics Department, University of New Brunswick, 2.Astronomical Institute, Slovak Academy of Sciences, 3.Northern Ontario School of Medicine)

[AAS02-P04] **Climate change initiated variation in the tracks of typhoons in the North West Pacific basin**

*Ravi Shankar Pandey[1], Yuei-An Liou[1] (1.National Central University)

[J] Oral | A (Atmospheric and Hydrospheric Sciences)：A-AS Atmospheric Sciences, Meteorology & Atmospheric Environment

9:00 AM - 10:30 AM JST | 12:00 AM - 1:30 AM UTC | Ch.08 Zoom Room 08

[A-AS05] Atmospheric Chemistry

convener:Tomoki Nakayama(Graduate School of Fisheries and Environmental Sciences, Nagasaki University), Naoko Saitoh(Center for Environmental Remote Sensing), Sakae Toyoda(Department of Chemical Science and Engineering, Tokyo Institute of Technology), Risa Uchida(Japan Automobile Research Institute), Chairperson:Risa Uchida(Japan Automobile Research Institute), Kei Sato(National Institute for Environmental Studies)

9:00 AM - 9:30 AM JST | 12:00 AM - 12:30 AM UTC

[AAS05-01] Cryosphere-atmosphere biogeochemical cycles: Insights from Arctic Ocean drifting campaign

★Invited Papers

*Daiki Nomura[1] (1.Field Science Center for Northern Biosphere, Hokkaido University)

9:30 AM - 9:45 AM JST | 12:30 AM - 12:45 AM UTC

[AAS05-02] Embedding of HCl droplets on ice crystal surfaces under atmospheric-concentration HCl gas

*Ken Nagashima[1], Ken-ichiro Murata[1], Gen Sazaki[1] (1.The Institute of Low Temperature Science, Hokkaido University)

9:45 AM - 10:00 AM JST | 12:45 AM - 1:00 AM UTC

[AAS05-03] A new method for quantifying sodium sulfate, sodium nitrate, and sodium chloride aerosols

*Yuya Kobayashi[1], Nobuyuki Takegawa[1] (1.Graduate School of Science, Tokyo Metropolitan University)

10:00 AM - 10:15 AM JST | 1:00 AM - 1:15 AM UTC

[AAS05-04] Investigation of gaseous and heterogeneous reactions of RO_2 radicals using FAGE-LIF method

*Nanase Kohno[1], Jiaru Li[1], Yosuke Sakamoto[1,2], Yoshizumi Kajii[1,2] (1.Kyoto University, 2.National Institute for Environmental Studies)

10:15 AM - 10:30 AM JST | 1:15 AM - 1:30 AM UTC

[AAS05-05] Real-time measurement of HO_2 and RO_2 uptake loss rate onto ambient particles during AQUAS-Kyoto summer campaign in 2020

*Yosuke Sakamoto[1,2], Bai Yu[1], Jiaru Li[1], Kohno Nanase[1], Yoshizumi Kajii[1,2] (1.Kyoto University , 2.National Institute for Environmental Studies)

[J] Oral | A (Atmospheric and Hydrospheric Sciences)：A-AS Atmospheric Sciences, Meteorology & Atmospheric Environment

10:45 AM - 12:15 PM JST | 1:45 AM - 3:15 AM UTC | Ch.08 Zoom Room 08

[A-AS05] Atmospheric Chemistry

convener:Tomoki Nakayama(Graduate School of Fisheries and Environmental Sciences, Nagasaki University), Naoko Saitoh(Center for Environmental Remote Sensing), Sakae Toyoda(Department of Chemical Science and Engineering, Tokyo Institute of Technology), Risa Uchida(Japan Automobile Research Institute), Chairperson:Nobuyuki Takegawa(Graduate School of Science, Tokyo Metropolitan University)

10:45 AM - 11:00 AM JST | 1:45 AM - 2:00 AM UTC

[AAS05-06] **Understanding of Volatile Organic Compound Emissions from Western US Wildfires**

*Kanako Sekimoto[1], Matthew M Coggon[2,3], Georgios Gkatzelis[2,3], Carsten Warneke[2,3] (1.Yokohama City University, 2.NOAA Earth System Research Laboratory, 3.Cooperative Institute for Research In Environmental Sciences)

11:00 AM - 11:15 AM JST | 2:00 AM - 2:15 AM UTC

[AAS05-07] New particle formation from ozonolysis of 2-methyl-2-butene and *trans*-2-butene

*Satoshi Inomata[1], Jun Hirokawa[2], Yosuke Sakamoto[3] (1.National Institute for Environmental Studies, 2.Hokkaido University, 3.Kyoto University)

11:15 AM - 11:30 AM JST | 2:15 AM - 2:30 AM UTC

[AAS05-08] Structural elucidation of a-pinene originating $C_{10}H_{17}O_6S$ organosulfates from CCS values derived from ion mobility mass spectrometry and theoretical structural modelling

*Yoshiteru Iinuma[1], Satoshi Inomata[2], Kei Sato[2] (1.Okinawa Institute of Science and Technology Graduate University, 2.National Institute for Environmental Studies)

11:30 AM - 11:45 AM JST | 2:30 AM - 2:45 AM UTC

[AAS05-09] Wet Deposition of Black Carbon at Ny-Ålesund, Svalbard

*Tatsuhiro Mori[1], Yutaka Kondo[2], Sho Ohata[3,4], Kumiko Goto-Azuma[2,5], Kaori Fukuda[2], Yoshimi Ogawa[2], Nobuhiro Moteki[6], Atsushi Yoshida[6], Makoto Koike[6], Puna Ram Sinha[7], Naga Oshima[8], Hitoshi MATSUI[9], Yutaka Tobo[2,5], Masanori Yabuki[10], Wenche Aas[11] (1.Tokyo University of Science, 2.National Institute of Polar Research, 3.Institute for Space–Earth Environmental Research, Nagoya University, 4.Institute for Advanced Research, Nagoya University, 5.The Graduate University for Advanced Studies, SOKENDAI, 6.Department of Earth and Planetary Science, Graduate School of Science, The University of Tokyo, 7.Department of Earth and Space Sciences, Indian Institute of Space Science and Technology, 8.Meteorological Research Institute, 9.Graduate School of Environmental Studies, Nagoya University, 10.Research Institute for Sustainable Humanosphere, Kyoto University, 11.Norwegian Institute for Air Research)

11:45 AM - 12:00 PM JST | 2:45 AM - 3:00 AM UTC

[AAS05-10] Improved simulations of global black carbon distributions by modifying wet scavenging processes in convective and mixed-phase clouds

*Mingxu Liu[1], Hitoshi Matsui[1] (1.Graduate school of environmental studies, Nagoya University)

12:00 PM - 12:15 PM JST | 3:00 AM - 3:15 AM UTC

[AAS05-11] High potential of Asian dust to act as ice nucleating particles in mixed-phase clouds simulated with a global model

*Kei Kawai[1], Hitoshi Matsui[1], Yutaka Tobo[2,3] (1.Nagoya University, 2.National Institute of Polar Research, 3.SOKENDAI (The Graduate University for Advanced Studies))

[J] Oral | A (Atmospheric and Hydrospheric Sciences)：A-AS Atmospheric Sciences, Meteorology & Atmospheric Environment

1:45 PM - 3:15 PM JST | 4:45 AM - 6:15 AM UTC | Ch.08 Zoom Room 08

[A-AS05] Atmospheric Chemistry

convener:Tomoki Nakayama(Graduate School of Fisheries and Environmental Sciences, Nagasaki University), Naoko Saitoh(Center for Environmental Remote Sensing), Sakae Toyoda(Department of Chemical Science and Engineering, Tokyo Institute of Technology), Risa Uchida(Japan Automobile Research Institute), Chairperson:Chika Minejima(International Christian University)

1:45 PM - 2:00 PM JST | 4:45 AM - 5:00 AM UTC

[AAS05-12] Validation and correction of TROPOMI tropospheric NO_2 column density data using 4AZ-MAXDOAS at Chiba, Japan

*Hikaru Saito[1], Hitoshi Irie[1], Alessandro Damiani[1] (1.University of Chiba)

2:00 PM - 2:15 PM JST | 5:00 AM - 5:15 AM UTC

[AAS05-13] **NO_X emission estimation over Japan based on satellite data with wind field divergence**

*Masahiro Yamaguchi[1], Yugo Kanaya[1] (1.Japan Agency for Marine-Earth Science and Technology)

2:15 PM - 2:30 PM JST | 5:15 AM - 5:30 AM UTC

[AAS05-14] Introducing new lightning schemes to a chemistry climate model CHASER (MIROC)

*Yanfeng He[1], Kengo Sudo[1] (1.Nagoya University)

2:30 PM - 2:45 PM JST | 5:30 AM - 5:45 AM UTC

[AAS05-15] Methane emissions from populated areas of Tokyo and five prefectures: Emission ratios with NOx and their trends over 2009-2018

*Yugo Kanaya[1], Kanami Saima[2], Akira Fukuike[2] (1.JAMSTEC, 2.MURATA Keisokuki Service Co., Ltd.)

2:45 PM - 3:00 PM JST | 5:45 AM - 6:00 AM UTC

[AAS05-16] An impact of tropospheric air pollution changes over Japan due to future climate and emission change

*Natsumi Kawano[1], Tatsuya Nagashima[1], Masayuki Hara[2], Satoru Chatani[1], Syuichi Itahashi[3] (1.National Institute for Environmental Studies, 2.Center for Environmental Science in Saitama, 3.Central Research Institute of Electric Power Industry)

3:00 PM - 3:15 PM JST | 6:00 AM - 6:15 AM UTC

[AAS05-17] An Empirical Approach toward the Reduction Targets of CH4 and O3 as SLCP: For Asia as an example

*Hajime Akimoto[1], Tatsuya Nagashima[1], Hiroshi Tanimoto[1], Zbigniew Klimont[2], Markus Amann[2] (1.National Institute for Environmental Studies, 2.International Institute for Applied System Analysis)

[J] Oral | A (Atmospheric and Hydrospheric Sciences)：A-AS Atmospheric Sciences, Meteorology & Atmospheric Environment

3:30 PM - 5:00 PM JST | 6:30 AM - 8:00 AM UTC | Ch.08 Zoom Room 08

[A-AS05] Atmospheric Chemistry

convener:Tomoki Nakayama(Graduate School of Fisheries and Environmental Sciences, Nagasaki University), Naoko Saitoh(Center for Environmental Remote Sensing), Sakae Toyoda(Department of Chemical Science and Engineering, Tokyo Institute of Technology), Risa Uchida(Japan Automobile Research Institute), Chairperson:Naoko Saitoh(Center for Environmental Remote Sensing), Shigeyuki Ishidoya(Advanced Industrial Science and Technology)

3:30 PM - 4:00 PM JST | 6:30 AM - 7:00 AM UTC

[AAS05-18] **Earth system modeling on interactions between ecosystem and atmospheric chemistry**

★Invited Papers

*Tomohiro Hajima[1], Manabu Abe[1], Akinori Ito[1], Akihiko Ito[2], Rumi Ohgaito[1], Kazuyuki Saito[1], Kengo Sudo[3], Michio Kawamiya[1], Maki Noguchi Aita[1], Prabir Patra[1], Akitomo Yamamoto[1], Tokuta Yokohata[2], Shingo Watanabe[1], Michio Watanabe[1] (1.Japan Agency for Marine-Earth Science and Technology, 2.National Institute for Environmental Studies, 3.Nagoya University)

4:00 PM - 4:15 PM JST | 7:00 AM - 7:15 AM UTC

[AAS05-19] **Seasonal variations of methane sources in South Asia inferred from observations of stable carbon isotope ratio of atmospheric methane**

*Yukio Terao[1], Taku Umezawa[1], Manish Naja[2], Md. Kawser Ahmed[3], Shohei Nomura[1], Toshinobu Machida[1], Motoki Sasakawa[1], Hitoshi Mukai[1], Prabir Patra[4] (1.National Institute for Environmental Studies, 2.Aryabhatta Research Institute of Observational Sciences, 3.Department of Oceanography, Faculty of Earth & Environmental Sciences, University of Dhaka, 4.Research Institute for Global Change, JAMSTEC)

4:15 PM - 4:30 PM JST | 7:15 AM - 7:30 AM UTC

[AAS05-20] The interhemispheric transport pathways of methane as observed by GOSAT and simulated by ACTM

*Dmitry Belikov[1], Naoko Saitoh[1], Prabir Patra[1,2] (1.Center for Environmental Remote Sensing, Chiba University, 2.Research Institute for Global Change (RIGC), JAMSTEC)

4:30 PM - 4:45 PM JST | 7:30 AM - 7:45 AM UTC

[AAS05-21] **Signal of CO_2 emitted from 2020 Western U. S. wildfire captured by commercial airliner observations**

*Kentaro Ishijima[1], Toshinobu Machida[2], Taku Umezawa[2], Yosuke Niwa[2,1], Kazuhiro Tsuboi[1], Ryo Fujita[1], Hidekazu Matsueda[3,1], Taichu Y Tanaka[1], Takashi Maki[1], Takashi Nakamura[4] (1.Meteorological Research Institute, 2.National Institute for Environmental Studies, 3.Dokkyo University, 4.Japan Meteorological Agency)

4:45 PM - 5:00 PM JST | 7:45 AM - 8:00 AM UTC

[AAS05-22] Secular trend of atmospheric N_2O isotopocule ratios observed at Syowa staion, Antarctica

*Sakae Toyoda[1], Tsutomu Mizuno[1], Daisuke Goto[2], Shinji Morimoto[3] (1.School of Materials and Chemical Technology, Tokyo Institute of Technology, 2.National Institute of Polar Research, 3.Center for Atmospheric and Oceanic Studies, Tohoku University)

[J] Poster | A (Atmospheric and Hydrospheric Sciences)：A-AS Atmospheric Sciences, Meteorology & Atmospheric Environment

5:15 PM - 6:30 PM JST | 8:15 AM - 9:30 AM UTC | Ch.07_2

[A-AS05] Atmospheric Chemistry

convener:Tomoki Nakayama(Graduate School of Fisheries and Environmental Sciences, Nagasaki University), Naoko Saitoh(Center for Environmental Remote Sensing), Sakae Toyoda(Department of Chemical Science and Engineering, Tokyo Institute of Technology), Risa Uchida(Japan Automobile Research Institute)

[AAS05-P01] The Relation between HONO Emission and the Amount of Carbon and Nitrogen Compounds in the Activated Sludge

*Chika Minejima[1], Yuta Orii[1], Ryosuke Fujinuma[1], Toshikazu Suenaga[2], Shohei Riya[2], Akihiko Terada[2], Masayuki Ohyama[4], Norimichi Takenaka[5], Keiichi Sato[3] (1.International Christian University, 2.Tokyo University of Agriculture and Technology, 3.Asia Center for Air Pollution Research (ACAP), 4.Osaka Institute of Public Health, 5.Osaka Prefecture University)

[AAS05-P02] Constraining the origin of tropospheric nitrous acid using triple oxygen isotopes as tracers

*Fumiko Nakagawa[1], Peng Lai[1], Kazuya Hirano[1], Masanori Ito[1], Urumu Tsunogai[1] (1.Graduate School of Environmental Studies, Nagoya University)

[AAS05-P03] **Changes in tropospheric nitrogen dioxide vertical column densities over Japan and Korea during the COVID-19 using Pandora and MAX-DOAS**

*Yongjoo Choi[1], Yugo Kanaya[1], Hisahiro Takashima[2], Kihong Park[3], Haebum Lee[3], Jihyo Chong[3,4], Jae Hwan Kim[5] (1.Japan Agency for Marine-Earth Science and Technology, 2.Faculty of Science, Fukuoka University, 3.Gwangju Institute of Science and Technology, 4.Environmental Management Division, Yeongsan River Basin Environmental Office, Gwangju 61945, Korea, 5.Pusan National University)

[AAS05-P04] Estimation of emission source of CO from biomass burning observed with ground-based FTIR spectrometers at Tsukuba since 2010

Daisuke Suzuki[2], *Hideaki Nakajima[1,2], Isao Murata[2], Isamu Morino[1] (1.National Institute for Environmental Studies, 2.Graduate School of Environmental Studies, Tohoku University)

[AAS05-P05] Evaluation of NICAM-TM CO data using MOPITT CO data

*Miyajima Hiroshi[1], Naoko Saitoh[1], Yosuke Niwa[2] (1.Center for Environmental Remote Sensing, Chiba University, 2.National Institute for Environmental Studies)

[AAS05-P06] **Evaluation of the global chemistry transport model CHASER utilizing TROPOMI formaldehyde measurements**

*Hossain Mohammed Syedul Hoque[1], Kengo Sudo[1,3], Hitoshi Irie[2], Takashi Sekiya[3] (1.Graduate School of Environmental Studies, Nagoya University, Japan, 2.Center for Environmental Remote Sensing (CEReS), Chiba University, Japan, 3.Japan Agency for Marine-Earth Science and Technology (JAMSTEC), Yokohama, Japan)

[AAS05-P07] Ozone steady-state at the semi-urban region, Shadnagar, in Southern India

*Vijay Kumar Sagar[1] (1.National Remote Sensing Centre, Hyderabad, ISRO)

[AAS05-P08] A relationship between surface oxidant concentration and daily maximum temperature, and its long-term variability

*Atsushi Shimizu[1], Tatsuya Nagashima[1] (1.National Institute for Environmental Studies)

[AAS05-P09] Analysis of tropospheric ozone budgets in CMIP6 experiments

*Paul T Griffiths[1], Lee T Murray[2], Guang Zeng[3], Vaishali Naik[4], Prodromos Zanis[5], Alexander T Archibald[1] (1.National Centre for Atmospheric Science, Cambridge University, 2.University of Rochester, Rochester, NY, USA, 3.National Institute of Water and Atmospheric Research, Wellington, New Zealand, 4.NOAA Geophysical Fluid Dynamics Laboratory, Princeton, NJ, USA, 5.Department of Meteorology and Climatology, Aristotle University of Thessaloniki, Thessaloniki, Greece)

[AAS05-P10] Study of tropospheric CS_2 photooxidation chemistry

*Yuanzhe Li[1], Kazuki Kamezaki[2], Sebastian Danielache[2] (1.Green Science And Engineering Division, Graduate School Of Science And Technology, Sophia University, 2.Department of Materials & Sciences, Faculty of Science & Technology, Sophia University)

[AAS05-P11] **Effects of hydroxyl radical exposure on chemical composition of secondary organic aerosol formed from sabinene ozonolysis**

*Kei Sato[1,2], Yu Morino[1], Takashi Imamura[1], Yoshizumi Kajii[1,2] (1.National Institute for Environmental Studies, 2.Kyoto University)

[AAS05-P12] Impact of nighttime aging on optical properties of toluene secondary organic aerosol

*Tomoki Nakayama[1], Kei Sato[2], Sathiyamurthi Ramasamy[2], Takashi Imamura[2], Yoshizumi Kajii[3,2] (1.Nagasaki University, 2.NIES, 3.Kyoto University)

[AAS05-P13] Volatility of nanoparticles generated from jet engine lubrication oil

*Nobuyuki Takegawa[1], Anna Nagasaki[1] (1.Graduate School of Science, Tokyo Metropolitan University)

[AAS05-P14] Vertical structural measures of atmospheric pollutants using XU-S

*Kazuyo Yamaji[1], Tetsuya Miyakoshi[2], Satoshi Komatsu[2], Isao Kanda[3] (1.Kobe University, 2.ShinMaywa Industries, Ltd. , 3.Japan Meteorological Corporation)

[AAS05-P15] **Continuous and multi-wavelength measurement of aerosol extinction coefficient by long-path propagation of LED light at Chiba, Japan**

*Ikuya Nishiwaki[1], Hitoshi Irie[2], Nofel D. Lagrosas[1], Hiroaki Kuze[2] (1.Chiba University, 2.Center for Environmental Remote Sensing, Chiba University)

[AAS05-P16] Aerosol type classification of ground-based remote sensing data by k-means clustering

*Hiroyasu Kobayashi[1], Hitoshi Irie[2], Masahiro Momoi[1] (1.Chiba University, 2.Center for Environmental Remote Sensing, Chiba University)

[AAS05-P17] Validation of MERRA-2 Reanalysis Aerosol Products Using Ground-based Observations in Phimai, Thailand, and Factors that Affect Aerosol Optical Depth over the Indochina Peninsula

*Takeru Ohno[1], Hitoshi Irie[1], Arlindo M da Silva[2], Ravi C Govindaraju[2] (1.Center for Environmental Remote Sensing, Chiba University, 2.Global Modeling and Assimilation Office, NASA Goddard Space Flight Center, Greenbelt, Maryland)

[AAS05-P18] Exploring ground-based aerosol optical properties to improve satellite estimates of surface particulate matter concentrations

*Alessandro Damiani[1], Hitoshi Irie[1], Kodai Yamaguchi[1], Hossain Mohammed Syedul Hoque[2], Tomoki Nakayama[3], Yutaka Matsumi[2], Yutaka Kondo[4] (1.CEReS, Chiba University, 2.Nagoya University, 3.Nagasaki University, 4.National Institute of Polar Research)

[AAS05-P19] Development of international air quality and sky research remote sensing (A-SKY) network

*Hitoshi Irie[1], Alessandro Damiani[1], Toshihiko Takemura[2], Thanawat Jarupongsakul[3], Manish Naja[4] (1.Center for Environmental Remote Sensing, Chiba University, 2.Research Institute for Applied Mechanics, Kyushu University, 3.Department of Geology, Faculty of Science, Chulalongkorn University, 4.Aryabhatta Research Institute of Observational Sciences (ARIES))

[AAS05-P20] Prediction of changes in DSS emission using the Earth System Model of the Meteorological Research Institute

*Takashi Maki[1], Taichu Y Tanaka[1], Thomas Sekiyama[1], Mizuo Kajino[1], Naga Oshima[1], Tsuyoshi Koshiro[1] (1.Meteorological Research Institute)

[AAS05-P21] Methane emission trends of China in 2009-2018 induced by atmospheric observations

*Fenjuan Wang[1], Shamil S Maksyutov[1], Rajesh Janardanan[1], Akihiko Ito[2], Isamu Morino[1], Yukio Yoshida[1], Yasunori Tohjima[1], Johannes W. Kaiser[3], Greet Janssens-Maenhout[4], xin Lan[5], Ivan Mammarella[6], Jost V. Lavric[7], Tsuneo Matsunaga[1] (1.NIES National Institute of Environmental Studies, 2.Finnish Meteorological Institute, 3.Deutscher Wetterdienst, 4.European Commission Joint Research Centre, 5.Earth System Research Laboratory, 6.University of Helsinki, 7.Max Planck Institute for Biogeochemistry)

[AAS05-P22] **Characteristics of methane vertical distributions over India**

*Dingkun Zhang[1], Naoko Saitoh[1], Dmitry Belikov[1], Prabir Patra[2], Naveen Chandra[3] (1.Center for Environmental Remote Sensing, Chiba University, 2.Japan Agency for Marine-Earth Science and Technology, 3.National Institute for Environmental Studies)

[AAS05-P23] Temporal and spatial variations of the mole fraction, carbon and hydrogen isotope ratios of atmospheric methane in the Western Pacific region

*Yasuda Mahito[1], Shinji Morimoto[1], Shuji Aoki[1], Ryo Fujita[2], Taku Umezawa[3] (1.Center for Atmospheric and Oceanic Studies, Graduate School of Science, Tohoku University, 2.Department of Climate and Geochemistry Research, Meterorological Reserach Research Institute, Tsukuba Japan, 3.National Institute for Environmental Studies, Tsukuba, Japan)

[AAS05-P24] Variations of atmospheric carbon dioxide and its radioisotope in the arctic region

*Hikaru Sekine[1], Shinji Morimoto[1], Chinatsu Yamada[1], Daisuke Goto[2], Masayo Minami[3], Toshio Nakamura[3], Shuji Aoki[1] (1.Center for Atmospheric and Oceanic studies, 2.National Institute of Polar Research, 3.Institute for Space-Earth Environmental Research)

[AAS05-P25] Preparation of O_2/N_2 dataset from the surface to the middle stratosphere around Japan traceable to NMIJ gravimetric scale

*Shigeyuki Ishidoya[1], Shinji Morimoto[2], Kazuhiro Tsuboi[3], Satoshi Sugawara[4], Daisuke Goto[5], Nobuyuki Aoki[1], Shohei Murayama[1], Yosuke Niwa[6], Shuji Aoki[2], Hidekazu Matsueda[3], Kentaro Ishijima[3] (1.Advanced Industrial Science and Technology, 2.Tohoku University, 3.Meteorological Research Institute, 4.Miyagi University of Education, 5.National Institute of Polar Research, 6.National Institute for Environmental Studies)

[AAS05-P26] Temporal variation of the ozone profile observed with FTIR at Tsukuba

*Isao Murata[1], Hideaki Nakajima[2], Isamu Morino[2], Masanori Takeda[1,2] (1.Graduate School of Environmental Studies, Tohoku University, 2.National Institute for Environmental Studies)

[E] Poster | A (Atmospheric and Hydrospheric Sciences)：A-OS Ocean Sciences & Ocean Environment

5:15 PM - 6:30 PM JST | 8:15 AM - 9:30 AM UTC | Ch.08_1

[A-OS08] Ocean renewable energy: resource, impacts and technologies

convener:Bahareh Kamranzad(The Hakubi Center for Advanced Research/Graduate School of Advanced Integrated Studies in Human Survivability, Kyoto University)

[AOS08-P01] FINE SCALE SENSITIVITY MAP OF SEABIRDS FOR OFFSHORE WIND FARM

*Yutaka Watanuki[1], Katsura Mikami[1], Kentaro Kazama[2], Mami T Kazama, Rui Ma[1] (1.Faculty of Fisheries Sciences, Hokkaido University, 2.School of Human Sciences, Waseda University)

[J] Oral | A (Atmospheric and Hydrospheric Sciences)：A-HW Hydrology & Water Environment

9:00 AM - 10:30 AM JST | 12:00 AM - 1:30 AM UTC | Ch.12 Zoom Room 12

[A-HW23] Isotope Hydrology 2021

convener:Masaya Yasuhara(Rissho Univ.), Kohei Kazahaya(Geological Survey of Japan, AIST), Shinji Ohsawa(Institute for Geothermal Sciences, Graduate School of Science, Kyoto University), Kazuyoshi Asai(Geo Science Laboratory), Chairperson:Masaya Yasuhara(Rissho Univ.), Takashi Nakamura(International Research Center for River Basin Environment, University of YAMANASHI), Kazuyoshi Asai(Geo Science Laboratory), Shinji Ohsawa(Institute for Geothermal Sciences, Graduate School of Science, Kyoto University)

9:00 AM - 9:05 AM JST | 12:00 AM - 12:05 AM UTC

[AHW23-01] Introduction

9:05 AM - 9:30 AM JST | 12:05 AM - 12:30 AM UTC

[AHW23-02] Seasonal and spatial variations of chemical weathering in the Mekong Basin: From the headwaters to the lower reaches

★Invited Papers

*Hiroto Kajita[1], Yuki Ota[2], Toshihiro Yoshimura[3], Daisuke Araoka[2], Takuya Manaka[4], Ziyu Ouyang[1], Shinya Iwasaki[3], Takuya Yanase[1], Akihiko Inamura[2], Etsuo Uchida[5], Hongbo Zheng[6], Qing Yang[6], Ke Wang[1], Atsushi Suzuki[2], Hodaka Kawahata[1] (1.The University of Tokyo, 2.National Institute of Advanced Industrial Science and Technology, 3.Japan Agency for Marine-Earth Science and Technology, 4.Forestry and Forest Products Research Institute, 5.Waseda University, 6.Yunnan University)

9:30 AM - 9:45 AM JST | 12:30 AM - 12:45 AM UTC

[AHW23-03] Stable Isotope Dynamics of Hydrological Interactions in The Chao Phraya River System in Thailand

*Jeerapong Laonamsai[1], Kimpei Ichiyanagi[1] (1.Deaprtment of Earth and Environmental Sciences, Graduate School of Science and Technology, Kumamoto University)

9:45 AM - 10:10 AM JST | 12:45 AM - 1:10 AM UTC

[AHW23-04] Groundwater in the area where ground flow with long displacement occurred due to the 2018 Sulawesi Island Earthquake in Indonesia

★Invited Papers

*Susumu Yasuda[1], Hisashi Furuichi[2] (1.Tokyo Denki University, 2.Yachiyo Engineering Co., Ltd.)

10:10 AM - 10:25 AM JST | 1:10 AM - 1:25 AM UTC

[AHW23-05] The formation of a temporary pond, Akaike, at the Northern Foot of Mount Fuji, Japan, in 2020

*Shinya Yamamoto[1], Takashi Nakamura[2], Seongwon Lee[3], Masaya Yasuhara[3] (1.Mount Fuji Research Institute, Yamanashi Prefectural Government, 2.International Research Center for River Basin Environment, University of Yamanashi, 3.Faculty of Geo-Environmental Science, Rissho University)

10:25 AM - 10:30 AM JST | 1:25 AM - 1:30 AM UTC

[AHW23-06] Discussion

[J] Oral | A (Atmospheric and Hydrospheric Sciences)：A-HW Hydrology & Water Environment

10:45 AM - 12:15 PM JST | 1:45 AM - 3:15 AM UTC | Ch.12 Zoom Room 12

[A-HW23] Isotope Hydrology 2021

convener:Masaya Yasuhara(Rissho Univ.), Kohei Kazahaya(Geological Survey of Japan, AIST), Shinji Ohsawa(Institute for Geothermal Sciences, Graduate School of Science, Kyoto University), Kazuyoshi Asai(Geo Science Laboratory), Chairperson:Kazuyoshi Asai(Geo Science Laboratory), Masaya Yasuhara(Rissho Univ.), Noritoshi Morikawa(Geological Survey of Japan, AIST), Kohei Kazahaya(Geological Survey of Japan, AIST)

10:45 AM - 11:10 AM JST | 1:45 AM - 2:10 AM UTC

[AHW23-07] Supply processes of dissolved inorganic carbon and flow system of groundwater in Fukui-Ohno Basin

★Invited Papers

*Yamanaka Masaru[1], Seongwon Lee[2], ZHAO MINGZHE[1], Takanori Nakano[3] (1.Department of Earth and Environmental Sciences, College of Humanities and Sciences, Nihon University, 2.Rissho University, 3.The Research Institute for Humanity and Nature)

11:10 AM - 11:25 AM JST | 2:10 AM - 2:25 AM UTC

[AHW23-08] Origin and hydro-chemical evolution of geothermal waters from Nozawa-Onsen hydrothermal springs in the northern Nagano Prefecture, central Japan

*Shunsuke Akazawa[1], Madhusoodhan Satish-Kumar[2], Naoki Watanabe[3], Cheibany Ould-Elemine[4], Masaki Yuhara[5] (1.Graduate School of Science and Technology, Niigata University, Japan, 2.Department of Geology, Faculty of Science, Niigata University, Japan , 3.Research Institute for Natural Hazards and Disaster Recovery, Niigata University, Japan, 4.Ensero Solutions, Canada, 5.Department of Earth System Science, Faculty of Science, Fukuoka University, Japan)

11:25 AM - 11:40 AM JST | 2:25 AM - 2:40 AM UTC

[AHW23-09] Composition of ammonium nitrogen isotope in Oita Plain, eastern Kyushu Island, Japan

*Takashi Nakamura[1], Kazuhiro Amita[2], Shinji Ohsawa[3] (1.Interdisciplinary Center for River Basin Environment, University of Yamanashi, 2.Research Center for Engineering Science, Akita University, 3.Beppu Geothermal Research Laboratory, Kyoto University)

11:40 AM - 12:05 PM JST | 2:40 AM - 3:05 AM UTC

[AHW23-10] The continuing story of mathmatical modelling for nitrogen pollution analysis in groundwater

★Invited Papers

*Kei Nishida[1], Ken Yokozawa[2], Bijjay Man Shakya[1], Hiroshi Ishidaira[1], Tadashi Toyama[1], Takashi Nakamura[1] (1.Interdisciplinary Centre for River Basin Environment, Interdisciplinary Graduate School, University of Yamanashi, 2.Shizuoka Prefecture)

12:05 PM - 12:15 PM JST | 3:05 AM - 3:15 AM UTC

[AHW23-11] Discussion

[J] Poster | A (Atmospheric and Hydrospheric Sciences)：A-HW Hydrology & Water Environment

5:15 PM - 6:30 PM JST | 8:15 AM - 9:30 AM UTC | Ch.08_2

[A-HW23] Isotope Hydrology 2021

convener:Masaya Yasuhara(Rissho Univ.), Kohei Kazahaya(Geological Survey of Japan, AIST), Shinji Ohsawa(Institute for Geothermal Sciences, Graduate School of Science, Kyoto University), Kazuyoshi Asai(Geo Science Laboratory)

[AHW23-P01] Detection of slab-derived fluid in saline ground water collected from coastal area of Seto Inland Sea, Japan

★Invited Papers

*Yoko Togo[1], Kohei Kazahaya[1], Yuki Tosaki[1], Masaaki Takahashi[1], Noritoshi Morikawa[1], Hiroshi A Takahashi[1], Yuri Nakamura[1], Akihiko Inamura[1], Hinako Shimizu[1], Hiroyuki Matsuzaki[2] (1.National Institute of Advanced Industrial Science and Technology, 2.University of Tokyo)

[AHW23-P02] Geochemical characteristics and origins of saline groundwater in the southern Boso Peninsula, Chiba, Japan

*Masaya Yasuhara[1], Akihiko Inamura[2], Ryotaro Mabuchi[3], Seongwon Lee[1], Noritoshi Morikawa[2] (1.Rissho University, 2.Geological Survey of Japan, AIST, 3.Out-Sourcing Technology Co., Ltd.)

[AHW23-P03] Isotope and water quality compositions of groundwater in the bedrock and sediment deposits in Kofu basin

*Ruri Isobe[1], Takashi Nakamura[2] (1.Interdisciplinary Center for River Basin Environment, University of YAMANASHI, 2.Interdisciplinary Centre for River Basin Environment, University of YAMANASHI)

[AHW23-P04] **The influence of weathering and hydrological cycles on Li isotopic compositions in river water and groundwater of the Ganges–Brahmaputra–Meghna River system in Bangladesh**

*Toshihiro Yoshimura[1], Daisuke Araoka[2], Hodaka Kawahata[3], Zakir Hossain[4], Naohiko Ohkouchi[1] (1.Japan Agency for Marine-Earth Science and Technology, 2.National Institute of Advanced Industrial Science and Technology, 3.Atmosphere and Ocean Research Institute, The University of Tokyo, 4.Jashore University of Science and Technology)

[AHW23-P05] Numerical modeling on the spatial distribution of d-excess values in river water in Japan

*Masaaki Takahashi[1], Hinako Shimizu[1], Akihiko Inamura[1], Noritoshi Morikawa[1] (1.The National Institute of Advanced Industrial Science and Technology)

[AHW23-P06] Temporal variation of stable isotopes in precipitation based on the intermittent sampling for 1998-2018 at Tiksi, northeastern Siberia

*Kimpei Ichiyanagi[1], Hotaek Park[2], Masahiro Tanoue[3] (1.Kumamoto University, 2.JAMSTEC, 3.National Institute for Environmental Studies)

[AHW23-P07] Tritium concentration in recent precipitation in central Japan

*Kazuyoshi Asai[1] (1.Geo Science Laboratory)

[AHW23-P08] An isotopic study on the role of groundwater in streamflow generation in the concrete-lined Nomi-gawa river, Ohta Ward, Tokyo, Japan

*Masaya Yasuhara[1], Seongwon Lee[1], Yuki Itoh[2], Akihiko Inamura[3], Noritoshi Morikawa[3], Takashi Nakamura[4] (1.Rissho University, 2.Saitama Agricultural Cooperatives, 3.Geological Survey of Japan, AIST, 4.University of Yamanashi)

[AHW23-P09] Inorganic nitrogen concentrations and nitrogen and oxygen isotope ratios of nitrate in shallow groundwater in an urban area, Shinagawa, Tokyo, Japan

*Yuki Itoh[1], Masaya Yasuhara[2], Seongwon Lee[2], Takashi Nakamura[3], Akihiko Inamura[4] (1.Saitama Agricultural Cooperatives, 2.Rissho Univ., 3.Yamanashi Univ., 4.Geological Survey of Japan, AIST)

[J] Oral | A (Atmospheric and Hydrospheric Sciences)：A-CG Complex & General

10:45 AM - 12:15 PM JST | 1:45 AM - 3:15 AM UTC | Ch.10 Zoom Room 10

[A-CG38] Dynamics of Oceanic and Atmospheric Waves, Vortices, and Circulations

convener:Yuki Tanaka(Faculty of Marine Science and Technology, Fukui Prefectural University), Kunihiro Aoki(Japan Agency for Marine Earth Science and Technology), Yukiharu Hisaki(University of the Ryukyus), Norihiko Sugimoto(Keio University, Department of Physics), Chairperson:Kunihiro Aoki(Japan Agency for Marine Earth Science and Technology), Yukiharu Hisaki(University of the Ryukyus), Yuki Tanaka(Faculty of Marine Science and Technology, Fukui Prefectural University)

10:45 AM - 11:00 AM JST | 1:45 AM - 2:00 AM UTC

[ACG38-01] Toward numerical modeling systems that seamlessly link coastal seas to open oceans

★Invited Papers

*Hiroyasu Hasumi[1] (1.Atmosphere and Ocean Research Institute, The University of Tokyo)

11:00 AM - 11:15 AM JST | 2:00 AM - 2:15 AM UTC

[ACG38-02] Long-term variability of sea level along the coast of Japan during the 20th century reproduced by an eddy resolving model

*Hideyuki Nakano[1], Shogo Urakawa[1], Kei Sakamoto[1], Takahiro Toyoda[1], Goro Yamanaka[1] (1.Meteorological Research Institute)

11:15 AM - 11:30 AM JST | 2:15 AM - 2:30 AM UTC

[ACG38-03] Dynamics of the estern-boundary currents

★Invited Papers

*Ryo Furue[1] (1.APL/JAMSTEC)

11:30 AM - 11:45 AM JST | 2:30 AM - 2:45 AM UTC

[ACG38-04] Impacts of bottom topography on the formation of the North Pacific subtropical-subarctic frontal zone

*Humio Mitsudera[1], Hayato Ashida[2], Toru Miyama[3] (1.Institute of Low Temperature Science, Hokkaido University, 2.Graduate School of Environmental Science, Hokkaido University, 3.JAMSTEC)

11:45 AM - 12:00 PM JST | 2:45 AM - 3:00 AM UTC

[ACG38-05] Stability of a Flow over Bottom Topography: A General Condition and a Linear Analysis in a Two-Layer Quasi-Geostrophic Model

*Yuki Tanaka[1] (1.Faculty of Marine Science and Technology, Fukui Prefectural University)

12:00 PM - 12:15 PM JST | 3:00 AM - 3:15 AM UTC

[ACG38-06] Eddy-mean flow interactions and vertical energy redistribution associated with the standing meander in the Antarctic Circumpolar Current

*Takuro Matsuta[1], Yukio Masumoto[1] (1.Graduate School of Science, The University of Tokyo)

[J] Oral | A (Atmospheric and Hydrospheric Sciences)：A-CG Complex & General

1:45 PM - 3:15 PM JST | 4:45 AM - 6:15 AM UTC | Ch.10 Zoom Room 10

[A-CG38] Dynamics of Oceanic and Atmospheric Waves, Vortices, and Circulations

convener:Yuki Tanaka(Faculty of Marine Science and Technology, Fukui Prefectural University), Kunihiro Aoki(Japan Agency for Marine Earth Science and Technology), Yukiharu Hisaki(University of the Ryukyus), Norihiko Sugimoto(Keio University, Department of Physics), Chairperson:Yukiharu Hisaki(University of the Ryukyus), Norihiko Sugimoto(Keio University, Department of Physics), Yuki Tanaka(Faculty of Marine Science and Technology, Fukui Prefectural University)

1:45 PM - 2:00 PM JST | 4:45 AM - 5:00 AM UTC

[ACG38-07] Irreversible energy extraction from negative temperature two-dimensional turbulence

*Yohei Onuki[1] (1.Ocean Modeling Group, Center for Oceanic and Atmospheric Research, Research Institute for Applied Mechanics, Kyushu University)

2:00 PM - 2:15 PM JST | 5:00 AM - 5:15 AM UTC

[ACG38-08] Near-inertial oceanic internal waves observed by LADCP (lowered acoustic Doppler current profiler)

*Katsuro Katsumata[1] (1.JAMSTEC)

2:15 PM - 2:30 PM JST | 5:15 AM - 5:30 AM UTC

[ACG38-09] The pathway of the Indonesian Throughflow transport increase due to tidal mixing

*Shiraishi Takeki[1], Shinichiro Kida[2], Hideharu Sasaki[3], Ryo Furue[3] (1.Kyushu University Interdisciplinary Graduate School of Engineering Sciences, 2.Research Institute for Applied Mechanics, Kyushu University, 3.Application Laboratory , Japan Agency for Marine-Earth Science and Technology)

2:30 PM - 2:45 PM JST | 5:30 AM - 5:45 AM UTC

[ACG38-10] Biogeophysical Interactions in transport of marine organisms

★Invited Papers

*Atsushi Fujimura[1] (1.University of Guam)

2:45 PM - 3:00 PM JST | 5:45 AM - 6:00 AM UTC

[ACG38-11] Wave resolving numerical simulation of non-breaking wave-induced mixing

*Haruka Imamura[1], Yutaka Yoshikawa[1], Yasushi Fujiwara[2] (1.Graduate School of Science, Kyoto University, 2.Graduate School of Frontier Sciences, the University of Tokyo)

3:00 PM - 3:15 PM JST | 6:00 AM - 6:15 AM UTC

[ACG38-12] Origin of swells propagated into small bays on the Sanriku rias coast facing the western North Pacific

*Kosei Komatsu[1,2], Takaki Fujii[3], Kiyoshi Tanaka[2] (1.Graduate School of Frontier Sciences, University of Tokyo, 2.Atmosphere and Ocean Research Institute, University of Toky, 3.Bank of Japan)

[J] Oral | A (Atmospheric and Hydrospheric Sciences)：A-CG Complex & General

3:30 PM - 4:45 PM JST | 6:30 AM - 7:45 AM UTC | Ch.10 Zoom Room 10

[A-CG38] Dynamics of Oceanic and Atmospheric Waves, Vortices, and Circulations

convener:Yuki Tanaka(Faculty of Marine Science and Technology, Fukui Prefectural University), Kunihiro Aoki(Japan Agency for Marine Earth Science and Technology), Yukiharu Hisaki(University of the Ryukyus), Norihiko Sugimoto(Keio University, Department of Physics), Chairperson:Norihiko Sugimoto(Keio University, Department of Physics), Kunihiro Aoki(Japan Agency for Marine Earth Science and Technology), Yuki Tanaka(Faculty of Marine Science and Technology, Fukui Prefectural University)

3:30 PM - 3:45 PM JST | 6:30 AM - 6:45 AM UTC

[ACG38-13] Formulation and application of phase-independent energy conversion terms for quasi-geostrophic eddies on a zonally-varying basic flow

★Invited Papers

*Takaya Koutarou[1] (1.Kyoto Sangyo University)

3:45 PM - 4:00 PM JST | 6:45 AM - 7:00 AM UTC

[ACG38-14] Recirculation of atmospheric wave energy associated with idealized MJO events

*Hidenori AIKI[1], Yoshiki Fukutomi[1], Yuki Kanno[2], Tomomichi Ogata[3], Takahiro Toyoda[4], Hideyuki Nakano[4] (1.Nagoya University, 2.Central Research Institute of Electric Power Industry, 3.Japan Agency for Marine-Earth Science and Technology, 4.Meteorological Research Institute)

4:00 PM - 4:15 PM JST | 7:00 AM - 7:15 AM UTC

[ACG38-15] Extratropical forcing of intraseasonal equatorial Kelvin waves over the Indian and Pacific Oceans

*Fukutomi Yoshiki[1], Hidenori Aiki[1] (1.Institute for Space-Earth Environmental Reasearch, Nagoya University)

4:15 PM - 4:30 PM JST | 7:15 AM - 7:30 AM UTC

[ACG38-16] Influence of marginal seas' hotspot on extratropical cyclones: explosive and binary cyclogenesis in idealized experiments

*Masaru Yamamoto[1] (1.Research Institute for Applied Mechanics, Kyushu University)

4:30 PM - 4:45 PM JST | 7:30 AM - 7:45 AM UTC

[ACG38-17] Discussion

[J] Poster | A (Atmospheric and Hydrospheric Sciences)：A-CG Complex & General

5:15 PM - 6:30 PM JST | 8:15 AM - 9:30 AM UTC | Ch.08_3

[A-CG38] Dynamics of Oceanic and Atmospheric Waves, Vortices, and Circulations

convener:Yuki Tanaka(Faculty of Marine Science and Technology, Fukui Prefectural University), Kunihiro Aoki(Japan Agency for Marine Earth Science and Technology), Yukiharu Hisaki(University of the Ryukyus), Norihiko Sugimoto(Keio University, Department of Physics)

[ACG38-P01] A statistical mechanics of phytoplankton diversity

*Kunihiro Aoki[1], Yoshio Masuda[2] (1.Japan Agency for Marine Earth Science and Technology, 2.Faculty of Environmental Earth Science, Hokkaido University)

[ACG38-P02] Essential spectrum of internal waves arising in rotating stratified fluid

*andrei giniatoulline[1] (1.Department of Mathematics, Los Andes University, Bogota, Colombia, South America)

[ACG38-P03] Statistical analysis of ocean waves in the sea of Japan

*Yukiharu Hisaki[1] (1.University of the Ryukyus)

[ACG38-P04] Observing system simulation experiments for new satellite observation missions on Venus

*Yukiko Fujisawa[1], Norihiko Sugimoto[1], Mirai Abe[1], Asako Hosono[2], Mimo Shirasaka[3], Hiroki Ando[4], Masahiro Takagi[4], Chi Ao[5], Itziar Garate Lopez[6], Sebastien Lebonnois[7], Tomotaka Yamamoto[8], Yosuke Kawabata[8], Satoshi Ikari[8], Takeshi Imamura[8], Masaru Yamamoto[9], Shin-ya Murakami[1], Masataka Imai[10], Toru Kouyama[10] (1.Keio University, 2.Toshimagaoka Women High School, 3.Seisen Senior High School, 4.Kyoto Sangyo University, 5.Jet Propulsion Laboratory, California Institute of Technology, 6.Bilboko Ingeniaritza Eskola (UPV/EHU), 7.Sorbonne Universite, 8.Tokyo University, 9.Research Institute for Applied Mechanics, Kyushu University, 10.National Institute of Advanced Industrial Science and Technology)

[J] Oral | H (Human Geosciences)：H-DS Disaster geosciences

1:45 PM - 3:15 PM JST | 4:45 AM - 6:15 AM UTC | Ch.15 Zoom Room 15

[H-DS08] Human environment and disaster risk

convener:Tatsuto Aoki(School of Regional Development Studies, Kanazawa University), Hiroshi, P. Sato(College of Humanities and Sciences, Nihon University), Chairperson:Tatsuto Aoki(School of Regional Development Studies, Kanazawa University), Hiroshi Sato(College of Humanities and Sciences, Nihon University)

1:45 PM - 1:50 PM JST | 4:45 AM - 4:50 AM UTC

[HDS08-01] Introduction

1:50 PM - 2:05 PM JST | 4:50 AM - 5:05 AM UTC

[HDS08-02] Measurement of landslide deformation velocity at Jure in Sunkoshi River Wateshed, Nepal using LiCSBAS

*Hiroshi, P. Sato[1] (1.College of Humanities and Sciences, Nihon University)

2:05 PM - 2:20 PM JST | 5:05 AM - 5:20 AM UTC

[HDS08-03] Map of Earthquake-induced Landslides Potential on Artificially Transformed Hills in the Depositional Area of Tephric Soil Deposits

*Takehiko Suzuki[1], Masahiro Chigira[2], Yuki Matsushi[3], Daichi Nakayama[1] (1.Faculty of Urban Environmental Sciences, Tokyo Metropolitan University, 2.Fukada Geological Institute, 3.Disaster Prevention Research Institute Kyoto University)

2:20 PM - 2:35 PM JST | 5:20 AM - 5:35 AM UTC

[HDS08-04] **Elucidation of the cause that the H / L value of volcanic sector collapse is very small compared to non-volcanic landslides**

*Shunichi Sato[1] (1. Graduate School of Frontier Science, The University of Tokyo)

2:35 PM - 2:50 PM JST | 5:35 AM - 5:50 AM UTC

[HDS08-05] Natural disasters and countermeasures in Ratnapura, Sri Lanka

*Takahito Kuroki[1], Kensuke Goto[2], Panditharathne N. G. S. [3] (1.Faculty of Letters, Kansai University, 2.Faculty of Education, Osaka Kyoiku Univ., 3.Health Service Rathnapura, Ministry of Health, Government of Sri Lanka)

2:50 PM - 3:05 PM JST | 5:50 AM - 6:05 AM UTC

[HDS08-06] Policy for creating a liquefaction trend map based on geomorphologic classification for recognition of regional liquefaction risk

*Takayuki Nakano[1], Ryo Endo[1], Hiroyuki Inoue[2], Nozomi Yamashina[2], Shingo Watanabe[3], Keita Takada[3], Takuma Fujita[3] (1.Geospatial Information Authority of Japan, 2.City Bureau, Ministry of Land, Infrastructure, Transport and Tourism, 3.Fukken Co., Ltd.)

3:05 PM - 3:15 PM JST | 6:05 AM - 6:15 AM UTC

[HDS08-07] Discussion

[J] Oral | H (Human Geosciences)：H-DS Disaster geosciences

3:30 PM - 4:30 PM JST | 6:30 AM - 7:30 AM UTC | Ch.15 Zoom Room 15

[H-DS08] Human environment and disaster risk

convener:Tatsuto Aoki(School of Regional Development Studies, Kanazawa University), Hiroshi, P. Sato(College of Humanities and Sciences, Nihon University), Chairperson:Tatsuto Aoki(School of Regional Development Studies, Kanazawa University), Hiroshi Sato(College of Humanities and Sciences, Nihon University)

3:30 PM - 3:45 PM JST | 6:30 AM - 6:45 AM UTC

[HDS08-08] Current problems of submarine geological risks

*Kiichiro Kawamura[1] (1.Yamaguchi University)

3:45 PM - 4:00 PM JST | 6:45 AM - 7:00 AM UTC

[HDS08-09] **Verification of “Past” seismic intensity and estimation of “Future” ground motion by “Present-day” seismic observation: The Yanesen area**

*Motoko Ishise[1], Ryoichi Nakamura[1], Jun Muragishi[3], Shin'ichi Sakai[2,1] (1.Earthquake Reseach Institute, University of Tokyo, 2.Thr university of Tokyo III/GSII, 3.Yashima Gakuen University)

4:00 PM - 4:15 PM JST | 7:00 AM - 7:15 AM UTC

[HDS08-10] Characteristics of International Risk Communication over Trans-boudary Volcanic Disaster-The Case of 2010 Iceland Volcano Erution

*Mayumi Sakamoto[1], Haruhisa Nakamichi[2], Wakana Takahashi[3], Chizu Arashima[4], Masaru Arakida[5] (1.Graduate School of Disaster Resilience and Governance, University of Hyogo, 2.Disaster Prevention Research Institute, Kyoto University, 3.School of International Studies, Utsunomiya University, 4.Faculty of Global Communication, Kobe Gakuin University, 5.Asian Disaster Reduction Center)

4:15 PM - 4:30 PM JST | 7:15 AM - 7:30 AM UTC

[HDS08-11] Discussion

[J] Poster | H (Human Geosciences)：H-DS Disaster geosciences

5:15 PM - 6:30 PM JST | 8:15 AM - 9:30 AM UTC | Ch.09_1

[H-DS08] Human environment and disaster risk

convener:Tatsuto Aoki(School of Regional Development Studies, Kanazawa University), Hiroshi, P. Sato(College of Humanities and Sciences, Nihon University)

[HDS08-P01] The role of residents' resilience on the recovery process in a torrential rain

*Shoji Ohtomo[1], Reo Kimura[2] (1.Kanto Gakuin University, 2.University of Hyogo)

[HDS08-P02] Flood damage mapping of 2020 Typhoon Ulysses in the Philippines

*Naoko Nagumo[1], Kentaro Aida[1], Miho Ohara[1], Masakazu Fujikane[1] (1.International Centre for Water Hazard and Risk Management, PWRI)

[HDS08-P03] An example of using Google Earth Engine in providing and sharing information on wide-area typhoon disasters in international joint research projects

*Kentaro Aida[1], Naoko Nagumo[1], Miho Ohara[1] (1.International Centre for Water Hazard and Risk Management, PWRI)

[HDS08-P04] Estimating the amount of waste treatment units in the event of a disaster with self-help and mutual support

*Yoshinobu MIZUI[1,2] (1.University of Tsukuba, 2.NationalResearch Institute for Earth Science and Disaster Resilience)

[HDS08-P05] Possibility of support for disaster victims by accommodation facilities-Advance evacuation and acceptance in the event of a disaster-

Yuka SUZUKI[1], *Tatsuto Aoki[2] (1.Kanazawa University, 2.School of Regional Development Studies, Kanazawa University)

[HDS08-P06] Effect of synchrony bias on excitation of evacuation behavior during tsunami-From the evacuation behavior of residents in Noto Town, Ishikawa Prefecture during the 2019 Yamagata-oki Earthquake-

Mayu KITAMURA[1], *Tatsuto Aoki[2] (1.Kanazawa University, 2.School of Regional Development Studies, Kanazawa Univ.)

[HDS08-P07] Status of provision of disaster prevention information and learning to international students at national and public universities and their issues

*CHENYUE LU[1], Kiyomi HAYASHI[2], Tatsuto AOKI[2] (1. Division of Regional Development Studies,Graduate School of Human and Sociology-Environmental Studies,Kanazawa University, 2.School of Regional Development Studies, Kanazawa University)

[E] Oral | H (Human Geosciences)：H-TT Technology & Techniques

1:45 PM - 3:15 PM JST | 4:45 AM - 6:15 AM UTC | Ch.14 Zoom Room 14

[H-TT14] Geographic Information Systems and Cartography

convener:Takashi Oguchi(Center for Spatial Information Science, The University of Tokyo), Yoshiki Wakabayashi(Graduate School of Urban Environmental Sciences, Tokyo Metropolitan University), Yuei-An Liou(National Central University), C. Ronald Estoque(National Institute for Environmental Studies, Japan), Chairperson:Takashi Oguchi(Center for Spatial Information Science, The University of Tokyo), Yoshiki Wakabayashi(Graduate School of Urban Environmental Sciences, Tokyo Metropolitan University)

1:45 PM - 2:00 PM JST | 4:45 AM - 5:00 AM UTC

[HTT14-01] A GIS-based study on accessibility of public bus system in Sapporo

*ZITONG XU[1], Yuichi S. Hayakawa[2,3] (1.Graduate School of Environmental Science, Hokkaido University, 2.Faculty of Environmental Earth Science, Hokkaido University., 3.Center for Spatial Information Science, The University of Tokyo.)

2:00 PM - 2:15 PM JST | 5:00 AM - 5:15 AM UTC

[HTT14-02] **Comparative study of visitors' perceptions of places by analyzing visual content of photographs in Shinjuku, Tokyo**

*Bochra Bettaieb[1], Yoshiki Wakabayashi[1] (1.Tokyo Metropolitan University)

2:15 PM - 2:30 PM JST | 5:15 AM - 5:30 AM UTC

[HTT14-03] **Geo-phenomenology: A Qualitative GIS Approach for Understanding People's Lived Experiences**

★Invited Papers

*Yuki Iwai[1] (1.Graduate School, University of Tsukuba)

2:30 PM - 2:45 PM JST | 5:30 AM - 5:45 AM UTC

[HTT14-04] UAS Surveys for Identifying Vacant Houses using Night Light and Thermal Information

★Invited Papers

*Kotaro Iizuka[1], Yuki Akiyama[1,2], Nobuyuki Imafuku[3], Satoru Sugita[4] (1.Center for Spatial Information Science, University of Tokyo, 2.Graduate School of Integrative Science and Engineering, Tokyo City University, 3.Urban Development Dept., Building and Housing Division, Omuta City, 4.International Digital Earth Applied Science Research Center, Chubu University)

2:45 PM - 3:00 PM JST | 5:45 AM - 6:00 AM UTC

[HTT14-05] Impacts of urbanization on the ecosystem services of the Muthurajawela Marsh and Negombo Lagoon, Sri Lanka

*SUMUDU DARSHANA ATHUKORALA ARACHCHIGE[1], Yuji Murayama[2], Bunkei Matsushita[2], Ronald C. Estoque[3] (1.Graduate School of Life and Environmental Sciences, University of Tsukuba, Tsukuba, Ibaraki, Japan, 2. Faculty of Life and Environmental Sciences, University of Tsukuba, Tsukuba, Ibaraki, Japan, 3.National Institute for Environmental Studies, Tsukuba City, Ibaraki, Japan)

3:00 PM - 3:15 PM JST | 6:00 AM - 6:15 AM UTC

[HTT14-06] **Evaluating land use change with urban development and its impact on habitat quality**

*BINGYU WANG[1], Takashi Oguchi[1,2], Kotaro Iizuka[2], Xun Liang[3] (1.Department of Natural Environment Studies, The University of Tokyo, 2.Center for Spatial Information Science, The University of Tokyo, 3.School of Geography and Information Engineering, China University of Geosciences)

[E] Oral | H (Human Geosciences)：H-TT Technology & Techniques

3:30 PM - 5:00 PM JST | 6:30 AM - 8:00 AM UTC | Ch.14 Zoom Room 14

[H-TT14] Geographic Information Systems and Cartography

convener:Takashi Oguchi(Center for Spatial Information Science, The University of Tokyo), Yoshiki Wakabayashi(Graduate School of Urban Environmental Sciences, Tokyo Metropolitan University), Yuei-An Liou(National Central University), C. Ronald Estoque(National Institute for Environmental Studies, Japan), Chairperson:Yuei-An Liou(National Central University), Ronald C. Estoque(National Institute for Environmental Studies, Japan)

3:30 PM - 3:45 PM JST | 6:30 AM - 6:45 AM UTC

[HTT14-07] Assessing the effect of landscape composition on land surface temperature in Tsukuba city, Japan

★Invited Papers

*RUCI WANG[1], Yuji Murayama[1], Takehiro Morimoto[1] (1.University of Tsukuba)

3:45 PM - 4:00 PM JST | 6:45 AM - 7:00 AM UTC

[HTT14-08] **Spatiotemporal Characterization and Evolution of Surface Urban Heat Islands in Tokyo: A Perspective from Land Cover/Use Layouts and Variations**

*Fei LIU[1] (1.University of Tsukuba)

4:00 PM - 4:15 PM JST | 7:00 AM - 7:15 AM UTC

[HTT14-09] Microclimate simulation of Doshisha University Kyotanabe campus with ENVI-met model

★Invited Papers

*XINGYU WANG[1] (1. Department of Environmental Systems Science, Doshisha University)

4:15 PM - 4:30 PM JST | 7:15 AM - 7:30 AM UTC

[HTT14-10] **Recent LULC change in Vietnamese Mekong Delta and its relation to land subsidence after implementation of the Resolution No.120/NQ-CP**

*Kim-Anh Nguyen[1], Yuei-An Liou[1], Phan Duong Cao[2], Philip Mindehoud[3] (1.National Central University, 2.University of Tsukuba, 3.University of Padova)

4:30 PM - 4:45 PM JST | 7:30 AM - 7:45 AM UTC

[HTT14-11] Locations of historical and archaeological sites in Japan and China in relation to geography

*Yuan Wang[1], Takashi Oguchi[1] (1.The University of Tokyo)

4:45 PM - 5:00 PM JST | 7:45 AM - 8:00 AM UTC

[HTT14-12] **Online Education of Disaster Risk Reduction using Web GIS: Applications to Chinese Secondary Schools**

*Jiali Song[1], Takashi Oguchi[2] (1.Graduate School of Frontier Sciences, The University of Tokyo, 2.Center for Spatial Information Science, The University of Tokyo)

[E] Poster | H (Human Geosciences)：H-TT Technology & Techniques

5:15 PM - 6:30 PM JST | 8:15 AM - 9:30 AM UTC | Ch.09_2

[H-TT14] Geographic Information Systems and Cartography

convener:Takashi Oguchi(Center for Spatial Information Science, The University of Tokyo), Yoshiki Wakabayashi(Graduate School of Urban Environmental Sciences, Tokyo Metropolitan University), Yuei-An Liou(National Central University), C. Ronald Estoque(National Institute for Environmental Studies, Japan)

[HTT14-P01] Using remote sensing and GIS to track vegetation changes at Unzen Volcano, Kyushu, Japan

*Roxanne Lai[1], Takashi Oguchi[1] (1.University of Tokyo)

[HTT14-P02] Analysis of Human-Environment Interactions in the Last Glacial Period Using the Ecological Niche Model and the Agent-Based Model

*Yuji Sakairi[1], Takashi Oguchi[2] (1.Department of Earth and Planetary Science, School of Science, The University of Tokyo, 2.Center for Spatial Information Science, The University of Tokyo)

[HTT14-P03] **GIS-based frequency ratio, logistic regression and artificial neural network models for landslide and sinkhole susceptibility analysis in central Shenzhen, South China**

*DI LU[1], Takashi Oguchi[1,2] (1.Dept. of Natural Environmental Studies, Graduate School of Frontier Sciences, The University of Tokyo, 2.Center for Spatial Information Science, The University of Tokyo)

[HTT14-P04] Online Workshop for Educating Disaster Risk Reduction using a Simplistic Digital Map with Basic GIS functions

*Hiroyuki Yamauchi[1], Jiali Song[1], Takashi Oguchi[2,1] (1.Department of Natural Environmental Studies, Graduate School of Frontier Sciences, The University of Tokyo, 2.Center for Spatial Information Science, The University of Tokyo)

[HTT14-P05] Remotely sensed tree canopy cover-based indicators for monitoring global sustainability and environmental initiatives

★Invited Papers

*Ronald C. Estoque[1], Brian A Johnson[2], Yan Gao[3], Rajarshi DasGupta[2], Makoto Ooba[1], Takuya Togawa[1], Yasuaki Hijioka[1], Yuji Murayama[6], Lilito D Gavina[4], Rodel D Lasco[5], Shogo Nakamura[1] (1.National Institute for Environmental Studies, Japan, 2.Institute for Global Environmental Strategies, Japan, 3.Universidad Nacional Autónoma de México, México, 4.Don Mariano Marcos Memorial State University, Philippines, 5.World Agroforestry Centre (ICRAF), Philippines, 6.University of Tsukuba, Japan)

[HTT14-P06] Application of network analysis to visualize residential preferences and its changes in Japan

★Invited Papers

*Yoshiki Wakabayashi[1] (1.Graduate School of Urban Environmental Sciences, Tokyo Metropolitan University)

[HTT14-P07] Mapping Inbound Package Tours Visiting Countryside of Japan - - A Case of Toyama Prefecture

*Yennan U[1] (1.Tokyo Metropolitan University)

[J] Oral | H (Human Geosciences)：H-TT Technology & Techniques

9:00 AM - 10:30 AM JST | 12:00 AM - 1:30 AM UTC | Ch.14 Zoom Room 14

[H-TT19] Geographic Information System and Cartography

convener:Mamoru Koarai(Earth Science course, College of Science, Ibaraki University), Kazunari Tanaka(Department of Civil Engineering and Urban Design, Faculty of Engineering, Osaka Institute of Technology), W. Kazuhiko Nakamura(The University of Tokyo), Chairperson:Mamoru Koarai(Earth Science course, College of Science, Ibaraki University), Kazunari Tanka(Department of Civil Engineering and Urban Design, Faculty of Engineering, Osaka Institute of Technology)

9:00 AM - 9:15 AM JST | 12:00 AM - 12:15 AM UTC

[HTT19-01] Introduction

9:15 AM - 9:30 AM JST | 12:15 AM - 12:30 AM UTC

[HTT19-02] Map representation of estimated concentration distribution of $PM_{2.5}$ using WebGIS

*Junji Yamakawa[1] (1.Graduate School of Natural Science and Technology, Okayama University)

9:30 AM - 9:45 AM JST | 12:30 AM - 12:45 AM UTC

[HTT19-03] Proposal of nocturnal light data as a proxy variable for building height

*Go Kazawa[1], Daikichi SEKI[1], Yosuke Alexandre Yamashiki[1], Fusanori Iwasaki[2], Keola Souknilanh[3] (1. Graduate School of Advanced Integrated Studies in Human Survivability, 2.Economic Research Institute for ASEAN and East Asia, 3.Institute of Developing Economies, Japan External Trade Organization)

9:45 AM - 10:00 AM JST | 12:45 AM - 1:00 AM UTC

[HTT19-04] A Consideration of the Spatio-Temporal Expansion of "Deep Wonder" Evoked by Forest Image Archives

*Kazuhiko W. Nakamura[1] (1.The University of Tokyo)

10:00 AM - 10:15 AM JST | 1:00 AM - 1:15 AM UTC

[HTT19-05] An analysis of Children’s school route with GPS: A case study of 30 elementary schools in Toyama city

*Koji Ohnishi[1] (1.Department of Humanities, University of Toyama)

10:15 AM - 10:30 AM JST | 1:15 AM - 1:30 AM UTC

[HTT19-06] Red Relief Image Map using Hyper Resolution DEM, New Development of Topography recognition

*Tatsuro Chiba[1], Makoto Ohashi[1] (1.Asia Air Survey Co., Ltd.)

[J] Oral | H (Human Geosciences)：H-TT Technology & Techniques

10:45 AM - 12:15 PM JST | 1:45 AM - 3:15 AM UTC | Ch.14 Zoom Room 14

[H-TT19] Geographic Information System and Cartography

convener:Mamoru Koarai(Earth Science course, College of Science, Ibaraki University), Kazunari Tanaka(Department of Civil Engineering and Urban Design, Faculty of Engineering, Osaka Institute of Technology), W. Kazuhiko Nakamura(The University of Tokyo), Chairperson:Mamoru Koarai(Earth Science course, College of Science, Ibaraki University), Kazuhiko W. Nakamura(The University of Tokyo)

10:45 AM - 11:00 AM JST | 1:45 AM - 2:00 AM UTC

[HTT19-07] Relationship between the Image of the Town and the Seams of Asphalt Pavement Works

*Kazunari Tanaka[1], Miku Ogawa[1], Hitomi Tsukioka[1] (1.Department of Civil Engineering and Urban Design, Faculty of Engineering, Osaka Institute of Technology)

11:00 AM - 11:15 AM JST | 2:00 AM - 2:15 AM UTC

[HTT19-08] On Spatial Cognition of Children by Distortion and Color on the Cognitive Map

*Ami Hasegawa[1], Kazunari Tanaka[1] (1.Osaka Institute of Technology)

11:15 AM - 11:30 AM JST | 2:15 AM - 2:30 AM UTC

[HTT19-09] On Evaluation of Environmental Sound by Degree of Human Concentration

*Haru Kanda[1] (1.Osaka Institute Technology)

11:30 AM - 11:45 AM JST | 2:30 AM - 2:45 AM UTC

[HTT19-10] On the Meaning of Affordance and Personal-Space in the COVID-19

*Kazuki Miyake[1], Shota Tanaka[1], Kazunari Tanaka[1] (1.Osaka Institute of Technology)

11:45 AM - 12:15 PM JST | 2:45 AM - 3:15 AM UTC

[HTT19-11] Discussion

[J] Poster | H (Human Geosciences)：H-TT Technology & Techniques

5:15 PM - 6:30 PM JST | 8:15 AM - 9:30 AM UTC | Ch.09_3

[H-TT19] Geographic Information System and Cartography

convener:Mamoru Koarai(Earth Science course, College of Science, Ibaraki University), Kazunari Tanaka(Department of Civil Engineering and Urban Design, Faculty of Engineering, Osaka Institute of Technology), W. Kazuhiko Nakamura(The University of Tokyo)

[HTT19-P01] Susceptibility assessment of post-seismic landslides with an index representative of seismic cracks

*Shui Yamaguchi[1], Mio Kasai[2] (1.Graduate School of Agriculture, Hokkaido University, 2.Research Faculty of Agriculture, Hokkaido University)

[HTT19-P02] Development of information platform for topographical recognition by CS topographic map

*Hiromu Daimaru[1], Kenichiro Toda[2], Wataru Murakami[1], Ryuichi Sekoguchi[3], Yoichi Kayama[3], Keichi Katsube[3], Hiroo Imaki[4], Koji Ijima[4], Ryosuke Wayama[5] (1.Forestry and Forest Products Research Institute, 2.Nagano Prefecture Forestry Research Center, 3.Aero Asahi Corporation, 4.Pacific Spatial Solutions Co., Ltd., 5.Northern System Service Co., Ltd.)

[J] Oral | H (Human Geosciences)：H-CG Complex & General

10:45 AM - 12:15 PM JST | 1:45 AM - 3:15 AM UTC | Ch.15 Zoom Room 15

[H-CG26] Adaptation to climate change and its social implementation

convener:Hiroya Yamano(National Institute for Environmental Studies), Yoichi Ishikawa(JAPAN Agency for Marine-Earth Science and Technology), KOJI DAIRAKU(University of Tsukuba), Makoto Tamura(Global and Local Environment Co-creation Institute, Ibaraki University), Chairperson:Hiroya Yamano(National Institute for Environmental Studies), Yoichi Ishikawa(JAPAN Agency for Marine-Earth Science and Technology), KOJI DAIRAKU(University of Tsukuba), Makoto Tamura(Global and Local Environment Co-creation Institute, Ibaraki University)

10:45 AM - 11:00 AM JST | 1:45 AM - 2:00 AM UTC

[HCG26-01] Enhancing resilience of atoll islands against sea level rise

★Invited Papers

*Hajime Kayanne[1], Masafumi Fujita[2], Nori Fujita[1], Takashi Hosono[3], Yoich Ide[4], Yuji Kuwahara[2], Fumiko Matsudate[13], Satoru Mimura[5], Nobuko Nakamura[6], Susumu Onaka[7], Daisaku Sato[8], Tomoko Takeda[9], Koji Yamada[10], Toru Yamaguchi[11], Hiroya Yamano[12], Hiromune Yokoki[2] (1.the University of Tokyo, 2.Ibaraki Univ., 3.JAMSTEC, 4.Oceanic Planning Corp., 5.JICA, 6.Sasakawa Peace Foundation, Ocean Policy Res. Inst., 7.Nippon Koei, 8.Setsunan Univ., 9.IGES, 10.Japan Construction Information Center Found., 11.Keio Univ., 12.National Inst. Environmental Studies, 13.Heart Biz)

11:00 AM - 11:15 AM JST | 2:00 AM - 2:15 AM UTC

[HCG26-02] **Developments of future climate scenario selection method for impact and adaptation studies**

*Hideo Shiogama[1], Noriko N. Ishizaki[1], Naota Hanasaki[1], Kiyoshi Takahashi[1], Seita Emori[1], Rui Ito[2,3], Toshiyuki Nakaegawa[3], Izuru Takayabu[3], Yasuaki Hijioka[1], Yukari N. Takayabu[4], Ryosuke Shibuya[4] (1.National Institute for Environmental Studies, 2.Japan Meteorological Business Support Center, 3.Meteorological Research Institute, 4.Atmosphere and Ocean Research Institute, The University of Tokyo)

11:15 AM - 11:30 AM JST | 2:15 AM - 2:30 AM UTC

[HCG26-03] Added values of regional multi-ensemble statistical downscaling approach in CORDEX Asia

*KOJI DAIRAKU[1] (1.University of Tsukuba)

11:30 AM - 11:45 AM JST | 2:30 AM - 2:45 AM UTC

[HCG26-04] Temperature rises and extreme rainfall intensity derived from observations and d4PDF in Japan

*Sayaka Yoshikawa[1,3], Megumi Watanabe[2], Shinjiro Kanae[3] (1.Ibaraki university, 2.The university Tokyo, 3.Tokyo institute of technology)

11:45 AM - 12:00 PM JST | 2:45 AM - 3:00 AM UTC

[HCG26-05] Adaptation measures based on future projections of corals and macroalgae, use/conservation status on the southwest coast of Shikoku

*Hiroya Abe[1], Haruka Suzuki[1], Yuko F Kitano[1], Naoki H Kumagai[1], Satomi Mitsui[1], Hiroya Yamano[1] (1.National Institute for Environmental Studies)

12:00 PM - 12:15 PM JST | 3:00 AM - 3:15 AM UTC

[HCG26-06] Workshop on Disaster Prevention Training to Improve Disaster Preparedness of Local Governments and Staff: As Part of Social Implementation of Disaster Prevention Policy for Climate Change Adaptation

*kouhei yoshimura[1,2], Seigo Nasu[2], Shingen Horiuchi[3] (1.Nippon Koei, 2.Kochi University of Technology, 3.Kochi City)

[J] Poster | H (Human Geosciences)：H-CG Complex & General

5:15 PM - 6:30 PM JST | 8:15 AM - 9:30 AM UTC | Ch.09_4

[H-CG26] Adaptation to climate change and its social implementation

convener:Hiroya Yamano(National Institute for Environmental Studies), Yoichi Ishikawa(JAPAN Agency for Marine-Earth Science and Technology), KOJI DAIRAKU(University of Tsukuba), Makoto Tamura(Global and Local Environment Co-creation Institute, Ibaraki University)

[HCG26-P01] ASSESSMENT OF WIND/SOLAR ENERGY POTENTIAL AS A POWER GENERATION SOURCES AT SOME SELECTED LOCATIONS IN PAKISTAN

*Muhammad Abid KHAN[1], KOJI DAIRAKU[1] (1.University of Tsukuba)

[J] Oral | H (Human Geosciences)：H-CG Complex & General

9:00 AM - 10:30 AM JST | 12:00 AM - 1:30 AM UTC | Ch.15 Zoom Room 15

[H-CG29] Advanced life support systems with closed bio-ecosystems and thier applications

convener:Masanori Shinohara(Teikyo University of Science), Hiroshi Katoh(Division of Plant Functional Genomics, Advanced Science Research Promotion Center, Organization for the Promotion of Regional Innovation, Mie University), Shunta Kimura(Institute of Space and Astronautical Science / Space Exploration Innovation Hub Center, Japan Aerospace Exploration Agency), Midori Ong(University of Tsukuba), Chairperson:Midori Ong(University of Tsukuba), Hiroshi Katoh(Division of Plant Functional Genomics, Advanced Science Research Promotion Center, Organization for the Promotion of Regional Innovation, Mie University), Masanori Shinohara(Teikyo University of Science)

9:00 AM - 9:05 AM JST | 12:00 AM - 12:05 AM UTC

[HCG29-01] Introduction

9:05 AM - 9:20 AM JST | 12:05 AM - 12:20 AM UTC

[HCG29-02] Recent Trends of Advanced and Closed Ecological Life Support System.

*Masanori Shinohara[1], Tamiyasu Shimamiya[2] (1.Teikyo University of Science, 2.Japan Manned Space Systems Corporation)

9:20 AM - 9:45 AM JST | 12:20 AM - 12:45 AM UTC

[HCG29-03] Establishment of food self-sufficiency system for functional space foods to support manned space activities

★Invited Papers

*Takeshi Nikawa[1] (1.Institute of Nutrition, Tokushima University Graduate School)

9:45 AM - 10:00 AM JST | 12:45 AM - 1:00 AM UTC

[HCG29-04] Searching for gene related to environments adaptation

*Hiroshi Katoh[1] (1.Mie University)

10:00 AM - 10:25 AM JST | 1:00 AM - 1:25 AM UTC

[HCG29-05] Current status of planetary protection and its importance in closed eco-systems

★Invited Papers

*Shunta Kimura[1,2], Shino Suzuki[1,2], Yuko Inatomi[1,2] (1.Institute of Space and Astronautical Science, Japan Aerospace Exploration Agency, 2.Space Exploration Innovation Hub Center, Japan Aerospace Exploration Agency)

10:25 AM - 10:30 AM JST | 1:25 AM - 1:30 AM UTC

[HCG29-06] Discussion

[J] Poster | H (Human Geosciences)：H-CG Complex & General

5:15 PM - 6:30 PM JST | 8:15 AM - 9:30 AM UTC | Ch.09_5

[H-CG29] Advanced life support systems with closed bio-ecosystems and thier applications

convener:Masanori Shinohara(Teikyo University of Science), Hiroshi Katoh(Division of Plant Functional Genomics, Advanced Science Research Promotion Center, Organization for the Promotion of Regional Innovation, Mie University), Shunta Kimura(Institute of Space and Astronautical Science / Space Exploration Innovation Hub Center, Japan Aerospace Exploration Agency), Midori Ong(University of Tsukuba)

[HCG29-P01] Growth of cyanobacterium, *Nostoc* sp. HK-01, after exposure to several harsh environments.

*Miku Tokita[1], Midori Ong[1], Hiroshi Katoh[2], Kaori Tomita-Yokotani[1] (1.University of Tsukuba, 2.University of Mie)

[HCG29-P02] Relationship between seed formation during tomato growth and microgravity generated by a hand-made 3D-clinostat.

*Yuan Takase[1], Kaori Totami-Yokotani[1] (1.University of Tsukuba)

[HCG29-P03] Identification of *Nostoc* sp. HK-01 proteins found in dry environment

*Hiroko Tanaka[1], Tomoko Abe[1], Hiroshi Katoh[2], Midori Ong[3], Kaori Tomita-Yokotani[3] (1.Graduate School of Science and Engineering, University of Tokyo Denki, 2.Organization for the Promotion of Regional Innovation, Mie University, 3.Faculty of Life and Environmental Sciences, University of Tsukuba)

[HCG29-P04] History of biological systems in closed-ecological systems

*Hiroshi Katoh[1] (1.Mie University)

[HCG29-P05] Advanced use of potatoes (*Solanum tuberosum* L.) for manned space activities

*Yota Tsukizaki[1], Toshisada Suzuki[2], Kaori Tomita-Yokotani[1] (1.University of Tsukuba, 2.Kagawa University)

[J] Poster | S (Solid Earth Sciences)：S-SS Seismology

5:15 PM - 6:30 PM JST | 8:15 AM - 9:30 AM UTC | Ch.10_1

[S-SS04] Earthquake prediction and forecast

convener:Shingo Watada(Division of Monitoring Science, Earthquake Research Institute, University of Tokyo), Masayuki Obayashi(Japan Agency for Marine-Earth Science and Technology)

[SSS04-P01] **Effects of Earth tides on the mainshock of the 2011 Tohoku Earthquake**

*Yoshiki SUE[1] (1.none)

[SSS04-P02] Statistical Study and Probability of Foreshocks on the Japan Mainland

*Hong Peng[1], James Mori[1] (1. Earthquake Hazards Division, Disaster Prevention Research Institute, Kyoto University)

[SSS04-P03] Comments on the Brownian Passage Time model for recurrent earthquakes with uncertain origin times

*Masajiro Imoto[1], Nobuyuki Morikawa[1], Hiroyuki Fujiwara[1] (1.National Research Institute for Earth Science and Disaster Resilience)

[SSS04-P04] Relationship between the Moderate Repeating Earthquakes and the Larger-scale Earthquakes on the trench side

*Masayuki Tanaka[1] (1.Meteorological Research Institute)

[SSS04-P05] Validation of forecast experiment on the Kamaishi repeating earthquakes based on numerical simulations

*Shingo Yoshida[1], Jun'ichi Fukuda[1], Toshihiro Igarashi[1] (1.Earthquake Research Institute, University of Tokyo)

[J] Oral | S (Solid Earth Sciences)：S-SS Seismology

9:00 AM - 10:30 AM JST | 12:00 AM - 1:30 AM UTC | Ch.18 Zoom Room 18

[S-SS11] Strong Ground Motion and Earthquake Disaster

convener:Kazuhiro Somei(Geo-Research Institute), Yasuhiro Matsumoto(Kozo Keikaku Engineering), Chairperson:Kenichi Tsuda(Institute of Technology, Shimizu Corporation), Asako Iwaki(National Research Institute for Earth Science and Disaster Prevention)

9:00 AM - 9:15 AM JST | 12:00 AM - 12:15 AM UTC

[SSS11-07] Development of data-driven strong motion model and common integrated database

*Hiroyuki Fujiwara[1], Nobuyuki Morikawa[1], Asako Iwaki[1], Takahiro Maeda[1], Shinichi Akiyama[1], Kenichi Kato[2], Toshiaki Sato[3], Takayuki Hayashi[4] (1.National Research Institute for Earth Science and Disaster Resilience, 2.KOBORI RESEARCH COMPLEX INC., 3.Ohsaki Research Institute, Inc., 4.Tokio Marine & Nichido Risk Consulting Co., Ltd.)

9:15 AM - 9:30 AM JST | 12:15 AM - 12:30 AM UTC

[SSS11-08] Consideration of Uncertainty in Seismic Hazard Assessment Based on Strong Motion Observation Record Database

*Nobuyuki Morikawa[1], Hiroyuki Fujiwara[1], Asako Iwaki[1], Takahiro Maeda[1] (1.National Research Institute for Earth Science and Disaster Resilience)

9:30 AM - 9:45 AM JST | 12:30 AM - 12:45 AM UTC

[SSS11-09] On applicabiltiy of ground-motion simulation data to data-driven ground-motion prediction model

*Asako Iwaki[1], Hiroyuki Fujiwara[1], Nobuyuki Morikawa[1], Takahiro Maeda[1] (1.National Research Institute for Earth Science and Disaster Prevention)

9:45 AM - 10:00 AM JST | 12:45 AM - 1:00 AM UTC

[SSS11-10] Spatial complexity characteristics of faut parameters based on self-similar models - Comparison of earthquake slip of Japan and all over the world-

*Fumino Suzuki[1], Kenichi Kato[1], Tetsushi Watanabe[1] (1.KOBORI RESEARCH COMPLEX INC.)

10:00 AM - 10:15 AM JST | 1:00 AM - 1:15 AM UTC

[SSS11-11] A scaling relation of crustal earthquakes assuming constant stress drop - in a case when fault width is used as a parameter -

*Kazuhito Hikima[1], Akihiro Shimmura[1] (1.Tokyo Electric Power Company Holdings, Inc.)

10:15 AM - 10:30 AM JST | 1:15 AM - 1:30 AM UTC

[SSS11-12] **Correlation of Kinematic Source Parameters from Rupture Models Simulated by the Full Dynamic Earthquake Cycles**

*Anatoly Petukhin[1], Percy Galvez[2,3], Paul Somerville[4], Ken Miyakoshi[1], Kojiro Irikura[5] (1.Geo-Research Institute, 2.ETH Zurich, Earth Science, 3.KAUST University, 4.AECOM, Los Angeles, 5.Aichi Institute of Technology)

[J] Oral | S (Solid Earth Sciences)：S-SS Seismology

10:45 AM - 12:15 PM JST | 1:45 AM - 3:15 AM UTC | Ch.18 Zoom Room 18

[S-SS11] Strong Ground Motion and Earthquake Disaster

convener:Kazuhiro Somei(Geo-Research Institute), Yasuhiro Matsumoto(Kozo Keikaku Engineering), Chairperson:Hisahiko Kubo(National Research Institute for Earth Science and Disaster Resilience), Hongjun Si(Seismological Research Institute Inc.)

10:45 AM - 11:00 AM JST | 1:45 AM - 2:00 AM UTC

[SSS11-13] Long-period incident waves to the Echigo basin during the 2011 off the Pacific coast of Tohoku Earthquake

*Tomiichi Uetake[1] (1.R&D Department, TEPCO research Institute, Tokyo Electric Power Company)

11:00 AM - 11:15 AM JST | 2:00 AM - 2:15 AM UTC

[SSS11-14] On the attenuation characteristics of peak ground motion from three M_W7 class intraplate earthquakes along the Japan Trench

*Hongjun Si[1] (1.Seismological Research Institute Inc.)

11:15 AM - 11:30 AM JST | 2:15 AM - 2:30 AM UTC

[SSS11-15] Comparison of seismic wave fields from the earthquakes off Fukushima prefecture, northeastern Japan

*Yasumaro Kakehi[1] (1.Department of Planetology, Graduate School of Science, Kobe University)

11:30 AM - 11:45 AM JST | 2:30 AM - 2:45 AM UTC

[SSS11-16] ESTIMATE TIME AND SPATIAL EVOLUTION OF THE RUPTURE PROCESS OF THE 2021 OFF-FUKUSHIMA BASED ON THE FINITE-FAULT SOURCE INVERSION

*Kenichi Tsuda[1], Chen Ji[3], Ralph J Archuleta[3,4], Toshiaki Sato[2] (1.Institute of Technology, Shimizu Corporation, 2.Ohsaki Research Institute, Inc., 3.University of California, Santa Barbara, 4.RJA Ground Motion Analysis, Inc.)

11:45 AM - 12:00 PM JST | 2:45 AM - 3:00 AM UTC

[SSS11-17] Source process of the 2021 off Fukushima, Japan, intraslab earthquake derived from strong motion data

*Hisahiko Kubo[1], Wataru Suzuki[1], Shin Aoi[1], Haruko Sekiguchi[2] (1.National Research Institute for Earth Science and Disaster Resilience, 2.Disaster Prevention Research Institute, Kyoto University)

12:00 PM - 12:15 PM JST | 3:00 AM - 3:15 AM UTC

[SSS11-18] Strong motion characteristics at MYGH10 (KiK-net), Yamamoto, during the Off Fukushima pref. earthquake of 13th Feb., 2021

*Tomotaka Iwata[1] (1.Disaster Prevention Research Institute, Kyoto University)

[J] Poster | S (Solid Earth Sciences)：S-SS Seismology

5:15 PM - 6:30 PM JST | 8:15 AM - 9:30 AM UTC | Ch.10_2

[S-SS11] Strong Ground Motion and Earthquake Disaster

convener:Kazuhiro Somei(Geo-Research Institute), Yasuhiro Matsumoto(Kozo Keikaku Engineering)

[SSS11-P01] Elasto-plastic soil-water coupling seismic response analysis of a sedimentary basin with a three-dimensional geometry

*Toshihiro Noda[1], Tomohiro Toyoda[1], Shuhei Iwai[2], Akira Asaoka[3] (1.Disaster Mitigation Research Center, Nagoya University, 2.Graduate School of Engineering, Nagoya University, 3.Association for the Development of Earthquake Prediction)

[SSS11-P02] Identification of potential problems for disaster mitigation using “the Nankai Trough Earthquake Extra Information”, a new Japanese earthquake forecast information -how to communicate the "uncertainty" of science to society-

*Sayaka Irie[1], Ryu Ohtani[2], Mamoru Hyodo[3], Yoshinari Hayashi[4], Manabu Hashimoto[5], Takane Hori[6], Nobumasa Kawabata[7], Kunihiko Kumamoto[8], Takayoshi Iwata[9], Takashi Yokota[10], Kazunori Tanihara[11], Yo Fukushima[12] (1.NHK Broadcasting Culture Research Institute , 2.National Institute of Advanced Industrial Science and Technology, 3.Osaka Regional Headquarters, Japan Meteorological Agency, 4.Kansai University, 5.Disaster Prevention Research Institute, Kyoto University (DPRI), 6. Japan Agency for Marine-Earth Science and Technology (JAMSTEC) , 7.Crisis and Environment Management Policy Institute(CeMI), 8.Edogawa University, 9.Center for Integrated Research and Education of Natural Hazards,Shizuoka University, 10.Disaster Prevention Research Center,Aichi Institute of Technology, 11.Nippon Television Network, 12.International Research Institute of Disaster Science,Tohoku University, (IRIDeS))

[SSS11-P03] Research Project for Disaster Prevention on the great Earthquakes along the Nankai trough

*Shuichi Kodaira[1], Hiroyuki Fujiwara[2], Narumi Takahashi[1,2] (1. Japan Agency for Marine-Earth Science and Technology, 2.National Research Institute for Earth Science and Disaster Resilience)

[SSS11-P04] Formulas for using simple array to determine Love-wave characteristics based on rotational component of microtremors

*Ikuo Cho[1], Kunikazu Yoshida[2], Hirotoshi Uebayashi[3] (1.National Institute of Advanced Industrial Science and Technology, 2.Geo-Research Institute, 3.Institute for Integrated Radiation and Nuclear Science, Kyoto University)

[SSS11-P05] Assessment of applicability of a proposed method to estimate phase velocity using arbitrary 5-site arrays

*Huan Zhang[1], Kahori Iiyama[2], Hitoshi Morikawa[1] (1.Department of Civil and Environmental Engineering, Tokyo Institute of Technology, 2.KAJIMA Technical Research Institute)

[SSS11-P06] Comprehensive Research Project for the Nara-bonchi-toen Fault Zone

*Tomotaka Iwata[1] (1.Disaster Prevention Research Institute, Kyoto University)

[SSS11-P07] Small-aperture Microtremor Array Surveys in the Nara Basin, Japan

*Kimiyuki Asano[1], Tomotaka Iwata[1], Haruko Sekiguchi[1] (1.Disaster Prevention Research Institute, Kyoto University)

[SSS11-P08] Dense Microtremor Surveys on the Eastern Part of the Nara Basin, Japan

*Masayuki Yoshimi[1], Kimiyuki Asano[2], Tomotaka Iwata[2], Hiro Nimiya[1], Takeshi Sugiyama (1.Geological Survey of Japan, AIST, 2.DPRI, Kyoto Univ.)

[SSS11-P09] Microtremor characteristics and subsurface structure in the vicinity of the Shikano-Yoshioka Fault, Tottori, Japan

*Tatsuya Noguchi[1], Kazuki Kobayashi[2], Ryo Ashida[1], Isamu Nishimura[3], Takao Kagawa[1] (1.Faculty of Engineering, Tottori University, 2.Graduate School of Sustainability Science, Tottori University, 3.Graduate School of Engineering, Tottori University)

[SSS11-P10] Determination of 3-D subsurface structure model in central Tottori, Japan

*Tatsuya Noguchi[1], Masaki Yamamuro[1], Isamu Nishimura[2], Takao Kagawa[1] (1.Faculty of Engineering, Tottori University, 2.Graduate School of Engineering, Tottori University)

[SSS11-P11] Estimation of Subsurface Structure and Ground Motion Characteristics in the Landslide Areas from Microtremor Observations – Case of Nawashiro and Amedaki, Kokufu-cho, Tottori City –

*Isamu Nishimura[1], Atsushi Shimada[2], Tatsuya Noguchi[2], Takao Kagawa[2] (1.Graduate School of Engineering Department of Social Infrastructure Engineering, Tottori University, 2.Social Systems and Civil Engineering, Department of Engineering, Tottori University)

[SSS11-P12] Modeling of subsurface velocity structures from seismic bedrock to ground surface for Yamanashi region

*Shigeki Senna[1], Atsushi Wakai[1], Yatagai Atsushi[2], Tadashi Sato[2], Hisanori Matsuyama[2], Hiroyuki Fujiwara[1] (1.National Research Institute for Earth Science and Disaster Resilience, 2.OYO Corporation)

[SSS11-P13] Modeling of subsurface velocity structures from seismic bedrock to ground surface for Kumamoto region

*Shigeki Senna[1], Atsushi Wakai[1], Yatagai Atsushi[2], Yoshiaki Inagaki[2], Hisanori Matsuyama[2], Hiroyuki Fujiwara[1] (1.National Research Institute for Earth Science and Disaster Resilience, 2.OYO Corporation)

[SSS11-P14] Basic study of a real-time damage estimation system for liquefaction

*Shohei Naito[1], Hiromitsu Nakamura[1], Shigeki Senna[1], Yoshinori Iwanami[2] (1.National Research Institute for Earth Science and Disaster Resilience, 2.MITSUBISHI SPACE SOFTWARE CO.,LTD.)

[SSS11-P15] Estimation of subsurface motion from surface seismic records: investigation on evaluation at deep levels

*Tomotsugu Watanabe[1], Hiroshi Takenaka[1], Masanao Komatsu[1], Mitsutaka Oshima[2] (1.Okayama University , 2.Shimizu Corporation)

[SSS11-P16] Estimation of seismic ground motions on the surface ground at MeSO-net stations

*Atsushi Wakai[1], Shigeki Senna[1] (1.National Research Institute for Earth Science and Disaster Resilience)

[SSS11-P17] Strong motion simulation of an intraslab earthquake beneath Kanto region using MeSO-net observation data

*Wataru Suzuki[1], Takeshi Kimura[1], Hisahiko Kubo[1], Takayuki Miyoshi[1] (1.National Research Institute for Earth Science and Disaster Resilience)

[SSS11-P18] Ground-motion simulation for the 2016 Kumamoto earthquake (Mj7.3) based on the strong-motion prediction recipe

*Asako Iwaki[1], Nobuyuki Morikawa[1], Takahiro Maeda[1], Hiroyuki Fujiwara[1] (1.National Research Institute for Earth Science and Disaster Prevention)

[SSS11-P19] Characterized source model of M7.3 2016 Kumamoto eq. by 3D reciprocity GFs inversion with special reference to velocity pulse at KMMH16

*Anatoly Petukhin[1], Hiroshi Kawase[2], Fumiaki Nagashima[2], Eri Ito[2] (1.Geo-Research Institute, 2.DPRI, Kyoto University)

[SSS11-P20] Evaluation of near-source ground motion during the 2008 Iwate-Miyagi Nairiku earthquake by using stochastic slip models and three-dimensional velocity structures

*Takeshi Nakamura[1], Masataka Sawada[1] (1.Central Research Institute of Electric Power Industry)

[SSS11-P21] **Source rupture process of the 2018 Hokkaido eastern Iburi earthquake estimated from waveform inversion with empirical Green's functions**

*SHUANGLAN WU[1], Atsushi Nozu[1], Yosuke Nagasaka[1] (1.PORT AND AIRPORT RESEARCH INSTITUTE)

[SSS11-P22] Calibrating Thailand's local magnitude scale: a preliminary result

*Mongkolchai Sukmee[1], Sutthipong Noisagool[1,2], Satoru Tanaka[3], Weerachai Siripunvaraporn[1,2], Songkhun Boonchaisuk[4,2], Yasushi Ishihara[5], Taewoon Kim[6], Hitoshi Kawakatsu[7], Nozomu Takeuchi[7], Kenji Kawai[8], Yuki Suzuki[8] (1.Department of Physics, Faculty of Science, Mahidol University , 2.Thailand Center of Excellence in Physics, Ministry of Higher Education, Science, Research and Innovation, 3.Volcanoes and Earth's Interior Research Center (VERC), Research Institute for Marine Geodynamics (IMG), Japan Agency for Marine-Earth Science and Technology (JAMSTEC), 4.Geoscience Program, Mahidol University, Kanchanaburi Campus, 5.Research Institute for Marine Geodynamics (IMG), Japan Agency for Marine-Earth Science and Technology (JAMSTEC), 6.Subduction Dynamics Research Center (SDR), Research Institute for Marine Geodynamics (IMG), Japan Agency for Marine-Earth Science and Technology (JAMSTEC), 7.Earthquake Research Institute, The University of Tokyo, 8.Department of Earth and Planetary Science, School of Science, The University of Tokyo)

[SSS11-P23] Strong ground motion simulation of the Fukushima-ken Oki earthquake of February 13, 2021 (M_J 7.3)

*Yosuke Nagasaka[1] (1.Port and Airport Research Institute)

[SSS11-P24] Strong Motion Generation Area for the 2021 off Fukushima, Japan, Earthquake Estimated based on the Empirical Green's Function Method

*Kazuhiro Somei[1], Ken Miyakoshi[1] (1.Geo-Research Institute)

[J] Oral | S (Solid Earth Sciences)：S-EM Earth's Electromagnetism

1:45 PM - 3:15 PM JST | 4:45 AM - 6:15 AM UTC | Ch.21 Zoom Room 21

[S-EM13] Geomagnetism, paleomagnetism and rock magnetism

convener:Chie Kato(Faculty of Social and Cultural Studies, Kyushu University), Tetsuro Sato(Earthquake Research Institute, The University of Tokyo), Chairperson:Chie Kato(Faculty of Social and Cultural Studies, Kyushu University), Tetsuro Sato(Earthquake Research Institute, The University of Tokyo), Yutaka Yoshimura(Faculty of Social and Cultural Studies, Kyushu University)

1:45 PM - 2:00 PM JST | 4:45 AM - 5:00 AM UTC

[SEM13-01] **Revised magnetostratigraphy and eruption timing of Afro-Arabian Large Igneous Province using new $^{40}Ar/^{39}Ar$ ages**

*Yutaka Yoshimura[1], Osamu Ishizuka[2], Toshitsugu Yamazaki[1], Yuhji Yamamoto[3], Hyeon-Seon Ahn[3], Tesfaye Kidane[4], Yo-ichiro Otofuji[5,6] (1.Atmosphere and Ocean Research Institute, The University of Tokyo, 2.Institute of Earthquake and Volcano Geology, Geological Survey of Japan, AIST, 3.Center for Advanced Marine Core Research, Kochi University, 4.School of Agricultural, Earth, and Environmental Sciences, University of KwaZulu Natal, 5.Institute of GeoHistory, 6.Kobe University)

2:00 PM - 2:15 PM JST | 5:00 AM - 5:15 AM UTC

[SEM13-02] Palaeomagnetism of ca. 3-4 Ma lavas from Borgarfjordur, Iceland - magnetostratigraphy and paleosecular variation of direction

Maxwell Christopher Brown[1,2], *Yuhji Yamamoto[3], Hiroyuki Hoshi[4], Masaru Kono[5], Hidefumi Tanaka[3], Takehiro Koyaguchi[6], Brian Jicha[7], Kohei Masaoka[3,8], Vivian Sinnen[2], Justin Tonti-Filippini[2,9], Hiroto Ishikawa[3], Richard Bono[10] (1.University of Minnesota, 2. University of Iceland, 3.Kochi University, 4.Aichi University of Education, 5.Tokyo Institute of Technology, 6.University of Tokyo, 7.University of Wisconsin-Madison, 8.Kyushu University, 9.Ludwig Maximilian University of Munich, 10.University of Liverpool)

2:15 PM - 2:30 PM JST | 5:15 AM - 5:30 AM UTC

[SEM13-03] Archeointensity variation for the past millennium from Reunion Island

*Koji Fukuma[1], Hisatoshi Ito[2] (1.Department of Environmental System Science, Faculty of Science and Engineering, Doshisha University, 2.Central Research Institute for Electric Power Industry)

2:30 PM - 2:45 PM JST | 5:30 AM - 5:45 AM UTC

[SEM13-04] Analyzing the early 19th century's geographical points in latitude and longitude of 0.2 second level and geomagnetic declination through Japan from Tadataka Inoh's magnetic survey azimuth ledger simultaneously.

*Motohiro Tsujimoto[1] (1.none)

2:45 PM - 3:00 PM JST | 5:45 AM - 6:00 AM UTC

[SEM13-05] Effects of cooling from the CMB on geodynamo with different Rayleigh numbers and inner core radii

*Yuki Nishida[1], Yuto Katoh[1], Hiroaki Matsui[2], Masaki Matsushima[3], Takumi Kera[1], Atsushi Kumamoto[1] (1.Department of Geophysics, Graduate School of Science, Tohoku University, 2.Dept. of Earth and Planetary Sciences, University of California, Davis, 3.Department of Earth and Planetary Sciences, School of Science, Tokyo Institute of Technology)

3:00 PM - 3:15 PM JST | 6:00 AM - 6:15 AM UTC

[SEM13-06] An attempt to detect a stratified layer at the core surface from a geomagnetic field model

*Masaki Matsushima[1] (1.Department of Earth and Planetary Sciences, School of Science, Tokyo Institute of Technology)

[J] Oral | S (Solid Earth Sciences)：S-EM Earth's Electromagnetism

3:30 PM - 5:00 PM JST | 6:30 AM - 8:00 AM UTC | Ch.21 Zoom Room 21

[S-EM13] Geomagnetism, paleomagnetism and rock magnetism

convener:Chie Kato(Faculty of Social and Cultural Studies, Kyushu University), Tetsuro Sato(Earthquake Research Institute, The University of Tokyo), Chairperson:Chie Kato(Faculty of Social and Cultural Studies, Kyushu University), Tetsuro Sato(Earthquake Research Institute, The University of Tokyo), Yutaka Yoshimura(Faculty of Social and Cultural Studies, Kyushu University)

3:30 PM - 4:00 PM JST | 6:30 AM - 7:00 AM UTC

[SEM13-07] **Unmixing complex sedimentary magnetic mineral assemblages**

★Invited Papers

*Andrew P Roberts[1], Jinhua Li[2,3,4,5], Yan Liu[2,3,4,5], Shuangchi Liu[2,5], Hongmiao Pan[4,6], Tian Xiao[4,6], Yongxin Pan[2,3,4,5] (1.Research School of Earth Sciences, Australian National University, Canberra, ACT 2601, Australia, 2.Key Laboratory of Earth and Planetary Physics, Institute of Geology and Geophysics, Innovation Academy for Earth Sciences, Chinese Academy of Sciences, Beijing 100029, China, 3.Laboratory for Marine Geology, Qingdao National Laboratory for Marine Science and Technology, Qingdao 266061, China, 4.International Associated Laboratory of Evolution and Development of Magnetotactic Multicellular Organisms (LIA-MagMC), CNRS-CAS, Beijing 100029, China, 5.College of Earth and Planetary Sciences, University of Chinese Academy of Sciences, Beijing 100049, China, 6.Key Laboratory of Marine Ecology and Environmental Sciences, Institute of Oceanology, Chinese Academy of Sciences, Qingdao 266071, China)

4:00 PM - 4:15 PM JST | 7:00 AM - 7:15 AM UTC

[SEM13-08] Examination of the properties of remanent magnetization carried by magnetotactic bacteria in the early stages of sediment formation; example of mixed system with magnetic particles of inorganic origin

*Kohei Masaoka[1], Yuki Morono[2], Naotaka Tomioka[2], Go-Ichiro Uramoto[3], Yuhji Yamamoto[3], Masao Ohno[1] (1.Kyushu University, 2.Kochi Institute for Core Sample Research, Japan Agency for Marine-Earth Science and Technology, 3.Kochi University)

4:15 PM - 4:30 PM JST | 7:15 AM - 7:30 AM UTC

[SEM13-09] Analysis of magnetic mineral composition of a sediment core taken from the Ontong-Java Plateau and its implications to relative paleointensity estimations

*Jiaxi Li [1], Toshitsugu Yamazaki[1], Yoichi Usui[2], Takuya Sagawa[3], Junichiro Kuroda[1] (1.Atmosphere and Ocean Research Institute, The University of Tokyo, 2.Japan Agency for Marine-Earth Science and Technology, 3.Kanazawa University)

4:30 PM - 4:45 PM JST | 7:30 AM - 7:45 AM UTC

[SEM13-10] **Environmental magnetic study of a Holocene sediment core from the Yeongsan Estuary, Southwest Korea**

*Hyeon-Seon Ahn[1], Jaesoo Lim[2] (1.Kochi University, 2.Korea Institute of Geoscience and Mineral Resources)

4:45 PM - 5:00 PM JST | 7:45 AM - 8:00 AM UTC

[SEM13-11] **Relationship between the abundance of the exsolved magnetite and the valence state of iron in single plagioclase crystal separated from Doshi gabbro**

*Yujiro Tamura[1], Masahiko Sato[2], Ryoichi Nakada[3], Chie Kato[4], Shinji Yamamoto[1] (1.Yokohama National University, 2.The University of Tokyo, 3.Japan Agency for Marine-Earth Science and Technology, 4.Kyushu University)

[J] Poster | S (Solid Earth Sciences)：S-EM Earth's Electromagnetism

5:15 PM - 6:30 PM JST | 8:15 AM - 9:30 AM UTC | Ch.11_1

[S-EM13] Geomagnetism, paleomagnetism and rock magnetism

convener:Chie Kato(Faculty of Social and Cultural Studies, Kyushu University), Tetsuro Sato(Earthquake Research Institute, The University of Tokyo)

[SEM13-P01] Brunhes-Matuyama geomagnetic reversal record from Terasaki, Boso Peninsula

*Hirokuni Oda[1], Hiroomi Nakazato[2], Futoshi Nanayama[1], Yumiko Harigane[1] (1.Institute of Geology and Geoinformation, Geological Survey of Japan, AIST, 2.National Agriculture and Food Research Organization)

[SEM13-P02] Plaeomagnetic study of the Kusatsu-Shirane volcano, Gunma, Japan

*Nagisa Sawada[1], Nobuko Kametani[2], Kazuo Kawasaki[1], Yasuo Ishizaki[1], Akihiko Terada[3] (1.University of Toyama, 2.Mount Fuji Research Institute, Yamanashi Prefectural Government, 3.Tokyo Institute of Technology)

[SEM13-P03] The Laschamp and a new post-Laschamp excursions repeating directional swings from Lake Suigetsu varved sediments

*Masayuki Hyodo[1,2], Takeshi Nakagawa[3], Hayato Matsushita[2], Ikuko Kitaba[3], Keitaro Yamada[3], Shota Tanabe[2], Balazs Bradak[1,4], Danielle McLean[5], Richard A. Staff[6], Victoria C. Smith[5], Paul G. Albert[5], Akiteru Yamasaki[7], Junko Kitagawa[8,7] (1.Research Center for Inland Seas, Kobe University, 2.Department of Planetology, Kobe University, 3.Research Centre for Palaeoclimatology, Ritsumeikan University, 4.Department of Physics, University of Burgos, 5.School of Archaeology, University of Oxford, 6.Scottish Universities Environmental Research Centre (SUERC), University of Glasgow, 7.Fukui Prefectural Satoyama-Satoumi Research Institute, 8.Varve Museum)

[SEM13-P04] Rock-magnetic properties of topmost sediments in Omura Bay, Nagasaki Prefecture

*Naoto Ishikawa[1], Yoriko Yokoo[2], Kazumi Matsuoka[3] (1.Faculty of Sustainable Design, Toyama University, 2.Faculty of Scinece and Engineering, Doshisha University, 3.Institute for East China Sea Research, Nagasaki University)

[SEM13-P05] Paleomagnetic Dating on Tsunami Boulders from the Kingdom of Tonga

*Tetsuro Sato[1], Norihiro Nakamura[2], Hiroyuki Nagahama[3], Masahiko Sato[4], Kazuhisa Goto[4], Masashi Watanabe[5], Akira Ikeda[3], Kenji Satake[1], Taaniela Kula[6] (1.Earthquake Research Institute, The University of Tokyo, 2.Institute for Excellence in Higher Education, Tohoku University, 3.Department of Earth Science, Tohoku University, 4.Department of Earth and Planetary Science, The University of Tokyo, 5.Faculty of Science and Engineering, Chuo University, 6.Ministry of Lands and Natural Resources)

[SEM13-P06] Influence of biogenic magnetite on paleointensity estimations inferred from FORC-PCA of sediments from the western equatorial Pacific

Kosuke Inoue[1], *Toshitsugu Yamazaki[1], Yoichi Usui[2] (1.Atmosphere and Ocean Research Institute, The University of Tokyo, 2.Japan Agency for Marine-Earth Science and Technology)

[SEM13-P07] Solitary magnetostrophic Rossby waves

*Kumiko Hori[1,2], Steve M Tobias[2], Chris A Jones[2] (1.Graduate School of System Informatics, Kobe University, 2.Department of Applied Mathematics, University of Leeds)

[SEM13-P08] Effects of driving mode of convection on a spherical dynamo action with a small inner core

*Futoshi Takahashi[1], Hinami Taniguchi[2] (1.Faculty of Science, Kyushu University, 2.School of Science, Kyushu University)

[SEM13-P09] Rock-magnetic and mineralogical properties of the exsolved magnetite in plagioclase crystal

*Masahiko Sato[1], Masashi Ushioda[2], Ryoichi Nakada[3], Yujiro Tamura[4], Shinji Yamamoto[4] (1.The University of Tokyo, 2.Shikoku Research Institute Inc., 3.Japan Agency for Marine-Earth Science and Technology, 4.Yohohama National University)

[SEM13-P10] Rock-magnetic properties of isocubanite from submarine hydrothermal deposits in the Okinawa Trough

*Chie Kato[1], Masao Ohno[1], Yoshihiro Kuwahara[1], Tadahiro Hatakeyama[2], Yasuhiro Yamada[3], Shuhei Totsuka[4], Kazuhiko Shimada[1], Jun-ichiro Ishibashi[1], Toshiro Nagase[5] (1.Kyushu University, 2.Okayama University of Science, 3.Tokyo University of Science, 4.National Institute of Advanced Industrial Science and Technology, 5.Tohoku University)

[SEM13-P11] Contribution of equatorially antisymmetric buoyancy to polarity reversals in geodynamo models

*Takumi Kera[1], Hiroaki Matsui[3], Masaki Matsushima[2], Yuki Nishida[1], Yuto Katoh[1] (1.Department of Geophysics, Graduate School of Science, Tohoku University, 2.Tokyo Institute of Technology, 3.Dept. of Earth and Planetary Sciences, University of California, Davis)

[SEM13-P12] **Simultaneous observation of the geomagnetic field at different sites using two SQUID magnetometer systems**

*Jun Kawai[1], Miki Kawabata[1], Masakazu Miyamoto[1] (1.Applied Electronics Laboratory, Kanazawa Institute of Technology)

[E] Poster | S (Solid Earth Sciences)：S-IT Science of the Earth's Interior & Techtonophysics

5:15 PM - 6:30 PM JST | 8:15 AM - 9:30 AM UTC | Ch.11_2

[S-IT19] East Asia geodynamics: New perspectives, top to bottom

convener:B Timothy Byrne(University of Connecticut), Asuka Yamaguchi(Atomosphere and Ocean Research Institute, The University of Tokyo), Jonny Wu(University of Houston), Kyoko Okino(Atmosphere and Ocean Research Institute, The University of Tokyo)

[SIT19-P01] Strain localization and development of deformation bands in a forearc coal-bearing Paleogene fold and thrust belt, Hokkaido, northern Japan

Hiromi Kaji[1,2], *Toru Takeshita[1] (1.Department of Natural History Sciences, Graduate School of Science, Hokkaido University, 2.Oyo Co. Ltd.)

[SIT19-P02] Comparison of paleostress and paleotemperature analysis at Roof Thrust and Out-of-Sequence Thrust of subduction zone : The Minami Awa Fault and Mizoochi Fault, The Mugi area in the Shimanto Belt

*Yu Sogawa[1], Arito Sakaguchi[1] (1.Graduate School of Sciences and Technology for Innovation, Yamaguchi University)

[SIT19-P03] Coseismic Fault Model for the Thabeikkyin earthquake in 2012 determined from GNSS Observation

*Tha Zin Htet Tin[1,5], Takuya NISHIMURA[2], Manabu Hashimoto[2], Eric LINDSEY[3,4], Yutaro Okada[1], Lin Thu Aung -[3], Myo Thant -[5,6] (1.Graduate School of Science, Kyoto University, Kyoto, Japan, 2.Disaster Prevention Research Institute, Kyoto University, Kyoto, Japan, 3.Earth Observatory of Singapore, Nanyang Technological University, Singapore, 4.University of New Mexico, Albuquerque, United States, 5.Department of Geology, University of Yangon, Myanmar, 6.Myanmar Earthquake Committee, Yangon, Myanmar)

[SIT19-P04] Estimation of postseismic effects of 2013 Okhotsk Sea M_w8.3 deep-focus earthquake

*Grigorii Viktorovich Nechaev[1,2], Nikolai Shestakov[1,2], Hiroaki Takahashi[3], Evgenii Lialiushko[2] (1.Institute for Applied Mathematics FEB RAS, 2.Far Eastern Federal University, 3.Institute of Seismology and Volcanology, Hokkaido University)

[J] Oral | S (Solid Earth Sciences)：S-MP Mineralogy & Petrology

9:00 AM - 10:30 AM JST | 12:00 AM - 1:30 AM UTC | Ch.20 Zoom Room 20

[S-MP25] Deformed rocks, Metamorphic rocks and Tectonics

convener:Yumiko Harigane(Geological Survey of Japan, National Institute of Advanced Industrial Science and Technology (AIST)), Yoshihiro Nakamura(Geological Survey of Japan, National Institute of Advanced Industrial Science and Technology), Chairperson:Yumiko Harigane(Geological Survey of Japan, National Institute of Advanced Industrial Science and Technology (AIST)), Yoshihiro Nakamura(Geological Survey of Japan, National Institute of Advanced Industrial Science and Technology)

9:00 AM - 9:15 AM JST | 12:00 AM - 12:15 AM UTC

[SMP25-01] Prolonged subduction metamorphism and deep forearc accumulation of Sanbagawa Complex: an example from Okawara district, southern Japanese Alps

*Kazuhiro Miyazaki[1], Yoshihiro Nakamura[1], Hiroshi Makimoto[1] (1.Institute of Geology and Geoinformation, Geological Survey of Japan/National Institute of Advanced Industrial Science and Technology)

9:15 AM - 9:30 AM JST | 12:15 AM - 12:30 AM UTC

[SMP25-02] High mobility of Sr and Ba in subduction-related metamorphism: Application of Machine-learning mass transfer analyses to mafic shists, the Sanbagawa belt

*Matsuno Satoshi[1], Masaoki Uno[1], Atsushi Okamoto[1], Noriyoshi Tsuchiya[1] (1.Graduate School of Environmental Studies Tohoku University)

9:30 AM - 9:45 AM JST | 12:30 AM - 12:45 AM UTC

[SMP25-03] U–Pb garnet dating of HP marble from the Eastern Iratsu body, Sanbagawa metamorphic terrane: decoupled isotopic signature and compositional zoning

*Sota Niki[1], Kenta Yoshida[2], Hikaru Sawada[2], Ryosuke Oyanagi[2], Takafumi Hirata[1] (1.Geochemical Research Center, Graduate School of Science, The University of Tokyo, 2.Japan Agency for Marine-Earth Science and Technology)

9:45 AM - 10:00 AM JST | 12:45 AM - 1:00 AM UTC

[SMP25-04] **Crystal size distribution of garnet formed by two-stage growth in the Kotsu eclogite, Sanbagawa belt**

*OTGONBAYAR DANDAR[1], Atsushi Okamoto[1], Masaoki Uno[1] (1.Graduate School of Environmental Studies, Tohoku University)

10:00 AM - 10:15 AM JST | 1:00 AM - 1:15 AM UTC

[SMP25-05] A shape change model of isolated K-feldspar inclusions within a micro-shear zone developed in Teshima granite, the Ryoke metamorphic belt

*Tae-Hoon Uhmb[1], Katsuyoshi Michibayashi[1] (1.Department of Earth and Planetary Sciences, Research group of Petrology and Mineralogy, Nagoya University)

10:15 AM - 10:30 AM JST | 1:15 AM - 1:30 AM UTC

[SMP25-06] C-O-H fluid was present during garnet-forming partial melting reaction in a pelitic migmatite from the Ryoke belt, Japan

*Natsumi Yoshimoto[1], Tetsuo Kawakami[1] (1.Kyoto University)

[J] Oral | S (Solid Earth Sciences)：S-MP Mineralogy & Petrology

10:45 AM - 12:15 PM JST | 1:45 AM - 3:15 AM UTC | Ch.20 Zoom Room 20

[S-MP25] Deformed rocks, Metamorphic rocks and Tectonics

convener:Yumiko Harigane(Geological Survey of Japan, National Institute of Advanced Industrial Science and Technology (AIST)), Yoshihiro Nakamura(Geological Survey of Japan, National Institute of Advanced Industrial Science and Technology), Chairperson:Yumiko Harigane(Geological Survey of Japan, National Institute of Advanced Industrial Science and Technology (AIST)), Yoshihiro Nakamura(Geological Survey of Japan, National Institute of Advanced Industrial Science and Technology)

10:45 AM - 11:00 AM JST | 1:45 AM - 2:00 AM UTC

[SMP25-07] Rheological and metamorphic evolutions of high-grade Shimanto accretionary complex in Kerama islands, Ryukyu

*Ippei Yamamoto[1], Yoshihiro Nakamura[2], Yumiko Harigane[2], Yui Kouketsu[3], Kenichiro Tani[4], Asuka Yamaguchi[1] (1.Atmosphere and Ocean Research Institute, The University of Tokyo, 2.National Institute of Advanced Industrial Science and Technology, 3.Nagoya University, 4.National Museum of Nature and Science)

11:00 AM - 11:15 AM JST | 2:00 AM - 2:15 AM UTC

[SMP25-08] Rheological Properties of Ductile Shear Zone Developed in Mado Megamullion, Shikoku Basin, Philippine Sea

*Kohei Nimura[1], Katsuyoshi Michibayashi[2], Yumiko Harigane[3], Yasuhiko Ohara[4,5] (1.Department of Earth and Planetary Science, Faculty of Science, Nagoya University , 2.Department of Earth and Planetary Sciences, Graduate School of Environmental Studies, Nagoya University, 3.Research Institute of Geology and Geoinformation, Geological Survey of Japan, AIST, 4.Hydrographic and Oceanographic Department of Japan, 5.JAMSTEC)

11:15 AM - 11:30 AM JST | 2:15 AM - 2:30 AM UTC

[SMP25-09] Possibility of CPO development during diffusion creep of the lower crustal minerals

*Bunrin Natsui[1], Kosuke Yabe[1], Takehiko Hiraga[1] (1.Earthquake Research Institute, University of Tokyo)

11:30 AM - 11:45 AM JST | 2:30 AM - 2:45 AM UTC

[SMP25-10] **The effect of fluid compositions on pore formation during plagioclase replacement under supercritical conditions**

*Astin Nurdiana[1], Atsushi Okamoto[1], Masaoki Uno[1], Noriyoshi Tsuchiya[1] (1.Tohoku University)

11:45 AM - 12:00 PM JST | 2:45 AM - 3:00 AM UTC

[SMP25-11] Garnet–aluminosilicate–spinel–plagioclase geobarometer

*Toshiaki Shimura[1], Yuki Harada[1,2], Geoffrey L. Fraser[3], Noriyoshi Tsuchiya[4] (1.Yamaguchi University, 2.i-SHOT Inc., 3.Geoscience Australia, 4.Tohoku University)

12:00 PM - 12:15 PM JST | 3:00 AM - 3:15 AM UTC

[SMP25-12] Porosity wave and mineral banding in the metamorphism

*mitsuhiro toriumi[1] (1.Japan agency of marine science and technology)

[J] Oral | S (Solid Earth Sciences)：S-MP Mineralogy & Petrology

1:45 PM - 3:15 PM JST | 4:45 AM - 6:15 AM UTC | Ch.20 Zoom Room 20

[S-MP25] Deformed rocks, Metamorphic rocks and Tectonics

convener:Yumiko Harigane(Geological Survey of Japan, National Institute of Advanced Industrial Science and Technology (AIST)), Yoshihiro Nakamura(Geological Survey of Japan, National Institute of Advanced Industrial Science and Technology), Chairperson:Yumiko Harigane(Geological Survey of Japan, National Institute of Advanced Industrial Science and Technology (AIST)), Yoshihiro Nakamura(Geological Survey of Japan, National Institute of Advanced Industrial Science and Technology)

1:45 PM - 2:00 PM JST | 4:45 AM - 5:00 AM UTC

[SMP25-13] Different entrapment timings of melt inclusions in garnet and quartz in an UH *T* granulite from Rundvågshetta

*Kota Suzuki[1], Tetsuo Kawakami[1] (1.Department of Geology and Mineralogy, Graduate School of Science, Kyoto University)

2:00 PM - 2:15 PM JST | 5:00 AM - 5:15 AM UTC

[SMP25-14] **Effect of syn-metamorphic fluids on HP-LT chloritoid-bearing assemblages: a study case from the Monti Romani (Italy)**

*Samuele Papeschi[1], Alessio Pontesilli[2], Claudia Romano[3], Federico Rossetti[3] (1.Kochi (X-Star), JAMSTEC, Japan, 2.INGV, Roma, Italy, 3.University Roma Tre, Italy)

2:15 PM - 2:30 PM JST | 5:15 AM - 5:30 AM UTC

[SMP25-15] **Newly discovered eclogite in the Khungui zone, Zavkhan terrane, Western Mongolia: P-T evolution and tectonic implication**

*Manzshir Bayarbold[1], Atsushi Okamoto[1], OTGONBAYAR DANDAR[1], Masaoki Uno[1], Noriyoshi Tsuchiya[1] (1.Graduate School of Environmental Studies, Tohoku University)

2:30 PM - 2:45 PM JST | 5:30 AM - 5:45 AM UTC

[SMP25-16] Serpentinization and Carbonation processes of Ultramafic rocks in Manlay Ophiolite, Southern Mongolia

*Nomuulin Amarbayar[1], Atsushi Okamoto[1], Masaoki Uno[1], OTGONBAYAR DANDAR[1], Noriyoshi Tsuchiya[1] (1.Graduate School of Environmental Studies, Tohoku University)

2:45 PM - 3:00 PM JST | 5:45 AM - 6:00 AM UTC

[SMP25-17] Petrological characteristics of the slab-mantle interface during incipient subduction: insights from Dalrympole Amphibolite, Palawan, Philippines

*Gabriel Theophilus Vinalay Valera[1], Tetsuo Kawakami[1], Betchaida Duetes Payot[2] (1.Graduate School of Science, Kyoto University, 2.National Institute of Geological Sciences, University of the Philippines)

3:00 PM - 3:15 PM JST | 6:00 AM - 6:15 AM UTC

[SMP25-18] New deformation proxy for alkaline felsic rocks: Na-K zoning of alkali feldspar in syenites from the Wadi Dib alkaline ring complex, Eastern Desert, Egypt

*Kazuhito Ozawa[1], Eman Saad Hassan[2], Hideto Yoshida[1], Ali Abdel-Kader Khudeir[2] (1.Department of Earth and Planetary Science, Graduate School of Science, University of Tokyo, 2.Geology Department, Assiut University)

[J] Poster | S (Solid Earth Sciences)：S-MP Mineralogy & Petrology

5:15 PM - 6:30 PM JST | 8:15 AM - 9:30 AM UTC | Ch.12_1

[S-MP25] Deformed rocks, Metamorphic rocks and Tectonics

convener:Yumiko Harigane(Geological Survey of Japan, National Institute of Advanced Industrial Science and Technology (AIST)), Yoshihiro Nakamura(Geological Survey of Japan, National Institute of Advanced Industrial Science and Technology)

[SMP25-P01] Multiple igneous activities recorded in the Nidar ophiolite complex, eastern Ladakh

*Akinori Sato[1], Takeshi Imayama[1], Dripta Dutta[2] (1.Okayama University of Science, 2.Indian Institute of Technology Bombay)

[SMP25-P02] Geology and missing tectonics in the Inashi-Hase area of the eastern part of the Ryoke belt, central Japan

*Akira Ono

[SMP25-P03] Kinematics of North Almora Thrust estimated from mylonite, India

*Hirotoshi Kotama[1], Jun-ichi Ando[1], Kaushik Das[1], Dyuti Prakash Sarkar[1] (1.Hiroshima University)

[SMP25-P04] Illite crystallization and faulting caused by hydrothermal fluid

*Jun-ichi Ando[1], Kota Kojima[1], Kaushik Das[1], Naotaka Tomioka[2], Seiichiro Uehara[3] (1.Department of Earth and Planetary Systems Science, Hiroshima University, 2.Kochi Institute for core sample research, Japan Agency for Marine-Earth Science and Technology, 3.The Kyushu university museum)

[SMP25-P05] Episodic fluid explosion in shallow and middle crust revealed by hydrothermal brecciation

*Geri Agroli[1], Atsushi Okamoto[1], Masaoki Uno[1], Noriyoshi Tsuchiya[1] (1.Tohoku University)

[SMP25-P06] Pseudotachylyte in a marble from the Takine Group (Abukuma Terrane) and its similarity to pseudotachylyte from the Higo Mertamorphic Rocks

*Tadao Nishiyama[1], Ebo Adou Douha[1] (1.Department of Earth and Environmental Sciences, School of Science, Graduate School of Science and Technology, Kumamoto University)

[SMP25-P07] **Frictional melting process during formation of pseudotachylyte, Sarwar-Junia fault zone, India**

*Jun-ya Okazaki[1], Jun-ichi Ando[1], Kaushik Das[1] (1.Earth and Planetary Systems Science Program, Division of Advanced Science and Engineering, Hiroshima University)

[SMP25-P08] Neoarchean magmatism and Paleoproterozoic high-pressure granulite-facies metamorphism from the southern Motloutse Complex, eastern Botswana: Implications for the western extension of the Central Zone of the Limpopo Complex

*Thembiso Otladisang Basupi[1,2], Toshiaki Tsunogae[1,3], Kazuki Takahashi[1], Yukiyasu Tsutsumi[4] (1.Graduate of Life and Environmental Sciences, University of Tsukuba, 2.Department of Earth and Environmental Sciences, Botswana International University of Science and Technology, 3.Department of Geology, University of Johannesburg, 4.Department of Geology and Paleontology, National Museum of Nature and Science)

[SMP25-P09] Petrography of a sulfide-rich garnet-sillimanite-biotite gneiss from Brattnipene, Sør Rondane Mountains, East Antarctica

*Hayato Ikeda[1], Tetsuo Kawakami[1] (1.Kyoto University)

[SMP25-P10] Microstructural characteristics of ultra-high pressure metamorphic rocks from the Dabie-Shan, eastern China

*Katsuyoshi Michibayashi[1], Kouhei Asano[1] (1.Department of Earth and Planetary Sciences, Graduate School of Environmental Studies, Nagoya University)

[SMP25-P11] Metamorphic history of the Suo metamorphic rocks inferred from two-stage garnet in pelitic schist

*Shunsuke Endo[1], Maki Ito[1] (1.Department of Earth Science, Interdisciplinary Faculty of Science and Engineering, Shimane University)

[SMP25-P12] Hidden intact coesite in deeply subducted rocks and its geological implications

*Tomoki Taguchi[1], Yui Kouketsu[2], Yohei Igami[3], Tomoyuki Kobayashi[4], Akira Miyake[3] (1.Department of Earth Sciences, Faculty of Education and Integrated Arts and Sciences, Waseda University, 2.Department of Earth and Planetary Science, Graduate School of Environmental Studies, Nagoya University, 3.Department of Geology and Mineralogy, Graduate School of Science, Kyoto University, 4.Faculty of Health and Sports, Nagoya Gakuin University)

[SMP25-P13] Metamorphic zoning and *P–T* conditions of contact metamorphic rocks in the Unai area, Yamaguchi prefecture, Japan.

*Kakeru Sakamoto[1], Toshiaki Shimura[1] (1.Graduate School of Sciences and Technology for Innovation, Yamaguchi University)

[SMP25-P14] Progressive metamorphism of the Ryoke metamorphic rocks from No-jima Island, South of Yamaguchi Prefecture

*ZEJIN LU[1] (1.Graduate School of Science and Engineering for Innovation, Yamaguchi University)

[SMP25-P15] *P–T–t* path of Ryoke metamorphic rocks in Kitsuki area, Kunisaki Peninsula, Oita prefecture, Japan.

*Kentaro Mutabaru[1], Toshiaki Shimura[1] (1.Yamaguchi University)

[SMP25-P16] *P-T* estimations of Ryoke metamorphic rocks in the Takato-Ohshika area, Nagano, Japan

*Yoshihiro Nakamura[1], Kazuhiro Miyazaki[1], Yutaka Takahashi[1] (1.Geological Survey of Japan, National Institute of Advanced Industrial Science and Technology)

[SMP25-P17] Ultrahigh-temperature HP granulite facies stage of the Early Jurassic pre-Sanbagawa metamorphism

*Kenta Yoshida[1], Sota Niki[3], Hikaru Sawada[1], Ryosuke Oyanagi[1], Takafumi Hirata[3], Kenji Asakura[2], Takao Hirajima[2] (1.Japan Agency for Marine-earth Science and Technology, 2.Kyoto University, 3.The University of Tokyo)

[SMP25-P18] **Meliorating the spatial resolution of SEM-EBSD**

*Thomas Jing Yi Yeo[1], Norio Shigematsu[1] (1.Research Institute of Earthquake and Volcano Geology, Geological Survey of Japan, National Institute of Advanced Industrial Science and Technology)

[SMP25-P19] Strain in quartz inclusion probed by Raman spectroscopy

*Yui Kouketsu[1], Yuki Tomioka[1], Tomoki Taguchi[2] (1.Department of Earth & Planetary Sciences, Graduate School of Environmental Studies, Nagoya University, 2.Department of Earth Sciences, Faculty of Education and Integrated Arts and Sciences, Waseda University)

[J] Oral | S (Solid Earth Sciences)：S-MP Mineralogy & Petrology

10:45 AM - 11:50 AM JST | 1:45 AM - 2:50 AM UTC | Ch.23 Zoom Room 23

[S-MP26] Physics and Chemistry of Minerals

convener:Masahiro KAYAMA(Department of General Systems Studies, Graduate School of Arts and Sciences, The University of Tokyo), Itaru Ohira(Department of Chemistry, Faculty of Science, Gakushuin University), Chairperson:Masahiro KAYAMA(Department of General Systems Studies, Graduate School of Arts and Sciences, The University of Tokyo), Itaru Ohira(Department of Chemistry, Faculty of Science, Gakushuin University)

10:45 AM - 11:00 AM JST | 1:45 AM - 2:00 AM UTC

[SMP26-01] **Skew-normal peak fitting of cathodoluminescence on shocked quartz: a statistical model for impact pressure estimation**

Yu Chang[2], Shintaro Kadoya[3], *Keisuke Yano[1], Masahiro KAYAMA[2], Eiichi Tajika[2], Yasuhito Sekine[4], Toshimori Sekine[5], Hirotsugu Nishido[6], Takamichi Kobayashi[7] (1.The Institute of Statistical Mathematics, 2.The University of Tokyo, 3.University of Washington , 4.Tokyo Institute of Technology, Earth-Life Science Institute (ELSI), 5.Osaka University, 6.Okayama University of Science, 7.National Institute for Materials Science)

11:00 AM - 11:15 AM JST | 2:00 AM - 2:15 AM UTC

[SMP26-02] Magnetite oxidation investigated by synchrotron X-ray diffraction and X-ray absorption spectroscopy

*Atsushi Kyono[1], Ibuki Kinebuchi[1] (1.Division of Earth Evolution Sciences, Faculty of Life and Environmental Sciences, University of Tsukuba)

11:15 AM - 11:30 AM JST | 2:15 AM - 2:30 AM UTC

[SMP26-03] *P-T* dependence of hydrogen-bond geometry of β-CrOOD

Chikara Shito[1], *Hiroyuki Kagi[1], Asami Sano-Furukawa[2,3], Sho Kakizawa[4], Kazuki Komatsu[1], Riko Iizuka-Oku[1], Katsutoshi Aoki[1], Jun Abe[5], Shinichi Machida[5], Takashi Saito[3], Takashi Kamiyama[3], Noboru Furukawa[6], Akio Suzuki[7] (1.Graduate School of Science, University of Tokyo, 2.Japan Atomic Energy Agency, 3.High Energy Accelerator Research Organization, 4.Graduate School of Advanced Science and Engineering, Hiroshima University, 5.Comprehensive Research Organization for Science and Society, 6.Graduate School of Science, Chiba University, 7.Graduate School of Science, Tohoku University)

11:30 AM - 11:50 AM JST | 2:30 AM - 2:50 AM UTC

[SMP26-04] Discussion

[J] Poster | S (Solid Earth Sciences)：S-MP Mineralogy & Petrology

5:15 PM - 6:30 PM JST | 8:15 AM - 9:30 AM UTC | Ch.12_2

[S-MP26] Physics and Chemistry of Minerals

convener:Masahiro KAYAMA(Department of General Systems Studies, Graduate School of Arts and Sciences, The University of Tokyo), Itaru Ohira(Department of Chemistry, Faculty of Science, Gakushuin University)

[SMP26-P01] Pressure-induced phase transitions in wülfingite (Zn(OH)2): Raman spectroscopic and First-principles study

*Masami Kanzaki[1], Longli Guan[1], Ran Wang[1] (1.Institute for Planetary Matereials, Okayama University)

[SMP26-P02] Elastic wave velocity of ε-FeOOH across the pressure-induced spin transition of iron

*Osamu Ikeda[1], Tatsuya Sakamaki[1], Hiroshi Fukui[2,3], Hiroshi Uchiyama[4], Alfred Q.E. Baron[3,4], Akio Suzuki[1] (1.Department of Earth Science, Graduate School of Science, Tohoku University, 2.Graduate School of Material Science, University of Hyogo, 3.RIKEN SPring-8 Center, 4.Japan Synchrotron Radiation Research Institute)

[SMP26-P03] Phase transition of M3+OOH-type oxyhydroxides under high pressure

*Akio Suzuki[1] (1.Department of Earth Science, Graduate School of Science, Tohoku University)

[SMP26-P04] Density measurement of silicate melt by the buoyancy test under high pressure

*Akio Suzuki[1] (1.Department of Earth Science, Graduate School of Science, Tohoku University)

[SMP26-P05] Structural study on the $Ca_2MgAl_2Si_4O_{14}$ composition melt under pressure

*Natsumi Adachi[1], Satoru Urakawa[1], Hidenori Terasaki[1] (1.OKAYAMA UNIVERSITY)

[SMP26-P06] Unique luminescence of rhodochrosite at low temperature

*Reina Masuda[1], Ayane Asano[1], Nobuhiro Kusano[1], Hirotsugu Nishido[1] (1.Biosphere-Geosphere Science, Okayama University of Science)

[SMP26-P07] Amesite and Al-serpentine accompanied with the serpentinite in Yakiyama, Iizuka, Fukuoka

*Yuki Isshiki[1], Seiichiro Uehara[2], Yuya Takeda[1] (1.Department of Earth and Planetary Sciences Faculty of Science, Kyushu University, 2.The Kyushu University Museum)

[SMP26-P08] Phase transitions and pressure calibration points

*Shigeaki Ono[1] (1.Japan Agency for Marine-Earth Science and Technology)

[SMP26-P09] The study on stability and properties of N-doped spinel Based on CGCNN and DFT

*SOK I TAM[1], CHI PUI TANG[1], Pak Kin Leong[1], Kin Tak U[1] (1.Macau University of Science and Technology)

[J] Oral | S (Solid Earth Sciences)：S-VC Volcanology

10:45 AM - 12:15 PM JST | 1:45 AM - 3:15 AM UTC | Ch.25 Zoom Room 25

[S-VC27] Mitigation of volcanic disasters - basic and applied researches

convener:Shinji Takarada(Geological Survey of Japan, National Institute of Advanced Industrial Science and Technology), Mitsuhiro Yoshimoto(Mount Fuji Research Institute, Yamanashi Prefectural Government), Tatsuro Chiba(Asia Air Survey Co., Ltd.), Yousuke Miyagi(National Research Institute for Earth Science and Disaster Resilience), Chairperson:Shinji Takarada(Geological Survey of Japan, National Institute of Advanced Industrial Science and Technology), Mitsuhiro Yoshimoto(Mount Fuji Research Institute, Yamanashi Prefectural Government)

10:45 AM - 11:00 AM JST | 1:45 AM - 2:00 AM UTC

[SVC27-01] Ash Fall Hazard Map using Newly Developed Simulation Model

*Tsuyoshi Nakatani[1], Toshiyuki Asano[1] (1.The Research and Education Center for Natural Hazards, Kagoshima University)

11:00 AM - 11:15 AM JST | 2:00 AM - 2:15 AM UTC

[SVC27-02] On the Effects of the Inertial Forces of the Falling Volcano Ash on the Ash absorption by an External Unit of Building Air Conditioning

*Kiyotoshi Otsuka[1], Arihide Nobata[1], Hitoshi Suwa[1], Tomohiro Kubo[2], Yosuke Miyagi[3], Masamitsu Miyamura[3] (1.Obayashi Corporation, 2.Mount Fuji Research Institute, Yamanashi Prefectural Government , 3.National Research Institute for Earth Science and Disaster Resilience)

11:15 AM - 11:30 AM JST | 2:15 AM - 2:30 AM UTC

[SVC27-03] Experimental Study on Safety of Wooden Building Roofs Against Impact of Ballistic Ejecta

*Kohei Tateyama[1], Hiroyuki Yamada[2], Ryo Honda[3], Tomohiro Kubo[3], Mitsuhiro Yoshimoto[3] (1.Ritsumeikan University, 2.National Defense Academy, 3.Mount Fuji Research Institute, Yamanashi Prefectural Government)

11:30 AM - 11:45 AM JST | 2:30 AM - 2:45 AM UTC

[SVC27-04] **A trajectory analysis of a rockfall on a steep slope at Mt. Fuji to determine the possible source area of the falling rock**

*Taishi Sakurada[1], Ryodo Hemmi[2], Yasuhiro Ishimine[3], Hideaki Miyamoto[1] (1.The University of Tokyo, 2.The University Museum, The University of Tokyo, 3.Mount Fuji Research Institute, Yamanashi Prefectural Government)

11:45 AM - 12:00 PM JST | 2:45 AM - 3:00 AM UTC

[SVC27-05] Improvement of Proto-type Educational Web Contents for the Municipalities' Disaster Response Staff.

*Tomohiro Kubo[1], Mitsuhiro Yoshimoto[1], Yosuke Miyagi[2], Ryo Honda[1], Yasuhiro Ishimine[1] (1. Mount Fuji Research Institute, 2.National Research Institute for Earth Science and Disaster Resilience)

12:00 PM - 12:15 PM JST | 3:00 AM - 3:15 AM UTC

[SVC27-06] Training of the human resource development for volcanic disaster management officers at Mt Fuji

*Mitsuhiro Yoshimoto[1], Tomohiro Kubo[1], Ryo Honda[1], Yasuhiro Ishimine[1], Kenji Niihori[2], Makoto Kanano[2] (1.Mount Fuji Research Institute, Yamanashi Prefectural Government, 2.Organization of Volcanic Disaster Mitigation, NPO.)

[J] Poster | S (Solid Earth Sciences)：S-VC Volcanology

5:15 PM - 6:30 PM JST | 8:15 AM - 9:30 AM UTC | Ch.13_1

[S-VC27] Mitigation of volcanic disasters - basic and applied researches

convener:Shinji Takarada(Geological Survey of Japan, National Institute of Advanced Industrial Science and Technology), Mitsuhiro Yoshimoto(Mount Fuji Research Institute, Yamanashi Prefectural Government), Tatsuro Chiba(Asia Air Survey Co., Ltd.), Yousuke Miyagi(National Research Institute for Earth Science and Disaster Resilience)

[SVC27-P01] Disaster-stricken vehicles dug up for the first time in 30 years and characteristics of pyroclastic surge deposits in 1991 on Unzen Volcano

*Daisuke Nagai[1], Shinichi Sugimoto[2] (1.Mt.Unzen disaster memorial hall, 2.Unzen volcanic area global geopark)

[SVC27-P02] Selective pulverization of pumiceous groundmass in pumice pulverization processes in a laboratory

*Shingo Takeuchi[1] (1.Central Research Institute of Electric Power Industry, Civil Engineering Research Laboratory, Geosphere Sciences)

[SVC27-P03] A case of sediment-related disaster in a volcanic area due to an earthquake off the coast of Fukushima Prefecture on February 13, 2021

*Takayama Toko[1], Tatsuro Chiba[1], Hiromichi Moriike[1], Tatsuya Ochiai[1] (1.Asia Air Survey Co.,Ltd.)

[SVC27-P04] Accelerating Two-Dimensional Lava Flow Simulations with OpenACC

*Yasuhiro Ishimine[1] (1.Mount Fuji Research Institute, Yamanashi Prefectural Government)

[SVC27-P05] Present situation of water pollution problem caused by 2018 Iwo-Yama volcano eruption in Kirishima volcanic complex

*Yoshikazu Kikawada[1], Haruka Yamamoto[2] (1.Faculty of Science and Technology, Sophia University, 2.Graduate School of Science and Technology, Sophia University)

[SVC27-P06] Training program of the human resource development for volcanic disaster management officers in JAPAN -Preliminary report-

*Kenji Niihori[1], Akio Sato[1], Maokoto Konno[1], Mitsuhiro Yoshimoto[2] (1.Organization of Volcanic Disaster Mitigation, NPO., 2.Mount Fuji Research Institute, Yamanashi Prefectural Government)

[SVC27-P07] Experiment for understanding of climber’s movement and tendency in Nasu Volcano

*Yousuke Miyagi[1], Mitsuhiro Yoshimoto[2], Yasuhiro Ishimine[2], Ryo Honda[2], Tomohiro Kubo[2] (1.National Research Institute for Earth Science and Disaster Resilience, 2.Mount Fuji Research Institute, Yamanashi Prefectural Government)

[SVC27-P08] **Eruption Sequences and Precursory Activities of Large-scale Volcanic Eruptions, and Construction of Large-scale Volcanic Eruption Database**

*Shinji Takarada[1], Yasuaki Kaneda[1], Fumihiko Ikegami[1], Yuki Nishino[1], Nobuo Geshi[1] (1.Geological Survey of Japan, National Institute of Advanced Industrial Science and Technology)

[J] Oral | S (Solid Earth Sciences)：S-VC Volcanology

1:45 PM - 3:15 PM JST | 4:45 AM - 6:15 AM UTC | Ch.25 Zoom Room 25

[S-VC29] Hydrothermal systems of volcanoes

convener:Yasuhiro Fujimitsu(Department of Earth Resources Engineering, Faculty of Engineering, Kyushu University), Wataru Kanda(Volcanic Fluid Research Center, School of Science, Tokyo Institute of Technology), Takeshi Ohba(Department of chemistry, School of Science, Tokia University), Chairperson:Takeshi Ohba(Department of chemistry, School of Science, Tokia University), Wataru Kanda(Volcanic Fluid Research Center, School of Science, Tokyo Institute of Technology)

1:45 PM - 2:00 PM JST | 4:45 AM - 5:00 AM UTC

[SVC29-01] Compositional variability of rare earth elements in spring waters around Aso Volcano

*Hitomi Nakamura[1], Noritoshi Morikawa[1], Hikaru Iwamori[2], Shuhei Sakata[2], Qing Chang[3] (1.Geological Survey of Japan, National Institute of Advanced Industrial Science and Technology, 2.The University of Tokyo, 3.Japan Agency for Marine-Earth Science and Technology)

2:00 PM - 2:15 PM JST | 5:00 AM - 5:15 AM UTC

[SVC29-02] Deep-seated fluid supply around Kusatsu-Shirane volcano revealed by helium and carbon isotope ratios

*Hirochika Sumino[1], Takiguchi Takahiro[2], Tomoya Obase[1], Kotaro Toyama[3], Akihiko Terada[4] (1.Department of General Systems Studies, Graduate School of Arts and Sciences, The University of Tokyo, 2.Department of Integrated Science, College of Arts and Science, The University of Tokyo, 3.Atmosphere and Ocean Research Institute, The University of Tokyo, 4.Volcanic Fluid Research Center, Tokyo Institute of Technology)

2:15 PM - 2:30 PM JST | 5:15 AM - 5:30 AM UTC

[SVC29-03] Evolution of the magmatic-hydrothermal system of Mendeleev volcano (Kunashir Island)

*Alexey Andreevich Kotov[1], Sergey Zakharovich Smirnov[2], Noriyoshi Tsuchiya[1], Masaoki Uno[1] (1.Graduate School of Environmental Studies, Tohoku University, 2.Institute of Geology and Mineralogy SB RAS, Novosibirsk, Russia)

2:30 PM - 2:45 PM JST | 5:30 AM - 5:45 AM UTC

[SVC29-04] Volcanic unrests after the 2015 phreatic eruption of Hakone volcano and its hydrothermal system

*Kazutaka Mannen[1], Yuki Abe[1], Ryosuke Doke[1], Yohei Yukutake[1] (1.Hot Springs Research Institute of Kanagawa Prefecture)

2:45 PM - 3:00 PM JST | 5:45 AM - 6:00 AM UTC

[SVC29-05] Structure of the shallow hydrothermal system in Hakone volcano inferred from InSAR analysis

*Ryosuke Doke[1], Kazutaka Mannen[1], Kazuhiro Itadera[1] (1.Hot Springs Research Institute of Kanagawa Prefecture)

3:00 PM - 3:15 PM JST | 6:00 AM - 6:15 AM UTC

[SVC29-06] Ground deformations at Kuju volcano, Japan, revealed by PALSAR-2 InSAR

*Shohei Narita[1], Takahiro Ohkura[1] (1.Aso Volcanological Laboratory, Institute for Geothermal Science, Graduate School of Science, Kyoto University)

[J] Oral | S (Solid Earth Sciences)：S-VC Volcanology

3:30 PM - 5:00 PM JST | 6:30 AM - 8:00 AM UTC | Ch.25 Zoom Room 25

[S-VC29] Hydrothermal systems of volcanoes

convener:Yasuhiro Fujimitsu(Department of Earth Resources Engineering, Faculty of Engineering, Kyushu University), Wataru Kanda(Volcanic Fluid Research Center, School of Science, Tokyo Institute of Technology), Takeshi Ohba(Department of chemistry, School of Science, Tokia University), Chairperson:Wataru Kanda(Volcanic Fluid Research Center, School of Science, Tokyo Institute of Technology), Yasuhiro Fujimitsu(Department of Earth Resources Engineering, Faculty of Engineering, Kyushu University)

3:30 PM - 3:45 PM JST | 6:30 AM - 6:45 AM UTC

[SVC29-07] The plumbing system of a Miyakejima volcano: insights into magmatic-hydrothermal interactions

*Marceau Gresse[1], Makoto Uyeshima[1], Takao Koyama[1], Hideaki Hase[2], Koki Aizawa[3], Yusuke Yamaya[4], Yuichi Morita[1], Derek Weller[1], Tawat Rung-Arunwan[5], Takayuki Kaneko[1], Yoichi Sasai[6], Jacques Zlotnicki[7], Tsuneo Ishido[8], Hideki Ueda[9], Maki Hata[1] (1.Earthquake Research Institute, The University of Tokyo, Tokyo, Japan, 2.Geothermal Energy Research & Development Co., Ltd., Tokyo, Japan, 3.Institute of Seismology and Volcanology, Faculty of Science, Kyushu University, Fukuoka, Japan, 4.National Institute of Advanced Industrial Science and Technology (AIST), Renewable Energy Research Center, Fukushima, Japan, 5.Curl-E Geophysics Co., Ltd., Thailand, 6.Earthquake Prediction Research Center, Tokai University, Shizuoka, Japan, 7.CNRS, EMSEV, OPGC-UMR6524, Aubière, France, 8.Geological Survey of Japan, National Institute of Advanced Industrial Science and Technology (AIST), Tsukuba, Japan, 9.National Research Institute for Earth Science and Disaster Resilience (NIED), Tsukuba, Japan)

3:45 PM - 4:00 PM JST | 6:45 AM - 7:00 AM UTC

[SVC29-08] Ability of the magnetotelluric method to image a deep conductor: Exploration of a supercritical geothermal system

*Keiichi Ishizu[1], Yasuo Ogawa[1], Toru Mogi[1], Yusuke Yamaya[2], Toshihiro Uchida[2] (1.Tokyo Institute of Technology, 2.National Institute of Advanced Industrial Science and Technology)

4:00 PM - 4:15 PM JST | 7:00 AM - 7:15 AM UTC

[SVC29-09] Analysis and interpretation of DAS-seismic results obtained at the Ohnuma geothermal field in the Hachimantai volcanic region, in Japan

*Junzo Kasahara[1,2], Yoko Hasada[1,3], Kuzume Haruyasu[1] (1.ENAA, 2.Shizuoka University, 3.Daiwa Exploration and Consulting Co. Ltd.)

4:15 PM - 4:30 PM JST | 7:15 AM - 7:30 AM UTC

[SVC29-10] Thermal property measurements by drilling cuttings obtained from a geothermal well in the Hachimantai area and thermal structure analysis

*Haruto Sugamoto[1], Kazuya Ishitsuka[1], Weiren Lin[1], Takemi Sakai[2] (1. Graduate School of Engineering, Kyoto University, 2.Geothermal Engineering Co., Ltd.)

4:30 PM - 4:45 PM JST | 7:30 AM - 7:45 AM UTC

[SVC29-11] Characteristics of eruption periodicity observed at Shikabe geyser and estimation of the factor of long term periodicity change

*Ayuta Tsuge[1], Hiroshi Aoyama[2] (1.Institute of Seismology and Volcanology, Graduate School of Sciences, Hokkaido University, 2.Institute of Seismology and Volcanology, Fuculty of Science, Hokkaido University)

4:45 PM - 5:00 PM JST | 7:45 AM - 8:00 AM UTC

[SVC29-12] Modeling of multidisciplinary observations during an inter-eruptive period by using a hydrothermal simulation with post-processors

*Ryo Tanaka[1], Takeshi Hashimoto[1], Shohei Narita[2] (1.Hokkaido University,Institute of Seismology and Volcanology, 2.Kyoto University, Graduate School of Science, Institute for Geothermal Sciences, Aso Volcanological Laboratory)

[J] Poster | S (Solid Earth Sciences)：S-VC Volcanology

5:15 PM - 6:30 PM JST | 8:15 AM - 9:30 AM UTC | Ch.13_2

[S-VC29] Hydrothermal systems of volcanoes

convener:Yasuhiro Fujimitsu(Department of Earth Resources Engineering, Faculty of Engineering, Kyushu University), Wataru Kanda(Volcanic Fluid Research Center, School of Science, Tokyo Institute of Technology), Takeshi Ohba(Department of chemistry, School of Science, Tokia University)

[SVC29-P01] Groundwater composition around the Aso caldera: multivariate statistical analysis and its implications for independent variables and geographical variations

*Hikaru Iwamori[1], Hitomi Nakamura[2], Noritoshi Morikawa[2], Masaaki Takahashi[2], Akihiko Inamura[2], Satoru Haraguchi[1], Tatsuji Nishizawa[3], Shuhei Sakata[1] (1.Earthquake Research Institute, The University of Tokyo, 2.AIST, 3.TITECH)

[SVC29-P02] Temporal variation of chemical composition of hot spring waters at Ebinokogen Ioyama Volcano in Kirishima Volcanic Group

*Keigo Mori[1], Jun-ichiro Ishibashi[1], Takeshi Matsushima[1], Harue Masuda[2], Syogo Oshima[3], Saki Tsutsumi[3], Yasuhisa Tajima[4] (1.Graduate School of Science, Kyushu University, 2.Graduate school of Science, Osaka City University, 3.West Japan Engineering Consultants, Inc,, 4.Nippon Koei Co., Ltd,)

[SVC29-P03] Temporal variations of helium and carbon isotopic compositions of fumarolic gases from Kusatsu-Shirane volcano

*Tomoya Obase[1], Hirochika Sumino[1], Kotaro Toyama[1], Takeshi Ohba[2], Muga Yaguchi[3], Akihiko Terada[4] (1.Department of General Systems Studies, Graduate School of Arts and Sciences, University of Tokyo, 2.Department of chemistry, School of Science, Tokai University, 3.Meteorological Research Institute, Japan Meteorological Agency, 4.Volcanic Fluid Research Center, Tokyo Institute of Technology)

[SVC29-P04] Change in fluoride ion concentration in Bandaiko hot spring at east flank of Kusatsu-Shirane volcano and its relationship with volcanic activity

*Haruka Yamamoto[1], Yoshikazu Kikawada[2] (1.Graduate School of Sophia University, 2.Faculty of Science and Technology, Sophia University)

[SVC29-P05] Volcanic ash from the June 17, 1962 eruption of Yakedake volcano, and its water-soluble components

*Muga Yaguchi[1], Yasuo Hirayama[2], Takeshi Ohba[3], Nozomi Numanami[3] (1.Meteorological Research Institute, JMA, 2.Nagano Meteorological Office, JMA, 3.School of Science, Tokai University)

[SVC29-P06] Tectonic controlled and hydrothermal alterations of geothermal reservoirs in El Salvador

*JOSE ANIBAL ERAZO[1], Noriyoshi Tsuchiya[1], Masaoki Uno[1], Arturo Quezada[2], Pedro Antonio Santos[2], Ryoichi Yamada[1], Hiroyuki Yamagishi[1], Shinichi Yamasaki[1], Alvaro Josue Amaya[3] (1.Graduate school of environmental studies , 2.LaGeO _ El Salvador, 3.UES _ El Salvador)

[SVC29-P07] **DAS-Seismic and temperature data acquisition using DAS and DTS measurements at the Ohnuma, geothermal field, Tohoku, Japan**

*Junzo Kasahara[1,2], Yoko Hasada[1,3], Kuzume Haruyasu[1], Hitoshi Mikada[4], Yoshihiro Fujise[5] (1.ENAA, 2.Shizuoka University, 3.Daiwa Exploration and Consulting Co. Ltd., 4.Graduate School of Kyoto University, 5.WELMA)

[SVC29-P08] **Ground surface Heat balance measurements at Izu-Oshima volcano**

*Shin'ya Onizawa[1], Nobuo Matsushima[2] (1.Volcanology Research Department, Meteorological Research Institute, JMA, 2.Geological Survey of Japan, National Institute of Advanced Industrial Science and Technology)

[SVC29-P09] Behavior of magmatic hydrothermal system of Kusatsu-Shirane Volcano inferred from numerical simulations

*Yasuo Matsunaga[1], Wataru Kanda[1] (1.School of Science, Tokyo Institute of Technology)

[SVC29-P10] Comprehension of hydrothermal systems in the East African Rift System –Collaborative Research with Kenya by SATREPS–

*Yasuhiro Fujimitsu[1], Jun Nishijima[1], Takeshi Tsuji[1], Kotaro Yonezu[1], Tatsuya Wakeyama[2], Ryuichi Itoi[3] (1.Department of Earth Resources Engineering, Faculty of Engineering, Kyushu University, 2.Platform of Inter-/Transdisciplinary Energy Research, Kyushu University, 3.School of Engineering, Kyushu University)

[E] Oral | S (Solid Earth Sciences)：S-CG Complex & General

9:00 AM - 10:30 AM JST | 12:00 AM - 1:30 AM UTC | Ch.21 Zoom Room 21

[S-CG39] Science of slow earthquakes: Toward unified understandings of whole earthquake process

convener:Satoshi Ide(Department of Earth an Planetary Science, University of Tokyo), Hitoshi Hirose(Research Center for Urban Safety and Security, Kobe University), Kohtaro Ujiie(Faculty of Life and Environmental Sciences, University of Tsukuba), Takahiro Hatano(Department of Earth and Space Science, Osaka University), Chairperson:Satoshi Ide(Department of Earth an Planetary Science, University of Tokyo)

9:00 AM - 9:15 AM JST | 12:00 AM - 12:15 AM UTC

[SCG39-19] Systematics and heterogeneity of deep and shallow slow earthquakes

*Kazushige Obara[1] (1.Earthquake Research Institute, The University of Tokyo)

9:15 AM - 9:30 AM JST | 12:15 AM - 12:30 AM UTC

[SCG39-20] Extraction of fine space-time structures in deep low-frequency tremor using the Hough transform

*Kodai Sagae[1], Hisashi Nakahara[1], Takeshi Nishimura[1], Kazutoshi Imanishi[2] (1.Solid Earth Physics Laboratory,Department of Geophysics,Graduate School of Science,Tohoku University, 2.National Institute of Advanced Industrial Science and Technology (AIST))

9:30 AM - 9:45 AM JST | 12:30 AM - 12:45 AM UTC

[SCG39-21] Comprehensive detection of tremor migration using multiple time windows beneath Kii Peninsula

*Takuya Maeda[1], Kazushige Obara[1], Akiko Takeo[1], Takanori Matsuzawa[2] (1. Earthquake Research Institute, The University of Tokyo, 2.National Research Institute for Earth Science and Disaster Resilience)

9:45 AM - 10:00 AM JST | 12:45 AM - 1:00 AM UTC

[SCG39-22] Focal mechanism and radiated energy from shallow tremors in the Guerrero seismic gap.

*Raymundo Omar Plata Martinez[1], Yoshihiro Ito[2], Kazuaki Ohta[4], Masanao Shinohara[5], Satoshi Ide[3] (1.Graduate School of Science, Kyoto University, 2.Disaster Prevention Research Institute, Kyoto University, 3.Department of Earth and Planetary Science, University of Tokyo, 4.National Research Institute for Earth Science and Disaster Resilience, 5.Earthquake Research Institute, University of Tokyo)

10:00 AM - 10:15 AM JST | 1:00 AM - 1:15 AM UTC

[SCG39-23] Seismicity around the subducted seamount in the trench-trench junction, southern off Hokkaido, by a broadband OBS array

*Ryosuke Azuma[1], Susumu Kawakubo[1], Hidenobu Takahashi[1], Ryota Hino[1], Yusaku Ohta[1], Ryota Takagi[1], Syuichi Suzuki[1], Makiko Sato[1], Tanaka Shinichi[2], Masanao Shinohara[2] (1.Recearch Center for Prediction of Earthquake and Volcanic Eruption, Graduate School of Science, Tohoku University, 2.Earthquake Research Institute, University of Tokyo)

10:15 AM - 10:30 AM JST | 1:15 AM - 1:30 AM UTC

[SCG39-24] Discussion

[E] Oral | S (Solid Earth Sciences)：S-CG Complex & General

10:45 AM - 12:15 PM JST | 1:45 AM - 3:15 AM UTC | Ch.21 Zoom Room 21

[S-CG39] Science of slow earthquakes: Toward unified understandings of whole earthquake process

convener:Satoshi Ide(Department of Earth an Planetary Science, University of Tokyo), Hitoshi Hirose(Research Center for Urban Safety and Security, Kobe University), Kohtaro Ujiie(Faculty of Life and Environmental Sciences, University of Tsukuba), Takahiro Hatano(Department of Earth and Space Science, Osaka University), Chairperson:Kimihiro Mochizuki(Earthquake Prediction Research Center, Earthquake Research Institute, University of Tokyo)

10:45 AM - 11:00 AM JST | 1:45 AM - 2:00 AM UTC

[SCG39-25] Spatio-temporal variation of fluid migration associated with slow earthquakes in the shallow Nankai subduction zone

*Takashi Tonegawa[1], Shunsuke Takemura[2] (1.Japan Agency for Marine-Earth Science and Technology, 2.Earthquake Research Institute, The University of Tokyo)

11:00 AM - 11:15 AM JST | 2:00 AM - 2:15 AM UTC

[SCG39-26] Land and marine long-term magnetotelluric observations around the western Nankai slow slip area

*Hiroshi Ichihara[1,2], Makoto Uyeshima[3], Hayato Nakamura[1], Maki Hata[3], Tada-nori Goto[4], Noriko Tada[2], Tetsuo Matsuno[5], Shinya Sato[6], Yoshiya Usui[3], Ryokei Yoshimura[7], Koki Aizawa[8] (1.Graduate school of Environmental Studies, Nagoya University, 2.JAMSTEC, 3.ERI, University of Tokyo, 4.University of Hyogo, 5.KOBEC, Kobe University, 6.Graduate school of Engineering, Kyoto University, 7.DPRI, Kyoto University, 8.Graduate school of Science, Kyushu Univeristy)

11:15 AM - 11:30 AM JST | 2:15 AM - 2:30 AM UTC

[SCG39-27] Active source seismic experiment investigating structural characteristics associated with slow earthquake activities in the Hyuga-nada, southwestern Japan

*Seiichi Miura[1], Kimihiro Mochizuki[2], Ryuta Arai[1], Yasuyuki Nakamura[1], Yuka Kaiho[1], Gou Fujie[1], Shuichi Kodaira[1], Rie Nakata[2], Yanxue Ma[2], Masataka Kinoshita[2], Yoshitaka Hashimoto[3], Yohei Hamada[1] (1.Japan Agency for Marine-Earth Science and Technology, 2.Earthquake Research Institute, University of Tokyo, 3.Kochi University)

11:30 AM - 11:45 AM JST | 2:30 AM - 2:45 AM UTC

[SCG39-28] Seismic characteristics of the northern Hikurangi subduction zone revealed by offshore seismic observations

*Kimihiro Mochizuki[1], Yusuke Yamashita[2], Emily Warren-Smith[3], Martha K Savage[4], Laura M Wallace[3], Stuart Henrys[3] (1.Earthquake Prediction Research Center, Earthquake Research Institute, University of Tokyo, 2.Disaster Prevention Research Institute, Kyoto University, 3.GNS Science, 4.Victoria University of Wellington)

11:45 AM - 12:00 PM JST | 2:45 AM - 3:00 AM UTC

[SCG39-29] **Temporal velocity variations in the northern Hikurangi margin and their relation to slow slip**

*Weiwei Wang[1], Martha Savage[1], Alec Yates[1,2], Hubert Zal[1], Carolyn Boulton[1], Megan Kortink[3], Tim Stern[1], Bill Fry[3], Kimihiro Mochizuki[4], Spahr Webb[5], Wallace Laura[3] (1.Victoria University of Wellington, 2.Université Grenoble Alpes, Université Savoie Mont Blanc, 3.GNS Science, 4.Earthquake Research Institute, University of Tokyo, 5.Lamont-Doherty Earth Observatory, Columbia University)

12:00 PM - 12:15 PM JST | 3:00 AM - 3:15 AM UTC

[SCG39-30] Discussion

[E] Poster | S (Solid Earth Sciences)：S-CG Complex & General

5:15 PM - 6:30 PM JST | 8:15 AM - 9:30 AM UTC | Ch.14_1

[S-CG39] Science of slow earthquakes: Toward unified understandings of whole earthquake process

convener:Satoshi Ide(Department of Earth an Planetary Science, University of Tokyo), Hitoshi Hirose(Research Center for Urban Safety and Security, Kobe University), Kohtaro Ujiie(Faculty of Life and Environmental Sciences, University of Tsukuba), Takahiro Hatano(Department of Earth and Space Science, Osaka University)

[SCG39-P01] Migration characteristics of shallow very low frequency earthquake episodes southeast off the Kii Peninsula

*Shunsuke Takemura[1], Kazushige Obara[1], Katsuhiko Shiomi[2], Akiko Takeo[1], Satoru Baba[1] (1.Earthquake Research Institute, the University of Tokyo, 2.National Research Institiute for Earth Science and Disaster Resilience)

[SCG39-P02] **Complementary distribution between very-low-frequency earthquakes and interplate-coupled area in the southwestern Ryukyu Trench**

Ren Yakabu[1], *Mamoru Nakamura[1] (1.Faculty of Science, University of the Ryukyus)

[SCG39-P03] **Spatio-temporal distribution of very low-frequency earthquakes activity in the north Ryukyu Trench**

*Mamoru Nakamura[1], Shuichi Kodaira[2], Yasushi Ishihara[2], Ban-Yuan Kuo[3], PeiYing Patty Lin[4] (1.Faculty of Science, University of the Ryukyus, 2.JAMSTEC, 3.Academia Sinica, 4.National Taiwan Normal University)

[SCG39-P04] Attenuation effect on observed frequency characteristics of broadband slow earthquakes

*Koki Masuda[1], Satoshi Ide[1], Takanori Matsuzawa[2] (1.Department of Earth an Planetary Science, University of Tokyo, 2.National Research Institute for Earth Science and Disaster Resilience)

[SCG39-P05] **Frictional coefficient and its velocity dependence of cuttings retrieved from the Nankai accretionary prism at IODP Site C0002**

*Riho Fujioka[1], Ikuo Katayama[1], Manami Kitamura[2], Hanaya Okuda[3], Takehiro Hirose[4] (1.Department of Earth and Planetary Systems Science, Hiroshima University, 2.National Institute of Advanced Industrial Science and Technology, 3.Department of Ocean Floor Geoscience, Atmosphere and Ocean Research Institute, University of Tokyo, 4.Kochi Institute for Core Sample Research, Japan Agency for Marine-Earth Science and Technology)

[SCG39-P06] Shallow tremor activity in the Hyuga-nada revealed by the seafloor observation of "*Science of Slow earthquakes*"

*Yusuke Yamashita[1], Masanao Shinohara[2], Hiroko Sugioka[3], Aki Ito[4], Tsutomu Takahashi[4], Daisuke Suetsugu[4] (1.Disaster Prevention Research Institute, Kyoto University, Japan, 2.Earthquake Research Institute, University of Tokyo, Japan, 3.Graduate School of Science, Kobe University, Japan., 4.Japan Agency for Marine-Earth Science and Technology, Japan.)

[SCG39-P07] **Extension of aseismic slip propagation theory to slow earthquake migration**

*Keisuke Ariyoshi[1], Roland Burgmann[2], Ampuero Jean-Paul[3] (1.Japan Agency for Marine-Earth Science and Technology, 2.University of California, Berkeley, 3.Institut de Recherche pour le Développement, Université Côte d'Azur)

[SCG39-P08] **Increase of tremor-rate in Marlborough region (New Zealand) after the 2016 Mw 7.8 Kaikōura earthquake.**

*Pierre Romanet[1], Florent Aden-Antoniow[2], Ryosuke Ando[1], Stephen C Bannister[3], Calum John Chamberlain[4], Yoshihisa Iio[5], Satoshi Matsumoto[6], Tomomi Okada[7], Richard H. Sibson[8], Akiko Toh[1], Satoshi Ide[1] (1.The University of Tokyo, School of Science, Earth and Planetary Science , Japan, 2.Department of Earth, Atmospheric and Planetary Sciences, Massachusetts Institute of Technology, Cambridge, MA, USA, 3.GNS Science, PO Box 30-368, Lower Hutt 5040, New Zealand, 4.School of Geography, Environment and Earth Sciences, Victoria University of Wellington, Wellington, New Zealand, 5.Disaster Prevention Research Institute, Kyoto University, Uji 611-0011, Japan, 6.Faculty of Sciences, Kyushu University, 2-5643-29 Shin'yama, Shimabara, Nagasaki 855-0843, Japan, 7.International Research Institute of Disaster Science (IRIDeS), Tohoku University, Sendai 980-0845, Japan, 8.Department of Geology, University of Otago, PO Box 56, Dunedin 9054, New Zealand)

[SCG39-P09] Modeling slow earthquakes by competing time scale of rupture propagation, stress loading and strength healing

*Kota Fukuda[1], Takahiro Hatano[2], Kimihiro Mochizuki[1] (1.Earthquake Research Institute The University of Tokyo, 2.Department of Earth and Space Science Osaka University)

[SCG39-P10] Scaled energy of shallow slow earthquakes in Hyuga-nada, southwest Japan

*Satoru Baba[1], Shunsuke Takemura[1], Kazushige Obara[1], Akiko Takeo[1], Yusuke Yamashita[2], Masanao Shinohara[1] (1.Earthquake Research Institute, The University of Tokyo, 2.Disaster Prevention Research Institute, Kyoto University)

[SCG39-P11] Tectonic tremors influenced by characteristic of structure and pore pressure in the Nankai subduction zone, Japan

*Andri Hendriyana[1], Takeshi Tsuji[2,3,4] (1.Geophysical Engineering, Institute of Technology Bandung, Indonesia, 2.International Institute for Carbon-Neutral Energy Research (I2CNER), Kyushu University, Fukuoka, Japan, 3.Department of Earth Resources Engineering, Kyushu University, Fukuoka, Japan, 4.Disaster Prevention Research Institute, Kyoto University, Kyoto, Japan)

[SCG39-P12] Impact of metasomatism on fluid overpressure in source depths of deep slow earthquakes

*Yasushi Mori[1], Kohtaro Ujiie[2], Miki Shigeno[1], Kazuya Noro[2], Tadao Nishiyama[3] (1.Kitakyushu Museum of Natural History and Human History, 2.University of Tsukuba, 3.Kumamoto University)

[SCG39-P13] Observation of localized slip events using viscoelastic fluids incorporating beads

Rinya Miyakawa[1], Kota Kamijo[1], Tatsuya Nishikubo[1], *Yutaka Sumino[1] (1.Tokyo University of Science)

[SCG39-P14] A trial digitization of analog seismograms of the Kanto-Tokai Observation Network for the analysis of tectonic tremor

*Takanori Matsuzawa[1], Tetsuya Takeda[1] (1.National Research Institute for Earth Science and Disaster Resilience)

[SCG39-P15] Slow slip events in the Bungo Channel and Hyuganada areas from May 2018 to June 2019 detected by a GNSS observation network

*Hitoshi Hirose[1], Takeshi Matsushima[2], Takao Tabei[3], Takuya NISHIMURA[4] (1.Research Center for Urban Safety and Security, Kobe University, 2.Faculty of Science, Kyushu University, 3.Research and Education Faculty, Natural Sciences Cluster, Sciences Unit, Kochi University, 4.Disaster Prevention Research Institute, Kyoto University)

[SCG39-P16] A Bayesian inversion for slip distribution of slow slip events beneath the Bungo Channel based on ensemble modeling of the uncertainty of underground structure

*Ryoichiro Agata[1], Ryoko Nakata[2], Yuji Yagi[3], Takeshi Iinuma[1] (1.Japan Agency for Marine-Earth Science and Technology, 2.Graduate School of Science, Tohoku University, 3.Graduate School of Life and Environmental Sciences, University of Tsukuba)

[SCG39-P17] Spontaneous extension of viscoelastic fluids confined between rotating parallel plates

*Tatsuya Nishikubo[1], Hiroki Ishikawa[1], Shoma Kato[1], Yutaka Sumino[1] (1.Department of Applied Physics, Graduate School of Science, Tokyo University of Science)

[SCG39-P18] **Pattern of injected fluid into a cell filled with swelling gel particles—effect of pressure**

*Kojiro Otoguro[1], Yutaka Sumino[1] (1.Tokyo University of Science)

[SCG39-P19] Detailed mapping of the subducting seamount and deformation structure in the Nankai Trough off the eastern Shikoku region deduced from densely acquired seismic profiles

*Yasuyuki Nakamura[1], Shuichi Kodaira[1], Yuka Kaiho[1], Tetsuo No[1], Kazuya Shiraishi[1], Gou Fujie[1], Seiichi Miura[1], Gaku Kimura[2] (1.Japan Agency for Marine Earth Science and Technology, 2.Tokyo University of Marine Science and Technology)

[SCG39-P20] **Distribution of Very-Low Frequency Earthquake in the Central Ryukyu Trench**

Hiromu Furugen[1], *Mamoru Nakamura[1] (1.Faculty of Science, University of the Ryukyus)

[SCG39-P21] Activity of low-frequency tremors and regular earthquakes off Erimo, Hokkaido from 2006 to 2007, by a tremor investigation based on waveform information

*Susumu Kawakubo[1], Ryosuke Azuma[1], Ryota Hino[1], Hidenobu Takahashi[2,1], Kazuaki Ohta[2], Masanao Shinohara[3] (1.Graduate School of Science Tohoku University, 2.National Research Institute for Earth Science and Disaster Resilience, 3.Earthquake Research Institute, University of Tokyo)

[SCG39-P22] Detecting short-term slow slip events using six-year records of ocean bottom pressure in Hikurangi subduction zone offshore New Zealand

*Tomohiro Inoue[1], Yoshihiro Ito[2], Laura M Wallace[3,4], Takuya Nishimura[2], Spahr Webb[7], Emmanuel Soliman M Garcia[2], Tomoya Muramoto[5], Syuichi Suzuki[6], Ryota Hino[6] (1.Graduate school of science, Kyoto University, 2.Disaster Prevention Research Institute, Kyoto University, 3.GNS Science, Lower Hutt, New Zealand, 4.Institute for Geophysics, University of Texas at Austin, Austin, TX, USA, 5.National Institute of Advanced Industrial Science and Technology, 6.Tohoku University, 7.Lamont-Doherty Earth Observatory, Columbia University)

[SCG39-P23] Variations of source characteristics of shallow tectonic tremor, Nankai trough, inferred from changes of the event size distribution

*Masaru Nakano[1], Suguru Yabe[2] (1.Japan Agency for Marine-Earth Science and Technology, 2.Geological Survey of Japan, AIST)

[SCG39-P24] Moment tensor inversion of shallow very low-frequency earthquakes in the northern Ryukyu subduction zone and the Hyuga-nada region

*Aki Ito[1], Hiroko Sugioka[2], Masaru Nakano[1], Yusuke Yamashita[3], Masanao Shinohara[4], Tsutomu Takahashi[1], Daisuke Suetsugu[1], Takashi Tonegawa[1] (1.Japan Agency for Marine-Earth Science and Technology, 2.Graduate School of Science, Kobe University, 3.Miyazaki Observatory, Disaster Prevention Research Institute, Kyoto University, 4.Earthquake Research Institute, University of Tokyo)

[SCG39-P25] Along-trench structural variation of the Philippine Sea plate subducting in the Hyuga-nada region and its relation to slow earthquakes

*Ryuta Arai[1], Seiichi Miura[1], Yasuyuki Nakamura[1], Gou Fujie[1], Yuka Kaiho[1], Shuichi Kodaira[1], Kimihiro Mochizuki[2], Rie Nakata[2] (1.Japan Agency for Marine-Earth Science and Technology, 2.Earthquake Research Institute, The University of Tokyo)

[SCG39-P26] Gravity data analysis to extract temporal gravity anomalies associated with slow slip events in the Ryukyu Trench

*Yuichi Hiramatsu[1], Yoshiyuki Tanaka[1], Akio Kobayashi[2] (1.Department of Earth Planetary Science , The University of Tokyo, 2.Meteorological Research Institute, JMA)

[SCG39-P27] Lithosphere properties along North-Central Chile subduction region and Relation to slow slip

*POUSALI MUKHERJEE[1], Yoshihiro Ito[1], Emmanuel Soliman M. Garcia[1], Kajaljyoti Borah[2] (1.Disaster Prevention Research Institute, Kyoto University, 2.Indian Institute of Science Education and Research, Kolkata)

[SCG39-P28] A comparison of the source areas in Hyuganada among afterslip of two interplate earthquakes in 1996 and successive slow slip events

Sawako Teshiba[1], *Hitoshi Hirose[1,2] (1.Department of Planetology, Graduate School of Science, Kobe University, 2.Research Center for Urban Safety and Security, Kobe University)

[SCG39-P29] Development of microseismicity catalog near the Japan Trench shallow slow earthquake region using a deep learning module

*Shukei Ohyanagi[1], Kazuaki Ohta[3], Yoshihiro Ito[2], Ryota Hino[4], Yusaku Ohta[4], Ryosuke Azuma[4], Masanao Shinohara[5], Kimihiro Mochizuki[5], Toshinori Sato[6], Yoshio Murai[7] (1.Graduate School of Science, Kyoto University, 2.Disaster Prevention Research Institute, Kyoto University, 3.National Research Institute for Earth Science and Disaster Resilience, 4.Tohoku University, 5.Earthquake Research Institute, The University of Tokyo, 6.Chiba University, 7.Hokkaido University)

[E] Oral | S (Solid Earth Sciences)：S-CG Complex & General

1:45 PM - 3:15 PM JST | 4:45 AM - 6:15 AM UTC | Ch.24 Zoom Room 24

[S-CG40] Active Tectonics and Seismic Hazards in the Himalayan Region

convener:Kazuki Koketsu(Earthquake Research Institute, University of Tokyo), Nath Soma Sapkota(Nepal Geological Society), Srinagesh Davuluri(CSIR-National Geophysical Research Institute), Chairperson:Kazuki Koketsu(Earthquake Research Institute, University of Tokyo), Hiroe Miyake(Earthquake Research Institute, University of Tokyo)

1:45 PM - 2:00 PM JST | 4:45 AM - 5:00 AM UTC

[SCG40-01] Seismic Hazard Assessment Studies in Uttarakhand Himalaya

*Srinagesh Davuluri[1], Suresh Gudapati[1], Srinivas Dakuri[1] (1.CSIR-National Geophysical Research Institute)

2:00 PM - 2:15 PM JST | 5:00 AM - 5:15 AM UTC

[SCG40-02] **Active Tectonics & Seismological Research in Nepal Himalaya: Preliminary results from SATREPS project**

*Soma Nath Sapkota[1], Kazuki Koketsu[2], Hiroe Miyake[3], Koji Okumura[4], Prakash Pokhrel[5] (1.Retired Director General, Department of Mines and Geology, Kathmandu Nepal, 2.Professor, Earthquake Research Institute, University of Tokyo, Tokyo Japan, 3.Associate Professor, Earthquake Research Institute, University of Tokyo, Tokyo Japan, 4.Professor, Graduate School of Humanities and Social Sciences, Hiroshima University, Japan, 5.Geologist, Department of Mines and Geology, Kathmandu Nepal)

2:15 PM - 2:30 PM JST | 5:15 AM - 5:30 AM UTC

[SCG40-03] Interseismic coupling on the Main Himalayan Thrust in Nepal derived from GNSS displacement rate field

*Takao Tabei[1], Mako Ohzono[2], Bishow Raj Silwal[3], Rajendra Bhandari[3], Janak B. Cahnd[3], Soma Nath Sapkota[4], Hiroe Miyake[2], Kazuki Koketsu[2] (1.Faculty of Science and Technology, Kochi University, 2.Earthquake Research Institute, University of Tokyo, 3.Department Mines and Geology, Nepal, 4.Nepal Geological Society)

2:30 PM - 2:45 PM JST | 5:30 AM - 5:45 AM UTC

[SCG40-04] Geodetic Observation for Evaluation of Earthquake Generation Potential in Nepal after the 2015 Gorkha Earthquake

*Bishow Raj Silwal[1], Rajendra Prasad Bhandari[1], Janak Bahadur Chand[1], Mako Ohzono[2], Takao Tabei[3] (1.Department of Mines and Geology, Nepal, 2.Earthquake Research Institute, University of Tokyo, Japan, 3.Kochi University, Kochi, Japan)

2:45 PM - 3:00 PM JST | 5:45 AM - 6:00 AM UTC

[SCG40-05] Rupture History of the Himalayan Frontal Thrust near Bagmati River crossing in Central Nepal

*Koji Okumura[1], Prakash Pokhrel[3], Hisao Kondo[2], Tomoru Yamanaka[1], Soma Nath Sapkota[3] (1.Graduate School of Letters, Hiroshima University, 2.Research Institute of Earthquake and Volcano Geology, GSJ, AIST, 3.Department of Mines and Geology, Nepal)

3:00 PM - 3:15 PM JST | 6:00 AM - 6:15 AM UTC

[SCG40-06] Strong Motion Observation Network for Earthquake Disaster Mitigation in the Kathmandu Valley, Nepal

*Nobuo Takai[1], Michiko Shigefuji[2], Hiroe Miyake[3], Kazuki Koketsu[3], Mukunda Bhattarai[4], Chintan Timsina[4], Shova Singh[4], Subeg Bijukchhen[5] (1.Hokkaido University, 2.Kyushu University, 3.University of Tokyo, 4.Department of Mines and Geology, Nepal, 5.Khwopa Engineering College, Nepal)

[E] Oral | S (Solid Earth Sciences)：S-CG Complex & General

3:30 PM - 5:00 PM JST | 6:30 AM - 8:00 AM UTC | Ch.24 Zoom Room 24

[S-CG40] Active Tectonics and Seismic Hazards in the Himalayan Region

convener:Kazuki Koketsu(Earthquake Research Institute, University of Tokyo), Nath Soma Sapkota(Nepal Geological Society), Srinagesh Davuluri(CSIR-National Geophysical Research Institute), Chairperson:Hiroe Miyake(Earthquake Research Institute, University of Tokyo), Kazuki Koketsu(Earthquake Research Institute, University of Tokyo)

3:30 PM - 3:45 PM JST | 6:30 AM - 6:45 AM UTC

[SCG40-07] 2D FDM simulation of seismic ground motions and inversion of velocity structure models in the Kathmandu Valley, Nepal

*Hongqi Diao[1], Kazuki Koketsu[1], Kazuhito Hikima[2] (1.Earthquake Research Institute, University of Tokyo, 2.Tokyo Electric Power Company Holdings)

3:45 PM - 4:00 PM JST | 6:45 AM - 7:00 AM UTC

[SCG40-08] Microtremor observation in the Kathmandu valley, Nepal: Past, Present, and Future perspectives

*Mukunda Bhattarai[1], Rajesh Sharma[3], Sunita Bhattarai[2], Tara Pokrarel[1], Chintan Timsina[1], Suresh Shrestha[2], Dinesh Nepali[2], Manoj Nakarmi[4], Prakirna Tuladhar[4], Takumi Hayashida[5], Toshiaki Yokoi[5], Hiroe Miyake[6], Koichi Kusunoki[6] (1.National Earthquake Monitoring and Research Center, Department of Mines and Geology, Nepal, 2.Department of Mines and Geology, Nepal, 3.Seismological Center Surkhet, Department of Mines and Geology, Nepal, 4.Department of Urban Development and Building Construction, Nepal, 5.International Institute of Seismology and Earthquake Engineering, Building Research Institute,Japan, 6.Earthquake Research Institute, The University of Tokyo, Japan)

4:00 PM - 4:15 PM JST | 7:00 AM - 7:15 AM UTC

[SCG40-09] **BROADBAND MICROTREMOR ARRAY EXPLORATION IN THE KATHMANDU VALLEY, NEPAL**

*Toshiaki Yokoi[1], Takumi Hayasida[1], Mukunda Bhattarai[3], Tara Pokharel[2], Suresh Shrestha[2], Chintan Timsina[3], Sunita Bhattarai[2], Rajesh Sharma[3], Dinesh Nepali[2] (1.International Institute of Seismology and Earthquake Engineering, Building Research Institute, Japan, 2.Department of Mines and Geology, Nepal, 3.National Earthquake Monitoring and Research Centre, NEMRC/DMG, Nepal)

4:15 PM - 4:30 PM JST | 7:15 AM - 7:30 AM UTC

[SCG40-10] **Seismic observation and automatic hypocenter location system in Nepal**

*Shigeki Horiuchi[1], Masumi Yamada[3], Koji MIYAKAWA[2], Hiroe Miyake[2], Tadashi Yamashina[4], Chintan Timsina[5], Mukunda Bhattarai[5], Bharat Prasad Koirala[5], Monika Jha[5], Lok Bijaya Adhikari[5] (1.Home Seismometer Corporation, 2.ERI, 3.DPRI, 4.Kochi University, 5.DMG, Nepal)

4:30 PM - 4:45 PM JST | 7:30 AM - 7:45 AM UTC

[SCG40-11] Upper-Crustal Structure of Central Nepal inferred from Local Earthquake Tomography

*Chintan Timsina[1], James Mori[2], Masumi Yamada[2] (1.Graduate School of Science, Kyoto University, 2.Disaster Prevention Research Institute, Kyoto University)

4:45 PM - 5:00 PM JST | 7:45 AM - 8:00 AM UTC

[SCG40-12] Towards the Further Development of the Education and Research on Earthquakes in Nepal

*Mai Suzuki[1], Binil Aryal[2], Kazuki Koketsu[1] (1.Earthquake Research Institute, The University of Tokyo, 2.Central Department of Physics, Tribhuvan University)

[E] Poster | S (Solid Earth Sciences)：S-CG Complex & General

5:15 PM - 6:30 PM JST | 8:15 AM - 9:30 AM UTC | Ch.15_1

[S-CG40] Active Tectonics and Seismic Hazards in the Himalayan Region

convener:Kazuki Koketsu(Earthquake Research Institute, University of Tokyo), Nath Soma Sapkota(Nepal Geological Society), Srinagesh Davuluri(CSIR-National Geophysical Research Institute)

[SCG40-P01] **The Timing and Extent of the Last Surface Rupture Event on the Himalayan Frontal Thrust in western Nepal around Butwal-Tribeni area**

*Prakash Pokhrel[1], Koji Okumura[2], Soma Nath Sapkota[1], Hisao Kondo[3], - - (1.Department of Mines and Geology, Nepal, 2.Hiroshima University, Japan, 3.Geological Survey of Japan)

[SCG40-P02] A future scenario earthquake for seismic hazard analysis in Kathmandu, Nepal

*Kazuki Koketsu[1], Hiroe Miyake[1], Koji Okumura[2] (1.Earthquake Research Institute, University of Tokyo, 2.Graduate School of Humanities and Social Sciences, Hiroshima University)

[SCG40-P03] **3D velocity structure model of the Kathmandu valley for ground motion simulation**

*Suzuki Haruhiko[1], Hisanori Matsuyama[1], Kazuki Koketsu[2], Toshiaki Yokoi[3] (1.OYO Corp., 2.Earthquake Research Institute, The University of Tokyo , 3.Building Research Institute)

[SCG40-P04] Measuring surface-wave phase velocities (< 0.2 Hz) using teleseismic/ambient noise data in the Kathmandu Valley, Nepal

*Takumi Hayashida[1], Toshiaki Yokoi[1], Mukunda Bhattarai[2], Tara Pokharel[2], Suresh Shrestha[2], Chintan Timsina[2], Sunita Bhattarai[2], Rajesh Sharma[2], Dinesh Nepali[2] (1.International Institute of Seismology and Earthquake Engineering, Building Research Institute, 2.Department of Mines and Geology, Nepal)

[SCG40-P05] Characterization of Extreme Ground Motions

*Hiroe Miyake[1] (1.Earthquake Research Institute, University of Tokyo)

[E] Oral | S (Solid Earth Sciences)：S-CG Complex & General

9:00 AM - 10:30 AM JST | 12:00 AM - 1:30 AM UTC | Ch.19 Zoom Room 19

[S-CG41] Hard-Rock Drilling Science: From Continental to Deep Sea Drilling, and Oman Project

convener:Eiichi TAKAZAWA(Department of Geology, Faculty of Science, Niigata University), Katsuyoshi Michibayashi(Department of Earth and Planetary Sciences, Nagoya University), Keishi Okazaki(Japan Agency for Marine-Earth Science and Technology), Chairperson:Keishi Okazaki(Japan Agency for Marine-Earth Science and Technology), Sayantani Chatterjee(Niigata University, Department of Geology, Faculty of Science)

9:00 AM - 9:15 AM JST | 12:00 AM - 12:15 AM UTC

[SCG41-01] The structure of magma chamber below a fast-spreading ridge based on field and core analyses of the Oman ICDP drilling

*Susumu Umino[1], Yuki Kusano[3], Osamu Ishizuka[3], Takahiro Fudai[4], Akihiro Tamura[1], Tomoaki Morishita[1,2] (1.Department of Earth Sciences, Kanazawa University, 2.JAMSTEC, 3.GSJ-AIST, 4.Taiheiyo Cement Corrperation)

9:15 AM - 9:30 AM JST | 12:15 AM - 12:30 AM UTC

[SCG41-02] **Oxidation controlled symplectitic formation in olivine gabbros from Oman ophiolite, Oman Drilling Project, Hole GT2A**

*Sayantani Chatterjee[1], Debaditya Bandyopadhyay[2,3], Eiichi Takazawa[1,4], Katsuyoshi Michibayashi[5] (1.Department of Geology, Faculty of Science, Niigata University, Niigata 950–2181, Japan, 2.Department of Geology, University of North Bengal, Darjeeling 734013, India, 3.Department of Geology, University of Calcutta, Kolkata 700019, India, 4.Japan Agency for Marine–earth Science and Technology, Yokosuka 237–0061, Japan, 5.Graduate School of Environmental Studies, Nagoya University, Nagoya 464–8602, Japan)

9:30 AM - 9:45 AM JST | 12:30 AM - 12:45 AM UTC

[SCG41-03] Effect of pore geometry on ultrasonic velocity of epidosites collected from the Oman Drilling Project

*Kumpei Nagase[1], Ikuo Katayama[1], Kohei Hatakeyama[1], Keishi Okazaki[2] (1.Earth and Planetary Systems Science Program, Graduate School of Advanced Science and Engineering, Hiroshima University, 2.Kochi Institute for Core Sample Research, Japan Agency for Marine-Earth Science and Technology)

9:45 AM - 10:00 AM JST | 12:45 AM - 1:00 AM UTC

[SCG41-04] Mineral mode of listvenite from ICDP Oman Drilling Project Hole BT1B inferred from X-ray CT core images

*Keishi Okazaki[1], Katsuyoshi Michibayashi[2], Kohei Hatakeyama[3], Natsue Abe[4], Kevin Johnson[5], Peter B Kelemen[6] (1.Kochi Institute for Core Sample Research, Japan Agency for Marine-Earth Science and Technology, 2.Department of Earth and Planetary Sciences, Nagoya University, 3.Department of Earth and Planetary Systems Sciences, Hiroshima University, 4.Mantle Drilling Promotion Office, Japan Agency for Marine-Earth Science and Technology, 5.Department of Earth Sciences, University of Hawai‘i at Mānoa, 6.Lamont Doherty Earth Observatory, Columbia University)

10:00 AM - 10:30 AM JST | 1:00 AM - 1:30 AM UTC

[SCG41-05] Serpentinization and Fe(III) distribution along the crust-mantle section of the oceanic lithosphere: insights from the Oman Drilling CM1A site

★Invited Papers

*Atsushi Okamoto[1], Kazuki Yoshida[1], Ryosuke Oyanagi[2], Yasuhiro Niwa[3], Yasuo Takeichi[3], Masao Kimura[3] (1.Graduate School of Environmental Studies, Tohoku University, 2.Japan Agency For Marine-Earth Science and Technology, 3.High Energy Accelerator Research Organization (KEK))

[E] Oral | S (Solid Earth Sciences)：S-CG Complex & General

10:45 AM - 12:15 PM JST | 1:45 AM - 3:15 AM UTC | Ch.19 Zoom Room 19

[S-CG41] Hard-Rock Drilling Science: From Continental to Deep Sea Drilling, and Oman Project

convener:Eiichi TAKAZAWA(Department of Geology, Faculty of Science, Niigata University), Katsuyoshi Michibayashi(Department of Earth and Planetary Sciences, Nagoya University), Keishi Okazaki(Japan Agency for Marine-Earth Science and Technology), Chairperson:Katsuyoshi Michibayashi(Department of Earth and Planetary Sciences, Nagoya University), Eiichi TAKAZAWA(Department of Geology, Faculty of Science, Niigata University)

10:45 AM - 11:00 AM JST | 1:45 AM - 2:00 AM UTC

[SCG41-06] Heterogeneity in the mantle section of the Oman ophiolite in terms of spinel and clinopyroxene compositions

*Eiichi TAKAZAWA[1,2] (1.Department of Geology, Faculty of Science, Niigata University, 2.Japan Agency for Marine-Earth Science and Technology)

11:00 AM - 11:15 AM JST | 2:00 AM - 2:15 AM UTC

[SCG41-07] Systematics of minor and trace element chemistry of olivine in peridotites

*Ikuya Nishio[1], Tomoaki Morishita[1], Keita Itano[1], Akihiro Tamura[1], Asyraf Muhamad[1] (1.Kanazawa University)

11:15 AM - 11:30 AM JST | 2:15 AM - 2:30 AM UTC

[SCG41-08] **ICDP DSeis project: compilation of borehole logging and recovered core information at the seismogenic zone of the M5.5 Orkney earthquake with lower crustal intrusives**

*Hiroshi Ogasawara[1], Shunsuke Yoshida[2], Mitsuya Higashi[2], Kensuke Sakaguchi[1], Yuki Yokoyama[4], Yasuo Yabe[3], Tetsuro Hirono[4], Dakalo Ligaraba[5], Nandipha Masondo[5], Yuhji Yamamoto[6], Team ICDP DSeis (1.College of Science and Engineering, Ritsumeikan University, 2.Graduate School of Science and Engineering, Ritsumeikan University, 3.Graduate School of Science, Tohoku University, 4.Graduate School of Science, Osaka University, 5.Graduate School of Geoscience, University of the Witwatersrand, 6.Kochi Core Center, Kochi University)

11:30 AM - 12:00 PM JST | 2:30 AM - 3:00 AM UTC

[SCG41-09] Volcanism along the eastern margin of the Ontong Java Plateau: More reasons to test the Ontong Java Nui hypothesis by scientific ocean drilling

★Invited Papers

*Maria Luisa Tejada[1], Takashi Sano[2], Takeshi Hanyu[1], Anthony A. P. Koppers[3], Masao Nakanishi[4], Akira Ishikawa[5], Takashi Miyazaki[1], Kenichiro Tani[2], Shoka Shimizu[6], Qing Chang[1], Bogdan Stefanov Vaglarov[1] (1.Volcano and Earth Interior Research Center, Institute for Marine Geodynamics, Japan Agency for Marine-Earth Science and Technology, 2-15 Natsushima, Yokosuka 237-0061, Japan, 2.Department of Geology and Paleontology, National Museum of Nature and Science, Amakubo 1-1-1, Tsukuba, Ibaraki 305-0005, Japan, 3.College of Earth, Ocean and Atmospheric Sciences, Oregon State University, Corvallis, OR 97331, U.S.A., 4.Graduate School of Science, Chiba University, Chiba 263-8522, Japan, 5.Department of Earth and Planetary Sciences, Tokyo Institute of Technology, 2-12-1 Ookayama, Meguro, Tokyo 152-8550, Japan , 6.Graduate School of Science and Engineering, Chiba University, Chiba 263-8522, Japan)

12:00 PM - 12:15 PM JST | 3:00 AM - 3:15 AM UTC

[SCG41-10] New Developments in Hard Rock Drilling Project: Horoman and Forearc Mantle drilling

*Katsuyoshi Michibayashi[1], Eiichi Takazawa[2], Tomoaki Morishita[3], Mikiya Yamashita[4,5], Gou Fujie[4], Shigeaki Ono[4] (1.Nagoya University, 2.Niigata University, 3.Kanazawa University, 4.JAMSTEC, 5.AIST)

[E] Poster | S (Solid Earth Sciences)：S-CG Complex & General

5:15 PM - 6:30 PM JST | 8:15 AM - 9:30 AM UTC | Ch.15_2

[S-CG41] Hard-Rock Drilling Science: From Continental to Deep Sea Drilling, and Oman Project

convener:Eiichi TAKAZAWA(Department of Geology, Faculty of Science, Niigata University), Katsuyoshi Michibayashi(Department of Earth and Planetary Sciences, Nagoya University), Keishi Okazaki(Japan Agency for Marine-Earth Science and Technology)

[SCG41-P01] Oeanic lithosphere production and the Earth's surface environments

★Invited Papers

*Junichiro Kuroda[1], Kosuke T. Goto[2], Akira Ishikawa[3], Azumi Kuroyanagi[4] (1.Atmosphere and Ocean Research Institute, the University of Tokyo, 2.Geological Survey of Japan, National Institute of Advanced Industrial Science and Technology, 3.Department of Earth and Planetary Sciences, Tokyo Institute of Technology, 4.The Tohoku University Museum)

[SCG41-P02] Water Content in Nominally Anhydrous Mineral of Crust/Mantle Boundary Recovered by International Oman Drilling Project

*Muhamad Asyraf Aminuddin[1], Tomoaki Morishita[1,2], Kenji Shimizu[3], Takayuki Ushikubo[3], Juan Miguel Ramirez Guotana[1], Keita Itano[1] (1.Kanazawa University Graduate School Natural Science and Technology, 2.Oman drilling project phase 2, 3.Kochi Institute for Core Sample Research,JAMSTEC)

[SCG41-P03] Sr isotopic and trace element variations of gabbros and peridotites at the CM1A drilling site of Wadi Tayin massif in the Oman ophiolite

*Masako Yoshikawa[1], Tomoaki Morishita[2], Asyraf Muhamad Aminuddin[2], Ryoko Senda[3], Tomoyuki Shibata[1] (1.Department of Earth and Planetary systems Science, Hiroshima University, 2.Geosciences and Civil Engineering, College of Science and Enginiering, Kanazawa University, 3.Facutly of Social and Cultural Studies, Kyushu University)

[SCG41-P04] Sr-Nd-Pb isotope systematics of proto-arc volcanic rocks in the Oman ophiolite

*Tsuyoshi Ishikawa[1], Kazuya Nagaishi[2], Kyoko Kanayama[3], Keitaro Kitamura[4], Shigeyuki Wakaki[1], Yuki Kusano[5], Susumu Umino[6] (1.Kochi Institute for Core Sample Research, JAMSTEC, 2.Marine Works Japan Ltd., 3.San'in Kaigan Geopark Museum of the Earth and Sea, 4.Asia Air Survey Co., Ltd., 5.Geological Survey of Japan, AIST, 6.College of Science and Engineering, Kanazawa University)

[SCG41-P05] Peridotites beneath the ophiolite: Petrology and chemistry of peridotite bodies located below the metamorphic sole of the Oman ophiolite

*Main Tokinaga[1], Marie Python[1], Georges Ceuleneer[2], Tomoya Suzuki, Jean-Paul Breton[3] (1.Hokkaido University Department of Natural History Science Division of Earth and Planetary Systems Sciences, 2.GET – Observatoire Midi-Pyrénées - CNRS, 3.French Bureau de Recherches Géologiques et Minières (BRGM))

[SCG41-P06] Vein permeability structure of the crustal section in the Oman Drilling Project inferred from the X-ray CT image analysis

*Yuya Akamatsu[1], Ikuo Katayama[1], Keishi Okazaki[2], Katsuyoshi Michibayashi[3], Oman Drilling Project Phase I Science Party (1.Hiroshima University, 2.Japan Agency for Marine-Earth Science and Technology, 3.Nagoya University)

[SCG41-P07] Serpentinization in the Salahi mantle section, the Oman Ophiolite

*Yohki YOSHIBA[1], Eiichi TAKAZAWA[1,2] (1.Faculty of Science Niigata University, 2.Japan Agency for Marine-Earth Science and Technology)

[J] Oral | S (Solid Earth Sciences)：S-CG Complex & General

1:45 PM - 3:15 PM JST | 4:45 AM - 6:15 AM UTC | Ch.23 Zoom Room 23

[S-CG44] Petrology, Mineralogy & Resource Geology

convener:Koichi Momma(National Museum of Nature and Science), Yu Nishihara(Geodynamics Research Center Ehime University), Tatsuo Nozaki(Submarine Resources Research Center, Research Institute for Marine Resources Utilization, Japan Agency for Marine-Earth Science and Technology), Nobutaka Tsuchiya(Department of Geology, Faculty of Education, Iwate University), Chairperson:Yu Nishihara(Geodynamics Research Center Ehime University), Koichi Momma(National Museum of Nature and Science), Tatsuo Nozaki(Submarine Resources Research Center, Research Institute for Marine Resources Utilization, Japan Agency for Marine-Earth Science and Technology)

1:45 PM - 2:00 PM JST | 4:45 AM - 5:00 AM UTC

[SCG44-01] Consolidation anisotropy of Mio–Pleistocene sedimentary soft rocks in the eastern part of the Boso Peninsula, central Japan

*Nana Kamiya[1], Masahiro Miyazaki[1], Weiren Lin[1] (1.Graduate School of Engineering, Kyoto University)

2:00 PM - 2:15 PM JST | 5:00 AM - 5:15 AM UTC

[SCG44-02] Prograde and progressive metamorphism of low-pressure and high-temperature terrane in the Tenzan area, Saga prefecture, north Kyusyu, Southwest Japan

*Yusaku Tanaka[1], Masaaki Owada[1] (1.Yamaguchi University)

2:15 PM - 2:30 PM JST | 5:15 AM - 5:30 AM UTC

[SCG44-03] ZIRCON U–Pb AGES AND GEOCHEMISTRY OF GRANITOIDS FROM SOUTHWEST MONGOLIA

*Dolzodmaa Boldbaatar[1], Yasuhito Osanai[1], Nobuhiko Nakano[1], Tatsuro ADACHI[1], Ippei Kitano[1], Kundyz Syeryekhan[2] (1.Kyushu University, 2.Golden Hill LLC)

2:30 PM - 2:45 PM JST | 5:30 AM - 5:45 AM UTC

[SCG44-04] Zircon U–Pb ages of plutonic rocks from Iwafune area, Ibaraki Prefecture

*Haruki Yamazaki[1], Terumi Ejima[1], Yoshiaki Kon[2], Yuki Tsunazawa[2] (1.Shinshu University Faculty of Science Department of Geology, 2.National Institute of Advanced Industrial Science and Technology)

2:45 PM - 3:00 PM JST | 5:45 AM - 6:00 AM UTC

[SCG44-05] Petrogenetic study on the cretaceous granitoids on the Takanawa Peninsula, northwest Shikoku, southwest Japan

*Kazuya Shimooka[1], Satoshi SAITO[1], Kenichiro Tani[2], Toshiro Takahashi[3] (1.Graduate School of Science and Engineering, Ehime University, 2.Department of Geology and Paleontology, National Museum of Nature and Science, 3.Graduate School of Science and Technology, Niigata University)

3:00 PM - 3:15 PM JST | 6:00 AM - 6:15 AM UTC

[SCG44-06] The kinetics and heat conduction model of thermoluminescence of orthoclase

*Takahiro Sato[1], Nobuo Hirano[1], Noriyoshi Tsuchiya[1] (1.Tohoku University)

[J] Oral | S (Solid Earth Sciences)：S-CG Complex & General

3:30 PM - 5:00 PM JST | 6:30 AM - 8:00 AM UTC | Ch.23 Zoom Room 23

[S-CG44] Petrology, Mineralogy & Resource Geology

convener:Koichi Momma(National Museum of Nature and Science), Yu Nishihara(Geodynamics Research Center Ehime University), Tatsuo Nozaki(Submarine Resources Research Center, Research Institute for Marine Resources Utilization, Japan Agency for Marine-Earth Science and Technology), Nobutaka Tsuchiya(Department of Geology, Faculty of Education, Iwate University), Chairperson:Tatsuo Nozaki(Submarine Resources Research Center, Research Institute for Marine Resources Utilization, Japan Agency for Marine-Earth Science and Technology)

3:30 PM - 3:45 PM JST | 6:30 AM - 6:45 AM UTC

[SCG44-07] Formation of bipyramidal quartz within the hydrothermal vents: inights from Kuroko samples and hydrothermal experiments

*Jumpei Sugioka[1], Atsushi Okamoto[1], Ryoichi Yamada[1] (1.Tohoku University)

3:45 PM - 4:00 PM JST | 6:45 AM - 7:00 AM UTC

[SCG44-08] Copper mobilization systems associated with the Neogene magmatism in the Northeast Japan arc

*Shota Satori[2,1], Yoshiaki Kon[2], Yasushi Watanabe[1], Takuya Echigo[1] (1.Graduate School of International Resource Sciences, Akita University, 2.Geological Survey of Japan, National Institute of Advanced Industrial Science and Technology)

4:00 PM - 5:00 PM JST | 7:00 AM - 8:00 AM UTC

[SCG44-09] Discussion

[J] Poster | S (Solid Earth Sciences)：S-CG Complex & General

5:15 PM - 6:30 PM JST | 8:15 AM - 9:30 AM UTC | Ch.15_3

[S-CG44] Petrology, Mineralogy & Resource Geology

convener:Koichi Momma(National Museum of Nature and Science), Yu Nishihara(Geodynamics Research Center Ehime University), Tatsuo Nozaki(Submarine Resources Research Center, Research Institute for Marine Resources Utilization, Japan Agency for Marine-Earth Science and Technology), Nobutaka Tsuchiya(Department of Geology, Faculty of Education, Iwate University)

[SCG44-P01] Intrusive and emplacement process of the Tono plutonic complex: Constraints from dating and isotopic analysis of zircons

*Yasuhiro Ogita[1], Kazusa Sando[2], Kozue Ishibashi[3], Shuhei Sakata[4], Takeshi Ohno[5], Satoshi Suzuki[3], Tatsunori Yokoyama[1], Saya Kagami[1], Mitsuhiro Nagata[1], Takashi Yuguchi[2] (1.Tono Geoscience Center, Japan Atomic Energy Agency, 2.Faculty of Science, Yamagata University, 3.Graduate school of Science and Engineering, Yamagata University, 4.Earthquake Research Institute, University of Tokyo, 5.Faculty of Science, Gakushuin University)

[SCG44-P02] Whole-rock chemical composition of the Nojima granodiorite in northern part of Awaji Island, southwestern Japan

*Akihiro Ishihara[1], Motohiro Tsuboi[1] (1.Kwansei Gakuin University)

[SCG44-P03] Influence of inclusions on hydrogen generated during low temperature serpentinization

*Asuka Sugawara[1], Ryohei Kawakita[1], Tsubasa Otake[2], Tsutomu Sato[2] (1.Graduate school of Engineering, Hokkaido University, 2.Faculty of Engineering, Hokkaido University)

[SCG44-P04] **Detailed characteristics of Raman spectra of carbonaceous materials in fault rocks nearby the Median Tectonic Line**

*Hiroshi Mori[1], Yuki Nobe[1], Ken Yamaoka[2], Yosuke Tomooka[1], Yui Kouketsu[3], Tetsuya Tokiwa[1] (1.Shinshu University, 2.The University of Tokyo, 3.Nagoya University)

[SCG44-P05] Trace element composition of chromian spinel in the Sanbagawa ultramafic rocks

*Yuki Aoshima[1], Yuji Ichiyama[1], Jung-Woo Park[2] (1.Chiba University, 2.Seoul National University)

[SCG44-P06] The trace element composition of sapphire in the xenolith of garnet-bearing andesitic tuff of the Donzurubo Formation, the Nijo Group, Japan.

*Mayuko Fukuyama[1], Masatsugu Ogasawara[2] (1.Graduate School of Engineering Science, Akita University, 2.Geological Survey of Japan, National Institute of Advanced Industrial Science and Technology)

[SCG44-P07] **Microstructures of spherical pyrite in the Kuroko deposits: possible mechanism of pyrite growth on bubble**

*Atsushi Okamoto[1], Yoeri van de Ridder[2], Oliver Plumper[2], Markus Ohl[2], Ryoichi Yamada[1] (1.Tohoku University, 2.Utrecht University)

[SCG44-P08] **The mineral occurrence of kaolinitic saprolite beneath the sedimentary kaolin deposit at Seto district**

*Haruna Asai[1], Kikuchi Ryosuke[1], Tsubasa Otake[1], Tsutomu Sato[1] (1.Hokkaido University)

[SCG44-P09] Borate concentration processes in modern evaporitic and hydrothermal environments: Constraints on the formation of a boron-rich environment on prebiotic earth

*Sara Rinka Christensen [1], Akizumi Ishida[1], Takeshi Kakegawa[1] (1.Department of Earth Science, Graduate School of Science, Tohoku University)

[SCG44-P10] Experimental study on propagation of elastic wave in supercritical geothermal reservoirs

*Katsuya Mizuno[1], Noriyoshi Tsuchiya[1], Nobuo Hirano[1] (1.Tohoku university)

[J] Oral | S (Solid Earth Sciences)：S-CG Complex & General

1:45 PM - 3:15 PM JST | 4:45 AM - 6:15 AM UTC | Ch.18 Zoom Room 18

[S-CG53] Reducing risks from earthquakes, tsunamis & volcanoes: new applications of realtime geophysical data

convener:Masashi Ogiso(Meteorological Research Institute, Japan Meteorological Agency), Masumi Yamada(Disaster Prevention Research Institute, Kyoto University), Yusaku Ohta(Research Center for Prediction of Earthquakes and Volcanic Eruptions, Graduate School of Science, Tohoku University), YAMAMOTO Naotaka CHIKASADA(National Research Institute for Earth Science and Disaster Resilience), Chairperson:Naotaka YAMAMOTO CHIKASADA(National Research Institute for Earth Science and Disaster Resilience), Yusaku Ohta(Research Center for Prediction of Earthquakes and Volcanic Eruptions, Graduate School of Science, Tohoku University)

1:45 PM - 2:00 PM JST | 4:45 AM - 5:00 AM UTC

[SCG53-01] An advanced system for automatic strong gust detection and warning for railroads using deep learning

★Invited Papers

*Kusunoki Kenichi[1], Toru Adachi[1], Hanako Inoue[1], Osamu Suzuki[1], Naoki Ishitsu[2], Ken-ichiro Arai[2], Chusei Fujiwara[3], Hiroto Suzuki[3] (1.Meteorological Research Institute, 2.Alpha-denshi Co., Ltd., 3.East Japan Railway Company)

2:00 PM - 2:15 PM JST | 5:00 AM - 5:15 AM UTC

[SCG53-02] Tsunami observation and development of real-time tsunami detection by using ocean surface radar

★Invited Papers

*Ryotaro Fuji[1], Kohei Ogata[2], Hirofumi Hinata[3] (1.Kokusai Kogyo Co., Ltd., Ehime University, 2.Kokusai Kogyo Co., Ltd., 3.Ehime University)

2:15 PM - 2:30 PM JST | 5:15 AM - 5:30 AM UTC

[SCG53-03] Preliminary comparison of strong-motion parameters at the land & ocean bottom sites for the 2021 Mw 7.1 Off Fukushima Prefecture earthquake

*Yadab Prasad Dhakal[1], Wataru Suzuki[1], Takashi Kunugi[1], Takeshi Kimura[1], Shin Aoi[1] (1.National Research Institute for Earth Science and Disaster Resilience)

2:30 PM - 2:45 PM JST | 5:30 AM - 5:45 AM UTC

[SCG53-04] Development of GNSS Real-time analysis including QZSS

*Satoshi ABE[1], Keitaro Ohno[1], Naofumi Takamatsu[1], MURAMATSU Hiroki[1], Tomoaki FURUYA[1], Yohei HIYAMA[1] (1.Geospatial Information Authority of Japan)

2:45 PM - 3:00 PM JST | 5:45 AM - 6:00 AM UTC

[SCG53-05] IPFx: extended integrated particle filter method for earthquake early warning and visualization of its results with social networking service

*Masumi Yamada[1], Koji Tamaribuchi[2], Stephen Wu[3] (1.Disaster Prevention Research Institute, Kyoto University, 2.Meteorological Research Institute, 3.Institute of Statistical Mathematics)

3:00 PM - 3:15 PM JST | 6:00 AM - 6:15 AM UTC

[SCG53-06] Near real-time estimation of hypocenter distribution from seismic amplitudes

*Masashi Ogiso[1] (1.Meteorological Research Institute, Japan Meteorological Agency)

[J] Poster | S (Solid Earth Sciences)：S-CG Complex & General

5:15 PM - 6:30 PM JST | 8:15 AM - 9:30 AM UTC | Ch.16_1

[S-CG53] Reducing risks from earthquakes, tsunamis & volcanoes: new applications of realtime geophysical data

convener:Masashi Ogiso(Meteorological Research Institute, Japan Meteorological Agency), Masumi Yamada(Disaster Prevention Research Institute, Kyoto University), Yusaku Ohta(Research Center for Prediction of Earthquakes and Volcanic Eruptions, Graduate School of Science, Tohoku University), YAMAMOTO Naotaka CHIKASADA(National Research Institute for Earth Science and Disaster Resilience)

[SCG53-P01] High precision of Realtime tsunami prediction based on the amplification

*Narumi Takahashi[1], Kentaro Imai[2] (1.National Research Institute for Earth Science and Disaster Resilience, 2.Japan Agency for Marine-Earth Science and Technology)

[SCG53-P02] Generation Requirements of PL Waves for Shallow Earthquakes around Japan-Possibility of Immediate Tsunami Prediction

*Keishi Osuga[1], Takashi Furumura[1] (1.Department of Earth and Planetary Science, School of Science, The University of Tokyo)

[SCG53-P03] Evaluation of simple source time function in rapid source parameter determination system (AQUA)

*Hisanori Kimura[1], Youichi Asano[1] (1.National Research Institute for Earth Science and Disaster Resilience (NIED))

[J] Oral | S (Solid Earth Sciences)：S-CG Complex & General

9:00 AM - 10:30 AM JST | 12:00 AM - 1:30 AM UTC | Ch.17 Zoom Room 17

[S-CG54] Ten years from the 2011 Tohoku Earthquake: A milestone of Solid Earth Science

convener:Ryota Hino(Graduate School of Science, Tohoku University), Shuichi Kodaira(Research Institute of Marine Geodynamics, Japan Agency for Marine-Earth Science and Technology), Toru Matsuzawa(Research Center for Prediction of Earthquakes and Volcanic Eruptions, Graduate School of Science, Tohoku University), Takeshi Iinuma(National Research and Development Agency Japan Agency for Marine-Earth Science and Technology), Chairperson:Takeshi Iinuma(National Research and Development Agency Japan Agency for Marine-Earth Science and Technology), Toru Matsuzawa(Research Center for Prediction of Earthquakes and Volcanic Eruptions, Graduate School of Science, Tohoku University)

9:00 AM - 9:05 AM JST | 12:00 AM - 12:05 AM UTC

[SCG54-01] Introduction

9:05 AM - 9:30 AM JST | 12:05 AM - 12:30 AM UTC

[SCG54-02] **Modeling stress field and deformation associated with the Tohoku-Oki earthquake: Understanding the dynamics of the northeastern Japan islands arc-trench system**

★Invited Papers

*Bunichiro Shibazaki[1], Ryohei Sasajima[2] (1.International Institute of Seismology and Earthquake Engineering, Building Research Institute, 2.Research Center for Earthquake Prediction, Disaster Prevention Research Institute, Kyoto University)

9:30 AM - 9:45 AM JST | 12:30 AM - 12:45 AM UTC

[SCG54-03] Temporal evolution of seafloor crustal deformation obtained by the 10-year-long GNSS-A observations after the 2011 Tohoku-oki earthquake

*Shun-ichi Watanabe[1], Tadashi Ishikawa[1], Yuto Nakamura[1], Yusuke Yokota[2] (1.Hydrographic and Oceanographic Department, Japan Coast Guard, 2.Institute of Industrial Science, University of Tokyo)

9:45 AM - 10:00 AM JST | 12:45 AM - 1:00 AM UTC

[SCG54-04] The slow earthquake spectrum in the Japan Trench illuminated by the S-net seafloor observatories

★Invited Papers

*Tomoaki Nishikawa[1], Takanori Matsuzawa[2], Kazuaki Ohta[2], Naoki Uchida[3], Takuya NISHIMURA[1], Satoshi Ide[4] (1.Disaster Prevention Research Institute, Kyoto University, 2.National Research Institute for Earth Science and Disaster Resilience, 3.Graduate School of Science and International Research Institute of Disaster Science, Tohoku University, 4.Department of Earth and Planetary Science, University of Tokyo)

10:00 AM - 10:15 AM JST | 1:00 AM - 1:15 AM UTC

[SCG54-05] A Decade of Lessons Learned from the 2011 Tohoku-oki Earthquake

*Naoki Uchida[1], Roland Bürgmann[2] (1.Research Center for Prediction of Earthquakes and Volcanic Eruptions Graduate School of Science, Tohoku University, 2.Department of Earth and Planetary Science, University of California, Berkeley)

10:15 AM - 10:30 AM JST | 1:15 AM - 1:30 AM UTC

[SCG54-06] Temporal and spatial variations in background seismicity after the 2011 Tohoku-Oki earthquake estimated from HIST-ETAS model

*Taku Ueda[1], Aitaro Kato[1] (1.Earthquake Research Institute, the University of Tokyo)

[J] Oral | S (Solid Earth Sciences)：S-CG Complex & General

10:45 AM - 12:15 PM JST | 1:45 AM - 3:15 AM UTC | Ch.17 Zoom Room 17

[S-CG54] Ten years from the 2011 Tohoku Earthquake: A milestone of Solid Earth Science

convener:Ryota Hino(Graduate School of Science, Tohoku University), Shuichi Kodaira(Research Institute of Marine Geodynamics, Japan Agency for Marine-Earth Science and Technology), Toru Matsuzawa(Research Center for Prediction of Earthquakes and Volcanic Eruptions, Graduate School of Science, Tohoku University), Takeshi Iinuma(National Research and Development Agency Japan Agency for Marine-Earth Science and Technology), Chairperson:Shuichi Kodaira(Research Institute of Marine Geodynamics, Japan Agency for Marine-Earth Science and Technology), Ryota Hino(Graduate School of Science, Tohoku University)

10:45 AM - 11:00 AM JST | 1:45 AM - 2:00 AM UTC

[SCG54-07] **Seismic Imaging and Physical Properties of Underthrust Sediments at the Japan Trench Subduction Zone**

*Ehsan Jamali Hondori[1], Jin-Oh Park[1] (1.The University of Tokyo, Atmosphere and Ocean Research Institute)

11:00 AM - 11:15 AM JST | 2:00 AM - 2:15 AM UTC

[SCG54-08] Inputs to the Japan Trench subduction zone and its implications for the subduction zone processes

★Invited Papers

*Gou Fujie[1], Shuichi Kodaira[1], Yasuyuki Nakamura[1], Seiichi Miura[1] (1.Japan Agency for Marine-Earth Science and Technology)

11:15 AM - 11:30 AM JST | 2:15 AM - 2:30 AM UTC

[SCG54-09] Frictional properties of incoming sediments and rocks at shallow conditions of the Japan Trench subduction zone

*Kyuichi Kanagawa[1], Sayumi Sagano[2], Takuma Hayashi[3], Junya Fujimori[2], Michiyo Sawai[1] (1.Graduate School of Science, Chiba University, 2.Graduate School of Science and Engineering, Chiba University, 3.Faculty of Science, Chiba University)

11:30 AM - 11:45 AM JST | 2:30 AM - 2:45 AM UTC

[SCG54-10] **Earthquake faulting in the Japan Trench subduction zone: lessons learned from deep ocean drilling and the fault rocks in the exhumed accretionary complex**

*Kohtaro Ujiie[1], Keisuke Ito[2], Ayaka Nagate[2], Hiroki Tabata[2] (1.Faculty of Life and Environmental Sciences, University of Tsukuba, 2.Graduate School of Life and Environmental Sciences, University of Tsukuba)

11:45 AM - 12:00 PM JST | 2:45 AM - 3:00 AM UTC

[SCG54-11] Development of near-field tsunami forecasting method using ocean-bottom pressure sensor network (S-net)

*Yuichiro Tanioka[1] (1.Hokkaido University, Institute of Seismology and Volcanology)

12:00 PM - 12:15 PM JST | 3:00 AM - 3:15 AM UTC

[SCG54-12] Real-time Tsunami Inundation Forecast in Japan - Present and Future

*Shunichi Koshimura[1,5], Ryota Hino[2,5], Yusaku Ohta[2,5], Akihiro Musa[3,5], Takayuki Suzuki[5], Takashi Abe[1], Hiroaki Kobayashi[4,5] (1.International Research Institute of Disaster Science, Tohoku University, 2.Graduate School of Science, Tohoku University, 3.Cyberscience Center, Tohoku University, 4.Graduate School of Information Sciences, Tohoku University, 5.RTi-cast, Inc.)

[J] Poster | S (Solid Earth Sciences)：S-CG Complex & General

5:15 PM - 6:30 PM JST | 8:15 AM - 9:30 AM UTC | Ch.16_2

[S-CG54] Ten years from the 2011 Tohoku Earthquake: A milestone of Solid Earth Science

convener:Ryota Hino(Graduate School of Science, Tohoku University), Shuichi Kodaira(Research Institute of Marine Geodynamics, Japan Agency for Marine-Earth Science and Technology), Toru Matsuzawa(Research Center for Prediction of Earthquakes and Volcanic Eruptions, Graduate School of Science, Tohoku University), Takeshi Iinuma(National Research and Development Agency Japan Agency for Marine-Earth Science and Technology)

[SCG54-P01] Ground motion waveforms in the epicentral area of the 2011 Tohoku-Oki earthquake with large displacements, retrieved from ocean-bottom dynamic pressure change data

*Tatsuya Kubota[1], Tatsuhiko Saito[1], Hiroaki Tsushima[2], Ryota Hino[3], Yusaku Ohta[3], Syuichi Suzuki[3], Daisuke Inazu[4] (1.National Research Institute for Earth Science and Disaster Resilience, 2.Meteorological Research Institute, Japan Meteorological Agency, 3.Tohoku University, 4.Tokyo University of Marine Science and Technology)

[SCG54-P02] Detectability of short-term seafloor deformation by S-net pressure observation

*Ryota Hino[1], Tatsuya Kubota[2], Naotaka YAMAMOTO CHIKASADA[2], Yusaku Ohta[1], Hideto Otsuka[1] (1.Graduate School of Science, Tohoku University, 2.National Research Institute for Earth Science and Disaster Resilience)

[SCG54-P03] Vertical seafloor movement after the 2011 Tohoku earthquake and remarkable uplift near the trench axis off Sanriku

*Chie Honsho[1], Motoyuki Kido[2], Fumiaki Tomita[3], Ryota Hino[1] (1.Research Center for Prediction of Earthquakes and Volcanic Eruptions, Graduate School of Science, Tohoku University, 2.International Research Institute of Disaster Science, Tohoku University, 3.Japan Agency for Marine-Earth Science and Technology)

[SCG54-P04] Improvement of spatial resolution and evaluation of uncertainty for the coseismic slip distribution of the 2011 Tohoku-oki Earthquake

*Fumiaki Tomita[1], Takeshi Iinuma[1], Motoyuki Kido[2], Ryota Hino[3], Yusaku Ohta[3], Ryoichiro Agata[1], Takane Hori[1], Naoki Uchida[3] (1.Japan Agency for Marine-Earth Science and Technology, 2.International Research Institute of Disaster Science, Tohoku University, 3.Graduate School of Science, Tohoku University)

[SCG54-P05] Resolving 3D rheology of northeastern Japan using postseismic deformation following the 2011 Tohoku-oki earthquake

*Jun Muto[1], Dhar Sambuddha[1], James Daniel Paul Moore[2], Satoshi Miura[3], Yusaku Ohta[3], Takeshi Iinuma[4] (1.Department of Earth Sciences, Tohoku University, 2.Earth Observatory of Singapore, Nanyang Technological University, Singapore, 3.Department of Geophysics, Tohoku University, 4.Japan Agency for Marine-Earth Science and Technology)

[SCG54-P06] Numerical simulation of earthquake generation cycles along the Japan Trench

*Ryoko Nakata[1], Takane Hori[2], Seiichi Miura[2], Ryota Hino[1] (1.Graduate School of Science, Tohoku University, 2.Research Institute for Marine Geodynamics, Japan Agency for Marine-Earth Science and Technology)

[SCG54-P07] Seismicity near the trench axis and in the outer rise region of southern Japan Trench: Results from ocean bottom seismograph observations

*Koichiro Obana[1], Gou Fujie[1], Yojiro Yamamoto[1], Yuka Kaiho[1], Yasuyuki Nakamura[1], Seiichi Miura[1], Shuichi Kodaira[1] (1.Research Institute for Marine Geodynamics, Japan Agency for Marine-Earth Science and Technology)

[SCG54-P08] Microseismicity prior to the 2011 Tohoku-Oki earthquake around the mainshock hypocenter

*Hirofumi Goto[1], Ryota Hino[1] (1.Graduate School of Science, Tohoku University)

[SCG54-P09] Characteristics of tectonic tremor activity along the Japan Trench before the 2011 Tohoku Oki earthquake

*Hidenobu Takahashi[1,2], Ryota Hino[1], Naoki Uchida[1], Ryosuke Azuma[1], Susumu Kawakubo[1], Kazuaki Ohta[3], Masanao Shinohara[4] (1.Graduate school of Science Tohoku University , 2.Central Research Institute of Electric Power Industry, 3.National Research Institute for Earth Science and Disaster Resilience, 4.Earthquake Research Institute, The university of Tokyo)

[SCG54-P10] Application of ensemble learning noise classifier to automatically determined earthquake catalog after the 2011 Tohoku Earthquake

*Koji Tamaribuchi[1] (1.Meteorological Research Institute)

[SCG54-P11] **Core-Mantle boundaries state estimation applying the strain analysis on frequency domain**

seiji matsumura[2], *Makoto OKUBO[1] (1.Natural Science Cluster, Kochi University, 2.Faculty of Science and Technology)

[SCG54-P12] Tomography and megathrust earthquakes in the Tohoku forearc

*Dapeng Zhao[1] (1.Department of Geophysics, Tohoku University)

[SCG54-P13] Trench fill and graben fill sediments on the incoming plate around the Japan trench

*Yasuyuki Nakamura[1], Shuichi Kodaira[1], Gou Fujie[1], Seiichi Miura[1], Koichiro Obana[1], Mikiya Yamashita[2] (1.Japan Agency for Marine Earth Science and Technology, 2.National Institute of Advanced Industrial Science and Technology)

[J] Oral | S (Solid Earth Sciences)：S-CG Complex & General

1:45 PM - 3:15 PM JST | 4:45 AM - 6:15 AM UTC | Ch.19 Zoom Room 19

[S-CG55] Oceanic plate as inputs to subduction zone: from oceanic spreading ridge to subduction trench

convener:Gou Fujie(Japan Agency for Marine-Earth Science and Technology), Makoto Yamano(Earthquake Research Institute, the University of Tokyo), Tomoaki Morishita(School of Geoscience and Civil Engineering, College of Science and Technology, Kanazawa University), Takanori Kagoshima(University of Toyama), Chairperson:Gou Fujie(Japan Agency for Marine-Earth Science and Technology), Takanori Kagoshima(University of Toyama)

1:45 PM - 2:00 PM JST | 4:45 AM - 5:00 AM UTC

[SCG55-01] The Earth recycle and verification of ocean extinction hypothesis - New development in ocean plate research

★Invited Papers

*Katsuyoshi Michibayashi[1] (1.Department of Earth and Planetary Sciences, Graduate School of Environmental Studies, Nagoya University)

2:00 PM - 2:15 PM JST | 5:00 AM - 5:15 AM UTC

[SCG55-02] Prolonged mantle history recorded in zircons from the Horoman peridotite, Hokkaido, Japan

*Shinji Yamamoto[1], Yibing Li[2], Kiyoaki Niida[3], Shuhei Sakata[4], Takeshi Ohno[5] (1.Graduate School of Environment and Information Sciences, Yohohama National University, 2.Institute of Geology Chinese Academy of Geological Science, 3.Hokkaido University Museum, 4.Earthquake Research Institute, The University of Tokyo, 5.Gakushuin University)

2:15 PM - 2:30 PM JST | 5:15 AM - 5:30 AM UTC

[SCG55-03] Depth profile of hydration along the crust - mantle section of the Oman ophiolite: insights from holes CM1A and CM2B

*Kazuki Yoshida[1], Atsushi Okamoto[1], Ryosuke Oyanagi[2], Noriyoshi Tsuchiya[1], Oman Drilling Project Phase2 Science Party (1.Tohoku university, 2.Japan Agency for Marine-Earth Science and Technology)

2:30 PM - 2:45 PM JST | 5:30 AM - 5:45 AM UTC

[SCG55-04] The geochemical structure of pre-subducting oceanic lithosphere explored from petit-spot volcano

*Kazuto Mikuni[1], Naoto Hirano[1], Norikatsu Akizawa[2], Shiki Machida[3] (1.Tohoku University , 2.University of Tokyo, 3.Chiba Institute of Technology)

2:45 PM - 3:00 PM JST | 5:45 AM - 6:00 AM UTC

[SCG55-05] Rejuvenated extension of the Philippine Sea plate and its effect on subduction dynamics in the Nankai Trough

*Gaku Kimura[1], Yasuyuki Nakamura[2], Kazuya Shiraishi[2], Gou Fujie[2], Shuichi Kodaira[2], Asuka Yamaguchi[3], Rina Fukuchi[4], Yoshitaka Hashimoto[5] (1.Tokyo University of Marine Science and Technology, 2.JAMSTEC, 3.Atmosphere and Ocean Research Institute, The University of Tokyo, 4.Dia Consultants Co., Ltd., 5.Kochi University)

3:00 PM - 3:15 PM JST | 6:00 AM - 6:15 AM UTC

[SCG55-06] Thermal structure of the Tohoku subduction zone: effects of plate cooling models

*Manabu Morishige[1] (1.Earthquake Research Institute, the University of Tokyo)

[J] Oral | S (Solid Earth Sciences)：S-CG Complex & General

3:30 PM - 5:00 PM JST | 6:30 AM - 8:00 AM UTC | Ch.19 Zoom Room 19

[S-CG55] Oceanic plate as inputs to subduction zone: from oceanic spreading ridge to subduction trench

convener:Gou Fujie(Japan Agency for Marine-Earth Science and Technology), Makoto Yamano(Earthquake Research Institute, the University of Tokyo), Tomoaki Morishita(School of Geoscience and Civil Engineering, College of Science and Technology, Kanazawa University), Takanori Kagoshima(University of Toyama), Chairperson:Takanori Kagoshima(University of Toyama), Tomoaki Morishita(School of Geoscience and Civil Engineering, College of Science and Technology, Kanazawa University)

3:30 PM - 3:45 PM JST | 6:30 AM - 6:45 AM UTC

[SCG55-07] Interpretation for variation in the incoming Pacific Plate structure around the Kuril Trench axial region by an OBS/MCS seismic survey

★Invited Papers

*Ryosuke Azuma[1], Shuichi Kodaira[2], Ryota Hino[1], Gou Fujie[2], Koichiro Obana[1], Fumiaki Tomita[2], Yusaku Ohta[1] (1.Recearch Center for Prediction of Earthquake and Volcanic Eruption, Graduate School of Science, Tohoku University, 2.Japan Agency for Marin-Earth Science and Technology)

3:45 PM - 4:00 PM JST | 6:45 AM - 7:00 AM UTC

[SCG55-08] **Characteristics of normal faults developing in the outer rise of the Japan Trench**

*YUE SUN[1], Ehsan Jamali Hondori[1], Jin-Oh Park[1] (1.Atmosphere and Ocean Research Institute, The University of Tokyo)

4:00 PM - 4:15 PM JST | 7:00 AM - 7:15 AM UTC

[SCG55-09] Complicated fault geometry of outer-trench normal-faulting earthquakes based on the ocean bottom seismograph observations

*Koichiro Obana[1], Tsutomu Takahashi[1], Yojiro Yamamoto[1], Yasuyuki Nakamura[1], Gou Fujie[1], Seiichi Miura[1], Shuichi Kodaira[1] (1.Research Institute for Marine Geodynamics, Japan Agency for Marine-Earth Science and Technology)

4:15 PM - 4:30 PM JST | 7:15 AM - 7:30 AM UTC

[SCG55-10] Mantle-derived helium released through the Japan Trench bend-faults

★Invited Papers

*Jin-Oh Park[1], Naoto Takahata[1], Ehsan Jamali Hondori[1], Asuka Yamaguchi[1], Takanori Kagoshima[2], Tetsuro Tsuru[3], Gou Fujie[4], Yue Sun[1], Juichiro Ashi[1], Makoto Yamano[5], Yuji Sano[1] (1.Atmosphere and Ocean Research Institute, University of Tokyo, 2.Department of Environmental Biology and Chemistry, University of Toyama, 3.Department of Marine Resources and Energy, Tokyo University of Marine Science and Technology, 4.Japan Agency for Marine-Earth Science and Technology, 5.Earthquake Research Institute, University of Tokyo)

4:30 PM - 4:45 PM JST | 7:30 AM - 7:45 AM UTC

[SCG55-11] Heat flow distribution seaward of the Japan and Kuril trenches: Implications for fluid circulation in the oceanic crust

*Makoto Yamano[1], Yoshifumi Kawada[2], Kouta Sasaki[3], Masataka Kinoshita[1] (1.Earthquake Research Institute, the University of Tokyo, 2.Japan Agency for Marine-Earth Science and Technology, 3.Kozo Keikaku Engineering Inc.)

4:45 PM - 5:00 PM JST | 7:45 AM - 8:00 AM UTC

[SCG55-12] Resistivity imaging around the Japan trench based on ocean bottom electromagnetic surveys

★Invited Papers

*Hiroshi Ichihara[1], Takafumi Kasaya[2], Tada-nori Goto[3], Kiyoshi Baba[4], Shinya Sato[5], Makoto Yamano[4] (1.Graduate school of environmental studies, Nagoya University, 2.JAMSTEC, 3.ERI, University of Tokyo, 4.University of Hyogo, 5.Graduate School of Engineering, Kyoto University)

[J] Poster | S (Solid Earth Sciences)：S-CG Complex & General

5:15 PM - 6:30 PM JST | 8:15 AM - 9:30 AM UTC | Ch.16_3

[S-CG55] Oceanic plate as inputs to subduction zone: from oceanic spreading ridge to subduction trench

convener:Gou Fujie(Japan Agency for Marine-Earth Science and Technology), Makoto Yamano(Earthquake Research Institute, the University of Tokyo), Tomoaki Morishita(School of Geoscience and Civil Engineering, College of Science and Technology, Kanazawa University), Takanori Kagoshima(University of Toyama)

[SCG55-P01] Compilation of bathymetry and seismic reflection data to characterize outer rise faults in the Kuril Trench

*Shuichi Kodaira[1], Tetsuo No[1], Yasuyuki Nakamura[1], Gou Fujie[1], Koichiro Obana[1], Seiichi Miura[1] (1.Research Institute for Marine Geodynamics, Japan Agency for Marine-Earth Science and Technology)

[SCG55-P02] Characteristics of the oceanic plate near the Nosappu fracture zone revealed by the extensive seismic structure studies

*Gou Fujie[1], Koichiro Obana[1], Shuichi Kodaira[1], Katsuyoshi Michibayashi[2] (1.Japan Agency for Marine-Earth Science and Technology, 2.Nagoya University)

[SCG55-P03] Hydrothermal experiments in olivine-orthopyroxene-H2O system at 200-400C: implications for hydrogen generation at high temperatures

*Shuhei Tanaka[1], Atsushi Okamoto[2], OTGONBAYAR DANDAR[2], Masaoki Uno[2], Masakazu Fujii[3] (1.Tohoku University, 2.Graduate school of environmental studies, Tohoku University, 3.National institute of Polar research and SOKENDAI)

[SCG55-P04] Hydration processes of a forearc mantle wedge inferred from the Takadomari serpentinite body in the Kamuikotan Belt, central Hokkaido, Japan

*Shun Takamizawa[1], Yuji Ichiyama[1], Shusaku Yamazaki[2], Akihiro Tamura[3], Tomoaki Morishita[3] (1.Chiba University , 2.Civil Engineering Research Institute for Cold Region, 3.School of Geoscience and Civil Engineering, College of Science and Technology, Kanazawa University)

[SCG55-P05] Petrological features and formation processes of lower crustal cumulate xenoliths from Oki-Dogo Island: A possibility of mantle plume origin

*Rio Higuchi[1], Yuji Ichiyama[1], Akihiro Tamura[2], Tomoaki Morishita[2] (1.Chiba University, 2.Faculty of Geosciences and Civil Engineering, Kanazawa University)

[E] Oral | B (Biogeosciences) : B-PT Paleontology

1:45 PM - 3:15 PM JST | 4:45 AM - 6:15 AM UTC | Ch.26 Zoom Room 26

[B-PT01] Biomineralization and Geochemistry of Proxies

convener:Takashi Toyofuku(Japan Agency for Marine-Earth Science and Technology (JAMSTEC)), Hiroshi Kitazato(Tokyo University of Marine Science and Technology (TUMSAT)), Jelle Bijma(Alfred-Wegener-Institut Helmholtz-Zentrum für Polar- und Meeresforschung), Kotaro Hirose(Faculty of Science and Engineering, Waseda University), Chairperson:Takashi Toyofuku(Japan Agency for Marine-Earth Science and Technology (JAMSTEC)), Hiroshi Kitazato(Tokyo University of Marine Science and Technology (TUMSAT)), Kotaro Hirose(Faculty of Science and Engineering, Waseda University), Jelle Bijma(Alfred-Wegener-Institut Helmholtz-Zentrum für Polar- und Meeresforschung)

1:45 PM - 1:48 PM JST | 4:45 AM - 4:48 AM UTC

[BPT01-01] Introduction

1:48 PM - 2:03 PM JST | 4:48 AM - 5:03 AM UTC

[BPT01-02] Seascape ecological view as a new insight of benthic foraminiferal community

*Hiroshi Kitazato[1] (1.Tokyo University of Marine Science and Technology (TUMSAT))

2:03 PM - 2:21 PM JST | 5:03 AM - 5:21 AM UTC

[BPT01-03] Macromolecular analysis of modern aquatic palynomorphs using micro-Raman spectroscopy

*Takuto Ando[1], Tatsuyuki Yamamoto[2], Mika Ishigaki[3], Kazumi Matsuoka[4] (1.Estuary Research Center, Shimane University, 2.Faculty of Life and Environmental Sciences, Shimane University, 3.Center for Promotion of Project Research. Shimane University, 4.Institute for East China Sea Research, Nagasaki University, Japan)

2:21 PM - 2:39 PM JST | 5:21 AM - 5:39 AM UTC

[BPT01-04] **The spatial distribution and the origin of heavy metals in bottom sediments from Lake Shinji and Nakaumi**

*Hanye ZHANG[1], Kotaro Hirose[1], Kazuo Kamura[1], Minami Aoki[1], Koji Seto[2] (1.Faculty of Science and Engineering, Waseda University, 2.Estuary Research Center, Shimane University)

2:39 PM - 2:57 PM JST | 5:39 AM - 5:57 AM UTC

[BPT01-05] Sedimentary geochemical record of human-induced environmental changes in the estuarine lake Nakaumi, southwest Japan

*Kotaro Hirose[1], Minami Aoki[4], Akira Tsujimoto[3], Koji Seto[2], Kazuo Kamura[1] (1.Faculty of Science and Engineering, Waseda University, 2.Estuary Research Center, Shimane University, 3.Faculty of Education, Shimane Universit, 4.Faculty of Science and Engineering, Waseda University (currently Seikei Gakuen))

2:57 PM - 3:15 PM JST | 5:57 AM - 6:15 AM UTC

[BPT01-06] Calcification depths of planktic foraminifers constrained using geochemical signatures in the sediment trap samples collected from the Bay of Bengal

*Ayumi Maeda[1], Azumi Kuroyanagi[2], Toshihiro Yoshimura[3], Birgit Gaye[4], Tim Rixen[5], Atsushi Suzuki[1], Hodaka Kawahata[6] (1.National Institute of Advanced Industrial Science and Technology, 2.Tohoku University Museum, The Center for Academic Resources and Archives, Tohoku University, 3.Japan Agency for Marine-Earth Science and Technology, 4.Institute for Geology, Universität Hamburg, 5.Leibniz Centre for Tropical Marine Research, 6.Atmosphere and Ocean Research Institute, The University of Tokyo)

[E] Oral | B (Biogeosciences) : B-PT Paleontology

3:30 PM - 5:00 PM JST | 6:30 AM - 8:00 AM UTC | Ch.26 Zoom Room 26

[B-PT01] Biomineralization and Geochemistry of Proxies

convener:Takashi Toyofuku(Japan Agency for Marine-Earth Science and Technology (JAMSTEC)), Hiroshi Kitazato(Tokyo University of Marine Science and Technology (TUMSAT)), Jelle Bijma(Alfred-Wegener-Institut Helmholtz-Zentrum für Polar- und Meeresforschung), Kotaro Hirose(Faculty of Science and Engineering, Waseda University), Chairperson:Hiroshi Kitazato(Tokyo University of Marine Science and Technology (TUMSAT)), Kotaro Hirose(Faculty of Science and Engineering, Waseda University), Takashi Toyofuku(Japan Agency for Marine-Earth Science and Technology (JAMSTEC)), Jelle Bijma(Alfred-Wegener-Institut Helmholtz-Zentrum für Polar- und Meeresforschung)

3:30 PM - 3:48 PM JST | 6:30 AM - 6:48 AM UTC

[BPT01-07] Long term size changes of the Middle Miocene planktonic foraminifera in the western equatorial Pacific

*Takuma Suzuki[1], Hiroki Hayashi[1] (1.Shimane University)

3:48 PM - 4:06 PM JST | 6:48 AM - 7:06 AM UTC

[BPT01-08] High-resolution minor element concentration records in modern brachiopod *Pictothyris picta* shells and their controlling factors

*Kazuma Oikawa[1], Hideko Takayanagi[1], Ryuichi Shinjo[2], Kazuyoshi Endo[3], Masa-aki Yoshida[4], Yasufumi Iryu[1] (1. Institute of Geology and Paleontology Graduate School of Science Tohoku University, 2.Department of Physics and Earth Sciences, University of the Ryukyus, 3.Department of Earth and Planetary Science, Tokyo University, 4.Shimane University Faculty of Life and Environmental Science)

4:06 PM - 4:24 PM JST | 7:06 AM - 7:24 AM UTC

[BPT01-09] Evolution of Mg transporters and their possible effects on coral skeletal proxies in geochemistry

*Tomoko Bell[1], Akira Iguchi[2], Kazuhiko Sakai[3], Yusuke Yokoyama[4] (1.WERI, Univ. of Guam, 2.AIST, 3.TBRC, Univ. of Ryukyus, 4.AORI, Univ. of Tokyo)

4:24 PM - 4:42 PM JST | 7:24 AM - 7:42 AM UTC

[BPT01-10] **The coral reef-dwelling *Peneroplis* spp. shows calcification resilience to ocean acidification conditions - results from culture experiments**

*Laurie Charrieau[1], Katsunori Kimoto[1], Delphine Dissard[2], Beatrice Below[2,3], Kazuhiko Fujita[4], Yukiko Nagai[1,5], Takashi Toyofuku[1,6] (1.Jamstec, 2.IRD/UMR LOCEAN, 3.UMR CR2P, 4.University of the Ryukyus, 5.Yokohama National University, 6.TUMSAT)

4:42 PM - 4:57 PM JST | 7:42 AM - 7:57 AM UTC

[BPT01-11] Can Irregular Observations Provide the Next Clue for the Ecology of Foraminifera?

*Takashi Toyofuku[1,2], Yukiko Nagai[1,3] (1.Japan Agency for Marine-Earth Science and Technology (JAMSTEC), 2.Tokyo University of Marine Science and Technology (TUMSAT), 3.National Museum of Nature and Science,Tokyo)

4:57 PM - 5:00 PM JST | 7:57 AM - 8:00 AM UTC

[BPT01-12] Discussion

[E] Poster | B (Biogeosciences)：B-PT Paleontology

5:15 PM - 6:30 PM JST | 8:15 AM - 9:30 AM UTC | Ch.17_1

[B-PT01] Biomineralization and Geochemistry of Proxies

convener:Takashi Toyofuku(Japan Agency for Marine-Earth Science and Technology (JAMSTEC)), Hiroshi Kitazato(Tokyo University of Marine Science and Technology (TUMSAT)), Jelle Bijma(Alfred-Wegener-Institut Helmholtz-Zentrum für Polar- und Meeresforschung), Kotaro Hirose(Faculty of Science and Engineering, Waseda University)

[BPT01-P01] Ultrafine structure and elemental compositions of Acantharian (Radiolarian) skeleton from Kashiwajima Island, southwestern Shikoku, Japan

*Mao Fujii[1], Rie S Hori[2], Hiroaki Ohfuji[5], Yasuhide Nakamura[3], Mariko Nagashima[4] (1.Graduate School of Agricultural and Life Science, The University of Tokyo, 2.Graduate School of Science and Engineering, Ehime University, 3.Estuary Research Center, Shimane University, 4.Graduate School of Science and Technology for Innovation, Yamaguchi University, 5.Department of Earth Science, Graduate School of Science, Tohoku University)

[BPT01-P02] Ultra-microstructure observation of miliolid foraminifera (*Sorites* sp.) during shell formation process

*Yukiko Nagai[1,2], Remi Tsubaki[5], Kazuhiko Fujita[4], Takashi Toyofuku[2,3] (1.National Museum of Nature and Science of Tokyo, 2.JAMSTEC, 3.TUMSAT, 4.The University of Ryukyu , 5.The University of Tokyo)

[J] Oral | B (Biogeosciences)：B-PT Paleontology

10:45 AM - 12:15 PM JST | 1:45 AM - 3:15 AM UTC | Ch.26 Zoom Room 26

[B-PT02] Biotic History

convener:Isao Motoyama(Faculty of Science, Yamagata University), Takao Ubukata(Division of Geology & Mineralogy, Department of Earth & Planetary Sciences, Kyoto University), Kazuyoshi Moriya(Department of Earth Sciences, Faculty of Education and Integrated Arts and Sciences, Waseda University), Chairperson:Isao Motoyama(Faculty of Science, Yamagata University), Takao Ubukata(Division of Geology & Mineralogy, Department of Earth & Planetary Sciences, Kyoto University), Kazuyoshi Moriya(Department of Earth Sciences, Faculty of Education and Integrated Arts and Sciences, Waseda University)

10:45 AM - 11:00 AM JST | 1:45 AM - 2:00 AM UTC

[BPT02-01] Reconstruction of paleovegetation changes by pollen, palynomorph, and kerogen analyses of the Late Cretaceous sediments from the Kotanbetsu area, Hokkaido, Japan

*Maho Hayakawa[1], Ken Sawada[2], Masashi A. Ikeda[1], Reishi Takashima[3], Hiroshi Nishi[4] (1.Graduate School of Science, Hokkaido University, 2.Department of Earth and Planetary Sciences, Faculty of Science, Hokkaido University, 3.The Center for Academic Resources and Archives, The Tohoku University Museum, Tohoku University, 4.Institute of Dinosaur Research, Fukui Prefectural University)

11:00 AM - 11:15 AM JST | 2:00 AM - 2:15 AM UTC

[BPT02-02] Depth habitat of the late Eocene planktic foraminifers

*Kazuyoshi Moriya[1], Taku Oyama[2], Toyoho Ishimura[3] (1.Department of Earth Sciences, Faculty of Education and Integrated Arts and Sciences, Waseda University, 2.Major in Earth Sciences, Resources and Environmental Engineering, Graduate School of Creative Science and Engineering, 3.Department of Interdisciplinary Environment, Graduate School of Human and Environmental Studies, Kyoto University)

11:15 AM - 11:30 AM JST | 2:15 AM - 2:30 AM UTC

[BPT02-03] Micro sensory organs reveal the perception system and ecology of the Cretaceous cockroach

*Ryo Taniguchi[1], Yasuhiro Iba[1], Hiroshi Nishino[2], Hidehiro Watanabe[3], Kosuke Tateishi[3] (1.Faculty of Science, Hokkaido University, 2.Research Institute for Electronic Science, Hokkaido University, 3.Department of Earth System Science, Faculty of Science, Fukuoka University)

11:30 AM - 11:45 AM JST | 2:30 AM - 2:45 AM UTC

[BPT02-04] Computed tomography scanning reveals morphological development of a burrow produced by the tiger pistol shrimp *Alpheus bellulus*

*Miyu Umehara[1], Koji Seike[2], Seishiro Furuyama[1] (1.Tokyo University of Marine Science and Technology, 2.National Institute of Advanced Industrial Science and Technology)

11:45 AM - 12:00 PM JST | 2:45 AM - 3:00 AM UTC

[BPT02-05] Shell microstructure of extinct protobranch bivalves

*Kei Sato[1] (1.Faculty of Education and Integrated Arts and Sciences, Waseda University)

12:00 PM - 12:15 PM JST | 3:00 AM - 3:15 AM UTC

[BPT02-06] A unification of absolute growth, allometric, and theoretical morphologic models: a case of molluscan shells

*Takao Ubukata[1] (1.Department of Geology & Mineralogy, Division of Earth & Planetary Sciences, Kyoto University)

[J] Poster | B (Biogeosciences)：B-PT Paleontology

5:15 PM - 6:30 PM JST | 8:15 AM - 9:30 AM UTC | Ch.17_2

[B-PT02] Biotic History

convener:Isao Motoyama(Faculty of Science, Yamagata University), Takao Ubukata(Division of Geology & Mineralogy, Department of Earth & Planetary Sciences, Kyoto University), Kazuyoshi Moriya(Department of Earth Sciences, Faculty of Education and Integrated Arts and Sciences, Waseda University)

[BPT02-P01] Preliminary reports on the ecology of Cretaceous pantrionychian turtles based on the carapace bone histology

*Haruka Fukasawa[1], Kohei Tanaka[1], Yasuhisa Nakajima[2] (1.University of Tsukuba, 2.Tokyo City University)

[BPT02-P02] Asexual reproduction of planktonic foraminifera: Discovery and its significance

*Haruka TAKAGI[1], Atsushi KURASAWA[2], Katsunori KIMOTO[3] (1.Chiba University, 2.Marine Works Japan Ltd., 3.JAMSTEC)

[BPT02-P03] Oceanic anoxic event 2 observed in Southwestern Newfoundland Ridge

*Kazuyoshi Moriya[1], Yasuko Miyakura[2], Takashi Hasegawa[3], Akiko S. Goto[4] (1.Department of Earth Sciences, Faculty of Education and Integrated Arts and Sciences, Waseda University, 2.Major in Earth Sciences, Resources and Environmental Engineering, Graduate School of Creative Science and Engineering, 3.Faculty of Earth Science and Civil Engineering, Institute of Science and Engineering, Kanazawa University, 4.Center for Ecological Research, Kyoto University)

[BPT02-P04] Radiolarians from the upper Neogene Tatsunokuchi Formation, Miyagi Prefecture: An attempt to research depth-related distribution of extinct species.

*Isao Motoyama[1], Mizuho Aizawa[1] (1.Faculty of Science, Yamagata University)

[J] Oral | G (General) : General

3:30 PM - 5:00 PM JST | 6:30 AM - 8:00 AM UTC | Ch.02 Zoom Room 02

[G-01] Disaster prevention education

convener:Hitoshi Nakai(Kobuchisawa Research Institute for Nature and Education), Jiro Komori(Teikyo Heisei University), Shintaro Hayashi(Akita University Graduate School of Education), Tetsuhiko Asano(Senshu University Matsudo Junior High School High School), Chairperson:Shintaro Hayashi(Akita University Graduate School of Education), Tetsuhiko Asano(HunabashiKeimei High School), Jiro Komori(Teikyo Heisei University), Hitoshi Nakai(Kobuchisawa Research Institute for Nature and Education)

3:30 PM - 3:45 PM JST | 6:30 AM - 6:45 AM UTC

[G01-01] Subjects on science education based on lower secondary school Students' cognition of triggers and first causes of natural disasters caused by flood and earthquake: A case of F City, Japan

*Norihito Kawamura[1] (1.School of Regional Resource Management, Graduate School, University of Hyogo)

3:45 PM - 4:00 PM JST | 6:45 AM - 7:00 AM UTC

[G01-02] School education of disaster prevention through stone monuments for historical natural disasters and SfM technique

*Wataru Tanikawa[1], Go-Ichiro Uramoto[2], Kazuhisa Iwaka[3], Group General Affairs Division[1] (1.Japan Agency for Marine-Earth Science and Technology, Kochi Instutute for Core Sample Research, 2.Kochi University, 3.Tokushima University)

4:00 PM - 4:15 PM JST | 7:00 AM - 7:15 AM UTC

[G01-03] A Teaching Material as an Education for Volcanic Disaster Prevention in No Active Volcanic Area - Kikai-Akahoya Volcanic Ash at Tarumi-Hyuga Site in Kobe -

*Tatsuya KODA[1], Eiichi Sato[2] (1.Yanagi Gakuen Soukai Senior High School, 2.Hokkaido University of Education at Asahikawa)

4:15 PM - 4:30 PM JST | 7:15 AM - 7:30 AM UTC

[G01-04] Disaster prevention education on volcanic disasters
Development of Sakurajima version HUG

*Yuko Matsunari[1], Yasuhiro Ishimine[2], Tatsuo Takama[3], Hideaki Yoshihara[4], Tsuyoshi Nakatani[1], kaori Kaimoto[5], Keiko Imamura[1], Mitsuhito Sato[4], Naoyuki Hironiwa[6] (1.Kagoshima University, 2.Mount Fuji Research Institute, Yamanashi Prefectural Government, 3.Kagoshima prefecture Hospital , 4.Kagoshima City Hospital , 5.Kagoshima Women's College, 6.Minami-Nippon Shimbun)

4:30 PM - 4:45 PM JST | 7:30 AM - 7:45 AM UTC

[G01-05] The Necessity of Expanding Disaster Literacy toward the Era of "Society 5.0" "SDGs"

*Mamoru Hayashi[1] (1.University of TOYAMA)

4:45 PM - 5:00 PM JST | 7:45 AM - 8:00 AM UTC

[G01-06] Disaster prevention education through on-demand classes at universities

*Shintaro Hayashi[1] (1.Akita University Graduate School of Education)

[J] Poster | G (General) : General

5:15 PM - 6:30 PM JST | 8:15 AM - 9:30 AM UTC | Ch.03_1

[G-01] Disaster prevention education

convener:Hitoshi Nakai(Kobuchisawa Research Institute for Nature and Education), Jiro Komori(Teikyo Heisei University), Shintaro Hayashi(Akita University Graduate School of Education), Tetsuhiko Asano(Senshu University Matsudo Junior High School High School)

[G01-P01] Considering limits of hazard map: A case of a debris flow disaster that struck a village at the southern foot of Yatsugatake in September 1898.

*Hitoshi Nakai[1] (1.Kobuchisawa Research Institute for Nature and Education)

[G01-P02] **A Quantitative Analysis of Nationwide Municipalities' Disaster Prevention Portals**

*Haruka Matsuoka[1], Ami Mori[1], Kei Takashima[1], Tsukasa Sano[1], Asako Sano[2], Seiji Hori[1], Minako Noda[1] (1.Department of Business and Informatics, Tsukuba Gakuin University, 2.Faculty of Home Economics, Otsuma Women's University)

[J] Oral | G (General) : General

9:00 AM - 10:30 AM JST | 12:00 AM - 1:30 AM UTC | Ch.03 Zoom Room 03

[G-02] Outreach and geoscience education

convener:Jiro Komori(Teikyo Heisei University), Naoko HASEGAWA(Ochanomizu University), Ken Tsukada(Hiratsuka City Museum), Satoko Oki(Faculty of Environment and information Studies), Chairperson:Ken Tsukada(Hiratsuka City Museum), Jiro Komori(Teikyo Heisei University), Naoko HASEGAWA(Ochanomizu University), Satoko Oki(Faculty of Environment and information Studies)

9:00 AM - 9:30 AM JST | 12:00 AM - 12:30 AM UTC

[G02-01] The strategy and implementation of the Hayabusa2 outreach activities during the phase of the near asteroid operation

★Invited Papers

*Chisato Ikuta[1] (1.Japan Aerospace Exploration Agency)

9:30 AM - 10:00 AM JST | 12:30 AM - 1:00 AM UTC

[G02-02] How to activate discussion on on-line science cafe: Case study of "Science Agora 2020"

★Invited Papers

*Harufumi Tamazawa[1,2], Yuko Ikkatai[3], Junya Terazono[4] (1.Kyoto City University of Arts, 2.Kyoto University, 3.University of Tokyo, 4.National Institute of Information and Communications Technology)

10:00 AM - 10:15 AM JST | 1:00 AM - 1:15 AM UTC

[G02-03] A practical report of virtual field activities with high-resolution panorama (GigaPans) at multiple scales and live broadcasting

*Norihito Kawamura[1], Takashi Sawaguchi[2], Jiro Komori[3] (1.School of Regional Resource Management, Graduate School, University of Hyogo, 2.Toyo Univ., 3.Teikyo Heisei Univ.)

10:15 AM - 10:30 AM JST | 1:15 AM - 1:30 AM UTC

[G02-04] Verification of demands for a location-based geological site interpretation service

*Keisuke Ito[1] (1.Geokatsu Inc.)

[J] Oral | G (General) : General

10:45 AM - 12:15 PM JST | 1:45 AM - 3:15 AM UTC | Ch.03 Zoom Room 03

[G-02] Outreach and geoscience education

convener:Jiro Komori(Teikyo Heisei University), Naoko HASEGAWA(Ochanomizu University), Ken Tsukada(Hiratsuka City Museum), Satoko Oki(Faculty of Environment and information Studies), Chairperson:Naoko HASEGAWA(Ochanomizu University), Ken Tsukada(Hiratsuka City Museum), Jiro Komori(Teikyo Heisei University), Satoko Oki(Faculty of Environment and information Studies)

10:45 AM - 11:00 AM JST | 1:45 AM - 2:00 AM UTC

[G02-05] History of public understanding of global warming -When were we able to recognize it?-

★Invited Papers

*Jiro Komori[1] (1.Teikyo Heisei University)

11:00 AM - 11:15 AM JST | 2:00 AM - 2:15 AM UTC

[G02-06] Visual demonstration of greenhouse gas using 15μm absorption band of carbon dioxide.

*Akira Yamamoto

11:15 AM - 11:30 AM JST | 2:15 AM - 2:30 AM UTC

[G02-07] Class proposals and practices for remote learning of chemistry experiments for earth science students.

*Mana Yasui[1], Taisei Fujimura[2], Chiharu Tano[3], Fumitaka Kondo[3], Kenji Yonemochi[3] (1.Waseda research institute for science and engineering, 2.The department of resources and environmental engineering, Waseda University, 3.Faculty of Education and Integrated Arts and Sciences, Waseda University)

11:30 AM - 11:45 AM JST | 2:30 AM - 2:45 AM UTC

[G02-08] Trial of composing a melody using ground motion records of the 2013 earthquake near Awaji Island

*Nobuyuki Yamada[1], Shiina Yamamoto[1] (1.Kochi University)

11:45 AM - 12:00 PM JST | 2:45 AM - 3:00 AM UTC

[G02-09] Education for awareness about sediment related disasters and trial of providing risk information at an elementary school

*Shusuke Miyata[1], Kensuke Takenouchi[2], Ryoko Shimasaki[1], Akira Kamata[2], Daizo Tsutsumi[3], Kotaro Ichida[1], Masaharu Fujita[1] (1.Kyoto University, 2.Kagawa University, 3.Mie University)

12:00 PM - 12:15 PM JST | 3:00 AM - 3:15 AM UTC

[G02-10] Discussion

[J] Poster | G (General) : General

5:15 PM - 6:30 PM JST | 8:15 AM - 9:30 AM UTC | Ch.03_2

[G-02] Outreach and geoscience education

convener:Jiro Komori(Teikyo Heisei University), Naoko HASEGAWA(Ochanomizu University), Ken Tsukada(Hiratsuka City Museum), Satoko Oki(Faculty of Environment and information Studies)

[G02-P01] Astronomy outreach with multiple perspectives by music, painting, and tourism

★Invited Papers

*Uenoyama Sachiyo[1], Akihiko Tomita[1], Masami Okyuudo[1] (1.Wakayama University)

[G02-P02] Astronomical environment in which outreach targets are interested and outreach methods utilizing it

*Miyuki Tsuchiya, Mie Enomoto

[J] Oral | G (General) : General

1:45 PM - 3:15 PM JST | 4:45 AM - 6:15 AM UTC | Ch.03 Zoom Room 03

[G-03] Geoscience education from elementary school to university students

convener:Masatsune Hatakeyama(Seiko Gakuin High School), Yoshihiro Niwa(Center for Ocean Literacy and Education, Graduate School of Education, The University of Tokyo), Chairperson:Masatsune Hatakeyama(Seiko Gakuin High School), Yoshihiro Niwa(Center for Ocean Literacy and Education, Graduate School of Education, The University of Tokyo)

1:45 PM - 2:00 PM JST | 4:45 AM - 5:00 AM UTC

[G03-01] Authentic learning from perspective of aerospace - JAXA space education material "Earth Observation Coloring" -

*Yusuke Koga[1], Kenta Nomura[1] (1.Japan Aerospace Exploration Agency)

2:00 PM - 2:15 PM JST | 5:00 AM - 5:15 AM UTC

[G03-02] Home Science of Astronomy and Earth Science for Childcare Educators and Elementary School Teachers

*Akihiko Tomita[1] (1.Wakayama University)

2:15 PM - 2:30 PM JST | 5:15 AM - 5:30 AM UTC

[G03-03] Promotion of STEAM education (focus on space) with public-private partnership using an online tool.

*Norika Numa[1,3], Yoshiki Teramoto[2], Kaori Shoda[2], Asuki Yokoyama[3] (1.School of science, The University of Tokyo, 2.NPO Ikeda eco staff, 3.math channel Co., Ltd)

2:30 PM - 2:45 PM JST | 5:30 AM - 5:45 AM UTC

[G03-04] Visualization of crustal deformations in Japan -10 years before and after the 2011 Tohoku Earthquake viewed with GNSS dates.-

*Tadayoshi Kato[1] (1.Moegino Junior High School)

2:45 PM - 3:00 PM JST | 5:45 AM - 6:00 AM UTC

[G03-05] A case study of bringing online field tip closer to reality
- how to deliver the online excursion with on-site live broadcasting-

*Jiro Komori[1], Norihito Kawamura[2], SAWAGUCHI TAKASHI[3] (1.Teikyo Heisei University, 2.University of Hyogo, 3.Toyo University)

3:00 PM - 3:15 PM JST | 6:00 AM - 6:15 AM UTC

[G03-06] Geoscience・Geography education experiences at seven Japanese universities during the COVID-19 pandemic.

*Wonsuh SONG[1] (1.Waseda University)

[J] Oral | G (General) : General

3:30 PM - 5:00 PM JST | 6:30 AM - 8:00 AM UTC | Ch.03 Zoom Room 03

[G-03] Geoscience education from elementary school to university students

convener:Masatsune Hatakeyama(Seiko Gakuin High School), Yoshihiro Niwa(Center for Ocean Literacy and Education, Graduate School of Education, The University of Tokyo), Chairperson:Masatsune Hatakeyama(Seiko Gakuin High School), Yoshihiro Niwa(Center for Ocean Literacy and Education, Graduate School of Education, The University of Tokyo)

3:30 PM - 3:45 PM JST | 6:30 AM - 6:45 AM UTC

[G03-07] **A study of the cognition regarding natural disasters of junior high school students in Kobe City, Japan.**

*Toshio Arimichi[1,2], Norihito Kawamura[2] (1.Kobe Municipal Ibukidai Junior High School, 2.Graduate School of Regional Resource Management, University of Hyogo)

4:00 PM - 4:15 PM JST | 7:00 AM - 7:15 AM UTC

[G03-09] Thin-Section Making Recipe in a classroom Ver3.0 -using 3D printer-

*Yoshio Okamoto[1] (1.Osaka-Kyoiku University (temporary lecturer))

4:15 PM - 4:30 PM JST | 7:15 AM - 7:30 AM UTC

[G03-10] Development to teaching materials related to GIGA school

*Iida Kazuya[1] (1.Komaba-Toho Junior and Senior High School)

4:30 PM - 4:45 PM JST | 7:30 AM - 7:45 AM UTC

[G03-11] The report of the International Earth Science Olympiad (IESO) ,2021

*Norihito Kawamura[1], Yutaka Takigami[2] (1.School of Regional Resource Management, University of Hyogo, 2.JESOC)

4:45 PM - 5:00 PM JST | 7:45 AM - 8:00 AM UTC

[G03-12] Discussion

[J] Poster | G (General) : General

5:15 PM - 6:30 PM JST | 8:15 AM - 9:30 AM UTC | Ch.03_3

[G-03] G03Geoscience education from elementary school to university students

[G03-P01] Practice of Inquiry Activities based on the Field of Earth Science in High School

*Kazuya Kawakatsu[1] (1.Hyogo Prefectural Himeji Higashi senior high school)

[E] Oral | M (Multidisciplinary and Interdisciplinary) : M-IS Intersection

9:00 AM - 10:30 AM JST | 12:00 AM - 1:30 AM UTC | Ch.13 Zoom Room 13

[M-IS01] Environmental, socio-economic, and climatic changes in Northern Eurasia

convener:Pavel Groisman(NC State University Research Scholar at NOAA National Centers for Environmental Information, Asheville, North Carolina, USA), Shamil Maksyutov(National Institute for Environmental Studies), A Dmitry Streletskiy(George Washington University), Yoshihiro Iijima(Graduate School of Bioresources, Mie University), Chairperson:Pavel Groisman(NC State University Research Scholar at NOAA National Centers for Environmental Information, Asheville, North Carolina, USA), Yoshihiro Iijima(Graduate School of Bioresources, Mie University), Shamil Maksyutov(National Institute for Environmental Studies)

9:00 AM - 9:15 AM JST | 12:00 AM - 12:15 AM UTC

[MIS01-01] Evaluation of a revised global high-resolution inverse model with CO_2 observations over Siberia.

*Shamil Maksyutov[1], Motoki Sasakawa[1], Toshinobu Machida[1], Tomohiro Oda[2], Jiye Zeng[1], Tsuneo Matsunaga[1], Johannes W Kaiser[3], Mikhail Arshinov[4], Boris Belan[4], Ed Dlugokencky[5] (1.National Institute for Environmental Studies, 2.Universities Space Research Association, 3.Deutscher Wetterdienst, 4.Inst. Atmospheric Optics, 5.Global Monitoring Laboratory, NOAA)

9:15 AM - 9:30 AM JST | 12:15 AM - 12:30 AM UTC

[MIS01-02] Co-production of environmental education material "Permafrost and Culture"

*Yoshihiro Iijima[1], Hiroki Takakura[2], Vanda Ignatyeva[3], Aleksandr Fedorov[4], Masanori Goto[5], Toshikazu Tanaka[6] (1.Graduate School of Bioresources, Mie University, 2.Center for Northeast Asian Studies, Tohoku University, 3.Institute of Humanities and Indigenous Studies of the North, SB RAS, 4.Melnikov Permafrost Institute, SB RAS, 5.Slavic-Eurasian Research Center, Hokkaido University, 6.Faculty of Economics, Ryukoku University)

9:30 AM - 9:45 AM JST | 12:30 AM - 12:45 AM UTC

[MIS01-03] Permafrost Degradation Threatens Arctic Communities and Infrastructure

*Dmitry A Streletskiy[1], Nikolay I Shiklomanov[1], Kelsey Nyland[1] (1.George Washington University)

9:45 AM - 10:00 AM JST | 12:45 AM - 1:00 AM UTC

[MIS01-04] Monthly precipitations for South Siberia derived from bias-corrected reanalysis

Nadezhda Voropay[1,2], *Anna Ryazanova[1], Egor Dyukarev[1,3] (1.Institute of Monitoring of Climatic and Ecological Systems of the Siberian Branch of the Russian Academy of Sciences, 2.V B Sochava Institute of Geography of the Siberian Branch of the Russian Academy of Sciences, 3.Yugra State University)

10:00 AM - 10:15 AM JST | 1:00 AM - 1:15 AM UTC

[MIS01-05] Fuel load mapping in central Siberia

★Invited Papers

*Elena Kukavskaya[1], Ludmila Buryak[2], Evgeny Shvetsov[1], Sergey Zhila[1] (1.V.N. Sukachev Institute of Forest of the Siberian Branch of the Russian Academy of Sciences - separate subdivision of the FRC KSC SB RAS, 2.The Branch of FBU VNIILM “Center of Forest Pyrology”)

10:15 AM - 10:30 AM JST | 1:15 AM - 1:30 AM UTC

[MIS01-06] New data on the state and changes of glaciers in mountain and Polar Regions of Russia

*Tatiana Khromova[1], Gennady Nosenko, Andrey Glazovsky, Stanislav Nikitin, Anton Muraviev, Ivan Lavrentiev (1.Institute of Geography Russian Academy of Sciences)

[E] Oral | M (Multidisciplinary and Interdisciplinary) : M-IS Intersection

10:45 AM - 12:15 PM JST | 1:45 AM - 3:15 AM UTC | Ch.13 Zoom Room 13

[M-IS01] Environmental, socio-economic, and climatic changes in Northern Eurasia

convener:Pavel Groisman(NC State University Research Scholar at NOAA National Centers for Environmental Information, Asheville, North Carolina, USA), Shamil Maksyutov(National Institute for Environmental Studies), A Dmitry Streletskiy(George Washington University), Yoshihiro Iijima(Graduate School of Bioresources, Mie University), Chairperson:Yoshihiro Iijima(Graduate School of Bioresources, Mie University), Shamil Maksyutov(National Institute for Environmental Studies), Pavel Groisman(NC State University Research Scholar at NOAA National Centers for Environmental Information, Asheville, North Carolina, USA)

10:45 AM - 11:00 AM JST | 1:45 AM - 2:00 AM UTC

[MIS01-07] Quantification of the water vapor transport between the northern Eurasia and Arctic ocean considering the water vapor origin

*Tomonori Sato[1], Tetsu Nakamura[1], Yoshihiro Iijima[2], Tetsuya Hiyama[3] (1.Hokkaido University, 2.Mie University, 3.Nagoya University)

11:00 AM - 11:15 AM JST | 2:00 AM - 2:15 AM UTC

[MIS01-08] The hydrological cycle over the three great Siberian rivers from reanalyses and observations

*Ambroise Dufour[1], Martin Wegmann[2], Olga Zolina[3,1], Sergey Gulev[1] (1.P.P. Shirshov Institute of Oceanology, Russian Academy of Science, 2.Oeschger Centre for Climate Change Research, University of Bern, 3.Institut des Géosciences de l'Environnement, Université Grenoble Alpes)

11:15 AM - 11:30 AM JST | 2:15 AM - 2:30 AM UTC

[MIS01-09] Dark conifer forests dieback at mid-to-highlands in the southern Siberia's mountains is not caused by drought stress

*Nadezhda Tchebakova[1], Elena I. Parfenova[1], Elena V. Bazhina[1], Amber J. Soja[2], Pavel Groisman[3] (1.Institute of Forests of FRC KSC, Siberian Branch, Russian Academy of Sciences, 2.National Institute of Aerospace, NASA Langley Research Center, Hampton, VA, USA , 3.NC State University Research Scholar at National Centers for Environment Information Federal Building, 151 Patton Avenue Asheville, NC 28801, USA)

11:30 AM - 11:45 AM JST | 2:30 AM - 2:45 AM UTC

[MIS01-10] Changing climate of the Western Siberia and socio-economic risks

*Daria Aleksandrovna Konstantinova[1], Valentina Petrovna Gorbatenko[1], Olga Vladimirovna Nosyreva[1], Marina Aleksandrovna Volkova[1], Irina Valer'evna Kuzhevskaia[1] (1.Tomsk State University)

11:45 AM - 12:00 PM JST | 2:45 AM - 3:00 AM UTC

[MIS01-11] Long-term temporal trends in water chemistry of lakes in response to decreases in acidic deposition and climate warming of the Kola arctic region

★Invited Papers

Tatyana I Moiseenko[1], *Marina I Dinu[1], Maria M Bazova[1] (1.Russian Institute of Geochemistry and Analytical Chemistry RAS)

12:00 PM - 12:15 PM JST | 3:00 AM - 3:15 AM UTC

[MIS01-12] Wildfires in boreal eastern Siberia: Reconstructing the past to predict the future

*Ramesh Glueckler[1], Stefan Kruse°[1], Ulrike Herzschuh[1,2,3], Elisabeth Dietze°[1] (1.Alfred Wegener Institute Helmholtz Centre for Polar and Marine Research, Potsdam, Germany , 2.Institute for Environmental Science and Geography, University of Potsdam, Potsdam, Germany, 3.Institute for Biochemistry and Biology, University of Potsdam, Potsdam, Germany)

[E] Poster | M (Multidisciplinary and Interdisciplinary)：M-IS Intersection

5:15 PM - 6:30 PM JST | 8:15 AM - 9:30 AM UTC | Ch.18_1

[M-IS01] Environmental, socio-economic, and climatic changes in Northern Eurasia

convener:Pavel Groisman(NC State University Research Scholar at NOAA National Centers for Environmental Information, Asheville, North Carolina, USA), Shamil Maksyutov(National Institute for Environmental Studies), A Dmitry Streletskiy(George Washington University), Yoshihiro Iijima(Graduate School of Bioresources, Mie University)

[MIS01-P01] NORTHERN EURASIA FUTURE INITIATIVE (NEFI), UPDATE

*Pavel Groisman[1,2,3] (1.NC State University Research Scholar at NOAA National Centers for Environmental Information, Asheville, North Carolina, USA, 2.Shirshov Institute of Oceanology, Russian Academy of Sciences, Moscow, Russia , 3.Hydrology Science & Services Corporation, Asheville, North Carolina, USA)

[MIS01-P02] Statistical approach on geochemical records from Lake Olgoy, Valley of the Gobi Lakes, Mongolia

*Uyangaa Udaanjargal[1], Noriko Hasebe[2], Davaadorj Davaasuren, Yudai Igarashi[1], Hitoshi Hasegawa[3], Baasansuren Gankhurel[1], Nagayoshi Katsuta[4], Shuukhaaz Ganbat[1], Ichinnorov Niiden, Keisuke Fukushi[2] (1.Department of Earth Sciences, Kanazawa University, Kakuma, Kanazawa 920-1192, Japan, 2.Institute of Nature and Environmental Technology, Kanazawa University, Kakuma, Kanazawa 920-1192, Japan, 3.Faculty of Science and Technology, Kochi University, Kochi 780-8520, Japan, 4.Faculty of Education, Gifu University, Gifu 501-1193, Japan)

[MIS01-P03] The Lacustrine Sediment Analysis to Understand the Past Environmental Changes and the Effect of Ongoing Global Warming in Valley of The Gobi Lakes, Mongolia: Analyses of Tsagaan Lake Sediment

*Shuukhaaz Ganbat[1], Noriko Hasebe[2], Davaadorj Davaasuren[3], Uyangaa Udaanjargal[1], Yudai Igarashi[1] (1.Department of Earth Sciences, Kanazawa University, Kakuma, Kanazawa 920-1192, Japan, 2.Institute of Nature and Environmental Technology, Kanazawa University, Kakuma, Kanazawa 920-1192, Japan, 3.Department of Geography, School of Art& Science, National University of Mongolia, Ulaanbaatar 210646, Mongolia)

[MIS01-P04] Development of a New Drought Index Using SMOS Satellite Soil Moisture Products: Case Study in Southwestern Mongolia

*Oyudari Vova[1], Martin Kappas[1], Pavel Groisman[2], Tsolmon Renchin[3], Steven Fassnacht[1,4,5,6] (1.University of Göttingen, Göttingen, Germany, 2.NC State University Research Scholar at National Centers for Environment Information, Asheville, USA, 3.Department of Physics, National University of Mongolia, Ulaanbaatar, Mongolia, 4.Department of Ecosystem Science and Sustainability – Watershed Science, Colorado State University, Fort Collins, United States, 5.Cooperative Institute for Research in the Atmosphere, CSU, Fort Collins, USA, 6.Natural Resources Ecology Lab, Colorado State University, Fort Collins, USA)

[MIS01-P05] Fire and Logging Disturbances in the Angara Region, Central Siberia

*Evgeny Shvetsov[1], Elena Kukavskaya[1], Tatiana Shestakova[2], Brendan Rogers[2] (1.V.N. Sukachev Institute of Forest of the Siberian Branch of the Russian Academy of Sciences, 2.Woodwell Climate Research Center)

[MIS01-P06] Shifts in mountain vegetation reveal ecological responses to changing environmental conditions in Central Asian highlands

*Munavar Zhumanova[1], Geoffrey M Henebry[2,1] (1.Center for Global Change and Earth Observations, Michigan State University, 2.Department of Geography, Environment, and Spatial Sciences, Michigan State University)

[MIS01-P07] Ice-free period duration changes in the coastal zone of the Kara sea using satellite data

*Pavel Shabanov[1] (1.Shirshov Institute of Oceanology, Russian Academy of Sciences)

[E] Oral | M (Multidisciplinary and Interdisciplinary)：M-IS Intersection

9:00 AM - 10:30 AM JST | 12:00 AM - 1:30 AM UTC | Ch.26 Zoom Room 26

[M-IS04] Evolution and variability of the Asian Monsoon and Indo-Pacific climate during the Cenozoic Era

convener:Takuya Sagawa(Institute of Science and Engineering, Kanazawa University), Kenji Matsuzaki(Atmosphere and Ocean Research Institute, The university of Tokyo), Chairperson:Takuya Sagawa(Institute of Science and Engineering, Kanazawa University), Kenji Matsuzaki(Atmosphere and Ocean Research Institute, The university of Tokyo)

9:00 AM - 9:15 AM JST | 12:00 AM - 12:15 AM UTC

[MIS04-01] Orbital- to millennial-scale variability of the East Asian monsoon and the Kuroshio Current during periods of low orbital eccentricity and precessional change in the Pleistocene

★Invited Papers

*Yoshimi Kubota[1], Yuki Haneda[2], Koji Kameo[3], Takuya Itaki[2], Hiroki Hayashi[4], Kizuku Shikoku[4], Kentaro Izumi[5], Martin J Head[6], Yusuke Suganuma[7], Makoto Okada[8] (1.National Museum of Nature and Science, 2.Geological Survey of Japan, AIST, 3. Department of Earth Sciences, Faculty of Science, Chiba University, 4.Interdisciplinary Faculty of Science and Engineering, Shimane University, 5. Faculty & Graduate School of Education, Chiba University, 6.Brock University, 7.National Institute of Polar Research, 8.Department of Earth Sciences, Ibaraki University)

9:15 AM - 9:30 AM JST | 12:15 AM - 12:30 AM UTC

[MIS04-02] Effect of orbitally-driven insolation changes on East Asian monsoon rainfall over the past 450,000 years

*Taiga Matsushita[1], Mariko Harada[1], Hiroaki Ueda[1], Takeshi Nakagawa[2], Yoshimi Kubota[3], Yoshiaki Suzuki[4] (1.University of Tsukuba, 2.Ritsumeikan University, 3.National Museum of Nature and Science, 4.National Institute of Advanced Industrial Science and Technology)

9:30 AM - 9:45 AM JST | 12:30 AM - 12:45 AM UTC

[MIS04-03] Quantification of Asian dust multi-source contributions to silt and clay fractions in the Japan Sea sediments at IODP Site U1425 since 10 Ma by the Parallel Factor (PARAFAC) end-member modelling

*Mui Fa Alison Lee[1], Airi Maruyama[1], Tomohisa Irino[2] (1.Graduate School of Environmental Science, Hokkaido University, 2.Faculty of Environmental Earth Science, Hokkaido University)

9:45 AM - 10:00 AM JST | 12:45 AM - 1:00 AM UTC

[MIS04-04] Cyclostratigraphy and orbitally-paced paleo-productivity records of the Miocene Onnagawa Formation in Akita Prefecture, Northern Japan

*Jumpei Yoshioka[1,2], Junichiro Kuroda[2], Kenji Matsuzaki[2], Ryuji Tada[1,3,4] (1.Department of Earth and Planetary Science, the University of Tokyo, 2.Atmosphere and Ocean Research Institute, the University of Tokyo, 3.Yunnan University, 4.Chiba Institute of Technology)

10:00 AM - 10:15 AM JST | 1:00 AM - 1:15 AM UTC

[MIS04-05] Sedimentary features and isotope records of the upper Eocene travertine-lacustrin carbonate in the SE Tibet and implication for hte monsoon climate

★Invited Papers

*Aki Sakuma[1], Akihiro Kano[1], Yoshihiro Kakizaki[1], Ryuji Tada[2,3], Hongbo Zheng[3] (1.Department of Earth and Planetary Science, School of Science, the University of Tokyo, 2.Institute for Geo-Cosmology, Chiba Institute of Technology, 3.Yunnan Key Laboratory of Earth System Science, Yunnan University)

10:15 AM - 10:30 AM JST | 1:15 AM - 1:30 AM UTC

[MIS04-06] Impact of long-term monsoon dynamics on Cenozoic-Mesozoic climate and ecosystems

*Masayuki Ikeda[1], Kazumi Ozaki[2], LEGRAND Julien[3] (1.University of Tokyo, 2.Toho University, 3.Shizuoka University)

[E] Poster | M (Multidisciplinary and Interdisciplinary)：M-IS Intersection

5:15 PM - 6:30 PM JST | 8:15 AM - 9:30 AM UTC | Ch.22_1

[M-IS04] Evolution and variability of the Asian Monsoon and Indo-Pacific climate during the Cenozoic Era

convener:Takuya Sagawa(Institute of Science and Engineering, Kanazawa University), Kenji Matsuzaki(Atmosphere and Ocean Research Institute, The university of Tokyo)

[MIS04-P01] Tropical Western Pacific hydrology during the last 6,000 years based on wildfire charcoal records from Borneo

*Masanobu Yamamoto[1], Takafumi Kikuchi[1], Hiromischi Sakurai[1], Ryoma Hayashi[2], Osamu Seki[3], Takayuki Omori[4], Abdullah Sulaiman[5], Hasrizal Shaari[6], Mohd Zulhilmy Abdhllah[7], Lulie Melling[7] (1.Faculty of Environmental Earth Science, Hokkaido University, 2.Lake Biwa Museum, 3.Institute of Low Temperature Science, Hokkaido University, 4.The University Museum, The University of Tokyo, 5.Department of Mineral and Geoscience of Malaysia, 6.Universiti Malaysia Terengganu, 7.Sarawak Tropical Peat Reserach Institute)

[MIS04-P02] Similarities and disparities between radiolarian-based Sea Surface Temperature (SST) estimates with foraminifera Mg/Ca SST in monsoon influenced area

*Kenji Matsuzaki[1], Yoshimi Kubota[2] (1.Atmosphere and Ocean Research Institute, The university of Tokyo, 2.Department of Geology and Paleontology, National Museum of Nature and Science)

[MIS04-P03] Major re-organisation in marine ecosystem during the Late Miocene Global Cooling caused by changes in major monsoonal mode

*Kenji Matsuzaki[1], Masayuki Ikeda[2], Ryuji Tada[2] (1.Atmosphere and Ocean Research Institute, The university of Tokyo, 2.Graduate School of Science, The University of Tokyo)

[MIS04-P04] Evolution of meridional and zonal sea surface temperature gradients in the Pacific Ocean during the Quaternary period

*Takuya Sagawa[1], Risako Makino[2], Yukimi Kubota[2], Yoshimi Kubota[3], Yair Rosenthal[4] (1.Institute of Science and Engineering, Kanazawa University, 2.Collage of Science and Engineering, Kanazawa University, 3.National Museum of Nature and Science, 4.Rutgers University)

[MIS04-P05] Pliocene thermocline stability in the western Pacific warm pool inferred from the individual foraminifera analysis

Fumito Mizuno[2], *Takuya Sagawa[1] (1.Institute of Science and Engineering, Kanazawa University, 2.Graduate School of Natural Science and Technology, Kanazawa University)

[E] Oral | M (Multidisciplinary and Interdisciplinary)：M-IS Intersection

10:45 AM - 12:15 PM JST | 1:45 AM - 3:15 AM UTC | Ch.11 Zoom Room 11

[M-IS05] Global climate change driven by the Southern Ocean and the Antarctic Ice Sheet

convener:Osamu Seki(Institute of Low Temperature Science, Hokkaido University), Yoshifumi Nogi(National Institute of Polar Research), Akira Oka(Atmosphere and Ocean Research Institute, The University of Tokyo), Yusuke Suganuma(National institute of Polar Research), Chairperson:Takashi Obase(Atmosphere and Ocean Research Institute, the University of Tokyo)

10:45 AM - 11:05 AM JST | 1:45 AM - 2:05 AM UTC

[MIS05-01] Modelling the Stability of Antarctic ice sheet for investigating the link between the past and future

★Invited Papers

*Ayako Abe-Ouchi[1], Kaho Harada[1], Takashi Obase[1], Fuyuki SAITO[2], Ralf Greve[3], Christopher Chambers[3], Osamu Seki[3], Kenji Kawamura[4], Jun'ichi Okuno[4] (1.Atmosphere and Ocean Research Institute, The University of Tokyo, 2.JAMSTEC, 3.Hokkaido University, 4.NIPR)

11:05 AM - 11:25 AM JST | 2:05 AM - 2:25 AM UTC

[MIS05-02] Carbon and nutrient cycles in and around the Cape Darnley polynya

★Invited Papers

*Michiyo Yamamoto-Kawai[1], Yoshihiko Ohashi[1] (1.Graduate School of Marine Science and Technology, Tokyo University of Marine Science and Technology)

11:25 AM - 11:45 AM JST | 2:25 AM - 2:45 AM UTC

[MIS05-03] MONACA: The hot explorer under ice

★Invited Papers

*Toshihiro Maki[1], Hirokazu Yamagata[1], Hiroshi Yoshida[2], Yoshifumi Nogi[3] (1.The University of Tokyo, 2.Japan Agency for Marine-Earth Science and Technology, 3.National Institute of Polar Research)

11:45 AM - 12:00 PM JST | 2:45 AM - 3:00 AM UTC

[MIS05-04] **Development of the Under Ice AUV “MONACA”**
- Autonomous Navigation Trial in Under Ice Environment -

*Hirokazu Yamagata[1], Shuma Kochii[1], Hiroshi Yoshida[2], Yoshifumi Nogi[3], Toshihiro Maki[1] (1.Institute of Industrial Science, The University of Tokyo, 2.Japan Marine Science and Technology Center, 3.National Institute of Polar Research)

12:00 PM - 12:15 PM JST | 3:00 AM - 3:15 AM UTC

[MIS05-05] Long-term future projections for the Antarctic ice sheet with the model SICOPOLIS

*Christopher Chambers[1], Ralf Greve[2,1], Takashi Obase[3], Fuyuki SAITO[4], Kaho Harada[3], Ayako Abe-Ouchi[3] (1.Institute of Low Temperature Science, Hokkaido University, 2.Arctic Research Center, Hokkaido University, 3.Atmosphere and Ocean Research Institute, University of Tokyo, 4.Japan Agency for Marine-Earth Science and Technology)

[E] Oral | M (Multidisciplinary and Interdisciplinary) : M-IS Intersection

1:45 PM - 3:15 PM JST | 4:45 AM - 6:15 AM UTC | Ch.11 Zoom Room 11

[M-IS05] Global climate change driven by the Southern Ocean and the Antarctic Ice Sheet

convener:Osamu Seki(Institute of Low Temperature Science, Hokkaido University), Yoshifumi Nogi(National Institute of Polar Research), Akira Oka(Atmosphere and Ocean Research Institute, The University of Tokyo), Yusuke Suganuma(National institute of Polar Research), Chairperson:Hiroki Matsui(Graduate School of International Resource Sciences, Akita University), Takeshige Ishiwa(National Institute of Polar Research)

1:45 PM - 2:00 PM JST | 4:45 AM - 5:00 AM UTC

[MIS05-06] Beryllium isotope records from sectors of the West and East Antarctic Ice sheet reveal Holocene melting related to the incursion of Circumpolar Deep Water

*Adam David Sproson[1,2], Yusuke Yokoyama[1,2], Yoshinori Takano[2], Rebecca Minzoni[3], Bethany Behrens[1], Yosuke Miyairi[1], Takahiro Aze[1] (1.Atmosphere and Ocean Research Institute, University of Tokyo, 5-1-5 Kashiwanoha, Kashiwa, Chiba 277-8564, Japan. , 2.Department of Biogeochemistry, Japan Agency for Marine-Earth Science and Technology, 2-15 Natsushima, Yokosuka, Kanagawa 237-0061, Japan. , 3.Department of Geological Sciences, The University of Alabama, USA.)

2:00 PM - 2:15 PM JST | 5:00 AM - 5:15 AM UTC

[MIS05-07] Abrupt Holocene ice-sheet retreat in Lutzow-Holm Bay, East Antarctica

*Yusuke Suganuma[1,2], Yuki Haneda[3], Takuya Itaki[3], Osamu Seki[4], Takeshige Ishiwa[1], Moto Kawamata[2], Masakazu Fujii[1,2], Kazuya Kusahara[8], Daisuke Hirano[4], Masao Iwai[9], Yuji Kato[9], Hiroki Matsui[6], Atsuko Amano[3], Kota Katsuki[5], Takayuki Omori[7], Motohiro Hirabayashi[1], Hiroyuki Matsuzaki[7], Takeyasu Yamagata[7], Masato Ito[8], Shin Sugiyama[4], Naohisa Nishida[10], Jun'ichi Okuno[1,2], Minoru Ikehara[9], Hideki Miura[1,2] (1.National institute of Polar Research, 2.The Graduate University for Advanced Studies (SOKENDAI), 3.Geological Survey of Japan, AIST, 4.Hokkaido University, 5.Shimane University, 6.Akita University, 7.University of Tokyo, 8.JAMSTEC, 9.Center for Advanced Marine Core Research, Kochi University, 10.Tokyo Gakugei University)

2:15 PM - 2:30 PM JST | 5:15 AM - 5:30 AM UTC

[MIS05-08] Paleoenvironmental reconstruction using lake sediment cores from Lake Nurume in Lützow Holm Bay

*Takeshige Ishiwa[1], Yuki Tokuda[2], Takuya Itaki[3], Satoshi Sasaki[4], Kota Katsuki[4], Yusuke Suganuma[1,5] (1.National Institute of Polar Research, 2.Tottori University of Environmental Studies, 3.National Institute of Advanced Industrial Science and Technology, 4.Shimane University, 5.The Graduate University for Advanced Studies (SOKENDAI))

2:30 PM - 2:45 PM JST | 5:30 AM - 5:45 AM UTC

[MIS05-09] Assessing dust-magnetic correlation in the Indian sector of the Southern Ocean

*Hiroki Matsui[1], Minoru Ikehara[2], Yusuke Suganuma[3,4], Osamu Seki[5], Ikumi Oyabu[3], Kenji Kawamura[3,4] (1.Graduate School of International Resource Sciences, Akita University, 2.Center for Advanced Marine Core Research, Kochi University, 3.National Institute of Polar Research, Research Organization of Information and Systems, 4.Department of Polar Science, School of Multidisciplinary Sciences, The Graduate University for Advanced Studies (SOKENDAI), 5.Institute of Low Temperature Science, Hokkaido University)

2:45 PM - 3:00 PM JST | 5:45 AM - 6:00 AM UTC

[MIS05-10] Antarctic warmth in the last interglacial driven by Northern insolation and deglaciation

*Takashi Obase[1], Ayako Abe-Ouchi[1,2], Fuyuki SAITO[3] (1.Atmosphere and Ocean Research Institute, the University of Tokyo, 2.National Institute of Polar Research, Japan, 3.Japan Agency for Marine-Earth Science and Technology)

3:00 PM - 3:15 PM JST | 6:00 AM - 6:15 AM UTC

[MIS05-11] Modeling the ocean carbon cycle during the last deglaciation

*Hidetaka Kobayashi[1], Akira Oka[1], Takashi Obase[1], Ayako Abe-Ouchi[1] (1.Atmosphere and Ocean Research Institute, The University of Tokyo)

[E] Oral | M (Multidisciplinary and Interdisciplinary) : M-IS Intersection

3:30 PM - 5:00 PM JST | 6:30 AM - 8:00 AM UTC | Ch.11 Zoom Room 11

[M-IS05] Global climate change driven by the Southern Ocean and the Antarctic Ice Sheet

convener:Osamu Seki(Institute of Low Temperature Science, Hokkaido University), Yoshifumi Nogi(National Institute of Polar Research), Akira Oka(Atmosphere and Ocean Research Institute, The University of Tokyo), Yusuke Suganuma(National institute of Polar Research), Chairperson:Hidetaka Kobayashi(Atmosphere and Ocean Research Institute, The University of Tokyo)

3:30 PM - 3:45 PM JST | 6:30 AM - 6:45 AM UTC

[MIS05-12] **Last Glacial Maximum Antarctic sea ice linked with global mean ocean temperature: evidence from PMIP3, PMIP4 and MIROC-4m simulations**

*Tristan Vadsaria[1], Sam Sherriff-Tadano[2,1], Ayako Abe-Ouchi[1], Takashi Obase[1], Wing-Le Chan[1], Xavier Crosta[3] (1.Atmosphere and Ocean Research Institute, The University of Tokyo, Japan, 2.School of Earth and Environment, The University of Leeds, Leeds, UK, 3.Environnements et Paléoenvironnements Océanique et Continentaux, Pessac, France)

3:45 PM - 4:00 PM JST | 6:45 AM - 7:00 AM UTC

[MIS05-13] **Antarctic Slope Current modulates warm ocean heat intrusions towards Totten Glacier**

*Yoshihiro Nakayama[1], Chad A Greene[2], Fernando S Paolo[2], Vigan Mensah[1], Hong Zhang[2], Haruhiko Kashiwase[3], Daisuke Simizu[3], Jamin S Greenbaum[4], Donald D Blankenship[5], Ayako Abe-Ouchi[6], Shigeru Aoki[1] (1.Institute of Low Temperature Science, Hokkaido University, Japan, 2.NASA Jet Propulsion Laboratory, California, USA, 3.National Institute of Polar Research, Tokyo, Japan, 4.Scripps Institution of Oceanography, University of California, California USA, 5.Institute for Geophysics, University of Texas at Austin, Texas, USA, 6.Atmosphere and Ocean Research Institute, The University of Tokyo, Tokyo, Japan.)

4:00 PM - 4:15 PM JST | 7:00 AM - 7:15 AM UTC

[MIS05-14] Sea Ice Variations in Coastal Amundsen Sea Affected by Ice Shelf Meltwater

*KOFAN LU[1] (1.Japan Agency for Marine-Earth Science and Technology)

4:15 PM - 4:30 PM JST | 7:15 AM - 7:30 AM UTC

[MIS05-15] Observation of plagic system using a drifter off Wilkes land during sea ice melting season

*Ryosuke Makabe[1,5,2], Keigo Takahashi[2], Shintaro Takao[3], Ryo Matsuda[4], Masayoshi Sano[1], Kohei Mizobata[5], Norio Kurosawa[4], Masato Moteki[5,1], Tsuneo Odate[1,2] (1.National Institute of Polar Research, 2.The Graduate University for Advanced Studies (SOKENDAI), 3.National Institute for Environmental Studies, 4.Soka University, 5.Tokyo University of Marine Science and Technology)

4:30 PM - 4:45 PM JST | 7:30 AM - 7:45 AM UTC

[MIS05-16] Primary production and carbon export related to sub-surface chlorophyll maximum off Wilkes land during post bloom season

*Norio Kurosawa[1], Ayuko Kagesawaa[2], Ryosuke Makabe[3,2,4], Shintaro Takao[5], Masayoshi Sano[3], Kohei Mizobata[4], Masato Moteki[4,3], Tsuneo Odate[2,3] (1.Soka University, 2.The Graduate University for Advanced Studies (SOKENDAI), 3.National Institute of Polar Research, 4.Tokyo University of Marine Science and Technology, 5.National Institute for Environmental Studies)

4:45 PM - 5:00 PM JST | 7:45 AM - 8:00 AM UTC

[MIS05-17] Contribution of fecal pellet-like dinoflagellates to the carbon sequestration in the seasonal ice zone of the Southern Ocean

*Ryo Matsuda[1], Jaekyeng Han[1], Shinya Okano[1], Masayoshi Sano[2], Shintaro Takao[3], Ryosuke Makabe[2,4,5], Masato Moteki[4,5], Tsuneo Odate[2,4], Norio Kurosawa[1] (1.Soka University, 2.National Institute of Polar Research, 3.National Institute for Environmental Studies, 4.The Graduate University for Advanced Studies (SOKENDAI), 5.Tokyo University of Marine Science and Technology)

[E] Poster | M (Multidisciplinary and Interdisciplinary)：M-IS Intersection

5:15 PM - 6:30 PM JST | 8:15 AM - 9:30 AM UTC | Ch.20_1

[M-IS05] Global climate change driven by the Southern Ocean and the Antarctic Ice Sheet

convener:Osamu Seki(Institute of Low Temperature Science, Hokkaido University), Yoshifumi Nogi(National Institute of Polar Research), Akira Oka(Atmosphere and Ocean Research Institute, The University of Tokyo), Yusuke Suganuma(National institute of Polar Research)

[MIS05-P01] Summary of the Year 2020 Activities of the Project on the Interaction of the solid Earth and the Antarctic Ice Sheet

*Yoichi Fukuda[1], Jun Nishijima[2], Takahito Kazama[3], Kazuki Nakamura[4], Koichiro Doi[1], Yusuke Suganuma[1], Jun'ichi Okuno[1], Akito Araya[5], Heitaro Kaneda[6], Yuichi Aoyama[1], Hideki Miura[1] (1.National Institute of Polar Research, 2.Graduate School of Engineering, Kyushu University, 3.Graduate School of Science, Kyoto University, 4.Faculty of Engineering, Nihon University, 5.ERI, University of Tokyo, 6.Faculty of Science and Engineering, Chuo University)

[MIS05-P02] Vertical crustal motion induced by GIA in Lützow-Holm Bay, East Antarctica

*Jun'ichi Okuno[1,2], Akihisa Hattori[2], Takeshige Ishiwa[1], Yoshiya Irie[1], Koichiro Doi[1,2] (1.National Institute of Polar Research, 2.SOKENDAI)

[MIS05-P03] Multibeam bathymetry off East Antarctica: 2010s Japanese observations

*Masakazu Fujii[1,2], Yoshifumi Nogi[1,2] (1.National Institute of Polar Research, 2.SOKENDAI (The Graduate University for Advanced Studies))

[MIS05-P04] Development of Research Instruments for unexplored frontiers in the Southern Ocean and Antarctica

*Yoshifumi Nogi[1], Shigeru Aoki[2], Hiroshi Yoshida[3], Toshihiro Maki[4], Kyoko Okino[5], Yuichi Aoyama[1], Tetsuo Sueyoshi[1], Takeshi Tamura[1], Hirokazu Yamagata[4], Masakazu Fujii[1] (1.National Institute of Polar Research, 2.Institute of Low Temperature Science, Hokkaido University, 3.Japan Agency for Marine-Earth Science and Technology, 4.Institute of Industrial Science, the University of Tokyo, 5.Atmosphere and Ocean Research Institute, the University of Tokyo)

[MIS05-P05] Lake Environmental change since little ice age in Antarctic ice-free area, Skarvsnes, East Antarctica

*Kota Katsuki[1], Yuito Kamada[2], Hanna Wakabayashi[2], Moemi Kawagishi[2], Akira Tsujimoto[6], Yusuke Suganuma[3], Daisuke Shibata[4], Moto Kawamata[5] (1.Estuary Research Center, Shimane University, 2.Interdisciplinary Faculty of Science and Engineering, Shimane University, 3.National Institute of Polar Research, 4.Shimoda Marine Research Center, Tsukuba Univeristy , 5.The Graduate University for Advanced Studies, 6.Faculty of Education, Shimane University)

[MIS05-P06] Application of AI-based classification to planktic foraminifera assemblage in the Southern Ocean

*Hiroki Matsui[1], Takuya Itaki[2], Minoru Ikehara[3] (1.Graduate School of International Resource Sciences, Akita University, 2.Geological Survey of Japan, AIST, 3.Center for Advanced Marine Core Research, Kochi University)

[MIS05-P07] Lateral migration of a flowstripe on the ice shelf of Shirase Glacier, East Antarctica

*Ken Kondo[1,2], Shin Sugiyama[1] (1.Institute of Low Temperature Science, Hokkaido University, 2.Graduate School of Environmental Science, Hokkaido University)

[MIS05-P08] Vertical fluctuation area of ice shelf due to tidal fluctuations in the Langhovde Glacier using DDInSAR.

*Chiyuki Narama[1], Tsutomu Yamanokuchi[2], Shin Sugiyama[3] (1.Niigata University, Program of Field Research in the Environmental Sciences, 2.RESTEC, 3.Hokkaido University, Institute of Low Temperature Science)

[MIS05-P09] Climatic and atmospheric changes over the last three Terminations from O_2/N_2,$d^{18}O_{atm}$ and CH_4 records of the Dome Fuji ice core, Antarctica

*Ikumi Oyabu[1], Kenji Kawamura[1,2,3], Kyotaro Kitamura[1], Anais Orsi[4], Frederic Parrenin[5], Christo Buizert[6] (1.National Institute of Polar Research, Research Organization of Information and Systems, 2.SOKENDAI (The Graduate University of Advanced Studies), 3.Japan Agency for Marine Science and Technology (JAMSTEC), 4.Laboratory for Sciences of Climate and Environment (LSCE), 5.Institut des Géosciences de l'Environnement (IGE), 6.Oregon State University)

[MIS05-P10] Periods of local melt during the Holocene at Terre Adelie, East Antarctica revealed by beryllium isotope ratios

*Bethany Behrens[1,2], Yusuke Yokoyama[1,2,4,5], Yosuke Miyairi[1], Adam David Sproson[1], Masako Yamane[3] (1.Atmosphere and Ocean Research Institute, University of Tokyo, Japan, 2.Graduate Program on Environmental Science, University of Tokyo, Japan, 3.Institute for Space-Earth Environmental Research, Nagoya University, Japan, 4.Department of Earth and Planetary Science, Graduate School of Science, University of Tokyo, Japan, 5.Japan Agency for Marine-Earth Science and Technology (JAMSTEC), Natsushimacho, Japan)

[MIS05-P11] **The Antarctic ice sheet and Southern Ocean dynamics during the Last Interglacial**

*Mutsumi Iizuka[1], Osamu Seki[1], Masanobu Yamamoto[1], Takuya Itaki[2], Michael E. Weber[3], Maureen E. Raymo[4], Victoria L. Peck[5], Trevor Williams[6], IODP Expedition 382 scientists (1.Hokkaido university, 2.National Institute of Advanced Industrial Science and Technology, 3.University of Bonn, 4.Lamont-Doherty Earth Observatory of Columbia University, 5.British Antarctic Survey, 6.Texas A&M University)

[MIS05-P12] Reconstruction of ice sheet dynamics in Totten Glacier/Aurora Subglacial Basin, East Antarctica during the Last Interglacial

*Osamu Seki[1], Mutsumi Iizuka[1], Keiji Horikawa[1], Tina van De Flierdt[2], Minoru Ikehara[3], Tomohisa Irino[4], Takuya Itaki[5], Saiko Sugisaki[5] (1.Institute of Low Temperature Science, Hokkaido University, 2.Imperial College London, 3.Kochi University, 4.Faculty of Earth and Environmental Science, Hokkado University, 5.National Institute of Advanced Industrial Science and Technology)

[MIS05-P13] Analysis of the abrupt climate change during the last deglaciation

*Ren Shimura[1], Ayako Abe-Ouchi[2] (1.Department of Earth and Planetary Science, The University of Tokyo, 2.Atmosphere and Ocean Research Institute (AORI), University of Tokyo)

[MIS05-P14] Incorporation of grounding line parameterizations in the ice sheet model SICOPOLIS and its application to Antarctica

*Takashi Obase[1], Ayako Abe-Ouchi[1,2], Fuyuki SAITO[3], Ralf Greve[4], Kaho Harada[1] (1.Atmosphere and Ocean Research Institute, The University of Tokyo, 2.National Institute of Polar Research, Japan, 3.Japan Agency for Marine-Earth Science and Technology, 4.Institute of Low Temperature Science, Hokkaido University)

[MIS05-P15] Numerical experiment of Antarctic ice sheet using a coupled ice-sheet/earth rebound model

*Fuyuki SAITO[1], Jun'ichi Okuno[2], Ayako Abe-Ouchi[3] (1.Japan Agency for Marine-Earth Science and Technology, 2.National Institute of Polar Research, 3.Atmosphere and Ocean Research Institute, The University of Tokyo)

[MIS05-P16] A linkage between Antarctic sea-ice extent and ice-shelf basal melting in summer: A circumpolar model study

*Kazuya Kusahara[1] (1.Japan Agency for Marine-Earth Science and Technology)

[MIS05-P17] Ocean circulation in the shelf-slope region of East Antarctica as suggested by satellite radar altimetry

*Kohei Mizobata[1], Mao Mori[1] (1.Tokyo University of Marine Science and Technology)

[MIS05-P18] Quantification of water mass age of Antarctic Bottom Water off Cape Darnley in East Antarctica, using chlorofluorocarbon and sulfur hexafluoride

*Yoshihiko Ohashi[1], Michiyo Yamamoto-Kawai[1], Kazuya Kusahara[2], Kenichi Sasaki[2], Narimi Baba[1], Naoyuki Tamura[1], Natsumi Nojiro[1], Kay I. Ohshima[3] (1.Tokyo University of Marine Science and Technology, 2.Japan Agency for Marine Earth Science and Technology, 3.Institute of Low Temperature Science, Hokkaido University)

[MIS05-P19] Seasonal flux and morphological changes in silicoflagellates in the Indian sector of the Southern Ocean

*Ryota Hayashi[1], Yusuke Okazaki[2], Koshiro Matsuo[2], Takahito Ikenoue[3], Takuya Itaki[4], Minoru Ikehara[5] (1.Department of Earth and Planetary Sciences, School of Science, Kyushu University, 2.Department of Earth and Planetary Sciences, Graduates School of Science, Kyushu University, 3.Marine Ecology Research Institute, 4.Geological Survey of Japan, AIST, 5.Center for Advanced Marine Core Research, Kochi University)

[MIS05-P20] Molecular analysis of individual fecal pellets collected by using gel sediment traps in the Indian sector of the Southern Ocean

*Masayoshi Sano[1], Ryosuke Makabe[1,2,3], Norio Kurosawa[4], Masato Moteki[2,1], Tsuneo Odate[1,3] (1.National Institute of Polar Research, 2.Tokyo University of Marine Science and Technology, 3.The Graduate University for Advanced

Studies, 4.Soka University)

[E] Oral | M (Multidisciplinary and Interdisciplinary)：M-IS Intersection

10:45 AM - 12:15 PM JST | 1:45 AM - 3:15 AM UTC | Ch.22 Zoom Room 22

[M-IS08] Interdisciplinary studies on pre-earthquake processes

convener:Katsumi Hattori(Department of Earth Sciences, Graduate School of Science, Chiba University), Dimitar Ouzounov(Center of Excellence in Earth Systems Modeling & Observations (CEESMO) , Schmid College of Science & Technology Chapman University, Orange, California, USA), Jann-Yenq LIU(Department of Space Science and Engineering, National Central University, Taiwan), Qinghua Huang(Peking University), Chairperson:Katsumi Hattori(Department of Earth Sciences, Graduate School of Science, Chiba University), Dimitar Ouzounov(Center of Excellence in Earth Systems Modeling & Observations (CEESMO) , Schmid College of Science & Technology Chapman University, Orange, California, USA)

10:45 AM - 11:00 AM JST | 1:45 AM - 2:00 AM UTC

[MIS08-01] The spatiotemporal evolution of pre-earthquake anomalies and their association with the activation zone

*Dimitar Ouzounov[1], Sergey Pulinets[2], J.Y Liu[3], Katsumi Hattori[4], Patrick Taylor[5] (1.Center of Excellence in Earth Systems Modeling & Observations (CEESMO) , Schmid College of Science & Technology Chapman University, Orange, California, USA, 2.Space Research Institute, Russian Academy of Sciences, Moscow, Russia, 3.Center for Space and Remote Sensing Research, National Central University, Taoyuan, Taiwan, 4.Department of Earth Sciences, Graduate School of Science, Chiba University, Chiba, Japan, 5.NASA GSFC, Greenbelt, MD, USA)

11:00 AM - 11:20 AM JST | 2:00 AM - 2:20 AM UTC

[MIS08-02] The multi observations on electromagnetic emissions and plasma perturbations around Yutian Earthquakes in China

★Invited Papers

*Xuemin Zhang[1], Jing Liu[1], Angelo De Santis[2], Loredana Perrone[2], Xuhui Shen[3], Jianping Huang[3] (1.Institute of Earthquake Forecasting, China Earthquake Administration, 2.Istituto Nazionale di Geofisica e Vulcanologia, 3.Institute of Crustal Dynamics, China Earthquake Administration)

11:20 AM - 11:35 AM JST | 2:20 AM - 2:35 AM UTC

[MIS08-03] Bizarre “earthquake weather” immediately before and after the 1995 Kobe earthquake

*Yuji Enomoto[1], Tsuneaki Yamabe[1], Shigeki Sugiura[2], Hitoshi Kondo[2] (1.Shinshu Univeristy, Ueda Campus Fii, 2.Genesis Research Institute Inc.)

11:35 AM - 11:50 AM JST | 2:35 AM - 2:50 AM UTC

[MIS08-04] A system of the Monitoring Vibrations and Propagations in the Lithosphere, Atmosphere, and Ionosphere

*Chieh-Hung Chen[1], Yang-Yi Sun[1], Kai Lin[1], Huaizhong Yu[2] (1.Institute of Geophysics and Geomatics, China University of Geosciences, Wuhan, Hubei, China, 2.China Earthquake Networks Center, Beijing, China)

11:50 AM - 12:10 PM JST | 2:50 AM - 3:10 AM UTC

[MIS08-05] Assessing the potential earthquake precursory information in ULF magnetic data recorded in Kanto, Japan during 2000 – 2010: distance and magnitude dependences

★Invited Papers

*Peng Han[1], Jiancang Zhuang[2], Katsumi Hattori[3], Chieh-Hung Chen[4], Febty Febriani[5], Hongyan Chen[1] (1.Southern University of Science and Technology, Shenzhen, China, 2.The Institute of Statistical Mathematics, Tokyo, Japan, 3.Graduate School of Science, Chiba University, Chiba, Japan, 4.Institute of Geophysics and Geomatics, China University of Geosciences, Wuhan 430074, China, 5.Research Center for Physics, Indonesian Institute of Sciences, Tangerang, Banten, Indonesia)

12:10 PM - 12:15 PM JST | 3:10 AM - 3:15 AM UTC

[MIS08-06] Discussion

[E] Oral | M (Multidisciplinary and Interdisciplinary) : M-IS Intersection

1:45 PM - 3:15 PM JST | 4:45 AM - 6:15 AM UTC | Ch.22 Zoom Room 22

[M-IS08] Interdisciplinary studies on pre-earthquake processes

convener:Katsumi Hattori(Department of Earth Sciences, Graduate School of Science, Chiba University), Dimitar Ouzounov(Center of Excellence in Earth Systems Modeling & Observations (CEESMO) , Schmid College of Science & Technology Chapman University, Orange, California, USA), Jann-Yenq LIU(Department of Space Science and Engineering, National Central University, Taiwan), Qinghua Huang(Peking University), Chairperson:Peng Han(Southern University of Science and Technology, Shenzhen, China), Xuemin Zhang(Institute of Earthquake Forecasting, China Earthquake Administration)

1:45 PM - 2:00 PM JST | 4:45 AM - 5:00 AM UTC

[MIS08-07] Seismo-ionospheric anomalies before the 11 March 2011 M9.0 Tohoku Earthquake

*Jann-Yenq LIU[1,2,3], FU-YUAN CHANG[1], I-Te Lee[4], Katsumi Hattori[5], Yuh-Ing Chen[6] (1.Center for Astronautical Physics and Engineering, National Central University, Taoyuan, TAIWAN, 2.Department of Space Science and Engineering, National Central University, TAIWAN, 3.Center for Space and Remote Sensing Research, National Central University, Taoyuan, TAIWAN, 4.Center Weather Bureau, Taipei, TAIWAN, 5.Department of Earth Sciences, Graduate School of Science, Chiba University, Chiba, JAPAN, 6.Institute of Statistics, National Central University, Taoyuan, TAIWAN)

2:00 PM - 2:15 PM JST | 5:00 AM - 5:15 AM UTC

[MIS08-08] 3D Tomography of the Ionospheric Anomalies Before the 2010 Maule Earthquake, Chile: Comparison with the 2011 Tohoku-oki and 2015 Illapel Earthquakes

*Ihsan Naufal Muafiry[1], Kosuke Heki[1] (1.Hokkaido University, Japan)

2:15 PM - 2:30 PM JST | 5:15 AM - 5:30 AM UTC

[MIS08-09] Spatiotemporal Distribution Characteristics of Conductivity Anomalies before Ms > 6 Earthquakes in the North-South Seismic Belt of China during 2014 – 2019

*Zhiqiang Mao[1], Chieh-Hung Chen[1], Suqin Zhang[2], Qi Li[2], Aisa Yisimayili[3] (1.China University of Geosciences (Wuhan), 2.Institute of Geophysics, China Earthquake Administration, 3.Earthquake Agency of Xinjiang Uygur Autonomous Region)

2:30 PM - 2:45 PM JST | 5:30 AM - 5:45 AM UTC

[MIS08-10] **Possible stimulation of seismic activity by geomagnetically induced currents generated by ionizing radiation of solar flare in the illuminated hemisphere**

*Victor A. Novikov[1], Valery M. Sorokin[2], Alexey K. Yaschenko[2], Georgy Yu. Mushkarev[2] (1.Joint Institute for High Temperatures of Russian Academy of Sciences, 2.Pushkov Institute of Terrestrial Magnetism, Ionosphere and Radio Wave Propagation of Russian Academy of Sciences)

2:45 PM - 3:00 PM JST | 5:45 AM - 6:00 AM UTC

[MIS08-11] **Detecting the ionospheric disturbances in Japan using the three-dimensional computerized tomography**

*Rui Song[1], Katsumi Hattori[1], Xuemin Zhang[2] (1.Graduate School of Science and Engeering, Chiba University, 2.Institute of Earthquake Forecasting, China Earthquake Administration)

3:00 PM - 3:15 PM JST | 6:00 AM - 6:15 AM UTC

[MIS08-12] A Statistical Study of the Correlation Between Geomagnetic Storms and M>7.0 Global Earthquakes During 1957–2020

*Hongyan Chen[1], Rui Wang[1], Miao Miao[1], Xiaocan Liu[2], Yonghui Ma[3], Katsumi Hattori[4], Peng Han[1] (1.Southern University of Science and Technology, Shenzhen, China, 2.The Institute of Geophysics China Earthquake Administration, Beijing, China, 3.School of Science, Harbin Institute of Technology, Shenzhen, China, 4.Graduate School of Science, Chiba University, Chiba, Japan)

[E] Oral | M (Multidisciplinary and Interdisciplinary)：M-IS Intersection

3:30 PM - 5:00 PM JST | 6:30 AM - 8:00 AM UTC | Ch.22 Zoom Room 22

[M-IS08] Interdisciplinary studies on pre-earthquake processes

convener:Katsumi Hattori(Department of Earth Sciences, Graduate School of Science, Chiba University), Dimitar Ouzounov(Center of Excellence in Earth Systems Modeling & Observations (CEESMO) , Schmid College of Science & Technology Chapman University, Orange, California, USA), Jann-Yenq LIU(Department of Space Science and Engineering, National Central University, Taiwan), Qinghua Huang(Peking University), Chairperson:Jann-Yenq LIU(Department of Space Science and Engineering, National Central University, Taiwan), Qinghua Huang(Peking University)

3:30 PM - 3:50 PM JST | 6:30 AM - 6:50 AM UTC

[MIS08-13] Italian contribution to the CSES satellite mission

★Invited Papers

*Livio Conti[1], Group the CSES-Limadou Collaboration (1.Uninettuno University)

3:50 PM - 4:10 PM JST | 6:50 AM - 7:10 AM UTC

[MIS08-14] A focus on the capability of the RST-based satellite TIR anomalies for the short-term seismic hazard assessment in Japan

★Invited Papers

*Nicola Genzano[1], Roberto Colonna[1], Carolina Filizzola[2], Katsumi Hattori[3,4], Mariano Lisi[2], Nicola Pergola[2], Valerio Tramutoli[1] (1.School of Engineering, University of Basilicata, Via dell' Ateneo Lucano, 10, 85100 Potenza, Italy, 2.National Research Council, Institute of Methodologies for Environmental Analysis, C. da S. Loja, 85050 Tito Scalo (Pz), Italy, 3.Graduate School of Science, Chiba University, Yayoi 1-33, Inage, Chiba, 263-8522, Japan, 4.Center for Environmental Remote Sensing, Chiba University, Yayoi 1-33, Inage, Chiba, 263-8522, Japan)

4:10 PM - 4:30 PM JST | 7:10 AM - 7:30 AM UTC

[MIS08-15] Radon Monitoring in the Gulf of Corinth, Greece

★Invited Papers

*VASSILIOS KARASTATHIS[1], G Elefteriou[1], M. Kafatos[2], K. Tsinganos[3], G Tselentis[1], D. Ouzounov[2], E Mouzakiotis[1] (1.National Observatory of Athens, 2.Chapman University, 3.National and Kapodistrian University of Athens)

4:30 PM - 4:50 PM JST | 7:30 AM - 7:50 AM UTC

[MIS08-16] Earth's crust as a new element of the LAIC model within the Global Electric Circuit concept

★Invited Papers

*Sergey A Pulinets[1], V. Gavrilov[2], V. Bogdanov[3], N. Blaustein[4] (1.Space Research Institute of the Russian Academy of Sciences, 2.Institute of Volcanology and Seismology, Far-East Branch of the Russian Academy of Sciences, 3.Institute of Cosmophysical Research and Radio Wave Propagation, Far-East Branch of the Russian Academy of Sciences, 4.Ben-Gurion University of the Negev, Israel)

4:50 PM - 5:00 PM JST | 7:50 AM - 8:00 AM UTC

[MIS08-17] Discussion

[E] Poster | M (Multidisciplinary and Interdisciplinary)：M-IS Intersection

5:15 PM - 6:30 PM JST | 8:15 AM - 9:30 AM UTC | Ch.19_1

[M-IS08] Interdisciplinary studies on pre-earthquake processes

convener:Katsumi Hattori(Department of Earth Sciences, Graduate School of Science, Chiba University), Dimitar Ouzounov(Center of Excellence in Earth Systems Modeling & Observations (CEESMO) , Schmid College of Science & Technology Chapman University, Orange, California, USA), Jann-Yenq LIU(Department of Space Science and Engineering, National Central University, Taiwan), Qinghua Huang(Peking University)

[MIS08-P01] Detecting clustered pre-earthquake anomalies of borehole strain network by Receiver Operating Characteristic Curve

★Invited Papers

*Zining Yu[1,2], Katsumi Hattori[3,4], Kaiguang Zhu[1,2], Mengxuan Fan[1,2], Dedalo Marchetti[2,5] (1.Key Laboratory of Geo-Exploration Instrumentation, Ministry of Education, Jilin University, Changchun 130061, China, 2.The College of Instrumentation and Electrical Engineering, Jilin University, Changchun 130061, China, 3.Graduate School of Science, Chiba University, Inage, Chiba 263-8522, Japan, 4.Center for Environmental Remote Sensing, Chiba University, Inage, Chiba 263-8522, Japan, 5.Istituto Nazionale di Geofisica e Vulcanologia, Via di Vigna Murata, 605 Rome, 00143, Italy)

[MIS08-P02] Statistical Analysis of Pre-seismic Ionospheric Electron Density Anomalies and Investigation of the Efficiency of Earthquake Forecasting

*Shunya Mitsuishi[1], Chie Yoshino[2], Katsumi Hattori[2,3], Jann-Yenq LIU[4] (1.Department of Earth Sciences, Faculty of Science, Chiba University, Japan, 2.Graduate School of Science, Chiba University, Japan, 3.Center for Environmental Remote Sensing, Chiba University, Japan , 4.National Central University, Taiwan)

[MIS08-P03] The fluctuation of the underground Rn flux near the surface

*Kazuhide Nemoto[1], Haruna Kojima[2], Chie Yoshino[3], Shu Kaneko[2], Katsumi Hattori[3], Toshiharu Konishi[4], Ryuichi Huruya[5] (1.Faculty of Science, Chiba University, 2.Graduate School of Science and Engineering, Chiba University, 3.Graduate School of Science, Chiba University, 4.OHYO KOKEN KOGYO Company Limited, 5.COM SYSTEM Incorporated)

[MIS08-P04] Development of Broadband Antenna System for Observation of Pre-Earthquake Electromagnetic Phenomena in LF range and Its Initial Observations

*Miura Kenshin[1], Katsumi Hattori[1], Chie Yoshino[1], Notiyuki Imazumi[2], Takeshi Morimoto[3], Yoshitaka Nakamura[4] (1.Chiba University, 2.The Institution of Professional Engineers, Japan, Chiba Chapter, 3.Kindai University, 4.Kobe City Collage of Technology)

[MIS08-P05] Numerical estimation of source current intensity causing ULF emission associated with earthquakes and correlation with the earthquake magnitude

*Ryota Kimura[1], Yoshiaki Ando[1], Masashi Hayakawa[2], Katsumi Hattori[3] (1. The University of Electro-Communications, 2.Hayakawa Institute of Seismo ElectroMagnetics Co. Ltd., 3.Chiba University)

[MIS08-P06] Development of Noise Reduction Method using two-stage MSSA (Multichannel Singular Spectrum Analysis) for MT data in Boso, Japan, Evaluation in Time series

*Shu Kaneko[1], Katsumi Hattori[2], Toru Mogi[2], Chie Yoshino[2] (1.Chiba University Graduate School of Science and Engineering, 2.Chiba University Graduate School of Science)

[MIS08-P07] Correlations between geomagnetic *Sq* external and internal equivalent current systems in East-Asia and Oceania regions

*Xiaocan Liu[1], Peng Han[4], Katsumi Hattori[2,3], Huaran Chen[1], Chie Yoshino[2] (1.Institute of geophysics China Earthquake Administrition, 2.Graduate School of Science, Chiba University, Chiba, Japan, 3.Center for Environmental Remote Sensing, Chiba University, Chiba, Japan, 4.Department of Earth and Space Sciences, Southern University of Science and Technology, ShenZhen, China)

[J] Oral | M (Multidisciplinary and Interdisciplinary)：M-IS Intersection

9:00 AM - 10:30 AM JST | 12:00 AM - 1:30 AM UTC | Ch.25 Zoom Room 25

[M-IS13] Dynamics of eruption cloud and cumulonimbus; modelling and observation

convener:Eiichi Sato(Meteorological Research Institute), Fukashi Maeno(Earthquake Research Institute, University of Tokyo), Takeshi Maesaka(National Research Institute for Earth Science and Disaster Resilience), Chairperson:Eiichi Sato(Meteorological Research Institute)

9:00 AM - 9:15 AM JST | 12:00 AM - 12:15 AM UTC

[MIS13-01] Radar Meteorological Study on Falling Volcaic Ash Particles

★Invited Papers

*Masayuki Maki[1] (1.Research and Education Center for Natural Hazards, Kagoshima University)

9:15 AM - 9:30 AM JST | 12:15 AM - 12:30 AM UTC

[MIS13-02] PUFF Model Prediction of Volcanic Ash Plume Dispersal for Sakurajima Using MP Radar Observation

*Hiroshi Tanaka[1], Haruhisa Nakamichi[2], Masato Iguchi[2] (1.Center for Computational Sciences, University of Tsukuba, 2.Sakurajima Volcano Research Center, DPRC, Kyoto University, Kagoshima)

9:30 AM - 9:45 AM JST | 12:30 AM - 12:45 AM UTC

[MIS13-03] Numerical simulation of wind flow around Sakurajima with eruption

*Takashi Maruyama[1], Masato Iguchi[1] (1.Disaster Prevention Research Institute, Kyoto University)

9:45 AM - 10:00 AM JST | 12:45 AM - 1:00 AM UTC

[MIS13-04] Highspeed image observation of ballistic projectiles at Sakurajima volcano and a numerical model of ballistics

*Kae Tsunematsu[1], Saruta Shusaku[1], Taishi Yamada[2], Masato Iguchi[2] (1.Yamagata University, 2.Kyoto University)

10:00 AM - 10:15 AM JST | 1:00 AM - 1:15 AM UTC

[MIS13-05] Pattern classification of parent clouds of tornadoes in Tosa Bay

*Koji Sassa[1], Kotarou Fujii[2] (1.Natural Science Cluster, Kochi University, 2.Graduate School of Integrated Arts and Sciences, Kochi University)

10:15 AM - 10:30 AM JST | 1:15 AM - 1:30 AM UTC

[MIS13-06] Cloud-Scientific Study of Volcano Eruption -perspective-

★Invited Papers

*Yasushi Fujiyoshi[1] (1.Emeritus Prof. of Hokkaido University)

[J] Poster | M (Multidisciplinary and Interdisciplinary)：M-IS Intersection

5:15 PM - 6:30 PM JST | 8:15 AM - 9:30 AM UTC | Ch.19_2

[M-IS13] Dynamics of eruption cloud and cumulonimbus; modelling and observation

convener:Eiichi Sato(Meteorological Research Institute), Fukashi Maeno(Earthquake Research Institute, University of Tokyo), Takeshi Maesaka(National Research Institute for Earth Science and Disaster Resilience)

[MIS13-P01] Estimation of ash refractive index and improvement of Himawari-8 volcanic ash algorithm

★Invited Papers

*Hiroshi Ishimoto[1], Masahiro Hayashi[1], Yuzo Mano[1], Rei Kudo[1] (1.Meteorological Research Institute)

[MIS13-P02] Multi-sensor observation of cloud evolution from cumulus to cumulonimbus in Tokyo metropolitan area

*Takeshi Maesaka[1], Tadayasu Ohigashi[1], Koyuru Iwanami[1], Shin-ichi Suzuki[1], Namiko Sakurai[1], Yukari Shusse[1], Kaori Kieda[1], Shingo Shimizu[1], Yasushi Uji[1], Nobuhiro Takahashi[2], Hiroshi Hanado[3], Katsuhiro Nakagawa[3], Tomoo Ushio[4] (1.National Research Institute for Earth Science and Disaster Resilience, 2.Nagoya University, 3.National Institute of Information and Communications Technology, 4.Osaka University)

[MIS13-P03] Application to the volcanic ash obserbation of the X-band solid state marine radar

*Takaaki NISHI[1], Masayuki MAKI[1], Takehiko KOBORI[1], Kanji ENDO[2], Kazuhiko KAIGA[2], Masato IGUCHI[3] (1.Kagoshima Univ., 2.Koden Electronics Co., Ltd, 3.Kyoto Univ.)

[MIS13-P04] Modification of probabilistic estimation method for eruption plume height using weather radars

*Eiichi Sato[1] (1.Meteorological Research Institute)

[MIS13-P05] Ash fall observation using 2D-Video Disdrometer (2)

*Eiichi Sato[1], Kosei Takishita[2], Masato Iguchi[3] (1.Meteorological Research Institute, 2.Division of Earth and Planetary Sciences, Graduate School of Science, Kyoto University, 3.Sakurajima Volcano Research Center, Disaster Prevention Research Institute, Kyoto University)

[MIS13-P06] Sedimentary process of ash deposits from long-term activity of repeated vulcanian eruptions at Sakurajima volcano, Japan

*Takahiro Miwa[1], Futoshi Nanayama[2] (1.National research institute for earth science and disaster resilience, 2.Geological Survey of Japan, AIST)

[J] Oral | M (Multidisciplinary and Interdisciplinary)：M-IS Intersection

1:45 PM - 3:15 PM JST | 4:45 AM - 6:15 AM UTC | Ch.17 Zoom Room 17

[M-IS15] Tsunami deposit: research progress after the 2011 Tohoku-oki earthquake and prospects

convener:Masaki Yamada(Department of Geology, Faculty of Science, Shinshu University), Takashi Ishizawa(International Research Institute of Disaster Science, Tohoku University), Masashi Watanabe(Chuo University), Koichiro Tanigawa(Geological Survey of Japan, National Institute of Advanced Industrial Science and Technology), Chairperson:Masaki Yamada(Department of Geology, Faculty of Science, Shinshu University), Takashi Ishizawa(International Research Institute of Disaster Science, Tohoku University)

1:45 PM - 2:15 PM JST | 4:45 AM - 5:15 AM UTC

[MIS15-01] Sedimentation and erosion by the 2011 Tohoku-oki tsunami

★Invited Papers

*Kazuhisa Goto[1] (1.Department of Earth and Planetary Science, The University of Tokyo)

2:15 PM - 2:45 PM JST | 5:15 AM - 5:45 AM UTC

[MIS15-02] How much we had understood a history of giant earthquakes along the Japan trench - progress and remaining problems-

★Invited Papers

*Yuki Sawai[1] (1.Geological Survey of Japan, AIST)

2:45 PM - 3:15 PM JST | 5:45 AM - 6:15 AM UTC

[MIS15-03] Advances in tsunami numerical modeling after the 2011 Tohoku earthquake and future challenges related to tsunami deposit research

★Invited Papers

*Daisuke Sugawara[1] (1.International Research Institute of Disaster Science, Tohoku University)

[J] Oral | M (Multidisciplinary and Interdisciplinary)：M-IS Intersection

3:30 PM - 5:00 PM JST | 6:30 AM - 8:00 AM UTC | Ch.17 Zoom Room 17

[M-IS15] Tsunami deposit: research progress after the 2011 Tohoku-oki earthquake and prospects

convener:Masaki Yamada(Department of Geology, Faculty of Science, Shinshu University), Takashi Ishizawa(International Research Institute of Disaster Science, Tohoku University), Masashi Watanabe(Chuo University), Koichiro Tanigawa(Geological Survey of Japan, National Institute of Advanced Industrial Science and Technology), Chairperson:Masashi Watanabe(Chuo University), Koichiro Tanigawa(Geological Survey of Japan, National Institute of Advanced Industrial Science and Technology)

3:30 PM - 4:00 PM JST | 6:30 AM - 7:00 AM UTC

[MIS15-04] **Application of DNN inverse model to large scale tsunamis to reconstruct the flow conditions of modern and ancient tsunamis**

★Invited Papers

*Rimali Mitra[1], Hajime Naruse[1], Tomoya Abe[2], Shigehiro Fujino[3], Daisuke Sugawara[4] (1.Kyoto University, Graduate School of Science, 2.Research Institute of Geology and Geoinformation, Geological Survey of Japan, National Institute of Advanced Industrial Science and Technology (AIST), Tsukuba, Japan, 3.University of Tsukuba, 4.Tohoku University, IRIDeS)

4:00 PM - 4:15 PM JST | 7:00 AM - 7:15 AM UTC

[MIS15-05] Analysis of the Response of Tsunami Sediment Transport Numerical Simulation to Parameter Uncertainty

*Hidetoshi Masuda[1], Daisuke Sugawara[2], Shuro Yoshikawa[3], Hideyuki Sakurai[3], Fumihiko Imamura[2] (1.Division of Geoenviromental Science, Faculty of Science, Tohoku University, 2.International Research Institute of Disaster Science, Tohoku University, 3.Institute of Technology, Shimizu Corporation)

4:15 PM - 4:30 PM JST | 7:15 AM - 7:30 AM UTC

[MIS15-06] Event deposits in Lake Jusan, western part of Aomori Prefecture, NE Japan

*Fumika Hirano[1], Atsushi Urabe[2] (1.Faculty of Science, Niigata University, 2.Research Institute for Natural Hazards and Disaster Recovery, Niigata University)

4:30 PM - 4:45 PM JST | 7:30 AM - 7:45 AM UTC

[MIS15-07] Features of 17th-century tsunami deposits formed by tsunami crossing river channel and detection using X-ray computed tomography

*Kohei Iwaki[1], Yasuhiro Takashimizu[2], Yuichi Nishimura[3], Takashi Chiba[4] (1.Graduate School of Science and Technology, Niigata University, 2.Mathematical and Natural Sciences, Institute of Humanities, Social Sciences and Education, Niigata University, 3.Graduate School of Science, Hokkaido University, 4.Faculty of Bioresource Sciences, Akita Prefectural University)

4:45 PM - 5:00 PM JST | 7:45 AM - 8:00 AM UTC

[MIS15-08] Identification of invisible tsunami deposits formed by the 2011 Tohoku-oki tsunami

*Tetsuya Shinozaki[1], Yuki Sawai[1], Dan Matsumoto[1], Koichiro Tanigawa[1] (1.Geological Survey of Japan, National Institute of Advanced Industrial Science and Technology)

[J] Poster | M (Multidisciplinary and Interdisciplinary)：M-IS Intersection

5:15 PM - 6:30 PM JST | 8:15 AM - 9:30 AM UTC | Ch.19_3

[M-IS15] Tsunami deposit: research progress after the 2011 Tohoku-oki earthquake and prospects

convener:Masaki Yamada(Department of Geology, Faculty of Science, Shinshu University), Takashi Ishizawa(International Research Institute of Disaster Science, Tohoku University), Masashi Watanabe(Chuo University), Koichiro Tanigawa(Geological Survey of Japan, National Institute of Advanced Industrial Science and Technology)

[MIS15-P01] A study for correlation of mega-tsunami in the Kuril Trench based on the tsunami deposits in the Erimo area, Hokkaido

*RYO NAKANISHI[1], Juichiro Ashi[1,2], Yosuke Miyairi[1], Yusuke Yokoyama[1,3] (1.Atmosphere and Ocean Research Institute, The University of Tokyo, 2.Graduate School of Frontier Science, The University of Tokyo, 3.Department of Earth and Planetary Sciences, Graduate School of Science, The University of Tokyo)

[MIS15-P02] Characteristics of event deposits and their distributions based on a drilling survey in Sekine-hama, the northern part of the Shimokita Peninsula, Aomori Prefecture

*Daisuke Ishimura[1], Masaki Yamada[2], Takashi Ishizawa[3], Kaori Aoki[4], Kai Sato[2] (1.Department of Geography, Tokyo Metropolitan University, 2.Department of Geology, Faculty of Science, Shinshu University, 3.International Research Institute of Disaster Science, Tohoku University, 4. Research Center for Volcanic Hazards and Their Mitigation, Tokyo Metropolitan University)

[MIS15-P03] Tsunami source estimation of paleotsunami deposits formed in the 17th century at Sekinehama, northern Shimokita Peninsula, Aomori Prefecture

*Kai Sato[1], Masaki Yamada[1], Daisuke Ishimura[2], Takashi Ishizawa[3], Toshitaka Baba[4] (1.Depatment of Geology, Faculty of Science, Shiushu University, 2.Department of Geography, Tokyo Metropolitan University , 3.International Research Institute of Disaster Science, Tohoku University, 4.Graduate School of Science and Technology, Tokushima University)

[MIS15-P04] Revised paleotsunami history at Kirikiri, Northeast Japan

*Takashi Ishizawa[1], Yusuke Yokoyama[2], Yosuke Miyairi[2] (1.International Research Institute of Disaster Science, Tohoku University, 2.Atmosphere and Ocean Research Institute, the University of Tokyo)

[MIS15-P05] Distribution and characteristics of the 1983 Nihonkai-chubu earthquake tsunami deposit along the Akita coastal area, Japan

*Takashi Chiba[1], Yuichi Nishimura[2] (1.Faculty of Bioresource Sciences, Akita Prefectural University, 2.Institute of Seismology and Volcanology (ISV), Faculty of Science, Hokkaido University)

[MIS15-P06] Event deposits in a coastal lake at Minami-ise Town, Mie Prefecture during the last 3000 years

*Yumi Shimada[1], Yuki Sawai[1], DAN MATSUMOTO[1], Koichiro Tanigawa[1], Yuichi Namegaya[1], Masanobu Shishikura[1], Kazumi Ito[1], Toru Tamura[1], Shigehiro Fujino[2] (1.Geological Survey of Japan, AIST, 2.Faculty of Life and Environmental Sciences, University of Tsukuba)

[MIS15-P07] Distributions and occurrences of sandy tsunami deposits in caves located along the East Coast of Ishigaki Island, Okinawa Prefecture

*Yoshiro Ishihara[1], Miyu Kitahara[1], Yuuka Okita[1], Ayano Shimabukuro[2], Hajime Naruse[3], Chiaki Katagiri[4], Rintaro Ono[5], Kazuhisa Yoshimura[6] (1. Fukuoka Univ., 2.Yaeyama Museum, 3.Kyoto Univ., 4.Okinawa Prefectural Archaeological Center, 5.National Museum of Ethnology, 6.Kyushu Univ.)

[MIS15-P08] Examining grain-size changes in sediment transport modeling of the 2011 Tohoku-oki tsunami in the Sendai Plain

*Wataru Nakamura[1], Daisuke Sugawara[1] (1.Tohoku University)

[MIS15-P09] Comparison of Observations and Numerical Simulations of Sediment Transport Using the 1707 CE Hoei Tsunami Source Model: Application to Kanigaike Pond in Kochi Prefecture, Japan

*Satoshi Kusumoto[1], Kentaro Imai[1], Narumi Takahashi[2,1], Takane Hori[1], Daisuke Sugawara[3] (1.JAMSTEC, 2.NIED, 3.Tohoku University)

[MIS15-P10] Uncertainty of geological information used in identification of tsunami deposit - Preliminary assessment –

*Takumi Yoshii[1], Takaomi Hamada[1], Yuki Ito[1], Shiro Tanaka[1], Masafumi Matsuyama[1] (1.Central Research Institute of Electric Power Industry)

[J] Oral | M (Multidisciplinary and Interdisciplinary)：M-IS Intersection

9:00 AM - 10:30 AM JST | 12:00 AM - 1:30 AM UTC | Ch.16 Zoom Room 16

[M-IS22] Geopark

convener:Takayuki Arima(Yokohama City University), Keiichi Tadokoro(Research Center for Seismology, Volcanology and Earthquake and Volcano Research Center, Nagoya University), Marekazu OHNO(Unzen Volcanic Area Geopark Promotion Office), Takayuki Ogata(Graduate School of Engineering and Science, University of the Ryukyus), Chairperson:Tatsuto Aoki(School of Regional Development Studies, Kanazawa University), Noritaka Matsubara(Graduate School of Regional Resource Management, University of Hyogo), Takayuki Arima(Yokohama City University)

9:00 AM - 9:15 AM JST | 12:00 AM - 12:15 AM UTC

[MIS22-01] Academic Support for Geoparks: Efforts of the Geopark Assistance Committee, the Seismological Society of Japan

★Invited Papers

*Yoshihiro Hiramatsu[1] (1.School of Geosciences and Civil Engineering, College of Science and Engineering, Kanazawa University)

9:15 AM - 9:30 AM JST | 12:15 AM - 12:30 AM UTC

[MIS22-02] Preservation and utilization of earth heritage in Japan's natural monument system

★Invited Papers

*Tadahiro Shibata[1] (1.The Unit of Natural Monuments, Monuments and Sites Division, Cultural Properties Department, Agency for Cultural Affaire)

9:30 AM - 9:45 AM JST | 12:30 AM - 12:45 AM UTC

[MIS22-03] Developing virtual field experience with high-resolution panorama (GigaPans) at multiple scales: Constructing a core technology for online geotours

*Norihito Kawamura[1], Takashi Sawaguchi[2] (1.School of Regional Resource Management, Graduate School, University of Hyogo, 2.Toyo University)

9:45 AM - 10:00 AM JST | 12:45 AM - 1:00 AM UTC

[MIS22-04] Subaqueous volcanic rocks as the object for the geo tourism-related to NHK Buratamori and geoparks

*Hiromitsu Yamagishi[1], Yoshiaki Matsuda[1], Kazuo Shimura[2] (1.NPO Hokkaido Research Center of Geology(HRCG), 2.Shin Engineering Consultant)

10:00 AM - 10:15 AM JST | 1:00 AM - 1:15 AM UTC

[MIS22-05] Disaster risk reduction in Geopark from social geographical approach : focusing on social capital for community resilience

*Akifumi Nakamura[1] (1.Muroto Geopark Promotion Committee)

10:15 AM - 10:30 AM JST | 1:15 AM - 1:30 AM UTC

[MIS22-06] The Land Use Change and Socio-economic Impact of Baiyankeng Geo-cultural Village, China

*Wenqi ZHAO[1] (1.University of Tsukuba)

[J] Poster | M (Multidisciplinary and Interdisciplinary)：M-IS Intersection

5:15 PM - 6:30 PM JST | 8:15 AM - 9:30 AM UTC | Ch.22_2

[M-IS22] Geopark

convener:Takayuki Arima(Yokohama City University), Keiichi Tadokoro(Research Center for Seismology, Volcanology and Earthquake and Volcano Research Center, Nagoya University), Marekazu OHNO(Unzen Volcanic Area Geopark Promotion Office), Takayuki Ogata(Graduate School of Engineering and Science, University of the Ryukyus)

[MIS22-P01] Scientific Roles of the JpGU Session "Geopark"

*Takayuki Ogata[1] (1.Graduate School of Engineering and Science, University of the Ryukyus)

[MIS22-P02] Discussion

[J] Oral | M (Multidisciplinary and Interdisciplinary)：M-IS Intersection

9:00 AM - 10:30 AM JST | 12:00 AM - 1:30 AM UTC | Ch.10 Zoom Room 10

[M-IS24] Geophysical fluid dynamics-Transfield approach to geoscience

convener:Keita Iga(Atmosphere and Ocean Research Institute, The University of Tokyo), Shigeo Yoshida(Department of Earth and Planetary Sciences, Faculty of Sciences, Kyushu University), Takatoshi Yanagisawa(Research Institute for Marine Geodynamics, Japan Agency for Marine-Earth Science and Technology), Hidenori AIKI(Nagoya University), Chairperson:Kensuke Nakajima(Department of Earth and Planetary Sciences,Flculty of Sciences,Kyushu University)

9:00 AM - 9:15 AM JST | 12:00 AM - 12:15 AM UTC

[MIS24-01] Balance of baroclinicity and restoring force due to stable temperature stratification in developing horizontal convection in a finite fluid layer

*Tomomi Terada[1], Daisuke Noto[1], Yuji Tasaka[2], Takatoshi Yanagisawa[3,2], Takehiro Miyagoshi[3], Yuichi Murai[2] (1.Graduate School of Engineering, Hokkaido University , 2.Faculty of Engineering, Hokkaido University, 3.Japan Agency for Marine-Earth Science and Technology)

9:15 AM - 9:30 AM JST | 12:15 AM - 12:30 AM UTC

[MIS24-02] Quasi-periodic oscillations of convection patterns and heat transport in horizontally finite geometries

*Takatoshi Yanagisawa[1], Megumi Akashi[2], Yuji Tasaka[3], Ataru Sakuraba[4] (1.Research Institute for Marine Geodynamics, Japan Agency for Marine-Earth Science and Technology, 2.Institute of Fluid Dynamics, Helmholtz-Zentrum Dresden-Rossendorf, 3.Faculty of Engineering, Hokkaido University, 4.Department of Earth and Planetary Science, University of Tokyo)

9:30 AM - 9:45 AM JST | 12:30 AM - 12:45 AM UTC

[MIS24-03] Cyclonic-anticyclonic asymmetry on maintained vortices near the westerlies focused on external vortices

*Koryu Yamamoto[1], Keita Iga[1] (1.Atmosphere and Ocean Research Institute, The University of Tokyo)

9:45 AM - 10:00 AM JST | 12:45 AM - 1:00 AM UTC

[MIS24-04] High-frequency measurement of a double helical vortex with a sonic anemometer thermometer for laboratory use

*Toshihisa Itano[1] (1.National Defense Academy)

10:00 AM - 10:15 AM JST | 1:00 AM - 1:15 AM UTC

[MIS24-05] Numerical experiments of surface flows on giant planets produced by forcings representing thunderstorms

Ryoma Suzuki[2], *Youhei SASAKI[1], Masaki Ishiwatari[3] (1.Institute of Fundamental Sciences, Faculity of Science and Engineering, Setsunan University, 2.Department of Cosmosciences, Graduate School of Science, Hokkaido University, 3.Department of Earth and Planetary Sciences, Faculty of Science, Hokkaido University)

10:15 AM - 10:30 AM JST | 1:15 AM - 1:30 AM UTC

[MIS24-06] Discussion

[J] Poster | M (Multidisciplinary and Interdisciplinary)：M-IS Intersection

5:15 PM - 6:30 PM JST | 8:15 AM - 9:30 AM UTC | Ch.18_2

[M-IS24] Geophysical fluid dynamics-Transfield approach to geoscience

convener:Keita Iga(Atmosphere and Ocean Research Institute, The University of Tokyo), Shigeo Yoshida(Department of Earth and Planetary Sciences, Faculty of Sciences, Kyushu University), Takatoshi Yanagisawa(Research Institute for Marine Geodynamics, Japan Agency for Marine-Earth Science and Technology), Hidenori AIKI(Nagoya University)

[MIS24-P01] Two-dimensional ideal MHD waves and the continuous Alfvén spectrum on a rotating sphere with a background toroidal magnetic field

*Ryosuke Nakashima[1], Shigeo Yoshida[2] (1.Faculty of Science, Kyushu University, 2.Department of Earth and Planetary Sciences, Faculty of Science, Kyushu University)

[MIS24-P02] Development of sea surface wave breaking observation system using industrial millimeter radar and optical particle size counter

*Hidenori AIKI[1], Fumiyoshi Kondo[2], Haruya Minda[1] (1.Nagoya University, 2.Japan Coast Guard Academy)

[MIS24-P03] Axisymmetric flows and non-axisymmetric phenomena in a cylindrical tank with a rotating bottom

*Keita Iga[1] (1.Atmosphere and Ocean Research Institute, The University of Tokyo)

[MIS24-P04] We examined **Origin of Great Red Spot of Jupiter, Deep Ocean Floor, Pacific Rim Arcuate Archipelago, Origin of Gomagnetic Reversal, and Origin of Asteroid Belt.**

*Akira Taneko[1] (1.SEED SCIENCE Lab.)

[J] Oral | M (Multidisciplinary and Interdisciplinary)：M-IS Intersection

9:00 AM - 10:30 AM JST | 12:00 AM - 1:30 AM UTC | Ch.11 Zoom Room 11

[M-IS25] Atmospheric electricity: Electrical phenomena associated with extreme weather

convener:Yasuhide Hobara(Graduate School of Information and Engineering Department of Communication Engineering and Informatics, The University of Electro-Communications), Daohong Wang(Gifu University), Chairperson:Yasuhide Hobara(Graduate School of Information and Engineering Department of Communication Engineering and Informatics, The University of Electro-Communications), Daohong Wang(Gifu University)

9:00 AM - 9:15 AM JST | 12:00 AM - 12:15 AM UTC

[MIS25-01] Understanding of fine structure of cumulonimbus using new observational method

★Invited Papers

*Fumiaki Kobayashi[1] (1.National Defense Academy)

9:15 AM - 9:30 AM JST | 12:15 AM - 12:30 AM UTC

[MIS25-02] Various common meteorological characteristics obtained by multiple observation results of downburst

*Hisato Iwashita[1], Fumiaki Kobayashi[2] (1.Meisei Electric Co.,Ltd, 2.National Defense Academy)

9:30 AM - 9:45 AM JST | 12:30 AM - 12:45 AM UTC

[MIS25-03] Observations of summer thunderstorms using dual polarized phased array weather radar and three-dimensional lightning location system using LF band in Kanto area

*Hiroshi Kikuchi[1], Yuhei Kamei[1], Yoshitaka Nakamura[3], Eiichi Yoshikawa[5], Takeshi Morimoto[4], Tomoo Ushio[2], Yasuhide Hobara[1] (1.The University of Electro Communications, 2.Osaka University, 3.Kobe City College of Technology, 4.Kinki University, 5.Japan Aerospace Exploration Agency)

9:45 AM - 10:00 AM JST | 12:45 AM - 1:00 AM UTC

[MIS25-04] 3D characteristics of lightning activity in Typhoon Faxai (2019)

*Namiko Sakurai[1], Hironori Fudeyasu[2], Paul R. Krehbiel[3], Ronald J. Thomas[3], William Rison[4], Daniel Rodeheffer[4] (1.National Research Institute For Earth Science and Disaster Prevention, 2.Yokohama National University, 3.New Mexico Tech, 4.LMA technologies)

10:00 AM - 10:15 AM JST | 1:00 AM - 1:15 AM UTC

[MIS25-05] Citizen science "Thundercloud project" for mapping observations of gamma rays from thunderstorms

*Teruaki Enoto[1], Yuko Ikkatai[2], Yuuki Wada[1], Gabriel Diniz[1], Masaki Numazawa[1], Yo Kato[1], Shoko Miyake[3], Kazuhiro Nakazawa[4], Shohei Hisadomi[4], Yuna Tsuji[4], Takayuki Yuasa, Harufumi Tsuchiya[5], Takeshi Morimoto[6], Yoshitaka Nakamura[7], Masashi Kamogawa[8] (1.RIKEN, 2.The University of Tokyo, 3.National Institute of Technology, Ibaraki College, 4.Nagoya University, 5.JAEA, 6.Kinki University, 7.Kobe City College of Technology, 8.Global Center for Asian and Regional Research, University of Shizuoka)

10:15 AM - 10:30 AM JST | 1:15 AM - 1:30 AM UTC

[MIS25-06] Radioluminescence appeared above the epicenter immediately before and after the 1995 Kobe earthquake

*Yuji Enomoto[1], Tsuneaki Yamabe[1], Shigeki Sugiura[2], Hitoshi Kondo[2] (1.Shinshu Univeristy, Ueda Campus Fii, 2.Genesis Research Institute Inc.)

[J] Poster | M (Multidisciplinary and Interdisciplinary)：M-IS Intersection

5:15 PM - 6:30 PM JST | 8:15 AM - 9:30 AM UTC | Ch.18_3

[M-IS25] Atmospheric electricity: Electrical phenomena associated with extreme weather

convener:Yasuhide Hobara(Graduate School of Information and Engineering Department of Communication Engineering and Informatics, The University of Electro-Communications), Daohong Wang(Gifu University)

[MIS25-P01] X-band radar and disdrometer observations of winter thunderclouds emitting gamma rays

*Yuuki Wada[1], Teruaki Enoto[1], Mamoru Kubo[2], Kazuhiro Nakazawa[3], Taro Shinoda[3], Daisuke Yonetoku[2], Tatsuya Sawano[2], Takayuki Yuasa, Tomoo Ushio[4], Yousuke Sato[5], Gabriel Sousa Diniz[1], Harufumi Tsuchiya[6] (1.RIKEN, 2.Kanazawa University, 3.Nagoya University, 4.Osaka University, 5.Hokkaido University, 6.JAEA)

[MIS25-P02] Observation of thundercloud gamma-rays in FY2020 with the GOOSE detector aiming at altitude measurements

*Yuuna Tsuji[1], Kazuhiro Nakazawa[1], Shohei Hisadomi[1], Yusaku Ikami[1], Daiki Odani[1], Teruaki Enoto[2], Yuuki Wada[2], Takayuki Yuasa, Harufumi Tsuchiya[3], Taro Shinoda[4], Keigo Ookuma[1], Gabriel Diniz[2] (1.Nagoya University, 2.RIKEN, 3.JAEA, 4.ISEE. Nagoya Univ.)

[MIS25-P03] Hydrometeor distribution in a thundercloud related to a gamma-ray emission event

*Takemoto Kiyomichi[1], Taro Shinoda[1], Masaya Kato[1], Shohei Hisadomi[2], Yuuna Tsuji[2], Kazuhiro Nakazawa[2], Yuuki Wada[3], Teruaki Enoto[3] (1.Institute for Space-Earth Environmental Research, Nagoya University, 2.Department of Physics, Nagoya University, 3.Institute of Physical and Chemical Research)

[MIS25-P04] A Study of 3D Precipitation Core Tracking Method Using Multi-Parameter Phased Array Weather Radar

*Keitaro Asai[1], Hiroshi Kikuchi[1], Yasuhide Hobara[1], Tomoo Ushio[2] (1.The University of Electro Communications, 2.Osaka University)

[MIS25-P05] Special negative lightning strokes in winter with extremely short preceding discharges

*Ting Wu[1], Daohong Wang [1], Nobuyuki Takagi[1] (1.Gifu University)

[MIS25-P06] **Simultaneous Observations of a Winter Lightning Flash in Japan**

*Haitao Huang[1], Daohong Wang[1], Ting Wu[1], Nobuyuki Takagi[1] (1.Gifu University)

[MIS25-P07] Spatio-temporal characteristics of lightning energy in Southeast Asia deduced from ELF observations

*Shunsuke Akama[1], Shu Hirai[1], Yasuhide Hobara[1], Hiroshi Kikuchi[1], Amir Izzani Mohamed[2], Chandima Gomes[3], Kazuo Shiokawa[4], Michael Stock[5] (1.The University of Electro-Communications, 2.University of Malaysia, Pahang, 3.University of the Witwatersrand, Johannesburg, 4.Institute for Space–Earth Environmental Research, 5.Earth Networks)

[MIS25-P08] Sprites observed from the summit of Mt. Fuji and their parent thunderstorm

*Suzuki Tomoyuki[1], Masashi Kamogawa[1], Syugo Hayashi[2] (1.University of Shizuoka, 2.Meteorological Research Institute)

[MIS25-P09] Coupling process of large-scale atmospheric disturbances to the ionosphere through typhoon

*Shu Hirai[1], Yasuhide Hobara[1], Hiroshi Kikuchi[1], Michael Stock[2] (1.The University of Electro-Communications, 2.Earth Networks)

[J] Oral | M (Multidisciplinary and Interdisciplinary)：M-IS Intersection

1:45 PM - 3:15 PM JST | 4:45 AM - 6:15 AM UTC | Ch.12 Zoom Room 12

[M-IS26] Gas hydrates in environmental-resource sciences

convener:Hitoshi Tomaru(Department of Earth Sciences, Chiba University), Akihiro Hachikubo(Kitami Institute of Technology), Atsushi Tani(Department of Human Environmental Science, Graduate School of Human Development and Environment, Kobe University), Shusaku Goto(Institute for Geo-Resources and Environment National Institute of Advanced Industrial Science and Technology), Chairperson:Hitoshi Tomaru(Department of Earth Sciences, Chiba University), Shusaku Goto(Institute for Geo-Resources and Environment National Institute of Advanced Industrial Science and Technology)

1:45 PM - 2:05 PM JST | 4:45 AM - 5:05 AM UTC

[MIS26-01] Massive seafloor methane release near the edge of the gas hydrate stability zone in southern Brazil

★Invited Papers

*Marcelo Ketzer[1], Daniel Praeg[2], Luiz F. Rodrigues[3], Adolpho Augustin[3], Maria A. G. Pivel[4], Mahboubeh Rahmati-Abkenar[1], Dennis J. Miller[5], Adriano R. Viana[5], José A. Cupertino[3] (1.Department of Biology and Environmental Science, Faculty of Health and Life Sciences, Linnaeus University, 2.Géoazur, 3.Petroleum and Natural Resources Institute, Pontificia Universidade Catolica do Rio Grande do Sul, 4.Instituto de Geociências, Universidade Federal do Rio Grande do Sul, 5.Petrobras)

2:05 PM - 2:25 PM JST | 5:05 AM - 5:25 AM UTC

[MIS26-02] **Experimental Verification of CH_4-CO_2 Replacement Occurring in Natural Gas Hydrates for Energy Recovery and CO_2 Sequestration**

★Invited Papers

*Yongwon Seo[1] (1.Ulsan National Institute of Science and Technology, Republic of Korea)

2:25 PM - 2:45 PM JST | 5:25 AM - 5:45 AM UTC

[MIS26-03] **Gashydrate accumulations in the Asian Seas and perspective on comparable research in the Indo-Pacific Region**

★Invited Papers

*Renat B. Shakirov[1], Hitoshi Tomaru[2], Pawan Dewangan[3], Prakash Kumar[4], Anatoly Obzhirov[1], Ryo Matsumoto[5] (1.POI FEB RAS, 2.Chiba University, 3.CSIR-NIO, 4.CSIR-NGRI, 5.Meiji University)

2:45 PM - 3:00 PM JST | 5:45 AM - 6:00 AM UTC

[MIS26-04] High-resolution seafloor observation of a shallow methane hydrate area off Sakata, eastern margin of the Sea of Japan, using a three-dimensional pictorial mapping system

*Miho Asada[1], Mikio Satoh[1], Manabu Tanahashi[1], Toshiyuki Yokota[1], Shusaku Goto[1] (1.NATIONAL INSTITUTE OF ADVANCED INDUSTRIAL SCIENCE AND TECHNOLOGY (AIST))

3:00 PM - 3:15 PM JST | 6:00 AM - 6:15 AM UTC

[MIS26-05] Survey of methane hydrate off Tokachi, Pacific Ocean

*Satoshi Yamashita[1], Akihiro Hachikubo[1], Hirotoshi Sakagami[1], Masaaki Konishi[1], Kzutaka Tateyama[1], Hirotsugu Minami[1] (1.Kitami Institute of Technology)

[J] Oral | M (Multidisciplinary and Interdisciplinary)：M-IS Intersection

3:30 PM - 5:00 PM JST | 6:30 AM - 8:00 AM UTC | Ch.12 Zoom Room 12

[M-IS26] Gas hydrates in environmental-resource sciences

convener:Hitoshi Tomaru(Department of Earth Sciences, Chiba University), Akihiro Hachikubo(Kitami Institute of Technology), Atsushi Tani(Department of Human Environmental Science, Graduate School of Human Development and Environment, Kobe University), Shusaku Goto(Institute for Geo-Resources and Environment National Institute of Advanced Industrial Science and Technology), Chairperson:Akihiro Hachikubo(Kitami Institute of Technology), Atsushi Tani(Department of Human Environmental Science, Graduate School of Human Development and Environment, Kobe University)

3:30 PM - 3:45 PM JST | 6:30 AM - 6:45 AM UTC

[MIS26-06] Geochemical processes in surface sediments in a shallow gas hydrate reserve area off Sakata, eastern margin of the Japan Sea

*Yuki Ota[1], Masahiro Suzumura[1], Ayumi Tsukasaki[1], Atsushi Suzuki[1] (1.National Institute of Advanced Industrial Science and Technology)

3:45 PM - 4:00 PM JST | 6:45 AM - 7:00 AM UTC

[MIS26-07] Vp anomalies of gas hydrate-bearing sediments inferred from BSR and BGHS

*Ryo Matsumoto[1], Shiro Ohkawa[1] (1.Meiji University)

4:00 PM - 4:15 PM JST | 7:00 AM - 7:15 AM UTC

[MIS26-08] Purity and specific surface area of methane hydrate synthesized from fine ice powder and gas

*Daisuke Yahagi[1], Akihiro Hachikubo[1], Satoshi Takeya[2] (1.Kitami Institute of Technology, 2.National Institute of Advanced Industrial Science and Technology)

4:15 PM - 4:30 PM JST | 7:15 AM - 7:30 AM UTC

[MIS26-09] Three-dimensional nondestructive observation of natural methane hydrate

*Satoshi Takeya[1], Akihiro Hachikubo[2], Satoshi Yamashita[2], Hirotsugu Minami[2], Hirotoshi Sakagami[2], Kazuyuki Hyodo[3], Akio Yoneyama[4] (1.National Institute of Advanced Industrial Science and Technology, 2.Kitami Institute of Technology, 3.High Energy Accelerator Research Organization, 4.SAGA Light Source)

4:30 PM - 4:45 PM JST | 7:30 AM - 7:45 AM UTC

[MIS26-10] Concentration of helium at the formation of methane and helium mixed-gas hydrate

*Yuki Moriya[1], Hiromi Kimura[1], Akihiro Hachikubo[1], Satoshi Takeya[2] (1.Kitami Institute of Technology, 2.National Institute of Advanced Industrial Science and Technology)

4:45 PM - 5:00 PM JST | 7:45 AM - 8:00 AM UTC

[MIS26-11] **Simulation of methane hydrate formation in coarse-/fine-grained sediments in the Nankai Trough, Japan**

*CHAO XU[1] (1.Chiba University)

[J] Poster | M (Multidisciplinary and Interdisciplinary)：M-IS Intersection

5:15 PM - 6:30 PM JST | 8:15 AM - 9:30 AM UTC | Ch.21_1

[M-IS26] Gas hydrates in environmental-resource sciences

convener:Hitoshi Tomaru(Department of Earth Sciences, Chiba University), Akihiro Hachikubo(Kitami Institute of Technology), Atsushi Tani(Department of Human Environmental Science, Graduate School of Human Development and Environment, Kobe University), Shusaku Goto(Institute for Geo-Resources and Environment National Institute of Advanced Industrial Science and Technology)

[MIS26-P01] **Geochemical characteristics of headspace gas and pore water in shallow sediment from the Tatar Trough**

*Musashi Yokoyama[1], Ryo Murata[1], Hitoshi Tomaru[1], Ryo Matsumoto[2], A.V. Yatsuk[3], D.A. Shvalov[3] (1.Chiba University, 2.Meiji University, 3.V.I.Ilichev Pacific Oceanological Institute)

[MIS26-P02] Gas hydrate survey at the gas seepage area off Abashiri, the Sea of Okhotsk

*Yuki Moriya[1], Hiromi Kimura[1], Akihiro Hachikubo[1], Satoshi Yamashita[1], Hirotoshi Sakagami[1], Masaaki Konishi[1], Hirotsugu Minami[1], Yasuhito Uchida[2], Hiroshi Yamaguchi[3] (1.Kitami Institute of Technology, 2. Research Institute of Energy, Environment and Geology, Hokkaido Research Organization, 3.Kushiro Fisheries Research Institute, Hokkaido Research Organization)

[MIS26-P03] Total organic carbon and its carbon isotope ratio in subsurface sediments off Hokkaido area

*Daisuke Yahagi[1], Akihiro Hachikubo[1], Masaaki Konishi[1], Hirotoshi Sakagami[1], Hirotsugu Minami[1], Satoshi Yamashita[1], Yasuhito Uchida[2], Hiroshi Yamaguchi[3] (1.Kitami Institute of Technology, 2.Research Institute of Energy, Environment and Geology, Hokkaido Research Organization, 3.Kushiro Fisheries Research Institute, Hokkaido Research Organization)

[MIS26-P04] Characteristics of gas hydrate crystals and their hydrate-bound gases retrieved at the seepage field off Tokachi (the Pacific Ocean)

*Hiromi Kimura[1], Ryoya Kamata[1], Daisuke Yahagi[1], Yuki Moriya[1], Akihiro Hachikubo[1], Masaaki Konishi[1], Hirotoshi Sakagami[1], Hirotsugu Minami[1], Satoshi Yamashita[1] (1.Kitami Institute of Technology)

[MIS26-P05] Gas hydrate survey at the gas seepage area off Hidaka, the Pacific Ocean

*Ryoya Kamata[1], Hiromi Kimura[1], Akihiro Hachikubo[1], Hirotoshi Sakagami[1], Satoshi Yamashita[1], Masaaki Konishi[1], Hirotsugu Minami[1] (1.Kitami Institute Of Technology)

[MIS26-P06] Emission of hydrated gas from seafloor to water column in the western Oki Trough

*Hitoshi Tomaru[1], Tianyou Ze[1], Sonoka Ikemoto[1], Minori Chikada[1] (1.Department of Earth Sciences, Chiba University)

[MIS26-P07] Isotope fractionation between hydrate-bound and ambient gases - case study in Lake Baikal gas hydrates -

*Hiromi Kimura[1], Akihiro Hachikubo[1], Oleg Khlystov[2], Gennadiy Kalmychkov[3], Marc De Batist[4], Hirotoshi Sakagami[1], Hirotsugu Minami[1], Satoshi Yamashita[1] (1.Kitami Institute of Technology, 2.Limnological Institute, SB RAS, 3.Vinogradov Institute of Geochemistry, SB RAS, 4.Ghent University)

[MIS26-P08] Carbon isotope fractionation of carbon monoxide hydrate between gas and hydrate phases

*Hiromi Kimura[1], Akihiro Hachikubo[1], Satoshi Takeya[2] (1.Kitami Institute of Technology, 2.National Institute of Advanced Industrial Science and Technology (AIST))

[MIS26-P09] Hydrogen isotopic fractionation of methane at the formation of synthetic structure I and II gas hydrates

*Ryoya Kamata[1], Akihiro Hachikubo[1], Satoshi Takeya[2] (1.Kitami Institute Of Technology, 2.National Institute of Advanced Industrial Science and Technology (AIST))

[MIS26-P10] Experimental study of CO2 hydrate phase equilibrium in sediments

*Tatsuki Iwamoto[1], Hitoshi Tomaru[1] (1.Chiba University)

[MIS26-P11] Effect of temperature and pressure on hydration number of methane hydrate

*Akihiro Hachikubo[1], Ryoya Kamata[1], Hiromi Kimura[1], Yuta Komagata[1], Go Fuseya[1], Satoshi Takeya[2] (1.Kitami Institute of Technology, 2.National Institute of Advanced Industrial Science and Technology (AIST))

[J] Oral | M (Multidisciplinary and Interdisciplinary)：M-IS Intersection

1:45 PM - 3:15 PM JST | 4:45 AM - 6:15 AM UTC | Ch.16 Zoom Room 16

[M-IS27] History X Earth and Planetary Science

convener:Yasuyuki Kano(Earthquake Research Institute, The University of Tokyo), Hiroaki Isobe(Faculty of Fine Arts, Kyoto City University of Arts), Kei Yoshimura(Institute of Industrial Science, The University of Tokyo), kiyomi iwahashi(National Institute of Japanese Literature), Chairperson:Yasuyuki Kano(Earthquake Research Institute, The University of Tokyo), kiyomi iwahashi(National Institute of Japanese Literature)

1:45 PM - 2:15 PM JST | 4:45 AM - 5:15 AM UTC

[MIS27-01] Sharing historical materials: An example of multi-disciplinal examination of historical materials in Edo period

★Invited Papers

*Hirotaka Terashima[1] (1.National Archives of JAPAN)

2:15 PM - 2:30 PM JST | 5:15 AM - 5:30 AM UTC

[MIS27-02] Improvement of climate reconstruction by focusing on the degree of detailed description of historical daily weather record

*Kenjiro Sho[1], Yoshimi Ikeda[2], Mika Ichino[3], Junpei Hirano[4], Kooiti Masuda[5], Asanobu Kitamoto[3,6] (1.Nagoya Institute of Technology, 2.Ikeda Gakuen Ikeda Senior High School, 3.Center for Open Data in the Humanities, 4.Teikyo University, 5.Tokyo Metropolitan University, 6.National Institute of Informatic)

2:30 PM - 3:00 PM JST | 5:30 AM - 6:00 AM UTC

[MIS27-03] Historical atmospheric analyses by weather information assimilation using Gaussian transformation

★Invited Papers

*Xiaoxing Wang[1], Kei Yoshimura[2], Kinya Toride[2] (1.Graduate School of Frontier Sciences, The University of Tokyo, 2.Institute of Industrial Science, The University of Tokyo)

3:00 PM - 3:15 PM JST | 6:00 AM - 6:15 AM UTC

[MIS27-04] Descriptions of natural phenomena in textbooks and people's perceptions

*Harufumi Tamazawa[1,2] (1.Kyoto City University of Arts, 2.Kyoto University)

[J] Oral | M (Multidisciplinary and Interdisciplinary)：M-IS Intersection

3:30 PM - 5:00 PM JST | 6:30 AM - 8:00 AM UTC | Ch.16 Zoom Room 16

[M-IS27] History X Earth and Planetary Science

convener:Yasuyuki Kano(Earthquake Research Institute, The University of Tokyo), Hiroaki Isobe(Faculty of Fine Arts, Kyoto City University of Arts), Kei Yoshimura(Institute of Industrial Science, The University of Tokyo), kiyomi iwahashi(National Institute of Japanese Literature), Chairperson:Kei Yoshimura(Institute of Industrial Science, The University of Tokyo), Harufumi Tamazawa(Kyoto City University of Arts)

3:30 PM - 4:00 PM JST | 6:30 AM - 7:00 AM UTC

[MIS27-05] Accomplishments and Potential Applications of Historical GIS: Researching Old Maps and Contributing Locally

★Invited Papers

*Akihiro Tsukamoto[1] (1.Tokushima Univ.)

4:00 PM - 4:15 PM JST | 7:00 AM - 7:15 AM UTC

[MIS27-06] Analysis of aftershocks of the 1855 Ansei Edo Earthquake using old documents discovered around Kanto Ko-Shinetsusing old documents discovered around Kanto Ko-Shinetsu

*Baba Michito[1], Yasuyuki Kano[1] (1.Earthquake Research Institute,University of Tokyo)

4:15 PM - 4:30 PM JST | 7:15 AM - 7:30 AM UTC

[MIS27-07] A historical record of frequent felt earthquakes on 1870 May and the destructive earthquake on 1870 May 13 felt in Yokohama

*Kentaro Hattori[1], Junzo Ohmura[2] (1.Kyoto Univ., 2.Tokyo Univ.)

4:30 PM - 4:45 PM JST | 7:30 AM - 7:45 AM UTC

[MIS27-08] Integrated IDP catalog considering the continuity of historical and modern earthquake catalog

*Yasuyuki Kano[1,2], Junzo Ohmura[1,2] (1.Earthquake Research Institute, The University of Tokyo, 2.Collaborative Research Organization for Historical Materials on Earthquakes and Volcanoes, UTokyo)

4:45 PM - 5:00 PM JST | 7:45 AM - 8:00 AM UTC

[MIS27-09] Discussion

[J] Poster | M (Multidisciplinary and Interdisciplinary)：M-IS Intersection

5:15 PM - 6:30 PM JST | 8:15 AM - 9:30 AM UTC | Ch.22_3

[M-IS27] History X Earth and Planetary Science

convener:Yasuyuki Kano(Earthquake Research Institute, The University of Tokyo), Hiroaki Isobe(Faculty of Fine Arts, Kyoto City University of Arts), Kei Yoshimura(Institute of Industrial Science, The University of Tokyo), kiyomi iwahashi(National Institute of Japanese Literature)

[MIS27-P01] An attempt to convert historical seismic data into GIS data and its challenges

*Junzo Ohmura[1,4], Miki Hamano[2], Yuta Hashimoto[3], Yasuyuki Kano[1,4] (1.Earthquake Research Institute,The University of Tokyo, 2.Graduate School of Letters, Ritsumeikan University, 3.National Museum of Japanese History, 4. Collaborative Research Organization for HistoricalMaterials on Earthquakes and Volcanoes, UTokyo)

[MIS27-P02] Historical materials of unlisted destructive earthquakes at Izu-Bonin Islands in the Meiji period: the 1873 Toshima earthquake and so on

*Kentaro Hattori[1] (1.Kyoto Univ.)

[MIS27-P03] Investigation of the stone monuments related to the hail and frost damage in the southern part of Gunma Prefecture

*Masafumi Aoyama[1] (1.Gunma University)

[E] Oral | M (Multidisciplinary and Interdisciplinary) : M-AG Applied Geosciences

3:30 PM - 5:00 PM JST | 6:30 AM - 8:00 AM UTC | Ch.20 Zoom Room 20

[M-AG37] CTBT IMS Technologies for Detecting Nuclear Explosion and Their Applications to Earth Science

convener:Nurcan Meral Ozel(Comprehensive Nuclear-Test-Ban Treaty Organization), Hiroyuki Matsumoto(Japan Agency for Marine-Earth Science and Technology), Dirk Metz(Japan Agency for Marine-Earth Science and Technology), Yosuke Naoi(Japan Atomic Energy Agency), Chairperson:Nurcan Meral Ozel(Comprehensive Nuclear-Test-Ban Treaty Organization), Hiroyuki Matsumoto(Japan Agency for Marine-Earth Science and Technology), Dirk Metz(Japan Agency for Marine-Earth Science and Technology)

3:30 PM - 3:45 PM JST | 6:30 AM - 6:45 AM UTC

[MAG37-01] **IMS Network Resilience and Business Continuity During Lockdown**

*Nurcan Meral Ozel[1] (1.Comprehensive Nuclear-Test-Ban Treaty Organization)

3:45 PM - 4:00 PM JST | 6:45 AM - 7:00 AM UTC

[MAG37-02] I30JP station repair following damage by typhoon “FAXAI”

*Takanari Fujii[1], Takayuki Otsu[1], Makiko Iwakuni[1], Masashi Motohashi[1] (1.Japan Weather Association)

4:00 PM - 4:15 PM JST | 7:00 AM - 7:15 AM UTC

[MAG37-03] Long-range acoustic measurements of the 2004 submarine eruption near Nightingale Island: Insights from hydrophone triplet array data recorded at IMS station H01W, Cape Leeuwin

*Dirk Metz[1], Julien Vergoz[2], Ingo Grevemeyer[3] (1.JAMSTEC, 2.CEA, 3.GEOMAR)

4:15 PM - 4:30 PM JST | 7:15 AM - 7:30 AM UTC

[MAG37-04] Operation of IMS radionuclide stations in Japan

*Yutaka Tomita[1], Yuichi Kijima[1], Akiko FURUNO[1], Yoichi Yamamoto[1] (1.Japan Atomic Energy Agency)

4:30 PM - 4:45 PM JST | 7:30 AM - 7:45 AM UTC

[MAG37-05] Atmospheric dispersion analysis for source term estimation of Xe-133 high-concentration detection events observed at the noble gas monitoring station in Takasaki regarding CTBT and two temporary experimental systems

*Akiko FURUNO[1], Yuichi Kijima[1], Yutaka Tomita[1], Yoichi Yamamoto[1] (1.Japan Atomic Energy Agency)

4:45 PM - 5:00 PM JST | 7:45 AM - 8:00 AM UTC

[MAG37-06] Discussion on how the CTBT IMS contributes to Earth and environmental sciences

Nurcan Meral Ozel[1], *Hiroyuki Matsumoto[2], Dirk Metz[2], Yosuke Naoi[3] (1.Comprehensive Nuclear-Test-Ban Treaty Organization, 2.Japan Agency for Marine-Earth Science and Technology, 3.Japan Atomic Energy Agency)

[E] Poster | M (Multidisciplinary and Interdisciplinary)：M-AG Applied Geosciences

5:15 PM - 6:30 PM JST | 8:15 AM - 9:30 AM UTC | Ch.21_2

[M-AG37] CTBT IMS Technologies for Detecting Nuclear Explosion and Their Applications to Earth Science

convener:Nurcan Meral Ozel(Comprehensive Nuclear-Test-Ban Treaty Organization), Hiroyuki Matsumoto(Japan Agency for Marine-Earth Science and Technology), Dirk Metz(Japan Agency for Marine-Earth Science and Technology), Yosuke Naoi(Japan Atomic Energy Agency)

[MAG37-P01] The upgrade of the CTBT Auxiliary Seismic Stations in Japan

*RYOHEI EMURA[1], Masashi Motohashi[1], Takayuki Otsu[1], Toyomi Sakamoto[1], Mami Nogami[1], Soshi Iwata[1] (1.Japan Weather Association)

[MAG37-P02] Detections of hydrocoustic signals associated with volcanic eruptions at Kadovar Island, Papua New Guinea, using CTBT IMS hydrophones

*Hiroyuki Matsumoto[1], Mario Zampolli[2], Georgios Haralabus[2], Jerry Stanley[2], James Robertson[2], Nurcan Meral Özel[2] (1.Japan Agency for Marine-Earth Science and Technology, 2.Comprehensive Nuclear-Test-Ban Treaty Organization)

[MAG37-P03] Characteristics of seismic signals associated with the hydrothermal system beneath a giant submarine caldera

*Hiroko Sugioka[1] (1.Department of Planetology, Kobe University)

[J] Oral | M (Multidisciplinary and Interdisciplinary)：M-AG Applied Geosciences

1:45 PM - 3:15 PM JST | 4:45 AM - 6:15 AM UTC | Ch.09 Zoom Room 09

[M-AG38] Ten years after the Fukushima Dai-ichi NPP Accident : Dynamics of radionuclides in the environment

convener:Daisuke Tsumune(Central Research Institute of Electric Power Industry), Yuichi Onda(Center for Research on Isotopes and Environmental Dynamics, University of Tsukuba), Kazuyuki Kita(Faculty of Science, Ibaraki University), Yoshio Takahashi(Department of Earth and Planetary Science, Graduate School of Science, The University of Tokyo), Chairperson:Yuichi Onda(Center for Research on Isotopes and Environmental Dynamics, University of Tsukuba), Daisuke Tsumune(Central Research Institute of Electric Power Industry)

1:45 PM - 2:00 PM JST | 4:45 AM - 5:00 AM UTC

[MAG38-01] New X-ray spectroscopic methods for the speciation of cesium in environment

★Invited Papers

*Yoshio Takahashi[1], Hikaru Miura[3], Daisuke Tsumune[3], Yuichi Kurihara[2] (1.Department of Earth and Planetary Science, Graduate School of Science, The University of Tokyo, 2.JAEA, 3.CRIEPI)

2:00 PM - 2:15 PM JST | 5:00 AM - 5:15 AM UTC

[MAG38-02] 10-year variation of atmospheric Cs radioactivity concentration observed at highly polluted area in Fukushima

*Kazuyuki Kita[1], Naho Hayashi[1], Peng Tang[1], Kotaro Hatanaka[1], Takeshi Kinase[2], Kouji Adachi[2], Yuji Zaizen[2], Ishizuka Masahide[5], Jun Furukawa[3], Yuko Hatano[3], Keisuke Sueki[3], Yuichi Onda[3], Kazuhiko Ninomiya[4], SHINOHARA ATSUSHI[4], Sakae Toyoda[6], Keita Yamada[6], Naohiro Yoshida[6], Yukihiko Satou[7], Yasuhito Igarashi[8] (1.Faculty of Science, Ibaraki University, 2.Meteorological Research Instutite, 3.Tsukuba University, 4.Osaka University, 5.Kagawa University, 6.Tokyo Institute of Technology, 7.JAEA, 8.University of Kyoto)

2:15 PM - 2:30 PM JST | 5:15 AM - 5:30 AM UTC

[MAG38-03] Temporal variations and future estimations of ^{90}Sr and ^{137}Cs in atmospheric depositions after the Fukushima Daiichi Nuclear Power Plant accident with long-term observations

★Invited Papers

*Takeshi Kinase[1,2], Kouji Adachi[2], Thomas Sekiyama[2], Mizuo Kajino[2], Yuji Zaizen[2], Yasuhito Igarashi[3,4] (1.Japan Agency for Marine-earth Science and Technology, 2.Meteorological Research Institute, 3.Institute for Integrated Radiation and Nuclear Science, Kyoto University, 4.Ibaraki University)

2:30 PM - 2:45 PM JST | 5:30 AM - 5:45 AM UTC

[MAG38-04] Comprehensive evaluation on wet scavenging schemes for ^{137}Cs transport modeling following the Fukushima Daiichi accident

*Shuhan Zhuang[1], sheng fang[1] (1.Tsinghua University)

2:45 PM - 3:00 PM JST | 5:45 AM - 6:00 AM UTC

[MAG38-05] Migration and distribution of radiocesium in forest 10 years after the Fukushima nuclear accident

*Hiroaki Kato[1], Yuichi Onda[1], Zul Hilmi Saidin[1], Hikaru Iida[1], Satoru Akaiwa[1], Tomoki Shinozuka[1] (1.Center for Research in Isotopes and Environmental Dynamics, University of Tsukuba)

3:00 PM - 3:15 PM JST | 6:00 AM - 6:15 AM UTC

[MAG38-06] Discussion

[J] Oral | M (Multidisciplinary and Interdisciplinary)：M-AG Applied Geosciences

3:30 PM - 5:00 PM JST | 6:30 AM - 8:00 AM UTC | Ch.09 Zoom Room 09

[M-AG38] Ten years after the Fukushima Dai-ichi NPP Accident : Dynamics of radionuclides in the environment

convener:Daisuke Tsumune(Central Research Institute of Electric Power Industry), Yuichi Onda(Center for Research on Isotopes and Environmental Dynamics, University of Tsukuba), Kazuyuki Kita(Faculty of Science, Ibaraki University), Yoshio Takahashi(Department of Earth and Planetary Science, Graduate School of Science, The University of Tokyo), Chairperson:Yoshio Takahashi(Department of Earth and Planetary Science, Graduate School of Science, The University of Tokyo), Kazuyuki Kita(Faculty of Science, Ibaraki University)

3:30 PM - 3:45 PM JST | 6:30 AM - 6:45 AM UTC

[MAG38-07] 10-year monitoring of ^{137}Cs transport in 30 river monitoring sites in 80km from the Fukushima Daiichi nuclear power plant

★Invited Papers

*Keisuke Taniguchi[1], Yuichi Onda[1], Kazuki Fujita[2], Yukio Takeuchi[2], Kazumi Katsuno[2], Hirotsugu Arai[2], Kouki Nasu[2] (1.Center for Research in Isotopes and Environmental Dynamics, University of Tsukuba, 2.Fukushima Prefectural Centre for Environmental Creation)

3:45 PM - 4:00 PM JST | 6:45 AM - 7:00 AM UTC

[MAG38-08] Impact of different land use along the Kasumigaura lake on suspended sediment delivery and particulate ^{137}Cs discharge

*Bin FENG[1], Yuichi Onda[1], Manabu Motohashi[1], Keisuke Taniguchi[1] (1.Center for research in isotopes and environmental dynamics, University of Tsukuba)

4:00 PM - 4:15 PM JST | 7:00 AM - 7:15 AM UTC

[MAG38-09] Ten years behavior of radiocaesium derived from TEPCO Fukushima Dai-ichi Nuclear Power Plant accident in surface water in the adjacent seas of the North Pacific Ocean

*Michio Aoyama[1,2], Yasunori Hamajima[3], Yayoi Inomata[3], Yuichiro Kumamoto[4], Hyoe Takata[2] (1.Center for Research in Isotopes and Environmental Dynamic, Faculty of Life and Environmental Sciences, University of Tsukuba, 2.Institute of Environmental Radioactivity, Fukushima University, 3.The Institute of Nature and Environmental Technolog, Kanazawa University, 4.Research Institute of Global Change, The Japan Agency for Marine-Earth Science and Technology)

4:15 PM - 4:30 PM JST | 7:15 AM - 7:30 AM UTC

[MAG38-10] On large-scale transport of suspended particulate matter on the continental shelf break off Fukushima, Japan.

*Kohei Kawano[1], Yusuke Uchiyama[1], Yuki - Kamidaira[2] (1.Graduate school of Engineering Faculty of Engineering, Kobe University, 2.Japan Atomic Energy Agency)

4:30 PM - 4:45 PM JST | 7:30 AM - 7:45 AM UTC

[MAG38-11] **Long-term simulation of oceanic ^{137}Cs with direct release and river discharge after the Fukushima Dai-ichi Nuclear Power Plant accident**

*Daisuke Tsumune[1], Tsubono Takaki[1], Kazuhiro Misumi[1], Hikaru Miura[1], Yutaka Tateda[1], Michio Aoyama[2] (1.Central Research Institute of Electric Power Industry, 2.University of Tsukuba)

4:45 PM - 5:00 PM JST | 7:45 AM - 8:00 AM UTC

[MAG38-12] Discussion

[J] Poster | M (Multidisciplinary and Interdisciplinary)：M-AG Applied Geosciences

5:15 PM - 6:30 PM JST | 8:15 AM - 9:30 AM UTC | Ch.21_3

[M-AG38] Ten years after the Fukushima Dai-ichi NPP Accident : Dynamics of radionuclides in the environment

convener:Daisuke Tsumune(Central Research Institute of Electric Power Industry), Yuichi Onda(Center for Research on Isotopes and Environmental Dynamics, University of Tsukuba), Kazuyuki Kita(Faculty of Science, Ibaraki University), Yoshio Takahashi(Department of Earth and Planetary Science, Graduate School of Science, The University of Tokyo)

[MAG38-P01] Effects of preferential flow on the spatial heterogeneity and chemical form of Cs-137 in a forest soil

*Junko Takahashi[1], Tetsuya Ono[1], Takuya Sasaki[1], Yuichi Onda[1] (1.Center for Research in Isotopes and Environmental Dynamics, University of Tsukuba)

[MAG38-P02] Contribution of fungal hyphal elongation to radiocesium transfer in deciduous broad-leaved litter

*Yoshito Sasaki[1], Tadafumi Niizato[1], Hiroki Amamiya[2], Kaori Yoshida[1] (1.Japan Atomic Energy Agency, 2.QJ science)

[MAG38-P03] The ^{137}Cs dynamics in a pond of urban area after decontamination

*Honoka Kurosawa[1], Misaki Usuki[1], Shota Moritaka[1], Kenji Nanba[2], Toshihiro Wada[2], Yoshifumi Wakiyama[2] (1.Graduate School of Symbiotic Systems Science and Technology, Fukushima University, 2.Institute of Environmental Radioactivity, Fukushima University)

[MAG38-P04] Variations in riverine ^{137}Cs concentration and its exportation to the ocean during high-flow events at three rivers in Hamadori area

Takuya Niida[1], *Yoshifumi Wakiyama[2], Hyoe Takata[2], Kazuki Fujita[3], Keisuke Taniguchi[4], Alexei Konoplev[2] (1.Graduate School of Symbiotic System and Technology, Fukushima Universiy, 2.Institute of Environmental Radioactivity, Fukushima Universiy, 3.Fukushima Prefectural Centre for Environmental Creation, 4.Center for Research in Isotope and Environmental Dynamics, University of Tsukuba)

[MAG38-P05] Comparison of cesium-bearing microparticles from marine and terrestrial sources

*Hikaru Miura[1], Atsushi Kubo[2], Takashi Ishimaru[3], Yukari Ito[3], Jota Kanda[3], Daisuke Tsumune[1], Yoshio Takahashi[4] (1.Central Research Institute of Electric Power Industry, 2.Shizuoka University, 3.Tokyo University of Marine Science and Technology, 4.The University of Tokyo)

[J] Oral | M (Multidisciplinary and Interdisciplinary)：M-TT Technology & Techniques

1:45 PM - 3:15 PM JST | 4:45 AM - 6:15 AM UTC | Ch.13 Zoom Room 13

[M-TT43] Brand-new scope of coupling geophysics being established by infrasound and associated waves

convener:Masa-yuki Yamamoto(Department of systems engineering, Kochi University of Technology), Takayuki Otsu(Japan Weather Association), Mie Ichihara(Earthquake Research Institute, University of Tokyo), Nobuo Arai(Disaster Mitigation Research Center, Nagoya University), Chairperson:Yoshihiro Kakinami(Hokkaido Information University), Masa-yuki Yamamoto(Department of systems engineering, Kochi University of Technology)

1:45 PM - 2:00 PM JST | 4:45 AM - 5:00 AM UTC

[MTT43-01] HTV Infrasound Phase Identification in Near and Far Field Records

*I. H. HAMAMA[1,2], Masa-yuki Yamamoto[1] (1.School of Systems Engineering, Kochi University of, Japan, 2.National Research Institute of Astronomy and Geophysics, NRIAG, Egypt)

2:00 PM - 2:15 PM JST | 5:00 AM - 5:15 AM UTC

[MTT43-02] An estimation of acoustic velocity in lower thermosphere using GNSS TEC after the foreshock of the 2011 Tohoku Earthquake

*Yoshihiro Kakinami[1], Hiroaki Saito[2], Tetsuo Yamamoto[2], Chia-Hung Chen[3], Masa-yuki Yamamoto[4], Kensuke Nakajima[5], Jann-Yenq LIU[6], Shigeto Watanabe[1] (1.Hokkaido Information University, 2.Hokkaido University, 3.National Cheng Kung University, 4.Kochi University of Technology, 5.Kyushu University, 6.National Central University)

2:15 PM - 2:30 PM JST | 5:15 AM - 5:30 AM UTC

[MTT43-03] Evaluation of prototype miniature microphones for observing infrasound

*Ryouichi Nishimura[1], Taira Itoh[2], Dai Adachi[2], Yasutaka Nakajima[2], Kenichi Kidokoro[2], Toshiyuki Hasumi[2], Yôiti Suzuki[1] (1.National Institute of Information and Communications Technology, 2.RION Co., Ltd.)

2:30 PM - 2:45 PM JST | 5:30 AM - 5:45 AM UTC

[MTT43-04] A prompt report of multiple-site infrasound observation by the nation-wide infrasound observation consortium for M 7.3 Fukushima offshore earthquake on Feb. 13, 2021

*Masa-yuki Yamamoto[1], Nobuo Arai[2], Takayuki Otsu[3], Ryouichi Nishimura[4], Takuma Oi[5], Kensuke Nakajima[6], Hideki Ueda[7], Makiko Iwakuni[3], Yoshihiro Kakinami[8], Kosuke Heki[9], Islam H. HAMAMA[1] (1.Kochi University of Technology, 2.Nagoya University, 3.JWA, 4.NICT, 5.Toho Merchantile, 6.Kyushu University, 7.NIED, 8.Hokkaido Information University, 9.Hokkaido University)

2:45 PM - 3:00 PM JST | 5:45 AM - 6:00 AM UTC

[MTT43-05] Three-dimensional large-scale numerical simulation of infrasound associated with tsunami generation considering wave source and atmospheric models

*Yoshiki Saito[1], Kan Okubo[1], Kentaro Uehara[2], Hidee Tatehata[2], Hiromu Yokosu[3] (1.Tokyo Metropolitan University, 2.Japan Weather Association, 3.Chubu Electric Power Company)

3:00 PM - 3:15 PM JST | 6:00 AM - 6:15 AM UTC

[MTT43-06] Continuous excitation of atmospheric free oscillation by cumulus heating

★Invited Papers

*Kensuke Nakajima[1] (1.Department of Earth and Planetary Sciences,Flculty of Sciences,Kyushu University)

[J] Poster | M (Multidisciplinary and Interdisciplinary)：M-TT Technology & Techniques

5:15 PM - 6:30 PM JST | 8:15 AM - 9:30 AM UTC | Ch.20_2

[M-TT43] Brand-new scope of coupling geophysics being established by infrasound and associated waves

convener:Masa-yuki Yamamoto(Department of systems engineering, Kochi University of Technology), Takayuki Otsu(Japan Weather Association), Mie Ichihara(Earthquake Research Institute, University of Tokyo), Nobuo Arai(Disaster Mitigation Research Center, Nagoya University)

[MTT43-P01] Infrasound detection of mining blasts from eastwards and westwards

*Mami Nogami[1], Takayuki Otsu[1], Makiko Iwakuni[1] (1.Japan Weather Association)

[MTT43-P02] The Infrasound signals excited by a bolide on 29th November 2020

*Makiko Iwakuni[1], Masa-yuki Yamamoto[2], Hiroaki Saito[3], Islam HAMAMA[2], Nobuo Arai[4], Takayuki Otsu[1], Mami Nogami[1], Takahiko Murayama[1] (1.Japan Weather Association, 2.Department of systems engineering, Kochi University of Technology, 3.Cosmosciences, Hokkaido University, 4.Disaster Mitigation Research Center, Nagoya University)

[MTT43-P03] Atmospheric wave energy of the 2020 August 4 explosion in Beirut, Lebanon, from ionospheric disturbances

*Ai Matsushita[1], Bhaskar Kundu[2], Batakrushna Senapati[2], Kosuke Heki[1] (1.Hokkaido University Graduate School of Science, 2.National Institute of Technology, Rourkela)

[MTT43-P04] Infrasound and seismic multiple-site observation of shock waves induced by hypersonic reentry of HAYABUSA-2 sample return capsule on Dec. 6, 2020

*Masa-yuki Yamamoto[1], Yoshihiro Hiramatsu[2], Shinsuke Abe[3], Yoshihiro Kakinami[4], Norihisa Segawa[5], Hiroshi Katao[6], Yoshiaki Ishihara[7], Taichi Kawamura[8], Satoshi Nozawa[9], Muneyoshi Furumoto[10], Phil Bland[11], Eleanor Sansom[11], Hadrien Devillepoix[11], Martin Towner[11], Yuichiro Inoue[1], Islam H. Hamama[1], Masato Yazawa[12], Kazuhisa Fujita[7], Makoto Yoshikawa[7] (1.Kochi University of Technology, 2.kanazawa University, 3.Nihon University, 4.Hokkaido Information University, 5.Kyoto Sangyo University, 6.Kyoto University, 7.JAXA, 8.Institut de Physique du Globe de Paris, 9.Ibaraki University, 10.Tono Research Institute of Earthquake Science, 11.Curtin University, 12.Mathematical Assist Design Laboratory)

[J] Poster | M (Multidisciplinary and Interdisciplinary)：M-ZZ Others

5:15 PM - 6:30 PM JST | 8:15 AM - 9:30 AM UTC | Ch.22_4

[M-ZZ44] Studies of Geoscience : historical, philosophical and STS studies

convener:Michiko Yajima(Tokyo Metropolitan University), Shigeyuki Aoki(Faculty of Letters, Chuo University), Toshihiro Yamada(Taisho University), Akira Yamamoto

[MZZ44-P01] The begining of lady earth scientists in Japan

*Michiko Yajima[1] (1.Tokyo Metropolitan University)

[MZZ44-P02] Finding Geoscientific Evidence in Nuclear Disaster Trials 2: Is Not "responsibility of the government" Scientific?

*Mamoru Hayashi[1] (1.University of TOYAMA)

[MZZ44-P03] Wilkins’s lunar world

*Shigeyuki Aoki[1] (1.Faculty of Letters, Chuo University)

[MZZ44-P04] The Popularization of Science and the Geo-power: Cosmic Evolution, China, and Buddhism in 1920s Shinjo Shinzo

*Toshihiro Yamada[1] (1.Taisho University)

[MZZ44-P05] Japan's first female meteorologist

*Akira Yamamoto

[J] Oral | M (Multidisciplinary and Interdisciplinary)：M-ZZ Others

10:45 AM - 12:15 PM JST | 1:45 AM - 3:15 AM UTC | Ch.16 Zoom Room 16

[M-ZZ48] Geology and culture

convener:Hisashi Suzuki(Otani University), Tohru Sakiyama(Institute of Geo History, Japan Geochronology Network), Naoki Takahashi(Natural History Museum and Institute, Chiba), Chairperson:Tohru Sakiyama(Institute of Geo History, Japan Geochronology Network), Naoki Takahashi(Natural History Museum and Institute, Chiba)

10:45 AM - 11:00 AM JST | 1:45 AM - 2:00 AM UTC

[MZZ48-01] A use of tuff beds in strata for natural resources at the Boso Peninsula – ‘Bosyu white clay’ or ‘Bosyu sand’

*Naoki Takahashi[1], Junichi Ohki[1] (1.Natural History Museum and Institute, Chiba)

11:00 AM - 11:15 AM JST | 2:00 AM - 2:15 AM UTC

[MZZ48-02] Change of usage patterns of Innai Tuff Member from Yuzawa City, Akita prefecture, northeast Japan: From ‘rolling stones‘ in early modern to ‘Innai Ishi’ in modern

*Norihito Kawamura[1] (1.School of Regional Resource Management, Graduate School, University of Hyogo)

11:15 AM - 11:30 AM JST | 2:15 AM - 2:30 AM UTC

[MZZ48-03] Japanese marbles used in some historic western style houses in Tokyo

*Mutsuko Inui[1], Shoji Nishimoto[2] (1.School of Science and Engineering, Kokushikan University, 2.Nagoya City Science Museum)

11:30 AM - 11:45 AM JST | 2:30 AM - 2:45 AM UTC

[MZZ48-04] Brewing culture and geology in Japan: examples of Satsuma shochu spirits and Koshu wine

*Hisashi Suzuki[1] (1.Otani University)

11:45 AM - 12:00 PM JST | 2:45 AM - 3:00 AM UTC

[MZZ48-05] The investigation of the relationship between the artificial terrain change of medieval mountain castles and the landslides in 2018

*Masami Inomata[1] (1.National University Corporation Hiroshima University)

12:00 PM - 12:15 PM JST | 3:00 AM - 3:15 AM UTC

[MZZ48-06] **Historical distribution of granitic stone materials from Setouchi area in the San-in and Hokuriku regions, Southwest Japan**

*Tohru Sakiyama[1] (1.Institute of Geo History, Japan Geochronology Network)

[J] Poster | M (Multidisciplinary and Interdisciplinary)：M-ZZ Others

5:15 PM - 6:30 PM JST | 8:15 AM - 9:30 AM UTC | Ch.22_5

[M-ZZ48] Geology and culture

convener:Hisashi Suzuki(Otani University), Tohru Sakiyama(Institute of Geo History, Japan Geochronology Network), Naoki Takahashi(Natural History Museum and Institute, Chiba)

[MZZ48-P01] Rock species of the cornerstone of the earthen wall in the northeastern part of Ninomaru earthworks of Yamagata Castle

*Ohtomo Yukiko[1], Saito Hitoshi[2] (1.Yamagata University, 2.Yamagata City Board of Education)

[J] Oral | EVENT：EVENT

12:20 PM - 1:00 PM JST | 3:20 AM - 4:00 AM UTC | Ch.01 Zoom Room 01

[EV-25] Lunchtime Special Lecture

12:20 PM - 1:00 PM JST | 3:20 AM - 4:00 AM UTC

[E-11-26] Chemical constraints on the origin and early evolution of the Solar System

[J] Oral | EVENT：EVENT

3:30 PM - 4:15 PM JST | 6:30 AM - 7:15 AM UTC | Ch.13 Zoom Room 13

[EV-26] Exhibitors' Seminar

3:30 PM - 4:15 PM JST | 6:30 AM - 7:15 AM UTC

[E-11-27] GRC virtual lab tour & the making of a diamond powder with Hime-diamond mortar

[J] Poster | U (Union)：Union

Sun. Jun 6, 2021 5:15 PM - 6:30 PM JST | Sun. Jun 6, 2021 8:15 AM - 9:30 AM UTC | Ch.01_1

[U-04] Promotion of SDGs in JpGU

convener:Yukihiro Takahashi(Department of Cosmosciences, Graduate School of Science, Hokkaido University), Chiaki T. Oguchi(Institute for Environmental Science and Technology, Graduate School of Science and Engineering, Saitama University), Richard Simon Wallis(The University of Tokyo), Eiichi Tajika(Department of Earth and Planetary Science, Graduate School of Science, The University of Tokyo)

The United Nations' Sustainable Development Goals (SDGs) have come to be widely recognized as a common goal for humankind, involving the international community. For many of the 17 goals and 169 targets, earth and planetary science has a significant potential role. It is also important for us, as one of the largest academic societies in Japan, to develop activities in line with the spirit of the SDGs. In this session, we will discuss how the research activities of earth and planetary science are related to the SDGs, how to expand our contributions in the future, and how JpGU itself should be in accordance with the SDGs.

[U04-P01] SDGs and academic researches in the Solid Earth Science Section

*Michihiko Nakamura[1], Yo Fukushima[2] (1.Department of Earth Science, Graduate School of Science, Tohoku University, 2.Disaster Science Division, International Research Institute of Disaster Science, Tohoku University)

[U04-P02] Ongoing research in Human Geosciences and its possible contributions to SDGs

*Reiichiro Ishii[1], Makoto Taniguchi[1], Naoki Masuhara[1], Sanghyun Lee[1] (1.Research Institute for Humanity and Nature)

[U04-P03] Contribution of SDGs in Subtropical Islands

*Jun Yasumoto[1] (1.University of the Ryukyus, Faculty of Agriculuture)

[U04-P04] Education for Sustainable Development (ESD) and environmental studies promoted by Seikei Gakuen

*Hitoshi Fujiwara[1], Atsushi MIYASHITA[1], Masumi Zaiki[2], Hironobu Oda[2], Atsuko Ikegami[1] (1.Education and Research Center for Sustainable Development/Faculty of Science and Technology, Seikei University, 2.Education and Research Center for Sustainable Development/Faculty of Economics, Seikei University)

SDGs and academic researches in the Solid Earth Science Section

*Michihiko Nakamura[1], Yo Fukushima[2]

1. Department of Earth Science, Graduate School of Science, Tohoku University, 2. Disaster Science Division, International Research Institute of Disaster Science, Tohoku University

Solid Earth sciences play an important role in achieving the SDGs in securing mineral, energy, and water resources, carbon capture and storage, geological disposal of high-level radioactive waste, disaster mitigation for earthquakes, volcanic eruptions, and landslides. Integrated viewpoints of SDGs are, in turn, suggestive for the development of Earth and planetary science as a system science. The closer connection of academia to economic and social activities such as ESG investment will strengthen international competitiveness. Based on this recognition, we would like to provide topics that match the scope of this session.

Keywords: SDGs, ESG investment, disaster mitigation

©2021. Japan Geoscience Union. All Right Reserved.

Ongoing research in Human Geosciences and its possible contributions to SDGs

*Reiichiro Ishii[1], Makoto Taniguchi[1], Naoki Masuhara[1], Sanghyun Lee[1]

1. Research Institute for Humanity and Nature

We will share some example topics from ongoing research in Human Geosciences field in Japan, partitularly conducted at Reasearch Institute for Humanity and Nature, and discuss its possible future contributions to the related SDGs

Keywords: SDGs, Resource Use, Ecosystem, Hydrological Cycle

©2021. Japan Geoscience Union. All Right Reserved.

Contribution of SDGs in Subtropical Islands

*Jun Yasumoto[1]

1. University of the Ryukyus, Faculty of Agriculuture

In this paper, we will briefly introduce the project "Watershed Governance Based on Participation and Consensus for
Sustainable Water Resource Use in Subtropical Islands" which is being implemented with the support of JST and aims to solve the SDGs.

Keywords: Watershed Governance, Sustainable Water Resource Use, Subtropical Islands

©2021. Japan Geoscience Union. All Right Reserved.

Education for Sustainable Development (ESD) and environmental studies promoted by Seikei Gakuen

*Hitoshi Fujiwara[1], Atsushi MIYASHITA[1], Masumi Zaiki[2], Hironobu Oda[2], Atsuko Ikegami[1]

1. Education and Research Center for Sustainable Development/Faculty of Science and Technology, Seikei University,
2. Education and Research Center for Sustainable Development/Faculty of Economics, Seikei University

Seikei Gakuen is an educational corporation which includes elementary school, junior high school, high school, and university (graduate school). From the beginning of Seikei Gakuen (1912), we have had educations and learning for ESD; e.g., practical training/studies of agricultural works and observations of nature. In particular, the meteorological observatory has continued weather-monitoring at Kichijoji/Tokyo since 1926. In order to increase the ESD activities, Seikei Education and Research Center for Sustainable Development (ERCS) has been established in April 2018. Seikei Gakuen has also joined the UNESCO Associated Schools Project Network in November 2019.
In this presentation, we will introduce our ESD activities, in particular, environmental studies to exchange information about study programs, educational tools, and so on with participants in the session. We hope enhancement of organized activities in the field of the Earth and Planetary Sciences for SDGs.

Keywords: Education for Sustainable Development, environmental studies, UNESCO Associated Schools Project Network, practical training/studies

©2021. Japan Geoscience Union. All Right Reserved.

[J] Poster | U (Union) : Union

Sun. Jun 6, 2021 5:15 PM - 6:30 PM JST | Sun. Jun 6, 2021 8:15 AM - 9:30 AM UTC | Ch.01_2

[U-09] Advancing SDGs through inclusive partnerships II: Engaging with communities

convener:Hidenroi Nakamura(Toyama Prefectural University), Vincent Tong(University College London), Mika Shimizu(Kyoto University), Fumiko Noguchi(United Nations University, Institute for the Advanced Study of Sustainability)



Sustainable Development Goals (SDGs) provide a comprehensive framework underpinning a wide range of interdisciplinary initiatives in Earth Sciences. With interconnected objectives and impact across natural, social and human sciences, inclusive partnerships between academics, students, citizens, industry, businesses and other stakeholders are critical to the success of these initiatives. Such partnerships involving academics and students across all types of higher education institutions and high schools have profound impact on the local communities across Japan. In this session, we examine the significance of inclusive partnerships in SDG-aligned research, outreach and education initiatives in Japan. We will focus on ways to engage with local communities and the wider Japanese society, including marginalised individuals and groups. We welcome contributions based on i) critical reflections on research and education projects from the perspectives of academics, students and non-academic partners, ii) theoretical examination of the nature of inclusive partnerships in the Japanese cultural contexts, and iii) evidencing impact of inclusive practices in SDG initiatives.

[U09-P01] SDGs community and social engagement in education and research: Implication for JpGU

*Hidenroi Nakamura[1] (1.Toyama Prefectural University)

SDGs community and social engagement in education and research: Implication for JpGU

*Hidenroi Nakamura[1]

1. Toyama Prefectural University

Community engagement in education and research activities of higher education institutions is crucial for SDGs promotion. I reflect and introduce own cases of education and research in Chubu region of Japan, including Toyama, to share the idea and implication for JpGU activities toward inclusive partnership. The cases include education under the COVID-19 in collaboration with a citizen organization promoting SDGs, citizen-led backcasting-based scenario making with a student and researchers, clinical volcano disaster management study in collaboration with local governments, and citizen dialogue study in collaboration with scientists. Implications to JpGU include promoting identification of linkage between three aspects of SDGs, i.e., economy, society and environment, and each discipline and field of activity. Moreover, it is desirable to strive strategic partnership development intentionally and experimentally: linking research and community, linking education and community, and linking research, education and community.

Keywords: SDGs, community engagement, partnership, collaboration, linkage

©2021. Japan Geoscience Union. All Right Reserved.

[J] Oral | O (Public)：Public

Sun. Jun 6, 2021 3:30 PM - 5:00 PM JST | Sun. Jun 6, 2021 6:30 AM - 8:00 AM UTC | Ch.01 Zoom Room 01

[O-02] Natural disasters and people -Listen to the voice of the Earth on the Japanese Geoparks-

convener:Noritaka Matsubara(Graduate School of Regional Resource Management, University of Hyogo), Kyohei Sano(Graduate School of Regional Resource Management, University of Hyogo), Suzuka Koriyama(Itoigawa city), Hikaru Yokoyama(Hokusho University), Chairperson:Kyohei Sano(Graduate School of Regional Resource Management, University of Hyogo), Suzuka Koriyama(Itoigawa city), HIROKO IMAI(Com Support Office /Wakayama University Center for Tourism Research), Hokuto Obara(Mine-Akiyoshidai Karst Plateau Geopark Promotion Council), Hikaru Yokoyama(Hokusho University)

People benefit from the earth, while sometimes geological activities bring disaster to human society. Geoparks aim to reconnect human society at all levels to our home planet and to celebrate how the planet with 4.6 billion years long history has shaped every aspect of our lives and society. Many geoparks in tectonically active areas of the world have a crucial role in helping mitigate geo-hazards through awareness-raising and constructing disaster response strategies. In this session, we discuss how people have lived with geological activities and natural hazards, and how to deal with new threats, including COVID-19, in nature through geoparks.

3:30 PM - 4:00 PM JST | 6:30 AM - 7:00 AM UTC

[O02-04] Achievements and issues of online program development at Hagi Geopark

*Takaaki Shirai[1] (1.Hagi Geopark Promotion Council)

4:00 PM - 4:30 PM JST | 7:00 AM - 7:30 AM UTC

[O02-05] Our ancestors who overcame natural disasters: A case study focused on Toya-Usu UNESCO Global Geopark

★Invited Papers

*Asami Nakaya[1] (1.Toya-Usu UNESCO GLobal Geopark Council)

4:30 PM - 5:00 PM JST | 7:30 AM - 8:00 AM UTC

[O02-06] The case of One Geopark damaged by 2018 Japan floods -The 3 years for reconstruction of Seiyo City, Ehime Prefecture and the Shikoku Seiyo Geopark-

★Invited Papers

*Takumi Sakakiyama[1] (1.Seiyo City)

Achievements and issues of online program development at Hagi Geopark

*Takaaki Shirai[1]

1. Hagi Geopark Promotion Council

Hagi Geopark has systematically conducted lectures and geotours that emphasize experiences such as outdoor experiences and cooking classes. However, we were forced to stop these activities due to the influence of COVID-19. Therefore, after April 2020, we started to develop a new method for the purpose of continuing educational activities and tourism activities in the with COVID-19 era. As a result, we have begun full-scale operation of programs that utilize the Internet, such as holding regular online tours once a month. I will share the process of these efforts and the challenges for the post COVID-19 era.

Keywords: geopark, online tour, with CORONA, after CORONA

©2021. Japan Geoscience Union. All Right Reserved.

Our ancestors who overcame natural disasters: A case study focused on Toya-Usu UNESCO Global Geopark

*Asami Nakaya[1]

1. Toya-Usu UNESCO GLobal Geopark Council

Toya-Usu UNESCO Global Geopark is located in the southwestern part of Hokkaido (the northernmost island of Japan). The geopark includes Mt.Usu, an active volcano, as a major geosite as shown by its major theme of coexistence with the volcano. The area to the south of Mt.Usu faces the sea and has been inhabited by people since the prehistoric Jomon period. Inhabitants of the area have been supported by abundant seafood and spring water from the volcano. Many settlements were formed along the coast, but the volcano's eruption during the Edo period (17th to 19th centuries) cost many lives. The indigenous Ainu of Hokkaido, who were living in the Mt. Usu area, described the volcanic eruption and their aftermath in epics (known as *yukar* in the Ainu language) and passed them down to ensure their descendants would be prepared for another possible eruption.
This presentation will focus on Ainu epics and archaeological sites that remain in the coastal area to highlight the history of those who have overcome natural disaster, such as repeated volcanic eruptions and tsunami. We will also share information about disaster mitigation efforts that have been under way at the geopark.

Keywords: Geopark, Eruption disaster, Ainu People

©2021. Japan Geoscience Union. All Right Reserved.

The case of One Geopark damaged by 2018 Japan floods -The 3 years for reconstruction of Seiyo City, Ehime Prefecture and the Shikoku Seiyo Geopark-

*Takumi Sakakiyama[1]

1. Seiyo City

The Shikoku Seiyo Geopark located in the southwestern part of Ehime Prefecture, has many geological landscapes of the Chichibu Belts, contained the Kurosegawa Tectonic Zone, various landforms from the ria coast at 0m above sea level to the Shikoku Karst at an altitude of about 1,400m and climates and the traditional culture, within an area of about 50 km east to west.During 2018 Japan floods, a lot of houses and buildings were damaged by flooding of rivers and landslides in various places. Particularly, a large-scale flood damage occurred in a residential area in the Nomura district of Nomura Town. Six precious lives were lost in a series of disasters in Seiyo City. In addition, out of 23 sites, a total of 5 sites were damaged to prevent access in the Geopark. Four of them have been restored, but the Katsuragawa Valley is still restricted except near the entrance. Our secretariat of the Shikoku Seiyo Geopark Counsil had to be suspended for a while after the disaster. Fortunately, we were supported such as receiving donations from Japanese Geoparks Network (JGN) and related people based on the Disaster Response Guidelines of JGN. In addition, Japanese Geopark Officers and researchers conduct disaster surveys about once a year and provide advice the recovery and course of actions on future.
After the disaster, the inhabitants became more interested in disaster prevention and the landforms around them. Following his, we have carried out many disaster prevention and programs such as "Seiyo Nature and Culture College" consisted mainly field excursions, the lectures with hazard maps, geography map, "NIED Quake map!" for elementary and junior high schools, public halls, labor unions, and so on. In October 2020, Disaster Tradition Exhibition Room was opened in the room renovated Otoi Kaikan. The aim to pass down the records and memories of the disaster, and its exhibition is incorporated the perspectives of Geoparks, such as the history of the earth and the blessings of the earth. In addition, we have devised ways to make various uses, such as providing guidance by the "Disaster Storyteller" and preparing disaster VR / AR content. And these efforts have been disseminated at Bosai Kokutai sponsored the secretariat of isaster prevention promotion mass meeting Japan, the National Conference of JGN, and many other workshops and lectures.
Looking back on the three years since the disaster, the disaster prevention awareness of past in this area has focused on the measure to act in the event of a disaster such as disaster drills. I realized that people are not able to fully acquire the disaster risk they had due to the characteristics of the landforms. Creating and distributing hazard maps is not enough to foster that perspective, and it is important to bring awareness through field excursions that actually follow the formation of the earth. In fact, these activities are being actively promoted in Geoparks around the world, and their experience has been accumulated. Geopark are an international certification system that started with the purpose of conservating geological heritage, but I supposed that it will make a great contribution to society in terms of disaster prevention and reduction.

Keywords: Shikoku Seiyo Geopark, Seiyo City, 2018 Japan floods, Disaster Prevention and Reduction, Disaster Tradition

©2021. Japan Geoscience Union. All Right Reserved.

[J] Poster | O (Public)：Public

Sun. Jun 6, 2021 5:15 PM - 6:30 PM JST | Sun. Jun 6, 2021 8:15 AM - 9:30 AM UTC | Ch.02_1

[O-02] Natural disasters and people -Listen to the voice of the Earth on the Japanese Geoparks-

convener:Noritaka Matsubara(Graduate School of Regional Resource Management, University of Hyogo), Kyohei Sano(Graduate School of Regional Resource Management, University of Hyogo), Suzuka Koriyama(Itoigawa city), Hikaru Yokoyama(Hokusho University)

People benefit from the earth, while sometimes geological activities bring disaster to human society. Geoparks aim to reconnect human society at all levels to our home planet and to celebrate how the planet with 4.6 billion years long history has shaped every aspect of our lives and society. Many geoparks in tectonically active areas of the world have a crucial role in helping mitigate geo-hazards through awareness-raising and constructing disaster response strategies. In this session, we discuss how people have lived with geological activities and natural hazards, and how to deal with new threats, including COVID-19, in nature through geoparks.

[O02-P01] New coronavirus response in Fossa Magna Museum

*Takahiko Ogawara[1], Ko Takenouchi[1], Yousuke Ibaraki[1], Takeo Kobayashi[2], Takuma Katori[2] (1.Fossa Magna Museum, 2.Itoigawa City Hall Geopark Promotion Office)

[O02-P02] Short-Term Effects of SNS Marketing: a Case Study in Hakusan Tedorigawa Geopark

*Susan May[1] (1.Hakusan Tedorigawa Geopark Promotion Council)

[O02-P03] Activities to promote the local sustainable development - Report at the time of spread of COVID-19 infection from Mt.Kurikoma Area Geopark -

*Yui Hasegawa[1], Rie Nakagawa[1], Seiya Tanaka[1], Jun Nagao[1] (1.Mt.Kurikoma Area Geopark Promotion Committee)

[O02-P04] Geotourism in Corona (COVID-19) related crisis - Advantage of being outdoors : In case of San'in Kaigan UNESCO Global Geoprk -

*Noritaka Matsubara[1], NAGAHAMA SATOSHI[1] (1.Graduate School of Regional Resource Management, University of Hyogo)

[O02-P05] Operation of geo-tours using online delivery tools under COVID-19

*Taku Morimoto[1] (1.Unzen Volcanic Area Geopark Promotion Office)

[O02-P06] Holding of event the Lake Shikaribetsu Igloo Village under COVID-19 measures

*Kanamori Syosaku[1], Hiroki Matsumoto[1], Onishi Jun[1] (1.Tokachi-Shikaoi Geopark Promotion Council)

[O02-P07] Stay-at-home Project with Local Students in Toya-Usu UNESCO Global Geopark

*NIRE KAGAYA[1], Yoshiaki Hata[1], Akihito Kato[2], Kiyono Kuroda[2], Koki Takagi[2], Kazuma Iwamura[2], Kanako Kitada[2], Koki Tomita[2], Mina Shionoya[2] (1.Toya-Usu UNESCO Global Geopark Council, 2.Date-Midorigaoka Highschool)

[O02-P08] Developing the San’in Kaigan Geopark Trail and the promotion of geotourism during COVID-19 Pandemic

*Hiroshi Nakase[1] (1.San'in Kaigan Geopark Promotion Council)

[O02-P09] A comparative study of educational on-site and online geotours in Hamamatsu-Hamanako Aspiring Geopark, Japan

*Hiroki Nagano[1], Masato Koyama[2], Yusuke Suzuki[2], Megumi Fukuyama[2] (1.Hamamatsu Technical High School, 2.Shizuoka University)

[O02-P10] Topographic evolution after the Aso-4 pyrocrastic flow and the meaning for disaster prevention in the Oita Bungoono Geopark, Japan

*Toshikazu Yoshioka[1] (1.Oita Bungoono Geopark Promotion Council)

[O02-P11] Conservation and Utillization of Natural Disaster Monument on Tosashimizu Geopark Plan

*Moriguchi Natsuki[1], Satoru Imai[1], Aika Sakuda[1], Kouichi Saruta[1], Michiru Sakai[1] (1.Tosashimizu Geopark Promotion Council)

[O02-P12] Records and countermeasure of disasters in Shimokita Geopark

*Satoshi Ishikawa[1], Kirika Kitagawa[1] (1.Shimokita geopark promotion council)

[O02-P13] Inform of weather disasters in geoparks

*Hiroshi Sato[1,2], Shinichi Sugimoto[3], Makoto Aoi[4], Shinya Miura[4], Hinako Suzuki[4] (1.Mt.Bandai Museum, 2.Bandaisan Geopark Council, 3.Unzen Volcanic Area Global Geopark, 4.National Research Institute for Earth Science and Disaster Resilience)

[O02-P14] How to Prevent Elderly People from Natural Disasters - An Example in Unzen Volcanic Area UNESCO Global Geopark -

Shunsei OGATA[1], Hiyori KADOHATA[1], Tasuku KONDO[1], Miraku TANAKA[1], Kosei HASHIDA[1], Shinsho FUJIO[1], Mizuho IWANAGA[1], Aiko ENGUCHI[1], Seren OTA[1], Rika TANAKA[1], Toru YAMAUCHI[2], Hiroaki OSAKO[2], *Marekazu OHNO[3] (1.Glocal Course of Nagasaki Prefectural Koka High School, 2.Nagasaki Prefectural Koka High School , 3.Unzen Volcanic Area Geopark Promotion Office)

[O02-P15] Disaster and Disaster Prevention Learning in the Naeba-Sanroku Geopark

*Kouhei Nakano[1] (1.Naeba-sanroku Geopark Promotion Council)

[O02-P16] Lives of the local people on the collapsing land and the flowing land by river water - Think about geohazard program of Miyoshi geopark project-

*Azusa Tonotani[1], Katsunori Ozakai[1], Mizuki Tochitani[1], Hiroyuki Ohnishi[1], Toshiaki Matsumoto[1] (1.Geopark Promotion office in Miyoshi city)

[O02-P17] Toward restoration of Geosites damaged by natural disaster with reaching consensus in local community: a case of Suzaki Coast in Seiyo City, Japan.

*Takumi Sakakiyama[1], Kazunari Kimura[2], Yuya Kato[3], Masahito Ono[1], Tsukasa Takahashi[1] (1.Seiyo City, 2.NAIBA Co. Ltd., 3.Noyama Company)

[O02-P18] Let's investigate the earth activity from Shimonita Geopark

*Hara Hideo[1] (1.Geopark Shimonita council)

[O02-P19] **The foundations of Yuzawa Geopark: a unification and a compilation of six geological maps published by the Geological Survey of Japan and Akita Prefecture**

*Akio Sasaki[1], Kohei Yamawaki[1], Yukio Fujimoto[1], Syoichi Goi[1], Shoei Chiba[1] (1.Network of Earth Science Museum for Akita)

[O02-P20] Conservation concerns in Yuzawa Geopark: Distributions and seasonal variation in blood-sucking flies and an invasive plant species

*Haruki Takayanagi[1] (1.Yuzawa City Geopark Promotion Council)

[O02-P21] The relationship between the former plate boundary and residents, especially the signboard production process

*Kato Satomi[1] (1.Mt. Apoi Geopark Promotion Council)

[O02-P22] Fossil collecting experience to solve summer vacation indipendent study in Itoigawa UNESCO Global Geopark

*Yousuke Ibaraki[1], Yutaka Furumi, Emma Longhorn, Takahiko Ogawara[1], Ko Takenouchi[1], Takuma Katori[2], Takeo Kobayashi[2] (1.Fossa Magna Museum, 2.Itoigawa Geopark Council)

[O02-P23] Geosite Map and Card in a Fun and Interesting Way by Local Elementary School Students: a Case Study of Geosite in Nankikumano Geopark with Takaike Elementary School

*Hiroko Shibasaki[1] (1.Nanki-Kumano GeoPark Guide Club)

[O02-P24] **Examples of joint projects (or joint events) between a museum and Sado Island Geopark**

*Takeyoshi SADAKANE[1], Mituhisa AIDA[1] (1.Sado Geopark Promotion Council)

[O02-P25] A Guide program that promote Proactive learning in School trip
- Practice at Toya-Usu UNESCO Global Geopark -

*Hikaru Yokoyama[1] (1.Hokusho University)

[O02-P26] Educational Program on spring water of Aso UNESCO Global Geopark related with elcetrical conductivity (Part 2)
Cooperated Research on Minamiaso Spring Water

*Tsuneomi Kagiyama[1], Koki Nagata[2], Toshikazu Maeda[3], Yuto Takeuchi[3], Haruki Watanabe[3], Kozue Inoue[3] (1.Aso Geopark Promotion Council, 2.Aso Volcano Museum, 3.Takamori Senior High School)

[O02-P27] Looking back on 11 years of the educational activities of the Dinosaur Valley Fukui Katsuyama Geopark

*Sumiaki Machi[1] (1.Dinosaur Valley Fukui Katsuyama Geopark Promotion Council)

New coronavirus response in Fossa Magna Museum

*Takahiko Ogawara[1], Ko Takenouchi[1], Yousuke Ibaraki[1], Takeo Kobayashi[2], Takuma Katori[2]

1. Fossa Magna Museum, 2. Itoigawa City Hall Geopark Promotion Office

Itoigawa Fossa Magna Museum is a core facility of the Itoigawa UNESCO Global Geopark. The museum opened in 1994 and was renovated in 2015. The museum's main exhibits are jade, limestone fossils, Itoigawa-Shizuoka Tectonic Line and formation of the Japanese archipelago. 90,270 people visited the museum in 2019.
The number of visitors in 2020 is 49.4% of the previous year's level (April to November), and the Fossa Magna Museum has implemented the following measures. (1) Corona prevention and three densification measures that allow visitors to visit the museum with peace of mind. (2) Development of a website that provides virtual tours of the museum and introduces the highlights of outdoor exhibits. (3) Introducing the museum remotely using Zoom and other tools.

Corona prevention and three densification measures at the Fossa Magna Museum

The following measures have been implemented at the Fossa Magna Museum: Prohibition of visitors from seven prefectures (April 8 to April 24, 2020). Temperature check and entry into the museum (April 8 to June 18, 2020; temperature check is ongoing). Temporary closure of the museum in response to the spread of infection (April 25 to May 30, 2020). Entry restricted to residents of non-Niigata Prefecture (June 1 to June 18, 2020). Stone appraisal service will be suspended (from March 9, 2020 to March 2021). The use of the Fossil Valley will be suspended (April 1, 2020 to June 30, 2020).
The temperature of each visitor was taken by a staff member using a non-contact thermometer when entering the museum. In order to solve this problem, the museum introduced an automatic temperature-taking device equipped with AI. This device automatically measures the body temperature of each visitor and calls for attention if the visitor is not wearing a mask.
Stone appraisal service is the museum's own promotion activity, in which visitors can bring in up to five stones and have their names appraised free of charge. As a countermeasure against the three densities of the corona disaster, the museum considered distributing numbered tickets and making advance reservations via the Internet or telephone. However, it has been decided to suspend these measures until the end of March 2021.
Therefore, the Fossa Magna Museum held an outdoor appraisal class (1,000 yen per class) during the summer vacation as an alternative to stone appraisal. For this event, we used the stone specimen kit "Hirokko" created by the Itoigawa City Tourism Association. Total of 16 workshops were held, with 122 participants from inside and outside the city.

Development of a website to introduce virtual tours of the museum and highlights of the outdoor exhibits

The Fossa Magna Museum was faced with the challenge of how to enjoy the museum when it is closed. In the fall of 2019, the Itoigawa Geopark Council conducted photography and virtual tours of the exhibition rooms using Matterport, a 3D model camera developed by Hokkaido Map Co. And a local cable TV station filmed a video of a curator giving a tour of the museum and posted it on the website.

Museum Introduction Using Zoom

Since the Corona disaster, the use of web conferencing systems such as Zoom has been developing rapidly. The Fossa Magna Museum conducted an online virtual tour of the museum using Zoom at the University Festival of the Faculty of Science of Niigata University (October 18) and the Chubu Block

©2021. Japan Geoscience Union. All Right Reserved.

Conference of the Japanese Geoparks Network (November 21). This was achieved by using a smartphone and a gimbal to connect to the Zoom conference room via a cell phone line. At the Chubu Block Conference, we not only provided a tour of the museum, but also broadcasted real-time indoor experiments and videos that we had taken in advance.
Virtual tours have the potential to make it possible to visit places that have been difficult to visit in large groups, such as conventional tours.

Keywords: Itoigawa UNESCO Global Geopark, Fossa Magna Museum, Countermeasures against new coronavirus infectious

©2021. Japan Geoscience Union. All Right Reserved.

Short-Term Effects of SNS Marketing: a Case Study in Hakusan Tedorigawa Geopark

*Susan May[1]

1. Hakusan Tedorigawa Geopark Promotion Council

Hakusan Tedorigawa Geopark, located in Hakusan City, Ishikawa Prefecture, is located near Kanazawa City –a famous and popular tourist destination. With the aim of increasing the number of tourists to the Geopark, from August 2020 we began a Social Network marketing campaign using the paid advertisement functions of Facebook and Instagram.

Online ads can be made to target certain areas, and we targeted Ishikawa Prefecture and the surrounding prefectures. From August to November we excluded the two prefectures directly neighboring Ishikawa Prefecture. As a result, views from Ishikawa Prefecture were the highest, with views becoming less frequent further from Ishikawa. This was also evident in views to the website, with the majority being from Ishikawa, with an increase in views from nearby prefectures.

As a result of the campaign we saw an immediate, but short-lived increase in views to our website as a result of advertisement clicks, which gradually decreased over time. Our Instagram account went from 302 followers in July, to 827 in February –a 174% increase. We noticed that advertisements containing pictures of scenery had high click rates, and advertisements were most popular with middle-aged people. As expected, advertisements concerning education and activities for children were most popular with middle aged women.

In addition to the effects to our website views, we also saw a small effect in the field. During September we conducted a survey at several key sights in the Geopark, and 2 people of the 168 people surveyed said that they came as a result of the advertisement, proving that although small, the advertisements had an effect. However, after running a campaign for approximately one month, where visitors were encouraged to visit a museum in exchange for a discount coupon, no visitors came to receive the coupon. Therefore it is believed that an instant response from viewers requires a greater reward and/or a longer run time.

As we continue this campaign we will continue to measure the effects both through online analysis and in-field surveys. Not only do we hope to see an increase in tourists, but also an increase in awareness of the Geopark.

Keywords: SNS, Marketing, Facebook, Instagram, Geopark, Tourism

©2021. Japan Geoscience Union. All Right Reserved.

Activities to promote the local sustainable development - Report at the time of spread of COVID-19 infection from Mt.Kurikoma Area Geopark -

*Yui Hasegawa[1], Rie Nakagawa[1], Seiya Tanaka[1], Jun Nagao[1]

1. Mt.Kurikoma Area Geopark Promotion Committee

Due to the effects of the spread of COVID-19, it became difficult to hold events where people could gather and various projects that had been previously planned. However, we worked to find projects that we could carry out only because our normal activities were restricted.
In conservation activities, we made use of the grant system and cooperated with researchers from universities and research institutes to promote research on disaster prevention education, social services, ecology, etc., and actively engaged in research activities that are at the root of Mt.Kurikoma Area Geopark.
In educational activities, we received requests from teachers to conduct learning activities as usual, mainly at elementary schools in the city, and implemented Geopark learning programs 50 times after taking sufficient measures to spread the disease. We also provided online information on Mt.Kurikoma Area Geopark Visitor Center and guidebooks were distributed free of charge to support learning.
In economic activities, we prepared guidelines for guiding activities to prevent the spread of COVID-19 infection, and studied and implemented safety management measures such as setting a limit on the number of guides and guiding with masks.
With regard to the "Kurikoma Sanroku no Megumi," an initiative to certify products that take advantage of the location and regional characteristics of Mt.Kurikoma Area Geopark, an e-commerce site was set up in the summer as part of support for certified businesses whose sales have declined due to the spread of COVID-19. For about three months, the EC site was set up to sell an assortment of partially certified products in the confectionery category. After that, the site was revised based on the sales results, and at the end of the year, sales for year-end gifts were conducted and 62 applications were received. At present, a stamp rally is being held until June 30, 2021, in which 17 stores, including stores in the food (restaurant) sector, are participating.
From these, we will consider sustainable regional development using Geoparks in COVID-19.

Keywords: Mt.Kurikoma Area Geopark, Geopark, Sustainable Development, Local Participation, Empowerment

©2021. Japan Geoscience Union. All Right Reserved.

Geotourism in Corona (COVID-19) related crisis - Advantage of being outdoors : In case of San'in Kaigan UNESCO Global Geoprk -

*Noritaka Matsubara[1], NAGAHAMA SATOSHI[1]

1. Graduate School of Regional Resource Management, University of Hyogo

The Corona (COVID-19) has a great impact on tourism in the world. UNWTO reports international tourist numbers could fall 60-80% in 2020. The other hand, number of tourists increased on some geosite and activity group in the San'in Kaigan UNESCO Global Geopark. We discuss why the number of tourists has increased or not changed in some sites and activities.

Keywords: geopark, tourism, COVID-19

©2021. Japan Geoscience Union. All Right Reserved.

Operation of geo-tours using online delivery tools under COVID-19

*Taku Morimoto[1]

1. Unzen Volcanic Area Geopark Promotion Office

1. Introduction

The COVID-19 has greatly affected social activities around the world. In the geopark programs, many activities and events had to be postponed or cancelled. While it has become difficult to conduct activities in the “face-to-face” style, the “online” forms of activities have gained the attention.

In 2020-2021, the Council of Unzen Volcanic Area Geopark (hereinafter called Unzen Geopark) conducted learning activities for secondary schools and took part in the exchange program for primary schools with the Oita Bungoono Geopark, using a web-meeting system “Zoom”. As these activities were held indoors, it was found that they could be easily conducted as long as the Internet environment (e.g., wired LAN) was stable.

As for the online geo-tours delivered from outdoors, they required a great deal of effort, compared to the indoor activities, including the selection of delivery tools, checking the Internet environment at each site of the tour, and acquiring camera techniques. This presentation will share the experience of online geo-tours conducted by the Unzen Geopark in 2020, and report on the types of delivery tools, and advantages, points of concern and issues in different methods.

2. Tools used for the online geo-tours

The online geo-tours were conducted in 2 ways: both ways used a mobile Wi-Fi router, but one in combination with Zoom (smartphone ver.) only, and the other with GoPro video camera and Zoom (PC ver.) together. The former method is to use a smartphone with Zoom app and an image stabilizer with anti-shake function. This method has an advantage of enabling interaction via smartphone screen and having a Q&A session during the tour. Its disadvantage is that the camera and sound-collection functions depend on the performance of smartphone. The latter method is to use the live-streaming function of GoPro and a platform for online streaming such as YouTube and Twitch. For the platform, Twitch is recommended as its transmission delay is short. An advantage of this method is that it can deliver sharp images of the sites to viewers, while it requires an initial cost for purchasing equipment. Since GoPro allows only one-way communication from the host to viewers, it is necessary to connect the Zoom from other devices if a Q&A session is conducted during the tour.

3. Issues and points of concern in conducting online geo-tours

The Unzen Geopark conducted online geo-tours guided by official Geopark Guides during the evaluation for revalidation of geopark status by the Japan Geopark Committee and in the event hosted by Oita Prefecture. One of the issues faced in the tours was that even if the Wi-Fi router was within the coverage area of the carrier used, there was a problem with Internet connectivity at some sites. Even in open fields with no geographical distance or obstacles, there were cases that Wi-Fi connection did not work. Therefore, when conducting online tours, it is important to carefully check the Wi-Fi connection at each site in advance and set the tour route including where to place the Wi-Fi router.

It is also necessary to have the camerawork that prevents viewers from getting screen sickness, and to put “pauses” for viewers to enjoy the scenery. During the tours, staff of the Unzen Geopark operated the

©2021. Japan Geoscience Union. All Right Reserved.

camera while the Guides explained about the site, but due to the fast pace of Guides switching the explaining subjects and walking, there were times when a “gap” occurred between the scenery shown and the contents of explanation. If the camera moves fast, it will elicit screen sickness from viewers and will not fully covey the appeal of the tour. It is important to always remember to guide the tour from the standpoint of the viewers watching through the screen.

In the event hosted by Oita Prefecture, it was planned to live-stream “a walk” in hot-spring town of Obama. However, due to an error caused by updating the GoPro app just before the event, it became impossible to live-stream a walking tour. We had to give up the walking tour, and changed to conduct the tour using the built-in camera of a PC connected to Zoom and showing the scenery that could be delivered without moving the PC. This kind of sudden trouble happens anytime, so it is important to always make an alternative plan when conducting an online tour.

4. Future prospects

It was found that anyone can easily start online tours if they become familiar with equipment and delivery tools. If more geoparks start conducting online geo-tours, it will be possible to deliver geo-tours jointly with other geoparks under common themes in the future.

Keywords: Live streaming, online geo-tours, Zoom, GoPro, mobile Wi-Fi router

©2021. Japan Geoscience Union. All Right Reserved.

Holding of event the Lake Shikaribetsu Igloo Village under COVID-19 measures

*Kanamori Syosaku[1], Hiroki Matsumoto[1], Onishi Jun[1]

1. Tokachi-Shikaoi Geopark Promotion Council

Tokachi Shikaoi Geopark is a geopark that covers the entire area of Shikaoi Town in the Tokachi region of Hokkaido. Theme of the geopark is “The story of life developed by volcanoes and freezing.” There are several geopark sites related to the cold climate. Lake Shikaribetsu in the northern part of Shikaoi Town is a representative site of Tokachi Shikaoi Geopark, and it freezes completely in winter. Since 1980, an event entitled "Shikaribetsuko-Kotan",which means “Lake Shikaribetsu Igloo Village”, has been held at Lake Shikaribetsu in winter. Kotan means village in Ainu language. At this event, many buildings called igloos are built using snow and ice on the frozen lake. There are many interesting activities such as ice bars, open-air bath, concerts in the igloos. This "Shikaribetsuko-Kotan" is also an important “site” of Tokachi Shikaoi Geopark.
"Shikaribetsuko-Kotan" in 2021 is held for about two months from January 30, 2021 under measures against COVID-19, while many domestic events have been canceled due to the influence of the corona disaster. In this presentation, we will report how the event was and discuss the ideal way of events under the influence of COVID-19.

Keywords: COVID-19, geopark

©2021. Japan Geoscience Union. All Right Reserved.

Stay-at-home Project with Local Students in Toya-Usu UNESCO Global Geopark

*NIRE KAGAYA[1], Yoshiaki Hata[1], Akihito Kato[2], Kiyono Kuroda[2], Koki Takagi[2], Kazuma Iwamura[2], Kanako Kitada[2], Koki Tomita[2], Mina Shionoya[2]

1. Toya-Usu UNESCO Global Geopark Council, 2. Date-Midorigaoka Highschool

In 2020, it was almost impossible to hold group events and outdoor activities as COVID-19 raged in Japan, and brown bears were spotted in our community more often than ever.
Under such a challenging circumstance, we sought to organize activities in different ways. In this presentation, we would like to give you one of the activities we did while observing the social distancing policy. We will present an educational project, “Let’s make together Lake Toya’s underwater model!”, which was carried out in collaboration with local elementary school pupils and junior and senior high school students.
This project was designed to make a 1/1,000 scale (1.3 m x 1.3 m) model of Lake Toya that reproduces the lake’s topography with local children. The model has been exhibited at the Lake Toya Tourist Information Center.
The nine-month project was developed as follows.
-Stage 1 (‘Stay-at-home event’): Participants made 148 layered model parts (37 layers x 4 divisions);
-Stage 2: Students of Date Midorigaoka High School Geography Course assembled the parts and painted the model; and
-Stage 3: The students made a presentation, and the model exhibition began.
If you ask a professional to make this kind of model, no one can be involved in the process. We designed this project as a participatory event for the people in the area. A total of 150 people (and their families) participated in making the model, and the completed work will be a symbolic exhibit of the Geopark in the future. We plan to use the model for teaching the history of regional topography formation and the risk reduction of geological disasters.
The COVID-19 pandemic will trigger significant changes to the communication and values that we appreciate. Each Geopark must think of what role the world expects from Geoparks and what contributions we can make to the world. To this end, Geoparks in Japan and the world have done various practices while being aware of the world after COVID-19, which have given us many thoughtful insights and new ideas.
Geoparks in Japan have domestic and international networks such as JGN, APGN, and GGN. These networks’ significance is represented in the diversity that encourages us to simultaneously address multiple challenges based on each region’s unique characteristics, and the oneness that unites us to promote such diverse activities by sharing “failures” and “know-how on success”. In our presentation, we will share with you one of our various practices by talking about our trials, errors, and the resulting success.

Keywords: Geopark, Geomorphology, Disaster Risk Reduction Education, Education for Sustainable Development

©2021. Japan Geoscience Union. All Right Reserved.

Developing the San’in Kaigan Geopark Trail and the promotion of geotourism during COVID-19 Pandemic

*Hiroshi Nakase[1]

1. San'in Kaigan Geopark Promotion Council

The establishing a long trail route, 230km long east-west route connecting Tottori City, Tottori Prefecture and Kyotango City, Kyoto Prefecture was completed in February 2020.

Even during the time of sharp drop down of number of tourist and a severe decline of tourism industry because of COVID-19 pandemic, the trail walk activity was safely conducted in 2020 using the newly completed trail, under the title of "Now is the time to return to nature! To the San'in Kaigan Geopark Trail!", with regional campaigns to revitalize the local economy, maintain and secure employment and consumption, maintain the health of local residents, promote the use of national parks, and foster awareness of environmental protection.

In implementing the activity, a system was established so that visitor centers, geoguides, outdoor activity businesses, retailers, and restaurants can cooperate to conserve geosites and provide services in order to strengthen geotourism after COVID-19 pandemic.

Through poster session, we will introduce the contents of this campaign, its results of 2020, and future developments of it.

Keywords: San’in Kaigan Geopark, tourism, protection and conservation

©2021. Japan Geoscience Union. All Right Reserved.

A comparative study of educational on-site and online geotours in Hamamatsu-Hamanako Aspiring Geopark, Japan

*Hiroki Nagano[1], Masato Koyama[2], Yusuke Suzuki[2], Megumi Fukuyama[2]

1. Hamamatsu Technical High School, 2. Shizuoka University

We made a practical study of on-site and online geotours in Hamamatsu-Hamanako Aspiring Geopark, central Japan, to clarify and compare educational effects of each type of tours. In August and October of 2019, we made two on-site bus tours (tours 1a and 1b), both of which were based on the same scenario focusing on the geological formation of Lake Hamanako and its deformation by the AD1498 tsunami disaster. In September and November of 2020, we made two online tours (tours 2 and 3) using the internet meeting application Zoom because of restriction under the COVID-19 pandemic. While tour 2 focused on the same scenario as tours 1a and 1b, tour 3 was based on the different scenario, which focused on the geological formation, historical floods, and relating agricultural/industrial products in the alluvial plain of the Tenryugawa River. All of the on-site and online tour participants were children and their parents, which were recruited by advertisement in elementary schools in the City of Hamamatsu. Main results of pre- and post-tour questionnaire surveys are as follows: (1) Understanding level of geological process (L1), pride level for regional geosites (L2), motivation level for further learning (L3), and total satisfaction level (L4) all show significant increases after tour 3, comparing with those before the tour. (2) L1 and L4 after tour 3 show significant increases comparing with those after tour 2. This is probably resulted from the decrease of connection troubles during tour 3 by improvement of networking instruments, (3) L1 and L4 after tour 3 are similar with those after tour 1a/1b. This may mean that educational effects of good online tours are equivalent as those of on-site tours.

Keywords: Geopark education, Online tour, Educational effect

表１　オンラインツアー第２回事後アンケート結果と，同オンライン第１回及び対面ツアーとの比較

質問項目		全体 (n=37)	第１回比	対面比	児童等 (n=27)	第１回比	対面比	大人 (n=10)	第１回比	対面比
1	浜名湖（天竜川）の地形の成り立ちを説明できるようになった	3.3	**+0.6	-0.3	3.2	**+0.8	-0.2	3.5	+0.4	-0.3
2	地域に浜名湖（天竜川）があることを誇りに思うようになった	3.7	+0.2	+0.0	3.6	+0.1	-0.0	3.9	+0.5	+0.2
3	自分の住んでいる地域にについて自分から勉強したくなった	3.3	+0.0	-0.0	3.1	-0.0	-0.1	3.7	+0.0	+0.2
4	ツアー全体の満足度	3.7	**+0.4	-0.1	3.5	*+0.5	-0.2	3.9	**+0.5	-0.0

（表中の＊は$p<0.1$，＊＊は$p<0.05$であり，前者は有意傾向，後者は有意差があることを示している。）

©2021. Japan Geoscience Union. All Right Reserved.

Topographic evolution after the Aso-4 pyrocrastic flow and the meaning for disaster prevention in the Oita Bungoono Geopark, Japan

*Toshikazu Yoshioka[1]

1. Oita Bungoono Geopark Promotion Council

The southwestern part of Oita Prefecture, where the Oita Bungoono Geopark is located east of the Aso v olcano, and the plateau formed by the Aso-4 pyroclastic flow that erupted about 90,000 years ago is spreading. The plateau was dissected by the Ono River and other rivers, and the remaining part of the plateau is called "Haru" and is used as a vast agricultural land. Of the dissected valleys, the valley bottom of the basin formed by relatively small rivers has been used as a residential area because it is easy to obtain water for living. On the other hand, the Ono River, which is one of the longest rivers in Kyushu, forms a deep valley while meandering, and although several river terraces can be seen along the river, the alluvial plain is hardly distributed.
The central city area of Mie Town, where the Bungo Ono City Hall is located, is located near the confluence of the Mie River and Tamada River, which are tributaries of the Ono River. After merging with the Tamada River, the Mie River does not head toward the main stream, the Ono River, but flows southeast toward the mountains, and after merging with the Matsuo River, flows north and joins the Ono River. The area near the confluence with the Matsuo River is a constriction, and upstream of it is accompanied by a wide alluvial lowland, but after the confluence it forms a deep valley.
These topographic features are greatly related to the characteristics of disasters in this area. First of all, along the Ono River, there is a disaster caused by the rise in water level during rainfall. The Ono River has a large basin area, and the upstream area includes areas with high rainfall such as the Aso, Kuju, and Sobo-Katamuki mountains. In addition, dencely welded tuff of the Aso-4 pyroclastic flow is distributed along the main stream, and the valley bottom plain is narrow because lateral erosion is hindered, and the water level rises at once when the water level rises. On the other hand, the lowlands along the tributary Mie River have their exits blocked, so once flooding occurs and the surrounding lowlands are flooded, drainage may become difficult. In addition, the small tributaries that flow into the Mie River are relatively steep and the valley width is narrow, so it can be pointed out that a disaster may occur due to debris flow. Furthermore, on the slope of the plateau edge, the base may be eroded by the gushing of groundwater, and the upper part of the slope may easily collapse.
The content of this presentation was given at the Association of Disaster Prevention Expert of Miemachi in October 2020, and efforts are being made to help with disaster prevention activities in the region.

Keywords: Oita Bungoono Geopark, Aso-4 pyroclastic flow, Ono River, topographic evolution, disaster prevention

©2021. Japan Geoscience Union. All Right Reserved.

Conservation and Utillization of Natural Disaster Monument on Tosashimizu Geopark Plan

*Moriguchi Natsuki[1], Satoru Imai[1], Aika Sakuda[1], Kouichi Saruta[1], Michiru Sakai[1]

1. Tosashimizu Geopark Promotion Council

Tosashimizu City in Kochi Prefecture, which corresponds to the area of the Tosashimizu Geopark plan, is facing the Pacific Ocean, and there are concerns about damage caused by the Nankai Trough earthquake and the resulting massive tsunami. In the past Earthquakes, such as the Hakuho, Hōei, Ansei Nankai, and Showa Nankai earthquakes, the city was severely damaged by earthquakes and tsunamis, which have been recorded in documents and monuments. In the Tosashimizu Geopark plan, seven stone monuments with records of Nankai Trough earthquakes and tsunamis existing in the area were designated as "Earthquake and Tsunami Related Monuments" as a cultural site. However, it was pointed out in the 2017 review for membership in the Japanese Geoparks Network that there was no legal basis for conservation. In addition, the use of the site for disaster prevention education was not sufficiently advanced.
In order to solve these problems, the Tosashimizu Geopark Promotion Council, in cooperation with citizens' groups and Tosashimizu City, conducted an exhaustive survey of the existing monuments recording past natural disasters in the area in 2019. As a result, 13 monuments related to other natural disasters, such as floods, were found, in addition to the earthquake and tsunami monuments that had already been designated as sites. These monuments were registered as "Natural Disaster Monuments" by the Geospatial Information Authority of Japan, and those with particularly high historical value were registered as tangible cultural properties designated by the city.
The Tosashimizu Geopark Promotion Council has reorganized these monuments as "Monuments to Natural Disasters," which include not only about earthquake and tsunami disasters, but also flood and typhoon disasters, and is promoting their use for disaster prevention education and awareness-raising about disaster prevention and mitigation. We conducted disaster prevention studies using the natural disaster monument at local elementary schools last year, and the monument will be included in a supplementary reader for social studies issued by the Board of Education. In addition, in cooperation with the Crisis Management Division, the division in charge of disaster prevention in Tosashimizu City, we are working to realize integrated disaster prevention and mitigation activities.
We will report on our action to preserve and utilize the stone monuments that record natural disasters in the Tosashimizu Geopark Plan. We will also discuss the prospects for disaster prevention and mitigation activities based on the use of natural disaster monuments in cooperation with citizens and local governments.

Keywords: Natural Disaster Monument, earthquakes, tsunamis, floods

©2021. Japan Geoscience Union. All Right Reserved.

Records and countermeasure of disasters in Shimokita Geopark

*Satoshi Ishikawa[1], Kirika Kitagawa[1]

1. Shimokita geopark promotion council

In Shimokita Geopark, local resident did not have enough disaster prevention awareness because of relatively much countermeasure for assumed disasters. So Shimokita Geopark Promotion Council strives to maintain and improve local resident's disaster prevention awareness by explanation of the example of hazards and countermeasures in other area and the disaster occurrence mechanism.

Keywords: Shimokita Geopark, Disaster, disaster prevention awareness

©2021. Japan Geoscience Union. All Right Reserved.

Inform of weather disasters in geoparks

*Hiroshi Sato[1,2], Shinichi Sugimoto[3], Makoto Aoi[4], Shinya Miura[4], Hinako Suzuki[4]

1. Mt.Bandai Museum, 2. Bandaisan Geopark Council, 3. Unzen Volcanic Area Global Geopark, 4. National Research Institute for Earth Science and Disaster Resilience

The land of Japan is prone to earthquakes and volcanic disasters, but the most frequent disasters are meteorological disasters. Typhoon-Vera class disasters are rare, but in recent years, rainfall caused by line-shaped precipitation system and river bank failures due to flooding. Especially in 2018 and 2019, meteorological disasters occurred in many parts of Japan. These disasters are not unique to others, but can also occur in geopark areas.

Therefore, the disaster prevention working group of the Japan Geopark Network (hereinafter referred to as JGN) thought that these disasters should be communicated in all geopark areas, and consulted with the National Research Institute for Earth Science and Disaster Resilience (hereinafter referred to as NIED). JGN and NIED signed an agreement on comprehensive cooperation in 2018, and have been working on a system called the "Earthquake!" to communicate the real-time occurrence of earthquakes in each region.

We have also decided to collaborate on weather-related disasters that have occurred frequently in recent years. The content of the collaboration is to create explanatory display panels on recent weather disasters and to display these panels in the Geopark area.The purpose of this project is to improve disaster literacy by viewing disasters as a personal challenge.

As the JGN, which has proposed putting more efforts into disaster prevention at UNESCO Geopark, we would like to continue to strengthen activities to inform of various disasters in geopark regions throughout Japan.

Keywords: weather disaster, disaster prevention, Geopark

©2021. Japan Geoscience Union. All Right Reserved.

How to Prevent Elderly People from Natural Disasters - An Example in Unzen Volcanic Area UNESCO Global Geopark -

Shunsei OGATA[1], Hiyori KADOHATA[1], Tasuku KONDO[1], Miraku TANAKA[1], Kosei HASHIDA[1], Shinsho FUJIO[1], Mizuho IWANAGA[1], Aiko ENGUCHI[1], Seren OTA[1], Rika TANAKA[1], Toru YAMAUCHI[2], Hiroaki OSAKO[2], *Marekazu OHNO[3]

1. Glocal Course of Nagasaki Prefectural Koka High School, 2. Nagasaki Prefectural Koka High School , 3. Unzen Volcanic Area Geopark Promotion Office

There are a lot of active faults in the areas recognized as Unzen Volcanic Area Geopark. These group of active faults are estimated to cause earthquakes with the possibilities of 0.5 - 1 % in 30 years and 0.8 - 2 % in 50 years (The Headquarters for Earthquake Research Promotion, 2006), and these numbers are relatively high in Japan, where earthquakes often happen. In addition, in the great Shimabara earthquake in 1992, 26 people were killed and 39 people are injured (Ota, 1984), and Tachibana bay area, which is located to the west of Shimabara peninsula, sometimes has series of volcanic earthquakes including ones with a seismic intensity of 5. These facts show that in Shimabara Peninsula, not only volcanic eruptions but also earthquakes which cause extensive damage can happen.

In this area, aging problem is also serious. The percentage of people who are over 65 years old is as much as 36.2 %, which is clearly high compared with the national average (28.1 %). Therefore, it is highly possible that a large number of elderly people will need to evacuate when a large earthquake occurs. Thus, we set our goal to establish a disaster prevention plan to protect the elderly.

In order to find out the difference of the awareness of disaster prevention among different generations, we conducted a research by sending out a questioner on their awareness of disaster prevention in daily lives to our school’ s students and their elderly family members: 409 people in total. We also examined the route from their residential areas to the evacuation center and compared it with the information put on the existing hazard map.

The result of the questioner showed that the elderly family members are more likely to be aware of disaster prevention than the students. This is equivalent to the result of a research conducted on university students and their family (Cabinet Office, 2016; Shimizu, 2011). Also, by examining the route to evacuate from their houses to the nearest evacuation center, we found out that the following three points are not put in the existing hazard map: (1) It has a long gentle slope, which is tough for the elderly to walk. (2) It has deep gutters at the side, which require extra caution if it is dark. (3) It has walls which can break down if an earthquake with a seismic intensity of 5 occurs.

These two results indicate that it is possible that the elderly people, who have greater awareness of disaster prevention, have difficulty in their evacuation. Therefore, we concluded that one way to prevent many elderly people from natural disasters is to make a detailed hazard map for each region, and raise young people’ s awareness of disaster prevention to make them “leading evacuees” when needed.

Keywords: Unzen Volcanic Area UNESCO Global Geopark, Nagasaki Prefectural Koka High School, Earthquake Hazards, Disaster Prevention

©2021. Japan Geoscience Union. All Right Reserved.

Disaster and Disaster Prevention Learning in the Naeba-Sanroku Geopark

*Kouhei Nakano[1]

1. Naeba-sanroku Geopark Promotion Council

Under the theme of "Natural Disasters and People", we will introduce two practices that we have already done in 2020. (Practice1 and Practice 2) One is for the general public, the other is for certified geo-guide members.

Practice 1:
We conducted a field tour called "Treasure Tour" for the general public by visiting some scars of disaster in the Naeba-Sanroku Geopark area. The followings are places we visited during this tour.
1) The Chikuma River Outcrops
・Located in front of the Sakae Village Office.
・It emerged after the 2019 East Japan Typhoon(Hagibis);
2) Aokura Avalanche Site
・It occurred in 1961 and killed 11 people.
・We visited the cenotaph during the tour.
3) The Nakajo River Collapse
・ It is scar of the 2011 Nagano North Earthquake.
4) The North Nagano Prefecture Earthquake Memorial Museum "Kizuna".
・We conducted this tour for not be forgotten of the fact that happened in March.12.2011.

Practice 2:
As a part of the guide training, a workshop was held by the disaster prevention section of Tsunan Town Office to understand the utility of hazard maps and create an evacuation plan called "Time Line" for just in case.

In order to raise awareness of disaster prevention among residents, we will continue to strengthen collaborative relations between the Geopark and the disaster prevention section of the local government.

©2021. Japan Geoscience Union. All Right Reserved.

Lives of the local people on the collapsing land and the flowing land by river water -Think about geohazard program of Miyoshi geopark project-

*Azusa Tonotani[1], Katsunori Ozakai[1], Mizuki Tochitani[1], Hiroyuki Ohnishi[1], Toshiaki Matsumoto[1]

1. Geopark Promotion office in Miyoshi city

Japan is known as one of the tectonic belt in the world. Therefore, various geohazards are caused such as the earthquake (subduction-zone and inland), volcanic eruption, the collapse of land (ex. land slide) and a heavy rain in Japan.

Miyoshi geopark project area is located in Tokushima prefecture and consists of all over the Miyoshi city area. As a feature of mainly geosciences are ;
1. Japanese median tectonic line (MTL) runs to east- west detection in this area. The south area of MTL is Shikoku Moutains and the north area is located Sanuki Mountain Range.
2. The south area mostly consists of Sambagawa metamorphic rock, and high mountains rise around 1500 m.
3. The average annual rainfall of Shikoku Mountains area in Miyoshi is about 2500 mm (heavy rain condition).
4. The Sanuki Mountain Range mainly consists of layers of sand stones and mud stones. Those layers often show the dip slope structure.
5. Yoshino river flows in Miyoshi area, sometimes cause floods at the middle and lower Yoshino-river area.

Those features triggered to cause the various geohazard such as the collapse of land (ex. land slide) and flood in past. Local people in this area lives together with distinctive geohazard for a long time, and we can see various those life style in local area even today. By way of example, Yokai stories (the oral tradition) in Miyoshi area are deeply associated with life style in a steeply and dangerous mountains area. Other example, local area name such as “Shima” area. Shima area is located in Ikeda town, and is often flooded because is located in the lowest river terrace.

Thus, a lot of original life style together with distinctive geohazard have been handed down in Miyoshi geopark project area. However, local area people don’t understand about each geohazard mechanism enough.

In this poster, we will introduce about the life style together with distinctive geohazard for a long time, and approach to various geohazards in Miyoshi geopark project area.

Keywords: Miyoshi geopark project, Geohazard, Land slide, Flood, MTL

©2021. Japan Geoscience Union. All Right Reserved.

Toward restoration of Geosites damaged by natural disaster with reaching consensus in local community: a case of Suzaki Coast in Seiyo City, Japan.

*Takumi Sakakiyama[1], Kazunari Kimura[2], Yuya Kato[3], Masahito Ono[1], Tsukasa Takahashi[1]

1. Seiyo City, 2. NAIBA Co. Ltd., 3. Noyama Company

In Japanese archipelago located in the deformation zone, we are always in the risk of catastrophic natural disasters that cause serious and widespread damage to society. The measures for these disasters will be carried out based on risk assessments and disaster prevention plans led by the government and institutes. The National Research Institute for Earth Science and Disaster Resilience (NIED) and the Volcanological Society of Japan cooperated to compile Database on Volcanic Hazard Maps and Reference Material.(1) The risk of huge earthquake occurrence is evaluated at Nankai Trough Earthquake Evaluation Study Group(2) sponsored by the Japan Meteorological Agency. On the other hand, it should be promoted the disaster prevention and reduction for Landslide Disaster in local communities by creating the Community Disaster Management Plan. However, the collapsed slopes are quickly covered because of ensuring lifeline and safety are taken the priorities during emergency. Therefore, it is difficult to educate inhabitants through field observations for slope failures. In this case, the slope failures occurred at a distance from the living area, such as natural heritage and geological heritage may be a good opportunity to understand the mechanism and talk about the restoration and utilization.

There is acidic tuff layer with vertical stripes in the Kurosegawa Tectnic Zone on the outcrops of the Suzaki Coast in Mikame, Seiyo City, Ehime Prefecture, Southwest Japan. The Suzaki Coast is one of the Geosites conservated by the Shikoku Seiyo Geopark. There are a cliff-shaped outcrops along the coast, and the path is maintained at this foot. Due to the rain from July 6th to the morning of 7th, 2020, The slope collapse occurred on a part of the slope on the mountain side of the path on the Suzaki Coast. The width of the slope failure is about 10 m, and the height from the coast to the collapse head is about 55 m. In addition, according to the results of a simple survey conducted in August, the amount of sediment deposited was estimated to be about 800 m^3. Although the collapsed sediment contains some acidic tuff gravel, it is considered to be a surface collapse of the sediment part existing at the upper part of the cliff because the weathered soil originating from the acidic tuff is the main component. The path is still restricted. It is difficult to remove the collapsed soil by heavy machinery or human power because the location of the path is not suitable to berth ships. Here, we have taken aerial photographs about once a month using a small drone, and simply monitored change in the amount of collapsed soil. As a result, after the passage of Typhoon Haishen in September, the collapsed soil deposited under the path moved due to the waves, and the collapsed soil deposited on the path also decreased slightly. In contrast, the amount of change was insignificant from October to February. Consequently, it is supposed that the movement of colluvium is more affected by waves than rainfall. If we experience waves caused by typhoons that reach the upper part of the path several times in the future, it is expected that the amount of soil will be reduced to a scale where restoration of the original can be started.

Furthermore, our group is going to present the educational program named "Seiyo Nature and Culture College" at March 13th, 2021 and the reactions of the participants and staffs. This program is going to plan the excursion to watch the collapsed soil mass in the Suzaki Coast and take the meeting about this.

Referred websites

(1) NIED "Database on Volcanic Hazard Maps and Reference Material":

©2021. Japan Geoscience Union. All Right Reserved.

http://vivaweb2.bosai.go.jp/v-hazard/ (last access on 2021.02.08)
(2) Japan Meteorological Agency "Nankai Trough Earthquake Evaluation Study Group":
https://www.data.jma.go.jp/svd/eqev/data/nteq/assessment.html (last access on 2021.02.08)

Keywords: Shikoku Seiyo Geopark, Suzaki Coast, Slope Failure, Drone, Disaster Prevention and Reduction

©2021. Japan Geoscience Union. All Right Reserved.

Let's investigate the earth activity from Shimonita Geopark

*Hara Hideo[1]

1. Geopark Shimonita council

Intro

The Shimonita town of Southwest Gunma is the town which is full of located nature. Shimonita basin is a plateau of Shinshu and a basin in during Kanto plains.It is two major special products such as "Shimonita-negi" and the konjac.
Shimonita-machi is the place that ever prospered as a course linking Edo to Shinshu.It is dotted with industrial inheritances using nature, the topography in a town.For examle,world helitage Arfune colad strage.It is one of the Japanese Geoparks that are 43 places in Japan.Typhoon Hagibis in 2019, It brought the damage such as floods in our area.The guide of the Shimonita Geopark tells the lesson of the flood in a guided tour.I discuss it about the story of the Shimonita Geopark and guide who introduce the lesson of the disaster by the main subject.

Three stories of Shimonita Geopark

Story.1 Great upheavals from the bottom of the sea to the land
Story.2 The ancient volcanic activity that separated plateau and Kanto plains
Story.3 The town of the course along the median tectonic line

Geopark Promoting activity and Disaster Resilience Education

We work on guide tourism, school education, disaster prevention education, activation of the local industry. The guide conveys an activity of the dynamic earth from nature of Shimonita. The typhoon Hagibis in caused a flood and changed the scenery. The guide tells a photograph and the damage situation at the time of the flooding in the case of the typhoon. And they convey about nature's wrath behind the scenery of beautiful nature to a tour visitor.
A tour visitor understands nature through this activity definitely, and we hope that it comes to be prepared for a disaster.

Keywords: Geodiversity, Geotourism, Education of Geology, Geopark, education for disaster prevention

©2021. Japan Geoscience Union. All Right Reserved.

The foundations of Yuzawa Geopark: a unification and a compilation of six geological maps published by the Geological Survey of Japan and Akita Prefecture

*Akio Sasaki[1], Kohei Yamawaki[1], Yukio Fujimoto[1], Syoichi Goi[1], Shoei Chiba[1]

1. Network of Earth Science Museum for Akita

The Yuzawa Geopark consists of approximately 300 geosites in the Yuzawa city, which are covered by six geological maps published by the Geological Survey of Japan and the Akita Prefecture.

It is difficult to understand geological events in this region using these maps alone, because of the different formation names at the same period, no-radiometric dates of volcanic rocks, and various coloration in these maps.

We began to work the project of the unification and compilation of six geological maps in 2017. During this project, we gathered the published papers including radiometric dates, preformed the geological field survey, collected fossils and rocks, and reconstructed the standard stratigraphic column for the study region. Based on these data, we compiled the distributions of formations from the same age in the study region.

The seamless geological map (B0 size) and a corresponding 226 page report were completed in 2020. These works provide valuable information including eruption ages of volcanic rocks from the Oligocene to the Pleistocene, and also newly discovered locations of molluscan and plant fossils. The seamless geological map and the report are useful for making the geo-story of geosites in the Yuzawa Geopark in near future.

References

Ozawa A. et.al. (1961)Uzenkanayama, (1979) Yuzawa, (1979) Asamai published by Geological Survey of Japan.
Usuta M. et.al. (1979)Yokote, (1981) Inaniwa, (1982) Akinomiya-Kurikomasan published by Akita Prefecture.
Takashima K. et.al. (1999) J. Min. Petr. Econ. Geol. Vol.94, p.1-10,
Kondo H.et.al. (2004) Island Are.vol.13, p.18-46.

Keywords: Geopark, Formation names, Fossil, Pyroclastic rock, Radiometric dating, Seamless geological map

©2021. Japan Geoscience Union. All Right Reserved.

Conservation concerns in Yuzawa Geopark: Distributions and seasonal variation in blood-sucking flies and an invasive plant species

*Haruki Takayanagi[1]

1. Yuzawa City Geopark Promotion Council

Yuzawa Geopark, located in Yuzawa City, Akita, Japan, is subject to two conservation issues that are common to many urban greenspaces: pest species are of concern for sustainable tourism, and invasive species threaten the integrity of the satoyama landscape. The first step in the management of both of these species groups is to clarify their distribution and seasonal variation. Here, we focused on blood-sucking flies (*Hirosia* spp.) in tourism hotspots, and on the invasive *Rudbeckia laciniata* in areas where it has colonized the satoyama landscape. Using dry ice traps, we found that blood-sucking flies were most abundant in early August, and that *Hirosia iyoensis* and *Hirosia sapporoensis* may have mutually exclusive spatial distributions. Visual surveys for *R. laciniata* confirmed that these plants occupy orchards, mined areas, and areas around silos at high densities, and have a patchy distribution in downstream areas. Appropriate mitigative measures are presented and discussed based on these results.

Keywords: blood-sucking flies, conservation, invasive species

©2021. Japan Geoscience Union. All Right Reserved.

The relationship between the former plate boundary and residents, especially the signboard production process

*Kato Satomi[1]

1. Mt. Apoi Geopark Promotion Council

Themes of Mt. Apoi Geopark is A Story of gifts from deep inside the earth connecting land and people together. Mt. Apoi is made up of peridotite that was thrust up from the depths of the earth by global-scale dynamic ground movement. Mt. Apoi Geopark is a stage featuring narratives that connect the planet’ s constitution, nature and people.

Sub- theme A: Peridotites- the interior and dynamic movement of the earth

The Hidaka Mountains formed as a result of a collision between two continental plates 13 million years ago. At that time, part of the mantle under the crust was thrust up onto the earth's surface to form the Horoman peridotite complex, which includes Mt. Apoi. The relatively fresh peridotites on and around the mountain contain valuable information from deep inside the earth's mantle, making them the subject of global attention. Mt. Apoi Geopark provides a variety of opportunities to learn about and enjoy phenomena relating to the earth's transformation. These include its status as the site of a plate collision, oddly shaped masses made of cooled and solidified magma, and rocks from far-off southern seas.

Sub- theme B: Alpine Plants- scarcity and the natural environment

Despite its low altitude, Mt. Apoi provides habitats for alpine vegetation due to its unique soil, weather and geographical conditions. Hidakaso (Callianthemum miyabeanum) and a host of other endemic species grow here, and the area's alpine plant communities have been collectively designated as a Special Natural Monument of Japan. In addition to alpine plants, the area is also home to the endemic Apoimaimai snail (Paraegista apoiensis) and Himechamadaraseseri (Pyrgus malvae; a butterfly not found anywhere else in Japan), as well as the Japanese pika (a relict species from the Ice Age). Mt. Apoi Geopark's valuable and diverse ecosystem provides opportunities to learn about and enjoy the natural environment.

Sub- theme C: Human History- the community of the nature and human life

The beautiful scenery of oddly shaped rocks (including masses called Oyako-iwa, Sobira-iwa and Cape Enrumu) along the Samani coast is a highlight of Hidaka's coastal road. Legends handed down by indigenous Ainu people in Samani, where Mt. Apoi Geopark is located, often feature these rocks. Cape Enrumu has long been known as a favorable natural harbor thanks to an ideal landform that shelters ships from strong winds, helping Samani to prosper as an important trading hub for Kitamaebune merchant vessels from the Edo period (1603 - 1868) onward. The rich history of people living with Mt. Apoi and the

©2021. Japan Geoscience Union. All Right Reserved.

sea continues to the present day in Mt. Apoi Geopark, making it an ideal place to learn about and enjoy the symbiosis between humans and nature.

Keywords: Former plate boundary, signboard

©2021. Japan Geoscience Union. All Right Reserved.

Fossil collecting experience to solve summer vacation indipendent study in Itoigawa UNESCO Global Geopark

*Yousuke Ibaraki[1], Yutaka Furumi, Emma Longhorn, Takahiko Ogawara[1], Ko Takenouchi[1], Takuma Katori[2], Takeo Kobayashi[2]

1. Fossa Magna Museum, 2. Itoigawa Geopark Council

Itoigawa UNESCO Global Geopark had held many education and outreach activities before 2009, when the Itoigawa Geopark was authorized as a member of the Global Geoparks Network. In 2020, many activities had to be cancelled because of the COVID-19 pandemic, but we held an education and outreach event with fossils using the grant for science museum activities from the Japanese Council of Science Museums.

The activity contains four events, using variable geology of Itoigawa Geopark, to search for fossils of Paleozoic, Mesozoic and Cenozoic in Itoigawa City, and fossil collecting experience and museum tour in Fukui Prefecture Dinosaur Museum.

This activity catered to elementary and junior high school students and their parents. To prevent new coronavirus infection, we limited the numbers of participants of each event to under 10.

The notice of the activity are, to distribute a flyer for all elementary and junior high school students, to publish the article of the participation offer of the activity in the public information paper of Itoigawa City, and to announce the participation offer in Itoigawa Geopark official Facebook. Applications were made to the Fossa Magna Museum, with applications only accepted by telephone to secure equitableness.

In the Itoigawa Geopark, Jade, Fossa Magna and many kinds of rocks on the beach are treated as main themes and used for promotion. But the fossils are treated as one of many themes.

Fossils are an interesting theme for not only children but adults, and useful for familiarization with geology. In the sign-up period for this activity, we received many calls from the morning of the first day. The number of applications exceeded our expectation. However, even with many events cancelled because of the pandemic, it is evidence of the high popularity of fossils.

Through the activity, participants look for and find fossils themselves, and received an explanation, and they may thought about ancient times when the creatures which became fossils lived. Perhaps there are children who would like to be a paleontologist. Fossil collecting of the dinosaur age was done in Ichiburi, Itoigawa City and in Fukui Prefecture, but no dinosaur fossils were found. However all of the participants found fossils of the dinosaur age, so the participants were satisfied to join the activity.

In 2020 fiscal year, we are planning an activity to make fossil replicas in March using the remainder of the grant for science museum activities from the Japanese Council of Science Museums. We would like to further promote the fossils of Itoigawa Geopark for education and outreach activities.

Keywords: Itoigawa UNESCO Global Geopark, Fossa Magna Museum, fossil collecting, education and outreach activity, geo-diversity

©2021. Japan Geoscience Union. All Right Reserved.

©2021. Japan Geoscience Union. All Right Reserved.

Geosite Map and Card in a Fun and Interesting Way by Local Elementary School Students: a Case Study of Geosite in Nankikumano Geopark with Takaike Elementary School

*Hiroko Shibasaki[1]

1. Nanki-Kumano GeoPark Guide Club

Cooperation with local schools is important for Geopark activities.

A good way to do this is to implement them in community studies and integrated learning.

(Takenouchi et al. 2014, Teramoto et al. 2017, Ueki 2019, etc.).

Ideally, children should choose Geopark activities as a means of learning because they want to learn independently. This is what leads to "fostering the qualities and abilities to find issues on their own, learn on their own, think on their own, make independent decisions, and solve problems better," which leads to the development of human resources to support sustainable regions.

The governing body of the Nanki-Kumano Geopark has a program to dispatch certified Geopark guides and specialists to schools. The presenter, a certified Geopark guide, has a relationship with local elementary and junior high schools and the Board of Education, and was able to collaborate on this project.

In this presentation, we will introduce an example of one of the activities conducted from July to December 2020 with 5th graders of Takaike Elementary School in Kozagawa Town, Wakayama Prefecture. The town is dotted with major villages along the Kozagawa River system, a second-class river running through the southern part of Wakayama Prefecture. In the middle to lower reaches of the mainstream, there are geosites such as the " Ichimai-iwa(monoliths) of Kozagawa River " and the " The Mushikui-iwa(insect-eating) Rock in Takaike " along the river, and the " Taki-no-hai (waterfall) " in a tributary stream. These are composed of the " Kozagawa arc-shaped dike", which is considered to be a part of the ring dike of the Kumano caldera (Miura, 1999) that was active during the Miocene of the Neogene period, and rocks related to siliciclastic igneous activity during the same period. The students in the same grade have been learning about these rock formations and landscapes that are characteristic of Kozagawa Town in their comprehensive studies every year.

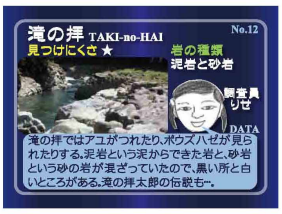
In order to deepen their study, they requested the cooperation and guidance of a Geopark guide, and took advantage of the aforementioned system.

In this way, this activity started with the school and the children as the main actors, both in setting the theme of the integrated study and in the way of interacting with the Geopark guide. Therefore, the presenter respected the independence and will of the children as much as possible during the activity. The results are reported here.

Keywords: Geo-education, integrated learning, community studies, geosite card, geosite pamphlet

©2021. Japan Geoscience Union. All Right Reserved.







上：パンフレット

右：カード一例

©2021. Japan Geoscience Union. All Right Reserved.

Examples of joint projects (or joint events) between a museum and Sado Island Geopark

*Takeyoshi SADAKANE[1], Mituhisa AIDA[1]

1. Sado Geopark Promotion Council

Sado Museum is one of the main facilities of Sado Island Geopark.
Active collaboration between this museum and Sado Island Geopark has been a challenge for many years, and during the revalidation process in 2019, it was suggested that the museum could be used as a place of "learning-based exhibits that would interest children about Geopark".

Two events for children jointly held at Sado Museum in 2020 were the first step towards this goal.
First of all, the exhibition was collaborated with a stamp rally. The stamp rally is organized every year under the initiative of Niigata University. A stamp rally means going to different locations to collect stamps on a card. In many rallies you can win prizes according to the number of stamps you collect. The stamp rally is a themed event designed to encourage people to visit Geoparks in Niigata Prefecture. The theme for 2020 was "Microfossils in Geoparks," and Sado Museum held a mini exhibition in line with this theme. Also, we participated in the "Sado Museum Festival" organized by this museum as an event for children. In our program, entitled "Rock Garden Treasure Hunt", visitors were asked to solve quizzes about rocks on display while walking around the museum's courtyard.

Through these activities, we believe that we were able to increase the number of children who visit the museum and introduce Sado Island Geopark to younger children. Sado Island Geopark has been steadily promoting cooperation by holding special exhibitions at Sado Museum and by having Geopark guides show visitors around the museum.
In this presentation, I will describe the details, effects, and challenges of the various events held at Sado Museum.

Keywords: geopark, Sado-Island, Museum

©2021. Japan Geoscience Union. All Right Reserved.

A Guide program that promote Proactive learning in School trip - Practice at Toya-Usu UNESCO Global Geopark -

*Hikaru Yokoyama[1]

1. Hokusho University

The area around Lake Toya in the southwestern part of Hokkaido was certified as a "Global Geopark" in 2009. This area is known as a place where you can not only enjoy the scenery and hot springs, but also learn about valuable geology and volcanic disaster prevention. Many schools visit the area as a place to visit for school trip, and in recent years, they have been seen learning outdoors as part of disaster prevention learning.

Now, the practice of "Proactive, Interactive and Deep learning" has been required in the field of education. Therefore, I wondered if it would be possible to provide a program that encourages students to learn independently even on school trips to Geoparks. So I assumed that the student would take the initiative in learning by changing from a learning style in which the guide "tells" to a style in which the student's "awareness of natural things / events" is valued.

Last year, I was able to practice this guide program in an elementary school's school trip. As a result of the practice, many children enjoyed "thinking" through quizzes and Interact based on the discovered events. In addition, a questionnaire one week later revealed that most of the tours left an impression on students. In this presentation, I will report on the programs that I practiced and how the students participated learned.

Part of this work was supported by JSPS KAKENHI Grant Number JP17K01041.

Keywords: Proactive, Interactive and Deep learning, School trip, Disaster prevention learning, Guide program

©2021. Japan Geoscience Union. All Right Reserved.

Educational Program on spring water of Aso UNESCO Global Geopark related with elcetrical conductivity (Part 2) Cooperated Research on Minamiaso Spring Water

*Tsuneomi Kagiyama[1], Koki Nagata[2], Toshikazu Maeda[3], Yuto Takeuchi[3], Haruki Watanabe[3], Kozue Inoue[3]

1. Aso Geopark Promotion Council, 2. Aso Volcano Museum, 3. Takamori Senior High School

Spring water is one of the important components of Aso UNESCO Global Geopark. We made an education program for local community to have more understandings on spring water of Aso Geopark. This poster presents a reslt on cooperated research with Takamori Senior High School.
We carried out water survey around Minamiaso Spring Waters. We found three types of waters; spring water around the caldera wall about 10 mS/m, spring water around the southern caldera floor about 23 mS/m (
just near from the foot of the central cones about 30 mS/m), and hotspring water more than 100 mS/m. This means waters have different relation with Aso volcanic system. Citizens use this low conductivity water for sake-making, and high conductivity water for bread making, etc.
We made educational programs how to understand the difference of electrical conductivity of spring waters; at first for high school students, and for kids and citizens later. We introduce our program briefly.
We have to express thanks to Kumamoto Prefecture for supporting us.

Keywords: Aso UNESCO Global Geopark, Spring water, Electrical conductivity

©2021. Japan Geoscience Union. All Right Reserved.

Looking back on 11 years of the educational activities of the Dinosaur Valley Fukui Katsuyama Geopark

*Sumiaki Machi[1]

1. Dinosaur Valley Fukui Katsuyama Geopark Promotion Council

The Dinosaur Valley Fukui Katsuyama Geopark became a member of the Japanese Geopark Network 11 years ago. We will look back on the 11 years of our educational activities.
Educational activities at geoparks have many meanings: encouraging understanding of the area and geoparks, fostering the people who leads the next generation of the area and also the world, giving a chance to study geology and so on. There are 12 schools (9 elementary schools + 3 junior high schools) in the geopark area. These schools are the member of UNESCO Asocciated Schools, base for ESD (Education for Sustainable Development) promotion.
We will analize the changes of the educational activities in this 11 years and discuss about the prospects and challenges.

Keywords: Geopark, Education, Dinosaur Valley Fukui Katsuyama Geopark, Katsuyama city

©2021. Japan Geoscience Union. All Right Reserved.

[J] Oral | O (Public)：Public

Sun. Jun 6, 2021 9:00 AM - 10:30 AM JST | Sun. Jun 6, 2021 12:00 AM - 1:30 AM UTC | Ch.02 Zoom Room 02

[O-03] How to cope with meteorological disasters under rapidly changing climate

convener:Jun Matsumoto(Deaprtment of Geography, Tokyo Metropolitan University), Akira Wada(Tokyo Institute of Technology), Yukihiro Takahashi(Department of Cosmosciences, Graduate School of Science, Hokkaido University), Chairperson:Yukihiro Takahashi(Department of Cosmosciences, Graduate School of Science, Hokkaido University), Akira Wada(Tokyo Institute of Technology), Jun Matsumoto(Deaprtment of Geography, Tokyo Metropolitan University)

In September 2018, we experienced severe storm damages over West Japan which paralyzed the Kansai International Airport. In September 2019, we also experienced severe storm damages by Typhoon No. 15 over East Japan, and huge electric power was down over wide areas in Chiba Prefecture. In October 2019, another Typhoon No. 19 caused extensive flood disasters over central Japan. In July 2020, severe flood disasters occurred in many places in Kyushu, Southwest Japan as well as in central Japan. We will discuss how to cope with such severe meteorological disasters under changing climate including participants. All the oral presentations are invited talks by the specialists in the Japan Geoscience Union (JpGU), and the Japan Academic Network for Disaster Reduction (JANET-DR) which was established in 2016.

9:00 AM - 9:15 AM JST | 12:00 AM - 12:15 AM UTC

[O03-01] Development of typhoon hazard map and typhoon-shot project; Change the "threat" of a typhoon into a "grace" by 2050!

★Invited Papers

*Fudeyasu Hironori[1] (1.Yokohama National University)

9:15 AM - 9:30 AM JST | 12:15 AM - 12:30 AM UTC

[O03-02] Recent trends in storm and flood damage and the latest efforts on JMA's weather warnings and information

★Invited Papers

*Takahashi Kenichi[1] (1.Japan Meteorological Agency)

9:30 AM - 9:45 AM JST | 12:30 AM - 12:45 AM UTC

[O03-03] Utilization of typhoon data before the middle 20th century

★Invited Papers

*Fumiaki Fujibe[1] (1.Department of Geography, Tokyo Metropolitan University)

9:45 AM - 10:00 AM JST | 12:45 AM - 1:00 AM UTC

[O03-04] Why was coastal damage due to T1915 concentrated in the Port of Yokohama?

★Invited Papers

*Hitoshi Tamura[1] (1.Port and Airport Research Institute)

10:00 AM - 10:15 AM JST | 1:00 AM - 1:15 AM UTC

[O03-05] Development of coastal monitoring method immediately after typhoon by remote sensing

★Invited Papers

*Yuji Sakuno[1] (1.Graduate School of Advanced Science and Engineering, Hiroshima University)

10:15 AM - 10:30 AM JST | 1:15 AM - 1:30 AM UTC

[O03-06] Proposal of Build Back Better “insurance” scheme for future wind-related disaster risk reduction

★Invited Papers

*Kazuyoshi Nishijima[1] (1.Disaster Prevention Research Institute, Kyoto University)

Development of typhoon hazard map and typhoon-shot project; Change the "threat" of a typhoon into a "grace" by 2050!

*Fudeyasu Hironori[1]

1. Yokohama National University

Typhoon Faxai, also known as “Reiwa 1 Boso Peninsula Typhoon”, made landfall in the Kanto region in September 2019. It was the strongest typhoon to make landfall in the region since 1991, the year the Japan Meteorological Agency (JMA) began to keep such records. The extreme winds of this typhoon left scars that exposed the vulnerabilities of the metropolitan area in Japan. A year earlier, the extremely powerful Typhoon Jebi in 2018 passed through western Japan, causing devastation to the Kinki area. According to the General Insurance Association of Japan (GIAJ), the damage caused by Typhoon Jebi resulted in the highest claims ever paid for wind and flooding damage in Japan. Typhoons remain a serious threat despite recent advances in science and technology. We meteorologists are working on the new challenges highlighted by typhoons in recent years. My presentation will introduce the typhoon hazard map developed by the latest research results and new project for typhoons, typhoon-shot project; change the "threat" of a typhoon into a "grace" by 2050.

Keywords: Typhoon, hazard map

©2021. Japan Geoscience Union. All Right Reserved.

Recent trends in storm and flood damage and the latest efforts on JMA’ s weather warnings and information

*Takahashi Kenichi[1]

1. Japan Meteorological Agency

Japan Meteorological Agency issues Emergency Warnings, Warnings and Advisories in response to the significance of possible disasters in association with meteorological phenomena so that disaster management authorities and residents can take appropriate measures to mitigate possible disasters.

During the "Heavy Rainfall in July 2018", JMA issued warnings from an early stage through the announcement of disaster prevention weather information, support to municipalities, and a press conference. However, the announcement of such information did not necessarily lead to evacuation behavior of residents. Based on this, in fiscal 2018, JMA held a “Review Committee on Dissemination of Disaster Prevention Weather Information” with the participation of the media, local government officials, and related ministries and agencies.

Keywords: Disaster mitigation information, Severe weather

©2021. Japan Geoscience Union. All Right Reserved.

Utilization of typhoon data before the middle 20th century

*Fumiaki Fujibe[1]

1. Department of Geography, Tokyo Metropolitan University

There were a number of strong typhoons that caused wind and rain disaster in Japan before the middle 20th century. For example, a typhoon attacked southern Kyushu on 15 August 1899, destroying sixteen thousand houses in Kagoshima Prefecture. On 28 September 1902, another typhoon attacked the Kanto area, destroying twenty thousand houses in Ibaraki Prefecture. Issues in using data from typhoons before the mid-20th century as lessons for future disasters will be discussed.

Keywords: typhoon, database, data collection

©2021. Japan Geoscience Union. All Right Reserved.

Why was coastal damage due to T1915 concentrated in the Port of Yokohama?

*Hitoshi Tamura[1]

1. Port and Airport Research Institute

Typhoon Faxai (T1915), which occurred in September 2019, was one of the strongest typhoons on record to make landfall in the Tokyo metropolitan area and it caused extensive damage along the coast in Tokyo Bay. Two intriguing phenomena are reported by a post-event survey, which motivated this study. The first was that although the storm impacted the whole bay, significant damage was concentrated in a small area near the Port of Yokohama. The second was about the direction of the hazardous waves, which came from both the northeast and the southeast. The underlying wave dynamics that lead to these events were unknown. Here, we elucidate characteristics of the waves incident to the Port of Yokohama that caused a concentration of severe damage, and we clarify the mechanism responsible for the two disparate wave directions observed.

Keywords: Typhoon1915, Coastal damage, Tokyo Bay

©2021. Japan Geoscience Union. All Right Reserved.

Development of coastal monitoring method immediately after typhoon by remote sensing

*Yuji Sakuno[1]

1. Graduate School of Advanced Science and Engineering, Hiroshima University

Heavy rains in recent years, represented by the western Japan region in July 2018, the Kanto region in September 2019, and the Kyushu region in July 2020, occur almost every year. The Remote Sensing Society of Japan is working on immediate disclosure of the damage situation using satellites and aircraft in the event of such a disaster. However, in most cases, land is the priority for such efforts. Therefore, even if there is a serious impact on the aquaculture industry, little is known about the damage situation in coastal waters and changes in the water quality environment. On the other hand, in recent years, the GCOM-C SGLI sensor with 250 spatial resolution and Himawari-8 AHI sensor with 2.5-minute observation cycle increase the possibility of coastal surveillance in the event of a disaster. Therefore, in this presentation, I will introduce the development of a disaster turbidity monitoring method using both SGLI and AHI sensors in order to monitor the outflow route of seafloor sediments during a disaster.

Keywords: satellite, turbidity, disaster

©2021. Japan Geoscience Union. All Right Reserved.

Proposal of Build Back Better “insurance” scheme for future wind-related disaster risk reduction

*Kazuyoshi Nishijima[1]

1. Disaster Prevention Research Institute, Kyoto University

This presentation proposes a Build Back Better “insurance” scheme for future wind-related disaster risk reduction, identifies and reports current progress on challenges in the proposed insurance scheme. It also introduces a simple study on the impact of the proposed insurance scheme on future wind-related disaster risk reduction in Japan.

Keywords: Residential house, Insurance, Strong wind

©2021. Japan Geoscience Union. All Right Reserved.

[J] Oral | O (Public)：Public

Sun. Jun 6, 2021 10:45 AM - 12:15 PM JST | Sun. Jun 6, 2021 1:45 AM - 3:15 AM UTC | Ch.02 Zoom Room 02

[O-03] How to cope with meteorological disasters under rapidly changing climate

convener:Jun Matsumoto(Deaprtment of Geography, Tokyo Metropolitan University), Akira Wada(Tokyo Institute of Technology), Yukihiro Takahashi(Department of Cosmosciences, Graduate School of Science, Hokkaido University), Chairperson:Akira Wada(Tokyo Institute of Technology), Yukihiro Takahashi(Department of Cosmosciences, Graduate School of Science, Hokkaido University), Jun Matsumoto(Deaprtment of Geography, Tokyo Metropolitan University)

In September 2018, we experienced severe storm damages over West Japan which paralyzed the Kansai International Airport. In September 2019, we also experienced severe storm damages by Typhoon No. 15 over East Japan, and huge electric power was down over wide areas in Chiba Prefecture. In October 2019, another Typhoon No. 19 caused extensive flood disasters over central Japan. In July 2020, severe flood disasters occurred in many places in Kyushu, Southwest Japan as well as in central Japan. We will discuss how to cope with such severe meteorological disasters under changing climate including participants. All the oral presentations are invited talks by the specialists in the Japan Geoscience Union (JpGU), and the Japan Academic Network for Disaster Reduction (JANET-DR) which was established in 2016.

10:45 AM - 11:00 AM JST | 1:45 AM - 2:00 AM UTC

[O03-07] Wind-induced damage to buildings and future risk reduction

★Invited Papers

*Yukio Tamura[1] (1.Chongqing University)

11:00 AM - 11:15 AM JST | 2:00 AM - 2:15 AM UTC

[O03-08] Behaviors of infrastructures under extreme wind and future challenges

★Invited Papers

*Tomomi Yagi[1] (1.Kyoto University)

11:15 AM - 11:30 AM JST | 2:15 AM - 2:30 AM UTC

[O03-09] Simultaneous multiple accident cases and their countermeasures for electric power system against Typhoon

★Invited Papers

*Yoshiharu Shumuta[1] (1.Central Research Institute of Electric Power Industry)

11:30 AM - 11:45 AM JST | 2:30 AM - 2:45 AM UTC

[O03-10] Fires Caused by Strong Winds and Storm Surges

★Invited Papers

*U HIROI[1] (1.The University of Tokyo)

11:45 AM - 12:15 PM JST | 2:45 AM - 3:15 AM UTC

[O03-11] Discussion

Wind-induced damage to buildings and future risk reduction

*Yukio Tamura[1]

1. Chongqing University

Wind pressures act on the surfaces of buildings, and the majority of wind-induced damage to buildings is initiated by damage to claddings and components, rather than to main frames. Small damage to eaves or breakage of windows can develop into larger damage to roofs and entire buildings. Therefore, “cladding and component design” is critical in the wind resistant design of buildings. Broken metal roof sheets, clay tiles, and other parts of buildings can be blown off, creating “wind-borne debris” that attacks downstream buildings and other structures, causing a chain of damage. “Damage chain” is a special feature of wind-induced damage. The impact of wind-borne debris is much higher than that of wind pressure, and claddings and components should have resistance to debris impacts, not only to strong wind pressures. Wind resistant design of buildings is basically made by comparing “wind action (load)” and “structural performance (resistance)”, but almost all past studies in the wind engineering field have focused on accurate estimations of wind actions (loads) on buildings and structures. Structural performance has not been sufficiently studied.

Many structures damaged by severe local storms are categorized as temporary ones such as construction site offices, and some of them, such as scaffoldings or movable roof structures, are designed assuming appropriate operation based on site wind speed. However, design criteria and maintenance discipline for these structures have not been well established.

This presentation describes recent examples of building damage due to typhoons and severe local storms resulting from the above mentioned problems. It also discusses the need for a full-scale storm simulator (FSSS) to cope with hypothesized future increase in wind-related disaster risks.

Keywords: Typhoon, Tornado, Wind Resistance, Claddings and components, Wind-borne Debris, Full-scale Storm Simulator

©2021. Japan Geoscience Union. All Right Reserved.

Behaviors of infrastructures under extreme wind and future challenges

*Tomomi Yagi[1]

1. Kyoto University

Behaviors of long-span bridges under the extreme wind speed and future challenges for the wind resistant design of bridges and their maintenance under the extreme weather due to the climate change will be discussed.

Keywords: Bridge, Wind registant design, Wind-induced vibration

©2021. Japan Geoscience Union. All Right Reserved.

Simultaneous multiple accident cases and their countermeasures for electric power system against Typhoon

*Yoshiharu Shumuta[1]

1. Central Research Institute of Electric Power Industry

In Japan, meteorological severe disasters including typhoon have recently continued to occur and have been intensifying damage to infrastructures. On the basis of recent disaster experiences, particular attention is paid to issues related to “Resilience” as a key concept of disaster control measures for electric power systems. This presentation introduces simultaneous multiple accident cases and their countermeasures for electric power system against Typhoon. At first, as typical typhoon disaster in metropolitan area, the damage and emergency restoration process of the electric power distribution equipment, caused by Typhoons occurred in 2018, 2019, and 2020, are illustrated. In addition, electric power resilience working group, organized by METI, suggests that in order to increase regional disaster mitigation performance (regional resilience), a disaster information collecting and sharing system, and damage prediction system are needed for wide-area collaboration among power transmission and distribution network companies. As an example of resilience improvement of electric power system, recent our research and practical use cases including a damage prediction tool for electric power distribution equipment, are also illustrated.

Keywords: Typhoon, disaster measures, electric power transmission and distribution equipment, resilience, local disaster prevention

©2021. Japan Geoscience Union. All Right Reserved.

Fires Caused by Strong Winds and Storm Surges

*U HIROI[1]

1. The University of Tokyo

This paper presents an overview of fires caused by typhoon-related storm winds, storm surges and power restoration after power outages, using the Typhoon No. 21 in 2018 and the Typhoon Boso Peninsula in 2019 as specific examples.

Keywords: fires, typhoon, storm surges

©2021. Japan Geoscience Union. All Right Reserved.

[J] Oral | O (Public) | Public

[O-03] How to cope with meteorological disasters under rapidly changing climate

convener:Jun Matsumoto(Deaprtment of Geography, Tokyo Metropolitan University), Akira Wada(Tokyo Institute of Technology), Yukihiro Takahashi(Department of Cosmosciences, Graduate School of Science, Hokkaido University), Chairperson:Akira Wada(Tokyo Institute of Technology), Yukihiro Takahashi(Department of Cosmosciences, Graduate School of Science, Hokkaido University), Jun Matsumoto(Deaprtment of Geography, Tokyo Metropolitan University)

Sun. Jun 6, 2021 10:45 AM - 12:15 PM Ch.02 (Zoom Room 02)

In September 2018, we experienced severe storm damages over West Japan which paralyzed the Kansai International Airport. In September 2019, we also experienced severe storm damages by Typhoon No. 15 over East Japan, and huge electric power was down over wide areas in Chiba Prefecture. In October 2019, another Typhoon No. 19 caused extensive flood disasters over central Japan. In July 2020, severe flood disasters occurred in many places in Kyushu, Southwest Japan as well as in central Japan. We will discuss how to cope with such severe meteorological disasters under changing climate including participants. All the oral presentations are invited talks by the specialists in the Japan Geoscience Union (JpGU), and the Japan Academic Network for Disaster Reduction (JANET-DR) which was established in 2016.

11:45 AM - 12:15 PM

[O03-11]Discussion

©Japan Geoscience Union

[J] Oral | O (Public)：Public

Sun. Jun 6, 2021 9:00 AM - 10:30 AM JST | Sun. Jun 6, 2021 12:00 AM - 1:30 AM UTC | Ch.01 Zoom Room 01

[O-04] Suggestion to teaching Earth science under GIGA school from online lesson

convener:Iida Kazuya(Komaba-Toho Junior and Senior High School), Iwata Makoto(Hiroshima Prefectural Ogaki High School), Satoshi Miyajima(Saitama Prefectural Kumagaya High School), Hiroaki Akimoto(Faculty of Economics,Dokkyo University), Chairperson:syo uranaka(Osaka Institute of Technology Graduate School), Hiroaki Akimoto(Faculty of Economics,Dokkyo University), Satoshi Miyajima(Saitama Prefectural Kumagaya High School), Iida Kazuya(Komaba-Toho Junior and Senior High School)

In this session, we will discuss teaching Earth science under GIGA school. GIGA school means Global and Innovation Gateway for All, which aims to provide computer and internet environment for all students in the school. In the online lessons due to the epidemic of the COVID-19, many practices using computer and internet were conducted. Based on suggestions from both online and face-to-face classes using computers, we will discuss teaching Earth science under GIGA school.

9:00 AM - 9:10 AM JST | 12:00 AM - 12:10 AM UTC

[O04-01] Introduction

9:10 AM - 9:25 AM JST | 12:10 AM - 12:25 AM UTC

[O04-02] The Potential of Online Learning to Realize "Independent and Interactive Deep Learning" in Elementary School Social Studies.

★Invited Papers

*Keiko Nakaya[1] (1.Elementary School Affiliated to the Faculty of Education chiba university)

9:25 AM - 9:40 AM JST | 12:25 AM - 12:40 AM UTC

[O04-03] Utilization of a digital globe system, Dagik Earth, in elementary schools

★Invited Papers

*Akinori Saito[1], Takuya Tsugawa[2], Miho Yamamori[3] (1.Department of Geophysics, Graduate School of Science, Kyoto University, 2.National Institute of Information and Communications Technology, 3.Tsuru University)

9:40 AM - 9:55 AM JST | 12:40 AM - 12:55 AM UTC

[O04-04] Effective use of online lesson and integrate with face to face lesson

★Invited Papers

*Hiroki Ushigome[1] (1.Otsuma nakano Junior and Senior High School)

9:55 AM - 10:10 AM JST | 12:55 AM - 1:10 AM UTC

[O04-05] Student presentations using digital devices In GIGA School Concept

★Invited Papers

*Hidenori Takemura[1] (1.Johoku Junior and Senior high school)

10:10 AM - 10:30 AM JST | 1:10 AM - 1:30 AM UTC

[O04-06] Discussion

[J] Oral | O (Public) | Public

[O-04] Suggestion to teaching Earth science under GIGA school from online lesson

convener:Iida Kazuya(Komaba-Toho Junior and Senior High School), Iwata Makoto(Hiroshima Prefectural Ogaki High School), Satoshi Miyajima(Saitama Prefectural Kumagaya High School), Hiroaki Akimoto(Faculty of Economics,Dokkyo University), Chairperson:syo uranaka(Osaka Institute of Technology Graduate School), Hiroaki Akimoto(Faculty of Economics,Dokkyo University), Satoshi Miyajima(Saitama Prefectural Kumagaya High School), Iida Kazuya(Komaba-Toho Junior and Senior High School)

Sun. Jun 6, 2021 9:00 AM - 10:30 AM Ch.01 (Zoom Room 01)

In this session, we will discuss teaching Earth science under GIGA school. GIGA school means Global and Innovation Gateway for All, which aims to provide computer and internet environment for all students in the school. In the online lessons due to the epidemic of the COVID-19, many practices using computer and internet were conducted. Based on suggestions from both online and face-to-face classes using computers, we will discuss teaching Earth science under GIGA school.

9:00 AM - 9:10 AM

[O04-01]Introduction

©Japan Geoscience Union

The Potential of Online Learning to Realize "Independent and Interactive Deep Learning" in Elementary School Social Studies.

*Keiko Nakaya[1]

1. Elementary School Affiliated to the Faculty of Education chiba university

The new coronavirus pandemic forced schools to close temporarily. In our school, we started online learning for the whole school using a groupware called "Microsoft Teams" (hereinafter referred to as "Teams") during the school closure period in March.

In addition, the period from July 13th to July 31st was designated as the "online school period," and online learning was conducted in the same way as during the closed period. During this period, the third-grade social studies class focused on the city of Chiba and worked on the following topics: *"Scenes in Chiba City"* and *"Changes in Scenes in Chiba City"*. The students did not use the online learning methods of "synchronous classes" or "real-time interaction where students communicate with each other. But instead we have used the asynchronous class where students do not communicate in real time, but present and submit assignments using videos, worksheets, and the face-to-face class during the online school period and after the summer vacation.

Furthermore, we designed a hybrid type unit by efficiently combining face-to-face classes during the online school period and after the summer vacation.

Through this practice, it became clear that online learning is highly compatible with social studies teaching and learning, as materials and tasks can be easily shared and viewed, and research and study can be conducted without any time restrictions.

In the case of online learning, children who were not good at speaking found it enjoyable to interact with their friends in the form of chats and comments. We were able to provide a new way of interaction.

Nevertheless, it was also very effective to have the students take the time to research and study online, which would lead to discussion and learning during the school day. It was also unexpected that many of the children took advantage of the online classes to go to museums and libraries with their parents during the summer vacation. This was also an unexpected outcome. However, in case, when the school is forced to close again for a long period of time due to a sudden disaster or other reasons, a major issue will be how to realize the discussion activities and cooperative learning that had been conducted in face-to-face classes.

Keywords: Online learning, Hybrid learning, Microsoft Teams, Elementary school social studies

©2021. Japan Geoscience Union. All Right Reserved.

Utilization of a digital globe system, Dagik Earth, in elementary schools

*Akinori Saito[1], Takuya Tsugawa[2], Miho Yamamori[3]

1. Department of Geophysics, Graduate School of Science, Kyoto University, 2. National Institute of Information and Communications Technology, 3. Tsuru University

Dagik Earth, a digital globe system, is an educational digital tool that displays various earth and planetary data in a three-dimensional format, allowing users to view the data in a way that is not possible with ordinary photographs or videos. It has been developed since 2007 and is being used in schools, science museums, and others. In elementary school science, content and instructional plans are being developed for use in "Weather" (5th grade) and "The Moon and the Sun" (6th grade), and are also being used in the "Planets" unit, although it is a developmental topic. The software can be used in elementary schools in two ways: (A) three-dimensional display using a spherical screen, and (B) flat display using a tablet or other device. In usage (A), a PC projector is used to project images of the earth and planets onto a spherical screen for a three-dimensional display. It is used not only in the classroom, but also in events in auditoriums where large screens with diameters of 2m or 4m are used for display. This presentation make students to have the feeling of looking down on the earth from space. In usage (B), students can manipulate and view the contents of "Dagik Earth" by using digital textbooks and applications. This allows for independent learning, as learners can select content, rotate, zoom in, and still/play the earth. In addition to these digital learning materials, the materials for hand-made globes and origamis are provided. These are used in "demae" classes and science events. In the lecture, we will also discuss the challenges of using teaching materials developed by university researchers in elementary schools.

Keywords: digital globe, science class, elementary school, digital text book, application

©2021. Japan Geoscience Union. All Right Reserved.

Effective use of online lesson and integrate with face to face lesson

*Hiroki Ushigome[1]

1. Otsuma nakano Junior and Senior High School

Many schools introduced online lessons after the epidemic of the COVID-19. There are many online lesson methods. For example, it is one-way or interactive communication. In the future, it will be necessary to use it properly effectively what to learn online and what to learn face-to-face. In addition, online lessons are not limited to school. Therefore, online lessons are restricted by the Internet environment of the students' homes. When we do online lessons, it is necessary to consider not only the lesson content but also internet capacity and communication speed. Every student owns a PC in our school. And I have practiced lessons that incorporate interactive communication using Internet.In this presentation, I will report on the use of ICT in our junior high school geography classes. And I propose how to cultivate students' proactive learning using both face-to-face and online classes.

Keywords: online lesson, proactive learning

©2021. Japan Geoscience Union. All Right Reserved.

Student presentations using digital devices In GIGA School Concept

*Hidenori Takemura[1]

1. Johoku Junior and Senior high school

The junior high school learning guidance guideline (notification in March 2017) says that the following three points should be realized without bias.
"(1) To acquire knowledge and skills."
"(2) To develop thinking ability, judgment ability, expressive ability, etc."
"(3) To cultivate the ability to learn and humanity."
Especially recently, due to the reform of university entrance examinations, universities are trying to evaluate not only (1) but also other abilities.

In order to realize the above (1) to (3) without bias, the science item of the learning guidance guideline say "time for sufficient observation and experiment, time for exploration to solve problems, etc." ". At that time, it says, "Enrich your language activities." To achieve this, we have been conducting experiments and group work. But we've done much with paper.
In GIGA School Concept, each student would have one computer. This has expanded the range of experiments and group work we have conducted so far, and has enabled us to conduct lessons different from the past. As an example, I will use a digital device to summarize the observation results and give a presentation.

Keywords: GIGA School Concept, ICT, presentation, Loilo Note, group work

©2021. Japan Geoscience Union. All Right Reserved.

[J] Oral | O (Public) | Public

[O-04] Suggestion to teaching Earth science under GIGA school from online lesson

convener:Iida Kazuya(Komaba-Toho Junior and Senior High School), Iwata Makoto(Hiroshima Prefectural Ogaki High School), Satoshi Miyajima(Saitama Prefectural Kumagaya High School), Hiroaki Akimoto(Faculty of Economics,Dokkyo University), Chairperson:syo uranaka(Osaka Institute of Technology Graduate School), Hiroaki Akimoto(Faculty of Economics,Dokkyo University), Satoshi Miyajima(Saitama Prefectural Kumagaya High School), Iida Kazuya(Komaba-Toho Junior and Senior High School)

Sun. Jun 6, 2021 9:00 AM - 10:30 AM Ch.01 (Zoom Room 01)

In this session, we will discuss teaching Earth science under GIGA school. GIGA school means Global and Innovation Gateway for All, which aims to provide computer and internet environment for all students in the school. In the online lessons due to the epidemic of the COVID-19, many practices using computer and internet were conducted. Based on suggestions from both online and face-to-face classes using computers, we will discuss teaching Earth science under GIGA school.

10:10 AM - 10:30 AM

[O04-06]Discussion

©Japan Geoscience Union

[J] Oral | O (Public)：Public

Sun. Jun 6, 2021 10:45 AM - 12:15 PM JST | Sun. Jun 6, 2021 1:45 AM - 3:15 AM UTC | Ch.01 Zoom Room 01

[O-04] Suggestion to teaching Earth science under GIGA school from online lesson

convener:Iida Kazuya(Komaba-Toho Junior and Senior High School), Iwata Makoto(Hiroshima Prefectural Ogaki High School), Satoshi Miyajima(Saitama Prefectural Kumagaya High School), Hiroaki Akimoto(Faculty of Economics,Dokkyo University), Chairperson:Hiroaki Akimoto(Faculty of Economics,Dokkyo University), syo uranaka(Osaka Institute of Technology Graduate School), Satoshi Miyajima(Saitama Prefectural Kumagaya High School), Iida Kazuya(Komaba-Toho Junior and Senior High School)

In this session, we will discuss teaching Earth science under GIGA school. GIGA school means Global and Innovation Gateway for All, which aims to provide computer and internet environment for all students in the school. In the online lessons due to the epidemic of the COVID-19, many practices using computer and internet were conducted. Based on suggestions from both online and face-to-face classes using computers, we will discuss teaching Earth science under GIGA school.

10:45 AM - 11:00 AM JST | 1:45 AM - 2:00 AM UTC

[O04-07] Report on the Online Teaching Experience with WebGIS in the High School Geography Classes under the COVID-19 Pandemic

★Invited Papers

*Yoshihiko Shibata[1] (1.Tokyo Metropolitan KOKUBUNJI Highschool)

11:00 AM - 11:15 AM JST | 2:00 AM - 2:15 AM UTC

[O04-08] Development of Educational Materials for the Kanagawa version of “Geological Fieldworks conducted in a Classroom" appling for High School Subject "Basic Earth Science" —Using Strata from Ikuta Ryokuchi Park—

★Invited Papers

*Yasushi Fujiwara[1], Shungo Kawagata[2] (1.Graduate School of Education, Yokohama National University, 2.College of Education, Yokohama National University)

11:15 AM - 11:30 AM JST | 2:15 AM - 2:30 AM UTC

[O04-09] Supporting school teachers with GSI’s Toolbox for geography education in the era of Society 5.0

★Invited Papers

*Yuki Kurisu[1] (1.Geospatial Information Authority of Japan)

11:30 AM - 11:45 AM JST | 2:30 AM - 2:45 AM UTC

[O04-10] The trial and error of on-line bidirectional lecture

★Invited Papers

*Yukari Kido[1] (1.Japan Agency for Marine-Earth Science and Technology)

11:45 AM - 12:15 PM JST | 2:45 AM - 3:15 AM UTC

[O04-11] General Discussion

★Invited Papers

*Iida Kazuya[1], Hiroaki Akimoto[2], Iwata Makoto[3], Satoshi Miyajima[4] (1.Komaba-Toho Junior and Senior High School, 2.Faculty of Economics, Dokkyo University, 3.Hiroshima Prefectural Ogaki High School, 4.Saitama Prefectural Kumagaya High School)

Report on the Online Teaching Experience with WebGIS in the High School Geography Classes under the COVID-19 Pandemic

*Yoshihiko Shibata[1]

1. Tokyo Metropolitan KOKUBUNJI Highschool

In April 2020, schools across the country were suddenly required to offer online lessons due to the state of emergency associated with the Corona disaster.

However, the ICT environment of public schools at that time was extremely low quality and the security was excessively strict, and schools could hardly do anything.

However, in the spare time of the work-at-home system, many geography teachers were able to actually operate WebGIS such as Geographical Survey Institute maps, Google Earth, and GSMaP, and realize their effectiveness.

For this reason, some teachers have used them to conduct online geography lessons from home, and their effects, issues, and know-how have been showed to islands where they cannot usually participate in workshops through online conferences that were explosively spread at the time, and shared with teachers who were on maternity leave.

In addition, we realized that digital teaching materials are easy to copy and spread, and launched a geography teaching materials sharing project to deliver useful geographic information to non-specialized teachers when geography becomes compulsory in 2022.

At this time, we will report on the merits and demerits of online lessons and the project to share geography teaching materials, and talk about geography education during the GIGA school era.

Keywords: Geography, WebGIS, Online lesson

©2021. Japan Geoscience Union. All Right Reserved.

Development of Educational Materials for the Kanagawa version of “Geological Fieldworks conducted in a Classroom" appling for High School Subject "Basic Earth Science" —Using Strata from Ikuta Ryokuchi Park—

*Yasushi Fujiwara[1], Shungo Kawagata[2]

1. Graduate School of Education, Yokohama National University, 2. College of Education, Yokohama National University

Purpose

The next Japanese High School Curriculum Guideline emphasizes the importance of Experiential learning for the Subject Area "Science" including "Basic Earth Science". However, this is not easy for not well-trained teachers in geoscience to teach the local geology for real by field observation. Thus, we develop a package of educational materials containing digital learning and hands-on training materials for geology which those teachers allow students to easily experience outdoor geological observations in classrooms and facilitate hands-on activities with sediment samples.

Target of research: Mt.Masugata in Ikuta Ryokuchi Park

In Kanagawa Pref., the Quaternary terrestrial sediments of the Kanto Loam cover the underlying marine deposits (Kazusa and Sagami Groups). These strata are well exposed along the 1 km circuit course in the Mt. Masugata in the Ikuta Ryokuchi Park, Kawasaki City, where we can observe the Iimuro Formation of Kazusa Group uncomformably overlain by the Oshinuma Sand and Gravel Formation of Sagami Group, and conformably overlying terrestrial Kanto Loam, in ascending order. The Iimuro Fm. yields fossil molluscs and fossil foraminifera, and the Kanto Loam interbeds wide-spread tephra. Therefore, these strata are suitable for students to learn a part of the Quaternary formation history in Kanagawa Pref. even at 1 location.

Developed Educational Materials

We have developed three digital materials, as follows; (1) "Ikuta Ryokuchi Park Fieldwork" for students to experience outdoor geological observations in classrooms, (2) "Fossil Foraminifera from the Iimuro Fm." and (3) "Rock-Minerals in Key Tephra". Each material involves worksheet and taxonomic search list for classification of foraminifera and rock-minerals for students, digital learning materials for students by operating with electronic devices of tablet terminals and smartphones, digital teaching materials for teachers and real sediment samples". These materials are expected to be used in the classes as shown below.

(1) Ikuta Ryokuchi Park Fieldwork (Estimated time: 1 to 2 class hours)

Students observe the overview of strata by moving the images of the 6 outcrops obtained by a 360 degrees camera around in any direction by themselves, and the details of sediment characters by enlarging the high-resolution spot images. They can compare their observations to images of boling sediment-core samples exhibited in Kawasaki Municial Science Museum and summarize the name of stratum in each outcrop and its characteristics, then draw geological columnar section.

(2) Fossil Foraminifera from the Iimuro Fm. (Estimated time: 2 class hours)

Students can wash sediments from the Iimuro Fm. within minutes using tea filter bags and obtain fossil

©2021. Japan Geoscience Union. All Right Reserved.

foraminifera from the residues (ca. >250 μm in size). They identify foraminifera by using the digital taxonomic search catalog named "Foraminifera search card". Based on the species lists compiled all results of classmates, they try to reconstract the past environment and depositional age of the sediments.

(3) Rock-Minerals in Key Tephra (Estimated time: 1 class hour)

Students can wash tephra sediments from the Kanto Loam in a short time using tea filter bags and can extract rock-minerals from the "Hakone Tokyo Tephra (Hk-TP)" and "Ontake Daiichi Tephra (On-Pm1) ". They identify rock-minerals by using taxonomic search catalog named "Mineral Search Card". Based on the observations, they estimate the type of magma for each tephra.

Summary

We have developed educational materials that help geologically not well-trained high school science teachers to teach the local geology for real by field observation in the Subject.
By three materials using the Parks with samples from the same strata in the other areas, students can deepen the understanding of formation history of the common land of Kanagawa Pref. with spatial relationships among strata.
Every student can operate the digital materials. So, they can do fieldwork in a regular classroom, which enables them to understand the scale of the entire outcrop and the geological formation using regional materials. They can extract the desired material from the sediment sample low cost and short time processes, and then identify fossils and minerals. Hence, those teachers can allow students to spend much time in observing and considering. Classes with these developed materials could shorten the necessary class times about an hour compared with traditional classes. "Fossil Foraminifera from the Iimuro Fm." is also a new material, which can lead to the understanding of depositional age.
We plan to distribute our newly developed materials and give a lecture on this package to teachers.

Keywords: Digital Educational Material, Non Geoscience-Based Teacher, Experiential Learning, Local Geology, Geological Fieldwork, Real Sediment Sample

©2021. Japan Geoscience Union. All Right Reserved.



図1. 教室で行う野外実習デジタル教材「生田緑地フィールドワーク」の操作例
生徒たちは、各露頭の360° カメラ(RICOH THETA V)による全天球画像とデジタル一眼レフカメラ等による詳細な画像を、自らの操作によって、模擬野外観察を行う。

Fig1. Operation example of the digital educational material named "Ikuta Ryokuchi Park Fieldwork" for students to experience outdoor geological observations in classrooms
Students observe the overview of strata by moving the images of outcrops obtained by a 360 degrees camera around in any direction by themselves, and the details of sediment characters by enlarging the high-resolution spot images.



図2. デジタル教材も併用した実物実習教材「有孔虫化石の観察」で、プロジェクター等で表示する授業進行用(教員用)資料の画面例(左)と、生徒が分類・同定に用いるデジタル教材「有孔虫 検索カード」の画面例(右)

Fig2. Screen example of materials for class progress (for teachers) displayed on a projector (left) and screen example of the digital taxonomic search catalog named "Foraminifera search card" (right) , in the educational material named "Fossil Foraminifera from the Iimuro Fm." using real sediment samples

©2021. Japan Geoscience Union. All Right Reserved.

Supporting school teachers with GSI’s Toolbox for geography education in the era of Society 5.0

*Yuki Kurisu[1]

1. Geospatial Information Authority of Japan

It is important for children to develop ICT skills in daily life as well as learning opportunities in the era of Society5.0: a new society which incorporates advanced technologies into every industry and social life, seeking for balanced solution between social agenda and economic development. GIGA school, which realizes a classroom provided with high-speed internet connection and individual ICT device such as tablet, and STEAM education, which enriches cross-curricular learning by integrating each subject such as Science, Technology, Engineering, liberal Arts, and Mathematics for solving the problems in the real world, have been well recognized for developing children’s ICT skills. Realizing GIGA school is further hoped as online teaching has imperatively prevailed in response to COVID-19 pandemic.
On the other hand, increased burden on teachers for preparation is concerned, if online education contents are not sufficient, resulting in insufficient learning experience of children. In this regard, Geospatial Information Authority of Japan (GSI) launched the Toolbox for geographic education (https://www.gsi.go.jp/CHIRIKYOUIKU/) (here in after “the Toolbox”) in support of school teachers in June 2016. In this article, we report the advantage of educational contents in the Toolbox, with a view to fully utilizing them in GIGA school and STEAM education.
First; data and cross-media accessibility. We posted all the contents on the Toolbox website so that anyone can easily download them through a web browser: an anticipated environment in GIGA school classrooms. We provided the contents as images and PDF files so that teachers can easily prepare their teaching materials for an online class. With easy links to "GSI maps" included in the contents, we also help teachers develop adequate story-telling for their teaching subject. Further, embedding attractive SNS postings in the contents is intended to make students feel closer to geography subjects.
Second; contents classification according to national school curricula. We first classified the contents into grade levels (3-4G(grade), 5G, 7-9G and 10-12G). Further we classified those according to themes such as neighborhood, Japanese landform and natural disasters in Japan. This classification help teachers find appropriate contents easily and quickly.
Third; contents for cross-curricular learning for STEAM education. Geography should not only be regarded us a subject, but can also be used as a connector to promote cross-curricular learning. For example, we developed a content which relates a section of a three-dimensional object (mathematics) to topographic sectional profile (geography). Another one relates three primary colors of light (visual art) to topographic/cartographic representation (geography).
Fourth; contents with story-telling aspects. These contents are intended to attract students for animating class teachings. For example, a character in a content poses a question toward students about the important points in understanding a hazard map. Another example is a cartoon style content where student can learn relationship between disaster and landform.
We asked 28 teachers about the possibility of utilizing contents in the Toolbox. Most teachers answered that the contents can be useful. Some respondents suggested the possibility of saving time for class preparation by using the contents in the Toolbox.
GSI will continuously support promotion of geography education through the Toolbox and introduce features and effectiveness of the contents in the Toolbox in various opportunities to help school teachers.

©2021. Japan Geoscience Union. All Right Reserved.

Keywords: Toolbox for geography education, cross-curricular learning, GIGA school, STEAM education

©2021. Japan Geoscience Union. All Right Reserved.

The trial and error of on-line bidirectional lecture

*Yukari Kido[1]

1. Japan Agency for Marine-Earth Science and Technology

The UN decade of Ocean Science for Sustainable Development (2021–2030, hereafter the UN Decade) by the United Nations Educational, Scientific, and Cultural Organization (UNESCO) began in January, 2021. We are involved in the marine research and technology field and would like to provide access to “Ocean, Marine, and Sea” to the general public. “Ocean, Marine, and Sea” contains information on the latest oceanographic investigations, future global environmental problems and their impacts on human lives, and the continuation of development objectives worldwide. Sustainable development goals are directed at men and women of all ages. Thus, we perform education and outreach activities at schools and conduct ongoing research expeditions. In this session, under the GIGA school framework, we conducted trial and error activities with student and teachers from the Saitama Prefectural Kumagaya High School during COVID-19 circumstances. We focused on outreach activities and provided online information that participants accessed using their tablets. Our online education and outreach activities are associated with three SSH schools of Shizuoka in collaboration with the Drilling Vessel "Chikyu" which are currently conducting operations in an accretionary prism in the Nankai Trough. We addressed the state of operations aboard the ship, which hosts international participants, in January, 2019. During a voyage on the American scientific drilling vessel "Joides Resolution" on Exp. 378 in the South Pacific Ocean in January 2020. Using a narrow internet network connection, students and teachers at Meijyo University Senior High School received online instruction and vivid real-time access to a drilling field. We would like to thank all the participants, supporting schools, and onboard researchers.

Keywords: GIGA network connection, Online lecture, bidirectional

©2021. Japan Geoscience Union. All Right Reserved.

General Discussion

*Iida Kazuya[1], Hiroaki Akimoto[2], Iwata Makoto[3], Satoshi Miyajima[4]

1. Komaba-Toho Junior and Senior High School, 2. Faculty of Economics, Dokkyo University, 3. Hiroshima Prefectural Ogaki High School, 4. Saitama Prefectural Kumagaya High School

Based on the presentations in this session, we will exchange opinions on future issues and how to use them in class.

©2021. Japan Geoscience Union. All Right Reserved.

[J] Oral | O (Public)：Public

Sun. Jun 6, 2021 1:45 PM - 3:15 PM JST | Sun. Jun 6, 2021 4:45 AM - 6:15 AM UTC | Ch.01 Zoom Room 01

[O-05] How to become a scientist? What can they do?

convener:Natsue Abe(Mantle Drilling Promotion Office, MarE3, Japan Agency for Marine-Earth Science and Technology), Rie Hori, S.(Department of Earth Science, Faculty of Science, Ehime University), Chairperson:Rie Hori(Department of Earth Science, Faculty of Science, Ehime University), Mayumi ARAI(National Museum of Emerging Science and Innovation), Natsue Abe(Mantle Drilling Promotion Office, MarE3, Japan Agency for Marine-Earth Science and Technology), Chiaki T. Oguchi(Institute for Environmental Science and Technology, Graduate School of Science and Engineering, Saitama University)

The earth and planetary sciences deal with many issues that are very close to our daily lives. Such researchers in this area are active in many parts of Japan. In this session, we introduce such researchers and people involved in this field and their activities, how they landed their current position. Many people may not know how to become a scientist. Either many of students may wonder how they apply their learned in university and their skills to society? We will have presentations on what they have learned and how they can use the skills they have acquired during their studies at universities and graduate schools in society.
Junior and senior high school students who want to go into the field of earth and planetary sciences are welcome to participate in this session and ask questions. We also welcome submissions from people who develop human resources and expand their colleagues.

1:45 PM - 1:50 PM JST | 4:45 AM - 4:50 AM UTC

[O05-01] Introduction

1:50 PM - 2:05 PM JST | 4:50 AM - 5:05 AM UTC

[O05-02] Why do you need a PhD?

★Invited Papers

*Manabe Makoto[1] (1.National Museum of Nature and Science)

2:05 PM - 2:20 PM JST | 5:05 AM - 5:20 AM UTC

[O05-03] From Organic Chemistry, Coral Study to Ocean Policy, My Journey through Carbon

★Invited Papers

*Nobuko Nakamura[1,2] (1.The Ocean Policy Research Institute of The Sasakawa Peace Foundation, 2.Keio Univ.)

2:20 PM - 2:35 PM JST | 5:20 AM - 5:35 AM UTC

[O05-04] Living with solar sytem exploration

★Invited Papers

*Takeshi Imamura[1] (1.Graduate School of Frontier Sciences, The University of Tokyo)

2:35 PM - 2:50 PM JST | 5:35 AM - 5:50 AM UTC

[O05-05] Introduction to IODP and the works inside

★Invited Papers

*Michiko Yamamoto[1] (1.Scripps Institution of Oceanography, UCSD)

2:50 PM - 3:05 PM JST | 5:50 AM - 6:05 AM UTC

[O05-06] I’m working as a nature guide, an environmental activist, and a facilitator.

★Invited Papers

*hisashi Oiwane[1] (1.Musuhi LLC)

3:05 PM - 3:15 PM JST | 6:05 AM - 6:15 AM UTC

[O05-07] Discussion

[J] Oral | O (Public) | Public

[O-05] How to become a scientist? What can they do?

convener:Natsue Abe(Mantle Drilling Promotion Office, MarE3, Japan Agency for Marine-Earth Science and Technology), Rie Hori, S.(Department of Earth Science, Faculty of Science, Ehime University), Chairperson:Rie Hori(Department of Earth Science, Faculty of Science, Ehime University), Mayumi ARAI(National Museum of Emerging Science and Innovation), Natsue Abe(Mantle Drilling Promotion Office, MarE3, Japan Agency for Marine-Earth Science and Technology), Chiaki T. Oguchi(Institute for Environmental Science and Technology, Graduate School of Science and Engineering, Saitama University)
Sun. Jun 6, 2021 1:45 PM - 3:15 PM Ch.01 (Zoom Room 01)

The earth and planetary sciences deal with many issues that are very close to our daily lives. Such researchers in this area are active in many parts of Japan. In this session, we introduce such researchers and people involved in this field and their activities, how they landed their current position. Many people may not know how to become a scientist. Either many of students may wonder how they apply their learned in university and their skills to society? We will have presentations on what they have learned and how they can use the skills they have acquired during their studies at universities and graduate schools in society.

Junior and senior high school students who want to go into the field of earth and planetary sciences are welcome to participate in this session and ask questions. We also welcome submissions from people who develop human resources and expand their colleagues.

1:45 PM - 1:50 PM

[O05-01]Introduction

©Japan Geoscience Union

Why do you need a PhD?

*Manabe Makoto[1]

1. National Museum of Nature and Science

You do not need a PhD to get your work published. Why do you need a PhD? During a PhD program at a graduate school, you will find out if you really like to do research for the rest of your life. Even if you do not get a research job in your field after a PhD, your experience of finishing the PhD will help you in your next phase of life. (Photo by Matsuichi YOKOTA)

Keywords: Vertebrate Palaeontology, Dinosaurs, PhD, Graduate School



©2021. Japan Geoscience Union. All Right Reserved.

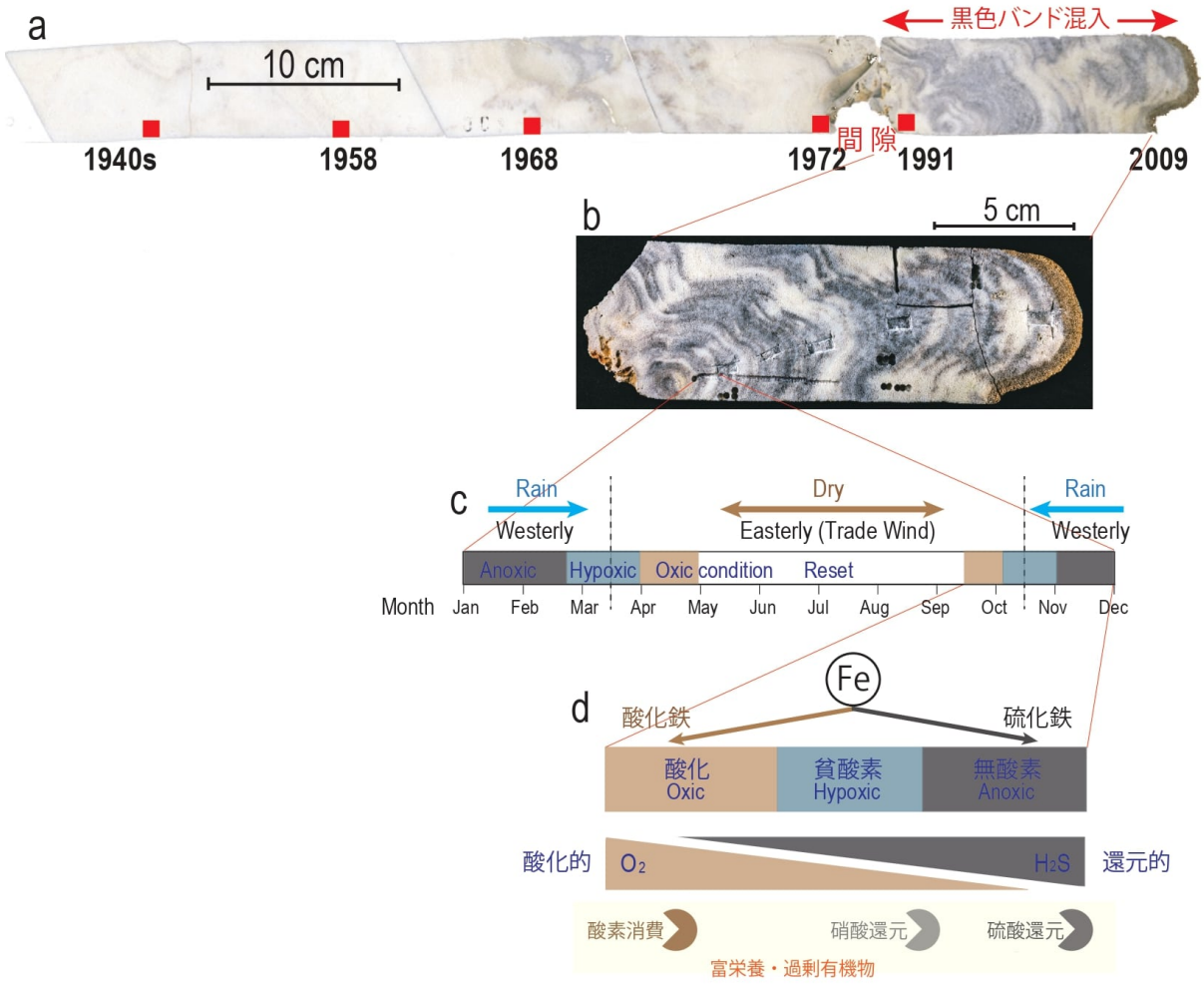
From Organic Chemistry, Coral Study to Ocean Policy, My Journey through Carbon

*Nobuko Nakamura[1,2]

1. The Ocean Policy Research Institute of The Sasakawa Peace Foundation, 2. Keio Univ.

I am currently looking at the world of "ocean policy". Around me there are various people who know about coral reefs and mangrove ecosystems, people who have conducted research on the ecology of sea turtles and whales by attaching sensors to them, people who have observed the Arctic Ocean, and experts in ocean climatology modeling and underwater noise. There are not only researchers in natural science and fisheries. There are professor of maritime culture and ethnology, people who have worked in maritime affairs such as transporting, ships, and ports, researchers in law and economics, experts in international relations and security, and people who have worked for the United Nations. It was like a cross-cultural exchange, a very unique place. I was reminded that the oceans, which I had seen in the natural sciences, were really a place of human activity. And I understand that if humans are to use the ocean, there must be rules. Strangely enough, however, there are not many experts in "ocean policy". It's a field where people with various backgrounds come together to think and build. I used to think that policy was in a different dimension for me, but I don't know how I ended up looking into this world . . . Let me tell you a little about the path I have taken so far. The starting point was studying chemistry at university. I was interested in pharmaceuticals, so I studied synthetic organic chemistry. Organic reagents and organic solvents are petroleum products. At that time, while using a lot of solvents such as hexane, I vaguely wondered how much more oil could be drilled. Next, I taught science in junior high and high school. The "science" part of the teaching license was relentless, and I was required to take physics, chemistry, biology, and geology. However, at that time, I was not familiar with the planetary space-time scale, and it was difficult for me to understand the subject and communicate it in my own words. I had always been interested in field science, so I dove into the world of earth science. There I encountered the science of coral reefs and the study of reconstruction of paleoclimate and paleoenvironment using coral annual rings. Annual rings are a visible measure of time. I was shocked to learn that the annual rings of calcium carbonate coral skeletons record information on seawater temperature and salinity, the flow of materials from the land through rivers, and even traces of human activity and waste. From the Kenyan coral rings I reconstructed the climatic mode of the Indian Ocean over the past 115 years, and clearly showed the rise in sea temperature in the Indian Ocean. The coral rings of Tuvalu in the South Pacific, which is threatened by sea level rise, have been showing black contamination since the 1990s. From the annual rings, we were able to elucidate the process by which the increase in domestic wastewater due to population growth affected the coral reef ecosystem. Through these jobs, I came to have a closer look at the issues of climate change and global warming related to increasing CO_2, and environmental changes. Looking around at Earth science, I became familiar with its spatio-temporal scale, and came to see my own position in the 4.6 billion years of planetary evolution.
And now, besides science, what else can I do? . . The journey continues.

©2021. Japan Geoscience Union. All Right Reserved.



ツバルのサンゴ年輪が記録する人為影響

(**a**) ツバル フォンガファレ島のサンゴ年輪, 成長停止により年輪が途切れ, 放射性炭素 (14C) 年代測定を行った. 1991 年に成長開始するが, その後 黒色バンドの混入が見られる (**b**) 黒色バンド部分拡大
(**c**) 月単位の酸素同位体比 (δ18O) 測定から年輪内に季節を入れ, 黒色バンドの位置を重ねた結果, 11 月から翌年 3 月頃にかけて, 西風の雨季に混入することが分かった.
(**d**) 黒色バンドには赤褐色 - 灰青色 - 黒色のグラデーションがある. また黒色部は鉄を多く含み, 色グラデーションは鉄の酸化還元状態を反映していた. 黒色部からは外部由来の有機物と嫌気性バクテリアの遺伝子断片も検出された. 過剰有機物のバクテリア分解過程で, 硫酸還元まで進行し, 無酸素環境下 硫化鉄がサンゴ骨格に沈殿する.

Nakamura, N., Kayanne, H., Takahashi, Y., Sunamura, M., Hosoi, G., & Yamano, H. (2020),
Anthropogenic Anoxic History of the Tuvalu Atoll Recorded as Annual Black Bands in Coral. Sci Rep 10, 7338,
https://doi.org/10.1038/s41598-020-63578-4
東京大学　ツバルのサンゴが記録していたサンゴ礁劣化の歴史 サンゴ年輪に黒色バンドとして記録された無酸素環境
UTOKYO FOCUS　https://www.u-tokyo.ac.jp/focus/ja/articles/z0508_00048.html

©2021. Japan Geoscience Union. All Right Reserved.

Living with solar sytem exploration

*Takeshi Imamura[1]

1. Graduate School of Frontier Sciences, The University of Tokyo

As one of the researchers involved in solar system exploration, I will talk about how I came to this research field, how I spend my life in my lab, and what I try to do in my life as a researcher. I will also introduce paths to the field of solar system exploration where various researchers and engineers with different skills cooperate.

Keywords: solar system exploration, researcher

©2021. Japan Geoscience Union. All Right Reserved.

Introduction to IODP and the works inside

*Michiko Yamamoto[1]

1. Scripps Institution of Oceanography, UCSD

International Ocean Discovery Program (IODP) has been a very successful international Earth science program over the past five decades with many scientific accomplishments in paleoclimatology, microbiology, marine geology, geophysics, and more. If you will major in Earth science at university or you are doing now in undergraduate, you wouldn't miss seeing the name in textbooks or papers or presentations at least once in your study life even if you are not directly participated in the program as IODP has been one of the largest data sources for the scientists in this field to study on or refer to. In this presentation, I will introduce the program and inside management work as sample of non-research role in academia, and I hope it will be helpful for you to broaden your perspective of possible career after PhD or MS and could be any hint in your future career planning.

©2021. Japan Geoscience Union. All Right Reserved.

I’ m working as a nature guide, an environmental activist, and a facilitator.

*hisashi Oiwane[1]

1. Musuhi LLC

I’ m working as a nature guide, an environmental activist, and a facilitator.

©2021. Japan Geoscience Union. All Right Reserved.

[J] Oral | O (Public) | Public

[O-05] How to become a scientist? What can they do?

convener:Natsue Abe(Mantle Drilling Promotion Office, MarE3, Japan Agency for Marine-Earth Science and Technology), Rie Hori, S.(Department of Earth Science, Faculty of Science, Ehime University), Chairperson:Rie Hori(Department of Earth Science, Faculty of Science, Ehime University), Mayumi ARAI(National Museum of Emerging Science and Innovation), Natsue Abe(Mantle Drilling Promotion Office, MarE3, Japan Agency for Marine-Earth Science and Technology), Chiaki T. Oguchi(Institute for Environmental Science and Technology, Graduate School of Science and Engineering, Saitama University)
Sun. Jun 6, 2021 1:45 PM - 3:15 PM Ch.01 (Zoom Room 01)

The earth and planetary sciences deal with many issues that are very close to our daily lives. Such researchers in this area are active in many parts of Japan. In this session, we introduce such researchers and people involved in this field and their activities, how they landed their current position. Many people may not know how to become a scientist. Either many of students may wonder how they apply their learned in university and their skills to society? We will have presentations on what they have learned and how they can use the skills they have acquired during their studies at universities and graduate schools in society.

Junior and senior high school students who want to go into the field of earth and planetary sciences are welcome to participate in this session and ask questions. We also welcome submissions from people who develop human resources and expand their colleagues.

3:05 PM - 3:15 PM

[O05-07]Discussion

©Japan Geoscience Union

[J] Poster | O (Public)：Public

Sun. Jun 6, 2021 5:15 PM - 6:30 PM JST | Sun. Jun 6, 2021 8:15 AM - 9:30 AM UTC | Ch.02_2

[O-05] How to become a scientist? What can they do?

convener:Natsue Abe(Mantle Drilling Promotion Office, MarE3, Japan Agency for Marine-Earth Science and Technology), Rie Hori, S.(Department of Earth Science, Faculty of Science, Ehime University)

The earth and planetary sciences deal with many issues that are very close to our daily lives. Such researchers in this area are active in many parts of Japan. In this session, we introduce such researchers and people involved in this field and their activities, how they landed their current position. Many people may not know how to become a scientist. Either many of students may wonder how they apply their learned in university and their skills to society? We will have presentations on what they have learned and how they can use the skills they have acquired during their studies at universities and graduate schools in society.
Junior and senior high school students who want to go into the field of earth and planetary sciences are welcome to participate in this session and ask questions. We also welcome submissions from people who develop human resources and expand their colleagues.

[O05-P01] Only Ph.D. holders can work in the research and science field?

*Natsue Abe[1,2], Rie Hori, S.[3] (1.Mantle Drilling Promotion Office, MarE3, Japan Agency for Marine-Earth Science and Technology , 2.Graduate School of Natural Science & Technology, Kanazawa University, 3.Ehime University)

[O05-P02] Skills required to work at the science museum

★Invited Papers

*Mayumi ARAI[1] (1.National Museum of Emerging Science and Innovation)

[O05-P03] Discussion

Only Ph.D. holders can work in the research and science field?

*Natsue Abe[1,2], Rie Hori, S.[3]

1. Mantle Drilling Promotion Office, MarE3, Japan Agency for Marine-Earth Science and Technology , 2. Graduate School of Natural Science & Technology, Kanazawa University, 3. Ehime University

The earth and planetary sciences deal with many issues that are very close to our daily lives. Such researchers in this area are active in many parts of Japan. We introduce such researchers and people involved in this field and their activities, how they landed their current position. Many people may not know how to become a scientist. Either many students may wonder how they apply their learned in university and their skills to society? We are going to explain their career pass, how to receive a Ph.D., how to get the position, and what they have learned, and how they can use the skills they have acquired during their studies at universities and graduate schools in society. Junior and senior high school students who want to go into the field of earth and planetary sciences are welcome to participate in this session and ask questions.

Keywords: Ph.D. holders, career pass, Earth and Planetary Sciences

©2021. Japan Geoscience Union. All Right Reserved.

Skills required to work at the science museum

*Mayumi ARAI[1]

1. National Museum of Emerging Science and Innovation

A variety of human resources work at the Science Museum. There are not only people who plan permanent exhibitions, special exhibitions, events, programs for schools, but also people who perform demonstrations and explanations, technical staff, receptionists, public relations, general affairs, accounting, and information system personnel. Shops, restaurants, cafes, security, cleaning, etc. may be outsourced to external organizations / institutions, but such tenant staff are also important to support the science museum. And unlike employees, human resources such as volunteers are also indispensable to science museums. In this way, the science museum is consist of human resources with various roles. Therefore, staffs working at the science museum are not only the person have a doctor's degree or a master's degree, but also those who have bachelor's degree from liberal arts or those who have professional skills.
In this presentation, we will consider the skills required to work at the science museum and propose the skills that will be needed more in the future.

©2021. Japan Geoscience Union. All Right Reserved.

[J] Poster | O (Public) | Public

[O-05] How to become a scientist? What can they do?

convener:Natsue Abe(Mantle Drilling Promotion Office, MarE3, Japan Agency for Marine-Earth Science and Technology), Rie Hori, S.(Department of Earth Science, Faculty of Science, Ehime University)

Sun. Jun 6, 2021 5:15 PM - 6:30 PM Ch.02

The earth and planetary sciences deal with many issues that are very close to our daily lives. Such researchers in this area are active in many parts of Japan. In this session, we introduce such researchers and people involved in this field and their activities, how they landed their current position. Many people may not know how to become a scientist. Either many of students may wonder how they apply their learned in university and their skills to society? We will have presentations on what they have learned and how they can use the skills they have acquired during their studies at universities and graduate schools in society.

Junior and senior high school students who want to go into the field of earth and planetary sciences are welcome to participate in this session and ask questions. We also welcome submissions from people who develop human resources and expand their colleagues.

5:15 PM - 6:30 PM

[O05-P03]Discussion

©Japan Geoscience Union

[J] Oral | O (Public)：Public

Sun. Jun 6, 2021 1:45 PM - 3:15 PM JST | Sun. Jun 6, 2021 4:45 AM - 6:15 AM UTC | Ch.02 Zoom Room 02

[O-06] Let's talk about "the 10 years of reconstruction from the Great East Japan Earthquake"

convener:Hitoshi Nakai(Kobuchisawa Research Institute for Nature and Education), Mamoru Hayashi(University of TOYAMA), Tetsuhiko Asano(Senshu University Matsudo Junior High School High School), Chairperson:Mamoru Hayashi(University of TOYAMA), Tetsuhiko Asano(HunabashiKeimei High School), Hitoshi Nakai(Kobuchisawa Research Institute for Nature and Education)

The year 2021 marks the 10th anniversary of the Great East Japan Earthquake. The severity and scale of the damage also shocked people who lived outside the disaster area. However, since earthquakes and floods have occurred regularly in various places since then, anyone who is not directly affected has tended to become oblivious of how reconstruction is progressing following the massive quake. The government designated the first five years after the disaster as an intensive reconstruction period, and the next five years, that is, the years up to March 2021, as the first period of reconstruction and creation. According to the "Roadmap and Prospects for Reconstruction from the Great East Japan Earthquake" posted on the Reconstruction Agency website, both private housing and public housing for disaster victims are now 99% complete. It states that most of the infrastructure was restored by the end of the intensive reconstruction period. In addition, it is reported that, as of August 2020, the number of evacuees has decreased from the initial 470,000 to 43,000. However, the lives of these 43,000 people under the conditions of evacuation are still severely impaired. Of these, 37,000 in Fukushima Prefecture (as of July 2020) are still unable to return to the towns and villages where they used to live. However, these numerical data cannot clearly convey a realistic picture of how people work and live, the status of their physical and mental health, and cannot evoke in us a sense of empathy for the victims. Therefore, the convenors would like to make this session an opportunity to get to know the current situation of the victims by inviting those involved in reconstruction to give lectures. We believe this session will provide useful information for recovery from future catastrophes.

1:45 PM - 2:15 PM JST | 4:45 AM - 5:15 AM UTC

[O06-01] Overview of reconstruction status for the 10th anniversary of the Great East Japan Earthquake

★Invited Papers

*Yoshihiro Okumura[1] (1.Kansai University)

2:15 PM - 2:45 PM JST | 5:15 AM - 5:45 AM UTC

[O06-02] Problems caused by and positive lessons to be inherited from the reconstruction of the Great East Japan Earthquake

★Invited Papers

*Hiromi ENSHU

2:45 PM - 3:15 PM JST | 5:45 AM - 6:15 AM UTC

[O06-03] One decade after the earthquake, reconstruction still not complete

★Invited Papers

*YUKIKO KIKUCHI[1] (1.general incorporated association Otsuchi Shimbun)

Overview of reconstruction status for the 10th anniversary of the Great East Japan Earthquake

*Yoshihiro Okumura[1]

1. Kansai University

Ten years have passed since the Great East Japan Earthquake, and it seems that the affected peoples are recovering their daily lives. However, there are many challenges. I will overview the current state of reconstruction, focusing on the disaster areas of Miyagi Prefecture.

Keywords: Great East Japan Earthquake, recovery, reconstruction

©2021. Japan Geoscience Union. All Right Reserved.

Problems caused by and positive lessons to be inherited from the reconstruction of the Great East Japan Earthquake

*Hiromi ENSHU

1 The current state of reconstruction in Miyagi prefecture
In March 2020, Miyagi Prefecture released the results of a review of the prefecture's earthquake recovery plan. It provides a glimpse into the current state of disaster recovery in Miyagi Prefecture.
The verification is based on the evaluation of the progress rate of 24 items in 7 fields included in the earthquake recovery plan, and those are categorized in the following 4 levels; A: certainty of achievement, B: achievement of 80% or more, C: achievement of less than 80%, and N: unmeasurable.
The following are the main points that can be read from the report.
(1) The selection of verification indicators is arbitrary, and there are no indicators that allow us to correctly grasp the progress in rebuilding the lives of disaster victims.
(2) Highly evaluated items are easily to control for local governments and biased to construction projects.
(3) Difficult to achieve are those that are beyond the control of local governments, in which private businesses and disaster victims are involved.
(4) Delaying in rebuilding livelihoods is obvious.
(5) The recovery plan in agricultural production that intends to introduce large-scale and entrepreneurial management has not been successful.
(6) Employment of disaster victims cannot be verified.
(7) Delays in the construction of seawalls, especially in the improvement of river levees for tsunami countermeasures are serious, whose main causes are skyrocketing construction costs caused by massive construction projects themselves.

2 Problem of victims living in poorly repaired houses and difficulties in community formation
685 households in Ishinomaki City were officially identified that they had been living in poorly repaired houses. Furthermore, based on the number of households with reduced property tax, not repaired houses may exceed 10,000 in Sendai City.
In addition, only less than one-third of households living in former villages moved in small-scale housing complexes constructed in remote peninsular areas, making community formation impossible and marginalization inevitable. The residents of public disaster housing are aging and becoming increasingly impoverished, and the formation and maintenance of a community is becoming a heavy burden on the leaders of neighborhood associations.

3 Characteristics of the recovery process in Miyagi Prefecture

The reconstruction process in Miyagi Prefecture can be characterized in the following three points. First, the rebuilding of the lives of the victims was neglected and massive civil engineering development was carried out to take advantage of the disaster. Secondly, the destruction of communities and self-governance proceeded, and thirdly, neoliberal structural reforms under the name of "creative reconstruction" were enforced, leaving "human reconstruction" behind and causing the selection and division of the victims in the project process.

4 What the Great Earthquake Left Behind
(1) What should be inherited

©2021. Japan Geoscience Union. All Right Reserved.

The following is a list of possible candidates. (1) Development of disaster case management, (2) Group subsidies for small and medium-sized enterprises, (3) Mandatory maintenance of registers of disaster victims and those who need support for evacuation, (4) Expansion of support for rebuilding the lives of disaster victims to medium scale collapses, (5) Lifting of the ban on moving into temporary housing during emergency repairs, (6) Use of existing rental houses as temporary housing and provision of wooden temporary housing, (7) Establishment of a comprehensive subsidy for supporting disaster victims.

(2) Possible negative legacy of the earthquake reconstruction
i. Arbitrary use of inundation simulations.
ii. Promotion of huge land readjustment with special exceptions and special zones for reconstruction.
iii. Relaxation of requirements for disaster prevention group relocation projects.

Keywords: reconstruction of earthquake disaster, creative reconstruction, unfair selection and division in disaster victims, human reconstruction, disaster case management

©2021. Japan Geoscience Union. All Right Reserved.

One decade after the earthquake, reconstruction still not complete

*YUKIKO KIKUCHI[1]

1. general incorporated association Otsuchi Shimbun

It has been ten years since the Great East Japan Earthquake. The media often report that reconstruction projects are a waste of taxpayers’ money and that the victims still lead difficult lives. What does “reconstruction” of a town mean? When can we say that reconstruction is complete? Did you know that the concept, "reconstruction," conveys an idea that is "more than simple disaster recovery"?

Otsuchi Town (Kamihei District, Iwate Prefecture) was devastated by the earthquake and tsunami that occurred on March 11, 2011. After the disaster, the townspeople lacked the information they needed just to survive. Given this situation, in 2012, I (the author) decided to publish a weekly newspaper, the "Otsuchi Shimbun." I had never before attempted to compile and publish a newspaper. I did everything by myself from interviewing to editing. Starting in the following year, the weekly newspaper was distributed free of charge to all households in the town. I have learned a lot about the town and thought more deeply about it as a consequence of publishing the newspaper. Initially, the newspaper was intended to deliver reconstruction information to the townspeople, but gradually it began to uncover problems that arose in the process of reconstruction.

Immediately after the earthquake, Otsuchi Town set up a disaster response headquarters in front of the town office building. However, the tsunami struck the headquarters, killing 38 local government employees including the mayor with the result that it was not possible to issue the evacuation order. Among Otsuchi Town’s population of 15,276 (according to the 2010 census), 1,286 died, including disaster-related deaths. Otsuchi is often referred to as "a town where 1 in 10 people died" in the disaster. It is one of the municipalities with the highest percentage of victims in the three affected prefectures: Iwate, Miyagi, and Fukushima. With about 70% of the houses damaged by the tsunami and subsequent fires, the town’s urban area was virtually destroyed. Most hardware projects covered by reconstruction budgets were completed by the end of 2019. New seawalls, floodgates, bridges, etc. have been constructed. Regarding the housing reconstruction to accommodate victims, 967 lots were created in the land readjustment area project, 422 residences were relocated in the disaster prevention group relocation project, and 876 disaster public housing units were built. The main current issues are restoring the town office organization, which suffers from a shortage of human resources, utilizing vacant lots, and investigating the effects of the earthquake disaster and what was lacking in the disaster prevention measures that were in place before the tsunami hit the town.

There is a concern that reports that are rooted in the media’s stereotyped perception that the reconstruction budget is a "waste of taxpayers’ money" may rob people of the memory of the disaster. Reconstruction has focused on hardware projects until now. However, budgets were additionally allocated to software projects, such as psychological support for the victims. The national "Basic Law for Reconstruction from the Great East Japan Earthquake" states the following reconstruction principles: "Take drastic measures with a view to revitalizing Japan beyond mere disaster recovery," and “carry out what should be accomplished now with a vision of what form Japan should take by the middle of the 21st century." We must achieve creative reconstruction that will remain valid for Japan 30 years from now. There are able people in Otsuchi who are working hard to make the town better than it was before the disaster, although the town government constantly suffers from a shortage of human resources. What is

©2021. Japan Geoscience Union. All Right Reserved.

most needed now is to revisit the principles of reconstruction without being swept away by the ongoing processes of reconstruction.

Keywords: earthquake, tsunami, Otsuchi Shimbun, reconstruction, restoration

©2021. Japan Geoscience Union. All Right Reserved.

[J] Oral | O (Public)：Public

Sun. Jun 6, 2021 12:30 PM - 1:30 PM JST | Sun. Jun 6, 2021 3:30 AM - 4:30 AM UTC | Ch.02 Zoom Room 02

[O-07] Poster presentations by senior high school students

Chairperson:Tatsuhiko Hara(International Institute of Seismology and Earthquake Engineering, Building Research Institute), Katsuyoshi Michibayashi(Department of Earth and Planetary Sciences, Nagoya University), Miwa Kuri(Japan Meteorological Agency), Keiko Konya(Japan Agency for Marine-Earth Science and Technology)

Senior high school students provide poster presentations on subjects in fields of earth and planetary sciences. This session provides an opportunity for senior high school students to give their presentations in the JpGU meeting and to have discussions with researchers. This session has been conducted as a public outreach session since 2006.

12:30 PM - 1:30 PM JST | 3:30 AM - 4:30 AM UTC

Poster presentations by senior high school students

[J] Poster | O (Public)：Public

Sun. Jun 6, 2021 1:45 PM - 3:15 PM JST | Sun. Jun 6, 2021 4:45 AM - 6:15 AM UTC | Ch.27

[O-07] Poster presentations by senior high school students

convener:Tatsuhiko Hara(International Institute of Seismology and Earthquake Engineering, Building Research Institute), Katsuyoshi Michibayashi(Department of Earth and Planetary Sciences, Nagoya University), Miwa Kuri(Japan Meteorological Agency), Keiko Konya(Japan Agency for Marine-Earth Science and Technology)

Senior high school students provide poster presentations on subjects in fields of earth and planetary sciences. This session provides an opportunity for senior high school students to give their presentations in the JpGU meeting and to have discussions with researchers. This session has been conducted as a public outreach session since 2006.

[O07-P01] Weather in Fukuoka Prefecture in the Edo period from the Nakamura Heizaemon diary

*Rui ANDOU[1], *Rio HAYASHIDA[1], *Hikari ARASE[1], *Mira EGUCHI[1], *Touko HAGIHARA[1] (1.Ikeda Senior High School)

[O07-P02] Discussion on Economic Effects of Muroto Deep Sea Water – How Does Deep Sea Water Industry Contribute to Revitalize the Community? –

*Kaede Yauoka[1] (1.Muroto High School)

[O07-P03] Observation of Columnar Joints and Research on its Origin

Atsushi Watanabe[1], *Iroha Kawaguchi[1], *Ryosuke Sugioka[1], *Mizuki Hukumuro[1], *Akihiro Amamiya[1], *Towa Serizawa[1] (1.Nirayama Highschool)

[O07-P04] A study of microplastics that is included in the rivers and coast of the Izu Peninsula

Atsushi Watanabe[1], *Namiki Kawai[1], *Koji Sadakane[1], *Yuichirou Takahashi[1], *Mayuko Toriikouji[1], *Daisuke Yamamoto[1], *Miori Yabuta[2], *Tubasa Ozawa[2], *Takaya Nishida[2], *Haruki Mimura[2], *Nanami Hujii[2], Ryosuke Yoshida[2] (1.Nirayama Highschool, 2.Shimoda Highschool)

[O07-P05] Consideration of method to increase artificial ruby

Atsushi Watanabe[1], *Yuichirou Nagatsu[1], *Moe Hatakeyama[1], *Koutarou Matsumoto[1], *Yudai Komiyama[1] (1.Nirayama Highschool)

[O07-P06] Earthquake prediction by Electric magnetic wave

*Masayuki Masa[1], *Nozomu Sakai[1], Michiya Sasaki[1], Souhei Kato[1], Ousuke Yagasaki[1], Mizuho Fujiwara[1], Maika Yashima[1] (1. Tokyo Metropolitan Tama High School of Science and Technology)

[O07-P07] Comparison of heated products of glucose with citric acid added

*Takumi Ohtsu[1] (1.Tokyo Metropolitan Tama High School of Science and Technology)

[O07-P08] Development of iron (II) phosphate lithium-ion battery using the adsorption power of Aso loess

*Ayumi Hoshi[1], *Sora Nozaki[1] (1.Tokyo Metropolitan Tama High School of Science and Technology)

[O07-P09] Method of Recovering Perfluorinated Compounds by coffee grounds

*Kouki Morimoto[1], *Issei Yamazeki[1], *Renon Shimizu[1] (1.Tokyo Metropolitan Tama High School of Science and Technology)

[O07-P10] Research into Moriya Formation Formed in Northen Fossa Magna

*Yusuke Morozumi[1] (1.Suwa Seiryo high school)

[O07-P11] A Consideration of a Landing Exploration on Europa

*Taichi Ito[1] (1.Seishin Gakuen High School)

[O07-P12] Relationship between five gigantic jets in the past and cloud-to-ground lightning

*Fuga Suzuki[1], *Yuya Takahashi[1], Sorachi Nishibori[1], Yuki Ito[1], Takumi Miyamoto[1] (1.Shizuoka Prefectural Iwata Minami High School)

[O07-P13] Examination of the fall position by the light emission of the Narashino meteorite fireball

*Ryunosuke Kamiya[1], *Haruka Sato[1], Kosuke Arimura[1], Saki Ozawa[1], Hana Miki[1], Yuka Ogawa[1], Honoka Tanabe[1] (1.Shizuoka Prefectural Iwata Minami High School)

[O07-P14] The Change of Microtopography of Samejima Coast Caused by the Storm Surge Brought by Hagibis

*Takeshi Totsuka[1], Yuya Takahashi[1], *Kosuke Arimura[1], Koki Suzuki[1], Shun Ichikawa[1], Rabu Kato[1] (1.Shizuoka Prefectural Iwata Minami High School)

[O07-P15] Putting legs on snake swimming robot going to be useless?Seeking truth of Tetrapodophis

*Ryoya Sato[1], *Kokoro Ikeda[1], *Ryota Ogawa[1], *Riko Tomioka[1], *Akari Hitomi[1], *Kanon Yamaguchi[1] (1.Tokyo Tech High School of Science and Technology)

[O07-P16] Consideration of snowmelt type lahar at Mt. Katta, Zao

*Haruya Shishido[1], *Reiki Syoji[1], *Ryo Hikichi[1] (1.Miyagi Prefectural Tagajo Senior High School)

[O07-P17] Geological structure of Urato Katsurashima Island and Nonoshima Island, Shiogama City

*Asahi Oyama[1], *Hikaru Sasaki[1], *Yuhi Suzuki[1], *Hayato Murakami[1], *Misaki Kuga[1] (1.Miyagi Prefectural Tagajo Senior High School)

[O07-P18] Threats and impacts of urban tsunami
-Simulate a tsunami when a Nankai Trough giant earthquake occurs using a tsunami generator-

*Misaki Suda[1], *Kenshin Okazaki[1], *Zen Sato[1], *Yusei Niinuma[1], *Kousei Matsuura[1], *Ayaka Akisawa[1] (1.Miyagi Prefectural Tagajo Senior High School)

[O07-P19] Countermeasures against Heat Island Phenomenon: Proposal for a New Building System

*Hiroaki HAYASHI[1] (1.Yokohama Science Frontier High School)

[O07-P20] An evaluation of artificial landform in Chiba prefecture called “Kawamawashi”

*Kodai SHIBUYA[1] (1.Yokohama Science Frontier High School)

[O07-P21] The relationship between sunspot number and typhoons

*Takeru TODA[1] (1.Yokohama Science Frontier High School)

[O07-P22] On the study of Fukui Earthquake Fault IX

*Kazuho Kuwajima[1], *Ryouhei Matta[1], *Youhei Morise[1], *Ayano Yashima[1] (1.Fujishima High School of Fukui prefecture)

[O07-P23] **Approach to the current situation and issues of geothermal power generation utilization based on field surveys**

*Kisho Kurosawa[1], *Tatsuki Miyamoto[1], *Nozomi Kawaharata[1], *Shoki Yashima[1], *Yusuke Oba[1] (1.FurukawaReimei High School)

[O07-P24] Study of mechanism of Light Emission by Spectroscopic Observation of Meteor

*Yui Sato[1], *Yuki Kato[1] (1.Miyagi Prefectual Furukawa Reimei Senior High School)

[O07-P25] Relationship between mineral crystallization and impurities.

*Usami Kenta[1], *Ryo Nakane[1], *Hiroyuki Sueno[1], Syotaro Kawana[1], Ryota Naito[1], Kazuhiko Hoshi[1], Mitsuhide Sai[1], Takuma Watanabe[1] (1.Johoku high school)

[O07-P26] Analysis of water quality of irrigation ponds focused on land use, irrigation systems and periodic pond draining

*Ayane INOUE[1], *Haruto TAKEYAMA[1], *Kousuke MANO[1], *Rio YAMANO[1] (1.Hyogo Prefectural Kakogawa Higashi High School)

[O07-P27] The Process of Raised-Bed River Formation and Factors that Affect It

*Natsuki KAMISASA[1], *Yuta KONDO[1], *Haruto TAKEYAMA[1], *Yasuharu TOMITA[1], *Rikushi NAGAO[1], *Naka NOHAMA[1] (1.Hyogo Prefectural Kakogawa Higashi High School)

[O07-P28] Studies of the SDGs on the Sanriku Geopark. The sea urchin spread trench in the Taneichi Formation.

*Kyougo Sakashita[1], *Asahi Sekibata[1], *Rina Nakajo[1], *Yuto Kugoi[1], *Hikaru Sasaki[1] (1.Marient Chikyu-tanken club senier)

[O07-P29] Studies of the SDGs on the Sanriku Geopark. The Aoba Lake and Shimamori Basin.

*Mizuki Kimura[1], * Naho Simodate[1], *Kahono Hinata[1], *Yuma Keicho[1], *Kouki Takahashi[1] (1.Marient Chikyu-tanken club senier)

[O07-P30] Proposal of Hachinohe Canyon to Sanriku Geopark Geosite.

*Sarina Shinohe[1], * Miyu Abe[1], * Akari Nakamura[1], *Yukihito Yasuhara[1], *Kensuke Shimomura[1] (1.Marient Chikyu-tanken club senier)

[O07-P31] Proposal of an index for estimating the distance from the source rock

*Ayaka Mitsui[1], *Reiji Iwamoto[1], *Keishi Okumi[1], *Mayu Naito[1], *Yamato Yasuhara[1], *Natsuki Yamamoto[1], *Naoko Kodama[1], *Akito Sasaki[1], *Akira Tada[1], *Takuto Nakanou[1], *Tomohiko Maeda[1], *Yuya Muromoto[1], *Ryusei Moriyama[1] (1.Hyogo Prefectural Himejihigashi Senior High School)

[O07-P32] Energy calibration of a cosmic-ray detector

*moe kimura[1] (1.Tokyo Metropolitan Hibiya High School)

[O07-P33] Floating waterdrops using a straw commutator

*Aoba Takahara[1], Yuri Yasui[1], Takaya Sato[1] (1.Niigata Prefectural Takada high school)

[O07-P34] The rotating-Water-tank that is replaced hot water tank and ice water tank

*Masamune Minou[1] (1.Niigata Prefectural Takada high School)

[O07-P35] Comparison of the surface of Mars with the previous one in the approach of Mars Spread of dust storm on November 17th

*Sayaka Mizutani[1], *Takumi Uchiyama[1], Riho Kagami[1], Aoi Takemoto[1] (1.Ichinomiya High School)

[O07-P36] Tumulus inspection project by using cosmic-ray muon

*Tomoyo Ishizawa[1], *Satoshi Ono[1], *Asahi Shiozaki[1], *Wakana Yanagimoto[1], *Kenshiro Aoki[1], *Yuna Ishii[1], *Sogo Kimura[1], *Yuki Shimada[1], *Aoi Soga[1], *Yuga Takemori[1], *Rino Tomiku[1], *Kana Hashizume[1], Miki Ohtsuka[1] (1.Waseda University Honjo Senior High School)

[O07-P37] Calculating the nebula density from the size of the emission nebula

*Yuki Shirai[1] (1.Totsuka High School)

[O07-P38] Strength evaluation of structures by making and improving quake-vibration generators

*Runaya Igari[1], *Yuto Meguro[1], *Rin Goto[1], Kenshiro Kamata[1] (1.Miyagi Rifu high school)

[O07-P39] Time dependence of ocean salinity

*Honami Hashimoto[1], Annu Ito[1] (1.Miyagi Rifu highschool)

[O07-P40] Toward "Solid-State Version Chromatography" Second Report

*Yuichiro Okuno[1], *Akihisa Wada[1], *Yudai Kozono[1], *Ryota Iwamoto[2], *Mai Fujitani[2], *Kyoya Okada[3], *Kusunori Sumi[3], *Arata Fujimoto[3] (1.Imamiya Technology Senior High School of Osaka Prefecture:The evening course, 2.Otemae Senior High School of Osaka Prefecture:The evening course, 3.Kasugaoka Senior High School of Osaka Prefecture:The evening course)

[O07-P41] How to extract bioethanol effectively by distillation.

*Ataru Kunihisa[1] (1.Wakasa high school)

[O07-P42] Confusion of the people in the northwestern area of Saitama Prefecture due to rumors after the 1923 Kanto Earthquake

*Miharu Shinoda[1] (1.Sakae Higashi High School)

[O07-P43] A quest for the best condition of a crystal radio's detection

*Motoaki Osone[1] (1.Yashiro High School)

[O07-P44] What cause columner joint changes?

*Yugo Sakurai[1], *Yuki Enomoto[1], *Kanta Hayashibe[1] (1.Yashiro High School)

[O07-P45] Preliminary analysis of HAYABUSA-2’s Doppler-Shift

*Azumi Sofue[1], *Naoko Nishino[1], *Riri Iida[1], *Riri Numata[1] (1.Wakayama Shin-ai Senior High School)

[O07-P46] Estimation of a ceiling thickness using the muography technique with a small cosmic-ray detector

*Nana Kobayashi[1] (1.Kaichi High School)

[O07-P47] A proposal of an inverse analysis method for ballistic ejecta flying focusing on crater shape in phreatic eruption

*Kouki Nishino[1], Neo Suzuki[1], Natsumi Waki[1] (1.Kanagawa Prefectural Yokosuka Senior High School)

[O07-P48] The survey of Micro-Plastics included in River sediments.

*Taichi Ichikawa[1], Ryuke Kawai[1], Suzuka Fukunaga[1], Tessho Yamamoto[1], Takumi Sato[1] (1.GIZAN SENIOR HIGH SCHOOL)

[O07-P49] Relationship between sprites and the lightning charge moment

*syunsuke nakao[1], *sora wake[1] (1.Prefectural Kochi Ozu High School)

[O07-P50] Potential Small Hydropower Generation in Kamikawa Basin -Hydro Energy Map Visualizing Power Generation-

*Airi Takei[1], *Akira Tamaki[1], *Naoki Kudo[1], *Asahi Takahashi[1], *Hikaru Kawashima[1] (1.Hokkaido Asahikawa Nishi High School)

[O07-P51] Consideration of brachiopod biota change events in the Kuzu limestone layer

*Omi Kono[1], Tokio Chiba[1] (1.Kaijo senior high school)

[O07-P52] Estimation of the variation in mechanism in the amount of spring water in Otomeyama Park, Shinjuku City

*Kuya Aoyama[1], Taichi Shimokobe[1], Masamune Kanou[1] (1.Kaijo high school)

[O07-P53] Modeling the earthquake damage in adeveloped land

*Shungo Kokubun[1], *Satoru Takahashi[1], *Hiroshi Takeuchi[1], *Haruki Tamakawa[1], *Masafumi Kaneko[1], Takumi Nanbu[1] (1.Miyagi Prefecture Sendai Daisan High School)

[O07-P54] Influence of Calcium chloride on frost columns

*Manaka Oya[1], Shohei Nanri[1] (1.Ichikawa gakuen Ichikawa senior high school)

[O07-P55] Differences in fog generation conditions in the Edogawa estuary -Examples of Edogawa-ku and Ichikawa-shi-

*Kenta Torii[1], Shohei Nanri[1] (1.Ichikawa gakuen Ichikawa senior high school)

[O07-P56] Development of variable slope type underwater embankment

*Kei Omura[1], Shohei Nanri[1] (1.Ichikawa gakuen Ichikawa senior high school)

[O07-P57] Environmental impact assessment of air and soil substances using spring water of Minowa as an index

*Mari Taki[1], Shohei Nanri[1] (1.Ichikawa gakuen Ichikawa senior high school)

[O07-P58] Development of an automatic meteor shower observation and the notification system
~Web broadcast of meteor appearance~

*Koichi Sato[1], *Koshi Ri[1], *Shunsuke Isoda[1], *Honoka Ohno[1] (1.Chuo University Junior and Senior High School)

[O07-P59] Meteorological and geographical conditions of river flooding-Comparison of the past and present of the Miyata River-

*Eri Yoshida[1], *Minami Oikawa[1], *Kotomi Shibata[1], *Chihiro Terazaki[1], *Kurumi Yabe[1] (1.Ibaraki prefectural Hitachi first senior high school)

[O07-P60] Where are solar panels actually used? Research on the present situation of Kashiwa City, Chiba prefecture, Japan.

*Souri Mizukami[1] (1.SHIBYA SENIOR HIGH SCHOOL)

[O07-P61] Decline and Fall of Martian Polar Capse; Whether the Dast Storm Is Warm the Polar Cap

*Kei Inoue[1], Hibiki Aminaka[1], Yuho Takagi[1], Nanami Yasuda[1], Yuki Tanaka[1], Tomoki Ugawa[1], Rio Mogi[1], Kyouka Miyake[1], Momoha Takashima[1], Mako Misumi[1], Kaho Okada[1] (1.Kumamoto Prefectural Daiichi High School)

[O07-P62] Spacial correlation between slow earthquake and mantle- derived hot spring in Southwest Japan

*Yui Kobayashi[1] (1.Shizuoka Higashi High School)

[O07-P63] **Visualize water current using vitamin B_2**

*Mutsuki Kamata[1], *Yuuma Nakagawa[1], *Io Kato[1], *Tokito Hirose[1], *Yuuki Matsui[1], *Kosuke Mafune[1], *Akihito Yamada[1], Kazumi Igawa[1] (1.Zushi-Kaisei Senior High School)

[O07-P64] Designe of lunar crater exploration rover

*Kosuke Kameoka[1] (1.Meikei High School)

[O07-P65] Distribution of Gravel in the Sakawa River and Factors Affecting the Distribution

*Nozomi Uemachi[1], *Misaki Yamamiya[1], Yosuke Saito[1] (1.Tokyo Gakugei University Senior High School)

[O07-P66] Detection of Cherenkov light with acrylic and photodetecto

*Juri Urano[1], *Yuka Kuze[1], *Kaho Kubota[1] (1.Toshimagaoka Joshigakuen senior high school)

[O07-P67] Research the View of Mt.Fuji with a Self-Made Observation Device

*Ryoo Niigawa[1], *Rin Takezoe[1] (1.Tokyo Metropolitan Tachikawa High School)

[O07-P68] Bad visibility in the past at Tachikawa High School

*Tomoya Ushizaka[1] (1.Tokyo Metropolitan Tachikawa High School)

[O07-P69] Analysis of visibility around Tachikawa High School

*Takumi Yasuhara[1] (1.Tokyo Metropolitan Tachikawa High School)

[O07-P70] The relationship between the shape and power generation amount of the simple wind power generators

*Sora Fukui[1] (1.Tokyo Metropolitan Tachikawa High School)

[O07-P71] **Is « evacuate to rise » the Right Action?**
Research and Proposition of Major Evacuation Routes to Shelters in Shibuya

*Sakura Oona Marie Sueoka[1] (1.Tokyo Metropolitan Kokusai High School)

[O07-P72] Mechanism of how the Shirata river looks blue

*Shuhei Sugai[1], *Ryosuke Yoshida[1] (1.Shimoda high school)

[O07-P73] Determining the Properties of Seyfert Galaxies

*Kuya ABE[1], *Kuranosuke IEHATA[1], *Koki TANII[1], *Tamotsu FUJIMOTO[1] (1.Nara Prefectural Seisho High School)

[O07-P74] Observation of Radio Waves from the Moon

*Koya YAMASHITA[1], *Ichika TSUTSUMI[1], *Atsushi HIRANUMA[1], *Ikumi MATSUYOSHI[1] (1.Nara Prefectural Seisho High School)

[O07-P75] Making Snow Meter Using Neutron Cosmic Rays Observation Data Collected By Cosmic Watch

*Kei Ikushima[1], Rikako Kono[2], Kaduo Tanaka[2], Akita Yuji[1] (1.Hiroo Gakuen High School, 2.Touhoku University)

[O07-P76] Water storage capacity of the green dam – Role of forest soil -

*Nanami Aoki[1] (1.Kyoto Prefectural Sagano High School)

[O07-P77] Measurement of Radon Concentration for Earthquake Prediction in the Woods for Field Practice Owned by Sagano H. S.

*Ayaka Kawabata[1], *Takahiro Kawabata[2] (1.Kyoto Prefectural Sagano High School, 2.Graduate School of Science, Osaka University)

Weather in Fukuoka Prefecture in the Edo period from the Nakamura Heizaemon diary

*Rui ANDOU[1], *Rio HAYASHIDA[1], *Hikari ARASE[1], *Mira EGUCHI[1], *Touko HAGIHARA[1]

1. Ikeda Senior High School

Motivation for research

We have been restoring the climate data for the Edo period in Japan from historical documents which were written before the official weather observation records were started in the 16th year of the Meiji period. This year, we analyzed the historical document called the "Nakamura Heizaemon diary" from Kitakyushu.The diary contains information about the actual conditions of people's lives and daily events and was written in the 55 years from 1812 to 1866.

The purpose of the research

1.To create a database in conjunction with the historical documents that we examined in the last few years.

2.Therefore, based on the previous research,we examined the relationship between the “weather appearance rate” and the “detail rate" which measures the accuracy of the records.

The research method

We classified the weather in the historical documents to make the classifications closer to the definitions currently used by Japan Meteorological Agency and the weather was classified as snowy, rainy, cloudy, or sunny.

Data#1 Weather appearance rate(graph1)

The annual trend of the weather appearance rate is as shown in the graph. The sunny appearance rate was the highest at 64.1% in 1828, and the lowest was 39.3% in 1860.The rainy appearance rate was highest at 41.2% in 1860 and lowest at 20.9% in 1813.

Data#2 The weather appearance rate according to the season(graph2)

Looking at the seasonal weather appearance rate , in 1836, when severe damage to crops caused the Tenpo famine, the rainy appearance rate in the summer was 45.7% and the sunny appearance rate was 32.6%. In fact, the usual sunny and rainy appearance rate was reversed.In 1860, the sunny appearance rate fell in the period from spring to autumn, and the sunny and rainy appearance rate in spring and summer were reversed.

Data#3 Annual composition ratio of descriptions of rain(graph3)

The Nakamura Heizaemon diary was written by one person who focused on recording rain .In the all of descriptions, weather described as only “rain” was 79.9%, and other records described the weather as “rainy weather”, “white rain”, “light rain”, “sprinkles of rain”, “light showers”, “drizzle”. The description of “heavy rain” or “strong rain” in 1836 was 10.2%.

Data#4 Summer rain by description / annual composition ratio(graph4)

Looking at the ratio of summer rain, 1836,which is considered to have been a year when heavy rain fell all through the summer, 20.9% of the rain was recorded as “heavy rain” combined with “strong rain”.In the summer of 1831, the record of “strong rain” was remarkable at 23.5%.

detail rate(reference)

Here, we decided to examine the accuracy of recording using the “detail rate” we found in a paper by Professor Sho Kenjiro of Nagoya Institute of Technology.

Data#5 The “detail rate” 1811 to 1866(graph5)

The average for the entire period was 29.9%, the highest rate was 46.2% in 1865 and the lowest rate was 3.6% in 1814.From 1812 to 1866 at the end of the Tokugawa shogunate, the weather records became

©2021. Japan Geoscience Union. All Right Reserved.

more detailed and correlated with the rainy appearance rate .The line of dashes shows the trend of the graph.

Data#6 The “detail rate” for four seasons(graph6)

The “detail rate” for all the four seasons increased towards the end of the Edo period.The “detail rate” of the Nakamura Heizaemon diary for the entire period was 29.9%, which was the same as the Joubu diary, which we had researched previously. The trend of the rainy appearance rate and the trend of the “detail rate” for 55 years are in agreement.

Data#6 Comparison of weather appearance rate every 30 years between the historical documents(graph7)

Comparing the historical documents, "Nijoke diary" and "Myohoin diary" are records of the same place, Kyoto. The "Nijōke diary" is uncomplicated and the rainy appearance rate during the same period is low.

Discussion1

(1)The “detail rate” of the Nakamura Heizaemon diary for the entire period was 29.9%, which was the same as the Joubu diary, which we had researched previously. The trend of the rain appearance rate and the trend of the “detail rate” for 55 years are in agreement.

It is suggested that "rain appearance rate" can be corrected by "detail rate".

Discussion2

In 1836, when the annual composition ratio of heavy rain was 10.2%, it was described as “heavy rain” only in the summer, and the composition ratio of heavy rain was 20.9%.

Summary of the study

1.The composition ratio of “heavy rain” in 1836 was 10.2%, and it is considered that it was the summer when heavy rain fell.

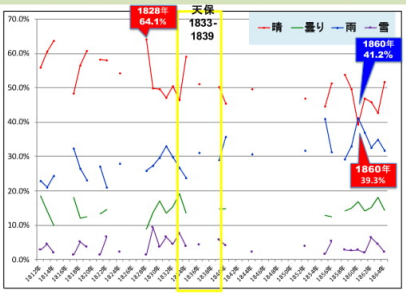
2.The “detail rate” for the entire period is 29.9%, which is higher than the previous research.It is said that the higher the detail rate, the higher than the rainy appearance rate ,and the Nakamura Heizaemon diary also shows a correlation as in previous studies.

Keywords: Nakamura Heizaemon diary, detail rate

©2021. Japan Geoscience Union. All Right Reserved.

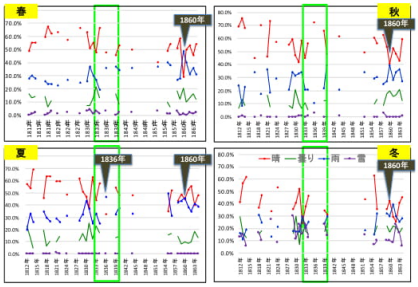
天気の出現率　1812年～1864年(全期間)

Graph1



四季の天気の出現率　1812～1866年

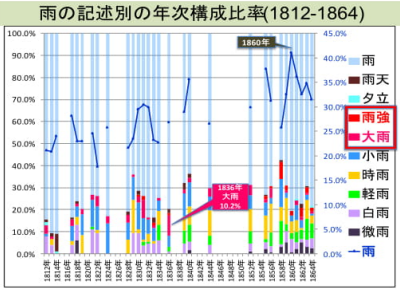
Graph2



天気の出現率の年次推移は左上の graph1 のとおりで、1828 年の晴れの出現率が 64.1%で最高で、最低は 1860 年の 39.3%であった。右上の graph2 のように四季の天気の出現率は「天保の飢饉」で一番被害が苛烈であった 1836 年は雨の出現率が晴れの出現率を逆転している。

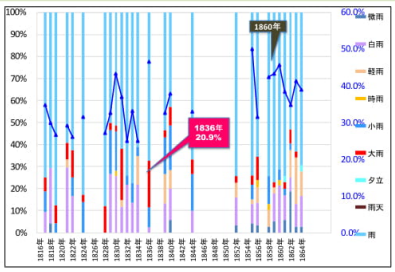
雨の記述別の年次構成比率(1812-1864)

Graph3



夏(6月～8月)の雨の記述別・年次構成比率(1812-1864)

Graph4

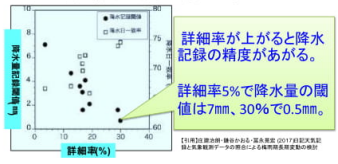


雨の記述別の年次構成比率をみると、1836 年は大雨の比率が高く、さらに、季節ごとの構成比率をみると 1831 年と 1836 年は夏季に大雨の降った年だったとわかった。

詳細率

reference

【定義】天気記録で「晴れ」や「雨」と1語の記録されているのではなく、複数種類の天気が併記されたり、時間変化に関する記述や「大雨」などの降水規模の記述がある日数の比率

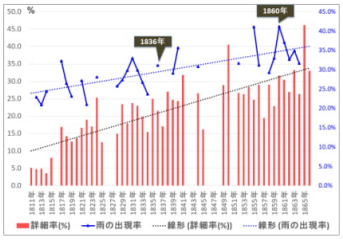


詳細率が上がると降水記録の精度があがる。

詳細率5%で降水量の閾値は7mm、30%で0.5mm。

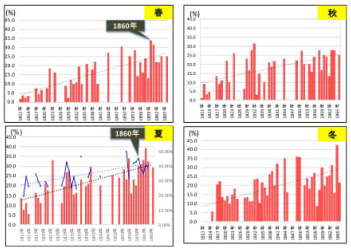
詳細率　1811年~1866年

Graph5



四季の詳細率

Graph6



古文書の30年ごとの天気の出現率の比較

Graph7



中村平左衛門日記の全期間の「詳細率」の平均は 29.9%で、最高は 1865 年の 46.2%で、最低は 1814 年で 3.6%であった。1812 年から幕末の 1866 年に行くに従い天気記録が詳細になり、雨の出現率の傾向と一致する。

graph7 のように、過年度に調べた古文書間で比較すると、「二條家内々御番所日次記」「妙法院日次記」は同じ京都の記録であるが、「二條家内々御番所日次記」は記述が単純で、同一期間の雨の出現率は低くなっている。一方「妙法院日次記」は記録が詳細で雨の出現率が高い結果となっている。詳細率と雨の出現率が関係することを示唆している。

このことから、詳細率で雨の出現率が補正できると考える。

©2021. Japan Geoscience Union. All Right Reserved.

Discussion on Economic Effects of Muroto Deep Sea Water –How Does Deep Sea Water Industry Contribute to Revitalize the Community? –

*Kaede Yauoka[1]

1. Muroto High School

This research will reveal how much deep sea water industry contributes to economic development in Muroto City, Kochi Prefecture.
Muroto City has a very unique underwater topography especially in the west coast of the City. Approximately 2 to 3 km off the land, a steep cliff is formed and the ocean depth suddenly falls into about 1,000m. Due to the cliff underwater, deep sea water upwells and approaches to the land. It allows Muroto to intake deep sea water easily with low coast, compared with other area in the world. In 1989, Kochi Prefectural Deep Sea Water Laboratory was established in Muroto City. That was the very first research facility on deep sea water in Japan then. Since the establishment of the facility, the number of deep sea water-related companies and facilities has been increased in the City. The biggest number of such companies and facilities is 14 in 2010, 2012, and 2014. The latest survey shows that those numbers are 11 as of 2019.
Those deep sea water industry development has been recognized as a new local industry in the area. Deep sea water products, such as bottled water and cosmetics, has been publicized and commercialized all over Japan. It is predicted that the industry brought a big economic effect to Muroto City. This research utilizes 1) the number of companies and facilities, 2) creation of new employment, 3) the number of visitors to deep sea water-related facilities as data to analyze a scale of economic effect and a level of contribution to Muroto City’ s economic development. In order to obtain precise data, this research is implemented with a collaboration with Muroto City Industrial Promotion Section, Deep sea water-related companies, and Muroto Geopark Promotion Committee.
This research will also compare the scale of economic effect of deep sea water industry with other local industry, fishery and agriculture. If a result can be determined that deep sea water industry plays a more significant role in terms of local economic development than other industry, this research will also analyze main cause of it. According to surveys and interviews implemented so far, any specific studies or analysis has not been done to find why deep sea water industry has been success in Muroto. It is expected that a reason will be a key for local revitalization in this City.

©2021. Japan Geoscience Union. All Right Reserved.

Observation of Columnar Joints and Research on its Origin

Atsushi Watanabe[1], *Iroha Kawaguchi[1], *Ryosuke Sugioka[1], *Mizuki Hukumuro[1], *Akihiro Amamiya[1], *Towa Serizawa[1]

1. Nirayama Highschool

It is widely known that hexagonal columnar joints is more than others. From our previous studies which use data from the Izu Peninsula and overseas columnar joints, it is known that ‘The complicated shapes of columnar joints mean the magma solidified quickly, and the more simple the shapes are, the slower the magma sets’. There is a positive correlation between the rapidity of magma’s solidification and the complexity of columnar joints’ shapes.

We conducted an analysis which investigated discovers this relationship in terms of circularity. Using the standard deviation of circularity and the kurtosis of heptagonal number distribution, we made one graph of columnar joints and distinguished it into three areas: upper left, lower left, and lower right. In this graph, the vertical axis is ‘deviation of circularity’ and the horizontal axis is ‘kurtosis of heptagonal number distribution’.The upper left’s rock was made in a thin dyke and the cooling was heterogeneous. As for the lower right, the magma was solidified underground, and the other’s magma was so thick that it set slowly. This magma’s cooling was homogeneneous under natural conditions. This history and the feature of this graph are similar, so according to this graph and circumstances, the kurtosis of circularity decreases, as the homogeneity of cooling magma increases and vice versa.

We pictured the procedure of forming starch columnar joints every three minutes. We finally found that cracks occur from one point and continuously, and columnar joints which stick to the container were larger than those which lie in the center. From this observation, we established a hypothesis that natural columnar joints which were made of magma adjacent to rock are relatively larger.

We once tried to make rock columnar joints, using an electric furnace(AS ONE HTR-1010). This purpose was to make the model of occuring columnar joints. As a result, there were quenching edges on the surface and irregular joints inside, however we weren’t able to make ‘columnar’ joints. We believe this was because the time of cooling was very short and that the experiment was small, compared to natural formations.

Keywords: Columnar Joints, Izu Peninsula

©2021. Japan Geoscience Union. All Right Reserved.

A study of microplastics that is included in the rivers and coast of the Izu Peninsula

Atsushi Watanabe[1], *Namiki Kawai[1], *Koji Sadakane[1], *Yuichirou Takahashi[1], *Mayuko Toriikouji[1], *Daisuke Yamamoto[1], *Miori Yabuta[2], *Tubasa Ozawa[2], *Takaya Nishida[2], *Haruki Mimura[2], *Nanami Hujii[2], Ryosuke Yoshida[2]

1. Nirayama Highschool, 2. Shimoda Highschool

The reseach of microplastics of Nirayama Highschool

Taking over the research of our seniors, we aimed to establish a method for collecting microplastics that could be used by high school students, and to investigate the extent of microplastics in the seas and rivers around the Izu Peninsula.

The experimental procedure is as follows. First, 500 L of water is collected, filtered, dried, and added to a potassium hydroxide solution. After 2 days, sodium iodide solution is added and the overflow method is performed, and the supernatant is collected. The collected supernatant is filtered, dried, and observed using a microscope and blue light.

Experimental results and discussion. Many small microplastics were discovered in Kano River, Ganyudo and Numazu Port. The percentage of small microplastics was higher in Ganyudo than in Kano River. It is thought that the microplastics are being scraped off while flowing through the river. In addition, the number of microplastics was higher in Ganyudo and Numazu Port, which are located at the mouth of the Kano River. The main reason for this is thought to be that microplastics contained in the three rivers that flow into the Kano River, the Daiba, Raikou, and Kise Rivers, flowed into the Kano River.

Next, the Kakita River. Since the Kakita River is fed by a spring, we thought that there would be no microplastics collected in the middle reaches.

However, the collection results showed that there were more microplastics in the middle reaches, but small amounts were also collected in the lower reaches.

The reason why microplastics were discovered in the Kakita River is that there are culvert channels as well as clear channels around the Kakita River, which causes domestic wastewater to flow into the Kakita River. There is a water purification facility upstream of the water sampling point in the middle of the river, and we thought that a small amount of microplastics remaining there were discovered this time. In order to improve the detection accuracy of microplastics, we tried fluorescence observation with blue light and observation with a polarizing microscope. The sample was stained with Nile-Red and fluorescence was observed. As a result, fluorescence was observed in polypropylene and polyethylene. In addition, when the shrimp shells and bark were dyed with Nile Red, it was found that they were not stained with Nile Red. A polarizing microscope showed a difference in polarization between plastic and shrimp shells and bark. From this, it is considered that the detection accuracy of microplastics can be improved by observation with a fluorescence and polarizing microscope.

The reseach of microplastics of Shimoda Highschool

We have studied a method for analyzing microplastics in a short time without using expensive potassium iodide. Sampling was performed mainly on microplastics on the Izu Peninsula.

Sampling was performed at two locations on the Shirahama coast, and comparisons were made before and after the typhoon at the same location. Specific gravity separation using sodium chloride was performed, and the type of plastic was detected using a self-made hydrometer.

When sand was collected on the Shirahama coast and the composition of the plastic pieces was confirmed, the sand on the Shirahama coast had a very high polypropylene content, followed by polystyrene contained in Styrofoam. We compared the differences between the two sampling points, but

©2021. Japan Geoscience Union. All Right Reserved.

no significant difference was detected in the composition or number of plastics. When the number of microplastics was compared between before the typhoon approached and on the day when the typhoon approached, there was a 14-fold difference in the number. The sand was collected from the high tide line so that it would not be affected by anything other than weather conditions. As the approaching typhoon increased the amount of microplastic detected, it was found that strong winds increased the amount of microplastic carried to the coast. Due to the color and shape of the MP, there were many relatively large pieces of green and blue plastic pieces, some of which were thought to be related to marine leisure. We thought that our research would lead to environmental protection on the Izu Peninsula because of the lack of MP data on the Izu Peninsula. In this study, we succeeded in discriminating the type of plastic by a new method. In the future, we will explore ways to reduce polypropylene, which was the most common on the Shirahama coast. We also want to compare the proportion of plastic contained in seawater and the proportion of plastic contained in sand.

Keywords: Izu Peninsula, Micro Plastics, Shirahama coast, Kano river

©2021. Japan Geoscience Union. All Right Reserved.

Consideration of method to increase artificial ruby

Atsushi Watanabe[1], *Yuichirou Nagatsu[1], *Moe Hatakeyama[1], *Koutarou Matsumoto[1], *Yudai Komiyama[1]

1. Nirayama Highschool

Gemstones have always fascinated many people. There are only a small number of gemstones produced by the movement of the earth's interior, compared to the large demand. For this reason, the technology to produce gems by hand has developed.

Rubies are one of the gems for which there is an artificial process. Today, they are used not only as gemstones but also as abrasives.

There have been many previous studies on the generation of artificial rubies by the flux method, but most of them were done using platinum crucibles. The platinum crucible is expensive, so there are many obstacles to using it for research by high school students.

So, in this study, we focused on the generation and enlargement of artificial rubies without using a platinum crucible by the flux method. Instead of platinum crucibles, we used alumina crucibles

This research is a continuation of the research done at our school last year. In contrast to last year's research, which focused on the relationship between crystal size and temperature changes during crystal formation (heating, holding, and cooling temperatures, etc.), this research focused on two new aspects to increase crystal size: enlargement by condensation nuclei and enlargement by changes in evaporation inhibitors.

The flow of the experiment is as described below. Aluminum oxide, molybdenum oxide, sodium carbonate, lithium carbonate, and chromium oxide were weighed, placed in an alumina crucible, stirred so that each material was evenly distributed, and heated in an electric furnace. After heating, we scraped out the crystals that had formed in a way that they adhered to the inner wall of the crucible, and measured their size using a microscope and a micrometer. The color of the crystals was also recorded in photographs.

We experimented with varying the aforementioned materials. Specifically, we varied the evaporation inhibitor by 0 and 2 times, and added gypsum, calcium oxide, calcium hydroxide, and lithium sulfate, respectively.

As a result of repeated experiments, it was found that gypsum was involved in the enlargement of crystals, that sulfate may be involved in the enlargement of crystals because it was the only substance other than gypsum that produced crystals when mixed with potassium sulfate, and that there is a correlation between the evaporation inhibitor and the enlargement of crystals, and that the optimal amount of evaporation inhibitor is between 0 and 2 times.

Keywords: ruby, flux method

©2021. Japan Geoscience Union. All Right Reserved.

Earthquake prediction by Electric magnetic wave

*Masayuki Masa[1], *Nozomu Sakai[1], Michiya Sasaki[1], Souhei Kato[1], Ousuke Yagasaki[1], Mizuho Fujiwara[1], Maika Yashima[1]

1. Tokyo Metropolitan Tama High School of Science and Technology

This research detects a presage phenomenon by earthquake and done Electric magnetic wave radiation, and to assume that earthquake prediction is possible, Electric magnetic wave radiation observation by an earthquake presage is performed and seismic magnitude and an area in the epicenter are predicted the signal strength from a relation of duration and data in the radiation direction. A presage phenomenon with earthquake is caught.

The Electric magnetic wave radiation measurement generates at space, I'm doing every second record of the signal strength by 2 receivers. An antenna is used for judgment of area specification using omni-directional and a directivity antenna. I judge as signal intensity data including thunderbolt data, the ionosphere data and solar activity data, etc. and decide as a presage of an earthquake. It's confirmed whether the phenomenon which occurred to the time of an eastern Japan great earthquake is detected.

It was possible to catch a presage of the big earthquake which occurred at Miyagi, Fukushima and Ibaraki during March 20 from February 13, 2021. I resembled a signal fluctuation of an eastern Japan great earthquake of 2011/3 closely, and time signal-less reference signal level was also fluctuating. There was also little fluctuation range by a short time for reduced level. When shaking isn't felt big by an observation point, this phenomenon is also the phenomenon which doesn't show.

This research would like to increase an observation point and elucidate a mechanism of occurrence.

Keywords: earthquake, prediction, Electric magnetic wave radiation

©2021. Japan Geoscience Union. All Right Reserved.

Comparison of heated products of glucose with citric acid added

*Takumi Ohtsu[1]

1. Tokyo Metropolitan Tama High School of Science and Technology

Currently,there are problems with the method of disposing of plastic and the depletion of petroleum, which is the raw material of plastic, so we use lemon juice (citric acid) and sugar (sucrose) to make plastic into polyester.
I wondered if I could do it. However, since there are many factors to consider such as sucrose having glycosidic bonds, first, while changing the mixing ratio of cirtic acid and glucose, observe what each heating product will be regular.
I wondered if there was.

Keywords: cirtic acid, glucose

©2021. Japan Geoscience Union. All Right Reserved.

Development of iron (II) phosphate lithium-ion battery using the adsorption power of Aso loess

*Ayumi Hoshi[1], *Sora Nozaki[1]

1. Tokyo Metropolitan Tama High School of Science and Technology

Now, the depletion of phosphorus is regarded as a problem worldwide. In order to solve this problem, we wondered if phosphorus could be adsorbed from surplus fertilizer in fields and reused. Adsorption is performed using Aso loess. Aso ocher is the ocher-colored soil that can be found in the mountains of Aso, and is also known as "limonite." About 70% of its constituents are made of iron. In addition, it has high binding properties with various gases and harmful substances, and is demonstrating its adsorptive power in a lot of fields. When phosphoric acid is adsorbed on Aso loess, the phosphoric acid and iron contained in Aso loess combine to form iron phosphate. The ultimate goal is to utilize the iron phosphate as a positive electrode material for iron (II) phosphate lithium-ion batteries. As a first step, this time we conducted an experiment to confirm the adsorption power of Aso loess.

Keywords: Aso loess, Iron (II) Phosphate Lithium Ion Battery

©2021. Japan Geoscience Union. All Right Reserved.

首都圏オープン2021（TSEF2021）2021314

肥料から流出したリン酸の阿蘇黄土による回収

東京都立都立多摩科学技術高等学校
1年　星歩実・野崎昊

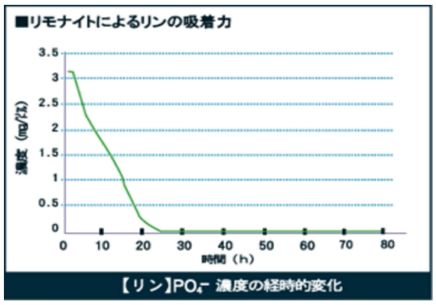
1．背景

今、リンの枯渇が世界的に問題視されている。その問題を解決するため、畑等の余剰肥料からリンを吸着し、再利用できないかと考えた。吸着は阿蘇黄土を使って行う。
阿蘇黄土とは、阿蘇の山の中でとれる黄土色の土のことで、別名を「リモナイト」という。その成分の約7割は鉄分でできている。また、様々なガスや有害物質との結合性が高く、その吸着力をあらゆる分野で発揮している。



2．先行研究

先行研究により、阿蘇黄土が水溶液中のリンの吸着が可能であるということがわかっている。



株式会社日本リモナイトホームページより

3．仮説

阿蘇黄土でリン酸を吸着すると、リン酸と阿蘇黄土内に含まれる鉄が結合しリン酸鉄という形になる。そのリン酸鉄をリン酸鉄（Ⅱ）リチウムイオンバッテリーの正極材料として活用することができるのではないか。

4．研究計画

私達は、肥料から吸着したリン酸を使ってリン酸鉄リチウムイオンバッテリーを作ることを目標にしている。

Step1
阿蘇黄土を使用して、肥料からリン酸の吸着を行う。

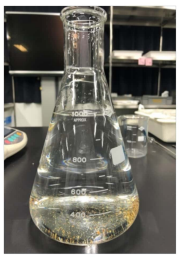
Step 2
吸着したリン酸を何らかの方法でリン酸鉄のまま取り出す。

Step 3
取り出したリン酸鉄を利用してリン酸鉄リチウムイオンバッテリーの正極材料を作る。

6．実験法方

今回は阿蘇黄土の吸着力を確かめることを目的に、以下の実験を行った。
（1）肥料と純水の混濁液を作る
（2）混濁液の上澄みに阿蘇黄土を混ぜ、リンを回収する
（3）黄土を混ぜる前と後のリン酸の濃度でどれほど回収したかを調べる
※リン酸の濃度を調べる方法として、パックテスト使用する。

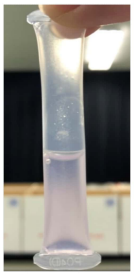
（1）　（2）　（3）



肥料と純水の混濁液

上澄み液と阿蘇黄土

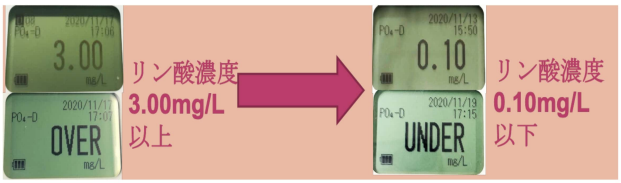




パックテスト

5．結果

阿蘇黄土を混ぜる前と後では、混ぜた後のほうがリン酸の濃度は小さくなった。



（上：デジタルリン酸パックテスト数値）

5．結果

結果から、阿蘇黄土によりリン酸は吸着されたことがわかった。今回の実験で、先行研究にもある通り、阿蘇黄土にはリンを吸着する作用があることを確認することができた。

5．今後の展望

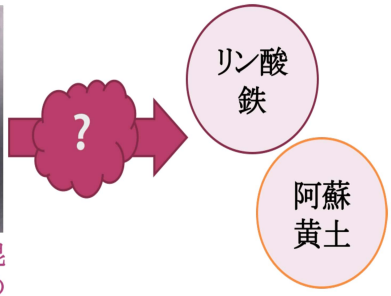
今回の実験で、阿蘇黄土による肥料中のリンの吸着力を確認できた。今後の課題として

1．リンを吸着した阿蘇黄土からどのようにリン酸鉄を取り出すか
2．取り出したものがリン酸鉄であることの証明はどのように行うのか

の２つが挙げられる。



阿蘇黄土を混ぜた混濁液をろ過したもの



©2021. Japan Geoscience Union. All Right Reserved.

Method of Recovering Perfluorinated Compounds by coffee grounds

*Kouki Morimoto[1], *Issei Yamazeki[1], *Renon Shimizu[1]

1. Tokyo Metropolitan Tama High School of Science and Technology

There are organofluorine compounds that are potentially carcinogenic, bioaccumulative, and persistent. Among them,perfluorooctane sulfonic acid (PFOS) and perfluorooctanoic acid (PFOA) were widely used in the life related products. Until recently, organofluorine compounds have been widely used mainly in products related to daily life due to their chemical stability, and are used especially for water-repellent coating processing, but many of them have flowed into the environment. Due to this, in recent years, there have been many reports on the environmental pollution of organic fluorine compounds. Coffee, on the other hand, is a beverage consumed around the world and its consumption is increasing year by year. However, most of coffee bean residue, which is the extraction residue, is incinerated as food waste. Therefore, as one of the effective uses of coffee grounds, the use of coffee grounds as an adsorbent for harmful substances is being sought. In this study, coffee grounds are known to have adsorption capacity for toxic substances, but their effectiveness against organofluorine compounds is not known. Therefore, an adsorbent using coffee bean residue is prepared, and the presence or absence of an adsorbing ability for PFOS and PFOA, in particular, is clarified this time. As a result, we believe it would be better if we could find new reuse values for coffee grounds and reduce environmental pollution and food waste. In this experiment, we conducted a water passing experiment using coffee bean dregs that had been subjected to untreated, boiling, bleaching and carbonization (240 ˚C, 400 ˚C), and environmental water (well water) that contained a large amount of activated carbon and PFOA. For each treatment, it was considered that the adsorption capacity would change by adding the treatment to the coffee grounds, and the bean grounds samples were prepared under the above four treatment conditions. In the water passing experiment, the column tube equipment for the water passing experiment was made by collecting and preparing materials suitable for the experiment conducted this time, and fine adjustment was carried out. The results obtained showed that coffee grounds had adsorption ability for PFOA. It was also found that addition of each treatment could improve the adsorption ability of most coffee grounds. In the carbonization treatment, it was found that the adsorption capacity was improved by the treatment at a higher temperature.

Keywords: Coffee grounds, Perfluorinated Compounds , Adsorption

©2021. Japan Geoscience Union. All Right Reserved.

Research into Moriya Formation Formed in Northen Fossa Magna

*Yusuke Morozumi[1]

1. Suwa Seiryo high school

1.Research motive
There is Moriya Formation around Mt.Moriya in Suwa. It didn’t investigate its details such as geological age or connection with other areas. So I thought I wanted to investigate them.
2.Research wayI did research in 13 places across Moriya Formation and I recorded fossil, lithofacies, and strike and dip. Based on the results of my research, I drew a geological map or make a conjecture about Moriya Formation’s geological age. And I compared with Shimonita Formation.
3.Research results
Research results and Geological map

Based on the results of my research, I drew a geological map. However, Shell fossils were produced from two outcrops, and these were called outcrops A and B. Outcrop A deposits volcanic ash gravel layer, gravel layer, and silt layer from the bottom, and outcrop B deposits volcanic ash gravel layer, coarse-grained sand layer, fine-grained sand layer, coarse-grained sand layer, and silt layer from the bottom.
Fossils of Moriya Formation

The fossils produced from outcrops A and B and the age of development of the major fossil species produced are shown in the figure. The fossils produced are divided into four types: those that inhabited the gradual Miocene, those that inhabited the Early Miocene and Middle Miocene, and those that inhabited after the Miocene.

Shimonita Formation’s Research

Since the Shimonita Formation is certified as a Japanese Geopark, I compared mainly the materials and literature surveys of previous studies. From Kurihara(2005), the Shimonita Formation has developed early Miocene species as a whole. And Sr isotope analysis using Mytilus tichanovitchi showed 20.4 ±0.2 Ma, and the upper limit was around 16.8 Ma from the production of planktonic foraminifera.

4.Considration
Based on the research results, I drew columnar maps of the Moriya outcrops A and B and the Shimonita Formation. Comparing them, it is considered that there is no big difference in the geological ages of the two layers because they have something in common, such as the production of Macoma and Mytilus tichanovitchi, which were developed from the Oligocene. In addition, the Moriya Formation has many mid-Miocene development species, but it is not found in the Shimonita Formation, and the Shimonita Town Formation shows 16.8 Ma, so the geological age of the Moriya Formation is 16 Ma, which is a little newer than the Shimonita Formation. Presumed. Matsumaru (1962) reported the production of large higher foraminifera in warm waters from the Moriya Formation, and it is believed that the Moriya Formation was formed in warm waters. We collected Kimura scallops and Anadara genus, which are characteristic of the Miocene Kadonosawa fauna, which developed from the Moriya Formation in the warm sea. However, Mytilus tichanovitchi from the Moriya class is considered to be evidence of the early Miocene cooling event. In that case, the Moriya Formation is considered to have been deposited in the

©2021. Japan Geoscience Union. All Right Reserved.

cold sea, which is inconsistent with the results of previous studies. However, Anadara and others are not effective phase-indicating fossils, and it is possible that they could adapt to the cold sea. However, no other strata, such as the Moriya Formation, where fossils of the Early Miocene cooling event period and the Middle Miocene Kadonosawa Animal Group coexist have been confirmed at this time. From the above, it is considered that the Moriya Formation was deposited during the transition period from the cold Miocene to the warm Miocene around the Early Miocene and the Middle Miocene.

Keywords: Moriya Formation, Fossa Magna

©2021. Japan Geoscience Union. All Right Reserved.



図1：①守屋層と②下仁田層の位置



図2：産出したMytilus tichanovitchi
上：守屋層産　下：下仁田層産

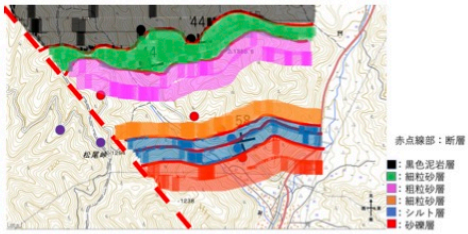


図3：作成した守屋層下部の地質図



図4：守屋層から産出した主な化石種の生息した年代

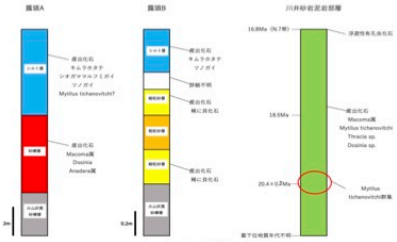


図5：作成した柱状図

©2021. Japan Geoscience Union. All Right Reserved.

A Consideration of a Landing Exploration on Europa

*Taichi Ito[1]

1. Seishin Gakuen High School

Europa, a Jovian moon, is said to have a huge ocean under its ice-surface, drawing attention as a major target of astrobiological research. Although NASA plans to send a probe and to do many flybys of Europa in 2020s, no landing project exists. So, I concentrated my research on a landing exploration.

Because a landing exploration on Europa can give us crucial information about the essence of lives, I regard this research extraordinarily significant.

Europa’ s atmosphere is rarefied. Therefore, I thought that parachutes would not be effectual. Hence, the purpose of this research is to consider the way to land softly with reverse thrust for an astrobiological exploration. The hypotheses I made are as follows:

[the Hypotheses]
The lander will be loaded onto a mother machine and undock at a height of 20km above Europa. The landing engine: hydrazine thruster (specific impulse: approx. 220 to 235s) The undocked lander whose initial velocity is 0m/s starts free fall, starts reverse thrust at an altitude, and comes to halt on the surface. The lander moves only vertically. The thrust, the effective exhaust velocity, and the propellant mass flow rate are constant.

In launching, they accelerate an object from 0 to a velocity, while, in reverse thrust, they decelerate an object from 0 to a velocity. In other words, you can think of soft landing as playing launching backwards. Grounded on this similarity, I thought if I could apply the derivation of the Tsiolkovsky rocket equation related to launching of rockets.

$\Delta V = c \ln(1/\mu)$

Provided that, ΔV: velocity change due to jetting, c: effective exhaust velocity, μ: mass ratio. In addition, based on relational expressions I created, I input a concrete condition,

Let

g as the gravitational acceleration of the target of landing
m_Max as the maximum mass of the lander
μ as the mass ratio of the lander
c as the effective exhaust velocity of the thruster
F as the thrust of the thruster
Then,

the Total Fall Altitude: $x_{total}=c^2/F*m_{Max}(\mu \ln(1/\mu)-(1-\mu))+c^2/2g*(\ln(1/\mu))^2$
the Altitude to Start Reverse Thrust: $x_{jet}=c^2/F*m_{Max} (\ln(1/\mu)-(1-\mu)-m_{Max}/2F*g(1-\mu)^2)$
the Altitude of Free Fall: $x_{free}=1/2g*(c \ln(1/\mu)-(c\ m_{Max} (1-\mu))/F*\ g)^2$
the Total Fall Time: $t_{total}=c/g*\ln(1/\mu)$

©2021. Japan Geoscience Union. All Right Reserved.

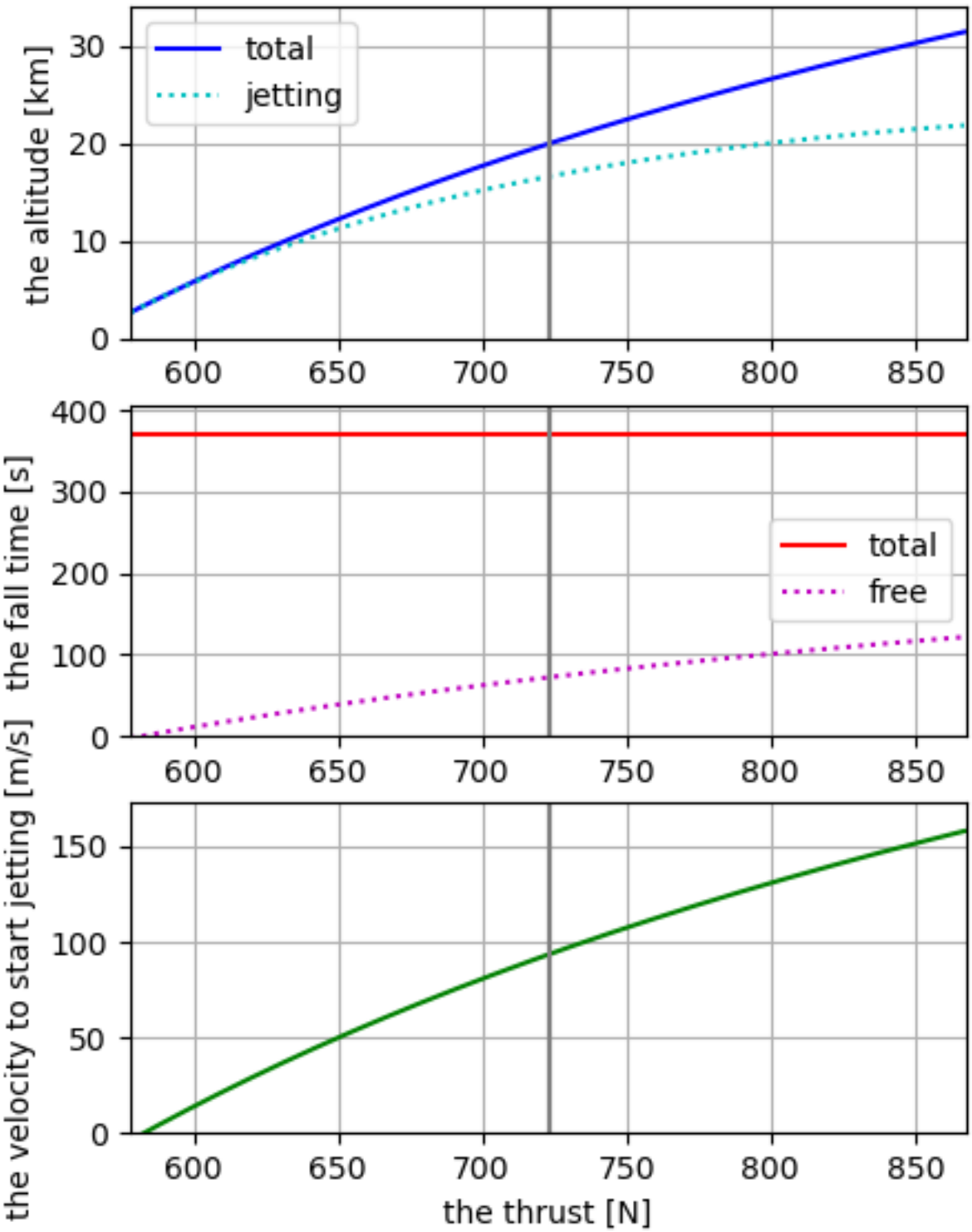
the Time of Reverse Thrust: t_jet=(c m_Max (1-μ))/F
the Time of Free Fall: t_free=c/g ln(1/μ)-(c m_Max (1-μ))/F
the Velocity to Start Reverse Thrust: v_Max=c ln(1/μ)-(c m_Max (1-μ))/F*g

Here, I made a Python program which outputs an approximate value of the thrust by using the bisection method with any accuracy, calculates each altitudes and times of reverse thrust, free fall and total, and draws graphs. If I run the program by taking 9.8m/s^2 for the gravitational acceleration of the Earth, 1.3m/s^2 for the gravitational acceleration of Europa, 500kg for the maximum mass, 220s for the specific impulse, 0.8 for the mass ratio, and 20km for the altitude to start falling, it outputs these approximate values:
F = 723.46875 ±0.03125 [N] x_total = 19.9992723959987 ±0.002981374671238882 [km] x_jet = 16.623466418409254 ±0.0017754098712466657 [km] x_free = 3.3758059775894473 ± 0.0012059647999922163 [km] t_total = 370.0749974103356 [s] t_jet = 298.0087258810587 ± 0.012872391079497447 [s] t_free = 72.06627152927692 ±0.012872391079469025 [s] v_Max = 93.68615298805997 ±0.016734108403312575 [m/s]
and following graphs.

As a result, I could set when and where to start falling, start reverse thrust and reach the surface by deciding the performance of the lander.

Keywords: Europa, Landing Exploration, Lives, Probe, Space Exploration, Reverse Thrust

©2021. Japan Geoscience Union. All Right Reserved.



©2021. Japan Geoscience Union. All Right Reserved.

Relationship between five gigantic jets in the past and cloud-to-ground lightning

*Fuga Suzuki[1], *Yuya Takahashi[1], Sorachi Nishibori[1], Yuki Ito[1], Takumi Miyamoto[1]

1. Shizuoka Prefectural Iwata Minami High School

Four gigantic jets have been observed from our school. According to previous studies, before and after the gigantic jet in 2017 occurred, the number of cloud-to-ground lightnings and the amount of their energy had been prone to decrease (Yamashita, 2017). This study aims to examine whether the other gigantic jets have a similar tendency. We investigated the positional relationship between the gigantic jets and cumulonimbus with infrared images, and the numeral one between cloud-to-ground lightnings with observational data. Based on the results, the tendency mentioned in the previous study was confirmed. Gigantic jets also tend to occur at the edge of huge cumulonimbus and the area cloud-to-ground lightnings were observed remarkably in. This indicates that gigantic jets occur if numerous charges are stored there.

Keywords: Transient Luminous Events, Gigantic Jet, Cloud-to-Ground Lightning

©2021. Japan Geoscience Union. All Right Reserved.

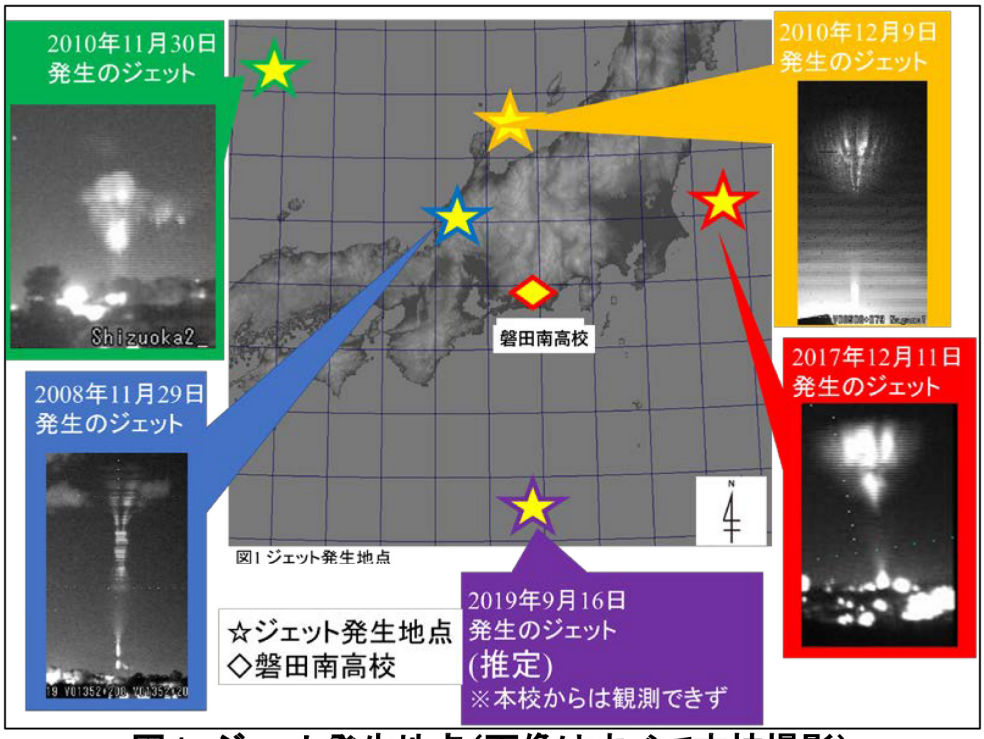


図1　ジェット発生地点（画像はすべて本校撮影）

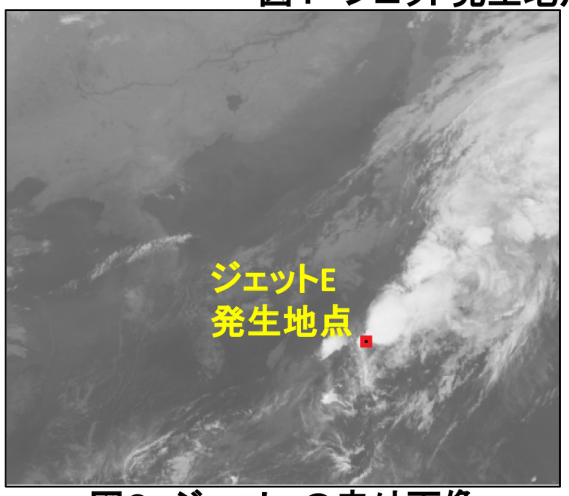


図2　ジェットEの赤外画像

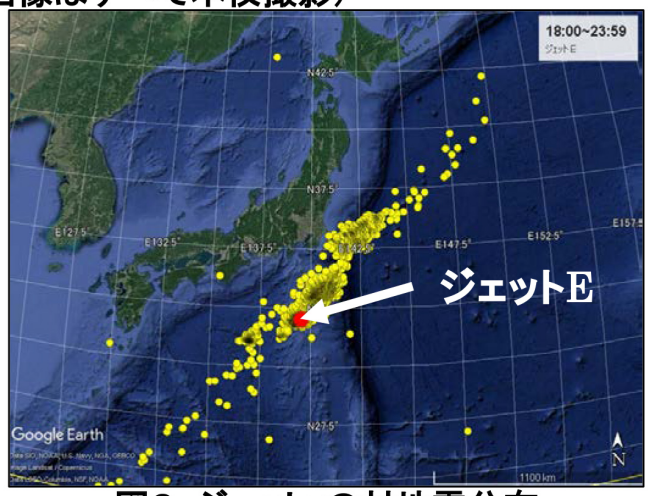


図3　ジェットEの対地雷分布

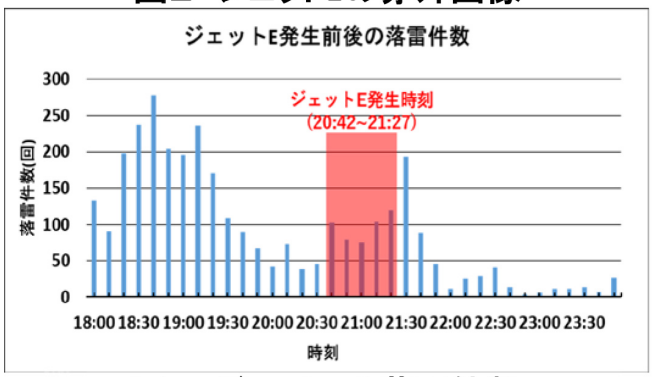


図4　ジェットEの落雷件数

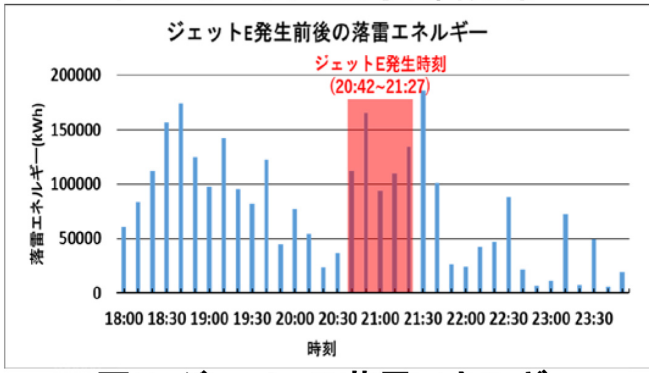


図5　ジェットEの落雷エネルギー

表1　5つのジェットの赤外雲画像と対地雷の比較

	A	B	C	D	E
赤外雲画像	積乱雲南西端	積乱雲南端	積乱雲南寄り	積乱雲南端	積乱雲南西端
空間分布	対地雷群南端	対地雷群南端	対地雷群北東端	対地雷群南西端	対地雷群南西端
対地雷時間変化	10分前から対地雷なし	不明	20分前から対地雷なし	1時間前から対地雷減少傾向	2時間前から対地雷減少傾向

©2021. Japan Geoscience Union. All Right Reserved.

Examination of the fall position by the light emission of the Narashino meteorite fireball

*Ryunosuke Kamiya[1], *Haruka Sato[1], Kosuke Arimura[1], Saki Ozawa[1], Hana Miki[1], Yuka Ogawa[1], Honoka Tanabe[1]

1. Shizuoka Prefectural Iwata Minami High School

At 2:32 a.m. on July 2, 2020, a fireball was observed flowing from west to east over the Kanto region. The fireball turned out to be a meteorite that had fallen in Narashino City, Chiba Prefecture.We conducted this research based on the video taken at our school.
We identified the trajectory of the fireball and the latitude, longitude, and altitude of the start and end points of its emission from it, and then examined the location of the fall.
As a result, we found that the fireball continued to fall while being subjected to physical factors, and fell in a parabolic motion after the emission ended.The total horizontal distance traveled by the fireball was close to the linear distance between the start of the emission and Narashino City. In other words, we found that the the location of the fall of the fireball can be estimated from the video taken.

Keywords: Narashino meteorite fireball, The location of the fall

©2021. Japan Geoscience Union. All Right Reserved.



図1.本校観測の習志野隕石火球の連続写真
（2020年7月2日2時32分）

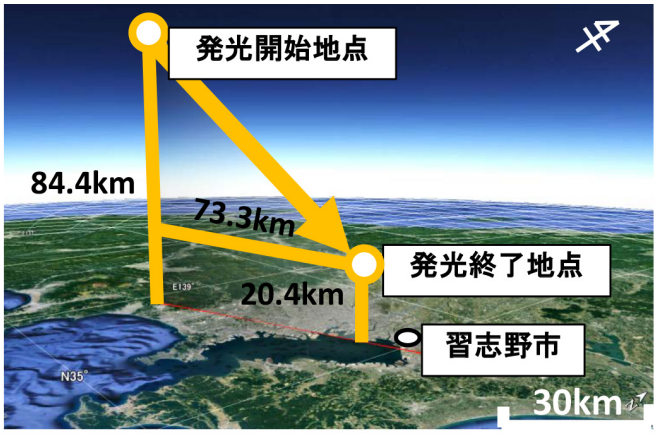


図2.立体的な習志野隕石火球の軌道

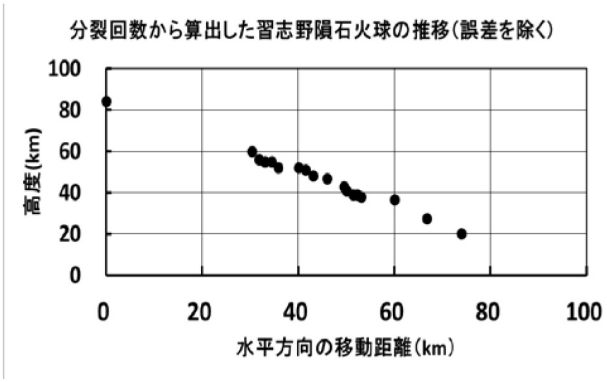


図3.誤差を除いた習志野隕石火球の推移

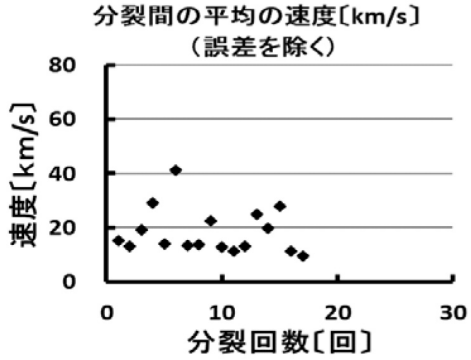


図4.誤差を除いた分裂間の平均の速度

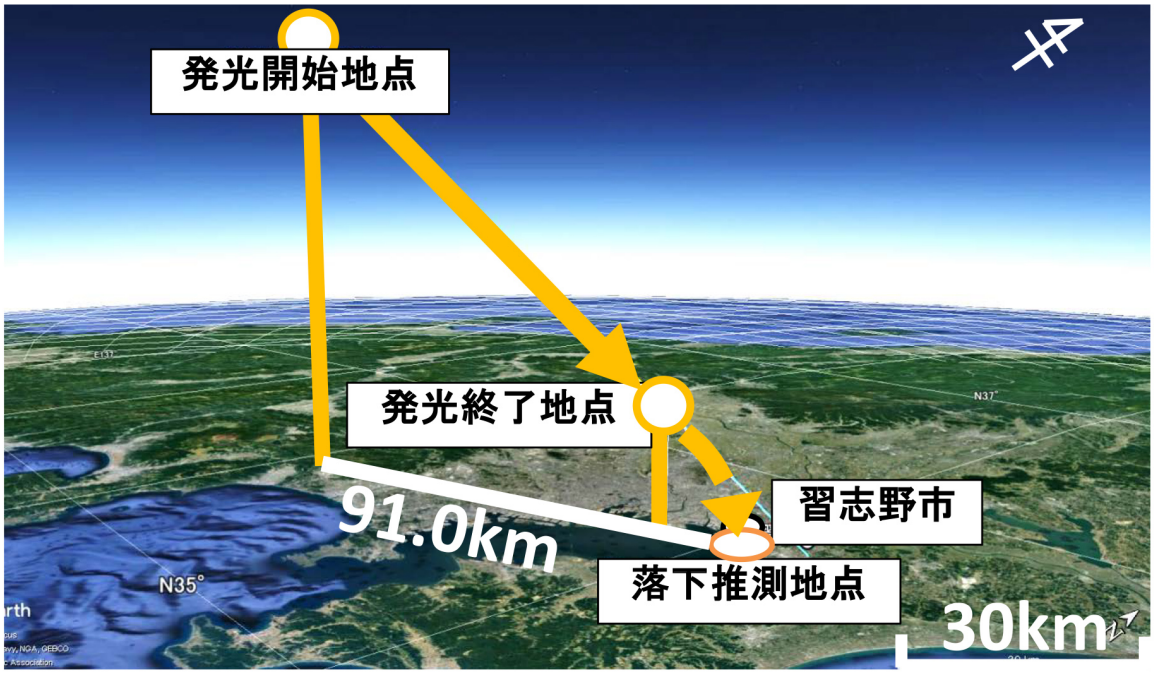


図5.物理的要因を受けた場合の落下推測地点

©2021. Japan Geoscience Union. All Right Reserved.

The Change of Microtopography of Samejima Coast Caused by the Storm Surge Brought by Hagibis

*Takeshi Totsuka[1], Yuya Takahashi[1], *Kosuke Arimura[1], Koki Suzuki[1], Shun Ichikawa[1], Rabu Kato[1]

1. Shizuoka Prefectural Iwata Minami High School

The Enshu Sea Samejima coast, where our school conducts regular surveying, showed significant coastal erosion on October 17, 2019, with the shoreline receding and the boardwalk destroyed. A study was conducted to elucidate the extent and cause of this damage.

We conducted meteorological observations, aerial photography, level surveying, mineral analysis, grain size analysis, and trench surveys to determine the cause of coastal erosion.

As a result, it was found that the topographic cross-sectional area decreased significantly after the passage of Hagibis, the average grain size of the sand became finer as it moved away from the coast, and the sediments showed a tendency toward upward finer grainedness and a structure that appeared to be a hummocky diagonal stratification. This indicates that the seaward side of Samejima Beach was eroded by the storm surge of Hagibis, and that storm surge sediments were deposited behind the landward side of the beach.

Keywords: Samejima coast, Hagibis, level surveying, grain size analysis, trench surveys

©2021. Japan Geoscience Union. All Right Reserved.

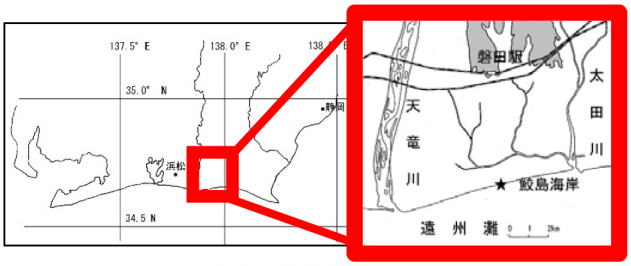


図1. 鮫島海岸の位置



図2. 台風通過前の海岸入口西側の空撮



図3. 台風通過後の海岸入口西側の空撮

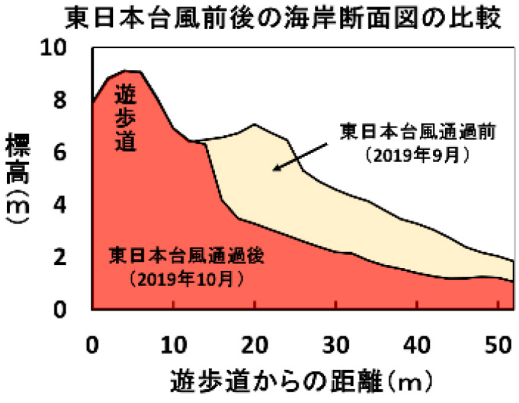


図4. 東日本台風前後の海岸断面図の比較

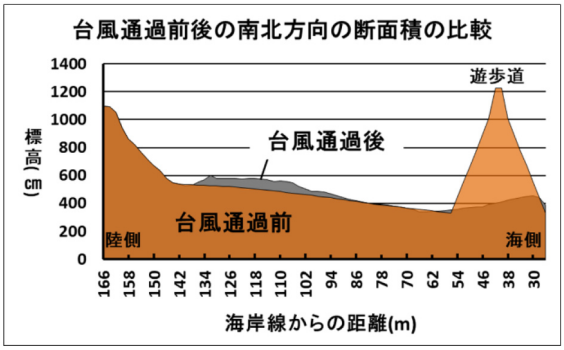


図5. 台風通過前後の地形断面図の重ね合わせ

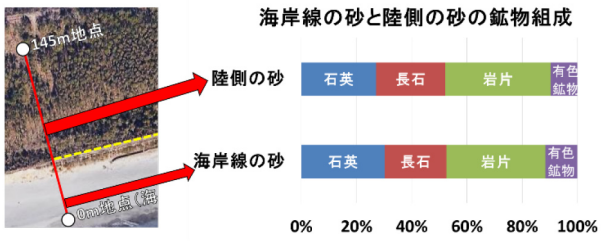


図6. 陸側(100m地点)と海側(0m地点)の鉱物組成

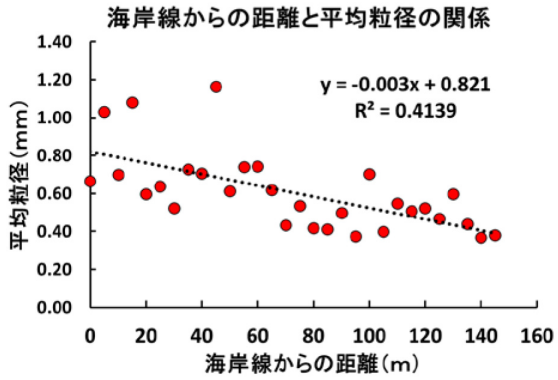


図7. 南北方向の平均粒径の変化

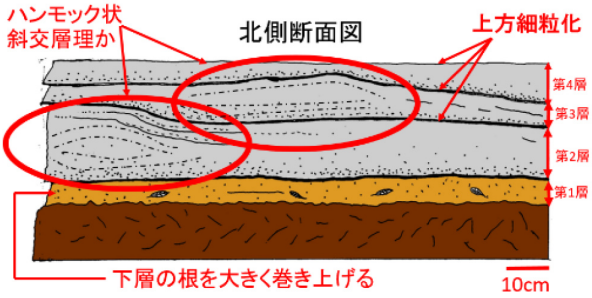


図8. 堆積物のスケッチ

©2021. Japan Geoscience Union. All Right Reserved.

Putting legs on snake swimming robot going to be useless? Seeking truth of Tetrapodophis

*Ryoya Sato[1], *Kokoro Ikeda[1], *Ryota Ogawa[1], *Riko Tomioka[1], *Akari Hitomi[1], *Kanon Yamaguchi[1]

1. Tokyo Tech High School of Science and Technology

Our team heard a new way to research ancient creatures called Robokaseki. Our research target is Tetorpodophis. Tetoraodophis is a snake-shaped creature, which lived 110 to 120 millions years ago. We are building a robot that moves like Tetoraodophis as robot and studying about how legs has been used. Ancient creatures are in the course of evolution, so their movement is considered to be simple and efficient. In the study of Tetrapodophis, we think we can elucidate the movement and ecology.
One of the most important studies in palaeontology is creatures evolution. Fossil is the only evidence that shows a real evolution pattern. On the other hand, fossil has only small information. Then, imitating movement of the robot can help predict the soft tissue and their movement and speed. Collecting data of robots speed and movement can be useful.Therefore, it is possible to predict their abilities and this will help to study creatures evolution.
There are several hypotheses of the roles of Tetrapodophis’ s legs. To catch prey or copulation partner, to swim and paddle. However there is no conclusion of theirs legs.
There are several theories about the role of legs that have been found in the literature on Tetrapodophis. The first theory is that the legs were used to hunt prey or mate with partners during life on land. The second theory is that they were used for swimming in the form of paddles during life in the water. Therefore, no conclusions have been drawn as to how the legs of Tetrapodophis were used.
Tetorapodophis which has found is 20cm long and their limbs are 1.5cm long. Fossil shows that hind legs are supported by strong bones than forefoot, so it is considered that hind legs are more used than forefoot. Limbs have something like finger, and that can be considered as they had same size or bigger than palm wedding.
To study more about Tetorapodophis’ s legs, in experiment we made a snake-shaped under water robot by reference to Tetorapodophis fossil. As a result, it is easy to change direction with forefeet and a way of swimming can be stabilized by using hind legs. Forefeet are too small to produce propulsive effect, but it can make instantaneous power, so it can be said that they have great effect on hind legs.
Also, moving hind legs and tail can stabilize robot and more propulsive. For those reasons putting legs on a snake-shaped underwater robot is making sense.
There are three issues that we would like to solve in the future. The first is to make the snake- shaped robot behave more like a real living thing. Our robot cannot dive or surface. If our robot become able to dive and surface, we would find more ways to use their legs and investigate its usefulness.
The second is to identify the habitat. The stratum where the fossil was found is thought to have been a shallow inland sea. Therefore, we expect that it was an aquatic organism. In order to prove this, we are going to investigate whether the robot can walk on land or not. And that will reveal whether it could have been active on land or not.
The third is to prove the reconstructions. If a robot cannot swim or moves in a way that does not fit the expected living environment, it is not a correct reproduction. Therefore, we believe that the shape of the robot with reasonable movements will prove the reconstructions.
We hope that this study will solve these three issues and that the use of robots in the study of palaeontology will become widespread.
There are several theories about the role of legs that have been found in the literature on Tetrapodophis.

©2021. Japan Geoscience Union. All Right Reserved.

The first theory is that the legs were used to hunt prey or mate with partners during life on land. The second theory is that they were used for swimming in the form of paddles during life in the water. Therefore, no conclusions have been drawn as to how the legs of Tetrapodophis were used.

Keywords: Tetrapodophis, Imagine a creature from a fossil and reproduce as robot, Restore

©2021. Japan Geoscience Union. All Right Reserved.

水中蛇型ロボットに脚をつけたら蛇足か
古代の化石から生物を再現して実証する

東京工業大学附属科学技術高等学校

佐藤諒弥　池田こころ　雄川綾太　人見あかり　富岡りこ　山口海音

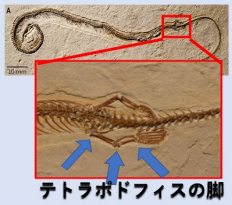
指導教諭　岩城純

10 mm

1. 研究目的







海に囲まれた日本では、海洋研究は重要であり未知の事柄が多い。水中探査ロボットは、海中調査を行う上で不可欠である。私達は、脚を持った蛇の**化石テトラポドフィスの形状を参考にした水中蛇型ロボット**を作成し、その動きを検証して、新たな水中蛇型ロボットの形を提案することが目的である

ロボットによる化石復元の意義

化石の復元は間違った形や生態にされてしまうこともある。そこでロボットを用いて形や生態を再現する。

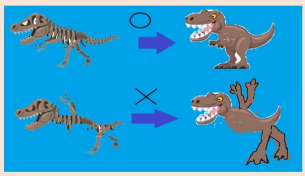
正確に復元しないとロボットは不自然な動作をして動かない

↓

自然に動くとき、その動きは実物に近いと類推

↓

新たな動作方法の発見



2　研究方法

テトラポドフィス（図1）は、脚を持った蛇型生物である。この生物は、陸上で生活していると考えられていたが、近年は水中で四肢をパドルのように使って生活していたと考えられている。そこで本研究では、テトラポドフィスの脚の使い方を推測し実験をすることで、従来の蛇型ロボットに脚をつけると機能性が上がる可能性があるのではないかという仮説を立てた。ここでは、図2に示すテトラポドフィスと似た生物のホライモリを参考に、テトラポドフィスの骨格を基にした脚付き蛇型ロボットを作成し、脚の役割について検証した。

・1億1000万年前に生息
・生息環境不明
・全長約20cm,
手足は約1.5cm
⇒手足の用途は不明



図1

・現在生息
・真洞穴性
・全長約20～30cm,
手足約2cm
⇒手足では地を這う
ことなどに使用

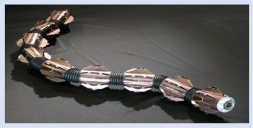


図2

化石からだけではテトラポドフィスの動きがわからないため、類似している生物のホライモリの動きを参考にロボットを製作した

先行研究例　蛇型水中ロボット

○ ACM-R5
ー東京工業大学 広瀬茂男名誉教授ら



体をくねらせるヘビのほふく推進を取り入れた水陸両用の口ボット

瓦礫が散乱する福島第一原子力発電所内部の探査において、高い適正を発揮した

先行研究例　ロボ化石

日本地質学会 **「ジオルジュ」**2019後期号
「水中で動く化石」 P7～9

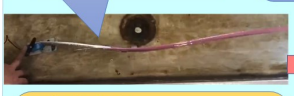
NPO日本水中ロボネット　水中ビークル・フリーミーティングの技術報告
9.7 ロボ化石工作マニュアル
「生体模倣(Biomimetic)水中ロボットの検討　ウミサソリ ロボ化石を作る」（2018）
文と写真 AFK研究所(同) 近藤敏康 イラスト よ志
http://uwr.sakura.ne.jp/oppama/tech-info/UmisasoriRobot_r2.pdf



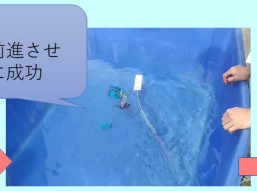
近藤氏のマニュアルを元に作成したロボ化石
＜シンダーハーネスを再現＞

3. ロボットの製作過程

1号機
蛇型ロボットを試作
バタつくだけで進まなかった。



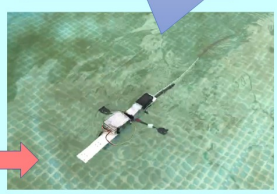
2号機
蛇型を前進させることに成功



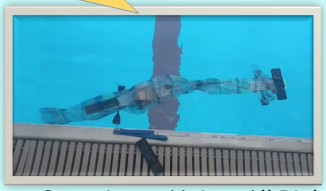
3号機
浮力調整を行い蛇型ロボットしてはスムーズに動くようになった



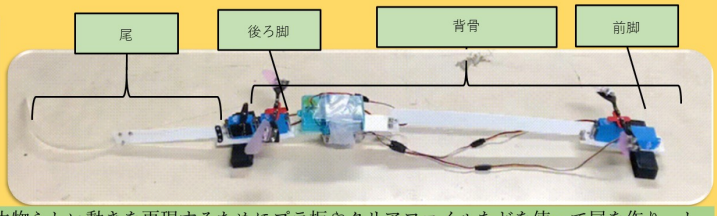
4号機
前脚付き蛇型ロボットを試作　計測実験を開始。



最終完成機
化石の骨格を基に四肢をつけ、外装をつけて泳がせることに成功！



ロボットの仕組み



生物らしい動きを再現するためにプラ板やクリアファイルなどを使って尾を作り、しなやかな動きを実現した。脚ヒレは水を掻くときにヒレが立ち、脚が前に戻るときは倒れこんで水の抵抗が小さくなるようにした。

©2021. Japan Geoscience Union. All Right Reserved.

©2021. Japan Geoscience Union. All Right Reserved.

Consideration of snowmelt type lahar at Mt. Katta, Zao

*Haruya Shishido[1], *Reiki Syoji[1], *Ryo Hikichi[1]

1. Miyagi Prefectural Tagajo Senior High School

Miyagi Prefecture is blessed with fine weather in the summer and snows in the winter. And it is a land that has developed with many benefits from active volcanoes such as Mt. Zao and Mt. Kurikoma. Therefore, we investigated and examined the damage caused by the snowmelt type lahar, targeting Mt. Zao, which has been active in recent years.
It was found that the pyroclastic surge calculated from the amount of eruption has the ability to prepare a large amount of snowmelt water. Even if all the 2m of snow in the pot is melted, there is still room. Damage is expected to increase in years with heavy snowfall, such as the year of the La Nina phenomenon.

Keywords: Lahar, Zao

©2021. Japan Geoscience Union. All Right Reserved.

Geological structure of Urato Katsurashima Island and Nonoshima Island, Shiogama City

*Asahi Oyama[1], *Hikaru Sasaki[1], *Yuhi Suzuki[1], *Hayato Murakami[1], *Misaki Kuga[1]

1. Miyagi Prefectural Tagajo Senior High School

We were interested in the fact that the two strata, the Matsushima Formation and the Otsuka Formation, were clearly exposed during the Urato Geological training in 2019, and considered the geological structure of Nonoshima Island.
In this study, as a continuation of the study, we decided to expand the scope of the study to Katsurashima Island on the west side and interpret the geological structure of the Urato Islands in a wider range.
[Results] It was found that a syncline structure exists in the eastern part of Katsura Island. The syncline axis was south-southeast and the plunge angle was 2 ˚. As a result of drawing, it was found that there are anticline structures and syncline structures with gentle slopes from Nonoshima to Katsurashima. It was also confirmed that the stratum was lying on its side.
[Discussion] In the history of the formation of the Japanese archipelago, the Matsushima Formation was brought about by volcanic activity and crustal movements caused by the expansion of the Sea of Japan. The location of the slump structure was confirmed in the Matsushima Formation due to the earthquake during deposition. In addition, a normal fault was confirmed as the condition of the pulling field continued. In addition, it is probable that at the point where the overturned stratum was confirmed, the earthquake motion at the stage where this tension field was generated caused a collapse or a submarine landslide in the water.

Keywords: Formation

©2021. Japan Geoscience Union. All Right Reserved.

Threats and impacts of urban tsunami -Simulate a tsunami when a Nankai Trough giant earthquake occurs using a tsunami generator-

*Misaki Suda[1], *Kenshin Okazaki[1], *Zen Sato[1], *Yusei Niinuma[1], *Kousei Matsuura[1], *Ayaka Akisawa[1]

1. Miyagi Prefectural Tagajo Senior High School

The Great East Japan Earthquake that occurred on March 11, 2011 caused a tsunami of up to 4.6 m in the city of Tagajo, killing 188 people. One of the factors that caused many casualties in Tagajo City is the characteristic of the urban tsunami, "the tsunami rushed in from unexpected directions." Based on this feature, we are conducting research on what kind of measures can be taken to suppress wave height, wave speed, and wave power.
The urban tsunami observed in Tagajo City is thought to be observed in the "Nankai Trough Giant Earthquake". In order to prevent such damage, we thought that it would be possible to minimize the damage caused by the tsunami by simulating the urban area at the time of the tsunami using tsunami generators, water source devices, building models, etc. ..

Keywords: Tsunami, Urban Tsunami, The Great East Japan Earthquake

©2021. Japan Geoscience Union. All Right Reserved.

Countermeasures against Heat Island Phenomenon: Proposal for a New Building System

*Hiroaki HAYASHI[1]

1. Yokohama Science Frontier High School

Introduction

Recently, the heat island phenomenon has become more serious and environmental problem peculiar to cities. The main causes are artificialization due to ground surface cover and high density of urban forms. Therefore, the heat island effect appears mainly in urban areas and needs to be considered separately from global warming. As a countermeasure, the reduction of artificial exhaust heat and the use of wind from the sea to create Wind Path have been mentioned. This time, I focused on the Wind Path and devised an environmentally friendly building structure and system to efficiently cool and utilize the harmful building wind, even in places where no wind reaches from the sea.

Methods and Results

1. Design of a cooling system using endothermic reaction of chemicals: (a) ammonium sulfate, (b) citric acid, (c) baking soda, and (d) urea were selected as relatively safe chemicals that undergo endothermic reaction when dissolved in water, and dissolved in water (100 cc, 35˚C) at different concentrations. The time course of temperature decrease was compared. When 5 mol of (a) was dissolved, the water temperature dropped to 24.5˚C. When 4 mol of (b) was dissolved, the water temperature dropped rapidly to 19˚C. (c) the water temperature dropped only to a maximum of 28˚C. The cooling effect of (a), (b), and (d) among the four types was high, and among them, the cooling effect of (d) was the highest. Therefore, two mixtures of (a) + (d) and (b) + (d) were dissolved in water, expecting a synergistic effect. However, all of them dropped to around 13˚C and there was no difference, and the expected synergistic effect compared to urea alone could not be obtained.

2. Relationship between walls and wind speed: A model of a cylindrical building was built with side and front walls, and the change in wind speed under the building was measured. The results showed that the buildings with side walls had stable wind speeds overall. In particular, the wind speeds at the 5-25 cm point were all above the average wind speed of 2.0 m/s. In addition, buildings with side and front walls had average wind speeds above 3.0 m/s at the 5 cm point, which were above the average wind speed values for buildings with only side walls at all points.

3. Building Wind-Based Cooling System: A building model with side and front walls was constructed, and wind was applied to the building to measure the ground surface temperature under the following three conditions; (a) building only, (b) radiator filled with water at 23˚C, and (c) radiator filled with cooled urea water. The average wind speed through the radiator was 1.2 m/s. The ground surface temperatures at 10, 15, and 20 cm distances from the radiator were (a) 39.7, 37.8, and 35.7˚C, (b) 38.0, 37.2, and 36.2˚C, and (c) 34.6, 35.1, and 35.2˚C, respectively, a decrease of about 5˚C at 10 cm and about 3˚C at 15 cm. There was not much difference in the surface temperature at 20 cm. When radiators filled with urea water were used, the temperature increase over time was suppressed and the surface temperature under the building was cooled down to the 15 cm point.

©2021. Japan Geoscience Union. All Right Reserved.

Summary and Discussion

As for the structure of the building, it was found that the wind was more concentrated when the side and front walls were attached to the surface of the building. As the cooling water for the wind, several chemicals that cause endothermic reactions when dissolved in water were investigated, and urea, used alone, provides an efficient and strong cooling effect. Urea is safe for the human body and is widely used in skin creams and fertilizers, etc. After cooling the building air, urea can be dissolved and diluted after filtered from the waste water, which is environmentally friendly and can be used as a fertilizer for plants. In devising a building system, it would be even better for the environment if urea could be extracted directly from the urine in the building effluent and sewage. It is said that humans discharge about 30 g of urea per day. There are reports of recovering urea through direct filtration by osmotic urea separation using a dialyzer used for artificial kidneys, and there are proposals to recover urine directly from underground septic tanks in cities. In future, specific methods to extract urea from urine discharged from buildings should be studied. In order to consolidate the complex building wind, the direction and the building structure need to be studied in more detail. In this experiment, a cylindrical building with only one side wall and one front wall in a small area was tested. For realization, experiments should be conducted to expand the area of walls to be attached to the building, or to have multiple buildings densely packed like a city, in order to construct a new Wind Path.

Keywords: heat island phenomenon, Wind Path, urea

©2021. Japan Geoscience Union. All Right Reserved.

An evaluation of artificial landform in Chiba prefecture called “Kawamawashi”

*Kodai SHIBUYA[1]

1. Yokohama Science Frontier High School

Kawamawashi landform is an artificial landform constructed in the Kazusa region of central Chiba Prefecture, where the curved part of a river is cut off and the detached old river channel is used as a paddy field. As the man-made landforms peculiar to the Kazusa region, including the Kawamawashi landforms, are gradually being lost, we attempted to evaluate them in order to utilize the Kawamawashi landforms. The geological features and locations in the Kazusa area were summarized by literature survey, and a field survey was conducted to one of the Kawamawashi landforms, and a comparison of the Kawamawashi landforms was made using a rapid survey map and past aerial photographs. As a result, it became clear that it is difficult to evaluate the geological features of the river-forming landforms more than "mainly mudstone".

Keywords: Kawamawashi, artificial landform, Kazusa region, mudstone

©2021. Japan Geoscience Union. All Right Reserved.

千葉県上総地方における川廻し地形の評価

横浜市立横浜サイエンスフロンティア高等学校
2-6 17 澁谷耕大

川廻しとは

千葉県中部の房総丘陵からの河川沿いに見られる人工地形であり、曲流を短絡し旧河道を田地として用いるために江戸時代から行われた、治水工事と新田開発を兼ねた工事及びそれによって形成された地形。

目的

田地の減少？ → 利活用のための評価

- 希少地形の荒廃
- 旧河道→活用しづらい可能性？
- そもそも評価が少ない

方法

- 地形図により川廻し地形の特徴を調査
  - ➢ 場所や規模
  - ➢ 航空写真による確認
- フィールドワークにおいて実際の使用状況を確認

結果①

1. 規模は多様
2. 面積は70000㎡程度が多い
3. 水田もしくは荒れ地
4. 養老川と夷隅川沿い双方に

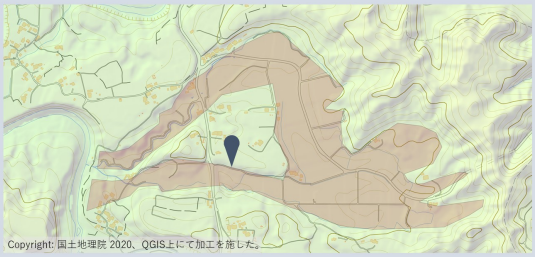


結果②



年月日: 2020/09/22
場所: 千葉県市原市

水田 / 一部休耕地
滑走斜面に泥岩



結論

川廻し地域は、基本的に泥岩を主とした田地であることが明らかとなった。フィールドワークにおいては基本的に水田が見られたものの、耕作が行われていない土地も見られた。また、地図上では荒れ地も見られた。

よって以下の結論が得られた。

- 泥岩を主体としており、軟弱地盤といえる
- 大規模な建設を行うには向かない
- 様々な規模を持つため評価は一定に出来ない

主な参考文献

- 八木 令子, 吉村 光敏, 小田島 高之, 房総丘陵を水源とする河川の地域特性と地形誌, 2017, 千葉県立中央博物館自然誌研究報告, 特別号第10号, p. 21-44
- 白井 哲之, 半固結地層地域の地形形成-1-小櫃川沿岸の段丘地形形成に関する予察的研究, 2017,千葉大学教育学部研究紀要 25(第1部), p. 159-169

今後

地誌学的な検討が不足しており、施工背景についての調査が行われていなかったことがある。

また評価基準の客観性が不足しているため、評価基準の明確化が必要であると考える。

©2021. Japan Geoscience Union. All Right Reserved.

The relationship between sunspot number and typhoons

*Takeru TODA[1]

1. Yokohama Science Frontier High School

Introduction

I wanted to connect meteorological phenomena and astronomy. Then I focused on the sun. The sun has been giving a huge amount of energy to the earth. And it should have effect on meteorological phenomena. On the other hand, typhoon is disaster that cause great damage to Japan every year. If it can be predicted, the damage can be reduced. For that reason, this study’ s goal is to show that solar activity has effect on the number and power of typhoons.

Method

Sunspot number was used to see the solar activity. Sunspot number is index that shows how active the sun with sunspots that appear on it. Assuming that the relative number of sunspots is R, the observation method, observation device, and the coefficient for correcting individual differences between observers is k, the number of sunspot groups is g, and the total number of sunspots is s, it is defined this.

R=k10g+s (1)

The definition of typhoon is tropical cyclone with maximum wind speed of over 34 knots in western pacific. On this report it means that in the global. ACE (Accumulated Cyclone Energy) is index shows lifespan and power of tropical cyclone. In order to see the transition over a long period of time, the relative number of black spots, the number of typhoons, and the ACE from 1951 to 2020 are summarized with using the data published on the Internet.

Conclusion

Figure 1 shows the relationship between the sunspot number and the number of typhoons in the western pacific from 1951 to 2020, and Figure 2 shows the two-year time lag correlation since 1990. From these figures, it can be seen that the number of typhoons has changed two years later than sunspot number since 1990. The correlation coefficient was 0.47 at this time. Figure 3 shows the relationship between the sunspot number and the number of typhoons in the globe from 1951 to 2020, but the two-year time lag correlation seen in the western pacific was not found. Also relationship between sunspot number and ACE was not found. From these, It cannot be concluded that solar activity directly affects the typhoon, but at least it seems to be related. The two-year time lag correlation seen since 1990 was very weak, but clearly stronger than the others. However, it is limited in western pacific. Possible causes are factors that affect typhoons other than solar activity. For example, the El Nino phenomenon is known to be related to ACE. By examining the differences between the western pacific since 1990 that has two-year time lag correlation and other regions and times, we can investigate the effects of the sun in detail. The problem for the future is to consider other factors as well. Therefore, we will first investigate the meteorological difference between the time when there is a time lag correlation and the time when there is not it.

Acknowledgments

I would like to thank Ms. Sato for giving us appropriate advice from the beginning to the end and for her polite guidance.

©2021. Japan Geoscience Union. All Right Reserved.

References
National Astronomical Observatory of Japan https://www.nao.ac.jp/

Japan Meteorological Agency https://www.jma.go.jp/jma/index.html

Sunspot Index and Long-term Solar Observations www.sidc.be/silso/

International Best Track Archive for Climate Stewardship https://www.ncdc.noaa.gov/ibtracs/

National Hurricane Center
https://www.ncdc.noaa.gov/ibtracs/

Hiroko Miyahara 2009-12 Solar activity, cosmic rays, and climate change

Keywords: typhoon, sun, sunspot

図1　黒点相対数と西太平洋の台風数

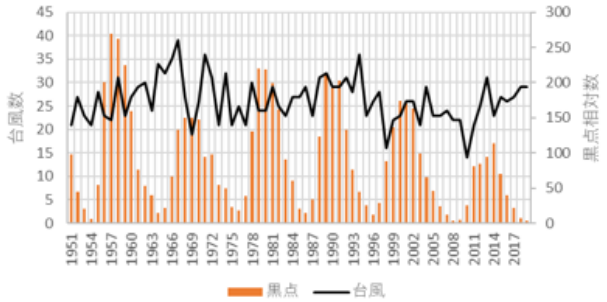


図2　黒点相対数と1990年以降のタイムラグ相関

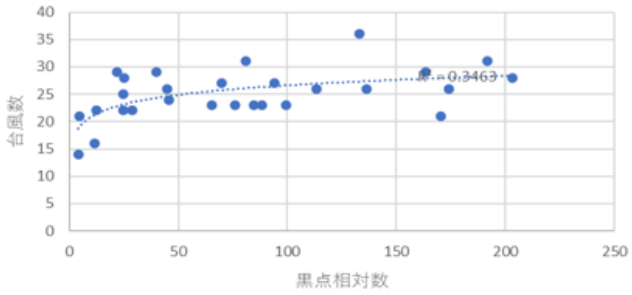
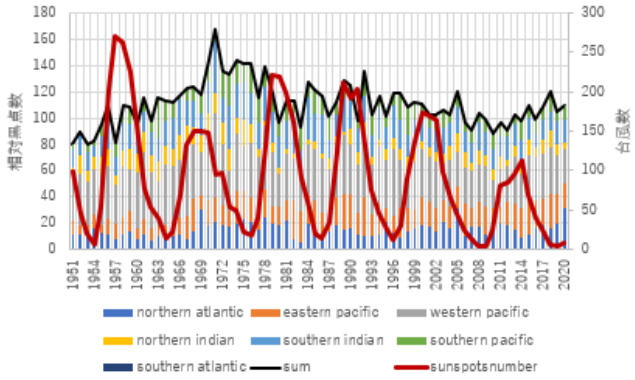


図3　全球の台風数と相対黒点数



©2021. Japan Geoscience Union. All Right Reserved.

On the study of Fukui Earthquake Fault IX

*Kazuho Kuwajima[1], *Ryouhei Matta[1], *Youhei Morise[1], *Ayano Yashima[1]

1. Fujishima High School of Fukui prefecture

The purpose of our research is identifying the main shock fault surface, which caused the M5.0 event on september 4 in 2020. The important point to understand this research is that there are a lot of reverse faults in
Japan. In addition, a character of the land-form by the fault is a straight structure. According to previous studies,a varied fault expected in the west side of Fukui plain. In this study we thought that the main shock might occured on the expected faults. We desided hypocenter of event by the Win-system. Win-system is a software to identify the hypocenters. With this system, we detected 44 hypocenters of the main shocks and aftershocks. We found that the decided epicenters concentrated on the west side of Fukui plain.Hypocenters of the first 13 aftershocks that occurred just after the main shock distributed like a plane. Therefore, these aftershocks occurred on the fault plane which had caused the main shock. We define this plane as a main shock fault surface. On the other hand, the other aftershocks were scattered outside from the main shock fault surface. We define these as extended type aftershocks.From the initial 13 aftershocks distribution,it was found that the main shock surface runs from West-southwest to East-northeast and incline North-northwest. After 30 aftershock epicenters show the distribution from east to west more widely than aftershocks of mainshock fault surface.

Keywords: Fukui Earthquake, fault, intensity of lower 5

©2021. Japan Geoscience Union. All Right Reserved.

Approach to the current situation and issues of geothermal power generation utilization based on field surveys

*Kisho Kurosawa[1], *Tatsuki Miyamoto[1], *Nozomi Kawaharata[1], *Shoki Yashima[1], *Yusuke Oba[1]

1. FurukawaReimei High School

Our electricity energy consumption is steadily increasing. Currently, most of the energy continues to depend on thermal power generation, but the fact that most fossil fuels depend on imports and the emission of large amounts of greenhouse gases such as CO2 have been regarded as problems. While investigating and learning about the "effective utilization of geothermal resources," which is a characteristic of the region, geothermal power generation has major advantages such as low power generation costs and low environmental impact, while resources in Japan. I learned the fact that the penetration rate is low for the amount. Regarding geothermal power generation, which is an energy resource peculiar to the region, we will clarify the current situation and issues regarding geothermal energy and its utilization based on site tours and references, and the ideal scientific approach to the utilization of geothermal energy. Practical training and surveys were conducted with the aim of finding out. Based on the results, I worked on this research to approach scientifically.

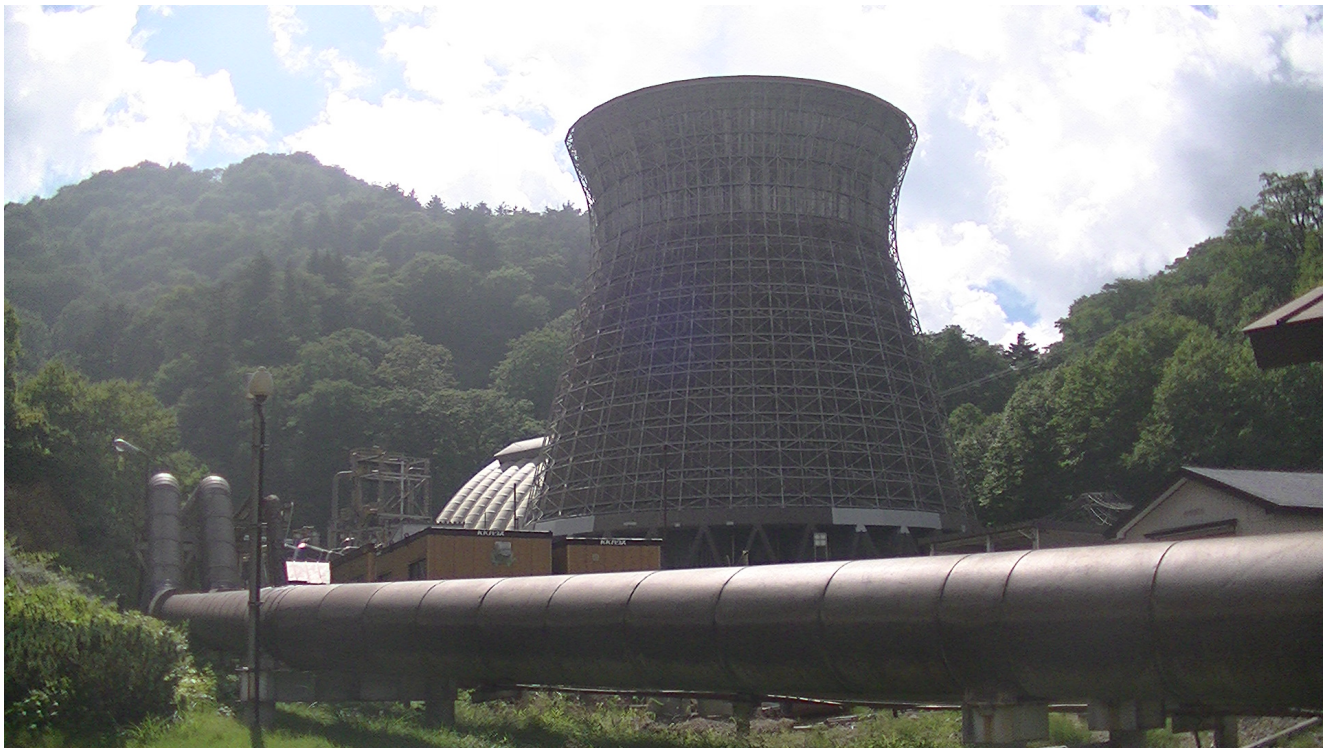
On August 23, 2020, we visited two contrasting and distinctive power plants in the neighboring Iwate prefecture. Japan's first commercial power plant, Matsukawa Geothermal Power Plant, and Matsuo Hachimantai Geothermal Power Plant, a new style run by the private sector, which started full-scale operation in 2019. After completing the on-site training, we thought that each power plant was almost unmanned and the labor cost for operation was overwhelmingly lower than that of thermal power and nuclear power. For that reason, I felt that geothermal power generation, which has a large amount of power generation, does not impose a burden on the environment, and has a low power generation cost itself, is a power generation method that matches the coming era. Despite this, the introduction of geothermal power plants seems to be stagnant, as the Matsuo Hachimantai geothermal power plant went into full-scale operation in Japan for the first time in 22 years. Considering the reason, I was interested in the balance between the size of the construction cost and the sales revenue for it, such as the excavation of additional production wells seen at the Matsukawa Geothermal Power Plant, and the cost of geothermal power generation using the Matsukawa Geothermal Power Plant as an example. I made a trial calculation.

It cannot be said that the construction of geothermal power plants in Japan is saturated. It is mainly concentrated in Hokkaido, Tohoku, and Kyushu, and it is essential that there is a stable hydrothermal system underground, which is thought to be due to the limited location, but it is also necessary to consider other reasons.

A hot spring binary power generation is being carried out at a hot spring inn in Naruko, Osaki City, and we are considering a future site visit. In addition, we are making a geothermal power generation model to solve the problems that became clear from this survey. The geothermal power generation model uses corrugated cardboard to create the image of a volcano, and a pressure cooker is installed inside to reproduce the production well. A turbine is attached to the outside to reproduce the power plant. Using this, I would like to conduct experiments on the current power generation efficiency due to the shape of the turbine and the loss of thermal energy associated with power generation. It also aims to disseminate energy education to local junior high school students using these models.

©2021. Japan Geoscience Union. All Right Reserved.

Keywords: Geothermal power generation, energy



©2021. Japan Geoscience Union. All Right Reserved.

Study of mechanism of Light Emission by Spectroscopic Observation of Meteor

*Yui Sato[1], *Yuki Kato[1]

1. Miyagi Prefectual Furukawa Reimei Senior High School

1. Purposes
The purpose of this study is to infer the type of elements related to the emission from the spacing of emission lines on the spectroscopic image of meteors, and to clarify the relationship between the altitude and the intensity of the emission lines by observing a meteor simultaneously at multiple points.

2. Hypothesis
・By determining the type and percentage of elements that make up the meteor material from the type and intensity of emission lines, we can clarify the characteristics and tendencies of each meteor shower
・Since the parent bodies of meteor showers are different, the elements detected by observation tend to be different in each meteor shower
・The relationship between the intensity of emission lines and the altitude of the meteor's emission can be derived by simultaneous observations at multiple points, and the mechanism and conditions of meteor emission can be clarified

3. Method
The process of identifying the elements is in the following order.
(1)Take a picture of a meteor with an SLR camera equipped with a diffraction grating and determine the scale of the diffraction grating and the number of pix to each emission line.
(2) Identify the wavelength of each emission line and determine the element from which the emission originates by referring to the literature.

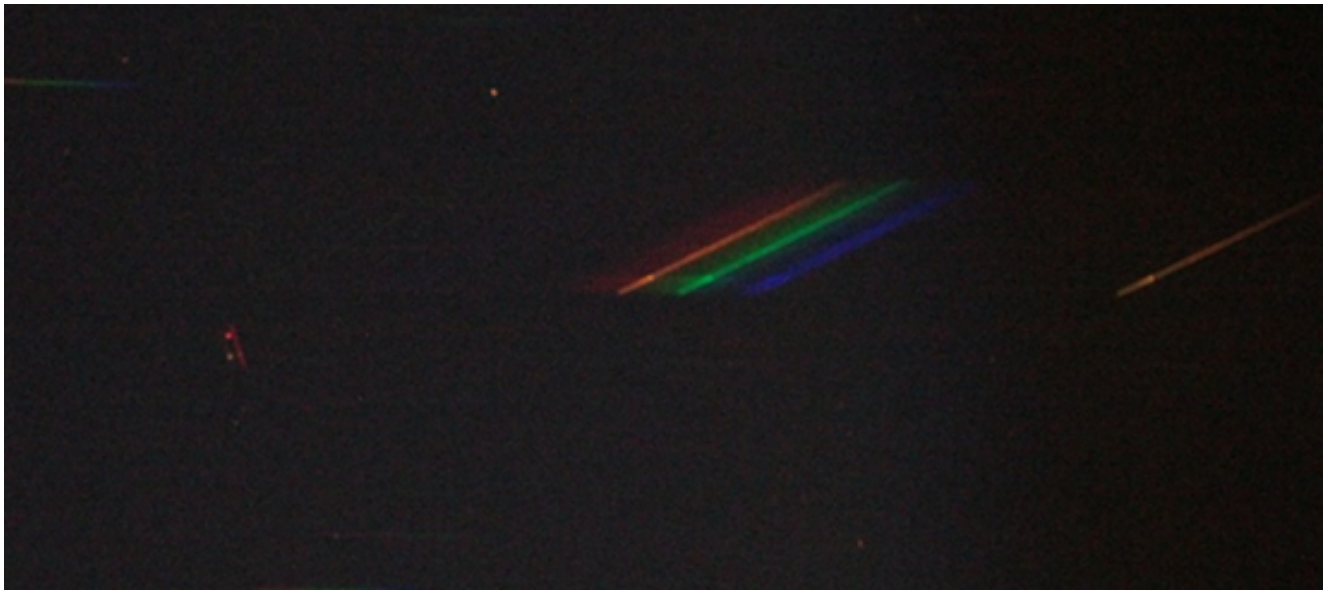
4. Results・Consideration
From the start of the study in 2014 until now, about 570,000 images have been taken and 58 spectral images have been obtained.
One spectroscopic image was obtained for the 2020 Orion meteor shower. Although we estimated three elements from the image, Mg, Na, and Fe, they showed an error of about 10 nm in the measured values. In addition, the emission line estimated to be Fe (529 nm) appeared to be emitted at a slightly earlier than the other two emission lines, suggesting that it may be an oxygen forbidden line (558 nm). These errors may have been caused by incomplete focusing, which obscured the image.
In order to improve the accuracy, we will reconsider the observation method, such as focus adjustment before starting observation and measures against condensation on the lens, especially in winter. Thus, the incident angle of the meteor was tilted to the diffraction grating, which may be the reason for the large error. Therefore, it is necessary to keep the angle of the diffraction grating perpendicular to the radiant point of the meteor shower by rotating the camera by 15 degrees every hour to improve the spectral accuracy.

5. Prospects
We would like to clarify the tendencies of elements in each meteor shower by continuous observation, because there are few meteor showers observed in the same year. We will continue to estimate the altitude and pursue the relationship between the oxygen forbidden line emission and the altitude,

©2021. Japan Geoscience Union. All Right Reserved.

because it is difficult to collect the data by simultaneous observation at multiple points at the same time.

Keywords: Meteors, Diffraction grating, Spectroscopic observation



©2021. Japan Geoscience Union. All Right Reserved.

Relationship between mineral crystallization and impurities.

*Usami Kenta[1], *Ryo Nakane[1], *Hiroyuki Sueno[1], Syotaro Kawana[1], Ryota Naito[1], Kazuhiko Hoshi[1], Mitsuhide Sai[1], Takuma Watanabe[1]

1. Johoku high school

Crystals produced by crystallizing from hot water or magma come in various sizes, lengths, and thicknesses. As a factor that changes these, the presence of impurities that are not related to the components of the product can be considered. However, it is not known how impurities affect the crystallized minerals. In this study, $NH_4H_2PO_4$ is crystallized with NaCl as an impurity.

Keywords: mineral , impurities, crystal



©2021. Japan Geoscience Union. All Right Reserved.

Analysis of water quality of irrigation ponds focused on land use, irrigation systems and periodic pond draining

*Ayane INOUE[1], *Haruto TAKEYAMA[1], *Kousuke MANO[1], *Rio YAMANO[1]

1. Hyogo Prefectural Kakogawa Higashi High School

Recently, irrigation ponds have had poor water quality. Therefore, we focused on land use around the ponds and “Ikeboshi” or regularly draining pond water, and researched the water quality of ponds in the Higashi Harima region. We measured COD, NH4-N, NO2-N, and PO4-P in August and December. It was found that fertilizing rice fields plays a large factor in increasing nitrogen concentration. Nitrogen and phosphorus levels in the ponds in residential areas weren’ t high because runoff of household effluents has decreased due to improvements in running drainpipes. Also, Ikeboshi may restrain the increase in concentration of nitrogen and phosphorus.

Keywords: irrigational ponds, analysis of water quality, land use , irrigation systems, periodic pond draining

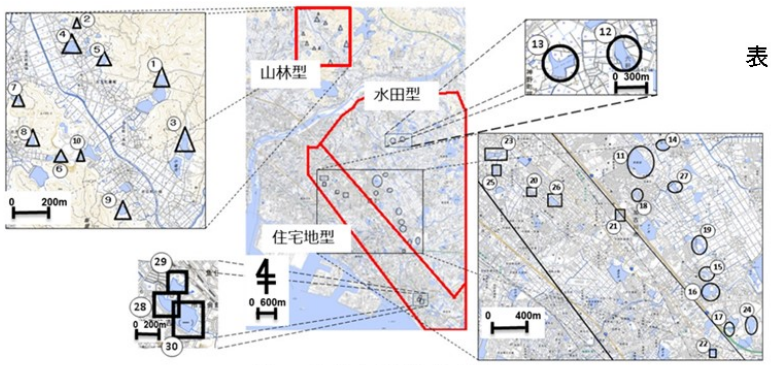


図1 対象ため池の分布

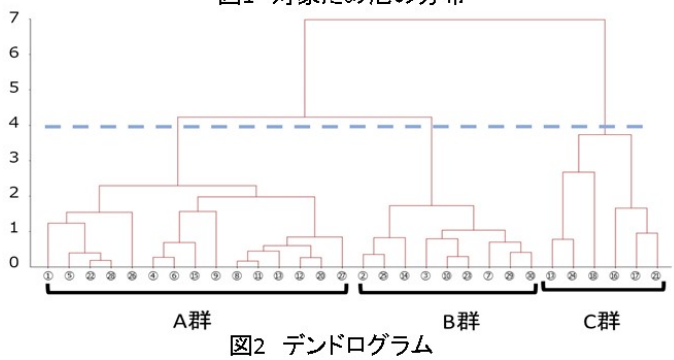


図2 デンドログラム

表1 クラスターごとの平均濃度 （単位はmg/l）

	リン酸態リン	COD	亜硝酸態窒素	アンモニウム態窒素
A	0.054	23	0.052	0.51
B	0.047	43	0.029	0.25
C	0.44	23	0.13	1.8

表2 クラスターごとのため池の内訳

A群	池干し有	池干し無
山林型	3	3
水田型	2	3
住宅地型	4	0

B	池干し有	池干し無
山林型	2	2
水田型	0	1
住宅地型	4	0

C群	池干し有	池干し無
山林型	0	0
水田型	1	4
住宅地型	0	1

©2021. Japan Geoscience Union. All Right Reserved.

The Process of Raised-Bed River Formation and Factors that Affect It

*Natsuki KAMISASA[1], *Yuta KONDO[1], *Haruto TAKEYAMA[1], *Yasuharu TOMITA[1], *Rikushi NAGAO[1], *Naka NOHAMA[1]

1. Hyogo Prefectural Kakogawa Higashi High School

In this study, features of raised-bed rivers in Japan were measured using GSI Maps and some other kinds of maps in order to clarify ‘in what kinds of areas’ and ‘how’ raised-bed rivers are formed. As a result, two things were found; 1.The bed of a raised-bed river rises as sediment accumulates near the point at which the slope greatly changes so that the slope becomes more gentle, and that point moves downstream as the riverbed rises over time. 2.Some raised-bed rivers are wide in the upstream alluvial fan sections and get narrower in the downstream floodplain sections. It became clear that the formation of raised-bed rivers is related not only to human influence but also to landforms.

Keywords: raised-bed river, alluvial fan, cross-sectional view, longitudinal view, overhead view

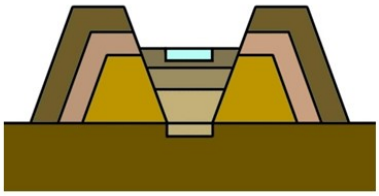


図1

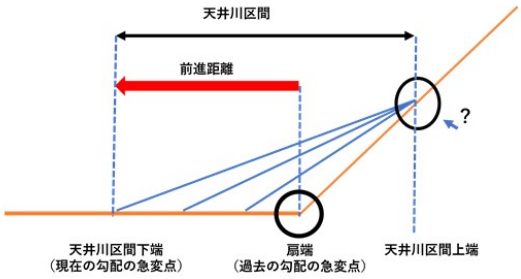


図2

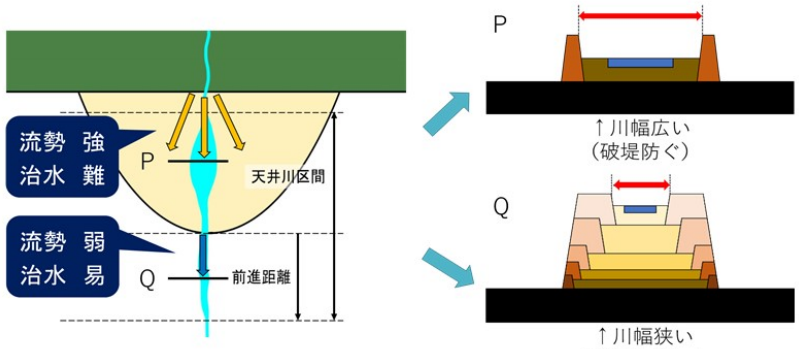


図3

©2021. Japan Geoscience Union. All Right Reserved.

Studies of the SDGs on the Sanriku Geopark. The sea urchin spread trench in the Taneichi Formation.

*Kyougo Sakashita[1], *Asahi Sekibata[1], *Rina Nakajo[1], *Yuto Kugoi[1], *Hikaru Sasaki[1]

1. Marient Chikyu-tanken club senier

The Sanriku Geopark covers the area from Aomori Prefecture through the coast of Iwate Prefecture and down to Miyagi Prefecture. Hachinohe City Marine Science Museum is located on the northern edge of that and to that belongs to the Mariento Chikyu Tanken club. We learned about Sanriku Geopark from 2019. And we announced this activity at the jpGU2019 and the Japanese Geoparks Network Meeting at Ohoita and jpGU2020.

SDO (Sustainable Development Objectives), a set of targets adopted by the United Nations in September 2015. Now, we must strive to achieve SDGs with society as a whole for the future of humanity. Geopark activity is very compatible with the SDGs. We felt that Sanriku Geoparks efforts toward SDGs were few. And so we examined the relationship between each geosite and the SDGs with GEO-KAMISHIBAI. GEO-KAMISHIBAI helps us understand the history of the land and people's lives.

The Geosite of Taneichi seaside park contains the sea urchin spread trench. The sea urchins grown in the trenches of the Hirono town are the best in Honshu in terms of quality and production.

We investigated the reason and found the following: Nanbu-Moguri is diving to a depth of 20 meters, taking the sea urchin and moving it to the trenches. Fresh seawater is constantly circulating in the trenches that that extend off the coast. The trenches are full of tides, so it is rich in seaweed. Working in shallow grooves is safer than diving off the coast.

The secret to the success was the co-operation between Nanbu-Moguri, the Taneichi Formation, and its trenches.

We made 3GEO-KAMISHIBAI. The titles are as follows: What does a sea urchin eating? The secret of the algae growing in the trench. The Taneichi Formation and sea urchin spread trench.

These are all related to 3Goal of SDGs; Goal 2: Zero hunger. Goal 12: Responsible consumption and production. Goal 14: Life below water.
Unfortunately, we can't exhibit GEO-KAMISHIBAI because of an Corona-Virus (COVID-19) problem. We understood the relationship between sea urchin, geocite and SDGs in Hirono town by conducting a survey and the making of GEO-KAMISHIBAI. We would like to publicize what we have learned using GEO-KAMISHIBAI.

Keywords: Sanriku、Geopark, Geosites, Taneichi Formation, Regional activity, Club activities

©2021. Japan Geoscience Union. All Right Reserved.



図１　種市層ウニ増殖溝の位置



図２　ジオ紙芝居　種市層ウニ増殖溝

©2021. Japan Geoscience Union. All Right Reserved.

Studies of the SDGs on the Sanriku Geopark. The Aoba Lake and Shimamori Basin.

*Mizuki Kimura[1], * Naho Simodate[1], *Kahono Hinata[1], *Yuma Keicho[1], *Kouki Takahashi[1]

1. Marient Chikyu-tanken club senier

The Sanriku Geopark covers the area from Aomori Prefecture through the coast of Iwate Prefecture and down to Miyagi Prefecture. Hachinohe City Marine Science Museum is located on the northern edge of that and to that belongs to the Mariento Chikyu Tanken club. We learned about Sanriku Geopark from 2019. And we announced this activity at the jpGU2019 and the Japanese Geoparks Network Meeting at Ohoita and jpGU2020.

The Aoba Lake and Shimamori Basin are located south of Hachinohe City (Figuer1). These were newly registered on the Sanriku Geopark in 2020. The history of geology and water control can be seen at the Aoba Lake and Shimamori Basin has beautiful countryside and history of agricultural cultivation.

SDO (Sustainable Development Objectives), a set of targets adopted by the United Nations in September 2015. Now, we must strive to achieve SDGs with society as a whole for the future of humanity. Geopark activity is very compatible with the SDGs. We felt that Sanriku Geoparks efforts toward SDGs were few. And so we examined the relationship between each geosite and the SDGs with GEO-KAMISHIBAI. GEO-KAMISHIBAI helps us understand the history of the land and people's lives.

We made 3GEO-KAMISHIBAI. The titles are as follows: Rice from Yomari-Dam? Meander in Niidagawa. Water springs of Shimamori Basin (Pictur1). The relationship between each title and SDGs is shown below.

Rice from Yomasari-Dam ? : Goal 6: Clean water and sanitation. Goal 2: Zero hunger.

Meander in Niidagawa : Goal 6: Clean water and sanitation. Goal 15: Life on land.

Water springs of Shimamori Basin: Goal 6: Clean water and sanitation. Goal 11: Sustainable cities and communities.
Unfortunately, we can't exhibit GEO-KAMISHIBAI because of a Corona-Virus (COVID-19) problem. We understood the relationship between people's lives and their history, geocite and SDGs in here by conducting a survey and the making of GEO-KAMISHIBAI. We would like to publicize what we have learned using GEO-KAMISHIBAI.

Keywords: Geosites, Shimamori Basin, Aoba Lake, Yomasari-Dam, Regional activity, Club activities

©2021. Japan Geoscience Union. All Right Reserved.



図１ 島守盆地と青葉湖の位置



写真１ ジオ紙芝居 島守湧水群

©2021. Japan Geoscience Union. All Right Reserved.

Proposal of Hachinohe Canyon to Sanriku Geopark Geosite.

*Sarina Shinohe[1], * Miyu Abe[1], * Akari Nakamura[1], *Yukihito Yasuhara[1], *Kensuke Shimomura[1]

1. Marient Chikyu-tanken club senier

The Sanriku Geopark covers the area from Aomori Prefecture through the coast of Iwate Prefecture and down to Miyagi Prefecture. Hachinohe City Marine Science Museum is located on the northern edge of that and to that belongs to the Mariento Chikyu Tanken club. We learned about Sanriku Geopark from 2019. And we announced this activity at the jpGU2019 and the Japanese Geoparks Network Meeting at Ohoita and jpGU2020.

Hachinohe Canyon is an open-pit limestone mine. (Fig.1) Its official name is The Hachinohe Limestone Mine. The quarry is 1,000 meters from east to west and 1800 meters from north to south. The mine’s lowest point is currently 170 meters below sea level. It is said to be the furthest place from the sky in Japan. They are shown in Figures 1 and Picture 1. This mine contributed to a Hachinohe city's becoming an industrial city. And its wonderful view is also a tourist attraction. But this isn't authorized by Geosite category in Sanriku Geopark.

SDO (Sustainable Development Objectives), a set of targets adopted by the United Nations in September 2015. Now, we must strive to achieve SDGs with society as a whole for the future of humanity. Geopark activity is very compatible with the SDGs. We felt that Sanriku Geoparks efforts toward SDGs were few. And so we examined the relationship between each geosite and the SDGs with GEO-KAMISHIBAI. GEO-KAMISHIBAI helps us understand the history of the land and people's lives.

We made 3GEO-KAMISHIBAI. The titles are as follows: Where did the Megalodon come from? Long belt conveyer. How to use the huge hole?

These are all related to Goal of SDGs; Goal 12: Responsible consumption and production. Goal 11: Sustainable cities and communities. Goal 13: Climate action.

In particular, there was a lively discussion of the title of How to use the huge hole?. There were many opinions, including tourist attractions, theme parks, garbage disposal facilities and disaster prevention facilities. We chose the idea of building a huge facility that combines those opinions.

Unfortunately, we can't exhibit GEO-KAMISHIBAI because of a Corona-Virus (COVID-19) problem. We understood the relationship between people's lives and their history, geocite and SDGs in Hachinohe Canyon by conducting a survey and the making of GEO-KAMISHIBAI.
It is strongly recommended that the Hachinohe Canyon be a geo-site for Sanriku Geopark. And we would like to publicize what we have learned using GEO-KAMISHIBAI.

Keywords: Sanriku Geopark, Geosites, Limestone, Megalodon, Regional activity, Club activities

©2021. Japan Geoscience Union. All Right Reserved.

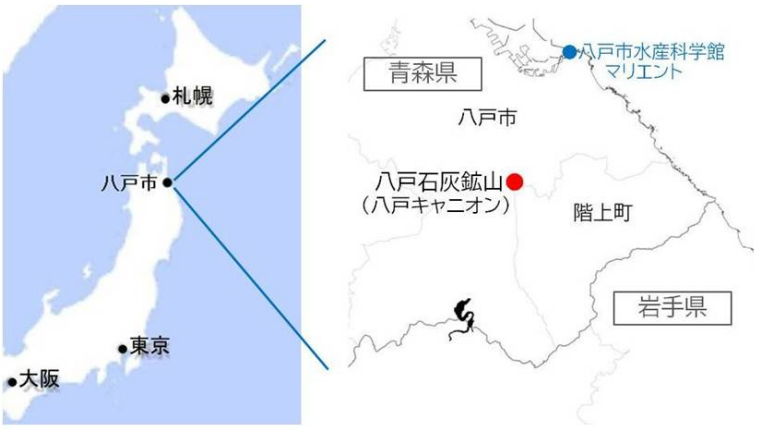


図１　八戸石灰鉱山の位置

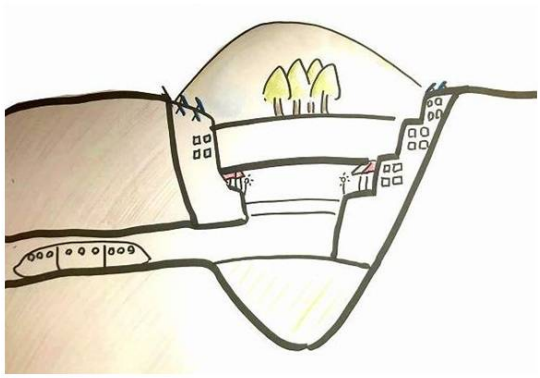


図２　八戸キャニオンの再利用案

©2021. Japan Geoscience Union. All Right Reserved.

Proposal of an index for estimating the distance from the source rock

*Ayaka Mitsui[1], *Reiji Iwamoto[1], *Keishi Okumi[1], *Mayu Naito[1], *Yamato Yasuhara[1], *Natsuki Yamamoto[1], *Naoko Kodama[1], *Akito Sasaki[1], *Akira Tada[1], *Takuto Nakanou[1], *Tomohiko Maeda[1], *Yuya Muromoto[1], *Ryusei Moriyama[1]

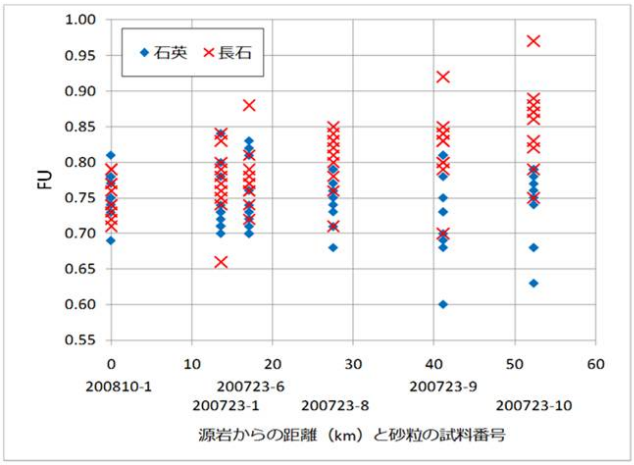
1. Hyogo Prefectural Himejihigashi Senior High School

The volume ratio of quartz / feldspar was calculated from the quartz and feldspar of the Ibo River flowing in the southwestern part of Hyogo prefecture.

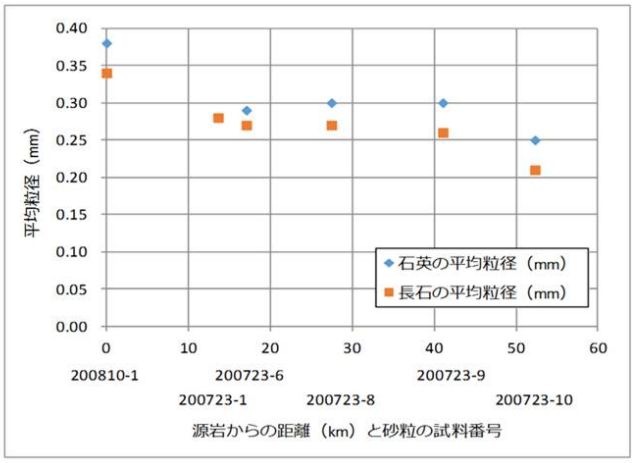
In the Ibo River basin, the average grain sizes of quartz and feldspar are almost the same. The FU value of quartz does not change much, but the FU value of feldspar increases downstream because feldspar melts very quickly. The volume ratio y of quartz / feldspar to the distance x from the source rock is indicated by an approximate straight line of y = 0.024x + 0.58. These show that the distance from the source rock can be estimated mathematically. Everyone intuitively knows that the particles are rounder and the quartz / feldspar is larger toward the downstream, but this study showed that it can be expressed by an equation for the first time.

Keywords: Ibo River , FU value, volume ratio of quartz / feldspar, source rock

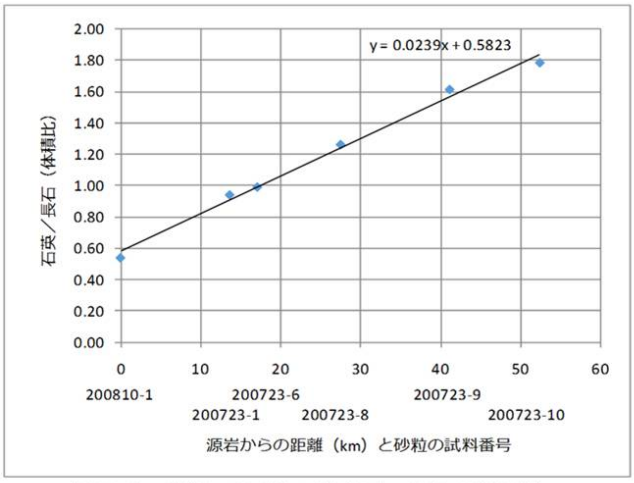
©2021. Japan Geoscience Union. All Right Reserved.



源岩からの距離と石英と長石のFU（各試料10粒ずつ）



源岩からの距離と砂粒の粒径



源岩からの距離と石英／長石（体積比）（直線は近似直線）

©2021. Japan Geoscience Union. All Right Reserved.

Energy calibration of a cosmic-ray detector

*Moe Kimura[1]

1. Tokyo Metropolitan Hibiya High School

CosmicWatch, a cosmic ray detector used in our research group, converts cosmic ray-derived fluorescence in a plastic scintillator into electrical signals using a semiconductor detector.

Cosmic rays are high-energy radiation from space, and CosmicWatch mainly detects muons.

CosmicWatch detects mainly muons. However, the correspondence between the signal value obtained by CosmicWatch and the energy value has not been investigated.

Therefore, we used Co60 and Cs137 radiation sources to investigate the correspondence between the signal values of the obtained peaks and the energy values.

The energy of the γ-rays emitted by the decay of radiation sources Co60 and Cs137 are known and are 318 keV and 662 keV, respectively.

Usually, plastic scintillators are used, but in this study, we also investigated using CsI scintillators, which are more specialized for detecting γ-rays.

CsI scintillators were chosen because they have higher energy sensitivity than plastic scintillators and are relatively inexpensive and easy to handle among inorganic scintillators.

In addition, the CsI scintillator had a larger fluorescence than the plastic scintillator, and the obtained signal value exceeded the upper limit of the analog-to-digital conversion in the circuit.

Therefore, we intentionally attenuated the signal value by delaying the acquisition time of the signal value while measuring.

This method was used to calibrate the energy of CosmicWatch.

In addition to the above, we measured and compared the frequency of radiation exposure when the detector was placed directly on the ground and when it was indoors, and considered the radiation exposure of the ground near our house.

Keywords: Radiation, CsI scintilator, Cosmic rays

©2021. Japan Geoscience Union. All Right Reserved.

Floating waterdrops using a straw commutator

*Aoba Takahara[1], Yuri Yasui[1], Takaya Sato[1]

1. Niigata Prefectural Takada high school

At the previous research,the experiment of floating a seed of Acer Rubrum was done. We thought of floating waterdrops in the same way.We replaced a sirocco fan with a blower in order to increase the wind speed,and we did the experiment. After controlling the wind speed by changing the length of straws,we found that the wind speed which could float waterdrops was about from 6.5m/s to 8.2m/s. However the wind speed distribution was far from our expectation because we made a lot of error. From now on, we need to devise the wind speed and the distribution so that we can float waterdrops for a long time.

Keywords: Meteorology

©2021. Japan Geoscience Union. All Right Reserved.

The rotating-Water-tank that is replaced hot water tank and ice water tank

*Masamune Minou[1]

1. Niigata Prefectural Takada high School

The rotating-water-tank experiment is the one to cause the meandered flow of water that is similar to westerlies by rotating tanks and difference of temperature. But in an intricate movement of a fluid, it is difficult to know phenomena that was caused by a specific factor. I studied effects that are caused by the difference of temperature through observation of the whole difference and thew common point between two kinds of rotating-water-tanks. As a result, I knew that difference of temperature affects the shape of waveform and the direction of the level flow and causes the rise and the fall of water. In the future, I want to give thorough cosideration by using substantial figure.

©2021. Japan Geoscience Union. All Right Reserved.

Comparison of the surface of Mars with the previous one in the approach of Mars Spread of dust storm on November 17th

*Sayaka Mizutani[1], *Takumi Uchiyama[1], Riho Kagami[1], Aoi Takemoto[1]

1. Ichinomiya High School

Observations of Mars were carried out from June 26 in conjunction with the 2020 Mars semi-major approach, and with the information that a dust storm had occurred since November 11, a comparison was made between the global dust storm that occurred during the 2018 major approach and the 2020 dust storm. For the comparison, we devised an image processing method and used the difference of the development maps.
The equipment used was a CMOS camera (made by ZWO),3x Barlow lens, 20cm Schmidt-Cassegrain telescope, ADC (Atmospheric Dispersion Compensation System) and IRVB filter.

Keywords: Mars, dust storm

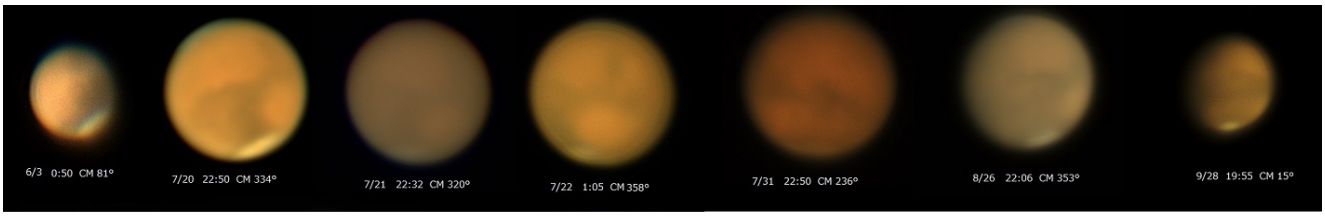


図1　2018年大接近観測画像

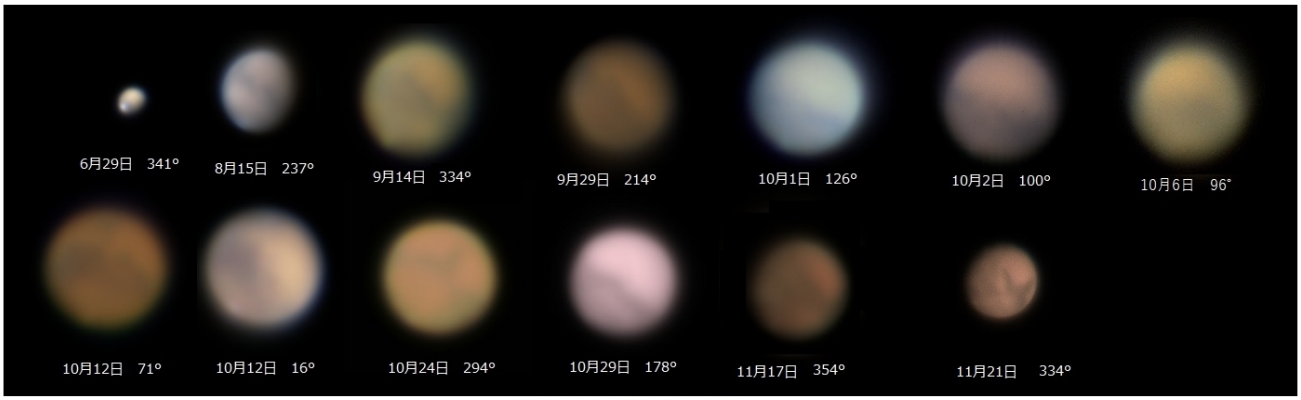


図2　2020年準大接近観測画像

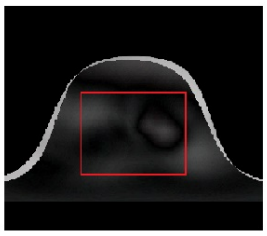


図3　10.12と11.17の展開図の差の絶対値

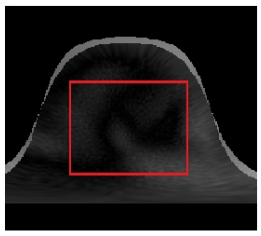


図4　9.14と11.21の展開図の差の絶対値

©2021. Japan Geoscience Union. All Right Reserved.

Tumulus inspection project by using cosmic-ray muon

*Tomoyo Ishizawa[1], *Satoshi Ono[1], *Asahi Shiozaki[1], *Wakana Yanagimoto[1], *Kenshiro Aoki[1], *Yuna Ishii[1], *Sogo Kimura[1], *Yuki Shimada[1], *Aoi Soga[1], *Yuga Takemori[1], *Rino Tomiku[1], *Kana Hashizume[1], Miki Ohtsuka[1]

1. Waseda University Honjo Senior High School

Higashiyatsu tumulus is a round barrow that has a horizontal stone chamber,which is located in our school. We are interested in the tumulus and want to know the details of the inside structure. Since it has great historical value, we decided to use a new method of imaging internal objects without destructing called muography. We have developed a new detector that detects cosmic-ray muons, and the prototype has been constructed. We first set it inside the school building and took data on the time when muons were thought to have passed through the detector.We evaluated the detector performance analyzing the data, and then measured the zenith angle distribution of cosmic-ray muons. In addition to those studies, we have proceeded the investigation of the tumulus itself by searching the historical records. We would like to improve the detector and install it in the tumulus to reconstruct the internal structure in three dimensions in the future.

Keywords: muography, integration of arts and sciences, cosmic ray, muon, archeology, interdisciplinary

©2021. Japan Geoscience Union. All Right Reserved.

Calculating the nebula density from the size of the emission nebula

*Yuki Shirai[1]

1. Totsuka High School

This study is a survey of the nebula density of the Emission Nebula-especially the M42 Orion Nebula, the M43, the M8 Lagoon Nebula, the M20 Trifid Nebula. I will compare and examine the nebula densities of the above four objects from the size of the emission nebula by analysis and calculation.
Visible light images were taken using a 400mm telephoto lens. The radius of the nebula was calculated by analyzing the visible light images using the graph function of Subaru image analysis software Makali`i. The density was calculated from the radius, temperature, and spectral type of the ionized star.
As one of the results, the density of the Orion Nebula , with the density obtained by calculation being 411cm^{-3}, compared to the density of 410cm^{-3}(nebula cluster series-emission nebula) obtained by observing the 21cm radio emission line. As described above, I got the result which has a very small error.

Keywords: emission nebula, density of emission nebula, evolution of HII region



©2021. Japan Geoscience Union. All Right Reserved.

Strength evaluation of structures by making and improving quake-vibration generators

*Runaya Igari[1], *Yuto Meguro[1], *Rin Goto[1], Kenshiro Kamata[1]

1. Miyagi Rifu high school

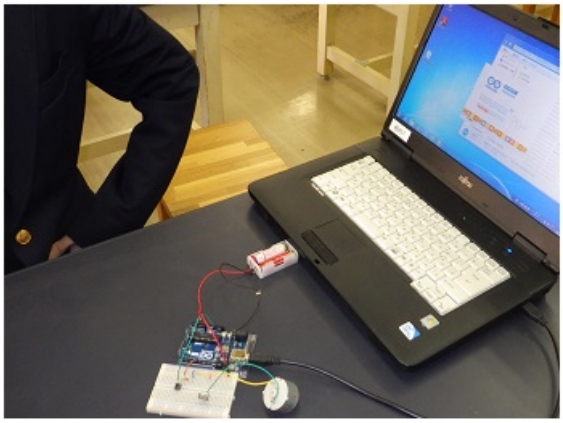
We made a simple seismic motion generator using empty cans and motors around us, and made a model of how the structures on the stratum due to the multi-layer structure are affected. In order to bring this vibration closer to the actual one, we are attempted reproduce it while electronically controlling it using Arduino. In order to construct layer, biscuits powder was used to reduce the weight and we conducted an experiment to observe how the structures such as houses would be affected and damaged in addition to the results of the earthquake by constructing the wooden framework on the stratum model.

In addition, we also observed how the shaking of earthquakes caused by heavy objects is involved by conducting experiments on the structures on the stratum with the weight of metal bodies such as iron, copper, and brass. Among them, we are trying to reproduce the shaking caused by the occurrence of a motor-controlled earthquake using Arduino programming.

There are still issues with the motor output and vibration frequency, but we plan to discuss how to make the quaking model closer to reality.

Keywords: Quaking model, Electric controlle, Geotechnical Engineering





©2021. Japan Geoscience Union. All Right Reserved.

Time dependence of ocean salinity

*Honami Hashimoto[1], Annu Ito[1]

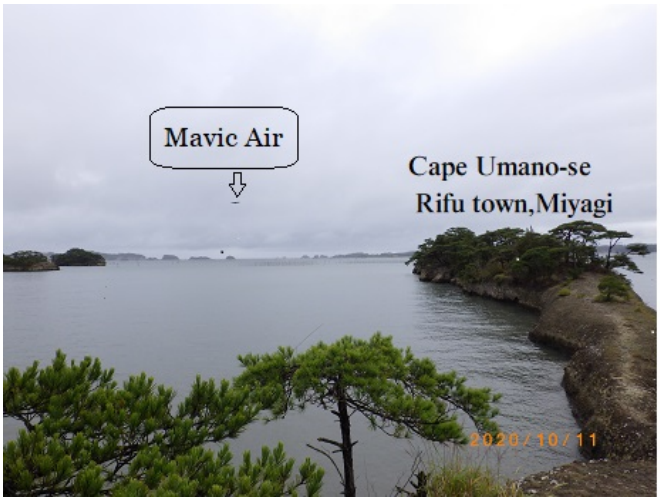
1. Miyagi Rifu highschool

Since 2018, the Natural Science club of Rifu High School has been conducting a monitoring activities on seasonal changes in the salt content of seawater in various shoe of Matsushima Bay. The survey are concentrated to the total salt content (%) and the amount of each cation of Na + / K + / Ca2 + (mg / L = ppm).

The seawater sampling locations are set in Shichigahama town Miyagi Prefecture, which is close to the outer ocean, Higashi-Shiogama at the bay front, cape Umanose in Matsushima Town, and Oshima in the back of the bay. We have found that the closer to the open sea, the larger the changes in cation content and saline content, while the closer to the inner bay, the more affected by land water and fine topography.
As a major tendency, the total saline components increases as expected in the summer when the amount of evaporation rate is higher. But according to the survey up to last year, when we observed each cation, only Na + cation increases in January in the winter.

This year, we will consider how small changes in topography and coastal distances bring about differences in seawater salt content, which taking into account the effects of topography and organisms based on the water sampling activity by highschool students drone operation up to about 200m.

Keywords: Ocean Saline components, Drone techniques, Year-term changing of ocean saline





©2021. Japan Geoscience Union. All Right Reserved.

Toward "Solid-State Version Chromatography" Second Report

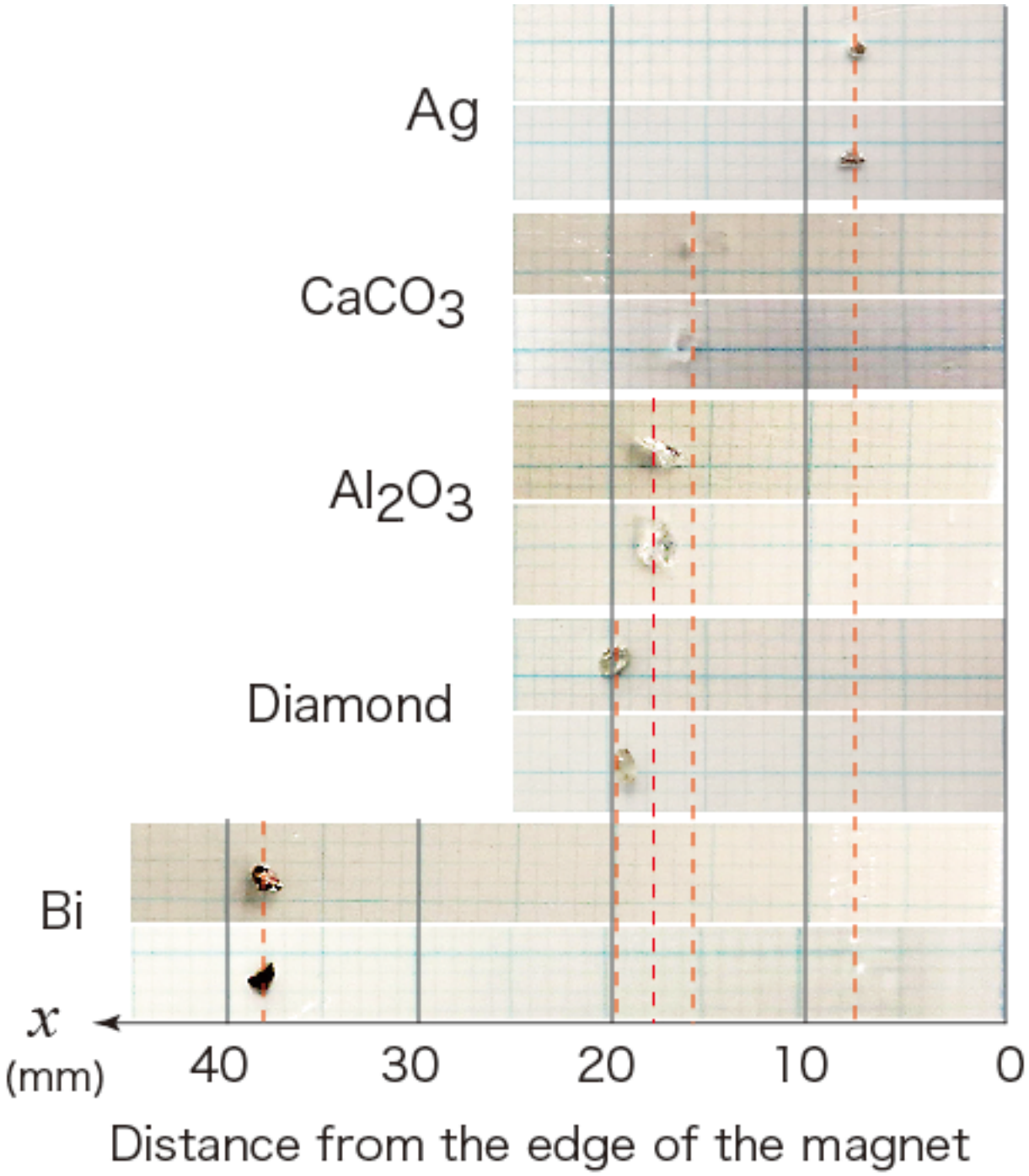
*Yuichiro Okuno[1], *Akihisa Wada[1], *Yudai Kozono[1], *Ryota Iwamoto[2], *Mai Fujitani[2], *Kyoya Okada[3], *Kusunori Sumi[3], *Arata Fujimoto[3]

1. Imamiya Technology Senior High School of Osaka Prefecture:The evening course, 2. Otemae Senior High School of Osaka Prefecture:The evening course, 3. Kasugaoka Senior High School of Osaka Prefecture:The evening course

Last year, we proposed the principle of separating and collecting a mixture of diamagnetic solid particles by material. In order to demonstrate this principle, we constructed an apparatus and conducted experiments. As a result, particles of six inorganic materials and six organic materials were collected on the collection plate as a group of particles that differed by material. We were able to verify the effectiveness of the apparatus based on this principle. This time, in order to further improve the separation accuracy of the apparus, we designed three types of magnetic circuits and conducted comparison experiments. As a result, we were able to separate corundum and calcite, which could not be separated by last year's apparatus. The resolution of the magnetic susceptibility was 0.4×10^{-7} emu/g. This technique has potential as a solid-state version of chromatography for separating solid mixtures by material.

Keywords: microgravity, magnetic separation, diamagnetic material, solid chromatography, translational motion

©2021. Japan Geoscience Union. All Right Reserved.



©2021. Japan Geoscience Union. All Right Reserved.

How to extract bioethanol effectively by distillation.

*Ataru Kunihisa[1]

1. Wakasa high school

In Japan, the number of Solidago altissima is increasing, and it is rampant.Therefore, we have been researching whether bioethanol can be used as a new energy resource by producing bioethanol from Solidago altissima.Mix crushed Solidago altissima and sulfuric acid and sterilize with autograve.Then, it was centrifuged, activated carbon was added, and the mixture was filtered, and then cultured for 3 days to try to produce ethanol.At present, ethanol has not been recovered yet.In the future, we will carry out experiments by changing the amount of sulfuric acid added. Ultimately, we would like to discover the possibility that Solidago altissima will become a new energy resource with the goal of efficiently extracting ethanol.

Keywords: Solidago altissima, bioethanol, a new energy resource

©2021. Japan Geoscience Union. All Right Reserved.

Confusion of the people in the northwestern area of Saitama Prefecture due to rumors after the 1923 Kanto Earthquake

*Miharu Shinoda[1]

1. Sakae Higashi High School

In the northwestern area of Saitama Prefecture, no damage was caused by the 1923 Kanto Earthquake. But a massacre of Koreans occurred due to false rumors in these areas. In this study, we surveyed stone monuments and other literature. In the Ohara grave of Yukokuji Temple located in Kumagaya City, Saitama Prefecture, there is a stone monument for the 1923 Kanto Earthquake. It says that a false rumor occurred and people were confused. According to Matsubara (2013), on September first after the main shock, the trains and telegraphs stopped between Tokyo and Urawa. On September third, an extra newspaper had false information about Koreans and it spread to many areas. The newspaper said that Koreans set on fire. As a result, about 150 Koreans were killed in Kumagaya and Honjo Cities in Saitama Prefecture. Later it was found that the rumor was false. Today still with the development of technology, life has become very convenient. But the false rumors are likely to occur. That is why, more than ever, we need to think about the credibility of the various information we get in our daily lives, and we should deal with emergencies calmly so that we will not be misled by false rumors.

Keywords: The 1923 kanto Earthquake, False rumor , The northwestern area of Saitama Prefecture

©2021. Japan Geoscience Union. All Right Reserved.



【「供養塔」の裏面に記されている碑文】　／は改行部分を示す

噫大正十二年九月一日午前十一時五十八分突如帝都ヲ中心トシテ勃發シタル大惨禍関東大震災ハ／瞬時ニシテ幾万ノ生霊ト幾百億ノ財貨トヲ奪ヒ去リシ振古未曽有ノ大惨害ナリキ當時我國ハ歐州／大戦ノ影響ヲ受ケ國内景気ハ非常ナル好調時代ニ在リ一般的ニ放縦ト贅澤ノ弊ヲ露呈シ吾世ノ春／ヲ謳歌シツヽアリシ時ナリシカハ恐怖モ一入大ニ狼狽又甚シカリシナリ一時全ク交通機関ハ素ヨ／リ通信機関ノ杜絶流言蜚語ノ百出其真相ヲ知ルニ由ナク或ハ此儘暗黒世界ヲ現出スルニアラサル／ナキヤヲ思ハシムルノ状態ナリキ此事實ヨリ災後ノ國民ハ俄然強キ反省ニ目覚メ此惨害ハ天ノ下／シ給ヘル戒ナリ天譴ナリトシテ異常ナル緊張ニ立戻リ専ラ復興ノ気魂ニ燃ヘ懸命ノ努力ヲ奮ヒ極／メテ迅速ニ其實ヲ擧クルヲ得タリシモ此災禍ノ為ニ犠牲トナリシ多クノ生霊ニ對シテハ誠ニ痛恨／哀惜ノ情ニ禁ヘサル所ナリ本市ニ於テ遭難セル生霊ハ熊谷寺及圓光寺ノ両墓地ニ埋葬シ季節ノ放養ヲ怠ラサリシモ将来其荒廢センコトヲ虞レ且ツ分葬シアルコトノ不便ヲ除カンカ爲メ今回ノ市内／有志胥謀リ両墓地ノ遺骨ヲ一ニシ茲ニ熊谷寺墓地内ニ地ヲ相シテ本供養塔ヲ建立シ以テ生霊ノ瞑／福ヲ祈ラントス　犠牲ノ霊不慮ノ遭難慰ムルニ由ナシト雖モ此尊キ犠牲カ同胞國民ノ自覺反省ヲ／促シ緊張堅實ナル風氣作興ニ寄興セル済世ノ供徳ハ盖シ大ナルモノアリト謂フヘク豈誰カ徒死ナ／リトセンヤ聊當時ノ概況ヲ録シテ誌トス／

昭和十三年七月　埼玉縣熊谷市長　勲六寺　新井良作書／坂群熊　水友勝　刻

図 1. 熊谷市熊谷寺の大原墓地に建つ供養塔(写真)とその裏面に記されている碑文

Fig.1 The photo of surface of the stone monument built in the Ohara Grave of Yukokuji Temple, Kumagaya City and inscription on the back.

表 1. 関東地震の発生から埼玉県北西部での事件が起こるまでの経緯

Table.1 Background to the incident in the northwestern area of Saitama Prefecture after occurrence of the Kanto Earthquake.

<table>
<tr><th></th><th>9月1日</th><th>9月2日</th><th>9月3日</th><th>9月4日</th><th>9月5日</th><th>9月6日</th><th>9月7日</th></tr>
<tr><td>地震と震災</td><td>本震発生（11時58分）
東京で大火災</td><td colspan="5">大小の余震の継続</td></tr>
<tr><td>東京から熊谷方面への交通機関</td><td>浦和以北の（現在の）高崎線が運転再開</td><td colspan="2"></td><td>東京と埼玉の都県境の荒川鉄橋が開通</td><td colspan="2"></td></tr>
<tr><td>東京方面から埼玉県北西部への避難</td><td colspan="3">浦和まで徒歩でたどり着いた避難民が熊谷方面へ列車で移動</td><td colspan="3">東京方面より鉄道を利用した避難が可能</td></tr>
<tr><td>新聞社の動向</td><td colspan="2">東京の新聞社は全て発行が不可能</td><td>東京の1社が流言を掲載した号外を発行</td><td colspan="2"></td><td>各新聞社が発行を再開</td></tr>
<tr><td>埼玉県北西部に広がった流言</td><td></td><td>東京にて、「放火」等の流言が発生</td><td colspan="4">埼玉県内にも流言が波及</td></tr>
<tr><td rowspan="2">埼玉県北西部での事件</td><td rowspan="2"></td><td colspan="2" rowspan="2">埼玉県内に在住していたあるいは東京方面から避難してきた朝鮮人の拘束</td><td colspan="3">朝鮮人の虐殺</td><td rowspan="2">事件の終息</td></tr>
<tr><td>深谷市（3日の夜より）
本庄市・熊谷市・上里町</td><td>上里町</td><td>寄居町</td></tr>
</table>

©2021. Japan Geoscience Union. All Right Reserved.

A quest for the best condition of a crystal radio's detection

*Motoaki Osone[1]

1. Yashiro High School

This research was designed to see both electric and chemical features of minerals. It was found that the differences of sounds among various types of materials were caused by their direct and alternative I-V curve character. Moreover, it was also revealed that the increase in oxygen on minerals' surfaces is one of the main causes of their rectifying effect. For the future study, since there can be other causes of rectifying effect, this research should be deepened by further experiments such as examining more species and changing the direction of voltage toward crystal orientation.

©2021. Japan Geoscience Union. All Right Reserved.

What cause columner joint changes?

*Yugo Sakurai[1], *Yuki Enomoto[1], *Kanta Hayashibe[1]

1. Yashiro High School

“Columnar joint” mean a hexagonal prism made from lava. When lava touch ground and is rapidly cooled causing volume contraction, they change into columnar joint. Even though scientists are making progress, there is no exact answer why there are difference in size and length between each columnar joint. We thought we may prove the environment of old period by discovering the answer, so we conducted experiments to clarify the causes.

It’s hard to do experiment using lava, so we used cornstarch as a model of columnar joint. It’s said most of their features are common with columnar joint because both them relate to volume contraction.

We named each container A~H and put cornstarch mixed with water, and dried.

A water:70g starch:30g container’s depth : shallow way : Incubator 40°

B water:70g starch:50g container’s depth : shallow way : Incubator 40°

C water:100g starch:140g container’s depth : deep way : Incubator 70°

D water:50g starch:70g container’s depth : shallow way : Incubator 70°

E water:50g starch:70g container’s depth : deep way : Incubator 70°

F water:50g starch:70g container’s depth : shallow way : Incubator 70°

G water:50g starch:70g container’s depth : deep way : light bulb

H water:50g starch:70g container’s depth : shallow way : light bulb

Comparing C with E, we found that the form of crack don’t depend on the depth of container.

Comparing D and E and F, there are few differences between drying incubator and light bulb. However, comparing F and H, there are obvious differences between them.

Comparing A with B, we found that the more it contains cornstarch, the more crock become complex.

Therefore, we supposed the gap of ease of warming caused these differences. the more it’s hard to warm, the more crocks become complex.

In conclusion, we made a hypothesis that “whether lave become columnar jointing is depend on the gap of ease of warming between inside and outside”. It’s still debatable, but it will contribute the development of geoscience.

©2021. Japan Geoscience Union. All Right Reserved.

©2021. Japan Geoscience Union. All Right Reserved.

Preliminary analysis of HAYABUSA-2’s Doppler-Shift

*Azumi Sofue[1], *Naoko Nishino[1], *Riri Iida[1], *Riri Numata[1]

1. Wakayama Shin-ai Senior High School

The school previously analyzed the data received for one day during Hayabusa2’s first Earth swing-by and found that the received frequency was Doppler-shifted. We concluded that this was caused by the change in relative motion between Hayabusa2 and the Earth due to the Earth’s rotation. On the occasion of Hayabusa2’s return, we were able to obtain much longer reception data than that mentioned above, including three days the re-approach and nine days after it started to move away from the Earth. Not only the large effect of the Earth’s rotation, but we also challenged the quantitative analysis of the relatively small effect on the Doppler shift caused by the change in the relative motion between the orbital motion of the Earth and that of Hayabusa2.

©2021. Japan Geoscience Union. All Right Reserved.

Estimation of a ceiling thickness using the muography technique with a small cosmic-ray detector

*Nana Kobayashi[1]

1. Kaichi High School

Since cosmic-ray muons are shielded by the ceiling inside a building, the detection rate of penetrated cosmic-ray muons is decreased on a lower level. It has been applied as muography e.g. observation of the interior of pyramids. I estimated the thickness of the ceiling of the school building by using this technique with the handmade cosmic-ray detector and I also confirmed the consistency between the measured result and value from the drawing of the building.
First, we measured the arrival rate of cosmic-ray muons on the 1st to 5th floors of the school and in the schoolyard (0 floors) using a cosmic-ray detector so-called Cosmic Watch. Two Cosmic Watch detectors were stacked on top of each other, and only the cosmic rays that passed through both upper and lower detectors were counted to limit the solid angle to the direction perpendicular to the ground. I confirmed that the frequency of arrival of cosmic rays decreased as the floor was lowered.
Then, we simulated the correlation between the thickness of concrete, which is the main component of the ceiling, and the arrival rate of cosmic-ray muons, and compared the simulation results with the arrival rates at each floor. I obtained the path length of the cosmic-ray muons with the averaged energy of muons and the stopping power of the concrete.
The total thickness of the ceiling from the measurement was 253 cm and from the drawing was 290 cm.

Keywords: cosmic-ray

©2021. Japan Geoscience Union. All Right Reserved.

A proposal of an inverse analysis method for ballistic ejecta flying focusing on crater shape in phreatic eruption

*Kouki Nishino[1], Neo Suzuki[1], Natsumi Waki[1]

1. Kanagawa Prefectural Yokosuka Senior High School

In recent years, many of the casualties has increased in sudden phreatic eruption. As its countermeasure, the experimental research on the safty of shelters for volcanic disaster prevention is being conducted. However, experimental conditions such as impact velocity of lapilli and block ejecta (ballistic ejecta), which are important in shelter design, largely depend on the experience of expert for volcanology. This is because the actual scattering behavior of the ballistic ejecta is not well understood. Therefore, in this study, we focus on the shape of the crater caused by the impact of the ballistic ejecta. We understand the characteristics of the crater shape that change depending on the impact conditions by the free fall test and the indentation test, and propose an inverse analysis method of the ballistic ejecta scattering behavior.

©2021. Japan Geoscience Union. All Right Reserved.

The survey of Micro-Plastics included in River sediments.

*Taichi Ichikawa[1], Ryuke Kawai[1], Suzuka Fukunaga[1], Tessho Yamamoto[1], Takumi Sato[1]

1. GIZAN SENIOR HIGH SCHOOL

"Micro-Plastics(MP)",recently taken up as a problem,inflow from also rivers.Most of the research on MP in the river are that for analyzing river water.Therefore,we think that if we can make clear the amount of MP in river sediments on the basis of this research,we can estimate the amount of MP that flowed from upstream or flow out to downstream or to the ocean.

Keywords: Micro-Plastics, River sediments, River environment

©2021. Japan Geoscience Union. All Right Reserved.

Relationship between sprites and the lightning charge moment

*syunsuke nakao[1], *sora wake[1]

1. Prefectural Kochi Ozu High School

We are studying the phenomenon of sprites. Sprites are a kind of Transient Luminous Events, and Transient Luminous Events are luminescence phenomena that occur with lighting in the mesosphere at an altitude of about 50 to 100 kilometers. The mechanism of sprites is as follows. A positive polarity lightning strike neutralizes the positive charge in the upper layers of the cloud, and a downward electric field is generated from the ionosphere toward the upper cloud layer. The electric field causes electrons at an altitude of around 60 kilometers to rise and collide with nitrogen atoms, putting them in an excited state. Sprites occur as a result of the release of energy when these nitrogen atoms return to their ground state. However, not all positive polarity lightning strikes produce sprites. We investigated relationship between the charge moment of the lightning and sprites to clarify the conditions for its occurrence. The charge moment is a value defined as the product of the amount of charge discharged by lightning and the altitude, and there is a paper that says this value is large for lightning that generates sprites. We tested whether this was also true for our own data. We have data on the images and locations of sprites when they occurred. By acquiring the data, the time and location of the lightning, and the magnetic field data from the electromagnetic waves generated by the lightning, we analyzed the charge moments of the lightning that generated sprites and the lightning that did not, and compared them to see if there was any difference.

As a method of verification, we first identified the location of the sprite's occurrence using data taken from multiple observation points. The next step was to identify the lightning, the thunderbolt that generated the sprite. Finally, we compared the size of the lightning charge moment at the time of sprite generation. It is not possible to directly determine the value of the lightning charge moment but the strength of the magnetic field of electromagnetic waves generated by lightning is proportional to the lightning charge moment. Therefore, we analyzed the relationship between the magnitude of the magnetic field strength and the magnitude of the lightning charge moment.

This section describes how to analyze the location of sprite generation. We are observing the high-altitude luminescence phenomenon together with 32 high schools in Japan. And in the observed data, there are successful events observed simultaneously from two or more locations. The position and direction of these sprites were identified by referring to the stars in the same location.

Next, we found the lightning at the time when the sprite occurred and timed the two data sets to identify the lightning. We obtained information on lightning from several companies and research institutes, and identified lightning from lightning that occurred at the same time when the sprites occurred.

Then, Chubu University provided us with data on the strength of the magnetic field of the electromagnetic waves generated by lightning. Thanks to the data, we compared the integrated magnetic field values for lightning with sprites and without them.

Keywords: TLEs, Lightning

©2021. Japan Geoscience Union. All Right Reserved.

Potential Small Hydropower Generation in Kamikawa Basin -Hydro Energy Map Visualizing Power Generation-

*Airi Takei[1], *Akira Tamaki[1], *Naoki Kudo[1], *Asahi Takahashi[1], *Hikaru Kawashima[1]

1. Hokkaido Asahikawa Nishi High School

In recent years, greenhouse gas has been generated by fossil fuel consumption. Power generation using renewable energy is become popular in order to reduce greenhouse gas. Renewable energy's merits are that it is undepletable and help eliminate CO_2 generation. On the other hand, renewable energy's demerits are its unstable generation. Small hydropower generation has those merits, and moreover, stable generation. Asahikawa has many rivers and aqueducts. Also, Asahikawa has a place where small hydropower is already generated, so we think that Asahikawa can be developed as a small hydropower town if we use the data. However, Asahikawa is a few case and a few suitable locations. In order to overcome this, we found a small hydro energy map. It is a map that the installable area of small hydropower generation and the estimated power generation is shown on the order of one-fifty thousand scale about the particular river. Originally, the small hydro energy map used the river, however, we will use the aqueducts developed for agriculture. We can find suitable places if we can create a small hydro energy map using aqueducts located in Kamikawa basin and expected power generation.
In order to make a small hydro energy map, we need the correct calculation method of power generation. So we compared actual planned power generation of Toei power plant with our estimated theoretical power generation. And these values matches within an error of 3 percent. We calculated the estimated power generation of the three aqueducts at a total of 23 points. By creating this map, we could see the energy distribution latent in the aqueduct. We think that it is possible to more exactness locate and choose a site the best point for power generation.

Keywords: Small Hydropower Generation

©2021. Japan Geoscience Union. All Right Reserved.

Consideration of brachiopod biota change events in the Kuzu limestone layer

*Omi Kono[1], Tokio Chiba[1]

1. Kaijo senior high school

In Kuzuu, Sano City, Tochigi Prefecture, which is the area covered in this study, the restoration of the sedimentary environment of upper limestone and lower limestone has been elucidated using rock flakes. However, the cause and timing of dolomite formation in the central layer has remained unclear for a long time, and conditions directly indicating deposition environment have not been confirmed. Therefore, we investigated the species of limestone limbs of the upper and lower layers, which had been suggested to have been of different species, using formic acid treatment, and examined the presence or absence of differences in the upper and lower layers. We will clarify the change events of species during deposition and ultimately identify the factors of dolomite formation in the middle layer.

Keywords: Geology, Fossil, Paleoenvironmental estimation

図 1

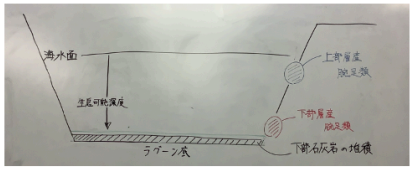


図 2

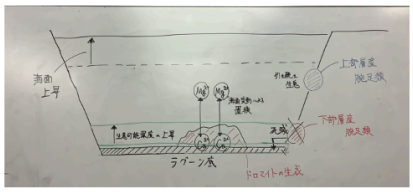
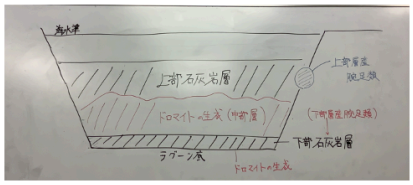
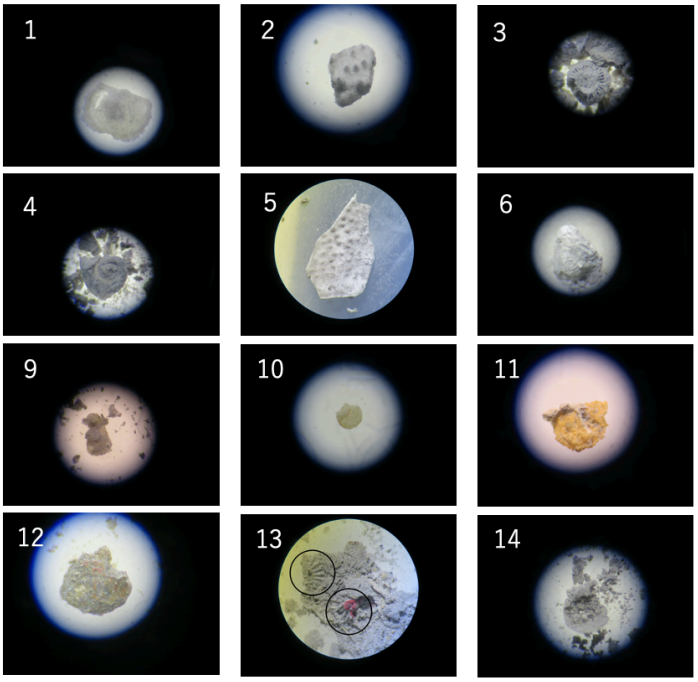


図 3



腕足類一覧（番号は予稿の番号と同一）
7、8に関しては同定後破壊されてしまったため写真は無い



©2021. Japan Geoscience Union. All Right Reserved.

Estimation of the variation in mechanism in the amount of spring water in Otomeyama Park, Shinjuku City

*Kuya Aoyama[1], Taichi Shimokobe[1], Masamune Kanou[1]

1. Kaijo high school

In this study, we estimated the fluctuation mechanism in the amount of spring water at Otomeyama Park in Shinjuku by comparing it with the groundwater level and water temperature in wells.

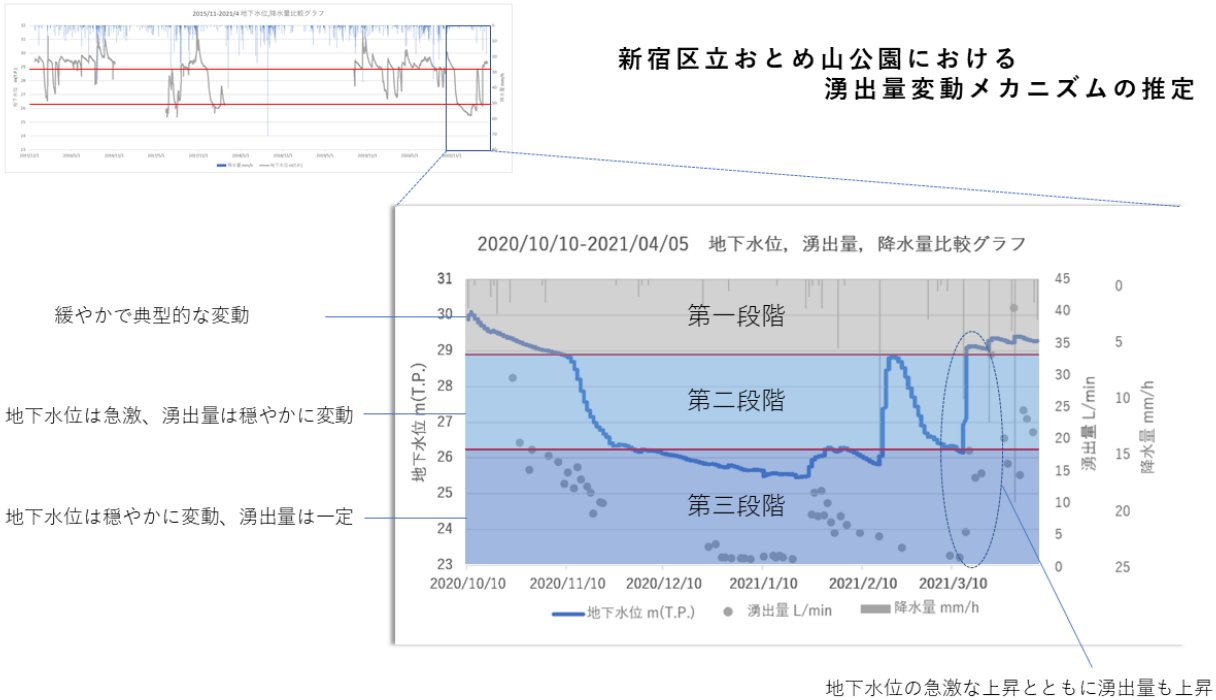
From October 2020 to January 2021, there was a period when there was only 16 mm of total rainfall in 90 days. At this time, the amount of spring water decreased by 87% compared to a normal year, and according to the groundwater level that decreased at the same time, it was classified into the following three stages with different water levels.

The first stage is when the groundwater level declines slowly but the amount of spring water reaches 1L/min, which is considered to be the base flow rate; the second stage is when the groundwater level fluctuates but the amount of spring water does not change; and the third stage is when the amount of spring water increases rapidly.

It can be said that the amount of spring water inflow, groundwater level, and water temperature in the well are controlled in these three stages.

This is thought to be due to the difference in strata.

Keywords: meteorology, hydrology, geology



©2021. Japan Geoscience Union. All Right Reserved.

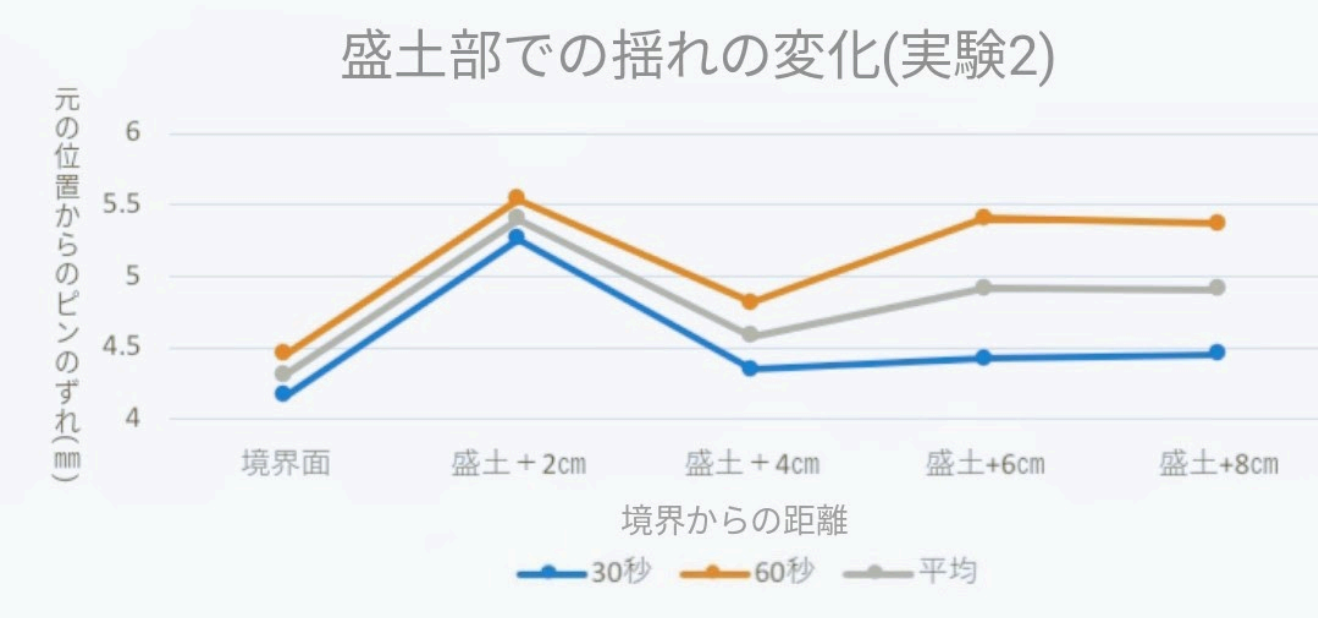
Modeling the earthquake damage in adeveloped land

*Shungo Kokubun[1], *Satoru Takahashi[1], *Hiroshi Takeuchi[1], *Haruki Tamakawa[1], *Masafumi Kaneko[1], Takumi Nanbu[1]

1. Miyagi Prefecture Sendai Daisan High School

We search about the relationship between banking and the effect of earthquake is close thing to our lives.And there are many secondly disaster.We focus on collapse of buildings.From previous research,on the embankment,earthquake damage is heavy.Purpose of research,we make model which reproduce closer to actual movement.We used shaking machine and took a video.In the result only on the border represent actual movement.

Keywords: earthquake, Analog experiment, Embankment



©2021. Japan Geoscience Union. All Right Reserved.

Influence of Calcium chloride on frost columns

*Manaka Oya[1], Shohei Nanri[1]

1. Ichikawa gakuen Ichikawa senior high school

The purpose of this research is to investigate the effect of calcium chloride on frost columns. In order to begin the investigation, an environment which allows the growth of frost columns was made. Frost columns grow when the air temperature is below 0℃, the temperature inside the dirt is above 0℃, and the dirt must be moist. To meet these conditions, the cool incubator was set below 0℃, and an instrument to incubate the dirt(Kanuma pumice) was made. After adjusting the temperature inside the cool incubator, soil particle size, and the temperature of the water used for incubation, the conditions for the growth of frost columns were observed. Next, the effect of calcium chloride on frost columns based on its molar concentration was researched. As a result, frost columns were observed when the cool incubator was set at -10℃, and took 4 hours for it to be detected. After applying calcium chloride upon the frost columns, the lowest molar concentration of calcium chloride in the dirt to prevent the growth of frost columns was 12.9×10-3mol/L.

Keywords: Frost columns, Calcium chloride

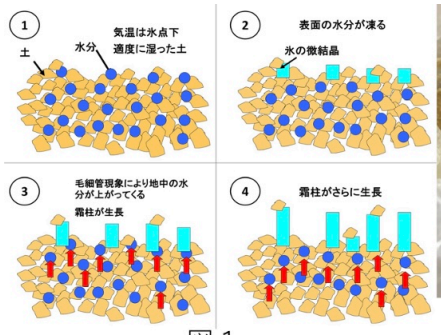


図 1



図 3

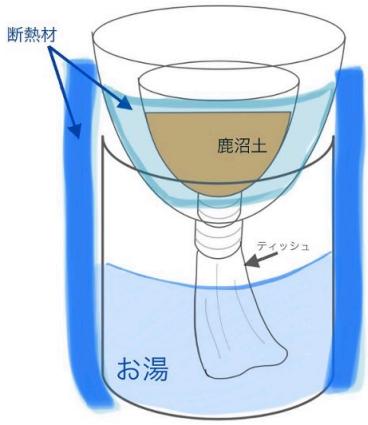


図 2 霜柱作成装置

出典: (NGKサイエンスサイト)

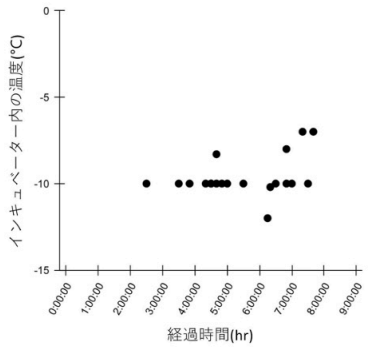


図 4 室温と経過時間の関係

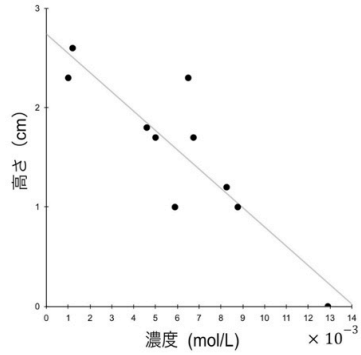


図 5 塩化カルシウムの濃度と霜柱の高さの関係

©2021. Japan Geoscience Union. All Right Reserved.

Differences in fog generation conditions in the Edogawa estuary -Examples of Edogawa-ku and Ichikawa-shi-

*Kenta Torii[1], Shohei Nanri[1]

1. Ichikawa gakuen Ichikawa senior high school

The aim of this research is clarifying the reason why fog of Ichikawa City, Chiba is a little thicker than that of Edogawa City, Tokyo.

Firstly, I checked the conditions for fog to occur, and they turned out to be as follows:
(1)The air contains a lot of water vapor.
(2)The temperature is high.
(3)The altitude is high. (Limited to areas of plains)

Ichikawa City and Edogawa City has geographical continuity that is why I selected Condition 1 as one relevant to this research.

Secondly, I focused on wind as the factor which makes a difference to the amount of water vapor. Examining directions of the winds at various points in southern Kanto on the morning of November 26th, 2020, I found a certain regular pattern of wind, that means, the larger current of wind proved to be. These currents turned out to meet around the area of Ichikawa City and Funabashi City, which Ichikawa City is bordered on the east by, and differ in volumetric humidity and temperature. These differences make fog occur in Ichikawa City firstly.

In conclusion, it is a natural consequence that the fog of Ichikawa City is thicker than that of the other areas including Edogawa City because Ichikawa City is the source of the fog.

Keywords: Fog, Edogawa river

©2021. Japan Geoscience Union. All Right Reserved.

Development of variable slope type underwater embankment

*Kei Omura[1], Shohei Nanri[1]

1. Ichikawa gakuen Ichikawa senior high school

We conducted research on variable slope type underwater embankment with the aim of developing underwater embankment that have a higher energy-reducing effect on tsunamis than conventional types. The research was conducted by combining a demonstration experiment in a laboratory using a small model and a computer simulation. In the demonstration experiment, waveforms were collected using an ultrasonic sensor, and the effect of the variable slope type underwater embankment was verified as compared with the case where a normal fixed underwater embankment was installed and where there was no underwater embankment. In addition, in the demonstration experiment, by using BB bullets as a tracer, the distance traveled by the waves of water molecules was estimated, and the changes in the amount of energy possessed by the waves were also compared. In the simulation, two-dimensional physics software, Algodoo, was used, and the accuracy of the demonstration experiment was verified using the discrete element method by reproducing the environment of the demonstration experiment. As a result of the experiment, it was found that the energy of the waves passing through the variable slope type underwater embankment tended to be dispersed over a wide area. In addition, the total amount of energy possessed by waves decreased the most when the conventional fixed underwater breakwater was installed. From these facts, the variable slope type underwater embankment reduces the load on the embankment compared to the conventional breakwater and disperses the wave energy over a wide area to reduce the amount of energy that rushes to the ground in a certain period of time, and the breakwater on the ground collapses. Ultimately, we would like to connect not only the variable slope type but also the curved underwater embankment whose shape itself changes.

Keywords: tsunami, Underwater embankment

©2021. Japan Geoscience Union. All Right Reserved.

Environmental impact assessment of air and soil substances using spring water of Minowa as an index

*Mari Taki[1], Shohei Nanri[1]

1. Ichikawa gakuen Ichikawa senior high school

In this study, air temperature, water temperature, pH, RpH, electrical conductivity, and COD were measured in the spring water of Minowa, Ichikawa City, Chiba Prefecture.
The pH value was lower than the RpH value, and it was found that the electrical conductivity depends on the amount of precipitation. COD was measured from September 18, 2020 to December 11, 2020. As a result, although there are some fluctuations, it was clarified that the water quality is generally good according to the graph of the environmental standard (lakes) regarding the conservation of the living environment of the Ministry of the Environment.

Keywords: Spring water, Ichikawa, Chiba

©2021. Japan Geoscience Union. All Right Reserved.

Development of an automatic meteor shower observation and the notification system
~Web broadcast of meteor appearance~

*Koichi Sato[1], *Koshi Ri[1], *Shunsuke Isoda[1], *Honoka Ohno[1]

1. Chuo University Junior and Senior High School

Introduction

Radio meteor observation is a worldwide method using a receiver and antenna for receiving a specific radio wave frequency (*i.e.,* HRO or FRO method). Meteors traversing the ionosphere create ionizing trails. The HRO or FRO method is based on the characteristic that ionized meteor trail reflects radio waves in a certain frequency band transmitted from the ground. The audio data obtained by this method is output as image files by HROFFT or MROFFT software. The conventional method of radio meteor observation requires expensive devices such as receivers, and it is needed to construct the observation system. Therefore, we have developed an automatic observation system and a quick notification system of meteor appearance so that anyone can easily observe meteor showers. In our previous study, we have succeeded in constructing an automatic meteor observation system with HRO, completely automating the process from detection of meteor appearance signals to data output, and stably collecting quantitative data and meteor appearance information. The system we have developed was equipped with a function to broadcast only the analyzed values of audio data, which is recorded during meteor observation. Furthermore, it could be more user-friendly and practical when the system automatically detects the meteor appearance signals from the audio data and broadcasts the signals. In this study, we aimed to upgrade our system with a new function of “quick notification of meteor appearances.”

Method

Our system consists of three sections: 1) the radio meteor observation section using a 2-element antenna and radio wave receiver, 2) the analysis section using a computer with Arduino, and 3) the bot-transmitting section made by Python running on a computer. We carried on three experiments in this study: 1) transmitting the audio (recorded) data of meteor observation to the devices, 2) transmitting the audio (in real-time) data of meteor observation to the devices, and 3) analyzing the audio (recorded) data and notifying the meteor appearance to the devices when a meteor appearance signal was detected.

Results and Discussion

The meteor audio data was analyzed by the Fast Fourier Transform (FFT) library in Arduino in order to extract the specific data observed at the time of meteor appearance (data with a frequency of approximately 495 Hz where the volume increases significantly). And then, we converted the meteor appearance data into the text data. The text data was shared and broadcasted to the bots created on Discord and LINE platforms.

In Experiment 1, the data transmitted by the bot running on Python was consistent with the received data

©2021. Japan Geoscience Union. All Right Reserved.

on the devices. It means that a “quick notification of meteor appearance system” was available. In Experiment 2, we succeeded in transmitting the data in real-time without any significant difference. In Experiment 3, we demonstrated a function to analyze the audio data and notify the meteor appearance to the devices when the meteor appearance signal was detected. Therefore, we succeeded in completely automating the procedure from the radio meteor observation section to the bot-transmitting section with a low-cost and simple method.

This system automatically distinguishes the meteor appearance signal from noises by analyzing the audio data collected during the radio meteor observation. When a meteor appearance signal is detected, the signal is broadcasted simultaneously to the devices as meteor appearance information. Our new system is expected to obtain the meteor appearance information easier with personal devices (*e.g.,* smartphones).

Conclusion

Our system with new functions allows us to broadcast the meteor appearance information to the individual devices in real-time at low-cost, instead of the conventional high-cost method. Our next goal is to provide “meteor shower forecasting” using our detecting system of the meteor appearance signals and the data storage system.

Keywords: Radio meteor observation, Automatic web broadcasting, Arduino, Python

©2021. Japan Geoscience Union. All Right Reserved.

Meteorological and geographical conditions of river flooding-Comparison of the past and present of the Miyata River-

*Eri Yoshida[1], *Minami Oikawa[1], *Kotomi Shibata[1], *Chihiro Terazaki[1], *Kurumi Yabe[1]

1. Ibaraki prefectural Hitachi first senior high school

In recent years, heavy rain disasters have occurred frequently all over the country. During the 2019 typhoon in East Japan, the Naka River (Mito City, Ibaraki) and Kuji River (Hitachiomiya City, Ibaraki) were flooded, but the Miyata River (Hitachi City, Ibaraki) did not flood. We investigated if the Miyata River was resistant to flooding, and as a result, we found that if flooded when Typhoon Kathleen approached the Kanto region in 1946.

Therefore, we wanted to consider the cause of river flooding geologically, categorize the conditions under which flood damage occurs, grasp the causes of disasters in advance, and utilize this knowledge for disaster mitigation.

Currently, we are investigating flood damage during the period from 2010 to July 2020, and investigating the relationship between the average slope of flooded rivers and precipitation per unit time, but no typified relationship was found. In the future, we plan to further analyze flooded rivers nationwide and conduct a field survey of the flooded areas of the Miyata River.

©2021. Japan Geoscience Union. All Right Reserved.

Where are solar panels actually used? Research on the present situation of Kashiwa City, Chiba prefecture, Japan.

*Souri Mizukami[1]

1. SHIBYA SENIOR HIGH SCHOOL

The purpose of this study is to find out where the solar panels are widely used. I comparedthe land-cover map created by JAXA with Google Earth to see the distribution of solar panels. I analyzed the data with QGIS to find where the solar panels are actually used.

Keywords: Land use, Agricultural land, solar panels



©2021. Japan Geoscience Union. All Right Reserved.

Decline and Fall of Martian Polar Capse; Whether the Dast Storm Is Warm the Polar Cap

*Kei Inoue[1], Hibiki Aminaka[1], Yuho Takagi[1], Nanami Yasuda[1], Yuki Tanaka[1], Tomoki Ugawa[1], Rio Mogi[1], Kyouka Miyake[1], Momoha Takashima[1], Mako Misumi[1], Kaho Okada[1]

1. Kumamoto Prefectural Daiichi High School

Mars in 2020 approached the earth for the first in two years. According to our previous research, Mars in 2018 had a global dust storm which cover Mars. It turned out that the dust storm promoted increasing in temperature and it decreased Martian polar ice cup’s surface area earlier than usual. Therefore, we set up a hypothesis that a dust storm warms up Mars’s atmosphere. The purposes of this study are researching Martian south polar ice cup’s surface area change in 2020 and we reveal the effect of the dust storm on Mars’s atmosphere through the experiment.

We collected 169 photos of Mars taken in all over the world from Internet, and we calculated Martian polar ice cup’s surface area. As a result, we found the area change is the same as Mars without a dust storm. We can say that the dust heats up Mars’s atmosphere. Moreover, we found Mars in 2020 had a dust storm from November 12 but it had nothing to the area change because the polar cap had been very small.

In the second place, we tried the experiment to consider atmospheric effects by using pyranometers and incandescent light bulb. We prepared the following four models. “Dust floating in the high altitude”, “Dust floating in the low altitude”, “There is no dust”, “Volcanic ash covering the earth”. We substituted the rock wool for the dust and volcanic ash. We observed temperature change through warming each model with incandescent light bulb.

The following are result of the experiment. Model with the largest temperature rise was “Dust floating in the low altitude”. In addition, this kept holding heat even after turning off the light. Model with the second largest temperature rise was “There is no dust”. However there was sudden temperature drop. “Dust floating in high altitude” hardly increased in temperature compared to the above two. “Volcanic ash covering the earth” had very little change. This is most unaffected by solar radiation.

According to results of the experiment, dust storm in 2018 corresponds to “Dust floating in low altitude”. Volcanic ash reduces temperature then there are dusts in the sky. (Parasol effect) On the other hand, the global dust storm has the ability to increase temperature.(Greenhouse effect) In this way, there is the exact opposite temperature change. We consider the cause is dusts rise from the surface of Mars.

We want to keep continuing this study. Future prospects are elucidation of the dust storm mechanism and occurrence condition. In addition, we will use the experimental methods. For example, not only Mars, but also phenomena on earth.

©2021. Japan Geoscience Union. All Right Reserved.

Spacial correlation between slow earthquake and mantle- derived hot spring in Southwest Japan

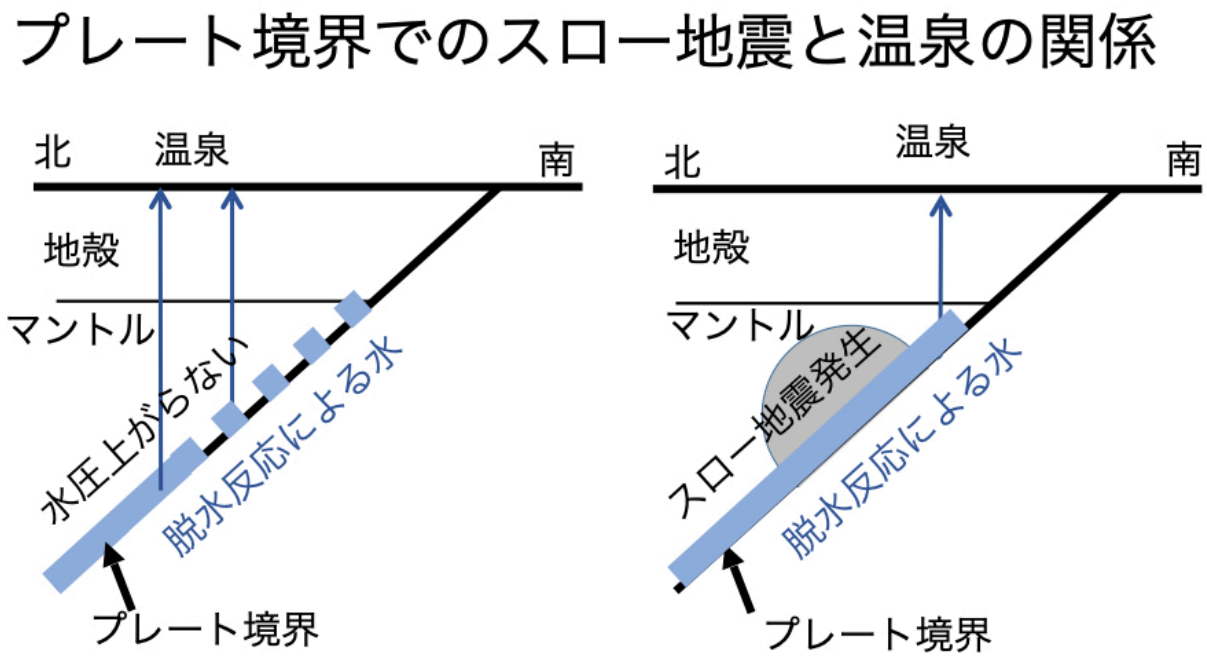
*Yui Kobayashi[1]

1. Shizuoka Higashi High School

Slab-derived fluids cause slow earthquakes and mantle-derived hot springs in Southwest Japan arc. In this study, the relationship between the locations of slow earthquakes and the mantle-derived hot springs in Southwest Japan is studied. Spacial correlation is evaluated between the number of slow earthquakes (National Research Institute for Earth Science and Disaster Prevention database) and Li/Cl values ratios of mantle-derived hot springs (AIST Deep Groundwater database). When the locations of slow earthquake are shifted 7 km to the south, the correlation is the largest. This indicates that the mantle-derived hot springs are located to the south of the region where the slow earthquakes are occurring (Figure).

Explanation of figure.
Schematic diagram showing the slow-earthquake occurring in the fluid-filled region in the slab-mantle boundary and the mantle-derived hot springs coming from the margins of the slow-earthquake region.

Keywords: slow earthquakes, Slab-derived fluid, mantle-derived hot springs



©2021. Japan Geoscience Union. All Right Reserved.

Visualize water current using vitamin B_2

*Mutsuki Kamata[1], *Yuuma Nakagawa[1], *Io Kato[1], *Tokito Hirose[1], *Yuuki Matsui[1], *Kosuke Mafune[1], *Akihito Yamada[1], Kazumi Igawa[1]

1. Zushi-Kaisei Senior High School

The deep ocean current mainly sinks in the polar regions such as off the coast of Greenland and in the Weddell Sea in the south pole. Then, it comes up to the surface in the Pacific and the Indian Ocean after making a circuit of Earth. Therefore, this current plays one of the important roles in long-term heat transportation in the polar regions, low latitudes and middle latitudes and has a great influence on Earth climate. However, there are many things that haven't been solved yet. The mechanism of upwelling is a prime example. The reasons for its sinking in the polar regions are low temperature and the high salinity of water. Nevertheless, the mechanism of its upwelling in the Pacific and the Indian ocean hasn’t been solved yet and people have been still studying.

These days global warming clearly begins to have an influence on our lives, so it is necessary to take measures against it. However, it is important to understand Earth’s potential climate control function more deeply to make global warming slower and realize the best living environment for all living things, including human beings.

For this reason, we have experimented by reproducing submarine topographies in an aquarium on the basis of a hypothesis that they have an influence on upwelling, and we have searched into what causes upwelling to discover the mechanism of its upwelling. Concretely, we set ices on the left end of the aquarium to reproduce low seawater temperature at polar regions and set mimicked seamounts made of plaster to reproduce submarine topography such as ridge, hotspots in Indian ocean. Also, we visualized water current using aqueous solution dissolved blue ink and try watching turbulence caused by current’s hitting seamounts and upwelling water. In addition to those, not only visualization but also measurement did we make by setting High speed Response Temperature Progs (given by Shimazu-Rika) one by one and changing their height to measure water temperature by 0.01℃ every 0.1 second, and try quantifying water current too detail for us to watch.

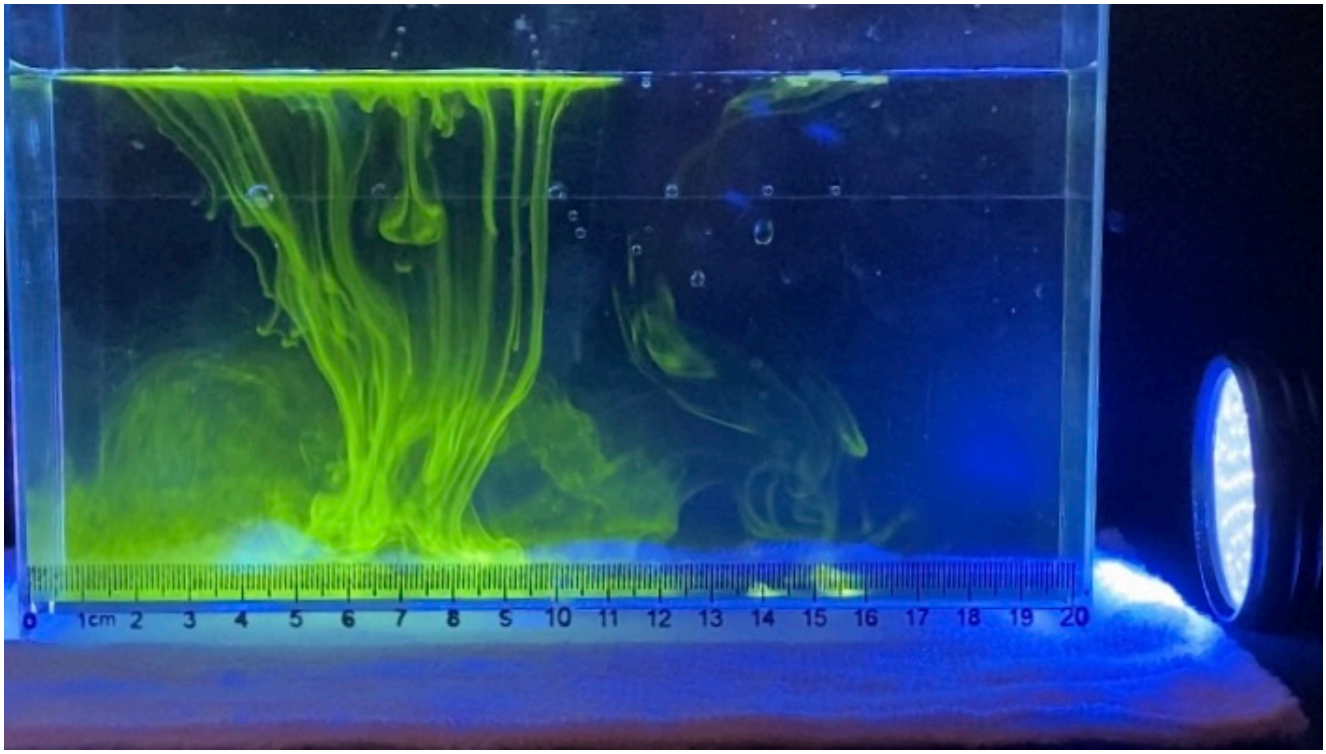
However, visualizing with ink has various problems. For example, because of aqueous solution’s uniformity, ink will spread all over the aquarium and the ink’s concentration is getting lower, so it gets more difficult to perceive ink. Besides, from the beginning, ink is difficult to perceive. Therefore, we focused on vitamin B_2’s fluorescent action and thought that we can improve such ink’s defect if we use powdered vitamin B_2 instead of ink. For this reason, we tried to visualize water current using vitamin B_2. Also, we groped for a method to use powdered vitamin B_2 for almost indefinite time without consuming powder by putting ingenuity into powder as it has advantages.

The new visualization method found through this study will be very useful in making a consideration about the deep ocean current from now on, this will make it easier to visualize sea turbulence and will be possible to observe accurately. Also, the way we present this time is considered that it can be applied to various fields on visualizing the current, at this conference, nothing is more pleasing if the way we use vitamin B_2 becomes popular from now on. We will announce visualization of sea turbulence we

©2021. Japan Geoscience Union. All Right Reserved.

experiment using vitamin B_2 we mentioned above and the ability of vitamin B_2.

Keywords: Sea



©2021. Japan Geoscience Union. All Right Reserved.

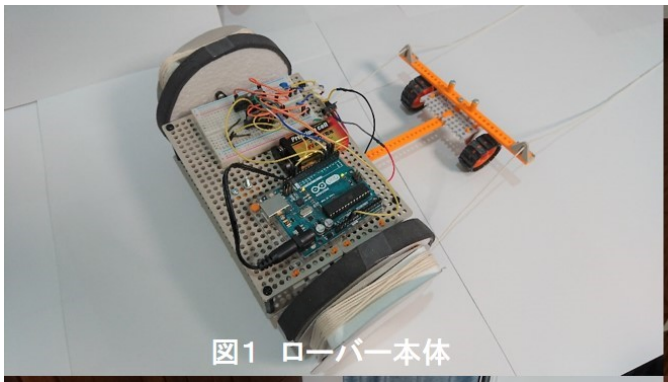
Designe of lunar crater exploration rover

*Kosuke Kameoka[1]

1. Meikei High School

The purpose of this study is to design a lunar rover that runs stably and securely on the sloping surface of lunar craters. First, I produced a rover of specification to keep the balance of the body with a rope. Second, I sent the rover in three courses that imitated the slope of the lunar craters. It ran under the three conditions; slope angle, surface relief and gravity, and evaluated the performance with two standards. Results of three type of driving experiments showed that the rover could run safely on the course. It is concluded that the rover have the potential to drive stably on the slopes of lunar craters.

Keywords: driving test, Arduino, simulated track


図1　ローバー本体

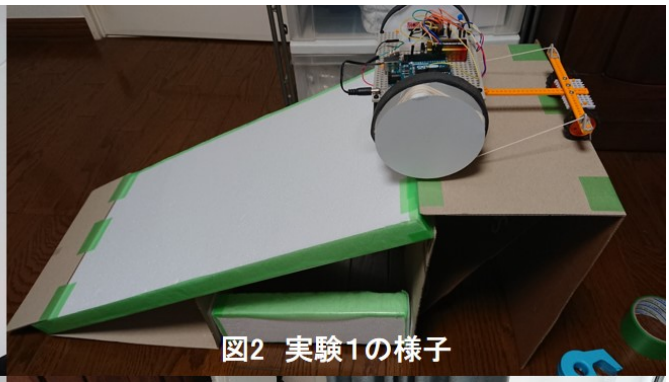

図2　実験1の様子


図3　実験2の様子


図4　実験4の様子

©2021. Japan Geoscience Union. All Right Reserved.

Distribution of Gravel in the Sakawa River and Factors Affecting the Distribution

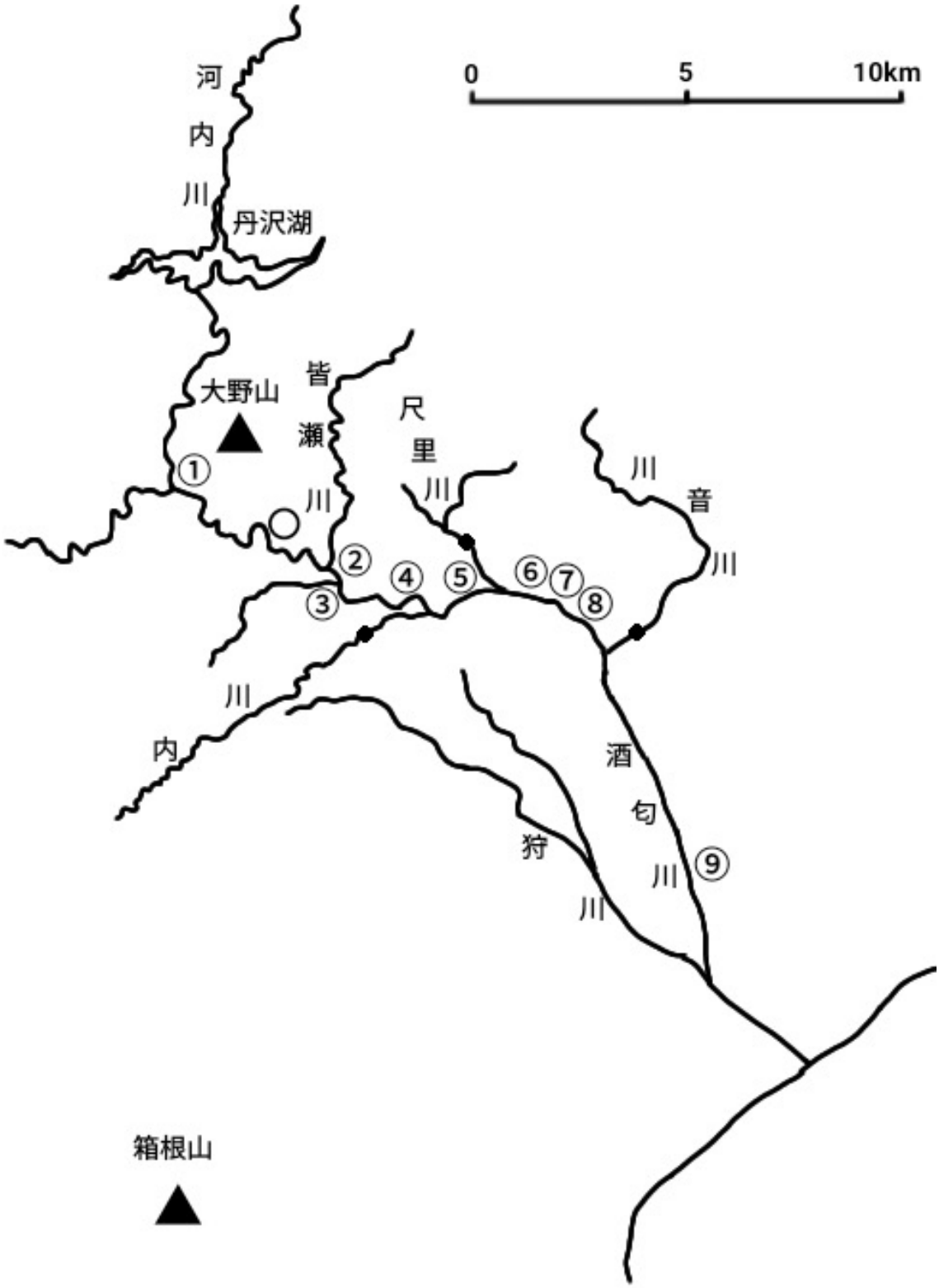
*Nozomi Uemachi[1], *Misaki Yamamiya[1], Yosuke Saito[1]

1. Tokyo Gakugei University Senior High School

The distribution of rock in the midstream and downstream of the Sakawa River was studied.
In this study, two types of samples were taken at nine points: the first was 200 rocks collected in order of size from the surface of a 1m x 1m frame; the second was the 10 largest rocks within 10m from the frame. The investigation has been done three times. In the first stage, the rock distribution in the midstream and downstream of the river was surveyed at points 1, 6 and 9 in the attached map. The result was that several kinds of gravel decreased We hypothesized that this was due to the topographical characteristics of the fan and the valley bottom plain, and conducted the second stage of the survey at points 3, 4, and 5 shown in the attached figure, sandwiched between the valley bottom plain and the fan edge, respectively. In the third stage, to confirm these hypotheses, the surveys were conducted at point 2 in the attached map, which is upstream of the weir at point 3, and at points 7 and 8, which are the middle and lower parts of the same sandbar as point 6.
In conclusion, in addition to the armoring and the feature of the grain size distribution of the sandbar, the following four things were found from the first and second stages of the survey. First, large rocks were deposited due to selective transport in the two sections where the river gradient and depositional topography changed. The average grain size and weight percentage of tonalite and green schist decreased rapidly between points 3 and 4. These types of rocks were deposited by selective transport because of their large average grain size at point 3. Andesite, basalt, and fine-grained tuff were deposited by the same principle between points 4 and 5. Secondly, sandstone and conglomerate were rarely found in the area after point 6, suggesting that clastic rocks were susceptible to abrasion. Third,as there was almost no increase in the number of rocks that could be supplied by the tributaries at the points after the tributary confluence, it can be said that the tributaries in the middle and lower reaches did not affect the gravel distribution in the mainstream. Finally, the weight percentage of andesite and basalt and the grain size of the largest rock increased at point 4. The possibility that the andesite and basalt are supplied by the Sekimoto Hills and Asama Mountain in the vicinity of this point is under investigation. The results of the third stage of the survey are currently being analyzed. We would like to make a presentation including these results.

Keywords: The Sakawa River, river bed stones, sorting, abrasion, sandbars, armoring

©2021. Japan Geoscience Union. All Right Reserved.



©2021. Japan Geoscience Union. All Right Reserved.

Detection of Cherenkov light with acrylic and photodetecto

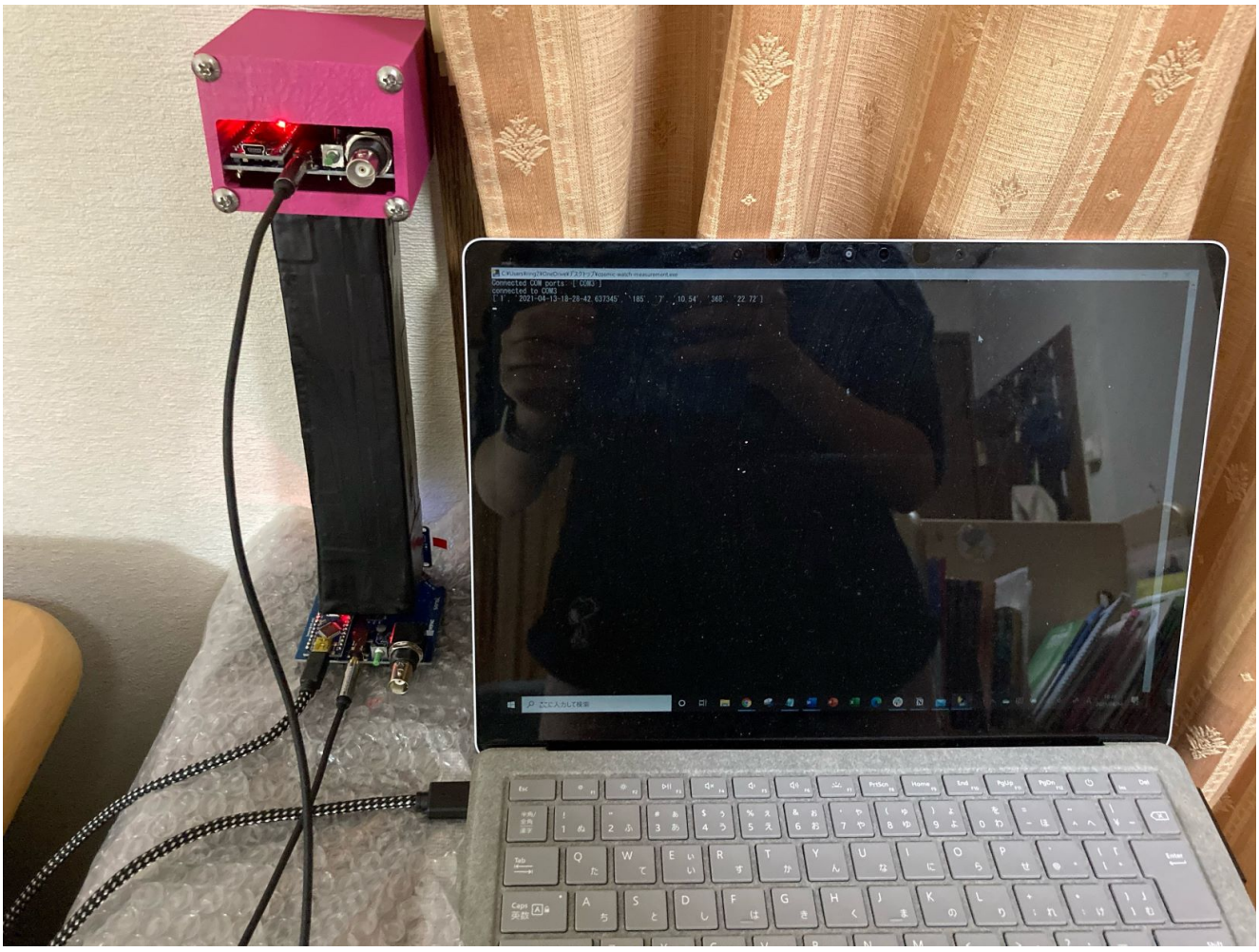
*Juri Urano[1], *Yuka Kuze[1], *Kaho Kubota[1]

1. Toshimagaoka Joshigakuen senior high school

We detected Cherenkov light with a handmade cosmic-ray detector so-called "Cosmic Watch". Cherenkov light is observed when cosmic ray goes through the substances which have a large refractive index. In this research, we used acrylic (4 cm * 4 cm * 20 cm). We flattened the surface of the acrylic with some pieces of sandpaper and abrasive to improve the transmission of the Cherenkov light to the photodetector sensor. We covered the acrylic with aluminum foil and black plastic tape to shading and shielding from electrical noise and light leakage. We put another Cosmic Watch with a plastic scintillator on the Cosmic Watch with acrylic and measured signal coincidences to prevent noise detection.

In this research, we succeeded in detecting a Cherenkov light in a certain condition. We would like to optimize for detection of Cherenkov light by changing conditions like material or its size.

Keywords: Cosmic Rays



©2021. Japan Geoscience Union. All Right Reserved.

Research the View of Mt.Fuji with a Self-Made Observation Device

*Ryoo Niigawa[1], *Rin Takezoe[1]

1. Tokyo Metropolitan Tachikawa High School

The astronomy meteorology club at our school has been making meteorological observations including visibility for more than 70 years. Visibility is the maximum distance at which objects can be clearly seen with the naked eye, and has been used as an indicator of air pollution. 4 years ago, a senior started a study to analyze visibility observation data for the past 50 years. Last year, a senior developed a new visibility observation device that uses a camera controlled by a small computer to take pictures regularly. In this study, we made a similar device to photograph around Mt. Fuji, and investigated the relationship between the view of Mt. Fuji and surrounding clouds and meteorological phenomena.
Analysis of past visual visibility observation data showed that the ratio of the number of days Mt. Fuji was visible per month was more than 50% in winter and less than 10% in summer.
The cloud characteristic of Mt. Fuji was noticed and analyzed from the photographing data for 6 months. As a result, most apron clouds occurred in midwinter, and they were associated with low temperatures at the top of Mt. Fuji. Cap clouds occurred three or four times a month, and they were associated with high humidity at the top of Mt. Fuji.

Keywords: Mt.Fuji, Visibility, Cap clouds, Apron clouds

©2021. Japan Geoscience Union. All Right Reserved.

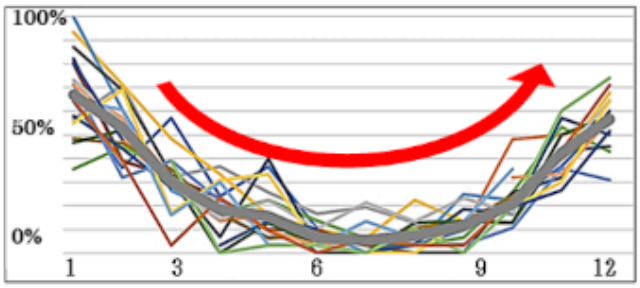


図1　過去の富士山が見えた日数の
1年間の変化(1959～1985年)



図2　観測装置が撮影した前掛け雲(上)と笠雲(下)

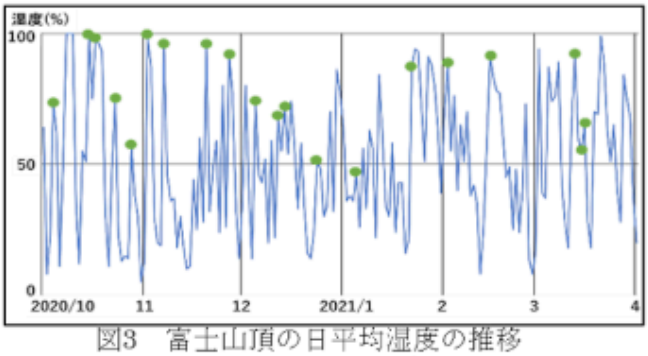


図3　富士山頂の日平均湿度の推移
（笠雲発生日に丸）

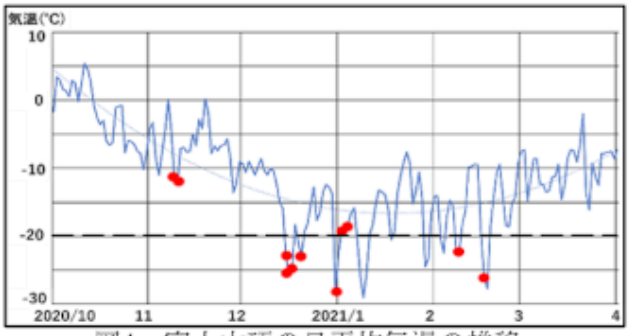
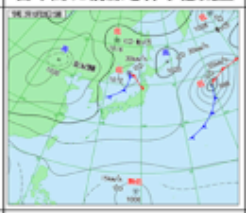
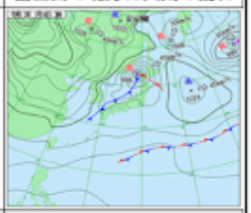


図4　富士山頂の日平均気温の推移
（前掛け雲発生時に丸）

表1　それぞれの気圧配置の例と
当てはまる事例の割合

	日本海に前線を伴う低気圧	富士山の北方に大気の乱れ
天気図の例		
日本大学の研究 2002/9/28～ 2003/3/31	9回/31回 ＝ 29%	18回/31回 ＝ 58%
我々の観測 2020/9/25～ 2021/3/31	5回/ 21回＝ 24%	13回/21回 ＝ 62%

©2021. Japan Geoscience Union. All Right Reserved.

Bad visibility in the past at Tachikawa High School

*Tomoya Ushizaka[1]

1. Tokyo Metropolitan Tachikawa High School

Transitions of visibility in the past for 10years in TachikawaVisibility is a meteorological term indicating the distance with which an object can be identified from the observation site and is information to measure how far we can see.
It is used as an indicator of air pollution.
Tachikawa high school astronomy meteorological club have been observing visibility for about 70 years since the 1950s.
A senior of the club conducted a survey focused on visibility and analyzed data.
The results show the condition of visibility was very bad in Tachikawa in the past.
In this study, the cause of visibility was investigated by comparing the data of visual range data for about 10 years from 1957 when visibility was the worst with recorded meteorological phenomena (smoke, haze, fog, inversion layer, and wind dust).
For the survey, we used monthly reports written in the past and interviewed our alumni.
The data of visibility showed that visibility tended to be poor in winter especially in the morning and phenomena such as soot, haze and inversion layer were more frequent during the same period than the present.
After 1965, the number of soot and haze decreased and the visibility tended to improve accordingly.
Also, unlike the soot and haze generated by the soaring dust and dirt, the inversion layer and fog caused by changes in temperature did not increase nor decrease throughout the 10 years.
The author discovered that the poor visibility and the occurrence of meteorological phenomena related to visibility are associated with each other.

Keywords: visibility , meteorological, air pollution

©2021. Japan Geoscience Union. All Right Reserved.

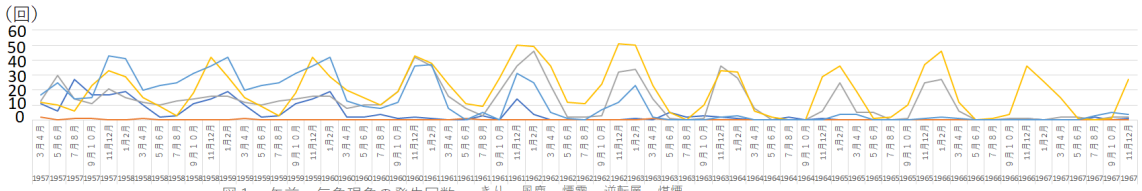


図１　午前　気象現象の発生回数

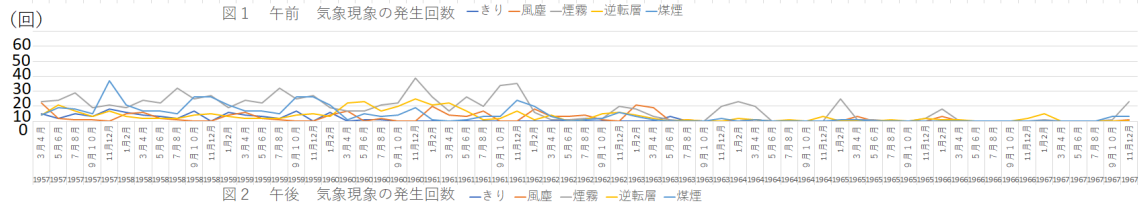


図２　午後　気象現象の発生回数

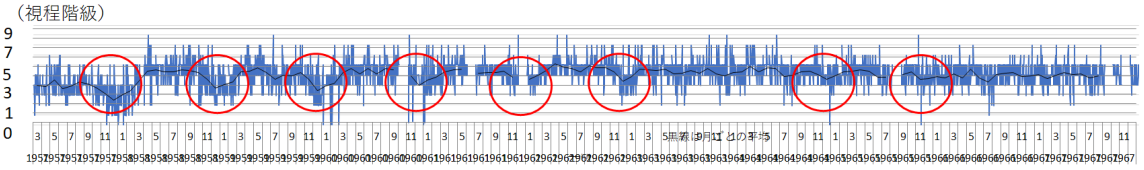


図３　午前の視程階級

赤丸で囲った部分は視程が悪化していた部分

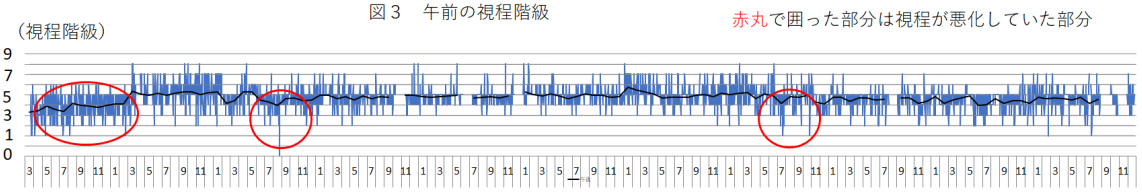


図４　午後の視程階級

視程階級	目標物を認めることができる最大距離
0	50m未満
1	50m以上　200m未満
2	200m以上 500m未満
3	500m以上　1km未満
4	1km以上　2km未満
5	2km以上　4km未満
6	4km以上　10km未満
7	10km以上　20km未満
8	20km以上　50km未満
9	50km以上

図５　先行研究にて作成された本校オリジナルの視程階級表

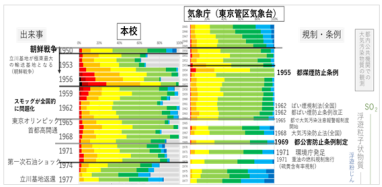


図６　先行研究にて作成した本校の視程のデータと気象庁のデータ



図７　当時の記録が残っている月報



図８　立川基地新聞

©2021. Japan Geoscience Union. All Right Reserved.

Analysis of visibility around Tachikawa High School

*Takumi Yasuhara[1]

1. Tokyo Metropolitan Tachikawa High School

In Tachikawa high school, we have continued weather observations including visibility for about 70years, but the number of missing data has been increasing since 1985. The visibility observation was resumed several years ago. However, because it was difficult to continue the observation on time, a senior person made an observation device for visibility by himself. In this study, the relationship between weather phenomena or air pollution and visibility was investigated by analyzing the tendency of visibility. As a result, it was found that changes in visibility were affected by weather and seasons. It was also found that the visibility in the morning is worse than in the afternoon due to the influence of forward scattering. In the future, we aim to automate visibility judgement by deep learning.

Keywords: Meteorology, Visibility, Visibility Observations

©2021. Japan Geoscience Union. All Right Reserved.

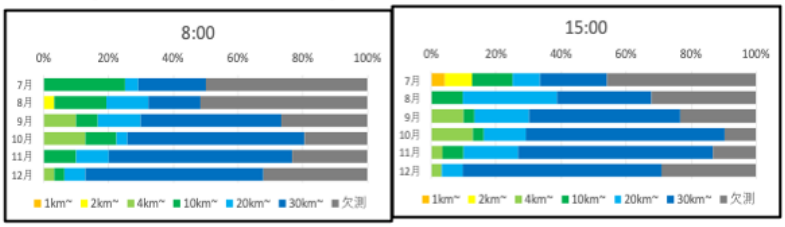
視程階級表

視程階級	視程距離	番号	目標物
1	0.1km	①	目の前のマンション
2	0.45km	②	YAZAWA Deux Bldg.
3	0.75km	③	立川病院
4	1.0km	④	ラポール西国立
5	3.0km	⑤	一橋大学法人本部棟
6	4.3km	⑥	多摩総合医療センター(府中病院)
6	4.9km	⑦	ライオンズガーデン西国分寺
7	13km	⑧	グレーシアタワー三鷹
8	25km	⑨	新宿ビル群
8	36km	⑩	東京スカイツリー

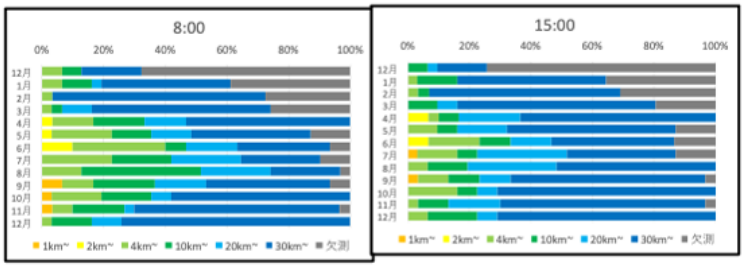


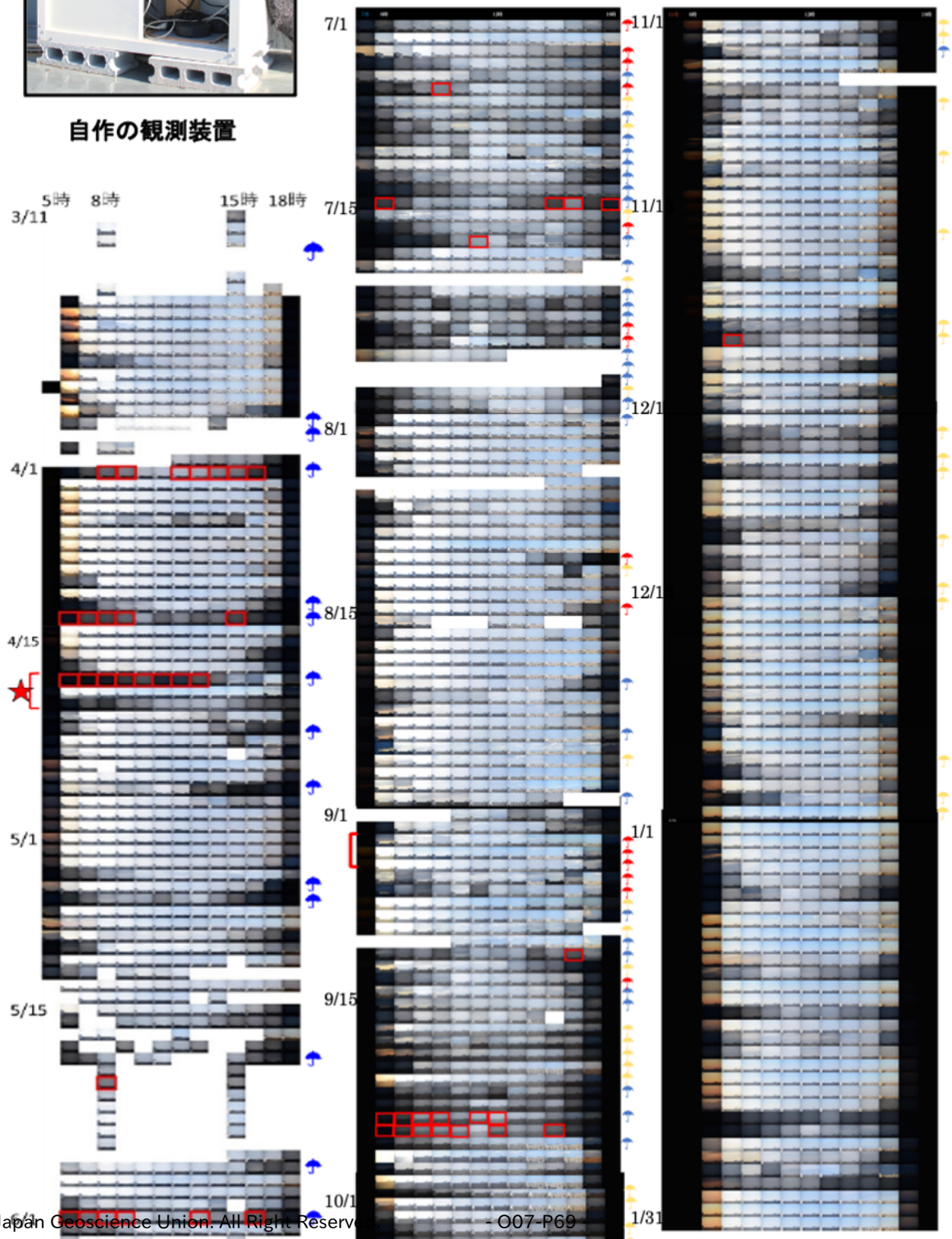
自作の観測装置

目視による月ごとの視程(8時・15時)



画像による月ごとの視程(8時・15時)





©2021. Japan Geoscience Union. All Right Reserv

©2021. Japan Geoscience Union. All Right Reserved.

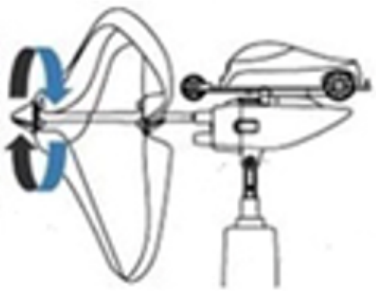
The relationship between the shape and power generation amount of the simple wind power generators

*Sora Fukui[1]

1. Tokyo Metropolitan Tachikawa High School

Since I was interested in the relationship between the shape of the wind power generator and the generated power, I conducted three experiments using a simple wind power generator of my own making and examined the relationship between the shape of the generator and the generated power. In the first experiment, the amount of power generated at each constant wind speed was measured using the loopwing type, and the value was smaller than the ideal value as the wind speed increased. This calls for more efficient use of power. In the second experiment, a multi-wing type generator and a savonius type generator were made. The savonius type was made by reusing discarded bicycles and unused buckets. Using these data, the wind velocity at the time of maximum power generation and minimum power generation was measured, and the power generation per unit wind-receiving area was calculated. On the other hand, the multi-winged wind generator had the advantage of starting to spin in a weak wind than the savonius type generator. In the third experiment, the generated power and the wind velocity were measured on the roof of the school using the wind power generator. As a result, the problem of stable electricity supply became clear.

Keywords: wind power generator, hub dynamo, stable supply



図ループウィング型



図 多翼型



図 サボニウス型

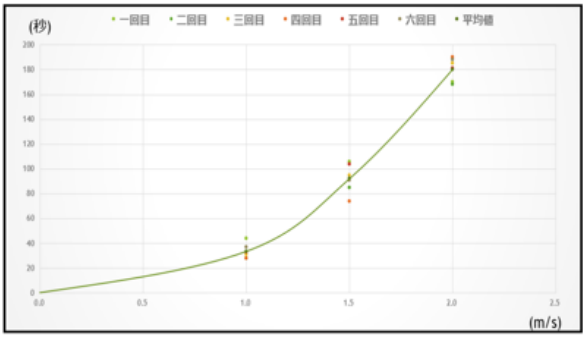


図 ループリング型を用いた実験結果

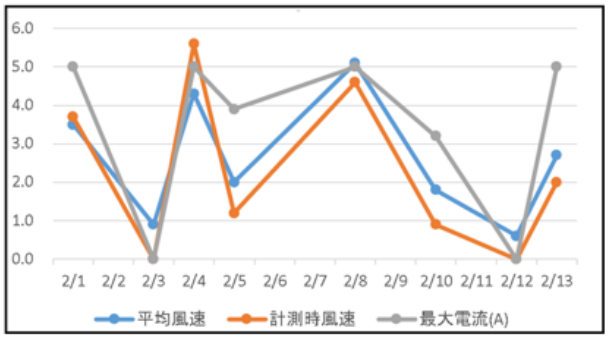


図 屋上での多翼型を用いた実験結果

©2021. Japan Geoscience Union. All Right Reserved.

Is «evacuate to rise »the Right Action?

Research and Proposition of Major Evacuation Routes to Shelters in Shibuya

*Sakura Oona Marie Sueoka[1]

1. Tokyo Metropolitan Kokusai High School

Is «evacuate to rise »always the right action?
In this research, I have verified the famous phrase "evacuate to rise". Furthermore, I have evaluated 15 shelters certified by the Shibuya City, and proposed major routes to these shelter from different points.

Keywords: Earthquake, Evacuate, Natural Disaster

©2021. Japan Geoscience Union. All Right Reserved.

Mechanism of how the Shirata river looks blue

*Shuhei Sugai[1], *Ryosuke Yoshida[1]

1. Shimoda high school

The Izu Peninsula, which faces Suruga Bay on the east side and Sagami Bay on the west side, is located at the eastern end of Shizuoka Prefecture. The Shirata River flows through the Izu Peninsula, and there was a sulfur mining trace upstream. We began our research with an interest in the pale-blue-looking points downstream, and eventually verified the sulfur production and also conducted a water quality survey of the surrounding area. At the site, pH was measured at each point of the mainstream and tributaries of Shirata River. We brought back the clay from the sulfur mining trace, and our analysis showed that the sulfer was contained 30% of the mass of the clay. The Shirata River, which supports the water supply in Higashiizu Town, was also the place that caused the oldest pollution in Japan from the Edo period to the Meiji period. We need to know more the Sirata River in order to coexist with peace of mind.

Keywords: Shirata River, Izu Peninsula, sulfur, colloid, water

©2021. Japan Geoscience Union. All Right Reserved.



©2021. Japan Geoscience Union. All Right Reserved.

Determining the Properties of Seyfert Galaxies

*Kuya ABE[1], *Kuranosuke IEHATA[1], *Koki TANII[1], *Tamotsu FUJIMOTO[1]

1. Nara Prefectural Seisho High School

Spectroscopic observations of ten Seyfert galaxies were performed at the Bisei Observatory in Okayama Prefecture and the data was analyzed using “BeSpec” software. The width and intensity of Hα, Hβ, He II, [N II], [O III] and [S II] emission lines were calculated. The result was the, type 1 galaxies products the so wide emission lines of hydrogen and helium. In contrast, it was found that type 2 galaxies produced emission lines for helium, sulfur and nitrogen which were slightly longer than the overall sample mean. In conclusion, it was determined that hydrogen and helium are found in the cores of Seyfert galaxies whereas there oxygen, nitrogen and sulfur are distributed throughout the fringe areas of Seyfert galaxies. Furthermore, we categorized the type of 6 galaxies again.

Keywords: Spectroscopic observation, Emission line, Active galactic nucleus

表　観測データから求めた各銀河の輝線幅（FWZI）

銀河名	型		観測日	輝線幅				
				He II	Hβ	[O III]	Hα	[S II]
NGC2782	–	1	2020.04.10	—	—	—	70.6	36.4
NGC3516	1.5	1	2020.04.10	—	50.0	28.1	139.2	24.0
NGC4151	1.5	1.5	2016.12.09	114.4	122.6	48.2	279.8	32.2
			2020.04.10	96.5	130.5	44.1	272.8	32.2
NGC5548	1.5	1	2020.04.10	16.5	107.6	36.3	258.0	43.0
NGC7469	1.2	1	2019.11.16	115.1	109.4	36.3	220.0	18.5
			2020.09.05	—	—	—	197.0	23.2
			2020.09.05	118.4	98.7	44.2	212.6	27.8
			2020.09.05	123.7	86.5	56.2	239.6	23.1
			2020.09.05	124.4	107.6	40.2	221.4	18.5
			2020.09.05	127.7	82.9	40.2	219.2	18.5
NGC3227	1.5	1.5	2020.04.10	84.4	96.1	44.1	159.3	27.6
NGC4051	1.5	1.5	2020.04.10	84.0	72.3	40.1	155.4	32.2
NGC1275	2	1.9	2016.10.21	45.6	69.7	44.5	148.6	25.0
			2019.11.16	58.2	57.3	60.2	131.5	23.9
NGC4258 （M106）	1.9	1.9	2020.04.10	—	—	26.5	36.4	28.7
NGC1068 （M77）	2	2	2016.10.21	78.4	54.7	72.3	136.7	44.4
			2019.11.16	71.4	44.1	67.8	116.0	32.2
			2020.09.05	—	49.4	—	—	—
			2020.09.05	68.1	53.8	68.2	138.9	41.4
			2020.09.05	72.8	51.2	64.1	132.0	36.8
			2020.09.05	78.1	55.6	72.4	143.0	31.0

©2021. Japan Geoscience Union. All Right Reserved.

Observation of Radio Waves from the Moon

*Koya YAMASHITA[1], *Ichika TSUTSUMI[1], *Atsushi HIRANUMA[1], *Ikumi MATSUYOSHI[1]

1. Nara Prefectural Seisho High School

There are radio waves from familiar things such as smartphone. These from the sun has already observed few years ago. However, these from the moon hasn’ t done yet. So, our research project is to survey relationship between intensity of the radio waves and moon age. On the other hand, we researched the apparent temperature too. First, we turned the antenna directly to the moon, sky and radio wave absorber. Second, we recorded these data which displayed by tester randomly, and analyzed them. As a result, Value of the moon radio waves were 0.109 0.272 0.270 0.245, and the moon age which is at that time were 13.4 4.9 7.9 11.9. In conclusion, the value of the full moon radio waves bear no relation to moon age, and surface temperature too. The cause of the result is difference of the moon`s altitude and the amount of cloud.

Keywords: Radio telescope, Moon age, Surface temperature

表　月齢と電波強度・月の表面温度の関係

	2020/12/28 18:36	2021/1/18 18:28	2021/1/21 18:23	2021/1/25 18:14
月の形（月齢）	小望月（13.4） 	三日月（4.9） 	半月（7.9） 	十日夜の月（11.9） 
気温Ta（℃）	8.0	2.0	7.0	9.0
高度（° ）	37.1	38.4	65.3	53.5
電波強度 $\frac{Vmoon-Vsky}{Va-Vsky}$	0.109	0.272	0.270	0.245
Tmoon（℃）	30.6	75.1	75.7	69.1

©2021. Japan Geoscience Union. All Right Reserved.

Making Snow Meter Using Neutron Cosmic Rays Observation Data Collected By Cosmic Watch

*Kei Ikushima[1], Rikako Kono[2], Kaduo Tanaka[2], Akita Yuji[1]

1. Hiroo Gakuen High School, 2. Touhoku University

One of the methods to observe volcanic activity is to measure the change in gravity, but in winter, snow falls on the gravity measuring instruments and affects the measurement due to the gravity of the snow. In order to correct for this, it is necessary to measure the amount of snowfall and modify the data. The use of cosmic rays has been attracting attention as a method to measure the amount of snow cover. In this method, a cosmic ray detector is placed under the snow, and the amount of snow cover is calculated from the decay of the cosmic ray energy. In this study, we aimed to reduce the cost of this method by using Cosmic Watch, an inexpensive and compact cosmic ray detector. The cosmic ray detector consists of two main components: a scintillator and a photomultiplier. The scintillator emits a small amount of light when a cosmic ray penetrates it, and this light is measured and recorded as an electrical signal using a photomultiplier. The voltage value of the electrical signal obtained is proportional to the energy of the cosmic ray. In this study, two cosmic ray detectors are stacked on top of each other and only the data detected simultaneously by the two detectors are recorded. By using the coincidence measurement, the noise data other than cosmic rays can be reduced drastically.
When neutron cosmic rays pass through snow, the energy of the cosmic rays decays in proportion to the amount of snow cover, so the amount of snow cover can be calculated by measuring the energy of the cosmic rays. However, Cosmic Watch can observe many other cosmic rays in addition to neutrons, so it is necessary to collect only the neutron data needed for the snow meter. To do this, we need to perform Pulse Shape Discrimination (PSD), which is a cosmic ray analysis method to determine the type of cosmic ray by integrating the voltage decay of the waveform data of the electrical signal obtained from the photomultiplier. This method is based on the fact that the attenuation of the electric signal is different for each type of cosmic ray depending on the characteristics of the scintillator. I installed a scintillator called EJ276, which can easily perform PSD of neutrons, in Cosmic Watch to collect data of neutron cosmic rays. In order to obtain a waveform outline, the voltages were acquired continuously over a number of times. Now that we are able to obtain neutron data through PSD, we would like to conduct experiments using actual snow and water tanks to see if we can correctly calculate the amount of snow and water from neutron cosmic rays.

Keywords: Cosmic rays, Neutron, Arduino, Snow meter

©2021. Japan Geoscience Union. All Right Reserved.

Water storage capacity of the green dam –Role of forest soil -

*Nanami Aoki[1]

1. Kyoto Prefectural Sagano High School

In the Sagano High School Woods for Field Studies (SWFS), we have been conducting research about the water source recharge function and flood mitigation function of the forest (Matsuki, 2019). The purpose of this study was to find out the water retention capacity of forest soil by conducting a soil profile investigation and a soil physical properties investigation at SWFS and three other locations with different pedogenic factors. As a result of the surveys, the soil of SWFS was classified as brown forest soil (wet) and those of Umihoshi Park, in northern Kyoto Prefecture, were classified into brown forest soil (slightly dry), reddish brown forest soil, and grey soil. It was discovered that the water retention capacity of the soils was greatly influenced by topographical factors. The survey of the soil in the valley of Umihoshi Park showed the gas phase rate was low and water permeability was poor, suggesting that rainfall could easily lead to Horton overland flow.

Keywords: Soil Profile, Hydraulic conductivity, Three phases of distribution, Soil penetration strength, Soil classification

©2021. Japan Geoscience Union. All Right Reserved.

Measurement of Radon Concentration for Earthquake Prediction in the Woods for Field Practice Owned by Sagano H. S.

*Ayaka Kawabata[1], *Takahiro Kawabata[2]

1. Kyoto Prefectural Sagano High School, 2. Graduate School of Science, Osaka University

Radon is a gaseous, radioactive isotope formed in the decay chains of elements such as thorium and uranium. It has been identified that the atmospheric concentration of radon increases before earthquakes because it is released from the ground through cracks caused by the seismic stress.
In the present study, we measured the atmospheric radon concentration in the Woods for Field Studies owned by Sagano High School in order to examine the relationship between earthquakes and the atmospheric radon concentration. We acquired a "Radon Scout Professional" radon detector and tested its performance using two samples containing thorium and uranium. After the test, we placed it in a well-ventilated, water-proof container and installed it in the school forest. The measurements are still on-going. In this presentation, we will report the details of the measurements and our results.

Keywords: Experiment forest, Forest, Earthquake, Radon

©2021. Japan Geoscience Union. All Right Reserved.

[J] Poster | O (Public)：Public

Sun. Jun 6, 2021 1:45 PM - 3:15 PM JST | Sun. Jun 6, 2021 4:45 AM - 6:15 AM UTC | Ch.28

[O-07] Poster presentations by senior high school students

convener:Tatsuhiko Hara(International Institute of Seismology and Earthquake Engineering, Building Research Institute), Katsuyoshi Michibayashi(Department of Earth and Planetary Sciences, Nagoya University), Miwa Kuri(Japan Meteorological Agency), Keiko Konya(Japan Agency for Marine-Earth Science and Technology)

Senior high school students provide poster presentations on subjects in fields of earth and planetary sciences. This session provides an opportunity for senior high school students to give their presentations in the JpGU meeting and to have discussions with researchers. This session has been conducted as a public outreach session since 2006.

[E] Oral | P (Space and Planetary Sciences)：P-PS Planetary Sciences

Sun. Jun 6, 2021 9:00 AM - 10:30 AM JST | Sun. Jun 6, 2021 12:00 AM - 1:30 AM UTC | Ch.04 Zoom Room 04

[P-PS04] Small Solar System Bodies: A New Insight from Hayabusa2, OSIRIS-REx and Other Space Missions

convener:Tatsuaki Okada(Institute of Space and Astronautical Science, Japan Aerospace Exploration Agency), Taishi Nakamoto(Tokyo Institute of Technology), Daisuke Kuroda(Kyoto University), Chairperson:Tatsuaki Okada(Institute of Space and Astronautical Science, Japan Aerospace Exploration Agency), Taishi Nakamoto(Tokyo Institute of Technology), YACHEN YANG(Center for Space and Remote Sensing Research)

Small Solar System bodies, including asteroids, comets, satellites, and interplanetary dust particles, are notably important for understanding the origin and evolution of our Solar System, as well as investigating the sources of building blocks of life. Many new discoveries on small bodies have been carried out by observations from ground-based and space-based observatories, and explorations by spacecraft rendezvous and flyby. New perspectives on solar system evolution have been paved by analyses of extraterrestrial materials such as meteorites, IDPs, and return samples by space missions. Numerical and laboratory simulation studies have helped interpretations for those results and proposed new insights on these topics. In this session, new results of scientific studies and new ideas of methodology for investigating small solar system bodies are highly welcome, especially the topics on the remote sensing, surface experiments, and analysis of return sample in the Hayabusa2 and OSIRIS-REx missions, as well as the expectations and preparations for future missions including MMX, Destiny+, Hera, Comet Interceptor, and Hayabusa2-Extended missions.

9:00 AM - 9:05 AM JST | 12:00 AM - 12:05 AM UTC

[PPS04-01] Introduction

9:05 AM - 9:20 AM JST | 12:05 AM - 12:20 AM UTC

[PPS04-02] Interdisiplinary Science of Hayabusa2 Mission

*Sei-ichiro WATANABE[1], Hikaru Yabuta[2], Koji Wada[3], Naru Hirata[4], Naoyuki Hirata[5], Yuri Shimaki[7], Rina Noguchi[7], Seiji Sugita[6], Kohei Kitazato[4], Tatsuaki Okada[7], Noriyuki Namiki[8], Shogo Tachibana[6,7], Masahiko Arakawa[5], Satoshi Tanaka[7] (1.Nagoya University, 2.Hiroshima University, 3.Chiba Institute of Technology, 4.University of Aizu, 5.Kobe University, 6.University of Tokyo, 7.JAXA/ISAS, 8.National Astronomical Observatory)

9:20 AM - 9:35 AM JST | 12:20 AM - 12:35 AM UTC

[PPS04-03] Progress report of initial description of the C-type asteroid Ryugu samples returned by Hayabusa2

*Toru Yada[1], Masanao Abe[1], Aiko Nakato[1], Kasumi Yogata[1], Akiko Miyazaki[1], Kazuya Kumagai[2], Kentaro Hatakeda[2], Tatsuaki Okada[1], Masahiro Nishimura[1], Shizuho Furuya[1], Yoshitake Miwa[1], Ayako Iwamae[2], Lucie Liu[1], Lionel Lourit[3], Cedric Pilorget[3], Vincent Hamm[3], Jean-Pierre Bibring[3], Yuichiro Cho[4], Koki Yumoto[4], Yuna Yabe[4], Seiji Sugita[4], Shogo Tachibana[4], Hirotaka Sawada[1], Sakamoto Kanako[1], Tasuku Hayashi[1], Daiki Yamamoto[1], Ryota Fukai[1], Haruna Sugahara[1], Hisayoshi Yurimoto[5], Tomohiro Usui[1], Sei-ichiro WATANABE[6], Yuichi Tsuda[1] (1.Japan Aerospace Exploration Agency, 2.Marine Works Japan, 3.Institut D'Astrophysique Spatiale, 4.University of Tokyo, 5.Hokkaido University, 6.Nagoya University)

9:35 AM - 9:50 AM JST | 12:35 AM - 12:50 AM UTC

[PPS04-04] EXPERIMENTAL STUDY ON IMPACT CRATERS FORMED ON MOUNTAIN-LIKE SURFACE TOPOGRAPHY OF ASTEROIDS

*Yusaku Yokota[1], Masahiko Arakawa[1], Minami Yasui[1], Yuya Yamamoto[1], Sunao Hasegawa[2], Hatsune Okawa[1] (1.Graduate School of Science, Kobe University, 2.Japan Aerospace Exploration Agency)

9:50 AM - 10:10 AM JST | 12:50 AM - 1:10 AM UTC

[PPS04-05] The collisional history in the Main Belt
★Invited Papers

*Hiroshi Kobayashi[1] (1.Department of Physics, Nagoya University)

10:10 AM - 10:30 AM JST | 1:10 AM - 1:30 AM UTC

[PPS04-06] Internal structure of pebble-pile comets inferred from thermal and mechanical properties of dust aggregates
★Invited Papers

*Sota ARAKAWA[1] (1.National Astronomical Observatory of Japan)

[E] Oral | P (Space and Planetary Sciences) | P-PS Planetary Sciences

[P-PS04] Small Solar System Bodies: A New Insight from Hayabusa2, OSIRIS-REx and Other Space Missions

convener:Tatsuaki Okada(Institute of Space and Astronautical Science, Japan Aerospace Exploration Agency), Taishi Nakamoto(Tokyo Institute of Technology), Daisuke Kuroda(Kyoto University), Chairperson:Tatsuaki Okada(Institute of Space and Astronautical Science, Japan Aerospace Exploration Agency), Taishi Nakamoto(Tokyo Institute of Technology), YACHEN YANG(Center for Space and Remote Sensing Research)

Sun. Jun 6, 2021 9:00 AM - 10:30 AM Ch.04 (Zoom Room 04)

Small Solar System bodies, including asteroids, comets, satellites, and interplanetary dust particles, are notably important for understanding the origin and evolution of our Solar System, as well as investigating the sources of building blocks of life. Many new discoveries on small bodies have been carried out by observations from ground-based and space-based observatories, and explorations by spacecraft rendezvous and flyby. New perspectives on solar system evolution have been paved by analyses of extraterrestrial materials such as meteorites, IDPs, and return samples by space missions. Numerical and laboratory simulation studies have helped interpretations for those results and proposed new insights on these topics. In this session, new results of scientific studies and new ideas of methodology for investigating small solar system bodies are highly welcome, especially the topics on the remote sensing, surface experiments, and analysis of return sample in the Hayabusa2 and OSIRIS-REx missions, as well as the expectations and preparations for future missions including MMX, Destiny+, Hera, Comet Interceptor, and Hayabusa2-Extended missions.

9:00 AM - 9:05 AM

[PPS04-01]Introduction

©Japan Geoscience Union

Interdisiplinary Science of Hayabusa2 Mission

*Sei-ichiro WATANABE[1], Hikaru Yabuta[2], Koji Wada[3], Naru Hirata[4], Naoyuki Hirata[5], Yuri Shimaki[7], Rina Noguchi[7], Seiji Sugita[6], Kohei Kitazato[4], Tatsuaki Okada[7], Noriyuki Namiki[8], Shogo Tachibana[6,7], Masahiko Arakawa[5], Satoshi Tanaka[7]

1. Nagoya University, 2. Hiroshima University, 3. Chiba Institute of Technology, 4. University of Aizu, 5. Kobe University, 6. University of Tokyo, 7. JAXA/ISAS, 8. National Astronomical Observatory

Asteroid explorer *Hayabusa2* completed its proximity operation around C-type asteroid Ryugu and returned to Earth with surface sample. More than 5 g of the particles in the sample catchers were successfully retrieved and wait for analyses. We will review the interdisciplinary science of *Hayabusa2* mission based on the proximity observations through visible and thermal IR imaging, NIR spectrometer, LIDAR, and the Small Carry-on Impactor (SCI) experiment, which will give a strategy of the return sample analyses. The SCI experiment reveals crater-to-impactor size ratio on Ryugu is more than 60 [1], contrast to the lower value of 10 derived from the size-frequency distributions of the main-belt asteroids and craters on the asteroids already explored [2]. This will change the chronology of the material transport process from the main asteroid belt to the Earth region. Based on the SCI scaling law, the surface age of Ryugu is estimated to be ~16 Ma, which is much shorter than the estimated ages (100 Ma to 1 Ga) of the candidate source collisional families in the inner asteroidal belt. This suggests that Ryugu is a product of a higher generation of the parent body disruption [3] or global resurfacing due to YORP induced past rapid rotation [4]. Visible color variations on Ryugu suggest the reddening of surface material by solar heating and/or space weathering under a temporal excursion near the Sun [5]. These hypotheses based on remote-sensing observations and the SCI experiment will be confirmed through return sample analyses.

Another important issue is the reconstruction of the properties of the parent body. Proximity observations using NIRS3 reveals the presence of global OH bearing minerals on Ryugu [6], whereas the amount is relatively small compared with hydrated carbonaceous chondrites and Bennu [7]. Both partial dehydration and incipient aqueous alteration will produce the weak OH absorption [3], which will be distinguished by return sample analyses. High porosity of Ryugu could be ascribed to loss of water ice during or after the formation of the rubble pile, if its parent body was an icy asteroid [4]. Water-rock ratio of the parent planetesimal with ^{26}Al heating will determine the set of coexisting minerals, which will also be determined by return sample analyses. Size-frequency distribution of surface particles as well as aggregate's constituent particles are important for identifying what kind of dust grains planetesimals are consist of. We will discuss the vision of exploration-based reconstruction of planetesimals.

[1] Arakawa et al. (2020), *Science* **368**, 268; [2] Bottke et al. (2020), *Astron. J.* **160**, 14; [3] Sugita et al. (2019), *Science* **364**, eaaw0422, [4] Watanabe et al. *Science* **364**, 268; [5] Morota et al. (2020), *Science* **368**, 654; [6] Kitazato et al. (2019) *Science* **364**, 272; [7] Hamilton et al. (2019), *Nature Astron.* **3**, 332.

Keywords: planetary exploration, material transport in the Solar System, planetary accretion process, planetesimals

©2021. Japan Geoscience Union. All Right Reserved.

Progress report of initial description of the C-type asteroid Ryugu samples returned by Hayabusa2

*Toru Yada[1], Masanao Abe[1], Aiko Nakato[1], Kasumi Yogata[1], Akiko Miyazaki[1], Kazuya Kumagai[2], Kentaro Hatakeda[2], Tatsuaki Okada[1], Masahiro Nishimura[1], Shizuho Furuya[1], Yoshitake Miwa[1], Ayako Iwamae[2], Lucie Liu[1], Lionel Lourit[3], Cedric Pilorget[3], Vincent Hamm[3], Jean-Pierre Bibring[3], Yuichiro Cho[4], Koki Yumoto[4], Yuna Yabe[4], Seiji Sugita[4], Shogo Tachibana[4], Hirotaka Sawada[1], Sakamoto Kanako[1], Tasuku Hayashi[1], Daiki Yamamoto[1], Ryota Fukai[1], Haruna Sugahara[1], Hisayoshi Yurimoto[5], Tomohiro Usui[1], Sei-ichiro WATANABE[6], Yuichi Tsuda[1]

1. Japan Aerospace Exploration Agency, 2. Marine Works Japan, 3. Institut D' Astrophysique Spatiale, 4. University of Tokyo, 5. Hokkaido University, 6. Nagoya University

The Hayabusa2 spacecraft reached the C-type near-Earth asteroid 162173 Ryugu in June 2018 and observed the asteroid with onboard instruments and from the landers [1-8], and accomplished two touchdown samplings on 22 Feb. and 12 Jul. 2019 [9]. After the 2nd touchdown, the sample catcher which contains samples was transferred into its reentry capsule. The spacecraft left the asteroid in Nov. 2019 and returned the capsule to the Woomera Prohibited Area in South Australia on 6 Dec. 2020. The handling processes for the capsule and the sample container in it after its landing have been detailed in a previous report [10].

The clean chambers in the Extraterrestrial Sample Curation Center of JAXA Sagamihara campus are composed of five chambers; CC3-1~3 and CC4-1~2 [12]. The container was installed into CC3-1 on 11 Dec. 2020 and opened after evacuated to high vacuum. The sample catcher was extracted from the container, and transported to CC3-2. The catcher is composed of three small chambers A, B and C. The chambers A and C contain sample obtained by the 1st and 2nd touchdowns, respectively. As the cover of the chamber A was opened in vacuum in CC3-2, a large number of black particles were observed inside the chamber A, as shown in the Fig. 1. Two particles inside the chamber A were picked up and placed on a quartz glass dish for future science. The catcher with the greater part of samples was transferred to CC3-3, and the gate valve between CC3-2 and CC3-3 was closed. Then, CC3-3 was slowly purged with purified nitrogen gas to the atmospheric pressure, in which the catcher was handled with Viton-coated butyl gloves.

The catcher containing samples was transferred to CC4-2 and its bulk weight was measured with an electronic balance. The total weight of the samples inside the catcher is 5.4g, subtracting the designed weight of the catcher and a tare weight of an attached jig. The catcher was then dismantled to extract samples from the chambers A, B and C to sapphire glass dishes in CC4-1. The bulk samples held in the dishes were photographed with an optical microscope installed above CC4-2. The same microscope was used to take images of the samples with illumination through five filters (0.40 μm (ul), 0.48 μm (b), 0.55 μm (v), 0.59 μm (Na), and 0.70 μm (w)) matched to the ONC-T camera of Hayabusa2 [2]. The weight of each dish was measured with the balance in CC4-2. The bulk samples in the dishes were measured with the FT-IR (JASCO VIR-300) installed to CC4-2 for their average spectra from 1 to 5 μm and were also measured with MicrOmega installed to CC3-3, a noncontact version of the hyperspectral microscope onboard the MASCOT lander [11], to investigate spectral features from 0.99 to 3.65 μm of the samples. After the bulk initial description, individual particles >1mm in size are handpicked one by one with a vacuum tweezer to be enclosed into individual particle containers. They are to be characterized in the

©2021. Japan Geoscience Union. All Right Reserved.

same manner as the bulk samples.

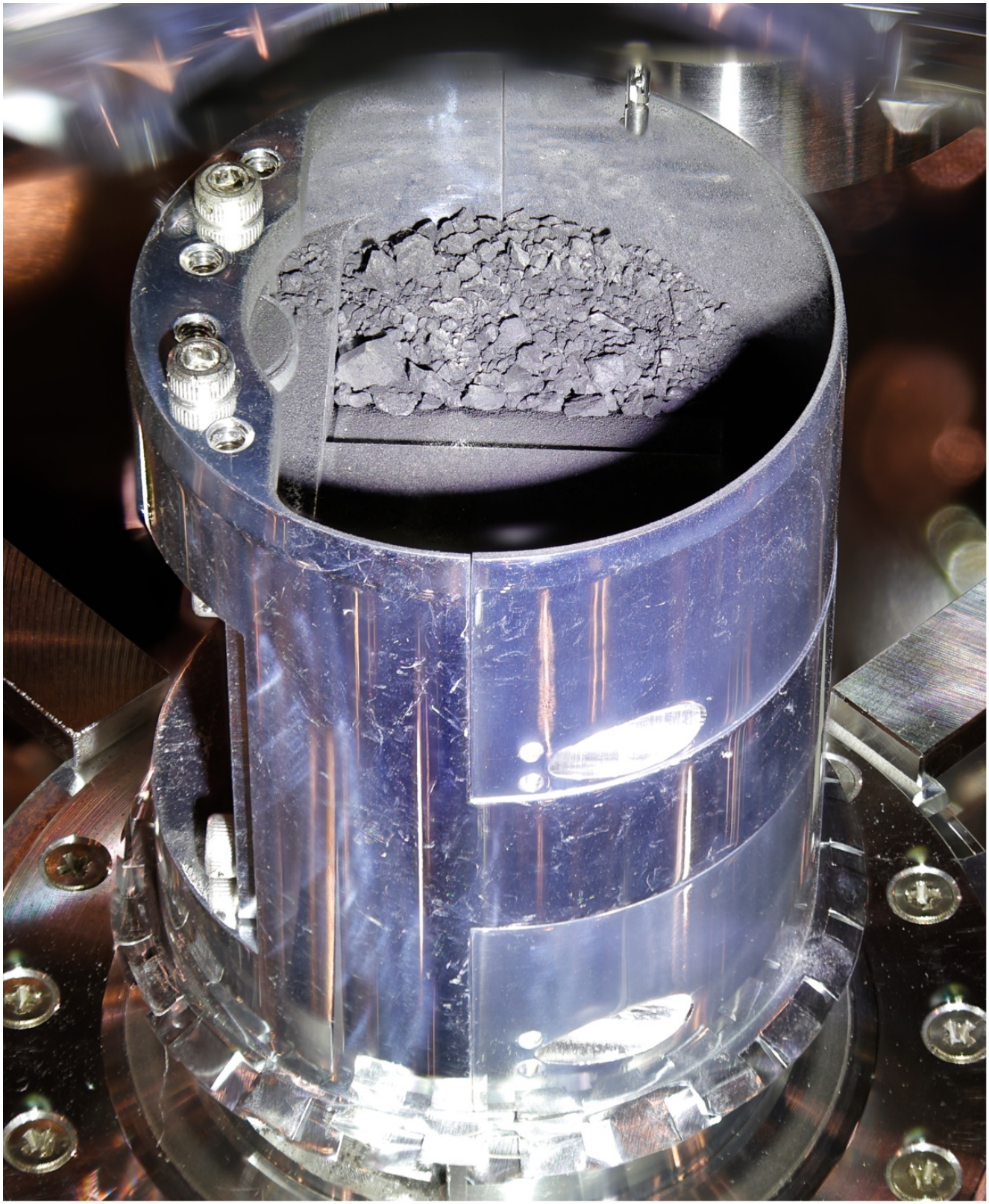
The sample distribution plan was detailed in [12]. JAXA plans to release the announcement of opportunity for the Hayabusa2 samples to the international science community with the sample catalog after 18 months from their return to the Earth.

References: [1] Watanabe S. et al. (2019) Science 364, 268. [2] Sugita S. et al. (2019) Science 364, 252. [3] Kitazato K. et al. (2019) Science 364, 272. [4] Jaumann R. et al. (2019) Science 365, 817. [5] Grott M. et al. (2019) Nat. Astron. [6] Okada T. et al. (2020) Nature 579, 518. [7] Morota T. et al. (2020) Science 368, 654. [8] Arakawa M. (2020) Science 368, 67. [9] Tachibana S. et al. (2020) 51st LPSC, #2027. [10] Tachibana S. et al. (2021) 52nd LPSC, #1289. [11] Bibring J.-P. et al. (2017) Space Sci. Rev. 208, 401. [12] Yada T. et al. (2021) 52nd LPSC, #2008.

Figure 1. A photograph of the sample catcher of Hayabusa2 after opening its chamber A in CC3-2. A large number of black particles are observed inside the chamber. An outer diameter of the catcher is 48mm.

Keywords: Hayabusa2, Ryugu, asteroid, return samples, carbonaceous chondrite, C-type asteroid

©2021. Japan Geoscience Union. All Right Reserved.



©2021. Japan Geoscience Union. All Right Reserved.

EXPERIMENTAL STUDY ON IMPACT CRATERS FORMED ON MOUNTAIN-LIKE SURFACE TOPOGRAPHY OF ASTEROIDS

*Yusaku Yokota[1], Masahiko Arakawa[1], Minami Yasui[1], Yuya Yamamoto[1], Sunao Hasegawa[2], Hatsune Okawa[1]

1. Graduate School of Science, Kobe University, 2. Japan Aerospace Exploration Agency

Impact craters are one of the major geological features on solid bodies such as asteroids and satellites. A crater formed on a flat surface is observed to be a circle but a crater formed on a slope is ellipse. In particular, various topographic features such as slope, bulge, and canyon have been observed on asteroids and small satellites. Recently, Hayabusa2 and OSIRIS-REx revealed that Ryugu and Bennu have a large bulge on their equatorial regions. Furthermore, some craters with asymmetric profiles were found on the bulge of Ryugu. However, the conventional crater scaling laws based on the results of laboratory experiments conducted on the targets having the flat surface. In order to apply the scaling laws to the cratering process on the mountain-like surface topography of asteroids, it is necessary to improve the crater scaling laws including the effect of the surface topography. In this study, we conducted the impact cratering experiments on granular targets simulating the mountain-like surface topography of asteroids, and we investigated the effects of the surface topography on the crater size scaling law and the ejecta growth process.

We prepared two types of targets to simulate the surface topography of asteroids: they are granular targets having the shape of a mountain range and a cone. The inclination (θ) of the mountain range target was set to be 20° and 30°, and that of the cone target was ~30°. We also prepared the target having the flat surface (that is, $\theta = 0°$). We changed the impact point d for the mountain range target; the d was defined as the horizontal distance between the impact point and the summit. In the case of the cone target, we changed the foot width of the target w.

We conducted impact experiments by using a one-stage vertical gas gun at Kobe University and a two-stage vertical gas gun at ISAS. The impact velocities ranged from 69 to 202 m/s for the mountain range target, and from 41 m/s to 4.21 km/s for the cone target. In order to analyze the crater morphology, we constructed the 3D shape model by using the software of PhotoScan Pro.

For the mountain range target, we observed that the crater had an elliptical shape: the width of the crater on the ridge direction (major axis) was always larger than that on the slope direction (minor axis). Furthermore, the elevated crater rim was observed on the ridge direction but it was not observed on the slope direction. The asymmetry of the crater shape strongly depends on the d. Now, the crater asymmetry is shown by the aspect ratio defined as the ratio of major axis length to minor axis length. We found that the aspect ratio increases with the increase of the major axis length at the constant d value, and furthermore, it increases more rapidly with the decrease of d. These characteristics were also found on the target with the slope of $\theta = 20°$ but the aspect ratio for the target with the slope of $\theta = 30°$ was larger than that of $\theta = 20°$ at the same d and the major axis length. Also, we constructed the crater size scaling law described by π-scaling for the mountain range target. The normalized crater radius, π_R, clearly depends on the slope θ, that is, they are ~1.3 times larger than that of the flat surface, $\theta = 0°$.

For the cone target, we observed the ratio of the initial target height to the impacted target height. We investigated the relationship between the height ratio and the v^* at different impact velocities. The v^* is defined as the velocity derived from the projectile momentum divided by the cone mass. At $v^* < 0.5$ m/s, the height ratio decreases exponentially with the increase of the v^*, irrespective of the impact velocity. This means that the height ratio could be controlled by the projectile momentum. At $v^* > 0.5$ m/s, most of the cone was excavated so the height ratio was almost zero. We also measured the crater diameter formed

©2021. Japan Geoscience Union. All Right Reserved.

on the cone target and it was almost the same as that formed on the flat surface at the same projectile kinetic energy.

Keywords: crater

©2021. Japan Geoscience Union. All Right Reserved.

The collisional history in the Main Belt

*Hiroshi Kobayashi[1]

1. Department of Physics, Nagoya University

Asteroids in the Main Belt Mean collisional velocity between them is estimated to be about 5 km/s so that collisions lead to fragmentation. The collisional timescale for 100 km-sized or larger asteroids is estimated to be much longer than the age of the Solar System, while smaller asteroids are expected to have experience of catastrophic disruption. This estimate is consistent with the fraction of asteroids in collisional families. Therefore, such large asteroids may have formed in the planet formation era. The mass distribution of 100km-sized or larger main belt asteroids is explained by the onset of runaway growth of planetesimals. On the other hand, smaller bodies are
fragmented into still smaller bodies. The mass distribution of 10km-sized or smaller asteroids is in the quasi steady state of the collisional cascade. However, the collisional lifetimes of such small asteroids highly depend on collisional outcome models. According to the collisional theory, we may discuss the possible histories of
kilometer sized asteroids.

Keywords: Asteroids, planetesimals, Collisions

©2021. Japan Geoscience Union. All Right Reserved.

Internal structure of pebble-pile comets inferred from thermal and mechanical properties of dust aggregates

*Sota ARAKAWA[1]

1. National Astronomical Observatory of Japan

The *Rosetta* mission has provided new data to better understand what comets are made of. The weak tensile strength of the cometary surface materials suggests that comet 67P/Churyumov–Gerasimenko is a hierarchical dust aggregate formed through gravitational collapse of a bound clump of small dust aggregates so-called `pebbles' in the gaseous solar nebula. Recently, we calculated the thermal inertias and thermal skin depths as functions of the size of pebbles (Arakawa & Ohno 2020). We found that the thermal properties of the comet are consistent with the hierarchical aggregate of cm- to dm-sized pebbles. This estimate is also consistent with the mechanical strength of the nucleus. In addition, we reanalyzed the stickiness of icy dust particles using a viscoelastic contact model. Our results indicate that not only H_2O ice but also CO_2 ice particles could easily grow into cm-sized large pebbles in the solar nebula (Arakawa & Krijt 2021), and this size estimate may be consistent with that from thermal and mechanical analyses on comet 67P.

Keywords: Comet, Thermal inertia, Dust growth

©2021. Japan Geoscience Union. All Right Reserved.

[E] Oral | P (Space and Planetary Sciences)：P-PS Planetary Sciences

Sun. Jun 6, 2021 10:45 AM - 12:15 PM JST | Sun. Jun 6, 2021 1:45 AM - 3:15 AM UTC | Ch.04 Zoom Room 04

[P-PS04] Small Solar System Bodies: A New Insight from Hayabusa2, OSIRIS-REx and Other Space Missions

convener:Tatsuaki Okada(Institute of Space and Astronautical Science, Japan Aerospace Exploration Agency), Taishi Nakamoto(Tokyo Institute of Technology), Daisuke Kuroda(Kyoto University), Chairperson:Tatsuaki Okada(Institute of Space and Astronautical Science, Japan Aerospace Exploration Agency), Taishi Nakamoto(Tokyo Institute of Technology), YACHEN YANG(Center for Space and Remote Sensing Research)

Small Solar System bodies, including asteroids, comets, satellites, and interplanetary dust particles, are notably important for understanding the origin and evolution of our Solar System, as well as investigating the sources of building blocks of life. Many new discoveries on small bodies have been carried out by observations from ground-based and space-based observatories, and explorations by spacecraft rendezvous and flyby. New perspectives on solar system evolution have been paved by analyses of extraterrestrial materials such as meteorites, IDPs, and return samples by space missions. Numerical and laboratory simulation studies have helped interpretations for those results and proposed new insights on these topics. In this session, new results of scientific studies and new ideas of methodology for investigating small solar system bodies are highly welcome, especially the topics on the remote sensing, surface experiments, and analysis of return sample in the Hayabusa2 and OSIRIS-REx missions, as well as the expectations and preparations for future missions including MMX, Destiny+, Hera, Comet Interceptor, and Hayabusa2-Extended missions.

10:45 AM - 11:00 AM JST | 1:45 AM - 2:00 AM UTC

[PPS04-07] Predicted strength, microporosity, thermal conductivity and grain density of Ryugu rock samples

*Jens Biele[1], Matthias Grott[2], Patrick Michel[3], Tatsuaki Okada[4], Seiji Sugita[5], Naoya Sakatani[6], Wladimir Neumann[2,7], Shingo Kameda[6], Tatsuhiro Michikami[8], Chikatoshi Honda[9] (1.German Aerospace Center, Cologne, Germany, 2.German Aerospace Center, Berlin, Germany, 3.Université Côte d'Azur, Observatoire de la Côte d'Azur, CNRS, Laboratoire Lagrange, Nice, France , 4.Japan Aerospace Exploration Agency, ISAS, Sagamihara, Japan, 5.University of Tokyo, Tokyo, Japan, 6.Rikkyo University, Tokyo, Japan, 7.Klaus-Tschira-Labor für Kosmochemie, Institut für Geowissenschaften, Universität Heidelberg, Heidelberg, Germany, 8.Kindai University, Hiroshima, Japan, 9.University of Aizu, Aizu-Wakamatsu, Japan)

11:00 AM - 11:15 AM JST | 2:00 AM - 2:15 AM UTC

[PPS04-08] Analysis of the temperature distributions of boulders on C-type asteroid 162173 Ryugu observed in low altitude operation of the asteroid explorer Hayabusa2

*Ayumu Ohsugi[1,2], Naoya Sakatani[3], Yuri Shimaki[2], Hiroki Senshu[4], Takehiko Arai[5], Hirohide Demura[6], Toru Kouyama[7], Tomohiko Sekiguchi[8], Satoshi Tanaka[2], Tetsuya Fukuhara[3], Tatsuaki Okada[1,2] (1.Graduate School of Science, The University of Tokyo, 2.Institute of Space and Astronautical Science, Japan Aerospace Exploration Agency, 3.Department of Physics, College of Science, Rikkyo University, 4.Planetary Exploration Research Center, Chiba Institute of Technology, 5.Faculty of Engineering, Department of Innovative Engineering, Division of Systems and Information Engineering,Ashikaga University, 6.Department of Computer Science and Engineering, University of Aizu, 7.National Institute of Advanced Industrial Science and Technology, 8.Hokkaido University of Education)

11:15 AM - 11:30 AM JST | 2:15 AM - 2:30 AM UTC

[PPS04-09] Surface Age of Ryugu's Boulders Based on Small Crater Statistics

*Yudai Takai[1], Tomokatsu Morota[1], Koki Yumoto[1], Rie Honda[2], Shingo Kameda[3], Eri Tatsumi[1,4], Yuichiro Cho[1], Kazuo Yoshioka[1], Hirotaka Sawada[5], Yasuhiro Yokota[2,5], Naoya Sakatani[3], Masahiko Hayakawa[5], Moe Matsuoka[5], Manabu Yamada[6], Toru Kouyama[7], Hidehiko Suzuki[8], Chikatoshi Honda[9], Kazunori Ogawa[5,10], Seiji Sugita[1] (1.University of Tokyo, 2.Kochi University, 3.Rikkyo University, 4.Instituto de

Astrofísica de Canarias, 5.JAXA, 6.Chiba Institute of Technology, 7.National Institute of Advanced Industrial Science and Technology, 8.Meiji University, 9.The University of Aizu, 10.Kobe University)

11:30 AM - 11:45 AM JST | 2:30 AM - 2:45 AM UTC

[PPS04-10] Space weathering of bright boulders inferred from the spectral comparison between SCI crater and blue regions on Ryugu

*Minami Aoki[1], Chiho Sugimoto[1], Koki Yumoto[1], Naofumi Takaki[1], ERI TATSUMI[2,1], Tomokatsu Morota[1], Yasuhiro Yokota[3], Masahiko Arakawa[4], Seiji Sugita[1] (1.Department of Earth and Planetary Science, Graduate School of Science, The University of Tokyo, 2.Instituto de Astrofísica de Canarias, 3.JAXA/ISAS, 4.Kobe University)

11:45 AM - 12:00 PM JST | 2:45 AM - 3:00 AM UTC

[PPS04-11] Estimation of space weathering timescale using the number of mottles on the boulder in Hayabusa/AMICA images

*Sunho Jin[1], Masateru Ishiguro[1] (1.Seoul National University)

12:00 PM - 12:15 PM JST | 3:00 AM - 3:15 AM UTC

[PPS04-12] The Chemical Composition of Interstellar Dust in Light of the DESTINY^{+} Mission: A Novel Tool to Measure the Elemental Abundances and Ionization of the Local Interstellar Cloud

*Hiroshi Kimura[1], Masanori Kobayashi[1], Tomoko Arai[1], DDA Team / DESTINY+ (1.Planetary Exploration Research Center, Chiba Institute of Technology)

Predicted strength, microporosity, thermal conductivity and grain density of Ryugu rock samples

*Jens Biele[1], Matthias Grott[2], Patrick Michel[3], Tatsuaki Okada[4], Seiji Sugita[5], Naoya Sakatani[6], Wladimir Neumann[2,7], Shingo Kameda[6], Tatsuhiro Michikami[8], Chikatoshi Honda[9]

1. German Aerospace Center, Cologne, Germany, 2. German Aerospace Center, Berlin, Germany, 3. Université Côte d'Azur, Observatoire de la Côte d'Azur, CNRS, Laboratoire Lagrange, Nice, France , 4. Japan Aerospace Exploration Agency, ISAS, Sagamihara, Japan, 5. University of Tokyo, Tokyo, Japan, 6. Rikkyo University, Tokyo, Japan, 7. Klaus-Tschira-Labor für Kosmochemie, Institut für Geowissenschaften, Universität Heidelberg, Heidelberg, Germany, 8. Kindai University, Hiroshima, Japan, 9. University of Aizu, Aizu-Wakamatsu, Japan

In this presentation, we summarize the findings and interpretations of the physical and thermophysical properties of C-type asteroid 162173 Ryugu obtained from Hayabusa2 remote sensing as well as from MASCOT radiometer (MARA) data. For a typical rock on Ryugu's surface, we find a thermal inertia of 295 ± 18 $Jm^{-2}K^{-1}s^{-1/2}$ (Hamm+ 2020), a microporosity of 50 ±3% (Grott+ 2020, Hamm+, 2020), and assuming a CM chondrite composition and thus an inferred specific heat capacity of cp=890 J/kg/K (±10%, at an average temperature of 277K), we estimate a thermal conductivity of 0.069 ±0.012 J/m/K at ~277 K. These estimates are based on MARA surface brightness temperature measurements of an arguably (Biele et al, 2019) dust-free boulder at MASCOT's landing site obtained over a full diurnal cycle. Those values are consistent with the TIR instrument's global findings (Okada+ 2020). The very high deduced microporosity lets us reasonably estimate the tensile strength of those abundant "cauliflower rocks" (Jaumann+ 2019), ~200-280 kPa (Grott+, 2019).

Furthermore, also from orbital data (ONC imaging and counting, plus radiometric data for GM), we have estimated the macroporosity of Ryugu, assumed to be a homogeneous rubble pile, based on granular mixing theory and the size-frequency distribution of boulders ranging from ~0.1 m to ~100 m diameter. We find (Grott+, 2020) that the macroporosity of Ryugu is very low, 16 ±3% and that if the underlying homogeneity assumption is true, taken together with Ryugu's bulk density and the average microporosity of its boulders, the average grain density can be estimated as 2.85 ±0.15 g/cm^3, consistent with the mineralogy of CM meteorites or the ungrouped carbonaceous chondrite Tagish Lake.

It will now be extremely exciting to compare these values with actual laboratory measurements of the returned samples. For example, if our values for Ryugu's macroporosity and rock microporosity (and/or grain density) do not agree with what is found from the samples, the assumption of homogeneity might be wrong. This would mean that the surface of Ryugu has a significantly different boulder SFD than its interior. Or, simpler, the assumed relationship between rock porosity and thermal conductivity is incorrect.

As for the strength of rock pieces, besides possible size (scale) dependencies and sampling bias, a higher strength than predicted here would have to be reconciled with the very low thermal conductivity of Ryugu's blocks, which dictates rather small grain-to-grain (sinter or volatile condensate or 'salt') neck diameters.

References

Hamm, M., et al. (2020). "Thermophysical modelling and parameter estimation of small Solar system

©2021. Japan Geoscience Union. All Right Reserved.

bodies via data assimilation." Monthly Notices of the Royal Astronomical Society **496**(3): 2776-2785.

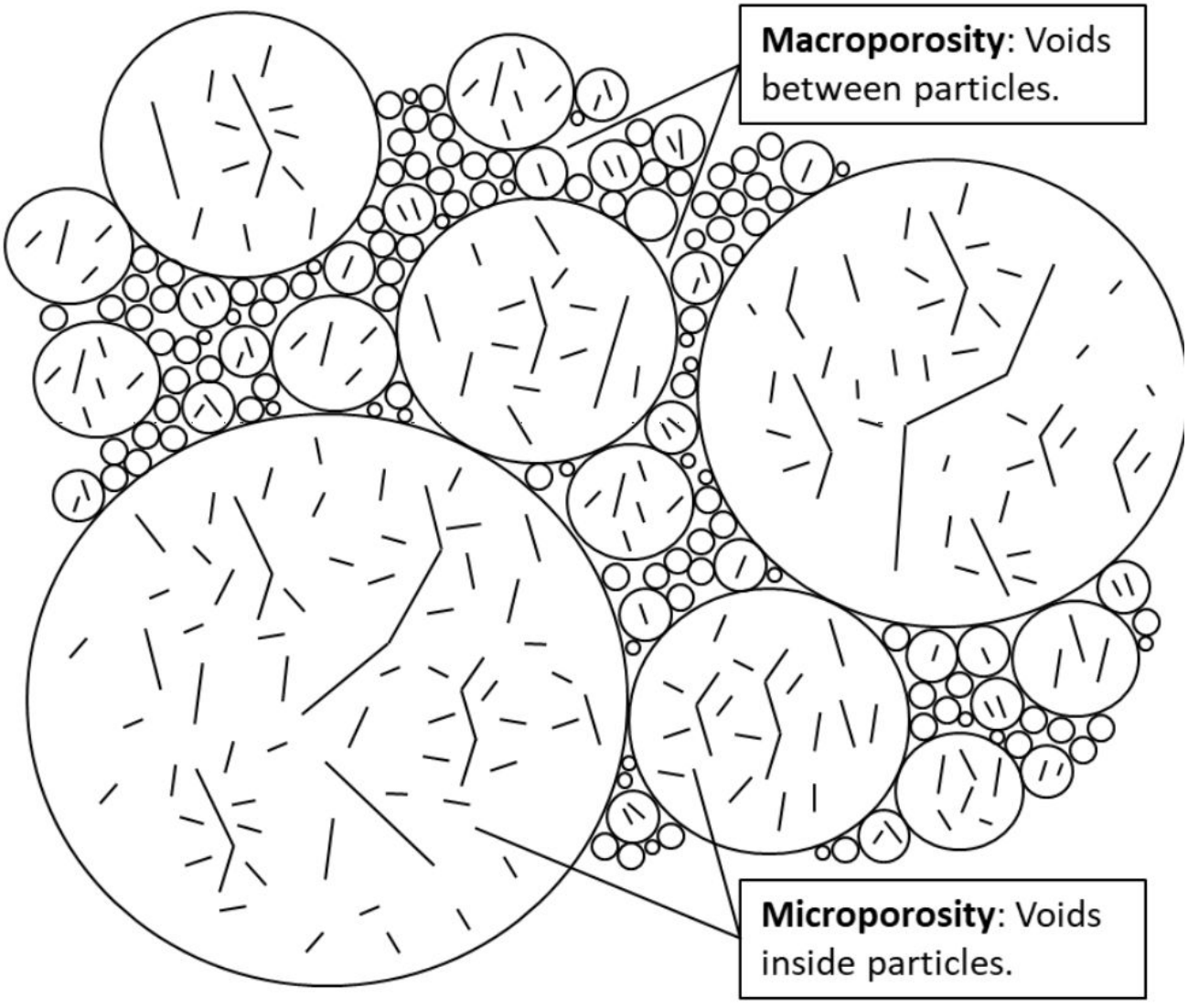
Grott, M., et al. (2019). "Low thermal conductivity boulder with high porosity identified on C-type asteroid (162173) Ryugu." Nature Astronomy **3**(11): 971-976.

Biele, J., et al. (2019). "Effects of dust layers on thermal emission from airless bodies." Progress in Earth and Planetary Science **6**(1): 48.

Okada, T., et al. (2020). "Highly porous nature of a primitive asteroid revealed by thermal imaging." Nature **579**(7800): 518-522.

Jaumann, R., et al. (2019). "Images from the surface of asteroid Ryugu show rocks similar to carbonaceous chondrite meteorites." Science **365**(6455): 817-820.

Keywords: rubble pile asteroid, Ryugu, material properties



©2021. Japan Geoscience Union. All Right Reserved.

Analysis of the temperature distributions of boulders on C-type asteroid 162173 Ryugu observed in low altitude operation of the asteroid explorer Hayabusa2

*Ayumu Ohsugi[1,2], Naoya Sakatani[3], Yuri Shimaki[2], Hiroki Senshu[4], Takehiko Arai[5], Hirohide Demura[6], Toru Kouyama[7], Tomohiko Sekiguchi[8], Satoshi Tanaka[2], Tetsuya Fukuhara[3], Tatsuaki Okada[1,2]

1. Graduate School of Science, The University of Tokyo, 2. Institute of Space and Astronautical Science, Japan Aerospace Exploration Agency, 3. Department of Physics, College of Science, Rikkyo University, 4. Planetary Exploration Research Center, Chiba Institute of Technology, 5. Faculty of Engineering, Department of Innovative Engineering, Division of Systems and Information Engineering,Ashikaga University, 6. Department of Computer Science and Engineering, University of Aizu, 7. National Institute of Advanced Industrial Science and Technology, 8. Hokkaido University of Education

The asteroid explorer Hayabusa2 [1] has the Thermal Infrared Imager (TIR) [2,3] which obtains the digital thermal images to indicate the thermal radiation from C-type asteroid 162173 Ryugu. In this study, to obtain detailed thermal properties of boulders at Ryugu, we analyzed TIR images taken below the altitude of 500 m and investigated temperature variations of boulders and their physical state in the specific regions.
TIR has a field of view (FOV) of 16.7˚×12.7˚ and the effective pixels of the detector of 328×248, resulting in the spatial resolution about of 0.051˚ per pixel [2]. The temperature range which TIR covers is 150 to 460 K and the well-calibrated temperature range is 230 to 420 K. We used TIR images taken during the release paths for the MINERVA rover (MNRV) and the MASCOT lander (MSCT). We identified boulders taken with more than 100 pixels and calculated the temperatures. The total numbers of detected boulders were 355 (MNRV) and 312 (MSCT), and the detection errors were obtained as ±5.2 % and ±5.5 % by Wald inequality [4]. In MNRV, the averages and the standard deviations of minimum, average, and maximum temperatures were 286 ±11.2 K, 314 ±5.65 K, and 332 ±5.74 K, respectively. In MSCT, the averages and the standard deviations of minimum, average, and maximum temperatures were 287 ±11.0 K, 313 ±5.53 K, and 332 ±5.99 K, respectively. From the normal Q-Q plots, where the x-axis is the observed value and the y-axis is the expected value which is assumed the detected value follows a normal distribution, the temperatures could follow the normal distribution. The YORP effect [1,5] might lead to the normality of the temperature distributions. Furthermore, the calculated slopes of the size-frequency distributions (SFD) divided by measured altitudes were in the range of 0.30 to 4.0 and these values were consistent with those investigated by Michikami T et al., (2019) [6], who suggested the existence of boulders formed when Ryugu's parent body was destroyed and those covered with regolith layers. Moreover, the range of thermal inertias [7] was calculated as low as 34.6-385 J m^{-2} $s^{-0.5}$ K^{-1} (hereafter, tiu) with the one-dimensional heat diffusion equation [8]. Our results are consistent with that of the global average estimated as 225 ±45 tiu by Shimaki et al. (2020) [9]. In this study, we assumed that the surfaces of boulders were confronted to the images so that further detailed study considering the surface local slopes is needed to estimate more accurately.
In summary, the total numbers of detected boulders were 355 (MNRV) and 312 (MSCT) and the normal Q-Q plots suggested that the average temperature distributions of boulders were close to the normal distribution. Moreover, the values of slopes of SFD and thermal inertias suggested the existence of boulders formed when Ryugu's parent body was destroyed, boulders covered with regolith layers, and porous and fluffy boulders. In the future, we will investigate other areas taken at low-altitudes.

Acknowledgments

©2021. Japan Geoscience Union. All Right Reserved.

The authors appreciate Dr. Koji Matsumoto and Kyoko Yamamoto at the National Astronomical Observatory of Japan for the use of the LIDAR corrected trajectory of the Hayabusa2 spacecraft. This study is partly supported by the JSPS Kakenhi No. JP17H06459 (Aqua Planetology) and the JSPS Core-to-Core Program “International Network of Planetary Sciences”.

References

[1] Watanabe S. et al., Science 364, 268-272 (2019), [2] Okada, T. et al., Space Sci. Rev., 208, 255-286 (2017), [3] Okada, T. et al., Nature 579, 518-522 (2020), [4] Kurihara, S., Introduction to statistics: from testing to multivariate analysis and experimental design, Ohmsha Ltd., pp.336 (2011), [5] Walsh et al., Nature 454, 188-191 (2008), [6] Michikami, T et al., Icarus 331, 179-191(2019), [7] Okada, T. et al, 13th Space Science Symposium, ISAS/JAXA, P2-117 (2013), [8] Takita, J. et al., Space Sci Rev, 208, 287-315 (2017), [9] Shimaki Y. et al., Icarus 348, 113835 (2020).

Keywords: Hayabusa2, Temperature, boulder, Ryugu

©2021. Japan Geoscience Union. All Right Reserved.

Surface Age of Ryugu's Boulders Based on Small Crater Statistics

*Yudai Takai[1], Tomokatsu Morota[1], Koki Yumoto[1], Rie Honda[2], Shingo Kameda[3], Eri Tatsumi[1,4], Yuichiro Cho[1], Kazuo Yoshioka[1], Hirotaka Sawada[5], Yasuhiro Yokota[2,5], Naoya Sakatani[3], Masahiko Hayakawa[5], Moe Matsuoka[5], Manabu Yamada[6], Toru Kouyama[7], Hidehiko Suzuki[8], Chikatoshi Honda[9], Kazunori Ogawa[5,10], Seiji Sugita[1]

1. University of Tokyo, 2. Kochi University, 3. Rikkyo University, 4. Instituto de Astrofísica de Canarias, 5. JAXA, 6. Chiba Institute of Technology, 7. National Institute of Advanced Industrial Science and Technology, 8. Meiji University, 9. The University of Aizu, 10. Kobe University

The Hayabusa2 spacecraft arrived at the asteroid Ryugu on June, 2018. Detailed observations by Hayabusa2 have revealed a large number of boulders on Ryugu's surface and its low bulk density of 1,190 kg/m^3, suggesting its "rubble-pile" structure [Watanabe et al., 2019; Michikami et al., 2019; Hirabayashi et al., 2019]. Unraveling the lifetime of boulders is important for understanding the surface processes, such as thermal fatigue, impacts and surface flow, and its timescale on Ryugu's surface.

During two touchdown rehearsal operations on October 15 and 25, 2018 (Japan Standard Time) before the first touchdown operation, the Optical Navigation Camera (ONC) onboard the Hayabusa2 spacecraft [Sugita et al., 2019; Kameda et al., 2017; Suzuki et al., 2018; Tatsumi et al., 2019], which took multiple high-resolution images (~1 cm/pixel). Moreover, during the touchdown operations on February 22, 2019 and July 11, 2019, the ONC took even higher-resolution images (~0.1 cm/pixel), showing topographic features of Ryugu's surface on the scale of a few centimeters. Because the characteristic size of the Ryugu's boulder is estimated to be 3 m [Sugita et al., 2019], low-altitude imaging allowed us to observe small craters on the boulder surface.

Using these high-resolution images of Ryugu's surface, we investigated 2,152 boulders and identified 22 several-centimeter-sized circular depressions on the boulder surfaces that are candidates for small impact craters. We also built a cratering chronology model of small craters on Ryugu's boulders, based on the Pi-group crater scaling law under the strength regime [Holsapple, 1993] and the size-frequency distribution model of near-Earth object population [Brown et al., 2002; Suggs et al., 2014].

Based on the size-frequency distributions of small crater candidates and the cratering chronology model for Ryugu's small craters, the surface age of Ryugu's boulders was estimated to 0.01 to 1 Myr, younger than the global surface age of Ryugu (~8 Myr) [Sugita et al., 2019; Morota et al., 2020; Cho et al., submitted]. Moreover, Ryugu's boulders have lower crater density than Bennu's boulders, whose surface age was estimated to be 1.75 ±0.75 Myr [Ballouz et al., 2020]. We will discuss the disruption and resurfacing processes of boulders, based on the estimated survival time of boulders and comparisons with the crater densities of large craters on Ryugu and mini craters on boulder surface of asteroid Bennu.

Keywords: Ryugu, Hayabusa2, crater, boulder

©2021. Japan Geoscience Union. All Right Reserved.

Space weathering of bright boulders inferred from the spectral comparison between SCI crater and blue regions on Ryugu

*Minami Aoki[1], Chiho Sugimoto[1], Koki Yumoto[1], Naofumi Takaki[1], ERI TATSUMI[2,1], Tomokatsu Morota[1], Yasuhiro Yokota[3], Masahiko Arakawa[4], Seiji Sugita[1]

1. Department of Earth and Planetary Science, Graduate School of Science, The University of Tokyo, 2. Instituto de Astrofísica de Canarias, 3. JAXA/ISAS, 4. Kobe University

Boulders with reflectance ≧1.5 times the surrounding background have been discovered on Ryugu [1-4]. These are called bright boulders (BBs). Based on spectral features, they are classified into S-type and C-type BBs. The former is likely exogenous, and the latter is likely endogenous [2-4]. Detailed spectral analysis using principal component analysis have revealed that S-type boulders on Ryugu experienced different degrees of space weathering. However, the degrees and patterns of space weathering of C-type bright boulders on Ryugu have not been understood well yet. Because Hayabusa2 collected samples near the SCI crater, which excavated fresh materials from depth that is not intensively influenced by either space weathering or solar heating [5], optical navigation camera telescope (ONC-T) have captured many high-resolution images of fresh materials. Analysis of 13 BBs inside the SCI crater indicate that all these 13 turned to be C-type BBs [6]. In this study, we extend our analysis of C-type BBs inside the SCI crater to understand the nature of space weathering on these C-type materials.

First, we compared the spectra of C-type BBs inside and outside the SCI crater with those of the heated carbonaceous chondrites [7, 8] in v-x slope/ul-index space. Results showed that the distribution of BBs inside the SCI crater is generally consistent with that of BBs outside the SCI crater. Also found is that the spectral trend of C-type BBs in v-x slope/ul-index space is generally similar to the trend formed by heating experiments with carbonaceous chondrites (CCs). However, there is significant difference between C-type BB trend and that of heated CCs; some BBs inside the SCI crater have a high ul-index value that is not found in BBs outside the SCI crater. Thus, this spectral feature may be lost due to space weathering.

Second, we further investigated whether the new spectral shape (e.g., excess ul-index) not seen in BBs outside the SCI crater is unique to BBs that have not undergone space weathering. Previous studies have found that Ryugu surface have both reddish and blueish regions [1]. Results of geologic analysis have shown that the reddish regions may have been exposed for a long time and experienced solar heating and/or solar wind irradiation [9]. Blueish regions are stratigraphically younger than reddish regions; they probably experienced some kind of resurfacing relatively recently [1, 9]. Thus, BBs in blue regions may be less affected by space weathering than those in reddish regions. Then, we have three different stages of solar heating and/or space weathering on Ryugu. Comparison of spectral properties of C-type BBs in these three different regions would give us important clue for understanding space weathering on C-type BBs. Preliminary analysis results suggest that C-type bright boulders on bluish regions, whose surface exposure ages are estimated to be ~0.3 to ~8 Myr [9], do not exhibit statistically significant excess ul-index. Thus, if the decrease in ul-index excess is caused by space weathering, then this mode of space weathering may occur at such short timescales. In the presentation, we will present the up-to-date results of our analyses of this comparison.

[1] Sugita, S. et al. (2019) Science, 364, eaaw0422 1-11.
[2] Tatsumi, E. et al. (2021) Nature Astron. 5, 39-45.
[3] Sugimoto, C. et al. (2021a) Icarus in review.
[4] Sugimoto, C. et al. (2021b) Icarus in review.
[5] Arakawa, M. et al. (2020) Science, 368, 67-71.
[6] Aoki, M. et al. (2021) LPSC, #1989.

©2021. Japan Geoscience Union. All Right Reserved.

[7] Hiroi, T. et al. (1996a) LPSC XXVII, 551-552.
[8] Hiroi, T. et al. (1996b) Meteorit. Planet. Sci, 31, 321–27.
[9] Morota, T. et al. (2020), 368, 654-659.

Keywords: asteroid, SCI Crater, Bright Boulder

©2021. Japan Geoscience Union. All Right Reserved.

Estimation of space weathering timescale using the number of mottles on the boulder in Hayabusa/AMICA images

*Sunho Jin[1], Masateru Ishiguro[1]

1. Seoul National University

The remote-sensing images of the Hayabusa mission target asteroid (25143) Itokawa (Sq-type) indicates the coexistence of both matured terrains by space weathering and fresh regions with newly exposed materials. Several resurfacing mechanisms (e.g., tidal interaction with terrestrial planets) [1] are proposed to explain the formation of these regions. The estimation of space weathering timescale is essential to constrain the possible mechanisms to rejuvenate the asteroid.

Note that there is an unignorable discrepancy between the timescale derived from different techniques. The timescale estimated from the solar flare track density and the weathered rim thickness of regolith samples acquired by Hayabusa spacecraft range from 10^2 to 10^4 years [2][3], while those estimated from laboratory simulations range from 10^4 to 10^6 years [4][5]. Besides, there are inherent insufficiencies of these age estimation methods. Since evidence of regolith migration is found on the surface of Itokawa [6], particles on the very surface would be rejuvenated by granular convection. Meanwhile, laboratory experiments are indirect stimulations of the space weathering process, which would have possibilities to be different from the actual process present in the asteroid. Thus, we focus on estimating the surface exposure age using bright mottles on the large boulders, where the materials are insusceptible to the regolith migration. These mottles are expected to be formed by impacts of mm to cm-sized interplanetary particles.

In this work, we used three AMICA (Asteroid Multi-band Imaging Camera) v-band images. These images were taken on November 12th, 2005, during the close approach to the asteroid. First, we masked boulders large enough to detect mottles. Then, we determined the size distribution of these mottles. We also derived theoretical size distribution with various timescales of space weathering with the well-known size distribution of interplanetary dust particles (e.g., Grün, 1985 [7]). By comparing these two distributions, we estimated the time needed to form mottles before becoming dark again by space weathering.

As a result, we found surface exposure timescales of these boulders are an order of 10^3 –10^4 years, consistent with those previously estimated from laboratory simulation with light ions, such as Hydrogen and Helium. We also plan to discuss possible resurfacing scenarios to expose fresh materials during such short time intervals at this meeting.

[1] Binzel et al. (2010), Nature, Volume 463, Issue 7279, p. 331-334.
[2] Keller and Berger (2014), Earth, Planets and Space, Volume 66, article id.71
[3] Noguchi et al. (2014), Meteoritics & Planetary Science, Volume 49, Issue 2, p. 188-214.
[4] Bonal et al. (2015), Meteoritics & Planetary Science, Volume 50, Issue 9, p. 1562-1576.
[5] Brunetto et al. (2006), Icarus, Volume 184, Issue 2, p. 327-337.
[6] Miyamoto et al. (2007), Science, Volume. 316, Issue 5827, p. 1011-1014.
[7] Grün (1985), Icarus, Volume 62, Issue 2, p. 244-272.

©2021. Japan Geoscience Union. All Right Reserved.

Keywords: Asteroids, Space Weathering, Itokawa, Hayabusa

©2021. Japan Geoscience Union. All Right Reserved.

The Chemical Composition of Interstellar Dust in Light of the DESTINY+ Mission: A Novel Tool to Measure the Elemental Abundances and Ionization of the Local Interstellar Cloud

*Hiroshi Kimura[1], Masanori Kobayashi[1], Tomoko Arai[1], DDA Team / DESTINY+

1. Planetary Exploration Research Center, Chiba Institute of Technology

The chemical composition of interstellar dust is directly linked to the depletion of elements in the gas phase of the interstellar medium (ISM), owing to the complementarity of elements in the solid and gas phases of the ISM. It has, therefore, been common practice to derive the elemental abundance of interstellar dust from the measured depletion of dust-forming elements in the gas phase of the ISM. The chemical composition of both solid and gas phases in the ISM would be a crucial factor for the evolution of the presolar molecular cloud, from which the Sun and the Solar System formed about 4.5 billion years ago. In particular, the organic and rocky components of interstellar dust would provide seeds for the origin of life and habitable planets.

On the one hand, the determination of elemental abundances in the solid and gas phases of the ISM is not a straightforward task if partially ionized, unless the ionization fractions of every elements are known a priori. This is exactly the case for the Local Interstellar Cloud (LIC) around the Sun, which is known to be a partially ionized warm cloud with an extension of several parsecs. On the other hand, recent technological advances in space missions have provided us direct information on the chemical composition of dust in the LIC by means of laboratory analyses (Stardust) and in situ measurements (Cassini).

The DESTINY$^+$ Dust Analyzer (DDA) onboard DESTINY$^+$ is a successor of Cassini’s Cosmic Dust Analyzer (CDA) equipped with an impact ionization detector and a time-of-flight mass spectrometer. The DDA will measure the chemical composition of interstellar dust streaming into the inner Solar System from the LIC, similar to the CDA, but with an elevated performance in terms of mass resolution and sensitive area. We have analyzed astronomical deta on the depletion of elements in the gas phase of the LIC and the ionization states of the elements, derived the elemental abundances of dust in the LIC from the depletion, and compared them with space mission data. We found that DDA’s data on the chemical composition of interstellar dust will constrain the gas-phase abundances and ionization states of elements undetectable by remote astronomical observations. In this talk, we will demonstrate that the DDA is a novel tool to measure the composition and ionization of the LIC.

Keywords: DESTINY+, interstellar dust, in-situ analysis, chemical composition, Local Interstellar Cloud, ionization state

©2021. Japan Geoscience Union. All Right Reserved.

[E] Oral | P (Space and Planetary Sciences)：P-PS Planetary Sciences

Sun. Jun 6, 2021 1:45 PM - 3:15 PM JST | Sun. Jun 6, 2021 4:45 AM - 6:15 AM UTC | Ch.04 Zoom Room 04

[P-PS04] Small Solar System Bodies: A New Insight from Hayabusa2, OSIRIS-REx and Other Space Missions

convener:Tatsuaki Okada(Institute of Space and Astronautical Science, Japan Aerospace Exploration Agency), Taishi Nakamoto(Tokyo Institute of Technology), Daisuke Kuroda(Kyoto University), Chairperson:Tatsuaki Okada(Institute of Space and Astronautical Science, Japan Aerospace Exploration Agency), Taishi Nakamoto(Tokyo Institute of Technology), YACHEN YANG(Center for Space and Remote Sensing Research)

Small Solar System bodies, including asteroids, comets, satellites, and interplanetary dust particles, are notably important for understanding the origin and evolution of our Solar System, as well as investigating the sources of building blocks of life. Many new discoveries on small bodies have been carried out by observations from ground-based and space-based observatories, and explorations by spacecraft rendezvous and flyby. New perspectives on solar system evolution have been paved by analyses of extraterrestrial materials such as meteorites, IDPs, and return samples by space missions. Numerical and laboratory simulation studies have helped interpretations for those results and proposed new insights on these topics. In this session, new results of scientific studies and new ideas of methodology for investigating small solar system bodies are highly welcome, especially the topics on the remote sensing, surface experiments, and analysis of return sample in the Hayabusa2 and OSIRIS-REx missions, as well as the expectations and preparations for future missions including MMX, Destiny+, Hera, Comet Interceptor, and Hayabusa2-Extended missions.

1:45 PM - 2:00 PM JST | 4:45 AM - 5:00 AM UTC

[PPS04-13] Regional photometric properties on asteroid Ryugu in visible wavelength

*Yasuhiro Yokota[1], Rie Honda[2], Eri Tatsumi[3], Deborah Domingue[4], Stefanus E. Schröder[5], Moe Matsuoka[1], Lucie Riu[1], Seiji Sugita[6], Tomokatsu Morota[6], Naoya Sakatani[7], Chikatoshi Honda[8], Yuichiro Cho[6], Shingo Kameda[7], Toru Kouyama[9], Manabu Yamada[10], Masahiko Hayakawa[1], Hiroki Senshu[10], Hidehiko Suzuki[11], Kazuo Yoshioka[6], Hirotaka Sawada[1], Kazunori Ogawa[1] (1.ISAS/JAXA, Japan, 2.Kochi Univ., Japan, 3.Instituto de Astrofisica de Canarias, Univ. of La Laguna, Spain, 4.Planetary Science Institute, USA, 5.DLR, Germany, 6.Univ. of Tokyo, Japan, 7.Rikkyo Univ., Japan, 8.Univ. of Aizu, Japan, 9.AIST, Japan, 10.Chiba Inst. Tech, Japan, 11.Meiji Univ., Japan)

2:00 PM - 2:15 PM JST | 5:00 AM - 5:15 AM UTC

[PPS04-14] Spectrophotometric behavior of Ryugu's surface as inferred from the Hayabusa2/NIRS3 data

*Andrea Longobardo[1], Ernesto Palomba[1,2], Anna Galiano[1], Fabrizio Dirri[1], Angelo Zinzi[2], Mario D'Amore[3], Deborah Domingue[4], Kohei Kitazato[5], Takahiro Iwata[6], Moe Matsuoka[6], Takahiro Hiroi[7], Driss Takir[8], Tomoki Nakamura[9], Masanao Abe[5], Makiko Ohtake[5], Shuji Matsuura[10], Sei-ichiro WATANABE[6,11], Makoto Yoshikawa[6], Takanao Saiki[6], Tatsuaki Okada[6], Yukio Yamamoto[6], Yoh Takei[6], Kei Shirai[6], Naru Hirata[5], Naoyuki Hirata[12], Koji Matsumoto[13], Yuichi Tsuda[6] (1.Istituto Nazionale di Astrofisica - Istituto di Astrofisica e Planetologia Spaziali, Rome, Italy, 2.ASI-SSDC, Rome, Italy, 3.German Aerospace Center, Institute of Planetary Research, Berlin, Germany, 4.PSI, Tucson, AZ, USA, 5.University of Aizu, Aizu-Wakamatsu 965-8580, Fukushima, Japan, 6.ISAS-JAXA, Japan, 7.Department of Earth, Environmental and Planetary Sciences, Brown University, Providence, RI 02912, USA, 8.Jacobs/NASA Johnson Space Center, USA, 9.Tohoku University, Miyagi, Japan, 10.Kwansei Gakuin University, Hyogo, Japan, 11.Nagoya University, Nagoya 464-8601, Japan, 12.Kobe University, Kobe 657-8501, Japan, 13.National Astronomical Observatory of Japan, Mitaka 181-8588, Japan)

2:15 PM - 2:30 PM JST | 5:15 AM - 5:30 AM UTC

[PPS04-15] Laboratory spectral constraints on the composition and origin of Phobos: Reconciling the Vis-NIR/Mid-IR contradictions

*Matthew Izawa[1], Sandra Potin[2], Edward Cloutis[2] (1.Institute for Planetary Materials, 2.University of Winnipeg)

2:30 PM - 2:45 PM JST | 5:30 AM - 5:45 AM UTC

[PPS04-16] UNSUPERVISED LEARNING OF NIRS3 DATA: RYUGU SPECTRAL SURFACE REGIONS CLASSIFICATION

*Mario D'Amore[1], E. Palomba[2,3], A. Galiano[2], A. Zinzi[3], F. Dirri[2], A. Longobardo[2], K. Kitazato[4], T. Iwata[5], M. Matsuoka[5], T. Hiroi[6], D. Takir[7], T. Nakamura[8], M. Abe[5], M.y Ohtake[5], S. Matsuura[9], S. Watanabe[10], M. Yoshikawa[5], T. Saiki[5], S. Tanaka[5], T. Okada[5], Y. Yamamoto[5], Y. Taikei[5], K. Shirai[5], N. Hirata[11,4], K. Matsumoto[12], Y. Tsuda[5] (1.German Aerospace Center, Institute of Planetary Research, Berlin, Germany, 2.INAF-IAPS, Rome, Italy, 3.SSDC-ASI, Rome, Italy, 4.University of Aizu, Aizu-Wakamatsu 965-8580, Fukushima, Japan, 5.Institute of Space and Astronautical Science (ISAS), Japan Aerospace Exploration Agency, Sagamihara, 252-5210, Japan, 6.Department of Earth, Environmental and Planetary Sciences, Brown University, Providence, RI 02912, USA, 7.Jacobs/NASA Johnson Space Center, USA, 8.Tohoku University, Miyagi, Japan, 9.Kwansei Gakuin University, Hyogo, Japan, 10.Nagoya University, Nagoya 464-8601, 11.Kobe University, Kobe 657-8501, Japan, 12.National Astronomical Observatory of Japan, Mitaka 181-8588, Japan.)

2:45 PM - 3:00 PM JST | 5:45 AM - 6:00 AM UTC

[PPS04-17] Quantitative analysis of spectral evolution of craters, boulders, and regolith on Ryugu and Bennu

*Koki Yumoto[1], Eri Tatsumi[2,1], Tatsuki Ebihara[1], DellaGiustina Daniella[3], Naofumi Takaki[1], Tomokatsu Morota[1], Yuichiro Cho[1], Golish Dathon[3], Rie Honda[4], Shingo Kameda[5], Yasuhiro Yokota[6], Naoya Sakatani[5], Toru Kouyama[7], Sawada Hirotaka[6], Masahiko Hayakawa[6], Matsuoka Moe[6], Manabu Yamada[8], Hidehiko Suzuki[9], Chikatoshi Honda[10], Kazunori Ogawa[11,12], Kazuo Yoshioka[1], Seiji Sugita[1] (1.University of Tokyo, 2.Instituto de Astrofísica de Canarias, 3.Lunar and Planetary Laboratory, Univ. of Arizona, 4.Kochi Univ., 5.Rikkyo Univ., 6.ISAS/JAXA, 7.Inst. of Adv. Ind. Sci. and Tech., 8.Chiba Inst. of Tech., 9.Meiji Univ., 10.Univ. of Aizu, 11.JSEC/JAXA, 12.Kobe Univ.)

3:00 PM - 3:15 PM JST | 6:00 AM - 6:15 AM UTC

[PPS04-18] Bennu's Global Geologic Map Reveals the Last Epoch of Resurfacing

*Erica R Jawin[1], Timothy J McCoy[1], Kevin John Walsh[2], Harold C Connolly[3], Ronald L Ballouz[4], Andrew Joseph Ryan[4], Maurizio Pajola[5], Olivier S Barnouin[6], Hannah H kaplan[7], Vicky E Hamilton[2], Josh P Emery[8], Daniella N Dellagiustina[4], Daniel Jay Scheeres[9], Michael G Daly[10], Carina A Bennett[4], Dathon R Golish[4], Mark Perry[6], R Terik Daly[6], E Beau Bierhaus[11], Michael C Nolan[4], Heather L Enos[4], Dante S Lauretta[4] (1.Smithsonian National Museum of Natural History, 2.Southwest Research Institute, 3.Rowan University, 4.University of Arizona, 5.INAF-Astronomical Observatory of Padova, 6.Johns Hopkins University Applied Physics Laboratory, 7.Goddard Space Flight Research Center, 8.Northern Arizona University, 9.University of Colorado, Boulder, 10.York University, 11.Lockheed Martin Space)

Regional photometric properties on asteroid Ryugu in visible wavelength

*Yasuhiro Yokota[1], Rie Honda[2], Eri Tatsumi[3], Deborah Domingue[4], Stefanus E. Schröder[5], Moe Matsuoka[1], Lucie Riu[1], Seiji Sugita[6], Tomokatsu Morota[6], Naoya Sakatani[7], Chikatoshi Honda[8], Yuichiro Cho[6], Shingo Kameda[7], Toru Kouyama[9], Manabu Yamada[10], Masahiko Hayakawa[1], Hiroki Senshu[10], Hidehiko Suzuki[11], Kazuo Yoshioka[6], Hirotaka Sawada[1], Kazunori Ogawa[1]

1. ISAS/JAXA, Japan, 2. Kochi Univ., Japan, 3. Instituto de Astrofisica de Canarias, Univ. of La Laguna, Spain, 4. Planetary Science Institute, USA, 5. DLR, Germany, 6. Univ. of Tokyo, Japan, 7. Rikkyo Univ., Japan, 8. Univ. of Aizu, Japan, 9. AIST, Japan, 10. Chiba Inst. Tech, Japan, 11. Meiji Univ., Japan

Introduction: Hayabusa2 revealed the detailed shape of the Cb-type asteroid 162173 Ryugu. The surface of Ryugu is divided into east and west regions by a trough [1,2,3]. The western region (160 - 290˚E) is called the Western bulge, and the wider eastern region is called the Eastern Hemisphere. Ryugu has an equatorial ridge, and the ridge spans across both east and west regions [1,2,3]. A model for the evolution of the ridge has been proposed, in which pebbles/regolith from the ridge have migrated towards the mid-latitudes [4]. The Western bulge has fewer craters [5] and fewer boulders (D>5 m) [6] than the Eastern hemisphere. The photometric analysis of Hayabusa2 Telescopic Onboard Navigation Camera (ONC-T) data reported that the Western bulge has a slightly higher v-band (0.55 μm) reflectance than the Eastern hemisphere when observed at a solar phase angle of 19˚ [2]. However, the ONC-T opposition observations (zero phase angle observations) show a similar range of values in both regions for the normal albedo [7]. We therefore hypothesize that this difference in optical properties between the east and west regions may be due to surface properties other than the albedo of the surface materials. To help understand the evolutionary history of these regions (Eastern hemisphere, Western bulge, and Equatorial ridge), we conducted a regional photometric analysis of the ONC-T data using the Hapke photometric model [8,9].

Data and method: We used seven sets of Ryugu global observations (2.1 m/pixel) acquired in the ONC-T v-band. The phase angles of the observations ranged from 0 to 42˚. In order to reduce the number of free parameters, we fixed three of the five parameters of the Hapke photometric model [8,9]. The fixed parameters were: opposition surge strength B_0 = 0.98, opposition surge width h = 0.075, and phase function parameter b = 0.388. These values are the global averages from a recent photometric study [10]. The two free parameters were the single scattering albedo, w, and the macroscopic roughness, θ-bar. A 32 x 32 m (4x4˚) mesh was defined on the Ryugu surface, and values of the radiance factor (I/F) and photometric angles (incident (i), emission (e), and phase (α) angles) were collected from the ONC images from the pixels within each mesh. Averaging binning was used to mitigate the bias of the data distribution in the three dimensional photometric angle space (Binning width: $\Delta i = \Delta e = 1$˚; $\Delta \alpha = 0.1$˚ for α = 0-2˚, $\Delta \alpha = 0.2$˚ for α = 2-5˚, and $\Delta \alpha = 1$˚ for α >5˚). Finally, Hapke model fitting (Levenberg-Marquardt method) was performed for each mesh to determine w and θ-bar.

Results: The spatial distribution of w appears similar to that of the normal albedo. On the other hand, the spatial distribution of θ-bar was similar to the reflectance map in [2], which was made from observations at α=19˚. This suggests that a difference in surface roughness/texture at small scales (cm to μm order) may exist between the east and west regions. We also found that the ridge has smaller θ-bar values than the Eastern hemisphere. This feature is consistent with the pebbles/regolith migration hypothesis [4]. The present analysis shows that the regional differences in photometric properties can be detected in the

©2021. Japan Geoscience Union. All Right Reserved.

ONC-T data. Further investigation of the history of the Eastern hemisphere, Western bulge, and ridge will require comparison with other roughness-related studies (e.g., densities of crater/boulder, thermal infrared data, and LIDAR data).

References: [1] Watanabe S. et al. (2019) Science 364, 268. [2] Sugita S., et al. (2019) Science 364, 252. [3] Hirabayashi M. et al. (2019) ApJL 874, L10. [4] Morota T. et al. (2020) Science 368, 654–659. [5] Cho et al., submitted. [6] Michikami T. et al. (2019) Icarus 331, 179–191. [7] Yokota Y. et al. submitted. [8] Hapke B. (1981) JGR 86(B4), 3039–3054. [9] Hapke B. (2012) Theory of Reflectance and Emittance Spectroscopy (2nd ed.). Cambridge Univ. Press. [10] Tatsumi E., et al. (2020) A&A 639, A83.

Keywords: Asteroid, Ryugu, Photometry

©2021. Japan Geoscience Union. All Right Reserved.

Spectrophotometric behavior of Ryugu’s surface as inferred from the Hayabusa2/NIRS3 data

*Andrea Longobardo[1], Ernesto Palomba[1,2], Anna Galiano[1], Fabrizio Dirri[1], Angelo Zinzi[2], Mario D'Amore[3], Deborah Domingue[4], Kohei Kitazato[5], Takahiro Iwata[6], Moe Matsuoka[6], Takahiro Hiroi[7], Driss Takir[8], Tomoki Nakamura[9], Masanao Abe[5], Makiko Ohtake[5], Shuji Matsuura[10], Sei-ichiro WATANABE[6,11], Makoto Yoshikawa[6], Takanao Saiki[6], Tatsuaki Okada[6], Yukio Yamamoto[6], Yoh Takei[6], Kei Shirai[6], Naru Hirata[5], Naoyuki Hirata[12], Koji Matsumoto[13], Yuichi Tsuda[6]

1. Istituto Nazionale di Astrofisica - Istituto di Astrofisica e Planetologia Spaziali, Rome, Italy, 2. ASI-SSDC, Rome, Italy, 3. German Aerospace Center, Institute of Planetary Research, Berlin, Germany, 4. PSI, Tucson, AZ, USA, 5. University of Aizu, Aizu-Wakamatsu 965-8580, Fukushima, Japan, 6. ISAS-JAXA, Japan, 7. Department of Earth, Environmental and Planetary Sciences, Brown University, Providence, RI 02912, USA, 8. Jacobs/NASA Johnson Space Center, USA, 9. Tohoku University, Miyagi, Japan, 10. Kwansei Gakuin University, Hyogo, Japan, 11. Nagoya University, Nagoya 464-8601, Japan, 12. Kobe University, Kobe 657-8501, Japan, 13. National Astronomical Observatory of Japan, Mitaka 181-8588, Japan

We studied the photometric behavior of the main spectral parameters describing the Ryugu near-infrared spectrum as measured by the Hayabusa2/NIRS3 spectrometer with a focus on albedo at 1.9 um, the band depths at 2.7 um, band depth at 2.8 um, spectral slope between 1.2 and 1.9 um.

We applied the same empirical model used to examine the surfaces of other small bodies such as Vesta, Lutetia. Ceres, Churyumov-Gerasimenko (Longobardo et al., 2014, 2016, 2017, 2019). The model methodology involves removing the topographic influence by dividing the radiance factor by a disk function and deriving the phase function by means of a statistical analysis approach.

In the following we summarize the results.

Albedo. Due to the small phase angle coverage (15˚-40˚), we approximated the phase function as a straight line and compared its slope with the slope of the phase function of other asteroids retrieved in the infrared range. We found a similarity between Ceres and Ryugu and flatter phase functions for Eros and Vesta, confirming the well known anti-correlation between albedo and phase function steepness.

Band depths. Band depths are observed to decrease with increasing phase angle. This is a unique behavior that has not been observed on any other small body visited by a space mission. This behavior can be ascribed to Ryugu’s very dark surface (~2% of incident light is reflected from the surface, Sugita et al., 2019; Kitazato et al., 2019), in which the role of multiple scattering is negligible and the large absorption properties of the surface reduces the radiation reflected at larger phase angles.

Infrared slope. A small phase reddening is observed, very similar to that observed by the ONC camera in the visible range (Tastumi et al., 2020), suggesting a constant particle phase function between visible and near-infrared and/or microscopically smooth particles.

©2021. Japan Geoscience Union. All Right Reserved.

References:
Kitazato, K. et al., 2019. Science 364, 6437, 272-275; Longobardo, A. et al., 2014. Icarus 240, 20-35; Longobardo, A. et al., 2016. Icarus 259, 72-90; Longobardo, A. et al., 2017. MNRAS 469, 2, S346-S356; Longobardo, A. et al., 2019. Icarus 320, 97-109; Sugita, S. et al., 2019. Science 364, 6437, 252; Tatsumi, E. et al., 2020. A&A 639, A83.

Keywords: Hayabusa2, Ryugu Asteroid, Photometry, Spectroscopy

©2021. Japan Geoscience Union. All Right Reserved.

Laboratory spectral constraints on the composition and origin of Phobos: Reconciling the Vis-NIR/Mid-IR contradictions

*Matthew Izawa[1], Sandra Potin[2], Edward Cloutis[2]

1. Institute for Planetary Materials, 2. University of Winnipeg

The origin and compositional makeup of Phobos, the larger and innermost satellite of Mars, remains uncertain. Phobos will be targeted by the Mars Moon eXplorer mission currently scheduled for a 2024 launch. In preparation for the upcoming exploration of Phobos, we have undertaken an investigation of various proposed spectral and compositional analogues of Phobos surface material. Fundamentally, Phobos presents a contradiction in that at visible and near-infrared wavelengths, Phobos is spectrally similar to D-type asteroids –possibly represented by meteorites like Tagish Lake –but at longer wavelengths, Phobos is more consistent with anhydrous silicate mixtures similar to basalts. Each wavelength range is therefore suggestive of different formation mechanisms: gravitational capture versus reaccretion of Martian ejecta. By investigating mixtures of various analogue materials, we are attempting to determine if any plausible mixtures of known components such as Martian regolith breccia, Tagish Lake carbonaceous chondrite, or their constituent phases, can reproduce the spectrum of Phobos over both the visible-near infrared and mid-infrared wavelength ranges.

Keywords: Phobos, Reflectance spectroscopy

©2021. Japan Geoscience Union. All Right Reserved.

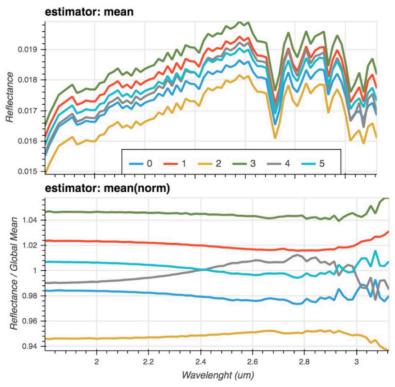
UNSUPERVISED LEARNING OF NIRS3 DATA: RYUGU SPECTRAL SURFACE REGIONS CLASSIFICATION

*Mario D'Amore[1], E. Palomba[2,3], A. Galiano[2], A. Zinzi[3], F. Dirri[2], A. Longobardo[2], K. Kitazato[4], T. Iwata[5], M. Matsuoka[5], T. Hiroi[6], D. Takir[7], T. Nakamura[8], M. Abe[5], M.y Ohtake[5], S. Matsuura[9], S. Watanabe[10], M. Yoshikawa[5], T. Saiki[5], S. Tanaka[5], T. Okada[5], Y. Yamamoto[5], Y. Taikei[5], K. Shirai[5], N. Hirata[11,4], K. Matsumoto[12], Y. Tsuda[5]

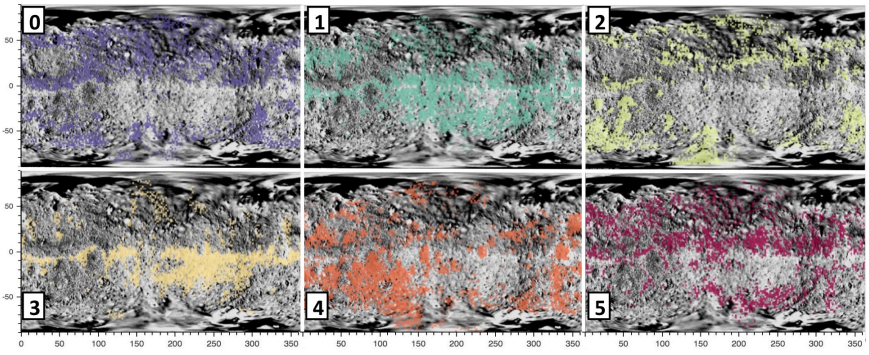
1. German Aerospace Center, Institute of Planetary Research, Berlin, Germany, 2. INAF-IAPS, Rome, Italy, 3. SSDC-ASI, Rome, Italy, 4. University of Aizu, Aizu-Wakamatsu 965-8580, Fukushima, Japan, 5. Institute of Space and Astronautical Science (ISAS), Japan Aerospace Exploration Agency, Sagamihara, 252-5210, Japan, 6. Department of Earth, Environmental and Planetary Sciences, Brown University, Providence, RI 02912, USA, 7. Jacobs/NASA Johnson Space Center, USA, 8. Tohoku University, Miyagi, Japan, 9. Kwansei Gakuin University, Hyogo, Japan, 10. Nagoya University, Nagoya 464-8601, 11. Kobe University, Kobe 657-8501, Japan, 12. National Astronomical Observatory of Japan, Mitaka 181-8588, Japan.

The 27th of June 2018 the Japanese Hayabusa2 spacecraft approached the C-type Near Earth asteroid 162173 Ryugu. Hayabusa2 is equipped with three remote sensing instruments such i.e. as the Thermal Infrared Imager TIR, the NIRS 3 spectrometer and the Optical Navigation Camera-Telescopic (ONC-T) with a wideband and seven narrow band filters. A Lidar instrument allowed to reconstruct the shape model of the asteroid and to measure the altimetry, in order to perform a precise touchdown in sampling the asteroidal regolith. Additionally, by using the robotic landers Minerva-II and Mascot, Hayabusa 2 has conducted in situ surface experiments. Ryugu is a top-shaped Cb type asteroid and is covered by a large number of boulders. It is one of the darkest object in our Solar System with a quite homogenous composition, including OH-rich materials. In conclusion, we find an automated approach to extract spatially coherent region on Ryugu surface based only on spectral data using almost the whole NIRS3 spectral range. Those classes show a significant spatial correlation with geomorphological feature and different spectral trends.

Keywords: unspuervised, machine learning , spectral surface regions



Classes average (top) and normalized to global mean.



Classes distribution on the surface of Ryugu

©2021. Japan Geoscience Union. All Right Reserved.

Quantitative analysis of spectral evolution of craters, boulders, and regolith on Ryugu and Bennu

*Koki Yumoto[1], Eri Tatsumi[2,1], Tatsuki Ebihara[1], DellaGiustina Daniella[3], Naofumi Takaki[1], Tomokatsu Morota[1], Yuichiro Cho[1], Golish Dathon[3], Rie Honda[4], Shingo Kameda[5], Yasuhiro Yokota[6], Naoya Sakatani[5], Toru Kouyama[7], Sawada Hirotaka[6], Masahiko Hayakawa[6], Matsuoka Moe[6], Manabu Yamada[8], Hidehiko Suzuki[9], Chikatoshi Honda[10], Kazunori Ogawa[11,12], Kazuo Yoshioka[1], Seiji Sugita[1]

1. University of Tokyo, 2. Instituto de Astrofísica de Canarias, 3. Lunar and Planetary Laboratory, Univ. of Arizona, 4. Kochi Univ., 5. Rikkyo Univ., 6. ISAS/JAXA, 7. Inst. of Adv. Ind. Sci. and Tech., 8. Chiba Inst. of Tech., 9. Meiji Univ., 10. Univ. of Aizu, 11. JSEC/JAXA, 12. Kobe Univ.

Spectral evolution of C-complex asteroids [1] needs to be identified to understand the implications for parent-body materials from telescopic observations. Spectroscopy of near-Earth C-complex asteroids Ryugu and Bennu provide data to identify the predominant weathering effects on the respective asteroids, which could be potentially extrapolated to main belt C-complex bodies. For instance, the spectral change of craters with increasing size showed a darkening/reddening effect for Ryugu [2, 3], whereas brightening/bluing was derived for Bennu [4]. In this study, we quantify the spectral evolution tracks of craters, boulders, and regolith to further constrain the weathering effects on Ryugu and Bennu.

Evidence of boulder breakdown on the surfaces of Ryugu and Bennu [5, 6] suggests a shorter lifetime for smaller boulders. Thus, a size-dependent spectral trend among boulders may reflect their spectral/physical evolution. For regolith, dependence on geopotential height should represent spectral evolution since regolith can migrate in the direction of local downslopes [7]. Moreover, for all geologic features, spectral evolution could be further deduced from latitude-dependent trends [8, 9]. To quantify the trends, we established spectral catalogues of craters and boulders on Ryugu based on images acquired by the Optical Navigation Camera [10]. For Bennu, we analyzed the catalogue based on images acquired by the mid-field multispectral imager MapCam [11] established in [4].

The trends we find from spectral analysis of both craters and regolith showed darkening/reddening on Ryugu and brightening/bluing on Bennu. Their significance was confirmed by t-tests with p-value <.01. The spectral evolution of these asteroids exhibits diverging tracks in spectral feature space. The rates of spectral change were estimated by combining the size-dependency of craters and their model ages with spectral measurements [12]. The weathering rate (/$\log_{10}$ time; time range ~10^3–10^7 yr) of albedo was quantified to be $-2.9(5)\times10^{-4}$ for Ryugu and $+3.5(6)\times10^{-4}$ for Bennu. As for the 480-to-850 nm spectral slope, the weathering rate (/um/$\log_{10}$ time; time range ~10^3–10^7 yr) was +0.006(2) for Ryugu and −0.009(2) for Bennu. The observed bluing rate on Bennu is smaller than that estimated from main-belt asteroids [13] by an order of magnitude. These rates provide observational constraints for weathering experiments of returned samples. Also, comparison of the magnitude of the maturation between craters and regolith shows that weathering heterogeneity on the surface is produced mainly by surface migrations on Ryugu, and crater formations on Bennu.

However, boulder color trends show significant darkening/reddening for both asteroids. Although size-dependent trends of boulders may be due to the difference in material properties, the consistency with latitude-dependent trends supports the association with weathering processes. The possible difference in spectral evolution of boulders compared with that of regolith is consistent with the presence

©2021. Japan Geoscience Union. All Right Reserved.

of fine particles, which may be produced by thermal disaggregation of boulder surfaces [3, 14]. Possible spectral alteration of boulders by the presence/absence of fines could be tested with reflectance measurements of returned samples.

[1] Lantz et al., 2018, *Icarus*, *302*, 10-17. [2] Sugita et al, 2019, *Science*, *364*(6437), eaaw0422. [3] Morota et al., 2020, *Science*, *368*(6491), 654-659, aaz6306. [4] DellaGiustina et al., 2020, *Science*, *370* (6517), eabc3660. [5] Molaro et al., 2020, *Nat. Commun.*, *11*(1), 2913. [6] Ballouz et al., 2020, *Nature*, *587*(7833), 205-209. [7] Jawin et al., 2020, *JGR: Planets*, *125*(9). [8] Hemingway et al., 2015, *Icarus*, 261, 66-79. [9] Sen et al., 2021, LPSC, #2548. [10] Kameda et al., 2017, *SSR*, *208*(1), 17-3. [11] Rizk et al., 2018, *SSR*, *214*(1), 26. [12] Takaki et al., submitted to *Icarus.* [13] Nesvorný et al., 2005, *Icarus*, *173*(1), 132-152. [14] Johnson & Fanale, 1973, *J. Geophys. Res. 78*, 8507–8518.

Keywords: Space weathering, Asteroids

©2021. Japan Geoscience Union. All Right Reserved.

Bennu's Global Geologic Map Reveals the Last Epoch of Resurfacing

*Erica R Jawin[1], Timothy J McCoy[1], Kevin John Walsh[2], Harold C Connolly[3], Ronald L Ballouz[4], Andrew Joseph Ryan[4], Maurizio Pajola[5], Olivier S Barnouin[6], Hannah H kaplan[7], Vicky E Hamilton[2], Josh P Emery[8], Daniella N Dellagiustina[4], Daniel Jay Scheeres[9], Michael G Daly[10], Carina A Bennett[4], Dathon R Golish[4], Mark Perry[6], R Terik Daly[6], E Beau Bierhaus[11], Michael C Nolan[4], Heather L Enos[4], Dante S Lauretta[4]

1. Smithsonian National Museum of Natural History, 2. Southwest Research Institute, 3. Rowan University, 4. University of Arizona, 5. INAF-Astronomical Observatory of Padova, 6. Johns Hopkins University Applied Physics Laboratory, 7. Goddard Space Flight Research Center, 8. Northern Arizona University, 9. University of Colorado, Boulder, 10. York University, 11. Lockheed Martin Space

Asteroid (101955) Bennu, the target of NASA’s OSIRIS-REx mission, is a rubble-pile asteroid with a surface dominated by boulders. We mapped its global geology to better understand its global characteristics and surface evolution. Our global geologic map of Bennu will facilitate future analyses of the asteroid and will contextualize the returned sample. We present the results of our analysis and the implications for the heterogeneous evolution of Bennu’s surface.

Bennu’s small size and rubble-pile nature have led to subdued topography with few distinct stratigraphic contacts. As such, our mapping methodology included first mapping major topographic features, geologic features, and surface texture variation, and then integrating these three products to define geologic units.

Bennu’s topographic features include two dominant structures: the equatorial bulge, between approximately 20°N and S latitude, and four longitudinal ridges (dorsa) and adjacent troughs (fossae) that span both hemispheres and the equator. The geologic features of Bennu that we mapped include craters >10 m in diameter, boulders >20 m in diameter, lineaments, particle ejection source regions, and morphologies associated with mass movement (e.g., imbricated or buried boulders). Craters are abundant on the equatorial bulge, which suggests that the bulge is an old feature. There are more large boulders in the southern hemisphere than the northern hemisphere or the equatorial region. Mass movement features appear to be spatially correlated with large boulders (many large boulders are partly buried) and are concentrated in fossae bound by lineaments. Bennu’s surface texture variation is controlled by the abundance of boulders. The surface can be divided into two dominant morphologies: (1) smooth or knobby with few boulders, and (2) rugged with abundant boulders.

To define geologic units, we integrated the maps of topographic features, geologic features, and surface texture variation, resulting in two geologic units we refer to as the “Smooth Unit” and the “Rugged Unit”. The Smooth Unit contains few large boulders or mass movement features and can occur on both dorsa and fossae. The mission’s sample collection site (Nightingale) and several particle ejection source regions are located in the Smooth Unit. The Rugged Unit contains 89% of the mapped large boulders and 85% of mass movement features, which are mostly located in fossae. The surface of Bennu can therefore be effectively characterized by only two geologic units that represent end-member characteristics. The two units are also distinct in other global maps of Bennu, including surface roughness, slopes, and certain spectral maps.

The relative concentration of mass movement features in the Rugged Unit, which likely formed in the last few hundred thousand years, suggests that resurfacing may have been more concentrated in the Rugged

©2021. Japan Geoscience Union. All Right Reserved.

Unit than the Smooth Unit. In addition, the distribution of the reddest (believed to be the youngest) craters on Bennu shows that the Rugged Unit contains fewer red craters, by a factor of ~3 per unit area relative to the Smooth Unit. This difference suggests the Rugged Unit may have experienced more resurfacing in the recent past (~500,000 years) relative to the Smooth Unit, which may have been less active.

The equatorial bulge, dorsa, and fossae appear to be the oldest features on Bennu due to their crater abundance. Both geologic units cross the equatorial bulge, suggesting that it has not greatly affected Bennu's surface evolution. Large boulders are abundant in fossae and may be linked to their evolution, but some large boulders are also present on dorsa, which suggests that topography is not the only control on the boulder distribution. Surface modification in the form of impact cratering, mass movement, and particle ejection continued after the formation of the equatorial bulge, dorsa, and fossae, and over time, enhanced resurfacing in certain regions led to the formation of the Rugged Unit.

Keywords: Bennu, OSIRIS-REx, Resurfacing, Geology, Mapping

©2021. Japan Geoscience Union. All Right Reserved.

[E] Oral | P (Space and Planetary Sciences)：P-PS Planetary Sciences

Sun. Jun 6, 2021 3:30 PM - 5:00 PM JST | Sun. Jun 6, 2021 6:30 AM - 8:00 AM UTC | Ch.04 Zoom Room 04

[P-PS04] Small Solar System Bodies: A New Insight from Hayabusa2, OSIRIS-REx and Other Space Missions

convener:Tatsuaki Okada(Institute of Space and Astronautical Science, Japan Aerospace Exploration Agency), Taishi Nakamoto(Tokyo Institute of Technology), Daisuke Kuroda(Kyoto University), Chairperson:Tatsuaki Okada(Institute of Space and Astronautical Science, Japan Aerospace Exploration Agency), Taishi Nakamoto(Tokyo Institute of Technology), YACHEN YANG(Center for Space and Remote Sensing Research)

Small Solar System bodies, including asteroids, comets, satellites, and interplanetary dust particles, are notably important for understanding the origin and evolution of our Solar System, as well as investigating the sources of building blocks of life. Many new discoveries on small bodies have been carried out by observations from ground-based and space-based observatories, and explorations by spacecraft rendezvous and flyby. New perspectives on solar system evolution have been paved by analyses of extraterrestrial materials such as meteorites, IDPs, and return samples by space missions. Numerical and laboratory simulation studies have helped interpretations for those results and proposed new insights on these topics. In this session, new results of scientific studies and new ideas of methodology for investigating small solar system bodies are highly welcome, especially the topics on the remote sensing, surface experiments, and analysis of return sample in the Hayabusa2 and OSIRIS-REx missions, as well as the expectations and preparations for future missions including MMX, Destiny+, Hera, Comet Interceptor, and Hayabusa2-Extended missions.

3:30 PM - 3:50 PM JST | 6:30 AM - 6:50 AM UTC

[PPS04-19] Impact histories inferred from exogenic boulders on asteroids Ryugu and Bennu

★Invited Papers

*ERI TATSUMI[1,2], Chiho Sugimoto[2], Seiji Sugita[2], Marcel Popescu[4], Humberto Campins[11], Julia de León[3], Amy A. Simon[5], Hannah H. Kaplan[6], Yuichiro Cho[2], Tomokatsu Morota[2], Rie Honda[7], Shingo Kameda[8], Yasuhiro Yokota[3], Koki Yumoto[2], Minami Aoki[2], Daniella N. DellaGiustina[10], Dathon R. Golish[10], Javier Licandro[1], Juan Luis Rizos[1], Takahiro Hiroi[12], Deborah Domingue[13], Michel Patrick[14], Dante S. Lauretta[10], Manabu Yamada[15], Naoya Sakatani[8], Toru Kouyama[9], Chikatoshi Honda[16], Masahiko Hayakawa[3], Moe Matsuoka[3], Hidehiko Suzuki[17], Kazunori Ogawa[3], Hirotaka Sawada[3] (1.Instituto de Astrofisica de Canarias, 2.Univ. of Tokyo, 3.ISAS/JAXA, 4.Astronomical Institute of the Romanian Academy, 5.NASA Goddard Space Flight Center, 6.Southwest Research Institute, 7.Kochi Univ., 8.Rikkyo Univ., 9.AIST, 10.Univ. of Arizona, 11.Univ. of Central Florida, 12.Brown Univ., 13.Planetary Science Institute, 14.Observatoire de la Côte d'Azur, 15.Chiba Institute of Tech., 16.Univ. of Aizu, 17.Meiji Uni.)

3:50 PM - 4:10 PM JST | 6:50 AM - 7:10 AM UTC

[PPS04-20] The ESA Hera mission: rendezvous with a binary asteroid, planetary defense and science

★Invited Papers

*Patrick Michel[1], Michael Kueppers[2], Alan Fitzsimmons[3], Simon F. Green[4], Monica Lazzarin[5], Stephan Ulamec[6], Ian Carnelli[7], Paolo Martino[7] (1.Universite Côte D'Azur, Observatoire De La Côte D'Azur, CNRS, Laboratoire Lagrange, 2.ESA-European Space Astronomy Centre, 3.Queen's University Belfast, 4.The Open University, 5.Padova University, 6.DLR RB-MUSC, 7.ESA-ESTEC)

4:10 PM - 4:25 PM JST | 7:10 AM - 7:25 AM UTC

[PPS04-21] Hayabusa2 Extended Mission to rendezvous with Asteroid 1998 KY26: Investigations of an extremely small fast rotator for planetary defense

*Masatoshi Hirabayashi[1], Y. Mimasu[2], N. Sakatani[3], S. Watanabe[4], Y. Tsuda[2], T. Saiki[2], S. Kikuchi[2], T. Kouyama[5], M. Yoshikawa[2], S. Tanaka[2], S. Nakazawa[2], Y. Takei[2], F. Terui[2], H. Takeuchi[2], A. Fujii[2], T. Iwata[2], K. Tsumura[6], S. Matsuura[7], Y. Shimaki[2], S. Urakawa[8], Y. Ishibashi[9], S. Hasegawa[2], M. Ishiguro[10], D. Kuroda[11], S. Okumura[8], S. Sugita[12], T. Okada[2], S. Kameda[3], S. Kamata[13], A. Higuchi[14], H. Senshu[15], H.

Noda[16], K. Matsumoto[16], R. Suetsugu[17], T. Hirai[15], K. Kitazato[18] (1.Auburn University, 2.Japan Aerospace Exploration Agency, 3.Rikkyo University, 4.Nagoya University, 5.National Institute of Advanced Industrial Science and Technology, 6.Tokyo City University, 7.Kwansei Gakuin University, 8.Japan Spaceguard Association, 9.Hosei University, 10.Seoul National University, 11.Kyoto University, 12.University of Tokyo, 13.Hokkaido University, 14.University of Occupational and Environmental Health, 15.Chiba Institute of Technology, 16.National Astronomical Observatory of Japan, 17.National Institute of Technology, 18.University of Aizu)

4:25 PM - 4:40 PM JST | 7:25 AM - 7:40 AM UTC

[PPS04-22] **Highly Time-Resolved Photometric Observations of Tiny Near Earth Objects with the Tomo-e Gozen Camera**

*Jin Beniyama[1], Shigeyuki Sako[1], Ryou Ohsawa[1], Satoshi Takita[1], Naoto Kobayashi[1], Shin-ichiro Okumura[2], Seitaro Urakawa[2], Fumihiko Usui[3], Fumi Yoshida[4,5], Makoto Yoshikawa[3] (1.Institute of Astronomy, Graduate School of Science, The University of Tokyo, 2.Japan Spaceguard Association, 3.Institute of Space and Astronautical Science, Japan Aerospace Exploration Agency, 4.University of Occupational and Environmental Health, 5.Planetary Exploration Research Center, Chiba Institute of Technology)

4:40 PM - 4:55 PM JST | 7:40 AM - 7:55 AM UTC

[PPS04-23] Color and size distributions of main belt asteroids obtained by the Subaru/Hyper Suprime-Cam

*Natsuho Maeda[1], Tsuyoshi Terai[2], Keiji Ohtsuki[1], Fumi Yoshida[3,4], Kosuke Ishihara[1,2,5], Takuto Deyama[1,6] (1.Graduate school of science, Kobe University , 2.National Astronomical Observatory of Japan, 3.Chiba Institute of Technology, 4.University of Occupational and Environmental Health, 5.The Graduate University for Advanced Studies, 6.NTT Data MSE Corporation)

4:55 PM - 5:00 PM JST | 7:55 AM - 8:00 AM UTC

[PPS04-24] Discussion

Impact histories inferred from exogenic boulders on asteroids Ryugu and Bennu

*ERI TATSUMI[1,2], Chiho Sugimoto[2], Seiji Sugita[2], Marcel Popescu[4], Humberto Campins[11], Julia de León[3], Amy A. Simon[5], Hannah H. Kaplan[6], Yuichiro Cho[2], Tomokatsu Morota[2], Rie Honda[7], Shingo Kameda[8], Yasuhiro Yokota[3], Koki Yumoto[2], Minami Aoki[2], Daniella N. DellaGiustina[10], Dathon R. Golish[10], Javier Licandro[1], Juan Luis Rizos[1], Takahiro Hiroi[12], Deborah Domingue[13], Michel Patrick[14], Dante S. Lauretta[10], Manabu Yamada[15], Naoya Sakatani[8], Toru Kouyama[9], Chikatoshi Honda[16], Masahiko Hayakawa[3], Moe Matsuoka[3], Hidehiko Suzuki[17], Kazunori Ogawa[3], Hirotaka Sawada[3]

1. Instituto de Astrofisica de Canarias, 2. Univ. of Tokyo, 3. ISAS/JAXA, 4. Astronomical Institute of the Romanian Academy, 5. NASA Goddard Space Flight Center, 6. Southwest Research Institute, 7. Kochi Univ., 8. Rikkyo Univ., 9. AIST, 10. Univ. of Arizona, 11. Univ. of Central Florida, 12. Brown Univ., 13. Planetary Science Institute, 14. Observatoire de la Côte d'Azur, 15. Chiba Institute of Tech., 16. Univ. of Aizu, 17. Meiji Uni.

Rubble-pile asteroids, such as (162173) Ryugu and (101955) Bennu, are formed as a result of catastrophic disruption of a parent body and re-accumulation of the fragments by self-gravity Michel and Ballouz et al. 2020). Therefore, reaccumulated rubble piles could include mixtures of materials from both the parent body and its catastrophic impactor, as they did in the case of 2008 TC_3 and the Almahata Sitta meteorites (Jenniskens et al. 2009). Indeed, six unusually bright, basaltic, meter-scale boulders were recently identified on Bennu's dark surface (DellaGiustina et al. 2021), and their close spectral matches to the Howardite-Eucrite-Diogenite (HED) meteorites and Vesta family members indicate that they originated from asteroid (4) Vesta. In parallel, bright exogenic anhydrous-silicate–rich materials were found on Ryugu (Tatsumi et al. 2021). The bright boulders on Ryugu are consistent with ordinary chondrite meteorites, based on their albedo and the weak or even absent absorption band at 2 μm. These exogenous materials on the surfaces of rubble-pile asteroids could be a key to constraining their specific impact conditions and collisional evolution.

In this study, we report further study of the visible spectrophotometry and morphology of exogenic boulders on Ryugu and Bennu using two multi-band cameras: the telescopic Optical Navigation Camera (ONC-T) onboard the Hayabusa2 spacecraft, and MapCam onboard the Origins, Spectral Interpretation, Resource Identification, and Security–Regolith Explorer (OSIRIS-REx) spacecraft, respectively.

For Ryugu, we first detected objects with peak reflectance brighter by a factor of >1.5 than the surrounding area. Tatsumi et al. (2021) found two spectral groups among the bright boulders: S-type with an absorption near 1 μm and C/X-type with a flat spectrum. That study found 6 S-types and 15 C/X-types, and here we report the additional finding of two S-types and ~70 C/X-types. We found that S-type bright boulders follow two parallel trends consistent with space weathering of ordinary chondrites. Fragments from projectiles suggest that Ryugu may not have formed directly from the original parent body, i.e., it is from a second or higher generation of collisional descendants (Sugimoto et al. in revision).

For Bennu, we directly surveyed the absorption near 1 μm, which is indicative of anhydrous silicates. We propose 77 objects of exogenic origin including 6 boulders previously reported by DellaGiustina et al. (2021). We find that proposed exogenic objects follow two mixing trends with respect to the average spectrum of Bennu (Tatsumi and Popescu et al. submitted). One trend can be explained by mixing with HEDs, as discussed in DellaGiustina et al. (2021), and the other trend can be explained by mixing with

©2021. Japan Geoscience Union. All Right Reserved.

another, of olivine-rich composition. Near-infrared spectra also support the possibility of multiple compositions among exogenic objects on Bennu. Le Corre et al. (submitted) also reached to the similar conclusion with a different methodology. Thus, similar to Ryugu, Bennu could represent a second or higher generation collisional fragment.

Using high-resolution images, we found that more than half of the exogenic objects that we identified on Bennu have breccia-like or inclusion-like morphologies. We do not observe a correlation between morphology and spectral shape.

Direct comparison of reflectance spectra of exogenic ,materials between Ryugu and Bennu suggests a compositional difference. Furthermore, the number density of exogenic objects > 0.5 m on Bennu is ˜40 times that on Ryugu (Tatsumi and Popescu et al. submitted). Bennu exhibits much more contamination from exogenic materials than Ryugu, which likely reflects differences in impact conditions, such as impact velocity and impactor size.

Michel and Ballouz et al. (2020) Nat. Commun. 11, 2655
Jenniskins et al. (2009) Nature 458, 485-488.
DellaGiustina et al. (2021) Nat. Astron. 5, 31-38.
Tatsumi et al. (2021) Nat. Astron. 5, 39-45.
Sugimoto et al. (in revision) Icarus.
Tatsumi and Popescu et al. (submitted) MNRAS.
Le Corre et al. (submitted) PSJ.

Keywords: Asteroids, Hayabusa2, OSIRIS-REx, Ryugu, Bennu

©2021. Japan Geoscience Union. All Right Reserved.

The ESA Hera mission: rendezvous with a binary asteroid, planetary defense and science

*Patrick Michel[1], Michael Kueppers[2], Alan Fitzsimmons[3], Simon F. Green[4], Monica Lazzarin[5], Stephan Ulamec[6], Ian Carnelli[7], Paolo Martino[7]

1. Universite Côte D'Azur, Observatoire De La Côte D'Azur, CNRS, Laboratoire Lagrange, 2. ESA-European Space Astronomy Centre, 3. Queen's University Belfast, 4. The Open University, 5. Padova University, 6. DLR RB-MUSC, 7. ESA-ESTEC

The Hera mission is in Phase C for launch in 2024 in the ESA Space Safety Programme. Hera will contribute to the first deflection test of an asteroid, in the framework of the international Asteroid Impact and Deflection Assessment (AIDA) collaboration, supported by NASA and ESA

Hera will rendezvous for the first time with a binary asteroid, (65803) Didymos, and take particular emphasis on its
secondary, Dimorphos, of only 160 m in diameter. So far, no mission has visited such a small rock in space. Moreover, for the first time, internal and subsurface properties will be directly measured. As a crucial contribution to planetary defense, Hera will perform the measurements necessary to understand the effect of the NASA DART impact on Didymos' secondary in 2022, in particular its mass, its internal structure, the direct determination of the momentum transfer and the detailed characterization of the crater left by DART.

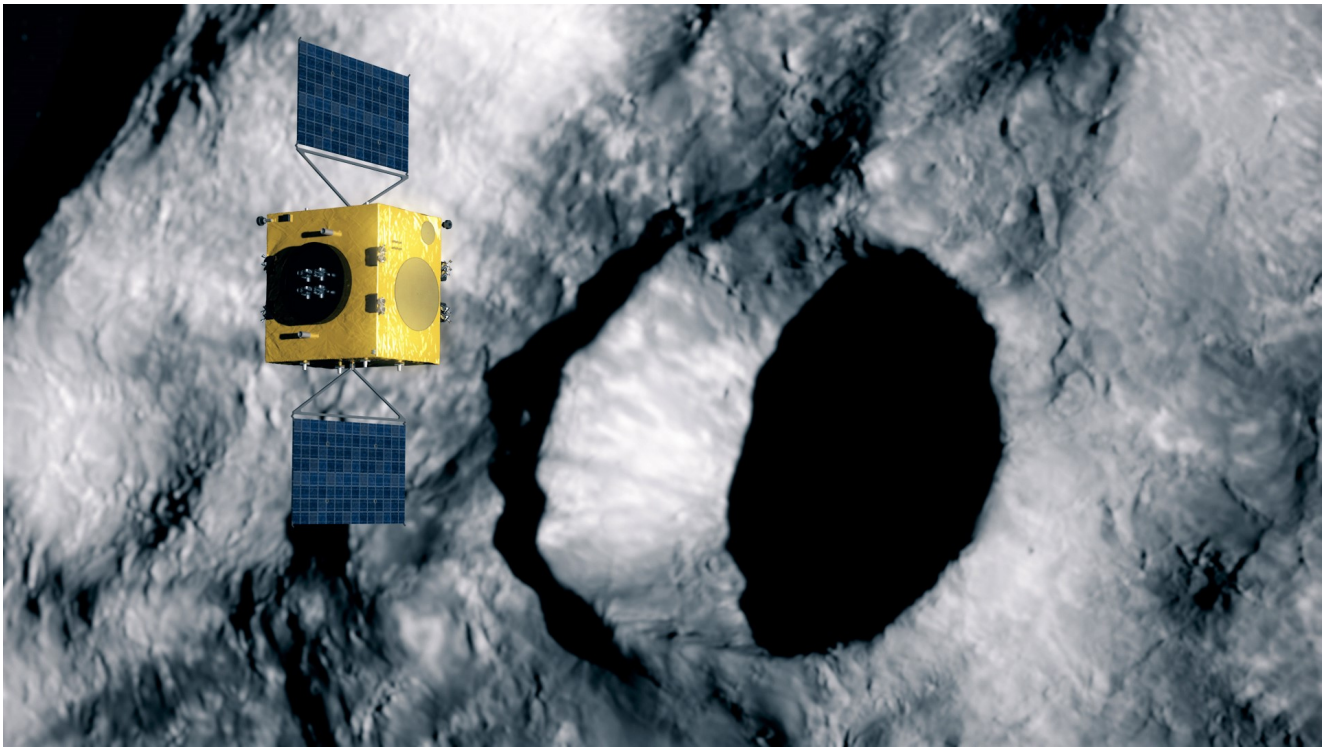
How do binaries form? What does a 160 m-size rock in space look like? What is the surface composition? What are its internal properties? What are the surface structure and regolith mobility on both Didymos and Dimorphos? What are the surface geophysical properties of two objects of different size and surface gravity, which probably formed from the same material? And what will be the size and the morphology of the crater left by DART, which will provide the first impact experiment at full asteroid scale using an impact speed close to the average speed between asteroids? What will be the exact momentum transferred by DART, which needs the precise measurement of the mass of the target by Hera? These questions and many others will be addressed by Hera as a natural outcome of its investigations focused on planetary defense.

The measurements performed by Hera will thus provide unique information on many current issues in asteroid science and therefore, the scientic legacy of the Hera mission will extend far beyond the core aims of planetary defense. Hera is, thus, the main European contribution to the current international asteroid exploration era.

Acknowledgement: Funding support from ESA and from the European Union's Horizon 2020 research and innovation programme under grant agreement No 870377 (project NEO-MAPP) is acknowledged.

Keywords: Asteroids, Binary Asteroids, Impact Physics, Planetary defense, Cubesat, Space mission

©2021. Japan Geoscience Union. All Right Reserved.



©2021. Japan Geoscience Union. All Right Reserved.

Hayabusa2 Extended Mission to rendezvous with Asteroid 1998 KY26: Investigations of an extremely small fast rotator for planetary defense

*Masatoshi Hirabayashi[1], Y. Mimasu[2], N. Sakatani[3], S. Watanabe[4], Y. Tsuda[2], T. Saiki[2], S. Kikuchi[2], T. Kouyama[5], M. Yoshikawa[2], S. Tanaka[2], S. Nakazawa[2], Y. Takei[2], F. Terui[2], H. Takeuchi[2], A. Fujii[2], T. Iwata[2], K. Tsumura[6], S. Matsuura[7], Y. Shimaki[2], S. Urakawa[8], Y. Ishibashi[9], S. Hasegawa[2], M. Ishiguro[10], D. Kuroda[11], S. Okumura[8], S. Sugita[12], T. Okada[2], S. Kameda[3], S. Kamata[13], A. Higuchi[14], H. Senshu[15], H. Noda[16], K. Matsumoto[16], R. Suetsugu[17], T. Hirai[15], K. Kitazato[18]

1. Auburn University, 2. Japan Aerospace Exploration Agency, 3. Rikkyo University, 4. Nagoya University, 5. National Institute of Advanced Industrial Science and Technology, 6. Tokyo City University, 7. Kwansei Gakuin University, 8. Japan Spaceguard Association, 9. Hosei University, 10. Seoul National University, 11. Kyoto University, 12. University of Tokyo, 13. Hokkaido University, 14. University of Occupational and Environmental Health, 15. Chiba Institute of Technology, 16. National Astronomical Observatory of Japan, 17. National Institute of Technology, 18. University of Aizu

Hayabusa2, led by the Japan Aerospace Exploration Agency (JAXA), brought material samples from asteroid Ryugu back to Earth. On December 6, 2020, the Hayabusa2 team successfully collected the re-entry capsule, while the spacecraft departed from Earth, again. As of January 2021, the spacecraft is reported to have no critical issues.

Based on the spacecraft’s healthy condition and remaining fuel, the Hayabusa2 extended mission development team has evaluated the feasibility of an additional mission. Here, we introduce an extended mission in which the spacecraft will explore Asteroid 1998 KY26, a ~30 m - ~40 m in diameter asteroid rotating at a spin period of ~10 m, after a ~10-year cruise phase. Rendezvous operations are planned to detail the physical properties and surrounding environments of this target, one of the smallest elements of small planetary bodies.

In the planned mission schedule, the spacecraft will rendezvous with 1998 KY26 in late 2031. During this cruise phase, the spacecraft may fly by 2001 CC21 in middle 2026. It will approach the asteroid at high speed (~ 5 km/sec) during the flyby, and thus sophisticated guidance, navigation, and control technologies will be necessary. We also plan to conduct long-term monitoring of the zodiacal light and the transits of exoplanets. After two Earth swing-by operations in late 2027 and early 2028, the spacecraft will arrive at the target asteroid. The planned trajectory will need an additional delta-V of 1.09 km/sec, given the 2,900-sec Isp. The distance from the sun is ~1 AU when the spacecraft arrives at this asteroid.

There are key challenges that need to be resolved in Planetary Defense.
Extremely small bodies (especially smaller than 100 m in diameter) are the most common in the solar system and may have a high probability to influence our societies. Ground- and space-based-telescopes still have technical difficulties in observing these asteroids. Therefore, the physical properties of these objects are poorly understood. Successful planetary defense strategies strongly depend on the physical conditions of asteroids. Extremely small asteroids, which may be the largest pieces within rubble pile asteroid elements, will strongly constrain these conditions.
Given the planned observations, the Hayabusa2 extended mission will significantly contribute to advancing science and engineering knowledge about Planetary Defense by exploring an extremely small body.

©2021. Japan Geoscience Union. All Right Reserved.

Finally, we note that the Hayabusa2 extended mission was approved by the science-engineering space exploration mission assessment committee in Japan, which evaluated the scientific and engineering significance of the mission, and is currently waiting for official approval by the government for budgeting. Also, this abstract is also presented at the Planetary Defense Conference in 2021.

Keywords: Asteroids, Planetary defense, Space exploration mission

©2021. Japan Geoscience Union. All Right Reserved.

Highly Time-Resolved Photometric Observations of Tiny Near Earth Objects with the Tomo-e Gozen Camera

*Jin Beniyama[1], Shigeyuki Sako[1], Ryou Ohsawa[1], Satoshi Takita[1], Naoto Kobayashi[1], Shin-ichiro Okumura[2], Seitaro Urakawa[2], Fumihiko Usui[3], Fumi Yoshida[4,5], Makoto Yoshikawa[3]

1. Institute of Astronomy, Graduate School of Science, The University of Tokyo, 2. Japan Spaceguard Association, 3. Institute of Space and Astronautical Science, Japan Aerospace Exploration Agency, 4. University of Occupational and Environmental Health, 5. Planetary Exploration Research Center, Chiba Institute of Technology

Near Earth Objects (NEO) are solar system bodies whose perihelion distances are smaller than 1.3 au. NEOs are thought to have their origin in the main-belt region between Mars and Jupiter. In addition to the gravitational interaction with the Sun and planets, nongravitational effect which arise from solar radiation plays an important role in their dynamical evolution. YORP effect is one of the nongravitational effects that affects the spin state of an asteroid. YORP effect strongly changes the rotation periods of tiny asteroids (smaller than 100 m in diameter) on a shorter timescale than that of the orbital evolution. Fast rotators suffer from strong centrifugal force and may experience deformation or rotational fission when its rotation period reaches the critical value by YORP spin-up. Therefore the strength of tiny bodies could be inferred using rotation periods of tiny NEOs. Recently, large survey projects have discovered 2,000–3,000 NEOs per year and some fast rotators with rotation periods below a minute have been discovered. Highly time-resolved observations are needed to accurately detect fast rotation because the lower-limit of rotation period which can be detected depends on the overhead time of the instrument. Since the past instruments did not have enought time-resolution, the distribution of rotation periods of NEOs with periods below a minute is still unclear.

We obtained highly time-resolved light curves of 37 tiny NEOs whose diameters are 3–86 m using Tomo-e Gozen camera equipped with 105 cm Schmidt telescope at Kiso Observatory, the University of Tokyo. The observation cadence was 2 fps. We derived the rotation periods of 22 NEOs, of which 5 NEOs show the rotation periods shorter than 20 seconds. The shortest rotation period of our NEOs was about 11 seconds. In spite of high-cadence observations, we found no asteroid rotating shorter than 10 seconds. The lack of tiny fast rotating NEOs has never been reported before our systematic highly time-resolved observation. We discuss the diameter-rotation period relation derived from our observation in terms of YORP spin-up. The observed rotation period distribution is consistent with the senario that the strength of tiny NEOs are weaker than those of meteorites. We also discuss another possible senario that most tiny NEOs are newly-formed in the near-earth region instead of the main-belt.

Keywords: asteroid, near earth objects, solar system, light curve, YORP effect

©2021. Japan Geoscience Union. All Right Reserved.

Color and size distributions of main belt asteroids obtained by the Subaru/Hyper Suprime-Cam

*Natsuho Maeda[1], Tsuyoshi Terai[2], Keiji Ohtsuki[1], Fumi Yoshida[3,4], Kosuke Ishihara[1,2,5], Takuto Deyama[1,6]

1. Graduate school of science, Kobe University , 2. National Astronomical Observatory of Japan, 3. Chiba Institute of Technology, 4. University of Occupational and Environmental Health, 5. The Graduate University for Advanced Studies, 6. NTT Data MSE Corporation

S-type and C-type asteroids are two of the most major types in the main asteroid belt (e.g., DeMeo & Carry 2014). S-type asteroids are thought to have a stony composition, while C-type asteroids are characterized by carbonaceous composition and hydrous minerals (e.g, DeMeo et al. 2015; Usui et al. 2019). Although S-type asteroids and C-type asteroids are thought to have different compositions and origins in this way, their evolution paths are still not well understood.

The size distribution of a population of asteroids strongly reflects the process of their collisional evolution (e.g., Bottke et al. 2015). In the collision equilibrium, the size distribution is primarily determined by the size dependence of impact strength (O’ Brien & Greenberg 2003). Therefore, by comparing size distributions of asteroids with different spectral types, we can obtain information about the relation between their type and their impact strength. This is essential information to reveal their collisional evolution. Although some previous observational works studied size distributions of asteroids with different spectral types (Ivezić et al. 2001; Yoshida & Nakamura 2007), the understanding is still far from complete.

In this work, we performed a survey observation of small main-belt asteroids with the wide-field camera, Hyper Suprime-Cam installed on the 8.2 m Subaru Telescope. Using data acquired with two types of filters, *g*-band (0.40-0.55 μm wavelength) and *r*-band (0.55-0.70 μm wavelength), we measured *g-r* color for 3459 main-belt asteroids detected in 14 deg^2 of the sky. From the asteroids we obtained above, we selected a statistical sample consisting of 1814 asteroids with absolute magnitude brighter than 20.3 mag to remove a detection bias. We classified them into two groups, i.e., reddish “S-like” asteroids and bluish “C-like” asteroids based on the boundary color derived from the previous survey data (The fourth release of Sloan Digital Sky Survey Moving Object Catalog, Ivezić et al. 2010). We converted the absolute magnitude of each sample into a diameter assuming an albedo of 0.21 for S-like and 0.07 for C-like asteroids, respectively, which are the mean values of the S- and C-type main-belt asteroids measured by the infrared astronomical satellite AKARI (Usui et al. 2013). We found that the shapes of the size distributions of the S-like and C-like samples agree well with each other within statistical errors for the diameter range from 0.4 km to 1.5 km. The similarity between the size distributions of the S-like and C-like asteroids indicates that their size dependences of impact strength are also similar at least in the size range from several hundred meters to several kilometers. Namely, the impact strength of asteroids in this size range is likely to be dominated by any other factors rather than their compositions. On the other hand, spin periods of most asteroids in this size range have an upper limit of 2.2 hours, the so-called “spin-barrier” (e.g., Chang et al. 2015). This is interpreted as showing that the asteroids in this size range are rubble-piles, i.e., they consist of numerous pieces of components held together by their self-gravity. The similarity of the size distributions between the S-like and C-like asteroids seems to support the view that most of them have a rubble-pile structure. Also, Itokawa and Ryugu, which were explored by Hayabusa/Hayabusa2, are both several hundred meters in diameter and are considered to

©2021. Japan Geoscience Union. All Right Reserved.

have a rubble-pile structure (Fujiwara et al. 2006; Watanabe et al. 2019). Our result is also consistent with this view.

Keywords: asteroids, survey, size distributions

©2021. Japan Geoscience Union. All Right Reserved.

[E] Oral | P (Space and Planetary Sciences) | P-PS Planetary Sciences

[P-PS04] Small Solar System Bodies: A New Insight from Hayabusa2, OSIRIS-REx and Other Space Missions

convener:Tatsuaki Okada(Institute of Space and Astronautical Science, Japan Aerospace Exploration Agency), Taishi Nakamoto(Tokyo Institute of Technology), Daisuke Kuroda(Kyoto University), Chairperson:Tatsuaki Okada(Institute of Space and Astronautical Science, Japan Aerospace Exploration Agency), Taishi Nakamoto(Tokyo Institute of Technology), YACHEN YANG(Center for Space and Remote Sensing Research)

Sun. Jun 6, 2021 3:30 PM - 5:00 PM Ch.04 (Zoom Room 04)

Small Solar System bodies, including asteroids, comets, satellites, and interplanetary dust particles, are notably important for understanding the origin and evolution of our Solar System, as well as investigating the sources of building blocks of life. Many new discoveries on small bodies have been carried out by observations from ground-based and space-based observatories, and explorations by spacecraft rendezvous and flyby. New perspectives on solar system evolution have been paved by analyses of extraterrestrial materials such as meteorites, IDPs, and return samples by space missions. Numerical and laboratory simulation studies have helped interpretations for those results and proposed new insights on these topics. In this session, new results of scientific studies and new ideas of methodology for investigating small solar system bodies are highly welcome, especially the topics on the remote sensing, surface experiments, and analysis of return sample in the Hayabusa2 and OSIRIS-REx missions, as well as the expectations and preparations for future missions including MMX, Destiny+, Hera, Comet Interceptor, and Hayabusa2-Extended missions.

4:55 PM - 5:00 PM

[PPS04-24]Discussion

©Japan Geoscience Union

[E] Poster | P (Space and Planetary Sciences)：P-PS Planetary Sciences

Sun. Jun 6, 2021 5:15 PM - 6:30 PM JST | Sun. Jun 6, 2021 8:15 AM - 9:30 AM UTC | Ch.04_1

[P-PS04] Small Solar System Bodies: A New Insight from Hayabusa2, OSIRIS-REx and Other Space Missions

convener:Tatsuaki Okada(Institute of Space and Astronautical Science, Japan Aerospace Exploration Agency), Taishi Nakamoto(Tokyo Institute of Technology), Daisuke Kuroda(Kyoto University)

Small Solar System bodies, including asteroids, comets, satellites, and interplanetary dust particles, are notably important for understanding the origin and evolution of our Solar System, as well as investigating the sources of building blocks of life. Many new discoveries on small bodies have been carried out by observations from ground-based and space-based observatories, and explorations by spacecraft rendezvous and flyby. New perspectives on solar system evolution have been paved by analyses of extraterrestrial materials such as meteorites, IDPs, and return samples by space missions. Numerical and laboratory simulation studies have helped interpretations for those results and proposed new insights on these topics. In this session, new results of scientific studies and new ideas of methodology for investigating small solar system bodies are highly welcome, especially the topics on the remote sensing, surface experiments, and analysis of return sample in the Hayabusa2 and OSIRIS-REx missions, as well as the expectations and preparations for future missions including MMX, Destiny+, Hera, Comet Interceptor, and Hayabusa2-Extended missions.

[PPS04-P01] Comparison of original orbits of Oort Cloud new comets given in various catalogues II. Different solutions from different observations

*Takashi Ito[1] (1.National Astronomical Observatory of Japan, National Institutes of Natural Science)

[PPS04-P02] Characteristics of high-albedo C-complex asteroids

*Sunao Hasegawa[1], Toshihiro Kasuga[2], Fumihiko Usui[1,3], Kuroda Daisuke[4] (1.Japan Aerospace Exploration Agency, 2.National Astronomical Observatory of Japan, 3.Kobe University, 4.Kyoto University)

[PPS04-P03] Thermal Radiation Pressure as a Possible Mechanism for Losing Small Particles from Near-Sun Asteroids

*Yoonsoo P. Bach[1], Masateru Ishiguro[1] (1.Department of Physics and Astronomy, Seoul National University)

[PPS04-P04] Implications of High Polarization Degree for the Surface State of Ryugu

*Daisuke Kuroda[1], Jooyeon Geem[2], Hiroshi Akitaya[3], Sunho Jin[2], Jun Takahashi[4], Koki Takahashi[5], Hiroyuki Naito[6], Kana Makino[7], Tomohiko Sekiguchi[5], Yoonsoo P. Bach[2], Jinguk Seo[2], Shuji Sato[8], Hiroshi Sasago[9], Koji S. Kawabata[3], Aoi Kawakami[4], Miyako Tozuka[4], Makoto Watanabe[10], Seiko Takagi[11], Kiyoshi Kuramoto[11], Makoto Yoshikawa[12], Sunao Hasegawa[12], Masateru Ishiguro[2] (1.Kyoto University, 2.Seoul National University, 3.Hiroshima University, 4.University of Hyogo, 5.Hokkaido University of Education, 6.Nayoro Observatory, 7.Nayoro City University, 8.Nagoya University, 9.Sasago Co.,Ltd., 10.Okayama University of Science, 11.Hokkaido University, 12.Japan Aerospace Exploration Agency)

[PPS04-P05] Three-dimensional tracking of ejecta particle: Effects of boulder size on ejecta velocity distribution

*Hatsune Okawa[1], Mizuno Toda[2], Masahiko Arakawa[1], Minami Yasui[1], Sunao Hasegawa[3], Yusaku Yokota[1], Yuya Yamamoto[1] (1.Graduate School of Science, Kobe University, 2.Science Department, Kobe University, 3.Japan Aerospace Exploration Agency)

[PPS04-P06] Experimental study on momentum transfer in high-velocity impact on asteroid

Kazuhiro Horikawa[1], *Masahiko Arakawa[1], Minami Yasui[1], Kei Shirai[1], Sunao Hasegawa[2] (1.Graduate School of Science, Kobe Univ., 2.ISAS, JAXA)

[PPS04-P07] Reconstruction of the past rotation state of asteroid (162173) Ryugu from a crater shape analysis

*Riona Yamada[1], Sei-ichiro Watanabe[1], Tomokatsu Morota[2], Naru Hirata[3], Naoyuki Hirata[4], Yuri Shimaki[5], Rina Noguchi[5], Rie Honda[6], Shingo Kameda[7], Manabu Yamada[8], Naoya Sakatani[7], Eri Tatsumi[9], Toru Kouyama[10], Yasuhiro Yokota[5,6], Yuichiro Cho[2], Hidehiko Suzuki[11], Masahiko Hayakawa[5], Moe Matsuoka[5], Chikatoshi Honda[3], Kazuo Yoshioka[2], Hirotaka Sawada[5], Kazunori Ogawa[5], Seiji Sugita[2] (1.Nagoya University, 2.University of Tokyo, 3.University of Aizu, 4.Kobe University, 5.JAXA, 6.Kochi University, 7.Rikkyo University, 8.Chiba Institute of Technology, 9.La Laguna University, 10.AIST, 11.Meiji University)

[PPS04-P08] Thermally Controlled Crack Orientation of Boulders on Ryugu: N-S Preference and Exfoliation Structure

*Sho Sasaki[1], Shiho Kanda[1], Hiroshi Kikuchi[2], Tatsuhiro Michikami[3], Tomokatsu Morota[4], Chikatoshi Honda[5], Hideaki Miyamoto[4], Ryodo Hemmi[4], Seiji Sugita[4], ERI TATSUMI[4,6], Masanori Kanamaru[2], Sei-ichiro WATANABE[7], Noriyuki Namiki[8], Patrik Michel[9], Masatoshi Hirabayashi[10], Naru Hirata[5], Tomoki Nakamura[11], Takaaki Noguchi[12], Takahiro Hiroi[13], Koji Matsumoto[8], Hirotomo Noda[8], Naoya Sakatani[14], Shingo Kameda[14], Toru Kouyama[15], Hidehiko Suzuki[16], Manabu Yamada[17], Rie Honda[18], Yuichiro Cho[4], Kazuo Yoshioka[4], Masahiko Hayakawa[2], Moe Matsuoka[2], Rina Noguchi[2], Hirotaka Sawada[2], Yasuhiro Yokota[2,18], Makoto Yoshikawa[2] (1.Department of Earth and Space Sciences, School of Science, Osaka University, 2.ISAS/JAXA, 3.Kindai University, 4.The University of Tokyo, 5.University of Aizu, 6.Instituto de Astrofisica de Canarias, 7.Nagoya University, 8.National Astronomical Observatory of Japan, 9.Observatoire de la Cote d'Azur, 10.Auburn University, 11.Tohoku University, 12.Kyushu University, 13.Brown University, 14.Rikkyo University, 15.The National Institute of Advanced Industrial Science and Technology, 16.Meiji University, 17.PERC, Chiba Institute of Technology, 18.Kochi University)

[PPS04-P09] **Orientation of Boulders and Rerationship with Gravitational Slope on Asteroid Rryugu: Implications for Surface Evolution.**

*Tatsuki Ebihara[1], Koki Yumoto[1], Seiji Sugita[1], Rie Honda[2], Shingo Kameda[3], ERI TATSUMI[1,4], Yuichiro Cho[1], Kazuo Yoshioka[1], Hirotaka Sawada[5], Yasuhiro Yokota[2,5], Naoya Sakatani[3], Masahiko Hayakawa[5], Moe Matsuoka[5], Manabu Yamada[6], Toru Kouyama[7], Hidehiko Suzuki[8], Chikatoshi Honda[9], Kazunori Ogawa[10,11], Tatsuhiro Michikami[12], Hideaki Miyamoto[1], Tomokatsu Morota[1] (1.The University of Tokyo, 2.Kochi University, 3.Rikkyo University, 4.Instituto de Astrofisica de Canarias, 5.Japan Aerospace Exploration Agency, 6.Planetary Exploration Research Center Chiba Institute of Technology, 7.National Institute of Advanced Industrial Science and Technology, 8.Meiji University, 9.University of Aizu, 10.Japan Aerospace Exploration Agency, JAXA Space Exploration Center, 11.Kobe University, 12.Kindai University)

[PPS04-P10] Apparently Layered Boulders with Multiple Textures on Bennu's Surface

*Kana Ishimaru[1], Dante S Lauretta[1], Nick Porter, Dathon Golish[1], Manar Al Asad[2], Ronald Ballouz[1], Olivier S Barnouin[3], Keara Burke[1], Mike Daly[4], Dani DellaGiustina[1], Kevin John Walsh[5] (1.Lunar and Planetary Laboratory, University of Arizona, 2.Department of Earth Ocean and Atmospheric Sciences, University of British Columbia, 3.The Johns Hopkins University, Applied Physics Laboratory, 4.The Centre for Research in Earth and Space Science, York University, 5.Southwest Research Institute)

[PPS04-P11] High-resolution global thermal images of Ryugu acquired from the dawn side

*Yuri Shimaki[1], Hiroki Senshu[2], Naoya Sakatani[3], Tatsuaki Okada[1,4], Tetsuya Fukuhara[3], Satoshi Tanaka[1,5], Takehiko Arai[6], Hirohide Demura[7], Tomohiko Sekiguchi[8], Toru Kouyama[9], Jun Takita[10], Sunao Hasegawa[1] (1.Institute of Space and Astronautical Science, Japan Aerospace Exploration Agency, 2.Planetary Exploration Research Center, Chiba Institute of Technology, 3.Rikkyo University, 4.The University of Tokyo, 5.The Graduate University for Advanced Studies, SOKENDAI, 6.Ashikaga University, 7.The University of Aizu, 8.Hokkaido University of Education, 9.National Institute of Advanced Industrial Science and Technology (AIST), 10.Hokkaido Kitami Hokuto High School)

[PPS04-P12] High-resolved temperature map of Ryugu surface observed with Thermal Infrared Imager onboard Hayabusa2

*Takehiko Arai[1], Tatsuaki Okada[2], Satoshi Tanaka[2], Tetsuya Fukuhara[3], Hirohide Demura[4], Toru Kouyama[5], Naoya Sakatani[3], Yuri Shimaki[2], Hiroki Senshu[6], Tomohiko Sekiguchi[7], Jun Takita[8] (1.Ashikaga University, 2.JAXA, 3.Rikkyo University, 4.The University of Aizu, 5.AIST, 6.Chiba Institute of Technology, 7.Hokkaido University of Education, 8.Hokkaido Kitami Hokuto High School)

[PPS04-P13] Current status and future plan of Hayabusa2 Science Data Archive in PDS4

*Shin-ya Murakami[1], Yukio Yamamoto[2], M. Katherine Crombie[3], Carol Neese[4], Yoshiaki Ishihara[2] (1.Keio University, 2.Japan Aerospace Exploration Agency, 3.Indigo Information Services, LLC, 4.Planetary Science Institute)

[PPS04-P14] **Assessing the debris generated by the small carry-on impactor operated from the *Hayabusa2* mission**

*Motoo Ito[1], Yoshinori Takano[2], Yoko Kebukawa[3], Takuji Ohigashi[4], Moe Matsuoka[5], Kento Kiryu[3], Masayuki Uesugi[6], Tomoki Nakamura[7], Hayato Yuzawa[4], Keita Yamada[8], Hiroshi Naraoka[9], Toru Yada[5], Masanao Abe[5], Masahiko Hayakawa[5], Takanao Saiki[5], Shogo Tachibana[10] (1.Kochi Institute for Core Sample Research, JAMSTEC, 2.Biogeochemistry Research Center, JAMSTEC, 3.Yokohama National University, 4.UVSOR, IMS, 5.ISAS, JAXA, 6.JASRI/SPring-8, 7.Tohoku University, 8.Tokyo Institute of Technology, 9.Kyushu University, 10.University of Tokyo)

[PPS04-P15] X-ray nanotomography of CM and CI chondrites and their heated samples: as a rehearsal of Hayabusa2 sample analysis.

*Mingqi Sun[1], Akira Tsuchiyama[1,2], Megumi Matsumoto[3], Yuri Fujioka[3], Tomoki Nakamura[3], Junya Matsuno[2], Akira Miyake[4], Shota Okumura[4], Naotaka Tomioka[5], Motoo Ito[5], Yu Kodama[6], Stefano Rubino[7], Naoto Nakano[4], Kentaro Uesugi[8], Akihisa Takeuchi[8], Masahiro Yasutake[8] (1.CAS Key laboratory of Mineralogy and Metallogeny, Guangzhou Institute of Geochemistry, Chinese Academy of Science, Guangzhou 510640, China, 2.Research Organization of Science and Technology, Ritsumeikan University, Japan, 3.Graduate School of Science, Tohoku University, Japan, 4.Graduate School of Science, Kyoto University, Japan, 5.Kochi Institute for Core Sample Research, Japan, 6.Marine Works Japan Ltd., Japan, 7.Institut d'Astrophysique Spatiale, Université Paris-Saclay, France, 8.JASRI/SPring-8, Japan)

[PPS04-P16] **Assessing the irradiation effects by a synchrotron X-ray micro-computed tomography on the organic materials in carbonaceous chondrite: Examination at SPring-8 facility**

*Haruna Sugahara[1], Yoshinori Takano[2], Toshihiro Yoshimura[2], Nanako O Ogawa[2], Naohiko Ohkouchi[2], Masayuki Uesugi[3], Akira Tsuchiyama[4], Hayabusa2 project team (1.Institute of Space and Astronautical Science, Japan Aerospace Exploration Agency (ISAS/JAXA), 2.Japan Agency for Marine-Earth Science and Technology (JAMSTEC), 3.Japan Synchrotron Radiation Research Institute, 4.Ritsumeikan University)

[PPS04-P17] Description of return sample from C-type asteroid Ryugu using the MicrOmega hyperspectral microscope in JAXA Curation Facility

*Tatsuaki Okada[1,2], KaKasumi Yogata[1], Aiko Nakato[1], Kentaro Hatakeda[1,3], Toru Yada[1], Lucie Riu[1], Akiko Miyazaki[1], Kazuya Kumagai[1,3], Masahiro Nishimura[1], Masanao Abe[1], Tomohiro Usui[1,2], Cedric Pilorget[4], Rosario Brunetto[4], Vincent Hamm[4], Lionel Lourit[4], Jean-Pierre Bibring[4] (1.Institute of Space and Astronautical Science, Japan Aerospace Exploration Agency, 2.University of Tokyo, 3.Marine Works Japan Ltd., 4.Institue d'Astrophysique Spaciale)

[PPS04-P18] Significant role of Asteroids: One step of purified rocks and minerals and life to final water planet

*Yasunori Miura[1] (1.Visiting (Yamaguchi University, EUA-Al. Univ. Toronto, LPI-NPPf))

[PPS04-P19] Simulation of Phobos internal density structure estimation by orbit determination of MMX

*Keiko Yamamoto[1], Koji Matsumoto[1], Hitoshi Ikeda[2], Hiroki Senshu[3] (1.National Astronomical Observatory of Japan, 2.Japan Aerospace Exploration Agency, 3.Chiba Institute of Technology)

[PPS04-P20] MMX InfraRed Spectrometer (MIRS) imaging spectrometer

*Jean-Michel Reess[1], Maria Antonella Barucci, Pernelle Bernardi, Michel Le Du, Eric Sawyer, Takahiro Iwata[2], Hiromu Nakagawa[3], Tomoki Nakamura[4], Alain Doressoundiram, Sonia Fornasier (1.J.-M. Reess, LESIA, Observatoire de Paris, Université PSL, CNRS, Université de Paris, Sorbonne Université, 92190 Meudon, France, 2.T. Iwata, ISAS, JAXA, Sagamihara 252-5210, Japan, 3.H. Nakagawa, JAXA, Sagamihara 252-5210, Japan, 4.T. Nakamura, JAXA, Sagamihara 252-5210, Japan)

[PPS04-P21] Thermophysical Properties of S-type Binary Didymos by Thermal Imaging in Hera Mission

*Tatsuaki Okada[1,2], Satoshi Tanaka[1,2], Naoya Sakatani[3], Yuri Shimaki[1], Takehiko Arai[4], Hiroki Senshu[5], Hirohide Demura[6], Toru Kouyama[7], Tomohiko Sekiguchi[8] (1.Institute of Space and Astronautical Science, Japan Aerospace Exploration Agency, 2.University of Tokyo, 3.Rikkyo University, 4.Ashikaga University, 5.Chiba Institute of Technology, 6.University of Aizu, 7.National Institute of Advanced Industrial Science and Technology, 8.Hokkaido University of Education)

[PPS04-P22] Current status and science of DESTINY+

*Tomoko Arai[1], Masanori Kobayashi[1], Ko Ishibashi[1], Hiroshi Kimura[1], Takayuki Hirai[1], Peng Hong[1], Fumi Yoshida[2], Naoya Ozaki[3], Takayuki Yamamoto[3], Hiroyuki Toyota[3], Kazutaka Nishiyama[3], Hiroshi Imamura[3], Takeshi Takashima[3], DESTINY+ science team (1.Planetary Exploration Research Center, Chiba Institute of Technology, 2.University of Occupational and Environmental Health, Japan, 3.ISAS, JAXA)

[PPS04-P23] Progress report of development and ground calibration of DESTINY$^+$ Dust Analyser

*Takayuki Hirai[1], Masanori Kobayashi[1], Tomoko Arai[1], Hiroshi Kimura[1], Sho Sasaki[2], Hikaru Yabuta[3], Amano Sui[3], Sachio Kobayashi[4], Motoo Ito[4], Akira Yamaguchi[5], Hajime Yano[6], Mario Trieloff[7], Jon Hillier[8], Nozair Khawaja[8], Lisa Eckart[8], Harald Krueger[9], Jonas Simolka[10], Ralf Srama[10] (1.Chiba Institute of Technology, Planetary Exploration Research Center, 2.Osaka University, 3.Hiroshima University, 4.Japan Agency for Marine-Earth Science and Technology, 5.National Institute of Polar Research, 6.Japan Aerospace Exploration Agency, 7.Heidelberg University, 8.Free University of Berlin, 9.Max Planck Institute for Solar System Research, 10.University of Stuttgart)

[PPS04-P24] Study of asteroid tracking mirror of telescopic camera onboard DESTINY+

*Peng Hong[1], Ko Ishibashi[1], Takayuki Hosonuma[2], Ozaki Naoya[3], Shunsuke Sato[3], Hiroyuki Toyota[3], Kazutaka Nishiyama[3], Masatsugu Otsuki[3], Osamu Okudaira[1], Takeshi Takashima[3] (1.Planetary Exploration Research Center, Chiba Institute of Technology, 2.Department of Aeronautics and Astronautics, The University of Tokyo, 3.Institute of Space and Astronautical Science, Japan Aerospace Exploration Agency)

[PPS04-P25] Development status of DESTINY$^+$ onboard cameras TCAP and MCAP

*Ko Ishibashi[1], Peng Hong[1], Takaya Okamoto[2], Takahiro Ishimaru[2], Manabu Yamada[1], Naoya Ozaki[2], Takayuki Hosonuma[3], Shunsuke Sato[2], Osamu Okudaira[1], Tomoko Arai[1], Fumi Yoshida[1,4], Masato Kagitani[5], Shingo Kameda[6], Takeshi Miyabara[2], Masayuki Ohta[2], Takeshi Takashima[2] (1.Chiba Institute of Technology, 2.Japan Aerospace Exploration Agency, 3.The University of Tokyo, 4.University of Occupational and Environmental Health, 5.Tohoku University, 6.Rikkyo University)

[PPS04-P26] A Ground-based Optical Calibration Plan for DESTINY$^+$ on-board Cameras, TCAP and MCAP

*Takaya Okamoto[1], Ko Ishibashi[2], Manabu Yamada[2], Peng Hong[2], Fumi Yoshida[2,3], Tomoko Arai[2], Takahiro Ishimaru[1], Masayuki Ohta[1], Takeshi Miyabara[1], Takeshi Takashima[1] (1.Japan Aerospace Exploration Agency, Institute of Space and Astronautical Science, 2.Chiba Institute of Technology, Planetary Exploration Research Center, 3.University of Occupational and Environmental Health, School of Medicine)

[PPS04-P27] Twinkle: a low-Earth orbit, visible and infrared observatory for exoplanet and solar system spectroscopy

*Billy Edwards[1] (1.Blue Skies Space Ltd)

Comparison of original orbits of Oort Cloud new comets given in various catalogues II. Different solutions from different observations

*Takashi Ito[1]

1. National Astronomical Observatory of Japan, National Institutes of Natural Science

Recent observational and theoretical studies have greatly revealed the dynamical nature of the Oort Cloud and its evolutionary history. However, many issues are yet to be known. Our goal is to understand current structure of this cloud as well as its dynamical origin. For estimating the current structure of the Oort Cloud, key information lies in the original orbit of the Oort Cloud new comets (OCNCs) that are defined at a distance where these objects do not receive gravitational perturbation from major planets (such as at r = 250 au from the Sun before comets enter into the planetary region). There have been several attempts to obtain OCNC's original orbits, but it never has been an easy task. This requires numerical orbit propagation of the observed comets with high accuracy including perturbation from major disturbing bodies. In addition, non-gravitational forces often play significant roles here. First and foremost, the orbit determination of OCNC includes substantially large uncertainty because of limited number of observational arcs and very large eccentricity of the comets (~1). Here I show our result of comparison of various catalogues of OCNCs' original orbital elements at r = 250 au: So-called the Warsaw catalogue by Krolikowska, the ephemeris given by MPC (Minor Planet Center), and that given by Horizons/JPL. In particular, I pay attention to the difference of the original semimajor axis among the several different solutions that the Warsaw catalogue and the MPC ephemeris have in comparison with the solutions given by Horizons/JPL - such as the difference between the solution 1 in the Warsaw catalogue and the solution from Horizons/JPL, the solutions 1 and 2 in the Warsaw catalogue, the solutions 2 and 3 in the MPC ephemeris and so forth. The resulting orbits that these solutions yield look overall similar, but sometimes they show stark difference for some reason.

Keywords: comet, Oort Cloud, catalogue, dynamics

©2021. Japan Geoscience Union. All Right Reserved.

Characteristics of high-albedo C-complex asteroids

*Sunao Hasegawa[1], Toshihiro Kasuga[2], Fumihiko Usui[1,3], Kuroda Daisuke[4]

1. Japan Aerospace Exploration Agency, 2. National Astronomical Observatory of Japan, 3. Kobe University, 4. Kyoto University

Almost C-complex asteroids have albedo values lower than 0.1, but there are some high-albedo C-complex asteroids with albedo values exceeding 0.1.
To clarify the nature and origin of high-albedo C-complex asteroids, we conducted spectroscopic observations of the asteroids in at visible and near-infrared wavelength regions.
The Bus B-, C-, and Ch-type asteroids with high-albedo values, which are subclasses of the Bus C-complex asteroids, are classified as DeMeo C-type asteroids with concave curvature, B-, Xn-, and K-type asteroids.
Analogue material such as CV/CK chondrites, enstatite chondrites/achondrites, and salts related with these spectral types of high-albedo asteroids are thought to be composed of minerals and material exposed to high temperatures.
A comparison of the results obtained in this study with the SDSS photometric data suggests the following three possibilities.
High-albedo C-complex asteroids that do not belong to any families are likely to be impact-metamorphosed carbonaceous chondrites, CV/CK chondrites, or enstatite chondrites/achondrites.
The high-albedo C-complex asteroids in other C-complex families were likely sourced by impact heating.
Salts may have occurred in the parent bodies of 24 Themis and 10 Hygiea, as well as 2 Pallas.

©2021. Japan Geoscience Union. All Right Reserved.

Thermal Radiation Pressure as a Possible Mechanism for Losing Small Particles from Near-Sun Asteroids

*Yoonsoo P. Bach[1], Masateru Ishiguro[1]

1. Department of Physics and Astronomy, Seoul National University

Recently space explorations of near-Earth asteroids (NEA) (25143) Itokawa, (162173) Ryugu, and (101955) Bennu have indicated a paucity of micron-sized fine-grains on the surface, which is likely different from that of larger asteroids, such as (4) Vesta and (433) Eros. Meanwhile, meteoritic samples show granular structures of size scales down to mm or even sub-micron scale. It is, therefore, expected that mechanisms including thermal fatigue or micrometeoroid impacts would supply a myriad of sub-micron to sub-mm debris particles on the asteroid surfaces. Then how have these continuously-supplied-micron-sized grains been lost from the NEA's surfaces? Among the NEAs, (3200) Phaethon has been showing recurrent activities at its perihelion, i.e., the dust cloud consisting of an effective particle radius ~ 1 micron. This is a hint that such small grains are not only being generated, but also being removed by ejection, although the ejection mechanism is unknown.

In this work, we suggest a unique idea that thermal radiation from the asteroidal regolith, viz., thermal radiation pressure (TRP), can play a dominant role in removing those small particles selectively. Our model predicts TRP is stronger at a smaller heliocentric distance while almost negligible at a distance of >~ 0.8 au. It is also shown that TRP is the most effective for particles of radius ~ 1 μm. Our theoretical estimate of the size is well consistent with the previous observational studies of Phaethon's dust cloud (radius ~ 1 μm). In the JpGU 2021 meeting, we will compare our TRP model with other mechanisms such as electrostatic dust levitation and discuss the future application of this theory to Phaethon to investigate a scientific case for JAXA's DESTINY+ mission.

Keywords: Minor planets, asteroids

©2021. Japan Geoscience Union. All Right Reserved.

Implications of High Polarization Degree for the Surface State of Ryugu

*Daisuke Kuroda[1], Jooyeon Geem[2], Hiroshi Akitaya[3], Sunho Jin[2], Jun Takahashi[4], Koki Takahashi[5], Hiroyuki Naito[6], Kana Makino[7], Tomohiko Sekiguchi[5], Yoonsoo P. Bach[2], Jinguk Seo[2], Shuji Sato[8], Hiroshi Sasago[9], Koji S. Kawabata[3], Aoi Kawakami[4], Miyako Tozuka[4], Makoto Watanabe[10], Seiko Takagi[11], Kiyoshi Kuramoto[11], Makoto Yoshikawa[12], Sunao Hasegawa[12], Masateru Ishiguro[2]

1. Kyoto University, 2. Seoul National University, 3. Hiroshima University, 4. University of Hyogo, 5. Hokkaido University of Education, 6. Nayoro Observatory, 7. Nayoro City University, 8. Nagoya University, 9. Sasago Co.,Ltd., 10. Okayama University of Science, 11. Hokkaido University, 12. Japan Aerospace Exploration Agency

We present the linear polarization measurements of the near-Earth asteroid (162173) Ryugu [1]. The asteroid exploration project "Hayabusa2" has been investigated in detail by the in-situ observations of Ryugu and successfully returned samples from Ryugu in December 2020. However, polarimetry had not been conducted so far.

The polarization degree of asteroids varies with phase angle (Sun-target-observer's angle), and near-Earth asteroids are observable up to the region of their maximum. This study performed polarimetric observations of Ryugu with four ground-based telescopes from September 27 to December 25, 2020, covering a wide-phase angle from 28˚ to 104˚.

We acquired polarimetric data for a total of 24 nights (23 nights in R-band and one night in V-band). The polarization degree of Ryugu reached 53% around the phase angle of 100˚, the highest value among all asteroids and comets reported in the previous studies. The polarimetric phase curve of Ryugu is similar to that of (152679) 1998 KU_2 [2]. It is slightly different from (101955) Bennu [3], which is the target of the OSIRIS-REx mission.

This high degree of polarization occurs on the surface layer and is attributed to the scattering properties of the surface material. Scattered light from a low albedo object is qualitatively consistent with a high degree of polarization because the contribution of multiple-scattering light, which reduces the polarization degree, is small [4]. The low light scattering frequency implies that the grain size of the surface layer is large. By analogy with the polarimetric measurements on the pulverized meteorite samples [5, 6], we can infer that there are submillimeter-sized grains on the surface layer of the very low albedo Ryugu [7, 8]. This grain size may also reflect a larger aggregate component, e.g., the cauliflower-like structures on the rock appearances observed by MASCOT [9].

The sample recovered by Hayabusa2 seems to have a very brittle structure. Our polarimetric data will also contribute to reconstructing the surface structure of Ryugu, which has already been lost in the recovered samples.

[1] Kuroda et al., ApJL, submitted; [2] Kuroda et al., 2018, A&A, 611, A31; [3] Cellino et al., 2018, MNRAS, 481, L49; [4] Bohren and Huffman, 1998, Absorption and Scattering of Light by Small Particles, Wiley; [5] Worms et al., 2000, Planet. Space Sci., 48, 493; [6] Hadamcik et al., 2011, JQSRT, 112, 1881; [7] Sugita et al., 2019, Science, 364, 252; [8] Tatsumi et al., 2020, A&A, 639, A83; [9] Jaumann et al., 2019, Science, 365, 817

©2021. Japan Geoscience Union. All Right Reserved.

Keywords: asteroid, polarimetry

©2021. Japan Geoscience Union. All Right Reserved.

Three-dimensional tracking of ejecta particle: Effects of boulder size on ejecta velocity distribution

*Hatsune Okawa[1], Mizuno Toda[2], Masahiko Arakawa[1], Minami Yasui[1], Sunao Hasegawa[3], Yusaku Yokota[1], Yuya Yamamoto[1]

1. Graduate School of Science, Kobe University, 2. Science Department, Kobe University, 3. Japan Aerospace Exploration Agency

The ejection process during the crater formation is important to consider the resurfacing process on solid bodies, so there are many studies related to the ejection process. Many of them were based on the experimental results for the targets composed of homogeneous sized regolith particles and they did not include the effect of the target particle size. However, recent asteroid explorations revealed that the boulders on the asteroid surface had a size frequency distribution in a wide range of the boulder size. The impact cratering experiment by Hayabusa2 spacecraft, which actually observed the crater formation process on the asteroid surface by DCAM3, resulted in the formation of the asymmetric and heterogeneous ejecta curtain. In this study, we carried out impact cratering experiments on granular particles with various sizes to investigate the ejecta velocity distribution, and we then discussed the effect of the ejecta particle size on the π-scaling law for ejecta velocity distribution. Moreover, we estimated the maximum size of the boulder which could be ejected out of the final crater.

Impact experiments were conducted by using a one-stage vertical gas gun at Kobe Univ., and a two-stage vertical gas gun at ISAS. We used glass beads with the median grain diameter of about 100 μm, as a target. In order to obtain the three-dimensional trajectory of the ejected beads, we recorded the ejection process by two synchronized high-speed cameras with a framing rate of 2000 to 10000 fps. We set the tracer beads with the size of 3–30 mm on the target surface before the shot and tracked them each image. Their traces in the three-dimensional coordinate system were determined based on the calibration.

We found the difference of the ejection process depending on the size and the buried volume of the tracer bead. First, we studied the ejecta velocity distribution which is defined as the relationship between the ejection velocity and the initial position of ejecta particle, which is the distance between the impact point and the center of the tracer bead, and found that the ejection velocity of the larger tracer bead was slower than that of the smaller one. We then rescaled it by using another initial position which is the distance between the impact point and the outside edge of the tracer bead. As a result, the size dependence of the tracer bead was almost disappeared, so that the redefined initial position enabled us to refine the ejecta velocity scaling law for large tracer beads.
The refined scaling law was theoretically analyzed by using the Z-model. Since the ejection velocity varied with the initial position according to the Z-model, the large tracer bead on the target surface could be pushed by target beads with the velocity depending on the initial position: A tracer bead was pushed at the inner edge by higher velocity than that at the outer edge. Thus, we assume that the ejection velocity of a large tracer bead could be roughly calculated as the average velocity of the target beads excavated from the area of a large tracer bead. More detail analysis showed us that the twice of the diameter of the tracer bead centered at the outer edge could be most suitable area for calculating the average ejection velocity applicable to large tracer beads.
Next, we investigated the effect of the buried volume of the large tracer bead on the ejection process. We found that the buried volume was larger as the ejection velocity was higher while the volume buried was

©2021. Japan Geoscience Union. All Right Reserved.

larger as the moved distance was smaller. Finally, we applied our refined scaling law for the ejecta velocity distribution and calculated the maximum size of the boulder which can be ejected outside the final crater. As a result, we found that the boulders with the radius larger than 0.3 times the crater radius could not be ejected outside the final crater.

Keywords: cratering, ejecta velocity distribution, crater scaling law, asteroids, boulders, size frequency distribution

©2021. Japan Geoscience Union. All Right Reserved.

Experimental study on momentum transfer in high-velocity impact on asteroid

Kazuhiro Horikawa[1], *Masahiko Arakawa[1], Minami Yasui[1], Kei Shirai[1], Sunao Hasegawa[2]

1. Graduate School of Science, Kobe Univ., 2. ISAS, JAXA

Asteroid Impact and Deflection Assessment (AIDA) mission is scheduled by NASA and ESA. This mission is constituted by two separate missions which are DART (Double Asteroid Redirection Test) by NSAS and Hera by ESA. The impactor with the mass of 500 kg will be impacted on the moon of the asteroid Didymos named Dimorphos with the size of 160 m in DART mission, then the deflection of the trajectory of Dimorphos caused by the impact will be detected by astronomical observations to study the effiects of the kinetic impactor on the small asteroid. Especially, the momentum transfer efficiency of the impactor onto the asteroid is the most important parameter to control the asteroid deflection and defined as β-1= P/mv, where m and v are the impactor mass and the velocity, respectively; P is the momentum of ejecta accompanied by the crater formation. The β-1 is strongly dependent on the subsurface mechanical properties [1], so the theoretical and numerical studies have been conducted to obtain β-1 for various subsurface properties of asteroids [1, 2, 3]. These studies give us a chance to elucidate the subsurface properties of Dimorphos by AIDA mission. However, the experimental study is still limited to confirm and improve these theories and the numerical models, then we conducted the high-velocity impact experiments to study β-1 by using the targets with various impact strength simulating small porous asteroids.

The impact experiments were conducted by using a horizontal type two-stage light gas gun at the impact velocity (v) from 0.6 to 3.6 km/s. The projectile was a spherical polycarbonate with the size from 2 to 7 mm. The target was a spherical porous sand-gypsum mixture with the porosity of 40 % and the static tensile strength (Y) from 800 kPa to 100 kPa; the size was from 30 to 90 mm. The target was set in a recovery box and hung from the ceiling by a string. A small crater was formed on the target by the head-on collision and the target was accelerated toward the impact direction, then it swung like a pendulum. The target movement after the impact was observed by a highspeed camera with the framing rate of 10^5 FPS, and the velocity of the center of the mass for the target was measured on these recorded images. The β-1 was found to increase with the impact velocity and it almost proportional to the velocity for 100 and 300 kPa targets; it is proportional to $v^{1.6}$ for 800 kPa targets. The β-1also increased with the decrease of the strength, so the target with the strength of 100 kPa had the largest β-1 value for all targets in this velocity range. According to the previous study [1, 3], the β-1 is scaled by the characteristic velocity (v*) written by $(Y/\rho)^{0.5}$, where ρ is the target density. We then applied this v^* to our results and found that the β-1 for 100 and 300 kPa targets were well merged by using v/v^*, but the β-1 for 800 kPa was slightly higher than that for others. This difference might be caused by the difference of the ejection angle of fragments excavated from the crater. The ejection angle for 800 kPa targets measured from the impact surface was observed to be higher than that of others. Since the velocity component parallel to the impact direction was larger for the ejected material with a high ejection angle, the β-1 for 800 kPa might be larger than others.

[1]Holsapple and Housen, Icarus 221,875–887, 2012. [2]Raducan et al., Icarus 329, 282–295, 2019. [3]Jutzi and Michel, Icarus 229, 247–253, 2014.

Keywords: Planetary defense, Near earth asteroids, Impact crater

©2021. Japan Geoscience Union. All Right Reserved.

©2021. Japan Geoscience Union. All Right Reserved.

Reconstruction of the past rotation state of asteroid (162173) Ryugu from a crater shape analysis

*Riona Yamada[1], Sei-ichiro Watanabe[1], Tomokatsu Morota[2], Naru Hirata[3], Naoyuki Hirata[4], Yuri Shimaki[5], Rina Noguchi[5], Rie Honda[6], Shingo Kameda[7], Manabu Yamada[8], Naoya Sakatani[7], Eri Tatsumi[9], Toru Kouyama[10], Yasuhiro Yokota[5,6], Yuichiro Cho[2], Hidehiko Suzuki[11], Masahiko Hayakawa[5], Moe Matsuoka[5], Chikatoshi Honda[3], Kazuo Yoshioka[2], Hirotaka Sawada[5], Kazunori Ogawa[5], Seiji Sugita[2]

1. Nagoya University, 2. University of Tokyo, 3. University of Aizu, 4. Kobe University, 5. JAXA, 6. Kochi University, 7. Rikkyo University, 8. Chiba Institute of Technology, 9. La Laguna University, 10. AIST, 11. Meiji University

Background

Proximity observations from the Hayabusa2 spacecraft reveal that Ryugu has a spinning-top shape [1] with 86 craters that have been reported on its surface [2]. The average surface tilt angle with respect to the net force of gravitational attraction and centrifugal force is nearly 35˚ when the rotation rate is 2.2 times the present value (period of 3.5 h), so that Ryugu's shape was formed by deformation induced by that high-speed rotation [1]. Owing to the YORP effect, the thermal torque changing the rotation state of small asteroids [3][4], Ryugu spun down from its past high-speed rotation state to its current low-speed (period of 7.63 h) on a timescale of about 10 million years. Therefore, craters on Ryugu must have been formed continuously under various rotation speeds. Laboratory experiments to investigate the shape of craters by varying the tilt angle and impact angle showed that the crater ellipse elongates in the tilt direction and the crater cavity moves downward when the tilt angle exceeds 20˚ at any impact angle [5]. In addition, the impact angle has little effect on the axial ratio of the ellipse [5]. Thus, we could constrain the change of rotation state of Ryugu by studying the shape of craters formed at various times in detail.

Method

We have measured the external shape of the craters in the existing list of craters on Ryugu [2]. We used the Small Body Mapping Tool (SBMT) to extract each crater profile from an 800,000-polygon shape model of Ryugu. Candidate points on the rim were extracted from the profiles of eight orientations through the crater center, and the crater outline that passed through them most consistently was determined and approximated by an outline ellipse. Craters with major to minor axis ratios (R) greater than 1.1 were considered elliptical craters, and those with $R < 1.1$ were considered circular craters. Craters with an angle of less than 45˚ between the meridian and the major axis of the ellipse were classified as north-south major axis craters, and those with an angle of more than 45˚ were classified as east-west major axis craters. The deepest point from the mean plane fitting through the rim was considered as the lowest point of the crater, and the deviation from the center of the ellipse was measured.

Results and discussion

Of the 22 craters measured so far, 8 (36%) are circular, 6 (27%) are east-west major axis ones, and 8 (36%) are north-south major axis ones. Further, 3 of the east-west major axis craters had $R > 1.2$, and only 1 of the north-south major axis craters had $R > 1.2$. Two craters have the deepest points shifted in the high-latitude direction, i.e., downward of the present tilt, and one was shifted in the low-latitude direction, i.e., downward of the tilt during the past fast rotation. The rest have no significant shift of the deepest point in the latitudinal direction relative to the center of each ellipse.

As for the north-south major-axis craters, which account for about 30% of the total, the elliptical shape may have been caused by the surface tilt with respect to the direction of the net forces of gravitational

©2021. Japan Geoscience Union. All Right Reserved.

attraction and centrifugal force. We will conduct detailed topographic analysis and compare the results with laboratory experiments. On the other hand, the formation of the east-west major-axis crater cannot be explained by the tilt angle, and the possible formation mechanisms are low-angle impacts, impacts to the equatorial ridge, and anisotropy of the subsurface structure of Ryugu. In the artificial cratering experiment using Small Carry-on Impactor (SCI), it is estimated that the bedrock in the southern part of the crater inhibited the growth of the crater, resulting in a semicircular shape [7]. The east-west major-axis craters may reflect the anisotropy of the subsurface structure of Ryugu, which inhibits crater growth in the north-south direction.
We will increase the number of craters measured, removing large boulders from the surface topography, which may cause errors in determining the crater shape, in order to obtain a more accurate understanding of the crater shape. Then, we will also discuss the formation scenario of the east-west major-axis craters and constrain the past rotation state of Ryugu from the crater shape analysis.

References
[1] Watanabe+. (2019), Science 364, 268; [2] Hirata+ (2020), Icarus 338, 113527; [3] Rubincam (2000), Icarus 148, 2; [4] Bottke+ (2006), Annu. Rev. Earth Planet. Sci. 2006. 34, 157; [5] Takizawa and Katsuragi (2020), Icarus 335, 113409; [6] Yokota+ (2019), 2019 Japan Geoscience Union Meeting, PPS03-P13; [7] Arakawa+ (2020), Science 368, 67.

Keywords: Hayabusa2, planetary exploration, spin state

©2021. Japan Geoscience Union. All Right Reserved.

Thermally Controlled Crack Orientation of Boulders on Ryugu: N-S Preference and Exfoliation Structure <gdiv></gdiv>

*Sho Sasaki[1], Shiho Kanda[1], Hiroshi Kikuchi[2], Tatsuhiro Michikami[3], Tomokatsu Morota[4], Chikatoshi Honda[5], Hideaki Miyamoto[4], Ryodo Hemmi[4], Seiji Sugita[4], ERI TATSUMI[4,6], Masanori Kanamaru[2], Sei-ichiro WATANABE[7], Noriyuki Namiki[8], Patrik Michel[9], Masatoshi Hirabayashi[10], Naru Hirata[5], Tomoki Nakamura[11], Takaaki Noguchi[12], Takahiro Hiroi[13], Koji Matsumoto[8], Hirotomo Noda[8], Naoya Sakatani[14], Shingo Kameda[14], Toru Kouyama[15], Hidehiko Suzuki[16], Manabu Yamada[17], Rie Honda[18], Yuichiro Cho[4], Kazuo Yoshioka[4], Masahiko Hayakawa[2], Moe Matsuoka[2], Rina Noguchi[2], Hirotaka Sawada[2], Yasuhiro Yokota[2,18], Makoto Yoshikawa[2]

1. Department of Earth and Space Sciences, School of Science, Osaka University, 2. ISAS/JAXA, 3. Kindai University, 4. The University of Tokyo, 5. University of Aizu, 6. Instituto de Astrofisica de Canarias, 7. Nagoya University, 8. National Astronomical Observatory of Japan, 9. Observatoire de la Cote d'Azur, 10. Auburn University, 11. Tohoku University, 12. Kyushu University, 13. Brown University, 14. Rikkyo University, 15. The National Institute of Advanced Industrial Science and Technology, 16. Meiji University, 17. PERC, Chiba Institute of Technology, 18. Kochi University

Hayabusa 2 revealed that a small carbonaceous asteroid 162173 Ryugu is a rubble pile [1]. The surface of Ryugu is covered with various sizes of numerous boulders [2-4]. Thermal fatigue has been advocated for the disintegration process of surface rocks [5], where diurnal (and annual) thermal cycle may promote crack growth in the rocks on regolith over various spatial and temporal scales [6]. Growth of crack is rapid enough to fracture a few 10 cm size rock [7].

In early data analysis, we noticed that cracks on Ryugu boulders have preferred orientation. Cracks/fractures with meridional (north-south) direction are frequently observed [8] in high resolution images where boulder size is between a few tens cm and a few tens m. Desert rocks of the Earth and Mars have preferred orientation of cracks [9,10]. This would be explained by thermal process. We analyzed 777 cracks on Ryugu boulders and checked their orientations.

We analyzed 101 images by Hayabusa-2 ONC-T. Image resolution is 3mm –4m/pixel. Hayabusa 2 usually observes the surface from the direction of the sun, which provide low phase angle data with short shadow width. We carefully check images so that we do not pick up the shadowed surface structure as a crack. We classified cracks into four types (Fig.1):

(a) Straight cracks: Cracks running linearly without bending or branching.

(b) Sinuous cracks: Cracks with bowing, bending, and wavy structure.

(c) Arrested cracks: Incomplete cracks.

(d) Complex (typically branched) cracks typically for different directions.

We separated the strike of cracks into 18 directions with 10deg bin. We analyzed 538 boulders (777 cracks) and found 60% of their cracks have the meridional direction (±15deg from N-S) except complex type. This trend is common among crack types as well as rock size.

Since Ryugu’ s rotational axis inclination is 172 degree, solar irradiation would produce E-W asymmetry

©2021. Japan Geoscience Union. All Right Reserved.

in temperature. So far, solar-induced thermal stress on a surface boulder by diurnal rotation and annual revolution of Ryugu might be a possible process for the growth of boulder cracks in the meridional direction, as discussed for the preferred crack orientation of desert rocks of the Earth and Mars [7,9,10]. However, we need to explain why large boulders (> 10m, much larger than thermal length scale) have preferred crack orientation. Preferred orientation of cracks is also observed on boulders of Bennu [11]; they would be driven by solar-induced thermal stress.

Another type of thermally-driven cracks is exfoliation [12]. Stress fields induced in boulders from diurnal thermal cycle cause crack propagation in different directions at different times of day. When boulder size is smaller than 2 m, peak stress may exceed 1 MPa, leading to onion-like exfoliation in boulders of Bennu [12]. We also check cracked boulders on Ryugu and found that a couple of boulders with sinuous cracks can be interpreted by exfoliation. Two examples are shown in Figure 3: sinuous boundaries would have formed by exfoliation of surface layer.

References: [1] Watanabe, S. et al (2019) Science 364. [2] Sugita, S. et al (2019) Science 364. [3] Michikami, T. et al (2019) Icarus, 331, 179-191 [4] Nakamura et al. (2008) Earth Planets Space 60, 7-12. [5] El-Maarry, M. R., et al. (2015) Geophys. Res. Lett., 42, 5170–5178. [6] Delbo M. et al. (2014) Nature 508, 233–236. [7] Molaro, J. L. et al. (2017) Icarus 294, 247-261. [8] Sasaki, S. et al. (2019) LPSC L, #1368. [9] MacFadden et al., (2005) Geol. Soc. Am. Bull. 117, 161-173. [10] Eppes, M. C. et al. (2015) Nature Comm., 6, 6712, [11] Delbo, M. et al (2019) EPSC-DPS-176-2. [12] Molaro, J. L. et al. (2020) Nature Comm., 11, 1-11.<gdiv></gdiv>

Keywords: asteroid, thermal fatigue, boulder cracks, crack orientation, exfoliation

©2021. Japan Geoscience Union. All Right Reserved.

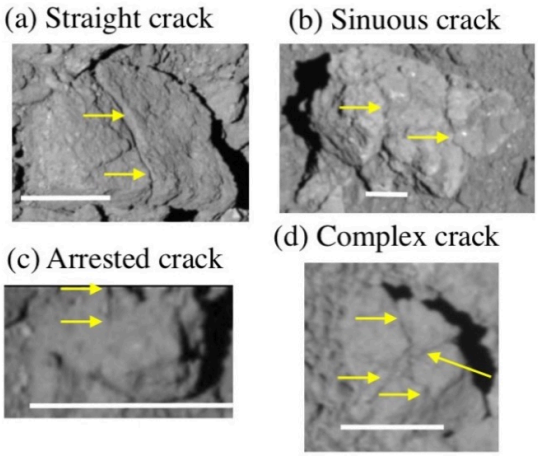


Figure 1 Examples of 4 types of cracks which are indicated by yellow arrows. White scale bars in the images indicate 1m.

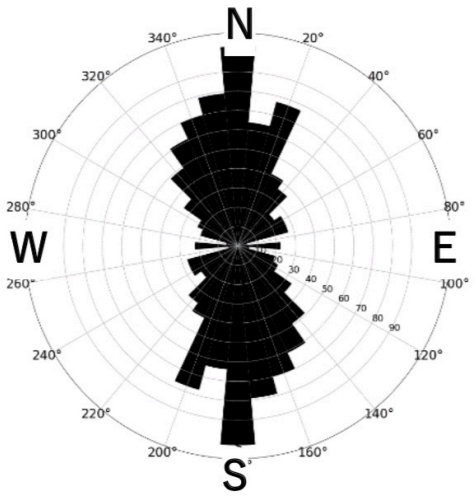


Figure 2 Distribution of crack orientation of boulders on Ryugu in a rose diagram. Each orientation bin of the rose diagram is 10 deg. The total number of cracks is 777.

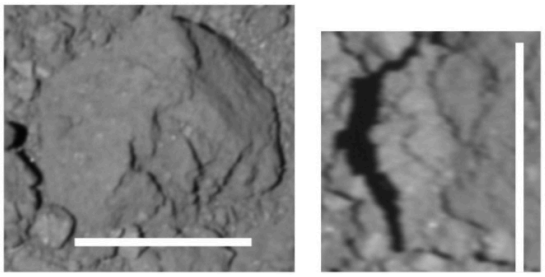


Figure 3 Exfoliation feature candidates on Ryugu. White scale bars in the images indicate 1m.

©2021. Japan Geoscience Union. All Right Reserved.

Orientation of Boulders and Rerationship with Gravitational Slope on Asteroid Rryugu: Implications for Surface Evolution.

*Tatsuki Ebihara[1], Koki Yumoto[1], Seiji Sugita[1], Rie Honda[2], Shingo Kameda[3], ERI TATSUMI[1,4], Yuichiro Cho[1], Kazuo Yoshioka[1], Hirotaka Sawada[5], Yasuhiro Yokota[2,5], Naoya Sakatani[3], Masahiko Hayakawa[5], Moe Matsuoka[5], Manabu Yamada[6], Toru Kouyama[7], Hidehiko Suzuki[8], Chikatoshi Honda[9], Kazunori Ogawa[10,11], Tatsuhiro Michikami[12], Hideaki Miyamoto[1], Tomokatsu Morota[1]

1. The University of Tokyo, 2. Kochi University, 3. Rikkyo University, 4. Instituto de Astrofisica de Canarias, 5. Japan Aerospace Exploration Agency, 6. Planetary Exploration Research Center Chiba Institute of Technology, 7. National Institute of Advanced Industrial Science and Technology, 8. Meiji University, 9. University of Aizu, 10. Japan Aerospace Exploration Agency, JAXA Space Exploration Center, 11. Kobe University, 12. Kindai University

Hayabusa2 spacecraft conducted close investigation at asteroid 162173 Ryugu from June 2018 to November 2019. Detailed observations by Hayabusa2 revealed numerous boulders on Ryugu’s surface [1, 2] and its low bulk density (1190 kg/m3), suggesting that Ryugu has a rubble pile structure [3, 4]. The distribution of visible spectral slope on Ryugu’s surface and stratigraphic relationship suggest that surface mass movement might have occurred from the equator and polar regions to the mid-latitude regions [1, 5]. In addition, morphological evidences for mass movement, such as imbricated boulders and asymmetric regolith deposits along boulders, have been reported [1]. However, the surface flows toward the mid-latitude regions on Ryugu has not been quantitatively characterized.
The spatial arrangement and orientation of clasts have been used for analyses of past flow directions [e.g., 6]. On the surface of rubble-pile asteroid Itokawa, the organized orientations of gravels were found in the boundary regions between the smooth and rough terrains, indicating gravel migration in the direction of local gravitational slopes [7]. To understand the direction and spatial scale of the mass movement, we measured the shape of boulders and investigated the relationship between their orientations (azimuth of major axis) and direction of gravitational slope on Ryugu. Based on these results, we discuss the mode of surface mass movement and the thickness of surface flow layer.
In order to measure the shape of boulders, we analyzed the images taken by Optical Navigation Camera Telescope (ONC-T) onboard Hayabusa2 [1, 8-11] during the MASCOT deployment operation (resolutions ~0.3 m/pixel), and created the catalog of boulders larger than 1 m in mean diameter near the equator (from 20˚N to 30˚S). This catalog includes size, axial ratio, azimuth angle of major axis of boulders. Considering the accuracy of shape measurement and identification of major axis of boulders, we used nearly 500 boulders larger than 4 m in the mean diameter and the minor axis/major axis ratio less than 0.7 and observed in emission angle less than 30˚. We also measured the shape of 792 small boulders and pebbles with diameters od 0.1 m to 7 m using close-up images obtained in the low-altitude operations (resolutions 0.013 m/pix and 0.033 m/pix). We calculated the angle between local gravitational slopes and major axes of boulders. To calculate local gravitational slopes, we used the SPC shape model of Ryugu [3] and took centrifugal force at the current rotation period (7.63 hours; [3]) into account.
The small boulders and pebbles exhibits its major axis tend to be preferentially perpendicular to the local slope direction than parallel ones, while boulders larger than 4 m do not show clearly such trend. Mass movement such as rolling of boulders can results in such transverse orientation to the local slope [e.g., 12]. The stronger arrangement of small boulders and pebbles suggest that they has more frequently experienced mass movement than larger boulders. This means that small boulders are relatively easy to move on Ryugu, which leads to segregation of small particles similar to asteroid Itokawa [7].
References: [1] S. Sugita et al. (2019) *Science*, aaw0422. [2] T. Michikami et al. (2019) *Icarus, 331*,

©2021. Japan Geoscience Union. All Right Reserved.

179-191. [3] S. Watanabe et al. (2019) *Science*, aav8032. [4] M. Hirabayashi et al. (2019) *ApJL, 874*, L10. [5] T. Morota et al. (2020) *Science*, aaz6306. [6] K. Yamamoto (1990), *Geograph. Rev. of Japan, Ser. A, 63.5*, 285-314. [7] H. Miyamoto et al. (2007) *Science*, 1134390. [8] S. Kameda et al. (2015) *ASR, 56.7*, 519-1524. [9] S. Kameda et al. (2017) *SSR, 208*, 17-31. [10] H. Suzuki et al. (2018) *Icarus, 300*, 341-359. [11] E. Tatsumi et al. (2019) *Icarus, 325*, 153-195. [12] K. Yamamoto (1996), *Geograph. Rev. of Japan, Ser. A, 69.3*, 165-183.

Keywords: Asteroid, Boulder, Surface Evolution

©2021. Japan Geoscience Union. All Right Reserved.

Apparently Layered Boulders with Multiple Textures on Bennu's Surface

*Kana Ishimaru[1], Dante S Lauretta[1], Nick Porter, Dathon Golish[1], Manar Al Asad[2], Ronald Ballouz[1], Olivier S Barnouin[3], Keara Burke[1], Mike Daly[4], Dani DellaGiustina[1], Kevin John Walsh[5]

1. Lunar and Planetary Laboratory, University of Arizona, 2. Department of Earth Ocean and Atmospheric Sciences, University of British Columbia, 3. The Johns Hopkins University, Applied Physics Laboratory, 4. The Centre for Research in Earth and Space Science, York University, 5. Southwest Research Institute

Introduction: Asteroid Bennu is a carbonaceous near-Earth asteroid explored by the OSIRIS-REx mission, which discovered that Bennu's surface is covered with boulders as large as tens of meters in long axis [1]. Bennu is a top-shaped, rubble-pile asteroid with diameter about 500 m [2]. Because of its small size, the collisional lifetime of Bennu is much shorter than the age of the solar system [3]. Bennu is thought to be an accumulation of fragments of a ~100-km-diameter parent body that experienced aqueous alteration [4]. The OSIRIS-REx Camera Suite (OCAMS) [5] has provided high-resolution images (<2 cm/pix) of the surface of Bennu. We discovered some boulders that exhibit multiple, apparently layered textures that are divided by linear boundaries [6]. The layered structures might have formed by geologic activity within a parent body [1, 7]; hence, they reflect its geologic history. In this work, linearly layered boulders on the asteroid surface were identified and categorized by texture and average normal albedo.

Methods: We searched for layered boulders were searched in a global mosaic of Bennu that was projected on a lidar-based global shape model (OLA v16; [10–12]) using the Small Body Mapping Tool [8]. Detailed observation and measurements of layered boulders were performed using OCAMS PolyCam [5] images with pixel scales of 2 –5 cm/pix that had been converted into reflectance [9]. All the lidar scans available (typically 10 or more scans for each boulder) were registered using a Poisson reconstruction method to create a digital terrain model (DTM) covering the entire surface of the boulder. The PolyCam images were registered to the corresponding DTM using reconstructed SPICE kernels in USGS's ISIS3 software [10]. Normal albedo was calculated in the method described in [11, 12]. Three large boulders—Gargoyle, KLR1, and KLR2—were selected for detailed analysis.

Results: Normal albedo of units can be largely divided into two texture groups: one is rough and dark (4 –5 % normal albedo), and the other is smooth and bright (5 –7% normal albedo). The layers are ~1–10 m thick. Gargoyle's dark, rough unit includes more than 100 visible clasts with an average length of 23 cm in the longest dimension. Clast size will be looked into closely because the clasts could be the individual particle that was present in the hydrothermal convection.

Future work: [13] modeled a mud convection in a 100-km asteroid parent body and showed that particle size sorting could occur. Catastrophic disruption of a parent body with a size-sorted interior could produce some rock fragments that include a boundary between two textures. The thickness of the layers observed in the boulders suggests that the size sorting could have occurred at scales of 1 to 10 m. By mapping and characterizing the layering in some boulders on Bennu, we will be able to give some constraints on the interior environment of the parent body. Using the results of physical measurements, we will develop a model of sedimentation in hydrothermal convection to reproduce the layered boulders.

[1] DellaGiustina D. N. et al. (2019) *Nature Astronomy, 3,* 341-351. [2] Barnouin O. S. et al. (2019) *Nature Geoscience, 12,* 247-252. [3] Bottke W. F. et al. (2005) *Icarus, 179,* 63-94. [4] Lauretta D. S. (2015)

©2021. Japan Geoscience Union. All Right Reserved.

Meteoritics & Planetary Science, 50, 834849. [5] Rizk B. et al. (2018) *Space Sci Rev, 214*, 26. [6] Molaro J. L. et al. (2020) *Nat. Commun. 11,* 2913. [7] Walsh K. J. et al. (2019) *Nature Geoscience, 12*, 242-246. [8] Ernst C. M. et al. (2018) *Lunar and Planetary Science Conference, 49,* Abstract #1043. [9] Golish D. R. et al. (2020) *Space Sci Rev, 216,* 12. [10] DellaGiustina et al. (2018) *Earth and Space Science*, 5, 929– 949. [11] Golish D. R. et al. (2020) *Icarus, 113724.* [12] Ishimaru K. et al. (2021) *Lunar and Planetary Science Conference, 52,* Abstract #1154. [13] Bland P. A. & Travis B. J. (2017) *Sci. Adv., 3,* e1602514.

Keywords: Bennu, OSIRIS-REx, Asteroid

©2021. Japan Geoscience Union. All Right Reserved.

High-resolution global thermal images of Ryugu acquired from the dawn side

*Yuri Shimaki[1], Hiroki Senshu[2], Naoya Sakatani[3], Tatsuaki Okada[1,4], Tetsuya Fukuhara[3], Satoshi Tanaka[1,5], Takehiko Arai[6], Hirohide Demura[7], Tomohiko Sekiguchi[8], Toru Kouyama[9], Jun Takita[10], Sunao Hasegawa[1]

1. Institute of Space and Astronautical Science, Japan Aerospace Exploration Agency, 2. Planetary Exploration Research Center, Chiba Institute of Technology, 3. Rikkyo University, 4. The University of Tokyo, 5. The Graduate University for Advanced Studies, SOKENDAI, 6. Ashikaga University, 7. The University of Aizu, 8. Hokkaido University of Education, 9. National Institute of Advanced Industrial Science and Technology (AIST), 10. Hokkaido Kitami Hokuto High School

The thermal infrared imager (TIR) on Hayabusa2 acquired high-resolution thermal images of Ryugu during the Mid-altitude observation on August 1, 2018. By comparing the temperature profiles of Ryugu and the results of a thermophysical model, we estimated the thermal inertia and surface roughness maps of Ryugu. The global average of the thermal inertia was calculated to be 225 J m^{-2} K^{-1} $s^{-0.5}$, with a surface roughness of 47˚ in the RMS slope [1]. However, we failed to determine the thermal inertia in the northern hemisphere due to temperature profiles' limitations. To assess the thermophysical properties of these areas, here we report other high-resolution thermal images of Ryugu acquired during Box-C observations in 2019, where the observational geometries were different from the Mid-altitude observation.
We used three high-resolution global observations with different sub-solar latitudes (L_s), solar phase angles (t_s), and heliocentric distances (r). They are the Mid-altitude on 2018-08-01 (L_s = -8.4˚, t_s = -20˚, r = 1.06 AU), the Box-C4 on 2019-07-25 (L_s = 4.6˚, t_s = 37, r = 1.05 AU), and the Box-C5 observations on 2019-10-24 (L_s = -7.6˚, t_s = 33˚, r = 1.00 AU). The brightness temperature images were obtained using a calibration method described in [2]. We assumed an emissivity of 0.9. The brightness temperature images were projected onto a shape model of Ryugu using the SPICE kernels; thus, we obtained three temperature profiles for each polygon of the shape model.
We prepared temperature profiles expected for the three observations by TPM2 with various thermal inertia and surface roughness. Since the dawn-side observations yield temperature rise in the morning but are hard to determine temperature peak in the afternoon, we directly compared observed and calculated temperature profiles to estimate thermal inertia and surface roughness. Our analysis suggests that global thermal inertia of 200-300 J m^{-2} K^{-1} $s^{-0.5}$ and with a surface roughness of 40-47˚ in the RMS slope could satisfy observation results.
[1] Shimaki Y. et al. (2020) *Icarus* 348, 113835. [2] Okada T. et al. (2020) *Nature* 579, 518-522.

Keywords: Hayabusa2, Thermal Infrared Imager, Asteroid Ryugu

©2021. Japan Geoscience Union. All Right Reserved.

High-resolved temperature map of Ryugu surface observed with Thermal Infrared Imager onboard Hayabusa2

*Takehiko Arai[1], Tatsuaki Okada[2], Satoshi Tanaka[2], Tetsuya Fukuhara[3], Hirohide Demura[4], Toru Kouyama[5], Naoya Sakatani[3], Yuri Shimaki[2], Hiroki Senshu[6], Tomohiko Sekiguchi[7], Jun Takita[8]

1. Ashikaga University, 2. JAXA, 3. Rikkyo University, 4. The University of Aizu, 5. AIST, 6. Chiba Institute of Technology, 7. Hokkaido University of Education, 8. Hokkaido Kitami Hokuto High School

The thermal infrared imager (TIR) onboard the Hayabusa2 spacecraft performed thermographic observations of the asteroid 162173 Ryugu (1999 JU3) from June 2018 to November 2019. Our previous report (Shimaki et al., 2020) indicated that the global thermal inertia of the Ryugu surface, obtained by the middle altitude observation of TIR (~5km), was 225 ±45 J m^{-2} $s^{-0.5}$ K^{-1}. This result implies that the surface is homogeneously filled in porous materials. On the other hand, boulders, which have high thermal inertia, have been founded by proximity observations of TIR (<1km). Therefore, local areas of the surface have various thermal inertia values and may not be homogeneous. In this study, we constructed high-resolved temperature maps of 0.5˚ by 0.5˚ gridded using the shape model of Ryugu (Watanabe et al., 2018). This study estimates the local thermal inertia, comparing the numerical simulation with the observed temperature.

Keywords: Asteroid, Hayabusa2, Thermal Infrared Imager, Temperature map

©2021. Japan Geoscience Union. All Right Reserved.

Current status and future plan of Hayabusa2 Science Data Archive in PDS4

*Shin-ya Murakami[1], Yukio Yamamoto[2], M. Katherine Crombie[3], Carol Neese[4], Yoshiaki Ishihara[2]

1. Keio University, 2. Japan Aerospace Exploration Agency, 3. Indigo Information Services, LLC, 4. Planetary Science Institute

The Hayabusa2 spacecraft collected many scientific data of the asteroid (162173) Ryugu in the asteroid proximity phase. These scientific data and engineering data which are thought to be useful for understanding of scientific data will be archived in PDS4 format. We are currently preparing following PDS4 bundles: the Mission Information bundle, the ONC bundle, the TIR bundle, the NIRS3 bundle, the LIDAR bundle, and the SPICE bundle. Some of these are under review process, and will be open to the public via web sites of DARTS at ISAS/JAXA and PDS Asteroid/Dust Subnode of PDS Small Bodies Node at PSI after finishing review process. This will be the first case of providing the PDS4-compliant archive for JAXA's mission.

We will show current status of the archiving and will also present future plans of the archive.

Keywords: Hayabusa2, (162173) Ryugu, PDS4, Planetary Data System, Data Archive

©2021. Japan Geoscience Union. All Right Reserved.

Assessing the debris generated by the small carry-on impactor operated from the *Hayabusa2* mission

*Motoo Ito[1], Yoshinori Takano[2], Yoko Kebukawa[3], Takuji Ohigashi[4], Moe Matsuoka[5], Kento Kiryu[3], Masayuki Uesugi[6], Tomoki Nakamura[7], Hayato Yuzawa[4], Keita Yamada[8], Hiroshi Naraoka[9], Toru Yada[5], Masanao Abe[5], Masahiko Hayakawa[5], Takanao Saiki[5], Shogo Tachibana[10]

1. Kochi Institute for Core Sample Research, JAMSTEC, 2. Biogeochemistry Research Center, JAMSTEC, 3. Yokohama National University, 4. UVSOR, IMS, 5. ISAS, JAXA, 6. JASRI/SPring-8, 7. Tohoku University, 8. Tokyo Institute of Technology, 9. Kyushu University, 10. University of Tokyo

We have analyzed the carbonaceous materials generated by the explosion of an HMX (high-melting explosive) mixture in an Ar atmosphere in a laboratory simulation of the SCI (small carry-on Impactor) experiment. We used both non-destructive and destructive analytical techniques to identify the chemical nature of the materials. From SEM–EDS, we found the materials to be composed mainly of carbon, nitrogen, and oxygen, with a detectable amount of metals. Suitable parameters for identifying these materials are a FTIR peak at 1520 cm^{-1}, low reflectance and gentle red slope of FTIR spectrum compared with a Murchison CM2 chondrite, the Raman D and G bands, and the H, C, and N isotopic compositions and their spatial distributions. The scanning transmission X-ray microscopy (STXM)–XANES results provided the molecular nature of these highly aromatic materials, which was supported by results from TD–GC/MS. These results suggest that it is possible to distinguish either Ryugu samples or SCI materials as potential contaminants in a sample container by using proper combinations of analytical techniques. This assessment provides information useful for the analysis of the Ryugu asteroidal samples.

Keywords: C-type asteroid Ryugu, Hayabusa2 mission, Off-nominal assessment, Small carry-on Impactor, Carbonaceous materials

©2021. Japan Geoscience Union. All Right Reserved.

X-ray nanotomography of CM and CI chondrites and their heated samples: as a rehearsal of Hayabusa2 sample analysis.

*Mingqi Sun[1], Akira Tsuchiyama[1,2], Megumi Matsumoto[3], Yuri Fujioka[3], Tomoki Nakamura[3], Junya Matsuno[2], Akira Miyake[4], Shota Okumura[4], Naotaka Tomioka[5], Motoo Ito[5], Yu Kodama[6], Stefano Rubino[7], Naoto Nakano[4], Kentaro Uesugi[8], Akihisa Takeuchi[8], Masahiro Yasutake[8]

1. CAS Key laboratory of Mineralogy and Metallogeny, Guangzhou Institute of Geochemistry, Chinese Academy of Science, Guangzhou 510640, China, 2. Research Organization of Science and Technology, Ritsumeikan University, Japan, 3. Graduate School of Science, Tohoku University, Japan, 4. Graduate School of Science, Kyoto University, Japan, 5. Kochi Institute for Core Sample Research, Japan, 6. Marine Works Japan Ltd., Japan, 7. Institut d'Astrophysique Spatiale, Université Paris-Saclay, France, 8. JASRI/SPring-8, Japan

The Hayabusa2 spacecraft has successfully returned to Earth on 6th of Dec. 2020, carrying samples of the C-type near-Earth asteroid 162173 Ryugu. It is highly expected that the samples are similar to carbonaceous chondrites, which play a significant role in water and organic material delivery to the earth [1]. SR-based X-ray nanotomography (nanoXCT) is a powerful technique to characterize nondestructively the detailed 3D structures including external shapes and constituent phases of a small particle (<~100 mm). We have analyzed extraterrestrial samples by combining two types of nanoXCT (e.g., [2]): dual-energy tomography (DET) [3] and scanning-imaging X-ray microscopy (SIXM) [4] with the resolution of ~100 nm at SPring-8, SR facility in Japan (DET-SIXM). We consider that the DET-SIXM method could be beneficial to recognize the mineralogical features and estimate the heated condition of the asteroid Ryugu samples.

As a rehearsal of the initial analysis for the Hayabusa2 samples, we performed the DET-SIXM analysis of small particles (20~80 mm in size) from different groups of carbonaceous chondrites; Murchison, Murray and Mighei CM chondrites and Orgueil CI chondrites. Murchison samples heated at different temperatures from 400 to 990°C for 50 hrs., Murray samples heated at 600°C for different durations from 10 to 1000 hrs. and Orgueil samples at 500°C for 50 hrs. were also analyzed to examine the effect of heating, which is expected to occur on the Ryugu samples. We obtained 3D distribution of the linear attenuation coefficients (LAC) and X-ray refractive index decrement (RID) of the samples by DET and SIXM, respectively, for phase discrimination. In this paper, we focused on the mineralogy based on the LAC and RID values of the CM and CI samples to understand the variations in the same meteorites and among different groups (CM and CI) and the effect of heating. The textural variations will be also reported by Matsuno et al. and TEM observation of specific phases in one of the nanoXCT sample by Matsumoto et al. in this meeting.

We obtained the peak(s) of the 3D histogram of the LAC and RID values as the representative(s) of the constituent material(s) in each sample grain by image analysis. The first peaks generally come from the matrix of the meteorites and correspond to Fe-bearing hydrous silicates, which should be serpentine in CM and saponite and/or serpentine in CI (note that we cannot discriminate between serpentine and saponite in DET-SIXM). We usually obtained the second and sometimes third peaks in CM, corresponding tochilinite-cronstedtite intergrowth (TCI) or TCI-like objects, forsterite and/or enstatite and calcite. The Mg# of the hydrous silicates has some variations among different grains of the same meteorite and we cannot distinguish between the three different CM meteorites by their Mg#. In contrast, the Mg# of CI is slightly smaller than that of CM.

©2021. Japan Geoscience Union. All Right Reserved.

In Murchison (CM), the serpentine peak positions heated at 400°C for 50 hrs. are almost similar to the unheated samples while that at 600°C for 50 hrs. becomes poor in the Mg# and partially dehydrated. The peak position at 990°C for 50 hrs. suggests that this contains heavy elements like Ca as well as Fe probably due to partial melting. In Orgueil (CI), the hydrous silicate peak positions heated at 500°C for 50 hrs. shows slight decrease in the Mg# and the degree of dehydration. In Murray (CM), the matrix became poor in the Mg# and partially dehydrated at 600°C for 10 hrs. but the Mg# and the degree of dehydration were almost the same even by increasing the heating duration. Based on the above results, it is concluded that by the DET-SIXM method (1) we may recognize the carbonaceous chondrite groups, CM and CI, (2) we can recognize samples heated at temperatures larger than ~500°C, and (3) estimation of heating duration may not be sensitive.

[1] K. Kitazato et al. (2019) *Science*, **364**, 272-275. [2] M. Matsumoto et al. (2019) *Science Advances*, **5**, eaax5078. [3] A. Tsuchiyama et al. (2013) *Geochim. Cosmochim. Acta*, **116**, 5-16. [4] A. Takeuchi, (2013) *J. Synchrotron Rad.* **20**, 793–800.

Keywords: Hayabusa2, carbonaceous chondrites, nanoXCT, DET-SIXM

©2021. Japan Geoscience Union. All Right Reserved.

Assessing the irradiation effects by a synchrotron X-ray micro-computed tomography on the organic materials in carbonaceous chondrite: Examination at SPring-8 facility

*Haruna Sugahara[1], Yoshinori Takano[2], Toshihiro Yoshimura[2], Nanako O Ogawa[2], Naohiko Ohkouchi[2], Masayuki Uesugi[3], Akira Tsuchiyama[4], Hayabusa2 project team

1. Institute of Space and Astronautical Science, Japan Aerospace Exploration Agency (ISAS/JAXA), 2. Japan Agency for Marine-Earth Science and Technology (JAMSTEC), 3. Japan Synchrotron Radiation Research Institute, 4. Ritsumeikan University

X-ray micro-computed tomography (μCT) using a synchrotron light source is a strong tool to reveal the three-dimensional (3D) structure of the small particle including its mineralogy and the textures. It was applied to the regolith particles on the asteroid Itokawa, which were returned by the Hayabusa spacecraft, and helped to understand the origin and the evolution of the particles [1]. The subsequent Hayabusa2 mission succeeded in returning the samples (> 5 gram for a twice touchdown [2]) from the carbonaceous-type asteroid Ryugu in December 2020. The μCT is planned as one of the initial analysis procedures of the Ryugu samples [3]. However, there is a concern about the effect of X-ray irradiation caused by μCT on the organic materials in the Ryugu samples. The organic materials are generally sensitive to X-ray irradiation due to potential alteration and/or degradation processes. Thus, we performed an assessment to examine the effect of the μCT procedure prior to the initial analysis. Friedrich et al. (2016) examined the effects of X-ray irradiation by μCT to amino acids in Murchison meteorite (CM2) at the GeoSoilEnviroCARS (GSECARS) facility at the Advanced Photon Source (APS), Argonne National Laboratory and reported that there was no significant effect observed for the abundance of the amino acids [4].

The purpose of the study is to investigate the potential effect on the soluble organic materials, inorganic ions, and bulk element profiles in a carbonaceous chondrite caused by the X-ray irradiation of μCT at the synchrotron SPring-8 [3]. We conducted the two sets of the irradiation experiments using a homogenized Murchison meteorites (CM2) powder. The one sample was irradiated with the typical condition as the usual μCT analysis. The total irradiation time was around 5 minutes. The second sample was irradiated for a longer time (8.5 hours) at the same energy. These irradiated samples and the non-irradiated control samples were investigated using several analytical techniques. We analyzed the concentration of the amino acids, which are labile but important target molecules in Ryugu samples. We also analyzed the soluble ion components using ion chromatograph and inductively coupled plasma-mass spectrometry (ICP-MS) and the bulk carbon and nitrogen abundances using an elemental analyzer connected to isotope ratio mass spectrometer (EA/IRMS). In this presentation, we will overview the present organic and inorganic assessments for the sampling process of the μCT description at SPring-8.

References:

[1] Tsuchiyama A. et al. (2011) Science, 336, 1125-1128.

[2] Tachibana S. et al. (2021) Abstract for the 52nd Lunar and Planetary Science Conference (LPSC).

©2021. Japan Geoscience Union. All Right Reserved.

[3] Tsuchiyama A. et al. (2020) Abstract for Spring-8 symposium 2020.

[4] Friedrich J. M. et al. (2016) Meteorit. Planet. Sci. 51, 429-437.

Keywords: Hayabusa2, Sample analysis, μCT, SPring-8, Organic materials, Carbonaceous chondrite

©2021. Japan Geoscience Union. All Right Reserved.

Description of return sample from C-type asteroid Ryugu using the MicrOmega hyperspectral microscope in JAXA Curation Facility

*Tatsuaki Okada[1,2], KaKasumi Yogata[1], Aiko Nakato[1], Kentaro Hatakeda[1,3], Toru Yada[1], Lucie Riu[1], Akiko Miyazaki[1], Kazuya Kumagai[1,3], Masahiro Nishimura[1], Masanao Abe[1], Tomohiro Usui[1,2], Cedric Pilorget[4], Rosario Brunetto[4], Vincent Hamm[4], Lionel Lourit[4], Jean-Pierre Bibring[4]

1. Institute of Space and Astronautical Science, Japan Aerospace Exploration Agency, 2. University of Tokyo, 3. Marine Works Japan Ltd., 4. Institue d' Astrophysique Spaciale

Sample from C-type asteroid 162173 Ryugu has been returned by Hayabusa2, and now treated in the Hayabusa2 Curation Facility. One of the tasks in the facility is to characterize the sample and describe its feature as the sample catalogue for further analysis by the initial analysis teams, the second-stage curation activity, NASA sample curation, and the future AO researches. The MicrOmega is a hyperspectral microscope developed by IAS and applied to characterize the sample as bulk properties and as individual particles, with the wavelength range scanning from 0.99 to 3.65 μm using AOTF and with four visible to near infrared LEDs, and with the area of 5 x 5 mm square at the spatial resolution of 22 μm per pixel. The sample has to be kept in the clean chamber under an ultra-purified nitrogen condition to avoid from contamination by terrestrial materials and from exposure to the terrestrial atmosphere, while the instrument is mounted outside of the clean chamber. Therefore, the sample observation must be conducted through the sapphire window with the MicrOmega. During the observation, the instrument is kept at about 10 ℃ for stable operation. The specially developed sample holder is mounted on the XYZ-R stage in the clean chamber which can be cooled down to ~0 ℃ during the observation to reduce thermal radiation from the sample. The stage is moved in three directions in micron steps to adjust the surface of the sample at the focal position, and is rotated around 360 ˚to enable the observation from various directions, while the incident angle is 35 ˚and the emission angle is 0 ˚. The MicrOmega and the dedicated chamber with these functions has been setup, tested, and calibrated by the team from IAS and ISAS Curation Facility. Many kindes of scripts for the observations are used for the observations to detemine the suitable methods of analyis. The catalogue information will include the images obtained at several wavelengths, a few color ratio images, and the spectra of several specific areas, and some brief description from MicrOmega, along with the data from other measurements in the Curation Facility such as optical microscope, FTIR, and weighing. The status and performance of MicrOmega activity will be presented in more detail.

Keywords: Hayabusa2, Sample return, hyperspectral microscope, asteroid

©2021. Japan Geoscience Union. All Right Reserved.

Significant role of Asteroids: One step of purified rocks and minerals and life to final water planet

*Yasunori Miura[1]

1. Visiting (Yamaguchi University, EUA-Al. Univ. Toronto, LPI-NPPf)

Introduction: We have been established "the Solar System movement" from "the geo-centered theory Helio-centered theory". However, we have been interpreted extraterrestrial materials from the terrestrial database collected by our longer and sensitive analytical methods. In this paper, author points out new development of extraterrestrial samples from the individual database in each Asteroids and planets.
Earth’ s Heliocentrism to the comparison of solid spheres: We require now new view from astronomical observations to material analysis with individual data base The solid sphere also changes to one case of celestial body. To the biosphere is considered as a one-state sphere though there are many life system on water planet Earth.
Total systems of gas-solid-liquid systems: Three systems are observed on planet Earth. Two systems of global air and solid systems ate found on Mars and Venus etc., though one system (solid) is known on Mercury, the moon and asteroids. This suggests that liquid system (global ocean) is obtained only in the three system spheres.
Carbon-bearing materials: Stable existence of the three systems also present in extreme conditions. These materials are remained in the solid sphere with all celestial bodies even at low temperature and low pressure conditions.
Biosphere with carbon-molecules: Water planet Earth composes of three systems largely as one unit of celestial body system, which can coexist and generate in the global three systems with ocean water system.
System theory consideration: Multi-changes of carbon-bearing materials are possible in the three systems which generates life system with carbon-component molecules mainly on the surface, though it remains in the global solid materials as the "fossil stones" as the relicts of life system sphere, where solid rocks (mainly inorganic solids) are included in all other celestial bodies as main igneous activity.
Problems of the global and regional states: All celestial bodies have global system of one celestial body totally with many regional site.
Significant role of Asteroids: Asteroids shows one step of the purified rocks and minerals (with clear crystal structure) and life (clear organic molecules) of final water planet.

Keywords: Asteroids, Water planet Earth, System consideration

©2021. Japan Geoscience Union. All Right Reserved.

Simulation of Phobos internal density structure estimation by orbit determination of MMX

*Keiko Yamamoto[1], Koji Matsumoto[1], Hitoshi Ikeda[2], Hiroki Senshu[3]

1. National Astronomical Observatory of Japan, 2. Japan Aerospace Exploration Agency, 3. Chiba Institute of Technology

The Martian Moons eXploration (MMX) mission aims to clarify the origin of Martian moons, the evolution of the Martian sphere, and the formation of solar system planets by remote-sensing observations and sample returns. For studying their origins and evolution processes, i t is important to obtain information on the internal structures of the Mars moons. In this study, we simulated estimations of Phobos' gravity field and internal density structure by the precise orbit determination of the MMX spacecraft. In the vicinity of Phobos, the orbit of the spacecraft is disturbed by the gravity of Phobos. Therefore, it is possible to estimate the gravity field and internal density structure of Phobos by orbit analysis of the spacecraft.
Based on the exploration plan, we first assumed some types of the orbit of the spacecraft: ascending orbit after landing on the surface of Phobos and Quasi-Satellite Orbits (QSO). Then, simulated data sets of Doppler observations, imaging observations and laser altimetry (LIDAR) was created. Using these data sets as observed values, we performed the following simulations. 1) Estimation of the depth of the density change boundary or the density of each layer of Phobos from the data of the ascending orbit after surface landing. 2) Estimation of regionally different density structures from the data of ascending orbit after surface landing. 3) Estimation of Phobos' gravity field coefficients from QSOs with different altitudes. In the presentation, we will show the results of these simulations and discuss how much constraints can be given to the internal density structure of Phobos.

Keywords: MMX, Phobos, Orbirt determination, gravity field

©2021. Japan Geoscience Union. All Right Reserved.

MMX InfraRed Spectrometer (MIRS) imaging spectrometer

*Jean-Michel Reess[1], Maria Antonella Barucci, Pernelle Bernardi, Michel Le Du, Eric Sawyer, Takahiro Iwata[2], Hiromu Nakagawa[3], Tomoki Nakamura[4], Alain Doressoundiram, Sonia Fornasier

1. J.-M. Reess, LESIA, Observatoire de Paris, Université PSL, CNRS, Université de Paris, Sorbonne Université, 92190 Meudon, France, 2. T. Iwata, ISAS, JAXA, Sagamihara 252-5210, Japan, 3. H. Nakagawa, JAXA, Sagamihara 252-5210, Japan, 4. T. Nakamura, JAXA, Sagamihara 252-5210, Japan

MIRS (MMX InfraRed Spectrometer) is an imaging spectrometer (in the range 0.9 - 3.6 microns) onboard of MMX mission, which will allow to characterize the Martian system and contribute to evaluate and select sampling site candidates. One of the main mission goals is to decipher the origin of the moons, which will provide important clues on planetary formation and how water is delivered to inner planets.
MIRS instrument is built at LESIA-Paris Observatory in collaboration with four other French laboratories (LAB, LATMOS, LAM, IRAP-OMP), with collaboration and financial support of CNES and close collaboration with JAXA and MELCO.

The instrument is designed to fully accomplish MMX’ s scientific and measurement objectives. MIRS is expected to characterize Phobos and Deimos surfaces and Mars atmospheric composition by remotely identifying diagnostic features in the near-infrared range. MIRS is also expected to perform observations of dust storm, clouds, distributions of total amount of water vapor. These observations are expected to be performed over several successive days in different seasons.

MIRS performance requirement:
Spectral range: 0.9 –3.6 microns
Spectral resolution (sampled) < 20 (+10%) nm
Spectral sampling: 10 (+10%) nm
IFOV: less than 0.41 mrad, goal: 0.35 mrad
FOV: higher than ±1.65° SNR: higher than 100 in [2.7 - 3.2] microns in less than 2 sec integration, for 30 degrees solar incidence, at 1.5 au, with Lambertian albedo at 30 degree phase angle
Modulation Transfer Function shall be higher than 8% at Nyquist frequency in the spatial direction
MIRS boresight orientation with respect to MMX spacecraft shall be known with an accuracy better than +/-1.4 mrad.
MIRS boresight relative orientation between successive acquisitions of an observation sequence shall be known with an accuracy better than +/-0.17 mrad.

MIRS will be a fundamental instrument to evaluate sampling site candidates and support the selection of the two sampling sites on the Phobos surface. In conclusion, MIRS will allow compositional characterization of Phobos, Deimos and temporal characterization of particular phenomena of Mars atmosphere.

Keywords: MMX, Mars, Phobos, Spectrometer

©2021. Japan Geoscience Union. All Right Reserved.

Thermophysical Properties of S-type Binary Didymos by Thermal Imaging in Hera Mission

*Tatsuaki Okada[1,2], Satoshi Tanaka[1,2], Naoya Sakatani[3], Yuri Shimaki[1], Takehiko Arai[4], Hiroki Senshu[5], Hirohide Demura[6], Toru Kouyama[7], Tomohiko Sekiguchi[8]

1. Institute of Space and Astronautical Science, Japan Aerospace Exploration Agency, 2. University of Tokyo, 3. Rikkyo University, 4. Ashikaga University, 5. Chiba Institute of Technology, 6. University of Aizu, 7. National Institute of Advanced Industrial Science and Technology, 8. Hokkaido University of Education

A thermal infrared imager TIRI is being developed to investigate thermophysical properties of S-type binary asteroid Didymos and Dimorphos in the ESA Hera mission. As was proven in the Hayabusa2 mission to the C-type asteroid 162173 Ryugu, thermal imaging is an established and essential method to investigate the surface physical state at high spatial resolution discriminating region to region, and boulder to boulder (Okada+, Nature 2020; Shimaki+, Icarus 2020). Asteroids are primitive bodies which might have experienced somewhat low degree of alteration and consolidation during its formation and evolution processes compared with larger planetary bodies, so that the micro-porosity in rocks and boulders should be a barometer of evolution of solar system bodies. TIRI is based on an uncooled micro-bolometer array of 1024 x 768 pixels and has the field of view of 13.3˚ x 10.0˚, which covers the total Didymos-Dimorphos binary system from 20 km distance to trace the whole one-rotation. The angular resolution is 0.013˚ (0.23 mrad) per pixel or 4.6 m per pixel from the distance of 20 km, which can resolve the artificial crater excavated by the kinetic impact of NASA DART spacecraft. TIRI also has the function of multiband thermal imaging with 8-point filter wheel. The filter wheel has a wide band of 7-14 μm, six narrow bands with the center positions of 7.6, 8.6, 9.6, 10.6, 11.6, 13.1 μm. The last one position is closed to be used as a reference temperature or a shutter to avoid insolation. TIRI also obtains the surface compositional information from the color ratios of these multi-bands, especially from the Christensen Feature (CF) and the Reststrahlen Feature (RF) to classify the surface material. We will report the progress report of the development of TIRI.

Keywords: Thermal inertia, planetary defense, thermography, binary asteroid, Multi-band imaging

©2021. Japan Geoscience Union. All Right Reserved.

Current status and science of DESTINY+

*Tomoko Arai[1], Masanori Kobayashi[1], Ko Ishibashi[1], Hiroshi Kimura[1], Takayuki Hirai[1], Peng Hong[1], Fumi Yoshida[2], Naoya Ozaki[3], Takayuki Yamamoto[3], Hiroyuki Toyota[3], Kazutaka Nishiyama[3], Hiroshi Imamura[3], Takeshi Takashima[3], DESTINY+ science team

1. Planetary Exploration Research Center, Chiba Institute of Technology, 2. University of Occupational and Environmental Health, Japan, 3. ISAS, JAXA

DESTINY+ (Demonstration and Experiment of Space Technology for INterplanetary voYage with Phaethon fLyby and dUst Science) was selected in 2017 as a mission for JAXA/ISAS smallclass program. It will be launched in 2024 and fly by Phaethon in 2028. It is a joint mission of technology demonstration and scientific observation. The engineering mission is led by ISAS/JAXA and the science mission is led by PERC, Chiba Inst. of Technology (ChiTech). It will test high performance electric propelled vehicle technology and high-speed flyby of asteroid (3200) Phaethon and possibly asteroid 2005UD, a likely break-up body from Phaethon, as an extended mission. Engineering challenges include an up-close encounter at a distance of 500 km from Phaethon with radio-optical hybrid navigation guidance and control, and autonomous imaging based on optical information for target tracking during a high-speed flyby of about 35km/sec. The science goal is to understand the nature and origin of cosmic dust brought onto the Earth, in the context of exogenous contribution of carbon and organics for possible prebiotic seeds of the terrestrial life. Phaethon is a parent body of Geminid meteor shower, and thus a known source to periodically provide dust to the Earth, via the dust stream. The science objectives are two folded: (1) in-situ analyses of velocity, arrival direction, mass and chemical composition of interplanetary and interstellar dust particles around 1 au, the dust trail, and nearby Phaethon, and (2) flyby imaging of Phaethon to study its geology, for understanding dust ejection mechanism of active asteroid and the surface compositional variation. Science payloads include a panchromatic, telescopic camera with a tracking capability (TCAP), a visible-NIR multi-band camera with four bands of 425, 550, 500, 850 nm (MCAP), and a dust analyzer (DDA). While the two cameras are developed by PERC, Chitech, DDA is developed by Univ. of Stuttgart, as an international collaboration. Ground calibration for DDA is being performed with German/Japanese joint efforts. International observation campaign for Phaethon was conducted in December 2017, and that of asteroid 2005 UD in October, 2018. Also, international observation campaign for stellar occultation by Phaethon was performed in 2019. Here, we present the current status and science of DESTINY+ mission.

Keywords: DESTINY+, Phaethon, Geminid meteor shower, active asteroid, cosmic dust, Flyby

©2021. Japan Geoscience Union. All Right Reserved.

Progress report of development and ground calibration of DESTINY$^+$ Dust Analyser

*Takayuki Hirai[1], Masanori Kobayashi[1], Tomoko Arai[1], Hiroshi Kimura[1], Sho Sasaki[2], Hikaru Yabuta[3], Amano Sui[3], Sachio Kobayashi[4], Motoo Ito[4], Akira Yamaguchi[5], Hajime Yano[6], Mario Trieloff[7], Jon Hillier[8], Nozair Khawaja[8], Lisa Eckart[8], Harald Krueger[9], Jonas Simolka[10], Ralf Srama[10]

1. Chiba Institute of Technology, Planetary Exploration Research Center, 2. Osaka University, 3. Hiroshima University, 4. Japan Agency for Marine-Earth Science and Technology, 5. National Institute of Polar Research, 6. Japan Aerospace Exploration Agency, 7. Heidelberg University, 8. Free University of Berlin, 9. Max Planck Institute for Solar System Research, 10. University of Stuttgart

DESTINY$^+$ is a Solar System small body exploration mission led by JAXA to demonstrate multiple technologies for fast flyby exploration and conduct scientific observation of 3200 Phaethon and cosmic dust including ejecta particles from the body.
For dust science, DESTINY$^+$ Dust Analyser (DDA) will detect hypervelocity impacts of interplanetary and interstellar dust particles during the interplanetary cruising phase, and hopefully Phaethon ejecta particles at the flyby phase. DDA is a time-of-flight mass spectrometer measuring ions generated by hypervelocity impact ionization of dust particles. The development of DDA is led by University of Stuttgart while the ground calibration activity is being conducted by an international collaboration among multiple researchers and institutions in Europe, US, and Japan.
This presentation reports the progress of development and ground calibration activity of DDA. As of early 2021, the development status of DDA has proceeded to critical design phase during which the engineering model of DDA will be developed according to the interface condition agreed with the spacecraft system. For the ground calibration, a new dust accelerator is expected to be available at University of Stuttgart. In addition, development of new calibration methods has been proceeded utilizing some ionization techniques used in e.g. SIMS, LA-ICP-MS, and MALDI as alternative ways to dust accelerator i.e. microparticle impact ionization. These alternative calibration methods are expected to expand the type or number of available sample materials and calibration frequency.

Keywords: Cosmic dust, 3200 Phaethon, Impact ionization mass spectrometry

©2021. Japan Geoscience Union. All Right Reserved.

Study of asteroid tracking mirror of telescopic camera onboard DESTINY+

*Peng Hong[1], Ko Ishibashi[1], Takayuki Hosonuma[2], Ozaki Naoya[3], Shunsuke Sato[3], Hiroyuki Toyota[3], Kazutaka Nishiyama[3], Masatsugu Otsuki[3], Osamu Okudaira[1], Takeshi Takashima[3]

1. Planetary Exploration Research Center, Chiba Institute of Technology, 2. Department of Aeronautics and Astronautics, The University of Tokyo, 3. Institute of Space and Astronautical Science, Japan Aerospace Exploration Agency

DESTINY$^+$ (Demonstration and Experiment of Space Technology for INterplanetary voYage with Phaethon fLyby and dUst Science) mission plans to conduct high-resolution imaging during close flyby of asteroid (3200) Phaethon, which is considered as a parent body of Geminid meteor shower. The Telescopic CAmera for Phaethon (TCAP) is planned to perform high-resolution imaging of the surface of Phaethon with an imaging rate of more than 1 frame per second and with a spatial resolution down to 3.5 m/px at closest approach. Since the relative flyby speed and closest distance to Phaethon are expected to be 30 to 40 km/s and about 500 km, it is significantly difficult to track the asteroid only by the rotation of the spacecraft itself. Therefore, an asteroid tracking system is required for TCAP to obtain unblurred high-resolution images. We have conducted conceptual studies of the tracking mirror to satisfy scientific requirements. To realize the designed concept, we have developed a simple breadboard model of the actuator of tracking mirror. The breadboard model consists of a rotating mirror, a 2-phase stepping motor and its driver, a motor reducer, and a FPGA board to control the driver. We show that the pointing and tracking accuracy of the breadboard model generally satisfy the required performance and discuss further improvements based on motor dynamics model.

Keywords: DESTINY+, camera, motor, asteroid

©2021. Japan Geoscience Union. All Right Reserved.

Development status of DESTINY$^+$ onboard cameras TCAP and MCAP

*Ko Ishibashi[1], Peng Hong[1], Takaya Okamoto[2], Takahiro Ishimaru[2], Manabu Yamada[1], Naoya Ozaki[2], Takayuki Hosonuma[3], Shunsuke Sato[2], Osamu Okudaira[1], Tomoko Arai[1], Fumi Yoshida[1,4], Masato Kagitani[5], Shingo Kameda[6], Takeshi Miyabara[2], Masayuki Ohta[2], Takeshi Takashima[2]

1. Chiba Institute of Technology, 2. Japan Aerospace Exploration Agency, 3. The University of Tokyo, 4. University of Occupational and Environmental Health, 5. Tohoku University, 6. Rikkyo University

DESTINY$^+$ (Demonstration and Experiment of Space Technology for INterplanetary voYage with Phaethon fLy-by and dUst Science) is a mission proposed for JAXA/ISAS Epsilon class small program, scheduled to be launched in 2024 [1]. The flyby target of the DESTINY$^+$ mission is the near-Earth asteroid (3200) Phaethon, which is known as an active asteroid and a parent body of the Geminid meteor shower. The size of (3200) Phaethon is 5 to 6 km in diameter. The spacecraft will flyby (3200) Phaethon with a distance of 500±50 km at the closest approach and relative speeds of ~35 km/s. In this mission, spatially resolved images of (3200) Phaethon will be taken by two onboard cameras, the Telescopic CAmera for Phaethon (TCAP) and the Multiband CAmera for Phaethon (MCAP). These observations would help understand the nature of a meteor shower's parent body, one of the sources of interplanetary dust particles that are thought to be an important transport medium of organic matter to the Earth.

TCAP is a panchromatic camera that observes the global shape, the semi-global features, and local surface features of (3200) Phaethon. To achieve those observations TCAP has a tracking mirror that can change the boresight of TCAP and can keep (3200) Phaethon in the field of view (FOV) of TCAP all the time during the flyby. The focal length, aperture, FOV, and IFOV (FOV per pixel) of TCAP are 790 mm, ϕ 114 mm, 0.82 deg ×0.82 deg, and 7.0 μrad/pixel, respectively. TCAP also plays the role of the optical navigation camera for the flyby observation. The specifications above are required for both the scientific imaging and for achieving the flyby imaging sequence.

MCAP is a multiband camera, the wavelengths of which are 425, 550, 700, 850 nm. The focal length, aperture, FOV, and IFOV are 100 mm, ϕ21 mm, 6.5 deg ×6.5 deg, and 55 μrad/pixel, respectively, for all the bands. MCAP has multiple optical systems and sensors to take all band images simultaneously. We are considering a branching optical system for MCAP, which separates incident light into two imaging sensors using a dichroic prism. Thus, four bands can be covered with two branching optical systems. MCAP does not have a tracking mirror because of a strict weight limitation and will take images at the solar phase angles of around 10 deg, where the amount of the reflected light is enough to achieve high signal-to-noise ratios.

The observation for searching (3200) Phaethon will start 30 days before the encounter. We estimated the time of detection of (3200) Phaethon using the phase curve of (3200) Phaethon obtained by ground observation, and (3200) Phaethon will be detected by TCAP at least ten days before or earlier the encounter. The optical navigation using TCAP images to estimate relative trajectory will be conducted 5 to 2.5 days before the encounter. Then, the images of (3200) Phaethon will be taken around the closest approach for scientific objectives. Since the angular velocity at the closest approach is around 4 deg/s, which is too high to track by spacecraft attitude control only, the tracking mirror is required.

High pointing accuracy and pointing stability are required to keep the asteroid in the FOV of TCAP and image the asteroid without motion blur. We set the pointing accuracy requirement to ≦0.05 deg (1 σ) and

©2021. Japan Geoscience Union. All Right Reserved.

≦0.067 deg (1 σ) for the horizontal and vertical directions, respectively. The pointing stability requirement during 0.3 msec, the nominal exposure time of TCAP, is set to ≦4×10^{-4} deg/0.3 msec (1 σ), which corresponds to 1 pixel. The main error sources in TCAP include the tracking mirror motion [2] and the alignment among the telescope's boresight, the rotational axis of the tracking mirror, and the direction of the mirror. We have been evaluating those errors, and the preliminary results show that the requirements are satisfied.

References: [1] Arai, T. et al. (2020) *LPS LII*, Abstract #1896. [2] Hong, P. et al. (2020) *LPS LII*, Abstract #1741.

Keywords: DESTINY+, (3200) Phaethon, Camera, Flyby imaging

©2021. Japan Geoscience Union. All Right Reserved.

A Ground-based Optical Calibration Plan for DESTINY$^+$ on-board Cameras, TCAP and MCAP

*Takaya Okamoto[1], Ko Ishibashi[2], Manabu Yamada[2], Peng Hong[2], Fumi Yoshida[2,3], Tomoko Arai[2], Takahiro Ishimaru[1], Masayuki Ohta[1], Takeshi Miyabara[1], Takeshi Takashima[1]

1. Japan Aerospace Exploration Agency, Institute of Space and Astronautical Science, 2. Chiba Institute of Technology, Planetary Exploration Research Center, 3. University of Occupational and Environmental Health, School of Medicine

DESTINY$^+$ (Demonstration and Experiment of Space Technology for INterplanetary voYage with Phaethon fLyby and dUst Science) is a flyby mission to the asteroid (3200) Phaethon, planned to be launched in 2024 [1]. The two cameras will be installed at the spacecraft; one is a telescopic camera, TCAP (Telescopic Camera for Phaethon), and the other is a multi-band camera, MCAP (Multi-band Camera for Phaethon). The scientific goals using the cameras are (1) Obtaining the global shape of Phaethon; the contour and the light curve, (2) Obtaining the semi global features of Phaethon; Observation of the 3-D shape, (3) Obtaining the local features of Phaethon; topography of the surface such as dust ejection, (4) Observing the material distribution on Phaethon [2]. In order to achieve these goals the characteristics of the imaging data taken by the cameras should be correctly understood, and it is necessary to construct the way of the accurate optical calibration so as to extract scientifically valuable data from raw image data.

We listed the radiometric and geometric calibration tests for the optical systems and the image sensors of the cameras needed for achieving the goals. The measurement items of the optical calibration tests are followings: Dark current, bias, hot pixel, linearity, accuracy of conversion gain, dead pixel, flat field correction, sensitivity, point-spread function (PSF), distortion correction, confirming field of view (FOV), instantaneous field of view (IFOV), stray light. In addition to these common measurement items for a camera on spacecraft, full well capacities of the CMOS image sensors used in TCAP and MCAP, must be evaluated at different irradiation conditions because it is found that they depend on incident light flux and temperature of the sensors [3].

We first plan to conduct the following calibration tests using only the image sensors (or the image sensors equipped to the boards without the optical instruments such as lens). The dark current, bias, hot pixel, linearity, accuracy of conversion gain, dead pixel, full well capacity, and temperature dependencies on them will be evaluated. The calibration data of the Engineering Model (EM) and Proto Flight Model (PFM) of the cameras pertaining to the flat field, sensitivity, out-of-field stray light will be planned to be obtained by using the integrating sphere at JAXA/EORC and those pertaining to the PSF, distortion, FOV, IFOV, in-field stray light will be obtained by using the collimated light. These tests are basically conducted under atmospheric pressure at room temperature , which is around nominal temperature of the sensors during the flyby. On the other hand, computational simulations will be also planned to be performed in order to understand the temperature and ambient pressure dependencies on those calibration data. It will help for calibrations if the temperature of the sensors does not keep the nominal temperature. The detailed optical calibration methods and preliminary results of the characteristics of the sensors will be reported in the presentation.

©2021. Japan Geoscience Union. All Right Reserved.

References: [1] Arai, T. et al., (2021), LPSC 52, Abstract #1896. [2] Ishibashi, K. et al., (2021), LPSC 52, Abstract #1405. [3] Ishimaru, T. et al., (2019) Proceedings of the Space Sciences and Technology Conference 63, 3M06.

Keywords: Exploration of small bodies, DESTINY+, Calibration of cameras

©2021. Japan Geoscience Union. All Right Reserved.

Twinkle: a low-Earth orbit, visible and infrared observatory for exoplanet and solar system spectroscopy

*Billy Edwards[1]

1. Blue Skies Space Ltd

The Twinkle Space Mission is a space-based observatory that has been conceived to characterise exoplanets, stars and solar system objects. The satellite is based on a high-heritage platform and will carry a 0.45 m telescope with a visible and infrared spectrograph providing simultaneous wavelength coverage from 0.5 - 4.5 μm. The spacecraft will be launched into a Sun-synchronous low-Earth polar orbit and will operate in this highly stable thermal environment for a baseline lifetime of seven years.

Twinkle’s rapid pointing and non-sidereal tracking capabilities will enable the observation of a diverse array of Solar System objects, including asteroids and comets. Twinkle aims to provide a visible and near-infrared spectroscopic population study of asteroids and comets to study their surface composition and monitor activity. Its wavelength coverage and position above the atmosphere will make it particularly well-suited for studying hydration features that are obscured by telluric lines from the ground as well as searching for other spectral signatures such as organics, silicates and CO_2.

Twinkle is available for researchers around the globe in two ways:

1) joining its collaborative multi-year survey programme, which will observe hundreds of exoplanets and solar system objects; and
2) accessing dedicated telescope time on the spacecraft, which they can schedule for any combination of science cases.

I will present an overview of Twinkle’s capabilities and discuss the broad range of targets the mission could observe, demonstrating the huge scientific potential of the spacecraft.

Keywords: Visible and near-infrared spectroscopy, space-based telescope

©2021. Japan Geoscience Union. All Right Reserved.

[E] Oral | P (Space and Planetary Sciences)：P-EM Solar-Terrestrial Sciences, Space Electromagnetism & Space Environment

Sun. Jun 6, 2021 9:00 AM - 10:30 AM JST | Sun. Jun 6, 2021 12:00 AM - 1:30 AM UTC | Ch.05 Zoom Room 05

[P-EM09] Dynamics of Magnetosphere and Ionosphere

convener:Akiko Fujimoto(Kyushu Institute of Technology), Mitsunori Ozaki(Faculty of Electrical and Computer Engineering, Institute of Science and Engineering, Kanazawa University), Yuka Sato(Nippon Institute of Technology), Aoi Nakamizo(Applied Electromagnetic Research Institute, National Institute of Information and Communications Technology), Chairperson:Hiroshi Hasegawa(Institute of Space and Astronautical Science, Japan Aerospace Exploration Agency), Masaki N Nishino(Japan Aerospace Exploration Agency, Institute of Space and Astronautical Science)

This session provides an opportunity to present recent results from satellite and ground-based observations and theoretical and simulation studies on the magnetosphere, ionosphere, and their coupling processes. We invite talks and posters discussing various phenomena related to the magnetosphere-ionosphere system: solar wind-magnetosphere interaction, magnetosphere-ionosphere convection, field-aligned current, magnetic storms/substorms, neutral-plasma interaction, ionospheric ion inflow and outflow, aurora phenomena, and so forth. Discussions on planetary and satellite ionospheres and magnetospheres, future missions and instrument developments are also welcome.

9:00 AM - 9:05 AM JST | 12:00 AM - 12:05 AM UTC

[PEM09-01] Introduction

9:05 AM - 9:20 AM JST | 12:05 AM - 12:20 AM UTC

[PEM09-02] Magnetic Reconnection in a Sheared Magnetic Flux Tube: Slippage versus Tearing

*Hidetaka Kuniyoshi[1], Michael Hesse[2], Cecilia Nogren[3], Paul Tenfjord[3], Norah Kaggwa Kwagala[3] (1.The University of Tokyo, Department of Earth and Planetary Science, 2.NASA Ames Research Center, 3.University of Bergen, Space Plasma Physics Group)

9:20 AM - 9:35 AM JST | 12:20 AM - 12:35 AM UTC

[PEM09-03] Fast Magnetic-Field Annihilation in Electron-scale Current Sheet in Earth's Magnetotail

*Hiroshi Hasegawa[1], Richard E. Denton[2], Kevin J. Genestreti[3], Takuma Nakamura[4], Tai D. Phan[5], Rumi Nakamura[4], Kyoung-Joo Hwang[6], Narges Ahmadi[7], Quanqi Shi[8], Michael Hesse[9], James L. Burch[6], James M. Webster[6], Roy B. Torbert[10], Barbara L. Giles[11], Dan J. Gershman[11], Christopher T. Russell[12], Robert J. Strangeway[12], Hanying Wei[12], Per-Arne Lindqvist[13], Yuri V. Khotyaintsev[14], Robert E. Ergun[15], Yoshifumi Saito[1] (1.Institute of Space and Astronautical Science, Japan Aerospace Exploration Agency, 2.Department of Physics and Astronomy, Dartmouth College, 3.Southwest Research Institute, Durham, 4.Space Research Institute, Austrian Academy of Sciences, 5.Space Sciences Laboratory, University of California, Berkeley, 6.Southwest Research Institute, San Antonio, 7.Laboratory for Atmospheric and Space Physics, University of Colorado, 8.Shandong Provincial Key Laboratory of Optical Astronomy and Solar-Terrestrial Environment, Institute of Space Sciences, Shandong University, 9.Space Plasma Physics Group, University of Bergen, 10.Physics Department, University of New Hampshire, 11.NASA Goddard Space Flight Center, 12.Department of Earth, Planetary, and Space Sciences, University of California, Los Angeles, 13.Royal Institute of Technology, Stockholm, 14.Swedish Institute of Space Physics, 15.Department of Astrophysical and Planetary Sciences, University of Colorado)

9:35 AM - 9:50 AM JST | 12:35 AM - 12:50 AM UTC

[PEM09-04] Energy dependence of field-aligned anisotropy of electrons during dipolarization at Earth's tailside

*Kaiti Wang[1], Ching-Huei Lin[2], Zhuo-Ren Lang[3], Tohru Hada[4], Toshi Nishimura[5] (1.Tamkang Univ., 2.Chien-Hsin Univ. of Sci. & Tech., 3.National Cheng Kung Univ., 4.Kyushu Univ., 5.Boston Univ.)

9:50 AM - 10:05 AM JST | 12:50 AM - 1:05 AM UTC

[PEM09-05] On the origin of cold-dense plasmas in the dusk magnetotail plasma sheet: MMS and Geotail observations

*Masaki N Nishino[1], Yoshifumi Saito[1], Hiroshi Hasegawa[1], Naritoshi Kitamura[2], Yukinaga Miyashita[3,4], Tsugunobu Nagai[1], Shoichiro Yokota[5], Daniel J Gershman[6], Christopher T Russell[7], Barbara L Giles[6] (1.Japan Aerospace Exploration Agency, Institute of Space and Astronautical Science, 2.Graduate School of Science, The University of Tokyo, 3.Korea Astronomy and Space Science Institute, South Korea, 4.Korea University of Science and Technology, South Korea, 5.Graduate School of Science, Osaka University, 6.Goddard Space Flight Center, NASA, 7.University of California, Los Angeles)

10:05 AM - 10:20 AM JST | 1:05 AM - 1:20 AM UTC

[PEM09-06] **Substorm-like events related to magnetosheath plasma jets**

*ALEXEI DMITRIEV[1,2], ALLA SUVOROVA[2] (1.Institute of Space Science, National Central University, Jungli City, Taiwan, 2.Skobeltsyn Institute of Nuclear Physics, Lomonosov Moscow State University, Moscow, Russia)

10:20 AM - 10:30 AM JST | 1:20 AM - 1:30 AM UTC

[PEM09-07] Discussion

[E] Oral | P (Space and Planetary Sciences) | P-EM Solar-Terrestrial Sciences, Space Electromagnetism & Space Environment

[P-EM09] Dynamics of Magnetosphere and Ionosphere

convener:Akiko Fujimoto(Kyushu Institute of Technology), Mitsunori Ozaki(Faculty of Electrical and Computer Engineering, Institute of Science and Engineering, Kanazawa University), Yuka Sato(Nippon Institute of Technology), Aoi Nakamizo(Applied Electromagnetic Research Institute, National Institute of Information and Communications Technology), Chairperson:Hiroshi Hasegawa(Institute of Space and Astronautical Science, Japan Aerospace Exploration Agency), Masaki N Nishino(Japan Aerospace Exploration Agency, Institute of Space and Astronautical Science)

Sun. Jun 6, 2021 9:00 AM - 10:30 AM Ch.05 (Zoom Room 05)

This session provides an opportunity to present recent results from satellite and ground-based observations and theoretical and simulation studies on the magnetosphere, ionosphere, and their coupling processes. We invite talks and posters discussing various phenomena related to the magnetosphere-ionosphere system: solar wind-magnetosphere interaction, magnetosphere-ionosphere convection, field-aligned current, magnetic storms/substorms, neutral-plasma interaction, ionospheric ion inflow and outflow, aurora phenomena, and so forth. Discussions on planetary and satellite ionospheres and magnetospheres, future missions and instrument developments are also welcome.

9:00 AM - 9:05 AM

[PEM09-01]Introduction

©Japan Geoscience Union

Magnetic Reconnection in a Sheared Magnetic Flux Tube: Slippage versus Tearing

*Hidetaka Kuniyoshi[1], Michael Hesse[2], Cecilia Nogren[3], Paul Tenfjord[3], Norah Kaggwa Kwagala[3]

1. The University of Tokyo, Department of Earth and Planetary Science, 2. NASA Ames Research Center, 3. University of Bergen, Space Plasma Physics Group

Although it still remains controversial whether auroral acceleration is, in fact, a manifestation of a reconnection process, discussions of a different type of reconnection in this context began with 'reconnection type II' by Haerendel (Haerendel, 2007, 2011), which recognized early on that auroral acceleration may be a form of magnetic reconnection. According to the author, the reconnection process enhances the auroral acceleration by reducing the flux tubes' shear magnetic stress of field aligned current sheets. The process of magnetic reconnection in a flux tube can occur in a time-stationary fashion as slippage reconnection or in a time-dependent manner, for example, tearing instability. However, it is not well known how a system can be set up to sustain slippage reconnection, whether there is a combination of slippage reconnection and time-dependent reconnection. To investigate this question, using a 3D MHD simulation, we model a twisted flux tube, adding a spatially localized resistive region in the center of the simulation box. As a result, firstly, the Poynting flux injected at the boundary propagates to the resistive region and dissipates there. Secondly, tearing instability occurs with slippage reconnection in the resistive region when the resistivity is strong enough and the cross section of the flux tube is elliptical enough, otherwise only slippage reconnection occurs. Finally, magnetic field generated by tearing instability propagates to both ends of the flux tube.

Keywords: Magnetic Reconnection, Auroral acceleration, Magnetohydrodynamics

©2021. Japan Geoscience Union. All Right Reserved.

Fast Magnetic-Field Annihilation in Electron-scale Current Sheet in Earth's Magnetotail

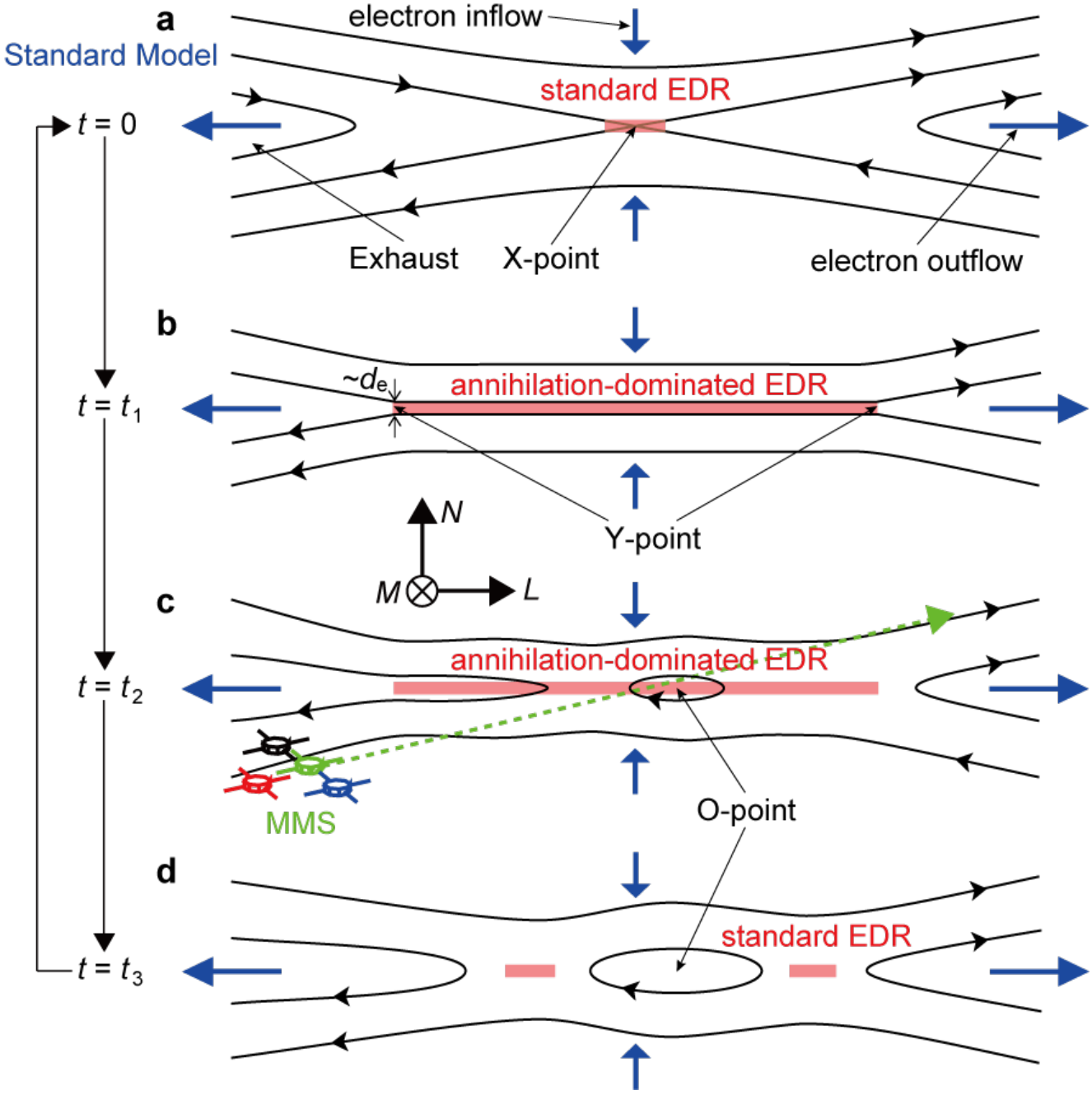
*Hiroshi Hasegawa[1], Richard E. Denton[2], Kevin J. Genestreti[3], Takuma Nakamura[4], Tai D. Phan[5], Rumi Nakamura[4], Kyoung-Joo Hwang[6], Narges Ahmadi[7], Quanqi Shi[8], Michael Hesse[9], James L. Burch[6], James M. Webster[6], Roy B. Torbert[10], Barbara L. Giles[11], Dan J. Gershman[11], Christopher T. Russell[12], Robert J. Strangeway[12], Hanying Wei[12], Per-Arne Lindqvist[13], Yuri V. Khotyaintsev[14], Robert E. Ergun[15], Yoshifumi Saito[1]

1. Institute of Space and Astronautical Science, Japan Aerospace Exploration Agency, 2. Department of Physics and Astronomy, Dartmouth College, 3. Southwest Research Institute, Durham, 4. Space Research Institute, Austrian Academy of Sciences, 5. Space Sciences Laboratory, University of California, Berkeley, 6. Southwest Research Institute, San Antonio, 7. Laboratory for Atmospheric and Space Physics, University of Colorado, 8. Shandong Provincial Key Laboratory of Optical Astronomy and Solar-Terrestrial Environment, Institute of Space Sciences, Shandong University, 9. Space Plasma Physics Group, University of Bergen, 10. Physics Department, University of New Hampshire, 11. NASA Goddard Space Flight Center, 12. Department of Earth, Planetary, and Space Sciences, University of California, Los Angeles, 13. Royal Institute of Technology, Stockholm, 14. Swedish Institute of Space Physics, 15. Department of Astrophysical and Planetary Sciences, University of Colorado

Magnetic reconnection in current sheets is the key to fast release of magnetic energy in many space and astrophysical plasma systems, such as during magnetospheric substorms, but observations to understand exactly how magnetic-to-electron energy conversion occurs in electron-scale diffusion regions (EDRs), where magnetic topology changes, have been lacking. It is generally believed that EDR has an X-type magnetic-field geometry around which the energy of anti-parallel magnetic fields is mostly converted to the bulk-flow energy of electrons by magnetic tension of reconnected field-lines. We present state-of-the-art analysis of multi-spacecraft observations in Earth's magnetotail of an electron-scale current sheet, which demonstrates that contrary to the standard model of reconnection with an X-type EDR geometry, the fast energy conversion in the detected EDR was caused mostly by magnetic-field annihilation, rather than reconnection. The experimental discovery of the annihilation-dominated EDR reveals a new form of energy conversion in the reconnection process that can occur when the EDR has evolved from the X-type to planar geometry.

Keywords: magnetic reconnection, magnetotail, magnetic field annihilation

©2021. Japan Geoscience Union. All Right Reserved.



©2021. Japan Geoscience Union. All Right Reserved.

Energy dependence of field-aligned anisotropy of electrons during dipolarization at Earth's tailside

*Kaiti Wang[1], Ching-Huei Lin[2], Zhuo-Ren Lang[3], Tohru Hada[4], Toshi Nishimura[5]

1. Tamkang Univ., 2. Chien-Hsin Univ. of Sci. & Tech., 3. National Cheng Kung Univ., 4. Kyushu Univ., 5. Boston Univ.

A specific pattern on energy-dependence of variations in field-aligned anisotropy (η) of electrons was found from hundreds of eV to thousands of eV during dipolarization time around 10 Earth radii near magnetic equator in the inner plasmasheet at tailside based on measurements of the instrument ESA (ElectroStatic Analyzer) onboard of THEMIS Mission. More exactly, in the beginning of dipolarization, η peaks at a lower energy and it shifts to a higher energy but with a smaller value when the dipolarization angle reaches maximum [*Wang et al.*, 2019]. In this study, by further analyzing the field-aligned anisotropies of electrons in both northward and southward directions at 62 dipolarization sites from the year of 2008 to 2011, we find that electrons observed at about two-thirds of these sites exhibit such a pattern and the energy range is largely associated with the ratio of bounce time to the dipolarization time. Furthermore, we find that this pattern hardly exists when the minimum AL index is less than -190nT or the maximum of y-component of electric field (E_y) measured by the onboard instrument EFI (Electric Field Instrument) is higher than 20mV/m during the dipolarization time analyzed. Hence, mechanisms affecting electron motions associated with the values of AL index and E_y as well as their influences on this energy-dependence will be assessed and discussed.

*References

Wang, K., Z. R. Lang, C. H. Lin, T. Hada, T. Nishimura (2019), Analysis on anisotropy variations for pitch angle distributions of electrons with various parameters at dipolarization sites in the inner plasma sheet, Paper No. PEM11-14, JpGU Meeting 2019, Chiba, Japan.

Keywords: dipolarizations in the inner plasmasheet, field-aligned anisotropy of electrons, energy-dependence, AL index, electric fields, observations of THEMIS mission

©2021. Japan Geoscience Union. All Right Reserved.

On the origin of cold-dense plasmas in the dusk magnetotail plasma sheet: MMS and Geotail observations

*Masaki N Nishino[1], Yoshifumi Saito[1], Hiroshi Hasegawa[1], Naritoshi Kitamura[2], Yukinaga Miyashita[3,4], Tsugunobu Nagai[1], Shoichiro Yokota[5], Daniel J Gershman[6], Christopher T Russell[7], Barbara L Giles[6]

1. Japan Aerospace Exploration Agency, Institute of Space and Astronautical Science, 2. Graduate School of Science, The University of Tokyo, 3. Korea Astronomy and Space Science Institute, South Korea, 4. Korea University of Science and Technology, South Korea, 5. Graduate School of Science, Osaka University, 6. Goddard Space Flight Center, NASA, 7. University of California, Los Angeles

The near-Earth plasma sheet becomes cold and dense under the northward interplanetary magnetic field (IMF) condition, which suggests entry of solar wind plasma into the magnetosphere across the magnetopause. The cold and dense characteristics of the plasma sheet are more evident in the magnetotail flank regions that are interface between cold solar wind plasma and hot magnetospheric plasma. Several physical mechanisms have been proposed to explain the entry of solar wind plasma across the magnetopause and resultant formation of the cold-dense plasma sheet (CDPS) in the tail flank regions. However, transport path of the cold-dense plasma inside the magnetotail has not been understood yet. Here we present a case study of the CDPS in the dusk magnetotail by Magnetospheric Multiscale (MMS) spacecraft under the conditions of the strongly northward IMF and the high-density solar wind. The ion distribution function consists of high- and low-energy components, and the low-energy one intermittently shows energy dispersion in the directions parallel and anti-parallel to the local magnetic field. Considering the time-of-flight effect of the energy-dispersed low-energy ions, we infer that these ions originate in the region down the tail, and move along the magnetic field toward the ionosphere and then come back to the magnetotail by the mirror reflection. The pitch-angle dispersion analysis gives consistent results on the travelling time and path length of the energy-dispersed ions. Interestingly, Geotail spacecraft detected large magnetic field fluctuations in the low-latitude boundary layer near the dusk terminator, which may be attributed to Kelvin-Helmholtz instability due to the velocity shear between the magnetosheath and the plasma sheet. Based on these observations, we discuss possible generation mechanisms of the energy-dispersed structure of the low-energy ions during the northward IMF.

Keywords: Magnetotail plasma sheet, Plasma transport, Northward IMF, Low-latitude boundary layer (LLBL), Magnetospheric Multiscale (MMS) spacecraft, Geotail spacecraft

©2021. Japan Geoscience Union. All Right Reserved.

Substorm-like events related to magnetosheath plasma jets

*ALEXEI DMITRIEV[1,2], ALLA SUVOROVA[2]

1. Institute of Space Science, National Central University, Jungli City, Taiwan, 2. Skobeltsyn Institute of Nuclear Physics, Lomonosov Moscow State University, Moscow, Russia

Fast and dense streams of magnetosheath plasma, so-called jets, can hit the dayside magnetopause. The interaction results in a localized compression of the magnetosphere and sometimes penetration of the magnetosheath plasma inside the magnetosphere. These effects produce intensification of the geomagnetic activity at high-latitudes on dayside with further propagation of the disturbances toward night side. These, so-called substorm-like events can occur even during quite geomagnetic conditions under northward orientation of interplanetary magnetic field. We present examples of substorm-like events under various conditions.

Keywords: substorms, auroral activity, magnetosheath plasma jets

©2021. Japan Geoscience Union. All Right Reserved.

[E] Oral | P (Space and Planetary Sciences) | P-EM Solar-Terrestrial Sciences, Space Electromagnetism & Space Environment

[P-EM09] Dynamics of Magnetosphere and Ionosphere

convener:Akiko Fujimoto(Kyushu Institute of Technology), Mitsunori Ozaki(Faculty of Electrical and Computer Engineering, Institute of Science and Engineering, Kanazawa University), Yuka Sato(Nippon Institute of Technology), Aoi Nakamizo(Applied Electromagnetic Research Institute, National Institute of Information and Communications Technology), Chairperson:Hiroshi Hasegawa(Institute of Space and Astronautical Science, Japan Aerospace Exploration Agency), Masaki N Nishino(Japan Aerospace Exploration Agency, Institute of Space and Astronautical Science)

Sun. Jun 6, 2021 9:00 AM - 10:30 AM Ch.05 (Zoom Room 05)

This session provides an opportunity to present recent results from satellite and ground-based observations and theoretical and simulation studies on the magnetosphere, ionosphere, and their coupling processes. We invite talks and posters discussing various phenomena related to the magnetosphere-ionosphere system: solar wind-magnetosphere interaction, magnetosphere-ionosphere convection, field-aligned current, magnetic storms/substorms, neutral-plasma interaction, ionospheric ion inflow and outflow, aurora phenomena, and so forth. Discussions on planetary and satellite ionospheres and magnetospheres, future missions and instrument developments are also welcome.

10:20 AM - 10:30 AM

[PEM09-07]Discussion

©Japan Geoscience Union

[E] Oral | P (Space and Planetary Sciences)：P-EM Solar-Terrestrial Sciences, Space Electromagnetism & Space Environment

Sun. Jun 6, 2021 10:45 AM - 12:15 PM JST | Sun. Jun 6, 2021 1:45 AM - 3:15 AM UTC | Ch.05 Zoom Room 05

[P-EM09] Dynamics of Magnetosphere and Ionosphere

convener:Akiko Fujimoto(Kyushu Institute of Technology), Mitsunori Ozaki(Faculty of Electrical and Computer Engineering, Institute of Science and Engineering, Kanazawa University), Yuka Sato(Nippon Institute of Technology), Aoi Nakamizo(Applied Electromagnetic Research Institute, National Institute of Information and Communications Technology), Chairperson:Hiroshi Hasegawa(Institute of Space and Astronautical Science, Japan Aerospace Exploration Agency), Masaki N Nishino(Japan Aerospace Exploration Agency, Institute of Space and Astronautical Science)

This session provides an opportunity to present recent results from satellite and ground-based observations and theoretical and simulation studies on the magnetosphere, ionosphere, and their coupling processes. We invite talks and posters discussing various phenomena related to the magnetosphere-ionosphere system: solar wind-magnetosphere interaction, magnetosphere-ionosphere convection, field-aligned current, magnetic storms/substorms, neutral-plasma interaction, ionospheric ion inflow and outflow, aurora phenomena, and so forth. Discussions on planetary and satellite ionospheres and magnetospheres, future missions and instrument developments are also welcome.

10:45 AM - 11:10 AM JST | 1:45 AM - 2:10 AM UTC

[PEM09-08] A Case Study of Transversely Heated Low-Energy Helium Ions by EMIC Waves in the Plasmasphere

★Invited Papers

*Khan-Hyuk Kim[1] (1.School of Space Research, Kyung Hee University)

11:10 AM - 11:25 AM JST | 2:10 AM - 2:25 AM UTC

[PEM09-09] CIR- and CME-driven magnetic storm effects on ion upflows in the low-altitude polar ionosphere

*Masayoshi Takada[1], Kanako Seki[1], Yasunobu Ogawa[2], Kunihiro Keika[1] (1.Tokyo University, 2.National Institute of Polar Research)

11:25 AM - 11:40 AM JST | 2:25 AM - 2:40 AM UTC

[PEM09-10] Science Objectives of FACTORS mission

*Yoshizumi Miyoshi[1], Naritoshi Kitamura[2], Kazushi Asamura[3], Takeshi Sakanoi[4], Takanori Nishiyama[6], Hirotsugu Kojima[5], Masahito Nose[1], Yuto Katoh[4], Kunihiro Keika[2], Atsuki Shinbori[4,1], Mizuki Fukizawa[4], Kiyoka Murase[6], Miki Kawamura[4] (1.Institute for Space-Earth Environmental Research, Nagoya University, 2.University of Tokyo, 3.JAXA, 4.Tohoku University, 5.Kyoto University, 6.NIPR)

11:40 AM - 11:55 AM JST | 2:40 AM - 2:55 AM UTC

[PEM09-11] **Development of a novel method for extracting the geometrical properties of the magnetic vector fields towards the era of multi-point satellite observations**

*Akimasa Yoshikawa[1], Tsubasa Hashimoto[2], Aoi Nakamizo[4], Shinichi Ohtani[3] (1.Department of Earth and Planetary Sciences, Kyushu University, 2.Gradient school of Earth and Planetary Sciences, Kyushu University, 3.JHU/APL, 4.NICT)

11:55 AM - 12:10 PM JST | 2:55 AM - 3:10 AM UTC

[PEM09-12] Dawn-dusk asymmetry in the mesoscale field-aligned currents embedded in the diminished large-scale Region 1 current

*Yoshihiro Yokoyama[1], Satoshi Taguchi[1], Toshihiko Iyemori[2] (1.Department of Geopysics, Graduate School of Science, Kyoto University, 2.Kyoto University)

12:10 PM - 12:15 PM JST | 3:10 AM - 3:15 AM UTC

[PEM09-13] Discussion

A Case Study of Transversely Heated Low-Energy Helium Ions by EMIC Waves in the Plasmasphere

*Khan-Hyuk Kim[1]

1. School of Space Research, Kyung Hee University

The Van Allen Probe A spacecraft observed strong ~0.5-Hz helium (He^+) band and weak ~0.8-Hz hydrogen (H^+) band EMIC waves on 17 April 2018, at L = ~4.5-5.2, in the dawn sector, near the magnetic equator, and close to the plasmapause. We examined low-energy ion fluxes observed by the Helium Oxygen Proton and Electron (HOPE) instrument onboard Van Allen Probe A during the wave interval and found that low-energy He^+ flux (< 10 eV) enhancements occur nearly simultaneously with He-band and H-band EMIC wave power enhancements in a direction mostly perpendicular to the background magnetic field without significant low-energy H^+ and O^+ flux variations. We suggest that cold He^+ ions (<1 eV) are preferentially and transversely heated up 10 eV through the interaction with EMIC waves inside the plasmasphere. The low-Earth orbit spacecraft observed localized precipitations of energetic protons in the upper ionosphere at subauroral latitudes near the magnetic field footprint of Van Allen Probe A. Our observations provide a clear evidence that EMIC waves play an important role in the overall dynamics in the inner magnetosphere, contributing to the high-energy particle loss and low-energy particle energization.

Keywords: EMIC waves, Low-energy ion heating, Plasmasphere

©2021. Japan Geoscience Union. All Right Reserved.

CIR- and CME-driven magnetic storm effects on ion upflows in the low-altitude polar ionosphere

*Masayoshi Takada[1], Kanako Seki[1], Yasunobu Ogawa[2], Kunihiro Keika[1]

1. Tokyo University, 2. National Institute of Polar Research

Molecular ions ($O_2^+/NO^+/N_2^+$) in the ring current of the terrestrial magnetosphere have been observed during the magnetic storms [e.g., Klecker et al., 1986; Seki et al., 2019]. These ions originate from the low-altitude ionosphere. In the ionosphere, upward ion transports (upflows) supply sources of the ions outflowing to the magnetosphere. Since the molecular ions usually exist in the low-altitude (< 300 km) ionosphere and can be affected by neutral winds, the generation mechanisms and properties of ion upflows to transport molecular ions are different from those of O^+ [e.g., Ogawa et al., 2010; Yamazaki et al., 2017]. In particular, their dependence on solar activities is one of the important properties to understand formation mechanisms of the ion upflows. In a previous study by Ogawa et al. [2019], the characteristics of O^+ ion upflows in the polar ionosphere were investigated during CIR- and CME-driven magnetic storms by using EISCAT radars. They reported that the upflows during CIR- and CME-driven storms have different dependence on magnetic local time. For the CIR-driven storms, upward ion flux around noon was pronounced, while it was enhanced around midnight during the CME-driven storms. Their study focused on the ion upflows in the altitude range between 400 and 500 km, where O^+ is the dominant species, and responses of the ion upflows to the different type of magnetic storms in the low-altitude ionosphere, where molecular ions exist, are far from understood. The purpose of this study is thus to understand effects of CIR- and CME-driven magnetic storms on ion upflows in the low-altitude ionosphere based on long-term observations of the EISCAT radars.

We used data from the EISCAT UHF radar at Tromsø and Svalbard radar at Longyearbyen from January 1, 1996 to January 1, 2016 and surveyed statistical properties of ion upflows and ionospheric conditions during CIR- and CME-driven magnetic storms. We used 1-minute time resolution data when the radar was looking along the local magnetic field line. The ionospheric parameters such as electron density, ion velocity, and ion and electron temperatures were averaged over three altitude range, i.e., 250-350, 300-400, and 400-500 km, respectively. We screened data to exclude unrealistic values with the following criteria: Absolute value of ion velocity was less than 1500 m/s, ion and electron temperatures were less than 10000 K, and electron density was more than 10^{10} m^{-3} and less than 10^{13} m^{-3}. To understand the similarity and difference between low and high altitude upflows, we compared data at different altitude ranges. The results show that the upward velocity in the nightside at Tromsø increased with increasing altitude in the main phase of both CIR- and CME-driven magnetic storms. On the other hand, the upward flux in the nightside at Longyearbyen was not enhanced at any altitude after CIR-driven storms, whereas it increased from the low-altitude region after CME-driven storms. It was also confirmed that any effect of the magnetic storms that was remarkable at the higher altitudes reported in the previous study [Ogawa et al., 2019] was not seen in the dayside low-altitude ionosphere at Longyearbyen.

References:

[1] B. Klecker et al., Discovery of energetic molecular ions (NO+ and O2+) in the storm time ring current, *Geophys. Res. Lett.*, 13, 632-635, 1986

[2] K. Seki et al., Statistical Properties of Molecular Ions in the Ring Current Observed by the Arase (ERG) Satellite, *Geophys. Res. Lett.*, 46, 8643–8651, 2019

©2021. Japan Geoscience Union. All Right Reserved.

[3] Y. Ogawa et al., Solar activity dependence of ion upflow in the polar ionosphere observed with the European Incoherent Scatter (EISCAT) Tromsø UHF radar, *J. Geophys. Res.,*115, A07310, 2010
[4] Y. Yamazaki et al., Average field-aligned ion velocity over the EISCAT radars, *J. Geophys. Res. Space Physics,*122, 5630-5642, 2017
[5] Y. Ogawa et al., Characteristics of CME- and CIR-driven ion upflows in the polar ionosphere, *J. Geophys. Res. Space Physics*, 124, 3637–3649, 2019

Keywords: ion upflow, corotating interaction region (CIR), coronal mass ejection (CME), magnetic stroms, polar ionosphere, EISCAT radars

©2021. Japan Geoscience Union. All Right Reserved.

Science Objectives of FACTORS mission

*Yoshizumi Miyoshi[1], Naritoshi Kitamura[2], Kazushi Asamura[3], Takeshi Sakanoi[4], Takanori Nishiyama[6], Hirotsugu Kojima[5], Masahito Nose[1], Yuto Katoh[4], Kunihiro Keika[2], Atsuki Shinbori[4,1], Mizuki Fukizawa[4], Kiyoka Murase[6], Miki Kawamura[4]

1. Institute for Space-Earth Environmental Research, Nagoya University, 2. University of Tokyo, 3. JAXA, 4. Tohoku University, 5. Kyoto University, 6. NIPR

FACTORS (Frontiers of Formation, Acceleration, Coupling and Transport Mechanisms Observed by the Outer Space Research System) is a future polar orbiting satellite mission to understand coupling processes between space and Earth’ s atmosphere including energy inputs from magnetosphere associated with aurora and ion outflow from ionosphere. FACTORS is a next-generation multi-satellite formation flight mission, and comprehensive plasma/particle and fields/waves instruments as well as visible/FUV imagers are installed. Major science objectives are 1) energy transport in the magnetosphere-ionosphere coupling system and their relationship to small-scale aurora phenomena, 2) particle transport in the magnetosphere-ionosphere system by ion outflow. In particular, we focus on the acceleration and/or heating of ions by plasma waves to the escaping energies. The team is now working for discussions about the science strategy. Moreover, the team conducts several simulation studies about orbit and measurements of waves. In this presentation, we report the science objectives and possible observation strategies.

Keywords: polar ionosphere/magnetosphere, future mission

©2021. Japan Geoscience Union. All Right Reserved.

Development of a novel method for extracting the geometrical properties of the magnetic vector fields towards the era of multi-point satellite observations

*Akimasa Yoshikawa[1], Tsubasa Hashimoto[2], Aoi Nakamizo[4], Shinichi Ohtani[3]

1. Department of Earth and Planetary Sciences, Kyushu University, 2. Gradient school of Earth and Planetary Sciences, Kyushu University, 3. JHU/APL, 4. NICT

We propose a new method for analyzing the evolution of a geomagnetic fields that enables us to extract the geometrical properties of the magnetic vector fields towards the era of multi-point satellite observations

In general, geometrical properties of magnetic fields (B-fields) can be represented by divergence and/or convergence of magnetic flux tube, gradient of magnetic flux density, curvature, and twist of magnetic field lines. Such geometries can be reconstructed from a dyadic tensor of B-field gradients that represents various spatial gradients of magnetic field components in a three-dimensional space. Furthermore, change of B-field can be characterized by a change of magnetic flux-density and a change of direction of B-field.

When a satellite cruse in space with finite velocity in the rest frame, the time-hysteresis of measured magnetic fields by this satellite includes contribution from a Euler differentiation of B-field at the satellite position in the rest frame and the change of B-field when the satellite moves across an inhomogeneous B-field region. In general, it is impossible to separate these two contributions from single satellite observation. To successfully measure the spatial gradients of B-field, we need an appropriate formation fright composed of multiple satellites. A formation flight composed of 4-satellites have already realized in the Cluster and the MMS missions and is a minimum configuration that enable to deduce a spatial gradient of B-field in the 3D system.

In this paper, we provide a methodology that derive the dyadic tensor of B-field in the triangular cone formed by 4-satellites, of which components describe averaged characteristic of spatial gradients of B-field. By using this methodology, we can extract the Euler differentiation of B-field at the centroid position of formation flight. This technique can be easily applied to formation flights of more than four satellites.

We also derive a novel expression of B-field development equation under any Ohm’ s law, which explicitly describes what type of plasma motion causes B-field development in the parallel and perpendicular direction to B-field. The former part corresponds to the development of magnetic flux density and the latter part corresponds to the changing ratio of B-field direction. By comparing extracted Euler differentiation of B-field from observational data and results deduced from new formulation, we can identify cause and results of B-field development under an arbitrary Ohm’ s law. Application to the MHD’ s Ohm’ s law will be discussed in the presentation.

Keywords: formation flight of satellites, Multi-point observation of magnetic field, magnetic gradient tensor

©2021. Japan Geoscience Union. All Right Reserved.

©2021. Japan Geoscience Union. All Right Reserved.

Dawn-dusk asymmetry in the mesoscale field-aligned currents embedded in the diminished large-scale Region 1 current

*Yoshihiro Yokoyama[1], Satoshi Taguchi[1], Toshihiko Iyemori[2]

1. Department of Geopysics, Graduate School of Science, Kyoto University, 2. Kyoto University

Irregular magnetic perturbations embedded in the diminished large-scale Region 1 current are observed in almost all MLT except for the near noon region during prolonged northward IMF conditions. Our recent statistical study for the dusk side sector has revealed that the mesoscale field-aligned currents that produce these irregular magnetic perturbations tend to occur under the northward IMF conditions and are possibly generated in the low-latitude boundary layer. Our study has also shown that the current density of the mesoscale field-aligned currents tends to increase as the solar wind proton density increases. To clarify whether or not there exist asymmetries in the mesoscale field-aligned currents between the dawn and dusk sector, by utilizing magnetic data obtained by Swarm satellites during the period from May 2014 to May 2017, we investigated the dependence of the dawn side field-aligned currents on the solar zenith angle, the IMF, and solar wind plasma parameters, and compared the results with those from the dusk side sector. We found that the occurrence ratio of the mesoscale field-aligned current in the dawn sector also shows a strong dependence on the northward IMF condition. Besides, we found that there are weak dawn-dusk asymmetries in the occurrence ratio against the Y component of IMF, and in the current density. From our proposed mechanism of the generation for the mesoscale field-aligned currents, which is associated with the cold dense ion regions in the low-latitude boundary layer, we interpret those dawn-dusk asymmetries.

Keywords: field-aligned currents, northward IMF

©2021. Japan Geoscience Union. All Right Reserved.

[E] Oral | P (Space and Planetary Sciences) | P-EM Solar-Terrestrial Sciences, Space Electromagnetism & Space Environment

[P-EM09] Dynamics of Magnetosphere and Ionosphere

convener:Akiko Fujimoto(Kyushu Institute of Technology), Mitsunori Ozaki(Faculty of Electrical and Computer Engineering, Institute of Science and Engineering, Kanazawa University), Yuka Sato(Nippon Institute of Technology), Aoi Nakamizo(Applied Electromagnetic Research Institute, National Institute of Information and Communications Technology), Chairperson:Hiroshi Hasegawa(Institute of Space and Astronautical Science, Japan Aerospace Exploration Agency), Masaki N Nishino(Japan Aerospace Exploration Agency, Institute of Space and Astronautical Science)

Sun. Jun 6, 2021 10:45 AM - 12:15 PM Ch.05 (Zoom Room 05)

This session provides an opportunity to present recent results from satellite and ground-based observations and theoretical and simulation studies on the magnetosphere, ionosphere, and their coupling processes. We invite talks and posters discussing various phenomena related to the magnetosphere-ionosphere system: solar wind-magnetosphere interaction, magnetosphere-ionosphere convection, field-aligned current, magnetic storms/substorms, neutral-plasma interaction, ionospheric ion inflow and outflow, aurora phenomena, and so forth. Discussions on planetary and satellite ionospheres and magnetospheres, future missions and instrument developments are also welcome.

12:10 PM - 12:15 PM

[PEM09-13]Discussion

©Japan Geoscience Union

[E] Oral | P (Space and Planetary Sciences)：P-EM Solar-Terrestrial Sciences, Space Electromagnetism & Space Environment

Sun. Jun 6, 2021 1:45 PM - 3:15 PM JST | Sun. Jun 6, 2021 4:45 AM - 6:15 AM UTC | Ch.05 Zoom Room 05

[P-EM09] Dynamics of Magnetosphere and Ionosphere

convener:Akiko Fujimoto(Kyushu Institute of Technology), Mitsunori Ozaki(Faculty of Electrical and Computer Engineering, Institute of Science and Engineering, Kanazawa University), Yuka Sato(Nippon Institute of Technology), Aoi Nakamizo(Applied Electromagnetic Research Institute, National Institute of Information and Communications Technology), Chairperson:Yuki Obana(Department of Engineering Science, Faculty of Engineering, Osaka Electro-Communication University), Yoshihiro Yokoyama(Department of Earth and Planetary Sciences, Graduate School of Science, Kyoto University)

This session provides an opportunity to present recent results from satellite and ground-based observations and theoretical and simulation studies on the magnetosphere, ionosphere, and their coupling processes. We invite talks and posters discussing various phenomena related to the magnetosphere-ionosphere system: solar wind-magnetosphere interaction, magnetosphere-ionosphere convection, field-aligned current, magnetic storms/substorms, neutral-plasma interaction, ionospheric ion inflow and outflow, aurora phenomena, and so forth. Discussions on planetary and satellite ionospheres and magnetospheres, future missions and instrument developments are also welcome.

1:45 PM - 2:10 PM JST | 4:45 AM - 5:10 AM UTC

[PEM09-14] Current and future perspectives on 3D analysis of aurora

★Invited Papers

*Yoshimasa Tanaka[1,2,3], Yasunobu Ogawa[1,2,3], Akira Kadokura[1,2,3], Bjorn Gustavsson[4], Kirsti Kauristie[5], Enell Carl-fredrik[6], Urban Brandstrom[7], Tima Sergienko[7], Alexander Kozlovsky[8], Tero Raita[8], Mizuki Fukizawa[9], Takeshi Sakanoi[9], Keisuke Hosokawa[10] (1.National Institute of Polar Research, 2.Polar Environment Data Science Center, Joint Support-Center for Data Science Research, Research Organization of Information and Systems, 3.The Graduate University for Advanced Studies, SOKENDAI, 4.The Arctic University of Norway, 5.Finnish Meteorological Institute, 6.EISCAT Scientific Association, 7.Swedish Institute of Space Physics, 8.Sodankyla Geophysical Observatory, 9.Planetary Plasma and Atmospheric Research Center, Graduate School of Science, Tohoku University, 10.Department of Communication Engineering and Informatics, University of Electro-Communications)

2:10 PM - 2:25 PM JST | 5:10 AM - 5:25 AM UTC

[PEM09-15] Reconstruction of the three-dimensional structure and precipitating electrons of pulsating auroral patches by Aurora Computed Tomography

*Mizuki Fukizawa[1], Takeshi Sakanoi[1], Yoshimasa Tanaka[2], Yasunobu Ogawa[2], Björn Gustavsson[3], Kirsti Kauristie[4], Carl-Fredrik Enell[5], Alexander Kozlovsky[6], Tero Raita[6], Urban Brändström[7], Tima Sergienko[7] (1.Planetary Plasma and Atmospheric Research Center, Graduate School of Science, Tohoku University, 2.National Institute of Polar Research, 3.University of Tromsø - The Arctic University of Norway, 4.Finnish Meteorological Institute, 5.EISCAT Scientific Association, 6.Sodankylä Geophysical Observatory, University of Oulu, 7.Swedish Institute of Space Physics)

2:25 PM - 2:40 PM JST | 5:25 AM - 5:40 AM UTC

[PEM09-16] A generation process of “Great Wall” aurora seen from ISS

*Sota Nanjo[1], Morio Tanaka[2], Natsuo Sato[3], Yuta Hozumi[1], Keisuke Hosokawa[1], Ryuho Kataoka[3,4], Yoshizumi Miyoshi[5], Shin-ichiro Oyama[3,5,6], Mitsunori Ozaki[7], Kazuo Shiokawa[5], Satoshi Kurita[2] (1.The University of Electro-Communications, 2.Kyoto University, 3.National Institute of Polar Research, 4.SOKENDAI, the Graduate University for Advanced Studies, 5.ISEE, Nagoya University, 6.University of Oulu, 7.Kanazawa University)

2:40 PM - 2:55 PM JST | 5:40 AM - 5:55 AM UTC

[PEM09-17] Exploring the Electron Acceleration Mechanism in the Poleward Boundary Intensification

*Hayato Higuchi[1], Akimasa Yoshikawa[2] (1.Department of Earth and Planetary Sciences, Graduate School of Science, Kyushu University, 2.Department of Earth and Planetary Sciences, Faculty of Science, Kyushu University)

2:55 PM - 3:10 PM JST | 5:55 AM - 6:10 AM UTC

[PEM09-18] **Antarctic large area network observation of auroral phenomena using unmanned system: Current status of project as of early 2021**

*Akira Kadokura[1], Yasunobu Ogawa[1], Yoshimasa Tanaka[1], Hisao Yamagishi[1], Masaki Okada[1], Ryuho Kataoka[1], Herbert Akihito Uchida[4], Yuichi Otsuka[2], Tetsuo Motoba[3], Natsuo Sato[1], Henri Robert[5], Ashwini K. Sinha[6], Jean Rasson[7] (1.National Institute of Polar Research, 2.Nagoya University, 3.Johns Hopkins University, Applied Physics Laboratory, 4.SOKENDAI, 5.International Polar Foundation, 6.Indian Institute of Geomagnetism, 7.Royal Meteorological Institute of Belgium)

3:10 PM - 3:15 PM JST | 6:10 AM - 6:15 AM UTC

[PEM09-19] Discussion

Current and future perspectives on 3D analysis of aurora

*Yoshimasa Tanaka[1,2,3], Yasunobu Ogawa[1,2,3], Akira Kadokura[1,2,3], Bjorn Gustavsson[4], Kirsti Kauristie[5], Enell Carl-fredrik[6], Urban Brandstrom[7], Tima Sergienko[7], Alexander Kozlovsky[8], Tero Raita[8], Mizuki Fukizawa[9], Takeshi Sakanoi[9], Keisuke Hosokawa[10]

1. National Institute of Polar Research, 2. Polar Environment Data Science Center, Joint Support-Center for Data Science Research, Research Organization of Information and Systems, 3. The Graduate University for Advanced Studies, SOKENDAI, 4. The Arctic University of Norway, 5. Finnish Meteorological Institute, 6. EISCAT Scientific Association, 7. Swedish Institute of Space Physics, 8. Sodankyla Geophysical Observatory, 9. Planetary Plasma and Atmospheric Research Center, Graduate School of Science, Tohoku University, 10. Department of Communication Engineering and Informatics, University of Electro-Communications

Aurora Computed Tomography (ACT) is an analysis method to reconstruct three-dimensional (3D) structure of auroral luminosity from monochromatic auroral images simultaneously taken by multi-point imager network on the ground. The ACT method enables us to derive the altitude profile of the auroral luminosity, corresponding to the energy distribution of precipitating electrons from the magnetosphere. Another advantage of the ACT is the capability to derive the 3D distribution of the electron density, resulting in the electrical conductivity, in the ionospheric E and F regions at high-time resolution. The auroras are the electromagnetic phenomena generated by the magnetosphere-ionosphere (M-I) coupling process, so it is essential to understand the 3D current system in the M-I system. The 3D current system can be estimated by using the ionospheric conductivity obtained from the ACT analysis, with the ionospheric electric field from the radars or the ionospheric equivalent current from the magnetometers. So far, we have applied the ACT analysis to several discrete aurora events to reconstruct the 3D distribution of the optical emission and the energy distribution of the precipitating electrons. It was demonstated that the altitude profile of the optical emission at the wavelength of 427.8 nm obtained by the ACT method is similar to the ionospheric density profile simultaneously observed with the EISCAT radar. Recently, we also succeeded in the 3D reconstruction of the pulsating auroral patches. In these case studies, the ionospheric electron density converted from the optical emission using the theoretical and empirical models was underestimated compared with that observed by the EISCAT radar. The radars and optical imagers are complementary to each other, because the radars have a high range resolution, while the imagers have a high angular resolution. In order to combine these different kinds of data effectively, we have developed the Generalized - Aurora Computed Tomography (G-ACT) method, which is capable of retrieving the differential number flux of precipitating electrons from multi-instrument data, such as the monochromatic images from the multiple imagers, the ionospheric electron density from the radars, and cosmic noise absorption from the imaging riometers. This method enables more accurate reconstruction of 3D aurora, even in case it is difficult to reconstruct by the optical data only. In particular, it is expected that the G-ACT method will be useful for the research on the auroral 3D structure by the EISCAT_3D, which is a multiple-site phased-array incoherent scatter radar system that is planned to be operated in 2022. We are planning to apply the G-ACT technique to data obtained from both the EISCAT_3D radar and the imager networks, which are being constructed by the international collaboration, to extract the 3D current system accompanied by various auroral phenomena.

Keywords: aurora, tomography analysis, discrete aurora, pulsating aurora, energy distribution of precipitating electrons, EISCAT_3D

©2021. Japan Geoscience Union. All Right Reserved.

Reconstruction of the three-dimensional structure and precipitating electrons of pulsating auroral patches by Aurora Computed Tomography

*Mizuki Fukizawa[1], Takeshi Sakanoi[1], Yoshimasa Tanaka[2], Yasunobu Ogawa[2], Björn Gustavsson[3], Kirsti Kauristie[4], Carl-Fredrik Enell[5], Alexander Kozlovsky[6], Tero Raita[6], Urban Brändström[7], Tima Sergienko[7]

1. Planetary Plasma and Atmospheric Research Center, Graduate School of Science, Tohoku University, 2. National Institute of Polar Research, 3. University of Tromsø - The Arctic University of Norway, 4. Finnish Meteorological Institute, 5. EISCAT Scientific Association, 6. Sodankylä Geophysical Observatory, University of Oulu, 7. Swedish Institute of Space Physics

Aurora Computed Tomography (ACT) is an inversion problem analysis method to reconstruct the auroral three-dimensional (3-D) structure from monochromatic auroral images obtained with multiple ground-based optical instruments which have common field of view by applying the Computed Tomography method (e.g., Aso et al., 1990). In addition, Generalized-Aurora Computed Tomography (G-ACT) is the analysis method developed from ACT to reconstruct the energy and spatial distribution of precipitating electrons by combining ionospheric electron density data observed by an Incoherent Scatter radar (Aso et al., 2008; Tanaka et al., 2011). These methods have been applied to discrete auroras whose structures have discrete boundaries such as auroral arcs. On the other hand, it is relatively difficult to reconstruct the 3-D structure of pulsating aurora (PsA) by ACT since the structure boundaries of PsA is generally blurred. Therefore, ACT and G-ACT have not been applied to PsA yet.

In this study, we evaluate the possibility applying ACT and G-ACT to the PsA patch and will finally investigate the temporal changes of the 3-D structure and precipitating electrons of PsA patches. We used monochromatic auroral images obtained with three all-sky images in Scandinavia (Skibotn (69.35˚N, 18.82˚E), Kilpisjärvi (69.05˚N, 20.36˚E), Abisko (68.36˚N, 18.82˚E)) during the substorm recovery phase in 0 –2 UT on 18 February 2018. The observation wavelength is 427.8 nm and temporal resolution is 2 s. We selected the isolated PsA patch observed by the three all-sky imagers to make the problem simple though PsA patches often occur in close proximity to each other. Then, we carried out to reconstruct its 3-D structure from only auroral images by ACT. The background diffuse auroral emission was subtracted from the auroral images as uniform emission to reduce noises before conducting ACT.

As a result, we obtained the auroral 3-D structure whose widths in the east-west, north-south, and altitude directions were 60 km, 42 km, and 14 km respectively. The accuracy of the reconstruction was evaluated by using a model aurora. We compared the auroral 3-D structure reconstructed from the pseudo images obtained by integrating model 3-D aurora in the line-of-sight directions to the model auroral 3-D structure and found that the peak altitude was correctly reconstructed but the peak value and altitude width of the reconstructed aurora were respectively ~18 % smaller and ~33 % larger than those of the model aurora. These errors would be caused by the horizontally wide structure of PsA patch which makes ambiguity in determining the lower- and upper-limit altitude from auroral images.

Next, we examined the events that a PsA patch was observed at the observation point of the EISCAT UHF radar in Tromsø (69.58˚N, 19.23˚E) and reconstructed the auroral 3-D structures from the three auroral images. The reconstructed 3-D volume emission rates were converted to electron densities to compare

©2021. Japan Geoscience Union. All Right Reserved.

with the altitude profiles of electron densities observed by the EISCAT UHF radar. As a result, the maximum values of reconstructed electron densities were ~32 –40 % smaller than those of observed ones. These errors might be caused by the subtraction of the background diffuse auroral emission from auroral images before conducting ACT, the error of reconstructing the 3-D volume emission rate by ACT, and the errors of the effective recombination coefficient and neutral atmospheric model which used to convert the volume emission rate to electron density.
We give the talk on the reconstruction of 3-D structure of PsA patches by G-ACT, and evaluate their accuracy. We also show the results on the temporal changes of 3-D structure and energy distribution of precipitating electrons that cause PsA patches.

Keywords: Pulsating aurora, Computed Tomography

©2021. Japan Geoscience Union. All Right Reserved.

A generation process of “Great Wall” aurora seen from ISS

*Sota Nanjo[1], Morio Tanaka[2], Natsuo Sato[3], Yuta Hozumi[1], Keisuke Hosokawa[1], Ryuho Kataoka[3,4], Yoshizumi Miyoshi[5], Shin-ichiro Oyama[3,5,6], Mitsunori Ozaki[7], Kazuo Shiokawa[5], Satoshi Kurita[2]

1. The University of Electro-Communications, 2. Kyoto University, 3. National Institute of Polar Research, 4. SOKENDAI, the Graduate University for Advanced Studies, 5. ISEE, Nagoya University, 6. University of Oulu, 7. Kanazawa University

By analyzing observations of the digital single-lens reflex cameras onboard the International Space Station, we have reported the morphology of the "Great Wall" aurora, which is a structure, embedded within the omega-band aurora, having wide distributions in the latitudinal and altitudinal directions and a narrow extent in the longitudinal direction. By studying the two case examples from both hemispheres, we found that the Great Wall auroras appeared in the western flank of the torch structure of the omega-band. We also showed the detailed structure of the Great Wall aurora at the JpGU-AGU meeting last year. However, we have not yet discussed their generation process in detail. To better understand the generation process of the Great Wall aurora, it is important to discuss the current system in the vicinity of the omega-band. Vanhamäki et al. (2009) derived the current system in the vicinity of the omega-band by combining model calculations with observations using optical instruments, a riometer, and magnetometers. Their results suggest that there is an upward field-aligned current (FAC) in the western flank of the torch structure due to the negative divergence of the electric field. The existence of the upward FAC is consistent with the appearance of the Great Wall aurora, but they did not discuss how the optical aurora forms in that region as a manifestation of FAC. In this study, we focus on the gradient of the conductance of the torch structure and discuss the possible generation process of the Great Wall aurora. Within the hole structure, a dark region between the consecutive torches, conductance is lower as compared to that in the torch structure; thus, the positive (negative) charges are accumulated along the western (eastern) flank to keep the westward flowing Hall current continuous. The positive potential along the western flank can increase the electron precipitation and drives the upward FAC, which can introduce the generation of Great Wall aurora. In the presentation, we will discuss the validity of this scenario by analyzing observations from the low-Earth orbiting satellites.

Keywords: Omega band, Field-Aligned Current, Magnetosphere-Ionosphere coupling

©2021. Japan Geoscience Union. All Right Reserved.

Exploring the Electron Acceleration Mechanism in the Poleward Boundary Intensification

*Hayato Higuchi[1], Akimasa Yoshikawa[2]

1. Department of Earth and Planetary Sciences, Graduate School of Science, Kyushu University, 2. Department of Earth and Planetary Sciences, Faculty of Science, Kyushu University

The auroral oval poleward boundary auroral intensification (PBI) had been regarded the result of “distant neutral line reconnection” effects in the ionosphere. On the other hand, Ohtani and Yoshikawa., [2016] proposed a model in which PBI is the result of polarization process caused by plasma flows due to “dayside reconnection” approaching the conductivity gradient region of auroral oval. This model is an application of the theory of ionospheric polarization-field-aligned current (FAC) proposed by Yoshikawa et al., [2013]. According to Ohtani and Yoshikawa., [2016], Alfven waves upwelling from the ionosphere to the magnetosphere accelerate electrons downward and generating explosive auroral intensification. This is a new concept of the auroral process that has never existed in magnetospheric physics before. To simulate above mentioned process, it is essential to consider the ionosphere-magnetosphere coupling via Alfven waves and kinetic effects based on wave-particle interactions, which can explain "how upward Alfven waves rising from the cold ionosphere as a result of ionospheric polarization can trigger explosive downward electron acceleration?.”
In this research, in order to reproduce the aurora acceleration process associated with "ionospheric polarization PBI", we try to develop a "3D Vlasov-PIC-Fluid electron acceleration simulation". This simulation scheme has advantages such as maximum kinetic effect and reduced computational cost in reproducing the electron acceleration process by Alfven waves of ionospheric origin.
In this presentation, we will introduce new model of PBI, and explain basic concept of our developing Vlasov-PIC-Fluid code.

Keywords: Poleward Boundary Intensification, Auroral electron acceleration mechanism, Kinetic effect, Vlasov simulation, M-I coupling system, Wave particle interaction

©2021. Japan Geoscience Union. All Right Reserved.

Antarctic large area network observation of auroral phenomena using unmanned system: Current status of project as of early 2021

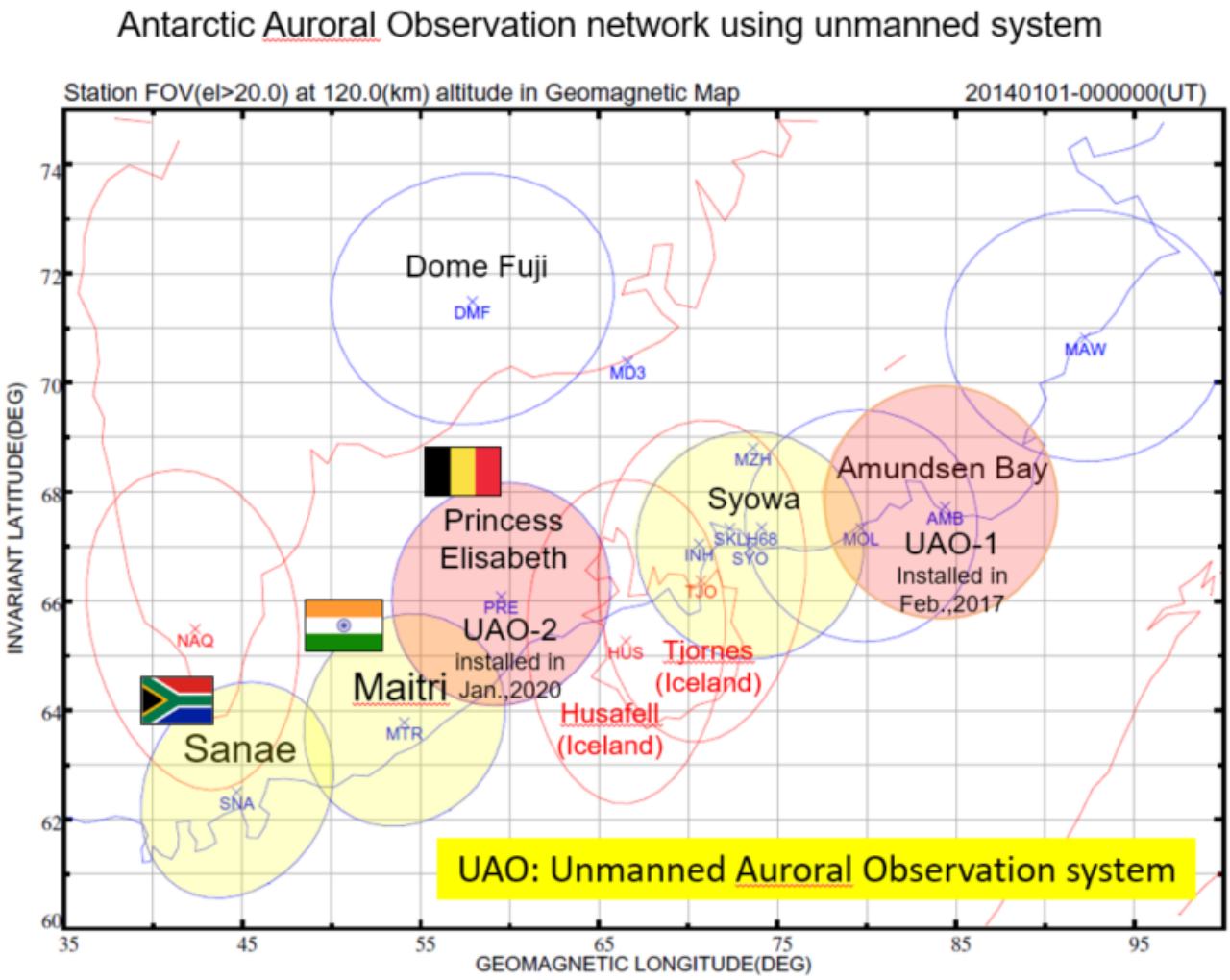
*Akira Kadokura[1], Yasunobu Ogawa[1], Yoshimasa Tanaka[1], Hisao Yamagishi[1], Masaki Okada[1], Ryuho Kataoka[1], Herbert Akihito Uchida[4], Yuichi Otsuka[2], Tetsuo Motoba[3], Natsuo Sato[1], Henri Robert[5], Ashwini K. Sinha[6], Jean Rasson[7]

1. National Institute of Polar Research, 2. Nagoya University, 3. Johns Hopkins University, Applied Physics Laboratory, 4. SOKENDAI, 5. International Polar Foundation, 6. Indian Institute of Geomagnetism, 7. Royal Meteorological Institute of Belgium

Space and upper atmospheric sciences group in the National Institute of Polar Research (NIPR) is now planning to construct an observation network for auroral phenomena along the coast of the Dronning Maud Land in the Antarctica including Japanese Syowa Station, and has developed a Unmanned Auroral Observation system (UAO), which is equipped with a 3-axis fluxgate magnetometer, all-sky auroral imager, GNSS/TEC receiver, and a data communication system using the Inmarsat satellite data link with a low power consumption. The first UAO (UAO-1) had been installed at Amundsen Bay area, which is located about 500 km eastward from Syowa Station, in February, 2017 in the summer operation of the 58th Japanese Antarctic Research Expedition (JARE-58). The second UAO (UAO-2) had been installed at Belgium Princess Elisabeth Antarctica (PEA) Station in January, 2020. Electric power of the UAO-1 is supplied by a hybrid natural energy electric generation system which consists of three sets of 192W wind generators and 8 sets of 62W solar panels, while that of the UAO-2 is supplied from the AC power source of the PEA Station which is generated by a power generation system of the station using nine big wind generators and solar panels. For the UAO, observed magnetometer data (1 sec resolution), GNSS BINEX data (30 sec resolution), daily Keogram and sample image data of the auroral imager, and House Keeping data (temperatures and power voltages) (1 min resolution) are transmitted at every 1 hour via the satellite link system to a server in Japan by FTP, and auroral image data of 1 sec resolution are stored in a memory card of the video encoder in the system. Sample interval and pixel resolution of the transmitted auroral image data are 1 hour (5 minutes) and 640x480 (160x120) for the UAO-1 (UAO-2), respectively. UAO-2 has the other USB memory in the system which can store auroral still image of 1 sec resolution with 640x480 pixel resolution and GNSS BINEX data of 1 sec resolution. PEA Station is maintained during summer season, and becomes an unmanned station during winter season, while the electric power to all the instruments at the station is supplied continuously all through the season. In January, 2020, we had also installed an auroral imager system at Indian Maitri Station, which consists of four sets of all-sky imager using Watec cameras: 1) Panchromatic (color) ; 2) Panchromatic (black&white); 3) filtered at 560nm (FWHM:10nm); 4) filtered at 632nm (FWHM:10nm), respectively. Maitri is a year-round station. The auroral imager system is run autonomously. We ask expedition members at Maitri to send daily summary files via E-mail to us. In our presentation, we will talk about current status of the project as of early 2021.

Keywords: aurora, network observation, Antarctic

©2021. Japan Geoscience Union. All Right Reserved.



©2021. Japan Geoscience Union. All Right Reserved.

[E] Oral | P (Space and Planetary Sciences) | P-EM Solar-Terrestrial Sciences, Space Electromagnetism & Space Environment

[P-EM09] Dynamics of Magnetosphere and Ionosphere

convener:Akiko Fujimoto(Kyushu Institute of Technology), Mitsunori Ozaki(Faculty of Electrical and Computer Engineering, Institute of Science and Engineering, Kanazawa University), Yuka Sato(Nippon Institute of Technology), Aoi Nakamizo(Applied Electromagnetic Research Institute, National Institute of Information and Communications Technology), Chairperson:Yuki Obana(Department of Engineering Science, Faculty of Engineering, Osaka Electro-Communication University), Yoshihiro Yokoyama(Department of Earth and Planetary Sciences, Graduate School of Science, Kyoto University)
Sun. Jun 6, 2021 1:45 PM - 3:15 PM Ch.05 (Zoom Room 05)

This session provides an opportunity to present recent results from satellite and ground-based observations and theoretical and simulation studies on the magnetosphere, ionosphere, and their coupling processes. We invite talks and posters discussing various phenomena related to the magnetosphere-ionosphere system: solar wind-magnetosphere interaction, magnetosphere-ionosphere convection, field-aligned current, magnetic storms/substorms, neutral-plasma interaction, ionospheric ion inflow and outflow, aurora phenomena, and so forth. Discussions on planetary and satellite ionospheres and magnetospheres, future missions and instrument developments are also welcome.

3:10 PM - 3:15 PM

[PEM09-19]Discussion

©Japan Geoscience Union

[E] Oral | P (Space and Planetary Sciences)：P-EM Solar-Terrestrial Sciences, Space Electromagnetism & Space Environment

Sun. Jun 6, 2021 3:30 PM - 5:00 PM JST | Sun. Jun 6, 2021 6:30 AM - 8:00 AM UTC | Ch.05 Zoom Room 05

[P-EM09] Dynamics of Magnetosphere and Ionosphere

convener:Akiko Fujimoto(Kyushu Institute of Technology), Mitsunori Ozaki(Faculty of Electrical and Computer Engineering, Institute of Science and Engineering, Kanazawa University), Yuka Sato(Nippon Institute of Technology), Aoi Nakamizo(Applied Electromagnetic Research Institute, National Institute of Information and Communications Technology), Chairperson:Yuki Obana(Department of Engineering Science, Faculty of Engineering, Osaka Electro-Communication University), Yoshihiro Yokoyama(Department of Earth and Planetary Sciences, Graduate School of Science, Kyoto University)

This session provides an opportunity to present recent results from satellite and ground-based observations and theoretical and simulation studies on the magnetosphere, ionosphere, and their coupling processes. We invite talks and posters discussing various phenomena related to the magnetosphere-ionosphere system: solar wind-magnetosphere interaction, magnetosphere-ionosphere convection, field-aligned current, magnetic storms/substorms, neutral-plasma interaction, ionospheric ion inflow and outflow, aurora phenomena, and so forth. Discussions on planetary and satellite ionospheres and magnetospheres, future missions and instrument developments are also welcome.

3:30 PM - 3:45 PM JST | 6:30 AM - 6:45 AM UTC

[PEM09-20] Seasonal dependence of dusk-side equatorial IHFACs polarity during solar cycle 23-24

Manjula Ranasinghe[2], *Akiko Fujimoto[1], Akimasa Yoshikawa[3], Chandana Jayaratne[2] (1.Kyushu Institute of Technology, 2.University of Colombo, 3.Kyushu University)

3:45 PM - 4:00 PM JST | 6:45 AM - 7:00 AM UTC

[PEM09-21] Development of the imaging receiver system for the SuperDARN Hokkaido East radar

*Nozomu Nishitani[1], Tomoaki Hori[1], Yoshiyuki Hamaguchi[1] (1.Institute for Space-Earth Environmental Research, Nagoya University)

4:00 PM - 4:15 PM JST | 7:00 AM - 7:15 AM UTC

[PEM09-22] Seasonal and longitudinal dependence of the Sub-Auroral Polarization Streams occurrence observed by the SuperDARN radars

Kento Oya[1], *Nozomu Nishitani[1], Tomoaki Hori[1], John Mike Ruohoniemi[2], William A. Bristow[3], Simon G. Shepherd[4], Bharat Kunduri[2] (1.Institute for Space-Earth Environmental Research, Nagoya University, 2.Virginia Tech Department of Electrical and Computer Engineering, 3.The Pennsylvania State University , 4.Thayer School of Engineering, Dartmouth College)

4:15 PM - 4:30 PM JST | 7:15 AM - 7:30 AM UTC

[PEM09-23] Investigation of the mid-latitude ionospheric response during substorm based on magnetic and electric field observations

*Moe Hayashi[1], Akimasa Yoshikawa[1], Akiko Fujimoto[2], Shinichi Ohtani[3] (1.Kyushu University, 2.Kyushu Institute of Technology , 3.The Johns Hopkins University Applied Physics Laboratory)

4:30 PM - 4:55 PM JST | 7:30 AM - 7:55 AM UTC

[PEM09-24] New results of auroral hiss observations on the ground at L=5.5 in Northern Europe

★Invited Papers

*Jyrki Manninen[1], Natalia G. Kleimenova[2,3], Yury Fedorenko[4], Olga Lebed[4], Alexander Kozlovsky[1], Alexander Nikitenko[4], Liudmila Gromova[5] (1.Sodankyla Geophysical Observatory, University of Oulu, Sodankylä, Finland, 2.Schmidt Institute of Physics of the Earth RAN, Moscow, Russia, 3.Space Research

Institute RAN, Moscow, Russia, 4.Polar Geophysical Institute, Apatity, Russia, 5.Pushkov Institute of Terrestrial Magnetism, Ionosphere and Radio Wave Propagation RAN, Moscow, Russia)

4:55 PM - 5:00 PM JST | 7:55 AM - 8:00 AM UTC

[PEM09-25] Discussion

Seasonal dependence of dusk-side equatorial IHFACs polarity during solar cycle 23-24

Manjula Ranasinghe[2], *Akiko Fujimoto[1], Akimasa Yoshikawa[3], Chandana Jayaratne[2]

1. Kyushu Institute of Technology, 2. University of Colombo, 3. Kyushu University

The east-west ward variation of MAGDAS/CPMN magnetometer 1-hour time resolution data at Davao (Philippines) station operated by International Center for Space Weather Science and Education, Kyushu University from August 1998 to July 2020 are used to investigate the characteristics of the long-term Inter-hemispheric field-aligned currents (IHFACs). The recent in-situ satellite and ground-based observations have reported the dusk-side current polarity of IHFACs are often inconsistent with the Fukushima’ s IHFACs model. We investigated whether the dusk-side IHFACs polarity is consistent or not with the current direction predicted by Fukushima’ s IHFACs model, by analyzing the time-series data of IHFACs variations. We confirmed that the solstices dusk IHFACs flow the same direction of noon IHFACs and the equinoxes dusk IHFACs disagree with Fukushima’ s model. Seasonal IHFACs variations exhibited remarkable asymmetry in both dawn and noon sectors. By contrast, the profile of dusk-side IHFACs intensity was symmetry. The difference between noon and dusk IHFACs intensity might be strongly related to the seasonal dependence of the dusk IHFACs polarity. In addition, we presented that solar cycle dependence can be seen in the peak-to-peak amplitude, monthly average and yearly integral intensity of IHFACs. In contrast to annual variations of IHFACs polarity in the dawn/noon sectors, there were multiple periodicities in the dusk sector: annual variation during the declining phase of solar cycle and semiannual or terannual variations during the increasing and maximum phase. The dusk-side IHFACs modulations were more related with F10.7 variability compared with the dawn and noon sectors. It suggests that the dusk IHFACs is affected by the solar cycle activities.

©2021. Japan Geoscience Union. All Right Reserved.

Development of the imaging receiver system for the SuperDARN Hokkaido East radar

*Nozomu Nishitani[1], Tomoaki Hori[1], Yoshiyuki Hamaguchi[1]

1. Institute for Space-Earth Environmental Research, Nagoya University

The Super Dual Auroral Radar Network (SuperDARN) is a network of High-Frequency (HF) radars located in the high- and mid-latitude regions of both hemispheres, operating continuously with a typical temporal resolution of 1 to 2 minutes. This resolution corresponds to the Nyquist frequency range of 4 to 8 mHz. In order to monitor any variations shorter than 1 min, such as Pc3 pulsations, the radar should choose a special beam scanning mode at the cost of the 1-min scanning period for the whole field of view.

In order to overcome this problem, several solutions have been proposed. One of them is the radar with imaging capability, which enables to sample data for multiple beam directions simultaneously. Several radars have adopted this method since 10 years ago. Meanwhile, traditional-style imaging radars adopted a costly A/D board so that the cost of building the radar system was high.

Software-Defined Radio (SDR), using a much less expensive A/D unit than the traditional A/D boards, is useful for the radar receiver system. A few imaging radars with the Universal Software Radio Peripheral (USRP), i.e., one of the SDR, are operating in the high latitude regions such as in Canada. In contrast, there is no imaging radar with the USRP in the mid-latitude region yet.

In this paper, we report on the present status and the future perspectives of an imaging receiver system that we plan to install for the SuperDARN Hokkaido East radar. We have developed a prototype (4-ch subset out of 20-ch array) of the SuperDARN imaging receiver system consisting mainly of USRP receiver units. This prototype set was attached to the SuperDARN Hokkaido East radar for testing in June-July 2020. With this 4-ch subset system, we succeeded in obtaining the data consistent with the preexisting receiver’ s data. Installation of the imaging receivers can significantly improve the spatial-temporal resolution of the radar data, and make it possible to examine several phenomena such as SAPS wave structures, Pc3 pulsations, and coseismic ionospheric disturbances, which have not been captured with sufficient spatial-temporal resolution by the preexisting receiver set.

Keywords: SuperDARN, imaging receiver

©2021. Japan Geoscience Union. All Right Reserved.

Seasonal and longitudinal dependence of the Sub-Auroral Polarization Streams occurrence observed by the SuperDARN radars

Kento Oya[1], *Nozomu Nishitani[1], Tomoaki Hori[1], John Mike Ruohoniemi[2], William A. Bristow[3], Simon G. Shepherd[4], Bharat Kunduri[2]

1. Institute for Space-Earth Environmental Research, Nagoya University, 2. Virginia Tech Department of Electrical and Computer Engineering, 3. The Pennsylvania State University , 4. Thayer School of Engineering, Dartmouth College

We conduct a statistical study on occurrence characteristics of Sub-Auroral Polarization Streams (SAPS), using the Super Dual Auroral Radar Network (SuperDARN) data. We use six years of mid-latitude SuperDARN data and study the seasonal dependence of SAPS type flows. We identify the equatorward auroral oval boundary using the precipitating energy flux data of the National Oceanic and Atmospheric Administration (NOAA) Polar Orbiting Environmental Satellites (POES) satellites. We use only ionospheric echoes sampled in the region equatorward of this boundary. We set the following criteria to identify SAPS events: 1. the flow speed should exceed 150 m/s [Nagano et al., 2015]. 2. the flow should be directed westward (-45 deg $< \Delta \theta <$ +45 deg).

Some past studies suggested the seasonal dependence of SAPS, e.g., SAPS-like high velocity flows occur over a larger magnetic local time (MLT) extent during winter months [Koustov et al., 2006], lower velocity flows are observed more often in the summer Northern Hemisphere than in the winter Southern Hemisphere [Kunduri et al., 2012]. These results are in slight disagreement with another interhemispheric study [Parkinson et al., 2005], which showed that summer Southern Hemisphere velocities are slightly higher than in the winter Northern Hemisphere. Nevertheless, there have been few comprehensive studies on the statistics of seasonal dependence.

One of the remarkable SAPS characteristics found in the present study is that the occurrence rate in spring and autumn are generally larger than other seasons for each radar, which can be interpreted in terms of the Russel-McPherron effect (Russell & McPherron, 1973). On the other hand, we see no consistent tendency among the radars regarding the summer-winter difference of the SAPS occurrence, but the peak MLT of SAPS occurrence in summer and winter depends on the radar's location. These results are interpreted in terms of the differences in the dipole tilt angle (DTA). To the best of our knowledge, this is the first result of the SAPS occurrence rate discussed as a function of the dipole tilt angle in addition to the solar zenith angle.

References

Koustov, A. V., et al., Ann. Geophys., https://doi.org/10.5194/angeo-24-1591-2006, 2006.

Kunduri, B. S. R., et al., J. Geophys. Res., https://doi.org/10.1029/2012JA017784, 2012.

©2021. Japan Geoscience Union. All Right Reserved.

Nagano, H., et al., Earth, Planets and Space, https://doi.org/10.1186/s40623-015-0299-7, 2015.

Parkinson, M. L., et al., Ann. Geophys., https://doi.org/10.5194/angeo-23-1371-2005, 2005.

Russell, C. T., & McPherron, R. L., J. Geophys. Res., https://doi.org/10.1029/ja078i001p00092, 1973.

Keywords: SuperDARN, Sub-Auroral Polarization Streams (SAPS), longitudinal dependence

©2021. Japan Geoscience Union. All Right Reserved.

Investigation of the mid-latitude ionospheric response during substorm based on magnetic and electric field observations

*Moe Hayashi[1], Akimasa Yoshikawa[1], Akiko Fujimoto[2], Shinichi Ohtani[3]

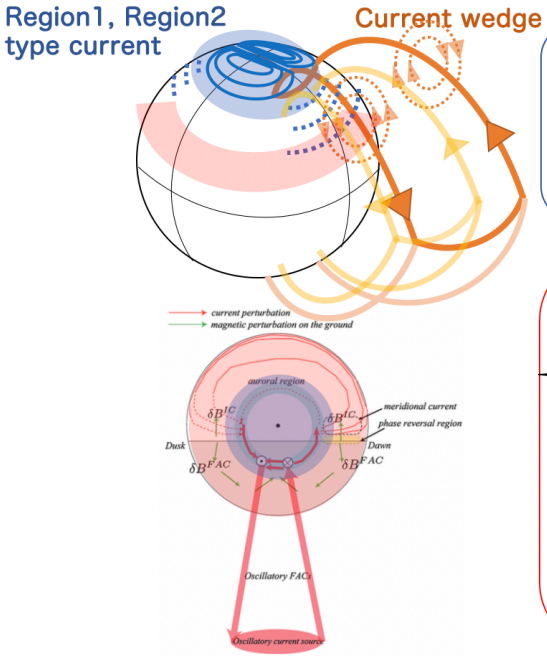
1. Kyushu University, 2. Kyushu Institute of Technology , 3. The Johns Hopkins University Applied Physics Laboratory

Investigation of the mid-latitude ionospheric response during substorm based on magnetic and electric field observations
The purpose of this study is to obtain a more comprehensive view and understanding of the formation process of global three-dimensional current system during auroral substorms.
It is known that there are two types of current systems in the polar ionosphere: the R1-current linked to the magnetospheric convection system and the R2-current linked to the pressure gradient region in the inner magnetosphere [Iijima and Potemra, 1976, 1978]. Substorms are caused by strong plasma injection in the near-earth region. The plasma vorticities that grow at the flow edge of the plasma injection forms a substorm current wedge (SCW) system of which current closure structure is the same of the R1 current system. At the lower latitude of the SCW system, the R2-type current system develops due to the increase in plasma pressure in the inner magnetosphere. Growth of the R2-type system and the SCW system don't always match. The R2-type current system causes not only a shielding effect that weakens the ionospheric current reaching low latitudes and equatorial regions due to the growth of the SCW system, but also an over-shielding effect that sometimes causes the growth of current systems in the opposite direction. (Kikuchi et al [1996]; Nishida [1968]).
The ground magnetic field disturbances observed during substorms are not only generated by the ionospheric currents, but also by the field-aligned currents (FACs) accompanied by the growth of the SCW. In the mid- and low-latitude regions, where this composite effect is particularly large, it is difficult to determine from the magnetic field data alone whether the magnetic field variation during substorms is due to the formation of the ionospheric current system or to the remote field effect of the current wedge current system. A direct comparison of ionospheric electric and magnetic field data is essential for a better understanding of the causes of magnetic disturbances.
In this presentation, we report the results of a study of mid-latitude ionospheric variability during auroral substorm using electric field data from the HF Doppler radar and magnetic field data from SuperMag and MAGDAS installed by Kyushu University in Palatunka, Russia. The analysis period was from October 2006 to May 2007, and the number of events was 100. As an initial result, two patterns of magnetic and electric field variations were identified in the mid-latitude night side. (i) A westward electric field was observed for 30 minutes to 1 hour after the magnetic and electric field fluctuation onset on the evening side of the SCW (14 out of 20 events). (ii) W-shaped oscillations and then westward electric field fluctuations were observed for 10 minutes before and after the SCW center magnetic field fluctuation and electric field fluctuation onset (4 out of 6 events). This may indicate the growth and extinction of the FAC pat of the SCW associated with the substorm. We report the results of a detailed global verification of this fact.

Keywords: Substorm, Field aligned current, current wedge, ionospheric current

©2021. Japan Geoscience Union. All Right Reserved.

1. Magnetic field variations in polar and mid-low latitudes



@ Magnetic field variations in the polar regions

・ Just below the ionosphere electric field
・ Region 1 and Region 2 types of ionospheric currents mainly cause magnetic field variations

@ Magnetic Field Fluctuations at Mid and Low Latitudes
Ionospheric currents of Region 1 and Region 2 types
＋
Substorm current wedge

These two things complicate the magnetic field fluctuations.
→During substorms, it is difficult to isolate the magnetic field variability given by the two from the magnetic field data alone.
→I want to compare magnetic and electric field data and distinguish between the two effects.

©2021. Japan Geoscience Union. All Right Reserved.

New results of auroral hiss observations on the ground at L=5.5 in Northern Europe

*Jyrki Manninen[1], Natalia G. Kleimenova[2,3], Yury Fedorenko[4], Olga Lebed[4], Alexander Kozlovsky[1], Alexander Nikitenko[4], Liudmila Gromova[5]

1. Sodankyla Geophysical Observatory, University of Oulu, Sodankylä, Finland, 2. Schmidt Institute of Physics of the Earth RAN, Moscow, Russia, 3. Space Research Institute RAN, Moscow, Russia, 4. Polar Geophysical Institute, Apatity, Russia, 5. Pushkov Institute of Terrestrial Magnetism, Ionosphere and Radio Wave Propagation RAN, Moscow, Russia

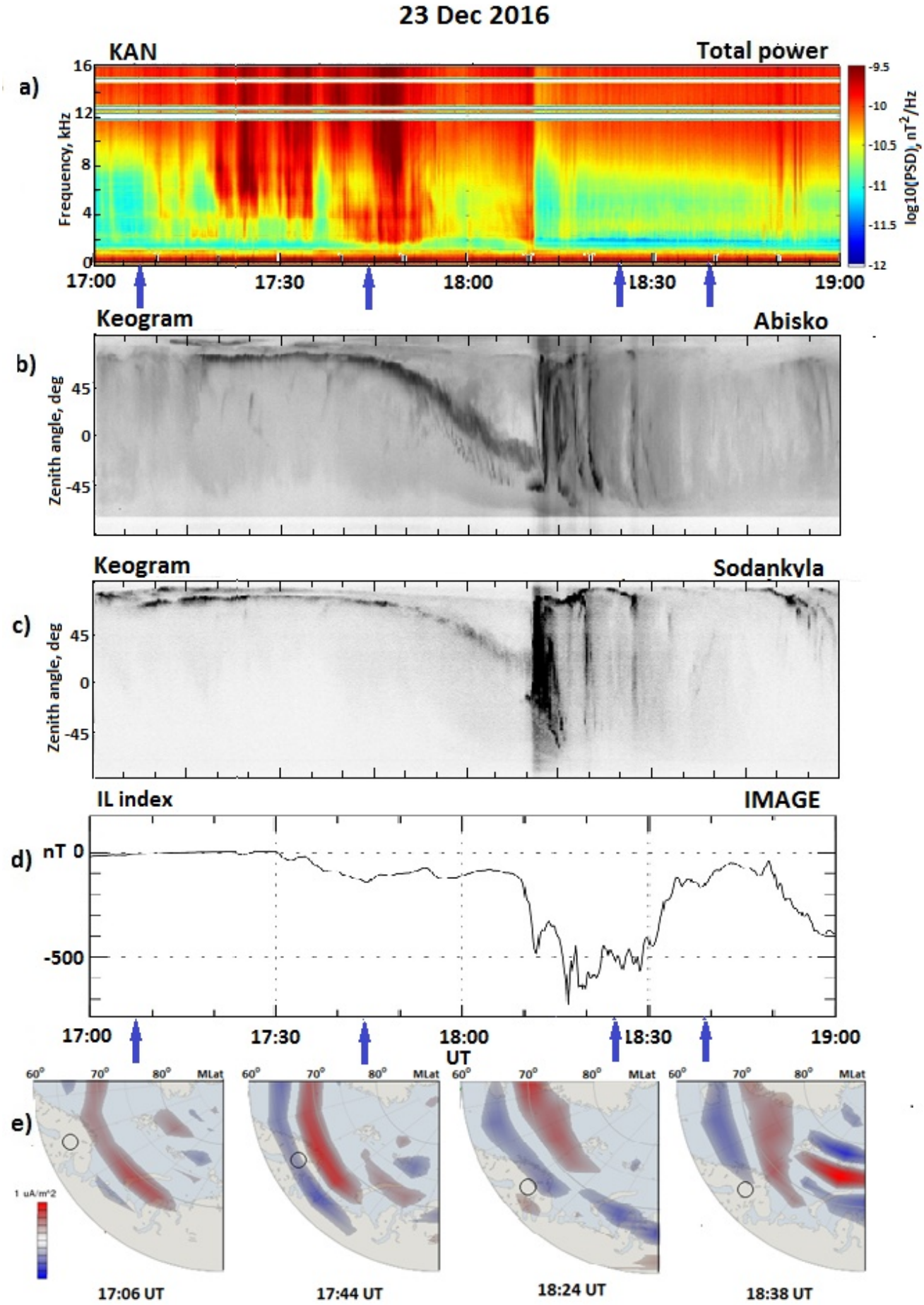
Auroral hiss is a well-known type of nighttime natural VLF emission with a noise-like structure generated by the Cherenkov instability of precipitating soft electrons above the ionosphere. Auroral hiss occurrence up to 39 kHz was studied in the equatorward region of the auroral oval at the Finnish station Kannuslehto (KAN, MLAT = 64.2˚N) during 11 winter months in 2015-2018. During this time interval, 98 isolated and rather powerful magnetic substorms were recorded over Scandinavia. In 93% of the substorms studied, an auroral VLF hiss was recorded at the same time as enhancement of field-aligned currents (FACs). FACs are caused by soft electron precipitation which could be a plausible source of the auroral VLF hiss generation. For the first time, it was found that auroral VLF hiss occurrence in the equatorward region of the auroral oval is a typical signature of the substorm growth phase.

Also a few examples of simultaneous auroral hiss observations at Lovozero, Russia (LOZ, MLAT = 64.2˚N) will be shown. LOZ is located at the same magnetic latitude as KAN, but 400 km to east from KAN. Simultaneous observations can be used for direction finding of auroral hiss events.

Figure presents a survey of the auroral hiss event on 23 December 2016 at 17-19 UT. From top to bottom: a) the auroral hiss spectrogram; b) the auroral keogram from Abisko; c) the auroral keogram from Sodankyla; d) the IL indicator of magnetic activity; and e) the south-west quarters of the global map (in geomagbnetic coordinate´s) of the field-aligned currents (FACs) according to the AMPERE data. Blue arrows point the time of these map of auroral hiss at KAN was accompanied by the upward FAC increasing in the premidnight sector constructions. The upward FACs are marked by red and the downward FACs, by blue. The small circles indicate the location of KAN.

Keywords: Auroral hiss, substorm, growth phase

©2021. Japan Geoscience Union. All Right Reserved.



©2021. Japan Geoscience Union. All Right Reserved.

[E] Oral | P (Space and Planetary Sciences) | P-EM Solar-Terrestrial Sciences, Space Electromagnetism & Space Environment

[P-EM09] Dynamics of Magnetosphere and Ionosphere

convener:Akiko Fujimoto(Kyushu Institute of Technology), Mitsunori Ozaki(Faculty of Electrical and Computer Engineering, Institute of Science and Engineering, Kanazawa University), Yuka Sato(Nippon Institute of Technology), Aoi Nakamizo(Applied Electromagnetic Research Institute, National Institute of Information and Communications Technology), Chairperson:Yuki Obana(Department of Engineering Science, Faculty of Engineering, Osaka Electro-Communication University), Yoshihiro Yokoyama(Department of Earth and Planetary Sciences, Graduate School of Science, Kyoto University)
Sun. Jun 6, 2021 3:30 PM - 5:00 PM Ch.05 (Zoom Room 05)

This session provides an opportunity to present recent results from satellite and ground-based observations and theoretical and simulation studies on the magnetosphere, ionosphere, and their coupling processes. We invite talks and posters discussing various phenomena related to the magnetosphere-ionosphere system: solar wind-magnetosphere interaction, magnetosphere-ionosphere convection, field-aligned current, magnetic storms/substorms, neutral-plasma interaction, ionospheric ion inflow and outflow, aurora phenomena, and so forth. Discussions on planetary and satellite ionospheres and magnetospheres, future missions and instrument developments are also welcome.

4:55 PM - 5:00 PM

[PEM09-25]Discussion

©Japan Geoscience Union

[E] Poster | P (Space and Planetary Sciences)：P-EM Solar-Terrestrial Sciences, Space Electromagnetism & Space Environment

Sun. Jun 6, 2021 5:15 PM - 6:30 PM JST | Sun. Jun 6, 2021 8:15 AM - 9:30 AM UTC | Ch.05_1

[P-EM09] Dynamics of Magnetosphere and Ionosphere

convener:Akiko Fujimoto(Kyushu Institute of Technology), Mitsunori Ozaki(Faculty of Electrical and Computer Engineering, Institute of Science and Engineering, Kanazawa University), Yuka Sato(Nippon Institute of Technology), Aoi Nakamizo(Applied Electromagnetic Research Institute, National Institute of Information and Communications Technology)

This session provides an opportunity to present recent results from satellite and ground-based observations and theoretical and simulation studies on the magnetosphere, ionosphere, and their coupling processes. We invite talks and posters discussing various phenomena related to the magnetosphere-ionosphere system: solar wind-magnetosphere interaction, magnetosphere-ionosphere convection, field-aligned current, magnetic storms/substorms, neutral-plasma interaction, ionospheric ion inflow and outflow, aurora phenomena, and so forth. Discussions on planetary and satellite ionospheres and magnetospheres, future missions and instrument developments are also welcome.

[PEM09-P01] Development of a 3-dimensional global ionospheric electrostatic potential solver using IGRF model

*Takuya Ijuin[1], Akimasa Yoshikawa[2] (1.Department of Earth and Planetary Sciences, Graduate School of Science, Kyushu University, 2.Department of Earth and Planetary Sciences, Kyushu University)

[PEM09-P02] Study on the Solar Flare Effect (SFE*) of equatorial electrojet around local noon

*Akihiro Yasunaga[1], Akiko Fujimoto[2], Akimasa Yoshikawa[1] (1.Department of Earth and Planetary Sciences, Kyushu University, 2.Kyushu Institute of Technology)

[PEM09-P03] Consideration of the CubeSat for Observation of IHFAC at LEO

*Kentarou Kitamura[1], Taku Takada[2], Kazumasa Imai[2], Manabu Shinohara[3], Makoto Wakabayashi[4], Akiko Fujimoto[1], Mariko Teramoto[1] (1.Kyushu Institute of Technology, 2.NIT, Koti College, 3.NIT, Kagoshima College, 4.NIT, Niihama College)

[PEM09-P04] Initial results of multi-event analysis of magnetosphere-ionosphere coupling for nighttime medium-scale traveling ionospheric disturbances

*Kouki Kawai[1], Kazuo Shiokawa[1], Yuichi Otsuka[1], Shin-ichiro Oyama[1,2,3], Martin G Connors[4], Yoshiya Kasahara[5], Yasumasa Kasaba[6], Atsuki Shinbori[1], Fuminori Tsuchiya[6], Atsushi Kumamoto[6], Masahiro Kitahara[1], Masafumi Shoji[1], Satoko Nakamura[1], Ayako Matsuoka[7], Shun Imajo[1], Yoichi Kazama[8], Shiang Yu Wang[8], Sunny W. Y. Tam[9], Tzu-Fang Chang[9], B J wang[8], Kazushi Asamura[10], Satoshi Kasahara[11], Shoichiro Yokota[12], Kunihiro Keika[11], Tomoaki Hori[1], Chae-Woo Jun[1], Iku Shinohara[10], Yoshizumi Miyoshi[1] (1.Institute for Space-Earth Environmental Research, Nagoya University, Japan, 2.University of Oulu, Oulu, Finland, 3.National Institute of Polar Research, Tokyo, Japan, 4.Athabasca University, Canada, 5.Kanazawa University, Kanazawa, Japan, 6.Tohoku University, Sendai, Japan, 7. Kyoto University, Kyoto, Japan, 8.Academia Sinica, Taipei, Taiwan, 9.National Cheng Kung University, Tainan, Taiwan, 10.Institute of Space and Astronautical Science, Japan Aerospace Exploration Agency, Sagamihara, Japan, 11.Tokyo University, Tokyo, Japan, 12.Osaka University, Osaka, Japan)

[PEM09-P05] Development of a new M-I coupling algorithm in global MHD magnetosphere simulation: Alfvénic-Coupling

*Aoi Nakamizo[1], Akimasa Yoshikawa[2], Hiroyuki Nakata[3], Keiichiro Fukazawa[4], Takashi Tanaka[2] (1.Applied Electromagnetic Research Institute, National Institute of Information and Communications Technology, 2.Faculty of Science, Kyushu University, 3.Faculty of Engineering, Chiba University, 4.Academic Center for Computing and Media Studies, Kyoto University)

[PEM09-P06] Understanding the 3-dimensional current between the magnetosphere and the ionosphere

*Yuto Yano[1], Yusuke Ebihara[1] (1.Research Institute for Sustainable Humanosphere, Kyoto University)

[PEM09-P07] Magnetospheric dynamics under northward IMF conditions surveyed by concurrent observations of TPA and omega-band aurora

*Motoharu Nowada[1], Yukinaga Miyashita[2,3] (1.Shandong Key Laboratory of Optical Astronomy and Solar-Terrestrial Environment, School of Space Science and Physics, Institute of Space Sciences, Shandong University at Weihai, P. R. China, 2.Korea Astronomy and Space Science Institute, Daejeon, South Korea, 3.Korea University of Science and Technology, Daejeon, South Korea)

[PEM09-P08] The terrestrial magnetosphere for zero interplanetary magnetic field

*Tsubasa Hashimoto[1], Masakazu Watanabe[2], Ryuho Kataoka[3], Shigeru Fujita[4], Takashi Tanaka[5] (1.Department of Earth and Planetary Sciences, Graduate School of Science, Kyushu University, 2.Department of Earth and Planetary Sciences, Faculty of Science, Kyushu University, 3.National Institute of Polar Research, 4.Meteorological College, Japan Meteorological Agency/ National Institute of Polar Research, 5.International Center for Space Weather Science and Education)

[PEM09-P09] Cusp ion precipitation for stably northward IMF and its relation to the magnetosheath flow

*Haruto Koike[1], Satoshi Taguchi[1] (1.Department of Geophysics, Graduate School of Science, Kyoto University)

[PEM09-P10] Topology and geometry of interchange-type reconnection in the terrestrial magnetosphere

*Masakazu Watanabe[1], Tomoya Asano[1], Dongsheng Cai[2], Peikun Xiong[2], Shigeru Fujita[3], Takashi Tanaka[1] (1.Kyushu University, 2.University of Tsukuba, 3.Meteorological College)

[PEM09-P11] **Understanding the behavior of charged particles in plasma by vector potential**

*Shinji Karasawa[1] (1.Miyagi National College of Technology Professor emeritus)

[PEM09-P12] Properties of dispersive Alfven waves and their roles in electron acceleration process in the terrestrial magnetosphere based on Plasma Distribution Solver

*Koseki Saito[1], Yuto Katoh[1], Atsushi Kumamoto[1], Tomoki Kimura[1], Yohei Kawazura[1] (1.Department of Geophysics, Graduate School of Science, Tohoku University)

[PEM09-P13] Equatorward development of electron precipitation in a longitudinally narrow region beyond the cusp

*Satoshi Taguchi[1], Keisuke Hosokawa[2], Yasunobu Ogawa[3] (1.Department of Geophysics, Graduate School of Science, Kyoto University, 2.Department of Communication Engineering and Informatics, University of Electro-Communications, 3.National Institute of Polar Research)

[PEM09-P14] Periodic variations of the high red aurora on the nightside

*kazuki yashima[1], Satoshi Taguchi[1], Keisuke Hosokawa[2] (1. Department of Geophysics, Graduate School of Science, Kyoto University, 2.Department of Communication Engineering and Informatics, The University of Electro-Communications)

[PEM09-P15] Initial study of a substorm onset auroral arc on 28 December 2018 by a ground EMCCD camera and the Arase satellite at L~5

*Liwei Chen[1], Kazuo Shiokawa[1], Yoshizumi Miyoshi[1], Shin-ichiro Oyama[1], Yasunobu Ogawa[2], Keisuke Hosokawa[12], Ryuho Kataoka[2], Yoichi Kazama[5], Shiang-Yu Wang[3], Sunny W. Y. Tam[5], Tzu-Fang Chang[1,4], Bo-Jhou Wang[5], Kazushi Asamura[6], Satoshi Kasahara[7], Shoichiro Yokota[8], Tomoaki Hori[1], Kunihiro

Keika[7], Yasumasa Kasaba[9], Masafumi Shoji[1], Yoshiya Kasahara[10], Ayako Matsuoka[11], Iku Shinohara[6] (1.Institute for Space-Earth Environmental Research, Nagoya University, 2.National Institute of Polar Research, 3.National Cheng Kung University, 4.Institute of Space and Plasma Sciences, National Cheng Kung University, 5.Institute of Astronomy and Astrophysics, Academia Sinica, 6.Institute of Space and Astronautical Science, Japan Aerospace Exploration Agency, 7.University of Tokyo, 8.Osaka University, 9.Tohoku University, 10.Kanazawa University, 11.Data Analysis Center for Geomagnetism and Space Magnetism, Graduate School of Science, Kyoto University, 12.The University of Electro-Communications)

[PEM09-P16] Ionospheric control of space weather: plasma injections arising out of dynamic ionosphere

*Osuke Saka[1] (1.Office Geophysik)

[PEM09-P17] Amplitude modulations of the flickering aurora

*Nomura Kazuki[1], Yoshizumi Miyoshi[1], Satoshi Kurita[2], Kohei Toyama[1], Ryuho Kataoka[3] (1.Institute for Space-Earth Environmental Research,Nagoya University, 2.Research Institite for Subtainable Humanosphere, 3.National Institue of Polar Research)

[PEM09-P18] Simultaneous pulsating aurora and microburst observation with ground-based fast auroral imagers and the Cubesat FIREBIRD-II

*Miki Kawamura[1], Takeshi Sakanoi[1], Mizuki Fukizawa[1], Yoshizumi Miyoshi[2], Keisuke Hosokawa[3], Fuminori Tsuchiya[1], Yuto Katoh[1], Yasunobu Ogawa[4], Kazushi Asamura[6], Harlan Spence[5] (1.Tohoku University, 2.ISEE, Nagoya University, 3.University of Electro-Communicants, 4.National Institute of Polar Research, 5.University of New Hampshire, USA, 6.JAXA/ISAS)

[PEM09-P19] Analysis of Langmuir waves caused by Chorus observed by the Arase satellite

*Towa Yoshida[1], Satoshi Kurita[2], Takahiro Zushi[1], Hirotsugu Kojima[2], Yoshiya Kasahara[3], Shoya Matsuda[4], Ayako Matsuoka[5] (1.National Institute of Technology, Nara College, 2.Research institute for sustainable humanosphere, Kyoto University, 3.Information Media Center, Kanazawa University, 4.Institute of Space and Astronautical Science/Japan Aerospace Exploration Agency, 5.Data Analysis Center for Geomagnetism and Space Magnetism, Graduate School of Science, Kyoto University)

[PEM09-P20] Mode identification of MHD waves observed by the SuperDARN radars using the Lomb-Scargle analysis

*Koki Morita[1], Nozomu Nishitani[1], Tomoaki Hori[1] (1.Institute for Space-Earth Environmental Research, Nagoya University)

[PEM09-P21] Progress in the full-automatic identification of FLR events in VLOS of multiple SuperDARN radars

*Hideaki Kawano[1,2], Akira Sessai Yukimatu[3,4], Nozomu Nishitani[5], Yoshimasa Tanaka[3,4], Satoko Saita[6], Tomoaki Hori[5] (1.Department of Earth and Planetary Sciences, Kyushu University, 2.ICSWSE, Kyushu University, 3.National Institute of Polar Research, 4.SOKENDAI, 5.ISEE, Nagoya University, 6.Kitakyushu College)

[PEM09-P22] Initial results from an induction magnetometer observation at Middlemarch (L = 2.7) in New Zealand

*Yuki Obana[1], Kaori Sakaguchi[2], Masahito Nose[3], Keisuke Hosokawa[4], Kazuo Shiokawa[3], Martin Connors[5], Akira Kadokura[6], Tsutomu Nagatsuma[2] (1.Department of Engineering Science, Faculty of Engineering, Osaka Electro-Communication University, 2.National Institute of Information and Communications Technology, 3.Institute for Space-Earth Environmental Research, Nagoya University, 4.Department of Communication Engineering and Informatics, University of Electro-Communications, 5.Centre for Science, Faculty of Science and Technology, Athabasca University, 6.National Institute of Polar Research)

[PEM09-P23] Detection of Pi2 geomagnetic pulsation by machine learning and development of real-time substorm warning system

Yusuke Sakai[1], *Masahito Nose[1], Hiroshi Ichihara[2], Genta Ueno[3], Naoto Nakano[4] (1.Institute for Space-Earth Environmental Research, Nagoya University, 2.Graduate school of environmental studies, Nagoya University, 3.Institute of Statistical Mathematics, Research Organization of Information and Systems, 4.Institute for Liberal Arts and Sciences, Kyoto University)

[PEM09-P24] Current Status of the FACTORS mission for the Space-Earth Coupling System Exploration

*Masafumi Hirahara[1], Yoshifumi Saito[2], Hirotsugu Kojima[3], Kazushi Asamura[2], Takeshi Sakanoi[4], Yoshizumi Miyoshi[1], Naritoshi Kitamura[5], Masatoshi Yamauchi[6], Yoshihide Sugimoto[7] (1.Nagoya Univ., 2.JAXA, 3.Kyoto Univ., 4.Tohoku Univ., 5.Univ. Tokyo, 6.IRF, 7.LSAS Tec Co., Ltd.)

[PEM09-P25] Future formation-flight satellite mission FACTORS: Development of far-ultra-violet imagers and simulation of Alfven wave observations

*Takeshi Sakanoi[1], Mizuki Fukizawa[1], Masafumi Hirahara[2], Yoshizumi Miyoshi[2], Kazushi Asamura[3], Yoshifumi Saito[3], Hirotsugu Kojima[4], Naritoshi Kitamura[5], Takanori Nishiyama[6], Kiyoka Murase[6], Miki Kawamura[1], Kaori Sakaguchi[7], Mamoru Ishii[7], Harald U Frey[8], Nick Schneider[9] (1.Planetary Plasma and Atmospheric Research Center, Graduate School of Science, Tohoku University, 2.ISEE, Nagoya University, 3.ISAS, JAXA, 4.RISH, Kyoto University, 5.Graduate School of Science, University of Tokyo, 6.NIPR, 7.NICT, 8.SSL, University of California, Berkeley, 9.LASP, University of Colorado Boulder)

[PEM09-P26] Future formation-flight mission FACTORS: Development of plasma particle instruments and evaluation of electric field measurements with short electric field sensors

*Kazushi Asamura[1], Hirotsugu Kojima[2], Taku Namekawa[1], Takefumi Mitani[1], Motoyuki Kikukawa[2], Ibuki Fukasawa[2], Satoshi Kurita[2], Yuki Miyake[2], Hideyuki Usui[3] (1.ISAS / JAXA, 2.RISH, Kyoto University, 3.Kobe University)

[PEM09-P27] Current status of development of multi-spectral auroral camera on the LAMP rocket experiment

*Miki Kawamura[1], Takeshi Sakanoi[1], Kazushi Asamura[2], Yoshizumi Miyoshi[3], Keisuke Hosokawa[4], Sarah Jones[5], Marc Lessard[6] (1.Tohoku University, 2.JAXA,ISAS, 3.ISEE, Nagoya University, 4.University of Electro-Communicants, 5.GSFC/NASA, USA, 6.University of New Hampshire, USA)

[PEM09-P28] Development of wideband impedance probe for measurement of the ion composition in the ionosphere and magnetosphere

*Atsushi Kumamoto[1] (1.Graduate School of Science, Tohoku University)

[PEM09-P29] Numerical design of double-shell electrostatic energy analyzer with hemispherical field of view

*Atsuya Takasu[1], Masafumi Hirahara[1], Shoichiro Yokota[2] (1.Institute of Space-Earth Environmental Research, Nagoya University, 2.Graduate School of Science, Osaka University)

[PEM09-P30] Development of SDR-based scintillation detector system and observation with magnetometer and radar

*Shuji Abe[1], Akiko Fujimoto[2], Akimasa Yoshikawa[3,1] (1.International Center for Space Weather Science and Education, Japan, 2.Kyushu Institute of Technology, 3.Department of Earth and Planetary Sciences, Kyushu University)

[PEM09-P31] Application of magneto-impedance sensor to geomagnetic field measurements for constructing Distributed Arrays of Small Instruments (DASI)

Nomura Hiroshi[1], *Masahito Nose[1], Hitoshi Aoyama[2], Takeshi Kawano[2], Hiroshi Ichihara[3], Masafumi Hirahara[1] (1.Institute for Space-Earth Environmental Research, Nagoya University, 2.Aichi Steel Corporation, 3.Graduate school of environmental studies, Nagoya University)

[PEM09-P32] Closure of the Onagawa Magnetic Field Observatory of Tohoku University

*Takahiro Obara[1], Takeshi Sakanoi[1], Yasumasa Kasaba[1], Fuminori Tsuchiya[1], Hiroaki Misawa[1], Masato Kagitani[1], Aya Otomo[1] (1.Planetary Plasma and Atmospheric Research Center,Tohoku University)

Development of a 3-dimensional global ionospheric electrostatic potential solver using IGRF model

*Takuya Ijuin[1], Akimasa Yoshikawa[2]

1. Department of Earth and Planetary Sciences, Graduate School of Science, Kyushu University, 2. Department of Earth and Planetary Sciences, Kyushu University

In order to investigate a magnetosphere-ionosphere-atmosphere coupling system, we developed a global ionospheric electrostatic potential solver that implements the international geomagnetic reference field (IGRF) model [e.g., Alken et al., 2020] as the background magnetic field structure by adopting the magnetic apex coordinates [VanZandt et al., 1972; Richmond, 1995]. By assuming equipotentiality of magnetic field lines, this solver can be reconstructed 3-demensional distribution of electric field and current density after solving electrostatic potentials with 2-demensional elliptic partial differential equations. Input parameters of the solver are the neutral wind that gives dynamo electric fields in the atmosphere-ionosphere coupled system, and distribution of field-aligned currents (FACs) at the high-latitudinal region (Region-1 FAC and Region-2 FAC) that gives boundary condition coupling to the magnetospheric dynamics. At the present stage, we calculate a distribution of conductivities by using NRLMSISE-00 [Picone et al., 2002] and IRI-2016 [Bilitza et al., 2017] for electron number densities and temperatures, and Ieda [2020] for collision frequencies.

Most of conventional potential solver has been adopted uniform and/or dipole magnetic field model. Moreover, ionosphere is regarded as an infinitely thin layer. Such approximation can be validated at high latitude ionosphere. However, at low and mid latitudinal region, there exist big differences between dipole field and realistic magnetic field and 3-dimensional coupling between ionosphere and atmosphere is inevitably required.

The newly developed solver is not only highly suitable for the MHD simulator through the magnetosphere-ionosphere coupling at high latitudes, but also enables us to reproduce the ionosphere-atmosphere coupling dynamics at mid and low latitudes. In this talk, we will introduce the details of the development process of this solver and report the initial results of numerical simulations.

Keywords: potential solver, ionospheric simulation, magnetosphere-ionosphere-atmosphere coupling

©2021. Japan Geoscience Union. All Right Reserved.

Study on the Solar Flare Effect (SFE*) of equatorial electrojet around local noon

*Akihiro Yasunaga[1], Akiko Fujimoto[2], Akimasa Yoshikawa[1]

1. Department of Earth and Planetary Sciences, Kyushu University, 2. Kyushu Institute of Technology

X-rays and ultraviolet rays associated with solar flares reach the Earth and stimulate an ionization of neutral particles in the daytime ionosphere, which changes the ionospheric current in a very short time, and this effect can be observed as drastically changing geomagnetic field perturbations [Campbell, 2003]. There are two types of magnetic field perturbations: positive SFE, in which the magnetic field becomes stronger than just before a solar flare, and negative SFE*, in which the magnetic field becomes weaker [Yamazaki et al., 2009].

Rastogi et al. (1996) stated that the positive variation of the magnetic field (SFE)through the equatorial region is a result of the enhanced equatorial electrojet (EEJ), while the negative variation (SFE*) the morning and evening side of dip-equator is a result of the enhanced counter electrojet (CEJ).

However, generation of SFE* around local noon dip equator is also reported [Rastogi et al., 2003; Yamazaki et al., 2009; Rastogi et al., 2013]. Yamazaki et al. (2009) reported two unique SFE*events. They suggested that this phenomenon may be caused by an increase in electrical conductivity in the lower part of the E layer due to X-class flares and the penetration of a westward electric field into the magnetic equatorial region due to the northward turning of the interplanetary magnetic field (IMF) Bz. On the other hand, Rastogi et al. (2013) examined the same event and proposed that this type of SFE* was enhanced partial CEJ by solar flares. However, reports on SFE* to date are limited, and it remains an open question what kind of ionospheric environment causes SFE*.

To clarify the generation mechanism of the unique SFE*, it is indispensable to understand the detailed structure of the ionospheric current system. The purpose of this study is to understand the generation mechanism of unique SFE* around noon time by developing a methodology that can quantitatively analyze the geomagnetic variations during solar flares times.

As a first step of this study, we visualize the ionospheric currents using the equivalent current method on MAGDAS/CPMN (Global Observation Network) geomagnetic data. Furthermore, by verifying the correlation between the Z-component and the fluctuation of the vector field of the Sq equivalent current system, we expect to understand the structure and development process of the current system before and after the SFE* occurrence. In this presentation, we will report the initial results of our analysis.

Keywords: Solar flare effect(SFE*), Equatorial Electrojet, Sq current

©2021. Japan Geoscience Union. All Right Reserved.



©2021. Japan Geoscience Union. All Right Reserved.

Consideration of the CubeSat for Observation of IHFAC at LEO

*Kentarou Kitamura[1], Taku Takada[2], Kazumasa Imai[2], Manabu Shinohara[3], Makoto Wakabayashi[4], Akiko Fujimoto[1], Mariko Teramoto[1]

1. Kyushu Institute of Technology, 2. NIT, Koti College, 3. NIT, Kagoshima College, 4. NIT, Niihama College

A current pattern in the dayside ionosphere during solar quiet time is well known as the Sq current system. The Sq current is mostly generated by the diurnal tidal mode of the neutral wind, also has an obvious seasonal variation on its current pattern due to the seasonal variations of ionospheric electric conductivities. In general, the vortex current is stronger (weaker) in the summer (winter) hemisphere. This feature indicates that the potential of the Sq current shows the north/south asymmetry depending on the seasons. In order to eliminate the potential asymmetry between the both hemispheres, Inter-Hemispheric Field Aligned Currents (IHFACs) is considered to flow between the both hemispheres. The IHFAC was first theoretically expected by Maeda [1974] and Fukushima [1979, 1991], then several observations by the satellites [Yamashita and Iyemori, 2002, and Park et al., 2002, 2020], and global ground magnetic observation networks [Yamazaki et al., 2009, Owolabi et al., 2018]. On the other hand, such 3D currents system is also strongly affected by the electric field imposed on the polar ionosphere which is consequence of the magnetosphere-ionosphere couplings. Therefore, the accurate monitoring of the 3D Sq current system is quite important to understand the comprehensive multi-scale coupling in the space weather sciences.

In this study, we propose the CubeSat project which make in-situ observation of the Sq current system including IHFAC at the LEO in the altitude of ~400km. The feasibility of CubeSat with 2U-size structure is considered for the electric power budget, communication capability, and specification of the magnetometer. In particular, the several kinds of magnetometer are considered to onboard the CubeSat for in-situ magnetic field measurement with an accuracy of less than 1 nT. The result of the feasibility study shows that the observation of the Sq current by CubeSat is enough considerable with a short duration of the development and quite low-cost.

Keywords: CubeSat, Interhemispheric FAC, Sq

©2021. Japan Geoscience Union. All Right Reserved.

Initial results of multi-event analysis of magnetosphere-ionosphere coupling for nighttime medium-scale traveling ionospheric disturbances

*Kouki Kawai[1], Kazuo Shiokawa[1], Yuichi Otsuka[1], Shin-ichiro Oyama[1,2,3], Martin G Connors[4], Yoshiya Kasahara[5], Yasumasa Kasaba[6], Atsuki Shinbori[1], Fuminori Tsuchiya[6], Atsushi Kumamoto[6], Masahiro Kitahara[1], Masafumi Shoji[1], Satoko Nakamura[1], Ayako Matsuoka[7], Shun Imajo[1], Yoichi Kazama[8], Shiang Yu Wang[8], Sunny W. Y. Tam[9], Tzu-Fang Chang[9], B J wang[8], Kazushi Asamura[10], Satoshi Kasahara[11], Shoichiro Yokota[12], Kunihiro Keika[11], Tomoaki Hori[1], Chae-Woo Jun[1], Iku Shinohara[10], Yoshizumi Miyoshi[1]

1. Institute for Space-Earth Environmental Research, Nagoya University, Japan, 2. University of Oulu, Oulu, Finland, 3. National Institute of Polar Research, Tokyo, Japan, 4. Athabasca University, Canada, 5. Kanazawa University, Kanazawa, Japan, 6. Tohoku University, Sendai, Japan, 7. Kyoto University, Kyoto, Japan, 8. Academia Sinica, Taipei, Taiwan, 9. National Cheng Kung University, Tainan, Taiwan, 10. Institute of Space and Astronautical Science, Japan Aerospace Exploration Agency, Sagamihara, Japan, 11. Tokyo University, Tokyo, Japan, 12. Osaka University, Osaka, Japan

Medium-scale traveling ionospheric disturbances (MSTIDs) are propagating fluctuations of the electron density in the F-region ionosphere and can cause significant influence in the positioning using satellites such as Global Positioning System (GPS). MSTIDs generated by the E-region–F-region coupling and Perkins instabilities show mirrored structures at magnetically conjugate points in the two hemispheres at middle latitudes [e.g., Otsuka et al., GRL, 2004]. In such a case, the electric field variations associated with the MSTIDs probably mapped to the other hemisphere along geomagnetic field lines and they can be observed by magnetospheric satellites. Previously we have reported one such event of the conjugate observation of MSTIDs with the Arase satellite (Kawai et al., JpGU-AGU2020, 2020; Kawai et al., submitted to JGR, 2021). On the other hand, this study reports initial results on the analysis of four events with simultaneous observations of MSTIDs made by the Arase satellite and airglow imagers operated at Athabasca (54.60˚N, 246.36˚E), Canada on February 25, 2020, at Gakona (62.39˚N, 214.78˚E), Alaska on February 26, 2019, and at Kapuskasing (49.39˚N, 277.81˚E), Canada on January 11 and 26, 2019. In the first event at Athabasca, the Arase satellite observed electric field variations associated with airglow intensity deviations, similar to that reported by Kawai et al. [2021]. We projected these electric field variations onto the ionosphere, the direction of the **E×B** drift derived with the background magnetic field showed the opposite senses between bright and dark structures of the airglow intensity deviation of the MSTIDs taken by the airglow camera. However, electron density fluctuations observed the Arase did not clearly correspond to the airglow intensity deviation of MSTIDs. Similar analyses for the other three events are underway. As preliminary results, we found that the Arase did not necessarily observe the characteristic variations of the magnetospheric electric field variations and electron density fluctuations associated with the MSTID structures. Based on these results, our scientific objective is to reveal the necessary conditions under which variations of the electric field and electron density associated with MSTIDs propagate to the magnetosphere.

Keywords: medium-scale traveling ionospheric disturbances, magnetosphere-ionosphere coupling, the Arase satellite, airglow imager

©2021. Japan Geoscience Union. All Right Reserved.

Development of a new M-I coupling algorithm in global MHD magnetosphere simulation: Alfvénic-Coupling

*Aoi Nakamizo[1], Akimasa Yoshikawa[2], Hiroyuki Nakata[3], Keiichiro Fukazawa[4], Takashi Tanaka[2]

1. Applied Electromagnetic Research Institute, National Institute of Information and Communications Technology, 2. Faculty of Science, Kyushu University, 3. Faculty of Engineering, Chiba University, 4. Academic Center for Computing and Media Studies, Kyoto University

Presently, most global MHD magnetosphere models equip ionospheric solvers at their inner boundaries and then simulate the magnetospheric and ionosphere (M-I) processes. Here the ionospheric solver is the so-called 'thin shell model' which solves the Ohm’s law under the thin shell approximated ionosphere with FACs in the polar region and the height-integrated ionospheric conductivity. With this solver, the global MHD models solve the inner boundary condition of electromagnetic field in the following manner. (1) The FAC distribution obtained from the rotation of the magnetic field at the inner boundary (usually placed at the altitude of 2–3 Re) is mapped to the ionospheric altitude. (2) The mapped FAC is inputted to the solvers equipped at the ionospheric altitude, then the ionospheric potential is calculated. (3) The potential is mapped back to the inner boundary and the bulk velocity is updated there.
On the other hand, Yoshikawa et al. [2010] proposed a new M-I coupling algorithm which guarantees the continuities of physical quantities between the magnetosphere and ionosphere and therefore the momentum and energy conservations by considering the incident and reflection process of shear Alfvén waves. We call the new algorithm ‘Alfvénic-coupling.’ We discuss in detail the characteristics of the traditional algorithm and the concept of Alfvénic-coupling algorithm. We report on the progress of the implementation of Alfvénic-coupling in a global MHD code and will show the preliminary results.

Reference

Yoshikawa, A., H. Nakata, A. Nakamizo, T. Uozumi, M. Itonaga, S. Fujita, K. Yumoto, and T. Tanaka, Alfvenic-coupling algorithm for global and dynamical magnetosphere-ionosphere coupled system, J. Geophys. Res., 115, A04211, 2010, dot:10.1029/2009JA014924.

Keywords: M-I Coupling, Global Magnetosphere Simulation, Alfven Mode, Algorithm

©2021. Japan Geoscience Union. All Right Reserved.

Understanding the 3-dimensional current between the magnetosphere and the ionosphere<gdiv></gdiv>

*Yuto Yano[1], Yusuke Ebihara[1]

1. Research Institute for Sustainable Humanosphere, Kyoto University

We developed a simplified 3-dimensional Hall-MHD simulation in order to understand the magnetosphere-ionosphere coupling in the polar region during the auroral substorm. The governing equations were derived from the law of conservation of momentum of ions and electrons, the equation of continuity of plasma, the law of Ohm, the law of Ampere, and the law of Faraday. The Hall effect is included because it retains the Hall term in the governing equations. The advection in the governing equations is solved by using the implicit scheme and the Lax-Wendroff scheme and the Superbee limiter function. We employed two different initial conditions, case 1 and case 2. In case 1, the density is uniform. In case 2, the density was enhanced in a longitudinally elongated region. An electric field perturbation is applied to the upper boundary of the simulation box, which represents a part of the magnetospheric convection with shear. The Alfven wave was launched by the shear, and propagated downward accompanied with field-aligned currents (FACs). In case 1, most of the FACs are closed primarily by the Pedersen current. A part of them are closed by the Hall current, which is presumably associated with the induction effect. In case 2, the FACs are closed by the Pedersen current and the Hall current as well. Additional FACs are generated at low altitudes, which are presumably associated with the polarization effect. We discuss the roles of the induction and the polarization effects in the 3-dimensional closure of the current<gdiv></gdiv>

Keywords: Polarization, Magnetosphere-Ionosphere Coupling

©2021. Japan Geoscience Union. All Right Reserved.

Magnetospheric dynamics under northward IMF conditions surveyed by concurrent observations of TPA and omega-band aurora

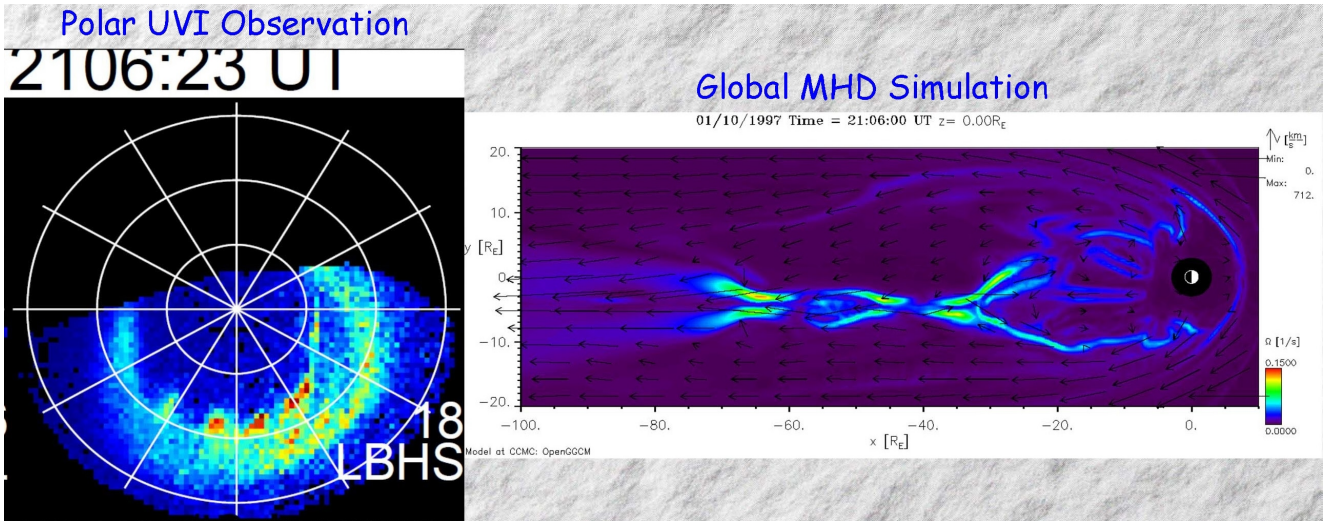
*Motoharu Nowada[1], Yukinaga Miyashita[2,3]

1. Shandong Key Laboratory of Optical Astronomy and Solar-Terrestrial Environment, School of Space Science and Physics, Institute of Space Sciences, Shandong University at Weihai, P. R. China, 2. Korea Astronomy and Space Science Institute, Daejeon, South Korea, 3. Korea University of Science and Technology, Daejeon, South Korea

Nightside magnetospheric processes (dynamics) directly reflect to auroral morphology and type. By investing type of auroras and the auroral morphological changes, we can expect to understand what physical processes would take place in the magnetotail. Under northward Interplanetary Magnetic Field (IMF) conditions, transpolar arcs (TPAs) and omega-band aurora can be observed. A source of TPA is considered as field-aligned currents induced by the plasma flow shear (including the plasma flow vortices) between the fast plasma flows generated by magnetotail magnetic reconnection and slower background magnetospheric plasma flows. On the other hand, it is well-known that omega-band aurora is also likely to be formed by the field-aligned current induced by the flow shear in the magnetotail, such as the Kelvin-Helmholtz instabilities. Based on the contemporaneous observations of TPA and omega-band aurora, we try to investigate (diagnose) how the plasma and its energy are transported in the nightside magnetosphere toward ionosphere under northward IMF conditions. On January 10th, 1997, transpolar arc (TPA) and omega-band aurora contemporaneously occurred for about 5.5 hours between 17:58 UT and 22:23 UT even when Interplanetary Magnetic Field (IMF) orientation changed from weakly southward to northward at ~21:00 UT. Because no in-situ magnetotail observations were unfortunately found in this day, we performed global MHD simulations based on the Open Geospace General Circulation Model (Open GGCM) distributed in the Community Coordinated Modeling Center (CCMC), and discussed the physical relation between two different auroral appearances and nightside magnetospheric processes. In this simulation, after the IMF-B_z orientation turned from weakly southward to northward, clear flow shear between fast earthward plasma flows triggered by magnetotail reconnection and slower tailward background magnetospheric flows was seen around X_{gsm} ~ -40 Re in the dawn sector, being consistent with the TPA and omega-band auroral brightening. These flow shears may be a “source” of field-aligned currents to form the TPA. Furthermore, they bifurcated toward dawn and dusk, and showed stronger vortices in the dusk region than those in the dawnward sector. These vortex(-like) structures, bifurcated duskward, and associated field-aligned currents would be linked to the formation of the omega-band aurora. In this presentation, we will discuss further the relation between the variations of these flow shear (vortex) structures, TPA and omega-band auroral formations under northward IMF conditions, followed by weak southward IMF intervals.

Keywords: Transpolar arc and omega band aurora, Solar wind-magnetotail-ionosphere coupling, Magnetospheric diagnosis, Magnetospheric dynamics under northward IMF conditions

©2021. Japan Geoscience Union. All Right Reserved.



©2021. Japan Geoscience Union. All Right Reserved.

The terrestrial magnetosphere for zero interplanetary magnetic field

*Tsubasa Hashimoto[1], Masakazu Watanabe[2], Ryuho Kataoka[3], Shigeru Fujita[4], Takashi Tanaka[5]

1. Department of Earth and Planetary Sciences, Graduate School of Science, Kyushu University, 2. Department of Earth and Planetary Sciences, Faculty of Science, Kyushu University, 3. National Institute of Polar Research, 4. Meteorological College, Japan Meteorological Agency/ National Institute of Polar Research, 5. International Center for Space Weather Science and Education

The solar wind energy is transported to the magnetosphere-ionosphere system via energy conversion. In particular, the interplanetary magnetic field (IMF) has a large effect on the solar wind-magnetosphere interaction. If the magnetosphere is totally closed in terms of magnetic field topology, in ideal magnetohydrodynamics, there is no solar wind energy flowing into the magnetosphere. One important element determining the energy inflow rate is the connectivity of the geomagnetic field and the IMF, namely, magnetic reconnection between the two fields. For southward IMF, reconnection occurs on the nose of the magnetosphere. The solar wind energy enters the magnetosphere effectively, producing magnetic storms, auroral substorms, and so forth. Meanwhile, for northward IMF, reconnection occurs on the high-latitude magnetopause. Though not so effective as for southward IMF, the solar wind energy also enters the magnetosphere, producing phenomena specific to northward IMF periods such as theta auroras. Thus, it is expected in the real magnetosphere that the energy inflow is minimized when the IMF is northward and extremely small (say B=0.1nT). However, prolonged periods of such IMF are of very rare occurrence, and consequently observational studies are virtually impossible. In this study, therefore, we performed a numerical simulation using the Reproduce Plasma Universe (REPPU) code (Tanaka, 2015) and reproduced a magnetosphere under northward and extremely small IMF conditions. We set the IMF magnitude to 0.1nT and the IMF clock angle (measured from due north) to 30°in the simulation. The conclusions of this study are summarized as follows.

(i) Reconnection occurs on the high-latitude magnetopause near the cusp. Although the IMF is northward, this reconnection is Dungey-type reconnection for southward IMF that converts the closed magnetic flux to open magnetic flux. We also found so-called merging cells in the ionosphere resulting from Dungey-type reconnection. However, the contribution of the merging cells to the cross polar cap potential is very small (a few kilovolts).

(ii) Ionospheric convection exhibits the normal twin-cell pattern. The cross polar cap potential (a few tens of kilovolts) is contributed mostly by the convection cells circulation exclusively in the closed field line region (so-called "viscous cells").

(iii)The main energy flow route from the solar wind to the ionosphere is similar to that for southward IMF conditions. The solar wind flow energy is first converted to the thermal energy in the magnetosheath. The thermal energy is then converted to the motional energy of a flow toward the cusp (mainly field-aligned), and then to the thermal energy of the cusp. At the high-latitude boundary layer behind the cusp, the thermal energy finally transmutes into the electromagnetic energy driving the R1 FAC system. Thus, the convection cells that appear in the closed field line region of the ionospheric are not the consequences of the viscous-like interaction in the low-latitude boundary layer between the solar wind and the magnetosphere, as conventionally thought to be the origin of the “viscous cells” (Axford & Hines, 1961). Instead, the energy supply mechanism for the “viscous cells” is basically the same as that for the merging cells for southward IMF. The role of reconnection is to make the magnetosphere topologically open to enable the entry of the solar wind energy into the magnetosphere and the subsequent formation

©2021. Japan Geoscience Union. All Right Reserved.

of the cusp. As long as the magnetosphere is topologically open, be it ever small, a closed magnetic flux circulation is formed in the magnetosphere-ionosphere system by the energy supply mechanism though the cusp.

Keywords: northward interplanetary magnetic field, viscous cell, cross polar cap potential

©2021. Japan Geoscience Union. All Right Reserved.

Cusp ion precipitation for stably northward IMF and its relation to the magnetosheath flow

*Haruto Koike[1], Satoshi Taguchi[1]

1. Department of Geophysics, Graduate School of Science, Kyoto University

Magnetic reconnection can occur at the high latitude of the cusp, where magnetosheath field lines and magnetospheric lobe field lines are antiparallel when the interplanetary magnetic field(IMF) is northward. Magnetosheath plasmas are injected into the cusp through this type of reconnection, i.e., lobe reconnection for northward IMF, and often produce localized aurora poleward of the usual auroral oval location. Previous studies have shown that the intensity of such proton auroras becomes greater as solar wind dynamic pressure increases, suggesting that the number flux of precipitating ions in the cusp increases as solar wind dynamic pressure increases. Since the quantity of solar wind dynamic pressure consists of solar wind density and solar wind velocity, the dynamic pressure dependence is due to the solar wind density dependence to a certain degree. For solar wind velocity, considering that lobe reconnection occurs in the presence of stronger shear flow as magnetosheath flow speed increases, it may be expected that solar wind velocity can also be a controlling parameter for the cusp ion injection. In this study, we examine how solar wind velocity is related to the cusp ion precipitation. We have analyzed precipitation particle data obtaind by DMSP F16 and F17 in the low-altitude cusp for 5 years, and identified more than 500 cusp events that occured during stably northward IMF periods, using our automated event identification method. The result of the analysis suggests that the ion outflow jet from reconnection tends to be strong as the sheath protons stream fast on lobe reconnection. We discuss how the streaming protons interact with the process in the lobe reconnection.

Keywords: cusp, northward IMF, lobe reconnection, ion precipitation, cold streaming protons

©2021. Japan Geoscience Union. All Right Reserved.

Topology and geometry of interchange-type reconnection in the terrestrial magnetosphere

*Masakazu Watanabe[1], Tomoya Asano[1], Dongsheng Cai[2], Peikun Xiong[2], Shigeru Fujita[3], Takashi Tanaka[1]

1. Kyushu University, 2. University of Tsukuba, 3. Meteorological College

Reconnection in which the topological regions of the two reconnecting field lines interchange at the time of reconnection is referred to as “interchange-type reconnection.” There exist two kinds of interchange-type reconnection in the terrestrial magnetosphere. One is reconnection of an interplanetary magnetic field (IMF) line and a lobe field line, and the other is reconnection of a lobe field line and a closed field line. For northward IMF, these two processes play a vital role in the convection system and form the “interchange cycle” associated with an ionospheric convection cell circulating exclusively in the closed field line region (called the “reciprocal cell”). Interchange-type reconnection occurs on a portion of the separatrix that is away from the separator, which contrasts with Dungey-type reconnection that occurs just on the separator. Despite of its importance, our understanding of the topological and geometrical nature of interchange-type reconnection is far from complete. The purpose of this study is to clarify the magnetic topology and geometry of interchange-type reconnection in the terrestrial magnetosphere using global magnetohydrodynamic (MHD) simulation. With the Reproduce Plasma Universe (REPPU) code, we obtained a quasi-steady magnetosphere associated with reciprocal cells under the IMF conditions of B=6nT (total intensity) and θ =20° (clock angle). The global magnetic topology of the magnetosphere is characterized by two magnetic null points and two separators connecting the nulls (which we call the separator circle). We tracked the separatrix surface emanating from each null, using the geodesic level set algorithm described by Krauskopf & Osinga (1999). The two diffusion regions on the separatrix surface (one to the dawnward of the separator circle and the other to the duskward of the separator circle) are both situated on a line passing through the null point elongating in the dawn-to-dusk direction. Each linear diffusion region corresponds to the so-called X line. The direction of the plasma flow passing through the separatrix surface reverses on the X line. We also determined the geometric configuration of the reconnecting and reconnected field lines near the X line. From the field line topology and the X line location, interchange-type reconnection is interpreted to be a variant of “fan reconnection” analytically modelled by Priest & Titov (1996).

Krauskopf & Osinga (1999). Chaos 9, 768–774. https://doi.org/10.1063/1.166450

Priest & Titov (1996). Phil. Trans. R. Soc. A.354, 2951–2992. http://doi.org/10.1098/rsta.1996.0136

Keywords: magnetic field topology, interchange reconnection, MHD simulation

©2021. Japan Geoscience Union. All Right Reserved.

Understanding the behavior of charged particles in plasma by vector potential

*Shinji Karasawa[1]

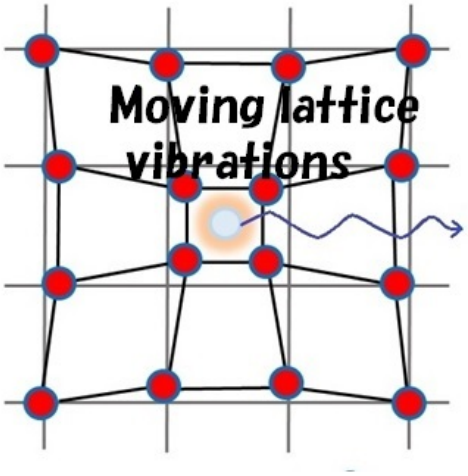
1. Miyagi National College of Technology Professor emeritus

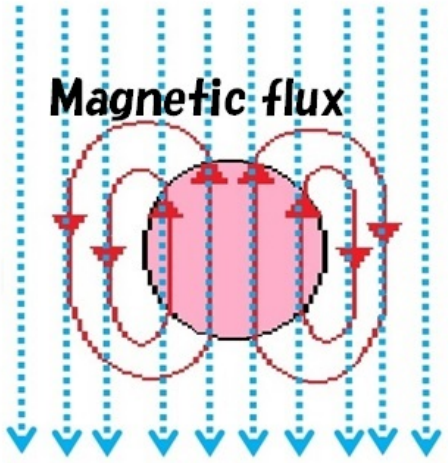
Geomagnetism is caused by the movement of charged particles. If the magnetic field is assumed at first, the effect of protons in solar wind on the Earth will be ignored. Because electrons are affected by the magnetic field and the electrons act as repulsive forces to protons. However, in practice, the behavior of protons will affect the motion of electrons. Aharonov–Bohm effect indicates that motion of particles must be considered first in a plasma. In a superconducting magnet, moving electrons are covered with positive ion lattice vibrations and the positive charges of vibration together with electrons and the lattice vibrations emits vector potentials. Although the magnetic field by the lattice vibration offsets internally, it exhibits a magnetic levitation [1].
The electrostatic potential (V) gives energy (U=q・V) for a charge (q), while the vector potential (**A**) gives energy (U= - **i** ・**A**) for a current (**i**). Since a line integral of (**B**) becomes **A**, **B**= rot **A**. Since d**B**/dt=- rot **E**, we get d**A**/dt=- **E**. In high-speed charged particles running side by side, if the polarity is the same particles, they attract each other as parallel currents, and when the polarity is different, they repel with anti-parallel currents. In the Sun's plasma, charged particles of high-speed motion create a structure. But the Sun has an escape rate of 617.5 km/sec, and most of the charged particles are pulled back by gravity to form an arc.
The Earth has Van Allen radiation belt, which consists of outer belt, slot region and inner belt. In addition, there is another slot region between the inner belt and ionosphere. Such layered structure is formed by high-speed charged particles.
Earth's gravity can't hold hydrogen. The Sun's electromagnetic waves ionize nitrogen and oxygen at the daytime hemisphere to form the ionosphere. The ionosphere with a lot of free electrons orbits the Earth, and it will form the geomagnetism. On the other hand, Jupiter and Saturn are covered with hydrogen, and hydrogen ions of the solar wind invade, and the atmosphere containing a lot of positive ions rotates counterclockwise direction. So, the geomagntism of Jupter and Saturn is oposite to the Earth.
On the Earth, auroras occur in the annular region around 75 degrees in the daytime hemisphere of the Earth and 65 degrees on the nighttime hemisphere. On the daytime hemisphere where there are many electrons generated by X-rays and ultraviolet rays from the Sun, auroral emission is weak and the area where auroras occur moves to the high latitude side. The area where the geomagnetic magnetic force line enters the ground perpendicularly is off the polar axis and it is an annular shape. The aurora always shakes. Such geomagnetism is not caused by the movement of material in the Earth's interior, but the current of electrons induced in the Earth's interior contributes to the geomagnetism.
[1] S. Karasawa, "Mechanism of superconducting magnet”, 2021, 3/Feb, https://www.youtube.com/watch?v=-ETMJ0Pr-8w

Keywords: Vector potential, Aharonov–Bohm effect,, Plasma, Geomagnetism , Van Allen radiation belt, Auroras

©2021. Japan Geoscience Union. All Right Reserved.

Mechanism of *superconducting magnet*





The principle of superconductivity has been elucidated by quantum mechanics, but the mechanism of superconducting magnets has not yet been elucidated. However, we are able to understand the mechanism by thinking about behaviors of charged particles involved.

©2021. Japan Geoscience Union. All Right Reserved.

Properties of dispersive Alfven waves and their roles in electron acceleration process in the terrestrial magnetosphere based on Plasma Distribution Solver

*Koseki Saito[1], Yuto Katoh[1], Atsushi Kumamoto[1], Tomoki Kimura[1], Yohei Kawazura[1]

1. Department of Geophysics, Graduate School of Science, Tohoku University

Observations from the FAST satellite revealed the downward electrons in the energy range from tens of eV to a few keV in the terrestrial high latitude region [Chaston et al., 2002]. It is suggested that “Alfvenic acceleration” process by dispersive Alfven waves is responsible for the auroral electron acceleration. Alfvenic acceleration has also attracted attention as the electron acceleration mechanism in Jupiter [e.g., Mauk et al., 2017; Saur et al., 2018], and the importance of Alfvenic acceleration in the auroral acceleration process in magnetized planets is increasing. While Alfvenic acceleration occurring in the terrestrial environment has been studied for decades [e.g., Chaston et al., 2002; Watt et al., 2006], physical processes controlling the characteristic energy and pitch angle distributions have been still unclear.

For the study of the efficiency and energy dependence of Alfvenic acceleration, understanding of the characteristics of dispersive Alfven waves is essential. In the present study, we quantitatively examine the characteristics of dispersive Alfven waves and their spatial variation in the magnetosphere by using originally developed “Plasma Distribution Solver”, which calculates the plasma and pressure distributions along a magnetic field line. We use results from three different conditions; Case 1 (L=4, Ne_eq=240 cm^{-3}), Case 2 (L=4, Ne_eq=24 cm^{-3}), and Case 3 (L=15, Ne_eq=12 cm^{-3}), where Ne_eq is the electron number density at the magnetic equator, and the background magnetic field is assumed to be a dipole field. First, the ratio of the plasma pressure to the magnetic pressure (plasma β) is calculated to determine whether kinetic or inertial Alfven wave dispersion relation should be used at each position along a magnetic field line. As a result, the characteristics of kinetic Alfven waves appears in the Case 1 in the region below 20 degrees of the magnetic latitude, and the kinetic Alfven wave region extends up to about 30 and 50 degrees of magnetic latitude in Cases 2 and 3, respectively.
Next, with the aim of considering the effect of Alfvenic acceleration on high-energy electrons, we investigate the relationship between the Larmor radius of energetic electrons and the perpendicular wavelength of dispersive Alfven waves, referring to the discussion in Chaston et al. (2004). Chaston et al. studied the relationship between the wavelength of the dispersive Alfven wave and the spatial scale of the cyclotron motion of ions, and showed that stochastic acceleration can occur when the wavelength perpendicular to the background magnetic field is smaller than the ion Larmor radius. In Case 1, the Larmor radius of electrons at 100 keV is larger than that thermal ions at the magnetic equator, and the effect of kinetic Alfven waves is expected to be significant. On the other hand, the Larmor radius of 100 keV electrons is smaller than that of thermal ions, suggests limited effect of kinetic Alfven waves in Case 2. In Case 3, the effect of kinetic/inertial Alfven waves is expected for 100 keV electrons in the region of 20-60 degrees magnetic latitude. In this presentation, we also discuss the energy dependence of the electron acceleration process with the results obtained by the Plasma Distribution Solver.

Keywords: Terrestrial magnetosphere, Alfven waves, Alfvenic acceleration, dispersive Alfven waves, electron acceleration mechanism, numerical experiment

©2021. Japan Geoscience Union. All Right Reserved.

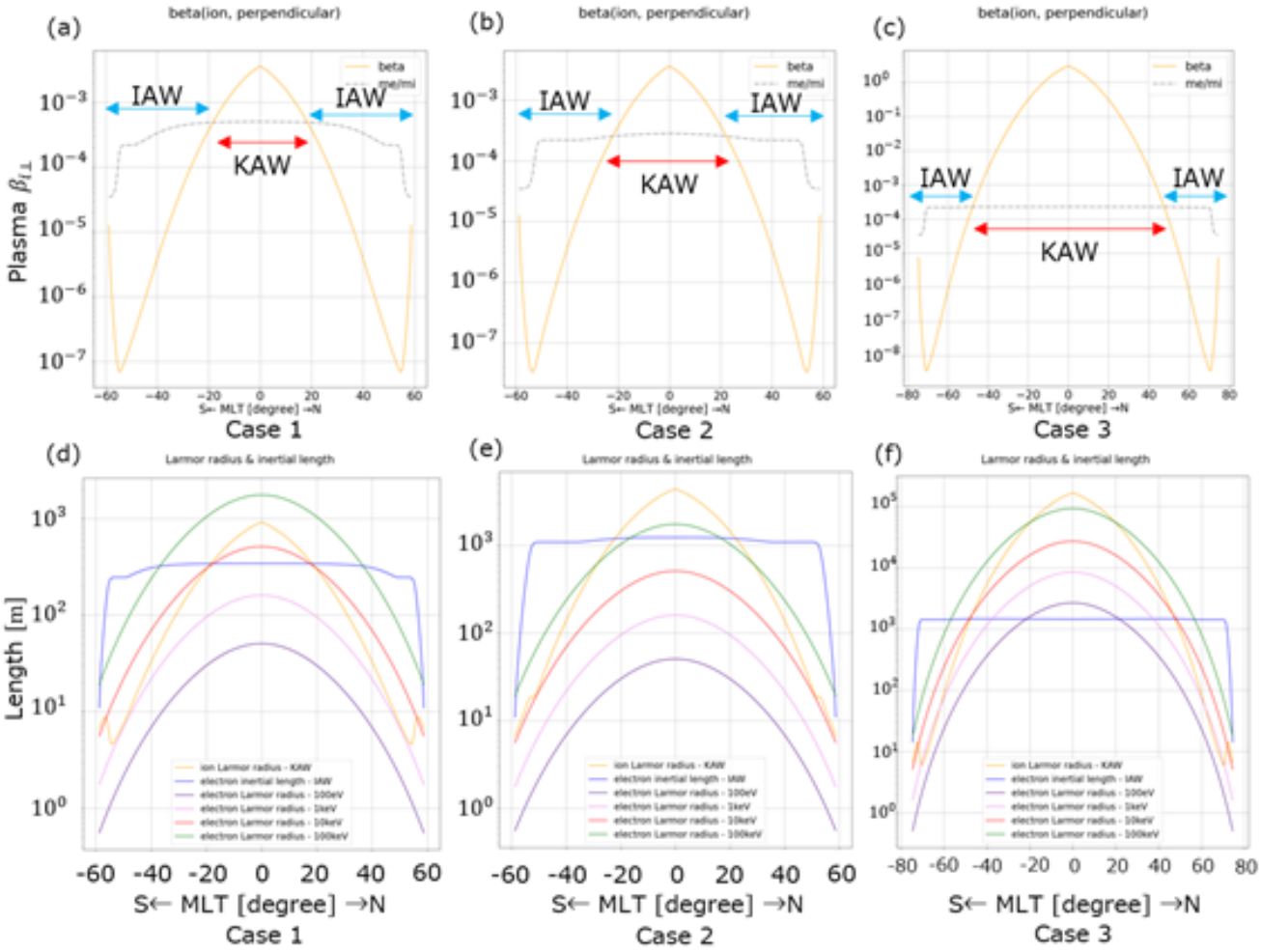


Fig. 1
(a)Plasma $\beta_{i\perp}$ profile for Case 1, (b) Profile of Case 2, (c) Profile for Case 3,
(d)Characteristic lengths profile for Case 1, (e) Profile of Case 2, (f) Profile for Case 3
IAW: inertial Alfven wave, KAW: kinetic Alfven wave

©2021. Japan Geoscience Union. All Right Reserved.

Equatorward development of electron precipitation in a longitudinally narrow region beyond the cusp

*Satoshi Taguchi[1], Keisuke Hosokawa[2], Yasunobu Ogawa[3]

1. Department of Geophysics, Graduate School of Science, Kyoto University, 2. Department of Communication Engineering and Informatics, University of Electro-Communications, 3. National Institute of Polar Research

Low energy elctron precipitation having relatively large flux produces clear red line auroras. This type aurora often appears in the cusp in a patchy manner. In this study we understand how the appearance of those electron precipitation spots in the cusp leads to the equatorward development of the electron precipitation beyond the cusp. On the basis of observations of the dayside auroras from an all-sky imager at Longyearbyen, Svalbard, in situ observations of precipitating particles and magnetic field from DMSP spacecraft that flew over the aurora, radar observations from EISCAT and SuperDARN, we identified an event in which intense electron precipitation occurred in the cusp, and immediately after that the electron precipitation developed equatorward in a longitudinally narrow region beyond the cusp. The result of the analysis from the event has shown that the intense electron precipitation occurred in the cusp periodically, and that at the same time as the stop of that periodic precipitation the electron precipitation region developed equatorward. We show detailed results from observations that were made with the multi-instruments simultaneously, and discuss the cause of the equatorward development of the electron precipitation region beyond the cusp.

Keywords: Cusp, Electron precipitation, Aurora

©2021. Japan Geoscience Union. All Right Reserved.

Periodic variations of the high red aurora on the nightside

*kazuki yashima[1], Satoshi Taguchi[1], Keisuke Hosokawa[2]

1. Department of Geophysics, Graduate School of Science, Kyoto University, 2. Department of Communication Engineering and Informatics, The University of Electro-Communications

A high red aurora can be produced by downgoing broadband electron associated with Alfvenic acceleration. Previous satellite observations have revealed the detailed characteristics of broadband electron precipitation, but we still do not understand how the broadband electron precipitation develops and decays. In this study, we have analyzed 630-nm auroral image data obtained in the nightside MLT sector by an all-sky imager (located at Longyearbyen, Svalbard), and examined how a high red aurora appears in a discrete auroral arc. To understand how tall the high red aurora is, we compared the auroral distribution with predicted red line emissions calculated by the Global Airglow model. The comparison shows that the height of the estimated volume emission rate for the discrete auroral arc have periodic variations during the course of the poleward motion of the discrete auroral arc. We discuss the reason for the periodic features of broadband electron precipitation.

Keywords: aurora, broadband electron precipitation

©2021. Japan Geoscience Union. All Right Reserved.

Initial study of a substorm onset auroral arc on 28 December 2018 by a ground EMCCD camera and the Arase satellite at L~5

*Liwei Chen[1], Kazuo Shiokawa[1], Yoshizumi Miyoshi[1], Shin-ichiro Oyama[1], Yasunobu Ogawa[2], Keisuke Hosokawa[12], Ryuho Kataoka[2], Yoichi Kazama[5], Shiang-Yu Wang[3], Sunny W. Y. Tam[5], Tzu-Fang Chang[1,4], Bo-Jhou Wang[5], Kazushi Asamura[6], Satoshi Kasahara[7], Shoichiro Yokota[8], Tomoaki Hori[1], Kunihiro Keika[7], Yasumasa Kasaba[9], Masafumi Shoji[1], Yoshiya Kasahara[10], Ayako Matsuoka[11], Iku Shinohara[6]

1. Institute for Space-Earth Environmental Research, Nagoya University, 2. National Institute of Polar Research, 3. National Cheng Kung University, 4. Institute of Space and Plasma Sciences, National Cheng Kung University, 5. Institute of Astronomy and Astrophysics, Academia Sinica, 6. Institute of Space and Astronautical Science, Japan Aerospace Exploration Agency, 7. University of Tokyo, 8. Osaka University, 9. Tohoku University, 10. Kanazawa University, 11. Data Analysis Center for Geomagnetism and Space Magnetism, Graduate School of Science, Kyoto University, 12. The University of Electro-Communications

While many substrom-related observations have been made, few conjugate observations of substorm auroral arcs have been reported in the inner magnetosphere at L~4-6. In this study we present a conjugate observation of a substorm brightening auroral arc during a substorm onset observed by the Arase satellite and a ground-bases EMCCD camera. The event was observed at Gakona, Alaska (62.39°N, 214.78°E) on 28 December 2018. The camera showed that a west-east auroral arc moved from the east at ~0730 UT and subsequently broke up poleward at ~0743 UT. The ionospheric footprint of the Arase satellite was moving equatorward from the northwest to the southeast around the center in the field-of-view of the EMCCD camera. The maximum AE index reached ~600 nT during the auroral breakup, indicating the occurrence of a substorm. The particle data of low energy electrons and medium energy ions show the characteristic variations and energizations around the timing of the arc crossing by Arase. The magnetic and electric field data presented a series of quasi-periodic fluctuations, and their cross products show a series of field-aligned Poynting flux flowing earthward and equator-ward alternately at the timing around the crossing. Based on these observations we will discuss the generation mechanisms of the substorm auroral arc in the source region in the inner magnetosphere.

Keywords: substorm, auroral arc, conjugate observation

©2021. Japan Geoscience Union. All Right Reserved.

Ionospheric control of space weather: plasma injections arising out of dynamic ionosphere

*Osuke Saka[1]

1. Office Geophysik

We propose that ionospheric plasma injections to the magnetosphere (ionospheric injection) represent a new plasma process in the polar ionosphere. The ionospheric injection is first triggered by westward electric fields transmitted from the convection surge in the magnetosphere in association with dipolarization onset. Localized westward electric fields result in local accumulation of ionospheric electrons because of differing electron and ion mobility in the E-layer. This charge imbalance was quickly reduced by polarization electric fields generated in the ionosphere. Meanwhile, ion/electron populations are partially released as injections to the magnetosphere to sustain quasi-neutral equilibrium of the ionosphere. Resultant geomagnetic field lines are not in equipotential equilibrium during ionospheric injections but instead develop field-aligned potentials to extract ions/electrons ejected from the ionosphere.

Ejected plasmas were transported along the field lines to higher altitudes above the ionosphere by conserving the total energy and first adiabatic invariant. Temperature anisotropies of the plasmas develop in these plasma flows and grow local field-aligned potentials. These potentials are initially localized above the ionosphere and become global varying monotonically from ionosphere to the equator. However, magnetic mirror force decreased rapidly above 10,000 km and a rate of parallel potential change (parallel electric fields) may drop at these altitudes. The formation of parallel potentials described above is consistent with fundamental plasma properties that require quasi-neutral equilibrium.

We suggest that ionospheric injection generated electrostatic potentials in the ionosphere in a manner consistent with those of the Harang Discontinuity (HD) and field-aligned current patterns matching those in HD. Equatorial projection of potentials may alter exsisting plasma convection patterns in the midnight magnetosphere. Although the substrom onset would be triggered initially by the magnetospheric convection enhancement, we suggest that the time of auroral onset and its location may be controlled and determined by the auroral ionosphere.

Keywords: Space weather, Substorm, Polar ionosphere

©2021. Japan Geoscience Union. All Right Reserved.

Amplitude modulations of the flickering aurora

*Nomura Kazuki[1], Yoshizumi Miyoshi[1], Satoshi Kurita[2], Kohei Toyama[1], Ryuho Kataoka[3]

1. Institute for Space-Earth Environmental Research,Nagoya University, 2. Research Institite for Subtainable Humanosphere, 3. National Institue of Polar Research

The flickering aurora appears during aurora breakup, and the average frequency is ~3-15 Hz. One of the possible origins of flickering aurora is that electromagnetic ion cyclotron (EMIC) waves that cause electron flux modulations at a few thousand kilometers. The flickering aurora has the amplitude modulations, and 10-20 % modulations to the background aurora intensity have been reported. In order to understand detail characteristics of the amplitude modulations of the flickering aurora, we analyze the s-CMOS camera at Poker Flat Research Range, Alaska and investigate distributions of the amplitude of the flickering aurora at different background aurora intensity. We analyzed the intense flickering aurora event at 06:40 UTC on February 8th, 2016. The frequency range of the observed flickering aurora was a few Hz. We derived the relative amplitudes to the background aurora arc. The average ratio was ~13 % and its standard deviation was ~10 % while the background aurora intensities are different. We suggest that the amplitudes and distribution to the background aurora arc do not depend on the background aurora arc. In this presentation, we will show the spatial and time variations of relative amplitude within the flickering aurora arcs.

Keywords: flickering aurora, high-speed camera observations, wave-particle interactions

©2021. Japan Geoscience Union. All Right Reserved.

Simultaneous pulsating aurora and microburst observation with ground-based fast auroral imagers and the Cubesat FIREBIRD-II

*Miki Kawamura[1], Takeshi Sakanoi[1], Mizuki Fukizawa[1], Yoshizumi Miyoshi[2], Keisuke Hosokawa[3], Fuminori Tsuchiya[1], Yuto Katoh[1], Yasunobu Ogawa[4], Kazushi Asamura[6], Harlan Spence[5]

1. Tohoku University, 2. ISEE, Nagoya University, 3. University of Electro-Communicants, 4. National Institute of Polar Research, 5. University of New Hampshire, USA, 6. JAXA/ISAS

We report the relationship between pulsating aurora and MeV-range high-energy electrons using simultaneous observations of ground-based pulsating aurora and the Cubesat FIREBIRD-II for the first time in the world. Although theory predicted that both the precipitation of several keV to several tens keV electrons that generate the pulsating aurora and the microburst (modulation of MeV electrons) are caused by the whistler-mode chorus (Miyoshi et al.,2020), there is no report of the observation. We examined data taken by ground-based all-sky EMCCD imagers (100 Hz sampling with a BG3 grass filter) installed at Sodankylä (67.37 ˚N, 26.63 ˚E) and Tjautjas (67.31 ˚N, 20.73 ˚E) and by the high-energy electron detector in the energy range from 219.7 keV to 984.95 keV on Cubesat FIREBIRD-II at low-altitudes (525 km). We found an event that simultaneous pulsating aurora and microburst was measured simultaneously when FIREBIRD-II (Flight Unit4: FU4) was located at 67.1 ˚N and longitude 23.1 ˚E in the geographical coordinates at 00:28:16-00:28:19 UT on October 8, 2018. Internal modulation with a period of less than 1 s was observed in the variations of pulsating aurora. Similar modulation was seen in the variation of high-energy electrons of FU4. We studied the observation results based on the model assuming that the chorus waves generate pulsating aurora and microburst simultaneously. We compared the variation of pulsating aurora with the timing of the electron precipitation in the energy range of more than 200 keV. The timing of the 200 keV electrons was ~300 ms ahead of pulsating aurora. From the model by Saito et al. (2012), the difference arrival timings of between 10 keV electrons and 200 keV electrons at the ionospheric altitude of 100 km is estimated to be 300 ms. Thus, the result is consistently explained by the model assuming that the pulsating aurora was generated by 10 keV electrons.

Keywords: pulsating aurora, microburst

©2021. Japan Geoscience Union. All Right Reserved.

Analysis of Langmuir waves caused by Chorus observed by the Arase satellite

*Towa Yoshida[1], Satoshi Kurita[2], Takahiro Zushi[1], Hirotsugu Kojima[2], Yoshiya Kasahara[3], Shoya Matsuda[4], Ayako Matsuoka[5]

1. National Institute of Technology, Nara College, 2. Research institute for sustainable humanosphere, Kyoto University, 3. Information Media Center, Kanazawa University, 4. Institute of Space and Astronautical Science/Japan Aerospace Exploration Agency, 5. Data Analysis Center for Geomagnetism and Space Magnetism, Graduate School of Science, Kyoto University

Langmuir waves caused by Chorus have been reported in the magnetosphere. In this event, a periodic Langmuir wave burst is observed with the $E_{//}$ component of the Chorus. In Li et al. (2017), the events observed by WFR, waveform receiver onboard Van Allen Probes, are analyzed. Since the Langmuir wave burst is observed in the phase where the $E_{//}$ component of the chorus is opposite to the propagation direction and the electron beam is observed at the same time, this event is thought to be due to the electron accelerated by the $E_{//}$ component of the Chorus.

In this presentation, we report a similar event observed by the Arase satellite. From the data observed by the WFC onboard the Arase satellite in May 2017, we confirmed a similar event 205 times. For these electric field waveforms, we extracted only the $E_{//}$ components of each of the chorus and Langmuir waves, and analyzed the relationship between the phase of the chorus and the intensity of the Langmuir waves. As a result, we were able to confirm an event in which a strong Langmuir wave was generated in a specific phase of the chorus, as in previous studies. In addition, we also found an example in which there was no relationship between the Langmuir wave intensity and the chorus phase, suggesting that there are multiple event generation mechanisms. In the presentation, we will report the details of these events and compare the parameters when observed for the two types of events.

References

Li, J., et al. (2017). Chorus wave modulation of Langmuir waves in the radiation belts. *Geophys. Res. Lett.*, 44, 11,713– 11,721. doi: 10.1002/2017GL075877

Keywords: The Arase satellite, Chorus, Langmuir wave

©2021. Japan Geoscience Union. All Right Reserved.

Mode identification of MHD waves observed by the SuperDARN radars using the Lomb-Scargle analysis

*Koki Morita[1], Nozomu Nishitani[1], Tomoaki Hori[1]

1. Institute for Space-Earth Environmental Research, Nagoya University

Ultralow frequency (ULF) waves are magnetohydrodynamic plasma waves. The ULF waves in the ionospheric plasma motion obtained by the Super Dual Auroral Radar Network (SuperDARN) can be categorized into toroidal and poloidal modes. Since different oscillation modes come from different generation mechanisms, the identification of the mode as a function of geomagnetic latitude (MLAT) and magnetic local time (MLT) might provide clues to the generation mechanisms of ULF waves. We analyzed Pc5 oscillation modes in ULF waves using the SuperDARN Hokkaido East high-frequency radar data. First, we applied the Lomb-Scargle frequency analysis method to the Doppler shifts of ionospheric irregularities obtained from the radar and identified Pc5 oscillation modes by comparing the Doppler velocity amplitude at one geomagnetic latitude with different beam directions. Next, we conducted statistical analysis on Pc5 oscillation modes in order to reveal the MLAT and MLT dependence of the dominant mode. As a result of the initial statistical analysis from Jan. 10 to Feb. 14 in 2008, we find the following characteristics: 1. The occurrence probability of the Pc5 oscillation is the highest at 0 to 1 MLT. 2. The Pc5 oscillation mode was poloidal at 51˚ to 52˚ MLAT and toroidal at 48˚ to 51˚ MLAT. The former result is explained by the difference in electrical conductivity between day and night. The latter result is interpreted in terms of the external oscillation propagating from higher magnetic latitudes and mode-converted to toroidal mode magnetic field line resonance.

Keywords: MHD waves, Pc5, toroidal, poloidal

©2021. Japan Geoscience Union. All Right Reserved.

Progress in the full-automatic identification of FLR events in VLOS of multiple SuperDARN radars

*Hideaki Kawano[1,2], Akira Sessai Yukimatu[3,4], Nozomu Nishitani[5], Yoshimasa Tanaka[3,4], Satoko Saita[6], Tomoaki Hori[5]

1. Department of Earth and Planetary Sciences, Kyushu University, 2. ICSWSE, Kyushu University, 3. National Institute of Polar Research, 4. SOKENDAI, 5. ISEE, Nagoya University, 6. Kitakyushu College

Where the frequency of waves coming into the magnetosphere matches the eigenfrequency of a geomagnetic field line, which runs through the ground, the ionosphere, and the magnetosphere, FLR (field-line resonance) can cause the eigen-oscillations of the field line. The FLR-generated eigen-oscillation of the magnetic field line, and of the plasma velocity frozen-in to the field line, can be identified by the combination of the maximum in the power and the steepest change in the phase at the eigen-frequency. From thus identified FLR frequency one can estimate the density along the magnetic field line, because, in a simplified expression, 'heavier' field line oscillates more slowly.
SuperDARN radars, which observe VLOS (Velocity along the Line of Sight), are expected to monitor the two-dimensional (2D) distribution of the FLR frequency, from which we can estimate 2D plasma-density distribution on the magnetospheric equatorial plane, including the location of the plasmapause. However, visual identification of the FLR in the VLOS data is time-consuming, and the visual identification could miss FLR events superposed by non-FLR oscillations of VLOS. In addition, there are lots of VLOS data to be analyzed. Thus, we started developing computer codes to automatically identify the FLR.
We have so far developed a set of computer codes to automatically identify the FLR for a beam of a radar by using the amplitude-ratio method and the cross-phase methods; these methods cancel out the superposed perturbations by dividing the data from a Range Gate (RG) by the data from a nearby RG along the same beam, because the FLR frequency tends to depend on the latitude more strongly than the superposed perturbations. Another advantage of applying these methods to the SuperDARN VLOS data is that we can choose any pair of RGs (along the same beam) with different distances, and thus can identify what distance is the best to identify the FLR. This distance reflects the resonance width, which is an important quantity reflecting the diffusion and dissipation of the FLR energy. This set of codes succeeded in identifying FLR events which we had visually identified in a few beams of a few radars by examining the raw amplitude and phase distribution along the beams.
We are now developing an all-in-one IDL code which unifies the above-stated set of codes and is applied to VLOS data of all the beams of a radar at once. The automatically identified FLR events would include events simultaneously observed at several locations by several radars, increasing the possibility of monitoring the 2D distributions of plasma density distribution on the magnetospheric equatorial plane and identify magnetospheric regions. We intend to show such events at the meeting.

©2021. Japan Geoscience Union. All Right Reserved.

Initial results from an induction magnetometer observation at Middlemarch (L = 2.7) in New Zealand

*Yuki Obana[1], Kaori Sakaguchi[2], Masahito Nose[3], Keisuke Hosokawa[4], Kazuo Shiokawa[3], Martin Connors[5], Akira Kadokura[6], Tsutomu Nagatsuma[2]

1. Department of Engineering Science, Faculty of Engineering, Osaka Electro-Communication University, 2. National Institute of Information and Communications Technology, 3. Institute for Space-Earth Environmental Research, Nagoya University, 4. Department of Communication Engineering and Informatics, University of Electro-Communications, 5. Centre for Science, Faculty of Science and Technology, Athabasca University, 6. National Institute of Polar Research

The plasmas in the inner magnetosphere have wide energy ranges from ~eV to ~MeV. Their interaction with plasma waves causes their acceleration and loss into the ionosphere. In order to establish that the loss of radiation belt particles due to EMIC waves occurs in the deep inner magnetosphere, we installed a new high-sensitivity all-sky camera and induction magnetometer at Middlemarch (L=2.7) in New Zealand where a fluxgate magnetometer has been operated.

So far, the following results have been obtained.
Ionospheric Alfvén Resonator (IAR) is found in a dynamic power spectrum of the geomagnetic field variations as spectral resonance structures in the frequency range of 0.1–10 Hz. We find IAR in the data from the induction magnetometer for three consecutive days of October 4–6, 2020. Lower harmonic modes are present throughout local nighttime, but higher harmonic modes with frequency of >~5 Hz suddenly disappear at the onset time of substorms. This may indicate that geomagnetic disturbances cause interference in the resonance condition of Alfvén waves in the ionospheric cavity between E and F2 layers, and the interference is effective only for the higher harmonic modes.

Unique Pc1 pulsations are found in a dynamic power spectrum of the geomagnetic field variations as a band-type structure in the frequency range of ~0.2–1 Hz before and after a small geomagnetic storm (minimum Dst = -40 nT). Before the geomagnetic storm, Pc1 events with different center frequencies were observed intermittently almost all day, regardless of local time. No pulsation was observed in frequency ranges of 0.2 to 30 Hz during the main phase and the early recovery phase after the occurrence of a sudden commencement of the geomagnetic storm, despite expecting to be observed at higher frequencies. During the recovery phase, four Pc1 events were observed at a periodic interval of about 3-4 hour following an IPDP (interval of pulsations of diminishing period) type Pc1 occurrence. It was found that these events were also observed at four stations in Canada and Iceland in the opposite hemisphere at the same time.

Keywords: ULF wave, ELF wave, Pc 1, ElectroMagnetic Ion Cyclotron (EMIC) wave, Ionospheric Alfvén Resonator (IAR)

©2021. Japan Geoscience Union. All Right Reserved.

Detection of Pi2 geomagnetic pulsation by machine learning and development of real-time substorm warning system

Yusuke Sakai[1], *Masahito Nose[1], Hiroshi Ichihara[2], Genta Ueno[3], Naoto Nakano[4]

1. Institute for Space-Earth Environmental Research, Nagoya University, 2. Graduate school of environmental studies, Nagoya University, 3. Institute of Statistical Mathematics, Research Organization of Information and Systems, 4. Institute for Liberal Arts and Sciences, Kyoto University

Pi2 geomagnetic pulsations are defined to have an irregular waveform with a period of 40-150 seconds. It is known that they appear during auroral breakups and intensifications, and the occurrence of Pi2 geomagnetic pulsations can be used to estimate the occurrence of auroral breakups, even at low latitudes where auroras cannot be seen directly. If Pi2 geomagnetic pulsations are detected in real time, we can nowcast disturbances in the polar regions where auroras occur and disturbances in the magnetosphere that provides the excitation energy of auroras. In this study, machine learning is used to automatically detect Pi2 pulsations from low latitude geomagnetic data.
The 1-sec geomagnetic field data are acquired at the Inabu observatory in Aichi prefecture. Geomagnetic coordinates of the Inabu observatory are 26.77˚N and 207.49˚E. We prepare 3000-5500 images by plotting the geomagnetic field data for the month of February 2020 and use them as training dataset for the machine learning. Visually scanning these images, we label them occurrence/no occurrence of Pi2 pulsations. Using these labeled images, we train a convolutional neural network (CNN), one of types of machine learning, as it can determine whether Pi2 pulsations are present or not in images. As CNN models, we use our own model and Resnet50. It is revealed that when the training dataset includes the equal numbers of occurrence/no occurrence of Pi2 images, CNN obtains a better learning result. The best performance is achieved by ResNet50 with 93% accuracy.
The future plan is to transfer geomagnetic field data continuously in real time from Inabu observatory to Nagoya University and to apply the developed CNN model to detect Pi2 pulsations in an automated way. By doing so we will construct a realtime substorm-warning system.

Keywords: machine learning, convolutional neural network, Pi2 pulsations, aurora, substorm

©2021. Japan Geoscience Union. All Right Reserved.

Current Status of the FACTORS mission for the Space-Earth Coupling System Exploration

*Masafumi Hirahara[1], Yoshifumi Saito[2], Hirotsugu Kojima[3], Kazushi Asamura[2], Takeshi Sakanoi[4], Yoshizumi Miyoshi[1], Naritoshi Kitamura[5], Masatoshi Yamauchi[6], Yoshihide Sugimoto[7]

1. Nagoya Univ., 2. JAXA, 3. Kyoto Univ., 4. Tohoku Univ., 5. Univ. Tokyo, 6. IRF, 7. LSAS Tec Co., Ltd.

The FACTORS mission opportunity has been investigated as the first Japanese multi-point space plasma exploration mission in a polar orbit of 400 km(perigee) to 4000 km(apogee) for integrated in-situ and remote-sensing observations in the space-Earth coupling system. We have been discussing the cutting-edge science goals, the state-of-the-art measurement methodologies with capabilities of high-time/spatial resolutions and direct evaluations on the energy transports between the plasma waves, and possibilities of international collaborations with the Swedish InnoSat program of the micro satellite series. We, here, present observation strategies and the current status of FACTORS.
The FACTORS mission consists of two identical compact satellites for realizing the formation flight configuration for the simultaneous multi-point observations by the adjacent satellites with their controllable separation distances of 1-50 km. In this mission, we focus on the demonstrative and quantitative investigations on the plasma acceleration/transport mechanisms and the electromagnetic coupling processes emerging in the terrestrial polar magnetosphere and ionosphere. In order to address these scientific targets, we apply some innovative measurement and operational approaches represented by identical six 5-m electric field antennas for three axial components, high time-resolution pitch-angle and gyro-phase captures of transversely accelerated ions, two-types of high-time/spatial resolving monochromatic auroral imaging cameras, and simultaneous multi-point observations with a satellite separation distance of 1 km at closest. While each FACTORS satellite carries a chemical propulsion system for large satellite orbit controls, the precise formation flight configuration could be kept by changing the satellite attitude which significantly affects the aerodynamics particularly near the perigee. These instrumentation and operation plans and developments are discussed in this presentation.

Keywords: multi-point simultaneous satellite observation, integrated satellite observation, formation flight observation, space-Earth coupling system

©2021. Japan Geoscience Union. All Right Reserved.

Future formation-flight satellite mission FACTORS: Development of far-ultra-violet imagers and simulation of Alfven wave observations

*Takeshi Sakanoi[1], Mizuki Fukizawa[1], Masafumi Hirahara[2], Yoshizumi Miyoshi[2], Kazushi Asamura[3], Yoshifumi Saito[3], Hirotsugu Kojima[4], Naritoshi Kitamura[5], Takanori Nishiyama[6], Kiyoka Murase[6], Miki Kawamura[1], Kaori Sakaguchi[7], Mamoru Ishii[7], Harald U Frey[8], Nick Schneider[9]

1. Planetary Plasma and Atmospheric Research Center, Graduate School of Science, Tohoku University, 2. ISEE, Nagoya University, 3. ISAS, JAXA, 4. RISH, Kyoto University, 5. Graduate School of Science, University of Tokyo, 6. NIPR, 7. NICT, 8. SSL, University of California, Berkeley, 9. LASP, University of Colorado Boulder

We report the science objectives, design of instruments, and recent updates of the development of the far-ultra violet (FUV) imager for the future polar orbiting satellite FACTORS. This design is also applicable to the FUV imager on a geostationary orbiting satellite. In addition, we report the simulation results of Alfven wave parameters obtained with a formation flight of FACTORS. FACTORS stands for Frontiers of Formation, Acceleration, Coupling, and Transport Mechanisms Observed by the Outer Space Research System, which is going to be proposed as a next-generation multi-satellite formation flight mission. Major scientific targets are: 1) energy transport in the magnetosphere-ionosphere (MI) coupling system and their relationship to small-scale auroral phenomena, 2) particle transport in the MI system by ion outflow, and 3) neutral-ion coupling in the auroral thermosphere. Multi-satellite observation of small-scale plasma parameters and simultaneous auroral imaging data in the altitude range from ~300 km to 4000 km enables us to understand dynamical spatial and time variations of Alfvenic wave acceleration, field-aligned current, particle distribution function and small-scale auroral emission.

We describe the design and development of visible and FUV imagers for this mission. Both visible and FUV images are required to have high-spatial and high-time resolution capability to observe the dynamical morphology of small-scale aurora. Therefore, we set the instrumental requirement for the visible imager to measure small-scale faint aurora with a spatial resolution of ~1km x 1km at apogee (~4000km altitude), a time resolution of ~10 frames/sec and sufficient sensitivity for auroral intensity of ~1 kR. The FUV imager is also required to have high-spatial and high-time resolutions, i.e., a few km x a few km, several frames/sec, to observe small-scale aurora, and sufficient sensitivity for auroral emission at ~1 kR. The candidate auroral emission is OI 135.6 nm, and/or N2 LBH band (140-180 nm). In contrast to the night-side operation of the visible imager, the FUV imager is required to be operated in the sunlit conditions, as the contribution of the FUV imager to the mission objectives is significant. Therefore, occulting optics may be a key in developing this instrument.

We designed and developed the test model of the FUV imager which consists of a commercial CCD detector which has a FUV sensitivity, objective lenses made of FUV-transparent CaF2 glass, rotational stage and vacuum chamber. We are going to carry out the accurate measurement of FUV spectroscopic sensitivity characteristics using the FUV-UV monochromator light source in ISAS/JAXA soon. In addition, we plan to perform a radiation test to the FUV detector in 2021, and demonstrate the performance required for the FUV imager. These technical issues are similar to the FUV imager designed to be on a geostationary satellite and are currently conducted by NICT, Japan.

Concerning the simulation of Alfven wave parameters obtained with a formation flight of FACTORS satellites, we investigated whether the frequency and wavelength of a propagating plasma wave could be derived by two satellites. The time series data of waveforms were produced by observing a pseudo plane

©2021. Japan Geoscience Union. All Right Reserved.

wave with the two satellites based on the orbital conditions at which the satellites are actually launched. The plane wave was assumed to be the Alfven wave in the polar region actually observed by the FACTORS satellites. The actual Alfven wave is a plane wave with a finite frequency width, but we assumed a monochromatic wave here. The initial placement conditions of the two satellites at the apogee were examined for three cases: horizontal distance of 10 km, travel distance of 10 km, and vertical distance of 10 km. The wave number vector was derived for the given monochromatic wave by applying the wave propagation direction analysis algorithm called the Means method to the data of the three magnetic field components observed by the two satellites. The instantaneous phase was obtained by applying the Hilbert transform to the waveforms observed by the two satellites. Then, we established a method to derive the frequency and wavelength of the wave in the inertial system by using the time series data of the derived wave number vector, the derived instantaneous phase, and the distance between the two satellites. It was shown that the wave frequency and wavelength can be derived under the three initial placement conditions of the two satellites without assuming the dispersion relation of the plasma wave, but the derivation was limited depending on the angle between the wave number vector and the inter-satellite distance vector.

Keywords: small-scale aurora, Alfven wave, instrument

©2021. Japan Geoscience Union. All Right Reserved.

Future formation-flight mission FACTORS: Development of plasma particle instruments and evaluation of electric field measurements with short electric field sensors

*Kazushi Asamura[1], Hirotsugu Kojima[2], Taku Namekawa[1], Takefumi Mitani[1], Motoyuki Kikukawa[2], Ibuki Fukasawa[2], Satoshi Kurita[2], Yuki Miyake[2], Hideyuki Usui[3]

1. ISAS / JAXA, 2. RISH, Kyoto University, 3. Kobe University

FACTORS is a multi-satellite formation flight mission to be proposed. Nominal trajectory of FACTORS is a polar orbit whose perigee and apogee are 400 and 4000km, respectively. Major scientific targets of the mission are to reveal physical mechanisms of (1) energy and particle transportations between the magnetosphere and the ionosphere, including small scales down to auroral fine-scale structures, (2) generation of ion outflow at polar ionosphere through plasma wave - particle interactions, (3) ion - neutral coupling in the thermosphere. Simultaneous multi-point measurements of in-situ plasma wave and particles in small scales provide us discrimination of temporal and spatial variations which are difficult to achieve with measurements by a single satellite. Therefore, each satellite carries plasma wave instruments, and particle instruments as well.

The model instruments onboard FACTORS contains three-axes sensors for electric and magnetic field fluctuations, ion energy-mass spectrometers (supra-thermal to a few tens of keV), and electron energy analyzers (10eV to 2MeV). Among these instruments, the supra-thermal ion energy mass spectrometer (SEP-IMS) is one of the key instruments for exploring the ion outflow phenomena. For measurements of ions in supra-thermal energy range, orbital motion of the satellite affects significantly (RAM effect), and it is important to measure particles coming from RAM direction. Therefore, SEP-IMS must have wide field-of-view with necessary angular resolution. On SEP-IMS design, we have implemented functions of changing the field-of-view by applying specific voltages on sensor electrodes. On the other hand, we have also implemented a sensitivity control mechanism on SEP-IMS, since estimated fluxes of supra-thermal ions in low (~400km) and high (~4000km) altitude are quite different.

For measuring plasma waves, the most challenging part is to observe three components of electric field oscillations using short electric field sensors. Electric field sensors show complicated characteristics in plasmas. In the case that wavelengths of plasma waves are comparable with sensor lengths, their characteristics should be considered carefully. A computer simulation is a useful tool for quantitatively examining the characteristics of sensors in plasmas. Full particle computer simulations targeting electric field measurements in the FACTORS mission show the characteristics of short electric field sensors with the lengths that are in the same order of wavelengths of plasma waves depending on relative angles between electric field sensors and ambient magnetic fields. The quantitative evaluation of electric field sensors is so crucial for meeting the objectives of the FACTORS mission.

We will report on the development status of plasma particle instruments and the evaluation of electric field sensors onboard the FACTORS mission.

Keywords: FACTORS, plasma particle instrument, electric field measurement

©2021. Japan Geoscience Union. All Right Reserved.

Current status of development of multi-spectral auroral camera on the LAMP rocket experiment

*Miki Kawamura[1], Takeshi Sakanoi[1], Kazushi Asamura[2], Yoshizumi Miyoshi[3], Keisuke Hosokawa[4], Sarah Jones[5], Marc Lessard[6]

1. Tohoku University, 2. JAXA,ISAS, 3. ISEE, Nagoya University, 4. University of Electro-Communicants, 5. GSFC/NASA, USA, 6. University of New Hampshire, USA

We report the current status of development and future plan of the multi-spectral auroral camera (AIC2) installed on the LAMP rocket which will be launched at Pokar Flat, Alaska in this winter period. Recent Arase satellite observations have revealed that chorus waves cause the pitch-angle scattering of several keV electrons, which produce pulsating aurora, near the magnetic equator. The chorus waves are theoretically thought to cause the pitch angle scattering of electrons in a wide energy range from several keV to MeV. Microburst is a high-speed modulation of MeV electrons at 1 Hz or higher and is generated by electron resonance with a chorus wave. Therefore, the positive relationship between pulsating aurora and microbursts is expected. However, there is no simultaneous observation between them. The purpose of the LAMP rocket is to clarify the relationship between pulsating aurora and microbursts with simultaneous particle, electromagnetic waves and imaging measurements. The project PI is Dr. Jones of NASA/GSFC. The instrumental package called PARM2 (Pulsating AuRora and Microburst 2) is provided by a Japanese team. AIC2 is a one of PARM2 which consists of two CMOS detectors called AIC-S1 and S2, and the data processing electrics AIC-E, and it will perform auroral imaging at two wavelengths simultaneously. AIC2 is characterized by a low noise (1.6 e-RMS) and wide dynamic range sampling capability (16bit A/D) using the consumer CMOS sensor (ZWO AS1183MM). AIC-S1 targets the N2 1PG aurora in the E region with the interference filter (Andover, CW 670 nm, FWHM 20 nm) and a fast objective lens (SpaceCom JF17095M, f= 17 mm. F/0.95, field of view 29 deg x 29 deg). AIC-S2 is designed to observe the OI 844.6 nm aurora in the F-region with an interference filer (Andover, CW 846 1 mm, FWHM 4.4 nm) and a wide-angle objective lens (SpacaCom HF3.5M-2, f= 3.5mm, F/1.6, field of view 106 deg x 106 deg). To gain S/N and reduce data size, binning is performed from an original 3660 pix x 3600 pix image to 60 bin x 60 bin (1bin=60pix x 60pix) image. AIC2 is mounted on the despun platform of the rocket to cancel a rocket spin. Combining the despun platform with the rocket attitude control, AIC-S1 will point to the magnetic footprint to observe the fine structure of pulsating aurora. AIC-S2 will point slantingly west to obtain the height profile of O 844.6 nm emission as well as the pulsating auroral distribution in the wide range. The time resolution of each camera is approximately 10 frames/s. At the apex altitude (~450km), the spatial resolution at nadir is 3.0 km x 3.0 km for AIC-S1 (the E-region), and 6.3 km x 6.3 km for AIC- S2 (the F-region). The AIC-E consists of two NanoPiM4V2 board computers, two FPGAs, and power supply to handle a large amount of image data produced by the two cameras. We use a heat pipe unit to cool the two CPUs of NanoPiM4V2. Total weight and power of AIC2 are 2.6 kg and 20 W, respectively. On the development of AIC2, we carried out the following tests: 1) time accuracy of image sampling, 2) sensitivity calibration, 3) data communication via rotational terminal of despun platform, 4) thermal vacuum test with the heat pipe, 5) focus adjustment, and 6) electrical interface between AIC-S1, S2 and AIC-E. As a result, 1) the time accuracy is 0.1 ms, which is sufficient to observe the internal modulation (~3 Hz) of pulsating aurora, 2) the dynamic range is 0-480 kR AIC-S1 and 0 - 360kR - for AIC-S2, 3) no data error happed via despun platform, 4) AIC operated normally in the vaccum conditions with temperatures of 0,10,20 ˚C for more than 30 minutes, and the heat pipes worked as designed, 5) focus adjustment was made with sims. On 6), there was an issue that the USB 3.0 connection between Nanopi M4V2 and ZWO camera electronics. To solve this, we improved the software to modify the

©2021. Japan Geoscience Union. All Right Reserved.

initialization of the Nanopi M4V2, and the timing of camera detection.

Keywords: pulsating aurora, LAMP sounding rocket, multi-spectral auroral camera

©2021. Japan Geoscience Union. All Right Reserved.

Development of wideband impedance probe for measurement of the ion composition in the ionosphere and magnetosphere

*Atsushi Kumamoto[1]

1. Graduate School of Science, Tohoku University

The performance of new wideband impedance probe system for observation of the ionospheric ion composition have been evaluated in the plasma chamber. Measurement system of Number density of Electron with Impedance probe (NEI) were developed by Oya [1966], and successfully utilized for many sounding rockets and spacecrafts such as Denpa, Taiyo, Jikiken, Hinotori, Ohzora, and Akebono [e.g. Wakabayashi et al., 2013]. NEI measures the equivalent capacitance of the probe immersed in the magnetized plasma. By applying RF signal to the probe, we can identify the minimum of equivalent capacitance at upper hybrid resonance (UHR) frequency. The frequency of RF signal is swept from 100 kHz to 25 MHz, in order to cover the UHR frequency range in the Earth’ s ionosphere. We can obtain accurate electron number density from the measured UHR frequency. NEI data obtained in several previous ionospheric sounding rockets are provided via DARTS maintained by JAXA/ISAS (https://www.darts.isas.jaxa.jp/ stp/rocket/index.html.en).
The effective capacitance of the probe in the magnetized plasma shows minimum not only at UHR frequency but also at another resonance frequency: Lower hybrid resonance (LHR). By measurement of LHR frequency, we can derive effective mass of ionospheric plasma and determine the ionospheric ion compositions. Since LHR frequency is about several kHz in the Earth's ionosphere, we have to extend the lower limit frequency of the current impedance probe system to 100 Hz.
The measurements of UHR frequency by NEI can be tested in the chamber experiments. However, due to high ion collision frequency in the chamber, it is difficult to demonstrate the measurements of LHR frequency by wideband NEI. So, the tests of the wideband NEI have to be performed in the ionosphere, where ion collision frequency is ~100 Hz, through the sounding rocket experiments. Wideband NEI will be installed on SS-520-3 and S-520-32 sounding rockets.
Acknowledgment: Development of NEI for SS-520-3 is supported by JAXA/ISAS. Development of NEI for S-520-32 was performed in the program titled "Training program of engineering skill of space instruments through the sounding rocket experiments" supported by MEXT Coordination Funds for Promoting AeroSpace Utilization; Grant Number JP000959. The NEI data was archived with support of Joint Research with JAXA/ISAS for Mission Data Archiving. The author expresses deep appreciation to all members of SS-520-3 and S-520-32 sounding rocket teams.

Keywords: Impedance probe, electron number density, ion composition, Lower hybrid resonance frequency, Sounding rocket

©2021. Japan Geoscience Union. All Right Reserved.

Numerical design of double-shell electrostatic energy analyzer with hemispherical field of view

*Atsuya Takasu[1], Masafumi Hirahara[1], Shoichiro Yokota[2]

1. Institute of Space-Earth Environmental Research, Nagoya University, 2. Graduate School of Science, Osaka University

The magnetospheres of the Earth and planets consist of regions with various structures due to the influence of the solar wind. In order to understand the physical phenomena occurring in these regions, it is important to obtain three-dimensional(3-D) velocity distribution functions through in-situ particle measurements. While the 3-D velocity distribution functions have been acquired by the analyzers with a fully planar field-of-view(FOV) on a spin-stabilized satellite, it is unrealistic to acquire the precise 3-D velocity distributions when this type of the analyzer is mounted on a three-axis stabilized satellite. Therefore, a hemispherical FOV analyzer is required to be mounted on a three-axis stabilized satellite for acquiring the 3-D velocity distribution functions.

The miniaturization of satellites has been promoted in these decades, and it is necessary to reduce the size and weight of particle analyzers for these small/micro satellites. In the case of observing ions and electrons in the conventional technology, two separate analyzers must be installed, one for ions and the other for electrons. However, it could be difficult to mount two analyzers due to the restriction for small/micro satellites. If these two sensor heads of the ion and electron analyzers can be combined into one, it is possible to reduce the total instrument size, weight, and power for the ion and electron observations on small/micro satellites. We have developed a hemispherical FOV double-shell electrostatic energy analyzer which enables to observe ions and electrons by one sensor head on a three-axis stabilized satellite.

The hemispherical FOV double-shell electrostatic energy analyzer is cylindrically symmetric and consists of an FOV deflection system, an ion/electron separator, a double-shell electrostatic energy analyzer, and detectors. The FOV deflectors have electrode shapes that achieve a hemispherical FOV of 2π [sr] by applying a high voltage to the upper or lower electrode, depending on deflection angle. The ion/electron separator is applied by a negative voltage so that ion and electron trajectories are separated into each of the analyzers.

The double-shell analyzer consists of an outer dome, a middle dome, and an inner dome. Ions enter the gap between the outer and middle domes, and electrons enter between the middle and inner domes. A negative voltage is applied only to the middle dome to produce an electric field that allows each species with appropriate energies to pass through the electrostatic energy analyzer.

Based on this instrumental concept, numerical simulations have been performed using a charged particle orbit calculation software, SIMION, and the performance of the hemispherical FOV double-shell electrostatic energy analyzer has been under evaluation. As evaluation criteria, the energy-elevation angle characteristics are particularly subject to investigation. The energies and incident angles of the particles that could reach the detector and the energy and angular resolutions should be evaluated. We report the simulation results of the performance for the hemispherical FOV double-shell electrostatic energy analyzer.

©2021. Japan Geoscience Union. All Right Reserved.

Keywords: Low-energy ion observation, Low-energy electron observation, Particle instrument, Electrostatic energy analyzer, Numerical design

©2021. Japan Geoscience Union. All Right Reserved.

Development of SDR-based scintillation detector system and observation with magnetometer and radar

*Shuji Abe[1], Akiko Fujimoto[2], Akimasa Yoshikawa[3,1]

1. International Center for Space Weather Science and Education, Japan, 2. Kyushu Institute of Technology, 3. Department of Earth and Planetary Sciences, Kyushu University

The upper part of Earth's atmosphere is ionized by solar ultraviolet and X-ray radiation. This region is called the ionosphere. It is located from about 60km to 1000km altitude and separated to some regions according to their characteristics. The ionosphere plays an important role for radio wave propagations. These propagations are dependent on the condition of the ionosphere because the ionosphere changes these conditions temporally and spatially by background fluctuations. Some disturbances are regular and repeated, such as daily, seasonal, and solar activity. In addition, some disturbances are irregular, such as sporadic E layer, and plasma bubbles. These disturbances cause the ionospheric scintillation, rapid intensity and phase changes of radio waves which pass through the ionosphere. Therefore, the observation of ionospheric scintillation is equivalent to observing the state of the ionosphere.

We developed the SDR (Software-Defined Radio) -based scintillation detector system for understanding the dynamics of ionosphere. We use the USRP N210 with WBX daughter board from Ettus research as the front end, and signal processing software based on some open source products. This system uses two GPS antennas, one is large antenna with multipath-mitigation and 30db gain, and the other is small antenna for GPS Disciplined Oscillator. For performance evaluation, we installed this system on the roof of the building. The data observed by our system have good correlation with others from a nearby GPS reference points. For the initial observation, we will install it at Sasaguri, Fukuoka, Japan (33.64N, 130.51E, in Geographic Coordinate). We operate magnetometers and a FM-CW radar at the station. Thus, our new device can observe GPS scintillation simultaneously with magnetic field variation recorded by magnetometer and ionosphere plasma density profile detected by FM-CW radar, which helps our understanding about magnetosphere and ionosphere coupling. In this paper, we will present the initial results of these observation.

©2021. Japan Geoscience Union. All Right Reserved.

Application of magneto-impedance sensor to geomagnetic field measurements for constructing Distributed Arrays of Small Instruments (DASI)

Nomura Hiroshi[1], *Masahito Nose[1], Hitoshi Aoyama[2], Takeshi Kawano[2], Hiroshi Ichihara[3], Masafumi Hirahara[1]

1. Institute for Space-Earth Environmental Research, Nagoya University, 2. Aichi Steel Corporation, 3. Graduate school of environmental studies, Nagoya University

Magneto-impedance (MI) effect was discovered about 25 years ago and micro-size magnetic sensors that utilizes this effect become commercially available. MI sensors are much less expensive than fluxgate sensors. We are developing a low-cost system to measure the geomagnetic field using the MI sensor, which is named MIM-Pi. MIM-Pi includes a Raspberry Pi, low-cost 24-bit AD converters, and power supply circuits for generating a stable power supply voltage.
For the period of June 17 to June 25, 2020, we conducted experimental observations of geomagnetic field variations with MIM-Pi at Inabu observation site in Japan (26.8˚, −152.5˚ in geomagnetic coordinates). Inabu observation site is operated by Nagoya University. Data obtained with MIM-Pi were compared with those from the fluxgate magnetometer that has been working at the site. Results showed that MIM-Pi recorded Sq variations and geomagnetic pulsations with amplitudes of ˜2 nT that were also detected with the fluxgate magnetometer.
In presentation, we will show long term observations by MIM-Pi and discuss the possibility of using this system for construction of Distributed Arrays of Small Instrument (DASI). We will also show the result of an attempt to remove artificial noises by placing multiple observation systems at neighboring observation points and performing independent component analysis.

Keywords: magneto-impedance sensor, geomagnetic field measurements, Distributed Arrays of Small Instruments (DASI), fluxgate magnetometer

©2021. Japan Geoscience Union. All Right Reserved.

Closure of the Onagawa Magnetic Field Observatory of Tohoku University

*Takahiro Obara[1], Takeshi Sakanoi[1], Yasumasa Kasaba[1], Fuminori Tsuchiya[1], Hiroaki Misawa[1], Masato Kagitani[1], Aya Otomo[1]

1. Planetary Plasma and Atmospheric Research Center,Tohoku University

The magnetic field observatory of Tohoku University at Onagawa Town in Miyagi Prefecture closed at the end of March in 2021with an illustrious history of over 60 years.

This observatory contributed immensely to research and education in the field of space science by providing a great deal of valuable magnetic field data over the decades of its operation.

This presentation will highlight the activities of the observatory during the past 60 years along with the scientific achievements of its research staffs.

Keywords: Onagawa Magnetic Field Observatory

©2021. Japan Geoscience Union. All Right Reserved.

[E] Oral | P (Space and Planetary Sciences)：P-EM Solar-Terrestrial Sciences, Space Electromagnetism & Space Environment

Sun. Jun 6, 2021 9:00 AM - 10:30 AM JST | Sun. Jun 6, 2021 12:00 AM - 1:30 AM UTC | Ch.06 Zoom Room 06

[P-EM10] Frontiers in solar physics

convener:Takaaki Yokoyama(School of Science, University of Tokyo), Shinsuke Imada(Institute for Space-Earth Environmental Research, Nagoya University), Shin Toriumi(Institute of Space and Astronautical Science, Japan Aerospace Exploration Agency), Alphonse Sterling(NASA/MSFC), Chairperson:Shin Toriumi(Institute of Space and Astronautical Science, Japan Aerospace Exploration Agency)

This session is for discussions on recent progress in solar and heliospheric physics, and related fields (including plasma physics and planetary physics). In 2020, we had several important milestones in this area. The Daniel K. Inouye Solar Telescope (DKIST operated by NSO) has taken its first image and its call for proposals in observation cycle 1 was announced. The Solar Orbiter was launched by ESAunder collaboration with NASA and released the first data to the public. In Japan, SOLAR-C(EUVST) was selected at ISAS/JAXA as 4th competitively-chosen middle-class mission. We will discuss what observational and theoretical studies achieved in the recent years and what should be addressed next in the coming mid-2020s. We welcome contributions not only by solar researchers but also those from related fields on observations, theories, numerical works, and experiments.

9:00 AM - 9:01 AM JST | 12:00 AM - 12:01 AM UTC

[PEM10-01] Introduction

9:01 AM - 9:23 AM JST | 12:01 AM - 12:23 AM UTC

[PEM10-02] Sun-to-Earth MHD Simulations of Geo-Effective CMEs

★Invited Papers

*Tibor Torok[1] (1.Predictive Science Inc.)

9:23 AM - 9:45 AM JST | 12:23 AM - 12:45 AM UTC

[PEM10-03] How To Trigger the Solar Flares?

★Invited Papers

*Yumi Bamba[1] (1.Nagoya University)

9:45 AM - 10:00 AM JST | 12:45 AM - 1:00 AM UTC

[PEM10-04] The Source Locations of Major Flares and CMEs in the Emerging Active Regions

*Liu Lijuan[1], Wang Yuming[2], Zhou Zhenjun[1] (1.School of Atmospheric Sciences, Sun Yat-sen University, Zhuhai, Guangdong, 519082, China, 2.Department of Geophysics and Planetary Sciences, University of Science and Technology of China, Hefei, Anhui, 230026, China)

10:00 AM - 10:15 AM JST | 1:00 AM - 1:15 AM UTC

[PEM10-05] Evaluation of horizontal flow velocity at the solar surface with machine learning and numerical simulation

*Hiroyuki Masaki[1], Hideyuki Hotta[2] (1.Graduate School of Science and Engineering, Chiba University, 2.Chiba University)

10:15 AM - 10:30 AM JST | 1:15 AM - 1:30 AM UTC

[PEM10-06] Satellite mission: *PhoENiX* (Physics of Energetic and Non-thermal plasmas in the X (= magnetic reconnection) region)

*Noriyuki Narukage[1], Mitsuo Oka[2], Yasushi Fukazawa[3], Keiichi Matsuzaki[4], Shin Watanabe[4], Taro Sakao[4], Kouichi Hagino[5], Ikuyuki Mitsuishi[6], Tsunefumi Mizuno[3], Iku Shinohara[4], Masumi Shimojo[1], Shinsuke Takasao[7], Tomoko Kawate[8], Takafumi Kaneko[6], Hiroshi Tanabe[9], Munetaka UENO[4], Tadayuki Takahashi[10], Takeshi Takashima[4], Masayuki Ohta[4] (1.National Astronomical Observatory of Japan, 2.University of California, Berkeley, 3.Hiroshima University, 4.Japan Aerospace Exploration Agency,

5.Tokyo University of Science, 6.Nagoya University, 7.Osaka University, 8.National Institute for Fusion Science, 9.The University of Tokyo, 10.Kavli Institute for the Physics and Mathematics of the Universe)

[E] Oral | P (Space and Planetary Sciences) | P-EM Solar-Terrestrial Sciences, Space Electromagnetism & Space Environment

[P-EM10] Frontiers in solar physics

convener:Takaaki Yokoyama(School of Science, University of Tokyo), Shinsuke Imada(Institute for Space-Earth Environmental Research, Nagoya University), Shin Toriumi(Institute of Space and Astronautical Science, Japan Aerospace Exploration Agency), Alphonse Sterling(NASA/MSFC), Chairperson:Shin Toriumi(Institute of Space and Astronautical Science, Japan Aerospace Exploration Agency)
Sun. Jun 6, 2021 9:00 AM - 10:30 AM Ch.06 (Zoom Room 06)
This session is for discussions on recent progress in solar and heliospheric physics, and related fields (including plasma physics and planetary physics). In 2020, we had several important milestones in this area. The Daniel K. Inouye Solar Telescope (DKIST operated by NSO) has taken its first image and its call for proposals in observation cycle 1 was announced. The Solar Orbiter was launched by ESAunder collaboration with NASA and released the first data to the public. In Japan, SOLAR-C(EUVST) was selected at ISAS/JAXA as 4th competitively-chosen middle-class mission. We will discuss what observational and theoretical studies achieved in the recent years and what should be addressed next in the coming mid-2020s. We welcome contributions not only by solar researchers but also those from related fields on observations, theories, numerical works, and experiments.

9:00 AM - 9:01 AM

[PEM10-01]Introduction

©Japan Geoscience Union

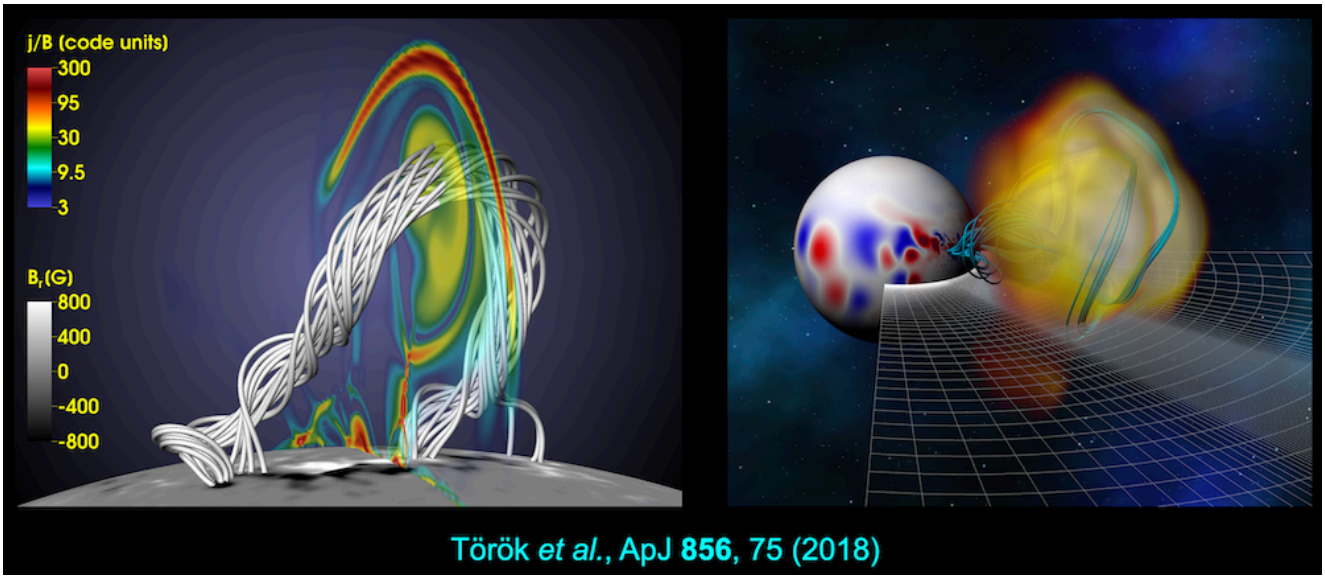
Sun-to-Earth MHD Simulations of Geo-Effective CMEs

*Tibor Torok[1]

1. Predictive Science Inc.

Coronal mass ejections (CMEs) are the main driver of space-weather disturbances in the terrestrial magnetosphere. Predicting the impact of CMEs before they arrive at Earth is one of the main challenges of solar and heliospheric physics. A candidate tool for this purpose are numerical simulations. State-of-the-art magnetohydrodynamic (MHD) simulations are capable of modeling CMEs all the way from Sun to Earth but computationally still too demanding to be used for real-time modeling. Presently, only a simplified model (WAS-ENLIL) is used for operational space-weather forecast. However, given the continuous increase of computing power, more sophisticated models may become available for this purpose in the near future, and first attempts are currently made to prepare such models for operational use. A specific task at hand is to evaluate their accuracy in reproducing in-situ measurements at Earth. In this presentation, I will discuss the predictive capabilities and limitations of state-of-the-art CME simulations. As an example, I will present a Sun-to-Earth simulation of the well-known 14 July 2000 "Bastille-Day" event, which produced a very strong geomagnetic storm. I will also briefly discuss a recent application of the simulation for a modeling of the solar particle event (SPE) associated with the eruption.

Keywords: Sun, Coronal Mass Ejections, Space Weather, Numerical Simulations, Magnetohydrodynamics



©2021. Japan Geoscience Union. All Right Reserved.

How To Trigger the Solar Flares?

*Yumi Bamba[1]

1. Nagoya University

Solar flares and coronal mass ejections, the largest energy-releasing events in the current solar system, are an excellent manifestation of ceaseless magnetohydrodynamic activity of the Sun. In particular, the question of when the flares occur and how they are triggered is not only crucial from the viewpoint of scientific curiosity but also directly linked to the space-weather forecasting, which is now increasingly demanded in tandem with ever-growing reliance of the modern society on information technology. To challenge this conundrum, it is of paramount importance to leverage state-of-the-art observational capabilities, such as spectroscopy in a variety of wavelength domains and polarimetry to derive the detailed magnetic information, and combine the observables with cutting-edge theoretical models that allow for exploration of coronal evolutions including the nonlinear force-free field extrapolations. In the last decade, we have seen a substantial improvement in understanding of flare-triggering mechanisms, facilitated by the development in the realm of both observation and theory. In this review, we first provide an overview of the status quo of flare-related studies. Then, we cast a spotlight on recent advancements by presenting some of our achievements, focusing especially on the series of analysis of the representative flares in Cycle 24 that unveil the physical mechanisms behind the photospheric evolution of the triggering field and its atmospheric response. Finally, the review concludes with discussing the future perspective.

Keywords: Solar flares, Coronal mass ejections, Magnetic fields

©2021. Japan Geoscience Union. All Right Reserved.

The Source Locations of Major Flares and CMEs in the Emerging Active Regions

*Liu Lijuan[1], Wang Yuming[2], Zhou Zhenjun[1]

1. School of Atmospheric Sciences, Sun Yat-sen University, Zhuhai, Guangdong, 519082, China, 2. Department of Geophysics and Planetary Sciences, University of Science and Technology of China, Hefei, Anhui, 230026, China

Major flares and coronal mass ejections (CMEs) tend to originate from the compact polarity inversion lines (PILs) in the solar active regions (ARs). Recently, a scenario named as "collisional shearing" is proposed by Chintzoglou, et. al, 2019 to explain the phenomenon, which suggests that the collision between different emerging bipoles is able to form the compact PIL, driving the shearing and flux cancellation that are responsible to the subsequent large activities. In this work, through tracking the evolution of 19 emerging ARs from their birth until they produce the first major flares or CMEs, we investigated the source PILs of the activities, i.e., the active PILs, to explore the generality of "collisional shearing". We find that none of the active PILs is the self PIL (sPIL) of a single bipole. We further find that 11 eruptions originate from the collisional PILs (cPILs) formed due to the collision between different bipoles, 6 from the conjoined systems of sPIL and cPIL, and 2 from the conjoined systems of sPIL and ePIL (external PIL between the AR and the nearby preexisting polarities). Collision accompanied by shearing and flux cancellation is found developing at all PILs prior to the eruptions, with 84% (16/19) cases having collisional length longer than 18~Mm. Moreover, we find that the magnitude of the flares is positively correlated with the collisional length of the active PILs, indicating that the intenser activities tend to originate from the PILs with severer collision. The results suggest that the "collisional shearing", i.e., bipole-bipole interaction during the flux emergence is a common process in driving the major activities in emerging ARs.

Keywords: Sun, Solar magnetic field, Solar active region, Flare, Coronal mass ejections

©2021. Japan Geoscience Union. All Right Reserved.

Evaluation of horizontal flow velocity at the solar surface with machine learning and numerical simulation

*Hiroyuki Masaki[1], Hideyuki Hotta[2]

1. Graduate School of Science and Engineering, Chiba University, 2. Chiba University

We develop a method to predict the horizontal velocity on the solar surface from snapshots of solar radiative intensity and vertical velocity using neural networks. The motion of solar plasma is related to many phenomena such as sunspot formation and flares. We can observe the line-of-sight (LOS) velocity field with the Doppler effect. In contrast, the velocity perpendicular to LOS is difficult to observe. Some methods estimate the horizontal velocity field by tracking the displacement of features on the solar surface, which require several images. Methods with a neural network for extracting the displacement are also proposed, but these methods also require images at two different times.

On the other hand, many numerical magnetohydrodynamic (MHD) simulations are carried out to explore the solar convection and magnetic field. They can reproduce the phenomena inside the sun with high accuracy thanks to recent improvements in computer performance. In this study, we develop a code for predicting the horizontal velocity field from the corresponding intensity and vertical velocity field by combining numerical MHD simulation and neural networks. We train the neural network using the results of our own MHD simulations. The networks output two components of the horizontal velocity field with the input of corresponding intensity and the vertical velocity field. The network is trained efficiently since we only use the convolutional neural network. As a result, the networks achieve a high correlation coefficient of 0.9 between the predicted and simulated velocity field. The horizontal velocity field can also be predicted from the image with any number of pixels.

Keywords: granulation

©2021. Japan Geoscience Union. All Right Reserved.

Satellite mission: *PhoENiX* (Physics of Energetic and Non-thermal plasmas in the X (= magnetic reconnection) region)

*Noriyuki Narukage[1], Mitsuo Oka[2], Yasushi Fukazawa[3], Keiichi Matsuzaki[4], Shin Watanabe[4], Taro Sakao[4], Kouichi Hagino[5], Ikuyuki Mitsuishi[6], Tsunefumi Mizuno[3], Iku Shinohara[4], Masumi Shimojo[1], Shinsuke Takasao[7], Tomoko Kawate[8], Takafumi Kaneko[6], Hiroshi Tanabe[9], Munetaka UENO[4], Tadayuki Takahashi[10], Takeshi Takashima[4], Masayuki Ohta[4]

1. National Astronomical Observatory of Japan, 2. University of California, Berkeley, 3. Hiroshima University, 4. Japan Aerospace Exploration Agency, 5. Tokyo University of Science, 6. Nagoya University, 7. Osaka University, 8. National Institute for Fusion Science, 9. The University of Tokyo, 10. Kavli Institute for the Physics and Mathematics of the Universe

We are planning a new solar satellite mission, "*PhoENiX*", for understanding of particle acceleration during magnetic reconnection. The main observation targets of this mission are solar flares. The scientific objectives of this mission are (1) to identify particle acceleration sites, (2) to investigate temporal evolution of particle acceleration, and (3) to characterize properties of accelerated particles, during solar flares. In order to achieve these science objectives, the *PhoENiX* satellite will obtain the information about individual X-ray and gamma-ray photons (i.e., position, time, energy and polarization) with three instruments of (1) photon-counting type Soft X-ray focusing Imaging-Spectrometer (SXIS; up to ~10 keV), (2) photon-counting type Hard X-ray focusing Imaging-Spectrometer (HXIS; up to ~30 keV), and (3) Soft Gamma-ray Spectro-Polarimeter (SGSP; spectroscopy is available in the energy range of from > 20 keV to < 600 keV; spectropolarimetry is available from >60 keV to < 600 keV). We plan to realize *PhoENiX* satellite in the Solar Cycle 26 (in 2030s). We emphasize that, thanks to above new observational approach for solar flares, *PhoENiX* is the first mission that can survey "accelerating" particles in the magnetic reconnection system. To maximize the scientific outputs from the new observations by *PhoENiX*, we are also promoting the sounding rocket project *FOXSI-4* (that aims to observe a solar flare in 2024) as a demonstration of *PhoENiX* and developing sophisticated numerical approach and interdisciplinary approach. In this presentation, we will introduce the *PhoENiX* mission and our trinity (observational, numerical, and interdisciplinary) approaches.

Keywords: particle acceleration, magnetic reconnection, solar flare, imaging spectroscopy in X-rays, PhoENiX, FOXSI-4

©2021. Japan Geoscience Union. All Right Reserved.

[E] Oral | P (Space and Planetary Sciences)：P-EM Solar-Terrestrial Sciences, Space Electromagnetism & Space Environment

Sun. Jun 6, 2021 10:45 AM - 12:14 PM JST | Sun. Jun 6, 2021 1:45 AM - 3:14 AM UTC | Ch.06 Zoom Room 06

[P-EM10] Frontiers in solar physics

convener:Takaaki Yokoyama(School of Science, University of Tokyo), Shinsuke Imada(Institute for Space-Earth Environmental Research, Nagoya University), Shin Toriumi(Institute of Space and Astronautical Science, Japan Aerospace Exploration Agency), Alphonse Sterling(NASA/MSFC), Chairperson:Takaaki Yokoyama(School of Science, University of Tokyo)

This session is for discussions on recent progress in solar and heliospheric physics, and related fields (including plasma physics and planetary physics). In 2020, we had several important milestones in this area. The Daniel K. Inouye Solar Telescope (DKIST operated by NSO) has taken its first image and its call for proposals in observation cycle 1 was announced. The Solar Orbiter was launched by ESAunder collaboration with NASA and released the first data to the public. In Japan, SOLAR-C(EUVST) was selected at ISAS/JAXA as 4th competitively-chosen middle-class mission. We will discuss what observational and theoretical studies achieved in the recent years and what should be addressed next in the coming mid-2020s. We welcome contributions not only by solar researchers but also those from related fields on observations, theories, numerical works, and experiments.

10:45 AM - 11:07 AM JST | 1:45 AM - 2:07 AM UTC

[PEM10-07] Spectroscopic and photometric observations of superflares and filament eruption on cool stars

★Invited Papers

*Kosuke Namekata[1,2], Hiroyuki Maehara[2], Ryo Sasaki[3], Hiroki Kawai[3], Yuta Notsu[4], Adam F. Kowalski[4], Joel C. Allred[5], Wataru Iwakiri[3], Yohko Tsuboi[3], Satoshi Honda[6], Soshi Okamoto[1], Kiyoshi Ichimoto[1], Daisaku Nogami[1], Kazunari Shibata[1], Katsuhiro L. Murata[7], Masafumi Niwano[7], Kazuki Shiraishi[7], Ryo Adachi[7], Kota Iida[7], Motoki Oeda[7], Miyako Tozuka[6], Noriyuki Katoh[6], Hiroki Onozuka[6], Keizuke Isogai[1], Mariko Kimura[8], Naoto Kojiguchi[1], Yasuyuki Wakamatsu[1], Yusuke Tampo[1], Futa Ogawa[7], Jun Takahashi[6], Takako T. Ishii[1], Masaki Takayama[6], Tomohito Ohshima[6], Tomoki Saito[6] (1.Kyoto Univ., 2.NAOJ, 3.Chuo Univ., 4.Colorado Univ., 5.NASA, 6.Univ. of Hyogo, 7.Tokyo Institute of Technology, 8.RIKEN)

11:07 AM - 11:29 AM JST | 2:07 AM - 2:29 AM UTC

[PEM10-08] The Solar Orbiter mission – Exploring the Sun and heliosphere

★Invited Papers

*Daniel Mueller[1] (1.European Space Agency)

11:29 AM - 11:44 AM JST | 2:29 AM - 2:44 AM UTC

[PEM10-09] Current Status of the Solar-C_EUVST Mission

*Shinsuke Imada[1], Toshifumi Shimizu[2], Tomoko Kawate[2], Shin Toriumi[2], Yukio Katsukawa[3], Masahito Kubo[3], Hirohisa Hara[3], Yoshinori Suematsu[3], Kiyoshi Ichimoto[4], Ayumi Asai[4], Kyoko Watanabe[6], Takaaki Yokoyama[5], Akiko Tei[2], Harry Warren[7], David Long[8], Louise Harra[8], Luca Teriaca[9], Sarah Matthews[8], Vincenzo Andrette[10], Frederic Auchere[11] (1.Institute for Space-Earth Environmental Research, Nagoya University, 2.ISAS, 3.NAOJ, 4.Kyoto University, 5.University of Tokyo, 6.NDA, 7.NRL, 8.UCL, 9.MPS, 10.Istituto Nazionale di Astrofisica,, 11.IAS)

11:44 AM - 11:59 AM JST | 2:44 AM - 2:59 AM UTC

[PEM10-10] Solar-C(EUVST)/SoSpIM development status and scientific studies

*Kyoko Watanabe[1], Louise Harra[2], Shinsuke Imada[3], Tomoko Kawate[4], Hirohisa Hara[5], Toshifumi Shimizu[6], Yoshizumi Miyoshi[3], Nozomu Nishitani[3], Tomoaki Hori[3], Akimasa Ieda[3], Toshiki Kawai[3], Hidekatsu Jin[7], Chihiro Tao[7], Shohei Nishimoto[1] (1.National Defense Academy of Japan, 2.Physical Meteorological Observatory in Davos, World Radiation Center, 3.Institute for Space-Earth Environmental Research, Nagoya University, 4.National Institute for Fusion Science, National Institutes of Natural

Sciences, 5.National Astronomical Observatory of Japan, National Institutes of Natural Sciences, 6.Institute of Space and Astronautical Science, Japan Aerospace Exploration Agency, 7.National Institute of Information and Communications Technology)

11:59 AM - 12:14 PM JST | 2:59 AM - 3:14 AM UTC

[PEM10-11] Cross-disciplinary study on heating, transport, and turbulence dynamics in solar/astrophysical and fusion/laboratory plasmas: SoLaBo-X

*Motoki Nakata[1], Ryohtaroh T Ishikawa[4], Yukio Katsukawa[2], Yohei Masada[5], Tatsuya Kobayashi[1], Munehito Shoda[2], Shinsuke Imada[3], Shin Toriumi[6], Kenichi Nagaoka[1], SoLaBo-X project[1,2] (1.National Institute for Fusion Science , 2.National Astronomical Observatory of Japan, 3.Institute for Space-Earth Environmental Research , 4.The Graduate University for Advanced Studies, 5.Aichi University of Education, 6.Japan Aerospace Exploration Agency Institute of Space and Astronautical Science)

Spectroscopic and photometric observations of superflares and filament eruption on cool stars

*Kosuke Namekata[1,2], Hiroyuki Maehara[2], Ryo Sasaki[3], Hiroki Kawai[3], Yuta Notsu[4], Adam F. Kowalski[4], Joel C. Allred[5], Wataru Iwakiri[3], Yohko Tsuboi[3], Satoshi Honda[6], Soshi Okamoto[1], Kiyoshi Ichimoto[1], Daisaku Nogami[1], Kazunari Shibata[1], Katsuhiro L. Murata[7], Masafumi Niwano[7], Kazuki Shiraishi[7], Ryo Adachi[7], Kota Iida[7], Motoki Oeda[7], Miyako Tozuka[6], Noriyuki Katoh[6], Hiroki Onozuka[6], Keizuke Isogai[1], Mariko Kimura[8], Naoto Kojiguchi[1], Yasuyuki Wakamatsu[1], Yusuke Tampo[1], Futa Ogawa[7], Jun Takahashi[6], Takako T. Ishii[1], Masaki Takayama[6], Tomohito Ohshima[6], Tomoki Saito[6]

1. Kyoto Univ., 2. NAOJ, 3. Chuo Univ., 4. Colorado Univ., 5. NASA, 6. Univ. of Hyogo, 7. Tokyo Institute of Technology, 8. RIKEN

Solar and stellar flares are caused by the release of magnetic energy on the surfaces. Solar flares produce strong emissions from radio to X-rays and mass ejections (known as filament eruptions or coronal mass ejections), which often affect the Earth's environment. In the case of stars other than the Sun, very large flares called `superflares' (more than 10 times the most energetic solar flares) have been observed not only on M-dwarfs and binaries but also on solar-type stars (G-type main-sequence stars). These can produce much larger X-ray/UV emission and huge mass ejection than those of solar flares, severely affecting the exoplanet habitability. Therefore, stellar superflares are getting more and more attention in terms of the exoplanet habitability as well as possible extreme space weather events on the current Sun (Maehara et al. 2012, Airapetian et al. 2020). The gigantic superflares are expected to share the same physics as solar flares, but the properties are not well known mostly because of the difficulty in observations.

Recently, we have started monitoring observations of stellar flares with our new 3.8m Seimei Telescope at Okayama Observatory in Japan (the largest optical and infrared telescope in East Asia), simultaneously with space/ground optical photometry (e.g. TESS). In this talk, I introduce interesting properties of the observed superflares on a solar-type star (G-dwarf) and an M-dwarf. First, we detected two superflares on an active young solar-type star named EK Draconis. Interestingly, one of them shows clear evidence for a stellar filament eruption associated with a superflare. After the superflare with radiated energy of 2.0×10^{33} erg, a blue-shifted Hα absorption component with a velocity of -510 km s^{-1} appeared. The temporal changes in the spectra greatly resemble those of solar filament eruptions and the erupted mass of 1.1×10^{18} g corresponds to those predicted from solar flare-energy/CME-mass relation. These discoveries imply that a huge stellar filament eruption occurred possibly in the same way as solar ones (Namekata et al. submitted). This fast eruption can lead to a coronal mass ejection, which enables further studies to estimate its impacts on planets and stellar mass loss.

We also detected one superflare on an active M-dwarf named AD Leonis. The time-resolved Hα line of the superflare shows symmetric line broadenings of 14 Åin association with the large white-light flare (2.0×10^{33} erg). The line broadening indicates very high electron density in the flaring chromosphere (cf. pressure or opacity broadening). The dense regions can be generated by flare heating of non-thermal high-energy particles that can penetrate into the lower chromosphere. We modeled the flaring M-dwarf atmosphere with the RADYN code (e.g. Kowalski et al. 2017) and found that the energy injection of high-energy particles with the flux of 10^{12} erg/s/cm^2 can well reproduce the observed Hα spectra (Namekata et al. 2020b, PASJ). The energy flux is much higher than the solar ones, which indicates the very efficient particle acceleration in the superflare. On the other hand, the superflare on M-dwarf and

©2021. Japan Geoscience Union. All Right Reserved.

another superflare on G-dwarf did not show any evidence of stellar filament eruptions. This may indicate the flare/mass-eruption association rates are not 100 % in stellar flares, although it should be noted that our detection is limited to the line-of-sight motions. Our studies provided how to investigate stellar mass eruption and high energy particles on stellar flares with the help of solar physics, and further solar-stellar connection will deepen our understanding of extreme events not only on active stars but also on the Sun.

Keywords: stellar flares, superflares, stellar mass ejection, Seimei telescope, optical spectroscopic observations

©2021. Japan Geoscience Union. All Right Reserved.

The Solar Orbiter mission –Exploring the Sun and heliosphere

*Daniel Mueller[1]

1. European Space Agency

Solar Orbiter, launched on 10 February 2020, is a space mission of international collaboration between ESA and NASA. It is exploring the linkage between the Sun and the heliosphere and has started to collect unique data at solar distances down to 0.49 au. By ultimately approaching as close as 0.28 au, Solar Orbiter will view the Sun with very high spatial resolution and combine this with in-situ measurements of the surrounding heliosphere. Over the course of the mission, the highly elliptical orbit will get progressively more inclined to the ecliptic plane. Thanks to this new perspective, Solar Orbiter will deliver images and comprehensive data of the unexplored Sun’ s polar regions and the side of the Sun not visible from Earth. This talk will highlight first science results from Solar Orbiter and provide a mission status update.

Keywords: the Sun, space mission

©2021. Japan Geoscience Union. All Right Reserved.

Current Status of the Solar-C_EUVST Mission

*Shinsuke Imada[1], Toshifumi Shimizu[2], Tomoko Kawate[2], Shin Toriumi[2], Yukio Katsukawa[3], Masahito Kubo[3], Hirohisa Hara[3], Yoshinori Suematsu[3], Kiyoshi Ichimoto[4], Ayumi Asai[4], Kyoko Watanabe[6], Takaaki Yokoyama[5], Akiko Tei[2], Harry Warren[7], David Long[8], Louise Harra[8], Luca Teriaca[9], Sarah Matthews[8], Vincenzo Andrette[10], Frederic Auchere[11]

1. Institute for Space-Earth Environmental Research, Nagoya University, 2. ISAS, 3. NAOJ, 4. Kyoto University, 5. University of Tokyo, 6. NDA, 7. NRL, 8. UCL, 9. MPS, 10. Istituto Nazionale di Astrofisica,, 11. IAS

Solar-C_EUVST (EUV High-Throughput Spectroscopic Telescope) is designed to comprehensively understand the energy and mass transfer from the solar surface to the solar corona and interplanetary space, and to investigate the elementary processes that take place universally in cosmic plasmas. As a fundamental step towards answering how the plasma universe is created and evolves, and how the Sun influences the Earth and other planets in our solar system, the proposed mission is designed to comprehensively understand how mass and energy are transferred throughout the solar atmosphere. Understanding the solar atmosphere, which connects to the heliosphere via radiation, the solar wind and coronal mass ejections, and energetic particles is pivotal for establishing the conditions for life and habitability in the solar system.

The two primary science objectives for Solar-C_EUVST are : I) Understand how fundamental processes lead to the formation of the solar atmosphere and the solar wind, II) Understand how the solar atmosphere becomes unstable, releasing the energy that drives solar flares and eruptions. Solar-C_EUVST will, A) seamlessly observe all the temperature regimes of the solar atmosphere from the chromosphere to the corona at the same time, B) resolve elemental structures of the solar atmosphere with high spatial resolution and cadence to track their evolution, and C) obtain spectroscopic information on the dynamics of elementary processes taking place in the solar atmosphere.

In this talk, we will first discuss the science target of the Solar-C_EUVST, and then discuss the current status of the Solar-C_EUVST mission.

©2021. Japan Geoscience Union. All Right Reserved.

Solar-C(EUVST)/SoSpIM development status and scientific studies

*Kyoko Watanabe[1], Louise Harra[2], Shinsuke Imada[3], Tomoko Kawate[4], Hirohisa Hara[5], Toshifumi Shimizu[6], Yoshizumi Miyoshi[3], Nozomu Nishitani[3], Tomoaki Hori[3], Akimasa Ieda[3], Toshiki Kawai[3], Hidekatsu Jin[7], Chihiro Tao[7], Shohei Nishimoto[1]

1. National Defense Academy of Japan, 2. Physical Meteorological Observatory in Davos, World Radiation Center, 3. Institute for Space-Earth Environmental Research, Nagoya University, 4. National Institute for Fusion Science, National Institutes of Natural Sciences, 5. National Astronomical Observatory of Japan, National Institutes of Natural Sciences, 6. Institute of Space and Astronautical Science, Japan Aerospace Exploration Agency, 7. National Institute of Information and Communications Technology

The Solar Spectral Irradiance Monitor (SoSpIM) has been developed by the Physical Meteorological Observatory in Davos World Radiation Center (PMOD/WRC) in Switzerland to be installed on the Solar-C(EUVST), the next solar observation satellite.

SoSpIM has two observation wavelength bands (170-215Å, 1115-1275Å) that are also covered by Solar-C(EUVST). By having a redundant system with three independent channels for each wavelength band, the instrument can monitor the degradation and contamination of Solar-C(EUVST). SoSpIM is expected to be used for calibration of the Solar-C(EUVST).

The extreme ultraviolet (EUV) emissions observed by SoSpIM play a main role in controlling the composition of the Earth's upper atmosphere. Both wavelength bands are mainly absorbed in the thermosphere and ionosphere, which are usually formed at altitudes > 80 km, and are thought to change the composition of the Earth's atmosphere around this altitude. In particular, it is known that sudden fluctuations in EUV emissions due to solar flares greatly change the composition and height profile of the ionosphere, causing space weather phenomena such as communication failures. Therefore, we set up the SoSpIM science team to study not only solar flare physics, but also discuss what kind of space weather research is feasible using SoSpIM data.

In this presentation, we will report on the current development status of SoSpIM and the scientific topics considered to be contributed by SoSpIM data.

Keywords: Solar-C(EUVST), Irradiance Monitor, Space Weather

©2021. Japan Geoscience Union. All Right Reserved.

Cross-disciplinary study on heating, transport, and turbulence dynamics in solar/astrophysical and fusion/laboratory plasmas: SoLaBo-X

*Motoki Nakata[1], Ryohtaroh T Ishikawa[4], Yukio Katsukawa[2], Yohei Masada[5], Tatsuya Kobayashi[1], Munehito Shoda[2], Shinsuke Imada[3], Shin Toriumi[6], Kenichi Nagaoka[1], SoLaBo-X project[1,2]

1. National Institute for Fusion Science , 2. National Astronomical Observatory of Japan, 3. Institute for Space-Earth Environmental Research , 4. The Graduate University for Advanced Studies, 5. Aichi University of Education, 6. Japan Aerospace Exploration Agency Institute of Space and Astronautical Science

A cross-disciplinary research activity for solar/astrophysical and fusion/laboratory plasmas “SoLaBo-X (Solar + Laboratory + Cross-disciplinary)” is presented. Multi-scale interactions and the energy transfer processes among the microscopic fluctuations and the macroscopic structures are key ingredients to elucidate long-standing issues, e.g., solar coronal heating, solar wind accelerations, and turbulence suppressions by spontaneously generated zonal flows in fusion plasmas. Beyond large difference of the mean plasma parameters, our joint-study project focuses on the turbulence dynamics and associated heating and transport processes in solar and magnetically confined plasmas. Two major directions have been specified, i.e., (1)Energy transfer analyses based on the higher order turbulence correlations in multi-component turbulent fields, and (2)Deep-learning-assisted fast and accurate evaluations/predictions of the spatio-temporal structures in the turbulent fields. In these directions, several research topics have been addressed: (i)Visualization experiments and the image analysis of electrically-driven turbulent convections in relevance to the dynamics in the solar tachocline, (ii)Statistical analysis and modeling of entropy-gradient-driven(local) and cooling-driven(nonlocal) turbulence in the solar convection zone, (iii)Multi-scale convolutional neural network modeling for the fast predictions of hardly-observable turbulence fields(e.g., horizontal velocity and/or magnetic fields, etc.) from the observables(e.g., continuum intensity and/or vertical velocity, etc.), and (iv)Extended modeling of the electron parallel energy transport and the experimental verification in a linear plasma device with the direct measurement of the electron energy distribution function.

Keywords: turbulence , solar plasmas , fusion plasmas , cross-disciplinary study

©2021. Japan Geoscience Union. All Right Reserved.

[E] Poster | P (Space and Planetary Sciences)：P-EM Solar-Terrestrial Sciences, Space Electromagnetism & Space Environment

Sun. Jun 6, 2021 5:15 PM - 6:30 PM JST | Sun. Jun 6, 2021 8:15 AM - 9:30 AM UTC | Ch.06_1

[P-EM10] Frontiers in solar physics

convener:Takaaki Yokoyama(School of Science, University of Tokyo), Shinsuke Imada(Institute for Space-Earth Environmental Research, Nagoya University), Shin Toriumi(Institute of Space and Astronautical Science, Japan Aerospace Exploration Agency), Alphonse Sterling(NASA/MSFC)

This session is for discussions on recent progress in solar and heliospheric physics, and related fields (including plasma physics and planetary physics). In 2020, we had several important milestones in this area. The Daniel K. Inouye Solar Telescope (DKIST operated by NSO) has taken its first image and its call for proposals in observation cycle 1 was announced. The Solar Orbiter was launched by ESAunder collaboration with NASA and released the first data to the public. In Japan, SOLAR-C(EUVST) was selected at ISAS/JAXA as 4th competitively-chosen middle-class mission. We will discuss what observational and theoretical studies achieved in the recent years and what should be addressed next in the coming mid-2020s. We welcome contributions not only by solar researchers but also those from related fields on observations, theories, numerical works, and experiments.

[PEM10-P01] Validation of solar flare emission spectra and their impact on the ionosphere

★Invited Papers

*Shohei Nishimoto[1], Kyoko Watanabe[1], Hidekatsu Jin[3], Toshiki Kawai[2], Shinsuke Imada[2], Tomoko Kawate[4] (1.National Defense Academy, 2.Institute for Space-Earth Environmental Research, Nagoya University, 3.National Institute of Information and Communications Technology, 4.National Institute for Fusion Science)

[PEM10-P02] Electron acceleration region in a small solar flare observed with Nobeyama Radioheliograph and MUSER

*Satoshi Masuda[1], Chengming Tan[2], Yihua Yan[2], Baolin Tan[2], Hiroaki Misawa[3] (1.Institute for Space-Earth Environmental Research, Nagoya University, 2.National Astronomical Observatories of China, 3.Graduate school of science, Tohoku University)

[PEM10-P03] Test particle simulation of high energy electrons during solar flare

*Takafumi Kaneko[1], Shinsuke Takasao[2] (1.Institute for Space-Earth Environmental Research, Nagoya University, 2.Department of Earth and Space Science, Graduate School of Science, Osaka University)

[PEM10-P04] Contribution of small-scale flares to coronal heating estimated by a spectroscopic observation of Hinode.

★Invited Papers

*Toshiki Kawai[1], Shinsuke Imada[1] (1.Institute for Space-Earth Environmental Research, Nagoya University)

[PEM10-P05] A Possible Generation Mechanism for “Switchbacks” Observed in the Solar Wind by the Parker Solar Probe (PSP)

*Alphonse Sterling[1], Ronald Moore[2,1] (1.NASA/MSFC, 2.University of Alabama Huntsville)

[PEM10-P06] MHD simulations of a coronal loop with effect of Alfven wave turbulence heating

Tatsuya Kai[1], *Takaaki Yokoyama[1], Munehito Shoda[2] (1.School of Science, University of Tokyo, 2.National Astronomical Observatory of Japan)

[PEM10-P07] Heating of the low-beta chromosphere by fast magnetic shock wave

*Yikang Wang[1], Takaaki Yokoyama[1], Haruhisa Iijima[2] (1.The University of Tokyo, 2.Nagoya University)

[PEM10-P08] Calculation of solar surface flow using a magnetic element tracking module

*Kengo Matoba[1], Shinsuke Imada[1], Haruhisa Iijima[1], Yoshizumi Miyoshi[1] (1.Institute for Space-Earth Environmental Research, Nagoya University)

[PEM10-P09] Prediction of latitude/longitude distribution of sunspot and tilt angle using machine learning

*Kento Michiwaki[1], Shinsuke Imada[1], Yoshizumi Miyoshi[1] (1.Institute for Space-Earth Environmental Research, Nagoya University)

[PEM10-P10] A numerical treatment for the unresolved transition region in the solar atmosphere

*Haruhisa Iijima[1], Shinsuke Imada[1] (1.Institute for Space-Earth Environmental Research, Nagoya University)

[PEM10-P11] EUV synthesis project for the Solar-C (EUVST) mission

*Akiko Tei[1], Takaaki Yokoyama[2], Shin Toriumi[1], Hirohisa Hara[3], Shinsuke Imada[4] (1.Institute of Space and Astronautical Science, 2.The University of Tokyo, 3.National Astronomical Observatory of Japan, 4.Nagoya University)

[PEM10-P12] Soalr-C(EUVST) coordination with and ground based and space observatories

*Shinichi Nagata[1], Ayumi Asai[2], Kiyoshi Ichimoto[2], Satoru UeNo[2], Toshifumi Shimizu[3], Shin Toriumi[3], Shinsuke Imada[4], Hirohisa Hara[5], Takaaki Yokoyama[6] (1.Hida Observatory, Astronomical Observatory, Graduate School of Science, Kyoto University, 2.Astronomical Observatory, Graduate School of Science, Kyoto University, 3.Institute of Space and Astronautical Science, JAXA, 4. Institute for Space–Earth Environmental Research, Nagoya University, 5.National Astronomical Observatory of Japan, 6.University of Tokyo)

[PEM10-P13] Comparison of the Optical Characteristics for Japanese Space Solar Telescopes: Hinode/XRT and Yohkoh/SXT

*Junho Shin[1], Ryouhei Kano[2], Takashi Sakurai[2], Yeon-Han Kim[3], Yong-Jae Moon[1] (1.Kyung Hee Univ., 2.NAOJ, 3.KASI)

Validation of solar flare emission spectra and their impact on the ionosphere

*Shohei Nishimoto[1], Kyoko Watanabe[1], Hidekatsu Jin[3], Toshiki Kawai[2], Shinsuke Imada[2], Tomoko Kawate[4]

1. National Defense Academy, 2. Institute for Space-Earth Environmental Research, Nagoya University, 3. National Institute of Information and Communications Technology, 4. National Institute for Fusion Science

Solar flares suddenly emit strong multi-wavelength electromagnetic emissions. Among these emissions, X-rays and extreme ultraviolet (EUV) emissions rapidly change the physical composition of the Earth's thermosphere and ionosphere, thereby causing space weather phenomena such as the sudden ionospheric disturbance etc. (Dellinger 1937).

To predict the effects of flare emissions on the Earth's upper atmosphere, empirical and physical models have been developed. We verify the extent of reproducing the flare emission spectra using a newly developed simple method based on the physical process of the flare loop (Kawai et al., 2020). In this method, we convert the soft X-ray light-curves observed during flare events into EUV emission spectra using a one-dimensional hydrodynamic calculation and the CHIANTI atomic database (Dere et al., 2019). We examined the “EUV flare time-integrated irradiance” and “EUV flare line rise time” of the EUV emissions for 21 the events by comparing the calculation results of the proposed method and observed EUV spectral data. Proposed method succeeded in reproducing the EUV flare time-integrated irradiance of the Fe VIII 13.1 nm, Fe XVIII 9.4 nm, and Fe XX 13.3 nm, as well as the 5.5-35.5 nm band. For the EUV flare line rise time, there was acceptable correlation between the proposed method estimations and observations for all Fe flare emission lines.

Furthermore, in order to examine the effect of flare EUV emission on the Earth’s ionosphere, we input our calculated flare EUV spectra that mentioned above to the Earth's atmospheric model GAIA (Ground-to-Topside Model of Atmosphere and Ionosphere for Aeronomy; Jin et al., 2011). We investigated the ionospheric response to solar flare emission by comparing the total electron content (TEC) variation in the ionosphere reproduced by GAIA with observations. This study statistically revealed which wavelengths in the solar flare emission spectrum affect which altitude in the ionosphere.
In this presentation, we will discuss the statistical analysis results of the ionospheric response due to differences in solar flare emission spectra.

Keywords: Solar flare, UV radiation, X-rays

©2021. Japan Geoscience Union. All Right Reserved.

Electron acceleration region in a small solar flare observed with Nobeyama Radioheliograph and MUSER

*Satoshi Masuda[1], Chengming Tan[2], Yihua Yan[2], Baolin Tan[2], Hiroaki Misawa[3]

1. Institute for Space-Earth Environmental Research, Nagoya University, 2. National Astronomical Observatories of China, 3. Graduate school of science, Tohoku University

Nobeyama Solar Radio Observatory, NAOJ, was closed at the end of March 2015. After that, Nobeyama Radioheliograph has been operated by the International Consortium for the Continued Operation of Nobeyama Radioheliograph (ICON). After the five-year extension of the operation by ICCON, finally, it was shut down at the end of March 2020. On the other hand, a new Chinese solar radio telescope, 'Mingantu Spectral Radioheliograph (MUSER)' was developed and started observations during this extension period. While NoRH observes the sun at two frequencies (17 and 34 GHz), MUSER observes at relatively lower, but much wider frequency range (0.4 –15 GHz). The observation using these two instruments provides us the information of the accelerated electrons with different energies and at different altitudes in the solar atmosphere. This is a great advantage to reveal the electron acceleration process in a solar flare.

At first, we made a list of the events which was simultaneously observed with NoRH and MUSER. The total number of the events was twenty-five. Among them, we analyzed a small solar flare with a duration of about 15 seconds on 22 November 2015. In this event, a group of weak type-III bursts appeared in the 1-2 GHz range. Its appearance frequency changed from low/high to high/low frequency before/after the peaktime of the 17 GHz flux. In addition, there was a blank (= no emission) frequency range between the type-III bursts with a negative and positive frequency drift, emitted by high-energy electrons moving upward and downward, respectively. In the frequency range higher/lower than the blank, the most of bursts show negative/positive frequency drift. This blank might correspond to the acceleration region and accelerated electrons move both upward and downward from that altitude. In addition, the frequency of the blank continuously moved to the higher frequency range at least until the peaktime. This indicates that the electron acceleration region gradually moved to the higher altitude during the flare. Here, there are two candidates as the acceleration region. One is the magnetic reconnection site, and the other is the fast shock region above the flare loop in the standard CSHKP-type flare scenario. Integrating the EUV imaging observations by SDO/AIA, we discuss which is more consistent with the observational results.

Keywords: solar flare, radio emission, particle acceleration

©2021. Japan Geoscience Union. All Right Reserved.

Test particle simulation of high energy electrons during solar flare

*Takafumi Kaneko[1], Shinsuke Takasao[2]

1. Institute for Space-Earth Environmental Research, Nagoya University, 2. Department of Earth and Space Science, Graduate School of Science, Osaka University

Solar energetic particles are generated by flares in the solar atmosphere and coronal mass ejections propagating in the interplanetary space. During solar flares, energetic electrons with an energy of 100 eV to 100 keV are commonly observed. The high energy electrons reaching 1 MeV or higher are also occasionally observed. The reconnection model of solar flare has been established by both numerous observations and MHD simulations. However, major electron acceleration processes have not been incorporated in the standard flare model yet. In MHD models, we can find multiple candidate sources of particle acceleration such as plasmoids, shocks, and turbulence. The remained issue is to specify the major acceleration site. In this study, we investigate possible sites of particle acceleration in a flare reconnection model using MHD simulations and test particle simulations for electrons based on the guiding center approximation. We quantitatively evaluated the electron energies in different locations in the framework of the standard flare model. We performed a MHD simulation of a solar flare including the thermal conduction and the gravitational stratification. We conducted test particle simulations using the numerical solution of the MHD simulation as the background field for the particles. As a result, high energy electrons with an energy of 10 keV to 1 MeV were reproduced. Our simulations show that the loop-top region is a strong accelerator: the particles around the termination shock were accelerated up to 1 MeV. In the other areas, the particles were accelerated up to 100 keV, consistent with observations. We found that electron energies around shock regions are larger than those in plasmoids. We discuss the link between MHD structures and major electron acceleration processes.

Keywords: solar flare, particle acceleration

©2021. Japan Geoscience Union. All Right Reserved.

Contribution of small-scale flares to coronal heating estimated by a spectroscopic observation of Hinode.

*Toshiki Kawai[1], Shinsuke Imada[1]

1. Institute for Space-Earth Environmental Research, Nagoya University

The mechanism of coronal heating is one of the long-standing problems in solar physics. Two primary mechanisms have been proposed to explain this problem, namely nanoflares and wave dissipation. In nanoflare model, it is crucial to accurately quantify the contribution of small-scale flares to the coronal heating. So far, spectroscopic observations succeeded in achieving many progress in physics of solar corona. One of the strengths of a spectral observation is capability to derive a line-of-site plasma velocity for each ion species. In this paper, we estimate a contribution of Doppler motion and non-thermal energies released during transient brightenings to the heating of an active region. We use Hinode/EUV Imaging Spectrometer and Solar Dynamics Observatory/Atmospheric Imaging Assembly for the energy estimation and detection of transient brightenings. As a result, the released Doppler motion and non-thermal energies are approximately 1 -- 10% and 10 -- 100% of a change amount of thermal energy in each enhancement, respectively. Using this ratio, we estimate a contribution of the energy flux of AIA transient brightenings as at most 10% of the loss flux.

Keywords: solar corona, spectroscopic observation, flare

©2021. Japan Geoscience Union. All Right Reserved.

A Possible Generation Mechanism for “Switchbacks” Observed in the Solar Wind by the Parker Solar Probe (PSP)

*Alphonse Sterling[1], Ronald Moore[2,1]

1. NASA/MSFC, 2. University of Alabama Huntsville

The Parker Solar Probe (PSP) has observed copious rapid magnetic field direction changes in the near-Sun solar wind. These features have been called "switchbacks," and their origin is a mystery. But their widespread nature suggests that they may be generated by a frequently occurring process in the Sun's atmosphere. We examine the possibility that the switchbacks originate from coronal jets. Recent work suggests that many coronal jets result when photospheric magnetic flux cancels, and forms a small-scale "minifilament" flux rope that erupts and reconnects with coronal field. We argue that the reconnected erupting-minifilament flux rope can manifest as an outward propagating Alfvenic fluctuation that steepens into an increasingly compact disturbance as it moves through the solar wind. Using previous observed properties of coronal jets that connect to coronagraph-observed white-light jets (a.k.a. "narrow CMEs"), along with typical solar wind speed values, we expect the coronal-jet-produced disturbances to traverse near-perihelion PSP in less than about 25 minutes, with a velocity of ~400 km/s. To consider further the plausibility of this idea, we show that a previously studied series of equatorial latitude coronal jets, originating from the periphery of an active region, generate white-light jets in the outer corona (seen in STEREO/COR2 coronagraph images; 2.5-15 solar radii), and into the inner heliosphere (seen in Solar-Terrestrial Relations Observatory (STEREO)/Hi1 heliospheric imager images; 15-84 solar radii). Thus it is tenable that disturbances put onto open coronal magnetic field lines by coronal-jet-producing erupting-minifilament flux ropes can propagate out to PSP space and appear as switchbacks. This work was supported through funding from NASA's Heliophysics Division.

Keywords: Solar coronal jets, Solar filament eruptions, Solar magnetic fields, Solar magnetic reconnection, Solar wind

©2021. Japan Geoscience Union. All Right Reserved.

MHD simulations of a coronal loop with effect of Alfven wave turbulence heating

Tatsuya Kai[1], *Takaaki Yokoyama[1], Munehito Shoda[2]

1. School of Science, University of Tokyo, 2. National Astronomical Observatory of Japan

Coronal heating is one of the most important but still unsolved problems in solar physics and heliophysics. Alfven wave is one of the candidate mechanisms that provide magnetic energy to the corona. However, detailed mechanisms of its thermalization are unclear. Non-linear conversion to the acoustic modes and their dissipation via shock generation are found to reproduce the hot corona in studies by one-dimensional MHD simulations (e.g. Moriyasu et al. 2004; Antolin et al. 2008, 2010). However, there remains some quantitative issues to be solved when one compares their results with observations. One is the dependence on the magnetic field strength of the corona. Since the amplitude of Alfven wave is sensitive to the distribution of Alfven speed, a prescribed coronal magnetic field has to be observationally acceptable one. The previous works assumed the strength to be a few Gauss that is rather small that infered from coronal seismology or potential field extraporation. Second is the consistency with the observed emission-line widths. For example, according to the Norikura observations, Hara & Ichimoto (1999) evaluated them to be less than 20 km/s in the lines with formation temperature of a few million Kelvin. The previous studies' amplitudes of the generated shock waves are larger than this observed value which must be investigated.

In this study, we conducted a series of one-dimensional MHD simulations to solve this line-width issue by including a noble effect: Alfven wave tubulence dissipation. Although turbulence is essentially a three-dimensional process, its heating rate was phenomenologically estimated in one-dimensional models and was implemented in the fast solar wind simulations by Shoda et al. (2018). Our present study adopted this phenomenological approximation to one-dimensional MHD equations and conducted simulations of a closed loop for applications to active-region loops in mind. We also updated the chromospheric cooling to a sophisticated model by Goodman and Judge (2012).

In the typical case with a coronal magnetic field of several tens of Gauss, the corona with 1 MK was successfully reproduced. The obtained wave amplitude was longitudinally 18.8 km/s and transversely 20.6 km/s that were consistent with the observed emission-line widths. Alfven wave turbulence heating was found to be more dominant than heating by shocks. Parameter survey gives a dependence of transverse velocity amplitude on the strength of coronal magnetic field as a broken power law with indices of -0.3 below 100 G and -1.0 above.

Keywords: Coronal heating, Alfven wave

©2021. Japan Geoscience Union. All Right Reserved.

Heating of the low-beta chromosphere by fast magnetic shock wave

*Yikang Wang[1], Takaaki Yokoyama[1], Haruhisa Iijima[2]

1. The University of Tokyo, 2. Nagoya University

The energy balance in the chromosphere is dominated by mechanical heating and radiative loss. Shock wave is one of the candidates for chromospheric heating. Previous researches provide different wave heating scenarios and comparison among them is necessary. However, it is difficult as the previous theoretical works usually use the artificial model that can include only one or a few mechanisms. On the other hand, previous studies using realistic simulations usually focus on synthesized observation without investigating the detailed physics about the heating mechanisms or the propagation of waves.

This study aims to investigate the propagation of MHD waves in realistic simulations and quantitatively determine the role of different wave modes in chromospheric heating. We perform two-dimensional MHD simulations from the convection zone to the corona with local thermodynamic equilibrium radiative transfer in the photosphere and approximated chromospheric and coronal radiative loss. From the simulation results, we identify the shocks by filtering the regions with large negative divergence of velocity. After identification of shocks, we separate fast and slow MHD waves by identifying the relation between magnetic pressure and gas pressure in the upstream and the downstream regions. We further calculate the contribution to chromospheric heating through the measurement of entropy jump. The results show that fast magnetic waves play a significant role in heating the low-beta chromosphere. The low-beta fast magnetic waves are generated by mode conversion from fast acoustic waves in the high-beta region.

Keywords: Sun, Chromosphere, MHD wave

©2021. Japan Geoscience Union. All Right Reserved.

Calculation of solar surface flow using a magnetic element tracking module

*Kengo Matoba[1], Shinsuke Imada[1], Haruhisa Iijima[1], Yoshizumi Miyoshi[1]

1. Institute for Space-Earth Environmental Research, Nagoya University

Solar flares have major impacts on the geospace electromagnetic environment. Flares are now believed to occur in conjunction with sunspot’ s activities. The number of sunspots increases and decreases periodically in about eleven years. For the long-term space weather forecast, it is important to predict the sunspot number for the next solar cycle. Recently, it has been suggested that the polar magnetic field during the cycle minimum is one of the good precursors for the solar activity of the next cycle. The surface flux transport (SFT) model has been used to predict the polar magnetic field prior to the cycle minimum. While the SFT model requires several parameters, such as meridional flow, differential rotation, and turbulent diffusion, these parameters are not fully understood, especially on their temporal variation and the behavior in the polar region.

In this study, we focused on two typical solar surface flows, differential rotation and meridional circulation, which are the parameters of the SFT model. We apply a magnetic element tracking (MET) module on the SDO/HMI magnetogram to estimate the solar surface velocities. The polar region is difficult to be observed in the low resolution HMI data. We use the high resolution Hinode/SOT magnetogram to measure the surface motion in the polar region. The alignment of the SOT data was performed in comparison with the HMI data. Because the HMI data is available since 2010, we calculated solar surface flows for the entire period of solar cycle 24. As a result, we obtained the latitudinal profile and time variation of the meridional flow and differential rotation rate. We find that the differential rotation/meridional flow is faster/slower at the latitude where the sunspots frequently emerge, respectively[YM1] . From the Hinode/SOT data, we calculated solar surface flow in the polar region with higher spatio-temporal resolution than ever before.

Keywords: Sun, Sunspot, Magnetic field

©2021. Japan Geoscience Union. All Right Reserved.

Prediction of latitude/longitude distribution of sunspot and tilt angle using machine learning

*Kento Michiwaki[1], Shinsuke Imada[1], Yoshizumi Miyoshi[1]

1. Institute for Space-Earth Environmental Research, Nagoya University

In space weather forecasting, it is important to estimate the solar activity in near future. Recent studies have shown that there is a correlation between the value of the polar magnetic field during the solar minimum and the next solar activity level. This means that the value of the polar magnetic field is one of the most important indicators for predicting the activity level. For this reason, many studies have tried to predict the polar magnetic field. The value of the polar field can be calculated using the surface flux transport model (SFT model). The SFT model consists of advection term due to differential rotation and meridional circulation, magnetic diffusion term, and flux emergence term. The advection and the diffusion coefficients are estimated by modern observations. On the other hand, estimation of future flux emergence is still very difficult without reliable information about these coefficients. Therefore, it is crucial problem about the solar cycle prediction to estimate when and where the sunspots will emerge.

In this study, we predict the latitude distribution (butterfly diagram) using 2D-CNN (two-dimensional Convolutional Neural Network), which is one of the machine learning technique. As a result, we can reproduce the transition and the periodicity of the appearance of the sunspot from the middle latitude to the low latitude. Furthermore, as a result of predicting cycle 25 using this model, the maximum sunspot number is slightly larger than cycle 24, and the structure of the butterfly diagram is similar to cycle 16. We present the prediction results on latitude distribution, longitude distribution, and tilt angle using 3D-CNN (three-dimensional Convolutional Neural Network) and LGB (Light Gradient Boosting) method.

Keywords: sun, sunspot, machine learning

©2021. Japan Geoscience Union. All Right Reserved.

A numerical treatment for the unresolved transition region in the solar atmosphere

*Haruhisa Iijima[1], Shinsuke Imada[1]

1. Institute for Space-Earth Environmental Research, Nagoya University

In the solar atmosphere, the transition region between the chromosphere and the corona is very thin compared to the typical spatial scale in the chromosphere and corona. To fully resolve the transition region in the numerical simulations of the quiet Sun, the grid size must be on the order of a kilo-meter or less, which is difficult to achieve in the multi-dimensional simulations. The requirement on the numerical resolution becomes even more stringent in the hotter atmosphere, like the active/flaring regions. In this study, we propose a new technique to numerically broaden the unresolved transition region without affecting the energy balance in the solar atmosphere. The performance of the proposed method is tested in terms of the time variation of the spectroscopic observables in the optically thin approximation. Using this method, the Doppler shift and non-thermal line width of the synthesized line emission are expected to agree with those of the high-resolution reference simulation within an error of a few km/s.

Keywords: Magnetohydrodynamics (MHD), Solar transition region, Numerical simulation

©2021. Japan Geoscience Union. All Right Reserved.

EUV synthesis project for the Solar-C (EUVST) mission

*Akiko Tei[1], Takaaki Yokoyama[2], Shin Toriumi[1], Hirohisa Hara[3], Shinsuke Imada[4]

1. Institute of Space and Astronautical Science, 2. The University of Tokyo, 3. National Astronomical Observatory of Japan, 4. Nagoya University

In the Solar-C (EUVST) mission, the Science Task Team (STT) develops strategies for achieving the science objectives, particularly through a coordination between the theory and observation. In 2020, the STT held a series of workshops and discussed, for each science objective, what observational and theoretical studies have achieved so far; what the remaining technical issues are in both theoretical and observational points of view; what we need for theoretically solving the science objectives; and what Solar-C (EUVST) would achieve observationally.

As a next step, we started a new project, where we synthesize EUV line emissions in the wavelength range covered by Solar-C (EUVST) from numerical simulation results. The purpose in this project is to study quantitative feasibility of EUVST for extraction of physical information from the observations. By employing the CHIANTI IDL package and assuming that the spectral lines are optically thin, we synthesize the EUV lines that form in the solar corona. We perform the line synthesis on the 3D model atmosphere produced from the magnetohydrodynamic simulation. For each snapshot of the model atmosphere, we extract the temperature, density, and velocity over lines of sight (LOS), and generate spectral line profiles across the field view, which can be directly compared with the observations. Then, we derive a LOS velocity and line width from each synthesized line profile, which can be utilized to discuss the origin of nonthermal width and dynamics.

At the moment, we adopt the above method to the 3D model atmosphere computed with the MPS/University of Chicago Radiative MHD (MURaM) code. In the presentation, we show the latest updates of our EUV synthesis project, with addressing the future outlook for the STT activities.

Keywords: Solar-C (EUVST), synthesis, CHIANTI

©2021. Japan Geoscience Union. All Right Reserved.

Soalr-C(EUVST) coordination with and ground based and space observatories

*Shinichi Nagata[1], Ayumi Asai[2], Kiyoshi Ichimoto[2], Satoru UeNo[2], Toshifumi Shimizu[3], Shin Toriumi[3], Shinsuke Imada[4], Hirohisa Hara[5], Takaaki Yokoyama[6]

1. Hida Observatory, Astronomical Observatory, Graduate School of Science, Kyoto University, 2. Astronomical Observatory, Graduate School of Science, Kyoto University, 3. Institute of Space and Astronautical Science, JAXA, 4. Institute for Space–Earth Environmental Research, Nagoya University, 5. National Astronomical Observatory of Japan, 6. University of Tokyo

Solar-C(EUVST) will make the most comprehensive spectroscopic observations of the solar atmosphere with an unprecedented combination of temperature coverage (5 kK –20 MK), spatial resolution (0.4″), and cadence (as high as 0.1˜s). To maximize the scientific output of EUVST, the coordination with ground based and space observatories such as Dnaiel K. Inouye Solar Telescope(US), Swedish Solar Telescope, (Sweden), Goode Solar Telescope (US), Hida Observatory, and Solar Orbiter is planned. The coordinated observations with ground based observatories will provide important information on the dynamics and energetics of plasma and magnetic fields in the photosphere and chromosphere. The in-situ measurements of solar wind plasma by Solar Orbiter and other space observatories will provide important information on solar wind acceleration. We will discuss the coordinated observation plans to achieve the goals such as (1) how to understand the formation of spicules and quantify their contribution to coronal heating, (2) how to identify signatures of global energy buildup and local triggering of the flare and eruption. We will also discuss the operations to achieve precise co-alignment between Solar-C and other observatories.

Keywords: Sun, Solar-C

©2021. Japan Geoscience Union. All Right Reserved.

Comparison of the Optical Characteristics for Japanese Space Solar Telescopes: Hinode/XRT and Yohkoh/SXT

*Junho Shin[1], Ryouhei Kano[2], Takashi Sakurai[2], Yeon-Han Kim[3], Yong-Jae Moon[1]

1. Kyung Hee Univ., 2. NAOJ, 3. KASI

Two Japanese Space Solar Telescopes, the Yohkoh Soft X-ray Telescope (SXT) and the Hinode X-Ray Telescope (XRT) have made great contributions for more than three decades to our research on three dimensional structures of coronal magnetic field. Aside from morphological studies, one of the main purposes of these instruments is to study the spatial and temporal variation of physical quantities of coronal plasma and interpret the mechanism of coronal activities. Both are so-called Wolter-type grazing incidence (GI) mirror telescopes with high resolution CCD cameras as a recording device. Astronomical telescopes are generally designed so that the quality of focusing reaches its best at or very close to the optical axis, and inevitably the optical performance becomes worse as it goes away from the center. However, the Sun is a large object about half degree in diameter almost fully filling in the field of view of these telescopes, and thus the targets near the limb of solar disk are usually placed in the off-axis region of full-disk synoptic images. For this reason, the optical design of an X-ray solar telescope should take into account the uniformity of image quality over a wide FOV. Together with an effort in designing the optics of the instrument, the imaging artefacts shown in the off-axis region should be calibrated carefully in order for the observed data to be properly interpreted.

Our presentation will introduce the results of comparison of the optical characteristics of Hinode/XRT and Yohkoh/SXT, especially for the scattered lights and the effect of vignetting. We have analyzed highly saturated in-flight images during the solar flare to estimate the amount of scattered light inherent in the observed data. It is revealed that the light scattered due to the roughness of GI mirror surface has a power-law distribution and its amount depends on the energy considered, which allows us to complete a PSF profile from the core to the scattering wing. Vignetting is also one of the important optical properties of a telescope, as it directly describes its ability to collect photons at different locations and with different energies. We have evaluated the vignetting effect by analyzing the 2D distribution of effective area in the FOV taken from pre-launch experiments and found that the overall pattern of vignetting in two instruments are quite different from each other. Detailed results on the interesting optical characteristics will be introduced in our presentation.

Keywords: Hinode/XRT, Yohkoh/SXT, Space Telescope, Optical Characteristics

©2021. Japan Geoscience Union. All Right Reserved.

[E] Oral | P (Space and Planetary Sciences)：P-AE Astronomy & Extrasolar Bodies

Sun. Jun 6, 2021 1:45 PM - 3:15 PM JST | Sun. Jun 6, 2021 4:45 AM - 6:15 AM UTC | Ch.06 Zoom Room 06

[P-AE16] Exoplanets

convener:Masahiro Ikoma(Division of Science, National Astronomical Observatory of Japan), Norio Narita(The University of Tokyo), Yuka Fujii(National Astronomical Observatory of Japan), Chairperson:Yuka Fujii(National Astronomical Observatory of Japan)

Exoplanetary science, which began with the discovery of a hot Jupiter in 1995, reached a significant turning point by the detection of countless super-Earths by the Kepler space telescope. In 2018, the new space telescope TESS was launched to conduct an extensive survey of exoplanets orbiting nearby bright stars, opening a new era of characterization of exoplanet atmospheres. Moreover, recent observations have identified a growing number of terrestrial planets in the so-called habitable zone. While exoplanets have been targeted mainly for astronomy until recently, it would be fair to say that Earth and planetary science is finally becoming a research field to make a central contribution. This session aims at allowing participants to share their research results and new ideas regarding exoplanets and also inform the current status of their projects. Exoplanet science is a growing, interdisciplinary research field. We welcome participants from various fields.

1:45 PM - 2:00 PM JST | 4:45 AM - 5:00 AM UTC

[PAE16-01] Exploring New Worlds: An Integrative, Probabilistic Analysis of Nearby Exoplanets and Exoplanetary Systems

★Invited Papers

*Daniel Apai[1] (1.The University of Arizona)

2:00 PM - 2:15 PM JST | 5:00 AM - 5:15 AM UTC

[PAE16-02] Global climate modeling of TRAPPIST-1e using MIROC for the model intercomparison

*Takeshi Kuroda[1], Yujie Zou[1,2], Arihiro Kamada[1], Takanori Kodama[2], Naoki Terada[1] (1.Department of Geophysics, Tohoku University, 2.Komaba Institute for Science, The University of Tokyo)

2:15 PM - 2:30 PM JST | 5:15 AM - 5:30 AM UTC

[PAE16-03] Global Mapping of the Surface Composition on an Exo-Earth using Sparse Modeling

*Atsuki Kuwata[1], Hajime Kawahara[1], Masataka Aizawa[2], Takayuki Kotani[3,4,5], Motohide Tamura[1,3,4] (1.The University of Tokyo, 2.Tsung-Dao Lee Institute, 3.Astrobiology center, 4.National Astronomical Observatory of Japan, 5.University for Advanced Studies (SOKENDAI))

2:30 PM - 2:45 PM JST | 5:30 AM - 5:45 AM UTC

[PAE16-04] Search for Extra-terrestrial Mother Planets Catalogue for influence of stellar activities on the extraplanetary system.

*Yosuke Alexandre Yamashiki[1], Hiroyuki Maehara[2], Vladimir Airapetian[3], Yuta Notsu[6], Kosuke Namekata[4], Riko Shimizu[5], Nami Kimura[1], Tatsuhiko Sato[7], Takanori Sasaki[4] (1.Earth & Planetary Water Resources Assessment Laboratory Graduate School of Advanced Integrated Studies in Human Survivability Kyoto University, 2.National Astronomical Observatory of Japan, 3.NASA's Goddard Space Flight Center, 4.Graduate School of Science, Kyoto University, 5.Faculty of Science, Kyoto University, 6.University of Colorado, 7.Japan Atomic Energy Agency)

2:45 PM - 3:00 PM JST | 5:45 AM - 6:00 AM UTC

[PAE16-05] Observational implications of atmospheric and orbital evolution of super-Earths

*Naho Fujita[1], Yasunori Hori[2,3], Takanori Sasaki[1] (1.Kyoto University, 2.Astrobiology Center, 3.National Astronomical Observatory of Japan)

3:00 PM - 3:15 PM JST | 6:00 AM - 6:15 AM UTC

[PAE16-06] Effects of H_2 pumping on hot Jupiter's atmospheric escape

*Hiroto Mitani[1], Riouhei Nakatani[2], Naoki Yoshida[1] (1.The University of Tokyo, 2.RIKEN)

Exploring New Worlds: An Integrative, Probabilistic Analysis of Nearby Exoplanets and Exoplanetary Systems

*Daniel Apai[1]

1. The University of Arizona

The number of known exoplanets is growing rapidly, opening a new era in astronomy, planetary science, and astrobiology. Yet, the detailed characterization of individual —and likely very complex —worlds will remain challenging: Even with future, ambitious space missions only limited information can be gained about a modest number of parameters. Some properties that likely impact the potential for habitability will remain not directly observable. While measurements of individual exoplanets and systems will be incomplete and will often carry significant uncertainties, our understanding of the exoplanet population and planet formation/evolution pathways deepens, opening an opportunity to enhance our interpretation of measurements of individual planets and systems.

In this talk I will describe a statistical framework that combines necessarily incomplete and somewhat uncertain measurements of individual planets and planetary systems with population-level statistical information (from exoplanet demographics and planet formation/evolution models), to provide a statistical, probabilistic assessment of nearby planetary systems. I will show how this approach can successfully predict the presence and properties of yet-undiscovered worlds in nearby multi-planet systems, such as tau Ceti, and how it can enhance the efficiency of next-generation, space-based direct imaging survey missions in their quest to characterize habitable worlds and identify biosignatures.

Keywords: Exoplanets

©2021. Japan Geoscience Union. All Right Reserved.

Global climate modeling of TRAPPIST-1e using MIROC for the model intercomparison

*Takeshi Kuroda[1], Yujie Zou[1,2], Arihiro Kamada[1], Takanori Kodama[2], Naoki Terada[1]

1. Department of Geophysics, Tohoku University, 2. Komaba Institute for Science, The University of Tokyo

TRAPPIST-1 is an ultra-cool red dwarf star (M-dwarf) with the size of slightly larger than Jupiter, located at about 40 light-years away from our Sun. It has been found that at least seven rocky planets are orbiting the star within the semi-major axis of ~0.06 AU, receiving the comparable irradiation to the terrestrial planets of our Solar System. Especially, the planet TRAPPIST-1e, whose size is estimated to be ~92% of the Earth orbiting with the semi-major axis of ~0.028 AU and the period of ~6.1 days (Gillon et al., 2017), would be favorable to keep the warm temperature which the surface liquid water may stably exist, with the estimated irradiation of ~900 W m^{-2} (~66% of the Earth). Also, it is highly probable that TRAPPIST-1e has a synchronous (tidally-locked with the same periods of rotation and revolution) orbit against TRAPPIST-1, like Ganymede against Jupiter with the similar size and positional relationship.

If TRAPPIST-1e has a suitable atmosphere, it is expected that its environment would be habitable, i.e. suitable for the existence of life. Several studies using global climate models (GCMs) have investigated the possible habitable climate of TRAPPIST-1e (Wolf, 2017; Turbet et al., 2018; Fauchez et al., 2019), and a model intercomparison project with several kinds of conditions is also ongoing (Fauchez et al., 2019, 2020). On this context, we also started GCM simulations of TRAPPIST-1e using MIROC (Model for Interdisciplinary Research on Climate), which has been developed in the Atmosphere and Ocean Research Institute of The University of Tokyo, National Institute for Environmental Studies and Japan Agency for Marine-Earth Science and Technology, to join the intercomparison project for the robust validation and understanding of the habitability of the extrasolar planet.

We have performed the simulations of the possible climate of TRAPPIST-1e with four kinds of ideal conditions with the surface pressure of 1 bar along with Fauchez et al. (2020): 1) Ben1: a dry land planet with a N_2 atmosphere including 400 ppm CO_2, 2) Ben2: a dry land planet with a pure CO_2 atmosphere, 3) Hab1: a slab ocean planet with a N_2 atmosphere including 400 ppm CO_2, and 4) Hab2: a slab ocean planet with a pure CO_2 atmosphere, and got preliminary results for each condition. In the presentation, we are showing the results and discussions in comparisons with other GCMs joining the intercomparison project (LMDG: the Laboratoire de Météorologie Dynamique Generic model, ROCKE-3D: the Resolving Orbital and Climate Keys of Earth and Extraterrestrial Environments with Dynamics, ExoCAM: the Exoplanet Community Atmospheric Model, and the Met Office Unified Model) for the validations of MIROC to adapt to tidally-locked exoplanets and the habitability of TRAPPIST-1e.

Keywords: Extrasolar planet, TRAPPIST-1, Global climate model

©2021. Japan Geoscience Union. All Right Reserved.

Global Mapping of the Surface Composition on an Exo-Earth using Sparse Modeling

*Atsuki Kuwata[1], Hajime Kawahara[1], Masataka Aizawa[2], Takayuki Kotani[3,4,5], Motohide Tamura[1,3,4]

1. The University of Tokyo, 2. Tsung-Dao Lee Institute, 3. Astrobiology center, 4. National Astronomical Observatory of Japan, 5. University for Advanced Studies (SOKENDAI)

In the exploration of extraterrestrial life, the characterization of exoplanets has been studied. Direct imaging is one of the fundamental observation methods for characterization. However, even for close terrestrial exoplanets from the solar system, a resolution of a few microarcseconds is required for spatially resolved observations, and even if direct imaging becomes possible, it will only be possible to observe point sources. Kawahara & Fujii (2010, 2011) proposed Spin-Orbit Tomography (SOT) to obtain the two-dimensional spatial distribution of a planet's surface from the temporal variation of observed reflected light without spatial resolution. Recently, Aizawa et al. (2020) obtained highly accurate spatial distribution maps by introducing sparse modeling to SOT.

In addition to the above methods, we focused on Spin-Orbit Unmixing (SOU), which was developed by introducing Spectral Unmixing, a remote sensing method, to SOT. SOU enables us to obtain the spatial distribution of the planet's surface and the reflection spectrum from the luminosity variations at multiple wavelengths (Kawahara 2020). In this study, we introduced sparse modeling to SOU. In SOU, we placed sparsity-inducing constraints and reformulated the solution into an appropriate form to use the proximal gradient method, one of the optimization algorithms. As a result, we obtain highly accurate and more sparse planetary surface distributions and reflection spectra. In this talk, we describe this method and show the results of tests using Earth data.

Keywords: Exoplanets, Mapping, Sparse Modeling

©2021. Japan Geoscience Union. All Right Reserved.

Search for Extra-terrestrial Mother Planets Catalogue for influence of stellar activities on the extraplanetary system.

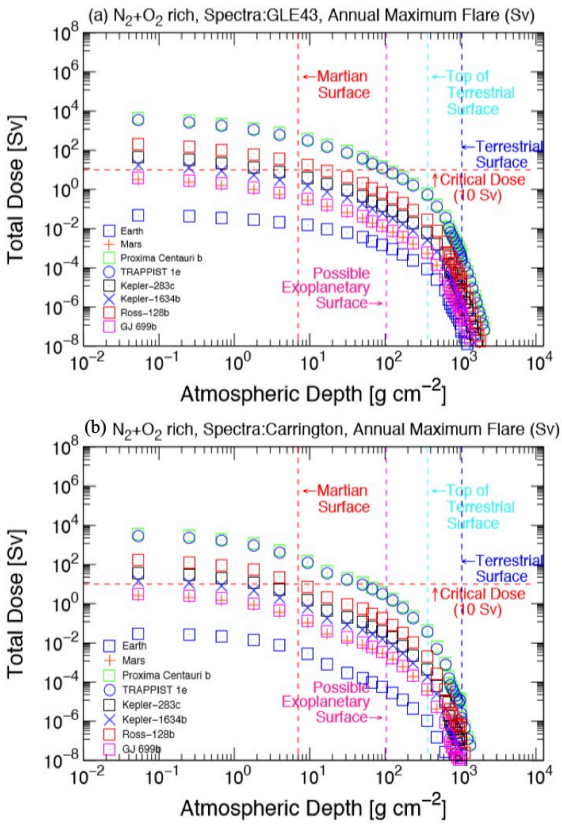
*Yosuke Alexandre Yamashiki[1], Hiroyuki Maehara[2], Vladimir Airapetian[3], Yuta Notsu[6], Kosuke Namekata[4], Riko Shimizu[5], Nami Kimura[1], Tatsuhiko Sato[7], Takanori Sasaki[4]

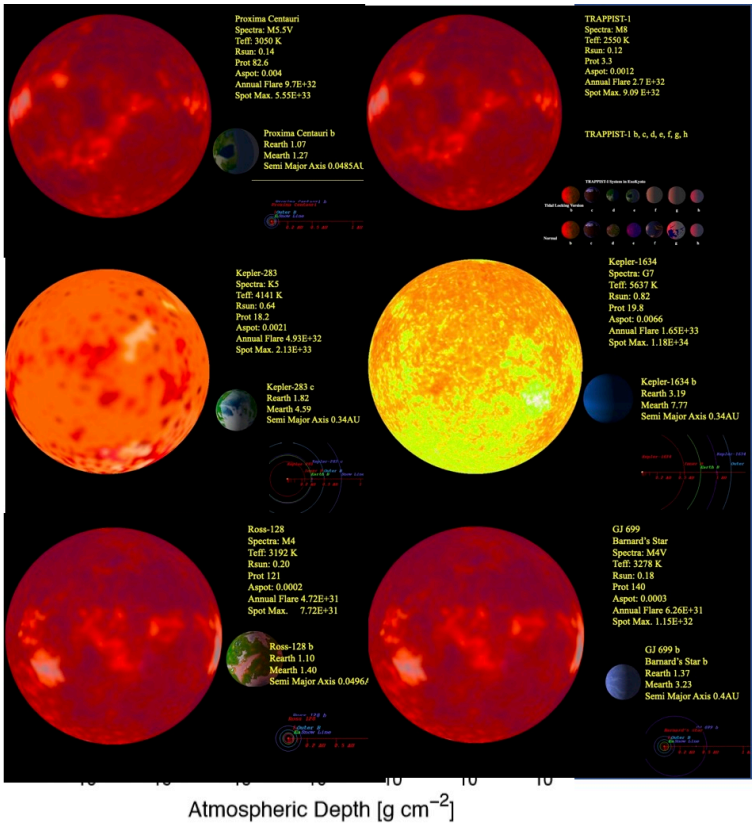
1. Earth & Planetary Water Resources Assessment Laboratory Graduate School of Advanced Integrated Studies in Human Survivability Kyoto University, 2. National Astronomical Observatory of Japan, 3. NASA's Goddard Space Flight Center, 4. Graduate School of Science, Kyoto University, 5. Faculty of Science, Kyoto University, 6. University of Colorado, 7. Japan Atomic Energy Agency

The Search for Extra-terrestrial Mother Planets Catalogue will be used to search for potentially habitable mother planets and to derive data on stellar activity of their host stars. The ultimate goal of the survey is to accomplish creating a full and original data catalogue of exoplanets at Kyoto University, based on the Exokyoto catalogue, while paying special attention to characterization of stellar activity of planet hosts. We presented the first quantitative impact evaluation system of stellar flares on the habitability factors with an emphasis on the impact of stellar proton events. We derive the maximum flare energy from stellar star spot sizes and examine the impacts of flare-associated ionizing radiation on CO_2, H_2, and N_2+ O_2-rich atmospheres of a number of well-characterized terrestrial type exoplanets. Our simulations based on the Particle and Heavy Ion Transport code System suggest that the estimated ground-level dose for each planet in the case of terrestrial-level atmospheric pressure (1 bar) for each exoplanet does not exceed the critical dose for complex (multicellular) life to persist, even for the planetary surface of Proxima Centauri b, Ross-128 b, and TRAPPIST-1 e. We re-conduct numerical simulation based on newely obtained spectra for the possible CME occurred in those planetary system, revailing higher and harder spectra may induce significant damage even for those "habitable"planets. Some thick atmosphere and hydrosphere may protect their habitability reducing exposure impact for those planet. Together with the observation for H-alpha for host stars we also are attempt to conduct developing database for those risk for potentially habitable planetary system.
In this presentation we will introduce how the energy spectra of potential CME may affect entire estimation of the possible dose at the surface environment of extrasolar planets with preliminary classification by stellar impact among "habitable" planets situated CHZ based on the conventional classification theory. According to our estimation, some planets with hardest energy spectra and higher atmospheric escape rate the surface environment become severe for terrestrial-type life system.

Keywords: extrasolar planetary catalogue, Stellar Energetic Particles, Mother planet

©2021. Japan Geoscience Union. All Right Reserved.





©2021. Japan Geoscience Union. All Right Reserved.

Observational implications of atmospheric and orbital evolution of super-Earths

*Naho Fujita[1], Yasunori Hori[2,3], Takanori Sasaki[1]

1. Kyoto University, 2. Astrobiology Center, 3. National Astronomical Observatory of Japan

There is a scarcity of close-in small planets with 1.5 to 2.0 times Earth radii and the orbital period of < 100 days in the radius distribution of Kepler planets around FGK stars (Fulton & Petigura 2018) and M dwarfs (Hirano et al. 2018). The so-called “radius gap” is considered as the radius boundary between planets with atmospheres and those without atmospheres. The atmospheric escape of small planets by photoevaporation can explain the origin of the observed radius gap (e.g., Owen & Wu 2017). Previous studies, however, assumed that evaporating planets stay in situ. Planets that undergo mass loss should move outward while conserving the total angular momentum of the star-planet system. In this study, we calculated the orbital evolution of close-in super-Earths that undergo hydrodynamic escape of their atmospheres driven by stellar X-ray and UV irradiations. We found that a radius gap, as seen in observations, appears in the orbital period-radius distribution of close-in super-Earths. Our results also suggest that the atmospheric escape of planets strongly affects the final orbital configuration of the planetary systems. More super-Earths orbiting M dwarfs are expected to be discovered by ongoing near-infrared doppler surveys, such as CFHT/SPIRou, Subaru/IRD, and VLT/CRIRES. Therefore, our theoretical study on the orbital evolution of close-in super-Earths helps understand their formation history and dynamical evolution.

Keywords: Exoplanets, Super-Earths, Atmospheric escape, Orbital evolution, Exoplanet observation, M dwarfs

©2021. Japan Geoscience Union. All Right Reserved.

Effects of H_2 pumping on hot Jupiter's atmospheric escape

*Hiroto Mitani[1], Riouhei Nakatani[2], Naoki Yoshida[1]

1. The University of Tokyo, 2. RIKEN

Observations have revealed atmospheric escape of hot Jupiters around various-type stars. Classically, extreme-ultraviolet (EUV; >13.6eV) radiation of the host stars is considered to be responsible for the atmospheric escape.
EUV radiation is particularly strong for low-mass young stars, while intermediate-mass stars are less luminous in EUV but have an intense far-ultraviolet (FUV; <13.6eV) radiation instead. Therefore, compared to EUV heating, FUV-associated heating can be relatively effective for hot jupiters around intermediate-mass stars. The Lyman-Werner photons can excite molecular hydrogen to upper vibrational states (so-called H_2 pumping), and subsequent collisional de-excitation can result in substantial heating to the gas. Recent observations have discovered planets around A-stars, which have FUV luminosity about five orders of magnitude higher than the solar value. It is expected that H_2 pumping is effective to drive atmospheric escape for such planets.
In this study, we investigate the heating effects on the dynamics of hot Jupiter's atmosphere, performing radiation hydrodynamic simulations with self-consistent thermochemistry. We found that H_2 pumping can yield a mass-loss rate of ~ 10^{13} g/s around hot A-stars, which is orders of magnitude larger than typical mass-loss rates for EUV-driven escape (~10^{10} g/s). We discuss the effect of H_2 pumping heating on the atmospheric escape process of hot Jupiters around various host stars.

Keywords: Exoplanet, Hot Jupiter, Atmospheric escape

©2021. Japan Geoscience Union. All Right Reserved.

[E] Oral | P (Space and Planetary Sciences)：P-AE Astronomy & Extrasolar Bodies

Sun. Jun 6, 2021 3:30 PM - 5:00 PM JST | Sun. Jun 6, 2021 6:30 AM - 8:00 AM UTC | Ch.06 Zoom Room 06

[P-AE16] Exoplanets

convener:Masahiro Ikoma(Division of Science, National Astronomical Observatory of Japan), Norio Narita(The University of Tokyo), Yuka Fujii(National Astronomical Observatory of Japan), Chairperson:Norio Narita(The University of Tokyo)

Exoplanetary science, which began with the discovery of a hot Jupiter in 1995, reached a significant turning point by the detection of countless super-Earths by the Kepler space telescope. In 2018, the new space telescope TESS was launched to conduct an extensive survey of exoplanets orbiting nearby bright stars, opening a new era of characterization of exoplanet atmospheres. Moreover, recent observations have identified a growing number of terrestrial planets in the so-called habitable zone. While exoplanets have been targeted mainly for astronomy until recently, it would be fair to say that Earth and planetary science is finally becoming a research field to make a central contribution. This session aims at allowing participants to share their research results and new ideas regarding exoplanets and also inform the current status of their projects. Exoplanet science is a growing, interdisciplinary research field. We welcome participants from various fields.

3:30 PM - 3:45 PM JST | 6:30 AM - 6:45 AM UTC

[PAE16-07] TESS legacy: the brightest, closest transiting planets for atmospheric studies.

★Invited Papers

*Rafael Luque[1] (1.Instituto de Astrofisica de Andalucia)

3:45 PM - 4:00 PM JST | 6:45 AM - 7:00 AM UTC

[PAE16-08] Development of multiband imager MuSCAT3 and its first results on followup observations of TESS transiting planets

*Akihiko Fukui[1], Norio Narita[1,2], Masahiro Ikoma[1], Keisuke Isogai[4], Kiyoe Kawauchi[1], Takanori Kodama[1], Seiya Kurita[1], Nobuhiko Kusakabe[2], Jerome Pitogo de Leon[1], John Livingston[1], Mayuko Mori[1], Taku Nishiumi[3], Motohide Tamura[1,2], Noriharu Watanabe[3], Tomoyasu Yamamuro[5], Daniel Harbeck[6], Mark Bowman[6], Mark Elphick[6], Jon Nation[6], James Armstrong[7], Jacqueline Han[7], Matt Daily[6] (1.The University of Tokyo, 2.Astrobiology Center, 3.SOKENDAI, 4.Kyoto University, 5.OptCraft, 6.Las Cumbres Observatory Global Telescope Network, 7.University of Hawaii)

4:00 PM - 4:15 PM JST | 7:00 AM - 7:15 AM UTC

[PAE16-09] New Validated Planets in Overlapping K2 Campaigns

*Jerome Pitogo de Leon[1], John Livingston[1], Michael Endl[4], William Cochran[5,4], Teruyuki Hirano[18], Masayuki Kuzuhara[15,14], Rafael Garcia[11], Savita Mathur[6,7], Fei Dai[10,9], Alessandro Trani[2], Judith Korth[6,7], Kristine Lam[8], Enrique Diez Alonzo[17], Amadeo Castro Gonzalez[17], Malcolm Fridlund[12,13], Akihiko Fukui[3], Rafa Luque[6,7], Norio Narita[16,2,15,14], Enric Palle[6,7], Motohide Tamura[1,14,15], KESPRINT team (1.Department of Astronomy, University of Tokyo, 7-3-1 Hongo, Bunkyo-ku, Tokyo 113-0033, Japan, 2.Department of Earth Science and Astronomy, College of Arts and Sciences, The University of Tokyo, 3-8-1 Komaba, Meguro-ku, Tokyo 153-8902, Japan, 3.Department of Earth and Planetary Science, University of Tokyo, 7-3-1 Hongo, Bunkyo-ky, Tokyo 113-0033, Japan, 4.Department of Astronomy and McDonald Observatory, University of Texas at Austin, 2515 Speedway, Stop C1400, Austin, TX 78712, USA, 5.Center for Planetary Systems Habitability, The University of Texas at Austin, Austin TX USA, 6.Instituto de Astrofisica de Canarias (IAC), 38205 La Laguna, Tenerife, Spain, 7.Departamento de Astrofisica, Universidad de La Laguna, 38206 La Laguna, Tenerife, Spain, 8.Center for Astronomy and Astrophysics, Technical University Berlin, Hardenbergstr. 36, 10623 Berlin, Germany, 9.Division of Geological and Planetary Sciences, California Institute of Technology, 1200 East California Blvd, Pasadena CA 91125, 10.Department of Astrophysical Sciences, Princeton University, 4 Ivy Lane, Princeton, NJ 08544, USA, 11.AIM, CEA, CNRS, Universite Paris-Saclay, Universite Paris Diderot, Sorbonne Paris Cité, F-91191 Gif-sur-Yvette, France, 12.Leiden Observatory, Leiden University, 2333CA Leiden, The Netherlands, 13.Department of Space, Earth and Environment, Chalmers University of Technology, Onsala Space Observatory, SE-439 92 Onsala,

Sweden, 14.Astrobiology Center, NINS, 2-21-1 Osawa, Mitaka, Tokyo 181-8588, Japan, 15.National Astronomical Observatory of Japan, NINS, 2-21-1 Osawa, Mitaka, Tokyo 181-8588, Japan, 16.JST, PRESTO, 3-8-1 Komaba, Meguro, Tokyo 153-8902, Japan , 17.Instituto Universitario de Ciencias y Tecnologias Espaciales de Asturias (ICTEA), C.Independencia 13, E-33004 Oviedo, Spain, 18.Department of Earth and Planetary Sciences, Tokyo Institute of Technology, 2-12-1 Ookayama, Meguro-ku, Tokyo 152-8551, Japan)

4:15 PM - 4:30 PM JST | 7:15 AM - 7:30 AM UTC

[PAE16-10] Spitzer and ground-based follow-up of the young transiting multi-planet system V1298 Tau

*John Livingston[1], Trevor David[2], Gudmundur Stefansson[3], Elisabeth Newton[4], Allyson Bieryla[5], Shreyas Vissapragada[6], Samuel Hadden[5], Erik Petigura[7], Eric Mamajek[8], Lynne Hillenbrand[6], David Ciardi[6], Charles Beichman[6], Luisa Rebull[6], John Stauffer[6], Varoujan Gorjian[6], Heather Knutson[6], Akihiko Fukui[1], Norio Narita[1], Motohide Tamura[1] (1.University of Tokyo, 2.Flatiron Institute, 3.Princeton University, 4.Dartmouth College, 5.Harvard-Smithsonian, 6.California Institute of Technology, 7.University of California, Los Angeles, 8.Jet Propulsion Laboratory)

4:30 PM - 4:45 PM JST | 7:30 AM - 7:45 AM UTC

[PAE16-11] **Twinkle: a low-Earth orbit, visible and infrared observatory for exoplanet and solar system spectroscopy**

*Billy Edwards[1] (1.Blue Skies Space Ltd)

4:45 PM - 5:00 PM JST | 7:45 AM - 8:00 AM UTC

[PAE16-12] Multi-planetary systems deduced from the observed ALMA disks: initial conditions and evolutionary outcomes

*Shijie Wang[1], Kazuhiro D Kanagawa[1,2], Toshinori Hayashi[1], Yasushi Suto[1] (1.University of Tokyo, 2.Ibaraki University)

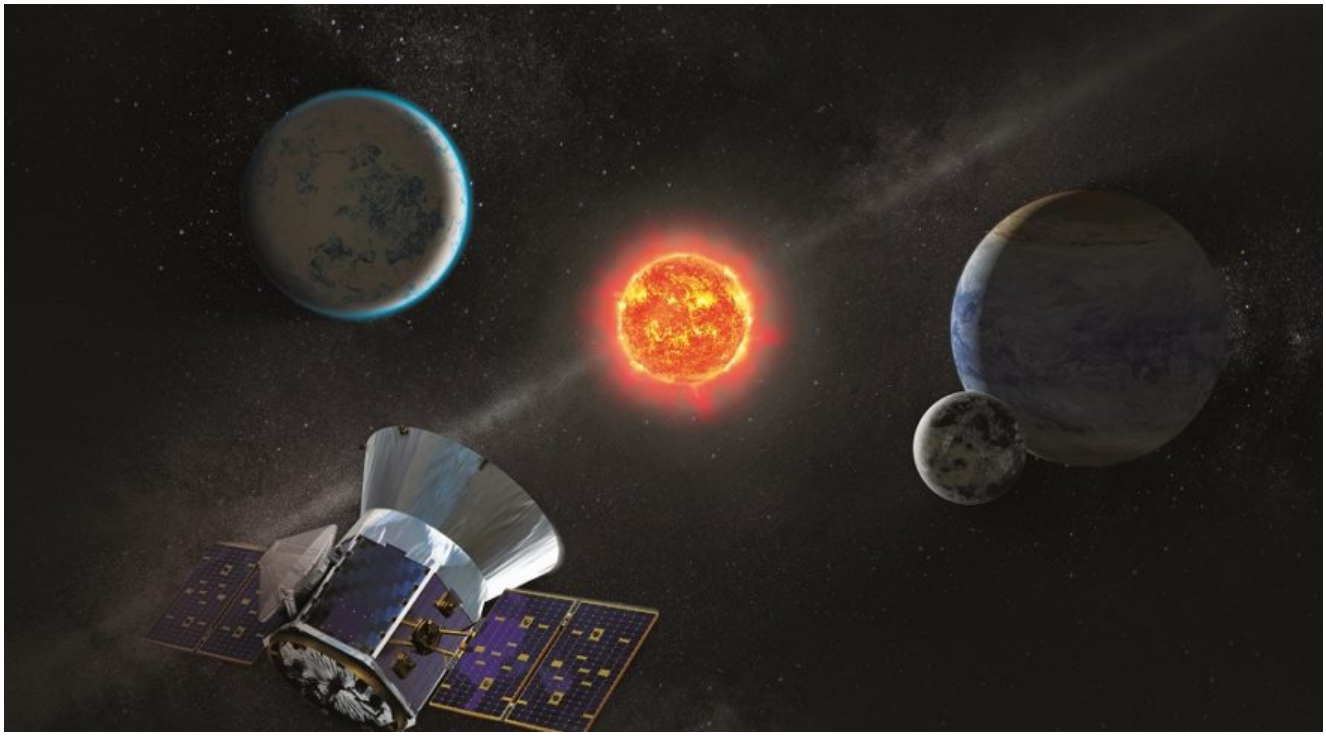
TESS legacy: the brightest, closest transiting planets for atmospheric studies.

*Rafael Luque[1]

1. Instituto de Astrofisica de Andalucia

Successfully launched in April 2018, NASA’s Transiting Exoplanet Survey Satellite (TESS) is well on its way to discovering thousands of exoplanets in orbit around the brightest stars in the sky. During its initial two-year survey mission, TESS has monitored more than 200,000 targeted bright stars in the solar neighborhood for drops in brightness caused by planetary transits, discovering more than a hundred planets already and with thousands of candidates pending confirmation. The brightness of TESS host stars makes TESS planets far easier to characterize with follow-up observations than planets from prior missions. TESS follow-up observations have already enabled measurements of the masses, sizes, densities, orbits, and atmospheres of a large cohort of small planets, including habitable zone rocky worlds. In this talk, I will review the ground-based efforts to perform those observations, the facilities and teams involved, and the prospects for atmospheric studies of the most promising targets with the new generation of ground- and space-based facilities such as the GSMTs and JWST.

Keywords: exoplanets, exoplanet atmospheres, radial velocity, transit, TESS



©2021. Japan Geoscience Union. All Right Reserved.

Development of multiband imager MuSCAT3 and its first results on followup observations of TESS transiting planets

*Akihiko Fukui[1], Norio Narita[1,2], Masahiro Ikoma[1], Keisuke Isogai[4], Kiyoe Kawauchi[1], Takanori Kodama[1], Seiya Kurita[1], Nobuhiko Kusakabe[2], Jerome Pitogo de Leon[1], John Livingston[1], Mayuko Mori[1], Taku Nishiumi[3], Motohide Tamura[1,2], Noriharu Watanabe[3], Tomoyasu Yamamuro[5], Daniel Harbeck[6], Mark Bowman[6], Mark Elphick[6], Jon Nation[6], James Armstrong[7], Jacqueline Han[7], Matt Daily[6]

1. The University of Tokyo, 2. Astrobiology Center, 3. SOKENDAI, 4. Kyoto University, 5. OptCraft, 6. Las Cumbres Observatory Global Telescope Network, 7. University of Hawaii

The successor of the Kepler space telescope, TESS, has been surveying ~80% of the entire sky to search for small planets transiting nearby stars, which can be prime targets for future atmospheric characterizasions. However, a large fraction of planetary candidates that TESS has been discovering are actually false positives, and ground-based followup observations are essential to identify true transiting planets. To validate such planetary candidates and further characterize them in detail, we have developed a new optical four-band imager MuSCAT3 for a 2m telescope at Haleakala Observatory in Hawaii. The first light of MuSCAT3 has scceeded in September 2020, and its science operation has started in November 2020. In this talk, we will introduce the characteristics of MuSCAT3, and show some scientific results obtained with this instrument, in coordination with two precedent instruments of MuSCAT in Japan and MuSCAT2 in Spain, for followup observations of TESS planetary candidates.

Keywords: transiting planet, TESS, multiband photometry

©2021. Japan Geoscience Union. All Right Reserved.

New Validated Planets in Overlapping K2 Campaigns

*Jerome Pitogo de Leon[1], John Livingston[1], Michael Endl[4], William Cochran[5,4], Teruyuki Hirano[18], Masayuki Kuzuhara[15,14], Rafael Garcia[11], Savita Mathur[6,7], Fei Dai[10,9], Alessandro Trani[2], Judith Korth[6,7], Kristine Lam[8], Enrique Diez Alonzo[17], Amadeo Castro Gonzalez[17], Malcolm Fridlund[12,13], Akihiko Fukui[3], Rafa Luque[6,7], Norio Narita[16,2,15,14], Enric Palle[6,7], Motohide Tamura[1,14,15], KESPRINT team

1. Department of Astronomy, University of Tokyo, 7-3-1 Hongo, Bunkyo-ku, Tokyo 113-0033, Japan, 2. Department of Earth Science and Astronomy, College of Arts and Sciences, The University of Tokyo, 3-8-1 Komaba, Meguro-ku, Tokyo 153-8902, Japan, 3. Department of Earth and Planetary Science, University of Tokyo, 7-3-1 Hongo, Bunkyo-ky, Tokyo 113-0033, Japan, 4. Department of Astronomy and McDonald Observatory, University of Texas at Austin, 2515 Speedway, Stop C1400, Austin, TX 78712, USA, 5. Center for Planetary Systems Habitability, The University of Texas at Austin, Austin TX USA, 6. Instituto de Astrofisica de Canarias (IAC), 38205 La Laguna, Tenerife, Spain, 7. Departamento de Astrofisica, Universidad de La Laguna, 38206 La Laguna, Tenerife, Spain, 8. Center for Astronomy and Astrophysics, Technical University Berlin, Hardenbergstr. 36, 10623 Berlin, Germany, 9. Division of Geological and Planetary Sciences, California Institute of Technology, 1200 East California Blvd, Pasadena CA 91125, 10. Department of Astrophysical Sciences, Princeton University, 4 Ivy Lane, Princeton, NJ 08544, USA, 11. AIM, CEA, CNRS, Universite Paris-Saclay, Universite Paris Diderot, Sorbonne Paris Cité, F-91191 Gif-sur-Yvette, France, 12. Leiden Observatory, Leiden University, 2333CA Leiden, The Netherlands, 13. Department of Space, Earth and Environment, Chalmers University of Technology, Onsala Space Observatory, SE-439 92 Onsala, Sweden, 14. Astrobiology Center, NINS, 2-21-1 Osawa, Mitaka, Tokyo 181-8588, Japan, 15. National Astronomical Observatory of Japan, NINS, 2-21-1 Osawa, Mitaka, Tokyo 181-8588, Japan, 16. JST, PRESTO, 3-8-1 Komaba, Meguro, Tokyo 153-8902, Japan , 17. Instituto Universitario de Ciencias y Tecnologias Espaciales de Asturias (ICTEA), C.Independencia 13, E-33004 Oviedo, Spain, 18. Department of Earth and Planetary Sciences, Tokyo Institute of Technology, 2-12-1 Ookayama, Meguro-ku, Tokyo 152-8551, Japan

We analysed 72 candidate planetary systems first identified during Campaigns 5 and 6 (C5 and C6) of the NASA K2 Mission. We set out to validate these systems using a suite of follow-up observations including adaptive optics, speckle imaging, and reconnaissance spectroscopy. The overlap between C5 with C16 and C18, and C6 with C17, yields light curves with longer baselines that allow us to measure the transit ephemeris very precisely, revisit single transit candidates identified in earlier campaigns, and search for additional transiting planets with longer periods not detected in previous works. Using vespa, we compute false positive probabilities less than 1% for 35 candidates and hence statistically validate them as planets. These planets have a typical size of 2.2R⊕ and orbital periods between 1.99 and 52.71 days. We highlight interesting systems including a sub-Neptune with the longest period with more than two transits detected from K2, sub-Saturns around F stars, and several multi-planetary systems in a variety of architectures, four of which are new discoveries. These results show that a wealth of planetary systems still remain in the K2 data, many ofwhich can be validated using minimal follow-up observations and taking advantage of analyses presented in previous catalogs.

Keywords: exoplanet, transit, imaging

©2021. Japan Geoscience Union. All Right Reserved.

Spitzer and ground-based follow-up of the young transiting multi-planet system V1298 Tau

*John Livingston[1], Trevor David[2], Gudmundur Stefansson[3], Elisabeth Newton[4], Allyson Bieryla[5], Shreyas Vissapragada[6], Samuel Hadden[5], Erik Petigura[7], Eric Mamajek[8], Lynne Hillenbrand[6], David Ciardi[6], Charles Beichman[6], Luisa Rebull[6], John Stauffer[6], Varoujan Gorjian[6], Heather Knutson[6], Akihiko Fukui[1], Norio Narita[1], Motohide Tamura[1]

1. University of Tokyo, 2. Flatiron Institute, 3. Princeton University, 4. Dartmouth College, 5. Harvard-Smithsonian, 6. California Institute of Technology, 7. University of California, Los Angeles, 8. Jet Propulsion Laboratory

We report on Spitzer IRAC2 and ground-based transit observations of the young (23 Myr) transiting multi-planet system V1298 Tau in the foreground of the Taurus-Auriga star-forming region. We find the transit depths at 4.5 microns of planets b, c, and d are consistent to within ~1-sigma of that measured at 0.42-0.90 microns from Kepler observations acquired during Campaign 4 of the K2 mission. The K2 data were acquired in early 2015 and were affected by a data gap as well as likely spot-crossings. We see no evidence for spot-crossings in the Spitzer light curves, consistent with the expectation of a lower spot-to-photosphere contrast at mid-IR wavelengths relative to the optical. Our revised ephemerides shrink the transit midpoint uncertainties from hours to minutes in mid-2021, when observations with JWST might be obtained. Our observations provide the first multi-wavelength view of the V1298 Tau system, an important benchmark for investigating the atmospheric properties of a moderately irradiated giant exoplanet shortly after its formation. Additionally, we publish individual transit times from K2, Spitzer, and our ground-based observations, along with dynamical investigations of transit timing variations. We measure very low dynamical masses consistent with the picture of low density young planets still undergoing significant radial contraction.

Keywords: Exoplanets, Young associations, Multi-planet systems, Transit photometry

©2021. Japan Geoscience Union. All Right Reserved.

Twinkle: a low-Earth orbit, visible and infrared observatory for exoplanet and solar system spectroscopy

*Billy Edwards[1]

1. Blue Skies Space Ltd

The Twinkle Space Mission is a space-based observatory that has been conceived to measure the atmospheric composition of exoplanets as well as characterising stars and solar system objects. The satellite is based on a high-heritage platform and will carry a 0.45 m telescope with a visible and infrared spectrograph providing simultaneous wavelength coverage from 0.5 - 4.5 μm. The spacecraft will be launched into a Sun-synchronous low-Earth polar orbit and will operate in this highly stable thermal environment for a baseline lifetime of seven years.

Twinkle will have the capability to provide high-quality infrared spectroscopic characterisation of the atmospheres of hundreds of bright exoplanets, covering a wide range of planetary types. It will also be capable of providing phase curves for hot, short-period planets around bright stars targets and of providing ultra-precise photometric light curves to accurately constrain orbital parameters, including ephemerides and TTVs/TDVs present in multi-planet systems.

Twinkle is available for researchers around the globe in two ways:

1) joining its collaborative multi-year survey programme, which will observe hundreds of exoplanets and solar system objects; and
2) accessing dedicated telescope time on the spacecraft, which they can schedule for any combination of science cases.

I will present an overview of Twinkle’s capabilities and discuss some example exoplanet surveys to highlight the broad range of targets the mission could observe, demonstrating the huge scientific potential of the spacecraft.

Keywords: Exoplanet atmospheres, Visible and near-infrared spectroscopy, Space-based telescope

©2021. Japan Geoscience Union. All Right Reserved.

Multi-planetary systems deduced from the observed ALMA disks: initial conditions and evolutionary outcomes

*Shijie Wang[1], Kazuhiro D Kanagawa[1,2], Toshinori Hayashi[1], Yasushi Suto[1]

1. University of Tokyo, 2. Ibaraki University

Since the discovery of the ring/gap substructure of the HL Tau disk in 2015, recent high-resolution ALMA/DSHARP observations have resolved more similar substructures on nearby protoplanetary disks. Theories have predicted that a massive planet can carve a gap in the disk as it grows, therefore these substructures were promisingly related to the planetary origin. Following this interpretation, it is possible to constrain the semi-major axis and even planetary mass from the morphology of the gaps. In Wang et al. 2020, we carried out N-body simulations to evolve the HL Tau planetary system from the current configuration up to 10 Gyrs after the disk dispersal, with implementation of both planetary migration and gas accretion schemes coupled with the the disk profile. By varying the disk parameters, we produced a variety of widely-separated planetary systems consisting of three super-Jupiters at the end of the disk dispersal. Most of the systems are found to be stable for at least 10 Gyr in a marginal resonance state. Our recent work expands the targets to other ALMA disks and considers alternative initial planetary mass estimates based on the dust-gap-only and gas-gap scenarios. We show it is possible to break the degeneracy for some gaps by considering the consistency of the predicted mass with the planetary formation model.

Keywords: Protoplanetary disks, Planet formation

©2021. Japan Geoscience Union. All Right Reserved.

[E] Poster | P (Space and Planetary Sciences)：P-AE Astronomy & Extrasolar Bodies

Sun. Jun 6, 2021 5:15 PM - 6:30 PM JST | Sun. Jun 6, 2021 8:15 AM - 9:30 AM UTC | Ch.06_2

[P-AE16] Exoplanets

convener:Masahiro Ikoma(Division of Science, National Astronomical Observatory of Japan), Norio Narita(The University of Tokyo), Yuka Fujii(National Astronomical Observatory of Japan)

Exoplanetary science, which began with the discovery of a hot Jupiter in 1995, reached a significant turning point by the detection of countless super-Earths by the Kepler space telescope. In 2018, the new space telescope TESS was launched to conduct an extensive survey of exoplanets orbiting nearby bright stars, opening a new era of characterization of exoplanet atmospheres. Moreover, recent observations have identified a growing number of terrestrial planets in the so-called habitable zone. While exoplanets have been targeted mainly for astronomy until recently, it would be fair to say that Earth and planetary science is finally becoming a research field to make a central contribution. This session aims at allowing participants to share their research results and new ideas regarding exoplanets and also inform the current status of their projects. Exoplanet science is a growing, interdisciplinary research field. We welcome participants from various fields.

[PAE16-P01] The research on the existence of helium in the atmosphere of small planets around M-type stars with Subaru/IRD

*Kiyoe Kawauchi[1], Norio Narita[1], Masayuki Kuzuhara[2,3], Teruyuki Hirano[2,3], Hiroki Harakawa[4], Sebastien Vievard[2,4], Aoi Takahashi[2,3], Takayuki Kotani[2,3], Motohide Tamura[1,2,3] (1.The University of Tokyo, 2.Natural Institute of Natural Sciences Astrobiology Center, 3.National Astronomical Observatory of Japan, NAOJ, 4.Subaru Telescope)

[PAE16-P02] Results of TESS follow-up observations by the MuSCAT series and the Subaru IRD intensive program

*Norio Narita[1,2], Akihiko Fukui[1], Masahiro Ikoma[1,3], Teruyuki Hirano[2,3], Takayuki Kotani[2,3], Motohide Tamura[1,2,3] (1.The University of Tokyo, 2.Astrobiology Center, 3.National Astronomical Observatory of Japan)

[PAE16-P03] Development of optical diffusers and the on-sky examination

*Taku Nishiumi[1,2], Norio Narita[3,2,7,8], Akihiko Fukui[3], Noriharu Watanabe[3], Kiyoe Kawauchi[3], Hideyuki Izumiura[4], Hiroyuki Maehara[4], Nobuhiko Kusakabe[2,4], Keisuke Isogai[5], Yuka Terada[6,9], John H Livingston[3], Mayuko Mori[3] (1.SOUKENDAI, 2.Astrobiology Center, 3.The University of Tokyo, 4.National Astronomical Observatory of Japan, 5.Kyoto University, 6.Academia Sinica, 7.Instituto de Astrof\'{i}sica de Canarias (IAC), 8.Japan Science and Technology Agency, 9.National Taiwan University)

[PAE16-P04] Measurement of Spin-orbit Obliquity of WASP-33b by Doppler Tomography and Transit Photometry

*Noriharu Watanabe[1], Norio Narita[1], Marshall C. Johnson[2], Akihiko Fukui[1], Nobuhiko Kusakabe[3], Enric Palle[4], John Livingston[1], Kiyoe Kawauchi[1], Jerome Pitogo de Leon[1], Taku Nishiumi[5], Mayuko Mori[1], Hannu Parviainen[4], Felipe Murgas[4], Pilar Montañes-Rodriguez[4] (1.The University of Tokyo, 2.Las Cumbres Observatory, 3.Astrobiology Center, NINS, 4.Instituto de Astrofisica de Canarias, 5.The Graduate University for Advanced Studies, SOKENDAI)

[PAE16-P05] Observation of Stellar Activities for the Planetary Hosted Stars

*Riko Shimizu[1], Yosuke Alexandre Yamashiki[1], Nami Kimura[1], Hiroyuki Maehara[2], Kosuke Namekata[1], Mikio Kurita[1], Vladimir Airapetian[3] (1.Kyoto Univ., 2.NAOJ, 3.NASA Goddard Space Flight Center)

[PAE16-P06] Climate for exo-terrestrial planets with a 3D high resolution cloud resolved climate model: Effect of obliquity

*Takanori Kodama[1], Daisuke Takasuka[2], Takeshi Kuroda[3], Tomoki Miyakawa[4], Masaki Satoh[4] (1.Komaba Institute for Science, The University of Tokyo, 2.Department of Information Science, Ochanomizu

University, 3.Department of Geophysics, Tohoku University, 4.Atmosphere and Ocean Research Institute, The University of Tokyo)

[PAE16-P07] **Possible Verifications for the Inner Void Model of Rapid Planet Formation**

*Masahiro Morikawa[1] (1.Department of Physics, Ochanomizu University)

[PAE16-P08] On the origin of metal-rich close-in gas giants: planetesimals vs pebbles

*Masahiro Ikoma[1,2], Kento Kikuchi[1], Tadahiro Kimura[1], Akifumi Nakayama[1], Sho Shibata[1] (1.Department of Earth and Planetary Science, The University of Tokyo, 2.Division of Science, National Astronomical Observatory of Japan)

The research on the existence of helium in the atmosphere of small planets around M-type stars with Subaru/IRD

*Kiyoe Kawauchi[1], Norio Narita[1], Masayuki Kuzuhara[2,3], Teruyuki Hirano[2,3], Hiroki Harakawa[4], Sebastien Vievard[2,4], Aoi Takahashi[2,3], Takayuki Kotani[2,3], Motohide Tamura[1,2,3]

1. The University of Tokyo, 2. Natural Institute of Natural Sciences Astrobiology Center, 3. National Astronomical Observatory of Japan, NAOJ, 4. Subaru Telescope

Many small planets, whose radius is between 1 and 4 Earth radius, were found by Kepler space telescope. It was found that these radii show a distribution of the bimodal (Fulton et al. 2017). From the observation with the ground-based telescopes, these masses have been estimated. The mean densities calculated by these estimated radii and masses can constrain the bulk composition and internal structure. However, we cannot constrain that the planet has a rocky core enveloped in the H-He gas (primary gas) or H2O dominated ices/fluids because they show the same mean density (Zeng et al. 2018). To resolve this degeneracy, we should research the atmosphere directly. The atmospheres of some small planets were already observed but it has been difficult for resolving them because the signals of the molecule lines become weak due to aerosols (e.g. Tsiaras et al. 2019). Helium is suitable for identifying whether the planets have a primary gas or not since it is abundant in the upper atmosphere above the aerosols layer if it presents and it is created in the protoplanetary disk only.

Recently, by the development of the high-resolution spectrograph in the near-infrared region, He triplet lines have been detected in the atmosphere of dozens hot Jupiters (e.g. Nortmann et al. 2018). He triplet lines in three small planets were investigated with high-resolution transmission spectroscopy on the ground by Kasper et al. 2020, but there are only a few small planets whose atmospheres are possible to be investigated as almost all discovered small planets are far from our solar system. However, more than 80 candidates of the small planets located near our solar system have been discovered by Transiting Exoplanet Survey Satellite (TESS) launched in 2018. It will be possible to search for the He triplet lines in many small planets.

We performed the high-resolution transmission spectroscopy of He triplet lines on three small planets discovered by TESS projects with Subaru/IRD. In this presentation, we will report on these results.

Keywords: exoplanet atmosphere, transmission spectroscopy, small planets

©2021. Japan Geoscience Union. All Right Reserved.

Results of TESS follow-up observations by the MuSCAT series and the Subaru IRD intensive program

*Norio Narita[1,2], Akihiko Fukui[1], Masahiro Ikoma[1,3], Teruyuki Hirano[2,3], Takayuki Kotani[2,3], Motohide Tamura[1,2,3]

1. The University of Tokyo, 2. Astrobiology Center, 3. National Astronomical Observatory of Japan

The Transiting Exoplanet Survey Satellite (TESS) was launched in April 2018 and has completed its 2-year prime mission. TESS is continuing its 3rd year survey as an extended mission. So far TESS has identified over 2000 candidate transiting planets. But the candidates include many false positives mainly due to eclipsing binaries. To discriminate false positives and identify the true planetary nature, it is necessary to conduct follow-up observations.
We are working on such follow-up observations using multi-color simultaneous camera series named MuSCAT/MuSCAT2/MuSCAT3 and a near-infrared radial velocimeter IRD on the Subaru 8.2 telescope. We have conducted follow-up observations for over 200 candidate transiting planets with the MuSCAT series and measured radial velocities of over 20 validated transiting planets around mid-late M dwarfs with the Subaru IRD in the Subaru IRD intensive program.
We present the results of TESS follow-up observations by the MuSCAT series and the Subaru IRD intensive program.

Keywords: Exoplanets, Transit, Radial velocity, TESS

©2021. Japan Geoscience Union. All Right Reserved.

Development of optical diffusers and the on-sky examination

*Taku Nishiumi[1,2], Norio Narita[3,2,7,8], Akihiko Fukui[3], Noriharu Watanabe[3], Kiyoe Kawauchi[3], Hideyuki Izumiura[4], Hiroyuki Maehara[4], Nobuhiko Kusakabe[2,4], Keisuke Isogai[5], Yuka Terada[6,9], John H Livingston[3], Mayuko Mori[3]

1. SOUKENDAI, 2. Astrobiology Center, 3. The University of Tokyo, 4. National Astronomical Observatory of Japan, 5. Kyoto University, 6. Academia Sinica, 7. Instituto de Astrof\'{i}sica de Canarias (IAC), 8. Japan Science and Technology Agency, 9. National Taiwan University

Over four thousands of exoplanets have been found to date. It is important to reveal the detailed physical properties of these exoplanets by various methods, including high-precision transit photometry from the ground. Some groups adopted diffusers and succeeded to observe transiting exoplanets for high-precise observation from the ground. Diffusers can enlarge light from stars and keep the shape of stars.We developed optical diffusers to observe transiting exoplanets for high precise photometry and equipped them to MuSCAT.
We examined the diffusers' capability compared with defocus and in-focus observing methods in the on-sky examination. We confirmed that the stability of diffusers are more stable than other observing methods.
We will report the details in this poster.

Keywords: exoplanets, photometry, diffuser, observation

©2021. Japan Geoscience Union. All Right Reserved.

Measurement of Spin-orbit Obliquity of WASP-33b by Doppler Tomography and Transit Photometry

*Noriharu Watanabe[1], Norio Narita[1], Marshall C. Johnson[2], Akihiko Fukui[1], Nobuhiko Kusakabe[3], Enric Palle[4], John Livingston[1], Kiyoe Kawauchi[1], Jerome Pitogo de Leon[1], Taku Nishiumi[5], Mayuko Mori[1], Hannu Parviainen[4], Felipe Murgas[4], Pilar Montañes-Rodriguez[4]

1. The University of Tokyo, 2. Las Cumbres Observatory, 3. Astrobiology Center, NINS, 4. Instituto de Astrofisica de Canarias, 5. The Graduate University for Advanced Studies, SOKENDAI

There are three major orbital evolution models of hot Jupiter. One model drops a hot Jupiter near its host star by the gravitational interaction between the planet and the gas disk (planet-disk interactive model) and often aligns the orbit with the stellar spin. Another model scatters more than three hot Jupiters by their mutual interactions (planet-planet scattering model), and the stellar rotation axis is inclined easily to the planetary orbital axis. The other model oscillates the orbit of hot Jupiter by the Kozai effect (Kozai-Lidov mechanism) and tends to make the obliquity distribution more widely than one via the planet-planet scattering. While the first model keeps an orbit circular, the second and the third ones make an orbit elliptic. Especially, the eccentric orbit gets circular by tidal evolution keeping its misaligned orbit.

However, a solar-like star, whose effective temperature is less than 6250K, is realigned with a planetary orbit because its thick convective has been affected by the tidal dissipation. On the other hand, a hot star, whose effective temperature is more than 7000K, has no convective zones and hardly undergoes realignment. Thus, the spin-orbit obliquity of hot Jupiter around the hot star is the clue to understanding its origin.

Doppler tomography is a powerful method to measure the spin-orbit obliquity of hot Jupiters around hot stars by transit spectroscopy. Nevertheless, a single observation can only measure the projected one and never detect the real one ϕ. The nodal precession occurs and moves the transit trajectory when a hot Jupiter revolves around a hot star, which tends to be oblate by its fast spin, in the misaligned orbit. The larger stellar quadrupole moment J_2, which is the index of the stellar oblateness, makes the speed of the nodal precession faster. This movement changes projected spin-orbit obliquity and impact parameter, which is available by more than one observation. In terms of measuring an impact parameter, transit photometry is also a valuable method for the nodal precession. Finally, we can measure the real spin-orbit obliquity ϕ by the two variations.

WASP-33b, a hot Jupiter around a hot star, is the only planet whose real spin-orbit obliquity ϕ has been measured by the nodal precession via Doppler tomographic observation. However, because the previous study measured it by only two-epoch Doppler tomographic datasets, it is not enough to confirm WASP-33b's nodal precession. Thus, we observed WASP-33b using HIgh Dispersion Echelle Spectrograph (HIDES) in 2019 by Doppler tomographic observation. We utilized this data from HIDES. We also analyzed Doppler tomographic data by High Dispersion Spectrograph (HDS) in 2011, and Robert G. Tull Coudé Spectrograph (TS23) in 2008, 2014, and 2016 to search the variations of its projected spin-orbit obliquity and its impact parameter. We also observed the hot Jupiter for adding data points of its impact parameters by Multicolor Simultaneous Camera for studying Atmospheres of Transiting exoplanets (MuSCAT) in 2017 and the second generation (MuSCAT2) in 2018. We calculated its ϕ and J_2 by MCMC with the time variation models of the two orbital parameters.

©2021. Japan Geoscience Union. All Right Reserved.

We confirmed the more precise WASP-33b's nodal precession with more extended and more observations than the previous study. We obtained WASP-33b's real spin-orbit obliquity, $\phi = 110.2^{+1.3}_{-1.4}$deg. This planetary orbit has evolved with the mechanisms which makes the orbit misaligned easily such as the planet-planet scattering and the Kozai migration. This research is the first step to make a histogram of the real spin-orbit obliquity ϕ by Doppler tomography and transit photometry. We also found $J_2 = 1.11^{+0.15}_{-0.11} \times 10^{-4}$, which is slightly smaller than the calculated one in theory. This may indicate the possibility that its actual stellar internal structure is different from the theoretical one. In the future, we will clarify how hot Jupiters have migrated by increasing the measured samples.

Keywords: Exoplanet, Planetary Orbit, Hot Jupiter, Hot star

©2021. Japan Geoscience Union. All Right Reserved.

Observation of Stellar Activities for the Planetary Hosted Stars

*Riko Shimizu[1], Yosuke Alexandre Yamashiki[1], Nami Kimura[1], Hiroyuki Maehara[2], Kosuke Namekata[1], Mikio Kurita[1], Vladimir Airapetian[3]

1. Kyoto Univ., 2. NAOJ, 3. NASA Goddard Space Flight Center

The Search for Extra-terrestrial Mother Planets Catalogue (SEMPAC) will be used to search for potentially habitable mother planets and to derive data on stellar activity about their host stars. We have conducted observation for the stellar activities for the planetary hosting stars in order to identify critical ionizing radiation for the planetary environment using Seimei Telescope. This activity may provide useful information for the dose of ionizing radiation and the estimation of atmospheric escape to secure planetary surface environment whether planets may preserve the aquatic environment. For the initiation of our observation, we observed the GJ180, GJ273, GJ357, GJ3293, GJ3323, Ross-128, and Kepler-1544. In additionwe also observed active young sun’ s analogues as Kappa1 Ceti and V993 Tau.

In this presentation we’ ll introduce the preliminary outcome throughout the observation activities via Seimeitelescope and input into SEMPAC, by focusing on their potential impact in their atmospheric environment of the host star.

©2021. Japan Geoscience Union. All Right Reserved.

Climate for exo-terrestrial planets with a 3D high resolution cloud resolved climate model: Effect of obliquity

*Takanori Kodama[1], Daisuke Takasuka[2], Takeshi Kuroda[3], Tomoki Miyakawa[4], Masaki Satoh[4]

1. Komaba Institute for Science, The University of Tokyo, 2. Department of Information Science, Ochanomizu University, 3. Department of Geophysics, Tohoku University, 4. Atmosphere and Ocean Research Institute, The University of Tokyo

A large number of exoplanets are detected and some of them are expected to be rocky planets with Earth-like bulk composition within the habitable zone. A characterization of atmospheres for exoplanets will start with new space telescopes. We are in a new era of exoplanetary science and will see more details for them. Recently, the climate for exoplanets in the habitable zone has been estimated with a three-dimensional climate mode. Thus, as observational information is accumulated, our understanding for the exoplanetary atmosphere gradually moves from the1D-averaged climate to the 3D climate which captures non-uniform distributions of components in the atmosphere.

In the atmospheric science for the Earth, the climate simulation incredibly developed and it can estimate cloud and water vapor distributions with explicit convection under the high-resolution horizontal mesh (~14km mesh). The distribution of clouds and water vapor should be significantly important in the exoplanetary atmosphere, especially tidally locked exoplanets. Thus, it will be good opportunity to apply their knowledge to the exoplanetary atmosphere. Do we really need such a high-resolution and cloud resolved GCM? We have not had the answer for this question yet.

Here, we introduce NICAM (Non-hydrostatic ICosahedral Atmospheric Model), known as a global cloud resolving model. This model can explicitly resolve cloud distributions and the vertical transport of water vapor. Additionally, we can simulate the climate with high resolution using FUGAKU. As a first step, we investigate the climate with different obliquity. We assumed aqua-planet configurations with 1 bar of air as a background atmosphere with 5 different obliquities (0º, 15º, 23.5º, 45º, and 60º). We ran three set of simulations: 1) low-resolution (~220km mesh as standard resolution of GCM for exoplanetary science) with parametrization for cloud formation, 2) low resolution + explicit cloud microphysics scheme, and 3) high-resolution (~14km mesh) + explicit cloud microphysics scheme. We will show the atmospheric circulation and meridional energy transport for an aqua planet with different obliquity and discuss water transport and the location of the ITCZ in this presentation.

Keywords: Exoplanets, Climates

©2021. Japan Geoscience Union. All Right Reserved.

Possible Verifications for the Inner Void Model of Rapid Planet Formation

*Masahiro Morikawa[1]

1. Department of Physics, Ochanomizu University

We have developed a new model of rapid planet formation. This model is based on the scenario that all the planets and cores are formed at the outer edge of the inner gas void at the radius of around 0.04AU, and then gravitationally shot toward the middle of the protoplanetary disk. In this paper, we improve this model with the results of possible verifications of this model.

The model avoids the general problem of the dust-fall toward the central star before planet formation. Due to the magnetorotational instability or any interaction with the central star, a gas-free region (void) with a radius of about 0.04 AU (astronomical unit) from the central star is assumed. Dust falls to its outer edge and accumulates there. Dense dust collides with each other a coherent Kepler motion is realized. Here, gas is involved and runaway accretion occurs, resulting in Hot Jupiter (HJ) and dust lumps of various sizes. The former heavy body sling-shots the latter light bodies in and out, which forms cold gas planet (CG) by the gas accretion. Lighter dust clumps are shot out to the outer edge of the disk and released to the outside of the system at a certain rate to become interstellar planets and dust lumps. On the other hand, dust that has fallen from the outside into the gas gap created by CG forms a lump of ice. (Arxiv 2007.15979). We verify our model based on the basic predictions of the model.
A rapid decrease of dust: This model promotes the rapid formation of planets: 50 years for dust fall, 200 years for dust accumulation in the dense environment, and less than 5000 years for the sling-shot. Thus the planets can have almost the same composition and are rapidly formed at the same time. This is compared with the observations such as C.F.Manara 2018, and μ54Fe verification by M. Schiller, et al., 2020. Verification from the magma ocean of the Earth. In our rapid formation model, the earth was also blown by a slingshot from 0.04 AU with an equilibrium temperature of less than 2000 K. Therefore, the Earth magma ocean has been there from the beginning. According to L. Piani et al., 2020, the Earth's hydrogen can be supplied from the Enstatite Chondrite in the mantle, and its chemical composition is consistent. In this case, the Earth's water has been naturally present, and the late heavy bombardment hypothesis would not be needed. The origin of the Moon. The Giant Impact hypothesis is popular but this cannot explain the similarity in composition of elements of the moon and the earth. On the other hand, the separation theory (the moon jumped out of the earth) best describes this elemental composition while the rotation was not sufficient for the separation. In our model, the tidal force of the slingshot gives 10 times the force required for the separation and enables the separation of the moon and the earth. The element composition ratio of all planets (cores) within a system is the same in our model. This result is compared with the observation by A. E. Doyle1 et al. 2019 which concludes the composition of six planets roasted by white dwarfs is the same as those for Earth, Mars, and Mercury. Planet cores and small dust masses are all undergoing thermal metamorphism in our model because the radius 0.04 AU corresponds to the equilibrium temperature 2000 K which naturally yields thermal metamorphism. In particular, smaller dust masses are blown to the outer periphery of the disk and bear a hot history of thermal metamorphism. On the other hand, at the outer edge of the gap created by the gas giant in the middle of the disk, the dust mass bears a cold history while adhering ice. These outer hot and inner cold sources mix to form meteorites, comets, and asteroids. This is compared with the results of the Stardust exploration (H. Bortman 2006). Further predictions of our model can be checked: A possibility of simple cooling of the earth; Many interstellar rogue planets; Origin of the spin of the planets and satellites.

©2021. Japan Geoscience Union. All Right Reserved.

Keywords: planet formation, unified model, solar system verifivation

©2021. Japan Geoscience Union. All Right Reserved.

On the origin of metal-rich close-in gas giants: planetesimals vs pebbles

*Masahiro Ikoma[1,2], Kento Kikuchi[1], Tadahiro Kimura[1], Akifumi Nakayama[1], Sho Shibata[1]

1. Department of Earth and Planetary Science, The University of Tokyo, 2. Division of Science, National Astronomical Observatory of Japan

According to observed mass-radius relationships for transiting exoplanets, many close-in gas giants contain large amounts of heavy elements (or metals). This fact may support the core accretion scenario for gas giant formation but brings a new challenge. Core accretion models suggest that such metals were likely injected into the gas giants after the core accretion stage. Here we explore the late accretion of metals for migrating gas giants based on two different scenarios: planetesimal accretion and pebble accretion. We show that metal-rich close-in gas giants like those detected so far can be formed under some conditions in both scenarios and, then, discuss the advantages and disadvantages of the two scenarios.

Keywords: Exoplanets, Formation, Interior

©2021. Japan Geoscience Union. All Right Reserved.

[E] Oral | A (Atmospheric and Hydrospheric Sciences)：A-AS Atmospheric Sciences, Meteorology & Atmospheric Environment

Sun. Jun 6, 2021 9:00 AM - 10:30 AM JST | Sun. Jun 6, 2021 12:00 AM - 1:30 AM UTC | Ch.07 Zoom Room 07

[A-AS02] Extreme Events: Observations and Modeling

convener:Sridhara Nayak(Disaster Prevention Research Institute, Kyoto University), Tetsuya Takemi(Disaster Prevention Research Institute, Kyoto University), Satoshi Iizuka(National Research Institute for Earth Science and Disaster Resilience), Chairperson:Satoshi Iizuka(National Research Institute for Earth Science and Disaster Resilience), Sridhara Nayak(Disaster Prevention Research Institute, Kyoto University), Tetsuya Takemi(Disaster Prevention Research Institute, Kyoto University)

The frequencies and intensities of extreme events such as heavy rainfall, flash floods, droughts, heat waves, tropical cyclones etc. have increased in many regions across the globe and are of serious concern due to their socio-economic and climate change connections. Thus, understanding of the patterns of such events and particularly their characteristics have been the focus of many recent studies. This session invites abstracts on observational and numerical modeling studies to enhance the understanding of the spatial and temporal characteristics and predictability of the extreme events. In particular, abstracts are encouraged on regional analysis of the extreme events in past years and in near or far future (30-100 years), which would assist the policy makers to build potentially more resilient societies to face the extreme event related disasters. This session also welcomes the submissions on model simulations and evaluations to advance the understanding of the physics and dynamics associated with the extreme events.

9:00 AM - 9:05 AM JST | 12:00 AM - 12:05 AM UTC

[AAS02-01] Introduction

9:05 AM - 9:25 AM JST | 12:05 AM - 12:25 AM UTC

[AAS02-02] Assessing the Impacts of Extreme Weather on Local-Scale Hazards under Climate Change

★Invited Papers

*Tetsuya Takemi[1] (1.Disaster Prevention Research Institute, Kyoto University)

9:25 AM - 9:45 AM JST | 12:25 AM - 12:45 AM UTC

[AAS02-03] **Estimation of moisture sources within an explosive cyclone over the Sea of Japan using an isotopic regional spectral model**

★Invited Papers

*Xiaoyang Li[1], Ryuichi Kawamura[1], Atsuko Sugimoto[2,3], Kei Yoshimura[4,5] (1.Department of Earth and Planetary Science, Faculty of Science, Kyushu University, 2.Arctic Research Center, Hokkaido University, 3.Graduate School of Environmental Science, Hokkaido University, 4.Atmosphere and Ocean Research Institute, The University of Tokyo, 5.Institute of Industrial Science, The University of Tokyo)

9:45 AM - 10:00 AM JST | 12:45 AM - 1:00 AM UTC

[AAS02-04] Influence of Warm SST in the Oyashio Region on Rainfall Distribution of Typhoon Hagibis (2019)

*Satoshi Iizuka[1], Ryuichi Kawamura[2], Hisashi Nakamura[3], Toru Miyama[4] (1.National Research Institute for Earth Science and Disaster Resilience, 2.Department of Earth and Planetary Sciences, Kyushu University, 3.Research Center for Advanced Science and Technology, University of Tokyo, 4.Japan Agency for Marine-Earth Science and Technology,)

10:00 AM - 10:15 AM JST | 1:00 AM - 1:15 AM UTC

[AAS02-05] Simulation of typhoon-induced heavy precipitation over the Philippines using the Multi-scale Kain-Fritsch Cumulus Scheme in WRF

*Jose Angelo Hokson[1], Shinjiro Kanae[1], Rie Seto[1] (1.School of Environment and Society, Tokyo Institute of Technology)

10:15 AM - 10:30 AM JST | 1:15 AM - 1:30 AM UTC

[AAS02-06] **Attribution of atmospheric circulation variations associated with winter temperature whiplash events over Northeast China**

*Zhen Liao[1], Panmao Zhai[1], Yang Chen[1] (1.LaSW, CAMS, China)

[E] Oral | A (Atmospheric and Hydrospheric Sciences) | A-AS Atmospheric Sciences, Meteorology & Atmospheric Environment

[A-AS02] Extreme Events: Observations and Modeling

convener:Sridhara Nayak(Disaster Prevention Research Institute, Kyoto University), Tetsuya Takemi(Disaster Prevention Research Institute, Kyoto University), Satoshi Iizuka(National Research Institute for Earth Science and Disaster Resilience), Chairperson:Satoshi Iizuka(National Research Institute for Earth Science and Disaster Resilience), Sridhara Nayak(Disaster Prevention Research Institute, Kyoto University), Tetsuya Takemi(Disaster Prevention Research Institute, Kyoto University)

Sun. Jun 6, 2021 9:00 AM - 10:30 AM Ch.07 (Zoom Room 07)

The frequencies and intensities of extreme events such as heavy rainfall, flash floods, droughts, heat waves, tropical cyclones etc. have increased in many regions across the globe and are of serious concern due to their socio-economic and climate change connections. Thus, understanding of the patterns of such events and particularly their characteristics have been the focus of many recent studies. This session invites abstracts on observational and numerical modeling studies to enhance the understanding of the spatial and temporal characteristics and predictability of the extreme events. In particular, abstracts are encouraged on regional analysis of the extreme events in past years and in near or far future (30-100 years), which would assist the policy makers to build potentially more resilient societies to face the extreme event related disasters. This session also welcomes the submissions on model simulations and evaluations to advance the understanding of the physics and dynamics associated with the extreme events.

9:00 AM - 9:05 AM

[AAS02-01]Introduction

©Japan Geoscience Union

Assessing the Impacts of Extreme Weather on Local-Scale Hazards under Climate Change

*Tetsuya Takemi[1]

1. Disaster Prevention Research Institute, Kyoto University

Understanding hazards and risks due to extreme weather phenomena is critically important in order to consider disaster risk reduction under climate change. Quantitative representations of meteorological hazards are critically important in order to assess the impacts of such hazards not only for past disastrous events but also as for anticipated extreme events under future global warming. Furthermore, hazard information at local-scales is required because the resulting phenomena occur depending on their local geographic features. Since the Innovative Program of Climate Change Projection for the 21st Century (KAKUSHIN Program, FY2007-2012) funded by the Japanese Government, we have been studying the impacts of extreme weather under future global warming under the subsequent Program for Risk Information on Climate Change (SOUSEI Program, FY2012-2017) and the latest Integrated Research Program for Advancing Climate Models (TOUGOU Program FY2017-). Meteorological hazards such as heavy rainfalls, strong winds, and tropical cyclones were quantitatively examined as case studies. In this presentation, we will talk about how the quantitative representation of meteorological hazards helps to assess the impacts of the hazards for climate change adaptation and disaster risk reduction. We will focus on tropical cyclones and heavy rainfalls as extreme weather and use a dynamical downscaling technique with the Weather Research and Forecasting (WRF) model for the impact assessment studies. Past extreme weather that caused severe disaster can be regarded as a baseline to consider local-scale hazards. The impacts of climate change are investigated with the use of pseudo-global warming technique in which warming increments are added to past meteorological fields. The results from case studies on tropical cyclones and heavy rainfalls are demonstrated in this presentation. Furthermore, the analysis of airflows downscaling to urban districts with the use of a building-resolving large-eddy simulation model is demonstrated. Strong wind hazards are quantitatively assessed by the building-resolving modelling technique.

Keywords: extreme weather, dynamical downscaling, climate change impact, urban disaster risk, global warming

©2021. Japan Geoscience Union. All Right Reserved.

Estimation of moisture sources within an explosive cyclone over the Sea of Japan using an isotopic regional spectral model

*Xiaoyang Li[1], Ryuichi Kawamura[1], Atsuko Sugimoto[2,3], Kei Yoshimura[4,5]

1. Department of Earth and Planetary Science, Faculty of Science, Kyushu University, 2. Arctic Research Center, Hokkaido University, 3. Graduate School of Environmental Science, Hokkaido University, 4. Atmosphere and Ocean Research Institute, The University of Tokyo, 5. Institute of Industrial Science, The University of Tokyo

In this study, we identified water origins and clarified moisture transport processes within the explosive cyclone migrating poleward across the Sea of Japan (SJ) on November 30, 2014, by using an isotopic regional spectral model. Regarding the total precipitable water and condensation in the vicinity of the cyclone center, a replacement of water origins occurred during the cyclone development, resulting from a shift of the moisture transport from the warm conveyor belt (WCB) to the cold conveyor belt (CCB) and dry intrusion (DI). At the early stage, the WCB transported large amounts of moisture from the East China Sea and Kuroshio (ECS & KS) into the cyclone’ s inner region. While at the rapidly developing stage, the CCB and DI conveyed more moisture from the Northwest Pacific Ocean (NWP) and SJ, respectively, to the cyclone center area. Compared with the local moisture, the contribution of remote moisture was dominant in the vicinity of the cyclone center. With respect to the water origins of condensation within the cyclone frontal system at the rapidly developing stage, the NWP vapors, principally transported by the CCB, contributed 35.5% of the condensation in the western warm front. The ECS & KS moisture, conveyed by the WCB, accounted for 32.4% of the condensation in the cold and eastern warm fronts. In addition, condensation from the SJ, which was mainly triggered by the DI and induced by the topography, occurred on the west coast of the mainland of Japan and near the cyclone center. The spatial distribution of the isotopic composition in condensation also supports the water origin results. These results point the way toward better understanding of where the moisture is evaporated, how the moisture is transported, and where the moisture is condensed. The findings can be used for weather forecasting, disaster preparedness, and allocation of water and energy resources in association with extratropical cyclones.

Keywords: explosive cyclone, water origins, warm conveyor belt, cold conveyor belt, isotopic regional spectral model, stable water isotopes

©2021. Japan Geoscience Union. All Right Reserved.

Influence of Warm SST in the Oyashio Region on Rainfall Distribution of Typhoon Hagibis (2019)

*Satoshi Iizuka[1], Ryuichi Kawamura[2], Hisashi Nakamura[3], Toru Miyama[4]

1. National Research Institute for Earth Science and Disaster Resilience, 2. Department of Earth and Planetary Sciences, Kyushu University, 3. Research Center for Advanced Science and Technology, University of Tokyo, 4. Japan Agency for Marine-Earth Science and Technology,

Typhoon Hagibis (2019) caused widespread flooding and damage over eastern Japan. The associated rainfall maxima were primarily observed on the windward mountain slopes along with the west of the leading edge of a low-level front. Concomitantly, a significant positive value in sea surface temperature anomalies (SSTAs) was observed in association with an ocean eddy over the Oyashio region, together with anomalous warmth over the entire western North Pacific. The present study examines the role of the SSTAs in the rainfall distribution associated with Hagibis, to deepen our understanding of the influence of the midlatitude ocean on tropical cyclones and associated rainfall. Our sensitivity experiments demonstrate that the observed warm SSTAs had the potential to displace the rainfall caused by Hagibis inland and thereby acted to increase precipitation along the Pacific coast of northeastern Japan. Our results suggest that midlatitude SSTAs on ocean-eddy scales can also influence the synoptic-scale atmospheric front and associated heavy rainfall.

Keywords: Typhoon, Rainfall, Sea Surface Temperature, Oyashio

©2021. Japan Geoscience Union. All Right Reserved.

Simulation of typhoon-induced heavy precipitation over the Philippines using the Multi-scale Kain-Fritsch Cumulus Scheme in WRF

*Jose Angelo Hokson[1], Shinjiro Kanae[1], Rie Seto[1]

1. School of Environment and Society, Tokyo Institute of Technology

Cumulus parameterization schemes, which handle convection processes such as those involving moisture and precipitation, have been indispensable in simulations using numerical weather prediction models such as the Weather Research and Forecasting (WRF) model. The Kain-Fritsch (KF) is one of the most-used schemes in WRF. An improved and scale-aware version of this scheme, called Multi-scale KF (MSKF), was produced to address overestimations of precipitation by KF. Studies in the Himalayas and the United States have proven that using MSKF brings improvement to the simulated precipitation values. However, the applicability and performance of MSKF over the Philippines in simulating precipitation, especially heavy precipitation, is yet to be verified. Herein, we examined these by simulating Typhoon Koppu and comparing the hourly and daily results with those of two other cumulus schemes –KF and Grell-Freitas (GF). Six simulations were conducted –three use cumulus schemes in high resolution (5 km, innermost domain), and three do not. Based on the results, the MSKF is applicable for use in simulating precipitations, including heavy precipitations, over the Philippines. It is best used when a typhoon is at its strongest but underperforms when the typhoon is weak and nearing dissipation. However, GF performs best among the three schemes. Additionally, the results show that using cumulus schemes in high resolution (5 km, using nests) does not always improve, sometimes even deteriorate, the performance of simulations in producing accurate precipitation values. Further investigations should be conducted regarding the performance of MSKF in simulating heavy precipitations over the Philippines and neighboring areas.

Keywords: typhoon-induced heavy precipitation, multi-scale Kain-Fritsch cumulus scheme, WRF, Typhoon Koppu, Philippines

©2021. Japan Geoscience Union. All Right Reserved.

Attribution of atmospheric circulation variations associated with winter temperature whiplash events over Northeast China

*Zhen Liao[1], Panmao Zhai[1], Yang Chen[1]

1. LaSW, CAMS, China

Based on the daily meteorological observations, reanalysis and model datasets, this study investigated the evolution and the causes of the extreme cold events in Northeast China via a ‘temperature whiplash’ index over 1980-2018 from the perspective of the temperature variability and associated circulation. Results indicate that winters in Northeast China have become increasingly volatile during 1980-2018 based on the interdiurnal temperature variation. Such enhanced volatility has a strong expression in significant increases in whiplash events, which characterizes rapid and drastic switches between warm and cold extremes within several days. And cold extremes in these areas are more likely to occur in the form of the whiplash events under global warming background. At the same time, the increased whiplash events in Northeast China have a good relationship with the enhanced winter 500 hPa geopotential height variance over the Sea of Okhotsk. Further, the attribution analysis of the associated circulation variance by using HadGEM3-A-N216 ensembles shows that the observed changes in the winter 500 hPa geopotential height variance over the Sea of Okhotsk can attribute to the anthropogenic forcing, implying that the anthropogenic forcing has an impact on the associated circulation and thus lead to the increased the whiplash events in Northeast China.

Keywords: attribution, compound event, circulation

©2021. Japan Geoscience Union. All Right Reserved.

[E] Oral | A (Atmospheric and Hydrospheric Sciences)：A-AS Atmospheric Sciences, Meteorology & Atmospheric Environment

Sun. Jun 6, 2021 10:45 AM - 12:15 PM JST | Sun. Jun 6, 2021 1:45 AM - 3:15 AM UTC | Ch.07 Zoom Room 07

[A-AS02] Extreme Events: Observations and Modeling

convener:Sridhara Nayak(Disaster Prevention Research Institute, Kyoto University), Tetsuya Takemi(Disaster Prevention Research Institute, Kyoto University), Satoshi Iizuka(National Research Institute for Earth Science and Disaster Resilience), Chairperson:Tetsuya Takemi(Disaster Prevention Research Institute, Kyoto University), Sridhara Nayak(Disaster Prevention Research Institute, Kyoto University), Satoshi Iizuka(National Research Institute for Earth Science and Disaster Resilience)

The frequencies and intensities of extreme events such as heavy rainfall, flash floods, droughts, heat waves, tropical cyclones etc. have increased in many regions across the globe and are of serious concern due to their socio-economic and climate change connections. Thus, understanding of the patterns of such events and particularly their characteristics have been the focus of many recent studies. This session invites abstracts on observational and numerical modeling studies to enhance the understanding of the spatial and temporal characteristics and predictability of the extreme events. In particular, abstracts are encouraged on regional analysis of the extreme events in past years and in near or far future (30-100 years), which would assist the policy makers to build potentially more resilient societies to face the extreme event related disasters. This session also welcomes the submissions on model simulations and evaluations to advance the understanding of the physics and dynamics associated with the extreme events.

10:45 AM - 10:50 AM JST | 1:45 AM - 1:50 AM UTC

[AAS02-07] Introduction

10:50 AM - 11:10 AM JST | 1:50 AM - 2:10 AM UTC

[AAS02-08] Observations and simulations of Typhoon Faxai over the Kanto area

★Invited Papers

*Woosub Roh[1], Masaki Satoh[1] (1.AORI, the university of Tokyo)

11:10 AM - 11:30 AM JST | 2:10 AM - 2:30 AM UTC

[AAS02-09] River discharge estimation of ungauged mountainous river basin using NIED Hi-net data

★Invited Papers

*Shakti P.C.[1], Kaoru Sawazaki[1] (1.National Research institute for Earth Science and Disaster Resilience (NIED))

11:30 AM - 11:45 AM JST | 2:30 AM - 2:45 AM UTC

[AAS02-10] **Increase in the strength of typhoons to Taiwan due to global warming**

*Ravi Shankar Pandey[1], Yuei-An Liou[1] (1.National Central University)

11:45 AM - 12:00 PM JST | 2:45 AM - 3:00 AM UTC

[AAS02-11] Investigation of Uncertainties in Regional Climate Information

*Saurabh Kelkar[1] (1.University of Tsukuba)

12:00 PM - 12:15 PM JST | 3:00 AM - 3:15 AM UTC

[AAS02-12] **Precipitation patterns in landfalling typhoons over Japan**

*Sridhara Nayak[1], Tetsuya Takemi[1] (1.Disaster Prevention Research Institute, Kyoto University)

[E] Oral | A (Atmospheric and Hydrospheric Sciences) | A-AS Atmospheric Sciences, Meteorology & Atmospheric Environment

[A-AS02] Extreme Events: Observations and Modeling

convener:Sridhara Nayak(Disaster Prevention Research Institute, Kyoto University), Tetsuya Takemi(Disaster Prevention Research Institute, Kyoto University), Satoshi Iizuka(National Research Institute for Earth Science and Disaster Resilience), Chairperson:Tetsuya Takemi(Disaster Prevention Research Institute, Kyoto University), Sridhara Nayak(Disaster Prevention Research Institute, Kyoto University), Satoshi Iizuka(National Research Institute for Earth Science and Disaster Resilience)
Sun. Jun 6, 2021 10:45 AM - 12:15 PM Ch.07 (Zoom Room 07)

The frequencies and intensities of extreme events such as heavy rainfall, flash floods, droughts, heat waves, tropical cyclones etc. have increased in many regions across the globe and are of serious concern due to their socio-economic and climate change connections. Thus, understanding of the patterns of such events and particularly their characteristics have been the focus of many recent studies. This session invites abstracts on observational and numerical modeling studies to enhance the understanding of the spatial and temporal characteristics and predictability of the extreme events. In particular, abstracts are encouraged on regional analysis of the extreme events in past years and in near or far future (30-100 years), which would assist the policy makers to build potentially more resilient societies to face the extreme event related disasters. This session also welcomes the submissions on model simulations and evaluations to advance the understanding of the physics and dynamics associated with the extreme events.

10:45 AM - 10:50 AM

[AAS02-07]Introduction

©Japan Geoscience Union

Observations and simulations of Typhoon Faxai over the Kanto area

*Woosub Roh[1], Masaki Satoh[1]

1. AORI, the university of Tokyo

A tropical cyclone is one of the extreme events to make heavy rainfall and strong winds. The typhoon Faxai generated in 1st Sep. 2019 and launched the Kanto area on 8th Sep. 2019. There are intensive observation stations over the Kanto area, whose domain size is 100 km×100 km. For example, the High Spectral Resolution Lidar (HSRL, 355 nm), Doppler lidar, and the Cloud Profiling Radar (CPR, 94 GHz) are located in Tokyo. Several polarimetric radars are available like C-band radar in two airports, X-band phased array radar in Saitama University, Ka-band radar in Tsukuba. The WInd profiler Network and Data Acquisition System (WINDAS) data is available in Kawaguchiko, Mito, and Kumagaya. The ULTIMATE (ULTra sIte for Measuring Atmosphere of Tokyo metropolitan Environment) is proposed to verify and improve high-resolution numerical simulations based on these observation data. The typhoon Faxai is one of the targets in the ULTIMATE project.

In this study, we analyzed these intensive observation data about the typhoon Faxai. We simulated typhoon Faxai using the Nonhydrostatic ICosahedral Atmospheric Model (NICAM, Satoh et al. 2014). We evaluate the performances of NICAM using a Joint simulator (Hashino et al. 2013) and discuss how to improve the microphysics in NICAM using the observation data.

Keywords: NICAM , Tropical cyclone , ULTIMATE, Joint simulator

©2021. Japan Geoscience Union. All Right Reserved.

River discharge estimation of ungauged mountainous river basin using NIED Hi-net data

*Shakti P.C.[1], Kaoru Sawazaki[1]

1. National Research institute for Earth Science and Disaster Resilience (NIED)

In Japan, flood events in mountainous river basins in recent years have resulted in significant loss of life and damage to infrastructure. Estimation of peak streamflow of rivers during flood events can be a good reference for flood disaster prevention and management. However, because there are no streamflow data for many of the small mountainous river basins in Japan –known as ungauged river basins –it takes considerably more effort to predict and estimate water-related disasters in such areas. To understand the flow rate of ungauged river basins during the extreme rain event, there are several direct and indirect approaches that have been applied and tested to estimate river discharge particularly during the period of an extreme rain event.
In this study, we considered High sensitivity seismograph network (Hi-net) observation to recognize the time and peak discharge during a heavy rain event. Hi-net is a nationwide high-sensitivity seismograph network, Japan, comprised of more than 800 seismograph stations distributed by approximately 20 km distance interval. They are also located in the mountainous region to measure earthquakes. Two Hi-net stations are located in a mountainous sub-basin of the Mogami River Basin, located in Yamagata prefecture of Japan. After validating the simulated discharge data of the Mogami River Basin with gauged data for the selected two past rain events (10-23 July 2004 and 7-16 September 2015), simulated discharge of a river was compared with noise data of the Hi-net stations. It was found that the noise data of those stations at a high-frequency level were followed a similar trend with the time series of simulated discharge at those two points for the selected events.

©2021. Japan Geoscience Union. All Right Reserved.

Increase in the strength of typhoons to Taiwan due to global warming

*Ravi Shankar Pandey[1], Yuei-An Liou[1]

1. National Central University

Detailed investigation on the tracks and cyclogenesis locations of all 77 typhoons that hit Taiwan in the last 40 years (1977 to 2016) during typhoon season (May to November) is carried out. Ten pathways of all typhoons that hit Taiwan are detected and statistical analysis is carried out on fundamental typhoon parameters, including the direction to enter Taiwan, ocean of cyclogenesis, and phases of El Niño Southern Oscillation (ENSO) at cyclogenesis. The majority (> half, 53 %) of typhoons strike Taiwan from the East direction, typically (78%) from the Philippine Sea. They are on average stronger than the rest two other directional (West, South) typhoons. Yet, typhoons from the West uniquely survive the longest hours with the highest curvy tracks, often (59%) from just bordering the ocean i.e., the South China Sea. They are on average relatively weaker. Further statistical analysis on relationships among all typhoon parameters through Fisher' s Exact and Chi-square (χ 2) tests supports the above crucial finding and reveals that the curvy nature of tracks of typhoons is more responsible for the longer survival of typhoons (r = 0.67) than its strength. 26% more cyclogenesis is detected during the warm phase of ENSO than the cold phase. In the last 4 decades during the warm phase of ENSO, the number of cyclogenesis is also observed slowly increasing. A significant rise in the Sea Surface Temperature (SST) by 0.4 ~ 0.7 ˚C is measured using decadal, 5-yearly, yearly, ENSO phase, and monthly-wise SST Anomalies (SSTA) for the whole typhoon season (May-November) during the last 40 years in comparison to base years (1941-1970) over the entire global ocean, North Pacific Ocean, Philippine Sea, South China sea, and Eastern China Sea. A 35% crucial increase in decadal-averaged strength of typhoons is observed by 0.4 ~ 0.7 ˚C rise in the SST in all study oceans that originate typhoons to hit Taiwan during the last 40 years (1977 to 2016). The role of El-Niño epochs is found very crucial for the major SSTA changes during the typhoon season. The climatological analysis is fully consistent with statistical findings and leads to global warming as the major cause of the rising strength of typhoons that hit Taiwan during the study period. The maximum SST change in the Eastern China Sea during the study period is potentially due to its proximity from mainland China. This fact opens new research opportunities for the future.

Keywords: Cyclogenesis, El Niño Southern Oscillation, Sea Surface Temperature, Sea Surface Temperature Anomaly

©2021. Japan Geoscience Union. All Right Reserved.

Investigation of Uncertainties in Regional Climate Information

*Saurabh Kelkar[1]

1. University of Tsukuba

Climate change is the change in the frequency, intensity, spatial extent, duration, and timing of extreme weather and climate events (IPCC, 2013). Its impacts have already been visible across the globe. People in coastal regions, high mountains as well as lower-income and other marginalised communities, have less capacity to prepare for and cope with the extreme events and thus experience a more significant impact. However, in order to respond to climate change, reliable climate information and projections are necessary. These projections are estimated with the help of global and regional climate models. Projecting the climate scenarios involves uncertainties such as systematic errors associated with structural differences in models and inconsistencies between observations. Addressing these is as crucial as responding to global warming. In this study, we attempt to explore the uncertainties involved in climate information on a regional scale. We use an ensemble of GCM and RCM to obtain regional climate information of Japan, and investigate the possible uncertainties by comparing the ensemble simulations with the statistical metrics. With the result of this research, we hope to contribute to existing knowledge on climate uncertainties.

Keywords: Regional Climate Modelling, Added Values, Ensemble

©2021. Japan Geoscience Union. All Right Reserved.

Precipitation patterns in landfalling typhoons over Japan

*Sridhara Nayak[1], Tetsuya Takemi[1]

1. Disaster Prevention Research Institute, Kyoto University

Typhoons are one of the most dangerous weather events in the world and some of them bring extensive precipitation, and cause widespread flooding on the regions along their track. Thus understanding the precipitation patterns in landfalling typhoons has a focus in many previous studies. In this study, the precipitation patterns in 120 landfalling typhoons around Japan during 2006-2019 are extensively analyzed. The best track data from the Regional Specialized Meteorological Center (RSMC) Tokyo are used to identify the typhoon tracks and the precipitation datasets from the Radar Automated Meteorological Data Acquisition System (Radar-AMeDAS) are used to analyze the precipitation patterns. The probabilities of the different spell durations of precipitation intensities over different regions of Japan with various radii from the typhoon center starting from 10 km to 300 km shows that the occurrence of typhoon induced heavier precipitations is higher compared to the typhoon induced lighter precipitations. The heavier precipitations last up to a day, while the lighter precipitations last about 12 hours. The long-lived precipitations are also noticed that last up to 2 days, but they don’ t occur so frequently. The results also indicate that the pattern of spell durations are mostly same over all the regions within 300 km radius.

Keywords: Precipitation pattern, Typhoon, Spell duration

©2021. Japan Geoscience Union. All Right Reserved.

[E] Poster | A (Atmospheric and Hydrospheric Sciences)：A-AS Atmospheric Sciences, Meteorology & Atmospheric Environment

Sun. Jun 6, 2021 5:15 PM - 6:30 PM JST | Sun. Jun 6, 2021 8:15 AM - 9:30 AM UTC | Ch.07_1

[A-AS02] Extreme Events: Observations and Modeling

convener:Sridhara Nayak(Disaster Prevention Research Institute, Kyoto University), Tetsuya Takemi(Disaster Prevention Research Institute, Kyoto University), Satoshi Iizuka(National Research Institute for Earth Science and Disaster Resilience)

The frequencies and intensities of extreme events such as heavy rainfall, flash floods, droughts, heat waves, tropical cyclones etc. have increased in many regions across the globe and are of serious concern due to their socio-economic and climate change connections. Thus, understanding of the patterns of such events and particularly their characteristics have been the focus of many recent studies. This session invites abstracts on observational and numerical modeling studies to enhance the understanding of the spatial and temporal characteristics and predictability of the extreme events. In particular, abstracts are encouraged on regional analysis of the extreme events in past years and in near or far future (30-100 years), which would assist the policy makers to build potentially more resilient societies to face the extreme event related disasters. This session also welcomes the submissions on model simulations and evaluations to advance the understanding of the physics and dynamics associated with the extreme events.

[AAS02-P01] Analysis of "Typhoon-class Strong Wind" During the Non-typhoon Period for 116 Years (1904-2019) after Weather Observation on the Korean Peninsula : Basic Analysis

*Woo-Sik JUNG[1] (1.Department of Atmospheric Environment Information Engineering, INJE University, Republic of Korea.)

[AAS02-P02] Development of the KTTI(Korean Typhoon Type Index) by Analyze the Characteristics of Typhoon Affecting the Korean Peninsula

*Woo-Sik JUNG[1], Gunwoo Kim[1] (1.Department of Atmospheric Environment Information Engineering, INJE University, Republic of Korea.)

[AAS02-P03] **High precipitation rates and floods: Relation to solar wind high-speed streams**

*Paul Prikryl[1], Vojto Rušin[2], Emil A. Prikryl[3] (1.Physics Department, University of New Brunswick, 2.Astronomical Institute, Slovak Academy of Sciences, 3.Northern Ontario School of Medicine)

[AAS02-P04] **Climate change initiated variation in the tracks of typhoons in the North West Pacific basin**

*Ravi Shankar Pandey[1], Yuei-An Liou[1] (1.National Central University)

Analysis of "Typhoon-class Strong Wind" During the Non-typhoon Period for 116 Years (1904-2019) after Weather Observation on the Korean Peninsula : Basic Analysis

*Woo-Sik JUNG[1]

1. Department of Atmospheric Environment Information Engineering, INJE University, Republic of Korea.

Global warming is accelerating due to climate change, and as global warming accelerates, the frequency and intensity of extreme weather on the Korean Peninsula are increasing. Recently, the frequency and intensity of strong winds during the non-typhoon period, not during the typhoon season, under the name of "Typhoon-class Strong Wind," is increasing, and the damage caused by it is gradually increasing. Several studies have been conducted related to strong winds accompanied by typhoons, but studies related to strong winds during the non-typhoon period are very lacking. Therefore, in this study, we would like to conduct a basic study of strong winds during the period of non-typhoon. To derive basic data, analysis was conducted on all points of the Automatic Synoptic Observation System (ASOS), BOUY, BEACON for a total of 116 years from 1904 to 2019 when meteorological observations began on the Korean Peninsula. In this study, the criteria for strong wind during non-typhoon period was selected and classified as 14 m/s, which is the Korea Meteorological Administration's strong wind warning standard. As a result of the analysis, the rate of strong winds during the non-typhoon is high in coastal and mountainous areas, and the wind speed is also high in coastal and mountainous areas, including Jeju. We analyzed the changes in the rate of strong winds and the speed of strong winds during the non-typhoon period, depending on the El Nino, La Nina, yearly, and monthly. The results of this study are believed to be able to reduce the damage of strong winds during the non-typhoon and use them as basic data for further analysis.

This work was supported by the National Research Foundation of Korea(NRF) grant funded by the Korea government(MSIT) (No. 2020R1F1A1068738)

Keywords: Non-Typhoon period, Strong wind, 116 years (1904~2019)

©2021. Japan Geoscience Union. All Right Reserved.

Development of the KTTI(Korean Typhoon Type Index) by Analyze the Characteristics of Typhoon Affecting the Korean Peninsula

*Woo-Sik JUNG[1], Gunwoo Kim[1]

1. Department of Atmospheric Environment Information Engineering, INJE University, Republic of Korea.

Recently, climate change has been strengthening the power of typhoons affecting the Korean Peninsula and increasing the resulting damage. According to the Ministry of the Interior and Safety's 'Statistical yearbook of natural disaster (2018)', out of all 361 typhoons that affected the Korean Peninsula from 1904 to 2018, 6 typhoons since 2000 have been recorded as the top 10 in property damage rankings. Therefore, this study has aimed to analyze the characteristics of typhoons affecting the Korean Peninsula and objectively quantify the extent of the effects of rain and wind on each typhoon. Typhoon represents the complex characteristics of rain and wind, and to analyze it objectively, it is necessary to quantify the degree of influence of rain and wind of each typhoon. The TTI is an index that quantifies the relationship between cumulative precipitation and strong winds within the impact period for all typhoons passing through one observation point. If the index calculated like this is positive, it can be classified as a wind typhoon that is heavily affected by the wind, or a rain typhoon that is heavily affected by rain if it is negative. And the closer the index is to 0, the more evenly influenced by rain and wind. As a result of analyzing the impact of typhoon on the Korean peninsula by applying the typhoon impact index to the Korean peninsula, the degree of impact of rain and wind on each typhoon could be expressed as an objective number. This study is a basic study to develop the Korean Typhoon Type Index (KTTI) for understand the characteristics of rain and wind.

This work was supported by the National Research Foundation of Korea(NRF) grant funded by the Korea government(MSIT) (No. 2020R1F1A1068738)

Keywords: Typhoon Type Index, Rain, Wind

©2021. Japan Geoscience Union. All Right Reserved.

High precipitation rates and floods: Relation to solar wind high-speed streams

*Paul Prikryl[1], Vojto Rušin[2], Emil A. Prikryl[3]

1. Physics Department, University of New Brunswick, 2. Astronomical Institute, Slovak Academy of Sciences, 3. Northern Ontario School of Medicine

Precipitation datasets based on rain-gauge and satellite-sensor measurements are used to examine the relationship between daily precipitation rates and the solar wind high-speed streams from coronal holes. The superposed epoch (SPE) analyses show increases in occurrence of high precipitation rates following arrivals of high-speed streams, including their recurrence with solar rotation period. The cross-correlation analysis of high precipitation rate occurrence, the SPE averages of the corona intensity in the emission line (Fe XIV, 530.3 nm) observed by ground-based coronagraphs and supplemented by a proxy measurement of green corona intensity based on the emission line at 28.4 nm (FeXV) [1], and solar wind parameters measured upstream from the Earth [2], show correlation peaks at lags spaced by the solar rotation period. When the SPE analysis is limited to years around the solar minimum, significant intermediate correlation peaks spaced by about 9 days are also found. These quantitative results are consistent with the observed tendency of heavy rainfall and flash floods to follow the arrivals of high-speed streams, which is demonstrated for different geographical regions, in Australia, Japan and the U.S. The role of the solar wind-magnetosphere-ionosphere-atmosphere coupling in severe weather occurrence mediated by aurorally generated atmospheric gravity waves is discussed. The gravity waves propagate globally from sources in the high-latitude lower thermosphere, both upward and downward [3]. In the upper atmosphere, the gravity waves are observed as traveling ionospheric disturbances [4,5]. In the lower atmosphere, they can reach the troposphere and be ducted to low latitudes. Despite significantly reduced wave amplitudes, the gravity waves, subject to amplification upon over-reflection in the upper troposphere, can trigger/release existing moist instabilities, initiating convection and latent heat release, the energy leading to intensification of storms [5].

[1] Dorotovič, I., et al., Sol. Phys. 289 (7), 2697–2703, 2014.
[2] King, J.H. and N.E. Papitashvili, J. Geophys. Res., 110, A02104, 2005.
[3] Mayr H.G., et al., J. Geophys. Res., 89, 10929–10959, 1984.
[4] Prikryl P., et al., Ann. Geophys., 23, 401–417, 2005.
[5] Prikryl P., et al., 2009, Ann. Geophys., 27, 31–57.

Keywords: Extreme weather, Precipitation, Flash floods, High-speed solar wind streams, Atmospheric gravity waves

©2021. Japan Geoscience Union. All Right Reserved.

Climate change initiated variation in the tracks of typhoons in the North West Pacific basin

*Ravi Shankar Pandey[1], Yuei-An Liou[1]

1. National Central University

Increasing sea surface temperature (SST) due to climate change is potentially linked with the increasing strength of typhoons especially in the North West Pacific (NWP) basin in recent years. This research aims to quantitatively and climatologically analyze the tracks and cyclogenesis locations of all typhoons that occurred after 1976 in the NWP basin. The International Best Track Archive for Climate Stewardship (IBTrACS) and Optimum Interpolation (OI) SST V2 data directly accessed by the National Oceanic and Atmospheric Administration (NOAA) of USA, and the Centennial in situ Observation-Based Estimates (COBE) SST2 data of Japan Meteorological Agency (JMA) indirectly accessed by NOAA are used. The level of curviness in the track of a typhoon makes forecasting rather challenging for the atmospheric models, resulting in more prospective damages. Statistical analysis is carried out on fundamental typhoon parameters like maximum wind speed and central pressure. Also, statistical analysis was done for the typhoons based on their ocean of cyclogenesis and phases of El Niño Southern Oscillation (ENSO) at cyclogenesis. The Chi-square (χ 2) test shows that the curvy nature of tracks of typhoons supersedes the strength as far as the relation with longer survival of typhoons is concerned. More than double cyclogenesis is detected during the warm phase of ENSO than the cold phase. A gradual rise is observed in the frequency of typhoons during the warm phase of ENSO in the last 40 years. The warm phase of Pacific Decadal Oscillation (PDO) is also associated with the warm phase of ENSO and assists in cyclogenesis in the NWP basin. Convectively active phases of Madden Julian Oscillation (MJO) (phases 4, 5, 6, and 7) cause almost double cyclogenesis than non-MJO or convectively inactive phases in the NWP basin. A significant rise in the SST by more than 0.4 ˚C is measured in typhoon originating oceans for the whole typhoon season during the last 40 years. The El-Niño years significantly contribute to higher SST Anomaly (SSTA) values. The climatological analysis and statistical results validate each other and indicate climate change as the main reason behind the increasing intensity of typhoons in the NWP basin.

Keywords: Cyclogenesis, El Niño Southern Oscillation, Sea Surface Temperature Anomaly, Pacific Decadal Oscillation, Madden Julian Oscillation

©2021. Japan Geoscience Union. All Right Reserved.

[J] Oral | A (Atmospheric and Hydrospheric Sciences)：A-AS Atmospheric Sciences, Meteorology & Atmospheric Environment

Sun. Jun 6, 2021 9:00 AM - 10:30 AM JST | Sun. Jun 6, 2021 12:00 AM - 1:30 AM UTC | Ch.08 Zoom Room 08

[A-AS05] Atmospheric Chemistry

convener:Tomoki Nakayama(Graduate School of Fisheries and Environmental Sciences, Nagasaki University), Naoko Saitoh(Center for Environmental Remote Sensing), Sakae Toyoda(Department of Chemical Science and Engineering, Tokyo Institute of Technology), Risa Uchida(Japan Automobile Research Institute), Chairperson:Risa Uchida(Japan Automobile Research Institute), Kei Sato(National Institute for Environmental Studies)

This session provides a forum for the presentation of the broad spectrum of tropospheric and stratospheric chemistry, including various research topics (e.g., dynamical processes, air quality and climate), approaches (modeling, field measurements, remote sensing, and laboratory studies), and species (gas and aerosol). This session also provides an opportunity for discussing possible future collaboration with other research fields relevant to atmospheric chemistry. We strongly encourage authors to prepare presentation slides and a poster in English.

9:00 AM - 9:30 AM JST | 12:00 AM - 12:30 AM UTC

[AAS05-01] Cryosphere-atmosphere biogeochemical cycles: Insights from Arctic Ocean drifting campaign

★Invited Papers

*Daiki Nomura[1] (1.Field Science Center for Northern Biosphere, Hokkaido University)

9:30 AM - 9:45 AM JST | 12:30 AM - 12:45 AM UTC

[AAS05-02] Embedding of HCl droplets on ice crystal surfaces under atmospheric-concentration HCl gas

*Ken Nagashima[1], Ken-ichiro Murata[1], Gen Sazaki[1] (1.The Institute of Low Temperature Science, Hokkaido University)

9:45 AM - 10:00 AM JST | 12:45 AM - 1:00 AM UTC

[AAS05-03] A new method for quantifying sodium sulfate, sodium nitrate, and sodium chloride aerosols

*Yuya Kobayashi[1], Nobuyuki Takegawa[1] (1.Graduate School of Science, Tokyo Metropolitan University)

10:00 AM - 10:15 AM JST | 1:00 AM - 1:15 AM UTC

[AAS05-04] Investigation of gaseous and heterogeneous reactions of RO_2 radicals using FAGE-LIF method

*Nanase Kohno[1], Jiaru Li[1], Yosuke Sakamoto[1,2], Yoshizumi Kajii[1,2] (1.Kyoto University, 2.National Institute for Environmental Studies)

10:15 AM - 10:30 AM JST | 1:15 AM - 1:30 AM UTC

[AAS05-05] Real-time measurement of HO_2 and RO_2 uptake loss rate onto ambient particles during AQUAS-Kyoto summer campaign in 2020

*Yosuke Sakamoto[1,2], Bai Yu[1], Jiaru Li[1], Kohno Nanase[1], Yoshizumi Kajii[1,2] (1.Kyoto University , 2.National Institute for Environmental Studies)

Cryosphere-atmosphere biogeochemical cycles: Insights from Arctic Ocean drifting campaign

*Daiki Nomura[1]

1. Field Science Center for Northern Biosphere, Hokkaido University

Sea ice has until now rarely been considered in estimates of global biogeochemical cycles, especially gas exchanges, because of the assumption that, in ice-covered oceans, sea-ice acts as a barrier for atmosphere–ocean exchange. In order to understand the effects of sea-ice growth and decay processes on the biogeochemical cycles in the polar oceans, field observations in the Arctic, Antarctic, and Sea of Okhotsk as well as laboratory experiments were carried out. Observations over recent decades suggest that sea ice plays a significant role in global biogeochemical cycles, providing an active biogeochemical interface at the cryosphere-atmosphere boundary. In this presentation, I will show preliminary results obtained during the international drift campaign MOSAiC in the central Arctic for the gas dynamics and exchange process between sea ice/water surface and atmosphere.

Keywords: biogeochemical cycles, gas exchange process, sea ice

©2021. Japan Geoscience Union. All Right Reserved.

Embedding of HCl droplets on ice crystal surfaces under atmospheric-concentration HCl gas

*Ken Nagashima[1], Ken-ichiro Murata[1], Gen Sazaki[1]

1. The Institute of Low Temperature Science, Hokkaido University

Surfaces of ice act as sites of various chemical reactions of atmospheric acidic gases, which cause serious environmental issues, such as the catalytic ozone depletion by hydrogen chloride (HCl) gas. As a means of direct observation of QLLs on ice surfaces, we and Olympus Engineering Co. Ltd., have developed laser confocal microscopy combined with differential interference contrast microscopy (LCM-DIM), which can directly visualize 0.37-nm-thick elementary steps [1] and QLLs on ice crystal surfaces [2].
Recently, we studied effects of HCl gas (10^2 Pa) on the behavior of QLLs on ice basal faces by LCM-DIM [3-4]. Then we found that the QLLs were not pure water but an HCl aqueous solution, whose HCl concentration was very close to that of a liquidus line of a binary phase diagram of water and HCl. Therefore, the HCl droplets did not disappear and were embedded in ice crystals stably without freezing [4]. However, in our previous studies, we used the HCl gas of 10^2 Pa HCl partial pressure, which is extremely higher than ordinary atmospheric partial pressure of HCl. Here, we show direct observations of ice basal faces by advanced optical microscopy under atmospheric-concentration HCl gases of from 10^{-4} to 10^{-2} Pa. Then, we investigated the appearance/disappearance of liquid water on ice surfaces and their effects on the growth of ice crystals [5].
Under atmospheric-concentration HCl gas, we found that liquid droplets and thin layers appeared/disappeared on the ice basal faces at about -1 ˚C with increasing/decreasing temperatures. These behaviors were similar to those in the absence of the HCl gases. In contrast, at temperatures below -10 ˚C, surprisingly we found that with decreasing temperature, the HCl gases induced the appearance of droplets of an HCl aqueous solution on the basal faces. In addition, the HCl droplets pinned the lateral advancement of spiral steps, resulting in the formation of bunched steps. The HCl droplets were finally embedded in the ice crystals by further growth of the bunched steps. In contrast, with increasing temperatures, the HCl droplets and the bunched steps disappeared at -10 ˚C.
These results indicate that a bulk of an ice crystal plays an important role in the uptake of HCl. So far, it has been believed that the contribution of a bulk of an ice crystal to the HCl uptake is less important than that of an ice surface, because of the small solubility of HCl and the slow diffusion of chloride ions in an ice crystal. Hence, the results found in this study suggest that the uptake of HCl in an ice crystal can be promoted via the bunching and embedding mechanism at temperatures below -10 ˚C. Our findings will give significant insights into various environmental issues caused by acidic gases in polar regions. However, it is crucially important to study whether the similar phenomena occur at -70 ˚C, at which temperature HCl on ice crystals plays an important role in the ozone depletion by the heterogeneous photochemical reactions in polar stratospheric clouds.

[1] Sazaki et al. (2010) PNAS 107, 19702.
[2] Sazaki et al. (2012) PNAS 109, 1052.
[3] Nagashima et al. (2016) Cryst. Growth Des. 16, 2225.
[4] Nagashima et al. (2018) Cryst. Growth Des. 18, 4117.
[5] Nagashima et al., Cryst. Growth Des. submitted.

We will present this study from other viewpoints in " M-IS17 Growth and dissolution of crystal".

©2021. Japan Geoscience Union. All Right Reserved.

Keywords: ice crystal, air-snow interaction, atmospheric-concentration HCl gas, bunched step, HCl uptake, advanced optical microscopy

©2021. Japan Geoscience Union. All Right Reserved.

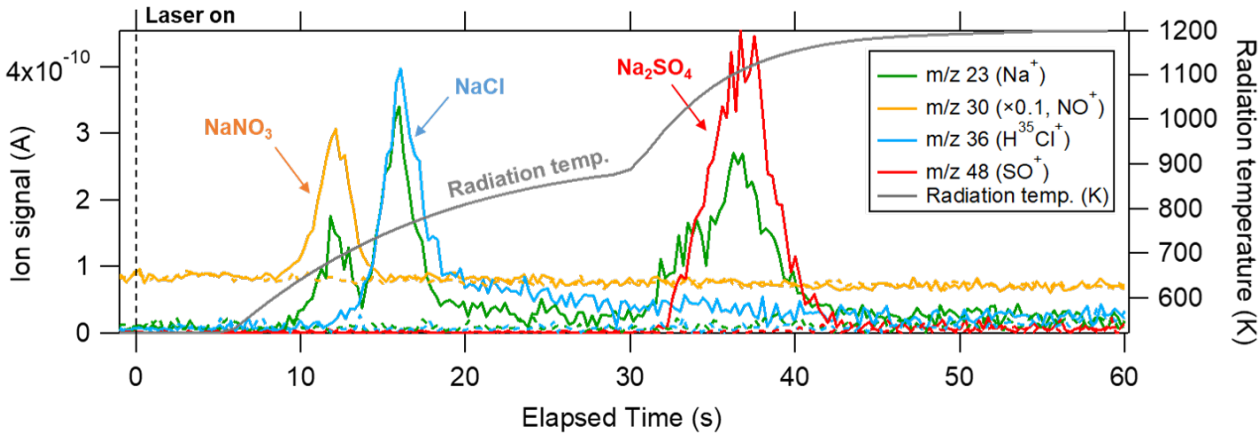
A new method for quantifying sodium sulfate, sodium nitrate, and sodium chloride aerosols

*Yuya Kobayashi[1], Nobuyuki Takegawa[1]

1. Graduate School of Science, Tokyo Metropolitan University

Sea salt aerosols are abundant in the marine boundary layer and have large influences on the Earth's radiative budget. Significant conversion of sodium chloride (NaCl) to sodium sulfate (Na_2SO_4) or sodium nitrate ($NaNO_3$) can take place via the reactions with sulfuric acid (H_2SO_4) or nitric acid (HNO_3) in polluted air exported from urban areas to coastal regions. In situ, continuous measurements of NaCl, Na_2SO_4, and $NaNO_3$ aerosols are needed to understand the chemical transformation of sea salt particles with air mass aging. However, there is no established method for quantifying these aerosol compounds with high time resolution. We have developed a new online particle mass spectrometer (refractory aerosol thermal desorption mass spectrometer; rTDMS) to quantify non-refractory and refractory sulfate aerosols. The combination of a graphite particle collector and a carbon dioxide (CO_2) laser enables high desorption temperature (radiation temperature > 1200 K). The evolved gas molecules are detected by using a quadrupole mass spectrometer. The purpose of this study is to develop a new method for quantifying the mass concentrations of NaCl, Na_2SO_4, and $NaNO_3$ aerosols by optimizing the laser desorption scheme of the rTDMS. Laboratory experiments were performed to test the instrument sensitivities to these aerosol compounds. The temporal evolution of ion signals at m/z 23 (Na^+), 30 (NO^+), 36 (HCl^+), and 48 (SO^+) during the laser desorption were monitored. Preliminary data indicate that ion signals originating from $NaNO_3$, NaCl, and Na_2SO_4 particles were clearly identified by three sequential peaks associated with an increase in the radiation temperature. The limit of detection, linearity of the instrument response, and potential artifacts under real world conditions are discussed.

Keywords: Sea salt aerosols, Online measurement, Quantification of each sodium salts



©2021. Japan Geoscience Union. All Right Reserved.

Investigation of gaseous and heterogeneous reactions of RO_2 radicals using FAGE-LIF method

*Nanase Kohno[1], Jiaru Li[1], Yosuke Sakamoto[1,2], Yoshizumi Kajii[1,2]

1. Kyoto University, 2. National Institute for Environmental Studies

Peroxy (RO_2) radicals are produced by oxidation of various volatile organic compounds (VOCs) in the atmosphere and play an important role. They are mainly removed by self-reactions under clean air conditions. On the other hand, they oxidize NO and produce NO_2. Since NO_2 produces O_3 via photochemical reactions, RO_2 radicals act as a part of the cyclic reaction producing tropospheric O_3. RO_2 radicals also react with NO_2 and generate a RO_2NO_2 complex, which can reproduce NO_2 via thermal decomposition and act as an atmospheric NOx reservoir. Furthermore, in recent years, it has been suggested that the loss processes of ROx radicals via heterogeneous reactions on the aerosol surface may be important. Despite these importance, there are limited kinetics data about RO_2. In particular, there were few reports of detection under atmospheric conditions, and it was limited to some RO_2 radicals. In this study, we improved a combination technique of Fluorescence Assay by Gas Expansion and Laser Induced Fluorescence (FAGE-LIF) system for detection of various RO_2 radicals and investigated their reactions including not only gaseous reactions but aerosol uptake processes.

All experiments were performed at 1 bar, 298 K. O_3/H_2O/sample VOC/N_2 carrier mixture were added into the reaction cell. By irradiation of pump laser pulses, OH radicals were generated by the photolysis of O_3 and subsequent reaction with H_2O. OH radicals reacted with VOC rapidly and generated RO_2 radicals. A part of main flow was added into the detection cell. In order to convert RO_2 radicals to OH radicals again, NO and O_2 were added into the detection cell. Then, OH radicals were detected by LIF method. The relative concentration of RO_2 radicals were measured from the LIF intensity of OH radicals.

Figure 1 shows time profiles of CH_3O_2 radicals, which were produced by the reaction of OH with CH_4, measured at various NO_2 concentrations. CH_3O_2 radicals decay single exponentially in the absence of NO_2. With the existence of NO_2, however, profiles include two decay components due to the reverse reaction. In order to determine the rate constants, double exponential fitting including the reverse reaction was performed. The fitting results are shown in figure as red lines. All lines reproduce the experimental results very well. The reaction rate constants including also reverse reaction have been determined from the NO_2 concentration dependence. Those rate constants agree with previous reported values. This indicates that the improved FAGE-LIF system allows us to measure the kinetics of RO_2 radicals appropriately. We also performed same experiments using $C_2H_5O_2$ radicals. We will discuss at the presentation.

Additionally, we investigated uptake processes of RO_2 radicals onto aerosols. Sample aerosols were deliquesced NaCl particles generated from 0.1 −0.3 g L^{-1} aqueous NaCl solutions via a collision-type atomizer. Those particles were added into the reaction cell with zero air carrier and another sample gases. The decay rates of RO_2 radicals due to aerosols were determined by the difference between the fitting results with and without aerosols. By using the decay rates due to the aerosols and aerosol size distributions, uptake coefficients have been determined for some RO_2 radicals (as shown in Fig.2). The aerosol size distributions were employed from the separate experiments under the almost same conditions. As a result, the increase of the uptake coefficients with the size of RO_2 radicals was observed for the first time. In addition, even small RO_2 radicals were uptaken into aerosols, although their values were small. This indicates that the heterogeneous reactions of RO_2 radicals can affect the O_3 production

©2021. Japan Geoscience Union. All Right Reserved.

mechanisms. Consequently, there is possibility that the considering the interaction between RO_2 radicals and aerosols should improve the accuracy of the atmospheric model.

This work was supported by JSPS KAKENHI Grant Nos. JP16H06305, JP18K18179, JP19J40218, and JP19H04255.

Keywords: RO2 radical, reaction rate coefficient, NO2, aerosol, uptake coefficient

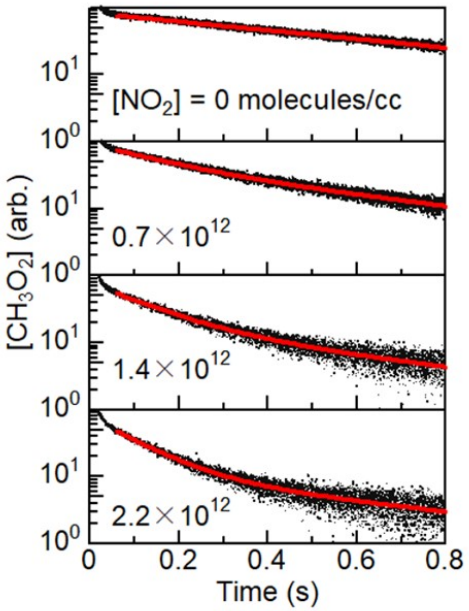


Figure 1. Time profiles of CH_3O_2 radicals.
Red lines show the fitting analysis results.

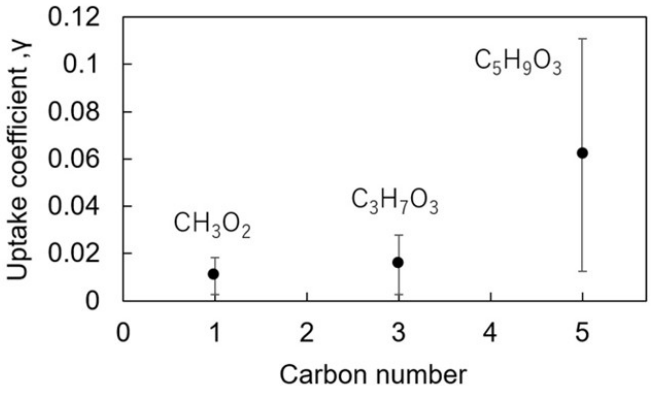


Figure 2. Radical size dependence of uptake coefficient.

©2021. Japan Geoscience Union. All Right Reserved.

Real-time measurement of HO_2 and RO_2 uptake loss rate onto ambient particles during AQUAS-Kyoto summer campaign in 2020

*Yosuke Sakamoto[1,2], Bai Yu[1], Jiaru Li[1], Kohno Nanase[1], Yoshizumi Kajii[1,2]

1. Kyoto University , 2. National Institute for Environmental Studies

Peroxy radicals, HO_2 and RO_2, play a central role in the daytime photochemistry in the troposphere, since they compose daytime radical recycling chain reaction through OH →RO_2 →HO_2 →OH, namely HO_x cycle, which dominate tropospheric O_3 formation. The gas phase reactions of peroxy radicals that produce non-radical species, e.g. HO_2 + HO_2 →H_2O_2 + O_2, HO_2 + RO_2 →ROOH + O_2, work as termination reaction of the HO_x cycle, and thus affect efficiency for O_3 formation. It has been suggested indirectly for decades that HO_2 uptake by ambient particles also work as termination process based on laboratory experiments with artificially produced particles. Recently, we achieved real-time measurement of HO_2 uptake kinetics onto ambient particles and reported the HO_2 loss rate and uptake coefficient for ambient particles during AQUAS-Kyoto summer campaign in 2018. [Zhou et al. 2020] In this study, we examined HO_2 uptake kinetics onto ambient particles in Kyoto again during AQUAS-Kyoto summer campaign in 2020, with the aim of investigating temporal variation of uptake kinetics from previous campaign. Additionally, we expanded the system to real-time measurement of isoprene-derived RO_2 (C_5H_8(OH)OO) uptake kinetics onto ambient particles. Daily average of HO_2 loss rate was similar but uptake coefficient was smaller compared with previous campaign. Observed loss rate was comparable to those of gas phase termination reactions. Temporal variation of aerosol components might be possible explanation of variation of uptake coefficient during the present campaign and difference from the previous campaign. We found that daily average of RO_2 loss rate and then uptake coefficient had significant values. Observed loss rate for RO_2 was also comparable to those of gas phase termination reactions as well as HO_2. Our results suggest that further investigations of not only HO_2 but also RO_2 uptake kinetics are required for complete understanding of O_3 formation in the troposphere.

Reference: Zhou et al. *Atmospheric Environment*, 223 (2020) 117189.
Acknowledgements: This work was supported by the Japan Society for the Promotion of Science (JSPS NO. 16H06305 and NO. JP19H04255). We would like to thank the technical support from KIMOTO ELECTRIC CO., LTD. in construction of aerosol enrichment system.

Keywords: heterogeneous reaction, aerosol, PM2.5, photochemical ozone, HOx cycle

©2021. Japan Geoscience Union. All Right Reserved.

[J] Oral | A (Atmospheric and Hydrospheric Sciences)：A-AS Atmospheric Sciences, Meteorology & Atmospheric Environment

Sun. Jun 6, 2021 10:45 AM - 12:15 PM JST | Sun. Jun 6, 2021 1:45 AM - 3:15 AM UTC | Ch.08 Zoom Room 08

[A-AS05] Atmospheric Chemistry

convener:Tomoki Nakayama(Graduate School of Fisheries and Environmental Sciences, Nagasaki University), Naoko Saitoh(Center for Environmental Remote Sensing), Sakae Toyoda(Department of Chemical Science and Engineering, Tokyo Institute of Technology), Risa Uchida(Japan Automobile Research Institute), Chairperson:Nobuyuki Takegawa(Graduate School of Science, Tokyo Metropolitan University)

This session provides a forum for the presentation of the broad spectrum of tropospheric and stratospheric chemistry, including various research topics (e.g., dynamical processes, air quality and climate), approaches (modeling, field measurements, remote sensing, and laboratory studies), and species (gas and aerosol). This session also provides an opportunity for discussing possible future collaboration with other research fields relevant to atmospheric chemistry. We strongly encourage authors to prepare presentation slides and a poster in English.

10:45 AM - 11:00 AM JST | 1:45 AM - 2:00 AM UTC

[AAS05-06] **Understanding of Volatile Organic Compound Emissions from Western US Wildfires**

*Kanako Sekimoto[1], Matthew M Coggon[2,3], Georgios Gkatzelis[2,3], Carsten Warneke[2,3] (1.Yokohama City University, 2.NOAA Earth System Research Laboratory, 3.Cooperative Institute for Research In Environmental Sciences)

11:00 AM - 11:15 AM JST | 2:00 AM - 2:15 AM UTC

[AAS05-07] New particle formation from ozonolysis of 2-methyl-2-butene and *trans*-2-butene

*Satoshi Inomata[1], Jun Hirokawa[2], Yosuke Sakamoto[3] (1.National Institute for Environmental Studies, 2.Hokkaido University, 3.Kyoto University)

11:15 AM - 11:30 AM JST | 2:15 AM - 2:30 AM UTC

[AAS05-08] Structural elucidation of a-pinene originating $C_{10}H_{17}O_6S$ organosulfates from CCS values derived from ion mobility mass spectrometry and theoretical structural modelling

*Yoshiteru Iinuma[1], Satoshi Inomata[2], Kei Sato[2] (1.Okinawa Institute of Science and Technology Graduate University, 2.National Institute for Environmental Studies)

11:30 AM - 11:45 AM JST | 2:30 AM - 2:45 AM UTC

[AAS05-09] Wet Deposition of Black Carbon at Ny-Ålesund, Svalbard

*Tatsuhiro Mori[1], Yutaka Kondo[2], Sho Ohata[3,4], Kumiko Goto-Azuma[2,5], Kaori Fukuda[2], Yoshimi Ogawa[2], Nobuhiro Moteki[6], Atsushi Yoshida[6], Makoto Koike[6], Puna Ram Sinha[7], Naga Oshima[8], Hitoshi MATSUI[9], Yutaka Tobo[2,5], Masanori Yabuki[10], Wenche Aas[11] (1.Tokyo University of Science, 2.National Institute of Polar Research, 3.Institute for Space–Earth Environmental Research, Nagoya University, 4.Institute for Advanced Research, Nagoya University, 5.The Graduate University for Advanced Studies, SOKENDAI, 6.Department of Earth and Planetary Science, Graduate School of Science, The University of Tokyo, 7.Department of Earth and Space Sciences, Indian Institute of Space Science and Technology, 8.Meteorological Research Institute, 9.Graduate School of Environmental Studies, Nagoya University, 10.Research Institute for Sustainable Humanosphere, Kyoto University, 11.Norwegian Institute for Air Research)

11:45 AM - 12:00 PM JST | 2:45 AM - 3:00 AM UTC

[AAS05-10] Improved simulations of global black carbon distributions by modifying wet scavenging processes in convective and mixed-phase clouds

*Mingxu Liu[1], Hitoshi Matsui[1] (1.Graduate school of environmental studies, Nagoya University)

12:00 PM - 12:15 PM JST | 3:00 AM - 3:15 AM UTC

[AAS05-11] High potential of Asian dust to act as ice nucleating particles in mixed-phase clouds simulated with a global model

*Kei Kawai[1], Hitoshi Matsui[1], Yutaka Tobo[2,3] (1.Nagoya University, 2.National Institute of Polar Research, 3.SOKENDAI (The Graduate University for Advanced Studies))

Understanding of Volatile Organic Compound Emissions from Western US Wildfires

*Kanako Sekimoto[1], Matthew M Coggon[2,3], Georgios Gkatzelis[2,3], Carsten Warneke[2,3]

1. Yokohama City University, 2. NOAA Earth System Research Laboratory, 3. Cooperative Institute for Research In Environmental Sciences

Biomass burning is a large source of volatile organic compounds (VOCs) and many other trace species to the atmosphere. These VOCs can act as precursors to formation of secondary pollutants such as ozone and fine particles, and some VOCs can also have direct effects on human and ecosystem health. Multiple different and complex processes take place in biomass burning, e.g., distillation, flaming, and smoldering combustion processes. In a given fire, most of these processes occur simultaneously, but the relative importance of each can change over the course of a fire. This gives rise to some of the variability in VOC emissions between different fires. To study gas-phase emissions from biomass burning in western US, a proton-transfer-reaction time-of-flight mass spectrometry (PTR-ToF-MS) was deployed during the FIREX 2016 laboratory intensive (at the US Forest Service Fire Sciences Laboratory in Missoula, Montana) and the FIREX-AQ field campaign (https://csl.noaa.gov/projects/firex-aq/). Measurements performed with the PTR-ToF-MS were analyzed with positive matrix factorization (PMF) to parameterize the VOC emissions. The results are summarized as follows:

1. Despite the complexity and variability of emissions, a PMF solution including just two emission profiles explained on average 85% of the VOC emissions across 15 different fuel types including pines, firs, spruce, grass, shrubs, chaparrals, and wood wool.
2. The two profiles were identified as resulting from high-temperature and low-temperature pyrolysis processes, and the profiles were remarkably similar (correlation coefficient $r > 0.9$) across nearly all the fuel types described in 1).
3. The VOC emissions from real-world wildfires were described on average of 80% by just three emission profiles, i.e., (i) high-temperature profile, (ii) low-temperature profile, and (iii) a profile related to chemical aging.
4. Contributions of high-temperature profile, low-temperature profile, and aging profile can be parameterized using fire radiation power and emissions of maleic anhydride and furan.

Keywords: Volatile organic compound, Wildfire, Proton-transfer-reaction mass spectrometry (PTR-MS)

©2021. Japan Geoscience Union. All Right Reserved.

New particle formation from ozonolysis of 2-methyl-2-butene and *trans*-2-butene

*Satoshi Inomata[1], Jun Hirokawa[2], Yosuke Sakamoto[3]

1. National Institute for Environmental Studies, 2. Hokkaido University, 3. Kyoto University

Atmospheric aerosols scatter and absorb incoming solar radiation, which directly impacts the global radiative balance of the atmosphere. If these aerosols are hydrophilic, they can act as cloud condensation nuclei (CCN) and have an indirect effect on the climate by modifying the properties of clouds. New particle formation (NPF) through nucleation is believed to contribute up to half of the global CCN concentrations. The nucleation and growth mechanisms of new particles in the atmosphere have therefore been topics of study in atmospheric research. Recently, we observed NPF during ozonolysis of isoprene (C_5H_8) and ethene (C_2H_4). We proposed that oligomeric hydroperoxides originated from stabilized Criegee intermediates (sCIs) that were generated during the ozonolysis of isoprene and ethene potentially contribute to the NPF. In the present work, we investigated the ozonolysis of 2-methyl-2-butene (C_5H_{10}) and *trans*-2-butene (C_4H_8), in order to investigate the role of C2-sCI ((CH_3)CHOO) on the new particle formation.

Keywords: 2-methyl-2-butene, trans-2-butene, ozonolysis, secondary organic aerosol,, Criegee intermediate

©2021. Japan Geoscience Union. All Right Reserved.

Structural elucidation of a-pinene originating $C_{10}H_{17}O_6S$ organosulfates from CCS values derived from ion mobility mass spectrometry and theoretical structural modelling

*Yoshiteru Iinuma[1], Satoshi Inomata[2], Kei Sato[2]

1. Okinawa Institute of Science and Technology Graduate University, 2. National Institute for Environmental Studies

Organosulfates (OS) are recognised as one of the important classes of marker compounds for atmospheric oxidation of biogenic volatile compounds (BVOCs) as it can account as high as 30% of the organic mass fraction in PM_{10} (Brüggemann et al., 2020). While a number of studies report the presence of OS in laboratory generated and ambient biogenic SOA based on LC/MS data, little is known about their formation mechanism and exact structures owing to a wide variety of possible formation mechanisms and structures. Nevertheless, several formation mechanisms are accepted in the community based on laboratory experimental data. These include the reaction of BVOC oxidation products with acidic sulfate or sulfoxy radical anion in the particle phase, and the reactions of unsaturated hydrocarbons and SO_2 in the gas phase (Brüggemann et al., 2020). The structural elucidation of OS species remains challenging owing to lack of authentic standard compounds.

In this work, we present the results from the structural elucidation experiments of *m/z* 265 ($C_{10}H_{17}O_6S^-$) organosulfates originating from the photo-oxidation and ozonolysis of a-pinene in the presence of neutral and acidic seed particles at two different temperatures. The resulting SOA were collected on Teflon filter, and extracted in acetonitrile, dried using a centrifugal evaporator, and reconstituted in a 50/50 (v/v) acetonitrile/water solution. The samples were analysed using high-performance liquid chromatography coupled to ion mobility spectrometry tandem time-of-flight mass spectrometry (Agilent 1290 HPLC and Bruker TimsTOF) to obtain collision cross section (CCS) values of *m/z* 265 organosulfates. To further evaluate the structures of *m/z* 265 compounds, the theoretical CCS value of a previously reported structure for *m/z* 265 organosulfate, specifically sulfated pinonaldehyde, was calculated with MobCal-MPI (Ieritano et al., 2019), and compared to the measured CCS values. The measured CCS values of *m/z* 265 compounds are in the range of 154 to 158 $Å^2$ that are much smaller than the theoretical CCS value of 164.7 $Å^2$. The theoretical CCS values of positional isomers of sulfated pionaldehyde (i.e. a sulfate group is attached at a different position than the previously reported structure) are also greater than those of measured CCS values, indicating that *m/z* 265 organosulfates likely have closed shell structures rather than open shell structures. To support this, theoretical CCS values of two of $C_{10}H_{17}O_6S^-$ compounds that are analogous to closed shell *m/z* 249 ($C_{10}H_{17}O_5S^-$) organosulfates were calculated and compared to measured values. The theoretical CCS values of both the closed shell *m/z* 265 compounds are in the order of 156 $Å^2$, suggesting that they are likely structures of *m/z* 265 organosulfates.

Brüggemann, M., Xu, R., Tilgner, A., Kwong, K.C., Mutzel, A., Poon, H.Y., Otto, T., Schaefer, T., Poulain, L., Chan, M.N., Herrmann, H., 2020. Organosulfates in Ambient Aerosol: State of Knowledge and Future Research Directions on Formation, Abundance, Fate, and Importance. Environ. Sci. Technol. 54, 3767–3782. https://doi.org/10.1021/acs.est.9b06751

Ieritano, C., Crouse, J., Campbell, J.L., Hopkins, W.S., 2019. A parallelized molecular collision cross section

©2021. Japan Geoscience Union. All Right Reserved.

package with optimized accuracy and efficiency. Analyst 144, 1660–1670. https://doi.org/10.1039/C8AN02150C

Keywords: SOA, Organosulfate, Ion mobility mass spectrometry, Collision Cross Section

©2021. Japan Geoscience Union. All Right Reserved.

Wet Deposition of Black Carbon at Ny-Ålesund, Svalbard

*Tatsuhiro Mori[1], Yutaka Kondo[2], Sho Ohata[3,4], Kumiko Goto-Azuma[2,5], Kaori Fukuda[2], Yoshimi Ogawa[2], Nobuhiro Moteki[6], Atsushi Yoshida[6], Makoto Koike[6], Puna Ram Sinha[7], Naga Oshima[8], Hitoshi MATSUI[9], Yutaka Tobo[2,5], Masanori Yabuki[10], Wenche Aas[11]

1. Tokyo University of Science, 2. National Institute of Polar Research, 3. Institute for Space–Earth Environmental Research, Nagoya University, 4. Institute for Advanced Research, Nagoya University, 5. The Graduate University for Advanced Studies, SOKENDAI, 6. Department of Earth and Planetary Science, Graduate School of Science, The University of Tokyo, 7. Department of Earth and Space Sciences, Indian Institute of Space Science and Technology, 8. Meteorological Research Institute, 9. Graduate School of Environmental Studies, Nagoya University, 10. Research Institute for Sustainable Humanosphere, Kyoto University, 11. Norwegian Institute for Air Research

Black carbon (BC) aerosol deposited in and onto Arctic snow increases the snow’s absorption of solar radiation and accelerates snowmelt. Concentrations of BC in the Arctic atmosphere and snow are controlled by wet deposition; however, details of this process are poorly understood owing to the scarcity of time-resolved measurements of BC in hydrometeors. We measured mass concentrations of BC in hydrometeors (C_{MBC}) and in air (M_{BC}) with 16% and 15% accuracies, respectively, at Ny-Ålesund, Svalbard during 2012–2019. Median monthly M_{BC} and C_{MBC} values showed similar seasonal variations, being high in winter-spring and low in summer. Median monthly BC wet deposition mass flux (F_{MBC}) was highest in winter and lowest in summer, associated with seasonal patterns of C_{MBC} and precipitation. Seasonally averaged BC size distributions in hydrometeors were similar except summer. Measurements of BC in air and hydrometeors in spring 2017 showed a size-independent removal efficiency, showing efficient activation of BC-containing particles into cloud droplets. These parameters observed at Ny-Ålesund were compared with those observed at Barrow, Alaska, during 2013–2017. The near surface M_{BC} at Ny-Ålesund and Barrow had similar seasonal patterns; however, they differed for C_{MBC} and F_{MBC}. In summer, C_{MBC} was low at Ny-Ålesund but moderate at Barrow, likely reflecting differences in M_{BC} in the lower troposphere. Seasonally averaged BC size distributions in hydrometeors were similar at both sites, suggesting similar BC size distributions in the Arctic lower troposphere, on average. Coating of BC particles at lower latitudes likely influence the BC size distributions in the Arctic.

Keywords: black carbon, wet deposition, Arctic, Seasonal variation, Laser-induced incandescence technique

©2021. Japan Geoscience Union. All Right Reserved.

Improved simulations of global black carbon distributions by modifying wet scavenging processes in convective and mixed-phase clouds

*Mingxu Liu[1], Hitoshi Matsui[1]

1. Graduate school of environmental studies, Nagoya University

In-cloud wet scavenging dominates the wet removal of aerosols in the atmosphere, but is not well represented in climate models. Aircraft measurements of black carbon (BC) concentrations suggest that models commonly overestimate BC concentrations in the upper troposphere of the tropics by more than one order of magnitude but underestimate BC burdens in polar latitudes. In this study, we improved the in-cloud wet scavenging parameterizations for convective clouds and mixed-phase clouds to better characterize BC abundances in the remote atmosphere (remote oceans and polar regions) with a global model, CAM5-ATRAS2. The modified wet scavenging processes in the model achieved a more realistic simulation of BC concentrations over both the tropics and the Arctic. The new, unified scheme for vertical transport and wet removal during deep convection generally reproduced the observed low mixing ratios (about 0.1 ng kg^{-1}) of BC in the middle and upper troposphere over the tropics, and the Wegener–Bergeron–Findeisen process lowered the wet removal efficiency of BC from mixed-phase clouds and consequently increased BC burdens in the Arctic by about a factor of 2. The BC direct radiative forcings increased by 20% globally (from 0.26 to 0.31 W m^{-2}), and more importantly by a factor of 2 in the Arctic (from 0.09 to 0.18 W m^{-2}). Our results indicated that good agreement between modeled and observed BC concentrations could be obtained in the remote atmosphere without requiring the relatively short global BC lifetime (~4 days) suggested by previous studies.

Keywords: Black carbon, Global climate model, Aerosol-cloud interactions, Deep convection, Mixed-phase clouds

©2021. Japan Geoscience Union. All Right Reserved.

High potential of Asian dust to act as ice nucleating particles in mixed-phase clouds simulated with a global model

*Kei Kawai[1], Hitoshi Matsui[1], Yutaka Tobo[2,3]

1. Nagoya University, 2. National Institute of Polar Research, 3. SOKENDAI (The Graduate University for Advanced Studies)

Mineral dust is recognized as the most important ice nucleating particle (INP) in mixed-phase clouds, which consist of supercooled water droplets and ice crystals. Dust INPs affect the microphysical and radiative properties of mixed-phase clouds and hence the radiative balance of the Earth. Although ice nucleating ability of dust has been measured with a cloud chamber, it is not well understood how much dust is transported to higher altitudes and acts as INPs. Asian dust (Kosa), which is emitted from arid and semi-arid regions of East Asia (e.g., the Gobi and Taklimakan Deserts), may have high potential to act as INPs because of high altitudes of the source regions and upward transport by cold frontal systems. In this study, we examined the contribution of Asian dust to global dust INP number and its effect on cloud radiative forcing (CRF) using a global aerosol model, CAM/ATRAS. We replaced the default ice nucleation scheme for mixed-phase clouds in the model with a parameterization that calculates INP number concentrations from the ambient temperature and dust number concentrations. We performed simulations for the years 2012–2017 and analyzed results for the last 5 years.
Our model well reproduces INP number concentrations measured at Tokyo Skytree during May 2017, when Asian dust was transported to Japan. The simulated emission flux of Asian dust is 283 Tg/yr, representing 7.1% of global dust emission flux. Asian dust extends from East Asia to the North Pacific, North America, and the Arctic. The annual mean atmospheric loading of Asian dust is 1.2 Tg, which accounts for 3.4% of global dust loading. In particular, this contribution increases to 13% for the temperature regimes relevant for the formation of mixed-phase clouds (i.e., between −38˚C and 0˚C). The contribution of Asian dust to global dust INP number is 15%, which is 2.1 times higher than the contribution to global dust emission flux and 4.4 times higher than the contribution to the global dust loading. These results show that Asian dust is efficiently transported into low-temperature regions and has high potential to act as INPs in mixed-phase clouds. According to sensitivity simulations, Asian dust INPs induce an annual mean positive CRF of 0.054–0.19 W/m^2 (cf. 0.092–1.0 W/m^2 for dust from other regions) in East Asia and the North Pacific.

Keywords: Asian dust, Kosa, ice nucleating particles, mixed-phase clouds, global aerosol model

©2021. Japan Geoscience Union. All Right Reserved.

[J] Oral | A (Atmospheric and Hydrospheric Sciences)：A-AS Atmospheric Sciences, Meteorology & Atmospheric Environment

Sun. Jun 6, 2021 1:45 PM - 3:15 PM JST | Sun. Jun 6, 2021 4:45 AM - 6:15 AM UTC | Ch.08 Zoom Room 08

[A-AS05] Atmospheric Chemistry

convener:Tomoki Nakayama(Graduate School of Fisheries and Environmental Sciences, Nagasaki University), Naoko Saitoh(Center for Environmental Remote Sensing), Sakae Toyoda(Department of Chemical Science and Engineering, Tokyo Institute of Technology), Risa Uchida(Japan Automobile Research Institute), Chairperson:Chika Minejima(International Christian University)

This session provides a forum for the presentation of the broad spectrum of tropospheric and stratospheric chemistry, including various research topics (e.g., dynamical processes, air quality and climate), approaches (modeling, field measurements, remote sensing, and laboratory studies), and species (gas and aerosol). This session also provides an opportunity for discussing possible future collaboration with other research fields relevant to atmospheric chemistry. We strongly encourage authors to prepare presentation slides and a poster in English.

1:45 PM - 2:00 PM JST | 4:45 AM - 5:00 AM UTC

[AAS05-12] Validation and correction of TROPOMI tropospheric NO_2 column density data using 4AZ-MAXDOAS at Chiba, Japan

*Hikaru Saito[1], Hitoshi Irie[1], Alessandro Damiani[1] (1.University of Chiba)

2:00 PM - 2:15 PM JST | 5:00 AM - 5:15 AM UTC

[AAS05-13] **NO_X emission estimation over Japan based on satellite data with wind field divergence**

*Masahiro Yamaguchi[1], Yugo Kanaya[1] (1.Japan Agency for Marine-Earth Science and Technology)

2:15 PM - 2:30 PM JST | 5:15 AM - 5:30 AM UTC

[AAS05-14] Introducing new lightning schemes to a chemistry climate model CHASER (MIROC)

*Yanfeng He[1], Kengo Sudo[1] (1.Nagoya University)

2:30 PM - 2:45 PM JST | 5:30 AM - 5:45 AM UTC

[AAS05-15] Methane emissions from populated areas of Tokyo and five prefectures: Emission ratios with NOx and their trends over 2009-2018

*Yugo Kanaya[1], Kanami Saima[2], Akira Fukuike[2] (1.JAMSTEC, 2.MURATA Keisokuki Service Co., Ltd.)

2:45 PM - 3:00 PM JST | 5:45 AM - 6:00 AM UTC

[AAS05-16] An impact of tropospheric air pollution changes over Japan due to future climate and emission change

*Natsumi Kawano[1], Tatsuya Nagashima[1], Masayuki Hara[2], Satoru Chatani[1], Syuichi Itahashi[3] (1.National Institute for Environmental Studies, 2.Center for Environmental Science in Saitama, 3.Central Research Institute of Electric Power Industry)

3:00 PM - 3:15 PM JST | 6:00 AM - 6:15 AM UTC

[AAS05-17] An Empirical Approach toward the Reduction Targets of CH4 and O3 as SLCP: For Asia as an example

*Hajime Akimoto[1], Tatsuya Nagashima[1], Hiroshi Tanimoto[1], Zbigniew Klimont[2], Markus Amann[2] (1.National Institute for Environmental Studies, 2.International Institute for Applied System Analysis)

Validation and correction of TROPOMI tropospheric NO_2 column density data using 4AZ-MAXDOAS at Chiba, Japan

*Hikaru Saito[1], Hitoshi Irie[1], Alessandro Damiani[1]

1. University of Chiba

To quantify and solve the reported negative bias in tropospheric nitrogen dioxide ($tropNO_2$) column data from the latest sensor TROPOspheric Monitoring Instrument (TROPOMI) aboard the Sentinel-5 Precursor satellite, we conducted ground-based four-different-azimuth-viewing multi-axis differential optical absorption spectroscopy (4AZ-MAXDOAS) observations at Chiba, Japan (35.63ºN, 140.10ºE, 21 m a.s.l.) in 2019. A comparison with simultaneous $tropNO_2$ observations by 4AZ-MAXDOAS enabled an evaluation of the spatial inhomogeneity of $tropNO_2$, which was considered responsible for a bias in results. Supported by inter-directional differences of up to 40% among 4AZ-MAXDOAS data, we found a significant horizontal spatial inhomogeneity in $tropNO_2$ around the observation site. We then compared 4AZ-MAXDOAS data with coincident TROPOMI data. TROPOMI data had a 53% smaller $tropNO_2$ column density as an annual average compared to 4AZ-MAXDOAS data, confirming the negative bias in TROPOMI data. However, the correlation between the magnitude of the bias and the coefficient of variance in four-azimuth directional data from 4AZ-MAXDOAS observations was not evident. This suggested that NO_2 horizontal inhomogeneity couldn't fully explain the observed bias. We also applied a correction using the $tropNO_2$ vertical profiles from 4AZ-MAXDOAS and the averaging kernels from TROPOMI. The correction reduced the bias to ~30% for annual average data, depending on the $tropNO_2$ profiles used, indicating that there was a significant contribution of $tropNO_2$ vertical profiles to the bias. These results not only quantified the reported negative bias but also emphasized the effectiveness of validation and correction using multi-directional ground-based data.

Keywords: Atmosphere, Satellite observation, Nitrogen dioxide, Atmospheric science, Atmospheric chemistry

©2021. Japan Geoscience Union. All Right Reserved.

NO_X emission estimation over Japan based on satellite data with wind field divergence

*Masahiro Yamaguchi[1], Yugo Kanaya[1]

1. Japan Agency for Marine-Earth Science and Technology

Nitrogen dioxide (NO_2) is a form of NO_X as important air pollutants, that leads to acid rain, ozone formation, and adverse impacts on human health. Anthropogenic activities involving the fossil fuel combustion such as vehicle engines and power plants are big sources of atmospheric NO_2. Despite their importance, it is not easy to create high-resolution emission maps with top-down estimation by direct measurement. In this study, we investigated the wide and detailed NO_2 emission map over Japan, based on the divergence of the NO_2 horizontal fluxes calculated from the datasets of satellite observation and meteorological model. According to the continuity equation for steady state, the divergence of NO_2 flux yields the net balance of sources and sinks. This approach has been demonstrated for the urban scale estimations (Shaiganfar et al., 2011, Shaiganfar et al., 2017, Beirle et al., 2019), and for a global catalog of point sources (Beirle et al., 2020). We also applied this local form of conservation laws to the NO_2 emission maps over Japan. Our method used datasets of tropospheric NO_2 vertical column density derived from the Sentinal-5P/TROPospheric Ozone Monitoring Instrument (TROPOMI) satellite and wind vector derived from The Meso-Scale Model (MSM). TROPOMI Level 2 data products has daily spatial coverage with high resolution for; 3.5 x 7.0 km^2 at beginning of mission in 2018, 3.5 x 5.5 km^2 since 6 August 2019. MSM which is one of the numerical weather prediction models operated by JMA provides 51-hour or 39-hour forecasts every 3 hours on 5 km grid all over Japan. Using these datasets, divergence calculations for daily estimation with high spatial resolution can be conducted. Our temporal averaged results showed well linear correlation with NO_X emission from EAGrid2010-Japan (Fukui et al., 2014) and revealed clear distribution of point sources.

Keywords: Nitrogen oxides (NOx), Emission estimation, Nitrogen dioxide (NO2), TROPOMI, Satellite data

©2021. Japan Geoscience Union. All Right Reserved.

Introducing new lightning schemes to a chemistry climate model CHASER (MIROC)

*Yanfeng He[1], Kengo Sudo[1]

1. Nagoya University

The formation of NO_x associated with lightning activities (hereinafter referred to as LNO_x) is estimated to contribute approximately 10% of the global NO_x source and is considered to be the most dominant NO_x source in the upper troposphere. NO_x, associated with many chemical reactions in the atmosphere, causes the production of tropospheric O_3 and OH radical which controls the oxidation capacity of the atmosphere. Consequently, LNO_x has significant influences on the atmospheric chemistry and global climate. Therefore, it is crucial to improve the prediction accuracy of lightning and LNO_x in chemical climate models.

This study implemented two new lightning schemes into a global chemical transport/climate model CHASER (MIROC). The first lightning scheme is based on upward cloud ice flux (hereinafter referred to as ICEFLUX scheme), while the second one, also adopted in the ECMWF forecasting system, calculates lightning flash rates as a function of frozen precipitation convective flux, CAPE, and convective cloud-base height (hereinafter referred to as ECMWF scheme). In the original version of CHASER (MIROC), lightning is initially parameterized by the widely-used cloud top height scheme (hereinafter referred to as CTH scheme). The lightning prediction accuracy by the ICEFLUX scheme, ECMWF scheme, and CTH scheme has been tested against the climatological lightning distributions by the LIS/OTD satellite observation.

Comparing the annual mean lightning flash rate of OTD 1996-2000 and the CHASER calculation for the years 2007-2011 exhibits spatial correlation coefficients of 0.80 and 0.79 for the ICEFLUX and ECMWF schemes respectively, which are slightly higher than that of the CTH scheme (0.78). In the case of the ECMWF scheme, by tuning the convective cloud-base height and factors for land and ocean (hereinafter referred to as modified ECMWF scheme), the spatial correlation is a bit more improved to 0.81. The RMSE of the ICEFLUX and modified ECMWF schemes are 3.30 fl./km^2/year and 3.39 fl./km^2/year respectively, which is slightly lower than that of the CTH scheme of 3.44 fl./km^2/year.

In conclusion, the new ICEFLUX lightning scheme and original/modified ECMWF lightning scheme both improved the prediction of global lightning in the CHASER model. This result suggests that LNO_x simulation in CHASER will be also improved with the new lightning schemes.

Keywords: Lightning scheme, Lightning NOx, Chemistry climate model, NOx

©2021. Japan Geoscience Union. All Right Reserved.

Methane emissions from populated areas of Tokyo and five prefectures: Emission ratios with NOx and their trends over 2009-2018

*Yugo Kanaya[1], Kanami Saima[2], Akira Fukuike[2]

1. JAMSTEC, 2. MURATA Keisokuki Service Co., Ltd.

Regarding methane as an important greenhouse gas, national reports on its annual emission fluxes are mandated. However, the reported fluxes, based on socioeconomical statistics of activities and assumed emission factors, have seldom been evaluated from atmospheric observations of methane concentrations. On the implementation of Paris Agreement/global stocktakes, efforts in the emission reduction have to be repeatedly quantified, particularly using ground/satellite-based observations. To obtain relevant scientific information, we focused on analysis of CH4 data included in the governmental air pollution monitoring. We identified positive correlations between methane and NOx in Tokyo during winter of 2018, indicating presence of urban sources of methane. Regarding the slope of the regression line (ΔCH4/ΔNOx = ca. 2.5 ppm/ppm) as the emission ratio, we preliminary estimated methane emissions of 36 kt/y from Tokyo Metropolitan area. We then extended the analysis to other five prefectures (Chiba, Saitama, Kanagawa, Osaka and Aichi) and found similar positive correlations with regression slopes ranging from 1.5 to 4.5 ppm/ppm, implying regional commonality. The slopes per sites showed a positive correlation with population densities. The emission ratio had a significant long-term increasing trend of ~4.1%/y over 2009-2018. Considering NOx concentrations had a ~4.0%/y decreasing trend over Tokyo, the methane flux was regarded as constant over the decade. Based on these analyses, we studied possibilities of leakage of methane distributed for residential use. As the upcoming satellite missions including GOSAT-GW aim combined, high-precision measurements of greenhouse gases and air pollutants, detectability of such sources from satellite CH4/NO2 measurements is also to be discussed.

Keywords: Atmospheric composition, Urban Area, GHG-AQ joint analysis, emissions

©2021. Japan Geoscience Union. All Right Reserved.

An impact of tropospheric air pollution changes over Japan due to future climate and emission change

*Natsumi Kawano[1], Tatsuya Nagashima[1], Masayuki Hara[2], Satoru Chatani[1], Syuichi Itahashi[3]

1. National Institute for Environmental Studies, 2. Center for Environmental Science in Saitama, 3. Central Research Institute of Electric Power Industry

Air pollutants and climate change, which are known as critical environmental issues, have inter-related closely (Jacob and Winner (2008)). Besides, an increase of anthropogenic emissions arising from future urban expansion, which are responsible for the emission of gaseous and particulate pollutants, is also concerned to have adverse influences on their surrounding environments (Fenger (1999); Martins (2012); Monks *et al.*, 2015). In order to address these issues, it is necessary for evaluating the impacts of change in climate and air pollutant emission in the future on regional air quality.
In this study, we investigated the projected changes in tropospheric ozone (O_3) and fine particulate matter ($PM_{2.5}$) concentrations over Japan by examining regional-scale chemical transport model with considering future climate and air pollutant emissions under future climate change scenarios. To predict the future climate in a specific region, the Pseudo global warming (PGW) method (Sato *et al.*, 2007), which is a tool to downscale future climate simulated by global circulation models (GCM), are widely used in regional to urban scale climate studies (Hara *et al.*, 2010; Kusaka *et al.*, 2014; Adachi *et al.*, 2018; Darmanto *et al.*, 2019). Here, we applied the PGW method to the regional-scale chemical transport modelling study as following steps. First, a PGW dataset is required which is calculated from the difference of decadal average monthly climatologies in the future climate (2030s, 2050s, 2090s) and present climate (2010s). The output of MIROC5 model in the 5th Coupled Model Intercomparison Project (CMIP5) datasets under the RCP 2.6 and RCP 8.5 climate scenarios was used to calculate climatologies in future. Second, the PGW dataset is added to the present initial and lateral boundary datasets (i.e. JRA-55, NCEP1, and RTGSST data). Moreover, the future change in air pollutant emission, which consist of emissions from vegetation sources (VG) and from anthropogenic sources (ANTH) were estimated from MIROC_CHEM as well as climatologies estimated from MIROC5.
To discuss the impact of future changes in climate and emission, we performed three different setups of experiments; one for the present climate with present VG and ANTH emission, second for the future climate with future VG and present ANTH emissions (for climate impact only), and the other for the future climate with future VG and ANTH emission (for both climate and emission impact). In the presentation, we plan to quantify the impacts on changes in tropospheric O_3 and $PM_{2.5}$ by dividing into seasons and day/night.

Keywords: ozone, fine particulate matter, regional air quality prediction, dynamical downscaling

©2021. Japan Geoscience Union. All Right Reserved.

An Empirical Approach toward the Reduction Targets of CH4 and O3 as SLCP: For Asia as an example

*Hajime Akimoto[1], Tatsuya Nagashima[1], Hiroshi Tanimoto[1], Zbigniew Klimont[2], Markus Amann[2]

1. National Institute for Environmental Studies, 2. International Institute for Applied System Analysis

Although importance of co-control of SLCPs together with the emission reduction of CO_2, has been well recognized for both of mid- and long-term climate change mitigation, discussion on the implementation into the policymaking process often meet difficulty due to the complexity ascribed to interrelationship between SLCPs and their precursors, particularly for CH_4 and O_3. The chemistry-climate model analysis usually used for presenting future scenarios which can treat such interaction scientifically, tends to give a “black box” for the contribution of each species of SLCPs. In order to deliver a more straightforward message on the effectiveness of the reduction of each SLCP to policymakers, we propose “top-down” method for determining reduction targets of CH_4 and tropospheric O_3 based on the historical levels of their radiative forcing (RF)*.

The increase of RF due to the increase of atmospheric concentration of CO_2 in mid-term future would reach e.g. ~0.80Wm^{-2}in 2040 regardless of the stringent emission control scenarios due to the long atmospheric lifetime more than 100 years. In order to compensate this, if the atmospheric concentrations of CH_4, and O_3 can be decreased to the levels of 1980, 1970, 1960, and 1950 from the 2010 level, RF of CH_4 and O_3 can be reduce to from 0.48 to 0.41, 0.34, 0.27, and 0.22 Wm^{-2}, and from 0.40 to 0.29, 0.23, 0.19, and 0.15 Wm^{-2}, respectively, according to the IPCC 2013 database. Thus, for example, if the atmospheric concentrations of CH_4 and O_3 can be reduced to their levels of 1970, the sum of RF for CH_4 and O_3 will be reduced by 0.31 Wm^{-2}, which can compensate the increase of RF due to CO_2 by 40%.

Here, the global reduction ratios of CH_4, NO_x, and NMVOC necessary to attain the 1970 levels of CH_4 and O_3 have been applied to Asia, and the estimated results were compared by sector with the GAINS model-based cost-beneficial reduction amount proposed by Solution Report (2018) prepared under UN Environment Asia and the Pacific Office. The results show that the emission reduction of CH_4 to the 1970 level is feasible for rice paddies and waste treatment, but for attaining the reduction of livestock emission, new technology/practice would be required. As for NO_x, the possibility of attaining the necessary reduction is high for transport sector. Also, the possibility of attaining the necessary reduction of NMVOC is high for the transport and waste treatment sectors. In contrast, the emission reduction of CH_4 and NMVOC from coal/natural gas/oil production sector, and NO_x from industry/power plant sector is not enough in Solution Report. It can be concluded that in order to attain these targeted reduced emission levels, energy transformation from fossil fuel to renewable energy sources would be highly advantageous.

* H. Akimoto, T. Nagashima, H. Tanimot1, Z. Klimont and M. Amann, An empirical approach toward the SLCP reduction targets in Asia for the mid-term climate change mitigation, Prog. Earth Planet, Sci., 7:73, https://doi.org/10.1186/s40645-020-00385-5, 2020.

Keywords: Short-lived Climate Pollutants , SLCP, CH4, O3, NOx, NMVOC

©2021. Japan Geoscience Union. All Right Reserved.

[J] Oral | A (Atmospheric and Hydrospheric Sciences)：A-AS Atmospheric Sciences, Meteorology & Atmospheric Environment

Sun. Jun 6, 2021 3:30 PM - 5:00 PM JST | Sun. Jun 6, 2021 6:30 AM - 8:00 AM UTC | Ch.08 Zoom Room 08

[A-AS05] Atmospheric Chemistry

convener:Tomoki Nakayama(Graduate School of Fisheries and Environmental Sciences, Nagasaki University), Naoko Saitoh(Center for Environmental Remote Sensing), Sakae Toyoda(Department of Chemical Science and Engineering, Tokyo Institute of Technology), Risa Uchida(Japan Automobile Research Institute), Chairperson:Naoko Saitoh(Center for Environmental Remote Sensing), Shigeyuki Ishidoya(Advanced Industrial Science and Technology)

This session provides a forum for the presentation of the broad spectrum of tropospheric and stratospheric chemistry, including various research topics (e.g., dynamical processes, air quality and climate), approaches (modeling, field measurements, remote sensing, and laboratory studies), and species (gas and aerosol). This session also provides an opportunity for discussing possible future collaboration with other research fields relevant to atmospheric chemistry. We strongly encourage authors to prepare presentation slides and a poster in English.

3:30 PM - 4:00 PM JST | 6:30 AM - 7:00 AM UTC

[AAS05-18] Earth system modeling on interactions between ecosystem and atmospheric chemistry

★Invited Papers

*Tomohiro Hajima[1], Manabu Abe[1], Akinori Ito[1], Akihiko Ito[2], Rumi Ohgaito[1], Kazuyuki Saito[1], Kengo Sudo[3], Michio Kawamiya[1], Maki Noguchi Aita[1], Prabir Patra[1], Akitomo Yamamoto[1], Tokuta Yokohata[2], Shingo Watanabe[1], Michio Watanabe[1] (1.Japan Agency for Marine-Earth Science and Technology, 2.National Institute for Environmental Studies, 3.Nagoya University)

4:00 PM - 4:15 PM JST | 7:00 AM - 7:15 AM UTC

[AAS05-19] Seasonal variations of methane sources in South Asia inferred from observations of stable carbon isotope ratio of atmospheric methane

*Yukio Terao[1], Taku Umezawa[1], Manish Naja[2], Md. Kawser Ahmed[3], Shohei Nomura[1], Toshinobu Machida[1], Motoki Sasakawa[1], Hitoshi Mukai[1], Prabir Patra[4] (1.National Institute for Environmental Studies, 2.Aryabhatta Research Institute of Observational Sciences, 3.Department of Oceanography, Faculty of Earth & Environmental Sciences, University of Dhaka, 4.Research Institute for Global Change, JAMSTEC)

4:15 PM - 4:30 PM JST | 7:15 AM - 7:30 AM UTC

[AAS05-20] The interhemispheric transport pathways of methane as observed by GOSAT and simulated by ACTM

*Dmitry Belikov[1], Naoko Saitoh[1], Prabir Patra[1,2] (1.Center for Environmental Remote Sensing, Chiba University, 2.Research Institute for Global Change (RIGC), JAMSTEC)

4:30 PM - 4:45 PM JST | 7:30 AM - 7:45 AM UTC

[AAS05-21] Signal of CO_2 emitted from 2020 Western U. S. wildfire captured by commercial airliner observations

*Kentaro Ishijima[1], Toshinobu Machida[2], Taku Umezawa[2], Yosuke Niwa[2,1], Kazuhiro Tsuboi[1], Ryo Fujita[1], Hidekazu Matsueda[3,1], Taichu Y Tanaka[1], Takashi Maki[1], Takashi Nakamura[4] (1.Meteorological Research Institute, 2.National Institute for Environmental Studies, 3.Dokkyo University, 4.Japan Meteorological Agency)

4:45 PM - 5:00 PM JST | 7:45 AM - 8:00 AM UTC

[AAS05-22] Secular trend of atmospheric N_2O isotopocule ratios observed at Syowa staion, Antarctica

*Sakae Toyoda[1], Tsutomu Mizuno[1], Daisuke Goto[2], Shinji Morimoto[3] (1.School of Materials and Chemical Technology, Tokyo Institute of Technology, 2.National Institute of Polar Research, 3.Center for Atmospheric and Oceanic Studies, Tohoku University)

Earth system modeling on interactions between ecosystem and atmospheric chemistry

*Tomohiro Hajima[1], Manabu Abe[1], Akinori Ito[1], Akihiko Ito[2], Rumi Ohgaito[1], Kazuyuki Saito[1], Kengo Sudo[3], Michio Kawamiya[1], Maki Noguchi Aita[1], Prabir Patra[1], Akitomo Yamamoto[1], Tokuta Yokohata[2], Shingo Watanabe[1], Michio Watanabe[1]

1. Japan Agency for Marine-Earth Science and Technology, 2. National Institute for Environmental Studies, 3. Nagoya University

Terrestrial ecosystems and ocean biogeochemistry interact with atmospheric chemistry –natural ecosystems can be source/sink of GHGs and sometimes get impacted from atmospheric deposition. Such ecosystem–atmosphere interactions are now being modeled and incorporated into Earth system models, which are realized by embedding atmosphere, land, and ocean chemical/biogeochemical components into climate models. Such models are first developed by incorporating ecosystem processes to represent climate-carbon cycle feedback, and now becoming a more complicated system by incorporating mutual interaction between ecosystems and atmospheric chemistry (e.g., nitrogen cycle). In this presentation, a brief introduction on the ecosystem role in the global carbon cycle will be made, based on CMIP6 (Coupled Model Intercomparison Project Phase6) simulations. The carbon sink/source of land and ocean play a crucial role in the global carbon cycle because of the quite long CO_2 life-time in the atmosphere, and recent studies suggest the importance to reduce the carbon cycle feedback uncertainties and sometimes focus on the long-term dynamics after the stoppage of anthropogenic emission (Arora et al. 2020; MacDougall et al. 2020). In addition, an ESM (MIROC-ES2L, Hajima et al. 2020 GMD) has been developed in which interactions between ecosystems and atmospheric processes are improved, by incorporating nutrient deposition on land/ocean ecosystems to alter the biogeochemical processes. In addition, we have started a modeling to include ecosystem feedback processes regarding CH_4 and N_2O, based on the model.

Keywords: Earth system models, Biogeochemistry, Atmospheric chemistry

©2021. Japan Geoscience Union. All Right Reserved.

Seasonal variations of methane sources in South Asia inferred from observations of stable carbon isotope ratio of atmospheric methane

*Yukio Terao[1], Taku Umezawa[1], Manish Naja[2], Md. Kawser Ahmed[3], Shohei Nomura[1], Toshinobu Machida[1], Motoki Sasakawa[1], Hitoshi Mukai[1], Prabir Patra[4]

1. National Institute for Environmental Studies, 2. Aryabhatta Research Institute of Observational Sciences, 3. Department of Oceanography, Faculty of Earth & Environmental Sciences, University of Dhaka, 4. Research Institute for Global Change, JAMSTEC

Various types of methane (CH_4) sources reside in South Asia, including ruminant, rice paddy, biomass burning, fossil fuel industry, and landfills. For effective reduction of CH_4 emissions, observations of stable carbon isotope ratio of CH_4 ($\delta^{13}C$-CH_4) play an important role. The $\delta^{13}C$-CH_4 data provide better understanding of CH_4 emission sources because of distinct $\delta^{13}C$-CH_4signatures for individual source types: −60‰ for microbial, −40‰ for fossil fuel, and −25‰ for biomass burning sources.

Here we present the first observations of atmospheric $\delta^{13}C$-CH_4 at two sites in South Asia. We have performed weekly air sampling at Nainital (29.36˚ N, 79.46˚ E, 1940 m a.s.l.) in the Himalaya mountain area, northern India since 2006 and at Comilla (23.43˚ N, 91.18˚ E, 30 m a.s.l.) in the paddy area, central Bangladesh since 2012. The air samples were analyzed for atmospheric GHGs and related tracers (Nomura et al., submitted to ACP). Using a newly developed measurement system for $\delta^{13}C$-CH_4 (Umezawa et al., JMSJ, 2020), we started $\delta^{13}C$-CH_4 analysis for air samples collected at both sites from August 2018. The observational data were grouped into three seasons for Comilla (from August to November (ASON), from December to March (DJFM) and from April to July (AMJJ)) and two seasons for Nainital (July and August (JA) and others) by considering the monsoon and agricultural cycles in the regions.

Large increases in the CH_4 concentration were observed during ASON and DJFM at Comilla. The relationship between $\delta^{13}C$-$CH_4$and the reciprocal of CH_4 concentration (Keeling plot) at Comilla inferred that the $\delta^{13}C$-CH_4 signature of the CH_4 source was −52‰ for ASON and −45‰ for DJFM, while no significant correlation was found for AMJJ. Our result suggested that 75% of CH_4emission come from microbial sources and 19% from biomass burning during ASON, while the estimated relative contributions are 55% and 39% during DJFM, by assuming that 6% of the total CH_4 emission was from fossil fuels in Bangladesh (EDGAR V4.3.2). These estimates of contribution of biomass burnings to the total CH_4 emission were much higher than those in the EDGAR inventory, suggesting that the EDGAR inventory underestimate the CH_4 emission from biomass burnings in Bangladesh. Our observation also showed higher carbon monoxide (CO) concentrations during DJFM than ASON, consistent with the above results suggesting the large contribution of biomass burnings during DJFM. At Nainital, increases in the CH_4 concentration and decreases in $\delta^{13}C$-CH_4 were observed during JA, although the ranges of variations in the CH_4 concentration and $\delta^{13}C$-CH_4 were much smaller than those at Comilla. The $\delta^{13}C$-CH_4 signature of the regional source was estimated to be −51‰ throughout the year, showing no seasonal variations of CH_4 sources. The Nainital data might represent a typical $\delta^{13}C$-CH_4 signature over the region.

Keywords: methane, carbon cycle, isotope, emission inventory

©2021. Japan Geoscience Union. All Right Reserved.

The interhemispheric transport pathways of methane as observed by GOSAT and simulated by ACTM

*Dmitry Belikov[1], Naoko Saitoh[1], Prabir Patra[1,2]

1. Center for Environmental Remote Sensing, Chiba University, 2. Research Institute for Global Change (RIGC), JAMSTEC

Observations of long-lived tracers indicate that mixing tropospheric air between the Northern Hemisphere (NH) and Southern Hemisphere (SH) extratropics is about 1–1.5 yr. The importance of the seasonal migration of the zonally averaged Hadley circulation and intertropical convergence zone (ITCZ) oscillation on interhemispheric (IH) transport of tracers has been recognized. The mechanisms for transport through the tropics and the role of the monsoonal circulation, however, are not well understood. This study aiming to identify the transport pathways that connect NH and SH by analyzing CH_4 global distributions as measured by thermal infrared (TIR) band observations by the Thermal And Near-infrared Sensor for carbon Observation-Fourier Transform Spectrometer (TANSO-FTS) onboard the Greenhouse gases Observation SATellite (GOSAT) and simulated by MIROC4.0-based Atmospheric Chemistry Tracer Model (MIROC4-ACTM) for the period 2010-2013.

We found several longitudinal zones of active IH transport located in the Upper Troposphere and Lower Stratosphere (UTLS) zone (levels of 400– 200hPa). The IH exchange over Amazonia and tropical Africa is active both for winter and summer, while in the Asia region there is significant seasonal variability. Presented results confirm the role of the Asian Summer Monsoon Anticyclone (ASMA) zonally asymmetric heating on IH transport and highlight that the monsoon-induced eddy circulation plays an important role in the interhemispheric transport of long-lived chemical constituents. The dual role of ASMA has been revealed. On the one hand, its influence blocks IH in the tropical zone of the Indian Ocean and Southeast Asia, on the other, it enhances vertical ventilation in northern India, where significant methane fluxes are concentrated. Fast convective transport caused by ASMA accelerates the saturation of the middle and upper troposphere in NH with methane-rich surface air. These stratospheric levels are the origin of two west-directed jets (TEJ and AEJ) transported air mass to tropical Africa and further to SH.

Keywords: interhemispheric transport, GOSAT, methane

©2021. Japan Geoscience Union. All Right Reserved.

Signal of CO_2 emitted from 2020 Western U. S. wildfire captured by commercial airliner observations

*Kentaro Ishijima[1], Toshinobu Machida[2], Taku Umezawa[2], Yosuke Niwa[2,1], Kazuhiro Tsuboi[1], Ryo Fujita[1], Hidekazu Matsueda[3,1], Taichu Y Tanaka[1], Takashi Maki[1], Takashi Nakamura[4]

1. Meteorological Research Institute, 2. National Institute for Environmental Studies, 3. Dokkyo University, 4. Japan Meteorological Agency

In 2020, the Western United States experienced a series of serious wildfires, ignited in August across California, Oregon, and Washington, followed by expansion of the burning in early September. In the early September, the color of the sky turned orange due to huge aerosols emitted from the wildfires in those regions. The preliminary estimate of the annual wildfire emission of CO_2 in California by the California Air Resources Board is more than twice of the largest emission in the past 20 years.

The Comprehensive Observation Network for TRace gases by AIrLiners (CONTRAIL) with Continuous Measuring Equipment (CME) onboard aircraft of Japan Airlines can continuously obtain atmospheric CO_2 mole fraction on the flight path. In 2020, considerable number of measurement flights to Los Angeles (~40 profiles) were carried out in September compared to previous years. Vertical profiles of CO_2 mole fraction obtained by CONTRAIL-CME over Los Angeles showed high magnitude of variability throughout the troposphere, in comparison to those in September of the preceding years. This resulted in exceptionally large median and mean values of the CO_2 mole fraction calculated from all profiles in September of 2020.

We also tried model simulations using the latest biomass burning emission inventory of GFED and GFAS. Preliminary simulations by an on-line atmospheric tracer transport model (GSAM-TM) reproduces some of CO_2 enhancement observed in relatively wide altitude range of more than a few kilometers in the vertical profile. More detailed analysis results will be prepared in our presentation.

Keywords: wildfire, co2, aircraft observation

©2021. Japan Geoscience Union. All Right Reserved.

Secular trend of atmospheric N_2O isotopocule ratios observed at Syowa staion, Antarctica

*Sakae Toyoda[1], Tsutomu Mizuno[1], Daisuke Goto[2], Shinji Morimoto[3]

1. School of Materials and Chemical Technology, Tokyo Institute of Technology, 2. National Institute of Polar Research, 3. Center for Atmospheric and Oceanic Studies, Tohoku University

Nitrous oxide (N_2O) is one of the increasing greenhouse gases in the troposphere and is the most important stratospheric ozone-depleting gas in the 21st century. Sources of atmospheric N_2O include oceans, natural soils, and human activity such as agriculture, fossil fuel combustion, and chemical industry. In addition to conventional concentration or flux measurements of N_2O, isotopocule ratios of N_2O, which include not only elemental $^{15}N/^{14}N$ and $^{18}O/^{16}O$ ratios but also site-specific $^{15}N/^{14}N$ ratio in asymmetric NNO molecule, have been used as parameters to infer the origin and production–consumption mechanisms of N_2O. Since secular trend of isotopocule ratios of atmospheric N_2O can be used to deduce relative contribution from each source, several efforts have been made by analyzing air trapped in the polar firn or air samples collected at monitoring stations. However, there have been only a few reports on long-term monitoring of atmospheric N_2O isotopocule ratios in the Southern Hemisphere. Moreover, the north-to-south gradient of isotopocule ratios remains uncertain because published data by different laboratories cannot be compared directly due to calibration problems.

In this study, we aimed at revealing isotopocule ratios of atmospheric N_2O and their trend in the Southern Hemisphere, and comparing with their counterparts in the Northern Hemisphere which were measured by the same laboratory. Surface air samples were collected into an aluminum cylinder at about 15MPa at Syowa station, Antarctica (69˚S, 40˚E) with 2–4 month interval in 1998–2020. They have been archived at NIPR, and were sub sampled to 1-L glass flasks for concentration and isotopic analyses of N_2O.
Isotopocule ratios of N_2O were measured using a GC-IRMS system which is also used to elucidate the secular trend of N_2O isotopes at three Northern Hemispheric sites, Hateruma Island, Japan (24˚N, 124˚E), Novosibirsk, Russia (55˚N, 83˚E), and Churchill, Canada (59˚N, 94˚W). Concentration was measured with GC-ECD.
Results showed that the bulk nitrogen isotope ratio ($\delta^{15}N^{bulk}$) in N_2O at Syowa station is decreasing at the similar rate (about -0.04‰ yr^{-1}) as observed in the Northern Hemispheric sites. When compared at the same year, the value of $\delta^{15}N^{bulk}$ is about 0.2‰ higher in the southern hemisphere. The oxygen isotope ratio ($\delta^{18}O$) also shows decreasing trend that is similar to the trend in the Northern Hemisphere, but north-to-south gradient is not detectable with the precision of the analysis. The ^{15}N-site preference in N_2O (SP) does not show secular increasing nor decreasing trend, and north-to-south gradient is not detectable.

These results suggest that contribution from southern hemispheric sources to atmospheric increase in N_2O is very small if we take into account the fact that concentration is higher in the Northern Hemisphere and that distributions of natural and anthropogenic sources are different between the two hemispheres. Further analysis of isotopic signature of N/S sources with simple model approaches will be discussed.

Keywords: Greenhouse gas, Stable isotope ratio, N2O, Southern Hemisphere

©2021. Japan Geoscience Union. All Right Reserved.

[J] Poster | A (Atmospheric and Hydrospheric Sciences)：A-AS Atmospheric Sciences, Meteorology & Atmospheric Environment

Sun. Jun 6, 2021 5:15 PM - 6:30 PM JST | Sun. Jun 6, 2021 8:15 AM - 9:30 AM UTC | Ch.07_2

[A-AS05] Atmospheric Chemistry

convener:Tomoki Nakayama(Graduate School of Fisheries and Environmental Sciences, Nagasaki University), Naoko Saitoh(Center for Environmental Remote Sensing), Sakae Toyoda(Department of Chemical Science and Engineering, Tokyo Institute of Technology), Risa Uchida(Japan Automobile Research Institute)

This session provides a forum for the presentation of the broad spectrum of tropospheric and stratospheric chemistry, including various research topics (e.g., dynamical processes, air quality and climate), approaches (modeling, field measurements, remote sensing, and laboratory studies), and species (gas and aerosol). This session also provides an opportunity for discussing possible future collaboration with other research fields relevant to atmospheric chemistry. We strongly encourage authors to prepare presentation slides and a poster in English.

[AAS05-P01] The Relation between HONO Emission and the Amount of Carbon and Nitrogen Compounds in the Activated Sludge

*Chika Minejima[1], Yuta Orii[1], Ryosuke Fujinuma[1], Toshikazu Suenaga[2], Shohei Riya[2], Akihiko Terada[2], Masayuki Ohyama[4], Norimichi Takenaka[5], Keiichi Sato[3] (1.International Christian University, 2.Tokyo University of Agriculture and Technology, 3.Asia Center for Air Pollution Research (ACAP), 4.Osaka Institute of Public Health, 5.Osaka Prefecture University)

[AAS05-P02] Constraining the origin of tropospheric nitrous acid using triple oxygen isotopes as tracers

*Fumiko Nakagawa[1], Peng Lai[1], Kazuya Hirano[1], Masanori Ito[1], Urumu Tsunogai[1] (1.Graduate School of Environmental Studies, Nagoya University)

[AAS05-P03] Changes in tropospheric nitrogen dioxide vertical column densities over Japan and Korea during the COVID-19 using Pandora and MAX-DOAS

*Yongjoo Choi[1], Yugo Kanaya[1], Hisahiro Takashima[2], Kihong Park[3], Haebum Lee[3], Jihyo Chong[3,4], Jae Hwan Kim[5] (1.Japan Agency for Marine-Earth Science and Technology, 2.Faculty of Science, Fukuoka University, 3.Gwangju Institute of Science and Technology, 4.Environmental Management Division, Yeongsan River Basin Environmental Office, Gwangju 61945, Korea, 5.Pusan National University)

[AAS05-P04] Estimation of emission source of CO from biomass burning observed with ground-based FTIR spectrometers at Tsukuba since 2010

Daisuke Suzuki[2], *Hideaki Nakajima[1,2], Isao Murata[2], Isamu Morino[1] (1.National Institute for Environmental Studies, 2.Graduate School of Environmental Studies, Tohoku University)

[AAS05-P05] Evaluation of NICAM-TM CO data using MOPITT CO data

*Miyajima Hiroshi[1], Naoko Saitoh[1], Yosuke Niwa[2] (1.Center for Environmental Remote Sensing, Chiba University, 2.National Institute for Environmental Studies)

[AAS05-P06] Evaluation of the global chemistry transport model CHASER utilizing TROPOMI formaldehyde measurements

*Hossain Mohammed Syedul Hoque[1], Kengo Sudo[1,3], Hitoshi Irie[2], Takashi Sekiya[3] (1.Graduate School of Environmental Studies, Nagoya University, Japan, 2.Center for Environmental Remote Sensing (CEReS), Chiba University, Japan, 3.Japan Agency for Marine-Earth Science and Technology (JAMSTEC), Yokohama, Japan)

[AAS05-P07] Ozone steady-state at the semi-urban region, Shadnagar, in Southern India

*Vijay Kumar Sagar[1] (1.National Remote Sensing Centre, Hyderabad, ISRO)

[AAS05-P08] A relationship between surface oxidant concentration and daily maximum temperature, and its long-term variability

*Atsushi Shimizu[1], Tatsuya Nagashima[1] (1.National Institute for Environmental Studies)

[AAS05-P09] Analysis of tropospheric ozone budgets in CMIP6 experiments

*Paul T Griffiths[1], Lee T Murray[2], Guang Zeng[3], Vaishali Naik[4], Prodromos Zanis[5], Alexander T Archibald[1] (1.National Centre for Atmospheric Science, Cambridge University, 2.University of Rochester, Rochester, NY, USA, 3.National Institute of Water and Atmospheric Research, Wellington, New Zealand, 4.NOAA Geophysical Fluid Dynamics Laboratory, Princeton, NJ, USA, 5.Department of Meteorology and Climatology, Aristotle University of Thessaloniki, Thessaloniki, Greece)

[AAS05-P10] Study of tropospheric CS_2 photooxidation chemistry

*Yuanzhe Li[1], Kazuki Kamezaki[2], Sebastian Danielache[2] (1.Green Science And Engineering Division, Graduate School Of Science And Technology, Sophia University, 2.Department of Materials & Sciences, Faculty of Science & Technology, Sophia University)

[AAS05-P11] **Effects of hydroxyl radical exposure on chemical composition of secondary organic aerosol formed from sabinene ozonolysis**

*Kei Sato[1,2], Yu Morino[1], Takashi Imamura[1], Yoshizumi Kajii[1,2] (1.National Institute for Environmental Studies, 2.Kyoto University)

[AAS05-P12] Impact of nighttime aging on optical properties of toluene secondary organic aerosol

*Tomoki Nakayama[1], Kei Sato[2], Sathiyamurthi Ramasamy[2], Takashi Imamura[2], Yoshizumi Kajii[3,2] (1.Nagasaki University, 2.NIES, 3.Kyoto University)

[AAS05-P13] Volatility of nanoparticles generated from jet engine lubrication oil

*Nobuyuki Takegawa[1], Anna Nagasaki[1] (1.Graduate School of Science, Tokyo Metropolitan University)

[AAS05-P14] Vertical structural measures of atmospheric pollutants using XU-S

*Kazuyo Yamaji[1], Tetsuya Miyakoshi[2], Satoshi Komatsu[2], Isao Kanda[3] (1.Kobe University, 2.ShinMaywa Industries, Ltd. , 3.Japan Meteorological Corporation)

[AAS05-P15] **Continuous and multi-wavelength measurement of aerosol extinction coefficient by long-path propagation of LED light at Chiba, Japan**

*Ikuya Nishiwaki[1], Hitoshi Irie[2], Nofel D. Lagrosas[1], Hiroaki Kuze[2] (1.Chiba University, 2.Center for Environmental Remote Sensing, Chiba University)

[AAS05-P16] Aerosol type classification of ground-based remote sensing data by k-means clustering

*Hiroyasu Kobayashi[1], Hitoshi Irie[2], Masahiro Momoi[1] (1.Chiba University, 2.Center for Environmental Remote Sensing, Chiba University)

[AAS05-P17] Validation of MERRA-2 Reanalysis Aerosol Products Using Ground-based Observations in Phimai, Thailand, and Factors that Affect Aerosol Optical Depth over the Indochina Peninsula

*Takeru Ohno[1], Hitoshi Irie[1], Arlindo M da Silva[2], Ravi C Govindaraju[2] (1.Center for Environmental Remote Sensing, Chiba University, 2.Global Modeling and Assimilation Office, NASA Goddard Space Flight Center, Greenbelt, Maryland)

[AAS05-P18] Exploring ground-based aerosol optical properties to improve satellite estimates of surface particulate matter concentrations

*Alessandro Damiani[1], Hitoshi Irie[1], Kodai Yamaguchi[1], Hossain Mohammed Syedul Hoque[2], Tomoki Nakayama[3], Yutaka Matsumi[2], Yutaka Kondo[4] (1.CEReS, Chiba University, 2.Nagoya University, 3.Nagasaki University, 4.National Institute of Polar Research)

[AAS05-P19] Development of international air quality and sky research remote sensing (A-SKY) network

*Hitoshi Irie[1], Alessandro Damiani[1], Toshihiko Takemura[2], Thanawat Jarupongsakul[3], Manish Naja[4] (1.Center for Environmental Remote Sensing, Chiba University, 2.Research Institute for Applied Mechanics, Kyushu University, 3.Department of Geology, Faculty of Science, Chulalongkorn University, 4.Aryabhatta Research Institute of Observational Sciences (ARIES))

[AAS05-P20] Prediction of changes in DSS emission using the Earth System Model of the Meteorological Research Institute

*Takashi Maki[1], Taichu Y Tanaka[1], Thomas Sekiyama[1], Mizuo Kajino[1], Naga Oshima[1], Tsuyoshi Koshiro[1] (1.Meteorological Research Institute)

[AAS05-P21] Methane emission trends of China in 2009-2018 induced by atmospheric observations

*Fenjuan Wang[1], Shamil S Maksyutov[1], Rajesh Janardanan[1], Akihiko Ito[2], Isamu Morino[1], Yukio Yoshida[1], Yasunori Tohjima[1], Johannes W. Kaiser[3], Greet Janssens-Maenhout[4], xin Lan[5], Ivan Mammarella[6], Jost V. Lavric[7], Tsuneo Matsunaga[1] (1.NIES National Institute of Environmental Studies, 2.Finnish Meteorological Institute, 3.Deutscher Wetterdienst, 4.European Commission Joint Research Centre, 5.Earth System Research Laboratory, 6.University of Helsinki, 7.Max Planck Institute for Biogeochemistry)

[AAS05-P22] **Characteristics of methane vertical distributions over India**

*Dingkun Zhang[1], Naoko Saitoh[1], Dmitry Belikov[1], Prabir Patra[2], Naveen Chandra[3] (1.Center for Environmental Remote Sensing, Chiba University, 2.Japan Agency for Marine-Earth Science and Technology, 3.National Institute for Environmental Studies)

[AAS05-P23] Temporal and spatial variations of the mole fraction, carbon and hydrogen isotope ratios of atmospheric methane in the Western Pacific region

*Yasuda Mahito[1], Shinji Morimoto[1], Shuji Aoki[1], Ryo Fujita[2], Taku Umezawa[3] (1.Center for Atmospheric and Oceanic Studies, Graduate School of Science, Tohoku University, 2.Department of Climate and Geochemistry Research, Meterorological Reserach Research Institute, Tsukuba Japan, 3.National Institute for Environmental Studies, Tsukuba, Japan)

[AAS05-P24] Variations of atmospheric carbon dioxide and its radioisotope in the arctic region

*Hikaru Sekine[1], Shinji Morimoto[1], Chinatsu Yamada[1], Daisuke Goto[2], Masayo Minami[3], Toshio Nakamura[3], Shuji Aoki[1] (1.Center for Atmospheric and Oceanic studies, 2.National Institute of Polar Research, 3.Institute for Space-Earth Environmental Research)

[AAS05-P25] Preparation of O_2/N_2 dataset from the surface to the middle stratosphere around Japan traceable to NMIJ gravimetric scale

*Shigeyuki Ishidoya[1], Shinji Morimoto[2], Kazuhiro Tsuboi[3], Satoshi Sugawara[4], Daisuke Goto[5], Nobuyuki Aoki[1], Shohei Murayama[1], Yosuke Niwa[6], Shuji Aoki[2], Hidekazu Matsueda[3], Kentaro Ishijima[3] (1.Advanced Industrial Science and Technology, 2.Tohoku University, 3.Meteorological Research Institute, 4.Miyagi University of Education, 5.National Institute of Polar Research, 6.National Institute for Environmental Studies)

[AAS05-P26] Temporal variation of the ozone profile observed with FTIR at Tsukuba

*Isao Murata[1], Hideaki Nakajima[2], Isamu Morino[2], Masanori Takeda[1,2] (1.Graduate School of Environmental Studies, Tohoku University, 2.National Institute for Environmental Studies)

The Relation between HONO Emission and the Amount of Carbon and Nitrogen Compounds in the Activated Sludge

*Chika Minejima[1], Yuta Orii[1], Ryosuke Fujinuma[1], Toshikazu Suenaga[2], Shohei Riya[2], Akihiko Terada[2], Masayuki Ohyama[4], Norimichi Takenaka[5], Keiichi Sato[3]

1. International Christian University, 2. Tokyo University of Agriculture and Technology, 3. Asia Center for Air Pollution Research (ACAP), 4. Osaka Institute of Public Health, 5. Osaka Prefecture University

Introduction & Research Purpose

OH radical is a strong oxidant and an essential component in the earth’ s atmosphere. However, quantification is very difficult because of its extremely high reactivity and low concentrations (Akimoto et al., 2002). Therefore, measuring precursor concentrations of OH radical is used to estimate its concentration. Gaseous nitrous acid, HONO, is one of the major OH precursors (Kleffmann, 2007).

$HONO + h\nu\ (\lambda < 400nm) \rightarrow NO + OH$

Despite the importance of HONO, its source is still not well understood. Soil was suggested as one of the missing sources (Su et al., 2011); thus, we use activated sludge to surrogate soil as it contains various organisms the same as any soil. Activated sludge is used in most of wastewater treatment plants. This study aims to elucidate the relation between HONO emission under aerobic conditions with carbon content, nitrogen content, and concentrations of inorganic nitrogen species such as NH_4^+, NO_2^-, and NO_3^-.

Experiments and Results

HONO fluxes from activated sludge were measured every 3 hours during daytime (AM9:00~PM6:00), October 6th, 2020 to 9:00, October 8th, 2020 using the filter pack method and ion chromatography. The measurement was started from the point of feeding the activated sludge. The filter pack was replaced every 3 hours. At night, samples were taken continuously for 15 hours from PM6:00 to AM9:00. Non-Purgeable Organic Carbon (NPOC) as carbon content and Total Nitrogen (TN) were also measured at the same time using TOC instrument (SHIMADZU TOC-V CSH). Secondly, NH_4^+, NO_2^-, NO_3^-, NPOC and TN concentration measurement was tried from the time of feeding on a separate day in order to find the change in chemical forms of nitrogen.

The result suggests that the HONO flux has strong relation with the carbon content under aerobic conditions. Further details will be discussed at the presentation.

Keywords: nitrous acid, activated sludge, soil

©2021. Japan Geoscience Union. All Right Reserved.

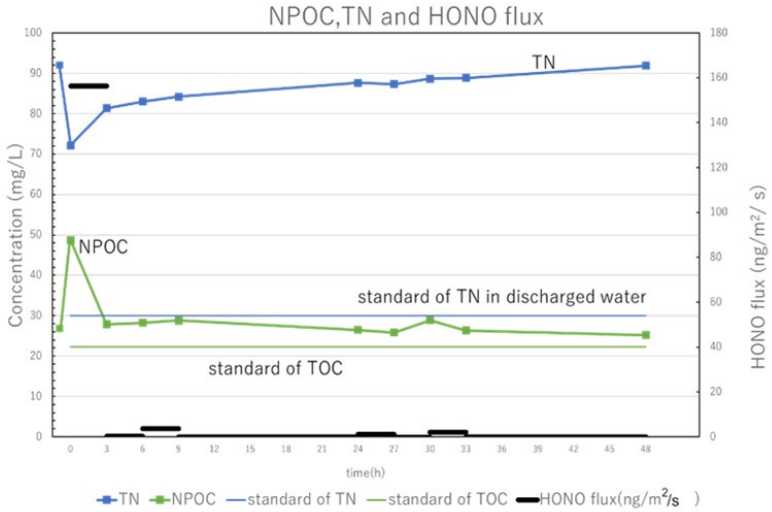


Figure 1. Time series of HONO fluxes, Carbon content (Non-Purgeable Organic Carbon (NPOC)) and Total Nitrogen (TN). Standards of Total Organic Carbon (TOC) and TN indicate the concentrations of TOC and TN in the released water from a wastewater treatment plant in Tokyo (TOC 22.2 mg/L, TN 30 mg/L). Feeding time was at the hour 0.

©2021. Japan Geoscience Union. All Right Reserved.

Constraining the origin of tropospheric nitrous acid using triple oxygen isotopes as tracers

*Fumiko Nakagawa[1], Peng Lai[1], Kazuya Hirano[1], Masanori Ito[1], Urumu Tsunogai[1]

1. Graduate School of Environmental Studies, Nagoya University

The photolysis of nitrous acid (HONO) has been recognized as a potentially important source of OH radicals, which is known as a major oxidant in the atmosphere removing reductive trace gases such as methane and NMHCs. Atmospheric HONO originates from both primary sources (direct emissions) and secondary sources (chemical formation in the atmosphere), however, their contributions to the atmospheric HONO production have not been well understood. Here, we determined a $\Delta^{17}O$ value of HONO together with $\Delta^{17}O$ value of $NO_2$and NO, because $\Delta^{17}O$ value of HONO produced via “secondary formation” is expected to have highly positive values as those of NO_2, while no $\Delta^{17}O$ anomaly should be observed for HONO which is emitted directly from various sources on the ground, making it possible to quantify their contribution to the atmospheric HONO production with $\Delta^{17}O$ measurement.

$\Delta^{17}O$ values of HONO, $NO_2$and NO was determined by combining sensitive determination method on isotope compositions of NO_2^-(Komatsu *et al.*, 2008; Tsunogai *et al.*, 2010) with a slightly modified filter-pack method (Noguchi *et al.*, 2007), in which HONO, $NO_2$and NOxwere collected as NO_2^-on alkaline (K_2CO_3) impregnated filter, triethanolamine (TEA)-coated filter, and mixture of 2-Phenyl-4,4,5,5-tetramethylimidazoline-3-oxide-1-oxyl (PTIO) and TEA-coated filter, respectively. Atmospheric HONO, $NO_2$and NO were collected at Nagoya University, which is located in a suburban area of Nagoya City. The sample collection period was fixed to three days with a flow rate of 10 L/min for HONO or $NO_2$and 1 L/min for NO, respectively.The $\Delta^{17}O$ values of $NO_2$and HONO showed similar diurnal variations; higher value on the day time than the night time. The result suggests that the atmospheric HONO is formed mainly by both direct emission and chemical reaction of NO_2 in the urban atmosphere.

Keywords: nitrous acid, triple oxygen isotopes, urban air, nitrogen dioxide, nitrogen monoxide

©2021. Japan Geoscience Union. All Right Reserved.

Changes in tropospheric nitrogen dioxide vertical column densities over Japan and Korea during the COVID-19 using Pandora and MAX-DOAS

*Yongjoo Choi[1], Yugo Kanaya[1], Hisahiro Takashima[2], Kihong Park[3], Haebum Lee[3], Jihyo Chong[3,4], Jae Hwan Kim[5]

1. Japan Agency for Marine-Earth Science and Technology, 2. Faculty of Science, Fukuoka University, 3. Gwangju Institute of Science and Technology, 4. Environmental Management Division, Yeongsan River Basin Environmental Office, Gwangju 61945, Korea, 5. Pusan National University

Using the measurements from ground-based remote sensing instruments, we investigated the changes in tropospheric nitrogen dioxide vertical column densities (NO_2 TropVCD) over Japan and Korea before and after the COVID-19 pandemic. Three sites for MAX-DOAS (Yokosuka, Cape Hedo, and Gwangju) and one site for Pandora (Busan) were selected for this study because these sites have been in operation for more than five years, allowing the results caused by COVID-19 in 2020 to be compared with previous reference years, 2015–2018 (2016–2018 for Busan) and 2019. To elucidate the relationship of NO_2 TropVCD with human activity during 2020, Google mobility data was also used as a proxy of transportation and industry activity. Because the behavior of NO_2 also depends on the meteorological variables, we also investigated the difference in meteorological fields from ERA5 along with spatial distribution of NO_2 TropVCD from Ozone Monitoring Instrument (OMI) satellite. During the Chinese New Year holidays, the NO_2 TropVCDs at three urban sites showed a rapid decrease due to less business and industry activities, then the level of NO_2 VCD slowly recovered but was consistently lower than the level of before the Chinese New Year holidays due to shorten NO_2 lifetime or low emission rate. During the periods of spontaneous social distancing in Korea (March–May) and Japan (April–May), decreasing activities of transportation and industry, especially in Japan, was obvious. NO_2 TropVCD in Busan and Gwangju showed a moderate correlation with the industrial sector, whereas that in Yokosuka showed moderate correlation with both the transportation and industrial sector. The monthly difference between reference years and 2020 showed that the average reduction in three urban sites was pronounced in May to September with high mean normalized bias (MNB; −48% to −32%) compared to the cold season (−27% to −11%). The difference in monthly variation of NO_2 TropVCD with reference years will be discussed in terms of meteorological variables, such as wind speed, temperature, and downward UV radiation.

Keywords: Tropospheric nitrogen dioxide vertical column densities , MAX-DOAS, Pandora, COVID-19

©2021. Japan Geoscience Union. All Right Reserved.

Estimation of emission source of CO from biomass burning observed with ground-based FTIR spectrometers at Tsukuba since 2010

Daisuke Suzuki[2], *Hideaki Nakajima[1,2], Isao Murata[2], Isamu Morino[1]

1. National Institute for Environmental Studies, 2. Graduate School of Environmental Studies, Tohoku University

Carbon monoxide (CO) is mainly produced by fossil fuels burning, biomass burning, and oxidization of hydrocarbons. CO is a precursor of tropospheric ozone generation and is an extremely important substance in atmospheric chemistry because it affects the abundance of various atmospheric trace components by reacting with OH radicals. It has a lifespan of several weeks to two months in the atmosphere, and there is a large regional ununiformity in its abundance and source. In recent years, it has been found that the emission of CO from the Asian region has a great influence on the global concentration, and it is desired to improve the estimation of its source. In Tsukuba (36.1N, 140.1E), since December 1998, we have been observing atmospheric trace components using solar infrared spectra with Bruker's high-resolution Fourier transform infrared spectrometer (FTIR). In this study, in order for clarifying the source of CO measured above Tsukuba, the altitude distribution of CO and hydrogen cyanide (HCN) was derived from the infrared spectra obtained by this FTIR. In this analysis, the source of CO was estimated using CO-HCN correlation. HCN has a lifetime of several years in the atmosphere and is mainly produced by biomass combustion. In this analysis, HCN was used as a proxy for biomass combustion.

For the period from April 2010 to May 2019, the altitude distribution of CO and HCN was analyzed from the observed spectra of FTIR in Tsukuba using the inversion analysis program of SFIT4. For the obtained altitude distribution, the partial column amounts of CO and HCN in the two layers 0-5 km and 5-18 km were obtained, and the correlations between them were analyzed. As a result, a significant positive correlation was confirmed between CO and HCN column amount at 5-18 km in spring. From the CO/HCN ratio obtained from the correlation analysis, the ratio of biomass combustion-derived CO in the atmospheric CO partial column was calculated, and the average value from March to May was about 70%. In addition, the air mass observed by FTIR in this season was subjected to backward trajectory analysis using METEX. We extracted cases where those air mass trajectories passed within 100 km from the forest fire observed by the MODIS sensor onboard the satellites Terra/Aqua. At an altitude of 5-18 km in the spring, the extracted trajectories mainly originated from northeastern China to the Eurasian continent. The results suggest that the observed enhanced CO over Tsukuba may have originated from forest fires in the area of latitude 50-60 N.

Keywords: carbon monoxide, Fourier transform infrared spectrometer , hydrogen cyanide, biomass burning, trajectory analysis, FTIR

©2021. Japan Geoscience Union. All Right Reserved.

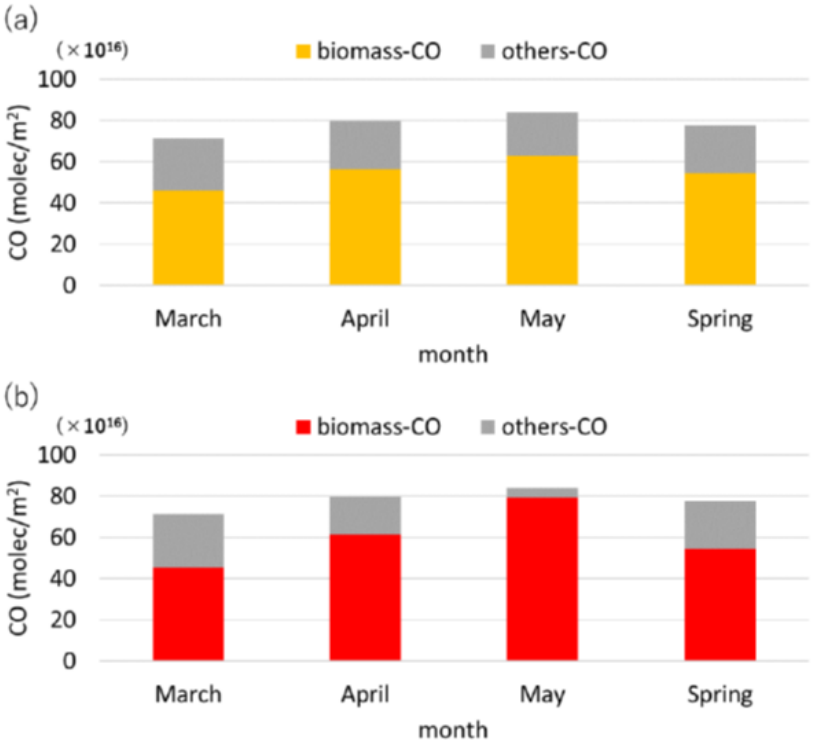


図１．高度5-18 km、バイオマス燃焼起源COのパーシャルカラム量。(a) すべての月のCO/HCN Biomass比に、春季の回帰直線の傾きの値を使用。(b) 各月のCO/HCN Biomass比に、各月の回帰直線の傾きの値を使用

Figure 1. Biomass burning-origin CO partial column for 5-18 km. (a) Calculated by annual averaged CO/HCN ratio and spring residual line's slope. (b) Calculated by monthly CO/HCN ratio and monthly residual line's slope.

©2021. Japan Geoscience Union. All Right Reserved.

Evaluation of NICAM-TM CO data using MOPITT CO data

*Miyajima Hiroshi[1], Naoko Saitoh[1], Yosuke Niwa[2]

1. Center for Environmental Remote Sensing, Chiba University, 2. National Institute for Environmental Studies

Carbon monoxide (CO) in the atmosphere is produced by incomplete combustion of carbonaceous materials and oxidation of hydrocarbons; biomass burning is one of the major sources of CO in the atmosphere. The main sink of atmospheric CO is a reaction with hydroxyl radical (OH). The lifetime of tropospheric CO is around two months, which results in its longer transport in hemispheric scale.

This study has compared CO concentrations simulated by Nonhydrostatic Icosahedral Atmospheric Model-based Transport Model (NICAM-TM) with CO concentrations observed by Measurement of Pollution In the Troposphere (MOPITT) on board the Terra satellite. Here, we have compared MOPITT CO data with NICAM-TM CO data with and without applying MOPITT CO averaging kernel functions (AK).

In the lower troposphere (850 hPa), NICAM-TM CO was lower than MOPITT CO in most regions except active biomass burning areas. NICAM-TM CO was significantly lower in the middle latitudes (30º–60ºN) where there are large anthropogenic CO emissions; the negative bias of NICAM-TM CO data against MOPITT CO data was about 30%. This implies the possibility of the underestimation of anthropogenic emissions in the NICAM-TM CO simulations. In the upper troposphere (250 hPa), NICAM-TM CO was lower than MOPITT CO in almost all regions; the negative bias of upper tropospheric NICAM-TM CO data was about 30% in low and mid-latitudes in both hemispheres in spring season.

In addition, seasonal variations in NICAM-TM CO data were much lower than those in MOPITT CO data in the upper troposphere. MOPITT CO there was largest in mid-latitude in spring and the differences between MOPITT and NICAM-TM CO was also largest in spring of all the season; these differences were also evident after applying MOPITT CO AK to NICAM-TM CO data. Comparisons with MOPITT CO data suggest that the negative bias in NICAM-TM CO data in the upper troposphere can be partly attributed to the underestimation of anthropogenic emissions and transport process from the surface to the upper troposphere in the NICAM-TM CO simulations.

Keywords: CO, satellite remote sensing, transport model

©2021. Japan Geoscience Union. All Right Reserved.

Evaluation of the global chemistry transport model CHASER utilizing TROPOMI formaldehyde measurements

*Hossain Mohammed Syedul Hoque[1], Kengo Sudo[1,3], Hitoshi Irie[2], Takashi Sekiya[3]

1. Graduate School of Environmental Studies, Nagoya University, Japan, 2. Center for Environmental Remote Sensing (CEReS), Chiba University, Japan, 3. Japan Agency for Marine-Earth Science and Technology (JAMSTEC), Yokohama, Japan

Tropospheric Monitoring Instrument (TROPOMI) has been providing observations of important atmospheric pollutants with an unprecedented horizontal resolution (~7×3.5 km^2) since August 2017. Such high-resolution global observations offer a unique opportunity to evaluate regional and global models at higher precision. In this study, TROPOMI formaldehyde (HCHO) measurements from June to December 2019 are used to evaluate the HCHO simulations from the global chemistry transport model CHASER-V4 (based on MIROC 5). In the evaluation's initial steps, the averaging kernel information from the TROPOMI HCHO measurements is applied to the CHASER HCHO. Overall, the CHASER simulations captured the observed global spatial variation of HCHO well, with a correlation coefficient (R) ~0.70. On a global scale, the mean bias error (CHASER –TROPOMI) and the root mean square error is -0.23 $\times 10^{16}$ and 0.31 $\times 10^{16}$ molecules cm^{-2}, respectively. The R values over eastern China, eastern and western US, and South America were ~ 0.9, indicating excellent agreement between the datasets. A negative correlation was observed over India and Southeast Asia during the monsoon season (June –August). One of the potential reasons for such disagreement could be the intense wet deposition of HCHO during the monsoon months, which the model might not capture well. However, previous studies reported that CHASER reproduced the OMI (Ozone Monitoring Instrument) nitrogen dioxide columns over India very well, including the monsoon season. Moreover, the lower TROPOMI HCHO columns over India and Southeast Asia during the monsoon are consistent with the ground-based MAX-DOAS (multi-axis differential optical absorption spectroscopy) HCHO observations in India and Thailand. Thus, the reason for the disagreement between CHASER and TROPOMI HCHO columns over India and Southeast Asia during the monsoon is not apparent yet. Other potential causes such as sources of HCHO other than biogenic emissions, high and low NOx conditions, etc., are required to be investigated.

Keywords: CHASER , TROPOMI , Formaldehyde (HCHO)

©2021. Japan Geoscience Union. All Right Reserved.

Ozone steady-state at the semi-urban region, Shadnagar, in Southern India

*Vijay Kumar Sagar[1]

1. National Remote Sensing Centre, Hyderabad, ISRO

The photo steady-state (PSS, $\phi=1$) of ozone (O_3) is considered when the production of O_3 (PO3) and sink of O_3 (S_{O3}) are in equilibrium. In the PSS, O_3 forms when NO_2 is destroyed and reform fast after reaction with O_3 in the sunlight. A hypothetical photo-stationary state (HPPS) can be assumed when the rate change of ozone balances with its net production (P_{netO3}) and net transport (T_{netO3}) in and out of small volume around the monitoring. The transport process is difficult to address without the set of spatial concentrations measurement, emissions inventories, and meteorological data for chemistry-transport modeling. Therefore the HPPS can be considered. However, detailed chemical observation and chemical transport models are used to study ozone production and its transport. In the real atmosphere, $\phi<1$ represents the involvement of transport and $\phi>1$ represents the involvement of peroxy radicals which converts NO to NO_2.
The Ozone concentration in PSS and HPPS framework were studied. The continuous observation of NO, NO_2, O_3 concentrations with a temporal resolution of 1 minute was hourly averaged during the August 2014 to April 2017 period. The hourly values of J_{NO2} were calculated using the radiative transfer model Tropospheric Ultraviolet and Visible (TUV) model. The average difference between the O_3 and O_{3HPPS} was observed 4.08 ppb while the difference between O_3 and O_{3pss} was observed -0.16 ppb in the daytime between 06:00 to 18:00 hours local through the study period. The net local transport was found at 52.78 ppb/h at the same time. The ozone that was transported was supported due to its long lifetime at the site. The study suggests that the site was ozone sink prominent and the ozone was transported at the site to balance the observed ozone throughout the study period.

©2021. Japan Geoscience Union. All Right Reserved.

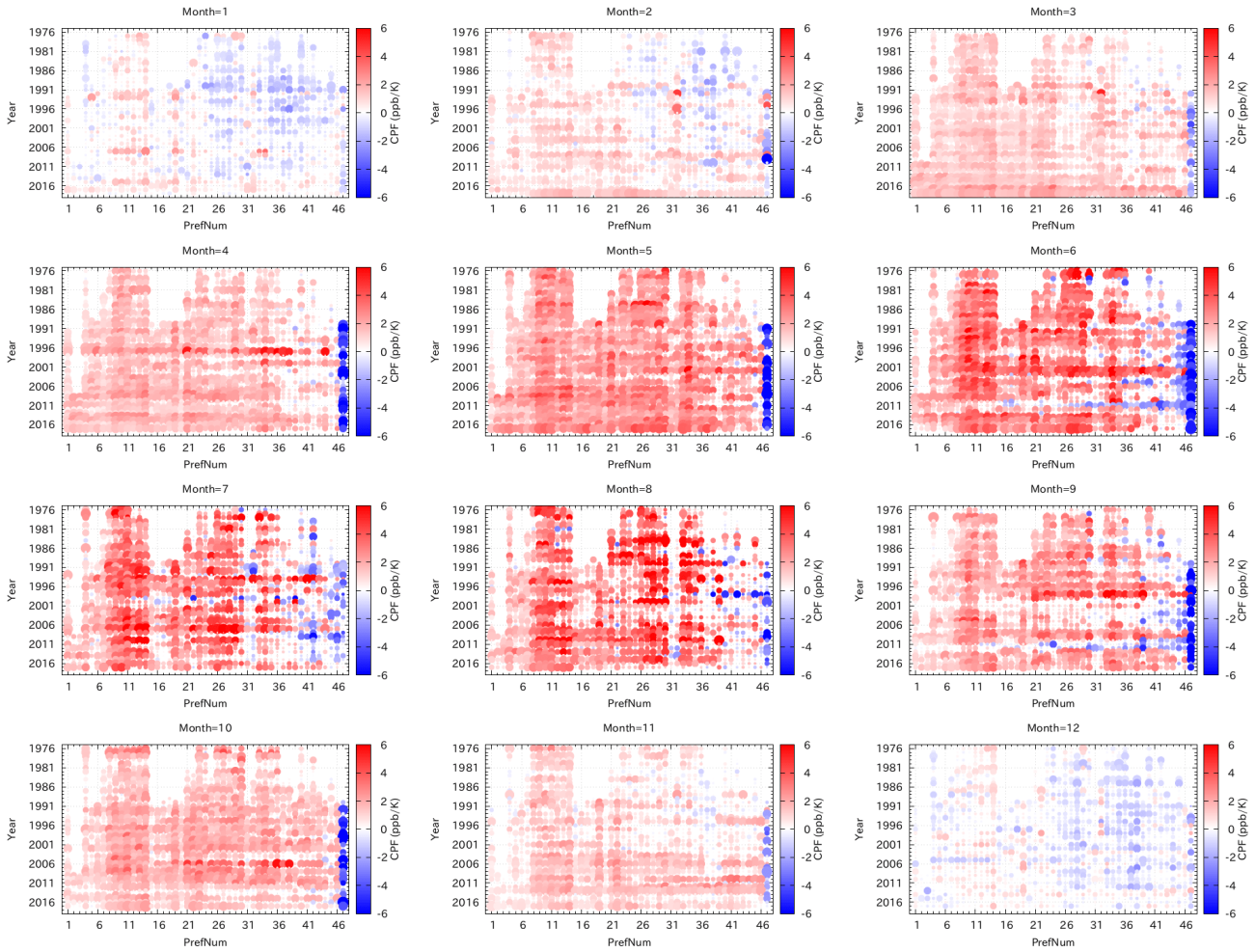
A relationship between surface oxidant concentration and daily maximum temperature, and its long-term variability

*Atsushi Shimizu[1], Tatsuya Nagashima[1]

1. National Institute for Environmental Studies

The climate penalty factor (CPF) for each prefecture and each month in last 42 years in Japan were estimated from mean 8 hours maximum surface oxidant and daily maximum temperature observations, and compared with CPF calculated by chemical transport model CMAQ. Opposite to general tendency of positive CPF all over Japan, negative CPF was confirmed in western part of Japan during winter. Large positive CPF was found during June and August around urbanized areas (Kanto and Kinki). Sporadic perturbations were dominant in several years/months. Horizontal variations of CPF calculated by CMAQ were dependent on the horizontal grid scale.

Keywords: oxidant, maximum temerature, climate penalty factor



©2021. Japan Geoscience Union. All Right Reserved.

Analysis of tropospheric ozone budgets in CMIP6 experiments

*Paul T Griffiths[1], Lee T Murray[2], Guang Zeng[3], Vaishali Naik[4], Prodromos Zanis[5], Alexander T Archibald[1]

1. National Centre for Atmospheric Science, Cambridge University, 2. University of Rochester, Rochester, NY, USA, 3. National Institute of Water and Atmospheric Research, Wellington, New Zealand, 4. NOAA Geophysical Fluid Dynamics Laboratory, Princeton, NJ, USA, 5. Department of Meteorology and Climatology, Aristotle University of Thessaloniki, Thessaloniki, Greece

A grand challenge in the field of chemistry-climate modelling is to understand the connection between anthropogenic emissions, atmospheric composition and the radiative forcing of trace gases and aerosols. The AerChemMIP model intercomparison project, part of CMIP6, focuses on calculating the radiative forcing of gases and aerosol particles over the period 1850 to 2100.

We present an analysis of the trends in tropospheric ozone budget in UKESM1 and other models from CMIP6 experiments. We discuss these trends in terms of chemical production and loss of ozone as well as physical processes such as transport and deposition. Where possible, AerChemMIP attribution experiments such as histSST-piCH4, will be used to quantify the effect of individual emissions and forcing changes on the historical ozone burden and budget. For future experiments, we focus on analogous experiments from the SSP3-70 scenario, a ‘regional rivalry’ shared socioeconomic pathway involving significant emissions changes.

Keywords: ozone, tropospheric, ozone budget

©2021. Japan Geoscience Union. All Right Reserved.

Study of tropospheric CS_2 photooxidation chemistry

*Yuanzhe Li[1], Kazuki Kamezaki[2], Sebastian Danielache[2]

1. Green Science And Engineering Division, Graduate School Of Science And Technology, Sophia University, 2. Department of Materials & Sciences, Faculty of Science & Technology, Sophia University

Abstract

Carbon disulfide (CS_2) is an atmospheric trace gas whose main sources in the atmosphere are from oceans and soils (Khalil et al., 1984). Anthropogenic emissions have increased in recent years, producing a strong regional distribution. CS_2 is a reactive atmospheric sulfur gas, and as such it has a relatively short lifetime, ranging from a few days to half a month (Khan et al., 2017). Its oxidation end products in the atmosphere are carbonyl sulfide (COS) and sulfur dioxide (SO_2). Therefore, CS_2 indirectly contributes to the production of sulfate aerosols, which influence atmospheric radiative properties and stratospheric ozone depletion.

The OH-initiated oxidation of CS_2 in the presence of O_2 is considered to be the main CS_2 sink pathway. By forming an intermediate SCSOH at first, followed by a series of oxidation reactions with O_2 to produce COS and SO_2, this process removes 75~88% of atmospheric CS_2 (Khan et al., 2017). The current literature suggests that the conversion ratio of CS_2 to COS is 0.83 (Stickel et al., 1993), but this result may be underestimated because only reaction with OH radicals considered and CS_2 photochemistry is neglected.

The mechanism of CS_2 photooxidation was first proposed by Wine et al. (1981). According to the CS_2 UV-Vis absorption spectrum, there is a strong absorption band at 280~360 nm, which would first photo excite CS_2 from ground state to $CS_2(^3A_2)$ state (usually presented as CS_2^* state). Then the majority of CS_2^* particles will be de-excited into CS_2 ground state molecules after collision with air molecules (N_2, O_2 and H_2O). Because of the rapid photochemical reaction rate of CS_2, a small portion of CS_2^* is oxidized with O_2 to produce COS and SO_2 during the pseudo-steady state process of continuous CS_2 photo excitation reaction and CS_2^* quenching reaction. In addition, the solar flux spectrum in the troposphere is strong enough to trigger the above CS_2 photochemistry.

In this study, an updated CS_2 photochemical network is studied by a 1-D atmospheric photochemical model (PATMO). Reaction path analysis is carried out using an open-source reaction network viewer (ReNView). From the simulated result, major reduced sulfur species (CS_2, COS and SO_2) reproduce field measurements. When the zenith angle of sunlight is 0°, our result shows that the conversion ratio of CS_2 to COS is 0.87. The reaction rate *r* for the net CS_2 photo-induced oxidation and CS_2 + OH reactions at 1 km are about 18 and 144 molecule cm^{-3} s^{-1} respectively. These results indicate that, under favorable light conditions photochemistry is a relevant tropospheric sink of CS_2.

References

Khalil, M. and Rasmussen, R. (1984). Global sources, lifetimes and mass balances of carbonyl 761 sulfide (OCS) and carbon disulfide (CS_2) in the earth’ s atmosphere. *Atmospheric Environment 762 (1967)*, 18(9):1805–1813.

©2021. Japan Geoscience Union. All Right Reserved.

Khan, A., Razis, B., Gillespie, S., Percival, C., Shallcross, D., Global analysis of carbon disulfide (CS2) using the 3-D chemistry transport model STOCHEM, *Aims Environ. Sci. (2017)*, *4*, 484–501.

Stickel, R. E. *et al.* (1993), *Journal of Physical Chemistry*, 97(51), pp. 13653–13661.

Wine, P. H., Chameides, W. L., Ravishankara, A. R., Potential role of CS2 photooxidation in tropospheric sulfur chemistry, *Geophys. Res. Lett. (1981)*, *8*, 543-546.

Keywords: CS2, Photochemistry, Modeling, PATMO, Sulfur chemistry

©2021. Japan Geoscience Union. All Right Reserved.

Effects of hydroxyl radical exposure on chemical composition of secondary organic aerosol formed from sabinene ozonolysis

*Kei Sato[1,2], Yu Morino[1], Takashi Imamura[1], Yoshizumi Kajii[1,2]

1. National Institute for Environmental Studies, 2. Kyoto University

Sabinene, a bicyclic monoterpene with an exocyclic double bond, is a major monoterpene emitted from Japanese cedar. We investigated OH initiated aging of secondary organic aerosol (SOA) formed from sabinene ozonolysis using a laboratory environmental chamber. SOA mass concentration and f43 and f44 ratios of SOA were monitored by an Aerodyne high-resolution time-of-flight aerosol mass spectrometer, where f43 and f44 are the ratios of *m/z* 43 and *m/z* 44 to total SOA mass, respectively. SOA mass concentration increased immediately after SOA was exposed to OH radicals due to photochemical aging. The f43 ratio, attributed to alcohols, carbonyls, and peroxides, increased only immediately after the start of exposure, whereas the f44 ratio, attributed to carboxylic acids, continuously increased during the exposure. Offline SOA samples collected before and after the exposure to OH radicals were analyzed by a liquid chromatograph negative-mode electrospray ionization mass spectrometer. Major products present in the particle phase were monomeric products, $C_{8\text{-}10}H_{12\text{-}18}O_{3\text{-}6}$, and dimeric products, $C_{17\text{-}19}H_{26\text{-}32}O_{7\text{-}9}$. Monomeric products include sabinic acid, norsabinic acid, and sabinalic acid as reported in previous studies. As a result of exposure to OH radicals highly functionalized eight to nine carbon products increased, whereas dimeric products decreased. Formation of highly functionalized products will be explained by gas phase OH initiated reaction of sabinaketone and nine carbon lactones, major gaseous products formed from sabinene ozonolysis. Decrease in dimeric products will be explained by decomposition of dimeric products due to OH initiated oxidation in the particle phase.

Keywords: Air pollution, Fine particulate matter, Biogenic volatile organic compound, Highly oxygenated molecule, Volatility basis-set model, Intramolecular hydrogen shift

©2021. Japan Geoscience Union. All Right Reserved.

Impact of nighttime aging on optical properties of toluene secondary organic aerosol

*Tomoki Nakayama[1], Kei Sato[2], Sathiyamurthi Ramasamy[2], Takashi Imamura[2], Yoshizumi Kajii[3,2]

1. Nagasaki University, 2. NIES, 3. Kyoto University

Toluene is known as an important precursor of anthropogenic secondary organic aerosol (SOA) in the troposphere. In the atmosphere, toluene is mainly oxidized by OH radical to generate gaseous oxidation products in addition to SOA. Whereas OH aging of the toluene-SOA will be negligible under dark conditions after sunset, a part of these oxidation products in gas-phase and/or SOA can be further oxidized with NO_3 or O_3 even in the nighttime. The SOA generated during OH oxidation of toluene in the presence of NO_x is known to have significant light absorption at the ultraviolet and shorter visible wavelengths (*i.e.*, known as brown carbon) [*e.g.*, Nakayama et al. 2013] and possibly contributes to the radiation balance and photochemical reactions in the atmosphere. In this work, the impact of NO_3 and O_3 aging on wavelength-dependent optical properties of the toluene SOA has been studied.

The SOA was generated during OH oxidation of toluene in the absence of NO_x in a 6 m^3 stainless steel photochemical chamber with Teflon coating. As sources of OH, either of photolysis of H_2O_2 or ozonolysis of tetramethylethylene was used. After enough amounts of SOA were generated, N_2O_5 (precursor of NO_3), O_3, or NO_2 was injected to the chamber under dark conditions. The NO_2 injection experiment was conducted to confirm the possible effects of NO_2 reactions, because both of NO_3 and NO_2 were generated during thermal decomposition of N_2O_5. Temporal variations of the optical properties of the SOA were measured by two photoacoustic spectrometers (absorption and scattering at 375, 405, 532, 781 nm) and a cavity ring-down spectrometer (extinction at 532 nm). Chemical properties and size distributions of SOA were measured by an Aerodyne aerosol mass spectrometer and a scanning mobility particle sizer, respectively. Gaseous reactants and products were monitored by a Fourier transform-infrared spectrometer and a proton transfer reaction time-of-flight mass spectrometer.

Mass concentrations of toluene-SOA were significantly enhanced and nitrocresols and nitrosalicylic alcohols were generated after NO_3 aging, but no clear enhancement was observed after O_3 aging [Ramasamy et al. 2019]. The toluene-SOA did not show light absorption properties at all wavelengths studied before NO_3 or O_3 aging. Significant light absorption was observed after NO_3 aging at 375 and 405 nm, but neither O_3 nor NO_2 additions. Nitro-aromatic compounds such as nitrocresols and nitrosalicylic alcohols generated from cresols during NO_3 aging are considered to be responsible for the observed light absorption. In the presentation, the atmospheric implications of the results will also be discussed.

References

Nakayama, T. et al., Wavelength and NO_x dependent complex refractive index of SOAs generated from the photooxidation of toluene, *Atmos. Chem. Phys.*, 13, 531-545, doi:10.5194/acp-13-531-2013 (2013).
Ramasamy, S. et al., Investigation of dark condition nitrate radical- and ozone-initiated aging of toluene secondary organic aerosol: Importance of nitrate radical reactions with phenolic products, *Atmos. Environ*., 219, 117049, doi:10.1016/j.atmosenv.2019.117049 (2019).

Keywords: Toluene, Secondary organic aerosol, Optical properties, Brown carbon

©2021. Japan Geoscience Union. All Right Reserved.

Volatility of nanoparticles generated from jet engine lubrication oil

*Nobuyuki Takegawa[1], Anna Nagasaki[1]

1. Graduate School of Science, Tokyo Metropolitan University

The characterization of particle emissions from jet aircraft equipped with turbofan engines is an important issue in the assessment of the impacts of aviation on climate and human health. The primary importance of aviation-produced aerosol particles in assessing the climate impacts is the formation of contrail cirrus clouds from black carbon (BC) emitted at aircraft cruising altitudes. In the method for measuring non-volatile particles (assumed to be equivalent with BC) from turbofan engines, a volatile particle remover (VPR) heated to 623 K is generally used to vaporize volatile compounds such as sulfate and organics. Tetracontane (n-$C_{40}H_{82}$) is used as a test compound for evaluating the removal efficiency of volatile particles in VPRs. Recent studies showed that the formation of nanoparticles from jet engine lubrication oil could be an important source of aerosol particles in aircraft emissions under real-world operating conditions (e.g., Fushimi et al. Atmos. Chem. Phys., 19, 6389-6399, 2019). The volatility of nanoparticles composed of jet engine lubrication oil has not been well characterized. The purpose of this study is to investigate the volatility of nanoparticles generated from unburned jet engine lubrication oil (Mobil Jet Oil II) and compare it with those from triacontane (n-$C_{30}H_{62}$) and tetracontane. The particle number fraction remaining downstream of a custom-made evaporation tube was measured for particle diameters of 30 and 50 nm. The temperature of the evaporation tube was varied from room temperature to 673 K, and the temperature dependency of the particle number fraction for jet engine lubrication oil, triacontane, and tetracontane particles was investigated. The results from the laboratory experiments were used for the interpretation of the volatility of aircraft exhaust particles under real-world operating conditions observed at Narita International Airport.

Keywords: Aerosol, Aircraft emission, Jet engine lubrication oil

©2021. Japan Geoscience Union. All Right Reserved.

Vertical structural measures of atmospheric pollutants using XU-S

*Kazuyo Yamaji[1], Tetsuya Miyakoshi[2], Satoshi Komatsu[2], Isao Kanda[3]

1. Kobe University, 2. ShinMaywa Industries, Ltd. , 3. Japan Meteorological Corporation

Vertical profiles of meteorological properties and atmospheric pollutant concentrations and these diurnal patterns were collected by using XU-S (Experimental Unmanned / Utility aircraft by ShinMaywa) over the northeast side of Awaji Island faced to the Osaka bey on early December, 2020, under a drone utilization promotion project by Hyogo prefecture and the New Industry Research Organization.In the early morning of 2nd December, monitoring data of the ground site indicated more chill and ground surface NO and NO_2 concentrations were increased, on the other hand, Oxidant (Ox) concentration became lower in comparison with the other days. Diurnal vertical profiles of O_3 and $PM_{2.5}$ concentrations and meteorological parameters were measured by POM (Personal Ozone Monitor), p-sensor, iMet-XQ2 mounted on XU-S, respectively. In the monitoring launched at 7:00 on 2nd December, atmospheric temperature profile suggested that the ground inversion layer was developed until around 50-100m alt. Meanwhile, O_3 concentrations were very low, less than 10 ppbv up to 50 m alt., but 20-40 ppbv in 50-500 m layers. $PM_{2.5}$ concentrations were around 13 mg/m^3 on the surface and were decreased to around 5 mg/m^3 in the upper layers from 50 m alt. Primary pollutants were trapped in the developed ground inversion layer within 50 m alt., where O_3 concentrations were depressed through the process of the NO titration until the early morning. During the second monitoring launched at 11:00, constructed atmospheric vertical gradient started to be disappearing and the vertical O_3 and $PM_{2.5}$ concentrations were close to constant values up to 500 m alt., respectively. In the afternoon, the atmospheric vertical gradient was mostly disappeared. Comparisons between observed and simulated vertical and diurnal profiles will be conducted to understand the uncertainties of simulated O_3.

Keywords: vertical profiles of atmospheric pollutants, vertical observations by using the fixed-wing unmanned aircraft, ozone, PM2.5

©2021. Japan Geoscience Union. All Right Reserved.

Continuous and multi-wavelength measurement of aerosol extinction coefficient by long-path propagation of LED light at Chiba, Japan

*Ikuya Nishiwaki[1], Hitoshi Irie[2], Nofel D. Lagrosas[1], Hiroaki Kuze[2]

1. Chiba University, 2. Center for Environmental Remote Sensing, Chiba University

It is well recognized that aerosols play a critical role in determining the Earth's radiation budget. Nevertheless, the accurate estimate of their direct and indirect radiative forcing is still challenging due to the complexity of their behavior in the ambient atmosphere. Ground-based remote sensing and optical observations have been conducted to characterize aerosol properties. A sunphotometer has widely been used for measuring the optical thickness of aerosols, but their data availability can be affected by clouds and time (usually daytime only). On the other hand, a visibility meter can provide visibility data and, consequently, aerosol extinction data even under cloudy conditions, whereas its operation is limited to a single wavelength (e.g., 875 nm). A nephelometer can provide aerosol scattering coefficients at multiple wavelengths, though the data often need corrections due to the relative humidity difference between the ambient and instrumental conditions. Under this circumstance, this study proposes a long-path measurement of aerosol extinction coefficients using a three-color, light-emitting diode (LED) light source emitting at 405, 455, and 505 nm. This approach realizes continuous and multi-wavelength observation (both day and night) of aerosol extinction coefficients near the ground surface level. A near-horizontal light path with a round-trip distance of around 600 m has been established inside the campus of Chiba University. A Newtonian telescope with a diameter of 130 mm collimates the LED light and directs it to a retro-reflector set up about 300 m away from the LED. The reflected light is condensed by a 130 mm diameter Newtonian telescope, and the light emitted from the eyepiece is introduced to the center of the optical fiber and detected by a UV-visible spectrometer. To remove background signals especially during the daytime, a square wave modulation to the LED light source is applied. Using this method, background signals are collected when the LED is off. These background signals are subtracted from the signals when the LED is on. With this instrument, test observations were performed from November 27 to December 5, 2020, together with a visibility meter (Vaisala, PWD52), a nephelometer (TSI3563), and a weather monitor. As expected, the raw signal was found to be directly proportional to the visibility but inversely proportional to the scattering coefficient and relative humidity. The extinction coefficient calculated from the visibility using the Koschmeider equation was compared with that derived from our instrument (at 505 nm). While the data from the visibility meter ranged up to 0.0006 km-1[LND1], our instrument indicated significant underestimation. However, their temporal variations were highly correlated (R = 0.88). This also implies that by using the long-path LED light, extinction coefficients for higher visibility (> 35 km) can be estimated.

Keywords: aerosol extinction coefficient, spectrometer, LED

©2021. Japan Geoscience Union. All Right Reserved.

Aerosol type classification of ground-based remote sensing data by k-means clustering

*Hiroyasu Kobayashi[1], Hitoshi Irie[2], Masahiro Momoi[1]

1. Chiba University, 2. Center for Environmental Remote Sensing, Chiba University

Aerosols, microscopic particles suspended in the air, are known to affect climate through their direct effects of scattering and absorbing solar radiation and indirect effects of altering the radiation budget via the role of cloud condensation nuclei. Since the effects on climate are different depending on the type of aerosols, it is important to classify the observation data into aerosol types. SKYNET is an international ground-based remote sensing observation network focusing mainly on aerosol observations by the skyradiometer. Data from more than 100 observation sites are available. This study attempts to develop a k-means clustering algorithm in order to classify normalized aerosol parameters retrieved from skyradiometer observations at SKYNET sites (e.g., complex refractive index, single scattering albedo, and asymmetry parameters) into different aerosol types for characterizing each observation site. To check our developed clustering algorithm and parameters used, we first applied our method to more than 120,000 AERONET data obtained for the past 10 years and compared the results of classification with those from previous studies. Especially for the biomass burning and urban clusters indicated by our method, the sites were classified into almost the same clusters as expected from previous studies, and their mean parameters were also found to be similar. This suggests that our method is reasonable particularly for biomass burning and urban clusters. In addition, our classification results for SKYNET sites will be presented in this presentation.

Keywords: Aerosol classification, SKYNET, Clustering algorithm

©2021. Japan Geoscience Union. All Right Reserved.

Validation of MERRA-2 Reanalysis Aerosol Products Using Ground-based Observations in Phimai, Thailand, and Factors that Affect Aerosol Optical Depth over the Indochina Peninsula

*Takeru Ohno[1], Hitoshi Irie[1], Arlindo M da Silva[2], Ravi C Govindaraju[2]

1. Center for Environmental Remote Sensing, Chiba University, 2. Global Modeling and Assimilation Office, NASA Goddard Space Flight Center, Greenbelt, Maryland

Biomass burning (BB) occurs during the dry season (December–April) over the Indochina Peninsula (ICP), resulting in poor air quality. We validated the Modern-Era Retrospective analysis for Research and Applications, Version 2 (MERRA-2) aerosol optical depth (AOD) and absorption aerosol optical depth (AAOD) data using a sky radiometer, and aerosol extinction coefficient (AEC) data using Multi-Axis Differential Optical Absorption Spectroscopy (MAX-DOAS) at the SKYNET Phimai site (15.18˚N, 102.56˚E) from 2009 to 2019. The validation analysis showed high correlation coefficients for the three MERRA-2 aerosol products. Compared with ground-based observations, the AOD, AAOD, and AEC were underestimated by 17%, 38%, and 62%, respectively. During the dry season, the height of the maximum AEC value near the ground from MERRA-2 was higher than that from MAX-DOAS. This was likely caused by uncertainty in the MERRA-2 model, such as its vertical profile simulation. Therefore, we expect that the validation analysis could contribute to the accuracy of MERRA-2 simulations conducted in regions affected by BB and anthropogenic emissions. We also analyzed factors that influence AOD over northwest ICP (NWIC), northeast ICP (NEIC), and south ICP (SIC) based on the validated MERRA-2 AOD data. Seasonal variation analysis showed that the major drivers of seasonal variation over the three regions were the organic carbon (OC) AOD and sulfate AOD. The OC AOD was dominant during the dry season, accounting for up to 50% of total AOD in March. The sulfate AOD was high throughout the year, accounting for more than 25% of the total AOD. In particular, the sulfate AOD over the NEIC was ~75% of the total AOD from September to November, indicating the strong impact of sulfate transport from China. Negative trends in AOD were found at Phimai and over the NEIC (1.0% and 1.2% $year^{-1}$, respectively).

Keywords: MERRA-2, Biomass Burning, AOD, Indochina Peninsula, Validation , SKYNET

©2021. Japan Geoscience Union. All Right Reserved.

Exploring ground-based aerosol optical properties to improve satellite estimates of surface particulate matter concentrations

*Alessandro Damiani[1], Hitoshi Irie[1], Kodai Yamaguchi[1], Hossain Mohammed Syedul Hoque[2], Tomoki Nakayama[3], Yutaka Matsumi[2], Yutaka Kondo[4]

1. CEReS, Chiba University, 2. Nagoya University, 3. Nagasaki University, 4. National Institute of Polar Research

Estimates of surface-level particulate matter (PM) concentrations from satellites, essential to complement surface network observations over extra-urban regions, mainly rely on the observed aerosol optical depth (AOD). Therefore, it is crucial exploring how column and profile optical properties are related to aerosol concentrations. Since this can be best achieved by using ground-based observations, we analyzed collocated observations of fine particulate matter (PM2.5), ambient black carbon (BC) as well as columnar aerosol optical properties from a skyradiometer and aerosol extinction profiles from multi-axis differential optical absorption spectroscopy (MAX-DOAS), with an emphasis on the ultraviolet (UV) spectral region. After accounting for the influence of the humidity and the different aerosol extinction profiles, we found that the partial column (i.e., the lowest 1 km layer) of the fine fraction aerosol optical depth ($fAOD_{pc}$), obtained by combing skyradiometer and MAX-DOAS retrievals, reproduced the variability of the PM2.5 better than the columnar fAOD. In the same way, although BC dominates the total absorption in the near-infrared (NIR) spectral range, we showed that the partial column aerosol absorption optical depth ($fAAOD_{pc}$) at UV wavelengths was related to the BC variability better than the corresponding column-based estimates. The observed relationship between the $fAAOD_{pc}$ and an estimated BC partial column was reproduced from Modern-Era Retrospective analysis for Research and Applications, Version 2 (MERRA-2) and resulted in an estimate close to a reasonable BC mass absorption cross-section. Overall, our results point to a right consistency among the used datasets and between them and MERRA-2, stress the well-known sensitivity to the aerosol absorption in the UV spectral region, and highlight the efficacy of combined MAX-DOAS & skyradiometer observations. We expect that these findings will allow a more in-depth evaluation of satellite estimates of surface particulate matter concentrations.

Keywords: aerosol, remote sensing, skyradiometer

©2021. Japan Geoscience Union. All Right Reserved.

Development of international air quality and sky research remote sensing (A-SKY) network

*Hitoshi Irie[1], Alessandro Damiani[1], Toshihiko Takemura[2], Thanawat Jarupongsakul[3], Manish Naja[4]

1. Center for Environmental Remote Sensing, Chiba University, 2. Research Institute for Applied Mechanics, Kyushu University, 3. Department of Geology, Faculty of Science, Chulalongkorn University, 4. Aryabhatta Research Institute of Observational Sciences (ARIES)

The international air quality and sky research remote sensing (A-SKY) network has been developed. The idea for this new network comes from simultaneous observations by the multi-axis differential optical absorption spectroscopy (MAX-DOAS) and the skyradiometer. Such unique simultaneous observations are currently in operation at 5 sites, namely, Chiba (Japan), Fukue (Japan), Kasuga (Japan), Phimai (Thailand), and Haldwani (India). The primary objectives of A-SKY are 1) to quantitatively evaluate long-term variations of important trace gases and aerosols and 2) to understand their interaction with climate. Furthermore, the validation of satellite observations, climate model simulations, and data assimilations are also within the scope of the A-SKY activity. Recent findings from each of our improved MAX-DOAS and skyradiometer technologies and their simultaneous observations are highlighted in this talk. For example, the long-term MAX-DOAS observation at Chiba revealed the presence of almost-constant annual variations in the planetary boundary layer ozone concentration from 2013 to 2019, whereas reductions in nitrogen dioxide (NO_2) and formaldehyde (HCHO) concentrations occurred at rates of approximately 6-10%/year. Under such dominant volatile-organic-compounds-limited conditions, the MAX-DOAS-derived concentration ratio of HCHO/NO_2 was found to be below unity for all months. Beside, the partial column (column below an altitude of 1 km) absorption aerosol optical depth at ultraviolet wavelengths derived from the simultaneous MAX-DOAS and skyradiometer observations was found to be correlated well with the surface black carbon mass concentration data. With such new findings, the potential contribution to atmospheric chemistry is discussed.

Keywords: network, MAX-DOAS, skyradiometer, trace gases, aerosols

©2021. Japan Geoscience Union. All Right Reserved.

Prediction of changes in DSS emission using the Earth System Model of the Meteorological Research Institute

*Takashi Maki[1], Taichu Y Tanaka[1], Thomas Sekiyama[1], Mizuo Kajino[1], Naga Oshima[1], Tsuyoshi Koshiro[1]

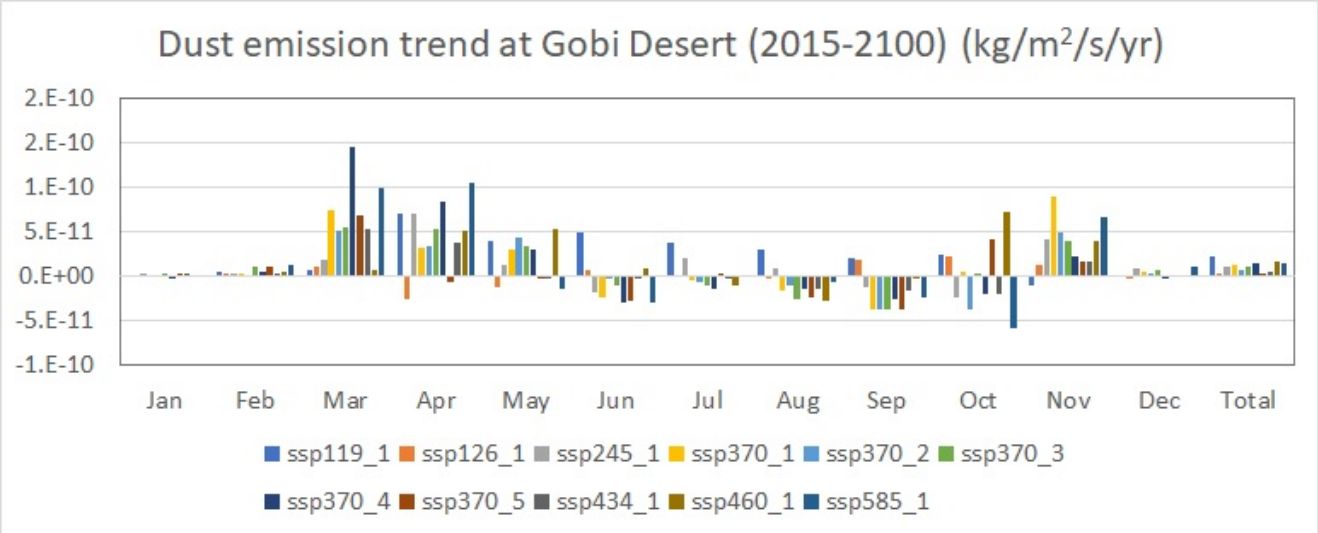
1. Meteorological Research Institute

1. Background
Yellow sand (DSS) is emitted in the arid regions of East Asia and arrives near Japan mainly in the springtime. The impact around Japan is limited to traffic disruptions and impact to people's lives, but near the source of the dust, it can have a significant social and economic impact, including human deaths. DSS is said to affect not only human activities but also climate and weather, and advanced numerical prediction centers are actively conducting tests to introduce aerosols including DSS into numerical models. Although DSS has such important social, economic, and scientific impacts, we do not yet have sufficient knowledge of how the amount of DSS emitted and transported to downstream areas will change with future climate change. This is because the generation of DSS is very sensitive to wind speed near the ground surface and ground surface conditions (snow cover, soil moisture, sand quality, vegetation, etc.), making accurate prediction of these factors extremely difficult. In this study, we attempted to analyze the results of future predictions of DSS emissions and various parameters related to it using the predictions of the Coupled Model Intercomparison Project (CMIP6) of the Earth System Model (MRI-ESM2) developed by the Meteorological Research Institute.
2. Method
MRI-ESM2 (Yukimoto et al., 2019) is an Earth system model that combines various modules such as atmosphere, ocean, land, aerosol, and atmospheric chemistry via couplers. The resolution of MRI-ESM2 in the CMIP6 experiment is TL159 (120 km horizontal grid spacing) for atmosphere, TL95 (180 km horizontal grid spacing) for aerosols, and T42 (280 km horizontal grid spacing) for atmospheric chemistry. The number of ensemble members is 5, and the past reproduction experiments were conducted from January 1850 to December 2014, and after that, 7 different SSP scenario experiments were conducted until December 2100 (of which only SSP370 has 5 ensemble members). The aerosol model is MASINGAR mk-2 (Tanaka et al., 2005), which has been developed by the Meteorological Research Institute. This model treats dust (DSS), sea salt, sulfate, black carbon, and organic aerosols assuming external mixing. For the natural aerosols, dust and sea salt, the model calculates the amount of dust and sea salt emitted based on the various surface conditions calculated by MRI-ESM2. For dust, which is the theme of this study, we adopt a scheme to calculate the amount of dust emission based on parameters such as friction velocity, soil moisture, vegetation, and snow cover.
3.Results and Discussion
The trend of DSS emission amount in the Gobi Desert is shown in Figure 1. Although there was a slight increase in many scenarios and ensembles throughout the entire period, an increasing trend was observed in many experiments during the spring season, which is the main period of DSS emission. In terms of correlations with factors closely related to DSS emission, the correlation with friction velocity was the largest throughout the entire period, and correlations with soil moisture and snow equivalent water were also observed in the spring season (Table omitted). Further analysis of these factors will be conducted and a presentation will be made on the presentation.
4. Acknowledgements
This work was supported by the Environment Research and Technology Development Fund of the Environmental Restoration and Conservation Agency of Japan (5-2001) and JSPS KAKENHI Grant Number

©2021. Japan Geoscience Union. All Right Reserved.

19H04316.

Keywords: Yellow sand (Dust and Sand Storm), Earth system model, Future prediction



©2021. Japan Geoscience Union. All Right Reserved.

Methane emission trends of China in 2009-2018 induced by atmospheric observations

*Fenjuan Wang[1], Shamil S Maksyutov[1], Rajesh Janardanan[1], Akihiko Ito[2], Isamu Morino[1], Yukio Yoshida[1], Yasunori Tohjima[1], Johannes W. Kaiser[3], Greet Janssens-Maenhout[4], xin Lan[5], Ivan Mammarella[6], Jost V. Lavric[7], Tsuneo Matsunaga[1]

1. NIES National Institute of Environmental Studies, 2. Finnish Meteorological Institute, 3. Deutscher Wetterdienst, 4. European Commission Joint Research Centre, 5. Earth System Research Laboratory, 6. University of Helsinki, 7. Max Planck Institute for Biogeochemistry

The reduction of methane emissions of China causes great interest as its significant increase in the last decade. Accuracy quantification of methane budgets of China plays a critical role in implementing national mitigation strategies. In this study, we present top-down estimates of methane emissions of China from 2009-2018 deduced from atmospheric inversions using the high-resolution (0.1° ×0.1°) global inverse model NIES-TM-FLEXPART-VAR. Surface observations, GOSAT retrieval, and a combination of surface observations and GOSAT are used to constrain inversions and the results are compared. Prior fluxes contained the latest Emission Database for Global Atmospheric Research (EDGAR v5) emissions, augmented by biomass burning emissions from the Global Fire Assimilation System (GFASv1.2) and wetland emissions from the Vegetation Integrative Simulator for Trace Gases (VISIT) model. The estimated results are further analyzed for a ten-year period and two five-year periods, which can serve as an independent evaluation of the coming global stock under the Paris Agreement.

Keywords: GOSAT, methane emissions, China, high-resolution inverse model

©2021. Japan Geoscience Union. All Right Reserved.

Characteristics of methane vertical distributions over India

*Dingkun Zhang[1], Naoko Saitoh[1], Dmitry Belikov[1], Prabir Patra[2], Naveen Chandra[3]

1. Center for Environmental Remote Sensing, Chiba University, 2. Japan Agency for Marine-Earth Science and Technology, 3. National Institute for Environmental Studies

Methane, the second most important greenhouse gas after carbon dioxide, accounts for 27% of India's greenhouse gas emissions [Garg et al., 2011]. Methane emissions from South Asia including India have a great contribution to global methane emissions [e.g., Patra et al., 2013]. Chandra et al. [2017] discussed the seasonal variations of methane columns over India by using methane column amounts data from the short-wave infrared (SWIR) band of Thermal and Near-infrared Sensor for Carbon Observation (TANSO)-Fourier Transform Spectrometer (FTS) on board Greenhouse gases Observing SATellite (GOSAT) and simulations by an Atmospheric General Circulation Model-based Atmospheric Chemistry-Transport Model (AGCM-ACTM). In this study, we have analyzed seasonal variations of methane vertical profiles over India by using MIROC4.0-based ACTM (MIROC4-ACTM) [Patra et al., 2018] and GOSAT/TANSO-FTS thermal infrared (TIR) band (hereafter referred as “GOSAT-TIR”).

Following the method proposed by Chandra et al. [2017], we calculated total column methane (XCH_4) and partial column methane ($XpCH_4$) from MIROC4-ACTM σ-pressure coordinates; here, $\sigma = 1.0–0.8$ is defined as Lower Troposphere (LT), $\sigma = 0.8–0.6$ as Mid-Troposphere 1 (MT1), $\sigma = 0.6–0.4$ as Mid-Troposphere 2 (MT2), $\sigma = 0.4–0.2$ as Upper Troposphere (UT), and $\sigma = 0.2–0.0$ as Upper Atmosphere (UA). In the MIROC4-ACTM simulations, two schemes of for emissions from wetlands and rice paddies are adapted [Cao et al., 1996 and Walter et al., 2001].

First, comparisons of XCH_4 and $XpCH_4$ between the Cao and WH schemes showed large differences over India in summer and autumn. Overall, seasonal variations of $XpCH_4$ derived from the Cao schemes of MIROC4-ACTM showed better agreements to the seasonal variations based on GOSAT-TIR than those based on the previous work (AGCM-ACTM) in the three regions over India: Arid India (AI), Eastern Indo-Gangetic Plain (EIGP), and Southern Peninsula (SP). In the UA layer, MIROC4-ACTM $XpCH_4$ values were closer to GOSAT-TIR $XpCH_4$ values in the all three regions. In the LT layer, MIROC4-ACTM $XpCH_4$ values were much higher than $XpCH_4$ values from the other two data in the all three regions. In the MT1 layer, MIROC4-ACTM $XpCH_4$ were closer to $XpCH_4$ in contrast to AGCM-ACTM presented in the previous work in the AI and SP regions. As for the EIGP region, variations in XCH_4 and $XpCH_4$ were relatively large due to variations in elevations, which makes it difficult to draw meaningful conclusions.

Keywords: methane, India, MIROC4-ACTM

©2021. Japan Geoscience Union. All Right Reserved.

Temporal and spatial variations of the mole fraction, carbon and hydrogen isotope ratios of atmospheric methane in the Western Pacific region

*Yasuda Mahito[1], Shinji Morimoto[1], Shuji Aoki[1], Ryo Fujita[2], Taku Umezawa[3]

1. Center for Atmospheric and Oceanic Studies, Graduate School of Science, Tohoku University, 2. Department of Climate and Geochemistry Research, Meterorological Reserach Research Institute, Tsukuba Japan, 3. National Institute for Environmental Studies, Tsukuba, Japan

To understand atmospheric CH_4 variations in the Western Pacific region, we have conducted systematic observations of the CH_4 mole fractions and its carbon and hydrogen isotope ratios ($d^{13}C$ and dD) using air samples collected on board container ships that regularly sail between Japan and Australia/New Zealand. In this study, we analyzed the observation data from 2006 to 2019.
In the temperate zones of both hemispheres, clear seasonal cycles in the CH_4 mole fractions, $d^{13}C$ and dD were observed. Using an atmospheric four-box model with prescribed CH_4 sink, we estimated the contribution of CH_4 sources to the seasonal CH_4 change. The results suggest that the seasonal change in the northern hemisphere is caused by the balance between CH_4 release from biogenic CH_4 sources such as wetlands in summer and CH_4 destruction by the reaction with OH radicals that become maximum also in summer. On the other hand, the seasonal CH_4 change in the southern hemisphere is almost determined by the seasonal changes in the amount of the CH_4 destruction by OH radicals.
In the Western Pacific, the CH_4 mole fractions, $d^{13}C$ and dD showed clear latitudinal gradients, with CH_4 mole fraction increasing and $d^{13}C$ and dD decreasing from south to north throughout a year. These observational facts suggest that there are isotopically lighter CH_4 sources (microbial origin) in the northern hemisphere. The latitudinal distributions of the CH_4 mole fractions and $d^{13}C$ obtained in this study were compared with those observed by the National Oceanic and Atmospheric Administration (NOAA/GMD) at background sites far from CH_4 source region (hereafter called as NOAA sites). During the boreal summer, the CH_4 and $d^{13}C$ in the Western Pacific showed lower and higher values, respectively, compared to those at the NOAA sites, suggesting that the Western Pacific region could be more strongly affected by the destruction by OH radicals. On the other hand, in the boreal winter, the CH_4 mole fractions were higher in the Western Pacific than the background NOAA sites. This would be due to the prevailing westerly winds in the winter season, which transported the air-mass strongly influenced by land CH_4 sources into the Western Pacific region.
The CH_4 mole fractions observed in the Western Pacific, at Syowa Station(69.0˚ S, 39.4˚ E) and Ny-Alesund(78.6˚ N, 11.6˚ E) showed increasing trends after 2006. In contrast, $d^{13}C$ and dD decreased after 2006.We employed the four-box model to investigate the cause of the long-term CH_4 variability. When the CH_4 destruction rate by reaction with OH radical is fixed after 2006, an increase in CH_4 emission after 2006 and decreases in $d^{13}C$ and dD of aggregated CH_4 sources in all latitudinal bands after 2007 are required to reproduce the observed CH_4, $d^{13}C$ and dD values. This suggests that biogenic CH_4 emission has increased since 2006.

Keywords: Methane, Isotopic ratio, Western Pacific

©2021. Japan Geoscience Union. All Right Reserved.

Variations of atmospheric carbon dioxide and its radioisotope in the arctic region

*Hikaru Sekine[1], Shinji Morimoto[1], Chinatsu Yamada[1], Daisuke Goto[2], Masayo Minami[3], Toshio Nakamura[3], Shuji Aoki[1]

1. Center for Atmospheric and Oceanic studies, 2. National Institute of Polar Research, 3. Institute for Space-Earth Environmental Research

To elucidate fossil fuel CO_2 input into the atmosphere, we analyzed temporal variations of CO_2, O_2 and CO concentration and $^{14}CO_2$ at Ny Alesund, Svalbard (79˚N, 13˚E) since 2012. Short-term variations of the atmospheric CO_2 concentration on the scale of hours to days were extracted from the Ny Aleusnd data at first and the durations of higher CO_2 with higher CO and lower O_2 were defined as CO_2 event in this study. Then, using a Lagrangian particle dispersion model and fossil fuel CO_2 emission database, we estimated the amount of CO_2 increase during the CO_2 events and compared it with the observation. As a result, the modeled values well reproduced the observations for the CO_2 events with air mass inflow from European regions, but the modeled values were lower than the observed values for CO_2 events from northern Russia. Using the flask observations of atmospheric $^{14}CO_2$ in the case of the CO_2 event from northern Russia, we estimated that the fossil fuel CO_2 was responsible to the CO_2 event. In order to evaluate the amount and distribution of the CO_2 emission by fossil fuel combustion, continuous observations of CO_2, O_2 and CO and systematic $^{14}CO_2$ observation are valuable.

Keywords: carbon dioxide, global warming, atmospheric observations

©2021. Japan Geoscience Union. All Right Reserved.

Preparation of O_2/N_2 dataset from the surface to the middle stratosphere around Japan traceable to NMIJ gravimetric scale

*Shigeyuki Ishidoya[1], Shinji Morimoto[2], Kazuhiro Tsuboi[3], Satoshi Sugawara[4], Daisuke Goto[5], Nobuyuki Aoki[1], Shohei Murayama[1], Yosuke Niwa[6], Shuji Aoki[2], Hidekazu Matsueda[3], Kentaro Ishijima[3]

1. Advanced Industrial Science and Technology, 2. Tohoku University, 3. Meteorological Research Institute, 4. Miyagi University of Education, 5. National Institute of Polar Research, 6. National Institute for Environmental Studies

Atmospheric delta(O_2/N_2), defined by $[(O_2/N_2)_{sample}/(O_2/N_2)_{ref} -1]x10^6$, has been widely used to evaluate the global CO_2 budget and air-sea O_2 flux (e.g. Manning and Keeling, 2006; Tohjima et al., 2015). However, an absolute value of $(O_2/N_2)_{ref}$ has not been determined by each laboratory with required high-precision, which prevent a direct comparison of the observed delta(O_2/N_2) among the laboratories. To resolve the problem, Aoki et al. (2019) developed O_2, N_2, Ar and CO_2 standard mixtures with sufficient precision (less than 5 per meg in delta(O_2/N_2)) to determine the absolute value of $(O_2/N_2)_{ref}$ traceable to gravimetric scale of National Metrology Institute of Japan (NMIJ/AIST scale). For the direct comparison of delta(O_2/N_2), it is also known that natural and artificial molecular-diffusive fractionations must be considered especially for the aircraft and scientific balloon observations (e.g. Ishidoya et al., 2013, 2014; Stephens et al., 2021). In the present study, we prepare the tropospheric and stratospheric O_2/N_2 dataset around Japan traceable to NMIJ/AIST scale. For this purpose, we corrected an effect of the diffusive fractionations on delta(O_2/N_2) by using the simultaneously measured delta(Ar/N_2) and stable isotopic ratios of N_2, O_2 and Ar. The correction is applied to the air samples collected onboard MD90, B737, CRJ, ERJ and C130 aircrafts (updated from Ishidoya et al., 2012, 2014) and a stratospheric scientific balloon (updated from Ishidoya et al., 2013) over Japan; some air samples were measured by Environmental Management Research Institute of AIST (EMRI/AIST) and the others were by Tohoku University (TU) on their own scales. Then, we converted the corrected delta(O_2/N_2) to the NMIJ/AIST scale based on the inter-comparison experiments using our gravimetric standard mixtures (Aoki et al., 2021). We also applied the scale conversion to the delta(O_2/N_2) observed at some surface stations; Takayama, Minamitorishima and Ryori, Japan (updated from Ishidoya et al., 2017 and our unpublished data). From the prepared delta(O_2/N_2) dataset, we found secular decreasing trends of delta(O_2/N_2) for the period 1999-2020 both for the tropospheric and the stratospheric data, of which change rates were consistent with those reported by Scripps O_2 program (Keeling and Manning, 2014). We also confirmed that the spatial variations in the tropospheric and the stratospheric delta(O_2/N_2) were generally consistent with those expected from the surface O_2 flux and the atmospheric transport. These results suggest that we can compare each laboratory’ s delta(O_2/N_2) values, obtained by analyzing the air samples collected at various observational platforms, with a traceability to NMIJ/AIST.

Acknowledgements

We thank crews and staffs of Japan Airlines and J-Air for their kind cooperation to the air sampling on board MD90, CRJ, B737 and ERJ and staffs of Tohoku University for their works to analyze the air samples. We also thank staffs of Japan Meteorological Agency for their works to collect the air samples on board C130 and maintain the continuous measurements at Minamitorishima and Ryori. We would like to acknowledge many staffs of Japan Ministry of Defense for supporting the C-130H aircraft observation.

©2021. Japan Geoscience Union. All Right Reserved.

This study was partly supported by the JSPS KAKENHI Grant Number 15H02814, 18H03365, 19H01975, 19K03963 and 19K05554, and the Global Environment Research Coordination System from the Ministry of the Environment, Japan (grant nos. METI1454 and METI1953).

Keywords: atmospheric O2/N2 ratio, aircraft observation, scientific balloon, diffusive fractionation of O2 and N2, gravimetric standard gas

©2021. Japan Geoscience Union. All Right Reserved.

Temporal variation of the ozone profile observed with FTIR at Tsukuba

*Isao Murata[1], Hideaki Nakajima[2], Isamu Morino[2], Masanori Takeda[1,2]

1. Graduate School of Environmental Studies, Tohoku University, 2. National Institute for Environmental Studies

Vertical profile of ozone was observed with solar infrared spectroscopy using a Fourier transform spectrometer (FTIR) at Tskuba from 2014 to 2020. SFIT4 spectral fitting program was used to derive the profile. We use the microwindow of 1000.0 - 1005.0 cm^{-1} and parameters recommended by the Network for the Detection of Atmospheric Composition
Change/InfraRed Working Group (NDACC/IRWG). The degrees of freedom for signal (DOFS) is around 5 for this analysis, which means that we can get 5 independent vertical information of the retrieved target gas profile.
Brewer and ozonesonde observations at Tateno were used to validate the retrieved total column and profile for the observation on same days in 2019. Tsukuba site has an advantage, in that the Tateno (JMA’s aerological observatory) is located close to our site. The total columns by FTIR show 4.9 % higher in average than Brewer and the standard deviation is 2.4 %, which agree with Vigouroux, et al.[2008]. This 5 % of bias may due to the uncertainty of the line intensity. After the height resolution matching, the profiles from FTIR and ozonesonde agree within 10% between 18 and 35 km. Comparison for the 15-day (58 spectra) observations shows the FTIR/sonde partial column ratio of 1.02 ±0.05, 1.11 ±0.19, and 1.03 ±0.05 for 0 - 9.8 km, 9.8 - 18.3 km, and 18.3 - 27.7 km, respectively, indicating good agreement within ~10%.
Linear trends were fitted to the temporal variations of total column, partial columns for 0 - 9.8 km, 9.8 - 18.3 km, 18.3 - 27.7 km, and 27.7 - 120 km and all shows negative values between -0.4 and -2.8 % for the period of 2014 - 2020. We don't know why but the total ozone in Japan (Sapporo, Tsukuba, and Naha) observed by Japan Meteorological Agency also shows decrease after 2014. We will investigate the mechanism.

Keywords: FTIR, ozone, height profile

©2021. Japan Geoscience Union. All Right Reserved.

[E] Poster | A (Atmospheric and Hydrospheric Sciences)：A-OS Ocean Sciences & Ocean Environment

Sun. Jun 6, 2021 5:15 PM - 6:30 PM JST | Sun. Jun 6, 2021 8:15 AM - 9:30 AM UTC | Ch.08_1

[A-OS08] Ocean renewable energy: resource, impacts and technologies

convener:Bahareh Kamranzad(The Hakubi Center for Advanced Research/Graduate School of Advanced Integrated Studies in Human Survivability, Kyoto University)

The development of renewable energy technologies is a vital part of mitigating the negative impacts related to the combustion of fossil fuels, such as global warming and climate change. More than 70% of the surface of the Earth is covered by water, and the oceans hold more than 96% of all water on the Earth. In addition, two-thirds of the population of the world live within 100 km of the coast. Hence, ocean renewable energies (such as wave, tidal, current and offshore wind) present a sustainable solution to address current and future demand for electricity, particularly in areas that are adjacent to coastal zones. However, the ocean renewable energy resource is not only affected by intra-annual variability, but also longer-term variability due to changes in the climate. Accordingly, as well as quantifying the available resources, it is also important to assess variability over various time scales such as inter- and intra-annual, decadal, etc. Moreover, development of advanced wave and current energy converters that operate efficiently under various ocean conditions and minimizing the potential environmental impacts is crucial to the success of harvesting ocean renewable energy. The levelized cost of energy (LCOE) of ocean renewable energy has been gradually decreasing due to technology advancement. However, much more effort is required to reduce it more compared to other renewable energy resources. In this session, we welcome presentations across a wide-range of themes related to ocean renewable energy, including resource, impacts and technologies.

[AOS08-P01] FINE SCALE SENSITIVITY MAP OF SEABIRDS FOR OFFSHORE WIND FARM

*Yutaka Watanuki[1], Katsura Mikami[1], Kentaro Kazama[2], Mami T Kazama, Rui Ma[1] (1.Faculty of Fisheries Sciences, Hokkaido University, 2.School of Human Sciences, Waseda University)

FINE SCALE SENSITIVITY MAP OF SEABIRDS FOR OFFSHORE WIND FARM

*Yutaka Watanuki[1], Katsura Mikami[1], Kentaro Kazama[2], Mami T Kazama, Rui Ma[1]

1. Faculty of Fisheries Sciences, Hokkaido University, 2. School of Human Sciences, Waseda University

Development of infrastructure of renewable energy in the ocean is one of urgent issues in Japan. One option is wind farm. Before construction of offshore wind farms, assessments of the impact on marine wildlife are essential but have not been fully investigated. A number of seabirds are known to hit the blades and avoid the area of wind farms. Therefore, potential risks of collision and displacement have been a concern for planning of offshore wind farms. Mapping the fine scale sensitivity of species of seabirds is required most urgently. Recently Environmental Agency provides sensitivity map of seabirds basing on the location of colonies, foraging distance, and density along transects made by air plain. The map is globally useful but resolution is not accurate enough for planning the setting of the each windmill.

To explore environmental factors that increase the possibility of collision and displacement risk at fine scale, we 3D GPS tracked, at 1s to 15 min intervals, 117 Black-tailed gulls *Larus crassirostris* that nested in six colonies in two areas in northern Hokkaido in 2016 –2019. With GPS position moving speed was calculated. Birds were assumed to fly when they moved faster than 15 km/h and to sit on the water so feed or rest when they moved slower than this criterion. Detailed body movement measured by accelerometers on 5 of these birds confirmed this criterion was reliable.

With these data, we constructed spatial model explaining the time of flying, especially at the altitude of 20-140m height of blades and time of sitting water (feeding or resting), at 1km spatial scale to evaluate the risk of collision and displacement, respectively. Although the environmental factors and its effect size varied between colonies, Black-tailed Gulls showed higher risk of collision near the colony, shallow sea depth and near the coast line. The gulls showed higher risk of displacement in grid cells distant from the colony, with relatively cold water, with larger number of fishing ports in general. Thus areas with high risk of collision and those of displacement differed often.

Accuracy of the model was relatively high ($r>0.6$) and well predicted the distribution of birds from the own colony and year. However, a model constructed in a colony each year was hardly applicable to the other colonies in different years. This indicates that the sensitivity map made for a colony by this procedure can’ t be expanded easily to the other regions. Nevertheless with some sampling effort at major colonies, we made fine scale sensitivity map of Black-tailed Gulls over northern Honshu and Hokkaido.

Keywords: Habitat modelling, Biologging, collision risk

©2021. Japan Geoscience Union. All Right Reserved.

[J] Oral | A (Atmospheric and Hydrospheric Sciences)：A-HW Hydrology & Water Environment

Sun. Jun 6, 2021 9:00 AM - 10:30 AM JST | Sun. Jun 6, 2021 12:00 AM - 1:30 AM UTC | Ch.12 Zoom Room 12

[A-HW23] Isotope Hydrology 2021

convener:Masaya Yasuhara(Rissho Univ.), Kohei Kazahaya(Geological Survey of Japan, AIST), Shinji Ohsawa(Institute for Geothermal Sciences, Graduate School of Science, Kyoto University), Kazuyoshi Asai(Geo Science Laboratory), Chairperson:Masaya Yasuhara(Rissho Univ.), Takashi Nakamura(International Research Center for River Basin Environment, University of YAMANASHI), Kazuyoshi Asai(Geo Science Laboratory), Shinji Ohsawa(Institute for Geothermal Sciences, Graduate School of Science, Kyoto University)

The purpose of the session is to review the present state of knowledge of isotope hydrology, by bringing together hydrologists, geologists, volcanologists, geochemists, agronomists, ecologists, engineers and so on.

9:00 AM - 9:05 AM JST | 12:00 AM - 12:05 AM UTC

[AHW23-01] Introduction

9:05 AM - 9:30 AM JST | 12:05 AM - 12:30 AM UTC

[AHW23-02] Seasonal and spatial variations of chemical weathering in the Mekong Basin: From the headwaters to the lower reaches

★Invited Papers

*Hiroto Kajita[1], Yuki Ota[2], Toshihiro Yoshimura[3], Daisuke Araoka[2], Takuya Manaka[4], Ziyu Ouyang[1], Shinya Iwasaki[3], Takuya Yanase[1], Akihiko Inamura[2], Etsuo Uchida[5], Hongbo Zheng[6], Qing Yang[6], Ke Wang[1], Atsushi Suzuki[2], Hodaka Kawahata[1] (1.The University of Tokyo, 2.National Institute of Advanced Industrial Science and Technology, 3.Japan Agency for Marine-Earth Science and Technology, 4.Forestry and Forest Products Research Institute, 5.Waseda University, 6.Yunnan University)

9:30 AM - 9:45 AM JST | 12:30 AM - 12:45 AM UTC

[AHW23-03] Stable Isotope Dynamics of Hydrological Interactions in The Chao Phraya River System in Thailand

*Jeerapong Laonamsai[1], Kimpei Ichiyanagi[1] (1.Deaprtment of Earth and Environmental Sciences, Graduate School of Science and Technology, Kumamoto University)

9:45 AM - 10:10 AM JST | 12:45 AM - 1:10 AM UTC

[AHW23-04] Groundwater in the area where ground flow with long displacement occurred due to the 2018 Sulawesi Island Earthquake in Indonesia

★Invited Papers

*Susumu Yasuda[1], Hisashi Furuichi[2] (1.Tokyo Denki University, 2.Yachiyo Engineering Co., Ltd.)

10:10 AM - 10:25 AM JST | 1:10 AM - 1:25 AM UTC

[AHW23-05] The formation of a temporary pond, Akaike, at the Northern Foot of Mount Fuji, Japan, in 2020

*Shinya Yamamoto[1], Takashi Nakamura[2], Seongwon Lee[3], Masaya Yasuhara[3] (1.Mount Fuji Research Institute, Yamanashi Prefectural Government, 2.International Research Center for River Basin Environment, University of Yamanashi, 3.Faculty of Geo-Environmental Science, Rissho University)

10:25 AM - 10:30 AM JST | 1:25 AM - 1:30 AM UTC

[AHW23-06] Discussion

[J] Oral | A (Atmospheric and Hydrospheric Sciences) | A-HW Hydrology & Water Environment

[A-HW23] Isotope Hydrology 2021

convener:Masaya Yasuhara(Rissho Univ.), Kohei Kazahaya(Geological Survey of Japan, AIST), Shinji Ohsawa(Institute for Geothermal Sciences, Graduate School of Science, Kyoto University), Kazuyoshi Asai(Geo Science Laboratory), Chairperson:Masaya Yasuhara(Rissho Univ.), Takashi Nakamura(International Research Center for River Basin Environment, University of YAMANASHI), Kazuyoshi Asai(Geo Science Laboratory), Shinji Ohsawa(Institute for Geothermal Sciences, Graduate School of Science, Kyoto University)

Sun. Jun 6, 2021 9:00 AM - 10:30 AM Ch.12 (Zoom Room 12)

The purpose of the session is to review the present state of knowledge of isotope hydrology, by bringing together hydrologists, geologists, volcanologists, geochemists, agronomists, ecologists, engineers and so on.

9:00 AM - 9:05 AM

[AHW23-01]Introduction

©Japan Geoscience Union

Seasonal and spatial variations of chemical weathering in the Mekong Basin: From the headwaters to the lower reaches

*Hiroto Kajita[1], Yuki Ota[2], Toshihiro Yoshimura[3], Daisuke Araoka[2], Takuya Manaka[4], Ziyu Ouyang[1], Shinya Iwasaki[3], Takuya Yanase[1], Akihiko Inamura[2], Etsuo Uchida[5], Hongbo Zheng[6], Qing Yang[6], Ke Wang[1], Atsushi Suzuki[2], Hodaka Kawahata[1]

1. The University of Tokyo, 2. National Institute of Advanced Industrial Science and Technology, 3. Japan Agency for Marine-Earth Science and Technology, 4. Forestry and Forest Products Research Institute, 5. Waseda University, 6. Yunnan University

Chemical weathering in the Himalayan river basins is among the highest in the world and has received vast research attention related to past climate change. Many early estimates of chemical weathering are based on a small number of water property data, that ignore those spatial and seasonal variations. Therefore, this study analyzed spatial and seasonal variations in chemical weathering in the Mekong River, where the geology, climate, and hydrologic cycle of the basin vary significantly from the lower to upper reaches, and from dry to rainy seasons. We separately estimated the origins of dissolved elements and potential CO_2 consumption rates using the numerous chemical compositions of river water throughout the entire basin and in both seasons. The CO_2 consumption rate in the rainy season is three to five times that in the dry season, which may be due to the high temperature and precipitation. Despite the low temperatures and dryness of the upper and middle basins, the CO_2 consumption rate is approximately twice that in the lower reaches; this can be attributed to active physical denudation in steep mountainous areas which increases the surface area for water-rock interactions. The total CO_2 consumption obtained by combining each season and basin was 48~70*10^9 mol/a and 148~159*10^9 mol/a for silicate and carbonate weathering, respectively, which are almost half the values of previous estimates. Our results suggest that seasonally and spatially separated evaluations are important for generating estimates of chemical weathering in large Himalayan rivers.

Keywords: Mekong River, Chemical weathering, Carbon cycle, Seasonal variation, Spatial variation

©2021. Japan Geoscience Union. All Right Reserved.







©2021. Japan Geoscience Union. All Right Reserved.

Stable Isotope Dynamics of Hydrological Interactions in The Chao Phraya River System in Thailand

*Jeerapong Laonamsai[1], Kimpei Ichiyanagi[1]

1. Deaprtment of Earth and Environmental Sciences, Graduate School of Science and Technology, Kumamoto University

The present study focuses on a detailed seasonally varying interaction study and flux quantification between the river and monsoon precipitation and groundwater in the Chao Phraya River system which is the main river system that feeds an enormous population. Contributing parameters to the total river discharge on a temporal scale are estimated through three-component hydrograph separation and end-member mixing analysis using high-resolution water isotope ($\delta^{18}O$ and $\delta^{2}H$). This model reports groundwater discharge in the river to be the highest in monsoon (30%), whereas the contribution lowers to 15% during the dry season. During peak monsoon, the monsoon precipitation directly generates river runoff which is also justified using isotopic amplitude damping approach of both river water and precipitation. The mean water transit time is about 26 days. Furthermore, hydrological interaction reflects quantitative variability depending on river morphometry. The current study also provides insight into aquifer vulnerability due to chemical mixing through interaction and reasonable water resources management efforts.

Keywords: Hydrology, Isotopic interactions, Tropical catchment, Water transit time

©2021. Japan Geoscience Union. All Right Reserved.

Groundwater in the area where ground flow with long displacement occurred due to the 2018 Sulawesi Island Earthquake in Indonesia

*Susumu Yasuda[1], Hisashi Furuichi[2]

1. Tokyo Denki University, 2. Yachiyo Engineering Co., Ltd.

The earthquake that struck Sulawesi, Indonesia on September 28, 2018 caused flow of the ground with long displacement in several areas in Palu City. A large amount of groundwater also spouted out with the earthquake. Similar damage has occurred in the past in this area, and it is called "Nalodo". For the purpose of elucidating the mechanism of damage and disaster prevention in the future, JICA has been studying it as part of the investigation of " Project for Development of Regional Disaster Risk Resilience Plan in Central Sulawesi in the Republic of Indonesia", and the authors have participated in it. So, we would like to report based on the study report by JICA[1)].

This area is the triple junction of the three plates and rotates clockwise. This causes a Palu-Koro left strike-slip fault, the displacement rate of which is very fast. A long and narrow pull-apart sedimentary basin is formed between the faults from north-northwest to south-southeast. The Palu River runs from south to north in the center, and gently sloping grounds of 1 to 3% spreads from the river to both sides. There is a hot spring near the area where Nalodo occurred.

Due to the earthquake, surface soil with a length of 1 to 3 km and a width of several hundred meters slipped and flowed toward the downstream side on the gently sloping ground in one area on the west side and four areas on the east side. According to interviews with several residents in and near Narodo, (1) a large vertical shaking and swelling occurred at the same time as the horizontal shaking of the earthquake ended, and (2) groundwater spouted and the ground started to flow at the same time as the horizontal shaking ended or within about 2 minutes. There was also testimony that hot water spouted out in some sites.

In the area where Nalodo occurred, spring belts crossed in the north-south direction before the earthquake. In order to study the origin of this spring, groundwater was sampled from the spring belts and others to test water quality. However, several months have passed since the earthquake, and the groundwater spouted by the earthquake has not been collected. Water was sampled at 29 locations, including springs in Nalodo, boring holes, a hot spring resort, deep wells, shallow wells, and rivers. A total of 37 samples were collected. Of these, 2 samples of spring water in the hot spring resort and 2 samples of deep wells are hot water with a temperature above 40 ˚C. When the results were shown by the relationship between the oxygen isotope ratio $\delta^{18}O$ and the hydrogen isotope ratio δD (δ diagram), they were plotted on the meteoric water line except for three points. On the other hand, the water of the hot spring is plotted to the right of the meteoric water line, and if it is extended, it will be between the “Arima-type” slab-related deep-seated fluid and the paleo-seawater (Yasuhara, personal communication). The other two points were spring water from a Nalodo and water from a deep well (120 m), which were plotted between the hot spring water and the meteoric water line.

It is thought that the groundwater spouted just after the shaking generated long-displacement flow. There are three possible eruption mechanisms: (1) the shallow ground is liquefied and groundwater is ejected, (2) the shallow groundwater flowing from the mountains spouted out, and (3) the pressurized deep groundwater in the fault fracture zones erupted. However, although various ground surveys and analyzes

©2021. Japan Geoscience Union. All Right Reserved.

have been conducted, it is complicated and no conclusion has been reached yet.

Reference 1) JICA : Project for Development of Regional Disaster Risk Resilience Plan in Central Sulawesi in the Republic of Indonesia / Japanese support committee for liquefaction - landslide (inland) / Technical Report / (in progress).

Keywords: groundwater, earthquake, flow of the ground, fault

©2021. Japan Geoscience Union. All Right Reserved.

The formation of a temporary pond, Akaike, at the Northern Foot of Mount Fuji, Japan, in 2020

*Shinya Yamamoto[1], Takashi Nakamura[2], Seongwon Lee[3], Masaya Yasuhara[3]

1. Mount Fuji Research Institute, Yamanashi Prefectural Government, 2. International Research Center for River Basin Environment, University of Yamanashi, 3. Faculty of Geo-Environmental Science, Rissho University

Akaike is a small, temporary pond that appears about 1 km east of Lake Shoji following heavy precipitation events at the northern foot of Mt. Fuji. It is widely accepted that the pond is connected to Lake Shoji by groundwater. However, such a connection has not yet been established because of the lack of water quality and isotopic data from both the Akaike Pond and Lake Shoji. In this study, we measured the major dissolved ion and trace element contents, the hydrogen (dD) and oxygen ($d^{18}O$) stable isotope ratios of water, and the nitrogen and oxygen stable isotope ratios of nitrate ions in water samples from the Akaike Pond in July 2020, and compared these data with surface water and precipitation samples collected from the surrounding area to identify the source of Akaike Pond water. The water qualities and isotopic compositions of Akaike Pond are clearly different from those of Lake Shoji, and showed close proximity in the dD and $d^{18}O$ values to the precipitation. These results suggest that the water in the Akaike Pond is likely derived from recent precipitation. The major dissolved ion compositions in the Akaike Pond showed lower Ca^{2+} and HCO_3^- concentrations than the water samples around the pond. This suggests that the water in the Akaike Pond accumulates in a relatively short period (within a few days) after precipitation, without deep underground percolation.

Keywords: Mount Fuji, temporary pond, water quality, stable isotopes

©2021. Japan Geoscience Union. All Right Reserved.



©2021. Japan Geoscience Union. All Right Reserved.

[J] Oral | A (Atmospheric and Hydrospheric Sciences) | A-HW Hydrology & Water Environment

[A-HW23] Isotope Hydrology 2021

convener:Masaya Yasuhara(Rissho Univ.), Kohei Kazahaya(Geological Survey of Japan, AIST), Shinji Ohsawa(Institute for Geothermal Sciences, Graduate School of Science, Kyoto University), Kazuyoshi Asai(Geo Science Laboratory), Chairperson:Masaya Yasuhara(Rissho Univ.), Takashi Nakamura(International Research Center for River Basin Environment, University of YAMANASHI), Kazuyoshi Asai(Geo Science Laboratory), Shinji Ohsawa(Institute for Geothermal Sciences, Graduate School of Science, Kyoto University)

Sun. Jun 6, 2021 9:00 AM - 10:30 AM Ch.12 (Zoom Room 12)

The purpose of the session is to review the present state of knowledge of isotope hydrology, by bringing together hydrologists, geologists, volcanologists, geochemists, agronomists, ecologists, engineers and so on.

10:25 AM - 10:30 AM

[AHW23-06]Discussion

©Japan Geoscience Union

[J] Oral | A (Atmospheric and Hydrospheric Sciences)：A-HW Hydrology & Water Environment

Sun. Jun 6, 2021 10:45 AM - 12:15 PM JST | Sun. Jun 6, 2021 1:45 AM - 3:15 AM UTC | Ch.12 Zoom Room 12

[A-HW23] Isotope Hydrology 2021

convener:Masaya Yasuhara(Rissho Univ.), Kohei Kazahaya(Geological Survey of Japan, AIST), Shinji Ohsawa(Institute for Geothermal Sciences, Graduate School of Science, Kyoto University), Kazuyoshi Asai(Geo Science Laboratory), Chairperson:Kazuyoshi Asai(Geo Science Laboratory), Masaya Yasuhara(Rissho Univ.), Noritoshi Morikawa(Geological Survey of Japan, AIST), Kohei Kazahaya(Geological Survey of Japan, AIST)

The purpose of the session is to review the present state of knowledge of isotope hydrology, by bringing together hydrologists, geologists, volcanologists, geochemists, agronomists, ecologists, engineers and so on.

10:45 AM - 11:10 AM JST | 1:45 AM - 2:10 AM UTC

[AHW23-07] Supply processes of dissolved inorganic carbon and flow system of groundwater in Fukui-Ohno Basin

★Invited Papers

*Yamanaka Masaru[1], Seongwon Lee[2], ZHAO MINGZHE[1], Takanori Nakano[3] (1.Department of Earth and Environmental Sciences, College of Humanities and Sciences, Nihon University, 2.Rissho University, 3.The Research Institute for Humanity and Nature)

11:10 AM - 11:25 AM JST | 2:10 AM - 2:25 AM UTC

[AHW23-08] Origin and hydro-chemical evolution of geothermal waters from Nozawa-Onsen hydrothermal springs in the northern Nagano Prefecture, central Japan

*Shunsuke Akazawa[1], Madhusoodhan Satish-Kumar[2], Naoki Watanabe[3], Cheibany Ould-Elemine[4], Masaki Yuhara[5] (1.Graduate School of Science and Technology, Niigata University, Japan, 2.Department of Geology, Faculty of Science, Niigata University, Japan , 3.Research Institute for Natural Hazards and Disaster Recovery, Niigata University, Japan, 4.Ensero Solutions, Canada, 5.Department of Earth System Science, Faculty of Science, Fukuoka University, Japan)

11:25 AM - 11:40 AM JST | 2:25 AM - 2:40 AM UTC

[AHW23-09] Composition of ammonium nitrogen isotope in Oita Plain, eastern Kyushu Island, Japan

*Takashi Nakamura[1], Kazuhiro Amita[2], Shinji Ohsawa[3] (1.Interdisciplinary Center for River Basin Environment, University of Yamanashi, 2.Research Center for Engineering Science, Akita University, 3.Beppu Geothermal Research Laboratory, Kyoto University)

11:40 AM - 12:05 PM JST | 2:40 AM - 3:05 AM UTC

[AHW23-10] The continuing story of mathmatical modelling for nitrogen pollution analysis in groundwater

★Invited Papers

*Kei Nishida[1], Ken Yokozawa[2], Bijjay Man Shakya[1], Hiroshi Ishidaira[1], Tadashi Toyama[1], Takashi Nakamura[1] (1.Interdisciplinary Centre for River Basin Environment, Interdisciplinary Graduate School, University of Yamanashi, 2.Shizuoka Prefecture)

12:05 PM - 12:15 PM JST | 3:05 AM - 3:15 AM UTC

[AHW23-11] Discussion

Supply processes of dissolved inorganic carbon and flow system of groundwater in Fukui-Ohno Basin

*Yamanaka Masaru[1], Seongwon Lee[2], ZHAO MINGZHE[1], Takanori Nakano[3]

1. Department of Earth and Environmental Sciences, College of Humanities and Sciences, Nihon University, 2. Rissho University, 3. The Research Institute for Humanity and Nature

A combination of carbon stable isotopic compositions, $d^{13}C$, and chemical compositions of groundwater in the lowland of the Fukui-Ohno Basin, FOB, was employed to elucidate supply processes of dissolved inorganic carbon, DIC, and additionally to give some constraints on groundwater flow systems in the FOB. Ca-HCO_3 type groundwater is dominated with relatively high concentrations of Ca^{2+} and HCO_3^-, which can be attributed to weathering processes of anorthite and partially of peridot in the aquifer with partial CO_2 pressure as typically observed in soil. Moreover, $d^{13}C$ values for the CO_2 gas initially equilibrated with DIC in the FOB groundwater are calculated to be -28.6~-22.8‰, indicating that the FOB groundwater has two carbon sources; one is C3 organic material mainly distributed in mountainous area, ≈-28‰, and another is organic materials in lacustrine deposits in the lowland, ≈-15‰. Considering a model calculation that 20~50% of DIC is lacustrine deposit origin, the FOB groundwater is likely composed of two components; 20~50% of penetrated precipitation in the lowland and 50~80% of groundwater which has been recharged mainly in mountainous area and horizontally transported in the aquifer.

Keywords: groundwater, carbon isotope

©2021. Japan Geoscience Union. All Right Reserved.

Origin and hydro-chemical evolution of geothermal waters from Nozawa-Onsen hydrothermal springs in the northern Nagano Prefecture, central Japan

*Shunsuke Akazawa[1], Madhusoodhan Satish-Kumar[2], Naoki Watanabe[3], Cheibany Ould-Elemine[4], Masaki Yuhara[5]

1. Graduate School of Science and Technology, Niigata University, Japan, 2. Department of Geology, Faculty of Science, Niigata University, Japan , 3. Research Institute for Natural Hazards and Disaster Recovery, Niigata University, Japan, 4. Ensero Solutions, Canada, 5. Department of Earth System Science, Faculty of Science, Fukuoka University, Japan

Nozawa-Onsen hydrothermal springs are located between the northern segment in the active fault zone along the western margin of the Nagano basin and the Quaternary Kenashi Volcano that was active during the period from 1.7 to 1.0 Ma at approximately 40 km northeast of Nagano City, central Japan. Geothermal waters have temperatures ranging from 85.4 to 26.4 degree centigrade, pH values from 8.1 to 9.2 and electric conductivity from 47.6 to 149.0 mS/m, which is correlated to the total ion concentration. They are categorized as sodium-sulfate type, even though respective waters have different temperatures and concentrations. In this study we have carried out hydro-chemical and isotopic analyses to better understand the origin and evolution of geothermal waters. The isotopic results of delta O-18 and delta D values reveals that these waters are meteoric in origin. In addition, delta S-34 values of sulfate indicate that volcanic fluids did not contribute to the formation of geothermal waters. Relationship between chloride concentration and water temperature suggest that several waters were diluted with low-temperature groundwater. Variations of sulfate and hydrogen sulfide concentration in these waters can be explained by the precipitation of native sulfur. It is likely that the calcite was removed as precipitates from some geothermal waters during transportation through faults on the basis of the relationship between Sr-87/Sr-86 and Rb-87/Sr-86 ratios. In conclusion, the evolution process of geothermal waters from Nozawa-Onsen hydrothermal springs are closely related to (1) the recharge of meteoric waters to deep zone, (2) dissolution of soluble minerals such as plagioclase, gypsum and pyrite in Neogene sediments, (3) removal of calcite from these waters during transportation through faults, (4) dilution with low-temperature groundwaters around shallow aquifers and (5) precipitation of the small amount of native sulfur near the earth surface.

Keywords: Nozawa-Onsen, Geothermal water, Isotope composition, Hydrological geochemistry, Fault

©2021. Japan Geoscience Union. All Right Reserved.

Composition of ammonium nitrogen isotope in Oita Plain, eastern Kyushu Island, Japan

*Takashi Nakamura[1], Kazuhiro Amita[2], Shinji Ohsawa[3]

1. Interdisciplinary Center for River Basin Environment, University of Yamanashi, 2. Research Center for Engineering Science, Akita University, 3. Beppu Geothermal Research Laboratory, Kyoto University

To identify the composition of ammonium nitrogen isotope in hot spring water, the water samples from hot spring, as well as deep groundwater wells and surface spring, were collected from Oita city in Kyusyu island, Japan. Major dissolved ions were then analyzed from the collected samples, while the ammonium nitrogen isotope from the samples was determined by the ammonium diffusion method (Cao et al., 2018). The Cl^- and NH_4-N concentrations in hot spring samples were detected ranging from 2506 to 19395 mg/L and 14.4 to 53.9 mg/L, respectively. The positive relationship between Cl^- and NH_4-N concentrations (R^2 =0.49) suggests the nitrogen load from deep-seated saline layers. The $d^{15}N\text{-}NH_4$ values of the hot spring range from -2.6 to +2.0 per mil. On the other hand, a relatively high isotopic value (+5.5 per mil) was detected in the groundwater sample collected from a deep tube well. These nitrogen isotope values showed relatively low values in high Cl^- concentration (>13000mg/L) and high values samples in low Cl^- concentrations. Similarly, the highest isotopic values obtained from the collected deep well samples were located close to the end-member of the trend line observed between Cl^- concentration, and $d^{15}N\text{-}NH_4$ values. These results presumably suggest the origin of the ammonium nitrogen in hot spring as mixed water from deep-seated layer and surface layer.

Acknowledgment: This study was financially supported by Grants-in-Aid for Scientific Research (KAKENHI No.19H0199, PM: Takao Hirashima).

Reference: Thi Thuy Hai Cao et al. (2018) Effect of dissolved organic nitrogen contamination on $d^{15}N\text{-}NH^4$ determination in water samples by modification of the diffusion method with gas-phase trapping. Rapid Communications in Mass Spectrometry. DOI: 10.1002/rcm.8091

Keywords: Oita Plain, Hot spring water, Nitrogen isotope in Ammonium

©2021. Japan Geoscience Union. All Right Reserved.

The continuing story of mathmatical modelling for nitrogen pollution analysis in groundwater

*Kei Nishida[1], Ken Yokozawa[2], Bijjay Man Shakya[1], Hiroshi Ishidaira[1], Tadashi Toyama[1], Takashi Nakamura[1]

1. Interdisciplinary Centre for River Basin Environment, Interdisciplinary Graduate School, University of Yamanashi, 2. Shizuoka Prefecture

We will update the results of analysis on groundwater nitrogen pollution in Kathmandu Valley, Nepal.

Keywords: nitrate, stable isotope ratio, microbial reaction, source mixing

©2021. Japan Geoscience Union. All Right Reserved.

[J] Oral | A (Atmospheric and Hydrospheric Sciences) | A-HW Hydrology & Water Environment

[A-HW23] Isotope Hydrology 2021

convener:Masaya Yasuhara(Rissho Univ.), Kohei Kazahaya(Geological Survey of Japan, AIST), Shinji Ohsawa(Institute for Geothermal Sciences, Graduate School of Science, Kyoto University), Kazuyoshi Asai(Geo Science Laboratory), Chairperson:Kazuyoshi Asai(Geo Science Laboratory), Masaya Yasuhara(Rissho Univ.), Noritoshi Morikawa(Geological Survey of Japan, AIST), Kohei Kazahaya(Geological Survey of Japan, AIST)

Sun. Jun 6, 2021 10:45 AM - 12:15 PM Ch.12 (Zoom Room 12)

The purpose of the session is to review the present state of knowledge of isotope hydrology, by bringing together hydrologists, geologists, volcanologists, geochemists, agronomists, ecologists, engineers and so on.

12:05 PM - 12:15 PM

[AHW23-11]Discussion

©Japan Geoscience Union

[J] Poster | A (Atmospheric and Hydrospheric Sciences)：A-HW Hydrology & Water Environment

Sun. Jun 6, 2021 5:15 PM - 6:30 PM JST | Sun. Jun 6, 2021 8:15 AM - 9:30 AM UTC | Ch.08_2

[A-HW23] Isotope Hydrology 2021

convener:Masaya Yasuhara(Rissho Univ.), Kohei Kazahaya(Geological Survey of Japan, AIST), Shinji Ohsawa(Institute for Geothermal Sciences, Graduate School of Science, Kyoto University), Kazuyoshi Asai(Geo Science Laboratory)

The purpose of the session is to review the present state of knowledge of isotope hydrology, by bringing together hydrologists, geologists, volcanologists, geochemists, agronomists, ecologists, engineers and so on.

[AHW23-P01] Detection of slab-derived fluid in saline ground water collected from coastal area of Seto Inland Sea, Japan

★Invited Papers

*Yoko Togo[1], Kohei Kazahaya[1], Yuki Tosaki[1], Masaaki Takahashi[1], Noritoshi Morikawa[1], Hiroshi A Takahashi[1], Yuri Nakamura[1], Akihiko Inamura[1], Hinako Shimizu[1], Hiroyuki Matsuzaki[2] (1.National Institute of Advanced Industrial Science and Technology, 2.University of Tokyo)

[AHW23-P02] Geochemical characteristics and origins of saline groundwater in the southern Boso Peninsula, Chiba, Japan

*Masaya Yasuhara[1], Akihiko Inamura[2], Ryotaro Mabuchi[3], Seongwon Lee[1], Noritoshi Morikawa[2] (1.Rissho University, 2.Geological Survey of Japan, AIST, 3.Out-Sourcing Technology Co., Ltd.)

[AHW23-P03] Isotope and water quality compositions of groundwater in the bedrock and sediment deposits in Kofu basin

*Ruri Isobe[1], Takashi Nakamura[2] (1.Interdisciplinary Center for River Basin Environment, University of YAMANASHI, 2.Interdisciplinary Centre for River Basin Environment, University of YAMANASHI)

[AHW23-P04] The influence of weathering and hydrological cycles on Li isotopic compositions in river water and groundwater of the Ganges–Brahmaputra–Meghna River system in Bangladesh

*Toshihiro Yoshimura[1], Daisuke Araoka[2], Hodaka Kawahata[3], Zakir Hossain[4], Naohiko Ohkouchi[1] (1.Japan Agency for Marine-Earth Science and Technology, 2.National Institute of Advanced Industrial Science and Technology, 3.Atmosphere and Ocean Research Institute, The University of Tokyo, 4.Jashore University of Science and Technology)

[AHW23-P05] Numerical modeling on the spatial distribution of d-excess values in river water in Japan

*Masaaki Takahashi[1], Hinako Shimizu[1], Akihiko Inamura[1], Noritoshi Morikawa[1] (1.The National Institute of Advanced Industrial Science and Technology)

[AHW23-P06] Temporal variation of stable isotopes in precipitation based on the intermittent sampling for 1998-2018 at Tiksi, northeastern Siberia

*Kimpei Ichiyanagi[1], Hotaek Park[2], Masahiro Tanoue[3] (1.Kumamoto University, 2.JAMSTEC, 3.National Institute for Environmental Studies)

[AHW23-P07] Tritium concentration in recent precipitation in central Japan

*Kazuyoshi Asai[1] (1.Geo Science Laboratory)

[AHW23-P08] An isotopic study on the role of groundwater in streamflow generation in the concrete-lined Nomi-gawa river, Ohta Ward, Tokyo, Japan

*Masaya Yasuhara[1], Seongwon Lee[1], Yuki Itoh[2], Akihiko Inamura[3], Noritoshi Morikawa[3], Takashi Nakamura[4] (1.Rissho University, 2.Saitama Agricultural Cooperatives, 3.Geological Survey of Japan, AIST,

4.University of Yamanashi)

[AHW23-P09] Inorganic nitrogen concentrations and nitrogen and oxygen isotope ratios of nitrate in shallow groundwater in an urban area, Shinagawa, Tokyo, Japan

*Yuki Itoh[1], Masaya Yasuhara[2], Seongwon Lee[2], Takashi Nakamura[3], Akihiko Inamura[4] (1.Saitama Agricultural Cooperatives, 2.Rissho Univ., 3.Yamanashi Univ., 4.Geological Survey of Japan, AIST)

Detection of slab-derived fluid in saline ground water collected from coastal area of Seto Inland Sea, Japan

*Yoko Togo[1], Kohei Kazahaya[1], Yuki Tosaki[1], Masaaki Takahashi[1], Noritoshi Morikawa[1], Hiroshi A Takahashi[1], Yuri Nakamura[1], Akihiko Inamura[1], Hinako Shimizu[1], Hiroyuki Matsuzaki[2]

1. National Institute of Advanced Industrial Science and Technology, 2. University of Tokyo

Southwest Japan is a place where slab-derived fluid supplies as hydrothermal fluids in the forearc region, as typified by the Arima hot springs (Kazahaya et al., 2014). In this study, oxygen and hydrogen isotope ratios, Li/Cl, Br/Cl, I/Cl ratios, and iodine isotope ratios of saline groundwater and spring water collected in Hiroshima, Hyogo, and Kagawa prefectures (Shodo-shima) were analyzed to investigate halogen characteristics of slab-derived fluid.

The chlorine concentrations in the groundwater samples ranged from 1760 to 16600 mg/L. Oxygen and hydrogen isotope ratios indicated that the samples from the western area with high chlorine concentrations were mainly seawater, while the samples from the eastern area with low chlorine concentrations were mainly meteoric water. According to Kazahaya et al. (2014), high Li/Cl ratios of groundwater are characteristic of slab-derived fluids. The Li/Cl ratio of groundwater was higher in the eastern area, suggesting the presence of slab-derived fluid. The samples with high Li/Cl ratios were characterized by low Br/Cl ratios and high I/Cl ratios compared to seawater. In addition, iodine isotope ratios ($^{129}I/^{127}I$) showed relatively lower in the eastern region (i.e., older iodine age), suggesting that low iodine isotope ratios are characteristic of slab-derived fluids in this region. The characteristics of halogen ratios and iodine isotope ratios of slab-derived fluids should be investigated and compared in various regions for further investigation.

Keywords: Slab-derived fluid, Halogen, Groundwater

©2021. Japan Geoscience Union. All Right Reserved.

Geochemical characteristics and origins of saline groundwater in the southern Boso Peninsula, Chiba, Japan

*Masaya Yasuhara[1], Akihiko Inamura[2], Ryotaro Mabuchi[3], Seongwon Lee[1], Noritoshi Morikawa[2]

1. Rissho University, 2. Geological Survey of Japan, AIST, 3. Out-Sourcing Technology Co., Ltd.

Ascent of deep-seated saline water toward the ground surface and its mixing with local shallow groundwater and river water has long been recognized to take place in and around the shallow well, *Kanamari Kobo Ido* (Tateyama City) and *Yunotani* (Futtsu City), both in the southern Boso Peninsula, Chiba, Japan. The saline water in this region is characterized by its high chloride ion (Cl^-) concentration of about 5,100-5,800 mg/L and 1,000-1300 mg/L for the *Kanamari Kobo Ido* and *Yunotani*, respectively. The oxygen and hydrogen isotopes, Li/Cl ratio, and $^3He/^4He$ ratio support an assumption that saline water is of see water origin which was subjected to sediment-water solute exchange to a large extent. On the other hand, we attempted to quantify the amount of Cl^- brought to the ground surface from the depth by the ascent of deep-seated saline water. As the result, its Cl^- amount was estimated at about 120 kg/day in November 2019 for the *Kanamari Kobo Ido* and its vicinity. Taking into account the Cl^- concentration of *Kanamari Kobo Ido* groundwater, the volume of deep-seated saline water mixed with river water and shallow groundwater in the area was estimated to be 24 m^3/day.

Keywords: deep-seated saline water, saline water ascent, river water, mixing, chloride ion, isotope

©2021. Japan Geoscience Union. All Right Reserved.

Isotope and water quality compositions of groundwater in the bedrock and sediment deposits in Kofu basin

*Ruri Isobe[1], Takashi Nakamura[2]

1. Interdisciplinary Center for River Basin Environment, University of YAMANASHI, 2. Interdisciplinary Centre for River Basin Environment, University of YAMANASHI

Nationwide, Kofu basin in Japan is well renowned for the presence of natural hot water springs. The extraction depth of the hot water in this basin varies while it is also found that the water is being extracted both from the bedrock and sedimentary deposits. However, the exact mechanism of the groundwater recharge process in this basin is yet unknown. Thus, this study is primarily focused in identifying the isotope and water quality compositions of groundwater in the bedrock and sediment deposits and understand the deep groundwater recharge processes in this basin.

For the purpose of the study, 485 borehole data and 307 hot spring water samples were collected from Kofu basin. The lithological analysis using the boreholes estimated bedrock distribution (granite) from surface to 1000+m deep, extending from the north to the central part of Kofu. The distribution of the deep groundwater isotope showed inverse relationship with topography i.e. altitude effect is found prevalent for isotopic variations. Those results suggest the possibility of mountains as the main area for the groundwater recharge to the basin floor. Thus, the presentation will show the isotope and water quality compositions of groundwater in the bedrock and sediment deposits and find the inter-relation between them.

©2021. Japan Geoscience Union. All Right Reserved.

The influence of weathering and hydrological cycles on Li isotopic compositions in river water and groundwater of the Ganges–Brahmaputra–Meghna River system in Bangladesh

*Toshihiro Yoshimura[1], Daisuke Araoka[2], Hodaka Kawahata[3], Zakir Hossain[4], Naohiko Ohkouchi[1]

1. Japan Agency for Marine-Earth Science and Technology, 2. National Institute of Advanced Industrial Science and Technology, 3. Atmosphere and Ocean Research Institute, The University of Tokyo, 4. Jashore University of Science and Technology

The silicate weathering of continental rocks plays a vital role in determining ocean chemistry and global climate. Spatiotemporal variations in Li isotope ratio (δ^7Li) in terrestrial waters identify regimes of current and past weathering processes. Here we examine (1) monthly dissolved δ^7Li variation in the Ganges River' s lower reaches, and (2) spatiotemporal variation of river water of the Brahmaputra, Meghna rivers, and groundwater in Bangladesh. From the beginning to maximum flood discharges of the rainy season (i.e., from June to September), Li concentrations and δ^7Li in the Ganges River show remarkable changes, with a large influence from the Himalayan sources. However, most Li discharge across the rainy season is a steady-state condition and strongly influenced by the secondary mineral formation in the low-altitude floodplain. For groundwater samples shallower than ~60 m depth, both δ^7Li and Li/Na are highly scattered regardless of the sampling region, suggesting the variable extent of fractionation. For deep groundwater (70–310 m) with a long residence time of about 3,000 to 20,000 years, the lower δ^7Li values indicate more congruent weathering. These results suggest that Li isotope fractionation in rivers and groundwater depends on the timescale of water-mineral interaction, which plays an essential role in determining the isotopic signature of terrestrial Li inputs to the ocean.

Keywords: Weathering, Bangladesh, Lithium isotope ratios, Groundwater, Ganges River

©2021. Japan Geoscience Union. All Right Reserved.

Numerical modeling on the spatial distribution of d-excess values in river water in Japan

*Masaaki Takahashi[1], Hinako Shimizu[1], Akihiko Inamura[1], Noritoshi Morikawa[1]

1. The National Institute of Advanced Industrial Science and Technology

There are many studies on the spatial distribution of δD and δ^{18}O values in river water in Japan, and numerical modeling are also shown. Latitude, altitude, annual mean temperature, distance from the coastline, precipitation amount, etc. are used as topographical and geographical parameters. On the other hand, there are many studies on the spatial distribution of d-excess values (δD−8xδ^{18}O) in river water, such as Katsuyama et al. (2015), but no numerical modeling has been shown, yet. From previous studies on the spatial distribution of d-excess values in river water, it is clarified that it does not depend on latitude, altitude, distance from the coastline, etc., and is also recognized that d-excess values change extremely at the (central) watershed.

This study presents the effect of "summer" and "winter" precipitation amounts on the spatial distribution of d-excess values in river water.

Keywords: river water, d-excess value, spatial distribution, numerical modeling

©2021. Japan Geoscience Union. All Right Reserved.

Temporal variation of stable isotopes in precipitation based on the intermittent sampling for 1998-2018 at Tiksi, northeastern Siberia

*Kimpei Ichiyanagi[1], Hotaek Park[2], Masahiro Tanoue[3]

1. Kumamoto University, 2. JAMSTEC, 3. National Institute for Environmental Studies

Recent global warming affects significant impacts on air temperature and sea ice extent through the atmospheric hydrological cycle in the Arctic region. Stable water isotopes are useful tracer for estimating the moisture source and transportation pathway in the atmospheric hydrological cycle. From 1998 to 2018, daily precipitation samples were intermittently collected at Tiksi, northern Siberia, Russia. Totally 1,519 samples for $\delta^{18}O$ and 1,024 samples for $\delta^{2}H$ were analyzed by the Isotope Ratio Mass Spectrometry (IRMS) by the 10th September 2007 and by the Cavity Ring-Down Spectroscopy (CRDS) after 11th September 2007. At the last JpGU meeting (abstract ID; AHW34-P10), we reported the depleting trend of deuterium excess (d-excess) in precipitation. Comparing with another isotopic data from July 2015 to June 2017 observed at Samoylov Island near Tiksi (Bonne et al., 2020), annual mean values of surface air temperature, $\delta^{2}H$, and $\delta^{18}O$ were matching well. However, annual mean d-excess at Samoylov Island was more than 10‰ higher than the observation at Tiksi. This fact indicates the depleting trend of d-excess at Tiksi might be caused by the insufficient quality check of observation data. Therefore, new quality control method by using relationships between $\delta^{18}O$ or $\delta^{2}H$ in precipitation samples analyzed by the IRMS and surface air temperature at Tiksi were adapted to the samples analyzed by the CRDS. The temperature effects for $\delta^{18}O$ and $\delta^{2}H$ by the IRMS were 0.47‰ and 3.15‰, respectively. Finally, 1,257 samples for $\delta^{18}O$ and 820 samples for $\delta^{2}H$ were selected to calculate monthly mean values. From the monthly mean surface air temperature at Tiksi from 1998 to 2018, long-term increasing trends in March, April, October, and November were significant (0.24-0.42℃/month within 5% statistically significance). Furthermore, the difference in air temperature, evaporation, and 850hPa winds fields between first 5 years (1998-2002) and last 5 years (2014-2018) of the observation period were investigated by using the NCEP reanalysis. The positive anomalies in air temperature, evaporation, and southwesterly (northerly) wind anomalies were found in the northern Siberian continent (along the coast of the Arctic Ocean) in March and April (October and November). On the other hand, the relationships between surface air temperature and $\delta^{18}O$ in precipitation were found only in April (0.50‰/℃) and October (0.73‰/℃) within 5% statistically significance. The difference in temperature effect between April and October might be caused by the difference in moisture source evaporated from land and open water in the Arctic Ocean.

Keywords: isotopic composition, precipitation, northeastern Siberia

©2021. Japan Geoscience Union. All Right Reserved.

Tritium concentration in recent precipitation in central Japan

*Kazuyoshi Asai[1]

1. Geo Science Laboratory

Tritium is a effective age-dating tracer in classifying groundwater into old (>70 y) and young (<70 y) water. Sustainable use of this age tracer requires a long-term record of precipitation tritium concentrations. In this presentation, we will introduce the tritium concentration of monthly precipitation measured in Nagoya City from 2010 to the present.

Keywords: precipitation, tritium, Nagoya city

©2021. Japan Geoscience Union. All Right Reserved.

An isotopic study on the role of groundwater in streamflow generation in the concrete-lined Nomi-gawa river, Ohta Ward, Tokyo, Japan

*Masaya Yasuhara[1], Seongwon Lee[1], Yuki Itoh[2], Akihiko Inamura[3], Noritoshi Morikawa[3], Takashi Nakamura[4]

1. Rissho University, 2. Saitama Agricultural Cooperatives, 3. Geological Survey of Japan, AIST, 4. University of Yamanashi

A role of groundwater in streamflow generation in a concrete-lined urban river was studied for the days of no rainfall from July 2015 to September 2019 in the Nomi-gawa river, Ohta Ward, Tokyo, Japan. Although the entire surface of side walls and riverbed is covered with concrete, groundwater seeps out through discharge pipes on the concrete walls and gaps in the riverbed concrete plates, making a considerable contribution in the river runoff formation. A two-component mixing analysis on the basis of oxygen isotope ratio of water made it clear that this kind of groundwater seepage accounts for in the range between 20% and 30% for the wet season and about 10% for the dry season, of the discharge in the Nomi-gawa river. These estimates are in accordance with those in our previous report (Fujioka et al., 2018) based on electric conductivity of water. The difference of groundwater contribution in the formation of river runoff can be attributed to the different groundwater levels in the vicinity of the river for the wet summer and dry winter seasons.

Keywords: urban river, concrete-lined channel, groundwater seepage, streamflow generation, oxygen isotope of water

©2021. Japan Geoscience Union. All Right Reserved.

Inorganic nitrogen concentrations and nitrogen and oxygen isotope ratios of nitrate in shallow groundwater in an urban area, Shinagawa, Tokyo, Japan

*Yuki Itoh[1], Masaya Yasuhara[2], Seongwon Lee[2], Takashi Nakamura[3], Akihiko Inamura[4]

1. Saitama Agricultural Cooperatives, 2. Rissho Univ., 3. Yamanashi Univ., 4. Geological Survey of Japan, AIST

A geochemical study on shallow groundwater of the densely-populated Kitashinagawa district in Shinagawa City, in the heart of Tokyo was carried out from January 2019 through February 2020, when water samples were collected from 7 shallow wells once every two months. In Kitashinagawa district, despite quite a small area of about 60 m (N-S) by 100 m (E-W), its shallow groundwater represents a wide range of nitrate (NO_3^-) concentration: for example1.6-34.1 mg/L NO_3^- in February 2019 (dry season) and 0.0-34.8 mg/L NO_3^- in July 2019 (wet season). Nitrogen ($d^{15}N$) and oxygen ($d^{18}O$) isotope ratios of nitrate also show a large range of values, about 10-25‰ and 2-20‰ for $d^{15}N$ and $d^{18}O$, respectively. For many wells, the ratio of enrichment of oxygen to nitrogen is found close to 1:2 for $d^{18}O$ and $d^{15}N$ plots, and on $d^{15}N$ vs. ln [NO_3-N] plots they yield a straight line, which can be explained using the Rayleigh equation and is indicative of the occurrence and progress of denitrification. In contrast, some wells fall on a straight line for $d^{15}N$ vs. 1/[NO_3-N] plots, indicating mixtures of two or three sources (water bodies). An overall conclusion is then that nitrate in shallow groundwater in the study area is primarily of sewage leakage origin (Itoh et al., 2020), but its concentration is subject to alternation to a large extent by the denitrification and/or by the mixing with other water bodies such as rainfall infiltration (natural recharge) and water supply leakage with different nitrogen characteristics.

Keywords: densely-populated urban area, shallow groundwater, inorganic nitrogen concentration, nitrogen and oxygen isotopes, mixing, denitrification

©2021. Japan Geoscience Union. All Right Reserved.

[J] Oral | A (Atmospheric and Hydrospheric Sciences)：A-CG Complex & General

Sun. Jun 6, 2021 10:45 AM - 12:15 PM JST | Sun. Jun 6, 2021 1:45 AM - 3:15 AM UTC | Ch.10 Zoom Room 10

[A-CG38] Dynamics of Oceanic and Atmospheric Waves, Vortices, and Circulations

convener:Yuki Tanaka(Faculty of Marine Science and Technology, Fukui Prefectural University), Kunihiro Aoki(Japan Agency for Marine Earth Science and Technology), Yukiharu Hisaki(University of the Ryukyus), Norihiko Sugimoto(Keio University, Department of Physics), Chairperson:Kunihiro Aoki(Japan Agency for Marine Earth Science and Technology), Yukiharu Hisaki(University of the Ryukyus), Yuki Tanaka(Faculty of Marine Science and Technology, Fukui Prefectural University)

Oceanic and atmospheric dynamics aims at abstracting general principles from observed phenomena and constructing a system of mathematical models, thereby leading to the understanding, prediction, and parameterization of those phenomena. It provides perspectives for the advancement of sciences in various areas such as turbulence, wind waves, internal waves, Rossby waves, tides, coastal and equatorial boundary processes, mesoscale and submesoscale eddies, meandering of jets and fronts, general circulation, and ocean-atmosphere coupled modes. It has also been and will continue to be benefited by new uses of ideas and methods from such theories as resonance, nonlinear interaction, stability analysis, spectral analysis, probability, statistics, and dynamical systems. In this session, we solicit presentations on observational, experimental, numerical, and theoretical studies of oceanic and atmospheric dynamics and on exploratory use of new ideas and methods. We also welcome presentations on interdisciplinary studies in fields such as ecosystems, climate, and environment.

10:45 AM - 11:00 AM JST | 1:45 AM - 2:00 AM UTC

[ACG38-01] Toward numerical modeling systems that seamlessly link coastal seas to open oceans

★Invited Papers

*Hiroyasu Hasumi[1] (1.Atmosphere and Ocean Research Institute, The University of Tokyo)

11:00 AM - 11:15 AM JST | 2:00 AM - 2:15 AM UTC

[ACG38-02] Long-term variability of sea level along the coast of Japan during the 20th century reproduced by an eddy resolving model

*Hideyuki Nakano[1], Shogo Urakawa[1], Kei Sakamoto[1], Takahiro Toyoda[1], Goro Yamanaka[1] (1.Meteorological Research Institute)

11:15 AM - 11:30 AM JST | 2:15 AM - 2:30 AM UTC

[ACG38-03] Dynamics of the estern-boundary currents

★Invited Papers

*Ryo Furue[1] (1.APL/JAMSTEC)

11:30 AM - 11:45 AM JST | 2:30 AM - 2:45 AM UTC

[ACG38-04] Impacts of bottom topography on the formation of the North Pacific subtropical-subarctic frontal zone

*Humio Mitsudera[1], Hayato Ashida[2], Toru Miyama[3] (1.Institute of Low Temperature Science, Hokkaido University, 2.Graduate School of Environmental Science, Hokkaido University, 3.JAMSTEC)

11:45 AM - 12:00 PM JST | 2:45 AM - 3:00 AM UTC

[ACG38-05] Stability of a Flow over Bottom Topography: A General Condition and a Linear Analysis in a Two-Layer Quasi-Geostrophic Model

*Yuki Tanaka[1] (1.Faculty of Marine Science and Technology, Fukui Prefectural University)

12:00 PM - 12:15 PM JST | 3:00 AM - 3:15 AM UTC

[ACG38-06] Eddy-mean flow interactions and vertical energy redistribution associated with the standing meander in the Antarctic Circumpolar Current

*Takuro Matsuta[1], Yukio Masumoto[1] (1.Graduate School of Science, The University of Tokyo)

Toward numerical modeling systems that seamlessly link coastal seas to open oceans

*Hiroyasu Hasumi[1]

1. Atmosphere and Ocean Research Institute, The University of Tokyo

Studies on the ocean have traditionally been separated into those on coastal seas and open oceans, and numerical modeling of the ocean has also developed separately. That is because the spatio-temporal scales are significantly different between these two targets. Recent advancement in observational technologies and computers, however, has led studies on open oceans to cover small scale phenomena such as submesoscales. Studies on coastal seas, on the other hand, have becoming to deal with not only individual bays but interactions between bays or with open oceans. Furthermore, the need is growing for such studies that synthetically deal with coastal seas and open oceans due to our awareness of the influence of global warming on human societies and the oceanic environmental problems caused by human activities. In this regard, we need numerical ocean modeling systems that seamlessly link coastal seas to open oceans. Development and application of such systems are attempted by many groups now, but there remain various problems to be solved because of the large difference between the spatio-temporal scales which control each of them. In this presentation, I would like to show my personal view on the objectives, requirements, and problems in “seamless ocean modeling systems”.

Keywords: ocean modeling, seamless modeling

©2021. Japan Geoscience Union. All Right Reserved.

Long-term variability of sea level along the coast of Japan during the 20th century reproduced by an eddy resolving model

*Hideyuki Nakano[1], Shogo Urakawa[1], Kei Sakamoto[1], Takahiro Toyoda[1], Goro Yamanaka[1]

1. Meteorological Research Institute

Long-term changes in sea level along the coast of Japan during the 20th century are characterized by decadal variations: a peak in the 1950s and a decline in the 1980s, followed by a consistent upward trend since 1980s. There are also weak fluctuations of sea level with a period of 10 to 20 years. In order to elucidate the mechanism of these coastal sea level variations, we drive an ocean general circulation model that can reproduce the Kuroshio/Kuroshio Extension and coastal trapped waves (CTWs) using multiple reanalysis data for the 20th century. This is the first experiment that uses an eddy-resolving model forced by reanalysis data for the entire 20th century. Since the effect of adjustment by longshore trapped waves is important in coastal areas, we also condust ideal experiments on CTWs. Although the ocean model is based on the Boussinesq approximation, the sea level rise due to thermal expansion of seawater can be diagnosed by its global mean because its local contribution spreads rapidly around the world. This global average sea level rise has been a major contributor to rising coastal sea levels since the 1980s. Prior to the 1980s, the contribution of the thermal expansion was small, with variations due to the change in wind stress curl dominating. The high coastal sea levels in the 1950s, with similar amplitudes along the northern coast of Honshu and Hokkaido, are found to be caused by the arrival of high sea level anomaly on the eastern coast of Hokkaido and their adjustment by CTWs. Since the 1980s, the sea level variation around Hokkaido is smaller than that of Honshu, except for the contribution of thermal expansion, suggesting that the sea level change around Japan was largely related to the path variability of the Kuroshio Current.

Keywords: coastal sea level rise, Kuroshio/Kuroshio Extension, Eddy resolving model

©2021. Japan Geoscience Union. All Right Reserved.

Dynamics of the estern-boundary currents

*Ryo Furue[1]

1. APL/JAMSTEC

This presentation is mostly a review of the eastern boundary structure with emphasis on the Leeuwin Current System along the west coast of Australia. Some preliminary descriptive results will also be shown about the annual variability of LCS.

Baroclinic coastal Kelvin waves propagate poleward along the eastern boundary of the ocean basin. If there is some forcing along the coast or a flow into or out of the eastern boundary, such as Ekman drift, pressure anomaly is generated and is propagated by the coastal Kelvin wave. This process establishes a coastal current in the wake of the wave.

Equatorward of the critical latitude, however, pressure anomaly along the eastern boundary is carried away offshore by Rossby waves. For this reason, for a narrow current to exist along the eastern boundary, some mechanism is necessary to arrest the propagation of Rossby waves. One potentially powerful mechanism is the bottom slope (topographic beta). The Leeuwin Current (LC), a shallow, permanent, poleward-flowing eastern boundary current anchored to the shelf break, owes its existence to the bottom slope.

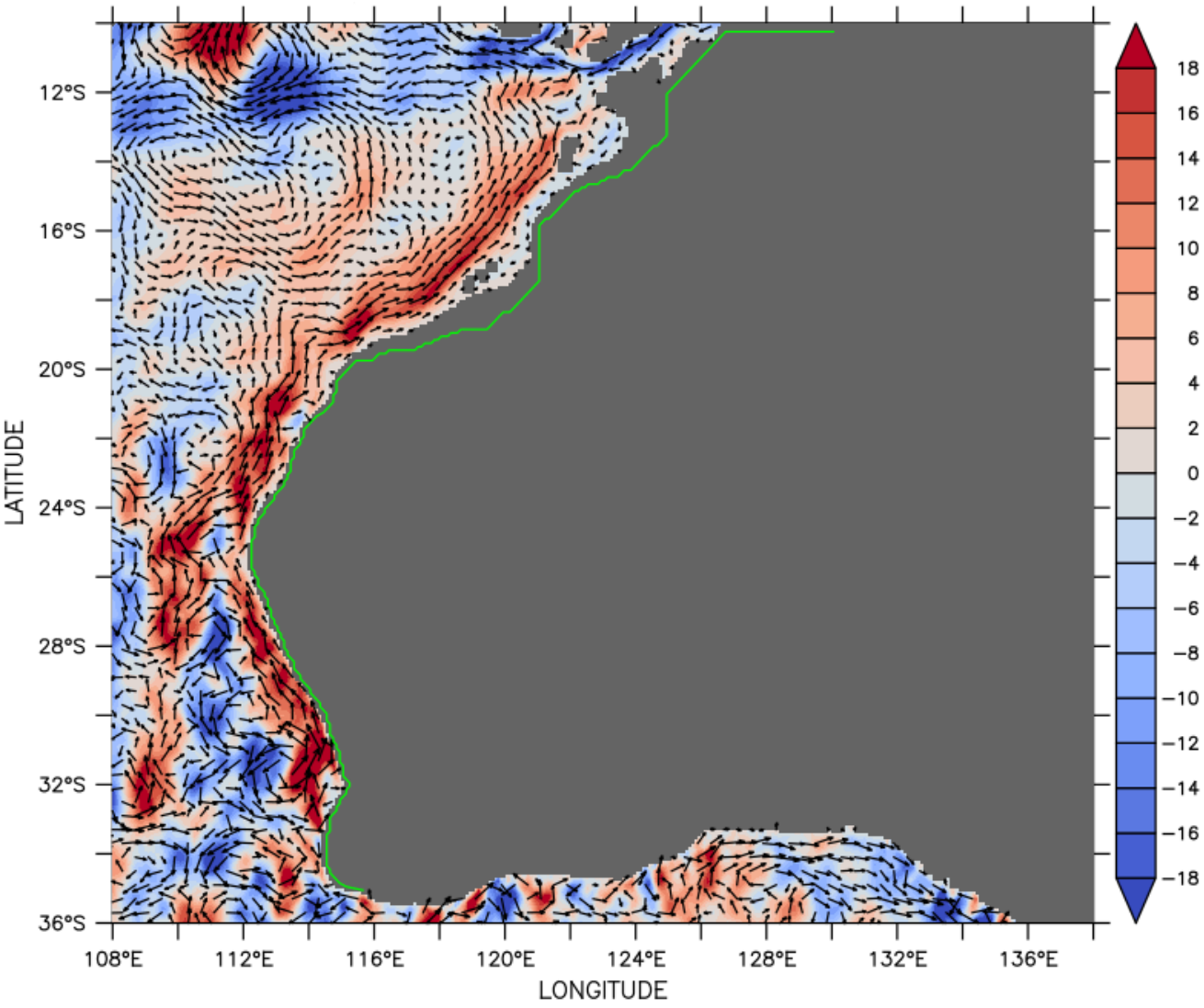
There is a permanent undercurrent flowing equatorward hugging the continental slope beneath the LC. The mechanism of its generation is a mystery. Qualitatively the pair of the LC and the undercurrent looks like a baroclinic mode of the coastal trapped wave. Can such a mode, however, remain trapped against the Rossby waves? If it can, what is the forcing?

There is also variability at various time scales. It is not known whether or not baroclinic variability due to the various modes of coastal trapped waves can remain trapped to the eastern boundary. There have been reports that during its normal annual cycle, the LC sheds eddies when it is strong. This may be a mechanism for the LCS to lose energy into the interior.

The structure of the eastern-boundary current system is crucial to determine the baroclinic structure of the interior ocean as its structure propagates as Rossby waves.

Keywords: coastal trapped waves, planetary Rossby waves, eastern boundary currents, baroclinic flow

©2021. Japan Geoscience Union. All Right Reserved.



©2021. Japan Geoscience Union. All Right Reserved.

Impacts of bottom topography on the formation of the North Pacific subtropical-subarctic frontal zone

*Humio Mitsudera[1], Hayato Ashida[2], Toru Miyama[3]

1. Institute of Low Temperature Science, Hokkaido University, 2. Graduate School of Environmental Science, Hokkaido University, 3. JAMSTEC

The subtropical-subarctic frontal zone in the North Pacific exhibits a complex water mass structure because the water of Kuroshio origin and the water of Oyashio origin are confluent, stirred there and mixed. Despite this complexity, two quasi-stationary fronts form in this region that characterize the frontal zone, which are the subarctic front (SAF), recognized by potential temperature of 4 ℃ contour at a depth of 100 m, and the subarctic boundary (SAB), recognized by salinity of 34 contour at a depth of 100 m; the so-called transition domain forms in between. This frontal zone is generally considered as a wind-driven gyre boundary between the subtropical and subarctic gyres. However, the frontal zone is located around 40 ˚N, which is further south than the location of the Sverdrup gyre boundary that forms at approximately ~45 ˚N. Here, we study the effects of bottom topography on the formation of the subtropical-subarctic frontal zone in the western North Pacific, with a particular attention to the Emperor Seamounts. We conducted an eddy-resolving two-layer modeling with a realistic topography of the ETOPO1, forced by a zonally-averaged wind stress derived from the JRA-55 do. The model exhibits a realistic frontal zone structure of the North Pacific comprising the SAF and SAB, as well as the transition domain. Eddy driven bottom currents are generated over topography, which in turn causes substantial impacts on the formation of upper layer frontal-zone structures. By conducting topography on/off experiments, we found that the Emperor Seamounts bring the subarctic thin layer southward across the Sverdrup gyre boundary. The thinner layer of the subarctic origin and thicker layer of the subtropical origin meet and mix there, leading to the formation of the SAB and the transition domain.

Keywords: subtropical-subarctic frontal zone, Emperor Seamounts, transition domain, quasi-stationary jets

©2021. Japan Geoscience Union. All Right Reserved.

Stability of a Flow over Bottom Topography: A General Condition and a Linear Analysis in a Two-Layer Quasi-Geostrophic Model

*Yuki Tanaka[1]

1. Faculty of Marine Science and Technology, Fukui Prefectural University

Bottom topography is an essential factor that controls the pattern and variability of ocean currents. In the present study, the stability of a two-layer quasi-geostrophic flow over bottom topography is examined by combining a method of obtaining a sufficient condition for stability and a linear stability analysis. First, using a conserved quantity referred to as pseudoenergy that is proportional to the square of the disturbance amplitude, a sufficient condition for stability is derived for the simplest steady background field in which the potential vorticity and the stream function are proportional to each other. The obtained stability condition is unique in that no specific form is assumed for the background field except for the linear relationship between the potential vorticity and the stream function, and that it depends on the minimum possible wavenumber of the disturbance. These features enable us to judge the stability of various background fields by explicitly taking into account the limitation imposed on the disturbance scale by the domain size and/or boundary conditions. Applying the stability condition to a special case of a sinusoidal background field shows that the stable range extends to the area where the currents flow with shallower water on their right in both the upper and lower layers. The stable range is broadened as the disturbance becomes limited to smaller horizontal scales, mainly due to the suppression of barotropic instability which works effectively at large scales. Finally, a linear stability analysis confirms the validity of the stability condition for background fields with a wide range of parameters.

Keywords: Two-Layer Quasi-Geostrophic Flow, Bottom Topography, Stability Theory, Barotropic and Baroclinic Instability

©2021. Japan Geoscience Union. All Right Reserved.

Eddy-mean flow interactions and vertical energy redistribution associated with the standing meander in the Antarctic Circumpolar Current

*Takuro Matsuta[1], Yukio Masumoto[1]

1. Graduate School of Science, The University of Tokyo

A remarkable feature of the Antarctic Circumpolar Current (ACC) is its insensivity to changes in surface forcing. This feature is explained by balances between a wind-driven overturning circulation and an eddy-driven circulation in the zonally averaged framework. However, the residulal mean theories miss the representation of the ACC's heterogeneity in eddy distributions. Active eddy activities are confined near the vicinity of standing meanders associated with the large topography. In this presentation, local eddy-mean flow interactions are discussed from the Lorentz diargram framework using a realistic eddy-resolution model. Our finding is that large amount of the wind energy input is locally dispersed near the standing meanders through baroclinic instability. Eddy energy is generated in the upper 3000m and dispersed near the bottom. This mismatch between the depth of energy production and dispersion is reconciled by the downward vertical energy flux.

Keywords: eddy-mean flow interactions, Antarctic Circumpolar Current, Lorentz diagram, energy flux

©2021. Japan Geoscience Union. All Right Reserved.

[J] Oral | A (Atmospheric and Hydrospheric Sciences)：A-CG Complex & General

Sun. Jun 6, 2021 1:45 PM - 3:15 PM JST | Sun. Jun 6, 2021 4:45 AM - 6:15 AM UTC | Ch.10 Zoom Room 10

[A-CG38] Dynamics of Oceanic and Atmospheric Waves, Vortices, and Circulations

convener:Yuki Tanaka(Faculty of Marine Science and Technology, Fukui Prefectural University), Kunihiro Aoki(Japan Agency for Marine Earth Science and Technology), Yukiharu Hisaki(University of the Ryukyus), Norihiko Sugimoto(Keio University, Department of Physics), Chairperson:Yukiharu Hisaki(University of the Ryukyus), Norihiko Sugimoto(Keio University, Department of Physics), Yuki Tanaka(Faculty of Marine Science and Technology, Fukui Prefectural University)

Oceanic and atmospheric dynamics aims at abstracting general principles from observed phenomena and constructing a system of mathematical models, thereby leading to the understanding, prediction, and parameterization of those phenomena. It provides perspectives for the advancement of sciences in various areas such as turbulence, wind waves, internal waves, Rossby waves, tides, coastal and equatorial boundary processes, mesoscale and submesoscale eddies, meandering of jets and fronts, general circulation, and ocean-atmosphere coupled modes. It has also been and will continue to be benefited by new uses of ideas and methods from such theories as resonance, nonlinear interaction, stability analysis, spectral analysis, probability, statistics, and dynamical systems. In this session, we solicit presentations on observational, experimental, numerical, and theoretical studies of oceanic and atmospheric dynamics and on exploratory use of new ideas and methods. We also welcome presentations on interdisciplinary studies in fields such as ecosystems, climate, and environment.

1:45 PM - 2:00 PM JST | 4:45 AM - 5:00 AM UTC

[ACG38-07] Irreversible energy extraction from negative temperature two-dimensional turbulence

*Yohei Onuki[1] (1.Ocean Modeling Group, Center for Oceanic and Atmospheric Research, Research Institute for Applied Mechanics, Kyushu University)

2:00 PM - 2:15 PM JST | 5:00 AM - 5:15 AM UTC

[ACG38-08] Near-inertial oceanic internal waves observed by LADCP (lowered acoustic Doppler current profiler)

*Katsuro Katsumata[1] (1.JAMSTEC)

2:15 PM - 2:30 PM JST | 5:15 AM - 5:30 AM UTC

[ACG38-09] The pathway of the Indonesian Throughflow transport increase due to tidal mixing

*Shiraishi Takeki[1], Shinichiro Kida[2], Hideharu Sasaki[3], Ryo Furue[3] (1.Kyushu University Interdisciplinary Graduate School of Engineering Sciences, 2.Research Institute for Applied Mechanics, Kyushu University, 3.Application Laboratory , Japan Agency for Marine-Earth Science and Technology)

2:30 PM - 2:45 PM JST | 5:30 AM - 5:45 AM UTC

[ACG38-10] Biogeophysical Interactions in transport of marine organisms

★Invited Papers

*Atsushi Fujimura[1] (1.University of Guam)

2:45 PM - 3:00 PM JST | 5:45 AM - 6:00 AM UTC

[ACG38-11] Wave resolving numerical simulation of non-breaking wave-induced mixing

*Haruka Imamura[1], Yutaka Yoshikawa[1], Yasushi Fujiwara[2] (1.Graduate School of Science, Kyoto University, 2.Graduate School of Frontier Sciences, the University of Tokyo)

3:00 PM - 3:15 PM JST | 6:00 AM - 6:15 AM UTC

[ACG38-12] Origin of swells propagated into small bays on the Sanriku rias coast facing the western North Pacific

*Kosei Komatsu[1,2], Takaki Fujii[3], Kiyoshi Tanaka[2] (1.Graduate School of Frontier Sciences, University of Tokyo, 2.Atmosphere and Ocean Research Institute, University of Toky, 3.Bank of Japan)

Irreversible energy extraction from negative temperature two-dimensional turbulence

*Yohei Onuki[1]

1. Ocean Modeling Group, Center for Oceanic and Atmospheric Research, Research Institute for Applied Mechanics, Kyushu University

Large-scale motions of the atmosphere and ocean are idealized as two-dimensional turbulence. Energy transfer and structure formation of two-dimensional turbulence have attracted attention for a long time, and many past studies have analyzed them within an open domain or surrounded by a fixed lateral boundary. In this study, to extend our understanding of two-dimensional turbulence, we consider a flow system in a bounded domain whose shape is distorted by an externally imposed force. Unlike fixed boundary cases, this system exchanges energy with the external system via pressure work through the moving boundary. At the same time, the flow field is still constrained by vorticity conservation. When the vorticity equation is expanded onto the Laplacian eigenfunctions and truncated at a finite number, it satisfies Liouville's theorem. Consequently, based on energy and enstrophy constraints, a grand-canonical ensemble (GCE) with the temperature either positive or negative sign is defined. Starting from GCE, when one distorts the domain from one to another in a finite time, the Jarzynski equality establishes. The pressure work exerted on the system is thus related to the difference in the Helmholtz free energy. The direction of the inequality derived from the Jarzynski equality depends on the sign of the initial temperature. For a negative-temperature state, the moving boundary irreversibly extracts turbulence energy from the system via pressure work. This peculiar result gives a new interpretation for the inter-scale energy transfer in geophysical flows.

Keywords: Two-dimensional turbulence, Statistical mechanics, Jarzynski equality

©2021. Japan Geoscience Union. All Right Reserved.

Near-inertial oceanic internal waves observed by LADCP (lowered acoustic Doppler current profiler)

*Katsuro Katsumata[1]

1. JAMSTEC

Frequency spectra of oceanic internal waves often show peaks around the inertial frequency of the observed location. These near-inertial waves are ubiquitous as many generation machnisms are possible such as surface wind, ocean currents interacting with bottom topography, and spontaneous break down of eddies. On the other hand, observation data of near-inertial waves are limited because of their intermittency, due partly to the transient and unsteady nature of their generation. The polarisation relationship of the internal wave constrains the particle movements of near-inertial waves within a horizontal plane which makes near-inertial wavs "invisible" to conventional conductivity temperature depth profilers (CTD) observations. Here, we attemp to observe these waves by using lowered acoustic Doppler current profiler (LADCP) used with CTDs in ship-based hydrographic observations. Since the near-inertial waves are peaks, we boldly assume that observed horizontal velocity is inertial waves, superposed upon which are other components (e.g. internal waves at other frequencies and geostrophic flows). At one station, the sensor package passes a depth twice, decent and ascent, giving meridional and zonal components of horizontal velocities each, which enables estimate of amplitude and phase of the inertial wave.
We applied this method to several sections in the Indian Ocean. On a section nominally along 55˚E, one CTD station lasting about 4 hours could capture inertial waves at poleward of about 30˚S where the inertial period is 24 hours. Their group velocity was more often downward than upward, not inconsistent with surface generation. Many had wavelengths longer than 2000 m, suggesting vertical structures of gravest modes. The magnitude was of the order of cm/s. On the other hand, there were unnegligible waves with upward group velocity with depths scatterd around the water column; suggesting contribution from other generation mechanims than wind.

Keywords: oceanic internal waves, inertial waves, ocean observation

©2021. Japan Geoscience Union. All Right Reserved.

The pathway of the Indonesian Throughflow transport increase due to tidal mixing

*Shiraishi Takeki[1], Shinichiro Kida[2], Hideharu Sasaki[3], Ryo Furue[3]

1. Kyushu University Interdisciplinary Graduate School of Engineering Sciences, 2. Research Institute for Applied Mechanics, Kyushu University, 3. Application Laboratory , Japan Agency for Marine-Earth Science and Technology

Indonesian through-flow (ITF) is an ocean current that passes through the Indonesian Seas from the Pacific Ocean to the Indian Ocean. In this area, vertical mixing is believed to be actively excited by the tide because the seafloor topography of the Indonesian Seas is complex. In Sakaki et al. (2018), the presence of a tidal mixing scheme was suggested to increase the ITF transport by 0.88 Sv. However, the mechanism of this increase. The mass balance of the increased transport due to tidal mixing was estimated by dividing the region around the Indonesian Seas into seven sections, such as the Celebes Sea, Makassar Strait, and the Molucca Sea. As a result, it was found that there are two main routes for the ITF increase. The first route is the upwelling that occurs within the Indonesian Seas (lower layer to upper layer). The second route is the upper layer flow from the eastern coast of the Philippines to the Makassar Strait. This second route is likely induced by tidal mixing that occurred in the Pacific Ocean.

Keywords: Indonesian Throughflow, Tidal mixing, OFES2

©2021. Japan Geoscience Union. All Right Reserved.

Biogeophysical Interactions in transport of marine organisms

*Atsushi Fujimura[1]

1. University of Guam

Population dynamics of marine organisms largely depend on transport of larvae, propagules and holoplankton. A number of factors influence their transport and multiple biological and geophysical processes are involved in various spatiotemporal scales. These processes and scales are often taxa specific, making it difficult to understand transport mechanisms as species-specific information may be required. Moreover, observing transport of such tiny planktonic organisms is challenging since they cannot be tagged and tracked effectively. Some techniques and methods were developed to describe transport mechanisms of the organisms over the last decades, and biological-physical coupling models are used more and more. The current status of our understanding of the transport processes and study methods will be discussed, and some results from recent research will be presented. For example, a biophysical simulation models indicate that cross-shore transport of larvae and phytoplankton in the surf zone are controlled by wave/wind-driven currents, turbulence, vertical positions of plankton, and bathymetric features. The study indicates that physical dynamics, biological traits, and geological characteristics are all important to understand plankton transport in coastal areas.

Keywords: Biophysical interaction, Larval transport, Coastal oceanography, Surf zone, Modeling, Plankton

©2021. Japan Geoscience Union. All Right Reserved.

Wave resolving numerical simulation of non-breaking wave-induced mixing

*Haruka Imamura[1], Yutaka Yoshikawa[1], Yasushi Fujiwara[2]

1. Graduate School of Science, Kyoto University, 2. Graduate School of Frontier Sciences, the University of Tokyo

Recent studies suggest that non breaking surface waves induce vertical mixing in the ocean surface layer. Langmuir circulations (LCs), generated by the interaction between surface waves and wind-driven shear flow, are one example of the processes that cause mixing without wave breaking. Some laboratory and numerical experiments, on the other hand, showed the mixing caused only by the non-breaking wave without wind-induced shear (hereafter referred as the non-breaking wave-induced mixing). Dai et al. (2010) observed that initially stratified water in their windless laboratory tank was homogenized under the monochromatic surface waves with wave steepness ak = 0.08 ~ 0.21. Savelyev et al. (2012) conducted windless laboratory experiments and identified an elongated streaky structure at the water surface in the presence of surface waves. Wave resolving numerical simulations showed that counterrotating streamwise vortex pairs like LCs (Tsai et al.,2015, 2017, Fujiwara et al.,2020) and elongated surface streaks (Tsai et al.,2015,2017) were formed even without wind stress at the surface. These numerical studies suggested that the structures can be formed by the CL2 instability mechanism, the interaction between surface waves and the sheard current as in LCs, but the current is produced by the wave viscous attenuation (Tsai et al.,2017, Fujiwara et al.,2020). However, there remain several issues to be resolved. For example, the numerical experiments used steeper waves (ak = 0.25; Tsai et al.,2015,2017) than the laboratory experiments (ak = 0.08 ~ 0.21; Dai et al.,2010) and larger viscosity than that of water (Fujiwara et al.,2020). The magnitude of mixing caused by this vortex structure was not evaluated in the studies. Furthermore, the velocity characteristics are different from those of LCs. Thus, the condition, magnitude, and mechanism of non-breaking wave-induced mixing need to be clarified.

The purpose of this study is to examine whether the non-breaking surface waves with relatively small steepness can induce the mixing in the water with molecular viscosity and to evaluate how strong it is. To this aim, we conduct the numerical experiments under the similar condition as the laboratory experiment by Dai et al. (2010). A sigma-coordinate free-surface nonhydrostatic model similar to Tsai and Hung (2007) and Yang and Shen (2011) was used. We considered a surface wave with a wavelength of λ = 75cm and an amplitude of 1cm (ak = 0.08) propagating on the surface of homogeneous water with an average depth of 20cm. The length and width of the computational domain are λ and $\lambda/2$ respectively with periodic boundary condition in both directions. No tangential stress at the surface was imposed. Initial surface elevation and velocity were set as those of the third-order Stokes wave. To visualize motion of water, a passive tracer with a linear vertical profile was distributed in the initial field. The domain was discretized with 256× 128× 64 grid points. The simulated wave kept propagating until at least 100 wave periods with less deformation from the stokes wave (except for the wave viscous attenuation).

Simulated velocity field showed that convergent (divergent) zones of the spanwise velocity at the surface and divergent (convergent) zones at depth correspond with the zones of downward (upward) velocity and acceleration (deceleration) of the streamwise (downwave) velocity. Tracer distribution at the surface was also characterized by elongated streaks. These features can be explained by the formation of streamwise vortices near the water surface. The vertical diffusivity estimated from the tracer distribution was O(10^{-5})m

©2021. Japan Geoscience Union. All Right Reserved.

^{2}/s, with its maximum at about 2cm depth and becoming almost zero at and below about 6cm depth.

Magnitude of the estimated diffusivity is similar to that of Dai et al. (2010). More detailed analysis about the mechanism of this mixing and dependences of vertical diffusivity on wave parameters and stratification will be presented.

Keywords: ocean surface mixing, streamwise vortex pairs, wave viscous attenuation

©2021. Japan Geoscience Union. All Right Reserved.

Origin of swells propagated into small bays on the Sanriku rias coast facing the western North Pacific

*Kosei Komatsu[1,2], Takaki Fujii[3], Kiyoshi Tanaka[2]

1. Graduate School of Frontier Sciences, University of Tokyo, 2. Atmosphere and Ocean Research Institute, University of Toky, 3. Bank of Japan

Real-time monitoring of wind and surface waves in Otsuchi Bay, a ria located in the northeastern portion of Japan, had been continued over four years since October 2012, using a mooring buoy with an ultrasonic anemometer and a single-mode GPS wave sensor. The monitoring revealed that waves in the bay were dominated by swells propagated from the northeastern offshore region in all seasons. Time-lag correlation coefficient between the significant wave height in the bay and the offshore wind velocity component blowing in the direction to the bay was maximized in the region approximately 300 km northeast of the bay, from which waves developed by the local wind are accessible within the corresponding time-lag to the bay at a speed of the group velocity of the swell observed in the bay. As an interesting feature common to swell-dominant waves observed in the rias bays adjacent to Otsuchi Bay, the region of the significant correlation between the wave height and the offshore wind velocity extends to the direction that faces the bay mouth. It implies that the source region of the swell depends heavily on the coastal shape of the bay. Consequently, the relation between the offshore wind field and the decay-rate of the swells propagating to Otsuchi Bay indicates that the source region of the swell influential in the bay is located in the offshore region several hundreds of kilometers northeast of the bay, which is on the typical migration route of high and low pressures in the Northern temperate zone.

Keywords: swell, rias coast, western North Pacific

©2021. Japan Geoscience Union. All Right Reserved.

[J] Oral | A (Atmospheric and Hydrospheric Sciences)：A-CG Complex & General

Sun. Jun 6, 2021 3:30 PM - 4:45 PM JST | Sun. Jun 6, 2021 6:30 AM - 7:45 AM UTC | Ch.10 Zoom Room 10

[A-CG38] Dynamics of Oceanic and Atmospheric Waves, Vortices, and Circulations

convener:Yuki Tanaka(Faculty of Marine Science and Technology, Fukui Prefectural University), Kunihiro Aoki(Japan Agency for Marine Earth Science and Technology), Yukiharu Hisaki(University of the Ryukyus), Norihiko Sugimoto(Keio University, Department of Physics), Chairperson:Norihiko Sugimoto(Keio University, Department of Physics), Kunihiro Aoki(Japan Agency for Marine Earth Science and Technology), Yuki Tanaka(Faculty of Marine Science and Technology, Fukui Prefectural University)

Oceanic and atmospheric dynamics aims at abstracting general principles from observed phenomena and constructing a system of mathematical models, thereby leading to the understanding, prediction, and parameterization of those phenomena. It provides perspectives for the advancement of sciences in various areas such as turbulence, wind waves, internal waves, Rossby waves, tides, coastal and equatorial boundary processes, mesoscale and submesoscale eddies, meandering of jets and fronts, general circulation, and ocean-atmosphere coupled modes. It has also been and will continue to be benefited by new uses of ideas and methods from such theories as resonance, nonlinear interaction, stability analysis, spectral analysis, probability, statistics, and dynamical systems. In this session, we solicit presentations on observational, experimental, numerical, and theoretical studies of oceanic and atmospheric dynamics and on exploratory use of new ideas and methods. We also welcome presentations on interdisciplinary studies in fields such as ecosystems, climate, and environment.

3:30 PM - 3:45 PM JST | 6:30 AM - 6:45 AM UTC

[ACG38-13] Formulation and application of phase-independent energy conversion terms for quasi-geostrophic eddies on a zonally-varying basic flow

★Invited Papers

*Takaya Koutarou[1] (1.Kyoto Sangyo University)

3:45 PM - 4:00 PM JST | 6:45 AM - 7:00 AM UTC

[ACG38-14] Recirculation of atmospheric wave energy associated with idealized MJO events

*Hidenori AIKI[1], Yoshiki Fukutomi[1], Yuki Kanno[2], Tomomichi Ogata[3], Takahiro Toyoda[4], Hideyuki Nakano[4] (1.Nagoya University, 2.Central Research Institute of Electric Power Industry, 3.Japan Agency for Marine-Earth Science and Technology, 4.Meteorological Research Institute)

4:00 PM - 4:15 PM JST | 7:00 AM - 7:15 AM UTC

[ACG38-15] Extratropical forcing of intraseasonal equatorial Kelvin waves over the Indian and Pacific Oceans

*Fukutomi Yoshiki[1], Hidenori Aiki[1] (1.Institute for Space-Earth Environmental Reasearch, Nagoya University)

4:15 PM - 4:30 PM JST | 7:15 AM - 7:30 AM UTC

[ACG38-16] Influence of marginal seas' hotspot on extratropical cyclones: explosive and binary cyclogenesis in idealized experiments

*Masaru Yamamoto[1] (1.Research Institute for Applied Mechanics, Kyushu University)

4:30 PM - 4:45 PM JST | 7:30 AM - 7:45 AM UTC

[ACG38-17] Discussion

Formulation and application of phase-independent energy conversion terms for quasi-geostrophic eddies on a zonally-varying basic flow

*Takaya Koutarou[1]

1. Kyoto Sangyo University

A new formulation of energy conversion terms for quasi-geostrophic disturbances is proposed under an assumption that an eddy is almost a plane wave in the WKB sense. Estimating energy conversions could be valid to explore dynamics of low-frequent variability of the disturbances. A traditional form of the energy conversion terms contains quadratic terms in disturbance amplitudes, such as a momentum transport u’v’ and a heat transport v’T’. Therefore, it inherently includes an oscillatory component of one-half wavelength of the disturbances. For transient eddies, time-averaging longer than one wave period can be equivalent to eliminating the half-wavelength oscillatory components in the energy conversion terms, so that the traditional form of the terms may be available. However, for stationary waves, time-averaging is not equivalent to phase-averaging and therefore inappropriate. A new form of the energy conversion proposed in this study can be proved to be phase-independent of the eddies without any spatial- and time-averaging taken, and thus can represent a “snapshot” distribution of the energy conversion terms. Therefore, the new formulation can be applicable to estimating energy conversions for stationary eddies or snapshot features of transient eddies.

Actual applications of the new form of the energy conversions to some teleconnection patterns will also be given. Our analysis based on the new formulation suggests that energy extraction from the basic state and energy dispersion by group velocity can be essential for formation and/or maintenance mechanisms of the teleconnection patterns.

Keywords: energy conversion, Rossby wave

©2021. Japan Geoscience Union. All Right Reserved.

Recirculation of atmospheric wave energy associated with idealized MJO events

*Hidenori AIKI[1], Yoshiki Fukutomi[1], Yuki Kanno[2], Tomomichi Ogata[3], Takahiro Toyoda[4], Hideyuki Nakano[4]

1. Nagoya University, 2. Central Research Institute of Electric Power Industry, 3. Japan Agency for Marine-Earth Science and Technology, 4. Meteorological Research Institute

A recent analytical study has derived an exact universal expression for the energy flux which can indicate the direction of the group velocity for linear shallow-water waves at all latitudes. This analytical result is extended in the present study to a height-dependent framework for three-dimensional waves in the atmosphere. This is achieved by investigating the classical analytical solution of both equatorial and midlatitude waves in a Boussinesq fluid. For the horizontal component of the energy flux, the same expression has been obtained between equatorial waves and midlatitude waves in the height-dependent framework, which is linked to a scalar quantity inverted from the isentropic perturbation of Ertel's potential vorticity (EPV). This EPV-inverted scalar quantity reduces to the geostrophic streamfunction for midlatitude Rossby waves and vanishes for gravity waves, a novel aspect for considering the universal expression of the energy flux. The expression of the vertical component of the energy flux requires computation of another scalar quantity which may be interpreted as the zonal integral of a variant of streamfunction and may be obtained by the time integration of a prognostic equation. The new energy flux diagnosis scheme, mentioned above, has been tested for three-dimensional Rossby and equatorial Kelvin waves induced by an idealized MJO-like heat forcing. The horizontal recirculation of wave energy is identified in each hemisphere with a smooth transition between equatorial and off-equatorial regions. The vertical flux of wave energy is mostly revealed by the pressure flux component of the energy flux, as it is maintained mainly by equatorial Kelvin waves.

©2021. Japan Geoscience Union. All Right Reserved.

Extratropical forcing of intraseasonal equatorial Kelvin waves over the Indian and Pacific Oceans

*Fukutomi Yoshiki[1], Hidenori Aiki[1]

1. Institute for Space-Earth Environmental Reasearch, Nagoya University

Equatorial Kelvin waves (KWs) are major convective disturbances accompanying tropical super cloud clusters (SCCs) which propagate eastward along the equatorial belt. KWs generally span the broad range from synoptic to intraseasonal time scales and they have horizontal scales of about zonal wavenumber 1-10. This study examines characteristics and origins of intraseasonal equatorial KWs which have periods of about 10-20 days in the Indian Ocean-western Pacific region during Austral winter. They are distinguished from synoptic-scale (about 2-8 days) KWs. An extended empirical orthogonal function (EEOF)-based composite analysis is performed on 8-25-day filtered outgoing longwave radiation and atmospheric circulation fields during June-August 1979-2018. The analysis results reveal the structure and evolution of the KWs and associated extratropical-tropical interactions. The composite KW patterns exhibit a zonal wave number 3 structure with eastward phase speed of around 12-16m/s. The KWs initially develop over the Indian Ocean, then they propagate eastward into the eastern Pacific after passing through the Maritime Continent (MC). Initiation mechanisms of KWs due to Southern Hemisphere extratropical wave activity is explored by identifying precursor wave signals in the extratropics. Southerly surge-like flows in the lower troposphere are identified over the western Indian Ocean and the western Pacific close to the MC associated with the KW development. These two southerly flows are linked to initiation of KWs at each location. They are originated in the extratropical wave train which progress eastward into the central-eastern South Pacific. There is strong evidence that equatorward advection of westerly momentum is enhanced by the southerly surge-like flow. This equatorward transport of westerly momentum plays a vital role in initiating KWs at these two locations.

Keywords: Equatorial Kelvin waves, Intraseasonal variability, Extratropical-tropical interaction

©2021. Japan Geoscience Union. All Right Reserved.

Influence of marginal seas' hotspot on extratropical cyclones: explosive and binary cyclogenesis in idealized experiments

*Masaru Yamamoto[1]

1. Research Institute for Applied Mechanics, Kyushu University

Over the marginal seas of the western North Pacific, the active region of extratropical cyclones is divided into two (the Sea of Japan and the southern coast of the Japanese main islands) and some cyclones often develop explosively. In addition, binary extratropical cyclones, called twin extratropical cyclones, are also often observed. A few works have studied cases of binary lows associated with (i) upper-level double jets (Ogura et al. 2006; Hitsuma 2006), (ii) the formation of binary lows in single jets (Yamamoto 2012, 2018), and (iii) transition from double jets to single jets (Yokoyama & Yamamoto 2019). At the present stage, one does not fully understand why binary cyclone structures often form around Japan. In winter, high sea surface heat fluxes are concentrated into the marginal seas of the western North Pacific. Recently, such a localized, strong surface heat flux at midlatitudes is called a "hotspot" in the climate system (e.g., Nakamura et al. 2015). The atmospheric response to the hotspots in the marginal seas has been studied in idealized atmospheric general circulation models from the viewpoint of geophysical fluid dynamics, to discuss the temperature decrease around the east coast of the continent and cyclonic activity over the North Pacific Basin (e.g., Kaspi & Schneider 2011).

The purposes of this study are to reconsider the atmospheric response to localized heating over marginal seas of the western North Pacific, and to clarify the impact of the sea hotspot on binary cyclones near Japan. In idealized experiments used, the setup of Held & Suarez (1994) was applied to the global Weather Research and Forecasting model (e.g., Dias Pinto & Mitchell, 2014). The present work assumed that the North Pacific marginal seas' hotspot heats the lower atmosphere. The steady and localized heating was given by the triangular region. Several sensitivity experiments were conducted by changing the location and thickness of this heating region.

In the area of enhanced westerly, the baroclinicity and short-period disturbance activity at low levels are enhanced by the hotspot. In addition, the frequency of explosive cyclones increases around the hotspot. Over the marginal seas of the western North Pacific, a pressure trough extends in a north-south direction and two maxima of cyclone activity (intensity of short-period disturbances) forms. These two maxima form even when the heating parameters are altered, and thus the hotspot is an important factor in forming the bifurcation of the cyclone activity area around Japan (Japan Sea path and south coast path). In the time-latitude cross-section of sea level pressure over the hotspot, a binary cyclone appears under the condition that a deep pressure trough has developed. A binary cyclone system appears in the early stage of the cyclone development, and the contact cyclone pair merges during the fully developed stage. This is consistent with several case studies of explosive, binary cyclones (Yamamoto 2018; Yokoyama & Yamamoto 2019).

A simple framework for investigating the atmospheric response to an oceanic hotspot in the western North Pacific shows that the heating of the lower atmosphere by the hotspot leads to the formation of a north-south bifurcation of the active cyclone area and increases the frequency of explosive cyclones. The formation of binary lows in the absence of the Japanese Islands suggests the importance of enhanced pressure troughs associated with heating over the marginal seas' hotspot.

©2021. Japan Geoscience Union. All Right Reserved.

Keywords: extratropical cyclone, binary cyclone, marginal seas' hotspot

©2021. Japan Geoscience Union. All Right Reserved.

[J] Oral | A (Atmospheric and Hydrospheric Sciences) | A-CG Complex & General

[A-CG38] Dynamics of Oceanic and Atmospheric Waves, Vortices, and Circulations

convener:Yuki Tanaka(Faculty of Marine Science and Technology, Fukui Prefectural University), Kunihiro Aoki(Japan Agency for Marine Earth Science and Technology), Yukiharu Hisaki(University of the Ryukyus), Norihiko Sugimoto(Keio University, Department of Physics), Chairperson:Norihiko Sugimoto(Keio University, Department of Physics), Kunihiro Aoki(Japan Agency for Marine Earth Science and Technology), Yuki Tanaka(Faculty of Marine Science and Technology, Fukui Prefectural University)

Sun. Jun 6, 2021 3:30 PM - 4:45 PM Ch.10 (Zoom Room 10)

Oceanic and atmospheric dynamics aims at abstracting general principles from observed phenomena and constructing a system of mathematical models, thereby leading to the understanding, prediction, and parameterization of those phenomena. It provides perspectives for the advancement of sciences in various areas such as turbulence, wind waves, internal waves, Rossby waves, tides, coastal and equatorial boundary processes, mesoscale and submesoscale eddies, meandering of jets and fronts, general circulation, and ocean-atmosphere coupled modes. It has also been and will continue to be benefited by new uses of ideas and methods from such theories as resonance, nonlinear interaction, stability analysis, spectral analysis, probability, statistics, and dynamical systems. In this session, we solicit presentations on observational, experimental, numerical, and theoretical studies of oceanic and atmospheric dynamics and on exploratory use of new ideas and methods. We also welcome presentations on interdisciplinary studies in fields such as ecosystems, climate, and environment.

4:30 PM - 4:45 PM

[ACG38-17]Discussion

©Japan Geoscience Union

[J] Poster | A (Atmospheric and Hydrospheric Sciences)：A-CG Complex & General

Sun. Jun 6, 2021 5:15 PM - 6:30 PM JST | Sun. Jun 6, 2021 8:15 AM - 9:30 AM UTC | Ch.08_3

[A-CG38] Dynamics of Oceanic and Atmospheric Waves, Vortices, and Circulations

convener:Yuki Tanaka(Faculty of Marine Science and Technology, Fukui Prefectural University), Kunihiro Aoki(Japan Agency for Marine Earth Science and Technology), Yukiharu Hisaki(University of the Ryukyus), Norihiko Sugimoto(Keio University, Department of Physics)

Oceanic and atmospheric dynamics aims at abstracting general principles from observed phenomena and constructing a system of mathematical models, thereby leading to the understanding, prediction, and parameterization of those phenomena. It provides perspectives for the advancement of sciences in various areas such as turbulence, wind waves, internal waves, Rossby waves, tides, coastal and equatorial boundary processes, mesoscale and submesoscale eddies, meandering of jets and fronts, general circulation, and ocean-atmosphere coupled modes. It has also been and will continue to be benefited by new uses of ideas and methods from such theories as resonance, nonlinear interaction, stability analysis, spectral analysis, probability, statistics, and dynamical systems. In this session, we solicit presentations on observational, experimental, numerical, and theoretical studies of oceanic and atmospheric dynamics and on exploratory use of new ideas and methods. We also welcome presentations on interdisciplinary studies in fields such as ecosystems, climate, and environment.

[ACG38-P01] A statistical mechanics of phytoplankton diversity

*Kunihiro Aoki[1], Yoshio Masuda[2] (1.Japan Agency for Marine Earth Science and Technology, 2.Faculty of Environmental Earth Science, Hokkaido University)

[ACG38-P02] Essential spectrum of internal waves arising in rotating stratified fluid

*andrei giniatoulline[1] (1.Department of Mathematics, Los Andes University, Bogota, Colombia, South America)

[ACG38-P03] Statistical analysis of ocean waves in the sea of Japan

*Yukiharu Hisaki[1] (1.University of the Ryukyus)

[ACG38-P04] Observing system simulation experiments for new satellite observation missions on Venus

*Yukiko Fujisawa[1], Norihiko Sugimoto[1], Mirai Abe[1], Asako Hosono[2], Mimo Shirasaka[3], Hiroki Ando[4], Masahiro Takagi[4], Chi Ao[5], Itziar Garate Lopez[6], Sebastien Lebonnois[7], Tomotaka Yamamoto[8], Yosuke Kawabata[8], Satoshi Ikari[8], Takeshi Imamura[8], Masaru Yamamoto[9], Shin-ya Murakami[1], Masataka Imai[10], Toru Kouyama[10] (1.Keio University, 2.Toshimagaoka Women High School, 3.Seisen Senior High School, 4.Kyoto Sangyo University, 5.Jet Propulsion Laboratory, California Institute of Technology, 6.Bilboko Ingeniaritza Eskola (UPV/EHU), 7.Sorbonne Universite, 8.Tokyo University, 9.Research Institute for Applied Mechanics, Kyushu University, 10.National Institute of Advanced Industrial Science and Technology)

A statistical mechanics of phytoplankton diversity

*Kunihiro Aoki[1], Yoshio Masuda[2]

1. Japan Agency for Marine Earth Science and Technology, 2. Faculty of Environmental Earth Science, Hokkaido University

.

Keywords: Biodiversity, Statistical mechanics, Ocean ecosystem, Ocean circulation, Maximum entropy method

©2021. Japan Geoscience Union. All Right Reserved.

Essential spectrum of internal waves arising in rotating stratified fluid

*andrei giniatoulline[1]

1. Department of Mathematics, Los Andes University, Bogota, Colombia, South America

For viscous and inviscid compressible fluid, we consider the three-dimensional models which involve simultaneously the stratification and rotation of the fluid. The rotation corresponds to the rotation of the Earth over the vertical axis, and the stratification corresponds to the non-homogeneous distribution of density due to the gravitational force. We find the structure and the localization of spectrum of normal vibrations of the inner waves for various boundary conditions. We prove that, when the spectral parameter belongs to the essential spectrum, there arises the resonance effect of non-uniqueness of the limit amplitude of internal waves. The results may find application in the study of the Ocean and Atmosphere.

Keywords: Dynamical systems, Internal waves, Resonance effect, Rotational fluid, Stratified fluid, Essential spectrum

©2021. Japan Geoscience Union. All Right Reserved.

Statistical analysis of ocean waves in the sea of Japan

*Yukiharu Hisaki[1]

1. University of the Ryukyus

Wave climate is important for marine disaster prevention. The Sea of Japan is a semi-enclosed sea that connects the Tsushima Strait and the Mamiya Strait to other sea areas. Therefore, waves in the Japan Sea are more influenced by local winds than by distant swells. In this study, we investigated the interannual variability of the wave height distribution using the ERA5 reanalysis data. First, we compared the wave heights by ERA5 with those by GPS buoys around Japan. The agreement between them is good. Next, the difference in the accuracy of the ERA5 wave height was compared between the short and long fetch cases. In the short fetch case, the accuracy of the ERA5 wave heights is significantly lower than that of the long fetch case.
Wave heights by ERA5 and those by JMA (Japan Meteorological Agency) moored buoys (1990 to 2000) were compared. The agreement between them was good. In addition, the accuracy of ERA5 wave height after incorporating altimeter data into ERA5 wave data from 1992 was compared with those of wave height before that. The difference in the accuracy between them was small.
Next, the spatial distribution of ERA5 monthly mean wave height anomalies from climatological values from 1979 to 2019 was examined by empirical orthogonal function (EOF) analysis. The first mode is a pattern of variability in the central region of the sea of Japan (around 40N, 135E). The second mode is a pattern that fluctuates alternately in the north and south of the Sea of Japan (around 35N, 131E and 45N, 140E). The correlation between the EOF time series of monthly mean wind anomalies and the EOF time series of wave height anomalies was investigated. The first mode of wave height anomalies is correlated with the second mode of EOF wind anomalies over almost the entire Japan Sea area. The second EOF mode of wave height anomaly is correlated with the first EOF mode of wind anomaly in the northern part of the sea of Japan.
The monthly wave height anomaly maps were classified by self-organizing map analysis. Some frequent wave height anomaly maps corresponded to the distributions of EOF first and second modes of wave height anomaly. The frequency of the distribution patterns with high wave height anomaly in the central area of the sea of Japan has been increasing in recent years. This is consistent with the trend of the EOF first mode time series of wave height anomalies. In addition, wave height anomalies in the northern and southern areas of the sea of Japan corresponded most closely to the distribution patterns of wind anomalies in the northern area of the sea of Japan. This is consistent with the result that the second EOF mode of wave height anomalies is correlated with the first EOF mode of wind anomalies in the northern part of the sea of Japan.

Keywords: wave height, Sea of Japan

©2021. Japan Geoscience Union. All Right Reserved.

Observing system simulation experiments for new satellite observation missions on Venus

*Yukiko Fujisawa[1], Norihiko Sugimoto[1], Mirai Abe[1], Asako Hosono[2], Mimo Shirasaka[3], Hiroki Ando[4], Masahiro Takagi[4], Chi Ao[5], Itziar Garate Lopez[6], Sebastien Lebonnois[7], Tomotaka Yamamoto[8], Yosuke Kawabata[8], Satoshi Ikari[8], Takeshi Imamura[8], Masaru Yamamoto[9], Shin-ya Murakami[1], Masataka Imai[10], Toru Kouyama[10]

1. Keio University, 2. Toshimagaoka Women High School, 3. Seisen Senior High School, 4. Kyoto Sangyo University, 5. Jet Propulsion Laboratory, California Institute of Technology, 6. Bilboko Ingeniaritza Eskola (UPV/EHU), 7. Sorbonne Universite, 8. Tokyo University, 9. Research Institute for Applied Mechanics, Kyushu University, 10. National Institute of Advanced Industrial Science and Technology

Observation system simulation experiment (OSSE) is a method for testing a virtual observation system using a data assimilation method, which enables us to evaluate planned observation by reproducibility of a target phenomenon. On Earth, it is actively used for objective evaluation of meteorological forecasting skill when new observations, such as satellite observations, are introduced (e.g., Masutani et al., 2010) [1]. However, there are few examples of OSSE for planetary satellite observation missions. Since a planetary satellite mission is limited in time and resources, it would be quite useful to investigate its effectiveness by using OSSE in advance to optimize its instruments and observation plans.

To implement OSSE, we need both a data assimilation system and a reliable meteorological model which can reproduce the atmospheric phenomena realistically. We have developed “AFES-Venus” (Sugimoto et al., 2014a) [2] which is based on AFES (Atmospheric GCM For the Earth Simulator) optimized for the Earth simulator, and “ALEDAS-V” (AFES LETKF Data Assimilation System for Venus) (Sugimoto et al., 2017) [3] which is the first data assimilation system for the Venus atmosphere using AFES-Venus and Local Ensemble Transform Kalman Filter (LETKF). In this presentation, we show an overview of four OSSEs conducted by this assimilation system (Table).

The radio occultation measurements mission between multiple small satellites is expected as a method to observe the vertical temperature distribution at altitudes in about 40-90km penetrating a thick cloud cover at altitudes in about 48–70 km. In addition, the observation frequency and coverage would be significantly improved compared to the radio occultation between the Earth and satellites. In this study, OSSE was performed for the observation points by actual orbit calculation[4], and the effectiveness of the orbit was investigated from (1) the reproducibility of “cold collar” [5,6] and (2) the improvement of the speed of “super rotation”, which are notable atmospheric phenomena on Venus.

Observations of the Venus Orbiter "Akatsuki" provide us horizontal distributions of the horizontal wind derived from cloud tracking of the UVI camera and of temperature observed by the LIR camera. In this study, the observational limits of Akatsuki were reduced, and OSSE was performed for various observation coverages (day and night side, or latitude area) and observation frequencies, and the effectiveness of the observations was investigated from (3) the reproducibility of “planetary-scale equatorial Kelvin waves with 4-day period” [7] and (4) the improvement of phases of “thermal tides”.

[1] Masutani, M., J. S. Woollen, S. J. Lord, G. D. Emmitt, T. J. Kleespies, S. A. Wood, S. Greco, H. Sun, J. Terry, V. Kapoor, R. Treadon, and K. A. Campana (2010), J. Geophys. Res., 115.
[2] Sugimoto, N., M. Takagi, and Y. Matsuda (2014a), J. Geophys. Res. Planets, 119, 1950–1968.

©2021. Japan Geoscience Union. All Right Reserved.

[3] Sugimoto, N., A. Yamazaki, T. Kouyama, H. Kashimura, T. Enomoto, and M. Takagi (2017), Scientific Reports, 7(1), 9321.
[4] Yamamoto, T., S. Ikari, H. Ando, T. Imamura, A. Hosono, M. Abe, Y. Fujisawa, N. Sugimoto, Y. Kawabata, R. Funase, and S. Nakasuka, (2021), Journal of the Japan Society for Aeronautical and Space Sciences, submitted.
[5] Sugimoto, N., M. Abe, Y. Kikuchi, A. Hosono, H. Ando, M. Takagi, I. Garate-Lopez, S. Lebonnois, and C. Ao (2019b), Journal of Japan Society of Civil Engineers A2: Applied Mechanics, 75(2), 477–486.
[6] Fujisawa, Y., N. Sugimoto, C. Ao, A. Hosono, H. Ando, M. Takagi, I. Garate-Lopez and S. Lebonnois, in preparation.
[7] Sugimoto, N., Y. Fujisawa, M. Shirasaka, A. Hosono, M. Abe, H. Ando, M. Takagi, M. Yamamoto, (2021), Atmosphere, Vol.12, No.1, 14, 16pp.

Keywords: Venus atmosphere, Data assimilation, Observing system simulation experiment

©2021. Japan Geoscience Union. All Right Reserved.

Experimental Case	Virtual observation data	Orbit
I. Radio Occultation Measurement Among Small Satellites		
① Reproduction of cold collar	temperature (IPSL Venus GCM)	Orbit with many observations near the poles
② Improvement of super-rotation	temperature (AFES-Venus)	Orbit with many observations in low latitudes
II. Camera images (assuming Akatsuki UVI or LIR)		
③ Reproduction of 4-day equatorial Kelvin wave	horizontal wind (CCSR/GCM)	Varying observation latitude and frequency
④ Improvement of phases of thermal tides	temperature (AFES-Venus)	Varying observation longitude and frequency

Table: Cases of observing system simulation experiments, virtual observation data and orbit used in the experiments

実験	仮想の観測データ	軌道
Ⅰ小型衛星を用いた衛星間電波掩蔽観測		
① コールドカラー再現	温度 (IPSL Venus GCM)	極付近にも多く観測が存在する軌道
② スーパーローテション速度改善	温度(AFES-Venus)	低緯度に多く観測が存在する軌道
Ⅱカメラ観測（e.g.あかつき UVI LIR 観測）		
③ 4 日周期ケルビン波再現	水平風速(CCSR/GCM)	複数の観測緯度や観測頻度
④ 熱潮汐波の位相改善	温度(AFES-Venus)	複数の観測経度や観測頻度

表: 観測システムシミュレーション実験の種類、及び実験に用いた仮想観測データと軌道

©2021. Japan Geoscience Union. All Right Reserved.

[J] Oral | H (Human Geosciences)：H-DS Disaster geosciences

Sun. Jun 6, 2021 1:45 PM - 3:15 PM JST | Sun. Jun 6, 2021 4:45 AM - 6:15 AM UTC | Ch.15 Zoom Room 15

[H-DS08] Human environment and disaster risk

convener:Tatsuto Aoki(School of Regional Development Studies, Kanazawa University), Hiroshi, P. Sato(College of Humanities and Sciences, Nihon University), Chairperson:Tatsuto Aoki(School of Regional Development Studies, Kanazawa University), Hiroshi Sato(College of Humanities and Sciences, Nihon University)

This session discusses disaster risks being inherent in the natural and human environment, which sometimes happen to appear at a disaster, from the viewpoint of not only natural sciences but also social and human sciences. Examples of discussion subjects are as follows: uncertainty of forecasting disaster and problems of huge disaster with low frequency that raised from the 2011 Tohoku earthquake, the methodology for improving hazard maps, national recovery plans considering probable changes or sustainability of the society, international cooperation for disaster mitigation, problems of active faults or liquefaction, adjusting disaster mitigation plan to the regional characteristics, technical development for supporting disaster prevention, education for the disaster mitigation.

1:45 PM - 1:50 PM JST | 4:45 AM - 4:50 AM UTC

[HDS08-01] Introduction

1:50 PM - 2:05 PM JST | 4:50 AM - 5:05 AM UTC

[HDS08-02] Measurement of landslide deformation velocity at Jure in Sunkoshi River Wateshed, Nepal using LiCSBAS

*Hiroshi, P. Sato[1] (1.College of Humanities and Sciences, Nihon University)

2:05 PM - 2:20 PM JST | 5:05 AM - 5:20 AM UTC

[HDS08-03] Map of Earthquake-induced Landslides Potential on Artificially Transformed Hills in the Depositional Area of Tephric Soil Deposits

*Takehiko Suzuki[1], Masahiro Chigira[2], Yuki Matsushi[3], Daichi Nakayama[1] (1.Faculty of Urban Environmental Sciences, Tokyo Metropolitan University, 2.Fukada Geological Institute, 3.Disaster Prevention Research Institute Kyoto University)

2:20 PM - 2:35 PM JST | 5:20 AM - 5:35 AM UTC

[HDS08-04] **Elucidation of the cause that the H / L value of volcanic sector collapse is very small compared to non-volcanic landslides**

*Shunichi Sato[1] (1. Graduate School of Frontier Science, The University of Tokyo)

2:35 PM - 2:50 PM JST | 5:35 AM - 5:50 AM UTC

[HDS08-05] Natural disasters and countermeasures in Ratnapura, Sri Lanka

*Takahito Kuroki[1], Kensuke Goto[2], Panditharathne N. G. S. [3] (1.Faculty of Letters, Kansai University, 2.Faculty of Education, Osaka Kyoiku Univ., 3.Health Service Rathnapura, Ministry of Health, Government of Sri Lanka)

2:50 PM - 3:05 PM JST | 5:50 AM - 6:05 AM UTC

[HDS08-06] Policy for creating a liquefaction trend map based on geomorphologic classification for recognition of regional liquefaction risk

*Takayuki Nakano[1], Ryo Endo[1], Hiroyuki Inoue[2], Nozomi Yamashina[2], Shingo Watanabe[3], Keita Takada[3], Takuma Fujita[3] (1.Geospatial Information Authority of Japan, 2.City Bureau, Ministry of Land, Infrastructure, Transport and Tourism, 3.Fukken Co., Ltd.)

3:05 PM - 3:15 PM JST | 6:05 AM - 6:15 AM UTC

[HDS08-07] Discussion

[J] Oral | H (Human Geosciences) | H-DS Disaster geosciences

[H-DS08] Human environment and disaster risk

convener:Tatsuto Aoki(School of Regional Development Studies, Kanazawa University), Hiroshi, P. Sato(College of Humanities and Sciences, Nihon University), Chairperson:Tatsuto Aoki(School of Regional Development Studies, Kanazawa University), Hiroshi Sato(College of Humanities and Sciences, Nihon University)

Sun. Jun 6, 2021 1:45 PM - 3:15 PM Ch.15 (Zoom Room 15)

This session discusses disaster risks being inherent in the natural and human environment, which sometimes happen to appear at a disaster, from the viewpoint of not only natural sciences but also social and human sciences. Examples of discussion subjects are as follows: uncertainty of forecasting disaster and problems of huge disaster with low frequency that raised from the 2011 Tohoku earthquake, the methodology for improving hazard maps, national recovery plans considering probable changes or sustainability of the society, international cooperation for disaster mitigation, problems of active faults or liquefaction, adjusting disaster mitigation plan to the regional characteristics, technical development for supporting disaster prevention, education for the disaster mitigation.

1:45 PM - 1:50 PM

[HDS08-01]Introduction

©Japan Geoscience Union

Measurement of landslide deformation velocity at Jure in Sunkoshi River Wateshed, Nepal using LiCSBAS

*Hiroshi, P. Sato[1]

1. College of Humanities and Sciences, Nihon University

Jure landslide at the west side slope of Sunkoshi river occurred on 2 Aug 2014, 70 km E away from Kathmandu. And now the denuded slope surface appears on the ground. Ao et al. (2020) has already reported that deformation at the speed of -100 mm/yr along LoS in Jure landslide using time-series analysis on C-band Sentinel-1 SAR data. Anyway, Morishita et al. (2020) provided the free analysis tool of 100-m-resolution “LiCSBAS” using the Sentinel-1 SAR data. This study found the result of LoS change of -28 mm/yr at the source site (27.77128˚N, 85.866˚E) of the landslide using this tool, as analyzing the SAR data measured from 7 Oct 2017 to 8 Sep 2018.

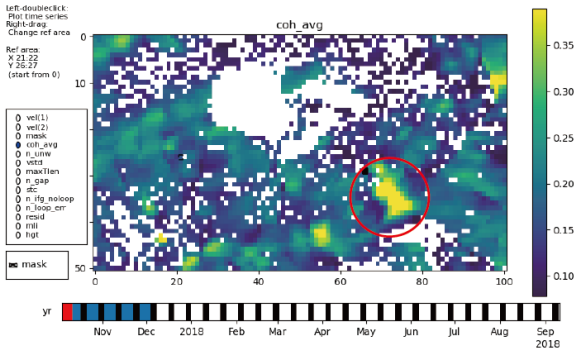
Acknowledgement
This study was supported by KAKEN 18KK0027.

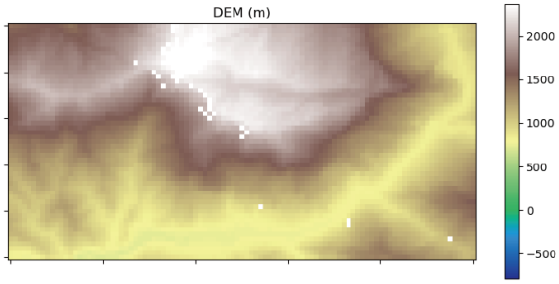
References
Ao et al., 2020: Characterizing the evolution life cycle of the Sunkoshi landslide in Nepal with multi-source SAR data. Nature Scientific Report, 10: 17988.
Morishita et al., 2020: LiCSBAS: An Open-source InSAR time series analysis package integrated with the LiCSAR Automated Sentinel-1 InSAR Processor. Remote Sensing, 12: 424.

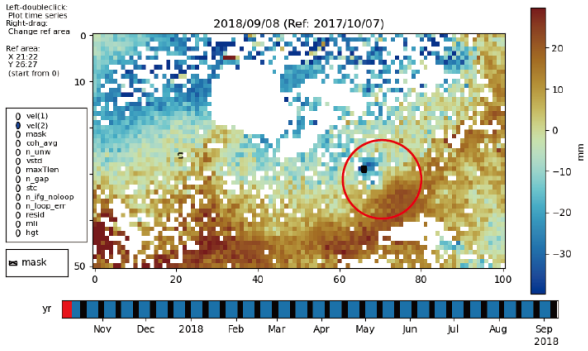
Keywords: LiCSBAS, Sentinel-1, Nepal, landslide

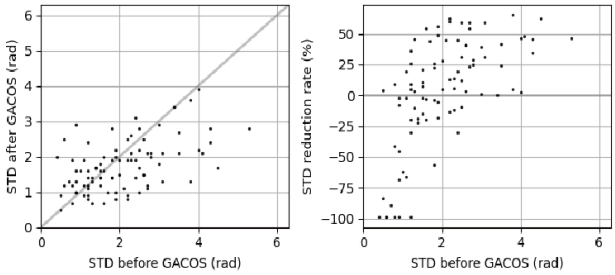
©2021. Japan Geoscience Union. All Right Reserved.

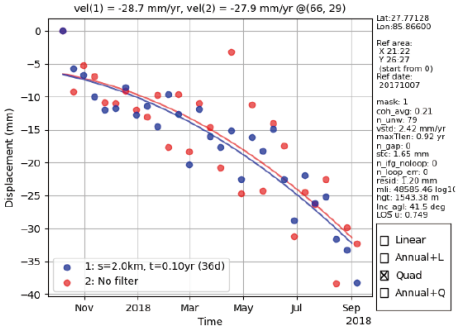


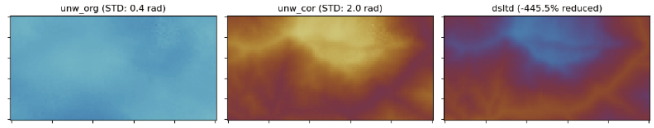




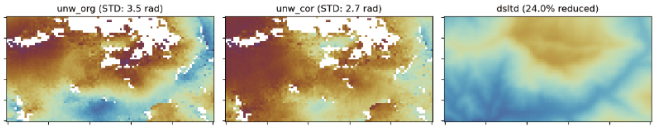




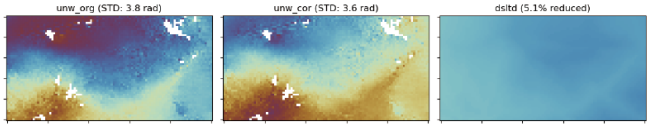




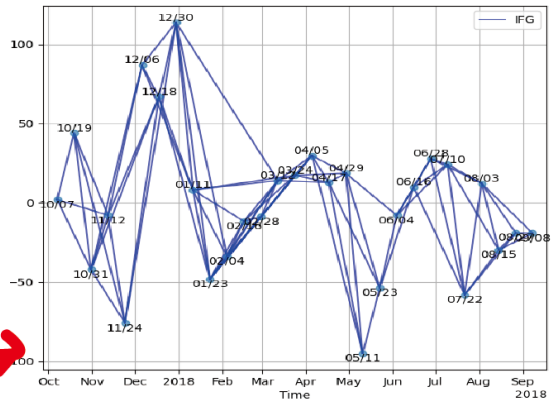
20180216-20180228.gacos

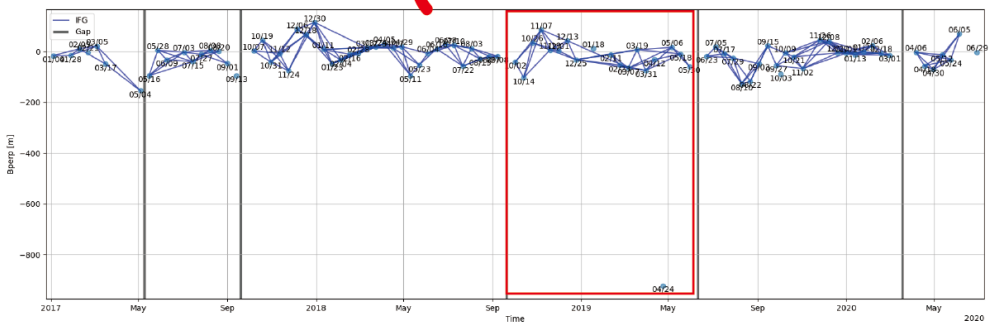


20180511_20180523.gacos



20180827_20180908.gacos





©2021. Japan Geoscience Union. All Right Reserved.

Map of Earthquake-induced Landslides Potential on Artificially Transformed Hills in the Depositional Area of Tephric Soil Deposits

*Takehiko Suzuki[1], Masahiro Chigira[2], Yuki Matsushi[3], Daichi Nakayama[1]

1. Faculty of Urban Environmental Sciences, Tokyo Metropolitan University, 2. Fukada Geological Institute, 3. Disaster Prevention Research Institute Kyoto University

So-called “loam” composed of primary fall-out tephras and tephric soil deposits (tephric loess) is one of the factors causes earthquake-induced landslides on hills where thick loam is preserved. To evaluate potential of slope failure by this condition in the Japanese Island, the distribution of map of loam has been reported. To assess possibilities of earthquake-induced landslides in hilly areas heavily modified by human activities, man-made landforms should be modelled at the micro-landform scale considering original loam thickness. We estimated elevation changes by cutting and fill operation in the Gotentoge and Karakida areas in the Tama Hills where the Tama New Town was built using 1:3,000 topographical maps published in 1950s and present digital elevation model (DEM) with 5 to 2 m mesh. Also, 1:10,000 geological map of loam was used for estimation of thickness distribution of preserved loam. By this method, we tentatively mapped earthquake-induced landslides potential for the Tama Hills, artificially transformed hills in the depositional area of thick tephric soil deposits.

Keywords: earthquake-induced landslide, artificially transformed landform, hills, tephric soil, Tama Hills

©2021. Japan Geoscience Union. All Right Reserved.

Elucidation of the cause that the H / L value of volcanic sector collapse is very small compared to non-volcanic landslides

*Shunichi Sato[1]

1. Graduate School of Frontier Science, The University of Tokyo

On case of volcanic sector collapse of stratovolcanoes, it has a ratio (H / L value) of the reach distance L of the debris avalanche and the height difference H, which is a very small value that can never be realized by general non-volcanic land sliding. Namely, it is known from previous studies that it has an very large flow distance L, but the cause is still unknown(Iguchi 2005, Moriwaki 1987). Therefore, I aim to elucidate the cause and mechanism, and to use it for the prediction and prevention of large-scale volcanic disasters due to the expected collapse of stratovolcanoes around the world in the future, including Mt. Fuji. Based on the verification results of the ballistic emission mechanism from the magma phreatic crater at the Izu Oshima’ s Habuminato explosion crater in 838, I applied the mechanism by simulation to following three cases, that is, (1) 1952 Myojinsho shallow submarine collapse, (2) 1888 Bandai collapse, and (3)1980 Mount St. Helens one. As a result, in each case, a part of the crater edge of the mountaintop was lifted vertically by the initial steam explosion, and almost at the same time, the slope of the collapse side started to slide down like a rigid plate. Therefore, it has been foreseen that by the reaction of the explosion will gain momentum and kinetic energy. And then, I came to think that the possibility of elucidating mystery of the small value H / L at the time of the sector collapse may become to rearise. Furthermore, there is a possibility that my assumption can well explain some field survey results of topographical changes, for example, Avalanche valley and so on.

Keywords: sector collapse, stratovolcano, H/L value, equivalent coefficient of friction, mechanism of ballistic explosion, steam explosion

©2021. Japan Geoscience Union. All Right Reserved.

Natural disasters and countermeasures in Ratnapura, Sri Lanka

*Takahito Kuroki[1], Kensuke Goto[2], Panditharathne N. G. S. [3]

1. Faculty of Letters, Kansai University, 2. Faculty of Education, Osaka Kyoiku Univ., 3. Health Service Rathnapura, Ministry of Health, Government of Sri Lanka

The purpose of this study is to investigate the basics of disaster countermeasure that can be used for disaster prevention education and that is flexible against nature and sustainable. We started to investigate them in the study area of Ratnapura district in southern Sri Lanka. Residents' awareness of the danger of natural disasters is still low there, so disaster prevention education has recently started in some areas. The education is conducted by the staff of the Ministry of Health, Government of Sri Lanka. In September 2019, we carried out a field survey on the natural disasters and the countermeasures for flood and landslide. In the survey, we received the support by them. Geologic map data of the US Department of Interior, Global Map data, ASTER GDEM, SRTM1and Landsat data were used as basic geographic data. From these geographic information, we were able to roughly understand the distribution of roads, water systems, land covers, altitudes, slopes, drainage basins, and geology.

The geology is Precambrian metamorphosed sedimentary rock, which is gneiss. Mountains, hills and lowlands can be seen there. The altitude is several tens of meters in the lowlands and around 500 m in the mountain areas. The mountains are widely covered with forests and have steep slopes, but there are also gentle slopes in some places. The landform with gentle slope is widely used as a tea plantation, and public facilities such as hospitals are often located in landform with such conditions. We were able to observe a lot of cracks in the foundation of a hospital building that indicated landslide is occurring. The landslides occurred on steep slopes in the mountain areas. This makes it difficult for roads in mountainous areas to pass. Most of the landslides which we investigated were slide-type slope failures caused by highly weathered basement rocks. The lowland is subdivided into alluvial plain and upland. Residential areas and agricultural lands are widely distributed in the alluvial plain. We confirmed that flood damage is likely to occur in lower elevation areas of the plain. There, the pedestals of the Buddha statue are unusually raised to escape flooding. High-class residential areas and public facilities such as hospitals are often located on the uplands. The hills are widely covered with forests. In urban areas, residential areas also develop at the foot of the hills with gentle slopes.

From the field survey, we understood some flexible responses of local people to natural disasters in their society. We confirmed countermeasures to use gentle slopes against landslide, and to use higher landforms or to raise the foundation against flood. However, the basic geographic data used was not able to represent the landform conditions in which the likelihood of landslide and flood could be estimated. In the next stage, we would like to examine in detail the safety landform condition and its land use from the analysis of large scale topographic maps and high resolution satellite data based on field surveys.

Keywords: landslide, flood, Sri Lanka, disaster prevention education

©2021. Japan Geoscience Union. All Right Reserved.

Policy for creating a liquefaction trend map based on geomorphologic classification for recognition of regional liquefaction risk

*Takayuki Nakano[1], Ryo Endo[1], Hiroyuki Inoue[2], Nozomi Yamashina[2], Shingo Watanabe[3], Keita Takada[3], Takuma Fujita[3]

1. Geospatial Information Authority of Japan, 2. City Bureau, Ministry of Land, Infrastructure, Transport and Tourism, 3. Fukken Co., Ltd.

1. Introduction

Ministry of Land, Infrastructure, Transport and Tourism conducted the General Technology Development Project "Study on liquefaction hazard map creation method for risk communication" in order to promote pre-disaster prevention of liquefaction and reduce its damage from FY2018 to 2020. In order to reduce the damage caused by liquefaction, residents/businesses and the government have a common understanding of the tendency of liquefaction in the area. It is important to think together about the necessity, i.e., to take risk communication.

As the first step in risk communication, in order to confirm and share the liquefaction occurrence tendency of the area between residents/businesses and the government, it is necessary information for understanding the tendency of liquefaction in the area. As the information, the "liquefaction trend map" that evaluates and classifies the liquefaction occurrence tendency for each geomorphologic classification based on the relationship between the liquefied points and the geomorphology in the past earthquakes is effective. In this presentation, we report on the policy for creating this "liquefaction trend map".

2. Basic policy and creation procedure of "Liquefaction trend map"

The "liquefaction trend map" is created based on information such as geomorphologic classification as a material showing the liquefaction occurrence tendency of the target area. In the map, the liquefaction occurrence tendency of the target area is evaluated and classified in 5 stages based on the geomorphology, man-made land, and the occurrence history of liquefaction in past earthquakes. The map scale is about 1:25,000 or larger, and the shape and distribution of geomorphology and man-made land are shown by polygon data.

The creating procedure of the "liquefaction trend map" is as follows. (1) Collection of materials, (2) Creation of geomorphologic classification maps, etc., (3) Evaluation/classification of liquefaction occurrence tendency, (4) Creation of “liquefaction trend map”.

3. Key points when creating "Liquefaction trend map"

(1) Collection of materials

- It collects previous geomorphologic classification maps, aerial photographs, old maps, man-made land creation materials, materials related to past liquefaction occurrence history, and ground information such as borehole data.

(2) Creation of geomorphologic classification maps, etc.

1) Creation of geomorphologic classification map by topography interpretation

- If there is no geomorphologic classification map, the map must be created by topography interpretation using topographic maps, DEMs, aerial photographs, etc.
- If there is a previous geomorphologic classification map, it may be possible to simplify the creation of the

©2021. Japan Geoscience Union. All Right Reserved.

map by referring to them.
2) Extraction and arrangement of man-made land
- With reference to old maps, aerial photographs, and construction materials, the area of reclaimed land in the water, backfills land after gravel collection, etc. is extracted as much as possible.
3) Arrangement of liquefaction occurrence history in past earthquakes
- The history of liquefaction in the target area is organized based on books, research papers, and materials.

(3) Evaluation/classification of liquefaction occurrence tendency
- Based on the geomorphologic classification map and the information of man-made land created in above (2), the liquefaction occurrence tendency is evaluated and classified using the five stages evaluation criteria shown in Table 1.

(4) Creation of “liquefaction trend map”
- Based on the evaluation result of the liquefaction occurrence tendency in above (3), “Liquefaction trend map” as map information is created at a scale of about 1:25,000.

4. Summary

The "liquefaction trend map" reported in this presentation will be posted as map information of the liquefaction hazard map and will be used together with other disaster learning information.

Keywords: liquefaction trend map, geomorphologic classification, liquefaction hazard map

©2021. Japan Geoscience Union. All Right Reserved.

表-1　微地形分類に基づく液状化発生傾向の評価区分
Table 1 Evaluation criteria for liquefaction tendency based on geomorphologic classification

液状化発生傾向 Liquefaction tendency		微地形（自然地形）・人工改変地 Geomorphology (natural) / man-made land	
Strong 強		微地形 Geomorphology	**旧河道**（former river channel）、**砂丘縁辺部**（margin of sand dune）、**砂丘間低地・砂州間低地**（lowland between costal dunes and/or bars）
		人工改変地 man-made land	**埋立地**（filled land）、**砂利(砂鉄)採取後の埋戻地**（Backfilled site after collecting gravel and/or iron sand）、**低地(湿地)上の盛土造成地**（filled-up land on lowland and/or marsh）
		微地形 Geomorphology	**三角州・海岸低地**（delta and costal lowland）、**自然堤防**（natural levee）、**砂州上・砂丘上の凹地**（depression on sand dunes and/or bars）
		人工改変地 man-made land	**干拓地**（reclaimed land）、**浅い谷や凹地の盛土地**（filled-up land of shallow valley and/or depression）、**谷埋め盛土造成地**（filled-up valley）
		微地形 Geomorphology	**砂州・砂礫州**（marine sand and gravel bars）、**氾濫低地**（flood plain）、**後背低地**（back marsh）
		微地形 Geomorphology	**砂丘(砂丘縁辺部、砂丘間低地を除く)**（sand dune）、**扇状地**（alluvial fan）※1、**谷底低地**（Valley bottom lowland）
弱 Weak		微地形 Geomorphology	**山地・丘陵**（Mountain and hill）、**山麓堆積地形**（Mountain footslope）、**台地**（Terrace）※2

※1：盛土造成されていない「扇状地上の旧河道」を含む.
(Including the unfilled-up former river channel on the alluvial fan)
※2：盛土造成されていない「台地上の浅い谷・凹地」を含む.
(Including the unfilled-up shallow valley and/or depression on the terrace)

©2021. Japan Geoscience Union. All Right Reserved.

[J] Oral | H (Human Geosciences) | H-DS Disaster geosciences

[H-DS08] Human environment and disaster risk

convener:Tatsuto Aoki(School of Regional Development Studies, Kanazawa University), Hiroshi, P. Sato(College of Humanities and Sciences, Nihon University), Chairperson:Tatsuto Aoki(School of Regional Development Studies, Kanazawa University), Hiroshi Sato(College of Humanities and Sciences, Nihon University)

Sun. Jun 6, 2021 1:45 PM - 3:15 PM Ch.15 (Zoom Room 15)

This session discusses disaster risks being inherent in the natural and human environment, which sometimes happen to appear at a disaster, from the viewpoint of not only natural sciences but also social and human sciences. Examples of discussion subjects are as follows: uncertainty of forecasting disaster and problems of huge disaster with low frequency that raised from the 2011 Tohoku earthquake, the methodology for improving hazard maps, national recovery plans considering probable changes or sustainability of the society, international cooperation for disaster mitigation, problems of active faults or liquefaction, adjusting disaster mitigation plan to the regional characteristics, technical development for supporting disaster prevention, education for the disaster mitigation.

3:05 PM - 3:15 PM

[HDS08-07]Discussion

©Japan Geoscience Union

[J] Oral | H (Human Geosciences)：H-DS Disaster geosciences

Sun. Jun 6, 2021 3:30 PM - 4:30 PM JST | Sun. Jun 6, 2021 6:30 AM - 7:30 AM UTC | Ch.15 Zoom Room 15

[H-DS08] Human environment and disaster risk

convener:Tatsuto Aoki(School of Regional Development Studies, Kanazawa University), Hiroshi, P. Sato(College of Humanities and Sciences, Nihon University), Chairperson:Tatsuto Aoki(School of Regional Development Studies, Kanazawa University), Hiroshi Sato(College of Humanities and Sciences, Nihon University)

This session discusses disaster risks being inherent in the natural and human environment, which sometimes happen to appear at a disaster, from the viewpoint of not only natural sciences but also social and human sciences. Examples of discussion subjects are as follows: uncertainty of forecasting disaster and problems of huge disaster with low frequency that raised from the 2011 Tohoku earthquake, the methodology for improving hazard maps, national recovery plans considering probable changes or sustainability of the society, international cooperation for disaster mitigation, problems of active faults or liquefaction, adjusting disaster mitigation plan to the regional characteristics, technical development for supporting disaster prevention, education for the disaster mitigation.

3:30 PM - 3:45 PM JST | 6:30 AM - 6:45 AM UTC

[HDS08-08] Current problems of submarine geological risks

*Kiichiro Kawamura[1] (1.Yamaguchi University)

3:45 PM - 4:00 PM JST | 6:45 AM - 7:00 AM UTC

[HDS08-09] **Verification of “Past” seismic intensity and estimation of “Future” ground motion by “Present-day” seismic observation: The Yanesen area**

*Motoko Ishise[1], Ryoichi Nakamura[1], Jun Muragishi[3], Shin'ichi Sakai[2,1] (1.Earthquake Reseach Institute, University of Tokyo, 2.Thr university of Tokyo III/GSII, 3.Yashima Gakuen University)

4:00 PM - 4:15 PM JST | 7:00 AM - 7:15 AM UTC

[HDS08-10] Characteristics of International Risk Communication over Trans-boudary Volcanic Disaster-The Case of 2010 Iceland Volcano Erution

*Mayumi Sakamoto[1], Haruhisa Nakamichi[2], Wakana Takahashi[3], Chizu Arashima[4], Masaru Arakida[5] (1.Graduate School of Disaster Resilience and Governance, University of Hyogo, 2.Disaster Prevention Research Institute, Kyoto University, 3.School of International Studies, Utsunomiya University, 4.Faculty of Global Communication, Kobe Gakuin University, 5.Asian Disaster Reduction Center)

4:15 PM - 4:30 PM JST | 7:15 AM - 7:30 AM UTC

[HDS08-11] Discussion

Current problems of submarine geological risks

*Kiichiro Kawamura[1]

1. Yamaguchi University

I show current problems of submarine geological risks in terms of off-shore wind powers in this presentation. Please discuss about them in this presentation.

Keywords: Submarine slides, Turbidity current, Mud volcano, Off-shore wind farm

©2021. Japan Geoscience Union. All Right Reserved.

Verification of “Past” seismic intensity and estimation of “Future” ground motion by “Present-day” seismic observation: The Yanesen area

*Motoko Ishise[1], Ryoichi Nakamura[1], Jun Muragishi[3], Shin'ichi Sakai[2,1]

1. Earthquake Reseach Institute, University of Tokyo, 2. Thr university of Tokyo III/GSII, 3. Yashima Gakuen University

We aim to clarify the details of “Future” disastrous earthquakes and ground motions in the Tokyo metropolitan area based on the investigation of “Past” ground motion by using “Present-dat” seismic observation (e.g., Ishise et al., 2020).

In the last fiscal year, we surveyed and collected various historical documents on earthquake damage caused by the 1855 Ansei-Edo Earthquake in the Hokuso area. Then, based on the results of the survey, we conducted seismic observations in the area and reported that the regional variation in seismic intensity of moderate-size earthquakes is consistent with that of the Ansei-Edo Earthquake (Ishise et al., 2021). And since last fall, we have been conducting the same kind of survey and seismic observation in the Yanesen area, as in the Hokuso area. In this study, we introduce the observational study and share a vision of the future.

“Past” ground motion

(1) Survey of historical documents:

Through this survey, we discovered new historical document about the earthquake damage to Tennoji temple cause by the 1855 Anse-Edo earthquake. The newly discovered document includes 13 descriptions of the damage within the temple.

(2) Re-examination of reported historical documents:

We re-examined historical documents used to estimate the seismic intensity map of the Ansei-Edo earthquake. As a result, we found out that some of the location information needed to be corrected.

“Present-day” seismic observation

Since last September, we have been conducting temporary seismic observations using 19 seismometers in the Yanesen area. The locations of seismometers were selected based on analyses of historical documents. Seismic observations will continue until March 2021.

Tentative waveform analysis using some of data shows regional variations in amplitude and frequency components at each site. After the completion of the temporary observation, we plan to quantitatively examine the relative seismic intensity distribution obtained from this observation and the seismic intensity distribution inferred from the analyses using historical documents.

“Future” earthquakes and the ground motion:

©2021. Japan Geoscience Union. All Right Reserved.

The seismological objective of this study is to predict the ground motion of future disastrous earthquakes, such as M7-class earthquakes in the Tokyo metropolitan area. To help with this, we plan to estimate detail site amplifications based on the present-day seismic observations to help make more realistic seismic intensity predictions. To do this, it is essential to develop a seismic observation network. Therefore, we are considering the construction of a super dense seismic network using seismic data obtained by Meso-net and SUPREME.

It is also important to know the distribution of strong motion caused by earthquakes as soon as possible after the occurrence of an earthquake. If seismometers are installed in advance at each site, they will be useful for in determining evacuation routes and priority of rescue operations. Furthermore, it is possible to start rebuilding livelihoods without survey by experts. In order to consider the construction of such a seismological observation system, we are conducting a pilot observation, which will be reported later.

Keywords: observational seismology, historical earthquake, estimation of seismic intensity

©2021. Japan Geoscience Union. All Right Reserved.

Characteristics of International Risk Communication over Trans-boudary Volcanic Disaster-The Case of 2010 Iceland Volcano Erution

*Mayumi Sakamoto[1], Haruhisa Nakamichi[2], Wakana Takahashi[3], Chizu Arashima[4], Masaru Arakida[5]

1. Graduate School of Disaster Resilience and Governance, University of Hyogo, 2. Disaster Prevention Research Institute, Kyoto University, 3. School of International Studies, Utsunomiya University, 4. Faculty of Global Communication, Kobe Gakuin University, 5. Asian Disaster Reduction Center

This study tries to identify characteristics of international risk communication over trans-boundary volcanic disaster. By analyzing policy making processes over international air traffic disturbances caused by 2010 Icelandic volcano Eyjafjallajökull eruption, it tries to describe its characteristics.

The 2010 Icelandic volcanic eruption caused airport closures or flight cancelations in Europe which resulted in huge socio-economic damages. The International Civil Aviation Organization (ICAO) had prepared Volcanic Ash Contingency Plan for EUR Region in 2009, however the plan was not sufficient to solve the problem caused by eruption. ICAO set “zero tolerance” for aircraft flying over volcanic eruptions in order to avoid the risk of jet engine shutdowns. In order to solve the problem, "acceptable tolerance" was discussed based on science and technology data, suchg as in-situ ash forecast over Europe or jet engine tolerance to airborne particles were required.

This case demonstrated difficulty of international policy making under an emergent situation regarding to the issue which was not defined in existing systems, but requires precise science and technological data. As for the case of 2010 eruption, the following points were discussed.
The first was the improvement of a communication system to revise volcanic ash forecast. As for the 2010 eruption, the disaster response was decided based on the forecast by the London VAAC, which observes atmospheric volcanic ash clouds including Iceland. However, international communication systems among volcano monitoring institutes were vulnerable. After the eruption, interenational communication system was revised.

Second, the importance of science and technological data regarding to the jet engine tolerance to airborne particles. After the eruption, governments, air plane companies and research institutes examined the effect of volcanic ash to jet engines and discussed engine tolerance.

Third, the necessity of an international policy-making mechanism. After the eruption, video conferences were held by the Ministers of Transportation of EU member states, led by the European Commission, and provisional standards were discussed. After this disaster, the European Commission established the European Aviation Crisis Coordination Cell (EACCC) as a permanent institute for the risk management. The experience demonstrated the necessity of the international risk communication system to share in-situ information among different actors such as countries where volcanoes are located, countries which suffers by volcanic ash dispersion or organizations which monitor volcanic ash.

Keywords: trans-boundary volcanic disaster, Eyjafjallajökull, risk communication

©2021. Japan Geoscience Union. All Right Reserved.

©2021. Japan Geoscience Union. All Right Reserved.

[J] Oral | H (Human Geosciences) | H-DS Disaster geosciences

[H-DS08] Human environment and disaster risk

convener:Tatsuto Aoki(School of Regional Development Studies, Kanazawa University), Hiroshi, P. Sato(College of Humanities and Sciences, Nihon University), Chairperson:Tatsuto Aoki(School of Regional Development Studies, Kanazawa University), Hiroshi Sato(College of Humanities and Sciences, Nihon University)

Sun. Jun 6, 2021 3:30 PM - 4:30 PM Ch.15 (Zoom Room 15)

This session discusses disaster risks being inherent in the natural and human environment, which sometimes happen to appear at a disaster, from the viewpoint of not only natural sciences but also social and human sciences. Examples of discussion subjects are as follows: uncertainty of forecasting disaster and problems of huge disaster with low frequency that raised from the 2011 Tohoku earthquake, the methodology for improving hazard maps, national recovery plans considering probable changes or sustainability of the society, international cooperation for disaster mitigation, problems of active faults or liquefaction, adjusting disaster mitigation plan to the regional characteristics, technical development for supporting disaster prevention, education for the disaster mitigation.

4:15 PM - 4:30 PM

[HDS08-11]Discussion

©Japan Geoscience Union

[J] Poster | H (Human Geosciences)：H-DS Disaster geosciences

Sun. Jun 6, 2021 5:15 PM - 6:30 PM JST | Sun. Jun 6, 2021 8:15 AM - 9:30 AM UTC | Ch.09_1

[H-DS08] Human environment and disaster risk

convener:Tatsuto Aoki(School of Regional Development Studies, Kanazawa University), Hiroshi, P. Sato(College of Humanities and Sciences, Nihon University)

This session discusses disaster risks being inherent in the natural and human environment, which sometimes happen to appear at a disaster, from the viewpoint of not only natural sciences but also social and human sciences. Examples of discussion subjects are as follows: uncertainty of forecasting disaster and problems of huge disaster with low frequency that raised from the 2011 Tohoku earthquake, the methodology for improving hazard maps, national recovery plans considering probable changes or sustainability of the society, international cooperation for disaster mitigation, problems of active faults or liquefaction, adjusting disaster mitigation plan to the regional characteristics, technical development for supporting disaster prevention, education for the disaster mitigation.

[HDS08-P01] The role of residents' resilience on the recovery process in a torrential rain

*Shoji Ohtomo[1], Reo Kimura[2] (1.Kanto Gakuin University, 2.University of Hyogo)

[HDS08-P02] Flood damage mapping of 2020 Typhoon Ulysses in the Philippines

*Naoko Nagumo[1], Kentaro Aida[1], Miho Ohara[1], Masakazu Fujikane[1] (1.International Centre for Water Hazard and Risk Management, PWRI)

[HDS08-P03] An example of using Google Earth Engine in providing and sharing information on wide-area typhoon disasters in international joint research projects

*Kentaro Aida[1], Naoko Nagumo[1], Miho Ohara[1] (1.International Centre for Water Hazard and Risk Management, PWRI)

[HDS08-P04] Estimating the amount of waste treatment units in the event of a disaster with self-help and mutual support

*Yoshinobu MIZUI[1,2] (1.University of Tsukuba, 2.NationalResearch Institute for Earth Science and Disaster Resilience)

[HDS08-P05] Possibility of support for disaster victims by accommodation facilities-Advance evacuation and acceptance in the event of a disaster-

Yuka SUZUKI[1], *Tatsuto Aoki[2] (1.Kanazawa University, 2.School of Regional Development Studies, Kanazawa University)

[HDS08-P06] Effect of synchrony bias on excitation of evacuation behavior during tsunami-From the evacuation behavior of residents in Noto Town, Ishikawa Prefecture during the 2019 Yamagata-oki Earthquake-

Mayu KITAMURA[1], *Tatsuto Aoki[2] (1.Kanazawa University, 2.School of Regional Development Studies, Kanazawa Univ.)

[HDS08-P07] Status of provision of disaster prevention information and learning to international students at national and public universities and their issues

*CHENYUE LU[1], Kiyomi HAYASHI[2], Tatsuto AOKI[2] (1. Division of Regional Development Studies,Graduate School of Human and Sociology-Environmental Studies,Kanazawa University, 2.School of Regional Development Studies, Kanazawa University)

The role of residents' resilience on the recovery process in a torrential rain

*Shoji Ohtomo[1], Reo Kimura[2]

1. Kanto Gakuin University, 2. University of Hyogo

Disasters linked to natural hazards have increased sharply in the last 20 years (UNDR, 2020). Despite the massive disasters that have occurred, there are limitations to the national disaster prevention and mitigation frameworks that aim to reduce the impact of disasters. In recent times, the strategy of promoting resilient communities that have the ability to recover from disasters has become of interest. The study examined the relationships between the recovery process and residents' resilience in the torrential rain in western Japan in 2018.

High infrastructural damages and fatalities were recorded in Okayama and Hiroshima prefecture in the torrential rain. The study conducted a web-based questionnaire from January 31 to February 12 2019, about 6 months after the torrential rain hit western Japan in 2018. Target areas were in 13 districts in Hiroshima prefecture and 6 districts in Okayama prefecture that suffered damage caused by the torrential rain. The result of the analysis of the recovery calendar (Kimura, 2005) indicated that recovery was progressed in the "disaster utopia" (up to 1.5 ~ 2 months after) and "reentry to everyday life" (up to 6 ~ 12 months after) phases (Figure 1). Next, to examine the difference in residents' life-recovery progress up to the "disaster utopia" and "reentry to everyday life" phase, GLM analysis was implemented using count data of recovery calendar for each period. Firstly, a Bayesian GLM with Poisson distribution was conducted to predict the count data for life recovery up to the "disaster utopia" phase, with gender, age, the level of flooding damage, and human suffering as interactive terms with psychological resilience, and psychological resilience and other variables were taken as the independent variables. As a result, the main effects of gender, dummy variable of flooding damage (vs. flooded above the floor), human suffering, and the interaction effect of age ×psychological resilience were found. Concerning these effects, male residents' life-recovery scores were higher than female residents' (Figure 2_a). Moreover, the life recovery of residents with flooding above the floor level was lower than other residents (Figure 2_b). The more human suffering the poorer the life-recovery scores (Figure 2_c). Moreover, although older residents' life recovery was lowest when their psychological resilience was low, older residents' life recovery was the highest when their psychological resilience was high (Figure 2_d). Secondly, when examining changes up to the "reentry to everyday life" phase, the difference in life-recovery count data from the "disaster utopia" phase to the "reentry to everyday life" phase was calculated. In addition, a similar Bayesian GLM with Poisson distribution was conducted to predict the difference in life-recovery count data. We found the main effects of gender and the dummy variable of flooding damage (vs. flooded above the floor), and the interaction effect of psychological resilience ×the dummy variable of flooding damage (vs. flooded above the floor). Concerning these effects, female residents' life-recovery scores were higher than male residents (Figure 4_a). Moreover, the life-recovery scores of residents with flooding above the floor level were higher than other residents (Figure 4_b). Contrary to our expectation, the weaker the psychological resilience of residents with flooding above the floor level, the greater their tendency to perceive life recovery.

Thus, residents' recovery from disasters differed depending on the level of damage and the time phase. The "disaster utopia" phase up to 2 months after the disaster is the stage where residents who have experienced less damage begin recovering. Even older residents or residents who have suffered serious

©2021. Japan Geoscience Union. All Right Reserved.

damage are more able to overcome the adverse situation and recover soon, if they have strong psychological resilience. The “reentry to everyday life” phase up to 6 months after the disaster is the stage when residents who have experienced serious damage begin recovering. Residents with weaker resilience are more likely to engage in recovery activities during this stage. Although psychological resilience does not have a direct impact on life recovery, it may increase the pace of life recovery. The study suggests the importance of resource of the community for disaster risk management, such as residents’ resilience, in addition to the level of damage and the time phase after the disaster, to fully understand recovery.

Keywords: Disaster risk management, Recovery calendar, Resilience, Torrential rain

©2021. Japan Geoscience Union. All Right Reserved.

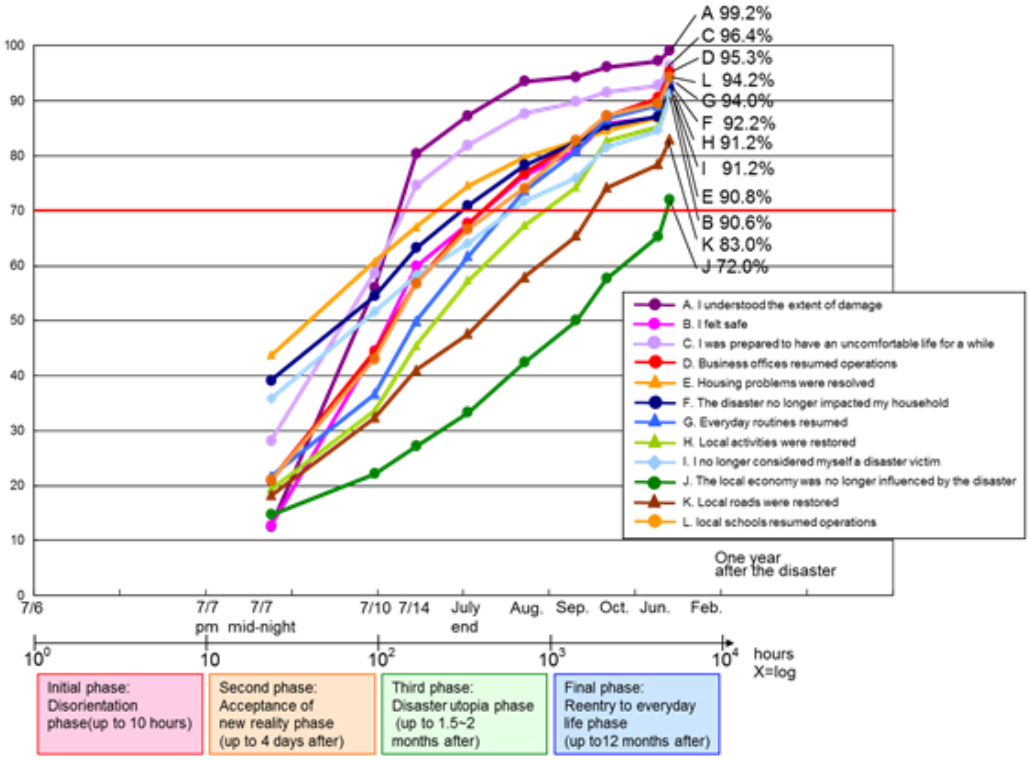


Figure 1 Life-recovery calendar of the torrential rain in western Japan in 2018

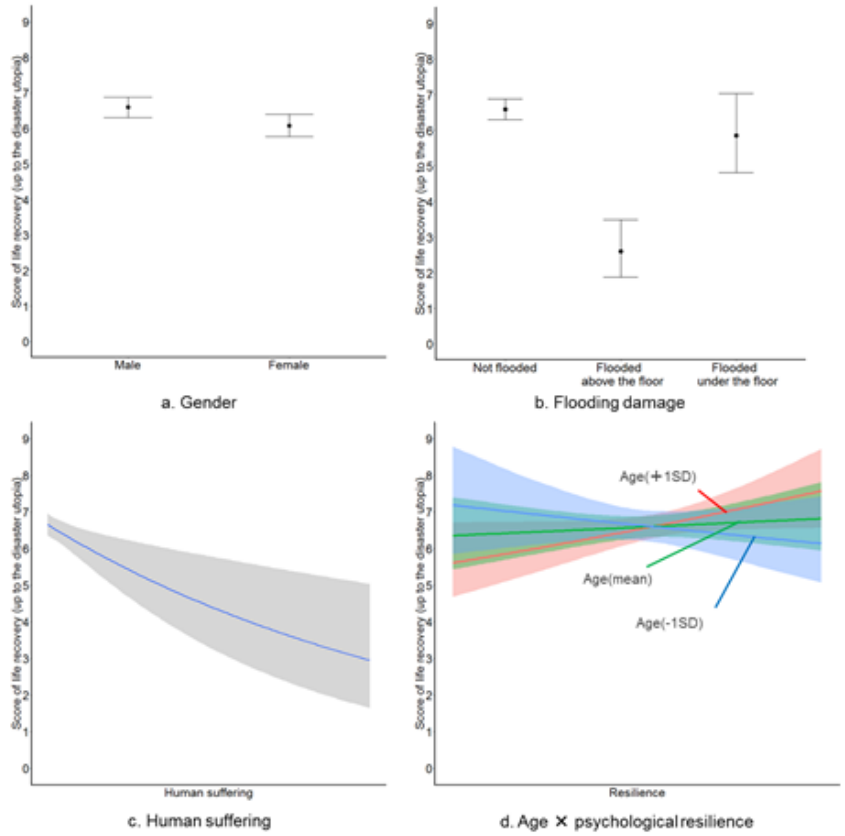
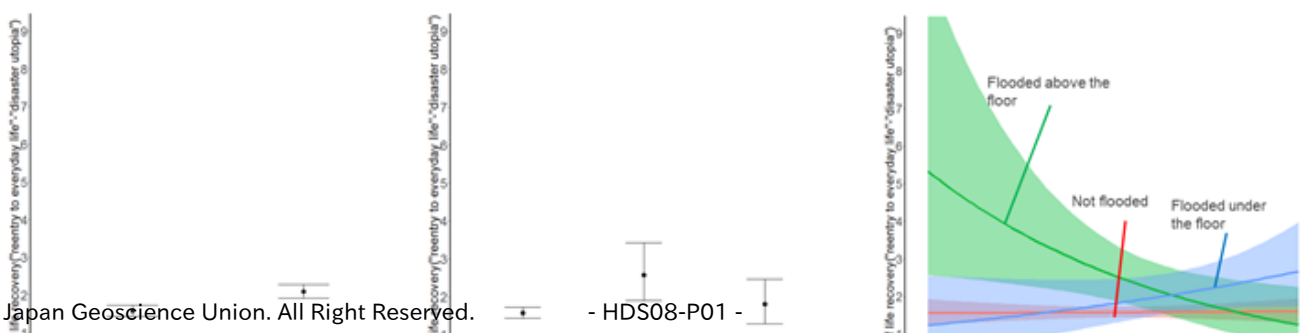


Figure 2 The plots of the posterior distribution of parameters of gender, flooding damage, human suffering, age × psychological resilience (changes in life recovery up to the "disaster utopia" phase).



©2021. Japan Geoscience Union. All Right Reserved.

©2021. Japan Geoscience Union. All Right Reserved.

Flood damage mapping of 2020 Typhoon Ulysses in the Philippines

*Naoko Nagumo[1], Kentaro Aida[1], Miho Ohara[1], Masakazu Fujikane[1]

1. International Centre for Water Hazard and Risk Management, PWRI

Typhoon Ulysses (international name: Vamco) crossed the Central Luzon Region of the Philippines in November 2020, bringing strong winds and torrential rainfall and causing 101 casualties throughout the country. The numbers of flooding and landslide/soil collapse were 264, while affected municipalities/cities reached 541 and affected persons were 5,184,824 in total (as of 13 January 2021). Also, the maximum numbers of evacuees reached to 556,318 (as of 15 November 2020). In flood-prone countries such as the Philippines, hazards and damage should be carefully investigated, and the collected data should be systematically sorted out for future disaster response, recovery and flood risk assessment. However, it is often difficult to get a whole picture of a disaster, especially when it is a widespread event. In addition, the recent worldwide pandemic of COVID-19 has made it difficult for experts to conduct sufficient field surveys. Therefore, this study conducted flood-related data mapping using satellite observation rainfall, satellite images and reports released on the web by the National Disaster Risk Reduction Management Council (NDRRMC) of the Philippines to understand the floods and damage caused by Typhoon Ulysses. Rainfall due to Typhoon Ulysses was particularly intense in the eastern part of Luzon Island; the 3-day-rainfall reached over 300 mm between 11 and 14 November. As a result, several rivers flooded at different locations of the island. The flood events of the Pasig-Marikina River in Metro Manila and the Cagayan River in Cagayan Valley Region, Northern Luzon, have been considered the most serious since the 2009 flood by Typhoon Ondoy and the 1980 flood by Typhoon Aring, respectively. Large numbers of people were reported to be affected in the regions of Central Luzon, Cagayan Valley, Bicol and Metro Manila as they lived along the typhoon course, while the house damage was concentrated in the regions of Central Luzon and Bicol. Also, 2991 evacuation centers were opened three days after the typhoon landed and 324,617 persons were evacuated inside the evacuation centers along with the other 231,701 persons evacuated outside the centers across the country, and more than 30-40 % of the population was evacuated in some municipalities. Mapping both hazard and damage data can be instrumental in understanding the characteristics of a disaster spatiotemporally, and such analytic understanding will be useful not only for recording disasters but also for sharing a common view of a disaster and identifying the needs for further support.

Keywords: typhoon, satellite image, flood, damage, Philippines

©2021. Japan Geoscience Union. All Right Reserved.

An example of using Google Earth Engine in providing and sharing information on wide-area typhoon disasters in international joint research projects

*Kentaro Aida[1], Naoko Nagumo[1], Miho Ohara[1]

1. International Centre for Water Hazard and Risk Management, PWRI

ICHARM has been conducting the SATREPS project with Philippine research members since 2020. The project's objective is to research disaster assessment to contribute to hydrology, agriculture, and water management under climate change. However, field surveys and local activities have been restricted even by local researchers due to the pandemic of COVID-19. In these circumstances, Typhoon Ulysses hit Luzon Island in early November 2020, and heavy rainfall caused large-scale floods in various parts of the country. According to the National Disaster Risk Reduction and Management Council (NDRRMC) of the Philippines, a large number of people were forced to evacuate because so many houses were severely damaged as a result of flooding. However, the overall picture of the damage caused or to be caused by the typhoon remained unknown during the disaster.

In such a case, earth observations (EO) by satellites have been proven extremely useful. Among various current operational EO-satellites, the Sentinel series by the European Space Agency (ESA) and the Landsat series by the National Aeronautics and Space Administration (NASA) provide satellite images of different areas on the planet free of charge. Sentinel-1 synthetic aperture radar (SAR) images and Sentinel-2 optical images are frequently acquired at intervals of 5 or 6 days, respectively. Such operations are beneficial for ground monitoring.

Similar to these satellite data, the information provided by government agencies is also essential for understanding the whole picture of a disaster. Information such as the number of victims, shelters, and evacuees of each municipality is regularly released by NDRRMC through the Internet. Though such information itself is very useful, it can be even more useful to understand the entire situation if visualized on a map.

Therefore, this project used the Google Earth Engine (GEE) to share the overall picture of the disaster situation due to Typhoon Ulysses. GEE is a cloud-type mapping application provided by Google. Using global satellite data and geographic information stored on Google's server, a special computer program is applied to process such data and information to help users understand them visually while looking at the screen. In other words, the most significant merit of GEE is that it can quickly launch a system that can collect and share information anywhere in the world without depending on the area of residence or human and economic resources. And, the application can visualize information for mapping, making it ready to be shared easily by many people with user-friendly functions such as enlarging and reducing images, as long as they have an Internet environment.

The information shared among the members in this project is disaster information released by NDRRMC, inundation area estimated based on Sentinel-1 SAR images, visible images and the estimated inundation area from the Sentinel-2 optical sensor, and precipitation products from satellites. The precipitation products are hourly and cumulative precipitation distributions using the satellite global precipitation map (GSMaP) provided by the Japan Aerospace Exploration Agency (JAXA) and the Integrated Multi-satellitE

©2021. Japan Geoscience Union. All Right Reserved.

Retrievals for GPM (IMERG) provided by NASA. These products were applied to the Pampanga River basin, Pasig River, Laguna Lake, Marikina River basin, and Cagayan River in the three main watersheds in northern Luzon Island.

Visualization with these GEE systems is considered to have the following significance from the viewpoint of disaster response: 1) Although the whole picture of the disaster could not be understood due to a widespread disaster, visualization of information was useful to capture a rough image of the damage distribution. To have an idea of the disaster makes it possible to predict how it may further develop or which areas need support more urgently than other areas; 2) Although, due to COVID-19, researchers from both countries could not go to the target site and meet each other, information shared among the members created a foundation for discussions on disaster response and recovery; 3) Although satellite-based visible images only offer inundation area, adding a land-use map to the inundation area map produced a useful tool for disaster response and restoration efforts; and 4) By increasing the number of information layers, the resultant map can be used not only immediately after a disaster but also at various subsequent stages, for example, to show the progress of restoration and reconstruction.

Keywords: Flood, Satellite data , Information sharing, Google Earth Engine, Philippines, Typhoon

©2021. Japan Geoscience Union. All Right Reserved.

Estimating the amount of waste treatment units in the event of a disaster with self-help and mutual support

*Yoshinobu MIZUI[1,2]

1. University of Tsukuba, 2. NationalResearch Institute for Earth Science and Disaster Resilience

1. Introduction

In recent years, regional disasters that cause enormous damage have occurred almost every year in various parts of Japan. As a self-help activity, there is a labor shortage due to the work of cleaning up the victim's house, but there are also disaster volunteers who voluntarily participate from inside and outside the area to make up for the shortage.
Since the Great East Japan Earthquake on March 11, 2011, I have been involved in the operation of disaster volunteer centers in various places, but I found it difficult to adjust the actual amount of work and the number of victims in the disaster area. To solve this problem, it is important to understand the amount of work required for self-help and mutual support and the total number of activists, and to clarify the breakdown of the total number of mutual support.
T In this study, we will grasp the total amount of self-help and mutual support. We first examined the total number of activities including self-help and mutual support in past disasters. We also calculated the amount of disaster waste treated in units of 100 people, which is the unit of the amount of treatment required to make a rough estimate.

2. Survey method

It is necessary to grasp the total amount of disaster waste caused by a disaster and clarify the breakdown amount for which self-help and mutual support are in charge of processing work. The target disaster waste is waste that can be manually cleaned on the premises of private land. The Ministry of the Environment investigates and reports on the breakdown of waste for each disaster.
Self-help / mutual support targets cleanup waste in disaster waste (waste discharged when citizens clean up damaged items at home), and cleanup waste includes combustibles and wood chips, Tatami, incombustibles, household waste, etc.
By dividing the amount of cleanup waste by the amount of self-help and mutual support activities, the unit amount of cleanup waste disposal work by self-help and mutual support can be obtained.

3. result

In 2015, the flood damage in Joso City, Kinugawa basin, was used as a model. The Joso City Disaster Volunteer Center was active for 58 days.
Assuming that one-quarter of the residents in the area where the evacuation order was issued were self-help volunteers, the total number of volunteers was 504,842 in 58 days. The total amount of disaster waste from floods in 2015 was 52,400 tons.
It was assumed that the waste to be cleaned up was combustibles, incombustibles, and earth and sand, and as condition (1), it was assumed that combustibles were almost 100% as household waste and incombustibles and earth and sand were 50%. In addition, as condition (2), a trial calculation was made assuming that combustibles are 100% and incombustibles and earth and sand are 25%. The weight ratio of combustibles and incombustibles / earth and sand will be ignored this time.
In the case of condition (1), combustibles account for 6.4% of the total amount of waste. Incombustibles account for 35.25%. Sediment is 6.0%. The ratio and weight of the target cleanup waste are
6.4 + 35.25 + 6.0 = 47.65%

©2021. Japan Geoscience Union. All Right Reserved.

52,400t ×47.65 = 24,968.6t
Assuming that this cleanup waste was processed by 504,842 people, 4.946 tons can be processed per 100 people.
In the case of condition (2), combustibles account for 6.4% of the total amount of waste. Incombustibles account for 17.625%. Sediment is 3.0%. The ratio and weight of the target cleanup waste are
6.4 + 17.625 + 3.0 = 30.025%
52,400t ×30.025 = 15,733.1t
Assuming that this cleanup waste was processed by 504,842 people, 3.116 tons can be processed per 100 people.
Also, using the estimation formula of the Ministry of the Environment, the total amount is estimated to be about 9541.933 tons. Assuming that this cleanup waste was processed by 504,842 people, 1.890 tons can be processed per 100 people.
As a result, it was found that the disaster waste treatment unit that can be treated in one day is 3t (2-5t) / 100 people.

Keywords: Self-help, mutual support, disaster volunteers, disaster waste, waste disposal

©2021. Japan Geoscience Union. All Right Reserved.

Possibility of support for disaster victims by accommodation facilities-Advance evacuation and acceptance in the event of a disaster-

Yuka SUZUKI[1], *Tatsuto Aoki[2]

1. Kanazawa University, 2. School of Regional Development Studies, Kanazawa University

Background

In order for Japan, where many natural disasters occur, to become a tourism-oriented country, it is essential to have a disaster prevention plan that keeps in mind that tourists who do not know the land will be affected.

The purpose of this study is the following two. One is to clarify the disaster prevention situation of tourists in Kanazawa City, and the other is to examine the possibility of supporting evacuees in the event of a large-scale disaster by accommodation facilities. To discuss this, we conducted interviews with the Crisis Management Division of Kanazawa City Hall, interviews and conducted a questionnaire survey with hotels (24 facilities) in Kanazawa City.

Kanazawa is one of the major tourist destinations in Japan. In addition, the Morimoto-Togashi fault zone, which is said to have a high probability of earthquake occurrence, exists in the center of the city, and it is assumed that a wide area of the city center will be flooded even with a planned-scale flood.

As an evacuation site in the event of a disaster

The regional disaster prevention plan of Kanazawa City does not specify how to deal with tourists and people who have difficulty returning home in the event of a disaster. Kanazawa City has signed an agreement with a cooperative of accommodation facilities for the purpose of utilizing accommodation facilities as a temporary evacuation site for tourists and those who have difficulty returning home. However, in the interviewed to the Crisis Management Division of the city hall, regular meetings were not held after the conclusion of the agreement, and the disaster management plan of the accommodation facility was not grasped. At present, it is hard to say that the agreement is effective.

On the other hand, there is also a problem on the accommodation facility side that accepts tourists. None of the facilities answered that they have a good understanding of earthquakes originating from the Morimoto-Togashi fault zone. It became clear that the awareness of the disaster assumption was low. Reflecting this, 42% (10/24 facilities) have not formulated a disaster prevention manual. Only 13% (3/24 facilities) have prepared manuals for both earthquakes and floods. 33% (8/24 facilities) do not expect to open the facilities as evacuation shelters in the event of a disaster. Even among facilities that are expected to accept evacuees, only 25% (6/24 facilities) are expected to accept tourists other than the guests of their own facilities.

In addition, 42% (10/24 facilities) of facilities that can accept evacuees for about 3 days, and 21% (5/24

©2021. Japan Geoscience Union. All Right Reserved.

facilities) that can accept evacuees for 1 week or more. It was. This indicates that the Kanazawa city government needs to evacuate tourists out of the city in a short period of time.

As an evacuation site for preventive evacuation

In the case of floods, preventive evacuation is important. 54% (13/24 facilities) answered that they could accept evacuees for preventive evacuation in some way. In the hearing for the facility, "if there is a request of the city government, acceptance of the citizens is also taken into account," there was some hotels that answered. On the other hand, another hotel said that it is difficult to distinguish evacuees from general guests before a disaster occurs, and they will be provided for a fee based on the reservations made by the guests. It was shown that there are certain difficulties in accepting preventive evacuation by accommodation facilities.

One hotel considering accepting preventive evacuees said, "Proactively providing evacuation shelters, will lead to the improvement of the hotel brand and disaster prevention can be monetized as our main business." The provision of shelters for accommodation facilities was a disaster response as CSR in response to government requests. This result shows that this could be developed into a model of responding to disasters as a social business and connecting it to the original business.

Conclusion

It was confirmed that the effectiveness of the disaster prevention agreement between Kanazawa City and accommodation facilities is currently questionable. In order to make it more effective, various types of support from the government will be required.

Accommodation facilities are also required to actively understand the disaster risks of their own facilities and the surrounding area. In preventive evacuation, it will be possible to take disaster prevention measures as an opportunity for social business and actively take measures. We would like to point out that introducing such a perspective into the BCP can be beneficial to companies, governments, and citizens.

Keywords: Accommodations, Evacuee, Preventive evacuation, Shelter, Social business

©2021. Japan Geoscience Union. All Right Reserved.

Effect of synchrony bias on excitation of evacuation behavior during tsunami-From the evacuation behavior of residents in Noto Town, Ishikawa Prefecture during the 2019 Yamagata-oki Earthquake-

Mayu KITAMURA[1], *Tatsuto Aoki[2]

1. Kanazawa University, 2. School of Regional Development Studies, Kanazawa Univ.

Research objectives

Japan is one of the world's highest affected countries by disaster. Within those disaster, the tsunami disaster is one of the most damaging. As a characteristic of disaster prevention actions against tsunami disasters, it may be possible to reduce human damage by evacuating using seismic motion and/or tsunami information prior to the arrival of the tsunami. and there are many studies and activities have been done to encourage evacuation.

In previous studies, psychological studies have also been conducted on the relationship between evacuation behavior and disaster experience / disaster prevention awareness. According to them, it has been clarified that human cognitive bias has a great influence as one of the factors that cause "evacuation delay" and "people who do not evacuate".

Therefore, in this study, we conducted a questionnaire survey of residents living in the tsunami inundation area of Noto Town, located in the northern part of the Noto Peninsula, Ishikawa Prefecture. And we investigated and analyzed how cognitive bias affected the evacuation behavior. At the time of the Yamagata-oki earthquake (M_{JMA}6.7), Noto Town are shaken of seismic scale 3 by JMA and only a tsunami advisory was issued. However, more than 500 residents moved to evacuation site. The area around the study area is the area where one-sixth of the seismic intensity was observed in the Noto Hanto earthquake in 2007. And the tsunami hazard map revised after the Great East Japan Earthquake in 2011.

Result

The questionnaire was distributed and collected by mail to 999 households in the district. The number of collections was 255 (25.5%), 55% for men (N = 141), 40% for women (N = 103), and 4% for others (N = 11). By age, the elderly aged 60 and over account for 65% (N = 165). The fact that household representatives are respondents to the questionnaire and that the aging rate in the target area is close to 50% influences the high proportion of elderly respondents in the questionnaire.

As a result, it was found that 25% of the respondents were evacuated from the tsunami. Respondents were classified into the following four patterns. (1) Evacuated during both of the Noto Hanto and the Yamagata-Oki earthquakes, (2) Evacuated only during the Noto Hanto earthquake, (3) Evacuated during the Yamagata-oki earthquake even though did not evacuated during Noto Hanto earthquake, ④ Did not evacuated during both the earthquakes. The composition of the respondents was (1) 4% (N = 9), (2) 3% (N = 6), (3) 19% (N = 43), and (4) 75% (N = 174). The important point is there were some cases where people who did not evacuate during the Noto Hanto earthquake evacuated this time.

Focusing on the residents who responded as (3), we asked for them multiple answers about the reasons for evacuation. As a result, the answers were obtained that "due to earthquake motion (20 people)", "due to tsunami information (19 people)", and "because they live in the inundation area (16 people)". In addition, the following answers followed. "Because I was instructed to evacuate (8 people)" "Because my neighbors were evacuating (8 people)" "Because someone told me to evacuate (7 people)". These results mean that in addition to the sense of crisis and information, "synchronization bias" such as "evacuation behavior of surrounding people and voices from others" acted positively. Furthermore, among the

©2021. Japan Geoscience Union. All Right Reserved.

categories (1) to (4), the highest percentage of those with synchronization bias affected was in (3), and the percentage was 30%.

Discussion

In the context of disaster prevention, synchronization bias is often cited along with normalcy bias as a reason for residents not to evacuate. However, the results of this study showed that by intentionally biasing the population in synchronization, people who did not evacuate voluntarily may be able to evacuate. It is also able to pointed out the importance of social capital to enhance disaster prevention capabilities, such as community disaster prevention leaders who calling for evacuation in emergencies and communities where residents can communicate on a daily basis.

In disaster prevention and mitigation, not only physical measures such as stockpiling but also psychological measures are important. As part of education for disaster prevention, we need to learn about cognitive bias.

Keywords: Tsunami, Evacuation, Synchronous bias, 2019 Yamagata-oki Earthquake

©2021. Japan Geoscience Union. All Right Reserved.

Status of provision of disaster prevention information and learning to international students at national and public universities and their issues

*CHENYUE LU[1], Kiyomi HAYASHI[2], Tatsuto AOKI[2]

1. Division of Regional Development Studies,Graduate School of Human and Sociology-Environmental Studies,Kanazawa University, 2. School of Regional Development Studies, Kanazawa University

In this study, we will clarify the status of dissemination of disaster prevention information and the implementation and support of disaster prevention to international students learning at national and public universities. Questionnaires were distributed by mail to departments that support international students at 179 universities nationwide (collection number 78, collection rate 43.6%).

Results

1) Status of provision of disaster prevention information at orientation

52.6% of univ. provide disaster information at orientation, and 55.1% of univ. distribute and post disaster information issued by local governments. 44.9% of univ. provide disaster information in languages other than Japanese. The languages used was English (100%), Simplified Chinese (54.3%), Korean (37.1%), Traditional Chinese (14.3%), and other languages (11.4%).

2) Status of learning opportunities related to disaster prevention

When it comes to safety confirmation systems and training for their use between univ. and international students, only 30 univ. "have system, and are training". Regarding "evacuation drills at univ.", 34 univ. "conducted and many international students participated" and 16 univ. "conducted but the participation rate of international students was low". At 66 univ., there were no disaster prevention events in collaboration with the local community. Only 15 univ. provided guidance on disaster drills of local community and encouraged international students to participate.

18 univ. have "established" classes for international students studying disasters and disaster prevention of Japan, and 4 of them "take many international students". There were 58 universities that did not provide Japanese language education including vocabulary and expressions of a disaster.

3) Issues felt by the university

The following issues were raised as problems in disaster prevention support and guidance for international students.

Insufficient communication and Japanese proficiency (43 univ.)
Unrecognized possibility of disaster (30 univ.)
Influence of culture and lifestyle of country of origin (28 univ.)
Incomprehensible jargon (28 univ.)
Insufficient understanding and image of disasters and disaster prevention caused by the lack of disaster experience and learning opportunities in the home country (26 univ.)

The following issues were also raised.

International students do not fully understand the characteristics of the natural environment and the

©2021. Japan Geoscience Union. All Right Reserved.

structure of the town in their area (22 univ.)
Undeveloped information provision routes and venues (22 s univ.)
Difficulty in collaboration between international students and the community at the time of the disaster (21 univ.)
Weak connection between international students and the community (21 univ.)

In addition, we asked each university's views on the need for learning support, guidance and information provision for community-related disasters for international students. 45 universities replied, "We should not only disseminate and train information on disaster prevention on campus, but also support and provide information on disasters related to the region, but we have not fully implemented it."

Issues and improvement measures considered from the results of the questionnaire
When international students begin their college life in Japan where the high-risk area in disaster, information provision, training, events, orientation and classes at univ. can be an important opportunity to recognize and prepare for disaster risks.

The departments in charge of international students at many univ. are aware of the following. Problems with Japanese language proficiency, low knowledge and awareness of disaster due to lack of experience and learning, differences in lifestyle, inadequate understanding of the region and inadequate cooperation with the region. In addition, they feel that it is necessary to devise environmental improvement and disaster prevention learning in order to improve these problems. However, they are struggling to be unable to fulfill. There are various things that need to be dealt with in support of international students, and it is difficult to devote a lot of time, labor, cost, and human resources to the enhancement of disaster prevention learning and activities. However, there are some aspects in which the situation can be improved and improved with a little ingenuity and consideration, and it is desirable to start from there.

Keywords: international students, study for disaster prevention, information of disaster prevention, university, questionnaire survey

©2021. Japan Geoscience Union. All Right Reserved.

[E] Oral | H (Human Geosciences)：H-TT Technology & Techniques

Sun. Jun 6, 2021 1:45 PM - 3:15 PM JST | Sun. Jun 6, 2021 4:45 AM - 6:15 AM UTC | Ch.14 Zoom Room 14

[H-TT14] Geographic Information Systems and Cartography

convener:Takashi Oguchi(Center for Spatial Information Science, The University of Tokyo), Yoshiki Wakabayashi(Graduate School of Urban Environmental Sciences, Tokyo Metropolitan University), Yuei-An Liou(National Central University), C. Ronald Estoque(National Institute for Environmental Studies, Japan), Chairperson:Takashi Oguchi(Center for Spatial Information Science, The University of Tokyo), Yoshiki Wakabayashi(Graduate School of Urban Environmental Sciences, Tokyo Metropolitan University)

This session discusses various methods which acquire, store, analyze and visualize geospatial data, and presents the outcomes of empirical studies using GIS or mapping methods. The session also deals with applications of digital data, and GIS, and mapping to various fields of earth and planetary science and human society. All presentations and discussion of this session are made in English.

1:45 PM - 2:00 PM JST | 4:45 AM - 5:00 AM UTC

[HTT14-01] A GIS-based study on accessibility of public bus system in Sapporo

*ZITONG XU[1], Yuichi S. Hayakawa[2,3] (1.Graduate School of Environmental Science, Hokkaido University, 2.Faculty of Environmental Earth Science, Hokkaido University., 3.Center for Spatial Information Science, The University of Tokyo.)

2:00 PM - 2:15 PM JST | 5:00 AM - 5:15 AM UTC

[HTT14-02] **Comparative study of visitors' perceptions of places by analyzing visual content of photographs in Shinjuku, Tokyo**

*Bochra Bettaieb[1], Yoshiki Wakabayashi[1] (1.Tokyo Metropolitan University)

2:15 PM - 2:30 PM JST | 5:15 AM - 5:30 AM UTC

[HTT14-03] **Geo-phenomenology: A Qualitative GIS Approach for Understanding People's Lived Experiences**

★Invited Papers

*Yuki Iwai[1] (1.Graduate School, University of Tsukuba)

2:30 PM - 2:45 PM JST | 5:30 AM - 5:45 AM UTC

[HTT14-04] UAS Surveys for Identifying Vacant Houses using Night Light and Thermal Information

★Invited Papers

*Kotaro Iizuka[1], Yuki Akiyama[1,2], Nobuyuki Imafuku[3], Satoru Sugita[4] (1.Center for Spatial Information Science, University of Tokyo, 2.Graduate School of Integrative Science and Engineering, Tokyo City University, 3.Urban Development Dept., Building and Housing Division, Omuta City, 4.International Digital Earth Applied Science Research Center, Chubu University)

2:45 PM - 3:00 PM JST | 5:45 AM - 6:00 AM UTC

[HTT14-05] Impacts of urbanization on the ecosystem services of the Muthurajawela Marsh and Negombo Lagoon, Sri Lanka

*SUMUDU DARSHANA ATHUKORALA ARACHCHIGE[1], Yuji Murayama[2], Bunkei Matsushita[2], Ronald C. Estoque[3] (1.Graduate School of Life and Environmental Sciences, University of Tsukuba, Tsukuba, Ibaraki, Japan, 2. Faculty of Life and Environmental Sciences, University of Tsukuba, Tsukuba, Ibaraki, Japan, 3.National Institute for Environmental Studies, Tsukuba City, Ibaraki, Japan)

3:00 PM - 3:15 PM JST | 6:00 AM - 6:15 AM UTC

[HTT14-06] **Evaluating land use change with urban development and its impact on habitat quality**

*BINGYU WANG[1], Takashi Oguchi[1,2], Kotaro Iizuka[2], Xun Liang[3] (1.Department of Natural Environment Studies, The University of Tokyo, 2.Center for Spatial Information Science, The University of Tokyo, 3.School of Geography and Information Engineering, China University of Geosciences)

A GIS-based study on accessibility of public bus system in Sapporo

*ZITONG XU[1], Yuichi S. Hayakawa[2,3]

1. Graduate School of Environmental Science, Hokkaido University, 2. Faculty of Environmental Earth Science, Hokkaido University., 3. Center for Spatial Information Science, The University of Tokyo.

It is commonly known that one of the most important keys to realize a compact city is to develop convenient urban public transportation. According to the second Sapporo city planning master plan in March, 2016, there is a trend of population decreasing, super-aged society, and the shrinkage of the productive age population in Sapporo. With this background, it is desired to have thorough assessments of accessibility covering the residential areas for the sustainable development of the city. This study focuses on the accessibility in Sapporo city with a particular interest in the public bus system and its spatial relationships to the population and point of interest (POI) data. For this purpose, the specific population in every block is estimated and the POI index is obtained. More specifically, by analyzing the population and POI distribution around the bus system (every stop and route), we evaluate the accessibility of the bus system in Sapporo. The network analysis and spatial analysis are performed to provide the objective assessment of the accessibility which will be supportive information for the future urban planning.

Keywords: Sapporo, Population, Point of interest, Spatial analysis, Accessibility

©2021. Japan Geoscience Union. All Right Reserved.

Comparative study of visitors' perceptions of places by analyzing visual content of photographs in Shinjuku, Tokyo

*Bochra Bettaieb[1], Yoshiki Wakabayashi[1]

1. Tokyo Metropolitan University

Photographs taken by tourists have the potential to play an important role in understanding visitors' behaviors and perceptions in tourist destinations. The authors had analyzed geocoded photographs taken in central Tokyo to compare the behavior patterns of foreign visitors. However, our previous study could not identify the contents of photographs. To resolve this issue, the present study employed a machine learning method to analyze the visual contents of photographs. The data obtained were geocoded photos in 2018, taken within 1 km from Shinjuku. We analyzed 1,940 photos taken by visitors from four major countries (e.g., USA, UK, Taiwan and Singapore) to Shinjuku who posted their pictures on Flickr. The images of photographs were analyzed by using Google Cloud' s Vision API that enables us to assign labels to images and automatically classify them into predefined categories. Based on the labels assigned to the photographs, we manually classified them into 8 categories. By employing the locational information of Flickr data, each photograph was geocoded as an input to GIS. The spatial distribution of photographs by category was compared between visitors' home countries to capture the variation in perception and behavior of visitors. The results indicated that the visitors' perceptions of Shinjuku varied with home countries of visitors. While all visitors showed a common perception of Shinjuku characterized by urbanism, some differences were observed among the other categories. Analysis of the spatial distribution of photos revealed that the photos categorized as urbanism widely distributed in and around Shinjuku station, whereas the photos categorized as culture concentrated at the east or south side of the station.

Keywords: Flickr, photo image, machine learning, GIS

©2021. Japan Geoscience Union. All Right Reserved.

Geo-phenomenology: A Qualitative GIS Approach for Understanding People’ s Lived Experiences

*Yuki Iwai[1]

1. Graduate School, University of Tsukuba

Ⅰ. Introduction

Although geographic information systems (GIS) were used worldwide, there has been remarkably little debate about an applicability to understanding qualitative aspects of geographical phenomena. The aim of this study is to contribute methodological advances in GIS at the intersection of quantitative methods and qualitative analysis. The approach to GIS-based phenomenology developed in this study, called "Geo-phenomenology," is based on the integration of spatial analysis and interpretation to understand participants' lived experiences. The three central elements of this approach are (1) go-along interviews to obtain the lived experiences of participants; (2) spatial analysis and exploratory spatial data analysis (ESDA) in GIS; (3) interpretative phenomenological analysis as a qualitative approach. A case study of the commuting route of a female graduate student, Ms. J, attending a national university in Japan, is used to illustrate the approach.

Ⅱ. Research Method

Ms. J was asked to speak spontaneously about her memories and impressions on the way to school. The semi-structured interview is known as an appropriate method for interpretative phenomenological analysis because the participants narrate their experiences from their perspective. The survey was conducted over two consecutive days. On the first day, an overview of the survey was given, and we conducted the go-along interview from her school building to her house in the evening. The second day's survey was conducted in the morning, and the go-along interview was conducted from Ms. J's home to her school building along the same route as last night. During go-along interviews, the GPS (10-second intervals) and voice recorder were used.

Ⅲ. Results and Discussion

Combing the obtained narratives with locational information, Ms. J’ s lived experiences could be visualized spatially and temporally. From the quantitative point of view, the number of words was interpreted for where she was interacting with locations. Conversely, what content of narratives changed where was shown by ESDA in the qualitative perspective. Removing previous geographic knowledge and preconceptions (i.e., Epoché), the relationship between J's narratives and the environment on the way to school was analyzed. As a result, the number of words was highly distributed around the waterfront and the park. Focusing on the content in narratives, Ms. J recognized the area around the university as a rich natural environment. Moreover, an overall discussion of Ms. J's responses, the central theme of her experiences on the commuting route was closely related to youth. Geo-phenomenology makes it possible to find spatiotemporal patterns and rules of his (her) world regarding the way he (she) interacts with the various facilities, natural environments, people, and places. In addition, the method of this approach allows various spatiotemporal analyses because the narrative data is directly combined with the attribute table of the vector data. This is one of contributes that the development of analytical methods for qualitative GIS that is relying on visualization. Previous GIS research has been dominated by objective analysis using large amounts of data. In contrast, geo-phenomenology proves that using GIS is also useful even when the sample size is N=1.

©2021. Japan Geoscience Union. All Right Reserved.

Keywords: phenomenological analysis, qualitative data analysis, exploratory spatial data analysis (ESDA), qualitative GIS

©2021. Japan Geoscience Union. All Right Reserved.

UAS Surveys for Identifying Vacant Houses using Night Light and Thermal Information

*Kotaro Iizuka[1], Yuki Akiyama[1,2], Nobuyuki Imafuku[3], Satoru Sugita[4]

1. Center for Spatial Information Science, University of Tokyo, 2. Graduate School of Integrative Science and Engineering, Tokyo City University, 3. Urban Development Dept., Building and Housing Division, Omuta City, 4. International Digital Earth Applied Science Research Center, Chubu University

Changes of the social environment such as the population decline has led to the increasing number of vacant houses in Japan. According to the Housing and Land Survey conducted by the Ministry of Internal Affairs and Communications, approximately 13.6 % of total housing units are vacant across Japan. Japanese government has enforced a new law, regarding the special law about the promotion of vacant houses. The law encourages the local governments to identify and record the situation of the vacant houses. However, the current situation of the identification method relies only on direct observation of the houses, estimating if it is vacant or not. The approach takes massive time and labor costs, which is inefficient to conduct such survey for the whole city and frequently. Situation always changes for house rents, people’ s activity, movements, etc., and difficulty rises to grasp the condition up to date.

This work considers the utilization of the Unmanned Aerial Systems (UAS) or hereafter drones, to spatially survey the necessary sites and identify the houses if they are vacant or not. Multiple aerial imageries were collected at different time of the day with a RGB camera. The Structure from Motion technique develops the 3D model of the residential areas which can be used to check through the 3D space. Nighttime flight was also conducted to collect the aerial imageries at nights. The data is processed to spatially identify the night lights that is observed from each home, which can be a direct measurement to identify the human activity. Finally, the thermal information simultaneously collected through the aerial survey was also image processed to observe the heat emission of each home, which also can be an indicator for human activities, hence, it would imply that vacant houses should have less heat transfer. We would like to present and discuss our proposed method for collecting the data and interpreting the developed data for understanding the situation.

Keywords: UAV, thermal, night light, remote sensing, vacant house

©2021. Japan Geoscience Union. All Right Reserved.

Impacts of urbanization on the ecosystem services of the Muthurajawela Marsh and Negombo Lagoon, Sri Lanka

*SUMUDU DARSHANA ATHUKORALA ARACHCHIGE[1], Yuji Murayama[2], Bunkei Matsushita[2], Ronald C. Estoque[3]

1. Graduate School of Life and Environmental Sciences, University of Tsukuba, Tsukuba, Ibaraki, Japan, 2. Faculty of Life and Environmental Sciences, University of Tsukuba, Tsukuba, Ibaraki, Japan, 3. National Institute for Environmental Studies, Tsukuba City, Ibaraki, Japan

This study examines the impacts of urbanization on the ecosystem services of the Muthurajawela Marsh and Negombo Lagoon (MMNL), a critical urban wetland ecosystem (UWE) in Sri Lanka. We developed a framework to estimate the changes in the ecosystem service value (ESV) of the MMNL based on land use/cover (LUC) changes in the area from 1997 to 2017. This framework encompasses various sub-disciplines, including environmental history, urban ecology, wetland science, GIScience, and remote sensing. Considering a business as usual scenario (BAU) and an ecological protection scenario (EPS) and using a set of spatial variables (driving factors of LUC changes), we simulated the future LUC changes (2017-2030) in the MMNL and examined the consequent projected future changes in its ESV. The results showed that the total ESV of the MMNL has decreased by LKR 7,005.85 million, or about 66%, from 1997 to 2017, in which about 98% was due to the loss of marshlands and mangroves. The scenario analysis revealed that if the current LUC change pattern continued, marshlands would continue to decrease by 2030 under the BAU scenario. However, under the EPS scenario, the marshland would increase. The scenario analysis also revealed that the total ESV of the MMNL would also continue to decrease by LKR 3570 million under the BAU scenario. However, under the EPS scenario, there would only be about a decrease of LKR 2120 million. In this study, LUC management strategies and environmental engineering measures are discussed to provide scientific guidance for improving the ecosystem services of MMNL and other UWEs in the country.

Keywords: Wetland ecosystem service, Muthurajawela Marsh, Negombo Lagoon, Socio-ecological scenarios, Land Change Modeler, Urban ecology

©2021. Japan Geoscience Union. All Right Reserved.

Evaluating land use change with urban development and its impact on habitat quality

*BINGYU WANG[1], Takashi Oguchi[1,2], Kotaro Iizuka[2], Xun Liang[3]

1. Department of Natural Environment Studies, The University of Tokyo, 2. Center for Spatial Information Science, The University of Tokyo, 3. School of Geography and Information Engineering, China University of Geosciences

Land use/and Cover Change (LUCC) is the core topic of the global environment, which significantly influences the structure and function of the ecosystem, including biodiversity, natural habitats, and resource usage. Accompanied by rapid population growth and socio-economic development, the world has undergone large-scale urban expansion. Therefore, seeking sustainable urban planning is essential to balance urban growth and environmental conservation. The concept of a compact city has been proposed globally as a critical strategy to establish sustainable urban forms. Whether a compact city is compelling for preserving the natural environment under urban development needs should be carefully examined considering regional differences.

Existing research has recognized the influences of landscape change on habitat quality by integrating ecosystem assessment tools and land use information. The Integrated Valuation of Ecosystem Services and Trade-offs model (InVEST) with intuitive spatial virtualization and less prior knowledge can improve the understanding and interpretation of ecosystem functioning. Spatiotemporal land use modeling is effective and reproducible for analyzing both causes and consequences of landscape dynamics. A growing body of land use simulation approaches with future scenarios such as the Cellular Automata (CA) model, which has been widely applied to illustrate landscape dynamics, with the fundamental expression of geospatial processes through cell states and their neighborhood space.

This research has adopted a patch-generating land-use simulation model (PLUS), which couples the CA model with a Random Forest algorithm of data mining technology, considering driving factors including topography and climate conditions, locational factors and traffic networks, and distribution of protected areas. This study proposes a framework to explore different urban patterns and their impact on habitat quality by incorporating the PLUS and InVEST models. Two coastal areas with urban agglomerations are selected for different urbanization levels, the National Capital Region (NCR) in the Tokyo Metropolitan Area of Japan and the Guangdong-Hong Kong-Macao Greater Bay Area (GBA) of China. Three future compact city scenarios with the urban layout evolution of high-compact cities, medium-compact cities, and low-compact cities are designed along with the corresponding habitat quality evaluation.

The results imply that under the scenario of high-compact cities, both significant improvement and degradation of habitat quality are observed within the study areas, and the total decline in habitat quality across each area is the largest. The scenario of low-compact cities depicts scattered urban growth with mixed land use patterns and have the least habitat quality variation in both areas. The scenario of medium-compact cities improves habitat quality more than that of low-compact cities in the NCR, and habitat quality decline is less than the scenario of high-compact cities. Therefore, conserving green space with medium-compact cities could be sustainable urban planning in the NCR. In the GBA, the scenario of medium-compact cities has average habitat quality variation compared with other scenarios. Here, macro-control of land use demand to prevent excessive urban growth and over-dense urban structure should be considered for long-term strategy.

©2021. Japan Geoscience Union. All Right Reserved.

Keywords: land use change, habitat quality, compact city, urban simulation, future scenarios

©2021. Japan Geoscience Union. All Right Reserved.

[E] Oral | H (Human Geosciences)：H-TT Technology & Techniques

Sun. Jun 6, 2021 3:30 PM - 5:00 PM JST | Sun. Jun 6, 2021 6:30 AM - 8:00 AM UTC | Ch.14 Zoom Room 14

[H-TT14] Geographic Information Systems and Cartography

convener:Takashi Oguchi(Center for Spatial Information Science, The University of Tokyo), Yoshiki Wakabayashi(Graduate School of Urban Environmental Sciences, Tokyo Metropolitan University), Yuei-An Liou(National Central University), C. Ronald Estoque(National Institute for Environmental Studies, Japan), Chairperson:Yuei-An Liou(National Central University), Ronald C. Estoque(National Institute for Environmental Studies, Japan)

This session discusses various methods which acquire, store, analyze and visualize geospatial data, and presents the outcomes of empirical studies using GIS or mapping methods. The session also deals with applications of digital data, and GIS, and mapping to various fields of earth and planetary science and human society. All presentations and discussion of this session are made in English.

3:30 PM - 3:45 PM JST | 6:30 AM - 6:45 AM UTC

[HTT14-07] Assessing the effect of landscape composition on land surface temperature in Tsukuba city, Japan

★Invited Papers

*RUCI WANG[1], Yuji Murayama[1], Takehiro Morimoto[1] (1.University of Tsukuba)

3:45 PM - 4:00 PM JST | 6:45 AM - 7:00 AM UTC

[HTT14-08] **Spatiotemporal Characterization and Evolution of Surface Urban Heat Islands in Tokyo: A Perspective from Land Cover/Use Layouts and Variations**

*Fei LIU[1] (1.University of Tsukuba)

4:00 PM - 4:15 PM JST | 7:00 AM - 7:15 AM UTC

[HTT14-09] Microclimate simulation of Doshisha University Kyotanabe campus with ENVI-met model

★Invited Papers

*XINGYU WANG[1] (1. Department of Environmental Systems Science, Doshisha University)

4:15 PM - 4:30 PM JST | 7:15 AM - 7:30 AM UTC

[HTT14-10] **Recent LULC change in Vietnamese Mekong Delta and its relation to land subsidence after implementation of the Resolution No.120/NQ-CP**

*Kim-Anh Nguyen[1], Yuei-An Liou[1], Phan Duong Cao[2], Philip Mindehoud[3] (1.National Central University, 2.University of Tsukuba, 3.University of Padova)

4:30 PM - 4:45 PM JST | 7:30 AM - 7:45 AM UTC

[HTT14-11] Locations of historical and archaeological sites in Japan and China in relation to geography

*Yuan Wang[1], Takashi Oguchi[1] (1.The University of Tokyo)

4:45 PM - 5:00 PM JST | 7:45 AM - 8:00 AM UTC

[HTT14-12] **Online Education of Disaster Risk Reduction using Web GIS: Applications to Chinese Secondary Schools**

*Jiali Song[1], Takashi Oguchi[2] (1.Graduate School of Frontier Sciences, The University of Tokyo, 2.Center for Spatial Information Science, The University of Tokyo)

Assessing the effect of landscape composition on land surface temperature in Tsukuba city, Japan

*RUCI WANG[1], Yuji Murayama[1], Takehiro Morimoto[1]

1. University of Tsukuba

In recent years, Urban Heat Island (UHI) phenomenon, which causes excessive energy consumption, environmental deterioration, and health damage, has become prevalent in many cities. Urban planners have been challenging to reduce UHI by effective city planning and policies. However, because of the complicated nature of causes in the urban environment changes, it is still challenging to measure their effectiveness on the UHI reduction. Therefore, this study takes Tsukuba city, a planned city, as an example, to assess the effect of landscape composition on Land Surface Temperature (LST) and evaluates the distribution of building height (3D) and functions (e.g., residential, commercial) on LST. This study uses Esri City Engine and ArcGIS software to conduct spatial analysis using remote sensing data, open street map data, and Zenrin data. The regression analysis examines the relationships between LST and land use/cover, building height, building function, and other variables (e.g., distance to the road). Our results show that green space management and control could be significant to harmonize demand growth, environment protection, economic development, and healthy urban establishment. The enhanced theoretical underpinning on sustainable cities can further promote city dwellers' environmental awareness and help the city make an orderly urban development.

Keywords: Geographical information science, Urban heat island, Land surface temperature, Land use/cover, Tsukuba city

©2021. Japan Geoscience Union. All Right Reserved.

Spatiotemporal Characterization and Evolution of Surface Urban Heat Islands in Tokyo: A Perspective from Land Cover/Use Layouts and Variations

*Fei LIU[1]

1. University of Tsukuba

The surface urban heat islands (SUHI) phenomenon in the urban context has gained considerable attention due to the climate crisis and environmental health issues. Targeting Tokyo Metropolitan Area (TMA) as a critical case, this study profiled and clarified the spatial variations, relationships, and trends between land surface temperature (LST) and land cover/use from 2001 to 2015 based on multi-source spatial data. Toward an in-depth understanding of SUHI dynamics in TMA for mitigation solutions and appropriate urban policies, this study conducted an integrative investigation by examining the spatiotemporal evolution of thermal gradients between the urban and non-urban fabric areas and delineating the layouts of thermal cores in TMA. The spatial interconnections between SUHI and its potential driving forces were explored and identified by incorporating spatial regression analysis. Results indicate that Tokyo was recognized as a polynucleated-structure metropolitan area distributing multiple intense thermal island clusters over space. Thermal islands densely emerged in the compact low/middle-rise residential quarters and renovating regions, rather than in the central business districts of TMA. High-rise buildings shielding solar radiation, the contributions of large-scale water bodies and urban afforestation, and sea breezes' impacts might result in this phenomenon. In light of this, this study suggests that the local authorities consider delineating the thermal cores areas, alleviating the magnitude of persistent thermal islands area, and controlling the emergence and formation of new thermal cores, coupled with partitioned or location-specified landscape-designing and green measures. Findings from this study can strive to tackle the urban climate issues and contribute to broader planning considerations on future sustainable development.

Keywords: Land Cover/Use, Land Surface Temperature, Tokyo Metropolitan Area, Urban Sustainability, Surface Urban Heat Island

©2021. Japan Geoscience Union. All Right Reserved.

Microclimate simulation of Doshisha University Kyotanabe campus with ENVI-met model

*XINGYU WANG[1]

1. Department of Environmental Systems Science, Doshisha University

Microclimate refers to small-scale meteorology, ranging from a few meters to a few kilometers, and directly affects our daily activities. The microclimate formed in a certain place is strongly influenced by the surrounding environment, such as topography, land-use, and type of vegetation, which are provided within standard GIS datasets. Recently, the microclimate simulations have been performed with the boundary conditions generated from GIS datasets to get the information on local climate, such as daily maximum/minimum temperature, humidity, and wind speed. One of the microclimate models used in the world is ENVI-met, which calculates mass, momentum, and energy budgets in a 3-dimensional space through the Eulerian approach, developed by Michael Bruse (Bruse 1999; see www.envi-met.com). Many researchers have studied the simulation capabilities of ENVI-met (e.g., Crank et al., 2018; Lopez-Cabeza et al., 2018), and compared ENVI-met with other models (e.g., Paas and Schneider, 2016; Liu et al., 2020; Gal and Kantor, 2020). It has been found that the ENVI-met simulations are relatively precise, while there are situations where it cannot highlight the difference of solar radiation in space and time (Liu et al., 2020; Gal and Kantor, 2020). This research focuses on the verification of the numerical stability of ENVI-met model through the microclimate simulation of Doshisha University Kyotanabe campus, and explores the capability of ENVI-met to produce the useful information on the local climate and the impact of different environment layout on the microclimate.

Microclimate simulations of Kyotanabe campus for a period from 0:00 to 24:00 on December 1, 2020 are conducted with ENVI-met model. The simulation area is 300 m×170 m×73.29 m, and grid number 300×170×28. The locations and heights of buildings come from KML data generated by Google Earth. The vegetation types are selected from the ENVI-met database, according to the actual vegetation. The soil moisture and temperature are based on the observations by Kyoto-city (2018) and Kinouchi and Yoshitani (2001). Meteorological conditions for the simulations, including surface air temperature, wind speed, and wind direction, are provided by the observations at Kyotanabe AMeDAS of Japan Meteorological Agency. We compare the meteorological observations on the lawn in Kyotanabe campus with the ENVI-met simulations, and explore the relationship between the simulated microclimate and the surrounding environment.

Simulated surface air temperature shows the daily variations similar to those of the observed temperature, although the simulated temperature is about 2 degrees lower than the observed temperature in the daytime. This may be due to the setting of excessive cloud cover, resulting in less solar radiation. Simulated relative humidity is lower than the observed relative humidity in the nighttime, and opposite in the daytime. Simulated wind speed fluctuates little and is much larger than the observed wind speed. The deviation may be caused by inappropriate model settings. The simulated air temperature and wind speed show the dependence on the degree of closed environment by buildings and trees. The enclosure degree affects the flow of air and the amount of received solar radiation and lost heat. It is found that the closed

©2021. Japan Geoscience Union. All Right Reserved.

environment has better heat conservation capability. The ENVI-met is basically good at microclimate simulations, and shows a significant impact of different environments on the microclimate. The enclosure degree of environment has a negative correlation with wind speed and relative humidity, and a positive correlation with air temperature.

Keywords: Microclimate, Urban environment, Numerical simulation

©2021. Japan Geoscience Union. All Right Reserved.

Recent LULC change in Vietnamese Mekong Delta and its relation to land subsidence after implementation of the Resolution No.120/NQ-CP

*Kim-Anh Nguyen[1], Yuei-An Liou[1], Phan Duong Cao[2], Philip Mindehoud[3]

1. National Central University, 2. University of Tsukuba, 3. University of Padova

Vietnamese Mekong Delta (VMD) is known as the second largest granary in the world, while its rice paddy yield has been seriously threatened by the alarmingly enhanced extreme weathers and human intervention in the upstream. After serious drought in 2016, the Vietnamese government enforced the Resolution No.120/NQ-CP on 17/11/2017 and Directive No. 04/CT-TTg on 4/2/2016 aiming for sustainable development of the Mekong Delta to adapt to climate change. These introduced strategies with new visions and strategic directions that lead the economic development of VMD focusing on aquaculture, fruit, and rice products, corresponding to transformation in land use and land cover (LULC). Consequently, LULC change in the Mekong Delta from paddy rice field to aquaculture has been observed significant, and LULC change has been found to accelerate the subsidence over aquaculture lands and wetlands. This paper presents the LULC change in the VMD, land subsidence and their relationship in the timeframe from 2014 to 2019. Land subsidence map and its value were generated from Sentinel-1 imagery from ESA (European Space Agency), LULC maps were created from the Landsat data time series. The accuracy of the LULC classification is 95% with Kappa coefficient 0.94. The land subsidence was validated with measured data. Results show that significant land subsidence generally occurred in aquaculture land, open water and mangrove wetland, which were significantly increased in terms of areas from the LULC change analysis. LULC change and its relationship with land subsidence in the VMD were also discussed. Results of the study provide useful information for the authorities to design plans to mitigate human impacts and reduce the risk while dealing with climate change.

Keywords: land subsidence;, land use, land cover; , Mekong Delta , Sentinel-1, Landsat

©2021. Japan Geoscience Union. All Right Reserved.

Recent LULC change in Vietnamese Mekong Delta and its relation to land subsidence after implementation of the Resolution No.120/NQ-CP

Kim-Anh Nguyen[1,2], Yuei-An Liou*[1], and Phan Duong Cao[3] and Philip Mindehoud[4]

[1]Center for Space and Remote Sensing Research National Central University

[2]Institute of Geography, Vietnam Academy of Science and Technology

[3]University of Tsukuba, Japan

[4]University of Padova, Department of Civil, Environmental and Architectural Engineering (ICEA), Via Marzolo, 9–35131, Padova, Italy.

Abstract:

Vietnamese Mekong Delta (VMD) is known as the second largest granary in the world, while its rice paddy yield has been seriously threatened by the alarmingly enhanced extreme weathers and human intervention in the upstream. After serious drought in 2016, the Vietnamese government enforced the Resolution No.120/NQ-CP on 17/11/2017 and Directive No. 04/CT-TTg on 4/2/2016 aiming for sustainable development of the Mekong Delta to adapt to climate change. These introduced strategies with new visions and strategic directions that lead the economic development of VMD focusing on aquaculture, fruit, and rice products, corresponding to transformation in land use and land cover (LULC). Consequently, LULC change in the Mekong Delta from paddy rice field to aquaculture has been observed significant, and LULC change has been found to accelerate the subsidence over aquaculture lands and wetlands. This paper presents the LULC change in the VMD, land subsidence and their relationship in the timeframe from 2014 to 2019. Land subsidence map and its value were generated from Sentinel-1 imagery from ESA (European Space Agency), LULC maps were created from the Landsat data time series. The accuracy of the LULC classification is 95% with Kappa coefficient 0.94. The land subsidence was validated with measured data. Results show that significant land subsidence generally occurred in aquaculture land, open water and mangrove wetland, which were significantly increased in terms of areas from the LULC change analysis. LULC change and its relationship with land subsidence in the VMD were also discussed. Results of the study provide useful information for the authorities to design plans to mitigate human impacts and reduce the risk while dealing with climate change.

Keywords: land subsidence; land use/land cover; Landsat data; Sentinel-1; Mekong Delta; Vietnam

©2021. Japan Geoscience Union. All Right Reserved.

Locations of historical and archaeological sites in Japan and China in relation to geography

*Yuan Wang[1], Takashi Oguchi[1]

1. The University of Tokyo

The remains of historical/archaeological sites exist all over the world. Their existence provides the basis of researches for many disciplines such as Archaeology, History, and Geography, as they can reflect activities and thinking of ancient people who built them as well as related environmental factors. In previous studies about the relationship between ancient sites and their surroundings, local topography is considered to be one of the most important factors that determine what kind of features to build, and several topographic factors such as elevation, slope and aspect have been analyzed. However, such research is still uncomprehensive, and the quantitative expression of relationships between the ancient sites and related topographic factors needs to be explored further. Therefore, this research utilizes GIS and DEMs (Digital Elevation Models) to investigate topographic factors more comprehensively as well as surface hydrological conditions in relation to historical and archaeological sites in Japan and China. It employs machine learning methods for quantitative analyses and compare the results from the two countries. The results were interpreted based on geographical, historical, and archaeological knowledge. It was found that the ancient sites in different study areas are sensitive to different topographic factors, and the distance between the ancient sites and major rivers also influence their distribution. Finally predictive maps of historical/archaeological sites were produced according to the obtained quantitative results.

Keywords: GIS, Topographic factors, Ancient sites

©2021. Japan Geoscience Union. All Right Reserved.

Online Education of Disaster Risk Reduction using Web GIS: Applications to Chinese Secondary Schools

*Jiali Song[1], Takashi Oguchi[2]

1. Graduate School of Frontier Sciences, The University of Tokyo, 2. Center for Spatial Information Science, The University of Tokyo

Use of Web GIS for DRR (Disaster Risk Reduction) has received attention in recent years. In 2022, a new subject of geography will become compulsory in Japanese high schools, and the guideline for the subject was provided by the Ministry of Education, Culture, Sports, Science, and Technology. The guideline shows that the new subject focuses on maps, GIS, ESD (Education for Sustainable Development), international understanding, regional surveys, and DRR. Introducing Web GIS to DRR education in school classrooms will be essential for students to develop knowledge and skills of DRR. There have been Web GIS systems for school education in Japan. For example, ESRI Japan provides the ArcGIS Online service to Japanese schools for learning geography with GIS technology. As a disaster-prone country, Japan puts emphasis on pre-DRR actions, and has relatively strong DRR countermeasures. Therefore, the United Nations Development Programme (UNDP) has allowed Japan to share the lessons learned from past earthquakes and other disasters. However, even in Japan, there are still no well-established guidelines for teaching DRR in schools, and it is still unknown whether students can understand DRR and improve their ability of DRR thinking by using GIS. Therefore, this study utilizes Web GIS technology to support geospatial thinking of students, and investigates factors influencing the learning effects of students. For this purpose, we developed materials for systematic DRR education and designed curricula to utilize the material effectively. This approach was implemented multiple times for students in Chinese secondary schools as online courses during the COVID-19 pandemic. Questionnaire surveys were also conducted during the courses to collect information useful for evaluating the educational effects of our educational materials and curricula. Important findings from the questionnaire surveys are: 1) students who can pay more attention to disaster information tend to feel easier to learn DRR, whereas the past learning experience of Web hazard maps is only weakly related; 2) experience of using Web maps makes students easier to learn about hazard maps; and 3) ability of using electronic products helps students learn GIS.

Keywords: Disaster risk reduction education, Web GIS, Learning effects

©2021. Japan Geoscience Union. All Right Reserved.

[E] Poster | H (Human Geosciences)：H-TT Technology & Techniques

Sun. Jun 6, 2021 5:15 PM - 6:30 PM JST | Sun. Jun 6, 2021 8:15 AM - 9:30 AM UTC | Ch.09_2

[H-TT14] Geographic Information Systems and Cartography

convener:Takashi Oguchi(Center for Spatial Information Science, The University of Tokyo), Yoshiki Wakabayashi(Graduate School of Urban Environmental Sciences, Tokyo Metropolitan University), Yuei-An Liou(National Central University), C. Ronald Estoque(National Institute for Environmental Studies, Japan)

This session discusses various methods which acquire, store, analyze and visualize geospatial data, and presents the outcomes of empirical studies using GIS or mapping methods. The session also deals with applications of digital data, and GIS, and mapping to various fields of earth and planetary science and human society. All presentations and discussion of this session are made in English.

[HTT14-P01] Using remote sensing and GIS to track vegetation changes at Unzen Volcano, Kyushu, Japan

*Roxanne Lai[1], Takashi Oguchi[1] (1.University of Tokyo)

[HTT14-P02] Analysis of Human-Environment Interactions in the Last Glacial Period Using the Ecological Niche Model and the Agent-Based Model

*Yuji Sakairi[1], Takashi Oguchi[2] (1.Department of Earth and Planetary Science, School of Science, The University of Tokyo, 2.Center for Spatial Information Science, The University of Tokyo)

[HTT14-P03] GIS-based frequency ratio, logistic regression and artificial neural network models for landslide and sinkhole susceptibility analysis in central Shenzhen, South China

*DI LU[1], Takashi Oguchi[1,2] (1.Dept. of Natural Environmental Studies, Graduate School of Frontier Sciences, The University of Tokyo, 2.Center for Spatial Information Science, The University of Tokyo)

[HTT14-P04] Online Workshop for Educating Disaster Risk Reduction using a Simplistic Digital Map with Basic GIS functions

*Hiroyuki Yamauchi[1], Jiali Song[1], Takashi Oguchi[2,1] (1.Department of Natural Environmental Studies, Graduate School of Frontier Sciences, The University of Tokyo, 2.Center for Spatial Information Science, The University of Tokyo)

[HTT14-P05] Remotely sensed tree canopy cover-based indicators for monitoring global sustainability and environmental initiatives

★Invited Papers

*Ronald C. Estoque[1], Brian A Johnson[2], Yan Gao[3], Rajarshi DasGupta[2], Makoto Ooba[1], Takuya Togawa[1], Yasuaki Hijioka[1], Yuji Murayama[6], Lilito D Gavina[4], Rodel D Lasco[5], Shogo Nakamura[1] (1.National Institute for Environmental Studies, Japan, 2.Institute for Global Environmental Strategies, Japan, 3.Universidad Nacional Autónoma de México, México, 4.Don Mariano Marcos Memorial State University, Philippines, 5.World Agroforestry Centre (ICRAF), Philippines, 6.University of Tsukuba, Japan)

[HTT14-P06] Application of network analysis to visualize residential preferences and its changes in Japan

★Invited Papers

*Yoshiki Wakabayashi[1] (1.Graduate School of Urban Environmental Sciences, Tokyo Metropolitan University)

[HTT14-P07] Mapping Inbound Package Tours Visiting Countryside of Japan - - A Case of Toyama Prefecture

*Yennan U[1] (1.Tokyo Metropolitan University)

Using remote sensing and GIS to track vegetation changes at Unzen Volcano, Kyushu, Japan

*Roxanne Lai[1], Takashi Oguchi[1]

1. University of Tokyo

Constraining the effects of vegetation on landform evolution is one of the biggest challenges in modern geomorphological studies. While there are many existing landform evolution models, not many studies have attempted to incorporate vegetation data explicitly due to difficulties in obtaining constructive quantitative data for integration into geomorphic transport functions. Quantification of the patterns and speeds of vegetation regrowth is integral to understanding the effects of vegetation on hillslope and other landform development. With time-robust remotely-sensed optical data and new platforms that allow for faster computation and processing, new opportunities to quantify vegetation changes at over larger areas and finer temporal scales are now available.

Using the study area of Unzen Volcano in Japan, this study aims to quantify vegetation regrowth on volcanic hillslopes. Unzen Volcano is the name of a cluster of volcanoes located on the Shimabara Peninsula in Nagasaki Prefecture, Kyushu. In its latest eruption sequence from 1991 –1995, large pyroclastic flows emerged from Fugendake volcano, resulting in destruction of vegetation and infrastructure. Therefore, vegetation recovery from the period 1985 –2011 was tracked over time. Satellite imagery from months June to August in the years of interest from the Landsat 5 Surface Reflectance Tier 1 dataset was processed in Google Earth Engine, and Normalized Difference Vegetation Index (NDVI) and fractional vegetation cover (FVC) time series analyses were performed with help of GIS.

Results from NDVI and FVC show that although all examined areas exhibited positive vegetation recovery rates, there are clear differences in vegetation recovery rate due to initial amount of damage and the location of vegetation. For areas in which vegetation returned to or close to pre-eruption levels, the rate of vegetation recovery was significantly quicker in the first five years of post-eruption.

Keywords: Google Earth Engine, Remote sensing, Vegetation changes, GIS

©2021. Japan Geoscience Union. All Right Reserved.

Analysis of Human-Environment Interactions in the Last Glacial Period Using the Ecological Niche Model and the Agent-Based Model

*Yuji Sakairi[1], Takashi Oguchi[2]

1. Department of Earth and Planetary Science, School of Science, The University of Tokyo, 2. Center for Spatial Information Science, The University of Tokyo

During the last glacial period, the Japanese Archipelago had a cold and dry climate. Accordingly, flora and fauna were different from those at present: the cool-temperate coniferous forest and large mammals were widely distributed over Japan. Empirical archaeological records have demonstrated that the early humans at that time lived based on hunting-gathering and adapted to environmental changes. However, there are only a few quantitative studies about human ecological adaptation to environmental changes in Japan in this period. This study aims to quantitatively analyze the human-environment interactions in the last glacial period using the ecological niche model (ENM) and the agent-based model (ABM), along with Geographical Information Systems (GIS).

The ENM is a computer-based method to simulate species' ecological niche based on environmental conditions and known location of species' occurrence. It is possible to quantitatively evaluate the influence of environmental factors that constrain human activities on the basis of percentage of environmental factors used in model calculations. The ABM is a computational model for simulating the actions and interactions of autonomous agents in order to assess their effects on the overall system. The ENM is suitable for static analysis, while the ABM is suitable for dynamic analysis; therefore, a deeper discussion becomes possible by combining the outcomes of the two models. This study applied both ENM and ABM to hunter-gatherers in the Kyushu region of western Japan during the last glacial period.

The results of ENM analysis suggest that topographical conditions were highly influential in human niche constructions during the last glacial period. In addition, climate change in this period is considered to have been the driving force of environmental changes which also influenced human behavior. We assumed that differences in topographical conditions had provoked different human ecological behaviors in response to the climatic cooling and warming during the last glacial period. The outcomes of the ABM analysis indicate many types of human dynamics interacting with the environment, and that elevation had a large influence on behavioral strategies of early humans as also shown by the ENM analysis. It is also suggested that hunting behavior was more sensitive to environmental conditions than gathering.

Keywords: human-environment interactions, hunter-gatherer, ecological niche model, agent-based model

©2021. Japan Geoscience Union. All Right Reserved.

GIS-based frequency ratio, logistic regression and artificial neural network models for landslide and sinkhole susceptibility analysis in central Shenzhen, South China

*DI LU[1], Takashi Oguchi[1,2]

1. Dept. of Natural Environmental Studies, Graduate School of Frontier Sciences, The University of Tokyo, 2. Center for Spatial Information Science, The University of Tokyo

As major geologic hazards, landslides and sinkhole formation account for a great number of human casualties, an enormous amount of property loss, and significant damage to natural ecosystems and human-built infrastructures, especially in urban areas. Therefore, risk evaluation and reduction of such hazards are massive challenges for researchers and engineers to prevent disasters. Although many previous studies have attempted to conduct susceptibility maps to portray hazards' spatial distribution, only a small number of them focused on both landslides and sinkholes in an urbanized area.

This study is to assess and compare the performances of three typical models for hazard susceptibility mapping, namely the frequency ratio model, the logistic regression model, and the artificial neural networks model for the study area in Shenzhen, south China. To focus on potential damage in populated areas, a typical area with high susceptibility values and high population density was chosen as the main target area for analyzing the susceptibility mapping results. For the artificial neural networks model, the radial basis function (RBF) algorithm was applied to construct the networks. The conditioning factors such as elevation, slope inclination, slope aspect, lithology, land cover, and NDVI were derived from various data sources to generate the geospatial database. Precipitation was chosen as the triggering factor of hazards. According to the available hazard inventory, 268 landslide events and 172 sinkhole events were identified and recorded. In addition, 400 points without geological hazards were randomly chosen to provide the absence data for susceptibility modeling.

Subsequently, for the evaluation and comparison of susceptibility models and resultant maps, the confusion matrix and the receiver operating characteristics (ROC) curve with the area under the curve (*AUC*) were used to evaluate the model performance. The results of landslide susceptibility analysis using land conditions indicate that the values of overall accuracy for the frequency ratio model, the logistic regression model, and the RBF neural networks model were 0.764, 0.803, and 0.810, respectively, and the values of *AUC* were 0.787, 0.815, and 0.850. In sinkhole susceptibility analysis, the values of overall accuracy for these three models were 0.648, 0.672, and 0.735, respectively, and the values of *AUC* were 0.707, 0.745, and 0.757. To discuss the probability of landslide or sinkhole occurrence, it is necessary to combine triggering factors like rainfall with land susceptibility. Logistic regression was employed to determine the relative weights of rainfall and land susceptibility, and the modified susceptibility maps considering the effect of precipitation were produced.

The results of this study demonstrate that the RBF neural networks model gave the best results in both landslide susceptibility analysis and sinkhole susceptibility analysis in terms of the values of *AUC* and the overall accuracy. Moreover, the RBF usually performed better than other commonly used artificial neural network algorithms, especially BP (back propagation). This study also has some advantages over previous studies conducted in the same city of Shenzhen.

©2021. Japan Geoscience Union. All Right Reserved.

Keywords: Landslide, Sinkhole, Susceptibility analysis, Frequency ratio, Logistic regression, Artificial neural network

©2021. Japan Geoscience Union. All Right Reserved.

Online Workshop for Educating Disaster Risk Reduction using a Simplistic Digital Map with Basic GIS functions

*Hiroyuki Yamauchi[1], Jiali Song[1], Takashi Oguchi[2,1]

1. Department of Natural Environmental Studies, Graduate School of Frontier Sciences, The University of Tokyo, 2. Center for Spatial Information Science, The University of Tokyo

Although people may understand disaster risks by using GIS, existing GIS products with many functions are difficult to use for those without specialized knowledge. Therefore, we developed a simplistic online digital map with basic GIS functions such as switching layers and measurement tools, using ArcGIS API for JavaScript. We had an online workshop using this digital map and taught how to use GIS to understand disaster risks. The workshop consisted of the lecture part for about 35 min and the exercise part using the digital map for about 80 min. Eighteen participants at ages from 10s to 60s joined the workshop. In the lecture part, we explained the usefulness of GIS in disaster risk reduction based on some cases of past disasters. In the exercise part, we firstly explained how to use the digital map. Then the participants were asked to answer five quizzes related to flood risks in Tokyo using the digital map. At the end of the workshop, we conducted a questionnaire survey to verify usability and educational effects of the digital map. Although the participants had various ages and professions, almost all of them could interpret information about evacuate shelters and high-risk areas from the digital map without feeling strong difficulties. These observations indicate that simplistic GIS functions in the digital map are useful for basic education of disaster risk reduction than existing GIS products with many professional functions. We plan to provide learning materials for those who like to create similar digital maps for educational purposes.

Keywords: WebGIS, disaster risk reduction education, exercise, questionnaire survey

©2021. Japan Geoscience Union. All Right Reserved.

Remotely sensed tree canopy cover-based indicators for monitoring global sustainability and environmental initiatives

*Ronald C. Estoque[1], Brian A Johnson[2], Yan Gao[3], Rajarshi DasGupta[2], Makoto Ooba[1], Takuya Togawa[1], Yasuaki Hijioka[1], Yuji Murayama[6], Lilito D Gavina[4], Rodel D Lasco[5], Shogo Nakamura[1]

1. National Institute for Environmental Studies, Japan, 2. Institute for Global Environmental Strategies, Japan, 3. Universidad Nacional Autónoma de México, México, 4. Don Mariano Marcos Memorial State University, Philippines, 5. World Agroforestry Centre (ICRAF), Philippines, 6. University of Tsukuba, Japan

With the intensifying challenges of global sustainability and biodiversity conservation, the monitoring of the world’ s remaining forests has become more important than ever. Today, Earth observation technologies, particularly remote sensing, are at the forefront of forest cover monitoring worldwide. Given the current conceptual understanding of what a forest is, canopy cover threshold values are used to map forest cover from remote sensing imagery and produce categorical data products such as forest/non-forest (F/NF) maps. However, multi-temporal categorical map products have important limitations because they inadequately represent the actual status of forest landscapes and the trajectories of forest cover changes as a result of the thresholding effect. Here, we examined the potential of using remotely sensed tree canopy cover (TCC) datasets, which are continuous data products, to complement F/NF maps for forest cover monitoring. We developed a conceptual analytical framework for forest cover monitoring using both types of data products and applied it to the forests of Southeast Asia. We conclude that TCC datasets and the statistics derived from them can be used to complement the information provided by categorical F/NF maps. TCC-based indicators (i.e. losses, gains, and net changes) can help in monitoring not only deforestation but also forest degradation and forest cover enhancement, all of which are highly relevant to the 2030 Agenda for Sustainable Development and other global forest cover monitoring-related initiatives. We recommend that future research should focus on the production, application, and evaluation of TCC datasets to advance the current understanding of how accurately these products can capture changes in forest landscapes across space and time.

Keywords: remote sensing , Earth observation, mapping, forest cover monitoring, tree canopy cover, sustainable development goal indicators

©2021. Japan Geoscience Union. All Right Reserved.

Application of network analysis to visualize residential preferences and its changes in Japan

*Yoshiki Wakabayashi[1]

1. Graduate School of Urban Environmental Sciences, Tokyo Metropolitan University

Visualization of the subjective evaluation of regional environment began in human geography as a study of mental maps in the 1960s. Studies on the mental map in terms of residential desirability have conducted at a variety of scales of regions around the world. However, since few studies have examined the change in space preference, the stability of space preference is unknown. In addition, maps representing space preference cannot capture the connection between regions in detail. To resolve these issues, this study aims is to examine variability of space preference by employing the method of network analysis. Data used in this research are derived from an attitude survey on the character of the people by prefecture conducted by Nippon Hoso Kyokai in 1978 and 1996. An analysis of the answers to questions on residential desirability of prefectures other than the present residence. A comparison of the residential preference on the map produced with GIS between 1978 and 1996 revealed that there are stable and variable components of residential desirability. Close examination with the network analysis method clarifies some local trends hidden in the map representing space preferences.

Keywords: residential preference, mental map, network analysis, GIS

©2021. Japan Geoscience Union. All Right Reserved.

Mapping Inbound Package Tours Visiting Countryside of Japan -- A Case of Toyama Prefecture

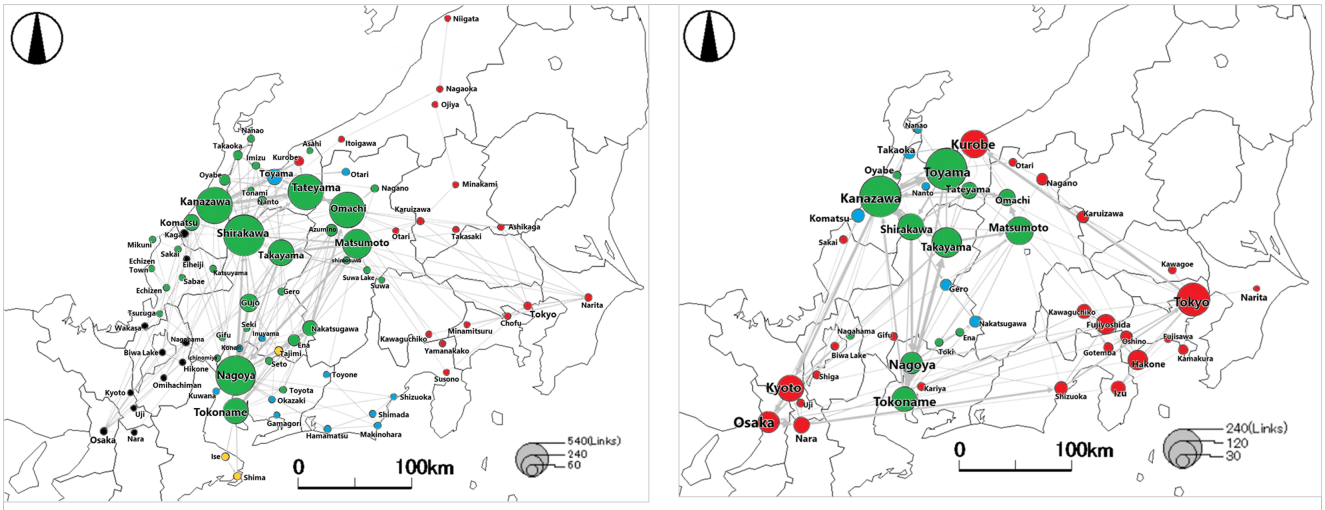
*Yennan U[1]

1. Tokyo Metropolitan University

Japan has seen a marked increase in inbound tourists since the start of the 2000s. However, foreign tourists are travelling unevenly across the country. Previous studies have made great effort to investigate the spatial travel pattern of foreign tourists, but detailed picture of countryside visitation has not been clarified enough. Moreover, inbound tourism in Japan heavily relies on two markets, Taiwan and mainland China accounted for half of the foreign arrivals. This case study aims to understand the spatial structure of inbound tours visiting the countryside of Japan from Taiwan and mainland China.
Toyama prefecture, a case of a countryside area which has the second-highest percentage of tourists visiting by package tours (according to Japan Tourism Agency “International Visitor Survey 2019”). In this study, City/village scale tour destination maps were visualized, which were generated from Taiwan (389) and Mainland China (258) package tours collected by web crawler in 2019. Each destination posted in tours was represented by nodes, the movement flow was represented by links, and the tour networks were analyzed by multiple network analysis methods.
The result can be summarized in two points: 1) The range of destinations posted in Taiwanese tours was as wide as 80 places, besides the number in mainland tours was 44 places. Especially numerous small countryside cities were contained in Taiwanese tours. But centrality indicators showed that some key infrastructure nodes were common, such as Kanazawa and Shirakawa occupied a central position both to Taiwan and mainland China. 2) Different patterns were also found in the touring routes detected by *modularity*-based classification. The most outstanding difference appeared to be the presence/absence of Tokyo-Osaka route, suggesting Taiwanese tours preferred countryside while mainland tours were orientated toward the metropolis even in the countryside visitation. This empirical study explored inbound tour networks by multiple methods and provided a detailed picture in ways of visiting the countryside of Japan. The result is meaningful to future tourism promotion.

Keywords: inbound tourism, countryside, network analysis

©2021. Japan Geoscience Union. All Right Reserved.



Note: Left graph stands for Taiwan network and right one stands for mainland network. Different color refers to divided communities by *modularity*. The size of nodes indicates the number of links between nodes.

Fig 1 Distribution of destinations in inbound package tours, 2019

©2021. Japan Geoscience Union. All Right Reserved.

[J] Oral | H (Human Geosciences)：H-TT Technology & Techniques

Sun. Jun 6, 2021 9:00 AM - 10:30 AM JST | Sun. Jun 6, 2021 12:00 AM - 1:30 AM UTC | Ch.14 Zoom Room 14

[H-TT19] Geographic Information System and Cartography

convener:Mamoru Koarai(Earth Science course, College of Science, Ibaraki University), Kazunari Tanaka(Department of Civil Engineering and Urban Design, Faculty of Engineering, Osaka Institute of Technology), W. Kazuhiko Nakamura(The University of Tokyo), Chairperson:Mamoru Koarai(Earth Science course, College of Science, Ibaraki University), Kazunari Tanka(Department of Civil Engineering and Urban Design, Faculty of Engineering, Osaka Institute of Technology)

This session discusses various methods which acquire, store, analyze and visualize geospatial data, and presents the outcomes of empirical studies using GIS or mapping methods. The session also deals with applications of digital data, GIS, and mapping to various fields of earth and planetary science and human society. All presentations and discussion of this session are made in Japanese.

9:00 AM - 9:15 AM JST | 12:00 AM - 12:15 AM UTC

[HTT19-01] Introduction

9:15 AM - 9:30 AM JST | 12:15 AM - 12:30 AM UTC

[HTT19-02] Map representation of estimated concentration distribution of $PM_{2.5}$ using WebGIS

*Junji Yamakawa[1] (1.Graduate School of Natural Science and Technology, Okayama University)

9:30 AM - 9:45 AM JST | 12:30 AM - 12:45 AM UTC

[HTT19-03] Proposal of nocturnal light data as a proxy variable for building height

*Go Kazawa[1], Daikichi SEKI[1], Yosuke Alexandre Yamashiki[1], Fusanori Iwasaki[2], Keola Souknilanh[3] (1. Graduate School of Advanced Integrated Studies in Human Survivability, 2.Economic Research Institute for ASEAN and East Asia, 3.Institute of Developing Economies, Japan External Trade Organization)

9:45 AM - 10:00 AM JST | 12:45 AM - 1:00 AM UTC

[HTT19-04] A Consideration of the Spatio-Temporal Expansion of "Deep Wonder" Evoked by Forest Image Archives

*Kazuhiko W. Nakamura[1] (1.The University of Tokyo)

10:00 AM - 10:15 AM JST | 1:00 AM - 1:15 AM UTC

[HTT19-05] An analysis of Children’s school route with GPS: A case study of 30 elementary schools in Toyama city

*Koji Ohnishi[1] (1.Department of Humanities, University of Toyama)

10:15 AM - 10:30 AM JST | 1:15 AM - 1:30 AM UTC

[HTT19-06] Red Relief Image Map using Hyper Resolution DEM, New Development of Topography recognition

*Tatsuro Chiba[1], Makoto Ohashi[1] (1.Asia Air Survey Co., Ltd.)

[J] Oral | H (Human Geosciences) | H-TT Technology & Techniques

[H-TT19] Geographic Information System and Cartography

convener:Mamoru Koarai(Earth Science course, College of Science, Ibaraki University), Kazunari Tanaka(Department of Civil Engineering and Urban Design, Faculty of Engineering, Osaka Institute of Technology), W. Kazuhiko Nakamura(The University of Tokyo), Chairperson:Mamoru Koarai(Earth Science course, College of Science, Ibaraki University), Kazunari Tanka(Department of Civil Engineering and Urban Design, Faculty of Engineering, Osaka Institute of Technology)

Sun. Jun 6, 2021 9:00 AM - 10:30 AM Ch.14 (Zoom Room 14)

This session discusses various methods which acquire, store, analyze and visualize geospatial data, and presents the outcomes of empirical studies using GIS or mapping methods. The session also deals with applications of digital data, GIS, and mapping to various fields of earth and planetary science and human society. All presentations and discussion of this session are made in Japanese.

9:00 AM - 9:15 AM

[HTT19-01]Introduction

©Japan Geoscience Union

Map representation of estimated concentration distribution of $PM_{2.5}$ using WebGIS

*Junji Yamakawa[1]

1. Graduate School of Natural Science and Technology, Okayama University

Interval estimation is important information in the examination of $PM_{2.5}$ concentration distribution estimated by geostatistical methods. Especially when comparing the estimated concentration with other geographical information and statistical information such as national census, it is indispensable to examine the probability of the impact of the estimated concentration. In the study, a method of expressing the estimated concentration distribution of $PM_{2.5}$ and its confidence interval in Okayama city obtained by the Kriging method, which is one of the methods of geostatistics, using the WebGIS application was examined.
The target area in the study was the entire area of Okayama City, Okayama Prefecture, and the $PM_{2.5}$ estimation was base on the observation data were for 2017 FY (monthly values) published by the National Institute for Environmental Studies (http: //www.nies.go.jp/igreen/). JPGIS (Geographical Survey Institute, 2020), which is government-affiliated open data, was used as the geographic information data required for the analysis. GNU R (R core team, 2020) and Google Colab (Google, 2020) were used for geostatistical analysis. The jSTAT MAP (Statistics Bureau, Ministry of Internal Affairs and Communications, 2020) was used as the WebGIS in the study.
The spatial dependence of $PM_{2.5}$ observation data was estimated using a variogram, and the $PM_{2.5}$ estimated concentration distribution and its variance throughout Okayama City were obtained by the Kriging method. The mesh grid used for estimation used the Japanese 3rd Mesh code. Then, the estimated concentration distribution and its confidence interval were mapped using the jSTAT MAP. The exposure risk examined together with the census data was also expressed in the jSTAT MAP.
Since jSTAT MAP has built-in various geographic information and statistical information, it was possible to perform easily the qualitative comparison with the estimated concentration of $PM_{2.5}$, its confidence interval, and exposure risk with it. Also, since jSTAT MAP is a WebApp, no proprietary GIS application is required to mapping the $PM_{2.5}$ exposure risk assessment data. It is expected that it will be used more as one of the information disclosure means expressed on a map.

Keywords: WebGIS, jSTAT MAP, Kriging, PM2.5, Google Colab

©2021. Japan Geoscience Union. All Right Reserved.

Proposal of nocturnal light data as a proxy variable for building height

*Go Kazawa[1], Daikichi SEKI[1], Yosuke Alexandre Yamashiki[1], Fusanori Iwasaki[2], Keola Souknilanh[3]

1. Graduate School of Advanced Integrated Studies in Human Survivability, 2. Economic Research Institute for ASEAN and East Asia, 3. Institute of Developing Economies, Japan External Trade Organization

In this study, we examine whether night light can be a proxy for building height.

The height of the building is a very important value for the damage situation of the city at the time of disaster and the urban design. However, building height data can only be obtained for high-rise buildings such as landmarks on Open Street, and it is necessary to purchase data to obtain height data including low-rise buildings nationwide. Another major disadvantage is that it is difficult to acquire data in chronological order. Building height data can be confirmed in chronological order, and user verification can be performed for various studies only after the aging of cities and towns.
In this study, we verified whether it is possible to estimate the height of a building with a high cost by using night light data whose time scale has been released in detail for free in recent years.

So far, active research has been conducted to estimate GDP using Night-Time Light Data. In particular, developing countries with low reliability of statistical data and rural poor areas that have not been surveyed in the first place have achieved very great results in the study area.
On the other hand, economic forecasts using satellite images in urban areas are not very active due to the coarseness of the spatial resolution of satellite images and the complex urban structure. In addition, since it is necessary to verify the accuracy of night light GDP estimation using data based on the presentations of each country, the difficulty of accuracy verification is described in various papers in developing countries due to its low reliability. It has been mentioned as an issue. When using night light to estimate GDP in this way, there is a strong tendency to choose a region.

In this study, we will verify whether it can be a proxy for the height of a building as a new usage of night light.
This takes advantage of the fact that the more floors a building have, the more light it has per unit area. Since this law is universal, it is possible to replace the height of buildings around the world with night light if the correlation between night light and building height can be found.
In this study, we used the 1m-resolution 3D data set released by Hyogo Prefecture for the first time in Japan on January 10, 2020, and the nighttime light data of the Suomi NPP satellite jointly managed by NOAA and NASA, which has been in operation since 2011. Correlation analysis was performed. Among the aerial laser survey results, it is obtained by the difference between the digital elevation model, which is a digital elevation model of the ground surface with buildings, vegetation, etc. removed from the digital surface model of the entire Hyogo prefecture, which is the numerical surface layer including the ground surface and buildings, vegetation, etc. Data on the height of buildings and vegetation above the ground surface. The observation period is from 2012 to 2013. In addition, there were no missing values in each of the Digital Surface Model and Digital Elevation Model. Since the observation period of Hyogo prefecture was from 2012 to 2013, the annual data of 2014 was used for the night light. The spatial resolution was about 450 meters, excluding outliers of the night light and setting the non-light areas to zero.

In order to classify the building as vegetation, the outer circumference data of the building was acquired

©2021. Japan Geoscience Union. All Right Reserved.

from the basic map information of the Geographical Survey Institute, and the data of only the height of the building was extracted. The night light was layered, and the pixels with 70% or more of the buildings in the 450m square were selected, and the average height of the buildings in those pixels was correlated with the luminous intensity of the night light. The x-axis is the value of night light weighted and averaged by the number of observations in each month for the pixel, and the y-axis is the average height of the buildings in the pixel.

As a result of the correlation analysis, the number of data was 1028 and the coefficient of determination was 0.392. The null hypothesis was rejected because the P-value was well below the significance level of 0.05. In this way, it was found that the night light has a certain correlation with the height of the building. This can be evaluated as having a correlation even if the building uses data with a roughness of 70% or more in Pixel. We calculated more than 50%, more than 60%, more than 80%, and more than 90% of buildings in Pixel, but 70% or more was the most accurate result. In the future, we would like to conduct verification in other regions and countries to investigate whether there is any regional difference in the correlation between night light and building height.

Keywords: Night Time Light, Digital Surface Model, Suomi NPP

©2021. Japan Geoscience Union. All Right Reserved.

A Consideration of the Spatio-Temporal Expansion of "Deep Wonder" Evoked by Forest Image Archives

*Kazuhiko W. Nakamura[1]

1. The University of Tokyo

In recent years, awareness of the importance of the connection between human society and natural environments, including forests, has been increasing. In this regard, it has become difficult to present the desirable state of this increasingly complex relationship based only on scientific evidence. Within this context, the significance of facing natural phenomena, which includes scientific uncertainty, is sometimes discussed in terms of the concept of wonder, especially in the field of pedagogy from the perspective of fostering the next generation. Schinkel (2017) has discussed the educational importance of wonder not only as a motivational effect but also as a way of making us aware of the limits of our understanding and has distinguished the latter as “deep wonder.” From a similar perspective, L’ Ecuyer (2014) considered the scope of wonder to be beyond mere curiosity and mentioned the visible expression called “beauty” as one of the properties of the environment that evokes wonder. When addressing issues at large spatio-temporal scales, such as climate change and biodiversity, which are important aspects for building a sustainable society, the perspective of "deep wonder" is important because it is difficult to avoid scientific uncertainty in this regard. However, it is extremely difficult to directly experience “deep wonder” as a visual expression. In this presentation, I will discuss the possibility of a virtual expansion of “deep wonder” using forest image archives since 1995. This is a case study of a method used to visualize phenomena virtually at a large temporal and spatial scale.

References:
L’ Ecuyer, C. (2014): The Wonder Approach to learning. *Front. Hum. Neurosci.* 8:764. doi: 10.3389/fnhum.2014.00764
Schinkel, A. (2017): The Educational Importance of Deep Wonder. *Journal of Philosophy of Education*, 51: 538-553. doi: 10.1111/1467-9752.12233

Keywords: Cyberforest, environmental education, image archive

©2021. Japan Geoscience Union. All Right Reserved.

An analysis of Children’ s school route with GPS: A case study of 30 elementary schools in Toyama city

*Koji Ohnishi[1]

1. Department of Humanities, University of Toyama

In Toyama City, a wireless network using LPWA was constructed in 2018 as a smart city project. Using this IoT, Toyama city is conducting a project to watch over children on school routes. Every elementary school districts will be surveyed the school routes safety by GPS sensors. These sensors are curried by children with their bags, so that we can grasp the state of going to and from school. The purpose of this study is that I analyze the relationship between regional characteristics and the expansion of children's activity spaces with the data of this project from 2018 to 2020. 30 schools data was obtained in the project from 2018 to 2020. The GPS data is obtained at 1-minute intervals, and was visualized and analyzed on GIS. It was found that most elementary schools go to school in groups, and they use the school route to go to school around at 7:45 when the school entrance opens. As a result, there were places where children stayed around the school, and that it was necessary to give consideration to traffic safety in those areas. In addition, it can be seen that children stay at pedestrian bridges and large intersections. It was also found that when the school district is wide, there is a difference in the morning commuting start time of children. On the other hand, it was found that the time of leaving school differs. It depends on the grade, and the start time of transportation to and from after-school care and lessons. In areas differences, far from the city center, they often are taken out by their parents to go some kinds of lessens to city center area or shopping center especially lower grades. At schools near the city center, it was found that these activities could start after they return to their home. In this way, it became clear that the quality and extent of the children's after-school activity space differed depending on the distance from the central city area.

Keywords: GPS, Children, school route

©2021. Japan Geoscience Union. All Right Reserved.

Red Relief Image Map using Hyper Resolution DEM, New Development of Topography recognition

*Tatsuro Chiba[1], Makoto Ohashi[1]

1. Asia Air Survey Co., Ltd.

1. Introduction

Precise resolution DEM made by airborne LiDAR measurement is getting available. Elevation data of Well distributed Fundamental Geospatial Data (DEM) 5 m Mesh made by LiDAR of Geospatial Information Authority of Japan has been useful for understanding topography. Red Relief Image Map, hereinafter called RRIM (Chiba et al., 2004) is a visualization method which is improved slope map, but not include altitude information. RRIM with overlapping contour map make topography understanding more easily. The problem when overlapping RRIM with 5m DEM and GSI Map of level 15 is that RRIM looks significantly jaggy and is difficult to grasp topography. The resolution of GSI Map level 15 is around 50cm, but DEM 5m ten times lower. It does not solve the issue to make higher resolution DEM by image processing.
This study reports that RRIM with hyper resolution DEM applying interpolation and moving average is decreasing jaggy and increasing three-dimensional effect. Fundamental work-flow of this methodology and several case studies are described.

2. Methodology

Matrix data is split by n times both for X and Y direction. It is desirable that n is odd number. By linear interpolation is acceptable experientially. Loop process for moving average is applied until jaggy becoming inconspicuous. Too much loop process make the result smooth, but deviate from initial value. RRIM is made using hyper resolution DEM. When n equal 9, data volume is 81 times bigger. Since considering mesh number of positive openness and negative openness are becoming n times, computing time is getting longer.

3. Case studies

The comparison between RRIM using 5m resolution DEM and RRIM using Hyper resolution DEM on Asahi-ku, Yokohama City are shown (Fig. 1).Orthogonal roads in the developed residential area and slope feature in the surround hill area are clearly seen as well. The topography of terrace paddy field is better reproduced by Hyper resolution DEM, which was open to the public as WebGIS at Map Gallery of Esri User Conference 2020.[2)]

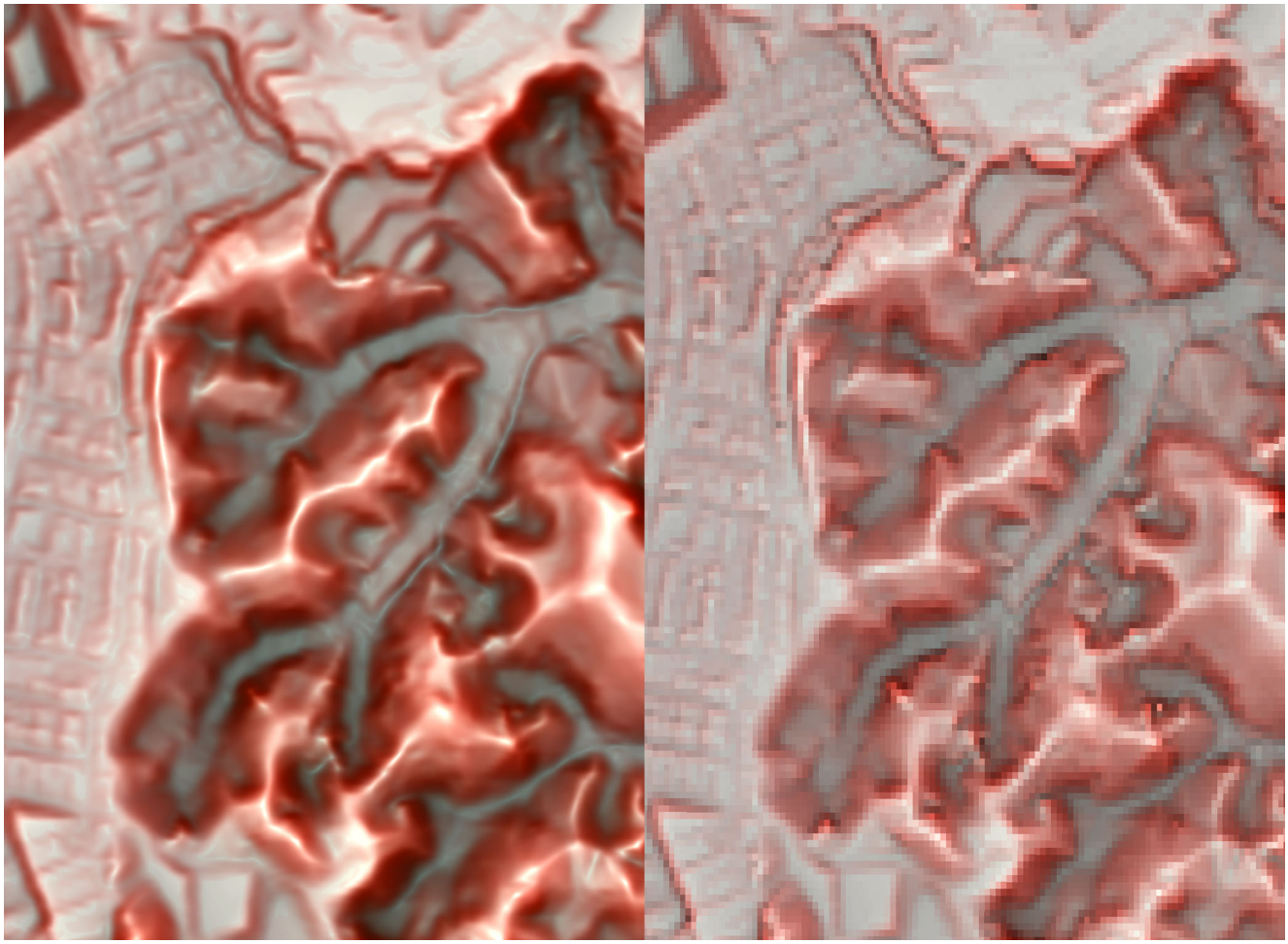
4. Conclusion

RRIM using Hyper resolution DEM visualize topography more smooth and easy to understand, and having high visibility when overlapping with GSI Map.The difficulty is that computing time is 100 times longer than previous method.

©2021. Japan Geoscience Union. All Right Reserved.

Reference
1) Tatsuro Chiba and Yusuke Suzuki (2004) Red relief image map,new topographical expression method, Proceedings of Applied Surveys, 15, 81-89.
2) Chiba T. and Ohashi M. (2020) Red Relief Image Map using Hyper Resolution DEM, ESRI map gallery 2020 User Conference, https://mapgallery.esri.com/map-detail/5efa4698f3b616cb34d9e11e

Keywords: RED RELIEF IMAGE MAP, Terrain visualization, GIS



©2021. Japan Geoscience Union. All Right Reserved.

[J] Oral | H (Human Geosciences)：H-TT Technology & Techniques

Sun. Jun 6, 2021 10:45 AM - 12:15 PM JST | Sun. Jun 6, 2021 1:45 AM - 3:15 AM UTC | Ch.14 Zoom Room 14

[H-TT19] Geographic Information System and Cartography

convener:Mamoru Koarai(Earth Science course, College of Science, Ibaraki University), Kazunari Tanaka(Department of Civil Engineering and Urban Design, Faculty of Engineering, Osaka Institute of Technology), W. Kazuhiko Nakamura(The University of Tokyo), Chairperson:Mamoru Koarai(Earth Science course, College of Science, Ibaraki University), Kazuhiko W. Nakamura(The University of Tokyo)

This session discusses various methods which acquire, store, analyze and visualize geospatial data, and presents the outcomes of empirical studies using GIS or mapping methods. The session also deals with applications of digital data, GIS, and mapping to various fields of earth and planetary science and human society. All presentations and discussion of this session are made in Japanese.

10:45 AM - 11:00 AM JST | 1:45 AM - 2:00 AM UTC

[HTT19-07] Relationship between the Image of the Town and the Seams of Asphalt Pavement Works

*Kazunari Tanaka[1], Miku Ogawa[1], Hitomi Tsukioka[1] (1.Department of Civil Engineering and Urban Design, Faculty of Engineering, Osaka Institute of Technology)

11:00 AM - 11:15 AM JST | 2:00 AM - 2:15 AM UTC

[HTT19-08] On Spatial Cognition of Children by Distortion and Color on the Cognitive Map

*Ami Hasegawa[1], Kazunari Tanaka[1] (1.Osaka Institute of Technology)

11:15 AM - 11:30 AM JST | 2:15 AM - 2:30 AM UTC

[HTT19-09] On Evaluation of Environmental Sound by Degree of Human Concentration

*Haru Kanda[1] (1.Osaka Institute Technology)

11:30 AM - 11:45 AM JST | 2:30 AM - 2:45 AM UTC

[HTT19-10] On the Meaning of Affordance and Personal-Space in the COVID-19

*Kazuki Miyake[1], Shota Tanaka[1], Kazunari Tanaka[1] (1.Osaka Institute of Technology)

11:45 AM - 12:15 PM JST | 2:45 AM - 3:15 AM UTC

[HTT19-11] Discussion

Relationship between the Image of the Town and the Seams of Asphalt Pavement Works

*Kazunari Tanaka[1], Miku Ogawa[1], Hitomi Tsukioka[1]

1. Department of Civil Engineering and Urban Design, Faculty of Engineering, Osaka Institute of Technology

In general, civil engineering work, based on various underlying plans in the city is carried out as a different project. Therefore, the attractiveness of the completed cityscape may be totally canceled even if a part of areas or individual buildings are good.

Attractive urban development has been considered for buildings and structures on the ground. For example, the undergrounding of buildings and electric wires with a sense of unity, and the maintenance of green spaces such as rows of trees. However, much attention has not been paid to the road surface of the road asphalt that has been peeled off and buried when each construction.

The purpose of this study is to explore the relationship between the condition of this asphalt and the image of the city.

In this study, we focus on the traces of general asphalt pavement work. We will explore the image that people have without noticing, focusing on the state of seams where the difference in texture of asphalt pavement is conspicuous, the size of construction marks, and the difference in color. In addition, by conducting psychological experiments on the consistency between the frontage of surrounding buildings and the size of the pavement, we extract the images which we have without knowing it daily.

In this study, we conducted three experiments to grasp the state of the seams of asphalt pavement, which makes us feel uncomfortable, to extract the sense of harmony due to the slight difference in color of the road surface, and to see the relationship between the building and the pavement traces.

By the experiment using the samples arranging two asphalt pavements with different textures in close contact with each other, we extracted a range that does not feel strange. As a result of conducting experiments on 180 subjects for 7 samples, it was found that the difference in aggregate particle size was within 25%, and that no discomfort was felt when the particle size was fine.

Next, for color combinations, an experiment using 30 colors extracted from actual pavement was conducted on 180 subjects. As a result, it was clarified that although no clear result was obtained, it felt natural in cases other than the contrasting colors.

Finally, a psychological experiment was conducted by the Paired Comparison Method on the relationship between the frontage of the building and the size of the asphalt pavement trace. Based on the results of the experiments so far, we compared the psychological amount of the consistency between the size and the frontage using the preferred pavement. As a result, it became clear that the size of the construction site and the consistency with the frontage affect the impression of a good cityscape.

Keywords: Asphalt, Road surface, Cityscape, Street

©2021. Japan Geoscience Union. All Right Reserved.

On Spatial Cognition of Children by Distortion and Color on the Cognitive Map

*Ami Hasegawa[1], Kazunari Tanaka[1]

1. Osaka Institute of Technology

With the development of transportation means by improving road and railway spaces, our lives have developed remarkably. On the other hand, traffic spaces may deprive children of playgrounds outside and have negative physical and mental impact on them. In order to solve such problems in public spaces, by clarifying the differences in objects and places that adults and children find attractive, urban space design that both adults and children find attractive is created. I think it should be suggested. In addition, I think it is important for future town development to clarify whether the intentions of adults are being conveyed to children.

While creating a city where adults feel comfortable and comfortable to live in, and the scenery is good, to create a livable city or town, it is important to conserve attractive places for children to play. One of the tasks of urban planning is to create a town where children want to continue living even when they grow up. For this, we need to understand in what ways children find it attractive. Regarding the parks, streets, rivers, etc., it is necessary to know how children perceive the space.

The purpose of this study is to identify the parts of the city that appeal to children, analyzing the cognitive maps drawn by them. Ultimately, the goal is to propose an urban space that will be enjoyable, fun, comfortable and safe for children and adults as well.

There are two research methods for this study. One is a route selection experiment based on the Paired Comparison Method using photographs. By grasping the components of each photograph, the “taste” of the road is analyzed. The other is to conduct a survey using the Basic Drawing Method, where we extract elements that are recognized.

As a research method, I conduct a survey using the Basic Drawing Method, where we extract elements and the colors. I explore the size of the cognitive space and the place where consciousness is easy to direct that are recognized.

From the results of the Basic Drawing Method, it was found that children perceived what they usually see more honestly than adults.

Keywords: Cognitive Map, Distortion, Color, Image

©2021. Japan Geoscience Union. All Right Reserved.

On Evaluation of Environmental Sound by Degree of Human Concentration

*Haru Kanda[1]

1. Osaka Institute Technology

Currently, COVID-19 is changing the learning environment of students and the working environment of office workers. In this study, we focus on the environmental sound, clarify the difference in the environment of residential areas, which is different from schools, companies, educational districts and office areas, from the viewpoint of concentration. In this study, we clarify the factors that lead to comfort from the two points of deep psychology and physiological response. This result should be useful for future design. In the physiological response experiment, brain waves, which are closely related to concentration, were measured and analyzed.
Before conducting the psychological experiment, the environmental sounds used in the experiment were collected from the subjects as a preliminary survey, and the representative sounds were selected after grouping the environmental sounds. The subjects were shown a limited environmental sound and evaluated the degree to which they could concentrate in five stages. The average value of human speech was 2.89 indoors at home and 2.19 during university lectures. A possible cause for this is the difference in the recognition range of environmental sounds obtained from the preliminary survey, and the number of people who recognize human speech as environmental sounds is higher during university lectures. Furthermore, since it was confirmed from some environmental sounds that the results were divided into two, the cause was analyzed. In addition, as a result of considering the correlation of the average values, regularity was found.
Experiments on physiological reactions were performed using a simple electroencephalograph (EMOTIV EPOC X). EMOTIV EPOC X can measure β wave by dividing it into two types, High β and Low β, and this time, we measured α wave and Low β wave, which are considered to be particularly affected. In the experimental method, the subjects were asked to solve 12 simple arithmetic operations by mental arithmetic, and at that time, the subjects were asked to listen to the sound source created as a sound stimulus at the same time as each environmental sound. The brain waves at that time were measured and compared with psychological experiments for analysis. Comparing the data obtained from the electroencephalogram measurement with the data obtained from the psychological experiment, the four things that actually matched were the sound of turning paper, the clock, the chirping of birds, and the voice of a person. It was found that the most human voice among them hindered concentration.It was also found that the sound of turning paper and the chirping of clocks and birds are environmental sounds that do not interfere with concentration.
In this study, experiments were conducted from two directions: psychological experiments and physiological experiments. Although there was some discrepancy between the auditory image and the response from the sound stimulus, it was noticeable that human speech had an adverse effect on concentration. In this experiment, we fixed the space and let the subject listen to it, and considered the effect of only sound on concentration, but it is also necessary to investigate how changing the space affects concentration.

Keywords: Sound, Pollution, Brain waves

©2021. Japan Geoscience Union. All Right Reserved.

On the Meaning of Affordance and Personal-Space in the COVID-19

*Kazuki Miyake[1], Shota Tanaka[1], Kazunari Tanaka[1]

1. Osaka Institute of Technology

The chair affords to sit, and the pencil affords to write. Humans get information from the environment and change their behavior. For example, a seat in a university lecture, a seat in a train, a position in an elevator, and so on. In 2020 people's lives have changed due to the spread of telecommuting, online lessons, and delivery services due to the influence of the new covin-19.Behavior is restricted, such as restrictions on admission to shopping malls, stores that cannot be entered without disinfection and temperature measurement, and restrictions on the use of benches and chairs. However, I think that there were other restrictions on people's behavior. I think it is a constraint on psychological behavior such as the sense of distance between people (personal space). The purpose of this study is to investigate how the surrounding environment affects our behavioral choices and how they change.

We compare our behavioral choices before and after the outbreak of the new covin-19 and investigate affordances and changes in personal space during the covin-19. Investigate behavioral restrictions and affordance changes during the covin-19. As a result of the experiment of seat selection in the train by a questionnaire using the presence or absence of a mask, it was found that people's behavior choices changed depending on the presence or absence of a mask. Secondly, we investigate whether there was a difference in the distance between the waiting positions in the station yard of a person depending on the presence or absence of a mask. As a result, there was not much difference between the position of the person standing behind the person without the mask and the wearing the mask. The cause may be that the presence or absence of the mask is not recognized. Finally, we conducted a post-epidemic personal space survey of the new coronavirus with and without masks. There was no big difference in personal space However, the value of personal distance changed to the value of social distance due to the influence of covin-19.

Keywords: Personal-Space, Affordance, mask

©2021. Japan Geoscience Union. All Right Reserved.

[J] Oral | H (Human Geosciences) | H-TT Technology & Techniques

[H-TT19] Geographic Information System and Cartography

convener:Mamoru Koarai(Earth Science course, College of Science, Ibaraki University), Kazunari Tanaka(Department of Civil Engineering and Urban Design, Faculty of Engineering, Osaka Institute of Technology), W. Kazuhiko Nakamura(The University of Tokyo), Chairperson:Mamoru Koarai(Earth Science course, College of Science, Ibaraki University), Kazuhiko W. Nakamura(The University of Tokyo)
Sun. Jun 6, 2021 10:45 AM - 12:15 PM Ch.14 (Zoom Room 14)
This session discusses various methods which acquire, store, analyze and visualize geospatial data, and presents the outcomes of empirical studies using GIS or mapping methods. The session also deals with applications of digital data, GIS, and mapping to various fields of earth and planetary science and human society. All presentations and discussion of this session are made in Japanese.

11:45 AM - 12:15 PM

[HTT19-11]Discussion

©Japan Geoscience Union

[J] Poster | H (Human Geosciences)：H-TT Technology & Techniques

Sun. Jun 6, 2021 5:15 PM - 6:30 PM JST | Sun. Jun 6, 2021 8:15 AM - 9:30 AM UTC | Ch.09_3

[H-TT19] Geographic Information System and Cartography

convener:Mamoru Koarai(Earth Science course, College of Science, Ibaraki University), Kazunari Tanaka(Department of Civil Engineering and Urban Design, Faculty of Engineering, Osaka Institute of Technology), W. Kazuhiko Nakamura(The University of Tokyo)

This session discusses various methods which acquire, store, analyze and visualize geospatial data, and presents the outcomes of empirical studies using GIS or mapping methods. The session also deals with applications of digital data, GIS, and mapping to various fields of earth and planetary science and human society. All presentations and discussion of this session are made in Japanese.

[HTT19-P01] Susceptibility assessment of post-seismic landslides with an index representative of seismic cracks

*Shui Yamaguchi[1], Mio Kasai[2] (1.Graduate School of Agriculture, Hokkaido University, 2.Research Faculty of Agriculture, Hokkaido University)

[HTT19-P02] Development of information platform for topographical recognition by CS topographic map

*Hiromu Daimaru[1], Kenichiro Toda[2], Wataru Murakami[1], Ryuichi Sekoguchi[3], Yoichi Kayama[3], Keichi Katsube[3], Hiroo Imaki[4], Koji Ijima[4], Ryosuke Wayama[5] (1.Forestry and Forest Products Research Institute, 2.Nagano Prefecture Forestry Research Center, 3.Aero Asahi Corporation, 4.Pacific Spatial Solutions Co., Ltd., 5.Northern System Service Co., Ltd.)

Susceptibility assessment of post-seismic landslides with an index representative of seismic cracks

*Shui Yamaguchi[1], Mio Kasai[2]

1. Graduate School of Agriculture, Hokkaido University, 2. Research Faculty of Agriculture, Hokkaido University

An intense earthquake can cause numerous landslides over a broad area, causing damage to human lives, property, and infrastructure. The strong tremors weaken the ground strength and induce cracks on the ground surface. Thus, following the earthquake, identification of the ground cracks is rapidly carried out via field survey and/or examining aerial photographs or topographic maps to find slopes in danger of sliding and prevent from further disaster. However, this operation requires more time and effort as the magnitude of the earthquake is more extensive. Hence, we proposed an index (DCI: Dense Crack Index) representative of the density of co-seismic cracks, which can be quickly and easily calculated using airborne LiDAR data before and after the earthquake. This study applied the index to an area (6 km^2) located in the southwestern Aso Caldera, Kumamoto Prefecture, where the 2016 Kumamoto earthquake (Mw 7.0) struck, and the 198 co-seismic and 125 post-seismic slides were recognized in the following four months. They were categorized as shallow landslides. Then, we statistically estimated the susceptibility of post-seismic landslides and examined the improvement of the evaluation accuracy when DCI is incorporated in predictor variables.

First, we calculated the slope angle for each 1-m cell derived from LiDAR survey data acquired before and after the earthquake (Fig. 1-a), and then its standard deviation for 3 ×3 cells. We found that the standard deviation increased by more than 2 degrees after the earthquake in 75% of the locations where co-seismic cracks were identified (Fig. 1-b). The DCI was given as the spatial density of those cells, calculated by the kernel density with a nearby distance of 10 meters (Fig. 1-c).

Weight of Evidence (WoE) and Logistic Regression (LR) methods were applied to estimate the susceptibility for post-seismic slides. The response variable used in these two statistical models was the presence or absence of post-earthquake landslides on the cell, which was identified from aerial photographs and topographic maps obtained four months after the earthquake. Also, the slope angle, profile curvature, slope aspect, distance to edge of co-seismic landslides, distance to epicenter fault, and peak ground acceleration (PGA) were adopted as predictor variables in addition to DCI. This study considered the geology, vegetation, and rainfall conditions as the same due to the small size of the study area.

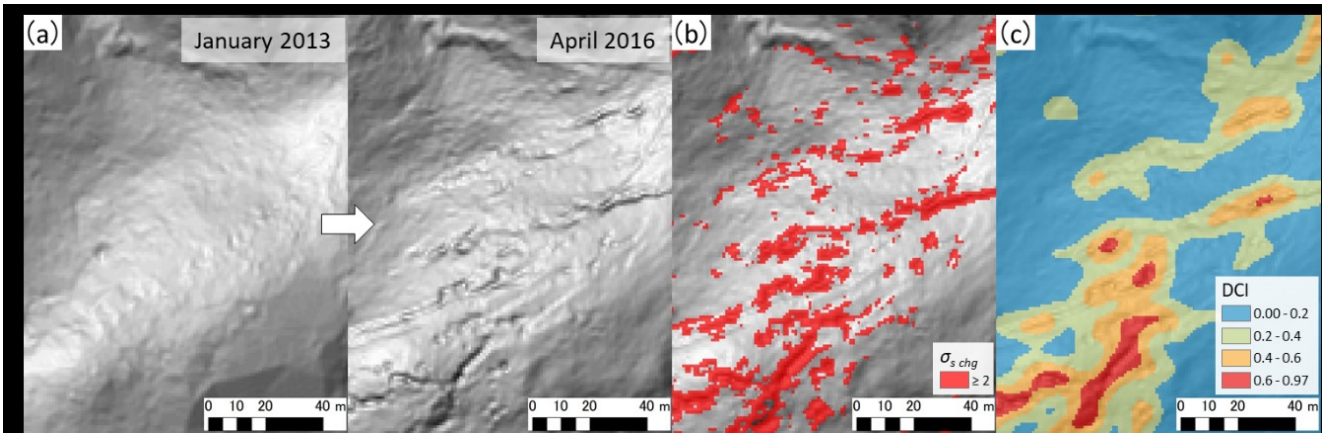
The analysis by the WoE method showed that steep slopes (slope: 40 - 55 degrees) near knick lines (profile curvature: -6 - -4 m^{-1}) affected by strong tremors (PGA: 1050 - 1150 gal) with dense crack appearance (DCI: 0.2 - 1.0) were more likely to slide after the earthquake. This result is in agreement with the report of the field survey conducted in the study area (Kumamoto Prefecture, 2019). The accuracy of the susceptibility assessment by the WoE and LR methods was slightly higher when DCI was included as a predictor variable, with an Area Under the Curve (AUC) value of 0.80 - 0.90 for the ROC curves, compared to the models without DCI (0.70 - 0.85).

As such, the inclusion of DCI in statistical susceptibility assessment improved the accuracy of the models and allowed the identification of slopes in danger of sliding that were consistent with those reported from the field. These results suggest that DCI is an important index for estimating slopes destabilized by seismic motion.

Fig.1:Step of DCI calculation (a: Slope maps of pre- and post- earthquake, b: red indicates the locations where the standard deviation of the slope increased by more than 2 after the earthquake , c: DCI map)

©2021. Japan Geoscience Union. All Right Reserved.

Keywords: post-seismic landslides, seismic cracks, landslide susceptibility assessment, WoE, Logistic regression



©2021. Japan Geoscience Union. All Right Reserved.

Development of information platform for topographical recognition by CS topographic map

*Hiromu Daimaru[1], Kenichiro Toda[2], Wataru Murakami[1], Ryuichi Sekoguchi[3], Yoichi Kayama[3], Keichi Katsube[3], Hiroo Imaki[4], Koji Ijima[4], Ryosuke Wayama[5]

1. Forestry and Forest Products Research Institute, 2. Nagano Prefecture Forestry Research Center, 3. Aero Asahi Corporation, 4. Pacific Spatial Solutions Co., Ltd., 5. Northern System Service Co., Ltd.

Topographical recognition is a fundamental process when considering land use plans for mountain areas. Airborne laser scanning, which has been widely used in recent years, has provided valuable data for landform recognition. We have developed an information system to support landform recognition in the mountain areas by distributing raster tile of CS topographic map, including a converting tool from Geotiff formatted DEM to CS topographic map image by using FME (Safe Software Inc.). This system includes the tool for LEM formatted data that is commonly used in Japan for LiDAR DEM.
The CS map images created by our system are displayed in seamless style and uniform tones. The metadata catalog of the CS map was provided to GKAN that was developed by adding spatial functions to the data catalog server CKAN. The platform enables GIS users to search for stored CS map database and distribute the raster tiles. Furthermore, we also developed a technology that automatically extract shallow landslide scarps and small forest roads from CS topographic maps by using AI.

Keywords: Landform, CS topographic map, Web GIS, GKAN, AI

©2021. Japan Geoscience Union. All Right Reserved.

[J] Oral | H (Human Geosciences)：H-CG Complex & General

Sun. Jun 6, 2021 10:45 AM - 12:15 PM JST | Sun. Jun 6, 2021 1:45 AM - 3:15 AM UTC | Ch.15 Zoom Room 15

[H-CG26] Adaptation to climate change and its social implementation

convener:Hiroya Yamano(National Institute for Environmental Studies), Yoichi Ishikawa(JAPAN Agency for Marine-Earth Science and Technology), KOJI DAIRAKU(University of Tsukuba), Makoto Tamura(Global and Local Environment Co-creation Institute, Ibaraki University), Chairperson:Hiroya Yamano(National Institute for Environmental Studies), Yoichi Ishikawa(JAPAN Agency for Marine-Earth Science and Technology), KOJI DAIRAKU(University of Tsukuba), Makoto Tamura(Global and Local Environment Co-creation Institute, Ibaraki University)

The impacts of climate change will increase in the risks to societies through increased intensities of typhoons and torrential rains, changes in the distribution of organisms, deterioration in quality and yield in the agriculture, forestry and fisheries, etc. In response to this, Japan enforced "Climate Change Adaptation Act" in 2018, aiming to minimize or avoid the damage caused by climate change, and to build a sustainable society.
In this session, toward planning adaptation to climate change and enhancing its social implementation based on scientific knowledge, we will discuss about generation of climate change projection data, assessment of the impacts and risks of climate change in various fields, as well as social implementation of adaptation plans by co-creation with stakeholders and/or by local climate change adaptation acts.

10:45 AM - 11:00 AM JST | 1:45 AM - 2:00 AM UTC

[HCG26-01] Enhancing resilience of atoll islands against sea level rise

★Invited Papers

*Hajime Kayanne[1], Masafumi Fujita[2], Nori Fujita[1], Takashi Hosono[3], Yoich Ide[4], Yuji Kuwahara[2], Fumiko Matsudate[13], Satoru Mimura[5], Nobuko Nakamura[6], Susumu Onaka[7], Daisaku Sato[8], Tomoko Takeda[9], Koji Yamada[10], Toru Yamaguchi[11], Hiroya Yamano[12], Hiromune Yokoki[2] (1.the University of Tokyo, 2.Ibaraki Univ., 3.JAMSTEC, 4.Oceanic Planning Corp., 5.JICA, 6.Sasakawa Peace Foundation, Ocean Policy Res. Inst., 7.Nippon Koei, 8.Setsunan Univ., 9.IGES, 10.Japan Construction Information Center Found., 11.Keio Univ., 12.National Inst. Environmental Studies, 13.Heart Biz)

11:00 AM - 11:15 AM JST | 2:00 AM - 2:15 AM UTC

[HCG26-02] Developments of future climate scenario selection method for impact and adaptation studies

*Hideo Shiogama[1], Noriko N. Ishizaki[1], Naota Hanasaki[1], Kiyoshi Takahashi[1], Seita Emori[1], Rui Ito[2,3], Toshiyuki Nakaegawa[3], Izuru Takayabu[3], Yasuaki Hijioka[1], Yukari N. Takayabu[4], Ryosuke Shibuya[4] (1.National Institute for Environmental Studies, 2.Japan Meteorological Business Support Center, 3.Meteorological Research Institute, 4.Atmosphere and Ocean Research Institute, The University of Tokyo)

11:15 AM - 11:30 AM JST | 2:15 AM - 2:30 AM UTC

[HCG26-03] Added values of regional multi-ensemble statistical downscaling approach in CORDEX Asia

*KOJI DAIRAKU[1] (1.University of Tsukuba)

11:30 AM - 11:45 AM JST | 2:30 AM - 2:45 AM UTC

[HCG26-04] Temperature rises and extreme rainfall intensity derived from observations and d4PDF in Japan

*Sayaka Yoshikawa[1,3], Megumi Watanabe[2], Shinjiro Kanae[3] (1.Ibaraki university, 2.The university Tokyo, 3.Tokyo institute of technology)

11:45 AM - 12:00 PM JST | 2:45 AM - 3:00 AM UTC

[HCG26-05] Adaptation measures based on future projections of corals and macroalgae, use/conservation status on the southwest coast of Shikoku

*Hiroya Abe[1], Haruka Suzuki[1], Yuko F Kitano[1], Naoki H Kumagai[1], Satomi Mitsui[1], Hiroya Yamano[1] (1.National Institute for Environmental Studies)

12:00 PM - 12:15 PM JST | 3:00 AM - 3:15 AM UTC

[HCG26-06] Workshop on Disaster Prevention Training to Improve Disaster Preparedness of Local Governments and Staff: As Part of Social Implementation of Disaster Prevention Policy for Climate Change Adaptation

*kouhei yoshimura[1,2], Seigo Nasu[2], Shingen Horiuchi[3] (1.Nippon Koei, 2.Kochi University of Technology, 3.Kochi City)

Enhancing resilience of atoll islands against sea level rise

*Hajime Kayanne[1], Masafumi Fujita[2], Nori Fujita[1], Takashi Hosono[3], Yoich Ide[4], Yuji Kuwahara[2], Fumiko Matsudate[13], Satoru Mimura[5], Nobuko Nakamura[6], Susumu Onaka[7], Daisaku Sato[8], Tomoko Takeda[9], Koji Yamada[10], Toru Yamaguchi[11], Hiroya Yamano[12], Hiromune Yokoki[2]

1. the University of Tokyo, 2. Ibaraki Univ., 3. JAMSTEC, 4. Oceanic Planning Corp., 5. JICA, 6. Sasakawa Peace Foundation, Ocean Policy Res. Inst., 7. Nippon Koei, 8. Setsunan Univ., 9. IGES, 10. Japan Construction Information Center Found., 11. Keio Univ., 12. National Inst. Environmental Studies, 13. Heart Biz

In the course of global warming, the sea level is projected to rise by 0.3 to 1.1 meters in this century, and by more than 5 meters in three centuries in the worst-case scenario. Atolls consist of low-lying land with an elevation of 1 to 4 meters, and are under threat of being submerged by rising sea levels. There are about 500 atolls globally, and about 400 of them are distributed in the Pacific Ocean. Tuvalu, Kiribati, and the Republic of the Marshall Islands in the Pacific Ocean, and the Maldives in the Indian Ocean are all atolls. These countries are in a critical situation due to global warming caused by CO_2, which they themselves emit little of. Therefore, they are appealing to the international community to join with other small island states to reduce global warming and support adaptation measures against sea level rise (Alliance of Small Island States). In response to this appeal, international support such as the Green Climate Fund (GCF) is being planned for adaptation to climate change. Atoll nations are anticipating sea walls and land reclamation as effective measures against sea level rise.

Atoll islands are formed by calcium carbonate skeletons of coral and foraminifera, which were washed up on the platform of coral reefs created by corals. The coral reefs were established 4,000 years ago, when sea level rise during the postglacial period stabilized, and atoll islands were constructed and inhabited as sea level fell by 1-2 m from 2,000 years ago (Yamaguchi et al., 2007; Kayanne et al., 2011). In atoll countries such as the Republic of the Marshall Islands and Tuvalu, the concentration of populations in the capital islands has led to the expansion of residential areas into low marshes and storm ridges, which are particularly vulnerable in atoll island landforms (Yamano et al., 2007). In addition, domestic wastewater from increasing population has created a reductive environment on the coast, degrading coral reef ecosystems and replacing coral communities with algae, thus reducing the resilience of the atoll islands against sea level rise (Fujita et al., 2013; Nakamura et al., 2020). Construction of causeways and dredge of shipping channels, piers, vertical seawalls by piling up stones also inhibit sand drift and accumulation.

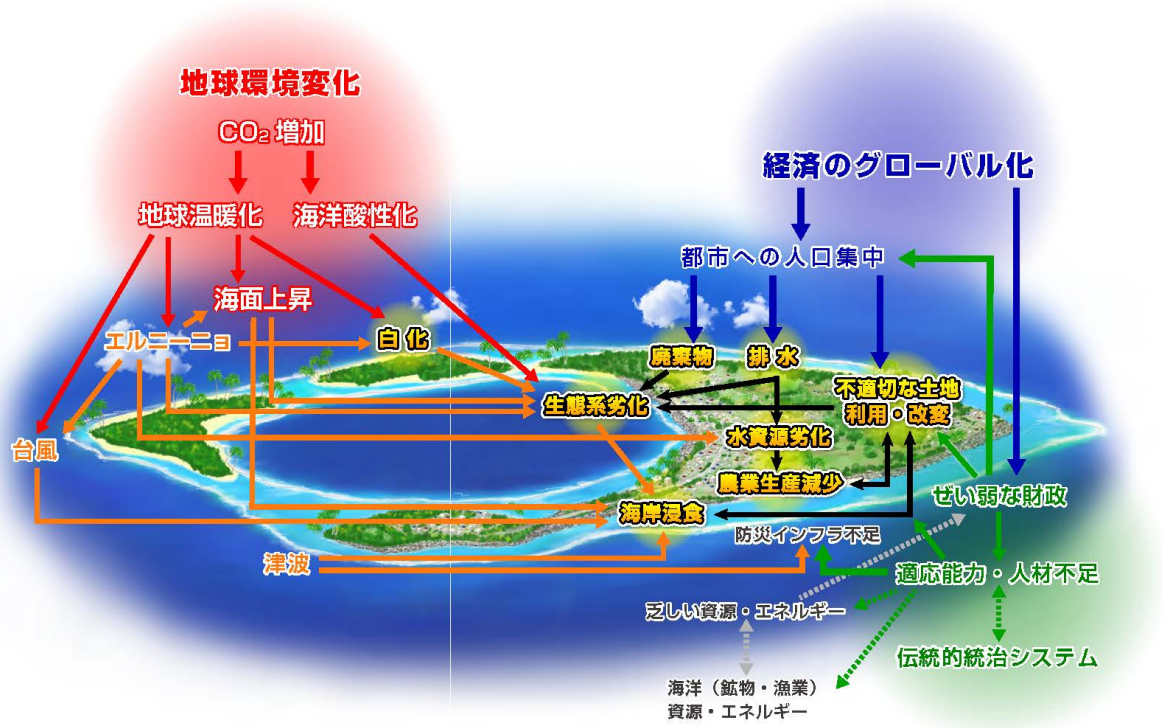
The problem of atolls is not as simple as submergence by sea level rise, but a complex problem caused by the expansion of inhabitable areas into vulnerable areas, the degradation of ecosystems due to environmental deterioration, and the diminishing restoration potential of the beach due to artificial coastal structures. In order to maintain atolls against future sea level rise, global warming and sea level rise must be suppressed as much as possible, and the resilience of the land must be rehabilitated through ecosystem restoration. The restoration of ecosystems will also contribute to the improvement of the basic environment of the atoll countries. From this perspective, Tuvalu implemented a beach reclamation project on Fongafale Island in Funafuti Atoll, the capital of Tuvalu, in 2015 with the technical cooperation of JICA (Onaka et al., 2017). Beach reclamation is a practical example of green infrastructure that does not interfere with the natural sand deposition process on the island.

However, Tuvalu has since planned a large-scale land reclamation project with the support of the GCF. Tuvalu's desire for short-term, tangible measures that will lead to the expansion of its small land area is

©2021. Japan Geoscience Union. All Right Reserved.

understandable. Green infrastructure as an ideal cannot be forced on them that do not yet have sufficient gray infrastructure. However, it is necessary to evaluate the stability of reclaimed land against external forces and the danger that reclamation will lead to environmental degradation in the long run, which is not sustainable and will inhibit the formation of atoll islands. The application of the best mix of green infrastructure and gray infrastructure such as seawalls and landfills, under a long-term perspective, must be based on the demands of the local government and residents, and an approach to gaining local understanding is essential for this purpose.

Keywords: atoll islands, sea level rise, resilience, Tuvalu



©2021. Japan Geoscience Union. All Right Reserved.

Developments of future climate scenario selection method for impact and adaptation studies

*Hideo Shiogama[1], Noriko N. Ishizaki[1], Naota Hanasaki[1], Kiyoshi Takahashi[1], Seita Emori[1], Rui Ito[2,3], Toshiyuki Nakaegawa[3], Izuru Takayabu[3], Yasuaki Hijioka[1], Yukari N. Takayabu[4], Ryosuke Shibuya[4]

1. National Institute for Environmental Studies, 2. Japan Meteorological Business Support Center, 3. Meteorological Research Institute, 4. Atmosphere and Ocean Research Institute, The University of Tokyo

Climate change impact assessment studies often use future projections of only a few global climate models (GCMs) due to limited research resources. Here we develop a novel method to select a small subset of GCMs that widely capture the uncertainty range of large ensemble. By applying this method, we select a subset of five GCM projections from the Coupled Model Intercomparison Project Phase 6 (CMIP6) ensemble for impact and adaptation studies in Japan. At first, we omit GCMs whose global warming projections have been evaluated to be overestimated in the recent literature. Then, we select a subset of five GCMs that widely captures the uncertainty ranges for 8 climate variables and have good performances in present-climate simulations. These selected GCM simulations will be used to provide better climate scenarios for impact and adaptation studies than those in the previous impact assessment project.

Keywords: Climate change, Adaptation, Climate scenarios

©2021. Japan Geoscience Union. All Right Reserved.

Added values of regional multi-ensemble statistical downscaling approach in CORDEX Asia

*KOJI DAIRAKU[1]

1. University of Tsukuba

To develop reliable regional climate information for climate change adaptation measures, we assess added values of regional multi-ensemble dynamical and statistical downscaling in collaboration with researchers of geoscience, social science and humanities, and officials of local governments in Japan and CORDEX Asia.

Though we have conducted dynamical downscaling experiments with horizontal grid spacing of 5km and 2km to reproduce regional climate information using database for Policy Decision making for Future climate change (d4PDF) to detect the climate change impact in this region, it is not enough to investigate its uncertainty caused by the structural differences in models.

Multi-model large ensemble regional climate scenarios over Japan and CORDEX Asia are developed by using CMIP5 GCMs and two statistical downscaling approaches (Bias Corrected Spatial Disaggregation (BCSD) and Bias Correction and Constructed Analogs(BCCA)) to investigate uncertainty of projected change associated with structural differences of the GCMs for the periods of historical climate (1950-2005) and near future climate (2026-2050).

This research for uncertainty information of the regional climate scenarios is intended to provide end-users to make an informed selection and decision making.

Keywords: Downscaling, Multi-model ensemble, CORDEX, Asia

©2021. Japan Geoscience Union. All Right Reserved.

Temperature rises and extreme rainfall intensity derived from observations and d4PDF in Japan

*Sayaka Yoshikawa[1,3], Megumi Watanabe[2], Shinjiro Kanae[3]

1. Ibaraki university, 2. The university Tokyo, 3. Tokyo institute of technology

The intensification of heavy rainfall in a warmer climate could follow the Clausius-Clapeyron (CC) relationship (7%/℃). Although there are studies which depict the intensification of heavy rainfall based on numerical climate model simulations, analyses based on observed records are limited in terms of whether the intensification eventually follows the CC relationship. In this study, we try to analyze whether the CC scaling can be applied to the intensification of heavy rainfall over Japan using observation data and a large-ensemble climate simulation database, namely d4PDF. We clarified the following three things. First, the intensification rate of sub-daily extremes is higher than that of daily extremes. Second, the intensification rate of rainfall extremes derived from climate models with a multiple ensemble coincides with that derived from observations. Third, the intensification rate of rainfall extremes under huge amounts of simulation results derived from climate models from the past to the future periods are less than those of the CC relationship. Although a large ensemble of climate simulations is a powerful tool for estimating extreme rainfall under climate change in the future, intensification rate of rainfall extremes derived from climate models in the future periods could be underestimated compared with those in the past periods.

Keywords: Clausius-Clapeyron, extreme rainfall, observations, climate model, warmer climate

©2021. Japan Geoscience Union. All Right Reserved.

Adaptation measures based on future projections of corals and macroalgae, use/conservation status on the southwest coast of Shikoku

*Hiroya Abe[1], Haruka Suzuki[1], Yuko F Kitano[1], Naoki H Kumagai[1], Satomi Mitsui[1], Hiroya Yamano[1]

1. National Institute for Environmental Studies

Range expansion of reef-building corals, a decline of macroalgal beds, and changes in constituent species for coral community and/or macroalgal beds have been reported in many temperate seas. Not only mitigation but also adaptation is important for the measures against climate change. Consideration of adaptation measures depending on local conditions such as the degree of environmental changes and industrial structure is necessary when the measures will be implemented. This study focused on the marine protected area (Ashizuri-Uwakai National Park) and its surrounding area on the southwest coast of Shikoku Island. This area is characterized by a very large north-south gradient in water temperature and the distribution of corals and macroalgae along with it. The main objective of this study was to consider what adaptation measures are desirable for each region and industry in response to the changes in coastal ecosystems (coral community and macroalgal bed). In order to achieve this objective, we assessed the underwater landscape with a focus on corals and macroalgae that dominates the study area and evaluated how these biological resources are used and conserved in the local tourism and fishery industries. The potential distribution of reef-building coral (*Acropora solitaryensis* complex, *A. hyacinthus* complex, *Pocillopora damicornis*), macroalgae (kelps: *Ecklonia cava kurome*, temperate *Sargassum S. hemiphyllum*, tropical *Sargassum S. ilicifolium*), and their predators (coral-eating seastars *Acanthaster* cf. *solaris* and herbivorous fish *Siganus fuscescens*) in the 2090s under the RCP2.6 and RCP8.5 scenarios were projected using a simulated sea surface temperature dataset with high-spatial-resolution (FORP-JPN02 by SI-CAT). After projecting the coastal ecosystem changes and organizing the current use/conservation of coastal ecosystems, we gave examples of what specific adaptation measures should be taken in each area for three fields, i.e., biodiversity conservation, fisheries, and tourism. Assuming the 2090s, though drastic changes in the coastal ecosystem are not projected compared to the present state under the RCP2.6 scenario, as coral distribution moves north, feeding damage by coral-eating seastars is projected to become a problem. Therefore, the expansion of protected areas and the promotion of conservation activities are a major task for coral ecosystem conservation. In municipalities where coral monitoring and conservation activities are not currently being carried out, it is necessary to establish a system for such activities. Also, the challenge is to utilize them as a new tourism resource and to develop tourism facilities in areas where corals are increasing. On the other hand, under the RCP8.5 scenario in the 2090s, it is important to take appropriate conservation measures for macroalgae and grazing pressure on macroalgae will be increased due to extremely elevated water temperature. Moreover, since coral growth becomes difficult to achieve, the creation of alternate or new tourism resources must be needed. Any of the emission scenarios may cause changes in vegetation, and adaptation measures such as changing the target species of fish catches in coastal fisheries and enhancing aquaculture of fish species tolerant to high water temperature may be necessary. This research could represent coastal ecosystem changes in the future with high spatial resolution and adaptation measures based on the changes for each municipality. In the future, we plan to improve methods for projecting the future distribution of corals and macroalgae, clarify connectivity, and identify areas that are less susceptible to climate change. This study was conducted as a part of “Regional Adaptation Consortium Project” by the Ministry of the

©2021. Japan Geoscience Union. All Right Reserved.

Environment, Japan.

Keywords: coral community, macroalgal bed, climate change, adaptation, utilization, conservation

©2021. Japan Geoscience Union. All Right Reserved.

Workshop on Disaster Prevention Training to Improve Disaster Preparedness of Local Governments and Staff: As Part of Social Implementation of Disaster Prevention Policy for Climate Change Adaptation

*kouhei yoshimura[1,2], Seigo Nasu[2], Shingen Horiuchi[3]

1. Nippon Koei, 2. Kochi University of Technology, 3. Kochi City

Disaster prevention policies as climate change adaptation are important. The government has modified laws to reflect climate change. Local governments that actually implement disaster prevention policies to protect citizens are now required to prepare for the largest flood events. However, it is difficult to protect against floods that will expand due to climate change.

Therefore, government-led soft measures, such as the provision of information through hazard maps in advance and evacuation guidance at the time of a disaster, will be the main solution.

Local governments are under pressure to cope with floods, which are expected to change more drastically than in the past, and are obliged to save lives, including those of the elderly and other vulnerable people. However, it is difficult for disaster management departments to conduct specialized simulations that take into account the effects of climate change.

Kochi University of Technology (KUT) and Kochi City Office have established a cooperative system as part of the SI-CAT, and cooperated to conduct a disaster prevention workshop style drill conducted by the Disaster Prevention Policy Division. This Division conducted a more practical drill using data on inundation analysis provided by KUT.

Under the current situation, staff members consider and implement countermeasures only after the damage is reported. Therefore, there was a time lag between the occurrence of damage and the implementation of countermeasures to demonstrate their effectiveness. If damage forecasts were shared and countermeasures were implemented in advance, the time lag would be reduced and evacuation orders and post-flood recovery activities can be carried out smoothly according to damage reports and damage expansion forecasts. In the discussions between KUT and division supervisor, we were able to find that this flow is the ideal image to aim for in disaster response.

In Kochi City, heavy rainfall is difficult to predict meteorologically, and it takes only a few hours for floodwaters to reach urban areas after heavy rains occur. Therefore, the government needs to protect the lives of citizens and respond quickly.

The purpose of the "Disaster Countermeasures Headquarters Workshop Training" is to improve disaster response capabilities as senior officials through imagining the damage and countermeasures. The two main points of the training were to "estimate future response items based on the situation at the time of the disaster" and "understand the necessity to start considering disaster response as early as possible. In February, as a test case, a trial drill was conducted with several groups of senior officials.

As a prologue, the recent torrential rain disasters were explained. Furthermore, as a common scenario,

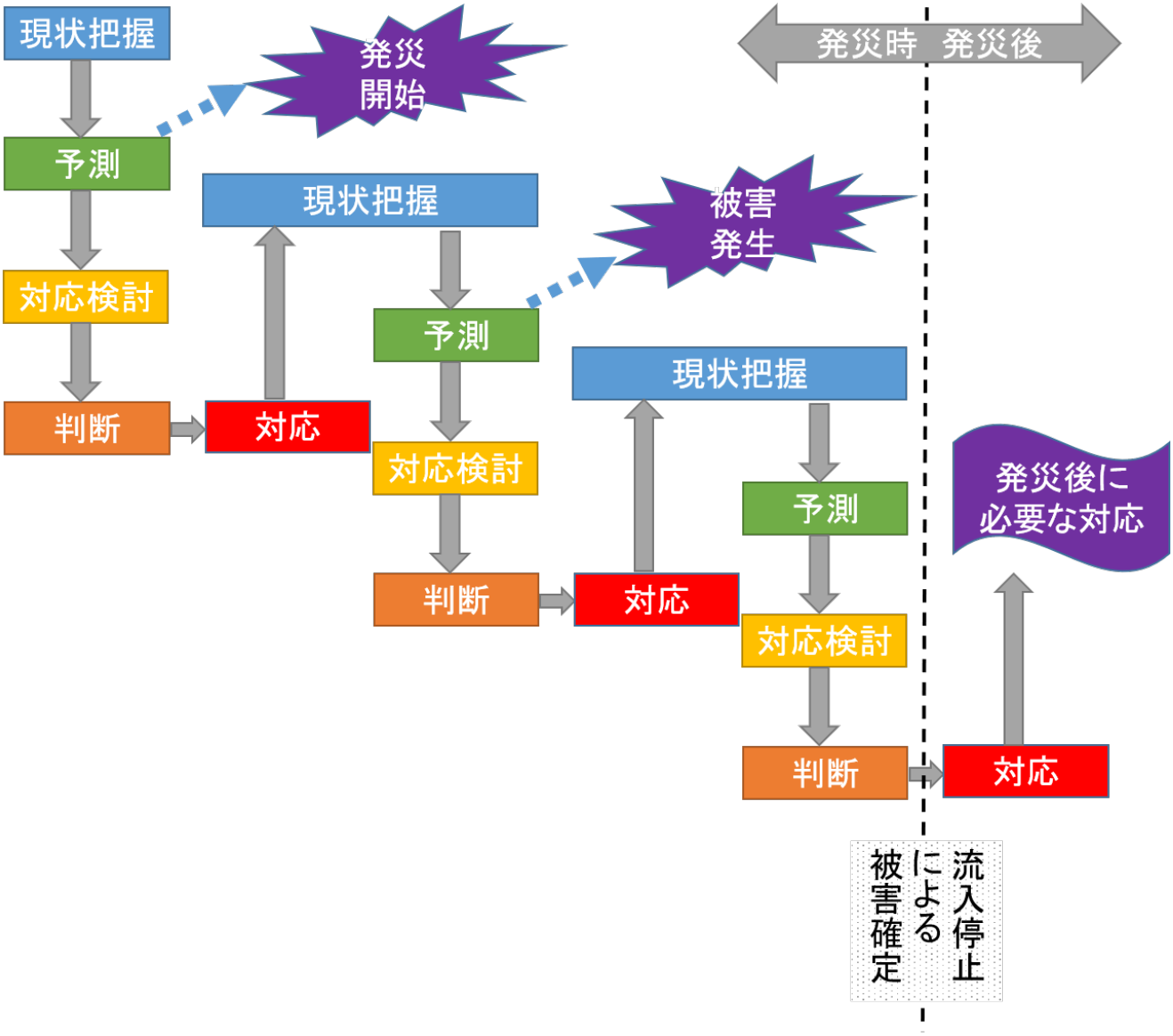
©2021. Japan Geoscience Union. All Right Reserved.

administrative responses such as the opening of evacuation centers, weather information such as typhoons, and data on flooding and the number of evacuees after the floods were presented.

Next, individual participants wrote down their responses from the first day to the third day and up to one week later. Next, each group did group work to organize and summarize their responses. In the final stage, the results were presented to each other.

The participants were able to experience and understand their roles in the time line. In addition, they were able to infer the phenomena that will occur in the future and come up with early responses. It is expected that the participating executives will expand their experience in their own departments.
We plan to develop the questions to reflect the change climate change, and to present the spread of inundation, the number of evacuees, and disaster waste in a way that participants cannot predict. In addition, we will continue to deepen operation process in the next year and beyond.

Keywords: climate change, adaptation, Regional disaster prevention, Flood analysis, River engineering, DIG



©2021. Japan Geoscience Union. All Right Reserved.

[J] Poster | H (Human Geosciences)：H-CG Complex & General

Sun. Jun 6, 2021 5:15 PM - 6:30 PM JST | Sun. Jun 6, 2021 8:15 AM - 9:30 AM UTC | Ch.09_4

[H-CG26] Adaptation to climate change and its social implementation

convener:Hiroya Yamano(National Institute for Environmental Studies), Yoichi Ishikawa(JAPAN Agency for Marine-Earth Science and Technology), KOJI DAIRAKU(University of Tsukuba), Makoto Tamura(Global and Local Environment Co-creation Institute, Ibaraki University)

The impacts of climate change will increase in the risks to societies through increased intensities of typhoons and torrential rains, changes in the distribution of organisms, deterioration in quality and yield in the agriculture, forestry and fisheries, etc. In response to this, Japan enforced "Climate Change Adaptation Act" in 2018, aiming to minimize or avoid the damage caused by climate change, and to build a sustainable society.
In this session, toward planning adaptation to climate change and enhancing its social implementation based on scientific knowledge, we will discuss about generation of climate change projection data, assessment of the impacts and risks of climate change in various fields, as well as social implementation of adaptation plans by co-creation with stakeholders and/or by local climate change adaptation acts.

[HCG26-P01] ASSESSMENT OF WIND/SOLAR ENERGY POTENTIAL AS A POWER GENERATION SOURCES AT SOME SELECTED LOCATIONS IN PAKISTAN

*Muhammad Abid KHAN[1], KOJI DAIRAKU[1] (1.University of Tsukuba)

ASSESSMENT OF WIND/SOLAR ENERGY POTENTIAL AS A POWER GENERATION SOURCES AT SOME SELECTED LOCATIONS IN PAKISTAN

*Muhammad Abid KHAN[1], KOJI DAIRAKU[1]

1. University of Tsukuba

The main objective of this research was to investigate the wind power potential and the feasibility of developing a solar PV plant at seven selected locations in Pakistan. In this study, wind speeds were collected over a period of 2005-16 and measured at 10m height. Ten dissemination functions were connected to analyze the wind speed characteristics of these chosen areas and assess the wind power density. In additions, the technical viability study of the proposed crystalline technology-based PV plants with different tracking systems in terms of Fixed, 1-axis, Inclined-axis, and Two-axis were analyzed using Photovoltaic Geographical Information Systems (PVGIS) and PV Watts' s software. The results showed that Kati Bandar has the highest annual wind speed of 4.04 m/s in comparison to other locations, while the lowest value of 1.33m/s was obtained in Islamabad Capital Territory. The maximum power density of 258.75W/m2 is occurred in July at Kati Bandar, while the lowest minimum wind power density of 1.68 W/m2 occurred in September at Islamabad at 10m height. Moreover, the simulation results showed that Two-axis performance is higher than as compared to another track system. Performance results, the performances of four small-scale wind turbines were evaluated. Based on the results, the Pitch wind/30kW Grid wind turbine had the highest annual capacity factor of 56.366%, whereas, WS-12/8kW wind turbine had the minimum at 15.416%. Consequently, the Minimum and the Maximum annual electricity cost in the studied locations are 0.005$/kWh and 0.032 $/kWh using Pitch wind/30kW Grid and WS-12/8kW, respectively. Moreover, the Levelized cost of electricity (LCOE) for PV Plants was estimated. It is found that, LCOE for fixed tilt, 1-axis, Inclined axis and 2-axis tracking modes PV plants for all locations were obtained in the range of 0.178 - 0.239 $/kWh, 0.14 –0.202 $/kWh, 0.145 –0.203 $/kWh and, 0.133 –0.191 $/kWh.

Keywords: Energy potential, probability distribution function, techno-economic, renewable energy, electricity cost

©2021. Japan Geoscience Union. All Right Reserved.

[J] Oral | H (Human Geosciences)：H-CG Complex & General

Sun. Jun 6, 2021 9:00 AM - 10:30 AM JST | Sun. Jun 6, 2021 12:00 AM - 1:30 AM UTC | Ch.15 Zoom Room 15

[H-CG29] Advanced life support systems with closed bio-ecosystems and thier applications

convener:Masanori Shinohara(Teikyo University of Science), Hiroshi Katoh(Division of Plant Functional Genomics, Advanced Science Research Promotion Center, Organization for the Promotion of Regional Innovation, Mie University), Shunta Kimura(Institute of Space and Astronautical Science / Space Exploration Innovation Hub Center, Japan Aerospace Exploration Agency), Midori Ong(University of Tsukuba), Chairperson:Midori Ong(University of Tsukuba), Hiroshi Katoh(Division of Plant Functional Genomics, Advanced Science Research Promotion Center, Organization for the Promotion of Regional Innovation, Mie University), Masanori Shinohara(Teikyo University of Science)

In this session, since 2011, we and invited researchers have been introducing and discussing about practical and useful life-support systems in closed bio-ecosystems for inhabitation on extraterrestrial environments. Not only biological studies but also engineering ones
including broad research fields are our target. And also, we assume that it is indispensable to discuss about these interdisciplinary fields beyond the generation for inheriting to our next generation and for developing our field. Theme from old and basic to current and applicative from senior to youth including undergraduate are welcomed.

9:00 AM - 9:05 AM JST | 12:00 AM - 12:05 AM UTC

[HCG29-01] Introduction

9:05 AM - 9:20 AM JST | 12:05 AM - 12:20 AM UTC

[HCG29-02] Recent Trends of Advanced and Closed Ecological Life Support System.

*Masanori Shinohara[1], Tamiyasu Shimamiya[2] (1.Teikyo University of Science, 2.Japan Manned Space Systems Corporation)

9:20 AM - 9:45 AM JST | 12:20 AM - 12:45 AM UTC

[HCG29-03] Establishment of food self-sufficiency system for functional space foods to support manned space activities

★Invited Papers

*Takeshi Nikawa[1] (1.Institute of Nutrition, Tokushima University Graduate School)

9:45 AM - 10:00 AM JST | 12:45 AM - 1:00 AM UTC

[HCG29-04] Searching for gene related to environments adaptation

*Hiroshi Katoh[1] (1.Mie University)

10:00 AM - 10:25 AM JST | 1:00 AM - 1:25 AM UTC

[HCG29-05] Current status of planetary protection and its importance in closed eco-systems

★Invited Papers

*Shunta Kimura[1,2], Shino Suzuki[1,2], Yuko Inatomi[1,2] (1.Institute of Space and Astronautical Science, Japan Aerospace Exploration Agency, 2.Space Exploration Innovation Hub Center, Japan Aerospace Exploration Agency)

10:25 AM - 10:30 AM JST | 1:25 AM - 1:30 AM UTC

[HCG29-06] Discussion

[J] Oral | H (Human Geosciences) | H-CG Complex & General

[H-CG29] Advanced life support systems with closed bio-ecosystems and thier applications

convener:Masanori Shinohara(Teikyo University of Science), Hiroshi Katoh(Division of Plant Functional Genomics, Advanced Science Research Promotion Center, Organization for the Promotion of Regional Innovation, Mie University), Shunta Kimura(Institute of Space and Astronautical Science / Space Exploration Innovation Hub Center, Japan Aerospace Exploration Agency), Midori Ong(University of Tsukuba), Chairperson:Midori Ong(University of Tsukuba), Hiroshi Katoh(Division of Plant Functional Genomics, Advanced Science Research Promotion Center, Organization for the Promotion of Regional Innovation, Mie University), Masanori Shinohara(Teikyo University of Science)

Sun. Jun 6, 2021 9:00 AM - 10:30 AM Ch.15 (Zoom Room 15)

In this session, since 2011, we and invited researchers have been introducing and discussing about practical and useful life-support systems in closed bio-ecosystems for inhabitation on extraterrestrial environments. Not only biological studies but also engineering ones
including broad research fields are our target. And also, we assume that it is indispensable to discuss about these interdisciplinary fields beyond the generation for inheriting to our next generation and for developing our field. Theme from old and basic to current and applicative from senior to youth including undergraduate are welcomed.

9:00 AM - 9:05 AM

[HCG29-01]Introduction

©Japan Geoscience Union

Recent Trends of Advanced and Closed Ecological Life Support System.

*Masanori Shinohara[1], Tamiyasu Shimamiya[2]

1. Teikyo University of Science, 2. Japan Manned Space Systems Corporation

Recent trends of bioregenerative LSS will be reviewed. Especially, results and lessons learned from Lunar Palace 365 project at Beihang University will be reported.

Keywords: LSS

©2021. Japan Geoscience Union. All Right Reserved.

Establishment of food self-sufficiency system for functional space foods to support manned space activities

*Takeshi Nikawa[1]

1. Institute of Nutrition, Tokushima University Graduate School

Nowaday, humankind is entering the Age of Discovery in the 21st century. The space environment causes various physical changes. One of the changes is muscle atrophy (sarcopenia). We aim to elucidate the mechanism of this weightless muscle atrophy and devise a nutritional treatment for it.

Previous studies have shown that ubiquitin ligase Cbl-b, of which expression is increased by microgravity, induced IRS-1 ubiquitination and degradation, resulting in impaired IGF-1 signal and muscular atrophy. However, it remains unclear how cells sense weightless stress and enhance Cbl-b expression. Therefore, to clarify the mechanism of gravity sensing by these cells, we conducted “Myolab” and “Cell Mechanosensing” space experiments, and 3D-Clinorotation, which is a simulated microgravity culture device on the ground. First, in the Myolab space experiment, we performed metabolome analysis of space samples cultured under microgravity conditions for a week. Then we found that microgravity accumulated oxidative stress in cells and changed the expression of proteins localized in mitochondria related to energy metabolism. It was also found that the oxidative stress regulates the expression of ubiquitin ligase Cbl-b via Egr1 / 2 and ERK1 / 2 pathways.

Therefore, we considered ubiquitin ligase Cbl-b and oxidative stress as targets for functional foods that can prevent muscle atrophy due to weightlessness.

1) Soy protein (anti-ubiquitinating effect)

We discovered a DG (p) YMP peptide (named Cblin peptide) that has an inhibitory activity on the binding of IRS-1, which is the target molecule of ubiquitin ligase Cbl-b. Furthermore, it was found that the soy protein glycinin has a similar sequence. These suppressed the ubiquitination of IRS-1 by Cbl-b and increased muscle mass in *in vitro* and *in vivo* experiments. In addition, the soy protein-added diet was also effective in suppressing muscle weakness in bedridden patients.

2) Polyphenol (antioxidant effect)

Polyphenols are attracting attention as a dietary ingredient that can reduce antioxidant stress. Antioxidant nutrients such as soy isoflavone and quercetin have been shown to suppress muscular atrophy due to tail suspension.

Because of the usefulness of these functional ingredients of soybeans for such muscle atrophy, we are advocating the construction of a plant factory that can make soybeans self-sufficient in the space environment.

Keywords: Functional Space Foods, Disuse muscle atrophy, Plant factory

©2021. Japan Geoscience Union. All Right Reserved.

Searching for gene related to environments adaptation

*Hiroshi Katoh[1]

1. Mie University

Living organisms are adapted to various environments. Previously, the author has been trying to search environmental adapted genes in cyanobacteria. In this presentation, the author will show to search result of environmental adapted gene in various living organisms.

Keywords: adaptation, environment, gene

©2021. Japan Geoscience Union. All Right Reserved.

Current status of planetary protection and its importance in closed eco-systems

*Shunta Kimura[1,2], Shino Suzuki[1,2], Yuko Inatomi[1,2]

1. Institute of Space and Astronautical Science, Japan Aerospace Exploration Agency, 2. Space Exploration Innovation Hub Center, Japan Aerospace Exploration Agency

In space missions, we have to avoid both forward and backward contamination. The Committee on Space Research (COSPAR) develop, maintain, and promote the Planetary Protection (PP) Policy. Space organizations of each country observe PP in their space missions. Japan Aerospace Exploration Agency (JAXA) has started the organizational PP activity. It is also necessary to confirm this issue in closed eco-systems for human habitation missions. Here, we review the current status of PP, and we want to discuss future plans.

Keywords: planetary protection, closed eco-systems

©2021. Japan Geoscience Union. All Right Reserved.

[J] Oral | H (Human Geosciences) | H-CG Complex & General

[H-CG29] Advanced life support systems with closed bio-ecosystems and thier applications

convener:Masanori Shinohara(Teikyo University of Science), Hiroshi Katoh(Division of Plant Functional Genomics, Advanced Science Research Promotion Center, Organization for the Promotion of Regional Innovation, Mie University), Shunta Kimura(Institute of Space and Astronautical Science / Space Exploration Innovation Hub Center, Japan Aerospace Exploration Agency), Midori Ong(University of Tsukuba), Chairperson:Midori Ong(University of Tsukuba), Hiroshi Katoh(Division of Plant Functional Genomics, Advanced Science Research Promotion Center, Organization for the Promotion of Regional Innovation, Mie University), Masanori Shinohara(Teikyo University of Science)

Sun. Jun 6, 2021 9:00 AM - 10:30 AM Ch.15 (Zoom Room 15)

In this session, since 2011, we and invited researchers have been introducing and discussing about practical and useful life-support systems in closed bio-ecosystems for inhabitation on extraterrestrial environments. Not only biological studies but also engineering ones
including broad research fields are our target. And also, we assume that it is indispensable to discuss about these interdisciplinary fields beyond the generation for inheriting to our next generation and for developing our field. Theme from old and basic to current and applicative from senior to youth including undergraduate are welcomed.

10:25 AM - 10:30 AM

[HCG29-06]Discussion

©Japan Geoscience Union

[J] Poster | H (Human Geosciences)：H-CG Complex & General

Sun. Jun 6, 2021 5:15 PM - 6:30 PM JST | Sun. Jun 6, 2021 8:15 AM - 9:30 AM UTC | Ch.09_5

[H-CG29] Advanced life support systems with closed bio-ecosystems and thier applications

convener:Masanori Shinohara(Teikyo University of Science), Hiroshi Katoh(Division of Plant Functional Genomics, Advanced Science Research Promotion Center, Organization for the Promotion of Regional Innovation, Mie University), Shunta Kimura(Institute of Space and Astronautical Science / Space Exploration Innovation Hub Center, Japan Aerospace Exploration Agency), Midori Ong(University of Tsukuba)

In this session, since 2011, we and invited researchers have been introducing and discussing about practical and useful life-support systems in closed bio-ecosystems for inhabitation on extraterrestrial environments. Not only biological studies but also engineering ones
including broad research fields are our target. And also, we assume that it is indispensable to discuss about these interdisciplinary fields beyond the generation for inheriting to our next generation and for developing our field. Theme from old and basic to current and applicative from senior to youth including undergraduate are welcomed.

[HCG29-P01] Growth of cyanobacterium, *Nostoc* sp. HK-01, after exposure to several harsh environments.

*Miku Tokita[1], Midori Ong[1], Hiroshi Katoh[2], Kaori Tomita-Yokotani[1] (1.University of Tsukuba, 2.University of Mie)

[HCG29-P02] Relationship between seed formation during tomato growth and microgravity generated by a hand-made 3D-clinostat.

*Yuan Takase[1], Kaori Totami-Yokotani[1] (1.University of Tsukuba)

[HCG29-P03] Identification of *Nostoc* sp. HK-01 proteins found in dry environment

*Hiroko Tanaka[1], Tomoko Abe[1], Hiroshi Katoh[2], Midori Ong[3], Kaori Tomita-Yokotani[3] (1.Graduate School of Science and Engineering, University of Tokyo Denki, 2.Organization for the Promotion of Regional Innovation, Mie University, 3.Faculty of Life and Environmental Sciences, University of Tsukuba)

[HCG29-P04] History of biological systems in closed-ecological systems

*Hiroshi Katoh[1] (1.Mie University)

[HCG29-P05] Advanced use of potatoes (*Solanum tuberosum* L.) for manned space activities

*Yota Tsukizaki[1], Toshisada Suzuki[2], Kaori Tomita-Yokotani[1] (1.University of Tsukuba, 2.Kagawa University)

Growth of cyanobacterium, *Nostoc* sp. HK-01, after exposure to several harsh environments.

*Miku Tokita[1], Midori Ong[1], Hiroshi Katoh[2], Kaori Tomita-Yokotani[1]

1. University of Tsukuba, 2. University of Mie

We previously reported that dried cells of the terrestrial cyanobacterium, *Nostoc* sp. HK-01, have a high tolerance to several cosmic environmental conditions. The dried cells of the species were used as materials in space exposure experiments. After exposure to harsh environments, there is a possibility that some cells may have suffered severe damage even if it is not evident in their appearance. Detailed observations of individual cells and their related chemical analyses are required by examining cells after exposure to harsh environments. In this study, we focused on the cell germination and continuous proliferation of *Nostoc* sp. HK-01 to confirm the damage.

Keywords: serious environments, terrestrial cyanobacteria, germination of akinetes, Nostoc sp. HK-01

©2021. Japan Geoscience Union. All Right Reserved.

Relationship between seed formation during tomato growth and microgravity generated by a hand-made 3D-clinostat.

*Yuan Takase[1], Kaori Totami-Yokotani[1]

1. University of Tsukuba

The circulationCirculation of foods is be an important matter for long–term manned space activity in extraterrestrial environments, such as on Mars. We have already confirmed that seed formation in tomato plants requires gravity. In this study, we will consider the gravity-required period and its mechanisms during seed formation under microgravity generated by a hand-made 3D-clinostat.

Keywords: Tomato growth, hand-made clinostat

©2021. Japan Geoscience Union. All Right Reserved.

Identification of *Nostoc* sp. HK-01 proteins found in dry environment

*Hiroko Tanaka[1], Tomoko Abe[1], Hiroshi Katoh[2], Midori Ong[3], Kaori Tomita-Yokotani[3]

1. Graduate School of Science and Engineering, University of Tokyo Denki, 2. Organization for the Promotion of Regional Innovation, Mie University, 3. Faculty of Life and Environmental Sciences, University of Tsukuba

Nostoc sp. HK-01, one of terrestrial cyanobacterium, could be used for bio-chemical circulation in a closed ecosystem including space. Furthermore, its high tolerance to desiccation stress has ability of usefulness as a food.
In this study, genes of *Nostoc* sp. HK-01 induced by desiccation stress were investigated.
Nostoc sp. HK-01 cells were dehydrated slowly. Proteins extracted from dehydrated HK-01 cells and wet HK-01 cells applied to SDS-polyacrylamide gel electrophoresis. In comparison with the wet cell proteins, significant abundance changes of some proteins in the dehydrated cells were detected. Further, expression analyses of genes encoding these proteins were performed by real-time PCR. The research will be expected to contribute to an effective utilization of food resources.

Keywords: cyanobacteria, desiccation tolerance, stress protein

©2021. Japan Geoscience Union. All Right Reserved.

History of biological systems in closed-ecological systems

*Hiroshi Katoh[1]

1. Mie University

It will be shown history of this session.

Keywords: closed, ecological systems, biological systems

©2021. Japan Geoscience Union. All Right Reserved.

Advanced use of potatoes (*Solanum tuberosum* L.) for manned space activities

*Yota Tsukizaki[1], Toshisada Suzuki[2], Kaori Tomita-Yokotani[1]

1. University of Tsukuba, 2. Kagawa University

Potato plants are very popular cultivated crops worldwide. Many studies related to the cultivation of potato plants under extraterrestrial environments exist, and here, we focus on the problems infor the cultivation of potato plants for manned space activities. In this study, we will propose the advanced use of potato plants in sever environments such as on Mars.

Keywords: Potato plants, cultivation, manned space activities

©2021. Japan Geoscience Union. All Right Reserved.

[J] Poster | S (Solid Earth Sciences)：S-SS Seismology

Sun. Jun 6, 2021 5:15 PM - 6:30 PM JST | Sun. Jun 6, 2021 8:15 AM - 9:30 AM UTC | Ch.10_1

[S-SS04] Earthquake prediction and forecast

convener:Shingo Watada(Division of Monitoring Science, Earthquake Research Institute, University of Tokyo), Masayuki Obayashi(Japan Agency for Marine-Earth Science and Technology)

This session provides the opportunity for presenting researches on prediction or forecasting of earthquake occurrences in wide sense, including times, places, sizes, or source mechanisms. Also, this session welcomes scientific discussions on possible causal relations to some other observation data, forecasting simulations based on theoretical models, developments and applications on statistical evaluation method for the verification of retrospective experiments, etc.

[SSS04-P01] **Effects of Earth tides on the mainshock of the 2011 Tohoku Earthquake**

*Yoshiki SUE[1] (1.none)

[SSS04-P02] Statistical Study and Probability of Foreshocks on the Japan Mainland

*Hong Peng[1], James Mori[1] (1. Earthquake Hazards Division, Disaster Prevention Research Institute, Kyoto University)

[SSS04-P03] Comments on the Brownian Passage Time model for recurrent earthquakes with uncertain origin times

*Masajiro Imoto[1], Nobuyuki Morikawa[1], Hiroyuki Fujiwara[1] (1.National Research Institute for Earth Science and Disaster Resilience)

[SSS04-P04] Relationship between the Moderate Repeating Earthquakes and the Larger-scale Earthquakes on the trench side

*Masayuki Tanaka[1] (1.Meteorological Research Institute)

[SSS04-P05] Validation of forecast experiment on the Kamaishi repeating earthquakes based on numerical simulations

*Shingo Yoshida[1], Jun'ichi Fukuda[1], Toshihiro Igarashi[1] (1.Earthquake Research Institute, University of Tokyo)

Effects of Earth tides on the mainshock of the 2011 Tohoku Earthquake

*Yoshiki SUE[1]

1. none

1. Introduction
In the 2011 Tohoku earthquake, a clear correlation between the earth tide and the earthquake occurrence was observed for about 10 years just before the main shock occurred near the rupture initiation zone of the main shock (Tanaka, 2012). So, the author reports effects of the earth tides possibly related to occurrence of the mainshock.

2. Effects of earth tides to foreshock-mainshock type earthquake
The largest foreshock occurred at 11:45 on March 9 and the main shock at 14:46 on March 11, with an interval of 51 hours 1 minute. The moon has the largest influence on the earth tides with an orbital period of 24 hours and 50 minutes, or roughly 25 hours. Therefore, the mainshock occurred just after the moon orbited twice. The equation with approximate number is as follows.

Time of mainshock = Time of foreshock + 2 orbits x 25 hours + approx. 1 hour (1)

The 2016 Kumamoto earthquake was also of the foreshock-mainshock type, with an interval of 27 hours and 59 minutes, i.e., one orbit x 25 hours + approx. 3 hours. With 2 data, we have the following equation.

Time of mainshock = time of largest foreshock + number of orbits x 25 hours ±several hours (2)

It is assumed that for the mainshock, the moon was in the same position as in the foreshock, and the moon caused similar deformation to the topography and triggered the earthquake.

In the case of the 2011 Tohoku earthquake, the time for the moon in the middle was 16:12, so the mainshock occurred 1 hour ad 30miutes before it. In the case of the 2016 Kumamoto earthquake, the time for the moon in the middle was 0:33, so the mainshock occurred about one hour after the moon in the middle. In both cases, the moon was almost directly above the epicenter.

3 Effects of the earth tides on the date of occurrence
3-1. 2011 Tohoku Earthquake (Fig. 1)
The lunar phases of the major earthquakes that occurred in the central off-Sanriku area are explained below. The phase of the moon is shown by the difference in ecliptic longitude between the moon and the sun, are 0 degrees at new moon, 90 degrees at first quarter moon and so on. In this area, there is an apparent dependency on 20 to 80 degrees, and the major damaging earthquakes have occurred during this period. Or, large earthquakes occurred around 3rd to 8th day of the lunar calendar (Sue, 2008).

The 2011 earthquake occurred on the 7th day of the lunar calendar, Or 70 degrees from the ecliptic longitude difference between the moon and the sun, which means that the earthquake occurred at the same lunar phase as before (Sue, 2011).

The 2008 survey was conducted in a rectangular area across the trench axis in the central part of Sanriku,

©2021. Japan Geoscience Union. All Right Reserved.

where the southern boarder is 39 degree north. The 2011 M9 earthquake, however, occurred at 38 degrees 6 minutes north, which is roughly 1 degree out of the boarder of the research area. Since the trench axis is running southward almost straight, I assume that the mechanical orientation is generally maintained. I have also conducted research to the southern area of this region, that is called land and offshore of Miyagi Prefecture. And I have confirmed that a cluster of occurrences at a lunar-solar ecliptic longitude difference of 70-95 degrees, and the 1793 earthquake (M8, 7th lunar day) occurred (Sue 2007) .

The case study of the central off-Sanriku area suggests that a area-by-area survey of past earthquakes is effective in estimating the date of occurrence of a new major earthquake that will occur in the same area later.

3-2. The 869 Jogan Earthquake
The 869 Jogan Earthquake is regarded as the similar earthquake of the 2011M9 earthquake. While this earthquake occurred on 26th of the lunar calendar, so the research shall be done carefully.

References
Sue, Y., 2007, Proc. of the Seismological Society of Japan, P2-056.
Sue, Y., 2008, JpGU, Preprints, S145-P004.
Sue, Y., 2011, JpGU, Preprints, MIS036-P87.
Tanaka, S., 2012, Geophys. Res. Lett., 39(7).

Keywords: Earthquake, Earth tides, 2011 Tohoku earthquake

©2021. Japan Geoscience Union. All Right Reserved.

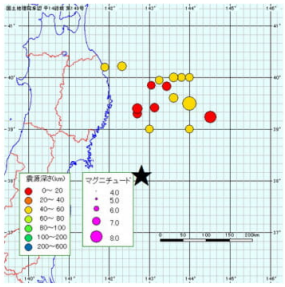
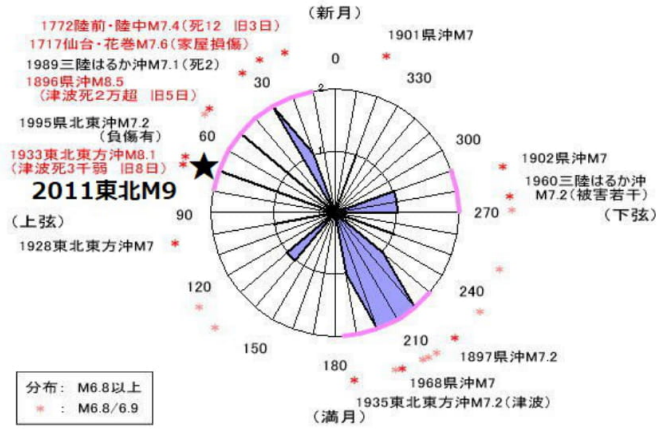
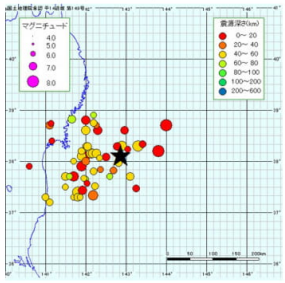
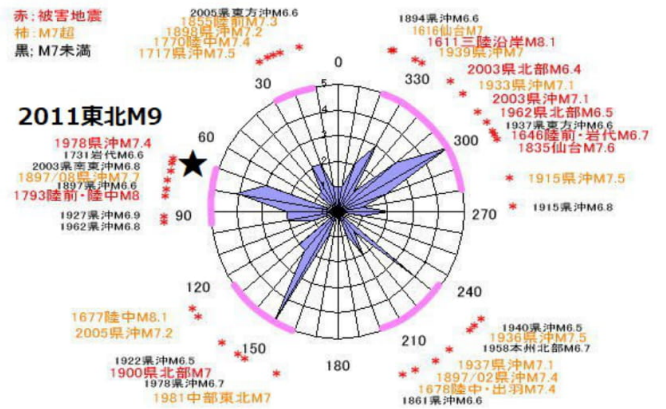
調査領域 Area	解析結果 Result
三陸沖中部 **Central off-Sanriku**  （図: KenMap）	
宮城県陸部及び沖合 （含三陸沖南部海溝寄り） **Land and offshore of Miyagi pref.** 	

図 1 地震発生時の月の位相の分布: データセット（左）と分布（右、中央は発生数、周囲は地震名、赤字は被害地震、2007-8 年作成）。分布は一様で無い。これに 2011 年東北 M9 地震（★）を追加した。大地震が発生した期間で今回も発生している。

Fig.1 The distribution of moon phases at earthquakes: Data set (left) and distribution (right, center is the number of occurrence, surrounding is the name of the earthquakes, and in red are the damaged earthquakes. Produced in 2007-8). The distribution is not uniform. The 2011 Tohoku M9 earthquake (*) is added. The earthquake occurred during the period when major earthquakes occurred so far.

©2021. Japan Geoscience Union. All Right Reserved.

Statistical Study and Probability of Foreshocks on the Japan Mainland

*Hong Peng[1], James Mori[1]

1. Earthquake Hazards Division, Disaster Prevention Research Institute, Kyoto University

Previous studies of foreshocks estimated the rate of foreshock occurrence before moderate and large earthquakes in high seismicity areas, such as California. The studies proposed that it is possible to calculate the probability that a larger earthquake follows a specific event. Here, we use the Japan Meteorological Agency (JMA) earthquake catalogue from 2001 to 2020 to check the temporal and spatial distributions of pairs of earthquakes where a smaller earthquake is followed by a larger earthquake. There is a clear peak for pairs of events which are located within 5 days and 2 km. . This time-space window is what we define as foreshocks. According to our results, it is possible to forecast the probability of a following larger event , but it is difficult to predict its magnitude . In order study the relation between the foreshock-mainshock distance, , we select about 200 mainshocks which have obvious foreshocks and use filtered P waveforms to relocate the foreshocks. This provides us with more accurate locations of foreshocks than the JMA catalog.

Keywords: Statistics, Foreshocks, Japan mainland

©2021. Japan Geoscience Union. All Right Reserved.

Comments on the Brownian Passage Time model for recurrent earthquakes with uncertain origin times

*Masajiro Imoto[1], Nobuyuki Morikawa[1], Hiroyuki Fujiwara[1]

1. National Research Institute for Earth Science and Disaster Resilience

Five recurrent great earthquakes along the Japan Trench off Tohoku (Tohoku-oki–type earthquakes) are reported through studies of tsunami deposits (Earthquake Research Committee; ERC report, 2019). For recurrent earthquakes with uncertain origin times, Ogata (JGR, 1999) formulated the likelihood function in a multiproduct form of a probability density function integrated with respect to origin times over uncertain intervals (ERC report, 2001). The ERC report (2019) estimates the long-term probability of a Tohoku-oki–type earthquake by using a method different from Ogata's. For the sake of comparison, we applied Ogata's formula with the Brownian Passage Time distribution to this earthquake sequence. This revealed that Ogata's formula leads to an extraordinarily small value, at most 0.03, for the shape parameter. A detailed calculation showed that sequences of lower likelihood, relatively larger shape parameters, are less weighted (even by orders of magnitude), and that sequences including the Keicho-Sanriku of the 1611 historical earthquake, one of two candidates for the fourth event, play no crucial role in the maximum likelihood estimation. This must be contrary to the idea that both historical earthquakes, Kyotoku of 1454 and Keichou-Sanriku, are listed with equal possibilities. Accordingly, Ogata's formula could not give a representative model parameter over all possible sequences.

Keywords: Great earthquake, Japan Trench, Probability, Inverse Gaussian distribution, Uncertain origin times

©2021. Japan Geoscience Union. All Right Reserved.

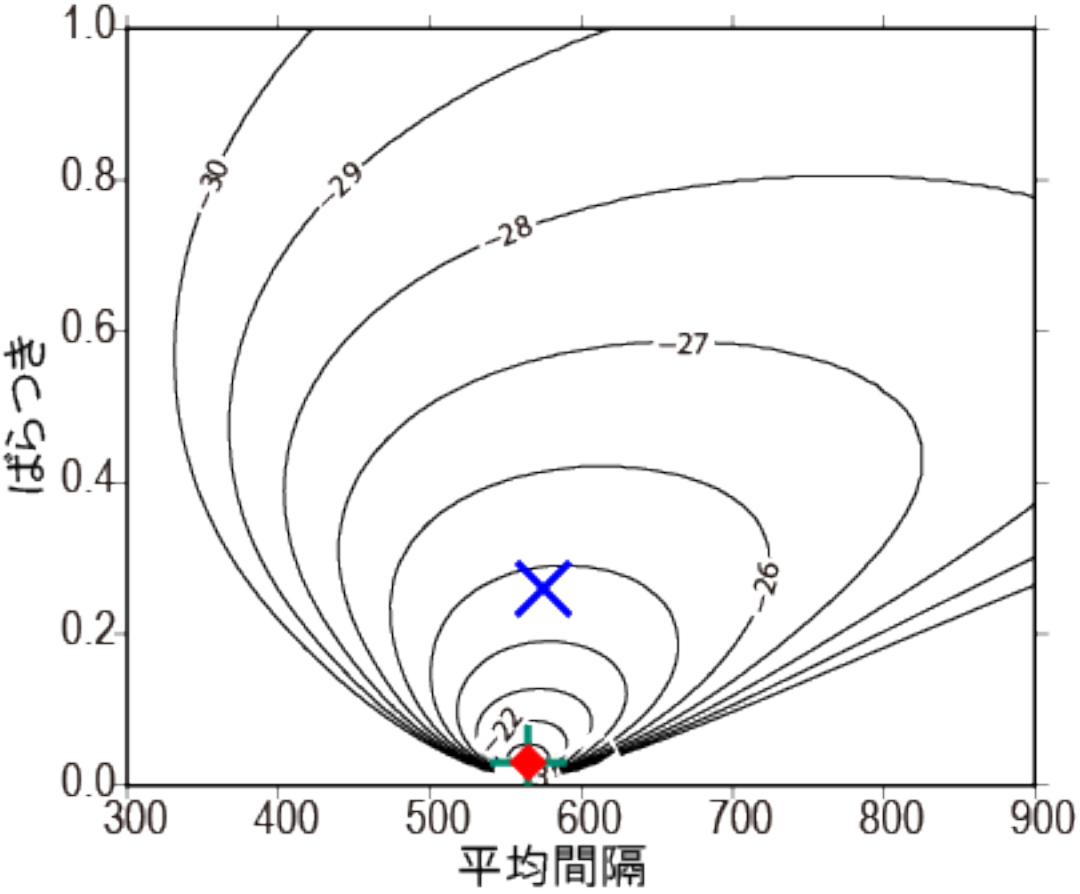


図　対数尤度の等値線
全地震(5回)を用いて，Ogataの方法により算出した対数尤度の等値線．
◆は最尤推定値．第4番が享徳地震あるいは慶長三陸地震で確定の場合には，
最尤推定値は ✚あるいは ✖となる．

©2021. Japan Geoscience Union. All Right Reserved.

Relationship between the Moderate Repeating Earthquakes and the Larger-scale Earthquakes on the trench side

*Masayuki Tanaka[1]

1. Meteorological Research Institute

Earthquakes with very similar waveforms (The Moderate Repeating Earthquakes) have been confirmed in various Japanese regions. Most occur at the plate boundaries and are considered to be closely related to regular slippage between plates. Comparing earthquakes of the same magnitude, it is considered that the slip speed between plates is fast when the interval between occurrences is short, and slow when the interval is long. We are tracking the moderate repeating earthquakes that occur repeatedly at almost the same location and have very similar waveforms, using seismic records observed by the Japan Meteorological Agency's velocity-type seismographs and accelerometers. On the other hand, tsunamis and large earthquakes with damage have occurred near the plate boundary. This time, we focused on the timing of occurrence of large-scale earthquakes in areas closer to the trench than where the moderate repeating earthquakes occurred, and investigated the relationship between the moderate repeating earthquakes and large-scale earthquakes.

Keywords: Moderate repeating earthquakes, Large-scale earthquakes, timing

©2021. Japan Geoscience Union. All Right Reserved.

Validation of forecast experiment on the Kamaishi repeating earthquakes based on numerical simulations

*Shingo Yoshida[1], Jun'ichi Fukuda[1], Toshihiro Igarashi[1]

1. Earthquake Research Institute, University of Tokyo

Repeating *M*5-class earthquakes occurred with a regular recurrence interval on the plate boundary offshore Kamaishi before the 2011 *M*9 Tohoku-oki earthquake. Since this event, repeating events of *M*5 to *M*6 occurred with shorter recurrence intervals than before the *M*9 event. We performed a forecast experiment on the Kamaishi repeaters after the Tohoku-oki earthquake based on numerical simulations assuming a large patch containing a small patch on a fault model that undergoes continuous afterslip.Simulations were conducted for various parameter values to produce time history of repeated ruptures.To forecast the *I*th event, we selected several modeled sequences that are able to accurately reproduce the observed event sequence up to the (*I*-1)th event. The averages of the occurrence times and magnitudes over the selected sequenceswere used as ensemble forecasts. Yoshida, Kato, and Fukuda (2016) attempted to predict the 7th event to the 11th event. In addition, the occurrence time of the 12th event, which did not occur before the publication of this paper, was forecasted. In this study, we discuss the forecast result.

Keywords: Kamaishi repeating earthquakes, forecast experiment

©2021. Japan Geoscience Union. All Right Reserved.

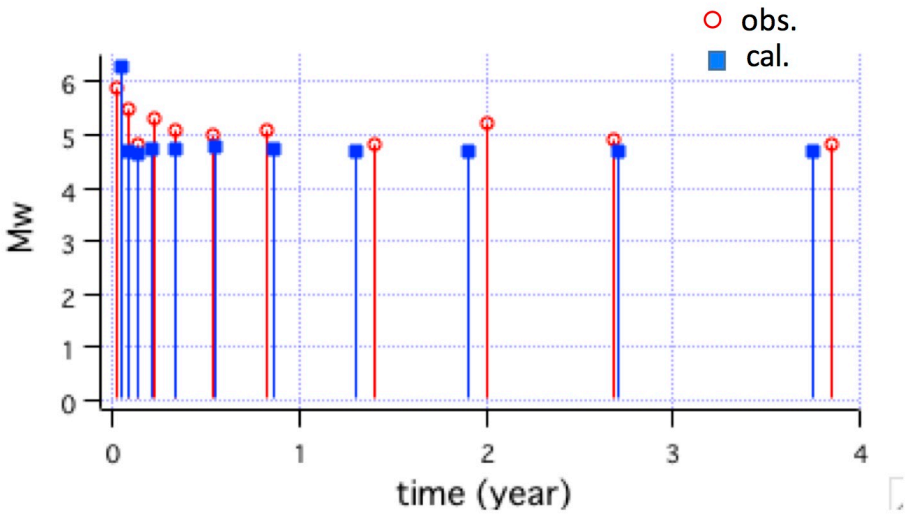


図1 釜石沖繰り返し地震のM-t図．t=0は東北沖地震発生時，赤丸は観測，青の四角はシミュレーション結果の1例．

©2021. Japan Geoscience Union. All Right Reserved.

[J] Oral | S (Solid Earth Sciences)：S-SS Seismology

Sun. Jun 6, 2021 9:00 AM - 10:30 AM JST | Sun. Jun 6, 2021 12:00 AM - 1:30 AM UTC | Ch.18 Zoom Room 18

[S-SS11] Strong Ground Motion and Earthquake Disaster

convener:Kazuhiro Somei(Geo-Research Institute), Yasuhiro Matsumoto(Kozo Keikaku Engineering), Chairperson:Kenichi Tsuda(Institute of Technology, Shimizu Corporation), Asako Iwaki(National Research Institute for Earth Science and Disaster Prevention)

Strong ground motion has social impacts as it induces earthquake disasters. We solicit contribution on any seismological topics related to strong ground motion that includes, but are not limited to, source processes, wave propagation, and site effects. We also welcome contribution on earthquake related disaster mitigation.

9:00 AM - 9:15 AM JST | 12:00 AM - 12:15 AM UTC

[SSS11-07] Development of data-driven strong motion model and common integrated database

*Hiroyuki Fujiwara[1], Nobuyuki Morikawa[1], Asako Iwaki[1], Takahiro Maeda[1], Shinichi Akiyama[1], Kenichi Kato[2], Toshiaki Sato[3], Takayuki Hayashi[4] (1.National Research Institute for Earth Science and Disaster Resilience, 2.KOBORI RESEARCH COMPLEX INC., 3.Ohsaki Research Institute, Inc., 4.Tokio Marine & Nichido Risk Consulting Co., Ltd.)

9:15 AM - 9:30 AM JST | 12:15 AM - 12:30 AM UTC

[SSS11-08] Consideration of Uncertainty in Seismic Hazard Assessment Based on Strong Motion Observation Record Database

*Nobuyuki Morikawa[1], Hiroyuki Fujiwara[1], Asako Iwaki[1], Takahiro Maeda[1] (1.National Research Institute for Earth Science and Disaster Resilience)

9:30 AM - 9:45 AM JST | 12:30 AM - 12:45 AM UTC

[SSS11-09] On applicabiltiy of ground-motion simulation data to data-driven ground-motion prediction model

*Asako Iwaki[1], Hiroyuki Fujiwara[1], Nobuyuki Morikawa[1], Takahiro Maeda[1] (1.National Research Institute for Earth Science and Disaster Prevention)

9:45 AM - 10:00 AM JST | 12:45 AM - 1:00 AM UTC

[SSS11-10] Spatial complexity characteristics of faut parameters based on self-similar models - Comparison of earthquake slip of Japan and all over the world-

*Fumino Suzuki[1], Kenichi Kato[1], Tetsushi Watanabe[1] (1.KOBORI RESEARCH COMPLEX INC.)

10:00 AM - 10:15 AM JST | 1:00 AM - 1:15 AM UTC

[SSS11-11] A scaling relation of crustal earthquakes assuming constant stress drop - in a case when fault width is used as a parameter -

*Kazuhito Hikima[1], Akihiro Shimmura[1] (1.Tokyo Electric Power Company Holdings, Inc.)

10:15 AM - 10:30 AM JST | 1:15 AM - 1:30 AM UTC

[SSS11-12] Correlation of Kinematic Source Parameters from Rupture Models Simulated by the Full Dynamic Earthquake Cycles

*Anatoly Petukhin[1], Percy Galvez[2,3], Paul Somerville[4], Ken Miyakoshi[1], Kojiro Irikura[5] (1.Geo-Research Institute, 2.ETH Zurich, Earth Science, 3.KAUST University, 4.AECOM, Los Angeles, 5.Aichi Institute of Technology)

Development of data-driven strong motion model and common integrated database

*Hiroyuki Fujiwara[1], Nobuyuki Morikawa[1], Asako Iwaki[1], Takahiro Maeda[1], Shinichi Akiyama[1], Kenichi Kato[2], Toshiaki Sato[3], Takayuki Hayashi[4]

1. National Research Institute for Earth Science and Disaster Resilience, 2. KOBORI RESEARCH COMPLEX INC., 3. Ohsaki Research Institute, Inc., 4. Tokio Marine & Nichido Risk Consulting Co., Ltd.

Strong motion observations in Japan have a history of nearly 70 years. In particular, due to the strengthening of the strong motion observation system after the Great Hanshin-Awaji Earthquake Disaster in 1995, a huge amount of strong motion observation data have been collected by many institutions and private companies, including more than 800,000 records by the strong motion observation networks K-NET and KiK-net of NIED. Information on underground structure exploration has been accumulated, and the construction of a nationwide subsurface velocity structure model for strong motion calculation is in progress. Strong motion prediction models (GMPEs) based on regression analysis of observation records have been developed and have contributed to the progress of seismic hazard assessment. The problem with strong motion prediction by GMPE is that the ability to predict rare and inexperienced events such as very large earthquakes is not guaranteed by observation records. In order to overcome these problems, a strong motion prediction method by physics-based simulation (PBS) using an advanced subsurface velocity structure model has also been developed. It is becoming possible to supplement the lack of observation records with simulation data based on theoretical models. In this study, we try to construct strong motion big data including inexperienced events by fusing observation data and PBS data based on theoretical model. We aim to develop strong motion prediction models that have high predictive performance and meet the needs of the practical side by using data-driven analysis that utilizes a common integrated strong motion database.

Seismic hazard and risk assessment are indispensable for ensuring safety and security against earthquake disasters. In seismic hazard assessment, there is "uncertainty" due to the natural variability of earthquakes and the limits of our human perception due to infrequent events. It is important for society to properly consider the “uncertainty” of seismic hazards to function risk management in preparation for earthquake disasters. Probabilistic seismic hazard analysis (PSHA) is one of the methods for such seismic hazard analysis. From the PSHA point of view, GMPE is currently the most practical strong motion prediction model in the world. In the United States, a unified observation database for the development of GMPE has been constructed, and based on this, multiple GMPEs are studied under the same conditions by multiple developers. Differences among multiple GMPEs are treated as epistemic uncertainty in PSHA and weighted according to the performance of each GMPE. On the other hand, GMPEs in Japan are developed by each developer under their own data set and conditions. Therefore, inadequate performance comparison and insufficient evaluation of epistemic uncertainty among multiple GMPEs have become a practical problem. It has also been pointed out that regression analysis based only on specific datasets has low prediction performance for events not included in the dataset. These are partly due to the lack of a unified strong motion database for the development of strong motion prediction models in Japan. To solve these problems, we have held a strong motion DB working group for the purpose of constructing an observation DB for the development of highly practical GMPE, and have been proceeding with trial production of the observation DB and formulation of GMPE specifications. The working group consists of GMPE researchers in Japan, NGA participants in the United States, and corporate researchers involved in structural design and risk assessment.

©2021. Japan Geoscience Union. All Right Reserved.

GMPE is a model secured by observation facts, but rare events that should be predicted have not yet been observed. In order to deal with this simple and fundamental problem, this research aims to construct "strong motion big data" by fusing observation data and PBS data. The goal of this study is to propose multiple new strong motion prediction models (GMM) with high prediction performance by analyzing strong motion big data based on various methods including machine learning by multiple teams with different specialties, and extracting the information hidden behind the data beyond the knowledge of strong motion research so far. Specifically, formulation of GMM requirement specifications from the viewpoint of utilization, development of fusion method of observation data and PBS data, GMM development by various methods, quantitative evaluation of GMM variation, area prediction by spatial interpolation, evaluation of GMM performance and epistemic uncertainty. In this presentation, we will introduce the current status of our research.

Keywords: strong ground motion, GMPE, GMM, database, simulation, machine learning

©2021. Japan Geoscience Union. All Right Reserved.

Consideration of Uncertainty in Seismic Hazard Assessment Based on Strong Motion Observation Record Database

*Nobuyuki Morikawa[1], Hiroyuki Fujiwara[1], Asako Iwaki[1], Takahiro Maeda[1]

1. National Research Institute for Earth Science and Disaster Resilience

In order to properly consider the epistemic uncertainties related to ground motion equations (GMPEs) in seismic hazard assessment, GMPEs based on various ideas for application of observation records to extrapolated regions. It is necessary to construct a framework for deriving the above and evaluating the performance of those models. Morikawa et al. (2020; JpGU) have prototyped a strong motion observation record database, which is the basis for this.

In order to evaluate the performance of GMPEs, it is necessary not only to use a common database in deriving the models, but also to be able to calculate ground motions under common conditions for earthquakes and site. In this study, from the viewpoint of applying to the seismic hazard assessment in Japan, the applicable conditions that can be the target of performance evaluation of the GMPE were determined as a tentative "specifications." It includes the condition that it is applied to the site very near source fault where the fault distance is within 1 km and to a mega-earthquake of magnitude 9. The analyst’ s concept regarding the modeling of extrapolation for which these observation records are not sufficiently obtained is clarified. Based on this prototype strong motion database and tentative specifications, we start to construct multiple GMPEs, including improvements to existing ones.

On the other hand, it is quite hard to verify the strong motion prediction results for a mega-earthquake along the Nankai Trough or near the source fault based on observation records. As the first step in the study to evaluate the reliability of such strong motion prediction results, we investigated strong motion intensity distribution for discretized magnitude-fault distance space in the strong motion observation record database. In the case with many records, it is close to the lognormal distribution. In the case with few records, however, it is close to the uniform distribution. We plan to further analyze the temporal changes in the distribution due to the accumulation of records. Such characteristic analysis of the database itself not only present the insufficiency of observation records, but also aims to formulate a method for evaluating the reliability of the added simulation data by changes in the distribution.

Keywords: Seismic Hazard Assessment, Uncertainty, Strong Motion Database, Ground Motion Prediction Equation (GMPE)

©2021. Japan Geoscience Union. All Right Reserved.

On applicabiltiy of ground-motion simulation data to data-driven ground-motion prediction model

*Asako Iwaki[1], Hiroyuki Fujiwara[1], Nobuyuki Morikawa[1], Takahiro Maeda[1]

1. National Research Institute for Earth Science and Disaster Prevention

Ground-motion simulation based on fault and wave-propagation models, often called physics-based simulation (PBS), has become a powerful tool for ground-motion prediction that can consider the effects of rupture propagation and wave propagation through complicated tectonics. On the other hand, ground-motion prediction equation (GMPE aka. GMM) is the most practical tool in probabilistic seismic hazard assessment (PSHA).

Our group has started a project to construct strong-motion database and data-driven GMPEs (Fujiwara et al. and Morikawa et al., 2021, this meeting), aiming to consider uncertainties in GMPEs to improve current PSHA in Japan. It has been pointed out that current GMPEs are not sufficient accurate at predicting ground motion with low probability, such as near-fault ground motion and ground motion from mega-earthquakes.

In this study, we attempt to merge PBS data with observation data in order to make up for the deficiency of the observation database especially in short distances and large magnitudes. We generated PBS data for scenario active fault earthquakes in Kanto area and performed statistical analysis to ensure the PBS data provide stable ground motion level and appropriate variability of ground motion.

Keywords: strong-motion prediction, seismic hazard assessment, ground-motion prediction equation, ground-motion simulation

©2021. Japan Geoscience Union. All Right Reserved.

Spatial complexity characteristics of faut parameters based on self-similar models -Comparison of earthquake slip of Japan and all over the world-

*Fumino Suzuki[1], Kenichi Kato[1], Tetsushi Watanabe[1]

1. KOBORI RESEARCH COMPLEX INC.

1. Introduction

Earthquake source parameters such as slip and stress drop on fault planes have spatially variable distributions. One of the models considered the complexity of the fault parameters is the self-similar model in which the spatially inhomogeneous distribution is characterized in the wavenumber domain (Hanks, 1979). As for the self-similar model, it was shown theoretically and numerically that the far field displacements follow the ω^{-2} decay assuming the "k-square" model in which the slip spectrum decays as k^{-2} beyond the corner wavenumber (Andrews, 1980, 1981; Herrero and Bernard, 1994). The slip complexities of past earthquakes around the world were characterized using the wavenumber spectra (Somerville et al. 1999; Mai and Beroza, 2002). The characterized complexities were utilized for strong motion simulations and validated by comparison with observation records of earthquakes around the world, such as in the SCEC BBP project. However, only four earthquakes in Japan were used for their evaluations, and validations of the complexities on Japan earthquakes are insufficient. In this study, the slip complexities are evaluated using the self-similar model for many earthquakes in Japan.

2. Methods

Targets are 38 earthquakes in Japan occurred from 1923 to 2016, and we used 61 fault slip models published on SRCMOD (http://equake-rc.info/srcmod/). One-segment fault models are used, since our targets are two-dimensional spatial distributions. In this study, 23 crustal earthquakes, 13 interplate earthquakes, and 2 intraplate earthquakes are used respectively.

The complexity evaluation method is similar to Mai and Beroza (2002). 2-D Fourier transform are applied to the fault slips to obtain 2-D wavenumber spectra. Then their spectra are fitted to the von Karman autocorrelation functions using grid-search, and the correlation distances and the Hurst exponents are estimated. Specifically, the correlation distances a_r and the Hurst exponents H are estimated from circular-averaged spectra. Next, the correlation distances a_x and a_y are estimated from along-strike spectra and downdip spectra respectively under conditions where H estimated from the circular-averaged spectra are fixed. These H, a_x, and a_y of earthquakes in Japan are compared with previous studies of earthquakes around the world. Differences between source types are also examined.

3. Results

Figure 1 shows the wavenumber spectra of all models.

©2021. Japan Geoscience Union. All Right Reserved.

Hurst exponents H estimated by circular-averaged spectra are independent of moment magnitude M_W, and differences between source types are small. The median of H is 0.77 and close to $H = 0.75$ by Mai and Beroza (2002). Next, Correlation distances a_x estimated by along-strike spectra have positive correlation with M_W, and differences between source types are small. Linear regression results of $\log(a_x)$ on M_W for all earthquakes, crustal earthquakes, and interplate earthquakes respectively are almost the same as those of Mai and Beroza (2002). Therefore, the difference of H and a_x characteristics between Japan and the world tends to be small.

Correlation distances a_y estimated by downdip spectra have positive correlation with M_W like a_x. On the other hand, there are differences between source types, and the a_y of interplate earthquakes are larger than that of crustal earthquakes. In addition, a_y tends to be constant for M_W 6 class or higher crustal earthquakes. The same tendency is also acknowledged for M_W 8 class or higher interplate earthquakes. These may indicate the saturation of the fault width due to the thickness of the seismogenic layer. Based on these trends, a_y are regressed for each source types with two segments of the following equation,

$\log(a_y) = bM_W + c \ (M_W <= M_{WC})$

$\log(a_y) = bM_{WC} + c \ (M_W > M_{WC})$.

As a result, M_{WC}, which is a break point, is 6.6 for crustal earthquakes and 8.4 for interplate earthquakes. These are consistent with the boundary between the 1st stage and the 2nd stage of 3-stage scaling relations by Irikura and Miyake (2001) and Tajima et al. (2013).

Keywords: self-similar, spatial complexity, fault slip, wavenumber domain

©2021. Japan Geoscience Union. All Right Reserved.

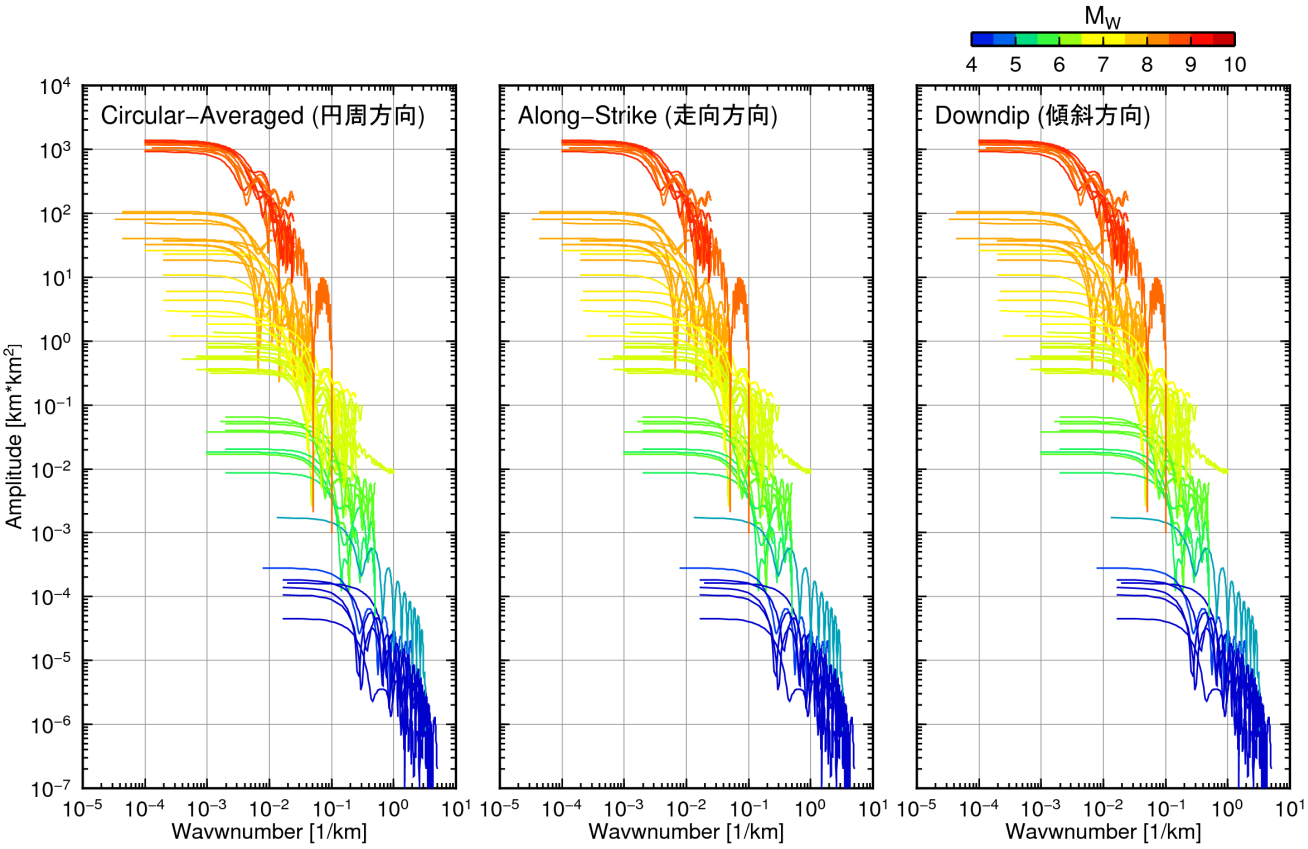


図1　すべり分布の全モデルの波数スペクトル

Figure 1 Wavenumber spectra for all models of fault slip

©2021. Japan Geoscience Union. All Right Reserved.

A scaling relation of crustal earthquakes assuming constant stress drop - in a case when fault width is used as a parameter -

*Kazuhito Hikima[1], Akihiro Shimmura[1]

1. Tokyo Electric Power Company Holdings, Inc.

- Outline -

In Japan, the Irikura and Miyake formula (Irikura and Miyake, 2001) and 3 stage model (Murotani *et al*, 2015) are the key of the “recipe for the strong motion prediction”. Those formulas take into account the limitation of crustal thickness and are basically considered physically reasonable. However, some defects are pointed out especially for long fault. In our previous study (Hikima and Shimmura, 2020; BSSA), we proposed the similar M_0-S scaling relation, which realizes constant stress drop from small to large fault models. Although the relation was consistent with existing parameters, it was necessary to examine using newly analyzed data.

In recent studies, fault parameters are estimated by inversion analyses, which are performed mostly assuming larger fault model than true slip area. Therefore, we have to extract major fault area from the inversion results. Somerville *et al*. (1999) proposed a method in that marginal rows and columns having relatively small slips are trimmed and rectangular main area is extracted. However, it seems that the physically clear criteria are not proposed and it is difficult automatically select the main target. Therefore, we proposed a procedure to extract an effective rectangular area based on wavenumber spectra of slip distribution (Hikima and Shimmura, 2020; JpGU).

In this study, we shortly explain the proposed trimming method again, because the explanation at the time of presentation was somewhat different from the published abstract. Then, we discuss scaling relations using the determined source parameters.

- Trimming method -

First, a slip distribution at 1 or 2 km intervals for length (X-direction) and for width (Y-direction) is made from an original slip model. Then, zero values are added outside of the fault area, and amplitude wavenumber spectra of these data are calculated using two-dimensional FFT. For these spectra, we consider that the spectrum at k_y=0 (k_y: wavenumber for Y-direction) is in length direction and the spectrum at k_x=0 (k_x: wavenumber for X-direction) is in width direction, respectively.

On the side, Fourier transform of a rectangular function having width as L is $f(\nu)=L\sin(\pi L\nu)/(\pi L\nu)$ [$\nu=1/\lambda$; λ: wavelength]. This sinc function crosses with zero line at $\nu=n/L$ [n=1, 2, …], and these correspond to trough of the spectrum in the case of amplitude spectrum.

We adopted following criteria to extract almost equal fault areas as those using Somerville *et al*. (1999). We focused on lower part than first trough (it corresponds to n=1) of sinc function, and we determined maximum L length not to exceed observed spectra from lower wavenumber side. We applied the same process to the spectrum of width direction. In the previous presentation, we confirmed that the determined fault areas are almost same as those by Somerville’s procedure.

- Scaling relation for crustal earthquakes -

We applied these analyses for the fault models in the SRCMOD (Mai and Thingbaijam, 2014) in last year. Following discussions are based on determined parameters.

First, we checked the relation between the fault length and the fault width (Fig. 1). Conventionally, it has been recognized that the width saturates for long faults. Although such a trend can be seen among the data, it is also observed that the fault width increased in the long fault. Such a tendency is particularly remarkable for longitudinal slip faults. On the other hand, when the stress drop was calculated considering the formulas of the rectangular fault, there was no obvious correlation between the

©2021. Japan Geoscience Union. All Right Reserved.

earthquake size and the stress drop (Fig. 2).
Considering these relations, we thought that the data could be explained more appropriately by treating the stress drop as a constant value and the fault width as a parameter. In Fig. 3, the fault widths of each earthquake are denoted according to the color table, and the curves show the M_O-S relations, assuming a constant stress drop of 2.5 MPa and with four saturation fault widths (W_{max}). The observed fault width becomes larger in larger earthquakes, and they are consistent with the relation with larger W_{max}.
These results may be affected by uniform treatment without considering various tectonic conditions in the world. However, it is shown that the relation for the crustal earthquakes can be basically scaled with constant stress drop condition. In addition, such as the area around Japan, where the tectonic environment is clear, W_{max} can be considered as almost constant in areas. Therefore, it may become possible to consider scaling with a single formula.
<Acknowledgment> We appreciate the SRCMOD and its related parties.

Keywords: Crustal earthquake, Scaling relation, Stress drop, Fault size, Fault width

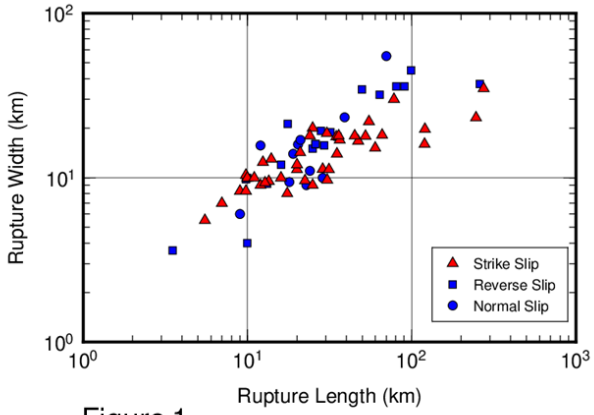


Figure 1

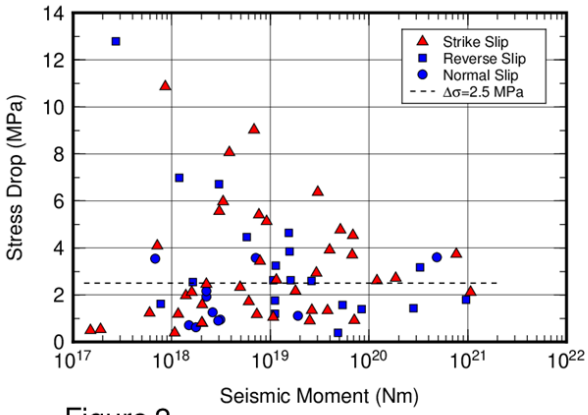


Figure 2

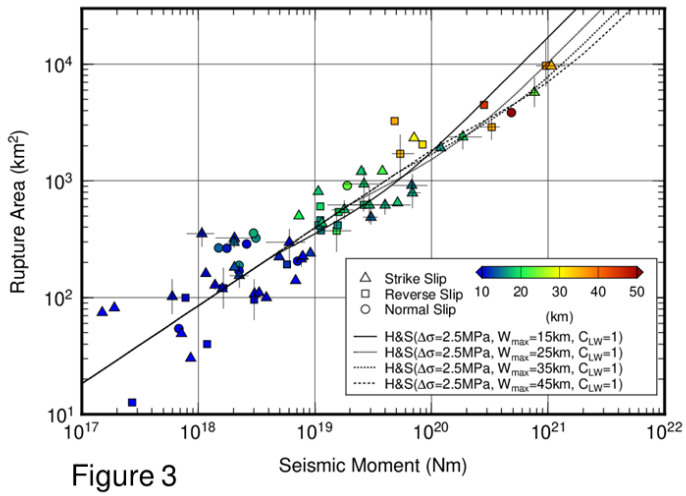


Figure 3

Fig. 1 Relation between rupture length and width.
Fig. 2 Relation between seismic moment and static stress drop. Stress drop values are calculated using formulae for rectangular faults.
Fig. 3 Scaling relation between seismic moment and rupture area. Color of each symbol indicates its fault width. Curves are scaling relations assuming constant stress drop by Hikima and Shimmura (2020), whose values are set as 2.5 MPa.
Fault models which have multiple slip models were plotted using averaged value. In figure 3, the bars indicate the corresponding ranges.

©2021. Japan Geoscience Union. All Right Reserved.

Correlation of Kinematic Source Parameters from Rupture Models Simulated by the Full Dynamic Earthquake Cycles

*Anatoly Petukhin[1], Percy Galvez[2,3], Paul Somerville[4], Ken Miyakoshi[1], Kojiro Irikura[5]

1. Geo-Research Institute, 2. ETH Zurich, Earth Science, 3. KAUST University, 4. AECOM, Los Angeles, 5. Aichi Institute of Technology

Realistic dynamic rupture modelling validated by observed earthquakes is necessary for estimating parameters, such as stress drop, rupture velocity and slip rate function, that are poorly resolved by seismic source inversion. Source inversions using forward dynamic modelling are frequently used to obtain rupture models. Alternatively, in this study, we use set of a hundred spontaneous physically self-consistent rupture models, whose rupture process is consistent with the spatio-temporal heterogeneity of previous earthquakes on the same fault, as the result of multicycle simulations under the rate-and-state friction law on strike-slip fault (Galvez et al., 2021). The magnitude range of the ruptures is *Mw*5.5-7.4. Models are validated by comparison with: (1) source scaling relations from seismic inversions, (2) ground motion preduction models, and (3) observed fault displacements.

From the heterogeneous rupture models, we analyzed distributions of *Slip*, peak slip rate (*PSR*), static stress drop (Ds), rupture velocity (*Vr*), parameters of the source time function (STF), as well as the rate-and-state critical distance *Dc*, the only initial heterogeneity parameter in the multicycle modeling. The dynamic rupture static stress drop tracks the evolution of stress during the rupture process. It is computed as the difference of final stress and initial stress at the rupture initiation moment. Dynamic STFs are well approximated by the regularized Yoffe function. This Kostrov-type STF is described by two parameters: smoothing time *Ts*, which is approximately equivalent to the peak delay time, and rise time *Tr* . Examples of parameter distributions are shown on the figure below. It seems that there are spatial correlations between parameters: high *PSR* areas correlate with areas of small *Dc*, large rupture velocity and small *Ts*-time, and areas of large *Tr* correlate with areas of small peak slip rate (*PSR)* and small Ds, although there can be a spatial offset in some cases.

On a 1x1 km mesh we studied one-point correlations between parameters. Additionally, we studied two-point cross-correlations considering possible spatial offset. The main findings are:

1. Strong positive correlations (correlation coef. > 0.4) are confirmed in the following pairs: Ds −*Slip*, *PSR* −*Vr*, *PSR* −1/*Ts*, *PSR* −Ds, *Ts* −*Dc*.

2. Minor positive correlations (correlation coef. < 0.4) are confirmed in the following pairs: *Tr* - *Slip*, *PSR* −1/*Dc*, *Vr* −1/*Dc*.

3. There is spatial correlation between *PSR* and *Slip*. However, where there is strong rupture directivity, high slip-rate areas are located on the outer edge of the large slip areas. Due to this effect, we could not confirm this correlation by the one-point method.

4. Spatial correlations between *PSR* and other parameters: 1/*Dc*, *Vr* and 1/*Ts*, have no spatial offset.

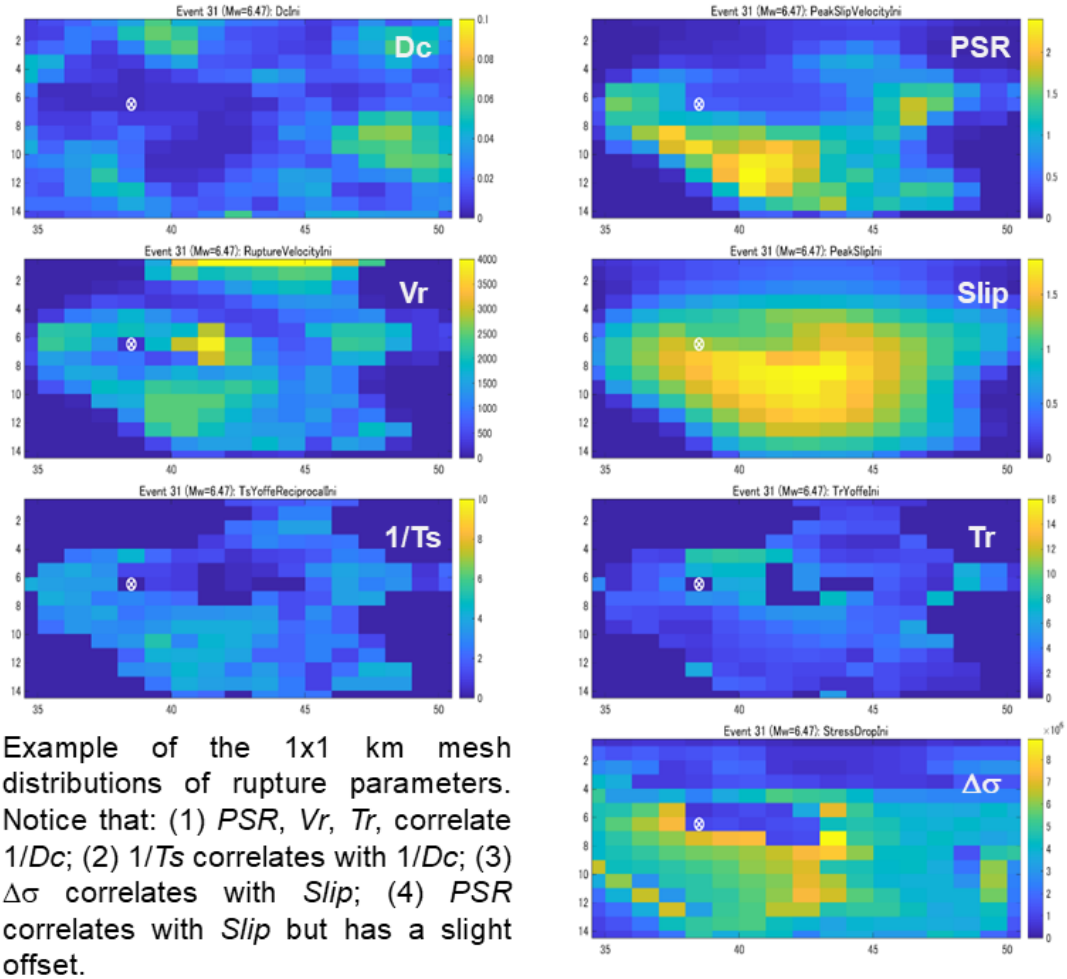
Although many of these correlations are as expected theoretically, it is important to confirm them by physics-based dynamic rupture simulations.

©2021. Japan Geoscience Union. All Right Reserved.

Acknowledgements. This study is based on the 2018 research project 'Examination for uncertainty strong ground motion prediction for inland earthquakes' by the Secretariat of Nuclear Regulation Authority (NRA), Japan.

Reference. Galvez, P., et al. (2021). Multi-cycle earthquake modeling for source scaling and near-source ground motion validation, *Bull.Seismol.Soc.Am.*, submitted.

Keywords: earthquake rupture dynamics, earthquake cycle simulation, source characterization, strong ground motion prediction



Example of the 1x1 km mesh distributions of rupture parameters. Notice that: (1) *PSR*, *Vr*, *Tr*, correlate 1/*Dc*; (2) 1/*Ts* correlates with 1/*Dc*; (3) $\Delta\sigma$ correlates with *Slip*; (4) *PSR* correlates with *Slip* but has a slight offset.

©2021. Japan Geoscience Union. All Right Reserved.

[J] Oral | S (Solid Earth Sciences)：S-SS Seismology

Sun. Jun 6, 2021 10:45 AM - 12:15 PM JST | Sun. Jun 6, 2021 1:45 AM - 3:15 AM UTC | Ch.18 Zoom Room 18

[S-SS11] Strong Ground Motion and Earthquake Disaster

convener:Kazuhiro Somei(Geo-Research Institute), Yasuhiro Matsumoto(Kozo Keikaku Engineering), Chairperson:Hisahiko Kubo(National Research Institute for Earth Science and Disaster Resilience), Hongjun Si(Seismological Research Institute Inc.)

Strong ground motion has social impacts as it induces earthquake disasters. We solicit contribution on any seismological topics related to strong ground motion that includes, but are not limited to, source processes, wave propagation, and site effects. We also welcome contribution on earthquake related disaster mitigation.

10:45 AM - 11:00 AM JST | 1:45 AM - 2:00 AM UTC

[SSS11-13] Long-period incident waves to the Echigo basin during the 2011 off the Pacific coast of Tohoku Earthquake

*Tomiichi Uetake[1] (1.R&D Department, TEPCO research Institute, Tokyo Electric Power Company)

11:00 AM - 11:15 AM JST | 2:00 AM - 2:15 AM UTC

[SSS11-14] On the attenuation characteristics of peak ground motion from three M_W7 class intraplate earthquakes along the Japan Trench

*Hongjun Si[1] (1.Seismological Research Institute Inc.)

11:15 AM - 11:30 AM JST | 2:15 AM - 2:30 AM UTC

[SSS11-15] Comparison of seismic wave fields from the earthquakes off Fukushima prefecture, northeastern Japan

*Yasumaro Kakehi[1] (1.Department of Planetology, Graduate School of Science, Kobe University)

11:30 AM - 11:45 AM JST | 2:30 AM - 2:45 AM UTC

[SSS11-16] ESTIMATE TIME AND SPATIAL EVOLUTION OF THE RUPTURE PROCESS OF THE 2021 OFF-FUKUSHIMA BASED ON THE FINITE-FAULT SOURCE INVERSION

*Kenichi Tsuda[1], Chen Ji[3], Ralph J Archuleta[3,4], Toshiaki Sato[2] (1.Institute of Technology, Shimizu Corporation, 2.Ohsaki Research Institute, Inc., 3.University of California, Santa Barbara, 4.RJA Ground Motion Analysis, Inc.)

11:45 AM - 12:00 PM JST | 2:45 AM - 3:00 AM UTC

[SSS11-17] Source process of the 2021 off Fukushima, Japan, intraslab earthquake derived from strong motion data

*Hisahiko Kubo[1], Wataru Suzuki[1], Shin Aoi[1], Haruko Sekiguchi[2] (1.National Research Institute for Earth Science and Disaster Resilience, 2.Disaster Prevention Research Institute, Kyoto University)

12:00 PM - 12:15 PM JST | 3:00 AM - 3:15 AM UTC

[SSS11-18] Strong motion characteristics at MYGH10 (KiK-net), Yamamoto, during the Off Fukushima pref. earthquake of 13th Feb., 2021

*Tomotaka Iwata[1] (1.Disaster Prevention Research Institute, Kyoto University)

Long-period incident waves to the Echigo basin during the 2011 off the Pacific coast of Tohoku Earthquake

*Tomiichi Uetake[1]

1. R&D Department, TEPCO research Institute, Tokyo Electric Power Company

During the 2011 off the Pacific coast of Tohoku Earthquake, the long-period ground motion was observed in the Echigo basin, Japan, and Rayleigh waves were predominant in periodic zones with a period of about 10 seconds or more [Uetake et al. (2016).)]. To know the characteristics of the incident wave are essential to consider the response of the basin structure. This report confirms whether the Rayleigh wave was predominant in the incident wave during the 2011 off the Pacific coast of Tohoku Earthquake.
To examine the incident wavefield to the Echigo basin, we selected 23 strong motion observation stations from the eastern part of Fukushima prefecture facing the Pacific Ocean to the Chuetsu region of Niigata prefecture. All of them are the observation stations of K-NET and KiK-net of the National Institute for Earth Science and Disaster Resilience and are lined up from east to west within the epicenter distance of the 2011 event in the range of 174 km to 347 km.
First, the Fourier spectrum characteristics of acceleration data were investigated. The spectral amplitude of the high-frequency band changes significantly due to the influence of ground characteristics, and at the observation point located west of the volcanic front, the spectral amplitude sharply decreases as the frequency increases. On the other hand, no significant change was observed at low frequencies below 0.1 Hz. Also, similarities were found in the spectral shapes of UD and EW in this frequency band.
Velocity waveforms were created by integrating the acceleration waveforms with a bandpass filter with a frequency of 0.05 to 0.2 Hz. Two wave groups propagating from east to west were observed in the EW- and the UD-component, continuous with the wave groups found in the Echigo Basin records. The apparent velocities of these two wave groups were approximately 3.4 km/s. When the particle locus was drawn with the EW- and the UD-component at observation stations other than the eastern part of Fukushima Prefecture, both wave groups have retrograde rotations characteristic of Rayleigh waves. The waveform of the NS component is different from that of the EW- and the UD-component. Next, the distance attenuation characteristics of the maximum value (PGV) of the velocity waveform concerning the epicenter distance (r) were investigated. For the UD-and EW-components, the attenuation curve of PGV shows the surface wave's attenuation characteristics. For the NS-component, the attenuation curve shows the body wave's attenuation characteristics.
Coherence analysis between the components was performed for each observation station. The coherence was calculated for 300 seconds from the head of the data. Focusing on the frequency of 0.05 to 0.1 Hz, the coherence between the UD-component and the EW- component was the highest, and the phase shift was about 90 degrees at many observation points. Also, coherence analysis was performed for 80 seconds from the start of recording and for the next 80 seconds, taking into account the two wave groups' appearance times confirmed in the velocity waveform, and similar results were obtained. Different results were obtained at the observation stations in the eastern part of Fukushima Prefecture.
It is considered that the Rayleigh wave component was predominant in the seismic motion with a period of 10 seconds or more that was incident on the Echigo Plain during the 2011 off the Pacific coast of Tohoku Earthquake. At least the seismic motions of the UD and EW components should be considered as Rayleigh waves propagating westward. The NS component is considered to be mainly body waves from the viewpoint of distance attenuation.

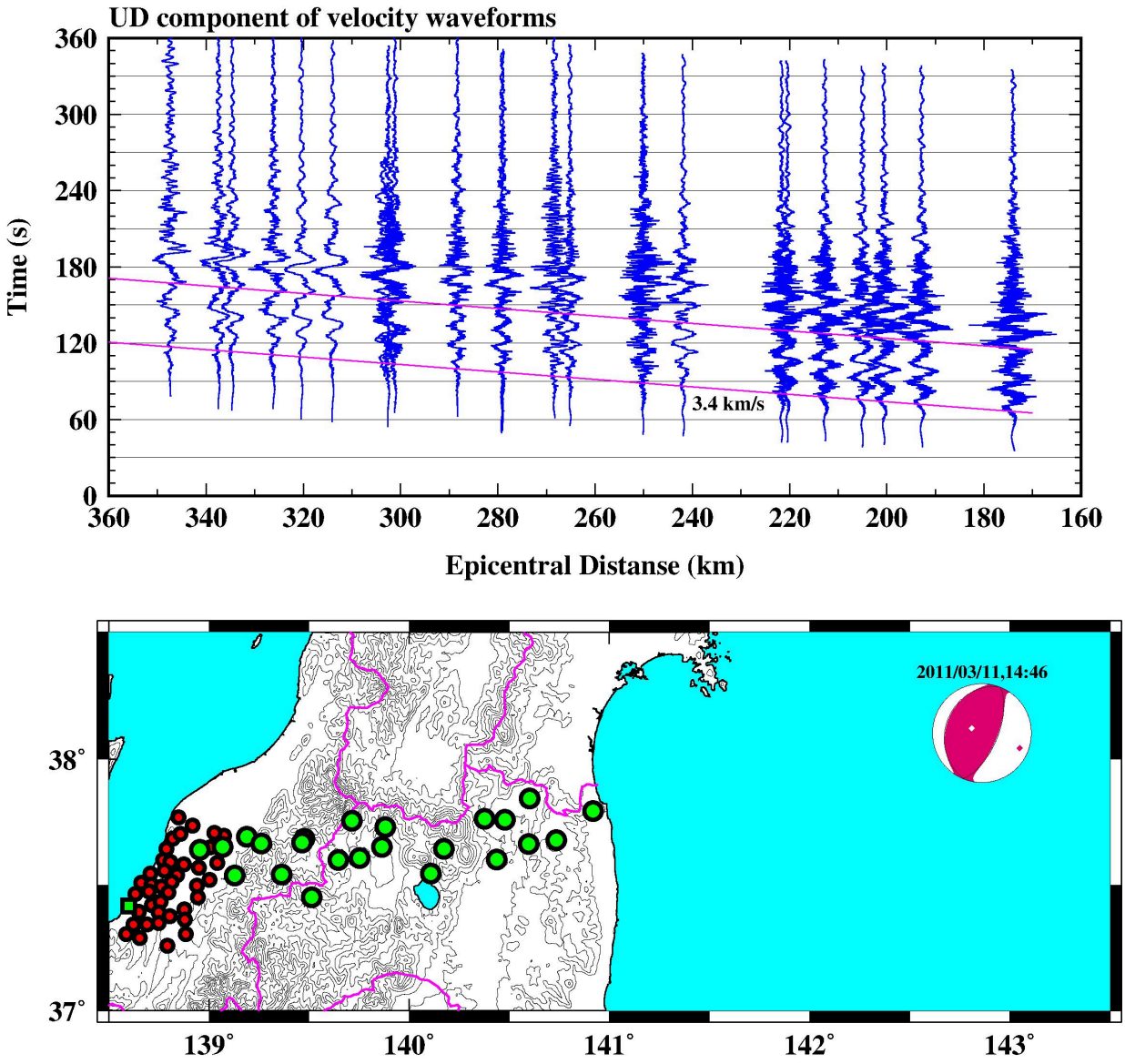
Acknowledgments: We used the strong motion data from K-NET and KiK-net of the National Research

©2021. Japan Geoscience Union. All Right Reserved.

Institute for Earth Science and Disaster Prevention.

Keywords: Rayleigh wave, Coherence analysis, Attenuation curve

©2021. Japan Geoscience Union. All Right Reserved.



Location of observation stations (green circles) and velocity waveforms

©2021. Japan Geoscience Union. All Right Reserved.

On the attenuation characteristics of peak ground motion from three M_w7 class intraplate earthquakes along the Japan Trench

*Hongjun Si[1]

1. Seismological Research Institute Inc.

Including the February 13, 2021 M_w 7.1 Fukushima-oki earthquake, there are three well recorded M_w 7 class intraplate earthquake that occurred along the Japan Trench. The other two earthquakes are the 2003 M_w 7.0 Miyagi-ken-oki earthquake and the 2011 M_w 7.1 Miyagi-ken-oki earthquake. In this study, we’ ll compare the attenuation characteristics of peak ground motions recorded during the three earthquakes and discuss the differences among them.

The data used in this study for all the three earthquakes are derived by K-NET and KiK-net. All the waveform data are processed by a bandpass filter with a lower cut off frequency at 0.1 Hz and higher one at 10 Hz. The acceleration waveforms are integrated to velocity waveforms. PGA and PGV are defined as the larger one between the two horizontal components. The closest distance from the seismic fault to the observation station is defined as the source distance. The source models used for the calculation of source distances are those proposed by Aoi et al. (2003), Harada and Kamae (2011) and the Kubo et al.(2021), respectively. M_w is adopted from the online catalog by the Global CMT Project. The source depth used here are 70km, 59km and 52km for the 2003 M_w 7.0 Miyagi-ken-oki earthquake, the 2011 M_w 7.1 Miyagi-ken-oki earthquake and the 2021 M_w 7.1 Fukushima-oki earthquake, respectively.
We compared the PGAs and PGVs observed during the 2021 M_w 7.1 Fukushima-oki earthquake with the 2003 M_w 7.0 Miyagi-ken-oki earthquake (shown in Figure 1), and with the 2011 M_w 7.1 Miyagi-ken-oki earthquake (shown in Figure 2). As a reference, in the figures, the values calculated by the GMPE proposed by Si and Midorikawa (1999) are also plotted. The figures show that, (1) the data for the 2021 Mw7.1 Fukushima-oki earthquake are generally similar to those for the 2003 M_w 7.0 Miyagi-ken-oki earthquake, but relatively weaker than those for the 2011 M_w 7.1 Miyagi-ken-oki earthquake at distances shorter than about 200 km; (2) the observations at distances farther than about 150 km are generally consistence with the prediction by GMPE, but stronger than GMPE at shorter distances; (3) higher attenuation for stations at far distances reported for the 2011 Geiyo earthquake are not significantly observed for all the three earthquakes in this study.

References

Aoi S., Sekiguchi H., Kunugi T., Honda R. and Fujiwara H.(2003), https://www.kyoshin.bosai.go.jp/kyoshin/news/miyagi/.

Harada and Kamae (2011) , https://www.rri.kyoto-u.ac.jp/jishin/eq/tohoku2/20110407miyagioki_slab.pdf.

Kubo H., Suzuki W., Aoi S. and Sekiguchi H. (2021) , https://www.kyoshin.bosai.go.jp/kyoshin/topics/FukushimakenOki_20210213/inversion/inv_index.html.

Si, H. and Midorikawa, S. (1999). J. Struct. Constr. Eng. AIJ. 523,63-70 (in Japanese with English Caption and Abstract).

Acknowledgements

©2021. Japan Geoscience Union. All Right Reserved.

The author thanks NIED to provide recordings by K-NET and KiK-net.

Keywords: Peak ground motion, Attenuation characteristics, Intraplate earthquake, 2021 Mw7.1 Fukushima-oki earthquake, Ground motion prediction equation (GMPE)

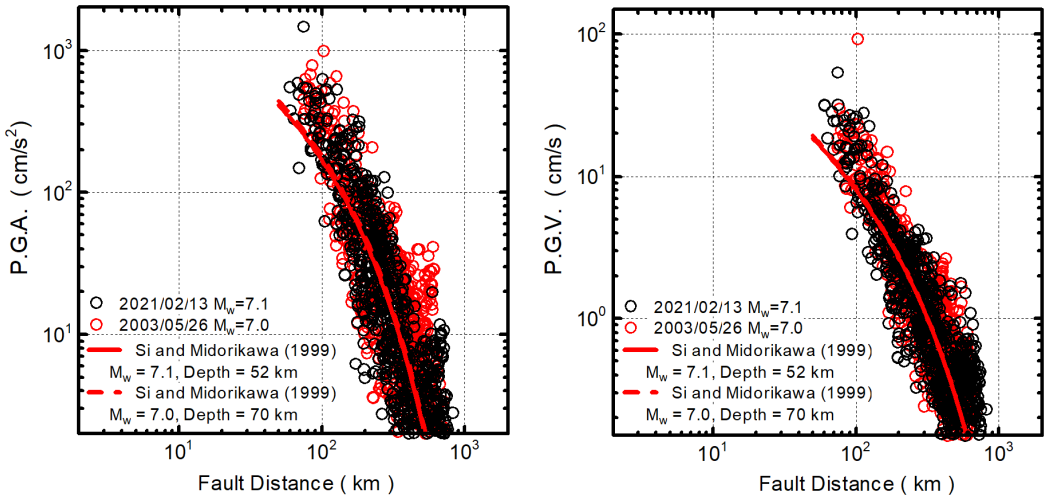


Fig.1.Comparison of peak ground motion for the 2021 Fukushima-oki earthquake (black open circle) and the 2003 Miyagiken-oki earthquake (red open circle)

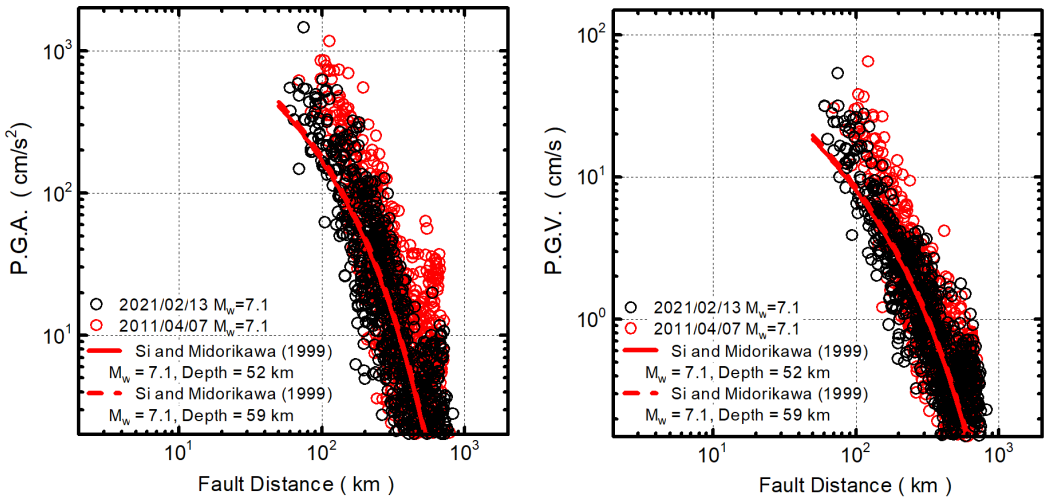


Fig.2.Comparison of peak ground motion for the 2021 Fukushima-oki earthquake (black open circle) and the 2011 Miyagiken-oki earthquake (red open circle)

©2021. Japan Geoscience Union. All Right Reserved.

Comparison of seismic wave fields from the earthquakes off Fukushima prefecture, northeastern Japan

*Yasumaro Kakehi[1]

1. Department of Planetology, Graduate School of Science, Kobe University

An M_W 7.1 earthquake occurred off Fukushima prefecture in northeastern Japan on Feb. 13, 2021. This (called event SU1 hereafter) is a down-dip compression type intraslab earthquake occurring on the upper plane of the double seismic zone, and its focal depth is 55km. The PGA (Peak Ground Acceleration) distribution based on NIED K-NET and KiK-net observation networks shows singular distribution, apart from concentric distribution, where high-frequency seismic wave amplitudes decay rapidly in the backarc side of the island arc, while large amplitudes of high-frequency seismic waves are observed in the forearc side. This phenomenon is a reflection of the attenuation structure with low-Q medium in the backarc side specific to island arc, and it comes from attenuation of high-frequency waves during propagation through the low-Q medium in the backarc side (Kakehi, 2015). In order to investigate the difference of seismic wave fields due to focal depths, strong ground motion data from following three M5 class earthquakes that have epicenters close to that of SU1 and various focal depths are analyzed: an interplate earthquake on Oct. 2, 2001 (M_W 5.5, 40.8km depth, event P hereafter), an intraslab (upper plane) earthquake on Aug. 4, 2013 (M_W 5.9, 58.0km depth, event SU2 hereafter), and an intraslab earthquake (lower plane) on Mar. 13, 2010 (M_W 5.5, 77.7km depth, event SL hereafter). The epicentral location and focal depth of SU2 are almost same as those of SU1. From the comparison of the PGA spatial distributions from these three earthquakes, a common feature that a clear contrast is seen between the forearc and backarc sides, where high-frequency seismic wave amplitudes decay rapidly in the backarc side, is observed among them, similar to the SU1 case. Although the focal depths of the three events have difference of about 20km among them, the incident angles of the seismic rays from the sources to the stations are commonly high angles, since the 40km depth of the shallowest P is sufficiently deep and the epicenter is close to the land area. Therefore, significant difference is not seen in the attenuation of high-frequency waves in the backarc side among the three events. On the other hand, a remarkable difference is seen between the shallowest event P and the deeper events of SU2 and SL, with regard to the absolute amplitude of overall PGA distribution. The amplitude level of the large acceleration area close to the epicenter of P is clearly lower than those of the deeper SU2 and SL. Additionally, while the spatial extents of the observed accelerations reach Hokkaido prefecture (= the accelerometers are triggered) in case of the deeper SU2 and SL, that of the shallowest P reaches only the southern part of Aomori prefecture at farthest. This indicates the overall acceleration level brought by the shallow P is lower than those by deeper SU2 and SL. This is an reflection of the finding by Kasatani and Kakehi (2014) based on the spectral inversion of strong ground motions of interplate and intraslab earthquakes in northeastern Japan: "high-frequency levers of source effects depend not on the tectonic environments but simply on the focal depths and the events with deeper focal depths have higher high-frequency levels."

Keywords: island arc, interplate earthquake, intraslab earthquake, attenuation

©2021. Japan Geoscience Union. All Right Reserved.

ESTIMATE TIME AND SPATIAL EVOLUTION OF THE RUPTURE PROCESS OF THE 2021 OFF-FUKUSHIMA BASED ON THE FINITE-FAULT SOURCE INVERSION

*Kenichi Tsuda[1], Chen Ji[3], Ralph J Archuleta[3,4], Toshiaki Sato[2]

1. Institute of Technology, Shimizu Corporation, 2. Ohsaki Research Institute, Inc., 3. University of California, Santa Barbara, 4. RJA Ground Motion Analysis, Inc.

The rupture process of large earthquakes is very essential to understand the physic of faulting process as well as to mitigate the seismic hazard for the future events. Furthermore, if such earthquake occurs on the ocean, the risk for generating tsunami needs to be considered. Usually, right after the occurrence of large earthquakes, many dislocation models to understand the rupture process have been released based on the analysis of various kinds of observed data, such as the seismic waveform including on the regional, near-field and the far-field data, the geodetic such as GPS and the geological field data. On other hand, these models are dependent on the assumption about how the fault ruptures, then, the choice of slip-rate functions that specify how fault ruptures is very important.
In this study, we have developed the source model of the mainshock of the 2021 Off-Fukushima earthquake (Mw 7.1) based on the finite-fault inversion method developed by Ji *et al.* (2002). We constructed the 1D velocity structure representing the source area of this event with consideration to the results by the seismic tomography (Matsubara *et al.,* 2019). We have used the waveform data at close stations by K-NET and KiK-net with the range of 0.05-0.2 Hz. Our preliminary results of the inversion show that the rupture extend to the southern side of the hypocenter.

Keywords: 2021 Off-Fukushima Earthquake, Finite-Fault-Inversion

©2021. Japan Geoscience Union. All Right Reserved.

Source process of the 2021 off Fukushima, Japan, intraslab earthquake derived from strong motion data

*Hisahiko Kubo[1], Wataru Suzuki[1], Shin Aoi[1], Haruko Sekiguchi[2]

1. National Research Institute for Earth Science and Disaster Resilience, 2. Disaster Prevention Research Institute, Kyoto University

The 2021 off Fukushima earthquake (Mjma 7.3) struck Tohoku and Kanto regions in Japan on February 13, 2021 (JST). This earthquake caused strong ground motions over a wide area with a maximum seismic intensity of 6+ on the JMA scale and a maximum PGA of approximately 1400 cm/s^2. The moment tensor solution of F-net and the spatial distribution of the mainshock and its aftershocks indicate that this event was an intraslab reverse-fault-type earthquake. In this study, we estimate the source process of this earthquake using strong motion waveforms.

We use velocity waveforms at 12 stations of K-NET and KiK-net of NIED. The waveforms are band-pass filtered between 0.05 and 0.5 Hz, resampled to 5 Hz, and windowed from 2 s before S-wave arrival for 30 s.

We assume a 32 km ×24 km rectangular fault model that has a strike of 24˚ and a dip of 34˚ based on the F-net moment tensor solution. The rupture starting point is set at 37.729˚N, 141.698˚E, and a depth of 55.4 km, which is the hypocenter determined by JMA.

The rupture process is spatially and temporally discretized following the multiple-time-window linear waveform inversion scheme (Olson and Apsel 1982; Hartzell and Heaton 1983; Sekiguchi et al. 2000). For the spatial discretization, the fault plane is divided into 8 subfaults along the strike direction and 6 subfaults along the dip direction, with a size of 4 km ×4 km each. For temporal discretization, the moment rate function of each subfault is represented by 4 smoothed-ramp functions (time windows) progressively delayed by 0.8 s and having a duration of 1.6 s each. The triggering velocity of first time window is set to 2.4 km/s to minimize the data-fit residual. Two orthogonal slips of each time window at each subfault are derived by minimizing the difference between the observed and synthetic waveforms using the non-negative least-squares scheme (Lawson and Hanson 1974). The slip angle is allowed to vary centered at 108˚, which is the rake angle of the F-net analysis. We impose a spatiotemporal smoothing constraint on slips (Sekiguchi et al. 2000).

Green's functions are calculated using the discrete wavenumber method (Bouchon 1981) and the reflection/transmission matrix method (Kennett and Kerry 1979) assuming 1-D velocity structure models. The structure models are obtained for each station from the 3-D structure model (Fujiwara et al. 2009). Logging information is also used for the KiK-net station. To consider the rupture propagation effect, 25 point-sources are uniformly distributed over each subfault in the calculation of Green’ s functions.

In the estimated source model, large slips are found south-west of the hypocenter and partly overlap the active-aftershock area. In the first 5 s, the rupture slowly grew around the hypocenter with small slips. Then, the rupture developed with the large moment release between 5 s and 10 s in the large slip area.

Keywords: The 2021 off Fukushima earthquake, Source process, Strong motion, Intraslab earthquake

©2021. Japan Geoscience Union. All Right Reserved.

©2021. Japan Geoscience Union. All Right Reserved.

Strong motion characteristics at MYGH10 (KiK-net), Yamamoto, during the Off Fukushima pref. earthquake of 13th Feb., 2021

*Tomotaka Iwata[1]

1. Disaster Prevention Research Institute, Kyoto University

We estimate ground motion characteristics of MYGH10 (KiK-net Yamamoto), south of Miyagi pref., during the 2021 Feb. 13th Off Fukushima Pref. earthquake (MJ7.3). The JMA seismic intensity of 6+ was estimated at this site. As this site is a KiK-net site, they have geological and velocity profile up to the downhole station whose depth is 208m. The superficial layer above the engineering bedrock is a cray one with 3.5m thickness and whose average S-wave velocity is about 150m/s. The predominant frequency of the observed horizontal accelerations at the surface station and those of the spectral ratio between the surface and the downhole is about 10Hz, during the weak motions, which is consistent with the predominant frequency of the superficial layer.

Nakano et al. (2019) separated the source, propagation-path, and site effects from strong motion data set and the predominant frequency of MYGH10 is about 10Hz for the weak motion S-waves. That is consistent to our results. On the contrary, during the mainshock, as the peak acceleration was 1,492cm/s/s (three comp. vectorial summation), the predominant frequency was about 4Hz. This would indicate the non-linear behavior of the superficial layer during the strong shaking. Those characteristics are similar to those at Nagomi site (Iwata et al., 2019).

Noguchi et al. (2016) analyzed the soil response recovery process at this site between 2007 and 2013 event data and pointed out that this kind of non-linear behavior occurs repeatedly during strong shakings and after the strong shaking the weak responses were stable. This paper will discuss the effect of non-linear response of the superficial layer on seismic intensity.

Acknowledgements

I used KiK-net strong motion data (NIED, 2019; doi:10.17598/NIED.0004).

References

Iwata et al. (2019) JpGU abstract, SSS11-P05.

Nakano et al. (2019) https://doi.org/10.5610/jaee.19.2_1 (in Japanese)

Noguchi et al. (2016) https://doi.org/10.5610/jaee.16.4_93 (in Japanese)

Keywords: the Off Fukushima pref. earthquake of 13th Feb., 2021, non-linear response of the superficial layer, KiK-net

©2021. Japan Geoscience Union. All Right Reserved.

©2021. Japan Geoscience Union. All Right Reserved.

[J] Poster | S (Solid Earth Sciences)：S-SS Seismology

Sun. Jun 6, 2021 5:15 PM - 6:30 PM JST | Sun. Jun 6, 2021 8:15 AM - 9:30 AM UTC | Ch.10_2

[S-SS11] Strong Ground Motion and Earthquake Disaster

convener:Kazuhiro Somei(Geo-Research Institute), Yasuhiro Matsumoto(Kozo Keikaku Engineering)

Strong ground motion has social impacts as it induces earthquake disasters. We solicit contribution on any seismological topics related to strong ground motion that includes, but are not limited to, source processes, wave propagation, and site effects. We also welcome contribution on earthquake related disaster mitigation.

[SSS11-P01] Elasto-plastic soil-water coupling seismic response analysis of a sedimentary basin with a three-dimensional geometry

*Toshihiro Noda[1], Tomohiro Toyoda[1], Shuhei Iwai[2], Akira Asaoka[3] (1.Disaster Mitigation Research Center, Nagoya University, 2.Graduate School of Engineering, Nagoya University, 3.Association for the Development of Earthquake Prediction)

[SSS11-P02] Identification of potential problems for disaster mitigation using “the Nankai Trough Earthquake Extra Information”, a new Japanese earthquake forecast information -how to communicate the "uncertainty" of science to society-

*Sayaka Irie[1], Ryu Ohtani[2], Mamoru Hyodo[3], Yoshinari Hayashi[4], Manabu Hashimoto[5], Takane Hori[6], Nobumasa Kawabata[7], Kunihiko Kumamoto[8], Takayoshi Iwata[9], Takashi Yokota[10], Kazunori Tanihara[11], Yo Fukushima[12] (1.NHK Broadcasting Culture Research Institute , 2.National Institute of Advanced Industrial Science and Technology, 3.Osaka Regional Headquarters, Japan Meteorological Agency, 4.Kansai University, 5.Disaster Prevention Research Institute, Kyoto University (DPRI), 6. Japan Agency for Marine-Earth Science and Technology (JAMSTEC) , 7.Crisis and Environment Management Policy Institute(CeMI), 8.Edogawa University, 9.Center for Integrated Research and Education of Natural Hazards,Shizuoka University, 10.Disaster Prevention Research Center,Aichi Institute of Technology, 11.Nippon Television Network, 12.International Research Institute of Disaster Science,Tohoku University, (IRIDeS))

[SSS11-P03] Research Project for Disaster Prevention on the great Earthquakes along the Nankai trough

*Shuichi Kodaira[1], Hiroyuki Fujiwara[2], Narumi Takahashi[1,2] (1. Japan Agency for Marine-Earth Science and Technology, 2.National Research Institute for Earth Science and Disaster Resilience)

[SSS11-P04] Formulas for using simple array to determine Love-wave characteristics based on rotational component of microtremors

*Ikuo Cho[1], Kunikazu Yoshida[2], Hirotoshi Uebayashi[3] (1.National Institute of Advanced Industrial Science and Technology, 2.Geo-Research Institute, 3.Institute for Integrated Radiation and Nuclear Science, Kyoto University)

[SSS11-P05] Assessment of applicability of a proposed method to estimate phase velocity using arbitrary 5-site arrays

*Huan Zhang[1], Kahori Iiyama[2], Hitoshi Morikawa[1] (1.Department of Civil and Environmental Engineering, Tokyo Institute of Technology, 2.KAJIMA Technical Research Institute)

[SSS11-P06] Comprehensive Research Project for the Nara-bonchi-toen Fault Zone

*Tomotaka Iwata[1] (1.Disaster Prevention Research Institute, Kyoto University)

[SSS11-P07] Small-aperture Microtremor Array Surveys in the Nara Basin, Japan

*Kimiyuki Asano[1], Tomotaka Iwata[1], Haruko Sekiguchi[1] (1.Disaster Prevention Research Institute, Kyoto University)

[SSS11-P08] Dense Microtremor Surveys on the Eastern Part of the Nara Basin, Japan

*Masayuki Yoshimi[1], Kimiyuki Asano[2], Tomotaka Iwata[2], Hiro Nimiya[1], Takeshi Sugiyama (1.Geological Survey of Japan, AIST, 2.DPRI, Kyoto Univ.)

[SSS11-P09] Microtremor characteristics and subsurface structure in the vicinity of the Shikano-Yoshioka Fault, Tottori, Japan

*Tatsuya Noguchi[1], Kazuki Kobayashi[2], Ryo Ashida[1], Isamu Nishimura[3], Takao Kagawa[1] (1.Faculty of Engineering, Tottori University, 2.Graduate School of Sustainability Science, Tottori University, 3.Graduate School of Engineering, Tottori University)

[SSS11-P10] Determination of 3-D subsurface structure model in central Tottori, Japan

*Tatsuya Noguchi[1], Masaki Yamamuro[1], Isamu Nishimura[2], Takao Kagawa[1] (1.Faculty of Engineering, Tottori University, 2.Graduate School of Engineering, Tottori University)

[SSS11-P11] Estimation of Subsurface Structure and Ground Motion Characteristics in the Landslide Areas from Microtremor Observations – Case of Nawashiro and Amedaki, Kokufu-cho, Tottori City –

*Isamu Nishimura[1], Atsushi Shimada[2], Tatsuya Noguchi[2], Takao Kagawa[2] (1.Graduate School of Engineering Department of Social Infrastructure Engineering, Tottori University, 2.Social Systems and Civil Engineering, Department of Engineering, Tottori University)

[SSS11-P12] Modeling of subsurface velocity structures from seismic bedrock to ground surface for Yamanashi region

*Shigeki Senna[1], Atsushi Wakai[1], Yatagai Atsushi[2], Tadashi Sato[2], Hisanori Matsuyama[2], Hiroyuki Fujiwara[1] (1.National Research Institute for Earth Science and Disaster Resilience, 2.OYO Corporation)

[SSS11-P13] Modeling of subsurface velocity structures from seismic bedrock to ground surface for Kumamoto region

*Shigeki Senna[1], Atsushi Wakai[1], Yatagai Atsushi[2], Yoshiaki Inagaki[2], Hisanori Matsuyama[2], Hiroyuki Fujiwara[1] (1.National Research Institute for Earth Science and Disaster Resilience, 2.OYO Corporation)

[SSS11-P14] Basic study of a real-time damage estimation system for liquefaction

*Shohei Naito[1], Hiromitsu Nakamura[1], Shigeki Senna[1], Yoshinori Iwanami[2] (1.National Research Institute for Earth Science and Disaster Resilience, 2.MITSUBISHI SPACE SOFTWARE CO.,LTD.)

[SSS11-P15] Estimation of subsurface motion from surface seismic records: investigation on evaluation at deep levels

*Tomotsugu Watanabe[1], Hiroshi Takenaka[1], Masanao Komatsu[1], Mitsutaka Oshima[2] (1.Okayama University , 2.Shimizu Corporation)

[SSS11-P16] Estimation of seismic ground motions on the surface ground at MeSO-net stations

*Atsushi Wakai[1], Shigeki Senna[1] (1.National Research Institute for Earth Science and Disaster Resilience)

[SSS11-P17] Strong motion simulation of an intraslab earthquake beneath Kanto region using MeSO-net observation data

*Wataru Suzuki[1], Takeshi Kimura[1], Hisahiko Kubo[1], Takayuki Miyoshi[1] (1.National Research Institute for Earth Science and Disaster Resilience)

[SSS11-P18] Ground-motion simulation for the 2016 Kumamoto earthquake (Mj7.3) based on the strong-motion prediction recipe

*Asako Iwaki[1], Nobuyuki Morikawa[1], Takahiro Maeda[1], Hiroyuki Fujiwara[1] (1.National Research Institute for Earth Science and Disaster Prevention)

[SSS11-P19] Characterized source model of M7.3 2016 Kumamoto eq. by 3D reciprocity GFs inversion with special reference to velocity pulse at KMMH16

*Anatoly Petukhin[1], Hiroshi Kawase[2], Fumiaki Nagashima[2], Eri Ito[2] (1.Geo-Research Institute, 2.DPRI, Kyoto University)

[SSS11-P20] Evaluation of near-source ground motion during the 2008 Iwate-Miyagi Nairiku earthquake by using stochastic slip models and three-dimensional velocity structures

*Takeshi Nakamura[1], Masataka Sawada[1] (1.Central Research Institute of Electric Power Industry)

[SSS11-P21] **Source rupture process of the 2018 Hokkaido eastern Iburi earthquake estimated from waveform inversion with empirical Green's functions**

*SHUANGLAN WU[1], Atsushi Nozu[1], Yosuke Nagasaka[1] (1.PORT AND AIRPORT RESEARCH INSTITUTE)

[SSS11-P22] Calibrating Thailand's local magnitude scale: a preliminary result

*Mongkolchai Sukmee[1], Sutthipong Noisagool[1,2], Satoru Tanaka[3], Weerachai Siripunvaraporn[1,2], Songkhun Boonchaisuk[4,2], Yasushi Ishihara[5], Taewoon Kim[6], Hitoshi Kawakatsu[7], Nozomu Takeuchi[7], Kenji Kawai[8], Yuki Suzuki[8] (1.Department of Physics, Faculty of Science, Mahidol University , 2.Thailand Center of Excellence in Physics, Ministry of Higher Education, Science, Research and Innovation, 3.Volcanoes and Earth's Interior Research Center (VERC), Research Institute for Marine Geodynamics (IMG), Japan Agency for Marine-Earth Science and Technology (JAMSTEC), 4.Geoscience Program, Mahidol University, Kanchanaburi Campus, 5.Research Institute for Marine Geodynamics (IMG), Japan Agency for Marine-Earth Science and Technology (JAMSTEC), 6.Subduction Dynamics Research Center (SDR), Research Institute for Marine Geodynamics (IMG), Japan Agency for Marine-Earth Science and Technology (JAMSTEC), 7.Earthquake Research Institute, The University of Tokyo, 8.Department of Earth and Planetary Science, School of Science, The University of Tokyo)

[SSS11-P23] Strong ground motion simulation of the Fukushima-ken Oki earthquake of February 13, 2021 (M_J 7.3)

*Yosuke Nagasaka[1] (1.Port and Airport Research Institute)

[SSS11-P24] Strong Motion Generation Area for the 2021 off Fukushima, Japan, Earthquake Estimated based on the Empirical Green's Function Method

*Kazuhiro Somei[1], Ken Miyakoshi[1] (1.Geo-Research Institute)

Elasto-plastic soil-water coupling seismic response analysis of a sedimentary basin with a three-dimensional geometry

*Toshihiro Noda[1], Tomohiro Toyoda[1], Shuhei Iwai[2], Akira Asaoka[3]

1. Disaster Mitigation Research Center, Nagoya University, 2. Graduate School of Engineering, Nagoya University, 3. Association for the Development of Earthquake Prediction

The seismic wave propagation is strongly affected by the ground non-uniformity. Especially in the sedimentary basin, the amplification in the sedimentary layer, the lens effect, and the edge effect due to the interference of the surface wave generated at the edge of the basin cause the strong ground motion. In this abstract, we conducted a single-phase elastic/two-phase (i.e., soil-water coupled) elasto-plastic seismic response analysis for the three-dimensional spherical basin shown in Table 1(d) and investigated the effects of three-dimensional structures, elasto-plasticity, and the presence of pore water.
First, a single-phase elastic analysis was performed on the three-dimensional mesh (conformed to Miyamoto et al.[1]) shown in Fig. 1. The analysis was conducted with the analysis code ***GEOASIA***[2] developed by the authors. Assuming a plane strain shear box test, the displacement of the front and back surfaces in *y*-direction was fixed and the periodic boundary was imposed on the left and right surfaces. At the bottom of the model, the vertical displacement was fixed and the viscous boundary condition was imposed in the horizontal direction. The EW component of the Kobe wave shown in Fig. 2 was applied in the *x*-direction as an input wave. As for the elastic material constants, we considered a clear rigidity contrast (11.4 times in the impedance ratio) between the sedimentary layer and the bedrock. As an analysis result, we confirmed the initial emergence of the ring-shaped strain concentration (Fig. 3), the occurrence of the three-dimensional waves and its long-term retention (Fig. 4).
Next, we compared the three-dimensional result with the reduced-dimensional model shown in Table 1(a)-(c) for evaluating the effect of the three-dimensionality of the sedimentary basin. Figure 5 shows the horizontal response on the ground surface at the center of the basin. As indicated in the figure, all reduced models underestimated the maximum acceleration and the residence time of seismic motion. The result suggests the limitation of the evaluation by the reduced-dimensional model. As for the spectral characteristics, the transfer function of the sedimentary layer at the center of the basin in the three-dimensional case in Fig. 6(d) indicated the amplification in the various frequency range, whereas the one-dimensional calculation in (a) just exhibited the theoretical solution.
Moreover, we conducted the two-phase elasto-plastic analysis. The SYS Cam-clay model [3] was used as the elasto-plastic constitutive equation. The typical parameters for consolidated rock and loose sand were assumed for the bedrock and the sedimentary layer, respectively. The analysis results for 1/10 amplitude of the Kobe wave indicated the decrease of the effective stress (liquefaction) in Fig. 7 and the sloshing behavior of the entire sedimentary layer in Fig. 8. The occurrence of liquefaction could also be confirmed in Fig. 9. Furthermore, the running transfer function in Fig. 10 indicated that the liquefaction reduced the transfer of the shear wave in the sedimentary layer.
(Acknowledgement) Numerical simulations were conducted by utilizing a supercomputer system in Kyoto University, Japan. And we received Grant-in-Aid for Scientific Research (Grant-in-Aid for Scientific Research (A): No. 17H01289).
[1] Miyamoto, T., Irihara, W., Suzuki, T., Fujita, K. and Ichimura, T. (2016): Analysis of strain concentration in alluvium using three dimensional nonlinear seismic ground response analysis (in Japanese), Proc. of JSCE, Vol.72, No.4, I_768-I_776.
[2] Asaoka, A., Noda, T., Yamada, E., Kaneda, K. and Nakano, M. (2002): An elasto-plastic description of two distinct volume change mechanisms of soils, Soils and Foundations, Vol.42, No.5, pp.47-57.

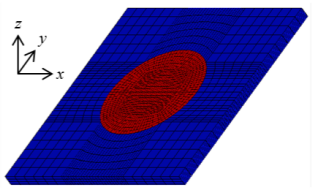
©2021. Japan Geoscience Union. All Right Reserved.

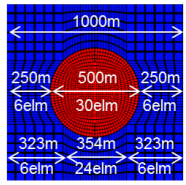
[3] Noda, T., Asaoka, A. and Nakano, M. (2008): Soil-water coupled finite deformation analysis based on a rate-type equation of motion incorporating the SYS Cam-clay model, Soils and Foundations, Vol.48, No.6, pp.771-790.

Keywords: Sedimentary basin, Seismic response analysis, Elasto-plasticity, Soil-water coupling, Three-dimensional

Table 1. Cases of the numerical simulation

Case	(a)	(b)	(c)	(d)
Model	1D	2D	2D	3D
Shear wave	Considered	Considered	Considered	Considered
Amplification	Considered	Considered	Considered	Considered
Reflection	Considered	Considered	Considered	Considered
Refraction	–	Considered	Considered	Considered
Rayleigh wave	–	Considered	–	Considered
Love wave	–	–	Considered	Considered





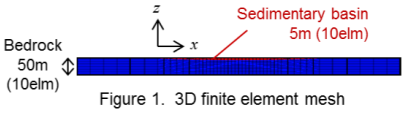


Figure 1. 3D finite element mesh

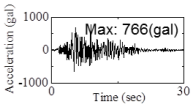


Figure 2. Input wave

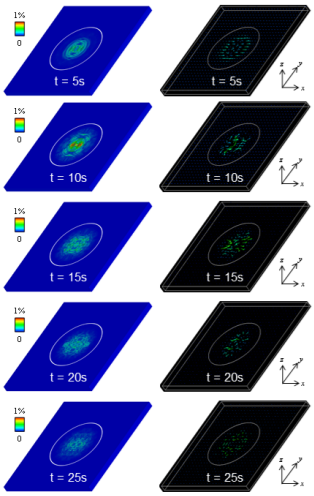


Figure 3. Shear strain (elastic)

Figure 4. Velocity (elastic)

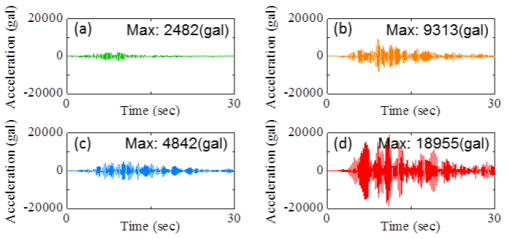


Figure 5 Surface acceleration in x-direction (elastic)

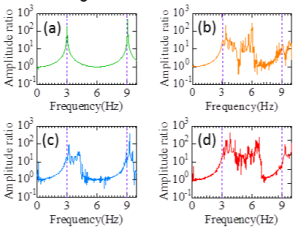


Figure 6 Transfer function of sedimentary basin in x-direction (elastic)

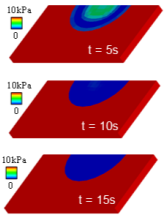


Figure 7. Mean effective stress (elasto-plastic)

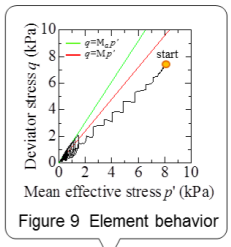


Figure 9 Element behavior

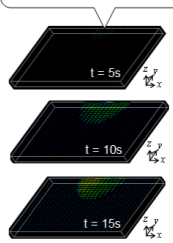


Figure 8. Veloity (elasto-plastic)

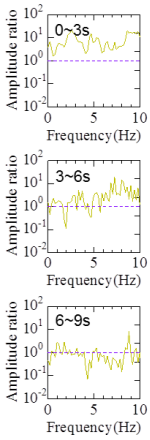


Figure 10. Transfer function (elasto-plastic)

©2021. Japan Geoscience Union. All Right Reserved.

Identification of potential problems for disaster mitigation using “the Nankai Trough Earthquake Extra Information”, a new Japanese earthquake forecast information -how to communicate the "uncertainty" of science to society-

*Sayaka Irie[1], Ryu Ohtani[2], Mamoru Hyodo[3], Yoshinari Hayashi[4], Manabu Hashimoto[5], Takane Hori[6], Nobumasa Kawabata[7], Kunihiko Kumamoto[8], Takayoshi Iwata[9], Takashi Yokota[10], Kazunori Tanihara[11], Yo Fukushima[12]

1. NHK Broadcasting Culture Research Institute , 2. National Institute of Advanced Industrial Science and Technology, 3. Osaka Regional Headquarters, Japan Meteorological Agency, 4. Kansai University, 5. Disaster Prevention Research Institute, Kyoto University (DPRI), 6. Japan Agency for Marine-Earth Science and Technology (JAMSTEC) , 7. Crisis and Environment Management Policy Institute(CeMI), 8. Edogawa University, 9. Center for Integrated Research and Education of Natural Hazards,Shizuoka University, 10. Disaster Prevention Research Center,Aichi Institute of Technology, 11. Nippon Television Network, 12. International Research Institute of Disaster Science,Tohoku University, (IRIDeS)

In 2017, the Japanese government introduced a new earthquake forecast information. When unusual seismic activity or crustal movements are observed around the Nankai trough extending from off the coast of central to the southwest Japanese Islands, the government will issue “the Nankai Trough Earthquake Extra Information” to let people prepare for the massive earthquake. However, with current seismological knowledge, it is difficult to accurately predict the time and magnitude of earthquakes. Therefore, while the information is expected to contribute to disaster mitigation, the information could also cause social disruption. The purpose of this research project is to identify the potential problems (or side effects) the information could bring to society through interdisciplinary collaboration among seismologists, disaster information studies researchers, and journalists. To this end, we apply a scenario method to construct a hypothetical scenario that describes how and when anomalous crustal deformation signals are observed, the information is issued by the government, and disseminated by TV media. Then, the scenario is displayed at scenario workshops where local stakeholders such as municipal officers and local residents discuss how they respond to the information to explore what kind of potential problems could arise. In this presentation, several findings will be introduced.

Keywords: Nankai Trough Earthquake, Nankai Trough Earthquake Extra Information, uncertainty, disaster information

©2021. Japan Geoscience Union. All Right Reserved.

Research Project for Disaster Prevention on the great Earthquakes along the Nankai trough

*Shuichi Kodaira[1], Hiroyuki Fujiwara[2], Narumi Takahashi[1,2]

1. Japan Agency for Marine-Earth Science and Technology, 2. National Research Institute for Earth Science and Disaster Resilience

In the Nankai Trough, where a future great earthquake would cause a national-scale crisis, recent research results revealed diversity and complexity of earthquake occurrence and slip behavior of the earthquake fault. To prepare for such a great earthquake in the Nankai Trough, this project aims to develop a system to rapidly and accurately evaluate crustal activities and distribute information on the current status of the Nankai Trough, including unusual slip behavior which has never observed previously, based on the latest scientific knowledge and data. Also, to maximize the use of the information, this project will investigate how local governments, communities, industries, etc., should take actions for hazard mitigation, particularly when unusual slip behavior is observed. Furthermore, in cooperation with local governments and other organizations, this project conducts a quantitative evaluation of how this project's research results have contributed to the improvement of hazard mitigation and identify practical research and development items for hazard mitigation plans. To achieve these goals, this project has the following three sub-themes. Generation and distribution of information on crustal activity: In this sub-theme, we construct an integrated 3D model of the Nankai Trough seismogenic zone and develop a system to rapidly process observed earthquake data to for evaluating crustal activities in the Nankai Trough by using the 3D model. We will also reanalyze the past observed data to understand the various seismic activities of the Nankai Trough earthquakes. Generation and distribution of information for hazard mitigation: In this sub-theme, we create an information infrastructure for disaster mitigation of earthquake and tsunami hazards and risks by incorporating a time evolution after a large earthquake or unusual slip behavior is observed. In addition, this sub-theme conducts a comprehensive research for "protecting lives," "protecting regional industrial activities," and "protecting metropolitan functions" by maximizing the use of disaster mitigation information. Hazard mitigation and risk communication: To improve knowledge and skill to use earthquake hazard information, we explore how to effectively use the latest information and knowledge about the earthquake hazard at each stage of pre-, during, and post-disaster response. For this purpose, we examine how to disseminate information to utilize the research results for disaster prevention and mitigation in communities and businesses.

Keywords: Nankai Trough, Earthquake Tsunami, Disaster resilience

©2021. Japan Geoscience Union. All Right Reserved.

Formulas for using simple array to determine Love-wave characteristics based on rotational component of microtremors

*Ikuo Cho[1], Kunikazu Yoshida[2], Hirotoshi Uebayashi[3]

1. National Institute of Advanced Industrial Science and Technology, 2. Geo-Research Institute, 3. Institute for Integrated Radiation and Nuclear Science, Kyoto University

Yoshida & Uebayashi (2018, 2020) demonstrated the effectiveness of using a rotational component (i.e., using spatial derivatives) in determining phase velocities of Love waves. Their method is based on a double triangular microtremor array. In this study, we present formulas to determine Love-wave characteristics using a rotational component based on a three-point array.

Cho et al. (2006) developed a general theory to analyze circular-array data of three-component microtremors. The titled formulation begins with equations (16) and (17) of their paper. These are equations representing the radial- and tangential-component waveforms recorded with a three-component seismometer located at (r, θ), where r is the distance from the origin and θ is the azimuthal angle from the x-axis to the y-axis. Taking the divergence and rotation of these waveforms, we can obtain

$D(t, r, \theta) = -\int\int\int ik \exp[-i\omega t - ikr\cos(\phi - \theta)] \zeta^{R}(d\omega, dk, d\phi)$, (divergent component) (1)

$C(t, r, \theta) = -\int\int\int ik \exp[-i\omega t - ikr\cos(\phi - \theta)] \zeta^{L}(d\omega, dk, d\phi)$, (rotational component) (2)

where t is time, i is the imaginary unit, k is the wavenumber, ω is the angular frequency, and ϕ is a wave arriving direction. We set r and θ to 0 in the above divergent- and rotational-component waveforms (D and C, respectively). Taking autocorrelation functions and then taking Fourier transforms yields

$PSD^{R}(\omega) = [c^{R}(\omega)]^{2} PSD^{D}(\omega)/\omega^{2}$, (3), $PSD^{L}(\omega) = [c^{L}(\omega)]^{2} PSD^{C}(\omega)/\omega^{2}$, (4)

where $PSD^{R}(\omega)$ and $PSD^{L}(\omega)$ is the power spectral densities (PSDs) for integrated spectra $\zeta^{R}(d\omega, dk, d\phi)$ and $\zeta^{L}(d\omega, dk, d\phi)$, respectively. $c^{R}(\omega)$ and $c^{L}(\omega)$ are the phase velocities of Rayleigh and Love waves, respectively.Taking the sum of equations (3) and (4), we obtain

$PSD^{R}(\omega) + PSD^{L}(\omega) = [c^{R}(\omega)]^{2} PSD^{D}(\omega)/\omega^{2} + [c^{L}(\omega)]^{2} PSD^{C}(\omega)/\omega^{2}$. (5)

We define the total powers of the horizontal components, $PSD^{H}(\omega)$, as the sum of the PSDs for Rayleigh and Love waves. i.e.,

$PSD^{H}(\omega) = PSD^{R}(\omega) + PSD^{L}(\omega)$. (6)

By the use of equations (5) and (6), we have

$c^{L}(\omega) = [(PSD^{H}(\omega)\omega^{2} - PSD^{D}(\omega)[c^{R}(\omega)]^{2})/PSD^{C}(\omega)]^{1/2}$. (7)

The use of equation (7) assumes that the observation of three-component microtremors was conducted using a triangular (three-point) array. On the right-hand side of equation (7), the phase velocity of

©2021. Japan Geoscience Union. All Right Reserved.

Rayleigh waves, $c^R(\omega)$, is obtained by applying the SPAC method to the vertical-component data from a three-point array, and $PSD^C(\omega)$ and $PSD^D(\omega)$ are obtained by processing two horizontal components of the three-point array (YU2020). $PSD^H(\omega)$ can be obtained from the two horizontal components at a single point (i.e., the sum of the PSDs for either the radial and tangential components or the east-west and north-south components). Therefore, the Love-wave phase velocity is obtained from a three-component three-point array. Once $c^L(\omega)$ is obtained, R/L (Amplitude ratio of Rayleigh to Love waves) of Arai and Tokimatsu (2004) can be obtained using equations (3) and (4). Alternatively, since $c^R(\omega)$ is already obtained, we can obtain the H/V ratio of Rayleigh waves via equation (3). It may be more convenient to use this quantity to model a velocity structure than to use R/L, as the calculation of theoretical values for a fitting becomes simple.

This research was supported by the Japan Society for the Promotion of Science (JSPS) KAKENHI Grant Numbers 19H02287.

Arai & Tokimatsu, 2004. *Bull. Seismol. Soc. Am.*, **94**, 53–63.
Cho, Tada, & Shinozaki, 2006. *Geophys. J. Int.,* **165**, 236–258.
Yoshida & Uebayashi, 2020. *Bull. Seismol. Soc. Am.,* doi://10.1785/0120200139.
Yoshida & Uebayashi, 2018. BUTSURI-TANSA, **71**, 15-23. (in Japanese)

Keywords: microtremor, Love wave , array, rotational component, spatial differentiation, phase velocity

©2021. Japan Geoscience Union. All Right Reserved.

Assessment of applicability of a proposed method to estimate phase velocity using arbitrary 5-site arrays

*Huan Zhang[1], Kahori Iiyama[2], Hitoshi Morikawa[1]

1. Department of Civil and Environmental Engineering, Tokyo Institute of Technology, 2. KAJIMA Technical Research Institute

To estimate earthquake ground motion, it’s necessary to model the ground structure. Then the use of array method was proposed by using microtremors because it’s an inexpensive and mobile means of estimating the phase velocity of surface waves. Based on the analytical solution of Lamb's problem for vertical components of Rayleigh wave, the relationship between two observation points, p and q for example, is given in a discrete representation with the Bessel function of the first kind and higher-order Bessel functions, which is called Complex Coherence Function (CCF) [4]. Zhang and Morikawa [5] extended the CCF to apply it to linear array situation. By adding an extra observation point s, the relationship between p and s can be expressed [6]. At last, the CCF equations have only 5 unknowns left, including the phase velocity. Therefore, we proposed a method [7] to estimate the phase velocity using Artificial Bee Colony (ABC) algorithm [8] under a constraint of kr belongs to [0, 5]. The selection of the constraint condition will affect the results and will be discussed.

The numerical simulations and the site observations’ results confirmed the availability of the proposed algorithm for array shapes with more free arrangement of sensors. When it comes to selecting the constraint condition, constraint condition is a better choice for most 3-site arrays if we expect a wider effective range. For 4-site arrays, we think acceptable results can be obtained with no constraint condition. After comparing with 4-site arrays without constraint condition and related 3-site arrays under r_{ave} constraint condition, we can see that the 4-site arrays' results are influenced by all of the 3-site arrays it contains, meaning that it might not be better than all of the 3-site arrays' results, especially the small regular 3-site array. However, they are better than most of other 3-site arrays which have irregular shapes.

Based on this method, we think the application to more-sites arrays, 5-site arrays for example, can further improve the results. If 5-site arrays were chosen, the 5 unknowns will remain the same but there will be 10 CCFs. On the other hand, since there will be 10 CCFs, we can extend the CCF’s application range and thus there will be 2 more unknowns, for example. In that case, the unknowns are still less than the CCFs and the constraint range, kr belongs to [0, 5], can be wider, too. However, similarly as 4-site arrays, adding more sites will inevitably extend the optimization time. And optimizing one phase velocity result to satisfy all of the CCF equations together will leave the result influenced by all of the CCFs. Still, numerical simulations and the application to ZRS field data using more-sites arrays, 5-site arrays for example, will be conducted to testify the validity of the proposed assumption. And comparisons with conventional methods will be conducted at the same time.

[1] Capon, J. (1969). *Proceedings of the IEEE*, 57(8), 1408-1418.
[2] Aki, K. (1957). *Bull. Earthq. Res. Inst.*, 35, 415-456.
[3] Cho, I., Tada, T., & Shinozaki, Y. (2006). *Journal of Geophysical Research: Solid Earth*, 111(B9).
[4] Shiraishi, H. & Matsuoka, T. (2005). *BUTSURI-TANSA,* 58(2), 137-146.
[5] Zhang, X. & Morikawa, H. (2014). *British Journal of Applied Science & Technology*, 6(4), 350–363.
[6] Morikawa, H. & Iiyama, K. (2015). *Program and Abstracts, The Seismological Society of Japan, Fall Meeting.*

©2021. Japan Geoscience Union. All Right Reserved.

[7] Zhang, H., Iiyama, K. & Morikawa, H. (2020). *17th World Conference on Earthquake Engineering.*
[8] Karaboga, D. & Basturk, B. (2007). *Journal of global optimization*, 39(3), 459-471.

Keywords: Arbitrary-shape array, phase velocity, Complex Coherence Function (CCF), Centerless Circular Array (CCA) method, Spatial Auto-correlation (SPAC) method, Artificial Bee Colony (ABC) algorithm

©2021. Japan Geoscience Union. All Right Reserved.

Comprehensive Research Project for the Nara-bonchi-toen Fault Zone

*Tomotaka Iwata[1]

1. Disaster Prevention Research Institute, Kyoto University

The Nara-bonchi-toen fault zone is south part of Kyoto and Nara basin faults, eastern margin of the Kyoto and Nara basins. Our research group has started to study this active fault zone in detail to get the information for developing the long-term earthquake evaluation and the strong ground motion prediction in 2019-2021FY.
This research group conducts an integrated research on long-term evaluation of earthquake occurrence of the active faults (Sub-theme 1), seismic activity and crustal structure (Sub-theme 2), strong ground motion prediction (Sub-theme 3) and outreach (Sub-theme 4). In 2019FY, Sub-theme 1 conducted to prepare the DEMs in this fault area, field surveys for trench site and height distribution of the basement of the Osaka group in the target area. Sub-theme 2 started the temporal seismic observations for obtaining the stress field in this area, and field surveys to obtain the characteristics of the micro faults. They also conducted the microtremor array observations with the member of Sub-theme 3. Sub-theme 3 conducted the seismic reflection surveys in the south Kyoto and the north Nara basins so as to image the basin and basin-basement structures. They also collected the geological boring well-logs and conducted microtremor array observations. Sub-theme 4 hosted a study group meeting on earthquake hazards in this area, that consists of the researchers, risk management members of local governments and companies in this area. We also show new findings in 2020FY and a research plan in 2021FY.

Keywords: Nara-bonchi-toen Fault Zone, long-term earthquake evaluation of active faults, strong ground motion prediction

©2021. Japan Geoscience Union. All Right Reserved.

Small-aperture Microtremor Array Surveys in the Nara Basin, Japan

*Kimiyuki Asano[1], Tomotaka Iwata[1], Haruko Sekiguchi[1]

1. Disaster Prevention Research Institute, Kyoto University

The Nara-Bonchi-Toen Fault Zone forms the eastern margin of the Kyoto and Nara basins, Japan. The Nara basin is mostly filled by the lower and lowermost parts of the Plio-Pleistocene Osaka Group. Alluvial and terrace deposits distributed over the Osaka Group inside the basin. Improvement on the velocity structure model from the superficial alluvial deposits to the seismic bedrock is quite important for advancing strong motion prediction for future earthquakes from nearby source faults. As a part of Comprehensive Research Project for the Nara-Bonchi-Toen Fault Zone funded by the Ministry of Education, Culture, Sports, Science and Technology (MEXT), Japan, we have carried out various kind of geophysical surveys to investigate the velocity structure in the Kyoto and Nara basins. Miniature to small aperture microtremor array surveys were carried out at 60 sites in the southern part of the Kyoto prefecture from Aug. 2019 to Mar. 2020 to obtain information on S-wave velocity of shallow subsurface sedimentary layers (Asano *et al.*, 2020). The surveyed area is extended to the whole part of the Nara basin in 2020. The total number of surveyed sites is 140 as of Jan. 29, 2021 (Fig. 1), and the field work is still undergoing to cover the whole area of the Nara basin. We will report our results in the Nara basin in this presentation.

We carried out miniature and small equilateral triangle array observations at each measurement. The circumradius is 0.6 m for a miniature array, and the circumradius for a small array depends on site in a range from 5 to 8 m. A portable integrated microtremor observation system HAKUSAN JU410 was installed at each apex of the equilateral triangle and the center of circumscribed circle. The microtremor was recorded continuously more than 15 minutes at a sampling rate of 200 Hz after amplified by 100 times (200V/G).

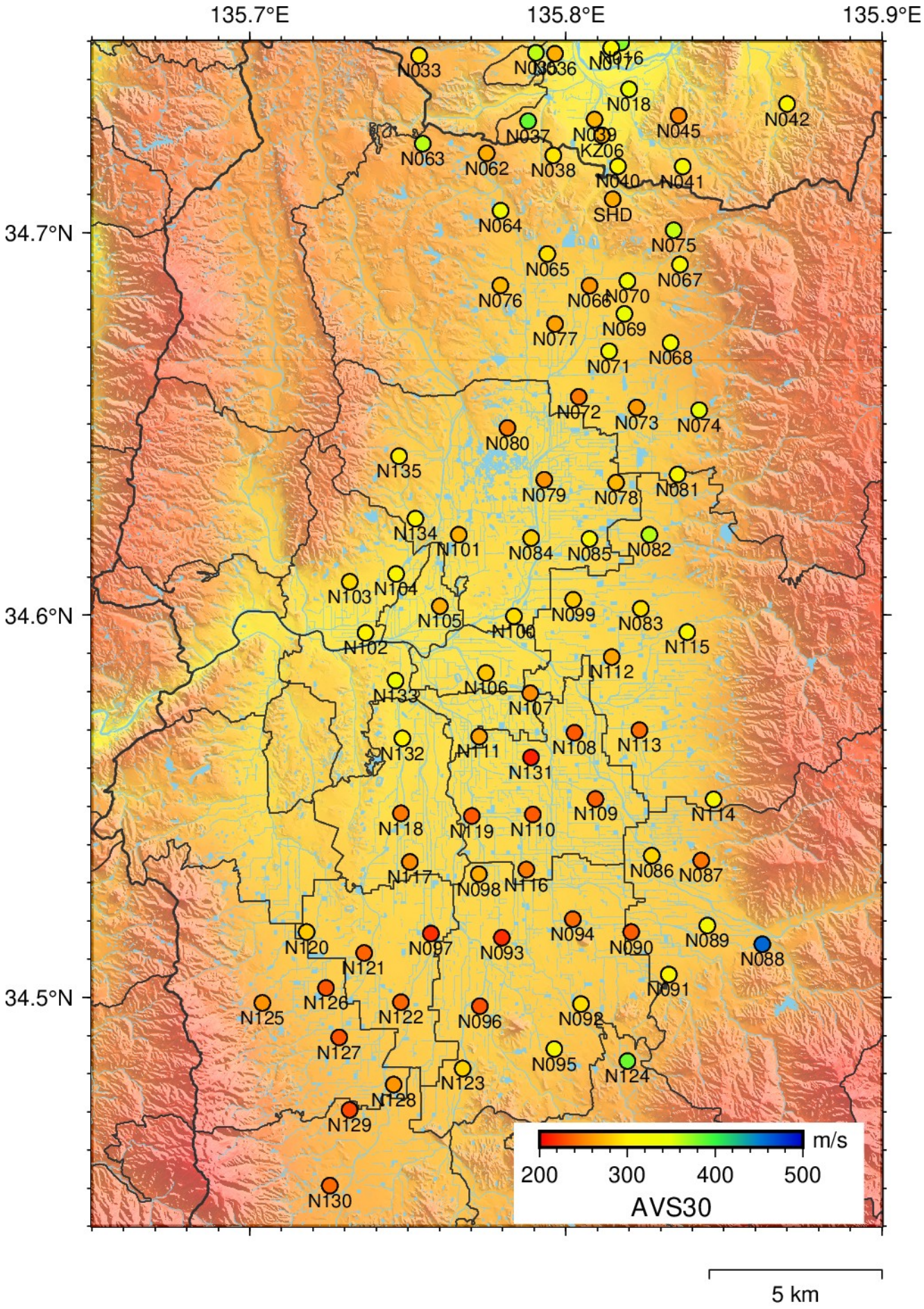
The vertical component of the observed microtremors were analyzed to obtain the spatial autocorrelation (SPAC) coefficients (Aki, 1957). The spatial autocorrelation function was calculated in the frequency domain, and the Fourier spectrum was smoothed by the technique of Konno and Ohmachi (1998). Finally, the phase velocity dispersion curve was estimated by the extended SPAC method (Ling and Okada, 1993; Okada, 2003).

The one-dimensional S-wave velocity structure model for each measurement site was estimated assuming the observed phase velocity dispersion curve as the fundamental mode of the Rayleigh wave using the Markov chain Monte Carlo method. The velocity structure model of deep sedimentary layers and the upper crust was given referring to the existing three-dimensional velocity structure models J-SHISV2 (Fujiwara *et al.*, 2012), and the velocity structure model from the lower crust to upper mantle was given referring to JIVSM (Koketsu *et al.*, 2012). The obtained S-wave velocity structure model will be discussed in terms of the spatial distribution of low-velocity layers with referring to surface geology and boring data information.

Acknowledgement: This work was conducted as a part of Comprehensive Research Project for the Nara-Bonchi-Toen Fault Zone of the Ministry of Education, Culture, Sports, Science and Technology, Japan. We appreciate many residents for cooperation of our survey.

Keywords: Nara Basin, microtremor array survey, velocity structure model

©2021. Japan Geoscience Union. All Right Reserved.



©2021. Japan Geoscience Union. All Right Reserved.

Dense Microtremor Surveys on the Eastern Part of the Nara Basin, Japan

*Masayuki Yoshimi[1], Kimiyuki Asano[2], Tomotaka Iwata[2], Hiro Nimiya[1], Takeshi Sugiyama

1. Geological Survey of Japan, AIST, 2. DPRI, Kyoto Univ.

We are conducting research on the Nara-bonchi-toen Fault Zone (Eastern Marginal Nara Basin Fault Zone). Since the location of these faults have been mainly determined by the topography, it is very important to clarify the depth distribution of the basement rocks to see if there is any depth difference at the fault locations. In this study, we conducted microtremor array surveys and single-point microtremor observations in the Nara Basin to estimate the location of the fault by clarifying depth of the basement. In the Nara Basin, the H/V spectra shows distinct peaks and the peak period changes in accordance with the depth of the basement (e.g., Morikawa et al., 1998). The peak period of the H/V spectrum has been used to develop a 3D velocity structure model of the Nara Basin (Sekiguchi et al., 2019).
Microtremor arrays with a maximum radius of 400 m were observed at five locations on the Narayama hill, two locations in the northern part of Nara City, three locations in the southern part of Nara City, and three locations in the central part of Tenri City. In addition, single-point microtremor observations were conducted at about 300 locations, mainly in the eastern Nara Basin. Six to eight seismometers were used for the single-point microtremor observations, with a spacing of about 100 m to 1 km, and simultaneous observation data of more than 30 minutes were obtained for the application of the two-point SPAC method. The instruments used are all the same, consisting of a three-component velocty-type seismometer (Tokyo Sokushin SE-321, 5V/kine, natural-period 10 seconds) and a data logger (Hakusan LS-8800, GPS time calibration, 24-bit AD conversion). The X direction of the microtremor was set to magnetic north. In addition to the 105 microtremor array stations reported in Yoshimi et al. (2020), we have accumulated more than 600 microtremor data points in total.
In this presentation, we explain the basement depth distribution estimated from the peak period of H/V spectra, along with the basement depth and velocity structure model estimated from the microtremor array. We also show the distribution of the eastern margin fault zone of the Nara Basin illustrated by the basement depth distribution.

Acknowledgments
This research was conducted as part of the "Comprehensive Research Project for the Nara-bonchi-toen Fault Zone" funded by the Ministry of Education, Culture, Sports, Science and Technology (MEXT). We would like to express our gratitude to Nara City, Tenri City, Yamato Koriyama City and local residents for their cooperation in the microtremor array observation.

References
Morikawa, H., Toki, K., Onoe, K., Akamatsu, J., and Takeuchi, T., Estimation of Deep Ground Structure in Northern Nara Basin using Microseism Array Record, 3rd Symposium on Urban Earthquake Hazards, a-26, 143-144, 1998.
Okumura, A., A. Samukawa, T. Sugai, M. Takada, and H. Soma, Comprehensive survey of the fault system at the eastern margin of the Nara Basin, 1996 Summary Report of the Research on Active Faults, Geological Survey of Japan, 51-62, 1997.
Haruko Sekiguchi, K. Asano, and T. Iwata, Three-dimensional velocity structure model of Nara Basin, Jour. Geol. Soc. Japan 125, 715-730, 2019.
M. Yoshimi, K. Asano, T. Iwata, K. Ninomiya, and L. Sugiyama, Microtremor array survey at the eastern

©2021. Japan Geoscience Union. All Right Reserved.

margin of the Nara Basin, JpGU, 2020.

Keywords: H/V spectra, active fault

©2021. Japan Geoscience Union. All Right Reserved.

Microtremor characteristics and subsurface structure in the vicinity of the Shikano-Yoshioka Fault, Tottori, Japan

*Tatsuya Noguchi[1], Kazuki Kobayashi[2], Ryo Ashida[1], Isamu Nishimura[3], Takao Kagawa[1]

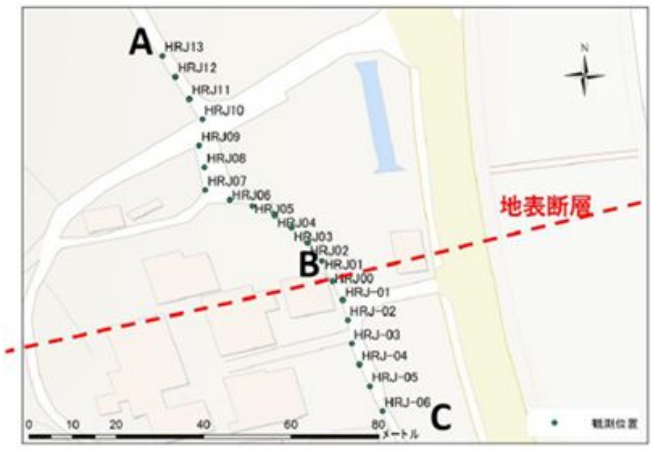
1. Faculty of Engineering, Tottori University, 2. Graduate School of Sustainability Science, Tottori University, 3. Graduate School of Engineering, Tottori University

The Shikano-Yoshioka fault is an earthquake fault that appeared due to the 1943 Tottori earthquake. At both faults, trench surveys, reconnaissance surveys, and interview surveys with residents are conduct-ed as fault displacement surveys. For the ground structure, microtremor exploration and gravity exploration were carried out. In addition, dense microtremor observations were also carried out at and near the fault displacement. However, the difference in ground motion characteristics due to irregularities such as crush zones and step structures due to faults has not been sufficiently investigated.

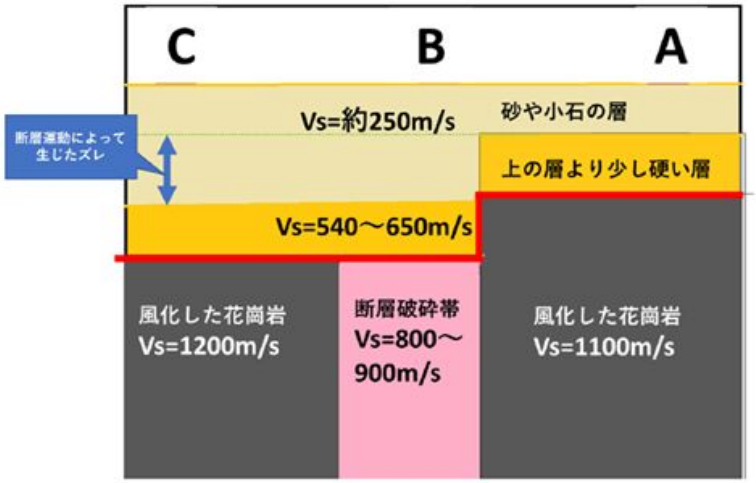
In this study, we grasped the ground motion characteristics in the vicinity of the fault by using the results of dense microtremor observations at the fault displacement location and in the vicinity. As a result, there was a difference in the shape of the microtremor H/V, predominate periods and particle motion of records between the front and the back of the fault displacement point. As the cause of this phenomenon, the correspondence between the results of microtremor observation and underground structure exploration suggests that the crush zone and step structure of the fault are in-volved in the characteristics of microtremor.

Keywords: Shikano-Yoshioka Fault, Microtremor characteristics, subsurface structure

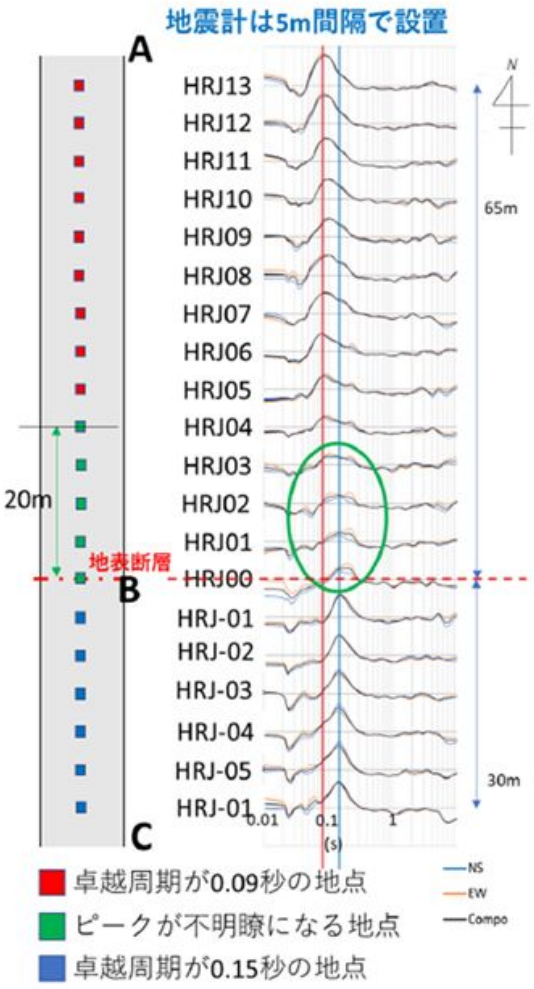
©2021. Japan Geoscience Union. All Right Reserved.



鹿野断層近傍（鹿野町末用地区）の微動観測点



S波反射法による地下構造モデルのイメージ図



微動のH/V

©2021. Japan Geoscience Union. All Right Reserved.

Determination of 3-D subsurface structure model in central Tottori, Japan

*Tatsuya Noguchi[1], Masaki Yamamuro[1], Isamu Nishimura[2], Takao Kagawa[1]

1. Faculty of Engineering, Tottori University, 2. Graduate School of Engineering, Tottori University

In central Tottori prefecture, there was the 2016 earthquake in central Tottori prefecture. This earthquake caused strong ground motion over a wide area and caused damage to buildings. Information on the underground structure is required to examine the causes of damage caused by this earthquake and evaluate the ground motion. In this area, microtremor, gravity observations, and temporary aftershock (strong ground motion) observations were carried out in central Tottori prefecture. Based on these data, an underground structure model has been obtained. In this study, new gravity observations were made mainly in the Hojo area in central Tottori, where many damages occurred. The underground structure was estimated by extending the underground structure model based on microtremor and aftershock observations to a two-dimensional or three-dimensional model using the new and the existing gravity data.

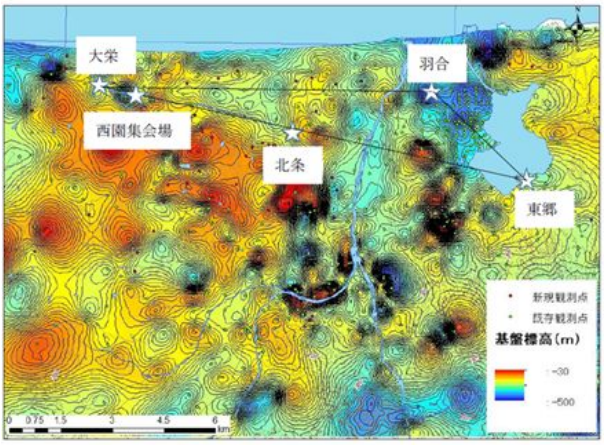
The analysis is as follows. First, a three-dimensional analysis was performed using a two-layer density structure model. The densities of the surface layer and the base layer of the two-layer model were set to 2.2g/cm^3 and 2.5g/cm^3, respectively. 8-seismic observation points with underground velocity structure models and 2-outcrop points of the basement were set as points to determine the depth to the basement. The depth to the basement controlled at the seismic station was the depth to the upper surface of the layer corresponding to Vs = 1700 m/s to 2200 m/s. As a result, it was possible to grasp the distribution of the basement surface in the target area, and it was found that the depth of the basement was 640 m at the deepest part.

Next, we assumed a three-layer density structure model and performed a two-dimensional analysis using gravity anomalies. The density of each layer was set to 2.0 g/cm^3 for the first layer, 2.3g/cm^3 for the second layer, and 2.5g/cm^3 for the third layer. In the velocity structure model, the first layer corresponds to Vs = 100 to 500 m / s layer, the second layer corresponds to Vs = 550 to 150m/s layer, and the third layer corresponds to Vs = 1700 to 3000m/s. The depth of the boundary between the first and second layers is based on the results of microtremor observation, and the depth of the boundary between the second and third layers is based on the results of three-dimensional analysis of the two-layer model. Under these conditions, the density structure model was estimated by trial and error to explain the gravity anomaly. As a result, the undulations of the layer boundaries of each layer could be grasped, and there were areas where the base shapes of the first and second layers were significantly different.

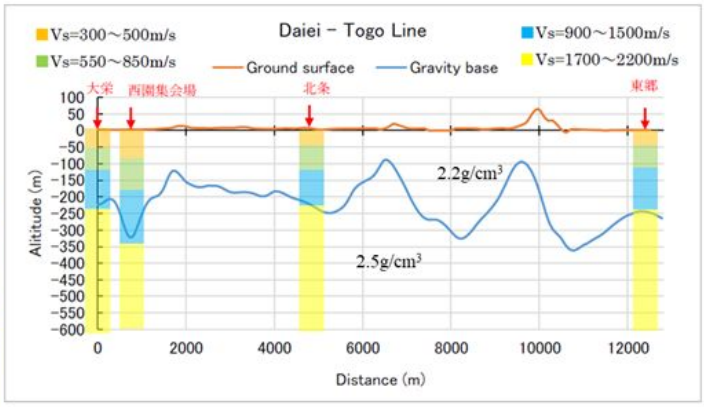
In the future, we plan to try a method of integrating the model of tremor and seismic motion and the model of gravity anomaly and expanding it to a three-dimensional structure. Furthermore, we will investigate the relationship between the undulations of the base surface of the obtained base structure and the damage distribution caused by the earthquake.

Keywords: central Tottori prefecture, 3-D subsurface structure model, gravity survey, microtremor survey, seismic observation

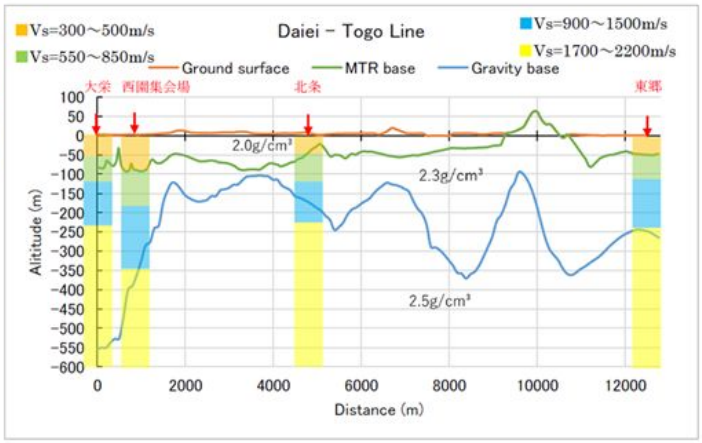
©2021. Japan Geoscience Union. All Right Reserved.



3次元解析結果



2次元解析結果(2層均質モデル)



2次元解析結果(3層均質モデル)

©2021. Japan Geoscience Union. All Right Reserved.

Estimation of Subsurface Structure and Ground Motion Characteristics in the Landslide Areas from Microtremor Observations –Case of Nawashiro and Amedaki, Kokufu-cho, Tottori City –

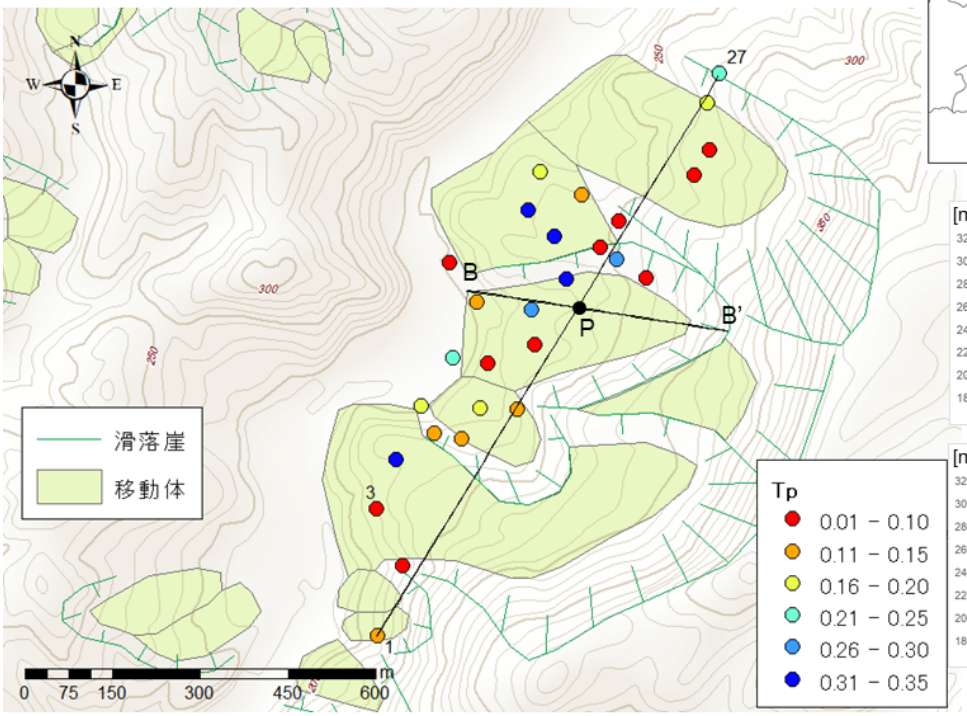
*Isamu Nishimura[1], Atsushi Shimada[2], Tatsuya Noguchi[2], Takao Kagawa[2]

1. Graduate School of Engineering Department of Social Infrastructure Engineering, Tottori University, 2. Social Systems and Civil Engineering, Department of Engineering, Tottori University

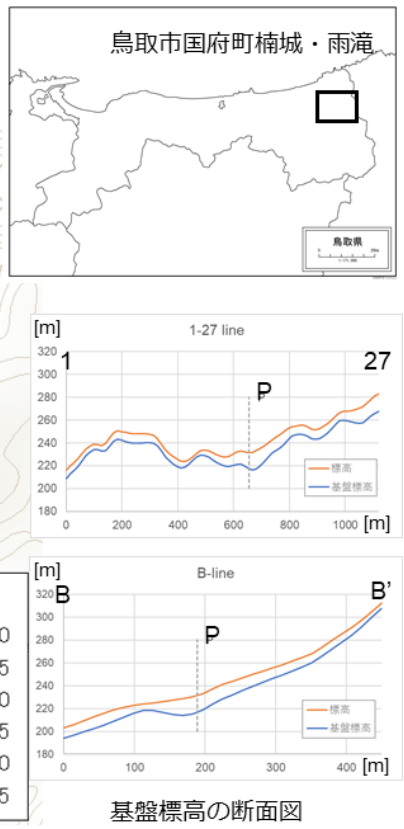
In recent years, landslides caused by earthquakes have resulted in large-scale damage. It is important to understand the ground motion characteristics of landslide areas because landslides often occur repeatedly in the same area based on past activity history. Microtremor surveys have been used to evaluate the ground motions in landslide areas because the sediments above the slip surface are very soft and the velocity contrast is likely to be distinct (e.g., Shima, 1981). In this study, we conducted microtremor observations in Nawashiro and Amedaki, Kokufu-cho, Tottori City, that are classified as landslide areas in the landslide topography map published by the National Research Institute for Earth Science and Disaster Resilience (NIED), and examined the extent to which landslide deposits can be evaluated.
From the landslide topography distribution map, the Nawashiro landslide is classified into three blocks, and the Amedaki landslide is one large body. As a result of the analysis, the predominant periods of microtremor H/V were 0.06-0.35 seconds in both regions. At Nawashiro, each block has its own characteristics of predominant periods. In some blocks, predominant periods of 0.1 seconds or less were widely distributed, while in other blocks, periods of 0.3 seconds were concentrated. At Amedaki, the predominant period tended to be longer at the sites identified as landslide bodies. From the array observation, it was estimated that the layer of Vs = 200 m/s is 6m at Nawashiro and the layer of Vs = 130 m/s is 5m at Amedaki. The S-wave velocities and the predominant periods were used to estimate the layer thicknesses. The layer thicknesses tend to be thicker at the center of the landslide bodies, that may reflect the landslide deposits.

Keywords: Microtremor observation, H/V spectra, Landslide, Subsurface structure

©2021. Japan Geoscience Union. All Right Reserved.



楠城の卓越周期分布



基盤標高の断面図

©2021. Japan Geoscience Union. All Right Reserved.

Modeling of subsurface velocity structures from seismic bedrock to ground surface for Yamanashi region

*Shigeki Senna[1], Atsushi Wakai[1], Yatagai Atsushi[2], Tadashi Sato[2], Hisanori Matsuyama[2], Hiroyuki Fujiwara[1]

1. National Research Institute for Earth Science and Disaster Resilience, 2. OYO Corporation

1. Introduction

The NIED has constructed a shallow and deep integrated underground structure model in the Kanto, Tokai, and Kumamoto regions in order to improve the accuracy of strong motion prediction. In this study, we will focus on the construction of a shallow and deep integrated underground structure model for the Yamanashi region, which is adjacent to the Kanto and Tokai regions. The model construction procedure basically follows the method of the Kanto region (for example, Senna et al., 2017) in which modeling is carried out in advance. Specifically, first, an initial underground structure model was created based on the existing underground model, borehole data and geological information collected so far. Then, the initial underground model was adjusted using the ground vibration characteristics obtained by conducting a dense microtremor array exploration. In this paper, we report the above contents and the features of the modified underground structure model.

2. Initial ground model

Of the initial underground models, the J-SHIS_V2 model of the NIED was basically used as the initial model for the deep underground structure model (deeper than Vs350 (m/s) defined as the engineering bedrock). For shallow underground, a underground model was connected to make it an initial model. After that, the upper surface of the engineering bedrock of the shallow underground was used as the upper surface of the first layer of the deep underground, and the two were integrated to form the initial integrated underground model. For the shallow underground structure model (shallower than Vs350 (m/s)), the geomorphologic classification of J-SHIS was reviewed and revised based on the hydraulic topography classification map, and then the borehole data in Yamanashi prefecture (about 3,000). This was organized and a 250m mesh model was created based on the modified geomorphologic classification.

3. Microtremor array observations and seismic records used

Microtremor array observations are large array observations (three points with array radii of 100, 200, 400m and L-shape with sides 25 to 75 m) at intervals of about 5 km in the lowlands and plateaus indicated by the geomorphologic divisions throughout Yamanashi prefecture. Microtremor observations (4 points with an array diameter of 60 cm and triangles with a side of 5 m to more than 10 m) were carried out at about 500 points at intervals of about 1 km (as of February 2021). The phase velocity and H/V spectrum ratio for each observation point were calculated. Seismic records are recorded using the K-NET and KiK-net seismic stations of the NIED and the JMA recorded in the Metropolitan Area Strong Motion

©2021. Japan Geoscience Union. All Right Reserved.

Network (SK-net) of the Earthquake Research Institute, the University of Tokyo. The R/V spectrum ratio for each observation point was calculated. Based on these ground vibration characteristic data and the initial ground model, joint inversion was performed to obtain a one-dimensional S wave velocity structure at each observation point.

4. Modification of initial ground model based on microtremor array observations and seismic observation results

Chapter 3. using the one-dimensional S-wave velocity structure obtained in the above, the initial deep ground model at each observation point was modified, and a three-dimensional S-wave velocity structure model was created by spatially interpolating each velocity layer in the horizontal direction. Based on the estimated S-wave velocity structure, the deep ground velocity structure (J-SHIS_V2) was modified. Since J-SHIS _V2 is uniformly shallow up to the S wave velocity of 1,000 m/s, the result is deep after correction (Figure 1). After the S-wave velocity of 1,200 m/s, it became shallower on the northwest side of Yamanashi prefecture after the model modification and deeper on the east side. How to modify the shallow underground model. It was created to match the AVS30 (C40 and S-wave velocity structure by inversion) obtained from the microtremor exploration at the point where the microtremor exploration is being carried out.

5. Summary

In this sutudy, we show an example of the construction and results of a shallow and deep integrated underground structure model for the Yamanashi region. In the future, we plan to verify the underground model using seismic records, such as the period and amplification characteristics at seismic stations.

Keywords: Underground structure model, Microtremors, Strong Ground Motion Prediction

©2021. Japan Geoscience Union. All Right Reserved.

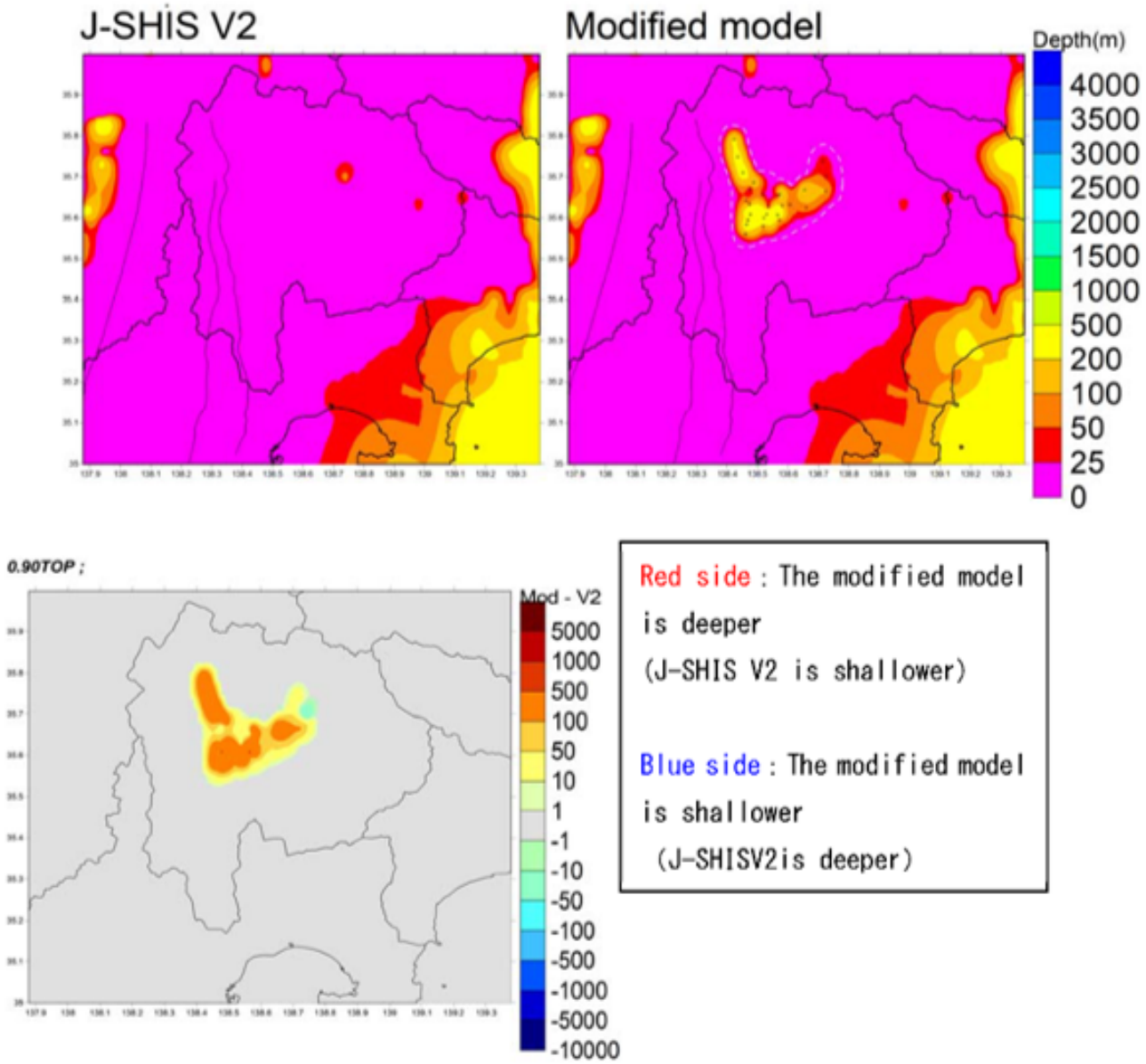


Figure 1. Top depth distribution of modified understructure model (Vs900 (m/s) top depth)

©2021. Japan Geoscience Union. All Right Reserved.

Modeling of subsurface velocity structures from seismic bedrock to ground surface for Kumamoto region

*Shigeki Senna[1], Atsushi Wakai[1], Yatagai Atsushi[2], Yoshiaki Inagaki[2], Hisanori Matsuyama[2], Hiroyuki Fujiwara[1]

1. National Research Institute for Earth Science and Disaster Resilience, 2. OYO Corporation

1. Introduction
The NIED has created a shallow and deep integrated ground structure model using the microtremor array exploration observed in the Kumamoto Plain (Senna et al., 2018). In this study, the range of the shallow and deep integrated underground structure model was expanded by significantly adding microtremor array exploration to the northern part of the Kumamoto Plain and the Aso area. In this study, we report the results of expanding the scope using the method proposed in the above paper.

2. Creation of initial ground model
Regarding the expansion range, of the initial ground models, the J-SHIS_V2 model of the NIED was basically used as the initial model for the deep underground model (deeper than Vs350 (m/s) defined as the engineering bedroock). For shallow underground, a ground model was connected to make it an initial model. After that, the upper surface of the engineering bedrock of the shallow underground was used as the upper surface of the first layer of the deep underground, and the two were integrated to form the initial integrated underground model. For the shallow underground model (shallow than Vs350 (m/s)), the geomorphologic classification of J-SHIS was reviewed and revised based on the flood control topography classification map, and Borehole data (about 12,000) were organized and a 250m mesh model was created based on the modified geomorphologic classification.

3. Microtremor array observations and seismic records used
Microtremor array observations are about 5 km of large array observations (three points with array radii of 100, 200, 400 m and L-shape with sides 25 to 75 m) in the lowlands and plateaus indicated by the geomorphologic in the northern part of Kumamoto Prefecture and the Aso area. 16 points were added at intervals. Including the 26 large array points in the past, there are a total of 42 points. On the other hand, extremely small and irregular array observations (4 points with an array diameter of 60 cm and triangles with a side of 5m to more than 10 m) were carried out at approximately 1 km intervals and in the Aso area at approximately 500 m intervals (2021. As of March). Including the 473 points of the existing microtremor array, the total number is 1327 points. The phase velocity and H/V spectrum ratio for each microtremor observation point were calculated. For the seismic records, the R/V spectrum ratio for each station was calculated using the K-NET and KiK-net seismic stations of the NIED, and the seismic records of local governments and the JMA. Based on these ground vibration characteristic data and the initial underground model, joint inversion was performed to obtain a one-dimensional S wave velocity structure at each observation point.

4. Modification of ground model based on microtremor array observations and seismic observation results
Using the one-dimensional S-wave velocity structure obtained in Chapter 3, the initial deep underground model at each observation point was modified, and a three-dimensional S-wave velocity structure model was created by spatially interpolating each velocity layer in the horizontal direction. Based on the estimated S-wave velocity structure, the deep underground velocity structure (J-SHIS_V2) was modified for the extension. Compared with the J-SHIS_V2 model created in this study, the top depth of the Vs900

©2021. Japan Geoscience Union. All Right Reserved.

layers (Figure1) more reflects the shape of the Aso caldera. There is. The top depth of the Vs2700 layers (Figure2) is deeper near the central crater hills of Aso volcano. This is in harmony with the results of the distribution map of the upward connection residuals of gravity. In the vicinity of Shimabara Bay, the model is based on the results of sound wave exploration and gravity. As a result of the above, we believe that we were able to construct a model that more clearly reflects the structure of the "Beppu-Shimabara Graben" from Oita to Aso, Kumamoto, and the Shimabara Peninsula. The modification of the shallow ground model was made to match the AVS30 (C40 and S-wave velocity structure by inversion) obtained from the microtremor exploration at the point where the microtremor exploration was carried out.

5. Summary

In this paper, we have extended the shallow and deep integrated ground structure model around the Kumamoto Plain that we have created so far, and showed the results. In the future, we plan to acquire past data such as active fault priority surveys, add microtremor array observations, build a underground model for the entire Kumamoto prefecture, and verify it with seismic records.

Keywords: Underground structure model, Microtremors, Strong Ground Motion Prediction

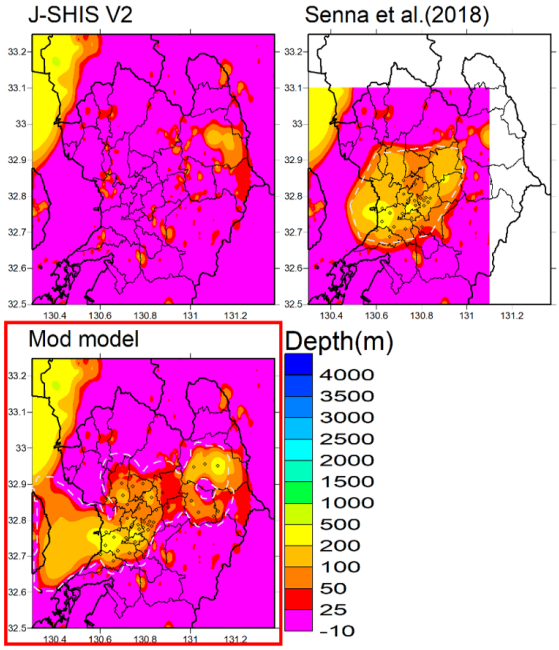


Figure 1. Top depth distribution of underground structure model (Vs900 m/s)
Upper left: J-SHIS V2
Upper right: Senna et al. (2018)
Lower left: Modified model

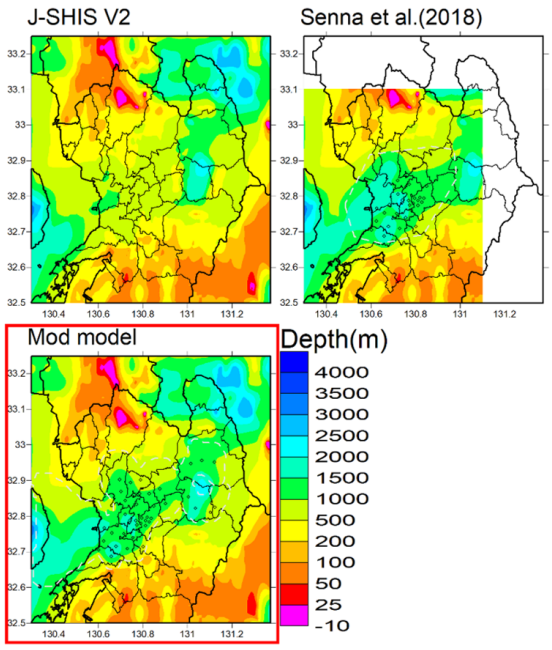


Figure 2. Top depth distribution of underground structure model (Vs2700 m/s)
Upper left: J-SHIS V2
Upper right: Senna et al. (2018)
Lower left: Modified model

©2021. Japan Geoscience Union. All Right Reserved.

Basic study of a real-time damage estimation system for liquefaction

*Shohei Naito[1], Hiromitsu Nakamura[1], Shigeki Senna[1], Yoshinori Iwanami[2]

1. National Research Institute for Earth Science and Disaster Resilience, 2. MITSUBISHI SPACE SOFTWARE CO.,LTD.

The real-time earthquake damage estimation system (Nakamura et al., 2013) makes it possible to immediately estimate damage to buildings, etc. due to earthquake motion in units of towns. It is being used for decision-making during disaster response. However, regarding the liquefaction that occurs due to earthquakes, it is not possible to provide damage estimation information of buildings for now, although there are development examples of liquefaction prediction systems such as Kamiya et al. (2013). Since the damage caused by liquefaction has many effects on various structures and lifelines, it is an urgent task to establish a damage estimation method for early recovery.

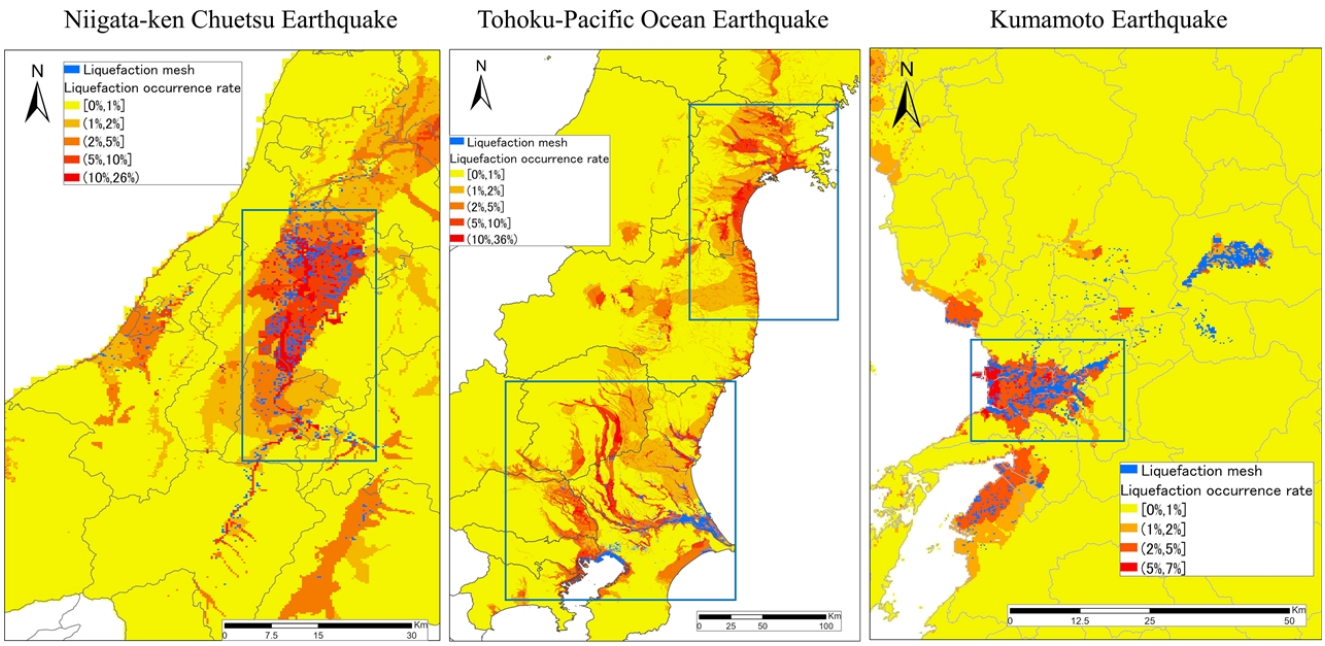
Therefore, we targeted three earthquakes, the Niigata-ken Chuetsu Earthquake, the Tohoku-Pacific Ocean Earthquake, and the Kumamoto Earthquake, and we developed the liquefaction estimation system mainly based on the liquefaction estimation method of Senna et al. (2018). After acquiring strong motion observation records on K-NET and KiK-net, an index deltals obtained from a 10-second integrated value of the real-time seismic intensity (Kunugi et al., 2008) exceeding a threshold (4.5) is calculated and interpolated by the IDW method. After that, a liquefaction occurrence probability in 250m mesh units is calculated by multiplying the regression coefficient α, which differs depending on a region and a microtopography classification group (Matsuoka et al., 2011). In addition, we developed the risk estimation system calculating the total destruction rate of the building due to liquefaction based on the method of Shimizu et al. (2016), by multiplying the liquefaction occurrence probability, the liquefaction area ratio (Yamamoto et al., 2009) and the total collapse rate of the building when liquefaction occurs (Cabinet Office, 2003). These estimation results are stored as a data file in netCDF format, and it is possible to visualize the spatial distribution on a Web browser or a GIS software (Fig. 1).

Next, as a result of comparing the distribution of the liquefaction occurrence rate of the 250 m mesh calculated by the system with the 250 m liquefaction mesh based on aerial photograph interpretation (Wakamatsu et al., 2017), it was confirmed that concerning each of the tree earthquakes, the mesh estimated to have a liquefaction occurrence rate of 2% or more contains about 80 to 90% of the liquefaction mesh within the blue frame area of Fig.1, and this method is effective in grasping the distribution of liquefaction damage. In addition, the 250m mesh was aggregated for each 10km mesh, and the average value of the estimation results by the system was compared with the ratio of the liquefied mesh to the 10km mesh. As a result, a certain correlation was confirmed between the two. On the other hand, in the Kumamoto earthquake, problems such as underestimation of the estimated value were confirmed, and it was found that more appropriate parameter setting is necessary in consideration of geomorphological factors.

In the future, in addition to developing a more precise prediction model of liquefaction occurrence rate based on recent earthquake damages, we are going to construct a real-time liquefaction damage estimation system that can be used for quick understanding of damage status and early restoration of social infrastructure. In addition, regarding building damage caused by liquefaction, sufficient observation data could not be obtained to verify the estimated value, but verification of the possibility of using it as data that contributes to risk evaluation will be an issue.

©2021. Japan Geoscience Union. All Right Reserved.

Keywords: liquefaction, damage estimation, real-time



©2021. Japan Geoscience Union. All Right Reserved.

Estimation of subsurface motion from surface seismic records: investigation on evaluation at deep levels

*Tomotsugu Watanabe[1], Hiroshi Takenaka[1], Masanao Komatsu[1], Mitsutaka Oshima[2]

1. Okayama University , 2. Shimizu Corporation

We need subsurface seismic motions or incident wavefields on a given subsurface level to evaluate the seismic stability of the shallow subsurface structure and the response of buildings through simulating the strong motion. It is conventional that the subsurface motion is estimated from the ground motion record at a free surface position by assuming a vertical plane-wave incidence. However, this approach requires that the vertical and horizontal components of the seismic wave independently propagate as P wave and S wave, respectively, which is theoretically incorrect, and could not represent the correct deformation in the subsurface structure. We have proposed a new method to evaluate the subsurface wavefields from a surface record without the assumption of the plane-wave incidence (Takenaka et al., 2019, SSJ Fall meeting) and applied the method to compare the evaluated motion with the subsurface records at shallow levels of around 100 –200 m (Watanabe et al., 2020, JpGU). The evaluation level is deeper, the actual wavefields could be more different from the conventionally estimated ones based on the assumption of the vertical incident plane wave, due to the oblique incident effect and so on. In this study, we check the effectiveness of our method and the conventional one by reproducing subsurface records in depth of more than 2 km.

Our method needs a horizontally-layered model including the earthquake source. We calculate the synthetic seismograms at the surface station and the subsurface evaluation point assuming the focal mechanism and impulsive source. We then deconvolve the surface record with the surface synthetic seismogram to derive the *effective source time function*. We apply the water level method for the stable deconvolution. The effective source time function has the substantial source time function and the unsimulated effects by the structural model, which are included in the surface record. Then, we convolve the effective source time function with the subsurface synthetic seismogram to derive the target motion at the evaluation point.

We apply our method and conventional one to the surface records observed at the KiK-net (NIED) TKYH02 station for a source of *Mj* 4.8, focal depth 83 km, and epicentral distance 53.73 km. Figure 1 shows the subsurface motion observed and evaluated by three methods, our method and methods based on vertical and oblique plane-wave incidence, respectively. We select the horizontal slowness of S-wave for the oblique plane-wave incidence so as to fit the estimated subsurface waveform of the transverse component to the observed one. We could successfully recover the subsurface motion by our method. In Fig. 1(a), it is found that there are differences in the amplitude of the P-wave coda and later phases on the radial component. The subsurface waveform estimated by our method is similar to one by the method based on the oblique plane-wave incidence. We confirmed that the subsurface acceleration spectra evaluated by three methods recovered the observed one around a few Hz, while our method underestimated the spectra in lower than 1 Hz because of the effect of the water level method. We will also report about the estimation of the subsurface motion using other events and records, the evaluation of incident wavefields, and the estimation at the subsurface evaluation points with horizontal offsets from the surface station and so on.

©2021. Japan Geoscience Union. All Right Reserved.

Keywords: seismic motion, plane wave, strong motion, subsurface wavefield

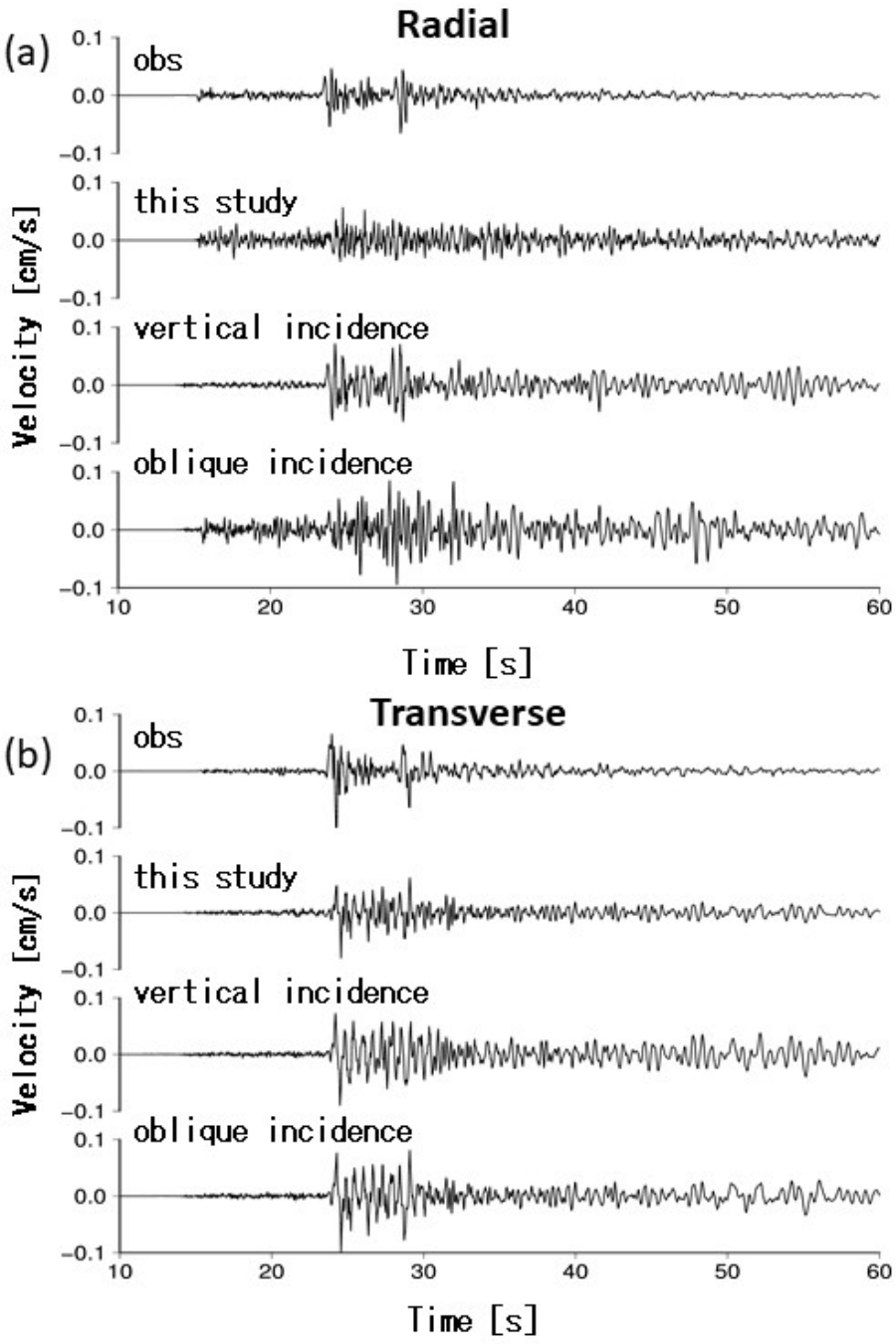


Fig1. Subsurface waveforms observed or estimated from surface records using three methods: (a) the radial and (b) transverse component.

©2021. Japan Geoscience Union. All Right Reserved.

Estimation of seismic ground motions on the surface ground at MeSO-net stations

*Atsushi Wakai[1], Shigeki Senna[1]

1. National Research Institute for Earth Science and Disaster Resilience

In the near future, it is concerned that a large earthquake will occur beneath the Tokyo metropolitan area and there will be severe damage for a lot of houses, buildings and infrastructures. Meanwhile, there are some earthquake observation networks in the area nowadays. Some of the networks provide us with the indexes of earthquake ground motions in a short time. Therefore, the information enables us to understand situation of earthquake ground motions in the area.

In the past national project of Japan, “Metropolitan Seismic Observation network” (hereinafter, referred to as “MeSO-net”) was constructed for the investigation of tectonic plate structures and the estimation of seismic source fault models in the Tokyo metropolitan area around ten years ago [1]. The MeSO-net has about 300 stations with sensors installed at around 20 meters underground in the area. Also, they are spatially distributed at intervals of 2 to 5 kilometers in the area. This network can provide us with the picture of earthquake ground motions with higher spatial resolution, provided that seismic records are acquired on the ground surface.

In recent years, we have worked a subproject of “acquisition of spatially very-high-resolution earthquake observation data and development of the database by private-public partnerships” as a member in a national project or “Tokyo Metropolitan Resilience Project [2].” As one of the issues, we have tackled estimation of seismic ground motions on the ground surface based on bore-hole seismic records observed at each MeSO-net station. This issue needs soil amplification factors between the ground surface and 20 meters below ground.

The procedure is as follows. First, a seismometer has installed on the ground surface at each MeSO-net station during two to three months and some earthquake observation records have been obtained in addition to the bore-hole records at each MeSO-net station. And then, an observed spectral ratio has been obtained by calculating Fourier spectra of seismic records on the ground surface and those in the bore-hole. Also, calculating JMA seismic intensity scale based on records on the ground surface and those in the borehole, increment of seismic intensity has been obtained by subtraction of them. Secondly, a miniature and centerless array microtremor exploration [3] was performed at each MeSO-net station. This method can be adopted principally for estimation of an S-wave velocity structure in the surface ground. It consists of 4-point miniature array with a radius of 60 centi-meters and 3-point centerless array with around 10 meters on a side. An S-wave velocity structure was estimated based on a disperse curve of phase velocity and an H/V spectral ratio calculated from microtremor data at each MeSO-net station. Then a transfer function was obtained using 1-dimensional multiple reflection theory based on the S-wave velocity structure at each MeSO-net station. Finally, an S-wave velocity structure can be enhanced by modifying a transfer function based on an observed spectral ratio at each MeSO-net station. Also, the existing S-wave velocity structures and other geotechnical information can be enhanced based on S-wave velocity structures at MeSO-net stations.

In this study, we will develop the scheme for estimation of earthquake ground motions at each MeSO-net station based on bore-hole seismic records by means of some soil amplification factors mentioned above.

©2021. Japan Geoscience Union. All Right Reserved.

In this presentation, we will report on the results in the analyses of seismic data and microtremor ones at this moment.

References
[1] MEXT (2011): https://www.mext.go.jp/a_menu/kaihatu/jishin/1319360.htm (in Japanese)
[2] NIED (2021): https://forr.bosai.go.jp/e/sub_b.html
[3] I. Cho, S. Senna, and H. Fujiwara (2013), “Miniature array analysis of microtremors,” Geophysics, Vol.78, No.1, pp. KS13-KS23, doi:10.1190/geo2012-0248.1.

Keywords: MeSO-net, soil amplification factor, seismic ground motion, microtremor exploration, S-wave velocity structure

©2021. Japan Geoscience Union. All Right Reserved.

Strong motion simulation of an intraslab earthquake beneath Kanto region using MeSO-net observation data

*Wataru Suzuki[1], Takeshi Kimura[1], Hisahiko Kubo[1], Takayuki Miyoshi[1]

1. National Research Institute for Earth Science and Disaster Resilience

MeSO-net (Metropolitan Seismic Observation network) conducted dense and real-time observation of seismic motion at approximately 300 stations in the metropolitan area. The network has contributed to researches of underground structure and seismic activity, and advancement of strong motion evaluation for the Kanto region. However, to authors' knowledge, the observed waveform itself has not been used for the strong motion simulation as empirical Green's function. We have noticed advantage of the observed MeSO-net data which contains the effects of the small heterogeneities of underground structure we cannot fully model. We, therefore, have performed strong motion simulation for an intraslab earthquake within the Philippine Sea plate beneath Tokyo by applying the empirical Green's function method to the MeSO-net observed waveforms.

We used waveforms recorded during an M_W5.0 intraslab earthquake that occurred at a depth of 57km on September 12, 2015 as empirical Green's functions. This event has a normal-fault-type mechanism of N-S and E-W striking nodal planes with high-dipping angle. We extended these two nodal planes to M7-class fault models for the strong motion simulation. The fault models have one strong motion generation area whose parameters were assumed considering the strong motion evaluation of Cabinet Office. Empirical Green's function simulation was conducted following the method proposed by Irikura (1986) and Irikura et al. (1997).

Simulated acceleration waveforms at MeSO-net E.TYPM station (Shinjuku, Tokyo) show the peak values of approximately 500gal and 250gal for horizontal and vertical components, respectively. The simulation results for N-S and E-W striking fault models are similar. Acceleration response spectra have the peak value at a period around 0.2 seconds and the spectral amplitude decreases as the period approaches to 1 second. It seems that the empirical Green's function used here lacks enough power for long-period components to simulate M7-class earthquake. Further examination to model the long-period components using the theoretical approach is necessary to simulate the strong motions that can be used to promote the disaster resilience in the metropolitan area.

Keywords: MeSO-net, Strong motion simulation, Empirical Green's function method, Strong motion generation area, Intraslab earthquake

©2021. Japan Geoscience Union. All Right Reserved.

Ground-motion simulation for the 2016 Kumamoto earthquake (Mj7.3) based on the strong-motion prediction recipe

*Asako Iwaki[1], Nobuyuki Morikawa[1], Takahiro Maeda[1], Hiroyuki Fujiwara[1]

1. National Research Institute for Earth Science and Disaster Prevention

The 2016 Kumamoto earthquake occurred on April 16, 01:46 JST (M_{JMA}7.3) revealed several issues on the strong-motion prediction in terms of fault size, seismic moment, etc. In this study, we attempt to “predict” the ground motion for the Kumamoto earthquake based on different fault models, aiming to clarify the key parameters and uncertainties to be considered for improving strong-motion prediction for active faults.

First, we set a reference fault model by following the procedure by the “recipe” (Headquarters for Earthquake Research Promotion of Japan, 2017) assuming the fault length was set to be a realistic number, 34 km a priori. The seismic moment calculated from the reference model via the S - M_0 (fault area –seismic moment) relation of the recipe is less than 50 % of the observation. We set two types of alternative models: (1) fault models with the same fault size as the reference model but with doubled seismic moment and (2) fault models with larger fault length but with the same S - M_0 relation.

Using the various fault models and a detailed 3-D velocity structure model (Senna et al. 2017), broadband ground motion was computed by a hybrid technique combining 3-D finite-difference method at long periods (> 1 s) and the stochastic Green’s function method at short periods (< 1 s). We show the effect of considering the uncertainties in S - M_0 relation, fault length, and the depth of fault top on the performance of the ground motion prediction.

Keywords: 2016 Kumamoto earthquake, strong motion, ground-motion simulation, active faults

©2021. Japan Geoscience Union. All Right Reserved.

Characterized source model of M7.3 2016 Kumamoto eq. by 3D reciprocity GFs inversion with special reference to velocity pulse at KMMH16

*Anatoly Petukhin[1], Hiroshi Kawase[2], Fumiaki Nagashima[2], Eri Ito[2]

1. Geo-Research Institute, 2. DPRI, Kyoto University

2016 Kumamoto earthquakes caused severe damage centering on Mashiki residential area. The velocity waveforms at KMMH16 station in Mashiki during the *M*7.3 event show a large velocity pulse observed both by the surface and downhole sensors. Kawase et al., 2017, found that severe damage in Mashiki may be result of strong westward velocity pulse. Question raised by the 2016 Kumamoto earthquakes is how the near-source ground motions with strong velocity pulses at KMMH16 were generated during *M*7.3 event.

In this study, we focus on the characterized SMGA source model. EGF method is widely used for source modelling in this case. However, in case of target site is located just near the fault in the nodal plane of the source mechanism (like KMMH16), the mechanism of the EGF event should perfectly fit the mechanism of the mainshock, which is a rare case. Otherwise, large variations of amplitudes in the vicinity of the nodal plane will produce large errors of ground motion synthetics. Instead, we will use theoretical 3D GFs.

Our approach is non-linear source inversion. This method requires calculation of waveforms and comparison with observations for many source models. To accelerate these calculations, we use precalculated Green’ s functions (GF) by the reciprocity method and the JIVSM velocity structure model. By comparison with aftershock record, we validated this structure for as short as 2 s in periods. For mainshock inversion we expand the target period to 1.5 sec. Target sites are limited to sites close to the fault: KMM005, KMM006, KMMH06, KMMH14, and KMMH16.

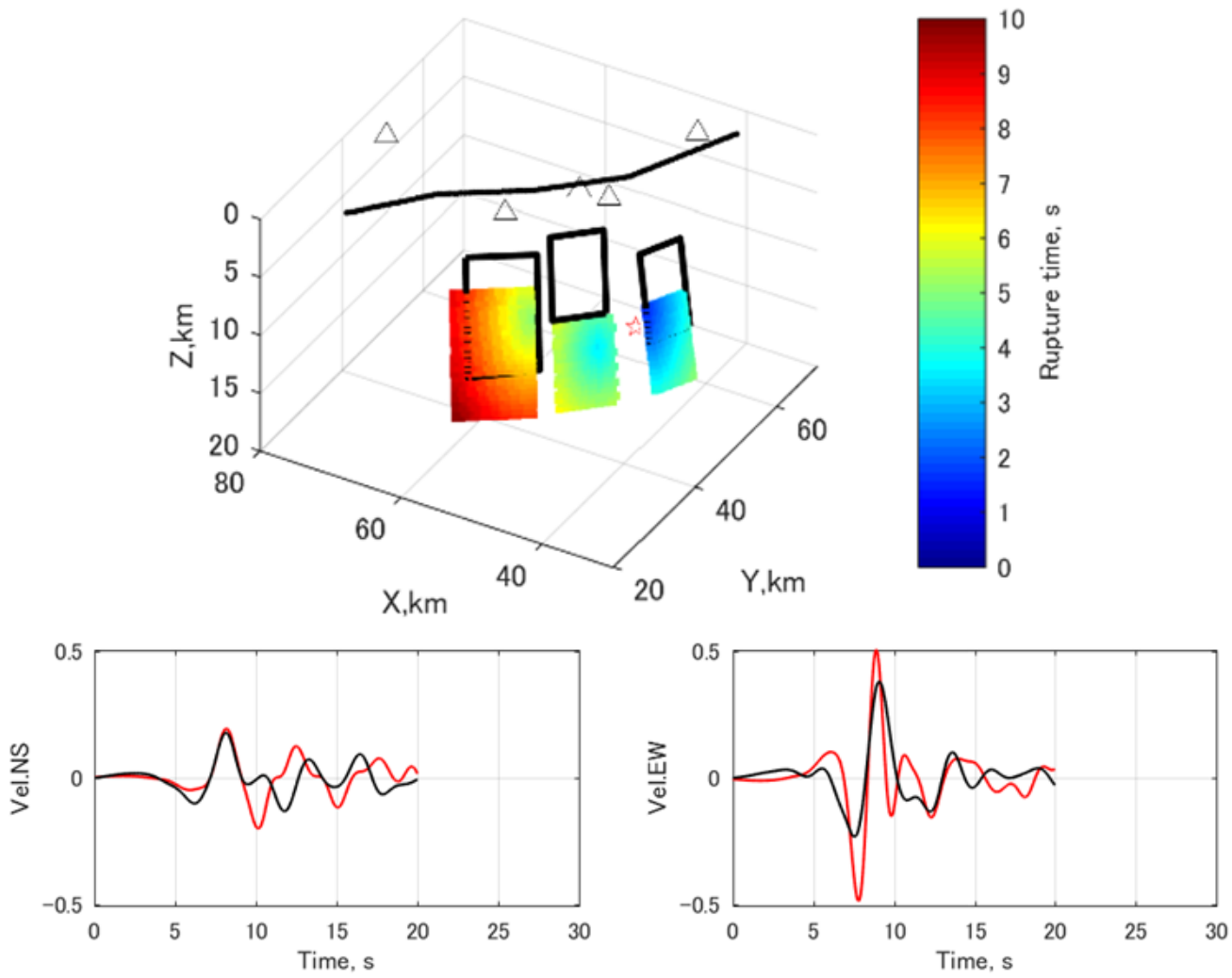
First, we explore the parameter space with the simplex search method with the initial SMGA model of Somei et al. (2019). In this process we were able to reduce a number of search parameters by limiting to effective parameters only. Also, necessary physical constraints for rupture velocity, rupture starting point, etc., as well as their strength, were estimated here. Then, we try to look for an alternative initial SMGA source model by the grid search method, and finally, estimate source model with the simplex search method again.

Resulting model and waveforms for KMMH16 are shown in figure below. Location of SMGAs is deeper than in initial model of Somei et al. (2019). For SMGA2 the deep location agrees well with other source inversions (e.g., Yoshida et al., 2017). SMGA rupture initiation points have physically reasonable location allowing outward propagation from the mainshock hypocenter, without any reverse ruptures. Waveform reproduces short period westward pulse at KMMH16.

Acknowledgements. We use strong motion data from K-NET, KiK-net, and CMT solutions from F-net, provided by the NIED.

©2021. Japan Geoscience Union. All Right Reserved.

Keywords: 2016 Kumamoto earthquake, source inversion, seismic reciprocity, characterised source model, strong motion generation area, Mashiki



Top - SMGA location and rupture time distribution; black rectangular – initial model SMGAs from left to right: SMGA1, SMGA2, SMGA3 for the Hinagu, Futagawa3 and Futagawa2 segments, respectively. Bottom - waveform fit at KMMH16 (black-observed, red-simulated).

©2021. Japan Geoscience Union. All Right Reserved.

Evaluation of near-source ground motion during the 2008 Iwate-Miyagi Nairiku earthquake by using stochastic slip models and three-dimensional velocity structures

*Takeshi Nakamura[1], Masataka Sawada[1]

1. Central Research Institute of Electric Power Industry

The detailed rupture process and heterogeneous subsurface structures should be considered in ground motion evaluations near the source fault at a large earthquake. Numerical simulation methods such as the finite difference method (FDM) and the finite element method (FEM) can incorporate the heterogenous fault slip and three-dimensional structure models into calculations and are useful for grasping seismic motion not only at individual points but also on whole ground surface and seafloor. However, these methods are computationally expensive because they treat a large number of grids and meshes in the computational domain when numerically solving the governing equation, which causes practical limitations on the number of models that can be used as inputs for simulations. However, in the case of a few number of receivers or stations to be evaluated, such as ground motion simulations at important facilities such as power plants, the Green's functions for many point sources can be efficiently calculated by interchanging the source and receiver locations based on the reciprocity theorem and the total number of numerical simulations for many source models can be significantly reduced compared with that by the straightforward approach (e.g., Eisner and Clayton). In this study, we evaluate the displacements including the static component and their deviations near the source fault of the 2008 Iwate-Miyagi Nairiku, Japan, earthquake by calculating waveforms with the reciprocal approach for various slip distribution models that are stochastically generated. We focus on KiK-net IWTH25 station that recorded the peak acceleration amplitude of 3866 gal and the static displacement of 140 cm in the vertical component at the earthquake (Aoi, et al., 2008; Aoi and Morikawa, 2009).
We calculated the Green's functions by using the 3D FDM developed by Nakamura et al. (2012). The finite-fault inversion result for the 2008 earthquake by Asano and Iwata (2011) was employed as a reference model to stochastically generate slip distributions on the fault plane. From their model, we generated 100 cases for the heterogeneous slip distribution based on the slip probability density function (SPDF) by Murphy et al. (2016). We used a point source on a subfault and set a total of 315,216 subfaults with a dense interval of 50 m on the fault plane. We assessed a smoothly spatial distribution of displacements near the fault by employing such dense interval in our simulations, whereas the distribution showed a periodic deformation pattern that is not observed by satellite geodetic surveys if the large subfault interval or size is employed. We used the same initial break point, rake angle, and rupture velocity as those presented in Asano and Iwata (2011). The rise time in subfault was set according to its subfault size. For subsurface velocity structures, we used the Japan Seismic Hazard Information Station (J-SHIS) model (Fujiwara et al., 2009). After confirming an excellent fitting of synthetic waveforms at the IWTH25 surface station for several cases between the straightforward simulation and the reciprocal approach, we generated synthetic waveforms for all slip distribution cases by postprocessing the reciprocal Green's functions.
Our calculation results show that the peak amplitude of the displacement waveform for the fault parallel and orthogonal components and the vertical one is 46±12 cm, 32±11 cm, and 88±26 cm, respectively. The static displacement, which is the mean value in a time window of 40-45 s in which the waveform amplitude converges to a constant value, for the three components is 32±13 cm, 4±10 cm, and 69±20 cm, respectively. Because the source mechanism of the reference model is a reverse fault with the rake

©2021. Japan Geoscience Union. All Right Reserved.

and dip angle of 108 and 51 degrees, respectively, and IWTH25 is located just above the fault plane, both of the static displacement and the peak displacement in the vertical component are larger than those in the horizontal ones in all cases except 5 ones. The static and peak displacement in the vertical component is 6.9 and 6.4 times difference among the cases, respectively, and the maximum value of these displacements is 112 cm and 144 cm, respectively. The peak displacement amplitude in the component is 1.3 times larger on average than the static displacement. Our results also show an attenuation feature of the displacement amplitudes according to the hypocentral distance from the maximum slip position in the source fault. Because IWTH25 is several kilometers away from the surface fault areas, this attenuation relation is significantly associated with the distance to the station location projected on the fault plane compared with the depth of the slip position.

Keywords: Iwate-Miyagi Nairiku earthquake, fault displacement, stochastic slip distribution, reciprocity theorem, finite-difference method

©2021. Japan Geoscience Union. All Right Reserved.

Source rupture process of the 2018 Hokkaido eastern Iburi earthquake estimated from waveform inversion with empirical Green’ s functions

*SHUANGLAN WU[1], Atsushi Nozu[1], Yosuke Nagasaka[1]

1. PORT AND AIRPORT RESEARCH INSTITUTE

The Hokkaido Eastern Iburi earthquake (M_{JMA}6.7) on September 6:03:08 (JST), 2018, occurred in the eastern Iburi region of Hokkaido, Japan, which is reported by the JMA (Japan Meteorological Agency). More than 6000 landslides occurred in the early hours after the earthquake (Yamagishi and Yamazaki, 2018). Tragically, more than 40 people lost their lives, along with 689 people injured (Fire and Disaster Management Agency, Japan, as of 5 October 2018). During this earthquake, large ground motions have been observed, e.g., ground motions at Kik-net Atsuma- (IBUH03) and K-net Mugawa (HKD126), the peak velocity is approximately 150cm/s, and ground motions in the frequency components 1~3Hz are predominant, which are very important to the engineering facilities. In general, the strong crustal earthquakes are with 5-20km depth, e.g., the mainshock of the 2016 Kumamoto earthquake (M_w7.1, depth 12km), the 1995 Kobe (M_w6.9 depth 16km); the 1989 Loma Prieta (M_w6.9, depth 19 km), the 1994 Northridge (M_w6.7, depth 18.2 km) earthquake. However, the 2018 Hokkaido eastern Iburi earthquake was in contrast to the usual situations; it is with Mj6.7 but with hypocentral depth of 37 km but caused large ground motions.

Such special characteristics, the large strong ground motions it generated, its impact on lifeline facilities and buildings, and the serious geological hazards it caused have motivated us to study its rupture features, especially focusing on the generation mechanism of the strong ground motions (e.g., the large pulse velocity). This event was well recorded by permanent strong-motion networks K-net and KiK-net, forming a rich waveform database, which enables us to investigate the rupture process of the earthquake in detail. Therefore, in this analysis, the source rupture process of this event was estimated from the waveform inversion of strong-motion data, and with the adoption of empirical Green’ s functions, which could avoid the possible uncertainties caused by the assumption of subsurface velocity structures, as well as to consider relatively higher frequency ranges of strong ground motions typically up to 2.0 Hz.

Our preferred slip model is illustrated in Figure 1, and the comparisons of observed and synthesized velocity waveforms (0.2 - 2.0 Hz) are illustrated in Figure 2. Figure 1(a) indicates that one large slip region with a maximum slip of approximately 3.4 m was centered ~ 2 km SE of the hypocenter; and in Figure 1(b), two regions with large peak slip velocity were identified, the first one with a peak value of 2.0 m/s was located ~ 6 km SE of the hypocenter, which was mainly contributed to the large pulse velocity of the K-net station HKD126, and the region with serious landslides; and the second one was centered ~ 5 km NW of the hypocenter. The large slip region (with 23~28km in depth) and both the regions with peak slip velocity (with 21~26 km in depth) are located shallower than the hypocenter. The rupture velocity of 2.0 km/s was identified, and the preferred source model corresponds to Mw 7.0 for this event.

The robustness of our preferred slip model was verified through different combinations of EGF events and near-fault stations, which resulted that the locations of the large slip regions are not significantly affected by the selection of the EGF events and the near-fault station. Additionally, based on the preferred source model, the ground motions are synthesized for strong-motion stations that were not used in the inversion

©2021. Japan Geoscience Union. All Right Reserved.

analyses, the synthesized ground motions are consistent with the observed ones. Furthermore, our preferred slip model is consistent very well with the broadband source model proposed by Satoh (2020).

Keywords: the 2018 Hokkaido eastern Iburi earthquake, rupture process, waveforms inversion, empirical Green’ s functions, strong ground motions, large pulse velocity

©2021. Japan Geoscience Union. All Right Reserved.

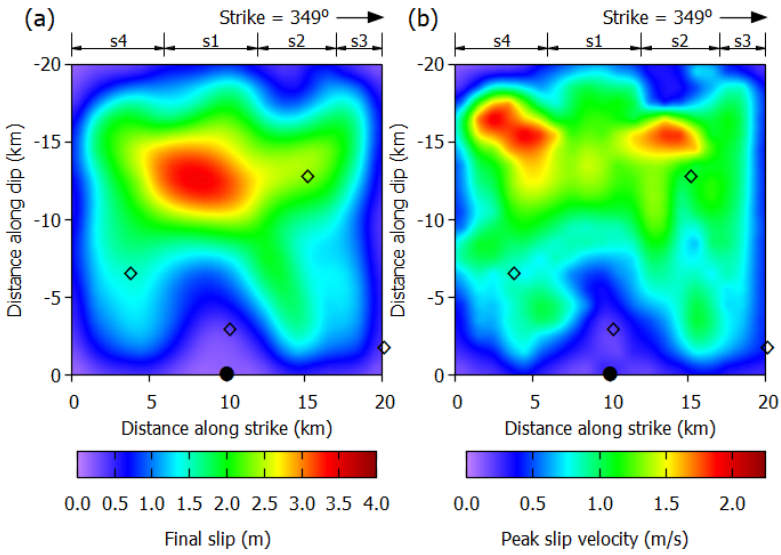


Figure 1. (a) The final slip distribution, and (b) the peak slip velocity of our preferred source model. In each panel, the black dot indicates the JMA hypocenter, which is the rupture starting point assumed for the waveform inversion. The allocation of the adopted 4 EGF events on the fault is also illustrated. The absolute values of the slip were obtained by using the moments of the EGF events.

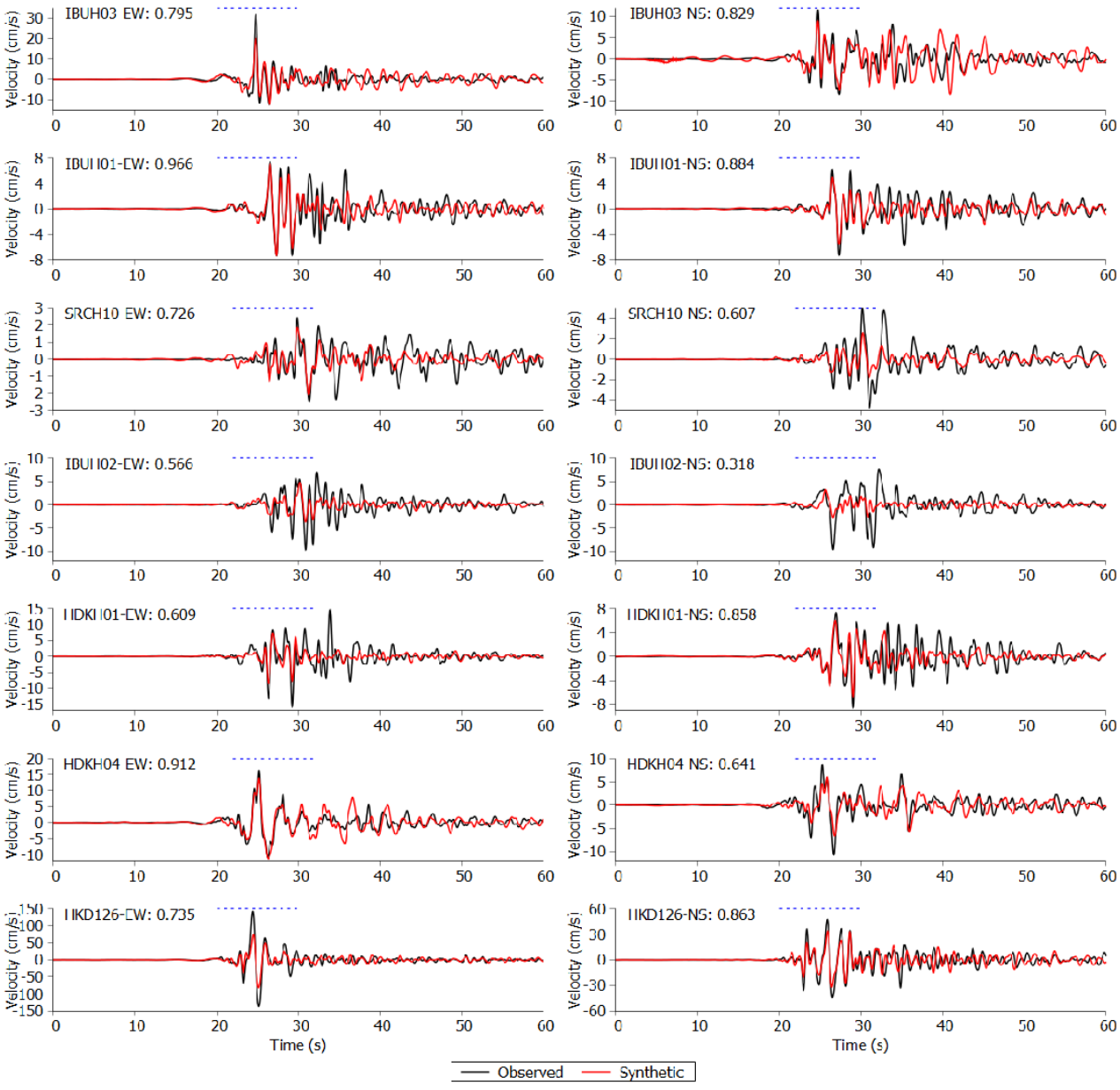


Figure 2. Comparisons of observed and synthesized velocity waveforms (0.2 - 2.0 Hz) based on our preferred source model, and the 10s waveform section under the blue dashed lines are the waveform data used in the inversion analysis. the numbers at the top left of each component are variance reduction (VR) values.

©2021. Japan Geoscience Union. All Right Reserved.

©2021. Japan Geoscience Union. All Right Reserved.

Calibrating Thailand’s local magnitude scale: a preliminary result

*Mongkolchai Sukmee[1], Sutthipong Noisagool[1,2], Satoru Tanaka[3], Weerachai Siripunvaraporn[1,2], Songkhun Boonchaisuk[4,2], Yasushi Ishihara[5], Taewoon Kim[6], Hitoshi Kawakatsu[7], Nozomu Takeuchi[7], Kenji Kawai[8], Yuki Suzuki[8]

1. Department of Physics, Faculty of Science, Mahidol University , 2. Thailand Center of Excellence in Physics, Ministry of Higher Education, Science, Research and Innovation, 3. Volcanoes and Earth's Interior Research Center (VERC), Research Institute for Marine Geodynamics (IMG), Japan Agency for Marine-Earth Science and Technology (JAMSTEC), 4. Geoscience Program, Mahidol University, Kanchanaburi Campus, 5. Research Institute for Marine Geodynamics (IMG), Japan Agency for Marine-Earth Science and Technology (JAMSTEC), 6. Subduction Dynamics Research Center (SDR), Research Institute for Marine Geodynamics (IMG), Japan Agency for Marine-Earth Science and Technology (JAMSTEC), 7. Earthquake Research Institute, The University of Tokyo, 8. Department of Earth and Planetary Science, School of Science, The University of Tokyo

The local magnitude scale (ML) or Richter scale is a fundamental measurement for the regional earthquake study. The backbone digital seismic record in Thailand started in 2007, although there is no study in the local magnitude scale and its calibration. Using the ML without its calibration may lead to large uncertainty in the statistical seismology and geodetic study. In this study, we use the new seismic data from Japanese-Thai joint observation project, Thai Seismic Array (TSAR), and Mahidol University private stations to measure the attenuation characteristic of regional seismic waves. The total number of data is 79 earthquakes with 364 records. The Thai Meteorological Department (TMD) local magnitude is used as an initial value for the iterative grid search optimization. The station correction factor of each station also statistically calculate. The synthetic test on the implemented algorithm and data distribution are satisfied with an error of about 1% from the true attenuation models. For the real data, the geometrical factor, α, is 0.043 and the anelastic attenuation, k, is 0.0017. A best-fit solution of the distance (R in km) correction function from this data set is

$-\log A0 = 1.043 \log R + 0.00171 R - 0.722.$

The calibrated local magnitude is slightly different from Southern California and nearby regions such as Northern Vietnam. This magnitude scaling will be improved and further calibrate with more regional data.

Keywords: Local magnitude, Thailand, Richter scale

©2021. Japan Geoscience Union. All Right Reserved.

Strong ground motion simulation of the Fukushima-ken Oki earthquake of February 13, 2021 (M_J 7.3)

*Yosuke Nagasaka[1]

1. Port and Airport Research Institute

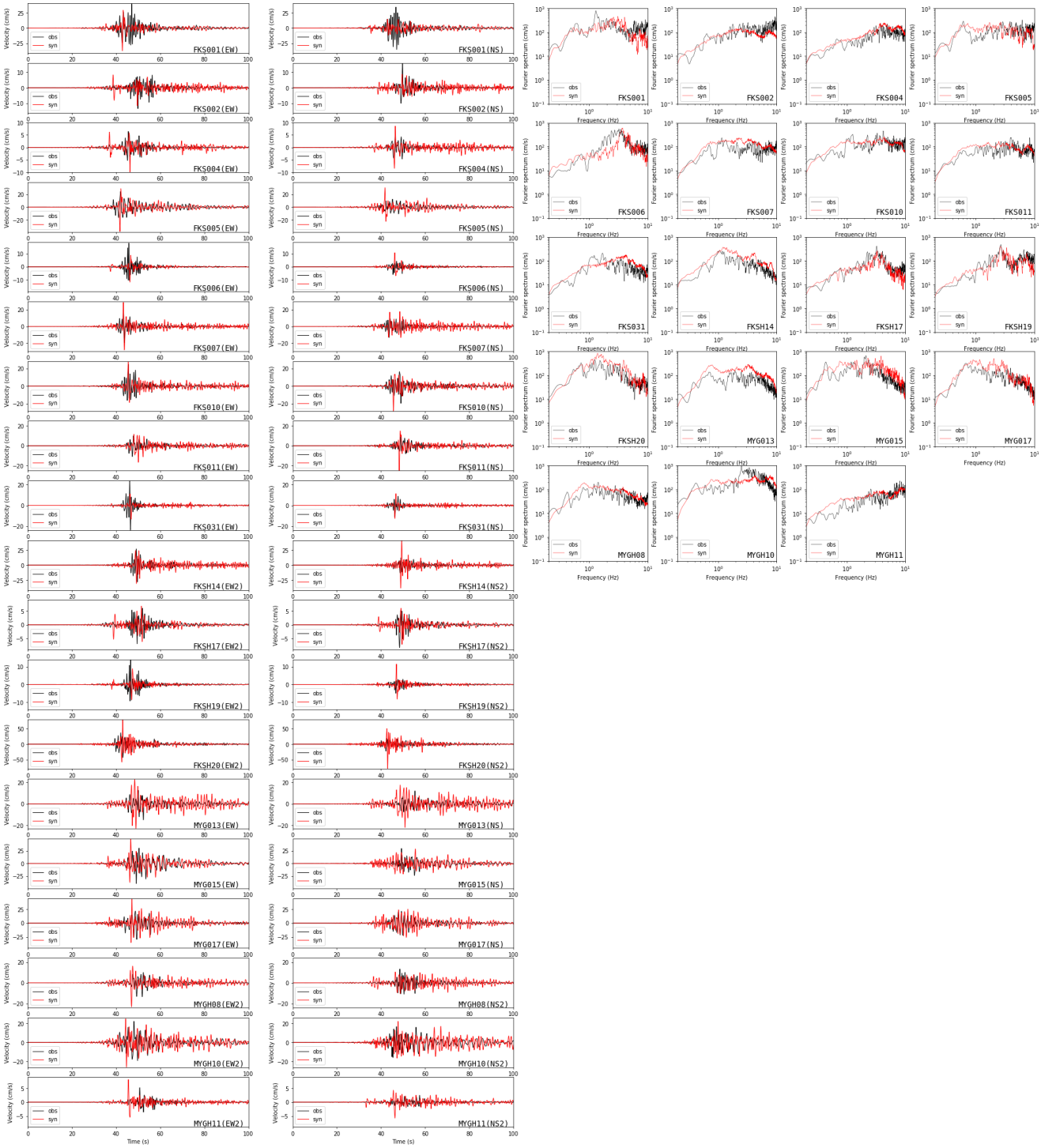
We conducted strong ground motion simulations of the Fukushima-ken Oki earthquake of February 13, 23:07 (JST) with M_J 7.3. As a preliminary model, we used a point source and corrected empirical Green's function method (Kowada et al., 1998; Nozu and Sugano, 2008; Nozu et al., 2009) for the simulation. This model uses the omega-square model as the source spectrum and considers path effect, empirical site amplifications, and empirical phase characteristics to synthesize strong motions. Nineteen K-NET and KiK-net stations are selected as the target. We used empirical site amplification factors by Nozu and Nagao (2005), and empirical site phase characteristics from the observed records of an aftershock occurred on February 15 at 21:26 JST (M_J 5.3).

We fixed the location of the subevent at the hypocenter and determined the seismic moment (=0.8e+19 Nm) and the corner frequency (0.9 Hz) by trial and error. Parameters to consider multiple nonlinear effects (Nozu and Sugano, 2008) are introduced to explain observed strong motions at some stations. Comparisons of observations and synthetics in terms of velocity time histories (0.2 to 2 Hz) and spectral accelerations are shown in the figure.

Good agreements are shown at most of the target stations. On the other hand, at FKS001 (K-NET Soma) where one of the biggest motions were recorded, the peak at 1-2 Hz and the duration of the strong motions are underestimated. We will work on improving the model, for example, by considering the directivity effect to Soma area, multiple asperities, and so on.

Keywords: Strong ground motion simulation, Fukushima-ken Oki earthquake of February 13, 2021, Source model

©2021. Japan Geoscience Union. All Right Reserved.



©2021. Japan Geoscience Union. All Right Reserved.

Strong Motion Generation Area for the 2021 off Fukushima, Japan, Earthquake Estimated based on the Empirical Green's Function Method

*Kazuhiro Somei[1], Ken Miyakoshi[1]

1. Geo-Research Institute

At 23:07 on 13 February 2021 (JST: UTC+9), an M_w 7.1 intra-slab earthquake with reverse faulting occurred off-shore Fukushima prefecture, northeastern Japan. The seismic intensity of 6+ and 6- in JMA scale were widely observed in the Fukushima and Miyagi prefectures. Within the nation-wide strong motion networks (K-NET and KiK-net) operated by NIED, strong ground motions with a peak acceleration 1426 cm/s^2 were recorded at MYGH10 (surface record of KiK-net Yamamoto). For understanding the mechanisms of strong motion generation processes during this event, we estimate the source model composed of strong motion generation area (SMGA) to explain the observed strong motion records in broadband frequency range between 0.3 and 10 Hz.

In this study, we use the empirical Green's function method to simulate the strong motion records at downhole sensors of 18 KiK-net stations located at Miyagi, Fukushima, and Ibaraki prefectures. The observed ground motion records of M_{JMA} 4.7 event (element event) occurring at 23:36 on 13 February 2021, are used as the empirical Green's functions. For an objective estimation of corner frequencies for the target and element events, we apply the source spectral ratio fitting method (Miyake et al., 1999). From the obtained corner frequencies, scaling parameters *N* and *C*, which required for the empirical Green's function method of Irikura (1986), are determined. Then, the parameters of each SMGA (e.g., the size, relative rupture starting point in SMGA, rise time, and rupture velocity) are estimated by trial and error method. Here we assume a squared SMGA on the fault plane with strike angle of N45°E and dip angle of 45°, according to the distribution of aftershocks occurring within 24 h after the mainshock.

As a provisional result, we construct the source model with SMGA located including the hypocenter. The rupture within SMGA mainly propagates southwest direction from the hypocenter. The size of SMGA is 108.2 km^2. The stress drop of SMGA is estimated to be 111.8 MPa. The short-period level of acceleration source spectrum calculated from the size and stress drop of SMGA is 1.2×10^{20} Nm/s^2, which is comparable to that expected from the empirical scaling relationship for intra-slab earthquakes occurring in the Pacific plate (Arai et al., 2015). Overall, the simulated ground motion generated from the SMGA explain well the observed acceleration, velocity, and displacement waveforms, however, there is still room to improve the reproducibility of observed ground motions. The fault geometry and parameters of SMGA need to be examined objectively in more detail.

Acknowledgements: We use the strong motion data of K-NET and KiK-net operated by NIED.

Keywords: 2021 off Fukushima earthquake, Strong motion generation area, Empirical Green's function method

©2021. Japan Geoscience Union. All Right Reserved.

[J] Oral | S (Solid Earth Sciences)：S-EM Earth's Electromagnetism

Sun. Jun 6, 2021 1:45 PM - 3:15 PM JST | Sun. Jun 6, 2021 4:45 AM - 6:15 AM UTC | Ch.21 Zoom Room 21

[S-EM13] Geomagnetism, paleomagnetism and rock magnetism

convener:Chie Kato(Faculty of Social and Cultural Studies, Kyushu University), Tetsuro Sato(Earthquake Research Institute, The University of Tokyo), Chairperson:Chie Kato(Faculty of Social and Cultural Studies, Kyushu University), Tetsuro Sato(Earthquake Research Institute, The University of Tokyo), Yutaka Yoshimura(Faculty of Social and Cultural Studies, Kyushu University)

We are going to discuss the issues on the magnetic fields of the Earth and planets, paleomagnetism, rock-magnetism, and their applications. This session includes following topics: (1) observation and analysis of the magnetic fields of the Earth and other planets, (2) paleomagnetic field variations obtained from natural and archaeological materials, (3) numerical simulations on the magnetic fields of the Earth and planets, (4) measurements and theories of magnetic properties of rocks, minerals, meteorites, and other materials, (5) climate changes and surface tectonics based on the paleomagnetic measurements of rocks and sediments, (6) observations of the magnetic anomalies and the crustal magnetization models of the Earth, planets, and satellites, and (7) developments of the measurement method and data analysis. We also encourage papers stimulating an interdisciplinary collaboration relating to establishment of the SEDI-Japan community. The presentations and discussions will be made in Japanese or English in this session.

1:45 PM - 2:00 PM JST | 4:45 AM - 5:00 AM UTC

[SEM13-01] Revised magnetostratigraphy and eruption timing of Afro-Arabian Large Igneous Province using new $^{40}Ar/^{39}Ar$ ages

*Yutaka Yoshimura[1], Osamu Ishizuka[2], Toshitsugu Yamazaki[1], Yuhji Yamamoto[3], Hyeon-Seon Ahn[3], Tesfaye Kidane[4], Yo-ichiro Otofuji[5,6] (1.Atmosphere and Ocean Research Institute, The University of Tokyo, 2.Institute of Earthquake and Volcano Geology, Geological Survey of Japan, AIST, 3.Center for Advanced Marine Core Research, Kochi University, 4.School of Agricultural, Earth, and Environmental Sciences, University of KwaZulu Natal, 5.Institute of GeoHistory, 6.Kobe University)

2:00 PM - 2:15 PM JST | 5:00 AM - 5:15 AM UTC

[SEM13-02] Palaeomagnetism of ca. 3-4 Ma lavas from Borgarfjordur, Iceland - magnetostratigraphy and paleosecular variation of direction

Maxwell Christopher Brown[1,2], *Yuhji Yamamoto[3], Hiroyuki Hoshi[4], Masaru Kono[5], Hidefumi Tanaka[3], Takehiro Koyaguchi[6], Brian Jicha[7], Kohei Masaoka[3,8], Vivian Sinnen[2], Justin Tonti-Filippini[2,9], Hiroto Ishikawa[3], Richard Bono[10] (1.University of Minnesota, 2. University of Iceland, 3.Kochi University, 4.Aichi University of Education, 5.Tokyo Institute of Technology, 6.University of Tokyo, 7.University of Wisconsin-Madison, 8.Kyushu University, 9.Ludwig Maximilian University of Munich, 10.University of Liverpool)

2:15 PM - 2:30 PM JST | 5:15 AM - 5:30 AM UTC

[SEM13-03] Archeointensity variation for the past millennium from Reunion Island

*Koji Fukuma[1], Hisatoshi Ito[2] (1.Department of Environmental System Science, Faculty of Science and Engineering, Doshisha University, 2.Central Research Institute for Electric Power Industry)

2:30 PM - 2:45 PM JST | 5:30 AM - 5:45 AM UTC

[SEM13-04] Analyzing the early 19th century's geographical points in latitude and longitude of 0.2 second level and geomagnetic declination through Japan from Tadataka Inoh's magnetic survey azimuth ledger simultaneously.

*Motohiro Tsujimoto[1] (1.none)

2:45 PM - 3:00 PM JST | 5:45 AM - 6:00 AM UTC

[SEM13-05] Effects of cooling from the CMB on geodynamo with different Rayleigh numbers and inner core radii

*Yuki Nishida[1], Yuto Katoh[1], Hiroaki Matsui[2], Masaki Matsushima[3], Takumi Kera[1], Atsushi Kumamoto[1] (1.Department of Geophysics, Graduate School of Science, Tohoku University, 2.Dept. of Earth and Planetary Sciences, University of California, Davis, 3.Department of Earth and Planetary Sciences, School of Science, Tokyo Institute of Technology)

3:00 PM - 3:15 PM JST | 6:00 AM - 6:15 AM UTC

[SEM13-06] An attempt to detect a stratified layer at the core surface from a geomagnetic field model

*Masaki Matsushima[1] (1.Department of Earth and Planetary Sciences, School of Science, Tokyo Institute of Technology)

Revised magnetostratigraphy and eruption timing of Afro-Arabian Large Igneous Province using new $^{40}Ar/^{39}Ar$ ages

*Yutaka Yoshimura[1], Osamu Ishizuka[2], Toshitsugu Yamazaki[1], Yuhji Yamamoto[3], Hyeon-Seon Ahn[3], Tesfaye Kidane[4], Yo-ichiro Otofuji[5,6]

1. Atmosphere and Ocean Research Institute, The University of Tokyo, 2. Institute of Earthquake and Volcano Geology, Geological Survey of Japan, AIST, 3. Center for Advanced Marine Core Research, Kochi University, 4. School of Agricultural, Earth, and Environmental Sciences, University of KwaZulu Natal, 5. Institute of GeoHistory, 6. Kobe University

We report four new $^{40}Ar/^{39}Ar$ ages on fresh groundmass grains of basalts from the 2 km thick Lima-Limo section in Ethiopia to construct magnetostratigraphy of the Afro-Arabian Large Igneous Province (AALIP). A succession of seven magnetozones (R4-N3-R3-N2-R2-N1-R1, from top to base) were identified by Ahn et al. (in press), which were tentatively correlated to Chron C11n.1r (29.477-29.527 Ma) (R4) - C11n.2n (29.527-29.970 Ma) (N3 to N2) - C11r (29.970-30.591 Ma) (R2 to R1) of the geomagnetic polarity time scale 2016 (GPTS 2016; Ogg et al., 2016).

New ages were obtained from the R4, N3, and N1 magnetozones. They have ~40 % higher precision than the previously reported ages (Coulie et al., 2003; Hofmann et al., 1997), and they are concordant with stratigraphy. We calibrated our ages using the FCs standard from Kuiper et al. (2008) and the ^{40}K decay constant of Min et al. (2000), which were used in GPTS 2016. We compared our calibrated ages and their uncertainties with GPTS 2016 and the revised GPTS model proposed by Sahy et al. (2017). The difference of the two ages obtained from the R4 magnetozone is 0.39 Myr. This supports that the R4 magnetozone belongs to Chron C11r rather than Chron C11n.1r; the former duration is 0.621 Myr and the latter 0.05 Myr (Ogg et al., 2016). The magnetozones from N1 to N3 are correlated to Chron C12n (31.23 to 30.41 Ma), which constrain that the R1 magnetozone is correlated to Chron C12r (33.09 to 31.23 Ma) (ages are based on Sahy et al., 2017).

From the duration of 0.5 Myr for C11r according to the GPTS model of Sahy et al. (2017) and the area of ~600,000 km^2 (Mohr, 1983), the average eruption rate within the R4 magnetozone is estimated to be 1.1 km^3/yr, which is about one third of the rate of the Siberian LIP (Pavlov et al., 2019). On the other hand, AALIP has large successive silicic components in the N3 magnetozone. Touchard et al. (2003) correlated them with tephra layers in ODP sediment cores of the Indian Ocean using magnetostratigraphy and geochemistry of volcanic glass, and suggested a linkage with the Oi-2 cooling event. However, based on our age determination, the tephra layers are not coeval with the AALIP silicic eruptions, and there was no tephra layer in the cores that could be correlated to the silicic eruptions (Touchard et al., 2003). This mismatch suggests that the AALIP silicic eruptions would not have caused the climate change.

Keywords: Afro-Arabian Large Igneous Province, magnetostratigraphy, 40Ar/39Ar dating, geomagnetic polarity time scale

©2021. Japan Geoscience Union. All Right Reserved.

Palaeomagnetism of ca. 3-4 Ma lavas from Borgarfjordur, Iceland - magnetostratigraphy and paleosecular variation of direction

Maxwell Christopher Brown[1,2], *Yuhji Yamamoto[3], Hiroyuki Hoshi[4], Masaru Kono[5], Hidefumi Tanaka[3], Takehiro Koyaguchi[6], Brian Jicha[7], Kohei Masaoka[3,8], Vivian Sinnen[2], Justin Tonti-Filippini[2,9], Hiroto Ishikawa[3], Richard Bono[10]

1. University of Minnesota, 2. University of Iceland, 3. Kochi University, 4. Aichi University of Education, 5. Tokyo Institute of Technology, 6. University of Tokyo, 7. University of Wisconsin-Madison, 8. Kyushu University, 9. Ludwig Maximilian University of Munich, 10. University of Liverpool

Iceland is a unique location for palaeomagnetism. Glacially and fluvially eroded valleys expose sequences of hundreds of easily accessible lavas that dip gently towards rift zones: ideal candidates for reconstructing past variations in Earth’ s magnetic field. In this study we present new palaeomagnetic directions from lavas spanning approximately 3.1-4.3 Ma from the Lundarreykjardalur valley in the Borgarfjörður region of western Iceland. In total ~1600 specimens from ~250 lavas spanning 14 sections along an 18 km transect of the Lundarháls ridge have been measured for palaeodirectional analysis. This provides one of the most detailed records of field changes recorded by lavas for this time.

This study is the culmination of two phases of field work and laboratory measurements. The first phase began in 1994 with the sampling and analysis of nine sections comprising the older half of the magnetostratigraphy. The second phase began in 2016, with an additional five sections expanding the magnetostratigraphy to younger ages. Through a combination of pilot K-Ar ages carried out in the 1990s and new $^{40}Ar/^{39}Ar$ ages we assigned a series of reversed and normal polarity lavas to chrons within the geomagnetic polarity time scale (GPTS) spanning approximately 4.3 to 3.1 Ma. $^{40}Ar/^{39}Ar$ ages confirm that the composite lava section records the reversal boundaries of C3n.1r/Cochiti (GPTS age, 4.300 Ma), Cochiti/C2Ar (4.187 Ma), C2Ar/C2An.3n (Gilbert/Gauss, 3.596 Ma) and C2An.2n/Kaena (3.116 Ma), but misses the Mammoth subchron.

Detailed variations in Earth's magnetic field can relate to changes in the geodynamo. We look at the distribution of virtual geomagnetic poles (VGPs), as well as their dispersion. Our analysis suggests the field recorded in the Lundarháls lavas is consistent with the geocentric axial dipole assumption, but that VGP dispersion may differ between chrons. This has implications for our understanding of the long-term variability of the field.

©2021. Japan Geoscience Union. All Right Reserved.

Archeointensity variation for the past millennium from Reunion Island

*Koji Fukuma[1], Hisatoshi Ito[2]

1. Department of Environmental System Science, Faculty of Science and Engineering, Doshisha University, 2. Central Research Institute for Electric Power Industry

Archeointensity variation for past one thousand years was obtained from volcanic rocks of Reunion Island in South Indian Ocean. Several geomagnetic field models such as gufm1 or cals-?k series have provided comprehensive global pictures of the geomagnetic field change for the past millennia. Although direct measurements for recent centuries form the basis of these models, for the more distant past archeomagnetic data are indispensable to construct the models. However, archeointensity data rely heavily on restricted regions and materials like archeological artifacts in Europe. This time we obtained reliable archeointensity data from lava flows of Piton de la Fournaise in Reunion Island. Hand samples of upper and lower clinkers were collected on twelve lava flows of archeomagnetic directional studies by Tanguy et al (2011). Emplacement ages are known based on historical records, 14C and archeomagnetic dating. An automated spinner magnetometer with thermal demagnetizer TSpin was utilized for Thellier measurements. Even strict selection criteria of TTA and curvature limit applied for the Thellier results still yielded paleointensity data for 64% samples and averaged paleointensities for 10/12 sites. Lava flows of recent centuries gave consistent archeointensity values with the presumed linear decay of gufm1. Reported lower g10 for 18th century seem restricted to Triaxe data on archeological artifacts. Older lava flows showed a monotonic decay of virtual dipole moment beginning at 1000 CE. Therefore the observed dipole moment decay after 1840 CE could have continued for the past millennium.

Keywords: archeointensity, Thellier method, geomagnetic field model

©2021. Japan Geoscience Union. All Right Reserved.

Analyzing the early 19th century's geographical points in latitude and longitude of 0.2 second level and geomagnetic declination through Japan from Tadataka Inoh's magnetic survey azimuth ledger simultaneously.

*Motohiro Tsujimoto[1]

1. none

The Santou-Houi-Ki is a national tresure of Japan recorded by cartographer Tadataka Inoh in 1800 to 1816 consist of 67 volumes magnetic survey azimuth ledger of Japan. In the Santou-Hou-Ki estimate 200,000 magnetic compass survey azimuth data by acculacy of 0 degree 05 minute unit were recrded with name or short description of magnetic compass survey excution reference point and target points . Inoh carried out the survey did not aplly the correction of magnetic declination<in Edo(ToKyo) was nearlyzero. It is able to calculte backward the precise position of survey excution reference point,where the value of geomagnetic declination,subtracting the magnetic survey azimuth from the true azimythto any target points are similar or approximate by using exce formula. Check the sourse books or maps of local history,and adjust the precise detail position. We must excute interdisciplinary and simultaneous analysis. This time,I will mention the transition of the geomagnetic declination in Nagasaki in the first half of the 19th century.

Keywords: Tadaataka Inoh, geomagnetic declination, inter disciplinary analysis

©2021. Japan Geoscience Union. All Right Reserved.

Effects of cooling from the CMB on geodynamo with different Rayleigh numbers and inner core radii

*Yuki Nishida[1], Yuto Katoh[1], Hiroaki Matsui[2], Masaki Matsushima[3], Takumi Kera[1], Atsushi Kumamoto[1]

1. Department of Geophysics, Graduate School of Science, Tohoku University, 2. Dept. of Earth and Planetary Sciences, University of California, Davis, 3. Department of Earth and Planetary Sciences, School of Science, Tokyo Institute of Technology

The geomagnetic field has been sustained for at least 3.5 billion years as revealed by paleomagnetic observations (Biggin et al., 2015; Tarduno et al., 2015). It is generated and maintained by dynamo action driven by convective motions of liquid iron alloy in the outer core. Studies of the thermochemical evolution of the Earth's core suggest that the solid inner core has been growing up for approximately on the last one billion years (Labrosse et al., 2001; Gubbins et al., 2004). Consequently, heat flow in the core has also been changing through the Earth's history (Driscoll and Bercovici, 2014; Patocka et al., 2020). While it is reported that sustained dynamos are dipolar-dominated in cooling from the core-mantle boundary (CMB) with an inner core smaller than the present in numerical dynamo simulations (Hori et al., 2010; Heimpel and Evans, 2013), a question remains how heat flux with relation to different inner core sizes have effects on properties of dynamo. Answers to the question are important to understand a physical state of the past Earth.

In the present study, using a numerical dynamo code Calypso (Matsui et al., 2014), we investigate the effects of cooling from the CMB on numerical dynamos with two inner core sizes. We fix the Ekman, Prandtl, and magnetic Prandtl numbers to be $E = 10^{-3}$, $Pr = 1$, and $Pm = 5$, respectively, and change the Rayleigh number (Ra) and the radius ratio of the inner core to the outer core, r_i/r_o, to be 0.25 and 0.35. To represent cooling from the CMB, fixed heat flux boundaries are set as different heat flow ratios: Q_i/Q_o = 0.5, 0.75, and 1, where Q_i and Q_o are the heat flow at the inner-core boundary (ICB) and CMB, respectively.

First, we perform numerical simulations of non-magnetic thermal convection to determine the critical Rayleigh number (Ra_{crit}), which represents the Rayleigh number for the onset of thermal convection, by the same method as Al-Shamali et al. (2004). While critical flux Rayleigh number based on the heat flux at the CMB increases with smaller Q_i/Q_o because of the decreasing the incoming heat flux at the ICB, the conventional critical Rayleigh number, which is based on the temperature difference between the ICB and CMB, is almost the same in various Q_i/Q_o. Property of onset of thermal convection can be understood in the same way regardless of different heat flow ratios in the range of $Q_i/Q_o \geqq 0.5$ by using the Ra based on the temperature.

Next, we perform dynamo simulations with the three heat flow ratios with changing the flux Ra. We find that kinetic and magnetic energy densities can be lined up based on Ra/Ra_{crit}. The parameter ranges are $2.4 \leqq Ra/Ra_{crit} \leqq 11.0$ at $r_i/r_o = 0.25$ and $2.5 \leqq Ra/Ra_{crit} \leqq 10.5$ at $r_i/r_o = 0.35$. The kinetic energy basically increases with increasing Ra/Ra_{crit}.The simulation results reveal that the change of the generated magnetic energy by Ra/Ra_{crit} is similar to the cases in the range of $Q_i/Q_o \geqq 0.5$. The change of the dipolar dominance by the Ra/Ra_{crit} is also the same as the behavior that we found in numerical dynamos in the fixed temperature boundary cases at $r_i/r_o = 0.25$ and 0.35, as we reported at JpGU Meeting 2019. Based on the simulation results and related discussion, in the range of $Q_i/Q_o \geqq 0.5$, we conclude that the

©2021. Japan Geoscience Union. All Right Reserved.

dynamo regime is determined by Ra/Ra_{crit} regardless of different heat flow ratios.

Keywords: geodynamo, the Rayleigh number, the inner core size, cooling

©2021. Japan Geoscience Union. All Right Reserved.

An attempt to detect a stratified layer at the core surface from a geomagnetic field model

*Masaki Matsushima[1]

1. Department of Earth and Planetary Sciences, School of Science, Tokyo Institute of Technology

A stably stratified layer at the top of the Earth's outer core can be present as suggested by recent seismic studies. If it is the case, upwelling and downwelling flows would not be present just below the core-mantle boundary (CMB); that is, only toroidal flows contribute to temporal changes in the geomagnetic field. Such fluid flows near the CMB can be estimated from a geomagnetic field model which provides information on the spatial distribution of the geomagnetic field and its temporal variation at the Earth's surface. The information at the CMB can be obtained through downward continuation of the geomagnetic potential field on the assumption that the mantle is an electrical insulator. Most of core flow models are estimated on the basis of the frozen-flux hypothesis. If a viscous boundary layer with finite thickness is present below the CMB, not only the motional induction but also the magnetic diffusion inside the boundary layer should cause temporal variations of the geomagnetic field. Hence core surface flows near the CMB can be estimated from a geomagnetic field model as follows; the magnetic diffusion contributing to temporal variations of the geomagnetic field is neglected below the boundary layer as in the frozen-flux approximation, whereas the magnetic diffusion is assumed to cause the temporal variations inside the boundary layer. Core surface flows below the boundary layer are assumed to be in the tangentially magnetostrophic state.

In this method to estimate a core surface flow, depths from the core surface are provided as parameters; one (ξ_1) is taken to be less than the thickness of the boundary layer, and the other (ξ_2) be larger than the thickness of the boundary layer. Hence, it might be possible to investigate the existence of a stably stratified layer at the top of the core in the following way. In case 1, only the toroidal flow is allowed inside the stratified layer, while in case 2, both the toroidal and poloidal flows are permitted there. Correlation coefficients and misfits between a temporal variation of the magnetic field obtained from a geomagnetic field model and that due to core surface flows in case 1 are calculated. Also correlation coefficients and misfits in case 2 are calculated. Then correlation coefficients and misfits thus obtained are compared with each other. The result provides information on the stratified layer at the top of the outer core.

Keywords: core surface flow, geomagnetic field, stratified layer

©2021. Japan Geoscience Union. All Right Reserved.

[J] Oral | S (Solid Earth Sciences)：S-EM Earth's Electromagnetism

Sun. Jun 6, 2021 3:30 PM - 5:00 PM JST | Sun. Jun 6, 2021 6:30 AM - 8:00 AM UTC | Ch.21 Zoom Room 21

[S-EM13] Geomagnetism, paleomagnetism and rock magnetism

convener:Chie Kato(Faculty of Social and Cultural Studies, Kyushu University), Tetsuro Sato(Earthquake Research Institute, The University of Tokyo), Chairperson:Chie Kato(Faculty of Social and Cultural Studies, Kyushu University), Tetsuro Sato(Earthquake Research Institute, The University of Tokyo), Yutaka Yoshimura(Faculty of Social and Cultural Studies, Kyushu University)

We are going to discuss the issues on the magnetic fields of the Earth and planets, paleomagnetism, rock-magnetism, and their applications. This session includes following topics: (1) observation and analysis of the magnetic fields of the Earth and other planets, (2) paleomagnetic field variations obtained from natural and archaeological materials, (3) numerical simulations on the magnetic fields of the Earth and planets, (4) measurements and theories of magnetic properties of rocks, minerals, meteorites, and other materials, (5) climate changes and surface tectonics based on the paleomagnetic measurements of rocks and sediments, (6) observations of the magnetic anomalies and the crustal magnetization models of the Earth, planets, and satellites, and (7) developments of the measurement method and data analysis. We also encourage papers stimulating an interdisciplinary collaboration relating to establishment of the SEDI-Japan community. The presentations and discussions will be made in Japanese or English in this session.

3:30 PM - 4:00 PM JST | 6:30 AM - 7:00 AM UTC

[SEM13-07] Unmixing complex sedimentary magnetic mineral assemblages

★Invited Papers

*Andrew P Roberts[1], Jinhua Li[2,3,4,5], Yan Liu[2,3,4,5], Shuangchi Liu[2,5], Hongmiao Pan[4,6], Tian Xiao[4,6], Yongxin Pan[2,3,4,5] (1.Research School of Earth Sciences, Australian National University, Canberra, ACT 2601, Australia, 2.Key Laboratory of Earth and Planetary Physics, Institute of Geology and Geophysics, Innovation Academy for Earth Sciences, Chinese Academy of Sciences, Beijing 100029, China, 3.Laboratory for Marine Geology, Qingdao National Laboratory for Marine Science and Technology, Qingdao 266061, China, 4.International Associated Laboratory of Evolution and Development of Magnetotactic Multicellular Organisms (LIA-MagMC), CNRS-CAS, Beijing 100029, China, 5.College of Earth and Planetary Sciences, University of Chinese Academy of Sciences, Beijing 100049, China, 6.Key Laboratory of Marine Ecology and Environmental Sciences, Institute of Oceanology, Chinese Academy of Sciences, Qingdao 266071, China)

4:00 PM - 4:15 PM JST | 7:00 AM - 7:15 AM UTC

[SEM13-08] Examination of the properties of remanent magnetization carried by magnetotactic bacteria in the early stages of sediment formation; example of mixed system with magnetic particles of inorganic origin

*Kohei Masaoka[1], Yuki Morono[2], Naotaka Tomioka[2], Go-Ichiro Uramoto[3], Yuhji Yamamoto[3], Masao Ohno[1] (1.Kyushu University, 2.Kochi Institute for Core Sample Research, Japan Agency for Marine-Earth Science and Technology, 3.Kochi University)

4:15 PM - 4:30 PM JST | 7:15 AM - 7:30 AM UTC

[SEM13-09] Analysis of magnetic mineral composition of a sediment core taken from the Ontong-Java Plateau and its implications to relative paleointensity estimations

*Jiaxi Li [1], Toshitsugu Yamazaki[1], Yoichi Usui[2], Takuya Sagawa[3], Junichiro Kuroda[1] (1.Atmosphere and Ocean Research Institute, The University of Tokyo, 2.Japan Agency for Marine-Earth Science and Technology, 3.Kanazawa University)

4:30 PM - 4:45 PM JST | 7:30 AM - 7:45 AM UTC

[SEM13-10] Environmental magnetic study of a Holocene sediment core from the Yeongsan Estuary, Southwest Korea

*Hyeon-Seon Ahn[1], Jaesoo Lim[2] (1.Kochi University, 2.Korea Institute of Geoscience and Mineral Resources)

4:45 PM - 5:00 PM JST | 7:45 AM - 8:00 AM UTC

[SEM13-11] **Relationship between the abundance of the exsolved magnetite and the valence state of iron in single plagioclase crystal separated from Doshi gabbro**

*Yujiro Tamura[1], Masahiko Sato[2], Ryoichi Nakada[3], Chie Kato[4], Shinji Yamamoto[1] (1.Yokohama National University, 2.The University of Tokyo, 3.Japan Agency for Marine-Earth Science and Technology, 4.Kyushu University)

Unmixing complex sedimentary magnetic mineral assemblages

*Andrew P Roberts[1], Jinhua Li[2,3,4,5], Yan Liu[2,3,4,5], Shuangchi Liu[2,5], Hongmiao Pan[4,6], Tian Xiao[4,6], Yongxin Pan[2,3,4,5]

1. Research School of Earth Sciences, Australian National University, Canberra, ACT 2601, Australia, 2. Key Laboratory of Earth and Planetary Physics, Institute of Geology and Geophysics, Innovation Academy for Earth Sciences, Chinese Academy of Sciences, Beijing 100029, China, 3. Laboratory for Marine Geology, Qingdao National Laboratory for Marine Science and Technology, Qingdao 266061, China, 4. International Associated Laboratory of Evolution and Development of Magnetotactic Multicellular Organisms (LIA-MagMC), CNRS-CAS, Beijing 100029, China, 5. College of Earth and Planetary Sciences, University of Chinese Academy of Sciences, Beijing 100049, China, 6. Key Laboratory of Marine Ecology and Environmental Sciences, Institute of Oceanology, Chinese Academy of Sciences, Qingdao 266071, China

Magnetic unmixing is an important part of environmental magnetic and sedimentary paleomagnetic studies because unambiguous magnetic mineral identification is usually a prerequisite for reconstructing magnetic signals of interest. Unmixing is an inverse problem that can have an infinite number of solutions, so magnetic studies tend to focus on identifying constituent magnetic minerals and their relative grain size variations through a series of magnetic measurements to minimize ambiguities by “supervised” unmixing. Supervised unmixing is normally achieved using bulk magnetic measurements that are used to indirectly interpret magnetic mineral components. Direct magnetic mineral observation using electron microscopy is a valuable addition to such studies, although it often raises questions about the representativeness of observed particles in relation to measured bulk magnetic properties. Challenges associated with magnetic unmixing are illustrated here from a detailed magnetic and electron microscopy study of a deep-sea surface sediment sample from the central Pacific Ocean. Magnetic analyses are interpreted to reveal the presence of 2-4 magnetic components depending on the type of mathematical functions used for fitting and whether the unmixing is unsupervised or supervised, while comprehensive electron microscope observations indicate the presence of 8 (titano-)magnetite particle types. Magnetite magnetofossils are also identified with extensive searching by transmission electron microscopy, but their contribution to the sediment magnetic properties is small. Combined results indicate that two particle types dominate the magnetic properties. This work illustrates the potential magnetic complexity of sediments and the need for detailed supervision of unmixing. Our results demonstrate the value of electron microscope observations in sedimentary magnetic studies and illustrate the potential magnetic complexity of sediments, which needs to be recognized to arrive at meaningful interpretations of conventional bulk magnetic data.

Keywords: Magnetic unmixing, Environmental magnetism, Paleomagnetism

©2021. Japan Geoscience Union. All Right Reserved.

Examination of the properties of remanent magnetization carried by magnetotactic bacteria in the early stages of sediment formation; example of mixed system with magnetic particles of inorganic origin

*Kohei Masaoka[1], Yuki Morono[2], Naotaka Tomioka[2], Go-Ichiro Uramoto[3], Yuhji Yamamoto[3], Masao Ohno[1]

1. Kyushu University, 2. Kochi Institute for Core Sample Research, Japan Agency for Marine-Earth Science and Technology, 3. Kochi University

Variation of the past geomagnetic field is recorded in marine sediments as a fossil magnetization, called natural remanent magnetization (NRM). The carrier of the NRM is not only detrital magnetic grains but also biogenic magnetic grains originated from magnetotactic bacteria. To investigate characters of NRM carried by biogenic magnetic grains we have cultured the magnetotactic bacteria *Magnetospirillum magnetotacticum* MS-1 (here under, MS-1) in laboratory. We made samples using them for remanent magnetization measurements to simulate the very early process of sediment formation.
Properties of the remanent magnetization carried by the samples used only MS-1 cells have been presented in Masaoka et al (2020JpGU). However, there is a difference from actual sediments containing magnetic particles of inorganic origin, and it is not possible to make a simple comparison. Various experiments and magnetic analysis were performed to fill this difference: we have made two types of samples containing reagent magnetite and MS-1 cells, and MS-1 cells crushed by ultrasonic. We will report and discuss the results.

©2021. Japan Geoscience Union. All Right Reserved.

Analysis of magnetic mineral composition of a sediment core taken from the Ontong-Java Plateau and its implications to relative paleointensity estimations

*Jiaxi Li [1], Toshitsugu Yamazaki[1], Yoichi Usui[2], Takuya Sagawa[3], Junichiro Kuroda[1]

1. Atmosphere and Ocean Research Institute, The University of Tokyo, 2. Japan Agency for Marine-Earth Science and Technology, 3. Kanazawa University

Marine sediments contain considerable amounts and different types of magnetic mineral particles. Magnetic minerals may be statistically aligned to the direction of the ambient geomagnetic field so that potentially preserve geomagnetic intensity records in the past. However, different types of magnetic minerals should preserve the remanent magnetization in different manners. And the compositional variation of magnetic mineral assemblages in marine sediments may hinder us from extracting reliable geomagnetic paleointensity records.

We studied a sediment core taken from the Ontong-Java plateau and managed to extract the geomagnetic paleointensity variation from it. The magnetic mineral assemblages of the sediment core are principally a two-component mixture of terrigenous and biogenic magnetite with changing amounts of carbonates. So it provides an opportunity to assess influence that compositional variations in marine sediments could bring to relative paleointensity (RPI) estimations and thus to distinguish different contributions of the biogenic and terrigenous components to paleointensity signal recording in marine sediments.

RPI obtained by normalizing natural remanent magnetization (NRM) with anhysteretic remanent magnetization (ARM) shows downcore decreases, and it has an inverse correlation with the ratio of ARM susceptibility (k_{ARM}) to saturation isothermal remanent magnetization (SIRM) (k_{ARM}/SIRM). This indicates that the RPI signal became apparently weaker with increasing proportion of biogenic to terrigenous magnetic minerals. Moreover, NRM-ARM demagnetization diagrams show curvature, which indicates that the coercivity distributions of NRM and ARM are different. Therefore, we tried to distinguish the different contributions of the biogenic and terrigenous components to the RPI record by recalculating NRM-ARM demagnetization slopes in relatively higher and lower coercivity intervals. If we assume that the magnetization of the higher coercivity interval is carried by biogenic magnetite while that of the lower coercivity interval is carried by the terrigenous component, RPI recording efficiency of the biogenic component may be lower than that of the terrigenous component. The validity of this assumption was investigated by first-order reversal curve (FORC) measurements, transmission electron microscope (TEM) observations, low-temperature measurements, and extraction of silicate-hosted magnetic inclusion from the sediments, and the results proved that NRM of the higher coercivity interval is carried mainly by biogenic magnetite. But our conclusion contradicts with the previous studies using a similar method; some previous studies suggested higher RPI recording efficiency of the biogenic magnetic component than the terrigenous component. Different concentrations of silicate-hosted magnetic inclusions due to different sedimentary environments might be a possible reason for the contradiction; the contribution of silicate-hosted magnetic inclusions to NRM is minor in our sediments. However, this contradiction remains to be studied further. The goal of our research is to figure out the mechanism how magnetic minerals derived from different sources contribute to remanent magnetizations of sediments. Then, it is expected that influences on RPI estimations brought by compositional variations of magnetic mineral assemblages in marine sediments will be able to be known.

©2021. Japan Geoscience Union. All Right Reserved.

Keywords: geomagnetic paleointensity, silicate-hosted magnetic mineral inclusion, biogenic magnetite, Ontong-Java plateau

©2021. Japan Geoscience Union. All Right Reserved.

Environmental magnetic study of a Holocene sediment core from the Yeongsan Estuary, Southwest Korea

*Hyeon-Seon Ahn[1], Jaesoo Lim[2]

1. Kochi University, 2. Korea Institute of Geoscience and Mineral Resources

The sensitivity of magnetic properties to environmental processes may provide useful information on paleoenvironmental changes in estuarine environments. Magnetic property studies of estuaries are less common than other environments. Owing to the west coast of South Korea having an abundance of estuaries, it can provide a good place to study these processes in estuarine environments. We analyzed a variety of magnetic properties based on magnetic susceptibility, hysteresis parameters, progressive acquisition of isothermal remanent magnetization (IRM), and first-order reversal curve data, in addition to electron microscopic observations of magnetic minerals, from a Holocene muddy sediment core recovered from the Yeongsan Estuary on the west coast of South Korea. The age of the studied sediment core was well constrained based on radiocarbon dates. We examined diagenetic effects on magnetic properties and tested their availability as proxies of paleoenvironmental change. The presence of generally low magnetic susceptibilities, ubiquitous authigenic magnetic components such as pyrite and greigite suggested that the analyzed sediments had undergone considerable early diagenetic alteration. Our results confirm that the use of initial bulk susceptibility as a stand-alone environmental change proxy is not recommended unless it is supported by additional magnetic analyses. We recognized the existence of ferromagnetic-based variabilities related to something besides the adverse diagenetic effects, and examined possible relationships with sea-level and some of major climate changes during the Holocene. The most remarkable finding of this study is the two distinct intervals with high values in magnetic coercivity (B_c), coercivity of remanence (B_{cr}), and ratio of remanent saturation moment to saturation moment (M_{rs}/M_s) that were well coincident with the respective abrupt decelerations in the rate of sea-level rise occurred at around 8.2 and 7 thousand years ago. Furthermore, it is inferred that such condition with abrupt drop in sea-level rise rate would be favorable for the abrupt modification of grain size distribution of ferromagnetic minerals toward more single-domain-like content.

Keywords: Holocene sediments, magnetic properties, estuary, paleoenvironments, diagenesis

©2021. Japan Geoscience Union. All Right Reserved.

Relationship between the abundance of the exsolved magnetite and the valence state of iron in single plagioclase crystal separated from Doshi gabbro

*Yujiro Tamura[1], Masahiko Sato[2], Ryoichi Nakada[3], Chie Kato[4], Shinji Yamamoto[1]

1. Yokohama National University, 2. The University of Tokyo, 3. Japan Agency for Marine-Earth Science and Technology, 4. Kyushu University

Paleomagnetic measurements using single silicate crystals such as quartz (Tarduno et al., 2010), zircon (Sato et al., 2015), and plagioclase (Kato et al., 2018) play a key role on the geomagnetic field study. Among them, the plagioclase crystal sometimes contains fine-grained and rod-shaped magnetite as exsolution lamellae, and the paleomagnetic record of exsolved magnetite likely provides reliable paleomagnetic information for a long era. However, the exsolved magnetite does not commonly exist in plagioclase crystals of various rock samples, and its formation mechanism has not been understood. It is expected that the formation of magnetite exsolution lamellae is caused by the decrease of maximum solubility of iron in plagioclase crystals during the cooling process of rocks under subsolidus conditions. Additionally, important factors controlling the exsolution of magnetite are the cooling speed of crystal, iron concentration, and valence state of iron in plagioclase should be important factors controlling the exsolution of magnetite. Then, to understand the exsolution mechanism, investigations of iron valence state and abundance of exsolved magnetite within a single plagioclase crystal are suitable because these factors are not significantly different in a single crystal. This study investigated the plagioclase crystal from the Doshi gabbro, northwest of the Tanzawa tonalitic complex, for microscopic observation and measurements of iron valence state. Thin sections with double-side polished were made for the observation by polarizing microscope and electron microscope. Subsequently, we analyzed the composition of plagioclase by Electron probe Micro-Analyzer and the valence state of iron within plagioclase by K-edge X-ray absorption fine structure analysis. The abundance of exsolved magnetite has estimated from backscattered electron images in the image analysis using the Image J software. The plagioclase crystal shows the clear zonal structure of exsolved magnetite parallel with the chemical zoning structure. In order to investigate the formation mechanism of magnetite exsolution, we compared the iron valence within plagioclase with the abundance of exsolved magnetite and iron concentration around the measured spot. The iron valence of plagioclase in each spot was approximately 2.5 to 2.6, and there is no clear relationship between the iron valence of plagioclase and the abundance of exsolved magnetite. We additionally estimated the iron valence state in plagioclase crystal before the magnetite exsolution from iron valence measurement and the abundance of exsolved magnetite. As a result, it was suggested that exsolved magnetite tends to form in the areas that originally had a high iron valence. The causes of the differences in iron valence in plagioclase will also be discussed.

Keywords: magnetite exsolution, plagioclase, iron valence

©2021. Japan Geoscience Union. All Right Reserved.

[J] Poster | S (Solid Earth Sciences)：S-EM Earth's Electromagnetism

Sun. Jun 6, 2021 5:15 PM - 6:30 PM JST | Sun. Jun 6, 2021 8:15 AM - 9:30 AM UTC | Ch.11_1

[S-EM13] Geomagnetism, paleomagnetism and rock magnetism

convener:Chie Kato(Faculty of Social and Cultural Studies, Kyushu University), Tetsuro Sato(Earthquake Research Institute, The University of Tokyo)

We are going to discuss the issues on the magnetic fields of the Earth and planets, paleomagnetism, rock-magnetism, and their applications. This session includes following topics: (1) observation and analysis of the magnetic fields of the Earth and other planets, (2) paleomagnetic field variations obtained from natural and archaeological materials, (3) numerical simulations on the magnetic fields of the Earth and planets, (4) measurements and theories of magnetic properties of rocks, minerals, meteorites, and other materials, (5) climate changes and surface tectonics based on the paleomagnetic measurements of rocks and sediments, (6) observations of the magnetic anomalies and the crustal magnetization models of the Earth, planets, and satellites, and (7) developments of the measurement method and data analysis. We also encourage papers stimulating an interdisciplinary collaboration relating to establishment of the SEDI-Japan community. The presentations and discussions will be made in Japanese or English in this session.

[SEM13-P01] Brunhes-Matuyama geomagnetic reversal record from Terasaki, Boso Peninsula

*Hirokuni Oda[1], Hiroomi Nakazato[2], Futoshi Nanayama[1], Yumiko Harigane[1] (1.Institute of Geology and Geoinformation, Geological Survey of Japan, AIST, 2.National Agriculture and Food Research Organization)

[SEM13-P02] Plaeomagnetic study of the Kusatsu-Shirane volcano, Gunma, Japan

*Nagisa Sawada[1], Nobuko Kametani[2], Kazuo Kawasaki[1], Yasuo Ishizaki[1], Akihiko Terada[3] (1.University of Toyama, 2.Mount Fuji Research Institute, Yamanashi Prefectural Government, 3.Tokyo Institute of Technology)

[SEM13-P03] The Laschamp and a new post-Laschamp excursions repeating directional swings from Lake Suigetsu varved sediments

*Masayuki Hyodo[1,2], Takeshi Nakagawa[3], Hayato Matsushita[2], Ikuko Kitaba[3], Keitaro Yamada[3], Shota Tanabe[2], Balazs Bradak[1,4], Danielle McLean[5], Richard A. Staff[6], Victoria C. Smith[5], Paul G. Albert[5], Akiteru Yamasaki[7], Junko Kitagawa[8,7] (1.Research Center for Inland Seas, Kobe University, 2.Department of Planetology, Kobe University, 3.Research Centre for Palaeoclimatology, Ritsumeikan University, 4.Department of Physics, University of Burgos, 5.School of Archaeology, University of Oxford, 6.Scottish Universities Environmental Research Centre (SUERC), University of Glasgow, 7.Fukui Prefectural Satoyama-Satoumi Research Institute, 8.Varve Museum)

[SEM13-P04] Rock-magnetic properties of topmost sediments in Omura Bay, Nagasaki Prefecture

*Naoto Ishikawa[1], Yoriko Yokoo[2], Kazumi Matsuoka[3] (1.Faculty of Sustainable Design, Toyama University, 2.Faculty of Scinece and Engineering, Doshisha University, 3.Institute for East China Sea Research, Nagasaki University)

[SEM13-P05] Paleomagnetic Dating on Tsunami Boulders from the Kingdom of Tonga

*Tetsuro Sato[1], Norihiro Nakamura[2], Hiroyuki Nagahama[3], Masahiko Sato[4], Kazuhisa Goto[4], Masashi Watanabe[5], Akira Ikeda[3], Kenji Satake[1], Taaniela Kula[6] (1.Earthquake Research Institute, The University of Tokyo, 2.Institute for Excellence in Higher Education, Tohoku University, 3.Department of Earth Science, Tohoku University, 4.Department of Earth and Planetary Science, The University of Tokyo, 5.Faculty of Science and Engineering, Chuo University, 6.Ministry of Lands and Natural Resources)

[SEM13-P06] Influence of biogenic magnetite on paleointensity estimations inferred from FORC-PCA of sediments from the western equatorial Pacific

Kosuke Inoue[1], *Toshitsugu Yamazaki[1], Yoichi Usui[2] (1.Atmosphere and Ocean Research Institute, The University of Tokyo, 2.Japan Agency for Marine-Earth Science and Technology)

[SEM13-P07] Solitary magnetostrophic Rossby waves

*Kumiko Hori[1,2], Steve M Tobias[2], Chris A Jones[2] (1.Graduate School of System Informatics, Kobe University, 2.Department of Applied Mathematics, University of Leeds)

[SEM13-P08] Effects of driving mode of convection on a spherical dynamo action with a small inner core

*Futoshi Takahashi[1], Hinami Taniguchi[2] (1.Faculty of Science, Kyushu University, 2.School of Science, Kyushu University)

[SEM13-P09] Rock-magnetic and mineralogical properties of the exsolved magnetite in plagioclase crystal

*Masahiko Sato[1], Masashi Ushioda[2], Ryoichi Nakada[3], Yujiro Tamura[4], Shinji Yamamoto[4] (1.The University of Tokyo, 2.Shikoku Research Institute Inc., 3.Japan Agency for Marine-Earth Science and Technology, 4.Yohohama National University)

[SEM13-P10] Rock-magnetic properties of isocubanite from submarine hydrothermal deposits in the Okinawa Trough

*Chie Kato[1], Masao Ohno[1], Yoshihiro Kuwahara[1], Tadahiro Hatakeyama[2], Yasuhiro Yamada[3], Shuhei Totsuka[4], Kazuhiko Shimada[1], Jun-ichiro Ishibashi[1], Toshiro Nagase[5] (1.Kyushu University, 2.Okayama University of Science, 3.Tokyo University of Science, 4.National Institute of Advanced Industrial Science and Technology, 5.Tohoku University)

[SEM13-P11] Contribution of equatorially antisymmetric buoyancy to polarity reversals in geodynamo models

*Takumi Kera[1], Hiroaki Matsui[3], Masaki Matsushima[2], Yuki Nishida[1], Yuto Katoh[1] (1.Department of Geophysics, Graduate School of Science, Tohoku University, 2.Tokyo Institute of Technology, 3.Dept. of Earth and Planetary Sciences, University of California, Davis)

[SEM13-P12] **Simultaneous observation of the geomagnetic field at different sites using two SQUID magnetometer systems**

*Jun Kawai[1], Miki Kawabata[1], Masakazu Miyamoto[1] (1.Applied Electronics Laboratory, Kanazawa Institute of Technology)

Brunhes-Matuyama geomagnetic reversal record from Terasaki, Boso Peninsula

*Hirokuni Oda[1], Hiroomi Nakazato[2], Futoshi Nanayama[1], Yumiko Harigane[1]

1. Institute of Geology and Geoinformation, Geological Survey of Japan, AIST, 2. National Agriculture and Food Research Organization

We report Brunhes-Matuyama geomagnetic reversal records from Terasaki, which is several km northeast of Chiba Section, Boso Peninsula. Oriented paleomagnetic drill core samples were taken from ~3.5m thickness silt layers at intervals of a few to ten centimeters. Three volcanic ash layers were identified and the middle ash layer could be recognized as Byk-E, which is assigned as a key bed for Chibanian. Paleomagnetic analyses were conducted using (1) stepwise alternating field demagnetization (AFD), (2) stepwise thermal demagnetization (ThD), (3) stepwise ThD up to 175-300˚C followed by stepwise AFD, etc. Although the third method was most successful in identifying primary magnetization, it is not always successful. In order to extract primary magnetization from most of the samples, we conducted combined analysis of remagnetization circles (McFadden&McElhinny, 1988) using a software paleomagnetism.org (Koymans et al., 2016). The calculated paleomagnetic directions (VGP latitudes) are consistent with those reported by Haneda et al. (2020). Correlation of VGP latitude in combination with rock magnetic results suggest the sedimentation rate at the studies site is about 3 times lower than that at Chiba Section. Further, we plan to discuss on the origin of magnetic minerals including magnetite and greigite, and its relation to decay/alterlation during thermal demagnetization.

Keywords: Paleomagnetism, Boso Peninsula, Geomagnetic Reversal, greigite, combined analysis of remagnetization circles

©2021. Japan Geoscience Union. All Right Reserved.

Plaeomagnetic study of the Kusatsu-Shirane volcano, Gunma, Japan

*Nagisa Sawada[1], Nobuko Kametani[2], Kazuo Kawasaki[1], Yasuo Ishizaki[1], Akihiko Terada[3]

1. University of Toyama, 2. Mount Fuji Research Institute, Yamanashi Prefectural Government, 3. Tokyo Institute of Technology

The ring of fire in Japan has 111 active volcanoes. Some have erupted frequently and caused serious loss of life and damages. The Kusatsu-Shirane volcano at Gunma prefecture, Japan is an active volcano and had a sudden phreatic eruption occurred with 12 casualties in 2018. Understandings of past volcanic eruptions are essential for minimizing future losses and therefore accurate age information of past eruptions is important. Paleomagnetic analyses were carried out on 36 volcanic ash specimens and 11 paleosoil specimens from 47 units. Rock magnetic analyses show that the major magnetic mineral in the specimens is likely pseudosingle-domain titanomagnetite. The characteristic remanent magnetization (ChRM) directions of individual specimens were isolated by alternating field demagnetization. The unit mean ChRM directions at which radius of 95% confidence circle is less than 8˚ were selected for estimating the palaeomagnetic age. The 19 unit mean ChRM directions are compared to the three different composite paleosecular variation curves from either Lake Biwa in Japan or the Tohoku-oki earthquake rupture zone, and found that the BIWA SV-3 curve from Lake Biwa is well-matched for the ChRM of the Kusatsu-Shirane sediments. The results indicate that the observed unit mean ChRM directions likely record the secular variation, giving palaeomagnetic ages for 18 units. The observed paleomagnetic ages show good agreements with radiocarbon dates and provided for previously-undated tephra layers at 11 units. Therefore, the paleomagnetic dating method for the volcaniclastic debris (volcanic ash) deposited on land at the Kusatsu-Shirane volcano is an effective method for directly dating the tephra layers to determine past volcanic eruptions.

Keywords: Paleomagnetic secular variation , Kusatsu-Shirane Volcano, Holocene, Tephra

©2021. Japan Geoscience Union. All Right Reserved.

The Laschamp and a new post-Laschamp excursions repeating directional swings from Lake Suigetsu varved sediments

*Masayuki Hyodo[1,2], Takeshi Nakagawa[3], Hayato Matsushita[2], Ikuko Kitaba[3], Keitaro Yamada[3], Shota Tanabe[2], Balazs Bradak[1,4], Danielle McLean[5], Richard A. Staff[6], Victoria C. Smith[5], Paul G. Albert[5], Akiteru Yamasaki[7], Junko Kitagawa[8,7]

1. Research Center for Inland Seas, Kobe University, 2. Department of Planetology, Kobe University, 3. Research Centre for Palaeoclimatology, Ritsumeikan University, 4. Department of Physics, University of Burgos, 5. School of Archaeology, University of Oxford, 6. Scottish Universities Environmental Research Centre (SUERC), University of Glasgow, 7. Fukui Prefectural Satoyama-Satoumi Research Institute, 8. Varve Museum

Geomagnetic excursions represent dynamic natures of the geodynamo during declined dipole-field periods. Many sedimentary records of excursions have been reported since 1970s, but none of them resolves sub-centennial scale field-changes. We report a tri-decadal resolution Laschamp Excursion record from Lake Suigetsu varved sediments that reveals many detailed features. A high resolution ^{14}C dates and varve chronology-based Bayesian age model reveals the Laschamp Excursion ranges from 42,340 to 41,410 IntCal13 (42,400 to 41,700 IntCal20) yr BP, consisting of five short (20 to 110 yr) excursional directional-swings. We found another excursion ranging from 38,580 to 38,030 IntCal13 (39,080 to 38,580 IntCal20) yr BP composed with similar swings. Both excursions coincided with the $\Delta^{14}C$ maxima in Lake Suigetsu as well as the ^{10}Be flux maxima in Greenland. We simulated how the high-frequency directional swings in the high sedimentation rate (s.r.) (72 cm/kyr) sediments are altered when recorded in sediments with lower s.r., by downsizing the data assuming response functions defined by a sample thickness and a half lock-in depth of post depositional remanent magnetization. As s.r. decreases, the short directional swings are gradually filtered-out and/or combined, which causes (1) stepwise decreases in the time duration of excursion, and (2) a drastic change of virtual geomagnetic pole (VGP)-pass from multiple linear swings between northern high-latitudes and northern mid-/southern latitudes to a large clockwise open loop with a precursory small episode. These features of the downsized Lake Suigetsu data are consistent with many previous observations in sediment with lower s.r. The excursional VGPs of Lake Suigetsu repeat swinging constrained by two longitudinal bands through the Pacific Ocean and the Indian Ocean-Africa. In addition, they make four clusters centered in the North Pacific, the South Pacific, the South Indian Ocean, and the eastern Africa in chronological order, which accounts for the apparent clockwise open loop of VGP-pass in low s.r. records. The clusters include the VGPs inferred from lava flows associated with the Laschamp Excursion from various regions of the world, which indicate dominance of non-axial dipolar fields whose sources located under the four clusters during the excursion.

Keywords: Paleomagnetism, Laschamp Excursion, dipolar field dominance, Lake Suigetsu, varved sediments, IntCal13/IntCal20 ages

©2021. Japan Geoscience Union. All Right Reserved.

Rock-magnetic properties of topmost sediments in Omura Bay, Nagasaki Prefecture

*Naoto Ishikawa[1], Yoriko Yokoo[2], Kazumi Matsuoka[3]

1. Faculty of Sustainable Design, Toyama University, 2. Faculty of Scinece and Engineering, Doshisha University, 3. Institute for East China Sea Research, Nagasaki University

We are analyzing magnetic properties of topmost sediments in Omura Bay, Nagasaki Prefecture, in order to differentiate magnetic signals from magnetic grains of different sources in the sediments. The bay is a highly enclosed bay with the water depth of 15-20m, connecting to East China Sea through two narrow channels. There is no large river loading to the bay. Sediments above 4.5 m below seafloor consists of homogenous silty clay with the medium grain size of 4 micrometer. Severe hypoxia expands every summer in bottom water (July-August). We are also examining the effect of such an anoxic condition in the bottom water on magnetic properties in the topmost sediments.
Sediment cores of about 15 cm long were sampled at the central part of the bay in July and October 2017 by a G.S. type-gravity core sampler. The cores were sliced at 1cm interval, and each slice was freeze-dried. Dry powder samples were packed into 1cc-plastic cubes. The cubes and remaining powder samples were subjected to rock magnetic experiments.
Results from thermo-magnetic analyses with magnetic balance and progressive thermal demagnetization experiments of composite isothermal remanences (IRMs) indicate the existence of magnetite, maghematized magnetite and hematite as principal magnetic minerals. Values of initial magnetic susceptibility, saturation magnetization and saturation remanent magnetization show no remarkable change through the cores. Downcore increase of the susceptibility of anhysteretic remanence and S-ratio (S_-0.1T) and downcore increase of the coercivity of remanence are detected. Results from coercivity distribution analyses of IRM acquisition and demagnetization curves suggest that the contribution of high-coercivity magnetic grain, probably hematite, to the whole of IRM increase downcore although its amount does not change. It may be implied that a downward selective dissolution of fine-grained magnetite by the effect of early diagenesis in the topmost sediments results in downward increases of magnetic grain size and contribution (relative amount) of hematite. We have not found any difference in magnetic properties and their variations mentioned above between the two cores of different month.

Keywords: rock-magnetic property, topmost marine sediment, origin of magentic minerals, eary diagenesis

©2021. Japan Geoscience Union. All Right Reserved.

Paleomagnetic Dating on Tsunami Boulders from the Kingdom of Tonga

*Tetsuro Sato[1], Norihiro Nakamura[2], Hiroyuki Nagahama[3], Masahiko Sato[4], Kazuhisa Goto[4], Masashi Watanabe[5], Akira Ikeda[3], Kenji Satake[1], Taaniela Kula[6]

1. Earthquake Research Institute, The University of Tokyo, 2. Institute for Excellence in Higher Education, Tohoku University, 3. Department of Earth Science, Tohoku University, 4. Department of Earth and Planetary Science, The University of Tokyo, 5. Faculty of Science and Engineering, Chuo University, 6. Ministry of Lands and Natural Resources

Viscous remanent magnetization partially overprints the natural remanent magnetization in reworked boulders. The magnitude of such magnetization depends on the time passed since reworking, as well as ambient temperature, for which there is a well-known theoretical time-temperature relationship of remanent magnetization. Most references used the paleomagnetic dating protocol, which is applicable to single-domain particle assemblages, while experimental data often disagree with other dating applications (e.g., radiocarbon and U-series dating). Here, we use modified time-temperature relationship based on a stretched exponential relaxation function that accounts for the complex magnetic structures. Samples of tsunami boulders from the Kingdom of Tonga have chemical-viscous remanent magnetization, and their non-exponential relaxation is well fitted by the stretched exponential relaxation function. Combining the modified time-temperature relationship of remanent magnetization, which considers the observed stretching exponent value, and sea level change data, we estimate the reworked age of the tsunami boulders.

Keywords: Tsunami boulder, Age estimation, Remanent magnetization

©2021. Japan Geoscience Union. All Right Reserved.

Influence of biogenic magnetite on paleointensity estimations inferred from FORC-PCA of sediments from the western equatorial Pacific

Kosuke Inoue[1], *Toshitsugu Yamazaki[1], Yoichi Usui[2]

1. Atmosphere and Ocean Research Institute, The University of Tokyo, 2. Japan Agency for Marine-Earth Science and Technology

Relative paleointensity (RPI) is estimated from sediments as normalized intensity: natural remanent magnetization (NRM) intensity divided by artificial magnetization intensity such as anhysteretic remanent magnetizaton (ARM). This method requires that magnetic particle composition is uniform and hence normalized intensity depends only on their abundance and geomagnetic intensity. Recent studies have shown wide occurrence of biogenic magnetite in marine sediments, which are originated from magnetotactic bacteria with magnetite chains in their cells. Difference of NRM and ARM acquisition efficiencies between biogenic and terrigenous magnetite needs to be understood for RPI estimations.

In this study, a relation between normalized intensity and magnetic mineral compositions was investigated using three sediment cores taken from the western equatorial Pacific, in which the average normalized intensities are largely different. In the western equatorial Pacific, high solar radiation makes sea surface temperature the highest in the world. The variations of precipitation in the western equatorial Pacific are related with the Inter Tropical Convergence Zone, whose southward migration causes increasing precipitation and fluvial discharge in New Guinea. Undercurrents deliver fluvial particles from New Guinea to the studied region. The ratio of biogenic to detrital magnetic particles is expected to vary with the distance from New Guinea, which helps to estimate the relation between normalized intensity and magnetic particle compositions.

First-order reversal curves (FORCs) are measured by sweeping the inside of a magnetic hysteresis loop, and magnetization (M) is given by function of a reversal field (Br) and a given field (B). FORC distribution ρ (B, Br) is defined as a mixed second derivative of M by B and Br, and plotted in the (Bc, Bu) axes to which (B, Br) is rotated -45°, called FORC diagram. Bc and Bu represent coercivity and magnetostatic interactions, respectively. In geological samples, biogenic and terrigenous magnetites are characterized by a narrow “central ridge” along the Bc axis and by a broad distribution with a significant vertical spread (background component), respectively. Bending and collapse of biogenic magnetite chains also contribute to the background component. This study conducted principal component analysis (PCA) of FORC diagrams and decomposed into the biogenic magnetite and the terrigenous input. It is revealed that the ratio of biogenic and terrigenous magnetite influences the normalized intensity. Larger contribution of biogenic magnetite causes lower relative paleointensity. Even when biogenic magnetite dominates, difference in chain bending could influence the normalized intensity. In conclusion, for estimating relative paleointensity, it is necessary to consider the effect of the variations of biogenic and terrigenous contributions and the difference in the preservation of biogenic-magnetite chain structure.

Keywords: FORC diagram, relative paleointensity, biogenic magnetite

©2021. Japan Geoscience Union. All Right Reserved.

Solitary magnetostrophic Rossby waves

*Kumiko Hori[1,2], Steve M Tobias[2], Chris A Jones[2]

1. Graduate School of System Informatics, Kobe University, 2. Department of Applied Mathematics, University of Leeds

Finite-amplitude hydromagnetic Rossby waves in the magnetostrophic regime are studied. We consider the slow mode, which travels in the opposite direction to the hydrodynamic or fast mode, in the presence of a toroidal magnetic field and zonal flow by means of quasi-geostrophic models for thick spherical shells. The weakly nonlinear long waves are derived asymptotically using a reductive perturbation method. The problem at the first order is found to obey a second-order ordinary differential equation, leading to a hypergeometric equation for a Malkus field and a confluent Heun equation for an electrical wire field, and is non-singular when the wave speed approaches the mean flow. Investigating its neutral non-singular eigensolutions for different basic states, we find the evolution is described by the Korteweg–de Vries equation. This implies that the nonlinear slow wave forms solitons and solitary waves. These may take the form of a coherent eddy, such as a single anticyclone. We speculate on the relation of the anticyclone to the asymmetric gyre seen in the Earth’ s fluid core, and in state-of-the-art dynamo direct numerical simulations.

Keywords: Magnetohydrodynamics, Waves in rotating fluids, Earth's core

©2021. Japan Geoscience Union. All Right Reserved.

Effects of driving mode of convection on a spherical dynamo action with a small inner core

*Futoshi Takahashi[1], Hinami Taniguchi[2]

1. Faculty of Science, Kyushu University, 2. School of Science, Kyushu University

Paleomagnetic studies suggest that the geodynamo has been working for ca. 4.2 billion years (Tarduno et al., 2020). During the long lifetime of the geodynamo it is often argued that the geomagnetic field is maintained without the solid inner core in the Hadean and Archean eons. Moreover, high electrical conductivity of the core material suggests a young age of the inner core (e.g., Ohta et al., 2016). Geomagnetic signature restored from paleomagnetic samples is possibly the only tool to infer the age of inner core nucleation based on observations (Biggin et al. 2016). However, we still have little knowledge how to properly interpret paleomagnetic data, which is, in part, ascribed to lack of the understanding of geodynamo behavior in an old era and the mechanisms controlling it. In order to enhance our understanding of the geodynamo, we have investigated basic features of convection and dynamos relying on numerical dynamo modeling. Also in this study, we will proceed along this line.

We focus on the buoyancy source distribution to drive convection in the Earth’s core. Light element ejection and latent heat release upon inner core growth fuels convection from the bottom, while various mechanisms such as uniformly distributed heat source, secular cooling of the core, iron-snow etc. provide negative buoyancy from the top. In fact, the geodynamo is driven by a mixture of the “bottom-up” and “top-down” buoyancy, strongly depending on the origin and evolution history of the Earth. Bearing the fact in mind, here we try to understand the effects of the individual driving mode on convection and magnetic field generation processes as a first step.

We consider a problem of an MHD dynamo in a rotating spherical shell, of which the inner to outer core radius ratio is 0.2. This geometry may suitably mimic that of the Earth’s core in the past well after inner core nucleation. The non-dimensional parameters are the Prandtl number (Pr = 1), the magnetic Prandtl number (Pm = 3), the Ekman number ($E = 10^{-4}$), and the Rayleigh number (Ra) kept close to the threshold for maintaining the dynamo, which is searched by trial and error. Note that equatorial symmetry (anti-symmetry) is assumed for the velocity (magnetic) field. The present results would be compared with the full 3-dimensional simulations to elucidate non-linear coupling between different symmetries. As a result of the runs, it is found that the minimum Rayleigh number required for a successful dynamo in terms of the critical value for the onset of convection, Ra_c, is substantially different between the two modes. Dynamo is not maintained even at 20 Ra_c for the bottom-up mode, while lower supercriticality of 4.5 Ra_c is sufficient for the top-down mode. In both cases, dipolarity is not as high as the present geomagnetic field, suggesting importance of symmetry-breaking interaction in maintaining a dipole-dominant dynamo (Takahashi et al., 2019). Analysis of kinetic energy budget reveals that the zonal flows are dominantly powered by the Reynolds stress in most of the runs. Furthermore, magnetic field morphology and characteristic force balance will be compared and discussed.

Acknowledgements: This work was supported by JSPS KAKENHI Grant Number JP18K03808.

©2021. Japan Geoscience Union. All Right Reserved.

Keywords: Dynamo, Convection, Core

©2021. Japan Geoscience Union. All Right Reserved.

Rock-magnetic and mineralogical properties of the exsolved magnetite in plagioclase crystal

*Masahiko Sato[1], Masashi Ushioda[2], Ryoichi Nakada[3], Yujiro Tamura[4], Shinji Yamamoto[4]

1. The University of Tokyo, 2. Shikoku Research Institute Inc., 3. Japan Agency for Marine-Earth Science and Technology, 4. Yohohama National University

Natural plagioclase crystals sometimes contain fine-grained magnetite inclusions, which are considered to be originated from exsolution at subsolidus condition. The exsolution process can crystalize and hold nearly pure fine-grained magnetite in deep crustal rocks, and natural remanent magnetizations (NRM) carried by the magnetite bearing plagioclase should play an important role in the source of magnetic anomaly. Therefore, to elucidate crystallization mechanism of magnetite in plagioclase crystal and to understand origin of its NRM is of prime importance in paleomagnetism and rock-magnetism, while the mechanism has been poorly understood yet. In this study, to precisely determine the chemical species of Fe in the plagioclase crystals and to better understand the crystallization mechanism of magnetite, magnetic measurements combined with microscopic observation and synchrotron radiation study were conducted for single grain plagioclase crystals. The plagioclase crystals were prepared from natural mafic-plutonic rocks. The plagioclase crystals were collected under a stereoscopic microscope and used for the measurements after a hydrochloric acid leaching. The main series of measurements for the single grain plagioclase crystals were as follows: (1) To estimate a content of magnetic mineral in the plagioclase crystals, magnetic hysteresis loop was measured using an Alternating Gradient Magnetometer. (2) To investigate the average valence state of Fe, L_{III}-edge X-ray absorption near edge structure (XANES) measurement was performed at synchrotron radiation facilities. (3) To investigate chemical compositions of the plagioclase crystals, microscopic observation was conducted using electron microprobes. The plagioclase crystals used in this study showed the Fe valence state of 2.5–2.9, and it was confirmed that there was inverse relationship between the magnetite content and average valence states of Fe. Combining the mineralogical properties with the rock-magnetic properties such as an intensity of thermal remanent magnetization, we will discuss the exsolved magnetite contribution to the crustal magnetization.

Keywords: Exsolved magnetite, Plagioclase

©2021. Japan Geoscience Union. All Right Reserved.

Rock-magnetic properties of isocubanite from submarine hydrothermal deposits in the Okinawa Trough

*Chie Kato[1], Masao Ohno[1], Yoshihiro Kuwahara[1], Tadahiro Hatakeyama[2], Yasuhiro Yamada[3], Shuhei Totsuka[4], Kazuhiko Shimada[1], Jun-ichiro Ishibashi[1], Toshiro Nagase[5]

1. Kyushu University, 2. Okayama University of Science, 3. Tokyo University of Science, 4. National Institute of Advanced Industrial Science and Technology, 5. Tohoku University

In recent years, submarine hydrothermal deposits have been attracting attention as a new mineral resource. To understand the nature of the deposits and constrain the possible area of hidden ore, it is necessary to gather information about the environment where deposits occur and grow based on investigations of mineral composition and texture of known deposits. Some of the ore minerals exhibit characteristic magnetic properties which potentially enable us a quick identification of such specific minerals. However, magnetic properties are not well documented except for a small number of minerals since they vary not only by mineral species but by chemical composition and texture.

In this study, we searched for ore minerals that can be identified by magnetic measurements from a series of samples collected at the Okinawa Trough submarine hydrothermal deposits and investigated the magnetic properties in detail. Samples were a suite of drilled subseafloor core samples and a block sample of a hydrothermal chimney collected from Noho site and Hakurei site in the Okinawa Trough under the framework of the Next-Generation Technology for Ocean Resources Exploration Project, Cross-ministerial Strategic Innovation Promotion Program (SIP) by the Japanese cabinet office.

First, low temperature magnetometry was conducted to seek for a characteristic signal which appear among different samples. In several samples we found a common feature that a magnetic transition occurs at ~100 K and below this temperature the magnetic moment is larger than at higher temperatures. On those samples or samples taken from nearby depth, we conducted XRD measurements, optical microscopic observation and EPMA analysis and found out that a Cu-Fe sulfide mineral isocubanite should be responsible for the magnetic feature. We further conducted detailed magnetic measurements and Mössbauer spectroscopy on a sample portion consisting almost exclusively of isocubanite that was separated from the chimney samples in which isocubanite appears most prominently. As a result, it was revealed that magnetic properties, Mössbauer spectrum, crystal structure, and the occurrence of intimate lamellar structure with chalcopyrite are generally consistent with ‘aged isocubanite’ which was originally collected at the Snake Pit, Mid-Atlantic Ridge, reported by Wintenberger et al. (1994). On the other hand, chemical composition and texture (with or without exsolution of chalcopyrite) varied among isocubanite samples indicating that the magnetic transition at 100 K is common to isocubanite in wide range of its solid solution, while the sharpness of the transition and the strength of the magnetic moment at low temperature seem to differ by Cu/Fe ratio.
From these results we conclude that low temperature magnetometry on ore samples may be effective to detect isocubanite and have the potential to make contribution to our understanding of the nature of submarine hydrothermal deposits.

Keywords: isocubanite, submarine hydrothermal deposits, low-temperature magnetometry

©2021. Japan Geoscience Union. All Right Reserved.

Contribution of equatorially antisymmetric buoyancy to polarity reversals in geodynamo models

*Takumi Kera[1], Hiroaki Matsui[3], Masaki Matsushima[2], Yuki Nishida[1], Yuto Katoh[1]

1. Department of Geophysics, Graduate School of Science, Tohoku University, 2. Tokyo Institute of Technology, 3. Dept. of Earth and Planetary Sciences, University of California, Davis

Paleomagnetic observations revealed that the geomagnetic field has reversed its polarity. Numerical dynamo simulations have represented dipole reversals and provided an insight into physical processes that give rise to polarity reversals. Both paleomagnetic observations and numerical dynamos have inferred that the equatorial symmetry of the magnetic and velocity fields is related to polarity reversals. The paleomagnetically inferred degree of the symmetry of the Earth's magnetic field during the past 150 Ma shows that geomagnetic field reversed polarity more frequently when the geomagnetic field was more symmetrical with respect to the equator (McFadden et al., 1991). Dynamo simulations revealed a strong inverse correlation between the stability and the equatorial symmetry of the magnetic field (Coe and Glatzmaier, 2006). Olson et al., (2004) proposed a process of magnetic polarity reversals in a dynamo model. In their model, the reversed magnetic field flux is produced locally in the convective plumes and transported from south to north by the meridional circulation. This result suggests that anti-symmetric flow with respect to the equator plays a role in reversals. However, it is an open question how to generate anti-symmetric flow under the condition of the strong rotation, in which symmetric flows with respect to the equator is dominant. In the present research, we investigate how anti-symmetric flow is growing and maintained in the dynamo in which reversals occur.

We perform three dynamo simulations using Calypso (Matsui et al., 2014) to represent dipole dominant dynamo with and without reversals and multipole dynamo, and compare the equatorial symmetry among the cases. In the present study, we set the fixed heat flux, non-slip, and connecting the potential field at the inner and outer boundaries as the boundary conditions for temperature, velocity, and magnetic field, respectively. For the dimensionless numbers, we fixed the three dimensionless numbers to $E = 6\times10^{-4}$, $Pr = 1$, and $Pm = 5$. We also set $Ra = 1500$, 2000, and 2700 for the non-reversal dipolar, dipolar with reversal, and multipolar cases, respectively. For each case, we investigate the structure of velocity and magnetic field in terms of the symmetricity with respect to the equator.

For dipolar dynamo with reversals, flow and magnetic field structure for axial components is similar to the structure of non-reversal dynamo, when the dipole magnetic field sustains stably. The symmetric component is dominant for the velocity field, while the anti-symmetric component is dominant for the magnetic field. On the other hand, during the reversal, the structure is very similar to the multipolar case. Outside the tangent cylinder, flow fields are nearly anti-symmetric and anti-symmetric component of the magnetic field is larger than the symmetric component in the entire domain. This dominance of flow energy of anti-symmetric component during reversals may be caused by buoyancy flux associated with anti-symmetric temperature field. We also give an investigation of buoyancy flux due to symmetric and anti-symmetric components with respect to the equator.

Keywords: dynamo, reversal, core, equatorial symmetry, geomagnetic field, buoyancy

©2021. Japan Geoscience Union. All Right Reserved.

Simultaneous observation of the geomagnetic field at different sites using two SQUID magnetometer systems

*Jun Kawai[1], Miki Kawabata[1], Masakazu Miyamoto[1]

1. Applied Electronics Laboratory, Kanazawa Institute of Technology

We performed simultaneous observation test of the geomagnetic field using two superconducting quantum interference devise (SQUID) magnetometer systems at different sites. The observation sites were Nishiyama (NSY : 36.16N, 136.6E) in Hakusan-city and Minazuki (MNZ : 37.36N, 136.76E) in Wajima-city. The observation period was from 2020.9.11 to 2020.11.25.

The field resolution and field sensitivity of the SQUID magnetometer system were ~ 30 fT/√Hz at 10 Hz and ~ 77 nT/V in a flux-locked loop operation, respectively. The observed data were acquired with a 27-bit data logger with a GPS function (HKS-9700, Keisokugiken Corp.), and the sampling frequency was 200 Hz.

We could observe the Ionospheric Alfvén resonator (IAR) in the night-time at both sites. The phase of IAR signals detected at both sites was almost the same, but the amplitude of IAR signals obtained at MNZ was bigger than that obtained at NSY. We speculate the difference in amplitude is because of the difference in latitude, as known according to the previous studies. From this result, we could confirm the reliability of the simultaneous geomagnetic observation using two SQUID magnetometer systems.

In this presentation, we show the summary of the observation test and discuss the data obtained at both sites.

Keywords: geomagnetic field, SQUID, ionospheric Alfvén resonator, high sensitivity

©2021. Japan Geoscience Union. All Right Reserved.

[E] Poster | S (Solid Earth Sciences)：S-IT Science of the Earth's Interior & Techtonophysics

Sun. Jun 6, 2021 5:15 PM - 6:30 PM JST | Sun. Jun 6, 2021 8:15 AM - 9:30 AM UTC | Ch.11_2

[S-IT19] East Asia geodynamics: New perspectives, top to bottom

convener:B Timothy Byrne(University of Connecticut), Asuka Yamaguchi(Atomosphere and Ocean Research Institute, The University of Tokyo), Jonny Wu(University of Houston), Kyoko Okino(Atmosphere and Ocean Research Institute, The University of Tokyo)

East Asia is one of the most tectonically active regions on Earth and includes the Eurasian continental margin, the western Pacific subduction zones and many of Earth's marginal seas. The region has a long history of subduction, collision, back-arc basin opening and closing, and other plate boundary interactions. In recent years, a wide range of new observations have been collected from the land, oceans and Earth interior, including detailed surface and bedrock geologic observations, earthquake data, high resolution crustal to mantle imaging and Big Data. These new data show that classic theories no long explain the detailed space-time evolution of subduction zones, mountain building, slab stagnation, crustal deformation, continental dynamics, back-arc spreading, and other East Asian geodynamics; new perspectives are needed. Here we seek to share new insights on the geologic history, paleomagnetism, and geophysical character of East Asia since the Paleozoic. We also invite geodynamic models that integrate diverse datasets into a more holistic view of the dynamic environment.

[SIT19-P01] Strain localization and development of deformation bands in a forearc coal-bearing Paleogene fold and thrust belt, Hokkaido, northern Japan

Hiromi Kaji[1,2], *Toru Takeshita[1] (1.Department of Natural History Sciences, Graduate School of Science, Hokkaido University, 2.Oyo Co. Ltd.)

[SIT19-P02] Comparison of paleostress and paleotemperature analysis at Roof Thrust and Out-of-Sequence Thrust of subduction zone : The Minami Awa Fault and Mizoochi Fault, The Mugi area in the Shimanto Belt

*Yu Sogawa[1], Arito Sakaguchi[1] (1.Graduate School of Sciences and Technology for Innovation, Yamaguchi University)

[SIT19-P03] Coseismic Fault Model for the Thabeikkyin earthquake in 2012 determined from GNSS Observation

*Tha Zin Htet Tin[1,5], Takuya NISHIMURA[2], Manabu Hashimoto[2], Eric LINDSEY[3,4], Yutaro Okada[1], Lin Thu Aung -[3], Myo Thant -[5,6] (1.Graduate School of Science, Kyoto University, Kyoto, Japan, 2.Disaster Prevention Research Institute, Kyoto University, Kyoto, Japan, 3.Earth Observatory of Singapore, Nanyang Technological University, Singapore, 4.University of New Mexico, Albuquerque, United States, 5.Department of Geology, University of Yangon, Myanmar, 6.Myanmar Earthquake Committee, Yangon, Myanmar)

[SIT19-P04] Estimation of postseismic effects of 2013 Okhotsk Sea M_w8.3 deep-focus earthquake

*Grigorii Viktorovich Nechaev[1,2], Nikolai Shestakov[1,2], Hiroaki Takahashi[3], Evgenii Lialiushko[2] (1.Institute for Applied Mathematics FEB RAS, 2.Far Eastern Federal University, 3.Institute of Seismology and Volcanology, Hokkaido University)

Strain localization and development of deformation bands in a forearc coal-bearing Paleogene fold and thrust belt, Hokkaido, northern Japan

Hiromi Kaji[1,2], *Toru Takeshita[1]

1. Department of Natural History Sciences, Graduate School of Science, Hokkaido University, 2. Oyo Co. Ltd.

Many studies have recently shown that deformation bands develop in porous sandstones constituting fold and thrust belts. We have analyzed microstructures of deformation bands in one such fold and thrust belt consisting of the Upper Eocence Urahoro Group, Hokkaido, northern Japan, which is typical forearc basin deposits. In the study area, the folds have a wavelength of c. 1-2 km, the axis of which trends NNE-SSW and plunges nearly horizontally, where the strata generally dip either east or west at moderate angles. However, there is one flexure in the eastern part of the study area, where deformation bands are pervasively developed only in the Shakubetsu Formation, which contains mudstones and coal layers other than sandstones. In the other parts of the Urahoro Group in the study area, only sandstones occur without the development of deformation bands. Deformation bands could have formed at the maximum burial depth around 1.5 km inferred from the thickness of overlying strata, which conforms to the one (1.5-2.5 km) inferred from the vitrinite reflectance values (%Ro) of the coal layers (c. 0.5) from the Shakubetsu Formation. The deformation bands are inferred to have originated as phyllosilicate bands, which developed into cataclastic bands with increasing strain in sandstones of the Shakubetsu Formation with up to c. 10 volume % of phyllosilicate. Coal seams, which flow into some deformation bands and smear them, also played a similar role to phyllosilicate in their development. In the cataclastic bands, the detrital grains in host sandstones are crushed into the sizes less than a half to one third of the original one, and also abrased during the formation of deformation bands. The latter fact can be revealed by a higher circularity of grains as well as its higher dependence on grain size in the deformation bands than in the host parts.

Keywords: Forearc basin deposits, Fold and thrust belts, Flexure, Deformation bands, Coal layers, Image analysis

©2021. Japan Geoscience Union. All Right Reserved.

Comparison of paleostress and paleotemperature analysis at Roof Thrust and Out-of-Sequence Thrust of subduction zone : The Minami Awa Fault and Mizoochi Fault, The Mugi area in the Shimanto Belt

*Yu Sogawa[1], Arito Sakaguchi[1]

1. Graduate School of Sciences and Technology for Innovation, Yamaguchi University

The duplex structure and out-of-sequence thrust (OST) of the hypocentral region in the of the deep subduction zone are typical structures. Many structures stated above result from repeating the underplating accretion which the thrust sheet overlaps by the step-down of the decollment which is the plate boundary. The old upper decollment is called roof thrust and the new lower decollment is called floor thrust. The OST is a large thrust at late stage that intersects with these accretionary topographies. The roof thrust has been considered inactive because the decollment forms the floor thrust at the bottom of the duplex structure. However, a number of pseudotachylytes have been found in the roof thrust. In this study area, “Mugi mélange”, the roof thrust as an earthquake source fault and the OST have been reported (Onishi and Kimura., 1995; Hashimoto and Kimura., 1999; Ujiie et al., 2000, etc.), which is the most suitable for comparing 2 major faults at the same burial depth in the identical mélange. The Minami-Awa fault (roof thrust) and the Mizoochi fault (OST) are located close together and may have splay fault.
Mugi mélange is located in the southeastern part of Shikoku and belongs to the southern margin of the northern Shimanto Belt. Mugi mélange is considered to be a tectonic mélange, a plate-boundary rock that appeared on the surface (Onishi and Kimura., 1995; Hashimoto and Kimura., 1999; Ujiie et al., 2000, etc.). Minami-Awa fault is a boundary fault (roof thrust) between Hiwasa Formation (turbidite) and Mugi mélange. Minami-Awa fault is the roof thrust containing pseudotachylyte (Kitamura et al., 2005; Ujiie et al., 2007 b). The cummulative displacement of Mizoochi fault (OST) is large as the depositional age and paleotemperature are different. The purpose of this study is to examine the difference in the stress concentration between the roof thrust and the OST using a calcite paleostress piezometer, and to estimate the paleotemperature and thermal diffusion from the vicinity of the fault to a distance using the vitrinite reflectance, and to estimate the roles of the 2 faults from them.

・Calcite paleostress piezometer: A geologic paleostress gauge that calcite in rocks records as twins when they undergo strain. In this study, we used calcite that cracks in boudin.
・Vitrinite reflectance paleothermometer: Vitrinite, a type of maceral, records the maximum heat exposure during the process of thermal maturation and carbonization of plant fragments.

The paleotemperature of the host rock of the Mizoochi fault (OST) is approximately 200 -244 ˚C in the hanging wall and approximately 150 -185 ˚C in footwall. This large thermal difference may indicate accumulative great offset to have repeated many slips.
The paleostress was obtained from calcite twin analysis. The value of the stress near the Minami Awa fault (roof thrust) ranged from 146 ±27 MPa to 183 ±24 MPa. The paleostress around the Mizoochi fault was 135 ±16 MPa to 179 ±22 MPa, and the paleostress decreases from 123 ±18 MPa with distance from the fault. This low value of the paleostress at distance from the fault may be background crustal stress. By contrast to this, the high shear stress around the faults may be due to the stress concentration during the rupture propagation from deep nucleation zone. The stress concentration at tip of the rupture front is the result of the resistance to failure of the locked fault. In this study, similar levels of the stress

©2021. Japan Geoscience Union. All Right Reserved.

concentrations were found at both of the roof thrust of the Minami-Awa fault and the OST of the Mizoochi fault. If one fault has stronger resistance from fracturing than the other in bifurcated fault, the rupture will propagate to weak fault any times. Two faults in this study experienced similar stress concentration, and the rupture can propagate either fault. This idea can explain that the rupture propagates to the roof thrust to reactivate the fault.

Keywords: Calcite, Shimanto belt, Vitrinite, Accretionary complex, Roof thrust, Out of sequence thrust

©2021. Japan Geoscience Union. All Right Reserved.

Coseismic Fault Model for the Thabeikkyin earthquake in 2012 determined from GNSS Observation

*Tha Zin Htet Tin[1,5], Takuya NISHIMURA[2], Manabu Hashimoto[2], Eric LINDSEY[3,4], Yutaro Okada[1], Lin Thu Aung -[3], Myo Thant -[5,6]

1. Graduate School of Science, Kyoto University, Kyoto, Japan, 2. Disaster Prevention Research Institute, Kyoto University, Kyoto, Japan, 3. Earth Observatory of Singapore, Nanyang Technological University, Singapore, 4. University of New Mexico, Albuquerque, United States, 5. Department of Geology, University of Yangon, Myanmar, 6. Myanmar Earthquake Committee, Yangon, Myanmar

The Sagaing Fault, a right-lateral strike slip fault, slip rate 18 –20 mm/yr, more than 1200km long which is north-south trending major active geological structure in Myanmar. Many significant historical earthquakes occurred along its fault. The recent 2012 Thabeikkyin earthquake, Myanmar occurred on 11 November 2012 at the Sagaing Fault in central Myanmar which claimed more than 20 fatalities and more than 200 injuries during in this earthquake.

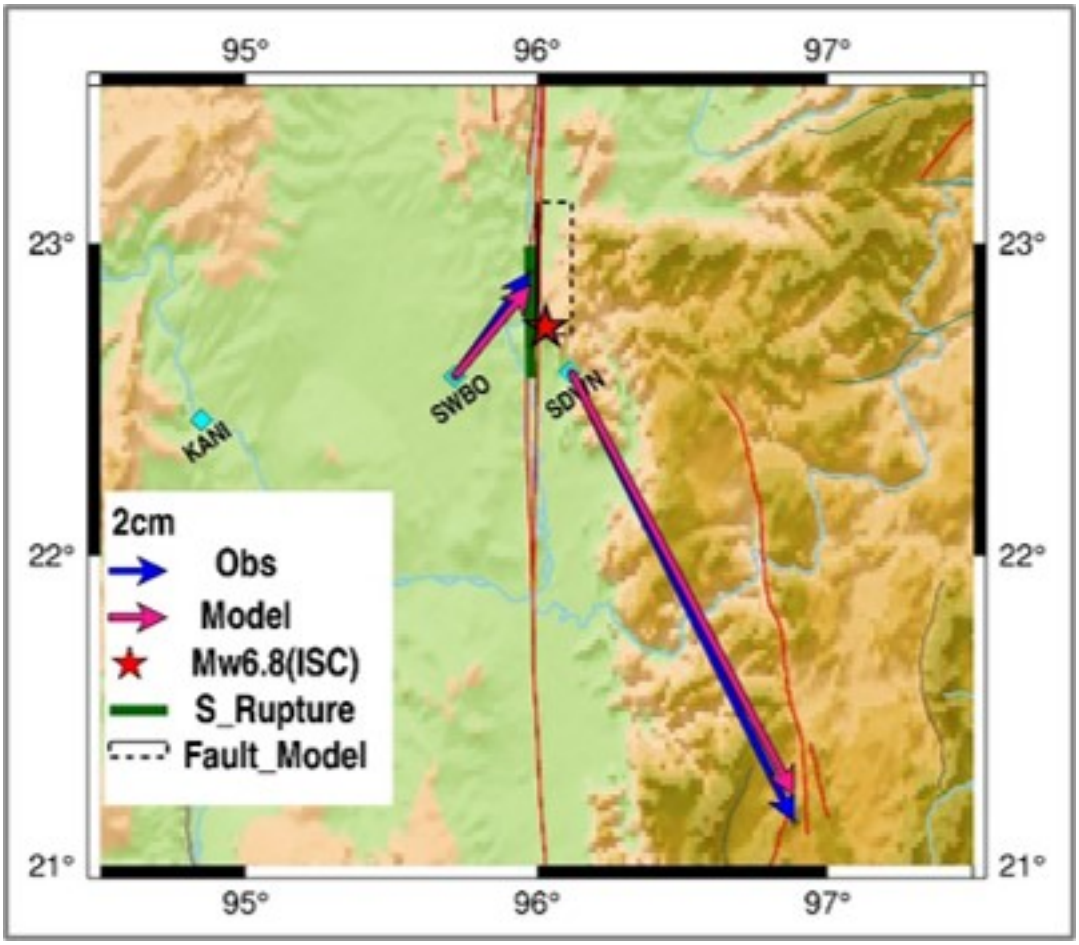
The GNSS (Global Navigation Satellite System) network was constructed under the collaboration between Earth Observatory of Singapore (EOS), Myanmar Earthquake Committee (MEC), Department of Meteorology and Hydrology, Myanmar (DMH) and Myanmar Survey Department (MSD) in 2011. We calculated velocities of GNSS stations by using GIPSY-OASIS ver 6.4 software from Jet Propulsion Laboratory (JPL) with latest realization of the International Terrestrial Reference Frame 2014 (ITRF2014). Ocean tide loading was calculated using FES2014b model by the Onsala Space Observatory (http://holt.oso.chalmers.se/loading/) with respect to the joint mass center of solid Earth and ocean combined. We also collected data for nearby 8 International GNSS Service (IGS) stations and estimated velocities of these stations in our processing. We subtracted the average positions for 10 days before the 2012 Thabeikkyin earthquake and from those for 10 days after the main shock to obtain coseismic displacement from GNSS surveyed data. We utilize observed coseismic displacements from GNSS data to estimate the coseismic slip of the 2012 earthquake by using Okada’ s (1992) elastic half-space dislocation model.

We estimate a rectangular fault model based on available GNSS continuous stations. In this study, we used two GNSS stations, SWBO and SDWN which recorded coseismic displacement during the earthquake. The calculated coseismic displacements show right lateral strike slip along the fault segment. SDWN showed large coseismic displacement up to 15 cm, while SWBO experienced 3.6 cm, respectively as shown in Fig. We assume a single fault plane with strike of 0˚, dip 71˚ (east-dipping) and rake of 178˚ based on CMT solution and that the fault plane is aligned on the Sagaing Fault. We search for fault parameters using a non-linear inversion method of Matsu’ ura and Hasegawa (1987). The initial parameters such as length, width, depth of the upper margin are assumed based on the field surface rupture length, that is, length: 45.185 km (SagaingFault.info), width: 10 km (Sun et al. 2013, Tun & Watkinson 2017, Hlaing et al. 2019) and depth: 0 km, respectively. The preliminary result of optimum geodetic data inversion suggested slip amount 1.5 m with seismic moment of 3.68×10^{19} Nm (Mw 6.9) and obtained fault size 46.8km x 17.2 km, at depth 2.3 km with strike 0˚, 44˚ east-dipping, rake 190˚, respectively. Our result of coseismic slip can explain very well the observed displacement of the Thabeikkyin earthquake although the available data is limited. Our estimated coseismic rectangle fault show east dipping which may be effected due to the clockwise rotation of the eastern himalayan synthesis in the northeastern part of Myanmar or roughly correspond to an intersection point of the Sagaing Fault,

©2021. Japan Geoscience Union. All Right Reserved.

Momeik fault and Shan scarp fault zone.
Fig. Coseismic displacement of the 2012 Thabeikkyin earthquake. The black rectangle denotes the fault plane. Blue and pink arrows show observed and model displacement, respectively.

Keywords: GNSS, Sagaing Fault, coseismic slip, Thabeikkyin earthquake



©2021. Japan Geoscience Union. All Right Reserved.

Estimation of postseismic effects of 2013 Okhotsk Sea M_w8.3 deep-focus earthquake

*Grigorii Viktorovich Nechaev[1,2], Nikolai Shestakov[1,2], Hiroaki Takahashi[3], Evgenii Lialiushko[2]

1. Institute for Applied Mathematics FEB RAS, 2. Far Eastern Federal University, 3. Institute of Seismology and Volcanology, Hokkaido University

The strong deep-focus earthquake M_w8.3 occurred beneath the Okhotsk Sea to the west of the Kamchatka Peninsula on 24 May 2013 at a depth of 620 km. This earthquake is the strongest deep-focus event ever instrumentally observed. Seismic shaking was registered at great distances from the epicenter almost over the World.

The earthquake generated surface coseismic displacements that were detected by GNSS-techniques for the first time for a deep-focus event. The regional GNSS-network revealed offsets up to 2 cm in both horizontal and vertical components [Shestakov et al. 2014]. Coseismic displacements affected all north-eastern Asia.

All regional GNSS-stations notable changed their secular movement directions and velocities after the event. Variations have systematic character and could be caused by postseismic processes. In such a case, in opposite to typical postseismic exponentially decaying motion caused by shallow earthquakes, Kamchatka GNSS-stations demonstrate linear postseismic drift.

Coordinate time series of Kamchatka GNSS-sites were carefully analysed for investigation of this effect. Coordinate sequences were divided into two parts –before and after the event. Each component was processed separately.

Obtained sites motion parameters were utilized for modeling by using Visco2.5D software [Pollitz, 2014]. Different sets of slab, crust and mantle rigidity and shape were tested. Finally, reasonable fit between the observed and calculated postseismic displacements was achieved.

References:

Shestakov, N. et al. Modeling of earth crustal coseismic movement initiated by deep-focus Okhotsk sea earthquakes on 24 May 2013, M_w8.3 // Reports of Academy of Sciences. 2014, vol. 457, 4, pp 471-476.

Pollitz, F. Post-earthquake relaxation using a spectral element method: 2.5-D case // Geophysical Journal International. 2014. 19 p.

This work was partially supported by the RFBR grant No. 20-05-00509 and JREX Fellowship.

Keywords: earthquake modeling, postseismic displacements, deep-focus earthquake

©2021. Japan Geoscience Union. All Right Reserved.

[J] Oral | S (Solid Earth Sciences)：S-MP Mineralogy & Petrology

Sun. Jun 6, 2021 9:00 AM - 10:30 AM JST | Sun. Jun 6, 2021 12:00 AM - 1:30 AM UTC | Ch.20 Zoom Room 20

[S-MP25] Deformed rocks, Metamorphic rocks and Tectonics

convener:Yumiko Harigane(Geological Survey of Japan, National Institute of Advanced Industrial Science and Technology (AIST)), Yoshihiro Nakamura(Geological Survey of Japan, National Institute of Advanced Industrial Science and Technology), Chairperson:Yumiko Harigane(Geological Survey of Japan, National Institute of Advanced Industrial Science and Technology (AIST)), Yoshihiro Nakamura(Geological Survey of Japan, National Institute of Advanced Industrial Science and Technology)

We invite all researchers who aim to understand the dynamics of the earth's crust and mantle at the plate boundaries, to discuss the latest results from various viewpoints. The scope will include contributions through petrology and structural geology as well as various techniques including rheology and transformation of heat and mass.

9:00 AM - 9:15 AM JST | 12:00 AM - 12:15 AM UTC

[SMP25-01] Prolonged subduction metamorphism and deep forearc accumulation of Sanbagawa Complex: an example from Okawara district, southern Japanese Alps

*Kazuhiro Miyazaki[1], Yoshihiro Nakamura[1], Hiroshi Makimoto[1] (1.Institute of Geology and Geoinformation, Geological Survey of Japan/National Institute of Advanced Industrial Science and Technology)

9:15 AM - 9:30 AM JST | 12:15 AM - 12:30 AM UTC

[SMP25-02] High mobility of Sr and Ba in subduction-related metamorphism: Application of Machine-learning mass transfer analyses to mafic shists, the Sanbagawa belt

*Matsuno Satoshi[1], Masaoki Uno[1], Atsushi Okamoto[1], Noriyoshi Tsuchiya[1] (1.Graduate School of Environmental Studies Tohoku University)

9:30 AM - 9:45 AM JST | 12:30 AM - 12:45 AM UTC

[SMP25-03] U–Pb garnet dating of HP marble from the Eastern Iratsu body, Sanbagawa metamorphic terrane: decoupled isotopic signature and compositional zoning

*Sota Niki[1], Kenta Yoshida[2], Hikaru Sawada[2], Ryosuke Oyanagi[2], Takafumi Hirata[1] (1.Geochemical Research Center, Graduate School of Science, The University of Tokyo, 2.Japan Agency for Marine-Earth Science and Technology)

9:45 AM - 10:00 AM JST | 12:45 AM - 1:00 AM UTC

[SMP25-04] **Crystal size distribution of garnet formed by two-stage growth in the Kotsu eclogite, Sanbagawa belt**

*OTGONBAYAR DANDAR[1], Atsushi Okamoto[1], Masaoki Uno[1] (1.Graduate School of Environmental Studies, Tohoku University)

10:00 AM - 10:15 AM JST | 1:00 AM - 1:15 AM UTC

[SMP25-05] A shape change model of isolated K-feldspar inclusions within a micro-shear zone developed in Teshima granite, the Ryoke metamorphic belt

*Tae-Hoon Uhmb[1], Katsuyoshi Michibayashi[1] (1.Department of Earth and Planetary Sciences, Research group of Petrology and Mineralogy, Nagoya University)

10:15 AM - 10:30 AM JST | 1:15 AM - 1:30 AM UTC

[SMP25-06] C-O-H fluid was present during garnet-forming partial melting reaction in a pelitic migmatite from the Ryoke belt, Japan

*Natsumi Yoshimoto[1], Tetsuo Kawakami[1] (1.Kyoto University)

Prolonged subduction metamorphism and deep forearc accumulation of Sanbagawa Complex: an example from Okawara district, southern Japanese Alps

*Kazuhiro Miyazaki[1], Yoshihiro Nakamura[1], Hiroshi Makimoto[1]

1. Institute of Geology and Geoinformation, Geological Survey of Japan/National Institute of Advanced Industrial Science and Technology

Sanbagawa and Chichibu complexes are distributed between the north-south trending MTL and BTL in the Okawara district, southern Japanese Alps. Both complexes were fragmented by some north-south trending vertical faults. Except for near MTL , dips of main schistosities ara gentle. Nearly horizontal structures are preserved within fault-bounded blocks. The Okawara district possesses about 2000 m difference of elevation, therefore this area is adequate for revealing geological architecture of the Sanbagawa Complex . The Sanbagawa Complex consists of Kurokawasawa (mainly pelitic schist), Kamasawa (mainly pelitic schist with small amount of marble), Mikabu (mainly ultramafic to mafic metamorphic rocks), and Terasawa units (mainly pelitic phyllite and metachert), in order from bottom to top with referring to the gentle-dipping main schistosity. The Mibugawa unit (mainly mixed rock, chert and basalt) of the Chichibu complex tectonically overlaps the Sanbagawa Complex.
Boundaries between Mikabu and Kurokamasawa units and between Kamaswa and Terasawa units are almost identical to 325 ˚C and 315 ˚C isotherms, restpectively. These planes were used as references. Using the references, lithological distribution, main schistosity, and RSCM isotherms, many geological cross sections generated by QGIS plug-in, mineral assemblages, solid solution composition of minerals, , bulk compositions, Gibbs free energy minimum modeling, and MCMC maximum likelihood estimation and information criterion of the youngest age component with detrital zircon U-Pb ages, we reconstruct geological architecture of the Sanbagawa Complex. The results show that thickness measured in the direction perpendicular to the main schistosity, peak temperatures and pressures, the youngest age components of detrital zircon are as follows; the Kurokawasawa unit: 1400 m, 325-400 ˚C, 6-8 kbar, 72.3 ±0.7 Ma (lower part), 96.3 ±2.8 Ma (middle part), 104.0 ±1.1 Ma (upper part); Kamasawa unit: 1200 m, 285-325 ˚C, 5.0-6.5 kbar, 105.7 ±1.2 Ma and 109.8 ±1.9 Ma; Mikabu unit: 285-325 ˚C, 5.0-6.5 kbar; Terasawa unit: 800 m, 135.8 ±1.8 Ma; Mibugawa unit: 1000 m, 280-305 ˚C, 4-5 kbar, 171.3 ±2.2 Ma. Using these values, we also estimate thermal gradient perpendicular to the main schistosity as follows; Kurokawasawa unit: 55 ˚C/km; Kamasawa unit: 40 ˚C/km; Mibugawa unit: 33 ˚C/km. These high values are possible in inverted thermal structure in subduction channel with descending cold slab. However, downward increases of temperatures in our case are opposite to what one expected for the inverted thermal structure. Assuming crustal density of 2.9 g/cm^3, our geological estimation of total thickness from the Kurokawasawa to Mibugawa units is about one third of the petrological estimation of pressure differences. This large discrepancy suggest large amount of crustal thinning took place with formation of main schistosity during exhumation.
P-T conditions from the Kurokawasawa to lower part of the Mibugawa units show linear array on P-T diagram, and are resemblant to those along subduction channel with shear heating (e.g. Ishii and Wallis, 2020). Metamorphic phengite K-Ar ages from bottom and top of the Kurokawasawa unit yield ca. 65 Ma (Shibata and Takagi, 1988) and 105 Ma (Watanabe et al., 1982), respectively. These metamorphic ages suggest at least 40 Myr duration of the Sanbagawa metamorphism. Our geological, petrological and geochronological results lead to the following formational picture for the Sanbagawa Complex; 1) steady-state P-T conditions observed by the Sanbagawa Complex was maintained along subduction

©2021. Japan Geoscience Union. All Right Reserved.

channel for at least 40 Myr duration, 2) protolith of the Sanbagawa Complex was continuously subducted to the subduction channel and suffered the Sanbagawa metamorphism, 3) metamorphic rocks were successively exhumed with thinning and formation of main schistosity, and 4) the exhumed metamorphic rocks accumulated from bottom at deeper depths of forearc in arc-trench system.

Keywords: Sanbagawa, Subduction zone, Metamorphism

©2021. Japan Geoscience Union. All Right Reserved.

High mobility of Sr and Ba in subduction-related metamorphism: Application of Machine-learning mass transfer analyses to mafic shists, the Sanbagawa belt

*Matsuno Satoshi[1], Masaoki Uno[1], Atsushi Okamoto[1], Noriyoshi Tsuchiya[1]

1. Graduate School of Environmental Studies Tohoku University

Regional mass transfer in subduction-related metamorphic rocks records fluid activities in subduction zones and serves as a key to understand fluid-related processes such as seismic activity (e.g., Hacker et al., 2003) and magma generation in island arcs (e.g., Pearce et al., 2005). Although geophysical observations suggest that such fluid distributions are in regional scales (i.e., 1–10km), the scales of quantitative mass transfer analyses are usually limited to outcrop scales. Mass transfer analysis on the regional scale has been investigated as chemical trends (e.g., John et al., 2004; Bebout 2007; Masters and Ague 2005); however, protolith heterogeneity hinders quantitative analyses of mass transfer in scales larger than outcrops (i.e., >100 m; e.g., Moss et al., 1995; Bebout 2007; Uno et al., 2014). To understand regional scale metamorphic mass transfer, it is required to determine protolith composition from metamorphic rock sample by sample.

To evaluate metamorphic mass transfer, we have developed protolith compositional estimation models using machine learning. The models were built by learning protolith basalt compositional dataset (Ocean Island basalt, Mid-ocean ridge basalt, and Island arc basalt), and designed to estimate trace element compositions from limited numbers of input trace element concentrations (i.e., 2–9 elements). Gradient Boosting Decision Tree was used as a machine learning algorithm, and models were evaluated by the Root Mean Squared Error in the log unit. With Zr, Th, Ti, and Nb as input elements and Rb, Ba, U, K, La, Ce, Pb, Sr, Nd, Y, Yb, and Lu as output elements, the developed models can reproduce protolith basalt compositions within errors of 10%–25% (i.e., <0.1 in log10 unit). As Zr, Th, Ti, and Nb are the most immobile element in typical regional metamorphism (e.g., Ague et al., 2017), these elements are adopted as input elements. It is noted that models with other input elements are also available. These models were applied to seafloor altered basalt for validation. Compositions of fresh glass remained in the seafloor altered basalt are compared to the estimated protolith compositions, which ensured the model reliability.

The protolith compositional estimation models were applied to the Sanbagawa metamorphic belt, SW Japan. Samples were collected from Asemigawa-river, Central Shikoku, where it crosses chlorite zone (CHZ), garnet zone (GTZ), albite-biotite zone (ABZ), and oligoclase-biotite (OBZ), with increasing metamorphic grade. Mafic rocks are exposed as lenticular bodies or layers, and are collected at each grade for mass transfer analyses. It has been revealed that mafic rocks in CHZ are N-MORB-like compositions, and those in GTZ and OBZ are E-MORB-like compositions (Uno et al., 2014), and such protolith heterogeneity inhibited direct comparisons of trace element compositions among metamorphic grades. To enable direct comparisons of mass transfer among metamorphic grades, the protolith compositional estimation models were applied to the mafic rock samples. It is revealed that both enrichment and depletion had occurred for Rb, K, Sr, and Y compared to their protoliths; Ba is depleted for most of the samples; Not a significant mass transfer was detected for La, Ce, and Nd. Although the degree of mass transfer varies within a metamorphic grade, maximum depletion of Ba and Sr at each grade correlates with metamorphic grades: Ba has been depleted more than 90% at the maximum, Sr has been enriched more than 200% at the maximum, while some samples have been depleted 50% at the

©2021. Japan Geoscience Union. All Right Reserved.

minimum. These results provide unique insights into elemental budgets and fluid activities in subduction zones.

Keywords: Mass transfer, Metamorphism, Regional scale, Machine-learning, Subduction zone

©2021. Japan Geoscience Union. All Right Reserved.

U–Pb garnet dating of HP marble from the Eastern Iratsu body, Sanbagawa metamorphic terrane: decoupled isotopic signature and compositional zoning

*Sota Niki[1], Kenta Yoshida[2], Hikaru Sawada[2], Ryosuke Oyanagi[2], Takafumi Hirata[1]

1. Geochemical Research Center, Graduate School of Science, The University of Tokyo, 2. Japan Agency for Marine-Earth Science and Technology

Generally, geochronological studies on metamorphic rocks have been dependent on the occurrence of specific minerals (e.g. mica and zircon). For these minerals, the relationships between the timing of mineral growth and metamorphic stages are often unclear [1, 2]. For the accurate reconstruction of the pressure-temperature-time (*P-T-t)* paths, geochronological data from in-situ dating while differentiating textures inside mineral grains should be linked to *P-T* conditions determined by co-existing inclusion minerals near the spots measured by in-situ dating methods.

Among metamorphic mineral species, grossular (Grs)-andradite (Adr) series garnet is a potential candidate to define both U–Pb ages and *P-T* conditions. The U–Pb isotopic system of garnet is robust against thermal events because of the high closure temperature (>800 ˚C [3]). The *P-T* conditions of garnet can also be deduced from the co-existing inclusion minerals.

In this study, U–Pb dating of metamorphic Grs garnet was first conducted using a laser ablation-ICP-mass spectrometry. The in-situ spot ages were linked to the *P-T* conditions deduced from the garnet itself. The garnet sample was collected from the eastern margin of the Eastern Iratsu body in the eclogite-unit of the Sanbagawa metamorphic terrane. Prior to the U–Pb isotopic analysis, the zoning texture inside the garnet sample was observed using backscattered electron images. The Grs grain showed a patchy texture with an almost pure Grs core ($Grs_{98}Adr_2$) and an Adr-rich rim ($Grs_{91}Adr_8Alm_{<2}$). The presence of aragonite in the core indicates formation during the eclogite-facies metamorphism while the rim was formed under the *P-T* conditions of the juxtaposition of the exhuming eclogite-unit and surrounding schists [4].

For U–Pb isotopic analysis, the 13 spots for the core and 13 spots for the rim were carefully selected. The obtained U–Pb isotopic results formed a regression line on the Tera and Wasserburg Concordia Diagram. The mean square weighted deviation (MSWD) of the regression line was greater than 2 (2.5 for core and 4.1 for rim). Since titanite in this sample recorded ages of an older stage (ca. 200 Ma [5]), the large MSWD can be attributed to the remnant of such old U–Pb isotopic signatures. By rejecting these “old” U–Pb isotopic data, the obtained age of the core was 95.8±8.9 (2 σ) with a MSWD = 0.70 and the obtained age of the rim was 95.3±8.3 (2 σ) with a MSWD =1.0.

The resulting U–Pb ages of the core were in good agreement with the timing of the eclogite-facies stage, such as 92.6±8.8 Ma of zircon U–Pb ages [6] and 88.8±0.6 Ma of garnet Lu–Hf isochron ages [7]. The core and rim were indistinguishable despite the obvious zoning texture inside the garnet and the difference in metamorphic *P-T* conditions constrained from co-existing inclusion minerals. The agreement of the U–Pb ages between the core and rim can be explained by two reasons. Firstly, the chemical compositions and the U–Pb isotopic system were decoupled because of coupled dissolution-reprecipitation processes [8]. The rim of Grs was produced through the series of dissolution-reprecipitation reactions among the Grs grains while the U–Pb isotopic system remains

©2021. Japan Geoscience Union. All Right Reserved.

unperturbed and partly preserved old (96 Ma) signature. Secondly, the time difference between core and rim formations was too small to detect by present analytical precision. The timing of the rim formation can be earlier than the peak (or cooling) ages of the surrounding schists, i.e. 90-85 Ma [7, 9]. This time period overlapped with the obtained ages in this study within the analytical errors.

References

[1] Itaya et al. 2009, *Isl. Arc.* [2] Kohn et al., 2015, *Am. Min.* [3] Mezger et al., 1991, *J. Geol.* [4] Yoshida et al., 2021, *JMPS.* [5] Yoshida et al., 2021, *JpGU2021.* [6] Aoki et al., 2020, *Lithos.* [7] Wallis et al., 2009, *J. Metamorph. Geol.* [8] Weinberg et al., 2020, *Geochim. Cosmochim. Acta.* [9] Dallmeyer and Takasu, 1991, *J. Metamorph. Geol.*

Keywords: garnet, U–Pb geochronology, Sanbagawa metamorphic terrane, LA-ICP-MS

©2021. Japan Geoscience Union. All Right Reserved.

Crystal size distribution of garnet formed by two-stage growth in the Kotsu eclogite, Sanbagawa belt

*OTGONBAYAR DANDAR[1], Atsushi Okamoto[1], Masaoki Uno[1]

1. Graduate School of Environmental Studies, Tohoku University

The nucleation and growth history of crystals during metamorphism are recorded both as crystal size distribution (CSD) and compositional zoning from core to rim. In particular, the crystal size distribution of garnet has been investigated and modeled by relative rate of nucleation and growth, and coupled with diffusion. As garnet is commonly formed during prograde metamorphism, the incremental amount of the garnet growth at individual P-T conditions is essential information to elucidate the water release at the subduction interfaces. Conventionally, there are two types of model on crystal size distribution; one is the nucleation and growth rates are defined as a function of time (e.g., Spillar and Dolejs 2013), and the other one is growth rate is defined as the size (e.g., Eberl et al., 1998). However, it is still uncertain which model is more appropriate, as the data aquations of CSD from thin sections and the composition of “true” core are very difficult due to the cut effects. In this contribution, we showed the detailed data showing the relationship between crystal size distribution and compositional zoning of garnet in the Kotsu eclogite in the Sanbagawa metamorphic belt, Japan. This eclogite sample is suitable to this trial, because garnet grains show euhedral shape and record two-stage growth history composed of the core containing abundant mineral inclusions (epidote, plagioclase, chlorite, carbonate, titanite, quartz, and omphacite) and poor-rim.

The detailed analyses were performed in the following steps. (1) We crashed the ~120 grams of eclogite samples by the system of high voltage pulse fragmentation (Selfrag), and picked up all garnet grains (n>4342). (2) We sieved the grains into five classes (>2 mm, >1 mm, >0.5 mm, >0.25 mm, and <0.25 mm). (3) In each class, garnet grains are embedded in epoxy resin, and we took the X-ray CT images for getting the crystal size distribution. (4) After taking X-ray CT, we polished the sample to section the real cores. (5) The two-stage growth is obtained based on the back-scattered images and get the compositional zoning from core to rim.
Combining the results of the crystal sizes taken from the X-ray CT images in all classes, we reveal that the garnet population shows pseudo-lognormal CSDs, which has a small shoulder at the medium grain size (~0.75 mm). The crystal growth is divided into two stages. The garnet grains are euhedral grains composed of the inclusion-rich core (stage 1) and poor-rim (stage 2). The core shows prograde zoning, characterized by decreases of X_{Mn} (0.025 to 0.005) and increase of X_{Mg} (0.06 to 0.12) from core to rim, and almost constant X_{Fe} (0.55-0.65) and X_{Ca} (0.27-0.35). The smaller grains have lower Mn and higher Mg contents, suggesting that nucleation at the later retrograde stages. All grains have an inclusion-poor rim showing Mn increase. One of the interesting observations is a positive relationship between the diameter of the inclusion-rich core and the growth width of the inclusion-poor rim, meaning that the growth rate is proportional to the grain size. We will construct the nucleation and growth model to reproduce the CSD and the trend of growth zoning, and discuss the mechanism and water production history.

Keywords: Garnet, Crystal size distribution, nucleation, growth, Kotsu eclogite

©2021. Japan Geoscience Union. All Right Reserved.

A shape change model of isolated K-feldspar inclusions within a micro-shear zone developed in Teshima granite, the Ryoke metamorphic belt

*Tae-Hoon Uhmb[1], Katsuyoshi Michibayashi[1]

1. Department of Earth and Planetary Sciences, Research group of Petrology and Mineralogy, Nagoya University

The isolated mineral inclusions possess many kinds of important information for geological history of natural rocks. Especially, shape change patterns (i.e. size versus aspect ratio pattern of the inclusion) of the inclusions were used as a tool to estimate deformation time and deformation conditions in some of previous studies. Toriumi [1981, 1987] firstly proposed mathematical equation representing shape change patterns of the isolated mineral inclusions. More recently, Okamoto and Michibayashi [2005] evaluated deformation time and deformation conditions of natural rock deformed in uniaxial deformation by modeling shape change patterns of garnet inclusions based on the mathematical equation. In this study, we present a numerical model explaining shape change of isolated K-feldspar inclusions within quartz host grain in micro-shear zone developed in Teshima granite, the Ryoke metamorphic belt based on the mathematical equation proposed by Toriumi [1987]. Moreover, we estimated deformation time and shear strain of the micro-shear zone on the basis of modeling and observing data of the K-feldspar inclusions.

To calculate shape change pattern according to various deformation conditions from the model, we estimated deformation temperature (~500-600 ˚C) and paleo-stress (156 MPa) based on deformed quartz microstructures within the micro-shear zone. Shape change patterns were obtained by calculating the model at the estimated temperature ranges from 500 to 600 ˚C with 25 ˚C of interval and at the estimated paleo-stress. Subsequently, the shape change patterns were corrected through combining shape change patterns in zero stress condition to compensate post-deformational annealing effects during exhumation stage of the micro-shear zone. Deformation time was measured by finding out the best-matched shape change pattern calculated by the model in comparison with a shape change pattern observed in the micro-shear zone and by cooling rate of the Ryoke belt proposed by Okudaira et al. [2001]. As a result, deformation time in the micro-shear zone is calculated as 2250-4000 yr under conditions of T = 540-550 ˚C, σ = 156 MPa. Shear strain in the micro-shear zone is 34-45.

Keywords: Micro-shear zone, Numerical modeling, K-feldspar inclusion, Deformation time

©2021. Japan Geoscience Union. All Right Reserved.

C-O-H fluid was present during garnet-forming partial melting reaction in a pelitic migmatite from the Ryoke belt, Japan

*Natsumi Yoshimoto[1], Tetsuo Kawakami[1]

1. Kyoto University

Partial melting of the crustal rocks has long been discussed based on the scheme of two end member concepts of vapor-present melting vs dehydration melting. Common textural characteristic of the incongruent melting is a coexistence of peritectic mineral(s) and leucosome, and this has long been considered as an evidence of dehydration melting. Existence of primary melt inclusions such as nanogranites in peritectic mineral(s) is also good evidence of incongruent melting. Recently, however, coexistence of melt inclusions and fluid inclusions are found from peritectic garnet in partially molten rocks (e.g., Carvalho et al., 2019), evidencing that fluid phase coexisted with partial melts when the peritectic garnet was formed. In order to investigate the presence/absence of such fluid phase during partial melting of the middle to lower crust beneath a volcanic arc, we carried out petrographic observation of pelitic migmatites from the Cretaceous Ryoke metamorphic belt (Aoyama area, SW Japan).

The sample used in this study is a pelitic diatexite that occur in the metatexite-dominant area of the Grt-Crd zone of the Aoyama area. The sample mainly consists of biotite + garnet + plagioclase + quartz, and minor K-feldspar and muscovite are also present in the matrix. The garnet is almost homogeneous in terms of major elements except for the grain margin in contact with biotite. Therefore, we utilized discontinuous zonings in terms of P and Y to define the isochronous surface within the garnet during its growth. As a result, garnet is divided into inner core, outer core, mantle, inner rim and outer rim. Inner and outer cores show higher Y concentration compared to other domains, and prograde xenotime is included in the outer core. In the mantle and the inner rim, sillimanite needles are included. Muscovite, plagioclase, K-feldspar are included in the vicinity of the sillimanite in the inner rim. The outer rim has abundant ilmenite inclusions and rare euhedral plagioclase inclusion indicative of partial melting. Fluid inclusions are seen throughout the garnet grain except for the inner rim. These fluid inclusions are composed of both fluid and solid phases. The fluid phase is mainly composed of CH_4 or CO_2 + CH_4, and the solid phases are siderite, chlorite, and clay minerals. Such a mode of occurrence of CH_4-bearing COH fluid inclusions is interpreted as a result of post-entrapment reaction between original COH fluid inclusion and host garnet that resulted in the formation of secondary daughter minerals (Carvalho et al., 2019).

Based on pieces of observation described above, the garnet-forming process is explained as follows. (1) High Y concentration and presence of prograde xenotime inclusion and COH fluid inclusion in the outer core of the garnet suggests that the garnet core grew at around 530-570°C (Kawakami et al., 2019) in the presence of COH fluid. (2) Sillimanite, muscovite, plagioclase and K-feldspar in the inner rim suggests that the inner rim grew at around the muscovite breakdown reaction Ms + Ab + Qtz = Sil + Kfs + melt. (3) The COH fluid inclusions, abundant ilmenite and rare euhedral plagioclase enclosed in the outer rim of garnet indicate that the biotite breakdown melting in the presence of COH fluid was responsible for the formation of the outer rim of garnet. Therefore, this study revealed that COH fluid was present during the biotite breakdown melting reaction to form garnet in the middle crust of the upper-amphibolite to granulite facies Ryoke metamorphic belt. Presence of fluid phase can be common even during the partial melting of graphite-bearing pelitic lithology that produces peritectic mineral(s).

©2021. Japan Geoscience Union. All Right Reserved.

Keywords: metamorphism, partial melting, crustal fluid

©2021. Japan Geoscience Union. All Right Reserved.

[J] Oral | S (Solid Earth Sciences)：S-MP Mineralogy & Petrology

Sun. Jun 6, 2021 10:45 AM - 12:15 PM JST | Sun. Jun 6, 2021 1:45 AM - 3:15 AM UTC | Ch.20 Zoom Room 20

[S-MP25] Deformed rocks, Metamorphic rocks and Tectonics

convener:Yumiko Harigane(Geological Survey of Japan, National Institute of Advanced Industrial Science and Technology (AIST)), Yoshihiro Nakamura(Geological Survey of Japan, National Institute of Advanced Industrial Science and Technology), Chairperson:Yumiko Harigane(Geological Survey of Japan, National Institute of Advanced Industrial Science and Technology (AIST)), Yoshihiro Nakamura(Geological Survey of Japan, National Institute of Advanced Industrial Science and Technology)

We invite all researchers who aim to understand the dynamics of the earth's crust and mantle at the plate boundaries, to discuss the latest results from various viewpoints. The scope will include contributions through petrology and structural geology as well as various techniques including rheology and transformation of heat and mass.

10:45 AM - 11:00 AM JST | 1:45 AM - 2:00 AM UTC

[SMP25-07] Rheological and metamorphic evolutions of high-grade Shimanto accretionary complex in Kerama islands, Ryukyu

*Ippei Yamamoto[1], Yoshihiro Nakamura[2], Yumiko Harigane[2], Yui Kouketsu[3], Kenichiro Tani[4], Asuka Yamaguchi[1] (1.Atmosphere and Ocean Research Institute, The University of Tokyo, 2.National Institute of Advanced Industrial Science and Technology, 3.Nagoya University, 4.National Museum of Nature and Science)

11:00 AM - 11:15 AM JST | 2:00 AM - 2:15 AM UTC

[SMP25-08] Rheological Properties of Ductile Shear Zone Developed in Mado Megamullion, Shikoku Basin, Philippine Sea

*Kohei Nimura[1], Katsuyoshi Michibayashi[2], Yumiko Harigane[3], Yasuhiko Ohara[4,5] (1.Department of Earth and Planetary Science, Faculty of Science, Nagoya University , 2.Department of Earth and Planetary Sciences, Graduate School of Environmental Studies, Nagoya University, 3.Research Institute of Geology and Geoinformation, Geological Survey of Japan, AIST, 4.Hydrographic and Oceanographic Department of Japan, 5.JAMSTEC)

11:15 AM - 11:30 AM JST | 2:15 AM - 2:30 AM UTC

[SMP25-09] Possibility of CPO development during diffusion creep of the lower crustal minerals

*Bunrin Natsui[1], Kosuke Yabe[1], Takehiko Hiraga[1] (1.Earthquake Research Institute, University of Tokyo)

11:30 AM - 11:45 AM JST | 2:30 AM - 2:45 AM UTC

[SMP25-10] The effect of fluid compositions on pore formation during plagioclase replacement under supercritical conditions

*Astin Nurdiana[1], Atsushi Okamoto[1], Masaoki Uno[1], Noriyoshi Tsuchiya[1] (1.Tohoku University)

11:45 AM - 12:00 PM JST | 2:45 AM - 3:00 AM UTC

[SMP25-11] Garnet–aluminosilicate–spinel–plagioclase geobarometer

*Toshiaki Shimura[1], Yuki Harada[1,2], Geoffrey L. Fraser[3], Noriyoshi Tsuchiya[4] (1.Yamaguchi University, 2.i-SHOT Inc., 3.Geoscience Australia, 4.Tohoku University)

12:00 PM - 12:15 PM JST | 3:00 AM - 3:15 AM UTC

[SMP25-12] Porosity wave and mineral banding in the metamorphism

*mitsuhiro toriumi[1] (1.Japan agency of marine science and technology)

Rheological and metamorphic evolutions of high-grade Shimanto accretionary complex in Kerama islands, Ryukyu

*Ippei Yamamoto[1], Yoshihiro Nakamura[2], Yumiko Harigane[2], Yui Kouketsu[3], Kenichiro Tani[4], Asuka Yamaguchi[1]

1. Atmosphere and Ocean Research Institute, The University of Tokyo, 2. National Institute of Advanced Industrial Science and Technology, 3. Nagoya University, 4. National Museum of Nature and Science

The Kerama Formation in the Ryukyu Arc is located at the southwestern edge of the Shimanto Belt, made up of repetition of greenstone, metasandstone, and pelitic schist. Sedimentation and metamorphic ages were estimated to be ca. 105 and ca. 91 Ma, respectively, based on zircon U-Pb and muscovite K-Ar ages (Yamamoto et al, submitted). Occurrence of terrigenous metasediment and N-MORB type greenstone contacts are intrusive in most places, suggesting ocean floor spreading occurred near the trench (Chinen et al., 2004; Yamamoto et al., submitted).

Although metamorphic mineral assemblage of greenstone (epidote + actinolite; Hashimoto, 1978) and the existence of mylonite originated from conglomerate (containing quartz, plagioclase, K-feldspar, muscovite and chlorite; Yamamoto et al., submitted) suggest metamorphism and deformation occurred at high temperature conditions, there have been few reports on the detailed metamorphic temperature estimations and deformation microstructures of the Kerara Formation before. In this study, we present results of Raman spectroscopy of carbonaceous material (RSCM) thermometry and electron backscatter diffraction (EBSD) analyses of the rocks of the Kerama Formation to constrain peak metamorphic temperature and rheological condition related to subduction of spreading center.

RSCM analyses were performed using a Raman spectrometer with a 532 nm Nd-YAG laser (system installed at Nagoya University). Peak metamorphic temperature of pelitic schist and conglomerate mylonite (originated from gravel sandstone) was estimated to be 470–525˚C, which is consistent with the temperature range of metamorphic facies proposed in the greenstone.

Measurement of grain size and crystallographic preferred orientations (CPO) in quartz were conducted by SEM-EBSD-EDS system in GSJ-Lab (HITACHI SU3500 SEM mounted with Oxford EBSD detector). Recrystallized quartz region from a sample of conglomerate mylonite shows type II crossed girdle CPO. According to the quartz c-axis fabric opening-angle thermometer of Faleiros et al (2017), it is suggested that the recrystallized quartz region from the sample of conglomerate mylonite was deformed under ~530˚C, which corresponds to the peak metamorphic temperature estimated from RSCM thermometry. The mean grain size of quartz in the mylonite is ~80 μm, which suggests the differential stress magnitudes of ~30 MPa (Cross et al. 2017).

In contrast to common occurrence of mylonite along fossil fault zones in continental lithosphere, mylonite in subduction setting is rare: no mylonite has reported from the Shimanto Belt so far. The geology of Kerama islands would be a strong constrain for rheology of subduction plate interface at high temperature condition.

©2021. Japan Geoscience Union. All Right Reserved.

Rheological Properties of Ductile Shear Zone Developed in Mado Megamullion, Shikoku Basin, Philippine Sea

*Kohei Nimura[1], Katsuyoshi Michibayashi[2], Yumiko Harigane[3], Yasuhiko Ohara[4,5]

1. Department of Earth and Planetary Science, Faculty of Science, Nagoya University , 2. Department of Earth and Planetary Sciences, Graduate School of Environmental Studies, Nagoya University, 3. Research Institute of Geology and Geoinformation, Geological Survey of Japan, AIST, 4. Hydrographic and Oceanographic Department of Japan, 5. JAMSTEC

Oceanic core complexes (OCCs) are domal bathymetric features that are found along intermediate-to ultraslow-spreading ridge (<55 mm/yr) and are characterized by exposed lower crust and mantle material. These domal bathymetric features are interpreted to be exposed on the seafloor over several million years by detachment faulting, but few studies have examined their properties from a rheological point of view. In this study, we investigate the kinematic features of detachment faulting in the Mado Megamullion, one of the OCCs in the Shikoku Basin of the Phillipine Sea, based on the deformation microstructure and crystallographic orientation fabric of the deformed gabbroic rocks.
Microstructural observations, crystallographic-preferred orientation (CPO) analysis and major element composition analysis of plagioclases and amphibole from 3 deformed gabbroic rocks (R10, R19a and R20) were studied among 10 rocks collected from the Mado Megamullion. The deformation mechanism was estimated based on the results of microstructural and CPO analyses. In addition, the deformation temperature was estimated by applying the chemical composition obtained from the major element composition analysis to the amphibole–plagioclase geothermometer.
Both plagioclase and the secondary amphibole show evidence of intracrystalline plastic deformation and were dynamically recrystallized. The CPOs of plagioclase and amphibole show a strong concentration of (001)[100] and (100)[001] patterns, respectively. The chemical compositions of plagioclase and amphibole are diverse, ranging from An_{41}–An_{76} and Hornblende–Pargasite, respectively. However, the equilibrium temperatures obtained for 3 samples were in the same temperature range (870–690˚C). Equilibrium temperatures of 690–610˚C were obtained from felsic veins penetrating the gabbros.
Based on microstructural observations and CPO analyses, the deformation mechanism of plagioclase and amphibole is assumed to be dislocation creep. Assuming that the equilibrium temperature is the temperature range during deformation, the analyzed gabbros were plastically deformed at 870–690˚C (granulite-facies) because the crystallographic slip planes of plagioclase and amphibole are the same.
In order to clarify the characteristics of the ductile shear zone, deformation mechanism maps of plagioclase deformed by dislocation creep were constructed from the dynamic recrystallized grain size, the equilibrium temperature and the flow law of plagioclase. The shear strain rate of the ductile shear zone of the Mado Megamullion was estimated to be more than 10^{-9} s^{-1} and its thickness to be about 20 cm. The values of shear strain rate and shear zone thickness estimated in this study mean that there are localized regions of high shear strain rate in the ductile shear zone. In other words, it suggests strain localization due to grain size reduction and fluid infiltration. We compared the deformation temperatures and shear strain rates obteined in this study with data from Godzilla Megamullion, the world's largest OCC in the Parece Vela Basin. The properties of the ductile shear zones of Mado Megamullion and Godzilla Megamullion show similarities. This suggests that there is a common feature in the formation process of Mado Megamullion and Godzilla Megamullion.

Keywords: Oceanic Core Complex, Ductile shear zone, Back-arc basin, lower oceanic crust, gabbro, flow law

©2021. Japan Geoscience Union. All Right Reserved.

©2021. Japan Geoscience Union. All Right Reserved.

Possibility of CPO development during diffusion creep of the lower crustal minerals

*Bunrin Natsui[1], Kosuke Yabe[1], Takehiko Hiraga[1]

1. Earthquake Research Institute, University of Tokyo

Olivine is a major constituent minerals of the upper mantle and is known for its crystal preferred orientations (CPO), where the crystal axis is oriented in a specific direction. CPO has been thought to develop only during dislocation creep, but recently the CPO development during diffusion creep and its mechanism have been experimentally demonstrated (Miyazaki et al., 2013; Maruyama and Hiraga, 2017). However, it is not clear that the similar CPO development process occurs in minerals other than olivine.

The CPO development of plagioclase in lower crustal rocks is well known. In this study, the mechanism of CPO development during deformation of plagioclase which is responsible for the lower crustal flow was investigated by pure shear deformation experiments at high temperatures. Polycrystalline anorthite ($CaAl_2Si_2O_8$), the Ca-rich end member of plagioclase, with an average grain size of ~2 μm and porosity of <0.01 vol% was synthesized using vacuum sintering technique. This polycrystalline material was placed in a carbon guide and deformed at atmospheric pressure, temperature of 1242℃ and stresses of 40~75 MPa. Microstructural analysis of the deformed samples revealed CPO development, and the stress-strain rate relationship during the deformation indicated the mechanism of diffusion creep. We discuss the possibility of CPO development during diffusion creep in the lower crust.

Keywords: diffusion creep, CPO, lower crust, anorthite

©2021. Japan Geoscience Union. All Right Reserved.

The effect of fluid compositions on pore formation during plagioclase replacement under supercritical conditions

*Astin Nurdiana[1], Atsushi Okamoto[1], Masaoki Uno[1], Noriyoshi Tsuchiya[1]

1. Tohoku University

Multistage feldspar replacement by Na-K rich fluid is frequently found in mid-crustal depth (e.g. Plümper et al., 2009; Yuguchi et al., 2019) at which micro- to nano- pores fluid pathways developed intensively. Such feldspar replacement was also found in mafic schist from Kinkasan Island, NE Japan, as a part of the South Kitakami Belt. Multiple plagioclase replacement by infiltration of Na-rich and K-rich fluid was recorded. In the K-rich fluid alteration, plagioclase (An35-60) was altered to Kfs (An0Ab1Or99) and albite (An4Ab94Or2) intergrowth along with pores development that increases bulk rock porosity up to 1.34± 0.14%. The replacement was induced by pegmatite-related Na-K-rich fluid and took place at 400-570˚C at 0.3–0.45 GPa. That shows that Na-K-rich fluid may induce multiple secondary feldspar and micro- to nano- pores generations. However, the role of these fluids governs the replacement process is still poorly understood.

We conduct feldspar replacement by Na-K rich fluids to see if the Na-K ratio may induce the secondary product and pore formations to compare to natural sample in Kinkasan. We carried out plagioclase replacement by aqueous 2M KCl and/or NaCl under 600˚C & 150 MPa for 4-8 days. Plagioclase starting materials are anorthite (An; An96Ab4), labradorite (Lab; An66Ab33Or1), and albite (Ab; An1Ab99) that each of them reacted with the fluid with and without silica presence to progress feldspar replacement. Reaction results show the dissolution-reprecipitation process with a sharp reaction front and induced pores formation up to ~7%. That micro-size pores are unlikely to always relate to the grain boundaries. Reactions of KCl-feldspar in undersaturated silica show a faster reaction rate and varied porosity properties compare to NaCl and/or KCl fluid with feldspar in silica saturated conditions. Labradorite-KCl reaction shows the most intense pore formations and alkali feldspar product which is the closest texture of plagioclase replacement by K-rich fluid in Kinkasan sample.

That result indicates the role of Na-K rich fluid ratio and silica saturation toward feldspar replacement. The reaction of feldspar with the higher K ratio fluid and limited silica leads to intense pore generations as the main fluid channel. The different ratios of Na-K and silica presence brought the feldspar replacement into different pore properties.

Keywords: Na-K rich fluid, feldspar replacement, fluid transport, hydrothermal experiment, Kinkasan

©2021. Japan Geoscience Union. All Right Reserved.

Garnet–aluminosilicate–spinel–plagioclase geobarometer

*Toshiaki Shimura[1], Yuki Harada[1,2], Geoffrey L. Fraser[3], Noriyoshi Tsuchiya[4]

1. Yamaguchi University, 2. i-SHOT Inc., 3. Geoscience Australia, 4. Tohoku University

Spinel series mineral, (Mg, Fe, Zn, Mn) Al_2O_4 solid solution is one of the rock-forming minerals in pelitic metamorphic rocks. It mainly occurs in the sillimanite field, but also occurs in the kyanite field and andalusite field. Many authors studied spinel-forming reactions of pelitic metamorphic rocks. Some of these were solved as net-transfer reactions, geobarometers. Many geobarometers have been proposed for spinel-bearing pelitic metamorphic rocks (e.g. Harris, 1981; Perchuk et al., 1989; Nichols et al., 1992). For example, such net-transfer reactions are;

(1) Grt + 2Als = Spl + Crd,
(2) Crd = 2Spl + 5Qz,
(3) Grt + 2Als = 3Spl + 5Qz.

The reaction (1) means that the product minerals are spinel and cordierite. As a result, the spinel must be in contact with cordierite. Such textures are well-known in the Hidaka metamorphic belt and Ryoke metamorphic belt. On the other hand, the reactions (2) and (3) mean that the product minerals are spinel and quartz. As a result, the spinel must be in contact with quartz directly. This mineral assemblage is one of the diagnostic UHT metamorphic mineral assemblages (e.g. Waters, 1991; Harley, 1998; Ganguly et al., 2017). Therefore, net-transfer reactions (2) and (3) geobarometers can be used only for the UHT conditions. Generally, almost all pelitic metamorphic rocks contain quartz. However, spinel does not occur in contact with quartz in the amphibolite facies and/or in the granulite facies (lower than the UHT) conditions. Geobarometers (2) and (3) cannot be used for such metamorphic conditions.

Spinel + plagioclase symplectites in pelitic metamorphic rocks have been reported from many localities. We report occurrence of such texture, from Lützow–Holm Complex (LHC), East Antarctica, Hidaka Metamorphic Belt, Japan, Uetsu area, Japan, and Ryoke Metamorphic Belt, Japan. For example, Tenmondai Rock of LHC lies approximately mid-way along the amphibolite- to granulite-facies progression (Shiraishi et al., 1984). In this example, spinel occurs in a garnet-sillimanite gneiss. It is mainly composed of garnet, spinel, biotite, sillimanite, plagioclase, K-feldspar, quartz, ilmenite, and rutile. Dark green spinel (hercynite) occurs as spinel + plagioclase symplectite. Spinel and quartz are always bounded by plagioclase and spinel is not in direct contact with quartz. Garnet near this texture is enveloped by plagioclase. These textures are produced by the following metamorphic reaction; garnet + sillimanite = spinel + plagioclase. This can be described as the following two net-transfer reactions;

For CFAS-system: 5Grs + Alm + 12Als = 3Hc + 15An, and
For CMAS-system: 5Grs + Prp + 12Als = 3Spl + 15An.

We employed thermodynamic data from Holland and Powell (2011) for these reactions. Consequently, we propose the following geobarometers:

$P_{[CFAS,\ sillimanite]} = (-155761 + 587.4\ T + RT \ln K_{Fe}) / 29.378$, and
$P_{[CMAS,\ sillimanite]} = (-132541 + 564.2\ T + RT \ln K_{Mg}) / 29.299$.

©2021. Japan Geoscience Union. All Right Reserved.

Where P is in bar, T is in K. The equilibrium constant K_{eq} is,

$K_{Fe} = (a_{Grs}^{5}\, a_{Alm}) / (a_{Hc}^{3}\, a_{An}^{15})$, and
$K_{Mg} = (a_{Grs}^{5}\, a_{Prp}) / (a_{Spl}^{3}\, a_{An}^{15})$.

Additionally, we will propose for kyanite and andalusite equations. Our proposed geobarometers are free from quartz, corundum, orthopyroxene, and cordierite within these equations. These are useful to analyze pressure conditions for spinel-bearing pelitic metamorphic rocks within a wide pressure–temperature range (andalusite, kyanite, and sillimanite fields).

References

Ganguly et al. (2017) *Jour. Petrol.*, **58**, 1941–1974.
Harley (1998) *Geol. Soc. London Spec. Publ.*, **138**, 81-107.
Harris (1981) *Contrib. Mineral. Petrol.*, **76**, 229-233.
Holland & Powell (2011) *Jour. Metamorphic Geol.*, **29**, 333-383.
Nichols et al. (1992) *Contrib. Mineral. Petrol.*, **111**, 362- 377.
Perchuk et al. (1989) *Jour. Metamorphic Geol.*, **7**, 599-617.
Shiraishi et al. (1984) *Mem. NIPR Spec. Issue*, **33**, 126-144.
Waters (1991) *European Jour. Mineral.*, **3**, 367-386.

Keywords: spinel, geobarometer, aluminosilicate, spinel + plagioclase symplectite

©2021. Japan Geoscience Union. All Right Reserved.

Porosity wave and mineral banding in the metamorphism

*mitsuhiro toriumi[1]

1. Japan agency of marine science and technology

Metamorphic and metasomatic banding are very common in the regional and contact metamorphic rocks. Mineral bands are composed mainly of retrograde assemblages of albite, chlorite, epidote, calcite and quartz in basic schists and quartz, albite, chlorite, calcite in pelitic schists of the low grade zones, although in the medium grade zones, albite, epidote, garnet, and amphiboles are common in basic schists. In many cases, bands both pelitic and basic schists together with low grade and medium grade metamorphic rocks exhibit monomineralic to bimineralic coarse grained texture compared with matrix. Besides, there is a significant difference in crystallographic orientation in matrix and bands. For examples, tabular grains of epidote occurs commonly perpendicular to the band boundary, suggesting the geometrical growth in the bands from the band wall.

By the way, in metamorphic bands abundant pores coated by oxides and hydroxide minerals appear in the central zone of the band. Those are considered to have been fluid filling pores but not pore after dissociation of carbonates, because of common existence of druse mineral of euhedral acicular quartz. Considering the periodic and parallel distribution of these metamorphic bands, it seems that there is a layered structure of fluid filling pore distribution during the retrograde metamorphism. Besides, such pores are surely considered to be the paths of metamorphic fluid. The pores in these bands also are thought to be derived from dissolution of constituent minerals.

In this paper, the author would like to proposes a theoretical model of banding distribution of the fluid filling pores during the metamorphism and metasomatism. It suggests that the banding distribution of these pores in the metamorphic rocks may result in the strain instability forming shear localization and large scale faults in the plate boundary metamorphic rocks.

Keywords: pore wave, mineral banding, metamorphism

©2021. Japan Geoscience Union. All Right Reserved.

[J] Oral | S (Solid Earth Sciences)：S-MP Mineralogy & Petrology

Sun. Jun 6, 2021 1:45 PM - 3:15 PM JST | Sun. Jun 6, 2021 4:45 AM - 6:15 AM UTC | Ch.20 Zoom Room 20

[S-MP25] Deformed rocks, Metamorphic rocks and Tectonics

convener:Yumiko Harigane(Geological Survey of Japan, National Institute of Advanced Industrial Science and Technology (AIST)), Yoshihiro Nakamura(Geological Survey of Japan, National Institute of Advanced Industrial Science and Technology), Chairperson:Yumiko Harigane(Geological Survey of Japan, National Institute of Advanced Industrial Science and Technology (AIST)), Yoshihiro Nakamura(Geological Survey of Japan, National Institute of Advanced Industrial Science and Technology)

We invite all researchers who aim to understand the dynamics of the earth's crust and mantle at the plate boundaries, to discuss the latest results from various viewpoints. The scope will include contributions through petrology and structural geology as well as various techniques including rheology and transformation of heat and mass.

1:45 PM - 2:00 PM JST | 4:45 AM - 5:00 AM UTC

[SMP25-13] Different entrapment timings of melt inclusions in garnet and quartz in an UH *T* granulite from Rundvågshetta

*Kota Suzuki[1], Tetsuo Kawakami[1] (1.Department of Geology and Mineralogy, Graduate School of Science, Kyoto University)

2:00 PM - 2:15 PM JST | 5:00 AM - 5:15 AM UTC

[SMP25-14] **Effect of syn-metamorphic fluids on HP-LT chloritoid-bearing assemblages: a study case from the Monti Romani (Italy)**

*Samuele Papeschi[1], Alessio Pontesilli[2], Claudia Romano[3], Federico Rossetti[3] (1.Kochi (X-Star), JAMSTEC, Japan, 2.INGV, Roma, Italy, 3.University Roma Tre, Italy)

2:15 PM - 2:30 PM JST | 5:15 AM - 5:30 AM UTC

[SMP25-15] **Newly discovered eclogite in the Khungui zone, Zavkhan terrane, Western Mongolia: P-T evolution and tectonic implication**

*Manzshir Bayarbold[1], Atsushi Okamoto[1], OTGONBAYAR DANDAR[1], Masaoki Uno[1], Noriyoshi Tsuchiya[1] (1.Graduate School of Environmental Studies, Tohoku University)

2:30 PM - 2:45 PM JST | 5:30 AM - 5:45 AM UTC

[SMP25-16] Serpentinization and Carbonation processes of Ultramafic rocks in Manlay Ophiolite, Southern Mongolia

*Nomuulin Amarbayar[1], Atsushi Okamoto[1], Masaoki Uno[1], OTGONBAYAR DANDAR[1], Noriyoshi Tsuchiya[1] (1.Graduate School of Environmental Studies, Tohoku University)

2:45 PM - 3:00 PM JST | 5:45 AM - 6:00 AM UTC

[SMP25-17] Petrological characteristics of the slab-mantle interface during incipient subduction: insights from Dalrympole Amphibolite, Palawan, Philippines

*Gabriel Theophilus Vinalay Valera[1], Tetsuo Kawakami[1], Betchaida Duetes Payot[2] (1.Graduate School of Science, Kyoto University, 2.National Institute of Geological Sciences, University of the Philippines)

3:00 PM - 3:15 PM JST | 6:00 AM - 6:15 AM UTC

[SMP25-18] New deformation proxy for alkaline felsic rocks: Na-K zoning of alkali feldspar in syenites from the Wadi Dib alkaline ring complex, Eastern Desert, Egypt

*Kazuhito Ozawa[1], Eman Saad Hassan[2], Hideto Yoshida[1], Ali Abdel-Kader Khudeir[2] (1.Department of Earth and Planetary Science, Graduate School of Science, University of Tokyo, 2.Geology Department, Assiut University)

Different entrapment timings of melt inclusions in garnet and quartz in an UH*T* granulite from Rundvågshetta

*Kota Suzuki[1], Tetsuo Kawakami[1]

1. Department of Geology and Mineralogy, Graduate School of Science, Kyoto University

The presence of melt during anatexis is considered to have profound effects on the rheology of middle to lower crustal rocks and thus the exhumation mechanisms of them (e.g., Jamieson et al., 2011). Therefore, precisely constraining the timings when melts coexisted in the pressure-temperature-time (*P-T-t*) evolutions of high-grade metamorphic rocks is important (e.g., Barich et al., 2014).
In this study, we report two types of melt inclusions (MI-g and MI-q) and discuss their entrapment timings in a clock-wise *P-T* evolution of an ultrahigh-*T* (UH*T*) granulite (sample TK2003010309) from Rundvå gshetta (Lützow-Holm Complex, East Antarctica). MI-g are enclosed in garnet porphyroblasts, while MI-q are in quartz grains in the matrix.
The occurrences of MI-g have been already reported by previous studies (e.g., Hiroi et al., 2019). They commonly consist of Qtz + Kfs + Pl + Bt. We recently reported that MI-g occur exclusively in the P-poor cores of garnet (Suzuki and Kawakami, 2020). In addition to MI-g, the P-poor cores of garnet commonly include biotite, sillimanite, quartz, rutile, and zircon monomineralic inclusions. Therefore, the P-poor cores of garnet and MI-g were probably formed by the following dehydration melting reaction; Bt + Sil + Qtz = Grt + Kfs + melt (e.g., Spear et al., 1999). By applying the Zr-in-rutile geothermometer (Tomkins et al., 2007) to rutile grains enclosed in the P-poor cores of garnet, the entrapment *P-T* condition of MI-g was constrained to be 892 ±11 ˚C/8.5 kbar to 914 ±10 ˚C/12.2 kbar in the sillimanite stability field. This corresponds to the prograde stage in the clock-wise *P-T* evolution of the UH*T* granulite. The peak metamorphic condition of 1026 °C/14.6 kbar was obtained by applying the same method to inclusion minerals enclosed in the P-rich mantles of garnet.
We newly found MI enclosed in quartz grains in the intervening matrix between garnet and sillimanite porphyroblasts. These MI-q are not aligned in the host quartz grains. Therefore, we interpret that they are primary ones. They commonly consist of Qtz +Kfs + Pl + Ms, without any mafic minerals. Some internal porosities were observed in MI-q, which were probably formed due to the increase of density during the melt crystallization in a constant cavity volume (e.g., Cesare et al., 2009). Quartz grains in MI-q are less luminescent under cathodoluminescence (CL) images compared to the host quartz grains. This might reflect the differences of Ti content in quartz and thus the crystallization *T* condition (e.g., Hiroi et al., 2020). However, there still exist some other possible factors that cause CL emissions of quartz (e.g., Okumura, 2005), and thus further analyses are needed to understand the cause.
It should be noted that in order to trap MI, host minerals must grow in the presence of melt. This can occur in two ways; (I) growth during melt-producing process and (II) melt-consuming process (e.g., Bartoli et al., 2013). As discussed above, MI-g were formed with the peritectic P-poor cores of garnet during the prograde dehydration melting reaction (I). On the other hand, MI-q and the host quartz grains in the matrix is not likely to be formed during process (I). This is because quartz is always consumed as a reactant mineral and its modal amount decreases during the prograde melt-producing process (e.g., Weinberg and Hasalová, 2015). Therefore, the host quartz grains in the matrix can grow and trap MI-q only during the retrograde melt-consuming process (II).
These results may indicate that melts coexisted from prograde into retrograde metamorphic stages and their composition might have changed to less mafic one during fractional crystallization. The melts coexisted in the prograde and retrograde stages of UH*T* metamorphism probably played an important role in weakening the metamorphic rocks (e.g., Rosenberg and Handy, 2005), and might have triggered and

©2021. Japan Geoscience Union. All Right Reserved.

promoted their exhumation, respectively (e.g., Jamieson et al., 2011).

Keywords: partial melting, melt inclusion, nanogranitoid, nanogranite inclusion, ultrahigh-temperature metamorphism

©2021. Japan Geoscience Union. All Right Reserved.

Effect of syn-metamorphic fluids on HP-LT chloritoid-bearing assemblages: a study case from the Monti Romani (Italy)

*Samuele Papeschi[1], Alessio Pontesilli[2], Claudia Romano[3], Federico Rossetti[3]

1. Kochi (X-Star), JAMSTEC, Japan, 2. INGV, Roma, Italy, 3. University Roma Tre, Italy

The Monti Romani Complex (Central Italy) exposes metapelitic –metapsammitic rocks that were metamorphosed during the Alpine Orogeny. HP-LT metamorphism is generally cryptic within these rocks, showing graphite-bearing white mica ±paragonite parageneses, where no Fe-Mg-silicate is evident. Only a handful of samples, collected in correspondence of quartz veins, lack graphite and contain chlorite or zoned chloritoid associated with hematite. Chloritoid zoning, in particular, ranges dramatically from XMg = 0.10-0.14 to XMg = 0.27. Raman Spectroscopy on Carbonaceous Material constraints the thermal peak to 340 –420 ˚C, excluding a possible contribution of temperature increase for chloritoid zoning.

Thermodynamic modelling in the system $MnO–Na_2O–K_2O–FeO–MgO–Al_2O_3–SiO_2–H_2O–TiO_2–O$ (MnNKFMASHTO) fails to reproduce the observed mineral chemistry, if all iron is considered as divalent. The introduction of ferric iron via P–T–X(Fe_2O_3) phase equilibria modelling reproduces the observed equilibria, mineral chemistry, and modes for values of X(Fe*) = Fe_2O_3/Fe_{TOT} ranging from 0.1 to 0.7. Chloritoid zoning can be explained by a change in the oxidation state of Fe at diminishing pressure and constant temperature, consistent with isothermal exhumation from P = 1.1–1.2 GPa to P = 0.6–0.7 GPa.

Our study suggests that the introduction of an oxidizing aqueous fluid in graphite-bearing metapelite deeply modified mineral stability, catalyzing the growth of Mg-Fe chloritoid and chlorite. This study highlights that the Fe_2O_3 content has a profound influence on the mineral assemblages that are stable in metapelites. The use of P–T–X(Fe_2O_3) phase equilibria diagrams is therefore fundamental to derive reliable P–T estimates from the analysis of greenschist- to blueschist-facies parageneses in metasedimentary rocks.

Keywords: HP/LT metamorphism, chloritoid, fluid/rock interaction, ferric iron, RSCM thermometry, pseudosection modelling

©2021. Japan Geoscience Union. All Right Reserved.

Newly discovered eclogite in the Khungui zone, Zavkhan terrane, Western Mongolia: P-T evolution and tectonic implication

*Manzshir Bayarbold[1], Atsushi Okamoto[1], OTGONBAYAR DANDAR[1], Masaoki Uno[1], Noriyoshi Tsuchiya[1]

1. Graduate School of Environmental Studies, Tohoku University

The Central Asian Orogenic belt (CAOB) is a significant site to understand the Paleo-subduction system (Neoproterozoic-Permian). The CAOB can be divided into southern and northern parts based on the distribution of ultrahigh-pressure and high-pressure rocks. Although the Paleo-subduction system in the south part of the CAOB has been studied in detail, the Paleo-subduction system in the northern part of the CAOB is not fully understood. A few details study has an occurrence of HP rock in the northern part of CAOB such as Chandman (Štípská et al., 2010), Gorny-Altai (Ota et al., 2007), and Kokecthav (Y et al., 2001). In this study, we present the P-T condition evolution, tectonic implication, and garnet micro-texture of the newly discovered Khungui eclogite from the Zavkhan terrane in western Mongolia, the northern part of the CAOB, and discuss its significance to the northern part of the CAOB. The geological character and metamorphic age of Khungui eclogite described by Naemure et al. (2020).

The seven eclogites collected from the Khungui zone, the Zavkhan terrane, western Mongolia were examined in detail. The geochemical signatures of eclogites manifest basaltic composition with a signature of continental arc basalt (Nb/La vs. La/Yb ratios). The eclogites are composed of garnet, omphacite, amphibole, Ti-rich phases (rutile, ilmenite, and sphene), phengite, quartz, epidote, plagioclase, and a small amount of zircon, chlorite, and feldspar. According to the modal abundance of minerals, the eclogites show two evident layers: Ti-rich phase-dominant and epidote-dominant layers. In Ti-rich phase-dominant layers, garnet occurs as the aggregates (>500 μm) composed of a large number of individual garnet grains (10-250 μm in size and xenomorphic shape), which are separated by high angle boundaries. In epidote-dominant layers, garnet appears as a euhedral crystal (>100 μm). In the Ti-rich phase-dominant layers, the individual garnet boundary is not controlled by compositional zoning. The garnet aggregate rim (bordered with the Ti-rich phase) is enriched in Mn. Garnet aggregate shows zoning core to rim: $Alm_{0.62\text{-}0.57}$, $Grs_{0.30\text{-}0.31}$, $Prp_{0.06\text{-}0.11}$, $Sps_{0.02\text{-}0.01}$ in the Ti-rich phase-dominant layers. The single euhedral garnet shows zoning core to rim: $Alm_{0.71\text{-}0.59}$, $Grs_{0.10\text{-}0.31}$, $Prp_{0.16\text{-}0.09}$, $Sps_{0.03\text{-}0.01}$ in the epidote-dominant layers. Jadeite content of the omphacite varies Xjd=0.32-0.38 in the matrix of the layers and Xjd=0.34-0.44 in the rim of garnets. The Si content of phengite is homogenous (3.23 - 3.49 a.p.f.u.) in a matrix of the layers and rim of garnets. Amphibole occurs as barroisite to taramite (core to rim) in the matrix of layers, hornblende in symplectite, and barroisite coexisted with the rim of garnets. Mineralogy of the eclogite suggests pre-peak (garnet core), peak (garnet rim), and retrograde (symplectite of hornblende + plagioclase) stages. The peak assemblage –garnet rim, omphacite, rutile, phengite, epidote, and barroisite, corresponds to T=445-610 ˚C and P=20-21 kbar. Taramite (barroisite rim), and the symplectite are interpreted as retrograde stages formed at T=541-615 ˚C and P=5-15 kbar.

The compositional and textural differences of garnets in the two layers suggest the aggregate formation of small garnets and heterogeneity of compositional zoning could be related to Ti- and Si-rich fluid. Garnet aggregate texture is not commonly observed in other northern parts of HP rocks of CAOB. Pressure-Temperature path based on mineralogy of the eclogites indicates clockwise metamorphism, which is similar to other HP rock in CAOB. The signature of continental arc basalt for eclogites in the Khungui zone (associated with orthogneisses) contrasts with other eclogite bodies (commonly related to

©2021. Japan Geoscience Union. All Right Reserved.

meta-ophiolite or ophiolite sequences) signatures (MORB type) in the CAOB. Outstanding microtexture, P-T path, protolith, and the surrounding rock of the eclogites in the Khungui zone imply the Paleo-collision type which is contrary to the eclogite bodies recording paleo-subduction system in the northern part of the CAOB.

Keywords: Eclogite, Metamorphic evolution , the Khungui zone, the CAOB

©2021. Japan Geoscience Union. All Right Reserved.

Serpentinization and Carbonation processes of Ultramafic rocks in Manlay Ophiolite, Southern Mongolia

*Nomuulin Amarbayar[1], Atsushi Okamoto[1], Masaoki Uno[1], OTGONBAYAR DANDAR[1], Noriyoshi Tsuchiya[1]

1. Graduate School of Environmental Studies, Tohoku University

Carbonation is a natural carbon-capturing process that silicate and hydroxide minerals of mafic and ultramafic rock react with CO_2 to form carbonate minerals such as magnesite, dolomite, and calcite as long-term carbon sequestration. One of the highly reactive materials for sequestering CO_2 is serpentinite formed by the hydration of olivine-rich ultramafic rocks. An ophiolite is a primary focus for studying carbonation and serpentinization, which is interpreted as remnants of oceanic crust and upper mantle suites of ultramafic, mafic, and felsic rocks. Numerous ophiolites are situated in the Central Asian orogenic belt (CAOB), which is one of the largest orogenic belts in the world. However, metamorphic processes of ophiolites in the CAOB have been insufficiently studied. This study aims to understand the mechanism of multi-stage alteration of ultramafic rock in the Manlay Ophiolite, southern Mongolia, which is located at the central part of the CAOB, in order to understand serpentinization and carbonation processes.

The mineral assemblage of collected samples suggests that ultramafic rocks from the Manlay ophiolite are divided into three types; (1) serpentinized ultramafic rock composed of the low-temperature serpentine phase of lizardite (mesh) and chrysotile (mesh, bastite, and vein) with calcite veins and a small amount of magnetite and spinel. Based on X-ray elemental mapping, mesh lizardite shows low Al content which could indicate that firstly it replaced the olivine, and Al and Fe rich chrysotiles were precipitated later. (2) The partially carbonated serpentinite (lizardite and chrysotile >50%) that replaced by calcite and cut by calcite and dolomite veins with a small amount of diopside, magnetite, and spinel, (3) completely carbonated serpentinite that entirely replaced by calcite and quartz, and contains a small amount of dolomite, magnetite and spinel. The completely carbonated sample includes quartz, calcite and dolomite that show zonal texture as dolomite inside the calcite and surrounded by quartz, as well as the remained mesh texture of serpentine is found which was replaced by quartz in the core and magnetite in the rim.

The relation of microtextures demonstrates three stages. The first stage, protolithic ultramafic rock consisted of olivine and orthopyroxene with a small amount of clinopyroxene and spinel. Secondly, the hydration of ultramafic rock produced serpentinite. The last stage is determined as the carbonation of serpentinites. The reactions of olivine to serpentine and serpentine to calcite and dolomite ±quartz suggest that ultramafic rock was hydrated with Si-rich fluid to form serpentine without brucite, and serpentinite was reacted with Ca and CO_2-rich fluid, and partially or completely carbonated by calcite and dolomite ±quartz. We are assuming that silica has dissolved during the continuous carbonation process, and pores have appeared due to volume change. After the serpentinite was completely carbonated, silica could precipitate in the pores which developed an uncommon texture. Therefore, the presence of carbonation in the Manlay ophiolite indicates that serpentinized ultramafic rocks could effectively capture and store CO2, and is an attractive occurrence to study calcium carbonate, especially calcite, dolomite and quartz assemblage.

Keywords: Serpentinization, Carbonation, Manlay Ophiolite, South Mongolia

©2021. Japan Geoscience Union. All Right Reserved.

©2021. Japan Geoscience Union. All Right Reserved.

Petrological characteristics of the slab-mantle interface during incipient subduction: insights from Dalrympole Amphibolite, Palawan, Philippines

*Gabriel Theophilus Vinalay Valera[1], Tetsuo Kawakami[1], Betchaida Duetes Payot[2]

1. Graduate School of Science, Kyoto University, 2. National Institute of Geological Sciences, University of the Philippines

The slab-mantle interface in the earliest stages of subduction are preserved in some ophiolites as thin slivers of amphibolite to granulite-facies rocks collectively referred to as metamorphic soles. Observation of most metamorphic soles reveal that they are composed of relatively coherent slices which preserve high geothermal gradients (~25 ˚C/ km) (e.g. Agard et al. 2018). The boundary between the subducting slab and the overlying mantle in a mature subduction zone on the other hand, is typically composed of eclogite-blueschist blocks surrounded by serpentine and/or chlorite- rich matrix (e.g. Bebout and Penniston-Dorland, 2016). The cooler gradients (4-10 ˚C/ km; Guillot et al., 2009) and fluid-rich nature of this setting, allows the extensive mixing of crustal and mantle components resulting in a hybridized matrix composition (e.g. Bebout and Penniston-Dorland, 2016).

In this study, we present the petrological characteristics and *P-T* history of the Dalrympole Amphibolite which correspond to the slab-mantle interface of an Eocene subduction zone in its infancy (Encarnacion et al., 1995). This unit underlies the residual mantle peridotites of the Palawan Ophiolite composed of harzburgite-dunite interlayers. Similar to other metamorphic soles (e.g. Oman), the Dalrympole amphibolite is predominantly composed of high grade metamafic blocks (i.e. amphibolites ±Grt, Ep) with only minor metasedimentary units. Unlike most soles which are preserved as coherent sheets however, the Dalrympole Amphibolites is a melange complex with 1-2 m blocks surrounded by a highly sheared matrix. The matrix apparently represents a hybridized composition (Ky-Hbl-Bt-Ilm±Grt) resulting from the mixing of sedimentary and mafic components derived from the downgoing slab.

Grt porphyroblasts in the garnet amphibolite block 214-TK9, preserves prograde zonation marked by a Mn-rich, Mg-poor core (= $Alm_{46-51}Prp_{10-19}Grs_{15-20}Sps_{15-25}$) and a Mn-poor, Mg-rich rim (= $Alm_{38-41}Prp_{30-35}Grs_{13-15}Sps_{13-17}$). Applying Zr-in-Rt thermometry (Tomkins et al., 2007) and Qz-in-Grt barometry (Angel et al., 2017) to Rt and Qz inclusions respectively, in the core and rim of the garnet porphyroblasts consistently reflect prograde metamorphism from the core (~625˚C, 11.5 kbar) towards the rim (~700˚C, 13 kbar). The same thermobarometric techniques were applied to the matrix sample 214-TK2 in order to constrain the *P-T* conditions leading to the formation of the matrix. Rutile inclusions in Ky, and Qz hosted in Grt which are in turn included in Ky were used. The Grt (=$Alm_{35-36}Prp_{28-32}Grs_{16-19}Sps_{16-19}$) in this sample are fine grained and do not preserve clear zonation. *P-T* conditions preserved in the matrix (~700˚C, 13 kbar) are comparable to the rim stage of the metamafic blocks.

The similar peak metamorphic conditions constrained in the matrix and the metamafic blocks in Dalrympole Amphibolite suggests that the matrix-forming deformation possibly started en route towards depths of around ~45 km (Jagoutz and Behn, 2013). Furthermore, the paleogeothermal gradient preserved in the Dalrympole Amphibolite (~16 ˚C/km) and its block-and-matrix structure are atypical of metamorphic soles but are also warmer than commonly observed for a developed subduction channel in a mature arc. These characteristics are more comparable to early high *T* melanges (e.g. Agard et al. 2018)

©2021. Japan Geoscience Union. All Right Reserved.

suggesting that the Dalrympole Amphibolite may correspond to the slab-mantle interface of a young subduction complex already transitioning from the much warmer conditions when subduction was first initiated.

Keywords: Slab-mantle interface, melange, Dalrympole amphibolite, Thermobarometry

©2021. Japan Geoscience Union. All Right Reserved.

New deformation proxy for alkaline felsic rocks: Na-K zoning of alkali feldspar in syenites from the Wadi Dib alkaline ring complex, Eastern Desert, Egypt

*Kazuhito Ozawa[1], Eman Saad Hassan[2], Hideto Yoshida[1], Ali Abdel-Kader Khudeir[2]

1. Department of Earth and Planetary Science, Graduate School of Science, University of Tokyo, 2. Geology Department, Assiut University

Deformation of rocks gives rise to diversities not only in microstructures but also chemical heterogeneity on various scales. These records in deformed rocks will conversely provide rich information on deformation conditions, such as strain, stress, and strain rate. Ozawa (1989) shows that Cr-Al zoning in spinel in deformed mantle peridotites formed by a diffusion creep driven by stress (kinetic demixing: Dimos and Kohlstedt 1987). The zoning is characterized by maxima of both Al and Cr on the grain surface and an intermediate value at the grain center. The shape of spinel and the strain predicted from diffusion creep is consistent: the Al maxima are found in the elongate direction and Cr on the shortest direction. The conditions for development of such zoning and morphology are: (1) notably smaller diffusivity of Cr than Al (Suzuki et al., 2008), (2) Cr and Al diffusion controls rate of deformation for given conditions of grain size and temperatures (Suzuki et al., 2008), (3) proper deformation conditions such as temperature, pressure, stress, and strain rate, and (4) deformation took place under lowering temperature to freeze the zoning pattern. If these conditions are fulfilled in other minerals and chemical components, similar chemical zoning in naturally deformed rocks may be expected. There are, however, no indisputable reports so far. We found such chemical zoning in intermediate alkali feldspar in terms of Na and K in fine-grained porphyritic trachyte and syenite from the 580Ma Wadi Dib alkaline ring complex, Eastern Desert, Egypt (Frisch and Abdel-Rahman, 1999). Deformation induced chemical zonings of feldspars have long been reported (e.g., White, 1975; Kramer and Seifert, 1991), but they mostly require involvement of open reaction processes and do not belong to kinetic demixing. The rocks from the Wadi Dib complex are composed dominantly of intermediate alkali feldspar, which underwent recrystallization by pyrometamorphism and deformation to grain size smaller than 200 microns. The above conditions (1) are satisfied because of a large difference in K and Na diffusivity in alkali feldspar by more than two orders of magnitude (Cherniak, 2010). The conditions of (2) - (4) might also be fulfilled because of high temperature and small grain size (Farver and Yund, 1995). In this talk, we will report microstructure and Na-K zoning in alkali feldspar to show that they formed by deformation, and we propose that the zoning may be a useful proxy of deformation.

Keywords: stress, chemical zoning, alkali feldspar, Na-K zoning

©2021. Japan Geoscience Union. All Right Reserved.

[J] Poster | S (Solid Earth Sciences)：S-MP Mineralogy & Petrology

Sun. Jun 6, 2021 5:15 PM - 6:30 PM JST | Sun. Jun 6, 2021 8:15 AM - 9:30 AM UTC | Ch.12_1

[S-MP25] Deformed rocks, Metamorphic rocks and Tectonics

convener:Yumiko Harigane(Geological Survey of Japan, National Institute of Advanced Industrial Science and Technology (AIST)), Yoshihiro Nakamura(Geological Survey of Japan, National Institute of Advanced Industrial Science and Technology)

We invite all researchers who aim to understand the dynamics of the earth's crust and mantle at the plate boundaries, to discuss the latest results from various viewpoints. The scope will include contributions through petrology and structural geology as well as various techniques including rheology and transformation of heat and mass.

[SMP25-P01] Multiple igneous activities recorded in the Nidar ophiolite complex, eastern Ladakh

*Akinori Sato[1], Takeshi Imayama[1], Dripta Dutta[2] (1.Okayama University of Science, 2.Indian Institute of Technology Bombay)

[SMP25-P02] Geology and missing tectonics in the Inashi-Hase area of the eastern part of the Ryoke belt, central Japan

*Akira Ono

[SMP25-P03] Kinematics of North Almora Thrust estimated from mylonite, India

*Hirotoshi Kotama[1], Jun-ichi Ando[1], Kaushik Das[1], Dyuti Prakash Sarkar[1] (1.Hiroshima University)

[SMP25-P04] Illite crystallization and faulting caused by hydrothermal fluid

*Jun-ichi Ando[1], Kota Kojima[1], Kaushik Das[1], Naotaka Tomioka[2], Seiichiro Uehara[3] (1.Department of Earth and Planetary Systems Science, Hiroshima University, 2.Kochi Institute for core sample research, Japan Agency for Marine-Earth Science and Technology, 3.The Kyushu university museum)

[SMP25-P05] Episodic fluid explosion in shallow and middle crust revealed by hydrothermal brecciation

*Geri Agroli[1], Atsushi Okamoto[1], Masaoki Uno[1], Noriyoshi Tsuchiya[1] (1.Tohoku University)

[SMP25-P06] Pseudotachylyte in a marble from the Takine Group (Abukuma Terrane) and its similarity to pseudotachylyte from the Higo Mertamorphic Rocks

*Tadao Nishiyama[1], Ebo Adou Douha[1] (1.Department of Earth and Environmental Sciences, School of Science, Graduate School of Science and Technology, Kumamoto University)

[SMP25-P07] Frictional melting process during formation of pseudotachylyte, Sarwar-Junia fault zone, India

*Jun-ya Okazaki[1], Jun-ichi Ando[1], Kaushik Das[1] (1.Earth and Planetary Systems Science Program, Division of Advanced Science and Engineering, Hiroshima University)

[SMP25-P08] Neoarchean magmatism and Paleoproterozoic high-pressure granulite-facies metamorphism from the southern Motloutse Complex, eastern Botswana: Implications for the western extension of the Central Zone of the Limpopo Complex

*Thembiso Otladisang Basupi[1,2], Toshiaki Tsunogae[1,3], Kazuki Takahashi[1], Yukiyasu Tsutsumi[4] (1.Graduate of Life and Environmental Sciences, University of Tsukuba, 2.Department of Earth and Environmental Sciences, Botswana International University of Science and Technology, 3.Department of Geology, University of Johannesburg, 4.Department of Geology and Paleontology, National Museum of Nature and Science)

[SMP25-P09] Petrography of a sulfide-rich garnet-sillimanite-biotite gneiss from Brattnipene, Sør Rondane Mountains, East Antarctica

*Hayato Ikeda[1], Tetsuo Kawakami[1] (1.Kyoto University)

[SMP25-P10] Microstructural characteristics of ultra-high pressure metamorphic rocks from the Dabie-Shan, eastern China

*Katsuyoshi Michibayashi[1], Kouhei Asano[1] (1.Department of Earth and Planetary Sciences, Graduate School of Environmental Studies, Nagoya University)

[SMP25-P11] Metamorphic history of the Suo metamorphic rocks inferred from two-stage garnet in pelitic schist

*Shunsuke Endo[1], Maki Ito[1] (1.Department of Earth Science, Interdisciplinary Faculty of Science and Engineering, Shimane University)

[SMP25-P12] Hidden intact coesite in deeply subducted rocks and its geological implications

*Tomoki Taguchi[1], Yui Kouketsu[2], Yohei Igami[3], Tomoyuki Kobayashi[4], Akira Miyake[3] (1.Department of Earth Sciences, Faculty of Education and Integrated Arts and Sciences, Waseda University, 2.Department of Earth and Planetary Science, Graduate School of Environmental Studies, Nagoya University, 3.Department of Geology and Mineralogy, Graduate School of Science, Kyoto University, 4.Faculty of Health and Sports, Nagoya Gakuin University)

[SMP25-P13] Metamorphic zoning and *P–T* conditions of contact metamorphic rocks in the Unai area, Yamaguchi prefecture, Japan.

*Kakeru Sakamoto[1], Toshiaki Shimura[1] (1.Graduate School of Sciences and Technology for Innovation, Yamaguchi University)

[SMP25-P14] Progressive metamorphism of the Ryoke metamorphic rocks from No-jima Island, South of Yamaguchi Prefecture

*ZEJIN LU[1] (1.Graduate School of Science and Engineering for Innovation, Yamaguchi University)

[SMP25-P15] *P–T–t* path of Ryoke metamorphic rocks in Kitsuki area, Kunisaki Peninsula, Oita prefecture, Japan.

*Kentaro Mutabaru[1], Toshiaki Shimura[1] (1.Yamaguchi University)

[SMP25-P16] *P-T* estimations of Ryoke metamorphic rocks in the Takato-Ohshika area, Nagano, Japan

*Yoshihiro Nakamura[1], Kazuhiro Miyazaki[1], Yutaka Takahashi[1] (1.Geological Survey of Japan, National Institute of Advanced Industrial Science and Technology)

[SMP25-P17] Ultrahigh-temperature HP granulite facies stage of the Early Jurassic pre-Sanbagawa metamorphism

*Kenta Yoshida[1], Sota Niki[3], Hikaru Sawada[1], Ryosuke Oyanagi[1], Takafumi Hirata[3], Kenji Asakura[2], Takao Hirajima[2] (1.Japan Agency for Marine-earth Science and Technology, 2.Kyoto University, 3.The University of Tokyo)

[SMP25-P18] **Meliorating the spatial resolution of SEM-EBSD**

*Thomas Jing Yi Yeo[1], Norio Shigematsu[1] (1.Research Institute of Earthquake and Volcano Geology, Geological Survey of Japan, National Institute of Advanced Industrial Science and Technology)

[SMP25-P19] Strain in quartz inclusion probed by Raman spectroscopy

*Yui Kouketsu[1], Yuki Tomioka[1], Tomoki Taguchi[2] (1.Department of Earth & Planetary Sciences, Graduate School of Environmental Studies, Nagoya University, 2.Department of Earth Sciences, Faculty of

Education and Integrated Arts and Sciences, Waseda University)

Multiple igneous activities recorded in the Nidar ophiolite complex, eastern Ladakh

*Akinori Sato[1], Takeshi Imayama[1], Dripta Dutta[2]

1. Okayama University of Science, 2. Indian Institute of Technology Bombay

The Nidar ophiolite complex (NOC) is exposed within the Indus suture zone (ISZ) in eastern Ladakh, India. The NOC comprises of a sequence of ultra-mafic rocks (*base to top*) gabbros, doleritic and basaltic rocks, and volcanic sedimentary assemblages. Previous studies considered that the NOC was formed by supra-subduction zone (SSZ) igneous activity in the early Cretaceous period (e.g. Ahmad et al. 2008), although multiple igneous activities from the late Jurassic to late Cretaceous periods are known in other ophiolites (e.g. Spongtang and Dras) from within the ISZ (e.g. Parsons et al., 2020). In this study, we identified the gabbro and dolerite of the NOC to be products of MORB, implying multiple igneous activities similar to that of the other ophiolites in the ISZ. In addition, metamorphic minerals are distinguished from the igneous ones based on detailed petrological work of the gabbro, dolerite, and basalt of the NOC. The gabbro mainly consists of clinopyroxene and plagioclase, and is subdivided into Type-1 and Type-2. The former is non-metamorphosed and clinopyroxene-rich, while the later is plagioclase-rich and contains epidote and chlorite. The Mg# [Mg/(Mg+Fe2+) ratio] of pyroxene in the rocks decrease down the stratigraphic level from gabbro (0.85-0.92) to dolerite (0.79), and basalt (0.66-0.77). The amphiboles in the dolerite show a compositional zoning –Mg-rich core (Mg#:0.73-0.90) surrounded by Fe-rich rim (Mg#:0.54-0.71). The Mg# of the actinolite and horblende grains in the basalt lie within 0.58-0.62. The plagioclase in the gabbro is bytownite (An: 70-90%), whereas the An content in the plagioclase grains of the dolerite varies from 5% to 89%. The euhedral plagioclase in the basalt are randomly oriented and rich in An (94-99%). In contrast, the anhedral grains are albitic (An: 0.2-2.2%). These indicate that the pyroxene and An-rich plagioclase are igneous minerals. The type-2 gabbro, dolerite and basalt experienced greenschist- to lower amphibolite-facies metamorphism to form An-poor plagioclase, Fe-rich hornblende, epidote, and chlorite. The SiO_2 content of Type-1 gabbro is 55 wt%, which is significantly higher than that of Type-2 gabbro (45 wt%). The Al_2O_3, MgO, and CaO contents decrease with increasing SiO_2, while that of the other major oxides increase. Six samples of the Type-1 gabbro yield flat REE patterns, which are consistent with those noted for SSZ-type igneous rocks (e.g. Ahmad et al. 2008). On the other hand, three samples of the Type-2 gabbro have low REE concentrations and are depleted in the LREE content, which is a characteristic of the MORB-type igneous rocks and not the SSZ rocks. Therefore, it is likely that the NOC is not a product of a single igneous event in the SSZ, but of multiple igneous activities including the formation of the MORB.

©2021. Japan Geoscience Union. All Right Reserved.

Geology and missing tectonics in the Inashi-Hase area of the eastern part of the Ryoke belt, central Japan

*Akira Ono

The Median Tectonic Line (MTL) in central Japan was formed during the opening of the Japan Sea, and large-scale tectonic movements and missing of geological bodies occurred near the MTL [1]. The eastern end of the Ryoke belt in the Ina-Valley area was strongly influenced by the missing tectonics [2, 3]. Here, we present an overview of the geology of the Hase-Ichinose area and confirm the missing tectonics.

Ryoke gneiss, Hiji tonalite and Awasawa metamorphic rocks are distributed in the Ryoke belt of the Hase-Ichinose area (Figure A). Many small meta-sediments derived from Ryoke metamorphic rocks are intercalated in the eastern margin of Hiji tonalite (the light blue region in Figure A). Regarding these xenoliths, pelitic and psammitic mylonites are distributed in Yamabuki Valley to the west of Awasawa village. On the other hand, chert and tuff-derived mylonites are common in the Magoi-Nakao area. The pelitic and psammitic mylonites near Yamabuki Valley are derived from Ryoke gneisses. This is based on the following geological facts. (1) Garnet-cordierite gneisses remain in two places (gneiss in Figure B). (2) Partialy resolved garnet porphyroclast (Figure C) is present in many rock samples, although garnet is not found in the matrix of mylonite.

For pelitic mylonites in and around Yamabuki Valley, the average grain sizes of matrix quartz and feldspar are about 20-30 μm in the upstream region and about 10-20 μm in the downstream region (Figure B). The increase of the grain sizes suggests the increase in metamorphic temperature. However, the metamorphic temperatures estimated by the feldspar geothermometer are almost the same for the two regions. That is, the Ab content of the matrix K-feldspar is almost constant for all the studied samples. Many tonalites in the upstream area are not suffered from mylonitization. For such tonalites, quartz and plagioclase of 70-100 μm in diameter are common.

Original rocks of meta-sediments in the Magoi-Nakao area are mainly mudstone, sandstone, chert, siliceous mudstone, siliceous tuff, conglomerate and mixed rock. These belong to the Hase unit of the accretionary complex [3]. Most of the pelitic mylonites derived from the Hase unit are very fine, and the grain sizes of quartz are about 5-15 μm. Moreover, fine sedimentary structure (Figure D) and radiolarian fossils (Figure E, H) were observed. It is reasonable to conclude that the meta-sediments were metamorphosed under lower temperatures than those of the garnet-cordierite zone. The main constituent minerals of the unaltered pelitic mylonites are biotite, muscovite, plagioclase and quartz. K-feldspar is rare and garnet is not recognized. However, fine garnets are present in calcite-rich pelitic mylonites. Coarse-grained andradite-rich garnets are found for a sample (Figure F).

The radiolarian fossils are not strongly deformed, and pressure shadows have not developed for many porphyroclasts (Figure G). Hence, shear deformation was not very strong as supposed before.

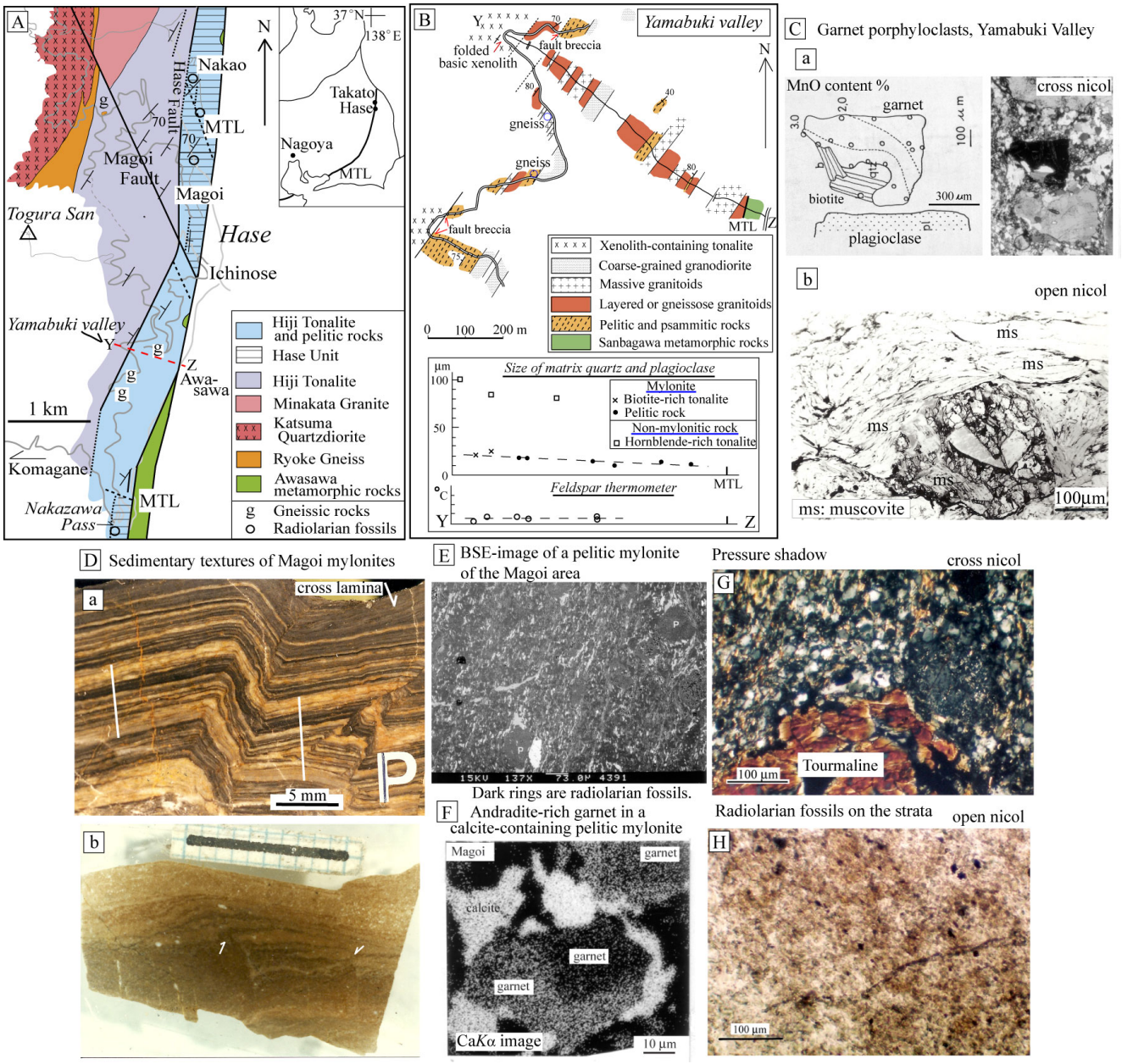
The Hase unit is distributed in the vicinity of MTL over a long distance from the Takato-Itayama area to the Hase-Awasawa area. However, the Hase unit is not confirmed in the Awasawa area, and it is presumed that the Hase unit in the Awasawa area was lost due to the Miocene tectonics. The Hase unit in the Magoi-Nakao area is narrow, and the strikes of foliations are significantly oblique to the directions of the MTL and Hase fault. The Hase unit was a large geological unit in the Paleogene, but most of it was lost by

©2021. Japan Geoscience Union. All Right Reserved.

the Miocene tectonics [1-3].

[1] Ono, 2020, JpGU-AGU Joint Meeting 2020, SGL33-P07. [2] Ono, 2016, JpGU Meeting, SGL37- P16. [3] Ono, 2018, GSJ Meeting, R15-P13.

Keywords: Ryoke belt, Inashi-Hase, Hase unit, Kashio mylonite, missing tectonics



©2021. Japan Geoscience Union. All Right Reserved.

Kinematics of North Almora Thrust estimated from mylonite, India

*Hirotoshi Kotama[1], Jun-ichi Ando[1], Kaushik Das[1], Dyuti Prakash Sarkar[1]

1. Hiroshima University

The purpose of this study is to clarify the faulting process of the North Almora Thrust (NAT) which belongs to a fault system of the Main Central Thrust, based on the characteristics of rock deformation microstructures. The study area lies in the north of Almora, Uttarakhand, India. The results obtained from the field study demonstrate that the granite and sandstone are mylonitized within ca. 7 km south of NAT. The mylonitization tends to change from "proto-mylonite" to "mylonite" closer to NAT, eventually to "ultramylonite". The strikes of these mylonite foliations are almost parallel to that of the NAT. The microstructures of mylonites are studied using an optical microscope, SEM, and SEM-EBSD. These methods combined with image analysis using ImageJ are used to measure the aspect ratio and grain size of dynamically recrystallized quartz. Similar measurements are also conducted using the orientation maps revealed by the SEM-EBSD analyses. The above microstructural observations helped us to determine 1) temperature, shear sense, three-dimensional strain field, and flow stress under which mylonitization occurred, and 2) the effect of phyllosilicate minerals on NAT faulting. In this presentation we shall report the faulting process of the NAT based on the above results.

Keywords: c-axis fabric, phyllosilicate minerals, mylonite

©2021. Japan Geoscience Union. All Right Reserved.

Illite crystallization and faulting caused by hydrothermal fluid

*Jun-ichi Ando[1], Kota Kojima[1], Kaushik Das[1], Naotaka Tomioka[2], Seiichiro Uehara[3]

1. Department of Earth and Planetary Systems Science, Hiroshima University, 2. Kochi Institute for core sample research, Japan Agency for Marine-Earth Science and Technology, 3. The Kyushu university museum

Based on the field survey and microstructural observations of massive chert block, we shall report that there is a strong possibility that illite crystallized from fluids contributed to fault formation.

The fault studied was developed in a massive chert block exposed in Watarai, Mie Prefecture, which belongs to the Southern Chichibu Belt. This massive chert block includes many stylolites and white bands, which develop parallel to the fault plane. The white band is particularly unique, and its width is about 0.5 mm to 1 cm. The massive chert is composed of trace amounts of chlorite along with quartz. On the other hand, the stylolite and white band are composed of quartz as well as trace amounts of chlorite and illite, and large amounts of illite, respectively. The white band also contains numerous voids less than a few μm in diameter, which might have caused due to pressure solution. These facts indicate that the illite was crystallized from a fluid. Furthermore, from the fact that a large amount of illite that was affected by fault slip can be seen on the fault plane, we summarize that the white band became a weak plane and acted finally as a fault plane in the massive chert block. The crystallinity of illite existing on the fault plane is better than those of stylolites and white bands. We propose that this is due to frictional heat caused by fault slip.

Keywords: Chert, Stylolite, Illite, Fluid, Fault

©2021. Japan Geoscience Union. All Right Reserved.

Episodic fluid explosion in shallow and middle crust revealed by hydrothermal brecciation

*Geri Agroli[1], Atsushi Okamoto[1], Masaoki Uno[1], Noriyoshi Tsuchiya[1]

1. Tohoku University

High energy released in the middle to shallow crust in the form of episodic fluid explosion. This phenomenon is triggered by several factors primarily an accumulation of fluid pressure from the dehydrated magmatic-hydrothermal system. The episodic fluid explosion is exemplified by intensive crustal failure through fracturing and brecciation. Further investigation of breccia elucidates the origin and characteristic of fluid and brecciation mechanism. Here we examined samples from 3 different locations to demonstrate how common fluid explosions occur in the middle to the shallow crust.

The Sør Rondane Mountains, in East Antarctica is part of the Pan-African collision zone between East and West Gondwana during Precambrian (650-500 Ma). Northeastern terrane of this mountain occupied by metamorphic sequence (granulite) and some locality of syn-metamorphic intrusion of old granite/diorite followed by younger granite which later makes up the breccia clast on this area and represents explosive activity in the middle crust. On the other hand, Breccia on porphyry deposit of Erdenet in Mongolia which occur in Mesozoic (245-235 Ma) and Cenozoic (9-7 Ma) volcanic breccia in Yuze, Japan represent brecciation processes in the shallow crust. The breccia in Sør Rondane Mountains (SRM) comprise of granulite clast cemented by carbonate rock (refer as carbonate breccia dyke) and subsequent granitic dyke which capture carbonate, granite, and gneiss as the clast. Estimated P-T conditions of this brecciation were P=200Mpa and T=580-700˚C which indicating middle crustal condition. Erdenet Porphyry (EP) comprises of 2 distinct breccia type of polymict-breccia which consist of granodiorite porphyry (with potassic alteration) cemented by biotite (phlogopite) located in the bottom part of the drilling-core and monomict-breccia which consist of quartz-porphyry (with sericite alteration) cemented by calcite, quartz, and gypsum occupied the middle and shallower part. We estimated this breccia occurs as multiple fluid processes during the evolution of ore processed. Phlogopite capture fluid temperature at ~700-750˚C with pressure <200Mpa and subsequent brecciation occur in lower temperature mark by low titanium content in quartz-matrix as well as the presence of gypsum which perhaps derived from hydration process of anhydrite indicate the ingress meteoric fluid in the system. Yuze breccia (YB) exhibit polymict breccia where volcanic and plutonic clasts cemented by aphanitic rock texture. Particle/Clast size distribution (PSD) shows that SRM clast primarily has boulder size (>5m) with an aspect ratio (Rs/Rl) of 0.4-0.5 and YB have cobble-pebble size ~50-100 mm with an aspect ratio of 0.5-0.6. As opposed to EP which represents hand specimen size breccia has a fine clast <5mm primarily with an aspect ratio of ~0.6 for all breccia types. Cumulative distribution for all breccia shows that fractal distribution with fractal dimension less or equal to two. And clast arrangement exhibit typical fluid assisted brecciation texture such as jigsaw and mosaic without significant rotation and subsequent wearing processes.

This suggests that brecciation due to overpressurized fluid commonly occurs from the middle to shallow part of the earth's crust. This overpressurized fluid follows by an episodic explosion which abruptly changes the crustal condition and enhanced permeability hence, the fluid can percolate and bring a high amount of energy or precipitate precious metal up to the shallower part of the crust.

Keywords: Fluid explosion, Breccia, Erdenet, Sør Rondane Mountains, Yuze

©2021. Japan Geoscience Union. All Right Reserved.

©2021. Japan Geoscience Union. All Right Reserved.

Pseudotachylyte in a marble from the Takine Group (Abukuma Terrane) and its similarity to pseudotachylyte from the Higo Mertamorphic Rocks

*Tadao Nishiyama[1], Ebo Adou Douha[1]

1. Department of Earth and Environmental Sciences, School of Science, Graduate School of Science and Technology, Kumamoto University

We have reported a pseudotachylyte in a marble from the Higo Metamorphic Rocks in central Kyushu (Nishiyama, et al., 2019 and 2020, JpGU Meeting). This time we investigated marbles in the Takine Group (Abukuma Terrane or Abukuma Belt), the Tohoku Region, and found pseudotachylytes which have characteristics very similar to those from the Higo Metamorphic Rocks. In this report, we present petrography of some pseudotachylytes in a marble at the Shin-Takine Mine (Asahi Koumatsu Co. Ltd.), Tamura City, Fukushima Prefecture, and discuss the possible genesis in comparison with pseudotachylytes from the Higo Metamorphic Rocks.

A large body (1×7 km^2) of marble associated with metasediments, metabasites, and metaperidotites occurs as an isolated mass (roof pendant) in a granitic pluton in Tamura City, about 20 km apart from the main body of the Abukuma Metamorphic Terrane. Ehiro et al. (1989) named them the Takine Group and gave detailed petrography for the metamorphic rocks, revealing that the Takine Group has undergone the contact metamorphism by Cretaceous granites. It is unknown whether it had undergone the regional metamorphism of the Abukuma Metamorphic Rocks prior to the contact metamorphism. It is also unknown to which geological unit the Takine Group belongs (Ehiro et al., 1989). The protolith age is not known, either.

In the Shin-Takine Mine, several metabasite dykes up to 2 meters thick occur in a massive marble. The metabasite dykes are strongly weathered and the mineral assemblage cannot be identified. The marble is a massive monomineralic rock consisting of coarse-grained calcite. However, a layered structure can be seen in part of the marble, in which grey layers several millimeters thick recurrently occur in the marble with a frequency of several centimeters. Quartz, diopside, tremolite and dolomite occur in the grey layers, but no wollastonite occurs. Apatite also occurs as an accessory mineral. These layers show intersecting relations in part, implying the origin not of original bedding but of fluid pathway (i.e., veins).

A quartz (1^{st}-stage quartz) vein develops along the contact between a metabasite dyke and a marble, and black veins 1 to 2 centimeters thick occur in this quartz vein and also in the marble, showing branching and layering. Observations with a SEM-EDS reveal following characteristics.

(a) The black vein consists mainly of dolomite, quartz (1^{st}- and 2^{nd}-stage), and kaolinite-group clay mineral (hereafter abbreviated as Al-Si clay) with a small amount of calcite. 1^{st}-stage quartz is anhedral and polycrystalline, partially dissolved by dolomite. Some quartz grains show fracturing. Quartz (2^{nd}-stage) also occurs as inclusions in dolomite, which have very irregular shape.
(b) Dolomite shows compositional heterogeneity with respect to Fe-Mg exchange. Some dolomite crystals show growth zoning.
(c) Al-Si clay rarely includes K-feldspar, indicating that the Al-Si clay is an alteration product of K-feldspar.
(d) Al-Si clay is frequently associated with quartz (2^{nd}-stage). In a rare case, an idiomorphic quartz (2^{nd}

©2021. Japan Geoscience Union. All Right Reserved.

-stage) crystal occurs within Al-Si clay.
(e) Pyrite occurs in dolomite, showing dissolution texture.
(f) Calcite occurs as inclusions with irregular shape in dolomite.

These characteristics indicate that this black vein is not a simple fault gouge. Because the country rock is a marble ($CaCO_3$), the occurrence of dolomite, Al-Si clay (originally K-feldspar) and 2nd-stage quartz implies mass transfer of Mg, Fe, Al, K, and Si from the exterior. Fracturing is only observed in 1st-stage quartz. Growth zoning in dolomite and an idiomorphic quartz (2^{nd}-stage quartz) crystal in Al-Si clay suggest crystallization of these minerals in fluid or melt. Dissolution texture of pyrite prefers reaction with dolomite melt rather than fluid. These lines of evidence indicate that this black vein represents a recrystallization product of dolomite and silicate melts formed by frictional melting associated with faulting, namely a kind of pseudotachylyte.

Reference
Ehiro, M., Kanisawa, S., and Teketani, Y. (1989) Pre-Tertiary Takine Group in the central Abukuma Massif. Bull. Fukushima Museum, No.3, 21-37.

Keywords: pseudotachylyte, marble, Abukuma Terrane, Takine Group, Higo Metamorphic Rocks

©2021. Japan Geoscience Union. All Right Reserved.

Frictional melting process during formation of pseudotachylyte, Sarwar-Junia fault zone, India

*Jun-ya Okazaki[1], Jun-ichi Ando[1], Kaushik Das[1]

1. Earth and Planetary Systems Science Program, Division of Advanced Science and Engineering, Hiroshima University

Introduction: Pseudotachylyte (Pst) is dark, aphanitic rock formed by frictional melting of host rock resulting from seismic rapid slip, and it develops along fault plane as vein and network. Therefore, Pst is a significant rock that preserves the information of the past seismic activity. Although Pst are generally formed in brittle deformation zone (or shallow crust), Pst deformed plastically and associated with mylonite are also reported (e.g., Chattopadhyay et al., 2008), and thus it suggests that seismic fault activity can occur in ductile deformation zone (or deep crust). Contributions of slip propagation from brittle deformation zone and plastic instabilities to fault generation mechanism in ductile deformation zone are suggested, but the mechanism is still not completely definite. In this study, it is the purpose that the frictional melting processes and the fault generation mechanism in ductile deformation zone are revealed by the results of microstructural observation and mineral phase identification using the two types of Pst samples within granitic gneiss from Sarwar-Junia Fault Zone, India.

Result: In the field observation, two types of Pst veins were observed in relation to the foliation of the host rock. One vein was parallel to the foliation (“P-Pst”) and another vein cut the foliation at a high angle (“C-Pst”). It is considered that “P-Pst” was formed in the same stress field as the ductile deformation of the host rock.

In the microstructural observation of the Pst veins, both veins have the black margins at both ends (chilled margin), and there were formed by the quench of the melt. The width of chilled margin of “P-Pst” is larger than the one of “C-Pst”. It is caused by the difference of the quench rates and indicates that “P-Pst” had the slower quench rate and “C-Pst” had the faster quench rate, respectively. Comparing the minerals survived as clasts within Pst veins, “P-Pst” mainly preserves quartz and sillimanite, while “C-Pst” mainly preserves quartz, sillimanite, plagioclase and K-feldspar. In addition, biotite grains, contained many in the host rock, don’t survive as clast within both veins, therefore it is considered that these grains were completely melted during Pst formation. On the other hand, especially in “P-Pst”, many acicular biotite grains are formed in the matrix, and it indicates the crystallization from the melt. The melting points of these minerals suggests that the maximum temperatures of melt were 1400-1726 ℃ for the “P-Pst” and 1200-1300 ℃ for the “C-Pst”, respectively. However, considering the non-equilibrium melting and the drop in melting point due to the dehydration of biotite, the actual temperature was probably lower than estimated. From the above, it is considered that “P-Pst” and “C-Pst” were formed in the ductile deformation zone and the brittle deformation zone, respectively, and their frictional melting processes are as follows. First, the host rock was fractured by fault activity, then the frictional melting occurred resulting from rapid slip. At this time, maximum melt temperature of “P-Pst” was higher than the temperature of “C-Pst”. Subsequently, because of slower quench rate of “P-Pst”, wider chilled margins were formed and acicular biotite grains crystallized from the melt.

In addition, it is considered that the formation of “P-Pst” in ductile deformation zone was contributed by the preferred orientation of biotite grains. However (001) plane of biotite grains in the host rock randomly directed, the preferred orientation of the (001) plane parallel to the foliation (or Pst vein) develop as approaching the Pst vein. The plane is bonded by van der Waals forces and has very low

©2021. Japan Geoscience Union. All Right Reserved.

strength. From the observation, the (001) plane of biotite grain works as weak plane, and concentration of stress and increasing of strain rate occurred on the plane, then brittle deformation (seismic fault activity) occurred in ductile deformation zone.

Keywords: Pseudotachylyte, Frictional melting, Plastic deformation, Biotite

©2021. Japan Geoscience Union. All Right Reserved.

Neoarchean magmatism and Paleoproterozoic high-pressure granulite-facies metamorphism from the southern Motloutse Complex, eastern Botswana: Implications for the western extension of the Central Zone of the Limpopo Complex

*Thembiso Otladisang Basupi[1,2], Toshiaki Tsunogae[1,3], Kazuki Takahashi[1], Yukiyasu Tsutsumi[4]

1. Graduate of Life and Environmental Sciences, University of Tsukuba, 2. Department of Earth and Environmental Sciences, Botswana International University of Science and Technology, 3. Department of Geology, University of Johannesburg, 4. Department of Geology and Paleontology, National Museum of Nature and Science

We provide the first record of the occurrence of high-pressure garnet-bearing amphibolite and mafic granulite hosted by the amphibolite of amphibolite facies –lower granulite facies from the Maope area of southern Motloutse Complex in eastern Botswana. Our results also provide for the first time Neoarchean magmatic age preserved in the mafic granulite. The mineral assemblages of the rocks are garnet + hornblende + plagioclase + ilmenite + rutile + quartz (garnet-bearing amphibolite), hornblende + orthopyroxene + clinopyroxene + plagioclase + quartz (mafic granulite), and hornblende + plagioclase + quartz + ilmenite + epidote + titanite (host amphibolite). The poikiloblastic garnet from the garnet-bearing amphibolite contains inclusions of hornblende, ilmenite, quartz, and plagioclase as prograde mineral and is mantled by hornblende + plagioclase coronae, which formed during retrograde metamorphism. In the mafic granulite, orthopyroxene is coarse-grained, and the hornblende occurs as a thin retrograde corona around the plagioclase and clinopyroxene. The geochemical signature of the mafic granulite and amphibolite, combined with the enrichment of large-ion lithophile elements and depletion of high-field strength elements (Nb and Ta), indicates subduction-related volcanic arc affinity, and the garnet-bearing amphibolite indicate subduction-related volcanic arc and within-plate basalt affinity. The peak metamorphic condition of the garnet-bearing amphibolite was obtained at 850˚C–910˚C at 10–10.5 kbar using phase equilibrium modeling in the Na_2O-CaO-FeO-MgO-Al_2O_3-SiO_2-H_2O-TiO_2-Fe_2O_3 (NCFMASHTO) system and was consistent with results from geothermobarometry. The conventional geothermobarometry results estimated from the mafic granulite and amphibolite are 745˚C–826˚C and 488˚C–736˚C at 7 kbar, respectively. The pressure-temperature (*P-T*) condition results suggest high-pressure garnet-bearing amphibolite, granulite-facies for the mafic granulite, and amphibolite-lower granulite facies for amphibolite. Zircon grains from the garnet-bearing amphibolite, with a discordance of <5% and Th/U of <2.5, recorded a metamorphic age of 2020.2 ±4.9 Ma whereas the zircon from mafic granulite with a discordance of <5% and Th/U of 0.44 to 0.86 recorded a magmatic age of 2648.8 ±9.8 Ma. The results of the *P-T* condition and the geochronology from the garnet-bearing amphibolite suggest that the southern Motloutse Complex is a high-pressure granulite terrane that underwent a single clockwise *P-T* evolution in the Paleoproterozoic Era (~2.02 Ga). Our results also suggested for a 2.6 Ga magmatic emplacement of mafic rocks recorded from the mafic granulite. The results further, suggest that the southern Motloutse Complex is nearly equivalent to the Beit Bridge Complex in the Central Zone of Limpopo Complex.

Keywords: Neoarchean, Paleoproterozoic, Motloutse Complex, High-pressure granulite, Garnet-bearing amphibolite, Mafic granulite

©2021. Japan Geoscience Union. All Right Reserved.

Petrography of a sulfide-rich garnet-sillimanite-biotite gneiss from Brattnipene, Sør Rondane Mountains, East Antarctica

*Hayato Ikeda[1], Tetsuo Kawakami[1]

1. Kyoto University

The Sør Rondane Mountains (SRM) is located in eastern Dronning Maud Land, East Antarctica, where the lower crust of the East-West Gondwana collision zone is exposed. The SRM is divided into the NE terrane and the SW terrane by the Main Tectonic Boundary (MTB) (Osanai et al., 2013). The NE terrane is characterized by clockwise pressure-temperature (*P-T)* path of granulite-facies metamorphic rocks and inherited zircons older than 1200 Ma, whereas the SW terrane is characterized by the counter-clockwise *P-T* path and inherited zircons younger than 1200 Ma. In Brattnipene, two counter-clockwise *P-T* paths have been proposed previously (Adachi et al., 2013; Baba et al.,2013). However, these studies have weakness of constructing the *P-T* path using boulder samples (Baba et al., 2013) or using samples from distant outcrops (Adachi et al., 2013). In this study, we utilized a pelitic gneiss sample from the Nakayubi-ridge, Brattnipene to constrain the retrograde *P-T* path.
The sample used in this study is a sulfide-rich garnet-sillimanite-biotite gneiss (sample TK2009120403D2) mainly composed of garnet, sillimanite, cordierite, biotite, Fe-sulfides (pyrite and pyrrhotite), plagioclase, K-feldspar, and quartz. Quartz ribbons are developed parallel to the gneissosity. Accessory minerals are rutile, apatite, zircon, monazite and graphite. Garnet (XMg ~ 0.53) includes abundant sillimanite in the core. Garnet rim (XMg ~ 0.27) is replaced by secondary cordierite (XMg ~ 0.85) + Fe-sulfide + sillimanite + quartz or cordierite (XMg ~ 0.88) + Fe-sulfide + biotite (XMg = 0.77-0.81) + quartz. The former mineral assemblage tends to appear near the garnet when both assemblages are observed. Common sulfide occurrence in the assemblage implies that infiltration of sulfur-bearing fluid/melt triggered the breakdown of garnet. The presence of sillimanite in the replacement assemblage suggests that the garnet breakdown took place under the sillimanite stability field, and the formation of cordierite probably represents decompression process. Rutile enclosed in the secondary cordierite is finer-grained and shows higher Cr, V and Al concentrations compared to matrix rutile. Therefore, inclusion rutile is likely a product formed during the garnet breakdown. Zr-in-rutile thermometry (Tomkins et al., 2007) applied to the inclusion rutile gave ~700 ^{o}C for the pressure of the sillimanite stability field, and this probably represents the temperature of the garnet breakdown. Although further detailed analysis is required, the observed decompression reaction texture in the sillimanite stability field contrasts with counter-clockwise *P-T* paths previously proposed for Brattnipene, and thus timing of the garnet breakdown reaction needs to be determined in order to understand its geological meaning in the tectonic framework proposed by Osanai et al. (2013).

Keywords: metamorphic rock, continental collision

©2021. Japan Geoscience Union. All Right Reserved.

Microstructural characteristics of ultra-high pressure metamorphic rocks from the Dabie-Shan, eastern China

*Katsuyoshi Michibayashi[1], Kouhei Asano[1]

1. Department of Earth and Planetary Sciences, Graduate School of Environmental Studies, Nagoya University

Ultrahigh-pressure (UHP) metamorphic rocks with their origin of continental material, which have formerly been subducted to mantle depths more than 80 km, are located in the Dabie-Shan, China. UHP rocks often record geodynamic processes during a series of subduction and exhumation. Deformation microstructures of UHP rocks at peak metamorphic conditions provide important information about rheological behavior of deeply subducted crustal material within subduction channel. However, it is pretty rare to preserve deformation microstructures of UHP rocks at peak metamorphic conditions due to subsequent retrograde metamorphism during exhumation. Here, we present deformation microstructures and crystallographic-preferred orientations (CPOs) of UHP rocks from the Dabie-Shan in order to study rheological behavior of deeply subducted continental material at UHP conditions. We investigated three mafic-ultramafic rocks: eclogite (garnet-omphacite-quartz), garnet-clinopyroxenite (garnet-Ca-pyroxene) and garnet peridotite (olivine-garnet-Ca-pyroxene) and one felsic rock: jadeite-quartzite (quartz-jadeite-garnet). Whereas the mafic-ultramafic rocks show distinctly high-strained microstructures such as intense elongated foliations with strong grain size reduction, the felsic rock preserves relatively low-strained microstructures such as weakly foliated granular texture, indicating that the jadeite-quartzite have been less deformed than mafic-ultramafic rocks. We argue that coesite occurrence after quartz in the felsic rock at the UHP condition can explain the deformation contrast between the mafic-ultramafic and the felsic rock. The presence of coesite with higher strength than quartz may result in increasing the bulk strength of felsic rocks, leading to strain localization in mafic-ultramafic rocks. EBSD analyses of the jadeite-quartzite revealed that the intracrystalline strains have been accumulated only within quartz grains, resulting in dense but irregular grain boundary formation, in contrast to the other minerals maintaining coarse grains with serrated grain boundaries. The formation of shear zones associated with strain localization at HP/UHP conditions can induce the detachment of subducted crustal material from subducting lithosphere, which is one of the necessary processes for exhumation of UHP rocks. We propose that strain localization in mafic-ultramafic rocks may trigger the exhumation of UHP rocks. Therefore, coesite could significantly influence rheological behavior of crustal material subducted to the depths where coesite is stable at UHP condition.

Keywords: Ultrahigh pressure metamorphic rock, Deformation microstructure, Rheology

©2021. Japan Geoscience Union. All Right Reserved.

Metamorphic history of the Suo metamorphic rocks inferred from two-stage garnet in pelitic schist

*Shunsuke Endo[1], Maki Ito[1]

1. Department of Earth Science, Interdisciplinary Faculty of Science and Engineering, Shimane University

Pelitic schist is the main lithology in coherent-type high-P/T metamorphic complexes such as the Sanbagawa and Suo metamorphic belts in SW Japan, and analyses of its subduction-exhumation records are important to constrain the thermal regime of subduction channels as well as spatial-temporal changes of force balance acting on the subduction interface. Since pelitic schist is generally subjected to high-strain ductile deformation and strong recrystallization during exhumation, subduction-stage records are only preserved within rigid minerals such as garnet. Here we report detailed petrological data on garnet-bearing pelitic schist from the Nichinan area in the Chugoku Mountains, where high-grade part of the Jurassic Suo metamorphic rocks is exposed. Detailed microstructural observations reveal that two stages of garnet growth punctuated by a garnet dissolution stage are common in the Nichinan pelitic schist. Euhedral garnet grains consist of a resorbed core and an overgrown rim. The garnet core preserves growth zoning and contains inclusions of quartz, rutile, zircon, phengite and box-shaped paragonite + clinozoisite aggregates (possible pseudomorph after lawsonite). Zr-in-rutile thermometry and pseudosection modelling (with garnet isopleths) reveal that the garnet core grew in the lawsonite stability field from ~1.8 GPa, 470℃ to ~1.6 GPa, 500℃. The garnet rim formed synchronous with the growth of titanite and albite porphyroblasts at ~0.8 GPa and 500℃. These microstructures and P-T evolution are very similar to those of pelitic schist in the eclogite unit of the Sanbagawa metamorphic belt. Onset of highly oblique subduction and shear heating at crustal levels may account for the decompression heating and Barrovian-type overprint during exhumation of coherent-type high-P/T metamorphic complexes, and this process largely obliterates subduction-stage high-P/T records.

Keywords: garnet, pelitic schist, Suo metamorphic rocks

©2021. Japan Geoscience Union. All Right Reserved.

Hidden intact coesite in deeply subducted rocks and its geological implications

*Tomoki Taguchi[1], Yui Kouketsu[2], Yohei Igami[3], Tomoyuki Kobayashi[4], Akira Miyake[3]

1. Department of Earth Sciences, Faculty of Education and Integrated Arts and Sciences, Waseda University, 2. Department of Earth and Planetary Science, Graduate School of Environmental Studies, Nagoya University, 3. Department of Geology and Mineralogy, Graduate School of Science, Kyoto University, 4. Faculty of Health and Sports, Nagoya Gakuin University

Coesite, a high-pressure phase of SiO_2, is a diagnostic indicator of ultrahigh-pressure (UHP) metamorphism, oftentimes implying subduction of a rock to a minimum depth of 80 km. Deciphering the petrology of UHP rocks will improve interpretations of not only the tectono-metamorphic evolution in ancient subduction and collision zones, but also the underlying framework of plate tectonics. Tracking the spatial extent of UHP metamorphic terranes within a convergent plate margin is the first step toward understanding the fluxes of subducted crust. Previous petrological studies indicate that metamorphic coesite rarely occurs as inclusions in rigid minerals, such as zircon and garnet (Chopin, 2003 and references therein). Most coesites are often partially or completely obscured owing to the formation of polycrystalline quartz grains surrounded by radial cracks (i.e., quartz pseudomorphs), driven by an increase in the volume during the exhumation process. In contrast, recent numerical modeling and deformation experiments show that UHP conditions may reach shallower depths in the lithosphere than previously estimated, presumably via overpressure at both microscopic and macroscopic scales (e.g., Schmalholz and Podladchikov, 2013; Richter et al., 2016). This debatable conflict between petrographic observations and theoretical notions has led to intense debate regarding the pressure-to-depth conversion of metamorphic rocks. Through integrated micro-Raman analyses and modern nano-observation techniques employing a focused ion beam system and transmission electron microscopy (FIB–TEM), this study reports the occurrence of minuscule coesite (<20 μm) as abundant inclusions in garnet-rich impure quartzites from the Lago di Cignana Unit (LCU) in the Italian Western Alps.

Coesite was identified by a strong Raman band at a wavenumber (ν) of 521 cm^{-1}. Representative bands of coesite inclusions completely sealed inside garnet grains showed slight shifts to higher frequencies (ν = ~522 cm^{-1}), which is indicative of residual pressures retained by the coesite inclusion in the garnet. Raman intensity maps revealed that these SiO_2 inclusions are composed entirely of coesite, with no quartz present. The results obtained via Raman intensity mapping of the LCU samples yielded residual pressure values for coesite inclusions of up to 0.5 GPa, with heterogeneous stress observed within the crystals. Bright-field TEM images show that the interface structures form notably sharp boundaries with no crystal defects, such as dislocations, stacking faults, or microcracks observed within either coesite or garnet. The high-resolution TEM image displays the lattice fringes of coesite along the [100] direction, corresponding to the lattice spacings of the (020) plane for coesite (d values = 0.62 nm). Our TEM results show only the lattice fringes of either coesite or garnet, further indicating that no quartz crystallized at the nano-interfaces.

We suggest that common coesite-derived quartz pseudomorphs are less typical structures in UHP metamorphic rocks. The discovery of such intact coesite inclusions may fill the gaps in the predicted and observed abundance of coesite worldwide. In addition, abundant intact minuscule coesite inclusions may be hidden in many established UHP localities, and overlooked because of their size. Our findings would play an essential role in reappraisal of the extent of deeply subducted rocks and their rheology.

©2021. Japan Geoscience Union. All Right Reserved.

Keywords: Coesite, Quartz pseudomorph, Phase transition, Raman spectroscopy, Transmission electron microscopy

©2021. Japan Geoscience Union. All Right Reserved.

Metamorphic zoning and *P–T* conditions of contact metamorphic rocks in the Unai area, Yamaguchi prefecture, Japan.

*Kakeru Sakamoto[1], Toshiaki Shimura[1]

1. Graduate School of Sciences and Technology for Innovation, Yamaguchi University

The Unai area lies near the boundary between Ube city and Mine city, Yamaguchi prefecture, belongs to the Suo Belt. Kishi et al. (2007) reported that this area was intruded by the plutonic complex composed of Amago intrusive rocks, Kurogoro plutonic rocks, and Iwago-yama granite. These K–Ar ages are 97.9 ±2.2 Ma, 94.0 ±4.8 Ma, and 92.8 ±2.0 Ma, respectively. The plutonic complex is exposed over an area of 14 × 8 km and its intrusion caused contact metamorphism to the Suo metamorphic rocks in the Unai area (Seo, 1976).
This study reports the metamorphic zoning, and *P–T* conditions of the contact metamorphism.

The Unai area is underlain by metamorphic rocks and granodiorites. Metamorphic rocks are composed of contact metamorphic rocks (dominant pelitic schist, and a small amount of calc-silicate schist) and the Suo metamorphic rocks (precursor).
In this area, granodiorites are distributed in the central part. Contact metamorphic rocks are distributed around the margin of granodiorite with a width of about 500 m, and most of them are pelitic schist, but calc-silicate schist also occurs as a small lens shape.

The dominant pelitic rocks had been used for zonal mapping in this area. It can be divided into six metamorphic zones. The critical mineral paragenesis are as follows.
For pelitic rocks,
Zone Ⅰ (Crd zone): Qz + Pl + Ms + Bt + Crd + (Chl)
Zone Ⅱ (And zone): Qz + Pl + Ms + Bt + And + Crd
Zone Ⅲ (Kfs zone): Qz + Pl + Bt + Ms + Kfs + Crn + And + Crd + Ilm
Zone Ⅳ (Grt zone): Qz + Pl + Bt + Kfs + Opx + Crd + And + Spl + Alm
Zone Ⅴ (Spl zone): Qz + Pl + Bt + Kfs + Opx + Crd + And + Spl
Zone Ⅵ (Sil zone): Bt + Opx + Pl + Kfs + Crd + Qz + Spl + Sil + Ilm
For calc-silicate rocks,
Zone Ⅵ (Sil zone): Pl + Cpx + Cal + Qz + Grs.

Zone Ⅰ pelitic rocks have a strong schistosity which originated precursor Suo metamorphic rocks. It is mainly composed by muscovite and biotite. This zone is characterized by the appearance of cordierite porphyroblast. Zone Ⅱ is characterized by andalusite porphyroblast. Zone Ⅲ is characterized by the occurrence of K-feldspar and euhedral corundum (up to 0.2 mm), they are coexisting with biotite. Zone Ⅳ is characterized by the appearance of orthopyroxene, which is coexisting with cordierite, biotite, and K-feldspar. Spinel (hercynite) also appear in this zone. Zone Ⅴ is almost same mineral paragenesis with that of Zone Ⅳ, but it is characterized by the disappearance of almandine. Zone Ⅵ pelitic rocks are characterized by the appearance of sillimanite (about 0.1 mm). The sillimanite is not fibrolite but is prismatic crystals. Calc-silicate rocks of Zone Ⅵ are mainly composed of calcite, clinopyroxene, and grossular.

The mineral chemistry of pelitic schist are as follows. In this abstract, we use X_{Mg} = Mg / (Fe + Mg) and X_{Mg^*} = Mg / (Mg + Fe^{2+} + Fe^{3+}). On spinel, Fe^{3+} and Fe^{2+} were calculated by stoichiometry. Plagioclase has

©2021. Japan Geoscience Union. All Right Reserved.

An = 4.1–43.9% in composition. Biotite has X_{Mg} = 0.34–0.62. Muscovite has X_{Mg} = 0.53–0.61. Orthopyroxene has X_{Mg} = 0.42–0.43. Spinel has X_{Mg^*} = 0.29–0.33, Zn = 0.002–0.007 apfu, and Cr = 0.005–0.020 apfu. Garnet has $Alm_{55.4–58.7}Prp_{41.0–44.3}Sps_{0.2–0.5}Grs_{0.1}$ in composition.
The mineral chemistry of calc-silicate rocks are as follows. Plagioclase has *An* = 91.0–96.8% in composition. Clinopyroxene has X_{Mg} = 0.68–0.79, diopside composition. Garnet has $Alm_{10.5–16.8}Prp_{1.3–2.2}Sps_{0.4–1.3}Grs_{80.1–87.5}$ in composition.

The variations of these mineral paragenesis and the variations in mineral chemical compositions reflect the metamorphic grade. The metamorphic pressure is about 0.8 kbar, and the metamorphic temperatures are about 500 ˚C for Zone Ⅰ, 500–550 ˚C for Zone Ⅱ, and 550–600 ℃ for Zone Ⅲ, 600–750 ˚C for Zone Ⅳ and Zone Ⅴ, and about 750 ˚C or higher for Zone Ⅵ. The highest metamorphic condition reached to the pyroxene hornfels facies.

References

Kishi et al. (2007) *Jour. Geol. Soc. Japan.*, **113**, 479-491.
Seo (1976) *Professor G. Kojima Memorial Volume*, 276-285.

Keywords: Unai area, contact metamorphism, metamorphic zoning, mineral chemistry

©2021. Japan Geoscience Union. All Right Reserved.

Progressive metamorphism of the Ryoke metamorphic rocks from No-jima Island, South of Yamaguchi Prefecture

*ZEJIN LU[1]

1. Graduate School of Science and Engineering for Innovation, Yamaguchi University

No-jima Island is located in the Seto Inland Sea, Yamaguchi Prefecture. It is thought to be the region that has undergone Cretaceous low-pressure type regional metamorphism (Ryoke metamorphism). No-jima Island is underlain by crystalline schists and metabasalts. Metabasalts show the geochemical character similar to the within plate basalts, for instance the green stones in the Mino-Tamba belt. Moreover, the metamorphic grade of the schists corresponds to the biotite zone of the Yanai region of the Ryoke belt, but the petrological character of the rocks from No-jima Island has been unclear. In addition, the geological correlation with the neighboring area, Kasado-jima Island, the Oshima peninsula, and Ohtsu-jima Island has not been understood yet. Therefore, the aim of this study, based on the mineral paragenesis of the pelitic schists, is to discuss the metamorphism of the rocks from No-jima Island, and also to unravel the thermal structure of the low-pressure type metamorphism, the Ryoke belt, in this region.

The metabasalts are mainly exposed on the northeastern part of the island but occur rarely in the west coast of the island. They are included in the schists of sedimentary origin as blocks. The metamorphic rocks are composed mainly of the pelitic schist and metamorphosed chert with bedded structure (siliceous schist hereafter) with trace amounts of calc-silicate schist as thin layers or lenses. The pelitic and siliceous schists are intermittently distributed on the western and southeastern coast of the island. Fold structures such as close folds often develop in the southern part of the island. Granite dikes with 1–2 m width intrude the schists on the western coast.

The metabasalt is porous and has a prominent pillow structure and often shows the amygdaloidal texture. Phenocryst minerals of igneous origin are of clinopyoroxene and plagioclase with minor amounts of amphibole. It contains recrystallized fibrous amphiboles partially coexisting with biotite. Calcite locally fill the amygdules and occurs as veins. The pelitic and siliceous schists show the repidoblastic texture. The calc-silicate schist is composed of Bt+Cal+Qtz. The mineral assemblage of the pelitic schists changes from north to south of the island; Bt+Ms+Chl+Pl±Grt in the north and Bt+Ms+Grt+Pl+Kfs in the south. On the other hand, the mineral assemblage of siliceous schist is mainly Ms+Bt+Grt+Pl.

The garnet of pelitic schist and siliceous schist shows a normal zoning with reduced spessartine toward the rim, probably formed during prograde metamorphism. The chemical composition of biotite depends on the mineral combination. Biotite that coexists with garnet and K-feldspar, has a high XFe in pelitie schist. Plagioclase is fine-grained and the zoning is not prominent. The composition differs for each rock such as politic schist and siliceous schist.

In addition to the change in mineral combination, the grain size becomes coarser in the south. A reaction is expected from the north to the south due to the symbiotic relationship with minerals. Therefore, the island can be divided into the biotite zone in north and the garnet zone in south in terms of the mineral paragenesis of the pelitic schists.

The geothermobarometers for garnet-biotite (Ferry and Spear, 1978) and garnet-pagioclase-biotite-quartz

©2021. Japan Geoscience Union. All Right Reserved.

(Hoish, 1990) are adapted to the pelitic schist. As a result, the peak metamorphic temperature and pressure conditions are estimated to be 480–530℃ and 180–300 MPa, respectively. According to the result, the thermal structures around the Seto Inland Sea region are discussed.

The metamorphic garnet zone of No-jima Island and its cordierite zone of Kasado-jima Island, Oshima peninsula and Ohtsu-jima Island show the same metamorphic conditions. Therefore, it is considered that the cause of garnet depends on the chemical composition of pelitic rocks. As a result of comparing the chemical composition of bulk and minerals, it is considered that the crystallization of garnet is affected not only by high XFe but also by XMn values.

Keywords: Ryoke metamorphism, Low-pressure type, Garnet isograd

©2021. Japan Geoscience Union. All Right Reserved.

P–T–t path of Ryoke metamorphic rocks in Kitsuki area, Kunisaki Peninsula, Oita prefecture, Japan.

*Kentaro Mutabaru[1], Toshiaki Shimura[1]

1. Yamaguchi University

The Kitsuki area of Oita prefecture belongs to the Ryoke metamorphic belt (Moriyama et al. 1983; Brown, 1998; Ishizuka et al., 2005; Isozaki et al., 2010). The Cretaceous Ryoke metamorphic rocks are less exposed in the Kitsuki area because they are widely covered by the Miocene volcanic and pyroclastic rocks. Ishizuka et al. (2005) indicated that the metamorphic grade of the Ryoke metamorphic rocks in this area corresponds to the sillimanite–K-feldspar zone in the Yanai area, Yamaguchi prefecture. This study discusses the *P–T–t* path of Ryoke metamorphic rocks in the Kitsuki area.
The Ryoke metamorphic rocks in Kitsuki area composed of pelitic gneiss, siliceous gneiss, and a few mafic metamorphic rocks. Ms–Bt granite and Hbl–Bt granodiorite are distributed around the Ushiyashiki and Kuranari area, respectively. Hbl–Bt granodiorite has weak foliation, and encloses pelitic gneiss as a xenolith.
The dominant mineral assemblages of pelitic gneiss in this area are the following.
Assemblage-I: And + Sil + Ms + Grt + Bt + Pl + Qz
Assemblage-II: Sil + Ms + Kfs + Grt + Bt + Pl + Qz
Assemblage-III: Sil + Kfs + Grt + Bt + Pl + Qz
Assemblage-I is recognized at the western part of this area. Assemblage-II is predominant in this area, and it contains tourmaline occurs as a minor phase. Assemblage-III is distributed in the eastern part in this area. Ti content of biotite increases from assemblages-I to III. Garnet grossular component of assemblage-I is poor than that of assemblages-II and III.
In this study area, the following two metamorphic reactions must be important. These are;
(1) And = Sil and
(2) Ms + Qz = Als + Kfs + H_2O.
Reaction curve (1) has negative slope, whereas (2) has positive slope. Because these two reaction curves are crossing each other in a *P-T* space, two bathozones or bathograds can be defined (e.g. Carmichael, 1978). In this study area, two bathozones (A and B) are recognized, and these two bathozones are further subdivided into three *P-T* fields (1, 2, and 3), as follows;

Bathozone-A (lower-*P* condition, ca. $P < 2.2$ kbar)
P–T field A-1 (lower-*T* condition): mineral assemblage is And + Ms
P–T field A-2 (middle-*T* condition): mineral assemblage is And + Kfs
P–T field A-3 (higher-*T* condition): mineral assemblage is Sil + Kfs
Bathozone-B (higher-*P* condition, ca. $P > 2.2$ kbar)
P–T field B-1 (lower-*T* condition): mineral assemblage is And + Ms
P–T field B-2 (middle-*T* condition): mineral assemblage is Sil + Ms
P–T field B-3 (higher-*T* condition): mineral assemblage is Sil + Kfs

These two prograde reactions can be observed as the following order;
And →Sil in the assemblage-I,
Ms + Qz →Sil + Kfs + H_2O in the assemblage-II.
On the other hand, these two retrograde reactions can be observed
Sil →And in the assemblage-I,

©2021. Japan Geoscience Union. All Right Reserved.

Sil (and And) + Kfs + H_2O →Ms + Qz in the assemblages-I and II.
These two retrograde reactions occurred almost at the same time. This *P–T* condition is the boundary between bathozones A and B, and it is about 620 ℃ and 2.2 kbar. Assemblage-I rocks passed through this point at the retrograde stage.
Metamorphic pressure condition was higher ($P > 2.2$ kbar) at the prograde stage, whereas it was lower (ca. 2.2 kbar) at the retrograde stage. Therefore, Ryoke metamorphic rocks in this study area was experienced a clockwise *P–T–t* path.

References

Brown, M. (1998) *Jour. Metamorph. Geol.*, **16**, 3–22.
Carmichael, D. M. (1978) *Amer. Jour. Sci.,* **278**, 769-797.
Ishizuka, Y. et al. (2005) *1:50,000 Geol. Map, Bungo-kitsuki. Geol. Surv. Japan.*, 11–18.
Isozaki, Y. et al. (2010) *Jour. Tokyo Geogr. Soc.*, **199**, 999–1053.
Moriyama, Z. et al. (1983) *Fac. Educ. Oita Univ.*, 29–62.

Keywords: Kitsuki area, Ryoke metamorphic belt, metamorphic P-T-t path, bathozone

©2021. Japan Geoscience Union. All Right Reserved.

P-T estimations of Ryoke metamorphic rocks in the Takato-Ohshika area, Nagano, Japan

*Yoshihiro Nakamura[1], Kazuhiro Miyazaki[1], Yutaka Takahashi[1]

1. Geological Survey of Japan, National Institute of Advanced Industrial Science and Technology

Low–*P/T* type metamorphism is closely related to the arc magmatism and the detailed *P–T–t–D* estimations of metamorphic rocks associated with granitoids lead to be understanding of the tectonic evolution of active convergent margin. Recently, a lot of U-Pb zircon ages from Ryoke granitoids and metamorphic rocks in Yanai and Mikawa regions were reported (e.g., Skrzypek et al. 2016; Takatsuka et al. 2018). These age data imply that the reconsideration of the classical intrusive relationship between gneissose older and massive younger Ryoke granitoids closely related to the low-*P/T* type metamorphism is required. Hence, we attempted to assess the detailed *P–T–D* estimations of mylonitic metasediments along the MTL in the Takato-Oshika area. The area is located in the eastern most part of the Ryoke metamorphic belt, where is suitable for comparison with other areas previously reported.

In the study area, the gneissose Hbl–Bt tonalite (the so-called Hiji tonalite) is widely exposed along the MTL, but there have been few reports on the Ryoke metamorphic rocks before. In this study, we conducted a detailed geologic field mapping survey, during which meter- and centimeter-scale blocks of Ryoke metamorphic rocks within the Ryoke granitic mylonite were successfully sampled. The mylonitic metasediments are locally associated with *C'* -type shear bands, suggesting sinistral shearing. The representative mineral assemblage of the mylonitic metasediments comprises garnet, biotite, muscovite, cordierite pseudomorphs (muscovite aggregates), plagioclase, and quartz, with minor amounts of apatite, zircon, tourmaline, sillimanite, and platy graphite. The highest-grade metamorphic rocks in the Grt–Crd zone of the Ryoke metamorphic belt are exposed at distances of ~1800 m from the MTL. Detailed petrological analyses coupled with conventional thermobarometers and *P–T* pseudosection modeling give estimated peak *P–T* conditions of 760–790 ˚C at 4.6–5.3 kbar. Likewise, the surrounding gneissose Ryoke granitoids were emplaced at around 680–710 ˚C and 4.6–5.8 kbar by Al in hornblende barometry and Hbl–Pl thermometry.

On the other hand, peak *P–T* estimations of mylonitic metasediments have been estimated to be 560 to 710 ˚C at 2.0–5.1 kbar, suggesting the decrease in peak *P–T* conditions with approaching the MTL. Such rocks correspond to the Kfs–Sill to Bt zone of the Ryoke metamorphic belt and are structurally upper unit to the highest-grade Ryoke metamorphic rocks. However, the present Ryoke metamorphic rocks and granitoids show a monoclinal structure with a dip of about 50–70˚W and the structurally upper unit in the Bt and Kfs–Sill zones of Ryoke belts were stacked at the lower portion of the highest-grade metamorphic rocks in the Grt–Crd zone. This suggests that the primary metamorphic zonation during the low-*P/T* type metamorphism has a tight asymmetric anticline at around the MTL. In addition, we revealed that a large pressure difference of >10 km was inferred from peak *P–T* conditions between the highest-grade metamorphic rocks and mylonitic rocks in a width of only ~1500m at around the MTL. These data suggest that a considerable amount of geologic mass in the middle crust was shortened or stretched, and upper units of Ryoke metamorphic rocks in the Bt and Kfs–Sill zones were selectively dragged into the deeper crust by ductile deformation related to the MTL.

[Reference]: Skrzypek et al. (2016), Lithos, 260, 9-27; Takatsuka et al. (2018), Lithos, 308-309, 428-445.

©2021. Japan Geoscience Union. All Right Reserved.

Keywords: Ryoke metamorphic rocks, MTL, Low-P/T type metamorphism

©2021. Japan Geoscience Union. All Right Reserved.

Ultrahigh-temperature HP granulite facies stage of the Early Jurassic pre-Sanbagawa metamorphism

*Kenta Yoshida[1], Sota Niki[3], Hikaru Sawada[1], Ryosuke Oyanagi[1], Takafumi Hirata[3], Kenji Asakura[2], Takao Hirajima[2]

1. Japan Agency for Marine-earth Science and Technology, 2. Kyoto University, 3. The University of Tokyo

The Sanbagawa metamorphic terrane records at least two distinct stages of metamorphism, i.e. the early metamorphism of granulite to epidote-amphibolite facies occurred at Early Cretaceous (c. 120 Ma) and the later high-pressure metamorphism covering eclogite facies, so-called Sanbagawa metamorphism, at Late Cretaceous (c. 90 Ma) (e.g., Aoya and Endo, 2017 and references therein). The evidence of the early Sanbagawa metamorphism is preserved in some coarse-grained mafic bodies in central Shikoku, such as the Western Iratsu body (Endo et al., 2009), and their protolith ages are considered to Early Jurrasic based on the U-Pb ages of zircon (c. 200 Ma) that represent the ages of the arc magmatism (Aoki et al., 2020).

We report the first evidence of the metamorphic event preceding the above ones (pre-Sanbagawa metamorphism), whose P-T conditions correspond to ultrahigh-temperature high-pressure (UHT-HP) granulite facies with the age of Early Jurrasic.

The studied sample is a high-pressure marble collected from the Eastern Iratsu body, which is composed of calcite, garnet, diopside, quartz, and minor minerals including titanite, and zircon. The eclogite facies metamorphism has been recognized by omphacite (jadeite content up to 50%) in the matrix garnet and within garnet-diopside aggregate (GDA), suggesting that diopside had become stable before the eclogite facies stage. In-situ U-Pb dating of the garnet in the quartz-rich domain yielded 96 +/- 9 Ma which is in good agreement with the previous estimates of the eclogite-facies metamorphism (Niki, Yoshida et al., JpGU2021). The sample records a unique evidence of fluid activity during the exhumation. The occurrence of datolite [$CaBSiO_4(OH)$] in a specific part of garnet, the P-T conditions of which were well constrained, indicates the boron-rich fluid activity during the juxtaposition of the eclogite unit to the surrounding non-eclogite rocks (Yoshida et al., 2021 JMPS).

The new evidence of the pre-Sanbagawa metamorphism was discovered using titanite in the same marble. Titanite occurs in the matrix and inter-grain minerals within GDA. Titanite grains in the matrix show spindle shape while those in GDA show irregular shape. In high-contrast back-scattered electron image (BSI), most titanite are homogeneous (Ttn1), but some grains have thin rim showing dark color in BSI (Ttn2). The formation P-T conditions of Ttn1 were well constrained by means of quartz-in-titanite Raman elastic barometer (Kohn, 2014) and Zr-in-titanite thermometer (Hayden et al., 2008), yielding 900-1100 degreeC and 1.5-1.8 GPa assuming a specific range of $aTiO_2$.

LA-ICP-MS U-Pb dating was performed for titanite and zircon. Zircon and Ttn1 yielded concordant age of Early Jurassic (200-180 Ma) while Ttn2 show a clear mixing line in the Terra-Wasserburg Concordia diagram whose lower intercept age was 126 Ma. In addition, few Ttn1 grains show intermediate ages around 164 Ma. All titanite and zircon analyzed show low Th/U ratios and thus are metamorphic origin. The Early Cretaceous age of Ttn2 is comparable to that of the early Sanbagawa metamorphism although P-T conditions were not constrained. On the contrary, Ttn1 and zircon preserved an Early Jurassic metamorphism of UHT-HP granulite conditions that has never reported from the Sanbagawa metamorphic terrane.

©2021. Japan Geoscience Union. All Right Reserved.

The oldest metamorphic ages of the Sanbagawa metamorphic terrane in the previous studies were c. 120 Ma of the early Sanbagawa metamorphism while our new data provide an evidence of the older metamorphic event. The 138 Ma of Nd-Sm age reported from the Nikubuchi peridotite body within the Eastern Iratsu body (Senda et al., 2006) was interpreted as either granulite facies metamorphism or magmatic event, which indicates that the Eastern Iratsu body records a longer history than other members of the Sanbagawa metamorphic terrane. The newly-reported pre-Sanbagawa metamorphism may provide a key to decipher tectonic evolution of the subducting Izanagi plate.

Keywords: Sanbagawa metamorphic terrane, HP granulite, U-Pb dating, high pressure metamorphism, titanite

©2021. Japan Geoscience Union. All Right Reserved.

Meliorating the spatial resolution of SEM-EBSD

*Thomas Jing Yi Yeo[1], Norio Shigematsu[1]

1. Research Institute of Earthquake and Volcano Geology, Geological Survey of Japan, National Institute of Advanced Industrial Science and Technology

Electron Backscatter Diffraction (EBSD) is a commonly applied analytical practice for quantitative analysis in the scanning electron microscope (SEM). The spatial resolutions of SEM-EBSD are known to be about a few μm for the tungsten filament electron gun SEM and a few tens of nm for the Schottky field-emission electron gun SEM.

Quartz grain size provides important information regarding the flow stress during the plastic deformation of mylonite (Stipp and Tullis, 2003). Some mylonite samples contains quartz grains with size of smaller than 1 μm (Okudaira and Shigematsu, 2012). It has been described that these quartz grains developed through dynamic recrystallisation mechanism. Thus, a higher spatial resolution is required during EBSD mapping in order to fully represent the microstructures of such sub-micro scale grains and techniques to meliorate the spatial resolution is essential for this purpose.

The SEM used for this study is located in the GSJ laboratory of AIST, Japan with a Hitachi SU-3500 (W filament gun SEM) and HKL Nordlys EBSD sensor. Quartz, a common mineral on the continental crust is first chemo-mechanically polished with colloidal silica before the analysis. The investigation was preformed with the sample coated with a 0.2 nm thick Osmium coating to reduce the charging effects.

There is a trade-off between the spatial resolution and the signal intensity of the EBSD, which is control by the probe diametre and accelerating voltage. This trade-off was investigated by adjusting the objective lens movable aperture, condenser lens and accelerating voltage to obtain the most optimal condition. The spatial resolution is qualitatively and quantitatively analysed from the kikuchi bands images obtained through a line profile. We investigated the spatial resolution for both X (parallel to the tilt axis) and Y axes (perpendicular to the tilt axis) as samples used for EBSD analysis are generally tilted at 70˚, thus yielding different spatial resolutions at both X and Y directions.

The knife-edge method was also applied to measure the beam diameter at different optical conditions. In this presentation, we show the preliminary results.

Keywords: SEM-EBSD, Spatial resolution, Quantitative microanalysis

©2021. Japan Geoscience Union. All Right Reserved.

Strain in quartz inclusion probed by Raman spectroscopy

*Yui Kouketsu[1], Yuki Tomioka[1], Tomoki Taguchi[2]

1. Department of Earth & Planetary Sciences, Graduate School of Environmental Studies, Nagoya University, 2. Department of Earth Sciences, Faculty of Education and Integrated Arts and Sciences, Waseda University

The residual pressure is maintained on the host–inclusion system that reflect the metamorphic conditions when the inclusion was trapped in the host mineral due to the difference in the volume change during their exhumation. In recent years, Raman geothermobarometers have been developed to estimate the metamorphic conditions from the peak shift of Raman spectra of inclusion minerals. The conventional Raman geothermobarometers have assumed that the inclusion minerals are uniformly stressed from the surrounding mineral under the hydrostatic pressure, but in reality, the inclusion minerals are under deviatoric stress due to the anisotropy of the elastic modulus of host and inclusion minerals, and are subjected to the different strains in each axial direction. Murri et al. (2018) proposed a method to estimate the strains from the peak shifts of Raman spectrum using the Grüneisen tensor. In this study, we used a strain calculation program based on this principle (stRAinMAN; Angel et al., 2019) to estimate the strains of quartz inclusions in garnet and kyanite host minerals.

Quartz eclogite from the Gongen area of the Sanbagawa belt, SW Japan, and Lawsonite eclogite from the Motagua Fault Zone, Guatemala, were used for analysis. In addition, we also used garnetite data from the Lago di Cignana unit in the Western Alps reported by van Schrojenstein Lantman et al. (2020). For all samples, the Raman spectra of quartz inclusions in garnet were obtained and the peak shifts from the standard quartz were calculated to estimate the strain. In addition to quartz inclusions in garnet, quartz inclusions in kyanite were also analyzed in quartz eclogite samples from the Sanbagawa belt. The strains were calculated using the values of the peak shifts at 464 cm^{-1}, 205 cm^{-1}, and 128 cm^{-1} and the Grüneisen tensor of quartz (γ_1+ γ_2, γ_3) reported by Murri et al. (2018), and the strains of ε_1+ε_2 and ε_3 were obtained.

Calculations of the strain of quartz inclusions in garnet show that quartz eclogite from the Sanbagawa belt shows ε_1+ε_2 ranging from -12×10^{-3} to -24×10^{-3} and ε_3 from $+1\times10^{-3}$ to -4×10^{-3}, whereas Lawsonite eclogite from Motagua Fault Zone shows ε_1+ε_2 ranging from -19×10^{-3} to -26×10^{-3} and ε_3 from -3×10^{-3} to -8×10^{-3}. In the garnetite of the Lago di Cignana unit reported in the previous study, ε_1+ε_2 ranges from -12×10^{-3} to -24×10^{-3} and ε_3 from $+1\times10^{-3}$ to -5×10^{-3}, which is almost the same range as that of quartz eclogite in the Sanbagawa belt. On the other hand, the calculated strains of quartz inclusions in kyanite in the quartz eclogite of the Sanbagawa belt show a range of ε_1+ε_2 from -5×10^{-3} to -21×10^{-3} and ε_3 from $+4\times10^{-3}$ to -4×10^{-3}.

The strains estimated from the Raman spectra of quartz inclusions tended to be retained closer to the hydrostatic conditions for the samples with lower peak temperature conditions. Conversely, the sample of the highest temperature condition, the quartz eclogite of the Sanbagawa belt, tended to show a smaller *c*-axis strain (ε_3) than under hydrostatic conditions. This result indicates that the higher the peak metamorphic temperature, the more easily the inclusion strain is relaxed, especially in the *c*-axis direction. In addition, the ε_3 tended to be more relaxed for quartz inclusions in kyanite host. This is due to the anisotropy of the elastic modulus of kyanite, which may lead to resolve the strain, depending on the relationship of the crystal orientation of host and inclusion. Strain analysis of inclusion minerals using Raman spectroscopy is expected to provide new clues to reconstruct the metamorphic history in more

©2021. Japan Geoscience Union. All Right Reserved.

detail.

References

Angel, R. J. et. al. (2019). *Zeitschrift Für Kristallographie - Crystalline Materials*, 234(2), 129–140.
Murri, M., et. al. (2018). *American Mineralogist*, 103(11), 1869–1872.
van Schrojenstein Lantman, H. W. et. al. (2020). *Journal of Metamorphic Geology*, 1–18.

Keywords: strain, inclusion mineral, Raman spectroscopy, quartz, garnet, kyanite

©2021. Japan Geoscience Union. All Right Reserved.

[J] Oral | S (Solid Earth Sciences)：S-MP Mineralogy & Petrology

Sun. Jun 6, 2021 10:45 AM - 11:50 AM JST | Sun. Jun 6, 2021 1:45 AM - 2:50 AM UTC | Ch.23 Zoom Room 23

[S-MP26] Physics and Chemistry of Minerals

convener:Masahiro KAYAMA(Department of General Systems Studies, Graduate School of Arts and Sciences, The University of Tokyo), Itaru Ohira(Department of Chemistry, Faculty of Science, Gakushuin University), Chairperson:Masahiro KAYAMA(Department of General Systems Studies, Graduate School of Arts and Sciences, The University of Tokyo), Itaru Ohira(Department of Chemistry, Faculty of Science, Gakushuin University)

Minerals are important constituent materials of the Earth and planetary bodies.
New results and findings of the physics and chemistry of minerals (including crystal, amorphous and melts) obtained from various analytical approaches, experimental methods (e.g, electron microscope, X-ray diffraction, FT-IR, and Raman spectroscopy), and computer simulations) will be discussed here.

10:45 AM - 11:00 AM JST | 1:45 AM - 2:00 AM UTC

[SMP26-01] **Skew-normal peak fitting of cathodoluminescence on shocked quartz: a statistical model for impact pressure estimation**

Yu Chang[2], Shintaro Kadoya[3], *Keisuke Yano[1], Masahiro KAYAMA[2], Eiichi Tajika[2], Yasuhito Sekine[4], Toshimori Sekine[5], Hirotsugu Nishido[6], Takamichi Kobayashi[7] (1.The Institute of Statistical Mathematics, 2.The University of Tokyo, 3.University of Washington , 4.Tokyo Institute of Technology, Earth-Life Science Institute (ELSI), 5.Osaka University, 6.Okayama University of Science, 7.National Institute for Materials Science)

11:00 AM - 11:15 AM JST | 2:00 AM - 2:15 AM UTC

[SMP26-02] Magnetite oxidation investigated by synchrotron X-ray diffraction and X-ray absorption spectroscopy

*Atsushi Kyono[1], Ibuki Kinebuchi[1] (1.Division of Earth Evolution Sciences, Faculty of Life and Environmental Sciences, University of Tsukuba)

11:15 AM - 11:30 AM JST | 2:15 AM - 2:30 AM UTC

[SMP26-03] *P-T* dependence of hydrogen-bond geometry of β-CrOOD

Chikara Shito[1], *Hiroyuki Kagi[1], Asami Sano-Furukawa[2,3], Sho Kakizawa[4], Kazuki Komatsu[1], Riko Iizuka-Oku[1], Katsutoshi Aoki[1], Jun Abe[5], Shinichi Machida[5], Takashi Saito[3], Takashi Kamiyama[3], Noboru Furukawa[6], Akio Suzuki[7] (1.Graduate School of Science, University of Tokyo, 2.Japan Atomic Energy Agency, 3.High Energy Accelerator Research Organization, 4.Graduate School of Advanced Science and Engineering, Hiroshima University, 5.Comprehensive Research Organization for Science and Society, 6.Graduate School of Science, Chiba University, 7.Graduate School of Science, Tohoku University)

11:30 AM - 11:50 AM JST | 2:30 AM - 2:50 AM UTC

[SMP26-04] Discussion

Skew-normal peak fitting of cathodoluminescence on shocked quartz: a statistical model for impact pressure estimation

Yu Chang[2], Shintaro Kadoya[3], *Keisuke Yano[1], Masahiro KAYAMA[2], Eiichi Tajika[2], Yasuhito Sekine[4], Toshimori Sekine[5], Hirotsugu Nishido[6], Takamichi Kobayashi[7]

1. The Institute of Statistical Mathematics, 2. The University of Tokyo, 3. University of Washington , 4. Tokyo Institute of Technology, Earth-Life Science Institute (ELSI), 5. Osaka University, 6. Okayama University of Science, 7. National Institute for Materials Science

Impact pressure is a key parameter to understand an impact cratering on celestial body, one of the ubiquitous processes on terrestrial planets, satellite and asteroidal bodies. Recent studies qualitatively revealed that cathodoluminescence (CL) spectra of shocked quartz depend on impact pressure [1, 2] as also found in alkali feldspar [3]. However, since CL spectra of shocked quartz have broad and skewed peaks, it has been difficult to obtain a quantitative relation between CL spectra and impact pressure by using spectral deconvolution.

In this study, we propose a statistical model that decomposes CL spectra of experimentally shocked quartz at various impact pressures into several peaks by utilizing skew-normal distributions, instead of normal distributions. The samples of shock-induced quartz were obtained by shock experiments done in Chang et al. (in prep). According to the experiments, the peak pressures of the samples reach 0 GPa to 40 GPa in 5 GPa increments. Also, the CL spectra of the samples were analyzed with SEM (JEOL: JSM-5410) combined with a grating monochromator (Oxford: Mono CL2) at the Okayama University of Science. The obtained CL spectra were corrected by standard lamp. Using Monte-Carlo sampling and Akaike information criterion, we estimate the number of skew-normal peaks and four parameters for each peak, i.e., location, scale, shape, and weight. A mixture of skew–normal distributions provides a better fitting model for CL spectrum of shocked quartz than a mixture of normal distributions. Moreover, it is statistically revealed that among the four parameters of a skew-normal distribution, weights of peaks change with impact pressure.

We also demonstrate that the quantitative relation between weights of CL peaks and impact pressure can be utilized for an estimate of impact pressure based on CL spectra of shocked quartz. Here, we divide the CL data of shocked quartz into two data sets, i.e., training and validation data sets. Then, we calculate a posterior probability of impact pressure of the validation data set by comparing posterior distributions of CL weights of the validation data sets with those of the training data sets. As a result, the actual pressure of the validation data set tends to have the highest posterior probability. The proposed method is as precise as a conventional impact pressure estimation via Planar Deformation Features (PDFs) while the dynamic range would be wider than the conventional method. Additionally, The proposed method is more convenient than the other. The improvement in the efficiency in estimation of paleo impact pressure would drive investigations of impact cratering processes. Also, a fitting via skew-normal distribution could contribute to deconvolution of spectra other than CL spectrum of shocked quartz.

[1] Chang et al., (2016) JpGU Meeting, PSS11-P21.

[2] Chang et al. (in prep)

[3] Kayama et al. (2012) JGR Planets 117 (E9).

©2021. Japan Geoscience Union. All Right Reserved.

Keywords: cathodoluminescence, impact, spectral deconvolution, Bayesian statistics

©2021. Japan Geoscience Union. All Right Reserved.

Magnetite oxidation investigated by synchrotron X-ray diffraction and X-ray absorption spectroscopy

*Atsushi Kyono[1], Ibuki Kinebuchi[1]

1. Division of Earth Evolution Sciences, Faculty of Life and Environmental Sciences, University of Tsukuba

The oxidation process from magnetite to hematite through maghemite was investigated by synchrotron X-ray diffraction and X-ray absorption spectroscopic analyses. The XRD pattern of magnetite heated at 100 °C showed a small peak corresponding to maghemite with partial Fe vacancy disorder structure (space group $P4_132$.) Diffraction peaks of hematite occurred from magnetite heated at 250 °C, in which maghemite and hematite coexisted with magnetite. Diffraction peaks of magnetite subsequently disappeared at 300 °C. Instead, maghemite and hematite dominated the XRD pattern, but the amount of maghemite reduced from 300 °C. Maghemite completely disappeared at 500 °C, and hematite finally dominated the XRD pattern. Rietveld fitting results clearly showed that the site occupancy of Fe at the octahedral sites in the oxidized magnetite continuously decreased from 1.000 to 0.3992(4) at the temperature range between 25 °C and 300 °C. The XANES result showed that the $Fe^{3+}/\Sigma Fe$ increased up to 300 °C and remained constant until 500 °C, indicating that the Fe^{2+} in magnetite was completely oxidized to Fe^{3+} at 300 °C. Furthermore, peaks derived from octahedrally coordinated Fe continuously reduced up to 300 °C. The fitting results of the first shells indicated that the coordination number and site occupancy factor at the octahedral site were continuously decreased at the temperature range between 25 °C and 300 °C, which were approximately consistent with those of Rietveld fitting analysis. It is therefore clearly confirmed that during oxidation from magnetite to maghemite Fe is continuously removed from the octahedral sites with keeping degree of vacancy ordering in the space group $P4_132$.

Keywords: magnetite, maghemite, oxidization, XRD, XANES

©2021. Japan Geoscience Union. All Right Reserved.

P-T dependence of hydrogen-bond geometry of β-CrOOD

Chikara Shito[1], *Hiroyuki Kagi[1], Asami Sano-Furukawa[2,3], Sho Kakizawa[4], Kazuki Komatsu[1], Riko Iizuka-Oku[1], Katsutoshi Aoki[1], Jun Abe[5], Shinichi Machida[5], Takashi Saito[3], Takashi Kamiyama[3], Noboru Furukawa[6], Akio Suzuki[7]

1. Graduate School of Science, University of Tokyo, 2. Japan Atomic Energy Agency, 3. High Energy Accelerator Research Organization, 4. Graduate School of Advanced Science and Engineering, Hiroshima University, 5. Comprehensive Research Organization for Science and Society, 6. Graduate School of Science, Chiba University, 7. Graduate School of Science, Tohoku University

The Earth's mantle contains a certain amount of high-pressure hydrous minerals. However, behaviors of hydrogen bonding and physical properties of such hydrous minerals at high-*PT* conditions have not been clarified. We focused on hydrogen-bond geometry and compression behavior of guyanaite (β-CrOOH). β-CrOOH is a distorted rutile-type hydrous mineral and isostructural to δ-AlOOH, one of the most promising hydrous phases for transporting hydrogen to the core–mantle boundary. In this study, X-ray and neutron diffraction experiments on β-CrOOD were carried out at various *P-T* conditions to clarify the *P-T* dependence of hydrogen-bond geometry in β-CrOOD. Crystal structure was refined using the Rietveld method.

The space group of β-CrOOD was determined to be $P2_1/c$, indicating that the hydrogen atoms are partially disordered at ambient condition. Above 450 K, however, the hydrogen atoms were fully disordered, and the space group was *Pnnm*. Thermal expansion anomaly was observed at temperature range of 300–500 K, where the phase transition ($P2_1/c$ – *Pnnm*) occurred. In high-pressure experiments, changes in compression behavior caused by phase transition from $P2_1/c$ to *Pnnm* were observed at about 3 GPa and 4.5 GPa at 300 K and 250 K, respectively. However, no significant change in compression behavior was observed at 450 K. Therefore, d*P*/d*T* of the phase boundary would have a negative slope. Assuming that the phase boundary of δ-AlOOH ($P2_1nm$–*Pnnm*) has the same tendency as that of β-CrOOD, δ-AlOOH would have a *Pnnm* structure in the Earth's mantle and would have higher seismic velocity than the major minerals in the mantle transition zone.

Keywords: neutron diffraction, hydrous mienerals, high pressure, hydrogen bonds

©2021. Japan Geoscience Union. All Right Reserved.

[J] Oral | S (Solid Earth Sciences) | S-MP Mineralogy & Petrology

[S-MP26] Physics and Chemistry of Minerals

convener:Masahiro KAYAMA(Department of General Systems Studies, Graduate School of Arts and Sciences, The University of Tokyo), Itaru Ohira(Department of Chemistry, Faculty of Science, Gakushuin University), Chairperson:Masahiro KAYAMA(Department of General Systems Studies, Graduate School of Arts and Sciences, The University of Tokyo), Itaru Ohira(Department of Chemistry, Faculty of Science, Gakushuin University)

Sun. Jun 6, 2021 10:45 AM - 11:50 AM Ch.23 (Zoom Room 23)

Minerals are important constituent materials of the Earth and planetary bodies.
New results and findings of the physics and chemistry of minerals (including crystal, amorphous and melts) obtained from various analytical approaches, experimental methods (e.g, electron microscope, X-ray diffraction, FT-IR, and Raman spectroscopy), and computer simulations) will be discussed here.

11:30 AM - 11:50 AM

[SMP26-04]Discussion

©Japan Geoscience Union

[J] Poster | S (Solid Earth Sciences)：S-MP Mineralogy & Petrology

Sun. Jun 6, 2021 5:15 PM - 6:30 PM JST | Sun. Jun 6, 2021 8:15 AM - 9:30 AM UTC | Ch.12_2

[S-MP26] Physics and Chemistry of Minerals

convener:Masahiro KAYAMA(Department of General Systems Studies, Graduate School of Arts and Sciences, The University of Tokyo), Itaru Ohira(Department of Chemistry, Faculty of Science, Gakushuin University)

Minerals are important constituent materials of the Earth and planetary bodies.
New results and findings of the physics and chemistry of minerals (including crystal, amorphous and melts) obtained from various analytical approaches, experimental methods (e.g, electron microscope, X-ray diffraction, FT-IR, and Raman spectroscopy), and computer simulations) will be discussed here.

[SMP26-P01] Pressure-induced phase transitions in wülfingite (Zn(OH)2): Raman spectroscopic and First-principles study

*Masami Kanzaki[1], Longli Guan[1], Ran Wang[1] (1.Institute for Planetary Matereials, Okayama University)

[SMP26-P02] Elastic wave velocity of ε-FeOOH across the pressure-induced spin transition of iron

*Osamu Ikeda[1], Tatsuya Sakamaki[1], Hiroshi Fukui[2,3], Hiroshi Uchiyama[4], Alfred Q.E. Baron[3,4], Akio Suzuki[1] (1.Department of Earth Science, Graduate School of Science, Tohoku University, 2.Graduate School of Material Science, University of Hyogo, 3.RIKEN SPring-8 Center, 4.Japan Synchrotron Radiation Research Institute)

[SMP26-P03] Phase transition of M3+OOH-type oxyhydroxides under high pressure

*Akio Suzuki[1] (1.Department of Earth Science, Graduate School of Science, Tohoku University)

[SMP26-P04] Density measurement of silicate melt by the buoyancy test under high pressure

*Akio Suzuki[1] (1.Department of Earth Science, Graduate School of Science, Tohoku University)

[SMP26-P05] Structural study on the $Ca_2MgAl_2Si_4O_{14}$ composition melt under pressure

*Natsumi Adachi[1], Satoru Urakawa[1], Hidenori Terasaki[1] (1.OKAYAMA UNIVERSITY)

[SMP26-P06] Unique luminescence of rhodochrosite at low temperature

*Reina Masuda[1], Ayane Asano[1], Nobuhiro Kusano[1], Hirotsugu Nishido[1] (1.Biosphere-Geosphere Science, Okayama University of Science)

[SMP26-P07] Amesite and Al-serpentine accompanied with the serpentinite in Yakiyama, Iizuka, Fukuoka

*Yuki Isshiki[1], Seiichiro Uehara[2], Yuya Takeda[1] (1.Department of Earth and Planetary Sciences Faculty of Science, Kyushu University, 2.The Kyushu University Museum)

[SMP26-P08] Phase transitions and pressure calibration points

*Shigeaki Ono[1] (1.Japan Agency for Marine-Earth Science and Technology)

[SMP26-P09] The study on stability and properties of N-doped spinel Based on CGCNN and DFT

*SOK I TAM[1], CHI PUI TANG[1], Pak Kin Leong[1], Kin Tak U[1] (1.Macau University of Science and Technology)

Pressure-induced phase transitions in wülfingite (Zn(OH)2): Raman spectroscopic and First-principles study

*Masami Kanzaki[1], Longli Guan[1], Ran Wang[1]

1. Institute for Planetary Matereials, Okayama University

$Zn(OH)_2$ has several polymorphs at ambient pressure, and one of which, epsilon phase, is known as the mineral wülfingite. Wülfingite has a cristobalite-like structure, and pressure-induced phase transitions were found at 1.1 and 2.1 GPa using in-situ X-ray diffraction study by Kusaba et al.[1] Since the coordination number of Zn is 4 in most of those polymorphs known so far, which is very different from that of brucite ($Mg(OH)_2$), the hydrogen bonding behavior is expected to be different. In this study, we investigated structural changes and the associated changes in hydrogen bonding using in-situ Raman spectroscopy and first-principles calculations.

Wülfingite was synthesized as follows. Zinc sulfate 7-hydrate was dissolved in water and sodium hydroxide solution was added to it to form a white precipitate. This precipitate was ZnO. When the filtered solution of the precipitate was left at room temperature for several weeks, large, transparent crystals grew, but small white crystals adhered to the surface. The clear crystals were identified as wülfingite and the white crystals as ZnO from powder X-ray diffraction and Raman spectroscopy. Clear crystal without ZnO was selected for DAC study. The pressure medium was a methanol-ethanol mixture, and ruby fluorescence method was used for pressure measurements.

In the high-pressure in situ Raman measurements, several new peaks appeared at about 1 GPa in addition to the previous Raman peak of wülfingite. According to Kusaba et al.[2], the transition at 1 GPa is reported to be a single-crystal-to-single-crystal transition from orthorhombic wülfingite to a tetragonal structure. This single-crystal-to-single-crystal transition was also confirmed by observation using a Raman microscopy. Wülfingite shows OH stretching peaks at 3190 and 3300 cm^{-1} at ambient pressure, but after the transition, the peaks shift to around 3410 cm^{-1} (with shoulders at 3350 and 3500) and the hydrogen bonding becomes weaker. As the pressure was further increased, the sharp Raman peaks disappeared at around 2 GPa and were replaced by broad peaks, which is consistent with previous X-ray studies showing a change to a broad X-ray pattern at 2.1 GPa. The OH stretching Raman peaks are observed at 3600 and 3650 cm^{-1}. The position of the 3650 cm^{-1} peak at is close to that of $Mg(OH)_2$, suggesting that the coordination number of Zn may have changed to 6. The Raman spectrum does not show a pattern characteristic of amorphous, and the OH peak is not particularly broad, suggesting poor crystallinity of the high-pressure phase rather than amorphization.

First-principles calculations were performed using Quantum-Espresso to optimize the known structures under pressure and to see the pressure changes in volume and enthalpy. Wülfingite, the tetragonal phase found at 1~2 GPa, and the brucite phase were performed. The phase found above 2 GPa could not be calculated due to its unknown structure. The enthalpies at 0 K predict a transition from wülfingite to the tetragonal phase at 4.5 GPa and from the tetragonal phase to the brucite phase at 9 GPa. The brucite phase has been reported to be synthesized at 11~14 GPa, but requires a certain temperature (~400 ^{o}C). In the compression of wülfingite, the transition to the tetragonal phase could not be reproduced, but a transition to a different structure was observed. In this structure, the coordination number of Zn was 5, which increased to 6 at further higher pressures. During decompression of this structure, another 4-coordinated structure was obtained. However, these structures could not explain the X-ray diffraction

©2021. Japan Geoscience Union. All Right Reserved.

patterns observed above 2 GPa, and their enthalpies did not seem to indicate that they could be stable phases. The hydrogen bond distances (O-H...O) of the tetragonal phase is longer than that of wülfingite, which is in agreement with the Raman results.

Both Raman and first-principles calculations show that the hydrogen bonding tends to weaken with pressure. The relatively stronger hydrogen bonding in the 4-coordinate compared to the 6-coordinate cannot be explained by bond strength or bond valence, but is due to the stronger covalent nature of Zn-O in the 4-coordinate. Since Raman spectra of the phases appearing above 2 GPa are very broad, we are planning to obtain good crystallinity data by using an external DAC with higher temperature.

1) Kusaba, K. et al., https://doi.org/10.1088/1742-6596/215/1/012001
2) Kusaba, K. et al., https://doi.org/10.1016/j.cplett.2007.02.009

Keywords: wulfingite, Zn(OH)2, pressure-induced phase transition, Raman spectroscopy, First-principles calculation

©2021. Japan Geoscience Union. All Right Reserved.

Elastic wave velocity of ε-FeOOH across the pressure-induced spin transition of iron

*Osamu Ikeda[1], Tatsuya Sakamaki[1], Hiroshi Fukui[2,3], Hiroshi Uchiyama[4], Alfred Q.E. Baron[3,4], Akio Suzuki[1]

1. Department of Earth Science, Graduate School of Science, Tohoku University, 2. Graduate School of Material Science, University of Hyogo, 3. RIKEN SPring-8 Center, 4. Japan Synchrotron Radiation Research Institute

ε-FeOOH is a high-pressure polymorph of α-FeOOH (goethite), and has been reported to be a crucial candidate of the water carriers into deep mantle via subduction (Nishi et al., 2019; Liu et al., 2019). Despite the importance of ε-FeOOH for water transportation, its elastic property is still unclear. At pressure of ~45 GPa, the phase shows the electronic high-spin to low-spin transition of iron which leads the density to higher along compression (Gleason et al., 2013). The elasticity is expected to be significantly affected by the spin transition.

We present the effect of the spin transition on the elastic wave velocity of ε-FeOOH under pressure. The sample was polycrystalline ε-FeOOH, which was synthesized in advance from a powder of α-FeOOH at a high-pressure and high-temperature condition. A pellet of the sample was enclosed in each sample chamber of a diamond anvil cell with either NaCl or glycerol as a pressure medium. The high-pressure experiments have been conducted at BL35XU in SPring-8 (Baron et al., 2000), and the longitudinal wave velocity, V_P, and density were measured up to a pressure 56 GPa at room temperature, combining non-resonant Inelastic X-ray scattering (IXS) spectroscopy and powder X-ray diffraction (XRD) method. Incident X-ray was monochromatized to 17.794 keV and focused to 16 ×16 μm. Scattered X-ray was analyzed by 12 analyzer crystals whose scattering angles correspond to the momentum transfer Q of 4.2–8.4 nm^{-1}, and the dispersion curve of the longitudinal acoustic phonon was determined. Diffracted X-ray was captured by a flat panel detector and the unit-cell parameters of the sample were obtained. V_P, which is the gradient of the dispersion curve at $Q \rightarrow 0$, was yielded by fitting the curve with a sine function. The pressure was calculated using the equations of state of the sample (Thompson et al., 2020).

In the pressure range below 20 GPa, V_P of ε-FeOOH in this study was consistent with that of a previous study using the ultrasonic method and multi-anvil apparatus (Ikeda et al., 2019). A ~4% drop in V_P was observed at pressures 40, 41, and 42 GPa, which is ~4 GPa below the spin transition in ε-FeOOH. This drop is considered to be the results of a decrease of shear modulus, or of an unstable state of electrons at around the transition pressure. V_P in the pressure range 45–56 GPa (the low-spin state) overlapped with the extrapolated V_P from the pressure below 40 GPa.

Reference:

Baron, A.Q.R., Tanaka, Y., Goto, S., Takeshita, K., Matsushita, T. and Ishikawa, T. (2000) An X-ray scattering beamline for studying dynamics. *Journal of Physics and Chemistry of Solids*, **61**, 461–465.
Gleason, A.E., Quiroga, C.E., Suzuki, A., Pentcheva, R. and Mao, W.L. (2013) Symmetrization driven spin transition in ε-FeOOH at high pressure. *Earth and Planetary Science Letters*, **379**, 49–55.
Ikeda, O., Sakamaki, T., Ohashi, T., Goto, M., Higo, Y. and Suzuki, A. (2019) Sound velocity measurements of ε-FeOOH up to 24 GPa. *Journal of Mineralogical and Petrological Sciences*, **114**, 155–160.
Liu, X., Matsukage, K.N., Nishihara, Y., Suzuki, T. and Takahashi, E. (2019) Stability of the hydrous phases of Al-rich phase D and Al-rich phase H in deep subducted oceanic crust. *American Mineralogist*, **104**,

©2021. Japan Geoscience Union. All Right Reserved.

64–72.
Nishi, M., Tsuchiya, J., Kuwayama, Y., Arimoto, T., Tange, Y., Higo, Y., Hatakeyama, T. and Irifune, T. (2019) Solid solution and compression behavior of hydroxides in the lower mantle. *Journal of Geophysical Research: Solid Earth*, **124**, 10231–10239.
Thompson, E.C., Davis, A.H., Brauser, N.M., Liu, Z., Prakapenka, V.B. and Campbell, A.J. (2020) Phase transitions in ε-FeOOH at high pressure and ambient temperature. *American Mineralogist*, **105**, 1769–1777.

Keywords: ε-FeOOH, High pressure, Spin transition, Inelastic X-ray scattering

©2021. Japan Geoscience Union. All Right Reserved.

Phase transition of M3+OOH-type oxyhydroxides under high pressure

*Akio Suzuki[1]

1. Department of Earth Science, Graduate School of Science, Tohoku University

Water is transported by the subducting slab into the Earth’s interior by hydrous phases. Suzuki et al. (2000) synthesized a high-pressure phase of AlOOH and named it the delta-phase. The crystal structure of the delta-phase is isostructural with InOOH. The study on the stability and transition of the M3+OOH-type oxyhydroxides is very important to investigate the transportation of hydrogen in the Earth’s interior. In this study, the phase transition of InOOH was investigated under high pressures and high temperatures. In situ X-ray diffraction study was carried out using multianvil techniques and synchrotron light source at the High Energy Accelerator Research Organization (KEK) in Japan. Based on the time-resolved diffraction measurements, we observed the phase transition from the distorted rutile structure to the pyrite structure of InOOH around 10 GPa.

Keywords: hydrous phase, mantle, high pressure, water, AlOOH, InOOH

©2021. Japan Geoscience Union. All Right Reserved.

Density measurement of silicate melt by the buoyancy test under high pressure

*Akio Suzuki[1]

1. Department of Earth Science, Graduate School of Science, Tohoku University

Density of magma (silicate melt) controls its transportation in the Earth’ s interior. Therefore, it is important to determine the density of silicate melts under high pressure. We adopted the buoyancy test of the density marker crystals in the silicate melt using a multianvil apparatus installed at Tohoku University. Based on the observation of sinking and flotation of the crystals in the melts, we determined the compression curves of sodium and potassium silicate melts.

Keywords: magma, density, mantle, high pressure, sink/float method

©2021. Japan Geoscience Union. All Right Reserved.

Structural study on the $Ca_2MgAl_2Si_4O_{14}$ composition melt under pressure

*Natsumi Adachi[1], Satoru Urakawa[1], Hidenori Terasaki[1]

1. OKAYAMA UNIVERSITY

Natural magmas are predominantly aluminosilicate in composition, and therefore the studies on structural properties of aluminosilicate under pressure is important for understanding the physical properties of magma at depth. The structure of the $Di_{50}An_{50}$ composition ($Ca_2MgAl_2Si_4O_{14}$) melt was studied by X-ray diffraction analysis and molecular dynamics simulations up to 7 GPa and 2200 K. The high pressure and temperature X-ray diffraction experiments were performed by MAX80 installed at AR-NE5C of PF, KEK. X-ray diffraction profiles were measured by energy dispersive X-ray diffractions method. The MD simulations were conducted with the MXDORTO code. The simulation system was composed of 2400 atoms.

Assuming the coordination number of Si is fixed to be four, we evaluated the coordination number of Al from the experimentally determined radial distribution function. It is increases to about five by 7 GPa. Increasing trend of the coordination number of Al with pressure is consistent with the results from the MD simulations. The FSDP of the structure factor shifts toward higher-*Q* side with increasing pressure, indicating shrinkage of intermediate range order by compression. The pressure dependence of the position of the FSDP changes around 4 GPa, showing intermediate range order does not change much above 4 GPa. Shrinkage of intermediate range order is thought to be correlated to the reorganization of TO_4 networks. These structural changes in the $Ca_2MgAl_2Si_4O_{14}$ melt were considered to correspond to the physical properties, such as viscosity, of the basaltic magma under pressure.

Keywords: magma, aluminosilicate, X-ray diffraction, molecular dynamics simulation

©2021. Japan Geoscience Union. All Right Reserved.

Unique luminescence of rhodochrosite at low temperature

*Reina Masuda[1], Ayane Asano[1], Nobuhiro Kusano[1], Hirotsugu Nishido[1]

1. Biosphere-Geosphere Science, Okayama University of Science

Cathodoluminescence (CL) of carbonate minerals has been widely applied in earth science as it has become a common method in carbonate sedimentology. In most cases of calcite-type carbonate minerals, their CL involve two types of impurity centers as activator of Mn^{2+} and quencher of Fe^{2+}. If the content of Fe^{2+} is low in the carbonates, the concentration of Mn^{2+} almost controls the CL emission intensity. It has been believed that the CL activated by Mn^{2+} should be quenched above ~50,000 ppm of Mn due to concertation quenching (e.g., Machel et al., 1991). Walker et al. (1989) reported that rhodochrosite ($MnCO_3$) emits an intense luminescence below 77 K, but extinction at room temperature. However, the mechanism of CL emission in high-Mn carbonates has not yet been elucidated. In this study, we have conducted to clarify the emission mechanism in rhodochrosite by spectral analyses of CL data obtained at various temperatures.

The single crystals of fourteen rhodochrosite from various localities were employed for CL measurements. The CL spectra were obtained by using an SEM-CL system (SEM combined with a grating monochromator) ranging from 300 to 800 nm under a control of sample temperature from −192 to 25 ºC with a cryo-stage. The digitized data were totally sensitive-corrected for all optical paths including grating and photomultiplier tube.

Most samples begin to emit CL in a red region below −100 ºC and increase rapidly during cooling down to near liquid nitrogen temperature, whereas no emission was detected in all samples at room temperature. The CL data were converted into energy unit from wavelength unit for quantitative spectral analysis. Each spectrum is composed of a broad emission band at ~700 nm, which shows clearly higher than previously reported values of calcite: Mn (~620 nm) and magnesite: Mn (~650 nm). It implies that the crystal-field strength (Dq) should be quite higher than other calcite-type carbonates due to a shorter distance between metal (Mn) and ligand in rhodochrosite. A drastic reduction of the CL intensity with increasing temperature can be well explained by a temperature quenching theory known as Mott-Seitz model based on an increase in the probability of non-radiative transition with the rise of temperature (calculated activation energy of ~0.03 eV). The fact suggests that a sample temperature strongly controls the travelling range of the energy, which causes concertation quenching by transfer to the adjacent Mn ions. Consequently, a unique CL in rhodochrosite should be understood as the result of the competition between the effects of temperature quenching and concertation quenching possibly by Förster energy transfer (FRET) model.

<references>
Machel, G., Mason, R., Mariano, N. and Mucci, A. (1991) Causes and emission of luminescence in calcite and dolomite, SEPM Short Course Notes, 25, 9-25.
Walker, G., Abumere, O. and Kamaluddin, B. (1989) Luminescence spectroscopy of Mn^{2+} centers in rock-forming carbonates, Mineralogical Magazine, 53, 103-140.

Keywords: Luminescence, Rhodochrosite, Temperature quenching, Concertation quenching

©2021. Japan Geoscience Union. All Right Reserved.

Amesite and Al-serpentine accompanied with the serpentinite in Yakiyama, Iizuka, Fukuoka

*Yuki Isshiki[1], Seiichiro Uehara[2], Yuya Takeda[1]

1. Department of Earth and Planetary Sciences Faculty of Science, Kyushu University, 2. The Kyushu University Museum

1.Introduction

Serpentine has an ideal chemical composition of Mg3Si2O5(OH)4, and generally contains small amounts of Fe and Al. Amesite (Mg, Al)3(Si, Al)2O5(OH)4 is one of the mineral that has a solid solution relationship with serpentine, and the intermediate composition is called Al-serpentine. Al-serpentine (7 Å) is polymorphic with clinochlore (14 Å) and is considered to be a low-temperature phase (metastable phase), which is mineralogically important. However, the occurrence of Al-serpentine and amesite is relatively rare, and detailed mineralogical descriptions are scarce. In this study, we found amesite and Al-serpentine in rodingites associated with serpentine bodies in this area, and investigated their occurrence and mineralogical properties.

2. samples and experiments

We observed rodingites in serpentinites and examined their constituent minerals in and around Yakiyama, Iizuka City. The samples were observed by naked eye and Stereoscopic microscopes followed by X-ray diffraction analysis (Rigaku Ultima IV, Rigaku RINT RAPID II), polarized light microscopy and scanning electron microscopy (SEM-EDS: JEOL JSM-7001F). TEM (JEOL JEM-3200FSK, JEM-ARM200CF) at the Research Center for Ultramicroscopic Analysis, Kyushu University was also used to observe the microstructure of thin film and powder samples.

3. results

Eleven rodingite outcrops were identified by field observations. Rodingites are composed of Ca- and Al-rich minerals such as epidote-clinozoisite, calcite, grossular, clinochlore, thomsonite, prehnite, and titanite. Amesite was found in three rodingite outcrops (samples Rod3, 7 and 9). Amesite and Al-serpentine are found in two types: veinlets in the rodingites and scattered with calcite and thomsonite around the veins.

Sample Rod3 contains white opaque Al-serpentine with associated light brown transparent amesite. The XRD analysis of both samples is consistent with the pattern of lizardite-$6T_1$. The white opaque part had very small crystals (about 50-300 nm) and was a mixture of plate-like, hollow cylindrical with plate-like crystals inside, fibrous, and irregularly shaped. The chemical composition of each crystalline particle was three phases: amesite, lizardite, and an excess of Si or Al than amesite-lizardite. Microstructural observation showed that these were mixed together. The hollow cylindrical part shows polygonal columnar lattice fringes by TEM observation, but the shape of the sectors is irregular and the lattice fringes at the sector boundaries cannot be confirmed, which is different from polygonal serpentine reported so far. In addition, the hollow cylindrical part has an Al cation number of about 1.3 (O=7), suggesting that it may be a mineral with a kaolin-like structure in which the size of the tetrahedral and octahedral sheets is reversed from that of ordinary serpentine, and the combination of the two sheets is reversed. Inside the hollow cylindrical section, there is a plate-like section bisecting the circle and parallel to the cylinder. The plate-part have an excess of Si or Al, and TEM observation shows a mixture of 7 Åand 14 Ålayers.

The light brown transparent part is coarse-grained (200 μm), and at the boundary with the white part,

©2021. Japan Geoscience Union. All Right Reserved.

there is a 1 μm filamentous crystal extending toward the white part. The composition of the crystals is non-uniform even within a single crystal, and EDS mapping revealed two types of crystals: one with a mosaic-like non-uniform composition and the other with a clear separation of Al concentration. The former was euhedral with a clear cleavage, while the latter was semi-euhedral, and the filamentous crystals described above were derived from this crystal. The composition of each is generally consistent with a solid solution of lizardite-amecite, but the Al-rich part tends to be Al or Si-rich, and may contain OH-rich material due to the low compound total.

Keywords: serpentine, amesite, rodingite, chlorite, Al-serpentine

©2021. Japan Geoscience Union. All Right Reserved.

Phase transitions and pressure calibration points

*Shigeaki Ono[1]

1. Japan Agency for Marine-Earth Science and Technology

Some phase transitions have been used as pressure calibration in high-pressure experiments, because reliable characterization of the pressure and temperature environment is of essential importance when we apply laboratory data to the study of the Earth's interior. In order to know reliable pressure environment, we can use the synchrotron X-ray source for the high-pressure studies. The in-situ pressure measurement has been accessible by the synchrotron X-ray technique. In the case of conventional laboratory experiments, this technique cannot be used and the conventional pressure calibration is of great interest to understand the Earth's interior. We have investigated several high-pressure phase transitions used as the pressure calibration points. Precise determinations of phase boundaries of SiO_2 [1], Fe_2SiO_4 [2], $CaGeO_3$ [3], ZnS [4], ZnSe [5], GaAs [6], GaP [7], Zr [8], and Bi [9] were performed by the multi-anvil press or the diamond anvil cell apparatuses combined with the synchrotron X-ray diffraction technique. Most transition pressures determined our studies were in general agreement with those reported by previous studies. However, some significant discrepancies for the pressure values or the slopes, dP/dT, of transitions between our and previous studies were confirmed. These discrepancies are due to the significant kinetics effect at the phase transition, because an apparent hysteresis was confirmed at relatively low temperature conditions. This indicates that the phase transitions accompanied with the significant hysteresis are not suitable for the pressure calibration.

[1] S. Ono et al. (2017) In situ determination of the phase boundary between coesite and stishovite in SiO_2, Phys. Earth Planet. Inter., 264, 1-6.

[2] S. Ono et al. (2013) In situ observation of a phase transition in Fe_2SiO_4 at high pressure and high temperature, Phys. Chem. Minerals, 40, 811-816.

[3] S. Ono et al. (2011) In situ observation of a garnet-perovskite transition in $CaGeO_3$, Phys. Chem. Minerals, 38, 735-740.

[4] S. Ono, T. Kikegawa, (2018) Determination of the phase boundary of ZnS, Phase Transition, 91, 9-14.

[5] S. Ono (2020) Phase transition in ZnSe at high pressures and high temperatures, J. Phys. Chem. Solids, 141, 109409.

[6] S. Ono, T. Kikegawa (2018) Phase transformation of GaAs at high pressures and temperatures, J. Phys. Chem. Solids, 113, 1-4.

[7] S. Ono, T. Kikegawa (2017) Determination of the phase boundary of GaP using in situ high-pressure and high-temperature X-ray diffraction, High Press. Res., 37, 28-35.

[8] S. Ono, T. Kikegawa (2015) Determination of the phase boundary of the omega to beta transition in Zr using in situ high-pressure and high-temperature X-ray diffraction, J. Solid State Chem., 225, 110-113.

©2021. Japan Geoscience Union. All Right Reserved.

[9] S. Ono (2020) High-pressure phase transition of bismuth, High Press. Res., 38, 414-421.

Keywords: Phase transformation, High-pressure experiment

©2021. Japan Geoscience Union. All Right Reserved.

The study on stability and properties of N-doped spinel Based on CGCNN and DFT

*SOK I TAM[1], CHI PUI TANG[1], Pak Kin Leong[1], Kin Tak U[1]

1. Macau University of Science and Technology

Spinel (AB_2X_4) is an essential mineral in geology and an important semiconductor and ceramic material. Doping with different atoms will change the properties of spinel and give them unique properties. The crystal graph convolutional neural network (CGCNN) developed by Xie et al. They use graphs to represent the crystal structure and apply neural graph networks to material performance prediction. Taking perovskite as an example, CGCNN has excellent prediction performance.

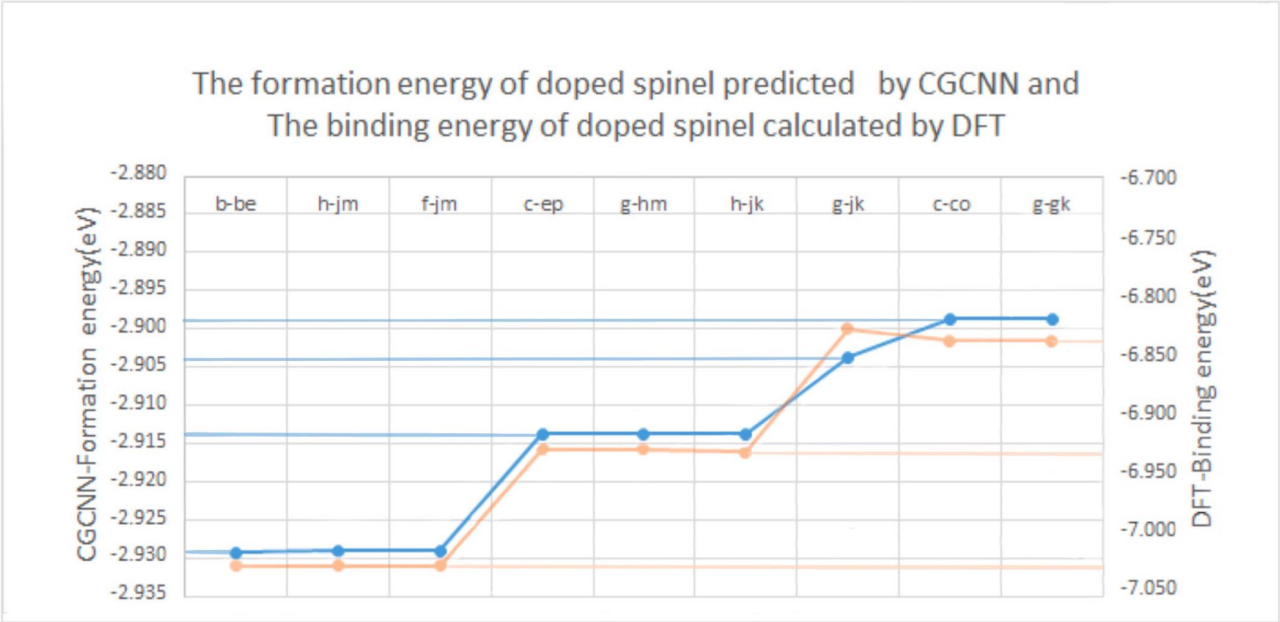
This study verified whether CGCNN is suitable for predicting the formation energy of doped spinel. The formation energy predicted by CGCNN is compared with the theoretical energy (binding energy) calculated by DFT.

From thousands of CGCNN predicted formation energies of doping Mg_2SiO_4 structure, which Mg is replaced by Si and O is replaced by N at different atomic ratios. We choose 3 data from the lowest, middle, and highest values respectively (9 data in total). And use DFT to calculate the binding energy at the corresponding structure of doping Mg_2SiO_4. The calculation results are shown that the changing trend between CGCNN and DFT is almost the same in Figure 1. It implies that CGCNN is suitable for predicting doped spinel. Through the auxiliary exploration of CGCNN. We found a possible nitrogen-doped oxygen structure of spinel ($MgAl_2O_{3.5}N_{0.5}$) in other work.

This work is supported by the Science and Technology Development Fund of Macau (File No. 0111/2020/A, 0042/2018/A2)

Keywords: CGCNN, DFT, Spinel

©2021. Japan Geoscience Union. All Right Reserved.



©2021. Japan Geoscience Union. All Right Reserved.

[J] Oral | S (Solid Earth Sciences)：S-VC Volcanology

Sun. Jun 6, 2021 10:45 AM - 12:15 PM JST | Sun. Jun 6, 2021 1:45 AM - 3:15 AM UTC | Ch.25 Zoom Room 25

[S-VC27] Mitigation of volcanic disasters - basic and applied researches

convener:Shinji Takarada(Geological Survey of Japan, National Institute of Advanced Industrial Science and Technology), Mitsuhiro Yoshimoto(Mount Fuji Research Institute, Yamanashi Prefectural Government), Tatsuro Chiba(Asia Air Survey Co., Ltd.), Yousuke Miyagi(National Research Institute for Earth Science and Disaster Resilience), Chairperson:Shinji Takarada(Geological Survey of Japan, National Institute of Advanced Industrial Science and Technology), Mitsuhiro Yoshimoto(Mount Fuji Research Institute, Yamanashi Prefectural Government)

Volcanic disasters are caused by wide range of volcanic phenomena including ash fall, pyroclastic flow, debris avalanche, lahar, and lava flow. To mitigate volcanic disasters, wide range of technologies including simulation, data processing on GIS, and communication techniques are required. Researches on volcanic hazards mapping, eruption scenarios, estimation of tephra falls, and probabilistic eruption assessments are getting important. This session invites presentations and broad reviews related to these topics. Contributions on database technology, case studies of social and school educations, the Next Generation Volcano Research, and specific examples of eruption crisis events are also encouraged.

10:45 AM - 11:00 AM JST | 1:45 AM - 2:00 AM UTC

[SVC27-01] Ash Fall Hazard Map using Newly Developed Simulation Model

*Tsuyoshi Nakatani[1], Toshiyuki Asano[1] (1.The Research and Education Center for Natural Hazards, Kagoshima University)

11:00 AM - 11:15 AM JST | 2:00 AM - 2:15 AM UTC

[SVC27-02] On the Effects of the Inertial Forces of the Falling Volcano Ash on the Ash absorption by an External Unit of Building Air Conditioning

*Kiyotoshi Otsuka[1], Arihide Nobata[1], Hitoshi Suwa[1], Tomohiro Kubo[2], Yosuke Miyagi[3], Masamitsu Miyamura[3] (1.Obayashi Corporation, 2.Mount Fuji Research Institute, Yamanashi Prefectural Government , 3.National Research Institute for Earth Science and Disaster Resilience)

11:15 AM - 11:30 AM JST | 2:15 AM - 2:30 AM UTC

[SVC27-03] Experimental Study on Safety of Wooden Building Roofs Against Impact of Ballistic Ejecta

*Kohei Tateyama[1], Hiroyuki Yamada[2], Ryo Honda[3], Tomohiro Kubo[3], Mitsuhiro Yoshimoto[3] (1.Ritsumeikan University, 2.National Defense Academy, 3.Mount Fuji Research Institute, Yamanashi Prefectural Government)

11:30 AM - 11:45 AM JST | 2:30 AM - 2:45 AM UTC

[SVC27-04] **A trajectory analysis of a rockfall on a steep slope at Mt. Fuji to determine the possible source area of the falling rock**

*Taishi Sakurada[1], Ryodo Hemmi[2], Yasuhiro Ishimine[3], Hideaki Miyamoto[1] (1.The University of Tokyo, 2.The University Museum, The University of Tokyo, 3.Mount Fuji Research Institute, Yamanashi Prefectural Government)

11:45 AM - 12:00 PM JST | 2:45 AM - 3:00 AM UTC

[SVC27-05] Improvement of Proto-type Educational Web Contents for the Municipalities' Disaster Response Staff.

*Tomohiro Kubo[1], Mitsuhiro Yoshimoto[1], Yosuke Miyagi[2], Ryo Honda[1], Yasuhiro Ishimine[1] (1. Mount Fuji Research Institute, 2.National Research Institute for Earth Science and Disaster Resilience)

12:00 PM - 12:15 PM JST | 3:00 AM - 3:15 AM UTC

[SVC27-06] Training of the human resource development for volcanic disaster management officers at Mt Fuji

*Mitsuhiro Yoshimoto[1], Tomohiro Kubo[1], Ryo Honda[1], Yasuhiro Ishimine[1], Kenji Niihori[2], Makoto Kanano[2] (1.Mount Fuji Research Institute, Yamanashi Prefectural Government, 2.Organization of Volcanic Disaster Mitigation, NPO.)

Ash Fall Hazard Map using Newly Developed Simulation Model

*Tsuyoshi Nakatani[1], Toshiyuki Asano[1]

1. The Research and Education Center for Natural Hazards, Kagoshima University

In 2020, Sakurajima volcano has recorded 432 times eruptions by counting cases of which column heights are more than 1000m, according to Kagoshima Local Meteorological Observatory. It should be noted that such an active volcano is located at just 6km west of the central city of Kagoshima having 600,000 population. In recent years, accumulation of magma in the underground pool is observed to be comparable to the 1914 Taisho eruption volume, and therefore, we are highly conscious of the precaution against large scale eruption in near future.

Not limited to large scale eruptions, smaller but more frequent eruptions may cause serious damages against infrastructure. In May and August 2020, 10 and 20 flights connecting to Kagoshima Airport respectively, were reported to be canceled due to ash fall from the eruptions. The Kagoshima Airport has many domestic flights to connect remote islands; some of them are also volcanic islands. Thus, it is important in this area to ensure the safety of aviation from the impact of ash fall.

The Research and Education Center for Natural Hazards, Kagoshima University, has been studying methodology for predicting ash fall transport in real time, and evaluating expected disaster risks to improve the resilience in Kagoshima area. In this presentation, ash fall hazard map using newly developed simulation model will be reported.

The simulation model was based on a two-dimensional convection-diffusion equation including a settling transport term of pyroclastic material, and a source term. The eruption column acts as the source term, where we adopted Suzuki(1983) model to describe the vertical mass distribution. The particle size distribution was assumed to be comprised of 11 classes ranging from -5 to 5 on the Φscale, which was equivalent to 32mm to 0.03125mm.
In the numerical algorithm, the advection term and the diffusion term were solved by the upwind difference scheme and the central difference scheme, respectively. The computational domain was taken horizontally about 150km square which covers the entire mainland of Kagoshima prefecture and taken vertically from 1500m to 20000m in the altitude. The number of computational grids was 169×169×38, which is about 1 million points totally. To reduce the computation time, non-equidistant grids were applied for the horizontal plane. As the results, the horizontal grid spacing around Sakurajima became 500m, meanwhile the spacing near the edge of the domain was 1330m. In the vertical direction, a constant grid spacing of 500m was taken, and the volume of ash fall passing through the grid of 1500m altitude was assumed to be accumulated on the ground.

The ash fall hazard map was made by the following scenarios.
1) The same magnitude of Taisho eruption is assumed to occur at 9 am every day in 2020.
2) The temporal variation of eruption column height is given as the same as Taisho eruption case. The eruption lasts for 39 hours.
3) The total amount of eruption volume is given as 600million m^3 equal to the Taisho case. The total amount is distributed to the instantaneous amount by referring the above assumed temporal variation.
4) Kagoshima Aerological Observatory has conducted observations on wind velocity and direction daily at 9am and 9pm. Using these data, the spatially interpolated dataset on the wind speeds of the east-west

©2021. Japan Geoscience Union. All Right Reserved.

and north-south components at every 500m altitude is constructed.
5) The simulation is carried out while updating the eruption height every hour, and the wind speed every 12 hours. The computational duration of one case simulation is set as 48 hours.
6) Computations are performed for 366 days from January 1 to December 31, 2020. For each calculation point, the maximum depth of ash deposition in one year period is analyzed.

The ash fall hazard map 2020 reveals that there are several vulnerable areas such as the coastal area of central Kagoshima city, where the deposition depths exceed 1m.

Keywords: Ash Fall Simulation, Hazard Map, Taisho Eruption, Sakurajima volcano



©2021. Japan Geoscience Union. All Right Reserved.

On the Effects of the Inertial Forces of the Falling Volcano Ash on the Ash absorption by an External Unit of Building Air Conditioning

*Kiyotoshi Otsuka[1], Arihide Nobata[1], Hitoshi Suwa[1], Tomohiro Kubo[2], Yosuke Miyagi[3], Masamitsu Miyamura[3]

1. Obayashi Corporation, 2. Mount Fuji Research Institute, Yamanashi Prefectural Government , 3. National Research Institute for Earth Science and Disaster Resilience

Explosive eruption of volcanos can affect infrastructures of the cities in many ways, even if they are situated far from the volcanos, say, more than 100km. Degradation of performances of the building air conditioning due to ashfall events is among such volcano impacts. In this context, we carried out experiments on ashfall influences on the operation of an open type cooling tower[1)], where the amount of the ashfall leading to the abnormal operation of it was investigated, showing the deviation from the normal operation of the cooling tower begins to be recognized when the cumulative ashfall depth exceeded around 20 to 30mm, mainly due to the intrusion of ash into the piping of the cooling water circulation. In their study, the amount of the ash absorbed into the cooling tower was related to the ashfall depth by assuming that the rate of the ash absorption at the air intake is expressed by the product of the air intake velocity and the airborne ash concentration which is directly related to ash fall rate when it is multiplied by bulk terminal fall velocities of ash particles. It is noted that ash particles falling in the vertical direction are assumed to quickly respond to the, usually horizontal, suctioning force of the air intake of the air conditioning system, which is usually set on the side walls of the devices or building walls. However, in reality, the inertia of the ash particles will more or less retard the response of the particle motion to the suctioning force near the air intakes, so it is possible that the relationships between the absorbed ash amount and the ash fall depth derived in our previous study will become somewhat different when the above mentioned inertia effects are taken into account.

In the present study, the effects of the inertia forces of the falling ash particles on the ash absorption rate at the air intake are investigated numerically. In reference to the method of the multi-phase flow simulations, the equations of motion of the ash concentration, which takes into account particle sizes and non-sphericities, are numerically integrated and the deviation of the ash flow from the air flow near the air intake due to inertia force are investigated for the simple cases where a rectangular exterior unit of the air conditioning device is placed at the bottom of the rectangular computational domain with ashfall from the ceiling of the domain. The air flow obtained from mass-consistent flow simulations with an incompressible continuity restriction condition is used to represent the air flow on which ash particles are laden. The results of the numerical calculation show that the inclusion of inertia effect tends, in general, to lessen the ash absorption rate at the air intake, and this tendency is more apparent for heavy particles than the light ones, and, in addition, for the particles with the same weight, the tendency is more of the case for the particles with small non-sphericity than with low non-sphericity. These results suggest the possibility of the ashfall depth at which the air conditioning begins to deviate from normal operation shift to somewhat larger side than the one indicated in our previous study.

Keywords: Ashfall, Functional Damage, Concentration, Inertial Force, Building Air Conditioning

©2021. Japan Geoscience Union. All Right Reserved.

Experimental Study on Safety of Wooden Building Roofs Against Impact of Ballistic Ejecta

*Kohei Tateyama[1], Hiroyuki Yamada[2], Ryo Honda[3], Tomohiro Kubo[3], Mitsuhiro Yoshimoto[3]

1. Ritsumeikan University, 2. National Defense Academy, 3. Mount Fuji Research Institute, Yamanashi Prefectural Government

Damages and destruction of the wooden buildings caused by volcanic activities are due to various factors. Especially, at the phreatic eruption of Mt. Ontake on September 27, 2014, most of the damages were caused by the impact of the ballistic ejecta.

In order to mitigation this damage, it is suggested that evacuation to a mountain hut is effective. Thus, evaluation of safety for wooden buildings (e.g. mountain huts) against ballistic ejecta impact is necessary. Previously, we reported the penetration boundary energy for the unreinforced 15 mm and 18 mm thick wooden building roof. In addition, it was found that by superimposing the cedar boards, impact absorption properties can be improved simply. In this study, we focused on the effect of pumice that are often installed on roofs in many mountain huts and investigated their impact absorption characteristics.

An impact test was carried out at the velocity of 10 to 90 m/s using a large-scale launching system. In this system, a projectile was accelerated by compressed air and then collided with the target. The projectile velocity was measured using two lasers and light receiving parts.

In case of normal phreatic eruptions, the ballistic ejecta with a diameter of approximately ϕ100 mm are scattered. Therefore, cylindrical abrasive materials similar to the common ballistic ejecta (density: 2400 kg/m^3, diameter: 90 mm, length: 170 mm, mass: 2.66 kg) was used as the projectile. A typical wooden roof structure (e.g., cedar boards, waterproof sheet, galvalume steel plate and cedar rafter) was used for the target. The thickness of the cedar board, waterproof sheet and galvalume steel plate were 18 mm, 1 mm and 0.4 mm, respectively. The components were fixed with nails and its spacing was approximately 150 mm. The dimensions of the specimen were 600 mm ×600 mm.

For the impact experiment, artificial pumice (hereafter referred to as pumice) in sandbags was placed in front of the specimen. The pumice with composition and specific gravity similar to natural pumice were used. The sandbag bag containing pumice is approximately 180 mm thick. The pumice used in this study was an inorganic porous material made from 96 % waste glass. Its particle size was approximately 2 to 75 mm and its shape was irregular. The density in oven-dry conditions was between 300 and 600 kg/m^3.

In previous study, it was known that the boundary between penetrating and non-penetrating impact energy was taken to be near 1.2 kJ in the unreinforced 15 mm thick wooden building roof.

As a result of the impact test, due to the installation of pumice on the roof structure, the boundary between penetrating and non-penetrating impact energy was taken to be near 3.7 kJ. Therefore, the impact absorption energy of pumice used in this study can be calculated as approximately 2.5 kJ.

Keywords: Ballistic ejecta, Wooden buildings roof , Artificial pumice

©2021. Japan Geoscience Union. All Right Reserved.

A trajectory analysis of a rockfall on a steep slope at Mt. Fuji to determine the possible source area of the falling rock

*Taishi Sakurada[1], Ryodo Hemmi[2], Yasuhiro Ishimine[3], Hideaki Miyamoto[1]

1. The University of Tokyo, 2. The University Museum, The University of Tokyo, 3. Mount Fuji Research Institute, Yamanashi Prefectural Government

Rockfalls are among the most active geologic events found on Earth, Mars, and the Moon. A newly detached mass of rock falling from a steep-slope often rolls down a slope until its break. It occurs most frequently in mountains or steep areas, especially crater and valley walls on Mars and the Moon (Bickel et al., 2020; Senthil Kumar et al., 2019). It is a kind of the fastest type of landslide often initiated by repeated freezing and thawing on Earth, while most extraterrestrial ones are likely caused by shaking induced by impacts (Bickel et al., 2020; Brown & Roberts, 2019). Complete monitoring of the phenomena is usually challenging, so the incidents are often recognized by the newly-formed tracks or debris fragments along the slope.
On September 9th, 2019, a rockfall occurred on the north-eastern flank of Mt. Fuji. No fatality or injured is involved with minor damage to a building reported. A notable characteristic of this incident is the clear boulder tracks along the rockfall route, which shows significant similarities to those found on Mars and the Moon. Thus, we studied the scale, distributions, and the possible route of the rockfall based on the field images obtained by Yoshikage Inoue (manager of Taishikan hut) and his observations, drone-based images, satellite images, as well as numerical modeling with a digital elevation model.
Our preliminary study shows that a boulder of a couple of meters in size may have detached from a region higher than 3,600 meters altitude and fall to the area of altitudes between 3,250-3400 meters, resulting in leaving 11 to 14 boulder tracks of about 30m intervals before it hit the other boulder, which would make the falling rock jump and fly more than 300m with a velocity of no less than about 50m/s. We find that the initial location of the boulder is essential in determining the exact route of a high-velocity boulder, which may imply that the boulder track analysis can be a useful method to determine the source area or the velocity of the boulder of a rockfall event.

References

Bickel, V. T., Aaron, J., Manconi, A., Loew, S., & Mall, U. (2020). Impacts drive lunar rockfalls over billions of years. *Nature Communications*, *11*(1), 1–7. https://doi.org/10.1038/s41467-020-16653-3
Brown, J. R., & Roberts, G. P. (2019). Possible Evidence for Variation in Magnitude for Marsquakes From Fallen Boulder Populations, Grjota Valles, Mars. *Journal of Geophysical Research: Planets*, *124*(3), 801–822. https://doi.org/10.1029/2018JE005622
Senthil Kumar, P., Krishna, N., Prasanna Lakshmi, K. J., Raghukanth, S. T. G., Dhabu, A., & Platz, T. (2019). Recent seismicity in Valles Marineris, Mars: Insights from young faults, landslides, boulder falls and possible mud volcanoes. *Earth and Planetary Science Letters*, *505*, 51–64. https://doi.org/10.1016/j.epsl.2018.10.008

Keywords: Mt.Fuji, rockfall, Discrete Element Method, boulder track

©2021. Japan Geoscience Union. All Right Reserved.

Improvement of Proto-type Educational Web Contents for the Municipalities' Disaster Response Staff.

*Tomohiro Kubo[1], Mitsuhiro Yoshimoto[1], Yosuke Miyagi[2], Ryo Honda[1], Yasuhiro Ishimine[1]

1. Mount Fuji Research Institute, 2. National Research Institute for Earth Science and Disaster Resilience

We develop the educational web contents which is funded by the D3 of the Integrated Program for Next Generation Volcano Research and Human Resource Development of MEXT. We conducted an interview survey on the proto-type educational web contents developed last year, against the municipalities' disaster response staff, we report on the result.

In the interview survey, we interviewed them the following issues.

1) The contents for their self-education

2) The contents and needs for public awareness activities to residents

3) How to use observation information in the event of a volcanic disaster

As a result, we found that they need the video education contents for about 15 minutes and the simulation contents, the semi-real-time photo data from volcano surveillance camera for observation. In addition, we report that we improved the educational web contents based on the above results.

Keywords: Web contents, Municipalities' disaster response staff, Volcano disaster mitigation

©2021. Japan Geoscience Union. All Right Reserved.

Training of the human resource development for volcanic disaster management officers at Mt Fuji

*Mitsuhiro Yoshimoto[1], Tomohiro Kubo[1], Ryo Honda[1], Yasuhiro Ishimine[1], Kenji Niihori[2], Makoto Kanano[2]

1. Mount Fuji Research Institute, Yamanashi Prefectural Government, 2. Organization of Volcanic Disaster Mitigation, NPO.

Since disaster prevention measures for active volcanoes differ for every volcano, it is difficult to imitate other volcanoes' disaster prevention plans and measures. On the other hand, disaster prevention officers will be changed every two to three years. As a result, knowledge and experience of volcanic disasters have not been accumulated, and disaster prevention measures have not progress.
In order to solve these problems, Yamanashi Prefecture has been considering an effective training program for volcano disaster prevention officers since 2017. In Yamanashi Prefecture, the Yamanashi Core Group Meeting of the Mt. Fuji Volcano Disaster Prevention Council is held about six times a year (four times in FY2020), and training is conducted once or twice a year using the framework of this meeting. The training was carried out five times before FY2020. In FY2020, the lecture about the volcanic disaster was held on July 22, 2020, and the tabletop exercise was held on January 20, 2021. In the FY 2020 tabletop exercise, each municipality's specific evacuation plan was examined based on new simulation results. If an eruption occurs, residents around Mt. Fuji must evacuate within the area or over a wide area, depending on the scale of the eruption. This exercise was conducted on the assumption that people would evacuate to neighboring municipalities. Eruption scenarios were prepared by experts belonging to the Volcano Disaster Prevention Council, and drills were conducted without distributing scenarios in advance.
In this exercise, we were able to extract problems that would occur by using realistic eruption scenarios and making realistic assumptions. It also revealed problems with the existing evacuation plan. In the future, it will be possible to improve the volcano disaster prevention officer's skills by conducting training in various patterns, changing the location of the crater, and other factors.

Keywords: Training, human resource development , volcanic disaster management officer, Mt Fuji

©2021. Japan Geoscience Union. All Right Reserved.

[J] Poster | S (Solid Earth Sciences)：S-VC Volcanology

Sun. Jun 6, 2021 5:15 PM - 6:30 PM JST | Sun. Jun 6, 2021 8:15 AM - 9:30 AM UTC | Ch.13_1

[S-VC27] Mitigation of volcanic disasters - basic and applied researches

convener:Shinji Takarada(Geological Survey of Japan, National Institute of Advanced Industrial Science and Technology), Mitsuhiro Yoshimoto(Mount Fuji Research Institute, Yamanashi Prefectural Government), Tatsuro Chiba(Asia Air Survey Co., Ltd.), Yousuke Miyagi(National Research Institute for Earth Science and Disaster Resilience)

Volcanic disasters are caused by wide range of volcanic phenomena including ash fall, pyroclastic flow, debris avalanche, lahar, and lava flow. To mitigate volcanic disasters, wide range of technologies including simulation, data processing on GIS, and communication techniques are required. Researches on volcanic hazards mapping, eruption scenarios, estimation of tephra falls, and probabilistic eruption assessments are getting important. This session invites presentations and broad reviews related to these topics. Contributions on database technology, case studies of social and school educations, the Next Generation Volcano Research, and specific examples of eruption crisis events are also encouraged.

[SVC27-P01] Disaster-stricken vehicles dug up for the first time in 30 years and characteristics of pyroclastic surge deposits in 1991 on Unzen Volcano

*Daisuke Nagai[1], Shinichi Sugimoto[2] (1.Mt.Unzen disaster memorial hall, 2.Unzen volcanic area global geopark)

[SVC27-P02] Selective pulverization of pumiceous groundmass in pumice pulverization processes in a laboratory

*Shingo Takeuchi[1] (1.Central Research Institute of Electric Power Industry, Civil Engineering Research Laboratory, Geosphere Sciences)

[SVC27-P03] A case of sediment-related disaster in a volcanic area due to an earthquake off the coast of Fukushima Prefecture on February 13, 2021

*Takayama Toko[1], Tatsuro Chiba[1], Hiromichi Moriike[1], Tatsuya Ochiai[1] (1.Asia Air Survey Co.,Ltd.)

[SVC27-P04] Accelerating Two-Dimensional Lava Flow Simulations with OpenACC

*Yasuhiro Ishimine[1] (1.Mount Fuji Research Institute, Yamanashi Prefectural Government)

[SVC27-P05] Present situation of water pollution problem caused by 2018 Iwo-Yama volcano eruption in Kirishima volcanic complex

*Yoshikazu Kikawada[1], Haruka Yamamoto[2] (1.Faculty of Science and Technology, Sophia University, 2.Graduate School of Science and Technology, Sophia University)

[SVC27-P06] Training program of the human resource development for volcanic disaster management officers in JAPAN -Preliminary report-

*Kenji Niihori[1], Akio Sato[1], Maokoto Konno[1], Mitsuhiro Yoshimoto[2] (1.Organization of Volcanic Disaster Mitigation, NPO., 2.Mount Fuji Research Institute, Yamanashi Prefectural Government)

[SVC27-P07] Experiment for understanding of climber's movement and tendency in Nasu Volcano

*Yousuke Miyagi[1], Mitsuhiro Yoshimoto[2], Yasuhiro Ishimine[2], Ryo Honda[2], Tomohiro Kubo[2] (1.National Research Institute for Earth Science and Disaster Resilience, 2.Mount Fuji Research Institute, Yamanashi Prefectural Government)

[SVC27-P08] Eruption Sequences and Precursory Activities of Large-scale Volcanic Eruptions, and Construction of Large-scale Volcanic Eruption Database

*Shinji Takarada[1], Yasuaki Kaneda[1], Fumihiko Ikegami[1], Yuki Nishino[1], Nobuo Geshi[1] (1.Geological Survey of Japan, National Institute of Advanced Industrial Science and Technology)

Disaster-stricken vehicles dug up for the first time in 30 years and characteristics of pyroclastic surge deposits in 1991 on Unzen Volcano

*Daisuke Nagai[1], Shinichi Sugimoto[2]

1. Mt.Unzen disaster memorial hall, 2. Unzen volcanic area global geopark

It has been 30 years since the eruption of Mt. Unzen Fugen killed 43 people. In the local area, the improvement plan of the disaster area is being made and the construction is being carried out. In the construction on February 8, 2021, 4 damaged cars were excavated and visited as they were 30 years ago. The vehicles will be installed on concrete foundations after volcanic ash and other soil is removed. Since the vehicle was salvaged by a heavy machine at the time of this excavation, we had an opportunity to investigate the damage of the entire vehicle which had not been investigated after the disaster, and the pyroclastic surge deposits accumulated in and around the vehicle body in 1991. The investigation was carried out in Kitakamikiba Town, Shimabara City, where many reporters called "fixed point" were present at that time, in a vehicle blown about 70 m downstream from a road by a pyroclastic flow generated on June 3, 1991. Two cars are placed close to each other at the same place, and the cars on the upstream side are placed facing the rear side with the north side facing the front, while the other cars on the downstream side are placed facing the obliquely rear side with the south side facing the front and are placed to lean against the cars on the upstream side. Judging from the testimonies at the time and the pictures and images left by the victims just before the disaster, it is assumed that the two taxis were chartered by the press. Through the excavation, license plates were dug up from cars on the mountain side, and it was discovered that the cars were "Koarashi Taxi".No license plate that could be read from the other car was found, but as a result of identifying the rest of the damaged cars, it was found that the car belonged to the "Maruzen Taxi". The body of the driver of Maruzen Taxi was found near the fixed point. On the other hand, it is probable that the driver of the Koarashi Taxi was in the taxi and suffered from the disaster because he was found somewhere between the fixed point and the excavated vehicle (About 30 m downstream from the fixed point) and communicated with his colleague's vehicle by radio until just before the excavation. In the aerial photograph taken on June 5, there was a damage on the wall surface of the gutter southeast of the location where both cars were supposed to have been, as if something had hit the wall surface, and further downstream, there was a cut mark of about 3 m in width and about 10 m in length, as if the ground had been dragged. Since there is a damaged vehicle on the extension of the cut mark, it is probable that this cut mark was made in the process in which the vehicle was transported by the impact of the pyroclastic surge. The entire engine section and the body of the vehicle were damaged so that they could be broken, and the bumpers, the bonnet, the roof, the bottom surface of the vehicle, and the entire body were found to have large dents that received an impact. It is presumed that the car body was carried rolling because there were relatively uniform dents in the whole car body and no falling marks on the ground. When the car body was dug out, an electric wire was caught around the body. It is known that there was a utility pole nearby, and it is known that the utility pole got entangled with electric wires and wound around the car body as the car moved. A pyroclastic surge deposit on June 3, 1991 around the vehicle was also found. The sediments are about 3 cm thick. The thickness diagram of the pyroclastic surge deposits including the surrounding observation sites suggests that the area was located near the major axis in the distribution basin. The excavated vehicles will be displayed on the site and will be used as a base for disaster learning by the local residents' association. It is hoped that the remains will enhance people's awareness of disaster prevention.

©2021. Japan Geoscience Union. All Right Reserved.

Keywords: pyroclastic surge, volcanic disaster, disaster prevention education



©2021. Japan Geoscience Union. All Right Reserved.

Selective pulverization of pumiceous groundmass in pumice pulverization processes in a laboratory

*Shingo Takeuchi[1]

1. Central Research Institute of Electric Power Industry, Civil Engineering Research Laboratory, Geosphere Sciences

The pulverization characteristics of volcanic rocks have recently been the subject of much experimental research from the viewpoint of volcanic ash generation during the eruption processes. The pulverization characteristics are also important for preparing artificial volcanic ash by pulverizing volcanic rocks and sieving the pulverized materials for experimental studies on the adverse effects of volcanic ash on equipment and facilities. The author has been experimentally investigating the pulverization characteristics of porous volcanic rocks for manufacturing artificial volcanic ash (Takeuchi, 2020). In this presentation, I investigate the variation in the ratio of crystal to glass at each ϕ-scale sieve class by pulverizing phenocryst-bearing pumice samples.

The Osumi pumice (Os), which is available in large quantities and is expected to produce pumiceous particles, was used as a raw material for the pulverization experiments. Lapilli with -1 ϕ (2000 μm) class were prepared as starting samples by a jaw crusher and manual sieving. The intensity of a disk mill used to pulverize the starting samples was varied by adjusting the slit width between the rotating metal discs. A Vibratory Sieve Shaker (FRITSCH A-3PRO) was used to sieve the pulverized material. The Vibratory Sieve Shaker is electro-magnetically controlled and can be loaded with vertical vibrations of 3000 times/min in the amplitude range of 0.1 to 3.0 mm, and the mass variation with the sieving time can also be confirmed to maintain objectivity in judging the end of sieving.

The difference in pulverization intensity produced a difference in the particle size distribution of the pulverized material as follows. For the wide and narrow slit widths, the median particle sizes (f_{50}) are -1.0 ϕ (2000 μm) and 1.5 ϕ (354 μm), and the mass fractions with a sieve class of less than 4 ϕ are 9% and 34%, respectively.

Based on the bulk rock composition obtained by XRF analysis and the average composition of each crystal and glass obtained by EPMA analysis, the mass fraction of crystal and glass for each class was quantified by mass balance calculation. As a result, the following characteristics of the crystal content, which changed during the pulverization and sieving processes, were clarified. Compared to crystal content (about 10%) of the raw material, the crystal content increases (up to ca. 30%) in the 1 ϕ (500 μm) to 3 ϕ (125 μm) particles. Crystal content decreases down to ca. 5% in the pulverized material of less than 4 ϕ (63 μm). Weak pulverization tended to result in a greater crystal content in sieve classes larger than 1 ϕ. The -1 ϕ (2000 μm) sieve class in the pulverized material has a lower crystal fraction than the starting sample (-1 ϕ, 2000 μm). The size distribution of the crystals (phenocryst) in the Os pumice obtained from image analysis of the elemental and electronic images of EPMA for the polished section of pumice lapilli was consistent with the crystal-rich sieve class of the pulverized material. I interpret that when the material is subjected to disk milling, the phenocryst in pumice is likely to be separated as free crystals, and the separated phenocryst is relatively difficult to be pulverized, and the pumiceous glassy matrix was selectively pulverized to a sieve class of less than 4 ϕ (63 μm). This variation in crystal content in pulverization and sieving processes of phenocryst-bearing pumices is an important note on the properties of artificial volcanic ash when using for experiments.

©2021. Japan Geoscience Union. All Right Reserved.

Keywords: pumice pulverization and sieving experiments, volcanic ash hazard, phenocryst, volcanic glass

©2021. Japan Geoscience Union. All Right Reserved.

A case of sediment-related disaster in a volcanic area due to an earthquake off the coast of Fukushima Prefecture on February 13, 2021

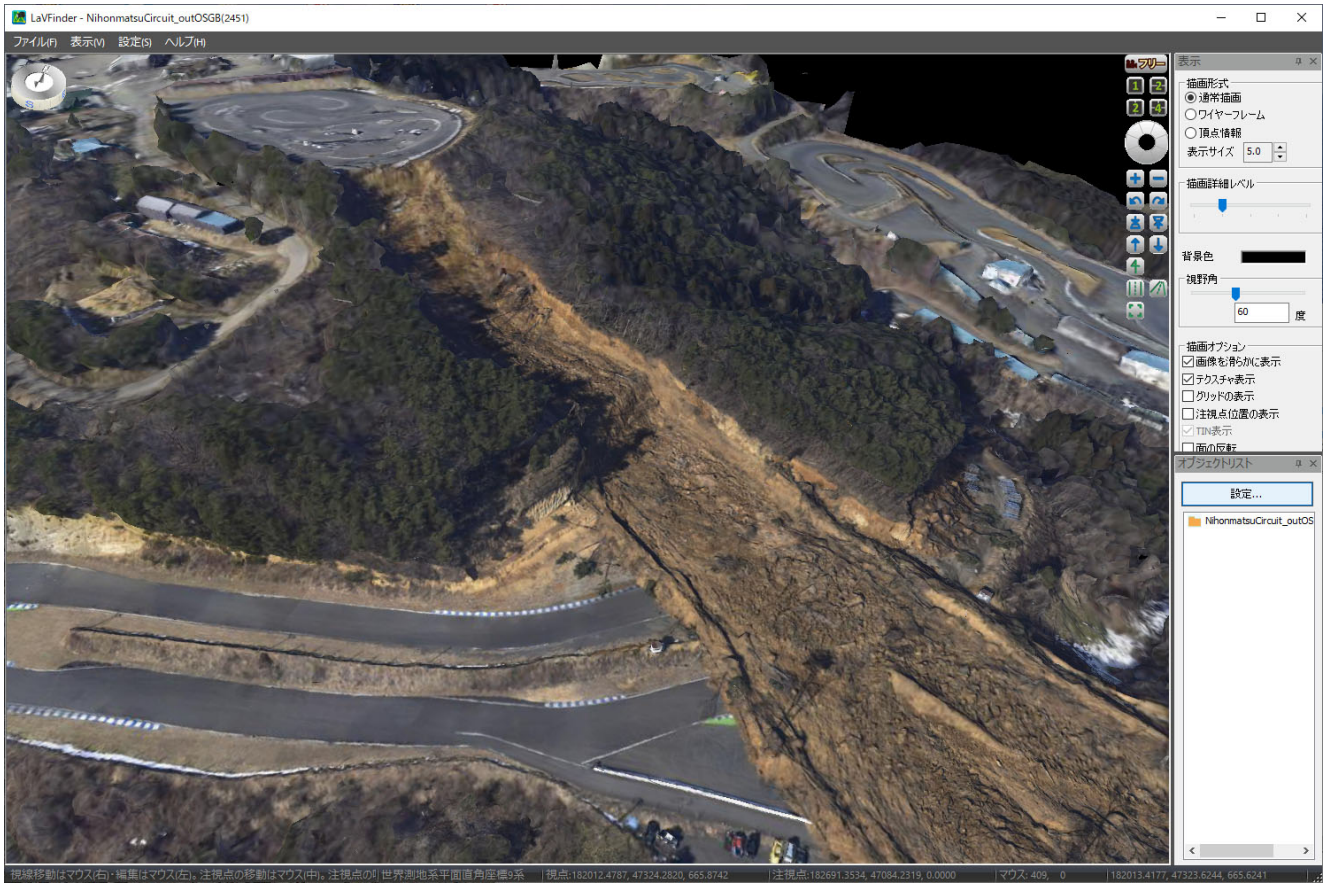
*Takayama Toko[1], Tatsuro Chiba[1], Hiromichi Moriike[1], Tatsuya Ochiai[1]

1. Asia Air Survey Co.,Ltd.

Sediment disasters were found in several places due to an earthquake that occurred off the coast of Fukushima Prefecture on February 13, 2021. In Nihonmatsu City, Fukushima Prefecture, a large-scale landslide occurred on the slope at the foot of Mt. Adatara in the volcanic area.

In order to grasp the scale of the collapse and to contribute to the mechanism analysis, aerial photogrammetry by the SfM-MVS method was carried out using the aerial oblique photograph taken on February 14, the following day of the earthquake, and generated a three-dimensional landform model. In addition, the authors created photographic map (simple orthographic image) and topographic map (Red Relief Image Map).
The authors report the results of analyzing about the landslides, such as the scale of landslide, using remote sensing data.

Keywords: Earthquake, Landslide, Tephra, Structure from Motion –Multi View Stereo, Three-dimensional terrain model



©2021. Japan Geoscience Union. All Right Reserved.

Accelerating Two-Dimensional Lava Flow Simulations with OpenACC

*Yasuhiro Ishimine[1]

1. Mount Fuji Research Institute, Yamanashi Prefectural Government

The performance of Graphics Processing Unit, or GPU, has been much grown in these few decades. While GPU has been originally developed for drawing 3D graphics for video games on computers, for example, at a high speed, GPU can be used for calculating double-precision floating-point values under certain conditions. That enhances General-Purpose Computing on GPUs, or GPGPU, in the field of high-performance computing. In particular, GPGPU research activities are rapidly expanding since the standardization of OpenACC has been initiated in 2011. Here, OpenACC is a directive-based programming model designed to provide a simple and effective approach.

Mount Fuji Research Institute has launched a research project entitled “Improvement of Numerical Simulation Techniques for Enhancing the Validity of Hazard Maps for Volcanic Eruptions” in 2020 and installed a computer with Titan V, which is a GPU developed by nVidia with a theoretical peak performance of 13.8 TFlops for single-precision floating-point calculations. We will present preliminary results of numerical simulations of lava flows that are performed with a numerical model developed by Ishihara (1990) and accelerated with OpenACC.

Keywords: Lava Flow, Numerical Simulation, GPGPU, OpenACC

©2021. Japan Geoscience Union. All Right Reserved.

Present situation of water pollution problem caused by 2018 Iwo-Yama volcano eruption in Kirishima volcanic complex

*Yoshikazu Kikawada[1], Haruka Yamamoto[2]

1. Faculty of Science and Technology, Sophia University, 2. Graduate School of Science and Technology, Sophia University

In April 2018, the first eruption in 250 years occurred at the Iwo-Yama volcano of the Kirishima volcanic complex. The newly opened vents with the phreatic eruptions gushed out the strongly acidic hydrothermal fluids containing toxic metal ions like lead and arsenic. The hydrothermal fluids were transported by a river to the Kakuto Basin at the volcano's foot and significantly impacted the agriculture and fishery in the lower reaches. The hydrothermal discharge from the volcano was prolonged, and the water pollution problem in the lower reaches finally came to an end near three years after the eruption. This study reviews the river water pollution in the Sendai River system caused by the 2018 Iwo-Yama volcano's eruption.

The new small craters opened on the south and west sides of the Iwo-Yama volcano summit area in April 2018, causing phreatic eruptions. There was one eruption at each crater, but a large amount of muddy thermal water discharged from the craters flowed into the Akago River, which originated from the area, and was carried to the Nagae River and the Sendai River. At this time, fish carcasses floated up in the river, and farmers had to give up paddy rice cultivation in the river basin. After that, the craters became thermal water pools, and a large amount of water that overflowed continued to be carried downstream, resulting in the water pollution problem in rivers for several years.

In May 2019, a demonstration experiment of a river neutralization system was started in the Akago River, and all river water, including thermal water from the craters of the Iwo-Yama volcano, began to flow down through the neutralization facility. The system works to reduce the solubility of metal ions dissolved in the river water and produces a neutralization product, resulting in a lower concentration of harmful dissolved components. The water quality of downstream rivers has improved significantly since the start of the neutralization demonstration experiment. At first glance thus, it seems that the effect of river neutralization has appeared. However, at that time, the hydrothermal activity of the Iwo-Yama volcano significantly decreased. The decreased activity resulted in lower acidity and lower concentrations of dissolved components in the crater pool. Besides, the amount of overflow from the pool also decreased at the same time. Consequently, it is unclear whether water quality improvement is due to river neutralization or decreased volcanic activity. On the other hand, referring to the data of river water quality monitoring by Miyazaki Prefecture [1], no significant fluctuations have been seen in river water quality in the downstream area since May 2019, which must be the effect of river neutralization.

As of the end of 2020, the Iwo-Yama volcano's volcanic activity is not so active, and there is little hydrothermal overflow from the thermal pool. The water quality of the Nagae River and the Sendai River in the Iwo-Yama volcano's lower reaches is stable and meets the environmental standard.

[1] Results of Water Quality Inspection of Akago River, Nagae River and Sendai River in Ebino City, https://www.pref.miyazaki.lg.jp/kankyokanri/kurashi/shizen/ebino.html (accessed 2021-02-12)

©2021. Japan Geoscience Union. All Right Reserved.

Keywords: Kirishima volcanic complex, Iwo-Yama volcano, phreatic eruption, water pollution, arsenic, thermal water pool

©2021. Japan Geoscience Union. All Right Reserved.

Training program of the human resource development for volcanic disaster management officers in JAPAN -Preliminary report-

*Kenji Niihori[1], Akio Sato[1], Maokoto Konno[1], Mitsuhiro Yoshimoto[2]

1. Organization of Volcanic Disaster Mitigation, NPO., 2. Mount Fuji Research Institute, Yamanashi Prefectural Government

There are many kinds of training program for natural disaster prevention officers in Japan. However, when it comes to volcanic disaster prevention, only few training programs exist because of the low frequent disaster. On the other hand, national and local government officers in Japan have to change their positions in a few years. Then it is very difficult for them to be specialists against volcanic hazard. In this research, we performed some types of training programs for volcanic disaster prevention officers from all over Japan, and questionnaire survey was conducted in the training programs. As a result, we could reveal the request from natural disaster prevention officers in Japan. From their request, we could re-build up a new type of training programs and method of volcanic disaster prevention.

Keywords: prevention of volcanic disaster, volcanic disaster management officers, training program

©2021. Japan Geoscience Union. All Right Reserved.

Experiment for understanding of climber’ s movement and tendency in Nasu Volcano

*Yousuke Miyagi[1], Mitsuhiro Yoshimoto[2], Yasuhiro Ishimine[2], Ryo Honda[2], Tomohiro Kubo[2]

1. National Research Institute for Earth Science and Disaster Resilience, 2. Mount Fuji Research Institute, Yamanashi Prefectural Government

Recently, many climbers are enjoying climbing in Japan, and can approach to an active vent in many volcanoes, for example Mt. Fuji or Mt. Nasu. In the tragic disaster of Ontake Volcano in 2014, it was difficult for local governments to grasp whereabouts of climbers and to conduct rescue and search for victims. The same issue was raised also in the 2019 eruption of Kusatsu-Shirane Volcano. Therefore, it is quite important to grasp whereabouts of climbers in the event of disaster for proper decision of rescue and search.

Experiments to acquire data of climbers have conducted in Mt. Nasu in 2020, named “Mt. Nasu Challenge”. In the experiment, we distribute 2,000 of beacons to climbers, and 15 of receivers which are set in mountain trails detect signals from the beacons, then we can grasp the number and location of climbers who have the beacons. And it took about two hours to grasp locations of 90% of climbers.

In this research, we are going to use the climber’ s data for disaster prevention. In the event of disaster, it is possible to reduce the time for grasping climber’ s information. In the normal time, local governments can refer the data to make evacuation plans, including establishment of shelters or evacuation routes. We evaluate exposures of climbers against volcanic hazards, including ash fall, volcanic materials, pyroclastic flow, mad flow, and lava flow, cited from Nasu volcano hazard map by using GIS software. First, we convert hazard map data that have been already published to GIS data, and make spatial analysis with the climber’ s data from the experiment. From results of the evaluation, we can make simple damage estimation of climbers.

Keywords: Nasu Volcano, experiment for understanding of climber's movement, evaluation of climber's exposures

©2021. Japan Geoscience Union. All Right Reserved.

Eruption Sequences and Precursory Activities of Large-scale Volcanic Eruptions, and Construction of Large-scale Volcanic Eruption Database

*Shinji Takarada[1], Yasuaki Kaneda[1], Fumihiko Ikegami[1], Yuki Nishino[1], Nobuo Geshi[1]

1. Geological Survey of Japan, National Institute of Advanced Industrial Science and Technology

Volcanic hazards can occur thousands of kilometers away from the volcano due to large-scale PDCs and tephra falls produced from the VEI 5-8 class large-scale eruptions. It is thus important to reveal the past eruption sequences of large-scale eruptions and their long-term and short-term precursory activities for an effective volcanic hazards mitigation measures. Many variations can be observed for the eruption sequences of large-scale eruptions and long-term and short-term precursory activities, which generally do not follow a common pattern. The Geological Survey of Japan, AIST, started a project to compile the characteristics of eruption products, eruption sequences, long-term and short-term precursory and post-caldera activities of large-scale volcanic eruptions. The contents and website of this large-scale eruption database are introduced in this presentation.

The long-term and short-term precursory activities, eruption sequences of main caldera-forming eruption, and post-caldera activities have been currently compiled for a total of 17 large-scale eruptions. These eruptions are the 946AD Chanbaishan-Tomakomai, 6.4 cal ka Ikeda caldera-forming, 7.3 cal ka Kikai-Akahoya, 7.6 cal ka Mashu Main-caldera-forming, 14.6 cal ka Nigorikawa, 15.5 cal ka Towada-Hachinohe, 30 cal ka Aira-Ito, 32 cal ka Towada-Ofudo, 40 cal ka Kutcharo I, 46 cal ka Shikotsu, 60 cal ka Daisen-Kurayoshi, 87-89 ka Aso-4, 95 ka Kikai-Nagase, 106 ka Toya, 108 ka Ata, 110-115 ka Sambe-Kisuki and 120 ka Kutchro IV eruptions. Part of descriptions of these eruptions are published in GSJ Openfile reports (no. 680 and 699; Nishino et al., 2019, Kaneda et al., 2020a).

The precursory activities of large-scale eruptions are categorized into two types: Type I, precursor activities were observed in the last 50 ka, and Type II, no precursor activities were observed. Type I precursory activities are subdivided into 3 types based on the average eruption rates until the main caldera-forming eruptions occur: increased (Type I-1), stayed constant (Type I-2) and decreased (Type I-3) (Kaneda et al., 2020b).

We have developed a Large-scale Eruption Database website, where users can browse and search the long-term and short-term precursory activities, sequences of main caldera-forming eruptions and post-caldera volcanic activities (Figure). Map of the distributions of major eruption products are displayed which could be zoomed in and zoomed out using WebGIS technology. The distributions of tephra falls and pyroclastic flows and the shape of caldera-rims are digitized and saved in GIS format and could be shown using the system. This website will be made accessible to the public within the fiscal year 2021, together with the Plinian Eruption Database, which is also currently developed.

Figure caption: Example of the website of the Large-scale Eruption Database (Aira-Tn Ash Fall descriptions during the main caldera-forming eruption).

©2021. Japan Geoscience Union. All Right Reserved.

Keywords: Large-scale, Eruption sequence, Precursor activities, Caldera, Database

姶良－入戸火砕流噴火

30 cal ka

Aira-Ito Pyroclastic Flow Eruption

総噴出量: 見かけ体積～700 km^3，700×10^{12} kg

姶良Tn火山灰

あいらてぃーえぬかざんばい

Aira Tn Volcanic Ash

年代: 30 cal ka –

Smith et al. (2013)

噴出源: 姶良カルデラ

▼ 噴火推移: プリニー式噴火→大規模火砕流発生 (カルデラ形成)

姶良－入戸火砕流噴火によって噴出し，遠方まで飛散した降下火山灰を姶良Tn火山灰 (AT)と呼ぶ．AT火山灰は姶良カルデラから約1,500 km離れた北海道や，北太平洋の海底からも報告されている．AT火山灰の見かけ体積は150 km^{3}以上と見積もられている (町田・新井，2003)．

AT火山灰は，その岩相からいくつかの降下ユニットに区分されている (Nagaoka, 1988, 河合・三宅，1999)．そのうち，基底のAT1層が大隅降下軽石の遠方相，AT2層 (Nagaoka, 1988のAT Ⅰ，町田・新井1992のA層) 妻屋火砕流の，AT3層及びf4層 (Nagaoka, 1988のAT Ⅱおよび Ⅲ，町田・新井1992のB及びC層) が入戸火砕流からのco-ignimbrite ashと考えられる (河合・三宅，1999)．

分布

日本列島全域を覆い，日本海全域・東シナ海・北太平洋の海底や朝鮮半島からも分布が報告されている (町田・新井，2003)．

噴出量

見かけの体積 > 150 km^3

構成要素体積 [km^3]

> 150

VEI

7

噴出量文献

町田・新井 (2003)

岩質

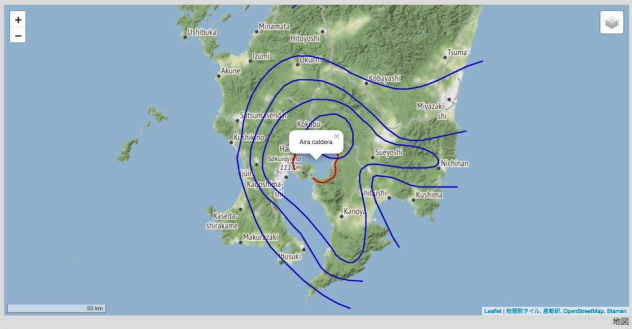
輝石流紋岩

構成物

主にバブルウォール型の火山ガラスからなるが，軽石型も含まれる．遊離結晶は主に輝石である (町田・新井，2003)．

岩相

複数の降下ユニットからなる降下火山灰層 (Nagaoka, 1988, 河合・三宅，1999)．



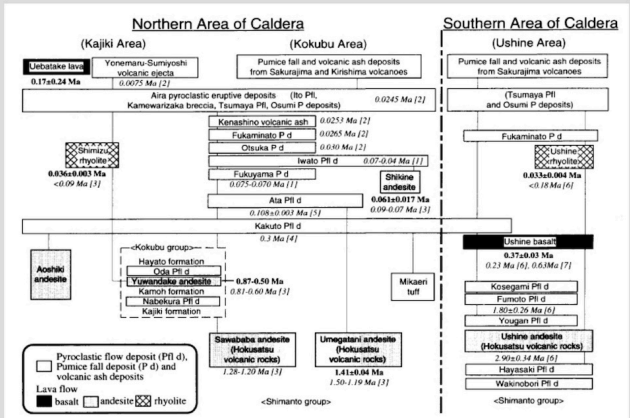


Fig. 3. Block diagrams showing the volcanic history of northern (Kajiki and Kokubu) and southern (Ushine) areas of Aira caldera summarized from Aramaki (1969), Hase *et al.* (1987), Kobayashi *et al.* (1977) Kobayashi and Iwamatsu (1980), Nagaoka *et al.* (1997), New Energy and Industrial Technology Development Organization (1987), Otsuka and Nishiinoue (1980) and Uto *et al.* (1997a). The ages obtained in this study (bold) and reported in the literatures (italic) are also indicated. The blocks whose stratigraphical relations are geologically observed each other are connected by thin lines. References: [1] Nagaoka *et al.*, 1997, [2] Okuno, 1997, [3] New Energy and Industrial Technology Development Organization, 1987, [4] Machida and Arai, 1992, [5] Matsumoto and Ui, 1997, [6] Kaneoka *et al.*, 1984, [7] Inoue, 1994 ms.

姶良カルデラ周辺の火山岩の年代 (周藤ほか，2000)

主要文献

Nagaoka (1988)

文献

Smith et al. (2013): https://www.sciencedirect.com/science/article/pii/S0277379113000413
町田・新井 (2003): http://www.utp.or.jp/book/b301896.html
Nagaoka (1988): https://ci.nii.ac.jp/naid/110008616087/
河合・三宅 (1999): https://www.jstage.jst.go.jp/article/geosoc1893/105/9/105_9_597/_article/-char/ja/

©2021. Japan Geoscience Union. All Right Reserved.

[J] Oral | S (Solid Earth Sciences)：S-VC Volcanology

Sun. Jun 6, 2021 1:45 PM - 3:15 PM JST | Sun. Jun 6, 2021 4:45 AM - 6:15 AM UTC | Ch.25 Zoom Room 25

[S-VC29] Hydrothermal systems of volcanoes

convener:Yasuhiro Fujimitsu(Department of Earth Resources Engineering, Faculty of Engineering, Kyushu University), Wataru Kanda(Volcanic Fluid Research Center, School of Science, Tokyo Institute of Technology), Takeshi Ohba(Department of chemistry, School of Science, Tokia University), Chairperson:Takeshi Ohba(Department of chemistry, School of Science, Tokia University), Wataru Kanda(Volcanic Fluid Research Center, School of Science, Tokyo Institute of Technology)

There is a diversity of hydrothermal systems between magmas and the ground surface in various geoscientific environments. Understanding of the hydrothermal systems contributes to understanding of the earth systems, and is essential for utilization of geothermal energy and prediction of volcanic eruption. In this session, we will discuss the topics on subsurface structures and heat and fluid flows of "hydrothermal systems of volcanoes" from the perspectives of geophysics, geochemistry, geology and geothermal reservoir engineering. Any research approaches, theoretical, observational and experimental, are welcome.

1:45 PM - 2:00 PM JST | 4:45 AM - 5:00 AM UTC

[SVC29-01] Compositional variability of rare earth elements in spring waters around Aso Volcano

*Hitomi Nakamura[1], Noritoshi Morikawa[1], Hikaru Iwamori[2], Shuhei Sakata[2], Qing Chang[3] (1.Geological Survey of Japan, National Institute of Advanced Industrial Science and Technology, 2.The University of Tokyo, 3.Japan Agency for Marine-Earth Science and Technology)

2:00 PM - 2:15 PM JST | 5:00 AM - 5:15 AM UTC

[SVC29-02] Deep-seated fluid supply around Kusatsu-Shirane volcano revealed by helium and carbon isotope ratios

*Hirochika Sumino[1], Takiguchi Takahiro[2], Tomoya Obase[1], Kotaro Toyama[3], Akihiko Terada[4] (1.Department of General Systems Studies, Graduate School of Arts and Sciences, The University of Tokyo, 2.Department of Integrated Science, College of Arts and Science, The University of Tokyo, 3.Atmosphere and Ocean Research Institute, The University of Tokyo, 4.Volcanic Fluid Research Center, Tokyo Institute of Technology)

2:15 PM - 2:30 PM JST | 5:15 AM - 5:30 AM UTC

[SVC29-03] Evolution of the magmatic-hydrothermal system of Mendeleev volcano (Kunashir Island)

*Alexey Andreevich Kotov[1], Sergey Zakharovich Smirnov[2], Noriyoshi Tsuchiya[1], Masaoki Uno[1] (1.Graduate School of Environmental Studies, Tohoku University, 2.Institute of Geology and Mineralogy SB RAS, Novosibirsk, Russia)

2:30 PM - 2:45 PM JST | 5:30 AM - 5:45 AM UTC

[SVC29-04] Volcanic unrests after the 2015 phreatic eruption of Hakone volcano and its hydrothermal system

*Kazutaka Mannen[1], Yuki Abe[1], Ryosuke Doke[1], Yohei Yukutake[1] (1.Hot Springs Research Institute of Kanagawa Prefecture)

2:45 PM - 3:00 PM JST | 5:45 AM - 6:00 AM UTC

[SVC29-05] Structure of the shallow hydrothermal system in Hakone volcano inferred from InSAR analysis

*Ryosuke Doke[1], Kazutaka Mannen[1], Kazuhiro Itadera[1] (1.Hot Springs Research Institute of Kanagawa Prefecture)

3:00 PM - 3:15 PM JST | 6:00 AM - 6:15 AM UTC

[SVC29-06] Ground deformations at Kuju volcano, Japan, revealed by PALSAR-2 InSAR

*Shohei Narita[1], Takahiro Ohkura[1] (1.Aso Volcanological Laboratory, Institute for Geothermal Science, Graduate School of Science, Kyoto University)

Compositional variability of rare earth elements in spring waters around Aso Volcano

*Hitomi Nakamura[1], Noritoshi Morikawa[1], Hikaru Iwamori[2], Shuhei Sakata[2], Qing Chang[3]

1. Geological Survey of Japan, National Institute of Advanced Industrial Science and Technology, 2. The University of Tokyo, 3. Japan Agency for Marine-Earth Science and Technology

Rare earth elements in spring waters may provide information on the origin and/or processes during water circulation; e.g., material and generation process at the source, interaction during the fluid migration through a crack or a vein with host rocks, mixing with meteoric water in a shallow aquifer. A large-scale circulation processes, including the dehydration from the subducted Philippine Sea slab and the subsequent interactions with surrounding basement rocks and meteoric waters, were distinguished by the rare earth element compositions of the spring waters in the Arima and the Kii areas, southwest Japan (Nakamura et al., 2015; 2016), with the aid of statistical analyses (Iwamori et al., 2020). To understand the origin and the upwelling processes, we have analyzed rare earth element composition of groundwaters including hot springs, river waters around the Aso volcano in Kyushu, Japan.

The Aso volcano has a caldera structure formed with four gigantic eruptions and numerous small eruptions (e.g., Kaneko et al., 2007). After the caldera formation, the central cone named Naka-dake has been and is active. The activity of Naka-dake and the related magma supply system have been studied by geophysical and petrological methods (e.g., Hata et al., 2018; Abe et al., 2017; AIST, 2016)). The northward-dipping conductive anomaly toward Naka-dake cone and several anomalies interpreted as an aqueous fluid flow have been detected by electromagnetic study (Hata et al., 2018). Both basaltic and dacitic magmas are thought to be involved in the magma supply system by petrological study, and the magma seems to have evolved during four gigantic eruptions (AIST, 2016). Alternatively, geochemical studies of groundwaters were performed to identify a magma related fluid (e.g., Kazahaya et al., 2019, Morikawa et al., 2019), and of which major solute elements are comprehensively analyzed by using statistical method (Iwamori et al., 2021). Statistical study has been revealed a spatial distribution of major solute elements which clearly decreases toward outside of caldera as a concentric structure (Iwamori et al., 2021).

In this study, we have classified the rare earth element compositions of groundwaters based on the result of statistical analysis of major solute elements, and newly found that the behavior of rare earth element is partly decoupled from major solute elements. Therefore, the dataset of rare earth elements would be expected to include unique information during fluid generation and upwelling. Combining geophysical, petrological, and geochemical studies, we aim to reveal the fluid circulation and the spatial extent of magmatic component at the Aso volcano.

This study was supported by the Secretariat of the Nuclear Regulation Authority, Japan, “Research on Knowledge Development of Giant Eruption Processes, FY 2020”.

©2021. Japan Geoscience Union. All Right Reserved.

Deep-seated fluid supply around Kusatsu-Shirane volcano revealed by helium and carbon isotope ratios

*Hirochika Sumino[1], Takiguchi Takahiro[2], Tomoya Obase[1], Kotaro Toyama[3], Akihiko Terada[4]

1. Department of General Systems Studies, Graduate School of Arts and Sciences, The University of Tokyo, 2. Department of Integrated Science, College of Arts and Science, The University of Tokyo, 3. Atmosphere and Ocean Research Institute, The University of Tokyo, 4. Volcanic Fluid Research Center, Tokyo Institute of Technology

In January 2018, a phreatic eruption occurred at Motoshirane, one of the three pyroclastic cones of Kusatsu-Shirane volcano. From September to December of the same year, a swarm of earthquakes was observed in Takayama Village, Nagano Prefecture, west of the volcano (Terada et al., JpGU-AGU Joint Meeting 2020). Both of these phenomena were caused not by magma itself but by deep hydrothermal fluids involving volatile components separated from magma. Therefore, it is important from the viewpoint of disaster prevention to obtain knowledge of the origin and migration path of deep-seated hydrothermal fluid in and around Kusatsu-Shirane volcano. In this study, we collected fumaroles, hot spring water, well water, and hot spring gas in the area, and measured the helium and carbon isotope ratios.

The $^{3}He/^{4}He$ ratio (defined as 1 Ra in the atmosphere and corrected for atmospheric contamination using the $^{4}He/^{20}Ne$ ratio) shows a decreasing trend with distance from the crater at the top of Shirane cone, where all documented (after 1882) phreatic eruptions have occurred until the 2018 eruption at Motoshirane cone. This suggests that the contribution of magmatic helium with a high $^{3}He/^{4}He$ ratio of about 8 Ra is diluted by the crustal helium with a low $^{3}He/^{4}He$ ratio during migration of the fluids. Based on the decreasing trend, degree of the dilution is more significant in the west than in the east. However, hot springs with almost constant $^{3}He/^{4}He$ ratios (4-5 Ra) are widely distributed from 9 to 15 km away from the volcano to the west. It is unlikely that fluids from the hydrothermal system beneath the volcano (e.g. Matsunaga et al., JVGR 2020) are supplied to the groundwater system in this region with a constant mixing ratio with crustal helium. The distribution of the $^{3}He/^{4}He$ ratio almost overlaps with the source distribution of the 2018 swarm of earthquakes, suggesting that deep hydrothermal fluid may have been efficiently supplied through the fault that may have been the epicenter. A higher $^{3}He/^{4}He$ ratio (6.1 Ra) was observed in the hot spring gas at a sampling site 26 km to the west, which is located near an active fault system on the western margin of the Nagano Basin, suggesting that deep-seated fluids are also supplied through this fault.

The carbon isotope ratios ($\delta^{13}C_{PDB}$) within 10 km from the crater were in the range of -1 to -8‰, but tended to become lower as the distance from the crater increased. At the farthest site in the west, a very low value of -76‰ was observed. The carbon in this hot spring gas is derived from methane, and since the Green Tuff is distributed in this area, there is a possibility that the natural gas reservoir in Green Tuff, which is reported to contain mantle-derived helium (Sakata, Sekiyu Gakkaishi 1997), is supplied from deep within the basin through the active fault system at the western margin of the Nagano Basin.

Keywords: helium isotope ratio, Kusatsu-Shirane volcano, hydrothermal fluids, carbon isotope ratio

©2021. Japan Geoscience Union. All Right Reserved.

Evolution of the magmatic-hydrothermal system of Mendeleev volcano (Kunashir Island)

*Alexey Andreevich Kotov[1], Sergey Zakharovich Smirnov[2], Noriyoshi Tsuchiya[1], Masaoki Uno[1]

1. Graduate School of Environmental Studies, Tohoku University, 2. Institute of Geology and Mineralogy SB RAS, Novosibirsk, Russia

Caldera eruption of Mendeleev volcano occurred about 39 thousand years ago on Kunashir Island. The volume of pyroclastic material is estimated at 60 km^3, which makes this eruption one of the largest eruptions of the Upper Pleistocene in the southern Kuril Islands. The pumice stones of the caldera eruption are dacitic. The proportion of porphyry phenocrysts in pumice is not higher than 20 vol. %. Phenocrysts are represented by plagioclase, augite, hypersthene, quartz, magnetite, and ilmenite, which are immersed in a glassy groundmass. Pumice stones do not contain amphibole phenocrysts; however, it was found in the form of crystalline inclusions in pyroxenes. Amphibole is Mg-Fe^{3+} hornblende (Al_2O_3 7-11 wt. %). To estimate pressures, we used an amphibole geobarometer (Ridolfi et al., 2010). We argue that the amphibole is a relic of a mineral association that formed during the partial melting of crustal metabasites of Kunashir Island. Thus, the estimates of the PT parameters correspond to the process of generation of the melt that participated in the formation of the upper crustal magmatic chamber. The maximum estimates of the PT parameters were about 3 kbar and 920˚C. Most of the compositions of amphibole correspond to 1-2 kbar and temperatures of 780 - 890˚C. Melts were formed at high fO_2 corresponding to the NNO +0.1-1.9 buffer.

Pumice phenocrysts often contain primary glassy melt inclusions (MI). Sometimes these MI’s contain empty shrinkage bubbles. The composition of MI corresponds to low-K_2O dacite-rhyodacite. MI’s differ from the bulk rocks by a higher SiO_2 content and do not differ in alkali content. The most important part of this study is to determine the content of volatile components in the melts that participated in the caldera eruption. By combining the methods of Raman spectroscopy and the measurement of oxygen by the EPMA EDS, we found that MI’s contain from 4.2 to 7.4 wt. % H_2O. At the same time, the water content in the glass of the groundmass does not exceed 4.5 wt% H_2O, which indicates significant losses of volatile melts during a caldera eruption. Comparison of the content of volatile components in glasses of the groundmass and in melt inclusions allows us to estimate the amount of volatile components emitted into the atmosphere during a caldera eruption.

Phenocrysts of plagioclase and clinopyroxene also contain primary and pseudo-secondary fluid inclusions (FI). The features of the composition and location of FI’s show that during the evolution the melt degassed. And this degassing is not associated with the final large eruption, as indicated by the presence of pseudo-secondary FI. Also, combined melt inclusions were found. They are represented by melt, trapped non-daughter crystals, and two-phase fluid segregations (liquid H_2O and gaseous CO_2). These inclusions indicate that the fluid pressure in the chamber could have exceeded the lithostatic one. An additional drop in lithostatic pressure (for example, due to the rise of magma) allowed additional portions of fluid to migrate from the glass of the melt inclusion into these segregations. The data obtained make it possible to accurately describe the evolution of magma from Mendeleev volcano before the caldera eruption and to compare it with other Pleistocene-Holocene calderas of the Southern Kuriles.

References

Ridolfi F., Renzulli A., Puerini M. Stability and chemical equilibrium of amphibole in calc-alkaline magmas:

©2021. Japan Geoscience Union. All Right Reserved.

an overview, new thermobarometric formulations and application to subduction-related volcanoes, 2010, Contrib. Mineral. Petrol. V. 160, P. 45–66.

Keywords: Caldera eruptions, Water content, Dacite pumice

©2021. Japan Geoscience Union. All Right Reserved.

Volcanic unrests after the 2015 phreatic eruption of Hakone volcano and its hydrothermal system

*Kazutaka Mannen[1], Yuki Abe[1], Ryosuke Doke[1], Yohei Yukutake[1]

1. Hot Springs Research Institute of Kanagawa Prefecture

Since the beginning of the 21st century, volcanic unrests detected as increase of seismic activity, increase of baseline length across the edifice, and frequent deep low-frequency earthquakes have been observed at Hakone volcano every few years. The most intensive volcanic unrest culminated in a small phreatic eruption in 2015 as the first eruption in the history of observation. Even after the eruption, volcanic unrests have been observed in 2017 and 2019. In this presentation, we compare the pre- and post-eruptive unrests, and discuss the status of the hydrothermal system just below the eruption center.

Volcanic unrests of Hakone volcano start with a deep inflation (6-10 km) and deep low-frequency events around 20 km below the surface, followed by volcano tectonic earthquakes (< 6 km below the sea level). At the same time, the component ratio of magmatic to hydrothermal in the fumarole such as CO2/H2S and He/ H2S increases. In addition, abnormal steam emission from steam production wells in Owakudani can be observed. In fact, Volcano Alert Level 2 for Hakone Volcano is defined are crustal movement, seismic activity, and fumarolic anomalies that exceed the specified level. This series of changes can be interpreted as the supply of magma or magmatic fluids to the deep inflation source, which increase pore pressure of the hydrothermal system.

The post eruptive volcanic unrests occurred in 2017 and 2019 also accompanied deep inflation, volcanic tectonic earthquakes, changes in volcanic gas ratios, and deep low-frequency earthquakes. However, the frequency of volcano tectonic earthquake during the post-eruptive unrests was significantly lower especially in the shallow immediately beneath Owakudani. Also rise of magmatic/hydrothermal gas ratio was less significant during the post-eruptive unrest. In this presentation, we attribute these phenomena to the 2015 eruption, which ruptured the hydrothermal system near the surface (cap-rock) and at the bottom (sealing zone near the brittle-ductile boundary).

Recent magnetotelluric surveys showed that volcano tectonic earthquakes at Hakone Volcano occur within the hydrothermal system, and seismic activity during the unrests was interpreted as intrusion of fluid and the pore pressure rise within the hydrothermal system. The decrease in seismic activity observed in the post-eruptive unrest beneath Owakudani may be due to the destruction of the caprock by the 2015 eruption which allows no significant pressure rise within the hydrothermal system. If so, the future volcanic unrests may not be accompanied by the significant increase in seismic activity and local uplift seen in 2015 near Owakudani, until the healing of the caprock.

©2021. Japan Geoscience Union. All Right Reserved.

Temperature profile beneath Owakudani can be constrained from the mineral assemblage of bore hole samples and the bottoming of seismicity. Assuming the temperature profile and isoenthalpy of pore water through the hydrothermal system, vapor static pore pressure beneath the bottom of the caprock can be inferred. In a liquid-dominated system, unload of surface deposit can cause explosion of hydrothermal water near the boiling temperature just beneath the surface and eject surrounding material. This ejection causes further unload and explosion progresses downward (8). The fact that the 2015 eruption resulted in a very small magnitude with the explosion source only around 100 m deep may be attributed to the pressure profile described above. In addition, paucity of volcanic tremors and low-frequency earthquakes at Hakone volcano can be attributed to the vapor dominated hydrothermal system.

Assuming healing of caprock in progress and the steam-dominated hydrothermal system, risk of phreatic eruption near Owakudani may be low at present, and phreatic eruption larger than that of 2015 can be highly unlikely. On the other hand, since the deep inflation has continued even after the eruption, magmatic fluid can accumulate in deep and its release may cause major phreatic eruption in future as observed at Ontake volcano.

1. Mannen et al. Earth, Planets Sp. 70, 68 (2018).

2. Abe et al. Bull. Hot Springs. Res. Inst. 50, 1–18 (2018). (in Japanese)

3. Mannen et al. Earth, Planets Sp. in review

4. Yoshimura et al. Earth, Planets Sp. 70, 66 (2018).

5. Yukutake, Y. et al. J. Geophys. Res. Solid Earth 116, 1–13 (2011).

6. Doke et al. Earth, Planets Sp. 70, (2018).

7. Kobayashiet al. Earth Planet. Sci. Lett. 491, 244–254 (2018).

8. Browne and Lowless Earth-Sci. Rev. 52, 229-331 (2001)

Keywords: Hakone volcano, hydrothermal system, volcanic unrest, phreatic eruption, pore pressure, caprock

©2021. Japan Geoscience Union. All Right Reserved.

Structure of the shallow hydrothermal system in Hakone volcano inferred from InSAR analysis

*Ryosuke Doke[1], Kazutaka Mannen[1], Kazuhiro Itadera[1]

1. Hot Springs Research Institute of Kanagawa Prefecture

During the 2015 unrest at Hakone volcano, satellite-based SAR observations captured surface deformation before, during, and after the phreatic eruption. Moreover, recent magnetotelluric surveys reveal the subsurface resistivity structure of the volcano. In this presentation, we introduce the surface displacement, which was considered to be related to activities of hydrothermal fluids, detected by InSAR analysis and these models. Furthermore, we will discuss the structure of the shallow hydrothermal system of Hakone volcano.

1. Surface Displacement at the Owakudani Fumarole Area during the 2015 Unrest

During the 2015 unrest, an abnormal blowout occurred at a steam production well (473 m deep) in Owakudani from May 3, and ALOS-2/PALSAR-2 repeatedly observed very local uplift (~200 m diameter) at Owakudani (Kobayashi et al., 2018; Doke et al. 2018). This surface displacement is explained by a Mogi source at an elevation of about 900 m (about 100 m deep). A magnetotelluric survey also confirms the existence of a small resistive body, which was interpreted as a vapor pocket locating almost at the Mogi source (Mannen et al., 2019).

2. Surface Displacement during the 2015 Phreatic Eruption and Intrusion of Fluid Crack

Observation of ALOS-2/PALSAR-2 before and after the phreatic eruption at Owakudani from June 29 to July 1, 2015, detected a surface displacement in an area about 1 km southeast of Owakudani (Doke et al., 2018). This displacement was explained by an NW-SE-trending crack opening and closing of a sill beneath the crack. The estimated crack location corresponds to a pre-existing fissure vent, suggesting that the crack was opened using the pre-existing structure. Moreover, a crater, which was considered the eruption center of a phreatic eruption that occurred in the past (Kobayashi et al., 2006; Kobayashi, 2008), is located on the estimated crack, and the opening of the crack is thought to have caused repeated phreatic eruptions. In the central cone of Hakone volcano, several crater chains with NW-SE strikes are distributed, suggesting the existence of similar cracks beneath the crater chains.

3. Surface Displacement during 2006-2011 by ALOS/PALSAR

The InSAR time series analysis (SBAS method) of ALOS/PALSAR showed steady subsidence on the west side of Owakudani (Doke et al., 2020), with a subsidence rate of 25 mm/yr estimated from the results of 2.5D analysis. This subsidence is explained by the contraction of a Mogi source at an elevation of 700 m (depth of 300 m), with about 10,000 m^3/yr. The existence of such contraction suggests that there is a similar vapor pocket to the 2015 unrest, although they differ in depth and behavior.

These results suggest that the hydrothermal system in the shallow part of Hakone volcano is characterized by plural NW-SE to WNW-ESE striking crack-like fluid supply paths and pocket-like fluid reservoirs distributed at depths of several hundred meters.

Acknowledgments

ALOS/PALSAR and ALOS-2/PALSAR-2 data were provided by JAXA via the Coordinating Committee for the Prediction of Volcanic Eruption as part of the project, “ALOS Domestic Demonstration on Disaster

©2021. Japan Geoscience Union. All Right Reserved.

Management Application," of the Volcano Working Group. The original ALOS/PALSAR data belong to JAXA and METI, and the original ALOS-2/PALSAR-2 data belong to JAXA.

Reference

Doke et al. (2018) *Earth, Planets and Space*, **70**, 63.
Doke et al. (2020) *Remote Sensing*, **12**, 2842.
Kobayashi (2008) *Research report of the Kanagawa Prefectural* Museum. Natural history, **13**, 43-60.
Kobayashi et al. (2006) *Bulletin of the Volcanological Society of Japan*, **51**, 245-256.
Kobayashi et al. (2018) *Earth and Planetary Science Letters*, **491**, 244-254.
Mannen et al. (2019) *Earth, Planets and Space*, **71**, 135.

Keywords: Hakone volcano, hydrothermal system, phreatic eruption, InSAR, surface displacement

©2021. Japan Geoscience Union. All Right Reserved.

Ground deformations at Kuju volcano, Japan, revealed by PALSAR-2 InSAR

*Shohei Narita[1], Takahiro Ohkura[1]

1. Aso Volcanological Laboratory, Institute for Geothermal Science, Graduate School of Science, Kyoto University

Kuju volcano is located in the western part of Oita prefecture in Kyushu Island, Japan. The latest eruption occurred in 1995 at Iwoyama, which is the most active area in Kuju volcano and has numerous active fumarolic vents. Post-eruptive ground deflation accompanying significant heat discharge started immediately after the eruption (Nakaboh et al., 2003), and continued until, at least, 2002 (Saito et al., 2003). From 2012, a continuous GNSS observation network installed in 2001 by Japan Metrological Agency (JMA), has recorded increases in the baseline length indicating ground inflation, which suggests a possibility of on-going magma intrusion or fluid migration into a shallow part of Kuju volcano.

To clarify the spatiotemporal evolution of this deformation in more detail, we analyzed PALSAR-2 data, which is L-band Interferometric Synthetic Aperture Radar (InSAR), operated by Japan Aerospace Exploration Agency (JAXA). We used two-track data; right-looking ascending and right-looking descending orbits, acquired from August 2014 to November 2019. We performed SAR interferometry using RINC software (Ozawa et al., 2016) and time series analysis using SBAS (Small Baseline Subset; Berardino et al., 2002) method implemented with GIAnT software (Agram et al., 2013).

SBAS results of both tracks show spatial patterns indicating ground deflation in Iwoyama and geothermal power plants of Hattyobaru and Otake (hereafter, Hattyobaru and Otake), which are located on the west side of Kuju volcano. The spatial extent of the deformation is less than 1 km at Iwoyama, while it is about 4 km in Hattyobaru and Otake. Quasi-eastward and vertical deformation maps show different spatial characteristics. At Iwoyama, there is a rather incomprehensible pattern; a combination of subsidence (1.4 cm/yr) and only eastward displacement (1.4 cm/yr), which is not likely to be modeled by only a simple deflation source. On the other hand, in Hattyobaru and Otake, a simple pattern indicating ground deflation can be recognized, and the maximum subsidence velocity is about 1.2 cm/yr at Hattyobaru and 0.4 cm/yr at Otake. These deformation characteristics are consistent with those of ALOS-derived deformation around Hattyobaru and Otake during 2007-2010 (Ishitsuka et al., 2016), suggesting that a common deflation source, such as the deflated geothermal reservoir just beneath Hattyobaru at 750-m depth (Nishijima et al., 2005), has consistently caused the deformation during 2007-2019.

Source modeling for the deformation at Iwoyama shows that a combination of a spherical deflation source and a right strike-slip fault with slight normal faulting better fits the observed deformation than only a single deflation source. The deflation source during 2014-2019, of which depth is 200-300 m, is clearly shallower than the deflation source during 1995-2002 at a depth of 500-600 m. On the other hand, the 2014-2019 deflation source is probably overlapped with the position of a demagnetized source from 2014, suggesting coeval progress of deflation and demagnetization. The combination of deflation and demagnetization is an unusual phenomenon because, in other volcanoes, only cases of coeval inflation-demagnetization and deflation-magnetization have frequently been reported (Hashimoto et al., 2019).

The ground deflation of Iwoyama observed in this study is opposed to the deformation observed by the GNSS network, i.e. ground inflation. In addition, GNSS baseline lengths (4-5 km) are longer than the

©2021. Japan Geoscience Union. All Right Reserved.

spatial scale of the Iwoyama deformation (less than 1 km), which suggests the existence of a deeper inflation source. To disclose the real nature of the ground inflation observed from 2012, it is necessary to further investigate GNSS data; remove several non-volcanic factors, such as post-seismic deformation of the Kumamoto earthquake and subsidence of Hattyobaru and Otake geothermal power plants.

Keywords: Interferometric Synthetic Aperture Radar, Kuju volcano, volcanic deformation, Hattyobaru geothermal power plant

©2021. Japan Geoscience Union. All Right Reserved.

[J] Oral | S (Solid Earth Sciences)：S-VC Volcanology

Sun. Jun 6, 2021 3:30 PM - 5:00 PM JST | Sun. Jun 6, 2021 6:30 AM - 8:00 AM UTC | Ch.25 Zoom Room 25

[S-VC29] Hydrothermal systems of volcanoes

convener:Yasuhiro Fujimitsu(Department of Earth Resources Engineering, Faculty of Engineering, Kyushu University), Wataru Kanda(Volcanic Fluid Research Center, School of Science, Tokyo Institute of Technology), Takeshi Ohba(Department of chemistry, School of Science, Tokia University), Chairperson:Wataru Kanda(Volcanic Fluid Research Center, School of Science, Tokyo Institute of Technology), Yasuhiro Fujimitsu(Department of Earth Resources Engineering, Faculty of Engineering, Kyushu University)

There is a diversity of hydrothermal systems between magmas and the ground surface in various geoscientific environments. Understanding of the hydrothermal systems contributes to understanding of the earth systems, and is essential for utilization of geothermal energy and prediction of volcanic eruption. In this session, we will discuss the topics on subsurface structures and heat and fluid flows of "hydrothermal systems of volcanoes" from the perspectives of geophysics, geochemistry, geology and geothermal reservoir engineering. Any research approaches, theoretical, observational and experimental, are welcome.

3:30 PM - 3:45 PM JST | 6:30 AM - 6:45 AM UTC

[SVC29-07] The plumbing system of a Miyakejima volcano: insights into magmatic-hydrothermal interactions

*Marceau Gresse[1], Makoto Uyeshima[1], Takao Koyama[1], Hideaki Hase[2], Koki Aizawa[3], Yusuke Yamaya[4], Yuichi Morita[1], Derek Weller[1], Tawat Rung-Arunwan[5], Takayuki Kaneko[1], Yoichi Sasai[6], Jacques Zlotnicki[7], Tsuneo Ishido[8], Hideki Ueda[9], Maki Hata[1] (1.Earthquake Research Institute, The University of Tokyo, Tokyo, Japan, 2.Geothermal Energy Research & Development Co., Ltd., Tokyo, Japan, 3.Institute of Seismology and Volcanology, Faculty of Science, Kyushu University, Fukuoka, Japan, 4.National Institute of Advanced Industrial Science and Technology (AIST), Renewable Energy Research Center, Fukushima, Japan, 5.Curl-E Geophysics Co., Ltd., Thailand, 6.Earthquake Prediction Research Center, Tokai University, Shizuoka, Japan, 7.CNRS, EMSEV, OPGC-UMR6524, Aubière, France, 8.Geological Survey of Japan, National Institute of Advanced Industrial Science and Technology (AIST), Tsukuba, Japan, 9.National Research Institute for Earth Science and Disaster Resilience (NIED), Tsukuba, Japan)

3:45 PM - 4:00 PM JST | 6:45 AM - 7:00 AM UTC

[SVC29-08] Ability of the magnetotelluric method to image a deep conductor: Exploration of a supercritical geothermal system

*Keiichi Ishizu[1], Yasuo Ogawa[1], Toru Mogi[1], Yusuke Yamaya[2], Toshihiro Uchida[2] (1.Tokyo Institute of Technology, 2.National Institute of Advanced Industrial Science and Technology)

4:00 PM - 4:15 PM JST | 7:00 AM - 7:15 AM UTC

[SVC29-09] Analysis and interpretation of DAS-seismic results obtained at the Ohnuma geothermal field in the Hachimantai volcanic region, in Japan

*Junzo Kasahara[1,2], Yoko Hasada[1,3], Kuzume Haruyasu[1] (1.ENAA, 2.Shizuoka University, 3.Daiwa Exploration and Consulting Co. Ltd.)

4:15 PM - 4:30 PM JST | 7:15 AM - 7:30 AM UTC

[SVC29-10] Thermal property measurements by drilling cuttings obtained from a geothermal well in the Hachimantai area and thermal structure analysis

*Haruto Sugamoto[1], Kazuya Ishitsuka[1], Weiren Lin[1], Takemi Sakai[2] (1. Graduate School of Engineering, Kyoto University, 2.Geothermal Engineering Co., Ltd.)

4:30 PM - 4:45 PM JST | 7:30 AM - 7:45 AM UTC

[SVC29-11] Characteristics of eruption periodicity observed at Shikabe geyser and estimation of the factor of long term periodicity change

*Ayuta Tsuge[1], Hiroshi Aoyama[2] (1.Institute of Seismology and Volcanology, Graduate School of Sciences, Hokkaido University, 2.Institute of Seismology and Volcanology, Fuculty of Science, Hokkaido University)

4:45 PM - 5:00 PM JST | 7:45 AM - 8:00 AM UTC

[SVC29-12] Modeling of multidisciplinary observations during an inter-eruptive period by using a hydrothermal simulation with post-processors

*Ryo Tanaka[1], Takeshi Hashimoto[1], Shohei Narita[2] (1.Hokkaido University,Institute of Seismology and Volcanology, 2.Kyoto University, Graduate School of Science, Institute for Geothermal Sciences, Aso Volcanological Laboratory)

The plumbing system of a Miyakejima volcano: insights into magmatic-hydrothermal interactions

*Marceau Gresse[1], Makoto Uyeshima[1], Takao Koyama[1], Hideaki Hase[2], Koki Aizawa[3], Yusuke Yamaya[4], Yuichi Morita[1], Derek Weller[1], Tawat Rung-Arunwan[5], Takayuki Kaneko[1], Yoichi Sasai[6], Jacques Zlotnicki[7], Tsuneo Ishido[8], Hideki Ueda[9], Maki Hata[1]

1. Earthquake Research Institute, The University of Tokyo, Tokyo, Japan, 2. Geothermal Energy Research & Development Co., Ltd., Tokyo, Japan, 3. Institute of Seismology and Volcanology, Faculty of Science, Kyushu University, Fukuoka, Japan, 4. National Institute of Advanced Industrial Science and Technology (AIST), Renewable Energy Research Center, Fukushima, Japan, 5. Curl-E Geophysics Co., Ltd., Thailand, 6. Earthquake Prediction Research Center, Tokai University, Shizuoka, Japan, 7. CNRS, EMSEV, OPGC-UMR6524, Aubière, France, 8. Geological Survey of Japan, National Institute of Advanced Industrial Science and Technology (AIST), Tsukuba, Japan, 9. National Research Institute for Earth Science and Disaster Resilience (NIED), Tsukuba, Japan

Phreatic and phreatomagmatic eruptions are difficult to predict with accuracy on volcanoes due to complex interactions at depth between heat, water, and magmatic fluids. To better understand such multifaceted interactions, we present here a multidisciplinary geophysical approach performed on Miyakejima, a 10-km wide stratovolcano in the Izu Bonin arc. Its plumbing system was highlighted by combining four geophysical methods: magnetotellurics, seismicity (hypocenters), self-potential, and thermal image (remote sensing). We thus propose the first large-scale interpretation of the volcanic structure in terms of rock properties, temperature, fluid content, and fluid flow. Our findings indicate that hot volatiles released from a *deep* magmatic reservoir (> 350 ˚C, 2.5–4.5 km depth) rise through a narrow permeable path, interact with the conductive hydrothermal system beneath the 2000 A.D. caldera (<250 ˚C, 0–2 km depth). This mixture of fluid is finally released in the fumarolic area in the southern part of the caldera at 181˚C. This combined approach allow us to: 1) delineate the water table of the volcano (300–700 m depth), 2) determine the general fluid flow circulation beneath the island, 3) characterize seismic signatures of long-period and volcano-tectonic events, and 4) elucidate the origin of the high water content of fumaroles developed since the last eruption in A.D. 2000.

Keywords: hydrothermal system, magnetotellurics, electrical resistivity, seismicity, self-potential, remote-sensing

©2021. Japan Geoscience Union. All Right Reserved.

Ability of the magnetotelluric method to image a deep conductor: Exploration of a supercritical geothermal system

*Keiichi Ishizu[1], Yasuo Ogawa[1], Toru Mogi[1], Yusuke Yamaya[2], Toshihiro Uchida[2]

1. Tokyo Institute of Technology, 2. National Institute of Advanced Industrial Science and Technology

Fluids trapped under supercritical conditions are attractive unconventional geothermal resources that can yield much higher well-productivity. The magnetotelluric (MT) method can image supercritical fluids as deep conductors. However, MT imaging of a deep conductor strongly depends on the conductor geometries and overlying clay layers. The MT ability to image a deep conductor should be clarified to understand the MT usefulness for exploring supercritical fluids and correctly relate the imaged conductor to supercritical fluids. Therefore, this study investigated the MT ability to image a deep conductor of supercritical fluids using numerical tests. The numerical tests used a conceptual resistivity model of a promising supercritical geothermal system in the Kakkonda area, northeast Japan. The test results prove that the MT method is useful for revealing the deep conductor of promising supercritical fluids. The results also showed that the MT ability to image deep conductors strongly depends on the size and depth of the target conductor and the thickness of overlying clay layers. The findings from the test results help to relate deep conductors imaged by the MT method to supercritical geothermal systems.

Keywords: Resistivity, Electromagnetic survey, Geothermal energy, supercritical geothermal system, Kakkonda

©2021. Japan Geoscience Union. All Right Reserved.

Analysis and interpretation of DAS-seismic results obtained at the Ohnuma geothermal field in the Hachimantai volcanic region, in Japan

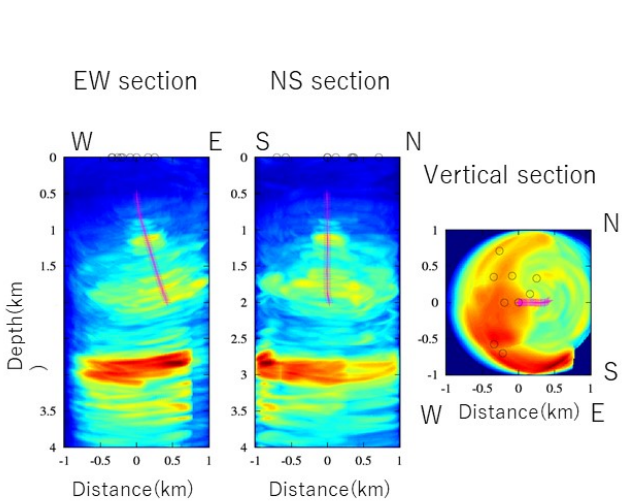
*Junzo Kasahara[1,2], Yoko Hasada[1,3], Kuzume Haruyasu[1]

1. ENAA, 2. Shizuoka University, 3. Daiwa Exploration and Consulting Co. Ltd.

We report seismic data analysis and preliminary interpretation for the distributed acoustic sensor (DAS)-seismic survey obtained at Ohunuma geothermal field in 2020. The New Energy and Industrial Technology Development Organization (NEDO) in Japan has promoted the use of supercritical water for geothermal power generation under a project called Research and Development of Supercritical Geothermal Resources. In September, we carried out a seismic survey as a part of this NEDO project using the DAS-seismic method using an optical fiber system. We deployed the optical fiber in the O-13R geothermal borehole at the Ohnuma power plant owned by Mitsubishi Materials Corporation. The Ohnuma geothermal filed is in Hachimantai volcanic region in the north-eastern part of Japan. We used a middle size active source at nine locations for the survey. In Ohnuma geothermal borehole, the optical fiber extended to 2,037 m-long along the borehole casing (vertical depth = c.a. 1,971 m). The DTS (distributed temperature sensor) temperature in the borehole obtained by the same optical fiber was 235 degree C at around 1,100m-depth. To enhance the signal to noise ratio (S/N) we applied the stacking of the DAS records by 480 times after the removal of outliners and source signature compensation. We separated the DAS records to down-going phases (direct arrivals) and up-going phases (reflected arrivals). We migrated the upgoing arrivals and made a composite migrated image of nine source locations in 3-D space (Fig. 1). We recognized several distinct reflection arrivals. The reflections occur at around 1.1 km, 1.5 km, 2 km and 2.8-3.0 km-depths. The amplitudes of reflected PP arrivals from the 2.8-3.0 km-depth is half of amplitude of direct P arrivals at C8 source location (~700 m distance in the south of O-13R wellhead). The depth of 1.1 km corresponds to the lithological boundary of the dacite welded tuff and the altered andesite, and the depth of 1.5 km does to another lithological boundary of the altered andesite and the silicious shale. The depth of the geothermal production of Ohnuma geothermal power plan is between approximately 1,200 m and 1,700 m depths. The migrated images have similarities to this production zone. We correlated fracture zones obtained by the drilling and logging data of geothermal boreholes (unpublished data of Mitsubishi Materials Co.) and the DAS seismic data, and some of reflections occur around the fracture zones. Because all geothermal boreholes in the Ohnuma geothermal power plant is down to 2,100 m, the distinct reflections from 2.8-3.0 km depth is not resolved by the lithological data of boreholes. One of interpretations for the reflections from the 2.8-3.0 km-depth is presence of hot fluids in fractures of granitic intrusive rock like Sumikawa geothermal field.
Acknowledgements This study was supported by the New Energy and Industrial Technology Development Organization (NEDO). We greatly appreciate Mitsubishi Materials Corporation for their kind permission for fieldwork in their power plant.We also express our great thanks to Mr. Iwasaki and his colleagues of Mitsubishi Materials Techno Corporation for their aggressive discussions.

Keywords: Geothermal exploration, supercritical water, DAS, seismic reflection, migration imaging, geothermal reservoir

©2021. Japan Geoscience Union. All Right Reserved.



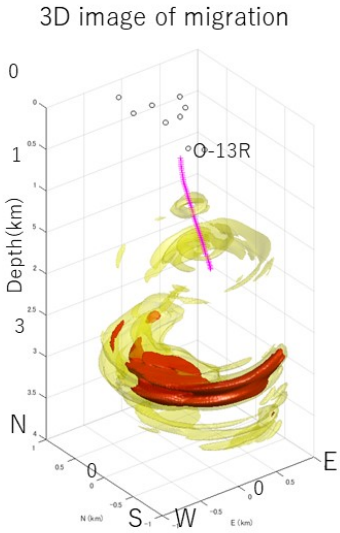


Fig. 1: Migrated image of reflection arrivals obtained by DAS-seismic survey in the O-13R geothermal borehole at the Ohnuma geothermal power plant

©2021. Japan Geoscience Union. All Right Reserved.

Thermal property measurements by drilling cuttings obtained from a geothermal well in the Hachimantai area and thermal structure analysis

*Haruto Sugamoto[1], Kazuya Ishitsuka[1], Weiren Lin[1], Takemi Sakai[2]

1. Graduate School of Engineering, Kyoto University, 2. Geothermal Engineering Co., Ltd.

It is important to identify the factors that influence the temperature depth profile of a well in order to investigate the presence of heat convection. Especially, the thermal conductivity of rocks of a well is a vital property for quantitatively analyzing temperature logs. In general, the thermal properties of rocks can be obtained by measuring core samples. However, rock cores are often not retrieved and only drilling cuttings are collected, thus thermal conductivity measurements of drilling cuttings are required. In this study, we measured the thermal conductivities by the drilling cuttings obtained in the N19-HA-1 well in the Hachimantai area, Japan, using a transient plane heat source method. We further estimated the core-equivalent thermal conductivities from the measurements of the drilling cuttings based on a thermal conduction mixing model, and the temperature profile was quantitatively examined from the viewpoint of heat conduction.

Firstly, to validate the method of estimating the core-equivalent thermal conductivity from the cuttings, we prepared cuttings by artificially grinding andesite cores in laboratory, and compared the thermal conductivities of the cuttings and the core sample. To select the best mixing model to convert measured thermal conductivity of cuttings to core-equivalent thermal conductivity, we tested five thermal conduction mixing models (i.e., arithmetic mean, harmonic mean, geometric mean, square root mean, and effective medium theory mean). After the validation, we applied the method to 18 cuttings samples of andesite and dacitic tuff in the Hachimantai area (5 samples from depth range of 120-220 m, 4 samples from 305-385 m, and 9 samples from 925-1165 m, respectively). The estimated core-equivalent thermal conductivities were used to examine the temperature log based on Fourier's law ($j = \lambda \, \mathrm{grad} T$, where j is the heat flux, λ is the thermal conductivity, and $\mathrm{grad} T$ is the temperature gradient). This analysis of temperature profile was performed under the assumption that the heat conduction is dominant in one dimension along the well and the heat flux is constant along the analyzed depth interval. In this analysis, the average thermal conductivity of each depth zone was obtained by taking the harmonic mean of the thermal conductivities at each depth, and the heat flux was calculated from the gradient of the temperature log data.

As a result of the validation using the andesite core and cuttings, we found that difference of the thermal conductivities between the core and cuttings was minimal (1.8%) when we applied the square root mean model. In conclusion of this validation, the core-equivalent thermal conductivity could be obtained using the square root mean model. We subsequently estimated the core-equivalent thermal conductivity from the cuttings samples in the Hachimantai area by using the square root mean model and calculated the conductive temperature profile using Fourier's law. The calculated temperature profile was then compared with the observed temperature log. As the result of this analysis, we found that the heat conduction is dominant between the 120-220 m depth range. In the case of the 305-385 m depth range, the measured temperature also agrees well with the estimated conductive profile especially below the depth of 330 m, indicating that the temperature pattern is determined mainly by heat conduction. In contrast, the temperature profile of some sections between 925 m and 1165 m could not be reproduced

©2021. Japan Geoscience Union. All Right Reserved.

from the present analysis. The fact that the temperature structure was not reproduced from the present analysis based on heat conduction may suggest the presence of heat convection in the depth intervals.

Keywords: Hachimantai area, Drilling cuttings, Thermal conductivity, Transient plane heat source method, Temperature profile

©2021. Japan Geoscience Union. All Right Reserved.

Characteristics of eruption periodicity observed at Shikabe geyser and estimation of the factor of long term periodicity change

*Ayuta Tsuge[1], Hiroshi Aoyama[2]

1. Institute of Seismology and Volcanology, Graduate School of Sciences, Hokkaido University, 2. Institute of Seismology and Volcanology, Fuculty of Science, Hokkaido University

The eruption periodicity of a geyser is not always regular but sometimes shows bimodal distribution or acts chaotically. Also, the eruption periodicity changes from short to long time scales. For example, the eruption periodicity at Old Faithful Geyser in Yellowstone National park was regular distribution in the 1800s, but gradually became bimodal distribution (Rinehart, 1969). Hurwitz *et al.* (2008) suggested that some geysers in Yellowstone National park may change their eruption periodicity due to the river discharge and precipitation. However, the mechanism of periodicity change has been discussed mainly statistically, so the physical parameters (hydraulic head, for example) controlling the eruption periodicity are not understood quantitatively.

In this study, we implemented observation at Shikabe geyser in southern Hokkaido to understand the mechanism of periodicity change of geyser, from November 26th, 2019 to February 24th, 2020 (first half) and from July 8th, 2020 to November 4th, 2020 (latter half). The intermittent cycle of the Shikabe geyser consists of the quiescence period—hot spring water does not discharge from the vent, the overflowing period—hot spring water overflows from the vent, and the eruption period. We measured the periodicity as the interval between the time of onset of overflow (IBO: Interval Between Overflow) from the temperature change of the Pt resistance thermometer attached at the vent. Then, we classified the periodicity into the quiescence time, overflowing time, and eruption time based on the acoustic pressure data which reflect onset and termination of eruption well, and investigated temporal change and the relative relationship of these times.

In the first half, IBO extended from approximately 12.5 min to 14.3 min, and the extending rate gradually decreased. We can find two distinctive modes of the periodicity: the stable mode distributing around the mean IBO, and the unstable mode fluctuating several minutes from the mean IBO. In particular, the unstable mode has a series of patterns in which once a long eruption occurs, the following quiescence time and the overflowing time are certainly extended, and the next quiescence time will be shortened. In the latter half, unlike the first half, the mean IBO decreased to approximately 11 min and changed to a double cycle. The quiescence time, overflowing time, and eruption time in the double cycle exhibit a pendulum-like behavior alternating back and forth around the mean IBO.

To understand the factor of the increase in mean IBO in the first half, we investigated the temporal change of the quiescence time, overflowing time and eruption time and found that the IBO extension is affected by the increase in both the quiescence time and overflowing time. Therefore, we made a hypothesis that the decrease in supply rate of the hot spring water to the geyser reservoir; the decrease in the hydraulic

©2021. Japan Geoscience Union. All Right Reserved.

head causes the decrease in mean IBO in the first half. We formulated the IBO change mathematically using the equation of water ascent in the well based on Darcy’ s law and calculated the hydraulic head change that explains the observed IBO change. As a result of the calculation, the IBO change in the first half can be explained by a decrease in the hydraulic head of about 0.7m. In the previous study, the pressure change in the aquifer was pointed out as one of the factors of periodicity change (Hurwitz *et al.*, 2008; Kiryukhin, 2016). The result of this study is quite significant in that the amount of change in aquifer pressure can be estimated from the model equation of the IBO.

The decrease in aquifer pressure suggested from the long-term IBO change may be affected locally by the increase in pumping at the nearby hot springs, or regionally by the decrease in aquifer pressure in the entire hot spring area or the seasonal changes. However, we only have data for about a year and have no information on nearby hot springs, so we have not yet been able to specifically distinguish these factors. Therefore, we should not only continue observing for several years, but also obtain information about the use of nearby hot springs and changes in the amount of spring discharge.

Keywords: geyser, eruption periodicity change

©2021. Japan Geoscience Union. All Right Reserved.

Modeling of multidisciplinary observations during an inter-eruptive period by using a hydrothermal simulation with post-processors

*Ryo Tanaka[1], Takeshi Hashimoto[1], Shohei Narita[2]

1. Hokkaido University,Institute of Seismology and Volcanology, 2. Kyoto University, Graduate School of Science, Institute for Geothermal Sciences, Aso Volcanological Laboratory

Recently, some volcanic unrest events in inter-eruptive periods have been observed with multidisciplinary monitoring (e.g. Tokachidake volcano, Kuchinoerabu-jima volcano, Kuju volcano). We focus on the simultaneous changes in ground deformation, total magnetic field, and thermal discharge rate, which are considered to be good indicators of subvolcanic hydrothermal activity. The ground deformation and total magnetic field mainly reflect the subsurface changes in pressure and temperature, respectively. Therefore, these observations are important to understand the activity of the hydrothermal system. In this study, we performed the simulation under several conditions to clarify the behavior of the hydrothermal system and the multidisciplinary observations by coupling the hydrothermal simulation with the post-processors which calculate a ground deformation and changes in the magnetic field.

The numerical simulation was carried out with the TOUGH2 geothermal simulator (Pruess et al. 1999). The calculation region was set axisymmetric 2D. A high permeability region (radius: 100 m, permeability: 1.0×10^{-12} m^2) was set near the symmetry axis to represent the fumarolic conduit. The rest of the calculation region represents the host rock and was set the permeability in two ways (1.0×10^{-14} m^2 and 5.0×10^{-15} m^2). For simplicity, the topography was assumed to be flat. In the subsequent simulations, the initial condition was obtained by simulating a constant injection of hydrothermal fluids (H_2O, 350 ºC, 1500 ton/day) from the bottom of the fumarolic conduit for 10k years, representing a quasi-steady state. After that, we imposed an elevated hydrothermal fluid input (3000 ton/day) from the bottom and/or a reduced permeability (1.0×10^{-14} m^2) at a particular depth in the middle of the conduit to monitor the subsequent changes.

The ground deformation was calculated by using the partial differential equation module of COMSOL Multiphysics (COMSOL, 2012). The ground deformation corresponding to changes in pressure and temperature was calculated following the extended Hooke’ s law (Jaeger et al., 2007), assuming the thermoporoelasticity. For the magnetic field changes, we take the thermomagnetic effect only and calculated the total magnetic field following the uniformly magnetized prism model (Bhattacharyya, 1964), where we assumed a temperature-dependence of the rock magnetization as 0.01 A/m/K. The heat discharge rate from the crater was calculated by summing up the heat discharge rate of the most upper cells of fumarolic conduit in the hydrothermal simulation.

When only an elevated injection rate was applied, the increase in the subsurface pressure and temperature resulted in the combination of inflation, demagnetizing field changes, and a larger heat discharge from the crater. In the case of a depleted permeability in the conduit, inflation, re-magnetizing field changes, and a reduced heat discharge was observed together. This combination was resulted from the simultaneous occurrence of cooling above the choked zone and pressurization below it. Subsequently, the cooled zone in the upper part of the conduit turned into heating and the continued pressurization below the choked point resulted in inflation, demagnetization, and recovery in the heat discharge.
As a next step, we will perform more calculations under various conditions to classify the simultaneous

©2021. Japan Geoscience Union. All Right Reserved.

changes in ground deformation, total magnetic field, and thermal activity, in which it is necessary to examine the effects of a caprock and topography. It enables us a direct comparison between hydrothermal simulations and field observations to better understand the behavior of a subvolcanic hydrothermal system during an inter-eruptive period.

This work was supported by MEXT “Integrated Program for Next Generation Volcano Research and Human Resource Development”.

Keywords: hydrothermal system, hydrothermal simulation, unrest event

©2021. Japan Geoscience Union. All Right Reserved.

[J] Poster | S (Solid Earth Sciences)：S-VC Volcanology

Sun. Jun 6, 2021 5:15 PM - 6:30 PM JST | Sun. Jun 6, 2021 8:15 AM - 9:30 AM UTC | Ch.13_2

[S-VC29] Hydrothermal systems of volcanoes

convener:Yasuhiro Fujimitsu(Department of Earth Resources Engineering, Faculty of Engineering, Kyushu University), Wataru Kanda(Volcanic Fluid Research Center, School of Science, Tokyo Institute of Technology), Takeshi Ohba(Department of chemistry, School of Science, Tokia University)

There is a diversity of hydrothermal systems between magmas and the ground surface in various geoscientific environments. Understanding of the hydrothermal systems contributes to understanding of the earth systems, and is essential for utilization of geothermal energy and prediction of volcanic eruption. In this session, we will discuss the topics on subsurface structures and heat and fluid flows of "hydrothermal systems of volcanoes" from the perspectives of geophysics, geochemistry, geology and geothermal reservoir engineering. Any research approaches, theoretical, observational and experimental, are welcome.

[SVC29-P01] Groundwater composition around the Aso caldera: multivariate statistical analysis and its implications for independent variables and geographical variations

*Hikaru Iwamori[1], Hitomi Nakamura[2], Noritoshi Morikawa[2], Masaaki Takahashi[2], Akihiko Inamura[2], Satoru Haraguchi[1], Tatsuji Nishizawa[3], Shuhei Sakata[1] (1.Earthquake Research Institute, The University of Tokyo, 2.AIST, 3.TITECH)

[SVC29-P02] Temporal variation of chemical composition of hot spring waters at Ebinokogen Ioyama Volcano in Kirishima Volcanic Group

*Keigo Mori[1], Jun-ichiro Ishibashi[1], Takeshi Matsushima[1], Harue Masuda[2], Syogo Oshima[3], Saki Tsutsumi[3], Yasuhisa Tajima[4] (1.Graduate School of Science, Kyushu University, 2.Graduate school of Science, Osaka City University, 3.West Japan Engineering Consultants, Inc,, 4.Nippon Koei Co., Ltd,)

[SVC29-P03] Temporal variations of helium and carbon isotopic compositions of fumarolic gases from Kusatsu-Shirane volcano

*Tomoya Obase[1], Hirochika Sumino[1], Kotaro Toyama[1], Takeshi Ohba[2], Muga Yaguchi[3], Akihiko Terada[4] (1.Department of General Systems Studies, Graduate School of Arts and Sciences, University of Tokyo, 2.Department of chemistry, School of Science, Tokai University, 3.Meteorological Research Institute, Japan Meteorological Agency, 4.Volcanic Fluid Research Center, Tokyo Institute of Technology)

[SVC29-P04] Change in fluoride ion concentration in Bandaiko hot spring at east flank of Kusatsu-Shirane volcano and its relationship with volcanic activity

*Haruka Yamamoto[1], Yoshikazu Kikawada[2] (1.Graduate School of Sophia University, 2.Faculty of Science and Technology, Sophia University)

[SVC29-P05] Volcanic ash from the June 17, 1962 eruption of Yakedake volcano, and its water-soluble components

*Muga Yaguchi[1], Yasuo Hirayama[2], Takeshi Ohba[3], Nozomi Numanami[3] (1.Meteorological Research Institute, JMA, 2.Nagano Meteorological Office, JMA, 3.School of Science, Tokai University)

[SVC29-P06] Tectonic controlled and hydrothermal alterations of geothermal reservoirs in El Salvador

*JOSE ANIBAL ERAZO[1], Noriyoshi Tsuchiya[1], Masaoki Uno[1], Arturo Quezada[2], Pedro Antonio Santos[2], Ryoichi Yamada[1], Hiroyuki Yamagishi[1], Shinichi Yamasaki[1], Alvaro Josue Amaya[3] (1.Graduate school of environmental studies , 2.LaGeO _ El Salvador, 3.UES _ El Salvador)

[SVC29-P07] DAS-Seismic and temperature data acquisition using DAS and DTS measurements at the Ohnuma, geothermal field, Tohoku, Japan

*Junzo Kasahara[1,2], Yoko Hasada[1,3], Kuzume Haruyasu[1], Hitoshi Mikada[4], Yoshihiro Fujise[5] (1.ENAA, 2.Shizuoka University, 3.Daiwa Exploration and Consulting Co. Ltd., 4.Graduate School of Kyoto University, 5.WELMA)

[SVC29-P08] **Ground surface Heat balance measurements at Izu-Oshima volcano**

*Shin'ya Onizawa[1], Nobuo Matsushima[2] (1.Volcanology Research Department, Meteorological Research Institute, JMA, 2.Geological Survey of Japan, National Institute of Advanced Industrial Science and Technology)

[SVC29-P09] Behavior of magmatic hydrothermal system of Kusatsu-Shirane Volcano inferred from numerical simulations

*Yasuo Matsunaga[1], Wataru Kanda[1] (1.School of Science, Tokyo Institute of Technology)

[SVC29-P10] Comprehension of hydrothermal systems in the East African Rift System –Collaborative Research with Kenya by SATREPS–

*Yasuhiro Fujimitsu[1], Jun Nishijima[1], Takeshi Tsuji[1], Kotaro Yonezu[1], Tatsuya Wakeyama[2], Ryuichi Itoi[3] (1.Department of Earth Resources Engineering, Faculty of Engineering, Kyushu University, 2.Platform of Inter-/Transdisciplinary Energy Research, Kyushu University, 3.School of Engineering, Kyushu University)

Groundwater composition around the Aso caldera: multivariate statistical analysis and its implications for independent variables and geographical variations

*Hikaru Iwamori[1], Hitomi Nakamura[2], Noritoshi Morikawa[2], Masaaki Takahashi[2], Akihiko Inamura[2], Satoru Haraguchi[1], Tatsuji Nishizawa[3], Shuhei Sakata[1]

1. Earthquake Research Institute, The University of Tokyo, 2. AIST, 3. TITECH

The compositional variability of groundwater (including hot/mineral spring waters) reflects the origin and circulation processes of groundwater, such as fluid sources, fluid-rock reactions, flow rates and residence times; e.g., identification of fluid sources by hydrogen-oxygen isotope ratio (Matsubaya et al., 1973), reaction with bedrock by Sr isotope ratio (Notsu et al., 1991), and evaluation of residence time of deep-seated fluid based on helium isotope ratio (Morikawa et al., 2005). By integrating these analyses, it is possible to forward our understanding of the origins of fluid and the circulation processes more comprehensively. Kusuda et al. (2014) integrated the geochemical data of the Arima spring waters with the dehydration simulation of the subducting plate to infer that the Arima-type brine is originated from the subducted Philippine Sea plate. Nakamura et al. (2016) and Iwamori et al. (2020) discussed the origin of Arima-type brine in the Arima-Kii Peninsula to be rooted from the subducting plate and geochemical processes during ascent to the surface, based on multivariate statistical analysis of the spring water compositions, including rare earth elements.

In this study, the existing composition data set of groundwater (Takahashi et al., 2018) is used to identify the geochemical sources and processes recorded in the groundwater composition over the area of about 120 km east-west and 80 km north-south surrounding the Aso caldera in central Kyushu. In particular, we aim to distinguish the volcanic and deep-seated fluid components from those related to meteoric water circulation, and ultimately to understand (1) fluid processes associated with magmatic activity under the Aso caldera, and (2) active tectonics and the large-scale fluid circulation from the subducting plate to the surface, including magmatism in central Kyushu.

As a pilot study for this purpose, in this presentation, we examine whether information on independent sources and processes can be extracted from the high-dimensional composition data set (590 samples containing 12 major dissolved elements of Na, K, Mg, Ca, Li, Cl, SO_4, HCO_3, F, NO_3, Br, and total C), based on multivariate statistical analyses. The statistical methods used were "whitened-data based k-means cluster analysis (KCA)" and "independent component analysis (ICA)" (Iwamori et al., 2017). Principal component analysis (PCA), a standard multivariate analysis, can extract information for independent sources and processes only if the data show a (joint) normal distribution. For data showing a non-normal distribution, the above KCA and ICA should be used. The data set used in this study shows clear non-normality, for which KCA and ICA are suitable. Based on the eigenvalue analysis of the data, we set the number of clusters and independent components to eight and attempted to detect statistically independent features in their compositional and geographical spaces.

As a result, a concentric spatial structure (distinguished with the 8 clusters) was found both in the Aso caldera and in the wide area surrounding the Aso volcano, with a broad decrease in the concentrations of Na, Li, Cl, HCO_3, Br, total C toward the outside. Even when focusing only on the inside of caldera, four clusters were mainly distributed concentrically, and two of them were distributed so as to surround basalt

©2021. Japan Geoscience Union. All Right Reserved.

and felsic rock bodies and lava. Except for the Aso caldera, the two clusters occur characteristically in the Kuju volcano centered around Mt. Kuju, which suggests that the two clusters are of magmatic origins.

The distribution and compositional characteristics of these clusters suggest that KCA and ICA are useful for the detection and identification of independent sources and processes involved in the origin of groundwater, especially the magmatic components. In the future, we plan to characterize the individual clusters with more elements and isotopic compositions, and to apply this statistical approach to other volcanic areas. This research was partly supported by JSPS KAKENHI Grant Numbers JP18H03747, JPJSBP120204804, JP17KK0018, JPJSBP120194830, and the Nuclear Regulation Authority "Research on Knowledge Development of Giant Eruption Processes, FY 2020".

Keywords: groundwater, composition, volcano, deep-seated fluid, statistical analysis

©2021. Japan Geoscience Union. All Right Reserved.

Temporal variation of chemical composition of hot spring waters at Ebinokogen Ioyama Volcano in Kirishima Volcanic Group

*Keigo Mori[1], Jun-ichiro Ishibashi[1], Takeshi Matsushima[1], Harue Masuda[2], Syogo Oshima[3], Saki Tsutsumi[3], Yasuhisa Tajima[4]

1. Graduate School of Science, Kyushu University, 2. Graduate school of Science, Osaka City University, 3. West Japan Engineering Consultants, Inc,, 4. Nippon Koei Co., Ltd,

Vigorous emanation of hot spring waters and fumarolic gases has been observed at Ebinokogen Ioyama Volcano, since the eruption in April 2018. We have conducted periodic sampling of hot waters emanating from the craters and fumarolic vents since July, 2018, and monitored temporal variation of their chemical composition which could be related to magmatic and hydrothermal activities. We report temporal variation of major cation compositions as well as anion compositions, to discuss factors which control fluid chemistry. Water samples were collected from W4 hot spring formed at the eruption crater located about 500 meters west from the Iwoyama crater, Y2a and Y2b hot springs formed at the eruption crater 50 meters south from the Iwoyama crater, and small fumarolic vents located in the area between them (Tajima et al., 2020). During the fluid sampling, water temperature, pH, ORP (oxidation-reduction potential) and EC (electrical conductivity) were measured on site using probes. Chemical composition of major cations (Na, K, Mg, Ca) and Si of the spring waters was determined by ICP-OES (inductivity coupled plasma optical emission spectrometry) and that of major anions (Cl, SO_4) was determined by IC (ion chromatography).

Long-term variation of major cations for two and half years duration basically follows the trend observed in that of major anions (such as Cl/SO_4 ratio). The most drastic change in W4 hot spring water chemistry was recognized at the early winter at year 2020; concentrations of major cations were high till Dec. 2019, while they significantly decreased since Feb. 2020. To characterize behavior of each cation, the observed concentration in the W4 hot spring water (defined as Ci) is compared with the concentration expected from complete dissolution of andesite from Ioyama by interaction with the acidic hot spring water (defined as Di), following the model proposed in Ohba et al. (2008). For Na and Mn, Ci was extremely high compared with Di in the duration till Dec. 2019, but Ci was decreased to comparable with Di after Feb. 2020. For Ca and Si, Ci was usually low compared with Di. For K, Ci was lower than Di till Dec. 2019, but Ci was higher than Di after Feb. 2020. These temporal variations are attributed to a shift of cation sources for W4 hot spring. After Feb. 2020, the cation composition can be explained by complete dissolution of andesite interaction with the acidic water and removal of some cations by formation of secondary minerals such as alunite. Whereas, the cation composition is likely to be dominantly controlled by other source till Dec. 2019, and hydrothermal aquifer had been developed beneath the volcano is presumed as the possible source. We discuss this model in detail from data of temporal variation of minor cations (Li, Rb, Cs) composition.

Keywords: fluid rock interaction, monitoring of time series change

©2021. Japan Geoscience Union. All Right Reserved.

Temporal variations of helium and carbon isotopic compositions of fumarolic gases from Kusatsu-Shirane volcano

*Tomoya Obase[1], Hirochika Sumino[1], Kotaro Toyama[1], Takeshi Ohba[2], Muga Yaguchi[3], Akihiko Terada[4]

1. Department of General Systems Studies, Graduate School of Arts and Sciences, University of Tokyo, 2. Department of chemistry, School of Science, Tokai University, 3. Meteorological Research Institute, Japan Meteorological Agency, 4. Volcanic Fluid Research Center, Tokyo Institute of Technology

Kusatsu-Shirane is an active stratovolcano consists of three pyroclastic cones, Mt. Shirane, Mt. Ainomine, and Mt. Motoshirane. A phreatic eruption occurred on 23 January 2018 at Mt. Motoshirane. Phreatic eruptions often occur without precursor geophysical signals, but chemical and isotopic compositions of volcanic gases may reflect some precursor events such as pressure rise at a gas reservoir. Helium ($^3He/^4He$) and carbon ($\delta^{13}C = (^{13}C/^{12}C)_{gas}/(^{13}C/^{12}C)_{PDB} - 1$) isotopic ratios are potential tracers of volcanic activity as they exhibit unique values corresponding to the origins. For example, $^3He/^4He$ ratios are ~8 Ra in the mantle (1 Ra equals to the atmospheric $^3He/^4He$) and <0.1 Ra in the crust, and $\delta^{13}C$ values are -6.5±2.5‰ in the mantle and <-20‰ for organic carbon. Pre-eruptive $^3He/^4He$ rises have been reported in some volcanoes, suggesting increase in magmatic He supply preceding the eruptions [e.g., 1]. Here we report $^3He/^4He$, $\delta^{13}C\text{-}CO_2$, and $^3He/CO_2$ of volcanic gases from five fumaroles at Kusatsu-Shirane volcano sampled from 2014 to 2020.

The $^3He/^4He$ ratios (corrected for atmospheric He contamination by $^4He/^{20}Ne$) of three Kitagawa fumaroles on the northern flank of Mt. Shirane roughly synchronized each other and temporally varied in the range of 7.1 to 8.1 Ra, suggesting that magmatic He supply changed during the sampling period. The temporal variations of $\delta^{13}C\text{-}CO_2$ values (-4.9 –-1.4‰) were inversely correlated to $^3He/^4He$, indicating low $\delta^{13}C\text{-}CO_2$ during high magmatic gas supply. On the other hand, the $\delta^{13}C$ values of the Sesshogawara and Manza fumaroles (located the east and west of Kusatsu-Shirane volcano, respectively) varied in the ranges of -4.5 –-0.8‰ and -3.7 –-0.5‰, respectively, were not correlated with each $^3He/^4He$ ratio.

The $^3He/CO_2$ ratios of Kitagawa fumaroles ($(0.3 – 2.0) \times 10^{-9}$) negatively correlated with $\delta^{13}C\text{-}CO_2$, indicating high $^3He/CO_2$ ratios in the periods of high magmatic gas supply. A trend for Manza fumarole is completely different that the $^3He/CO_2$ ratios show less variation ($(0.3 – 0.5) \times 10^{-9}$) that positively correlate with $\delta^{13}C\text{-}CO_2$. The $^3He/CO_2$ ratios of Sesshogawara fumarole ($(0.3 – 0.7) \times 10^{-9}$) were slightly higher than those of Manza fumarole and do not correlate with $\delta^{13}C\text{-}CO_2$. The $^3He/CO_2$ ratios of Sesshogawara and Manza fumaroles with high $\delta^{13}C\text{-}CO_2$ values were similar to the $^3He/CO_2$ ratios of Kitagawa fumaroles in the periods of low magmatic gas supply.

These trends can be explained by a mixing of two gas components with organic CO_2. One is the magmatic gas with high $^3He/CO_2$ and low $\delta^{13}C\text{-}CO_2$ values directly degassed from the magma. The other is probably the gas separated from hydrothermal fluids with low $^3He/CO_2$ and high $\delta^{13}C\text{-}CO_2$ values produced by addition of the crustal CO_2 with a high $\delta^{13}C$ value (~1.1‰ around Kusatsu-Shirane volcano [2]) to the magmatic gas. This model suggests that both magmatic and hydrothermal gases contribute to the fumarolic gases of Kitagawa. The Manza fumarole is fed by the hydrothermal fluid only, resulting in the small temporal variation of $^3He/CO_2$ ratios. The positive correlation between the $^3He/CO_2$ and $\delta^{13}C\text{-}CO_2$ values is attributable to the addition of the organic CO_2 to various extents. The Sesshogawara fumarole is mainly fed by the hydrothermal fluid with small contributions of the magmatic gas and organic CO_2.

©2021. Japan Geoscience Union. All Right Reserved.

The presence of a hydrothermal fluid reservoir at depths of 1-3 km broadly extending from beneath Mt. Shirane to Mt. Motoshirane was suggested by magnetotelluric investigation [3]. If the reservoir supplies fluids to the Sesshogawara and Manza fumaroles, the episodic drop of $^{3}He/^{4}He$ ratios following the 2018 phreatic eruption at Mt. Motoshirane [4] might be attributable to a decrease in the supply of fluids that carry magmatic He to both fumaroles, resulting in crustal He more apparent.

References

[1] Padrón et al. (2013) Geology. [2] Sano et al. (1994) Appl. Geochem. [3] Matsunaga et al. (2020) J. Volcanol. Geotherm. Res. [4] Sumino et al. JpGU2020.

Keywords: helium isotope, carbon isotope, volcanic gas, Kusatsu-Shirane volcano, temporal variation, hydrothermal system

©2021. Japan Geoscience Union. All Right Reserved.

Change in fluoride ion concentration in Bandaiko hot spring at east flank of Kusatsu-Shirane volcano and its relationship with volcanic activity

*Haruka Yamamoto[1], Yoshikazu Kikawada[2]

1. Graduate School of Sophia University, 2. Faculty of Science and Technology, Sophia University

In a phreatic eruption, apparent seismic activity and crustal movements that can be regarded as precursors of eruption may not be observed. Therefore, for volcanoes with extensive hydrothermal activity, geochemical observations on fumaroles and hot springs are important in addition to geophysical observations. Chloride ions and fluoride ions derived from HCl and HF in volcanic gas are dissolved into active crater lakes and volcanic hot spring water. Their dissolved concentrations and concentration ratios are often used as indicators of volcanic activity. In particular, HF reacts readily with rocks mainly composed of silicates and is easily incorporated into rocks. Thus, an increase in the concentration of fluoride ions in volcanic geothermal water can be a more remarkable indicator of volcanic activity than that of chloride ions.

On the other hand, due to fluoride ions' strong complex-forming ability, direct determination by using an ion chromatography or an ion-selective electrode may give erroneous results. Therefore, in volcanic geothermal water containing a high concentration of metal ions complex with fluoride ions, it is essential to isolate fluoride ions by distillation prior to the determination of fluoride ions. For example, a trimethylsilylating distillation method is known.[1)] However, since the distillation operation is troublesome and time-consuming, the determination of fluoride ions is often omitted. In this study, we investigated a simple method that directly determines fluoride ions with an ion-selective electrode without distillation by using a specific total ionic strength adjustment buffer and confirmed its precision and accuracy. After that, we applied the simple method to the water of Yugama, the crater lake of the Kusatsu-Shirane volcano, and the water of Bandaiko hot spring located on the eastern flank of the volcano stored in our laboratory, and reconstructed the time-series data of the fluoride ion concentrations over the past decades. Subsequently, we discussed the relationship between the fluoride ion concentrations and the activity of the Kusatsu-Shirane volcano.

The Kusatsu-Shirane volcano consists of three pyroclastic cones, Mt. Shirane, Mt. Moto-Shirane, and Mt. Ainomine. In January 2018, a phreatic eruption occurred at Mt. Moto-Shirane. The fluoride ion concentration of Bandaiko located on the eastern flank of Mt. Moto-Shirane gradually increased from 2012 to 2017, then increased significantly coincidently with the eruption at Mt. Moto-Shirane. After that, fluoride ion still maintains high concentration until 2020, while a small fluctuation in the concentration has been observed. In the case of chloride ion, which is also halide ion, a gradual increase in the concentration was observed from 2012 to 2017 as same as fluoride ion concentration. However, unlike fluoride ion, no increase in the concentration coincident with the eruption of Mt. Moto-Shirane was seen, and no increase was observed after that.
On the other hand, the concentrations of both fluoride and chloride ions in Yugama, the crater lake of Mt. Shirane, increased from 2014 to 2016 and then gradually decreased. There was no significant increase in their concentrations coincident with the eruption of Mt. Moto-Shirane in January 2018, unlike Bandaiko, but the concentrations began to increase from around June 2018. After that, the concentrations have remained at a high while a small fluctuation has been observed. The F/Cl concentration ratio also

©2021. Japan Geoscience Union. All Right Reserved.

increased significantly from June to September 2018 and has remained high since then.

Seismic activity and ground inflation have been observed around Yugama intermittently after the eruption at Mt. Moto-Shirane. The fluctuation of fluoride ion concentration in Yugama and Bandaiko occur to follow those volcanic activities. However, the change in fluoride ion concentration coincident with the eruption of Mt. Moto-Shirane in January 2018 is observed in Bandaiko, but not in Yugama. Accordingly, the chemistry of Yugama reflects volcanic activity around the summit area of Mt. Shirane, while Bandaiko may reflect the activities of the entire Kusatsu-Shirane volcano or that of Mt. Moto-Shirane, which do not appear in Yugama. Since the changes in halide ion concentrations are different between Bandaiko and Yugama, we would like to keep an eye on future changes.

1)Tsuchiya *et al.* (1985) Separation of microamounts of fluoride coexisting with large amounts of aluminum and silica by improved trimethylsilylating distillation. *Analytica Chimica Acta* **176,** 151-159.

Keywords: fluoride ion, Kusatsu Shirane Volcano, hydrothermal system, geothermal fluid, hot spring, active crater lake

©2021. Japan Geoscience Union. All Right Reserved.

Volcanic ash from the June 17, 1962 eruption of Yakedake volcano, and its water-soluble components

*Muga Yaguchi[1], Yasuo Hirayama[2], Takeshi Ohba[3], Nozomi Numanami[3]

1. Meteorological Research Institute, JMA, 2. Nagano Meteorological Office, JMA, 3. School of Science, Tokai University

Mt. Yakedake is one of the active volcanoes, and several phreatic eruptions have been recorded. The most recent eruptions occurred in 1962-1963. The ash fall from the June 17 eruption, the first eruption in the series of 1962-63 eruptions, was distributed mainly on the eastern flank of this volcano [1]. The volcanic ash from this eruption has already been analyzed by Ossaka and Ozawa, and it is considered that the 1962 eruption was not caused by ascending magma but by an explosion in a mud reservoir because volcanic ash does not contain essential materials but contains montmorillonite [2]. On the other hand, for example, microscopic images of the ash particles and analytical results of water-soluble components of the ash have not been available as far as we know. In this presentation, we present the results of microscopic observation and analysis of water-soluble components of the volcanic ash from the June 17, 1962 eruption.

The ash sample we analyzed in this study was collected from the roof of a house on the morning after the eruption on June 17, 1962, which was collected before being exposed to rainfall or contaminated by soil materials. Water-soluble Cl and SO4 were analyzed by ion-chromatography after the ultrasonic extraction into pure water. The ash after extraction was rinsed and dried for microscopic observation.

Under microscopic observation, most of the ash before ultrasonic extraction was less than 500 μm in size, covered with fine particles, and gray in color. On the other hand, the washed volcanic ash is dominated by particles smaller than 100-200 μm. Most of these particles are transparent to white, accompanied by altered rock and crystal fragments that appear to be pyrite. No particle that was clearly derived from fresh magma was found. On the other hand, as a result of the analysis of water-soluble components, 1,250 mg of Cl and 10,800 mg of SO4 were detected per 1 kg of ash sample. These amounts of water-soluble components are clearly higher than those of volcanic ashes discharged from typical magmatic eruptions (e.g., the 1707 Hoei eruption of Mt. Fuji and the 2017 eruption of Nishinoshima) and are consistent with the characteristics of volcanic ashes discharged from phreatic eruptions (e.g., the 1982-83 eruption of Kusatsu-Shirane volcano and the 2015 eruption of Hakone volcano). These results suggest that the June 17, 1962 eruption was not caused by fresh magma ascending but by a phreatic explosion in the hydrothermal alteration zone, and this suggestion is consistent with previous studies. In this presentation, we also show another analytical result, such as powder XRD analysis, and the geochemical characteristics of this ash will be discussed.

[1] Murai I. (1962) Bull. Earthq. Res. Inst., 40, 805-814. [2] Ossaka J. and Ozawa T. (1966) Bull. Volcanol. Soc. Japan, 11, 17-29.

Keywords: Yakedake volcano, the June 17, 1962 eruption, phreatic eruption, volcanic ash, water-soluble components

©2021. Japan Geoscience Union. All Right Reserved.

Tectonic controlled and hydrothermal alterations of geothermal reservoirs in El Salvador

*JOSE ANIBAL ERAZO[1], Noriyoshi Tsuchiya[1], Masaoki Uno[1], Arturo Quezada[2], Pedro Antonio Santos[2], Ryoichi Yamada[1], Hiroyuki Yamagishi[1], Shinichi Yamasaki[1], Alvaro Josue Amaya[3]

1. Graduate school of environmental studies , 2. LaGeO _ El Salvador, 3. UES _ El Salvador

A comparative study of magma-hydrothermal activities of main geothermal fields (Ahuachapán, Berlín, San Vicente, and Chinameca) was carried out in El Salvador/ Central America, where significant relationships were identified between volcanism and geothermal activities.

All geothermal fields are located north and/or northwest flank of the volcanic complex inside ESFZ (El Salvador Fault Zone). Geothermal reservoirs are controlled by fault system, which direction is mainly N-S, NE-SW, NW-SE, and E-W. The reservoirs are developed in the intersected area of those faults.

Most of the reservoir are developed in the San Salvador Cuscatlán and Bálsamo formation of Pliocene-Holocene in age.

The top depths of geothermal reservoirs are ranging from 600 to 2000 m. Ahuachapán is relatively shallow (below 600 to 1500 m, thickness around 800 to 1200 m), and Berlín (below 1500 m, thickness around 600 to 1000 m). Geothermal reservoirs of San Vicente and Chinameca were estimated around 1100 to 1400 m in depth. The temperatures of the reservoirs in the different geothermal fields range from 200 to 300˚C.

The mineral alteration facies in the four fields have a very similar distribution (Fig. 1), and Propylitic, Phyllitic-Propylitic, Phyllitic zones correspond to the geothermal reservoir. In the different facies, key minerals are Argillitic: Low-temperature clays like Smectites (Montmorillonite, Saponite); Argillitic-Phyllitic: Chloritic clays (mixed-layer clay minerals) like Corrensite; Phyllitic: Chlorite; Phyllitic-Propylitic: Incipient epidote or in very low percentages. Propylitic: key mineral: epidote. Other minerals are also present in each facie. In the shallow zone, the Argillic alteration is dominant and is in the range of temperatures of 50°C-120°C, the Argillic-Phyllitic mineral alteration is found in the temperature range of 100°C-180°C, Phyllitic-Propylitic mineral alteration type is found in the temperature range of 200°C-260°C and in the deepest zone, the Propylitic type mineral alteration is dominant, found it at temperatures ranging from 250°C to temperatures around 300°C.

The chemical composition of trace elements of volcanic rocks in El Salvador shows a subduction setting through Miocene to the present. The Miocene-Pliocene volcanoes located northward of ESFZ were similar to the back-arc setting. A wide range of mineral assemblages of volcanic rocks was observed (Mainly from the series calc-alkaline from basalts to rhyolites), however, it is rare to contain quartz.

In the case of Quaternary volcanoes distributed inside ESFZ (and parallel to the Middle America Trench), the magma chamber was presumed to be slightly shallower, and variation of geochemical behaviors may show that El Salvador is located as a transition zone of the subduction system of the Cocos Plate between Guatemala and Nicaragua

©2021. Japan Geoscience Union. All Right Reserved.

Keywords: hydrothermal, mineral alteration, geothermal reservoirs , magma

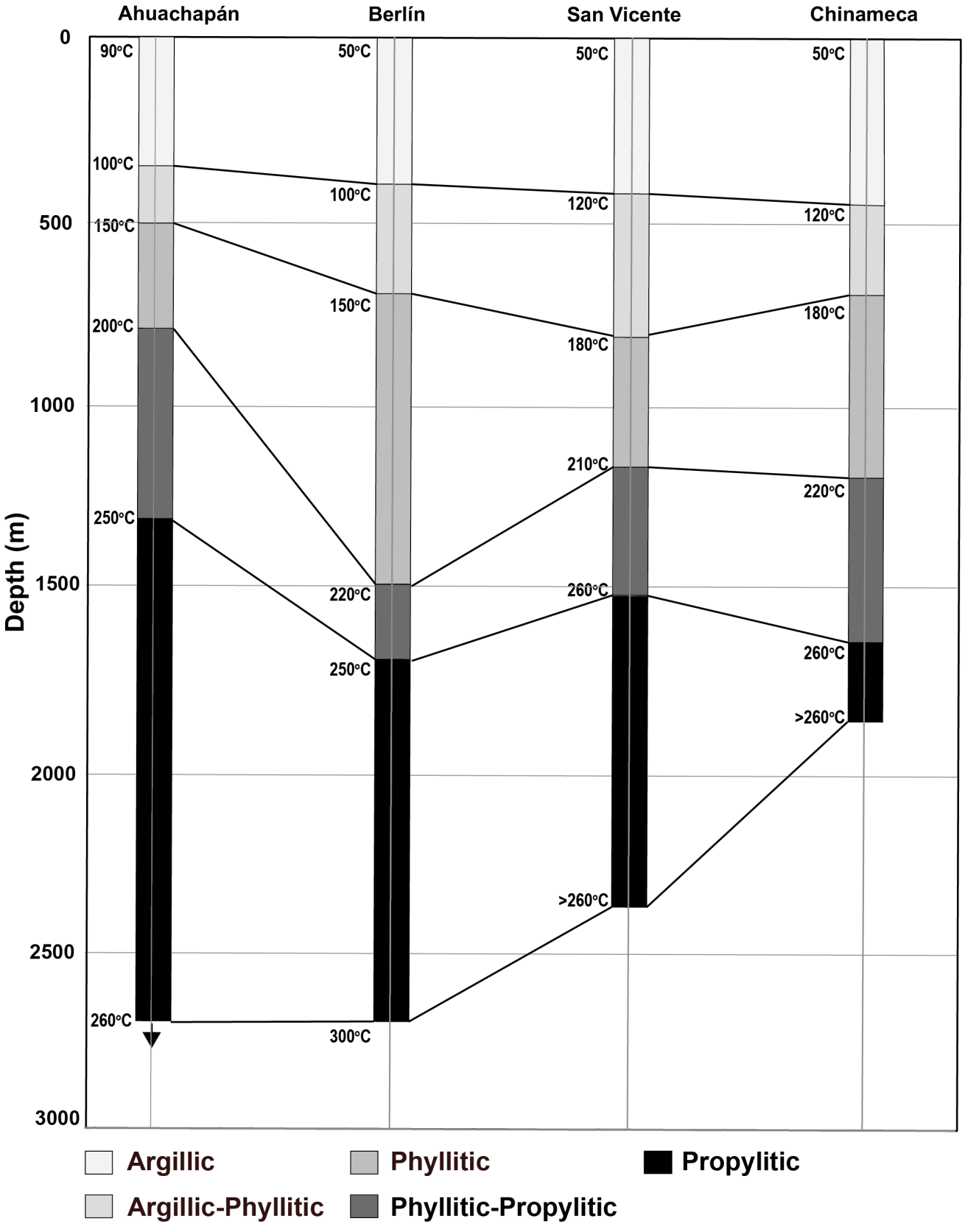


Fig. 1 Depth of mineral alteration facies in different geothermal fields in El Salvador.

©2021. Japan Geoscience Union. All Right Reserved.

DAS-Seismic and temperature data acquisition using DAS and DTS measurements at the Ohnuma, geothermal field, Tohoku, Japan

*Junzo Kasahara[1,2], Yoko Hasada[1,3], Kuzume Haruyasu[1], Hitoshi Mikada[4], Yoshihiro Fujise[5]

1. ENAA, 2. Shizuoka University, 3. Daiwa Exploration and Consulting Co. Ltd., 4. Graduate School of Kyoto University, 5. WELMA

The New Energy and Industrial Technology Development Organization (NEDO) in Japan has promoted the use of supercritical water for geothermal power generation under a project called “Research and Development of Supercritical Geothermal Resources. In September, 2020, we carried out a seismic survey as a part of this NEDO project using distributed acoustic sensor (DAS) method by an optical fiber system. We deployed an optical fiber system in the O-13R borehole at the Ohnuma geothermal power plant owned by Mitsubishi Materials Corporation. The Ohnuma geothermal power station, the third commercial geothermal power plant in Japan, was completed in 1974; its installed capacity is 9.5 MW. The optical fiber reached to the depth of 1,973 m. The temperature was measured as 235 ˚C at around 1,130 m depth using the DTS mode. We operated a medium size seismic source at nine locations. We repeated the frequency sweep of 10–75 Hz 480 times a day for nine days. To enhance the signal to noise ratio (S/N), we stacked the DAS data and correlated the seismic records with the source signature. By stacking for a long duration, we obtained excellent DAS records down to the bottom of the boreholes. Using the migration of observed and synthetic DAS seismic records, we recognized intense seismic reflections from 2.8–3.0 km depth, suggesting the possibility of geothermal reservoirs in or above basement rock and/or igneous intrusions (Fig. 1).

Acknowledgements

This study was supported by the New Energy and Industrial Technology Development Organization (NEDO). We greatly appreciate Mitsubishi Materials Corporation for their kind permission for fieldwork in their power plant. Mr. Kimura provided us with Schlumberger hDVS measurements. YK Engineering Co. and Fujitsu Research Institute Co. provided DAS data. WELMA Co. provided us with a borehole fiber-optic system and measured the temperatures in the borehole. The staff of the Kawasaki Geological Engineering Co. and Daiwa Exploration and Consulting Co. assisted our surface seismological measurements during the field study. The IVI EnviroVibe operation was performed by JGI Inc.

References

Kasahara, J., Hasada, Y., Kuzume, H., Mikada, H., and Fujise, Y. [2020a] The second seismic study at the geothermal field in southern Kyushu, Japan using an optical fiber system and surface geophones, 44th Workshop on Geothermal Reservoir Engineering, Stanford University, Stanford, CA.

Kasahara, J., Hasada, Y., and Kuzume, H. [2020b] Possibility of high Vp/Vs zone in the geothermal filed suggested by the P-to-S conversion, 44th Workshop on Geothermal Reservoir Engineering, Stanford University, Stanford, CA.

Kubota, Y. [1985] Conceptional model of the north Hachmantai-Yakeyama geothermal area, Journal of Geothermal Society of Japan, **7**(3), 231-245.

©2021. Japan Geoscience Union. All Right Reserved.

Kubota, Y., Hatakeyama, K., Banba, M., Kato, H. [1989] Chemical changes of Ohnuma geothermal fluid since operation and related reservoir management, Journal of JGEA (Japan Geothermal Energy Association), **26**(1), 1-20.

Yora, M., Wakita, K., and Honda, S. [1973] Exploration of Onuma geothermal field, northern Japan, Journal of JGEA (Japan Geothermal Energy Association), **10**(4), 27-44.

Yora, M, [1976] Drilling of Onuma geothermal wells, specially O-3Rb, Journal of JAPT (Japanese Association of Petroleum Technology), **41**(5), 13-19.

Yora, M., Watanabe, K., Ito, J., Wakita, K., Kubota, Y. [1977] On the geothermal system of the northern Hachimantai, Mining Geology, **27**, 233-244.

Keywords: Geothermal exploration, supercritical water, DAS, seismic reflection, migration imaging, geothermal reservoir

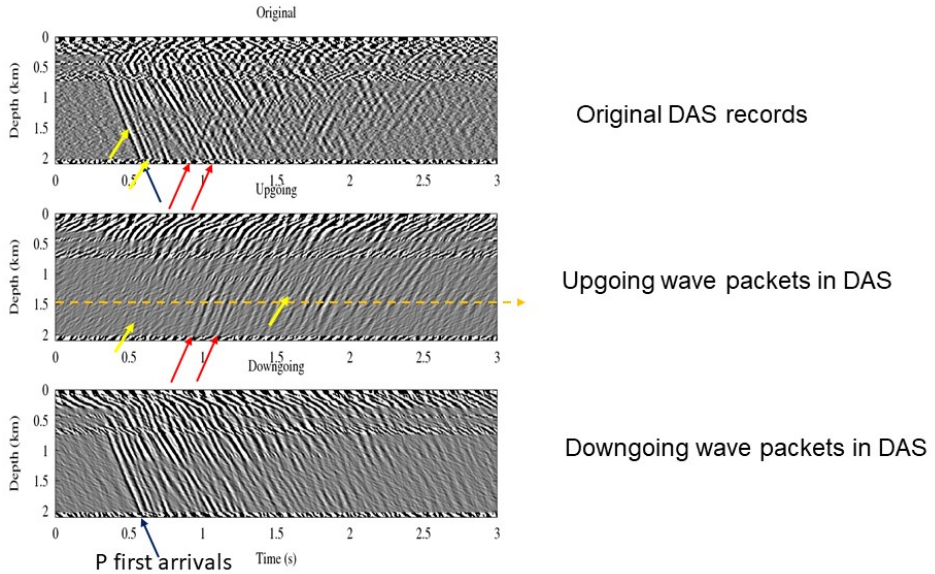


Fig. 1: Using original DAS records at the C8 seismic source, we calculated upgoing phases (reflection phases) and upgoing phases(direct waves). The Red and the yellow arrows indicate reflections. The yellow broken line is a possible layer boundary and fracture zone.

©2021. Japan Geoscience Union. All Right Reserved.

Ground surface Heat balance measurements at Izu-Oshima volcano

*Shin'ya Onizawa[1], Nobuo Matsushima[2]

1. Volcanology Research Department, Meteorological Research Institute, JMA, 2. Geological Survey of Japan, National Institute of Advanced Industrial Science and Technology

1. Introduction

During the 1986 eruption of Izu-Oshima volcano, phenomena suggesting the development of the underground hydrothermal system were observed. Thus, thermal observation is important for grasping such the transitions of volcanic activities. In order to understand the thermal activity, underground and surface temperature measurements are often performed. However, the temperature near the ground surface strongly affected by external factors such as radiation from the sun and atmosphere and meteorological factors. Therefore, in order to detect and quantify thermal signs associated with volcanic activity, it is necessary to understand the effect of these external factors. For the purpose of clarifying these factors, heat balance observation devices were installed at two locations in caldera area of the Izu-Oshima volcano.

2. Measurement System

The system consists of sensors that measure not only the surface and underground temperatures, but also the radiations from the sun and the atmosphere and meteorological factors that can affect them. Further, as auxiliary information, the soil moisture and the thermal conductivity in the ground are measured.

Sensors

T-type thermocouple thermometers (CHINO SCHS1-5) are installed at 5 depths (10, 30, 50, 70 and 100 cm) for the underground temperatures. For ground surface temperature, infrared radiation thermometer (Apogee SI-431) is installed. The meteorological parameters (wind speed and direction, atmospheric pressure, temperature, relative humidity, precipitation, and hail) are measured by the weather transmitter Vaisala WXT536. The albedometer (Hukseflux SRA01) is used to measure short-wave radiations (solar radiation and its reflection from the ground surface), and the long-wave radiometer (Hukseflux IR02) is used to measure atmospheric radiation (infrared radiation). The sensors of the soil moisture meter (Sentek EnviroSMART) were installed at the same depth of 5 as the underground temperature. In addition, the thermal properties sensor (Huluseflux TP01) is installed at a depth of about 20 to 30 cm in order to estimate the effective thermal conductivity of the medium.

Data Record and Transmission

Measurements were performed at a minimum interval of 10 seconds, and these were recorded with a data logger (Campbell Scientific CR-1000X). In addition, data is transmitted to the Meteorological Research Institute using a mobile phone line.

3. Observation

This device was installed at two locations inside the caldera of Izu-Oshima volcano. One is in a fumarolic area and the other is in a non-fumarolic area. Both were set up in March 2020.

HB01 (Eastern Crater Floor of Mt. Mihara)

It was installed in a steaming ground distributed along a crack in the eastern crater floor of Mt. Mihara. It is near a fixed point where the Japan Meteorological Agency has been continuously measuring fumarolic temperature since 1991. According to this, what was about 80 ˚C in 1991 has decreased over time, and has been around 45 to 50 ˚C in recent years.

HB02 (Southeastern Caldera Floor)

©2021. Japan Geoscience Union. All Right Reserved.

While HB01 was installed in a the fumarolic area, this site was selected from areas where thermal signs associated with volcanic activity were not observed, because the purpose was to understand the heat balance due to external factors such as radiation and meteorological conditions. It was installed in the bare land in the southeastern caldera floor. The ground surface is covered with scoriaceous silt, sand and lapilli.

4. Characteristics of Observed Data

Characteristics of changes in the surface and underground temperatures are totally different between two sites. At the HB02 in non-fumarolic area, diurnal and seasonal (that are considered to be annual) changes are clearly observed. In particular, it is strongly affected by solar radiation, and the amplitude of temperature changes attenuate and the phase is delayed as it gets deeper. On the other hand, at HB01 in the fumarolic area, such the changes are not prominent in the underground temperatures, although diurnal changes in temperature are observed on the ground surface. The underground temperatures are almost constant at about 45 to 48 ˚C at depths from 10 cm to 100 cm during the seasons. However, when the average wind speed for 10 minutes exceeds approximately 5 m/s, the temperature decreases from the surface to the deeper often occur, suggesting that sensible heat transport or latent heat transport is promoted.

In this presentation, we show the outlines of the measurements and characteristics of observed data.

Keywords: Izu-Oshima volcano, heat balance measurement

©2021. Japan Geoscience Union. All Right Reserved.

Behavior of magmatic hydrothermal system of Kusatsu-Shirane Volcano inferred from numerical simulations

*Yasuo Matsunaga[1], Wataru Kanda[1]

1. School of Science, Tokyo Institute of Technology

Kusatsu-Shirane Volcano (KSV) is an active volcano known for its significant hydrothermal activity and phreatic eruptions in recent years. According to geological studies, frequent magmatic eruptions were estimated at Mt. Motoshirane, which constitutes the southern part of KSV, until 1500 years ago. Therefore, it is expected that the magma produced at that time has not yet cooled and solidified.

To infer the extent of the magmatic-hydrothermal system of KSV, broadband magnetotelluric observations covering the entire region of KSV were conducted from 2015 to2020. The study found a remarkable conductive zone extending from a depth of ~1.5 km below the summit area to a depth of ~10 km northwest of the KSV. The lower part (5–10 km deep) of this conductor showed moderately low resistivities (~50 Ωm) and the upper part (1.5–5 km deep) showed extremely low resistivities (< ~1 Ω m)(Matsunaga et al., 2020). The lower half of the conductor can be explained as a zone containing hydrous silicate melt, because it exhibited low resistivities on the order of 10 Ωm (Pommier et al., 2011). Based on previous geochemical studies and the seismicity, we interpreted the upper half of this conductor as a fluid-rich zone strongly affected by magmatic volatiles.

Since the hypocenters of volcanic earthquakes are distributed from the top of this conductor to the summit area, it is likely that these conductive zones are involved in the various volcanic activities observed in KSV. Therefore, it is crucial to consult the behavior of hydrothermal fluids to understand the magmatic hydrothermal system of KSV. However, it is still difficult to estimate the exact position and volume of molten rocks because the MT data collected has low resolution and sensitivity, particularly in the lower part. Since the geothermal and geochemical processes observed near the surface are strongly influenced by the behavior of shallow hydrothermal systems, it is also difficult to infer the deep processes of volcanoes which have well-developed hydrothermal systems like KSV.

One possible way to estimate the thermal state and process inside a conductor is to numerically simulate the movement of geothermal fluids using the observed data and the inferred subsurface structure as constraints. To construct a hydrothermal fluid circulation model of KSV, we use a multi-phase and multi-component TOUGH3 model (Jung et al., 2017). In the presentation, we will show some of the simulation results.

Keywords: Kusatsu-Shirane, hydrothermal system, resistivity structure, numerical simulation

©2021. Japan Geoscience Union. All Right Reserved.

Comprehension of hydrothermal systems in the East African Rift System –Collaborative Research with Kenya by SATREPS–

*Yasuhiro Fujimitsu[1], Jun Nishijima[1], Takeshi Tsuji[1], Kotaro Yonezu[1], Tatsuya Wakeyama[2], Ryuichi Itoi[3]

1. Department of Earth Resources Engineering, Faculty of Engineering, Kyushu University, 2. Platform of Inter-/Transdisciplinary Energy Research, Kyushu University, 3. School of Engineering, Kyushu University

SATREPS is an acronym standing for Science and Technology Research Partnership for Sustainable Development, and is a joint research program for 3 to 5 years between Japan and developing countries that aims to find solutions to issues of a global scale. Japan Science and Technology Agency (JST) and Japan International Cooperation Agency (JICA) are responsible for the areas of Environment/Energy (Global-scale Environmental Issues, and Low Carbon Society/Energy), Bioresources and Disaster Prevention and Mitigation. The research topic “Comprehensive Solutions for Optimum Development of Geothermal Systems in East Africa Rift Valley” proposed by Kyushu University (Principal Investigator: Yasuhiro Fujimitsu; Research Period: FY2020 to FY2024; Partner Country: Kenya) was adopted in FY2019.

The participants Kyushu University (Faculty of Engineering, Faculty of Science, and Platform of Inter-/Transdisciplinary Energy Research) and West Japan Engineering Consultants, Inc. in Japan and Jomo Kenyatta University of Agriculture and Technology, The University of Nairobi, Kenya Electricity Generating Company and Geothermal Development Company in Kenya. It was scheduled that the project started from FY2020 with a preparation period in FY2019. However, the actual commencement becomes FY2021 caused by a worldwide pandemic of COVID-19. In order to obtain 4 outputs of this research topic (I: Development of high resolution geothermal reservoir models, II: Understanding of silica scale formation mechanism in highly alkaline hot water and examination of countermeasures, III: Proposal of a scenario for enhancement of social acceptance by the expansion of cascade use of geothermal energy, IV: Cultivation of human resources in geothermal development and research capability of the counterpart institutions), we conduct collaborative research of Olkaria and Menengai geothermal areas with the Kenyan institutions.

Keywords: East African Rift System, hydrothermal system, SATREPS

©2021. Japan Geoscience Union. All Right Reserved.

[E] Oral | S (Solid Earth Sciences)：S-CG Complex & General

Sun. Jun 6, 2021 9:00 AM - 10:30 AM JST | Sun. Jun 6, 2021 12:00 AM - 1:30 AM UTC | Ch.21 Zoom Room 21

[S-CG39] Science of slow earthquakes: Toward unified understandings of whole earthquake process

convener:Satoshi Ide(Department of Earth an Planetary Science, University of Tokyo), Hitoshi Hirose(Research Center for Urban Safety and Security, Kobe University), Kohtaro Ujiie(Faculty of Life and Environmental Sciences, University of Tsukuba), Takahiro Hatano(Department of Earth and Space Science, Osaka University), Chairperson:Satoshi Ide(Department of Earth an Planetary Science, University of Tokyo)

Accumulating observational studies on various types of slow deformation events, such as tectonic tremors, very low frequency events, and slow slip events, portrays some universal characteristics in generally complex behavior, including interaction among events and influence by various outer loading. Some of these phenomena seem to have causal relation with the occurrence of very large earthquakes. A unified understanding of these slow and fast earthquake processes requires an approach integrating geophysics, seismology, geodesy, geology, and non-equilibrium statistical physics. We welcome presentations based on, but not limited to, geophysical observation, data analysis, analytical theory, numerical simulation, field study, and laboratory experiments.

9:00 AM - 9:15 AM JST | 12:00 AM - 12:15 AM UTC

[SCG39-19] Systematics and heterogeneity of deep and shallow slow earthquakes

*Kazushige Obara[1] (1.Earthquake Research Institute, The University of Tokyo)

9:15 AM - 9:30 AM JST | 12:15 AM - 12:30 AM UTC

[SCG39-20] Extraction of fine space-time structures in deep low-frequency tremor using the Hough transform

*Kodai Sagae[1], Hisashi Nakahara[1], Takeshi Nishimura[1], Kazutoshi Imanishi[2] (1.Solid Earth Physics Laboratory,Department of Geophysics,Graduate School of Science,Tohoku University, 2.National Institute of Advanced Industrial Science and Technology (AIST))

9:30 AM - 9:45 AM JST | 12:30 AM - 12:45 AM UTC

[SCG39-21] Comprehensive detection of tremor migration using multiple time windows beneath Kii Peninsula

*Takuya Maeda[1], Kazushige Obara[1], Akiko Takeo[1], Takanori Matsuzawa[2] (1. Earthquake Research Institute, The University of Tokyo, 2.National Research Institute for Earth Science and Disaster Resilience)

9:45 AM - 10:00 AM JST | 12:45 AM - 1:00 AM UTC

[SCG39-22] Focal mechanism and radiated energy from shallow tremors in the Guerrero seismic gap.

*Raymundo Omar Plata Martinez[1], Yoshihiro Ito[2], Kazuaki Ohta[4], Masanao Shinohara[5], Satoshi Ide[3] (1.Graduate School of Science, Kyoto University, 2.Disaster Prevention Research Institute, Kyoto University, 3.Department of Earth and Planetary Science, University of Tokyo, 4.National Research Institute for Earth Science and Disaster Resilience, 5.Earthquake Research Institute, University of Tokyo)

10:00 AM - 10:15 AM JST | 1:00 AM - 1:15 AM UTC

[SCG39-23] Seismicity around the subducted seamount in the trench-trench junction, southern off Hokkaido, by a broadband OBS array

*Ryosuke Azuma[1], Susumu Kawakubo[1], Hidenobu Takahashi[1], Ryota Hino[1], Yusaku Ohta[1], Ryota Takagi[1], Syuichi Suzuki[1], Makiko Sato[1], Tanaka Shinichi[2], Masanao Shinohara[2] (1.Recearch Center for Prediction of Earthquake and Volcanic Eruption, Graduate School of Science, Tohoku University, 2.Earthquake Research Institute, University of Tokyo)

10:15 AM - 10:30 AM JST | 1:15 AM - 1:30 AM UTC

[SCG39-24] Discussion

Systematics and heterogeneity of deep and shallow slow earthquakes

*Kazushige Obara[1]

1. Earthquake Research Institute, The University of Tokyo

During the last two decades from the first discovery of slow earthquakes in southwest Japan around 2000, many types of slow earthquakes associated with different source depths and time scales have been discovered in such a way to fill gaps in space and spectral domains because of deployment of observation networks, continuous monitoring, and development of analyzing technology. As a result, composition of slow earthquakes in shallow and deep parts became common at present although different at the beginning. On the other hand, more quantitative and comprehensive analyses revealed more heterogeneous activity pattern of slow earthquakes rather than homogeneous. In this presentation, I would like to review the slow earthquake activity from points of view on systematics and heterogeneity.

Slow earthquakes in the Nankai trough region are separated into shallow and deep sides of the huge earthquake seismogenic zone along the subducting Philippine Sea plate interface. Deep slow earthquakes are systematically separated into Episodic Tremor and Slip (ETS), which is composed of tremor, very low frequency earthquake (VLF), and short-term slow slip event (SSE) at the deepest part and long-term SSE in between ETS and locked zones. Long-term SSEs have been detected in some places in this intervened zone as to fill the spatial gap recently although originally detected at two limited areas. These deep slow earthquakes are distributed at their own depths along-strike horizontally separated into some segments with different spatiotemporal pattern. This suggests that the type of slow earthquakes is systematically controlled by the environment as a function of depth.

On the other hand, the distribution pattern of shallow slow earthquakes is different from those of deep slow earthquakes. Although shallow VLF were originally detected at some spatiotemporal clusters along the Nankai trough, very recently shallow SSE, VLF and tremor has been detected simultaneously southeast off Kii Peninsula. This is an evidence for the occurrence of ETS in shallow side. Moreover, a long-term SSE was detected by acoustic GNSS measurement system near the Nankai trough. As a result, we have a common set of slow earthquakes in both shallow and deep sides; however, detail distribution pattern is different. Near the Nankai trough, shallow ETS and long-term SSE are aligned along-strike on the same depth contour line of the subducting plate. This indicates along-strike strong heterogeneity including different types of slow earthquakes and also strong/weak coupling portions. This along-strike heterogeneity is similar to the Japan trench.

Regarding spatiotemporal activity of slow earthquakes, there are two characteristic properties: migration and recurrence. Migration of ETS including slow speed main front migration and Rapid Tremor Reversal is common for shallow and deep sides. On the other hand, recurrence property is different. Deep ETS indicates beautiful periodic pattern at each segment; however, there is no clear periodicity in shallow ETS activity. This might be interpreted that shallow strong heterogeneity affects interaction between different neighboring phenomena and disturbs regular recurrence behavior. However, migration indicating rupture propagation of slow slip event is interpreted as a common process after initiation in both shallow and deep sides.

Keywords: Slow earthquake, tremor, very low frequency earthquake, slow slip event

©2021. Japan Geoscience Union. All Right Reserved.

©2021. Japan Geoscience Union. All Right Reserved.

Extraction of fine space-time structures in deep low-frequency tremor using the Hough transform

*Kodai Sagae[1], Hisashi Nakahara[1], Takeshi Nishimura[1], Kazutoshi Imanishi[2]

1. Solid Earth Physics Laboratory,Department of Geophysics,Graduate School of Science,Tohoku University, 2. National Institute of Advanced Industrial Science and Technology (AIST)

Tremor migration is one of the important features of deep low-frequency tremors. The characteristics of the tremor migration are classified into the following three types: (1) Long-term migration (Obara, 2010) for which tremor propagates along the strike of a subducting plate at approximately 10 km/day in synchronization with a slow slip event (SSE); (2) Rapid tremor reversal (RTR) for which tremor propagates along the strike into the reverse direction to the long-term migration with a speed of approximately 200 km/day (Houston et al., 2011); (3) Tremor streak which is a migration of tremor along the dip at approximately 1000 km/day (Ghosh et al., 2010). We usually investigate the temporal evolution of tremors by projecting tremor locations into an axis (Obara, 2010; Sagae et al., 2021, GJI). Therefore, it is necessary to study the three-dimensional behavior of tremors from the epicentral distribution and the time of occurrence. In the field of astronomy, Morii (2019) performed a detection of straight lines using the 3-D Hough transform (2D in space and 1D in time) to investigate movements of celestial bodies in the observed images. We called the method as “space-time Hough transform” to distinguish it from the conventional 3-D Hough transform in 3D spatial dimensions. As a previous study which applied Hough transform in seismology, Uchide and Imanishi (2017, SSJ) detected fault planes using hypocenter locations and focal mechanism information based on the conventional Hough transform. In this study, by slightly modifying the space-time Hough transform, we extract fine space-time structures in tremor migrations.

In this study, straight lines (tremor migrations) are detected in the three-dimensional space of the epicentral distribution and time. We set the positive x-axis, y-axis, and z-axis in the east, north, and time direction, respectively. Any straight line in the three-dimensional space is represented as $\rho = x(-\sin\phi \sin\psi + \cos\theta \cos\phi \cos\psi) + y(\sin\phi \cos\psi + \cos\theta \cos\phi \sin\psi) - z(\sin\theta \cos\phi)$, where ρ is the distance from the origin to the straight line, θ is the zenith angle, ϕ is the azimuth, and ψ is the rotation angle, respectively. In particular, $\tan\theta$ represents the migration speed, and the vector $(\cos\psi, \sin\psi)$ represents the direction vector in the x-y plane. In this study, the direction vector of a straight line is taken in the radial direction, whereas in Morii (2019), that is taken in a direction perpendicular to the radial direction. We set a “bin” for each parameter of $(\rho, \theta, \phi, \psi)$. Then, we calculate ρ while changing (θ, ϕ, ψ) for each event, and perform a “vote” to the corresponding “bin”. Finally, the “bin” $(\rho, \theta, \phi, \psi)$ with the largest number of votes is the best straight line that represents event data best. Furthermore, even if there are multiple straight lines in the space, these straight lines can be detected separately using the Hough transform because votes for different lines are cast on different “bins”. This enables to relax a constraint of one migration in one time-window used in previous studies (Obara et al., 2012; Maeda et al., 2020 SSJ). Our method has a potential to detect multiple migrations within a time window.

We analyzed a tremor catalog in which tremor epicenters were determined using a dense seismic array beneath the Kii Peninsula (Sagae et al., 2021, GJI). This catalog is suitable for investigating details of tremor migrations because it determined approximately 2.2 times more tremors than a catalog determined by the envelope correlation method (Obara, 2002). The analyzed period is from July 2012 to July 2014. We used every one hour time-window to detect migrations. The parameters “bins” were set

©2021. Japan Geoscience Union. All Right Reserved.

in increments of 10 degrees for ϕ and ψ, in the range of 1–40 km/hr for θ, and in an increment of 5 km for ρ in consideration of uncertainties in the tremor locations. The Hough transform was applied when the time-window contained more than 10 events, and a straight line with the largest number of votes was detected. Then, after removing events composing the straight lines already detected, other straight lines were detected iteratively until the number of unvoted events was less than 10 events.

As a result, we found that predominant directions of migrations differ depending on locations. In the place where along-strike migrations were predominant, we found a feature that tremor migrated into the opposite direction to the long-term migration. Moreover, locations of RTR and Tremor streak reported in Sagae et al. (2021, GJI) were similar to locations where migrations were predominant in the strike and dip directions, respectively. This result suggests that RTR and Tremor streak may occur repeatedly in the same locations.

Keywords: Deep low-frequency tremor,, Hough transform, Migration, Kii Peninsula

©2021. Japan Geoscience Union. All Right Reserved.

Comprehensive detection of tremor migration using multiple time windows beneath Kii Peninsula

*Takuya Maeda[1], Kazushige Obara[1], Akiko Takeo[1], Takanori Matsuzawa[2]

1. Earthquake Research Institute, The University of Tokyo, 2. National Research Institute for Earth Science and Disaster Resilience

Deep low-frequency tremors occur downdip of seismogenic zone along the subducting plate interface. Together with short-term slow slip events (SSEs), tremors constitute the Episodic Tremor and Slip (ETS; Rogers and Dragert, 2003). Tremors are known to migrate in the along-strike direction at a velocity of ~10 km/day. After main slip front associated with the ETS passes, relatively small-scale and high-velocity migrations like as Rapid Tremor Reversal (RTR ; Houston et al., 2011) and streak (Ghosh et al., 2010) are often observed. RTR propagates in the direction opposite to that of the ETS main front at a velocity of ~100 km/day, and streak propagates in the along-dip direction at a velocity of ~1000 km/day. Bletery et al. (2017) interpreted these migrations of tremors to represent secondary slip fronts (SSFs) and detected SSFs with wide timescales in Cascadia. In this study, we comprehensively detect SSFs using multiple time windows and estimate migration parameters beneath the Kii Peninsula, southwest Japan.

We use a tremor catalog derived by using the hybrid method based on the envelope correlation considering the spatial distribution of amplitude (Maeda and Obara, 2009). We analyze tremors included in not only major ETS but also minor episodes beneath the Kii Peninsula during 2001 to 2020. In order to detect various SSFs, we use seven different time windows (1 h, 2 h, 4 h, 8 h, 16 h, 32 h,64 h). In this analysis, we assume that all tremor sources in a SSF migrate in one direction in each fixed time window and the migration front extends perpendicularly to the migration direction. First, we estimate the direction of migration as follows: (i) remove spatial outliers from the tremors included in the time window, (ii) calculate the correlation coefficient between time and distance along temporary migration direction, (iii) find a direction which gives the maximum correlation coefficient by a grid search. Next, we estimate the velocity of migration as follows: (i) remove spatiotemporal outliers by the linear regression of space–time plot projected on the direction of migration, (ii) find the slope of the regression line of remaining points. Finally, assuming that SSF area is a rectangle here, we estimate the spatial dimension of SSF as follows: (i) calculate the migration length from the product of migration velocity and duration, (ii) locate the spatial center of SSF in each time window, (iii) calculate standard deviation (σ) of distance between the tremor sources and a straight line in the migration direction through the center, (iv) define the perpendicular width of SSF as 6σ.

As a result, the distribution of direction is isotropic in shorter time windows and is dominated in the along-strike direction as the time window becomes longer. This result is consistent with previous studies in the sense that SSF in the strike direction is dominant in longer time windows (Bletery et al., 2017; Ide, 2012; Obara et al., 2012). The velocity of SSFs becomes slower as the time window increases. For example, average velocity is 270 and 9 km/day for the time window of 1 and 64 h, respectively. Regarding the shape of the SSF, the perpendicular width is longer than the migration length in most of the SSFs. The area of SSFs does not change significantly in shorter time windows. The isotropic distribution of direction in shorter time windows suggest that short timescale migrations occur in a random direction. The along-strike direction in longer time window is interpreted to represent the main slip front. The result that most of the SSF migrates with a spread in the perpendicular direction to the migration direction suggests that migration is two-dimensional phenomena rather than one- dimensional phenomena like as streak.

©2021. Japan Geoscience Union. All Right Reserved.

Keywords: slow earhquake, tremor, migration

©2021. Japan Geoscience Union. All Right Reserved.

Focal mechanism and radiated energy from shallow tremors in the Guerrero seismic gap.

*Raymundo Omar Plata Martinez[1], Yoshihiro Ito[2], Kazuaki Ohta[4], Masanao Shinohara[5], Satoshi Ide[3]

1. Graduate School of Science, Kyoto University, 2. Disaster Prevention Research Institute, Kyoto University, 3. Department of Earth and Planetary Science, University of Tokyo, 4. National Research Institute for Earth Science and Disaster Resilience, 5. Earthquake Research Institute, University of Tokyo

Thanks to the recent development of offshore seismic networks monitoring shallow slow earthquakes have been reported in different subductions zones, such as the case of the Japan trench, New Zealand and most recently the Guerrero seismic gap at the Mexican subduction. In Guerrero, a good understanding of deep slow earthquakes has already been acquired, on the contrary, shallow slow earthquakes in Guerrero have been scarcely explored. A better knowledge of the shallow slow earthquakes in the Guerrero seismic gap is necessary to characterize the seismogenic zone at the shallow plate interface. Shallow tremors in the Guerrero seismic gap were observed using data from an array of ocean bottom seismometers (OBS). We analyzed this data to estimate source parameters, such as focal mechanisms and radiated seismic energies of shallow tremors. OBS data includes attenuation and site effects, predominantly from an offshore environment, which needs to be understood to unmask source properties of seismic events recorded. After correcting horizontal orientation of OBS, focal mechanism of shallow tremors and regular earthquakes were calculated by inverting observed S-wave polarization angles. Focal mechanisms for both shallow tremors and regular earthquakes trend to follow the subducting plate motion with a low thrust angle. Additionally, spectral inversion with regular earthquakes was done to estimate site effects and attenuation for the OBS region. By removing these two effects, source spectrum of shallow tremors will be available for comparison with regular earthquakes in the region. Describing shallow tremors in the Guerrero the seismic gap will bring a new perspective of the seismic behavior of the Guerrero seismic gap.

Keywords: Shallow tremor, Guerrero gap, Slow earthquakes, Focal mechanism, Seismic energy

©2021. Japan Geoscience Union. All Right Reserved.

Seismicity around the subducted seamount in the trench-trench junction, southern off Hokkaido, by a broadband OBS array

*Ryosuke Azuma[1], Susumu Kawakubo[1], Hidenobu Takahashi[1], Ryota Hino[1], Yusaku Ohta[1], Ryota Takagi[1], Syuichi Suzuki[1], Makiko Sato[1], Tanaka Shinichi[2], Masanao Shinohara[2]

1. Recearch Center for Prediction of Earthquake and Volcanic Eruption, Graduate School of Science, Tohoku University, 2. Earthquake Research Institute, University of Tokyo

Many shallow very-low-frequency earthquakes (sVLFE) have been observed in the Kuril and Japan trench-trench junction, southern off Erimo, Hokkaido, by the inland F-net (Asano et al., 2008). In this region, many tectonic tremors have been also discovered by the S-net after 2016 (Tanaka et al., 2019; Nishikawa et al., 2019) and the long-term offline ocean bottom seismometer (OBS) network between 2006 and 2007 (Kawakubo et al., 2020). These studies reported simultaneous occasion of sVLFE and tremors. Kawakubo et al. additionally indicated that intervals of activities and epicenters distribution are roughly consistent with that before and the 2011 Tohoku-oki earthquake. However, there is no broad-band observatory above sVLFEs, and known hypocenters only by F-net are less accurate. Therefore, a spatial comparison of sVLFEs with tremors and regular earthquakes is difficult. In addition, because a spatial relation between a seamount subduction from the junction (Tsuru et al., 2005; Makino, 2005) and sVLFE occasion is expected, a near-field observatory providing precise spatio-temporal distribution of earthquakes is essential for understanding a state of the slow earthquake activities. From above backgrounds, we aim to investigate a seismicity of slow and regular earthquakes by deploying a near-field broad-band OBSs array.

This study uses seismograms recorded by one broad-band (120 seconds) OBS and four shot-period (1 Hz) OBSs deployed around the subducted seamount during July 6th, 2019 to October 8th, 2020. The deployment and recovery of OBSs were operated by the R/V Shinsei-maru (KS19-12 and KS20-16 cruises), the Japan Agency for Marin-Earth Science and Technology, and the R/V Ryoufu-maru (RF20-07), the Japan Meteorological Agency. Seismograms were recorded by a recorder featuring a 24-bit A/D converter with a 200 Hz sampling rate.

To investigate sVLFE, we firstly search tremors occurring simultaneously with sVLFEs by an envelope correlation method (Ide, 2010) which calculates correlation between station pairs and estimates hypocenters by using residuals of arrival times between pairs with maximum correlation coefficient over an optional value. We calculated envelopes from three components of seismograms between 2–8 Hz, took the squared sum of components, low-pass filtered below 0.5 Hz, and finally resampled at 1 Hz. We then took cross correlation for each 120 s window with 60 s overlap and adopted events with a maximum correlation coefficient over 0.6 at all pairs of stations. Finally, we extracted reliable events in accordance with a hypocenter error < 5 km, and arrival time residual < 3 s.

As a preliminary result, we obtained 378 events satisfying thresholds for errors, and 176 of them have a duration over 20 seconds, identified as tremors referring to Ohta et al. (2019). Followings are of interest in our result.

(1) A time series of all events projected along the seismic survey line (Tsuru et al., 2005; Makino et al., 2005) shows a highly activating period accompanied by long duration events on middle February, 2020, so that simultaneous sVLFE occasion is expected. We will process a waveform analysis for this period as a

©2021. Japan Geoscience Union. All Right Reserved.

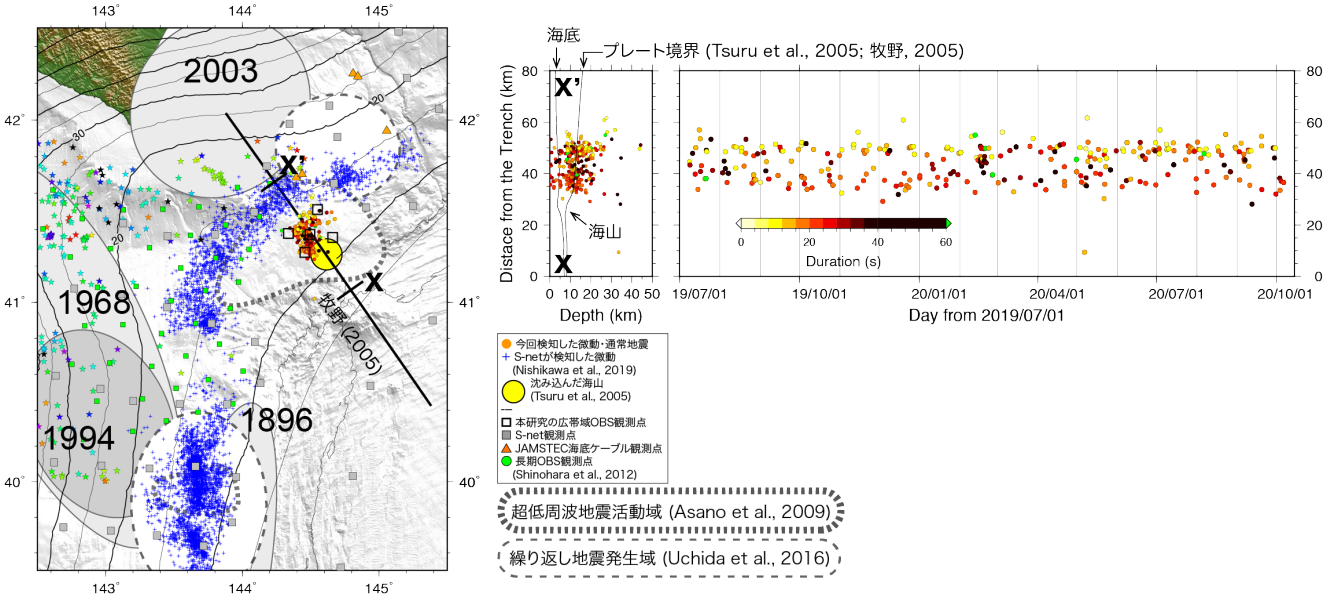
first step of sVLFE investigation.

(2) Most of determined events locate at the west half of the array, that is down-dip side of the subducted seamount. This may indicate a stress accumulation by the forearc–seamount collision.

(3) The resultant epicenter distribution seems to be isolated from that by previous works (Nishikawa et al., 2019; Kawakubo et al. 2020). Such a state of the seismic gap would be apparent related with a limit of detectable area of S-net and our arrays. Therefore, to discuss the isolation, the analysis with S-net data to expand the detectable area would be effective.

As future tasks, careful investigation of accuracy of hypocenter and duration, and confirmation of events on seismograms would bring an understanding of the state of seismic activity and the relationship with the subducted seamount.

Keywords: Shallow VLFEs and tremors around the Kuril and Japan trench-trench junction, Broadband ocean bottom seismometer array observation, Subducted seamount



©2021. Japan Geoscience Union. All Right Reserved.

[E] Oral | S (Solid Earth Sciences) | S-CG Complex & General

[S-CG39] Science of slow earthquakes: Toward unified understandings of whole earthquake process

convener:Satoshi Ide(Department of Earth an Planetary Science, University of Tokyo), Hitoshi Hirose(Research Center for Urban Safety and Security, Kobe University), Kohtaro Ujiie(Faculty of Life and Environmental Sciences, University of Tsukuba), Takahiro Hatano(Department of Earth and Space Science, Osaka University), Chairperson:Satoshi Ide(Department of Earth an Planetary Science, University of Tokyo)

Sun. Jun 6, 2021 9:00 AM - 10:30 AM Ch.21 (Zoom Room 21)

Accumulating observational studies on various types of slow deformation events, such as tectonic tremors, very low frequency events, and slow slip events, portrays some universal characteristics in generally complex behavior, including interaction among events and influence by various outer loading. Some of these phenomena seem to have causal relation with the occurrence of very large earthquakes. A unified understanding of these slow and fast earthquake processes requires an approach integrating geophysics, seismology, geodesy, geology, and non-equilibrium statistical physics. We welcome presentations based on, but not limited to, geophysical observation, data analysis, analytical theory, numerical simulation, field study, and laboratory experiments.

10:15 AM - 10:30 AM

[SCG39-24]Discussion

©Japan Geoscience Union

[E] Oral | S (Solid Earth Sciences)：S-CG Complex & General

Sun. Jun 6, 2021 10:45 AM - 12:15 PM JST | Sun. Jun 6, 2021 1:45 AM - 3:15 AM UTC | Ch.21 Zoom Room 21

[S-CG39] Science of slow earthquakes: Toward unified understandings of whole earthquake process

convener:Satoshi Ide(Department of Earth an Planetary Science, University of Tokyo), Hitoshi Hirose(Research Center for Urban Safety and Security, Kobe University), Kohtaro Ujiie(Faculty of Life and Environmental Sciences, University of Tsukuba), Takahiro Hatano(Department of Earth and Space Science, Osaka University), Chairperson:Kimihiro Mochizuki(Earthquake Prediction Research Center, Earthquake Research Institute, University of Tokyo)

Accumulating observational studies on various types of slow deformation events, such as tectonic tremors, very low frequency events, and slow slip events, portrays some universal characteristics in generally complex behavior, including interaction among events and influence by various outer loading. Some of these phenomena seem to have causal relation with the occurrence of very large earthquakes. A unified understanding of these slow and fast earthquake processes requires an approach integrating geophysics, seismology, geodesy, geology, and non-equilibrium statistical physics. We welcome presentations based on, but not limited to, geophysical observation, data analysis, analytical theory, numerical simulation, field study, and laboratory experiments.

10:45 AM - 11:00 AM JST | 1:45 AM - 2:00 AM UTC

[SCG39-25] Spatio-temporal variation of fluid migration associated with slow earthquakes in the shallow Nankai subduction zone

*Takashi Tonegawa[1], Shunsuke Takemura[2] (1.Japan Agency for Marine-Earth Science and Technology, 2.Earthquake Research Institute, The University of Tokyo)

11:00 AM - 11:15 AM JST | 2:00 AM - 2:15 AM UTC

[SCG39-26] Land and marine long-term magnetotelluric observations around the western Nankai slow slip area

*Hiroshi Ichihara[1,2], Makoto Uyeshima[3], Hayato Nakamura[1], Maki Hata[3], Tada-nori Goto[4], Noriko Tada[2], Tetsuo Matsuno[5], Shinya Sato[6], Yoshiya Usui[3], Ryokei Yoshimura[7], Koki Aizawa[8] (1.Graduate school of Environmental Studies, Nagoya University, 2.JAMSTEC, 3.ERI, University of Tokyo, 4.University of Hyogo, 5.KOBEC, Kobe University, 6.Graduate school of Engineering, Kyoto University, 7.DPRI, Kyoto University, 8.Graduate school of Science, Kyushu Univeristy)

11:15 AM - 11:30 AM JST | 2:15 AM - 2:30 AM UTC

[SCG39-27] Active source seismic experiment investigating structural characteristics associated with slow earthquake activities in the Hyuga-nada, southwestern Japan

*Seiichi Miura[1], Kimihiro Mochizuki[2], Ryuta Arai[1], Yasuyuki Nakamura[1], Yuka Kaiho[1], Gou Fujie[1], Shuichi Kodaira[1], Rie Nakata[2], Yanxue Ma[2], Masataka Kinoshita[2], Yoshitaka Hashimoto[3], Yohei Hamada[1] (1.Japan Agency for Marine-Earth Science and Technology, 2.Earthquake Research Institute, University of Tokyo, 3.Kochi University)

11:30 AM - 11:45 AM JST | 2:30 AM - 2:45 AM UTC

[SCG39-28] Seismic characteristics of the northern Hikurangi subduction zone revealed by offshore seismic observations

*Kimihiro Mochizuki[1], Yusuke Yamashita[2], Emily Warren-Smith[3], Martha K Savage[4], Laura M Wallace[3], Stuart Henrys[3] (1.Earthquake Prediction Research Center, Earthquake Research Institute, University of Tokyo, 2.Disaster Prevention Research Institute, Kyoto University, 3.GNS Science, 4.Victoria University of Wellington)

11:45 AM - 12:00 PM JST | 2:45 AM - 3:00 AM UTC

[SCG39-29] **Temporal velocity variations in the northern Hikurangi margin and their relation to slow slip**

*Weiwei Wang[1], Martha Savage[1], Alec Yates[1,2], Hubert Zal[1], Carolyn Boulton[1], Megan Kortink[3], Tim Stern[1], Bill Fry[3], Kimihiro Mochizuki[4], Spahr Webb[5], Wallace Laura[3] (1.Victoria University of Wellington, 2.Université Grenoble Alpes, Université Savoie Mont Blanc, 3.GNS Science, 4.Earthquake Research Institute, University of Tokyo, 5.Lamont-Doherty Earth Observatory, Columbia University)

12:00 PM - 12:15 PM JST | 3:00 AM - 3:15 AM UTC

[SCG39-30] Discussion

Spatio-temporal variation of fluid migration associated with slow earthquakes in the shallow Nankai subduction zone

*Takashi Tonegawa[1], Shunsuke Takemura[2]

1. Japan Agency for Marine-Earth Science and Technology, 2. Earthquake Research Institute, The University of Tokyo

Slow earthquakes in the subduction zones are potentially linked to fluids, and such observations have been recently reported in the shallow Nankai subduction zone through heterogeneous variations of seismic structure (Tonegawa et al. 2020, JpGU, AGU). However, the region of fluid migration has not been precisely identified yet. Because those studies have reported that fluid migration may occur before shallow slow earthquakes, the identification of the region of fluid migration is important to investigate the characteristics of shallow slow earthquakes. In this study, we estimated two-dimensional maps of the scattering coefficient by seismic heterogeneous variations through a non-linear inversion, i.e., simulated annealing, and investigated the relationship between the scattering coefficient changes, which reflects fluid migration, and slow earthquakes. Here, this technique was confirmed by synthetic waveforms calculated with a three-dimensional velocity structure incorporating heterogeneous structure and random sources at the sea surface.

In the numerical simulations, we set a region with a velocity reduction, and estimated scattering coefficient by using synthetic waveforms with and without the velocity reduction. We performed this test twice by changing the region of velocity reduction, and these tests showed that the anomalies of the scattering coefficient were suitably estimated at the regions of the velocity reductions.

We applied this technique to the following observed data. We calculated cross-correlation functions (CCFs) from ambient noise records in the vertical component observed at the DONET stations, and the stacked CCFs show ocean-acoustically coupled Rayleigh (ACR) waves at frequency band of 0.5–2.0 Hz. We further calculated cross correlation coefficients (CCs) between the reference CCF and individual CCF, which was corrected by temporal change in seismic velocity. Here, dCC is defined by the difference of the CCs (CCs) between the stable period and the period with a reduction. The dCCs for all of the station pairs were the observed data, and such dCCs were observed multiple times.
As a result, the anomaly of the scattering coefficient was estimated to be surrounding and partly overlapped with the region of slow earthquakes including slow slip event (SSE) observed by borehole pore pressure measurements and very low frequency earthquakes (VLFEs). Figure 1 shows an example of dCC occurred in 2012, and the anomaly region was estimated at the southern part of and around the SSE region estimated by Araki et al. (2017). This observation may indicate that a leakage of fluids around the edges of the source region of slow earthquakes is observed.

Keywords: Fluid migration, Spatial mapping, Slow earthquake, Scattering coefficient

©2021. Japan Geoscience Union. All Right Reserved.

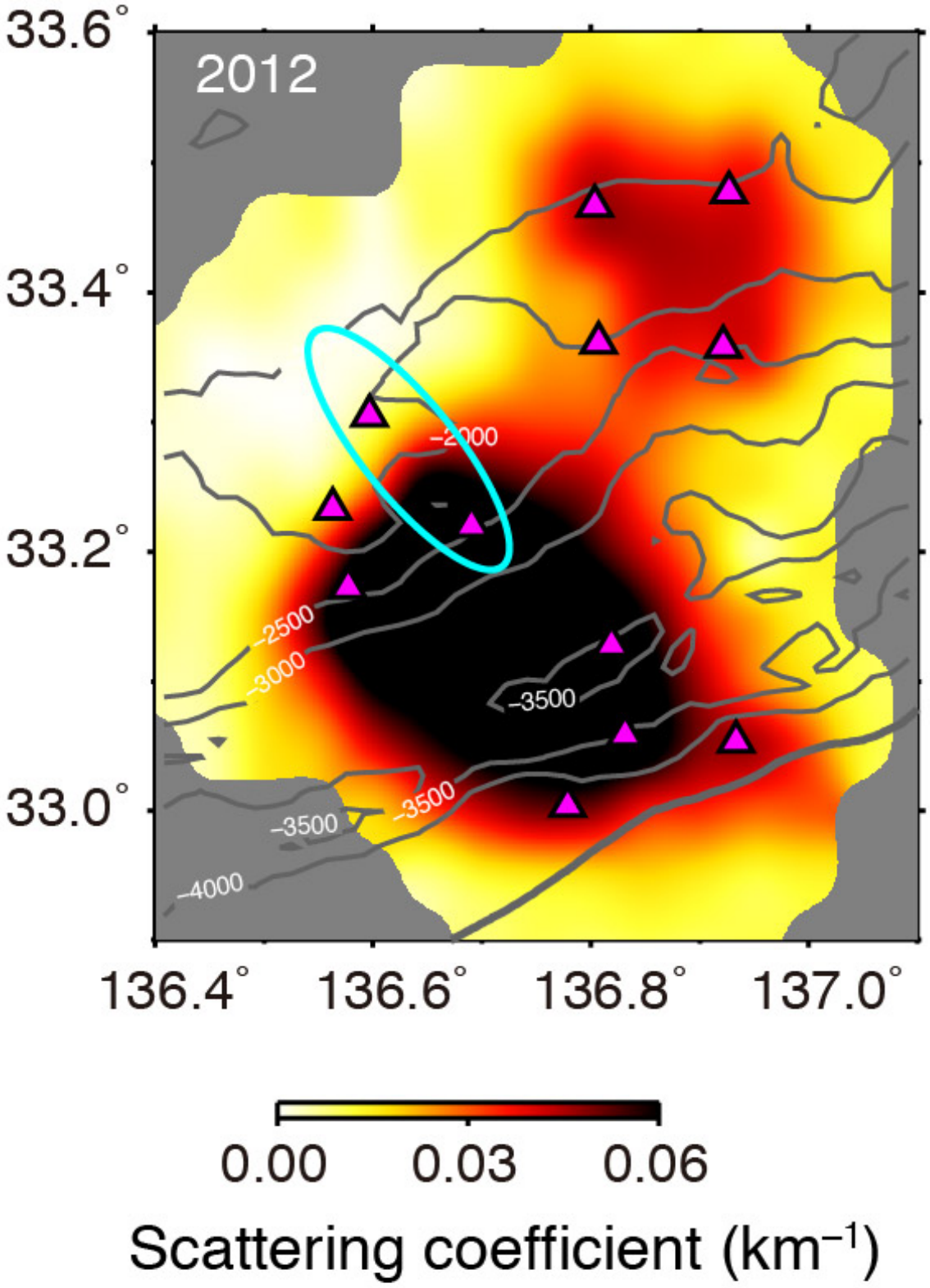


Figure 1. The anomaly of the scattering coefficient around the nodes of KMB, KMC and KMD of DONET for a case of dCC observed in 2012. Blue box roughly indicates the region of SSE detected by Araki et al. (2017).

©2021. Japan Geoscience Union. All Right Reserved.

©2021. Japan Geoscience Union. All Right Reserved.

Land and marine long-term magnetotelluric observations around the western Nankai slow slip area

*Hiroshi Ichihara[1,2], Makoto Uyeshima[3], Hayato Nakamura[1], Maki Hata[3], Tada-nori Goto[4], Noriko Tada[2], Tetsuo Matsuno[5], Shinya Sato[6], Yoshiya Usui[3], Ryokei Yoshimura[7], Koki Aizawa[8]

1. Graduate school of Environmental Studies, Nagoya University, 2. JAMSTEC, 3. ERI, University of Tokyo, 4. University of Hyogo, 5. KOBEC, Kobe University, 6. Graduate school of Engineering, Kyoto University, 7. DPRI, Kyoto University, 8. Graduate school of Science, Kyushu Univeristy

Imaging of resistivity distribution gives us fundamental information about fluid and lithological feature around focal area of slow earthquakes because it depends on the pore-fluid distribution, salinity, connectivity of fluid-filled rock pores, and clay minerals the crust and upper-most mantle. Resistivity distribution of the crust-mantle scale can be estimated based on long period magnetotelluric (MT) observations. In this study, we introduce results of long period MT observations around the slow earthquake zones in the western Nankai trough mainly conducted by the JSPS KAKENHI project "Science of Slow Earthquakes". The observations were carried out by the two research teams for marine and land MT surveys.

Marine MT surveys were conducted between 2017 and 2020 at fifteen sites around the off-Miyazaki and off-Kochi area, Japan, based on Ocean Bottom Electro-Magnetometers (OBEMs). The observation periods of each OBEM were between 5 and 12 months. The training ship “Fukae-maru” and research vessel “Kairei” owned by Kobe University and JAMSTEC, respectively, cooperated for deployment and recovery of OBEMs. The OBEMs also acquired absolute pressure in three sites to detect SSEs. Based on the observed electromagnetic data, we estimated magnetotelluric impedances using BIRRP code (Chave and Thomson, 2004). The estimated MT impedances showed strong coastal effect due to complicated bathymetry in the western Nanakai Trough area. Based on the impedances at the twelve OBEM site in middle and eastern side of study area, we conducted forward resistivity modeling to evaluate the coastal effect using the 3-D modelling code (Tada et al., 2012). A simple optimum model consisting of seawater, seabed conductive layer and underneath background area can explain the coastal effect. In addition, the forward modeling implied heterogenous resistivity structure in the background area. Thus we applied 3-D inversion using the forward model as initial model. The inverted model mostly explained observed MT impedances. The model showed resistive anomaly around the ruptured area of the 1968 Hyuga-nada earthquake (M7.5) (Yagi et al., 1998). The resistivity model also shows conductive area in the western area part of the study area. It may relate to structural heterogeneity dure to subducting Kyushu-Palao ridge.

The network-MT surveys have been carried out in the western part of Shikoku Island and eastern part of Kyushu Island since April, 2016 to discuss resistivity distribution and its time variation in the long-term slow slip events (L-SSE) area beneath the Bungo channel. We used metallic telephone line network of the Nippon Telegraph and Telephone (NTT) Corp. to measure the electrical potential difference with long baselines over several kilometers. The electrical potential differences measured in this way are known to be less affected by small scale near-surface lateral resistivity heterogeneities (e.g. Uyeshima, 2007). We also measure the geomagnetic field at two stations in the target region. We estimated the frequency-domain response functions in the western Shikoku area of good quality with the aid of the BIRRP code. After applying the 3-D DASOCC inversion code (Siripunvaraporn et al., 2004), which directly inverted the Network-MT response and obtain the 3-D resistivity structure in the western Shikoku area.

©2021. Japan Geoscience Union. All Right Reserved.

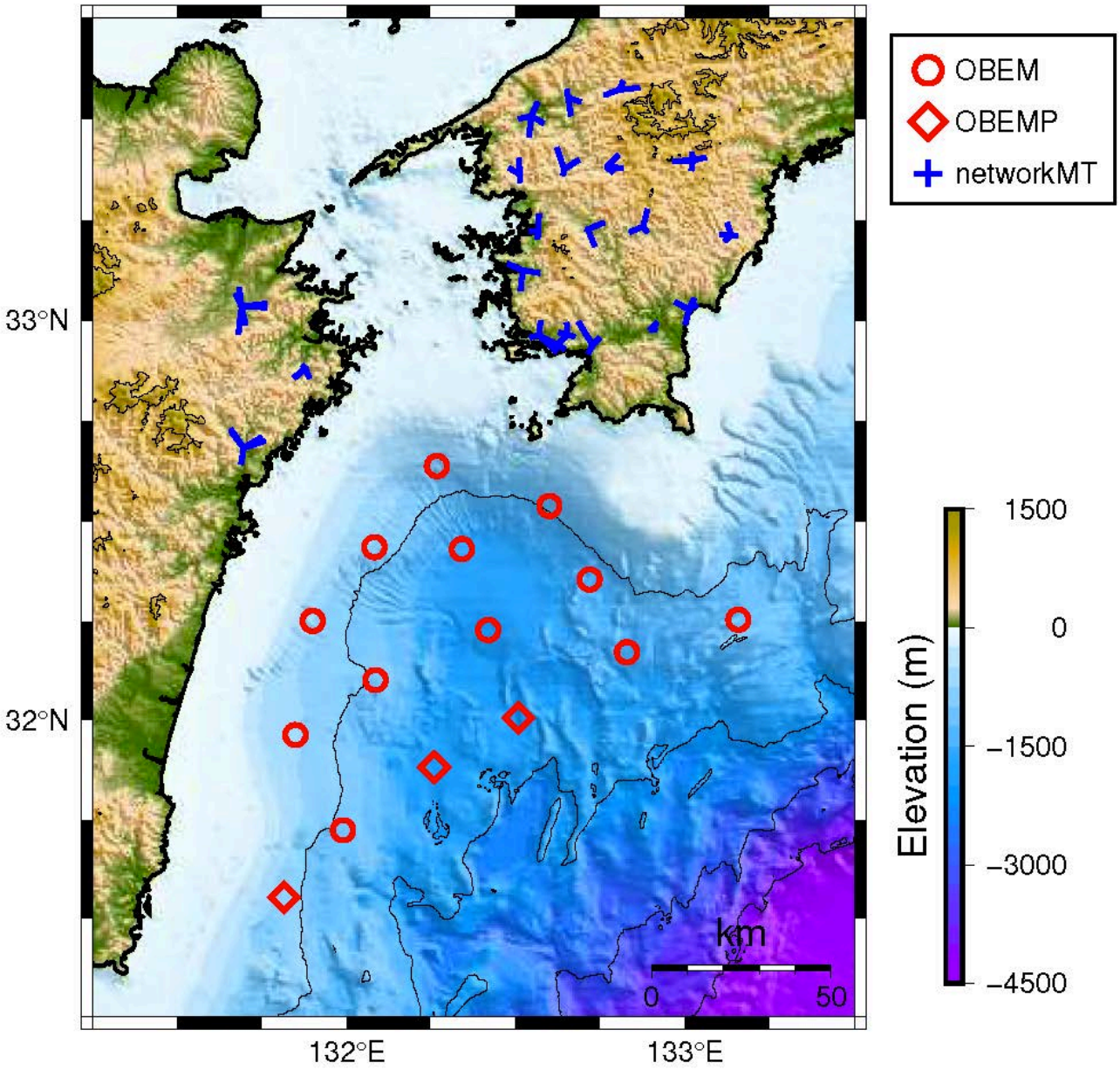
Remarkable low resistivity anomalies were detected in the middle crust of the hanging wall above the subducting Philippine Sea slab. However, no remarkable conductive anomaly was shown around the area of L-SSE in the Bungo channel region. Thus we also examined how the Network-MT responses are sensitive to temporal resistivity change along the slab because the L-SSE repeatedly occurred about every 6 or 7 years. In a test model, 10 km thick conductive layer is assigned just beneath the top surface of the slab. When the resistivity is set to be 20 Ohm-m (thus 500 S anomaly), RMS misfit was significantly increased from the best fit model. It indicates that temporal change could be detected due to current Network-MT survey.

We successfully obtained long-period MT impedances and preliminary resistivity distributions around western Nankai slow earthquake area based on the land and marine MT observations. Thus we plan to integrate the marine and land MT data in this study and past network-MT data in Kyushu Island (e.g. Hata et al., 2015) and estimate reliable 3-D resistivity structure covering the slow EQ areas in the western Nankai subduction zone.

Figure: Locations of OBEM sites and baselines of network-MT

Keywords: Slow earthquake, Bungo Channel, magnetotelluric, OBEM, Network-MT, 3-D resistivity

©2021. Japan Geoscience Union. All Right Reserved.



©2021. Japan Geoscience Union. All Right Reserved.

Active source seismic experiment investigating structural characteristics associated with slow earthquake activities in the Hyuga-nada, southwestern Japan

*Seiichi Miura[1], Kimihiro Mochizuki[2], Ryuta Arai[1], Yasuyuki Nakamura[1], Yuka Kaiho[1], Gou Fujie[1], Shuichi Kodaira[1], Rie Nakata[2], Yanxue Ma[2], Masataka Kinoshita[2], Yoshitaka Hashimoto[3], Yohei Hamada[1]

1. Japan Agency for Marine-Earth Science and Technology, 2. Earthquake Research Institute, University of Tokyo, 3. Kochi University

The Hyuga-nada is located in the westernmost part of the Nankai subduction zone, connecting to the Ryukyu Trench toward southwest. The Kyushu-Palau Ridge in the Philippine Sea Plate is now subducting in the Hyuga-nada region where the seafloor topography is very rough (e.g., Yamamoto et al. 2013). Magnitude (M) seven class large earthquakes have occurred in the Hyuga-nada such as 1961 (M7.0), 1968 (M7.5), and 1984 (M7.1), whereas no earthquake greater than M8 has occurred. Frequent slow slip events (SSE) are detected in the shallow part of the Hyuga-nada as well as low frequency tremors and very low-frequency earthquakes that exhibit spatial migration (e.g. Yamashita et al., 2015; Tonegawa et al., 2020; Yokota and Ishikawa, 2020).

To investigate the structural characteristics associated with the slow earthquake activity in the Hyuga-nada, we conducted two seismic cruises using R/Vs Kaimei and Kairei of Japan Agency for Marine-Earth Science and Technology (JAMSTEC) from August to September, 2020. These cruises are partly supported by KAKENHI “Science of Slow Earthquakes”, and also a part of site survey for IODP drilling proposal in Hyuga-nada. The seismic source was an airgun array with total volume of 10600 cu. in. of R/V Kaimei. Multi-channel seismic (MCS) hydrophone streamer cable with 6-km length was also towed by the R/V Kaimei to acquire seismic reflection profiles along the four seismic lines crossing tremor area (Yamashita et al, 2015): NE-SW (HYU01), WNW-ESE (HYU02), and two NW-SE (HYU18 and 22) directions. One hundred ocean bottom seismometers (OBS) were deployed by R/V Kaimei along two seismic lines (HYU01 and HYU02) with 2-km spacing to record wide-angle reflection and refraction signals and retrieved by R/V Kairei .

In our presentation, we will show the detail of the active source experiments, acquired MCS and OBS data, and preliminary processing results.

Keywords: Slow earthquake, Hyuga-nada, MCS, OBS

©2021. Japan Geoscience Union. All Right Reserved.

Seismic characteristics of the northern Hikurangi subduction zone revealed by offshore seismic observations

*Kimihiro Mochizuki[1], Yusuke Yamashita[2], Emily Warren-Smith[3], Martha K Savage[4], Laura M Wallace[3], Stuart Henrys[3]

1. Earthquake Prediction Research Center, Earthquake Research Institute, University of Tokyo, 2. Disaster Prevention Research Institute, Kyoto University, 3. GNS Science, 4. Victoria University of Wellington

Since 2012, we conducted marine seismic observations in the northern part of the Hikurangi subduction zone, where slow slip events have occurred regularly at an interval of 1.5 ~ 2 years. Owing to the shallow subduction of the Pacific Plate beneath the Australian Plate, the structural features of the plate interface have been well identified from seismic reflection sections and magnetic anomaly maps. Such structural features include subducted seamounts and high seismic reflectivity of the plate interface attributable to an abundance of fluid (Bell et al., 2010; Barker et al., 2018).

We started offshore seismic observations by deploying four ocean bottom seismometers (OBSs) for a year-long observation from April 2012 to March 2013. We successfully determined hypocenters of mostly offshore earthquakes and subsurface seismic velocity structures down to ~30 km depth and imaged detailed velocity variations (Mochizuki et al., 2021). We found that the seismicity is mainly distributed around a core of high Vp/Vs bodies within the subducted oceanic crust of ~12 km thickness and we interpreted those high Vp/Vs values representing abundance of fluid that has been produced by dehydration reactions during subduction of the oceanic crust. The seismically highly reflective plate interface is found to be located above such high Vp/Vs bodies, which is consistent with our interpretation. Therefore, the seismicity around the high Vp/Vs bodies coincides with the peripheries of the highly reflective plate interface.

During a 2014-15 observation period and through international collaboration, we captured for the first time offshore tectonic tremor activity accompanying a large SSE (Wallace et al., 2016; Todd et al., 2018). The tremors appear to be activated near the end of the SSE and continued for about two weeks. The envelope correlation method revealed that a total of 120 tremors were only distributed around one of the subducted seamounts.

Another deployment was undertaken between 2018 and 2019, during which a large SSE occurred in the same region as the 2014 SSE event (Woods et al., 2020). We also observed tremor activity over the subducted seamount, and it showed the same temporal relationship with the SSE occurrence as the 2014 activity (Yamashita et al., 2020).

These observations strongly suggest the involvement of cyclic fluid transfer around the plate interface in concordance with the occurrences of SSE and tremors. Indeed, the spatio-temoral distribution of focal mechanisms as well as changing seismic velocity and anisotropy, suggests the systematic changes of fluid pressure within the subducting oceanic crust (Warren-Smith et al., 2019; Zal et al., 2020; Wang et al., in preparation). Therefore, the fluid production rate within the subducting oceanic crust is possibly a major factor that controls the seismic behavior at the northern Hikurangi margin. Rolling ocean bottom seismograph deployments are improving our ability to evaluate seismic potential, by accounting for the influence of slow slip events.

©2021. Japan Geoscience Union. All Right Reserved.

Keywords: Slow slip events, Fluid transfer, High Vp/Vs bodies

©2021. Japan Geoscience Union. All Right Reserved.

Temporal velocity variations in the northern Hikurangi margin and their relation to slow slip

*Weiwei Wang[1], Martha Savage[1], Alec Yates[1,2], Hubert Zal[1], Carolyn Boulton[1], Megan Kortink[3], Tim Stern[1], Bill Fry[3], Kimihiro Mochizuki[4], Spahr Webb[5], Wallace Laura[3]

1. Victoria University of Wellington, 2. Université Grenoble Alpes, Université Savoie Mont Blanc, 3. GNS Science, 4. Earthquake Research Institute, University of Tokyo, 5. Lamont-Doherty Earth Observatory, Columbia University

Slow Slip Events (SSE) have been studied in increasing detail over the last 20 years, improving our understanding of subduction zone behavior. Although the relationship between SSEs and the physical properties of their surrounding materials is still not well-understood, the northern Hikurangi margin in New Zealand is the site of relatively shallow (<10 km deep), frequent SSEs, providing excellent opportunities for near-field investigations. From September to October 2014, an SSE occurred with more than 250 mm slip, and was recorded successfully by the Hikurangi Ocean Bottom Investigation of Tremor and Slow Slip (HOBITSS) deployment. This study applies coda wave interferometry to the ambient noise data acquired by nine HOBITSS ocean bottom seismometers (OBS) to study the seismic velocity variations related to the SSE. Single station cross-component correlations are computed and a period band of 2.5-14 s is used to calculate velocity variations, which focuses on the upper plate in our study region. The average velocity variations display a velocity decrease of approximate 0.05% during the SSE, followed by a velocity increase of approximate 0.05% afterward. We suggest that two possibilities exist to explain this: The first possibility is the velocity changes are related to changes in crustal strain during the slow slip cycle, whereby elastic strain accumulates prior to the SSE causing contraction and reduction of porosity above the SSE source (seismic velocity increase between SSEs). During the SSE the upper plate goes into extension as the elastic strain is released, which results in dilation and a porosity increase (seismic velocity reduction). After the SSE, stress and strain accumulate again, causing a porosity decrease and a velocity increase. The second possibility, which has been suggested by other seismological observations is that fluid migration into the upper plate during the SSE, due to breakage of a low-permeability seal on the plate boundary caused by the SSE, explains the seismic velocity decrease during the SSE. Under this model, after the SSE, the fluids in the upper plate diffuse gradually and the velocity increases again.

Keywords: slow slip event, the Hikurangi subduction zone, seismic velocity variations, ambient noise

©2021. Japan Geoscience Union. All Right Reserved.

[E] Oral | S (Solid Earth Sciences) | S-CG Complex & General

[S-CG39] Science of slow earthquakes: Toward unified understandings of whole earthquake process

convener:Satoshi Ide(Department of Earth an Planetary Science, University of Tokyo), Hitoshi Hirose(Research Center for Urban Safety and Security, Kobe University), Kohtaro Ujiie(Faculty of Life and Environmental Sciences, University of Tsukuba), Takahiro Hatano(Department of Earth and Space Science, Osaka University), Chairperson:Kimihiro Mochizuki(Earthquake Prediction Research Center, Earthquake Research Institute, University of Tokyo)

Sun. Jun 6, 2021 10:45 AM - 12:15 PM Ch.21 (Zoom Room 21)

Accumulating observational studies on various types of slow deformation events, such as tectonic tremors, very low frequency events, and slow slip events, portrays some universal characteristics in generally complex behavior, including interaction among events and influence by various outer loading. Some of these phenomena seem to have causal relation with the occurrence of very large earthquakes. A unified understanding of these slow and fast earthquake processes requires an approach integrating geophysics, seismology, geodesy, geology, and non-equilibrium statistical physics. We welcome presentations based on, but not limited to, geophysical observation, data analysis, analytical theory, numerical simulation, field study, and laboratory experiments.

12:00 PM - 12:15 PM

[SCG39-30]Discussion

©Japan Geoscience Union

[E] Poster | S (Solid Earth Sciences)：S-CG Complex & General

Sun. Jun 6, 2021 5:15 PM - 6:30 PM JST | Sun. Jun 6, 2021 8:15 AM - 9:30 AM UTC | Ch.14_1

[S-CG39] Science of slow earthquakes: Toward unified understandings of whole earthquake process

convener:Satoshi Ide(Department of Earth an Planetary Science, University of Tokyo), Hitoshi Hirose(Research Center for Urban Safety and Security, Kobe University), Kohtaro Ujiie(Faculty of Life and Environmental Sciences, University of Tsukuba), Takahiro Hatano(Department of Earth and Space Science, Osaka University)

Accumulating observational studies on various types of slow deformation events, such as tectonic tremors, very low frequency events, and slow slip events, portrays some universal characteristics in generally complex behavior, including interaction among events and influence by various outer loading. Some of these phenomena seem to have causal relation with the occurrence of very large earthquakes. A unified understanding of these slow and fast earthquake processes requires an approach integrating geophysics, seismology, geodesy, geology, and non-equilibrium statistical physics. We welcome presentations based on, but not limited to, geophysical observation, data analysis, analytical theory, numerical simulation, field study, and laboratory experiments.

[SCG39-P01] Migration characteristics of shallow very low frequency earthquake episodes southeast off the Kii Peninsula

*Shunsuke Takemura[1], Kazushige Obara[1], Katsuhiko Shiomi[2], Akiko Takeo[1], Satoru Baba[1] (1.Earthquake Research Institute, the University of Tokyo, 2.National Research Instituite for Earth Science and Disaster Resilience)

[SCG39-P02] **Complementary distribution between very-low-frequency earthquakes and interplate-coupled area in the southwestern Ryukyu Trench**

Ren Yakabu[1], *Mamoru Nakamura[1] (1.Faculty of Science, University of the Ryukyus)

[SCG39-P03] **Spatio-temporal distribution of very low-frequency earthquakes activity in the north Ryukyu Trench**

*Mamoru Nakamura[1], Shuichi Kodaira[2], Yasushi Ishihara[2], Ban-Yuan Kuo[3], PeiYing Patty Lin[4] (1.Faculty of Science, University of the Ryukyus, 2.JAMSTEC, 3.Academia Sinica, 4.National Taiwan Normal University)

[SCG39-P04] Attenuation effect on observed frequency characteristics of broadband slow earthquakes

*Koki Masuda[1], Satoshi Ide[1], Takanori Matsuzawa[2] (1.Department of Earth an Planetary Science, University of Tokyo, 2.National Research Institute for Earth Science and Disaster Resilience)

[SCG39-P05] **Frictional coefficient and its velocity dependence of cuttings retrieved from the Nankai accretionary prism at IODP Site C0002**

*Riho Fujioka[1], Ikuo Katayama[1], Manami Kitamura[2], Hanaya Okuda[3], Takehiro Hirose[4] (1.Department of Earth and Planetary Systems Science, Hiroshima University, 2.National Institute of Advanced Industrial Science and Technology, 3.Department of Ocean Floor Geoscience, Atmosphere and Ocean Research Institute, University of Tokyo, 4.Kochi Institute for Core Sample Research, Japan Agency for Marine-Earth Science and Technology)

[SCG39-P06] Shallow tremor activity in the Hyuga-nada revealed by the seafloor observation of "*Science of Slow earthquakes*"

*Yusuke Yamashita[1], Masanao Shinohara[2], Hiroko Sugioka[3], Aki Ito[4], Tsutomu Takahashi[4], Daisuke Suetsugu[4] (1.Disaster Prevention Research Institute, Kyoto University, Japan, 2.Earthquake Research Institute, University of Tokyo, Japan, 3.Graduate School of Science, Kobe University, Japan., 4.Japan Agency for Marine-Earth Science and Technology, Japan.)

[SCG39-P07] **Extension of aseismic slip propagation theory to slow earthquake migration**

*Keisuke Ariyoshi[1], Roland Burgmann[2], Ampuero Jean-Paul[3] (1.Japan Agency for Marine-Earth Science and Technology, 2.University of California, Berkeley, 3.Institut de Recherche pour le Développement, Université Côte d'Azur)

[SCG39-P08] **Increase of tremor-rate in Marlborough region (New Zealand) after the 2016 Mw 7.8 Kaikōura earthquake.**

*Pierre Romanet[1], Florent Aden-Antoniow[2], Ryosuke Ando[1], Stephen C Bannister[3], Calum John Chamberlain[4], Yoshihisa Iio[5], Satoshi Matsumoto[6], Tomomi Okada[7], Richard H. Sibson[8], Akiko Toh[1], Satoshi Ide[1] (1.The University of Tokyo, School of Science, Earth and Planetary Science , Japan, 2.Department of Earth, Atmospheric and Planetary Sciences, Massachusetts Institute of Technology, Cambridge, MA, USA, 3.GNS Science, PO Box 30-368, Lower Hutt 5040, New Zealand, 4.School of Geography, Environment and Earth Sciences, Victoria University of Wellington, Wellington, New Zealand, 5.Disaster Prevention Research Institute, Kyoto University, Uji 611-0011, Japan, 6.Faculty of Sciences, Kyushu University, 2-5643-29 Shin'yama, Shimabara, Nagasaki 855-0843, Japan, 7.International Research Institute of Disaster Science (IRIDeS), Tohoku University, Sendai 980-0845, Japan, 8.Department of Geology, University of Otago, PO Box 56, Dunedin 9054, New Zealand)

[SCG39-P09] Modeling slow earthquakes by competing time scale of rupture propagation, stress loading and strength healing

*Kota Fukuda[1], Takahiro Hatano[2], Kimihiro Mochizuki[1] (1.Earthquake Research Institute The University of Tokyo, 2.Department of Earth and Space Science Osaka University)

[SCG39-P10] Scaled energy of shallow slow earthquakes in Hyuga-nada, southwest Japan

*Satoru Baba[1], Shunsuke Takemura[1], Kazushige Obara[1], Akiko Takeo[1], Yusuke Yamashita[2], Masanao Shinohara[1] (1.Earthquake Research Institute, The University of Tokyo, 2.Disaster Prevention Research Institute, Kyoto University)

[SCG39-P11] Tectonic tremors influenced by characteristic of structure and pore pressure in the Nankai subduction zone, Japan

*Andri Hendriyana[1], Takeshi Tsuji[2,3,4] (1.Geophysical Engineering, Institute of Technology Bandung, Indonesia, 2.International Institute for Carbon-Neutral Energy Research (I2CNER), Kyushu University, Fukuoka, Japan, 3.Department of Earth Resources Engineering, Kyushu University, Fukuoka, Japan, 4.Disaster Prevention Research Institute, Kyoto University, Kyoto, Japan)

[SCG39-P12] Impact of metasomatism on fluid overpressure in source depths of deep slow earthquakes

*Yasushi Mori[1], Kohtaro Ujiie[2], Miki Shigeno[1], Kazuya Noro[2], Tadao Nishiyama[3] (1.Kitakyushu Museum of Natural History and Human History, 2.University of Tsukuba, 3.Kumamoto University)

[SCG39-P13] Observation of localized slip events using viscoelastic fluids incorporating beads

Rinya Miyakawa[1], Kota Kamijo[1], Tatsuya Nishikubo[1], *Yutaka Sumino[1] (1.Tokyo University of Science)

[SCG39-P14] A trial digitization of analog seismograms of the Kanto-Tokai Observation Network for the analysis of tectonic tremor

*Takanori Matsuzawa[1], Tetsuya Takeda[1] (1.National Research Institute for Earth Science and Disaster Resilience)

[SCG39-P15] Slow slip events in the Bungo Channel and Hyuganada areas from May 2018 to June 2019 detected by a GNSS observation network

*Hitoshi Hirose[1], Takeshi Matsushima[2], Takao Tabei[3], Takuya NISHIMURA[4] (1.Research Center for Urban Safety and Security, Kobe University, 2.Faculty of Science, Kyushu University, 3.Research and Education Faculty, Natural Sciences Cluster, Sciences Unit, Kochi University, 4.Disaster Prevention Research Institute, Kyoto University)

[SCG39-P16] A Bayesian inversion for slip distribution of slow slip events beneath the Bungo Channel based on ensemble modeling of the uncertainty of underground structure

*Ryoichiro Agata[1], Ryoko Nakata[2], Yuji Yagi[3], Takeshi Iinuma[1] (1.Japan Agency for Marine-Earth Science and Technology, 2.Graduate School of Science, Tohoku University, 3.Graduate School of Life and Environmental Sciences, University of Tsukuba)

[SCG39-P17] Spontaneous extension of viscoelastic fluids confined between rotating parallel plates

*Tatsuya Nishikubo[1], Hiroki Ishikawa[1], Shoma Kato[1], Yutaka Sumino[1] (1.Department of Applied Physics, Graduate School of Science, Tokyo University of Science)

[SCG39-P18] **Pattern of injected fluid into a cell filled with swelling gel particles—effect of pressure**

*Kojiro Otoguro[1], Yutaka Sumino[1] (1.Tokyo University of Science)

[SCG39-P19] Detailed mapping of the subducting seamount and deformation structure in the Nankai Trough off the eastern Shikoku region deduced from densely acquired seismic profiles

*Yasuyuki Nakamura[1], Shuichi Kodaira[1], Yuka Kaiho[1], Tetsuo No[1], Kazuya Shiraishi[1], Gou Fujie[1], Seiichi Miura[1], Gaku Kimura[2] (1.Japan Agency for Marine Earth Science and Technology, 2.Tokyo University of Marine Science and Technology)

[SCG39-P20] **Distribution of Very-Low Frequency Earthquake in the Central Ryukyu Trench**

Hiromu Furugen[1], *Mamoru Nakamura[1] (1.Faculty of Science, University of the Ryukyus)

[SCG39-P21] Activity of low-frequency tremors and regular earthquakes off Erimo, Hokkaido from 2006 to 2007, by a tremor investigation based on waveform information

*Susumu Kawakubo[1], Ryosuke Azuma[1], Ryota Hino[1], Hidenobu Takahashi[2,1], Kazuaki Ohta[2], Masanao Shinohara[3] (1.Graduate School of Science Tohoku University, 2.National Research Institute for Earth Science and Disaster Resilience, 3.Earthquake Research Institute, University of Tokyo)

[SCG39-P22] Detecting short-term slow slip events using six-year records of ocean bottom pressure in Hikurangi subduction zone offshore New Zealand

*Tomohiro Inoue[1], Yoshihiro Ito[2], Laura M Wallace[3,4], Takuya Nishimura[2], Spahr Webb[7], Emmanuel Soliman M Garcia[2], Tomoya Muramoto[5], Syuichi Suzuki[6], Ryota Hino[6] (1.Graduate school of science, Kyoto University, 2.Disaster Prevention Research Institute, Kyoto University, 3.GNS Science, Lower Hutt, New Zealand, 4.Institute for Geophysics, University of Texas at Austin, Austin, TX, USA, 5.National Institute of Advanced Industrial Science and Technology, 6.Tohoku University, 7.Lamont-Doherty Earth Observatory, Columbia University)

[SCG39-P23] Variations of source characteristics of shallow tectonic tremor, Nankai trough, inferred from changes of the event size distribution

*Masaru Nakano[1], Suguru Yabe[2] (1.Japan Agency for Marine-Earth Science and Technology, 2.Geological Survey of Japan, AIST)

[SCG39-P24] Moment tensor inversion of shallow very low-frequency earthquakes in the northern Ryukyu subduction zone and the Hyuga-nada region

*Aki Ito[1], Hiroko Sugioka[2], Masaru Nakano[1], Yusuke Yamashita[3], Masanao Shinohara[4], Tsutomu Takahashi[1], Daisuke Suetsugu[1], Takashi Tonegawa[1] (1.Japan Agency for Marine-Earth Science and Technology, 2.Graduate School of Science, Kobe University, 3.Miyazaki Observatory, Disaster Prevention Research Institute, Kyoto University, 4.Earthquake Research Institute, University of Tokyo)

[SCG39-P25] Along-trench structural variation of the Philippine Sea plate subducting in the Hyuga-nada region and its relation to slow earthquakes

*Ryuta Arai[1], Seiichi Miura[1], Yasuyuki Nakamura[1], Gou Fujie[1], Yuka Kaiho[1], Shuichi Kodaira[1], Kimihiro Mochizuki[2], Rie Nakata[2] (1.Japan Agency for Marine-Earth Science and Technology, 2.Earthquake Research Institute, The University of Tokyo)

[SCG39-P26] Gravity data analysis to extract temporal gravity anomalies associated with slow slip events in the Ryukyu Trench

*Yuichi Hiramatsu[1], Yoshiyuki Tanaka[1], Akio Kobayashi[2] (1.Department of Earth Planetary Science , The University of Tokyo, 2.Meteorological Research Institute, JMA)

[SCG39-P27] Lithosphere properties along North-Central Chile subduction region and Relation to slow slip

*POUSALI MUKHERJEE[1], Yoshihiro Ito[1], Emmanuel Soliman M. Garcia[1], Kajaljyoti Borah[2] (1.Disaster Prevention Research Institute, Kyoto University, 2.Indian Institute of Science Education and Research, Kolkata)

[SCG39-P28] A comparison of the source areas in Hyuganada among afterslip of two interplate earthquakes in 1996 and successive slow slip events

Sawako Teshiba[1], *Hitoshi Hirose[1,2] (1.Department of Planetology, Graduate School of Science, Kobe University, 2.Research Center for Urban Safety and Security, Kobe University)

[SCG39-P29] Development of microseismicity catalog near the Japan Trench shallow slow earthquake region using a deep learning module

*Shukei Ohyanagi[1], Kazuaki Ohta[3], Yoshihiro Ito[2], Ryota Hino[4], Yusaku Ohta[4], Ryosuke Azuma[4], Masanao Shinohara[5], Kimihiro Mochizuki[5], Toshinori Sato[6], Yoshio Murai[7] (1.Graduate School of Science, Kyoto University, 2.Disaster Prevention Research Institute, Kyoto University, 3.National Research Institute for Earth Science and Disaster Resilience, 4.Tohoku University, 5.Earthquake Research Institute, The University of Tokyo, 6.Chiba University, 7.Hokkaido University)

Migration characteristics of shallow very low frequency earthquake episodes southeast off the Kii Peninsula

*Shunsuke Takemura[1], Kazushige Obara[1], Katsuhiko Shiomi[2], Akiko Takeo[1], Satoru Baba[1]

1. Earthquake Research Institute, the University of Tokyo, 2. National Research Institute for Earth Science and Disaster Resilience

Recent studies revealed that slow earthquake activity patterns could be related to the tectonic environment, such as frictional conditions and stress accumulation on the plate boundary (e.g., Takemura, Noda et al., 2019; Baba et al., 2020). To reveal spatial heterogeneities on the shallow plate boundary off the Kii Peninsula, where shallow slow earthquakes actively occur, we conducted template matching and cross-correlation analysis of Takemura, Noda et al. (2019). In our analysis, to enhance VLFE signals at NIED F-net stations, we used filtered velocity waveforms with periods of 20-50 s.

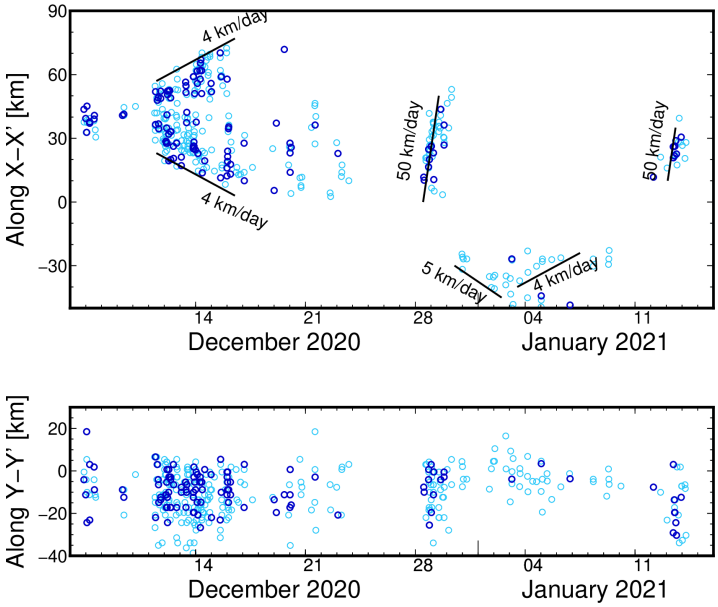
Takemura Noda et al. (2019) reported the large VLFE episodes in September 2004 and March 2009. We found another large shallow VLFE episode, which started on 6 December 2020. This episode started in the eastern side of the shallow VLFE active areas, and then VLFEs bilaterally migrated along the strike direction at a speed of approximately 4 km/day (Figure). Several rapid (~50 km/day) VLFE reverse migrations after passing the major migration front were found. Similar characteristics were confirmed in the episodes of 2004 and 2009, but the major fronts of both VLFE episodes were characterized by eastward migration with approximately 8 km/day from the western side of the activity area. These differences among each shallow VLFE episode may be related to local heterogeneities on the shallow plate boundary southeast off the Kii Peninsula.

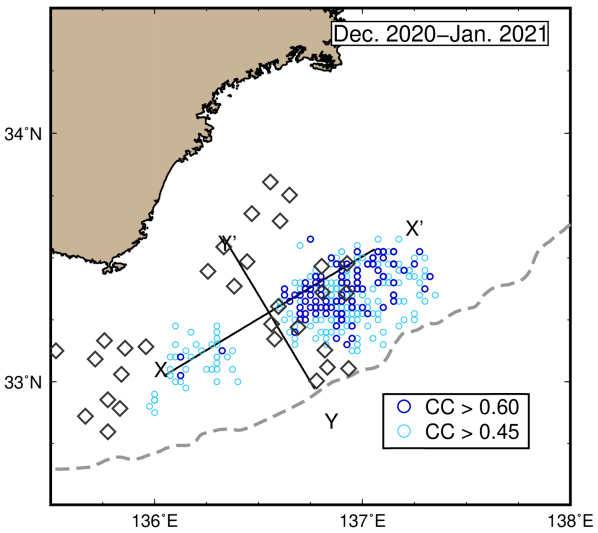
To investigate this episode more quantitatively, we evaluated moment rate functions of detected VLFEs via the simulated annealing method. Green’ s functions from sources to F-net stations in the regional 3D model were evaluated by the OpenSWPC (Maeda et al., 2017). We constructed the 3D model by combining Koketsu et al. (2012) and Tonegawa et al. (2017). Focal mechanisms and source depths were fixed as low-angle thrust-faulting mechanisms on the plate boundary (e.g., Baba et al., 2020). By using estimated moment rate functions, we depicted spatiotemporal characteristics of moment release during this VLFE episode. The total moment of this episode was 3.45×10^{17} Nm, which is about ten times larger than that of the episode in April 2016 estimated by DONET data (Nakano et al., 2018). The VLFEs with low moment release rates were dominant in the initiation phase of the episode, the VLFEs with high moment rates continuously occurred along the major and rapid reverse migration fronts. This feature is similar to the deep tremor episodes (e.g., Thomas et al., 2013; Yabe and Ide, 2014).

Acknowledgments: We used NIED F-net data https://doi.org/10.17598/NIED.0005. Numerical simulations were conducted on the Fujitsu PRIMERGY CX600M1/CX1640M1 (Oakforest-PAC) in the Information Technology Center, University of Tokyo. This study was also supported by the ERI JURP 2020-S-04

Keywords: slow earhquake, Nankai Trough, migration, source time function

©2021. Japan Geoscience Union. All Right Reserved.





©2021. Japan Geoscience Union. All Right Reserved.

Complementary distribution between very-low-frequency earthquakes and interplate-coupled area in the southwestern Ryukyu Trench

Ren Yakabu[1], *Mamoru Nakamura[1]

1. Faculty of Science, University of the Ryukyus

We investigated the distribution of very low-frequency earthquakes (VLFEs) in the southwestern Ryukyu Trench and clarified its relationship with the interplate-coupling area. In the southwest Ryukyu Trench, VLFEs are widely distributed from the Yaeyama Islands to near Taiwan (Nakamura and Sunagawa, 2015). In this region, slow slip events (SSEs), interplate locked zones (Hsu et al., 2012), and source fault of tsunami earthquake (Nakamura, 2009) are distributed. Distribution of these and VLFEs is important for understanding the frictional conditions in the plate interface subducted in the southwest Ryukyu Trench. However, the broadband seismic network (Fnet) of the National Research Institute for Earth Science and Disaster Prevention (NIED), which has been used in previous studies, has a linearly biased arrangement of seismic stations, which tends to cause large deviations in the determination of the epicenter. Furthermore, the error in determining the epicenter was as large as several tens of kilometers. In order to improve the accuracy of the location, the epicenters of the VLFEs were determined by adding data from Taiwan's Broadband Active Seismic Network (BATS) and temporary broadband seismometers by Association for the Development of Earthquake Prediction to Fnet data and using the semblance method and template method.

We used the semblance method to determine the locations of VLFEs using data for the periods 2005-2013 and 2015-2018. The template method used the data from the period January 2005 to December 2018 to determine the position of the VLFEs. A band-pass filter of 0.02-0.05 Hz was applied to the vertical component waveform in both cases. In the template method, a thrust-type earthquake south of Iriomote Island was used as a template.

The epicenters of the VLFEs determined by the semblance method were distributed in an elongated region along the trench axis. The VLFEs were further divided into three clusters. The clusters were distributed off the south coast of Miyako Island, off the southeast coast of Ishigaki Island, and the south coast of Iriomote Island and Yonaguni Island. The cluster off the southern coast of Iriomote Island and Yonaguni Island had a shape that extends along the trench axis. The slab depths at these epicenters were 10-15 km. The distribution of VLFEs determined by the template method was similar to the case of semblance method, with the epicenter of VLFEs distributed in an elongated region along the trench axis. The epicenter's distribution determined by the template method was 10-20 km north of the one by the semblance method. However, we could detect the clusters off the southern coast of Iriomote Island and Yonaguni Island in the template method. The distribution of clusters off the southeastern coast of Ishigaki Island was scattered. We determined the CMT solutions of the VLFEs and found that they were all reverse fault earthquakes that occurred at epicentral depths of 17-35 km.

The distribution and depths of the determined VLFEs were similar to those of the low-frequency earthquakes (LFEs) determined by OBS (Arai et al., 2016). It was also compatible with the location of LFEs accompanying with VLFEs (Nakamura, 2017). The VLFEs did not occur in the locked area in the southwestern part of the Ryukyu Trench. Similarly, it did not overlap with the region of the reverse fault earthquakes on the down-dip side of the locked area. This suggests that the areas where VLFEs and LFEs occur have a complementary relationship with the interplate locked area.

©2021. Japan Geoscience Union. All Right Reserved.

Keywords: slow earthquake, ryukyu trench, interplate coupling, very-low frequency earthquake

©2021. Japan Geoscience Union. All Right Reserved.

Spatio-temporal distribution of very low-frequency earthquakes activity in the north Ryukyu Trench

*Mamoru Nakamura[1], Shuichi Kodaira[2], Yasushi Ishihara[2], Ban-Yuan Kuo[3], PeiYing Patty Lin[4]

1. Faculty of Science, University of the Ryukyus, 2. JAMSTEC, 3. Academia Sinica, 4. National Taiwan Normal University

We investigated the Spatio-temporal changes in the activity of very low-frequency earthquakes (VLFEs) occurring in the northern Ryukyu Trench. We used broadband ocean-bottom seismometers (OBS) installed in the north Ryukyu Trench and the north Okinawa Trough, and broadband seismographs installed on land (F-net and temporary stations). The station intervals of the OBSs were approximately 20 to 60 km. The template matching method (Asano et al., 2015) was used to detect and the epicentral determination of the VLFEs. The vertical component waveforms were band-pass filtered at 0.05-0.1 Hz, and the cross-correlation with the template was calculated. Thrust-type earthquakes that occurred in the Ryukyu Trench were used as the template.

As a result of the analysis, active regions of the VLFEs were distributed off the northeast of Amami Island and from the southeast coast of Amami Island to the offshore of Okinoerabu Island. The errors of the epicentral position were 10-20 km. Off the northeast coast of Amami Island, the swarm of VLFEs started in November 2018. The swarm area corresponds to the slab depth of 10-30 km. The swarm activity concentrated around 28.6N and 130.6E, and the activity of the VLFEs spreaded to the west and south of the active area, avoiding the active area of regular earthquakes. In January 2019, the VLFE swarm activity was observed off the east of Amami Island. The VLFE activity was separated in several clusters along the trench in the east of Okinoerabu Island. The location of the clusters corresponded to a slab depth of 10-20 km.

The activity of these VLFEs did not overlap with the faults of slow slip events (SSEs). However, they tend to occur at the edge of the SSE faults near Kikai Island and Okinoerabu Island. The cluster of the VLFEs was complementary to the distribution of the thrust-type earthquakes.

The magnitude distribution of the VLFEs showed that the large-scale VLFEs occurred in the clusters of VLFEs in the east of Okinoerabu Island and east of Amami Island. The magnitude of VLFEs tended to be larger at shallower slab depths. Variation in the size of maximum earthquake was also observed along the trench axis. This suggests that the frictional condition is changing along the trench axis.

Keywords: slow earthquake, Ryukyu trench, interplate coupling, very-low frequency earthquake

©2021. Japan Geoscience Union. All Right Reserved.

Attenuation effect on observed frequency characteristics of broadband slow earthquakes

*Koki Masuda[1], Satoshi Ide[1], Takanori Matsuzawa[2]

1. Department of Earth an Planetary Science, University of Tokyo, 2. National Research Institute for Earth Science and Disaster Resilience

Slow earthquakes have been classified according to the observation frequency, or period, bands: such as low frequency earthquake (LFE) and tremor in 1-10 Hz, very low frequency earthquake (VLFE) in 20 to 100 s, and much longer slow slip event (SSE). This classification was popular because it is difficult to detect signals of slow earthquakes in 0.1-1 Hz due to large microseism noise. However, recent studies confirmed continuous signals from LFE and tremor to VLFE frequency bands, i.e., 0.01-10 Hz, by near-field observation at the shallow part of the subduction zone during low microseism activity (Kaneko et al., 2018), and by stacking records of many LFEs at the deep part of the subduction zone (Masuda et al., 2020). Therefore, it is time to redefine slow earthquakes as phenomena in a continuous broad frequency band, and investigate the characteristic of broadband slow earthquakes.
An important quantity characterizing a broadband slow earthquake is relative magnitude of seismic radiation among different frequency bands, which we investigate by using the maximum amplitude of the stacked waveforms aligned relative to the timing of LFEs. First, we detected LFEs using a two-step matched-filter analysis in three regions, Shikoku, Kii, and Tokai. The data used for this analysis is the velocity seismograms of Hi-net. The first step adopts templates from the observed waveforms of the selected LFE events in the JMA catalog referring the result of Kato & Nakagawa (2020). The stacked waveforms of detected events in the first step is used as templates for the second step. Then, we aligned broadband seismograms, which is the data of high sensitivity accelerometers of Hi-net, relative to the timing of the detected LFEs, stacked, integrated them to convert to velocity data, and normalized by the maximum amplitude. The maximum amplitude of stacked waves bandpass filtered in low frequency bands generally increases as distance from the hypocenter. This is due to the attenuation of seismic waves, i.e., low frequency waves are less attenuated than high frequency waves, which control the total amplitude in broad frequency band.

Keywords: slow earthquakes, broadband slow earthquakes, LFE, tremor, VLFE

©2021. Japan Geoscience Union. All Right Reserved.

Frictional coefficient and its velocity dependence of cuttings retrieved from the Nankai accretionary prism at IODP Site C0002

*Riho Fujioka[1], Ikuo Katayama[1], Manami Kitamura[2], Hanaya Okuda[3], Takehiro Hirose[4]

1. Department of Earth and Planetary Systems Science, Hiroshima University, 2. National Institute of Advanced Industrial Science and Technology, 3. Department of Ocean Floor Geoscience, Atmosphere and Ocean Research Institute, University of Tokyo, 4. Kochi Institute for Core Sample Research, Japan Agency for Marine-Earth Science and Technology

To understand the process of Nankai megathrust earthquakes, the Nankai Trough Seismogenic Zone Excavation Project (NanTroSEIZE) has been conducted as part of the IODP since 2007 to 2019. Previous studies of friction experiments were performed using core samples collected by ODP/IODP drilling project (e.g., Takahashi et al., 2014; Ikari et al., 2020), however, these samples were retrieved form the shallow parts of the Nankai accretional prism. In order to make detailed depth profile of frictional properties, we carried frictional experiments on cuttings samples, which were collected from 875 to 3262 meters below seafloor (mbsf) during riser operations in the IODP Expeditions 348 and 358.

Frictional tests (currently about 40 cuttings) were conducted by biaxial frictional machine at Hiroshima University under wet conditions (brine, 0.5 mol/L) at in-situ effective normal stress assuming the hydrostatic condition (σe = 9–34 MPa). The cuttings samples were ground and the grain size was adjusted to less than 106 μm. The gouge sample was sandwiched by gabbro blocks in double–direct configuration. After slip behavior reached a steady state at 3 μm/s, velocity was changed stepwise between 0.3, 3, and 33 μm/s. In these tests, frictional coefficient at a steady state and the velocity dependence parameters (a, b, and Dc) defined by the rate- and sate-dependent friction constitutive law were examined. To obtain the velocity dependence parameters, we used software “RSFit3000” (Skarbek and Savage,2019). The relationship between frictional properties and clay contents were also investigated using clay content data reported by Underwood 2017.

Frictional coefficient of the cuttings samples were ranging from 0.472 to 0.657, in which frictional coefficients tend to slightly as the depth increased. Frictional coefficients show a negative correlation with increasing smectite content, which is consistent with the pervious study (Takahashi et al., 2014). Velocity dependence of friction(a-b) were positive ranging from 0.001 to 0.006, indicating a velocity strengthening behavior. Dc tends to decrease with depth, which is likely related to decreasing smectite contents. From these experimental results, the frictional properties at Site C0002 are governed by the clay mineralogy and its content. The relatively large Dc and positive velocity dependence at shallow depth may favor the occurrence of slow slip that have been observed around the drilling site.

Keywords: friction, Nankai trough, clay minerals

©2021. Japan Geoscience Union. All Right Reserved.

Shallow tremor activity in the Hyuga-nada revealed by the seafloor observation of "*Science of Slow earthquakes*"

*Yusuke Yamashita[1], Masanao Shinohara[2], Hiroko Sugioka[3], Aki Ito[4], Tsutomu Takahashi[4], Daisuke Suetsugu[4]

1. Disaster Prevention Research Institute, Kyoto University, Japan, 2. Earthquake Research Institute, University of Tokyo, Japan, 3. Graduate School of Science, Kobe University, Japan., 4. Japan Agency for Marine-Earth Science and Technology, Japan.

In the Hyuga-nada region, the western part of Nankai Trough, after the first observation of shallow tremors in 2013, ocean bottom seismological observation in the shallow tremor focal region has been conducted continuously since 2014. In March 2017, the observation using ocean bottom seismometers and pressure gauges started as part of "*Science of Slow Earthquakes*". The instruments of the first observation were recovered in January-February 2019, and generally good records were obtained. During the first observation period from December 2017 to January 2018, shallow slow earthquake activity increased from off the east of Tanegashima to Hyuga-nada, and shallow tremors and VLFEs activity were recorded in our seismic network. The second observation started in August 2018, and the recovery was conducted in September 2020. During the second observation period, a M_J 6.3 earthquake (31.81˚N, 131.93˚E, 19km) occurred on May 10, 2019, and we succeeded in capturing the slow earthquake activity that may have been triggered by this earthquake. For these activities, we determined the location of the shallow tremors using almost the same method as Yamashita *et al.* [2015]. The depth of the hypocenter was fixed to the plate boundary model by Nakanishi *et al.* [2018], and the S-wave velocity structure was assumed to be homogeneous with 3.5 km/s. The source of the shallow tremor was determined by the ocean bottom seismological network including another project, which was conducting observations in the off east of Tanegashima Island at the same time.

As a result of the analysis, we found that the epicentral distribution of shallow tremors in the first observation is almost the same as that of the 2013 activity area up to the point where the epicentral distribution bends to the east. The distribution of the tremors coincides with the first migration episode seen in the 2013 activity. The clear migration was also confirmed, and the migration from south to north and the endpoint of the migration were almost the same as the first migration episode in the 2013 activity. The area where the migration stopped may correspond to the area where the Kyushu-Palau Ridge is subducting.

As for the second observation, the activity started a few hours after the Mj 6.3 earthquake near the northern end of the first observation activity, and the eastward and southward migration was confirmed. In the eastward migration, although the number of detectable stations was limited and the source location has not yet been determined in many events, the waveform record revealed that the activity continued until around May 25. Migration to the south was intermittent but slow, a few kilometers per day, and propagated to about 30.5˚N, off the east coast of Tanegashima, over a month and a half. The end of the migration was almost the same as that of the first observation, suggesting that the southern end of the shallow tremor from Hyuga-nada to the south is around 30.5˚N. Also, the direction of migration and the pattern of shallow tremor activity seem to change around 31˚N. This area is considered to be a subduction area of seamounts belonging to the Kyushu-Palau Ridge; the northward migration of shallow tremors is blocked by the NW-SW oriented subducting seamounts, and the migration direction is changed to the northwest. A similar pattern was observed in the first observation and 2013 activity, suggesting that

©2021. Japan Geoscience Union. All Right Reserved.

the active area of shallow tremors is strongly influenced by the subduction of the Kyushu-Palau Ridge.

Acknowledgments: This study is supported by the JSPS KAKENHI Grant Number JP16H06471, JP17K01328, and the research project for compound disaster mitigation on the great earthquakes and tsunami around the Nankai trough region, the MEXT of Japan.

Keywords: Slow earthquake, Shallow low-frequency tremor, Ocean bottom seismological observaion

©2021. Japan Geoscience Union. All Right Reserved.

Extension of aseismic slip propagation theory to slow earthquake migration

*Keisuke Ariyoshi[1], Roland Burgmann[2], Ampuero Jean-Paul[3]

1. Japan Agency for Marine-Earth Science and Technology, 2. University of California, Berkeley, 3. Institut de Recherche pour le Développement, Université Côte d’ Azur

Recent observations have revealed various types of migrating slow earthquake phenomena. Very low-frequency earthquakes, one of the major types of slow earthquake, have migration speed in the range of about 1-10 km/day, which is much lower than shear wave speeds. Slow earthquakes also have anomalous moment-duration scaling, compared to regular earthquakes, and they are one possible mechanism of precursory slip before large earthquakes. To model and improve our understanding of the migration process of slow earthquakes and their longer duration relative to regular earthquakes, we assume a chain reaction model of numerous asperities along the strike direction, governed by rate- and state-dependent friction on a 3-D subduction plate boundary. From the simulation results, we find that the migration speed is quantitatively explained by an analytical derivation of frictional properties. By applying the analytical results to the simulation and observational results, we conclude that (i) the migration speed of slow slip transients can increase before megathrust earthquakes due to an increase of the background slip velocity, (ii) the longer duration of slow earthquakes given their seismic moment may be explained by the chain reaction model with time delay for stress transfer between nearby asperities mediated by aseismic slip propagation, and (iii) the characteristic slip distance for very low-frequency earthquakes can be roughly estimated in the range of 0.1 μm~2 mm.

Keywords: rate- and state-dependent friction law, subduction zones, megathrust earthquakes

©2021. Japan Geoscience Union. All Right Reserved.

Increase of tremor-rate in Marlborough region (New Zealand) after the 2016 Mw 7.8 Kaikōura earthquake.

*Pierre Romanet[1], Florent Aden-Antoniow[2], Ryosuke Ando[1], Stephen C Bannister[3], Calum John Chamberlain[4], Yoshihisa Iio[5], Satoshi Matsumoto[6], Tomomi Okada[7], Richard H. Sibson[8], Akiko Toh[1], Satoshi Ide[1]

1. The University of Tokyo, School of Science, Earth and Planetary Science , Japan, 2. Department of Earth, Atmospheric and Planetary Sciences, Massachusetts Institute of Technology, Cambridge, MA, USA, 3. GNS Science, PO Box 30-368, Lower Hutt 5040, New Zealand, 4. School of Geography, Environment and Earth Sciences, Victoria University of Wellington, Wellington, New Zealand, 5. Disaster Prevention Research Institute, Kyoto University, Uji 611-0011, Japan, 6. Faculty of Sciences, Kyushu University, 2-5643-29 Shin'yama, Shimabara, Nagasaki 855-0843, Japan, 7. International Research Institute of Disaster Science (IRIDeS), Tohoku University, Sendai 980-0845, Japan, 8. Department of Geology, University of Otago, PO Box 56, Dunedin 9054, New Zealand

In a previous study, tremors have been detected in Marlborough (New Zealand) region using 6 stations from the national GEONET network during the period 2010-2017. This region hosted the 2016 Mw7.8 Kaikōura earthquake, and lies at the transition between the Alpine Fault and the Hikurangi subduction zone. The previous study detected 40 tremors in this region, however this work was limited by the scarcity of seismic stations and their distance from the tremor area. Here we conduct the same analysis, but in addition to 4 stations from the national network, we added 16 stations from a local campaign network that surrounds the tremor area. This composite network enabled the construction of an enhanced tremor catalogue for the region, composed of around 100 times more tremors than the previous study (4,699 tremors) during the period 2013-2019.

The tremor locations form two clusters, one that has a circular shape, and another one that as an elongated shape in the direction of the major upper-plate dextral (Hope and Clarence) faults of the Marlborough Fault system. The estimated depth of the tremor, as well as the shape of the cluster suggests that these tremors may be on the dextral strike-slip faults and not on the subduction interface although It needs to be confirmed by further study.

We observed that the tremor rate is almost constant before the Mw 7.8 Kaikōura earthquake. After the earthquake, we observed a huge increase in the tremor rate in both the clusters. At the end of our analysis in May 2019, more than 2 years after the earthquake, the tremor-rate has still not recovered to the pre-earthquake rate. This increase in tremor-rate appears unrelated to changes in seismic networks.

We were also able to observe several local migrations of tremors with jumps from one cluster to the other. Most of the migrations take place from the South-West to the North-East. We estimated the migration velocity to be of around ~50km/day.

©2021. Japan Geoscience Union. All Right Reserved.

This new tremor catalog provides unique information on the tectonic context of the Marlborough fault system and may help to better understand interaction of regular earthquakes with tremors.

Keywords: Slow-earthquake, Tremors

©2021. Japan Geoscience Union. All Right Reserved.

Modeling slow earthquakes by competing time scale of rupture propagation, stress loading and strength healing

*Kota Fukuda[1], Takahiro Hatano[2], Kimihiro Mochizuki[1]

1. Earthquake Research Institute The University of Tokyo, 2. Department of Earth and Space Science Osaka University

Slow earthquakes, which have been actively studied in recent years, are phenomena with a wide range of propagation velocities on the order of 0.1 m/s (SSE) to 10 m/s (LFE) and a duration of several years (SSE) to 0.1 s (LFE) with a wide range of time constants [Ide et al., 2007]. The purpose of this study is to investigate the possibility of using cellular automaton models to comprehensively model the behavior of a wide range of slow earthquakes using the widely varying propagation time constant as a parameter.

Conventional studies of cellular automata models have aimed at modeling regular earthquakes, and have assumed that the time constant of stress accumulation is negligible compared to the time constant of rupture propagation [Carlson and Langer,1989:Olami et al.,1992]. However, in slow earthquakes with slow rupture propagation, these two time constants may be in competition. In order to discuss how this effect affects the statistical properties, the Dynamic OFC model is an extension of the Olami_Feder_Christensen model that reproduces the GR law well. This model is incorporating a finite rupture chain time constant and a loading time constant. In the Dynamic OFC model, the competition between these two time constants is known to produce continuous events, and this behavior reproduces the point that the tremor is swarms of low-frequency earthquakes.

The Dynamic OFC model discussed so far incorporates the assumption that the rupture threshold (corresponding to the strength) does not change even at the end of one rupture step, which implies that the strength recovery is very fast in relation to the rupture chain (i.e., the rupture chain is slow). In this study, the model was extended to include a new parameter, the ratio of the time constant of loading and strength recovery to the time constant of the fracture chain. This model is capable of discussing slow phenomena (slow fracture propagation) and fast phenomena (fast fracture propagation) in a unified manner, using the competition between the two time constants of (1) fracture and stress accumulation, and (2) fracture and strength recovery as parameters.

In the parameter range of the slow phenomenon (slow fracture propagation) of the present model, a transition from continuous behavior such as the tremor to periodic behavior such as that seen in SSE was observed depending on the combination of the two parameters. We will also discuss whether such a model can comprehensively explain the characteristics of slow earthquakes with various time constants. The results of this model in the parameter range of fast phenomena (fast rupture propagation) will be presented in the S-SS06 session.

Keywords: Cellular automata models, Tremor, Low-frequency earthquakes, Slow Slip Event

©2021. Japan Geoscience Union. All Right Reserved.

Scaled energy of shallow slow earthquakes in Hyuga-nada, southwest Japan

*Satoru Baba[1], Shunsuke Takemura[1], Kazushige Obara[1], Akiko Takeo[1], Yusuke Yamashita[2], Masanao Shinohara[1]

1. Earthquake Research Institute, The University of Tokyo, 2. Disaster Prevention Research Institute, Kyoto University

Slow earthquakes, such as tremors, very low frequency earthquakes (VLFEs), and slow slip events, are fault slips with slower slip speed compared to regular earthquakes. Shallow slow earthquakes, which occur in the shallower extensions of seismogenic zones near trench axes, are very active in Hyuga-nada (Asano et al., 2008). Yamashita et al. (2015; 2017) revealed the spatiotemporal distribution of shallow tremors by using temporal ocean bottom seismometers (OBSs) deployed in Hyuga-nada in 2013 and 2015, respectively. To obtain more physical characteristics of shallow slow earthquakes, scaled energy of shallow slow earthquakes has been discussed by Yabe et al. (2019; 2021) in Nankai, off Tokachi and Tohoku. In this study, to clarify the characteristics of shallow slow earthquakes in Hyuga-nada and the differences with other regions, we estimated scaled energies using tremors of Yamashita et al. (2015; 2017) and accompanying VLFEs.

For the tremor analysis, we used OBS records in 2013 and 2015 (Yamashita et al., 2015; 2017), applied a band-pass filter of 2–8 Hz, and calculated root-mean-square envelope. After estimating site amplifications and attenuations based on the coda-normalization method, we estimated energy rate functions of tremors at each station by the method of Maeda and Obara (2009). The energy rate function of an event is estimated by averaging energy rate functions calculated at each station. The duration of the event is defined as the time window in which the value of the energy rate function exceeded 0.2 times the maximum value. The energy rate of the event is calculated by the ratio of integration of the energy rate function to the duration.

Next, we estimated seismic moments and source durations of VLFEs which correspond to tremors using NIED F-net seismograms in a frequency range of 0.02-0.05 Hz. We calculated Green’ s functions from the assumed source grids on the plate boundary by the OpenSWPC; (Maeda et al., 2017) using a three-dimensional velocity structure model, JIVSM (Koketsu et al., 2012). Based on the method of Yabe, Baba et al. (2021), the source duration with the highest cross-correlation coefficients between observed and synthetic waveforms was selected for each event and seismic moments were estimated by the relative amplitudes to synthetic waveforms. Scaled energy is calculated by the ratio of the seismic energy rate of a tremor to the seismic moment rate of accompanying VLFE.

The ranges of energy rates of tremors and moment rates of VLFEs are 10^{2}–10^{5} J/s and 10^{13}–10^{15} Nm/s, respectively. In 2013, tremors occurred from 30.3ºN to 31.7ºN, and events with large energy rates and large moment rates were concentrated in the south of 31ºN. Around 31.0ºN, the trench is bending, and the Kyushu-Palau ridge is subducting. The relationship between the geometrical characteristics and VLFE activity in Hyuga-nada was suggested in Tonegawa et al. (2020). In 2015, tremors occurred in the north of 31.0ºN, and events with large energy rates and large moment rates tended to locate in the east of 132.6º E, which is the shallower part of the plate boundary. The cumulative energy of tremors is larger in the 2015 episode than in the 2013 episode. The range of scaled energy in Hyuga-nada is 10^{-12}–10^{-10}, which is one to three orders smaller than that of shallow Nankai and shallow Tohoku. Smaller scaled energy may be related to weak interplate locking or complex geometry in Hyuga-nada.

©2021. Japan Geoscience Union. All Right Reserved.

Acknowledgements: The temporal seismological observations in Hyuga-nada were conducted as part of "Research project for compound disaster mitigation on the great earthquakes and tsunamis around the Nankai Trough region," a project of Ministry of Education, Culture, Sports, Science and Technology. We used NIED F-net broadband seismograms (https://doi.org/10.17598/NIED.0005). Numerical simulations were performed on the Fujitsu PRIMERGY CX600M1/CX1640M1 (Oakforest-PACS) at the Information Technology Center, the University of Tokyo.

Keywords: Slow earthquake, Low frequency tremor

©2021. Japan Geoscience Union. All Right Reserved.

Tectonic tremors influenced by characteristic of structure and pore pressure in the Nankai subduction zone, Japan

*Andri Hendriyana[1], Takeshi Tsuji[2,3,4]

1. Geophysical Engineering, Institute of Technology Bandung, Indonesia, 2. International Institute for Carbon-Neutral Energy Research (I2CNER), Kyushu University, Fukuoka, Japan, 3. Department of Earth Resources Engineering, Kyushu University, Fukuoka, Japan, 4. Disaster Prevention Research Institute, Kyoto University, Kyoto, Japan

Episodes of tectonic tremor are observed in the Nankai accretionary prism close to the trough axis; however, their non-impulsive signals and the distortion of seismic signals in the accretionary prism make it challenging to accurately estimate their locations. Reliable tremor locations would help to characterize geological conditions favourable for tremor generation. Here we report a new approach to pinpoint tremor locations based on seismic phase polarization. The estimated epicentres of tremor distribution mostly coincide with low velocity shear zone or thick underthrust sediments where high pore pressures are inferred, and the distribution of tremor appears to be controlled by characteristics of the shear zone. A tremor episode occurred a couple days after the off-Mie earthquake clearly shows migration. Migration of tremor initiated around the outer ridge where the estimated pore pressure is greatest. The spatio-temporal tremor distribution indicates that pore pressure relaxation could trigger the tremor migration. The occurrence of tremor thus may indicate a weak shallow plate interface that is prone to slip following large earthquakes. Based on the information of tremor migration, the permeability along the fault can be estimated as 3.7 ×10 −12 m2 .

Keywords: tectonic tremor, source estimation, tremor migration, pore pressure, Nankai trough

©2021. Japan Geoscience Union. All Right Reserved.

Impact of metasomatism on fluid overpressure in source depths of deep slow earthquakes

*Yasushi Mori[1], Kohtaro Ujiie[2], Miki Shigeno[1], Kazuya Noro[2], Tadao Nishiyama[3]

1. Kitakyushu Museum of Natural History and Human History, 2. University of Tsukuba, 3. Kumamoto University

Fluid overpressure in subduction plate boundaries is recognized as a key factor in generating deep slow earthquakes. However, the fluid source and geological environment remain unknown. Here we show that metasomatism (rock-alteration with substantial change in bulk chemical composition) in serpentinite mélanges is a potential source of the fluid overpressure, which results in shear strain localization in source depths of deep slow earthquakes.

The Nishisonogi unit of the Nagasaki Metamorphic Complex exposed on Kyushu, Southwest Japan, represents part of a Late Cretaceous subduction complex. It contains serpentinite mélanges formed within source depths of deep slow earthquakes (~35–45 km depth, ~470 ˚C). The serpentinite mélanges have characteristics of anastomosing shear zones composed of high-strain zones of chlorite-actinolite schist (CAS) that enclose relatively undeformed serpentinite, metabasites and metapelite. The sheared CAS contains the lenses of serpentinite commonly rimmed by the selvage of talc schist. The bulk chemical composition analysis suggests that the CAS is derived from mixture of the talc schist and the metabasites. These findings suggest that the serpentinite was replaced by the talc schist, which in turn was mixed with the metabasites resulting in the formation of CAS.

The replacement of the serpentinite by the talc schist involves significant dehydration. The chemical mass balance and composition–volume relationships indicate that the replacement has released about 150 g of H_2O per 1000 cm^3 of the serpentinite without changing the rock volume much; this is comparable to almost a half of H_2O in the serpentinite. The released H_2O could generate fluid overpressure. Talc, a major constituent of the talc schist, has known to be an extremely weak mineral and thus provides an important weakening effect on rock strength. The low shear strength of talc and metasomatism-derived fluid overpressure facilitate the mixing of talc schist and metabasites and shear localization along CAS. In addition, the replacement of serpentinite is described by the combination of two end-member reactions: antigorite + SiO_2(aqueous) →talc + H_2O and antigorite + H^+ →talc + Mg^{2+} + H_2O. The former reaction increases rock volume, whereas the latter reaction decreases it. The balance of these reactions could modulate porosity and pore fluid pressure in serpentinite mélange. Therefore, metasomatism in serpentinite mélange has a significant impact on fluid overpressure in source depths of deep slow earthquakes. If serpentinite mélange extensively develops along subduction plate boundaries, fluid overpressure due to metasomatism could facilitate the generation of deep slow earthquakes.alc schist, which in turn was mixed with the metabasites resulting in the formation of CAS.

Keywords: Metasomatism, Fluid overpressure, Serpentinite mélange, Deep slow earthquakes, Nagasaki Metamorphic Complex

©2021. Japan Geoscience Union. All Right Reserved.

Observation of localized slip events using viscoelastic fluids incorporating beads

Rinya Miyakawa[1], Kota Kamijo[1], Tatsuya Nishikubo[1], *Yutaka Sumino[1]

1. Tokyo University of Science

Slow earthquakes are distinctive quantized slip events with long duration and without seismic waves observed in regular earthquakes. Propagation of slip region in a single event and spatiotemporal coupling of these events, so-called migration, are noticeable features of slow earthquake. The fact that slow earthquakes are observed at the marginal region between seismogenic and aseismic steady sliding zones indicates brittle-ductile transition may be a key for the slow earthquake. This study intended to do an analog experiment using a mixture of beads and viscoelastic fluid situated between thin parallel plates. Here, viscoelastic fluids and beads are imitations of ductile and brittle rocks at a plate boundary.

The system was composed of zircon beads (ϕ=0.7 mm) dispersed in viscoelastic fluids. We used viscoelastic fluids consisting of (1) the mixture of emulsion and telechelic polymer and (2) wormlike micelles. These samples were placed between parallel acrylic plates, and the shear was applied by moving plates with a fixed speed or angular velocity. The gap between the plates was kept at 1 mm, so that the typical crack formation is constrained in the same order of this length. In this way, we could localized slip events and observe large-scale cooperative behavior between slip events. In the case of sample (1) that is known to produce fracture at low energy, we found spontaneous formation of lane structure through the appearance of localized crack in the sample. In the sample (2) with a large viscoelastic relaxation time, we found propagating behavior of the slip whose speed is less than the speed of the sound wave in the sample. In the talk, we will discuss the details of the experimental results and its theoretical interpretation.

Keywords: analog experiments, brittle-ductile mixture, viscoelastic fluids

©2021. Japan Geoscience Union. All Right Reserved.

A trial digitization of analog seismograms of the Kanto-Tokai Observation Network for the analysis of tectonic tremor

*Takanori Matsuzawa[1], Tetsuya Takeda[1]

1. National Research Institute for Earth Science and Disaster Resilience

Slow earthquakes have been studied by many researchers since the discovery of tectonic tremor (hereinafter, tremor) in the Nankai region (Obara, 2002, Science). However, the past activity of tremor in 20th century is still not clear. Continuous digital seismic data in this period is rare due to the cost of data storage. Thus, analog seismograms are essential dataset to reveal the tremor activity in such period. In addition, digitization of analog data is important for the waveform analysis of tremor. In terms of the analysis of tremor activity, manual digitization requires much time, as tremor episodes lasts several days, typically. Therefore, automatic digitization seems to be suitable. National Research Institute for Earth Science and Disaster Resilience has stored the paper recordings of seismograms of the Kanto-Tokai Observation Network, which started since late 1970s. In our previous study, we have reported the tremor activity in the Tokai region in 1980s, based on the visual inspection of analog seismograms (Matsuzawa and Takeda, 2020, JpGU). We aim to digitize these analog seismograms for the analysis of tremor, and tried to develop an automatic digitization tool of analog seismograms.

The analog seismograms are recorded by ink recorders. Two hours data are divided to four blocks in a sheet. Traces of seismograms in the left and right blocks are 0-35s, 30-65s in each minute, respectively. Upper and lower blocks correspond to the former and the latter hour, respectively. In each trace, time marks for each second are added as streaks. Short offset is added in each minute. We scanned these analog recordings and saved to files in the Portable Network Graphics (PNG) format (400dpi, grayscale).

We tried to develop a tool to digitize these data in the following procedure. At first, we converted the PNG format file to the PGM (Portable Gray Map) format, and handled bitmap data in our program. In our program, we locate four trace blocks, then set the analysis area for each trace, based on the sum of pixel values in the horizontal direction in each trace block. The horizontal, and vertical width of analysis area is set to the block length, and interval of baselines of traces, respectively. We calculated weighted sum in the vertical direction based on the distance from the baseline, and set to the value as the waveform amplitude.

To validate our developed program, we applied this tool to image data which simulate analog seismograms of the Kanto-Tokai Observation Network, using Hi-net digital data. The recovered digital data from images are generally similar to the original data in the case of small amplitude signal, although high frequency components are lacked. We compared power spectra between original and recovered data. The amplitude is similar below 10Hz, while peaks in 1Hz and overtones are found in the recovered data due to time marks for every second. This result supports that the analog seismograms and our tool can extract tremor signal, as the tremor signal is dominant at several Hz.

Our digitization method assumes that amplitude of waveforms is smaller than the vertical width of analysis area (i.e. the interval of traces). This means that larger signal than this width cannot be recovered, due to the saturation in the trace and contamination to the adjacent traces. Active tremor signals sometimes exceed this amplitude, while most tremor has small amplitude. Another problem is related to the time marks. Envelope correlation technique or matched filter techniques are frequently used in locating

©2021. Japan Geoscience Union. All Right Reserved.

tremor. As these are based on correlation functions, we need to develop a method to avoid the apparent effect of time marks.

Keywords: Slow Earthquakes, Analog Seismogram, Deep Tectonic Tremor

©2021. Japan Geoscience Union. All Right Reserved.

Slow slip events in the Bungo Channel and Hyuganada areas from May 2018 to June 2019 detected by a GNSS observation network

*Hitoshi Hirose[1], Takeshi Matsushima[2], Takao Tabei[3], Takuya NISHIMURA[4]

1. Research Center for Urban Safety and Security, Kobe University, 2. Faculty of Science, Kyushu University, 3. Research and Education Faculty, Natural Sciences Cluster, Sciences Unit, Kochi University, 4. Disaster Prevention Research Institute, Kyoto University

GNSS observations reveal that slow slip events (SSEs) that last for months--year have repeatedly occurred around the Bungo Channel area, southwest Japan (e.g., Hirose et al., 1999; Ozawa et al., 2020). These events have a similar size in seismic moment, but have different source slip evolutions. In the Hyuganada area, south of the Bungo Channel area, repeating SSE activities have also been reported (e.g., Yarai and Ozawa, 2013). It is important to better constrain a time development of an SSE because this provides not only critical constraints on the generation mechanisms of slow earthquakes in general, but also useful information for estimating the interplate strain budget, that is, strain accumulated by relative plate motions and one released by slip episodes. To do this, we have installed continuous GNSS stations around the Bungo Channel and Hyuganada areas since 2014. In this study, we estimate time evolution of slow slip sequences in these areas from May 2018 to June 2019, including a long-term SSE in the Bungo Channel and another long-term SSE in the Hyuganada area.

We used GNSS data from our stations in addition to GSI's GEONET stations located in Kyushu, Shikoku and southern Chugoku areas. These observed RINEX data were processed with GIPSY-OASIS 6.4 to estimate daily coordinates of these stations in ITRF2014. We selected five stations in the Chugoku area as reference sites. A constant velocity component (a linear trend) and an annual and a semi-annual components are estimated from the two one-year-long time windows before and after the slip sequences for each displacement component as a background, and are subtracted from the data of entire time period of each component of each station. Jumps caused by coseismic deformations and station maintenances are also removed.

These processed data from March 2018 to June 2019 are inverted by using a Network Inversion Filter technique (Segall and Matthews, 1997; Hirose et al., 2014). We assume that slip occurs on the plate interface and model the interface geometry by placing 19 x 11 square fault elements (15 km x 15 km each).

From the estimated slip history of the entire inverted time period, we identified at least four slip stages: (1) slip starts around the Oita--Miyazaki boundary area (hereafter, area A) near the east coast of Kyushu at May 2018 and continues until around September 2018 with the slip area expands to the south; (2) slip propagates from the area A to the Bungo Channel area following the slip (1) and continues until around May 2019; (3) the southern slip propagation described in (1) is followed by a long-term SSE around the Miyazaki Plain that lasts until around April 2019; (4) slip at the western Shikoku area appears from late September 2018 to October 2018, corresponding to a short-term SSE (event "201810" in Hirose and Kimura, 2020).

The northern end of the slow slip in the Bungo Channel corresponds to the "updip tremor belt" (Obara et al., 2010), suggesting that a tremor activity there is induced by slow slip in the Bungo Channel area. Northward slow slip propagations around the area A have been observed (e.g., Ozawa, 2017; Takagi et al.,

©2021. Japan Geoscience Union. All Right Reserved.

2019). This study shows clearer evidence of a southern propagation behavior there. Uchida et al. (2020) suggest a slow slip pathway from south to north of the Hyuganada area from repeating earthquakes activity. Our result shows that the Hyuganada slow slip pathway is not "one-way" but bi-directional.

Acknowledgments
The GEONET GNSS data were provided by Geospatial Authority of Japan. This research was supported by JSPS KAKENHI Grant Number JP16H06474 in Scientific Research on Innovative Areas "Science of Slow Earthquakes", the MEXT of Japan under its "The Second Earthquake and Volcano Hazards Observation and Research Program", and by ERI JURP 2014-A-01, 2015-A-01, 2016-A-01, 2017-A-01, 2018-A-01, 2020-A-03.

Keywords: slow earthquakes, subduction zone, interplate coupling, strain budget, Network Inversion Filter

©2021. Japan Geoscience Union. All Right Reserved.

A Bayesian inversion for slip distribution of slow slip events beneath the Bungo Channel based on ensemble modeling of the uncertainty of underground structure

*Ryoichiro Agata[1], Ryoko Nakata[2], Yuji Yagi[3], Takeshi Iinuma[1]

1. Japan Agency for Marine-Earth Science and Technology, 2. Graduate School of Science, Tohoku University, 3. Graduate School of Life and Environmental Sciences, University of Tsukuba

Because long-term slow slip events (L-SSE) are associated with relatively long duration and large magnitude, we can estimate slip distribution of L-SSE using geodetic displacement data. For instance, the L-SSE beneath the Bungo Channel is known to regularly occur in every six or seven years with the help of continuous GNSS observation in the land area. Most of geodetic slip inversions performed for this event were based on regularization using spatially uniform smoothing constraints. On the other hand, Nakata et al. (2017) introduced a sparse-promoting regularization for slip estimation for the past events. Their result of slip distribution with discontinuous boundaries obtained by introducing sparse-promoting constraint agreed better with the spatial distribution of deep nonvolcanic tremors and temperature structure at the plate boundary of Nankai Trough area. It also follows that the choice of empirical constraints for regularization to reduce the instability of estimation due to several error factors often largely affects the estimation results.

Geodetic slip inversion requires a prior assumption of the underground structure. Provided that we only have information on the underground structure with uncertainty, the assumption of “one model” of the underground structure may lead to a significant amount of model prediction errors, which essentially results in significant bias in slip estimation results. Several studies have addressed this problem by considering the contribution of the model prediction error due to the uncertainty of Green’s functions to the data covariance (e.g., Yagi & Fukahata 2008, 2011; Duputel et al. 2014). Agata et al. (2021) recently developed a new full Bayesian inference method for estimating fault slips, which considers the model prediction errors more generally without assumption of Gaussian distribution by incorporating the uncertainty of the underground structure using an ensemble consisting of many models of underground structure: It reduces the error factor associated with the assumption of “one model” by considering an ensemble of multiple underground structure models together. In this study, we apply the new method to estimation of slip distribution in the L-SSE in 2010 that occurred beneath the Bungo Channel, because this method may allow for estimating slip distribution without introducing such empirical constraint, relaxing the instability of estimation.

We use the homogeneous elastic half-space for the underground structure model, whose property is characterized by the plate boundary model to locate the fault slips and Poisson’s ratio of the media. We consider an ensemble of weight averages of three models of the geometry, namely, those provided in the models of Hayes et al. (2018), Iwasaki et al. (2015) and Koketsu et al. (2009, 2012). We assume that the stochastic property of the weights is characterized by the Dirichlet distribution with α=0.5. We also consider an ensemble of Poisson’s ratio calculated based on random samples of density from a uniform distribution between 2000 and 3400 kg/m^3 and the empirical relationship between density and other elastic parameters proposed by Brocher (2005). In such a manner, we compose 1,000 samples of underground structure models and incorporate them as an ensemble in the estimation method of Agata et al. (2021). We use the digital data for the observed vertical and horizontal displacements provided by

©2021. Japan Geoscience Union. All Right Reserved.

Yoshioka et al. (2015).

As a result, we obtained posterior PDFs for the slip distribution, in which the mean model presents a sharp slip distribution which is similar to that estimated in Nakata et al. (2017) rather than to those estimated based on spatially uniform smoothing constraints. In the conference, we would also like to show results incorporating uncertainty of one-dimensional heterogeneous elastic structure to consider a wider model space for the underground structure, which is expected to further reduce the bias in the estimation.

Keywords: Slow slip events , Bayesian inference, Uncertainty of the underground structure, Geodetic data inversion

©2021. Japan Geoscience Union. All Right Reserved.

Spontaneous extension of viscoelastic fluids confined between rotating parallel plates

*Tatsuya Nishikubo[1], Hiroki Ishikawa[1], Shoma Kato[1], Yutaka Sumino[1]

1. Department of Applied Physics, Graduate School of Science, Tokyo University of Science

Slow earthquakes are observed at a marginal region between seismogenic and steady sliding zones[1]. Subducting plate at a boundary can be recognized as brittle elastic solids and viscous liquids in the seismogenic and steady sliding zones, respectively. Therefore, the viscoelastic behavior of subducting plate, especially macroscopic spatio-temporal patterns, should be explored to understand slow earthquakes. To observe these behaviors in accessible time and space, we make an analog experimental system using viscoelastic fluids with shorter viscoelastic relaxation time. Here, we continuously sheared a brittle viscoelastic fluid using rotating parallel plates.

The sample, an analog for a rock, was a physical gel. It was made of thermodynamically stable oil-in-water microemulsion bridged by telechelic polymers. The microemulsion was decane droplet dispersed in 0.2 mol/L NaCl aqueous phase with cetylpyridinium chloride and octanol. Telechelic polymer was polyethylene glycol distearate, and its concentration was varied as a parameter[2]. In short, increasing the conectivity of telechelic polymer r leads to longer viscoelastic relaxation time.

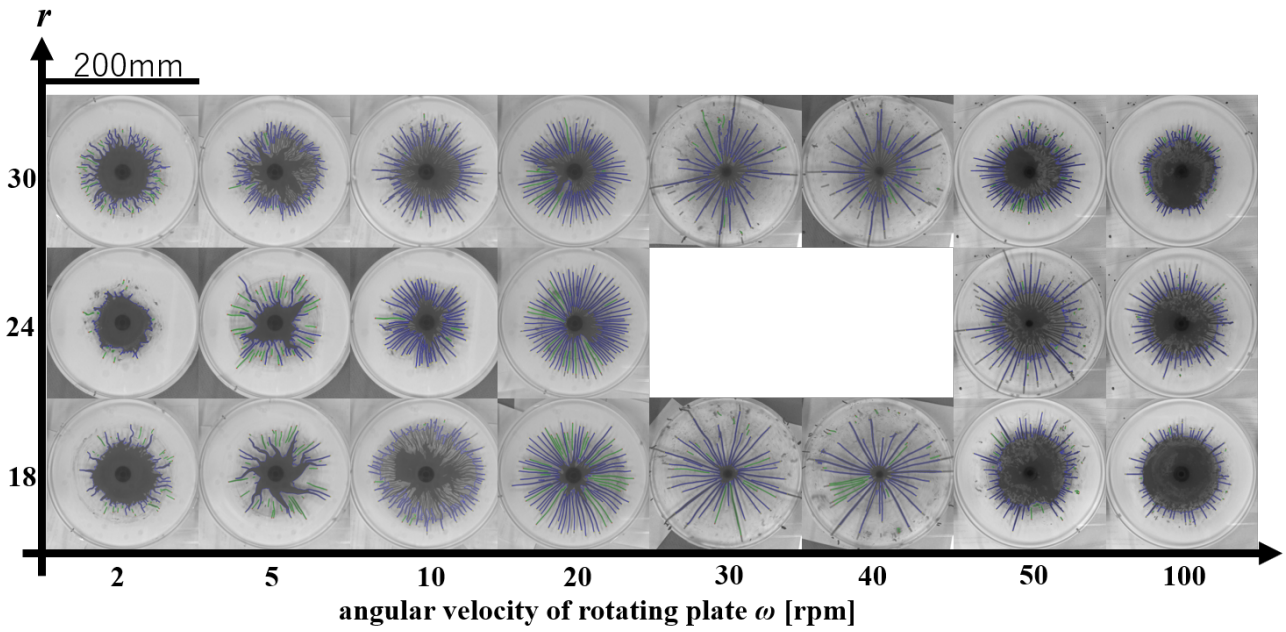
The sample was introduced at the central part of parallel circular plates whose gap was h, and the bottom plate was rotated with fixed angular velocity ω. The typical initial radius of a sample in the cell was R_0. The sample showed viscous flow at low ω, as seen in the case of ordinary liquids. However, when ω exceeds critical values determined by $\omega \sim h/R_0\tau$, the crack formation was observed in the sample. Furthermore, the sample starts to extend branches in the radial direction while their width continuously becomes smaller until the width reaches a steady value scaled with h. We anticipate this spontaneous extension of viscoelastic fluids is due to the first normal stress difference. To confirm this hypothesis, we measured the branch extension speed and took its statistics.

[1] K. Obara, A. Kato, *Science* **353**, 253-257 (2016).

[2] M. Filali and J. Appell, *J. Phys. Chem. B* **103**, 7293-7301 (1999).

Keywords: viscoelastic fluid, pattern formation, brittle ductile transition

©2021. Japan Geoscience Union. All Right Reserved.



©2021. Japan Geoscience Union. All Right Reserved.

Pattern of injected fluid into a cell filled with swelling gel particles—effect of pressure

*Kojiro Otoguro[1], Yutaka Sumino[1]

1. Tokyo University of Science

In the silica-rich subduction zone, silica dissolution induces enhanced permeability and pore-fluid pressure reduction, which leads to a higher frequency of slow slip events [1]. For a comprehensive understanding of slow earthquakes, the spatio-temporal pattern induced by variation of permeability due to chemical reaction is worthy of inspection. For this purpose, we explore the fluid dynamics in varying permeability by an analog injection experiment.

In this study, we injected an aqueous sodium chloride solution into gel particles packed in a thin 2-dimensional cell made of two acrylic plates. While fluid flows, gel particles swell and interrupt fluid flow. We imitated the fluid dynamics in varying permeability by conducting the experiment.

The gel particle is a so-called ionic gel particle. The typical radius is 350 μm in dry condition and can increase to be ten times by immersing in pure water. This increase is 1000 times in its volume corresponds to the one for gas-liquid transition. We should note that one can control the swelling rate of ionic gel particles by changing water’ s salinity [2]. We packed the particles into the cell whose gap between plates is 1 mm. The cell was tapped ten times to have particles packed well [3]. Then, we injected the aqueous phase from the bottom of the cell and measured fluid pressure in the injection-tube. As a control parameter, we changed the concentration of sodium chloride C and injection rate Q. The schematic illustration of the experimental setup is shown in Fig. 1.

We obtained a phase diagram of the flow pattern (shown in Fig.2). In the diagram, particles are displaced by fluid flow at the boundary of white areas, and fluid penetrates the pore of particles in deep black areas. At high C and Q, particles didn’ t swell significantly, and fluid percolated isotropically without interruption. On the contrary, at low C and Q, due to the swelling of gel particles, fluid flow was blocked, and the injection front branched. We explored the relationship between these patterns and fluid pressure.

[1] P. Audet and R. Burgmann, *Nature* **510**, 389-392(2014).

[2] T. Tanaka*, From gels to life, University of Tokyo Press* (2002).

[3] M. Suzuki, *J. Soc. Powder Technol., Japan*, **40**, 348-354(2003)

Keywords: analog experiments, fluid flow, fluid pressure

©2021. Japan Geoscience Union. All Right Reserved.

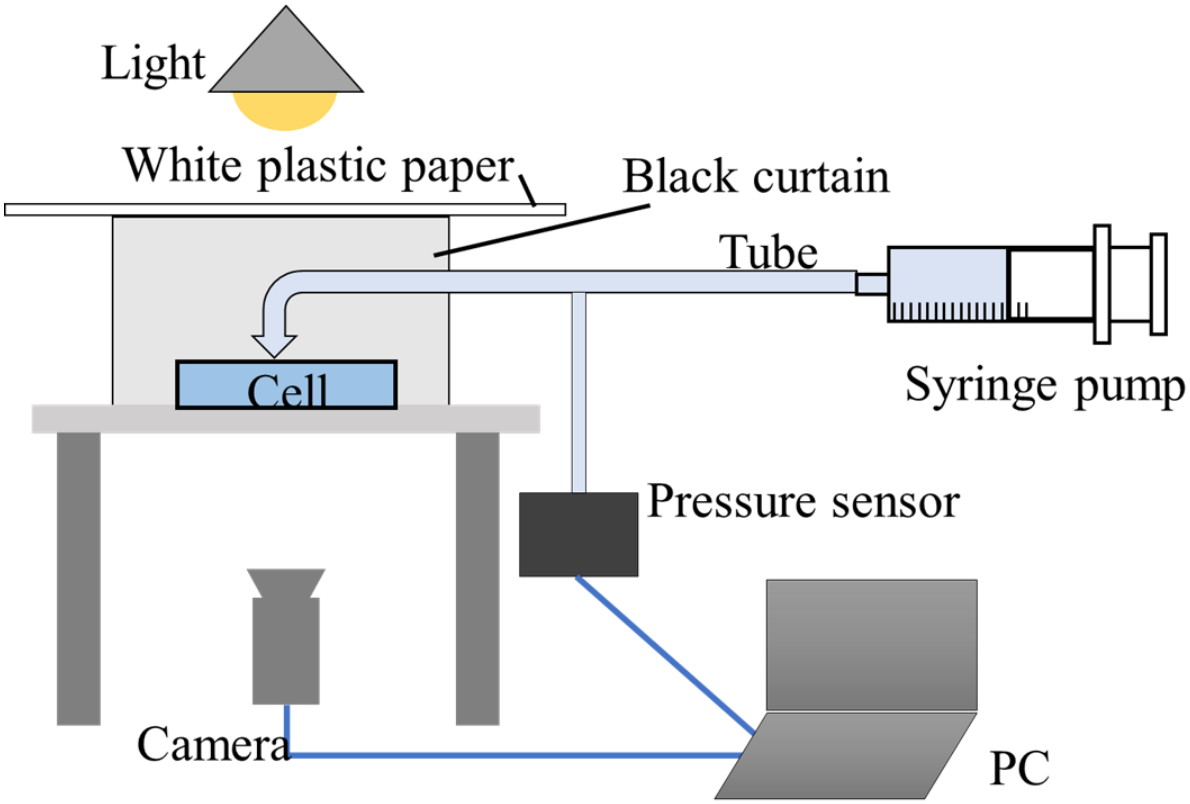


Fig.1 Schematic representation of experiment setup

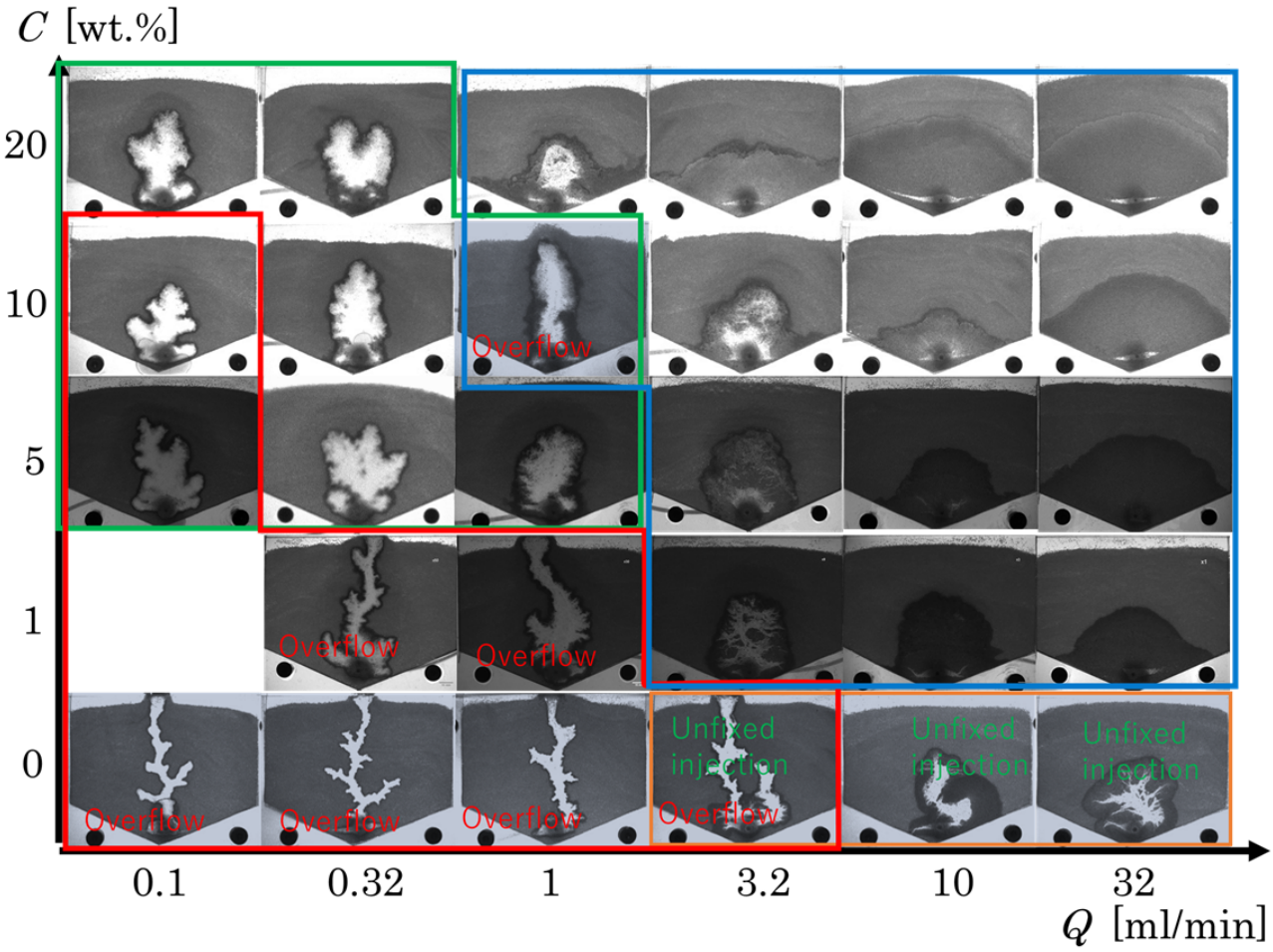


Fig.2 Phase diagram of injection behavior

©2021. Japan Geoscience Union. All Right Reserved.

©2021. Japan Geoscience Union. All Right Reserved.

Detailed mapping of the subducting seamount and deformation structure in the Nankai Trough off the eastern Shikoku region deduced from densely acquired seismic profiles

*Yasuyuki Nakamura[1], Shuichi Kodaira[1], Yuka Kaiho[1], Tetsuo No[1], Kazuya Shiraishi[1], Gou Fujie[1], Seiichi Miura[1], Gaku Kimura[2]

1. Japan Agency for Marine Earth Science and Technology, 2. Tokyo University of Marine Science and Technology

Nankai Trough off Muroto is one of the areas of interest from the subduction zone seismogenesis and tectonics viewpoints. Subduction of a seamount was suggested southeast off the Cape Muroto from refraction seismic data analysis (Kodaira et al. 2000). Shallow very low frequency earthquakes have been observed around this seamount using the cabled seafloor observation network, DONET (Nakano et al. 2018), and onshore stations (Takemura et al. 2019). Deformation and rebuilding of the accretionary prism probably due to the subduction of the seamount have been reported seaward of the suggested location of the subducting seamount (Gulick et al. 2004).

We conducted a reflection seismic survey in the Nankai Trough off the eastern Shikoku region in December 2019 and January 2020 using R/V Kairei. A 5500m-long streamer cable with 444 channels of hydrophones and an air gun array with a volume of 7800 inch^3 were used to obtain the seismic data along 21 and 6 survey lines running in dip and strike direction respectively. The total line length was ~ 2300 km, which covers the forearc area of the Nankai trough off the Kii channel to the east and off the Cape Muroto to the west, including seaward of the Tosa-bae. The pre-stack depth migration was applied to the data after the pre-conditioning, noise reduction, and iterative velocity analysis. Obtained depth migrated profiles show the characteristic structure in the subduction zone, e.g., top of the subducting Philippine Sea plate, decollement, fold-and-thrust deformation of the hanging wall sediments, bottom simulating reflection (BSR). The top of the Philippine Sea plate is traceable in most of the survey lines to create a detailed depth map of the subducting plate surface. The map shows a distinct shallow portion around the Tosa-bae, where the subduction of the seamount has been suggested. The map seems to show two peaks, not a single peak around the inferred seamount. The dip of the subducting plate is generally shallower off the eastern Shikoku than off the western Kii Peninsula. We can identify landward dipping clear reflections below the slope off the Cape Muroto, which are not clearly imaged off the western Kii peninsula and Kii channel. The decollement refection is clearly imaged with apparently negative polarity above the top of the subducting Philippine sea basement near the trough axis off the eastern Shikoku, however, the polarity of the decollement is positive off the Kii channel. These structural characteristics should be related to the plate boundary slip behavior difference between off Cape Muroto and off Kii peninsula.

Keywords: Nankai Trough, seismic reflection survey, subducting seamount, slow earthquakes

©2021. Japan Geoscience Union. All Right Reserved.

Distribution of Very-Low Frequency Earthquake in the Central Ryukyu Trench

Hiromu Furugen[1], *Mamoru Nakamura[1]

1. Faculty of Science, University of the Ryukyus

The distribution of very-low-frequency earthquakes (VLFEs), one type of slow earthquake, illuminates the heterogeneous stress accumulation at the subducting plate interface. VLFEs occurred along the Ryukyu Trench (Ando et al., 2012); however, their detailed distribution has not been clarified because few broadband seismic stations were deployed along the Ryukyu Islands. The detection capability is poor in the Miyako Strait, between Miyako Island and Okinawa Island, where the seismic stations' spacing is over 300 km. In this study, we determined the epicenters of the VLFEs in the Miyako Strait and Okinawa Island using the waveform data from temporary stations in the central Ryukyu arc. We used the F-net stations of the National Research Institute for Earth Science and Disaster Resilience and temporary stations on Okinoerabu Island, Kume Island, Miyako Island, Tarama Island, and Hateruma Island, which were set up by the Association for the Development of Earthquake Prediction. We performed band-pass filtering at a frequency range of 0.05–0.1 Hz for the vertical component waveforms. We then determined the epicenters of the VLFEs using the template matching method (Asano et al., 2015). We adopted the thrust events of regular earthquakes near the Ryukyu Trench in the Miyako Strait for the template. We analyzed the epicenters of VLFEs from January 2015 to December 2019.

The VLFE was distributed in a band along the trench axis near Okinawa Island. On the other hand, in the Miyako Strait, the VLFEs were distributed in spots along the trench axis. In the Miyako Strait, events that could not be detected by the conventional method (Nakamura and Sunagawa, 2015) were also detected. The horizontal location errors in VLFE near Okinawa Island and the Miyako Strait were both 10-12 km in error. The VLFE in the Miyako Strait occurred at a slab depth of 10-15 km. The distribution of VLFEs was complementary to that of reverse fault earthquakes. However, the active area of the VLFEs near Miyako Island was close to the distribution of the reverse fault type earthquakes.

On the other hand, the VLFE activity near Okinawa Island was concentrated at a 12-15 km slab depth. This area was located in a gap between the slow slip events (Nishimura, 2014) and the interplate locked area (Tadokoro et al., 2018). The distribution of activity and reverse fault earthquakes was complementary. This suggests the lateral heterogeneity of the frictional coefficient in the subducted plate interface.

Keywords: Ryukyu Trench, slow earthquake, very-low frequency earthquake, interplate coupling

©2021. Japan Geoscience Union. All Right Reserved.

Activity of low-frequency tremors and regular earthquakes off Erimo, Hokkaido from 2006 to 2007, by a tremor investigation based on waveform information

*Susumu Kawakubo[1], Ryosuke Azuma[1], Ryota Hino[1], Hidenobu Takahashi[2,1], Kazuaki Ohta[2], Masanao Shinohara[3]

1. Graduate School of Science Tohoku University, 2. National Research Institute for Earth Science and Disaster Resilience, 3. Earthquake Research Institute, University of Tokyo

Slow earthquakes implying slow fault slip have been discovered since 1990s, owing to development of seismological and geodetic observations. Low-frequency tremors, one of slow phenomena, excite seismic energy in the frequency band of 2–8 Hz and simultaneously occur with VLFEs (Very Low-Frequency Earthquakes) having energy in frequency band 0.01–0.1 Hz. Slow earthquakes are important research target, because their activities reflect the stress state at the plate boundary adjacent to the fault area of maegathrust earthquake (Obara & Kato, 2016). Off Erimo, southern Hokkaido, VLFEs have been active every several months to a year after the 2003 Tokachi-oki earthquake (Asano et al., 2003; Baba et al., 2020). On the other hand, because seismological amplitude of tremors is small, a near-field network is necessary to observe them. At the corresponding area, tremors have been observed after 2016 when the Seafloor observation network for earthquakes and tsunamis along Japan Trench (S-net) started operation (Tanaka et al., 2019; Nishikawa et al., 2019). However, in the corresponding area, there is no understanding for actual tremor activities before 2016. This study analyzes the records collected by a pop-up type ocean bottom seismometer array installed during 2006 to 2007 and tries to detect tremors. During the observation period, VLFE activities were reported off Erimo, Hokkaido, and it is probable that tremors were also active.

In our previous result, tremors with duration over 20 detected by an envelope cross-correlation method (e.g. Ide, 2010), after filtering according to epicenter errors and time residual were 1,172 events. Most of their epicenters distributes similar to tremors detected by S-net observation (Tanaka et al., 2019; Nishikawa et al., 2019). In addition, although there is some difference in the activity cycle and scale from results of S-net studies, we found 3 high activities followed by VLFE occasions (Asano et al., 2003; Baba et al., 2020) and their intermedial aseismic periods. This feature is commonly observed in S-net studies. On the other hand, we also detected tremors occurring constantly but less active between major active periods. There is a possibility mistaking regular earthquakes barely satisfying thresholds for detecting tremors. Therefore, we reinvestigated tremors by a discrimination based on the waveform and frequency analysis information.

For the discrimination, we determined regular earthquakes based on following features; (1) clear P and/or S wave arrivals in seismogram envelope, (2) exponential decay in amplitude and (3) having power even at 10 Hz or higher. We interpreted the event with (4) less difference in seismogram amplitudes between stations as a teleseismic event. We excluded the events with (5) power only at high frequency (over 8 Hz) and (6) low S/N ratio at the stations near the epicenter as noise. In order to improve the efficiency and objectivity of the discrimination that is currently being performed visually, we plan to study a method for automatically discriminating in the future.

The discrimination certified 201 events as regular earthquakes, 11 as noise, and 960 as tremors. The

©2021. Japan Geoscience Union. All Right Reserved.

improved catalog made a segregation of tremor distribution from regular earthquakes clearer than Kawakubo et al. (2020, JpGU). Most of the tremors in the new catalog occurred usually belong 3 known activities, and low and constant events are mostly recognized as regular earthquakes. We newly discovered very small-scale activities with short activity cycles at intervals of main active periods, and they distribute at down-dip side of main tremors activities. Because we have been able to classify tremors and regular earthquakes, we would like to investigate the relationship between tremors and regular earthquakes in the future.

Keywords: tremor, Off Erimo, Hokkaido, Slow earthquakes

©2021. Japan Geoscience Union. All Right Reserved.

Detecting short-term slow slip events using six-year records of ocean bottom pressure in Hikurangi subduction zone offshore New Zealand

*Tomohiro Inoue[1], Yoshihiro Ito[2], Laura M Wallace[3,4], Takuya Nishimura[2], Spahr Webb[7], Emmanuel Soliman M Garcia[2], Tomoya Muramoto[5], Syuichi Suzuki[6], Ryota Hino[6]

1. Graduate school of science, Kyoto University, 2. Disaster Prevention Research Institute, Kyoto University, 3. GNS Science, Lower Hutt, New Zealand, 4. Institute for Geophysics, University of Texas at Austin, Austin, TX, USA, 5. National Institute of Advanced Industrial Science and Technology, 6. Tohoku University, 7. Lamont-Doherty Earth Observatory, Columbia University

Over the last decades, ocean bottom pressure gauges (OBPG) have been widely deployed in the world to measure seafloor crustal deformation due to tectonic events, such as short-term slow slip events (SSE). However, adequate techniques to detect SSE in OBPG data have not been well-established, because some pressure changes due to oceanographic effects can be difficult to distinguish from those due to crustal deformation processes. A common approach to address this is a reference-station method which utilizes pressure records from a reference station outside of the deforming zone under the assumption that the non-tidal components are common-mode over a large region (e.g., Wallace et al., 2016). Fredrickson et al. (2019) recently demonstrated greater coherence in bottom pressure changes observed between sites in similar water depths offshore Cascadia, leading them to suggest a method of placing reference sites at common isobaths to achieve large reductions in oceanographic noise in OBP timeseries. Here, we attempt to develop a new method for the detection of SSE using the reference-station method in conjunction with onshore continuous GNSS and OBP records for data acquired for 6 years between 2014-2019. First, we obtain a continuous time series record calculating the difference between OBPG sites in the combination of all observation sites (hereinafter referred to as a site-pair) using the reference-station method. Next, the ΔAIC method (Nishimura et al., 2013) used in previous studies (e.g. Nishimura et al., 2013) is applied to the obtained differenced time series records (in conjunction with the continuous GNSS records) as a method to detect the seafloor crustal movement caused by SSE. A value of ΔAIC is calculated by subtracting a pair of AICs calculated from fitting with a simple linear trend and fitting with the combination of a linear trend and a step function(Akaike information criterion, Akaike 1974). The average ΔAIC for each day is calculated by averaging the daily ΔAICs for that day obtained from the time series records of all station pairs. We apply DEFNODE (McCaffrey, 1995, 2002) to use relative vertical displacements from the site pairs; we estimate a slip distribution from minimizing the reduced χ^2 value between the observed and model values. We use the average ΔAIC and χ^2 value as the detection thresholds, and classify the date as a Class 1 event if the average ΔAIC and χ^2 are less than -10 and 0.5, respectively. The dates with either threshold below -10 and 0.5 are classified as Class 2 events.

Two Class 1 events are detected twice in 2014 with a duration of less than a month (e.g., about 265-290 days in Julian dates of 2014); the 265-290-day event in 2014 is generally consistent with the duration of SSEs derived from land GNSS and ocean bottom pressure records (Wallace et al., 2016). Meanwhile, two Class 2 events are detected twice with a duration of a few tens of days. Some of the Class 2 events (e.g., 235-255 days and 300-310 days) are events that have not been reported in previous studies. These may be new seafloor crustal movements associated with SSEs that have not been previously identified from the onshore GNSS observation network alone, or they may represent regional oceanographic changes. In the future, we plan to conduct a quantitative evaluation of spatial resolution by means of resolution tests.

©2021. Japan Geoscience Union. All Right Reserved.

Keywords: ocean bottom pressure, seafloor crustal deformation, Slow slip events

©2021. Japan Geoscience Union. All Right Reserved.

Variations of source characteristics of shallow tectonic tremor, Nankai trough, inferred from changes of the event size distribution

*Masaru Nakano[1], Suguru Yabe[2]

1. Japan Agency for Marine-Earth Science and Technology, 2. Geological Survey of Japan, AIST

The event size distribution is one of the scaling relationships that characterize the source processes of seismic phenomena. In our previous study of shallow tectonic tremor along the Nankai trough (Nakano et al., 2019), we found that the event size distribution follows a tapered Gutenberg-Richter (TGR) distribution (Kagan, 2002), which is a GR-like distribution with an exponential taper for events larger than a cut-off magnitude (Mc). For ordinary earthquakes, the slope (b-value) of the GR distribution has been related to the stress level in the medium, and the cut-off magnitude (Mc) of TGR may be related to the fault dimension. For Nankai trough slow earthquakes, both b-value and Mc differ in activities during different time periods in the same source region, implying that the source characteristics of these events change with time, although the cause is poorly understood.

In this study, we analyzed the size distributions of shallow tectonic tremor along the Nankai trough during tremor episodes that occurred off Kumano in 2016 and off the Kii Channel in 2018, both activities lasted at least one month. By fitting the data with the TGR distribution, we found that the b-value increased as Mc decreased in the later part of the episode as the rate of events decreased. Because the tremor sources migrated during each episode, the changes in these parameters may represent spatial or temporal changes in the source characteristics.

We qualitatively interpreted the controlling factors of the size distribution of slow earthquakes using the 2D probabilistic cell automaton (PCA) model proposed by Ide and Yabe (2019). The 2D PCA model has three probabilistic parameters as pb, pl, and pv, where pb is a probability of interactions between adjacent cells, pl is a probability of the random ignition of slip in a cell, and pv is a probability related to energy dissipation during slip. We found that the b-value increase while Mc decrease as pl decrease or pv increase, and the observed changes of the b-value and Mc of shallow tremor can be qualitatively explained by a decrease in pl or an increase in pv.

In the following, we discuss the causes that change these probabilistic parameters. Accumulated stress on the causative fault drives the spontaneous activity of regular and slow earthquakes. Accumulated stress that is initially high is released gradually in slow earthquakes, which may decrease the event ignition probability pl that is consistent with the observations. Because the slip history of previous slow earthquakes may result in a heterogeneous distribution of accumulated stress, the migration of tremor sources may also affect the tremor size distributions. The degree of coupling along the plate interface may affect the stress accumulation rate and accordingly the slip ignition probability, and the spatial variations of the coupling ratio may also be related to the variations of the event size distributions.

Frictional resistance depends on the pore-fluid pressure on the fault interface. A decrease in pore-fluid pressure increases frictional resistance during slip and therefore increases the energy dissipation probability pv or decreases the slip ignition probability pl in the 2D PCA model. The observed b-value increase and Mc decrease can be explained by a decrease of pore-fluid pressure as tremor activity decreases in the later part of tremor episodes. Spatially heterogeneous distribution of pore-fluid pressure and frictional properties on the fault interface may change the event size distribution of tremor as it

©2021. Japan Geoscience Union. All Right Reserved.

migrates.

In summary, observed changes of the tremor event size distribution can be attributed to the release of accumulated stress by slow earthquakes or spatial-temporal variations of pore-fluid pressures during slow earthquakes.

Acknowledgments: This research was supported by JSPS KAKENHI Grant Number JP18K13639, JP19K04050, and 16H06477 in Scientific Research on Innovative Areas “Science of Slow Earthquakes”

Keywords: DONET, Nankai trough, earthquake size distributions, slow earthquakes

©2021. Japan Geoscience Union. All Right Reserved.

Moment tensor inversion of shallow very low-frequency earthquakes in the northern Ryukyu subduction zone and the Hyuga-nada region

*Aki Ito[1], Hiroko Sugioka[2], Masaru Nakano[1], Yusuke Yamashita[3], Masanao Shinohara[4], Tsutomu Takahashi[1], Daisuke Suetsugu[1], Takashi Tonegawa[1]

1. Japan Agency for Marine-Earth Science and Technology, 2. Graduate School of Science, Kobe University, 3. Miyazaki Observatory, Disaster Prevention Research Institute, Kyoto University, 4. Earthquake Research Institute, University of Tokyo

Shallow very low-frequency earthquakes (sVLFEs) have occurred in the northern Ryukyu subduction zone and the Nankai subduction zone (e.g., Ito and Obara 2006; Asano et al. 2015; Asano 2020). Observations using long-term ocean-bottom seismometers equipped with 1Hz seismometer have been conducted since 2014 in the Hyuga-nada region to investigate the shallow slow earthquake activities. Studies from the offshore data revealed the spatiotemporal distribution and migration of shallow low-frequency tremors (Yamashita et al. 2015; Yamashita et al. this session). Although the shallow low-frequency tremors and sVLEFs are considered as a coupled phenomenon, the sVLFE activities have not been studied in detail mainly because only a few broadband ocean bottom seismometers (BBOBSs) have been deployed in the northern Ryukyu subduction zone and the Hyuga-nada region before 2017. Use of offshore observation data from BBOBS is crucial to reveal the sVLFE activities.

We conducted four consecutive temporary seismic observations using BBOBSs off the east of Tanegashima Island and the Hyuga-nada region from August 2017 to August 2020 in order to study sVLFE activities. The BBOBSs are equipped with either a Guralp CMG-3T broadband sensor (Kanazawa et al. 2009) or a Trillium Compact 120s broadband sensor (Shinohara et al. 2018). We applied the centroid moment tensor (CMT) inversion method (SWIFT system; Nakano et al. 2008) to the sVLFE waveforms observed by the BBOBSs. The waveforms were band-pass filtered between 0.03 and 0.05 Hz in the analysis. The sVLFE signals were detected from the continuous records according to sVLFE catalog from land-based observations (Asano 2020), which includes the date and time of sVLFEs and their epicenters. We assumed the one-dimensional structure model by referring to the following two velocity structures off the east of Tanegashima Island for computations of the Green’ s functions. For depths shallower than 10 km, we referred to the S-wave velocity structure obtained by the method of Tonegawa et al. (2017). For depths deeper than 10 km, we referred to the three-dimensional P- and S- wave velocity structures estimated by seismic tomography (Yamamoto et al. 2020).

We determined the CMT solutions of approximately 15 sVLEFs so far. The preliminary results showed that the focal mechanisms of sVLFEs were mostly reverse faulting type, dipping to the direction of plate subduction. Moment magnitude were between 3.6 and 5.4. Although most sVLFEs occurred along the plate interface between subducting Philippine Sea plate and landward plate obtained by previous studies (Nakanishi et al. 2018; Yamamoto et al. 2020), some events seem to occur within the Philippine Sea plate. Increasing the event number is necessary to obtain further details of the characteristics of sVLFEs in this region. We will analyze more sVLEFs in the future and discuss the source processes of shallow slow activities.

Acknowledgments: This study is supported by the JSPS KAKENHI Grant Number JP16H06471 and the research project for compound disaster mitigation on the great earthquakes and tsunami around the Nankai trough region, the MEXT of Japan. We also use the data obtained as part of collaborative

©2021. Japan Geoscience Union. All Right Reserved.

researches with Association for the Development of Earthquake Prediction.

References:
Asano et al. (2015) Geophys. Res. Lett., 42, doi:10.1002/2014GL062165.
Asano (2020) Report of the Coordinating Committee for Earthquake Prediction, Japan, 1-2, 103.
Ito and Obara (2006) Geophys. Res. Lett., 33, L02311, doi:10.1029/2005GL025270.
Kanazawa et al. (2009) Zisin, 61, S55-S68.
Nakanishi et al. (2018) Geological Society of America Special Papers, 534, 69–86.
Nakano et al. (2008) Geophys. J. Int., 173,1000-1011, doi: 10.1111/j.1365-246X.2008.03783.x.
Shinohara et al. (2018) OCEANS-MTS/IEEE Kobe Techno-Ocean,
doi:10.1109/OCEANSKOBE.2018.8559338.
Tonegawa et al. (2017) Nature Communications, 8, 2048, doi:10.1038/s41467-017-02276-8.
Yamamoto et al. (2020) Earth Planet. Sci. Lett., doi:10.1016/j.epsl.2020.116143.
Yamashita et al. (2015) Science, 348, 676-679, doi: 10.1126/science.aaa4242.

Keywords: shallow very low-frequency earthquakes , nothern Ryukyu subduction zone, Hyuga-nada region

©2021. Japan Geoscience Union. All Right Reserved.

Along-trench structural variation of the Philippine Sea plate subducting in the Hyuga-nada region and its relation to slow earthquakes

*Ryuta Arai[1], Seiichi Miura[1], Yasuyuki Nakamura[1], Gou Fujie[1], Yuka Kaiho[1], Shuichi Kodaira[1], Kimihiro Mochizuki[2], Rie Nakata[2]

1. Japan Agency for Marine-Earth Science and Technology, 2. Earthquake Research Institute, The University of Tokyo

The Hyuga-nada subduction zone east off the Kyushu Island, southwest Japan, host active tectonic tremor and very low-frequency earthquakes (VLFEs) that presumably occur at the shallow plate boundary (e.g., Yamashita et al., 2015). The source region of the slow earthquakes is known to coincide with the subduction of the Kyushu-Palau Ridge (Yamamoto et al., 2013; Tonegawa et al., 2020). These seismogenic and tectonic environments allow us to examine physical controls on shallow slow earthquakes associated with the ridge subduction. In order to better understand structural properties controlling the seismogenic behaviors in the Hyuga-nada region, we conducted high-resolution seismic refraction experiments along two seismic lines and multi-channel seismic (MCS) reflection surveys in August-September 2020. In this presentation, we report preliminary results of P-wave velocity (Vp) modeling along one of the refraction profiles, trench-parallel HYU01 line, and discuss the subduction structure of the Philippine Sea plate and its relation to seismic activity in the region.
The HYU01 profile is located above the subducted part of the Kyushu-Palau Ridge and crosses the active area of tremor and VLFEs in the NE-SW direction. For acquisition of seismic refraction data, 50 ocean bottom seismographs (OBS) were deployed at 2 km interval during the research cruise KM20-05 and recorded over 3,800 signals generated at 50- and 200-m intervals by the 10,600-cubic-inch airgun arrays of the R/V Kaimei. We also acquired multichannel seismic reflection data on the coincident line using the 5.6-km-long, 444-channel streamer cable. Together with the preexisting MCS reflection data nearby (KR98-10-4), these data sets provide seismic constraints on the along-trench variation of the overriding and subducting Philippine Sea plates.
We applied traveltime tomography analysis to this dense OBS-airgun data and constructed a Vp model along the HYU01 profile. The preliminary result reveals that the overriding plate (forearc region) exhibits low-velocity ($Vp < 5.0$ km/s) on the whole without significant along-trench variation in velocity. On the other hand, the subducting plate shows a rapid lateral velocity change suggesting a structural transition from a typical oceanic crust to more arc-like feature indicating the subducted part of the Kyushu-Palau Ridge. This transition roughly corresponds to the location with active tectonic tremor. It is also indicated that tremor and VLFE activities are limited to the eastern part of the profile where the plate boundary is shallower than ~15 km depth.

Keywords: Hyuga-nada, Kyushu-Palau Ridge, Active-source seismic survey

©2021. Japan Geoscience Union. All Right Reserved.

Gravity data analysis to extract temporal gravity anomalies associated with slow slip events in the Ryukyu Trench

*Yuichi Hiramatsu[1], Yoshiyuki Tanaka[1], Akio Kobayashi[2]

1. Department of Earth Planetary Science , The University of Tokyo, 2. Meteorological Research Institute, JMA

Slow slip events (SSEs) have been detected at depths of 30-40 km along the plate subduction boundaries around the world, where different evidences have suggested the presence of high-pressure fluids such as seismic velocity structures, laboratory experiments and numerical simulations. Theoretically, temporal variations in the fluid pressure can change recurrence intervals of SSEs. However, few observational facts have been reported to support transient fluid flow during an SSE. Fluid migrations cause a subsurface mass redistribution and change the surface gravity. Therefore, this study is aimed at detecting fluid migrations by observing gravity.
In the Tokai area, gravity anomalies associated with the two long-term SSEs which occurred during 2001-2005 and 2013-2017 were detected by absolute gravimeters, suggesting that high-pressure fluids could migrate toward the shallow part of the plate interface during the SSEs. In the Ryukyu Trench, where a long-term SSE has occurred approximately every six months, relative gravimeters gPhoneX with a higher temporal resolution were installed last year. In this study, we analyzed one-year gravity data from January 2020 and examined various corrections to extract gravity changes during the long-term SSEs. We removed a long-term drift by a polynomial regression and tides and atmospheric pressure loading by BAYTAP-G. The residual short-term component with periods from a few to ten days was synchronized with precipitation and non-tidal sea level variations. The long-term component with periods longer than ten days included gravity changes with the order of magnitude of 1 microGal, which could not be explained by precipitation and crustal movements alone. To extract gravity anomalies during SSEs, we need to improve the method to remove the long-term drift, model the influence of groundwater which has not yet been considered, and correct for the effects of sea level changes including long- period tides.

Keywords: slow earthquakes, slow slip events, gravity, groundwater, crustal deformation, geodesy

©2021. Japan Geoscience Union. All Right Reserved.

Lithosphere properties along North-Central Chile subduction region and Relation to slow slip

*POUSALI MUKHERJEE[1], Yoshihiro Ito[1], Emmanuel Soliman M. Garcia[1], Kajaljyoti Borah[2]

1. Disaster Prevention Research Institute, Kyoto University, 2. Indian Institute of Science Education and Research, Kolkata

The Chile region in South America is one of the most active tectonic regions where the Nazca plate subducts beneath the South American plate. In addition to megathrust earthquakes, the region has also been reported to host slow slip earthquakes from shallow subsurface to deeper portions. Investigating the lithosphere of the slow slip and non slow slip area in Chile subduction zone is crucial in understanding the role of the internal structure to control slow slip. In this study, we are using teleseismic receiver function method to estimate the lithospheric parameters in northern and central Chile using in an around the slow slip region to estimate the shear wave velocity variation and the Vp/Vs ratio. The Vs and the Vp/Vs ratio is sensitive to the fluid distribution in the lithosphere. The results show differences in lithosphere properties in the continental and subducted oceanic lithosphere, indicating that they could have played a key role in occurrence of past slow slips in the region.

Keywords: Receiver Function, Chile Subduction System, Vs and Vp/Vs ratio, Lithosphere, Slow slip

©2021. Japan Geoscience Union. All Right Reserved.

A comparison of the source areas in Hyuganada among afterslip of two interplate earthquakes in 1996 and successive slow slip events

Sawako Teshiba[1], *Hitoshi Hirose[1,2]

1. Department of Planetology, Graduate School of Science, Kobe University, 2. Research Center for Urban Safety and Security, Kobe University

Around the Hyuganada in southwestern Japan, the Philippine Sea Plate (PHS) is subducting beneath the Amurian Plate. It is known that afterslip and long-term slow slip events (SSEs) occur on the plate interface around this region. Afterslip occurs following two interplate earthquakes in Hyuganada (both are Mw 6.7) in October and December, 1996 (Yagi et al., 2001) and SSEs repeatedly occur near the afterslip area (e.g., Yarai and Ozawa et al., 2013). However, little is known about the spatiotemporal relationship between the afterslip and the SSEs. In this study, we identify the time periods of aseismic slip episodes including the afterslip and SSEs that occurred from 1996 to 2011 and estimate detailed spatiotemporal evolutions from an inversion analysis based on GNSS data.

We use daily coordinates of GEONET GNSS stations operated by Geospatial Information Authority of Japan (GSI) (F3 solutions: Nakagawa et al., 2009). From the coordinate time-series data, we identify the slow transients and their time periods possibly of the afterslip and SSEs by reference to the transients of SSEs reported in previous studies (Yarai and Ozawa, 2013; Takagi et al., 2019).

Five transients are identified. One is afterslip from Oct .1996 to Nov. 1997 and the others are four SSEs: (1) Jun. 1998 - Mar. 1999; (2) Jan. 2005 - Mar. 2006; (3) Jan. 2007 - Nov. 2007; and (4) Apr. 2009 - Apr. 2010. For each transient, we apply an inversion method based on network inversion filter (Segall and Matthews, 1997; Hirose et al., 2014). In the inversion analysis, a spatial distribution of slip is represented by 8 ×7 small subfaults with a size of 20 km x 20 km. These subfaults are assumed to represent the geometry of the plate interface of the subducting PHS estimated by Shiomi et al. (2008) and Nakanishi et al. (2018).

Our result shows clear time variation of the afterslip area. In the time period between the first and the second earthquakes in 1996, slip area extends on the plate interface within the depth range from about 15 km to 50 km. But after the second earthquake, slip at shallower part near the epicenter of the first earthquake (< ~25 km depth) gradually decreases and ends around May 1997, whereas deeper slip continues until Nov 1997. In addition, source areas of the SSEs are located in and around the afterslip area. We also identified additional slip area in the offshore area of Cape Toi, south of the afterslip area, during the transient periods (1), (2), and (4). Among them, the southern slip area is spatially separated from the northern slip during (1) and (2). Comparing the obtained slip distribution of the afterslip with the cumulative slip distribution of the four SSEs, the SSE slip is located in the deeper part of the afterslip area and south of the afterslip.

From the above characteristics of the afterslip and the SSE slip, it is suggested that the deeper area of the afterslip may host longer (or slower) slip and SSE slip while the shallower area may host shorter (or faster) slip. Yamamoto et al. (2013) show the subducted Kyushu-Palau Ridge (KPR) in the PHS slab from a seismic exploration. Comparing the cumulative slip distribution of the SSEs with the location of subducted KPR, the main slip area of the SSEs is located deeper and outside of the KPR. This suggests that the subducted KPR controls the slip behavior on the plate interface.

©2021. Japan Geoscience Union. All Right Reserved.

Acknowledgments:
GNSS data were provided by Geospatial Authority of Japan. This research was supported by JSPS KAKENHI Grant Number JP16H06474 in Scientific Research on Innovative Areas "Science of Slow Earthquakes".

Keywords: GNSS, slow earthquakes, subduction zone, aseismic slip, Kyushu-Palau Ridge

©2021. Japan Geoscience Union. All Right Reserved.

Development of microseismicity catalog near the Japan Trench shallow slow earthquake region using a deep learning module

*Shukei Ohyanagi[1], Kazuaki Ohta[3], Yoshihiro Ito[2], Ryota Hino[4], Yusaku Ohta[4], Ryosuke Azuma[4], Masanao Shinohara[5], Kimihiro Mochizuki[5], Toshinori Sato[6], Yoshio Murai[7]

1. Graduate School of Science, Kyoto University, 2. Disaster Prevention Research Institute, Kyoto University, 3. National Research Institute for Earth Science and Disaster Resilience, 4. Tohoku University, 5. Earthquake Research Institute, The University of Tokyo, 6. Chiba University, 7. Hokkaido University

The Japan Trench subduction zone is a cradle for wide spectrum of seismic and aseismic activities, such as the Mw 9.0 Tohoku-Oki earthquake, slow slip event, very low frequency earthquakes, and tectonic tremors. In a past few years, the S-Net, the cabled network of ocean bottom seismometers (OBSs) and dense networks established by free-fall type OBSs reveal tectonic tremor in a shallow portion of the subduction zone [e.g. Nishikawa et al., 2019; Tanaka et al., 2019; Ohta et al. 2019]. However, abundant OBS data sets have not fully utilized to understand micro-seismicity of the same region in contrast to tectonic tremor activity. The OBS networks have often used to relocate hypocenters of earthquakes cataloged in the JMA unified catalog [e.g. Shinohara et al., 2012]. However, the JMA unified catalog is developed only using onshore seismic network, which has limited detectability and location capability on earthquakes occur offshore. Meanwhile, it is uncommon attempt to detect micro-earthquakes, which are exclusively visible from offshore seismic network despite of its necessity to fully-expose interplay between fast, standard seismicity and slow seismicity at the shallow trench; the attempt is definitely important to understand the wide spectrum of rupture processes in the subduction zone.

Here, we perform detection and phase picking of microearthquakes to a data set of an OBS network, which was deployed in offshore Fukushima near the trench to develop a high-quality offshore seismicity catalog, with applied the Earthquake Transformer (EQT) [Mousavi et al., 2020]. The EQT has already been trained with a set of onshore seismic and ambient noise signals [Mousavi et al., 2019]. We attempt to apply the trained model directly to the OBS data to examine its performance on offshore environment. Our OBS data set is composed of 3 dense arrays with a small aperture and 3 single station OBSs. First, we select one OBS from each array in the network as well as the single station OBSs. Seismograms of the selected stations are then filtered between 2 Hz and 30 Hz to suppress low frequency noise and increase signal-to-noise ratio. The filtered continuous waveforms are then used to detect and pick P- and S-wave arrivals from microearthquakes. The picked arrival times are finally used to estimate event hypocenters with hypomh [Hirata and Matsu’ura, 1987].

As a result of the experiment, the EQT detects more than 5000 microearthquakes, which is six times number of events than the earthquakes located by the JMA in the same region during the observation period. Although most of the detected events are located outside of the region where tectonic tremors have been observed [Nishikawa et al., 2019; Ohta et al., 2019], there are about 60 events located in close proximity of the tectonic tremors.

To evaluate closeness of the tectonic tremors and the microearthquakes, we perform array beamforming in the 3 arrays mentioned above to compare two different types of phenomena in slowness domain. It is generally unclear whether those microearthquakes occur within the tremorgenic region or completely separated from each other, because the tectonic tremors have relatively large error on their hypocenter compares to the microearthquakes because they are located with the envelope correlation method [e.g.,

©2021. Japan Geoscience Union. All Right Reserved.

Ide, 2010; Obara, 2002]. After filtering their waveform in 2 Hz and 8 Hz, the tectonic tremors are beamformed with the duration based on Ohta et al. (2019), and the microearthquakes are beamformed for 2 seconds S-wave arrival time. Comparison in the slowness domain suggests at least 3 ordinal, or fast earthquakes occur within the source region of tectonic tremors.

Keywords: Slow earthquake, Low frequency tremor, Deep Learning, Seismic array, Japan Trench, Ocean bottom seismometer

©2021. Japan Geoscience Union. All Right Reserved.

[E] Oral | S (Solid Earth Sciences)：S-CG Complex & General

Sun. Jun 6, 2021 1:45 PM - 3:15 PM JST | Sun. Jun 6, 2021 4:45 AM - 6:15 AM UTC | Ch.24 Zoom Room 24

[S-CG40] Active Tectonics and Seismic Hazards in the Himalayan Region

convener:Kazuki Koketsu(Earthquake Research Institute, University of Tokyo), Nath Soma Sapkota(Nepal Geological Society), Srinagesh Davuluri(CSIR-National Geophysical Research Institute), Chairperson:Kazuki Koketsu(Earthquake Research Institute, University of Tokyo), Hiroe Miyake(Earthquake Research Institute, University of Tokyo)

In the Himalayan region, the Indian and Eurasian plates collide, and the Indian lithosphere underthrusts beneath the Eurasian plate from the Main Frontal Thrust with a convergence rate of approximately 18 mm/year. This has historically caused large earthquakes such as the 1934 Bihar-Nepal earthquake, and seismic hazards in the region remain high. On April 25, 2015 (UTC), the Mw 7.8 Gorkha earthquake occurred along the plate boundary, and this affected the Main Frontal Thrust increasing the stress in possible source areas of future large earthquakes. Therefore, even after the Gorkha earthquake, studies on active tectonics and seismic hazards are still necessary in the Himalayan region. All kinds of studies on them are welcome for this session.

1:45 PM - 2:00 PM JST | 4:45 AM - 5:00 AM UTC

[SCG40-01] Seismic Hazard Assessment Studies in Uttarakhand Himalaya

*Srinagesh Davuluri[1], Suresh Gudapati[1], Srinivas Dakuri[1] (1.CSIR-National Geophysical Research Institute)

2:00 PM - 2:15 PM JST | 5:00 AM - 5:15 AM UTC

[SCG40-02] Active Tectonics & Seismological Research in Nepal Himalaya: Preliminary results from SATREPS project

*Soma Nath Sapkota[1], Kazuki Koketsu[2], Hiroe Miyake[3], Koji Okumura[4], Prakash Pokhrel[5] (1.Retired Director General, Department of Mines and Geology, Kathmandu Nepal, 2.Professor, Earthquake Research Institute, University of Tokyo, Tokyo Japan, 3.Associate Professor, Earthquake Research Institute, University of Tokyo, Tokyo Japan, 4.Professor, Graduate School of Humanities and Social Sciences, Hiroshima University, Japan, 5.Geologist, Department of Mines and Geology, Kathmandu Nepal)

2:15 PM - 2:30 PM JST | 5:15 AM - 5:30 AM UTC

[SCG40-03] Interseismic coupling on the Main Himalayan Thrust in Nepal derived from GNSS displacement rate field

*Takao Tabei[1], Mako Ohzono[2], Bishow Raj Silwal[3], Rajendra Bhandari[3], Janak B. Cahnd[3], Soma Nath Sapkota[4], Hiroe Miyake[2], Kazuki Koketsu[2] (1.Faculty of Science and Technology, Kochi University, 2.Earthquake Research Institute, University of Tokyo, 3.Department Mines and Geology, Nepal, 4.Nepal Geological Society)

2:30 PM - 2:45 PM JST | 5:30 AM - 5:45 AM UTC

[SCG40-04] Geodetic Observation for Evaluation of Earthquake Generation Potential in Nepal after the 2015 Gorkha Earthquake

*Bishow Raj Silwal[1], Rajendra Prasad Bhandari[1], Janak Bahadur Chand[1], Mako Ohzono[2], Takao Tabei[3] (1.Department of Mines and Geology, Nepal, 2.Earthquake Research Institute, University of Tokyo, Japan, 3.Kochi University, Kochi, Japan)

2:45 PM - 3:00 PM JST | 5:45 AM - 6:00 AM UTC

[SCG40-05] Rupture History of the Himalayan Frontal Thrust near Bagmati River crossing in Central Nepal

*Koji Okumura[1], Prakash Pokhrel[3], Hisao Kondo[2], Tomoru Yamanaka[1], Soma Nath Sapkota[3] (1.Graduate School of Letters, Hiroshima University, 2.Research Institute of Earthquake and Volcano Geology, GSJ, AIST, 3.Department of Mines and Geology, Nepal)

3:00 PM - 3:15 PM JST | 6:00 AM - 6:15 AM UTC

[SCG40-06] Strong Motion Observation Network for Earthquake Disaster Mitigation in the Kathmandu Valley, Nepal

*Nobuo Takai[1], Michiko Shigefuji[2], Hiroe Miyake[3], Kazuki Koketsu[3], Mukunda Bhattarai[4], Chintan Timsina[4], Shova Singh[4], Subeg Bijukchhen[5] (1.Hokkaido University, 2.Kyushu University, 3.University of Tokyo, 4.Department of Mines and Geology, Nepal, 5.Khwopa Engineering College, Nepal)

Seismic Hazard Assessment Studies in Uttarakhand Himalaya

*Srinagesh Davuluri[1], Suresh Gudapati[1], Srinivas Dakuri[1]

1. CSIR-National Geophysical Research Institute

The seismic Hazard Assessment studies in the Uttarakhand region has been undertaken with the installation of seismological network comprising of 53 Broad band seismographs, 32 Strong Motion Accelerometers and 4 Strong Motion Velocity meters to constrain the seismicity and characterize with the major tectonic features, record ground motion accelerations to characterize the ground motions in Uttarakhand both in terms of the Amplitude, Frequency and compare with the BIS Response spectra. During February 2017 –November 2020, around 700 earthquakes of magnitude ranging from 0.8 to 5.5 have been located. The main features of the seismicity patterns show they cluster both in space and depth. Majority of the earthquakes are coinciding with the Main Himalayan thrust, the interface between the Eurasian and Indian Plates was the locale for the past large earthquakes. Further, the strong motion and Broad band seismograph data past and present has contributed in the deriving the ground motion Prediction equations for this region which is the first of the kind for the continental continental plate collision.

Keywords: Uttarakhand Himalaya, Seismicity, Ground Motion Prediction Equations

©2021. Japan Geoscience Union. All Right Reserved.

Active Tectonics & Seismological Research in Nepal Himalaya: Preliminary results from SATREPS project

*Soma Nath Sapkota[1], Kazuki Koketsu[2], Hiroe Miyake[3], Koji Okumura[4], Prakash Pokhrel[5]

1. Retired Director General, Department of Mines and Geology, Kathmandu Nepal, 2. Professor, Earthquake Research Institute, University of Tokyo, Tokyo Japan, 3. Associate Professor, Earthquake Research Institute, University of Tokyo, Tokyo Japan, 4. Professor, Graduate School of Humanities and Social Sciences, Hiroshima University, Japan, 5. Geologist, Department of Mines and Geology, Kathmandu Nepal

Knowing the return period and possible impact of great and megaquake in Nepal Himalaya is key to mitigate impending seismic risk in this region. To understand and evaluate seismic risk, Deapartment of Mineas and Geology (DMG), Urban Development and Building Construction (DUDBC), and Tribhuwan University (TU) in collaboration with Japan International Cooperation Agency (JICA), Japan Science and Technology (JST) and Earthquake Research Institute (ERI) of Tokyo University are collaborating through Science and Technology Research Partnership for Sustainable Development (SATREPS) project for Seismic Hazard assessment of Kathmandu valley and quantifying central Himalayan seismic gap between 2015 Gorkha Earthquake and 1905 Kangra earthquake.

Many geological and geophysical survey are conducted in Kathmandu valley to calculate and predict the different parameter of thick sediment (approx. 600m) of Kathmandu valley during impending big earthquake. Permanent eight GNSS station of Global Positioning System and eight seismic stations are installed which are now connected to the national network and will enhance the monitoring capacity of Nepalese network. This will ultimately improve the location accuracy to report earthquake parameter to the government authority. Paeloseismological trenching is also conducted in Butwal, Tribeni, Bagmati and Kathmandu valley preliminary promising results are coming from different Geophysical campaign experiment in Kathmandu valley, Geomorphological and paleoseismological trenching in Himalayan front which will be discussed.

Keywords: Central Himalayan Seismic Gap , Return Period, Paleoseismology, GNSS stations

©2021. Japan Geoscience Union. All Right Reserved.

Interseismic coupling on the Main Himalayan Thrust in Nepal derived from GNSS displacement rate field

*Takao Tabei[1], Mako Ohzono[2], Bishow Raj Silwal[3], Rajendra Bhandari[3], Janak B. Cahnd[3], Soma Nath Sapkota[4], Hiroe Miyake[2], Kazuki Koketsu[2]

1. Faculty of Science and Technology, Kochi University, 2. Earthquake Research Institute, University of Tokyo, 3. Department Mines and Geology, Nepal, 4. Nepal Geological Society

Most of the land in Nepal is located on the hanging wall of the Indian-Eurasian plate convergent zone. We have deployed 10 continuous GNSS stations in central and mid-western Nepal since 2016 under the SATREPS/NERDiM project to enhance spatial resolution of geodetic observation network and better estimate earthquake generation potential in the Himalayan Frontal Zone (Silwal et al., 2021; this meeting). We focus especially on the “Central Seismic Gap” where no destructive event has been recorded for centuries. Data collected at each SATREPS/NERDiM GNSS site are transmitted to Kathmandu on a semi-daily basis via domestic cell phone network and then processed together with data from the pre-existing domestic GNSS stations and IGS reference stations. Highly automated data acquisition and baseline analysis system is implemented in a processing server.

As a preliminary analysis, we collect all available GNSS data in Nepal since 1995 through UNAVCO DAI v2 and process them using PPP-AR method of GIPSY/OASIS II ver.6.4. The result shows that the north-south contraction in Nepal is roughly 10-15 mm/yr, equivalent to a strain rate of 0.1 ppm/yr, implying that about 30-40% of the relative Indian-Eurasian plate motion (36-37 mm/yr) is taken up in crustal shortening across the Himalayan Frontal Zone. Next we estimate interseismic coupling on the Indian-Eurasian plate boundary using TDEFNODE (McCaffrey, 2009) and GNSS site displacement rates. Two plate boundary models are checked, the first one is characterized by down-dip variation of gently dipping fault planes and steeper ramps (Hubbard et al., 2016) and the second by rather flatter surface (Hayes, 2018). We constrain the lower limit of the plate interface to 35 km in depth and place nodes on the interface with a lateral spacing of 30-40 km along depth contours every 5 km. Then slip deficit rates are estimated on the interface. Plate coupling ratio (normalized slip deficit rate) seems corelate with structure of the interface, i.e., strong coupling on the gently dipping fault planes and week or null coupling on the steeper ramps. This pattern is in contrast with the previous result that shows coupling ratios nearly monotonously decreasing with depth on the flatter interface (e.g. Stevens and Avouac, 2015). Further investigation is needed to clarify current state of plate coupling on the Himalayan Frontal Zone.

Keywords: Nepal, GNSS, NERDiM

©2021. Japan Geoscience Union. All Right Reserved.

Geodetic Observation for Evaluation of Earthquake Generation Potential in Nepal after the 2015 Gorkha Earthquake

*Bishow Raj Silwal[1], Rajendra Prasad Bhandari[1], Janak Bahadur Chand[1], Mako Ohzono[2], Takao Tabei[3]

1. Department of Mines and Geology, Nepal, 2. Earthquake Research Institute, University of Tokyo, Japan, 3. Kochi University, Kochi, Japan

Nepal is prone to devastating earthquake disaster because it is located in the active collision zone between the Eurasian and Indian tectonic plates. Immediately after the 2015 Gorkha earthquake, Integrated Research on Great Earthquakes and Disaster Mitigation in Nepal Himalaya, SATREPS/NERDiM, was initiated under the collaboration of Nepalese and Japanese governments. One of the project teams is working with an objective of evaluating earthquake generation potential in central Nepal by means of geodetic data collected from Global Navigation Satellite System (GNSS) network, which is able to monitor 3-D site displacements caused by the plate interaction at a high precision of a few millimeters per year. Spatial and temporal variation of displacement field and converted strain accumulation pattern will be useful to reveal physical processes ongoing on the plate interface. Our new GNSS network, composed of ten permanent stations deployed in central and mid-western Nepal covering about 100 km north to south and 400 km east to west, have greatly improved detectability of crustal deformation in the plate convergent region. In addition, we have installed an automated GNSS data processing and archiving system in Kathmandu. Preliminary result shows that the north-south contraction in Nepal is as large as 10-15 mm/yr, equivalent to the strain rate of 0.1 ppm/yr. As the next step, we are preparing estimation of plate locking distribution using the latest plate boundary model. Strain build-up monitored by our system, in conjunction with data from other pre-existing GNSS stations in and around Nepal, will provide very fundamental and important information for evaluating earthquake generation potential in the near future.

Keywords: GNSS, Earthquake, Geodetic, Nepal

©2021. Japan Geoscience Union. All Right Reserved.

Rupture History of the Himalayan Frontal Thrust near Bagmati River crossing in Central Nepal

*Koji Okumura[1], Prakash Pokhrel[3], Hisao Kondo[2], Tomoru Yamanaka[1], Soma Nath Sapkota[3]

1. Graduate School of Letters, Hiroshima University, 2. Research Institute of Earthquake and Volcano Geology, GSJ, AIST, 3. Department of Mines and Geology, Nepal

The 2015 Golkha earthquake raised concern about the future large earthquake occurring in south of the 2015 source area. The 2015 earthquake ruptured 10 to 20 km deep portion of the plate boundary interface ~50 km away from the surface trace of the frontal thrust. It is necessary to evaluate the earthquake potential of the shallowest part of the Himalayan Frontal Thrust in central Nepal. After 5 years of intensive studies on the rupture history, now there are important questions about three large past earthquakes of 1934, 1344, and 1255 (or 13 century). They are, (1) the existence and extent of 1934 surface rupture, (2) the existence and extent of 1344 rupture, and (3) the extent and exact timing of 1255 (or 13th century) event. As to the 1934 surface rupture, Rizza et al. (2019) as well as Sapkota et al. (2012) demonstrated ruptures on fault exposures against Wesnousky et al. (2018) in Bardibas area. However, the west terminations of the 1255 and 1934 rupture have not been defined yet. We excavated two trenches on the Himalayan front in east and in west of Bagmati river to examine the terminations and to know the rupture history. At the Dumachaur Khola site 4 km east of Bagmati river, 3 or 4 events in 3500 years are excavated. The timing of the last event here is in the earlier half of the 2nd millennium C.E.. At the Gopalkoti-Dandatol site, 0.7 km west of Bagmati river, 2 or 3 events between 3rd and 14th century C.E. are recognized. 1934 ruptures do not appear in both trenches. This study is a part of the JICA-JST SATREPS project: Integrated Research on Great Earthquakes and Disaster Mitigation in Nepal Himalaya.

Keywords: Himalayan Frontal Thrust, paleoseismology, surface rupture

©2021. Japan Geoscience Union. All Right Reserved.

Strong Motion Observation Network for Earthquake Disaster Mitigation in the Kathmandu Valley, Nepal

*Nobuo Takai[1], Michiko Shigefuji[2], Hiroe Miyake[3], Kazuki Koketsu[3], Mukunda Bhattarai[4], Chintan Timsina[4], Shova Singh[4], Subeg Bijukchhen[5]

1. Hokkaido University, 2. Kyushu University, 3. University of Tokyo, 4. Department of Mines and Geology, Nepal, 5. Khwopa Engineering College, Nepal

The Himalayan continental collision zone of the Indian plate and the Eurasian plate have been causing many devastating earthquakes in the past. The Kathmandu Valley in Nepal is filled with soft soil of Plio-Pleistocene origin the thickness of the sediments is more than 600 m in the central part of the valley. Because of the site amplification of this sediment structure, many damages occurred not only by the near earthquakes (e.g., the 2015 Gorkha Nepal earthquake) but also by the far earthquakes (e.g., the 1934 Bihar-Nepal, the 2011 Taplejung-Sikkim earthquakes).

Moreover, the residential area in the Kathmandu Valley has been spread quickly in recent years by the explosive population growth. By this seismological and social environment, the earthquake damage risk of this metropolitan area in the valley is increasing. This risk must be reduced by a high precision prediction for the next great earthquake which has the potential to occur in the Central Seismic Gap of the Main Frontal Thrust in Nepal Himalaya.

There were six known seismic observation sites in the valley: one station by USGS, one station by the Department of Mines and Geology, Ministry of Industry, Commerce, and Supplies and four stations by the collaborative observation of Hokkaido University and Tribhuvan University (Takai et al., 2016). However, the density of these former stations was too low to know the site amplification variation in the valley whose diameter is about 25 km in detail.

“Integrated Research on Great Earthquake and Disaster Mitigation in Nepal Himalaya” is a project of the Science and Technology Research Partnership for Sustainable Development program supported by JST and JICA (SATREPS NERDiM, 2016-2021, Principal Investigator: Kazuki Koketsu). By this NERDiM project, in order to accumulate the strong motion data, the strong motion observation network was installed with ten strong-ground motion seismometers in Nov. 2016- May 2018. There was only one rock site station (Kirtipur) in the valley, therefore, we installed the instruments to north, west, and east rock site stations. Moreover, we selected the heavily damaged area (Balaju) during the 2015 Gorkha Nepal earthquake and the low-density observation area as observation sites.

Even the small amount of accumulated important data can show the difference of the amplification factor at each station in the valley. The north rock site Jhor and the east rock site Sanga have predominant periods in 0.25 - 0.3 s, on the other hand, other sedimentary sites have those in 1.2 - 5 s (2018 JpGU, 2019 SSJ). We have constructed the 1-D and 3-D deep sedimentary velocity structure models in the Kathmandu Valley (Bijukchhen et al., 2017, Bijukchhen, 2018) by using aftershock records of the 2015 Gorkha earthquake of existing stations. After installing these observation sites, we could compare the observed receiver function with the theoretical one (2020 JpGU, 2020 WCEE). In this comparison, the observed receiver functions agreed with the theoretical ones in most stations except stations on the center and marginal part of the valley, which is not used by the construction of that velocity model. Also, we made the correction term of the ground motion prediction equation (GMPE) for velocity response

©2021. Japan Geoscience Union. All Right Reserved.

spectra for this valley using aftershock records and depth to seismic bedrock of the valley (2020 SDEE). This will be a powerful tool for making the design spectrum for a long period of ground motion for high-rise buildings increasing in the valley.

The accumulation of the strong motion data by this new network will be able to upgrade this GMPE and the underground structure to contribute to the disaster mitigation planning for the Kathmandu metropolitan area, in the future.

Acknowledgments: A part of this research was supported by SATREPS of JST-JICA Grant Number JPMJSA1511, and JSPS KAKENHI.

Keywords: Strong Motion Observation Network, Nepal Himalaya, Kathmandu Valley

©2021. Japan Geoscience Union. All Right Reserved.

[E] Oral | S (Solid Earth Sciences)：S-CG Complex & General

Sun. Jun 6, 2021 3:30 PM - 5:00 PM JST | Sun. Jun 6, 2021 6:30 AM - 8:00 AM UTC | Ch.24 Zoom Room 24

[S-CG40] Active Tectonics and Seismic Hazards in the Himalayan Region

convener:Kazuki Koketsu(Earthquake Research Institute, University of Tokyo), Nath Soma Sapkota(Nepal Geological Society), Srinagesh Davuluri(CSIR-National Geophysical Research Institute), Chairperson:Hiroe Miyake(Earthquake Research Institute, University of Tokyo), Kazuki Koketsu(Earthquake Research Institute, University of Tokyo)

In the Himalayan region, the Indian and Eurasian plates collide, and the Indian lithosphere underthrusts beneath the Eurasian plate from the Main Frontal Thrust with a convergence rate of approximately 18 mm/year. This has historically caused large earthquakes such as the 1934 Bihar-Nepal earthquake, and seismic hazards in the region remain high. On April 25, 2015 (UTC), the Mw 7.8 Gorkha earthquake occurred along the plate boundary, and this affected the Main Frontal Thrust increasing the stress in possible source areas of future large earthquakes. Therefore, even after the Gorkha earthquake, studies on active tectonics and seismic hazards are still necessary in the Himalayan region. All kinds of studies on them are welcome for this session.

3:30 PM - 3:45 PM JST | 6:30 AM - 6:45 AM UTC

[SCG40-07] 2D FDM simulation of seismic ground motions and inversion of velocity structure models in the Kathmandu Valley, Nepal

*Hongqi Diao[1], Kazuki Koketsu[1], Kazuhito Hikima[2] (1.Earthquake Research Institute, University of Tokyo, 2.Tokyo Electric Power Company Holdings)

3:45 PM - 4:00 PM JST | 6:45 AM - 7:00 AM UTC

[SCG40-08] Microtremor observation in the Kathmandu valley, Nepal: Past, Present, and Future perspectives

*Mukunda Bhattarai[1], Rajesh Sharma[3], Sunita Bhattarai[2], Tara Pokrarel[1], Chintan Timsina[1], Suresh Shrestha[2], Dinesh Nepali[2], Manoj Nakarmi[4], Prakirna Tuladhar[4], Takumi Hayashida[5], Toshiaki Yokoi[5], Hiroe Miyake[6], Koichi Kusunoki[6] (1.National Earthquake Monitoring and Research Center, Department of Mines and Geology, Nepal, 2.Department of Mines and Geology, Nepal, 3.Seismological Center Surkhet, Department of Mines and Geology, Nepal, 4.Department of Urban Development and Building Construction, Nepal, 5.International Institute of Seismology and Earthquake Engineering, Building Research Institute,Japan, 6.Earthquake Research Institute, The University of Tokyo, Japan)

4:00 PM - 4:15 PM JST | 7:00 AM - 7:15 AM UTC

[SCG40-09] BROADBAND MICROTREMOR ARRAY EXPLORATION IN THE KATHMANDU VALLEY, NEPAL

*Toshiaki Yokoi[1], Takumi Hayasida[1], Mukunda Bhattarai[3], Tara Pokharel[2], Suresh Shrestha[2], Chintan Timsina[3], Sunita Bhattarai[2], Rajesh Sharma[3], Dinesh Nepali[2] (1.International Institute of Seismology and Earthquake Engineering, Building Research Institute, Japan, 2.Department of Mines and Geology, Nepal, 3.National Earthquake Monitoring and Research Centre, NEMRC/DMG, Nepal)

4:15 PM - 4:30 PM JST | 7:15 AM - 7:30 AM UTC

[SCG40-10] Seismic observation and automatic hypocenter location system in Nepal

*Shigeki Horiuchi[1], Masumi Yamada[3], Koji MIYAKAWA[2], Hiroe Miyake[2], Tadashi Yamashina[4], Chintan Timsina[5], Mukunda Bhattarai[5], Bharat Prasad Koirala[5], Monika Jha[5], Lok Bijaya Adhikari[5] (1.Home Seismometer Corporation, 2.ERI, 3.DPRI, 4.Kochi University, 5.DMG, Nepal)

4:30 PM - 4:45 PM JST | 7:30 AM - 7:45 AM UTC

[SCG40-11] Upper-Crustal Structure of Central Nepal inferred from Local Earthquake Tomography

*Chintan Timsina[1], James Mori[2], Masumi Yamada[2] (1.Graduate School of Science, Kyoto University, 2.Disaster Prevention Research Institute, Kyoto University)

4:45 PM - 5:00 PM JST | 7:45 AM - 8:00 AM UTC

[SCG40-12] Towards the Further Development of the Education and Research on Earthquakes in Nepal

*Mai Suzuki[1], Binil Aryal[2], Kazuki Koketsu[1] (1.Earthquake Research Institute, The University of Tokyo, 2.Central Department of Physics, Tribhuvan University)

2D FDM simulation of seismic ground motions and inversion of velocity structure models in the Kathmandu Valley, Nepal

*Hongqi Diao[1], Kazuki Koketsu[1], Kazuhito Hikima[2]

1. Earthquake Research Institute, University of Tokyo, 2. Tokyo Electric Power Company Holdings

Great and disastrous earthquakes have repeatedly occurred at the subduction interface along the Himalayan arc in the past and would continue to occur in the future due to the continuous collision between the Indian Plate and Eurasian Plate. And a recent example was the 2015 Mw7.8 Gorkha earthquake, which induced serious seismic disasters in the Kathmandu Valley, Nepal. The Kathmandu Valley sits on an ancient lake bed zone with irregular soft sedimentary layers of several hundred meters depth in the deep part. Previous studies of the tomography of the Kathmandu valley demonstrated that the velocity structure model in the Kathmandu Valley is highly spatially variable, with obvious difference of thickness of soft sedimentary layers within short distances. The gravity survey and seismic reflection experiment conducted in the Kathmandu Valley in latest years by the joint research team between Japan and Nepal has confirmed the high thickness gradients of sediments and obtained a preliminary 3D velocity structure model. Because seismic ground motions especially long-period ground motions that can be significantly amplified and reverberated due to the basin effect within the valley can pose a serious threat to the buildings and infrastructures in the Kathmandu Valley, it’s necessary to investigate the propagation effect and the amplification effect of seismic ground motions in the valley and to refine the preliminary velocity structure model for the strong ground motion simulations for seismic hazard assessment.

A collaboration between Japan and Nepal has begun since 2011 to study the strong motion characteristics in the Kathmandu Valley and several strong motion accelerometers have been installed within the valley since then. Three-component strong motions of several moderate regional and local earthquakes and small local earthquakes have been recorded by these strong motion stations. In this study, we performed 2D FDM simulations of seismic ground motions at the strong motion station sites in the Kathmandu Valley using the preliminary velocity structure model and compared with other researcher’s 3D FDM simulation results and the observation data for a moderate regional earthquake. The results showed that the source size effect of the moderate regional earthquake could not be ignored, and that the 2D FDM simulation could reproduce the early phases of the propagation effect but could not reproduce the later phases of the large surface waves generated in the deep part of the Kathmandu Basin. Due to the limited number of strong motion records accumulated in the Kathmandu Valley, we perform inversion of 2D velocity structure models based on the preliminary 3D model in the valley. To avoid the source size effect of the moderate regional or local earthquakes, we choose to use small local earthquakes which occurred near the Kathmandu Valley to perform inversion of 2D velocity structure models. The 2D velocity structure models along the lines connecting the epicenter of the small local earthquake and different strong motion station sites are inverted. The 2D FDM simulations of strong ground motions using the inverted velocity structure models in the Kathmandu Valley could reproduce the amplitudes of the main phases of the observation data. Our study on the strong motion simulations and inversion of velocity structure models in the Kathmandu Valley provides a basis for the seismic hazard assessment in this area.

Keywords: Kathmandu Valley, strong ground motion, 2D FDM simulation, inversion, velocity structure model

©2021. Japan Geoscience Union. All Right Reserved.

©2021. Japan Geoscience Union. All Right Reserved.

Microtremor observation in the Kathmandu valley, Nepal: Past, Present, and Future perspectives

*Mukunda Bhattarai[1], Rajesh Sharma[3], Sunita Bhattarai[2], Tara Pokrarel[1], Chintan Timsina[1], Suresh Shrestha[2], Dinesh Nepali[2], Manoj Nakarmi[4], Prakirna Tuladhar[4], Takumi Hayashida[5], Toshiaki Yokoi[5], Hiroe Miyake[6], Koichi Kusunoki[6]

1. National Earthquake Monitoring and Research Center, Department of Mines and Geology, Nepal, 2. Department of Mines and Geology, Nepal, 3. Seismological Center Surkhet, Department of Mines and Geology, Nepal, 4. Department of Urban Development and Building Construction, Nepal, 5. International Institute of Seismology and Earthquake Engineering, Building Research Institute,Japan, 6. Earthquake Research Institute, The University of Tokyo, Japan

Kathmandu valley falls in the Lesser Himalaya of central Nepal and is one of the largest intermontane basins of Nepal. It is prone to earthquake disasters due to its tectonic environment and local site conditions. Furthermore, accumulated piles of thick sediment above the basement rock, steep topography in basin outskirts, unplanned land use/settlements, rapid urbanization, and poor earthquake-resistant constructions have made this region highly vulnerable to earthquake disaster. These factors emphasize the need for subsurface structure studies and their applications to damage evaluation of Reinforced Concrete (RC) buildings. Not only the evaluation of site-specific seismic hazard where the dwelling is located using passive surface waves but also surveys inside the building itself is of great concern for the evaluation of future seismic risk, where about 3 million agglomerates are residing.

Passive microtremor measurement has been performed in the Kathmandu valley before the Gorkha earthquake using a single tri-axial seismometer (Pandey et al., 1996, Paudel et al., 2010, Bhandary et al, 2014). After the Gorkha earthquake, there exist few studies in the Kathmandu valley for the site-specific studies using microtremor (JICA, 2016, Poovarodom et al., 2017, Molnar et al., 2017). These studies also have the limitation of revealing the deep shear wave velocity structures up to the basin basement.

The project for “Integrated Research on Great Earthquakes and Disaster Mitigation in Nepal Himalaya” is a multidisciplinary research project (FY:2016-2021) in Nepal supported by Japan Science and Technology Agency (JST) and Japan International Cooperation Agency (JICA). The main objective of this project is to provide an advanced seismic risk assessment of the Kathmandu valley by subsurface explorations and establishing seismic observation networks targeting around the central seismic gap along the Main Himalayan Thrust (MHT) to contribute to disaster risk reduction of Nepal by utilizing data acquired from explorations/observations and their research findings.

There are five working groups in this project, group 3 (G3) where most of the authors belong is mainly involved in subsurface explorations of the Kathmandu valley, whereas group 5 (G5) which reflects the overall output of the project is mainly based on inputs from G1 to G4. Few outcomes of microtremor explorations have already been documented for e.g., Bhattarai et al., 2017a; 2017b, Yokoi et al., 2018; 19, Hayashida et al.,2018; 2019. However, most of these studies could not obtain the dispersion curve and consequently velocity structures in the frequency range from 0.1 to 0.2 Hz.

In this meeting, I will discuss the period verification of Nepalese RC buildings revealed from microtremor observations in some sampled RC buildings with the building codes and explain the application of shear wave velocity structures to building damage analysis as a potential output of (G5) and also emphasizes its importance on the future disaster mitigation of the Kathmandu valley.

©2021. Japan Geoscience Union. All Right Reserved.

Acknowledgments:

This research was supported by Science and Technology Research Partnership for Sustainable Development (SATREPS) from Japan Science and Technology Agency (JST) and Japan International Cooperation Agency (JICA). I highly acknowledge the Director General of the Department of Mines and Geology (DMG) for providing me an opportunity to join this scientific gathering remotely.

Keywords: Array deployment, Kathmandu valley, Shear wave velocity structure, Gorkha earthquake, RC buildings

©2021. Japan Geoscience Union. All Right Reserved.

BROADBAND MICROTREMOR ARRAY EXPLORATION IN THE KATHMANDU VALLEY, NEPAL

*Toshiaki Yokoi[1], Takumi Hayasida[1], Mukunda Bhattarai[3], Tara Pokharel[2], Suresh Shrestha[2], Chintan Timsina[3], Sunita Bhattarai[2], Rajesh Sharma[3], Dinesh Nepali[2]

1. International Institute of Seismology and Earthquake Engineering, Building Research Institute, Japan, 2. Department of Mines and Geology, Nepal, 3. National Earthquake Monitoring and Research Centre, NEMRC/DMG, Nepal

Strong ground motion of long duration and long predominant period around four seconds were observed during the 2015 Gorkha earthquake at the central part of the Kathmandu Valley (KTV), Nepal (e.g., [1], [2]). KTV is a tectonic basin formed during the Himalayan orogeny due to the collision of the Indian plate to the Eurasian plate (e.g., [3]). The research group to which the authors belong (Group3, SATREPS) has conducted the deep exploration using microtremor from Dec. 2016 to May 2019, with the aim to reveal the cause of the mentioned phenomena to make use it for bettering the seismic hazard assessment. In JPGU2019, we presented a partial report of the activities until Dec. 2018 ([4]). We will report the summary of the activities in JPGU2021.

We conducted the field observation of microtremor in KTV using four broadband seismographs to estimate mainly Vs structure of deep sediments. We used also short period seismometers, land geophones and multi-channel data logger for shallow exploration [4]. Due to the difficulty to set up a large regular polygon arrays in the densely built-up city, we had to deploy large irregular quadrilateral ones based on confirmation of the isotropic nature of coherence function of microtremor, whereas equilateral triangular ones for middle and small sizes. The maximum inter-station distances of each sites were about 900m, and at maximum 1,400 m. Recording duration was one night or longer per deployment. Then we applied 2ST-SPAC analysis to the records of these arrays in a combined way to estimate the dispersion curves.

We, however, had to take countermeasures to extend the analyzable frequency range. To fix the problem supposed to be caused by the insufficient power of microtremor in the frequency range lower than 0.2 Hz, we have combined the phase velocity of Rayleigh waves that was determined by [5] using surface waves components of tectonic earthquake records in the frequency range from 0.01 Hz to 0.13 Hz. To cover highest frequency range we have conducted shallow exploration using different methods, MASW, CCA of mini hexagon array, L-Shape SPAC, etc., using short period seismometers and geophones: from about 5 Hz to higher than 10 Hz.

Besides we filled the gap of dispersion curves appeared in some sites between 0.2 Hz and the lowest analyzable frequency of 2ST-SPAC, i.e., around 0.3 Hz, by applying CCA to the records of scalene triangle arrays extracted from the quadrilateral ones. However, the gap from 0.13 Hz to 0.2 Hz remained unfilled for all sites. We also filled other gaps at a few sites in higher frequency ranges, but lower than 1 Hz, using auxiliary the phase velocities calculated from zero crosses of the SPAC coefficient curves.

We, then, applied the inversion of Vs structure from the determined dispersion curves. The estimated Vs structure showed a sharp discontinuity at a depth of about 600 m at the central part of KTV. In addition, another Vs discontinuity was observed at a depth of about 400 m. According to the information from a few deep drilling in KTV, The former can be interpreted as the seismic bedrock, and the latter is speculated to be a buried terrace formed in an era of discharge of the paleo-Kathmandu lake.

©2021. Japan Geoscience Union. All Right Reserved.

We could show a sufficient efficacy and usefulness of irregular shape arrays, and a comparison of various methods for shallow exploration as a show case, based on these observational activities.

Acknowledgement: This study was supported by JST and JICA under SATREPS: “Integrated Research on Great Earthquakes and Disaster Mitigation in Nepal Himalaya (FY2016-2021)”.

REFERENCES: [1] Bhattarai et al. (2015): Seism. Res. Lett., 86, 40-48;
[2] Takai et al. (2016): Earth Planets and Space, 68(10),1-8;
[3] Sakai et al. (2016): Earth Planets and Space, 68, 31, 1-10;
[4] Yokoi et al. (2019): Proceedings of JPGU2019, Tokyo;
[5] Hayashida et al. (2018): Proceedings of SSJ Fall Meeting.

Keywords: Microtremor Array Exploration, Irregular Shape Array, Deep Sedimentary layers, Kathmandu Valley

©2021. Japan Geoscience Union. All Right Reserved.

Seismic observation and automatic hypocenter location system in Nepal

*Shigeki Horiuchi[1], Masumi Yamada[3], Koji MIYAKAWA[2], Hiroe Miyake[2], Tadashi Yamashina[4], Chintan Timsina[5], Mukunda Bhattarai[5], Bharat Prasad Koirala[5], Monika Jha[5], Lok Bijaya Adhikari[5]

1. Home Seismometer Corporation, 2. ERI, 3. DPRI, 4. Kochi University, 5. DMG, Nepal

1. Introduction

SATREPS program of Integrated Research on Great Earthquake and Disaster Mitigation in Nepal was started in 2015. One of the objectives of this project is to enhance the eismic observation system in Nepal. Our group installed eight seismic stations in the area called central Himalayan seismic gaps. Seismic waveform data are collected in near real-time. We developed an automatic location system, which determines hypocenter locations, magnitude, and seismic intensity distribution within a few minutes after the felt earthquake occurrence. The computed earthquake parameters are disclosed on a website for the damage reduction by a larger earthquake. We present our group activity and scientific results from this subject.

2. Seismic observation system

We installed 8 seismic stations with three-component velocity and acceleration sensors. Broadband velocity seismometers were installed at four stations and 1 Hz seismometers were installed at remaining four stations. A modem with a SIM card was installed in the seismic observation device and continuous waveform data is transmitted every minute to a server at the Department of Mines & Geology (DMG) in Kathmandu. The observation device operates with a solar panel and a built-in battery. There is a function to update the software remotely from the cental server.

3. Automatic processing system

Since the seismic stations were installed in the area of central Himalayan earthquake gap, seismicityinside and around the seismic network is relatively low. For security reasons, we need to install seismometers inside the public facilities, such as schools and parks. Therefore, the noise level during the daytime is relatively high for most of the stations. We found that the events created by noise are several ten times larger than seismic events without a noise filter. The low seismicity and high noise level require a good algorithm of noise signal discrimination.

Since the seismic stations are located on the premises of schools, etc., the main source of noises is human activity. The noise durations are mostly 1-2 seconds or less and high-frequency components are dominant. We set the following criteria for the noise-signal discrimination and removed noise events after hypocenter location.

The event is classified as noise if:

(1) Standard error of arrival time residual > 2.0 seconds.

(2) No P-wave readings at the closest 3 stations if the number of P-wave readings (Np) < 5.

(3) No P wave reading at the closest station if Np < 4.

(4) Nerr>Np, where Nerr is the number of the inappropriate stations with (a) (f-P) time <(S-P) time and (b) predominant period(Tp) and epicentral distance(D) are following combinations; Tp>1.2 and D>100km, Tp>0.7 and D<100km, Tp>0.3 and D<50km. These parameters are set empirically by checking noise events and seismic events to eliminate noise events.

4. Result

Hypocenters are located automatically when more than three P-wave arrival times are observed. Many noise events are included in events, which are located by three P wave arrivals.However, if the number of P wave readings is 4 or more, the event is most likely an earthquake and accurate location can be

©2021. Japan Geoscience Union. All Right Reserved.

determined. The processing results can be monitored on the website. When an earthquake with a magnitude > 4.5 occurs, our system displays the distribution of the MMI seismic intensity calculated from the epicenter location and magnitude.
In addition to the SATREPS seismic stations, DMG collects continuous waveform data from seismic stations installed by France, China, and RIMES in a mini-seed format. Currently, we are developing an automatic hypocenter location system using all the data.

Keywords: SATREPS Nepal, Seismic Observation, Automatic hypocenter location

©2021. Japan Geoscience Union. All Right Reserved.

Upper-Crustal Structure of Central Nepal inferred from Local Earthquake Tomography

*Chintan Timsina[1], James Mori[2], Masumi Yamada[2]

1. Graduate School of Science, Kyoto University, 2. Disaster Prevention Research Institute, Kyoto University

Central Nepal is one of the most studied sections of the Himalayas. Multiple geological and geophysical campaigns in central Nepal have proposed a variety of models for seismo-tectonics and geometries of the Main Himalayan Thrust (MHT). However, most of them focused on the two-dimensional model across the MHT. After the 2015 Gorkha earthquake (Mw 7.8), several studies have suggested considerable lateral variation on the crustal structure in both cross-strike and along-strike directions. In this study, we utilize the recordings of numerous local events by the dense network focusing on (1) imaging 3D physical heterogeneities of the upper crust in central Nepal and (2) its role in controlling the rupture of the 2015 earthquake.

We used manually picked P- and S- arrivals from around 1700 events of the Gorkha earthquake sequence for a simultaneous inversion of the seismic velocities and hypocenters using the local earthquake tomography technique. These events were recorded in central Nepal by a temporary network of 42 broadband and short-period stations from June 2015 to April 2016. We applied a gradational approach starting with inversion of a 1D velocity model and progressively updated to a detailed 3D model in several steps. This allows us to have a reasonable model even in areas where we have lower resolution. Moreover, we also obtained a Qp model of the region using vertical-component waveforms of relocated earthquakes and the Vp model. Our results not only provide a detailed velocity structure and aftershock distribution within the source region of the Gorkha earthquake but also are useful for other applications such as numerical simulations.

Preliminary results of our velocity model show three main domains. (1) Zone of low Vp and low Vs in the southern part of the area at shallow depth (<10 km). This zone is spatially well-correlated with sedimentary rocks of the sub-Himalaya. (2) A zone of remarkably low Vp/Vs ratio (<1.65) in the central-northern part of the area from surface to the depth of 10 km. This anomalously low ratio may represent bodies of felsic (quartz-rich) rocks as mapped at the surface. (3) A region of high Vp, at the depth of the Gorkha Earthquake rupture, coincides with the area of large (>4 m) co-seismic slip. This high-velocity zone may represent an asperity on the fault which possibly controlled the rupture of the mainshock.

©2021. Japan Geoscience Union. All Right Reserved.

Towards the Further Development of the Education and Research on Earthquakes in Nepal

*Mai Suzuki[1], Binil Aryal[2], Kazuki Koketsu[1]

1. Earthquake Research Institute, The University of Tokyo, 2. Central Department of Physics, Tribhuvan University

In order to mitigate the earthquake disaster, it is important to promote the public understanding of earthquakes and to foster an expert on earthquakes, and the various educational institutions provide the diverse curriculums related to earthquakes. In Nepal, where the latest large earthquake hit in 2015 and the risk of future big earthquakes is still high, the different types of earthquake related education and research are provided from the elementary education institutions to the higher education institutions. These curriculums contribute to nurturing people who have the precise knowledge on earthquakes and have the skills on disaster preparedness, however, there are still problems. Based on the interview and literature research at the educational institutions and the government agencies in Nepal, this presentation discusses the actual circumstances of the education and research on earthquakes in Nepal and suggests what is needed for the further development of it.

In Nepal, the primary and secondary schools provide the education on the earthquake disaster mitigation (e.g. how to evacuate in the event of an earthquake) and the higher education institutions offer the courses in geology, engineering, and social sciences related to earthquakes. In addition, the national ministries and NGOs provide training and advice to the builders on how to construct the earthquake-resistant buildings. While these various efforts are being made to mitigate the future earthquake damage, it is revealed that the earthquake-related education and research in the educational institutions mainly focuses on the general knowledge about earthquakes and hardly deals with the specific cases in Nepal, and that the course of seismology, one of the most important earthquake-related academic fields, is hardly provided in Nepal. These problems are shared by those involved in the earthquake education and research in Nepal, and in order to solve these problems, it is necessary to develop the educational curriculum for seismology that incorporates the examples of Nepal.

This research was supported by Science and Technology Research Partnership for Sustainable Development (SATREPS), Japan Science and Technology Agency (JST, JPMJSA1511) / Japan International Cooperation Agency (JICA).

Keywords: Seismology, Higher education, Nepal

©2021. Japan Geoscience Union. All Right Reserved.

[E] Poster | S (Solid Earth Sciences)：S-CG Complex & General

Sun. Jun 6, 2021 5:15 PM - 6:30 PM JST | Sun. Jun 6, 2021 8:15 AM - 9:30 AM UTC | Ch.15_1

[S-CG40] Active Tectonics and Seismic Hazards in the Himalayan Region

convener:Kazuki Koketsu(Earthquake Research Institute, University of Tokyo), Nath Soma Sapkota(Nepal Geological Society), Srinagesh Davuluri(CSIR-National Geophysical Research Institute)

In the Himalayan region, the Indian and Eurasian plates collide, and the Indian lithosphere underthrusts beneath the Eurasian plate from the Main Frontal Thrust with a convergence rate of approximately 18 mm/year. This has historically caused large earthquakes such as the 1934 Bihar-Nepal earthquake, and seismic hazards in the region remain high. On April 25, 2015 (UTC), the Mw 7.8 Gorkha earthquake occurred along the plate boundary, and this affected the Main Frontal Thrust increasing the stress in possible source areas of future large earthquakes. Therefore, even after the Gorkha earthquake, studies on active tectonics and seismic hazards are still necessary in the Himalayan region. All kinds of studies on them are welcome for this session.

[SCG40-P01] **The Timing and Extent of the Last Surface Rupture Event on the Himalayan Frontal Thrust in western Nepal around Butwal-Tribeni area**

*Prakash Pokhrel[1], Koji Okumura[2], Soma Nath Sapkota[1], Hisao Kondo[3], - - (1.Department of Mines and Geology, Nepal, 2.Hiroshima University, Japan, 3.Geological Survey of Japan)

[SCG40-P02] A future scenario earthquake for seismic hazard analysis in Kathmandu, Nepal

*Kazuki Koketsu[1], Hiroe Miyake[1], Koji Okumura[2] (1.Earthquake Research Institute, University of Tokyo, 2.Graduate School of Humanities and Social Sciences, Hiroshima University)

[SCG40-P03] **3D velocity structure model of the Kathmandu valley for ground motion simulation**

*Suzuki Haruhiko[1], Hisanori Matsuyama[1], Kazuki Koketsu[2], Toshiaki Yokoi[3] (1.OYO Corp., 2.Earthquake Research Institute, The University of Tokyo , 3.Building Research Institute)

[SCG40-P04] Measuring surface-wave phase velocities (< 0.2 Hz) using teleseismic/ambient noise data in the Kathmandu Valley, Nepal

*Takumi Hayashida[1], Toshiaki Yokoi[1], Mukunda Bhattarai[2], Tara Pokharel[2], Suresh Shrestha[2], Chintan Timsina[2], Sunita Bhattarai[2], Rajesh Sharma[2], Dinesh Nepali[2] (1.International Institute of Seismology and Earthquake Engineering, Building Research Institute, 2.Department of Mines and Geology, Nepal)

[SCG40-P05] Characterization of Extreme Ground Motions

*Hiroe Miyake[1] (1.Earthquake Research Institute, University of Tokyo)

The Timing and Extent of the Last Surface Rupture Event on the Himalayan Frontal Thrust in western Nepal around Butwal-Tribeni area

*Prakash Pokhrel[1], Koji Okumura[2], Soma Nath Sapkota[1], Hisao Kondo[3], - -

1. Department of Mines and Geology, Nepal, 2. Hiroshima University, Japan, 3. Geological Survey of Japan

The 2015 Gorkha earthquake ruptured only the deeper northern part of the thrust during the Mw 7.8 earthquake but did not rupture the surface and shallow portion of the Himalayan Frontal Thrust (HFT) in the south. Since then, the evaluation of the potential of the future surface rupture event on the HFT in central Nepal in the south of 2015 rupture became an important task for paleoseismology. Mishra et al. (2016), Bollinger et al. (2016), and Wesnousky et al. (2017) proposed respective 1100 CE, 1344 CE and/or 1408 CE, and 1221 CE to 1262 CE (possibly 1255 CE) for the timing of the last surface-rupture event. Each report eliminates the timing of the earthquake proposed by the other authors. Therefore, it is necessary to think over the possibility of multiple events in short (less than 100 km) segments or of misleading radiocarbon dates. Also, the existence and the east termination of 1505 CE Indian central seismic gap event (Malik et al., 2017) are not certain yet. In order to solve the rupture history and rupture extents in central and western Nepal, we excavated two trenches across the HFT around the city of Butwal. One is at 12 km west of Butwal at Sorauli (27.70˚N 83.36˚E) and another is at Tribeni which is 60 km ESE of Butwal at Susta (27.48˚N 83.86˚E). Around the Sorauli trench site, there is no clear continuous scarp along the Siwalik hill front, but ~100 m wide zone of the alluvial surface adjacent to the foot of the hills tilt toward the south and juxtaposed to flat alluvial surface. The boundary between the tilted surface and the flat plain is continuous and looks like the active front of a flexure scarp. The trench across a small scarp on the tilted surface did not expose any fault, but a fine sand layer was tilted towards the boundary. A Bayesian model of radiocarbon dates indicates the timing of tilting is between 1328 CE and 1435 CE. This period coincides with the 1344 CE earthquake (Bollinger et al., 2016). The Susta trench in the east of Butwal was dug into the foot of ~20 m high fault/flexure scarp below an uplifted terrace surface. In this trench also, 13˚ south-dipping fine sand layers appeared but the fault was below the water table and not exposed. The timing of the tilt in the Susta trench as well as results from an investigation in further west in the boundary area between 1344 CE and 1505 CE event will be reported.

Keywords: Himalaya, Active tectonics, western Nepal

©2021. Japan Geoscience Union. All Right Reserved.

A future scenario earthquake for seismic hazard analysis in Kathmandu, Nepal

*Kazuki Koketsu[1], Hiroe Miyake[1], Koji Okumura[2]

1. Earthquake Research Institute, University of Tokyo, 2. Graduate School of Humanities and Social Sciences, Hiroshima University

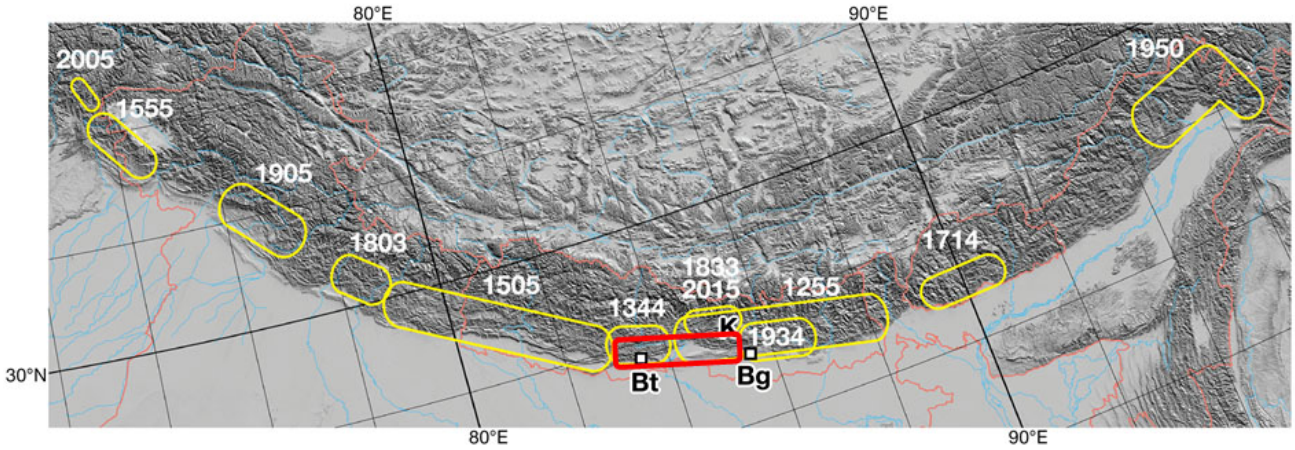
We propose a distribution of the source regions of great historical earthquakes in the Main Himalayan Thrust (Figure) using Bilham (2019) and the results of trench surveys (Bt and Bg in Figure). In this distribution, the red rectangle can be the source region of a future scenario earthquake for seismic hazard analysis in Kathmandu, Nepal. The rectangle is neighboring Kathmandu (K in Figure), and the previous events in the rectangle occurred in 1255 and 1344. They are the oldest among the great historical earthquakes in the Main Himalayan Thrust (MHT). The displacement rates observed by the GNSS are similar along the southern boundary of the MHT (Tabei *et al.*, 2020), and it can be assumed that the great historical earthquakes mostly released accumulated strain. Therefore, it is the most probable for the rectangle, where the previous events are the oldest, to generate a great future earthquake the soonest. The area of the rectangle is measured to be 17,600 km^2 with a length of 220 km and a width of 80 km.

The 2015 Gorkha earthquake recently occurred in the MHT. Kobayashi *et al.* (2016) performed a source inversion for this earthquake, obtaining a seismic moment M_0 of 7.4 x 10^{20} Nm (M_w 7.8) and the slip distribution. We trim insignificant slips off the slip distribution following the scheme of Somerville *et al.* (1999). This trimming results in a rupture area of 9,600 km^2. This rupture area corresponds to M_0 = 8.9 x 10^{20} Nm (M_w 7.9) using the formula of Somerville *et al.* (1999), while the area corresponds to M_0 = 5.2 x 10^{20} Nm (M_w 7.7) using the formula of Murotani *et al.* (2008). The actual M_0 of 7.4 x 10^{20} Nm (M_w 7.8) falls between these, so that we use the both formulas to determine two characterized source models for the future scenario earthquake with the rupture area of 17,600 km^2. The formula of Somerville *et al.* (1999) gives M_0 = 2.2 x 10^{21} Nm (M_w 8.2), an average stress drop $\Delta\sigma_c$ of 2.3 MPa, an asperity area S_a of 4,000 km^2, a stress drop on asperity σ_a of 10.1 MPa, and an effective stress in the background σ_b of 2.0 MPa. Meanwhile, the formula of Murotani *et al.* (2008) gives M_0 = 1.3 x 10^{21} Nm (M_w 8.0), $\Delta\sigma_c$ = 1.4 MPa, S_a = 4,400 km^2, σ_a = 5.6 MPa, and σ_b = 1.1 MPa.

This study partly includes the results of the SATREPS project with the Department of Mines and Geology, Nepal.

Keywords: scenario earthquake, seismic hazards, Kathmandu, characterized source models

©2021. Japan Geoscience Union. All Right Reserved.



©2021. Japan Geoscience Union. All Right Reserved.

3D velocity structure model of the Kathmandu valley for ground motion simulation

*Suzuki Haruhiko[1], Hisanori Matsuyama[1], Kazuki Koketsu[2], Toshiaki Yokoi[3]

1. OYO Corp., 2. Earthquake Research Institute, The University of Tokyo , 3. Building Research Institute

For evaluating seismic hazards in the Kathmandu valley after the 2015 Gorkha earthquqke, we are doing a joint research project with the Department of Mines and Geology, Nepal, under the SATREPS program of Japan Science and Technology Agency and Japan International Corporation Agency.
In this project, a 3D velocity structure model was constructed, using the results of reflection surveys (Kawasaki *et al*., 2019), boring explorations, microtremor surveys (Yokoi *et al*., 2019), gravity surveys (Pradhan *et al*., 2018), and R/V spectrum analyses. We performed joint inversion analysis of phase velocity and the R/V spectra (Senna et al,2013). We calculated phase velocity for fundamental mode. For theoretical H/V spectra, we calculated residuals with theoretical and observed values normalized to their maximum values to align peak shapes. We obtained theoretical H/V spectra of Rayleigh waves with medium response of Rayleigh waves of the fundamental to 4^{th} mode (Arai and Tokimatsu, 2004). The correlation between the basement depth and the gravity basement elevation by reflection survey and inversion results of microtremor survey was abour 0.9.
We performed the Sequential Gaussian Co-simulation (Remy *et al*., 2009; Pyrcz and Deutsch, 2014) to combine and interpolate these results. The model consists of several layers, and the boundary shape of each layer was estimated in 50 cases by the Sequential Gaussian Co-simulation(Figure 1). They were then averaged to obtain the final boundary shape of each layer. To confirm the obtained model, we simulated ground motions for moderate earthquakes using the 3D finite difference method. The simulated ground velocity waveforms almost agree with observed waveforms.

Keywords: 3D velocity structure model, gravity survey, microtremor array, R/V spectral ratio, 3D finite-difference method

©2021. Japan Geoscience Union. All Right Reserved.

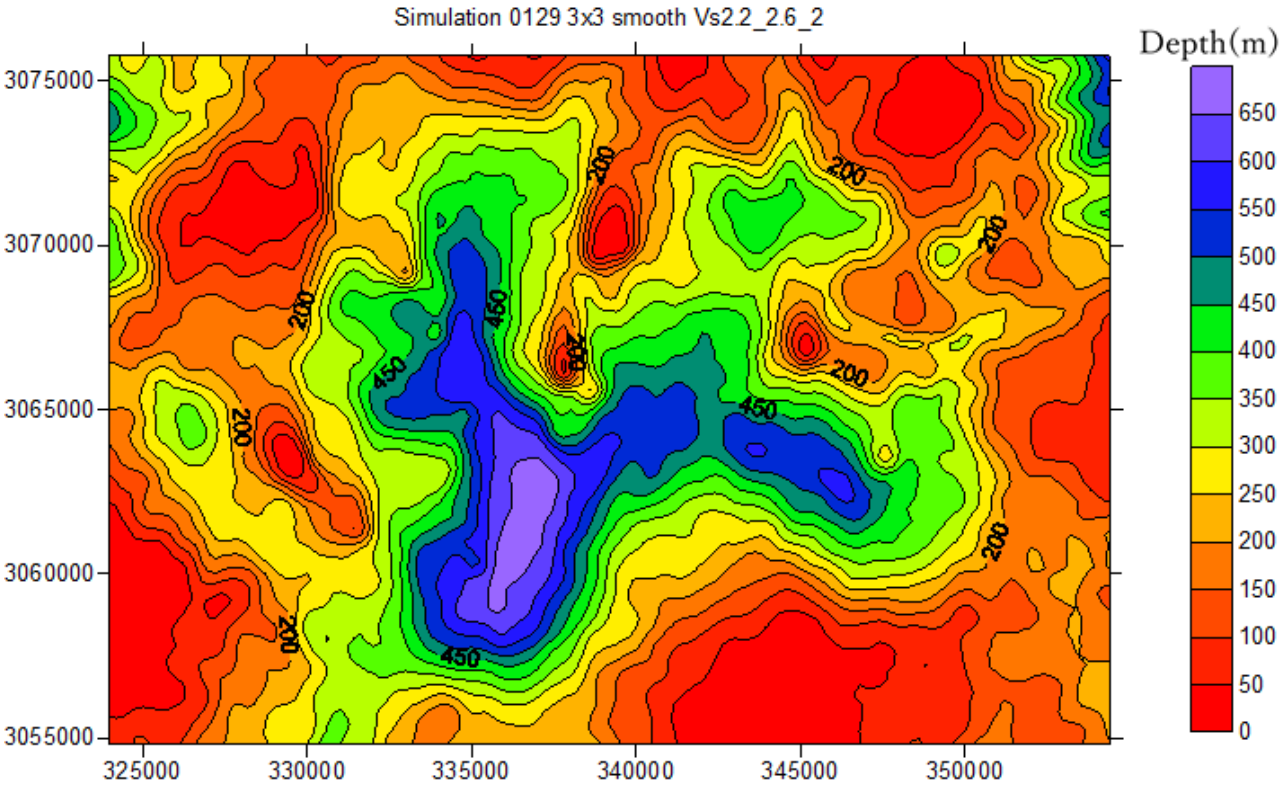


Figure1 Basement Depth(Vs2.2km/s)

©2021. Japan Geoscience Union. All Right Reserved.

Measuring surface-wave phase velocities (< 0.2 Hz) using teleseismic/ambient noise data in the Kathmandu Valley, Nepal

*Takumi Hayashida[1], Toshiaki Yokoi[1], Mukunda Bhattarai[2], Tara Pokharel[2], Suresh Shrestha[2], Chintan Timsina[2], Sunita Bhattarai[2], Rajesh Sharma[2], Dinesh Nepali[2]

1. International Institute of Seismology and Earthquake Engineering, Building Research Institute, 2. Department of Mines and Geology, Nepal

The S-wave velocity (Vs) structure of the Kathmandu Valley (KTV) has been investigated using gravity data (Moribayashi and Maruo, 1980; Pradhan et al., 2018), waveforms from local earthquakes (Dhakal et al., 2016; Bijukchhen et al., 2017), microtremor data (e.g., Poovarodom et al., 2017; Hayashida et al., 2019; Yokoi et al., 2021), and reflection survey (Koshika et al., 2019; Kawasaki et al., 2019). These results indicate the substantial seismic velocity contrast between sedimentary layers and bedrock (Vs > 2000 m/s) and the existence of thick sediments (> 600 m) in the central basin. We conducted microtremor array surveys using broadband seismometers (CMG-40T; Guralp Systems Ltd.) and determined the Rayleigh-wave phase velocities in the lower frequency range (< 1 Hz) to estimate the thickness of the sedimentary layers (Bhattarai et al., 2017; Yokoi et al., 2018, 2019), but the dispersion characteristics below 0.2 Hz were unclear due to the low ambient noise level. To clarify the dispersive characteristics of Rayleigh waves below 0.2 Hz and improve the accuracy of depth estimations, we conducted continuous seismic/microtremor at seven sites in the KTV from February 2018 to November 2020. The station-to-station intervals are 4.6 –14.7 km. First, we applied the seismic interferometry to the continuously recorded seismic ambient noise data and estimated phase/group velocities of the Rayleigh wave at the lower frequency side. Seismic signals from several local earthquakes (> ML=4.0) and distant large earthquakes were detected during the observation period, so we also used the surface-wave component of the recordings for the phase velocity estimations. The calculated phase velocities show dispersive characteristics between 0.03 and 0.2 Hz, connected to the dispersion curves (> 0.2 Hz) derived from existing microtremor results. The inverted one-dimensional seismic velocity structure indicates substantially higher S-wave velocities between 10 and 30 km depth compared with the model of Pandey et al. (1995). The model helps constraint the bedrock depths that better explain dominant frequencies of microtremor H/V spectral ratios in the lower frequencies.

Acknowledgments:

This study was conducted as an international research project, 'Integrated research on great earthquakes and disaster mitigation in Nepal Himalaya (FY2016-FY2021)', under the Science and Technology Research Partnership for Sustainable Development (SATREPS) program of the Japan Science and Technology Agency (JST) and Japan International Cooperation Agency (JICA).

Keywords: Kathmandu Valley, S-wave velocity structure, Surface wave, Seismic interferometry

©2021. Japan Geoscience Union. All Right Reserved.

Characterization of Extreme Ground Motions

*Hiroe Miyake[1]

1. Earthquake Research Institute, University of Tokyo

Ground motion time history is one of the most important factors to judge whether ground motion prediction works well in the scenario-based seismic hazard assessment. To link seismology and earthquake engineering, ground motion response spectra became the first priority to validate broadband ground motions. Although the duration and phase information are useful to separate near-fault ground motions with rupture directivity pulses and long-period ground motions for similar ground motion response levels, ground motion response spectra are helpful to direct use for design basis ground motions. It is well known that ground motion pulses increase the response at the dominant periods that largely affect structures. The significant impact of ground motion pulse on response spectra is indicated for the 1992 Landers, 1995 Kobe, 1999 Kocaeli, 1999 Chi-Chi, 2015 Gorkha, 2016 Kumamoto, and other earthquakes. In theory, both duration and amplitude of ground motion pulse increase as a function of earthquake magnitude, therefore the upper bounds of response spectra are increasing as a function of period. Due to the accumulation of extreme ground motions with dense strong motion observations, empirical upper bounds of peak ground accelerations and peak ground velocities are still increasing due to seismic source complexity and strong site amplification. However, this study found the empirical upper bounds of response spectra exist and can be shaped by a few extreme ground motions of crustal and collusion earthquakes. On the other hand, many simulated ground motions for subduction earthquakes exceed the current empirical upper bounds of response spectra.

©2021. Japan Geoscience Union. All Right Reserved.

[E] Oral | S (Solid Earth Sciences)：S-CG Complex & General

Sun. Jun 6, 2021 9:00 AM - 10:30 AM JST | Sun. Jun 6, 2021 12:00 AM - 1:30 AM UTC | Ch.19 Zoom Room 19

[S-CG41] Hard-Rock Drilling Science: From Continental to Deep Sea Drilling, and Oman Project

convener:Eiichi TAKAZAWA(Department of Geology, Faculty of Science, Niigata University), Katsuyoshi Michibayashi(Department of Earth and Planetary Sciences, Nagoya University), Keishi Okazaki(Japan Agency for Marine-Earth Science and Technology), Chairperson:Keishi Okazaki(Japan Agency for Marine-Earth Science and Technology), Sayantani Chatterjee(Niigata University, Department of Geology, Faculty of Science)

The IODP and ICDP have decided to launch a new international science framework, and hard rock drilling science is about to enter the preparatory period for the next phase. Therefore, drilling proposals from a new perspective and the production of scientific results based on existing drilling projects are expected. In this session, we invite presentations on the scientific results of hard-rock drilling. We also invite related studies of on-land geological investigations of Oman ophiolites and experimental studies. The session is intended to be interdisciplinary, including the fields of geophysics, geochemistry, petrology, engineering, and biology. This session is co-hosted with the focus group of hard rock drilling science.

9:00 AM - 9:15 AM JST | 12:00 AM - 12:15 AM UTC

[SCG41-01] The structure of magma chamber below a fast-spreading ridge based on field and core analyses of the Oman ICDP drilling

*Susumu Umino[1], Yuki Kusano[3], Osamu Ishizuka[3], Takahiro Fudai[4], Akihiro Tamura[1], Tomoaki Morishita[1,2] (1.Department of Earth Sciences, Kanazawa University, 2.JAMSTEC, 3.GSJ-AIST, 4.Taiheiyo Cement Corrperation)

9:15 AM - 9:30 AM JST | 12:15 AM - 12:30 AM UTC

[SCG41-02] Oxidation controlled symplectitic formation in olivine gabbros from Oman ophiolite, Oman Drilling Project, Hole GT2A

*Sayantani Chatterjee[1], Debaditya Bandyopadhyay[2,3], Eiichi Takazawa[1,4], Katsuyoshi Michibayashi[5] (1.Department of Geology, Faculty of Science, Niigata University, Niigata 950–2181, Japan, 2.Department of Geology, University of North Bengal, Darjeeling 734013, India, 3.Department of Geology, University of Calcutta, Kolkata 700019, India, 4.Japan Agency for Marine–earth Science and Technology, Yokosuka 237–0061, Japan, 5.Graduate School of Environmental Studies, Nagoya University, Nagoya 464–8602, Japan)

9:30 AM - 9:45 AM JST | 12:30 AM - 12:45 AM UTC

[SCG41-03] Effect of pore geometry on ultrasonic velocity of epidosites collected from the Oman Drilling Project

*Kumpei Nagase[1], Ikuo Katayama[1], Kohei Hatakeyama[1], Keishi Okazaki[2] (1.Earth and Planetary Systems Science Program, Graduate School of Advanced Science and Engineering, Hiroshima University, 2.Kochi Institute for Core Sample Research, Japan Agency for Marine-Earth Science and Technology)

9:45 AM - 10:00 AM JST | 12:45 AM - 1:00 AM UTC

[SCG41-04] Mineral mode of listvenite from ICDP Oman Drilling Project Hole BT1B inferred from X-ray CT core images

*Keishi Okazaki[1], Katsuyoshi Michibayashi[2], Kohei Hatakeyama[3], Natsue Abe[4], Kevin Johnson[5], Peter B Kelemen[6] (1.Kochi Institute for Core Sample Research, Japan Agency for Marine-Earth Science and Technology, 2.Department of Earth and Planetary Sciences, Nagoya University, 3.Department of Earth and Planetary Systems Sciences, Hiroshima University, 4.Mantle Drilling Promotion Office, Japan Agency for Marine-Earth Science and Technology, 5.Department of Earth Sciences, University of Hawai‘i at Mānoa, 6.Lamont Doherty Earth Observatory, Columbia University)

10:00 AM - 10:30 AM JST | 1:00 AM - 1:30 AM UTC

[SCG41-05] Serpentinization and Fe(III) distribution along the crust-mantle section of the oceanic lithosphere: insights from the Oman Drilling CM1A site

★Invited Papers

*Atsushi Okamoto[1], Kazuki Yoshida[1], Ryosuke Oyanagi[2], Yasuhiro Niwa[3], Yasuo Takeichi[3], Masao Kimura[3] (1.Graduate School of Environmental Studies, Tohoku University, 2.Japan Agency For Marine-Earth Science and Technology, 3.High Energy Accelerator Research Organization (KEK))

The structure of magma chamber below a fast-spreading ridge based on field and core analyses of the Oman ICDP drilling

*Susumu Umino[1], Yuki Kusano[3], Osamu Ishizuka[3], Takahiro Fudai[4], Akihiro Tamura[1], Tomoaki Morishita[1,2]

1. Department of Earth Sciences, Kanazawa University, 2. JAMSTEC, 3. GSJ-AIST, 4. Taiheiyo Cement Corrperation

The ICDP Oman Drilling Project drilled the lower crustal section of the Oman Ophiolite in Wadi Gideah, north of Ibra and recovered 400 m long cores each from Hole GT1A and GT2A. We report field observations of the lower crustal section along Wadi Gideah and reconstructed the vertical stratigraphy in reference to the Moho and describe the microstructures and major and trace element compositions of the whole rocks and constituent minerals. These observations enable us to estimate the amount of trapped melt in the lower crustal gabbro and discuss the conditions of magmatic and hypersolidus deformation that operated in the lower crustal magma chamber beneath the Oman paleoridge axis.

The lower crust attains 3.5 km in thickness, among which GT1A and GT2A holes range in stratigraphic height above the Moho from 0.4 to 0.8 km and from 2.0 to 1.6 km, respectively. Foliation and hypersolidus deformation structures are ubiquitous. Modal layering is locally present but is much less common. Well developed modal layering is present in the lowermost 125 m thick gabbro above the Moho.

Cored samples are predominantly olivine gabbros with deformed olivine aggregates and clinopyroxene with quarter structures embedded in granoblastic plagioclase and large euhedral plagioclases with resorbed turbid cores. These textures suggest deformation under the presence of melt, which assisted complete recovery of strain through recrystallization of fine-grained plagioclase and overgrowth of euhedral rims around magmatic plagioclase cores. Poikilitic and ophitic clinopyroxene occur sporadically throughout the holes, which are commonly present in the upper gabbros. Hypersolidus deformation structures are present irrespective to depth.

The lower GT1A and higher GT2A sections range in whole-rock Mg#s of 72-83 and 68-79, respectively. The lowest Mg#s overlap those of the sheeted dikes above. The whole-rock compositions are mainly controlled by accumulation of plagioclase, olivine, clinopyroxene and interstitial melts. The lower whole-rock Mg# and higher REEs and HFSEs of GT2A suggest larger amounts of trapped melt at stratigraphically higher levels. The amounts of trapped melt were estimated by LREE concentrations in the clinopyroxene cores, and by assuming LREE abundance in trapped melts to be equivalent to that of the sheeted dikes. Mass balance calculations yield the amount of trapped melt in gabbros to be 5 to 10 mass% in general and 25 mass% at most.

The drilled cores have common hypersolidus deformation with foliation but only limited modal layering, ubiquitous zoned cumulus minerals and common ophitic clinopyroxenes as well as the amount of trapped melt >5 mass% are all characteristics of foliated gabbros. In addition to this, field observations of the gabbros in Wadi Gideah show poorly develop modal layering but foliation defined by shape-preferred orientation of clinopyroxenes in the stratigraphic levels including both GT1A and GT2A holes. We concluded that both GT1A and GT2A holes sampled the thick foliated gabbros in Wadi Gideah section, which crystallized on the axial melt lens floor and were transported downward in the lower crust.

©2021. Japan Geoscience Union. All Right Reserved.

Keywords: Oman ICDP, lower oceanic crust, magma chamber, fast-spreading ridge, upper gabbro, layered gabbro

©2021. Japan Geoscience Union. All Right Reserved.

Oxidation controlled symplectitic formation in olivine gabbros from Oman ophiolite, Oman Drilling Project, Hole GT2A

*Sayantani Chatterjee[1], Debaditya Bandyopadhyay[2,3], Eiichi Takazawa[1,4], Katsuyoshi Michibayashi[5]

1. Department of Geology, Faculty of Science, Niigata University, Niigata 950–2181, Japan, 2. Department of Geology, University of North Bengal, Darjeeling 734013, India, 3. Department of Geology, University of Calcutta, Kolkata 700019, India, 4. Japan Agency for Marine–earth Science and Technology, Yokosuka 237–0061, Japan, 5. Graduate School of Environmental Studies, Nagoya University, Nagoya 464–8602, Japan

Symplectites are vermicular intergrowth of two or more mineral phases that inferred to be formed via melt-rock reaction, solid-state transformation, oxidation, or during different stages of magmatic crystallization. Here we report orthopyroxene-magnetite symplectitic intergrowth partly surrounding olivine within lower crustal olivine gabbros from Oman ophiolite recovered during Oman drilling project at Hole GT2A. The symplectites are found to be only associated with olivine and typically characterized by orthopyroxene groundmass hosting magnetite lamella. The width of the homogeneous grain of orthopyroxene ranges up to 300 μm whereas the width of vermicular intergrowth of magnetite within orthopyroxene ranges between 20-30 μm. The intergrowth of fine-grained magnetite rods is sometimes typified by the perpendicular arrangement with respect to the contact of adjacent olivine. Further, fine-grained lamella of magnetite within orthopyroxene generally grades away into irregular coarser-grained variety with increasing distance from olivine. From closer petrographic observation and previously inferred depth of formation of the sample (i.e., ~1kbar) we conclude this texture does not involve reaction (or significant material transfer) between two minerals (e.g., olivine and plagioclase). We thus infer such vermicular intergrowth is formed via olivine oxidation involving the reaction

Olivine + O_2 →Orthopyroxene + Magnetite

In order to test this hypothesis, we have adapted the equilibrium phase equilibria approach and computed several Temperature –Composition diagrams in a fixed pressure (1 kbar) to observe the oxidation effects in different olivine compositions. Our experiments predict the coexistence of olivine with Fo_{75-76} and Fo_{71} with the orthopyroxene (En_{79} and En_{76}) respectively; which is remarkably similar to the obtained mineral chemistry. Our result suggests the symplectite growth may have occurred between 600-1000˚C via subsolidus olivine oxidation and/or reaction with oxidizing melt.

References:

Connolly, J.A.D. (2005) Computation of phase equilibria by linear programming: A tool for geodynamic modeling and its application to subduction zone decarbonation. Earth and Planetary Science Letters, 236, 24–541.

Connolly, J.A.D. (2009) The geodynamic equation of state: What and how, Geochemistry. Geophysics, Geosystems, 10, 1–19.

Gallien, F., Mogessie, A., Hauzenberger, C.A., and Bjerg, E., et al. (2012) On the origin of multi-layer coronas between olivine and plagioclase at the gabbro–granulite transition, Valle Fertil–La Huerta Ranges, San Juan Province, Argentina. Journal of Metamorphic Geology, 30, 281–301.

©2021. Japan Geoscience Union. All Right Reserved.

Goode, A. (1974) Oxidation of natural olivines. Nature, 248, 500–501.

Holland, T.J.B. and Powell, R. (1998) An internally consistent thermodynamic data set for phases of petrological interest. Journal of Metamorphic Geology, 16, 309–343.

Joesten, R. (1986) The role of magmatic reaction, diffusion and annealing in the evolution of coronitic microstructure in troctolitic gabbro from Risor, Norway. Mineralogical Magazine, 50, 441–67.

Kelemen, P.B., Matter, J.M., Teagle, D.A.H., Coggon, J.A., and the Oman Drilling Project Science Team (2020) Site GT2: foliated to layered gabbro transition. Proceedings of the Oman Drilling Project: College Station, TX (International Ocean Discovery Program).

Klemme, S. Ivanic, T.J., Connolly, J.A.D., Harte, B. (2009) Thermodynamic modelling of Cr-bearing garnets with implications for diamond inclusions and peridotite xenoliths. Lithos, 112, 986–991.

Powell, R., & Holland, T. (1999) Relating formulations of the thermodynamics of mineral solid solutions: activity modeling of pyroxenes, amphiboles, and micas. American Mineralogist, 84, 1–14.

Keywords: Olivine gabbro, Orthopyroxene-magnetite symplectite, Lower crust, Oman ophiolite

©2021. Japan Geoscience Union. All Right Reserved.

Effect of pore geometry on ultrasonic velocity of epidosites collected from the Oman Drilling Project

*Kumpei Nagase[1], Ikuo Katayama[1], Kohei Hatakeyama[1], Keishi Okazaki[2]

1. Earth and Planetary Systems Science Program, Graduate School of Advanced Science and Engineering, Hiroshima University, 2. Kochi Institute for Core Sample Research, Japan Agency for Marine-Earth Science and Technology

Geophysical survey suggests a large amount of pore water exists in crack at the upper oceanic crust where seismic wave velocity is slow. However, anomalous low Vp/Vs ratio observed in central ridge and young oceanic crust (Spudich and Orcutt 1980; Kim et al., 2019), and such low Vp/Vs structure can't be explained by crack alone. Theorical model predict that crack with small aspect ratio increase Vp/Vs of rocks. On the other hand, pore with large aspect ratio decrease Vp/Vs (Kuster and Toksoz, 1974). Therefore, these anomalies can be explained by thick pore with large aspect ratio (shearer 1988). In this study, we focused on epidosite suggested to form on the hydrothermal alteration process of oceanic crust (Schiffman et al., 1987). We measured physical properties of epidosite and diabase collected from the Oman ophiolite, and we investigate pore aspect ratio from simultaneous measurement of velocity and porosity.

We developed simultaneous measurement system of ultrasonic velocity and porosity under hydrostatic pressure, using Intra-vessel deformation and fluid flow apparatus at Hiroshima University (Shimamoto et al., 2006). Ultrasonic velocity and porosity were measured under confining pressure up to 200 MPa at water-saturated condition. Pore pressure was fixed at 1 MPa. Ultrasonic velocity was measured by a pulse transmission method using both P- and S-wave piezoelectric transducers with a resonant frequency of 2 MHz. Porosity was calculated by initial porosity measured by pycnometer before compaction, and volume change of pore water after compaction using syringe pump. After each experiment, the measurement specimens were cored (10 mm in length, 6 mm in diameter) to perform X-ray microtomography in order to obtain 3D images of the pore shape. Microtomography analyses were performed using Xradia 410 Versa at Kochi Core Center. We used epidosite and diabase collected from gabbro-dike transition sections at Hole GT3A on the Oman Drilling project.

The experimental result shows that both P-wave and S-wave velocities increase with decreasing of porosity due to closing of pore. Diabase shows an increasing of Vp/Vs with increasing porosity whereas, sample with epidosite shows a decreasing of Vp/Vs with porosity. The microstructure of the measurement specimen showed that diabase is consisted crack-like pore shape, while the epidosite showed a porous pore shape.

We investigate pore aspect ratio from measured velocities and porosities based on application of effective medium theory by Kuster and Toksoz (1974). As a result, this implies that different aspect ratio in diabase and epidosite, pore aspect ratio is more than an order of magnitude higher in epidosite. This implies that there is possibility that anomalous low Vp/Vs observed in the central ridge and young oceanic crust might be explained by the effect of pore water in epidosite.

Keywords: Epidosite, Pore geometry, Vp/Vs, Aspect ratio

©2021. Japan Geoscience Union. All Right Reserved.

Mineral mode of listvenite from ICDP Oman Drilling Project Hole BT1B inferred from X-ray CT core images

*Keishi Okazaki[1], Katsuyoshi Michibayashi[2], Kohei Hatakeyama[3], Natsue Abe[4], Kevin Johnson[5], Peter B Kelemen[6]

1. Kochi Institute for Core Sample Research, Japan Agency for Marine-Earth Science and Technology, 2. Department of Earth and Planetary Sciences, Nagoya University, 3. Department of Earth and Planetary Systems Sciences, Hiroshima University, 4. Mantle Drilling Promotion Office, Japan Agency for Marine-Earth Science and Technology, 5. Department of Earth Sciences, University of Hawai ʻi at Mānoa, 6. Lamont Doherty Earth Observatory, Columbia University

To understand the global cycle of fluid flow from the surface to the deep of the Earth, it is important to constrain how and how much fluid is captured and released by metamorphic reactions following hydration/dehydration and carbonation/decarbonation. In the Oman Ophiolite, a fossil of an oceanic plate is widely exposed. Continuous drilling from the bottom of the ophiolite through the basal thrust to the footwall metamorphic sole was conducted in Hole BT1B by the ICDP Oman Drilling Project. Listvenite, completely carbonated former peridotite, is the main lithology in Hole BT1B also found in other ophiolite bodies. Listvenite is mainly composed of magnesite, quartz, dolomite and Fe-hydroxide with minor chromian spinel and chromian mica (fuchsite). Two serpentinite and ophicarbonate intervals were also found above the basal thrust. Below the basal thrust, the metamorphic sole composed by the greenschist/greenstone is the main lithology.

We evaluated the mineral mode of listvenite in BT1B from the X-ray Computed Tomography (XCT) images. XCT images was continuously obtained with a spacing of 0.625 mm along the Z-axis on all 401 whole-round core sections recovered from Hole BT1B. The X-Y resolution of XCT image is 0.125mm and an intensity of X-ray attenuation, “XCT number”, are computed for each voxel. The XCT number of a material depends on several factors such as density, element (e.g., atomic number), porosity, sample shape and sample volume. All listvenite and serpentinite core sections are nearly the same dimensions (~63.5 mm in diameter) and thus same volume, therefore, the XCT number provides information of physical and chemical properties of the core samples.

Each XCT number in XCT images and chemical mapping data of Mg, Si, Ca and Fe from the XRF core scanner in the same location as XCT images are compared for 27 sections including 9289 data points for each element. Multiple linear regression for XCT number and XRF quantified that XCT numbers of pure magnesite ($MgCO_3$), quartz (SiO_2), and dolomite ($CaMg(CO_3)_2$) grains in the cores are 3106, 2974 and 3415, respectively. Using these values, histograms of XCT number of each slice in each section is fitted assuming that the CT histogram (CT number >2500) of a slice is composed of three peaks with Gaussian distribution.

In most core sections, XCT data indicates that the matrix of listvenite is mainly composed of magnesite and quartz, and minor dolomite, consistent with discrete XRD and XRF data. Veins usually show high CT number (~3400), while the CT number in veins is fitted well with dolomite. Dolomite abundance in each core section is highly dependent on the intensity of veins. Dolomite abundance in most core sections within 15 m from the basal thrust is higher than 50%. This is consistent with higher vein intensity close to the basal thrust and could indicate that significant amounts of Ca were supplied from Ca- and CO_2-rich fluids along the basal thrust. Total MgO/SiO_2 ratio in BT1B is ~1.2. This value is slightly smaller than that

©2021. Japan Geoscience Union. All Right Reserved.

from onboard XRF data of listvenite (~1.3) and smaller than that estimated from the geochemical analysis of the Oman peridotite (~1.5). This suggest that Si enrichment or Mg loss during carbonation and/or following serpentinization of the ophiolite. Fe contents may also have significant effect on evaluating the modal abundance of minerals in listvenite and further investigation of compositional effects, especially Fe solid solutions in carbonate and hematite on the XCT number would be needed for an accurate assessment of the mineralogy in listvenite.

Keywords: Ophiolite, Mantle, Oceanic crust, Listvenite, Serpentinite, X-ray CT

©2021. Japan Geoscience Union. All Right Reserved.

Serpentinization and Fe(III) distribution along the crust-mantle section of the oceanic lithosphere: insights from the Oman Drilling CM1A site

*Atsushi Okamoto[1], Kazuki Yoshida[1], Ryosuke Oyanagi[2], Yasuhiro Niwa[3], Yasuo Takeichi[3], Masao Kimura[3]

1. Graduate School of Environmental Studies, Tohoku University, 2. Japan Agency For Marine-Earth Science and Technology, 3. High Energy Accelerator Research Organization (KEK)

Serpentinization of mantle peridotite causes the production of hydrogen and hydrocarbon, which provides energy for sustaining the microbial activities within the oceanic lithosphere. The total production of hydrogen energy depends on the extent of serpentinization and its reaction pathway. During serpentinization, Fe(II) in olivine or orthopyroxene is commonly oxidized to form magnetite Fe_3O_4, which is coupled with H_2O reduction to produce H_2. In contrast, the Fe(II)-rich brucite is often reported as a precursor of magnetite+serpentine, and Fe(III) can exist within serpentine minerals. Due to variable occurrences of iron-bearing minerals, the magnetic sustainability of the serpentinized peridotite within the oceanic lithosphere is not always linear relationship with the extent of serpentinization. The CM1site of the Oman Drilling Project provides us a good opportunity to understand where and how much amount of hydrogen produces within the oceanic lithosphere from the lower crust to upper mantle section. In this study, we reported the depth variation of serpentinization and the Fe(III)/Fe(II) ratios along the crust-mantle section, and the spatial and temporal variations on Fe(III), meaning that the hydrogen production. We conducted bulk measurement of Fe(III)/total Fe along the borehole, and micro XANES mapping at Photon Factory, KEK.

The CM1A site shows the complete continuous core with length of 404.15 m, from the lower crust composed of olivine gabbros and troctolite, crust-mantle transition zone composed of dunite, and mantle section mainly composed of harzburgite. All the core samples are highly serpentinized, but it has a variation along the depth. In the olivine gabbros, the extent of the serpentinization is relatively low (11-69%; Yoshida et al., 2021), but serpentinization of olivine grains with mesh texture are observed as black network veins. In the transition zone, dunite is almost 100% serpentinized, and the onboard X-ray CT images reveals that the network of distinct “bright (magnetite-rich)” vein networks. In the upper mantle section, olivine shows mesh texture and bastite formed around the Opx and 70-90% serpentinized. The serpentine minerals in the gabbroic rocks, dunite and hurzburgite are mostly lizardite and associated with brucite, but we found that blight vein network is composed of antigorite.

The bulk Fe(III)/total Fe ratio ranges from 0.21 to 0.66. we found two clear trends, and the ratio is higher in dunite and harzburgite than gabbroic crust, reflecting the extent of serpentinization. In the harzburgite, the local Fe(III)/total Fe ratio is higher in the mesh rim around the olivine, whereas it is low in bastite. Magnetite also preferentially occurs in olivine mesh texture, and it is absent around olivine, due to the difference in silica activity. This indicates that the olivine has higher potential of oxidation of iron to produce hydrogen. The other feature is that antigorite veins in dunite parts shows (1) magnetite was dissolved and reprecipitated at the margin of the veins, (2) the antigorite is high XMg value, and (3) high Fe(III)/total Fe ratio than the other lizardite. These features indicate that the low-temperature alteration characterized by lizardite + brucite occurred pervasively at the earlier stage to produce hydrogen, and the high-temperature oxidizing fluids would have infiltrated along the fracture networks from the deeper parts, probably related to the later obduction/subduction stage.

©2021. Japan Geoscience Union. All Right Reserved.

References: Yoshida, K., Okamoto, A., Oyanagi, R., Shimizu, H., Tsuchiya, N., Oman Drilling Project Science Party II, 2020. Journal of Geophysical Research, 125, e2020JB020268

Keywords: Oman ophiolite, Fe(III)/Fe(II) distribution, serpentinite, antigorite, magnetite, crust-mantle transition zone

©2021. Japan Geoscience Union. All Right Reserved.

[E] Oral | S (Solid Earth Sciences)：S-CG Complex & General

Sun. Jun 6, 2021 10:45 AM - 12:15 PM JST | Sun. Jun 6, 2021 1:45 AM - 3:15 AM UTC | Ch.19 Zoom Room 19

[S-CG41] Hard-Rock Drilling Science: From Continental to Deep Sea Drilling, and Oman Project

convener:Eiichi TAKAZAWA(Department of Geology, Faculty of Science, Niigata University), Katsuyoshi Michibayashi(Department of Earth and Planetary Sciences, Nagoya University), Keishi Okazaki(Japan Agency for Marine-Earth Science and Technology), Chairperson:Katsuyoshi Michibayashi(Department of Earth and Planetary Sciences, Nagoya University), Eiichi TAKAZAWA(Department of Geology, Faculty of Science, Niigata University)

The IODP and ICDP have decided to launch a new international science framework, and hard rock drilling science is about to enter the preparatory period for the next phase. Therefore, drilling proposals from a new perspective and the production of scientific results based on existing drilling projects are expected. In this session, we invite presentations on the scientific results of hard-rock drilling. We also invite related studies of on-land geological investigations of Oman ophiolites and experimental studies. The session is intended to be interdisciplinary, including the fields of geophysics, geochemistry, petrology, engineering, and biology. This session is co-hosted with the focus group of hard rock drilling science.

10:45 AM - 11:00 AM JST | 1:45 AM - 2:00 AM UTC

[SCG41-06] Heterogeneity in the mantle section of the Oman ophiolite in terms of spinel and clinopyroxene compositions

*Eiichi TAKAZAWA[1,2] (1.Department of Geology, Faculty of Science, Niigata University, 2.Japan Agency for Marine-Earth Science and Technology)

11:00 AM - 11:15 AM JST | 2:00 AM - 2:15 AM UTC

[SCG41-07] Systematics of minor and trace element chemistry of olivine in peridotites

*Ikuya Nishio[1], Tomoaki Morishita[1], Keita Itano[1], Akihiro Tamura[1], Asyraf Muhamad[1] (1.Kanazawa University)

11:15 AM - 11:30 AM JST | 2:15 AM - 2:30 AM UTC

[SCG41-08] **ICDP DSeis project: compilation of borehole logging and recovered core information at the seismogenic zone of the M5.5 Orkney earthquake with lower crustal intrusives**

*Hiroshi Ogasawara[1], Shunsuke Yoshida[2], Mitsuya Higashi[2], Kensuke Sakaguchi[1], Yuki Yokoyama[4], Yasuo Yabe[3], Tetsuro Hirono[4], Dakalo Ligaraba[5], Nandipha Masondo[5], Yuhji Yamamoto[6], Team ICDP DSeis (1.College of Science and Engineering, Ritsumeikan University, 2.Graduate School of Science and Engineering, Ritsumeikan University, 3.Graduate School of Science, Tohoku University, 4.Graduate School of Science, Osaka University, 5.Graduate School of Geoscience, University of the Witwatersrand, 6.Kochi Core Center, Kochi University)

11:30 AM - 12:00 PM JST | 2:30 AM - 3:00 AM UTC

[SCG41-09] Volcanism along the eastern margin of the Ontong Java Plateau: More reasons to test the Ontong Java Nui hypothesis by scientific ocean drilling

★Invited Papers

*Maria Luisa Tejada[1], Takashi Sano[2], Takeshi Hanyu[1], Anthony A. P. Koppers[3], Masao Nakanishi[4], Akira Ishikawa[5], Takashi Miyazaki[1], Kenichiro Tani[2], Shoka Shimizu[6], Qing Chang[1], Bogdan Stefanov Vaglarov[1] (1.Volcano and Earth Interior Research Center, Institute for Marine Geodynamics, Japan Agency for Marine-Earth Science and Technology, 2-15 Natsushima, Yokosuka 237-0061, Japan, 2.Department of Geology and Paleontology, National Museum of Nature and Science, Amakubo 1-1-1, Tsukuba, Ibaraki 305-0005, Japan, 3.College of Earth, Ocean and Atmospheric Sciences, Oregon State University, Corvallis, OR 97331, U.S.A., 4.Graduate School of Science, Chiba University, Chiba 263-8522, Japan, 5.Department of

Earth and Planetary Sciences, Tokyo Institute of Technology, 2-12-1 Ookayama, Meguro, Tokyo 152-8550, Japan , 6.Graduate School of Science and Engineering, Chiba University, Chiba 263-8522, Japan)

12:00 PM - 12:15 PM JST | 3:00 AM - 3:15 AM UTC

[SCG41-10] New Developments in Hard Rock Drilling Project: Horoman and Forearc Mantle drilling

*Katsuyoshi Michibayashi[1], Eiichi Takazawa[2], Tomoaki Morishita[3], Mikiya Yamashita[4,5], Gou Fujie[4], Shigeaki Ono[4] (1.Nagoya University, 2.Niigata University, 3.Kanazawa University, 4.JAMSTEC, 5.AIST)

Heterogeneity in the mantle section of the Oman ophiolite in terms of spinel and clinopyroxene compositions

*Eiichi TAKAZAWA[1,2]

1. Department of Geology, Faculty of Science, Niigata University, 2. Japan Agency for Marine-Earth Science and Technology

The tectonic environment during the formation of Oman ophiolite is still debated, but it becomes consensus that ridge spreading worked in the early stage [1, 2]. The age of the volcanic and plutonic rocks in the crustal section formed by the spreading ridge is 96-95 Ma, which is close to the oldest age (~ 95-94 Ma) of the metamorphic sole, indicating that the thrusting of ophiolite had started during or immediately after the formation of the crustal section [3, 4]. It is important to clarify the compositional modification that the residual mantle peridotite have received during thrusting/subduction following the partial melting in the spreading ridge. In this talk, I will summarize what has been clarified at this time.

Spinel's Cr# (= Cr/[Cr+Al] atomic ratio) and abundance of heavy rare earth elements in clinopyroxene (e.g., Yb) are used as an indicator to estimate the depletion of peridotites with upper mantle origin [5, 6, 7]. Research team at Niigata University has examined spatial compositional heterogeneity in the mantle section of the Oman ophiolite. The study area has been focused in the Fizh and Salahi massifs from the northern part and the Wadi Tayin massif from the southern part of the Oman ophiolite.

In the Fizh and Salahi massifs, the Cr# of spinels in harzburgite falls within the composition range of abyssal peridotites except for some areas. Areas where Cr# is higher than the composition range of abyssal peridotites exist locally as the "high refractory harzburgite zone" [8] in the northern part of the Fizh mantle section and as the ultramafic complex of the Salahi mantle section [9]. In the Wadi Tayin mantle section in the southern part of Oman ophiolite, Cr# of harzbergite spinel is mostly within the composition range of abyssal peridotite.

On the other hand, the Cr# of dunite spinel has a wide range from abyssal peridotite to forearc peridotite, and spinel with a high value of 0.7 or more widely distributed in the Fizh and Sarahi mantle section. The high Cr# region of the dunite spinel spreads finger-like in the mantle section, suggesting a reaction with melts (island arc tholeiite and boninite) derived from highly refractory peridotite. Even in the Wadi Tayin mantle section in the southern part of Oman ophiolite, some of the dunite spinel have high Cr#, and their distribution is limited to the shear zone and the vicinity of the basal thrust.

The rare earth element pattern of Cpx in the peridotites in the mantle section of the Oman ophiolite tends to change with the coexisting spinel Cr#. That is, as the Cr# of spinel increases, the Ce/Yb ratio of Cpx increases. There is a difference in the correlation between the northern part and the southern part of Oman ophiolite, and when comparing the peridotites with the same Cr# of spinel, the Ce/Yb ratio of Cpx is higher in the southern part. This is thought to represent a difference in the composition of the melt that reacted with harzburgite to form dunite, and while boninite melt was involved in the north, it is possible that MORB may be an island arc tholeiite in the south. The former is characterized by a higher amount of Cr and a lower abundance of rare earth elements than the latter.

References: [1] Nicolas et al., 1988, Tectonophysics, 151, 87–105; [2] Umino, 1995, Journal of Geography (Chigaku Zasshi), 104, 321–349; [3] Rioux et al., 2012, JGR, 117, B07201,

©2021. Japan Geoscience Union. All Right Reserved.

doi:10.1029/2012JB009273; [4] Rioux et al., 2013, JGR, 118, 2085-2101; [5] Dick and Bullen, 1984, CMP, 86, 54-76; [6] Arai, 1994, Chemical Geology, 113, 191-204; [7] Hellebrand et al., 2001, Nature, 410, 677-681; [8] Kanke and Takazawa, 2014, Geological Society, London, Special Publications, 392, 229–246; [9] Nomoto and Takazawa, 2013, JMMPS, 42, 123-135.

Keywords: Oman ophiolite, upper mantle, spreading ridge, thrusting, mantle-melt reaction

©2021. Japan Geoscience Union. All Right Reserved.

Systematics of minor and trace element chemistry of olivine in peridotites

*Ikuya Nishio[1], Tomoaki Morishita[1], Keita Itano[1], Akihiro Tamura[1], Asyraf Muhamad[1]

1. Kanazawa University

Upper mantle consists of mostly peridotites consisting mostly of olivine. Minor and trace element chemistry of olivine has received attention to understand mantle heterogeneity (Sobolev et al., 2007) and element mobility in subducted oceanic mantle (Scambelluri et al., 2004). Therefore, minor and trace element chemistry of olivine has been lately investigated for volcanic rocks (Foley et al., 2013), garnet-peridotite (De Hoog et al., 2010), deserpentinized peridotite (Garrido et al., 2005). However, those of residual spinel-peridotite after partial melting have not been well studied compared to those peridotites and also systematics of olivine minor and trace element chemistry is not well established. Therefore, a comprehensive study on minor and trace element chemistry of olivine from various origins is important as an indicator of constraining the origin of peridotite and understanding elements input/output during the secondary process such as metasomatism and serpentinization/deserpentinization.

We make a systematic inquiry into olivine trace elements of residual peridotites, cumulus ultramafic rocks, metasomatized and deserpentinized ultramafic rocks. We used previously well-studied samples for the trace element analyses: abyssal peridotites from the Atlantis Massif, the Central Indian Ridge, and Southwest Indian Ridge (Tamura et al., 2008; Morishita et al., 2007, 2009) and forearc peridotite from Izu-Bonin-Mariana arc (Morishita et al., 2011) for residual peridotite samples, and ultramafic xenolith from Takashima in the southwest Japan arc (Muroi and Arai, 2014), banded-dunite-harzburgite from Horoman peridotite complex (Matsufuji et al., 2006), and hornblende peridotite from Hakusan area for cumulative samples, respectively. Minor and trace elements in olivine of other origins such as lower dunite recovered by Oman Drilling Project, and metasomatized and/or deserpentinized ultramafic rocks from SW Greenland were analyzed to understand the secondary process.

The minor and trace element abundance in olivine was obtained by LA-ICP-MS analysis. The analysis was performed by an ablating spot of 100 μm in diameter and a repetition rate of 6-10 Hz. Each analysis consisted of 30 s measurement of gas bland and 30 s ablation. The following isotopes were measured: ^{7}Li, ^{11}B, ^{23}Na, ^{27}Al, ^{29}Si, ^{31}P, ^{43}Ca, ^{45}Sc, ^{49}Ti, ^{51}V, ^{53}Cr, ^{59}Co, ^{62}Ni, ^{63}Cu, ^{66}Zn, ^{75}As, ^{85}Rb, ^{88}Sr, ^{89}Y, ^{90}Zr, ^{93}Nb, ^{95}Mo, ^{118}Sn, ^{121}Sb, ^{137}Ba, ^{140}Ce, ^{181}Ta, ^{208}Pb, ^{209}Bi, ^{232}Th, and ^{238}U. Signals of certain elements such as B, Ba, Sr, Ba, Pb, Al, and Cr, which indicate the presence of cracks or inclusions such as serpentine and spinel, were carefully monitored. In this study, we did not obtain rare earth elements abundance because they are mostly the below detection limit.

The minor and trace element abundances in olivine primarily depend on the degree of depletion. However, the results suggest that Ca, Ti, Y, B, and Li can be used as proxies to discriminate the origin of ultramafic rocks. Those elements tend to be higher in olivine of cumulus, metasomatized and deserpentinized ultramafic rocks than in olivine of residual peridotites. Y concentration in olivine of residual peridotite presents good correlations with the degree of partial melting estimated by REE concentration in clinopyroxene and Cr# of spinel. We emphasize that the minor and trace element chemistry of olivine has the potential as an indicator of the mantle process.

©2021. Japan Geoscience Union. All Right Reserved.

Keywords: Olivine, Mantle, Peridotite, Trace element

©2021. Japan Geoscience Union. All Right Reserved.

ICDP DSeis project: compilation of borehole logging and recovered core information at the seismogenic zone of the M5.5 Orkney earthquake with lower crustal intrusives

*Hiroshi Ogasawara[1], Shunsuke Yoshida[2], Mitsuya Higashi[2], Kensuke Sakaguchi[1], Yuki Yokoyama[4], Yasuo Yabe[3], Tetsuro Hirono[4], Dakalo Ligaraba[5], Nandipha Masondo[5], Yuhji Yamamoto[6], Team ICDP DSeis

1. College of Science and Engineering, Ritsumeikan University, 2. Graduate School of Science and Engineering, Ritsumeikan University, 3. Graduate School of Science, Tohoku University, 4. Graduate School of Science, Osaka University, 5. Graduate School of Geoscience, University of the Witwatersrand, 6. Kochi Core Center, Kochi University

The ICDP DSeis project (ICDP, 2019, The Thrill to Drill) has accomplished a full core recovery with a total of 1.6 km length drilled from 2.9 km underground, probing the upper margin of the aftershock zone of the M5.5 Orkney sinistral earthquake (Ogasawara et al. Deep Mining 2019). It was known before drilling that the host rocks of this seismogenic zone were Archean metamorphosed sedimentary rocks (2.9 billion years old; West Rand group, including quartzite and etc.).

This presentation will report the results of the compilation of down-hole logging (gamma-rays, density, elastic wave velocity, magnetic susceptibility, water temperature and conductivity) performed in 2017-2018 and non-destructive analysis (e.g., MSCL) of a hundred-plus meter-long core imported to the Kochi Core Center in 2019.

Drilling and logging in 2017-2018 revealed not only that the densities and Vp of the metamorphosed sedimentary rocks of the West Rand group (Roodepoort, Crown, Babrosco formations) are comparable to the upper crust, but also that dolerite sills with densities and seismic velocities were comparable to the lower crust.

Lamprophyre dyke and fault gouge and breccia were recovered from the intersection with the aftershock zone of the M5.5 sinistral earthquake (Ogasawara et al. Deep Mining 2019), and talc was also detected (Yokoyama 2020 MSc thesis, Osaka University). Because the borehole collapsed and blocked at the intersection with the aftershock zone, it was not possible to conduct borehole logging at the intersection and beyond it. This section was imported to the Kochi Core Center for MSCL and X-ray CT in FY 2019.

In FY2020, these were compiled. As a result, the density of the intact part of the lamprophyre dyke intersected at the aftershock zone is significantly larger than that of the dolerite sill, and the magnetic susceptibility increases rapidly and Vp decreases sharply when approaching the fault zone.

At the other intersection of the dolerite sill and another mafic dyke, Wiersberg et al. (2019 EGU), Rusley et al. (2018 AGU), Nisson et al. (2019 AGU), Warr et al. (2020 AGU) also found hypersaline brine fissure and gases (similar to those near hydrothermal vents on oceanic ridges?) rich in dissolved organic hydrocarbons of non-meteoric or non-biogenic origins. Aftershock activity consists of several streaks, with direction in line with the intersection line between the aftershock plane and the dolerite sills (Tadokoro MSc thesis Ritsumeikan). Since it is well known that mafic intrusives affect the subsurface fluid flow, an integrated analysis of all of these will kick off discussions on the relationship between material, water, and rupture at a seismogenic zone.

©2021. Japan Geoscience Union. All Right Reserved.

The ICDP team consists of researchers from Japan, South Africa, USA, Germany, Switzerland, India, Israel, Australia, and practitioners from the mining industry in South Africa. The core members include Y. Yabe and T. Ito (Tohoku Univ.), J. Mori (Kyoto Univ.), T. Hirono (Osaka Univ.), Y. Yamamoto (Kochi Univ.), B. Liebenberg (Moab Khotsong mine), T.C. Onsott (Princeton Univ.), T.L. Kieft (New Mexico Tech), T. Wiersberg (GFZ), R.J. Durrheim (Wits Univ.). Durrheim (Wits Univ.), J. Castillo (Free State Univ.), M. Ziegler (ETH, Zurich), and their students.

This drilling program was built on the projects supported by JST-JICA SATREPS and JSPS Kakenhi. It is currently supported by AngloGold Ashanti, Harmony, Sibanye Stillwater, ICDP, JSPS Core-to-Core Program, JSPS-SA NRF bilateral Program, Ritsumeikan University, Kochi Core Center, Collaborative Research Program for Seismic Volcanic Observations to Mitigate Hazards, US NSF, German DFG, South African NRF, CSIR and CGS.

Keywords: Seismogenic zone, ICDP scientific drilling, Deep goold mines in South Africa, Altered intrusives as dense as lower crustal material

©2021. Japan Geoscience Union. All Right Reserved.

Volcanism along the eastern margin of the Ontong Java Plateau: More reasons to test the Ontong Java Nui hypothesis by scientific ocean drilling

*Maria Luisa Tejada[1], Takashi Sano[2], Takeshi Hanyu[1], Anthony A. P. Koppers[3], Masao Nakanishi[4], Akira Ishikawa[5], Takashi Miyazaki[1], Kenichiro Tani[2], Shoka Shimizu[6], Qing Chang[1], Bogdan Stefanov Vaglarov[1]

1. Volcano and Earth Interior Research Center, Institute for Marine Geodynamics, Japan Agency for Marine-Earth Science and Technology, 2-15 Natsushima, Yokosuka 237-0061, Japan, 2. Department of Geology and Paleontology, National Museum of Nature and Science, Amakubo 1-1-1, Tsukuba, Ibaraki 305-0005, Japan, 3. College of Earth, Ocean and Atmospheric Sciences, Oregon State University, Corvallis, OR 97331, U.S.A., 4. Graduate School of Science, Chiba University, Chiba 263-8522, Japan, 5. Department of Earth and Planetary Sciences, Tokyo Institute of Technology, 2-12-1 Ookayama, Meguro, Tokyo 152-8550, Japan , 6. Graduate School of Science and Engineering, Chiba University, Chiba 263-8522, Japan

The Ontong Java Nui hypothesis, which states that three Pacific oceanic plateaus, Ontong Java, Manihiki and Hikurangi, once formed a single super plateau has been around for more than a decade now. However, there are critical pieces of the Ontong Java Nui puzzle that either do not fit or are sorely missing. Two of the outstanding inconsistencies are the contrasting crustal thickness between Manihiki Plateau (MP) and Ontong Java Plateau (OJP) and the rather distinct geochemical composition of the former which is not found on the latter so far. During the R/V Kairei KR16-04 cruise, we conducted geological surveys and dredging on the ridges protruding from the eastern margin of the OJP, as well as from the capping seamounts. We found that the dredged rocks have a variety of chemical composition ranging from tholeiitic to transitional to alkalic affinities. The tholeiites show similar middle to heavy rare earth abundances to OJP tholeiites but have elevated highly incompatible element (Rb, Th, Nb, Ta) contents, somewhat forming U-shaped trace element patterns that resemble those of Danger Island Trough basalts. Alkalic basalt composition mimics the trace element patterns of the 44 Ma, 65 Ma, and 90 Ma transitional to strongly alkalic basalts from the Solomon Islands and the Lyra Basin that form the southern and western margins of the OJP, respectively. Indicative older ~96-116 Ma ^{40}Ar-^{39}Ar ages of the ridge samples dredged near or below the base of the seamounts contrast with the 67-68 Ma plateau ages of samples from a seamount atop one of the ridges. These ages indicate later formation of the ridges compared to the main OJP (~122 Ma) but match with those of dated samples from Rapuhia Scarp on the northern margin of Hikurangi Plateau. Isotope and trace element data provide the missing compositional link while the new age data tie together the younger ages among Ontong Java, Manihiki and Hikurangi plateau volcanism. These findings support but add complexity to the Ontong Java Nui jigsaw fit. Thus, drilling the basement around the Eastern Salient of the OJP is required to further probe the extent or existence of the Ontong Java Nui super plateau.

Keywords: Ontong Java Nui, Ontong Java Plateau, Manihiki Plateau, Hikurangi Plateau

©2021. Japan Geoscience Union. All Right Reserved.

New Developments in Hard Rock Drilling Project: Horoman and Forearc Mantle drilling

*Katsuyoshi Michibayashi[1], Eiichi Takazawa[2], Tomoaki Morishita[3], Mikiya Yamashita[4,5], Gou Fujie[4], Shigeaki Ono[4]

1. Nagoya University, 2. Niigata University, 3. Kanazawa University, 4. JAMSTEC, 5. AIST

Plate tectonics, which is the paradigm of modern earth science, has been based on the assumption of a homogeneous and dry oceanic plate. However, rapid progress in ocean bottom exploration in the last 20 years strongly suggests that oceanic plates are diverse and quite wet (water-bearing). The Oman Drilling Expedition (2016-2018) has clearly demonstrated that the oceanic plate is not only poorly understood, but also that a major feature of the oceanic plate is that it can be far more hydrous than currently thought. However, while the Oman drilling experiment is revealing the full picture of the wet oceanic plate, our understanding of the dry case is still lacking. The Horoman peridotite body, located near Cape Erimo in the southernmost part of the Hidaka Mountains in Hokkaido, Japan, is one of the rare dry oceanic plate fragments in the world. We are now planning to carry out Horoman peridotite drilling experiments to recover continuous samples of dry oceanic plate material. We will compare our results with those of the recent Oman ophiolite drilling experiments to develop a new lithostratigraphic model that accounts for the entire oceanic plate, taking into account magma production and water content. In addition, the results of the geophysical survey of the Ogasawara Trench performed on December 19, 2020 will be briefly presented for the forearc Mantle drilling project.

Keywords: Horoman Peridotite, Oman ophiolite, Forearc Mantle Drilling

©2021. Japan Geoscience Union. All Right Reserved.

[E] Poster | S (Solid Earth Sciences)：S-CG Complex & General

Sun. Jun 6, 2021 5:15 PM - 6:30 PM JST | Sun. Jun 6, 2021 8:15 AM - 9:30 AM UTC | Ch.15_2

[S-CG41] Hard-Rock Drilling Science: From Continental to Deep Sea Drilling, and Oman Project

convener:Eiichi TAKAZAWA(Department of Geology, Faculty of Science, Niigata University), Katsuyoshi Michibayashi(Department of Earth and Planetary Sciences, Nagoya University), Keishi Okazaki(Japan Agency for Marine-Earth Science and Technology)

The IODP and ICDP have decided to launch a new international science framework, and hard rock drilling science is about to enter the preparatory period for the next phase. Therefore, drilling proposals from a new perspective and the production of scientific results based on existing drilling projects are expected. In this session, we invite presentations on the scientific results of hard-rock drilling. We also invite related studies of on-land geological investigations of Oman ophiolites and experimental studies. The session is intended to be interdisciplinary, including the fields of geophysics, geochemistry, petrology, engineering, and biology. This session is co-hosted with the focus group of hard rock drilling science.

[SCG41-P01] Oeanic lithosphere production and the Earth's surface environments

★Invited Papers

*Junichiro Kuroda[1], Kosuke T. Goto[2], Akira Ishikawa[3], Azumi Kuroyanagi[4] (1.Atmosphere and Ocean Research Institute, the University of Tokyo, 2.Geological Survey of Japan, National Institute of Advanced Industrial Science and Technology, 3.Department of Earth and Planetary Sciences, Tokyo Institute of Technology, 4.The Tohoku University Museum)

[SCG41-P02] Water Content in Nominally Anhydrous Mineral of Crust/Mantle Boundary Recovered by International Oman Drilling Project

*Muhamad Asyraf Aminuddin[1], Tomoaki Morishita[1,2], Kenji Shimizu[3], Takayuki Ushikubo[3], Juan Miguel Ramirez Guotana[1], Keita Itano[1] (1.Kanazawa University Graduate School Natural Science and Technology, 2.Oman drilling project phase 2, 3.Kochi Institute for Core Sample Research,JAMSTEC)

[SCG41-P03] Sr isotopic and trace element variations of gabbros and peridotites at the CM1A drilling site of Wadi Tayin massif in the Oman ophiolite

*Masako Yoshikawa[1], Tomoaki Morishita[2], Asyraf Muhamad Aminuddin[2], Ryoko Senda[3], Tomoyuki Shibata[1] (1.Department of Earth and Planetary systems Science, Hiroshima University, 2.Geosciences and Civil Engineering, College of Science and Enginiering, Kanazawa University, 3.Facutly of Social and Cultural Studies, Kyushu University)

[SCG41-P04] Sr-Nd-Pb isotope systematics of proto-arc volcanic rocks in the Oman ophiolite

*Tsuyoshi Ishikawa[1], Kazuya Nagaishi[2], Kyoko Kanayama[3], Keitaro Kitamura[4], Shigeyuki Wakaki[1], Yuki Kusano[5], Susumu Umino[6] (1.Kochi Institute for Core Sample Research, JAMSTEC, 2.Marine Works Japan Ltd., 3.San'in Kaigan Geopark Museum of the Earth and Sea, 4.Asia Air Survey Co., Ltd., 5.Geological Survey of Japan, AIST, 6.College of Science and Engineering, Kanazawa University)

[SCG41-P05] Peridotites beneath the ophiolite: Petrology and chemistry of peridotite bodies located below the metamorphic sole of the Oman ophiolite

*Main Tokinaga[1], Marie Python[1], Georges Ceuleneer[2], Tomoya Suzuki, Jean-Paul Breton[3] (1.Hokkaido University Department of Natural History Science Division of Earth and Planetary Systems Sciences, 2.GET – Observatoire Midi-Pyrénées - CNRS, 3.French Bureau de Recherches Géologiques et Minières (BRGM))

[SCG41-P06] Vein permeability structure of the crustal section in the Oman Drilling Project inferred from the X-ray CT image analysis

*Yuya Akamatsu[1], Ikuo Katayama[1], Keishi Okazaki[2], Katsuyoshi Michibayashi[3], Oman Drilling Project Phase I Science Party (1.Hiroshima University, 2.Japan Agency for Marine-Earth Science and Technology,

3.Nagoya University)

[SCG41-P07] **Serpentinization in the Salahi mantle section, the Oman Ophiolite**

*Yohki YOSHIBA[1], Eiichi TAKAZAWA[1,2] (1.Faculty of Science Niigata University, 2.Japan Agency for Marine-Earth Science and Technology)

Oeanic lithosphere production and the Earth's surface environments

*Junichiro Kuroda[1], Kosuke T. Goto[2], Akira Ishikawa[3], Azumi Kuroyanagi[4]

1. Atmosphere and Ocean Research Institute, the University of Tokyo, 2. Geological Survey of Japan, National Institute of Advanced Industrial Science and Technology, 3. Department of Earth and Planetary Sciences, Tokyo Institute of Technology, 4. The Tohoku University Museum

It has been discussed that long-term changes in the production rates of oceanic plates have influenced on Earth's surface environments through Phanerozoic. For example, carbon cycles in the global oceans have been largely affected by CO_2 degassing along mid-ocean ridges and at hot spots, and precipitation of carbonate minerals through low-temperature hydrothermal alteration. Thus, the high/low rates of oceanic lithosphere production could be one of the major driving forces for the Greenhouse /Icehouse climate periods, which have occurred repeatedly on the scale of hundreds of millions of years. Because of the role of hydrothermal alteration as a removing process of Mg from seawater, large-scale changes in amplitude of hydrothermal activity associated with oceanic plate production have influenced on the secular variation of Mg concentrations in seawater, and thus also on carbonate biomineralization. Time periods in the late Cenozoic (Neogene and Quaternary) are classified as one of the "Icehouse" climatic episodes. The cooler climates may have been related to the relatively low rate of degassing associated with the reduced seafloor spreading rates for those time periods. In addition, the removal of Mg from seawater by hydrothermal alteration was relatively low, which resulted in relatively high concentrations of Mg remained in seawater in Neogene and Quaternary. On the other hand, Cretaceous represents one of the "Greenhouse" climate periods. Cretaceous is also characterized by relatively high rates of oceanic plate productions, and voluminous igneous province volcanisms, both of which may have maintained high degassing rates. The Mg removal rates were considered to be high, resulting in low Mg concentrations in seawater.

The likelihood of those classic hypotheses on the link between oceanic plate productions and surface environments have long been the subject of debate. Here, we introduce a new concept of wetness/dryness of oceanic lithospheres into the long-lasting discussions. "Dry" plates are less hydrated oceanic plates that were formed under conditions of higher production rates, as represented by the Pacific Plate, while "wet" plates are more hydrated ones formed under lower spreading rates. How those "dry" and "wet" oceanic plates have affected the surface environments throughout the Earth's history could become one of the major themes of the Earth sciences in the future. We discuss the validity and testability of the hypothesis that the differences between the "dry" and "wet" oceanic plates have caused variations in global seawater volumes and major (Ca, Mg etc.) and trace element (Sr, Os etc.) compositions of seawater, and also have affected the global climates and carbonate biomineralization.

Keywords: Oceanic lithosphere, Greenhouse/Icehouse climate periods

©2021. Japan Geoscience Union. All Right Reserved.

Water Content in Nominally Anhydrous Mineral of Crust/Mantle Boundary Recovered by International Oman Drilling Project

*Muhamad Asyraf Aminuddin[1], Tomoaki Morishita[1,2], Kenji Shimizu[3], Takayuki Ushikubo[3], Juan Miguel Ramirez Guotana[1], Keita Itano[1]

1. Kanazawa University Graduate School Natural Science and Technology, 2. Oman drilling project phase 2, 3. Kochi Institute for Core Sample Research,JAMSTEC

The presence of water in the Earth’ s mantle has been to have a prominent role in the volatile cycle of Earth’ s mantle but measuring water flux into the mantle proved to be difficult and not fully constraint. Nevertheless, measuring water content in the mantle have its importance. It is known that some portion of water can be stored in nominally anhydrous mineral (NAM) like olivine and pyroxene which support the presence of water in the deep mantle. The significance of water retained in such minerals are that it can cause deformation to the minerals such as olivine which is the most abundant mineral in the mantle. Measuring water content in the oceanic plate specifically in the crust-mantle section is the most practical as water retained in the oceanic plate should be nearly zero due to the upwelling of the asthenosphere causing partial melting to occur extracting water into the melt. Therefore, the objective of this study is to measure water content in the oceanic crust specifically in the crust-mantle boundary.

As direct sample from the crust-mantle section is unattainable, ophiolite is used for this water content analysis as samples with the idea of measuring water content in oceanic plate as ophiolite is tectonically originated from mid-ocean ridge. However, some studies showed ophiolite might be affected by a later subduction zone tectonic setting (Lippard *et al.,* 1986) where second stage magmatism occurred at the subduction zone during obduction process. Thus, a high-water content could prove that ophiolite might be affected by subduction metasomatism. Ophiolite samples were from core samples recovered by International Oman Drilling Project in Samail Ophiolite, Oman. The core recovered reached about 400m depth and consists of layered gabbro (160 m), dunite (150 m) and harzburgite (75 m) with a compositionally gradational zone of 15m between dunite and harzburgite. Samples from each sequence (gabbro, dunite and harzburgite) of the core were used for water content analysis.

Fourier transform infrared spectroscopy (FTIR) and Secondary Ion Mass Spectrometry (SIMS) is used for water content analyses (Shimizu et al., 2017). The disadvantage of FTIR is its sample preparation that need the samples to doubly polished are difficult for sample with small grains. SIMS have its disadvantage like high hydrogen background in low-concentration phases, but improved technique and procedure established by Hauri (Hauri et al., 2002; Koga et al., 2003: Shimizu et al., 2017) contributing for more reliable quantifications of low-level volatiles. Improved sample preparation technique and analytical sensitivity (Koga, 2003) are done like use of indium metal as embedment material instead of epoxy to limit the hydrogen background (Koga et al., 2003: Shimizu et al., 2017). IMS-1280HR of SIMS instrument is used which are installed in the Kochi Institute for Core Sample Research, JAMSTEC with 20 keV of Cs^+ ion beam bombarded to the sample surface with diameter 10-15 micrometer. Negative secondary ions of $^{12}C^-$, $^{16}OH^-$, $^{19}F^-$, $^{30}Si^-$, $^{32}S^-$ and ^{35}Cl signals will be collected from the center of analysis spot. The internally corrected data using ^{30} Si signal intensity were calibrated by the analyses of glass and olivine standard materials with known H2O concentrations.

Based on the result, $^{16}OH/^{30}Si$ signal intensities value on the layered gabbro sample are consistent with no significant changes of value on the rims and core of olivine. In contrast, $^{16}OH/^{30}Si$ signal intensities

©2021. Japan Geoscience Union. All Right Reserved.

value on the dunite and harzburgite showed uncertainties where high hydrogen background occurred due to the presence of serpentine in the sample that prevent water to be completely removed during degassing process prior analysis. Despite that, we can certain that the water content measured in gabbro sample is 34 ppm on average and the water content measured in dunite and harzburgite are on the range of 30-50 ppm. When comparing the value to the previous study of water content of olivine in natural peridotites obtained by Secondary Ion Mass Spectrometry (Kurosawa et. al., 1997, Warren & Hauri, 2014), the water content in olivine are significantly high (Fig 2). The explanation of high-water content of olivine is related to hydrous melting. Hydrous melting is where the presence of water in the mantle lower the solidus temperature allowing melts to be formed. The hydrous melting occurred in ophiolite support that subduction metasomatism might happened in ophiolite.

Keywords: oman drilling project, nominally anhydrous mineral, ophiolite

©2021. Japan Geoscience Union. All Right Reserved.

Sr isotopic and trace element variations of gabbros and peridotites at the CM1A drilling site of Wadi Tayin massif in the Oman ophiolite

*Masako Yoshikawa[1], Tomoaki Morishita[2], Asyraf Muhamad Aminuddin[2], Ryoko Senda[3], Tomoyuki Shibata[1]

1. Department of Earth and Planetary systems Science, Hiroshima University, 2. Geosciences and Civil Engineering, College of Science and Enginiering, Kanazawa University, 3. Facutly of Social and Cultural Studies, Kyushu University

Hydrothermal alteration processes of seawater occurring in oceanic crust impact the physical, chemical, and biological processes of the Earth system (Staudigel., 2003). Comprehensive research of hydrothermal circulation on direct oceanic crust is not sufficient due to the difficulty of obtaining samples. Petrological and geochemical characteristics caused by hydrothermal alteration have been studied from detailed observations of ophiolite, which is believed to be fragments of the oceanic lithosphere (e.g. Lanphere et al., 1986).

We analyzed Sr isotopic and trace element compositions of gabbros and peridotites (dunite and harzburgite) collected from the drilling CM1A site that penetrates the crustal-mantle boundary of the Wadi Tayin massif in the southern Oman ophiolite. The core sample is 404.15 m in length, composed mainly with olivine gabbro in the upper 160 m of the core (Layered Gabbro sequence: Sequence I), with massive dunite from 160 m to 310 m (Crust-Mantle Transition sequence) that is divided into the upper 90 m Dunite sequence (Sequence II) and the lower 60 m Dunite with Gabbro Sequence (Sequence III), and with deeper harzburgite (Mantle sequence; Sequence IV) (Tamura et al., 2018; Takazawa et al., 2019).

The Sr isotopic variations of eight gabbro samples in Sequence I is small ($^{87}Sr/^{86}Sr$ = 0.7030 to 0.7033). The $^{87}Sr/^{86}Sr$ ratios of dunites are higher than those of the gabbros and decrease from 0.7072 in sequence I to 0.7039 in lower part of Sequence II and Sequence III through 0.7042 in upper part of Sequence II. The harzburgite in the Sequence IV shows slightly higher $^{87}Sr/^{86}Sr$ ratio (0.7040) than the dunites in Sequence II and III.

The Sr isotopic variations of the gabbros of Sequence I is consistent with those of fresh gabbros in the Ibra massif of the southern part of the Oman ophiolite (0.7028 –0.7033; Lanphere et a., 1986; Zhilman et al., 2018), but the Sr isotopic ratio of the Sequence I dunite is higher than them. This difference might depend on degree of alteration (gabrros = 11 - 16 %, dunite = 80 %). The dunite of Sequence I shows extensive enrichment of Th and U compared than the gabbros. The estimated Sr isotope ratio of the solution circulated in the Sequence I dunite is 0.70821 using the equation (1) of Kawahata et al (2001). The Sr isotopic variations of dunites from Sequence II and III do not simply correlate with degree of serpentinization. Degree of serpentinization and multi-element primordial mantle (PM) normalized patterns of these dunites are similar to each other. These results suggest that the hydrothermal fluid circulating at different depths shows different Sr isotope ratios. The Sequence IV harzburgites show various PM-normalized patterns and slightly higher Sr isotopic ratios compared than upper sequence dunites. This feature may be due to the influence of fluids from the metamorphic sole.

References:

©2021. Japan Geoscience Union. All Right Reserved.

Kawahata et al., JGR, 206, 11083-11099, 2001.
Lanphere et al., JGR, 86, 2709-2720, 1986.
Staudigel, Treatise on Geochemistry, 3, 511–535, 2003.
Takazawa et al. Abs. of JpGU, SCG49-10, 2019.
Tamura et al., Abs. of JpGU, SCG54-P08, 2018.
Zhilman et al., Lithos, 323, 103–124, 2018.

Keywords: Oman Drilling Project samples, Sr isotopic ratios, trace element compositions, crust-mantle boundary

©2021. Japan Geoscience Union. All Right Reserved.

Sr-Nd-Pb isotope systematics of proto-arc volcanic rocks in the Oman ophiolite

*Tsuyoshi Ishikawa[1], Kazuya Nagaishi[2], Kyoko Kanayama[3], Keitaro Kitamura[4], Shigeyuki Wakaki[1], Yuki Kusano[5], Susumu Umino[6]

1. Kochi Institute for Core Sample Research, JAMSTEC, 2. Marine Works Japan Ltd., 3. San'in Kaigan Geopark Museum of the Earth and Sea, 4. Asia Air Survey Co., Ltd., 5. Geological Survey of Japan, AIST, 6. College of Science and Engineering, Kanazawa University

In the Oman ophiolite, spreading-ridge-derived lavas are covered by arc-like lavas after a short interval, possibly related to subduction initiation. The lavas with arc affinity include boninite, which is generally known to represent one of the most important products of proto-arc magmatism. Thus, the occurrence of boninites and related volcanic rocks in the Oman ophiolite has a key to understanding subduction initiation and concomitant proto-arc magmatism. However, currently only limited geochemical data are available for these volcanic rocks. In this study, we present Sr, Nd, and Pb isotope compositions of boninites in the Oman ophiolite, together with those of proto-arc tholeiites extruded prior to the boninites. The proto-arc tholeiites show slightly to moderately enriched Sr and Pb isotope compositions but almost identical Nd isotope compositions compared to axial lavas, consistent with melting of residual depleted mantle metasomatized by amphibolite-facies slab fluids. On the other hand, boninites show distinctly more radiogenic Sr, Nd, and Pb isotope compositions than axial lavas, which requires addition of slab fluids formed at higher temperatures as well as small amounts of mafic-sedimentary hybrid slab melt to the residual highly depleted mantle. The observed isotope variations suggest involvement of hotter slab in boninite magma genesis than in the case of proto-arc tholeiites, probably due to successive subduction of the slab after subduction initiation.

©2021. Japan Geoscience Union. All Right Reserved.

Peridotites beneath the ophiolite: Petrology and chemistry of peridotite bodies located below the metamorphic sole of the Oman ophiolite

*Main Tokinaga[1], Marie Python[1], Georges Ceuleneer[2], Tomoya Suzuki, Jean-Paul Breton[3]

1. Hokkaido University Department of Natural History Science Division of Earth and Planetary Systems Sciences, 2. GET –Observatoire Midi-Pyrénées - CNRS, 3. French Bureau de Recherches Géologiques et Minières (BRGM)

The Oman ophiolite is a large slab of Tethyan ocean floor obducted onto the Arabic peninsula, comprising one of the largest piece of exposed lithospheric peridotites. It is the last of several nappes thrusted onto the autochtonous units of the Arabian margin (Saih Hatat and Jebel Akhdar), and then the highest in the general stratigraphic column of Oman. The emplacement of the ophiolite resulted from intraoceanic subduction in North-northeast direction followed by a period of continental subduction leading to the Oman margin burying.

The Taww region is located at the northernmost border of the Jebel Akhdar, south to the Kahwad ophiolitic massif. It is characterised by the presence of small peridotite occurrences that are in direct contact with the Jebel Akhdar autochthonous units, and is located below the Hawasina nappes and the metamorphic sole (in this study, we call them the “Taww peridotites”). Similar peridotite bodies are found in various small regions around the Jebel Akhdar and the Saih Hatat. They crop out as a few meter to a few kilometre wide massifs, most of the time highly serpentinised or carbonated and deformed. They are characterized by the absence of magmatic veins and dykes, their stratigraphic location below the metamorphic sole of the ophiolite, and when found as ophiolitic melange, by the inclusion of limestone blocks. In these 3 points, they differ from the ophiolite mantle main body. In order to understand the petrogenesis of the Taww peridotites, we sampled several peridotite bodies from both location below and above the metamorphic sole and Hawasina units. Only one of our samples taken near Ibra had an unclear stratigraphic position (this sample is called “Ibra” in the present study).

The ophiolitic peridotites are all from the lowermost ophiolite, taken a few meter to a few tens of meter above the metamorphic sole. Their petrological characteristics are similar to what was described for basal peridotite by other researchers: they are mostly high depleted harzburgites containing 1 to 7% of Cpx (mostly from refertilised sources) with granular and porphyroclastic textures. The Taww peridotites seem to contain slightly less Cpx and more Opx but their texture are basically very similar to the usual ophiolite peridotites. The mineral chemistry shows that the Taww peridotites as well as the ophiolite peridotites are residual harzburgites. However, the Taww peridotites, instead more depleted in Cpx than the ophiolite peridotites, show lower Cr-spinel Cr# and higher Al content in Opx, suggesting a possible lower melting degree than in the ophiolite but also a relatively Al-rich chemical environment. In our study, Cpx in ophiolite lherzolites and Cpx-rich harzburgites (2 to 5% Cpx) show a relatively Na and Ti-rich chemistry showing that they are mainly from trapped melts and refertilisation processes. By contrast, ophiolite harzburgites and the Taww peridotites, independently of their lithology, show a very depleted chemistry suggesting that they are mostly melting residue. Cpx REE composition and calculation of the peridotites melting degree (Fmax) show that The Taww peridotites and the ophiolite peridotites had distinct melting history. Taww peridotites are richer in HREE and Al and less melted than the ophiolite harzburgites, (Fmax from 9 to 15% in the Taww peridotites vs 14-22% in the ophiolite), suggesting a possible higher melting pressure. They do botshow any traces of refertilisation or metasomatism and are unlikely to have

©2021. Japan Geoscience Union. All Right Reserved.

undergone any ridge-related processes (high degree of decompression melting, melt-rock reaction, refertilisation at low pressure, etc.). All these data, in addition to the Taww peridotites structural general context (Breton et al., 2004) led us to think that the Taww peridotites were not a part of the Tethys ocean mantle but they are more probably a piece of the mantle that have underlied the Arabian thinned margin.

Keywords: Oman ophiolite, Taww peridotite, Partial melting degree

©2021. Japan Geoscience Union. All Right Reserved.

Vein permeability structure of the crustal section in the Oman Drilling Project inferred from the X-ray CT image analysis

*Yuya Akamatsu[1], Ikuo Katayama[1], Keishi Okazaki[2], Katsuyoshi Michibayashi[3], Oman Drilling Project Phase I Science Party

1. Hiroshima University, 2. Japan Agency for Marine-Earth Science and Technology, 3. Nagoya University

Permeability is a key parameter that controls spatial and temporal changes in fluid circulation in the oceanic crust. Permeability is strongly dependent not only on the presence of fractures but also on the scale of fractures, which means that a few large fractures can control the fluid circulation in the oceanic plate. Such highly permeable features are often preserved as hydrothermal veins in the rocks. In this study, we developed a method to automatically characterize vein parameters in the recovered cores of the IODP Oman Drilling Project from the X-ray CT image analysis to calculate the vein permeability structure of the oceanic crust.

First, we prepared “unwrapped” images from the 3-D CT images which are cylindrical-shaped. In the unwrapped images planar fractures or veins appear as sinusoids. After edges that are possibly consist of veins are detected, we performed iterative Hough transform to determine automatically the vein parameters including amplitude, phase, depth, aperture, and CT number. Permeability was calculated by applying an equivalent channel model to the detected vein geometry. The analyses were conducted on >1,500 CT core images of Holes GT1A, GT2A, and GT3A, which represent the lower crustal section of the Oman ophiolite.

Approximately 2,000 veins were detected in each of the Holes GT1A, GT2A, and GT3A. More than 85% of veins had CT numbers less than 3300, and the other veins had CT numbers greater than 3500. In each hole, estimated maximum permeability is ~10^{-10} m^2, which is much larger than that estimated from laboratory measurements using mini-core samples. In the Hole GT3A, which represents the sheeted dike-gabbro transition zone in the Oman Drilling Project, the azimuthal orientation of the veins is nearly random. In the Holes GT1A and GT2A, which represent the middle-to-lower crustal section, the vein orientations are relatively anisotropic compared to that of GT1A. Given that the fracturing and fluid flow have occurred when the host rocks were at the ocean floor, permeability of the oceanic crust can be controlled by large fractures and become anisotropic at the deeper levels.

Keywords: Permeability, Vein, Oman ophiolite, X-ray CT, Image processing

©2021. Japan Geoscience Union. All Right Reserved.

Serpentinization in the Salahi mantle section, the Oman Ophiolite

*Yohki YOSHIBA[1], Eiichi TAKAZAWA[1,2]

1. Faculty of Science Niigata University, 2. Japan Agency for Marine-Earth Science and Technology

The Oman ophiolite is presumed to be an oceanic lithosphere formed in Neo-Tethys Sea during the late Cretaceous and settled at the eastern end of the Arabian Peninsula through an uplift process associated with subduction. The peridotites of the Oman ophiolite are subject to serpentinization with various degree, and the Salahi mantle section is no exception. In this study, we observed the process of serpentinization recorded in the peridotites from the central part of the Salahi mantle section to the Moho transition zone. The samples used in this study have a relatively low degree of serpentinization, which is suitable for studying the process of hydrothermal alteration of marine lithosphere at an earlier stage.

The results of microscopic observation of altered minerals and identification of mineral species by laser Raman spectroscopy indicated that all samples underwent low temperature type serpentinization. In addition, antigorite, a high-temperature serpentine and talc were widely distributed, and tremolite and chlorite were observed in some samples. These results suggest that there was hydrothermal alteration at 400-900 ˚C. Moreover, the preservation of the mesh structure and bastite, and the cutting of minerals stable at high temperatures by minerals stable at lower temperatures, suggest that these rocks underwent hydrothermal alteration with a gradual decrease in temperature and serpentinization beneath the ocean floor. The source of the water seems to be hydrous fluid infiltrated from the basal thrust, or seawater supplied along faults in the crustal section.

Keywords: Oman ophiolite, serpentinization, mantle section, hydrous alteration, antigorite

©2021. Japan Geoscience Union. All Right Reserved.

[J] Oral | S (Solid Earth Sciences)：S-CG Complex & General

Sun. Jun 6, 2021 1:45 PM - 3:15 PM JST | Sun. Jun 6, 2021 4:45 AM - 6:15 AM UTC | Ch.23 Zoom Room 23

[S-CG44] Petrology, Mineralogy & Resource Geology

convener:Koichi Momma(National Museum of Nature and Science), Yu Nishihara(Geodynamics Research Center Ehime University), Tatsuo Nozaki(Submarine Resources Research Center, Research Institute for Marine Resources Utilization, Japan Agency for Marine-Earth Science and Technology), Nobutaka Tsuchiya(Department of Geology, Faculty of Education, Iwate University), Chairperson:Yu Nishihara(Geodynamics Research Center Ehime University), Koichi Momma(National Museum of Nature and Science), Tatsuo Nozaki(Submarine Resources Research Center, Research Institute for Marine Resources Utilization, Japan Agency for Marine-Earth Science and Technology)

We widely invite presentations in the fields of petrology, mineralogy and resource geology. Especially description of minerals and rocks, investigation of their origin and evolution by field investigation and/or laboratory experiments, and development of new methods are accepted.

1:45 PM - 2:00 PM JST | 4:45 AM - 5:00 AM UTC

[SCG44-01] Consolidation anisotropy of Mio–Pleistocene sedimentary soft rocks in the eastern part of the Boso Peninsula, central Japan

*Nana Kamiya[1], Masahiro Miyazaki[1], Weiren Lin[1] (1.Graduate School of Engineering, Kyoto University)

2:00 PM - 2:15 PM JST | 5:00 AM - 5:15 AM UTC

[SCG44-02] Prograde and progressive metamorphism of low-pressure and high-temperature terrane in the Tenzan area, Saga prefecture, north Kyusyu, Southwest Japan

*Yusaku Tanaka[1], Masaaki Owada[1] (1.Yamaguchi University)

2:15 PM - 2:30 PM JST | 5:15 AM - 5:30 AM UTC

[SCG44-03] **ZIRCON U–Pb AGES AND GEOCHEMISTRY OF GRANITOIDS FROM SOUTHWEST MONGOLIA**

*Dolzodmaa Boldbaatar[1], Yasuhito Osanai[1], Nobuhiko Nakano[1], Tatsuro ADACHI[1], Ippei Kitano[1], Kundyz Syeryekhan[2] (1.Kyushu University, 2.Golden Hill LLC)

2:30 PM - 2:45 PM JST | 5:30 AM - 5:45 AM UTC

[SCG44-04] **Zircon U–Pb ages of plutonic rocks from Iwafune area, Ibaraki Prefecture**

*Haruki Yamazaki[1], Terumi Ejima[1], Yoshiaki Kon[2], Yuki Tsunazawa[2] (1.Shinshu University Faculty of Science Department of Geology, 2.National Institute of Advanced Industrial Science and Technology)

2:45 PM - 3:00 PM JST | 5:45 AM - 6:00 AM UTC

[SCG44-05] Petrogenetic study on the cretaceous granitoids on the Takanawa Peninsula, northwest Shikoku, southwest Japan

*Kazuya Shimooka[1], Satoshi SAITO[1], Kenichiro Tani[2], Toshiro Takahashi[3] (1.Graduate School of Science and Engineering, Ehime University, 2.Department of Geology and Paleontology, National Museum of Nature and Science, 3.Graduate School of Science and Technology, Niigata University)

3:00 PM - 3:15 PM JST | 6:00 AM - 6:15 AM UTC

[SCG44-06] The kinetics and heat conduction model of thermoluminescence of orthoclase

*Takahiro Sato[1], Nobuo Hirano[1], Noriyoshi Tsuchiya[1] (1.Tohoku University)

Consolidation anisotropy of Mio–Pleistocene sedimentary soft rocks in the eastern part of the Boso Peninsula, central Japan

*Nana Kamiya[1], Masahiro Miyazaki[1], Weiren Lin[1]

1. Graduate School of Engineering, Kyoto University

Consolidation generally progresses with an increase in the overburden by the thickness of the sediment. In tectonic stress field, such as a subduction zone, folding also progress with sedimentation, therefore it is necessary to consider the effects of tectonic stress on consolidation. In this study, consolidation tests were conducted using siltstone distributed on the Boso Peninsula, central Japan which is located at the subduction zone of the Sagami Trough to investigate the anisotropy of the consolidation.

The Boso Peninsula is located at the northern part of the Sagami Trough and had formed with the subduction of the Philippine Sea Plate. The Boso Peninsula is composed of the accretionary prisms, trench slope break, and forearc basin, in this study, siltstones were taken from the eastern part of the Boso forearc basin as samples for the consolidation tests. The Boso forearc basin is composed of the Miura Group (15-3 Ma) and the Kazusa Group (2.5-0.3 Ma) and the boundary of both groups is the Kurotaki Unconformity. The large scale folds are distributed in the Miura Group, but the Kazusa group is monocline to the north. In this study, siltstone block samples were taken from the eastern part of the Boso forearc basin composed of both groups to consider the characteristics of anisotropy of consolidation based on geological structure.

We made two types of specimens from a block sample: height direction is perpendicular or parallel to the bedding plane. Cylindrical specimens were put into a consolidation ring, loaded at a constant strain rate, and the consolidation yield stress (p_c) was obtained from the consolidation curve. As a result, the consolidation yield stress in the parallel direction was the same or larger than that in the perpendicular direction. K_{0pc} value which is the ratio of the stress of the parallel to the perpendicular was estimated as an indicator of the anisotropy of consolidation using the p_c of perpendicular and parallel directions. K_{0pc} of the Miura Group is approximately 1.1 and that of the Kazusa Group is approximately 1.2. Compared to the characteristics of anisotropy of consolidation between the two groups, there is no difference between the two groups. The K_0 value of sediment is generally 0.5-0.8 in the silence basin without tectonic stress. Therefore, considering the setting of the Boso forearc basin, it was suggested that the consolidation of the Boso forearc basin is affected by the tectonic compaction.

Keywords: Consolidation, Anisotropy, Sedimentary soft rock

©2021. Japan Geoscience Union. All Right Reserved.

Prograde and progressive metamorphism of low-pressure and high-temperature terrane in the Tenzan area, Saga prefecture, north Kyusyu, Southwest Japan

*Yusaku Tanaka[1], Masaaki Owada[1]

1. Yamaguchi University

Low-pressure and high-temperature type metamorphic rocks are exposed as mega blocks in the Cretaceous north Kyushu batholiths. Adachi et al. (2012) reported 120—100 Ma monazite Th—U—Pb chemical age and 105 Ma LA—ICP—MS zircon U—Pb ages from pelitic granulites in the Ukidake area, Fukuoka prefecture. This report is addressed with the petrological characters of the metamorphosed mafic rocks from the Tenzan area, Saga prefecture, and discussed in their temporal and spatial changes on the metamorphic grade.

The Tenzan area is underlain by the metamorphic rocks including ultramafic rocks and the Cretaceous granites and gabbros. The metamorphic rocks are exposed in the area covering 20 km in the east to west and 8 km in the north to south. The main structural features in the study area generally show east-west in strikes and dipping 50 to 80 degrees to the south or north. In the eastern part of the Tenzan area, the metamorphic rocks occur apart in the two areas with distance about 3 km, the Hiko-dake area in the north and the Ogi area in the south. The Cretaceous granitic rocks intruding the metamorphosed mafic rocks are situated between two areas.

The metamorphosed rocks consist mainly of amphibolite that are classified into Amphibolite-I and Amphibolite-II in terms of lithofacies. Amphibolite-I shows fine-grained and well foliated structures, and locally intercalates thin calc-silicate layers. On the other hand, Amphibolite-II has coarse-grained without any thin calc-silicate layers. Both Amphibolites-I and -II geochemically resemble N-MORB based on some discrimination diagrams. Amphibolite-I has a nematoblastic structure and is composed mainly of hornblende and plagioclase with a small amount of quartz. The hornblende shows a zonal structure with light green in cores to greenish brown in rims. Opaque minerals and titanite are included as accessory minerals. In addition to these minerals, clinopyroxene and epidote appear in the calc-siliceous thin layers. Amphibolite-II consists mainly of hornblende and plagioclase with a small amount of biotite, potassium feldspar and quartz. Hornblende possesses greenish brown in cores with light-green thin rims, and locally includes plagioclase and quartz with poikilitic textures indicating originally intrusive rocks. Potassium feldspar is produced as antiperthite. Opaque minerals, apatite, zircon and titanite are included as accessory minerals. In addition, Amphibolites-I and -II show granoblastic textures near the contact area of the Cretaceous granites.

Hornblende in Amphibolite-I compositionally shows actinolite in core and magnesio-hornblende or edenite in mantle to rim, and locally has thin actinolite rim, whereas that of Amphibolite-II has wide ferro-edenite in core to rim with locally associated with thin actinolite rim. Plagioclase grains are of Anorthite contents (An) 35 to 43 for both Amphibolites-I and -II with few chemical zoning. Zonal structures of hornblende grains in Amphibolite-I would reflect the prograde metamorphism from greenschist to amphibolite facies metamorphism, then finally greenschist facies again at the retrograde stage. The prograde change in Amphibolite-I can be explained by the reaction of tremolite and albite to form edenite and quartz. Since plagioclase in Amphibolite-I is of andesine, it is inferred that the low An

©2021. Japan Geoscience Union. All Right Reserved.

plagioclase stabled in the greenschist facies has been consumed by the above reaction. The estimated peak metamorphic temperatures of Amphibolite-I in the Ogi and Hiko-dake areas were 550—600℃ and 640—650℃, respectively. The results indicate that the metamorphic rocks in this area underwent the progressive metamorphism with increasing temperatures from south to north regardless of the distribution of granites. Overall, it is inferred that the metamorphism occurred at 100—105 Ma because of resembling its mode of occurrence and metamorphic features metamorphic style to those of the Ukidake area.

Keywords: Tenzan area, metamorphosed mafic rocks, MORB

©2021. Japan Geoscience Union. All Right Reserved.

ZIRCON U–Pb AGES AND GEOCHEMISTRY OF GRANITOIDS FROM SOUTHWEST MONGOLIA

*Dolzodmaa Boldbaatar[1], Yasuhito Osanai[1], Nobuhiko Nakano[1], Tatsuro ADACHI[1], Ippei Kitano[1], Kundyz Syeryekhan[2]

1. Kyushu University, 2. Golden Hill LLC

We present new petrographic, geochemical and geochronological data for granitic rocks emplaced in the Altai (Mongolian Altai) terrane of southwest Mongolia. The data are used to constrain their evolution and to discuss the tectonic implications for the Altai terrane. The zircon U–Pb ages indicate that the magmatism can be divided into three stages: stage 1 (397–366 Ma), stage 2 (340-300 Ma) and stage 3 (208-200 Ma). The stage 1 granitic rocks are divided into two types: Bt–Hbl granites having I-type affinity with volcanic arc signature and Crd–Grt bearing Bt–Ms granites having S-type affinity. On the other hand, Stage 2 Qz–Bt syenite having shoshonitic affinity and stage 3 Kfs-porphyritic Bt granites having high-K calc-alkaline affinity with intraplate tectonic setting.

Keywords: I-, S-type granite, zircon U–Pb age, SW Mongolia

©2021. Japan Geoscience Union. All Right Reserved.

Zircon U–Pb ages of plutonic rocks from Iwafune area, Ibaraki Prefecture

*Haruki Yamazaki[1], Terumi Ejima[1], Yoshiaki Kon[2], Yuki Tsunazawa[2]

1. Shinshu University Faculty of Science Department of Geology, 2. National Institute of Advanced Industrial Science and Technology

The Yamizo Mountains consist of Yamizo, Torinoko, Keisoku and Tsukuba Mountain Blocks. The Yamizo, Torinoko, and greater part of Keisoku Mountain Blocks consist of the Yamizo Group and several plutons. The diorites and gabbros of the plutons are of Early Cretaceous in age (109–102 Ma: Ejima et al., 2018; Ejima et al., 2019), and the granites of Late Cretaceous–Paleocene in age (69–63 Ma: Ejima et al., 2019). On the other hand, southern part of the Keisoku and Tsukuba Mountain Blocks mainly consist of plutonic rocks, such as granites and gabbros are of Late Cretaceous–Paleocene in age (66–61 Ma: Koike and Tsutsumi, 2017; Koike and Tsutsumi, 2018). The Iwafune pluton occurs in northern part of the Keisoku Mountain Block. The Iwafune pluton consists mainly of diorite with minor gabbroic diorite and granite which is distributed in southeast. Shibata et al. (1973) reported biotite K–Ar age of the Iwafune diorite is 64.5 ±2.5 Ma. However, the petrographic characteristics of the Iwafune diorite are similar to diorite of the Fukuroda pluton with about 100 Ma ages in the Torinoko Mountain Block.
Therefore, in order to reexamine age of igneous activity of the Iwafune pluton, U–Pb dating of zircons extracted from the Iwafune plutonic rocks was carried out using laser ablation inductively coupled plasma mass spectrometry combined with cathodoluminescence (CL) imaging on the zircons.
The CL images of zircons separated from diorite, gabbroic diorite and granite show that these zircons have oscillatory zoning and broad-banded zoning which are characteristic internal texture for magmatic zircon. The zircon U–Pb ages of the diorite, gabbroic diorite and granite are 64.4 ±0.6 Ma (n = 37), 64.5 ± 0.7 Ma (n = 24) and 64.6 ±0.8 Ma (n = 41), respectively. The diorite, gabbroic diorite and granite of the Iwafune pluton are same intrusive age, and there is no difference between these ages of the Iwafune pluton and the K–Ar age of previous study (Shibata et al.,1973). Moreover, the zircon U–Pb ages of the Iwafune pluton are same as those of granites in the Yamizo Mountain Block (69–63 Ma: Ejima et al., 2019), and granites and gabbros in the Tsukuba Mountain Block (66–61 Ma: Koike and Tsutsumi, 2017; Koike and Tsutsumi, 2018).

Keywords: U-Pb age of zircon, Iwafune pluton, Granite, Diorite, Gabbroic Diorite

©2021. Japan Geoscience Union. All Right Reserved.

Petrogenetic study on the cretaceous granitoids on the Takanawa Peninsula, northwest Shikoku, southwest Japan

*Kazuya Shimooka[1], Satoshi SAITO[1], Kenichiro Tani[2], Toshiro Takahashi[3]

1. Graduate School of Science and Engineering, Ehime University, 2. Department of Geology and Paleontology, National Museum of Nature and Science, 3. Graduate School of Science and Technology, Niigata University

In recent years, felsic igneous activity during magmatic anomalies in volcanic arcs has attracted much attention as a key to understanding the formation and growth processes of continental crust. This period of anomalous magma generation is called "flare-up" (e.g., Paterson and Ducea, 2015), and is recognized on a global scale, from North and South America to the Pacific Rim of Eurasia.
Takanawa Peninsula in northwestern Shikoku is composed of plutonic rocks and related rocks including granitoids, mafic rocks, metamorphic rocks formed druing the Cretaceous flare-up event. The granitoids, which are the most widely exposed in the area, consist of several granitoid plutons with different petrological characteristics such as occurrence, mineral constituents and mineral modal ratio. The mantle-derived mafic rocks and metamorphic rocks of accretionary complex are distributed in the area, making the Takanawa Peninsula the best field to investigate thermal and chemical effects of mantle activity on the crust during the flare-ups. However, although wide range of studies including petrological studies by Ochi (1982), isotopic studies by Kagami et al. (1985; 1988), and geochronological studies by Yoshikura et al. (2004) and Shimooka et al. (2019) have been reported, no comprehensive petrogenetic studies on the granitoids have been conducted to elucidate the magmatic processes during the flare-ups in the Takanawa Peninsula.
In this study, I obtained new data including whole-rock and mineral chemical compositions, zircon U-Pb ages and Sr-Nd isotope ratios for the granitoids and related rocks to investigate the magma process of granitoids in the Takanawa Peninsula.
The results suggest that the granitoids in the Takanawa peninsula were formed from multiple pulsed magmas generated by partial melting of the mafic lower crust in 99 Ma, 96-93 Ma, and 89 Ma, which intruded, emplaced, and solidified in the middle crust. Based on the isotopic compositions, assimilation of the host metasedimentary rocks into the granitoid magmas is limited. The differences in the chemical compositions observed in the granitoid plutons are attributed to the degree of partial melting of the mafic lower crust and/or the degree of fractional crystallization of evolving magmas.

Keywords: Cretaceous Granitoids, Petrogenetic study, Flare-ups, Takanawa Peninsula

©2021. Japan Geoscience Union. All Right Reserved.

The kinetics and heat conduction model of thermoluminescence of orthoclase

*Takahiro Sato[1], Nobuo Hirano[1], Noriyoshi Tsuchiya[1]

1. Tohoku University

One method of applying the thermoluminescence phenomenon of minerals such as quartz or feldspar to geothermal exploration is to estimate the underground temperature from the thermoluminescence intensity. In this study, we developed a model to relate the kinetics of thermoluminescence intensity to the heat conduction equation.
TL is a phenomenon in which the energy accumulated in a solid crystal due to the excitation and trapping of electrons by incident radiation is emitted as light by thermal stimulation. When the energy accumulation is caused by natural radiation, it is called natural TL (NTL), and when it is caused by artificial radiation, it is called artificial TL (ATL). A plot of TL intensity versus temperature is called a glow curve, and the Randall-Wilkins model exists as a simple model for drawing this glow curve (Randall and Wilkins., 1945). There is also a model that optimized Randall-Wilkins model using parameters obtained from experiments (Kitis et al., 1998). The integrated intensity of the glow curve is used to compare TL intensity. The kinetics of TL is expressed in terms of the decay of TL by thermal stimulation and the accumulation of TL by radiation. The decay term is described by a reaction rate equation and fitted to the results of isothermal heating experiments. We measured TL from a feldspar sample in a granitic pegmatite collected in Ishikawa-machi, Fukushima Prefecture, and separated several TL peak from glow curves using the Kitis model described above (hereinafter referred to as Peak). The glow curves of the samples whose TL was decayed by isothermal heating were also separated in the same way. The isothermal heating temperatures were 90, 125, and 150℃, and the heating times were 24, 168, 672, 1512, and 3360 hour. The results of the decay of TL intensity were plotted for each peak, and the curves drawn by the reaction rate equation with the frequency factor and reaction order as variables were fitted. The reaction was 2nd or 3rd order. The decay term in the kinetics of TL intensity was described by the reaction rate equation of the 2nd or 3rd order reaction. Next, To investigate the accumulation term, we performed ATL measurements. After artificially irradiating the feldspar samples with γ-rays, the ATL intensity was measured according to the radiation intensity, and the TL intensity per radiation intensity for each Peak was determined. The irradiation doses were 80, 500, 1000, and 2000 Gy. The annual dose received by the samples used was set to 15 mGy/year, and the annual accumulation intensity of each Peak was determined. From the above, the accumulation term could be expressed as a function of time with the annual accumulation intensity as a constant.
The temperature structure of a hypothetical heat source was set up using a heat conduction model, and the time variation of TL intensity was examined in a one-dimensional unsteady heat conduction model. The temperature at which the decay/accumulation of TL is switched is in the range of 20~30℃ at the lowest Peak, and the TL of the feldspar located far from the heat source is accumulated.

References

Randall, J. T. & Wilkins, M. H. F. (1945, November). Phosphorescence and electron traps. I. The study of trap distributions. In Proceedings of the Royal Society of London A: Mathematical, Physical and Engineering Sciences (Vol. 184, No. 999, pp. 365-389). The Royal Society.
Kitis, G., Gomez-Ros, J.M. and Tuyn J. W. N. (1998) Thermoluminescence glow-curve deconvolution functions for first, second and general orders of kinetics. J. Phys. D: Appl. Phys. 31 (1998) 2636–2641.

©2021. Japan Geoscience Union. All Right Reserved.

Keywords: Thermoluminescence, feldspar, Heat conduction

©2021. Japan Geoscience Union. All Right Reserved.

[J] Oral | S (Solid Earth Sciences)：S-CG Complex & General

Sun. Jun 6, 2021 3:30 PM - 5:00 PM JST | Sun. Jun 6, 2021 6:30 AM - 8:00 AM UTC | Ch.23 Zoom Room 23

[S-CG44] Petrology, Mineralogy & Resource Geology

convener:Koichi Momma(National Museum of Nature and Science), Yu Nishihara(Geodynamics Research Center Ehime University), Tatsuo Nozaki(Submarine Resources Research Center, Research Institute for Marine Resources Utilization, Japan Agency for Marine-Earth Science and Technology), Nobutaka Tsuchiya(Department of Geology, Faculty of Education, Iwate University), Chairperson:Tatsuo Nozaki(Submarine Resources Research Center, Research Institute for Marine Resources Utilization, Japan Agency for Marine-Earth Science and Technology)

We widely invite presentations in the fields of petrology, mineralogy and resource geology. Especially description of minerals and rocks, investigation of their origin and evolution by field investigation and/or laboratory experiments, and development of new methods are accepted.

3:30 PM - 3:45 PM JST | 6:30 AM - 6:45 AM UTC

[SCG44-07] Formation of bipyramidal quartz within the hydrothermal vents: inights from Kuroko samples and hydrothermal experiments

*Jumpei Sugioka[1], Atsushi Okamoto[1], Ryoichi Yamada[1] (1.Tohoku University)

3:45 PM - 4:00 PM JST | 6:45 AM - 7:00 AM UTC

[SCG44-08] Copper mobilization systems associated with the Neogene magmatism in the Northeast Japan arc

*Shota Satori[2,1], Yoshiaki Kon[2], Yasushi Watanabe[1], Takuya Echigo[1] (1.Graduate School of International Resource Sciences, Akita University, 2.Geological Survey of Japan, National Institute of Advanced Industrial Science and Technology)

4:00 PM - 5:00 PM JST | 7:00 AM - 8:00 AM UTC

[SCG44-09] Discussion

Formation of bipyramidal quartz within the hydrothermal vents: inights from Kuroko samples and hydrothermal experiments

*Jumpei Sugioka[1], Atsushi Okamoto[1], Ryoichi Yamada[1]

1. Tohoku University

Mineral precipitation from the hydrothermal vent fluids has been thought to occur in response to rapid cooling of hydrothermal fluids by mixing with cold seawater, but the mechanism of mineral precipitation still poorly understood. Kuroko is one of the typical massive sulfide deposits distributed along the western side of the central mountains of NE Japan, and formed at seafloor associated with rhyolitic magmatism. The Kuroko sample with the concentric structures represents the chimneys in submarine hydrothermal deposits (Shimazaki and Horikoshi, 1990). In addition to sulfides, bipyramidal quartz grains has been reported in such chimney-like structure, and is thought to be the key to understanding the physico-chemical conditions within chimneys. In this study, we analyzed the quartz-bearing Kuroko samples and conducted the hydrothermal flow-through experiments on silica precipitation. Comparing natural and experimental silica minerals, we discuss the formation and transport processes of quartz particles within the submarine hydrothermal vents.

We analyzed two Kuroko samples containing bipyramidal quartz grains collected from the Hanaoka mine (Doyashiki and Matsumine deposits) in the Hokuroku district, NE Japan. The samples show banded structure mainly composed of barite, galena, sphalerite, chalcopyrite, pyrite, and quartz. The quartz grains show euhedral bipyramidal shape with a long axial length of 0.07-0.45 mm and aspect ratio of 3-5. The bipyramidal quartz contains pyrite. The quartz contained fluid inclusions with size less than 5 micrometers, and showed homogenization temperature of 281-309℃. These features suggest that quartz crystals were formed from the high temperature fluids exceeding 300℃.

The silica precipitation experiments were conducted using the flow-through apparatus with vertical flow-path at constant pressure of 25 MPa with using high-silica aqueous solution (~300 mg/kgH_2O) by dissolution of granite. Within the cylindrical vessel, temperature increased from 350℃ to 430℃ along the flow-path, and silica minerals precipitation occur at around 390℃ within the inner tube in response to the drop of solubility of silica minerals. The silica precipitates were caught by 23 stainless steel nets placed at 10 mm intervals. We conducted two runs with flow rate of 0.1 ml/min and the different durations 1 h and 11 h, respectively. The precipitation of various silica minerals was observed along the flow-path. In the 1h run, amorphous silica occurred at 9-10 cm from the inlet of the alumina tube, cristobalite at 10-14 cm. In contrast, the 11h run, the precipitation of spherical amorphous silica were observed at 7 cm, and quartz particles at 8-10 cm. The quartz grained showed euhedral bipyramidal shape with size of 5.9-103 micrometers. These occurrences suggests that the silica nucleated as amorphous silica, in response to its low interfacial energy with water, and the silica particle grew and aggregated, and then transformed into more stable phases, such as cristobalite or quartz via heterogeneous nucleation on metastable silica phases (Okamoto et al., 2015). The Stokes' equation predict that the silica particles smaller than ~14 micrometers can move upward in ascending flow velocity of 0.01 m/s in the experiments, which is consistent with the particle size observed within the reaction vessel, suggesting that the bipyramidal quartz formation occurred in suspension. The bipyramidal quartz grains in the Kuroko samples were similar to that produced in the hydrothermal experiments. Because of the larger grain size of quartz grains, the fluid ascending velocity within the chimney was estimated to be 0.04-1.6 m/s, which is consistent with that inferred for the active submarine hydrothermal vents (Nozaki et al. 2016).

References Shimazaki, H., Horikoshi, E., 1990. Mining Geology, 40, 313-321. Okamoto, A., Kuwatani, T., et al. 2015. Physical Review E, 92, 042130. Nozaki T., Ishibashi, J.I., Shimada, K., et al. 2016. Scientific

©2021. Japan Geoscience Union. All Right Reserved.

Reports, 6, 22163.

Keywords: submarine hydrothermal vents, bipyramidal quartz, chimney, silica, kuroko, submarine hydrothermal deposits

©2021. Japan Geoscience Union. All Right Reserved.

Copper mobilization systems associated with the Neogene magmatism in the Northeast Japan arc

*Shota Satori[2,1], Yoshiaki Kon[2], Yasushi Watanabe[1], Takuya Echigo[1]

1. Graduate School of International Resource Sciences, Akita University, 2. Geological Survey of Japan, National Institute of Advanced Industrial Science and Technology

A large number of Neogene vein-type copper deposits are distributed in the Northeast Japan arc, which is a volcanic arc associated with subduction of the oceanic plate but lacks porphyry-type copper deposits. Those vein-type copper deposits associated with neighboring Miocene and Pliocene intrusive rocks. The purpose of this study is to clarify how copper mobilized and concentrated as an ore deposit in the magma supply system. Felsic intrusive rocks and included enclaves (MME; mafic magmatic enclave / mafic microgranular enclave) in the Arakawa area, which have been clarified to be temporally and spatially related to the Arakawa copper deposit. In order to estimate the amount of copper released with the fluid during magma solidification, the copper content of the melt estimated using the partition coefficient was compared with the whole rock copper content.

The three felsic intrusive rocks in the Arakawa area consist of plagiorhyolite and amphibole rhyodacite stocks. The MME contained in felsic intrusive rocks is basaltic to dacite and is mainly classified into two types: clinopyroxene-bearing hornblende gabbro and hornblende dacite. All plagioclase in basaltic MME is lath-shape with An 36-89 % and Cu 2.8-35.7 ppm. Felsic intrusive rocks mainly contain tabular-shaped plagioclase with An 11-38 % and Cu 0.5-5.1 ppm. The lath-shaped plagioclase contained in basaltic MME and dacitic MME shows a negative correlation between the An value and Cu content. In the An value vs. Cu diagram, the plot is linearly continuous regardless of the type of MME. Tabular-shaped plagioclase has a small An value and Cu content as a whole, and shows a clear compositional difference from lath-shaped plagioclase. The Cu content of the whole rock is 1 ppm for felsic intrusive rocks, 2 ppm for dacitic MME, and 65-106 ppm for basaltic MME.

The copper content in the melt estimated using the partition coefficient between plagioclase and melt is about 9-24 ppm for felsic intrusive rocks and about 120-150 ppm for basaltic MME. The melts that crystallize lath-shaped plagioclase and tabular-shaped plagioclase in dacitic MME are 74-138 ppm and 8-36 ppm, respectively.

Thus, these analytical results suggest that the dacitic MME with an intermediate composition was generated by the magma mixing of the differentiated mafic magma that formed the basaltic MME and felsic magma. It is suggested that the difference between the estimated copper content of the magma that formed the felsic intrusive rocks and dacitic MME and the whole rock copper content was distributed to the fluid phase during degassing process to form the ore forming fluid.

Keywords: copper mobilization system, magma mixing / mingling, Northeast Japan arc

©2021. Japan Geoscience Union. All Right Reserved.

[J] Oral | S (Solid Earth Sciences) | S-CG Complex & General

[S-CG44] Petrology, Mineralogy &Resource Geology

convener:Koichi Momma(National Museum of Nature and Science), Yu Nishihara(Geodynamics Research Center Ehime University), Tatsuo Nozaki(Submarine Resources Research Center, Research Institute for Marine Resources Utilization, Japan Agency for Marine-Earth Science and Technology), Nobutaka Tsuchiya(Department of Geology, Faculty of Education, Iwate University), Chairperson:Tatsuo Nozaki(Submarine Resources Research Center, Research Institute for Marine Resources Utilization, Japan Agency for Marine-Earth Science and Technology)

Sun. Jun 6, 2021 3:30 PM - 5:00 PM Ch.23 (Zoom Room 23)

We widely invite presentations in the fields of petrology, mineralogy and resource geology. Especially description of minerals and rocks, investigation of their origin and evolution by field investigation and/or laboratory experiments, and development of new methods are accepted.

4:00 PM - 5:00 PM

[SCG44-09]Discussion

©Japan Geoscience Union

[J] Poster | S (Solid Earth Sciences)：S-CG Complex & General

Sun. Jun 6, 2021 5:15 PM - 6:30 PM JST | Sun. Jun 6, 2021 8:15 AM - 9:30 AM UTC | Ch.15_3

[S-CG44] Petrology, Mineralogy & Resource Geology

convener:Koichi Momma(National Museum of Nature and Science), Yu Nishihara(Geodynamics Research Center Ehime University), Tatsuo Nozaki(Submarine Resources Research Center, Research Institute for Marine Resources Utilization, Japan Agency for Marine-Earth Science and Technology), Nobutaka Tsuchiya(Department of Geology, Faculty of Education, Iwate University)

We widely invite presentations in the fields of petrology, mineralogy and resource geology. Especially description of minerals and rocks, investigation of their origin and evolution by field investigation and/or laboratory experiments, and development of new methods are accepted.

[SCG44-P01] Intrusive and emplacement process of the Tono plutonic complex: Constraints from dating and isotopic analysis of zircons

*Yasuhiro Ogita[1], Kazusa Sando[2], Kozue Ishibashi[3], Shuhei Sakata[4], Takeshi Ohno[5], Satoshi Suzuki[3], Tatsunori Yokoyama[1], Saya Kagami[1], Mitsuhiro Nagata[1], Takashi Yuguchi[2] (1.Tono Geoscience Center, Japan Atomic Energy Agency, 2.Faculty of Science, Yamagata University, 3.Graduate school of Science and Engineering, Yamagata University, 4.Earthquake Research Institute, University of Tokyo, 5.Faculty of Science, Gakushuin University)

[SCG44-P02] Whole-rock chemical composition of the Nojima granodiorite in northern part of Awaji Island, southwestern Japan

*Akihiro Ishihara[1], Motohiro Tsuboi[1] (1.Kwansei Gakuin University)

[SCG44-P03] Influence of inclusions on hydrogen generated during low temperature serpentinization

*Asuka Sugawara[1], Ryohei Kawakita[1], Tsubasa Otake[2], Tsutomu Sato[2] (1.Graduate school of Engineering, Hokkaido University, 2.Faculty of Engineering, Hokkaido University)

[SCG44-P04] **Detailed characteristics of Raman spectra of carbonaceous materials in fault rocks nearby the Median Tectonic Line**

*Hiroshi Mori[1], Yuki Nobe[1], Ken Yamaoka[2], Yosuke Tomooka[1], Yui Kouketsu[3], Tetsuya Tokiwa[1] (1.Shinshu University, 2.The University of Tokyo, 3.Nagoya University)

[SCG44-P05] Trace element composition of chromian spinel in the Sanbagawa ultramafic rocks

*Yuki Aoshima[1], Yuji Ichiyama[1], Jung-Woo Park[2] (1.Chiba University, 2.Seoul National University)

[SCG44-P06] The trace element composition of sapphire in the xenolith of garnet-bearing andesitic tuff of the Donzurubo Formation, the Nijo Group, Japan.

*Mayuko Fukuyama[1], Masatsugu Ogasawara[2] (1.Graduate School of Engineering Science, Akita University, 2.Geological Survey of Japan, National Institute of Advanced Industrial Science and Technology)

[SCG44-P07] **Microstructures of spherical pyrite in the Kuroko deposits: possible mechanism of pyrite growth on bubble**

*Atsushi Okamoto[1], Yoeri van de Ridder[2], Oliver Plumper[2], Markus Ohl[2], Ryoichi Yamada[1] (1.Tohoku University, 2.Utrecht University)

[SCG44-P08] **The mineral occurrence of kaolinitic saprolite beneath the sedimentary kaolin deposit at Seto district**

*Haruna Asai[1], Kikuchi Ryosuke[1], Tsubasa Otake[1], Tsutomu Sato[1] (1.Hokkaido University)

[SCG44-P09] Borate concentration processes in modern evaporitic and hydrothermal environments: Constraints on the formation of a boron-rich environment on prebiotic earth

*Sara Rinka Christensen [1], Akizumi Ishida[1], Takeshi Kakegawa[1] (1.Department of Earth Science, Graduate School of Science, Tohoku University)

[SCG44-P10] Experimental study on propagation of elastic wave in supercritical geothermal reservoirs

*Katsuya Mizuno[1], Noriyoshi Tsuchiya[1], Nobuo Hirano[1] (1.Tohoku university)

Intrusive and emplacement process of the Tono plutonic complex: Constraints from dating and isotopic analysis of zircons

*Yasuhiro Ogita[1], Kazusa Sando[2], Kozue Ishibashi[3], Shuhei Sakata[4], Takeshi Ohno[5], Satoshi Suzuki[3], Tatsunori Yokoyama[1], Saya Kagami[1], Mitsuhiro Nagata[1], Takashi Yuguchi[2]

1. Tono Geoscience Center, Japan Atomic Energy Agency, 2. Faculty of Science, Yamagata University, 3. Graduate school of Science and Engineering, Yamagata University, 4. Earthquake Research Institute, University of Tokyo, 5. Faculty of Science, Gakushuin University

Introduction

Tono plutonic complex (TPC), northeast Japan, consists of adakitic rocks (central facies) and calk-alkaline rocks (main facies and marginal facies) surrounding the central facies [1,2]. Some previous studies have reported TPC zircon U-Pb ages; 117.5 ±2.4 Ma in the central facies; 118.9 ±2.6 Ma and 118.0 ±1.2 Ma in the main facies [3,4]. These ages are related to last stage of igneous activity in the Kitakami Mountains. Revealing the formation process of zonal granitic pluton such as TPC can constrain for the history of the Cretaceous igneous activities in the Kitakami Mountains. Although intrusive relations among the facies are estimated from field observations [5] and whole rock Nd and Sr isotopic compositions [6], there is no discussion regarding to zircon U-Pb ages associated with solidification temperature and origin of magma. Zircon collected from a granitic pluton provides its crystallization age and crystallization temperature [7] from zircon U-Pb dating and titanium (Ti) concentration analysis, respectively. The pairs of data enable to reveal the sequential formation process from intrusion through emplacement to crystallization/solidification of plutonic body [8]. Hafnium isotopic compositions of zircon provide us the information of their source of magma [4]. In this study, we estimated crystallization age and temperature of TPC zircons deduced from U-Pb isotopic analysis and quantitative analysis of Ti, respectively. Moreover, Hf isotopic analysis of TPC zircons are carried out to discuss their source magma.

Samples and methods

Zircons were separated from each rock samples of TPC three lithofacies, and observed through cathodoluminescence images using scanning electron microscope at Yamagata University to clarify the internal structures related to crystal growths. On the basis of the observation, we performed simultaneous determination of U-Pb age and Ti concentration by using laser ablation-inductively coupled plasma-mass spectrometry (LA-ICP-MS) [9] at Gakushuin University. Hf isotopic analysis are carried out at Tono Geoscience Center, Japan Atomic Energy Agency by using LA-ICP-MS.

Results and discussion

As the result of U-Pb isotopic analysis of zircons, age ranges of TPC three lithofacies overlap (**Table 1**). There are no significant age differences between core and rim of each zircon grain. Weighted means of U-Pb age are listed (**Table 1**). The zircon U-Pb age of central facies is older than reference age [3], whereas that of main facies is consistent with results of previous studies [3,4].

Ti concentrations have ranges between 1.96 ±0.28 ppm and 4.74 ±0.44 ppm for the central facies (9 grains, 23 spots), 4.07 ±0.42 ppm and 13.61 ±0.96 ppm for the main facies (12 grains, 32 spots), and 6.65 ±0.59 ppm and 8.81 ±0.71 ppm for the marginal facies (1 grain, 10 spots) (**Table 1**). Crystallization

©2021. Japan Geoscience Union. All Right Reserved.

temperature estimated by Ti-in-zircon geothermometer (assuming both SiO_2 activity and TiO_2 activity were 1.0.) [10] range 613 ±38 ℃ to 680 ±39 ℃ for the central facies, 668 ±39 ℃ to 775 ±43 ℃ for the main facies, and 709 ±40 ℃ to 734 ±41 ℃ for the marginal facies. Since these temperature conditions are close to solidus of granitic magma, zircon U-Pb age and crystallization temperature reflect the emplacement age and thermal condition in magma chamber, respectively. In future works, to make further consideration on intrusive and emplacement process of each TPC lithofacies, additional analysis and new perspective such as Hf isotope are required.

Acknowledgments

This study was carried out under a contract with the Ministry of Economy, Trade and Industry (METI), Japan, as part of its R&D supporting program titled “Establishment of Advanced Technology for Evaluating the Long-term Geosphere Stability (2020 Fy)”.

References

[1] Tsuchiya and Kanisawa, 1994, J. Geophysical Research, **99**, 205 –220. [2] Mikoshiba and Kanisawa, 2008, Earth Sci. (Chikyu Kagaku), **62**, 183 –201. (in Japanese with English abstract) [3] Tsuchiya et al., 2015, Japanese Magazine of Mineralogical and Petrological Sci., **44**, 69 –90. (in Japanese with English abstract) [4] Osozawa et al., 2019, J. Asian Earth Sci., **184**, e103968. [5] Nishimura et al., 1999, The Memoirs of the Geological Society of Japan, **53**, 177 –188. (in Japanese with English abstract) [6] Tsuchiya et al., 2007, J. Volcanology and Geothermal Reseach, **167**, 134 –159. [7] Watson et al., 2006, Contribution to Mineralogy and Petrology, **151**, 413 - 433. [8] Yuguchi et al., 2016, J. Mineralogical and Petrological Sci., **111**, 9 –34. [9] Yuguchi et al., 2020, Lithos, **372 –373**, e105682. [10] Ferry and Watson, 2007, Contribution to Mineralogy and Petrology, **154**, 429 –437.

Keywords: zircon, U-Pb age, Ti concentration, Hf isotope, Tono plutonic complex

©2021. Japan Geoscience Union. All Right Reserved.

Table 1. Zircon U-Pb age and titanium concentration in Tono plutonic complex.

lithology			Cetral fafies	Main facies	Marginal facies
U-Pb age			9 grains, 23 spots	12 grains, 32 spots	1 grain, 10 spots
		range	108.7 ± 9.0 Ma - 153.9 ± 12.2 Ma	96.1 ± 10.7 Ma - 135.0 ± 12.1 Ma	121.6 ± 7.6 Ma - 147.5 ± 10.3 Ma
		weighted mean	125.6 ± 2.0 Ma	116.8 ± 2.1 Ma	133.8 ± 2.7 Ma
	core		7 grains, 9 spots	8 grains, 12 spots	1 grain, 3 spots
		range	108.8 ± 9.0 Ma - 153.9 ± 12.2 Ma	100.2 ± 9.7 Ma - 134.2 ± 13.0 Ma	121.6 ± 7.6 Ma - 147.5 ± 10.3 Ma
		weighted mean	125.3 ± 3.4 Ma	112.17 ± 3.2 Ma	134.2 ± 5.0 Ma
	rim		9 grains, 14 spots	9 grains, 20 spots	1 grain, 7 spots
		range	114.6 ± 7.5 Ma - 146.4 ± 12.3 Ma	96.1 ± 10.7 Ma - 135.0 ± 12.1 Ma	130.8 ± 7.2 Ma - 140.2 ± 12.2 Ma
		weighted mean	125.8 ± 2.5 Ma	120.1 ± 2.7 Ma	133.6 ± 3.2 Ma
Ti concentration			9 grains, 23 spots	12 grains, 32 spots	1 grain, 10 spots
		range	1.96 ± 0.28 ppm - 4.74 ± 0.44 ppm	4.07 ± 0.42 ppm - 13.61 ± 0.96 ppm	6.65 ± 0.59 ppm - 8.81 ± 0.71 ppm
		weighted mean	2.86 ± 0.07 ppm	7.73 ± 0.11 ppm	7.65 ± 0.20 ppm
	core		7 grains, 9 spots	8 grains, 12 spots	1 grain, 3 spots
		range	1.96 ± 0.28 ppm - 4.74 ± 1.96 ppm	5.19 ± 0.50 ppm - 13.61 ± 0.96 ppm	7.63 ± 0.65 ppm - 8.81 ± 0.71 ppm
		weighted mean	3.00 ± 0.11 ppm	7.38 ± 0.18 ppm	7.98 ± 0.39 ppm
	rim		9 grains, 14 spots	9 grains, 20 spots	1 grain, 7 spots
		range	2.19 ± 0.27 ppm - 4.09 ± 0.40 ppm	4.07 ± 0.42 ppm - 12.19 ± 0.90 ppm	6.65 ± 0.59 ppm - 8.57 ± 0.68 ppm
		weighted mean	2.78 ± 0.08 ppm	7.96 ± 0.15 ppm	7.52 ± 0.24 ppm

©2021. Japan Geoscience Union. All Right Reserved.

Whole-rock chemical composition of the Nojima granodiorite in northern part of Awaji Island, southwestern Japan

*Akihiro Ishihara[1], Motohiro Tsuboi[1]

1. Kwansei Gakuin University

The Late Cretaceous to Paleogene granitic rocks in the inner belt of southwestern Japan is divided into three zones from north to south: the Sanin belt, the Sanyo belt, and the Ryoke belt (1). Granitic rocks in Awaji Island in Hyogo Prefecture belongs to the Ryoke or Sanyo belt. The granitoids of Awaji Island are divided into three groups (granitoids I, II, and III) and eleven rock types according to the intrusion sequences (2). The Nojima granodiorite is a medium-grained hornblende biotite granodiorite to granite that is classified as granitoids Ⅱ. The chemical compositions of whole-rocks and minerals of the granitoids of Awaji Island have been reported (3), however, the chemical compositions of rare earth elements are rarely reported. In this study, chemical composition of the Nojima granodiorite including rare earth elements were analyzed and the formation process and petrogenesis were investigated. Major and trace elements were measured by using wavelength-dispersive X-ray fluorescence spectrometer (XRF). Rare earth elements were determined by inductively coupled plasma mass spectrometer (ICP-MS). SiO_2 content is in the range of 58.7-72.8 wt%. Fe_2O_3, MnO, TiO_2, CaO, P_2O_5 and MgO decreases and K_2O increases with increasing SiO_2. Al_2O_3 and Na_2O shows almost constant. Alumina saturation index (Al_2O_3 /(CaO+Na_2O+K_2O)) ranges from 0.87 to 1.10. Alumina saturation index increases with increasing SiO_2. On the Chondrite normalized REE pattern diagram, the light rare earth elements (La, Ce, Pr, Nd, Sm, Eu) are more abundant than the heavy rare earth elements (Gd, Tb, Dy, Ho, Er, Tm, Yb, Lu). This may be due to the relationships between ionic radii of REE and differentiation process of parental magma. It shows negative Eu anomalies for three samples and positive Eu anomalies for two samples among six samples. Two samples show negative Ce anomalies among six samples.

(1)Ishihara, S. (1971) Modal and chemical compositions of the granitic rocks related to the major molybdenum and tungsten deposits in the Inner Zone of Southwest Japan. Jour. Geol. Soc. Japan, 77, 441-452.

(2)Takahashi, Y. and Hattori H. (1992) Granitic rocks in Awaji Island-with an emphasis on the foliated granites-. Bull. Geol. Surv. Japan, 43, 335-357.

(3)Takahashi, Y. (1995) Major element geochemistry and mineral chemistry of granitic rocks in Awaji Island-Implications for the zonal distribution of Cretaceous granitic rocks, Inner Zone of Southwest Japan-. Bull. Geol. Surv. Japan, 46, 23-40.

Keywords: granodiorite, X-ray fluorescence, inductively coupled plasma mass spectrometer, rare earth elements, Awaji Island

©2021. Japan Geoscience Union. All Right Reserved.

Influence of inclusions on hydrogen generated during low temperature serpentinization

*Asuka Sugawara[1], Ryohei Kawakita[1], Tsubasa Otake[2], Tsutomu Sato[2]

1. Graduate school of Engineering, Hokkaido University, 2. Faculty of Engineering, Hokkaido University

Low temperature serpentinization, a hydration reaction of ultramafic rocks occurring at < 100℃, may generate hydrogen near Earth’ s surface environment. Fluids containing abundant hydrogen and methane formed by low temperature serpentinization (e.g., Lost City at the Mid-Atlantic Ridge) may have played key roles in abiotic synthesis of organic materials and therefore the origin of life in the Earth. However, the detail mechanism of the hydrogen generation during the reaction is poorly understood. Previous experimental studies have demonstrated that fresh peridotites produced more hydrogen than serpentinites suggesting that dissolution of olivine and pyroxene generates hydrogen. On the other hand, Klein et al. (2019) suggests that olivine-hosted fluid inclusions in which serpentinization progresses during cooling from magmatic temperatures are the important reservoir of hydrogen and abiotic methane released during low temperature serpentinization in the Earth’ s surface environments.
The objective of this study is to evaluate olivine-hosted inclusions as a potential source for hydrogen released during low temperature serpentinization experiments using different ultramafic rocks from the previous studies.

Harzburgites from Konde Hill (Soroako), Sulawesi, Indonesia and Horoman, Hokkaido were used in this study since they are the two samples that generated the greatest amount of hydrogen by low temperature serpentinization experiments. Although, both samples are relatively fresh harzburgites (< 0.7 wt% of water content), the generated amount of hydrogen was higher in Konde Hill (322 μmol/kg) than Horoman (146 μmol/kg). We observed the occurrence of olivine-hosted inclusions in the thin section samples using petrographic microscope under transmitted light and analyzed their mineralogical and gaseous compositions by confocal Raman spectroscopy.
Raman spectroscopy indicated that olivine-hosted inclusions are predominantly composed of some secondary minerals (i.e., serpentine, brucite) as well as methane in both samples. None of the samples show inclusions containing water molecules. These results suggest that serpentinization had occurred in the fluid inclusions with exhausting water. Whereas 33% of the gas inclusions contain hydrogen in the Konde Hill sample, none of the gas inclusions contain hydrogen in the Horoman sample. Based on the Raman spectroscopic analysis, we estimated the possible contribution of hydrogen in the gas inclusions to hydrogen generated during low temperature serpentinization experiments, which account for 230 μmol/kg. This amount of hydrogen may actually explain the difference between the two samples in the generated amounts of hydrogen during the experiments which can cover all of the differences measured in the previous study.

Therefore, this study suggests that olivine-hosted inclusions are an important source for the hydrogen generated during low temperature serpentinization. However, since the Horoman sample does not have any inclusion containing hydrogen, a significant amount of hydrogen was also likely produced by dissolution of olivine at the low temperature.

Reference

Klein, F., Grozeva, N. G., & Seewald, J. S. (2019). Proc. Natl. Acad, Sci. U.S.A., 116, 17666–17672.

©2021. Japan Geoscience Union. All Right Reserved.

Keywords: low temperature serpentinization, hydrogen, inclusion

©2021. Japan Geoscience Union. All Right Reserved.

Detailed characteristics of Raman spectra of carbonaceous materials in fault rocks nearby the Median Tectonic Line

*Hiroshi Mori[1], Yuki Nobe[1], Ken Yamaoka[2], Yosuke Tomooka[1], Yui Kouketsu[3], Tetsuya Tokiwa[1]

1. Shinshu University, 2. The University of Tokyo, 3. Nagoya University

Based on sensitivity of Raman spectra of carbonaceous material (CM) to the degree of graphitization of CM and the close relationship between the graphitization and metamorphic temperature, the Raman CM geothermometry has been developed and well used to estimate the maximum attained temperature in sedimentary and metamorphic rocks. In contrast, some studies pointed out that the degree of graphitization of CM is modified by brittle shearing. Therefore, to obtain the reliable maximum temperatures from fault rocks by this method, it is important to clarify the effects of brittle shearing on the Raman spectra of CM and here we conducted the Raman spectral analyses of CM in pelitic fault rocks nearby the Median Tectonic Line (MTL)—which is the largest on-land fault in Japan—in the Mizoguchi outcrop, Nagano Prefecture, central Japan.

In the Mizoguchi outcrop, the MTL is well exposed and recognized as the geological boundary separating the high-P/T Sanbagawa and low-P/T Ryoke belts. Five pelitic samples within 13 m from the MTL in the Sanbagawa side and three pelitic samples within 3.5 m in the Ryoke side were collected. As microstructural characteristics, brittle deformation structures are well developed in all samples and CM are contained in highly sheared matrix parts and also as inclusions in rock fragments or in porphyroblasts. In addition, the intensity of brittle shearing increases towards the MTL. To compare these structural characteristics, we respectively analyzed CM of matrix parts (matrix-CM) and of inclusion parts (inclusion-CM) and estimated temperature for each Raman spectrum by using the Raman CM geothermometry to use this value as an index of the degree of graphitization.

The average temperatures of inclusion-CM are ~370–430 ºC in the Sanbagawa belt and ~400–520 ºC in the Ryoke belt while those of matrix-CM are ~360–380 ºC in the Sanbagawa belt and ~370–410 ºC in the Ryoke belt. Comparison the data between inclusion- and matrix-CM in same samples implies lower average temperatures and smaller heterogeneities of matrix samples than those of inclusion-CM. In addition, as the special trends of the average temperatures, inclusion-CM show decreasing of temperature towards the MTL on both sides of the MTL while those of matrix-CM show no clear change. Based on a characteristic that temperature estimated by the Raman CM geothermometry increases as increasing the degree of graphitization of CM and the observed close relationship between microstructural characteristic and estimated temperature, effects of secondary brittle shearing result in the lower values of matrix-CM, while inclusion-CM preserve metamorphic conditions recorded before brittle shearing although some parts of the inclusion-CM (especially in samples within ~1m from the MTL) suffered brittle shearing. These suggest not only that the Raman spectral analysis of CM in fault rock is a useful tool to extract the metamorphic temperature recorded before faulting also that importance of careful selection of CM based on comparing microstructures of the brittle deformation.

Keywords: Raman spectral analysis, carbonaceous material, Median Tectonic Line, Sanbagawa belt, Ryoke belt, fault rock

©2021. Japan Geoscience Union. All Right Reserved.

©2021. Japan Geoscience Union. All Right Reserved.

Trace element composition of chromian spinel in the Sanbagawa ultramafic rocks

*Yuki Aoshima[1], Yuji Ichiyama[1], Jung-Woo Park[2]

1. Chiba University, 2. Seoul National University

The Sanbagawa belt, which is distributed from the Kanto Mountains to the eastern part of Kyushu Island, is a Cretaceous high-pressure-type metamorphic terrane and records Cretaceous subduction zone tectonics. In the Higashi-Akaishi area, the central part of Shikoku Island, a large ultramafic body is exposed associated with metamorphic rocks (mafic gneiss, metagabbro, etc.), which experienced eclogite-facies metamorphism (e.g., Kugimiya and Takasu, 2002). Also, there are exotic rocks of ultramafic volcanic rocks in an ophiolitic belt (Mikabu belt) in the south of the Sanbagawa belt and serpentinite blocks in low-grade pelitic schist, as seen in the Fujiwara body. In this study, major- and trace-element analyses of chromian spinel for the Sanbagawa ultramafic rocks were performed to reveal the origin of various ultramafic rocks in the Sanbagawa belt. Chromian spinel in the Higashi-Akaishi dunites and chromitite show high Cr# (= Cr / [Cr + Al]; >0.6) and low TiO2 (<0.3 wt.%) content and are poor in Ga, Ti, and Ni in normalized elemental patterns. No positive anomaly in Ru is present in platinum-group element patterns. These results suggest that the Higashi-Akaishi dunites and chromitite formed as cumulates crystallized from the same parental magma, which is derived from the highly depleted mantle like boninite in an island arc setting. On the other hand, chromian spinel in the serpentinite in the Fujiwara body and picrite in the Mikabu belt show intermediate Cr# (0.4-0.6) and TiO2 (0.4-1.7 wt.%) content relative to those of the Higashi-Akaishi body rocks. The trace element patterns show enrichment in Ga, Ti, and Ni and the platinum-group element patterns are characterized by a significant positive anomaly in Ru. These results suggest that the Fujiwara serpentinite and Mikabu picrite are derived from the intraplate magma produced by the upwelling of a large mantle plume, as proposed by the previous studies (Ichiyama, 2014). The metamorphic rocks associated with the Higashi-Akaishi body were formed in an oceanic island arc in the Early Jurassic (Aoki et al., 2019; 2020). The Higashi-Akaishi ultramafic rocks would have been parts of the lower crust of an Early Jurassic oceanic island arc on the Izanagi plate, whereas the Fujiwara serpentinite and Mikabu picrite are probably fragments of a Late Jurassic oceanic plateau. These results imply that all ultramafic rocks in the Sanbagawa metamorphic belt were brought through the subduction process of the Izanagi plate.

Keywords: Sanbagawa belt, ultramafic rocks, chromian spinel, platinum group elements

©2021. Japan Geoscience Union. All Right Reserved.

The trace element composition of sapphire in the xenolith of garnet-bearing andesitic tuff of the Donzurubo Formation, the Nijo Group, Japan.

*Mayuko Fukuyama[1], Masatsugu Ogasawara[2]

1. Graduate School of Engineering Science, Akita University, 2. Geological Survey of Japan, National Institute of Advanced Industrial Science and Technology

The Donzurubo Formation is a member of the Middle Miocene Nijo Group in the Mt. Nijo, Japan. The Donzurubo Formation consists of three sub-formations, the Lower Donzurubo Formation: garnet-biotite rhyolitic welded tuff, the Middle Donzurubo Formation: garnet-biotite andesite (Ishikiriba Volcanics), garnet-biotite andesitic clastic rocks, garnet-hornblend-orthopyroxene andesite (Hata Volcanics), and the Upper Donzurubo Formation: garnet-biotite rhyolite (Medake Volcanics), garnet-biotite rhyolitic clastic rocks. The volcanic rocks in the Nijo Group are a typical Setouchi Volcanic Rocks which are characterized by the occurrence of high-Mg andesite in Miocene. The volcanic rocks in Nijo Group contains abundant garnets. The occurrence of corundum as a xenolith of garnet-bearing andesite were reported in previous studies (e.g. Omori, 1942, Morimoto, 1949). On the other hand, the euhedral sapphires and garnets are found in Takeda river which is downstream from Mt. Nijo.
In this study, we present the occurrence of corundum-bearing xenolith which is found in garnet-biotite andesitic tuff in the Lower Donzurubo Formation. The euhedral pastel blue sapphire grains are also collected from river sands in Takeda river. The mineral assemblage of corundum-bearing xenolith is corundum, orthopyroxene, plagioclase, sillimanite, garnet, spinel, zircon, monazite, and ilmenite. The corundum is replaced by sillimanite, spinel and plagioclase. The sillimanite and spinel are a product of metamorphic reaction as; 5 corundum + garnet = 3 sillimanite + 3 spinel. This reaction takes place at high temperature condition (> 750 ^{o}C).
The corundum in xenolith are Fe-poor (1178-1707 μg/g), Ga-poor (43-63 μg/g), Cr-poor (81-159 μg/g), Ti-rich (273-975 μg/g), and Mg-rich (114-240 μg/g). Some of sapphires from Takeda river shows similar trace element composition to the corundum in xenolith, but some of them shows the different compositions which may indicate the different origin of sapphires. Trace elements in corundum are often used for origin determination. In the case of blue sapphire, the discrimination diagram of sapphire is difficult to identify their origin (Groat et al., 2019) but trace element compositions of corundum and sapphires in this study clearly shows the metamorphic origin.
The basement rocks of the Nijo Group consist of granitoids and high-temperature metamorphic rocks of the Ryoke belt. The mineral assemblage of xenolith and trace elements of corundum indicate that the origin of xenolith could be lateritic metamorphic rock at high-T condition which might be the Ryoke metamorphic rocks.

Acknowledgement
We appreciate the Hikia Group for obtaining samples.

References
Groat at al. (2019) Gems & Gemology, 55, 512-535.
Morimoto (1949) The Journal of the Geological Society of Japan, 55, 38-43.
Omori (1942) The Journal of the Japanese Association of Mineralogists, Petrologists and Economic Geologists, 27, 27-58.

©2021. Japan Geoscience Union. All Right Reserved.

Keywords: sapphire, corundum, trace element, LA-ICP-MS, Mt. Nijo

©2021. Japan Geoscience Union. All Right Reserved.

Microstructures of spherical pyrite in the Kuroko deposits: possible mechanism of pyrite growth on bubble

*Atsushi Okamoto[1], Yoeri van de Ridder[2], Oliver Plumper[2], Markus Ohl[2], Ryoichi Yamada[1]

1. Tohoku University, 2. Utrecht University

The submarine hydrothermal vents are one of the most active sites of mineralization in the Earth. The Kuroko deposits provide the significant insights on the mineralization processes at the active submarine hydrothermal systems. It is known that various forms of pyrite exist within the Kuroko deposits, but the formation mechanism and controlling factor have not been fully understood. In this study, we show the microstructural features of the spherical pyrite of the Kuroko deposits by using the EBSD, EDX and micro X-ray CT analyses, and discuss the formation processes within the hydrothermal vent. The sample was a part of chimney collected from the Kannondo deposit in the Hanaoka mine, NE Japan. The sample show the banded structure mainly composed of pyrite, barite, sphalerite with lessor amount of chalcopyrite and aluminosilicate. The pyrite particles show a spherical shape with 10-100 micrometer in diameter. The spherical pyrite grains often have hollow at the center, and some of them are filled by later minerals (barite and Cu-rich phase). The detailed microstructural analyses revealed that the spherical pyrite is composed of needle-like pyrite crystals, all of which are oriented with <100> direction. The needles are wider outward, suggesting the growth from the center to the margin. These features suggest the growth of pyrite crystals on bubble template as follows. Pyrite nano particles were initially formed in fluids, and they were attracted to a bubble surface by electrostatic double-layer forces and hydrophobic forces in response to specific pH, pS and pFe conditions. The preferential faces were attached on the bubble, and developed their face to grow in <100> direction. Such particle with hollow could have advantages on transport with low particle density.

Keywords: spherical pyrite, Kuroko, bubble surface

©2021. Japan Geoscience Union. All Right Reserved.

The mineral occurrence of kaolinitic saprolite beneath the sedimentary kaolin deposit at Seto district

*Haruna Asai[1], Kikuchi Ryosuke[1], Tsubasa Otake[1], Tsutomu Sato[1]

1. Hokkaido University

Kaolin is the common clay minerals in the Earth’ s surface, and important non-metallic mineral commodity used for ceramics, refractories and paper filler. The cluster of sedimentary kaolin deposits distributed in the Seto-Tono district is the largest kaolin field in Japan. Kibushi clay (ligneous clayey sediment) and Gerome clay (unsorted sediment consisting of coarse-grained quartz and fine-grained kaolin) in this district resulted from granitic clastics and have been mined for many years owing to its high plasticity, refractoriness and whiteness after baking. Recently, however, it is concerned that remained resource is being exhausted, and thus, utilization of kaolinitic saprolite which is the weathered crust of the basement granite underlying the kaolin deposit has been considered. Moreover, the close relationship between this kaolinitic saprolite and kaolin deposit is expected as a window to elucidate the formation condition for high quality kaolin deposit[1]. In this study, we investigated mineralogical characteristics of kaolinitic saprolite and chemical forms of iron which is undesirable impurity for industrial uses.

The samples used were obtained from the active mining area in the northern Seto-city, Aichi prefecture, where the kaolin deposits are embedded in the lower Tokai Group, Seto porcelain clay formation (Late Miocene to Pliocene). Several samples were collected from Kibushi, Gaerome clays and kaolinitic saprolite (hereafter “Green saprolite”, named after its greenish grey color). Bulk and the elutriated clay fraction of 0.2 –2 μm size were analyzed by XRF, powder XRD and SEM-EDS to clarify the chemical and mineralogical compositions. All of three types of clays (Kibushi, Gaerome and Green saprolite) consist of quartz, feldspar and kaolinite, but SEM found the difference in kaolinite morphology: The kaolinite in Kibushi and Gaerome clays were fine particles, whereas Green saprolite contained both larger (~ several hundreds of μm), highly crystalline kaolinite grains and fine particles. Further analysis indicated that the fine kaolinite particles were derived from feldspar and the larger crystalline grains were formed by alteration of biotite. Dithionite-citrate-bicarbonate (DCB)[2] extractable Fe was measured to distinguish the free Fe from the structural Fe in the total Fe in both bulk and clay fraction of Green saprolite. More than the half of Fe in the clay fraction was extractable by the DCB method, while only ~ 25% of Fe in the bulk was extracted. This indicate that Fe in the clay fraction was distributed both in the structure of kaolinite and low crystalline, ferric iron hydroxides/oxides, and the bulk sample including the larger kaolinite grains contained structural Fe in the remnants of altered biotite. Further analysis using Mö ssbauer spectroscopy indicated that Fe valence ratio (Fe^{2+}/Fe^{3+}) in the fine kaolinite particles of the green saprolite was 7/5, and this Fe^{2+} is the possible cause of its greenish color. Our analysis suggests that the Green saprolite layer can be improved as a resource of kaolin commodity by separating clay fractions and removing free iron in hydroxides/oxides.

References

[1] Takagi, T., Shin, K. C., Jige, M., Hoshino, M., & Tsukimura, K. (2021). Microbial nitrification and acidification of lacustrine sediments deduced from the nature of a sedimentary kaolin deposit in central Japan. *Scientific Reports*, 1–17.

©2021. Japan Geoscience Union. All Right Reserved.

[2] Mehra, O. P., & Jackson, M. L. (1958). Iron oxide removal from soils and clays by a dithionite-citrate system buffered with sodium bicarbonate. *Clays and Clay Minerals*, *7*(1), 317–327.

Keywords: kaolinite, Green saprolite, SEM-EDS, DCB method

©2021. Japan Geoscience Union. All Right Reserved.

Borate concentration processes in modern evaporitic and hydrothermal environments: Constraints on the formation of a boron-rich environment on prebiotic earth

*Sara Rinka Christensen [1], Akizumi Ishida[1], Takeshi Kakegawa[1]

1. Department of Earth Science, Graduate School of Science, Tohoku University

Boron-rich environments are favored places for the evolution of prebiotic nucleotides. Modern evaporitic borate basins are often considered as modern analogs of ancient boron-rich environments. Despite this, the (1) source of highly concentrated boron, (2) factors in accumulation of boron, and (3) post-deposition modification of initial boron-bearing minerals in modern evaporitic borate basins are not yet decided.

In order to approach the above problems, the borate mine in Boron, California (= ‘Boron mine’, hereafter), and boron-enriched (up to 980 ppm) hot spring waters of Shin-appi hot spring, Iwate prefecture were studied. The Boron mine in California is one of the biggest boron-ore mines in the world. A huge borax occurs together with Miocene lake sediments. At Shin-appi hot spring in Iwate prefecture, which has the highest boron concentration in the region, aragonite and calcite precipitates rapidly around the discharging areas. Geochemical and mineralogical studies were performed on samples from Boron mine and Shin-appi hot spring which include mineral precipitate and water samples.

Shin-appi hot spring was abnormally enriched in bicarbonate, sodium, LILEs, REEs and radioactive elements. Measured $d^{13}C$ values of dissolved inorganic carbon ranged from -5 to -3 per mil. Such geochemical characteristics suggest that the source of boron-rich waters at Ninohe are deep magmatic brines evolved from felsic plutons. No boron-containing minerals were found in the precipitates, although the chemistry of the water seemingly allows for the formation of tourmalines and other boro-silicates. Instead, borax was found precipitating from an actively evaporating area with minor halite. This suggests the difficulty to precipitate boron-bearing minerals in aquatic environments, even with the high availability of boron.

Chemical analyses of borax and kernite samples from the Boron mine indicated that both were enriched in water-mobile heavy elements. These heavy metals were likely supplied by hydrothermal activity through the constraining faults of the mine. Magmatic brines formed by ancient felsic magma were considered as a source of boron-rich hydrothermal fluids at Boron mine, the same as in Shin-appi hot spring. Ancient boron-rich hydrothermal fluids were discharged into the evaporitic sedimentary basin at the Boron mine, where boron minerals initially precipitated with other chemical and clastic components. The texture of borax and kernite indicate that initial boron minerals were dissolved and reprecipitate as borax and kernite during later diagenesis, by separating other chemical and clastic components. Such later processes could further concentrate boron in a specific environment.

From the above, we found that evaporitic borate deposits may require (1) brine evolved from felsic plutons, (2) rapid separation of components other than borate, and (3) reprecipitation by diagenesis. This environment may have occurred on the surface of the proto-arc on the early Earth, which was likely ideal for the evolution of prebiotic nucleotides.

©2021. Japan Geoscience Union. All Right Reserved.

©2021. Japan Geoscience Union. All Right Reserved.

Experimental study on propagation of elastic wave in supercritical geothermal reservoirs

*Katsuya Mizuno[1], Noriyoshi Tsuchiya[1], Nobuo Hirano[1]

1. Tohoku university

Elastic wave velocity of rocks have been applied to the exploration of geothermal resources in geothermal development or the understanding of underground structures. Many laboratory scale studies have been conducted on elastic wave velocity measurements of rocks used to interpret seismic data measured in the field, but most of them were conducted under room temperature and pressure. However, Since the physical properties of rocks has changed by temperature and pressure, it is important to measure the elastic wave velocity of rocks under the in situ high temperature and pressure conditions of underground in order to achieve more accurate geothermal resource exploration. J.W. Spencer Jr & A.M. Nur, (1976), H.B. Morta & F. Wuttke, (2016) has measured elastic wave velocity in supercritical conditions of granite and amphibolite, respectively. In order to develop geothermal energy in more deep-seated regions in the future, elastic wave velocity measurements for other rocks will be necessary. The purpose of this study is to provide a new interpretation of seismic data through the measurement of elastic wave velocity of rocks under supercritical water conditions.

In this study, we started by measuring the elastic wave velocity of water as a function of temperature in order to prove that the elastic wave measurement data obtained from the experimental system for in situ measurements is correct. Then we measured the elastic wave velocity for gabbro, which is universally present in the lower crust, and compare it with the data for granite measured under the same conditions.

References

James W. Spencer Jr., Amos M. Nur, The effects of pressure, temperature, and pore water on velocities in westerly granite, JGR Vol.81, Issue5, 10 February 1976, 899-904

H.B. Morta & F. Wuttke, Temperature dependence of elastic P- and S-wave properties of rocks: Applications to geothermal reservoir evaluation, Energy Geotechnics (2016), 311-316

Keywords: Supercritical fluid, Supercritical geothermal reservoirs, Elastic wave

©2021. Japan Geoscience Union. All Right Reserved.

[J] Oral | S (Solid Earth Sciences)：S-CG Complex & General

Sun. Jun 6, 2021 1:45 PM - 3:15 PM JST | Sun. Jun 6, 2021 4:45 AM - 6:15 AM UTC | Ch.18 Zoom Room 18

[S-CG53] Reducing risks from earthquakes, tsunamis & volcanoes: new applications of realtime geophysical data

convener:Masashi Ogiso(Meteorological Research Institute, Japan Meteorological Agency), Masumi Yamada(Disaster Prevention Research Institute, Kyoto University), Yusaku Ohta(Research Center for Prediction of Earthquakes and Volcanic Eruptions, Graduate School of Science, Tohoku University), YAMAMOTO Naotaka CHIKASADA(National Research Institute for Earth Science and Disaster Resilience), Chairperson:Naotaka YAMAMOTO CHIKASADA(National Research Institute for Earth Science and Disaster Resilience), Yusaku Ohta(Research Center for Prediction of Earthquakes and Volcanic Eruptions, Graduate School of Science, Tohoku University)

As the number of population centers grows in regions with earthquake, tsunami and volcano hazards, the importance of improving methods for rapid, realtime estimates of activity increases. Realtime monitoring, analysis, and prediction of seismic ground motion, crustal movement and tsunami will be powerful tools to contribute to earthquake and tsunami disaster preparedness/mitigation. Tsunami and Earthquake Early Warning systems exist today in many locations around the world. Now JMA has started to promptly provide Eruption Notices to inform people of impending and beginning volcanic eruptions. Large events like the 2011 Tohoku Earthquake (Mw9.0) have demonstrated some of the shortcomings of existing techniques. In this session, we invite presentations on new ideas, methods and applications of (near) realtime analysis of seismic, geodetic and tsunami data, to the problem of realtime prediction aimed at improving disaster preparedness/mitigation in the fields of earthquake, tsunami and volcano observation. Presentation is encouraged to bring together scientists, engineers, and practitioners from a broad range of backgrounds from around the world, and to promote collaborative communication at the leading edge of the science and technologies.

1:45 PM - 2:00 PM JST | 4:45 AM - 5:00 AM UTC

[SCG53-01] An advanced system for automatic strong gust detection and warning for railroads using deep learning

★Invited Papers

*Kusunoki Kenichi[1], Toru Adachi[1], Hanako Inoue[1], Osamu Suzuki[1], Naoki Ishitsu[2], Ken-ichiro Arai[2], Chusei Fujiwara[3], Hiroto Suzuki[3] (1.Meteorological Research Institute, 2.Alpha-denshi Co., Ltd., 3.East Japan Railway Company)

2:00 PM - 2:15 PM JST | 5:00 AM - 5:15 AM UTC

[SCG53-02] Tsunami observation and development of real-time tsunami detection by using ocean surface radar

★Invited Papers

*Ryotaro Fuji[1], Kohei Ogata[2], Hirofumi Hinata[3] (1.Kokusai Kogyo Co., Ltd., Ehime University, 2.Kokusai Kogyo Co., Ltd., 3.Ehime University)

2:15 PM - 2:30 PM JST | 5:15 AM - 5:30 AM UTC

[SCG53-03] Preliminary comparison of strong-motion parameters at the land & ocean bottom sites for the 2021 Mw 7.1 Off Fukushima Prefecture earthquake

*Yadab Prasad Dhakal[1], Wataru Suzuki[1], Takashi Kunugi[1], Takeshi Kimura[1], Shin Aoi[1] (1.National Research Institute for Earth Science and Disaster Resilience)

2:30 PM - 2:45 PM JST | 5:30 AM - 5:45 AM UTC

[SCG53-04] Development of GNSS Real-time analysis including QZSS

*Satoshi ABE[1], Keitaro Ohno[1], Naofumi Takamatsu[1], MURAMATSU Hiroki[1], Tomoaki FURUYA[1], Yohei HIYAMA[1] (1.Geospatial Information Authority of Japan)

2:45 PM - 3:00 PM JST | 5:45 AM - 6:00 AM UTC

[SCG53-05] IPFx: extended integrated particle filter method for earthquake early warning and visualization of its results with social networking service

*Masumi Yamada[1], Koji Tamaribuchi[2], Stephen Wu[3] (1.Disaster Prevention Research Institute, Kyoto University, 2.Meteorological Research Institute, 3.Institute of Statistical Mathematics)

3:00 PM - 3:15 PM JST | 6:00 AM - 6:15 AM UTC

[SCG53-06] Near real-time estimation of hypocenter distribution from seismic amplitudes

*Masashi Ogiso[1] (1.Meteorological Research Institute, Japan Meteorological Agency)

An advanced system for automatic strong gust detection and warning for railroads using deep learning

*Kusunoki Kenichi[1], Toru Adachi[1], Hanako Inoue[1], Osamu Suzuki[1], Naoki Ishitsu[2], Ken-ichiro Arai[2], Chusei Fujiwara[3], Hiroto Suzuki[3]

1. Meteorological Research Institute, 2. Alpha-denshi Co., Ltd., 3. East Japan Railway Company

In 2007, the Meteorological Research Institute and the East Japan Railway company started a project to develop an automatic strong gust detection and warning system for railroads , which the decision to warn is based upon information from a single-Doppler radar at low elevation angles. Through over ten years of R&D, it had reached the stage of practical application with a reliable real-time performance and a comprehensive operational system has been implemented in some areas over the coast of the Sea of Japan (limited to Yamagata, Akita, and Niigata Prefectures) . In this presentation, we will introduce an overview of the project since the introduction of the operational system since 2017 and the recent progresses especially about the use of deep learning. Possibilities for further development of the sysytem and their application to other traffic systemss will be also discussed.

This study is partly supported by Cabinet Office, Government of Japan, Public/Private R&D Investment Strategic Expansion Program (PRISM).

Keywords: tornado, Doppler radar

©2021. Japan Geoscience Union. All Right Reserved.

Tsunami observation and development of real-time tsunami detection by using ocean surface radar

*Ryotaro Fuji[1], Kohei Ogata[2], Hirofumi Hinata[3]

1. Kokusai Kogyo Co., Ltd., Ehime University, 2. Kokusai Kogyo Co., Ltd., 3. Ehime University

Ocean surface radar is a land-based remote sensing instrument that emits radio waves toward the ocean and receives radio waves backscattered by ocean waves to measure ocean surface currents from the frequency difference between the transmitted and received waves. The advantage of this radar is that it enables observation from the vicinity of the continental shelf edge to a harbor area with high resolution (spatial resolution 0.5 to 3 km, time resolution 2 minutes). Ocean surface radar first succeeded in observing the flow velocity of the tsunami generated by the 2011 Tohoku-Oki earthquake (e.g., Hinata et al., 2011). Since this success, real-time tsunami detection using ocean surface radar has been developed (e.g., Grilli et al., 2016).

On the other hand, tsunami detection accuracy with ocean radar depends on the SNR (ratio of the intensity of the received signal to external noise), so the detection performance should be statistically evaluated based on tsunami measurement data under various SNR conditions. However, the only tsunamis for which observation data have been acquired by ocean surface radar thus far are the 2012 tsunami in Indonesia and the meteotsunami in the US, and the data were insufficient for statistical evaluation. To solve this problem, a method called a virtual tsunami observation experiment has been proposed (Fuji and Hinata, 2017), and real-time tsunami detection has been developed based on this method (Ogata et al., 2018).

In this presentation, we will introduce the method of tsunami observation using ocean surface radar and the development of real-time tsunami detection, and discuss the utilization of ocean radar in tsunami disaster mitigation.

Keywords: Ocean surface radar, Tsunami, Tsunami mitigtation

©2021. Japan Geoscience Union. All Right Reserved.

Preliminary comparison of strong-motion parameters at the land & ocean bottom sites for the 2021 Mw 7.1 Off Fukushima Prefecture earthquake

*Yadab Prasad Dhakal[1], Wataru Suzuki[1], Takashi Kunugi[1], Takeshi Kimura[1], Shin Aoi[1]

1. National Research Institute for Earth Science and Disaster Resilience

The 2021 Mw 7.1 Off Fukushima Prefecture earthquake is the largest magnitude earthquake in the Japan Trench area that was successfully recorded by all the 150 stations of S-net (Seafloor observation Network for Earthquake and Tsunami along the Japan Trench) after the start of the network. The Japan Meteorological Agency focal depth of the event was 55 km. The moment tensor solution of F-net (National Research Institute for Earth Science and Disaster Resilience, NIED) showed that the earthquake was a reverse fault event. The distribution of hypocenters of the aftershocks suggested that the event occurred inside the subducting Pacific Plate (NIED, 2021). This event was recorded by about 1060 strong-motion stations of MOWLAS acronym for Monitoring of Waves on Land and Seafloor operated by NIED, including the 150 stations of the S-net (Aoi et al. 2020). The largest peak ground acceleration (PGA) of approximately 1425 cm/s^2 was recorded at site MYGH10, located at the epicentral distance of about 70 km. This PGA value was larger than the PGA value of 1030 cm/s^2 recorded at the same site during the 2011 Mw 9.1 Tohoku-Oki earthquake. It is known that the cylindrical casings of S-net stations are prone to rotate during strong motions, adding artificial noises and offsets to the acceleration records. However, the X-component that is aligned along the long axis of the cylindrical casing is found to be generally less affected by the rotation of the cylindrical casing. The maximum X-component PGA of about 1100 cm/s^2 was recorded at the S-net S2N02 site at the epicentral distance of about 7 km. The X-component peak ground velocity (PGV) at the S2N02 site was about 50 cm/s, while the PGV at the MYGH10 was about 75 cm/s. We compared the X-component PGAs and PGVs from all the S-net sites with those on land recorded by K-NET and KiK-net of MOWLAS, operated by NIED, with respect to the ground motion prediction equation (GMPE) by Si and Midorikawa (1999). We found that the PGA values at the ocean bottom and land sites were, on average, similar within the hypocentral distance of 200 km. On the other hand, the X-component PGVs at the S-net sites were, on average, larger at the S-net sites. Dhakal et al. (2020) pointed out that the larger PGVs at the S-net sites were most probably due to the lower S-wave velocity of the subsea sediments. We also compared the absolute velocity response spectra (AVRS) in the period range of 1 to 10 s at the land and S-net sites with respect to the GMPE by Dhakal et al. (2015). The AVRS were computed from the two horizontal component records (see Dhakal et al. 2015 for details). We used the J-SHIS (Japan Seismic Hazard Information Station, Fujiwara et al. 2012) model to correct the deep soil amplification effect at both land and S-net sites. Similar to the case of PGVs, we found that the observed AVRS values at the S-net sites were, on average, larger than those at the land sites, and the root mean square errors (RMSE) for the S-net sites were slightly larger than those for the land sites. The RMSE values' differences are generally expected as the velocity model at the S-net sites is not well resolved compared with the velocity model on land. We are currently working on larger data set to understand the features of S-net strong-motion records for real-time application and report the results in future papers.

References:

©2021. Japan Geoscience Union. All Right Reserved.

Aoi et al. (2020). Earth Planets Space 72, 126.

Dhakal et al. (2020). Japan Geoscience Union Meeting, SSS04-10.

Dhakal et al. (2015). Journal of Japan Association for Earthquake Engineering, 15(6):91-111.

Fujiwara et al. (2012). Technical Note of the National Research Institute for Earth Science and Disaster Prevention, No. 379.

NIED (2021). The 2021-02-13 Off Fukushima Prefecture Earthquake (in Japanese), https://www.hinet.bosai.go.jp/topics/off-fukushima210213/?LANG=ja, accessed 2021/2/17.

Si H, S. Midorikawa (1999). Journal of Structural and Construction Engineering Transactions of AIJ 523:63–70.

Keywords: Ocean bottom seismographs, S-net, The 2021 Mw 7.1 off Fukushima Prefecture earthquake, MOWLAS, PGA, PGV, Long-period ground motions

©2021. Japan Geoscience Union. All Right Reserved.

Development of GNSS Real-time analysis including QZSS

*Satoshi ABE[1], Keitaro Ohno[1], Naofumi Takamatsu[1], MURAMATSU Hiroki[1], Tomoaki FURUYA[1], Yohei HIYAMA[1]

1. Geospatial Information Authority of Japan

Displacement obtained by real-time GNSS positioning isn't saturate for large earthquakes, which directly measure the amount of ground deformation. The Geospatial Information Authority of Japan (GSI) operates REGARD (REal-time GEONET Analysis system for Rapid Deformation monitoring), which estimates a finite fault model based on a continuous GNSS observation network called GEONET.

REGARD conducts real-time kinematic (RTK) analysis using data from two observation points, but if one of the observation stops, the solution cannot be obtained. In particular, if the observation stops at a reference station, the effect will spread to results of all other stations. In addition, earthquakes that occur in the vicinity of a reference station have the weakness of making it appear as if crustal movement has occurred all over Japan. In order to overcome these weaknesses of relative positioning, we attempted to introduce Precise Point Positioning (PPP), which does not have the disadvantages of relative positioning because PPP can perform positioning alone. However, various kinds of correction information is required for accurate PPP.

In this study, we performed real-time PPP positioning by estimating satellite orbits and clocks in real time, including the Japanese positioning satellite MICHIBIKI (QZSS), and generating correction information. In this presentation, we present the results of our research and report the evaluation of the accuracy of real-time PPP, the comparison result with REGARD.

Keywords: REGARD, GEONET, PPP, QZSS

©2021. Japan Geoscience Union. All Right Reserved.

IPFx: extended integrated particle filter method for earthquake early warning and visualization of its results with social networking service

*Masumi Yamada[1], Koji Tamaribuchi[2], Stephen Wu[3]

1. Disaster Prevention Research Institute, Kyoto University, 2. Meteorological Research Institute, 3. Institute of Statistical Mathematics

We improve the integrated particle filter (IPF) method, which is a new source determination algorithm recently incorporated into the Japanese earthquake early warning system. The problem of the current IPF method is that it uses specific trigger information as an input and is therefore applicable to only limited seismic networks. This study proposes the extended IPF (IPFx) method to deal with continuous waveforms and merge all Japanese real-time seismic networks into a single framework.

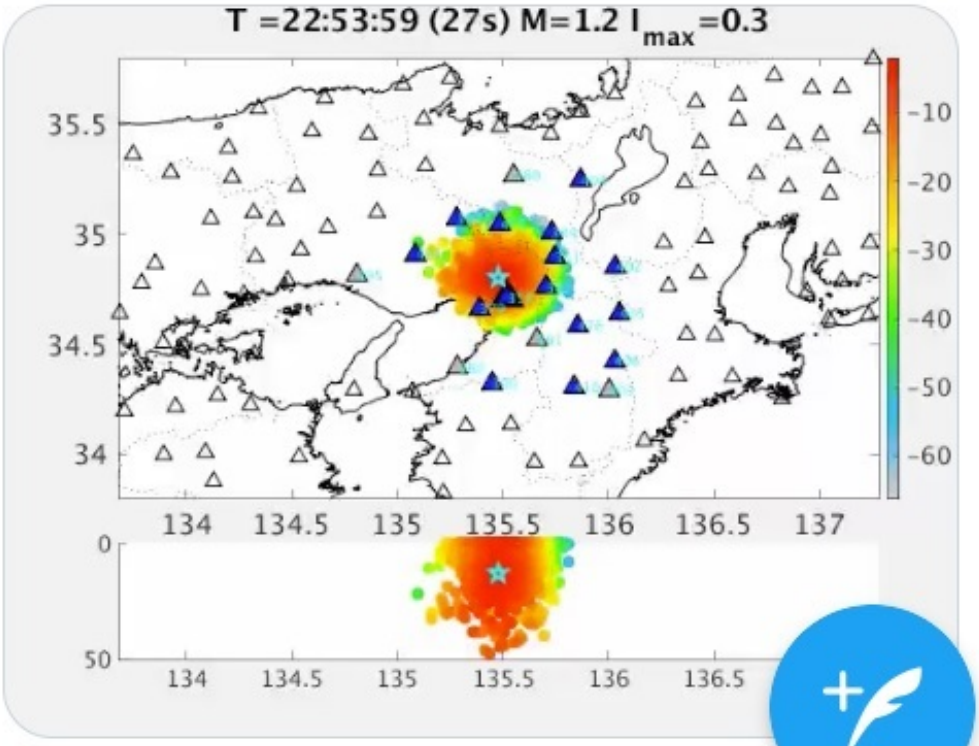
The new source determination algorithm processes seismic waveforms in two stages. The first stage (single-station processing) extracts trigger and amplitude information from continuous waveforms. The second stage (network processing) accumulates information from multiple stations and estimates the location and magnitude of ongoing earthquakes based on Bayesian inference. In a 10-month continuous online test, this method performed better than the JMA EEW method in detecting earthquakes with a maximum seismic intensity >=3 as per the JMA manual catalog. By merging multiple networks into a single method, both the P-wave detection and the event detection speeds were significantly improved compared to those of the current JMA EEW method.

We also developed an automatic processing system to visualize the results of the IPFx method in real-time. We use “Net::Twitter”, a perl interface to the Twitter API. The results of the IPFx method (time histories of the estimated source parameters, time histories of the trigger information, and waveforms aligned as a function of distance from the estimated location) are uploaded online a few minutes after the event detection. Currently, the tweets are protected by password and open for only limited users. The advantage of using twitter is that we can access the results anytime and anywhere. We can monitor the performance of the online IPFx system without accessing servers. The results will be uploaded automatically without human interactions. The tweets also work as a super-rapid earthquake report. The IPFx method can detect earthquakes as small as M=1 for inland, so we are able to monitor the seismicity of small earthquakes with only a few minutes latency.

Keywords: earthquake early warning, IPFx method, strong motion, source estimation

©2021. Japan Geoscience Union. All Right Reserved.

2020/08/27,22:53:54.5_34.80_135.48_13.0km_M1.2_15/1/0_1



©2021. Japan Geoscience Union. All Right Reserved.

Near real-time estimation of hypocenter distribution from seismic amplitudes

*Masashi Ogiso[1]

1. Meteorological Research Institute, Japan Meteorological Agency

Hypocenter distribution is important information for monitoring seismicity. In general, arrival times of seismic waves are used to determine hypocenters, but it is difficult to read arrival times when seismicity becomes active, resulting in a decrease in the numbers of hypocenters.

The amplitude source location (ASL) method uses seismic amplitudes to determine hypocenters. The ASL method does not require arrival times, but the precision of hypocenters is usually worse compared with that of arrival-time based hypocenters. Ogiso and Yomogida (2021, EPS) has proposed a method to estimate relative source locations of seismic events from seismic amplitude ratios. The relative source locations by their method show a good agreement with those estimated using phase arrival times. Hence, if the method of Ogiso and Yomogida (2021) could be applied in near real-time, the hypocenter distribution derived by the method would complement that derived by phase-arrival-time based automated hypocenter location method (e.g., Tamaribuchi, 2018, EPS), and the method would be useful for monitoring seismicities in real-time.

First, we applied the method to the continuous waveforms recorded on 29 September 2008 at Meakandake volcano. A volcanic tremor that occurred on 14:11 had activated seismicity at the volcano. The number of earthquakes that occurred from 14:00 to 16:00 was about 230 according to Sapporo District Meteorological Observatory, in which 34 earthquakes were estimated there hypocenters. We successfully estimated hypocenters of 103 earthquakes in that time window by applying the method.

Next, we conducted a synthetic test to investigate the applicability of the method in a wider region than in the case of volcanoes. The test was conducted in a focal region of the 2016 Kumamoto earthquake. At least an epicenter can be appropriately estimated for the earthquake about 26 km far from the reference event if we calculated amplitude at each station appropriately, that is, amplitude calculation considering the difference of arrival times between the reference and target events. This result implies that the method might be useful for hypocenter determination of aftershocks automatically after a large earthquake with an appropriate correction of arrival times when measuring the amplitude of each subevent at each station.

Keywords: seismic amplitude, hypocenter distribution, real-time analysis

©2021. Japan Geoscience Union. All Right Reserved.

[J] Poster | S (Solid Earth Sciences)：S-CG Complex & General

Sun. Jun 6, 2021 5:15 PM - 6:30 PM JST | Sun. Jun 6, 2021 8:15 AM - 9:30 AM UTC | Ch.16_1

[S-CG53] Reducing risks from earthquakes, tsunamis & volcanoes: new applications of realtime geophysical data

convener:Masashi Ogiso(Meteorological Research Institute, Japan Meteorological Agency), Masumi Yamada(Disaster Prevention Research Institute, Kyoto University), Yusaku Ohta(Research Center for Prediction of Earthquakes and Volcanic Eruptions, Graduate School of Science, Tohoku University), YAMAMOTO Naotaka CHIKASADA(National Research Institute for Earth Science and Disaster Resilience)

As the number of population centers grows in regions with earthquake, tsunami and volcano hazards, the importance of improving methods for rapid, realtime estimates of activity increases. Realtime monitoring, analysis, and prediction of seismic ground motion, crustal movement and tsunami will be powerful tools to contribute to earthquake and tsunami disaster preparedness/mitigation. Tsunami and Earthquake Early Warning systems exist today in many locations around the world. Now JMA has started to promptly provide Eruption Notices to inform people of impending and beginning volcanic eruptions. Large events like the 2011 Tohoku Earthquake (Mw9.0) have demonstrated some of the shortcomings of existing techniques. In this session, we invite presentations on new ideas, methods and applications of (near) realtime analysis of seismic, geodetic and tsunami data, to the problem of realtime prediction aimed at improving disaster preparedness/mitigation in the fields of earthquake, tsunami and volcano observation. Presentation is encouraged to bring together scientists, engineers, and practitioners from a broad range of backgrounds from around the world, and to promote collaborative communication at the leading edge of the science and technologies.

[SCG53-P01] High precision of Realtime tsunami prediction based on the amplification

*Narumi Takahashi[1], Kentaro Imai[2] (1.National Research Institute for Earth Science and Disaster Resilience, 2.Japan Agency for Marine-Earth Science and Technology)

[SCG53-P02] Generation Requirements of PL Waves for Shallow Earthquakes around Japan-Possibility of Immediate Tsunami Prediction

*Keishi Osuga[1], Takashi Furumura[1] (1.Department of Earth and Planetary Science, School of Science, The University of Tokyo)

[SCG53-P03] Evaluation of simple source time function in rapid source parameter determination system (AQUA)

*Hisanori Kimura[1], Youichi Asano[1] (1.National Research Institute for Earth Science and Disaster Resilience (NIED))

High precision of Realtime tsunami prediction based on the amplification

*Narumi Takahashi[1], Kentaro Imai[2]

1. National Research Institute for Earth Science and Disaster Resilience, 2. Japan Agency for Marine-Earth Science and Technology

We have developed a realtime tsunami prediction system based on the tsunami amplification. The system predicts tsunami arrival times, the heights, inundation area and inundation depth for each target points in turn, in proportion to observed pressure values on observatories of the oceanfloor network like Dense Oceanfloor Network system for Earthquakes and Tsunamis (DONET). The prediction information is extracted from a database of the system for the observatories, which composed of calculated waveforms using many fault models changing the magnitude, depth, dip angle and strike. The merits are simplified system using only one PC playing a roles data transmission, making prediction information and visualization, easy revise even though coastline changes, and robustness of the prediction under the local anomalies of tsunami by landslides on the seafloor. We implemented it on local government of Wakayama and Mie prefectures and an electric power company using DONET. Recently, it was implemented on Chiba prefecture using Seafloor observation network for earthquakes and tsunamis along the Japan trench (S-net).

The error of the prediction is brought by following items, which are noises on observatories of the oceanfloor network, complicated tsunami propagation for the local topography, and contamination of the crustal displacement on the observatories. S-net data sometimes includes large offset for the strong motion due to rotation and unstable posture of the sensor. Sometimes observatories subside by liquefaction on seafloor. We resolved this noise issue statistically by comparison of the observed data among the triggered sensor and dismissal of abnormal data. Second issue of dispersion of the tsunami height due to complicated tsunami propagation are resolved by specification of fault models using detected direction of the source. For the last issue of contamination of the composition of crustal displacement, we introduce distribution of the observed crustal displacement on the oceanfloor network and omit fault models with large difference of the composition of crustal displacement. In particular, The crustal displacement around the prediction target point brings large dispersion on the inundation areas. We realized the high precision of the tsunami prediction by devise on settings and extraction of the fault models.

Keywords: Oceanfloor network system, pressure data

©2021. Japan Geoscience Union. All Right Reserved.

Generation Requirements of PL Waves for Shallow Earthquakes around Japan-Possibility of Immediate Tsunami Prediction

*Keishi Osuga[1], Takashi Furumura[1]

1. Department of Earth and Planetary Science, School of Science, The University of Tokyo

PL is a long period phase with a period of several seconds to several tens of seconds, which is observed between P wave and S wave. P-waves emitted from shallow epicenters interfere with each other as they propagate through the crust by multiple wide-angle reflections, forming long-period wave groups. Sommville (1930) named this wave PL, meaning P-long wave, which was later interpreted by Oliver and Major (1960) as the leaking mode of Rayleigh waves. A longer-period (100-1000 s) phase generated by a similar mechanism in the upper mantle was named W-phase by Kanamori (1993) and is widely used for CMT analysis of large earthquakes and immediate tsunami prediction. Recently, W-phase analysis has also been applied to wave groups with periods of tens of seconds or less (i.e., PL waves) in near-field strong-motion records (e.g., Duputel et al., 2012; Hayes et al., 2009; Usui and Yamauchi, 2013). In this study, in order to utilize the PL waves in the near-field wavefield as an indicator to immediately determine the possibility of tsunami generation, the characteristics of PL waves in large trench earthquakes and their generation and propagation requirements were investigated based on seismic wave propagation simulations.

As an example of PL waves observation, Figure 1a shows the vertical motion velocity record of K-NET during the foreshock of the 2009/3/9 off the Pacific coast of the Eastern Japan Earthquake (M7.3, 8 km depth). At the AOM014 (K-NET Nenokuchi) station, located at the epicentral distance of 310 km, a wave group of PL waves with a period of about 20 s is clearly observed between the P and S phases of the Radial (R) and Vertical (Z) components. It is possible to evaluate the size and depth of the earthquake, namely the possibility of tsunami generation, from the seismic amplitude of PL waves in the near-field strong-motion records.

In order to confirm the generation and propagation characteristics of PL waves caused by shallow, large trench earthquakes, we performed seismic wave propagation simulations using the two-dimensional finite difference method. We selected a cross-sectional area from off Miyagi to northeast Japan (Fig. 2a), set up sedimentary layers, crust and mantle structures using the JIVSM (Koketsu et al., 2012) model, and calculated seismic wave propagation. The epicenter was set as a point source for simplicity, and seismic waves were radiated using a triangular source-time function with a period of 20 seconds based on the GCMT analysis results of the 2009/3/9 earthquake. The record section of the Z-component velocity waveform is shown in Figure 2b. The record section of the Z-component velocity waveform is shown in Figure 2b, and the waveforms at the epicenter distance of 310 km for different source depths of 1, 2, 4, 8, 16, 32, and 64 km are compared in Figure 2c. As a result, it is confirmed that PL waves with the same amplitude as S waves or Rayleigh waves are generated in earthquakes shallower than 8 km depth, and the amplitude weakens with depth.

©2021. Japan Geoscience Union. All Right Reserved.

Observations of PL waves with periods of about 20 s in large (>M7) and shallow (< 40 km) epicentral earthquakes occurring in the ocean may provide a simple assessment of tsunami generation potential prior to CMT inversion analysis of W-phase (PL waves) using far- and near-field waveform records. Earthquakes that occurred inland and propagated overland are dominated by short-period PL waves with periods around 7 s (Furumura and Kennett, 2018), which can be distinguished from earthquakes that occurred in the ocean. In this study, we focused on the Miyagi-oki earthquake. However, the propagation characteristics and prevailing period of PL waves are considered to be affected by deep structures such as the thickness of the crust, as shown by the difference in PL waves between land and sea propagation paths. It is necessary to confirm the regional characteristics of PL wave propagation by analyzing observed waveforms and simulating seismic wave propagation in other regions, such as along the Nankai Trough and the eastern margin of the Japan Sea.

Keywords: PL Waves, Seismic Wave Propagation, Difference Method, Immediate Tsunami Prediction

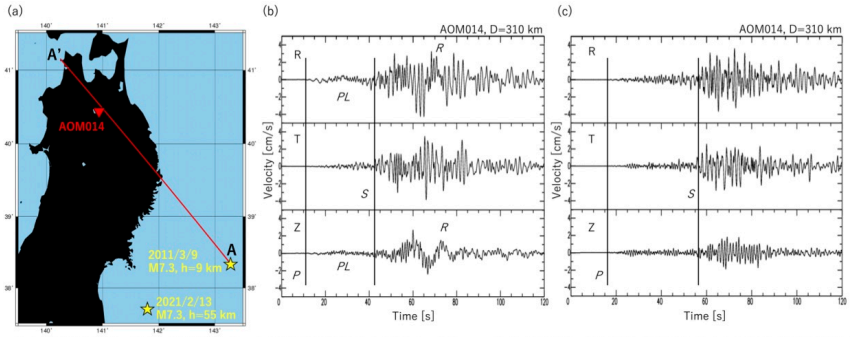


図１ 海溝型地震に見られるPL波の例。(a)震源と観測点およびスナップショットの水平位置。(b)2011/3/9東北地方太平洋沖地震の前震（M7.3、深さ8 km）の３成分速度波形と、Radial/Vertical成分のＰ～Sの間に見られる卓越周期20秒のPL波。(c) 2021/2/13福島県沖の地震（M7.3, 深さ55 km）。

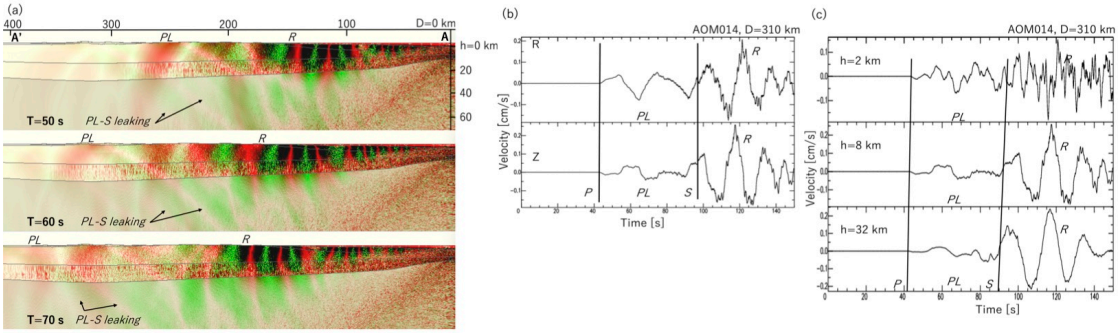


図２　２次元差分法による地震波伝播シミュレーション結果。(a) 地震波伝播のスナップショット（赤がP波、緑はS波を表す）。地震発生から、50、60、70秒後。
(b) AOM014観測点（震源距離310 km）におけるRadial/Vertical成分速度波形、(c)　震源の深さを2、8、32kmとした場合の、同観測点における上下動速度波形とPL波の波形変化。

©2021. Japan Geoscience Union. All Right Reserved.

Evaluation of simple source time function in rapid source parameter determination system (AQUA)

*Hisanori Kimura[1], Youichi Asano[1]

1. National Research Institute for Earth Science and Disaster Resilience (NIED)

In the rapid source parameter determination system called Accurate and QUick Analysis System for Source Parameters (AQUA), source parameters including location, size, and moment tensor (MT) are automatically determined with good accuracy. By incorporating the velocity type strong motion seismometer in the NIED full-range seismograph network (F-net) and changing the processing flow, it became possible to analyze the 2011 off the Pacific coast of Tohoku earthquake (M9.0)(Kimura et al., 2020). However, its size was underestimated as Mw8.6. Since appropriate estimation of the earthquake size is important for disaster mitigation including tsunami warning and initial damage assessment, the simple source time function (STF) in AQUA was evaluated, as suggested by Asano and Kimura (2012).

The isosceles triangle type STF is incorporated into the current processing flow after determining the MT solution with fixed horizontal location (called as ´AQUA-MT´) and its source duration is estimated by a grid search. Here, the centroid time and depth are fixed to those of AQUA-MT to shorten the processing time. When the variance reduction (VR) decreases, the source duration with the highest VR is used hereafter, including the horizontal location estimation (called as ´AQUA-CMT´). Based on this flow, we reanalyzed the 2011 Off Tohoku earthquake and its major aftershocks and earthquakes with Mw6.8 or greater. In addition, the 2003 Tokachi-oki Earthquake (Mjma8.0) and the 2004 Kii Peninsula and Tokaido-oki earthquake (Mjma7.4) were reanalyzed as past major earthquakes. For these two earthquakes, waveform data recorded by the F-net broadband seismometer with epicentral distance of 400 km or more is used.

In the 2011 Off Tohoku earthquake, selecting a 70 sec source duration increased VR from 67.0% to 81.4% and Mw from 8.6 to 8.8. The centroid time, depth, and the focal mechanism are almost the same. The additional processing time was estimated to be about 1 sec. The source duration of major aftershocks of the 2011 Off Tohoku earthquake (15:08 and 15:15, 11 March 2011 (JST); Mjma7.4 and 7.6; note that the latter is the largest aftershock) and two past major earthquakes were estimated as 50, 30, 40, and 40 sec, respectively. Mw increased from 7.4 to 7.6, 7.8 to 7.9, 7.8 to 8.0, and 7.4 to 7.5, respectively.

The incorporation of the STF reduced the underestimation of Mw for the 2011 Off Tohoku earthquake while its size is still underestimated. The source duration of 70 sec is comparable with analysis of rupture process (e.g., Suzuki et al., 2012) and can be considered to represent a major part of the slip history. This duration is not negligible compared to the bandwidth of the analysis (50-200 sec). Hence, we can consider that the incorporation of the STF improved size underestimation. Mw of GlobalCMT for the aftershock on 15:15 and the 2003 and 2004 earthquakes are 7.9, 8.3, and 7.4, respectively. Incorporation of the STF reduced difference from GlobalCMT in most cases.

A grid search of the source duration with a fixed centroid time and depth suppresses a significant increase in processing time. Since STF is introduced only when VR increases after determination of AQUA-MT, the determination ratio would be maintained. By incorporating STF, we can expect to be able to better estimate earthquake size while maintaining process speed and determination ratio.

©2021. Japan Geoscience Union. All Right Reserved.

Keywords: the 2011 off the Pacific coast of Tohoku earthquake, rapid source parameter determination system, Centroid moment tensor

©2021. Japan Geoscience Union. All Right Reserved.

[J] Oral | S (Solid Earth Sciences)：S-CG Complex & General

Sun. Jun 6, 2021 9:00 AM - 10:30 AM JST | Sun. Jun 6, 2021 12:00 AM - 1:30 AM UTC | Ch.17 Zoom Room 17

[S-CG54] Ten years from the 2011 Tohoku Earthquake: A milestone of Solid Earth Science

convener:Ryota Hino(Graduate School of Science, Tohoku University), Shuichi Kodaira(Research Institute of Marine Geodynamics, Japan Agency for Marine-Earth Science and Technology), Toru Matsuzawa(Research Center for Prediction of Earthquakes and Volcanic Eruptions, Graduate School of Science, Tohoku University), Takeshi Iinuma(National Research and Development Agency Japan Agency for Marine-Earth Science and Technology), Chairperson:Takeshi Iinuma(National Research and Development Agency Japan Agency for Marine-Earth Science and Technology), Toru Matsuzawa(Research Center for Prediction of Earthquakes and Volcanic Eruptions, Graduate School of Science, Tohoku University)

In the 2011 JpGU Meeting held immediately after the 2011 Tohoku-Oki Earthquake, an emergency session related to this earthquake was set up and 188 research results were reported. Not only was there a preliminary report of research and observations regarding this giant earthquake and tsunami, but also various important ideas indicating directions of subsequent solid-earth science researches were presented: the mechanism of earthquake generation including possible processes leading its large-scaled seismic rupture, the impact of the Tohoku-Oki earthquake on the inland crust, and limitations and effectiveness of early warning regarding earthquakes and tsunamis. Ten years after the 2011 JpGU, which was held just two months after the quake, how far has our understanding of these research themes progressed? In addition to the accumulation of 10 years of researches, our understanding of giant earthquakes and tsunamis has dramatically increased through the observations of post-Tohoku Earthquake phenomena of various kinds that have been progressing over a long period of time and through the newly developed observation networks in the offshore area. In this session, not only the researches on the Tohoku-Oki earthquake and tsunami itself, but also the research results in various solid-earth science fields that have clarified after this earthquake and tsunami will be brought together, to discuss the direction of research that should be aimed at in the future.

9:00 AM - 9:05 AM JST | 12:00 AM - 12:05 AM UTC

[SCG54-01] Introduction

9:05 AM - 9:30 AM JST | 12:05 AM - 12:30 AM UTC

[SCG54-02] **Modeling stress field and deformation associated with the Tohoku-Oki earthquake: Understanding the dynamics of the northeastern Japan islands arc-trench system**

★Invited Papers

*Bunichiro Shibazaki[1], Ryohei Sasajima[2] (1.International Institute of Seismology and Earthquake Engineering, Building Research Institute, 2.Research Center for Earthquake Prediction, Disaster Prevention Research Institute, Kyoto University)

9:30 AM - 9:45 AM JST | 12:30 AM - 12:45 AM UTC

[SCG54-03] Temporal evolution of seafloor crustal deformation obtained by the 10-year-long GNSS-A observations after the 2011 Tohoku-oki earthquake

*Shun-ichi Watanabe[1], Tadashi Ishikawa[1], Yuto Nakamura[1], Yusuke Yokota[2] (1.Hydrographic and Oceanographic Department, Japan Coast Guard, 2.Institute of Industrial Science, University of Tokyo)

9:45 AM - 10:00 AM JST | 12:45 AM - 1:00 AM UTC

[SCG54-04] The slow earthquake spectrum in the Japan Trench illuminated by the S-net seafloor observatories

★Invited Papers

*Tomoaki Nishikawa[1], Takanori Matsuzawa[2], Kazuaki Ohta[2], Naoki Uchida[3], Takuya NISHIMURA[1], Satoshi Ide[4] (1.Disaster Prevention Research Institute, Kyoto University, 2.National Research Institute for Earth Science and Disaster Resilience, 3.Graduate School of Science and International Research Institute of Disaster Science, Tohoku University, 4.Department of Earth and Planetary Science, University of Tokyo)

10:00 AM - 10:15 AM JST | 1:00 AM - 1:15 AM UTC

[SCG54-05] A Decade of Lessons Learned from the 2011 Tohoku-oki Earthquake

*Naoki Uchida[1], Roland Bürgmann[2] (1.Research Center for Prediction of Earthquakes and Volcanic Eruptions Graduate School of Science, Tohoku University, 2.Department of Earth and Planetary Science, University of California, Berkeley)

10:15 AM - 10:30 AM JST | 1:15 AM - 1:30 AM UTC

[SCG54-06] Temporal and spatial variations in background seismicity after the 2011 Tohoku-Oki earthquake estimated from HIST-ETAS model

*Taku Ueda[1], Aitaro Kato[1] (1.Earthquake Research Institute, the University of Tokyo)

[J] Oral | S (Solid Earth Sciences) | S-CG Complex & General

[S-CG54] Ten years from the 2011 Tohoku Earthquake: A milestone of Solid Earth Science

convener:Ryota Hino(Graduate School of Science, Tohoku University), Shuichi Kodaira(Research Institute of Marine Geodynamics, Japan Agency for Marine-Earth Science and Technology), Toru Matsuzawa(Research Center for Prediction of Earthquakes and Volcanic Eruptions, Graduate School of Science, Tohoku University), Takeshi Iinuma(National Research and Development Agency Japan Agency for Marine-Earth Science and Technology), Chairperson:Takeshi Iinuma(National Research and Development Agency Japan Agency for Marine-Earth Science and Technology), Toru Matsuzawa(Research Center for Prediction of Earthquakes and Volcanic Eruptions, Graduate School of Science, Tohoku University)

Sun. Jun 6, 2021 9:00 AM - 10:30 AM Ch.17 (Zoom Room 17)

In the 2011 JpGU Meeting held immediately after the 2011 Tohoku-Oki Earthquake, an emergency session related to this earthquake was set up and 188 research results were reported. Not only was there a preliminary report of research and observations regarding this giant earthquake and tsunami, but also various important ideas indicating directions of subsequent solid-earth science researches were presented: the mechanism of earthquake generation including possible processes leading its large-scaled seismic rupture, the impact of the Tohoku-Oki earthquake on the inland crust, and limitations and effectiveness of early warning regarding earthquakes and tsunamis. Ten years after the 2011 JpGU, which was held just two months after the quake, how far has our understanding of these research themes progressed? In addition to the accumulation of 10 years of researches, our understanding of giant earthquakes and tsunamis has dramatically increased through the observations of post-Tohoku Earthquake phenomena of various kinds that have been progressing over a long period of time and through the newly developed observation networks in the offshore area. In this session, not only the researches on the Tohoku-Oki earthquake and tsunami itself, but also the research results in various solid-earth science fields that have clarified after this earthquake and tsunami will be brought together, to discuss the direction of research that should be aimed at in the future.

9:00 AM - 9:05 AM

[SCG54-01]Introduction

©Japan Geoscience Union

Modeling stress field and deformation associated with the Tohoku-Oki earthquake: Understanding the dynamics of the northeastern Japan islands arc-trench system

*Bunichiro Shibazaki[1], Ryohei Sasajima[2]

1. International Institute of Seismology and Earthquake Engineering, Building Research Institute, 2. Research Center for Earthquake Prediction, Disaster Prevention Research Institute, Kyoto University

After the 2011 earthquake off the Pacific coast of Tohoku (Mw9.0) (Tohoku-Oki earthquake) the dynamics of the northeastern Japan islands arc- trench system were investigated, and as a result, our understanding of it was dramatically improved. Important issues investigated include stress changes due to the Tohoku-Oki earthquake and postseismic deformation that occurred after the Tohoku-Oki earthquake. This presentation reviews the research on stress changes and postseismic deformation after the Tohoku-oki earthquake considering the heterogeneous rheological structure of the islands arc-trench system.

Before the Tohoku-Oki earthquake, east-west compression reverse fault-type earthquakes occurred sparsely under the forearc sea area, but after the Tohoku-Oki earthquake, normal fault-type earthquakes occurred frequently. Hasegawa et al. (2011) pointed out that the amount of compressive stress along the subduction zone was small, and the Tohoku-Oki earthquake released the absolute stress. The sources of the stress field in the arc upper plate are the tensile stress field affected by gravity from the topography and density structure, the compressive stress field affected by the frictional force acting on the plate boundary, the bending stress field caused by steady subduction (e.g., Fukahata and Matsu'ura, 2016), and stress fields associated with mantle wedge convection. Sasajima et al. (2018) considered the effects of four sources by subducting of the oceanic plate beneath Northeastern Japan for 100,000 years, considering a realistic nonlinear elasto-visco-plastic material with reference to the temperature, water content distribution, and serpentinization as simulated by Horiuchi and Iwamori (2016). When low frictional strength (5-11MPa) is applied to the shallow brittle region along the plate boundary, a normal fault stress field of east-west tension in the shallow part of the upper plate under the forearc sea is developed, and so is a reverse fault stress field of east-west compression near the plate boundary. The results suggest that the major changes in the main mechanism before and after the Tohoku-Oki earthquake are the suppression of normal fault activity and the promotion of reverse fault activity during inter-plate coupling between megathrust earthquakes. Then, normal fault activity is promoted and reverse fault activity is suppressed due to the stress change resulting from the Tohoku-Oki earthquake.

During the Tohoku-Oki earthquake, upward movement was observed in the east-southeast direction under the forearc sea area, but in the postseismic deformation, subsidence was observed in the west-northwest movement. Sun et al. (2014) showed that the west-northwest movement was due to the viscoelastic relaxation process of the mantle. Numerous detailed analyses of postseismic deformation after the Tohoku-Oki earthquake were performed (Yamagiwa et al., 2015; Muto et al., 2016; Hu et al., 2016; Iinuma et al., 2016; Suito, 2017; Freed et al., 2017; Noda et al., 2018). Agata et al. (2019) performed a large-scale numerical simulation of postseismic deformation, including afterslip and viscoelastic deformation processes, by applying the rate- and state-dependent friction laws to the plate boundary. They also considered the nonlinear flow law for the viscoelastic element in the Burgers model for the surrounding material. Large stress changes resulting from the Tohoku-Oki earthquake have caused the viscosity to drop sharply and rapid motion to occur due to the non-linear flow law in the asenospheres

©2021. Japan Geoscience Union. All Right Reserved.

under the oceanic lithosphere and the forearc. The existence of a low-viscosity layer near the boundary between the oceanic lithosphere and the asenosphere has been pointed out in other studies (Sun et al., 2014), but its existence is inevitable when one considers the nonlinear flow law. In the presentation, we will also discuss the deformation processes during megathrust earthquake cycles.

Keywords: Tohoku-Oki earthquake, northeastern Japan islands arc-trench system, Geodynamics, Stress field, Postseismic deformation

©2021. Japan Geoscience Union. All Right Reserved.

Temporal evolution of seafloor crustal deformation obtained by the 10-year-long GNSS-A observations after the 2011 Tohoku-oki earthquake

*Shun-ichi Watanabe[1], Tadashi Ishikawa[1], Yuto Nakamura[1], Yusuke Yokota[2]

1. Hydrographic and Oceanographic Department, Japan Coast Guard, 2. Institute of Industrial Science, University of Tokyo

On March 11, 2011, the Tohoku-oki earthquake occurred in the western side of the Japan Trench. Seafloor geodetic observation using the GNSS-A technique detected the trench-ward seafloor movements of several tens of meters (Sato et al., 2011 Science; Kido et al., 2011 GRL). Differential bathymetric measurements revealed that the coseismic rupture had reached the trench axis in the off-Miyagi region (Fujiwara et al., 2011 Science), where the seafloor geodetic network in 2011 had no resolution. Additionally, tsunami data suggested that the shallow coseismic rupture had spread in wider area from the off-Iwate to off-Fukushima regions than the geodetically derived distributions (Satake et al., 2013 BSSA).

The stress induced by the coseismic slip causes transitional rock deformation following the mainshock. In the time scale of months to years, afterslip and viscoelastic relaxation are dominant in the postseismic crustal deformation (e.g., Wang et al., 2012 Nature). Whereas the afterslip consistently causes trench-ward surface motion, the viscoelastic relaxation drives land-ward and trench-ward movements above the source region and its downdip side, respectively. The viscoelastic relaxation additionally causes significant subsidence on and around the downdip edge of the main rupture (e.g., Luo and Wang, 2021 Nat. Geo.).

Because both the afterslip and viscoelastic relaxation similarly cause the trench-ward motion in the onshore region, it is difficult to evaluate the contributions of these processes. In contrast, the seafloor geodetic observation is capable of extracting the dominant source rather than the terrestrial observations. The landward and downward movements were detected at the sites above the main rupture using the three-year-long GNSS-A seafloor observations, which provided the definitive evidence for the dominance of viscoelastic relaxation (e.g., Watanabe et al., 2014 GRL, Sun et al., 2014 Nature). The spatial distribution of GNSS-A observation was improved by the Tohoku University in mid-2012 (Kido et al., 2015 GENAH), which lead to detecting more detailed deformation pattern in and around the whole source region (Tomita et al., 2015 GRL; Tomita et al., 2017 Sci. Adv.; Honsho et al., 2019 JGR). Many researchers had proposed the postseismic models (e.g., Sun et al., 2014 Nature; Sun and Wang, 2014 JGR; Iinuma et al., 2016 Nat. Commun.; Freed et al., 2017 EPSL), and consensus has reached that the viscoelastic relaxation was dominant in the main rupture area and that the afterslip less likely occurred in the downdip side of main rupture in the off-Miyagi region. On the other hand, there remain difficulties in decomposing the postseismic deformation sources in the northern and southern regions, because the geodetic data including the early postseismic stage are insufficient. Moreover, the lower resolution of the shallow coseismic slip in these areas increased uncertainty in the viscoelastic relaxation modeling. Although many postseismic models used the geodetically-constrained coseismic model (e.g., Iinuma et al., 2012 JGR) as an input, tsunami data indicated wider shallow slip in the north-south extensions which will significantly affect the viscoelastic deformation in the marginal areas.

Based on the decade of GNSS-A data after the event, we investigated the temporal evolution of

©2021. Japan Geoscience Union. All Right Reserved.

postseismic crustal deformation in this study especially in the northern and southern regions. Our results indicated (1) that the afterslip occurred on the rupture edges at depths near the epicenter, (2) that the northern afterslip had almost decayed in the first three years, and (3) that the shallow coseismic slip had taken place in the off-Fukushima region. We will present the decadal GNSS-A results and discuss the postseismic behaviors in the offshore region.

Keywords: GNSS-A, Seafloor geodetic observation, Postseismic deformation

©2021. Japan Geoscience Union. All Right Reserved.

The slow earthquake spectrum in the Japan Trench illuminated by the S-net seafloor observatories

*Tomoaki Nishikawa[1], Takanori Matsuzawa[2], Kazuaki Ohta[2], Naoki Uchida[3], Takuya NISHIMURA[1], Satoshi Ide[4]

1. Disaster Prevention Research Institute, Kyoto University, 2. National Research Institute for Earth Science and Disaster Resilience, 3. Graduate School of Science and International Research Institute of Disaster Science, Tohoku University, 4. Department of Earth and Planetary Science, University of Tokyo

Investigating slow earthquake activity in subduction zones provides insight into the slip behavior of megathrusts, which can provide important clues about the rupture extent of future great earthquakes. In the Japan Trench, which is a subduction zone located off the Pacific coast of eastern Japan, a pioneering study by Kawasaki et al. (1995) observed a M_w 7.3–7.7 aseismic slip transient accompanied by an earthquake swarm (seven M_j 6.0–6.9 events) far off the coast of Iwate Prefecture in July 1992. Furthermore, Kato et al. (2012) and Ito et al. (2013) revealed that one month before the March 2011 M_w 9.0 Tohoku-Oki earthquake, a slow slip event (SSE) accompanied by an earthquake swarm (four M_j 5.2–5.5 events) containing repeating earthquakes had occurred inside the Tohoku-Oki earthquake rupture area off Miyagi Prefecture. However, the distribution and activity of slow earthquakes across the entire Japan Trench have been unclear because the slow earthquakes occur far offshore and because ocean-bottom seismic or geodetic observations have been conducted only in limited areas and periods.

In 2016, the National Research Institute for Earth Science and Disaster Resilience (NIED) started the operation of the Seafloor Observation Network for Earthquakes and Tsunamis along the Japan Trench (S-net). The S-net consists of 150 seafloor observatories equipped with ocean-bottom seismometers and pressure gauges that are distributed over the Japan Trench and southern end of the Kuril Trench. Here, we used the S-net seismograms to map a detailed distribution of tectonic tremors from August 2016 to August 2018. The observed tremors coincided with very-low-frequency earthquakes (VLFEs) and an SSE. Compiling these and other related observations, including earthquake swarms containing repeating earthquakes, we found that the slow earthquake distribution is complementary to the Tohoku-Oki earthquake rupture. We then used our observations to divide the megathrust in the Japan Trench into three along-strike segments characterized by different slip behaviors: the northern (off Iwate Prefecture) and southern (off Ibaraki Prefecture) segments are characterized by a frequent occurrence of slow earthquakes, whereas the central (off Miyagi Prefecture) segment hosted the Tohoku-Oki earthquake and is characterized by a sparse distribution of slow earthquakes.

Very recently, there has been further progress in the study on the slow earthquake activity along the Japan Trench. Onshore seismic and geodetic observations have revealed the VLFE distribution across the entire Japan Trench (Baba et al., 2020) and the detailed SSE distribution in the southern segment (Nishimura, 2020) before and after the 2011 Tohoku-Oki earthquake. Moreover, Kubo & Nishikawa (2020) have pointed out the complementarity between the slow earthquake distribution and rupture areas of M_w -7-class interplate earthquakes that occurred before or after the 2011 Tohoku-Oki earthquake in the northern and southern segments.

Integrating the results of the S-net observations and these very recent studies, we suggest that the along-strike variation of the slow earthquake activity is a persistent feature that has existed since before the Tohoku-Oki earthquake. The VLFE distribution before the Tohoku-Oki earthquake well correlates with

©2021. Japan Geoscience Union. All Right Reserved.

the tremor distribution after the Tohoku-Oki earthquake, with sparse VLFE and tremor distributions inside the largest coseismic slip area of the Tohoku-Oki earthquake. Slow earthquakes and rupture areas of large interplate earthquakes are distributed in a complementary manner, although the SSE one month before the Tohoku-Oki earthquake in the central segment is a notable exception. On the basis of these integrated observations, we propose that the slow-earthquake-prone areas impede the rupture propagation of great earthquakes along the Japan Trench and limit their sizes. This insight may help us better estimate the rupture extent of future great earthquakes along the Japan Trench.

Keywords: The 2011 Tohoku-Oki earthquake, Slow earthquake, Subduction zone, Megathrust earthquake, S-net, The Japan Trench

©2021. Japan Geoscience Union. All Right Reserved.

A Decade of Lessons Learned from the 2011 Tohoku-oki Earthquake

*Naoki Uchida[1], Roland Bürgmann[2]

1. Research Center for Prediction of Earthquakes and Volcanic Eruptions Graduate School of Science, Tohoku University, 2. Department of Earth and Planetary Science, University of California, Berkeley

The moment magnitude Mw 9 Tohoku-oki earthquake was one of the most disastrous earthquakes in recent history. The large slip area and slip amount, including in the near-trench area, resulted in strong shaking and a huge tsunami that caused severe damage and casualties in Japan. In this presentation, we review the state of knowledge of the earthquake and tsunami potential of the Japan Trench before the earthquake, and the improved understanding after the earthquake. Pre-Tohoku-oki studies partly recognized the potential of Mw8 or larger earthquakes. However, the knowledge based on different types of observations was incomplete and the occurrence of such a great event was not considered in the governmental estimates of earthquake probabilities. The improved understanding of earthquake-cycle and rupture processes since the Tohoku-oki earthquake advanced the leading edge of efforts to characterize megathrust earthquake hazards. We can summarize the lessons as follows: 1) In addition to individual studies of a particular aspect of earthquakes, interdisciplinary research is essential to advance our understanding of the processes underlying the occurrence of earthquakes. 2) The recognition of earthquake potential informed by geologic evidence extending beyond available instrumental records is essential for assessing the largest possible earthquake in a subduction zone. 3) The development of advanced scientific infrastructure, especially near-source (ocean-bottom) observations is necessary to evaluate the locking state of subduction thrusts and to monitor dynamic megathrust fault-zone processes. 4) Although post-Tohoku-oki studies have better characterized the hazard and a number of possible precursors have been identified, the confident prediction of such events appears impossible in the near future.

©2021. Japan Geoscience Union. All Right Reserved.

Temporal and spatial variations in background seismicity after the 2011 Tohoku-Oki earthquake estimated from HIST-ETAS model

*Taku Ueda[1], Aitaro Kato[1]

1. Earthquake Research Institute, the University of Tokyo

Epidemic Type Aftershock Sequence (ETAS) model (e.g., Ogata, 1988, 1998) represents seismicity rate as a summation of background seismicity rate and rate of aftershock. The HIerarchical Space-Time ETAS (HIST-ETAS) model (e.g., Ogata, 2004) represents the parameters as a function of space. Therefore, we can discuss the spatial variations in seismicity characteristics using this model. In addition, the removal of the contribution of aftershock using the HIST-ETAS model provides us the evolution in background seismicity rate.

In this study, we applied the HIST-ETAS model to the seismicity > M4 after the 2011 Tohoku-Oki earthquake to overview the decadal evolution of the aftershocks. We estimated the spatial variations in background seismicity rate μ, the parameters of the Omori-Utsu law (K, p), and the other parameters. Using the estimated parameters, we calculated the probability that each earthquake occurred as background seismicity and investigated the spatial and temporal changes in the background seismicity rate.

Immediately after the 2011 Tohoku-Oki earthquake, the background seismicity rate was higher around the large-slip zone of the 2011 Tohoku-Oki earthquake, which is consistent with the rapid increase in inter-plate earthquakes (Asano et al., 2011; Kato and Igarashi, 2012). The spatial variation in aftershock productivity K is strongly heterogeneous compared with the other parameters (α, p, q). As for temporal variation, the background seismicity has decreased with time (1/t). This result is consistent with the spatial and temporal changes of repeating earthquakes detected by Igarashi (2020) and may reflect aseismic slip associated with the afterslip driven by the Tohoku-Oki earthquake.

©2021. Japan Geoscience Union. All Right Reserved.

[J] Oral | S (Solid Earth Sciences)：S-CG Complex & General

Sun. Jun 6, 2021 10:45 AM - 12:15 PM JST | Sun. Jun 6, 2021 1:45 AM - 3:15 AM UTC | Ch.17 Zoom Room 17

[S-CG54] Ten years from the 2011 Tohoku Earthquake: A milestone of Solid Earth Science

convener:Ryota Hino(Graduate School of Science, Tohoku University), Shuichi Kodaira(Research Institute of Marine Geodynamics, Japan Agency for Marine-Earth Science and Technology), Toru Matsuzawa(Research Center for Prediction of Earthquakes and Volcanic Eruptions, Graduate School of Science, Tohoku University), Takeshi Iinuma(National Research and Development Agency Japan Agency for Marine-Earth Science and Technology), Chairperson:Shuichi Kodaira(Research Institute of Marine Geodynamics, Japan Agency for Marine-Earth Science and Technology), Ryota Hino(Graduate School of Science, Tohoku University)

In the 2011 JpGU Meeting held immediately after the 2011 Tohoku-Oki Earthquake, an emergency session related to this earthquake was set up and 188 research results were reported. Not only was there a preliminary report of research and observations regarding this giant earthquake and tsunami, but also various important ideas indicating directions of subsequent solid-earth science researches were presented: the mechanism of earthquake generation including possible processes leading its large-scaled seismic rupture, the impact of the Tohoku-Oki earthquake on the inland crust, and limitations and effectiveness of early warning regarding earthquakes and tsunamis. Ten years after the 2011 JpGU, which was held just two months after the quake, how far has our understanding of these research themes progressed? In addition to the accumulation of 10 years of researches, our understanding of giant earthquakes and tsunamis has dramatically increased through the observations of post-Tohoku Earthquake phenomena of various kinds that have been progressing over a long period of time and through the newly developed observation networks in the offshore area. In this session, not only the researches on the Tohoku-Oki earthquake and tsunami itself, but also the research results in various solid-earth science fields that have clarified after this earthquake and tsunami will be brought together, to discuss the direction of research that should be aimed at in the future.

10:45 AM - 11:00 AM JST | 1:45 AM - 2:00 AM UTC

[SCG54-07] Seismic Imaging and Physical Properties of Underthrust Sediments at the Japan Trench Subduction Zone

*Ehsan Jamali Hondori[1], Jin-Oh Park[1] (1.The University of Tokyo, Atmosphere and Ocean Research Institute)

11:00 AM - 11:15 AM JST | 2:00 AM - 2:15 AM UTC

[SCG54-08] Inputs to the Japan Trench subduction zone and its implications for the subduction zone processes

★Invited Papers

*Gou Fujie[1], Shuichi Kodaira[1], Yasuyuki Nakamura[1], Seiichi Miura[1] (1.Japan Agency for Marine-Earth Science and Technology)

11:15 AM - 11:30 AM JST | 2:15 AM - 2:30 AM UTC

[SCG54-09] Frictional properties of incoming sediments and rocks at shallow conditions of the Japan Trench subduction zone

*Kyuichi Kanagawa[1], Sayumi Sagano[2], Takuma Hayashi[3], Junya Fujimori[2], Michiyo Sawai[1] (1.Graduate School of Science, Chiba University, 2.Graduate School of Science and Engineering, Chiba University, 3.Faculty of Science, Chiba University)

11:30 AM - 11:45 AM JST | 2:30 AM - 2:45 AM UTC

[SCG54-10] Earthquake faulting in the Japan Trench subduction zone: lessons learned from deep ocean drilling and the fault rocks in the exhumed accretionary complex

*Kohtaro Ujiie[1], Keisuke Ito[2], Ayaka Nagate[2], Hiroki Tabata[2] (1.Faculty of Life and Environmental Sciences, University of Tsukuba, 2.Graduate School of Life and Environmental Sciences, University of Tsukuba)

11:45 AM - 12:00 PM JST | 2:45 AM - 3:00 AM UTC

[SCG54-11] Development of near-field tsunami forecasting method using ocean-bottom pressure sensor network (S-net)

*Yuichiro Tanioka[1] (1.Hokkaido University, Institute of Seismology and Volcanology)

12:00 PM - 12:15 PM JST | 3:00 AM - 3:15 AM UTC

[SCG54-12] Real-time Tsunami Inundation Forecast in Japan - Present and Future

*Shunichi Koshimura[1,5], Ryota Hino[2,5], Yusaku Ohta[2,5], Akihiro Musa[3,5], Takayuki Suzuki[5], Takashi Abe[1], Hiroaki Kobayashi[4,5] (1.International Research Institute of Disaster Science, Tohoku University, 2.Graduate School of Science, Tohoku University, 3.Cyberscience Center, Tohoku University, 4.Graduate School of Information Sciences, Tohoku University, 5.RTi-cast, Inc.)

Seismic Imaging and Physical Properties of Underthrust Sediments at the Japan Trench Subduction Zone

*Ehsan Jamali Hondori[1], Jin-Oh Park[1]

1. The University of Tokyo, Atmosphere and Ocean Research Institute

Although 10 years has passed since the 2011 Tohoku earthquake (M 9.0) occurred in the Japan Trench subduction zone, still the physical properties of the underthrust sediments and plate boundary are poorly known. The stress pattern at the decollement level plays a key role in the seismic behavior of the plate boundary fault and rupture propagation of the megathrust earthquakes. In order to investigate the detailed structure of the Japan Trench underthrust sediments, we have conducted pre-stack depth migration (PSDM) using multichannel seismic reflection data which was acquired along line D13 by research vessel Kairei offshore Miyagi in 2011. After developing a reliable seismic velocity model which could plausibly image the subsurface geological features, we calculated vertical effective stress by using existing empirical relations between P-wave velocity and porosity, and data-fitting approaches. Then we calculated pore-fluid pressure and fluid overpressure ratio for the underthrust sediments. We also calculated shear stress by applying a friction coefficient provided by previous studies. The PSDM depth section revealed a backstop interface with a reverse-polarity reflection, implying on a low velocity zone which extends upward from the plate-boundary fault at a depth of 11 km and a distance of 40 km landward from the trench axis. We specially focused on this area, where the huge shallow slip occurred during the 2011 Tohoku event.

Our results showed that the effective stress at the decollement level is significantly lower than the expected effective stress (under normal consolidation). The very low effective stress might have enabled the 2011 Tohoku earthquake (M 9.0) rupture, which was nucleated at greater depth, to propagate along the shallow decollement up to the trench. JFAST temperature sensors across the fault zone have previously shown that the slip-averaged shear stress and the apparent coefficient of friction estimated from the temperature anomaly at the plate-boundary thrust are 0.54 MPa and 0.08, respectively. By applying a friction coefficient of 0.08 to our vertical effective stress we obtained a shear stress of 0.543 MPa at a location 6km far from the Trench axis, i.e. relatively at the same distance from the Trench axis as the JFAST site. In addition, we calculated fluid overpressure ratio (λ^*), which corresponds to the ratio between fluid overpressure and overburden pressure. When $\lambda^*=1$, it reflects undrained conditions or total fluid retention (the media is impermeable) and when $\lambda^*=0$, it indicates optimal drainage conditions for fluid evacuation (the media is totally permeable). We noticed an area with a dramatically low λ^* located between 7km to 15 km from the Trench axis. The PSDM section shows that there are several faults in this area which provide a drainage path for the sediments and the pore fluid pressure becomes nearly equal to hydrostatic pressure. On the other hand, we found bucket sediments trapped in the subducting grabens with a reflection polarity alteration, indicating that these sediments are fluid-rich and a considerable amount of pore fluid is trapped right below the decollement. The relatively low permeability results in a very low shear stress value and a mechanically weak behavior of the underthrust sediments. Our seismic velocity model, which is built by a layer stripping method and tuned by several iterations of grid-based tomography, has an uncertainty of less than 5% for a depth of 10 km at a location 30 km far from the trench axis. The uncertainty of the velocity model increases downdip to 10% at a location 40 km far from the trench axis. The uncertainty of Vp-porosity transformation is also around 3.5%. A curve fitting approach is used to derive the consolidation curve of the incoming sediments and a

©2021. Japan Geoscience Union. All Right Reserved.

normalized RMS error of 15% is estimated based on the goodness of the fitted curve to the data points. Since the propagated uncertainty of Vp model and Vp-porosity transform are already included in the data points prior to data fitting, we believe the 15% uncertainty is the maximum total uncertainty in our calculated stress values. The maximum vertical effective stress is around 63 MPa and the maximum expected effective stress is 114 MPa, which is almost 80% larger than effective stress. Compared to 80% of difference in the stress values, 15% of uncertainty is negligible.

Acknowledgments: The authors would like to thank JAMSTEC for providing the seismic reflection data. We also thank Paradigm/Emerson (http://www.pdgm.com) for providing seismic data processing software.

Keywords: Subduction, Japan Trench, Seismic Imaging, Stress, Pore Pressure

©2021. Japan Geoscience Union. All Right Reserved.

Inputs to the Japan Trench subduction zone and its implications for the subduction zone processes

*Gou Fujie[1], Shuichi Kodaira[1], Yasuyuki Nakamura[1], Seiichi Miura[1]

1. Japan Agency for Marine-Earth Science and Technology

The megathrust earthquakes in plate subduction zones, such as the 2011 Tohoku earthquake, occur along the boundary between the overriding plate and the subducting oceanic plate. Therefore, the nature of the incoming oceanic plate, such as surface topography, thermal state, lithology, and the water content, affects various processes in subduction zones.
However, the oceanic plate had been poorly studied before. One of the reasons was the difficulties in conducting extensive observations on the oceanic plate because the oceanic plate is generally far from land. However, with the advancement of the various studies in the plate subduction zone, the importance of revealing the nature of the incoming oceanic plate, as the inputs to the subduction zones, has been come to recognized.

Since 2009, We have conducted extensive controlled-source seismic surveys on the oceanic Pacific plate off northeastern Japan arc in order to reveal the nature and spatial variations of the inputs to the Japan Trench subduction zone. We have conducted eight 2-D wide-angle seismic reflection and refraction surveys using ocean bottom seismometers (OBSs) and a large volume airgun array of R/V Kairei and R/V Kaimei of JAMSTEC. The OBS spacing was basically 6-km and we have deployed about 400 OBSs in total. Along all the OBS survey lines, we have obtained multi-channel seismic (MCS) reflection data using a 6-km-long hydrophone streamer cable. In addition, we collected MCS data along more than a hundread of densely alighned short survey lines across the Japan Trench using a relatively small MCS reflection survey system.

Based on these large amount of seismic data, we have revealed systematic structural evolution of the oceanic plate prior to subduction due to the plate bending faulting. In addition, we found the oceanic plate is not laterally so uniform as previously thought. One of the notable spatial variations is the sediment thickness. In most area on the Pacific plate off northeastern Japan arc, the thickness of the sediments is roughly 400 meters. However, there are several areas with extremely thin sediment cover, e.g., ninety percent of the sediment seems to be missing. We investigated the detailed seismic structure beneath the thin sediment cover and found that the areas of thin sediments are heavily disturbed by recent magmatic activities related to the petit-spot.

Intriguingly, the along-trench variations in the sediment thickness on the incoming oceanic plate are well correlates with the extension of the large coseismic slip areas of the 2011 Tohoku earthquake. Therefore, we propose that post-spreading volcanic activities on the oceanic plate before subduction are factors controlling the size and the distribution of the interplate earthquakes after subduction through the disturbance and thermal metamorphism of the sediments.

Keywords: oceanic plate, Tohoku earthquake, petit-spot, seismic survey

©2021. Japan Geoscience Union. All Right Reserved.

Frictional properties of incoming sediments and rocks at shallow conditions of the Japan Trench subduction zone

*Kyuichi Kanagawa[1], Sayumi Sagano[2], Takuma Hayashi[3], Junya Fujimori[2], Michiyo Sawai[1]

1. Graduate School of Science, Chiba University, 2. Graduate School of Science and Engineering, Chiba University, 3. Faculty of Science, Chiba University

In order to examine the frictional properties of incoming sediments and rocks at shallow conditions of the Japan Trench subduction zone, we conducted triaxial friction experiments on gouges of the following samples at a confining pressure of 150 MPa, a pore-water pressure of 50 MPa, temperatures of 25–200℃, and axial displacement rates V_{axial} changed stepwise among 0.1, 1 and 10 μm/s. We used hemipelagic and pelagic clay samples cored from the cover sediments on the Pacific plate off Sanriku, a chert sample cored from the footwall of the plate boundary thrust near the Japan Trench, and a basalt sample cored from the oceanic basement of the Philippine Sea plate off Kii Peninsula.

The results show that the steady-state friction coefficient μ_{ss} decreases with increasing content of clay minerals at a given temperature. Although μ_{ss} of a given sample does not change noticeably with increasing temperature up to 100℃, it increases with increasing temperature from 100℃ to 200℃, which is more pronounced for samples with higher contents of amorphous silica. Fitting the friction data for each step change in V_{axial} by the rate-and state-dependent friction constitutive law reveals that ($a-b$) value (rate dependence of μ_{ss}) decreases with increasing temperature. ($a-b$) values are positive for all samples at temperatures ≦50℃, while they are negative for all samples at 200℃, where all samples showed stick-slip. However, the temperature at which ($a-b$) value becomes negative increases with increasing content of clay minerals; 50–100℃ for the chert sample, ≈100℃ for the basalt sample, 100–150℃ for the hemipelagic clay sample and 150–200℃ for the pelagic clay sample. This implies that the temperature of transition from aseismic faulting with $a-b>0$ to potentially seismic faulting with $a-b<0$ is different among incoming sediments and rocks according to the content of clay minerals, suggesting that a heterogeneous distribution of seismicity at the Japan Trench subduction zone possibly reflects the heterogeneous distribution of fault-zone materials along the plate boundary megathrust.

Keywords: incoming sediments and rocks, frictional properties, shallow conditions of the Japan Trench subduction zone

©2021. Japan Geoscience Union. All Right Reserved.

Earthquake faulting in the Japan Trench subduction zone: lessons learned from deep ocean drilling and the fault rocks in the exhumed accretionary complex

*Kohtaro Ujiie[1], Keisuke Ito[2], Ayaka Nagate[2], Hiroki Tabata[2]

1. Faculty of Life and Environmental Sciences, University of Tsukuba, 2. Graduate School of Life and Environmental Sciences, University of Tsukuba

Drilling into the shallow coseismic slip zone, which produced > 40 m of slip during the 2011 Tohoku-Oki earthquake, revealed that the earthquake faulting was localized along the smectite-rich pelagic clay. High-velocity friction experiments using the fault zone material demonstrated that large slip at the shallow portions of the Japan Trench subduction zone resulted from coseismic weakening of the fault due to the abundance of smectite and thermal pressurization. However, the actual conditions of earthquake faulting in the deeper portions of the Japan Trench subduction zone are largely unknown. The fault rocks in the Jurassic chert–clastic complex in central Japan provide windows to observe seismogenic processes in the deeper portions of the cold subduction zone, where pelagic sedimentary rocks were subducted at a temperature of ~220 ˚C. On the basis of structural and Raman spectroscopic analyses, we recognize the pseudotachylyte in the thrust fault branched from the plate-boundary décollement, which is marked by the preferential melting of illite, thermal erosion, wall-rock fracturing, and increased carbonization at temperatures higher than 900–1100 ˚C. The pseudotachylyte is derived from the frictional melting of black carbonaceous mudstone flanked with pelagic chert. The thermal modeling, the measurement of the fracture density in wall rocks, and the quartz-dominated mineral composition of the chert suggest that wall-rock fracturing is caused by thermal fracturing associated with the alpha–beta transition of quartz in chert. Such thermal fracturing tends to occur along the coseismic slip zone, flanked by rocks with high thermal diffusivities, and, thus, may be a characteristic process during seismic slip along the black carbonaceous mudstone flanked with chert. The thermal fracturing of wall rocks could lead to a dilatancy-induced fluid pressure drop in the coseismic slip zone and reduction in the stiffness of wall rocks, potentially contributing to the generation of frictional melt and acceleration of seismic slip. The seismic slip processes recorded in the Jurassic chert–clastic complex may be applicable to the deeper portions of the Japan Trench subduction zone, where pelagic clays are subducted with pelagic chert.

Keywords: Pelagic clay, JFAST, Accretionary complex, Pseudotachylyte, Thermal fracturing

©2021. Japan Geoscience Union. All Right Reserved.

Development of near-field tsunami forecasting method using ocean-bottom pressure sensor network (S-net)

*Yuichiro Tanioka[1]

1. Hokkaido University, Institute of Seismology and Volcanology

The 2011 Tohoku-oki earthquake (Mw9.0) generated a large tsunami along the Pacific coast of northern Japan. Although the Japan Meteorological Agency (JMA) issued a major tsunami warning along the Pacific coast of Japan immediately after the earthquake, the tsunami caused a catastrophic disaster with approximately 19,000 casualties. After this event, the development of a more accurate and rapid tsunami warning system became a high-priority focus area in Japan. For this purpose, the Japanese government installed a dense cabled observation network, called the seafloor observation network for earthquakes and tsunami around the Japan Trench (S-net), in 2017. The network is operated by the National Research Institute for Earth Science and Disaster Resilience (NEID). In this network, 150 observation stations consisting of ocean-bottom pressure sensors and seismometers are connected by cables at the 30-km intervals.

Tsunami forecasting methods that use the data collected from the ocean floor sensors were recently developed. Tsushima et al. (2012) developed a method called tsunami Forecasting based on Inversion for initial sea Surface Height (tFISH) which estimates the initial sea surface deformation from tsunami waveforms observed at ocean-bottom pressure gauges. Moreover, new tsunami computation methods based on the assimilation of tsunami observations without the tsunami source information were developed by Maeda et al. (2015), Tanioka (2018), and Tanioka and Gusman (2018). Gusman et al. (2016) applied the method developed by Maeda et al. (2015) to the tsunami generated by the 2012 Haida Gwaii earthquake and computed the tsunami wave field successfully by assimilating data observed at ocean-bottom pressure sensors in Cascadia. However, it is difficult to apply this method with ocean-bottom pressure data within the source area. The near-field tsunami inundation forecasting method developed by Tanioka (2018) and Tanioka and Gusman (2018) uses the time derivative of the pressure waveforms observed at the ocean-bottom pressure sensors near the source area. Therefore, tsunami computation by assimilating data can be performed without any tsunami source information as soon as the earthquake or tsunami generation is completed. Tanioka and Gusman (2018) tested ocean-bottom pressure sensors equally distributed at 15 min intervals or approximately 30 km apart. In reality, the S-net ocean-bottom sensors are not installed at uniform intervals, particularly in the north–south direction, and have a lesser number than those tested by Tanioka and Gusman (2018). They finally concluded that it is necessary to improve their method using the exact locations of the S-net sensors for real-time tsunami inundation forecasts.

To overcome its limitation, we developed an interpolation method to generate the appropriate data at the equally spaced positions for the assimilation from the data observed at sensors in S-net. The method was numerically tested for two large underthrust fault models, a giant earthquake (Mw8.8) and the Nemuro-oki earthquake (Mw8.0) models. Those fault models off Hokkaido in Japan are expected to be ruptured in the future. The weighted interpolation method, in which weights of data are inversely proportional to the square of the distance, showed good results for the tsunami forecast method with the data assimilation. Furthermore, results indicated that the method is applicable to the actual observed data at the S-net stations. The only limitation of the weighted interpolation method is that the computed tsunami wavelengths tend to be longer than the actual tsunamis wavelength.

©2021. Japan Geoscience Union. All Right Reserved.

References
Tanioka Y (2018) Tsunami simulation method assimilating ocean bottom pressure data near a tsunami source region. Pure Appl Geophys 175(2):721–729
Tanioka Y, Gusman AR (2018) Near-field tsunami inundation forecast method assimilating ocean bottom pressure data: a synthetic test for the 2011 Tohoku-oki tsunami. Phys Earth Planet Int. 283:82–91.

Keywords: Tsunami, real-time forecast

©2021. Japan Geoscience Union. All Right Reserved.

Real-time Tsunami Inundation Forecast in Japan - Present and Future

*Shunichi Koshimura[1,5], Ryota Hino[2,5], Yusaku Ohta[2,5], Akihiro Musa[3,5], Takayuki Suzuki[5], Takashi Abe[1], Hiroaki Kobayashi[4,5]

1. International Research Institute of Disaster Science, Tohoku University, 2. Graduate School of Science, Tohoku University, 3. Cyberscience Center, Tohoku University, 4. Graduate School of Information Sciences, Tohoku University, 5. RTi-cast, Inc.

The 2011 Great East Japan earthquake and tsunami disaster revealed many problems in Japan’s disaster management policies, and these have undergone reforms in the years since to promote initiatives for building national resilience in confronting any future disasters. One of the key challenges in the aftermath of tsunami disaster is identifying its impact and prioritizing disaster response and relief activities. Because of the widespread damage to infrastructure and communication networks, the impacted regions were hampered in addressing the overall damage, sometimes for months. This experience highlighted the need to develop technologies to forecast the regional impact of tsunamis. Recent advances in high-performance computing and large data sets comprising observations of tsunami emergence, propagation, and effects hold out the promise of dramatically improving our understanding of the whole picture of tsunami-affected areas in real-time.

Three approaches to real-time tsunami inundation forecast methods have been proposed in Japan. The first is the “Tsunami Scenario Database” approach: searching tsunami forecast data from pre-computed database connected with offshore tsunami observation. Once a tsunami is observed offshore, the pre-computed database starts searching for the best matching pair of offshore tsunami heights that fits the observations, then projects the tsunami inundation scenarios most likely to correctly forecast coastal tsunami heights.

The second is the “Data Assimilation” approach that assimilates tsunami wave field using dense offshore tsunami observation networks. This method estimates the tsunami wave field (tsunami height and tsunami velocity) in real-time by repeatedly assimilating dense tsunami observation data into a numerical simulation. Both are highly dependent on the configuration of offshore tsunami sensors.

The third is the “Real-time Forward Simulation” approach that runs simulations in real-time with estimation of tsunami source models based on seismic and geodetic observations. The real-time forward approach has the advantages in simulating tsunami inundation on land—if reliable tsunami source model information is obtained. None of the three methods was developed before the 2011 Great East Japan Earthquake. Some “Tsunami Scenario Database” methods are now being operated in some coastal areas, and the “Real-time Forward Simulation” method is now in operation as a part of the Japanese central government’s emergency response effort.

Throughout the case studies of modeling recent and potential tsunami events, we discuss advantages and drawbacks of those approaches with regard to applicabilities towards next generation tsunami inundation forecast system.

Keywords: Tsunami, Real-time Forecast, Disaster Response

©2021. Japan Geoscience Union. All Right Reserved.

[J] Poster | S (Solid Earth Sciences)：S-CG Complex & General

Sun. Jun 6, 2021 5:15 PM - 6:30 PM JST | Sun. Jun 6, 2021 8:15 AM - 9:30 AM UTC | Ch.16_2

[S-CG54] Ten years from the 2011 Tohoku Earthquake: A milestone of Solid Earth Science

convener:Ryota Hino(Graduate School of Science, Tohoku University), Shuichi Kodaira(Research Institute of Marine Geodynamics, Japan Agency for Marine-Earth Science and Technology), Toru Matsuzawa(Research Center for Prediction of Earthquakes and Volcanic Eruptions, Graduate School of Science, Tohoku University), Takeshi Iinuma(National Research and Development Agency Japan Agency for Marine-Earth Science and Technology)

In the 2011 JpGU Meeting held immediately after the 2011 Tohoku-Oki Earthquake, an emergency session related to this earthquake was set up and 188 research results were reported. Not only was there a preliminary report of research and observations regarding this giant earthquake and tsunami, but also various important ideas indicating directions of subsequent solid-earth science researches were presented: the mechanism of earthquake generation including possible processes leading its large-scaled seismic rupture, the impact of the Tohoku-Oki earthquake on the inland crust, and limitations and effectiveness of early warning regarding earthquakes and tsunamis. Ten years after the 2011 JpGU, which was held just two months after the quake, how far has our understanding of these research themes progressed? In addition to the accumulation of 10 years of researches, our understanding of giant earthquakes and tsunamis has dramatically increased through the observations of post-Tohoku Earthquake phenomena of various kinds that have been progressing over a long period of time and through the newly developed observation networks in the offshore area. In this session, not only the researches on the Tohoku-Oki earthquake and tsunami itself, but also the research results in various solid-earth science fields that have clarified after this earthquake and tsunami will be brought together, to discuss the direction of research that should be aimed at in the future.

[SCG54-P01] Ground motion waveforms in the epicentral area of the 2011 Tohoku-Oki earthquake with large displacements, retrieved from ocean-bottom dynamic pressure change data

*Tatsuya Kubota[1], Tatsuhiko Saito[1], Hiroaki Tsushima[2], Ryota Hino[3], Yusaku Ohta[3], Syuichi Suzuki[3], Daisuke Inazu[4] (1.National Research Institute for Earth Science and Disaster Resilience, 2.Meteorological Research Institute, Japan Meteorological Agency, 3.Tohoku University, 4.Tokyo University of Marine Science and Technology)

[SCG54-P02] Detectability of short-term seafloor deformation by S-net pressure observation

*Ryota Hino[1], Tatsuya Kubota[2], Naotaka YAMAMOTO CHIKASADA[2], Yusaku Ohta[1], Hideto Otsuka[1] (1.Graduate School of Science, Tohoku University, 2.National Research Institute for Earth Science and Disaster Resilience)

[SCG54-P03] Vertical seafloor movement after the 2011 Tohoku earthquake and remarkable uplift near the trench axis off Sanriku

*Chie Honsho[1], Motoyuki Kido[2], Fumiaki Tomita[3], Ryota Hino[1] (1.Research Center for Prediction of Earthquakes and Volcanic Eruptions, Graduate School of Science, Tohoku University, 2.International Research Institute of Disaster Science, Tohoku University, 3.Japan Agency for Marine-Earth Science and Technology)

[SCG54-P04] Improvement of spatial resolution and evaluation of uncertainty for the coseismic slip distribution of the 2011 Tohoku-oki Earthquake

*Fumiaki Tomita[1], Takeshi Iinuma[1], Motoyuki Kido[2], Ryota Hino[3], Yusaku Ohta[3], Ryoichiro Agata[1], Takane Hori[1], Naoki Uchida[3] (1.Japan Agency for Marine-Earth Science and Technology, 2.International Research Institute of Disaster Science, Tohoku University, 3.Graduate School of Science, Tohoku University)

[SCG54-P05] Resolving 3D rheology of northeastern Japan using postseismic deformation following the 2011 Tohoku-oki earthquake

*Jun Muto[1], Dhar Sambuddha[1], James Daniel Paul Moore[2], Satoshi Miura[3], Yusaku Ohta[3], Takeshi Iinuma[4] (1.Department of Earth Sciences, Tohoku University, 2.Earth Observatory of Singapore, Nanyang Technological University, Singapore, 3.Department of Geophysics, Tohoku University, 4.Japan Agency for Marine-Earth Science and Technology)

[SCG54-P06] Numerical simulation of earthquake generation cycles along the Japan Trench

*Ryoko Nakata[1], Takane Hori[2], Seiichi Miura[2], Ryota Hino[1] (1.Graduate School of Science, Tohoku University, 2.Research Institute for Marine Geodynamics, Japan Agency for Marine-Earth Science and Technology)

[SCG54-P07] Seismicity near the trench axis and in the outer rise region of southern Japan Trench: Results from ocean bottom seismograph observations

*Koichiro Obana[1], Gou Fujie[1], Yojiro Yamamoto[1], Yuka Kaiho[1], Yasuyuki Nakamura[1], Seiichi Miura[1], Shuichi Kodaira[1] (1.Research Institute for Marine Geodynamics, Japan Agency for Marine-Earth Science and Technology)

[SCG54-P08] Microseismicity prior to the 2011 Tohoku-Oki earthquake around the mainshock hypocenter

*Hirofumi Goto[1], Ryota Hino[1] (1.Graduate School of Science, Tohoku University)

[SCG54-P09] Characteristics of tectonic tremor activity along the Japan Trench before the 2011 Tohoku Oki earthquake

*Hidenobu Takahashi[1,2], Ryota Hino[1], Naoki Uchida[1], Ryosuke Azuma[1], Susumu Kawakubo[1], Kazuaki Ohta[3], Masanao Shinohara[4] (1.Graduate school of Science Tohoku University , 2.Central Research Institute of Electric Power Industry, 3.National Research Institute for Earth Science and Disaster Resilience, 4.Earthquake Research Institute, The university of Tokyo)

[SCG54-P10] Application of ensemble learning noise classifier to automatically determined earthquake catalog after the 2011 Tohoku Earthquake

*Koji Tamaribuchi[1] (1.Meteorological Research Institute)

[SCG54-P11] **Core-Mantle boundaries state estimation applying the strain analysis on frequency domain**

seiji matsumura[2], *Makoto OKUBO[1] (1.Natural Science Cluster, Kochi University, 2.Faculty of Science and Technology)

[SCG54-P12] Tomography and megathrust earthquakes in the Tohoku forearc

*Dapeng Zhao[1] (1.Department of Geophysics, Tohoku University)

[SCG54-P13] Trench fill and graben fill sediments on the incoming plate around the Japan trench

*Yasuyuki Nakamura[1], Shuichi Kodaira[1], Gou Fujie[1], Seiichi Miura[1], Koichiro Obana[1], Mikiya Yamashita[2] (1.Japan Agency for Marine Earth Science and Technology, 2.National Institute of Advanced Industrial Science and Technology)

Ground motion waveforms in the epicentral area of the 2011 Tohoku-Oki earthquake with large displacements, retrieved from ocean-bottom dynamic pressure change data

*Tatsuya Kubota[1], Tatsuhiko Saito[1], Hiroaki Tsushima[2], Ryota Hino[3], Yusaku Ohta[3], Syuichi Suzuki[3], Daisuke Inazu[4]

1. National Research Institute for Earth Science and Disaster Resilience, 2. Meteorological Research Institute, Japan Meteorological Agency, 3. Tohoku University, 4. Tokyo University of Marine Science and Technology

Introduction

Recent studies have shown that ocean-bottom pressure gauges (OBPs) can record seismic waves in addition to tsunamis and seafloor permanent displacements. Recently the method to numerically simulate more realistic OBP signals inside the focal area based on the theory of tsunami generation (Saito, 2013; 2019) has been established (e.g., Lotto et al., 2015; Saito et al., 2019; Maeda et al., 2020), although the method to appropriately decompose the OBP signal to the seismic and tsunami signals has not been established well (Saito & Tsushima, 2016). If the seismic waveforms inside the focal area are obtained, our understandings for the source process of earthquakes will be deepened, as well as the seismic wave propagation process inside the focal area. In this study, we develop a method to decompose the in-situ OBP records into the tsunami and seismic motion components based on the theory of tsunami generation and apply the method to the OBP data during the 2011 Tohoku-Oki earthquake.

How to extract ground motions from OBP data

When we focus on the low frequency band ($f < \sim 10^{-1}$ Hz) where the elasticity of the seawater can be ignored and we can suppose the seawater is incompressible, the ocean bottom pressure change $p(t)$ can be expressed as a sum of the hydrostatic pressure change $p(t) = \rho_0 g_0[\eta(t) - u(t)]$ (ρ_0: seawater density, g_0 : gravity acceleration, $\eta(t)$: sea surface height change, $u(t)$: seafloor vertical displacement) and the dynamic pressure change $p(t) = \rho_0 h_0 \partial^2 u / \partial t^2$ (h_0: seawater depth) (e.g., Saito, 2013). The seafloor pressure change inside the focal area at nth OBP $p_n(t)$ can be expressed as a superposition of the contributions by the Green's functions for the hydrostatic pressure ($G_{i,n}^{\text{hydrostatic}}(t)$) and dynamic pressure ($G_{i,n}^{\text{dynamic}}(t)$), generated by the seafloor vertical ground motion at ith element: $p_n(t) = \sum_i [m_i\{G_{i,n}^{\text{hydrostatic}}(t) + G_{i,n}^{\text{dynamic}}(t)\}]$. By estimating the amplitude of each unit source, m_i, based on this equation, we can obtain the time series of vertical ground motion.

Application to the 2011 Tohoku-Oki earthquake

We apply this method to the in-situ OBP records during the Tohoku-Oki earthquake, installed by Tohoku University and the University of Tokyo (Maeda et al. 2011; Hino et al. 2014). After removing the tidal component, we apply a low-pass filter with a cutoff of 0.05 Hz to remove the high-frequency acoustic component. The vertical displacement waveforms obtained by the analysis show large displacement offsets at stations GJT3, P08, and P09, located in the area where the seafloor displacement was extremely large (e.g., Saito et al. 2011). The final displacement offsets of these stations were in good agreement with the permanent displacements detected by the hydrostatic pressure offset change, indicating the validity of our proposed method. The velocity waveforms at stations P08 and P09 just above the epicenter showed two peaks, which suggests that the two moment releases near the epicenter during the rupture (e.g., Ide et al., 2011). In addition, the waveforms recorded by the nearest coastal seismographs from each station were similar, except for the arrival time delay.

©2021. Japan Geoscience Union. All Right Reserved.

High-sensitivity ocean bottom seismographs, commonly used for the offshore seismic observation, cannot record seismic waveforms correctly because of waveform saturation. Because of the broadband and broad dynamic range observations by the OBPs (Kubota et al., 2020), OBPs can observe high frequency seismic components without saturation. In addition to the tsunami early warning (e.g., Tsushima et al., 2012), the OBP installed inside the focal area is expected to make the important contribution as an instrument to record nearfield strong ground motion.

Keywords: Ocean bottom pressure gauge, Tsunami, Dynamic pressure change, The 2011 Tohoku-Oki earthquake, Seafloor ground motion

©2021. Japan Geoscience Union. All Right Reserved.

Detectability of short-term seafloor deformation by S-net pressure observation

*Ryota Hino[1], Tatsuya Kubota[2], Naotaka YAMAMOTO CHIKASADA[2], Yusaku Ohta[1], Hideto Otsuka[1]

1. Graduate School of Science, Tohoku University, 2. National Research Institute for Earth Science and Disaster Resilience

Long-term continuous observation of seafloor pressure is effective for detecting unsteady seafloor vertical deformations associated with transient tectonic phenomena such as slow slip event. A series of crustal vertical movements that occurred before and after the 2011 Tohoku-Oki Earthquake were captured by seafloor pressure observations and played significant roles in constraining the distributions of coseismic slip and aseismic slip preceded the mainshock, and the contribution of viscoelastic relaxation in the postseismic crustal deformation. Recently, number of new discoveries have been made in the slow earthquake activities along the Japan Trench. The continuous seismic records over a wide offshore area obtained by Seafloor observation network for earthquakes and tsunamis along the Japan Trench (S-net) showed that low-frequency tectonic tremors occurred repeatedly. It is expected that a slow slip event (SSE) occurs in the background of the tremor activity. If the crustal deformation caused by SSEs can be detected, it will greatly contribute to a comprehensive understanding of interplate coupling in the area. In this paper, we report quality of seafloor pressure data obtained by S-net in the geodetic frequency band, as the first step to capture the seafloor vertical motions associated with SSEs.
The characteristics of continuous records at all of the 150 stations from August 2016 to January 2020 were examined based on the RMS amplitudes of the pressure time series after the tidal components were removed. To remove the tidal components, a “tide killer filter”, a low-pass filter that effectively removes each tidal tide component. The filter output is composed of pressure variations with periods of two-days or more. Looking at the time series for about 3.5 years, it turned out that many records contain remarkable slow fluctuations with a time constant of several months or more. There are irregular variations of unknown cause that cannot be interpreted as fluctuations due to pressure sensor drift or transient fluctuations during the settlement of instruments on the seabed after the deployment. Since we can expect that the duration of SSE is about 1 to 2 weeks, which is the duration of low-frequency tremor activity episodes, the accompanying crustal movements may be detected even if long-period noise levels are high and we inspected the RMS amplitudes in a time window of 100 days. Only ~40 out of 150 stations provide pressure data with noise levels less than 10 hPa (10 cm in terms of vertical displacement), which is a guideline for detecting transient crustal movements, whereas about a half of the S-net stations show noise level more than 20 hPa. The noise level of the S-net pressure data is considerably higher than the data obtained by the pop-up type ocean bottom pressure gauge (OBP) used in many previous studies. It is thought that the difference in performance is related to the difference in the sensor installation method on the seafloor and also in the structure of the instruments. The longer path of pressure transmission to the sensor and the larger amount of self-heating of the device can raise noise level of pressure data. However, the noise level of the pressure data by DONET, another submarine cabled observation system, is not inferior to the data obtained by OBPs. We will inspect characteristics of the noises in S-net pressure data more in detail to identify the causes and also to find a way to reduce the noise so that the S-net pressure records can be used to monitor the SSEs along the Japan Trench.

Keywords: Seafloor pressure measurement, Slow Slip Event, noise characteristics

©2021. Japan Geoscience Union. All Right Reserved.

©2021. Japan Geoscience Union. All Right Reserved.

Vertical seafloor movement after the 2011 Tohoku earthquake and remarkable uplift near the trench axis off Sanriku

*Chie Honsho[1], Motoyuki Kido[2], Fumiaki Tomita[3], Ryota Hino[1]

1. Research Center for Prediction of Earthquakes and Volcanic Eruptions, Graduate School of Science, Tohoku University, 2. International Research Institute of Disaster Science, Tohoku University, 3. Japan Agency for Marine-Earth Science and Technology

We have continuously conducted GNSS-Acoustic observation since September 2012 at the 20 benchmarks distributed off Aomori to Ibaraki. Tomita et al. (2017) first revealed the broad distribution of horizontal seafloor movement and thereby discussed viscoelastic relaxation and afterslip of the 2011 Tohoku earthquake. The horizontal movement has been improving through revision of analysis method (Honsho and Kido, 2017; Honsho et al., 2019) and continued observation. Recently, by the application of a revised method for the traveltime determination in acoustic ranging (Honsho et al., 2021), the distribution of vertical movement has been revealed. Overall, it shows uplift to the east of a trench-parallel boundary ~20–30 km landward from the trench axis, along which little vertical movement occurs, and subsidence to the west; the uplift or subsidence becomes larger as it goes away from the boundary. Except for Site G06 off Sanriku, to be described later, the fastest uplift 3.2 cm/year was observed at Site G01, located on the Pacific plate and ~70 km away from the trench axis. The fastest subsidence was 3.5 cm/year at Site G14 located ~100 km landward from the trench axis.

The observed movement was compared with a model of postseismic deformation of the 2011 Tohoku earthquake by Agata et al. (2019). The model incorporates power-law viscoelastic flow, and the plate interface is considered as a frictional interface on which afterslip or backslip (fault locking) occurs according to frictional conditions. The calculation period of the model is 2.8 year after the earthquake and thus much shorter than the period of our observations (1.5–9.3 year after the earthquake). Nevertheless, the model surface movements become rather steady 2 years after the earthquake, and therefore, the model displacements during the period of 2.0–2.8 year were used to calculate the displacement rate to be compared with our observation. The overall pattern of resulting vertical movement was in excellent agreement with the observed one; uplift in the seaward and subsidence in the landward across a trench-parallel zero line located a little landward of the trench axis. However, the model magnitude of uplift or subsidence was generally two to three times as large as the observed one. Because the vertical movement is mainly caused by viscoelastic relaxation, the result would suggest that the model viscoelastic structure leave room for further adjustment.

Remarkable uplift was observed at the three adjacent sites off Sanriku: Site G04 (located at 39˚34'N, 2.6 cm/year), Site G06 (39˚18'N, 3.4 cm/year), and Site G07 (38˚57'N, 1.9 cm/year). Such significant uplift in this area cannot be explained by viscoelastic relaxation. The local uplift seems to exactly occur in the mid-slope terrace, a flat area ~4,500–5,000 m deep elongated parallel to the trench axis. Active slow earthquakes have been observed in the downdip of these sites (e.g., Nishikawa et al., 2019), and a slow slip event occurred in the early 2015 (Uchida et al., 2018; Honsho et al., 2019). Uplift of the seafloor can be qualitatively explained by fault slip only in the downdip side of these sites, or backslip only in the updip side, or both. Our observations are not frequent enough to determine whether the uplift is episodic or steady movement. However, our result suggests that fault slip in the downdip side, including the slow slip event in 2015, does not reach the trench axis but stops around these sites located ~20–30 km from the trench axis.

©2021. Japan Geoscience Union. All Right Reserved.

Keywords: GNSS-Acoustic, The 2011 Tohoku earthquake, Postseismic deformation

©2021. Japan Geoscience Union. All Right Reserved.

Improvement of spatial resolution and evaluation of uncertainty for the coseismic slip distribution of the 2011 Tohoku-oki Earthquake

*Fumiaki Tomita[1], Takeshi Iinuma[1], Motoyuki Kido[2], Ryota Hino[3], Yusaku Ohta[3], Ryoichiro Agata[1], Takane Hori[1], Naoki Uchida[3]

1. Japan Agency for Marine-Earth Science and Technology, 2. International Research Institute of Disaster Science, Tohoku University, 3. Graduate School of Science, Tohoku University

Due to the 2011Tohoku-oki earthquake, a large coseismic deformation was detected not only by the onland geodetic observational network but also by the seafloor geodetic observations (GNSS-Acoustic observations, ocean bottom pressure observations and differential bathymetry observations). These observations revealed that large coseismic slip reached to the Japan trench off Miyagi [e.g., Iinuma et al., 2012, JGR; Sun et al., 2016, Nat. Comm.]. However, southern and northern extent of the large coseismic slip along the trench was not well constrained due to low spatial resolution in the northern and southern areas because the seafloor geodetic observation sites mainly located in the central part (off-Miyagi region). Meanwhile, it is essential to evaluate uncertainties of the slip parameters to discuss the extent of the large coseismic slip. Although the linear slip inversion methods generally assume Gaussian distribution for the unknown parameters, this assumption was not necessarily right. Here, we examined the following two approaches: 1) Constraining the coseismic slip distribution by postseismic geodetic observational data via a viscoelastic inversion [Tomita et al., 2020, EPS], 2) Evaluating the uncertainties of the slip parameters by introducing a MCMC technique.

Introduction of the viscoelastic inversion: Viscoelastic relaxation, which is a transient deformation after the large earthquake, is caused by stress changes due to coseismic slips. Thus, postseismic geodetic observational data have information of the coseismic slip via the viscoelastic relaxation. Then, we tried to constrain the coseismic slip distribution from the postseismic geodetic observational data by simultaneously estimating the co- and post-seismic slip distribution via viscoelastic Green functions. We calculated the viscoelastic Green functions assuming a simple horizontally stratified viscoelastic structure [Fukahata & Matsu’ura, 2005; 2006, GJI]. As a result, the spatial resolution of the coseismic slip distribution can be improved using the seafloor geodetic observational data in the postseismic period (Tomita et al., 2017, Sci. Adv.). The conventional elastic inversion method showed that large coseismic rupture area was concentrated in the narrow region where the spatial resolution was high. By contrast, in the viscoelastic inversion method, the high spatial resolution region was relatively wide along the trench, and the large coseismic slip area was also extended. The northern and southern limits of the large coseismic slip (over 20 m) area were estimated as ~39.2°N and ~37.0°N, respectively.

Introduction of the MCMC technique: Using the MCMC technique, posterior probability density function (PDF) following a non-Gaussian distribution can be estimated by sampling unknown parameters. In this study, we divided the fault space using Voronoi cells and estimated number of the unknown parameters (number of the Voronoi cells) by a reversible-jump MCMC (rj-MCMC) technique to perform the slip inversion without using any spatial smoothing constraints. Note that we conducted the rj-MCMC analysis only using the coseismic geodetic data and investigated the performance of the rj-MCMC method. As a result, we successfully obtained the posterior PDFs following the non-Gaussian distributions for the slip parameters and found the region where large coseismic slip might occur in a low probability.

Through above two approaches, we successfully improved the inversion methods of the coseismic slip

©2021. Japan Geoscience Union. All Right Reserved.

distribution of the 2011 Tohoku-oki earthquake in terms of the spatial resolution and evaluation of uncertainties. We plan to perform the viscoelastic inversion assuming a realistic viscoelastic structure and to apply the rj-MCMC technique to the viscoelastic inversion method in the future.

Keywords: The 2011 Tohoku Earthquake, Viscoelastic relaxation, Reversible-jump MCMC technique, Seafloor geodesy

©2021. Japan Geoscience Union. All Right Reserved.

Resolving 3D rheology of northeastern Japan using postseismic deformation following the 2011 Tohoku-oki earthquake

*Jun Muto[1], Dhar Sambuddha[1], James Daniel Paul Moore[2], Satoshi Miura[3], Yusaku Ohta[3], Takeshi Iinuma[4]

1. Department of Earth Sciences, Tohoku University, 2. Earth Observatory of Singapore, Nanyang Technological University, Singapore, 3. Department of Geophysics, Tohoku University, 4. Japan Agency for Marine-Earth Science and Technology

In the ten years since the 2011 Tohoku-oki earthquake geodetic observations of the postseismic deformation, recorded both onshore and offshore, have revealed a highly complex rheological structure in the subsurface of Japan. In addition to the nation-wide geodetic network (GEONET), Tohoku University deployed dense networks of GNSS stations in the Miyagi-Yamagata and Fukushima-Niigata regions. Observations from these networks illustrate a pronounced heterogeneity in the surface deformation across northeastern (NE) Japan. In particular, the Miyagi-Yamagata region closer to the main rupture area exhibits intense forearc uplift with localized subsidence around the volcanic front (Muto et al., 2019, Sci. Adv.), whereas uplift has been observed throughout the volcanic front and forearc of the Fukushima-Niigata region.

Over the past decade, a number of studies have gleaned new insight from the postseismic deformation of NE Japan, shedding light on the subsurface rheology and the role of coupled interactions between viscoelastic flow in the mantle and stress-driven afterslip on the plate interface (e.g., Agata et al., 2019, Nat. Commun; Freed et al., 2017, EPSL; Hu et al., 2016, JGR; Muto et al., 2019, Sci.Adv.). Recent studies have not only highlighted the presence of small-scale low viscosity bodies beneath a number of Quaternary volcanoes (Muto et al., 2016, GRL), but also the stagnancy and ubiquity of the forearc mantle (Uchida et al., 2020, Nat. Commun). Furthermore, a strong contrast has been observed in the frictional behavior of the megathrust between central areas near Miyagi and southern areas near Fukushima (Nishikawa et al., 2019, Science).

We have taken advantage of newly acquired observations along the Fukushima-Niigata area and utilized these observations to explore three-dimensional rheological heterogeneities in the mantle wedge mechanically coupled to afterslip on the megathrust interface with variable frictional properties. We developed a numerical model using laboratory-derived constitutive laws to reproduce the geodetic observations (Ozawa et al., 2012, JGR; Tomita et al., 2015, Sci. Adv.; Watanabe et al., 2014, GRL). Our results suggest that the rapid uplift in the Miyagi forearc was caused by deep afterslip underlying a narrow cold nose in the mantle wedge, in contrast to a wider cold nose beneath the Fukushima forearc without significant deeper afterslip. The model resolves along-arc rheological heterogeneity in good agreement to the cumulative observations across ten years in both magnitude and azimuth, as well as their time-series over the 5 years. Our results illuminate the forearc mantle rheology highlighting the variability of cold nose geometry and frictional properties on the subduction zone plate boundary along the arc. Therefore, the dense geodetic network, as well as the numerical model based on the laboratory constrained flow laws of rocks contribute to resolve 3D rheological heterogeneity of the NE Japan imaged through the postseismic deformation of the 2011 Tohoku-oki earthquake.

Keywords: 2011 Tohoku-oki Earthquake, Postseismic deformation, Rheology, Viscoelastic relaxation, Afterslip

©2021. Japan Geoscience Union. All Right Reserved.

©2021. Japan Geoscience Union. All Right Reserved.

Numerical simulation of earthquake generation cycles along the Japan Trench

*Ryoko Nakata[1], Takane Hori[2], Seiichi Miura[2], Ryota Hino[1]

1. Graduate School of Science, Tohoku University, 2. Research Institute for Marine Geodynamics, Japan Agency for Marine-Earth Science and Technology

Seismic, geodetic and paleoseismological studies have demonstrated that the large coseismic slip in the shallow area which caused the 2011 Tohoku-Oki earthquake was limited to the middle segment of the Japan Trench [e.g., Iinuma et al., 2012; Ikehara et al., 2016]. In contrast, in the shallow area off the coast of Fukushima Prefecture, i.e. the southern segment of the trench, postseismic slips were predominant [Iinuma et al., 2016; Tomita et al., 2017]. The observed negative residual gravity anomaly area [Bassett et al., 2016] in the southern segment corresponds to the postseismic slip area. At the southern segment, slow earthquakes include low-frequency earthquakes, tectonic tremors, and very-low-frequency earthquakes, which are distributed complementary to the coseismic slip and overlapping the postseismic slip area of the Tohoku-Oki earthquake [Matsuzawa et al. 2015; Nishikawa et al., 2019; Ohta et al., 2019]. In the northern segment, slow-slips [Uchida et al., 2016] and tsunami earthquakes [Tanioka & Satake, 1996; Satake et al., 2017] occurred. We conducted numerical simulation of earthquake generation cycles along the Japan Trench. In the southern segment, we assumed evident frictional heterogeneity caused by a thick low-velocity channel layer in the shallow part of the off Fukushima [Tsuru et al, 2002; Miura et al., 2003; 2005]. Then, we efficiently reproduced M9 earthquakes recurring only in the middle, followed by evident postseismic slips in the south. In the northern segment, we are conducting the simulations to reproduce a situation in which the 2011 M~9 earthquake and the 1896 M~8 Meiji-Sanriku earthquake have occurred independently even though their source areas are adjacent to each other. In our presentation, we will discuss the factors that control these complementary spatial distributions of slips along the Japan Trench.

©2021. Japan Geoscience Union. All Right Reserved.

Seismicity near the trench axis and in the outer rise region of southern Japan Trench: Results from ocean bottom seismograph observations

*Koichiro Obana[1], Gou Fujie[1], Yojiro Yamamoto[1], Yuka Kaiho[1], Yasuyuki Nakamura[1], Seiichi Miura[1], Shuichi Kodaira[1]

1. Research Institute for Marine Geodynamics, Japan Agency for Marine-Earth Science and Technology

The 2011 Mw 9.0 Tohoku-oki earthquake ruptured the subduction mega-thrust fault in the central Japan Trench. The 2011 Tohoku-oki earthquake is characterized by large coseismic slip along the plate boundary fault reaching the trench axis. Based on the seismic and geodetic observations, main rupture area with the coseismic slip over 50 m occurred on the shallow subduction plate interface in the central Japan Trench. The post-seismic deformation following the 2011 earthquake shows along-trench variations. Westward post-seismic deformations were observed by seafloor geodetic measurements in the central Japan Trench, which can be explained by the viscoelastic relaxation. On the other hand, eastward post-seismic deformations were observed in the southern Japan Trench, south of the main rupture area. The eastward deformations suggest the afterslip on the shallow subduction zone near the trench. In contrast, normal-faulting earthquakes in the trench-outer rise region occurred in both central and southern Japan Trench. We investigate the aftershock activity in the southern Japan Trench to the south of the main rupture area by using ocean bottom seismographs deployed both landward and seaward of the trench. In the trench-outer rise region seaward of the trench axis, several ~100 km long linear earthquake trends both parallel and oblique to the southern Japan Trench have been identified. The trench-strike changes from N-S to NNE-SSW to the south of the main rupture area of the 2011 Tohoku-oki earthquake. The earthquake trend oblique to the southern Japan Trench is a southern extension of the trench-parallel linear earthquake trend in central to northern Japan Trench. This suggests that faults of large outer-trench normal-faulting earthquakes can extend linearly beyond the bend of the trench. The trench-oblique faults should be considered as a substantial part of the outer-rise earthquakes and related tsunamis. In the trench landward slope, we found regular earthquakes along the shallow plate interface near the trench of the southern Japan Trench, where the afterslip of the 2011 Tohoku-oki earthquake is expected from the eastward post-seismic deformations. The near-trench shallow earthquakes locate seaward of the episodic tremor activities reported by Ohta et al. (2019). Temporal correlations between the near-trench earthquakes and the tremor activities suggest that the slow-slip on the shallow subduction plate interface extends close to the trench axis. As indicated by the proximity of the regular earthquakes and slow slips, the diverse slip behavior in the shallow subduction zone is a distinct feature of the southern Japan Trench. The diverse slip behavior in the shallow subduction zone of the southern Japan Trench could be related to smaller scale structure heterogeneity, such as the thickness variation in the low-velocity interplate sedimentary unit imaged by seismic reflection surveys (Tsuru et al. 2002).

Keywords: Japan Trench, Outer rise, Tohoku-oki Earthquake

©2021. Japan Geoscience Union. All Right Reserved.

Microseismicity prior to the 2011 Tohoku-Oki earthquake around the mainshock hypocenter

*Hirofumi Goto[1], Ryota Hino[1]

1. Graduate School of Science, Tohoku University

It has been pointed out that slow earthquakes driving intense foreshock activities cause stress concentration on the epicenters of eventual large earthquakes and trigger mainshocks (e.g. Obara and Kato, 2016). In the 2011 Tohoku-oki Earthquake, foreshock activity thought to be accompanied by a slow earthquake was observed from about one month before the mainshock on March 11 (Kato et al., 2012). At that time, ocean bottom seismometers (OBSs) were installed in this area. In the seismic waveform records obtained by this observation, many events that seemed to be small earthquakes that were not the subject of the previous research were observed. By inspecting such numerous micro earthquakes, it is expected that we will be able to deepen our understanding of the spatiotemporal distribution of foreshock activity and clarify new features of processes preceding large earthquakes. Here, we detected foreshocks and estimated their hypocenter distribution prior to the Tohoku-oki earthquake including tiny events, to discuss the characteristics of the spatiotemporal development of the foreshock activity.

In this study, the waveforms obtained from the OBSs installed around the epicenter of the Tohoku-oki earthquake were used to detect the earthquake and estimate the epicenter by the envelope correlation method (Obara, 2002). As a result, 1963 events were detected during the three days of the analysis period, from March 9 to March 11, and about 70% of them were located with epicenter errors within 10 km. Using this result, the spatial distribution of foreshock activity was investigated in detail. It was found that microearthquakes were concentrated into two regions, separated by the coseismic rupture area of the largest foreshock (M 7.3, March 9 11:45 JST), on the northeastern and southwestern sides, respectively. This is in good agreement with the general picture pointed out for aftershock distributions of many large earthquakes, in which aftershock activities become low in the main coseismic slip area of mainshocks.

The onset timing of seismicity is different between these two active areas. On the northeastern side, activity began immediately after the occurrence of the largest foreshock, showing temporal expansion from the epicenter of the largest foreshock. On the southwest side, activity began about 9 hours after the occurrence of the largest foreshock. This activity expanded from the west side (down-dip side), and the second largest foreshock (M 6.8, March 10 06:24 JST) occurred on the east side (up-dip side).

The number of earthquakes in each active area showed a temporal variation; several increases associating large earthquakes (M> 6) occurrences. However, a sudden increase of the seismicity without any large earthquakes was observed in the northeastern active area. With this activation, the activity of the small repeating earthquakes (Kato et al., 2012) seem to have reactivated. It is suggested that there is a temporal fluctuation in the aseismic process behind the foreshock activity.

Keywords: 2011 Tohoku-Oki earthquake, foreshock activity

©2021. Japan Geoscience Union. All Right Reserved.

Characteristics of tectonic tremor activity along the Japan Trench before the 2011 Tohoku Oki earthquake

*Hidenobu Takahashi[1,2], Ryota Hino[1], Naoki Uchida[1], Ryosuke Azuma[1], Susumu Kawakubo[1], Kazuaki Ohta[3], Masanao Shinohara[4]

1. Graduate school of Science Tohoku University , 2. Central Research Institute of Electric Power Industry, 3. National Research Institute for Earth Science and Disaster Resilience, 4. Earthquake Research Institute, The university of Tokyo

Recently, slow earthquakes have been discovered in Tohoku-oki by using the Seafloor Observation Network for Earthquakes and Tsunamis along the Japan Trench (S-net) (Nishikawa et al., 2019). The characteristics of the slow earthquakes in Tohoku-oki differ from those in the Nankai Trough (Obara and Kato, 2016). Along the Nankai Trough, sources of slow earthquakes are continuously distributed along the deeper and shallower sides of the seismogenic zone, whereas those show complex spatial distribution along the Japan Trench (Nishikawa et al., 2019). In Tokachi-Oki, Tanaka et al. (2019) observed tremors within several kilometers from moderate-sized interplate earthquakes, suggesting small-scaled frictional heterogeneities on the plate interface in the area. Mixed distribution of regular earthquakes and tremors, as well as high regular earthquake activity, make the Japan trench ideal place to study the relationships between tremors and regular earthquakes.

Takahashi et al. (2020, AGU) detected tremors based on the ocean bottom observations from October 2007 to October 2008 along the Japan trench. As a result, tremors occurred before the 2011 Tohoku-Oki earthquake in Iwate-Oki (39.3–40.2˚N), Miyagi-Oki (38.7˚N–39.2˚N), Fukushima-Oki (36.5–37.0˚N), and Ibaraki-Oki (35.5–36.5˚N). In this study, we compare spatio-temporal relationships between tremors and regular earthquakes based on the same data set with those used in our previous study. We focused on if spatial complementarity of tremors and regular earthquakes distributions, and synchronicity of tremors and nearby regular earthquakes activation.
In the depth range between 10–20 km, where tremors are active, most of the regular earthquakes were concentrated in several clusters, like tremors, and these regular earthquake clusters were clearly separated from the tremor clusters. However, tremor and regular earthquake clusters are close to each other, and in many cases, both are adjacent to each other at a distance of a few kilometers or less.

The most active cluster of regular earthquakes during our observation period in Iwate–Oki is located in between two isolated tremor clusters. These regular earthquakes were concentrated in time and its timing is immediately after the nearby tremor episodes. The location of the regular earthquake cluster was located near the end of the tremor cluster where the tremor migration terminated. A similar pattern was observed in Ibaraki–Oki. The cluster of regular earthquakes was observed adjacent to the tremor sources, and this cluster also activated after the cessation of the tremor episode with source migration and was located near the terminal of the migrating. However, not all the tremor activities are accompanied by regular earthquake activity. In the case of tremor activity followed by the regular earthquake activity, tremor distribution tends to be broaden toward the regular earthquake cluster, suggesting variety of interaction between tremor and regular earthquake.

The spatial complementarity of tremors and regular earthquakes suggests that these occur in different conditions on the plate boundary, like other subduction zones, but their spatial closeness indicates that the frictional heterogeneity has a scale of several kilometers on the plate interface in the Japan Trench subduction zone. The observed synchronicity of tremor and regular earthquake activities can be

©2021. Japan Geoscience Union. All Right Reserved.

explained by a common phenomenon, SSEs. The variety of the association between tremors and regular earthquakes can be attributed to the fluctuation in the generation of SSEs: only when the SSEs, initiated from tremor sources, expanded to a nearby seismogenic area, the slip activates regular earthquakes.

Keywords: The Tohoku Oki earthquake, Slow earthquake

©2021. Japan Geoscience Union. All Right Reserved.

Application of ensemble learning noise classifier to automatically determined earthquake catalog after the 2011 Tohoku Earthquake

*Koji Tamaribuchi[1]

1. Meteorological Research Institute

A microseismic catalog is one of the big data that is important for earthquake research and disaster prevention. However, because the 2011 Mw 9.0 Tohoku earthquake caused an enormous number of aftershocks and induced earthquakes, it was impossible to process all the detectable earthquakes. Thus, the microseismic activity remains hidden. Tamaribuchi and Nakagawa [2020] applied the automatic hypocenter determination method to the continuous seismic waveform data for March 2011. The automatically determined earthquake catalog was more than twice in the JMA unified catalog.

On the other hand, it is necessary to remove the noise efficiently because the automatically determined catalog contains several percent of false detections due to noise. Therefore, Tamaribuchi et al. [2020, SSJ Fall Meeting] applied ensemble learning, a kind of supervised machine learning, to the automatically determined catalog and confirmed that we could remove about 80% of false detections. In this study, we apply the supervised ensemble learning to the aftershocks of the 2011 Tohoku earthquake and create a denoised earthquake catalog.

Tamaribuchi et al. [2020, SSJ Fall Meeting] created a training dataset of earthquakes and noise by visual inspection based on the data recorded in the automatically determined catalog from January to February 2020. We then created a noise classifier based on the supervised ensemble learning (Adaboost). The classifier uses hypocenter information such as magnitude, location, and the number of P- and S-phases at 20 stations near the epicenter for learning. In this study, we applied the classifier trained on the data from January to February 2020 to the March 2011 data. There were no living stations near the epicenter due to the lack of an observation network in some cases. Therefore, we used only alive stations when selecting the 20 stations near the epicenter.

For March 2011, the automatic process determined 122353 events all over Japan. As a result of applying the classifier, 119037 (97.3% of the total) and 3316 (2.7%) were classified as earthquakes and noises, respectively. The time taken for classification was 31 minutes (0.02 seconds per event). Most of the noises were in the aftershock areas and Ryukyu islands, and we can classify the noise appropriately in a realistic processing time. On the other hand, compared with the JMA unified catalog, 124 misclassified cases are in aftershock areas. We will consider improving the generalization performance, such as including data from 2011 in the training data.

Keywords: Earthquake catalog, Automatic hypocenter determination, The 2011 Tohoku Earthquake, Machine learning

©2021. Japan Geoscience Union. All Right Reserved.

Core-Mantle boundaries state estimation applying the strain analysis on frequency domain

seiji matsumura[2], *Makoto OKUBO[1]

1. Natural Science Cluster, Kochi University, 2. Faculty of Science and Technology

It is well known that seismic waves, especially surface waves, of a huge earthquake can go around on surface of the earth many times. Surface waves trace on a spherical earth surface many times and become a standing wave, deform the earth, such as to expand and contract or to twist, periodically. These periodical deformations of the earth are so called 'earth free oscillation.' Observing the amplitude and period of these oscillation mode of the earth, we can understand a condition of inner structure of the earth.

In this study, we applied strain analysis on the frequency domain (so called FSA; *c.f.* Okubo, 2007) to the dynamic strain records, which observed at the 2011 off the coast of Tohoku Earthquake. Originally, applying strain analysis, we can determine the principal strain magnitude and its direction from time series changes of the independent three horizontal components. on the other hands, FSA is able to estimate the principal strain azimuth for each frequency. Dynamic strain records we used (UWA1 belonging AIST) contain independent four horizontal components, thus the four principal strain directions can be determined independently, and can be evaluated the mean value, and determination accuracy from the deviations. We determined the natural frequencies of earth free oscillations, and Q values representing the attenuation of the amplitude corresponding to the state of Core-Mantle boundaries (CMB).
We first applied a Fourier analysis to each of the four horizontal components with a data length of 37 hours (133200 s) from 00:00 on March 11, 2011, and obtained amplitude-phase spectra. Next, we estimate averaged the principal strain azimuths and deviations from four spectra applying with Okubo (2009) procedure. Since the earth free oscillation phenomenon is a periodic global vibration, deviations of the determination should be small. Therefore, we set a threshold 5 degrees for deviation, and surveyed nearby frequencies predicted by PREM (Dziewonski and Anderson, 1980). As a result, three frequencies of 0.315 mHz, 0.382 mHz, and 0.818 mHz were obtained, corresponding to ${}_0S_2$, ${}_0T_2$ and ${}_0S_0$, respectively. These frequencies are almost same as the frequencies predicted by PREM. Furthermore, performing the same procedure with the start time shifted a hour, we determined the temporal changes in amplitude for the three frequencies. We finally estimated the Q^{-1} value corresponding to each frequency mode, fitting with the damped oscillation equation.

As a result, we obtained 378.5, 31.3, and 235.7, corresponding to ${}_0S_2$, ${}_0T_2$ and ${}_0S_0$, respectively. In PREM, these values were mentioned 509.6, 250.4, and 5327.6, our results seems to smaller than PREM.

Keywords: Q, Dynamic Strain, Earth Free Oscillation

©2021. Japan Geoscience Union. All Right Reserved.

Tomography and megathrust earthquakes in the Tohoku forearc

*Dapeng Zhao[1]

1. Department of Geophysics, Tohoku University

Tomographic studies have been made continuously for the Tohoku forearc region in the past two decades. Using P-wave arrival-time data recorded at land-based seismic stations of suboceanic earthquakes relocated with sP depth phases (Umino et al., 1995), Zhao et al. (2002) and Mishra et al. (2003) determined the first 3-D P-wave velocity (Vp) images of the Tohoku forearc from the Japan trench to the Pacific coast and found a correlation between the Vp variations of the megathrust zone and the hypocentral distribution of large megathrust earthquakes (M> 6.0). Later studies of both Vp and Vs tomography of the region have confirmed the first findings (Mishra & Zhao, 2004; Wang & Zhao, 2005; Zhao et al., 2007, 2009; Huang et al., 2011). Since the occurrence of the great 2011 Tohoku-oki earthquake (Mw 9.0), more tomographic studies have been made using P and S wave data of the aftershocks relocated with sP depth phases (Zhao et al., 2011; Huang & Zhao, 2013a,b; Liu et al., 2014; Zhao, 2015; Liu & Zhao, 2018). Zhao et al. (2011) relocated the Tohoku mainshock, 339 foreshocks and 5609 aftershocks during 9–27 March 2011 using a 3-D velocity model and local P and S wave arrival times, and suggested that the rupture nucleation of the largest events in the Tohoku-oki sequence, including the mainshock, was controlled by structural heterogeneities in the megathrust zone. Liu & Zhao (2018) constrained the structure of the Tohoku forearc using seismic tomography, residual topography, and gravity data, which reveal a close relationship between structural heterogeneities in and around the megathrust zone and rupture processes of the 2011 Tohoku-oki earthquake. They suggested that the structural heterogeneities in and around the megathrust zone originate from both the overriding Okhotsk plate and the subducting Pacific plate, which controlled the nucleation and rupture processes of the Tohoku-oki earthquake. Recently, P and S wave arrival-time data of suboceanic events recorded by the permanent ocean-bottom seismic network (S-net) have been used to improve the tomographic images of the Tohoku forearc, in particular, near the Japan trench (Hua et al., 2020; Yu & Zhao, 2020; Katayama et al., 2021). All these results indicate structural control on the generation of megathrust earthquakes in the Tohoku forearc.

References

Hua, Y., D. Zhao, G. Toyokuni, Y. Xu (2020). *Nature Communications 11*, 1163.
Huang, Z., D. Zhao, L. Wang (2011). *Geophys. J. Int.* 184, 1428-1444.
Huang, Z., D. Zhao (2013a). *Tectonophysics* 586, 35-45.
Huang, Z., D. Zhao (2013b). *J. Asian Earth Sci.* 70, 160-168.
Katayama, Y., D. Zhao, G. Toyokuni (2021). Joint Symposium of Sciences and Lift Science, Tohoku University on February 19, 2021.
Liu, X., D. Zhao, S. Li (2014). *J. Geophys. Res.* 119, 1094-1118.
Liu, X., D. Zhao (2018). *Science Advances* 4, eaat4396.
Mishra, O.P., D. Zhao et al. (2003). *Geophys. Res. Lett.* 30, GL017736.
Mishra, O.P., D. Zhao (2004). *Geophys. Res. Lett.* 31, L09610.
Umino, N., A. Hasegawa, T. Matzuzawa (1995). *Geophys. J. Int.* 120, 356–366.
Wang, Z., D. Zhao (2005). *Phys. Earth Planet. Inter.* 152, 144-162.
Yu, Z., D. Zhao (2020). *J. Geophys. Res.* 125, e2019JB018600.
Zhao, D., O.P. Mishra, R. Sanda (2002). *Phys. Earth Planet. Inter.* 132, 249-267.
Zhao, D. et al. (2007). *Bull. Seismol. Soc. Am.* 97, 1121-1132.
Zhao, D. et al. (2009). *Tectonophysics* 467, 89-106.

©2021. Japan Geoscience Union. All Right Reserved.

Zhao, D. et al. (2011). *Geophys. Res. Lett.* 38, L17308.
Zhao, D. (2015). *J. Asian Earth Sci.* 98, 26-49.

Keywords: Tohoku forearc, great earthquake, seismic tomography

©2021. Japan Geoscience Union. All Right Reserved.

Trench fill and graben fill sediments on the incoming plate around the Japan trench

*Yasuyuki Nakamura[1], Shuichi Kodaira[1], Gou Fujie[1], Seiichi Miura[1], Koichiro Obana[1], Mikiya Yamashita[2]

1. Japan Agency for Marine Earth Science and Technology, 2. National Institute of Advanced Industrial Science and Technology

The input material to the subduction trench is one of the key elements to the subduction zone processes like megathrust earthquakes and tsunamis. In the Japan Trench where the 2011 Tohoku earthquake occurred, the variation of the incoming sediment thickness correlates with the extent of the large shallow coseismic slip during the 2011 Tohoku earthquake (Fujie et al. 2020). We present the complete map of the incoming sediments in the Japan Trench and discuss characteristics of the seismic structure focusing on the trench and graben fill sediments.

Since the 2011 Tohoku earthquake, extensive seismic surveys have been conducted in the Japan Trench. More than 100 reflection seismic profiles were obtained in the vicinity of the trench axis off Ibaraki to the south and off Aomori to the north with 4-8 km survey line separation. The incoming sediments show generally weak semicontinuous reflections which parallel to the strong basement reflections. The seafloor reflection also generally parallels that of the basement, gently inclined landward. However, we also observe sediments which cover or onlap the inclined “original” sediments on the Pacific plate. These sediments are mostly distributed at the trench axis and trench-ward end of the grabens. Two types of seismic characters are observed on these fill sediments; one is chaotic, the other is horizontally stratified. The graben fills mostly show the stratified characters, but chaotic graben fills are also observed in some locations. These chaotic graben fills seem to be brought from the failure of the sediments on the horst edge located east of the graben. The trench fill sediments show chaotic character in many cases, which should be related to the failure of the slope immediately landward of the trench. In some locations, the stratified units are interbedded in the chaotic units in the trench fills. These trench fills and graben fills are identified in the southern and northern part of the Japan Trench, but not dominant in the central part where the shallow slip occurred during the 2011 Tohoku earthquake. The fill sediments increase the thickness of the input sediments to the subduction zone and could increase the water content of the input materials, which could be related to the plate boundary slip behavior.

Keywords: Japan Trench, input sediments, fill sediments

©2021. Japan Geoscience Union. All Right Reserved.

[J] Oral | S (Solid Earth Sciences)：S-CG Complex & General

Sun. Jun 6, 2021 1:45 PM - 3:15 PM JST | Sun. Jun 6, 2021 4:45 AM - 6:15 AM UTC | Ch.19 Zoom Room 19

[S-CG55] Oceanic plate as inputs to subduction zone: from oceanic spreading ridge to subduction trench

convener:Gou Fujie(Japan Agency for Marine-Earth Science and Technology), Makoto Yamano(Earthquake Research Institute, the University of Tokyo), Tomoaki Morishita(School of Geoscience and Civil Engineering, College of Science and Technology, Kanazawa University), Takanori Kagoshima(University of Toyama), Chairperson:Gou Fujie(Japan Agency for Marine-Earth Science and Technology), Takanori Kagoshima(University of Toyama)

As the inputs to subduction zone, the nature of the incoming oceanic plate, such as surface relief, thermal state, lithology, and the water content, affects various processes occurring in the subduction zone, including arc magmatism and interplate and intraplate seismic activities. The oceanic plate is formed in the oceanic spreading ridge and moves through the ocean basin for a long time and subducts from the oceanic trench. The nature of the incoming oceanic plate is determined by all the processes occurring from the spreading ridge to the subduction trench; e.g., hydrothermal circulation, sedimentation and diagenesis for more than millions years at the oceanic basin, and plate bending-related faulting near the subduction trench. Therefore, for studying the nature of the subduction inputs, it is essential to reveal the various evolution processes of the oceanic plate between the spreading ridge and the subduction trench.

We welcome contributions from a broad range of earth science (geophysics, geology, petrology, drilling science, and so on) discussing topics related to the inputs to subduction zones, such as tectonic process associated with the plate bending prior to subduction, post-spreading volcanic activities including large seamount formation and petit-spot volcanoes, and the nature of the "normal" or "typical" oceanic plate.

This session is supported by the focus group of hard rock drilling science.

1:45 PM - 2:00 PM JST | 4:45 AM - 5:00 AM UTC

[SCG55-01] The Earth recycle and verification of ocean extinction hypothesis - New development in ocean plate research

★Invited Papers

*Katsuyoshi Michibayashi[1] (1.Department of Earth and Planetary Sciences, Graduate School of Environmental Studies, Nagoya University)

2:00 PM - 2:15 PM JST | 5:00 AM - 5:15 AM UTC

[SCG55-02] Prolonged mantle history recorded in zircons from the Horoman peridotite, Hokkaido, Japan

*Shinji Yamamoto[1], Yibing Li[2], Kiyoaki Niida[3], Shuhei Sakata[4], Takeshi Ohno[5] (1.Graduate School of Environment and Information Sciences, Yohohama National University, 2.Institute of Geology Chinese Academy of Geological Science, 3.Hokkaido University Museum, 4.Earthquake Research Institute, The University of Tokyo, 5.Gakushuin University)

2:15 PM - 2:30 PM JST | 5:15 AM - 5:30 AM UTC

[SCG55-03] Depth profile of hydration along the crust - mantle section of the Oman ophiolite: insights from holes CM1A and CM2B

*Kazuki Yoshida[1], Atsushi Okamoto[1], Ryosuke Oyanagi[2], Noriyoshi Tsuchiya[1], Oman Drilling Project Phase2 Science Party (1.Tohoku university, 2.Japan Agency for Marine-Earth Science and Technology)

2:30 PM - 2:45 PM JST | 5:30 AM - 5:45 AM UTC

[SCG55-04] The geochemical structure of pre-subducting oceanic lithosphere explored from petit-spot volcano

*Kazuto Mikuni[1], Naoto Hirano[1], Norikatsu Akizawa[2], Shiki Machida[3] (1.Tohoku University , 2.University of Tokyo, 3.Chiba Institute of Technology)

2:45 PM - 3:00 PM JST | 5:45 AM - 6:00 AM UTC

[SCG55-05] Rejuvenated extension of the Philippine Sea plate and its effect on subduction dynamics in the Nankai Trough

*Gaku Kimura[1], Yasuyuki Nakamura[2], Kazuya Shiraishi[2], Gou Fujie[2], Shuichi Kodaira[2], Asuka Yamaguchi[3], Rina Fukuchi[4], Yoshitaka Hashimoto[5] (1.Tokyo University of Marine Science and Technology, 2.JAMSTEC, 3.Atmosphere and Ocean Research Institute, The University of Tokyo, 4.Dia Consultants Co., Ltd., 5.Kochi University)

3:00 PM - 3:15 PM JST | 6:00 AM - 6:15 AM UTC

[SCG55-06] Thermal structure of the Tohoku subduction zone: effects of plate cooling models

*Manabu Morishige[1] (1.Earthquake Research Institute, the University of Tokyo)

The Earth recycle and verification of ocean extinction hypothesis - New development in ocean plate research

*Katsuyoshi Michibayashi[1]

1. Department of Earth and Planetary Sciences, Graduate School of Environmental Studies, Nagoya University

Planet Earth is the only planet in the solar system where the warm surface environment and oceans that harbor life are stabilized by the long-term circulation (global recycling) of various materials such as rocks, water, and organic matter over tens of millions of years. However, 4.6 billion years after its birth, the Earth is now at a major turning point in global recycling, and the hypothesis of the complete disappearance of the oceans as early as 100 million years has been predicted as a possible future scenario. The key to this future is the infiltration of seawater into the oceanic plates. In this research area, we focus on the hydrophilic properties and inundation processes of oceanic plates, which play a major role in global recycling, and conduct comprehensive research to verify and clarify the oceanic extinction hypothesis on multiple scales. The objectives of this research area are (1) to elucidate the effects of inundation of the oceanic plate on global recycling, especially on the Earth's surface environment and life on Earth, and (2) to test the ocean extinction hypothesis triggered by increased inundation of the oceanic plate and water transport to the Earth's depths. This research area is a fundamental study of natural science that will create a new dynamic model of global recycling by reviewing the oceanic plate from multiple perspectives. The new vision of the future of the Earth, including the oceanic annihilation hypothesis, will bring about new changes and turning points in the field of earth and planetary science, including the redefinition of the discipline responsible for the future of humanity.

Keywords: Earth, recycle, ocean distinction hypothesis, oceanic plate, inundation

©2021. Japan Geoscience Union. All Right Reserved.

Prolonged mantle history recorded in zircons from the Horoman peridotite, Hokkaido, Japan

*Shinji Yamamoto[1], Yibing Li[2], Kiyoaki Niida[3], Shuhei Sakata[4], Takeshi Ohno[5]

1. Graduate School of Environment and Information Sciences, Yohohama National University, 2. Institute of Geology Chinese Academy of Geological Science, 3. Hokkaido University Museum, 4. Earthquake Research Institute, The University of Tokyo, 5. Gakushuin University

The Horoman peridotite complex, exposed at the southwestern end of the Hidaka metamorphic belt, is a well-preserved peridotite suites containing highly depleted spinel-harzburgite to fertile plagioclase-lherzolite with a large scale layered-structure coexisting with types of gabbro, pyroxenite and dunite (Niida, 2007). Geochemical studies have shown that the Horoman peridotite have complex and prolonged history from mid-ocean ridge (MOR) stage ca. 1.0 Ga (Yoshikawa and Nakamura, 2000; Ranaweera et al., 2018) to final stage of up-lifting from the mantle ca. 20 Ma (Yoshikawa et al., 1993; Kaneoka et al., 2001). We recovered sixteen zircon grains from lherzolite rock sample, and examined U-Pb age, trace elements and mineral inclusions in zircon to constraint their formation and age relationship previously reported. Rock samples of harzburgite and lherzolite were collected directly from quarry site of TOHO Olivine Industrial Company and cut them into plats on site, then transferred to the laboratory. To avoid any contaminations, all procedures mineral separation were conducted at newly built facilities in Yokohana National University.

Zircons are transparent or slightly pink in color and show subhedral to rounded shape. Analysis using Raman spectroscopy on zircon grains show relatively narrow and intense Raman peak indicating well-crystallinity, probably due to long annealing under the mantle conditions. Spot analyses with LA-IC-PMS, assisted by cathodoluminescence (CL) images gave a wide age range, from the early Miocene to the Mesoproterozoic (ca. 18–1055 Ma). Zircon CL images show unclear oscillatory zoning and relatively uniform and/or complex internal structure, and some grains have inherited old core (911 Ma) with younger rim (620 Ma). Zircons recovered often have mineral and or fluid inclusions within them. A young zircon with age of 18 Ma has Mg-hydrous silicate inclusion (phase not determined), which suggest that such zircons were formed by hydrous fluid/melt metasomatism at the mantle environment. It has been suggested that zircon U-Pb age retain under the mantle conditions (> 1000 ˚C) due to low Pb diffusion rate of host minerals such as orthopyroxene and olivine (Bea et al., 2020). The minimum ages of ca 18 Ma, plotted on the concordia curve, were consistent with the age of metasomatic event previously reported by Ar-Ar plateau age (20.6 ±0.5 Ma), and the maximum age of 1055 Ma in the study would correspond to that of MOR setting ca. 1.0 Ga.

Keywords: zircon, Horoman, peridotite, mantle metasomatism, recycling

©2021. Japan Geoscience Union. All Right Reserved.

Depth profile of hydration along the crust - mantle section of the Oman ophiolite: insights from holes CM1A and CM2B

*Kazuki Yoshida[1], Atsushi Okamoto[1], Ryosuke Oyanagi[2], Noriyoshi Tsuchiya[1], Oman Drilling Project Phase2 Science Party

1. Tohoku university, 2. Japan Agency for Marine-Earth Science and Technology

The extent of serpentinization of the oceanic lithosphere is a key factor for evaluating the water content brought into the Earth’ s interior. However, the distribution of the serpentinized peridotites is still poorly constrained. The Oman ophiolite is one of the best places showing the complete sections from the upper crust to mantle of the oceanic lithosphere. In this study, we investigated the water content, vein structures and hydration structures of the continuous drilling cores from lower crust to transition zone to upper mantle taken from the Oman Drilling Project at CM1A (404 m) and CM2B (300 m) sites, based on thermogravimetry, Raman spectroscopy and electron microbe analyses. The main lithologies are gabbroic rocks at the lower crust, dunites in the crust-mantle transition zone (CMTZ), and harzburgites in upper mantle section.

All parts of CM1A and CM2B are extensively altered, and mainly characterized by serpentinization of olivine grains. The olivine grains in the gabbroic rocks are serpentinized ranging from 11 to 69 % to produce radial cracks at the surrounding plagioclase and pyroxene. Dunite is completely serpentinized with lizardite + brucite + magnetite, and cut by later antigorite vein networks. Harzburgite from upper mantle section are highly serpentinized (70–90%). The matrix part (lizardite + brucite + less magnetite) of the harzburgites are cut by tremolite veins. The TG analysis shows homogeneous serpentinization along the depth. The higher temperature veins (antigorite vein in the dunties, tremolite vein in the harzburgites) after pervasive lower temperature alteration (lizardite + brucite) suggest that the pervasive serpentinization before or during intra-oceanic overthrust of the Oman ophiolite. 300 m length of the crust-mantle transition zone to upper mantle section of the CM2B are almost completely serpentinized with average water content of 12 wt%.

Given that the gabbro has a low permeability as estimated by the intact sample ($k=10^{-22}$ m^2), 25 Myr of fluid-supply are required to complete the serpentinization observed in the CM1A & CM2B cores. This estimate contradicts with the interval of the igneous activity at ridge center of the Oman ophiolite and obduction of 1-2 Myr (Hacker, 1991). In contrast, the discrete element numerical simulations revealed that microcrack network formation by reaction induced stress during serpentinization could be important for enhancement of the permeability by more than several order of magnitude (Yoshida et al., 2020). In case of intact gabbro with enhanced permeability ($k=10^{-20}$ m^2), the duration for sepentinization is estimated to be ~0.25 Myr. These results suggest that abundant of water for the lower temperature serpentinization is possibly supplied during intra-oceanic overthrust of the ophiolite. The fluid flow triggered by intraoceanic thrusting is enhanced by later reaction-induced fracturing, which results in fluid penetration through the lower crust to the upper mantle. After the low-temperature alteration, hot fluids came from the subducting slab to form antigorite vein networks.

References

1. Hacker (1991). *Tectonics*, *10*(2), 455–473. https://doi.org/10.1029/90TC02779
2. Yoshida et al. (2020). *J. Geophys. Res. : Solid Earth*, 125, 11. https://doi.org/10.1029/2020JB020268

©2021. Japan Geoscience Union. All Right Reserved.

Keywords: serpentinization, reaction-induced fracturing, hydrothermal alteration

©2021. Japan Geoscience Union. All Right Reserved.

The geochemical structure of pre-subducting oceanic lithosphere explored from petit-spot volcano

*Kazuto Mikuni[1], Naoto Hirano[1], Norikatsu Akizawa[2], Shiki Machida[3]

1. Tohoku University , 2. University of Tokyo, 3. Chiba Institute of Technology

Chemical composition of the oceanic lithosphere has been represented previously by “abyssal peridotite” exposed along transform faults in the mid-ocean ridge. However, nobody has ever seen the lithospheric mantle of the oldest part of Pacific Plate. A subseafloor petit-spot (small conical knoll) cluster was recently discovered in the south of Minamitorishima (Marcus) Island, where the age of Pacific Plate is estimated as 160 Ma. Peridotite and pyroxenite xenoliths, and pyroxene xenocrysts transported to the ocean floor through the petit-spot volcanism could directly provide petrological and geochemical information of the oldest Pacific lithosphere. This study presents in-situ chemical compositions, determined using an electron micro-probe, of quenched glasses, xenoliths and xenocrysts in petit-spot basalts on the oldest part of Pacific Plate. The whole-rock chemical compositions were analyzed using an inductively coupled plasma-mass spectrometry. Eruption ages were estimated from thickness of palagonite, an altered quenched glass rind by the interaction with seawater.

The eruption ages of eight petit-spot volcanoes in this region were dated at 0.03–2.2 Ma, suggesting recent eruptions due to lithospheric flexure of the subducting Pacific Plate into the Mariana Trench. The petrographic and geochemical features of petit-spot basalts obtained in this study are similar to those of previously reported petit-spot basalts in the northwestern Pacific Plate.
Most of clinopyroxenes of peridotite and pyroxenite xenoliths are Ti-rich Al-augite, indicating compositional difference with the depleted abyssal peridotite. Ti-rich Al-augite is possibly originated from phenocryst crystallized at high pressure, cumulate from alkalic magma or metasomatic vein in lithospheric mantle. However, the petrographic characteristics of clinopyroxene in these xenoliths (e.g., lamellae) specify the presence of metasomatic veins in the lithospheric mantle. The estimated temperature and pressure of pyroxenite and peridotite xenoliths peculiarly fit on a geotherm younger than 160 Ma. These results imply that the oldest Pacific Plate has a high geothermal gradient due to multiple petit-spot magma injections as previously indicated in the northwestern Pacific Plate. If petit-spot volcanism is ubiquitous phenomenon, the nature of subducting oceanic plate must be revised drastically in previous recognition.

Keywords: Petit-spot, Lithosphere, Metasomatism, Mantle Xenolith, Pacific Plate

©2021. Japan Geoscience Union. All Right Reserved.

Rejuvenated extension of the Philippine Sea plate and its effect on subduction dynamics in the Nankai Trough

*Gaku Kimura[1], Yasuyuki Nakamura[2], Kazuya Shiraishi[2], Gou Fujie[2], Shuichi Kodaira[2], Asuka Yamaguchi[3], Rina Fukuchi[4], Yoshitaka Hashimoto[5]

1. Tokyo University of Marine Science and Technology, 2. JAMSTEC, 3. Atmosphere and Ocean Research Institute, The University of Tokyo, 4. Dia Consultants Co., Ltd., 5. Kochi University

The Nankai Trough, Japan, is a subduction zone characterized by the recurrence of disastrous earthquakes and tsunamis. Slow earthquakes and associated tremor also occur intermittently and locally in the Nankai Trough. The causal relationship between slow earthquakes and large earthquakes is important to understanding subduction zone dynamics. The Nankai Trough off Muroto, Shikoku, near the southeast margin of the rupture segment of the 1946 Nankai earthquake, is one of three regions where slow earthquakes and tremor cluster in the Nankai Trough. On the Philippine Sea plate, the rifting of the central domain of the Shikoku Basin was aborted at ~15 Ma and underthrust the Nankai forearc off Muroto. Here, the Tosa-Bae seamount and other high-relief features, which are northern extension of the Kinan Seamount chain, have collided with and indented the forearc wedge. In this study, we analyzed seismic reflection profiles around the deformation front of accretionary wedge and stratigraphically correlated them to drilling sites off Muroto. Our results show that the previously aborted horst-and-graben structures, which were formed around the spreading center of the Shikoku Basin at ~15 Ma, was rejuvenated at ~ 6 Ma to ~3.3 Ma and has remained active since. The reactivated normal faulting has enhanced seafloor roughness and appears to affect the locations of slow earthquakes and tremors. Rejuvenated normal faulting is not limited to areas near the Nankai Trough, and extends more than 200 km into the Shikoku Basin to the south. This extension might be due to extensional forces applied to the Philippine Sea plate, which appear to be driven by slab-pull in the Ryukyu and Philippine trenches along the western margin of the Philippine Sea plate.

Keywords: Nankai Trough, slow earthquake, seamount subduction, Philippine Sea plate, Tosa-Bae, subduction

©2021. Japan Geoscience Union. All Right Reserved.

Thermal structure of the Tohoku subduction zone: effects of plate cooling models

*Manabu Morishige[1]

1. Earthquake Research Institute, the University of Tokyo

Recent studies have extensively investigated the effects of experimentally constrained thermal conductivity on the thermal structure of oceanic plates. However, little is known about how the updated cooling models affect the thermal structure of subduction zones. In this presentation I investigate the effects of plate cooling models on the thermal structure of the Tohoku subduction zone, with a particular focus on thermal conductivity. Three types of thermal conductivity were tested, including constant (Case 1), temperature-dependent (Case 2), and temperature- and material-dependent (Case 3) types. For each case, the parameters for the plate cooling models were inferred based on the observed variations in surface heat flow and seafloor depth with plate age using Bayes' theorem. It was found that the predicted locations of the blueschist-out boundaries in the oceanic crust and serpentinite-out boundaries in the slab mantle, which are possibly related to intermediate-depth earthquakes, can change by approximately 10 km depending on the assumed thermal conductivity. This may be significant when considering the causes of earthquakes. Therefore, it is desirable to take into account the variations in thermal conductivity when predicting the thermal structure of oceanic plates and subduction zones.

Keywords: Oceanic plate, Subduction zone, Thermal structure, Thermal conductivity

©2021. Japan Geoscience Union. All Right Reserved.

[J] Oral | S (Solid Earth Sciences)：S-CG Complex & General

Sun. Jun 6, 2021 3:30 PM - 5:00 PM JST | Sun. Jun 6, 2021 6:30 AM - 8:00 AM UTC | Ch.19 Zoom Room 19

[S-CG55] Oceanic plate as inputs to subduction zone: from oceanic spreading ridge to subduction trench

convener:Gou Fujie(Japan Agency for Marine-Earth Science and Technology), Makoto Yamano(Earthquake Research Institute, the University of Tokyo), Tomoaki Morishita(School of Geoscience and Civil Engineering, College of Science and Technology, Kanazawa University), Takanori Kagoshima(University of Toyama), Chairperson:Takanori Kagoshima(University of Toyama), Tomoaki Morishita(School of Geoscience and Civil Engineering, College of Science and Technology, Kanazawa University)

As the inputs to subduction zone, the nature of the incoming oceanic plate, such as surface relief, thermal state, lithology, and the water content, affects various processes occurring in the subduction zone, including arc magmatism and interplate and intraplate seismic activities. The oceanic plate is formed in the oceanic spreading ridge and moves through the ocean basin for a long time and subducts from the oceanic trench. The nature of the incoming oceanic plate is determined by all the processes occurring from the spreading ridge to the subduction trench; e.g., hydrothermal circulation, sedimentation and diagenesis for more than millions years at the oceanic basin, and plate bending-related faulting near the subduction trench. Therefore, for studying the nature of the subduction inputs, it is essential to reveal the various evolution processes of the oceanic plate between the spreading ridge and the subduction trench.

We welcome contributions from a broad range of earth science (geophysics, geology, petrology, drilling science, and so on) discussing topics related to the inputs to subduction zones, such as tectonic process associated with the plate bending prior to subduction, post-spreading volcanic activities including large seamount formation and petit-spot volcanoes, and the nature of the "normal" or "typical" oceanic plate.

This session is supported by the focus group of hard rock drilling science.

3:30 PM - 3:45 PM JST | 6:30 AM - 6:45 AM UTC

[SCG55-07] Interpretation for variation in the incoming Pacific Plate structure around the Kuril Trench axial region by an OBS/MCS seismic survey

★Invited Papers

*Ryosuke Azuma[1], Shuichi Kodaira[2], Ryota Hino[1], Gou Fujie[2], Koichiro Obana[1], Fumiaki Tomita[2], Yusaku Ohta[1] (1.Recearch Center for Prediction of Earthquake and Volcanic Eruption, Graduate School of Science, Tohoku University, 2.Japan Agency for Marin-Earth Science and Technology)

3:45 PM - 4:00 PM JST | 6:45 AM - 7:00 AM UTC

[SCG55-08] **Characteristics of normal faults developing in the outer rise of the Japan Trench**

*YUE SUN[1], Ehsan Jamali Hondori[1], Jin-Oh Park[1] (1.Atmosphere and Ocean Research Institute, The University of Tokyo)

4:00 PM - 4:15 PM JST | 7:00 AM - 7:15 AM UTC

[SCG55-09] Complicated fault geometry of outer-trench normal-faulting earthquakes based on the ocean bottom seismograph observations

*Koichiro Obana[1], Tsutomu Takahashi[1], Yojiro Yamamoto[1], Yasuyuki Nakamura[1], Gou Fujie[1], Seiichi Miura[1], Shuichi Kodaira[1] (1.Research Institute for Marine Geodynamics, Japan Agency for Marine-Earth Science and Technology)

4:15 PM - 4:30 PM JST | 7:15 AM - 7:30 AM UTC

[SCG55-10] Mantle-derived helium released through the Japan Trench bend-faults

★Invited Papers

*Jin-Oh Park[1], Naoto Takahata[1], Ehsan Jamali Hondori[1], Asuka Yamaguchi[1], Takanori Kagoshima[2], Tetsuro Tsuru[3], Gou Fujie[4], Yue Sun[1], Juichiro Ashi[1], Makoto Yamano[5], Yuji Sano[1] (1.Atmosphere and Ocean Research Institute, University of Tokyo, 2.Department of Environmental Biology and Chemistry, University of Toyama, 3.Department of Marine Resources and Energy, Tokyo University of Marine Science and Technology, 4.Japan Agency for Marine-Earth Science and Technology, 5.Earthquake Research Institute, University of Tokyo)

4:30 PM - 4:45 PM JST | 7:30 AM - 7:45 AM UTC

[SCG55-11] Heat flow distribution seaward of the Japan and Kuril trenches: Implications for fluid circulation in the oceanic crust

*Makoto Yamano[1], Yoshifumi Kawada[2], Kouta Sasaki[3], Masataka Kinoshita[1] (1.Earthquake Research Institute, the University of Tokyo, 2.Japan Agency for Marine-Earth Science and Technology, 3.Kozo Keikaku Engineering Inc.)

4:45 PM - 5:00 PM JST | 7:45 AM - 8:00 AM UTC

[SCG55-12] Resistivity imaging around the Japan trench based on ocean bottom electromagnetic surveys

★Invited Papers

*Hiroshi Ichihara[1], Takafumi Kasaya[2], Tada-nori Goto[3], Kiyoshi Baba[4], Shinya Sato[5], Makoto Yamano[4] (1.Graduate school of environmental studies, Nagoya University, 2.JAMSTEC, 3.ERI, University of Tokyo, 4.University of Hyogo, 5.Graduate School of Engineering, Kyoto University)

Interpretation for variation in the incoming Pacific Plate structure around the Kuril Trench axial region by an OBS/MCS seismic survey

*Ryosuke Azuma[1], Shuichi Kodaira[2], Ryota Hino[1], Gou Fujie[2], Koichiro Obana[1], Fumiaki Tomita[2], Yusaku Ohta[1]

1. Recearch Center for Prediction of Earthquake and Volcanic Eruption, Graduate School of Science, Tohoku University, 2. Japan Agency for Marin-Earth Science and Technology

The Pacific Plate subducting to the Japan and Kuril trenches is topographically characterized by bending-related faults, fracture zones, large seamounts, and therefore various heterogeneity seem to exist in the incoming plate. Previous seismic studies in these regions concluded that plate-bending faults at the trench outer slope is impactful for incoming plate hydration based on seismic velocity reduction. We have also analyzed an OBS seismic survey data newly collected in the Kuril Trench axial region to understand a state of the incoming plate development. Our previous model by first arrival and wide-angle PmP traveltime inversion proposed a low Vp (~7.5 km/s) mantle, expecting serpentinization of 40–50 %, quite larger than in the Japan and Kuril trenches (15–25 % serpentinization, Fujie et al., 2018), but similar to mantle Vp beneath the seamount (Kodaira et al., 2002; Nishizawa et al., 2009). Furthermore, a systematic difference in the estimated oceanic Moho depth was found between OBS and multi-channel seismic (MCS) data, meaning our model has the 8–10 km thick crustal-Vp (< 7 km/s) layer. We consider that this systematic difference can be explained by a presence of a zone with gradual increase of Vp beneath the MCS Moho; identified wide-angle phases seem to be not reflection but refraction in the corresponding zone. In this presentation, we quantitatively investigate the state of the low Vp anomaly around the Moho by an additional analysis based on traveltime data of the MCS profile in addition to OBS record sections.

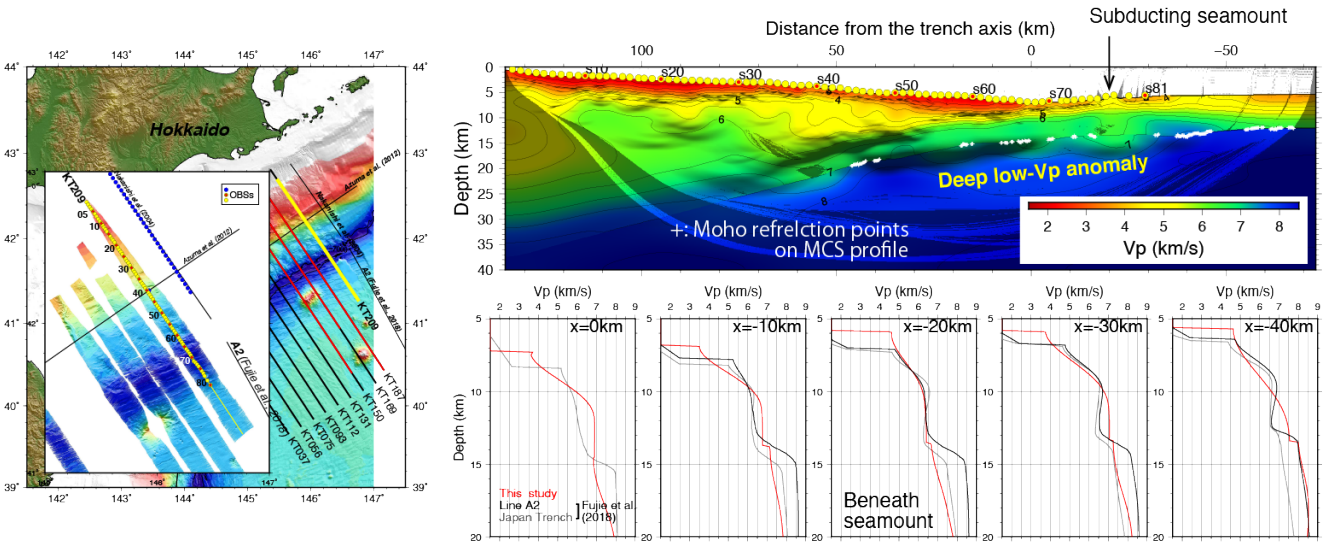
The survey was conducted by R/Vs Kairei and Yokosuka of JAMSTEC in 2019. A 208 km-length survey line KT209 runs from the land slope to the trench outer slope across bending-related faults and a seamount (call as the KT209 seamount). 80 of OBSs were deployed every ~2 km along the line. An airgun array with a total volume of 7,800 cu.in. was used as a controlled source and shoot every 200 m. Multi-channel seismic (MCS) reflection data was also collected by towing a 5.5 km-length multichannel hydrophone streamer cable. Observed first arrival traveltimes in OBS record sections and two-way-time of near-vertical oceanic Moho reflection were used for modeling P-wave velocity (Vp) structure by a 2-D traveltime tomographic inversion.

The revised Vp model is featured by a deep low-Vp anomaly in the incoming plate; the anomaly is less than 7 km/s and still reaches 10 kilometers depth from the seafloor same as the previous model. Because this anomaly expands beneath the oceanic Moho depth defined by the MCS profile, we interpret that the anomaly causes not in but beneath the crust. This anomaly is also significant and thickest beneath the KT209 seamount and continuously appears to at least 30 km landward from the trench. We understand above all features are close to crustal thickening beneath the Erimo and the Daiichi-Kashima Seamounts imaged from wide-angle data (Nishizawa et al., 2009). In addition, traveltimes of wide-angle PmP are projected along the bottom of low Vp anomaly in the revised model. We therefore interpret that low Vp anomaly beneath the oceanic crustal basement, that is the Moho, would be underplated magma material and wide-angle PmP seem to be reflections at the bottom of underplate layer. The age of the Erimo and Ryofu Seamounts near the KT209 are dated at ~100 Ma which are at least 20 Ma younger than surrounding seafloor, and produced by Cretaceous off-ridge volcanism (Takigami et al., 1989). Although an origin of the KT209 seamount is unknown, the fact of large seamounts distribution limitedly in the

©2021. Japan Geoscience Union. All Right Reserved.

southmost Kuril Trench implies that the KT209 seamounts would belong to these Cretaceous volcanoes. Tens of small seamounts can be also recognized on the bathymetric topography in the northwest Pacific. We suggest that the Pacific Plate in this region subducts with a strong spatial heterogeneity.

Keywords: Incoming Pacific Plate, Outer rise in the Kuril Trench subduction zone, Seamount, Seismic survey



©2021. Japan Geoscience Union. All Right Reserved.

Characteristics of normal faults developing in the outer rise of the Japan Trench

*YUE SUN[1], Ehsan Jamali Hondori[1], Jin-Oh Park[1]

1. Atmosphere and Ocean Research Institute, The University of Tokyo

There have been several large earthquakes occurred in the Japan Trench subduction zone and outer rise. Many previous studies have been conducted to elucidate the shallow crustal structure of the Japan Trench outer rise, but most of these studies depend on seafloor topographic maps and there are few studies focusing on the faults which cut the acoustic base in the Multi-Channel Seismic (MCS) survey profile. In order to investigate the characteristics of normal faults developing in the Japan Trench outer rise, the "Portable Multi-Channel Seismic Survey System" of the Atmosphere and Ocean Research Institute (AORI) of the University of Tokyo was mounted on the research vessel *Shinsei-maru*, for the survey KS-19-05 in April 2019 and survey KS-20-14 in September 2020, and a total number of 5 survey lines of MCS data were acquired. In this study, the data from three survey lines, KS19-05-1, KS19-05-5, and KS20-14-5 are used. Line KS19-05-5 of survey KS19-05 and line KS20-14-5 of survey KS20-14 generated strong noise due to bad sea conditions and poor equipment conditions. I succeeded in removing the noise by manually deleting the traces with spike noise and applying the Band-pass filter and FX deconvolution. Furthermore, the MCS data processing was performed with a Kirchhoff pre-stack depth migration (PSDM) and seismic depth sections were obtained. Three survey lines confirmed a clear Horst-Graben structure in the subducting Pacific plate. The results of investigating the normal faults, which are caused by plate bending and are imaged in the three survey lines, show that the normal faults of the survey line KS19-05-1 have a larger fault offset compared to the faults in the survey lines KS19-05-5 and KS20-14-5. However, the horizontal spatial distributions of these faults tend to be sparse. In addition, a number of young volcanic activities are observed near the trench axis in line KS19-05-1 and near the eastern side of line KS19-05-5 and line KS20-14-5. These young volcanic activities are referred to by Hirano et al. (2006) as petit spot volcanoes of site A and site C. In the PSDM section, petit spot volcanos and traces of magma intrusion were confirmed. In particular, on the line KS19-05-1, the reflection horizon of the chert layer is unclear within a range of 75 km from the trench axis to the seaside, and the existence of the chert layer cannot be confirmed. The sediment layer thickness was also clearly reduced in the petit spot volcanic area. I evaluated the formation time of the normal faults by calculating the difference between seafloor offset and the acoustic basement offset following the method of Ranero et al. (2003). In the line KS19-05-1, most of the normal faults are recent faults but in the line KS19-05-5 and the line KS20-14-5 both recent faults and older faults are seen on the seismic depth sections. Based on the above evaluations, the fault developing characteristics in the Japan Trench outer rise are organized into two models. In Model 1 the normal faults are not affected by the petit spot volcano, where older faults and recent faults are mixed and both are developing. In Model 2 the normal faults are affected by the petit spot volcano and only recent normal faults are developing. Model 1 applies to offshore Miyagi and model 2 applies to offshore Sanriku. The most important condition affecting the two models is the presence of the petit spot volcano.

Keywords: Japan Trench, Outer rise, Multi-Channel Seismic (MCS), Normal fault, Petit spot volcano

©2021. Japan Geoscience Union. All Right Reserved.

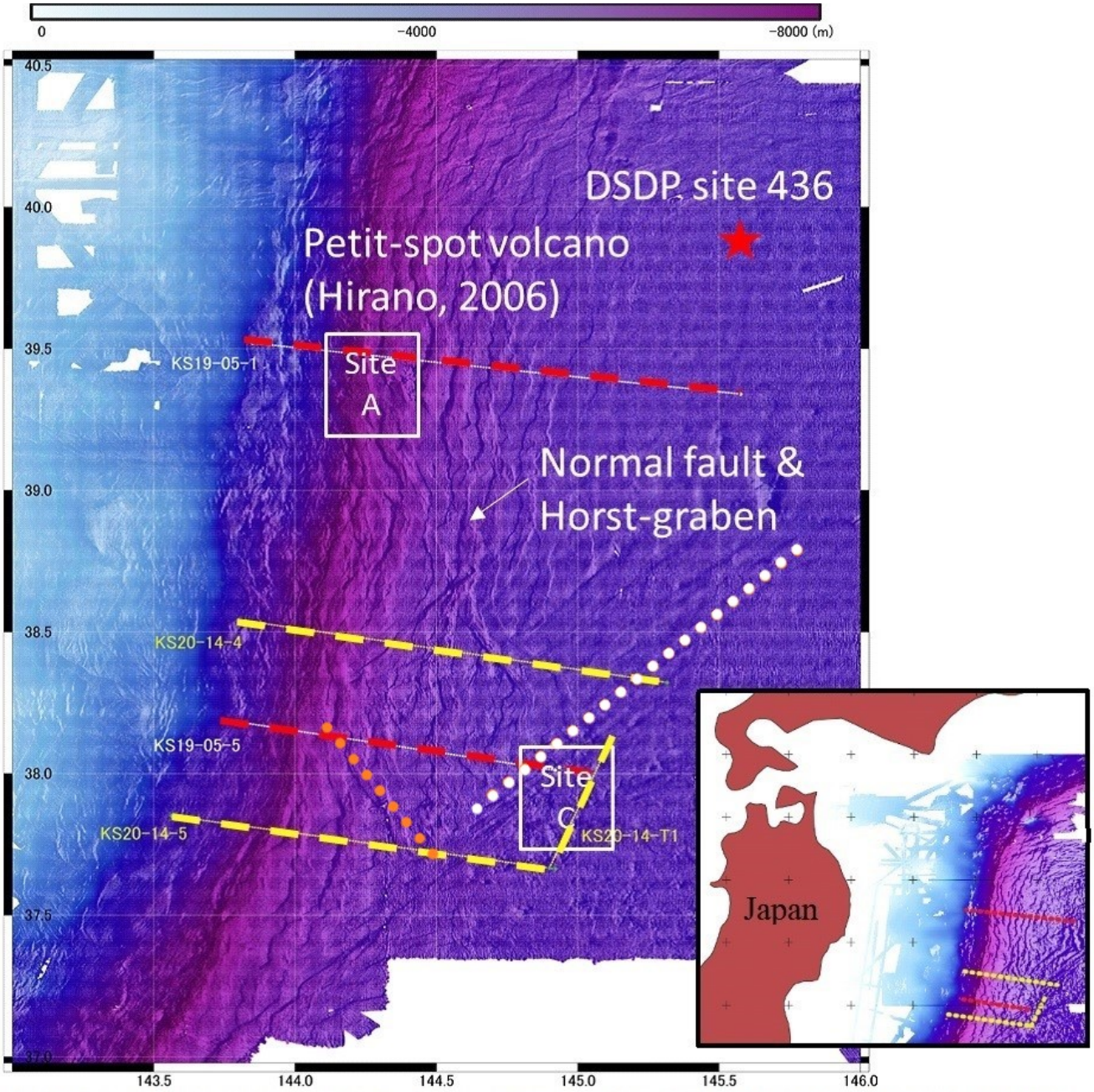


Fig.1 150m grid bathymetry map and seismic survey lines made from JCG & JAMSTEC (2011). Red dashed lines show two seismic survey lines of survey KS19-05 and yellow dashed lines show three seismic survey lies of survey of KS20-14. Two white squares show petit-spot volcanos site A and site C from Hirano (2006). The red star shows the location of DSDP (Deep Sea Drilling Project) Site 436. White dashed line shown faults that have different direction with trench axis. These faults parallel with paleomagnetic anomaly line. The orange dashed line perpendicular to the direction of the white line, shown the fracture zone direction. The lower right figure shows the relative position of study area and Japan.

©2021. Japan Geoscience Union. All Right Reserved.

Complicated fault geometry of outer-trench normal-faulting earthquakes based on the ocean bottom seismograph observations

*Koichiro Obana[1], Tsutomu Takahashi[1], Yojiro Yamamoto[1], Yasuyuki Nakamura[1], Gou Fujie[1], Seiichi Miura[1], Shuichi Kodaira[1]

1. Research Institute for Marine Geodynamics, Japan Agency for Marine-Earth Science and Technology

After the 2011 Mw 9.0 Tohoku-oki earthquake, intra-plate normal-faulting earthquakes, including several M7-class earthquakes, have occurred in the trench-outer rise region along the Japan Trench and concern of large outer-rise earthquakes and related tsunamis have been raised. Based on the aftershock distribution, earthquake ruptures consisting of multiple faults are suggested for some large outer rise earthquakes. For 1933 Showa-Sanriku earthquake, rupture along two roughly parallel faults dipping toward opposite direction (westward dipping and eastward dipping) are proposed by Uchida et al. (2016). In addition, aftershock distribution along two conjugate faults were observed for two M7-class earthquakes in 2005 and 2011 in the trench-outer rise region along the Japan Trench (Hino et al. 2009, Obana et al.). The aftershock distribution used in these studies are based on the far-filed observations or observations conducted in a month to a few years later from the mainshock. During the OBS observations conducted in the trench-outer rise region of the central Japan Trench from September 2017 to July 2018, three M6-class outer-rise normal-faulting earthquakes (M6.3 on Sep. 21, 2017, M6.3 on Oct. 6, 2017, and M6.0 on Nov. 13, 2017) occurred around the OBS network. The results from the OBS observations succeeded to locate the rupture initiation of the mainshocks and aftershock activities including immediately after the mainshocks. The aftershocks of M6.3 earthquake on October 6 occurred along several inclined planes with different dipping angles and directions. Focal mechanisms indicate both normal-faulting and strike-slip aftershocks. In the trench-outer rise region, there are horst-and-graben structures formed by normal-faults cutting through the oceanic crust. The M6.3 earthquake on October 6 occurred at a joint of segments of the horst-graben-structures. Complicated distribution of the aftershocks with both normal-faulting and strike-slip suggests a possible compound rupture of multiple faults during the intra-plate normal-faulting earthquake. The other two M6-class earthquakes also show the complicated distribution of the aftershocks and suggest the relation to multiple faults both apparent and obscure from the bathymetry. Such complicated fault geometry should be considered as a possible fault of large intra-plate normal-faulting earthquakes and related tsunamis.

Keywords: Japan Trench, outer rise

©2021. Japan Geoscience Union. All Right Reserved.

Mantle-derived helium released through the Japan Trench bend-faults <gdiv></gdiv>

*Jin-Oh Park[1], Naoto Takahata[1], Ehsan Jamali Hondori[1], Asuka Yamaguchi[1], Takanori Kagoshima[2], Tetsuro Tsuru[3], Gou Fujie[4], Yue Sun[1], Juichiro Ashi[1], Makoto Yamano[5], Yuji Sano[1]

1. Atmosphere and Ocean Research Institute, University of Tokyo, 2. Department of Environmental Biology and Chemistry, University of Toyama, 3. Department of Marine Resources and Energy, Tokyo University of Marine Science and Technology, 4. Japan Agency for Marine-Earth Science and Technology, 5. Earthquake Research Institute, University of Tokyo

Plate bending-related normal faults (i.e. bend-faults) develop at the outer trench-slope of the oceanic plate incoming into the subduction zone. Numerous geophysical and numerical simulation studies suggest that bend-faults play a key role by providing pathways for seawater to flow into the oceanic crust and upper mantle, thereby promoting hydration of the oceanic plate. However, deep penetration of seawater along bend-faults remains controversial because fluids that have percolated down into the mantle are difficult to detect. In this talk we presents anomalously high helium isotope (3He/4He) ratios and seismic reflection data which support fluid infiltration into the mantle and subsequent outflow through bend-faults across the outer slope of the Japan Trench. Almost constant 3He/4He and 4He/20Ne ratios with depth at sites near trench bend-faults suggest local seawater inflow. Our findings provide the first reported evidence for a potentially large-scale active hydrothermal circulation system through bend-faults across the Moho (crust-mantle boundary) in and out of the oceanic lithospheric mantle. Mantle fluids expelled from the oceanic plate before subduction, if found to be pervasive across most of the ocean trench slope, would necessitate reconsideration of the water budget between Earth’s surface and its interior in terms of the global water cycle. As a future study, time-series geochemical observations at additional sites are required to clarify detailed fluid flux and the water circulation pattern. Ocean drilling of the bend-faults, which enables us to define mechanical and hydrological properties of the faults and to observe the mantle fluids at deeper depths, would be useful for more comprehensive understanding of the mantle fluid flow.<gdiv></gdiv><gdiv></gdiv><gdiv></gdiv>

Keywords: Mantle-derived helium, bend-faults, Japan Trench

©2021. Japan Geoscience Union. All Right Reserved.

Heat flow distribution seaward of the Japan and Kuril trenches: Implications for fluid circulation in the oceanic crust

*Makoto Yamano[1], Yoshifumi Kawada[2], Kouta Sasaki[3], Masataka Kinoshita[1]

1. Earthquake Research Institute, the University of Tokyo, 2. Japan Agency for Marine-Earth Science and Technology, 3. Kozo Keikaku Engineering Inc.

Anomalous heat flow values, higher than that expected for the seafloor age of the incoming Pacific plate, are pervasively distributed on the outer rise of the Japan Trench. Overlapping the broad anomaly, local variations at a scale of several kilometers were detected through concentrated measurements along lines perpendicular to the trench. The broad high heat flow zone seaward of the trench can be attributed to pore fluid circulation in a permeable layer developed through fracturing of the oceanic crust due to plate bending, which efficiently pumps up heat from deeper part of the crust. Local variations may have arisen from heterogeneous development of fractures: higher surface heat flow is observed at sites where the crust has been fractured down to deeper part.

On the seaward slope of the Japan Trench, where normal faults are well developed, heat flow data has been rather sparse compared to dense data on the outer rise. We conducted heat flow measurements around faults with large surface displacement in the upper part of the seaward slope, on research cruises in 2015, 2016, and 2020. At around 39°N, heat flow values obtained at sites near faults are, on average, lower than the values on the outer rise, indicating that fluid circulation pattern in the oceanic crust may have changed associated with development of normal faults. Local heat flow variations were found in the vicinities of fault escarpments, possibly related to focused fluid flow along faults.

We also conducted heat flow measurements on the outer rise of the westernmost part of the Kuril Trench, adjacent to the Japan Trench, in 2018 and 2020. Most of the obtained values are normal for the seafloor age, in contrast to the high average heat flow on the Japan Trench outer rise. Local high heat flow anomalies were detected at two sites. One of them, at around 70 km from the trench axis, is rather broad, extending at least 5 km along a line perpendicular to the trench. We should make more measurements to delineate the shapes of local anomalies off the Kuril Trench for comparison with those off the Japan Trench.

These characteristics in the heat flow distribution provide information on fracturing process and fluid flow pattern in the oceanic crust. Nearly normal heat flow off the Kuril Trench may result from lower average permeability in less fractured crust, which suppresses development of large-scale fluid circulation. It is consistent with the observation that the anomaly in the seismic velocity structure is more significant off the Japan Trench than off the Kuril Trench. More detailed survey of the local anomalies would allow us to discuss heterogeneity in the oceanic crust and its regional variation along the trench.

Keywords: heat flow, oceanic crust, fluid circulation, heat transport, Japan Trench, Kuril Trench

©2021. Japan Geoscience Union. All Right Reserved.

Resistivity imaging around the Japan trench based on ocean bottom electromagnetic surveys

*Hiroshi Ichihara[1], Takafumi Kasaya[2], Tada-nori Goto[3], Kiyoshi Baba[4], Shinya Sato[5], Makoto Yamano[4]

1. Graduate school of environmental studies, Nagoya University, 2. JAMSTEC, 3. ERI, University of Tokyo, 4. University of Hyogo, 5. Graduate School of Engineering, Kyoto University

Electrical resistivity in the earth reflects amount, composition and connectivity of fluid, temperature, and lithology. Recent developments of seafloor observation instruments, data processing and inversion method allow us to obtain reliable images of resistivity distribution. Thus resistivity imaging is a powerful tool to discuss fluid and clay mineral distribution around the outer-rise (e.g. Naif et al., 2015) and subduction zone. In the Tohoku-oki area, Ocean Bottom Electro-magnetometers were deployed at 48 sites in order to obtain regional resistivity distribution based on magnetotelluric method. In the presentation, we introduce the OBEM surveys and resistivity models based on 2-D inversion procedures in the incoming plate zone and around the rupture zone of the 2011 Tohoku-oki earthquake (M9.0). Beneath the survey line along N39.4° across the incoming plate zone, the resistivity profile showed a conductive zone around a bending fault area. Sensitivity tests showed that the conductive zone may widely distributed near the Japan trench although depth range of the conductor were not constrained well. It implies hydration around the bending fualt. Beneath the survey line across rupture area of the 2011 Tohoku-oki earthquake (M9.0), the resistivity profile shows a low resistivity zone in the shallowest part of plate interface where huge fault slip over 80 m was reported (e.g. Iinuma et al., 2012; Fujiwara et al., 2011). On the other hand, resistivity is relatively high in the deeper plate interface that had been known as “asperity” and initial rupture zone was located. They indicate that the huge fault slip occurred in the pore fluid rich area that may affected by hydration in the incoming plate. However, especially in the incoming plate zone, MT impedances indicated strong three-dimensionality of resistivity structure and were not explained by a simple resistivity model including 3D bathymetry. It implies strong heterogeneity of the underground resistivity distribution and thus requires 3-D resistivity analyses.

Keywords: incoming plate, 2011 Tohoku-oki earthquake, OBEM, magnetotelluric

©2021. Japan Geoscience Union. All Right Reserved.

[J] Poster | S (Solid Earth Sciences)：S-CG Complex & General

Sun. Jun 6, 2021 5:15 PM - 6:30 PM JST | Sun. Jun 6, 2021 8:15 AM - 9:30 AM UTC | Ch.16_3

[S-CG55] Oceanic plate as inputs to subduction zone: from oceanic spreading ridge to subduction trench

convener:Gou Fujie(Japan Agency for Marine-Earth Science and Technology), Makoto Yamano(Earthquake Research Institute, the University of Tokyo), Tomoaki Morishita(School of Geoscience and Civil Engineering, College of Science and Technology, Kanazawa University), Takanori Kagoshima(University of Toyama)

As the inputs to subduction zone, the nature of the incoming oceanic plate, such as surface relief, thermal state, lithology, and the water content, affects various processes occurring in the subduction zone, including arc magmatism and interplate and intraplate seismic activities. The oceanic plate is formed in the oceanic spreading ridge and moves through the ocean basin for a long time and subducts from the oceanic trench. The nature of the incoming oceanic plate is determined by all the processes occurring from the spreading ridge to the subduction trench; e.g., hydrothermal circulation, sedimentation and diagenesis for more than millions years at the oceanic basin, and plate bending-related faulting near the subduction trench. Therefore, for studying the nature of the subduction inputs, it is essential to reveal the various evolution processes of the oceanic plate between the spreading ridge and the subduction trench.

We welcome contributions from a broad range of earth science (geophysics, geology, petrology, drilling science, and so on) discussing topics related to the inputs to subduction zones, such as tectonic process associated with the plate bending prior to subduction, post-spreading volcanic activities including large seamount formation and petit-spot volcanoes, and the nature of the "normal" or "typical" oceanic plate.

This session is supported by the focus group of hard rock drilling science.

[SCG55-P01] Compilation of bathymetry and seismic reflection data to characterize outer rise faults in the Kuril Trench

*Shuichi Kodaira[1], Tetsuo No[1], Yasuyuki Nakamura[1], Gou Fujie[1], Koichiro Obana[1], Seiichi Miura[1] (1.Research Institute for Marine Geodynamics, Japan Agency for Marine-Earth Science and Technology)

[SCG55-P02] Characteristics of the oceanic plate near the Nosappu fracture zone revealed by the extensive seismic structure studies

*Gou Fujie[1], Koichiro Obana[1], Shuichi Kodaira[1], Katsuyoshi Michibayashi[2] (1.Japan Agency for Marine-Earth Science and Technology, 2.Nagoya University)

[SCG55-P03] Hydrothermal experiments in olivine-orthopyroxene-H2O system at 200-400C: implications for hydrogen generation at high temperatures

*Shuhei Tanaka[1], Atsushi Okamoto[2], OTGONBAYAR DANDAR[2], Masaoki Uno[2], Masakazu Fujii[3] (1.Tohoku University, 2.Graduate school of environmental studies, Tohoku University, 3.National institute of Polar research and SOKENDAI)

[SCG55-P04] Hydration processes of a forearc mantle wedge inferred from the Takadomari serpentinite body in the Kamuikotan Belt, central Hokkaido, Japan

*Shun Takamizawa[1], Yuji Ichiyama[1], Shusaku Yamazaki[2], Akihiro Tamura[3], Tomoaki Morishita[3] (1.Chiba University , 2.Civil Engineering Research Institute for Cold Region, 3.School of Geoscience and Civil Engineering, College of Science and Technology, Kanazawa University)

[SCG55-P05] Petrological features and formation processes of lower crustal cumulate xenoliths from Oki-Dogo Island: A possibility of mantle plume origin

*Rio Higuchi[1], Yuji Ichiyama[1], Akihiro Tamura[2], Tomoaki Morishita[2] (1.Chiba University, 2.Faculty of Geosciences and Civil Engineering, Kanazawa University)

Compilation of bathymetry and seismic reflection data to characterize outer rise faults in the Kuril Trench

*Shuichi Kodaira[1], Tetsuo No[1], Yasuyuki Nakamura[1], Gou Fujie[1], Koichiro Obana[1], Seiichi Miura[1]

1. Research Institute for Marine Geodynamics, Japan Agency for Marine-Earth Science and Technology

It has been reported that stress changes in the oceanic plate associated with an interplate megathrust earthquakes cause to activate seismic activity in the oceanic plate before subduction, which is sometimes accompanied with a large normal fault earthquake. For example, along the Kuril Trench, an extensional earthquake (Mw=8.1) occurred within the oceanic plate in 2007, following a shallow megathrust event (Mw=8.3) at the plate boundary in 2006. In the Japan Trench region, normal fault earthquakes in the outer-rise have been activated immediately after the 2011 Tohoku-oki earthquake. Based on results of our previous earthquake observations and seismic imaging, it has been concluded that, i) the outer rise normal fault earthquakes dominantly occur along the horst-and-graben structure formed by plate bending, ii) the horst-and-graben structure is mainly developed oblique to the fabric of the oceanic plate, and iii) dip of the normal fault is as high as 70˚ at the depth of the crust and uppermost mantle. On the other hand, in the Kuril Trench, the trench axis and oceanic fabric run almost parallel, and the development of bend-related faults along the oceanic fabric can be confirmed from bathymetry data. In order to clarify the differences in a formation process of outer-rise faults and fault geometry between the Japan Trench, where new bend-related faults are dominantly formed, and the Kuril Trench, where bend-related faults develop along the oceanic fabric, this study compiles high resolution seismic reflection data, conventional seismic reflection data, and detailed bathymetry data, which have been acquired in the Kuril Trench by JAMSTEC since 2016. The results indicate that the half-graben fault structure formed by seaward trending high-angle normal faults is dominant in the Kuril Trench, unlike the Japan Trench where horst-and-graben faults dominantly develop. The conventional seismic reflection data also shows oceanic Moho, but the current processing of the data does not allow us to identify if there is an offset of the Moho associated with normal faulting. Reflection events indicating normal faults in the oceanic crust are not imaged, but it is still unknow whether this is due to structure or processing. Further data processing focusing on fault images in the oceanic crust and Moho offsets is necessary. We will use these data to describe the fault geometry and discuss the formation process of the outer rise fault. As a final goal of the project, we will also create a fault map of the offshore Kuril Trench to contribute mitigation of tsunami hazards.

Keywords: Kuril Trench, Outer rise earthquake, Bend-related fault

©2021. Japan Geoscience Union. All Right Reserved.

Characteristics of the oceanic plate near the Nosappu fracture zone revealed by the extensive seismic structure studies

*Gou Fujie[1], Koichiro Obana[1], Shuichi Kodaira[1], Katsuyoshi Michibayashi[2]

1. Japan Agency for Marine-Earth Science and Technology, 2. Nagoya University

The global compilation studies on the seismic structure of the oceanic crust, such as Christeson et al. (2019) and Grevemeyer et al. (2018), indicate that the fast spreading oceanic crust, in comparison with the slow spreading oceanic crust, is laterally uniform in thickness and seismic velocities, and has relatively higher seismic velocities within both the oceanic layer 2 and layer 3. The northwestern part of the oceanic Pacific plate off northeast Japan arc was formed at a fast spreading ridge more than 100 million years ago. We JAMSTEC have conducted extensive controlled-source seismic surveys in this region and confirmed that the oceanic crust is quite simple and laterally uniform in most areas. The typical thickness of the oceanic crust is approximately 7 km and the seismic velocities at the top of the oceanic layer 3 is 6.5 km/sec in most areas. These features are well consistent with the global compilation studies.

However, our data show that the oceanic crust become thinner when it approaches to the Nosappu fracture zone. As the crust become thinner, seismic velocities within the oceanic crust become lower and the boundary between the layer 2 and layer 3, which is estimated by the changes in the vertical velocity gradient, becomes unclear. These characteristics are not consistent with those of the fast spreading oceanic crust but somewhat similar to those of the slow spreading oceanic crust. In addition to the oceanic crust, we found that the oceanic mantle shows strange characteristics toward the Nosappu fracture zone. Generally, the topmost oceanic mantle formed at the fast spreading center shows strong seismic anisotropy, which can be explain by the alignments of the olivin crystal due to the fast mantle flow at the spreading center. Since the mantle flow is expected to be perpendicular to the ridge axis, the fast axis of the seismic anisotropy is perpendicular to the ancient ridge axis which is represented by the magnetic anomaly lineation. In the northwestern part of the oceanic Pacific plate, the topmost oceanic mantle shows a strong anisotropy, more than 8 percent, and the fast axis is perpendicular to the magnetic anomaly lineation in most areas (Kodaira et al., 2014). However, when it approaches to the Nosappu fracture zone, the direction of the fast axis seems to rotate by more than 45 degrees although the strength of the seismic anisotropy suggested by the shear wave splitting is roughly the same (about 8 percent). If the strong anisotropy is caused by the mantle flow at the spreading center, our observation implies that the mantle flow near the Nosappu fracture zone was oblique to the ridge axis when the oceanic plate was formed. The oblique mantle flow might be explained by the existence of the transform fault (the current Nosappu fracture zone) near the spreading center and might be responsible for the slow-spreading-like oceanic crust there.

In this presentation, we will show the existing seismic data and seismic structures that support our hypothesis. In addition, we would like to propose an integrated marine geophysical observation, including seismic, electromagnetic, and gravity, to test our hypothesis.

Keywords: oceanic plate, Fracture zone, seismic survey, mantle anisotropy

©2021. Japan Geoscience Union. All Right Reserved.

Hydrothermal experiments in olivine-orthopyroxene-H2O system at 200-400C: implications for hydrogen generation at high temperatures

*Shuhei Tanaka[1], Atsushi Okamoto[2], OTGONBAYAR DANDAR[2], Masaoki Uno[2], Masakazu Fujii[3]

1. Tohoku University, 2. Graduate school of environmental studies, Tohoku University, 3. National institute of Polar research and SOKENDAI

Hydrogen and hydrocarbon production during serpentinization provide significant impacts on microbial activities within the oceanic lithosphere. At the slow- to ultraslow spreading ridges, the alkaline hydrothermal vents with a special ecosystem has been discovered such as Lost City in Mid Atlantic Ridge. These hydrothermal vents are relatively low-temperatures, compared to the those in the fast-spreading ridges. Recently, it is suggested that serpentinization proceeds by seawater penetrating to the deep high-temperature fracture zones, and the bending faults, which potentially higher extent of hydration and hydrogen production. However, there has been few studies on serpentinization and hydrogen generation at temperature exceeding 300C.

In this study, we conducted hydrothermal experiments on serpentinization, focusing on (1) temperature, (2) silica (orthopyroxene) and (3) mass transport (batch vs. flow-through). The experiments were conducted in Ol-H_2O system and Ol-Opx-H_2O system. Batch type experiments were conducted for 576 hours at 200, 250, 280, 300, 350C at the vapor-saturated pressure and 400℃ at 30 MPa. Flow-through type experiments were conducted at 35 MPa and flow rate of 0.1 ml/min at 300C and 350C for the Ol-H_2O system and 300C and 380C for the Ol-Opx-H_2O system for 207-284 hours. After each run, the water content and magnetic susceptibility were measured, and microstructures were observed by using SEM.

In the Ol-H2O system, the extent of the serpentinization is highest at 300, and serpentinization did not proceed at 400C. In contrast, in the Ol-Opx-H_2O system, the rate of the serpentinization was 1.5 times larger at 300C and >10 times larger at 400C than in the Ol-H_2O system. In the flow-through type experiments, the reaction progress was 10 times larger than in the batch type experiments for both systems. These results indicates that the serpentinization proceeded after orthopyroxene faster in particular at high temperatures, and leaching of SiO_2 by flow-through systems. The EDS analyses suggest that serpentinine minerals do not contain Fe3+ in any conditions. In contrast, magnetite linearly increased with the progress of serpentinization in the Ol-H2O system, whereas it does not increase in the Ol-Opx-H2O system. This can be understood in the activity diagram of silica activity and oxygen fugacity that iron is included in serpentine minerals in high silica activity. Our results suggest that serpentinization proceeds in harzburgite even at high temperature of >350, but the iron contents in orthopyroxene does not contribute to the hydrogen production. The production of hydrogen energy occurs at olivine-rich rocks at relatively low temperature.

Keywords: serpentinization, hydrogen

©2021. Japan Geoscience Union. All Right Reserved.

Hydration processes of a forearc mantle wedge inferred from the Takadomari serpentinite body in the Kamuikotan Belt, central Hokkaido, Japan

*Shun Takamizawa[1], Yuji Ichiyama[1], Shusaku Yamazaki[2], Akihiro Tamura[3], Tomoaki Morishita[3]

1. Chiba University , 2. Civil Engineering Research Institute for Cold Region, 3. School of Geoscience and Civil Engineering, College of Science and Technology, Kanazawa University

Subduction zones are the place where the recycling of Earth's surface materials has been taking place. In particular, the water cycle, which is caused by the subduction of the hydrated oceanic crust, is thought to be related to hydration of mantle wedges and consequent igneous and hydrothermal activities in subduction zones, but the details of hydration processes have been unclear. The Kamuikotan Belt in central Hokkaido consists mainly of Cretaceous high-pressure metamorphic rocks and ultramafic rocks. Because the high-pressure metamorphic rocks are interpreted to be derived from ancient subducted slabs, the ultramafic rocks associated with them can be regarded as mantle wedge materials beneath a subduction zone. The Takadomari serpentinite body in the Kamuikotan Belt. Consist of highly depleted serpentinized peridotite, which is interpreted as the residual mantle after the release of high-Mg andesitic magma, such as boninite, beneath an oceanic island arc (Tamura et al., 1999). The Takadomari serpentinite body contact with the high-pressure metamorphic rocks by faults, and the degrees of antigoritization increase towards the boundary with the metamorphic rocks (e.g., Igarashi, 1985). The presence of amphibolite tectonic blocks with blueschist-facies overprints (e.g., Ishizuka and Imaizumi, 1980) suggests that high-pressure metamorphism also affected the Takadomari serpentinite body. In this study, field survey, petrographic observations, and major and trace element analyses of minerals for the Takadomari serpentinite body in the Kamuikotan Belt, were performed to understand the spatial and temporal hydration processes of a mantle wedge. In the Takadomari serpentinite body, highly depleted harzburgite and dunite (Spinel Cr# = 0.6-0.9) are highly serpentinized. In particular, antigoritization tends to be strong in the southern part of the body near the high-pressure metamorphic rocks. This trend is consistent with the observation of Igarashi (1985), but highly antigoriteized serpentinites are also broadly distributed the Takadomari serpentinite body. Antigoritization is more pronounced in dunite than harzburgite. The Takadomari serpentinites usually have talc and Ca amphibole with tremolite to magnesio-hornblende compositions, as replacements of pyroxene. The Ca amphibole in the Takadomari serpentinites can be divided into two types, based on the Na_2O content. Estimated temperatures and pressures using thermobarometries for the Na-rich Ca amphibole (ca. 830 ℃ and 1.2 GPa) are higher than those of the Na-poor Ca amphibole (ca. 780 ℃ and 0.5 GPa). The occurrence of the Na-rich Ca amphibole is restricted to the northern part of the Takadomari serpentinite body, and rare phlogopite-bearing serpentinite is also present. After the formation of Ca amphibole, subsequent cooling resulted in talc. Further cooling formed richterite, Fe-rich metamorphic olivine, and clinopyroxene in association with antigorite in serpentinites near the boundary with high-pressure schist. In these serpentinites, olivine with stripe structure or parting is also present. These mineral paragenesis indicate that the serpentinites experienced prograde and retrograde events at around 500-600 ℃. In contrast, Mg-rich metamorphic olivine associated with antigorite and magnetite, was formed by prograde events at lower temperatures (around 400 ℃). The petrological characteristics of the Takadomari serpentinites are closely similar to those of the Mariana forearc serpentinites, indicating that the Takadomari serpentinite body was part of a forearc mantle wedge. The trace element patterns of Ca amphibole and richterite are significantly enriched in fluid mobile elements, such as Cs, Rb, and Pb. Similar trends are also observed in

©2021. Japan Geoscience Union. All Right Reserved.

the Mariana forearc serpentinite (Ichiyama et al., 2021), implying that the metasomatic agent for the Takadomari serpentinites body would have been fluids derived from subducted slabs. The slab-derived fluids at high temperatures were probably K-rich, as implied by the presence of phlogopite, but those at low temperatures were Na-rich due to the formation of richterite. The Takadomari serpentinite body, was finally emplaced on land together with the high-pressure Kamuikotan metamorphic rocks as an ancient forearc mantle wedge and an underlying slab.

Keywords: Subduction zone, Mantle wedge, Slab-derived Fluid, Metasomatism, Kamuikotan Belt

©2021. Japan Geoscience Union. All Right Reserved.

Petrological features and formation processes of lower crustal cumulate xenoliths from Oki-Dogo Island: A possibility of mantle plume origin

*Rio Higuchi[1], Yuji Ichiyama[1], Akihiro Tamura[2], Tomoaki Morishita[2]

1. Chiba University, 2. Faculty of Geosciences and Civil Engineering, Kanazawa University

In Oki-Dogo Island, the northern part of Shimane Prefecture, Pliocene alkali basalts often include ultramafic and mafic xenoliths (e.g., Aoki, 1977; Takahashi, 1976). Takahashi(1976) reconstructed a petrologic structure from crust to upper mantle beneath Oki-Dogo Island, based on the lithofacies of the xenoliths. Abe et al. (2003) investigated lherzolitic mantle peridotite xenoliths from Oki-Dogo Island and revealed that they are characterized by Fe- and rare-earth element (REE)-enrichment and the presence of aluminous spinel. They also proposed that the Oki-Dogo peridotite xenoliths are involved with the Middle Miocene backarc spreading of the Japan Sea. In contrast to attention to the mantle peridotite xenoliths, mafic and ultramafic xenoliths derived from the lower crust have not yet been studied. In this study, the petrographic observation and major- and trace-element analyses for the lower crustal cumulate xenoliths, olivine-gabbro, orthopyroxene-gabbro, granulite, clinopyroxenite, and wehrlite were performed to examine the petrological features and formation processes and to reveal their source mantle composition and tectonic implications for the circum-Japan Sea region. The lower crustal xenoliths exhibit the cumulate texture of poikilitic plagioclase with olivine and clinopyroxene oikocrysts, and the estimated equilibrium temperatures (>700℃) indicate that they formed in the lower crust. Olivine Mg# [=Mg/(Mg+Fe)] in the cumulates is lower than those of MORB (0.7–0.8), at a given NiO content, and spinel Cr# [=Cr/(Cr+Al)] is significantly low (<0.1). The REE patterns of clinopyroxene show light REE-enrichment. These petrological characteristics indicate that the lower crust cumulates were crystallized from the magma that was produced by low degrees of partial melting of the source mantle. The estimated REE patterns of the parental magma of the cumulates are different from those of basalts formed during the Japan Sea backarc-spreading in the Middle Miocene but resemble those of the Late Miocene-Pliocene alkali basalts, formed by mantle plumes in the post-backarc-spreading magmatism. The lherzolite xenoliths can be the source mantle for the estimated parental magma of lower crustal cumulates. The Oki-Dogo spinel- lherzolite xenoliths are possibly enriched mantle material derived from the Late Miocene-Pliocene mantle plumes.

Keywords: Backarc-spreading, Backarc-spreading of the Japan Sea, Xenolith, Mantle plume, Lower crust, Southwest Japan

©2021. Japan Geoscience Union. All Right Reserved.

[E] Oral | B (Biogeosciences)：B-PT Paleontology

Sun. Jun 6, 2021 1:45 PM - 3:15 PM JST | Sun. Jun 6, 2021 4:45 AM - 6:15 AM UTC | Ch.26 Zoom Room 26

[B-PT01] Biomineralization and Geochemistry of Proxies

convener:Takashi Toyofuku(Japan Agency for Marine-Earth Science and Technology (JAMSTEC)), Hiroshi Kitazato(Tokyo University of Marine Science and Technology (TUMSAT)), Jelle Bijma(Alfred-Wegener-Institut Helmholtz-Zentrum für Polar- und Meeresforschung), Kotaro Hirose(Faculty of Science and Engineering, Waseda University), Chairperson:Takashi Toyofuku(Japan Agency for Marine-Earth Science and Technology (JAMSTEC)), Hiroshi Kitazato(Tokyo University of Marine Science and Technology (TUMSAT)), Kotaro Hirose(Faculty of Science and Engineering, Waseda University), Jelle Bijma(Alfred-Wegener-Institut Helmholtz-Zentrum für Polar- und Meeresforschung)

In order to reconstruct the Earth climate system, marine paleoclimatologists resort to transfer functions or geochemical proxies, which are produced or affected by organisms. The relationships used for reconstructions are generally based on field calibrations or derived from laboratory experiments. The danger of these so-called empirical relationships is that they may be valid only within the restricted parameter space of their calibration. Application of proxy relationships to very different environmental settings (e.g. high vs. low latitude or glacial vs. interglacial) requires a mechanistic understanding of these relationships. Much progress can be expected by a better understanding of the biomineralization mechanisms and the incorporation of proxy signals.
In this session we facilitate contributions related to the biomineralization, calibration and validation of marine proxies from field study, laboratory culture experiment and paleo-environmental reconstruction.

1:45 PM - 1:48 PM JST | 4:45 AM - 4:48 AM UTC

[BPT01-01] Introduction

1:48 PM - 2:03 PM JST | 4:48 AM - 5:03 AM UTC

[BPT01-02] Seascape ecological view as a new insight of benthic foraminiferal community

*Hiroshi Kitazato[1] (1.Tokyo University of Marine Science and Technology (TUMSAT))

2:03 PM - 2:21 PM JST | 5:03 AM - 5:21 AM UTC

[BPT01-03] Macromolecular analysis of modern aquatic palynomorphs using micro-Raman spectroscopy

*Takuto Ando[1], Tatsuyuki Yamamoto[2], Mika Ishigaki[3], Kazumi Matsuoka[4] (1.Estuary Research Center, Shimane University, 2.Faculty of Life and Environmental Sciences, Shimane University, 3.Center for Promotion of Project Research. Shimane University, 4.Institute for East China Sea Research, Nagasaki University, Japan)

2:21 PM - 2:39 PM JST | 5:21 AM - 5:39 AM UTC

[BPT01-04] **The spatial distribution and the origin of heavy metals in bottom sediments from Lake Shinji and Nakaumi**

*Hanye ZHANG[1], Kotaro Hirose[1], Kazuo Kamura[1], Minami Aoki[1], Koji Seto[2] (1.Faculty of Science and Engineering, Waseda University, 2.Estuary Research Center, Shimane University)

2:39 PM - 2:57 PM JST | 5:39 AM - 5:57 AM UTC

[BPT01-05] Sedimentary geochemical record of human-induced environmental changes in the estuarine lake Nakaumi, southwest Japan

*Kotaro Hirose[1], Minami Aoki[4], Akira Tsujimoto[3], Koji Seto[2], Kazuo Kamura[1] (1.Faculty of Science and Engineering, Waseda University, 2.Estuary Research Center, Shimane University, 3.Faculty of Education, Shimane Universit, 4.Faculty of Science and Engineering, Waseda University (currently Seikei Gakuen))

2:57 PM - 3:15 PM JST | 5:57 AM - 6:15 AM UTC

[BPT01-06] Calcification depths of planktic foraminifers constrained using geochemical signatures in the sediment trap samples collected from the Bay of Bengal

*Ayumi Maeda[1], Azumi Kuroyanagi[2], Toshihiro Yoshimura[3], Birgit Gaye[4], Tim Rixen[5], Atsushi Suzuki[1], Hodaka Kawahata[6] (1.National Institute of Advanced Industrial Science and Technology, 2.Tohoku University Museum, The Center for Academic Resources and Archives, Tohoku University, 3.Japan Agency for Marine-Earth Science and Technology, 4.Institute for Geology, Universität Hamburg, 5.Leibniz Centre for Tropical Marine Research, 6.Atmosphere and Ocean Research Institute, The University of Tokyo)

[E] Oral | B (Biogeosciences) | B-PT Paleontology

[B-PT01] Biomineralization and Geochemistry of Proxies

convener:Takashi Toyofuku(Japan Agency for Marine-Earth Science and Technology (JAMSTEC)), Hiroshi Kitazato(Tokyo University of Marine Science and Technology (TUMSAT)), Jelle Bijma(Alfred-Wegener-Institut Helmholtz-Zentrum für Polar- und Meeresforschung), Kotaro Hirose(Faculty of Science and Engineering, Waseda University), Chairperson:Takashi Toyofuku(Japan Agency for Marine-Earth Science and Technology (JAMSTEC)), Hiroshi Kitazato(Tokyo University of Marine Science and Technology (TUMSAT)), Kotaro Hirose(Faculty of Science and Engineering, Waseda University), Jelle Bijma(Alfred-Wegener-Institut Helmholtz-Zentrum für Polar- und Meeresforschung)

Sun. Jun 6, 2021 1:45 PM - 3:15 PM Ch.26 (Zoom Room 26)

In order to reconstruct the Earth climate system, marine paleoclimatologists resort to transfer functions or geochemical proxies, which are produced or affected by organisms. The relationships used for reconstructions are generally based on field calibrations or derived from laboratory experiments. The danger of these so-called empirical relationships is that they may be valid only within the restricted parameter space of their calibration. Application of proxy relationships to very different environmental settings (e.g. high vs. low latitude or glacial vs. interglacial) requires a mechanistic understanding of these relationships. Much progress can be expected by a better understanding of the biomineralization mechanisms and the incorporation of proxy signals.

In this session we facilitate contributions related to the biomineralization, calibration and validation of marine proxies from field study, laboratory culture experiment and paleo-environmental reconstruction.

1:45 PM - 1:48 PM

[BPT01-01]Introduction

©Japan Geoscience Union

Seascape ecological view as a new insight of benthic foraminiferal community

*Hiroshi Kitazato[1]

1. Tokyo University of Marine Science and Technology (TUMSAT)

Foraminifers secrete various chemicals for chamber walls. They are calcium carbonates such as calcite, aragonite, Mg-calcite, organic compounds for agglutinated chambers and/or organic cemented test walls. Foraminiferal test walls basically form according to genetic information. However, same test group is tended to gather at specific microenvironments. For instance, turf shaped algal microhabitat such as coralline algae at rocky shore is composed of both frond and thallus parts as microhabitat. Frond part is open space where fresh seawater moves inbetween one frond and to the other. *Elphidium crispum*, *Pararotalia nipponica* and *Patellina corrugate* and other calcareous foraminifers dwell at frondal surface. In contrast, thallus part is muddy and high concentration of organic matters. The thallus part shows less oxygenated than frondal part as the space is close. Microbial cascades are developed at thallus part. Minor elements such as Mg or Sr are relatively high in sediment. Soft-shelled forms such as *Allogromia*, gromiid, agglutinated forms and miliolids groups with high magnesian calcite tests flourish at the thallus part. Most of foraminifers dwelled at muddy environments are mobile mode of life.
Microhabitat segregation and microenvironmental differences may cause similar biomineralization of benthic foraminiferal tests. I would like to stress that micro-seascape should be important to characterize benthic foraminiferal communities.

Keywords: Seascape ecology, microhabitat, benthic foraminifers, biodiversity, biomineralization

©2021. Japan Geoscience Union. All Right Reserved.

Macromolecular analysis of modern aquatic palynomorphs using micro-Raman spectroscopy

*Takuto Ando[1], Tatsuyuki Yamamoto[2], Mika Ishigaki[3], Kazumi Matsuoka[4]

1. Estuary Research Center, Shimane University, 2. Faculty of Life and Environmental Sciences, Shimane University, 3. Center for Promotion of Project Research. Shimane University, 4. Institute for East China Sea Research, Nagasaki University, Japan

Palynomorphs are composed of resistant biomacromolecules and preserved partly in sedimentary rocks. Aquatic palynomorphs have great potential to reconstruct ecosystem or community composition of aquatic organisms in the past due to that they include several taxa with different ecological roles. For example, dinoflagellate cysts, ciliate cysts/loricas, foraminiferal linings, raphidophycean cysts, prasinophycean phycomata, flagments/eggs of zooplanktons, and acritarchs including *Micrhystridium ariakense* are deposited as aquatic palynomorphs in the sediments of Nakaumi Lagoon and Lake Shinji. However, production, preservation and distribution of these aquatic palynomorphs are not fully understood. Macromolecular analysis using micro-FTIR is common technique to know preservation/decomposition process of palynomorphs. In fact, we used micro-FTIR for chemotaxonomy and understanding preservation bias of several aquatic palynomorphs, and showed the results in this session at the last JpGU-AGU Meeting. Raman microscopy is another spectroscopic method to observe macromolecular structure and can analyze the area with micron- or submicron size. However, it is difficult to get good spectra due to emission of autofluorescence from targeted palynomorphs under the light with low wavelength (e.g., 532nm laser). In this presentation, we would like to introduce the results of micro-Raman analysis for aquatic palynomorphs succeeded by using the laser with higher wavelength (785 nm).

We analyzed authentic standards (e.g., cellulose and chitin) to compare with macromolecular structures of aquatic palynomorphs. IR spectra of polysaccharides are characterized by a dominant absorption band between 1200-1000 cm^{-1} (fingerprint region) related to the stretching vibration of C-O bond. On the other hand, Raman spectra of polysaccharides are more sharp and smaller number of peaks in the same region. The data using authentic standards suggested that IR and Raman spectra are sensitive to differences in the position of glycosidic bond (e.g., α-/β- and 1,3-/1,4-/1,6-) and the type of functional groups in fingerprint region, respectively. In fact, a shift in the Raman spectra around fingerprint region of chitin with acetamide groups was observed as compared with those of cellulose with hydroxyl groups. *Alexandrium catenella/pacificum* is one of causative dinoflagellates for paralytic shellfish poisoning and forms a translucent ellipsoidal cyst. The highest peak of IR spectra around fingerprint region in the cyst of *A. catenella/pacificum* is at ~1033cm^{-1} and lower than for cellulose (~1059cm^{-1}). On the other hand, there is no change in Raman spectra of cellulose and *A. catenella/pacificum* in fingerprint region. However, Raman spectra of the cyst wall in *A. catenella/pacificum* included the higher peaks around 1500-1200 cm^{-1} region characterized by polysaccharides with α-glucoside bond and mainly related to the scissoring vibration of C-H bond. We suggested the macromolecules in cyst wall of *A. catenella/pacificum* is possibly composed of polysaccharides with β-glucoside bonds including smaller number of α-glucoside bonds. The cysts of *A. catenella/pacificum* are more labile than the dinoflagellate cysts for degradation in the sediments, which might be resulted from higher α-/β-glucoside bonds ratio in macromolecule of cyst wall.

Keywords: micro-Raman, palynomorph, biomacromolecule, polysaccharide

©2021. Japan Geoscience Union. All Right Reserved.

©2021. Japan Geoscience Union. All Right Reserved.

The spatial distribution and the origin of heavy metals in bottom sediments from Lake Shinji and Nakaumi

*Hanye ZHANG[1], Kotaro Hirose[1], Kazuo Kamura[1], Minami Aoki[1], Koji Seto[2]

1. Faculty of Science and Engineering, Waseda University, 2. Estuary Research Center, Shimane University

The elemental composition of the surface sediment of the Hii River system estuary (Lake Shinji / Nakaumi), which straddles Shimane and Tottori prefectures, was clarified. Based on the results, mainly targeting the heavy metal elements, the spatial distribution and factors were investigated.

Using an Ekman-Birge grab, the surface sediment samples were collected from the bottom of Lake Shinji and Nakaumi and the related water systems during August and September 2016. The surface layers of the samples were separated by 2.3 cm square cube for the following analysis. Afterwards, the homogenized samples were lyophilized in order to be acid-decomposed with nitric acid and hydrochloric acid. Ultimately, the element concentration was measured by an Agilent 7700x ICP mass spectrometer.

Most of the surveyed elements show that it tends to be distributed at relatively high concentrations near the center of Lake Shinji and Nakaumi. On the contrary, low concentrations appear near the Ohashi River and its estuary and the Sakai Channel. This result has a good inverse correlation with the sand content of the sediment and is consistent with the research result by Matsumoto (2009). This tendency is thought to be due to the fact that debris brought from the catchment areas was separated according to particle size and specific gravity by the deposition process, and then particles containing each element accumulated near the center of the lake.

The spatial distribution of heavy metals in the surface sediments of the Lake Nakaumi obtained in this research is compared to the vertical change of the core sediments excavated in the center of the Lake Nakaumi (Aoki, 2019) and the spatial distribution in previous studies (Nakao et al., 1971; Kondo et al., 1986, etc.). Most of the heavy metal elements reflect the load of former mining activities, which were brought through the Ohashi and Iu rivers. Compared to the past results, the concentrations of heavy metals have been declining in recent decades, but still show a relatively high level in the western part of the Nakaumi. On the other hand, the sample of Yonago Bay in the eastern part of Nakaumi retains a relatively high concentration, among which the concentration of Mo is particularly remarkable. It is considered that Mo remains in the sediment as sulfide deposition. Possible causes include the effects of organic matter due to production activities and waste water from daily life around Yonago Bay, as well as the reducing environment caused by the obstruction of the bay and the depressions after dredging. Moreover, Mn shows a relatively high concentration from the central part of Lake Nakaumi to the area around Daikonshima and Ejima, and a relatively low concentration in Yonago Bay. It is considered that the reason why Mn is concentrated in the center of the lake rather than fixed in the sediment is probably that Mn does not form sparingly soluble sulfide.

Keywords: Lake Shinji and Nakaumi water system, surface sediment, heavy metals, spatial distribution, anthropogenic pollution, accumulation process

©2021. Japan Geoscience Union. All Right Reserved.

Sedimentary geochemical record of human-induced environmental changes in the estuarine lake Nakaumi, southwest Japan

*Kotaro Hirose[1], Minami Aoki[4], Akira Tsujimoto[3], Koji Seto[2], Kazuo Kamura[1]

1. Faculty of Science and Engineering, Waseda University, 2. Estuary Research Center, Shimane University, 3. Faculty of Education, Shimane Universit, 4. Faculty of Science and Engineering, Waseda University (currently Seikei Gakuen)

We investigated the distribution of organic- and abiotic- geochemical records in sediment from brackish lake Nakaumi to put the consequences of natural and artificial environmental factors affecting the lake environment into a larger context.

The eastern part of the Shimane Prefecture is a region of intense human activities since ancient times, and these activities are well documented in historical records. Lake Nakaumi is a brackish lagoon, which is located at the estuary of the Hii River system in the lower reaches of Lake Shinji-ko and is isolated from the Japan Sea by the Yumigahama peninsula. So, this maritime lake with geography enclosed setting is recording the effects of human activities in the lake sediments with a high temporal resolution.

We established the stratigraphy of bottom sediments at site Nk-3C in Lake Nakaumi based on three sediment cores using lithofacies, soft X-ray photography and CNS elemental analysis. Using the age model inferred from ^{137}Cs, ^{210}Pb and ^{14}C dating, the sediment is estimated to be deposited for the past 600 years, and the sedimentation rates ranges between 0.24 and 0.38 cm/yr.

The C/N, which follows a generally increasing trend in the 18th century, indicating a relative increase of terrestrial organic materials. We suggest that a displacement in river course of the Hii and/or Iinashi rivers in the middle 17th century and resulting progradation of their deltas enhanced the dilution effect on C and N due to an increase in sedimentation rate at the core site. The sharp rise of C, N, and S after late 19th century reflects the eutrophication of Lake Nakaumi, caused by an array of anthropogenic impacts, such as the rapid increase of nutrient inputs due to industrialization and population growth, and the semi-enclosure of the lake due to land reclamation in the Sakai Strait, the outlet of Lake Nakaumi.

We also investigated the vertical distribution of abiotic elements mainly heavy metals by using XRF analyzer and ICP-MS. There, we found a significant trend in Cu and Mo, which can be the distinct time indicators for the bottom sediment in Lake Nakaumi. Cu sharply increased from the 19th century, which is earlier than initiation of heavy metal increase in common sediments from Japanese urban bays (e.g. Yasuhara et al., 2007) due to industrial development at the beginning of 20th century. It reflects the Cu loads to the lake through the River Iu from Homan-zan copper mine which started in middle 19th century and reached their peak in early 20th century. Mo displayed three peaks in the early 1900s, 1940-50 and 1960-70, which indicated remarkable correspondence with the changes in domestic demand for molybdenum. Molybdenum, which was used as an additive element in steel, was mined in the Daito mine from 1912 to 1985 on the upper reaches of the Hii River. This mine accounted for most of the Mo supply in Japan at that period. Accordingly, these trends in Mo is considered to be reflected by the load from this mine.

The pollution in Lake Nakaumi can be linked to copper mining activity in the catchment area from the 18th century. Interestingly, the clear trend in heavy metal pollution (Cu, Pb, Zn and As) predates eutrophication and also nationwide trends of heavy metals. Most of the metals peaked around 1970 CE

©2021. Japan Geoscience Union. All Right Reserved.

and decreased in general due to the decline of industrial activities after the rapid economic growth and emission regulations, but Pb, Zn, As and In displays recent increasing trends. In our presentation we will also discuss the trends of other heavy metals, including the possibility of long-distance transport from Asian continents.

Reference:
Yasuhara, M. et al. (2007) Limnology and Oceanography, 52: 1633–1644.

Keywords: estuarine lake, bottom sediment, human induced pollution, CNS, heavy metals, Lake Nakaumi

©2021. Japan Geoscience Union. All Right Reserved.

Calcification depths of planktic foraminifers constrained using geochemical signatures in the sediment trap samples collected from the Bay of Bengal

*Ayumi Maeda[1], Azumi Kuroyanagi[2], Toshihiro Yoshimura[3], Birgit Gaye[4], Tim Rixen[5], Atsushi Suzuki[1], Hodaka Kawahata[6]

1. National Institute of Advanced Industrial Science and Technology, 2. Tohoku University Museum, The Center for Academic Resources and Archives, Tohoku University, 3. Japan Agency for Marine-Earth Science and Technology, 4. Institute for Geology, Universität Hamburg, 5. Leibniz Centre for Tropical Marine Research, 6. Atmosphere and Ocean Research Institute, The University of Tokyo

Mg/Ca and oxygen isotope ratios (δ^{18}O) of planktic foraminifers revealed the hydrological conditions from the surface to thermocline using multiple species. Knowledge of apparent calcification depth (ACD) of planktic foraminifers plays a key role in reconstructing past environment, while the ACDs showed seasonal variations and are different at regional scale. We pursued revealing ACDs of *Globigerinoides ruber*, *Trilobatus sacculifer*, and *Neogloboquadrina dutertrei* in the Bay of Bengal using multiyear sediment trap samples collected approximately 900 m depth. The sediment traps were moored in the southwestern Bay of Bengal at ~950 m depth and 17-42 days intervals. The estimated temperature using δ^{18}O and Mg/Ca patterns of *G. ruber*, *T. sacculifer* and *N. dutertrei* showed that *G. ruber* reflect the temperature within the surface mixed layer, whereas *N. dutertrei* precipitated tests in the upper thermocline and *T. sacculifer* calcify between them. The rapidly attenuating photosynthetically active radiation constrained living depth of the symbiont-bearing species within the euphotic zone of the upper 60 m in the southern Bay of Bengal. The flux-weighed δ^{18}O values of each species corresponded to the mean annual δ^{18}O values of respective species. Seasonal variations in species-specific test fluxes can be averaged out due to the recuring flux peaks in the NEM and the SWM.

Keywords: planktic foraminifera, Bay of Bengal, oxygen isotope ratio

©2021. Japan Geoscience Union. All Right Reserved.

[E] Oral | B (Biogeosciences) : B-PT Paleontology

Sun. Jun 6, 2021 3:30 PM - 5:00 PM JST | Sun. Jun 6, 2021 6:30 AM - 8:00 AM UTC | Ch.26 Zoom Room 26

[B-PT01] Biomineralization and Geochemistry of Proxies

convener:Takashi Toyofuku(Japan Agency for Marine-Earth Science and Technology (JAMSTEC)), Hiroshi Kitazato(Tokyo University of Marine Science and Technology (TUMSAT)), Jelle Bijma(Alfred-Wegener-Institut Helmholtz-Zentrum für Polar- und Meeresforschung), Kotaro Hirose(Faculty of Science and Engineering, Waseda University), Chairperson:Hiroshi Kitazato(Tokyo University of Marine Science and Technology (TUMSAT)), Kotaro Hirose(Faculty of Science and Engineering, Waseda University), Takashi Toyofuku(Japan Agency for Marine-Earth Science and Technology (JAMSTEC)), Jelle Bijma(Alfred-Wegener-Institut Helmholtz-Zentrum für Polar- und Meeresforschung)

In order to reconstruct the Earth climate system, marine paleoclimatologists resort to transfer functions or geochemical proxies, which are produced or affected by organisms. The relationships used for reconstructions are generally based on field calibrations or derived from laboratory experiments. The danger of these so-called empirical relationships is that they may be valid only within the restricted parameter space of their calibration. Application of proxy relationships to very different environmental settings (e.g. high vs. low latitude or glacial vs. interglacial) requires a mechanistic understanding of these relationships. Much progress can be expected by a better understanding of the biomineralization mechanisms and the incorporation of proxy signals.
In this session we facilitate contributions related to the biomineralization, calibration and validation of marine proxies from field study, laboratory culture experiment and paleo-environmental reconstruction.

3:30 PM - 3:48 PM JST | 6:30 AM - 6:48 AM UTC

[BPT01-07] Long term size changes of the Middle Miocene planktonic foraminifera in the western equatorial Pacific

*Takuma Suzuki[1], Hiroki Hayashi[1] (1.Shimane University)

3:48 PM - 4:06 PM JST | 6:48 AM - 7:06 AM UTC

[BPT01-08] High-resolution minor element concentration records in modern brachiopod *Pictothyris picta* shells and their controlling factors

*Kazuma Oikawa[1], Hideko Takayanagi[1], Ryuichi Shinjo[2], Kazuyoshi Endo[3], Masa-aki Yoshida[4], Yasufumi Iryu[1] (1. Institute of Geology and Paleontology Graduate School of Science Tohoku University, 2.Department of Physics and Earth Sciences, University of the Ryukyus, 3.Department of Earth and Planetary Science, Tokyo University, 4.Shimane University Faculty of Life and Environmental Science)

4:06 PM - 4:24 PM JST | 7:06 AM - 7:24 AM UTC

[BPT01-09] Evolution of Mg transporters and their possible effects on coral skeletal proxies in geochemistry

*Tomoko Bell[1], Akira Iguchi[2], Kazuhiko Sakai[3], Yusuke Yokoyama[4] (1.WERI, Univ. of Guam, 2.AIST, 3.TBRC, Univ. of Ryukyus, 4.AORI, Univ. of Tokyo)

4:24 PM - 4:42 PM JST | 7:24 AM - 7:42 AM UTC

[BPT01-10] **The coral reef-dwelling *Peneroplis* spp. shows calcification resilience to ocean acidification conditions - results from culture experiments**

*Laurie Charrieau[1], Katsunori Kimoto[1], Delphine Dissard[2], Beatrice Below[2,3], Kazuhiko Fujita[4], Yukiko Nagai[1,5], Takashi Toyofuku[1,6] (1.Jamstec, 2.IRD/UMR LOCEAN, 3.UMR CR2P, 4.University of the Ryukyus, 5.Yokohama National University, 6.TUMSAT)

4:42 PM - 4:57 PM JST | 7:42 AM - 7:57 AM UTC

[BPT01-11] Can Irregular Observations Provide the Next Clue for the Ecology of Foraminifera?

*Takashi Toyofuku[1,2], Yukiko Nagai[1,3] (1.Japan Agency for Marine-Earth Science and Technology (JAMSTEC), 2.Tokyo University of Marine Science and Technology (TUMSAT), 3.National Museum of

Nature and Science,Tokyo)

4:57 PM - 5:00 PM JST | 7:57 AM - 8:00 AM UTC

[BPT01-12] Discussion

Long term size changes of the Middle Miocene planktonic foraminifera in the western equatorial Pacific

*Takuma Suzuki[1], Hiroki Hayashi[1]

1. Shimane University

Planktonic foraminifera is an oceanic free-floating single celled protozoa. In the modern ocean, it is classified into approximately 50 species. The oldest planktonic foraminiferal fossil records are appeared from the Jurassic. Carbonate shells of planktonic foraminifera are well preserved into marine sediments especially from ocean drilled cores. The successive and rich appearance of the fossils provide good paleoenvironmental proxies with high special-temporal resolution by chemical and morphological analyses.

In this study, we focused “size” of planktonic foraminiferal shell to consider evolution models about size such as “Lilliput Effect” and “Giantism”. These models have a potential to make clear what the relationship between organism response and environmental fluctuation. The size analysis of planktonic foraminifera has a significant potential for investigation of “Lilliput Effect” and “Giantism” because a size analysis to investigate these evolution models require a lot of individuals of single taxon. Another reason should be pointed out that planktonic foraminifera shows accretion growth by adding a new chamber on its penultimate chamber, therefore the size of planktonic foraminifera well reflects the ontogenic pattern.

Our study is composed of two parts as described bellow:

1. This study aims to reconstruct the temporal size change of *Paragloborotalia siakensis* (LeRoy) during Middle Miocene in the western equatorial Pacific. The core samples we used in this study were drilled at ODP Site 807. The successive sediments well preserved foraminiferal shells, and recorded the transition from the relatively warm face (MMCO: Mid-Miocene Climatic Optimum) to the colder mode Mi-3 with the expansion of the Eastern Antarctica Ice Sheet.

2. In order to consider the model about “Dwarfing” and “Giantism” of *P. siakensis* in equatorial Pacific, we compared the size change at ODP Site 807 with those of IODP Sites U1337 and U1338 drilled at the eastern equatorial Pacific.

Keywords: body size, planktonic foraminifera, Lilliput Effect, Cope’s rule, Middle Miocene

©2021. Japan Geoscience Union. All Right Reserved.

High-resolution minor element concentration records in modern brachiopod *Pictothyris picta* shells and their controlling factors

*Kazuma Oikawa[1], Hideko Takayanagi[1], Ryuichi Shinjo[2], Kazuyoshi Endo[3], Masa-aki Yoshida[4], Yasufumi Iryu[1]

1. Institute of Geology and Paleontology Graduate School of Science Tohoku University, 2. Department of Physics and Earth Sciences, University of the Ryukyus, 3. Department of Earth and Planetary Science, Tokyo University, 4. Shimane University Faculty of Life and Environmental Science

Carbon ($\delta^{13}C$) and oxygen ($\delta^{18}O$) isotope composition of Rhynchonelliformea brachiopods (hereafter, called 'brachiopods') have been regarded as useful paleoenvironmental indicators throughout the Phanerozoic. However, variations of minor element concentrations in modern brachiopod shells and their relationships with environmental factors (e.g., temperature, salinity, and pH) and biological controls are not well understood. In this study, we measured $\delta^{13}C$ and $\delta^{18}O$ values and minor element concentrations of the primary (PL) and secondary (SL) layers of three *Pictothyris picta* shells (one male and two female individuals) collected at a water depth of 61 m off Okinoshima to clarify the factors controlling the isotopic and elemental variations. We obtained ontogenetic-series $\delta^{13}C$, $\delta^{18}O$, and minor element (i.e., Mg/Ca, Mn/Ca, Fe/Ca, and Sr/Ca) profiles from the PL (PL-Ont) and the uppermost SL (SL-Ont) at the sampling resolution of 3 days to 8 months per sample. We also obtained minor element concentrations as well as $\delta^{13}C$ and $\delta^{18}O$ from the innermost SL (SL-In). The SL-Ont was precipitated in oxygen isotopic equilibrium with ambient seawater regardless of the growth stage and the seasonal changes at the growth site. Mg/Ca profiles of the PL- and SL-Ont showed that the Mg uptake into the *P. picta* shells is related to the shell growth stages. This relationship likely indicates that Mg removal mechanism works during brachiopod shell precipitation, and the extent of the Mg removal varies with the growth stages. Consequently, we identified three growth stages (sectors 1 to 3) based on differences in Mg/Ca values between PL- and SL-Ont. A significant positive correlation between Sr/Ca and $\delta^{13}C$ values was found in the sectors 1 and 2 of PL- and SL-Ont profiles of the three shells. This correlation implies that the shell precipitation rate is likely to be influenced by the metabolic effect affecting the $\delta^{13}C$ values. The shell Mn and Fe concentrations were low and constant throughout the shells, respectively, except for Mn/Ca values from sectors 2 and 3 of the PL-Ont.

Keywords: brachiopod, carbon and oxygen isotope, minor element concentrations, calcification, vital effect

©2021. Japan Geoscience Union. All Right Reserved.

Evolution of Mg transporters and their possible effects on coral skeletal proxies in geochemistry

*Tomoko Bell[1], Akira Iguchi[2], Kazuhiko Sakai[3], Yusuke Yokoyama[4]

1. WERI, Univ. of Guam, 2. AIST, 3. TBRC, Univ. of Ryukyus, 4. AORI, Univ. of Tokyo

Corals have been used as geochemical proxies since the 1970's and they play prominent roles in paleoclimatology. However, it has not been well elucidated how minerals in seawater are transported and precipitated in aragonite coral skeleton. There are no foundational methods to differentiate and quantify biogenic and abiogenic effects during skeletal formation, thus it hampers corals from being fully reliable environmental proxies. To address these uncertainties, in this study, we attempt to evaluate biological complexity by investigating how coral genes evolved over geologic time scales (e.g. million years). In coral skeletons, Mg is an abundant element of coral skeleton (1000-2100ppm), and Mg can be concentrated by almost double that of modern seawater. Therefore, we decided to focus on coral Mg transporters of five coral species (*Acropora digitifera, Acropora hyacinthus, Acropora millepora, Acropora palmate* and *Acropora tenuis*) and investigated how Mg transporters have been evolving. Our preliminary result indicated that Mg transporter of *Acropora digitifera*, *Acropora hyacinthus and Acropora millepora* showed high similarity to Mg transporter of Japanese rice fish. On the other hand, *Acropora palmate* and *Acropora tenuis* did not show such a trend. According to the Coral Trait database, the three types of corals that showed high similarity to rice fish appeared on the earth less than 1 million years ago while the other two species showed ages older than 3 million years ago. Such difference could be possibly triggered by an environmental change such as the availability of Mg ion in seawater (seawater [Mg]). There have been continuous increases in seawater [Mg] from 5 Ma to present: from 50 mmol/L to 55 mmol/L. This increase (about 10%) of seawater [Mg] could potentially facilitate coral Mg transport systems to respond to the seawater chemistry change and evolve to develop more Mg specific transporters. Our result indicated a strong biogenic response and control (Mg transporter) to abiotic factors (seawater [Mg]). That is to say, using Mg ratio in coral skeletons might not be ideal due to vital effect. We suggest our approach to investigate gene evolution may guide us to identify the geochemical proxies with possible strong vital effects thus help us identify robust proxies.

Keywords: Coral, Evolution, Skeletal proxy, Mg transporter

©2021. Japan Geoscience Union. All Right Reserved.

The coral reef-dwelling *Peneroplis* spp. shows calcification resilience to ocean acidification conditions - results from culture experiments

*Laurie Charrieau[1], Katsunori Kimoto[1], Delphine Dissard[2], Beatrice Below[2,3], Kazuhiko Fujita[4], Yukiko Nagai[1,5], Takashi Toyofuku[1,6]

1. Jamstec, 2. IRD/UMR LOCEAN, 3. UMR CR2P, 4. University of the Ryukyus, 5. Yokohama National University, 6. TUMSAT

Ocean acidification is a consequence of the current climate changes, driven by anthropogenic activities. The concomitant decrease in pH and carbonate ion concentration in sea water may have severe impacts on marine life, and especially on calcifying organisms. Coral reefs were among the first ecosystems to be recognized as vulnerable to ocean acidification. Within coral reefs, large benthic foraminifera (LBF) are major calcium carbonate producers.

The aim of this work was to evaluate the impacts of varying pH on survival and calcification of the symbiont-bearing LBF species *Peneroplis* spp. We performed culture experiments to first study their resistance to ocean acidification conditions, and then their resilience once placed back under open ocean pH.

After three days, small signs of test decalcification were observed on specimens kept at pH 7.4, and severe test decalcification was observed on specimens kept at pH 6.9, with the inner organic lining clearly appearing. Similar strongly decalcified specimens were observed after 32 days under pH 7.4. All the specimens were alive at the end of the experiment. These results demonstrate the resistance of *P eneroplis* spp. to an acidified pH, at least on a short period of time.

After being partially decalcified, some of the living specimens were placed back at pH 7.9 (in situ value). After one month, the majority of the specimens showed recalcification features, mainly by addition of new chambers. The trace elements concentrations of the newly formed chambers were analysed by LA-ICPMS. Interestingly, more chambers were added when food was given, which highlights the crucial role of energy source in the recalcification process. Moreover, the newly formed chambers were most of the time abnormal, and the general structure of the tests was altered. These abnormalities have potential impacts on reproduction capacities and in situ survival of *Peneroplis* spp. In conclusion, if symbiont-bearing LBF show some resistance and resilience to lowered pH conditions, they will remain strongly affected by ocean acidification.

Keywords: Ocean acidification, Large Benthic Foraminifera, Culture experiments, Calcification process

©2021. Japan Geoscience Union. All Right Reserved.



©2021. Japan Geoscience Union. All Right Reserved.

Can Irregular Observations Provide the Next Clue for the Ecology of Foraminifera?

*Takashi Toyofuku[1,2], Yukiko Nagai[1,3]

1. Japan Agency for Marine-Earth Science and Technology (JAMSTEC), 2. Tokyo University of Marine Science and Technology (TUMSAT), 3. National Museum of Nature and Science,Tokyo

Calcareous foraminifera is major producers of carbonates in the ocean. By extracting foraminifera from sediments, analyzing their assemblages, and analyzing their elemental compositions, we can reconstruct the geologic time's past environment. The carbonate shells, called tests, deposited by foraminifera play a central role in paleoenvironmental reconstructions. Therefore, it is one of the centers of interest how the calcareous test is formed. This carbonate test is known to form intermittently as the foraminifera cell grows. As the foraminifera collect food and increase the volume of their cytoplasm, they repeatedly build the next chamber before the last one is full. In this process, new chambers are built using the existing chambers as footholds. The angle and size of the new chamber determine the overall shape of the test e.g., biserial, triserial, spiral, and others. Behind the scenes, the pseudopods, which control the foraminifera's locomotion, have been found to play a very diverse and important role in chamber formation. This is due to the repeated and detailed observation of the chamber formation process and the observation of its ultrastructure by electron microscopy. In our laboratory, we controlled the feeding conditions of foraminifera to derive the conditions that induce chamber formation. Therefore, we can control the timing of shell formation to some extent and prepare a system for reliable observation. The process of shell formation can be documented by, for example, time-lapse observation, recording foraminifera chamber formation, and the order in which they form (and sometimes reproduction to observe the birth of new offspring in detail). We can also use fluorescent indicators to label calcium, pH, and other intracellular organelles and observe how they are distributed during chamber formation and the rest of ecology.

On the other hand, if such observations are made for too long and too often, the observation may fail. For example, an individual may stop and run away when it seems to be forming a chamber, or it may return to a single cell even though it is dividing during reproduction. These observations are difficult to explain straight forward, so it is not easy to publish them in a paper very much. However, there are many interesting observations, and it would be a shame to keep them in storage, so we would like to introduce them to this opportunity.

Keywords: foraminifera, time-lapse microscopy, biomineralization, laboratory culture, fulorescnet obseervation, null negative

©2021. Japan Geoscience Union. All Right Reserved.

[E] Oral | B (Biogeosciences) | B-PT Paleontology

[B-PT01] Biomineralization and Geochemistry of Proxies

convener:Takashi Toyofuku(Japan Agency for Marine-Earth Science and Technology (JAMSTEC)), Hiroshi Kitazato(Tokyo University of Marine Science and Technology (TUMSAT)), Jelle Bijma(Alfred-Wegener-Institut Helmholtz-Zentrum für Polar- und Meeresforschung), Kotaro Hirose(Faculty of Science and Engineering, Waseda University), Chairperson:Hiroshi Kitazato(Tokyo University of Marine Science and Technology (TUMSAT)), Kotaro Hirose(Faculty of Science and Engineering, Waseda University), Takashi Toyofuku(Japan Agency for Marine-Earth Science and Technology (JAMSTEC)), Jelle Bijma(Alfred-Wegener-Institut Helmholtz-Zentrum für Polar- und Meeresforschung)

Sun. Jun 6, 2021 3:30 PM - 5:00 PM Ch.26 (Zoom Room 26)

In order to reconstruct the Earth climate system, marine paleoclimatologists resort to transfer functions or geochemical proxies, which are produced or affected by organisms. The relationships used for reconstructions are generally based on field calibrations or derived from laboratory experiments. The danger of these so-called empirical relationships is that they may be valid only within the restricted parameter space of their calibration. Application of proxy relationships to very different environmental settings (e.g. high vs. low latitude or glacial vs. interglacial) requires a mechanistic understanding of these relationships. Much progress can be expected by a better understanding of the biomineralization mechanisms and the incorporation of proxy signals.

In this session we facilitate contributions related to the biomineralization, calibration and validation of marine proxies from field study, laboratory culture experiment and paleo-environmental reconstruction.

4:57 PM - 5:00 PM

[BPT01-12]Discussion

©Japan Geoscience Union

[E] Poster | B (Biogeosciences)：B-PT Paleontology

Sun. Jun 6, 2021 5:15 PM - 6:30 PM JST | Sun. Jun 6, 2021 8:15 AM - 9:30 AM UTC | Ch.17_1

[B-PT01] Biomineralization and Geochemistry of Proxies

convener:Takashi Toyofuku(Japan Agency for Marine-Earth Science and Technology (JAMSTEC)), Hiroshi Kitazato(Tokyo University of Marine Science and Technology (TUMSAT)), Jelle Bijma(Alfred-Wegener-Institut Helmholtz-Zentrum für Polar- und Meeresforschung), Kotaro Hirose(Faculty of Science and Engineering, Waseda University)

In order to reconstruct the Earth climate system, marine paleoclimatologists resort to transfer functions or geochemical proxies, which are produced or affected by organisms. The relationships used for reconstructions are generally based on field calibrations or derived from laboratory experiments. The danger of these so-called empirical relationships is that they may be valid only within the restricted parameter space of their calibration. Application of proxy relationships to very different environmental settings (e.g. high vs. low latitude or glacial vs. interglacial) requires a mechanistic understanding of these relationships. Much progress can be expected by a better understanding of the biomineralization mechanisms and the incorporation of proxy signals.
In this session we facilitate contributions related to the biomineralization, calibration and validation of marine proxies from field study, laboratory culture experiment and paleo-environmental reconstruction.

[BPT01-P01] Ultrafine structure and elemental compositions of Acantharian (Radiolarian) skeleton from Kashiwajima Island, southwestern Shikoku, Japan

*Mao Fujii[1], Rie S Hori[2], Hiroaki Ohfuji[5], Yasuhide Nakamura[3], Mariko Nagashima[4] (1.Graduate School of Agricultural and Life Science, The University of Tokyo, 2.Graduate School of Science and Engineering, Ehime University, 3.Estuary Research Center, Shimane University, 4.Graduate School of Science and Technology for Innovation, Yamaguchi University, 5.Department of Earth Science, Graduate School of Science, Tohoku University)

[BPT01-P02] Ultra-microstructure observation of miliolid foraminifera (*Sorites* sp.) during shell formation process

*Yukiko Nagai[1,2], Remi Tsubaki[5], Kazuhiko Fujita[4], Takashi Toyofuku[2,3] (1.National Museum of Nature and Science of Tokyo, 2.JAMSTEC, 3.TUMSAT, 4.The University of Ryukyu , 5.The University of Tokyo)

Ultrafine structure and elemental compositions of Acantharian (Radiolarian) skeleton from Kashiwajima Island, southwestern Shikoku, Japan

*Mao Fujii[1], Rie S Hori[2], Hiroaki Ohfuji[5], Yasuhide Nakamura[3], Mariko Nagashima[4]

1. Graduate School of Agricultural and Life Science, The University of Tokyo, 2. Graduate School of Science and Engineering, Ehime University, 3. Estuary Research Center, Shimane University, 4. Graduate School of Science and Technology for Innovation, Yamaguchi University, 5. Department of Earth Science, Graduate School of Science, Tohoku University

Radiolarians are divided into two major groups based on the chemical composition of shell: the first group, Polycystine, has opal ($SiO_2 + nH_2O$) skeleton, preserved from Cambrian to Recent sediments, and the second one possessing celestite ($SrSO_4$) skeleton called Acantharia. Acantharia is one of the unicellular zooplankton taxa including ca. 50 genera and ca. 150 species. Acantharians are distributed in the oceans around the world, especially oligotrophic surface waters. However, the acantarian skeletons do not remain as fossils because they melt in seawater after died. Acantharia show high value in biomass and there are no other planktons that makes $SrSO_4$-skeletons. In this study, we examined of living Acantharian cells from surface seawater of Kuroshio Current off shore Kashiwa-jima Island, Kochi prefecture, Shikoku, Japan, and studied crystalline structure and chemical compositions of skeletons, in order to clarify its biomineralization process, using by TEM, FE-SEM, EDS (at Ehime University) and WDS analyses (at Yamaguchi University), combined with Focused Ion Beam (FIB) method at GRC (Ehime University).

Radiolarians were picked up from the plankton samples obtained from the surface seawater off Kashiwa-jima samples, and separated into 6 types of Acantharian Clade (A, B, C, D, E and F), under a binocular microscope. Skeletons of each Clade were put on the sample plate separately, and cut off by FIB after washed carefully by Milli-Q water. The thin films of Acantharian skeletons, in particular spines, were made and then observed with a field emission-transmission electron microscope to understand the ultrafine structure.

The crystal structure of Acantharian skeleton was confirmed as uniform Celestine minerals, possessing polarity parallel structure. However, we recognized different characters among SEM images of thin section of spines between Clade E&F and Clade D, which are probably concerned to skeletal forming process, also heterogeneous chemical compositions in the section of spines were detected. We will show these precise results of studies on Acantharia as a poster presentation.

Keywords: Radiolaria, Acantharia, skeletal composition

©2021. Japan Geoscience Union. All Right Reserved.

Ultra-microstructure observation of miliolid foraminifera (*Sorites* sp.) during shell formation process

*Yukiko Nagai[1,2], Remi Tsubaki[5], Kazuhiko Fujita[4], Takashi Toyofuku[2,3]

1. National Museum of Nature and Science of Tokyo, 2. JAMSTEC, 3. TUMSAT, 4. The University of Ryukyu , 5. The University of Tokyo

Foraminifera are unicellular organisms with calcareous shells that live mainly in the marine environment. The elemental composition of foraminiferal shells contributes significantly to paleoceanographic reconstruction analysis. Nowadays, there are many unclear points remained about foraminiferal shell formation process. There are two types of foraminifera with different shell structures: hyaline foraminifera and porcelaneous (miliolid) foraminifera. Regarding the process of forming a milky white porcelaneous shell called miliolid foraminifera, Hemleben et al. (1986) showed that needle-like crystals of calcium carbonate were formed in intracellular vesicles. Since then, research of this field was not progressing very much (with some exception.). Therefore, in this study, in order to clarify the shell formation process of the large benthic foraminifera *Sorites* sp., which is a member of miliolid foraminifera, the ultra-fine structure of the shell formation site was observed using a specimen during the calcification.

According to time-lapse observations by optical microscopy, the shell formation of *Sorites* sp. involves the formation of cytoplasm in the form of a new chamber, framed by two organic sheets. Crystals are deposited between these two sheets.

In SEM and FIB-SEM observations, we observed the specimen in the process of deposition of the crystals in the above shell formation process. The cross-sectional observation revealed a structure with five major layers. From the outermost to inner surfaces, a relatively thick layer of organic matter (layer a), sheet mixture of needle-like crystals and organic matter on the surface of the shell (layer b), a crystal-filled layer occupying most of the shell (layer c), a sheet of organic matter on the inner surface (layer d), and spherical cytoplasm distributed on the inner surface (layer e). The primary organic sheet is not present in layer c as seen in hyaline foraminifera.

In the layer a, there is a network structure of pseudopods woven together and a membrane with holes in places between them. Spherical organic structures are present on the sheet. The spherical structure has a variability of size about 0.1 μm-1 μm. The thickness of the layers also varies from 0.1-3 μm. Layer b was found that the outer side of the shell formation site. This was a thin organic film structure. This structure likely corresponds to the Outer Organic Lining (OOL) of hyaline foraminifera. However, its thickness seems thinner than hyaline species. The structure looks like a sheet of needle-like crystals with organic material as a binder. The crystals are arranged in a way that is sometimes random and sometimes flowing. The needle-like crystals was about 700 nm. The layer c is filled with needle-like material, but in some places it is spongy with low filling density and scattered voids. The electron density of this needle-like material seems to be somewhat lower than that of a normal crystal. Whether they are pseudopodia or crystals will require further analysis. Layer d is a few nanometers thick and appears to be lining the inside of the layer c, but its structure still needs to be examined. The structure and other details still need to be investigated. The layer e seems to have pseudopodia and cytoplasm attached to the layer d.
These findings will deepen our understanding of biomineralization of foraminifera and support to consider the conditions under which elemental partitioning and isotopic fractionation occur.

©2021. Japan Geoscience Union. All Right Reserved.

Keywords: Biomineralization, Foraminifera, Calcification, FIB, Microstructure

©2021. Japan Geoscience Union. All Right Reserved.

[J] Oral | B (Biogeosciences)：B-PT Paleontology

Sun. Jun 6, 2021 10:45 AM - 12:15 PM JST | Sun. Jun 6, 2021 1:45 AM - 3:15 AM UTC | Ch.26 Zoom Room 26

[B-PT02] Biotic History

convener:Isao Motoyama(Faculty of Science, Yamagata University), Takao Ubukata(Division of Geology & Mineralogy, Department of Earth & Planetary Sciences, Kyoto University), Kazuyoshi Moriya(Department of Earth Sciences, Faculty of Education and Integrated Arts and Sciences, Waseda University), Chairperson:Isao Motoyama(Faculty of Science, Yamagata University), Takao Ubukata(Division of Geology & Mineralogy, Department of Earth & Planetary Sciences, Kyoto University), Kazuyoshi Moriya(Department of Earth Sciences, Faculty of Education and Integrated Arts and Sciences, Waseda University)

The Biotic History session covers all aspects of ancient life and the history of biosphere through the geologic time. The study of ancient life is essential for unveiling mysteries of our planet earth. It also provides evidence for evolution of oceans, continents and island arcs. Modern progress in this field has been enhanced by interdisciplinary collaboration with allied sciences, such as paleoceanography and evolutionary biology. Our session intends to be a hub of communication amongst all earth scientists studying the biosphere; we welcome biological and biogeochemical approaches toward the understanding of the history of life.

10:45 AM - 11:00 AM JST | 1:45 AM - 2:00 AM UTC

[BPT02-01] Reconstruction of paleovegetation changes by pollen, palynomorph, and kerogen analyses of the Late Cretaceous sediments from the Kotanbetsu area, Hokkaido, Japan

*Maho Hayakawa[1], Ken Sawada[2], Masashi A. Ikeda[1], Reishi Takashima[3], Hiroshi Nishi[4] (1.Graduate School of Science, Hokkaido University, 2.Department of Earth and Planetary Sciences, Faculty of Science, Hokkaido University, 3.The Center for Academic Resources and Archives, The Tohoku University Museum, Tohoku University, 4.Institute of Dinosaur Research, Fukui Prefectural University)

11:00 AM - 11:15 AM JST | 2:00 AM - 2:15 AM UTC

[BPT02-02] Depth habitat of the late Eocene planktic foraminifers

*Kazuyoshi Moriya[1], Taku Oyama[2], Toyoho Ishimura[3] (1.Department of Earth Sciences, Faculty of Education and Integrated Arts and Sciences, Waseda University, 2.Major in Earth Sciences, Resources and Environmental Engineering, Graduate School of Creative Science and Engineering, 3.Department of Interdisciplinary Environment, Graduate School of Human and Environmental Studies, Kyoto University)

11:15 AM - 11:30 AM JST | 2:15 AM - 2:30 AM UTC

[BPT02-03] Micro sensory organs reveal the perception system and ecology of the Cretaceous cockroach

*Ryo Taniguchi[1], Yasuhiro Iba[1], Hiroshi Nishino[2], Hidehiro Watanabe[3], Kosuke Tateishi[3] (1.Faculty of Science, Hokkaido University, 2.Research Institute for Electronic Science, Hokkaido University, 3.Department of Earth System Science, Faculty of Science, Fukuoka University)

11:30 AM - 11:45 AM JST | 2:30 AM - 2:45 AM UTC

[BPT02-04] Computed tomography scanning reveals morphological development of a burrow produced by the tiger pistol shrimp *Alpheus bellulus*

*Miyu Umehara[1], Koji Seike[2], Seishiro Furuyama[1] (1.Tokyo University of Marine Science and Technology, 2.National Institute of Advanced Industrial Science and Technology)

11:45 AM - 12:00 PM JST | 2:45 AM - 3:00 AM UTC

[BPT02-05] Shell microstructure of extinct protobranch bivalves

*Kei Sato[1] (1.Faculty of Education and Integrated Arts and Sciences, Waseda University)

12:00 PM - 12:15 PM JST | 3:00 AM - 3:15 AM UTC

[BPT02-06] A unification of absolute growth, allometric, and theoretical morphologic models: a case of molluscan shells

*Takao Ubukata[1] (1.Department of Geology & Mineralogy, Division of Earth & Planetary Sciences, Kyoto University)

Reconstruction of paleovegetation changes by pollen, palynomorph, and kerogen analyses of the Late Cretaceous sediments from the Kotanbetsu area, Hokkaido, Japan

*Maho Hayakawa[1], Ken Sawada[2], Masashi A. Ikeda[1], Reishi Takashima[3], Hiroshi Nishi[4]

1. Graduate School of Science, Hokkaido University, 2. Department of Earth and Planetary Sciences, Faculty of Science, Hokkaido University, 3. The Center for Academic Resources and Archives, The Tohoku University Museum, Tohoku University, 4. Institute of Dinosaur Research, Fukui Prefectural University

The early Late Cretaceous (–Turonian) was characterized by one of the warmest paleoclimates, and subsequently the middle - late Late Cretaceous (Coniacian–Maastrichtian) is considered an interval of global cooling, possibly attributed by declining atmospheric CO_2concentration (e.g. Tabor et al., 2016). In the Cretaceous cooling condition, it is important to clarify the variation and evolution of paleovegetation adding angiosperm flora for understanding terrestrial paleoenvironment and paleoclimate. However, there have few reports for reconstructing long-time scale variation in paleovegetation during the Cretaceous. In the present study, we performed analyses of palynomorph including pollen and palynofacies (visual kerogen) of the sediments from the Upper Yezo Group (Hokkaido, Japan) to reconstruct the long-time scale variations in paleovegetation during the Late Cretaceous.

The mudstones of Saku Formation and Haborogawa Formation, Yezo Group, were sampled in the Kotanbetsu area, Hokkaido, Japan. In the Cretaceous Yezo Group, integrated bio- and carbon isotope stratigraphy have been well established in the studied section. We analyzed the Turonian–Santonian mudstone samples. We performed the treatments for separating pollen from sediments by 1) the common method for the Quaternary sediments, and 2) kerogen separation method. The palynomorphs including pollen and spore as well as kerogen were observed under transmitted and fluorescent light microscopes.

In the Coniacian–Santonian sediments, we identified trilete (fern origin), bisaccate (gymnosperm, especially Pinaceae), non-saccate gymnosperm pollen, and polyplicate (gymnosperm Ephedraceae). As angiosperm pollen, tricolpate, triporate, and tricolporate were ideintified. Interestingly, we found triprojectate, which is characteristically observed in the Late Cretaceous sediments from the Asia and North America. The angiosperm pollen/bisaccate ratios tended to decrease during the Coniacian, and subsequently increase during the Santonian. The bisaccate pollens are the most abundant, and could be divided to several types based on their sizes. The compositions of these bisaccate types varied, suggesting that the variations in coniferous vegetations can be reconstructed by using these bisaccate pollens. In addition, dinocysts were commonly observed. Microscopic observation of kerogen (palynofacies analysis) from sediments in the sediments from the Coniacian–Santonian Haborogawa Foramtion indicates that the kerogens mainly compose of wood and amorphous organic matter (AOM) such as fluorescent AOM (FA; plant cuticle origin) and non-fluorescent AOM (NFA; woody tissue origin), as well as sporomorphs (spore and pollen) and cuticle as minor component. The (Cuticle+FA)/(Wood+NFA) ratios, which is used as the proxy for herbaceous / woody vegetation ratios, tended to decrease from the early to middle Santonian, and slightly increased during late Santonian. However, the kerogen compositions by palynofacies analysis is thought to vary depending on sedimentological processes such as transport from land area, so that the sedimentological factors should be paid attention in the paleovegetation reconstruction by kerogen composition.

©2021. Japan Geoscience Union. All Right Reserved.

Keywords: paleovegetation, Yezo Group, pollen, palynomorph, Cretaceous

©2021. Japan Geoscience Union. All Right Reserved.

Depth habitat of the late Eocene planktic foraminifers

*Kazuyoshi Moriya[1], Taku Oyama[2], Toyoho Ishimura[3]

1. Department of Earth Sciences, Faculty of Education and Integrated Arts and Sciences, Waseda University, 2. Major in Earth Sciences, Resources and Environmental Engineering, Graduate School of Creative Science and Engineering, 3. Department of Interdisciplinary Environment, Graduate School of Human and Environmental Studies, Kyoto University

Planktic foraminifers (Rhizaria) are widely distributed in modern ocean from equatorial to sub-polar oceans. Especially for surface dwelling species, distribution of those species is related to sea surface temperatures. For example, *Globigerinoides sacculifer* and *Neogloboquadrina pachyderma* predominantly inhabit tropical and polar oceans, respectively. In addition to this geographic variation, depth of habitat is also segregated from species to species. *Globigerinoides ruber* is well known as the shallowest dwelling species, *Globorotalia menardii* is deeper, and *Globorotalia truncatulinoides* is the deepest dwelling species. When calcifying their tests, oxygen isotope ratio (δ^{18}O) of their test carbonates records temperature of their habitat. Therefore, δ^{18}O of each species occurred from a given sample shows variation from positive to negative, hence, cooler to warmer. Using this temperature segregation, we can identify the depth of habitat of each species. This temperature/isotope segregation can be found in fossils species as well. Here, we report isotope segregation of the late Eocene planktic foraminifers in north Atlantic Ocean. We have determined δ^{13}C and δ^{18}O of 15 species at most within one sediment sample. The difference in δ^{18}O between species showing the most negative and positive δ^{18}O is approximately 3‰, corresponding to 12 degree C. *Turborotalia ampliapertura* show the most negative δ^{18}O, indicating surface dwelling nature of this species. On the other hand, the most positive δ^{18}O is recorded by *Globorotaloides quadrocameratus*.

©2021. Japan Geoscience Union. All Right Reserved.

Micro sensory organs reveal the perception system and ecology of the Cretaceous cockroach

*Ryo Taniguchi[1], Yasuhiro Iba[1], Hiroshi Nishino[2], Hidehiro Watanabe[3], Kosuke Tateishi[3]

1. Faculty of Science, Hokkaido University, 2. Research Institute for Electronic Science, Hokkaido University, 3. Department of Earth System Science, Faculty of Science, Fukuoka University

Sensory organs play essential roles for animals in detecting information of the surrounding environment. Insects are the most diverse group in Animalia, and their sensory organs have a notable ability to process complicated information despite the small size restriction. Among insects, cockroaches have maintained the body plan for a long time since they appeared on the earth, and they possess relatively small eyes and well-developed antennae reflecting the nocturnal ecology. Therefore, cockroaches can be considered model organisms on evolution and diversity of the remarkable insect sensors in paleontology. Fossils are the only direct evidence for paleontological research of these organs. Insect organs, however, are hardly fossilized owing to the smallness and fragility. Although they are exceptionally well preserved in amber, existing non-destructive analysis such as X-ray computed tomography does not achieve enough resolution to observe the fossil microstructure. Here, we focused on and visualized micro-sensors of an extinct male cockroach in Cretaceous Myanmar amber (*Huablattula hui* Qiu et al., 2019), combining destructive and non-destructive methods. Furthermore, we reconstructed the perception system and ecology of the cockroach in high-resolution.

We measured the surface area of the ommatidia and compound eyes based on the macro photographs and 3D-model constructed via X-ray CT. From these data, we estimated the number of ommatidia composing the compound eyes. We applied the thin-sectioning method used in mineralogy to observe antennal sensilla that are sensors of multiple information and too small for non-destructive methods to visualize. In this process, the amber piece containing the right antenna was cut off and ground down to 200 μm thick. We observed the thin section with a confocal laser scanning microscope.

The compound eyes of *H. hui* are large and round, and they consist of about 6,000 ommatidia. This number is 1.5 times larger than extant nocturnal species whose body sizes are five times as large as *H. hui* . Many sensilla are well preserved with surface microstructure on the antenna. We were able to classify them based on the morphology and estimate their function: mechanoreception and multiple olfactions. Compared to extant species living in dark environments, these sensilla are small against the body size, and mechanoreceptive sensilla are markedly fewer. These holistic characters of sensors indicate that *H. hui* relied on light stimulation rather than contact or odors to perceive environmental cues. *H. hui* was probably the diurnal insect adapted to bright habitats opposite to many modern cockroaches. We also revealed that the abundant sensillum type on the *H. hui* antenna is similar to extant male mantises. The abundance of particular sensilla in males results from using sex pheromones, and therefore *H. hui* may have used mantis-like intersexual communication. We show that detailed observation of micro sensory organs with destructive analysis enables reconstructing ecology and behavior of fossil insects in high-resolution.

Keywords: micro sensory organ, cockroach, amber, ecological reconstruction, destructive analysis, Cretaceous

©2021. Japan Geoscience Union. All Right Reserved.

Computed tomography scanning reveals morphological development of a burrow produced by the tiger pistol shrimp *Alpheus bellulus*

*Miyu Umehara[1], Koji Seike[2], Seishiro Furuyama[1]

1. Tokyo University of Marine Science and Technology, 2. National Institute of Advanced Industrial Science and Technology

Trace fossils made by ancient animals provide information on the activities of their producers. However, improving our understanding of trace fossils requires the analysis of their modern analogs. In this study, we investigate morphology of a burrow produced by a modern benthic crustacean with computed tomography (CT) scanning to reveal its four-dimensional morphology. Because crustaceans are known to show a wide habitat range from shallow to deep sea and have lived since the Paleozoic era, they are suitable for burrow forming experiment as a modern analog of trace fossils.

The tiger pistol shrimp *Alpheus bellulus* used in this study was placed in each of the five tanks, and a light-shielding plate was set on the bottom to enable the shrimp to produce burrow easily. The CT images were taken at intervals of 10 to 30 minutes immediately after the start of burrowing by the shrimp. Then, morphological changes of the burrow were imaged with CT data processing, and we calculated surface area, volume, depth, diameter, and length of the burrow. Additionally, we calculated the growth rate of burrow surface area, volume, depth and length.

The surface area and volume of all burrows increased immediately after the start of the experiment, but the growth rates of them gradually decreased. The variation in the value of each diameter gradually got smaller. The depth sharply increased immediately after the start of the experiment and then moderately increased. The length of almost burrows significantly increased immediately after the start of, but then the growth rate gradually decreased. In addition, weak positive correlations were recognized between the carapace length and growth rates of the volume, depth, length, and surface area increase rate though there was almost no correlation between the carapace length and growth rates of the length.

The increase of the growth rate of surface area and volume immediately after the start of the experiment and no reactions by shrimp to food during burrowing indicate that a burrowing is high priority for shrimp. The increase of burrow depth growth rate immediately after the start of the experiment suggests that a hiding against predators is prioritized in the early stage of burrowing. Furthermore, the weak positive correlation between carapace length and volume indicates that larger shrimp produces larger burrow. Additionally, the growth rate of burrow to the shrimp size could be also positively correlated.

This study four-dimensionally observed burrow morphology of the tiger pistol shrimp *Alpheus bellulus*. The method used in this study can be applied to various burrowing organisms, and can contribute to further understandings of benthic ecology and paleoecology.

©2021. Japan Geoscience Union. All Right Reserved.

Shell microstructure of extinct protobranch bivalves

*Kei Sato[1]

1. Faculty of Education and Integrated Arts and Sciences, Waseda University

The shell microstructure is the micro-scale morphological trait of molluscan shells. It can be potentially preserved in fossils, and therefore is considered as a clue for inference on evolution and phylogeny of the past life. The presenter has described the shell microstructures of Recent protobranchs, the ancestral taxon of bivalve, using scanning electron microscopy. Furthermore, microstructural characters have been evaluated phylogenetically through molecular phylogenetic analysis using DNA sequences. Mapping of shell-microstructure characters on the phylogenetic tree confirmed that the composition of shell microstructures is conservative at the superfamily level and can be divided into three major groups; RESP (radially elongate simple prismatic structure), homogeneous, and nacreous groups. To assess the evolutional history of protobranch bivalves, the presenter newly described shell microstructures of fossil protobranchs mainly from the Mesozoic and revealed that several taxa changed their shell microstructural composition from homogeneous to nacreous group. This microstructural evolution can be one of the driving forces of their diversity modulation according to the paleobiological evidence.

Keywords: Shell microstructure, nacreous structure, bivalve, Protobranchia

©2021. Japan Geoscience Union. All Right Reserved.

A unification of absolute growth, allometric, and theoretical morphologic models: a case of molluscan shells

*Takao Ubukata[1]

1. Department of Geology & Mineralogy, Division of Earth & Planetary Sciences, Kyoto University

Study on growth and form of past creatures is a fundamental part of paleobiology. There are three types of approaches: absolute growth analysis, allometry, and theoretical morphology. An absolute growth curve describing the pattern of growth with time provides information about the life history strategy of the animal. However, such information is often unavailable for fossil specimens, and paleontologists commonly focus on the relationship of relative growth rate between measurable morphological traits. Allometric equations are commonly used to describe the relative growth. However, allometric models do not fully represent the geometric characteristics of biological forms and abstraction of geometric information prevents us to perform an inversion analysis of the properties of absolute growth curves from morphological data. A theoretical morphologic model which mimics growth and form of an organism represents the relationship between elementary growth processes and geometric properties. However, theoretical morphology has developed independently from absolute and relative growth analyses in terms of methodology. In the present study, I introduce a new theoretical morphologic model of molluscan shell growth which combines absolute growth and allometric models. It allows us to estimate the properties of absolute growth curves based on an inversion analysis from morphological measurements. A pilot inversion analysis was carried out using artificial data sets to assess reliability of the estimation.
The theoretical morphologic model introduced herein is based on a logistic growth model represented by a sigmoid function of time. It is approximately exponential in the early growth stage, but shows a convex upward curve in the later growth stage, and finally approaches the upper bound of the curve. The logistic function can be defined by its initial value, the intrinsic growth rate, and the inflection point of the logistic curve. These parameters describe the rate and timing of growth processes that underlie shell geometries. The theoretical morphologic model is represented by growth of a helicospiral tube which consists of increases in length of the helicospiral, radius of the spiral, height of the helix, and radii of the elliptic cross-section of the tube. Anisomorphic shell growth can be represented by the theoretical morphologic model if growth of each dimension is approximated by a logistic growth function. A total of 14 dimensionless parameters uniquely define the ontogenetic trajectory of a computer-generated shell form. When intrinsic growth rate and the inflection point of the logistic curve are equal among dimensions, shell shape remains constant throughout ontogeny, even though growth rate changes during growth. If the timing of the inflection point of the logistic curve is nearly equal between a pair of dimensions and the intrinsic growth rate is not greatly different between them, the relative growth between the two dimensions can be approximated by an allometric model. Various patterns of ontogenetic variation in shell shape observed in actual mollusks were reproduced by the theoretical model.
The theoretical morphologic model was designed as a forward model for inversion of parameters of the logistic growth function that are ecologically and developmentally important. A computer-generated planispiral shell form with known parameter values which mimics anisomorphic shell growth of an ammonoid was used to generate data for a pilot inversion analysis. A grid search over the 11-dimensional parameter space revealed that the topography of the parameter hyper-space is not intractably complicated, although the global minimum corresponding to the true values of parameters is in a narrow spike.

©2021. Japan Geoscience Union. All Right Reserved.

Keywords: theoretical morphology, absolute growth, allometry

©2021. Japan Geoscience Union. All Right Reserved.

[J] Poster | B (Biogeosciences)：B-PT Paleontology

Sun. Jun 6, 2021 5:15 PM - 6:30 PM JST | Sun. Jun 6, 2021 8:15 AM - 9:30 AM UTC | Ch.17_2

[B-PT02] Biotic History

convener:Isao Motoyama(Faculty of Science, Yamagata University), Takao Ubukata(Division of Geology & Mineralogy, Department of Earth & Planetary Sciences, Kyoto University), Kazuyoshi Moriya(Department of Earth Sciences, Faculty of Education and Integrated Arts and Sciences, Waseda University)

The Biotic History session covers all aspects of ancient life and the history of biosphere through the geologic time. The study of ancient life is essential for unveiling mysteries of our planet earth. It also provides evidence for evolution of oceans, continents and island arcs. Modern progress in this field has been enhanced by interdisciplinary collaboration with allied sciences, such as paleoceanography and evolutionary biology. Our session intends to be a hub of communication amongst all earth scientists studying the biosphere; we welcome biological and biogeochemical approaches toward the understanding of the history of life.

[BPT02-P01] Preliminary reports on the ecology of Cretaceous pantrionychian turtles based on the carapace bone histology

*Haruka Fukasawa[1], Kohei Tanaka[1], Yasuhisa Nakajima[2] (1.University of Tsukuba, 2.Tokyo City University)

[BPT02-P02] Asexual reproduction of planktonic foraminifera: Discovery and its significance

*Haruka TAKAGI[1], Atsushi KURASAWA[2], Katsunori KIMOTO[3] (1.Chiba University, 2.Marine Works Japan Ltd., 3.JAMSTEC)

[BPT02-P03] Oceanic anoxic event 2 observed in Southwestern Newfoundland Ridge

*Kazuyoshi Moriya[1], Yasuko Miyakura[2], Takashi Hasegawa[3], Akiko S. Goto[4] (1.Department of Earth Sciences, Faculty of Education and Integrated Arts and Sciences, Waseda University, 2.Major in Earth Sciences, Resources and Environmental Engineering, Graduate School of Creative Science and Engineering, 3.Faculty of Earth Science and Civil Engineering, Institute of Science and Engineering, Kanazawa University, 4.Center for Ecological Research, Kyoto University)

[BPT02-P04] Radiolarians from the upper Neogene Tatsunokuchi Formation, Miyagi Prefecture: An attempt to research depth-related distribution of extinct species.

*Isao Motoyama[1], Mizuho Aizawa[1] (1.Faculty of Science, Yamagata University)

Preliminary reports on the ecology of Cretaceous pantrionychian turtles based on the carapace bone histology

*Haruka Fukasawa[1], Kohei Tanaka[1], Yasuhisa Nakajima[2]

1. University of Tsukuba, 2. Tokyo City University

Pantrionychia is a group of non-marine, cryptodiran turtles that includes Nanhsiungchelyidae, Adocidae, and extant superfamily Trionychia (Trionychidae and Carettochelyidae). Pantrionychia originated in the Early Cretaceous of Asia and dispersed to North America during Cenomanian and Santonian. The Late Cretaceous turtle fauna in North America was thus likely influenced by the migration of Pantrionychia. Nevertheless of the importance, however, little is known about the ecology of Cretaceous Pantrionychia. Previous studies on bone/carapace morphology and/or taphonomic evidence suggest that extinct Adocidae was aquatic, whereas Nanhsiungchelyidae is still in debate between aquatic and fully terrestrial. Consequently, it is uncertain whether the clade Pantrionychia evolved from an aquatic or terrestrial form. The aim of this study therefore is to estimate their mode of lifestyles (i.e., terrestrial, freshwater, or marine) and discuss their evolutionally history.

The mode of lifestyle in tetrapods can be inferred based on bone histology. As a general trend, bone compactness is higher in freshwater animals than in terrestrial ones. Marine animals can acquire very high bone compactness (e.g., manatees) or very low (e.g., extant whales) according to animal’s swimming ecology. Such trends are also found in extant turtle limb bones, suggesting that the bone histology method can be applied for fossil Pantrionychia. Turtle limb bones, however, are relatively rare in the fossil record, comparing with abundant discoveries of carapace fragments. Thus, if the carapace histology reflects lifestyles, it can be an easy and powerful tool to infer the ecology of turtles.

In order to test whether the carapace bone histology can be used to infer the mode of lifestyles in turtles, we examined diverse extant taxa, including terrestrial, freshwater, and marine forms, before we applied the method to fossil taxa. Our results revealed that the carapace bone compactness is not necessarily correlated to their lifestyles, differing from previous speculations. However, we found that the size (cross-sectional area) of each intertrabecular space is correlated to the mode of lifestyles, at least between terrestrial and aquatic forms: the cross sectional area is significantly higher in terrestrial species than in aquatic species. The size of each intertrabecular space therefore can be an indicator of the lifestyles in turtles.

Based on the method above, we examined three fossil pantrionychian taxa discovered from the Late Cretaceous (Campanian) deposits in Alberta, Canada (Oldman and/or Dinosaur Park formations): *Basilemys* sp. (Nanhsiungchelyidae), *Adocus* sp. (Adocidae), and *Aspideletoides* sp. (Trionychidae). Our preliminary results revealed that *Basilemys* possesses a relatively large cross-sectional area of intertrabecular space, suggesting a terrestrial lifestyle. In contrast, *Adocus* and *Aspideletoides* show a relatively small cross-sectional area, suggesting an aquatic lifestyle. These results suggest that Pantrionychia changed their lifestyles though their evolutional history, which may be related to their radiation pattern.

Keywords: Pantrionychia, bone histology, ecology, Late Cretaceous, carapace, turtle

©2021. Japan Geoscience Union. All Right Reserved.

Asexual reproduction of planktonic foraminifera: Discovery and its significance

*Haruka TAKAGI[1], Atsushi KURASAWA[2], Katsunori KIMOTO[3]

1. Chiba University, 2. Marine Works Japan Ltd., 3. JAMSTEC

Marine protists have developed diverse modes of reproduction such as binary fission, multiple fission, and budding as means of asexual reproduction, and gametogamy and gamontogamy as means of sexual reproduction. Foraminifera, a group of protists in the Rhizaria, comprise mainly benthic species that generally reproduce both sexually and asexually alternately in their life cycles. However, for planktonic species, gamete release alone has been frequently observed in laboratory cultures. It has been taken as evidence that these organisms produce new generations exclusively by sexual reproduction. We report here the first observation of asexual reproduction in *Globigerinita uvula*, based on the evidence of the vertical transmission of their endosymbionts.
The foraminiferal sample was collected during Cruise MR13-04 of the R/V Mirai in the western North Pacific, July 2013. Four days after isolation, we found a matured individual releasing numerous two-chambered tests from its aperture. The juvenile specimens were immediately separated and utilized for either (1) DNA analysis, (2) culturing and observation, or (3) active fluorometric measurement to investigate photosymbionts. Based on the 18S rDNA analysis, the juveniles were identified to be *G. uvula*. Based on the morphological features, the reproduced matured individual was identified to be *G. uvula* as well, which convinced us that it is the parent of the juveniles. Chlorophyll active fluorescence was detected from the offspring through the culture period, and the intracellular algae were identified to be a pelagophyte alga phylogenetically closest to *Pelagomonas calceolata*. The presence of symbionts in the newborn, two-chambered offspring indicates that the symbionts were probably transferred vertically from the parent. The vertical transmission of symbionts cannot occur via sexual reproduction since the gametes are too small to hold symbionts. Therefore, our observation strongly suggests that the offspring were asexually reproduced by multiple fissions together with the symbionts.
The trigger for asexual reproduction and its ecological or evolutionary roles remain unknown. Considering that *G. uvula* is known to dominate opportunistically at times of high phytoplankton production, their ability of asexual reproduction may support their rapid population growth under changing environment.

Keywords: Planktonic foraminifera, Asexual reproduction, Symbiont transmission, Life cycle

©2021. Japan Geoscience Union. All Right Reserved.

Oceanic anoxic event 2 observed in Southwestern Newfoundland Ridge

*Kazuyoshi Moriya[1], Yasuko Miyakura[2], Takashi Hasegawa[3], Akiko S. Goto[4]

1. Department of Earth Sciences, Faculty of Education and Integrated Arts and Sciences, Waseda University, 2. Major in Earth Sciences, Resources and Environmental Engineering, Graduate School of Creative Science and Engineering, 3. Faculty of Earth Science and Civil Engineering, Institute of Science and Engineering, Kanazawa University, 4. Center for Ecological Research, Kyoto University

We have re-examined Oceanic Anoxic Event 2 (OAE2) at Southwestern Newfoundland Ridge. Mid-Cretaceous sequences including a major black shale approximately 40 cm thick and a few minor black shale layers were recovered by Integrated Ocean Drilling Program Expedition 342 at Site U1407. Shipboard and shore-based biostratigraphy indicates that the sections including these black shales are correlated to the Cenomanian through Turonian. Here, we report total organic carbon content (TOC), organic carbon/total nitrogen ratio (C/N ratio), and organic stable carbon isotope ratio ($\delta^{13}C_{org}$). Maximum TOC observed becomes more than 20 wt% at the major black shale, while background TOC is less than 1 wt%. $\delta^{13}C_{org}$ stratigraphy suggests well-known isotope signature at OAE2, namely, first build-up (FB), trough interval (TI), second build-up (SB), plateau (PT), and recovery (RV), is preserved at this site. At the PT interval, $\delta^{13}C_{org}$ shows an approximately 5‰ positive excursion from the pre-excursion background. The magnitude of this positive excursion is comparable to that observed in Oceanic Drilling Program Site 1276 at Newfoundland Basin. On the other hand, stratigraphic distribution of Black shales in Site U1407 is different from those in Site 1276. In Site 1276, the deposition of black shales started at the base of FB and continued up to PT. However, the major black shale in Site U1407 observed only at SB and PT. Estimated paleodepth at the mid-Cretaceous is deeper than 2000 m for both sites, indicating depths may not regulate the timing of the black shale deposition. Considering bathymetry of western north Atlantic and position of Grand Banks, we hypothesize that these two sites were under the different bottom water current system at the Cenomanian through Turonian.

©2021. Japan Geoscience Union. All Right Reserved.

Radiolarians from the upper Neogene Tatsunokuchi Formation, Miyagi Prefecture: An attempt to research depth-related distribution of extinct species.

*Isao Motoyama[1], Mizuho Aizawa[1]

1. Faculty of Science, Yamagata University

Radiolarians are marine micro-zooplanktons today living in a wide environmental range from tropic to polar regions as well as from shallow to great depths in the world ocean. Therefore, their fossil siliceous remains in sediments are stratigraphically and ecologically useful material to reconstruct the history of the Earth’ s life and surface environments. Going back in deep time, however, living species that are proxies of oceanographic environments become less and less frequent in geological records. Paleobiogeography of extinct species can be a key to understand oceanic biofacies and ecological realms but it is rather difficult to research depth-related distribution in the water column of extinct species.

The Tatsunokuchi Formation is dominated by marine fine-grained sediments deposited in a paleo-bay in northeastern Japan during the latest Miocene to the early Pliocene. This formation yields the Tatsunokuchi Fauna characterized by abundant, diversified fossils including mollusks, crabs, sharks, whales and seals, which indicate cool water condition and water depths shallower than 50 m. This formation provides an opportunity to study ancient planktonic fauna of shallow water environments.

We collected samples from the Tatsunokuchi Formation from the southernmost part of Miyagi Prefecture to the northern border. Most of the samples yielded radiolarian fossils. Some of these samples contain well-preserved extinct species including *Stichocorys peregrina*, *Stichocorys delmontensis*, *Didymoyrtis penultima* and *Cycladophora sphaeris*. *S. peregrina* is the commonest component among the samples and the others occurred in rare abundance from one or two samples. The occurred specimens of *S. peregrina* and *D. penultima* have well-developed siliceous skeletons. *S. peregrina* and *C. sphaeris* are known to be abundant in age-equivalent deep-sea sediments in offshore drilled sites (e.g., DSDP/ODP Sites 438, 1150, 1151). *D. penultima* is a zonal marker species of the *D. penultima* Zone. *Didymocyrtis tetrathalamus*, a modern descendant of the *Didymocyrtis* lineage, is known to be a surface water dweller.
Our results suggest that *S. peregrina* and *D. penultima* lived in surface waters shallower than 50 m. It is likely that both were shallow water taxa, although it cannot be excluded that they had wide depth ranges from the surface to deeper layers. It is not certain that *S. delmontensis* and *C. sphaeris* dwelt in abundance in the paleo-Tatsunokuchi bay because of their rare, sporadic occurrence.

Keywords: radiolarians, paleo-ecology, Tatsunokuchi Formation

©2021. Japan Geoscience Union. All Right Reserved.

[J] Oral | G (General)：General

Sun. Jun 6, 2021 3:30 PM - 5:00 PM JST | Sun. Jun 6, 2021 6:30 AM - 8:00 AM UTC | Ch.02 Zoom Room 02

[G-01] Disaster prevention education

convener:Hitoshi Nakai(Kobuchisawa Research Institute for Nature and Education), Jiro Komori(Teikyo Heisei University), Shintaro Hayashi(Akita University Graduate School of Education), Tetsuhiko Asano(Senshu University Matsudo Junior High School High School), Chairperson:Shintaro Hayashi(Akita University Graduate School of Education), Tetsuhiko Asano(HunabashiKeimei High School), Jiro Komori(Teikyo Heisei University), Hitoshi Nakai(Kobuchisawa Research Institute for Nature and Education)

This session, slated for the 2021 convention, will mark the 10th time the meeting has been convened since the first public session was held a year after the Great East Japan Earthquake. We have consistently focused on how to provide disaster prevention education that is universally and continuously applicable. Almost every year since the first session has been marked by earthquakes and meteorological disasters, and each time we discovered defects in our preparatory measures to mitigate the effects of disasters. The accumulation of such bitter experiences must lead to the creation of new disaster prevention measures. For this purpose, it is necessary to share the experiences of regions right across the country. In particular, people involved in disaster prevention education must extract, from what has been learned in individual regions, those lessons that are universally applicable to any region, and pass them on to future generations. The year 2021 will mark the 10th anniversary of the Great East Japan Earthquake, which resulted in the death or loss of more than 18,000 people, and many more injuries, within the space of just a few hours. The last 10 years has revealed a number of issues to be addressed in disaster prevention education. We would like to review and discuss these issues.

3:30 PM - 3:45 PM JST | 6:30 AM - 6:45 AM UTC

[G01-01] Subjects on science education based on lower secondary school Students' cognition of triggers and first causes of natural disasters caused by flood and earthquake: A case of F City, Japan

*Norihito Kawamura[1] (1.School of Regional Resource Management, Graduate School, University of Hyogo)

3:45 PM - 4:00 PM JST | 6:45 AM - 7:00 AM UTC

[G01-02] School education of disaster prevention through stone monuments for historical natural disasters and SfM technique

*Wataru Tanikawa[1], Go-Ichiro Uramoto[2], Kazuhisa Iwaka[3], Group General Affairs Division[1] (1.Japan Agency for Marine-Earth Science and Technology, Kochi Instutute for Core Sample Research, 2.Kochi University, 3.Tokushima University)

4:00 PM - 4:15 PM JST | 7:00 AM - 7:15 AM UTC

[G01-03] A Teaching Material as an Education for Volcanic Disaster Prevention in No Active Volcanic Area
- Kikai-Akahoya Volcanic Ash at Tarumi-Hyuga Site in Kobe -

*Tatsuya KODA[1], Eiichi Sato[2] (1.Yanagi Gakuen Soukai Senior High School, 2.Hokkaido University of Education at Asahikawa)

4:15 PM - 4:30 PM JST | 7:15 AM - 7:30 AM UTC

[G01-04] Disaster prevention education on volcanic disasters
Development of Sakurajima version HUG

*Yuko Matsunari[1], Yasuhiro Ishimine[2], Tatsuo Takama[3], Hideaki Yoshihara[4], Tsuyoshi Nakatani[1], kaori Kaimoto[5], Keiko Imamura[1], Mitsuhito Sato[4], Naoyuki Hironiwa[6] (1.Kagoshima University, 2.Mount Fuji Research Institute, Yamanashi Prefectural Government, 3.Kagoshima prefecture Hospital , 4.Kagoshima City Hospital , 5.Kagoshima Women's College, 6.Minami-Nippon Shimbun)

4:30 PM - 4:45 PM JST | 7:30 AM - 7:45 AM UTC

[G01-05] The Necessity of Expanding Disaster Literacy toward the Era of "Society 5.0" "SDGs"

*Mamoru Hayashi[1] (1.University of TOYAMA)

4:45 PM - 5:00 PM JST | 7:45 AM - 8:00 AM UTC

[G01-06] Disaster prevention education through on-demand classes at universities

*Shintaro Hayashi[1] (1.Akita University Graduate School of Education)

Subjects on science education based on lower secondary school Students' cognition of triggers and first causes of natural disasters caused by flood and earthquake: A case of F City, Japan

*Norihito Kawamura[1]

1. School of Regional Resource Management, Graduate School, University of Hyogo

The presenter review progress and subjects of study regarding natural hazards and disasters in scence education for elementary to upper secondary schools in Japan.

Keywords: flood disaster, earthquake disaster , questionnaire survey, elementary school, lower secondary school

©2021. Japan Geoscience Union. All Right Reserved.

School education of disaster prevention through stone monuments for historical natural disasters and SfM technique

*Wataru Tanikawa[1], Go-Ichiro Uramoto[2], Kazuhisa Iwaka[3], Group General Affairs Division[1]

1. Japan Agency for Marine-Earth Science and Technology, Kochi Instutute for Core Sample Research, 2. Kochi University, 3. Tokushima University

Natural disaster monuments are used not only to preserve records of past natural disasters, but also as icons to warn people to be prepared for future natural disasters. However, due to the weathering of natural disaster monuments over the years, damage to the monuments and illegibility of the inscriptions has become a problem. Therefore, solutions using digital technology have been devised. On the other hand, the use of natural disaster monuments for disaster prevention education for citizens and students is not sufficient. In this study, as part of the "Hirameki Tokimeki Science" project funded by the Grants-in-Aid for Scientific Research, we conducted a project to deepen understanding of natural disasters by learning about the background of natural disaster monuments and the contents of their inscriptions through the 3D digital technology. This project was designed for elementary to high school students, with two points in mind: practicality and spontaneity. The project was conducted in Tosashimizu City, Kochi Prefecture, which has been hit by earthquakes many times in the past and has many monuments to earthquakes and tsunamis.

A survey of natural disaster monuments in Tosa-Shimizu City revealed that there are not only earthquake and tsunami monuments that tell of the damage caused by the Nankai earthquake, but also many stone monuments that tell of flood damage. Monuments to the 1707 Hōei earthquake, the 1854 Ansei Nankai earthquake, and the 1946 Showa Nankai earthquake were found to exist as monuments to the Nankai earthquake, while monuments to flood damage were erected as a memorial to the August 1920 flood and a monument to the September 2001 torrential rain disaster in southwest Kochi Prefecture. Therefore, it is possible to examine the characteristics of the stone monuments according to the natural disaster and the period of their construction. This project consisted of (1) a lecture on natural disasters and disaster monuments, (2) a visit to a natural disaster monument at the site and data acquisition for building a 3D model, and (3) the use of SfM Structure-from-Motion Multi-View Stereo Photogrammetry (3) construction of 3D models using SfM (Structure-from-Motion Multi-View Stereo Photogrammetry) and production of miniatures using 3D printers, and (4) examination of natural disaster monuments to be produced in the future. In (2) and (3), students learned (A) how to clarify inscriptions that are difficult to see in the field due to sunlight or shade, and (B) how to create 3D digital models of stone monuments. Each group visited five to six natural disaster monuments and conducted (A) and (B) for two monuments.For (4), the following task was given to each group to think of a stone monument they would like to produce. For (4), we gave each group the following task: "X years from now, the Nankai Trough Earthquake will hit your city, causing great damage. A huge tsunami came rushing in, and the port, bridges, and elementary schools were severely damaged. As soon as the quake hit, everyone rushed to evacuate to a nearby shelter, which saved their lives. Afterwards, you were assigned the role of conveying the experience of this great earthquake to future generations through the use of stone monuments. Afterwards, you were assigned the role of conveying the experience of this great earthquake to future generations through the use of stone monuments. What kind of stone monument will you build?".

As a result of this project, we once again felt the difficulty of reading and understanding the inscriptions in the field. During our visit to the natural disaster monument, we were also able to hear from the people who managed and preserved the stone monument and those who experienced the flood disaster. We realized the importance of passing on disaster records using stone monuments as well as hearing from

©2021. Japan Geoscience Union. All Right Reserved.

people who were directly involved in the disasters and the monuments. The future stone monuments presented by students stood out by making it colorful, huge, and near the school. Since the SfM technology is not yet widely used, I felt that this technology could be used for educational activities other than learning about stone monuments.

Acknowledgements:
This program is funded by JSPS program (20HT0112).

Keywords: stone monuments for natural disasters, Nankai Earthquake, flood disaster, tradition, Structure from Motion, SfM

©2021. Japan Geoscience Union. All Right Reserved.

2020年 雨天決行 11月15日(日)
9:30~15:40
参加費無料(昼食付き)

3Dデジタル技術で地震津波災害の記録を未来へ残そう!



わたしたちの祖先は、過去に起きた大地震や台風による災害を伝えるために、巨大な石に文字を彫って記録を残しました。しかしその碑は長年の風化でダメージを受けて、文字が読めなくなりつつあります。そこで、3Dデジタル技術を用いて、文字を読みやすくして蘇らせた碑を保存する試みが行われています。このプログラムでは、実際の碑から過去に発生した大災害を知り、災害の記録を未来へ残す最先端の取り組みを学習・体験します。

対　　象:小学校5、6年・中学生
定　　員:15名(先着順)
会　　場:竜串ビジターセンター「うみのわ」
集合場所:8:45 土佐清水市役所前(バス送迎)
または
9:00 会場「うみのわ」

<スケジュール>
9:00 - 9:30 受付(うみのわ)
9:30 - 9:40 開会式・オリエンテーション
9:50 -10:10 講義① 地震津波碑から南海トラフ地震を理解しよう
10:20 -12:20 実習① 自然災害碑の観察(散策)
12:20 -13:20 昼食・休憩
13:20 -13:35 講義② 3Dデジタル技術を体験しよう
13:35 -14:20 実習② 3Dモデルからミニチュアの作成
14:30 -15:30 実習③ 自然災害ロールプレイング
15:30 -15:40 終了式・解散
＊野外での散策可能な服装と靴でお越しください。

講師:谷川　亘(海洋研究開発機構 高知コア研究所・主任研究員)
協力:浦本 豪一郎(高知大学・特任助教)
　　:井若　和久(徳島大学・学術研究員)

主催:海洋研究開発機構 高知コア研究所
協力:土佐清水ジオパーク推進協議会
　　高知大学

申込方法:「ひらめき★ときめき サイエンス」HPまたはQRコードからお申し込みください。
申込締切:2020年11月9日(月) https://www.jsps.go.jp/hirameki/

本プログラムは感染症予防対策を徹底し、安全に配慮して実施いたします。

<お問合せ>海洋研究開発機構 高知コア研究所(管理課)　メール:kochicore@jamstec.go.jp　電話:088-864-6705

©2021. Japan Geoscience Union. All Right Reserved.

A Teaching Material as an Education for Volcanic Disaster Prevention in No Active Volcanic Area
- Kikai-Akahoya Volcanic Ash at Tarumi-Hyuga Site in Kobe -

*Tatsuya KODA[1], Eiichi Sato[2]

1. Yanagi Gakuen Soukai Senior High School, 2. Hokkaido University of Education at Asahikawa

In recently many natural disasters happened for examples earthquake, typhoon, local heavy rain, volcanic eruption and so on. We asked to university students what do you think about the most worried disaster. As a result, the volcanic disaster was the most worried less than earthquake disaster and meteorological disaster. So we tried them to be anxious about the volcanic disaster in no active volcanic area such as Kobe and Osaka. We gave a lesson for volcanic disaster prevention observing the volcanic ash as a teaching material. This volcanic ash that is abundant in fresh volcanic glasses was collected at Kobe Tarumi-Hyuga site in 1997. The volcanic ash was identified as the widespread tephra named Kikai-Akahoya volcanic ash composed of bubble type glasses less than 1mm length. Consequently, most of university students changed their image of volcano and grew up their intension for the volcanic disaster by the lesson. The volcanic ash sample is quite able to be an effective teaching material as an education for volcanic disaster prevention in no active volcanic area

Keywords: Widespread tephra, Kikai-Akahoya volcanic ash, Tarumi-Hyuga site, Education for volcanic disaster prevention

©2021. Japan Geoscience Union. All Right Reserved.

Disaster prevention education on volcanic disasters Development of Sakurajima version HUG

*Yuko Matsunari[1], Yasuhiro Ishimine[2], Tatsuo Takama[3], Hideaki Yoshihara[4], Tsuyoshi Nakatani[1], kaori Kaimoto[5], Keiko Imamura[1], Mitsuhito Sato[4], Naoyuki Hironiwa[6]

1. Kagoshima University, 2. Mount Fuji Research Institute, Yamanashi Prefectural Government, 3. Kagoshima prefecture Hospital , 4. Kagoshima City Hospital , 5. Kagoshima Women's College, 6. Minami-Nippon Shimbun

The purpose of this research is to develop the Sakurajima version of HUG (an acronym for *hinanzyo unei* game, a game for managing evacuation shelters) as a part of the educational program for disaster prevention related to Sakurajima’ s volcanic disasters. Residents will understand the need for self-help and mutual assistance in the event of a disaster by experiencing the Sakurajima version of the evacuation center management game. The aim is to take action to gain self-help in disasters and to strengthen disaster prevention and mitigation measures in the region. At the Earthquake and Volcano Disaster Prevention Center of Kagoshima University, a working group was established in 2018 and started its activities. It was predicted that it would have a great impact on people's lives and livelihoods. In a volcanic disaster, Kagoshima City would be isolated due to the effects of ash- fall. The effects of volcanic disaster would be prolonged. It was concluded that living in a shelter would be inevitable. Then, measures residents should take were examined. After some consideration, it was thought that it was necessary to expand disaster prevention and disaster mitigation awareness activities for residents by having them experience the evacuation center (HUG) game developed by Shizuoka Prefecture. Consequently, the Sakurajima version of the evacuation center management game was developed. This shelter game is a game that simulates how to respond to various events that occur in the shelter. Currently, a prototype version of this Sakurajima evacuation center management game has been completed. This prototype version allows people in local governments and related occupations involved in disasters to gain knowledge and ways to respond during volcanic disasters. However, since the ultimate goal of this research project is to improve disaster prevention literacy for volcanic disasters of local residents, further activities are needed. Therefore, in order to spread disaster prevention literacy to the general public, elementary school students, and the elderly, teaching material which can be grasped visually and intuitively are needed. Thus, a card game with commentary was developed, which when played and completed, can lead to disaster prevention awareness. A prototype version of the Sakurajima evacuation center management game has been completed. First, we asked general participants to play the game during the Sakurajima evacuation drill, which is held once a year. We also recruited elementary and junior high school students who are interested in disasters and disaster prevention. We also asked the children who applied to play the game and observe it. Then, we asked for opinions on whether there were any words that they did not understand or if they had any problems. We also asked the elementary and junior high school teachers for their opinions on possible problems. Thus, the content was revised and led to the completed version of the modified Sakurajima evacuation center management game. The elementary school students were able to enjoy playing games and to increase their level of interest in disasters. The junior high school students gained confidence in leadership skills by explaining the game and taking care of the elementary school students. There is a danger that Sakurajima may erupt on the same scale as that of the Taisho eruption. By using this game, information about disaster prevention and mitigation can be disseminated to local residents in cities and the prefecture. This will raise awareness not only in volcanic disasters but also in other kinds of disasters. This game has not been developed exclusively for Sakurajima but also for other volcanic disasters. For example, possibility of a volcanic disaster on Mt. Fuji is not zero. Thus, measures to prevent and mitigate volcanic disasters should be a topic priority in a volcanic country

©2021. Japan Geoscience Union. All Right Reserved.

like Japan.

Keywords: Disaster prevention , education , volcano , shelter

©2021. Japan Geoscience Union. All Right Reserved.

The Necessity of Expanding Disaster Literacy toward the Era of "Society 5.0" "SDGs"

*Mamoru Hayashi[1]

1. University of TOYAMA

The junior high school textbook with the highest adoption rate in Japan (Tokyo-shoseki Edition), contained the geological cross-section of Rokko Ikoma since 1981, and it was introduced as a typical example of earthquake and crustal movement. In 1970's, Kobe City asked the group of researchers of Osaka City University for active fault investigation, and the result covered 1 side of the local paper as "Kobe May Hit by Earthquake". In 1990's, in the decision of the regional disaster prevention plan, the seismic intensity of 5 which is unnecessary in the earthquake resistant fire cistern was chosen through the discussion on which seismic intensity of 6 or seismic intensity of 5 is assumed. The Han-Shin Awaji Earthquake disaster is a typical example of causing the earthquake disaster without being utilized even if there is a knowledge with high probability.

The Ishinomaki plain, Sendai plain and the coastal area of Fukushima Prefecture was left unprotected, because it was not taken in the countermeasure, though there was an experience of the giant history tsunami of Jogan and Keicho.The Manual for the Creation of Tsunami Storm Hazard Maps by the Cabinet Office (2004) established the principle of indicating a wide inundation area for the purpose of soft disaster prevention, which protects people's lives by evacuation, even if the hardware could not prevent tsunami attacks. However, it did not even specify the possibility of inundation damage such as making the Fukushima Nuclear Power Plant an inundation area. It is thought that behind this was political pressure from the electric power companies (The details are summarized in the serial of 'Science' "and the tsunami that was buried" by Kunihiko Shimazaki who experienced a member of the Earthquake Research Committee of the Headquarters for Earthquake Research Promotion, a chairman of the Long-term Evaluation Subcommittee of the Headquarters, and an acting chairman of the Nuclear Regulation Authority.).

The SDGs target of "leave no one behind" is set, and in the "Society 5.0" for the realization, it can be said that the innovation is not only the industrial technology development but also the solution of the public problem by the cooperation of civil society. I would like to establish a social framework that does not bring about "unexpected" such as the Great Hanshin-Awaji Earthquake and the Great East Japan Earthquake as one of the pillars of literacy for disaster prevention education. To achieve this goal, the government will examine the need for public education and democracy.

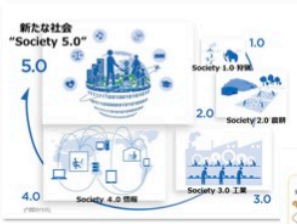
Keywords: Great Hanshin-Awaji Earthquake Disaster, Great East Japan Earthquake Disaster, soft disaster prevention, hazard map, Fukushima nuclear power plant, probability

©2021. Japan Geoscience Union. All Right Reserved.

狭義の防災教育を越えた論点

- 新自由主義的な能力選抜のための学校教育だった側面（差がつくようにできた試験点数重視）
- 学力は個人では決まらないのに，いまだに個人で測定→学校格差社会化→動機づけが限定
- 「誰一人取り残さない」（SDGs）公教育に変われるかどうかが問われている。。
- 全体の奉仕者のまちがいを正す「市民社会の主権者」のための知識･教育の重要性（社会科教育だけの問題ではないが社会科に限界あり）
- その一例として，中学理科でもマグニチュードを→原理がわかるので知識定着も高いはず

Society 5.0やSDGsのためのとしてGIGAスクール構想が語られる現在



SDGs→「誰一人取り残さない」

イノベーション→産業技術発展ではなく，知識･情報の共有，連係による社会問題解決としてのイノベーション概念の強調

美辞麗句に終わらせないために



内閣府：Society 5.0とは
https://www8.cao.go.jp/cstp/society5_0/

「知識があっても生かされない」問題



直下地震が神戸に起きる可能性を報じた１９７４年６月２６日付の本紙

神戸新聞連載「想定を問う　不作為の連鎖　災害列島に生きる」（2012年1月14日付）ネット版掲載写真から

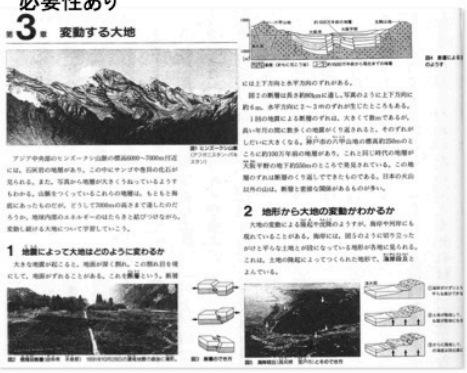


1996年4月刊

https://www.kobe-np.co.jp/rentoku/sinsai/17/rensai/201201/0005480235.shtml

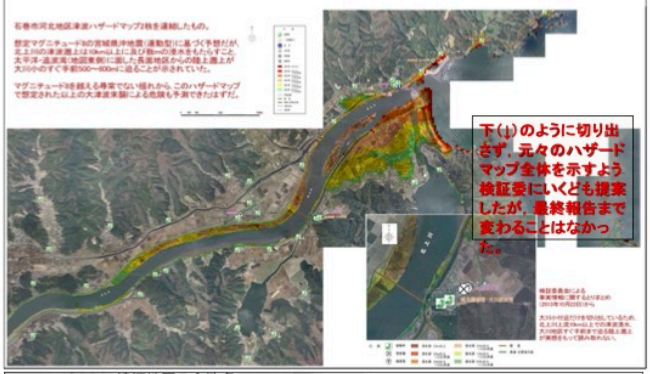


- 1981年から日本で一番採択率の高い東京書籍中学校理科の教科書に→“啓蒙”の最終段階？
- 主体性をうながすには，社会のしくみを問題にする必要性あり

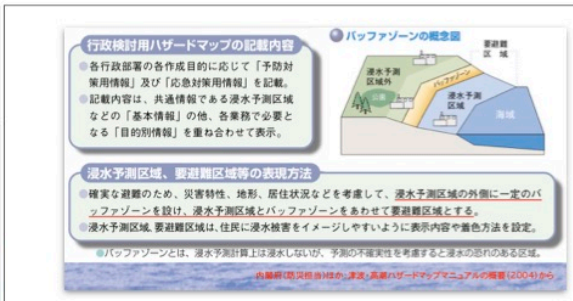


100万年で800m
1万年で8m
1250年で1m
600年で約50cm

3.5kmもの津波陸上遡上が予言マグニチュード8以上では明確に危険



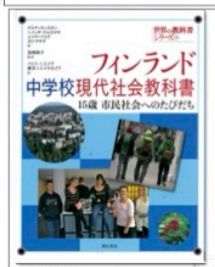
下（↓）のように切り出さず，元々のハザードマップ全体を示すよう検証委にいくども提案したが，最終報告まで変わることはなかった。



論点例その3：バッファゾーン明示義務の記録，検証は不要か。
ひとつの計算結果はひとつの結果にすぎず，ひとつの結果だけをもとに安全，危険を判断してはならないという認識は，防災研究者，政府の防災関係者らに2004年の段階で共有されていたといってよい。2004年の時点で，誤差や津波の多様性があるのを補うためにハザードマップにはバッファゾーン明示が求められていた。ところが，バッファゾーンが明示されないハザードマップが自治体によって繰り返し使われていた（右に続く）。

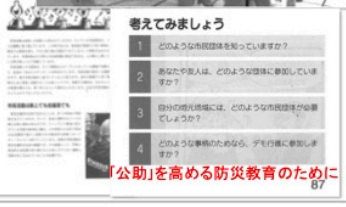


東北大学災害科学国際研究所展示
浪江町での津波堆積物はぎ取り標本。これら平野部への激しい浸水の証拠があったのに生かされなかったために東日本大震災の犠牲者数は倍加した。原発立地の影響があったのだろうか。









Cf.日本国憲法，フランス革命などの市民革命の説明から始まるのが日本の「公民」

「公助」を高める防災教育のために

©2021. Japan Geoscience Union. All Right Reserved.

©2021. Japan Geoscience Union. All Right Reserved.

Disaster prevention education through on-demand classes at universities

*Shintaro Hayashi[1]

1. Akita University Graduate School of Education

1) COVID-19 and Akita University

On January 16, 2020, the first person infected with COVID-19 by the new coronavirus was found in Japan. Since then, COVID-19 has spread rapidly, and on April 16th, a state of emergency was issued to all prefectures in Japan. In response to this, classes were rapidly brought online at many universities.

At Akita University, to which the speaker belongs, classes using the online conference system and class system (Zoom and WebClass in the case of Akita University) began on May 11. Akita University's 2020 classes can be divided into three types: time-space shared face-to-face classes, space-non-shared time-shared online conferencing systems, and time-space non-shared on-demand classes. Of these, especially in on-demand lessons, teachers and students do not share time and space, so it is necessary to devise ways to interact with students.

2) On-demand "natural disaster and disaster prevention education"

The class of "Natural disaster and disaster prevention education" (Hayashi, 2020) in the latter half of 2021 was offered as an on-demand class that does not share time and space. The class consists of four parts, STEP1,2,3 & 4.

The short lecture (STEP 1) is a explanation of basic knowledge that conveys only the main points in a compact manner. In the exercises (STEP2), exercises related to the theme of the lesson were given. We performed tasks such as reading through the relevant page of the designated textbook, investigating on the Internet, and making the situation of the disaster site considered from the prediction data of earthquake damage. These tasks were used by slightly revising what was done in group work until last year. The mini test (STEP 3) is a quiz-style four-choice question for confirming knowledge. Ask about 5 questions to strengthen the knowledge gained in the lecture. In Reflection (STEP4), we looked back on the learning tasks and made them think about their use in disaster prevention education at school.

3) Interaction with students in on-demand lessons

Of course, the diligent response to students was done online. There are two main methods: a) commenting on the assignment submitted to the lesson system, and b)summary of sudent answers were presented at the short lecture. a) Add simple comments to exercises and reflections at the same time as scoring. Students have seen this comment quite a bit, so it functions as a reaction from the teacher. It's much easier to comment than a paper-based submission. Here, we took the action of "praising" as much as possible and controlled the students to be active in disaster prevention education. b) We selected

©2021. Japan Geoscience Union. All Right Reserved.

excellent answers from the exercises and reflections submitted and introduced them at the beginning of the short lecture. Since group work cannot be used, the interaction between students had to rely on this part.

4) Class results

I will describe the impression that these classes were given (the lecture will give concrete examples of student reactions). Hayashi (2020) cited "knowledge about disaster factors," "knowledge about disasters," "quick judgment," "independent judgment," and "ability to respond before a disaster occurs" as the results of face-to-face lessons. Among these, I have the impression that they learned more about "quick judgment," "independent judgment," and "ability to respond before a disaster occurs" than in face-to-face lessons. In the final exam of this lecture, the question is how to act in a situation where a doctor who was hit by a direct earthquake calls for help from a collapsed house along the road on the way from his home to the clinic. It is a problem that must be solved in about 30 minutes, and of course there is no correct answer. In the student's answer, I could read the process of imagining the situation realistically, seriously imagining how to worry, and coming up with countermeasures. In the lecture, concrete examples of answers will be given for other problems.

Keywords: Disaster prevention education, On-demand class, Natural disaster, Online class, COVID-1

©2021. Japan Geoscience Union. All Right Reserved.

[J] Poster | G (General)：General

Sun. Jun 6, 2021 5:15 PM - 6:30 PM JST | Sun. Jun 6, 2021 8:15 AM - 9:30 AM UTC | Ch.03_1

[G-01] Disaster prevention education

convener:Hitoshi Nakai(Kobuchisawa Research Institute for Nature and Education), Jiro Komori(Teikyo Heisei University), Shintaro Hayashi(Akita University Graduate School of Education), Tetsuhiko Asano(Senshu University Matsudo Junior High School High School)

This session, slated for the 2021 convention, will mark the 10th time the meeting has been convened since the first public session was held a year after the Great East Japan Earthquake. We have consistently focused on how to provide disaster prevention education that is universally and continuously applicable. Almost every year since the first session has been marked by earthquakes and meteorological disasters, and each time we discovered defects in our preparatory measures to mitigate the effects of disasters. The accumulation of such bitter experiences must lead to the creation of new disaster prevention measures. For this purpose, it is necessary to share the experiences of regions right across the country. In particular, people involved in disaster prevention education must extract, from what has been learned in individual regions, those lessons that are universally applicable to any region, and pass them on to future generations. The year 2021 will mark the 10th anniversary of the Great East Japan Earthquake, which resulted in the death or loss of more than 18,000 people, and many more injuries, within the space of just a few hours. The last 10 years has revealed a number of issues to be addressed in disaster prevention education. We would like to review and discuss these issues.

[G01-P01] Considering limits of hazard map: A case of a debris flow disaster that struck a village at the southern foot of Yatsugatake in September 1898.

*Hitoshi Nakai[1] (1.Kobuchisawa Research Institute for Nature and Education)

[G01-P02] **A Quantitative Analysis of Nationwide Municipalities' Disaster Prevention Portals**

*Haruka Matsuoka[1], Ami Mori[1], Kei Takashima[1], Tsukasa Sano[1], Asako Sano[2], Seiji Hori[1], Minako Noda[1] (1.Department of Business and Informatics, Tsukuba Gakuin University, 2.Faculty of Home Economics, Otsuma Women's University)

Considering limits of hazard map: A case of a debris flow disaster that struck a village at the southern foot of Yatsugatake in September 1898.

*Hitoshi Nakai[1]

1. Kobuchisawa Research Institute for Nature and Education

Hazard maps that describe sediment disaster warning areas and inundation areas are extremely important sources of safety information for residents. For sediment-related disasters, the warning area (and the special warning area) due to collapse of steep slopes and those for debris flow are designated. The steep slopes mentioned here refer to slopes with an inclination of 30 degrees or more, but flat areas within 10 m from the upper end of each slope and flat areas within 50 m from the lower end of each slope are also included in the warning area (Sediment Disaster Prevention Law Enforcement Regulations). However, the designation is made for "the area of land where it is recognized that there is a risk of harm to the lives or bodies of residents, etc. in the event of a collapse of a steep slope" (Sediment Disaster Prevention Law). Therefore, steep slopes in the mountains are not generally designated as a warning area. However, if a slope collapse occurs when heavy rain continues for a long time in a mountainous area, the debris flow may extend with a plenty of water to a region that is not expected as a sediment disaster warning area. It may consequently occur a significant disaster. Since such a case of the slope collapse under continuing heavy rain is not assumed in the current hazard map, inhabitants have to know about past catastrophes occurred in their area in detail.

In this presentation, we will discuss one of the debris flow disasters that once occurred at the southern foot of Yatsugatake as an example. Around 1:30 am on September 7, 1898, heavy rain brought about by a typhoon caused a debris flow in the Yato Area of Oizumi Village (Hokuto-city Yamanashi) at the southern foot of Yatsugatake. Consequently, 57 were killed, and 51 were injured. The author identified the locations of the damaged houses based on the "Storm Damage Investigation Report" compiled in the Meiji era and archived in the Imperial Household Agency, and the records of the land register stored in the Legal Affairs Bureau. It was found that most of the damaged houses had been located along an agricultural canal that flowed through the village. The author also compared the distribution of damaged houses in the disaster area with the results of debris flow simulations, which was made using the Hyper KANAKO system, and found that the local topographic features were the primary cause of the concentration of victims in a specific group of houses.

Based on the investigation of this historic disaster, it is pointed out that the debris flow may extend beyond the warning area designated on the hazard map, and that a minimal topography of the residential area could cause enormous damage. Farther, these findings suggest that general commentaries on the hazard map is not only insufficient as the disaster prevention education, but it may instill a dangerous sense of security in the inhabitants.

Keywords: hazard map, sediment disaster, historical documents of disaster

©2021. Japan Geoscience Union. All Right Reserved.

A Quantitative Analysis of Nationwide Municipalities' Disaster Prevention Portals

*Haruka Matsuoka[1], Ami Mori[1], Kei Takashima[1], Tsukasa Sano[1], Asako Sano[2], Seiji Hori[1], Minako Noda[1]

1. Department of Business and Informatics, Tsukuba Gakuin University, 2. Faculty of Home Economics, Otsuma Women's University

Japan is a country of frequent natural disasters, with casualties tallied every year. Disaster prevention information and education are therefore very important to mitigate the human and material damages resulting from natural disasters.

One of the familiar disaster educational materials for people is the disaster prevention portal site in the prefecture where they reside. All prefectures in Japan have their own disaster prevention portal sites, which contains various information and educational contents pertaining to natural disaster prevention.

In this study, the disaster prevention portal sites from forty six prefectures were investigated. The results suggest that there is disparity concerning variety contents and structure, which makes it difficult to analyze comparatively or statistically. The twenty eight categories were therefore defined for the information and/or the functions that each portal contains. The value 0 or 1 were then applied to indicate the absence or presence of them. Using these numerical values, correlation analyses were conducted to evaluate the strength of the relationship between the variety among categories and some values or indexes associated with a natural disaster. Additionally, Quantification Method III was also used for multi-dimensional scaling to quantify the characteristics of the portal sites.

The variety of disaster prevention information and education seems to have almost no-correlation with both the index of susceptibility for disasters and the number of victims from disasters over the past five years. The characteristics of the portals possibly are indicated by two components involved in the information it containes, these being the degree of emergency and of concreteness for evacuation actions.

Keywords: Disaster Prevention, Disaster Education, Quantification Method of the Third Type

©2021. Japan Geoscience Union. All Right Reserved.

[J] Oral | G (General)：General

Sun. Jun 6, 2021 9:00 AM - 10:30 AM JST | Sun. Jun 6, 2021 12:00 AM - 1:30 AM UTC | Ch.03 Zoom Room 03

[G-02] Outreach and geoscience education

convener:Jiro Komori(Teikyo Heisei University), Naoko HASEGAWA(Ochanomizu University), Ken Tsukada(Hiratsuka City Museum), Satoko Oki(Faculty of Environment and information Studies), Chairperson:Ken Tsukada(Hiratsuka City Museum), Jiro Komori(Teikyo Heisei University), Naoko HASEGAWA(Ochanomizu University), Satoko Oki(Faculty of Environment and information Studies)

The aims of Outreach and geoscience education are to encourage developments that raise public awareness of geosciences through schools and/or public outreach by not only educators but also researchers. Therefore, any presentation related with these aims will be welcomed to this session. Depending on schedule and venue,some presentation will be changed to Poster presentations.

9:00 AM - 9:30 AM JST | 12:00 AM - 12:30 AM UTC

[G02-01] The strategy and implementation of the Hayabusa2 outreach activities during the phase of the near asteroid operation

★Invited Papers

*Chisato Ikuta[1] (1.Japan Aerospace Exploration Agency)

9:30 AM - 10:00 AM JST | 12:30 AM - 1:00 AM UTC

[G02-02] How to activate discussion on on-line science cafe: Case study of "Science Agora 2020"

★Invited Papers

*Harufumi Tamazawa[1,2], Yuko Ikkatai[3], Junya Terazono[4] (1.Kyoto City University of Arts, 2.Kyoto University, 3.University of Tokyo, 4.National Institute of Information and Communications Technology)

10:00 AM - 10:15 AM JST | 1:00 AM - 1:15 AM UTC

[G02-03] A practical report of virtual field activities with high-resolution panorama (GigaPans) at multiple scales and live broadcasting

*Norihito Kawamura[1], Takashi Sawaguchi[2], Jiro Komori[3] (1.School of Regional Resource Management, Graduate School, University of Hyogo, 2.Toyo Univ., 3.Teikyo Heisei Univ.)

10:15 AM - 10:30 AM JST | 1:15 AM - 1:30 AM UTC

[G02-04] Verification of demands for a location-based geological site interpretation service

*Keisuke Ito[1] (1.Geokatsu Inc.)

The strategy and implementation of the Hayabusa2 outreach activities during the phase of the near asteroid operation

*Chisato Ikuta[1]

1. Japan Aerospace Exploration Agency

The outreach activities for Hayabusa2 was great success due to frequent updates of information with the maximam transparency. Good access to video clips, and images contributed to increase the number of news articles and the visibility in media. Direct communication by using social media added a human dimension to the mission. Telling the risks openly helped the public to understand the challenge and dificulties of the space mission.

In this talk, we will describe our overall strategy and its implementation for the outreach activities of the phase of near asteroid operation of Hayabusa2. Analysing news articles and social media activities, we will share results, and lessons learned to utilize our experience for future missions.

Keywords: Hayabusa2, Outreach strategy, Science communication

©2021. Japan Geoscience Union. All Right Reserved.

How to activate discussion on on-line science cafe: Case study of "Science Agora 2020"

*Harufumi Tamazawa[1,2], Yuko Ikkatai[3], Junya Terazono[4]

1. Kyoto City University of Arts, 2. Kyoto University, 3. University of Tokyo, 4. National Institute of Information and Communications Technology

It has been a long time since the "science café" has been held in Japan to provide the general public with an opportunity to casually participate in and discuss science. However, despite their purpose and advantages, they often take the form of a lecture by the speaker and a question-and-answer session by the participants, and it is necessary to devise a way to facilitate discussion by both the speaker and the general participants. In recent years, various scientific events have shifted to online format, and the Science Café needs to be constructed in such a way that discussions can be held online. As for science cafés, the author and his colleagues have developed a "discussion-type science café" that aims to make discussion easier by clearly indicating the axes of discussion and having multiple topic providers (Tamazawa and Kazai 2020 jjsc accepted). We are also working on the online version. In the case of a format that does not involve an actual venue, it will be necessary to devise publicity strategies and facilitators that are unique to the online format. As an example, I will report on a science café on space development held as a part of Science Agora in November 2020.

©2021. Japan Geoscience Union. All Right Reserved.

A practical report of virtual field activities with high-resolution panorama (GigaPans) at multiple scales and live broadcasting

*Norihito Kawamura[1], Takashi Sawaguchi[2], Jiro Komori[3]

1. School of Regional Resource Management, Graduate School, University of Hyogo, 2. Toyo Univ., 3. Teikyo Heisei Univ.

We condcted a veirtual geotours using a GigaPan image and live broadcasting. The students could make observations through the web site. Outreach activities for students utilizing the high-resolution images and live broadcasting will be enable to teach studenst in distance areas geological field work skills .

Keywords: GigaPan, geology, Anden geosite, Ikuta Ryokuchi Park, lower secondary school student, upper secondary school students

©2021. Japan Geoscience Union. All Right Reserved.

Verification of demands for a location-based geological site interpretation service

*Keisuke Ito[1]

1. Geokatsu Inc.

Outreach in academia is very important for understanding the activities of academia in society. Earth and planetary science, in particular, is a field of research familiar to mankind, and can be a compass to show the state of mankind and what paths , beyond the framework of science, it should take in the future. The mission of Geokatsu Inc. is to create businesses that contribute to the solution of global issues by finding interfaces between the field of earth and planetary science, and society. G-Tour is designed for mobile devices. Users receive a push notification when they enter within a few meters of a geological site, and can read a description of the site by tapping on the push notification. Expected users are mountain climbers and campers. We are currently conducting a needs assessment in low mountains areas of the Kanto area, and will share the results of this needs assessment and knowledge gained at the conference.

Keywords: geological site, outreach, location information

©2021. Japan Geoscience Union. All Right Reserved.

[J] Oral | G (General)：General

Sun. Jun 6, 2021 10:45 AM - 12:15 PM JST | Sun. Jun 6, 2021 1:45 AM - 3:15 AM UTC | Ch.03 Zoom Room 03

[G-02] Outreach and geoscience education

convener:Jiro Komori(Teikyo Heisei University), Naoko HASEGAWA(Ochanomizu University), Ken Tsukada(Hiratsuka City Museum), Satoko Oki(Faculty of Environment and information Studies), Chairperson:Naoko HASEGAWA(Ochanomizu University), Ken Tsukada(Hiratsuka City Museum), Jiro Komori(Teikyo Heisei University), Satoko Oki(Faculty of Environment and information Studies)

The aims of Outreach and geoscience education are to encourage developments that raise public awareness of geosciences through schools and/or public outreach by not only educators but also researchers. Therefore, any presentation related with these aims will be welcomed to this session. Depending on schedule and venue,some presentation will be changed to Poster presentations.

10:45 AM - 11:00 AM JST | 1:45 AM - 2:00 AM UTC

[G02-05] History of public understanding of global warming -When were we able to recognize it?-

★Invited Papers

*Jiro Komori[1] (1.Teikyo Heisei University)

11:00 AM - 11:15 AM JST | 2:00 AM - 2:15 AM UTC

[G02-06] Visual demonstration of greenhouse gas using 15μm absorption band of carbon dioxide.

*Akira Yamamoto

11:15 AM - 11:30 AM JST | 2:15 AM - 2:30 AM UTC

[G02-07] Class proposals and practices for remote learning of chemistry experiments for earth science students.

*Mana Yasui[1], Taisei Fujimura[2], Chiharu Tano[3], Fumitaka Kondo[3], Kenji Yonemochi[3] (1.Waseda research institute for science and engineering, 2.The department of resources and environmental engineering, Waseda University, 3.Faculty of Education and Integrated Arts and Sciences, Waseda University)

11:30 AM - 11:45 AM JST | 2:30 AM - 2:45 AM UTC

[G02-08] Trial of composing a melody using ground motion records of the 2013 earthquake near Awaji Island

*Nobuyuki Yamada[1], Shiina Yamamoto[1] (1.Kochi University)

11:45 AM - 12:00 PM JST | 2:45 AM - 3:00 AM UTC

[G02-09] Education for awareness about sediment related disasters and trial of providing risk information at an elementary school

*Shusuke Miyata[1], Kensuke Takenouchi[2], Ryoko Shimasaki[1], Akira Kamata[2], Daizo Tsutsumi[3], Kotaro Ichida[1], Masaharu Fujita[1] (1.Kyoto University, 2.Kagawa University, 3.Mie University)

12:00 PM - 12:15 PM JST | 3:00 AM - 3:15 AM UTC

[G02-10] Discussion

History of public understanding of global warming -When were we able to recognize it?-

*Jiro Komori[1]

1. Teikyo Heisei University

In order for us to take action to limit global warming, it is important to understand "when the problem first became apparent" and "when we first learned about it". In this presentation, I will discuss the history of understanding by researchers, government agencies, mass media, and the general public, as revealed in compilations of literature (e.g., Weart (2019) The Discovery of Global Warming https://history.aip.org/climate/index.htm) and newspaper databases.

Researchers' understanding dates back to J. Fourier's study on the greenhouse effect in the Earth's atmosphere in 1824, but the 1938 report by G.S. Callender appears to be the first to present and predict specific warming data (Hawkins and Jones, 2013. RMetS, 139, 1961- 1963). In Japan, Yamamoto (1957, Meteorological Research Notes, 55, 113-117.) is considered to be an early report (Tomari, 2018. JpGU prep. MZZ40-02).
As a governmental organization, the Japan Meteorological Agency revised its long-term forecast from "colding" to "warming" in the late 1970s and early 1980s.
In terms of books for the general public, a boundary may be drawn between the sales of 80,000 copies of "The Ice Age is Coming" in 1976 and the publication of translated books on global warming in Japan in 1983 and 1984.
As for the mass media, the term "global warming" has been used in foreign newspapers since the 1960s, but it did not really increase until 1988, the year the IPCC was established. The term "global warming" has had several peaks since then, but the 1997 and 2007 peaks can be attributed to the Kyoto Protocol and A. Gore's "An Inconvenient Truth" respectively. In Japanese newspapers, the use of the term "global warming" increased slightly around 1975, and then increased rapidly from 1988, as in the case of foreign newspapers. On the other hand, the term "global cooling" was used from the 1960s to 1983.

Keywords: climate change, public understanding, awareness history, global warming skepticism, newspaper database, negative legacy

©2021. Japan Geoscience Union. All Right Reserved.

Visual demonstration of greenhouse gas using 15 μm absorption band of carbon dioxide.

*Akira Yamamoto

An uncooled infrared camera was made that visualizes the infrared radiation emitted by carbon dioxide, which is an important greenhouse gas. It has become possible to perform a demonstration with a consistent and clear physical meaning of global warming for the first time, that is: the generation of carbon dioxide by burning fossil fuels, the greenhouse effect that the infrared radiation emitted by carbon dioxide in the atmosphere warm the earth's surface, and the mechanism of global warming that the concentration in the atmosphere increases as infrared radiation that warm the earth surface temperature increases.

Figure

A gas included in a polyethylene bag was photographed by the infrared camera (a). The whiter the color, the stronger the infrared emission. Infrared emission by carbon dioxide (c) is much stronger than emission from a polyethylene bag only((b), the air included). The room temperature is around 25 degrees C, and the background is about 5 degrees C lower than the room temperature using wet Kent paper.

Keywords: Visual demonstration of greenhouse gas, infrared camera, thermography, infrared emission, carbon dioxcide



©2021. Japan Geoscience Union. All Right Reserved.

Class proposals and practices for remote learning of chemistry experiments for earth science students.

*Mana Yasui[1], Taisei Fujimura[2], Chiharu Tano[3], Fumitaka Kondo[3], Kenji Yonemochi[3]

1. Waseda research institute for science and engineering, 2. The department of resources and environmental engineering, Waseda University, 3. Faculty of Education and Integrated Arts and Sciences, Waseda University

The new coronavirus infection forced many universities to change all classes remotely during the spring 2020 semester. In the chemistry experiment course for students studying earth science, we tried a new proposal when remotening the experiment class. We will also report the results from the feedback from students.

The biggest concern in the remote learning of experiments is that the technique of experimental operation cannot be inherited.Regarding the remoteization of experimental subjects, we expected face-to-face lessons in the fall semester. For this reason, we have reorganized the annual experimental items as planned to be conducted after the fall semester, especially for those that require learning of experimental operations.For this reason, analytical experiments were actively placed in the spring semester. The aim is to cultivate the basic data handling and concepts required for analysis when using analytical instruments such as the calibration curve and least squares method. The lesson was organized by creating a video that handles analytical equipment, giving students dummy data, deriving analytical values from the data, and encouraging consideration. However, I thought that it would be very disadvantageous for students studying earth science to not be able to realize the connection between the actual substance and what they are analyzing, considering the future specialized education in earth science.Therefore, in the "water hardness analysis using chelatometric titration", the water used for the analysis was collected at actual sites such as rivers and springs. Then, the video of the water collection was prepared as a teaching material after adding explanations such as the hinterland and the origin of the spring water. Here, it was recognized that the feeling of imagining the relationship between actual substances and analysis results varies considerably from person to person.
In the fall semester, face-to-face communication was realized and wet phylogenetic analysis operations became possible, but due to the influence of the third wave of new coronavirus infection, we applied distance learning again.We tried to propose a lesson in which students infer and think by themselves from the numerical values read using difficult instrumental analysis.Regarding this, we will consult with TA (Master's Course Student of Earth Science) who is a member of this presentation, and ask junior students to actually think about the content (meteorite analysis) that is close to the theme of his master's thesis. Coincidentally, the sample of "Hayabusa2" had just arrived in Japan, so We think it was a good time to arouse interest. We also report the interesting characteristics of the submitted report.

Keywords: earth science students, chemistry experiments, remote learning

©2021. Japan Geoscience Union. All Right Reserved.

Trial of composing a melody using ground motion records of the 2013 earthquake near Awaji Island

*Nobuyuki Yamada[1], Shiina Yamamoto[1]

1. Kochi University

It is important to understand about the strong ground motion in order to protect ourselves from them. In this report, we attempted to express the ground motion records in a way other than the time history waveforms for the outreach of earthquake education and disaster prevention. In particular, we sought a method to convert the seismic motion records into a melody that enables us to "feel" the nature of seismic motion by listening to the melody. In this study, we modified the method of Yamada and Okubo (2012) for the 2013 earthquake near Awaji Island, and sought to express sensory to the differences of seismic wave propagation and seismic motion at each location.

In this paper, we show the spatial characteristics of the ground motion from the K-NET records of the 2013 Awaji Island earthquake (277 points), and introduce an attempt to create a melody using these data. For data processing, the Fourier spectrum of the velocity record for 20.48 s after the S-wave arrival time of the UD component was calculated, and the peak value and dominant frequency of the spectrum were extracted. From the results, we can see the trend of ground motion such as longer period in the sedimentary basins. In addition, we used them to create a musical score, using the strength, height, and placement of notes. To determine the pitch of a note, the relationship between the key number and the frequency of the note was retained and applied to the frequency characteristics of seismic motion. The maximum spectral amplitude was used for the intensity of the sound, and the maximum spectral amplitude was correlated with the reference value of the intensity symbol to create a musical score. In order to arrange the determined notes on the score, the temporal characteristics were retained and the order of S-wave arrival was set, with a time frame of 1 second and 0.01 second per note. In the 1 s case, there are points at which the S-wave arrives at almost the same time, resulting in a large number of overlapping scales in a single note, and in the 0.01 s case, there are many blank time slots, each of which creates its own problems, and there is room for ingenuity in the way the notes are arranged. The speed of the song and the type of sound are also issues that need to be addressed in the future. On the other hand, we have attempted to create a version of this report that is limited to the Shikoku region, where the number of observation records has been reduced. In the future, we believe that the combination of the melody we created and the visual representation method, as well as the process of creating the melody itself, will help us understand seismic motion in a fun way. Although it is impossible to judge the impressions and quality of the results because they are subjective, we would like to make further efforts based on the problems we encountered.

The contents of this report are based on the graduation research of the co-author, Ms. Shiina Yamamoto in 2020. And we used K-NET data provided by National Research Institute for Earth Science and Disaster Resilience. This research was supported in part by Grant-in-Aid for Scientific Research (C) (19K02615). I would like to express my gratitude to all of them.

Keywords: ground motion record, composing a melody, education for disaster mitigation

©2021. Japan Geoscience Union. All Right Reserved.

Education for awareness about sediment related disasters and trial of providing risk information at an elementary school

*Shusuke Miyata[1], Kensuke Takenouchi[2], Ryoko Shimasaki[1], Akira Kamata[2], Daizo Tsutsumi[3], Kotaro Ichida[1], Masaharu Fujita[1]

1. Kyoto University, 2. Kagawa University, 3. Mie University

Sediment related disasters such as landslide and debris flow occur locally and unexpectedly. More than 80 % of human damages and losses due to sediment related disasters took place in buildings, implying late evacuation actions during heavy storms. Therefore, it is essential to understand the disaster risks at one’s own place for early evacuation actions. Education of disaster mitigation can contribute to understanding the disasters and their risks, which has been referred in guidelines of disaster mitigations at schools. As available land is generally limited in mountainous areas, public facilities such as schools must be located at areas with danger of sediment related disasters. According to the guidelines above, schools are requested to establish disaster mitigations individually. Real-time risk information of sediment related disasters is useful for schools in mountainous areas. We will present an education program on precipitation and sediment related disasters and real-time risk information based on observation and a simple model at Tochio elementary school, Takayama city, Gifu prefecture.

Because Tochio elementary school is situated adjacent to steep slopes, the site of the school is specified as the high- and very high-risk areas of landslide and/or debris flows (as called as ‘yellow zone’ and ‘red zone’, respectively). A huge debris flow at a torrent close to the school caused casualties and damages in 1979. The adjacent steep slopes and the previous debris flow disaster indicate the risk of the school. Tochio elementary school has been tackled education on mitigation of sediment related disasters in which our lectures, 4 classes per year, have been included. Our education program consists of classes on 1) what are sediment related disasters, 2) precipitation and evacuation actions, 3) ‘Cross-road game’ drill, and 4) what are disasters in winter. To realize amount of precipitation, the relationship between precipitation observed at the school and students’ feeling of precipitation was recorded. The recorded results showed large variations of sensitivity on precipitation among the students, suggesting that the difference between criterions of precipitation for disaster alert and residents’ feeling of precipitation should be recognized and is critical for effective risk information.

To provide real-time risk information for the school, we try to establish a method for evaluating the risk of the adjacent steep slope in real time. Discharge of a spring in the adjacent slope is observed and simulated by a simple function model. The spring discharge is assumed to be correlated to the groundwater level in the slope. Thus, the greater spring discharge can be assumed as the higher risk level of the slope. The input data for the model is only observed precipitation at the school, so that the risk information can be estimated in real time at the school. This information can contribute avoiding human damages at the school.

Keywords: Landslide, Precipitation, Evacuation

©2021. Japan Geoscience Union. All Right Reserved.

[J] Oral | G (General) | General

[G-02] Outreach and geoscience education

convener:Jiro Komori(Teikyo Heisei University), Naoko HASEGAWA(Ochanomizu University), Ken Tsukada(Hiratsuka City Museum), Satoko Oki(Faculty of Environment and information Studies), Chairperson:Naoko HASEGAWA(Ochanomizu University), Ken Tsukada(Hiratsuka City Museum), Jiro Komori(Teikyo Heisei University), Satoko Oki(Faculty of Environment and information Studies)
Sun. Jun 6, 2021 10:45 AM - 12:15 PM Ch.03 (Zoom Room 03)
The aims of Outreach and geoscience education are to encourage developments that raise public awareness of geosciences through schools and/or public outreach by not only educators but also researchers. Therefore, any presentation related with these aims will be welcomed to this session. Depending on schedule and venue,some presentation will be changed to Poster presentations.

12:00 PM - 12:15 PM

[G02-10]Discussion

©Japan Geoscience Union

[J] Poster | G (General)：General

Sun. Jun 6, 2021 5:15 PM - 6:30 PM JST | Sun. Jun 6, 2021 8:15 AM - 9:30 AM UTC | Ch.03_2

[G-02] Outreach and geoscience education

convener:Jiro Komori(Teikyo Heisei University), Naoko HASEGAWA(Ochanomizu University), Ken Tsukada(Hiratsuka City Museum), Satoko Oki(Faculty of Environment and information Studies)

The aims of Outreach and geoscience education are to encourage developments that raise public awareness of geosciences through schools and/or public outreach by not only educators but also researchers. Therefore, any presentation related with these aims will be welcomed to this session. Depending on schedule and venue,some presentation will be changed to Poster presentations.

[G02-P01] Astronomy outreach with multiple perspectives by music, painting, and tourism

★Invited Papers

*Uenoyama Sachiyo[1], Akihiko Tomita[1], Masami Okyuudo[1] (1.Wakayama University)

[G02-P02] Astronomical environment in which outreach targets are interested and outreach methods utilizing it

*Miyuki Tsuchiya, Mie Enomoto

Astronomy outreach with multiple perspectives by music, painting, and tourism

*Uenoyama Sachiyo[1], Akihiko Tomita[1], Masami Okyuudo[1]

1. Wakayama University

As stated in the Strategic Plan 2020-2030 of the International Astronomical Union, astronomy is deeply related to and has a significant impact on the fields of “culture and society” in addition to “science and research” and “technology and skills.” Although the discussion here stands from a point of view of astronomy, the same point of view can be applied to any discipline and field in the broad field of earth and planetary sciences. In the area of “culture and society,” we would like to focus on the inspiration and the raising of awareness of the need to create communities for sustainable development that come from a sense of awe in contact with great nature. Music, painting, and tourism have a high affinity with astronomy, and many of such outreach activities have been conducted to acquire the above-mentioned power in the “culture and society” area. On the other hand, many researchers have been struggling with the methodology of how to measure and evaluate these powers.

The outreach that will be examined here is the practice at Deti, a facility for Japanese students to study English in Negros Island, Philippines. It is a residential school that aims to help students acquire English through encounters with local people, culture, and values. The schedule was 12 days, from August 5 to August 16, 2019. Participants included parents and their children studying abroad from Japan (5 adults and 7 children), Filipino English teachers (about 20), Japanese tourists (several), Japanese staff and their families (6), and Japanese interns of students and adults (7).

The practices included, (1) “Star storytelling and star-watching party” was held almost every day, (2) “Storytelling about constellations and the arpa” while playing the arpa (a South American harp), concerts at night pools while looking at the stars, self-help and healing music, “Obon” music ceremonies, etc, (3) Psychological counseling sessions to look at the way of life, (4) Mural painting on the wall of the child house in the Deti campus, (5) Projecting illustrations of picture books and reading them, and reading anti-war picture books with background music by a local harp player. The participants’ comments and actions during the practice were recorded in writing, and from the records, we found cases that led people to have a broader perspective and to think about their way of life and community, and examined the conditions of the environment in which the cases happened. This is the material and method we have adopted for the measurement and evaluation.

Twenty-four episodes were identified as examples to focus on. For example, they noticed that the night sky was different due to the difference in latitude, and became aware of the planet Earth. They also learned about each other’s thoughts and way of life, and at the same time, began to talk about the changes in each person’s behavior and mental attitude. For each case, we wrote down the timing of the case, the participants’ actions, and the educator’s impression and evaluation. The four physical environments needed for the cases are: (1) the good atmosphere and climate of the region, (2) the good physical settings (building, educational discipline), (3) the appropriate timing (period and time of year), and (4) a simple and highly functional astronomical software. The three human environments needed for the cases are: (1) the collaborative and ambitious mind of the staff (mediators and collaborators), (2) the high level of awareness of the participants, and (3) the educator’s wide range of skills and knowledge.

©2021. Japan Geoscience Union. All Right Reserved.

Keywords: astronomy outreach, astro-turism

©2021. Japan Geoscience Union. All Right Reserved.

Astronomical environment in which outreach targets are interested and outreach methods utilizing it

*Miyuki Tsuchiya, Mie Enomoto

This paper considers Tokyo Disney Sea as an astronomical environment in which outreach targets are of daily interest, and considers the specific astronomical environment by adding new knowledge, taking into consideration previous research. Next, we will take up Shuichiro Yoshioka's "The Relationship between Astrology and Astronomy, its History"(1943,The Heavens) and consider how astrologyshould be viewed. As an outreach method that takes advantage of the astronomical environment of interest, we propose to hold summits by organizations and organizations with the symbol "Foucault pendulum" currently installed in 59 locations nationwide, including TDS.@Points to keep in mind when using the astronomical environment at TDS for outreach.TDS is a daily source of interest to outreach targets, with an average of about 30 million visitors a year. Previous research by Hiroaki Ying, Reiji Hibara, and Sayaka Nabeshima "Utilizing Artificial Materials in Earth Science Education : A Utilizing Example of Earth Science Materials at TDS" (Education of earth science 61(4)," 133-139, 2008-07-25), Chii Shimomura, Noritsugu Takahashi, "Utilization of Geological Education Materials in TDS" (Research on Space Education, (1), 85-89, 2020-07-07)TDS already has 11 astronomical objects in its main case alone, and it is already well unders been unders been grasped in detail that it is a rich astronomical environment. However, only the fact is pointed out though one of the points pointed out there is a point where not only the earth movement theory but also the astronomical object according to the heavenly movement theory is installed. When using TDS as an outreach method, we propose to actively view it as a material to explain the history of astronomy from the theory of heaven to the earth movement theory. It should also be pointed out accurately to the outreach target that the stoned position of the ground indicating the age of the moon is reversed, even if the reason is not clear. @Shuichiro Yoshioka" The Relationship between Astrology and Astronomy, ItsHistory" (1943, Heaven), astrology as the history of astronomy.Shuichiro Yoshioka is a "relationship between astrology and astronomy, its history" (1943, Tenkai 23(268), In 305-310, 1943-10-25, and 23(269), 344-347, 1943-12-28), astrology born in Babylonia is one with astronomy, and what is born there is also utilized in the system of units and other fundamentals of modern life. Astrology, so to speak, is a living witness to astronomy and embodies the history of astronomy. And in light of modern standards, even if it is unscientific, it is certain that it has been passed down to modern society as a culture related to astronomical texts. In that respect, it is thought that it is near the religion, and it should be calmly caught as the same kind as the annual event of daily such as the new year's visit. @Proposal for holding the " Foucault pendulum " Summit as an Outreach Method As examined in @1 a huge " Foucault pendulum " is installed in TDS along with other astronomical objects. Looking at the number of " Foucault pendulum " currently installed nationwide, there are a total of 59 locations. Therefore, various organizations and organizations that have established this " Foucault pendulum " will set up a network and hold a summit with the symbol " Foucault pendulum ", and propose that it be an opportunity to widely interest in astronomical texts. The content of the summit is not only knowledge of the astronomical text itself, but also the participation of researchers in fields and fields that deal with astronomical events in various forms. Specifically, it assumes areas such as literature, painting, film, architecture, urban planning, calendar, annual events, naming, astrology, religion, politics, etc.

Keywords: Outreach, Foucault pendulum, Tokyo Disney Sea, Astrology

©2021. Japan Geoscience Union. All Right Reserved.

[J] Oral | G (General)：General

Sun. Jun 6, 2021 1:45 PM - 3:15 PM JST | Sun. Jun 6, 2021 4:45 AM - 6:15 AM UTC | Ch.03 Zoom Room 03

[G-03] Geoscience education from elementary school to university students

convener:Masatsune Hatakeyama(Seiko Gakuin High School), Yoshihiro Niwa(Center for Ocean Literacy and Education, Graduate School of Education, The University of Tokyo), Chairperson:Masatsune Hatakeyama(Seiko Gakuin High School), Yoshihiro Niwa(Center for Ocean Literacy and Education, Graduate School of Education, The University of Tokyo)

We will provide and discuss various educational practices (teachings and procedures)
for elementary, junior high school, high school, and university students. We also welcome ONLINE education, fieldwork reports, and outreach reports for all grades.
Besides, especially for liberal arts level geoscience education of undergraduate,
we will consider the problems, such as online education, contents, and prospects of our current geoscience situation.
Furthermore, we will also think about fundamental teaching material development and
the sharing of teaching material data.

1:45 PM - 2:00 PM JST | 4:45 AM - 5:00 AM UTC

[G03-01] Authentic learning from perspective of aerospace - JAXA space education material "Earth Observation Coloring" -

*Yusuke Koga[1], Kenta Nomura[1] (1.Japan Aerospace Exploration Agency)

2:00 PM - 2:15 PM JST | 5:00 AM - 5:15 AM UTC

[G03-02] Home Science of Astronomy and Earth Science for Childcare Educators and Elementary School Teachers

*Akihiko Tomita[1] (1.Wakayama University)

2:15 PM - 2:30 PM JST | 5:15 AM - 5:30 AM UTC

[G03-03] Promotion of STEAM education (focus on space) with public-private partnership using an online tool.

*Norika Numa[1,3], Yoshiki Teramoto[2], Kaori Shoda[2], Asuki Yokoyama[3] (1.School of science, The University of Tokyo, 2.NPO Ikeda eco staff, 3.math channel Co., Ltd)

2:30 PM - 2:45 PM JST | 5:30 AM - 5:45 AM UTC

[G03-04] Visualization of crustal deformations in Japan -10 years before and after the 2011 Tohoku Earthquake viewed with GNSS dates.-

*Tadayoshi Kato[1] (1.Moegino Junior High School)

2:45 PM - 3:00 PM JST | 5:45 AM - 6:00 AM UTC

[G03-05] A case study of bringing online field tip closer to reality
- how to deliver the online excursion with on-site live broadcasting-

*Jiro Komori[1], Norihito Kawamura[2], SAWAGUCHI TAKASHI[3] (1.Teikyo Heisei University, 2.University of Hyogo, 3.Toyo University)

3:00 PM - 3:15 PM JST | 6:00 AM - 6:15 AM UTC

[G03-06] Geoscience・Geography education experiences at seven Japanese universities during the COVID-19 pandemic.

*Wonsuh SONG[1] (1.Waseda University)

Authentic learning from perspective of aerospace - JAXA space education material "Earth Observation Coloring" -

*Yusuke Koga[1], Kenta Nomura[1]

1. Japan Aerospace Exploration Agency

JAXA Space Education Center support to take aerospace into education. As the philosophy of Education Center, the main goal is not learning about space, but learning with space. And it is most important to use the material of space to ignite the three hearts of “curiosity”, “adventure” and “craftmanship”.

Education Center widely covers various fields such as formal education, informal education and experience-based learning opportunities. In addition to that, Education Center develop and release space education materials which is over 300 currently. In this presentation, we introduce space education material named “Earth Observation Coloring” developed and released in 2020. We mention not only how to use, but also educational effect we expect. Finally we indicate issue and vision about this space education material from report a teacher who actually use this material wrote.

Keywords: JAXA, space education, earth obeservation

©2021. Japan Geoscience Union. All Right Reserved.

Home Science of Astronomy and Earth Science for Childcare Educators and Elementary School Teachers

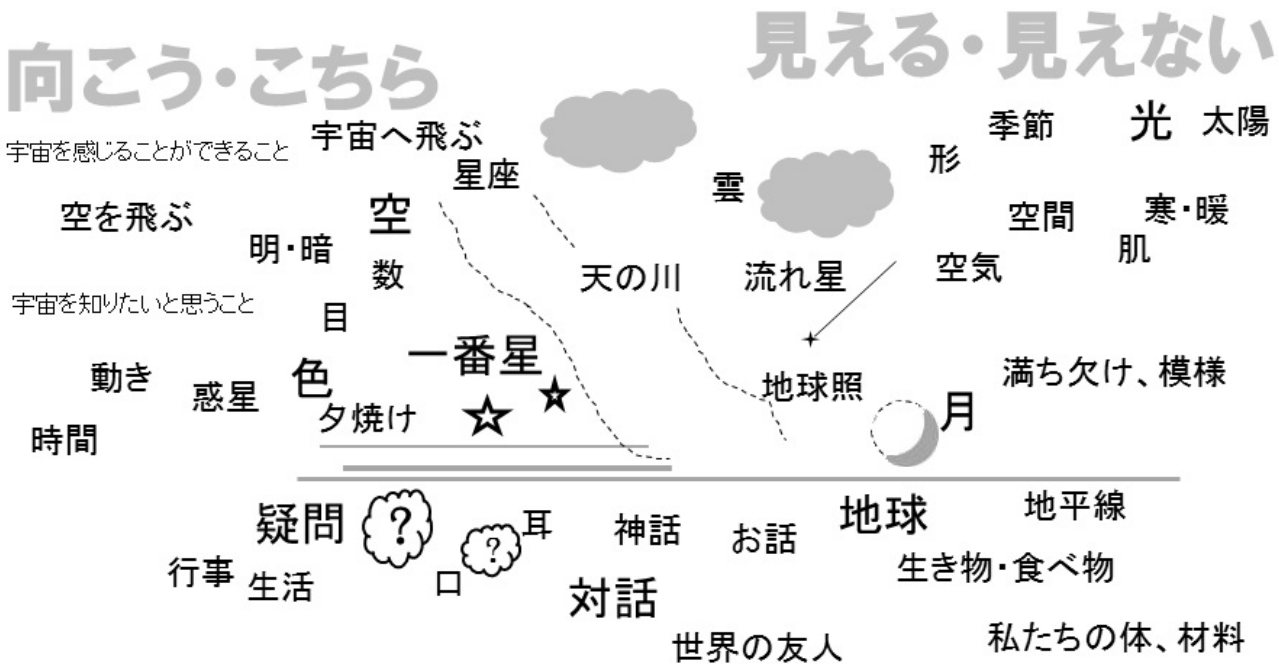
*Akihiko Tomita[1]

1. Wakayama University

The significance and importance of introducing children to the world around them, and the vast world of science, including astronomy and earth science, at all times, from infancy through elementary, middle, and high school, has been pointed out not only by researchers in science education but also by researchers in early childhood education. Various surveys have shown that many adults, even those who do not work in science, are interested in scientific topics, and would like to talk about science if given the chance. School teachers in elementary, middle, and high schools can have opportunities to train themselves in astronomy and earth science, although the problem of inadequate environment still needs to be tackled with. However, early childcare and after-school care educators have little time to do so due to not just the busy schedule of childcare, but the lack of understanding and environment for science education inside and outside the childcare actual site.
For this reason, the author has been working with researchers and practitioners of science education in childcare settings to implement activities that incorporate scientific play about the universe and the earth in everyday life (for convenience, I will call this "home science" in this presentation; e.g., the 73rd Annual Meeting of the Japan Society of Research on Early Childhood Care and Education, Symposium J-C-10 "Home Science, Home Math: What you need to encounter is always in the scenery, and you are the one who intervenes in the encounter!”).
In this presentation, I will introduce some examples of the practices and evaluation methods. Please refer to the following figure for the subject to be covered. The target age range is from 3 to 15 years old, from early childhood to school age. The practices include observation of the sky during the day, evening, and night, both outdoors and in the room; scientific play with light and color in the room; stories and awareness activities to notice the heavens throughout the year, especially the motion of the sun, and the accompanying changes of weather and living things throughout the year; and the yearly cycle of our lives.
The practices presented in this presentation are intended to be used by childcare educators (nurseries, kindergartens, preschools, and after-school care) and elementary school teachers. Although this practice is not an activity of formal education in a school classroom according to the official curriculum, it can serve as a foundation for increasing children's and students' interest in the astronomy and earth science, and for better connecting the formal educational content with life and society. There are many elementary school teachers who are interested in the field of astronomy and earth science but are not good at teaching in this field. Not only childcare educators but also such elementary school teachers will benefit from this study. In addition, it can provide good contents on astronomy and earth science, which are rarely covered in life classes for lower grades of elementary school. In response to the spread of infectious diseases, we are now in a social situation where we have no choice but to keep a physical distance from each other, and this is expected to continue for some time to come. Activities that do not require special equipment and can be done outdoors and in a relaxed indoor environment have the potential to be used in schools under these circumstances, as well as for independent learning by children and students. As an evaluation method, I will introduce the method of recording episodes in childcare settings. Although this is different from the official evaluation method used in formal school education, it is in the same direction in that it looks at thinking, expression, and proactive attitude, and expects the acquisition of knowledge and skills based on these. In addition, I will show how this activity has helped improve the confidence of teacher-training students who are not good at science teaching.

©2021. Japan Geoscience Union. All Right Reserved.

Keywords: Astronomy education, Early childhood education, Primary education



©2021. Japan Geoscience Union. All Right Reserved.

Promotion of STEAM education (focus on space) with public-private partnership using an online tool.

*Norika Numa[1,3], Yoshiki Teramoto[2], Kaori Shoda[2], Asuki Yokoyama[3]

1. School of science, The University of Tokyo, 2. NPO Ikeda eco staff, 3. math channel Co., Ltd

STEAM education is an education policy that includes the areas of science, technology, engineer, art (liberal arts) and mathematics as a form of creative education. Interdisciplinary learning is needed for critical-thinking and creating things. For example, we can see the importance of this policy playing part in our developing society. Society is changing rapidly due to technological advances, so the qualities and skills required for human resources in today’s society is changing. To adapt the changing society, creating new things as well as integrating skills and concepts from various disciplines are important.
One real-life example of STEAM education in action is at Shibaura Institute of Technology Junior High School. Second graders were tasked to create beetle-type robots in a day. This approach brings a sense of accomplishment and self-esteem to the students, as well as, improving their problem-solving abilities. However, human resources, time and platforms are still insufficient to carry out STEAM education, hence more time is still needed to promote STEAM education. In addition, education at schools abruptly came to a halt due to the outbreak of COVID-19. Thus, we believe STEAM education could be promoted as a means of being an online education tool to improve learning.
Last year, we promoted STEAM education as an environmental business promotion project at Ikeda City, Osaka Prefecture. This project was sponsored by Ikeda City, with the cooperation of the board of education of Ikeda City, and planned and operated by NPO Ikeda eco staff). STEAM education was promoted through environmental learning. Familiar things around us are “environment” and the “purpose of environmental learning” is to be aware of the relationships between oneself and familiar events. From here, thinking how actions and decisions can affect an outcome is important. In particular, Ikeda eco staff were interested in STEAM education focusing on space based on the findings of The Greenhouse Gases Observing Satellite “IBUKI”. On the other hand, I worked on STEAM education to promote about space and mathematics. I also conducted lectures on math channel Co., Ltd. This way, STEAM education focusing on space was implemented through the cooperation of the three parties.
The project was named “Have fun with Mathematics and Space at home”. There were around 52 participants. The participants participated from their homes, and each participant was connected with the online tool, Zoom. The contents of the project are as follow. First, the participants compared the size of different planets using things at home. Since the size of planets cannot measure directly, it is difficult to imagine their size by only using figures. Thus, by replacing the size of planets with things at home, the participants were able to feel the universe closer. After that, I introduced my recent study on meteorites, and I brought out interest in space by interacting with the participants through their questions. Through these exchanges, it made me ask questions about the universe, and think about the issues I could tackle in my research. Finally, small groups were formed (4-5 participants per groups) using the function of breakout room in Zoom for more interaction time between the participants.
By comparing the size of planets with familiar objects at home, participants could understand more on the universe qualitatively and quantitatively. Moreover, for the ‘Questions and Answers’ section, I received many good questions. As for the questionnaires, many participants answered the event was fun. There was also feedback such as future approaches. Based on the above results, STEAM education could be promoted with public-private partnership other than at school. In this presentation, the approach of STEAM education and how to promote STEAM education with public-private partnership will be introduced.

©2021. Japan Geoscience Union. All Right Reserved.

Keywords: STEAM education, public-private partnership, primary education, online

©2021. Japan Geoscience Union. All Right Reserved.

Visualization of crustal deformations in Japan -10 years before and after the 2011 Tohoku Earthquake viewed with GNSS dates.-

*Tadayoshi Kato[1]

1. Moegino Junior High School

March 11, 2021 marks the 10th anniversary of the 2011 Tohoku Earthquake. The earthquake, which observed the largest magnitude in Japan's observation history, was recorded by various observation networks and recording media, and was also captured by the “GNSS Earth Observation Network System” (GEONET). GEONET has accumulated coordinate value data from 1996 to the present, and has continued to observe daily crustal deformations associated with this earthquake with an observation network of about 1,400 points. This observational data is open to the public on the Geospatial Information Authority of Japan website and can be accessed by anyone. However, since it is difficult to process a huge amount of data and visualize the observation results, it is difficult for students to grasp the appearance of Japan. On the other hand, applications and tools that can display the earth and planets in 2D or 3D, such as “Dagke Earth” (http://earth.dagik.org), are appearing as digital teaching materials and have been emphasized in recent years. These can be used for active learning, which "not only gives students knowledge and information, but also allows students to observe problems and draw conclusions." The introduction of these kinds of ICT in schools and educational institutions has begun to gradually progress, and it is expected that the number of places where these teaching materials can be used will increase in the future.

Daily observation data is stored as GEONET data from 1996 to the present, and crustal deformations during any period can be displayed as vector diagrams or baseline length graphs. In addition, the analysis coordinate values (F3 solution and F4 solution) analyzed by the Geospatial Information Authority of Japan for general use are also open to the public. However, it is difficult to intuitively grasp how Japan is fluctuating by utilizing these databases and expressing baseline length graphs and maps, and there are aspects that can only be understood by people with some specialized knowledge. In this study, we created a map that can capture the temporal fluctuations of Japan by calculating the displacement amount of each electronic reference point using the F3 solution and exaggerating the crustal deformations.

The map created by exaggerating the amount of displacement (variable topographic map) changes the shape of Japan after that depending on the reference year. In particular, the change is remarkable when the base year is before and after a relatively large earthquake. In this study, we set three periods: 1996 to 2020, when GEONET began observing Japan, 1996 to 2010, and 2011 to 2020, with the 2011 Tohoku Earthquake as the boundary. By comparing the monthly crustal deformation maps of each month, we attempted to visualize the steady movements of Japan and the aftereffect movements that are prominent after a large earthquake.

In order to capture crustal deformations, there are many aspects that must be captured by continuous observation in units of several years to several decades, so in elementary and junior high school education, it is difficult to observe during class hours, as a huge amount of data is handled. However, effectively studying the use observations that GEONET has accumulated using the new method should help us to think about the appearance of the country in which we live. In addition, if students can freely change the analysis period and exaggeration ratio of the crustal deformation map created, it will be a tool

©2021. Japan Geoscience Union. All Right Reserved.

to help students learn independently.

Keywords: crustal deformation, Japan, Digital teaching material

©2021. Japan Geoscience Union. All Right Reserved.

A case study of bringing online field tip closer to reality - how to deliver the online excursion with on-site live broadcasting-

*Jiro Komori[1], Norihito Kawamura[2], SAWAGUCHI TAKASHI[3]

1. Teikyo Heisei University, 2. University of Hyogo, 3. Toyo University

1. Introduction
Due to the COVID-19 infection control measures, opportunities for "a real" field training and trips are decreasing. On the other hand, there are more chances to conduct online tours. Originally, classroom-to-classroom teleclasses and exchange classes using videoconferencing systems were conducted in the late 1980s (e.g., Shimizu, 1986; Kawamura, 1993). In the 2000s, the use of high-speed Internet connections led to an increase in the introduction of remote classes, and there have been cases of classroom-to-field connections (e.g., Soma et al., 2000; Kawamura et al., 2011).

Since 2010, the use of smartphones and satellite phones has contributed to the diversity of connectivity. However, these are online applications as part of a class, and there are probably no examples of "field trip" around research and learning targets. Hayakawa et al. (2015 JpGU abstract) are exploring the construction of online pilgrimage contents based on actual pilgrimages and maps on the Internet. However, since users use these contents on demand (at different times) after they are made public, there is no direct interaction between guides and participants.

After 2020, there are several projects called online field trip, such as a connecting with several museums ("Gakujyutu Yaei 2020". https://amane-project.jp/post-1111/). Among them, the group "Geography Plaza for Everyone! (https://geo-plaza.hatenablog.com/) is organizing an online tour of the city center based on Google Street View as a tour in the field of geography. This tour using Zoom is close to the original tour where the guide and participants communicate with each other.

In addition, the Izu Peninsula Geopark is providing a real-time tour guide via Zoom from before the outcrop as part of the "2nd Earth Science Week Japan in Shizuoka" (https://www.earthsciweekjp.org/).

The author conducted an online tour connecting participants with outdoor landforms and outcrops as part of a project sponsored by a high school geology club and the Japanese Geology Olympiad. The preparation for this project was done by a trials and errors, without knowing the precedents mentioned above. However, it was easy to implement with only one or a few people on the instructor side, and we obtained some knowledge that will be useful in the future for online field trips and field observation for school education and lifelong education.

2. Findings
The following points were clarified by the online excursion with on-site live broadcasting.

The number of people on the sending side: It was possible for one person to guide the participants from the field. However, it is very important to have a facilitator who can act as an intermediary between the participants in case of communication breakdowns and to encourage questions from the participants.

©2021. Japan Geoscience Union. All Right Reserved.

Whiteboards: In a normal tour, whiteboards are often used to explain terms and present overviews as a supplement to the handouts. On the other hand, in the online tour, it was possible to replace the whiteboard by writing on the tablet screen using a stylus pen. In particular, when explaining outcrop sketches, it was possible to overlay lines and text on the outcrop photos, and then erase only the photos. This is an innovation that could not be done with a whiteboard.

Fixing a smartphone on a camera stabilizer (gimbal): Fixing a smartphone on a gimbal absorbs large vibrations and prevents rapid rotation (panning) of the camera. This is useful when giving explanations while walking. It was very effective when moving by bicycle. However, when transmitting from in front of an outcrop, I often shoot with a smartphone or tablet in hand, and heavy gimbal makes my hands tired.

Microphone: Since we were participating in Zoom in the open air, the use of a microphone and earphones was essential to prevent noise. In order to avoid connection problems, we used wired microphones and earphones fixed to our heads. In addition, we used a microphone sponge as a windbreak.

Cell phone lines: Mobile phone lines were good at all sites during this "online excursion with on-site live broadcasting ". However, this is not always the case at outcrops and field trips around the country. It is necessary to confirm this in the preliminary inspection before implementation.

Keywords: remote lecture, field trip, tips introduction, outcrop definition, online meeting system, camera Stabilizer

©2021. Japan Geoscience Union. All Right Reserved.

Geoscience・Geography education experiences at seven Japanese universities during the COVID-19 pandemic.

*Wonsuh SONG[1]

1. Waseda University

Online lectures offer many benefits. However, it was a huge test for the freshmen who had never spent their time in college and started living alone without any acquaintance or friend as Japanese universities started in April. Such suffers apply not only to students, but also to lecturers who must bring all their lectures into online. Part-time lecturers had a hard time finding a place to shoot the lectures and had no financial support to get the equipment needed to shoot, which was a burden to the household. Here I would like to share my experience of giving online lectures at several universities and what I have learned from them.

First, adding virtual field trip in on-demand class is very effective. Japanese undergraduate students are gradually becoming accustomed to online lectures and prefer on-demand lectures. Students take on-demand lessons at double speed and rewind what they didn't understand. They can take the class from the beginning even if they are late or absent. Nocturnal students can also take 9 am classes at 9 pm. In addition to the on-demand class, I held an online meeting for a physical geography class which has a lot of freshmen. I set out a task for them to find interesting terrain on the Google Maps and to investigate its land formation process with a small group. Students felt satisfied a lot to find interesting place and communicate with their classmates. I convinced that a virtual field trip will be a very important and indispensable tool for future geoscience and geography education.

Second, active learning in university classes is becoming more and more important. It is also important to attract students' interest and broaden their horizons. People can search freely and get a lot of information easily. However, students who have just entered university do not know what to look for and how to search it. It is necessary to know the background of the knowledge that has been earned by simple memorization. Students should know where and how to get reliable information and how to apply it to their present and future life. The lecturer should give important keywords regarding to the content. The students should practice more to do active learning. The existence of lecturers who can move students and broaden their horizons will become more important.

Third, it is also important to make students aware of the current situation and raise their motivation. I explained the value of the class on the first day for every lecture. The cost can be calculated simply by using total cost paid by the student for 4 years, excluding the opportunity cost, and the number of credits required for graduation. Students pay for one class (fifteen classes in a semester) about $ 56 in private universities, and the half in national universities. All the students were very surprised at this number. Students felt that they had to be more concentrated on their study. I sometimes hear that universities may disappear in the future, but as long as the educational background is the simplest and fair standard to prove young student's value, no matter how the times change in the future, good universities will not disappear. Universities are valuable because they provide the place and time that students can learn thinking, problem-solving, and creativity rather than the knowledge. Students should learn and think a lot during their lifetime. This keeps students growing. Lecturers have to tell this fact to the students.

Today's students are getting smarter. Their learning speed is very fast. If the students are not interested in

©2021. Japan Geoscience Union. All Right Reserved.

the subject or the lecturer anymore, “natural selection” will be occurred in academic ecosystem. Universities are no longer a heaven. It's time for university executives, staff, faculty, and students to review and renew everything to be survived. Pandemics give us the opportunity to evolve. I hope everyone to do their best to change this crisis into an opportunity.

Keywords: Geoscience education, Geography education, Online education, University, Covid-19

©2021. Japan Geoscience Union. All Right Reserved.

[J] Oral | G (General)：General

Sun. Jun 6, 2021 3:30 PM - 5:00 PM JST | Sun. Jun 6, 2021 6:30 AM - 8:00 AM UTC | Ch.03 Zoom Room 03

[G-03] Geoscience education from elementary school to university students

convener:Masatsune Hatakeyama(Seiko Gakuin High School), Yoshihiro Niwa(Center for Ocean Literacy and Education, Graduate School of Education, The University of Tokyo), Chairperson:Masatsune Hatakeyama(Seiko Gakuin High School), Yoshihiro Niwa(Center for Ocean Literacy and Education, Graduate School of Education, The University of Tokyo)

We will provide and discuss various educational practices (teachings and procedures)
for elementary, junior high school, high school, and university students. We also welcome ONLINE education, fieldwork reports, and outreach reports for all grades.
Besides, especially for liberal arts level geoscience education of undergraduate,
we will consider the problems, such as online education, contents, and prospects of our current geoscience situation.
Furthermore, we will also think about fundamental teaching material development and
the sharing of teaching material data.

3:30 PM - 3:45 PM JST | 6:30 AM - 6:45 AM UTC

[G03-07] **A study of the cognition regarding natural disasters of junior high school students in Kobe City, Japan.**

*Toshio Arimichi[1,2], Norihito Kawamura[2] (1.Kobe Municipal Ibukidai Junior High School, 2.Graduate School of Regional Resource Management, University of Hyogo)

4:00 PM - 4:15 PM JST | 7:00 AM - 7:15 AM UTC

[G03-09] Thin-Section Making Recipe in a classroom Ver3.0 -using 3D printer-

*Yoshio Okamoto[1] (1.Osaka-Kyoiku University (temporary lecturer))

4:15 PM - 4:30 PM JST | 7:15 AM - 7:30 AM UTC

[G03-10] Development to teaching materials related to GIGA school

*Iida Kazuya[1] (1.Komaba-Toho Junior and Senior High School)

4:30 PM - 4:45 PM JST | 7:30 AM - 7:45 AM UTC

[G03-11] The report of the International Earth Science Olympiad (IESO) ,2021

*Norihito Kawamura[1], Yutaka Takigami[2] (1.School of Regional Resource Management, University of Hyogo, 2.JESOC)

4:45 PM - 5:00 PM JST | 7:45 AM - 8:00 AM UTC

[G03-12] Discussion

A study of the cognition regarding natural disasters of junior high school students in Kobe City, Japan.

*Toshio Arimichi[1,2], Norihito Kawamura[2]

1. Kobe Municipal Ibukidai Junior High School, 2. Graduate School of Regional Resource Management, University of Hyogo

In recent years, the number of natural disasters that cause many victims has increased. A natural disaster is a phenomenon in which a critical natural hazard causes loss of human life and damage to social infrastructure. To minimize the damage caused by natural disasters, it is important to understand both their causes and potential effects. In addition, it is necessary to treat natural disasters as teaching materials, so that the experience gained can be used to help prevent damage in the future. By studying examples of natural disasters, students are made to think about the relationship between human society and the environment, and what can be done to prevent or mitigate damage from natural disasters. Opportunities to deal with natural disasters can occur within science, social studies, health and physical education, technology and home economics, and integrated study lessons, however the most suitable place to learn about the phenomena that cause natural disasters is in science classes, particularly in the study of earth science.

Since the 1995 Southern Hyogo Prefecture Earthquake, disaster education for evacuation preparedness in the event of a disaster, and for minimizing damage in the event of a disaster has progressed considerably. However, education about earth science, particularly in relation to the causes and occurrence of natural disasters has not progressed. Few papers are published, and the cognition of the general public concerning natural hazards remains low. Many core principles such as the difference between typhoon and tropical cyclone, seismic intensity and earthquake magnitude, trench type earthquake and intraplate earthquake, how to interpret the probability of precipitation, and the existence of hazard maps are important topics that the general public has little recognition of. We think that it is the responsibility of science and earth science education to provide the general public with the basic knowledge needed to fully understand the principles and the importance of natural science and natural hazard awareness.

In the *Course of Study (Science) for Junior High School* (Ministry of Education, Culture, Sports, Science, and Technology, 2018), students are to learn that volcanic disasters, earthquake disasters and benefits from nature by learning “the formation and change of the earth”, meteorological disasters and benefits from nature by learning “weather and its changes”, and the local natural disasters by learning “nature and humans”.

In addition to the Southern Hyogo Prefecture Earthquake, Kobe City also frequently suffers damage from strong winds, or flooding caused by heavy rain (including debris flows, landslides, and floods). This is due to the tilted block of Mt. Rokko. The Mt. Rokko range is a massif located on the north side of the city of

©2021. Japan Geoscience Union. All Right Reserved.

Kobe. The rivers that flow from Mt. Rokko have a very short distance to the sea, so they are rapids with high flow rates. Moreover, since Mt. Rokko is made of weathered granite, it is easy for landslips and earthfalls to occur, often leading to debris flows. At the foot of Mt. Rokko, sand and stones carried by rivers from Mt. Rokko over the years have formed an alluvial fan on which the urban area of Kobe and its 2 million inhabitants are located, making it a heavily urbanized area with a high risk of sediment related disasters. However, in science classes at junior high school there are few opportunities to learn more about natural disasters that occur in the region. Therefore, we conducted a survey of junior high students in Kobe city concerning natural disaster cognition.

Survey Method

In November 2020, we conducted a questionnaire survey on disaster cognition for seventh grade students (987 students) and eighth grade students (1009 students) of junior high schools (13 schools) in Kobe City.

The survey consisted of eight questions:

Question 1 asked students to specify their opinion of the most frightening natural disaster.

Questions 2-4 asked students about their sources of information relating to natural disasters.

Questions 5-6 asked students to answer questions relating to the cause of earthquakes, and the ground shaking.

Questions 7-8 asked students about the causes of floods, and the places where floods can occur.

In this presentation, we will present the results of an analysis of the junior high school students' cognition of natural disasters and their learning experiences relating to them.

Keywords: questionnaire survey, junior high school students, natural disasters, earth science education, Mt.Rokko, Kobe City

©2021. Japan Geoscience Union. All Right Reserved.

Thin-Section Making Recipe in a classroom Ver3.0 -using 3D printer-

*Yoshio Okamoto[1]

1. Osaka-Kyoiku University (temporary lecturer)

We have been developing the method to make and observe rock thin-sections easily at a secondary school classroom. Our previous method is necessary to make some parts using a lathe-machine and employ metal processing skills. This process is quite challenging to realize in a standard school. Therefore, at this conference, we will present a new approach to promote the above purpose using plastic parts made by employing a 3D-printer as alternatives to metal parts, which is very popular in science rooms at secondary schools.

The base tools are not changed 1) Homemade rock saw employing a bench-grinder, 2) Homemade rock grinder based on a kitchen knife sharpener. 3) A standard binocular microscope + a homemade polarized unit

My updated methods are as follows; The plastic arbors as alternatives to metal arbors, which fix a diamond blade or a diamond plate on the motor rods, are made by a cheap 3D printer, Cleality Ender 3 Pro (250USD). Homemade polarized unit bodies (previously made of acrylic plates) for a standard microscope to use as a polarized microscope are similar. The bottom LED system for the USB microscope was also improved. The merit of such improvement using a 3D printer is that the 3D CAD data (.stl files) are freely distributable from our website. So, no other technical skills such as metalwork, which relies on special training and high-expensive tool, are needed, although some easy additional work is still necessary. For plastic printing, it is recommended to use filament like nylon or PET because they are strong under intense stress and/or water filling condition. However, we now use standard PLA filaments, cheap and widely used. There is no inconvenience on this use by this time.

One further trial is to use a kitchen knife sharpener as a rock-saw. We made a new arbor to hold a thin diamond blade on the knife sharpener's wet stone and try to use it as rock cutting instead of the bench-grinder-based tool. Because our previous developed rock-saw based on a bench-grinder has a fatal drawback of their structure; the water from the water tank is invaded to the inside through the motor rod and rusted the bearing; finally, the motor does not work. Our 3D printer also made this arbor used on the knife sharpener. Although the 3D CAD software (Autodesk Fusion 360) has the function of creating a screw trench coupled with the motor rod, the screw trench sometimes would not go well due to the thermal expansion. So, we need only some additional smooth tapping on this screw hole before use. In this new tool, the saw's clearance is not so broad, and the main motor of the knife sharpener has less torque and speed than a bench-grinder, so we can only cut a small tip by this saw. However, it is enough to make a small number of thin-sections, and this is suitable for geoscience club students to use in a classroom safely. The water-proof system works quite well. We can purchase the diamond blade (150mm diameter, 0.5mm thickness) from a Chinese net shop at around 4 USD, including the shipping cost!

Our making and observing methods are improving now based on our trial experience for a couple of years. The basic concept is to make it easier, use only cheap mass production tools, and avoid special skills and high-expensive tools. So the details of our plans are now available and updated on our website (http://www.yossi-okamoto.net/). The contents are written both in Japanese and English for school use in foreign countries. Our method was presented in the teacher share online meeting at KVIS-SIF2021

©2021. Japan Geoscience Union. All Right Reserved.

(Thailand), one of the best Thai science highschools I already taught as a visiting teacher.

Keywords: thin-section, rock-saw, rock-grinder, polarized unit, geoscience education

©2021. Japan Geoscience Union. All Right Reserved.

Development to teaching materials related to GIGA school

*Iida Kazuya[1]

1. Komaba-Toho Junior and Senior High School

According to the GIGA school plan, the infrastructure of each person's terminal and communication environment is about to be developed in the classroom. Since large-scale time and space scales are handled in the earth science fields of elementary, junior high and high schools, it is estimated from the results of the national academic ability survey that there is difficulty in learning due to the concept of space. In addition, many geological events have vast time and space scales, and unlike physics, chemistry, and biology, it is often difficult to conduct experiments in the classroom.
There are many apps on PCs and tablets that are excellent at grasping large-scale time and space scales (Google Map, Geographical Survey Map, etc.), and are compatible with earth science education. In addition, by using AR teaching materials, it is possible to capture the geological events in the field in a pseudo manner. In this presentation, we plan to report on the development of teaching materials and lesson practice using PCs and tablets for students.

Keywords: GIGA school plan, AR, development teaching material, GSI Maps, 3D printer

©2021. Japan Geoscience Union. All Right Reserved.

The report of the International Earth Science Olympiad (IESO) ,2021

*Norihito Kawamura[1], Yutaka Takigami[2]

1. School of Regional Resource Management, University of Hyogo, 2. JESOC

We report outline and history of Earth Science Olympiad.

Keywords: IESO, high school student

©2021. Japan Geoscience Union. All Right Reserved.

[J] Oral | G (General) | General

[G-03] Geoscience education from elementary school to university students

convener:Masatsune Hatakeyama(Seiko Gakuin High School), Yoshihiro Niwa(Center for Ocean Literacy and Education, Graduate School of Education, The University of Tokyo), Chairperson:Masatsune Hatakeyama(Seiko Gakuin High School), Yoshihiro Niwa(Center for Ocean Literacy and Education, Graduate School of Education, The University of Tokyo)

Sun. Jun 6, 2021 3:30 PM - 5:00 PM Ch.03 (Zoom Room 03)

We will provide and discuss various educational practices (teachings and procedures)
for elementary, junior high school, high school, and university students. We also welcome ONLINE education, fieldwork reports, and outreach reports for all grades.
Besides, especially for liberal arts level geoscience education of undergraduate,
we will consider the problems, such as online education, contents, and prospects of our current geoscience situation.
Furthermore, we will also think about fundamental teaching material development and
the sharing of teaching material data.

4:45 PM - 5:00 PM

[G03-12]Discussion

©Japan Geoscience Union

[J] Poster | G (General)：General

Sun. Jun 6, 2021 5:15 PM - 6:30 PM JST | Sun. Jun 6, 2021 8:15 AM - 9:30 AM UTC | Ch.03_3

[G-03] G03Geoscience education from elementary school to university students

We will provide and discuss various educational practices (teachings and procedures)
for elementary, junior high school, high school, and university students. We also welcome ONLINE education, fieldwork reports, and outreach reports for all grades.
Besides, especially for liberal arts level geoscience education of undergraduate,
we will consider the problems, such as online education, contents, and prospects of our current geoscience situation.
Furthermore, we will also think about fundamental teaching material development and the sharing of teaching material data.

[G03-P01] Practice of Inquiry Activities based on the Field of Earth Science in High School

*Kazuya Kawakatsu[1] (1.Hyogo Prefectural Himeji Higashi senior high school)

Practice of Inquiry Activities based on the Field of Earth Science in High School

*Kazuya Kawakatsu[1]

1. Hyogo Prefectural Himeji Higashi senior high school

1 Introduction
In order to revitalize the inquiry activities, in the first year (2019) when I was invited to the incumbent school, I was introduced the Themed Research to all 280 students in the first grade. Due to this achievement and expectations for new educational goals, it was designated as a Super Science High School (SSH) by the Ministry of Education, Culture, Sports, Science and Technology in 2020 (Received designation for 5 years). From now on, we will carry out research and development on the educational themes listed, and disseminate the results nationwide.

2 Goals of inquiry activities
The specific goals of our school's SSH agenda are the following.

(1) Challenge to international activities based on earth science and foster science girls who can work internationally
(A) In order to inherit the lessons learned from the Great Hanshin-Awaji Earthquake, it is necessary to learn both disaster prevention education and natural science understanding. But in the current high school education, education to understand disasters as a whole is not effectively conducted. Therefore, based on the field of earth science, we will educate the four fields of science in a cross-disciplinary manner ("Natural Science Inquiry Basics").
(B) All first-grade students conduct themed research and acquire the power of inquiry ("Basics of Inquiry in Science and Mathematics"). All subject teachers are in charge of themed research, and provide guidance and advice. In addition to scheduling and ensuring safety, the teacher will draw out new ideas from students by participating in discussions, and giving advice.
(C) The excellent students found in this process will proceed to the science course after 2021, and will spend two years doing full-scale themed research. Students who wish to conduct a field survey in southeastern Australia with the cooperation of the University of Sydney will present the results obtained at the international conference.
(D) Support the activities of female students who aspire to science. Next year, we will hold "Girl's Expo with Science Ethics" centered on female researchers and female students.

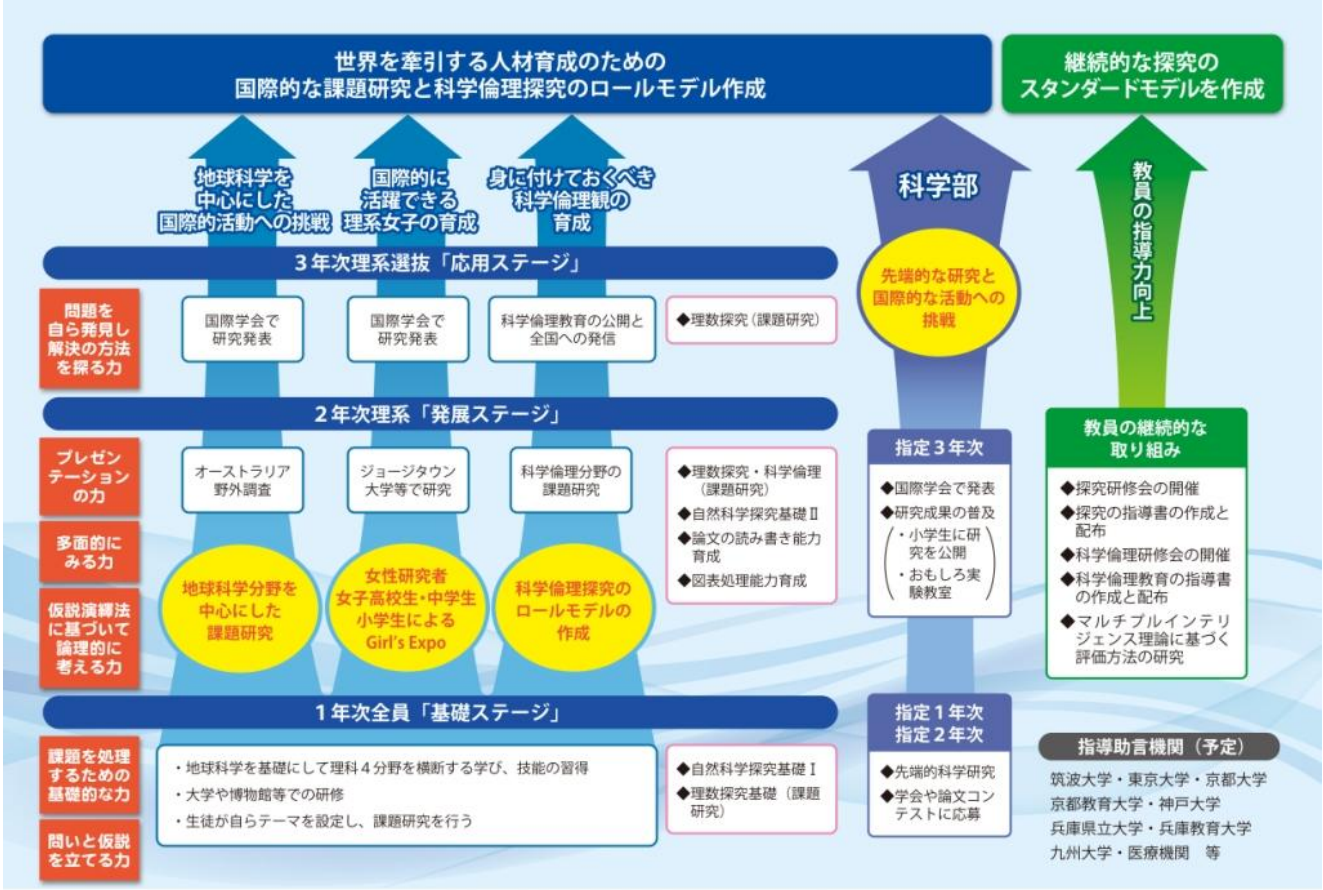
(2) Fostering science ethics that should be acquired for scientific research
(A) In order to learn the responsible behavior of scientists toward society and the science ethics that should be acquired as a member of society, we will conduct research on science ethics issues related to the research on natural science conducted by students. We will present it at the "Girl's Expo with Science Ethics".
(B) Through this activity, we will create a program for fostering science ethics and disseminate it nationwide. Students who are motivated to challenge the international arena will challenge research and presentation at international conferences at domestic and overseas universities such as Georgetown University.

(3) Support for cutting-edge research and challenges for international activities conducted by the Science

©2021. Japan Geoscience Union. All Right Reserved.

Club
(A) Rather than simply relying on advanced analytical equipment, we will conduct research with flexible ideas and ingenuity that are typical of high school students, and achieve excellent results that will lead the themed research of our students.
(B) Actively carry out dissemination activities in the region.

Keywords: Super Science High School, Inquiry Activities, Themed Research, Science Ethics



兵庫県立姫路東高等学校　SSH概要図

©2021. Japan Geoscience Union. All Right Reserved.

[E] Oral | M (Multidisciplinary and Interdisciplinary)：M-IS Intersection

Sun. Jun 6, 2021 9:00 AM - 10:30 AM JST | Sun. Jun 6, 2021 12:00 AM - 1:30 AM UTC | Ch.13 Zoom Room 13

[M-IS01] Environmental, socio-economic, and climatic changes in Northern Eurasia

convener:Pavel Groisman(NC State University Research Scholar at NOAA National Centers for Environmental Information, Asheville, North Carolina, USA), Shamil Maksyutov(National Institute for Environmental Studies), A Dmitry Streletskiy(George Washington University), Yoshihiro Iijima(Graduate School of Bioresources, Mie University), Chairperson:Pavel Groisman(NC State University Research Scholar at NOAA National Centers for Environmental Information, Asheville, North Carolina, USA), Yoshihiro Iijima(Graduate School of Bioresources, Mie University), Shamil Maksyutov(National Institute for Environmental Studies)

We invite presentations on the biogeochemical cycles, the surface energy budget and water cycle, and climate and ecosystem interactions in Northern Eurasia (land-cover/land-use change, atmospheric aerosols, soil, and permafrost changes that affect and are being affected by climate and ecosystem change), "human dimension", and tools to address the Northern Eurasia studies.

In environmental studies, our Session foci are on the permafrost changes in Siberia, Asian Mountains, and the Arctic coastal regions and on the carbon cycle of Northern Eurasia.

In the regional water cycle studies, our Session foci are on the changing distribution of precipitation intensity, frequency, form (solid versus liquid) and on the pattern and seasonal cycle changes of runoff.

In the "human dimension" studies, our Session foci are on assessments of impact of the ongoing environmental changes in Northern Eurasia on the human well-being and on mitigation strategies development in response to harmful consequences of these changes.

The particular foci of this Session will be the studies of changes that impacts regional sustainable development in the Arctic, Boreal zone, and the Drylands of Northern Eurasia.

We invite also early career scientists associated with (or interested in) the Northern Eurasia Earth Science Partnership Initiative and its continuation, Northern Eurasia Future Initiative (http://nefi-neespi.org/NEFI-WhitePaper.pdf).

9:00 AM - 9:15 AM JST | 12:00 AM - 12:15 AM UTC

[MIS01-01] Evaluation of a revised global high-resolution inverse model with CO_2 observations over Siberia.

*Shamil Maksyutov[1], Motoki Sasakawa[1], Toshinobu Machida[1], Tomohiro Oda[2], Jiye Zeng[1], Tsuneo Matsunaga[1], Johannes W Kaiser[3], Mikhail Arshinov[4], Boris Belan[4], Ed Dlugokencky[5] (1.National Institute for Environmental Studies, 2.Universities Space Research Association, 3.Deutscher Wetterdienst, 4.Inst. Atmospheric Optics, 5.Global Monitoring Laboratory, NOAA)

9:15 AM - 9:30 AM JST | 12:15 AM - 12:30 AM UTC

[MIS01-02] Co-production of environmental education material "Permafrost and Culture"

*Yoshihiro Iijima[1], Hiroki Takakura[2], Vanda Ignatyeva[3], Aleksandr Fedorov[4], Masanori Goto[5], Toshikazu Tanaka[6] (1.Graduate School of Bioresources, Mie University, 2.Center for Northeast Asian Studies, Tohoku University, 3.Institute of Humanities and Indigenous Studies of the North, SB RAS, 4.Melnikov Permafrost Institute, SB RAS, 5.Slavic-Eurasian Research Center, Hokkaido University, 6.Faculty of Economics, Ryukoku University)

9:30 AM - 9:45 AM JST | 12:30 AM - 12:45 AM UTC

[MIS01-03] Permafrost Degradation Threatens Arctic Communities and Infrastructure

*Dmitry A Streletskiy[1], Nikolay I Shiklomanov[1], Kelsey Nyland[1] (1.George Washington University)

9:45 AM - 10:00 AM JST | 12:45 AM - 1:00 AM UTC

[MIS01-04] Monthly precipitations for South Siberia derived from bias-corrected reanalysis

Nadezhda Voropay[1,2], *Anna Ryazanova[1], Egor Dyukarev[1,3] (1.Institute of Monitoring of Climatic and Ecological Systems of the Siberian Branch of the Russian Academy of Sciences, 2.V B Sochava Institute of Geography of the Siberian Branch of the Russian Academy of Sciences, 3.Yugra State University)

10:00 AM - 10:15 AM JST | 1:00 AM - 1:15 AM UTC

[MIS01-05] Fuel load mapping in central Siberia

★Invited Papers

*Elena Kukavskaya[1], Ludmila Buryak[2], Evgeny Shvetsov[1], Sergey Zhila[1] (1.V.N. Sukachev Institute of Forest of the Siberian Branch of the Russian Academy of Sciences - separate subdivision of the FRC KSC SB RAS, 2.The Branch of FBU VNIILM “Center of Forest Pyrology”)

10:15 AM - 10:30 AM JST | 1:15 AM - 1:30 AM UTC

[MIS01-06] New data on the state and changes of glaciers in mountain and Polar Regions of Russia

*Tatiana Khromova[1], Gennady Nosenko, Andrey Glazovsky, Stanislav Nikitin, Anton Muraviev, Ivan Lavrentiev (1.Institute of Geography Russian Academy of Sciences)

Evaluation of a revised global high-resolution inverse model with CO_2 observations over Siberia.

*Shamil Maksyutov[1], Motoki Sasakawa[1], Toshinobu Machida[1], Tomohiro Oda[2], Jiye Zeng[1], Tsuneo Matsunaga[1], Johannes W Kaiser[3], Mikhail Arshinov[4], Boris Belan[4], Ed Dlugokencky[5]

1. National Institute for Environmental Studies, 2. Universities Space Research Association, 3. Deutscher Wetterdienst, 4. Inst. Atmospheric Optics, 5. Global Monitoring Laboratory, NOAA

We apply a revised version of the global inverse model NTFVAR (NIES-TM-FLEXPART-variational) to make top-down estimates of regional carbon dioxide fluxes based on data from the Japan-Russia Siberian tall tower inland observation network (JR-STATION) in Siberia and NOAA's global monitoring network for 2008-2017. In the revised coupled modeling system, the global tracer transport model NIES-TM uses ERA-5 reanalysis winds interpolated to 42 hybrid-pressure levels with a horizontal resolution of 2.5 and 3.75 degrees, while the FLEXPART model uses 0.1-degree resolution and includes a diurnal cycle. Simulation of advection in the transport model and its adjoint was revised to a 3rd order upwind scheme. The land biosphere fluxes are provided by the global upscaling product based on tower flux data at a resolution of 0.1 degrees (Zeng et al. 2020). Fossil emissions are provided by ODIAC, fire emissions by GFAS, and oceanic fluxes by the upscaling product based on surface ocean pCO_2 observations (Landschü tzer et al. 2015). The diurnal cycle of biospheric CO_2 exchange is simulated by combining data for gross ecosystem production and ecosystem respiration. The respiration and oceanic fluxes are scaled to match the global CO_2 growth rate. Corrections to the prior fluxes are estimated on a bi-weekly time step for two sets of observational data, one includes only background observation sites of the global network and another adds JR-STATION data to it by taking afternoon averaged data once a day for each site. Flux optimization with the global background network results in a good match and strong correlation with JR-STATION data over West Siberia, demonstrating that the combination of accurate transport and prior fluxes make background observations useful for constraining large scale fluxes. Addition of the Siberian observations further reduces the bias of the CO_2 simulations at the sites and improves the match in the cold season. The comparison shows the importance of adding regional observations for improving regional carbon dioxide flux estimates.

Landschützer, P., et al. The reinvigoration of the Southern Ocean carbon sink, Science, 349, 1221-1224, 2015.
Zeng, J., et al. Global terrestrial carbon fluxes of 1999–2019 estimated by upscaling eddy covariance data with a random forest. Sci Data 7, 313, 2020.

Keywords: carbon dioxide, inverse modeling, Siberia

©2021. Japan Geoscience Union. All Right Reserved.

Co-production of environmental education material "Permafrost and Culture"

*Yoshihiro Iijima[1], Hiroki Takakura[2], Vanda Ignatyeva[3], Aleksandr Fedorov[4], Masanori Goto[5], Toshikazu Tanaka[6]

1. Graduate School of Bioresources, Mie University, 2. Center for Northeast Asian Studies, Tohoku University, 3. Institute of Humanities and Indigenous Studies of the North, SB RAS, 4. Melnikov Permafrost Institute, SB RAS, 5. Slavic-Eurasian Research Center, Hokkaido University, 6. Faculty of Economics, Ryukoku University

Co-production of environmental education material "Permafrost and Culture"

Iijima, Y., H. Takakura, V. Ignatieva, A.N. Fedorov, M. Goto, T. Tanaka

The Arctic has been facing enhanced climate change with intensified warming trend for the recent decades. Understanding the impact of the climate change on human societies in the Arctic/North emerges urgent importance from the standpoint of sustainability of the local population and indigenous culture. Based on the long-term collaborative researches between Japan and Arctic countries, in particular Siberia in Russia, interdisciplinary outcomes combining between natural sciences and social/humanitarian sciences have potential importance to introduce structured knowledges on present situation and future direction of environmental changes in the Arctic to local population. As for this challenge, the new collaboration has been conducted to compile an educational textbook entitled “Permafrost and Culture”. In this book, particular attention is paid to the Sakha (Yakut) people living in the Republic of Sakha (Yakutia), Russia. The life of the Sakha people is closely connected with permafrost. Scientific data clearly show that permafrost thawing resulting from climate change causes acute issues on a pan-Arctic scale. Although many published scientific papers confirm what is really happening in local communities inhabiting permafrost zones, the general public receives insufficient information on this. While climate change is a global phenomenon, it often manifests itself in regional and local natural disasters, so it is extremely important to consider it from a regional perspective. Focusing on regions and conducting a detailed study of individual specific situations allows us to discover the interconnections and attain a more accurate global picture of the changes that are occurring. This book was originally published in Russia under the same title and has been translated into English to expand the readership. The content is based on results of two international research projects, ArCS: Arctic Challenge for Sustainability (September 2015 to March 2020) and ArCS II:Arctic Challenge for Sustainability II (June 2020 to March 2025), which were jointly supported by the Ministry of Education, Culture, Sports, Science and Technology of Japan. In addition, this activity is supported by JSPS KAKENHI Grant Number JP19H00556 “Co-production of permafrost degradation impact assessment for permafrost environmental utilization and conservation” and Joint Russia and Japan bilateral project in JST-SICORPS (2019-2021) “ARCTIC Hydrological Cycle CHanges: Impacts on environment sustainability and natural resources (ARCTIC-CHI)”

Keywords: Arctic, climate change, permafrost, local population, interdisciplinary research

©2021. Japan Geoscience Union. All Right Reserved.

Permafrost Degradation Threatens Arctic Communities and Infrastructure

*Dmitry A Streletskiy[1], Nikolay I Shiklomanov[1], Kelsey Nyland[1]

1. George Washington University

Active layer thickness (ALT) is one of the essential climatic variables and is important for understanding many natural processes in the cold regions. ALT is also a required variable for land-use planning and construction on permafrost. The Circumpolar Active Layer Monitoring (CALM) program, part of Global Terrestrial Network for Permafrost (GTN-P), is the primary global archive of ALT data worldwide with more than 250 sites located in polar and high altitude permafrost environments. Some of the CALM sites go back to early 1970th, however the majority of sites were established in either in mid-1990s of after the fourth international polar year (2008). Three main measurement methods are employed by the CALM program include mechanical probing at the at grids ranging from 10 to 1000 square meters, thaw tubes, and shallow temperature boreholes, where ALT is obtained by interpolation of maximum depth of zero degree C isotherm. Using CALM data we temporal variability of ALT across circumpolar permafrost regions that have more than 10 years of data and were active over the last 5 years. The results show that absolute majority of CALM sites have increasing ALT trends over the last 20 years. The median rate is about 5 cm/decade, with majority of sites experiencing 2 to 8 cm/decade increase. Sites located in continuous permafrost generally show less changes relative to sites in discontinuous permafrost. Northern Eurasia regions, including Russian European North and North of Central Siberia were found to have highest regional rates of change. Changes in permafrost have negative impacts on communities and industrial facilities of the Northern Eurasia. Enhanced permafrost monitoring is urgently needed to address challenges associated with permafrost degradation in Northern Eurasia.

Keywords: permafrost, active layer, monitoring, climate change

©2021. Japan Geoscience Union. All Right Reserved.

Monthly precipitations for South Siberia derived from bias-corrected reanalysis

Nadezhda Voropay[1,2], *Anna Ryazanova[1], Egor Dyukarev[1,3]

1. Institute of Monitoring of Climatic and Ecological Systems of the Siberian Branch of the Russian Academy of Sciences, 2. V B Sochava Institute of Geography of the Siberian Branch of the Russian Academy of Sciences, 3. Yugra State University

The accuracy of global hydrometeorological data is important for regional and global climate studies. We compared the ERA5 reanalysis monthly precipitation data of the European Centre for Medium-range Weather Forecasts over South Siberia against observed precipitation data records from 132 ground weather stations for 1979–2015. The ERA5 reanalysis provides detailed fields reasonably reproducing features of mesoscale precipitation structures related to topography and synoptic-scale patterns. The linear correlation coefficients between reanalysis and weather station data are high but mean values are biased. The mean absolute error varies from -23 mm to 90 mm. A bias correction procedure was suggested to improve the precipitation data quality and reduce mean values error. The linear scaling coefficient for each month and weather station were calculated and extrapolated to the study area using the ordinary kriging method.

Finally, the maps of the Bias-**C**orrected **P**recipitation data for **S**outh **S**iberia (**CPSS**) were created and annual sums of precipitation were calculated. Multiply validation of bias correction was performed on the control test sets. The CPSS data fit the observation data very well. The mean error does not exceed 7 mm, the mean absolute error maximal value is 44 mm, and the mean relative error is less than 23%. The maximal biases are typical for mountain areas.

After bias correction for all months, in most cases, there is a decrease in monthly precipitation compared to the original ERA5 dataset. The precipitation decreases slightly in the winter months and significantly (by 10–13 mm) in the summer. The standard deviation also decreases for all months, but the changes are more pronounced in summer. The correction procedure almost eliminated the average error, the rest of the statistical characteristics also showed an improvement in the data quality.

The suggested approach of bias correction and downscaling is based on a combination of the physical-based high-resolution precipitation data field obtained in ERA5 reanalysis and spatially-irregular statistical correction using high-quality ground observation data. Taking into account the assessment of the scaling efficiency, the described approach can be recommended for correcting the monthly precipitation in territories with continental and sharply continental climates at territories with similar physical and geographical conditions.

Accordingly, this work forms part of a long-term effort to produce high-quality precipitation datasets across this region. High-resolution bias-corrected gridded precipitation data sets provide important information regarding precipitation conditions over different regions, especially for regions with very sparse meteorological stations. The dataset obtained could be useful for large-scale hydrological streamflow simulations, for studies of long-term precipitation variations at a higher scale, and analysis of droughts and water-logging events. The data is available for download from Zenodo in Network Common Data Form (NetCDF) format (https://zenodo.org/record/4472614).

©2021. Japan Geoscience Union. All Right Reserved.

The study was carried out with the financial support of the RFBR in the framework of scientific project 18-45-700015.

Keywords: precipitations, reanalysis, South Siberia, bias correction, downscaling

©2021. Japan Geoscience Union. All Right Reserved.

Fuel load mapping in central Siberia

*Elena Kukavskaya[1], Ludmila Buryak[2], Evgeny Shvetsov[1], Sergey Zhila[1]

1. V.N. Sukachev Institute of Forest of the Siberian Branch of the Russian Academy of Sciences - separate subdivision of the FRC KSC SB RAS, 2. The Branch of FBU VNIILM “Center of Forest Pyrology”

Fuel load and structure are fundamental drivers of fire behavior and are critical elements for strategic fire management interventions. Moreover, data on fuel loads are of high importance to accurately estimate wildland fire emissions and their contribution to the regional and global carbon balances. We have developed fuel loads maps for the Krasnoyarsk region, central Siberia by integrating satellite and ground-based data with respect to the forest-growing conditions and the disturbance of the territory by anthropogenic and natural factors (fires, loggings, insects). The maps obtained could be used to timely prepare and minimize the possible damage from fires ensuring the functional stability of forest ecosystems. The research was funded by the RFBR/KRFC Grant #20-44-242004.

Keywords: fuel load, Siberia, fire, logging

©2021. Japan Geoscience Union. All Right Reserved.

New data on the state and changes of glaciers in mountain and Polar Regions of Russia

*Tatiana Khromova[1], Gennady Nosenko, Andrey Glazovsky, Stanislav Nikitin, Anton Muraviev, Ivan Lavrentiev

1. Institute of Geography Russian Academy of Sciences

The new glacier inventory created recently at the Institute of Geography of the Russian Academy of Sciences is based on Sentinel 2 images obtained mainly in 2016-2019. This data made it possible to study the current state and recent changes of glaciers in Russia, where now there are 22 glacial systems. Glaciers are located on islands and archipelagoes of Russian Arctic and in mountain regions of continental part of the country and currently cover the area of 54,531 km2.

The largest glacial systems are located on archipelagoes of Russian Arctic. The next in area

glacial systems are located in the mountains of the temperate zone: the Caucasus, Kamchatka and Altai. The most numerous group is small glacial systems, the area of which does not exceed 100 km2. They are located in different glaciological zones. The De Long Islands and the Urals are in polar region. The Putorana Plateau, the Byranga Mountains, the Chersky Ridge, the Chukotka Upland, Northeast of the Koryak highlands are in subpolar area. Kodar Ridge and Eastern Sayan are in the temperate zone. Some glacier systems are very small. There area is less than 10 km2. Despite their small size, these glacial systems are important from indicative point of view, fixing the zone of spatial distribution of glaciation. They indicate the growth points in the event of a change in climatic conditions according to a scenario favorable for glaciers.

The glacier area has decreased since the compilation of the USSR glacier Inventory (1965-1982) by 5603.9 km2 or 9.3%. The area of polar glaciers has decreased less than glaciers in mountainous regions. Values range from 5.44% (Novaya Zemlya) to 19.11% (De Longa Islands). Small glaciers were not found in the Khibiny. Glaciers in the Urals have reduced their area by 63%. The subpolar glacier systems of the Orulgan (46.6%), Chersky (44.4%), and Suntar-Khayata (34%) ridges reduced the area a little less. Reduction in the area of glacial systems in the temperate zone ranges from 57% (Eastern Sayan) to 13% (Kodar). The largest glacial systems in the Caucasus, Kamchatka and Altai have reduced their areas by 25, 22 and 39 percent, respectively.

The results of our studies confirm the tendencies for the reduction of the glacier area throughout Russia. The exception is the glaciers of the volcanic regions of Kamchatka, which increased their size or remained stationary. The magnitude and rate of changes depend on the local climatic and orographic features.
The presentation includes the results obtained in the framework of the following research projects: №. 0148-2019-0004 of the Research Plan of the Institute of Geography of RAS, №. 18-05-60067 supported by RFBR.

Keywords: glaciers, climate change, Northern Eurasia

©2021. Japan Geoscience Union. All Right Reserved.

[E] Oral | M (Multidisciplinary and Interdisciplinary)：M-IS Intersection

Sun. Jun 6, 2021 10:45 AM - 12:15 PM JST | Sun. Jun 6, 2021 1:45 AM - 3:15 AM UTC | Ch.13 Zoom Room 13

[M-IS01] Environmental, socio-economic, and climatic changes in Northern Eurasia

convener:Pavel Groisman(NC State University Research Scholar at NOAA National Centers for Environmental Information, Asheville, North Carolina, USA), Shamil Maksyutov(National Institute for Environmental Studies), A Dmitry Streletskiy(George Washington University), Yoshihiro Iijima(Graduate School of Bioresources, Mie University), Chairperson:Yoshihiro Iijima(Graduate School of Bioresources, Mie University), Shamil Maksyutov(National Institute for Environmental Studies), Pavel Groisman(NC State University Research Scholar at NOAA National Centers for Environmental Information, Asheville, North Carolina, USA)

We invite presentations on the biogeochemical cycles, the surface energy budget and water cycle, and climate and ecosystem interactions in Northern Eurasia (land-cover/land-use change, atmospheric aerosols, soil, and permafrost changes that affect and are being affected by climate and ecosystem change), "human dimension", and tools to address the Northern Eurasia studies.

In environmental studies, our Session foci are on the permafrost changes in Siberia, Asian Mountains, and the Arctic coastal regions and on the carbon cycle of Northern Eurasia.

In the regional water cycle studies, our Session foci are on the changing distribution of precipitation intensity, frequency, form (solid versus liquid) and on the pattern and seasonal cycle changes of runoff.

In the "human dimension" studies, our Session foci are on assessments of impact of the ongoing environmental changes in Northern Eurasia on the human well-being and on mitigation strategies development in response to harmful consequences of these changes.

The particular foci of this Session will be the studies of changes that impacts regional sustainable development in the Arctic, Boreal zone, and the Drylands of Northern Eurasia.

We invite also early career scientists associated with (or interested in) the Northern Eurasia Earth Science Partnership Initiative and its continuation, Northern Eurasia Future Initiative (http://nefi-neespi.org/NEFI-WhitePaper.pdf).

10:45 AM - 11:00 AM JST | 1:45 AM - 2:00 AM UTC

[MIS01-07] Quantification of the water vapor transport between the northern Eurasia and Arctic ocean considering the water vapor origin

*Tomonori Sato[1], Tetsu Nakamura[1], Yoshihiro Iijima[2], Tetsuya Hiyama[3] (1.Hokkaido University, 2.Mie University, 3.Nagoya University)

11:00 AM - 11:15 AM JST | 2:00 AM - 2:15 AM UTC

[MIS01-08] The hydrological cycle over the three great Siberian rivers from reanalyses and observations

*Ambroise Dufour[1], Martin Wegmann[2], Olga Zolina[3,1], Sergey Gulev[1] (1.P.P. Shirshov Institute of Oceanology, Russian Academy of Science, 2.Oeschger Centre for Climate Change Research, University of Bern, 3.Institut des Géosciences de l'Environnement, Université Grenoble Alpes)

11:15 AM - 11:30 AM JST | 2:15 AM - 2:30 AM UTC

[MIS01-09] Dark conifer forests dieback at mid-to-highlands in the southern Siberia's mountains is not caused by drought stress

*Nadezhda Tchebakova[1], Elena I. Parfenova[1], Elena V. Bazhina[1], Amber J. Soja[2], Pavel Groisman[3] (1.Institute of Forests of FRC KSC, Siberian Branch, Russian Academy of Sciences, 2.National Institute of Aerospace, NASA Langley Research Center, Hampton, VA, USA , 3.NC State University Research Scholar at National Centers for Environment Information Federal Building, 151 Patton Avenue Asheville, NC 28801, USA)

11:30 AM - 11:45 AM JST | 2:30 AM - 2:45 AM UTC

[MIS01-10] Changing climate of the Western Siberia and socio-economic risks

*Daria Aleksandrovna Konstantinova[1], Valentina Petrovna Gorbatenko[1], Olga Vladimirovna Nosyreva[1], Marina Aleksandrovna Volkova[1], Irina Valer'evna Kuzhevskaia[1] (1.Tomsk State University)

11:45 AM - 12:00 PM JST | 2:45 AM - 3:00 AM UTC

[MIS01-11] Long-term temporal trends in water chemistry of lakes in response to decreases in acidic deposition and climate warming of the Kola arctic region

★Invited Papers

Tatyana I Moiseenko[1], *Marina I Dinu[1], Maria M Bazova[1] (1.Russian Institute of Geochemistry and Analytical Chemistry RAS)

12:00 PM - 12:15 PM JST | 3:00 AM - 3:15 AM UTC

[MIS01-12] **Wildfires in boreal eastern Siberia: Reconstructing the past to predict the future**

*Ramesh Glueckler[1], Stefan Kruse°[1], Ulrike Herzschuh[1,2,3], Elisabeth Dietze°[1] (1.Alfred Wegener Institute Helmholtz Centre for Polar and Marine Research, Potsdam, Germany , 2.Institute for Environmental Science and Geography, University of Potsdam, Potsdam, Germany, 3.Institute for Biochemistry and Biology, University of Potsdam, Potsdam, Germany)

Quantification of the water vapor transport between the northern Eurasia and Arctic ocean considering the water vapor origin

*Tomonori Sato[1], Tetsu Nakamura[1], Yoshihiro Iijima[2], Tetsuya Hiyama[3]

1. Hokkaido University, 2. Mie University, 3. Nagoya University

Arctic warming has been a pronounced feature of the recent climate change. Related changes in meridional thermal gradient and surface evaporation from the Arctic ocean could modulate the horizontal water vapor transport which may further affect the continental precipitation variability. The study develops the atmospheric water vapor transport model in which the spatiotemporal variation of water vapor fraction originated from the evaporation at the designated land and ocean surface areas is predicted. The model experiment driven by JRA-55 reanalysis dataset with bias correction reveals that the water vapor originated from the Arctic ocean can be transported southward, penetrating the northern coastal regions of the Eurasian continent. The monthly mean fraction of Arctic-originated water vapor relative to total precipitable water vapor becomes as high as 20% in northern Eurasia. The higher fraction of Arctic water vapor is partly attributable to the enhanced evaporation from the Arctic ocean in the low sea ice years. Besides that, the atmospheric circulation pattern is found to be an important factor for the high fraction because the high Arctic fraction is likely to occur in the area where monthly mean southward moisture flux is strong, like western Siberia in September 2017 and eastern Siberia in September 2011.

Keywords: Atmospheric water vapor, Water vapor transport model, Arctic

©2021. Japan Geoscience Union. All Right Reserved.

The hydrological cycle over the three great Siberian rivers from reanalyses and observations

*Ambroise Dufour[1], Martin Wegmann[2], Olga Zolina[3,1], Sergey Gulev[1]

1. P.P. Shirshov Institute of Oceanology, Russian Academy of Science, 2. Oeschger Centre for Climate Change Research, University of Bern, 3. Institut des Géosciences de l’ Environnement, Université Grenoble Alpes

The basins of the three great Siberian rivers –Ob, Yenisei, Lena –have come under scrutiny as symptomatic of the effects of Arctic amplification on regional water cycles. As the air moistens, Zhang et al. (2013) report more vapour convergence and greater discharges into the Arctic Ocean. The thawing permafrost is also extremely relevant. However, the warming signal can display counterintuitive patterns (Wegmann et al., 2018) and the consequences on moisture fluxes are not straightforward (Dufour et al., 2016).

This study draws on several reanalyses including ERA-5 (Hersbach et al., 2019) and discharge data (Shiklomanov et al., 2018).

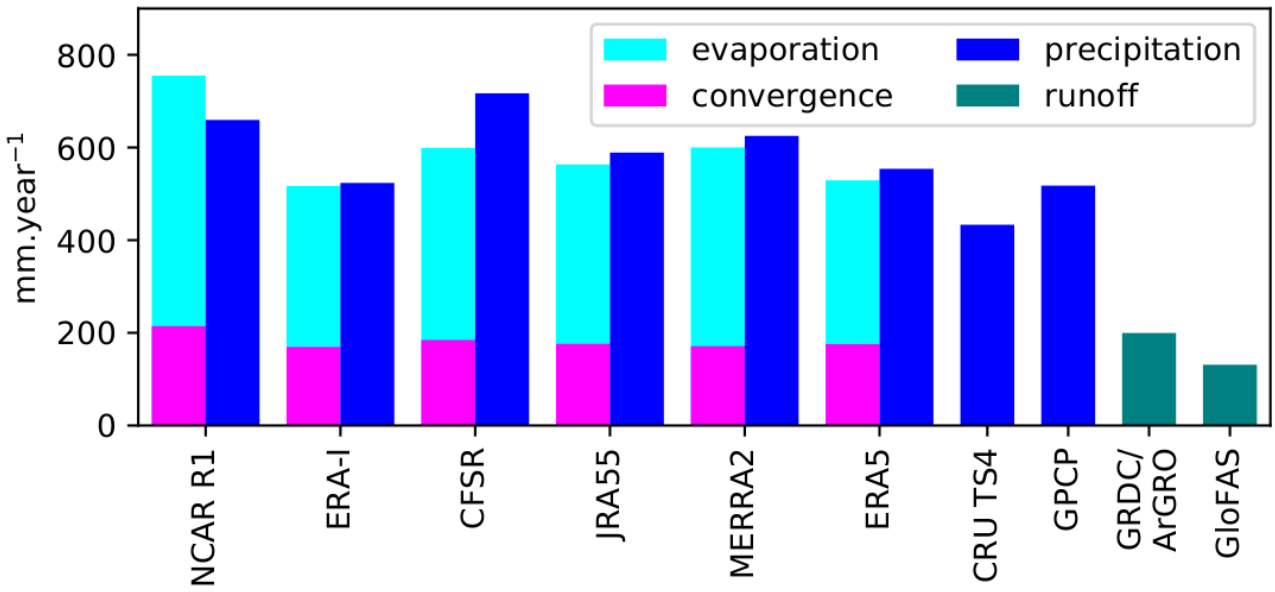
We replicate the significant moisture convergence trend found in Zhang et al., 2013 for the extended 1948-2018 period. However, the trend breaks down for the shorter 1979-2018 time windows and in other reanalyses except MERRA-2 over 1980-2018. The discharge observations summed over the mouths of all three rivers are significantly increasing in the long run but not during the satellite era. The weak increasing trend in convergence and discharge is indeed due to moister air but it is superimposed on strong atmospheric variability.

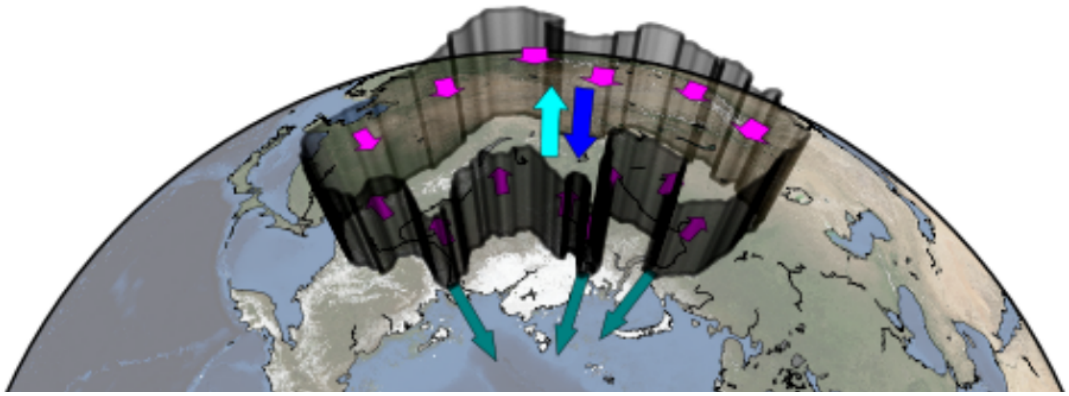
Nearly all reanalyses exhibit significant negative net precipitation trend over the satellite era with the exception of NCEP NCAR R1 and MERRA-2. Further analysis indicates that these trends are due to a decrease in precipitation rather than an increase in evaporation. The decrease in precipitation occurred mainly in summer and is absent in GPCP and CRU TS4 data. The conflicting trends between convergence and net precipitation indicate a severe unbalance of moisture budgets over Siberia.

Over the Siberian river basins, there are weak long-term increasing trends of moisture convergence and river discharge. The reanalyses show perplexing negative precipitation trends in contradiction with the increasing/constant moisture transport. The causes of either tendencies are likely atmospheric variability and non-stationary analysis increments.

Keywords: water cycle, Siberia, reanalyses

©2021. Japan Geoscience Union. All Right Reserved.





©2021. Japan Geoscience Union. All Right Reserved.

Dark conifer forests dieback at mid-to-highlands in the southern Siberia’s mountains is not caused by drought stress

*Nadezhda Tchebakova[1], Elena I. Parfenova[1], Elena V. Bazhina[1], Amber J. Soja[2], Pavel Groisman[3]

1. Institute of Forests of FRC KSC, Siberian Branch, Russian Academy of Sciences, 2. National Institute of Aerospace, NASA Langley Research Center, Hampton, VA, USA , 3. NC State University Research Scholar at National Centers for Environment Information Federal Building, 151 Patton Avenue Asheville, NC 28801, USA

Foresters and ecologists of the world register dieback of dark conifer (shade-tolerant, water-loving *Pinus sibirica, Abies sibirica* and *Picea obovata*) forests across the boreal zone since the 1960-x. This issue has become urgent since the 1970s across the southern Siberia’s mountains (west-east: Altai, Kuznetsky Alatau, West and East Sayans and southern Transbaikalia) in the most productive dark conifer forests. The damage was expressed through: necroses of branches with generative organs that cause microsporogenesis and pollen development irregularities followed by low pollen and seed vitality; chloroses and premature needle falls; the occurrence of stem rot; the linear and radial increment decrease etc.

To date, there are several hypotheses to explain dieback of dark conifers within the 50-56° N latitudes across Northern Eurasia associated with:

1. climate aridization supposedly taking place under global warming;

2. anthropogenic environmental pollution (various gas emissions, acid rainfall).;

3. phytopathogens (Armillaria mellea, Heterobasidion annosum, etc;

4. invasive insect pests;

5. increased hard ultraviolet radiation (UV-- caused by the troposphere ozone depletion and additionally amplified by the increased ozone concentration in the near-surface air layer).

Our goal was to concentrate only on one Hypothesis #1 and accept/reject that: 1. Has the climate across the southern Siberia’s Mts been drying for the last 60 years; 2. If the current climate is drying then whether it may cause dieback of dark conifer trees as referred in the literature. Finally, would be climate change predicted from the CMIP5 projections (AR5) dry enough to cause dieback hotspots within the range of climax dark conifer forests by the end of the 21st century.

To achieve our goals we investigated climate change trends of annual precipitation, summer monthly temperatures and aridity/moisture indices (annual moisture index, AMI, and standardized precipitation evapotranspiration index, SPEI) for 1961-2019; and modeled dark conifer forest distributions and their shifts in a changing climate using our mountain bioclimatic vegetation model.

Our examinations of damaged trees in dark conifer forests along four mountain transects in each mountain system across the southern Siberia’s Mts showed that most dieback was found in the mid-elevation taiga at 700-900 m and up to 1400 m in highland taiga. To identify whether those events were associated with climate droughts AMI, SAMI (standardized AMI) and water balance (precipitation

©2021. Japan Geoscience Union. All Right Reserved.

minus evapotranspiration), SPEI, were calculated for nine weather stations located in various ecosystem types (Fig. 1) and interpolated then for the lower border of decline/dieback occurrences. Climate trends for 1961-2019 demonstrated that moisture conditions have not changed much at these dieback sites and remained sufficient for dark conifer forests. Given the AMI limit for the lower/southern border of dark conifer forests was 2.25, AMI varied between 0.8-0.2 at 800-1200 m that indicated very wet conditions. Modeled moisture conditions would still remain satisfactory for dark conifers at the 2080s even for the extreme dry scenario RCP 8.5. Given the SPEI values <-1.5 were characteristic of extreme droughts, such moisture conditions occurred only 3-4 times for 1961-2019 (Fig. 1). Trees are known to survive occasional 1-2 drought years and then successfully recover. To state on a drought event for an ecosystem based only on SPEI is not ecologically sufficient. Dark conifers grow under positive annual water balance > 150 mm and true steppe –under negative. However, SPEI in these ecosystems varied within the same range ±2 (Fig. 1).

We conclude that Siberian pine and fir dieback observed mainly at the mid-to-high elevations were caused by reasons other than the drought stress as cited in the literature (Kharuk et al. 2020 et seq.). Other hypotheses are to be investigated to explain the phenomena.

Supported by RFBR grant 20-05-00540

Keywords: forest ecosystems, annual moisture index, SPEI, die-back, dark-needled species

©2021. Japan Geoscience Union. All Right Reserved.

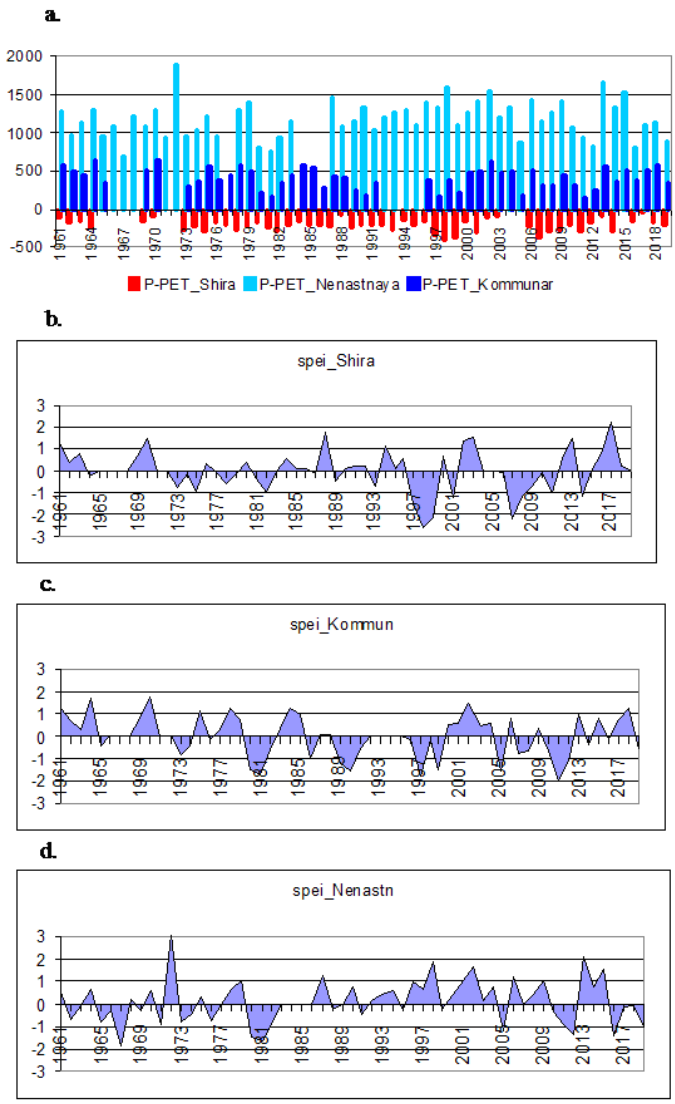


Fig. 1. Annual water balance (precipitation minus evapotranspiration, a) and SPEI (b, c, d) in different ecosystem types for 1961–2019: steppe (b), mountain dark conifer taiga (c), subalpine open taiga (d)

©2021. Japan Geoscience Union. All Right Reserved.

Changing climate of the Western Siberia and socio-economic risks

*Daria Aleksandrovna Konstantinova[1], Valentina Petrovna Gorbatenko[1], Olga Vladimirovna Nosyreva[1], Marina Aleksandrovna Volkova[1], Irina Valer'evna Kuzhevskaia[1]

1. Tomsk State University

Western Siberia belongs to the regions with the highest rate of climate warming. Despite the positive factor for the inhabitants of the region, such changes can cause significant socio-economic consequences. The sectors of the economy particularly dependent on meteorological conditions include agriculture complex, construction design, the electric power complex, and the transport sector. The aim of the paper is a comprehensive analysis of specialized climatic indicators of the most populated part of Western Siberia, necessary for the development of the economy sectors in the presence of global climate change. Indicators based on the values of air temperature, precipitation and include the frequency of thunderstorms, hail, and convective instability. In addition, the peculiarities of snow cover, blizzard and glaze-rime phenomena were analyzed for the cold period of the year, the duration of which is considerable in the investigated territory. Data of daily weather station observations of air temperature, precipitation and atmospheric phenomena from the RIHMI-WDC information database from 1961 to 2020 were analyzed for the research.
First of all, global warming is reflected in the values of climatic conditions used in applied calculations. The dates of the steady transition of the mean daily air temperature through 0 ˚C moved to an earlier date by 4-6 days, through 5 ˚C by 6-9 days. There is an increase in the extreme temperature of the cold half-year period in the south of Western Siberia. The “low temperatures” events observed more often. Withal, the “high temperatures” events conduct itself similarly during the warm half-year period, against the background of the most conspicuous warming and relatively moderate warming cycle. Studying of the precipitation regime has showed that in most of the territory, the number of days is increasing, both with continuous rainfall and without rainfall. The maximum continuous dry periods are generally greater than the duration of wet periods and increases at a rate of up to 0.8 days per decade. The duration of snow cover is on average 180 days. A decrease in the occurrence duration over the last 30 years is observed, which is due to a change in snow occurrence time and destruction of the snow cover. Over the past three decades, in both the number of days with a blizzard and the average duration of blizzards declined by 2-3 times. To study the frequency of glaze-rime phenomena, the numbers of days with an event and the sum of cases per year have been calculated. The intra-annual, diurnal courses and continuous duration of glaze-rime phenomena were considered. The frequent phenomenon –rime –is 84% of all cases of studied phenomena. The prevalent continuous duration of rime ranges from 7 to 12 hours, glaze and wet snow –within 6 hours. As a result of the study of meteorological conditions for the formation of ice covering on road surface have been determined that the number of anti-icing treatment with deicing materials used in practice is insufficient to ensure the required level of road maintenance and traffic safety on the road network of the northern regions. The number of cycles of anti-icing treatment applied on roads should be expanded by almost 1.5 times. Convective instability of the atmosphere over Western Siberia, evaluated by the temperature-humidity characteristics of the atmosphere in the layer to 500 hPa, has increased in the recent decade. The boundary of the zones of active convection has been gradually moving to the north. The duration of the thunderstorm season and number of days with a hail and thunderstorm have increased. Numbers of days with durable hail as well as with large hail have doubled. The range of values of climatic characteristics taken into account in the construction design, the development and operation of the highways network, housing and utilities sector, the agricultural complex of the region has changed against the global background of climate change.

©2021. Japan Geoscience Union. All Right Reserved.

Keywords: climate risks, socio-economic risks, changing climate

©2021. Japan Geoscience Union. All Right Reserved.

Long-term temporal trends in water chemistry of lakes in response to decreases in acidic deposition and climate warming of the Kola arctic region

Tatyana I Moiseenko[1], *Marina I Dinu[1], Maria M Bazova[1]

1. Russian Institute of Geochemistry and Analytical Chemistry RAS

Acidification of waters had been identified in acid-sensitive areas of many countries by the 1960s because of regional and global emissions of acid-forming gases. Although the emission of SO_2 and NO_x had notably diminished by the 1990s, the problem of water acidification remains pressing: the anticipated recovery of water chemistry does not occur in some lakes because of the effects of associated factors and climate warming. We studied the long-term response of water chemistry to reduced acid deposition and climate warming in the northern Kola part of Russia, based on the monitoring data on 75 lakes. The monitoring was carried out once every 4–5 years in 1990–2018, with analysis for major anions an cations, dissolved organic carbon (DOC), and heavy metals (Ni and Cu). Analysis of archive data on the weather allowed us to reliably identify trends toward a systematic temperature increase over the past 28 years (when our studies were carried out). The population of the lakes under study was proved to generally show a decrease in concentrations of anthropogenic sulfates and strengthening of the acid-neutralizing capacity (ANC) of the waters during this period of time. The lakes were analyzed in six subareas depending on the bedrock geology of the catchment areas and distances from the emission sources. The water chemistry of the lakes responded notably differently to a decrease in the influx of acids: in the most acid-sensitive areas, whose catchment bedrocks are granite and quartz sand, ANC did not increase, and acidification continued to develop. The concentrations of both DOC and nutrients in the lake waters were determined to increase. Simultaneously the P_{tot}/PO_4^{3-} and N_{tot}/NO_3^- ratios systematically increased, which indicates that bioavailable forms of nutrients are successively utilized in the ecosystems, which means that the lakes are eutotrophied. This phenomenon can be explained by the following two mechanisms: a decrease in the deposition of strong acids and climate warming. We suggest that the effects of multiple factors on the surface waters results in an irreversible evolution of the lakes, and hence, the term *recovery* does not adequately reflect the processes occurring in this industrially well-developed part of the Arctic.

The research was carried out with the financial support of the Russian Foundation for Basic Research 18-05-60012

Keywords: Acidification , Metals, Climate change

©2021. Japan Geoscience Union. All Right Reserved.

Wildfires in boreal eastern Siberia: Reconstructing the past to predict the future

*Ramesh Glueckler[1], Stefan Kruse°[1], Ulrike Herzschuh[1,2,3], Elisabeth Dietze°[1]

1. Alfred Wegener Institute Helmholtz Centre for Polar and Marine Research, Potsdam, Germany , 2. Institute for Environmental Science and Geography, University of Potsdam, Potsdam, Germany, 3. Institute for Biochemistry and Biology, University of Potsdam, Potsdam, Germany

Recent extreme fire seasons in many parts of the world have raised concern: How will wildfire activity change with a warming climate? And which consequences could this in turn bring to the environment and to society? The boreal forest of Siberia, where wildfires are a key ecological disturbance, experiences rapidly rising temperatures. This affects vegetation dynamics, permafrost stability and the predominant fire regimes. However, due to a lack of long-term data, the relationships between these processes yet remain to be fully understood. With the aim of improving predictions about impacts of future fire regimes in Siberia, this highlights the need for (I) new long-term paleoenvironmental fire reconstructions to assess the impacts of past fire regime changes and (II) a fire-vegetation model capable of reproducing observed and reconstructed fire activity, so that it can eventually be used to reliably predict future changes.

Here, we present the first results of a project that aims at providing new insights for both of those aspects in eastern Siberia. First, new lake-sedimentary macroscopic charcoal records from south-west Yakutia characterize Holocene fire regime changes in larch-dominated boreal forests. Second, a new fire module for the individual-based, spatially explicit vegetation model LAVESI (*Larix* Vegetation Simulator) allows for an evaluation of fine-scale fire-weather-vegetation interactions. The newly available fire reconstructions are a promising opportunity to help inform the model. Ongoing research will be continuing to add data from more sites, as well as looking into ways in which proxy-based fire characterization could be improved. A combination of paleoenvironmental reconstructions and the fire-vegetation model can serve as an important tool in order to more reliably evaluate wildfire risks and impacts in eastern Siberia.

°shared senior-authorships

Keywords: boreal, forest, siberia, yakutia, wildfire, larch

©2021. Japan Geoscience Union. All Right Reserved.

[E] Poster | M (Multidisciplinary and Interdisciplinary)：M-IS Intersection

Sun. Jun 6, 2021 5:15 PM - 6:30 PM JST | Sun. Jun 6, 2021 8:15 AM - 9:30 AM UTC | Ch.18_1

[M-IS01] Environmental, socio-economic, and climatic changes in Northern Eurasia

convener:Pavel Groisman(NC State University Research Scholar at NOAA National Centers for Environmental Information, Asheville, North Carolina, USA), Shamil Maksyutov(National Institute for Environmental Studies), A Dmitry Streletskiy(George Washington University), Yoshihiro Iijima(Graduate School of Bioresources, Mie University)

We invite presentations on the biogeochemical cycles, the surface energy budget and water cycle, and climate and ecosystem interactions in Northern Eurasia (land-cover/land-use change, atmospheric aerosols, soil, and permafrost changes that affect and are being affected by climate and ecosystem change), "human dimension", and tools to address the Northern Eurasia studies.

In environmental studies, our Session foci are on the permafrost changes in Siberia, Asian Mountains, and the Arctic coastal regions and on the carbon cycle of Northern Eurasia.

In the regional water cycle studies, our Session foci are on the changing distribution of precipitation intensity, frequency, form (solid versus liquid) and on the pattern and seasonal cycle changes of runoff.

In the "human dimension" studies, our Session foci are on assessments of impact of the ongoing environmental changes in Northern Eurasia on the human well-being and on mitigation strategies development in response to harmful consequences of these changes.

The particular foci of this Session will be the studies of changes that impacts regional sustainable development in the Arctic, Boreal zone, and the Drylands of Northern Eurasia.

We invite also early career scientists associated with (or interested in) the Northern Eurasia Earth Science Partnership Initiative and its continuation, Northern Eurasia Future Initiative (http://nefi-neespi.org/NEFI-WhitePaper.pdf).

[MIS01-P01] NORTHERN EURASIA FUTURE INITIATIVE (NEFI), UPDATE

*Pavel Groisman[1,2,3] (1.NC State University Research Scholar at NOAA National Centers for Environmental Information, Asheville, North Carolina, USA, 2.Shirshov Institute of Oceanology, Russian Academy of Sciences, Moscow, Russia , 3.Hydrology Science & Services Corporation, Asheville, North Carolina, USA)

[MIS01-P02] Statistical approach on geochemical records from Lake Olgoy, Valley of the Gobi Lakes, Mongolia

*Uyangaa Udaanjargal[1], Noriko Hasebe[2], Davaadorj Davaasuren, Yudai Igarashi[1], Hitoshi Hasegawa[3], Baasansuren Gankhurel[1], Nagayoshi Katsuta[4], Shuukhaaz Ganbat[1], Ichinnorov Niiden, Keisuke Fukushi[2] (1.Department of Earth Sciences, Kanazawa University, Kakuma, Kanazawa 920-1192, Japan, 2.Institute of Nature and Environmental Technology, Kanazawa University, Kakuma, Kanazawa 920-1192, Japan, 3.Faculty of Science and Technology, Kochi University, Kochi 780-8520, Japan, 4.Faculty of Education, Gifu University, Gifu 501-1193, Japan)

[MIS01-P03] The Lacustrine Sediment Analysis to Understand the Past Environmental Changes and the Effect of Ongoing Global Warming in Valley of The Gobi Lakes, Mongolia: Analyses of Tsagaan Lake Sediment

*Shuukhaaz Ganbat[1], Noriko Hasebe[2], Davaadorj Davaasuren[3], Uyangaa Udaanjargal[1], Yudai Igarashi[1] (1.Department of Earth Sciences, Kanazawa University, Kakuma, Kanazawa 920-1192, Japan, 2.Institute of Nature and Environmental Technology, Kanazawa University, Kakuma, Kanazawa 920-1192, Japan, 3.Department of Geography, School of Art& Science, National University of Mongolia, Ulaanbaatar 210646, Mongolia)

[MIS01-P04] Development of a New Drought Index Using SMOS Satellite Soil Moisture Products: Case Study in Southwestern Mongolia

*Oyudari Vova[1], Martin Kappas[1], Pavel Groisman[2], Tsolmon Renchin[3], Steven Fassnacht[1,4,5,6] (1.University of Göttingen, Göttingen, Germany, 2.NC State University Research Scholar at National Centers for Environment Information, Asheville, USA, 3.Department of Physics, National University of Mongolia, Ulaanbaatar, Mongolia, 4.Department of Ecosystem Science and Sustainability – Watershed Science, Colorado State University, Fort Collins, United States, 5.Cooperative Institute for Research in the Atmosphere, CSU, Fort Collins, USA, 6.Natural Resources Ecology Lab, Colorado State University, Fort Collins, USA)

[MIS01-P05] Fire and Logging Disturbances in the Angara Region, Central Siberia

*Evgeny Shvetsov[1], Elena Kukavskaya[1], Tatiana Shestakova[2], Brendan Rogers[2] (1.V.N. Sukachev Institute of Forest of the Siberian Branch of the Russian Academy of Sciences, 2.Woodwell Climate Research Center)

[MIS01-P06] Shifts in mountain vegetation reveal ecological responses to changing environmental conditions in Central Asian highlands

*Munavar Zhumanova[1], Geoffrey M Henebry[2,1] (1.Center for Global Change and Earth Observations, Michigan State University, 2.Department of Geography, Environment, and Spatial Sciences, Michigan State University)

[MIS01-P07] Ice-free period duration changes in the coastal zone of the Kara sea using satellite data

*Pavel Shabanov[1] (1.Shirshov Institute of Oceanology, Russian Academy of Sciences)

NORTHERN EURASIA FUTURE INITIATIVE (NEFI), UPDATE

*Pavel Groisman[1,2,3]

1. NC State University Research Scholar at NOAA National Centers for Environmental Information, Asheville, North Carolina, USA, 2. Shirshov Institute of Oceanology, Russian Academy of Sciences, Moscow, Russia , 3. Hydrology Science & Services Corporation, Asheville, North Carolina, USA

NEFI was conceived in 2015 as a successor of the Northern Eurasia Earth Science Partnership Initiative (NEESPI; **http://neespi.org**). In 2016, a NEFI White Paper was posted at **http://nefi-neespi.org/**. This White Paper was converted and expanded into two peer-reviewed programmatic NEFI Science Plan papers (Monier et al. 2017; Groisman et al. 2017). Being focused on the same region, the difference between two Initiatives stems from their major Science Questions:
NEESPI: How do Northern Eurasia' s terrestrial ecosystems dynamics interact with and alter the biosphere, atmosphere, cryosphere, and hydrosphere of the Earth? NEFI: How to provide in Northern Eurasia a sustainable societal development (economy well-being, activities, health, and strategic planning) in changing climate, ecosystems, and societies?
In other words, while NEESPI foci were on understanding of the processes that have and will be occurred over Northern Eurasia, NEFI foci are to answer questions about what should be done for the human well-being in the changing natural and social environments of the region. Currently, NEFI includes 35 international projects devoted to the Arctic, Eurasian Boreal Forest Zone, and the Dry Land Belt of Northern Eurasia (31 of them are new; Figure 1).

Each year, the NEFI active organizes three or more dedicated NEFI Sessions at the AGU, JpGU and SCERT Conferences. NEFI Special Issue of the *Environ. Res. Lett.* is being published (currently, the Issue has 47 papers accepted and a number of manuscripts are in the review process). The deadline for the article submissions of the NEFI Special Issue submissions is December 30, 2021. NEFI is open for joining of other research groups.

References:

Groisman et al. 2017: Northern Eurasia Future Initiative (NEFI): Facing the challenges and pathways of global change in the twenty-first century. *Progress in Earth and Planetary Science*, **4**:41.

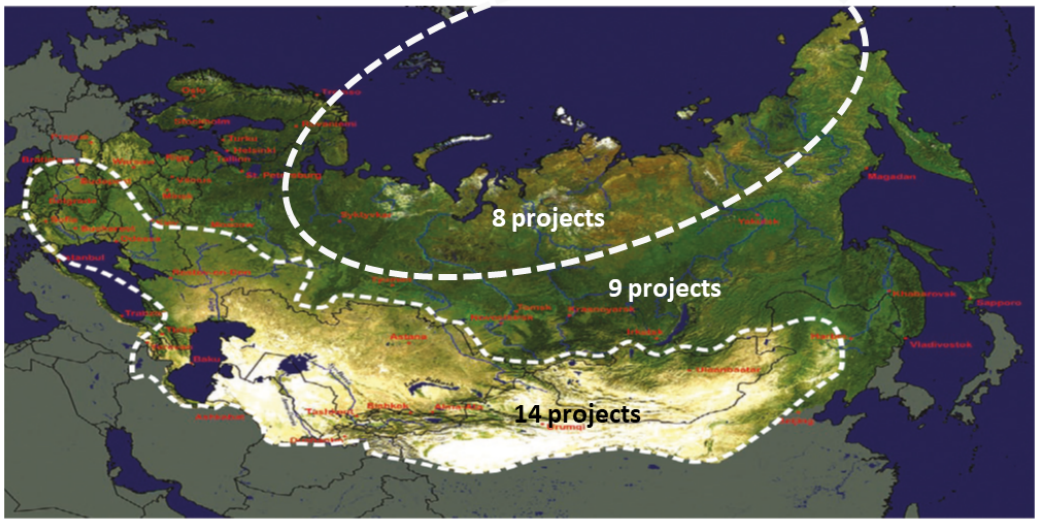
Monier et al. 2017: A Review of and Perspectives on Global Change Modeling for Northern Eurasia. *Environ. Res.Lett.*, **12**: 083001.

Keywords: Northern Eurasia, Environment and socio-economic changes, Climate change, NEFI, annual update

©2021. Japan Geoscience Union. All Right Reserved.

Regions of new NEFI studies are positioned in:

- **The Eurasian Arctic – the region of the most prominent natural changes**
- **Boreal Forest zone– the largest storage of terrestrial carbon. Ecosystems' boundaries here are unstable.**
- **Dry Latitudinal Belt of Northern Eurasia – the largest region with acute water deficit in the extratropics.**



©2021. Japan Geoscience Union. All Right Reserved.

Statistical approach on geochemical records from Lake Olgoy, Valley of the Gobi Lakes, Mongolia

*Uyangaa Udaanjargal[1], Noriko Hasebe[2], Davaadorj Davaasuren, Yudai Igarashi[1], Hitoshi Hasegawa[3], Baasansuren Gankhurel[1], Nagayoshi Katsuta[4], Shuukhaaz Ganbat[1], Ichinnorov Niiden, Keisuke Fukushi[2]

1. Department of Earth Sciences, Kanazawa University, Kakuma, Kanazawa 920-1192, Japan, 2. Institute of Nature and Environmental Technology, Kanazawa University, Kakuma, Kanazawa 920-1192, Japan, 3. Faculty of Science and Technology, Kochi University, Kochi 780-8520, Japan, 4. Faculty of Education, Gifu University, Gifu 501-1193, Japan

Mongolia is located in northern Central Asia and provides an important key archive for research on the past environment in the region. To assess the regional paleoenvironment, this study analyzed a 10.5 m sediment core retrieved from Olgoy lake in the west-central part of Mongolia. The sedimentary features are investigated as environmental proxies, including whole and mineral grain size, water, organic matter, carbonate, amorphous silica contents, and variations in elements analyzed by X-ray fluorescence. The core was divided into three units based on lithology and analytical results: Unit I with clayey sediment, Unit II with silty sediment, and Unit III with sand and gravel. Principal component analysis (PCA) was applied to the 18 major and trace elements, and they were divided into terrigenous (Al, Si, K, Rb, Zr, Cd, and Pb as the first principal component, and Cr, Fe, Zn, and Ti as the second principal component), authigenic (Ca, Mn, and Sr), and melting (S and Br) inputs. PCA provided insight on the correlation between the sediment characteristics and elemental data. PCA variables demonstrated that lithogenic elements transported by the alluvial or aeolian processes are the principal component through the whole core. The PCA score showed a significant difference in each unit. In-lake chemical productivity, indicated by elements found in authigenic materials, was most active during the LGM and, so far in early Pleistocene in the Olgoy lake sediment.

Keywords: major and trace elements, principal component analysis, sediment characteristics, Olgoy lake

©2021. Japan Geoscience Union. All Right Reserved.

The Lacustrine Sediment Analysis to Understand the Past Environmental Changes and the Effect of Ongoing Global Warming in Valley of The Gobi Lakes, Mongolia: Analyses of Tsagaan Lake Sediment

*Shuukhaaz Ganbat[1], Noriko Hasebe[2], Davaadorj Davaasuren[3], Uyangaa Udaanjargal[1], Yudai Igarashi[1]

1. Department of Earth Sciences, Kanazawa University, Kakuma, Kanazawa 920-1192, Japan, 2. Institute of Nature and Environmental Technology, Kanazawa University, Kakuma, Kanazawa 920-1192, Japan, 3. Department of Geography, School of Art& Science, National University of Mongolia, Ulaanbaatar 210646, Mongolia

Environmental change causes a large influence on a significant part of the world's population in the fragile ecological systems of arid central Asia concerning livestock husbandry, nomadic migration, irrigation farming, and stability of political societies (Pederson et al., 2014; Yu et al., 2017). For instance, a portion of the population depends on the nomadic husbandry in Mongolia. This lifestyle is under the direct impact on the natural disasters and vulnerable to environmental changes. One of the severe environmental issue is desertification, that is observed in 67% of the total area in Mongolia (Mongolian Environment, 2017).

The most parts of Mongolia are in arid and semi-arid region with extreme climate conditions. The air temperature fluctuates approximately between -40^{O}C /winter/ and 40^{O}C /summer/. The climate of Mongolia is controlled by Westerlies, East Asian Summer Monsoon (EASM), and Siberian anticyclone. Therefore, Mongolia is the suitable region to understand the past climate system in long or short-time series to predict future trends.

There are few studies conducted in this region. Komatsu et al., (2001) identified paleoshorelines on the east edge of the Tsagaan lake basin and other sites. For late Quaternary, the expanded lake had covered the greater part of the arid region including “The Valley of the Gobi Lakes” and “Great Valley of the lakes” in Mongolia *(Lehmkuhl & Lang, 2001).* However, the current condition has drastically altered and become drier for hydrology and climatic comparing to that time. However, the large lakes (e.g., Buuntsagaan and Orog lakes) are extant until nowadays fed by rivers originated in the Mountain area. For this study, Tsagaan lake (*^{45O}33'N, 100O2'E*) in “Valley of the Gobi lakes”, a small ephemeral lake in the arid region is studied.

Lacustrine sediment of the short core was taken at Tsagaan lake by a Russian peat sampler in order to reconstruct environmental changes of short time series of last 100-150 years in the drainage basin or region. The short core samples were divided into 3 parts that is being the upper part /0-50 cm/, the middle part /50-90 cm/, and the lower part /90-130 cm/. The upper part was predominantly greyish silt, interrupted 5 cm thick brownish sand layer between 38-45 cm. The middle part is dominated by whitish clay with intercalated sand spots at ~ 67 cm, ~75 cm, and ~82 cm. The lower part was dominated by greyish silt and sand layer with the spotted distribution. We cut the sample every 1 cm the multiproxy analysis including water content, organic matter, carbonate, amorphous silica, and grain size to reconstruct sedimentation and climatic process in the study area. The water content was measured by desiccating a given amount of the sediment at 105˚C. The samples of 50±3 mg were dried at 77˚C for 24 hours followed by the treatment with 10% hydrogen peroxides (H_2O_2) for 24 hours to estimate organic

©2021. Japan Geoscience Union. All Right Reserved.

matter concentration. Carbonate in the sediment was dissolved by 1-N hydrochloric acid (HCl) to calculate the concentration. The amorphous silica content was estimated by 0.1 ml solution taken after NA_2CO_3 treatment using the ICP-OES instrument. Mineral and Whole grain size were measured by SALD2200 laser diffraction particle size analyzer. The age dating of sediments was carried out by the RI method (210 Lead) due to the short time series of the sediment.

The accumulated sediment proxies can reconstruct the changes in regional climatic and hydrological conditions. For example, the whole and mineral grains size fraction can indicate the sedimentation process (river discharge changes, wind accumulation activity, and other factors), the change in carbonate deposit may associate with water level changes, the organic matter accumulation reflects organic productivity in the catchment area. Consequently, we’ re identifying the effect of ongoing global warming and future trend of climate changes in the arid region from the lacustrine sediment sequences in a short time scale.

Keywords: Lacustrine sediment, Short-time series, Environmental changes, Tsagaan lake

©2021. Japan Geoscience Union. All Right Reserved.

Development of a New Drought Index Using SMOS Satellite Soil Moisture Products: Case Study in Southwestern Mongolia

*Oyudari Vova[1], Martin Kappas[1], Pavel Groisman[2], Tsolmon Renchin[3], Steven Fassnacht[1,4,5,6]

1. University of Göttingen, Göttingen, Germany, 2. NC State University Research Scholar at National Centers for Environment Information, Asheville, USA, 3. Department of Physics, National University of Mongolia, Ulaanbaatar, Mongolia, 4. Department of Ecosystem Science and Sustainability –Watershed Science, Colorado State University, Fort Collins, United States, 5. Cooperative Institute for Research in the Atmosphere, CSU, Fort Collins, USA, 6. Natural Resources Ecology Lab, Colorado State University, Fort Collins, USA

A new drought index for meteorological and hydrological drought monitoring is presented, based on the integration of different remote sensing products and in situ observations. This research was conducted in the Bayankhongor Province. The Province is located in the southwest of Mongolia and covers an area of 116,000 square kilometers. It includes the southern region of the Khangai Mountain Range, the eastern ridges of the Altai Mountains, and the unique Gobi Desert to the south (Figure 1). The research area suffers from a scarcity of water and has an average annual precipitation of 80 --160 mm (Vova et al. 2020).

Multiple linear regression method was used for estimation of GDI drought index. The former includes the surface soil moisture from the Soil Moisture and Ocean Salinity (SMOS) mission, the Moderate Resolution Imaging Spectroradiometer (MODIS) derived land surface temperature (LST), normalized difference vegetation index (NDVI), and potential evapotranspiration (PET). The validation of the approach is based on the relationship between SPI and in-situ soil moisture (SM) observations, and their comparison to remote sensing -- derived indices. The GDI drought index combines the soil moisture and temperature conditions while including the sensitive response of arid and semi-arid vegetation. The GDI benefits are: (a) few data are required for its computation; (b) it is mostly a remote sensing product; (c) it is easily transferable and scalable over the entire globe; (d) it is a useful model in areas with scarce gauge coverage; and (e) it is an affordable tool since it can identify agrometeorological and hydrological droughts. The established new GDI index was retrieved at the 1 km spatial resolution for Southwest Mongolia from 2000 to 2018, and their two summer months (July, August) were used for monitoring drought and vegetation response to the varying soil/climatic conditions. Based on the assessment of drought severity, the new drought index allowed us to assess a large-scale spatial coherence of droughts across the Southwestern part of Mongolia.

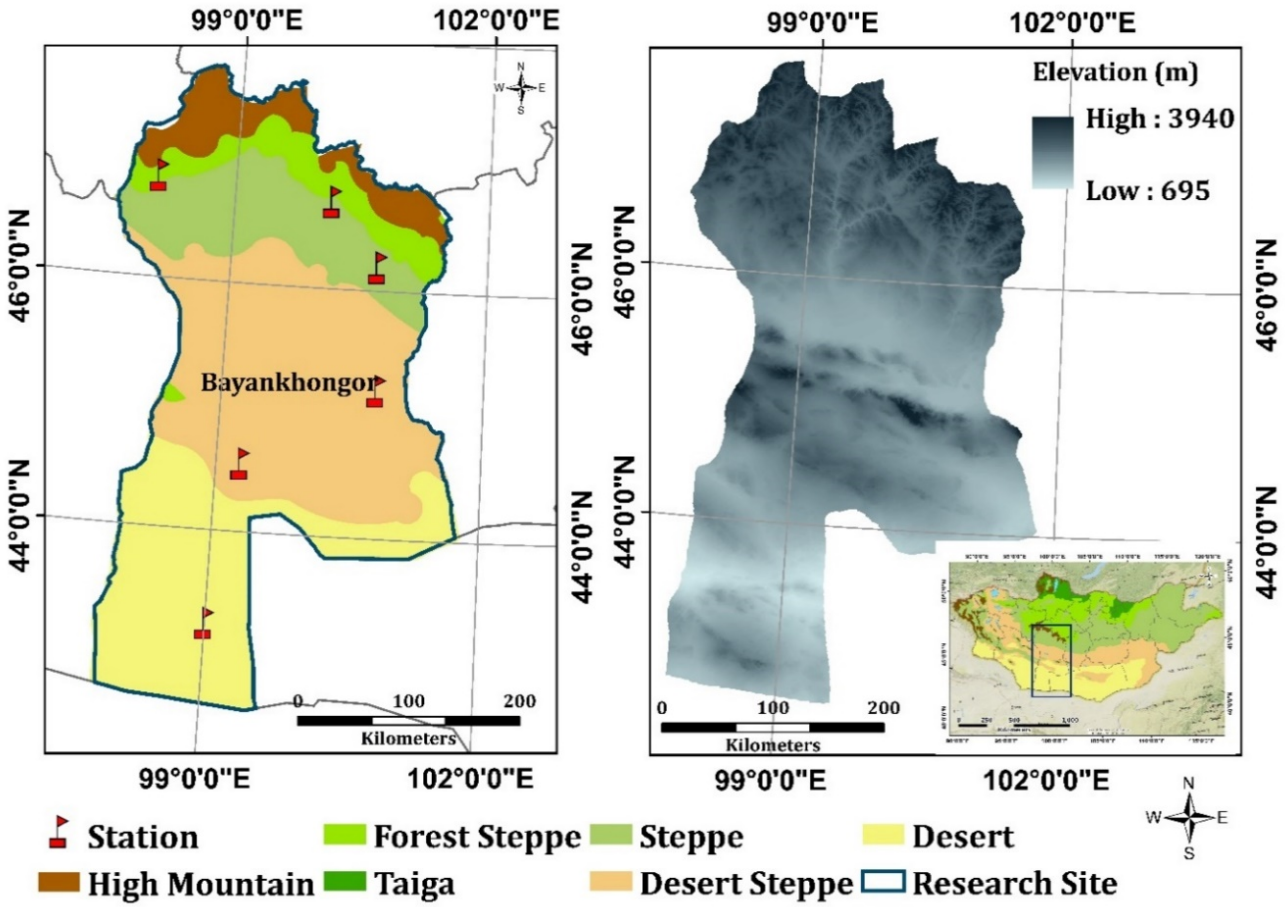
FIGURE 1 CAPTION. Geographical location and vegetation zone maps of Bayankhongor Province. (a) Meteorological station distribution and vegetation zones, data sourced from the Information and Research Institute of Meteorology, Hydrology, and Environment (IRIMHE) of Mongolia.

REFERENCE:

Vova, Oyudari, Martin Kappas, Tsolmon Renchin, and Steven Fassnacht. 2020: Extreme Climate Event and Its Impact on Landscape Resilience in Gobi Region of Mongolia. *Remote Sensing* 12 (18): 2881. https://doi.org/10.3390/rs12182881.

Keywords: drought, SMOS L2, MODIS products, in-situ soil moisture (SM), multiple regression

©2021. Japan Geoscience Union. All Right Reserved.



©2021. Japan Geoscience Union. All Right Reserved.

Fire and Logging Disturbances in the Angara Region, Central Siberia

*Evgeny Shvetsov[1], Elena Kukavskaya[1], Tatiana Shestakova[2], Brendan Rogers[2]

1. V.N. Sukachev Institute of Forest of the Siberian Branch of the Russian Academy of Sciences, 2. Woodwell Climate Research Center

Intensification of anthropogenic activities, logging and forest fires, together with climate change, can lead to significant disturbances in the functioning of boreal forests. In Russia, several million hectares of forested lands, mostly in Siberia, are exposed to fires annually. Apart from wildfires logging also is an important disturbing factor in several Siberian regions such as Irkutsk oblast and Krasnoyarsk krai. The territory of the Angara region located in the Central Siberia has experienced significant disturbances caused by fires and logging during the several past decades. Here we estimated fire and logging disturbances between 2002 and 2020 using MODIS and Landsat data. The total area disturbed by fires and loggings reached almost 45% of the region’ s area. More than 4.1 million hectares were affected by wildfires with mean annual fire disturbance rate increased twice during the last two decades: from 1% to 2% of the total region’ s area. The bulk of wildfires (more than 70%) ignited within 15 km from anthropogenic features such as settlements, roads and logged sites. Multiple successive disturbances were quite common in the study area, affecting about 650 thousand hectares between 2002 and 2020. Most of these disturbances were multiple fire events, affecting 514 thousand hectares (5% of the study area). We also found a shift to a longer fire season from 140±11 days in between 2002 and 2010 to 176± 20 days in 2011 –2020.

This study was supported by the Russian Foundation for Basic Research and Krasnoyarsk Regional Fund for Support of Scientific and Technical Activity project 20-44-242004.

Keywords: Siberia, wildfires, clear cuts

©2021. Japan Geoscience Union. All Right Reserved.

Shifts in mountain vegetation reveal ecological responses to changing environmental conditions in Central Asian highlands

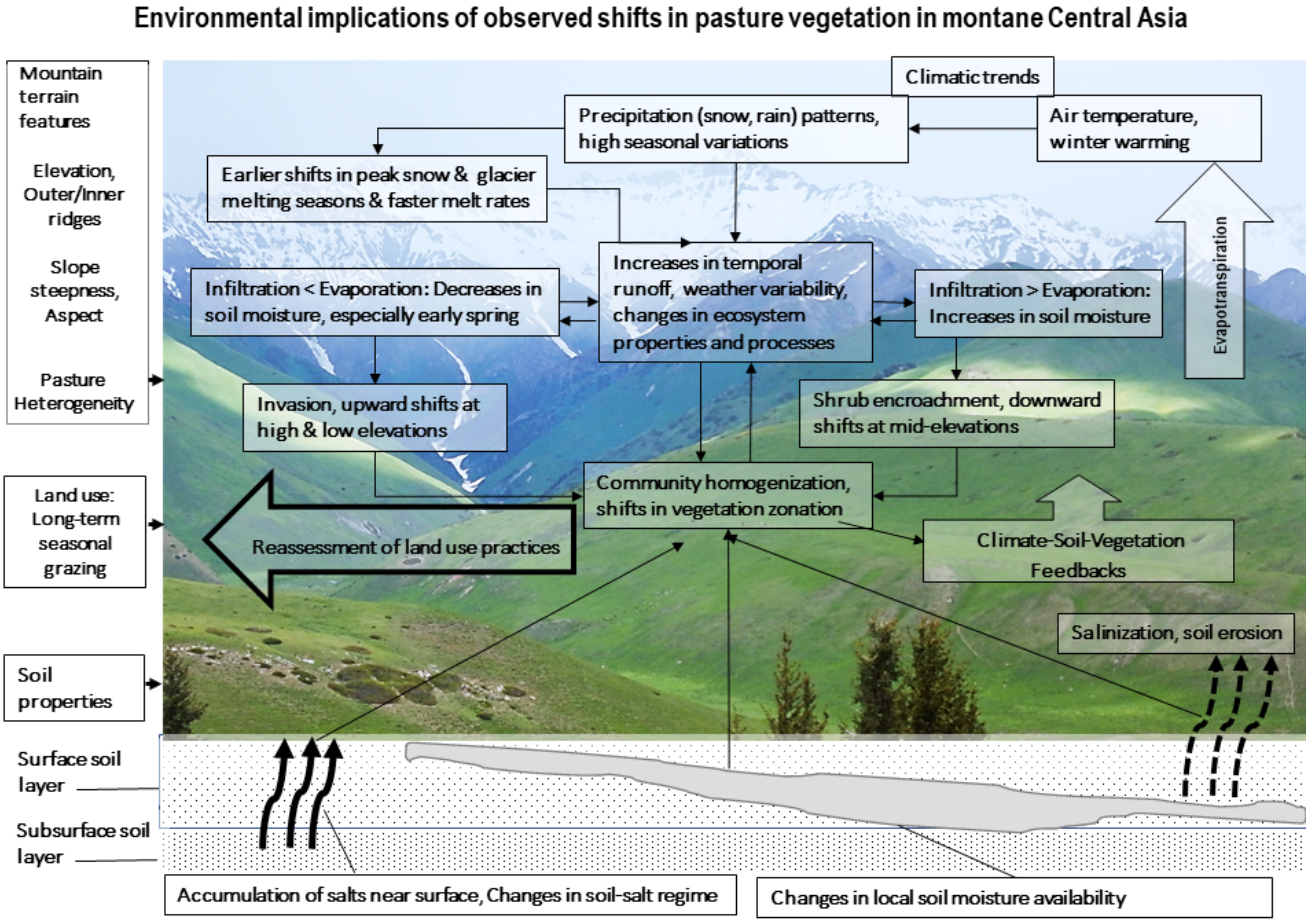
*Munavar Zhumanova[1], Geoffrey M Henebry[2,1]

1. Center for Global Change and Earth Observations, Michigan State University, 2. Department of Geography, Environment, and Spatial Sciences, Michigan State University

Mountain pastures feature complex terrain and experience harsh climatic conditions. The resulting vegetation formations are spatially heterogeneous, influenced by slope, aspect, and disturbance history. Studies on changing climate and mountain vegetation dynamics in Central Asia are few. We used nine species ecological indicators and three phytoindicators of environmental conditions to reveal species-specific, community, and landscape-level responses to changes in land use and ecological factors, and to identify limiting factors. Using a resurvey approach, we explored the responses of mountain vegetation communities to environmental changes in the Western Tien-Shan ranges in Kyrgyzstan. We assembled historic vegetation data (1973-1987) for 136 species in six vegetation types and then resurveyed the plots annually from 2008-2019. In response to global warming, mean elevation shifted significantly ($p<0.001$) for 35 out of 136 species, with 60% shifting >100 m. More species shifted upwards (mainly at lower and higher elevations) than downwards (mainly at mid-elevations). Overall, three patterns of vegetation homogenization within and among ecozones were observed. First, the mountain steppe, meadow-steppe, and subalpine meadows showed the strongest convergence towards the dominance of mesic shrubs, related to increasing precipitation, changing soil moisture, and the transient dominance of mesohalotrophic *Iris* spp. following changes in soil-salt regimes. Second, in high mountain steppe and alpine ecozones, keystone cushion dwarf shrubs expanded and shifting slightly upwards into areas of permanent snow belt shrinkage. Upward shifts of forbs into grass swards, driven by increased soil moisture from earlier and faster snowmelt but no precipitation changes during the growing season. Third, in the semidesert ecozone, drastic declines in *Artemisia* communities were linked to downward shifts of transient dominant, tropophytic species (e.g., *Prangos, Ferula, Inula*) from mid-elevation combined with upward shifts of desert ecozone species (e.g., *Alhagi, Aegilops, Koelpinia*) linked to highly variable soil moisture availability during spring. Current states of mountain ecosystems in the Western Tien-Shan are likely more mediated by precipitation variability that affects soil properties than warming. Accordingly, observed changes at high elevations may be an ephemeral effect in most cases; once the extent of permanent snow cover and small glaciers have greatly diminished or even totally disappeared, warmth-requiring or drought-tolerant species might expand upslope rapidly. Responses of mountain vegetation to global change may not always be direct: elevational shifts in one vegetation type may induce changes in neighboring vegetation communities. Adaptive management should consider vegetation responses to environmental changes and promote alternative land use options to maintain the productivity and resilience of mountain pastures. Advances in such analyses of combined datasets with remote sensing integration may derive valuable insights for interdisciplinary research groups working on climate change, deglaciation, snow cover loss, hazard, and the resulting ecological impacts in the regional and global context.

Keywords: precipitation patterns , vegetation resurvey , mountain pastures , Kyrgyzstan

©2021. Japan Geoscience Union. All Right Reserved.



©2021. Japan Geoscience Union. All Right Reserved.

Ice-free period duration changes in the coastal zone of the Kara sea using satellite data

*Pavel Shabanov[1]

1. Shirshov Institute of Oceanology, Russian Academy of Sciences

Rapid arctic sea ice reduction in the XXI century is a clear example of the global warming process. The seasonal evolution of Arctic sea ice could be described by the timing of key dates of sea ice concentration change during its annual retreat and advance cycle. Sea ice area decrease leads to an ice-free period duration increase in the Arctic ocean seas. Changes in the characteristics of the ice-free period, such as day of the retreat, day of advance, and total duration, significantly influence coastal infrastructure, navigation, and coastal ecosystems. Satellite datasets allow us to analyze the long-term state and dynamics of the sea ice cover in the arctic coastal zone in Russia.

In this paper, we explore whether and how the ice-free period characteristics over the Kara sea coastal zone have changed during the satellite data record period of 1979–2019 and examine the sensitivity decadal trends of ice-free period duration to sea ice concentration datasets in the Kara sea coastal zone.

The threshold-based ice-free period detection method was modified with a focus on seasonal gradients in the sea ice concentrations time series and adapted for the coastal data. The annual estimates of ice-free period characteristics for the coastal zone of the Kara sea were obtained using ensemble estimations, calculated from the satellite sea ice concentration datasets provided by JASMES, NSIDC, and OSI SAF services for the time period 1979-2019.

A detailed description of the Kara sea coastal zone of the means and trends in the ice-free period characteristics is performed. It was found that the duration of the ice-free period in the coastal zone of the Kara sea has increased significantly over the last decades. The duration increase is due to both dates of retreat shifts to earlier periods (the average rate is -8 days/decade) and dates of advance shifts to later periods (the average rate is +4+5 days/decade). The total ice-free period duration average rate was estimated as +12+13 days/decade during the period 1979-2019. At the same time, the leading contribution to the total duration of the ice-free period is made by the dates of retreat dynamics, which has high interannual variability and large spatial diversity over the Kara sea coast.

Keywords: sea ice, arctic coastal zone, climate change

©2021. Japan Geoscience Union. All Right Reserved.

[E] Oral | M (Multidisciplinary and Interdisciplinary) : M-IS Intersection

Sun. Jun 6, 2021 9:00 AM - 10:30 AM JST | Sun. Jun 6, 2021 12:00 AM - 1:30 AM UTC | Ch.26 Zoom Room 26

[M-IS04] Evolution and variability of the Asian Monsoon and Indo-Pacific climate during the Cenozoic Era

convener:Takuya Sagawa(Institute of Science and Engineering, Kanazawa University), Kenji Matsuzaki(Atmosphere and Ocean Research Institute, The university of Tokyo), Chairperson:Takuya Sagawa(Institute of Science and Engineering, Kanazawa University), Kenji Matsuzaki(Atmosphere and Ocean Research Institute, The university of Tokyo)

The Asian Monsoon (AM) is an inter-hemispheric atmospheric system driven by the thermal contrast between ocean and land and has a significant impact on the global climate. The uplift of Himalaya and Tibetan Plateau (HTP) has been considered to have played a significant role on the establishment and intensification of Asian monsoon, but its importance is still controversial. On the other hand, comparison of AM evolution process with global climatic changes suggests that AM evolution during Cenozoic is significantly affected by global climate changes most likely through pCO2. In addition, oceanic climate condition in areas adjacent to monsoon region is also essential for the land-ocean thermal contrast.
In this session, we promote understanding of AM evolution, variability at multiple time scale (millennial to tectonic time scale) as well as their controlling factors, and their interaction with global climate system. Presentations from various archives such as piston cores, DSDP/ODP/IODP cores as well as land sections relying on a wide panel of paleo-environmental proxy are welcome (e.g. Geochemistry, Geophysics, Sedimentology, Micropaleontology as well as modeling studies). We also welcome presentations from older time periods such as Mesozoic and Paleozoic for better understanding of the evolution of the monsoon system during the Phanerozoic.

9:00 AM - 9:15 AM JST | 12:00 AM - 12:15 AM UTC

[MIS04-01] Orbital- to millennial-scale variability of the East Asian monsoon and the Kuroshio Current during periods of low orbital eccentricity and precessional change in the Pleistocene
★Invited Papers

*Yoshimi Kubota[1], Yuki Haneda[2], Koji Kameo[3], Takuya Itaki[2], Hiroki Hayashi[4], Kizuku Shikoku[4], Kentaro Izumi[5], Martin J Head[6], Yusuke Suganuma[7], Makoto Okada[8] (1.National Museum of Nature and Science, 2.Geological Survey of Japan, AIST, 3. Department of Earth Sciences, Faculty of Science, Chiba University, 4.Interdisciplinary Faculty of Science and Engineering, Shimane University, 5. Faculty & Graduate School of Education, Chiba University, 6.Brock University, 7.National Institute of Polar Research, 8.Department of Earth Sciences, Ibaraki University)

9:15 AM - 9:30 AM JST | 12:15 AM - 12:30 AM UTC

[MIS04-02] **Effect of orbitally-driven insolation changes on East Asian monsoon rainfall over the past 450,000 years**

*Taiga Matsushita[1], Mariko Harada[1], Hiroaki Ueda[1], Takeshi Nakagawa[2], Yoshimi Kubota[3], Yoshiaki Suzuki[4] (1.University of Tsukuba, 2.Ritsumeikan University, 3.National Museum of Nature and Science, 4.National Institute of Advanced Industrial Science and Technology)

9:30 AM - 9:45 AM JST | 12:30 AM - 12:45 AM UTC

[MIS04-03] Quantification of Asian dust multi-source contributions to silt and clay fractions in the Japan Sea sediments at IODP Site U1425 since 10 Ma by the Parallel Factor (PARAFAC) end-member modelling

*Mui Fa Alison Lee[1], Airi Maruyama[1], Tomohisa Irino[2] (1.Graduate School of Environmental Science, Hokkaido University, 2.Faculty of Environmental Earth Science, Hokkaido University)

9:45 AM - 10:00 AM JST | 12:45 AM - 1:00 AM UTC

[MIS04-04] Cyclostratigraphy and orbitally-paced paleo-productivity records of the Miocene Onnagawa Formation in Akita Prefecture, Northern Japan

*Jumpei Yoshioka[1,2], Junichiro Kuroda[2], Kenji Matsuzaki[2], Ryuji Tada[1,3,4] (1.Department of Earth and Planetary Science, the University of Tokyo, 2.Atmosphere and Ocean Research Institute, the University of Tokyo, 3.Yunnan University, 4.Chiba Institute of Technology)

10:00 AM - 10:15 AM JST | 1:00 AM - 1:15 AM UTC

[MIS04-05] Sedimentary features and isotope records of the upper Eocene travertine-lacustrin carbonate in the SE Tibet and implication for hte monsoon climate

★Invited Papers

*Aki Sakuma[1], Akihiro Kano[1], Yoshihiro Kakizaki[1], Ryuji Tada[2,3], Hongbo Zheng[3] (1.Department of Earth and Planetary Science, School of Science, the University of Tokyo, 2.Institute for Geo-Cosmology, Chiba Institute of Technology, 3.Yunnan Key Laboratory of Earth System Science, Yunnan University)

10:15 AM - 10:30 AM JST | 1:15 AM - 1:30 AM UTC

[MIS04-06] Impact of long-term monsoon dynamics on Cenozoic-Mesozoic climate and ecosystems

*Masayuki Ikeda[1], Kazumi Ozaki[2], LEGRAND Julien[3] (1.University of Tokyo, 2.Toho University, 3.Shizuoka University)

Orbital- to millennial-scale variability of the East Asian monsoon and the Kuroshio Current during periods of low orbital eccentricity and precessional change in the Pleistocene

*Yoshimi Kubota[1], Yuki Haneda[2], Koji Kameo[3], Takuya Itaki[2], Hiroki Hayashi[4], Kizuku Shikoku[4], Kentaro Izumi[5], Martin J Head[6], Yusuke Suganuma[7], Makoto Okada[8]

1. National Museum of Nature and Science, 2. Geological Survey of Japan, AIST, 3. Department of Earth Sciences, Faculty of Science, Chiba University, 4. Interdisciplinary Faculty of Science and Engineering, Shimane University, 5. Faculty & Graduate School of Education, Chiba University, 6. Brock University, 7. National Institute of Polar Research, 8. Department of Earth Sciences, Ibaraki University

Marine Isotope Stages (MIS) 20–18, along with MIS 12–10, are the closest astronomical analogues of the present interglacial and last glacial period (MIS 2–1). Comparing MIS 20–18 with MIS 2–1 provides an excellent opportunity to investigate natural climate variability and constrain future climate change predictions in East Asia. A previous study on the Chinese Loess Plateau shows that the grain-size-inferred intensity of the East Asian winter monsoon (EAWM) remains weak during MIS 20 and 18 likely due to the less-severe summer insolation and resulting suppressed snow accumulation and weak Siberian High. Here, we reconstruct the paleoceanography of MIS 20–18 through multiple proxies including microfossil assemblage data, planktonic foraminiferal isotopes (δ^{18}O and δ^{13}C), and foraminiferal Mg/Ca-based temperature records, from the Chiba composite section (CbCS) exposed on the Boso Peninsula, east-central Japan to compare with the East Asian monsoon proxies. The boundary between the warm Kuroshio and cold Oyashio currents is presently situated just east of the Boso Peninsula. The fluctuating position of the boundary between the Kuroshio and Oyashio currents in the mid-latitude western North Pacific affects both heat transport and air–ocean interactions and has significant consequences for the East Asian climate. We use principal component analysis (PCA) to capture dominant patterns of the temporal variation in these marine records, and show that MIS 19b and 19a are represented by millennial-scale stadial/interstadial oscillations. The northerly positions for the gyre boundary during late MIS 19c, early MIS 18, and the interstadials of MIS 19a are inferred from the leading mode, which is consistent with a weak EAWM and consequent mild winter climate in East Asia. Glacial MIS 20 had significantly more mild winters than MIS 2. For the interglacial MIS 19 and following glacial MIS 18, the onset of winter cooling in East Asia lagged the summer/annual climate by 30–40 kyr, which is also seen in the leading mode of the CbCS marine proxies.

Keywords: Asian monsoon, Kuroshio, Chiba composite section, Pleistocene, Millennial-scale, Marine Isotope Stage (MIS) 19

©2021. Japan Geoscience Union. All Right Reserved.

Effect of orbitally-driven insolation changes on East Asian monsoon rainfall over the past 450,000 years

*Taiga Matsushita[1], Mariko Harada[1], Hiroaki Ueda[1], Takeshi Nakagawa[2], Yoshimi Kubota[3], Yoshiaki Suzuki[4]

1. University of Tsukuba, 2. Ritsumeikan University, 3. National Museum of Nature and Science, 4. National Institute of Advanced Industrial Science and Technology

Understanding orbital-scale changes in East Asian summer monsoon (EASM) precipitation is one of the fundamental issues in paleoclimate research, for determining the response of East Asian monsoon to different climate forcings such as insolation, ice volume, and greenhouse gases. Proxy records suggest that East Asian summer monsoon precipitation over the last hundreds of thousands of years has fluctuated associated with orbitally driven insolation changes and/or changes in global ice volume. However, due to the inconsistency between different proxies, it has been controversial what was the essential driving force for the EASM variability.

In the present study, we aim to evaluate the effect of insolation changes on the EASM based on numerical simulations. Using a climate model (MRI-CGCM 3.2), the global climate under given insolation changes for the past 450,000 years were calculated. The results showed that the summer precipitation in East Asia varies at the periodicities of precession (23 kyr) and obliquity (41 kyr), consistently with insolation changes. The calculated temporal changes in summer precipitation is highly consistent with cave speleothem $d^{18}O$ data in South East China, while the proxy data from North China (Chinese Loess Plateau) and Japan (Lake Biwa) cannot be fully explained by the calculation results. Importantly, the 100-kyr periodicity which dominates the variation in Chinese Loess Plateau was not found in our calculation results. We found a strong positive correlation between insolation and precipitation over the coastal area of China and a negative correlation between insolation and precipitation around Japan, which implies that EASM intensity is strongly affected by insolation intensity and but the effect can vary between regions.

The positive correlation between boreal summer insolation and summer precipitation over China results from the atmosphere-ocean interaction over the Indian Ocean and the western Pacific. Under strong insolation, northern shift of a monsoon front associated with intensification of the North Pacific subtropical high causes the increase in rainfall in the coastal area of China. Intensification of the subtropical high is caused by the integration of local Wind-Evaporation-Sea Surface Temperature (WES) feedback with Kelvin wave response to the warm Indian Ocean (IPOC mode). On the other hand, the correlation between insolation and precipitation around Japan affected by the strength of North Pacific High. Under strong insolation, the North Pacific High intensified, which causes decrease in summer precipitation around Japan.

Keywords: East Asian Summer Monsoon, Insolation, Global Ice Volume, Climate Modeling, Air-Sea Interactions

©2021. Japan Geoscience Union. All Right Reserved.

Quantification of Asian dust multi-source contributions to silt and clay fractions in the Japan Sea sediments at IODP Site U1425 since 10 Ma by the Parallel Factor (PARAFAC) end-member modelling

*Mui Fa Alison Lee[1], Airi Maruyama[1], Tomohisa Irino[2]

1. Graduate School of Environmental Science, Hokkaido University, 2. Faculty of Environmental Earth Science, Hokkaido University

A complete aeolian accumulation rates in silt and clay fractions from the Late Miocene to Pleistocene were reconstructed at the Integrated Ocean Drilling Program (IODP) Site U1425 in the Japan Sea. A total of 180 samples were collected from the Hole 1425D, which had 354 m in length and covered the last 9.76 m.y. Grain size separation was conducted to evaluate the mineral composition in silt (>4 μm) and clay (<4 μm) fractions by X-ray diffractometer (XRD). Mineral composition suggests the source variabilities in silt and clay fractions, which could be interpreted as provenance shifts occurring in 8 and 2.7 Ma.

Parallel factor analysis (PARAFAC) was applied to decompose X-ray diffractograms into individual subcomponents to identify the sources and quantify their contributions. Six-components PARAFAC model was established and 3 Asian dust sources (Taklimakan Desert, Gobi Desert and Ordos Plateau), a riverine source of Japan Island Arc, and 2 biogenic sources of Opal-A and Opal-CT were identified.

In the late Miocene, high riverine flux from Japan Islands reflected strong summer monsoon during 9.7-8 Ma. Provenance shift occurred between 8 and 7 Ma from Japan Islands source to aeolian source for a short period. Flux of materials from Japan decreased to the lowest of 0.2 g/cm^2/kyr in 8 Ma and aeolian flux was higher from 7.5 to 7 Ma. These data implied that Asian aridification was intensified at about 8 Ma coinciding with the late Miocene cooling. During this period, eolian flux was generally low with occasional increases to 1.4 and 1 g/cm^2/kyr in 6.7 and 5.64 Ma, respectively, indicating sporadic aridification of Asian interior and the intensification of the winter monsoon.

Aeolian flux increased dramatically in Pleistocene to the maximum of 4 g/cm^2/kyr, where the Gobi Desert, Taklimakan Desert and Ordos Plateau were the 3 main contributors of the aeolian flux to the Japan Sea since then. The abrupt increases of aeolian flux in Japan Sea were related to the Northern Hemisphere Glaciation (NHG) which established a very cold and dry environment to accelerate sediment erosion in the Central Asia Mountain ranges and strengthened the atmospheric circulation systems in northern hemisphere. However, aeolian flux decreased to 2.8 g/cm^2/kyr during Holocene due to decreasing fluxes from Gobi and Ordos Plateau.

The contribution of Taklimakan source to Japan Sea ranged from 10 to 50% and the dust flux increased gradually in Pleistocene to the highest of 1.74 g/cm^2/kyr at 0.13 Ma. Lower flux occurred in the Late Miocene to Pliocene of <0.6 g/cm^2/kyr. Mass accumulation rate (MAR) of Taklimakan aeolian in silt fraction was generally higher than clay fraction. The contribution of Gobi dust to Japan Sea ranged from 20 to 50% since 10 Ma. The highest MAR of 2.42 g/cm^2/kyr occurred in 1.02 Ma and the lowest in Pliocene. The MAR of Gobi dust in clay fraction was higher than silt fraction from 9.24 to 0.75 Ma. Taklimakan dust showed higher grain size index than Gobi, which could be controlled by the different pathways of westerly jet and winter monsoon from the source regions to the site.

©2021. Japan Geoscience Union. All Right Reserved.

Keywords: aeolian accumulation rate, Parallel factor analysis , Miocene to Pleistocene, Taklimakan Desert, Gobi Desert, Ordos Plateau

©2021. Japan Geoscience Union. All Right Reserved.

Cyclostratigraphy and orbitally-paced paleo-productivity records of the Miocene Onnagawa Formation in Akita Prefecture, Northern Japan

*Jumpei Yoshioka[1,2], Junichiro Kuroda[2], Kenji Matsuzaki[2], Ryuji Tada[1,3,4]

1. Department of Earth and Planetary Science, the University of Tokyo, 2. Atmosphere and Ocean Research Institute, the University of Tokyo, 3. Yunnan University, 4. Chiba Institute of Technology

Middle-to-Late Miocene is the time of the global climate transition from a relatively warm climate mode to a more glaciated mode. The global cooling in the earth history is highly related to changes in the Earth system dynamics such as tectonics, ocean circulation, and carbon cycling. During this epoch, diatomaceous sediments were widely deposited in the North Pacific margin and marginal basins including the Japan Sea, and deposition of these formations is supposed to have great influence on the global carbon cycling through the enhanced organic carbon burial that might have resulted in the global cooling. Despite years of efforts to study the role of the organic carbon burial associated with the formations of diatomaceous sediments along the North Pacific margins, a full consensus about their contributions on the Middle-to-Late Miocene cooling has not been reached.
The Onnagawa Formation, which is widely exposed in Akita Prefecture, northern Japan, is one of the representative expressions of the Miocene siliceous (diatomaceous) sediments deposited during Middle-to-Late Miocene, and known for its rhythmical sedimentary cycles in diagenetically recrystallized siliceous rocks. Since silica diagenesis prevents the construction of precise biostratigraphy, the periodicities of the sedimentary cycles have not been clarified.
We have obtained a numerical age of 11.18±0.37 Ma for the middle part of the Onnagawa Formation based on U-Pb dating of zircon grains obtained from volcanic ash layers (Yoshioka et al., submitted to Geochemical Journal). By integrating this age with the radiolarian biostratigraphy, we established the chronostratigraphy of the Onnagawa Formation. Then, we reconstructed the changes in the ratio of detritus to biogenic silica to apply cyclostratigraphic approach. The ratio of detritus to biogenic silica was estimated by using continuous and high-resolution records of mineralogical composition taken by an X-ray diffractometry (XRD) and major element composition taken by X-ray fluorescence (XRF) spectroscopy, and correlated with the short-eccentricity-tuned gamma ray attenuation (GRA) records of the deep-sea sediment cores at Integrated Ocean Drilling Program (IODP) Site U1430 in the Japan Sea. GRA is supposed to reflect the ratio of detritus to biogenic silica in the biosiliceous sediments. Continuous and high-resolution XRD and XRF records enabled not only the application of cyclostratigraphy to the Onnagawa Formation but also the discussion of paleoceanography. The age-tuned XRF data indicate that the cyclicities of outstanding sedimentary cycles derived from the biogenic silica productivity are those of obliquity and precession cycles and that the biogenic productivity was highly related to the supply of nutrients such as silicon and phosphorus. The detailed age model by cyclostratigraphy will promote research on paleoceanography of the Onnagawa basin.

Keywords: cyclostratigraphy, biogenic silica, orbital forcing, XRF, XRD

©2021. Japan Geoscience Union. All Right Reserved.

Sedimentary features and isotope records of the upper Eocene travertine-lacustrin carbonate in the SE Tibet and implication for hte monsoon climate

*Aki Sakuma[1], Akihiro Kano[1], Yoshihiro Kakizaki[1], Ryuji Tada[2,3], Hongbo Zheng[3]

1. Department of Earth and Planetary Science, School of Science, the University of Tokyo, 2. Institute for Geo-Cosmology, Chiba Institute of Technology, 3. Yunnan Key Laboratory of Earth System Science, Yunnan University

The Asian monsoon is one of the largest climatic systems in the world but estimates of its onset vary from the late Eocene to the Quaternary (e.g. Licht et al., 2014). We investigated the sedimentary environment of the late Eocene Jiuziyan Formation, a terrestrial limestone unit that occurs a few localities in the Jianchuan basin, Yunnan Province in China. Previously, this has been characterized as lacustrine carbonate and the transition to the palustrine deposit was interpreted as the appearance of wetter climate during the late Eocene (Sorrel et al., 2017). Our observations of macro- and microfacies revealed sedimentary fabrics indicating rapid $CaCO_3$ precipitation, such as dendritic calcite and calcified reed stems, which are unlikely to develop in a simple lacustrine setting. These fabrics, together with clearly higher $\delta^{13}C$ values (-0.7 to +6.9 ‰) and lower $\delta^{18}O$ values (-14.6 to -10.5 ‰) than those of lacustrine marlstone of the overlying Shuanghe Formation shown by Wu et al. (2018), indicate that the limestone was at least partly travertine, carbonate formed from thermogenic (endogenic) spring water. In addition, the occurrence of centimeter-scale lamination coupled with cyclic changes in $\delta^{13}C$ and $\delta^{18}O$ is almost identical with the modern travertine reported from Baishuitai in northern Yunnan Province (Sun and Liu, 2010). The centimeter-scale lamination is annual and the cyclic changes in $\delta^{13}C$ and $\delta^{18}O$ imply seasonal temperature and precipitation change, which have comparable amplitude to the record of the modern travertine at Baishuitai. Our results do not contradict late Eocene wetting and additionally suggest the development of a high-CO_2 aquifer in the underground, which was likely associated with a tectonic activity in the southeastern Tibetan Plateau. This might be related to the shift from the dry condition of the Baoxiangsi Fm. underlying the Jiuziyan Fm. to the wet condition of the Shuanghe Fm.

Keywords: late Eocene, travertine, lacustrine carbonate, annual lamination, carbon and oxygen isotopes, Asian monsoon

©2021. Japan Geoscience Union. All Right Reserved.

Impact of long-term monsoon dynamics on Cenozoic-Mesozoic climate and ecosystems

*Masayuki Ikeda[1], Kazumi Ozaki[2], LEGRAND Julien[3]

1. University of Tokyo, 2. Toho University, 3. Shizuoka University

Earth’ s orbital variations on timescales of 10^4 to 10^5 years, known as Milankovitch cycles, have played a critical role in pacing climate change and ecosystem dynamics during the Cenozoic and Mesozoic, through glacial and monsoon dynamics. However, the climatic and biotic consequences of these cycles on much longer 10^7 years timescales remain unclear, due to a lack of long proxy records with precise age constraints.
Here, we show 10 Myr scale variations in Triassic Jurassic records of lake level, desert distribution, biogenic silica burial flux, atmospheric CO2 levels, and sea surface temperature, SST. Their phase relationships, coupled with carbon cycle modeling results, suggest that orbitally paced summer monsoon dynamics modulates changes in terrestrial weatherability, affecting changes in pCO2 of up to 500 to 1000 ppmv and 3 to 7 C SST. We also infer that these 10 Myr scale climatic variations could have been causally linked to biotic turnover, size variations in dinosaur footprints, and tetrapod dispersal, potentially through spatio temporal variations in resource availability and arid hot climatic barriers at low middle latitudes.

Keywords: monsoon

©2021. Japan Geoscience Union. All Right Reserved.

[E] Poster | M (Multidisciplinary and Interdisciplinary)：M-IS Intersection

Sun. Jun 6, 2021 5:15 PM - 6:30 PM JST | Sun. Jun 6, 2021 8:15 AM - 9:30 AM UTC | Ch.22_1

[M-IS04] Evolution and variability of the Asian Monsoon and Indo-Pacific climate during the Cenozoic Era

convener:Takuya Sagawa(Institute of Science and Engineering, Kanazawa University), Kenji Matsuzaki(Atmosphere and Ocean Research Institute, The university of Tokyo)

The Asian Monsoon (AM) is an inter-hemispheric atmospheric system driven by the thermal contrast between ocean and land and has a significant impact on the global climate. The uplift of Himalaya and Tibetan Plateau (HTP) has been considered to have played a significant role on the establishment and intensification of Asian monsoon, but its importance is still controversial. On the other hand, comparison of AM evolution process with global climatic changes suggests that AM evolution during Cenozoic is significantly affected by global climate changes most likely through pCO2. In addition, oceanic climate condition in areas adjacent to monsoon region is also essential for the land-ocean thermal contrast.
In this session, we promote understanding of AM evolution, variability at multiple time scale (millennial to tectonic time scale) as well as their controlling factors, and their interaction with global climate system. Presentations from various archives such as piston cores, DSDP/ODP/IODP cores as well as land sections relying on a wide panel of paleo-environmental proxy are welcome (e.g. Geochemistry, Geophysics, Sedimentology, Micropaleontology as well as modeling studies). We also welcome presentations from older time periods such as Mesozoic and Paleozoic for better understanding of the evolution of the monsoon system during the Phanerozoic.

[MIS04-P01] Tropical Western Pacific hydrology during the last 6,000 years based on wildfire charcoal records from Borneo

*Masanobu Yamamoto[1], Takafumi Kikuchi[1], Hiromischi Sakurai[1], Ryoma Hayashi[2], Osamu Seki[3], Takayuki Omori[4], Abdullah Sulaiman[5], Hasrizal Shaari[6], Mohd Zulhilmy Abdhllah[7], Lulie Melling[7] (1.Faculty of Environmental Earth Science, Hokkaido University, 2.Lake Biwa Museum, 3.Institute of Low Temperature Science, Hokkaido University, 4.The University Museum, The University of Tokyo, 5.Department of Mineral and Geoscience of Malaysia, 6.Universiti Malaysia Terengganu, 7.Sarawak Tropical Peat Reserach Institute)

[MIS04-P02] Similarities and disparities between radiolarian-based Sea Surface Temperature (SST) estimates with foraminifera Mg/Ca SST in monsoon influenced area

*Kenji Matsuzaki[1], Yoshimi Kubota[2] (1.Atmosphere and Ocean Research Institute, The university of Tokyo, 2.Department of Geology and Paleontology, National Museum of Nature and Science)

[MIS04-P03] Major re-organisation in marine ecosystem during the Late Miocene Global Cooling caused by changes in major monsoonal mode

*Kenji Matsuzaki[1], Masayuki Ikeda[2], Ryuji Tada[2] (1.Atmosphere and Ocean Research Institute, The university of Tokyo, 2.Graduate School of Science, The University of Tokyo)

[MIS04-P04] Evolution of meridional and zonal sea surface temperature gradients in the Pacific Ocean during the Quaternary period

*Takuya Sagawa[1], Risako Makino[2], Yukimi Kubota[2], Yoshimi Kubota[3], Yair Rosenthal[4] (1.Institute of Science and Engineering, Kanazawa University, 2.Collage of Science and Engineering, Kanazawa University, 3.National Museum of Nature and Science, 4.Rutgers University)

[MIS04-P05] Pliocene thermocline stability in the western Pacific warm pool inferred from the individual foraminifera analysis

Fumito Mizuno[2], *Takuya Sagawa[1] (1.Institute of Science and Engineering, Kanazawa University, 2.Graduate School of Natural Science and Technology, Kanazawa University)

Tropical Western Pacific hydrology during the last 6,000 years based on wildfire charcoal records from Borneo

*Masanobu Yamamoto[1], Takafumi Kikuchi[1], Hiromischi Sakurai[1], Ryoma Hayashi[2], Osamu Seki[3], Takayuki Omori[4], Abdullah Sulaiman[5], Hasrizal Shaari[6], Mohd Zulhilmy Abdhllah[7], Lulie Melling[7]

1. Faculty of Environmental Earth Science, Hokkaido University, 2. Lake Biwa Museum, 3. Institute of Low Temperature Science, Hokkaido University, 4. The University Museum, The University of Tokyo, 5. Department of Mineral and Geoscience of Malaysia, 6. Universiti Malaysia Terengganu, 7. Sarawak Tropical Peat Reserach Institute

The forcing of multi-centennial climate variability in the Western Pacific Warm Pool (WPWP) region is not fully understood. Here we generated 6-ky long continuous charcoal records from five peatlands in Borneo. Peaks of charcoal abundance every several hundred years were identified at each site, indicating that the peatlands repeatedly experienced aridity and wildfires. Major fire events were identified at ~5.2, 4.7, 4.3, 3.7, 3.1, 2.5, 2.2, 1.6, 1.1, 0.6 and 0.2 ka. Most of these coincided with the maxima of Borneo speleothem $\delta^{18}O$, and occurred in the high solar activity periods soon after the solar minima. This suggests that the solar minima increased rainfall, leading to fuel accumulation, while the subsequent higher solar activity decreased rainfall, increasing aridity and wildfire frequency. This result challenges the hypothesis that high solar activity intensifies atmospheric convection in the WPWP area.

Keywords: Charcoal, Paleofire, Borneo, Holocene, Precipitation, Solar forcing

©2021. Japan Geoscience Union. All Right Reserved.

Similarities and disparities between radiolarian-based Sea Surface Temperature (SST) estimates with foraminifera Mg/Ca SST in monsoon influenced area

*Kenji Matsuzaki[1], Yoshimi Kubota[2]

1. Atmosphere and Ocean Research Institute, The university of Tokyo, 2. Department of Geology and Paleontology, National Museum of Nature and Science

Radiolarian microfossils-based sea surface temperature (SST) estimates relying on statistics such as an Imbrie and Kipp type transfer function were developed in the early 1970's and showed promising results. Since, micropaleontologists tried to increase the accuracy of their reconstruction relying on more advanced statistics such as the Modern Analogue Technique or Partial Least Square method, which is an improved transfer function. The accuracy of radiolarian SST estimates may be statistically correct, however it still has an error margin around 1.2 to 1.5℃, while SST estimated using geochemical methods on foraminifera shells Mg/Ca or alkenones shows an accuracy around or less than 1.0℃. Direct comparison between both statistics and geochemical methods are not often conducted because in general, sediments rich in radiolarians have a low preservation of foraminifera and vice-versa.

The East China Sea, an area directly under the influence of the East Asian Monsoon is a marginal sea of the northwest Pacific where foraminifera preservation state is good. In the Danjo basin in the northern East China Sea, previous studies showed that at the IODP Site U1249 drilled at water depths of about 700 m, radiolarians and foraminifera are both well-preserved and thus direct comparison are possible between radiolarian and foraminiferal Mg/Ca. In this study we propose to discuss similarities and disparities between the SST reconstructed using these two methods and also to discuss the sensitivity of each proxies to the East Asian Monsoon dynamic.

Keywords: East China Sea, Radiolarian, Foraminifer shell Mg/Ca, East Asian Monsoon

©2021. Japan Geoscience Union. All Right Reserved.

Major re-organisation in marine ecosystem during the Late Miocene Global Cooling caused by changes in major monsoonal mode

*Kenji Matsuzaki[1], Masayuki Ikeda[2], Ryuji Tada[2]

1. Atmosphere and Ocean Research Institute, The university of Tokyo, 2. Graduate School of Science, The University of Tokyo

The Late Miocene Global Cooling (LMGC) between 7.6 and 5.8 Ma corresponds to a shift from an East Asian Summer Monsoon (EASM) dominated climate to an East Asian Winter Monsoon (EAWM) dominated one. In the Japan Sea, one of the dominant plankton groups of the Neogene, radiolarians, is of interest because an endemic species dominate its assemblages, the species *Cycladophora nakasekoi*. This species occurred between 10 and 7.3 Ma and during the LMGC, co-existed for 500 kyr with a species of the same Genus *Cycladophora sphaeris*. Here, using sediment cores collected at Site U1425 of the Integrated Ocean Drilling Program (IODP) Expedition 346, we estimated *C. nakasekoi* and *C. sphaeris* accumulation rates for a better understanding on the variation of their fluxes during the LMGC and clarify the relationship between *C. nakasekoi* and *C. sphaeris* ecology and the LMGC. We interpreted changes in sediment physical properties collected at Site U1425 of the IODP Expedition 346 for reconstructing local hydrography. It is probable that under an EASM domination, strong summer monsoonal rainfalls caused a stratification of the water column in the Japan Sea by a strong riverine run-off delivering high amount of nutrient and dissolved silica to the shallow water, and favoured the blooming of *C. nakasekoi*. During the LMGC the EAWM strengthened likely because of both the establishment of an east Greenland Ice-sheet and decrease in height of the Iran Plateau, which would have strengthened the Siberian High and affected the path of tropical moist air respectively. Strong EAWM intensifies northerlies, and it is likely that the water column of the Japan Sea was well mixed during the LMGC and promoted the blooming of diatoms and *C. sphaeris*. In addition, the great marine predator, the shark *Carcharocles megalodon*, steadily disappears from the seas around Japan during the LMGC as well. Thus, the major re-organization in climate and marine nutrient systems during the LMGC is of a broad impact on marine micro to macro fauna.

Keywords: Summer Monsoonal Rainfalls, Japan Sea, Ecosystem response

©2021. Japan Geoscience Union. All Right Reserved.

Evolution of meridional and zonal sea surface temperature gradients in the Pacific Ocean during the Quaternary period

*Takuya Sagawa[1], Risako Makino[2], Yukimi Kubota[2], Yoshimi Kubota[3], Yair Rosenthal[4]

1. Institute of Science and Engineering, Kanazawa University, 2. Collage of Science and Engineering, Kanazawa University, 3. National Museum of Nature and Science, 4. Rutgers University

Long-term change of meridional and zonal temperature gradients in the Pacific Ocean is key to understanding the evolution of the global climate change. The asymmetric zonal SST pattern in the modern tropical Pacific, i.e. warm pool in the west and cold tongue in the east, has been gradually evolved since the Plio-Pleistocene climate transition. This zonal SST gradient has been attributed to a strengthening of the Walker Circulation. Here, we conduct planktonic foraminiferal Mg/Ca temperature reconstruction in the western Pacific warm pool (WPWP) using two species, Globigerinoides ruber sensu stricto and Trilobatus trilobus. In the modern tropical Pacific, both species calcify in mixed layer and show similar Mg/Ca temperature with a bit deeper signature in T. trilobus. Our temperature reconstruction using T. trilobus is consistent with that of ODP806, which is also in WPWP region, indicating regional representativeness. Temperature reconstruction using G. ruber is significantly higher than that using T. trilobus before 1.7 Ma, suggesting a deepening of the western thermocline at that time. This vertical temperature gradient change is accompanied by SST drop in the eastern equatorial Pacific. Therefore, our data support the strengthening of the Walker Circulation. Further, both northern and southern subpolar SST dropped at similar timing, which indicates a steepening of the meridional temperature gradient. We infer that the strengthening of the Walker Circulation at 1.7 Ma was induced by the steepening of meridional temperature gradient in the course of Northern Hemisphere Glaciation.

Keywords: Sea surface temperature, Tropical Pacific, Planktonic foraminifera

©2021. Japan Geoscience Union. All Right Reserved.

Pliocene thermocline stability in the western Pacific warm pool inferred from the individual foraminifera analysis

Fumito Mizuno[2], *Takuya Sagawa[1]

1. Institute of Science and Engineering, Kanazawa University, 2. Graduate School of Natural Science and Technology, Kanazawa University

Past behavior of the El Nino-Southern Oscillation (ENSO) has been investigated by the zonal sea surface temperature (SST) gradient in the tropical Pacific. Previous studies have shown that the zonal SST gradient was quite small during the Pliocene period, suggesting the permanent El Nino condition. However, since the SST reconstruction by “bulk” foraminiferal Mg/Ca analysis represents the average condition of each sample (a few centimeters thick), which generally includes several hundred years, the diminished zonal SST gradient does not necessarily mean El Nino condition in the year-to-year timescale. Here, we conducted the individual foraminiferal shell analysis (IFA) of *Pulleniatina obliuqiloculata* Mg/Ca picked from the sediment core IODP Site U1488. First, we compared Mg/Ca-based thermocline temperature (TT) variability of the late Holocene with SODA record and found that the TT variability is similar to that of SODA record at 150 m water depth. Then, we compared the Holocene variability with that of the mid-Pliocene warm period (MPWP). The TT variability during MPWP is approximately two-thirds of the Holocene, suggesting a more stable thermocline depth during MPWP. Considering a smaller difference between SST and TT, the stable thermocline is interpreted as a deeper and more stable condition during MPWP than the modern one.

Keywords: planktonic foraminifer, individual foraminifera analysis, Mg/Ca

©2021. Japan Geoscience Union. All Right Reserved.

[E] Oral | M (Multidisciplinary and Interdisciplinary)：M-IS Intersection

Sun. Jun 6, 2021 10:45 AM - 12:15 PM JST | Sun. Jun 6, 2021 1:45 AM - 3:15 AM UTC | Ch.11 Zoom Room 11

[M-IS05] Global climate change driven by the Southern Ocean and the Antarctic Ice Sheet

convener:Osamu Seki(Institute of Low Temperature Science, Hokkaido University), Yoshifumi Nogi(National Institute of Polar Research), Akira Oka(Atmosphere and Ocean Research Institute, The University of Tokyo), Yusuke Suganuma(National institute of Polar Research), Chairperson:Takashi Obase(Atmosphere and Ocean Research Institute, the University of Tokyo)

The Southern Ocean and Antarctic ice sheet, which are the giant reservoirs of heat, water, and materials, have a potential to play central roles in long-term global climate change. This system is composed of the following sub-systems; ice shelf which is a place of the interaction of ice sheet and ocean, flowing iceberg, seasonal sea ice zone, Antarctic bottom water which drives the thermohaline circulation, active biological production and Antarctic Circumpolar Current. These sub-systems are interacted with each other and have significant impact on changes in the global environmental system. This session aim to summarize recent observational and simulation studies from various fields relating to the past and present changes in the Antarctic Ice sheet and Southern Ocean, which are essential elements for unraveling the changes in the global climate system. Further, future science plans for understanding of the environmental changes of the Antarctic Cryosphere is also discussed.

10:45 AM - 11:05 AM JST | 1:45 AM - 2:05 AM UTC

[MIS05-01] Modelling the Stability of Antarctic ice sheet for investigating the link between the past and future

★Invited Papers

*Ayako Abe-Ouchi[1], Kaho Harada[1], Takashi Obase[1], Fuyuki SAITO[2], Ralf Greve[3], Christopher Chambers[3], Osamu Seki[3], Kenji Kawamura[4], Jun'ichi Okuno[4] (1.Atmosphere and Ocean Research Institute, The University of Tokyo, 2.JAMSTEC, 3.Hokkaido University, 4.NIPR)

11:05 AM - 11:25 AM JST | 2:05 AM - 2:25 AM UTC

[MIS05-02] Carbon and nutrient cycles in and around the Cape Darnley polynya

★Invited Papers

*Michiyo Yamamoto-Kawai[1], Yoshihiko Ohashi[1] (1.Graduate School of Marine Science and Technology, Tokyo University of Marine Science and Technology)

11:25 AM - 11:45 AM JST | 2:25 AM - 2:45 AM UTC

[MIS05-03] MONACA: The hot explorer under ice

★Invited Papers

*Toshihiro Maki[1], Hirokazu Yamagata[1], Hiroshi Yoshida[2], Yoshifumi Nogi[3] (1.The University of Tokyo, 2.Japan Agency for Marine-Earth Science and Technology, 3.National Institute of Polar Research)

11:45 AM - 12:00 PM JST | 2:45 AM - 3:00 AM UTC

[MIS05-04] Development of the Under Ice AUV “MONACA” - Autonomous Navigation Trial in Under Ice Environment -

*Hirokazu Yamagata[1], Shuma Kochii[1], Hiroshi Yoshida[2], Yoshifumi Nogi[3], Toshihiro Maki[1] (1.Institute of Industrial Science, The University of Tokyo, 2.Japan Marine Science and Technology Center, 3.National Institute of Polar Research)

12:00 PM - 12:15 PM JST | 3:00 AM - 3:15 AM UTC

[MIS05-05] Long-term future projections for the Antarctic ice sheet with the model SICOPOLIS

*Christopher Chambers[1], Ralf Greve[2,1], Takashi Obase[3], Fuyuki SAITO[4], Kaho Harada[3], Ayako Abe-Ouchi[3] (1.Institute of Low Temperature Science, Hokkaido University, 2.Arctic Research Center, Hokkaido University, 3.Atmosphere and Ocean Research Institute, University of Tokyo, 4.Japan Agency for Marine-Earth Science and Technology)

Modelling the Stability of Antarctic ice sheet for investigating the link between the past and future

*Ayako Abe-Ouchi[1], Kaho Harada[1], Takashi Obase[1], Fuyuki SAITO[2], Ralf Greve[3], Christopher Chambers[3], Osamu Seki[3], Kenji Kawamura[4], Jun'ichi Okuno[4]

1. Atmosphere and Ocean Research Institute, The University of Tokyo, 2. JAMSTEC, 3. Hokkaido University, 4. NIPR

Linking the paleo-ice sheet modelling studies and the future projection is challenging because of its millennial-scale long response time to external forcing which leads to its long commitment. Here in this study, in order to investigate the existence of threshold in the system which characterizes the irreversible behavior under climate changes, we use three-dimensional ice sheet model, SICOPOLIS, to investigate the Antarctic ice sheet response to atmospheric and oceanic warming, systematically. Ice sheet change is calculated for a given anomaly of surface temperature of 1 to 20 degree C as atmosphere forcing and basal melting beneath ice shelves of 1 to 400 m/a as ocean forcing. The response of ice sheet mass balance and volume for different time scales, 100, 1000, 10000 and 100, 000 years are analyzed for different initial conditions. We find that the collapse of West Antarctic ice sheet (WAIS) and the retreat of coastal areas of East Antarctic ice sheet (EAIS) such as Wilkes Subglacial Basin result in sea-level contributions of about 10m within 1kyr if an oceanic melt anomaly were around 5 to 10 m/a. The ice sheet change is little for the first 100 years, partly because of the compensation between the accumulation increase and the ice sheet retreat. Especially, continuous basal melting rate of 2-10m/a leads to Marine ice sheet instability (MISI) in a few hundred years before the major glacial rebound, while it takes much longer time for the recovery after eliminating the melting or warming. Implication for paleoclimate and ice sheet modelling as well as future projection will be further discussed.

Keywords: climate, ice sheet, modelling, Antarctic ice sheet, deglaciation

©2021. Japan Geoscience Union. All Right Reserved.

Carbon and nutrient cycles in and around the Cape Darnley polynya

*Michiyo Yamamoto-Kawai[1], Yoshihiko Ohashi[1]

1. Graduate School of Marine Science and Technology, Tokyo University of Marine Science and Technology

In polynyas around the Antarctic coast, cold dense shelf water (DSW), the precursor to Antarctic Bottom Water (AABW), is formed by enhanced sea-ice production. The outflow of this DSW into the abyss links biogeochemistry of the upper and deeper oceans. As part of the GRAntarctic project, we have investigated carbon and nutrient cycles in and around the Cape Darnley polynya region, where DSW and AABW are formed. Data of transient tracers CFCs and SF_6 are also used to estimate time-scale of AABW transport from the polynya to the deep ocean.

Ship-based and moored observations have shown large seasonal and interannual changes in carbon and nutrient concentrations in the polynya, due to production and decomposition of organic matter. Estimates of carbon and nutrient budgets in the polynya indicate the net removal of silicate and dissolved inorganic carbon (DIC) on the shelf. As a result, low DIC and silica concentrations characterize the newly formed AABW in this region. CFC and SF_6 showed a rapid transport of well-ventilated AABW from the Cape Darnley polynya region to the north and west. During this rapid transport, the effect of decomposition of organic matter was not evident in DIC or nutrient concentrations. These results revealed that Cape Darnley polynya acts as a significant sink of DIC and silicate, lowering DIC and silicate concentrations of AABW.

Keywords: carbon cylce, nutrient cycle, polynya, Southern Ocean

©2021. Japan Geoscience Union. All Right Reserved.

MONACA: The hot explorer under ice

*Toshihiro Maki[1], Hirokazu Yamagata[1], Hiroshi Yoshida[2], Yoshifumi Nogi[3]

1. The University of Tokyo, 2. Japan Agency for Marine-Earth Science and Technology, 3. National Institute of Polar Research

Autonomous Underwater Vehicles (AUVs) are now recognized as a convenient and high-performance tool for underwater survey. However, under ice observation is still challenging. Because the surface is packed with ice, AUVs cannot directly surface even in case of emergency. Support vessels cannot stay in close to the vehicle either. The vehicle mostly has to return to a pinpoint open water nearby the ship through long lonely journey home.
The AUV MONACA was developed for under ice survey of Antarctica, supported by JSPS Grant-in-Aid for Scientific Research on Innovative Areas No.4902. MONACA is 2 m long, 230 kg weigh, and it can cruise for about 8 hours. The vehicle is designed to go into ice covered oceans as far as 10 km. Although the survey range is limited compared with large AUVs, it can conduct a highly precise survey with lower costs. Its sensor unit consisting of a multi-beam sonar, an INS (Inertial Navigation System), and a DVL (Doppler Velocity Log) can be flipped upside down, so that the vehicle can survey both the ice and seafloor with minimum modification. In this presentation, the overview of the project is introduced. Results of open water and under ice experiments are also shown.

Keywords: Antarctica, Observation technology, Autonomous Underwater Vehicle

©2021. Japan Geoscience Union. All Right Reserved.



©2021. Japan Geoscience Union. All Right Reserved.

Development of the Under Ice AUV “MONACA” - Autonomous Navigation Trial in Under Ice Environment -

*Hirokazu Yamagata[1], Shuma Kochii[1], Hiroshi Yoshida[2], Yoshifumi Nogi[3], Toshihiro Maki[1]

1. Institute of Industrial Science, The University of Tokyo, 2. Japan Marine Science and Technology Center, 3. National Institute of Polar Research

This presentation introduces the AUV MONACA (Mobility Oriented Nadir AntarctiC Adventurer) and reports the results of autonomous navigation trials held in Oct. 2020 and Feb. 2021.

The AUV MONACA was developed for under ice survey of Antarctica, supported by JSPS Grant-in-Aid for Scientific Research on Innovative Areas No.4902, to measure the sea ice/shelf ice and seafloor for research of ice sheet-ocean interaction. MONACA is 2 m long, 230 kg weigh, and it can cruise for about 8 hours. Depth rating is 1500m. The vehicle is designed to go into ice covered oceans as far as 10 km. The flat body is filled with buoyancy materials at the top so that the battery units and main unit can be accessed from the side. The vehicle has five degrees of freedom (surge, heave, roll, pitch, and yaw) by 4 vertical thrusters and 2 horizontal thrusters. Although the survey range is limited compared with large AUVs, it can conduct a highly precise survey with lower costs. Its modular design enables the necessary and sufficient compositions for various survey needs. Its sensor unit consisting of a multi-beam sonar, an INS (Inertial Navigation System), and a DVL (Doppler Velocity Log) can be flipped upside down, so that the vehicle can survey both the ice and seafloor with minimum modification.

The first autonomous navigation trial was held in Oct. 2020 at Shimoda Bay, located in Sizuoka. MONACA was deployed, and its basic performance such as waypoint tracking and altitude control were veirfied at the open and calm water. The sensor unit was looking downward. Bathymetry data was also collected by the multibeam sonar. The second autonomous navigation trial is planned in Feb. 2021 at Mombetsu Port, located in Hokkaido and covered by ice. The sensor unit is looking upward to detect floating ice. The performance of ice-relative navigation and ice mapping is evaluated. The results of the trial will be shown in the presentation.

Keywords: Under-ice Survey, AUV

©2021. Japan Geoscience Union. All Right Reserved.



©2021. Japan Geoscience Union. All Right Reserved.

Long-term future projections for the Antarctic ice sheet with the model SICOPOLIS

*Christopher Chambers[1], Ralf Greve[2,1], Takashi Obase[3], Fuyuki SAITO[4], Kaho Harada[3], Ayako Abe-Ouchi[3]

1. Institute of Low Temperature Science, Hokkaido University, 2. Arctic Research Center, Hokkaido University, 3. Atmosphere and Ocean Research Institute, University of Tokyo, 4. Japan Agency for Marine-Earth Science and Technology

Ice-sheet simulations of extended versions of ISMIP6 (Ice Sheet Model Intercomparison Project for the Coupled Model Intercomparison Project Phase 6) future climate experiments for the Antarctic ice sheet until the year 3000 are used to investigate the long term impacts of 21st century projected warming. The simulations use climate projections from the beginning of 2015 until the end of 2100, after which no further climate trend is applied. Fourteen experiments are for the “unabated warming” pathway, and three are for the “reduced emissions” pathway. For the unabated warming path simulations, a large difference in the vulnerability of east and west Antarctica develops over hundreds of years (Figure 1 bottom), with west Antarctica suffering a much more severe ice loss than east Antarctica. In these cases, the mass loss amounts to a 14-experiment average of ~3.3 m sea-level equivalent by the year 3000 and ~5.3 m for the most sensitive experiment (Figure 1 top). For the reduced emissions pathway, the mean mass loss is ~0.25 m sea-level equivalent. The conclusions are quite different to ISMIP6, which saw only modest losses, or even gains, by the year 2100, demonstrating that the consequences of the unabated warming path are large and long term. Under the unabated 21st century warming scenario the ice sheet progresses through 4 phases, that are defined by differing rates of ice loss. The stages are attributable to how west Antarctica loses mass along the Siple Coast followed later by additional loss from the Thwaites/Pine Island region and an eventual leveling out in the rate of ice sheet loss once the majority of the west Antarctic ice sheet has melted. Simulations with and without bedrock rebound corroborate a negative feedback for ice loss found in previous studies. Limitations to the study, include the lack of accounting for local climatic changes in regions where ice sheet collapse occurs.

Keywords: Antarctica, ice sheet, climate change, cryosphere

©2021. Japan Geoscience Union. All Right Reserved.

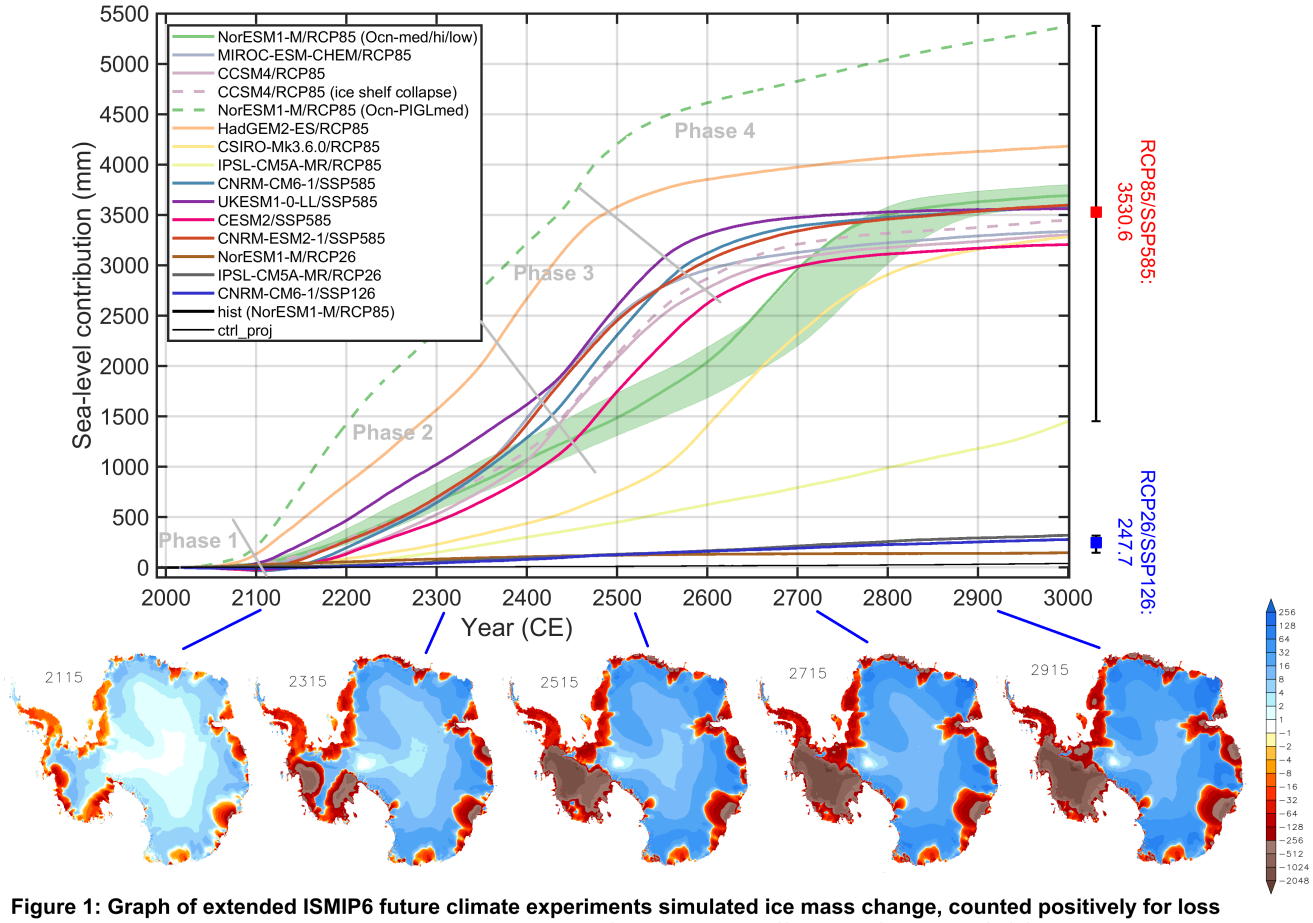


Figure 1: Graph of extended ISMIP6 future climate experiments simulated ice mass change, counted positively for loss and expressed as sea-level contribution. Below are ice surface elevation differences from 2015 (m) for the year indicated for case MIROC-ESM-CHEM/RCP85.

©2021. Japan Geoscience Union. All Right Reserved.

[E] Oral | M (Multidisciplinary and Interdisciplinary)：M-IS Intersection

Sun. Jun 6, 2021 1:45 PM - 3:15 PM JST | Sun. Jun 6, 2021 4:45 AM - 6:15 AM UTC | Ch.11 Zoom Room 11

[M-IS05] Global climate change driven by the Southern Ocean and the Antarctic Ice Sheet

convener:Osamu Seki(Institute of Low Temperature Science, Hokkaido University), Yoshifumi Nogi(National Institute of Polar Research), Akira Oka(Atmosphere and Ocean Research Institute, The University of Tokyo), Yusuke Suganuma(National institute of Polar Research), Chairperson:Hiroki Matsui(Graduate School of International Resource Sciences, Akita University), Takeshige Ishiwa(National Institute of Polar Research)

The Southern Ocean and Antarctic ice sheet, which are the giant reservoirs of heat, water, and materials, have a potential to play central roles in long-term global climate change. This system is composed of the following sub-systems; ice shelf which is a place of the interaction of ice sheet and ocean, flowing iceberg, seasonal sea ice zone, Antarctic bottom water which drives the thermohaline circulation, active biological production and Antarctic Circumpolar Current. These sub-systems are interacted with each other and have significant impact on changes in the global environmental system. This session aim to summarize recent observational and simulation studies from various fields relating to the past and present changes in the Antarctic Ice sheet and Southern Ocean, which are essential elements for unraveling the changes in the global climate system. Further, future science plans for understanding of the environmental changes of the Antarctic Cryosphere is also discussed.

1:45 PM - 2:00 PM JST | 4:45 AM - 5:00 AM UTC

[MIS05-06] Beryllium isotope records from sectors of the West and East Antarctic Ice sheet reveal Holocene melting related to the incursion of Circumpolar Deep Water

*Adam David Sproson[1,2], Yusuke Yokoyama[1,2], Yoshinori Takano[2], Rebecca Minzoni[3], Bethany Behrens[1], Yosuke Miyairi[1], Takahiro Aze[1] (1.Atmosphere and Ocean Research Institute, University of Tokyo, 5-1-5 Kashiwanoha, Kashiwa, Chiba 277-8564, Japan. , 2.Department of Biogeochemistry, Japan Agency for Marine-Earth Science and Technology, 2-15 Natsushima, Yokosuka, Kanagawa 237-0061, Japan. , 3.Department of Geological Sciences, The University of Alabama, USA.)

2:00 PM - 2:15 PM JST | 5:00 AM - 5:15 AM UTC

[MIS05-07] Abrupt Holocene ice-sheet retreat in Lutzow-Holm Bay, East Antarctica

*Yusuke Suganuma[1,2], Yuki Haneda[3], Takuya Itaki[3], Osamu Seki[4], Takeshige Ishiwa[1], Moto Kawamata[2], Masakazu Fujii[1,2], Kazuya Kusahara[8], Daisuke Hirano[4], Masao Iwai[9], Yuji Kato[9], Hiroki Matsui[6], Atsuko Amano[3], Kota Katsuki[5], Takayuki Omori[7], Motohiro Hirabayashi[1], Hiroyuki Matsuzaki[7], Takeyasu Yamagata[7], Masato Ito[8], Shin Sugiyama[4], Naohisa Nishida[10], Jun'ichi Okuno[1,2], Minoru Ikehara[9], Hideki Miura[1,2] (1.National institute of Polar Research, 2.The Graduate University for Advanced Studies (SOKENDAI), 3.Geological Survey of Japan, AIST, 4.Hokkaido University, 5.Shimane University, 6.Akita University, 7.University of Tokyo, 8.JAMSTEC, 9.Center for Advanced Marine Core Research, Kochi University, 10.Tokyo Gakugei University)

2:15 PM - 2:30 PM JST | 5:15 AM - 5:30 AM UTC

[MIS05-08] Paleoenvironmental reconstruction using lake sediment cores from Lake Nurume in Lützow Holm Bay

*Takeshige Ishiwa[1], Yuki Tokuda[2], Takuya Itaki[3], Satoshi Sasaki[4], Kota Katsuki[4], Yusuke Suganuma[1,5] (1.National Institute of Polar Research, 2.Tottori University of Environmental Studies, 3.National Institute of Advanced Industrial Science and Technology, 4.Shimane University, 5.The Graduate University for Advanced Studies (SOKENDAI))

2:30 PM - 2:45 PM JST | 5:30 AM - 5:45 AM UTC

[MIS05-09] Assessing dust-magnetic correlation in the Indian sector of the Southern Ocean

*Hiroki Matsui[1], Minoru Ikehara[2], Yusuke Suganuma[3,4], Osamu Seki[5], Ikumi Oyabu[3], Kenji Kawamura[3,4] (1.Graduate School of International Resource Sciences, Akita University, 2.Center for Advanced Marine Core Research, Kochi University, 3.National Institute of Polar Research, Research Organization of

Information and Systems, 4.Department of Polar Science, School of Multidisciplinary Sciences, The Graduate University for Advanced Studies (SOKENDAI), 5.Institute of Low Temperature Science, Hokkaido University)

2:45 PM - 3:00 PM JST | 5:45 AM - 6:00 AM UTC

[MIS05-10] Antarctic warmth in the last interglacial driven by Northern insolation and deglaciation

*Takashi Obase[1], Ayako Abe-Ouchi[1,2], Fuyuki SAITO[3] (1.Atmosphere and Ocean Research Institute, the University of Tokyo, 2.National Institute of Polar Research, Japan, 3.Japan Agency for Marine-Earth Science and Technology)

3:00 PM - 3:15 PM JST | 6:00 AM - 6:15 AM UTC

[MIS05-11] Modeling the ocean carbon cycle during the last deglaciation

*Hidetaka Kobayashi[1], Akira Oka[1], Takashi Obase[1], Ayako Abe-Ouchi[1] (1.Atmosphere and Ocean Research Institute, The University of Tokyo)

Beryllium isotope records from sectors of the West and East Antarctic Ice sheet reveal Holocene melting related to the incursion of Circumpolar Deep Water

*Adam David Sproson[1,2], Yusuke Yokoyama[1,2], Yoshinori Takano[2], Rebecca Minzoni[3], Bethany Behrens[1], Yosuke Miyairi[1], Takahiro Aze[1]

1. Atmosphere and Ocean Research Institute, University of Tokyo, 5-1-5 Kashiwanoha, Kashiwa, Chiba 277-8564, Japan. , 2. Department of Biogeochemistry, Japan Agency for Marine-Earth Science and Technology, 2-15 Natsushima, Yokosuka, Kanagawa 237-0061, Japan. , 3. Department of Geological Sciences, The University of Alabama, USA.

Glaciers and ice sheets in both mountain regions and the poles are losing mass, causing an increase in the rate of mean sea level rise whilst expanding an ever-warming ocean. Sea level rose globally by ~15 cm over the past ~100 years but that rate is currently accelerating, becoming twice as fast (3.6 mm yr^{-1}). Sea level rise could reach around 30 to 60 cm by 2100 if greenhouse gas emissions are sharply reduced and global warming is limited less than 2˚C but could rise to around 60 to 110 cm if greenhouse gas emissions continue to increase [1]. It is therefore imperative for Earth scientists to use the geological record to reconstruct the deglacial history of key regions relevant to sea level rise during past periods of extreme climate [e.g., 2]. This will allow better constraints on numerical models for future climate predictions and a greater understanding of the cryosphere response to future global warming. Here, we present the authigenic Be isotope composition of lake and marine sediments from the Lützow-Holm Bay and the Ferrero Bay, respectively [3-5].

Meteoric ^{10}Be is produced in the atmosphere by cosmic rays and delivered to the Earth and ocean surface via dust and precipitation. In Antarctica, these sources of ^{10}Be become locked up in ice sheets and are subsequently released to the continental shelf during periods of melting and freshwater discharge, where they adhere to suspended particles in the water column and subsequently accumulate on the basin floor [6]. Stable ^{9}Be is present in silicate rocks and is released during subglacial weathering, with little simultaneous release of ^{10}Be, and transported to the oceans via meltwater outflow [7]. When Be is incorporated into the authigenic phase of marine sediments, the $^{10}Be/^{9}Be$ reflects that of the overlying water column [8], which in turn reflects the relative dominance of freshwater flux and/or subglacial weathering.

New Be isotope records from Lakes Maruwan Oike and Lake Skallen, near Lützow-Holm Bay, and Ferrero Bay, the Amundsen Sea Embayment, reveal a large increase in ^{10}Be abundance and $^{10}Be/^{9}Be$ ratios between 4.1 to 3.6 Ka BP and 10 to 6 ka BP, respectively. This suggests widespread meltwater discharge and destabilisation of respective parts of the East and West Antarctic Ice Sheet during the Late and Early Holocene. Such events could be linked to a strengthening of the Southern Hemisphere westerlies which, in turn, would have caused enhanced upwelling of warm Circumpolar Deep Waters (CDW) onto the shelf leading to increased marine ice shelf instability and melting [9, 10] suggesting possible Antarctic contribution to global sea-level rise during the Holocene [11].

[1] Pörtner H.-O. et al. (2019) *IPCC Special Report on the Ocean and Cryosphere in a Changing Climate.* [2] Mackintosh et al. (2014) *Quaternary Science Reviews* **100**: p 10-30. [3] Takano, Y., et al. (2015) Progress in Earth and Planetary Science **2**(1): p. 8. [4] Takano, Y., et al. (2012) Applied Geochemistry **27** (12): p. 2546-2559. [5] Minzoni, R.T., et al. (2017) The Holocene **27**(11): p. 1645-1658. [6] Simon, Q., et

©2021. Japan Geoscience Union. All Right Reserved.

al. (2016) Quaternary Science Reviews **140**: p. 142-162. [7] Sjunneskog, C. et al. (2007) Nuclear Instruments and Methods in Physics Research Section B: Beam Interactions with Materials and Atoms **259** (1): p. 576-583. [8] von Blanckenburg, F. and J. Bouchez (2014) Earth and Planetary Science Letters **387**: p. 34-43. [9] Crosta, X., et al. (2018) *Global & Planetary Change* **166**: p. 62-74.
[10] Yokoyama, Y., et al. (2016) *Proceedings of the National Academy of Sciences* **113**(9): p. 2354. [11] Yokoyama, Y., et al. (2019) *Quaternary Science Reviews* **206**: p. 150-161.

Keywords: Beryllium isotopes, Holocene, Antarctica, Glacial discharge

©2021. Japan Geoscience Union. All Right Reserved.

Abrupt Holocene ice-sheet retreat in Lutzow-Holm Bay, East Antarctica

*Yusuke Suganuma[1,2], Yuki Haneda[3], Takuya Itaki[3], Osamu Seki[4], Takeshige Ishiwa[1], Moto Kawamata[2], Masakazu Fujii[1,2], Kazuya Kusahara[8], Daisuke Hirano[4], Masao Iwai[9], Yuji Kato[9], Hiroki Matsui[6], Atsuko Amano[3], Kota Katsuki[5], Takayuki Omori[7], Motohiro Hirabayashi[1], Hiroyuki Matsuzaki[7], Takeyasu Yamagata[7], Masato Ito[8], Shin Sugiyama[4], Naohisa Nishida[10], Jun'ichi Okuno[1,2], Minoru Ikehara[9], Hideki Miura[1,2]

1. National institute of Polar Research, 2. The Graduate University for Advanced Studies (SOKENDAI), 3. Geological Survey of Japan, AIST, 4. Hokkaido University, 5. Shimane University, 6. Akita University, 7. University of Tokyo, 8. JAMSTEC, 9. Center for Advanced Marine Core Research, Kochi University, 10. Tokyo Gakugei University

The Antarctic Ice Sheet (AIS) is one of the most significant potential contributors to future sea-level changes. Recently, the acceleration of AIS’ s mass loss has been reported based on satellite observations, such as radar altimetry, interferometer, and gravity measurements, and shipboard observations coupled with modeling studies. In these studies, the main cause of the modern ice mass loss is thought to be iceberg calving and basal melting due to an inflow of modified Circumpolar Deep Water (mCDW). However, the role of the mCDW for the large-scale deglaciation of the AIS, such as the deglaciation since the Last Glacial Maximum (LGM), remains unclear due to the lack of the geological data-based constraint. Therefore, marine and land-based reconstruction of the deglaciation process of the AIS since the LGM is essential to understand the role of the mCDW for a large-scale ice mass loss, which will be a useful analog to calibrate the climate and ice sheet models and to refine the future ice sheet retreat projection. In this presentation, we show an overview of our recent activities in the Lützow-Holm Bay (LHB), Dronning Maud Land, East Antarctica. Newly obtained sedimentary cores and legacy samples from the LHB are used for detailed lithofacies analysis, authigenic Be-10 measurement, hydrogen isotopic compositions analysis, and benthic foraminiferal assemblage of the sedimentary cores. And also, a hybrid age model is constructed by foraminiferal and calibrated bulk organic carbon AMS C-14 dates. These indicate that the East AIS rapidly retreated since the Early Holocene due to an intensified incision of the mCDW. This retreat propagated from the submarine trough to shallower vicinity and then ceased by the Mid-Holocene coincide with the weakening of the mCDW incision. This phenomenon is consistent with the abrupt ice sheet thinning observed along the eastern coast of the bay (Soya Coast) revealed by surface exposure ages and clear lithofacies change of lake sediments and its AMS C-14 dates. This is the first clear terrestrial and marine-based geological constraint for the large-scale deglaciation of the East AIS, driven by a modulation of the mCDW incision, since the LGM.

Keywords: Antarctica Ice Sheet and Southern Ocean, Giant Reservoirs - Antarctic, Solid Earth

©2021. Japan Geoscience Union. All Right Reserved.

Paleoenvironmental reconstruction using lake sediment cores from Lake Nurume in Lützow Holm Bay

*Takeshige Ishiwa[1], Yuki Tokuda[2], Takuya Itaki[3], Satoshi Sasaki[4], Kota Katsuki[4], Yusuke Suganuma[1,5]

1. National Institute of Polar Research, 2. Tottori University of Environmental Studies, 3. National Institute of Advanced Industrial Science and Technology, 4. Shimane University, 5. The Graduate University for Advanced Studies (SOKENDAI)

Lake sediment in Antarctica is a useful archive for paleoenvironmental reconstruction as sea-level and ice-sheet change. Various sediment cores have been collected from a large number of lakes in Lützow Holm Bay, East Antarctica (e.g., Takano et al., 2012; Verleryen et al., 2017; Suganuma et al., 2018; Ishiwa et al., 2020). However, the previous studies generally used one core sample for each lake in most cases, and it is necessary to proceed with an analysis of multiple core samples to reconstruct detailed environmental changes in the lake. Lake Nurume at Langhovde, Lützow Holm Bay is isolated from the sea by ~1 m sill, and a perennial snow patch is well developed in the southeast of the lake. In the geomorphological survey of the 61st Japanese Antarctic Research Expedition, we collected four sediment cores in Lake Nurume and also measured water column profiles (e.g., salinity, temperature, and turbidity) and detailed lake bathymetry (Ishiwa et al., in press). We will present preliminary results of these cores, such as radiocarbon dating, XRF, X-ray CT scanning, and microfossils analysis of the cores. Combining geological settings and obtained results in Lake Nurume provides significant insight into paleoenvironmental reconstruction around Lützow Holm Bay. Moreover, the dataset will be a valuable archive of paleoenvironmental studies using lake sediments in Antarctica.

Keywords: East Antarctica, Lake sediments

©2021. Japan Geoscience Union. All Right Reserved.

Assessing dust-magnetic correlation in the Indian sector of the Southern Ocean

*Hiroki Matsui[1], Minoru Ikehara[2], Yusuke Suganuma[3,4], Osamu Seki[5], Ikumi Oyabu[3], Kenji Kawamura[3,4]

1. Graduate School of International Resource Sciences, Akita University, 2. Center for Advanced Marine Core Research, Kochi University, 3. National Institute of Polar Research, Research Organization of Information and Systems, 4. Department of Polar Science, School of Multidisciplinary Sciences, The Graduate University for Advanced Studies (SOKENDAI), 5. Institute of Low Temperature Science, Hokkaido University

Understanding Antarctic climate change requires integration of marine and ice core records. Recent advances in transfer of ice core chronology to marine core by signal matching will eventually allow direct comparison between marine and ice core records. Dust-magnetic correlation which utilizes great similarity between magnetic susceptibility of marine cores and aeolian dust of ice cores has been increasingly used in the Scotia Sea and the Pacific sector of the Southern Ocean (SO). However, dust-magnetic correlation has rarely been assessed in the Indian sector of the SO, hampering circum-Antarctic application of the method. Here we test dust-magnetic correlation in the Indian sector of the SO through the last 400 kyrs by age-depth model comparison of dust-magnetic correlation, oxygen isotope correlation, and published radiocarbon dates. We discuss potential effect of age-depth errors and bioturbation process to integrate traditional marine core chronologies with ice core chronology.

Keywords: Dust-magnetic correlation, Age-depth model, Southern Ocean

©2021. Japan Geoscience Union. All Right Reserved.

Antarctic warmth in the last interglacial driven by Northern insolation and deglaciation

*Takashi Obase[1], Ayako Abe-Ouchi[1,2], Fuyuki SAITO[3]

1. Atmosphere and Ocean Research Institute, the University of Tokyo, 2. National Institute of Polar Research, Japan, 3. Japan Agency for Marine-Earth Science and Technology

The global mean sea level in the last interglacial (LIG, about 130,000 to 115,000 years before present) was very likely higher than the present level, driven mainly by mass loss of the Antarctic ice sheet. Some studies have suggested that this mass loss may have been caused by the warmer temperature over the Southern Ocean in the LIG compared with the present interglacial. However, the ultimate cause of the difference in Antarctic warming between the last and current interglacials has not been explained. Here, based on transient simulations of the last deglaciation using a fully coupled ocean–atmosphere model, we show that greater meltwater (by a factor of 1.5 relative to the last deglaciation) during the middle and later stages of the deglaciation could have produced the difference in Antarctic warmth. Northern Hemisphere ice sheet model experiments suggest that the difference in meltwater was caused by slightly smaller orbital eccentricity in our current interglacial than in the LIG, indicating that mass loss of the Antarctic ice sheet is influenced by the preceding northern summer insolation and disintegration of Northern Hemisphere ice sheets.

©2021. Japan Geoscience Union. All Right Reserved.

Modeling the ocean carbon cycle during the last deglaciation

*Hidetaka Kobayashi[1], Akira Oka[1], Takashi Obase[1], Ayako Abe-Ouchi[1]

1. Atmosphere and Ocean Research Institute, The University of Tokyo

Ice core records show that the atmospheric carbon dioxide concentration (pCO2) varied with an amplitude of about 100 ppm during glacial-interglacial cycles. Although not yet fully understood, it is recognized that the variation of atmospheric pCO2 is mainly due to changes in the ocean carbon cycle (e.g., sea surface temperature, biological carbon pump, ocean circulation, and carbonate inorganic chemistry). Recent studies, including those of the authors, point to the importance of changes in the Southern Ocean for the changes in the ocean carbon cycle. On the other hand, these consequences are mainly derived from comparisons of the carbon cycle under equilibrium climates, and more practically, the mechanisms of the transient responses of the carbon cycle that occur in the context of temporal changes in climate need to be finally clarified. Using the results of our modeling study, in which a complex coupled atmosphere-ocean general circulation model reproduces well the deep ocean circulation and surface temperature changes during the Bolling-Allerod (BA) transition, we investigate the transient response of the ocean carbon cycle during the last deglaciation between 21,000 and 11,000 years ago. We report the preliminary results of the transient simulation. In particular, we focus on the response of the ocean carbon cycle to rapid changes in the Atlantic meridional overturning circulation during the BA transition.

Keywords: ocean carbon cycle, last deglaciation, Atlantic meridional overturning circulation, Southern Ocean

©2021. Japan Geoscience Union. All Right Reserved.

[E] Oral | M (Multidisciplinary and Interdisciplinary)：M-IS Intersection

Sun. Jun 6, 2021 3:30 PM - 5:00 PM JST | Sun. Jun 6, 2021 6:30 AM - 8:00 AM UTC | Ch.11 Zoom Room 11

[M-IS05] Global climate change driven by the Southern Ocean and the Antarctic Ice Sheet

convener:Osamu Seki(Institute of Low Temperature Science, Hokkaido University), Yoshifumi Nogi(National Institute of Polar Research), Akira Oka(Atmosphere and Ocean Research Institute, The University of Tokyo), Yusuke Suganuma(National institute of Polar Research), Chairperson:Hidetaka Kobayashi(Atmosphere and Ocean Research Institute, The University of Tokyo)

The Southern Ocean and Antarctic ice sheet, which are the giant reservoirs of heat, water, and materials, have a potential to play central roles in long-term global climate change. This system is composed of the following sub-systems; ice shelf which is a place of the interaction of ice sheet and ocean, flowing iceberg, seasonal sea ice zone, Antarctic bottom water which drives the thermohaline circulation, active biological production and Antarctic Circumpolar Current. These sub-systems are interacted with each other and have significant impact on changes in the global environmental system. This session aim to summarize recent observational and simulation studies from various fields relating to the past and present changes in the Antarctic Ice sheet and Southern Ocean, which are essential elements for unraveling the changes in the global climate system. Further, future science plans for understanding of the environmental changes of the Antarctic Cryosphere is also discussed.

3:30 PM - 3:45 PM JST | 6:30 AM - 6:45 AM UTC

[MIS05-12] Last Glacial Maximum Antarctic sea ice linked with global mean ocean temperature: evidence from PMIP3, PMIP4 and MIROC-4m simulations

*Tristan Vadsaria[1], Sam Sherriff-Tadano[2,1], Ayako Abe-Ouchi[1], Takashi Obase[1], Wing-Le Chan[1], Xavier Crosta[3] (1.Atmosphere and Ocean Research Institute, The University of Tokyo, Japan, 2.School of Earth and Environment, The University of Leeds, Leeds, UK, 3.Environnements et Paléoenvironnements Océanique et Continentaux, Pessac, France)

3:45 PM - 4:00 PM JST | 6:45 AM - 7:00 AM UTC

[MIS05-13] Antarctic Slope Current modulates warm ocean heat intrusions towards Totten Glacier

*Yoshihiro Nakayama[1], Chad A Greene[2], Fernando S Paolo[2], Vigan Mensah[1], Hong Zhang[2], Haruhiko Kashiwase[3], Daisuke Simizu[3], Jamin S Greenbaum[4], Donald D Blankenship[5], Ayako Abe-Ouchi[6], Shigeru Aoki[1] (1.Institute of Low Temperature Science, Hokkaido University, Japan, 2.NASA Jet Propulsion Laboratory, California, USA, 3.National Institute of Polar Research, Tokyo, Japan, 4.Scripps Institution of Oceanography, University of California, California USA, 5.Institute for Geophysics, University of Texas at Austin, Texas, USA, 6.Atmosphere and Ocean Research Institute, The University of Tokyo, Tokyo, Japan.)

4:00 PM - 4:15 PM JST | 7:00 AM - 7:15 AM UTC

[MIS05-14] Sea Ice Variations in Coastal Amundsen Sea Affected by Ice Shelf Meltwater

*KOFAN LU[1] (1.Japan Agency for Marine-Earth Science and Technology)

4:15 PM - 4:30 PM JST | 7:15 AM - 7:30 AM UTC

[MIS05-15] Observation of plagic system using a drifter off Wilkes land during sea ice melting season

*Ryosuke Makabe[1,5,2], Keigo Takahashi[2], Shintaro Takao[3], Ryo Matsuda[4], Masayoshi Sano[1], Kohei Mizobata[5], Norio Kurosawa[4], Masato Moteki[5,1], Tsuneo Odate[1,2] (1.National Institute of Polar Research, 2.The Graduate University for Advanced Studies (SOKENDAI), 3.National Institute for Environmental Studies, 4.Soka University, 5.Tokyo University of Marine Science and Technology)

4:30 PM - 4:45 PM JST | 7:30 AM - 7:45 AM UTC

[MIS05-16] Primary production and carbon export related to sub-surface chlorophyll maximum off Wilkes land during post bloom season

*Norio Kurosawa[1], Ayuko Kagesawaa[2], Ryosuke Makabe[3,2,4], Shintaro Takao[5], Masayoshi Sano[3], Kohei Mizobata[4], Masato Moteki[4,3], Tsuneo Odate[2,3] (1.Soka University, 2.The Graduate University for Advanced Studies (SOKENDAI), 3.National Institute of Polar Research, 4.Tokyo University of Marine Science and Technology, 5.National Institute for Environmental Studies)

4:45 PM - 5:00 PM JST | 7:45 AM - 8:00 AM UTC

[MIS05-17] Contribution of fecal pellet-like dinoflagellates to the carbon sequestration in the seasonal ice zone of the Southern Ocean

*Ryo Matsuda[1], Jaekyeng Han[1], Shinya Okano[1], Masayoshi Sano[2], Shintaro Takao[3], Ryosuke Makabe[2,4,5], Masato Moteki[4,5], Tsuneo Odate[2,4], Norio Kurosawa[1] (1.Soka University, 2.National Institute of Polar Research, 3.National Institute for Environmental Studies, 4.The Graduate University for Advanced Studies (SOKENDAI), 5.Tokyo University of Marine Science and Technology)

Last Glacial Maximum Antarctic sea ice linked with global mean ocean temperature: evidence from PMIP3, PMIP4 and MIROC-4m simulations

*Tristan Vadsaria[1], Sam Sherriff-Tadano[2,1], Ayako Abe-Ouchi[1], Takashi Obase[1], Wing-Le Chan[1], Xavier Crosta[3]

1. Atmosphere and Ocean Research Institute, The University of Tokyo, Japan, 2. School of Earth and Environment, The University of Leeds, Leeds, UK, 3. Environnements et Paléoenvironnements Océanique et Continentaux, Pessac, France

Southern Ocean sea ice and oceanic fronts are known to play an important role on the climate system, carbon cycles, bottom ocean circulation, and Antarctic ice sheet. However, many models of the previous Past-climate Model Intercomparison Project (PMIP) underestimated sea-ice extent (SIE) for the Last Glacial Maximum (LGM)(Roche et al., 2012; Marzocchi and Jensen, 2017), mainly because of surface bias (Flato et al., 2013) that may have an impact on mean ocean temperature (MOT). Indeed, recent studies further suggest an important link between Southern Ocean sea ice and mean ocean temperature (Ferrari et al., 2014; Bereiter et al., 2018 among others). Misrepresent the Antarctic sea-ice extent could highly impact deep ocean circulation, the heat transport and thus the MOT. In this study, we will stress the relationship between the distribution of Antarctic sea-ice extent and the MOT through the analysis of the PMIP3 and PMIP4 exercise and by using a set of MIROC models. To date, the latest version of MIROC improve its representation of the LGM Antarctic sea-ice extent, affecting the deep circulation and the MOT distribution (Sherriff-Tadano et al., under review).

Our results show that available PMIP4 models have an overall improvement in term of LGM sea-ice extent compared to PMIP3, associated to colder deep and bottom ocean temperature. Focusing on MIROC (4m) models, we show that models accounting for Southern Ocean sea-surface temperature (SST) bias correction reproduce an Antarctic sea-ice extent, 2D-distribution, and seasonal amplitude in good agreement with proxy-based data. Finally, using PMIP-MIROC analyze, we show that it exists a relationship between the maximum SIE and the MOT, modulated by the Antarctic intermediate and bottom waters.

Keywords: Antartic sea-ice, Last Glacial Maximum , Mean Ocen Temperature, MIROC simulations, PMIP3 and PMIP4 simulations

©2021. Japan Geoscience Union. All Right Reserved.

Antarctic Slope Current modulates warm ocean heat intrusions towards Totten Glacier

*Yoshihiro Nakayama[1], Chad A Greene[2], Fernando S Paolo[2], Vigan Mensah[1], Hong Zhang[2], Haruhiko Kashiwase[3], Daisuke Simizu[3], Jamin S Greenbaum[4], Donald D Blankenship[5], Ayako Abe-Ouchi[6], Shigeru Aoki[1]

1. Institute of Low Temperature Science, Hokkaido University, Japan, 2. NASA Jet Propulsion Laboratory, California, USA, 3. National Institute of Polar Research, Tokyo, Japan, 4. Scripps Institution of Oceanography, University of California, California USA, 5. Institute for Geophysics, University of Texas at Austin, Texas, USA, 6. Atmosphere and Ocean Research Institute, The University of Tokyo, Tokyo, Japan.

The Totten Glacier in East Antarctica has received increasing attention in recent years for its ice loss and warm oceanographic conditions observed at the ice shelf front. Here, we developed satellite estimates of temporally varying Totten Ice Shelf (TIS) melt rates and a high-resolution ocean model. We show that the Antarctic Slope Current (ASC) impedes ocean heat intrusions onto the continental shelf, whereas on-shelf intrusions are enhanced when the ASC weakens. Our findings suggest that atmospheric and oceanic conditions beyond our regional model domain play a greater role than local wind stress curl or other factors in driving interannual variability of the ASC. We further show that heat intrusions towards the TIS are enhanced with coastal freshening, suggesting a positive feedback whereby even freshening due to ice loss in West Antarctica could start a chain reaction, leading to increased melt in East Antarctica, and further coastal freshening.

Keywords: Southern Ocean, Ice shelf-ocean interaction, Circumpolar Deep Water

©2021. Japan Geoscience Union. All Right Reserved.

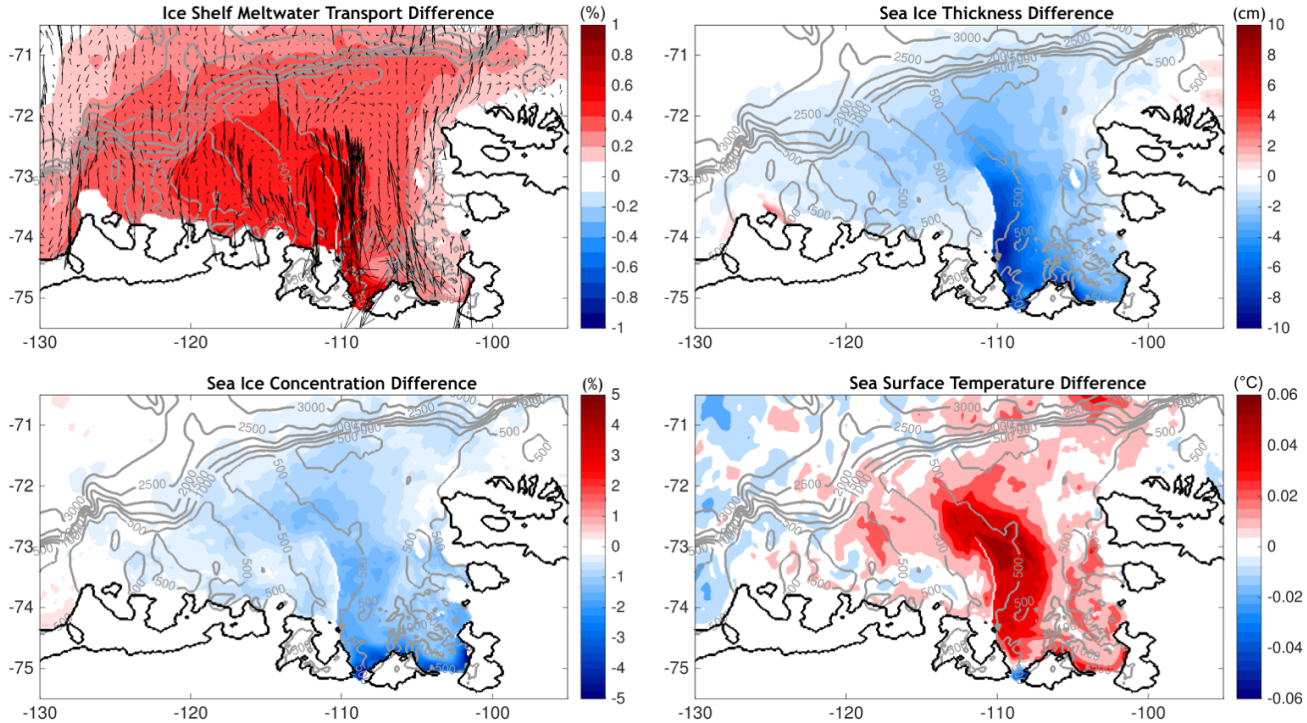
Sea Ice Variations in Coastal Amundsen Sea Affected by Ice Shelf Meltwater

*KOFAN LU[1]

1. Japan Agency for Marine-Earth Science and Technology

Meltwater outflows from Pine Island Embayment become more important in changing the ocean circulations in the coastal Amundsen along with the elevated basal melt of ice shelves. Sea ice variations in Amundsen Sea is modified by a combination of thermodynamic and dynamic processes, while in coastal areas dynamical process determined by ocean circulations is more dominant. A melt rate-controlled model set is developed to study the changes of the surface hydrography and sea ice distributions when double the melt rate (~ +135 Gt/yr in total) of Pine Island and Thwaites Glaciers. The increasing meltwater outflows from Pine Island Embayment transport westward and flush the sea ice drift, leading to both lower sea ice concentration and thickness along the coast. Sea ice concentration drops ~2% in average inthe coastal areas and sea ice thickness reduces ~10 cm in maximum. Due to the declined albedo that follows the lower sea ice concentration, the sea surface temperature increases ~0.06˚C in maximum. Although this surface warming occurs only in the upper layer (~100 m) and would not feedback to the ice shelf melt, the stored surface heat delays the sea ice formation and shorten freezing season. Changes of sea ice seasonal cycle by ice shelf meltwater are further investigated to evaluate the importance of thermodynamic and dynamic processes, which helps to assess the future sea ice trend under the climatological perturbations of surface heat budget in Amundsen Sea.

Keywords: Amundsen Sea sea ice, Pine Island Glacier, Thwaites Glacier, ice shelf meltwater



©2021. Japan Geoscience Union. All Right Reserved.

Observation of plagic system using a drifter off Wilkes land during sea ice melting season

*Ryosuke Makabe[1,5,2], Keigo Takahashi[2], Shintaro Takao[3], Ryo Matsuda[4], Masayoshi Sano[1], Kohei Mizobata[5], Norio Kurosawa[4], Masato Moteki[5,1], Tsuneo Odate[1,2]

1. National Institute of Polar Research, 2. The Graduate University for Advanced Studies (SOKENDAI), 3. National Institute for Environmental Studies, 4. Soka University, 5. Tokyo University of Marine Science and Technology

Ice edge phytoplankton bloom is one of the most important events to regulate primary production, which accelerates biological carbon pump in the seasonal ice zone in the Southern Ocean. Improvement of light condition and iron supply with sea ice melt are thought to be critical factors for development of the ice edge bloom. Thus, relationship between sea ice dynamics and biological activity is essential for understanding not only ecosystem structure and its dynamics but also carbon sequestration. Ice edge blooms were found only in situation with <40% sea ice cover. In that time, amount of sea ice had already melted, i.e. most of materials and algae in sea ice had already been released into water column. Therefore, time-series observation should be started at earlier phase of sea ice melt to understand dynamics of ice edge bloom and related biogeochemical cycles. We designed an ice guard GPS buoy for drifter observation attached with sensor frames and time series sediment traps at various depth to reveal surface condition and export flux during ice melting season.

A drifter observation was conducted in austral summer 2019/2020 during ice breaker *Shirase* cruise under 61st Japanese Antarctic Research Expedition. A drifter was deployed at 64.26˚S, 115.96˚E on 9th Dec., 2019 and retrieved at 64.55˚S, 104.79˚E on 16th Feb., 2020. All instruments, i.e. sensors attached to GPS frame and four sensor frames, two time-series sediment traps and an Acoustic Doppler Current Profiler (ADCP, 300 kHz) worked. At the deployment and retrieval sites, a CTD cast for vertical profiles of physical parameters and water sampling for determination of chlorophyll *a* (chl. *a*), particulate organic carbon/nitrogen (POC/N) and phytoplankton community structure. Three closing net tows for zooplankton analyses were conducted from 200-100, 100-50 and 50-0 m depth layers. Ten sea ice collections for analyzing sea ice components (salinity, chl. *a*, POC/N, taxonomic composition of ice algae) were also obtained at deployment site.
Less variability in depth of all instruments indicates that the drifter array was relatively stable even in dense sea ice situation. Sea ice concentration at deployment site was over 90%, which rapidly decreased from end of December to early January. Chlorophyll fluorescence at 20 m depth increased with decrease of sea ice concentration. However quite rapid increase in the fluorescence in higher (>50%) sea ice concentration. The euphotic layer depth (1% PAR) was still shallower than 20 m at the same time, and an increase in dissolved oxygen at 20 m depth occurred after the fluorescence peak. These suggested that the fluorescence peak at 20 m depth was caused by rather released ice algae than primary production in surface water column. After then, increase in fluorescence was also found at 30 m depth following the increase at 40 m depth. These changes in peak depth of fluorescence means that temporal changes of productive layer, i.e. transition from ice edge bloom to sub-surface chlorophyll maximum. Size composition of chl. *a* and taxonomic composition of algae in sea ice showed dominance of diatom. The abundance in the water column at deployment site was dominated by smaller taxa (<10 μm), and this was replaced by larger taxa (>10 μm) at retrieval site. Macro-nutrients at surface layer decreased indicates amount of diatom production as well as microbial degradation during the study period. We will also discuss zooplankton composition and the vertical migration pattern during ice melting season by using ADCP data.

©2021. Japan Geoscience Union. All Right Reserved.

Keywords: seasonal ice zone, sea ice melt, pelagic ecosystem

©2021. Japan Geoscience Union. All Right Reserved.

Primary production and carbon export related to sub-surface chlorophyll maximum off Wilkes land during post bloom season

*Norio Kurosawa[1], Ayuko Kagesawaa[2], Ryosuke Makabe[3,2,4], Shintaro Takao[5], Masayoshi Sano[3], Kohei Mizobata[4], Masato Moteki[4,3], Tsuneo Odate[2,3]

1. Soka University, 2. The Graduate University for Advanced Studies (SOKENDAI), 3. National Institute of Polar Research, 4. Tokyo University of Marine Science and Technology, 5. National Institute for Environmental Studies

In the Southern Ocean, ecological studies have mainly focused on ice edge phytoplankton blooms. This bloom is usually decline within 10-14 days, after then, sub-surface chlorophyll maximum (SCM) is often found widespread in the seasonal ice zone in austral summer. Structures and ecological roles of SCM have been reported especially in sub-tropical regions. Less is known in the seasonal ice zone in the Southern Ocean, although the important roles for trophic link and carbon cycling were implied by previous snap shots.

We conducted two time-series survey using a drifter array with series of ship based observation around the drifter to reveal the pelagic environment, net primary production (NPP) and export flux when SCM developed, during Southern Ocean cruises of T/RV Umitaka-maru of Tokyo University of Marine Science and Technology. The experiments were conducted off Vincennes Bay (63.5˚S, 110˚E) from January 17-18, 2017 and January 14-19, 2019. A drifter was composed of GPS buoy, 4 sensor frames (attached with CTD, Chl. sensor and PAR sensor), an upward looking ADCP (300 kHz) and sediment traps. Multiple CTD casts were also conducted to determine vertical profiles of physical parameters and to sample waters for measurements of macro-nutrients, chlorophyll *a* (chl. *a*), particulate organic matters (POC and PON) and phytoplankton abundance.

In 2017, SCM was found at 40-50 m depth with lower chl. *a* of less than 0.4 μg L^{-1}. NPP was vertically even ranged 0.4-5.5 mg C m^{-3}. Standing stock of POC highly decreased during 24 hours due to other than export flux, suggesting high microbial activity which was probably enhanced by small haptophytes dominant food web. On the other hand, marked high SCM, reached 2.0 μg L^{-1} was found in 2019. NPP was 4 times higher at 10 m depth than that at SCM depth, and surface (0-40 m depth) integrated NPP was higher in the latter period than the former. The temporal changes in NPP would be relation to increase in large diatom abundance (e.g. *Chaetoceros* spp.). Standing stock of POC was increased in the upper (0-60 m) layer in the latter period, and, at the same time, production-export (P-E) ratio also increased in the lower layer (60-150 m). Temporal changes in temperature at various depth indicates that nutrient supply by vertical mixing was higher in 2019 than in 2017, which would cause differences in biomass and NPP between two years. Increase in standing stock of silicic acid and low δ^{13}C values in POM at SCM in 2019 also supported strong influence of deeper waters. Southern Annular Mode (SAM) from November to January was positive in 2018/19 and negative in 2016/17, respectively. This might cause the difference in pelagic system in two seasons. By the way, diel vertical migration of meso- to macro-zooplankton detected by an ADCP back-scatter suggested strong relationship between SCM and zooplankton communities in 2019.

We found a bottom up regulation of SCM structures. SCM was mainly formed by accumulation of phytoplankton at thermocline, which would play roles as a hot spot of herbivorous and omnivorous feeding of zooplankton community. Further studies focusing on biogeochemical contribution of SCM with physico-chemical conditions relation to SAM are needed for understanding changing ecosystems with

©2021. Japan Geoscience Union. All Right Reserved.

climate changes in the Antarctic seasonal ice zone.

Keywords: Southern Ocean, phytoplankton bloom, seasonal ice zone, sub-surface chlorophyll maximum

©2021. Japan Geoscience Union. All Right Reserved.

Contribution of fecal pellet-like dinoflagellates to the carbon sequestration in the seasonal ice zone of the Southern Ocean

*Ryo Matsuda[1], Jaekyeng Han[1], Shinya Okano[1], Masayoshi Sano[2], Shintaro Takao[3], Ryosuke Makabe[2,4,5], Masato Moteki[4,5], Tsuneo Odate[2,4], Norio Kurosawa[1]

1. Soka University, 2. National Institute of Polar Research, 3. National Institute for Environmental Studies, 4. The Graduate University for Advanced Studies (SOKENDAI), 5. Tokyo University of Marine Science and Technology

Ice edge phytoplankton bloom is an important factor affecting on the food web and the carbon sequestration in the seasonal ice zone of the Southern Ocean. As a sinking particulate organic carbon (POC), zooplankton fecal pellets, marine snow, and phyto-detritus are known as important drivers for export carbon flux from surface layer. To investigate composition of sinking particles and those variability with sea ice melts, sinking particles have been recovered in off Wilkes land since the austral summer in 2016. In the preliminarily observation, we found a large number of fecal pellet (FP)-like dinoflagellates (FLDs) containing phytoplankton in the trap samples at 50 m taken in 2016. The export fluxes in this season would be underestimated to assess FLDs as FP. In the present study, we investigated on FLD's dynamics during the melting of sea ice.

Sediment traps were deployed at 50 m depth (63°52' S, 109°87' E) from December 10, 2016 to January 8, 2017, at 50 m and 80 m (63°29' S, 110°00' E) from January 17-18, 2017, at the 60 m and 150 m (63°29' S, 109°59' E) from January 14 to 19, 2019, at the 60 m and 150 m (64°16' S, 116°58' E) from December 10, 2019 to January 20, 2020. Sinking particle samples were fixed in neutral Lugol's solution (final conc. 5-20%) and stored at 4℃ until analysis. After removing zooplankton swimmers, FLDs and FPs were identified into several groups based on their morphological characteristics. Numbers and lengths of them were counted and measured under the optical microscope. POC fluxes were estimated using numbers and volumes of FLDs and FPs. To reveal the organisms predated by the FLDs, the eukaryotic community structures were analyzed by high throughput sequencing of 18S rRNA gene amplicons (V9 region) using the total DNA of FLDs. Taxonomic affiliations were assigned using PR2 database.

Based on morphological features such as protrusions and grid-like patterns on the cell membrane, FLDs were found in all samples except for short term observation in January 17-18, 2017. As similar cells have been found in the other Antarctic waters, which were tentatively identified to be dinoflagellates, the FLDs was also assumed to be a type of dinoflagellates. FLDs, which were covered by thin membrane were resolved and released ellipsoidal FPs. The POC fluxes of FLDs and its derived ellipsoidal FPs was 5.1 ±5.4 mg C m^{-2} day^{-1} in the spring of 2016 at depth of 50 m and were 1.3 ±0.8 mg C m^{-2} day^{-1} and 0.2 ±0.2 mg C m^{-2} day^{-1} in the summer of 2019 at depths of 60 m and 150 m. These values were almost equal to depths of 60 m and 150 m from the spring of 2019 to the summer of 2020. Those results indicate the melting sea ice season and the dynamics of FLDs are closely, and the FLDs still contribute to the carbon transport even one month after sea ice melting. In the analysis of the eukaryotic community structure of FLDs, 69 ±32% of the total OTU was identified to a dinoflagellate *Gyrodinium rubrum*, which was estimated to be FLDs itself. The remaining OTUs, the contents of the FLDs mainly consisted of other species of *Dinoflagellata* (37 ±25%), *Ochrophyta* (36 ±27%), unidentified Eukaryota (16 ±27%). The eukaryotic communities of the ellipsoidal FPs showed similar structures, suggesting that the ellipsoidal FPs were derived/discharged from FLDs, which is consistent with the microscopic observation as mentioned above. Comparison of the eukaryotic community structure of FLD contents with that in seawater indicated that FLDs were estimated to be an opportunistic feeder.

©2021. Japan Geoscience Union. All Right Reserved.

In this study, dinoflagellates, which are similar to fecal granules were found, and they contributed to carbon sequestration into the depth layers in conjugation with the occurrence of ice bloom. It is essential to further investigate the physiology and ecology of this species to deeply understand the carbon transport in the Southern Ocean.

Keywords: Southern Ocean, carbon sequestration, fecal pellet-like dinoflagellates, sediment trap, Gyrodinium rubrum

©2021. Japan Geoscience Union. All Right Reserved.

[E] Poster | M (Multidisciplinary and Interdisciplinary)：M-IS Intersection

Sun. Jun 6, 2021 5:15 PM - 6:30 PM JST | Sun. Jun 6, 2021 8:15 AM - 9:30 AM UTC | Ch.20_1

[M-IS05] Global climate change driven by the Southern Ocean and the Antarctic Ice Sheet

convener:Osamu Seki(Institute of Low Temperature Science, Hokkaido University), Yoshifumi Nogi(National Institute of Polar Research), Akira Oka(Atmosphere and Ocean Research Institute, The University of Tokyo), Yusuke Suganuma(National institute of Polar Research)

The Southern Ocean and Antarctic ice sheet, which are the giant reservoirs of heat, water, and materials, have a potential to play central roles in long-term global climate change. This system is composed of the following sub-systems; ice shelf which is a place of the interaction of ice sheet and ocean, flowing iceberg, seasonal sea ice zone, Antarctic bottom water which drives the thermohaline circulation, active biological production and Antarctic Circumpolar Current. These sub-systems are interacted with each other and have significant impact on changes in the global environmental system. This session aim to summarize recent observational and simulation studies from various fields relating to the past and present changes in the Antarctic Ice sheet and Southern Ocean, which are essential elements for unraveling the changes in the global climate system. Further, future science plans for understanding of the environmental changes of the Antarctic Cryosphere is also discussed.

[MIS05-P01] Summary of the Year 2020 Activities of the Project on the Interaction of the solid Earth and the Antarctic Ice Sheet

*Yoichi Fukuda[1], Jun Nishijima[2], Takahito Kazama[3], Kazuki Nakamura[4], Koichiro Doi[1], Yusuke Suganuma[1], Jun'ichi Okuno[1], Akito Araya[5], Heitaro Kaneda[6], Yuichi Aoyama[1], Hideki Miura[1] (1.National Institute of Polar Research, 2.Graduate School of Engineering, Kyushu University, 3.Graduate School of Science, Kyoto University, 4.Faculty of Engineering, Nihon University, 5.ERI, University of Tokyo, 6.Faculty of Science and Engineering, Chuo University)

[MIS05-P02] Vertical crustal motion induced by GIA in Lützow-Holm Bay, East Antarctica

*Jun'ichi Okuno[1,2], Akihisa Hattori[2], Takeshige Ishiwa[1], Yoshiya Irie[1], Koichiro Doi[1,2] (1.National Institute of Polar Research, 2.SOKENDAI)

[MIS05-P03] Multibeam bathymetry off East Antarctica: 2010s Japanese observations

*Masakazu Fujii[1,2], Yoshifumi Nogi[1,2] (1.National Institute of Polar Research, 2.SOKENDAI (The Graduate University for Advanced Studies))

[MIS05-P04] Development of Research Instruments for unexplored frontiers in the Southern Ocean and Antarctica

*Yoshifumi Nogi[1], Shigeru Aoki[2], Hiroshi Yoshida[3], Toshihiro Maki[4], Kyoko Okino[5], Yuichi Aoyama[1], Tetsuo Sueyoshi[1], Takeshi Tamura[1], Hirokazu Yamagata[4], Masakazu Fujii[1] (1.National Institute of Polar Research, 2.Institute of Low Temperature Science, Hokkaido University, 3.Japan Agency for Marine-Earth Science and Technology, 4.Institute of Industrial Science, the University of Tokyo, 5.Atmosphere and Ocean Research Institute, the University of Tokyo)

[MIS05-P05] Lake Environmental change since little ice age in Antarctic ice-free area, Skarvsnes, East Antarctica

*Kota Katsuki[1], Yuito Kamada[2], Hanna Wakabayashi[2], Moemi Kawagishi[2], Akira Tsujimoto[6], Yusuke Suganuma[3], Daisuke Shibata[4], Moto Kawamata[5] (1.Estuary Research Center, Shimane University, 2.Interdisciplinary Faculty of Science and Engineering, Shimane University, 3.National Institute of Polar Research, 4.Shimoda Marine Research Center, Tsukuba Univeristy , 5.The Graduate University for Advanced Studies, 6.Faculty of Education, Shimane University)

[MIS05-P06] Application of AI-based classification to planktic foraminifera assemblage in the Southern Ocean

*Hiroki Matsui[1], Takuya Itaki[2], Minoru Ikehara[3] (1.Graduate School of International Resource Sciences, Akita University, 2.Geological Survey of Japan, AIST, 3.Center for Advanced Marine Core Research, Kochi

University)

[MIS05-P07] Lateral migration of a flowstripe on the ice shelf of Shirase Glacier, East Antarctica

*Ken Kondo[1,2], Shin Sugiyama[1] (1.Institute of Low Temperature Science, Hokkaido University, 2.Graduate School of Environmental Science, Hokkaido University)

[MIS05-P08] Vertical fluctuation area of ice shelf due to tidal fluctuations in the Langhovde Glacier using DDInSAR.

*Chiyuki Narama[1], Tsutomu Yamanokuchi[2], Shin Sugiyama[3] (1.Niigata University, Program of Field Research in the Environmental Sciences, 2.RESTEC, 3.Hokkaido University, Institute of Low Temperature Science)

[MIS05-P09] Climatic and atmospheric changes over the last three Terminations from O_2/N_2,$d^{18}O_{atm}$ and CH_4 records of the Dome Fuji ice core, Antarctica

*Ikumi Oyabu[1], Kenji Kawamura[1,2,3], Kyotaro Kitamura[1], Anais Orsi[4], Frederic Parrenin[5], Christo Buizert[6] (1.National Institute of Polar Research, Research Organization of Information and Systems, 2.SOKENDAI (The Graduate University of Advanced Studies), 3.Japan Agency for Marine Science and Technology (JAMSTEC), 4.Laboratory for Sciences of Climate and Environment (LSCE), 5.Institut des Géosciences de l'Environnement (IGE), 6.Oregon State University)

[MIS05-P10] Periods of local melt during the Holocene at Terre Adelie, East Antarctica revealed by beryllium isotope ratios

*Bethany Behrens[1,2], Yusuke Yokoyama[1,2,4,5], Yosuke Miyairi[1], Adam David Sproson[1], Masako Yamane[3] (1.Atmosphere and Ocean Research Institute, University of Tokyo, Japan, 2.Graduate Program on Environmental Science, University of Tokyo, Japan, 3.Institute for Space-Earth Environmental Research, Nagoya University, Japan, 4.Department of Earth and Planetary Science, Graduate School of Science, University of Tokyo, Japan, 5.Japan Agency for Marine-Earth Science and Technology (JAMSTEC), Natsushimacho, Japan)

[MIS05-P11] **The Antarctic ice sheet and Southern Ocean dynamics during the Last Interglacial**

*Mutsumi Iizuka[1], Osamu Seki[1], Masanobu Yamamoto[1], Takuya Itaki[2], Michael E. Weber[3], Maureen E. Raymo[4], Victoria L. Peck[5], Trevor Williams[6], IODP Expedition 382 scientists (1.Hokkaido university, 2.National Institute of Advanced Industrial Science and Technology, 3.University of Bonn, 4.Lamont-Doherty Earth Observatory of Columbia University, 5.British Antarctic Survey, 6.Texas A&M University)

[MIS05-P12] Reconstruction of ice sheet dynamics in Totten Glacier/Aurora Subglacial Basin, East Antarctica during the Last Interglacial

*Osamu Seki[1], Mutsumi Iizuka[1], Keiji Horikawa[1], Tina van De Flierdt[2], Minoru Ikehara[3], Tomohisa Irino[4], Takuya Itaki[5], Saiko Sugisaki[5] (1.Institute of Low Temperature Science, Hokkaido University, 2.Imperial College London, 3.Kochi University, 4.Faculty of Earth and Environmental Science, Hokkado University, 5.National Institute of Advanced Industrial Science and Technology)

[MIS05-P13] Analysis of the abrupt climate change during the last deglaciation

*Ren Shimura[1], Ayako Abe-Ouchi[2] (1.Department of Earth and Planetary Science, The University of Tokyo, 2.Atmosphere and Ocean Research Institute (AORI), University of Tokyo)

[MIS05-P14] Incorporation of grounding line parameterizations in the ice sheet model SICOPOLIS and its application to Antarctica

*Takashi Obase[1], Ayako Abe-Ouchi[1,2], Fuyuki SAITO[3], Ralf Greve[4], Kaho Harada[1] (1.Atmosphere and Ocean Research Institute, The University of Tokyo, 2.National Institute of Polar Research, Japan, 3.Japan Agency for Marine-Earth Science and Technology, 4.Institute of Low Temperature Science, Hokkaido University)

[MIS05-P15] Numerical experiment of Antarctic ice sheet using a coupled ice-sheet/earth rebound model

*Fuyuki SAITO[1], Jun'ichi Okuno[2], Ayako Abe-Ouchi[3] (1.Japan Agency for Marine-Earth Science and Technology, 2.National Institute of Polar Research, 3.Atmosphere and Ocean Research Institute, The University of Tokyo)

[MIS05-P16] A linkage between Antarctic sea-ice extent and ice-shelf basal melting in summer: A circumpolar model study

*Kazuya Kusahara[1] (1.Japan Agency for Marine-Earth Science and Technology)

[MIS05-P17] Ocean circulation in the shelf-slope region of East Antarctica as suggested by satellite radar altimetry

*Kohei Mizobata[1], Mao Mori[1] (1.Tokyo University of Marine Science and Technology)

[MIS05-P18] Quantification of water mass age of Antarctic Bottom Water off Cape Darnley in East Antarctica, using chlorofluorocarbon and sulfur hexafluoride

*Yoshihiko Ohashi[1], Michiyo Yamamoto-Kawai[1], Kazuya Kusahara[2], Kenichi Sasaki[2], Narimi Baba[1], Naoyuki Tamura[1], Natsumi Nojiro[1], Kay I. Ohshima[3] (1.Tokyo University of Marine Science and Technology, 2.Japan Agency for Marine Earth Science and Technology, 3.Institute of Low Temperature Science, Hokkaido University)

[MIS05-P19] Seasonal flux and morphological changes in silicoflagellates in the Indian sector of the Southern Ocean

*Ryota Hayashi[1], Yusuke Okazaki[2], Koshiro Matsuo[2], Takahito Ikenoue[3], Takuya Itaki[4], Minoru Ikehara[5] (1.Department of Earth and Planetary Sciences, School of Science, Kyushu University, 2.Department of Earth and Planetary Sciences, Graduates School of Science, Kyushu University, 3.Marine Ecology Research Institute, 4.Geological Survey of Japan, AIST, 5.Center for Advanced Marine Core Research, Kochi University)

[MIS05-P20] Molecular analysis of individual fecal pellets collected by using gel sediment traps in the Indian sector of the Southern Ocean

*Masayoshi Sano[1], Ryosuke Makabe[1,2,3], Norio Kurosawa[4], Masato Moteki[2,1], Tsuneo Odate[1,3] (1.National Institute of Polar Research, 2.Tokyo University of Marine Science and Technology, 3.The Graduate University for Advanced Studies, 4.Soka University)

Summary of the Year 2020 Activities of the Project on the Interaction of the solid Earth and the Antarctic Ice Sheet

*Yoichi Fukuda[1], Jun Nishijima[2], Takahito Kazama[3], Kazuki Nakamura[4], Koichiro Doi[1], Yusuke Suganuma[1], Jun'ichi Okuno[1], Akito Araya[5], Heitaro Kaneda[6], Yuichi Aoyama[1], Hideki Miura[1]

1. National Institute of Polar Research, 2. Graduate School of Engineering, Kyushu University, 3. Graduate School of Science, Kyoto University, 4. Faculty of Engineering, Nihon University, 5. ERI, University of Tokyo, 6. Faculty of Science and Engineering, Chuo University

A five years research project funded by JSPS (Japan Society for the Promotion of Science) has been started in July 2017. The title of the project is "Giant reservoirs of heat/water/material: Global environmental changes driven by Southern Ocean and Antarctic Ice Sheet" and is aiming to establish a new research area for Antarctic environmental system science. The project consists of 7 research topics, including Antarctic ice sheet and Southern ocean sciences, new observation methodology, modeling and other interdisciplinary topics, and we are involved in the topic, "Interaction of the solid Earth and the Antarctic Ice Sheet".

So far, we have been conducting several field surveys in Antarctica, e.g., absolute gravity measurements, GNSS measurements, lake sediment coring, topographic surveys, geomorphological and other surveys near Japanese Syowa station and other foreign research stations as well. In parallel with these observations, we also have been conducting GIA model analyses, satellite data analyses, and ground data analyses, and these results have been reported at the previous JpGU meetings and other opportunities.

As the fourth year of the project, the year 2020 activities were unfortunately quite limited due to the COVID-19 pandemic situation. All most all field surveys were cancelled, and there were several inconveniences to conduct the research works. In the situation, we mainly focus on the data analyses and the model studies using the data so far obtained. In this presentation, we report the outline of these activities and the results. We also report the observation/research plans in 2021.

This study was partially supported by JSPS KAKENHI Grant No. 17H06321.

Keywords: Glacial Isostatic Adjustment, Ice sheet changes, Sea level rise, East Antarctica

©2021. Japan Geoscience Union. All Right Reserved.

Vertical crustal motion induced by GIA in Lützow-Holm Bay, East Antarctica

*Jun'ichi Okuno[1,2], Akihisa Hattori[2], Takeshige Ishiwa[1], Yoshiya Irie[1], Koichiro Doi[1,2]

1. National Institute of Polar Research, 2. SOKENDAI

Geodetic and geomorphological observations in the Antarctic coastal area generally indicate the uplift movement of the crust associated with the Antarctic Ice Sheet (AIS) change since the Last Glacial Maximum (LGM). This trend is called the glacial isostatic adjustment (GIA), the Earth's viscoelastic response due to the surface load changes. The current crustal motion, which the GNSS observation indicates, includes the elastic component due to the present-day surface mass balance of AIS in addition to the viscoelastic response. To reveal the secular crustal movement associated with the GIA, the separation of both components due to the current mass balance and last deglaciation is essential. Recently geomorphological study in the Lützow-Holm Bay region, East Antarctica, reported that the rapid ice thinning of about 400 m for 3000 years has occurred in the early-to-mid Holocene. This melting may influence the crustal deformation through the viscoelastic response due to rapid ice load change. Therefore, we examine the GIA component due to this melting on the current crustal deformation rate using the numerical modeling. Results indicate that the viscoelastic relaxation due to the abrupt ice thinning depends significantly on the upper mantle viscosity profile. This presentation will discuss the dependence of the AIS retreat history and mantle viscosity structure on the GIA-induced crustal movement based on the numerical experiments.

Keywords: Glacial Isostatic Adjustment, Antarctic Ice Sheet change, Viscosity of the mantle

©2021. Japan Geoscience Union. All Right Reserved.

Multibeam bathymetry off East Antarctica: 2010s Japanese observations

*Masakazu Fujii[1,2], Yoshifumi Nogi[1,2]

1. National Institute of Polar Research, 2. SOKENDAI (The Graduate University for Advanced Studies)

The seafloor covers two-thirds of the solid-earth surface, but most parts have not been explored because of acoustic observation difficulty, especially in polar regions. Significant records of glacial erosion and sedimentation as well as tectonic activities are preserved in the seafloor. Recent developments of ocean and ice sheet numerical modeling need better topographical boundary conditions for precise and high-resolution calculations. Therefore, further observations of acoustic bathymetry are essentially required. Since 2009, multibeam swath bathymetric mapping lead by Japanese scientists has started in the Japanese Antarctic Research Expeditions (JAREs) and several campaign observations. Here, we present preliminary results of these surveys on multibeam bathymetry off East Antarctica to show geomorphological structures from continental margin to ocean basins.

Multibeam bathymetric data were acquired by a 20 kHz frequency SeaBeam3020 system (L3 Communications ELAC Nautik) installed on the Japanese icebreaker Shirase, R/V Hakuho-maru, and R/V Mirai during fifteen expeditions in 2008–2020; KH-07-4, KH-09-5, KH-10-7, KH-16-1, KH-19-1, KH-20-1, JARE 51, JARE 52, JARE 53, JARE 54, JARE 55, JARE 61, MR12-05 leg2, MR12-05 leg3, and MR19-04 Leg3. The Shirase multibeam data was mainly provided by Japan Coast Guard for the utilization of scientific purposes. The sound velocity was corrected by real-time data of the surface water velocity meter, and seawater observations of conductivity, temperature, and depth. The CARIS HIPS and SIPS software (Teledyne CARIS Inc., Ltd., Fredericton, Canada) was used for raw data processing. In the Lü tzow-holm bay, multibeam data were merged with the point echo sounding data using sea ice drill holes acquired during the JARE 9, 14, 15, 18, and 22 (see Hirano et al., 2020; Kusahara et al., in revision).

The obtained bathymetric map covers the continental shelf of Lützow-holm bay (off Shirase glacier), Prytz Bay (off Amelie ice shelf), and off-Totten glacier. Observed landforms are likely associated with grounded ice flow, proglacial and subglacial erosion, and grounding line retreat. The continental slope was systematically investigated off Cape Darnley and off Lützow-holm bay, showing complex submarine channels. It is considered that asymmetric channel signatures are probably related to the spatial variation of sedimentation processes controlled by Antarctic slope current and bottom water. In the Gunnerus ridge, we newly identify volcanic edifices, which show 150-m topographic high and high amplitude of magnetic anomaly. Several series of depressional lineaments were observed in the south of the Southern Kerguelen plateau. Based on these results and descriptions, we would like to discuss the role of seafloor and interaction with ocean and ice sheet from the point of long-term geomorphological perspective.

Keywords: Multibeam bathymetry, Southern Ocean, East Antarctica

©2021. Japan Geoscience Union. All Right Reserved.

Development of Research Instruments for unexplored frontiers in the Southern Ocean and Antarctica

*Yoshifumi Nogi[1], Shigeru Aoki[2], Hiroshi Yoshida[3], Toshihiro Maki[4], Kyoko Okino[5], Yuichi Aoyama[1], Tetsuo Sueyoshi[1], Takeshi Tamura[1], Hirokazu Yamagata[4], Masakazu Fujii[1]

1. National Institute of Polar Research, 2. Institute of Low Temperature Science, Hokkaido University, 3. Japan Agency for Marine-Earth Science and Technology, 4. Institute of Industrial Science, the University of Tokyo, 5. Atmosphere and Ocean Research Institute, the University of Tokyo

The Antarctic ice sheet holds 90% of ice, equivalent to approximately 70 m height of sea level. On the other hand, the Southern Ocean produces the densest seawater, called the Antarctic bottom water, which drives ocean circulation. The Antarctic ice sheet and the Southern Ocean are the most significant components that control global climate and sea level changes. However, the field observation data around ice shelf and sea ice areas is very poor because of the observation difficulties. The acquisition of the field observation data in the unexplored frontiers such as under ice shelf is vital to understand the interactions between the Southern Ocean and the Antarctic ice sheet.

Unmanned research instruments and vehicles, especially underwater robots, namely ROV (Remotely Operated Vehicle) and AUV (Autonomous Underwater Vehicle), are required to acquire the field observation data in the unexplored area. The AUV is developing to obtain the oceanographical data in the border region between the ocean and the ice sheet. The ROV to assist the AUV operation and the acquisition of the oceanographic data is also customizing. The application of unmanned research vehicles and instruments is extended to the outcrops and ice sheet area in Antarctica. The present status of the observation instruments' development in the Southern Ocean and Antarctica is introduced, and the future application is also discussed.

Keywords: Southern Ocean, Antarctic ice sheet, unmanned research instrument, sea ice

©2021. Japan Geoscience Union. All Right Reserved.

Lake Environmental change since little ice age in Antarctic ice-free area, Skarvsnes, East Antarctica

*Kota Katsuki[1], Yuito Kamada[2], Hanna Wakabayashi[2], Moemi Kawagishi[2], Akira Tsujimoto[6], Yusuke Suganuma[3], Daisuke Shibata[4], Moto Kawamata[5]

1. Estuary Research Center, Shimane University, 2. Interdisciplinary Faculty of Science and Engineering, Shimane University, 3. National Institute of Polar Research, 4. Shimoda Marine Research Center, Tsukuba Univeristy , 5. The Graduate University for Advanced Studies, 6. Faculty of Education, Shimane University

Recently, there has been concern over the rapid melting of the Antarctic ice sheet due to increases in air and sea temperatures. Then, researches about instrumental and satellite ice sheet and ocean observations have been eagerly studied in recent. Furthermore, geological research for understanding the ice sheet melting history since the last glacial maximum has also been actively. On the other hand, unfortunately, there has been little research on the history of ice sheet changes and its effect on Antarctic lake ecosystems over the past few hundred years, when the effects of anthropogenic warming have become more pronounced. Therefore, we investigate the changes of Antarctic lake ecosystem since the little ice age based on the lowland and glacial lakes which may have the relatively high sedimentation rate. It is well used diatom remains for reconstructing the paleo lake ecosystem and environment. In Antarctic region, diatom distributions and ecology were reported from the fresh water and saline lake in ice free areas and outer sea, however it was rare reports for coast and gulf. In this study, the diatom distributions along the coast of Gulfs of Osen and Torinosu in Skalvsnes were investigated at first, then the diatom remains in sediment of the small lakes along the Gulf of Osen was analyzed. Skalvsnes is the one of the ice free area along the Soya Coast in East Antarctica. Lake Koike is the small fresh water lake, and fresh water diatom taxa has been dominated in the sediment. The number of diatom valves in the sediment has been highly fluctuated, and the peaks of diatom valves occur when the marine diatom increased. It probably means that the austral summer high tide event has been occurred in cyclic.

Keywords: Antactica, Ice free area, Diatom, Paleoenvironment

©2021. Japan Geoscience Union. All Right Reserved.

Application of AI-based classification to planktic foraminifera assemblage in the Southern Ocean

*Hiroki Matsui[1], Takuya Itaki[2], Minoru Ikehara[3]

1. Graduate School of International Resource Sciences, Akita University, 2. Geological Survey of Japan, AIST, 3. Center for Advanced Marine Core Research, Kochi University

Microfossils provide valuable information on past climate changes, although counting and picking of microfossils necessitate a large amount of effort and time. Recent development of a system for automated image collection and AI-based classification of microfossils thus can significantly contribute biostratigraphy and paleoceanography. Because Southern Ocean (SO) planktic foraminifera assemblage is characterized by generally low diversity (i.e., small number of species), it is suitable to develop AI-based classification. We utilize miCRAD (microfossil Classification and Rapid Accumulation Device) system to differentiate planktic foraminifera Globigerina bulloides, Neogloboquadrina pachyderma, other foraminifera species, and all other particles of a marine core in the SO. We report preliminary results of classification accuracy to the above four categories (81.3% on average). We discuss further improvements of classification model and potential application to SO paleoceanography.

Keywords: Automatic classification, Planktic foraminifera, Southern Ocean

©2021. Japan Geoscience Union. All Right Reserved.

Lateral migration of a flowstripe on the ice shelf of Shirase Glacier, East Antarctica

*Ken Kondo[1,2], Shin Sugiyama[1]

1. Institute of Low Temperature Science, Hokkaido University, 2. Graduate School of Environmental Science, Hokkaido University

The Antarctic ice sheet discharges ice into the ocean through outlet glaciers. On the surface of the outlet glaciers, surface structures prallel to flow direction are frequently observed and referred to "flowstripes". The flowstripes form in (1) a confluence area of tributaries, (2) lateral shear margins and (3) where glaciers flow over undurated bedrock (Glasser and Gudmundsson, 2012), suggesting the relevance with a glacier flow regime. Thus, studying flowstripes gives insight into the glacier dynamics. Here, we report recent dynamic behaviour of a flowstripe on Shirase Glacier in Antarctica.

Shirase Glacier is one of the fastest outlet glaciers in East Antarctica (Fig. 1). Ice flow converges from a vast accumulation basin into a ~10 km wide trough before feeding into the ocean, reaching a speed of 2200 m a^{-1} near the grounding line. We found on satellite imagery an intriguing lateral migration of a flowstripe near the margin of the ice shelf. The flowstripe located 4 km from the western ice margin began westward migration in 2013 and merged with another flowstripe generated at the confluence with a tributary (Fig. 2). The migration of the flowstripe was associated with a change in the ice flow pattern. Ice flow velocity across the ice shelf 10 km downstream from the grounding line showed an acceleration of a section 3–5 km from the western margin, where the flowstripe was observed (Fig. 3). Ice speed of the section increased from 2050 to 2400 m a^{-1} during the migration of the flowstripe in 2013–2018. We propose two possible drivers of this lateral migratin of the flowstripe as: (1) detachment of basal ice from underlying bedrock and (2) changes in the ice rheology. Numerical experiments with an ice flow model is planned to investigate the mechanism of the observed changes in the ice shelf dynamics.

(Figures are included in the PDF version of this abstract.)

Reference:
Glasser, N. F. and Gudmundsson, G. H. (2012), Longitudinal surface structures (flowstripes) on Antarctic glaciers, *The Cryosphere*, **6**, 383–391.

Keywords: Antarctica, Ice sheet, Glacier

©2021. Japan Geoscience Union. All Right Reserved.

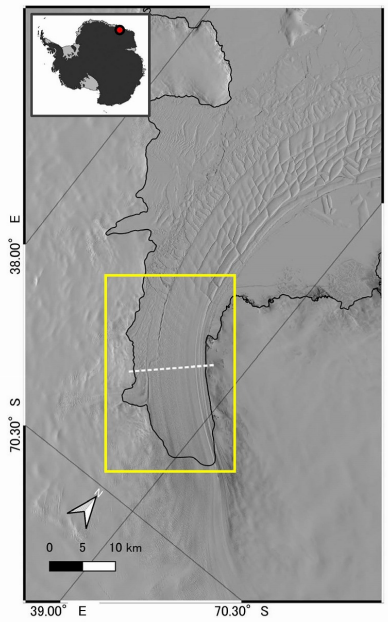


Figure 1. Landsat 8 OLI image on 26 November 2013 showing Shirase Glacier, East Antarctica. Dashed line shows the profile used in the velocity plot in Figure 3. A box indicates the area shown in Figure 2.

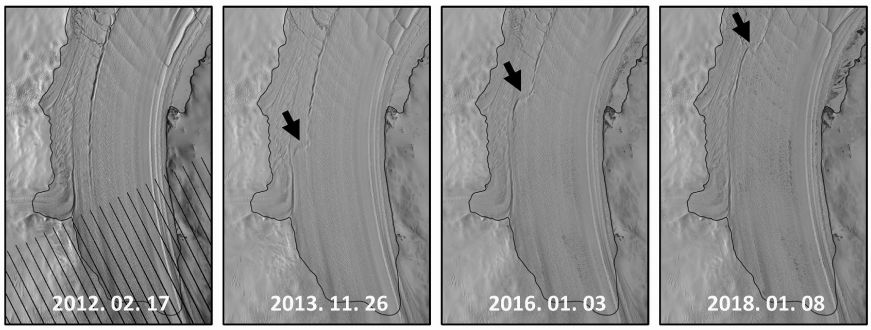


Figure 2. Landsat 7/8 imagery showing the migration of the flowstripe in 2013-2018 (black arrows).

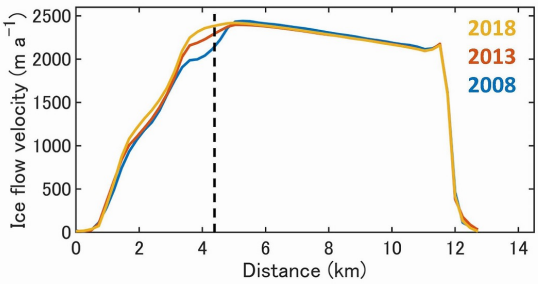


Figure 3. Annual ice flow velocity along the cross-sectional profile shown in Figure 1 (dashed line). Dashed line shows the location of the flowstripe before 2013.

©2021. Japan Geoscience Union. All Right Reserved.

Vertical fluctuation area of ice shelf due to tidal fluctuations in the Langhovde Glacier using DDInSAR.

*Chiyuki Narama[1], Tsutomu Yamanokuchi[2], Shin Sugiyama[3]

1. Niigata University, Program of Field Research in the Environmental Sciences, 2. RESTEC, 3. Hokkaido University, Institute of Low Temperature Science

The USAP and SCAR data show grounding line data in the East Antarctica based on optical images and Interferometric SAR (InSAR) data of ERS-1/2 data taken around 1995-1996 (Konrad et al., 2018). However, the accuracy of the positions is not perfect, because the grounding line may change on the tidal condition. In this study, we tried to detect a vertical fluctuation area of ice shelf in response to tidal fluctuations in the Langhovde Glacier, located on eastern part of Lützow-Holm Bay in East Antarctica based on satellite data. We used Double Differential InSAR (DDInSAR; Doi et al., 2011), analysis method in this study. This method can extract phase difference caused by tidal movement for detecting a grounding line by removal of the phases caused by the glacier flow and topography.

Keywords: ice shelf, tidal fluctuations , DDInSAR, grounding line

©2021. Japan Geoscience Union. All Right Reserved.

Climatic and atmospheric changes over the last three Terminations from O_2/N_2,$d^{18}O_{atm}$ and CH_4 records of the Dome Fuji ice core, Antarctica

*Ikumi Oyabu[1], Kenji Kawamura[1,2,3], Kyotaro Kitamura[1], Anais Orsi[4], Frederic Parrenin[5], Christo Buizert[6]

1. National Institute of Polar Research, Research Organization of Information and Systems, 2. SOKENDAI (The Graduate University of Advanced Studies), 3. Japan Agency for Marine Science and Technology (JAMSTEC), 4. Laboratory for Sciences of Climate and Environment (LSCE), 5. Institut des Géosciences de l' Environnement (IGE), 6. Oregon State University

Understanding the mechanisms of glacial terminations and associated global climatic changes is an important area of paleoclimatic research, because the terminations involve various interactions between the atmosphere, ocean, ice, and solid earth over multiple timescales. However, the climatic variations for the older terminations than the last one are relatively poorly reconstructed because of the limitations of available paleoclimatic proxies, time resolution, and chronological controls. Here, we revise the Dome Fuji chronology using newly measured O_2/N_2 ratio (a proxy of local summer insolation) combined with densification modeling and ice flow modeling, and discuss the timing of climatic and atmospheric variations including abrupt changes for Termination I, II and III, based on the records of CH_4 concentrations and $\delta^{18}O$ of O_2 in the Dome Fuji ice core.

Keywords: ice core, degraciation, Antarctica

©2021. Japan Geoscience Union. All Right Reserved.

Periods of local melt during the Holocene at Terre Adelie, East Antarctica revealed by beryllium isotope ratios

*Bethany Behrens[1,2], Yusuke Yokoyama[1,2,4,5], Yosuke Miyairi[1], Adam David Sproson[1], Masako Yamane[3]

1. Atmosphere and Ocean Research Institute, University of Tokyo, Japan, 2. Graduate Program on Environmental Science, University of Tokyo, Japan, 3. Institute for Space-Earth Environmental Research, Nagoya University, Japan, 4. Department of Earth and Planetary Science, Graduate School of Science, University of Tokyo, Japan, 5. Japan Agency for Marine-Earth Science and Technology (JAMSTEC), Natsushimacho, Japan

The West Antarctic Ice Sheet (WAIS) and East Antarctic Ice Sheet (EAIS) contain an amount of ice equivalent to 3-5 m and 53 m sea level rise, respectively (1). The WAIS, as a largely marine-based ice sheet, is susceptible to changes in ocean temperatures and prone to retreat. Recent research has revealed that areas of the EAIS situated below sea level are also very sensitive to atmospheric and oceanic temperature changes and vulnerable to retreat (2, 3). The two largest subglacial basins in East Antarctica, the Wilkes and Aurora basins, hold a total ice mass equivalent to 28 m sea level rise (4), demonstrating that even a partial collapse of the EAIS would have a major effect on global sea level.

While we know the general timing of post-LGM glacial retreat around Antarctica, there is scarce data on specific locations with detailed, high-resolution records of ice sheet dynamics during the Holocene. Here we present reactive beryllium-10 and beryllium-9 ratio ($^{10}Be/^{9}Be_{reac}$) analysis of a marine sediment core from the Adélie Basin, located on the continental shelf offshore the Wilkes Basin. The sediment record covers the most recent period of major Holocene ice sheet retreat, sea level rise, and increased atmospheric CO_2 since the Last Glacial Maximum ice sheet retreat (5). The beryllium isotope data suggest oceanic or climatic changes occurred at ca. 9.9 ka and from ca. 4 ka BP. From prior research, we can conclude our high meteoric ^{10}Be values at 9.9 ka BP are attributed to an open marine environment created by the retreat of grounded ice along with an increased influx of meltwater (6-8). The increasing concentration of reactive ^{10}Be values starting from ~4 ka indicates a change in regime, possibly linked to changes in climate.

(1) Wilson DJ, Bertram RA, Needham EF, van de Flierdt T, Welsh KJ, McKay RM, et al. Nature. 2018;561(7723):383-6.

(2) Hansen MA, Passchier S. Geo-Marine Letters. 2017;37(3):207-13.

(3) DeConto RM, Pollard D. Nature. 2016;531:591.

(4) Shen Q, Wang H, Shum C, Jiang L, Hsu HT, Dong J. Scientific reports. 2018;8(1):4477.

(5) Yokoyama Y, Esat TM, Thompson WG, Thomas AL, Webster JM, Miyairi Y, et al. Nature. 2018;559(7715):603-7.

©2021. Japan Geoscience Union. All Right Reserved.

(6) Yokoyama Y, Anderson JB, Yamane M, Simkins LM, Miyairi Y, Yamazaki T, et al. Proceedings of the National Academy of Sciences. 2016;113(9):2354.

(7) Valletta RD, Willenbring JK, Passchier S, Elmi C. Paleoceanography and Paleoclimatology. 2018;33(9):934-44.

(8) Behrens B, Miyairi Y, Sproson AD, Yamane M, Yokoyama Y. Journal of Quaternary Science. 2019;34(8):603-8.

Keywords: Wilkes Subglacial Basin, East Antarctica, Beryllium isotopes, Holocene, Glacial retreat

©2021. Japan Geoscience Union. All Right Reserved.

The Antarctic ice sheet and Southern Ocean dynamics during the Last Interglacial

*Mutsumi Iizuka[1], Osamu Seki[1], Masanobu Yamamoto[1], Takuya Itaki[2], Michael E. Weber[3], Maureen E. Raymo[4], Victoria L. Peck[5], Trevor Williams[6], IODP Expedition 382 scientists

1. Hokkaido university, 2. National Institute of Advanced Industrial Science and Technology, 3. University of Bonn, 4. Lamont-Doherty Earth Observatory of Columbia University, 5. British Antarctic Survey, 6. Texas A&M University

Melting of the Antarctic ice sheet (AIS) are very likely to lead to sea level rise in future warming scenarios. Recent observations indicate that AIS mass loss is mainly caused by oceanic forcing (e.g., ocean warming and intrusion of warm Circumpolar Deep Water (CDW) onto the continental shelf of Antarctica). Thus, it is crucial to better understand ocean-ice-sheet interactions to improve projections of sea level change in the future. A better understanding of AIS and Southern Ocean (SO) dynamics during the last interglacial (LIG: 130–115 ka), during which global mean surface air temperatures are estimated to be +1ºC warmer than the preindustrial level, provides useful insight into future sea level rise. Previous studies suggested significant AIS mass loss during the LIG. However, AIS and SO dynamics during the LIG are poorly understood due to a lack of high-resolution paleoclimate records in the LIG. Here we reconstruct variability of sea surface temperature (SST), meltwater discharge, and influence of CDW with high temporal resolution (170 years) during the LIG based on analyses of geochemical and micropaleontological proxies in the marine sediment core U1536 collected from the Scotia Sea in IODP Expedition 382. Our preliminary results suggest that during the LIG, significant meltwater events are resolvable when SST and contribution of CDW mass to the other water masses increased, suggesting a causal link between oceanic change and AIS retreat. Furthermore, the timing of individual AIS mass loss events are consistent with the reported reconstruction of sea level variability during the LIG, suggesting a substantial contribution of AIS mass loss to the sea level rise (6–9 m) in the LIG.

Keywords: Antarctic ice sheet , Southern Ocean, Circumpolar Deep Water, Last Interglacial

©2021. Japan Geoscience Union. All Right Reserved.

Reconstruction of ice sheet dynamics in Totten Glacier/Aurora Subglacial Basin, East Antarctica during the Last Interglacial

*Osamu Seki[1], Mutsumi Iizuka[1], Keiji Horikawa[1], Tina van De Flierdt[2], Minoru Ikehara[3], Tomohisa Irino[4], Takuya Itaki[5], Saiko Sugisaki[5]

1. Institute of Low Temperature Science, Hokkaido University, 2. Imperial College London, 3. Kochi University, 4. Faculty of Earth and Environmental Science, Hokkado University, 5. National Institute of Advanced Industrial Science and Technology

The Totten Glacier is one of the largest glaciers in East Antarctica. Recent observations suggest that the Totten Glacier is vulnerable to ocean warming. Ice mass loss in the Aurora Subglacial Basin, which locates behind and connects to Totten Glacier, could potentially cause a 3.5 m rise in global sea level. However, the sensitivity of the glacier-ice sheet system to ongoing global warming remains uncertain. A better understanding of Antarctic ice sheet dynamics in the warm past provides useful insights into projecting ice mass loss in the future. The Last Interglacial (LIG: 115-130 ka), which is characterized by temperatures 1 ºC warmer than the current interglacial climate, is often considered as a possible analogue for the future warm climate. Previous studies suggest significant ice mass loss in West Antarctica and the Wilkes Subglacial Basin during the LIG. However, ice sheet dynamics in the Aurora Subglacial Basin during the LIG remain an enigma. In this study, we attempt to reconstruct ice sheet dynamics in the Aurora Subglacial Basin during the LIG based on analysis of geochemical provenance proxies in two marine sediment cores, PC404 and PC504, collected off East Antarctica. Our data, together with Antarctic ice core isotope records in EDC and Vostok, suggest that the ice extent in the Aurora Subglacial Basin fluctuated dynamically during the LIG.

Keywords: Antarctic ice sheet, Aurora Subglacial Basin, Totten Glacier, Last Interglacial

©2021. Japan Geoscience Union. All Right Reserved.

Analysis of the abrupt climate change during the last deglaciation

*Ren Shimura[1], Ayako Abe-Ouchi[2]

1. Department of Earth and Planetary Science, The University of Tokyo, 2. Atmosphere and Ocean Research Institute (AORI), University of Tokyo

Abrupt climate changes in the deglaciation share many features with glacial abrupt climate changes, i.e. DO events. However, we do not know much about how global temperature changes in response to this, the exact changes in the interior of the ocean, or similarities between the deglaciation and DO events. In this study, we compared the experimental results of the last deglaciation and the DO oscillations using MIROC-4m, an atmosphere-ocean general circulation model (AOGCM), focusing on changes in the air surface temperature, ocean temperature and ocean salinity. By comparing model results to proxy records, we showed the challenges of interpreting model and proxy data, and by comparing the last deglaciation and the DO oscillations, we discussed the ocean-wide feedbacks, including those of the deep ocean.
As a result, a comparison of the model results and proxy data for the last deglacial period shows that the warming during the last deglaciation was moderate in the Southern Hemisphere but rapid in the Northern Hemisphere. The model also shows that the tropics warm gradually at first, like Antarctica, and then warm rapidly when the northern hemisphere warms rapidly. A comparison of mid-glacial and deglacial experiments shows that the rapid climate change during the deglaciation has much in common with those of the DO oscillations, specifically, in terms of how the temperature and ocean density change. In both experiments, the temperature changes in the sub-surface ocean due to the AMOC mode change spread eastward from the Atlantic Ocean to the Pacific Ocean via the Southern Ocean. Also, while the AMOC was in the same mode, the density change at the bottom ocean, which is caused by changes in sea ice formation over the Southern Ocean proceeded to affect the vertical density gradient in the Atlantic Ocean.
It is thought that the behavior of the Southern Ocean and the deep ocean is deeply involved not only in DO oscillation with a period of several thousand years but also in the AMOC oscillation during deglaciation. This suggests that the rapid climate change during deglaciation is part of the rapid climate change during glaciation and that similar mechanisms are at work.

Keywords: AMOC, deglaciation, Glacial climate, AOGCM

©2021. Japan Geoscience Union. All Right Reserved.

Incorporation of grounding line parameterizations in the ice sheet model SICOPOLIS and its application to Antarctica

*Takashi Obase[1], Ayako Abe-Ouchi[1,2], Fuyuki SAITO[3], Ralf Greve[4], Kaho Harada[1]

1. Atmosphere and Ocean Research Institute, The University of Tokyo, 2. National Institute of Polar Research, Japan, 3. Japan Agency for Marine-Earth Science and Technology, 4. Institute of Low Temperature Science, Hokkaido University

The flow of the Antarctic ice sheet in large-scale ice sheet modeling is often represented by the shallow ice approximation (SIA) , the shallow shelf approximation (SSA) or combinations of them. However, under a coarse horizontal resolution (O ~10 km), which is necessary for simulations of the paleoclimate and long-term future, a combined SIA/SSA model has limited performance in simulating the migration of grounding lines. In this study, a sub-grid grounding line parameterization is incorporated in the 3-dimensional ice sheet model SICOPOLIS to improve the representation of grounding line dynamics. We employed the grounding line parameterization by Schoof (2007), which computes the ice velocity based on the sub-grid horizontal ice flux across the grounding line.

First, we conduct the MISMIP2 experiments, which are hysteresis experiments under idealized bedrock topography and parameters to check the fundamental performance of grounding line migrations[GRG1] . The simulated grounding line positions exhibited hysteresis behavior to perturbations, which is largely in agreement with other ice sheet models.

Next, we conduct equilibrium experiments under a present-day climate condition with freely evolving ice sheet topography to examine the performance of the present-day simulation. The results indicate that the grounding line parameterization tends to increase the volume of the Antarctic ice sheet in total, but the simulated advances/retreats of the grounding line positions depend on the regions. We also conduct idealized atmospheric and oceanic warming experiments to examine the effect of grounding line parameterizations on the speed and extent of the retreat of the Antarctic ice sheet. The results suggest that the difference in the formulations in basal sliding could induce greater difference in the volume change of Antarctic ice sheet than the grounding line parameterization, but further analysis and careful treatments of the uncertain parameters are needed.

©2021. Japan Geoscience Union. All Right Reserved.

Numerical experiment of Antarctic ice sheet using a coupled ice-sheet/earth rebound model

*Fuyuki SAITO[1], Jun'ichi Okuno[2], Ayako Abe-Ouchi[3]

1. Japan Agency for Marine-Earth Science and Technology, 2. National Institute of Polar Research, 3. Atmosphere and Ocean Research Institute, The University of Tokyo

Feedback between changes in the ice-sheet and the earth's isostatic rebound is considered to be a crucial process for long-term evolution of the past ice-sheets in glacial cycles, and for short-term instability of marine ice sheets systems. We have been developing a coupled ice-sheet/earth rebound model: the Earth rebound model is based on a self-gravitating visco-elastic multi-layer model developed by Okuno and Nakada (2001), while the ice-sheet model is IcIES (Abe-Ouchi et al. 2013, Saito and Abe-Ouchi 2010, Saito et al 2016). We will report some basic sensitivity studies using the coupled model on Antarctic ice sheet, e.g., for technical aspects such as model resolution. The results are compared with the previous IcIES results coupled with a simple isostatic model (i.e., a local lithosphere/relaxing asthenosphere) which is controlled by two parameters (the mantle density and the time scale of isostatic response). Difference in model sensitivities to changes in environment will be reported.

Keywords: ice-sheets, isostatic rebounds

©2021. Japan Geoscience Union. All Right Reserved.

A linkage between Antarctic sea-ice extent and ice-shelf basal melting in summer: A circumpolar model study

*Kazuya Kusahara[1]

1. Japan Agency for Marine-Earth Science and Technology

Recent observations indicate that two cryospheric components, namely the Antarctic sea ice and ice shelf over the Southern Ocean, have been changing over the decades. Here we analyze results from an ocean–sea ice–ice shelf model to examine the relationship between the Antarctic sea-ice extent and ice-shelf basal melting. The model reproduces seasonal and interannual variability in the Antarctic sea-ice extent and indicates that summertime ice-shelf basal melting is closely anti-correlated with the sea-ice extent anomaly. For example, the unprecedented minimum of the Antarctic sea-ice extent in the 2016 spring was accompanied by a substantial increase in the Antarctic ice-shelf melting in the model. Detailed analysis of Antarctic coastal water masses flowing into the ice-shelf cavities reveals a possible physical link in the strong anti-correlation. This study suggests that the Antarctic sea-ice extent in summer can be a proxy for Antarctic coastal water masses and subsequent ice-shelf melting.

Keywords: ice shelf-ocean interaction, sea ice

©2021. Japan Geoscience Union. All Right Reserved.

Ocean circulation in the shelf-slope region of East Antarctica as suggested by satellite radar altimetry

*Kohei Mizobata[1], Mao Mori[1]

1. Tokyo University of Marine Science and Technology

The mass loss of ice shelf/sheet due to intrusion of warm Circumpolar Deep Water (CDW) has been pointed out. CDW is basically observed in the deep basin area, so that the transport mechanisms of CDW from deep basin to shelf is needed to be elucidated for understanding the future fate of ice shelf/sheet of Antarctica. However, because of the presence of sea ice, it is difficult to describe the spatio-temporal variability of ocean circulation using only hydrographic observations. The Dynamic Ocean Topography (DOT) derived from the satellite altimeters is another method to reveal the ocean circulation even in the sea ice area. Our previous DOT data showed four clockwise eddies, which contributes to poleward CDW transport, off the Sabrina coast. Here, we introduce newly developed DOT using the retrievals of satellite radar altimeters, the CryoSat-2/SIRAL, Sentinel-3A/SRAL, Sentinel-3B/SRAL, Jason-3/Posidon-3B, and Saral/AltiKa. Our products revealed the existence of the clockwise circulation at the continental slope area. In particular, stationary clockwise circulation was observed offshore of ice sheet/shelf such as Shirase Glacier, Amery Ice Shelf, and Totten Ice Shelf, where basal melting due to CDW has been suggested in recent years. Moreover, the increased number of radar altimeter retrievals made it possible to visualize the ocean circulation in the shelf-slope region that were unknown in the previous products. A clockwise circulation was also observed in the continental shelf region, and it was frequently coupled with the aforementioned circulation. In other words, this coupled circulation between the slope and shelf regions suggests that CDW in the ocean basin is efficiently transported to the continental shelf of East Antarctica, where the ACC is relatively far from the slope than in West Antarctica. On the other hand, a counterclockwise circulation was observed in the shallow region adjacent Cape Poinsett near Totten Glacier, where sea ice is present all year round. It is implied that this circulation may be preventing the sea ice flush out.

Keywords: Dynamic Ocean Topography, Ocean Circulation, Circumpolar Deep Water, Southern Ocean

©2021. Japan Geoscience Union. All Right Reserved.

Quantification of water mass age of Antarctic Bottom Water off Cape Darnley in East Antarctica, using chlorofluorocarbon and sulfur hexafluoride

*Yoshihiko Ohashi[1], Michiyo Yamamoto-Kawai[1], Kazuya Kusahara[2], Kenichi Sasaki[2], Narimi Baba[1], Naoyuki Tamura[1], Natsumi Nojiro[1], Kay I. Ohshima[3]

1. Tokyo University of Marine Science and Technology, 2. Japan Agency for Marine Earth Science and Technology, 3. Institute of Low Temperature Science, Hokkaido University

Antarctic Bottom Water (AABW), which is formed by the mixing of Dense Shelf Water (DSW) and Circumpolar Deep Water (CDW), spreads throughout the global ocean. This process has a crucial role in transporting heat, freshwater, and carbon from the continental shelf to the deep ocean. Off Cape Darnley (CD) in East Antarctica, a newly formed AABW was found (Ohshima et al., 2013). However, the spreading of AABW and its time scale off CD have not been clearly understood. To quantitatively understand its time scale, it is effective to use transient tracers of chlorofluorocarbon (CFC) and sulfur hexafluoride (SF_6). We carried out CTD observation and water sampling in the Indian sector of the Southern Ocean, including off CD, in the summers of 2019 and 2020. CFC-12 and SF_6 of the samples were measured by an analytical system based on Bullister and Wisegarver (2008). Additional data observed in 2013 (MR12-05) and 2016 (WHP I08S) were obtained from the Clivar and Carbon Hydrographic Data Office. A numerical experiment of transient tracers was also performed using a coupled ocean-sea ice-ice shelf model.

The model results showed that transient tracer concentrations of AABW can be explained by a two-endmember mixing of DSW formed in the previous winter and very old CDW (almost no CFC/SF_6). Based on the model results, the water mass age (the elapsed time since the water is in contact with the atmosphere) of AABW was quantified from observed concentrations of CFC/SF_6. Along the western canyons of CD and ~3500 m isobath near the bottom, the water mass age of AABW (~0–3 years) was younger than those on the eastern side and in the western offshore (~5–15 years). This distribution of new AABW is roughly consistent with the suggested pathway of new CD Bottom Water in the previous study. The old AABW on the eastern side and in the western offshore of CD reflect the effects of AABW inflow through the Princess Elizabeth Trough and from the Weddell Sea, respectively. Transient tracer measurements provide quantitative information on the time scale of AABW spreading.

Keywords: Antarctic Bottom Water , Transient tracer, Water mass age

©2021. Japan Geoscience Union. All Right Reserved.

Seasonal flux and morphological changes in silicoflagellates in the Indian sector of the Southern Ocean

*Ryota Hayashi[1], Yusuke Okazaki[2], Koshiro Matsuo[2], Takahito Ikenoue[3], Takuya Itaki[4], Minoru Ikehara[5]

1. Department of Earth and Planetary Sciences, School of Science, Kyushu University, 2. Department of Earth and Planetary Sciences, Graduates School of Science, Kyushu University, 3. Marine Ecology Research Institute, 4. Geological Survey of Japan, AIST, 5. Center for Advanced Marine Core Research, Kochi University

Seasonal silicoflagellate flux change was investigated in the Indian sector of the Southern Ocean. Time-series sediment trap was deployed at 3400m water depth of Station ECR-1 (55˚S, 45˚E, 4020m seafloor depth) near the Conrad Rise located in the southwest Indian sector of the Southern Ocean from February 2016 to February 2017. *Stephanocha speculum* was the dominant silicoflagellate species occupying greater than 95.4%. The silicoflagellate flux pattern corresponded to the biogenic opal mass flux exhibiting pronounced austral summer peaks. In the Southern Ocean, diatoms are the main contributor to the biogenic opal. However, onset of the silicoflagellate flux maximum in summer precede the diatoms. Detailed morphological investigation was performed on *S. speculum* skeletons. In austral summer, *S. speculum* var. *bispicata* with multiple apical pike was the most abundant morphotype. On the other hand, *S. speculum speculum* without apical pike was the abundant morphotype other seasons when flluxes of both silicoflagellates and biogenic opal were relatively low. This suggests that the number of the apical pikes have decreaced during diatom bloom. During the diatom bloom, diatoms consume most of dissolved silicic acid in the euphotic layer of the Southern Ocean. Earlier silicoflagellate summer peak may be due to silicic acid availability regulated by the subsequent diatom bloom, leading to the fine morphological changes in silicoflagellate skeletons.

Keywords: Southern Ocean, silicoflagellate, sediment trap

©2021. Japan Geoscience Union. All Right Reserved.

Molecular analysis of individual fecal pellets collected by using gel sediment traps in the Indian sector of the Southern Ocean

*Masayoshi Sano[1], Ryosuke Makabe[1,2,3], Norio Kurosawa[4], Masato Moteki[2,1], Tsuneo Odate[1,3]

1. National Institute of Polar Research, 2. Tokyo University of Marine Science and Technology, 3. The Graduate University for Advanced Studies, 4. Soka University

Sinking particles, an important contributor to biological carbon pump, consist of various types of particles. Export efficiencies and sinking speeds are different among types of sinking particles, for example, phytodetritus and fecal pellets. In the Southern Ocean, the contribution of fecal pellets to carbon flux is expected to be high because of the high abundance of the large zooplankton, such as salps and krills, which excrete fast-sinking large fecal pellets. However, in the Indian sector of the Southern Ocean, the krill-independent ecosystem is expected to be important. It is difficult to identify producer of fecal pellets based on morphological information, and fecal pellets contains large amounts of amorphous materials which are difficult to be identified by microscopic analysis. Little is yet known of the sinking process of fecal pellets. In this study, we applied molecular method to individual fecal pellets collected by gel sediment traps for estimating fecal pellet producers and the sinking process of fecal pellets.
Fecal pellet samples were collected from a station (63.5˚S, 110˚E) during the Southern Ocean cruise of the T/V *Umitaka Maru* of Tokyo University of Marine Science and Technology. The trap system consisted of gel-filled sediment traps deployed at 50, 200 and 500 m depths. Traps were left to drift for 24h (17 January 2019 to 18 January 2019). After recovery, each gel was preserved at <-60˚C until analysis. DNA was extracted from individual fecal pellets picked up from gel under a stereo microscope. Sizes of the fecal pellets were varied (<50 μm to 500 μm diameter). To assess the eukaryotic community structure of the fecal pellets, the 18S rRNA gene V9 region was amplified by using primers 1389F and 1510R and the amplicons were sequenced by high throughput sequencer. Bioinformatics analysis of the sequence data were performed using mothur (Schloss et al. 2009). For estimating zooplankton community structures in this station, VMPS and MOHT nets were towed. Collected zooplankton samples were sorted and counted under a stereo microscope.
Eukaryotic community composition of the fecal pellets in 50 m and 200 m mainly consist of Stramenopiles, Metazoa and Dinophyta. This result indicated that the fecal pellets were excreted by particle feeders. Metazoan community composition of the fecal pellets in 50 m and 200 m mainly consist of copepods (>90%) and were homogenized among all types of fecal pellets which were excreted by various species. Thus, it is considered that the fecal pellets were repackaged several times even in 50 m depth which was just under the Chlorophyll *a* maximum (40 m depth) and did not sink directly from 50 m to 200 m. Metazoan community composition also showed that potential producers of large fecal pellets were Malacostraca, which include Euphausiids, and Heterobranchia, which include *Limacina*, but Malacostraca was quite rare. Thus, producer of large fecal pellets is considered to be *Limacina*. Not only salps and krills, but also *Limacina* should be focused as fast-sinking large fecal pellet producer which will affect to the efficiency of the transport of POC in this area. We will also discuss zooplankton community structures as potential producers of fecal pellets.

Keywords: Sediment trap, Zooplankton, Southern Ocean, Sinking particles

©2021. Japan Geoscience Union. All Right Reserved.

[E] Oral | M (Multidisciplinary and Interdisciplinary)：M-IS Intersection

Sun. Jun 6, 2021 10:45 AM - 12:15 PM JST | Sun. Jun 6, 2021 1:45 AM - 3:15 AM UTC | Ch.22 Zoom Room 22

[M-IS08] Interdisciplinary studies on pre-earthquake processes

convener:Katsumi Hattori(Department of Earth Sciences, Graduate School of Science, Chiba University), Dimitar Ouzounov(Center of Excellence in Earth Systems Modeling & Observations (CEESMO) , Schmid College of Science & Technology Chapman University, Orange, California, USA), Jann-Yenq LIU(Department of Space Science and Engineering, National Central University, Taiwan), Qinghua Huang(Peking University), Chairperson:Katsumi Hattori(Department of Earth Sciences, Graduate School of Science, Chiba University), Dimitar Ouzounov(Center of Excellence in Earth Systems Modeling & Observations (CEESMO) , Schmid College of Science & Technology Chapman University, Orange, California, USA)

The year 2021 is the memorial year of the 2011 Tohoku Earthquake (M9.0). For the past decade, we have advanced our knowledge of precursors and earthquake preparation processes.
This session expands the interdisciplinary discussions on the preparation process of earthquake and earthquake predictability by presenting the latest progress in studying the physically based pre-earthquake phenomena. New observations from space and ground have provided evidence, enhancing a better understanding of the tectonic activity. The session anticipates talks that include but is not limited to observations and analyses of seismic, electrical, electromagnetic, electro-chemical, and thermodynamic processes related to stress changes in the lithosphere along with their statistical and physical validation. Presentations on the latest observational results associated with major earthquakes obtained by different methodologies are welcomed. The topics of the session are as follows but not limited.

-General discussion on earthquake preparation process and the physics of pre-earthquake signals
- Theory, modeling, laboratory experiments, computational simulation for generation and propagation of pre-earthquake signals and their connection with the seismic cycle
- Multi-parameter observations, detection, and validation of pre-earthquake signals
- Cross-disciplinary studies, practical and technical approaches for better understanding of earthquake preparation processes and their connection with seismicity.

10:45 AM - 11:00 AM JST | 1:45 AM - 2:00 AM UTC

[MIS08-01] The spatiotemporal evolution of pre-earthquake anomalies and their association with the activation zone

*Dimitar Ouzounov[1], Sergey Pulinets[2], J.Y Liu[3], Katsumi Hattori[4], Patrick Taylor[5] (1.Center of Excellence in Earth Systems Modeling & Observations (CEESMO) , Schmid College of Science & Technology Chapman University, Orange, California, USA, 2.Space Research Institute, Russian Academy of Sciences, Moscow, Russia, 3.Center for Space and Remote Sensing Research, National Central University, Taoyuan, Taiwan, 4.Department of Earth Sciences, Graduate School of Science, Chiba University, Chiba, Japan, 5.NASA GSFC, Greenbelt, MD, USA)

11:00 AM - 11:20 AM JST | 2:00 AM - 2:20 AM UTC

[MIS08-02] The multi observations on electromagnetic emissions and plasma perturbations around Yutian Earthquakes in China

★Invited Papers

*Xuemin Zhang[1], Jing Liu[1], Angelo De Santis[2], Loredana Perrone[2], Xuhui Shen[3], Jianping Huang[3] (1.Institute of Earthquake Forecasting, China Earthquake Administration, 2.Istituto Nazionale di Geofisica e Vulcanologia, 3.Institute of Crustal Dynamics, China Earthquake Administration)

11:20 AM - 11:35 AM JST | 2:20 AM - 2:35 AM UTC

[MIS08-03] Bizarre “earthquake weather” immediately before and after the 1995 Kobe earthquake

*Yuji Enomoto[1], Tsuneaki Yamabe[1], Shigeki Sugiura[2], Hitoshi Kondo[2] (1.Shinshu Univeristy, Ueda Campus Fii, 2.Genesis Research Institute Inc.)

11:35 AM - 11:50 AM JST | 2:35 AM - 2:50 AM UTC

[MIS08-04] A system of the Monitoring Vibrations and Propagations in the Lithosphere, Atmosphere, and Ionosphere

*Chieh-Hung Chen[1], Yang-Yi Sun[1], Kai Lin[1], Huaizhong Yu[2] (1.Institute of Geophysics and Geomatics, China University of Geosciences, Wuhan, Hubei, China, 2.China Earthquake Networks Center, Beijing, China)

11:50 AM - 12:10 PM JST | 2:50 AM - 3:10 AM UTC

[MIS08-05] Assessing the potential earthquake precursory information in ULF magnetic data recorded in Kanto, Japan during 2000 – 2010: distance and magnitude dependences

★Invited Papers

*Peng Han[1], Jiancang Zhuang[2], Katsumi Hattori[3], Chieh-Hung Chen[4], Febty Febriani[5], Hongyan Chen[1] (1.Southern University of Science and Technology, Shenzhen, China, 2.The Institute of Statistical Mathematics, Tokyo, Japan, 3.Graduate School of Science, Chiba University, Chiba, Japan, 4.Institute of Geophysics and Geomatics, China University of Geosciences, Wuhan 430074, China, 5.Research Center for Physics, Indonesian Institute of Sciences, Tangerang, Banten, Indonesia)

12:10 PM - 12:15 PM JST | 3:10 AM - 3:15 AM UTC

[MIS08-06] Discussion

The spatiotemporal evolution of pre-earthquake anomalies and their association with the activation zone

*Dimitar Ouzounov[1], Sergey Pulinets[2], J.Y Liu[3], Katsumi Hattori[4], Patrick Taylor[5]

1. Center of Excellence in Earth Systems Modeling & Observations (CEESMO) , Schmid College of Science & Technology Chapman University, Orange, California, USA, 2. Space Research Institute, Russian Academy of Sciences, Moscow, Russia, 3. Center for Space and Remote Sensing Research, National Central University, Taoyuan, Taiwan, 4. Department of Earth Sciences, Graduate School of Science, Chiba University, Chiba, Japan, 5. NASA GSFC, Greenbelt, MD, USA

We studied the temporal and spatial phenomenon between Thermal Radiation (TRA); Ionospheric total electron content (TEC); and; abnormal patterns of radon data and their relationship with earthquake activation zones (EAZ). For the estimates of each EAZ, we use Dobrovolsky et al. (1979) and Bowman et al. (1998), where the EAZ radius scales exponentially with earthquake magnitude, especially for Mw 6.0 and larger. This gives a broader study of larger magnitudes earthquakes and TRA and TEC anomalies. We analyzed 10 large (M6+) earthquakes (2004-2019) for TRA and TEC anomalies in each of the EAZ zones. Our results show evolutionally patterns in the appearance of pre-earthquake transient effects in the atmosphere and ionosphere, with a short time-lag, from hours up to a few days, and scalable with a magnitude estimate at their unusually far distance from the epicenter (for the M7+ events). The spatial characteristics of pre-earthquake anomalies were associated with the larger area but always inside the preparation-activation region estimated by Dobrovolsky-Bowman. The pre-earthquake pattern of the atmosphere and ionosphere signals, revealed by a simultaneous analysis of satellite, GPS/TEC, Satellite Earth observations, and ground data, all suggesting that these earthquakes follow a global recognizable spatial pattern of TRA and TEC.

Keywords: pre-earthquake, precursor, thermal anomaly, GPS/TEC

©2021. Japan Geoscience Union. All Right Reserved.

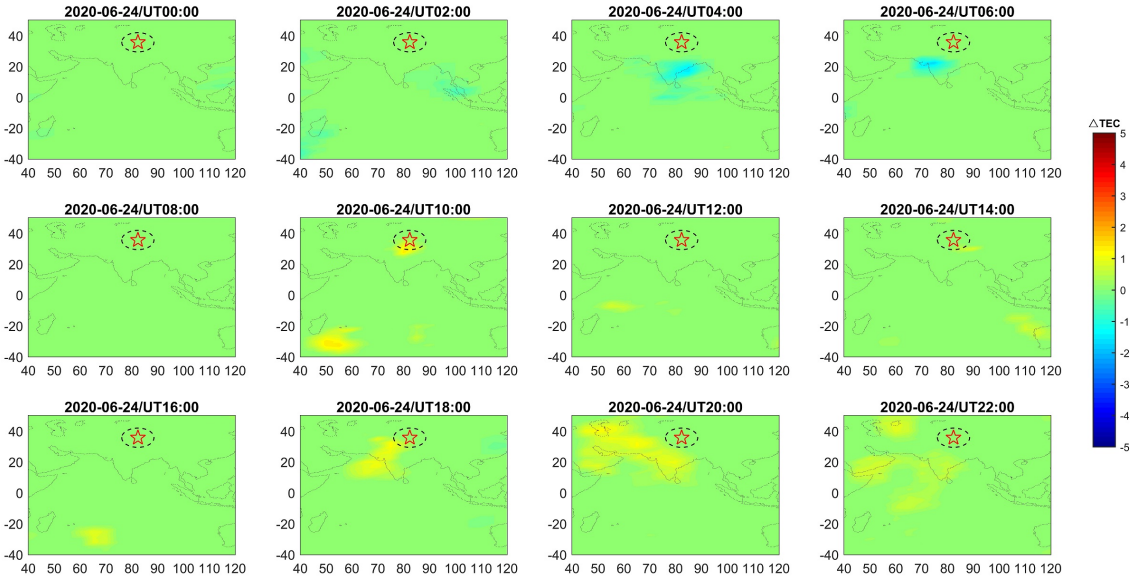
The multi observations on electromagnetic emissions and plasma perturbations around Yutian Earthquakes in China

*Xuemin Zhang[1], Jing Liu[1], Angelo De Santis[2], Loredana Perrone[2], Xuhui Shen[3], Jianping Huang[3]

1. Institute of Earthquake Forecasting, China Earthquake Administration, 2. Istituto Nazionale di Geofisica e Vulcanologia, 3. Institute of Crustal Dynamics, China Earthquake Administration

Based on the multi data of TEC inversed from GPS observations in China mainland, TEC mapping published by JPL, electron density from Zhangheng-1 satellite, electromagnetic data from ground geomagnetic observatories and ZH-1 satellite, the ionospheric perturbations were mainly analyzed around Yutian Ms6.4 earthquake on 26 June 2020, in Xinjiang Uygur Autonomous Region. The plasma perturbations were revealed from peak F2 layer to the topside ionosphere at satellite height about 507km. The electromagnetic emissions were enhanced before the earthquake, but its seasonal variations make it difficult to distinguish those anomalies possibly related to the earthquake. The consistence from ground and space-borne experiments may help to validate the earthquake-associated disturbances. Combined with the results for other three earthquakes in Yutian with magnitude larger than 6.0 during 2008-2020, it is found that the seismo-ionospheric disturbances concentrated 1 week before, mainly with increasing features and local effects, in which some showed simultaneous anomaly at its conjugate region. The comprehensive multi data analysis can improve the distinguishing capability for earthquake-related anomalies, and enhance their reliability. The solar activity and space magnetic disturbances will cause high frequent anomaly occurrence in the global maps, and influence heavily for abstracting the seismo-ionospheric signals. But a case study for solar eclipse on 21 June 2020 induced decreasing TEC anomalies, which is totally different with those related to Yutian earthquake, whatever in region or abnormal state. The LAIC couping process was discussed finally, and the effects from overlapped electric field were simulated by SAMI-2 model in high and low solar activity year.

Keywords: GPS TEC, CSES satellite, Ionospheric perturbation, LAIC model



©2021. Japan Geoscience Union. All Right Reserved.

Bizarre “earthquake weather” immediately before and after the 1995 Kobe earthquake

*Yuji Enomoto[1], Tsuneaki Yamabe[1], Shigeki Sugiura[2], Hitoshi Kondo[2]

1. Shinshu Univeristy, Ueda Campus Fii, 2. Genesis Research Institute Inc.

In the Kobe earthquake that occurred at 5:46 LT on January 17, 1995, the night sky, which should normally be dark immediately before and after, became bright and changed to bluish purple, white, and red. Among the many eyewitness testimonies (e.g. Sakaguchi, 2007), a series of photographs, taken by N. Yokota (lived in Izumiotsu, Osaka) in the direction of the epicenter[E1] , scientifically support this bizarre earthquake weather. (See Fig. 1). Radon emanation from faults, earthquake lights, and appearance of sporadic E in ionosphere have been reported associated with this earthquake. Based on this information, causal mechanisms of two kinds of the earthquake weather: whitish illuminants with extending streak clouds and bluish/purple- and red-colored clouds, are proposed as follows.

One is the radioluminescence that occurred in the atmosphere above around the epicenter due to emanation of a large amount of ^{222}Rn from the fault, that is, the ionization of nitrogen molecules and water molecules due to the α-ray irradiation during the radon decay, which resulted in EQL, the generation of high-frequency electromagnetic waves and generation of whitish streak clouds due the cloud chamber effect of γ-rays.

Secondly, regarding the origin of the blue-purple clouds and red clouds in the sky, we propose that the Sun light was color-dispersed due to the electro-optical interaction (Pockels/Kerr effect) between the sunlight shining into the ionosphere and the ionospheric electric field.

This is probably the first time in the world that such bizarre earthquake weather has been confirmed.

[E1]

Keywords: 1995Kobe earthquake, Earthquake weather, Radioluminescence, Electro-optical effect

©2021. Japan Geoscience Union. All Right Reserved.



Fig.1 a) Map, b) photo showing bizarre earthquake weather just after the 1995 Kobe EQ, c) the simulated night sky which should be dark (StellaNavigator ver.5)

©2021. Japan Geoscience Union. All Right Reserved.

A system of the Monitoring Vibrations and Propagations in the Lithosphere, Atmosphere, and Ionosphere

*Chieh-Hung Chen[1], Yang-Yi Sun[1], Kai Lin[1], Huaizhong Yu[2]

1. Institute of Geophysics and Geomatics, China University of Geosciences, Wuhan, Hubei, China, 2. China Earthquake Networks Center, Beijing, China

Scientists have reported that pre-earthquake anomalous phenomena can be observed in numerous distinct fields. These anomalous phenomena were classified into different groups based on promising relationships from potential mechanisms. However, the promising relationships among distinct parameters in a group are sometimes questionable due to that a certain distance exists between adjacent stations. A novel system was established in Leshan, Sichuan, China to monitor changes and/or waves propagations from the lithosphere to the ionosphere in 2021. The system monitors changes of more than 10 physical parameters at altitudes ranged from -5 meters to ~350 kilometers. A piezometer monitors changes of groundwater levels with a sampling interval of 2 seconds in a well. Variations of temperature and air pressure are continuously observed by utilizing thermometers and barometers in wells with depths of 5, 3 and 1 meters and 0.5 meters above the surface. Two broadband seismometers were set at opposite corners of the station to monitor ground motion with a sampling rate of 50 Hz. A ground-based GNSS receiver routinely receive signals from the BeiDou geosynchronous satellites to study ground vibrations and changes of the total electron content about 350 kilometers above the Earth’ s surface. A Sonic Detection And Ranging (SODAR) system and a Radio Acoustic Sounding System (RASS) were also employed in monitoring changes of temperature and winds from the surface to ~5 kilometers in altitude. To understand the disturbance of the acoustic-gravity waves on clouds, an all-sky camera is installed in the station. Two atmospheric electric field meters are utilized to monitor electric fields around the surface. A flux magnetometer was installed in the surrounded areas with horizontal distance of about 50 meters to study changes of the geomagnetic field and ionospheric current about 100 kilometers above the surface. Furthermore, the VHF coherent scattering radar and the Meteor radar were set about 20 kilometers away from the stations for monitoring changes 80-160 kilometers above the surface. Note that observations from the China Seismo-Electromagnetic Satellite (CSES) and Radio occultation can also be integrated together to sheds light on extending the monitoring upon 500 kilometer above the surface. In short, an MVP-LAI system was established to Monitors Vibrations and Propagations in the Lithosphere, Atmosphere, and Ionosphere and to examines the accuracy of those potential mechanisms.

Keywords: LAI coupling, Pre-earthquake anomalous phenomena

©2021. Japan Geoscience Union. All Right Reserved.

Assessing the potential earthquake precursory information in ULF magnetic data recorded in Kanto, Japan during 2000 –2010: distance and magnitude dependences

*Peng Han[1], Jiancang Zhuang[2], Katsumi Hattori[3], Chieh-Hung Chen[4], Febty Febriani[5], Hongyan Chen[1]

1. Southern University of Science and Technology, Shenzhen, China, 2. The Institute of Statistical Mathematics, Tokyo, Japan, 3. Graduate School of Science, Chiba University, Chiba, Japan, 4. Institute of Geophysics and Geomatics, China University of Geosciences, Wuhan 430074, China, 5. Research Center for Physics, Indonesian Institute of Sciences, Tangerang, Banten, Indonesia

In order to clarify the ULF seismo-magnetic phenomena, a sensitive geomagnetic network has been installed in Kanto, Japan since 2000. In previous studies, we have verified the correlation between ULF magnetic anomalies and local sizeable earthquakes. In this paper, we use Molchan’s error diagram to evaluate the potential earthquake precursory information in the magnetic data recorded in Kanto, Japan during 2000 –2010. We introduce the probability gain (*PG*) and the probability difference (*D*) to quantify the forecasting performance and to explore the optimal prediction parameters for a given ULF magnetic station. The results show that the earthquake predictions based on magnetic anomalies are significantly better than random guesses, indicating the magnetic data contain potential useful precursory information. Further investigations suggest that the prediction performance depends on the choices of the distance (*R*) and size of the target earthquake events (*Es*). Optimal *R* and *Es* are about (100 km, $10^{8.75}$) and (180 km, $10^{8.75}$) for Seikoshi (SKS) station in Izu and Kiyosumi (KYS) station in Boso, respectively.

Keywords: ULF magnetic data, earthquake precursory information, Molchan’s error diagram, Kanto, Japan

©2021. Japan Geoscience Union. All Right Reserved.

[E] Oral | M (Multidisciplinary and Interdisciplinary) | M-IS Intersection

[M-IS08] Interdisciplinary studies on pre-earthquake processes

convener:Katsumi Hattori(Department of Earth Sciences, Graduate School of Science, Chiba University), Dimitar Ouzounov(Center of Excellence in Earth Systems Modeling &Observations (CEESMO) , Schmid College of Science &Technology Chapman University, Orange, California, USA), Jann-Yenq LIU(Department of Space Science and Engineering, National Central University, Taiwan), Qinghua Huang(Peking University), Chairperson:Katsumi Hattori(Department of Earth Sciences, Graduate School of Science, Chiba University), Dimitar Ouzounov(Center of Excellence in Earth Systems Modeling &Observations (CEESMO) , Schmid College of Science &Technology Chapman University, Orange, California, USA)

Sun. Jun 6, 2021 10:45 AM - 12:15 PM Ch.22 (Zoom Room 22)

The year 2021 is the memorial year of the 2011 Tohoku Earthquake (M9.0). For the past decade, we have advanced our knowledge of precursors and earthquake preparation processes.
This session expands the interdisciplinary discussions on the preparation process of earthquake and earthquake predictability by presenting the latest progress in studying the physically based pre-earthquake phenomena. New observations from space and ground have provided evidence, enhancing a better understanding of the tectonic activity. The session anticipates talks that include but is not limited to observations and analyses of seismic, electrical, electromagnetic, electro-chemical, and thermodynamic processes related to stress changes in the lithosphere along with their statistical and physical validation. Presentations on the latest observational results associated with major earthquakes obtained by different methodologies are welcomed. The topics of the session are as follows but not limited.

-General discussion on earthquake preparation process and the physics of pre-earthquake signals
- Theory, modeling, laboratory experiments, computational simulation for generation and propagation of pre-earthquake signals and their connection with the seismic cycle
- Multi-parameter observations, detection, and validation of pre-earthquake signals
- Cross-disciplinary studies, practical and technical approaches for better understanding of earthquake preparation processes and their connection with seismicity.

12:10 PM - 12:15 PM

[MIS08-06]Discussion

©Japan Geoscience Union

[E] Oral | M (Multidisciplinary and Interdisciplinary)：M-IS Intersection

Sun. Jun 6, 2021 1:45 PM - 3:15 PM JST | Sun. Jun 6, 2021 4:45 AM - 6:15 AM UTC | Ch.22 Zoom Room 22

[M-IS08] Interdisciplinary studies on pre-earthquake processes

convener:Katsumi Hattori(Department of Earth Sciences, Graduate School of Science, Chiba University), Dimitar Ouzounov(Center of Excellence in Earth Systems Modeling & Observations (CEESMO) , Schmid College of Science & Technology Chapman University, Orange, California, USA), Jann-Yenq LIU(Department of Space Science and Engineering, National Central University, Taiwan), Qinghua Huang(Peking University), Chairperson:Peng Han(Southern University of Science and Technology, Shenzhen, China), Xuemin Zhang(Institute of Earthquake Forecasting, China Earthquake Administration)

The year 2021 is the memorial year of the 2011 Tohoku Earthquake (M9.0). For the past decade, we have advanced our knowledge of precursors and earthquake preparation processes.
This session expands the interdisciplinary discussions on the preparation process of earthquake and earthquake predictability by presenting the latest progress in studying the physically based pre-earthquake phenomena. New observations from space and ground have provided evidence, enhancing a better understanding of the tectonic activity. The session anticipates talks that include but is not limited to observations and analyses of seismic, electrical, electromagnetic, electro-chemical, and thermodynamic processes related to stress changes in the lithosphere along with their statistical and physical validation. Presentations on the latest observational results associated with major earthquakes obtained by different methodologies are welcomed. The topics of the session are as follows but not limited.

-General discussion on earthquake preparation process and the physics of pre-earthquake signals
- Theory, modeling, laboratory experiments, computational simulation for generation and propagation of pre-earthquake signals and their connection with the seismic cycle
- Multi-parameter observations, detection, and validation of pre-earthquake signals
- Cross-disciplinary studies, practical and technical approaches for better understanding of earthquake preparation processes and their connection with seismicity.

1:45 PM - 2:00 PM JST | 4:45 AM - 5:00 AM UTC

[MIS08-07] Seismo-ionospheric anomalies before the 11 March 2011 M9.0 Tohoku Earthquake

*Jann-Yenq LIU[1,2,3], FU-YUAN CHANG[1], I-Te Lee[4], Katsumi Hattori[5], Yuh-Ing Chen[6] (1.Center for Astronautical Physics and Engineering, National Central University, Taoyuan, TAIWAN, 2.Department of Space Science and Engineering, National Central University, TAIWAN, 3.Center for Space and Remote Sensing Research, National Central University, Taoyuan, TAIWAN, 4.Center Weather Bureau, Taipei, TAIWAN, 5.Department of Earth Sciences, Graduate School of Science, Chiba University, Chiba, JAPAN, 6.Institute of Statistics, National Central University, Taoyuan, TAIWAN)

2:00 PM - 2:15 PM JST | 5:00 AM - 5:15 AM UTC

[MIS08-08] 3D Tomography of the Ionospheric Anomalies Before the 2010 Maule Earthquake, Chile: Comparison with the 2011 Tohoku-oki and 2015 Illapel Earthquakes

*Ihsan Naufal Muafiry[1], Kosuke Heki[1] (1.Hokkaido University, Japan)

2:15 PM - 2:30 PM JST | 5:15 AM - 5:30 AM UTC

[MIS08-09] Spatiotemporal Distribution Characteristics of Conductivity Anomalies before Ms > 6 Earthquakes in the North-South Seismic Belt of China during 2014 – 2019

*Zhiqiang Mao[1], Chieh-Hung Chen[1], Suqin Zhang[2], Qi Li[2], Aisa Yisimayili[3] (1.China University of Geosciences (Wuhan), 2.Institute of Geophysics, China Earthquake Administration, 3.Earthquake Agency of Xinjiang Uygur Autonomous Region)

2:30 PM - 2:45 PM JST | 5:30 AM - 5:45 AM UTC

[MIS08-10] **Possible stimulation of seismic activity by geomagnetically induced currents generated by ionizing radiation of solar flare in the illuminated hemisphere**

*Victor A. Novikov[1], Valery M. Sorokin[2], Alexey K. Yaschenko[2], Georgy Yu. Mushkarev[2] (1.Joint Institute for High Temperatures of Russian Academy of Sciences, 2.Pushkov Institute of Terrestrial Magnetism, Ionosphere and Radio Wave Propagation of Russian Academy of Sciences)

2:45 PM - 3:00 PM JST | 5:45 AM - 6:00 AM UTC

[MIS08-11] **Detecting the ionospheric disturbances in Japan using the three-dimensional computerized tomography**

*Rui Song[1], Katsumi Hattori[1], Xuemin Zhang[2] (1.Graduate School of Science and Engeering, Chiba University, 2.Institute of Earthquake Forecasting, China Earthquake Administration)

3:00 PM - 3:15 PM JST | 6:00 AM - 6:15 AM UTC

[MIS08-12] A Statistical Study of the Correlation Between Geomagnetic Storms and M>7.0 Global Earthquakes During 1957–2020

*Hongyan Chen[1], Rui Wang[1], Miao Miao[1], Xiaocan Liu[2], Yonghui Ma[3], Katsumi Hattori[4], Peng Han[1] (1.Southern University of Science and Technology, Shenzhen, China, 2.The Institute of Geophysics China Earthquake Administration, Beijing, China, 3.School of Science, Harbin Institute of Technology, Shenzhen, China, 4.Graduate School of Science, Chiba University, Chiba, Japan)

Seismo-ionospheric anomalies before the 11 March 2011 M9.0 Tohoku Earthquake

*Jann-Yenq LIU[1,2,3], FU-YUAN CHANG[1], I-Te Lee[4], Katsumi Hattori[5], Yuh-Ing Chen[6]

1. Center for Astronautical Physics and Engineering, National Central University, Taoyuan, TAIWAN, 2. Department of Space Science and Engineering, National Central University, TAIWAN, 3. Center for Space and Remote Sensing Research, National Central University, Taoyuan, TAIWAN, 4. Center Weather Bureau, Taipei, TAIWAN, 5. Department of Earth Sciences, Graduate School of Science, Chiba University, Chiba, JAPAN, 6. Institute of Statistics, National Central University, Taoyuan, TAIWAN

In this paper, observations of the total electron content (TEC) of the global ionosphere map (GIM), radio occultation electron density profiles of FORMOSAT-3/COSMIC, and in situ plasma quantities probed by DMSP satellite are used to study seismo-ionospheric anomalies associated the 11 March 2011 M9.0 Tohoku earthquake, while the Thermosphere Ionosphere Electrodynamics General Circulation Model (TIEGCM) is applied to simulate and understand the observed anomalies. The observation shows that the GIM TEC over the epicenter significantly and continuously enhances on 6-8 March 2011, 4-2 days before the earthquake. The spatial analysis further demonstrates that the enhancement anomaly specifically and persistently appears in the northern epicenter area. Simulation results well agree with the observations, which suggest that the electric potential around the epicenter has been distorted and significantly affects the TEC during the earthquake preparation period.

Keywords: Tohoku Earthquake, GIM TEC, FORMOSAT-3/COSMIC, ionospheric earthquake precursor, TIEGCM, seismo-electric field

©2021. Japan Geoscience Union. All Right Reserved.

3D Tomography of the Ionospheric Anomalies Before the 2010 Maule Earthquake, Chile: Comparison with the 2011 Tohoku-oki and 2015 Illapel Earthquakes

*Ihsan Naufal Muafiry[1], Kosuke Heki[1]

1. Hokkaido University, Japan

This study compares the 3D structure of ionospheric electron density anomalies immediately before the three megathrust earthquakes, i.e. 2011 Mar. 11 Tohoku-Oki (Muafiry & Heki, JGR 2020), 2015 Sep.16 Illapel (He & Heki, JGR 2018), and the 2010 Feb. 27 Maule, Chile (new study), earthquakes, revealed using slant-TEC residuals as inputs to 3D tomographic inversion. For the Maule earthquake, we used 371 TEC data obtained using 7 satellites and 91 ground GNSS stations mainly in Chile and Argentine. The tomography results showed that the pre-seismic ionospheric anomaly in each case has following similarities; (1) They are composed of pairs of low-altitude positive and high-altitude negative electron density anomalies. (2) They occur above the land area close to the submarine faults. (3) They have clear onsets a few tens of minutes before earthquakes (~40 min before 2011 Tohoku-oki, and Maule, and ~20 minutes before the Illapel earthquakes) and grow with decaying rates. Muafiry & Heki (2020) hypothesized the physical process consistent with such 3D structure. We will also compare strengths and dimensions of the electron density anomalies before these three earthquakes.

Keywords: 3D tomography, GNSS, Pre-seismic Ionospheric Anomaly

©2021. Japan Geoscience Union. All Right Reserved.

Spatiotemporal Distribution Characteristics of Conductivity Anomalies before Ms > 6 Earthquakes in the North-South Seismic Belt of China during 2014 –2019

*Zhiqiang Mao[1], Chieh-Hung Chen[1], Suqin Zhang[2], Qi Li[2], Aisa Yisimayili[3]

1. China University of Geosciences (Wuhan), 2. Institute of Geophysics, China Earthquake Administration, 3. Earthquake Agency of Xinjiang Uygur Autonomous Region

The North-South Seismic Belt of China is one of the most active seismic areas on the Chinese continent. More than ten strong earthquakes (Ms > 6) have occurred in this region since 2010. However, Earthquake-related conductivity anomalies are rarely reported for those earthquakes. In this study, 3-component geomagnetic data recorded at sixty geomagnetic stations are selected to compute the Parkinson vectors to monitor the changes of conductivity before and after the earthquakes. Considering most fluxgate magnetometer have only been installed since 2014, we concentrate on six Ms > 6 earthquakes occurred during 2014–2019. To mitigate artificial disturbances, low noise data during the 00:00 –5:00 LT are utilized. We compute the background distribution and monitoring distribution using the azimuth of the Parkinson vectors at each station within six years (2014 –2019) and a 15-day moving window, respectively. The background distribution is subtracted from the monitoring distributions to mitigate the influences of underlying inhomogeneous tectonic structures. The obtained difference distributions binned by 10˚ within 400 km from each station are superimposed during 60 days before and after the earthquake to construct integrated maps. To analyze the potential frequency characteristics, we compute the results form low to high frequency band. The results show that for four earthquakes, the conductivity anomalies areas appear near the epicenter 10 to 20 days before earthquakes, while the rest two earthquakes have no anomaly. The conductivity anomalies appear at all study frequency band from 0.0005 Hz to 0.1 Hz, and significantly at 0.001 –0.005 Hz before earthquakes. Meanwhile, we find that the lower frequency band corresponds to larger anomalies area. These results suggest the change of underlying conductivity near the hypocenter is a possible phenomena for strong earthquakes, and the frequency characteristics of the seismo-conductivity anomaly during the earthquake are helpful to understand the pre-earthquake anomalous phenomena.

Keywords: Seismo-conductivity anomalies, Parkinson vector , Geomagnetic, The North-South Seismic Belt of China

©2021. Japan Geoscience Union. All Right Reserved.

Possible stimulation of seismic activity by geomagnetically induced currents generated by ionizing radiation of solar flare in the illuminated hemisphere

*Victor A. Novikov[1], Valery M. Sorokin[2], Alexey K. Yaschenko[2], Georgy Yu. Mushkarev[2]

1. Joint Institute for High Temperatures of Russian Academy of Sciences, 2. Pushkov Institute of Terrestrial Magnetism, Ionosphere and Radio Wave Propagation of Russian Academy of Sciences

In addition to traditional approach to the short-term earthquake (EQ) prediction based on a search of possible precursors of seismic event, the following steps towards EQ predictability look reasonable [Sobolev, 2011]: a) determination of an unstable area; (b) monitoring the triggering effects and assessment their impact on the unstable area; and (c) estimation of probability of location, time, and magnitude of impending EQ.

It is well-known that external factors like distant strong EQs, underground explosions, fluid injection, etc. can trigger EQ in the crust fault matured for dynamical rupture. Recently it was found that EQ triggering is possible during injection of DC pulses into the Earth crust by statistical analysis of regional seismicity during artificial electromagnetic impact [Tarasov & Tarasova] and laboratory experiments [Sobolev & Ponomarev, 2003; Novikov et al, 2017].

Numerical estimations based on a theoretical model of disturbance of electric filed, electric current, and heat release in lithosphere associated with variation of ionosphere conductivity caused by absorption of ionizing radiation of solar flares [Sorokin et al, 2019] demonstrated that solar flare can generate electric current density in lithosphere over 10^{-6} A/m^2, that is comparable with a current density generated in the Earth crust by artificial pulsed power systems, which provide regional earthquake triggering and spatiotemporal variation of seismic activity. Therefore, EQ triggering is possible not only by man-made pulsed power sources but also by the solar flares. The results obtained were confirmed by sharp increase of global seismicity after the strong solar flare of X9.3 class on September 6, 2017 [Novikov et al, 2020].

For application of the obtained results for EQ alarm immediately after the strong solar flare in the specific seismic-prone zones we need to select the areas, most sensitive to impact of solar flare, where the maximal density of geomagnetically induced currents (GIC) will be generated in the conductive crust faults. We present the numerical model of GIC generation by ionizing radiation of solar flare in the illuminated hemisphere. Calculations of disturbance of electromagnetic field and telluric current were performed for San Andreas fault (California), integral radiant flux density of 0.005 J/m^2, and the time of UTC 15:00 and 18:00 on July 20, 2020. It was found that ionosphere conductivity disturbance is 2 S and 4 S for UTC 15:00 and 18:00, respectively, that provides double increase of telluric current in the fault (1.5×10^{-7} and 3×10^{-7} A/m^2). Duration of the current pulse is about 40-50 s. These parameters are comparable with the DC pulse generated in the EQ sources by artificial power system (MHD generator "Pamir-2": current density 10^{-7} - 10^{-8} A/m^2 at depth of 5-10 km, DC pulse duration up to 10s) resulted in triggering of regional weak seismicity at Northern Tien Shan.

The reported study was funded by RFBR and NSFC, project number 21-55-53053.

References:

©2021. Japan Geoscience Union. All Right Reserved.

Sobolev G.A. (2011) Seismicity dynamics and earthquake predictability. Nat. Hazards Syst. Sci., 11, 445-458.

Tarasov N.T., Tarasova N.V. (2004) Spatial-temporal structure of seismicity of the North Tien Shan and its change under effect of high energy electromagnetic pulses. Annals of Geophysics, 47, 1, 199-212.

Sobolev G.A., Ponomarev A.V. (2003) Physics of earthquakes and precursors. Moscow, Nauka, 269 p (in Russian).

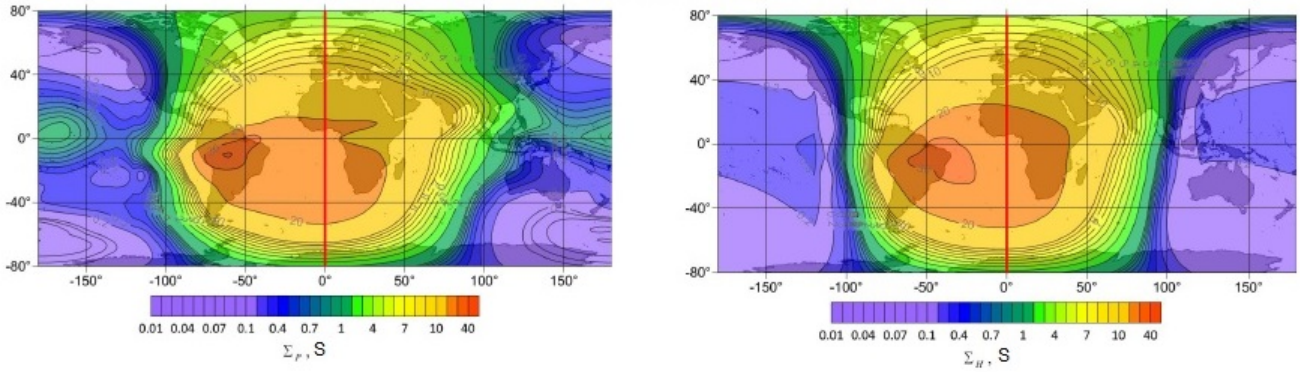
Novikov V.A., Okunev V.I., Klyuchkin V.N., Liu J., Ruzhin Yu.Ya., Shen X. (2017) Electrical triggering of earthquakes: results of laboratory experiments at spring-block models. Earthq. Sci. 30, 4, 167-172.

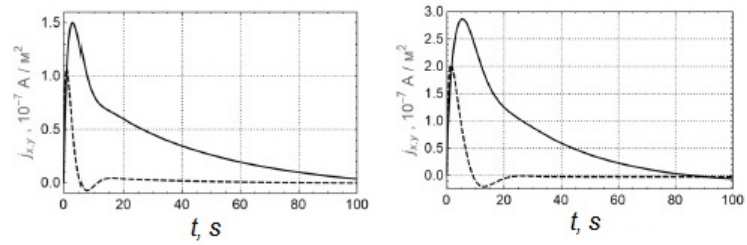
Sorokin V.M., Yashchenko A.K., Novikov V.A. (2019) A possible mechanism of stimulation of seismic activity by ionizing radiation of solar flares. Earthq. Sci., 32, 1, 26-34.

Novikov V., Ruzhin Yu., Sorokin V., Yaschenko A. (2020) Space weather and earthquakes: possible triggering of seismic activity by strong solar flares. Annals of Geophysics, 63, 5, PA554.

Keywords: solar flare, geomagnetically induced current, earthquake triggering, conductive fault

Spatial distriution of integral Pedersen (left panel) and Hall (right panel) ionosphere conductivities
vertical red line is undersolar meridian





Time dependence of telluric current density

Solid line - jx , dotted line - jy.

UTC 15:00 - left panel
UTC 18:00 - right panel

©2021. Japan Geoscience Union. All Right Reserved.

Detecting the ionospheric disturbances in Japan using the three-dimensional computerized tomography

*Rui Song[1], Katsumi Hattori[1], Xuemin Zhang[2]

1. Graduate School of Science and Engeering, Chiba University, 2. Institute of Earthquake Forecasting, China Earthquake Administration

To reconstruct the 3-D structures related to ionospheric irregularities in Japan, the improved constraint least-square fitting algorithm was adopted. Unlike the conventional least-square fitting, spatial restrictions in horizontal direction were removed for better reproducing the disturbances. Before the performance on imaging ionospheric irregularities was evaluated, common assessments for quiet ionospheric conditions were first implemented. Taking the day of March 22, 2012, as an example, the results indicated that the characteristics of IED could be well retrieved by the improved algorithm. Then, the temporal and spatial IEDs related to plasma depletions and MSTIDs were elaborated, respectively. Especially for the storm-time depletion occurred on July 27, 2004, although it exhibited equatorward propagating characteristic, considering the abrupt fracture of up to 15 TECU imaged by TEC mapping, we speculated it was the abnormal PBs generated by the combing effects from the equatorward TADs and eastward PPEF during an intense storm. However, whether such irregularities being related to PBs or storm-induced LSTIDs is still worth further study and discussion in the future work. Next, Ne reconstruction for the nighttime MSTIDs on June 23, 2012, was conducted. The upward and downward motions of Ne were found to be connected with the negative and positive disturbances. Moreover, the sinusoidal structure concerning such disturbances indicates that an east-west oscillating EF exists in F region, then drives the plasma drift via $\delta \mathbf{E} \times \mathbf{B}$. It is suggested that the electrodynamic process, as expected from the Perkins instability, plays an important role in generating the nighttime MSTIDs.

Keywords: Computerized Ionospheric Tomography, Total Electron Content, Plasma Depletion, Medium-scale Traveling Ionospheric Disturbance

©2021. Japan Geoscience Union. All Right Reserved.

A Statistical Study of the Correlation Between Geomagnetic Storms and M>7.0 Global Earthquakes During 1957–2020

*Hongyan Chen[1], Rui Wang[1], Miao Miao[1], Xiaocan Liu[2], Yonghui Ma[3], Katsumi Hattori[4], Peng Han[1]

1. Southern University of Science and Technology, Shenzhen, China, 2. The Institute of Geophysics China Earthquake Administration, Beijing, China, 3. School of Science, Harbin Institute of Technology, Shenzhen, China, 4. Graduate School of Science, Chiba University, Chiba, Japan

In order to find out whether the geomagnetic storms and large-mega earthquakes are correlated or not, statistical studies based on Superposed Epoch Analysis (SEA), significance analysis, and Z test have been applied to the Dst index data and M > 7.0 global earthquakes during 1957–2020. The results indicate that before M > 7.0 global earthquakes, there are clearly higher probabilities of geomagnetic storms than after them. Geomagnetic storms are more likely to be related to shallow earthquakes rather than deep ones. Further statistical investigations of the results based on cumulative storm hours show consistency with those based on storm days, suggesting that the high probability of geomagnetic storms prior to large-mega earthquakes is significant and robust. Some possible mechanisms such as a reverse piezoelectric effect and/or electroosmotic flow are discussed to explain the statistical correlation. The result might open new perspectives in the complex process of earthquakes and the Lithosphere-Atmosphere-Ionosphere (LAI) coupling.

Keywords: Statistical study, Geomagnetic storm, Earthquakes, Superposed epoch analysis

©2021. Japan Geoscience Union. All Right Reserved.

[E] Oral | M (Multidisciplinary and Interdisciplinary)：M-IS Intersection

Sun. Jun 6, 2021 3:30 PM - 5:00 PM JST | Sun. Jun 6, 2021 6:30 AM - 8:00 AM UTC | Ch.22 Zoom Room 22

[M-IS08] Interdisciplinary studies on pre-earthquake processes

convener:Katsumi Hattori(Department of Earth Sciences, Graduate School of Science, Chiba University), Dimitar Ouzounov(Center of Excellence in Earth Systems Modeling & Observations (CEESMO) , Schmid College of Science & Technology Chapman University, Orange, California, USA), Jann-Yenq LIU(Department of Space Science and Engineering, National Central University, Taiwan), Qinghua Huang(Peking University), Chairperson:Jann-Yenq LIU(Department of Space Science and Engineering, National Central University, Taiwan), Qinghua Huang(Peking University)

The year 2021 is the memorial year of the 2011 Tohoku Earthquake (M9.0). For the past decade, we have advanced our knowledge of precursors and earthquake preparation processes.
This session expands the interdisciplinary discussions on the preparation process of earthquake and earthquake predictability by presenting the latest progress in studying the physically based pre-earthquake phenomena. New observations from space and ground have provided evidence, enhancing a better understanding of the tectonic activity. The session anticipates talks that include but is not limited to observations and analyses of seismic, electrical, electromagnetic, electro-chemical, and thermodynamic processes related to stress changes in the lithosphere along with their statistical and physical validation. Presentations on the latest observational results associated with major earthquakes obtained by different methodologies are welcomed. The topics of the session are as follows but not limited.

-General discussion on earthquake preparation process and the physics of pre-earthquake signals
- Theory, modeling, laboratory experiments, computational simulation for generation and propagation of pre-earthquake signals and their connection with the seismic cycle
- Multi-parameter observations, detection, and validation of pre-earthquake signals
- Cross-disciplinary studies, practical and technical approaches for better understanding of earthquake preparation processes and their connection with seismicity.

3:30 PM - 3:50 PM JST | 6:30 AM - 6:50 AM UTC

[MIS08-13] Italian contribution to the CSES satellite mission

★Invited Papers

*Livio Conti[1], Group the CSES-Limadou Collaboration (1.Uninettuno University)

3:50 PM - 4:10 PM JST | 6:50 AM - 7:10 AM UTC

[MIS08-14] A focus on the capability of the RST-based satellite TIR anomalies for the short-term seismic hazard assessment in Japan

★Invited Papers

*Nicola Genzano[1], Roberto Colonna[1], Carolina Filizzola[2], Katsumi Hattori[3,4], Mariano Lisi[2], Nicola Pergola[2], Valerio Tramutoli[1] (1.School of Engineering, University of Basilicata, Via dell' Ateneo Lucano, 10, 85100 Potenza, Italy, 2.National Research Council, Institute of Methodologies for Environmental Analysis, C. da S. Loja, 85050 Tito Scalo (Pz), Italy, 3.Graduate School of Science, Chiba University, Yayoi 1-33, Inage, Chiba, 263-8522, Japan, 4.Center for Environmental Remote Sensing, Chiba University, Yayoi 1-33, Inage, Chiba, 263-8522, Japan)

4:10 PM - 4:30 PM JST | 7:10 AM - 7:30 AM UTC

[MIS08-15] Radon Monitoring in the Gulf of Corinth, Greece

★Invited Papers

*VASSILIOS KARASTATHIS[1], G Elefteriou[1], M. Kafatos[2], K. Tsinganos[3], G Tselentis[1], D. Ouzounov[2], E Mouzakiotis[1] (1.National Observatory of Athens, 2.Chapman University, 3.National and Kapodistrian University of Athens)

4:30 PM - 4:50 PM JST | 7:30 AM - 7:50 AM UTC

[MIS08-16] Earth's crust as a new element of the LAIC model within the Global Electric Circuit concept

★Invited Papers

*Sergey A Pulinets[1], V. Gavrilov[2], V. Bogdanov[3], N. Blaustein[4] (1.Space Research Institute of the Russian Academy of Sciences, 2.Institute of Volcanology and Seismology, Far-East Branch of the Russian Academy of Sciences, 3.Institute of Cosmophysical Research and Radio Wave Propagation, Far-East Branch of the Russian Academy of Sciences, 4.Ben-Gurion University of the Negev, Israel)

4:50 PM - 5:00 PM JST | 7:50 AM - 8:00 AM UTC

[MIS08-17] Discussion

Italian contribution to the CSES satellite mission

*Livio Conti[1], Group the CSES-Limadou Collaboration

1. Uninettuno University

We present a review of the research activity of the Italian team (Limadou Collaboration) within the CSES-1 mission. CSES-1 is a satellite of the China National Space Administration (CNSA) developed in collaboration with the Italian Space Agency (ASI). The mission is led by the Chinese Earthquake Administration from the Chinese side. The Italian Institute for Nuclear Physics (INFN) leads the Limadou collaboration that includes several other institutes (INGV, INAF-IAPS, CNR-IFAC) and Universities. The satellite - equipped with nine advanced instruments devoted to measure continuously and simultaneously data of electric and magnetic field, charged particles, and plasma parameters –has been designed for studying the near-Earth electromagnetic, plasma and particles environment. The main Italian contribution to the mission is the HEPD detector for measuring high-energy charged particles (O(1 MeV to O(100 MeV)) on board of CSES-1. We have also carried out measurement and validation test sessions of CSES-1 plasma instruments in the INAF-IAPS plasma chamber. CSES-1 aims at investigating the iono-magnetospheric phenomena induced by internal natural sources (such as earthquakes, volcanos, lightning, etc.) and external sources (Sun and cosmic rays) and by artificial emitters including radio emitters). Two case studies of strong earthquakes occurred in 2018 in Indonesia revealed some important anomalies in the electron density, preceding each seismic event occurrence. In addition, a preliminary systematic superposed space and time analysis between CSES-1 electron density data and earthquakes occurred in 2018 and 2019 has shown a significant robust correlation. The CSES-1 mission allows a detailed study of the structure and the dynamic of the topside ionosphere, the coupling mechanisms with the lower and higher plasma layers and the temporal variations of the geomagnetic field, in quiet and disturbed conditions. Data collected by the CSES-1 mission are extremely useful for investigating solar-terrestrial interactions and phenomena of solar physics, namely coronal mass ejections (CMEs), solar flares and cosmic ray solar modulation. CSES-1 is the first of a series of satellites that will be launched - with the same instruments suite and similar orbital parameters - in order to reduce the revisit time between consecutive observations. On board the CSES-2 satellite will be installed a particle detector and an electric field analyzer provided by the Limadou collaboration.

©2021. Japan Geoscience Union. All Right Reserved.

A focus on the capability of the RST-based satellite TIR anomalies for the short-term seismic hazard assessment in Japan

*Nicola Genzano[1], Roberto Colonna[1], Carolina Filizzola[2], Katsumi Hattori[3,4], Mariano Lisi[2], Nicola Pergola[2], Valerio Tramutoli[1]

1. School of Engineering, University of Basilicata, Via dell' Ateneo Lucano, 10, 85100 Potenza, Italy, 2. National Research Council, Institute of Methodologies for Environmental Analysis, C. da S. Loja, 85050 Tito Scalo (Pz), Italy, 3. Graduate School of Science, Chiba University, Yayoi 1-33, Inage, Chiba, 263-8522, Japan, 4. Center for Environmental Remote Sensing, Chiba University, Yayoi 1-33, Inage, Chiba, 263-8522, Japan

With the aim to evaluate the potentiality of the parameter "RST-based satellite TIR anomalies" in a space-time relation with large earthquakes (M>=6) occurred in Japan from 2005 to 2015, we have performed a long-term statistical correlation analysis (see Genzano et al., 2021).
To accomplish this purpose, we use the Robust Satellite Technique (RST; Tramutoli 1998, 2007), and the Robust Estimator TIR Anomalies (RETIRA; Tramutoli et al., 2005) index, to identify Significant Sequences of TIR Anomalies (SSTAs) over 11 years of night-time satellite images acquired by MTSAT satellites over Japan.
By applying empirical spatial-temporal rules, which are established also taking in account the physical models up to now proposed to explain seismic TIR anomalies appearances, the performed long-term correlation analysis put in relief that a non-casual relation exists between satellite TIR anomalies and the occurrence of the earthquakes.
Here, we summarize the achieved results and discuss them in the perspective of a multi-parameter system, which could improve our present knowledge on the earthquake-related processes and increase our capacity to assess the seismic hazard in the medium-short term (months to days).
Moreover, we will discuss the improvements to the RST approach, recently introduced, aimed to minimize the proliferation of the false positives (i.e. TIR anomalies independent to the seismic sources, but due to other causes, e.g. meteorological factors), as well as the exportation of the RST/RETIRA approach/index on the radiances collected by the next-generation satellite sensor Himawari-8/AHI.

Acknowledgments
This study was partly supported by joint research program of Center for Environmental Remote Sensing of Chiba University (Japan).

References
Genzano, N., C. Filizzola, K. Hattori, N. Pergola, and V. Tramutoli (2021), Statistical correlation analysis between thermal infrared anomalies observed from MTSATs and large earthquakes occurred in Japan (2005 - 2015). Journal of Geophysical Research: Solid Earth, 126, e2020JB020108. https://doi.org/10.1029/2020JB020108
Tramutoli, V. (1998), Robust AVHRR Techniques (RAT) for Environmental Monitoring: theory and applications, in Proceedings of SPIE, vol. 3496, edited by E. Zilioli, pp. 101–113, doi: 10.1117/12.332714
Tramutoli, V. (2007), Robust Satellite Techniques (RST) for Natural and Environmental Hazards Monitoring and Mitigation: Theory and Applications, in 2007 International Workshop on the Analysis of Multi-temporal Remote Sensing Images, pp. 1–6, IEEE. doi: 10.1109/MULTITEMP.
Tramutoli, V., V. Cuomo, C. Filizzola, N. Pergola, and C. Pietrapertosa (2005), Assessing the potential of thermal infrared satellite surveys for monitoring seismically active areas: The case of Kocaeli (Izmit)

©2021. Japan Geoscience Union. All Right Reserved.

earthquake, August 17, 1999, Remote Sens. Environ., 96(3–4), 409–426, doi:10.1016/j.rse.2005.04.006.

Keywords: Earthquakes, Satellite thermal anomalies, Seismic hazard, Statistical analysis, Multi-parametric system, Japan

©2021. Japan Geoscience Union. All Right Reserved.

Radon Monitoring in the Gulf of Corinth, Greece

*VASSILIOS KARASTATHIS[1], G Elefteriou[1], M. Kafatos[2], K. Tsinganos[3], G Tselentis[1], D. Ouzounov[2], E Mouzakiotis[1]

1. National Observatory of Athens, 2. Chapman University, 3. National and Kapodistrian University of Athens

Significant new findings on the relation between soil radon variations with the natural seismicity and forthcoming events have been obtained after continuous real-time monitoring of soil radon concentration in the area of the Gulf of Corinth, Greece through a five-year period. The Gulf of Corinth, one of Earth's most active continental rift systems is a high seismic hazard area with many catastrophic earthquakes in its history; however its seismicity rate is not as high comparing to others active tectonic systems such as the Hellenic Arc region. The long quiescent periods between the major seismic events essentially help to establish a safe correlation of possible pre-earthquake radon variations with the seismic events. The Gulf of Corinth has a high rate of crustal extension of up to 1.5 cm/yr at the western part and 0.5 at the eastern one.

Two permanent real-time and continuously operating gamma-ray spectrometers have been installed in the area as a part of a larger network of radon monitoring stations covering South and Western Greece. More specifically, in order to observe pre-earthquake anomalies in radon concentration before strong earthquakes we have installed soil radon concentration monitoring stations at high seismicity areas such as the Hellenic arc in Western Greece and the eastern part of the Gulf of Corinth. The installation of the stations began in May 2016 and in all sites a real-time monitoring was established. The network is currently expanding with new stations at Crete.

The radon network was mainly based on NaI(Tl) scintillation detectors for γ-spectrometry. A full spectrum analysis processing that is applied to the data, provides us with a good energy resolution. At all stations there is detailed information of meteorological parameters that could affect the radon concentration measurements such as temperature, pressure, humidity and wind speed.

The Loutraki station, which is installed at a site close to a large fault with significant hydrothermal flux, provided us with highly interesting insights about the correlation of the seismicity rate with radon level at the area. However, an even more noteworthy observation is that the radon level variations also seem to follow a pattern, related to the stronger events. This station shows a very high consistency in the measurements and is strongly insulated from exogenous factors such as temperature, pressure and humidity.
Our results appear to be compatible with the “dilatancy model” that proposes an inelastic volumetric increase of rocks prior to failure. Before earthquakes there is accumulation of tectonic strain that produces a slow, steady increase of effective stress.

Before the major events there is a steady and slow increase of radon due to the increase of cracks and porosity and/or an increase in the flow rate of pore water. In addition, before strong events there is a significant drop of radon level.
Several seismic events have been associated with soil radon variations in three local radon monitoring stations.

©2021. Japan Geoscience Union. All Right Reserved.

Keywords: Radon monitoring, pre-earthquake phenomena, earthquake precursors

©2021. Japan Geoscience Union. All Right Reserved.

Earth’s crust as a new element of the LAIC model within the Global Electric Circuit concept

*Sergey A Pulinets[1], V. Gavrilov[2], V. Bogdanov[3], N. Blaustein[4]

1. Space Research Institute of the Russian Academy of Sciences, 2. Institute of Volcanology and Seismology, Far-East Branch of the Russian Academy of Sciences, 3. Institute of Cosmophysical Research and Radio Wave Propagation, Far-East Branch of the Russian Academy of Sciences, 4. Ben-Gurion University of the Negev, Israel

Multiparameter analysis (deep borehole measurements, vertical ionospheric sounding, GPS TEC, meteorological parameters) for several strong (M≧7) earthquake in Kamchatka peninsula area demonstrated the self-organizing process characteristic to the critical stage approaching. The most striking fact was the synchronization of variations of the specific resistivity of the earth crust measured at different depths in several boreholes close to Petropavlovsk-Kamchatsky and night-time positive ionospheric variations several days before the mains shock of strong earthquake. The vertical sounding provided by the "Parus" ionosonde at Paratunka (close to Petropavlovsk-Kamchatsky) in addition to variations similar to GPS TEC demonstrated several features in E-region of the ionosphere which usually interpreted as particle precipitation. Increase of the crust resistivity could be interpreted as the serial resistance added to the resistance of the boundary layer in the Global Electric Circuit (GEC) blocking the vertical fair weather current and leading to generation of the vertical electric field, which through the GEC induced the positive anomaly in the ionosphere. For Zhupanovskoye M7.2 earthquake on 30 January 2016 the increase of the apparent resistivity reached 700%. The sporadic E effects could be interpreted as E-layer delamination stimulated by acoustic gravity waves. This delamination was clearly demonstrated at oblique sounding ionograms before earthquakes in Vrancea zone observation. It is assumed that a joint multiparameter analysis of borehole measurement data and monitoring data of the state of the ionosphere will improve the reliability of determining the start of the final stage of earthquake preparation, since significant changes in ionospheric parameters occur, in general, no more than five days before strong Kamchatka earthquakes.

©2021. Japan Geoscience Union. All Right Reserved.

[E] Oral | M (Multidisciplinary and Interdisciplinary) | M-IS Intersection

[M-IS08] Interdisciplinary studies on pre-earthquake processes

convener:Katsumi Hattori(Department of Earth Sciences, Graduate School of Science, Chiba University), Dimitar Ouzounov(Center of Excellence in Earth Systems Modeling &Observations (CEESMO) , Schmid College of Science &Technology Chapman University, Orange, California, USA), Jann-Yenq LIU(Department of Space Science and Engineering, National Central University, Taiwan), Qinghua Huang(Peking University), Chairperson:Jann-Yenq LIU(Department of Space Science and Engineering, National Central University, Taiwan), Qinghua Huang(Peking University)
Sun. Jun 6, 2021 3:30 PM - 5:00 PM Ch.22 (Zoom Room 22)

The year 2021 is the memorial year of the 2011 Tohoku Earthquake (M9.0). For the past decade, we have advanced our knowledge of precursors and earthquake preparation processes.
This session expands the interdisciplinary discussions on the preparation process of earthquake and earthquake predictability by presenting the latest progress in studying the physically based pre-earthquake phenomena. New observations from space and ground have provided evidence, enhancing a better understanding of the tectonic activity. The session anticipates talks that include but is not limited to observations and analyses of seismic, electrical, electromagnetic, electro-chemical, and thermodynamic processes related to stress changes in the lithosphere along with their statistical and physical validation. Presentations on the latest observational results associated with major earthquakes obtained by different methodologies are welcomed. The topics of the session are as follows but not limited.

-General discussion on earthquake preparation process and the physics of pre-earthquake signals
- Theory, modeling, laboratory experiments, computational simulation for generation and propagation of pre-earthquake signals and their connection with the seismic cycle
- Multi-parameter observations, detection, and validation of pre-earthquake signals
- Cross-disciplinary studies, practical and technical approaches for better understanding of earthquake preparation processes and their connection with seismicity.

4:50 PM - 5:00 PM

[MIS08-17]Discussion

©Japan Geoscience Union

[E] Poster | M (Multidisciplinary and Interdisciplinary)：M-IS Intersection

Sun. Jun 6, 2021 5:15 PM - 6:30 PM JST | Sun. Jun 6, 2021 8:15 AM - 9:30 AM UTC | Ch.19_1

[M-IS08] Interdisciplinary studies on pre-earthquake processes

convener:Katsumi Hattori(Department of Earth Sciences, Graduate School of Science, Chiba University), Dimitar Ouzounov(Center of Excellence in Earth Systems Modeling & Observations (CEESMO) , Schmid College of Science & Technology Chapman University, Orange, California, USA), Jann-Yenq LIU(Department of Space Science and Engineering, National Central University, Taiwan), Qinghua Huang(Peking University)

The year 2021 is the memorial year of the 2011 Tohoku Earthquake (M9.0). For the past decade, we have advanced our knowledge of precursors and earthquake preparation processes.
This session expands the interdisciplinary discussions on the preparation process of earthquake and earthquake predictability by presenting the latest progress in studying the physically based pre-earthquake phenomena. New observations from space and ground have provided evidence, enhancing a better understanding of the tectonic activity. The session anticipates talks that include but is not limited to observations and analyses of seismic, electrical, electromagnetic, electro-chemical, and thermodynamic processes related to stress changes in the lithosphere along with their statistical and physical validation. Presentations on the latest observational results associated with major earthquakes obtained by different methodologies are welcomed. The topics of the session are as follows but not limited.

-General discussion on earthquake preparation process and the physics of pre-earthquake signals
- Theory, modeling, laboratory experiments, computational simulation for generation and propagation of pre-earthquake signals and their connection with the seismic cycle
- Multi-parameter observations, detection, and validation of pre-earthquake signals
- Cross-disciplinary studies, practical and technical approaches for better understanding of earthquake preparation processes and their connection with seismicity.

[MIS08-P01] Detecting clustered pre-earthquake anomalies of borehole strain network by Receiver Operating Characteristic Curve

★Invited Papers

*Zining Yu[1,2], Katsumi Hattori[3,4], Kaiguang Zhu[1,2], Mengxuan Fan[1,2], Dedalo Marchetti[2,5] (1.Key Laboratory of Geo-Exploration Instrumentation, Ministry of Education, Jilin University, Changchun 130061, China, 2.The College of Instrumentation and Electrical Engineering, Jilin University, Changchun 130061, China, 3.Graduate School of Science, Chiba University, Inage, Chiba 263-8522, Japan, 4.Center for Environmental Remote Sensing, Chiba University, Inage, Chiba 263-8522, Japan, 5.Istituto Nazionale di Geofisica e Vulcanologia, Via di Vigna Murata, 605 Rome, 00143, Italy)

[MIS08-P02] Statistical Analysis of Pre-seismic Ionospheric Electron Density Anomalies and Investigation of the Efficiency of Earthquake Forecasting

*Shunya Mitsuishi[1], Chie Yoshino[2], Katsumi Hattori[2,3], Jann-Yenq LIU[4] (1.Department of Earth Sciences, Faculty of Science, Chiba University, Japan, 2.Graduate School of Science, Chiba University, Japan, 3.Center for Environmental Remote Sensing, Chiba University, Japan , 4.National Central University, Taiwan)

[MIS08-P03] The fluctuation of the underground Rn flux near the surface

*Kazuhide Nemoto[1], Haruna Kojima[2], Chie Yoshino[3], Shu Kaneko[2], Katsumi Hattori[3], Toshiharu Konishi[4], Ryuichi Huruya[5] (1.Faculty of Science, Chiba University, 2.Graduate School of Science and Engineering, Chiba University, 3.Graduate School of Science, Chiba University, 4.OHYO KOKEN KOGYO Company Limited, 5.COM SYSTEM Incorporated)

[MIS08-P04] Development of Broadband Antenna System for Observation of Pre-Earthquake Electromagnetic Phenomena in LF range and Its Initial Observations

*Miura Kenshin[1], Katsumi Hattori[1], Chie Yoshino[1], Notiyuki Imazumi[2], Takeshi Morimoto[3], Yoshitaka Nakamura[4] (1.Chiba University, 2.The Institution of Professional Engineers, Japan, Chiba Chapter,

3.Kindai University, 4.Kobe City Collage of Technology)

[MIS08-P05] Numerical estimation of source current intensity causing ULF emission associated with earthquakes and correlation with the earthquake magnitude

*Ryota Kimura[1], Yoshiaki Ando[1], Masashi Hayakawa[2], Katsumi Hattori[3] (1. The University of Electro-Communications, 2.Hayakawa Institute of Seismo ElectroMagnetics Co. Ltd., 3.Chiba University)

[MIS08-P06] Development of Noise Reduction Method using two-stage MSSA (Multichannel Singular Spectrum Analysis) for MT data in Boso, Japan, Evaluation in Time series

*Shu Kaneko[1], Katsumi Hattori[2], Toru Mogi[2], Chie Yoshino[2] (1.Chiba University Graduate School of Science and Engineering, 2.Chiba University Graduate School of Science)

[MIS08-P07] **Correlations between geomagnetic *Sq* external and internal equivalent current systems in East-Asia and Oceania regions**

*Xiaocan Liu[1], Peng Han[4], Katsumi Hattori[2,3], Huaran Chen[1], Chie Yoshino[2] (1.Institute of geophysics China Earthquake Administrition, 2.Graduate School of Science, Chiba University, Chiba, Japan, 3.Center for Environmental Remote Sensing, Chiba University, Chiba, Japan, 4.Department of Earth and Space Sciences, Southern University of Science and Technology, ShenZhen, China)

Detecting clustered pre-earthquake anomalies of borehole strain network by Receiver Operating Characteristic Curve

*Zining Yu[1,2], Katsumi Hattori[3,4], Kaiguang Zhu[1,2], Mengxuan Fan[1,2], Dedalo Marchetti[2,5]

1. Key Laboratory of Geo-Exploration Instrumentation, Ministry of Education, Jilin University, Changchun 130061, China, 2. The College of Instrumentation and Electrical Engineering, Jilin University, Changchun 130061, China, 3. Graduate School of Science, Chiba University, Inage, Chiba 263-8522, Japan, 4. Center for Environmental Remote Sensing, Chiba University, Inage, Chiba 263-8522, Japan, 5. Istituto Nazionale di Geofisica e Vulcanologia, Via di Vigna Murata, 605 Rome, 00143, Italy

The preparatory process and the occurrence of shallow earthquakes are usually accompanied by crustal deformation. In recent years, the correlation between monitoring strain anomalies and local major earthquakes has been verified, however, whether these anomalies contain precursory information and their use in forecasting of major earthquakes were not evaluated.

In this study, we evaluate the possibility of strain anomalies containing earthquake precursors by using Receiver Operating Characteristic (ROC) prediction. First, strain network anomalies were extracted in the borehole strain data recorded in Western China during 2010-2017. Then, we considered the clustering characteristics of the anomalies and proposed a new prediction strategy characterized by the number of network anomalies in an anomaly window, N_ano, and the length of alarm window, T_alm, as shown in Fig. 1. We assumed that clusters of network anomalies indicate a probability increase of an impending earthquake, and consequently, the alarm window would be the duration that a possible earthquake would occur. The Area Under the ROC Curve (AUC) between true predicted rate, *tpr*, and false alarm rate, *fpr*, is measured to evaluate the efficiency of the prediction strategies.

First, we found that the optimal strategy of short-term forecasts has been established with AUC=0.82, by setting the number of anomalies greater than 7 within 14 days and alarm window at 1 day, as shown in Fig. 2. The results further show the prediction strategy performs significantly better when there are frequent enhanced network anomalies prior to the larger earthquakes surrounding the strain network region. Next, we tested the influence of different proportions of anomalies in an anomaly window under the condition of N_ano=7 and T_alm=1. The results are as shown in Fig. 3, when there were more than half (2N) or a third (3N) of network anomalies in an anomaly window, the detection efficiency was more significant and stable. When there were few anomalies in an anomaly window, the detection efficiency was low and especially when T_ano=8 N_ano, the result seems to be accidental and irregular. This result shows that clusters of anomalies indicate an increased probability of an earthquake, which is also consistent with the physical assumption of the prediction model.

In summary, we discussed whether the prediction strategy can be used in short-term forecasting and further demonstrated the influences of different proportions of anomalies in an anomaly window on short-term earthquake forecasting using AUC values. We confirmed that clusters of network anomalies may contain precursory information related to the earthquakes, and highlighted the potential for short-term earthquake forecasting.

Keywords: clustered pre-earthquake anomalies, Receiver Operating Characteristic, short-term earthquake forecasting

©2021. Japan Geoscience Union. All Right Reserved.

©2021. Japan Geoscience Union. All Right Reserved.

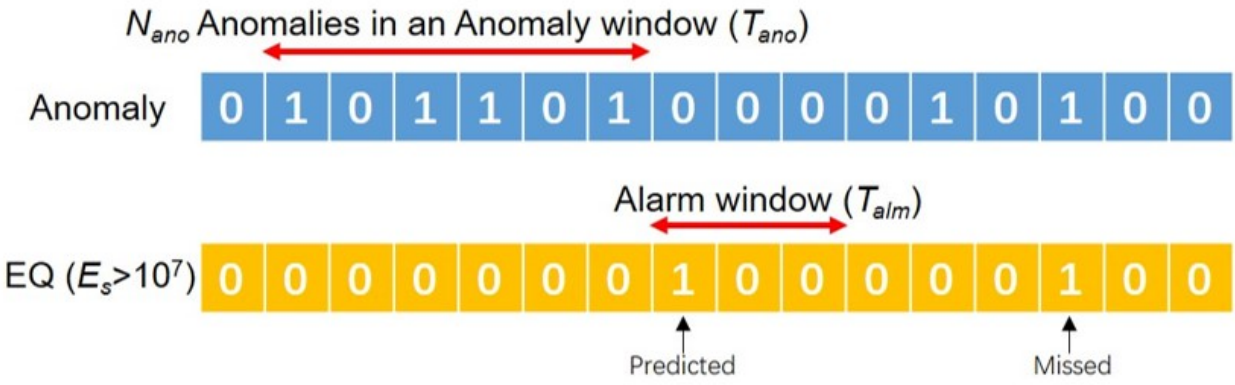


Fig. 1

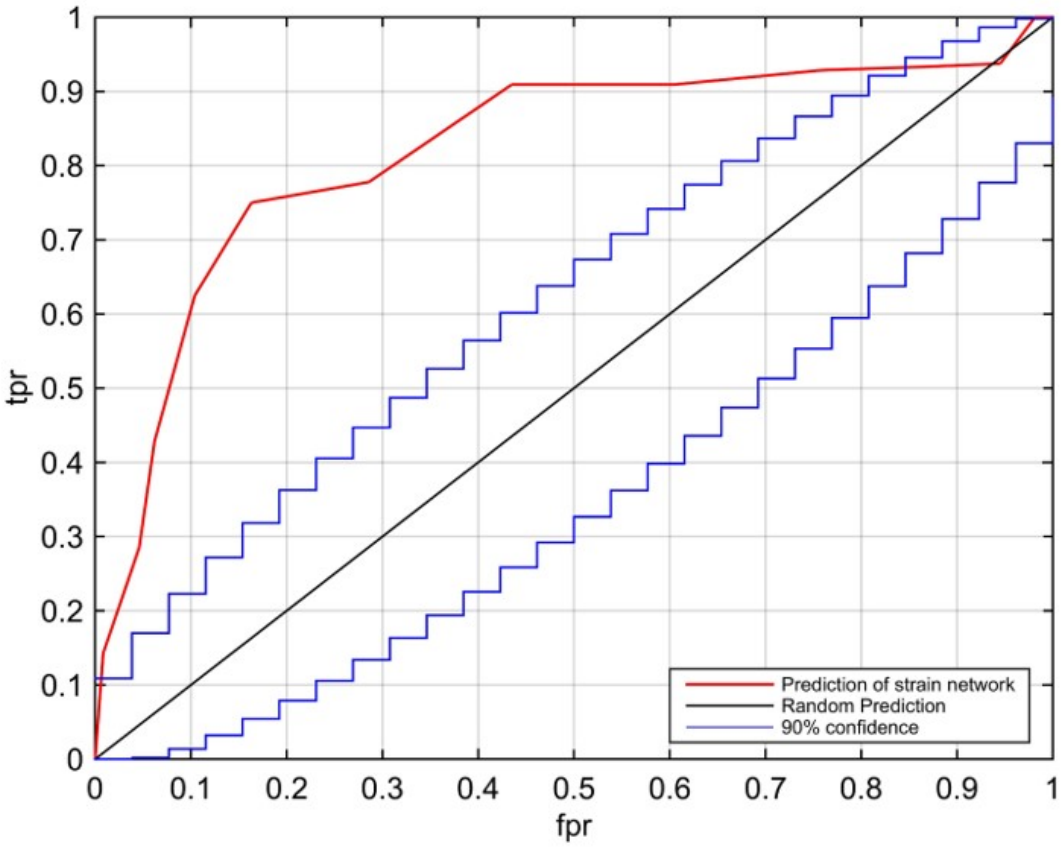
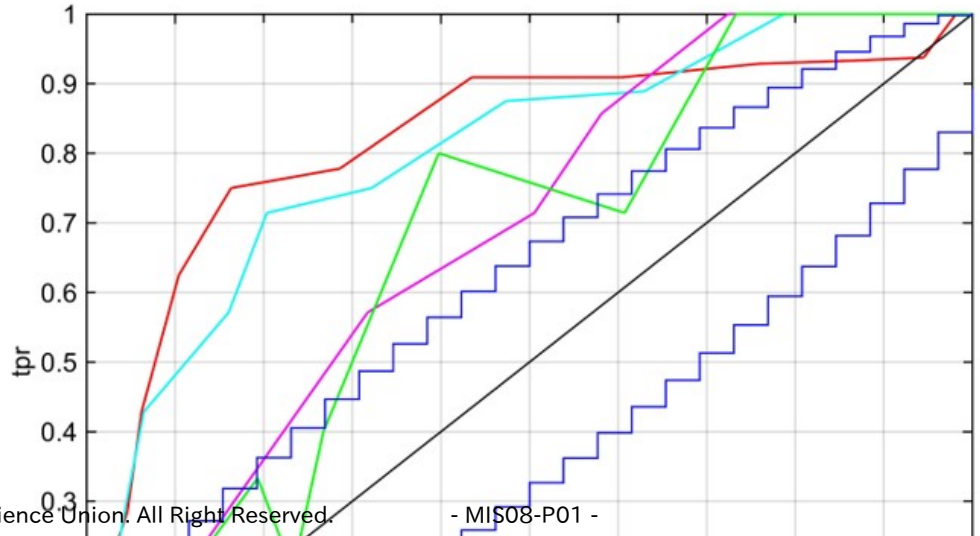


Fig. 2



©2021. Japan Geoscience Union. All Right Reserved.

©2021. Japan Geoscience Union. All Right Reserved.

Statistical Analysis of Pre-seismic Ionospheric Electron Density Anomalies and Investigation of the Efficiency of Earthquake Forecasting

*Shunya Mitsuishi[1], Chie Yoshino[2], Katsumi Hattori[2,3], Jann-Yenq LIU[4]

1. Department of Earth Sciences, Faculty of Science, Chiba University, Japan, 2. Graduate School of Science, Chiba University, Japan, 3. Center for Environmental Remote Sensing, Chiba University, Japan , 4. National Central University, Taiwan

Recently, ionospheric anomalies related to earthquakes have been reported and are considered promising for realizing short-term earthquake forecasting. In the Japan region, the previous statistical study during 1958-2017 shows a significant anomaly 1-10 days before the earthquakes with M>=6, depth D<=40 km, epicenter distance R<=350 km in NmF2, which indicates the maximum electron density in the F2 layer. However, the sensitivity of NmF2 anomalies for earthquakes is not clarified. Therefore, we performed statistical analysis to investigate the magnitude, depth, and epicenter distance dependences for earthquakes in which there is a significant positive anomaly in NmF2.
This study used ionosonde data observed at Kokubunji (35.71N, 139.49E), Japan, operated by the National Institute of Information and Communications Technology (NICT). We defined the threshold of the positive anomaly as the value of median + 1.5 IQR of the NmF2 at the same hour in the previous 15 days and the anomalous day as ten or more hours of the anomalies appear in one day. We performed the Superposed Epoch Analysis (SEA) to investigate statistical significance in the correlation between NmF2 anomalies and earthquakes. To evaluate the statistical significance, we repeated the random SEA test 100,000 times.
SEA results show that there is a significant NmF2 anomaly 6-10 days before the earthquakes. NmF2 anomalies have sensitivity for earthquakes with magnitude M>=5.8, depth D<=40 km, epicenter distance R<=350 km. Furthermore, these results indicated the magnitude, depth, and epicenter distance dependences of NmF2 anomalies.
We performed Molchan’ s Error Diagram (MED) analysis to evaluate the efficiency of NmF2 anomalies for earthquake forecasting. These results indicated that NmF2 anomalies are a precursor of earthquakes and it is more obvious for the shallower, the larger, and the closer earthquakes. We examined the optimum parameters for short-term earthquake forecast in lead time Δ, alarm window L, magnitude M, depth D, and epicenter distance R with NmF2 anomalies. The result indicated that the most effective forecast is given by M>=6.4, D<=20 km, R<=200 km, Δ=10, L=1. This set of parameters provides the detection of about 46% with the targeted earthquakes and the alarm rate is about 0.07.

©2021. Japan Geoscience Union. All Right Reserved.

The fluctuation of the underground Rn flux near the surface

*Kazuhide Nemoto[1], Haruna Kojima[2], Chie Yoshino[3], Shu Kaneko[2], Katsumi Hattori[3], Toshiharu Konishi[4], Ryuichi Huruya[5]

1. Faculty of Science, Chiba University, 2. Graduate School of Science and Engineering, Chiba University, 3. Graduate School of Science, Chiba University, 4. OHYO KOKEN KOGYO Company Limited, 5. COM SYSTEM Incorporated

In recent years, radon anomalies preceding large earthquakes have been reported, which are interpreted as modulation of Rn gas emanation due to stress changes in the earth’ s crust. For this verification, we are conducting continuous observations of underground radon concentration (GRC) in Asahi, Chiba Prefecture (N35.77, E140.69, June 2014-) and Miho Village, Ibaraki Prefecture (N35.99, E140.29, September 2020-), Japan. We have developed the method to estimate the underground Rn flux (GRF) by using the MSSA (Multi-channel Singular Spectrum Analysis) to remove the effects of weather factors of temperature and atmospheric pressure. GRF indicates the upward flow of Rn gas near the ground surface. However, GRF may be affected by heavy precipitations. We conducted a statistical analysis of the relationship between the fluctuation of GRF and precipitation. As a result, we found that GRF significantly increased after heavy rainfall events with 20 mm or more in 2 hours. This is caused by both the increase in load due to rainwater and the infiltration of rainwater near the station. Similar tendency is given for Miho station even though the data are very short. Excluding the influence of the above precipitation effects at the Asahi station, we compare the variation of GRF with the seismic activity near the station, we found there are cases where the GRF increases for reverse fault type earthquakes within an epicenter distance of 50 km from the station. This result suggests the possibility of GRF fluctuation due to the earthquake. In the future, it is necessary to quantitatively evaluate the relationship between the fluctuation of crustal stress fields and that of GRF at Miho and Asahi stations.

©2021. Japan Geoscience Union. All Right Reserved.

Development of Broadband Antenna System for Observation of Pre-Earthquake Electromagnetic Phenomena in LF range and Its Initial Observations

*Miura Kenshin[1], Katsumi Hattori[1], Chie Yoshino[1], Notiyuki Imazumi[2], Takeshi Morimoto[3], Yoshitaka Nakamura[4]

1. Chiba University, 2. The Institution of Professional Engineers, Japan, Chiba Chapter, 3. Kindai University, 4. Kobe City Collage of Technology

Increases in the electromagnetic pulse in the LF band have been reported as one of the electromagnetic phenomena preceding large earthquakes. Before the 1995 Hyogo-ken Nanbu Earthquake (M7.2), Oike et al. reported an increase in the number of pulses, and this phenomenon is considered to be the precursor for the earthquake. On the other hand, it has been suggested that some of these pulse increases are strongly affected by lightning. The issue is to distinguish between electromagnetic pulses caused by lightning and electromagnetic pulses that are precursors to earthquakes. Therefore, we developed the observation system for LF band electromagnetic waves, which can record detailed pulse waveforms, and investigated the relationship between the number of pulses and earthquakes, and analyzed their waveforms to extract the characteristics of the earthquake precursor pulse.

The observation system consists of a capacitive fast antenna with a circular flat plate, a 500 kHz low-pass filter, a 16-bit AD converter, and a PC for data recording. 100 ms data before and after the pulse waveform exceeding the trigger level (V_pp = 6000 [du]) is registered at 4 MHz sampling. The system was installed on the top of the roof of Science Building No. 5, Chiba University. The analyzed period is from May 1, 2018, to May 31, 2019.
First, the total number of pulses recorded in the system was counted and the amplitude histogram was created. We decided to investigate the temporal variation of the top 15% of pulses (V_pp ≧ 28880 [d.u.]). The mean value m and standard deviation σ for the entire analyzed period was calculated, and the anomaly in the number of pulses was defined as $m + 2\sigma$. Next, we identify well-known pulses related to the lightning with waveforms and products of lightning discharge (cloud to ground discharge only) location estimated by blitzortung.org. Then, we investigate the relationship between the temporal change of the number of the pulse and earthquakes. We selected seven earthquakes that occurred during the observation period within an epicenter distance of 100 km and satisfy log (Es)>8, where $Es=10^{1.5M+4.8}/r^2$, M and r are the magnitude and hypocenter distance, respectively. As a result, an abnormal increase in the number of pulses of $m + 2\sigma$ threshold and without lightning determined by blitzortung was observed four days before the M5.0 earthquake on November 27, 2018. Similar pulse waveforms did not exceed the $m + 2\sigma$ threshold but were also observed before the other 4 earthquakes with log (Es)>8 that occurred during the observation period. These pulses may be due to seismic precursor electromagnetic radiation. On the other hand, it is possible that the pulse waveform is due to the discharge in the clouds. It is found that the identification of the location of discharge should be completed by an interferometer system to distinguish between the cloud-cloud discharges and earthquake-related discharge.

Keywords: Earthquake, Lightning Discharge

©2021. Japan Geoscience Union. All Right Reserved.

Numerical estimation of source current intensity causing ULF emission associated with earthquakes and correlation with the earthquake magnitude

*Ryota Kimura[1], Yoshiaki Ando[1], Masashi Hayakawa[2], Katsumi Hattori[3]

1. The University of Electro-Communications, 2. Hayakawa Institute of Seismo ElectroMagnetics Co. Ltd., 3. Chiba University

For decades, many papers reported that the Ultra Low Frequency (ULF) emission associated with earthquakes were observed by magnetometers installed at the Earth's surface. In this study, we have developed the numerical simulation of the ULF wave propagation in the lithosphere, by using the the weighted Laguerre polynomial finite-difference time-domain (WLP-FDTD) method. The numerical simulation allows us to estimate the source current intensity from observed electromagnetic fields in the ULF band. The correlation between magnitude of earthquakes and the estimated source current intensity is deduced from the numerical simulation.

The observed ULF anomaly depends on the time before the main shock of earthquakes, which are classified as follows: (1) Preseismic anomaly occurs several days before the main shock and (2) Near-seismic ULF bursts are observed around several hours around the main shock.

We adopt Loma Prieta earthquake as a standard because both the preseismic and the near-seismic effects are observed for this event, and because the observation was performed over wide range of frequency bands. The different current intensity spectra are deduced from the observed magnetic fields.

The source current intensity of other earthquakes, such as Spitak(1988), Guam(1993), Biak(1996), and so on, are analyzed, considering their observed time preceding the main shock, and the relative intensity of their source currents are identified.

From the above analyses, it is found that the relative intensity of source currents shows good correlation with the magnitude of EQs.

Keywords: Ultra Low Frequency electromagnetic wave, Weighted Laguerre Polynomial FDTD, Seismo-electromagnetics

©2021. Japan Geoscience Union. All Right Reserved.

Development of Noise Reduction Method using two-stage MSSA (Multichannel Singular Spectrum Analysis) for MT data in Boso, Japan, Evaluation in Time series

*Shu Kaneko[1], Katsumi Hattori[2], Toru Mogi[2], Chie Yoshino[2]

1. Chiba University Graduate School of Science and Engineering, 2. Chiba University Graduate School of Science

There is a triple junction of the Pacific Plate, the Philippine Sea Plate, and the North American Plate off the coast of the Boso Peninsula and it is one of the most active areas of the crustal activity. To investigate the subsurface resistivity structure of the whole Boso area, magnetotelluric (MT) survey with 41 sites (inter-sites distance of 7 km) has been conducted in 2014-2016, using U43 (12 sites, 1 Hz sampling ; Tierra Technica) and MTU-5, 5A, net (41 sites, 15, 150, and 2400 Hz sampling; Phoenix Geophysics). However, the Boso area is greatly affected by leak current from DC-driven trains, factories, and power lines, so the observed data are severely contaminated by artificial noises. When we tried to apply the conventional noise reduction methods (e.g., remote reference (Gamble et al., 1979) and BIRRP (Chave and Thomson, 2004)) in frequency domain, the obtained MT sounding curve was not ideal. In particular, the phases between the periods of 20 and 400 sec were close to 0 degrees. It suggests that these conventional methods are insufficient to reduce the near-field effects for the Boso data. Thus, we developed a new noise reduction method using MSSA (Multi-channel Singular Spectrum Analysis) as a time domain pre-processing method.

The procedure is as follows;
(1) Decompose 6 component data (Hx, Hy, Ex, Ey, Hxr and Hyr: H and E means magnetic and electric field, respectively, x and y indicates NS and EW component, and r denotes the reference field observed at a quiet station) using MSSA into 6×L principal components (PCs). Here, L shows the window length of MSSA.
(2) Check each PC's contribution and periods and eliminate the PCs corresponding to the longer than 400 sec. That means "detrend" of the original data.
(3) Apply the second MSSA to the detrended time series data to separate signals and noises shorter than 400 sec.
(4) Calculate correlation coefficients between H and Hr and between E and Hr for each PC and select the PCs with higher correlation to "reconstruct" time series data to make MT analysis.

Then, we perform MT analysis by BIRRP to estimate MT response functions,
As a result, the MT sounding curve became smoother than those results by the conventional noise reduction methods. It indicates that the effectiveness of the proposed noise reduction.
In the presentation, we will discuss the evaluation of time series noise reduction in detail.

Keywords: MT method, Multi-channel Singular Spectrum Analysis, Noise reduction, Boso peninsula

©2021. Japan Geoscience Union. All Right Reserved.

Correlations between geomagnetic *S*q external and internal equivalent current systems in East-Asia and Oceania regions

*Xiaocan Liu[1], Peng Han[4], Katsumi Hattori[2,3], Huaran Chen[1], Chie Yoshino[2]

1. Institute of geophysics China Earthquake Administrition, 2. Graduate School of Science, Chiba University, Chiba, Japan, 3. Center for Environmental Remote Sensing, Chiba University, Chiba, Japan, 4. Department of Earth and Space Sciences, Southern University of Science and Technology, ShenZhen, China

Abstract Geomagnetic *S*q variation, namely the solar quiet daily variation [*Campbell,* 1989; *Xu*, 2003; *Yamazaki*, 2009], originates from the dynamo currents (external source current) at about an altitude of 100km in the ionosphere and the induced currents (internal source current) generated underground by the external source current [*Chapman and Bartels*, 1940; *Chapman*, 1951; *Kane*, 1976; *Xu*, 2003]. The *S*q variations recorded by the ground stations contain total geomagnetic effects produced by the two current systems. The *S*q currents deduced from the data of ground geomagnetic observatories are called *S*q equivalent current systems. Most previous studies focused on kinds of the variations for the two *S*q current systems. So far, we don't know what the consistency of the activities for the two parts current systems is, whether they are completely the same, or there are differences.

In present work, the absolute values of geomagnetic three components (XYZ) data from 20 observatories in East-Asia and Oceania regions were used to investigate the correlations between the external and internal *S*q current systems. The seasonal current models of D (northern winter) season, E (equinox) season, and J (northern summer) season have been constructed by SHA (Spherical Harmonic Analysis) respectively. The intra-seasonal correlations of the current vortex center parameters T (local time), Φ (latitude), J (current intensity) between the *S*q equivalent internal and external currents are analyzed. The results show that (1) in the E season, the correlation of T is the highest, the square of correlation coefficients is R^2=0.857 in the NH (northern hemisphere). (2) And in the local summer and winter, the correlation of J is the strongest. The square of correlation coefficients are R^2= 0.490 and 0.778, respectively, and also in the NH.

The mechanism for different seasonal correlations of different current vortex center parameters between the external and internal current systems is roughly considered. In fact, as two parts of the same current system, solar activity, ionospheric conductivity, neutral wind field, geomagnetic field and so on affect the internal and external current systems. At the same time, the variations of internal current are also controlled by the conductivity of underground conductive circle in the upper mantle. [*Schmucker* 1970; *Campbell* 1987, *Campbell and Schiffmacher*, 1988].

Keywords: Sq external current, Sq internal current, correlation, East-Asia and Oceania regions

©2021. Japan Geoscience Union. All Right Reserved.

[J] Oral | M (Multidisciplinary and Interdisciplinary)：M-IS Intersection

Sun. Jun 6, 2021 9:00 AM - 10:30 AM JST | Sun. Jun 6, 2021 12:00 AM - 1:30 AM UTC | Ch.25 Zoom Room 25

[M-IS13] Dynamics of eruption cloud and cumulonimbus; modelling and observation

convener:Eiichi Sato(Meteorological Research Institute), Fukashi Maeno(Earthquake Research Institute, University of Tokyo), Takeshi Maesaka(National Research Institute for Earth Science and Disaster Resilience), Chairperson:Eiichi Sato(Meteorological Research Institute)

Volcanic eruption clouds (eruption column, pyroclastic flow, and umbrella cloud) and cumulonimbus are similar phenomena in the atmosphere. Models that can precisely reproduce the physical processes in such phenomena, and accurate observations have been required. Recently, the development of remote sensing techniques such as weather radar and weather satellite are remarkable, and they are being adopted for volcanic eruption monitoring. However, it is indispensable to verify the results of modeling and remote sensing using in-situ observations. In this session, we will discuss the modelling and the observations of eruption clouds and cumulonimbus from the viewpoint of meteorology, volcanology, geology, and other related fields. The related phenomena such as ashfall, rainfall, snowfall, hail and volcanic block will also be discussed.

9:00 AM - 9:15 AM JST | 12:00 AM - 12:15 AM UTC

[MIS13-01] Radar Meteorological Study on Falling Volcaic Ash Particles

★Invited Papers

*Masayuki Maki[1] (1.Research and Education Center for Natural Hazards, Kagoshima University)

9:15 AM - 9:30 AM JST | 12:15 AM - 12:30 AM UTC

[MIS13-02] PUFF Model Prediction of Volcanic Ash Plume Dispersal for Sakurajima Using MP Radar Observation

*Hiroshi Tanaka[1], Haruhisa Nakamichi[2], Masato Iguchi[2] (1.Center for Computational Sciences, University of Tsukuba, 2.Sakurajima Volcano Research Center, DPRC, Kyoto University, Kagoshima)

9:30 AM - 9:45 AM JST | 12:30 AM - 12:45 AM UTC

[MIS13-03] Numerical simulation of wind flow around Sakurajima with eruption

*Takashi Maruyama[1], Masato Iguchi[1] (1.Disaster Prevention Research Institute, Kyoto University)

9:45 AM - 10:00 AM JST | 12:45 AM - 1:00 AM UTC

[MIS13-04] Highspeed image observation of ballistic projectiles at Sakurajima volcano and a numerical model of ballistics

*Kae Tsunematsu[1], Saruta Shusaku[1], Taishi Yamada[2], Masato Iguchi[2] (1.Yamagata University, 2.Kyoto University)

10:00 AM - 10:15 AM JST | 1:00 AM - 1:15 AM UTC

[MIS13-05] Pattern classification of parent clouds of tornadoes in Tosa Bay

*Koji Sassa[1], Kotarou Fujii[2] (1.Natural Science Cluster, Kochi University, 2.Graduate School of Integrated Arts and Sciences, Kochi University)

10:15 AM - 10:30 AM JST | 1:15 AM - 1:30 AM UTC

[MIS13-06] Cloud-Scientific Study of Volcano Eruption -perspective-

★Invited Papers

*Yasushi Fujiyoshi[1] (1.Emeritus Prof. of Hokkaido University)

Radar Meteorological Study on Falling Volcaic Ash Particles

*Masayuki Maki[1]

1. Research and Education Center for Natural Hazards, Kagoshima University

In the present study, we describe fundamental characteristics of falling volcanic ash particles such as the particle size distribution, fall velocity, shape, et al. from the radar meteorological view point. Because it is beneficial for the weather radar monitoring of ash fall to identify similarities and differences between rain drops and ash particles, we present the results of analyses of the rain drop data collected by two-dimensional video disdrometers, As for the volcanic ash particles, we presented the results of Maki et al. (2021) who analyzed the particle size distribution (PSD) of falling volcanic ash particles measured using optical disdrometers during six explosive eruptions of the Sakurajima volcano in Kagoshima Prefecture, Japan. We found that PSD for both rain drops and ash particles could be expressed by the gamma distribution, $N(D) = N_0 D^{\mu} \exp(-\Lambda D)$, where $N(D)$ is the particle size distribution, D is the particle diameter, N_0 is the intercept parameter, Λ is the slope parameter, and μ is the shape parameter. The relationships between each of the gamma PSD parameters were shown to be a characteristic of falling volcanic ash particles. The strong correlation between R_A/N_w and D_m suggests that the normalized intercept parameter N_w and mass-weighted mean diameter D_m are suitable for estimating the ash fall rate R_A. We also derived empirical power law relationships between pairs of integrated PSD parameters: R_A, the volcanic ash mass concentration C_A, the reflectivity factor Z, and the total number of the ash particles per unit volume N_T. The results of the present study provide essential information for studying microphysical processes in volcanic ash clouds, for developing a method for quantitative ash fall estimation using weather radar, and for improving ash transport and sedimentation models.

Keywords: particle size distribution, disdrometer, polarimetric radar parameters

©2021. Japan Geoscience Union. All Right Reserved.

PUFF Model Prediction of Volcanic Ash Plume Dispersal for Sakurajima Using MP Radar Observation

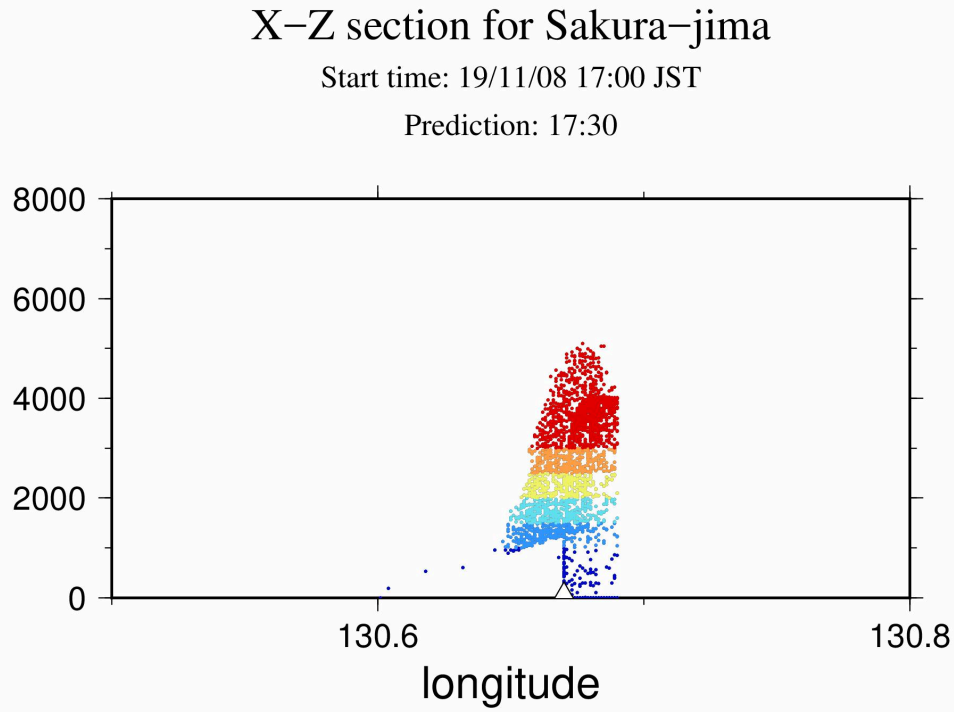
*Hiroshi Tanaka[1], Haruhisa Nakamichi[2], Masato Iguchi[2]

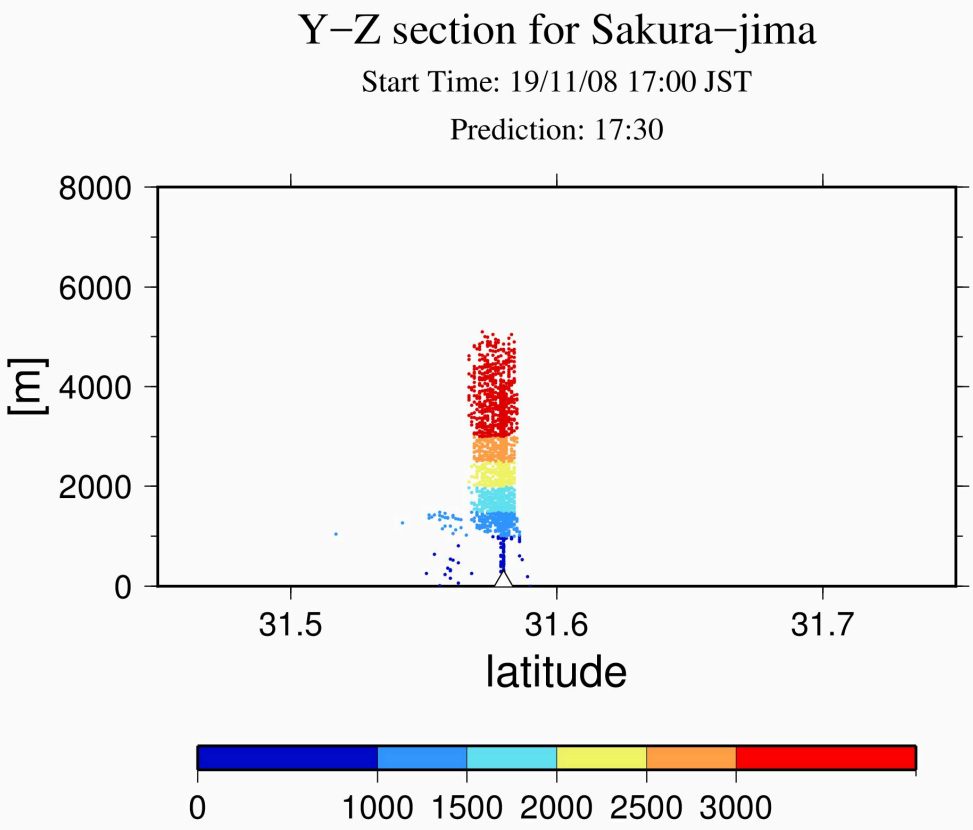
1. Center for Computational Sciences, University of Tsukuba, 2. Sakurajima Volcano Research Center, DPRC, Kyoto University, Kagoshima

In this study, a real-time volcanic ash plume prediction by the PUFF system was applied to the Sakurajima volcano (which erupted at 17:24 Japan Standard Time (JST) on 8 November, 2019), using the direct observation of the multi-parameter (MP) radar data installed at the Sakurajima Volcano Research Center. The MP radar showed a plume height of 5500 m a.s.l. around the volcano. The height was higher than the 4000 m by the PUFF system, but was lower than the observational report of 6500 m by the Japan Meteorological Agency in Kagoshima. In this study, ash particles by the MP radar observation were assimilated to the running PUFF system operated by the real-time emission rate and plume height, since the radar provides accurate plume height. According to the simulation results, the model prediction has been improved in the shape of the ash cloud with accurate plume top by the new MP radar observation. The plume top is corrected from 4000 m to 5500 m a.s.l., and the three-dimensional (3D) ash dispersal agrees with the observation. It was demonstrated by this study that the direct observation of MP radar obviously improved the model prediction, and enhanced the reliability of the prediction model.

Keywords: ash dispersion, Sakurajima volcano, data assimilation

©2021. Japan Geoscience Union. All Right Reserved.





©2021. Japan Geoscience Union. All Right Reserved.

Numerical simulation of wind flow around Sakurajima with eruption

*Takashi Maruyama[1], Masato Iguchi[1]

1. Disaster Prevention Research Institute, Kyoto University

1. Introduction
Volcanic eruption products such as ash, ciders, hazardous gas and so on sometimes cause disasters. Volcanic ash harms crops, traffics, transportations, human health and so on. Flying ciders, lapilli and volcanic blocks often cause loss of lives and structures so as the eruption of Mt. Ontake in September 2014 causing 63 deaths and missing persons [1]. Accurate prediction of the product’ s distribution is necessary for prevention and mitigation of the disaster. The distribution of flying products is affected by the air flow around the volcano, therefore the prediction of the flow field is essential for the prevention and mitigation of the volcanic disasters.
The trajectory of the volcanic smoke, ash and the flying product is directly affected by the wind flow, resulting in a distribution of the density of eruption products. The flow field around the volcano varies with the meteorological condition, the topography and the surface roughness. And fluctuation of the flow affects the distribution of the density.
2. Outline of Calculation
We designed a numerical simulation of wind flow around Sakurajima Volcano. The large eddy simulation using the Smagorinsky model was used for calculating the turbulent flow fields. The spatial averaging was conducted to the governing equation of the fluid and the effect of drag caused by the surface roughness such as plants and the buildings are added to the governing equations as a canopy model [2]. The curvilinear coordinate system was used for generating the topography. The meteorological condition was introduced as an inflow condition with wind velocity and temperature field obtained from the mesoscale numerical weather prediction model WRF. The eruption was expressed as a blowout of hot air and the effect of buoyancy was introduced by Boussinesq approximation. The volcanic ash was calculated as a diffusion of scalar density.
3. Calculated Results
Turbulent wind flow around Sakurajima volcano with eruption was simulated. The distribution of plants and buildings on the ground surface was obtained from the GIS data base and field survey. Space-time variation of wind velocity, temperature and ash density was obtained as shown in Figure 1.
4. Conclusions
Numerical method of turbulent flow field around a volcano with eruption was presented. The effect of surface roughness, topography, meteorological condition and eruption was reflected to the simulated turbulent wind fields.
Reference
1. Oikawa, T.; Yamaoka, K.; Yoshimoto, M.; Nakada, S.; Takeshita, Y.; Maeno, F.; Ishizuka, Y.; Komori, J.; Shimano, T.; Nakano, S. The 2014 Eruption of Ontake Volcano, Central Japan. Volcanol. Soc. Japan 2015, 60, 411–415.
2. Maruyama, T. (2008). Large eddy simulation of turbulent flow around a windbreak. Journal of Wind Engineering and Industrial Aerodynamics 96, 1998–2006.
Acknowledgments: This research was funded by Integrated Program for Next Generation Volcano Research and Human Resource Development・Issue D: Development of volcanic disaster countermeasure technology・Sub-theme 2: “Development of real-time volcanic ash hazard evaluation method”.

©2021. Japan Geoscience Union. All Right Reserved.

Keywords: numerical simulation, wind flow, eruption, Sakurajima

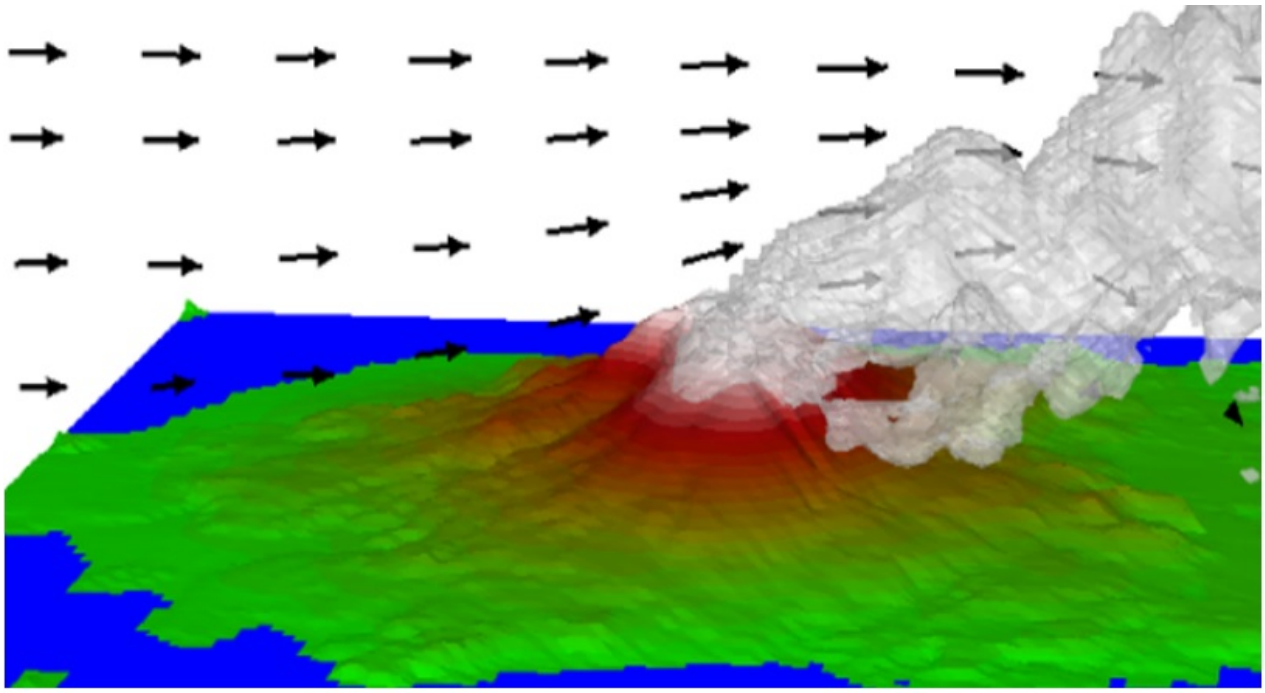


Fig. 1 Simulated diffusion of volcanic ash in the neutral wind condition

©2021. Japan Geoscience Union. All Right Reserved.

Highspeed image observation of ballistic projectiles at Sakurajima volcano and a numerical model of ballistics

*Kae Tsunematsu[1], Saruta Shusaku[1], Taishi Yamada[2], Masato Iguchi[2]

1. Yamagata University, 2. Kyoto University

Sakurajima is one of the most active volcanoes in Japan and in the world, erupting explosively. Vulcanian eruptions are the most frequent eruption type in Sakurajima, and ballistic blocks are often ejected during vulcanian eruptions. In Sakurajima, a ballistic block ejected during the eruption on June 4, 2020 and it landed in the resident area called “Yuno”, 3.4 km from the vent. This was an exceptional event that a block traveled so long distance (longer than 2.5 km) after the block landed also in the Yuno area in 1987. The impact crater due to the ballistic block was six meters in diameter. Moreover, near the block landing location, another block penetrated the roof of the hut. Thus, people living near the volcano have risks being hit by blocks, and it is important for assessing ballistic hazards using numerical models.

Recently, numerical models of ballistics were suggested by Tsunematsu et al. (2016), Biass et al. (2016) and Bertin (2017), while the models cannot express some characteristics of ballistic transport. Especially, the model consists mainly of gravity and air drag terms, but some phenomena, such as that larger particles travel shorter distance than smaller particles, are not reproduced by these models. It is necessary to elucidate another force by observations of experiments or real eruptions. In fact, based on the hypothesis that the ejection of ballistic projectiles is affected by the gas flow near the vent, we carried out experiments. However, we could not verify our hypothesis. Therefore, we have observed the vulcanian eruption in Sakurajima volcano and a numerical simulation result using a model Ballista (Tsunematsu et al., 2016) is compared with the block trajectories.

Campaign observation was carried out on Mt. Harutayama in Sakurajima from January 25 to January 29, 2021 using two highspeed cameras installed on a roof terrace of the Harutayama branch of Sakurajima Volcano Research Center. Mt. Harutayama is located approximately 2.7 km from the Sakurajima active vent “A” and “B”. One highspeed camera is for a monochrome shooting with an 800 mm zoom lens and another is for a color shooting with a 135 mm zoom lens.

During the campaign observation, the weather was sometimes unstable and sometimes the Harutayama region was covered by the ash clouds due to the Sakurajima continuous ash ejection. We successfully shoot an explosion at 16:48 (JST) on January 28. A seismic monitor showed the explosion waves, and the switch was turned on at the same time as the sound of the explosion. Although the color highspeed camera did not record any block as the magnification of this camera was not enough, the monochrome camera recorded seven blocks traveling in the air.
The vertical speed of these blocks was ~10 to 50 m/s, which was much smaller than the ejection speed recorded during the Strombolian eruptions (Taddeucci et al., 2017). As the crater wall around the vent A and B was ~400 m higher than the bottom of the craters, the blocks travelled this vertical interval. The smaller velocity was probably due to the velocity decay during the travel of this height difference. In our presentation, we would like to present the result of the image analysis of the explosion and discuss the ballistic transport mechanism based on the comparison of these result with simulated trajectories.

Keywords: Ballistic projectiles, Explosive eruptions, Sakurajima volcano, Numerical models

©2021. Japan Geoscience Union. All Right Reserved.

©2021. Japan Geoscience Union. All Right Reserved.

Pattern classification of parent clouds of tornadoes in Tosa Bay

*Koji Sassa[1], Kotarou Fujii[2]

1. Natural Science Cluster, Kochi University, 2. Graduate School of Integrated Arts and Sciences, Kochi University

The coast line of Tosa Bay in Kochi Prefecture is one of the area where tornadoes frequently occur. We have continuously made the radar observation with the radar network composed of six compact polarimetric radars of Kochi University. Most of parent clouds of tornadoes reported by JMA Kochi observatory were captured by our radars from 2014 to 2020. The present study aims to classify the parent clouds of tornadoes and to clarify their characteristics. Our final goal is the establishment of warning system automatically detecting the parent clouds with machine learning.
From the results of analysis, we found that the parent clouds could be classified to following 5 patterns; supercell, wavy cloud, cloud cluster, squall line and isolated cell. Fig.1 shows the example of supercell. The mesocyclone is shown in the southwest end of the high intensity echo region. Fig. 2 shows the example of wavy clouds appeared far away from the typhoon. The vortex is shown in the southwest end of the southern system. The example of cloud cluster composed of small cumulonimbi is shown in Fig.3 The moving velocity of the system was quite slow. Fig.4 shows the example of squall line. The moving direction was east and it has large angle with respect to the direction of the system. The example the one of the isolated cells passing through the radar was the parent cloud of a tornado is shown in Fig.5. The hook echo which shows the existence of a tornado vortex is clearly observed in the east end of the isolated cell, though its horizontal scale is small about 10 km in length.
The majority was the isolated cell. 11 cases were found to be it. The length of the isolated cells was less than 10 km in most cases. The length of the other systems exceeded 20km, but the width of wavy cloud and squall line was about 5km. The moving velocity of the supercell, wavy cloud and squall line was larger than the other systems. And we also found that the vortex located in the rear side of most of the parent clouds.
In the present study, we will discuss about the temporal change of the parent clouds.

Keywords: Radar observation, Tornado, Parent cloud

©2021. Japan Geoscience Union. All Right Reserved.

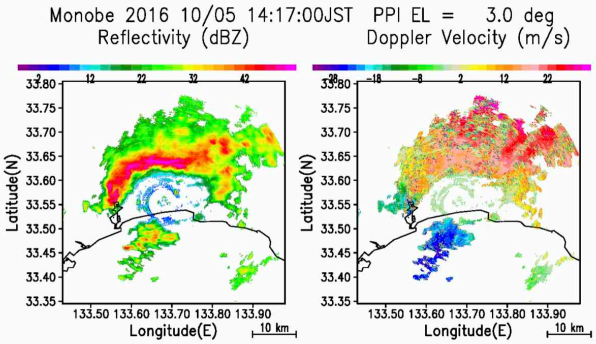


Fig.1 Example of supercell

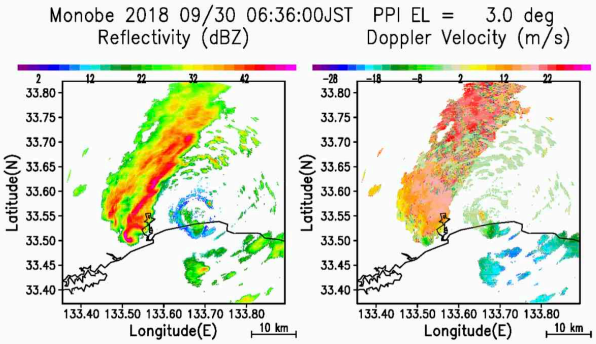


Fig.2 Example of wavy cloud

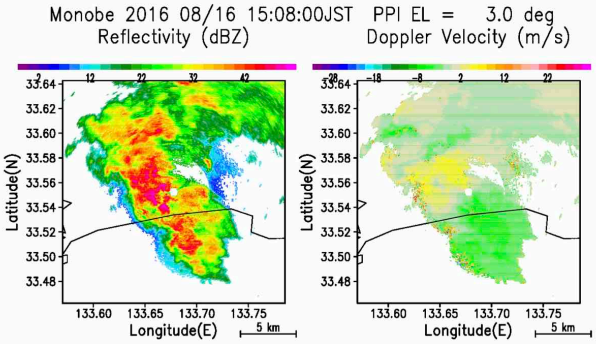


Fig.3 Example of cloud cluster

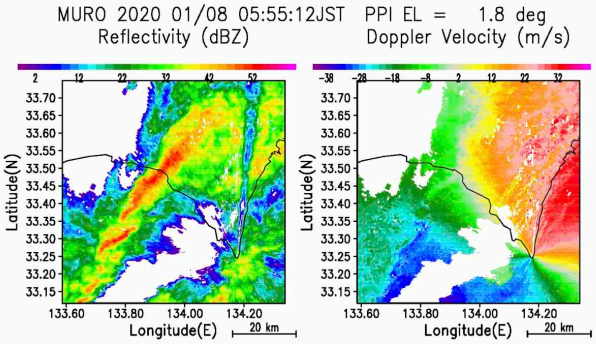


Fig.4 Example of squall line

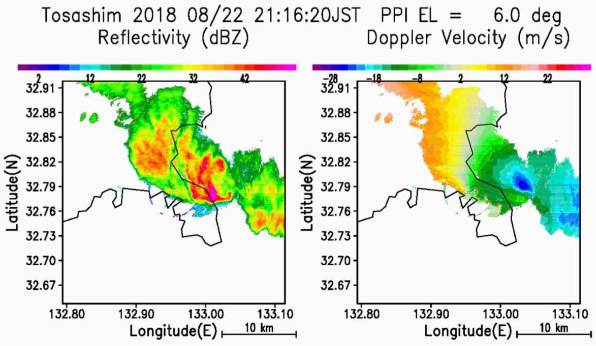


Fig.5 Example of isolated cell

©2021. Japan Geoscience Union. All Right Reserved.

Cloud-Scientific Study of Volcano Eruption -perspective-

*Yasushi Fujiyoshi[1]

1. Emeritus Prof. of Hokkaido University

This presentation aims to emphasize how cooperative observation and modeling of volcanic eruption clouds will result in mutual benefit.

Many numerical models can simulate atmospheric convective clouds if initial and environmental conditions (CCN, IN, vertical profiles of temperature, humidity, and winds, etc.) are given. However, it is almost impossible to observe these conditions, because natural clouds develop sporadically, move fast, and change rapidly. Indeed, strictly speaking, there are no numerical models verified by field observations. If we know where a cloud develops, we will be able to verify and improve the formula and parameters assumed in these cloud models.

Volcanic eruption clouds, on the other hand, develop at the same place. Therefore, observation of volcanic eruption clouds has the potential to validate numerical models. For example, using marine radars, we succeeded in estimating the high-temporal (2 sec.) and spatial (5 m) change of height, volume, and ascending speed of Sakurajima volcanic clouds (Maki et al., 2020). These data will be useful to study the dynamics of convection in the air. We also observed a small rain cloud originated from the volcanic eruption (Fig. 1). A small eruption occurred at 09:46 JST on 18 Sep. 2019, and the ash cloud reached 1800 m a.s.l.. A small cloud (condensation) began to develop at 9:50 JST, precipitation occurred at 09:51 JST, and raindrops reached the ground surface at 09:55 JST. These high-temporal and spatial data are also useful to validate microphysical processes used in cloud models.

On 5 Nov. 2019, rising volcanic ash began to fall rapidly (Fig. 2). A small eruption occurred at 12:41 JST, and the ash cloud reached 1900 m a.s.l.. The radar echo indicates that the ash cloud began to dissipate in its middle part at 12:45 JST. The lower part of the ash cloud went down to the ground very fast like a downburst. The upper air sounding data suggests that this downburst-like phenomenon was caused by dry air intrusion at the middle part level. This case clearly shows that vertical atmospheric stratification strongly affects volcanic ash transport and dispersion. We also compared electric potential gradient changes with the temporal change of radar echoes of eruption clouds. These surface and in-situ data will be useful to study the charging, charge separation, and lightning mechanisms of volcanic clouds as well as the electrification of natural clouds.

Modeling eruption clouds is challenging for meteorological researchers, although almost the same physical processes are involved both in eruption clouds and atmospheric clouds. For example, turbulence and updraft within eruption clouds are much stronger than those in atmospheric clouds. Components within eruption clouds are more complicated than those in atmospheric clouds. A larger size range of particles is included in eruption clouds than those in atmospheric clouds. Vertical profiles of temperature and updraft within eruption clouds are opposite to those within atmospheric clouds. Some volcanic ejecta is formed by fragmentation and solidification of liquid state lava. On the other hand, raindrops (liquid) are formed by melting and fragmenting snow particles (solid-state). Figure 3 shows 2DVD (2-Dimensional Video Distrometer) images of melting snow particles. It is quite interesting that these melting particles have almost the same shape as those of volcanic bombs (aggregates, spindle-shaped, ribbon-shaped, Peles’ s tear, etc.).

©2021. Japan Geoscience Union. All Right Reserved.

Reference
Maki, M., et al., 2020: Monitoring of Sakurajima Volcanic Eruption Columns with Marine Radar - Results of Observations in 2018 -, *Disaster Prevention Research Institute Annuals. B*, 2020, 63.B: 136-148.

Keywords: cloud science, volcanic eruption

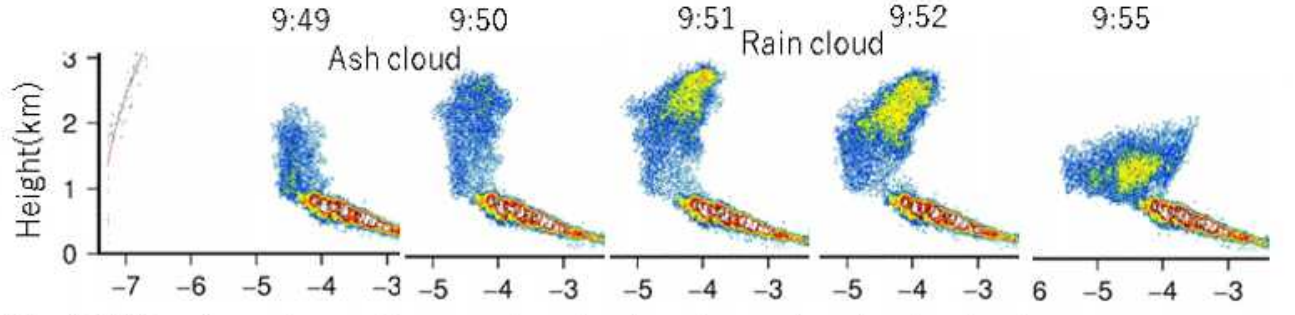


Fig.1 RHI radar echoes of an erupion cloud and associated rain cloud.

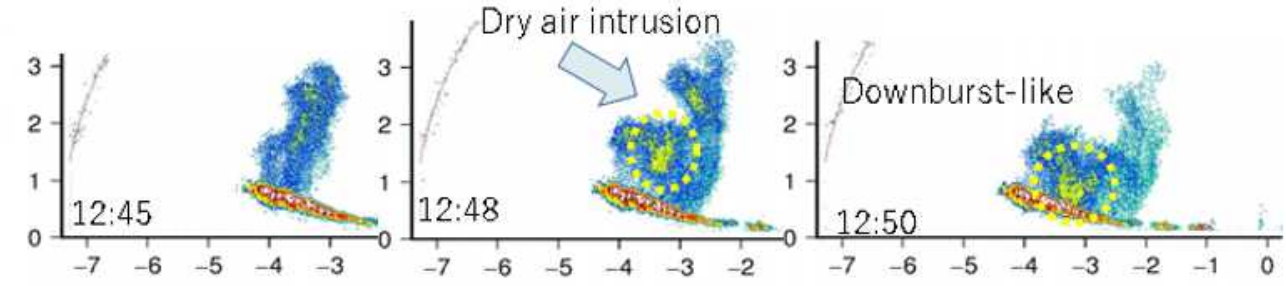


Fig. 2 RHI radar echoes of an ash cloud and associated downburst-like phenomenon.

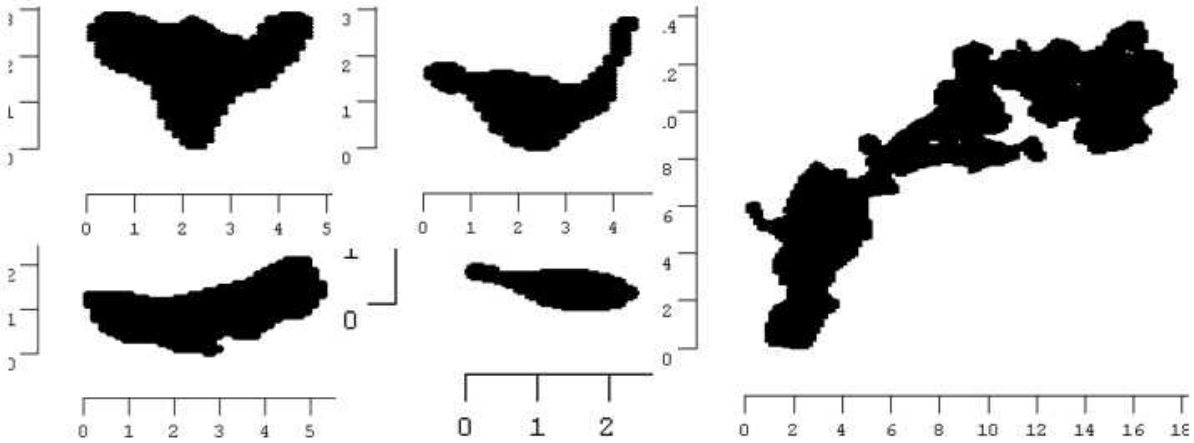


Fig. 3 2DVD-images of melting snow particles observed at Sapporo, Japan.

©2021. Japan Geoscience Union. All Right Reserved.

[J] Poster | M (Multidisciplinary and Interdisciplinary)：M-IS Intersection

Sun. Jun 6, 2021 5:15 PM - 6:30 PM JST | Sun. Jun 6, 2021 8:15 AM - 9:30 AM UTC | Ch.19_2

[M-IS13] Dynamics of eruption cloud and cumulonimbus; modelling and observation

convener:Eiichi Sato(Meteorological Research Institute), Fukashi Maeno(Earthquake Research Institute, University of Tokyo), Takeshi Maesaka(National Research Institute for Earth Science and Disaster Resilience)

Volcanic eruption clouds (eruption column, pyroclastic flow, and umbrella cloud) and cumulonimbus are similar phenomena in the atmosphere. Models that can precisely reproduce the physical processes in such phenomena, and accurate observations have been required. Recently, the development of remote sensing techniques such as weather radar and weather satellite are remarkable, and they are being adopted for volcanic eruption monitoring. However, it is indispensable to verify the results of modeling and remote sensing using in-situ observations. In this session, we will discuss the modelling and the observations of eruption clouds and cumulonimbus from the viewpoint of meteorology, volcanology, geology, and other related fields. The related phenomena such as ashfall, rainfall, snowfall, hail and volcanic block will also be discussed.

[MIS13-P01] Estimation of ash refractive index and improvement of Himawari-8 volcanic ash algorithm

★Invited Papers

*Hiroshi Ishimoto[1], Masahiro Hayashi[1], Yuzo Mano[1], Rei Kudo[1] (1.Meteorological Research Institute)

[MIS13-P02] Multi-sensor observation of cloud evolution from cumulus to cumulonimbus in Tokyo metropolitan area

*Takeshi Maesaka[1], Tadayasu Ohigashi[1], Koyuru Iwanami[1], Shin-ichi Suzuki[1], Namiko Sakurai[1], Yukari Shusse[1], Kaori Kieda[1], Shingo Shimizu[1], Yasushi Uji[1], Nobuhiro Takahashi[2], Hiroshi Hanado[3], Katsuhiro Nakagawa[3], Tomoo Ushio[4] (1.National Research Institute for Earth Science and Disaster Resilience, 2.Nagoya University, 3.National Institute of Information and Communications Technology, 4.Osaka University)

[MIS13-P03] Application to the volcanic ash obserbation of the X-band solid state marine radar

*Takaaki NISHI[1], Masayuki MAKI[1], Takehiko KOBORI[1], Kanji ENDO[2], Kazuhiko KAIGA[2], Masato IGUCHI[3] (1.Kagoshima Univ., 2.Koden Electronics Co., Ltd, 3.Kyoto Univ.)

[MIS13-P04] Modification of probabilistic estimation method for eruption plume height using weather radars

*Eiichi Sato[1] (1.Meteorological Research Institute)

[MIS13-P05] Ash fall observation using 2D-Video Disdrometer (2)

*Eiichi Sato[1], Kosei Takishita[2], Masato Iguchi[3] (1.Meteorological Research Institute, 2.Division of Earth and Planetary Sciences, Graduate School of Science, Kyoto University, 3.Sakurajima Volcano Research Center, Disaster Prevention Research Institute, Kyoto University)

[MIS13-P06] Sedimentary process of ash deposits from long-term activity of repeated vulcanian eruptions at Sakurajima volcano, Japan

*Takahiro Miwa[1], Futoshi Nanayama[2] (1.National research institute for earth science and disaster resilience, 2.Geological Survey of Japan, AIST)

Estimation of ash refractive index and improvement of Himawari-8 volcanic ash algorithm

*Hiroshi Ishimoto[1], Masahiro Hayashi[1], Yuzo Mano[1], Rei Kudo[1]

1. Meteorological Research Institute

For continuous near-real time monitoring of volcanic ash clouds (VAC) in both day and night, satellite observations by using infrared sensors are particularly useful. Because volcanic silicate has a characteristic absorption band around 10μm wavelength, VAC of fine ash particles can be easily detected and distinguished from water/ice clouds by measurements of brightness temperature difference between two channels in this absorption band. Applying further constraints for microphysical properties of the ash particles, such as particle size distribution, and for atmospheric profile, retrieval of physical properties for VAC (cloud height, particle effective radius, optical depth, and the associated ash mass loading) has been realized by adding the measurements of other infrared channels of high-resolution satellite imagers. These retrieval analyses are based on the results of numerical simulations for the measured infrared brightness temperature by radiative transfer calculations for VAC under the assumption of atmospheric profiles and surface condition, and therefore, optical properties of the ash particles are essential. In particular, the complex refractive index (RI) is one of the important and upstream parameters in estimation of the ash optical properties and their wavelength dependences.
From the data of satellite infrared sounder measurements for VAC and radiative transfer calculations, we estimate optimal refractive index models of the volcanic ash material to simulate the measured brightness temperature spectrum. In addition, we have developed an algorithm of 1DVAR analysis (OVAA) that estimates the physical properties of VAC from the data of multi-wavelength satellite imager such as Himawari-8. By using the optimal RI model estimated by the infrared sounder and using OVAA, high accuracy Himawari-8 analysis for the physical parameters of VAC is expected.

Keywords: volcanic ash clouds , refractive index, Himawari-8

©2021. Japan Geoscience Union. All Right Reserved.

Multi-sensor observation of cloud evolution from cumulus to cumulonimbus in Tokyo metropolitan area

*Takeshi Maesaka[1], Tadayasu Ohigashi[1], Koyuru Iwanami[1], Shin-ichi Suzuki[1], Namiko Sakurai[1], Yukari Shusse[1], Kaori Kieda[1], Shingo Shimizu[1], Yasushi Uji[1], Nobuhiro Takahashi[2], Hiroshi Hanado[3], Katsuhiro Nakagawa[3], Tomoo Ushio[4]

1. National Research Institute for Earth Science and Disaster Resilience, 2. Nagoya University, 3. National Institute of Information and Communications Technology, 4. Osaka University

Recently, weather radar network which consists of X- and C-band polarimetric radars has matured in Japan. This nationwide network enables Quantitative Precipitation Estimation (QPE) with high resolutions (1 minute and 250 m), and is used for a monitoring of localized heavy rain. So now a social request is shifting from the monitoring to the forecast of the heavy rain. This kind of forecast needs a seed of cumulonimbus development as an initial condition. The weather radar is a suitable instrument to find the seed. But when the ordinary weather radar finds it, the rainfall has already started. To make the lead time of the forecast longer, we should monitor the pre-stages of cumulonimbus, such as horizontal convergence and cumulus clouds. For this purpose, we installed microwave radiometers, Doppler lidars, Ka-band cloud radars around Tokyo metropolitan area. Furthermore, X-band Multi-Parameter Phased Array Weather Radar (MP-PAWR) also covers the area, and is a powerful instrument to capture the three-dimensional structure of precipitation system. In this presentation, an evolution from cumulus to cumulonimbus is analyzed by using multi-sensor data.

We analyzed the cloud activities on 3 August 2018. Many cumulus clouds appeared and dissipated, before the precipitation started, cloud size and its reflectivity gradually became larger with time. Finding the clouds in transition stage (reflectivity of about -5 dBZ, and echo size of about 5 km^2) is important for monitoring the evolution from cumulous to cumulonimbus. Cumulus activity moistened mid-troposphere, and this moistening may help the cumulonimbus development.

Keywords: Cumulus, Cumulonimbus, Cloud radar, MP-PAWR

©2021. Japan Geoscience Union. All Right Reserved.

Application to the volcanic ash obserbation of the X-band solid state marine radar

*Takaaki NISHI[1], Masayuki MAKI[1], Takehiko KOBORI[1], Kanji ENDO[2], Kazuhiko KAIGA[2], Masato IGUCHI[3]

1. Kagoshima Univ., 2. Koden Electronics Co., Ltd, 3. Kyoto Univ.

Volcanic ash Sakurazima and Kirishima has been observed by Ku band radar(Ku-RAD) of Kagoshima University. In addition, marine radar had shorter search time than Ku-RAD was able to observe volcanic ash. On the other hand, marine radar produced a transmission signal in magnetron which was necessary to change magnetron in a fixed period. This time, we borrowed solid state marine radar which was no necessary to change solidified transmission device and can observe volcanic ash. At first solid satate marine radar was installed on the Kagoshima University Shimoarata campus roof and measured the Sakurajima area in PPI and RHI. Furthrtmore, to move, and to observe eruption of Sakurajima, the marine solid state radar was installed in the boat, the volcanic ash of Sakurajima was observed under navigation. These observation methods were effective for volcanic ashes observation.

Keywords: X-band SSR, volcanic ash, PPI, RHI

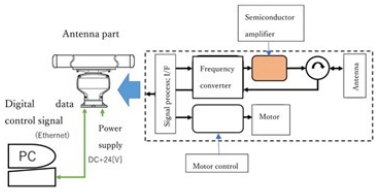
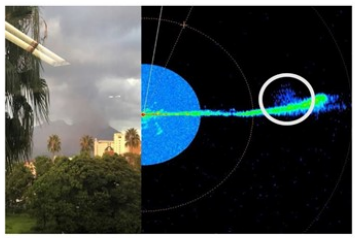
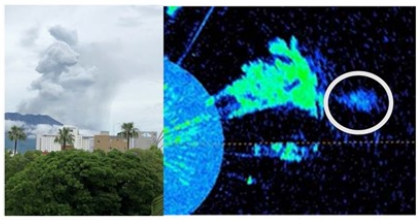


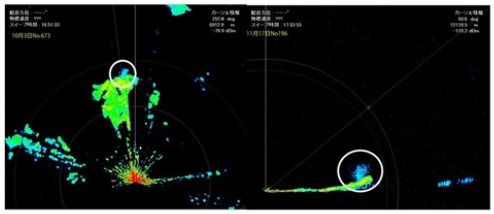
図1 船舶用固体化レーダ(SSR : solid-state marine radar) 基本構成



(a) 18:00 (b) 17:58 1400m
図3 9月17日2019年桜島噴煙の写真(a)とSSRによって観測された噴煙(b)



(a) 10:54 (b) 10:44 3200m
図2 7月4日2019年桜島噴煙の写真(a)とSSRによって観測された噴煙(b)



(a)10月 3 日16:51 1700m (b) 11月17日 17:33
図 4 2020年 SSRによって観測された桜島噴煙のPPI映像(a)とRHI映像(b)

©2021. Japan Geoscience Union. All Right Reserved.

Modification of probabilistic estimation method for eruption plume height using weather radars

*Eiichi Sato[1]

1. Meteorological Research Institute

Sato et al. (2018) developed a probabilistic estimation method for eruption plume height and applied it to the 2016 Mt. Aso eruption case.In this presentation, we will show the result of applying the improved probabilistic estimation method (MPE method) to the 2018 Kusatsu-Shirane (Motoshirane) eruption case.

The main improvements of the method are that the refractive index of the atmosphere was calculated from the GPV of the initial value of the Mesoscale Model (MSM) of the Japan Meteorological Agency, and that the effect of the earth ellipsoid was included. In addition, the correction of geoid altitude is also included.

As a result of applying the MPE method to the 2018 eruption of Mt. Kusatsu-Shirane (Mt. Motoshirane), the eruption plume height is estimated to be 5,580 m ±506 m (1 σ).

Based on this result, the author also tried to estimate the amount of ejecta by applying four methods for estimating the mass eruption rate from the eruption altitude.

The author also discusses the adequacy of applying these techniques to phreatic eruptions.

Keywords: weather radar, eruption plume height, probabilistic estimation method, refractivity, earth ellipsoid

©2021. Japan Geoscience Union. All Right Reserved.

Ash fall observation using 2D-Video Disdrometer (2)

*Eiichi Sato[1], Kosei Takishita[2], Masato Iguchi[3]

1. Meteorological Research Institute, 2. Division of Earth and Planetary Sciences, Graduate School of Science, Kyoto University, 3. Sakurajima Volcano Research Center, Disaster Prevention Research Institute, Kyoto University

Meteorological Research Institute (MRI) is conducting ash fall observations at Sakurajima Volcano using two-dimensional video disdrometers (2DVDs). 2DVD is originally a ground-based instrument that observes precipitation particles, and it is possible to obtain the three-dimensional shape and falling velocity of each target particle. This instrument is used in meteorology to verify polarimetric (dual-polarization) radar and to observe precipitation particles on the ground, but in volcanology there are few observations. MRI is developing a technology for estimating the amount of volcanic ash inside the eruption plume using a polarimetric radar. In addition, 2DVD observations are being conducted to obtain the “ground truth” data.
Here, we describe the main previous researches and current issues. Suh et al. (2019) conducted an indoor ash fall experiment to discuss the characteristics of volcanic ash particle shape, falling velocity, and canting angle, however, it is necessary to investigate the characteristics of the actual ash fall. Kozono et al. (2019) is an example of ash fall observation by a disdrometer in the natural environment. However, since the disdrometer used in this paper cannot recognize the shape of particles, it is not suitable for verification of dual-pol radar data.
In this presentation, we will report the outline of the quality control method of ash fall observation data by 2DVD and the verification method of the amount of volcanic ash retrieved using a polarimetric radar.

Keywords: 2D-Video Disdrometer, Sakurajima volcano, ash fall, dual-polarization/polarimetric radar

©2021. Japan Geoscience Union. All Right Reserved.

Sedimentary process of ash deposits from long-term activity of repeated vulcanian eruptions at Sakurajima volcano, Japan

*Takahiro Miwa[1], Futoshi Nanayama[2]

1. National research institute for earth science and disaster resilience, 2. Geological Survey of Japan, AIST

Ash deposit from a long-term activity of repeated vulcanian eruptions are important for understanding the development of a volcanic edifice. In this study we discussed the sedimentary system of ash deposits produced by long-term vulcanian activity from Showa crater of Sakurajima volcano, Japan, based on the grain size distributions of falling ash from individual eruptions. We sampled falling ash particles from 21 individual vulcanian eruptions between March 3–11, 2010. The grain size distributions of the ash samples were unimodal, bimodal, and trimodal characteristics. The median particle size of the main subpopulation decreases with distance from the Showa crater. The low standard deviation of the grain size of the main subpopulation implies deposition from transient volcanic plumes (Walker, 1971). For the finest subpopulation in the polymodal samples, the median particle size is very fine ash (<30 μm) which is difficult to fall as individual particles due to low terminal velocity, indicating that this subpopulation was originated from ash aggregates. Overall, the sedimentary process of the repeated vulcanian eruptions at Sakurajima volcano is explained by accumulation of ash particles from transient plumes and ash aggregation, and the latter controlled the behavior of the very fine ash. We consider the model proposed in this study reflects the long-term activity of repeated vulcanian eruptions, based on the following: (1) The vulcanian eruptions considered in this study were typical of Sakurajima volcano; (2) the Md–distance relationship of main subpopulation from this study are similar to those for the March 26 2016 vulcanian eruption (Miwa et al. 2020) and the July 28–August 3 2013 vulcanian eruptions at Sakurajima volcano (Gabellini et al. 2020). Deposition of ash particles during long-term vulcanian activity generates a close-concentric spatial distribution of ash grain size and thickness around the crater (Imura, 1995), and builds the volcanic edifice, along with the eruptive products from large-scale eruptions. Year-long monitoring of ash accumulation should be suggested for future research.

Keywords: Volcanic ash, Deposit, Vulcanian eruption, Sakurajima volcano

©2021. Japan Geoscience Union. All Right Reserved.

[J] Oral | M (Multidisciplinary and Interdisciplinary)：M-IS Intersection

Sun. Jun 6, 2021 1:45 PM - 3:15 PM JST | Sun. Jun 6, 2021 4:45 AM - 6:15 AM UTC | Ch.17 Zoom Room 17

[M-IS15] Tsunami deposit: research progress after the 2011 Tohoku-oki earthquake and prospects

convener:Masaki Yamada(Department of Geology, Faculty of Science, Shinshu University), Takashi Ishizawa(International Research Institute of Disaster Science, Tohoku University), Masashi Watanabe(Chuo University), Koichiro Tanigawa(Geological Survey of Japan, National Institute of Advanced Industrial Science and Technology), Chairperson:Masaki Yamada(Department of Geology, Faculty of Science, Shinshu University), Takashi Ishizawa(International Research Institute of Disaster Science, Tohoku University)

The 2011 off the Pacific coast of Tohoku Earthquake and associated tsunami have an influence on the development of tsunami deposit research. After the tsunami, a lot of findings have been reported in various research fields. However, it has been still uncertain how to use the tsunami deposit to estimate its size and source and the risk assessment. As it commemorates the 10th anniversary of the 2011 off the Pacific coast of Tohoku Earthquake, we would like to review research progress over the past decade and share in the vision of future researches. In this session, we welcome research from all aspects of sedimentary records of modern and paleo tsunamis and numerical and experimental modeling studies for risk assessment. We also include research on other event deposits, such as river floodings and storm surges, that they are considered important for identification of tsunami deposits in geological strata.

1:45 PM - 2:15 PM JST | 4:45 AM - 5:15 AM UTC

[MIS15-01] Sedimentation and erosion by the 2011 Tohoku-oki tsunami

★Invited Papers

*Kazuhisa Goto[1] (1.Department of Earth and Planetary Science, The University of Tokyo)

2:15 PM - 2:45 PM JST | 5:15 AM - 5:45 AM UTC

[MIS15-02] How much we had understood a history of giant earthquakes along the Japan trench -progress and remaining problems-

★Invited Papers

*Yuki Sawai[1] (1.Geological Survey of Japan, AIST)

2:45 PM - 3:15 PM JST | 5:45 AM - 6:15 AM UTC

[MIS15-03] Advances in tsunami numerical modeling after the 2011 Tohoku earthquake and future challenges related to tsunami deposit research

★Invited Papers

*Daisuke Sugawara[1] (1.International Research Institute of Disaster Science, Tohoku University)

Sedimentation and erosion by the 2011 Tohoku-oki tsunami

*Kazuhisa Goto[1]

1. Department of Earth and Planetary Science, The University of Tokyo

Sedimentation and erosion by the 2011 Tohoku-oki tsunami were investigated from various aspects not only by sedimentological and micropaleontological ways but also by geochemical and agricultural approaches. Since the possible predecessors including the AD869 Jogan event were well studied before the event, it was also possible to test the validity of the pre-event paleotsunami researches that had been done along the Pacific coast of Tohoku. Also, numerous data about tsunami such as flow depth and inundation area obtained by the efforts of tsunami researchers provided us a rare opportunity to quantitatively compare the tsunami deposit characteristics with flow dynamics. In these points, paleotsunami research after the 2011 Tohoku-oki event has drastically been changed both in its quality and quantity. Then, what did we actually learn from the 2011 Tohoku-oki event and how such knowledge has been incorporated in the paleotsunami research?

Lessons learned from the 2011 Tohoku-oki event can be classified into expected and unexpected results. For instance, sedimentary features such as grading and lamination and distribution pattern as well as the sedimentary process were more or less reasonable based on the pre-2011 knowledge since they are similar to those of other modern tsunami deposits formed by, e.g., the 2004 Indian Ocean tsunami. Also, sedimentary characteristics of the 2011 tsunami deposits were remarkably similar to that formed by paleotsunamis in this region so that identification procedures used in the pre-2011 paleotsunami researches can be evaluated as valid. As expected, diverse size of sedimentary grains from mud to meter-long boulders were transported depending on the sediment source and size of local tsunami. Considering the fact that over thousand tons of huge blocks were transported by the 2011 tsunami, even few thousand tons of enigmatic boulders reported in the world might be explained by large, but not extremely large, tsunami similar to the 2011 one.

On the other hand, some survey results were somewhat beyond the common knowledge of paleotsunami research at that time. For example, sandy deposits were not necessarily distributed up to the maximum tsunami inundation limit so that estimation of earthquake magnitude from paleotsunami research might have been underestimated. While, muddy deposits or geochemical signature, which had been generally overlooked, were important to appropriately estimate the inundation area from the deposits. Also, tsunami deposits were not necessarily of marine source so that absence of marine microfossils does not indicate the event deposit is not formed by the tsunami. These results commonly indicate that paleotsunami research before the 2011 Tohoku-oki event had a chance of underestimation for the estimation of recurrence interval and tsunami/earthquake size.

Now, ten years since the 2011 event, identification of tsunami deposit and its usage to understand paleotsunami events have been under improvement. Paleotsunami research should expand its research field to overcome the remaining difficulties. For example, scarce of modern examples of other water-related event deposits such as flood or storm deposits prevent us to understand the identification criteria of tsunami deposits. Also, technical improvements and reconsideration of research scheme might be essential for efficient, high-accuracy, and high-resolution estimation of paleotsunami recurrence interval and size.

©2021. Japan Geoscience Union. All Right Reserved.

©2021. Japan Geoscience Union. All Right Reserved.

How much we had understood a history of giant earthquakes along the Japan trench -progress and remaining problems-

*Yuki Sawai[1]

1. Geological Survey of Japan, AIST

The 2011 Tohoku earthquake disaster was broadcasted as “unexpected disaster” by non-geologists but also surprised them because it had been not well known that geologists had previously studied geological evidence for 869 Jogan earthquake and tsunami: a potential predecessor of the 2011 event.

The Jogan tsunami deposit was first reported in Sendai by Abe et al. (1990 Zishin) and Minoura and Nakaya (1991 J. Geol.). Sugawara et al. (2001 Research Report of Tsunami Engineering) later found a similar sand deposit in Soma, Fukushima prefecture. Building on their research, research groups of Geological Survey of Japan, AIST traced the Jogan sandy deposits using several hundred cores along leveled transects in Sendai, Ishinomaki, and Minami-Soma regions. On the basis of such geological records, the source of the Jogan tsunami was examined by comparison between simulated inundation areas and the observed extent of Jogan tsunami deposits (Namegaya et al., 2010 AFRC reports; Satake et al., 2008b AFRC reports). These results had been submitted to the Japanese government, but they were not employed by governmental assessments of subduction zone earthquakes until the 2011 Tohoku earthquake.

After the 2011 disaster, many researchers began to study tsunami geology along the Tohoku coast to extend tsunami history in millennium time scale. In Iwate and Aomori prefectures, they identified Jogan tsunami deposits as well as historical (Goto et al. 2015 Mar. Geol.) and prehistoric (Tanigawa et al. 2014 JQS) tsunami deposits. Also, a tsunami of 1454 in the Sendai plain was reexamined on the basis of historical documents (Namegaya and Yata, 2014 Zishin) and stratigraphic and geomorphological evidence (Sawai et al., 2015 GRL).

In the last two decades, tsunami geology has developed along the Pacific coast of Tohoku region, but there still remain issues that should be tackled. For example, the moment magnitude of the Jogan earthquake may have been greater than the present model proposed by Namegaya and Satake (2014 GRL). They constrained their fault parameters using distributions of tsunami deposits at multiple sites along the trench, but the modeled fault may be extended farther north or south if the recent geological data were involved. Also, a parent earthquake is still unknown for a tsunami deposit in 17th-century along the Pacific coast of Aomori prefecture (Tanigawa et al. 2014 JQS). These problems may be solved by future comprehensive research.
This presentation is based on description in Sawai (2020 ESR).

Keywords: subduction zone great earthquakes, tsunami deposit, Japan trench

©2021. Japan Geoscience Union. All Right Reserved.

Advances in tsunami numerical modeling after the 2011 Tohoku earthquake and future challenges related to tsunami deposit research

*Daisuke Sugawara[1]

1. International Research Institute of Disaster Science, Tohoku University

Tsunami numerical modeling, such as source modeling and hazard assessment, has been playing a crucial role in policy making and consensus building for disaster mitigation actions. While the 2011 Tohoku-oki earthquake tsunami brought unexpected disasters, it also left valuable lessons for improving tsunami numerical modeling. Since tsunamis cause not only surges and inundations of the seawater, but also induced phenomena such as sediment erosion and deposition, debris drift and structural damage, development of multi-physics model is a key challenge, in terms of improved hazard assessment. Verification and validation of such multi-physics models have been promoted with aids from the groundbreaking data of the Tohoku-oki earthquake and tsunami.

Tsunami numerical modeling has been used to estimate the source of past disastrous tsunamis by bridging the findings from different disciplines, such as seismology, geodesy, geology, geomorphology, ecology, coastal engineering, archaeology and history. An established approach is comparison of the spatial distribution of tsunami deposits, such as sand layers and boulders, and simulated tsunami inundation area. Although gaps between sediment distribution and inundation limit are a well-known concern, source models of paleotsunami events, such as the 869 Jogan earthquake tsunami in the Tohoku region, have been deduced based on such comparisons. Upgrading the ability of the source modeling is expected with aids from the sediment transport simulations. Numerical modeling of tsunami-induced sediment transport and morphological change due to the Tohoku-oki tsunami have been providing physical explanations for geological and geomorphological features of sandy tsunami deposits in Sendai Bay and Sanriku Coast. It encourages application of the tsunami sediment transport modeling to paleotsunami researches. A recent case study of the 1867 Keelung tsunami in the northern Taiwan demonstrated that the tsunami sediment transport modeling benefit interpreting sparse historical and geological records of the tsunami and estimating the mechanism and size of the tsunamigenic earthquake.

A key challenge of tsunami numerical modeling is quantification and reduction of uncertainty. Various factors are involving in the uncertainty in tsunami numerical modeling, such as inputs, formulations and model parameters. With regard to the modeling of paleotsunami deposits, the uncertainty due to inputs include the vegetation, sediment source and grain-size composition and sea level, in addition to the bathymetry and topography at that time. A numerical experiment showed that simulated thickness and inland extent of onshore sandy tsunami deposits may be several times larger or smaller, depending on the assumptions of the height of coastal sand dunes. A systematic framework to quantify the uncertainty is needed for further utilization of tsunami numerical modeling. The quantification of uncertainty provides the range of variability of the outputs, which is beneficial when comparing the simulations with sedimentary data. Efforts to collect contextual data, such as long-term change in coastal environment, annual and seasonal variation of beach topography and anthropogenic land modification, in addition to

©2021. Japan Geoscience Union. All Right Reserved.

reconstructed paleo-topographic and bathymetric data, will be needed to reduce the uncertainty in numerical modeling of paleotsunamis.

Keywords: source modeling, sediment transport modeling, uncertainty

©2021. Japan Geoscience Union. All Right Reserved.

[J] Oral | M (Multidisciplinary and Interdisciplinary)：M-IS Intersection

Sun. Jun 6, 2021 3:30 PM - 5:00 PM JST | Sun. Jun 6, 2021 6:30 AM - 8:00 AM UTC | Ch.17 Zoom Room 17

[M-IS15] Tsunami deposit: research progress after the 2011 Tohoku-oki earthquake and prospects

convener:Masaki Yamada(Department of Geology, Faculty of Science, Shinshu University), Takashi Ishizawa(International Research Institute of Disaster Science, Tohoku University), Masashi Watanabe(Chuo University), Koichiro Tanigawa(Geological Survey of Japan, National Institute of Advanced Industrial Science and Technology), Chairperson:Masashi Watanabe(Chuo University), Koichiro Tanigawa(Geological Survey of Japan, National Institute of Advanced Industrial Science and Technology)

The 2011 off the Pacific coast of Tohoku Earthquake and associated tsunami have an influence on the development of tsunami deposit research. After the tsunami, a lot of findings have been reported in various research fields. However, it has been still uncertain how to use the tsunami deposit to estimate its size and source and the risk assessment. As it commemorates the 10th anniversary of the 2011 off the Pacific coast of Tohoku Earthquake, we would like to review research progress over the past decade and share in the vision of future researches. In this session, we welcome research from all aspects of sedimentary records of modern and paleo tsunamis and numerical and experimental modeling studies for risk assessment. We also include research on other event deposits, such as river floodings and storm surges, that they are considered important for identification of tsunami deposits in geological strata.

3:30 PM - 4:00 PM JST | 6:30 AM - 7:00 AM UTC

[MIS15-04] **Application of DNN inverse model to large scale tsunamis to reconstruct the flow conditions of modern and ancient tsunamis**

★Invited Papers

*Rimali Mitra[1], Hajime Naruse[1], Tomoya Abe[2], Shigehiro Fujino[3], Daisuke Sugawara[4] (1.Kyoto University, Graduate School of Science, 2.Research Institute of Geology and Geoinformation, Geological Survey of Japan, National Institute of Advanced Industrial Science and Technology (AIST), Tsukuba, Japan, 3.University of Tsukuba, 4.Tohoku University, IRIDeS)

4:00 PM - 4:15 PM JST | 7:00 AM - 7:15 AM UTC

[MIS15-05] Analysis of the Response of Tsunami Sediment Transport Numerical Simulation to Parameter Uncertainty

*Hidetoshi Masuda[1], Daisuke Sugawara[2], Shuro Yoshikawa[3], Hideyuki Sakurai[3], Fumihiko Imamura[2] (1.Division of Geoenviromental Science, Faculty of Science, Tohoku University, 2.International Research Institute of Disaster Science, Tohoku University, 3.Institute of Technology, Shimizu Corporation)

4:15 PM - 4:30 PM JST | 7:15 AM - 7:30 AM UTC

[MIS15-06] Event deposits in Lake Jusan, western part of Aomori Prefecture, NE Japan

*Fumika Hirano[1], Atsushi Urabe[2] (1.Faculty of Science, Niigata University, 2.Research Institute for Natural Hazards and Disaster Recovery, Niigata University)

4:30 PM - 4:45 PM JST | 7:30 AM - 7:45 AM UTC

[MIS15-07] Features of 17th-century tsunami deposits formed by tsunami crossing river channel and detection using X-ray computed tomography

*Kohei Iwaki[1], Yasuhiro Takashimizu[2], Yuichi Nishimura[3], Takashi Chiba[4] (1.Graduate School of Science and Technology, Niigata University, 2.Mathematical and Natural Sciences, Institute of Humanities, Social Sciences and Education, Niigata University, 3.Graduate School of Science, Hokkaido University, 4.Faculty of Bioresource Sciences, Akita Prefectural University)

4:45 PM - 5:00 PM JST | 7:45 AM - 8:00 AM UTC

[MIS15-08] Identification of invisible tsunami deposits formed by the 2011 Tohoku-oki tsunami

*Tetsuya Shinozaki[1], Yuki Sawai[1], Dan Matsumoto[1], Koichiro Tanigawa[1] (1.Geological Survey of Japan, National Institute of Advanced Industrial Science and Technology)

Application of DNN inverse model to large scale tsunamis to reconstruct the flow conditions of modern and ancient tsunamis

*Rimali Mitra[1], Hajime Naruse[1], Tomoya Abe[2], Shigehiro Fujino[3], Daisuke Sugawara[4]

1. Kyoto University, Graduate School of Science, 2. Research Institute of Geology and Geoinformation, Geological Survey of Japan, National Institute of Advanced Industrial Science and Technology (AIST), Tsukuba, Japan, 3. University of Tsukuba, 4. Tohoku University, IRIDeS

The 2011 Tohoku-oki tsunami and 2004 Indian Ocean tsunami caused significant economic losses and fatalities in the coastal areas. These modern tsunamis could be traced back and linked to the ancient tsunamis such as 869 Jogan tsunami as a precursor for 2011 Tohoku-oki tsunami. The Deep Neural network (DNN) 1D inverse model has the potential to predict the values of hydraulic conditions such as maximum inundation distance, flow velocity and maximum flow depth, sediment concentration of different grain-size classes using the thickness and grain-size distribution of the tsunami deposit from the post-tsunami survey around Sendai plain and other locations. The DNN model incorporates the forward model, which was based on non-uniform, unsteady transport of suspended sediments during turbulent mixing. The forward model employs iterative random flow conditions as boundary conditions to produce artificial training data sets which represent depositional characteristics, such as, thickness and grain-size distribution. Then the DNN was trained to find relationships between simulation results and initial conditions using the artificial output datasets of forward model. Finally, the DNN model was applied to natural field data sets from different locations. The quantification of uncertainty of the model predicted results was also reported using the jackknife method. The model successfully reconstructed the flow conditions of 2011 Tohoku-oki tsunami from Sendai plain and Joban coast, 2004 Indian Ocean tsunami from Phra Thong island, Thailand and 869 Jogan tsunami from Sendai plain. The estimated of values maximum inundation distance flow velocity, maximum flow depth were reasonable and close to the measured or reported values from the study area. Despite having topographical complicacy and lesser sampling locations for ancient deposits, the DNN model have the potential to predict the flow characteristics from the deposits satisfactorily. These qualitative and quantitative estimations demonstrated that the DNN inverse model is a potential tool for evaluating tsunami hazard and mitigation strategies.

Keywords: Tsunami Deposit, DNN inverse model, Machine learning

©2021. Japan Geoscience Union. All Right Reserved.

Analysis of the Response of Tsunami Sediment Transport Numerical Simulation to Parameter Uncertainty

*Hidetoshi Masuda[1], Daisuke Sugawara[2], Shuro Yoshikawa[3], Hideyuki Sakurai[3], Fumihiko Imamura[2]

1. Division of Geoenviromental Science, Faculty of Science, Tohoku University, 2. International Research Institute of Disaster Science, Tohoku University, 3. Institute of Technology, Shimizu Corporation

Numerical simulation of tsunami-induced sediment transport is a powerful technique for improving our understanding of sedimentological characteristics of tsunami. Recently, validation of the simulation has been conducted using the vast amount of data obtained from the 2011 Tohoku-oki Tsunami (TOT) as a benchmark (Sugawara et al., 2014). Numerical simulations are generally affected by uncertainty related to input parameters for the model, however, few studies investigated the uncertainty systematically and comprehensively. In this study, sensitivity analyses using the TUNAMI-STM numerical model are conducted on the southern part of Sendai Bay, Miyagi Prefecture, where large-scale geomorphological changes due to the 2011 TOT were observed (Udo et al., 2013), in order to establish a systematic framework for evaluating the uncertainty in the simulation.

Sensitivity analysis was performed with ten parameters in total, such as grain size and settling velocity. A combination between grain size and other parameters, such as critical friction velocity and coefficient of transport formula, was taken into account in several cases. The area of comparison was divided into six segments, in which volumes of the tsunami-induced erosion and deposition varied significantly (Udo et al., 2013). The sensitivity was examined using simulated volumes of erosion and deposition for each case normalized by the outputs of a reference case.

The sensitivity was high in grain size and Manning’ s roughness coefficient, which exhibited larger change rates of the erosion and deposition volume to change rates of the parameter. Besides, change rates of the erosion and deposition volumes by single simulation showed variabilities among the segments. As a result of detailed analysis focusing on sensitivity to the grain size, significant correlations were identified among the changes of the volume of onshore deposition, offshore erosion, the survival rate of the coastal dike (i.e. the ratio of fixed bed and a total length of dike) and height of the dike. In addition, changes in the sensitivity corresponding to the dimension of the segments were analyzed using narrower segments. These results suggest that the magnitude of the effect of parameter uncertainty depends on the distribution of coastal dike and spatial scale of comparison between simulation and observation.

Keywords: Tohoku-oki tsunami, Sendai Bay, sediment transport , numerical modeling

©2021. Japan Geoscience Union. All Right Reserved.

Event deposits in Lake Jusan, western part of Aomori Prefecture, NE Japan

*Fumika Hirano[1], Atsushi Urabe[2]

1. Faculty of Science, Niigata University, 2. Research Institute for Natural Hazards and Disaster Recovery, Niigata University

In this study, the first boring survey was conducted in the central part of the Lake Jusan, a lagoon along the coast of the Japan Sea to analyze tsunami records on the coast of the Japan Sea in NE Japan. As a result of this survey, nine layers of tsunami deposits caused by the offshore tsunami were identified, and their ages were estimated.
The transport process was restored for tsunami deposits formed by tsunamis that entered the coastal lacustrine that are different from tsunami deposits that run up to land. Additionally, the formative process of the tsunami deposits in lacustrine was clarified by observing composition of particles and their roundness. The characteristics of the constituent particle indicated that tsunami deposits of the JSK-1 core were transported by backwash in a lacustrine environment. The results of this research contribute to the elucidation of tsunami records in the Japan Sea region and the analysis of the source faults distributed offshore of NE Japan.

Keywords: Japan Sea, tsunami deposit, Lake Jusan

©2021. Japan Geoscience Union. All Right Reserved.

Features of 17th-century tsunami deposits formed by tsunami crossing river channel and detection using X-ray computed tomography

*Kohei Iwaki[1], Yasuhiro Takashimizu[2], Yuichi Nishimura[3], Takashi Chiba[4]

1. Graduate School of Science and Technology, Niigata University, 2. Mathematical and Natural Sciences, Institute of Humanities, Social Sciences and Education, Niigata University, 3. Graduate School of Science, Hokkaido University, 4. Faculty of Bioresource Sciences, Akita Prefectural University

Tsunami deposits distributed during run-up show inland fining and thinning trends. However, the effect of abandoned river channels within the run-up area on deposit features is unknown and was investigated in this study. Tsunami deposits are an effective index by which to estimate the inundation area of historical and paleo tsunamis. However, the actual inundation area and distribution limit of tsunami deposits are distinct; the former is generally wider than the latter. Therefore, this study also verified the effectiveness of X-ray computed tomography (CT) analysis for reconstructing the actual distribution of the deposits. The study was conducted in a coastal lowland of the Yufutsu Plain in Hokkaido, Japan, interspersed with back marshes, ponds, and depressions (interpreted as traces of abandoned river channels) behind coastal sand dunes. Samples extracted using a geoslicer and peat sampler were used for core, X-ray CT, and grain size analyses, and the weight of clastic grain contents was measured using organic matter treatments. The lithofacies of the tsunami deposits changed from sand to sandy peat with gradually decreasing sand content. However, X-ray CT analyses identified the presence of clastic materials beyond the area in which sand was visually identifiable, and a positive correlation existed between the mean CT value and the clastic material content of the tsunami deposits, suggesting that the mean CT value could be used as a proxy for the tsunami deposit distribution. The thickness of the tsunami deposits along shore-normal transects generally presented inland thinning part with local coarsening trends in abandoned channels (topographical depressions), which was indicative of the sudden deposition of transported grains under tsunami deceleration during run-up into these channels. The mode grain size and mud content of the tsunami deposits along the shore-normal transect generally indicated inland fining and increasing trends, respectively, which also suggested deceleration of the tsunami run-up flow. However, the mode grain size became coarser after the tsunami flowed across abandoned channels. Thus, these coarse materials may have originated from the channel deposits, a possibility which should be explored in further research.

Keywords: Tsunami deposit, X-ray CT, Grain size distribution

©2021. Japan Geoscience Union. All Right Reserved.

Identification of invisible tsunami deposits formed by the 2011 Tohoku-oki tsunami

*Tetsuya Shinozaki[1], Yuki Sawai[1], Dan Matsumoto[1], Koichiro Tanigawa[1]

1. Geological Survey of Japan, National Institute of Advanced Industrial Science and Technology

We conducted a field survey at Oirase town, Aomori Prefecture, to examine the identification of invisible tsunami deposit. Evidence of paleo-tsunamis is not always preserved as a visible deposit. Near the inundation limit, tsunami deposits tend to be thin and fine-grained because the weakened tsunami flow cannot transport coarser particles and large amounts of sand; thus, tsunami deposits can be difficult to identify from underlying and overlying sediment by eye observation. Identification of invisible tsunami evidence as well as visible tsunami deposits is necessary for more accurate estimation of tsunami recurrence and its magnitude.

To examine the identification of invisible tsunami deposits, we focused on the 2011 Tohoku-oki tsunami because we have information on inundation area and sediment distribution. In October 2020, we set two transects that were nearly perpendicular to the shoreline. About 20 cm deep sediment samples were directly collected from walls of excavated pits at 12 locations. Based on the eye observation, sediments consist of an upper soil layer and a lower thick fine to medium sand layer. At the relatively seaward locations, 1.5 to 4 cm-thick fine to medium sand layer, which is considered as the 2011 tsunami deposit, was intercalated within the soil layer. On the other hand, no sand layer within the soil was found by eye observation at the relatively landward locations. As well as the eye observation, we could not identify event deposits by CT images and the depth profile of sand contents. In the study sites, wind may constantly transport sand particles from the beach to the landward sampling locations around the inundation limit (about 300 m from the shoreline and about 150 m from the beach). This setting made it difficult to identify evidence of tsunami inundation based on CT images and sand contents. In the presentation, we discuss about invisible tsunami deposits based on the data of CT, sand contents, and depth profile of grain size distribution and organic geochemistry.

Keywords: Invisible tsunami deposits, 2011 Tohoku-oki tsunami, Aomori, Grain-size distribution, Organic geochemistry

©2021. Japan Geoscience Union. All Right Reserved.

[J] Poster | M (Multidisciplinary and Interdisciplinary)：M-IS Intersection

Sun. Jun 6, 2021 5:15 PM - 6:30 PM JST | Sun. Jun 6, 2021 8:15 AM - 9:30 AM UTC | Ch.19_3

[M-IS15] Tsunami deposit: research progress after the 2011 Tohoku-oki earthquake and prospects

convener:Masaki Yamada(Department of Geology, Faculty of Science, Shinshu University), Takashi Ishizawa(International Research Institute of Disaster Science, Tohoku University), Masashi Watanabe(Chuo University), Koichiro Tanigawa(Geological Survey of Japan, National Institute of Advanced Industrial Science and Technology)

The 2011 off the Pacific coast of Tohoku Earthquake and associated tsunami have an influence on the development of tsunami deposit research. After the tsunami, a lot of findings have been reported in various research fields. However, it has been still uncertain how to use the tsunami deposit to estimate its size and source and the risk assessment. As it commemorates the 10th anniversary of the 2011 off the Pacific coast of Tohoku Earthquake, we would like to review research progress over the past decade and share in the vision of future researches. In this session, we welcome research from all aspects of sedimentary records of modern and paleo tsunamis and numerical and experimental modeling studies for risk assessment. We also include research on other event deposits, such as river floodings and storm surges, that they are considered important for identification of tsunami deposits in geological strata.

[MIS15-P01] A study for correlation of mega-tsunami in the Kuril Trench based on the tsunami deposits in the Erimo area, Hokkaido

*RYO NAKANISHI[1], Juichiro Ashi[1,2], Yosuke Miyairi[1], Yusuke Yokoyama[1,3] (1.Atmosphere and Ocean Research Institute, The University of Tokyo, 2.Graduate School of Frontier Science, The University of Tokyo, 3.Department of Earth and Planetary Sciences, Graduate School of Science, The University of Tokyo)

[MIS15-P02] Characteristics of event deposits and their distributions based on a drilling survey in Sekine-hama, the northern part of the Shimokita Peninsula, Aomori Prefecture

*Daisuke Ishimura[1], Masaki Yamada[2], Takashi Ishizawa[3], Kaori Aoki[4], Kai Sato[2] (1.Department of Geography, Tokyo Metropolitan University, 2.Department of Geology, Faculty of Science, Shinshu University, 3.International Research Institute of Disaster Science, Tohoku University, 4. Research Center for Volcanic Hazards and Their Mitigation, Tokyo Metropolitan University)

[MIS15-P03] Tsunami source estimation of paleotsunami deposits formed in the 17th century at Sekinehama, northern Shimokita Peninsula, Aomori Prefecture

*Kai Sato[1], Masaki Yamada[1], Daisuke Ishimura[2], Takashi Ishizawa[3], Toshitaka Baba[4] (1.Depatment of Geology, Faculty of Science, Shiushu University, 2.Department of Geography, Tokyo Metropolitan University , 3.International Research Institute of Disaster Science, Tohoku University, 4.Graduate School of Science and Technology, Tokushima University)

[MIS15-P04] Revised paleotsunami history at Kirikiri, Northeast Japan

*Takashi Ishizawa[1], Yusuke Yokoyama[2], Yosuke Miyairi[2] (1.International Research Institute of Disaster Science, Tohoku University, 2.Atmosphere and Ocean Research Institute, the University of Tokyo)

[MIS15-P05] Distribution and characteristics of the 1983 Nihonkai-chubu earthquake tsunami deposit along the Akita coastal area, Japan

*Takashi Chiba[1], Yuichi Nishimura[2] (1.Faculty of Bioresource Sciences, Akita Prefectural University, 2.Institute of Seismology and Volcanology (ISV), Faculty of Science, Hokkaido University)

[MIS15-P06] Event deposits in a coastal lake at Minami-ise Town, Mie Prefecture during the last 3000 years

*Yumi Shimada[1], Yuki Sawai[1], DAN MATSUMOTO[1], Koichiro Tanigawa[1], Yuichi Namegaya[1], Masanobu Shishikura[1], Kazumi Ito[1], Toru Tamura[1], Shigehiro Fujino[2] (1.Geological Survey of Japan, AIST, 2.Faculty of Life and Environmental Sciences, University of Tsukuba)

[MIS15-P07] Distributions and occurrences of sandy tsunami deposits in caves located along the East Coast of Ishigaki Island, Okinawa Prefecture

*Yoshiro Ishihara[1], Miyu Kitahara[1], Yuuka Okita[1], Ayano Shimabukuro[2], Hajime Naruse[3], Chiaki Katagiri[4], Rintaro Ono[5], Kazuhisa Yoshimura[6] (1. Fukuoka Univ., 2.Yaeyama Museum, 3.Kyoto Univ., 4.Okinawa Prefectural Archaeological Center, 5.National Museum of Ethnology, 6.Kyushu Univ.)

[MIS15-P08] Examining grain-size changes in sediment transport modeling of the 2011 Tohoku-oki tsunami in the Sendai Plain

*Wataru Nakamura[1], Daisuke Sugawara[1] (1.Tohoku University)

[MIS15-P09] Comparison of Observations and Numerical Simulations of Sediment Transport Using the 1707 CE Hoei Tsunami Source Model: Application to Kanigaike Pond in Kochi Prefecture, Japan

*Satoshi Kusumoto[1], Kentaro Imai[1], Narumi Takahashi[2,1], Takane Hori[1], Daisuke Sugawara[3] (1.JAMSTEC, 2.NIED, 3.Tohoku University)

[MIS15-P10] Uncertainty of geological information used in identification of tsunami deposit - Preliminary assessment –

*Takumi Yoshii[1], Takaomi Hamada[1], Yuki Ito[1], Shiro Tanaka[1], Masafumi Matsuyama[1] (1.Central Research Institute of Electric Power Industry)

A study for correlation of mega-tsunami in the Kuril Trench based on the tsunami deposits in the Erimo area, Hokkaido

*RYO NAKANISHI[1], Juichiro Ashi[1,2], Yosuke Miyairi[1], Yusuke Yokoyama[1,3]

1. Atmosphere and Ocean Research Institute, The University of Tokyo, 2. Graduate School of Frontier Science, The University of Tokyo, 3. Department of Earth and Planetary Sciences, Graduate School of Science, The University of Tokyo

In order to clarify the spatial diversity of the rupture mode of giant earthquakes with recurrence intervals of hundreds to thousands of years, it is necessary to obtain information from a geological record such a tsunami deposit, because observational data alone are insufficient. In the southern part of the Kuril Trench, the geological studies reveal the existence of giant earthquakes that cannot be explained by the earthquakes observed (Sawai, 2020). These giant earthquakes have intervals of several hundred years, and the last one is said to have occurred in the 17th century. However, there have been few cases of comparing the ages of sand layers at different sites, and the spatio-temporal distribution of fracture areas over long-time scales has not been clarified. In this study, we focused on the east coast of Erimo, which has not been investigated, and examined the magnitude of the 17th century tsunami and the possibility of contrasting older events. In the Erimo town, 8-10 sand layers were found during the past 4000 years, which were judged to be tsunami deposits based on their supply from the beach sand and anomalous distribution. Numerical simulations showed that the 17th-century tsunami can be explained by the same rupture zone as the 17th-century tsunami widely observed in eastern Hokkaido (Ioki and Tanioka, 2016). The ^{14}C dating results show that the depositional ages of the sand layers in this area are similar to those of the sites facing the Tokachi-oki segment, while some sand layers do not have candidates comparable to those of the sites facing the Nemuro-oki segment. The age of the sand layers in the area west of Erimo Cape also correlated with the age of the sand layers in the southern part of Hidaka, suggesting that the sand layers in the southern part of Hidaka are likely to have originated from the giant earthquake in the Kuril Trench.

Keywords: Tsunami deposits, Kuril Trench, Radiocarbon dating, Hokkaido, Numerical simulation

©2021. Japan Geoscience Union. All Right Reserved.

Characteristics of event deposits and their distributions based on a drilling survey in Sekine-hama, the northern part of the Shimokita Peninsula, Aomori Prefecture

*Daisuke Ishimura[1], Masaki Yamada[2], Takashi Ishizawa[3], Kaori Aoki[4], Kai Sato[2]

1. Department of Geography, Tokyo Metropolitan University, 2. Department of Geology, Faculty of Science, Shinshu University, 3. International Research Institute of Disaster Science, Tohoku University, 4. Research Center for Volcanic Hazards and Their Mitigation, Tokyo Metropolitan University

This study reports the event deposits found at Sekinehama, Aomori Prefecture, which is the northernmost part of the Shimokita Peninsula. Tsunamis associated with earthquakes along the Japan and Kuril trenches and volcanic activities in the 17th-18th century possibly could reach this site. Therefore, tsunami deposit research at this site provides information for the assessment of tsunami hazards in this area and understanding of the mechanism of earthquakes and tsunamis along the subduction zone.

Our study site, Sekinehama, is located between Omazaki and Shiriyazaki, and the late Pleistocene marine terraces and sand dunes were distributed behind the coast. In the 2011 Tohoku-oki earthquake, tsunami runup height of 2 to 6 m was reported (The 2011 Tohoku Earthquake Tsunami Joint Survey (TTJS) Group (http://www.coastal.jp/ttjt/)). The outcrops are exposed along the coastline and its height is ca. 5 m. In 2020, we conducted the coring survey with the Handy-Geoslicer (GS) and obtained nine cores at the lowland in the incised valley of the late Pleistocene marine terrace. In this study, we conducted core descriptions, X-ray CT imaging, grain size analysis, tephra analysis, and radiocarbon dating.

At the outcrops, we found more than 10 sandy event deposits interbedded within the soil and marsh sediments. Additionally, we identified two tephras; one is the Baegdusan-Tomakomai (B-Tm) tephra (AD946; Oppenheimer et al., 2017), another is the Towada-Chuseri (To-Cu) tephra (ca. 6 ka; Mclean et al., 2018; Ishimura and Hiramine, 2020). We identified four event deposits above the B-Tm tephra. One of them after 530-490 calBP (1420-1460 calAD) showed an erosional feature at the base, indicating a large flow speed. Below the B-Tm tephra, we also identified some event deposits with grading and erosive contact at the base.

In the preliminary research, we found one sandy event deposit after 530-490 calBP (1420-1460 calAD) at the lowland in the incised valley of the late Pleistocene marine terrace. From the grain analysis, this sandy deposit has a similar grain size distribution with the modern beach sediments. In the GS cores, drilled at 200-400 m distance from the coast, we traced this sandy layer up to 400 m from the coast. From this drilled survey, we confirmed that this sandy layer was only one event deposit above the B-Tm tephra. The sandy layers above the B-Tm tephra show multiple units in the seaside cores and its thickness decreases toward inland. These characteristics indicate that the sand layer is related to paleo-tsunami events after the 15th century. On the other hand, several event deposits were also identified below the B-Tm tephra and radiocarbon dates revealed that the GS cores cover the recent six thousand years. We will show the grain size analysis and additional radiocarbon dates in the presentation.

This work was supported by the Sasakawa Scientific Research Grant from The Japan Science Society. This study was partially performed under the cooperative research program of the Center for Advanced Marine Core Research, Kochi University (Accept No. 20B052).

©2021. Japan Geoscience Union. All Right Reserved.

Keywords: tsunami deposits, Shimokita Peninsula, B-Tm tephra

©2021. Japan Geoscience Union. All Right Reserved.

Tsunami source estimation of paleotsunami deposits formed in the 17th century at Sekinehama, northern Shimokita Peninsula, Aomori Prefecture

*Kai Sato[1], Masaki Yamada[1], Daisuke Ishimura[2], Takashi Ishizawa[3], Toshitaka Baba[4]

1. Depatment of Geology, Faculty of Science, Shiushu University, 2. Department of Geography, Tokyo Metropolitan University , 3. International Research Institute of Disaster Science, Tohoku University, 4. Graduate School of Science and Technology, Tokushima University

This study reports the source estimation based on tsunami deposits at Sekinehama, Aomori Prefecture, northern Japan. In the 17th century, it is known that two huge tsunamis, 1611 CE Keicho tsunami and 17th century earthquake tsunami, have occurred along Japan and Kuril trenches, but their source areas, especially 1611 CE Keicho tsunami, are not well constrained yet. Besides, it is also uncertain whether two tsunamis were generated by discrete earthquakes or identical one. Their tsunami deposits have been identified along Sanriku coast and Sendai Plain and Tokachi to Nemuro coast along the Pacific coast of Hokkaido, respectively. Since our study area, Sekinehma, northern Shimokita Peninsula, is located between Kuril and Japan trenches, geological surveys in such location will give a significant information to solve the relationship of two huge tsunamis. Previous investigations revealed that there are widely-distributed a sand layer that are probable tsuami deposit showing the depositional age of the 17th century at Sekinehama. In this study, we conducted numerical simulations on tsunamis occurred in the 17th century in order to clarify tsunami source of the paleotsunami deposits at Sekinehama.

We used existing ten fault models which reconstruct the 1611 CE Keicho tsunami occurred along Japan Trench, 1677 CE Enpo-Sanriku and 17th century tsunamis occurred along Kuril Trench, and the tsunami caused by uplift of offshore active fault located on northern Shimokita Peninsula. To examine tsunami influence on Sekinehama, the ratio of computed tsunami inundation to the coastal lowland (<300 m from shoreline) was roughly evaluated near the place where probable tsunami deposits were found. In this study, calculations were performed using JAGRUS with an assumption that the topography in the 17th century is not much different from the present at Sekinehama. It is interpretated from the computed inundation rate at Sekinehama that large influences at the study area were given by three models which have >25 m slip amount along the south part of the Kuril Trench (>Mw 8.8; Ioki and Tanioka, 2016; Okamura and Namegaya, 2011; The Hokkaido Disaster Prevention Council, 2012) and one model which has 80 m slip amount along the north part of the Japan Trench (1611 CE Keicho tsunami model with Mw 9.0; Fukuhara and Tanioka, 2017). This suggests the possibility that the study area is inundated by a tsunami when its source is placed off the Pacific coast of Hokkaido rather than off Sanriku coast.
We then compared the calculated inundation rate for tsunami deposits distributed at coastal lowlands along Iburi coast in Hokkaido and east coast of Aomori Prefecture. These tsunami deposits are thought to be deposited in the 17th century, but their sources are still unknown. According to the computation results, the Kuril–Japan trench interlocking model can only explain the distribution of these tsunami deposits as well as that at Sekinehama. In addition, 1640 CE tsunami caused by Mt. Komagatake collapse should be also taken into consideration as a tsunami source at Sekinehama. However, there is no model restored a detailed process from mountain collapse to tsunami. As the result of preliminary simulation used a simple model by Nakanishi and Okamura (2019), 90% inundation rate and 4.6 m maximum height were calculated at Sekinehama, suggesting that the 1640 CE tsunami is one of the possible sources for the tsunami deposits at Sekinehama.

©2021. Japan Geoscience Union. All Right Reserved.

We inferred the Interlocking earthquake model and 1640 CE tsunami model caused by Mt. Komagatake eruption as the source of tsunami deposits at Sekinehama. For future, we plan to create highly accurate source models by changing fault parameters of mainly these two models to recover tsunami deposit distribution at study area.

This work was partly supported by the Sasakawa Scientific Research Grant from The Japan Science Society.

©2021. Japan Geoscience Union. All Right Reserved.

Revised paleotsunami history at Kirikiri, Northeast Japan

*Takashi Ishizawa[1], Yusuke Yokoyama[2], Yosuke Miyairi[2]

1. International Research Institute of Disaster Science, Tohoku University, 2. Atmosphere and Ocean Research Institute, the University of Tokyo

Tsunami deposits are defined as reworked sediment which is transported by a tsunami. The distribution area of tsunami deposits is often related to the inundation area of the tsunami and thus is useful for the reconstruction of paleotsunami. In general, age correlations of tsunami deposits were performed to identify tsunami deposits that were formed by the same tsunami. However, several problems (e.g., erosion and re-sedimentation by a tsunami, sample selection for ^{14}C dating) make it difficult to accurately estimate the age of tsunami deposit. Herein, we conducted dating of tsunami deposits at Kirikiri, Iwate prefecture where paleotsunami history was not established well. ^{14}C dating was performed by a few sample types at the same stratigraphic horizon. Our results indicated that wood samples showed younger age than the age of overlying sediments. Moreover, sediment from the same stratigraphic horizon with the wood also showed younger age than the age of overlying sediments. The reversion of age might be due to penetration of younger wood and surrounded sediment of the wood might also be affected by the wood. From the results, we revised the ages of paleotsunami deposits and our results were well consistent with the paleotsunami history of the surrounded area. Such detailed re-examination of paleotsunami ages was crucially important for the correlation of widely distributed tsunami deposits.

Keywords: Tsunami deposit, Radiocarbon dating

©2021. Japan Geoscience Union. All Right Reserved.

Distribution and characteristics of the 1983 Nihonkai-chubu earthquake tsunami deposit along the Akita coastal area, Japan

*Takashi Chiba[1], Yuichi Nishimura[2]

1. Faculty of Bioresource Sciences, Akita Prefectural University, 2. Institute of Seismology and Volcanology (ISV), Faculty of Science, Hokkaido University

The Nihonkai-chubu earthquake occurred off the western coast of Noshiro City in Akita Prefecture, northeastern Japan on 26th May 1983. The tsunami due to the earthquake caused widespread damage to the west coastal area of the northeastern Japan, including Akita coastal region, depositing sand and mud transported by the tsunami. We conducted geological surveys from December 2019 to January 2020 within the pine-based coastal protecting forests planted along the coastal region of Akita Prefecture in the period of 1948 to 1970. Sand layers that exhibit inland thinning were observed in the soil at a depth of <10 cm at Happo Town, Noshiro City and Mitane Town, Akita Prefecture. As this sand layer contains well preserved brackish-marine diatoms such as *Fallacia* sp. and *Thalassiosira nanolineata*, it is highly probable that it was transported inland from the coast; a continuity distribution was confirmed from the coast to ~300 m inland only within the coastal protecting forest. According to historical records, we postulate that this sand layer is the result of deposition by the 1983 tsunami, as the area could not have been reached by any means other than the tsunami produced by the Nihonkai-chubu Earthquake. There are few reports of tsunami deposits with specific ages in Japan, so they are an important historical record of past disasters. It has been noted that tsunami deposits lose their sedimentary structures and constituents over time due to changes in weather conditions; therefore, the samples of these deposits can also be used to study the weathering processes of tsunamis deposits.

On the other hand, we also recognized another thin sand layer upper the tsunami deposits. There is a high probability that this sand layer was formed by the strong wind of the Typhoon 9119 reached in 28th September 1991, because no major floods or tsunamis caused damage to our study area have occurred after the 1983 tsunami event.

In this presentation, we report the distribution and characteristics of deposits from the tsunami generated by the 1983 Nihonkai-chubu earthquake and the eolian sand formed by the Typhoon 9119 recognized in coastal protecting forests planted along the Happo Town, Noshiro City and Mitane Town.

Keywords: 1983 Nihonkai-chubu earthquake, Tsunami deposit, Microfossils

©2021. Japan Geoscience Union. All Right Reserved.

Event deposits in a coastal lake at Minami-ise Town, Mie Prefecture during the last 3000 years

*Yumi Shimada[1], Yuki Sawai[1], DAN MATSUMOTO[1], Koichiro Tanigawa[1], Yuichi Namegaya[1], Masanobu Shishikura[1], Kazumi Ito[1], Toru Tamura[1], Shigehiro Fujino[2]

1. Geological Survey of Japan, AIST, 2. Faculty of Life and Environmental Sciences, University of Tsukuba

Sediment cores taken at Kogare-ike, a coastal lake in Minami-ise town facing the Nankai Trough, contain the sixteen event deposits likely representing tsunamis or storm surges. Nine of the event deposits were invisible but identified by computed tomography (CT) images. Depositional ages of the event deposits were estimated by combination of ^{137}Cs concentration and radiocarbon ages from pollens and plant macrofossils. An age-depth model was then established from these radiometric analyses was constructed using Bchron (Haslett & Parnell, 2008). This model revealed that the event deposits in the study site had settled during the last 3000 years. In order to detect environmental changes during the period, fossil diatom assemblages from the core taken at the center of the lake were identified and counted. Until the deposition of the youngest event deposit (E1), diatom assemblages were dominated by freshwater species such as *Tabellaria fenestrata* and *Staurosira* spp. After the deposition of the E1, however, assemblages were dominated by brackish species such as *Amphora coffeiformis*, *Bacillaria paxillifer*, *Navicula gregaria*.

There are some causes of event deposits in coastal lakes: tsunamis, storm surges and floods. However, the event deposits are likely to represent seawater inundation associated with tsunamis and/or storm surges, not river floods, because Kogare-ike has no significant fluvial input. The youngest event deposit (E1) exists above the lowest horizon occurrence of ^{137}Cs. Because the first occurrence of the cesium shows a timeline of 1940's, E1is likely to be correlated by the recent documents with the 1959 Isewan typhoon. The change in diatom assemblages before and after the E1 suggested breaching of the barrier generated with the storm surge that enabled more seawater to flow into the study site. As for the other event deposits at Kogare-ike, some of them may represent tsunami because there are the written documents and the tsunami monuments at Minami-ise town inferring the repetitive inundation by tsunamis associated with the earthquakes along the Nankai Trough (e.g. Nakata, 1991; Namegaya & Tsuji, 2005).

Keywords: event deposits, tsunami, storm, lacustrine sediments, fossil diatom assemblages, Nankai Trough

©2021. Japan Geoscience Union. All Right Reserved.

Distributions and occurrences of sandy tsunami deposits in caves located along the East Coast of Ishigaki Island, Okinawa Prefecture

*Yoshiro Ishihara[1], Miyu Kitahara[1], Yuuka Okita[1], Ayano Shimabukuro[2], Hajime Naruse[3], Chiaki Katagiri[4], Rintaro Ono[5], Kazuhisa Yoshimura[6]

1. Fukuoka Univ., 2. Yaeyama Museum, 3. Kyoto Univ., 4. Okinawa Prefectural Archaeological Center, 5. National Museum of Ethnology, 6. Kyushu Univ.

Many "tsunami-ishi" boulders are distributed along the east coast and coastal lowlands of Ishigaki Island, Yaeyama Islands, Okinawa Prefecture. Detailed investigations have revealed that the boulders were moved and settled by several tsunami events of different ages. The trench excavated near the coast also revealed several sandy tsunami deposits containing marine fossils. These boulders and deposits suggest that tsunamis originating from the Ryukyu Trench repeatedly struck the east coast of Ishigaki Island.
Along the coasts of the Yaeyama Islands, many limestone caves are located in marine terraces composed of limestone of the Ryukyu Group. These limestone caves are isolated from weathering of the surface environment and maintain a stable environment, which results in good preservation of sediments and fossils. As a result, these caves often include artifact remains and human bones and are sometimes recognized as archaeological sites. The speleothems found in the caves may also contain records of events such as tsunamis. In the cave deposits of the Shirahosaonetabaru Cave Site, a historic site located within the New Ishigaki Airport, a few tens of centimeters thick sandy gravel bed containing many corals and other marine fossils is presumed to be tsunami-derived deposits. This sandy graved bed was deposited about 1,800 years ago, and the cave entrance that in-flowed this sediment is estimated to have existed at an elevation of about 40 m. Therefore, it is considered evidence of a large-scale tsunami, comparable to the "Okinawa Sakishima Tsunami".
We investigate the cave sediments along the east coast of Ishigaki Island for artifacts and fossils, and tsunami event deposits in the cave sediments. In this presentation, we will show the distribution of the tsunami deposits in the caves. This work was supported by JSPS KAKENHI Grant Number JP20K04138.

Keywords: Ishigaki Island, Tsunami deposit, Cave, Archaeological site, speleothem

©2021. Japan Geoscience Union. All Right Reserved.

Examining grain-size changes in sediment transport modeling of the 2011 Tohoku-oki tsunami in the Sendai Plain

*Wataru Nakamura[1], Daisuke Sugawara[1]

1. Tohoku University

Information of past tsunami events inferred from tsunami deposits is useful in preparing for future tsunami disasters. Existing tsunami sediment transport modeling is intended to correlate characteristics of tsunami deposits with tsunami source from wave heights and source parameters. In such simulations, either single or multiple grain size class is assumed for particle composition. Although some studies conducted sediment transport modeling considering multiple grain-size classes, majorities have been performed with the single grain-size assumption. However, the single grain-size simulations cannot resolve lateral and horizontal variations of grain-size composition. Major sedimentological features of sandy tsunami deposits, such as landward and upward fining, cannot be used for comparison of field data and numerical simulations. In this study, we examined and compared the sediment transport simulations of the 2011 off the Pacific coast of Tohoku Earthquake Tsunami, considering single and multiple grain-size compositions. The study area is located in the neighborhood of the right bank of the Nanakita River in the Sendai Plain. A detailed field survey for the tsunami deposit was carried out previously (Abe et al., 2012) along a shore-normal transect (transect B). The Delft3D, which has been developed by Deltales, was used for the modeling. It includes cross-sectional simulations along transect B (1-D model) and two-dimensional horizontal simulations (2-D model) covering transect B. The fault parameters proposed by Imamura et al. (2012) was used to generate the initial water level of the 2-D tsunami simulations. Time series of the water level at 2 km offshore of transect B, generated by the 2-D simulation, was used for the input of the 1-D simulations. We assumed an initial thickness of 5 m for movable bed, which corresponds to the entire seafloor and the land areas from shoreline to the Teizan canal; meanwhile the areas further inland were assumed to be fixed bed (initial sediment thickness of zero). Four grain-size classes (sediment 1 to 4) were used to synthesize the grain-size distribution of the movable bed, based on the grain size data of the tsunami deposits (e.g., Szczuciński et al., 2012). The Manning’ s roughness coefficient map constructed by Sugawara et al. (2014) was used for the computation of the tsunami-induced flow.
Modeling results showed that inundation distance, flow depth and distribution of the tsunami deposit were generally consistent with those measured by Abe et al. (2012), although there were some discrepancy in the flow depth near the shoreline. The simulations with single grain size class (mode diameter) and the multiple grain-size classes were almost similar. This is probably because of the assumption of the normal distribution for the grain-size composition and higher percentage of the mode diameter. Comparison of the 2-D and 1-D simulations showed a slight difference, due to effects from topography that cannot be considered in the 1-D simulations.

Keywords: tsunami numerical simulation, multiple grain size, the 2011 Tohoku-oki tsunami

©2021. Japan Geoscience Union. All Right Reserved.

Comparison of Observations and Numerical Simulations of Sediment Transport Using the 1707 CE Hoei Tsunami Source Model: Application to Kanigaike Pond in Kochi Prefecture, Japan

*Satoshi Kusumoto[1], Kentaro Imai[1], Narumi Takahashi[2,1], Takane Hori[1], Daisuke Sugawara[3]

1. JAMSTEC, 2. NIED, 3. Tohoku University

The Nankai Trough subduction zone have repeatedly produced large earthquakes with tsunamis (e.g., Ando, 1975; Ishibashi, 2004). The 1707 CE Hoei Nankai earthquake and tsunami caused serious damages to the southwestern coast of Japan. Its damages have been described many historical documents and its tsunami deposits have been found from the coastal lowlands from Kyusyu to Tokai (e.g., Cabinet Office, 2011; Kitamura and Kobayashi, 2014). Therefore, it is considered that the 1707 CE Hoei earthquake was a M9-class event on the Nankai Trough subduction zone. The source models have been proposed based on its tsunami heights and its tsunami deposits (e.g., Furumura et al., 2011; Sugawara et al., 2019). However, they are still not enough. In this study, we examine the sedimentary process of the tsunami deposits from the comparison of observation and numerical simulation of tsunami sediment transport using the revised 1707 CE Hoei tsunami source model (Furumura et al., 2011).
Study site is a coastal pond (Kanigaike pond) in Kochi Prefecture, Japan. The sand movements were computed using a coupled numerical model of tsunami inundation and sediment transport developed by Takahashi et al. (1999). The saturation concentration of suspended sediments.was also adopted (e.g., Sugawara et al., 2014; Yamashita et al., 2016). The mean grain size of the sand was set to be 0.267 mm and grain-size dependent parameters (i.e., the coefficients of bedload rate and exchange rate, settling velocity, and critical shear stress) were provided by Takahashi et al. (2011).
Our results showed a sand deposition of ~1 m near the shoreline. However, few sand deposition took place in the pond. According to the tsunami deposit survey performed by Kochi University and Okamura and Matsuura (2012), the 1707 CE Hoei tsunami deposits were ~50 cm in thickness. Our results did not match the observations, suggesting the need of reevaluation with different slip amount and width of the subfaults.
We concluded that the 1707 CE Hoei tsunami source model should be reexamined based on geological evidences, although there are several uncertainties in tsunami sediment transport modeling (Jaffe et al., 2016; i.e., incompleteness of the theory, topographic and bathymetric changes, parameter setting). Further studies would lead to further understanding of the Nankai Trough megathrust earthquakes.

Keywords: 1707 CE Hoei earthquake, Tsunami deposit, Tsunami sediment transport simulation

©2021. Japan Geoscience Union. All Right Reserved.

Uncertainty of geological information used in identification of tsunami deposit - Preliminary assessment –

*Takumi Yoshii[1], Takaomi Hamada[1], Yuki Ito[1], Shiro Tanaka[1], Masafumi Matsuyama[1]

1. Central Research Institute of Electric Power Industry

Tsunami deposit can provide important information about the local history of tsunamis. The geological record of tsunamis has been used to improve hazard maps in coastal cities and to develop the countermeasures against tsunamis in important facilities, such as nuclear power plants. However, the identification of tsunami deposit has uncertainties inherent in geological analysis. To consider the uncertainties in the identification, the authors presented probabilistic identification method for deposit made by natural hazards including tsunami [1]. In this method, deposit with little geological information on its formation is attributed to potential several natural hazards. To utilize this identification method, we must assess the uncertainties of geological information obtained from deposit.

In this study, we assessed the uncertainties of the information obtained from diatom analysis, which is widely used to identify tsunami deposit. We analyzed tsunami deposits formed by the 2011 Tohoku-oki earthquake tsunami [2]. The result showed that the 31% of the tsunami deposit has no marine diatom and more than half of tsunami deposit has marine to brackish diatom (>10% in the total diatom assemblage). The only 8% of the tsunami deposit has no marine to brackish diatom. These results indicate that the fraction of marine to blackish diatom can be the useful proxy to infer the source of deposit. Although choice of better proxy helps reducing uncertainties in geological information inferred from the deposit, we still must take account of the persisting uncertainty on geological information.

[1] Yoshii, T., Tanaka, S., Ito, Y., Hamada, T., Matsuyama, M., Identification method of event deposits caused by natural hazards, JpGU meeting 2019, 2019.
[2] Yoshii, T., Hamada, T., Sasaki, T., Matsuyama, M., Tanaka, S., Ito, Y., Watanabe, M., Okuzawa, K., Sedimentological features of tsunami deposit caused by the 2011 Tohoku-oki earthquake tsunami, JpGU meeting 2014, 2014.

Keywords: Tsunami deposit, Identification method, Probabilistic assessment

©2021. Japan Geoscience Union. All Right Reserved.

[J] Oral | M (Multidisciplinary and Interdisciplinary)：M-IS Intersection

Sun. Jun 6, 2021 9:00 AM - 10:30 AM JST | Sun. Jun 6, 2021 12:00 AM - 1:30 AM UTC | Ch.16 Zoom Room 16

[M-IS22] Geopark

convener:Takayuki Arima(Yokohama City University), Keiichi Tadokoro(Research Center for Seismology, Volcanology and Earthquake and Volcano Research Center, Nagoya University), Marekazu OHNO(Unzen Volcanic Area Geopark Promotion Office), Takayuki Ogata(Graduate School of Engineering and Science, University of the Ryukyus), Chairperson:Tatsuto Aoki(School of Regional Development Studies, Kanazawa University), Noritaka Matsubara(Graduate School of Regional Resource Management, University of Hyogo), Takayuki Arima(Yokohama City University)

This session targets interdisciplinary and multidisciplinary discussion on geopark, involving geoheritage, geodiversity, geoconservation, geotourism, sustainable development, governance, risk management, science communication and geoscientific education. These topics contribute to scientific and attractive activities in geoparks.

9:00 AM - 9:15 AM JST | 12:00 AM - 12:15 AM UTC

[MIS22-01] Academic Support for Geoparks: Efforts of the Geopark Assistance Committee, the Seismological Society of Japan

★Invited Papers

*Yoshihiro Hiramatsu[1] (1.School of Geosciences and Civil Engineering, College of Science and Engineering, Kanazawa University)

9:15 AM - 9:30 AM JST | 12:15 AM - 12:30 AM UTC

[MIS22-02] Preservation and utilization of earth heritage in Japan's natural monument system

★Invited Papers

*Tadahiro Shibata[1] (1.The Unit of Natural Monuments, Monuments and Sites Division, Cultural Properties Department, Agency for Cultural Affaire)

9:30 AM - 9:45 AM JST | 12:30 AM - 12:45 AM UTC

[MIS22-03] Developing virtual field experience with high-resolution panorama (GigaPans) at multiple scales: Constructing a core technology for online geotours

*Norihito Kawamura[1], Takashi Sawaguchi[2] (1.School of Regional Resource Management, Graduate School, University of Hyogo, 2.Toyo University)

9:45 AM - 10:00 AM JST | 12:45 AM - 1:00 AM UTC

[MIS22-04] Subaqueous volcanic rocks as the object for the geo tourism-related to NHK Buratamori and geoparks

*Hiromitsu Yamagishi[1], Yoshiaki Matsuda[1], Kazuo Shimura[2] (1.NPO Hokkaido Research Center of Geology(HRCG), 2.Shin Engineering Consultant)

10:00 AM - 10:15 AM JST | 1:00 AM - 1:15 AM UTC

[MIS22-05] Disaster risk reduction in Geopark from social geographical approach : focusing on social capital for community resilience

*Akifumi Nakamura[1] (1.Muroto Geopark Promotion Committee)

10:15 AM - 10:30 AM JST | 1:15 AM - 1:30 AM UTC

[MIS22-06] The Land Use Change and Socio-economic Impact of Baiyankeng Geo-cultural Village, China

*Wenqi ZHAO[1] (1.University of Tsukuba)

Academic Support for Geoparks: Efforts of the Geopark Assistance Committee, the Seismological Society of Japan

*Yoshihiro Hiramatsu[1]

1. School of Geosciences and Civil Engineering, College of Science and Engineering, Kanazawa University

For the development and enhancement of geopark activities, organic cooperation between Geoparks in various regions and academic societies with academic expertise is indispensable. The Seismological Society of Japan established the Geopark Assistance Committee in 2017 to support geopark activities in Japan, to disseminate and raise awareness of seismological knowledge, and to promote seismological research.

The Seismological Society of Japan has been recommending members to the Japan Geopark Committee since the beginning of geopark activities in Japan. As a project of the Social Activity Fund, the Seismological Society of Japan has held seminars for residents in Sanriku (2011 off the Pacific coast of Tohoku Earthquake), Kurikoma (2008 Iwate-Miyagi Nairiku Earthquake), and Aso (2016 Kumamoto Earthquake) Geoparks. Children's Summer School on Earthquake and Volcanoes and Teacher's License Renewal Course have been held with the support of the geoparks in the areas.

Efforts to establish a committee to support geopark activities began in 2014 with the establishment of the Geopark Working Group. In addition, a series of articles on Japanese Geoparks began in "Nai Furu". In 2016, the Preparatory Working Group for the Geopark Assistance Committee was set up to study the support activities of the Seismological Society of Japan and the need for support. In 2017, The Geopark Support Committee was established.

The main activities of the Geopark Assistance Committee are earthquake seminar for geopark staffs and geopark tours for members of the Seismological Society of Japan. In 2017-2019, the earthquake seminar held in Makuhari during JpGU: in 2017, how to obtain and use seismic data obtained from Hi-net, K-NET, and KiK-net in real-time, and how to use seabed topographic map data, in 2018, the introduction of past damaging earthquakes (historical earthquakes) around Japanese Geoparks, and in 2019, demonstration of various functions and usage of GSI maps.

Geopark tours are conducted with the cooperation of geoparks after the Fall Meeting of Seismological Society of Japan: Aso Geopark and Mashiki Town in 2017, Bandaisan Geopark and Aizuwakamatsu City in 2018, and a tour of Abuyama Observatory, Kyoto University, and the Hanaore Fault withOike Guide, although those are not a geopark, in 2019.

The Geopark Assistance Committee discussed how to realize seismic activity at a geosite, and the NIED implemented the "NIED Quake map!". Itoigawa UNESCO Global Geopark introduced it with the reopening of Fossa Magna Park in July 2018, and as of February 2021, it has also been introduced in Hakusan Tedorigawa Geopark, Shikoku Seiyo Geopark, Happo-Shirakami Geopark, and Sanriku Geopark.

In 2020, the JpGU was postponed and held remotely, so that we held an online earthquake seminar in October. The main theme of the workshop was how to communicate seismic activity. There were presentations as follows: how to find out about historical earthquakes and disasters, how the Hot Spring Research Institute, Kanagawa Prefecture, as a home doctor, and the Hakone Geomuseum disseminates

©2021. Japan Geoscience Union. All Right Reserved.

information about the activities of the Hakone Volcano in 2015 to a local society, and examples of the use of the "NIED Quake map!" from five geoparks. The number of participants was 62, the largest number in the past. The results of the post-event questionnaire showed the usefulness of the online seminar.

We would like to improve the scientific value of Geopark activities and communicate with the local community through Geoparks, together with those in Geoparks, by continuing to support Geopark activities.

Acknowledgments: We are grateful to the Japanese Geoparks Network and those in the Geoparks for their cooperation to the activities of the Geopark Assistance Committee, the Seismological Society of Japan.

Keywords: earthquake, earthquake seminar, geopark tour, seismicity, visualization

©2021. Japan Geoscience Union. All Right Reserved.

Preservation and utilization of earth heritage in Japan's natural monument system

*Tadahiro Shibata[1]

1. The Unit of Natural Monuments, Monuments and Sites Division, Cultural Properties Department, Agency for Cultural Affaire

Geoparks evaluate and organize the legal protection of geoscientific heritage sites such as geosites. According to the "Guidelines for the Conservation of Natural Resources of the Japanese Geopark Network" (2018) formulated by the Japan Geopark Network Conservation Working Group, research and data collection on geosites to evaluate their scientific value and conservation plans It is stated that important geosites that have been formulated will be legally protected. The Natural Parks Act, the Law for the Protection of Cultural Properties, and the Law for the Protection of Cultural Properties of prefectures and municipalities are applied as general legal protection and security measures in Japan. Recently, the outcrops of the Itoigawa-Shizuoka Tectonic Line, which is the most important geosite of the Itoigawa UNESCO Global Geopark, and the Mizonokuchi Cave of the Kirishima Geopark are in early 2021. It is expected to be designated as a natural monument. In addition, in recent years, it has been designated as a natural monument in domestic geoparks such as Byobugaura in Choshi Geopark, Sedimentary layers and the marine mammal fossils in Paleo-Chichibu-Bay in Chichibu Geopark. On the other hand, there is an opinion that it is necessary to clarify the procedure by regulation accompanying the designation of natural monuments, and to support private organizations and local governments that promote the utilization of academic research, education, tourism use, etc. Therefore, this time, based on this situation in Japan, we will explain the natural monument system, and the status of support for natural monument designation standards and flows, laws and regulations, preservation and utilization plan formulation, surveys and maintenance before and after designation. Introducing.

Keywords: Natural monument, Geopark

©2021. Japan Geoscience Union. All Right Reserved.

Developing virtual field experience with high-resolution panorama (GigaPans) at multiple scales: Constructing a core technology for online geotours

*Norihito Kawamura[1], Takashi Sawaguchi[2]

1. School of Regional Resource Management, Graduate School, University of Hyogo, 2. Toyo University

GigaPan images are very useful for virtual geotour!

Keywords: GigaPan, mosaic composite image, virtual tour, Anden geosite, Oga Peninsula-Ogata Geopark

©2021. Japan Geoscience Union. All Right Reserved.

Subaqueous volcanic rocks as the object for the geo tourism-related to NHK Buratamori and geoparks

*Hiromitsu Yamagishi[1], Yoshiaki Matsuda[1], Kazuo Shimura[2]

1. NPO Hokkaido Research Center of Geology(HRCG), 2. Shin Engineering Consultant

Recently, Japanese geologic term "Suirei-hasaigan"(hyaloclastite) or "Suirei-hasaiyougan" as a composition of subaqueous volcanoes has been known to be public by NHK TV Program such as “NHK Buratamori Atami, Shiretoko and Muroran” and the other programs. Such subaqueous volcanic rocks have been shown in many geoparks (Fig.1) in Japan: particularly, pillow lavas are exhibited in geoparks of Shimokita, Oga, Sanriku, Sado, Itoigawa, Shimonita, Simane Peninsula, Seiyo, Muroto etc., but hyaloclastites ("Suirei-hasaigan" or "Suirei-hasaiyougan") are displayed only in Izu Peninsula, San-in and Shimane Hanto Shinjiko geopark.
During 1970 to 1980’s the discussions and studies on the genesis of “Kuroko” (Sulphide Ore Deposits) had been popular in Japan, but later almost of the metal mines have been abolishid and then the researching and studies have been declined.
On the otherhand, in engineering geological fields, such as highway and tunnel construction, investigation on the subaqueous volcanic rocks has been attention, for instance, rock classification is usually done by mechanical classification, however, the subaqueous volcanic rocks display variable and heterogeneous facies differently from the other rocks, namely the classification needs knowledges of the occurrence of the rocks. Namey, such subaqueous volcanic rocks show different physical properties such as porosity, alteration and weathering processes, from subaerial ones and others. In terms of disaster problem, these subaqueous volcanic rocks have been attention also. For examples, 1971 Shizuoka Ohkuzure Rock Falls and 1996 Hokkaido Shakotan Toyohama Rock falls generated from the subaqueous volcanic rocks.
In terms of basic geology, Dr Kazuo Amano, proposed “Green Tuff Renaissance” meaning re-evaluation of the Neogene tectonics studies which have been studied much in the 1970’s in Japan. While, in the field of current oceanography, the sea bottom black smoke related to marine resources, has necessity of knowledge of Black Ore Deposits (KurokoVMS) during 1970-1980’s. While, the new technology such as drone (UAV) mapping of seashore bench, and digital exploring of the current ocean volcanology needs much knowledge of ancient subaqueous volcanic rocks.
Backbones of the Japanese islands were formed by subaqueous volcanism since the 10M, therefore one to thirds of the Japanese islands have been developed on the basement of the subaqueous volcanic rocks.
In this presentation, We review the terminology of the subaqueous volcanic rocks such as hyaloclastite, and report aerial and cruising geo-tour for Muroran Etomo Peninsula (Fig.1) composed of variable shapes of felsic subaqueous volcanic rocks.

Keywords: Subaqueous volcanic rocks, Pillow lava, Hyaloclastite, Geopark, NHK Buratamori, Muroran Etomo Peninsula

©2021. Japan Geoscience Union. All Right Reserved.

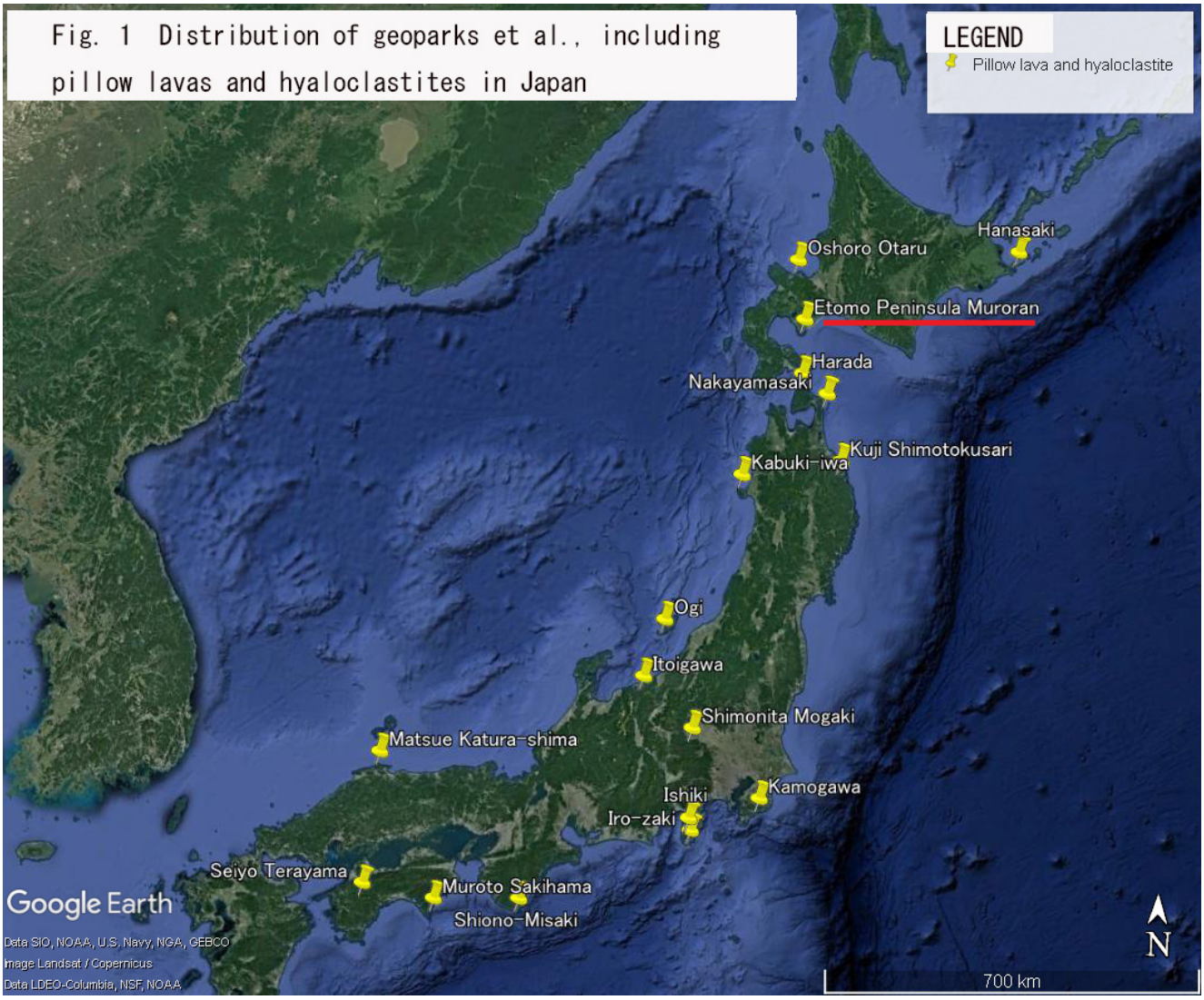


Fig. 1 Distribution of geoparks et al., including pillow lavas and hyaloclastites in Japan

©2021. Japan Geoscience Union. All Right Reserved.

Disaster risk reduction in Geopark from social geographical approach : focusing on social capital for community resilience

*Akifumi Nakamura[1]

1. Muroto Geopark Promotion Committee

In recent years, mesurements of disaster risk reduction is active in various Geoparks. In Muroto Geopark, structural measures such as ocean wave barriers, tsunami evacuation towers, tsunami shelters, and evacuation routes have been constructed for coming Nankai Trough earthquake. On the other hand, if we consider disaster risk reduction and mitigation as well as recovery and reconstruction after disaster, it is necessary to improve community resilience in total. This presentation considers disaster risk reduction in Geoparks based on social geographical approach. Shaw and Sharma (2011) classified risks into two categories : Shocks and Stresses. Shock is a threat to the region, referring to "low probability but rapid onset and high impact events that cause immediate and visible damage," such as natural hazards, epidemics, conflicts, and terror. Stresses refer to "slow onset and low impact processes that are of high probability in the context of a day-to-day continuum of hardships," such as poverty, public health, and sea level rise. In Muroto, there is high level interest on shocks caused by natural hazards such as earthquakes, tsunamis, and typhoons, but there seems to be little interest in chronic stresses such as population and birthrate decline, aging population, economic inequality, and infrastructure deterioration. Otherwise, even though locals recognize those are problems in itself, they do not notice that community resilience is weakend by such stresses. In social science research dealing with community resilience, the concept of social capital gives us clues to consider. Researches on the heat wave of Chicago, Hurricane Katrina, and the Great East Japan Earthquake showed that social capital as a resource to reduce damage during disaster and to enhance recovery after shocks. In addition, social capital is social networks, reciprocity, and trust that are built in daily life, and is expected to relieve daily and chronic stresses. This presentation discusses a case of Tanegashima, engaged in regional activities to maintain and enhance social capital. It also considers several characteristics of social capital in the island found on a questionnaire survey. As Geoparks, it is important to present comprehensive approach for disaster risk reduction including both social scientific and natural scientific perspectives.

Keywords: Disaster risk reduction, Resilience, Social capital, Island

©2021. Japan Geoscience Union. All Right Reserved.

The Land Use Change and Socio-economic Impact of Baiyankeng Geo-cultural Village, China

*Wenqi ZHAO[1]

1. University of Tsukuba

1. Introduction

Over the years, the three-dimensional rural issues concerning agriculture, countryside and farmers are long-standing problems in Chinese society. The government of China released a package of policies charting the roadmap for rural vitalization. Among the policies, the government of Zhejiang Province proposed a strategy of *Geo-cultural village* in 2013, on account of a lack of cultivated land for the large population in Zhejiang. The policy of Geo-cultural village is considered to be a model of endogenous development. Although most of the Geoparks in China are operated by the government, the policy of Geo-cultural village gives a top priority to self-governance by the villagers. This research aims to illustrate the land use change, industrial transformation and the impact on rural society and economy after Baiyankeng village has been registered as the first Geo-cultural village in China. The data of this research are collected from the interviews of the village committee, reports and statistical yearbooks of the local government.

2. Research Area

Baiyankeng village is one of the traditional villages in Kuaijishan mountains of middle Zhejiang, where Chinese Torreya trees have been cultivated through long periods of ancient grafting and artificial selection techniques from the weathering of Cretaceous volcanic rock strata. The project of Geo-cultural village has started here since Kuaijishan Ancient Chinese Torreya Community was registered as a *Globally Important Agricultural Heritage System* in 2013. By 2019, there are 251 families living here with a registered population of 760. The total area of the village is 6.03 square kilometers, 23.2% and 26.3% of which are respectively covered by Torreya forests and tea plantations. Other forests occupy 31.55% and only 4.5% is cultivated land. The villagers are mainly growing Chinese Torreya and Chinese tea for a living.

3. The Change of Land Use and Socio-economic Situation of Baiyankeng Village

The policy of Geo-cultural village caused many changes in the village from 2013 to 2019. The development of geo-tourism, homestay business, and Torreya production distinctly raised the income and increased the economic condition of the village. Although people are still going out of the village for part-time jobs, some people returned to the village to grow Chinese Torreya or to do some service jobs for geo-tourism. The land of planted Torreya trees is increasing, while the land of tea plantations is decreasing. In the meantime, however, some wild forests have been destroyed by cultivation of fields for Torreya. In addition, the fundamental facilities are constructed such as road and parking lot.

4. The Driving Forces behind the Change in Land Use and Socio-economic Situation

Initially the soil in the village is suitable to cultivate Torreya trees. Since Chinese tea is common around China but Chinese Torreya is distinctive, growing Torreya is easier to receive benefits than growing tea. The visitors would like to buy Torreya nuts rather than buying tea. Also, more labors are demanded and more chances for working in the village are provided due to the development of geo-tourism. After the improvement of the infrastructure, the living condition has become better. More and more previous villagers who took part-time jobs in the city would like to return to the village to work. Furthermore, the support of the local government and the enthusiastic members of the village committee give a big push to

©2021. Japan Geoscience Union. All Right Reserved.

this rural vitalization project.

5. Summary

Geo-cultural village aims to make use of the geological resources, inherit traditional ideas and rebuild cultures. It can be considered as a new model of endogenous development. The policy causes a positive impact on land use suitability, solving the three-dimensional rural issues and promoting social and economic development. Meanwhile, there are problems with self-governance, the prevention of over-development that should be considered for future research.

Keywords: Geo-cultural Village, Endogenous Development, Chinese Torreya, Land Use, Rural Vitalization, Baiyankeng Village

©2021. Japan Geoscience Union. All Right Reserved.

[J] Poster | M (Multidisciplinary and Interdisciplinary)：M-IS Intersection

Sun. Jun 6, 2021 5:15 PM - 6:30 PM JST | Sun. Jun 6, 2021 8:15 AM - 9:30 AM UTC | Ch.22_2

[M-IS22] Geopark

convener:Takayuki Arima(Yokohama City University), Keiichi Tadokoro(Research Center for Seismology, Volcanology and Earthquake and Volcano Research Center, Nagoya University), Marekazu OHNO(Unzen Volcanic Area Geopark Promotion Office), Takayuki Ogata(Graduate School of Engineering and Science, University of the Ryukyus)

This session targets interdisciplinary and multidisciplinary discussion on geopark, involving geoheritage, geodiversity, geoconservation, geotourism, sustainable development, governance, risk management, science communication and geoscientific education. These topics contribute to scientific and attractive activities in geoparks.

[MIS22-P01] Scientific Roles of the JpGU Session "Geopark"

*Takayuki Ogata[1] (1.Graduate School of Engineering and Science, University of the Ryukyus)

[MIS22-P02] Discussion

Scientific Roles of the JpGU Session "Geopark"

*Takayuki Ogata[1]

1. Graduate School of Engineering and Science, University of the Ryukyus

The session of "Geopark" has been held in JpGU meeting for 10 years. The author reviews 185 presentations from 2012 to 2020, and discusses scientific roles of this session and its future. The co-sponsored session with several society members of JpGU has provided as a collaborative session which targets interdisciplinary and multidisciplinary discussion on geopark, involving geoheritage, geodiversity, geoconservation, geotourism, sustainable development, governance, risk management, science communication and geoscientific education. Studies presented in this session seem to be classified into methodology on education, cases of outreach and geotourism, and geoscientific studies in geosites. The author especially expects field observation on regional geography and historical geology in many geoparks.

Keywords: geopark, geoscience, field observation

©2021. Japan Geoscience Union. All Right Reserved.

[J] Poster | M (Multidisciplinary and Interdisciplinary) | M-IS Intersection

[M-IS22] Geopark

convener:Takayuki Arima(Yokohama City University), Keiichi Tadokoro(Research Center for Seismology, Volcanology and Earthquake and Volcano Research Center, Nagoya University), Marekazu OHNO(Unzen Volcanic Area Geopark Promotion Office), Takayuki Ogata(Graduate School of Engineering and Science, University of the Ryukyus)

Sun. Jun 6, 2021 5:15 PM - 6:30 PM Ch.22

This session targets interdisciplinary and multidisciplinary discussion on geopark, involving geoheritage, geodiversity, geoconservation, geotourism, sustainable development, governance, risk management, science communication and geoscientific education. These topics contribute to scientific and attractive activities in geoparks.

5:15 PM - 6:30 PM

[MIS22-P02]Discussion

©Japan Geoscience Union

[J] Oral | M (Multidisciplinary and Interdisciplinary) : M-IS Intersection

Sun. Jun 6, 2021 9:00 AM - 10:30 AM JST | Sun. Jun 6, 2021 12:00 AM - 1:30 AM UTC | Ch.10 Zoom Room 10

[M-IS24] Geophysical fluid dynamics-Transfield approach to geoscience

convener:Keita Iga(Atmosphere and Ocean Research Institute, The University of Tokyo), Shigeo Yoshida(Department of Earth and Planetary Sciences, Faculty of Sciences, Kyushu University), Takatoshi Yanagisawa(Research Institute for Marine Geodynamics, Japan Agency for Marine-Earth Science and Technology), Hidenori AIKI(Nagoya University), Chairperson:Kensuke Nakajima(Department of Earth and Planetary Sciences,Flculty of Sciences,Kyushu University)

This session on geophysical fluid dynamics is open to discussions and researches on fluid phenomena in whatever fields of earth and planetary sciences, e.g., motions in the earth and planetary interior, oceans, atmospheres, volcanoes, and the ionosphere, conducted with whatever methods. Talks intending to stimulate exchange of ideas among multiple fields of researches or those identifying concepts that are commonly applicable to wide range of geophysical fluids are especially welcome.

9:00 AM - 9:15 AM JST | 12:00 AM - 12:15 AM UTC

[MIS24-01] Balance of baroclinicity and restoring force due to stable temperature stratification in developing horizontal convection in a finite fluid layer

*Tomomi Terada[1], Daisuke Noto[1], Yuji Tasaka[2], Takatoshi Yanagisawa[3,2], Takehiro Miyagoshi[3], Yuichi Murai[2] (1.Graduate School of Engineering, Hokkaido University , 2.Faculty of Engineering, Hokkaido University, 3.Japan Agency for Marine-Earth Science and Technology)

9:15 AM - 9:30 AM JST | 12:15 AM - 12:30 AM UTC

[MIS24-02] Quasi-periodic oscillations of convection patterns and heat transport in horizontally finite geometries

*Takatoshi Yanagisawa[1], Megumi Akashi[2], Yuji Tasaka[3], Ataru Sakuraba[4] (1.Research Institute for Marine Geodynamics, Japan Agency for Marine-Earth Science and Technology, 2.Institute of Fluid Dynamics, Helmholtz-Zentrum Dresden-Rossendorf, 3.Faculty of Engineering, Hokkaido University, 4.Department of Earth and Planetary Science, University of Tokyo)

9:30 AM - 9:45 AM JST | 12:30 AM - 12:45 AM UTC

[MIS24-03] Cyclonic-anticyclonic asymmetry on maintained vortices near the westerlies focused on external vortices

*Koryu Yamamoto[1], Keita Iga[1] (1.Atmosphere and Ocean Research Institute, The University of Tokyo)

9:45 AM - 10:00 AM JST | 12:45 AM - 1:00 AM UTC

[MIS24-04] High-frequency measurement of a double helical vortex with a sonic anemometer thermometer for laboratory use

*Toshihisa Itano[1] (1.National Defense Academy)

10:00 AM - 10:15 AM JST | 1:00 AM - 1:15 AM UTC

[MIS24-05] Numerical experiments of surface flows on giant planets produced by forcings representing thunderstorms

Ryoma Suzuki[2], *Youhei SASAKI[1], Masaki Ishiwatari[3] (1.Institute of Fundamental Sciences, Faculity of Science and Engineering, Setsunan University, 2.Department of Cosmosciences, Graduate School of Science, Hokkaido University, 3.Department of Earth and Planetary Sciences, Faculty of Science, Hokkaido University)

10:15 AM - 10:30 AM JST | 1:15 AM - 1:30 AM UTC

[MIS24-06] Discussion

Balance of baroclinicity and restoring force due to stable temperature stratification in developing horizontal convection in a finite fluid layer

*Tomomi Terada[1], Daisuke Noto[1], Yuji Tasaka[2], Takatoshi Yanagisawa[3,2], Takehiro Miyagoshi[3], Yuichi Murai[2]

1. Graduate School of Engineering, Hokkaido University , 2. Faculty of Engineering, Hokkaido University, 3. Japan Agency for Marine-Earth Science and Technology

Convection driven by a temperature gradient along a horizontal surface at the same level is termed horizontal convection and plays important roles in various fluid motions on the Earth, e.g. oceanic flows, atmospheric flows, liquid metal flows inside the outer core. Conventionally, horizontal convection has been studied on its equilibrium state, i.e. a flow state after a sufficiently long time for thermal diffusion. Both buoyancy and baroclinicity dominate the equilibrium horizontal convection. By contrast, during a temporal evolution from a certain initial state toward an equilibrium state, effect of restoring force becomes prominent instead of that of the buoyancy. The developing horizontal convection has been scarcely discussed, and it is worth investigating.

In this study, we aim to identify the contribution of stable temperature stratification on flow characteristics of developing horizontal convection, where the stratification relaxes with time. Visualization experiments were performed adopting a rectangular vessel where differential heating is imposed at the top and other boundaries are thermally insulated. We could observe formation of circulating flows owing to the baroclinicity of the horizontal temperature gradient. Using particle tracking velocimetry, various flow characteristics, e.g. stream functions, thickness of circulating flows, total kinetic energy, were quantified. It was found that the degree of stratification becomes a primary parameter determining the flow features of developing horizontal convection. This finding extends the conventional scalings of Rayleigh number applicable in the equilibrium state by adding the stratification parameter even in the developing state.

Keywords: Horizontal convection, Temporal evolution, Stable temperature stratification

©2021. Japan Geoscience Union. All Right Reserved.

Quasi-periodic oscillations of convection patterns and heat transport in horizontally finite geometries

*Takatoshi Yanagisawa[1], Megumi Akashi[2], Yuji Tasaka[3], Ataru Sakuraba[4]

1. Research Institute for Marine Geodynamics, Japan Agency for Marine-Earth Science and Technology, 2. Institute of Fluid Dynamics, Helmholtz-Zentrum Dresden-Rossendorf, 3. Faculty of Engineering, Hokkaido University, 4. Department of Earth and Planetary Science, University of Tokyo

Pattern of Rayleigh-Bernad convection at low Prandtl numbers has been a hot topic in recent years. In laboratory experiments, patterns existing in turbulent convection of liquid metals are observed and quantified by ultrasonic velocity measurements. In numerical simulations, calculations of convection in horizontally wide geometries are realized and so-called superstructures are identified in turbulence. We reported transitions from roll-like to cell-like structure in turbulent convection of a liquid metal experiment with the increase of the Rayleigh number (Ra) for a vessel having aspect ratio five (Akashi et al., 2019, Phys. Rev. Fluids). Both roll- and cell-like structures were marked by quasi-periodic oscillations whose periods are comparable to the turn-over time of the flow.
Here we studied the dependency of the features on aspect ratios of the square geometry confined by no-slip side walls by numerical simulations. The aspect ratio of the geometry (=A) is defined by the horizontal length of square vessel to its layer thickness, and we examined A from 0.5 to 20. The value of Prandtl number was fixed at 0.025 and Ra numbers were set around 10^5, where features of turbulence are clearly recognized. There exist organized flow structures in turbulence. When A < 4, the patterns are roll-like showing strong directionality. When 4 < A < 6, the patterns are cell-like with similar flow velocities for two horizontal directions. In both cases the patters are consist of a single or a pair of circulation and show quasi-periodic oscillations. For geometries with larger A, the patterns are composed of multiple cells and rolls; quasi-periodic oscillations are not observed any more. The degree of heat transport and its fluctuation in time are closely related to the convection pattern. We quantified them by using time averaged value of the Nusselt numbers (Nu) and their standard deviations. The dependence of Nu on A is not monotonic but complicated reflecting the transition of patterns. We found that Nu shows maximum where pattern changes from roll to cell, and that the fluctuation of Nu is very small at that point.

Keywords: convection pattern, quasi-periodic oscillation, heat transport

©2021. Japan Geoscience Union. All Right Reserved.

Cyclonic-anticyclonic asymmetry on maintained vortices near the westerlies focused on external vortices

*Koryu Yamamoto[1], Keita Iga[1]

1. Atmosphere and Ocean Research Institute, The University of Tokyo

The weather in mid- and high-latitude area including Japan is affected by the meandering westerlies. They occasionally result in vortices such as blocking anticyclones and cut-off cyclones. It is suggested by several previous studies that the way how anticyclones and cyclones sustain themselves for some days and maintain their position can be different between polarity. Few studies, however, have clarified the cyclonic-anticyclonic asymmetry by comparing them comprehensively. In the present study, we focus on maintained vortices near the westerlies, and we also analyzed their migration and how the potential vorticity flowed into them which can be one of the reasons of the migration. First, maintained anticyclonic and cyclonic non-dipole vortices are extracted from a global reanalysis as we symmetrically applied the previous and objective method to extract blocking anticyclones to cyclones. The analysis period is for 61 years, from March 1958 to February 2019. Geopotential height on 500hPa surface is used to extract them. A comparison of the anticyclones and cyclones extracted shows that several characteristics such as migration length of their center are suggested to be different with statistical significance. Furthermore, detailed examination of their migration during particular periods confirms that the cyclones exhibit larger movement in the east-west direction but smaller in the north-south direction than the anticyclones do. Next, composited maps which show how the potential vorticity into the vortices are made and analyzed in order to discover the differences in the migration. The results show that the maps are consistent with the migration. It is confirmed that air with high potential vorticity flows into the cyclones mainly from the west, whereas air with low potential vorticity doesn't show such a tendency for the anticyclones. Finally, in order to confirm the inflow and investigate the origins of the air into the vortices, we conducted a backward trajectory analysis. The result shows that the origins are migrating disturbances in the westerlies and vortices which existed in the previous time. Diabatic effects also contribute to the anomalous potential vorticity around the center of the vortices. It is confirmed that almost all the cyclones are accompanied with an area where the potential vorticity decreases due to strong convection to their south side, whereas the anticyclones are not. The present study has confirmed that anticyclones and cyclones can have different mechanisms for maintenance near the westerlies.

Keywords: cyclonic-anticyclonic asymmetry, potential vorticity, trajectory analysis

©2021. Japan Geoscience Union. All Right Reserved.

High-frequency measurement of a double helical vortex with a sonic anemometer thermometer for laboratory use

*Toshihisa Itano[1]

1. National Defense Academy

The multiple-vortex phenomenon, in which the core of a vortex is destabilized to split into a pairs of secondary vortices intertwined with each other and revolving around the radius of the maximum wind of the parent vortex, was discovered in the middle 1960’s and reproduced in a laboratory experiment in early 1970’s. Afterwards, in 1980’s, a similar kind of tornado simulators, which could reproduce the multiple-vortex phenomenon, were designed in several universities and the wind and pressure distributions, etc. were examined in addition to the condition for the formation. However, due to the restrictions on the instruments available at that time, direct measurement by one- or two-dimensional hot-wire anemometer and/or photometric analysis of stroboscopic photography visualized by smoke wire were simply carried out in most of the case. It should be noted that we can’t obtain the turbulent momentum transport and its cospectra by one- dimensional probe of the hot-wire anemometer. Also, even with the two- dimensional probe, two components of the wind velocity are not obtained necessarily: the measuring surface of the probe has to be turned parallel to the wind direction, and the fluctuations of the wind direction must be restricted within 90 degree. In this respect, to measure the multiple vortex phenomenon, where secondary vortices are embedded within the primary vortex, is quite difficult because the wind direction tends to be reversed frequently (Indeed, Monji (1985) gave up tp measure the core part of the multiple-vortex phenomenon.). Laser Doppler velocimeter (LDV) and Cobra probe, a kind of Pitot tube, were introduced for the measurement of laboratory tornadoes in 1990’s and after 2000, respectively. Especially, the latter is an attractive instrument, which can measure not only three components of wind velocity but also the pressure in the same time. Nevertheless, it could not be used for the multiple-vortex phenomenon since it can’t measure the flow from behind. By considering the above situations, we would like to introduce our attempt to measure the multiple-vortex phenomenon with a sonic anemometer thermometer (SAT) for laboratory use.

We focused on a “double helical vortex” which appears in our tornado simulator at National Defense Academy (1.9m<diameter>×0.95m<height>, aspect ratio a=0.857(=0.3m/0.35m)) when the inflow angle is θ=45 degree (i.e. the swirl ratio a (=tanθ/(2a)=0.58)) and the frequency of the fan is 10Hz (i.e. Reynolds number Re=16,800). We set 72 observation points, every 3cm and 5cm in the radial and vertical directions, respectively, within a vertical cross section of the simulator. The WA-790 <Sonic>, the probe of which has the base line of 3cm between a pair of its transducers, is adopted and high frequency observation is carried out for 10 minutes with 10Hz at each point. Results indicate that in most of the region, the basic swirling flow deviates inward (less than 10 degrees) from the tangential direction and the elevation angle increases with height. Meanwhile, the downward flow exists in the core part, where net wind speed is weak, forming an “eye”. Standard deviation of the wind speed is large at the shear region surrounding the “eye”, which indicates the existence of the secondary vortices. Covariance of the wind fluctuations implies the momentum of the basic swirling flow is transported both upward and outward in most of the region, but inward transported is detected around the radius of the maximum wind of the basic swirling flow.

Keywords: multiple-vortex, sonic anemometer thermometer, momentum transport

©2021. Japan Geoscience Union. All Right Reserved.

©2021. Japan Geoscience Union. All Right Reserved.

Numerical experiments of surface flows on giant planets produced by forcings representing thunderstorms

Ryoma Suzuki[2], *Youhei SASAKI[1], Masaki Ishiwatari[3]

1. Institute of Fundamental Sciences, Faculity of Science and Engineering, Setsunan University, 2. Department of Cosmosciences, Graduate School of Science, Hokkaido University, 3. Department of Earth and Planetary Sciences, Faculty of Science, Hokkaido University

It is known that the surfaces of giant planets have the banded structures consisting of equatorial jets with wide latitudinal widths and mid-latitudinal jets with narrow latitudinal widths, and the vortex structures in the polar regions.Large-scale structures such as banded structures and polar vortices can be formed from small-scale turbulence due to the inverse cascade effect (e.g. Showman et al., 2009). Thunderstorms are considered to be a candidate for causing such small-scale turbulence (e.g. Ingersoll et al., 2000). Showman (2007) and Brueshaber et al. (2019) performed calculations in the framework of the shallow water system with the mass forcing representing thunderstorms. Showman (2007) showed the formation of the banded structures with restricting the computational domain to the latitude range 0-70 degrees and the longitude range of 0-120 degrees. Brueshaber et al. (2019) found the polar vortex structures were formed in the computational domain from latitude 60 degrees to high latitude. In addition, their results showed that the number and size of polar vortices, and the sign of vorticity significantly depend on the value of Burger number (Bu=$(L_d/a)^2$, L_d: deformation radius, a: planetary radius). However, computational domains used by previous studies are restricted to a part of the sphere. In cases of calculation by regional model, the structure of jets and vortices may change due to momentum transport from regions outside the restricted computational domain.
The purpose of this study is to perform global calculations and to investigate whether the jet and polar vortex structures can be formed by the mass forcing representing thunderstorms. These structures are compared with the results obtained in previous studies to validate the domain calculations. The model used in this study is the Hierarchical Spectral Models for GFD (SPMODEL; Takehiro et al. 2006, Takehiro et al. 2013). The used equations are 1.5-layer shallow water equations with the mass forcing representing thunderstorms. The experiments are performed with changing values of the Burger number. In this presentation, the results of numerical experiments and the consistency with previous studies will be reported.

Keywords: Jovian planets, Banded structure, Polar vortex, Shallow water model

©2021. Japan Geoscience Union. All Right Reserved.

[J] Oral | M (Multidisciplinary and Interdisciplinary) | M-IS Intersection

[M-IS24] Geophysical fluid dynamics-Transfield approach to geoscience

convener:Keita Iga(Atmosphere and Ocean Research Institute, The University of Tokyo), Shigeo Yoshida(Department of Earth and Planetary Sciences, Faculty of Sciences, Kyushu University), Takatoshi Yanagisawa(Research Institute for Marine Geodynamics, Japan Agency for Marine-Earth Science and Technology), Hidenori AIKI(Nagoya University), Chairperson:Kensuke Nakajima(Department of Earth and Planetary Sciences,FIculty of Sciences,Kyushu University)
Sun. Jun 6, 2021 9:00 AM - 10:30 AM Ch.10 (Zoom Room 10)
This session on geophysical fluid dynamics is open to discussions and researches on fluid phenomena in whatever fields of earth and planetary sciences, e.g., motions in the earth and planetary interior, oceans, atmospheres, volcanoes, and the ionosphere, conducted with whatever methods. Talks intending to stimulate exchange of ideas among multiple fields of researches or those identifying concepts that are commonly applicable to wide range of geophysical fluids are especially welcome.

10:15 AM - 10:30 AM

[MIS24-06]Discussion

©Japan Geoscience Union

[J] Poster | M (Multidisciplinary and Interdisciplinary)：M-IS Intersection

Sun. Jun 6, 2021 5:15 PM - 6:30 PM JST | Sun. Jun 6, 2021 8:15 AM - 9:30 AM UTC | Ch.18_2

[M-IS24] Geophysical fluid dynamics-Transfield approach to geoscience

convener:Keita Iga(Atmosphere and Ocean Research Institute, The University of Tokyo), Shigeo Yoshida(Department of Earth and Planetary Sciences, Faculty of Sciences, Kyushu University), Takatoshi Yanagisawa(Research Institute for Marine Geodynamics, Japan Agency for Marine-Earth Science and Technology), Hidenori AIKI(Nagoya University)

This session on geophysical fluid dynamics is open to discussions and researches on fluid phenomena in whatever fields of earth and planetary sciences, e.g., motions in the earth and planetary interior, oceans, atmospheres, volcanoes, and the ionosphere, conducted with whatever methods. Talks intending to stimulate exchange of ideas among multiple fields of researches or those identifying concepts that are commonly applicable to wide range of geophysical fluids are especially welcome.

[MIS24-P01] Two-dimensional ideal MHD waves and the continuous Alfvén spectrum on a rotating sphere with a background toroidal magnetic field

*Ryosuke Nakashima[1], Shigeo Yoshida[2] (1.Faculty of Science, Kyushu University, 2.Department of Earth and Planetary Sciences, Faculty of Science, Kyushu University)

[MIS24-P02] Development of sea surface wave breaking observation system using industrial millimeter radar and optical particle size counter

*Hidenori AIKI[1], Fumiyoshi Kondo[2], Haruya Minda[1] (1.Nagoya University, 2.Japan Coast Guard Academy)

[MIS24-P03] Axisymmetric flows and non-axisymmetric phenomena in a cylindrical tank with a rotating bottom

*Keita Iga[1] (1.Atmosphere and Ocean Research Institute, The University of Tokyo)

[MIS24-P04] We examined **Origin of Great Red Spot of Jupiter, Deep Ocean Floor, Pacific Rim Arcuate Archipelago, Origin of Gomagnetic Reversal, and Origin of Asteroid Belt.**

*Akira Taneko[1] (1.SEED SCIENCE Lab.)

Two-dimensional ideal MHD waves and the continuous Alfvén spectrum on a rotating sphere with a background toroidal magnetic field

*Ryosuke Nakashima[1], Shigeo Yoshida[2]

1. Faculty of Science, Kyushu University, 2. Department of Earth and Planetary Sciences, Faculty of Science, Kyushu University

Two-dimensional magnetohydrodynamic (MHD) linear waves on a rotating sphere are investigated for perfectly conducting fluids permeated by an azimuthal magnetic field whose magnitude may depend on the colatitude θ. If the toroidal background field is expressed as $B_{0\Phi} = B_0 \sin\theta$, where B_0 is constant and Φ is the azimuth, two types of waves exist: westward-propagating fast magnetic Rossby waves and eastward-propagating slow counterparts. Except for this profile of the imposed field, the wave equation of this system can possess regular singular points at which the zonal phase velocity of an eigenmode is equal to a local Alfvén wave velocity devided by $\sin\theta$. Since the positions of critical latitudes depend on the azimuthal phase speed of a chosen eigenmode, this means that continuous spectra appear due to Alfvén resonance in spite of the closed region such as a sphere surface. Similar situations include the linear problem in the inviscid parallel shear flow, which can yield critical layers where the phase velocity coincides with a local mean flow velocity (e.g. Case, 1960).

We solved the eigenvalue problem for $B_{0\Phi} = B_0 \sin\theta\cos\theta$ numerically and confirmed the existence of the Alfvén continuum. Since the eigenfrequencies of continuous modes areally spread on the dispersion diagram, there is a possibility that the branches of discrete eigenmodes are buried under the continuous spectrum. We therefore scanned the buried branches by calculating the energy partition of each eigenmodes. Remarkably, discrete branches of slow magnetic Rossby waves were not found in the case of this main field configuration. Thus, the choice of the background field profile might have an influence of the appearance of these slow waves in the ideal MHD case.

Numerical study gives the structure of continuous eigenmodes and shows that these conform to the superposition of the two linearly independent solutions resulted from the Frobenius technique around a critical latitude and to their theoretical connection conditions. When the magnitude of the applied field is small, these eigenfunctions tend to be evanescent on the north side of the critical latitude in the north hemisphere for westward-propagating continuous modes and on the south side of the critical latitude in the north hemisphere for eastward-propagating continuous modes, although there is an exception. This feature is consistent with the WKBJ approximation in slowly varying magnetic shear (Acheson, 1972; Eltayeb & McKenzie, 1977), which suggests the critical level absorption of MHD waves with high wavenumber in rotating fluids. Although Acheson (1972) proposed the "valve" effect, which means that MHD waves can penetrate through the critical layer in limited circumstances, our problem is out of range of its condition, that is, horizontal angular velocity Ω_θ vanishes.

Keywords: MHD waves, critical latitude, magnetic shear, continuous Alfvén spectrum, rotating fluid

©2021. Japan Geoscience Union. All Right Reserved.

Development of sea surface wave breaking observation system using industrial millimeter radar and optical particle size counter

*Hidenori AIKI[1], Fumiyoshi Kondo[2], Haruya Minda[1]

1. Nagoya University, 2. Japan Coast Guard Academy

When a typhoon passes over the sea surface, strong winds cause waves to develop and countless whitecap waves are generated. Large and small droplets are simultaneously generated in the atmospheric boundary layer by the whitecap breaking waves. Large droplets play an important role in the transport of momentum, heat, and CO2 between the atmosphere and the ocean due to their large mass. The small droplets become oceanic aerosols that form cloud condensation nuclei a few kilometers above the surface and contribute to the radiation budget of the atmosphere. Conventional observation of whitecap breaking waves using a CCD camera was affected by fog and sunlight and was not suitable for continuous observation during stormy weather or day and night. In this study, we develop a system to measure the spatio-temporal structure of whitecap breaking waves at sea using millimeter-wave radar electronic circuit boards for automobile parts. Since the resolution of millimeter-wave radar is a few millimeters to a few centimeters, it is ideal for capturing the dynamics of individual whitecap waves and sea spray layer. Since the temporal variation of the particle size distribution is also important information, the optical particle size counter for marine observation developed by the authors is used in combination with the radar.

©2021. Japan Geoscience Union. All Right Reserved.

Axisymmetric flows and non-axisymmetric phenomena in a cylindrical tank with a rotating bottom

*Keita Iga[1]

1. Atmosphere and Ocean Research Institute, The University of Tokyo

In the terrestrial and planetary atmospheres, even under axisymmetric enviroenments, the symmetry is often broken to cause various non-axisymmetric phenomena. Such non-axisymmetric phenomena can be realized in a simple laboratory experiment in a cylindrical tank which is filled with water and whose bottom rotates rapidly.
These phenomena have been investigated by many researchers, mainly by laboratory experiments and by theoretical analyses. On the other hand, the same problem has been investigated using numerical calculations. However, due to the restirictions of the computational resources, the parameter range of the calculated situation has been apart from those used in the laboratory experiments, where the boundary layers play important roles in the interesting phenomena.
Recently, the numerical calculations with closer parameters are performed, and in some cases, we can discuss the boundary layers formed in the numerical calculations. We compare the structures of the numerical results and those obtaied in labotaroty experiments and theoretically.

Keywords: rotating flow, laboratory experiments, axisymmetry breaking, boundary layers

©2021. Japan Geoscience Union. All Right Reserved.

We examined Origin of Great Red Spot of Jupiter, Deep Ocean Floor, Pacific Rim Arcuate Archipelago, Origin of Gomagnetic Reversal, and Origin of Asteroid Belt.

*Akira Taneko[1]

1. SEED SCIENCE Lab.

Hypothesis can be tested by Abduction using Results (Features) of Evolution. More Results (Characteristics) of multiple Evolutions can be explained consistently with One Hypothesis, More True it becomes. First was a hypothesis explaining Origin of Moon. It also explains Origin of Earth's Plate Tectonics and Driving Forces in other Sessions.
In this time, we explained each the detailed reasons for Origin of Jupiter's Great Red Spot, Origin of Deep Ocean Floor, and Origin of Asteroid Belt using the multi-impact hypothesis. I believe that if we can explain Everything with Cosmic Law (Universal Gravitational Force) of Geophysical Fluid Dynamics and explain Three Themes of Origin of planets, Earth, and Solar System with One Hypothesis, we can attract Audience of SCIENTIST beyond Interdisciplinary.

1.Origin of **Jupiter's Great Red Spot**
From circumstantial evidence, the Shoemaker-Ninth Comet Jupiter collision occurred in 1993. Collision traces formed multiple small white spots and disappeared over time. In Previous Encounter, it collided with Comet Train in a Row in Same Orbit. A Collision Flash was also observed after being Photographed. In Malti-Impact hypothesis, assuming a Martian-sized Protoplanet CERRA at Ceres Position, CERRA Orbit was flattened into an Elliptical Orbit by Perturbation of Giant Mass Jupiter, which accumulated behind Outer Orbit.

In Multi-Impact Hypothesis, assuming a Mars-sized protoplanet CERRA at Ceres Position, CERRA Orbit flattened into an Elliptical Orbit due to Perturbation of Giant Mass Jupiter that accumulated behind Outer Orbit. At Point where Gravitational pulls of Sun and Jupiter are balanced, CERRA ruptures Tide and Orbits in a Row as Train Mantle rupture Fragments.
At Position where it intersects Earth's Orbit, it collides intermittently at Each Meeting Period. Inevitable Collision Mechanism of Mantle Impactor is completed. If it does not rupture, it is an Inevitable Collision of Giant Impact Mars. Here, Collision Velocity and Angle can be calculated from Theory, and their values are Same. **V=12.43km /s** and **36.45 ˚**.
At Time of this CERRA Rupture, Mantle Rupture that collided with Jupiter is a Fragment Larger than a Comet, pierces Liquid Core and Solid Core of Jupiter, and rotates with Jupiter Core. Naturally, **Birth of** Great Red Spot **Soliton**. If Material is different from that of Jupiter Core and Thermal Conductivity is low, Debris will become an Enlarged Vortex and will have a Long Life if it is not buried.

2.Origin of **Earth's Deep Ocean Floor**
Rupture of CERRA in Malti-Impact Hypothesis caused Intermittent Collisions of Train Mantle Fragments with Earth, resulting in Multiple Earth Mantle Ejections and Detachments. Largest of these is Lunar Ejection, a Defect in Pacific Ocean, Indian Ocean, Antarctic Ocean, and Arctic Ocean.

Theory that Crust Breaks due to thermal stress is Nonsense. There are No Planets in Solar System that are broken like Turtle Shell. There is No Mechanism to heat it even though it has Cooled Down. Pacific Ocean

©2021. Japan Geoscience Union. All Right Reserved.

is in more than Double Collision. Crust does not crack under Internal Forces such as Mantle Convection. Even with Pressure, it just spouts from One Point and does not last.

Earth's Mantle Cracks due to Impact Force from Outside and Melts when Pressure drops. Mantle is classified into Lithosphere (Plate), Asthenosphere (Rock Basin), partially melted and flowing, and Mesosphere (Lower Mantle Solid). In other words, when Crust is cracked and divided, a Layer called a Plate Easily moves on Fluidized Bed called Asthenosphere. Crustal Defects are balanced and interconnected at an Average Depth of 4 km by Isostasy, occupying **70%** of Earth's Surface.

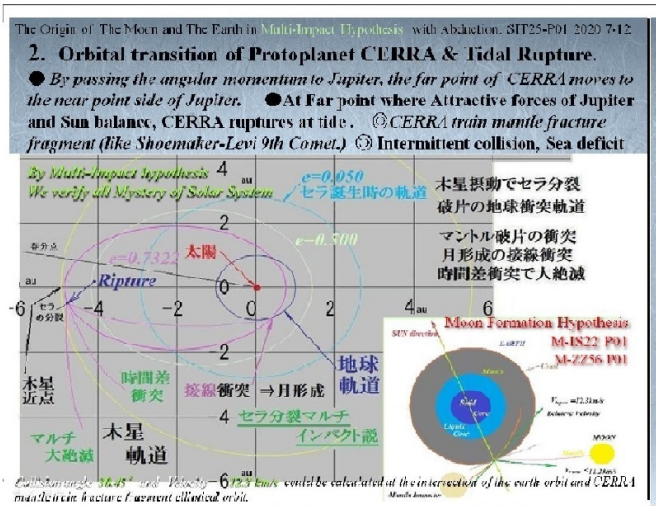
3.**Pacific Rim Arc Archipelago and Geomagnetic Reversal**
CERRA Fragment caused Lunar Ejection and Pacific mantle defect due to Earth's Collision. Isostasy uplifted Seafloor. Surrounding Mantle is dented to form an Ocean Basin, forming Pacific Rim Arcuate Archipelago. Liquid core was also Eccentric, and Van Allen Belt was also Eccentric. Rotation of Solid Core and Mantle deviated, Direction of Flow of Liquid Core was reversed, and Magnetic Poles were replaced.

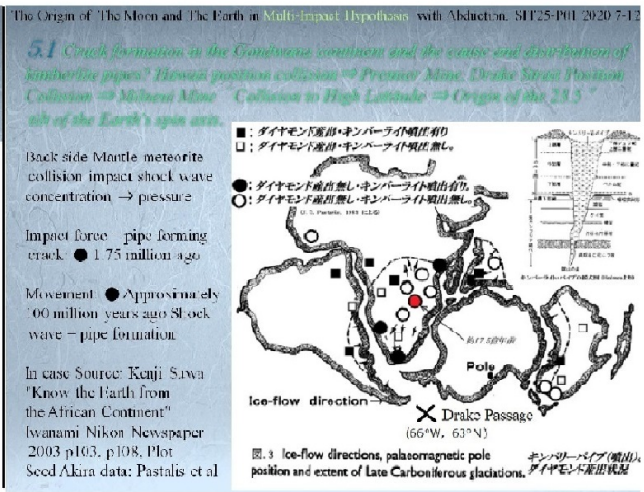
4.Origin of **Asteroid Belt**
Due to Rupture of CERRA in Malti-Impact Hypothesis, Mantle fragments scattered in all directions other than Train Mantle shards formed an Asteroid Belt and orbited Sun. Objects that collided and accumulated with each other became **Mantle-only Asteroids** (Itokawa and Ryugu) that differentiated as **Love Pile Objects**. **Most of Core + Mantle Fragments** became **Mercury (Core rich)** due to Decrease in Peripheral Speed due to Law of Energy Equipartition.

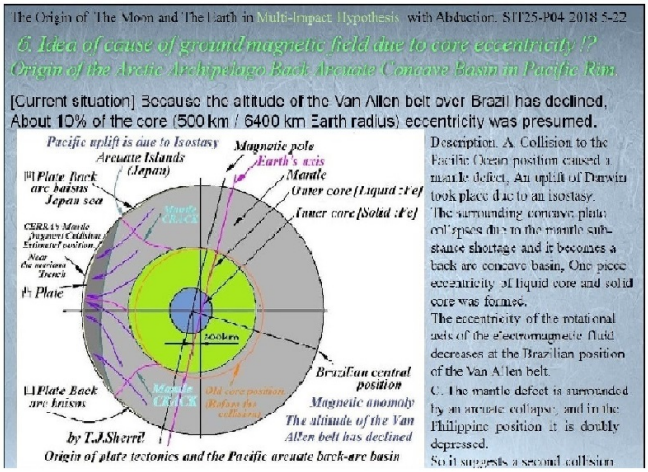
Evolution include fluid to gas, solid to collisional melting, tidal bursting, melt scattering and accumulation, etc.

Keywords: Multi-impact hypothesis, Abduction using Evolutionary Results , Origin of Jupiter's Great Red Spot , Origin of Earth's Deep Ocean Floor, Origin of Asteroid Belt, Origin of Asteroid, Origin of Mercury (Core Rich) , Titius-Bode's Law, Feeding Zone

©2021. Japan Geoscience Union. All Right Reserved.









©2021. Japan Geoscience Union. All Right Reserved.

[J] Oral | M (Multidisciplinary and Interdisciplinary)：M-IS Intersection

Sun. Jun 6, 2021 9:00 AM - 10:30 AM JST | Sun. Jun 6, 2021 12:00 AM - 1:30 AM UTC | Ch.11 Zoom Room 11

[M-IS25] Atmospheric electricity: Electrical phenomena associated with extreme weather

convener:Yasuhide Hobara(Graduate School of Information and Engineering Department of Communication Engineering and Informatics, The University of Electro-Communications), Daohong Wang(Gifu University), Chairperson:Yasuhide Hobara(Graduate School of Information and Engineering Department of Communication Engineering and Informatics, The University of Electro-Communications), Daohong Wang(Gifu University)

In recent years, extreme weather events have occurred frequently not only in Japan but also in other countries around the world. In particular, last year's typhoons 15 and 19 caused tremendous damage in Japan. This year's Atmospheric Electricity session will focus on observational and theoretical studies of atmospheric electrical phenomena associated with extreme weather.
This session will consist of invited presentations introducing above-mentioned fields by leading experts, and contributed presentations on the latest observational and theoretical research results in these fields. For example, we welcome lightning activity associated with many of extreme weather events such as typhoons, heavy rains, wind gusts, and their effects on the upper atmosphere/ionosphere. Besides, we certainly welcome papers regarding all topics on atmospheric electricity including lightning physics, lightning observation technology, electrical effects of thunderstorms, mesospheric transient luminous events (TLEs), lightning-related high-energy phenomena, global electric circuit, atmospheric ion, aerosol, fair-weather electricity, lightning protection, terrestrial electromagnetic noise environment (e.g. wave propagation in the magnetosphere and ionosphere).

9:00 AM - 9:15 AM JST | 12:00 AM - 12:15 AM UTC

[MIS25-01] Understanding of fine structure of cumulonimbus using new observational method

★Invited Papers

*Fumiaki Kobayashi[1] (1.National Defense Academy)

9:15 AM - 9:30 AM JST | 12:15 AM - 12:30 AM UTC

[MIS25-02] Various common meteorological characteristics obtained by multiple observation results of downburst

*Hisato Iwashita[1], Fumiaki Kobayashi[2] (1.Meisei Electric Co.,Ltd, 2.National Defense Academy)

9:30 AM - 9:45 AM JST | 12:30 AM - 12:45 AM UTC

[MIS25-03] Observations of summer thunderstorms using dual polarized phased array weather radar and three-dimensional lightning location system using LF band in Kanto area

*Hiroshi Kikuchi[1], Yuhei Kamei[1], Yoshitaka Nakamura[3], Eiichi Yoshikawa[5], Takeshi Morimoto[4], Tomoo Ushio[2], Yasuhide Hobara[1] (1.The University of Electro Communications, 2.Osaka University, 3.Kobe City College of Technology, 4.Kinki University, 5.Japan Aerospace Exploration Agency)

9:45 AM - 10:00 AM JST | 12:45 AM - 1:00 AM UTC

[MIS25-04] 3D characteristics of lightning activity in Typhoon Faxai (2019)

*Namiko Sakurai[1], Hironori Fudeyasu[2], Paul R. Krehbiel[3], Ronald J. Thomas[3], William Rison[4], Daniel Rodeheffer[4] (1.National Research Institute For Earth Science and Disaster Prevention, 2.Yokohama National University, 3.New Mexico Tech, 4.LMA technologies)

10:00 AM - 10:15 AM JST | 1:00 AM - 1:15 AM UTC

[MIS25-05] Citizen science "Thundercloud project" for mapping observations of gamma rays from thunderstorms

*Teruaki Enoto[1], Yuko Ikkatai[2], Yuuki Wada[1], Gabriel Diniz[1], Masaki Numazawa[1], Yo Kato[1], Shoko Miyake[3], Kazuhiro Nakazawa[4], Shohei Hisadomi[4], Yuna Tsuji[4], Takayuki Yuasa, Harufumi Tsuchiya[5], Takeshi

Morimoto[6], Yoshitaka Nakamura[7], Masashi Kamogawa[8] (1.RIKEN, 2.The University of Tokyo, 3.National Institute of Technology, Ibaraki College, 4.Nagoya University, 5.JAEA, 6.Kinki University, 7.Kobe City College of Technology, 8.Global Center for Asian and Regional Research, University of Shizuoka)

10:15 AM - 10:30 AM JST | 1:15 AM - 1:30 AM UTC

[MIS25-06] Radioluminescence appeared above the epicenter immediately before and after the 1995 Kobe earthquake

*Yuji Enomoto[1], Tsuneaki Yamabe[1], Shigeki Sugiura[2], Hitoshi Kondo[2] (1.Shinshu Univeristy, Ueda Campus Fii, 2.Genesis Research Institute Inc.)

Understanding of fine structure of cumulonimbus using new observational method

*Fumiaki Kobayashi[1]

1. National Defense Academy

Extreme weather, such as local heavy rain, tornado and downburst, and supertyhoon, is caused by developing cumulonimbus (e.g., supercell). Understanding of fine structure of cumulonimbus is important at the points of weather forecasting and disaster mitigation. In this lecture, the front of cumulonimbus observation using new observational method would be introduced.

Keywords: extreme weather, tornado, cumulonimbus, weather radar

©2021. Japan Geoscience Union. All Right Reserved.

Various common meteorological characteristics obtained by multiple observation results of downburst

*Hisato Iwashita[1], Fumiaki Kobayashi[2]

1. Meisei Electric Co.,Ltd, 2. National Defense Academy

In recent years, it is eminent that the very severe damage caused by not only a synoptic atmospheric phenomenon such as typhoon or linear precipitation zone but also a localized extreme weather such as downburst or tornado. The observation technology of ground surface radar and satellite radar had developed remarkably. The radar which can observe the spatial and temporal structure of a localized extreme weather has appeared. But, the ground surface meteorological observation network which can sufficiently validate the observation result of meteorological radar has not easily appeared.

The high density ground surface meteorological observation network (POTEKA) of the North Kanto plain area observed multiple gust events which included the 3 eminent downbursts of F1 category (Fujita scale) / JEF1 category (Japan enhanced Fujita scale). These observation results revealed the various meteorological characteristics, for example, the ground surface meteorological change characteristic just under a downburst, the cumulonimbus advancing characteristic which caused a downburst, the existence of the divergent wind by a downburst and the horizontal scale of a downburst.

Keywords: downburst, tornado, localized, extreme weather, high density, ground surface observation

©2021. Japan Geoscience Union. All Right Reserved.

Observations of summer thunderstorms using dual polarized phased array weather radar and three-dimensional lightning location system using LF band in Kanto area

*Hiroshi Kikuchi[1], Yuhei Kamei[1], Yoshitaka Nakamura[3], Eiichi Yoshikawa[5], Takeshi Morimoto[4], Tomoo Ushio[2], Yasuhide Hobara[1]

1. The University of Electro Communications, 2. Osaka University, 3. Kobe City College of Technology, 4. Kinki University, 5. Japan Aerospace Exploration Agency

In Japan, a X-band dual polarized phased array weather radar (DP-PAWR), which simultaneously transmits pulses of horizontal and vertical polarized radiation, was developed and installed in December 2017 at Saitama University. The DP-PAWR has a scanning scheme similar to the PAWR, which also performs mechanical and electronic scanning at azimuth and elevation angles, respectively. The DP-PAWR yields polarimetric precipitation measurements via three-dimensional volume scanning in less than 1 min, 10 sec at the shortest, in a range of up to 80 km. The DP-PAWR is also able to provide coverage of urban areas in Tokyo.
In 2020, our research group (Japan Aerospace Exploration Agency, Kobe City College of Technology, Osaka University, Kinki University, and UEC are included) has installed 13 LF sensor network to obtain the 3D location of lightning discharges in the Kanto area in Japan. The system provides the 3D location of lightning discharges using the time-of-arrival location technique. The mean distance between stations is approximately 20-30 km. The electric field antenna bandwidth is broad from 51 Hz to 550 kHz. Its signal is sampled at 5 MHz. The recorded waveforms allow detailed analysis of lightning discharge processes.
In this presentation, we will show the case study of simultaneous lightning and precipitation observations with the DP-PAWR and 3D Lightning location system. The relationship between the initiation of lightning discharges and hydrometer types in the thunderstorm is also discussed.

Keywords: Phased array weather radar , Lightning discharges

©2021. Japan Geoscience Union. All Right Reserved.

3D characteristics of lightning activity in Typhoon Faxai (2019)

*Namiko Sakurai[1], Hironori Fudeyasu[2], Paul R. Krehbiel[3], Ronald J. Thomas[3], William Rison[4], Daniel Rodeheffer[4]

1. National Research Institute For Earth Science and Disaster Prevention, 2. Yokohama National University, 3. New Mexico Tech, 4. LMA technologies

This study examined 3D characteristics of lightning activity associated with Typhoon Faxai (T1915) using Tokyo Lightning Mapping Array (Tokyo LMA) and JMA C-band Doppler radar. Lightning flashes were observed in the eyewall and outer-rainband in the typhoon. In the observation area of Tokyo LMA, the number of lightning in the eyewall were more observed than that in the outer-rainband. Most of lightning in the eyewall were observed when the typhoon center was located over the sea. On the other hand, lightning in the outer-rainband were observed when the typhoon center was approaching to Kanto region and passing over Tokyo bay or Kanto region. There were developed convective cells in the eyewall which had 10 km echo top height and lightning location sources were observed in the upper layer of the developed convective cells and surrounding upper stratiform region. Flash size in the eyewall was about 21 km in average off the coast of Ibaraki Prefecture.

Keywords: lightning, Typhoon, LMA

©2021. Japan Geoscience Union. All Right Reserved.

Citizen science "Thundercloud project" for mapping observations of gamma rays from thunderstorms

*Teruaki Enoto[1], Yuko Ikkatai[2], Yuuki Wada[1], Gabriel Diniz[1], Masaki Numazawa[1], Yo Kato[1], Shoko Miyake[3], Kazuhiro Nakazawa[4], Shohei Hisadomi[4], Yuna Tsuji[4], Takayuki Yuasa, Harufumi Tsuchiya[5], Takeshi Morimoto[6], Yoshitaka Nakamura[7], Masashi Kamogawa[8]

1. RIKEN, 2. The University of Tokyo, 3. National Institute of Technology, Ibaraki College, 4. Nagoya University, 5. JAEA, 6. Kinki University, 7. Kobe City College of Technology, 8. Global Center for Asian and Regional Research, University of Shizuoka

The Gamma-ray Observation of Winter Thunderclouds (GROWTH) collaboration has measured high-energy atmospheric phenomena along the Sea of Japan since 2006. This campaign observed prolonged bremsstrahlung radiations from relativistic electrons accelerated by thunderclouds' electric field and short bursts from photonuclear reactions induced by terrestrial gamma-ray flashes (TGFs). Since the gamma rays can fly only a few hundred meters in the atmosphere, mapping observations is essential to compare high-energy events with meteorological observations. We are now distributing portable radiation detectors to citizen supporters and establish a new extended mapping observation network at Kanazawa that incorporates the Citizen Science method. The device is named Cogamo (Compact Gamma-ray Monitor), which operates with a single button and automatically sends data over the network. We aim to have citizen supporters take pictures of gamma-ray emitting clouds and study whether relativistic electron flow in thunderclouds is involved in the initiation of lightning discharges.

Keywords: high-energy atmospheric physics, gamma rays from thunderstorms, citizen science

©2021. Japan Geoscience Union. All Right Reserved.

Radioluminescence appeared above the epicenter immediately before and after the 1995 Kobe earthquake

*Yuji Enomoto[1], Tsuneaki Yamabe[1], Shigeki Sugiura[2], Hitoshi Kondo[2]

1. Shinshu Univeristy, Ueda Campus Fii, 2. Genesis Research Institute Inc.

Immediately before and after the Kobe earthquake that occurred at 05:46 (LT) on January 17, 1995, the night sky, which should have been dark, became as bright as the daytime. While there were many eyewitness testimonies, photographs demonstrating this phenomena was taken by N. Yokota, who lives in Izumi-Ohtsu, Osaka. A total of 5 photographs were taken, and from these photographs, fairly bright illuminants can be seen in two places above near the epicenter. This illuminant stays at an altitude of about 0.7km-2.5km, and linear mottled clouds are emitted from the illuminants. This luminescence / streak cloud has almost no change during the shooting time of several minutes and thus has a long life. By referring to other electromagnetic and radon observation data, it was concluded that this illuminants should be attributed to radioluminescence (α-ray, γ-ray) due to the decay of radon emanated from the fault.

Keywords: 1995Kobe earthquake, Radioluminescence, Earthquake lights



図.1 地震直後の震源方向の光る夜空の写真5枚（泉大津市在住：横田安子氏提供）
Fig.1 Five photos of the glowing night sky in the direction of the epicenter immediately after the Kobe earthquake(provided by Yasuko Yokota,Izumi-Ohtsu city)

©2021. Japan Geoscience Union. All Right Reserved.

[J] Poster | M (Multidisciplinary and Interdisciplinary)：M-IS Intersection

Sun. Jun 6, 2021 5:15 PM - 6:30 PM JST | Sun. Jun 6, 2021 8:15 AM - 9:30 AM UTC | Ch.18_3

[M-IS25] Atmospheric electricity: Electrical phenomena associated with extreme weather

convener:Yasuhide Hobara(Graduate School of Information and Engineering Department of Communication Engineering and Informatics, The University of Electro-Communications), Daohong Wang(Gifu University)

In recent years, extreme weather events have occurred frequently not only in Japan but also in other countries around the world. In particular, last year's typhoons 15 and 19 caused tremendous damage in Japan. This year's Atmospheric Electricity session will focus on observational and theoretical studies of atmospheric electrical phenomena associated with extreme weather.
This session will consist of invited presentations introducing above-mentioned fields by leading experts, and contributed presentations on the latest observational and theoretical research results in these fields. For example, we welcome lightning activity associated with many of extreme weather events such as typhoons, heavy rains, wind gusts, and their effects on the upper atmosphere/ionosphere. Besides, we certainly welcome papers regarding all topics on atmospheric electricity including lightning physics, lightning observation technology, electrical effects of thunderstorms, mesospheric transient luminous events (TLEs), lightning-related high-energy phenomena, global electric circuit, atmospheric ion, aerosol, fair-weather electricity, lightning protection, terrestrial electromagnetic noise environment (e.g. wave propagation in the magnetosphere and ionosphere).

[MIS25-P01] X-band radar and disdrometer observations of winter thunderclouds emitting gamma rays

*Yuuki Wada[1], Teruaki Enoto[1], Mamoru Kubo[2], Kazuhiro Nakazawa[3], Taro Shinoda[3], Daisuke Yonetoku[2], Tatsuya Sawano[2], Takayuki Yuasa, Tomoo Ushio[4], Yousuke Sato[5], Gabriel Sousa Diniz[1], Harufumi Tsuchiya[6] (1.RIKEN, 2.Kanazawa University, 3.Nagoya University, 4.Osaka University, 5.Hokkaido University, 6.JAEA)

[MIS25-P02] Observation of thundercloud gamma-rays in FY2020 with the GOOSE detector aiming at altitude measurements

*Yuuna Tsuji[1], Kazuhiro Nakazawa[1], Shohei Hisadomi[1], Yusaku Ikami[1], Daiki Odani[1], Teruaki Enoto[2], Yuuki Wada[2], Takayuki Yuasa, Harufumi Tsuchiya[3], Taro Shinoda[4], Keigo Ookuma[1], Gabriel Diniz[2] (1.Nagoya University, 2.RIKEN, 3.JAEA, 4.ISEE. Nagoya Univ.)

[MIS25-P03] Hydrometeor distribution in a thundercloud related to a gamma-ray emission event

*Takemoto Kiyomichi[1], Taro Shinoda[1], Masaya Kato[1], Shohei Hisadomi[2], Yuuna Tsuji[2], Kazuhiro Nakazawa[2], Yuuki Wada[3], Teruaki Enoto[3] (1.Institute for Space-Earth Environmental Research, Nagoya University, 2.Department of Physics, Nagoya University, 3.Institute of Physical and Chemical Research)

[MIS25-P04] A Study of 3D Precipitation Core Tracking Method Using Multi-Parameter Phased Array Weather Radar

*Keitaro Asai[1], Hiroshi Kikuchi[1], Yasuhide Hobara[1], Tomoo Ushio[2] (1.The University of Electro Communications, 2.Osaka University)

[MIS25-P05] Special negative lightning strokes in winter with extremely short preceding discharges

*Ting Wu[1], Daohong Wang [1], Nobuyuki Takagi[1] (1.Gifu University)

[MIS25-P06] Simultaneous Observations of a Winter Lightning Flash in Japan

*Haitao Huang[1], Daohong Wang[1], Ting Wu[1], Nobuyuki Takagi[1] (1.Gifu University)

[MIS25-P07] Spatio-temporal characteristics of lightning energy in Southeast Asia deduced from ELF observations

*Shunsuke Akama[1], Shu Hirai[1], Yasuhide Hobara[1], Hiroshi Kikuchi[1], Amir Izzani Mohamed[2], Chandima Gomes[3], Kazuo Shiokawa[4], Michael Stock[5] (1.The University of Electro-Communications, 2.University of Malaysia, Pahang, 3.University of the Witwatersrand, Johannesburg, 4.Institute for Space–Earth Environmental Research, 5.Earth Networks)

[MIS25-P08] Sprites observed from the summit of Mt. Fuji and their parent thunderstorm

*Suzuki Tomoyuki[1], Masashi Kamogawa[1], Syugo Hayashi[2] (1.University of Shizuoka, 2.Meteorological Research Institute)

[MIS25-P09] Coupling process of large-scale atmospheric disturbances to the ionosphere through typhoon

*Shu Hirai[1], Yasuhide Hobara[1], Hiroshi Kikuchi[1], Michael Stock[2] (1.The University of Electro-Communications, 2.Earth Networks)

X-band radar and disdrometer observations of winter thunderclouds emitting gamma rays

*Yuuki Wada[1], Teruaki Enoto[1], Mamoru Kubo[2], Kazuhiro Nakazawa[3], Taro Shinoda[3], Daisuke Yonetoku[2], Tatsuya Sawano[2], Takayuki Yuasa, Tomoo Ushio[4], Yousuke Sato[5], Gabriel Sousa Diniz[1], Harufumi Tsuchiya[6]

1. RIKEN, 2. Kanazawa University, 3. Nagoya University, 4. Osaka University, 5. Hokkaido University, 6. JAEA

Strong electric fields in thunderclouds accelerate electrons to relativistic energy even in a dense atmosphere, and bremsstrahlung gamma rays are observed as gamma-ray glows by radiation monitors on aircraft and on the ground. Since gamma rays are absorbed by the atmosphere, it is difficult to observe gamma rays emitted from summer thunderclouds at sea-level, but gamma-ray glows during winter thunderstorms in the Hokuriku region can be observed on the ground because they develop at low altitudes. We are conducting the GROWTH experiments in Ishikawa and Niigata prefectures to observe high-energy atmospheric phenomena such as gamma-ray glows. During the three seasons from 2016 to 2018, a radiation monitor installed at Kanazawa University registered a total of 11 gamma-ray glows. In each case, it was confirmed by the X-band radar operated by the Ministry of Land, Infrastructure, Transport and Tourism that a thundercloud with strong echoes exceeding 35 dBZ developed at an altitude of 2 km or more (-10 degrees or less) passed over the detector. Also a disdrometer installed at the site detected graupel precipitation during the gamma-ray glows. Therefore, it is considered that the developed thundercloud accompanied by hail contributes to the occurrence of gamma-ray glows.

Keywords: gamma rays, winter thunderstorm, high energy atmospheric physics

©2021. Japan Geoscience Union. All Right Reserved.

Observation of thundercloud gamma-rays in FY2020 with the GOOSE detector aiming at altitude measurements

*Yuuna Tsuji[1], Kazuhiro Nakazawa[1], Shohei Hisadomi[1], Yusaku Ikami[1], Daiki Odani[1], Teruaki Enoto[2], Yuuki Wada[2], Takayuki Yuasa, Harufumi Tsuchiya[3], Taro Shinoda[4], Keigo Ookuma[1], Gabriel Diniz[2]

1. Nagoya University, 2. RIKEN, 3. JAEA, 4. ISEE. Nagoya Univ.

Lightning activity emitting gamma-rays has been observed on the coast of the Sea of Japan in winter season. Those gamma rays are due to bremsstrahlung from electrons accelerated by the electrostatic field in thundercloud, and their energy reaches 30 MeV. Specifically, the gamma-ray emission events observed in an instant of less than 1 ms are called gamma-ray flash, and those observed from the thundercloud itself for a few minutes are called gamma-ray glows. We have been observing thundercloud gamma rays in the coast of the Sea of Japan in winter since 2006. The project is named GROWTH (Gamma-ray Observation of Winter Thunderclouds). In this talk, I will report on the observations in FY2020, aiming to measure the altitude of the accelerator.
For the FY2020 observations, detectors were set up at two locations in Kanazawa City, each ~2 km away from each other. Kanazawa City is an area where lightning frequently occurs, and there have been many gamma-ray observations in the past. We deployed the detector called GOOSE (Gamma-ray Orientation Observing System with Electron-monitor), which consists of collimated detectors and an electron detector. The former consist of four detectors, three of which have lead plates limiting the field of view and also inclined; directly upward, 30° eastward, and 30° westward, respectively. When the size of the accelerator is smaller than the altitude, it can be approximated as a point source. The altitude of the accelerator can be estimated using the time difference in the count rates of the three collimator detectors as they are swept by the wind. When the altitude is less than 100 m, 30 MeV electrons can be detected directly on the ground because their range in the atmosphere is longer.
Observations for FY2020 began at the end of October, and gamma-ray glows were observed at around 18:00 on January 8, 2021, and at around 6:00 on January 9, 2021. It was snowing on both days, and there was a west-southwest wind of 16.6 m/s on the 8th and a west wind of 10 m/s on the 9th events. In the collimator detectors, the count rate observed in the detectors facing upwards was 1.5-2.5 times higher than that in the detectors tilted to the east and west. This is a clear evidence for the beaming effect of bremsstrahlung. In both events, the time difference between westward and eastward included detectors was generally less than 10 seconds, and the altitude was less than ~150 m in the point source approximation. The electron detector also detected an excess of charged particles synchronized with the gamma-ray glow. The origin of this excess is still under analysis.

Keywords: gamma rays from thunderstorms, altitude measurement of the electron accelerator, electron detector

©2021. Japan Geoscience Union. All Right Reserved.

Hydrometeor distribution in a thundercloud related to a gamma-ray emission event

*Takemoto Kiyomichi[1], Taro Shinoda[1], Masaya Kato[1], Shohei Hisadomi[2], Yuuna Tsuji[2], Kazuhiro Nakazawa[2], Yuuki Wada[3], Teruaki Enoto[3]

1. Institute for Space-Earth Environmental Research, Nagoya University, 2. Department of Physics, Nagoya University, 3. Institute of Physical and Chemical Research

Lightning events are frequently bought about by a shallow convective cloud in Hokuriku region during the cold-air outbreak in winter. Gamma-ray emission events have been simultaneously observed from thunderclouds in the region. The Gamma-ray Observation of Winter Thunderclouds (GROWTH) field campaign has been conducted to investigate gamma-ray events from thunderclouds by multiple sensors around Kanazawa City, Japan (Enoto et al. 2017, Wada et al. 2019).
The gamma-ray glow, which is a kind of gamma-ray emission, is lasting a few seconds to several minutes. The gamma-ray glow is considered that phenomena originate from relativistic runaway electron avalanches (RREAs) in strong electric fields due to positively charged particles in the lower part of the cloud and negatively charged ones in the upper part of it (Wada et al., 2019). Although several gamma-ray glow events have been observed in recent years by the GROWTH field campaign, microphysical properties in a thundercloud brought about gamma-ray emission events have not been clarified. Hisadomni et al. (2020) reported double gamma-ray glows in Kanawaza at 0203 and 0206 JST on 13 January 2020. This study shows 3-dimensional hydrometeor distributions in the thunderclouds brought about the gamma-ray emission event using a hydrometeor classification algorithm (Kouketsu et al. 2015). Polarimetric parameters, i.e., reflectivity, differential reflectivity, specific differential phase, correlation coefficient between horizontal and vertical polarizations, which are obtained by XRAIN radar at the Noumi site.
High reflectivity area that exceeds 40 dBZ is observed above the gamma-ray observation sites at least 5 minutes before the gamma-ray glow. At that time, the echo-top height reaches at a height of 6 km that is relatively higher than typical one of snow clouds. Wet graupel (0.5 ~ 2 km) and dry graupel (2 ~ 5.5 km) are detected with the high reflectivity area that should correspond to the convective core. The surface temperature is 6.6 degrees Celsius at Kanazawa Meteorological Observatory at 02:00 JST. Thus, graupel particles in the lower part of the thundercloud should be positively charged by the riming electrification (Takahashi, 1978).

Keywords: Hokuriku winter thundercloud, lightning discharge, gamma-ray glow

©2021. Japan Geoscience Union. All Right Reserved.

A Study of 3D Precipitation Core Tracking Method Using Multi-Parameter Phased Array Weather Radar

*Keitaro Asai[1], Hiroshi Kikuchi[1], Yasuhide Hobara[1], Tomoo Ushio[2]

1. The University of Electro Communications, 2. Osaka University

In Japan, a weather radar network, known as the extended radar information network (XRAIN), is operated to provide regular observations of rainfall and wind distribution. The network is comprised of 16 C-band radars and 39 X-band multi-parameter (X-MP) radars that are capable of conducting dual-polarization observations. X-MP radars have parabolic-type antennas, and they require about 5 min to complete a volume scan because both the azimuth and elevation angles are scanned mechanically. Only ten elevation angles (approximately) are scanned, and areas covered at high elevation angles are limited. The Multi-Parameter Phased Array Weather Radar (MP-PAWR) has been developed as the next generation dual-polarized weather radar to address the limitations of X-MP radars. When conducting a volume scan, the MP-PAWR uses electronic and mechanical scanning in the elevation and azimuth angles, respectively, to achieve 3D observation within a radius of 60 km and an altitude of about 15 km in 30 sec.

In order to discuss the distribution and temporal change of 3D precipitation data obtained by MP-PAWR, it is necessary to develop a method to classify and track precipitation cores. In this study, a density-based clustering method, DBSCAN (Density-based spatial clustering of applications with noise), was used for clustering and tracking of 3D precipitation cores.

In this presentation, we will introduce the developed clustering and tracking method for 3D precipitation cores. The distribution and temporal characteristics of convective and stratiform precipitation analyzed by the developed method are also discussed.

Keywords: Phased Array Weather Radar, Dual-polarization Observation, Precipitation Observation

©2021. Japan Geoscience Union. All Right Reserved.

Special negative lightning strokes in winter with extremely short preceding discharges

*Ting Wu[1], Daohong Wang [1], Nobuyuki Takagi[1]

1. Gifu University

The return stroke (RS) is the most well-studied process in lightning. The first RS in a negative cloud-to-ground (-CG) flash is usually preceded by the preliminary breakdown (also called initial breakdown) and the stepped leader, and the typical time difference between the start of a -CG flash and the first RS is from several to a few tens of ms. In winter, however, thunderclouds are much shallower and the time difference can be much shorter. -CG flashes with the time difference between the first RS and the start of the flash shorter than 1 ms have been reported. In this study, we will analyze negative strokes in winter with the duration of preceding discharges shorter than 1 ms based on the observation of FALMA (Fast Antenna Lightning Mapping Array). Particularlly, we will focus on strokes with the duration of preceding discharges shorter than 200 us, and we will demonstrate that these strokes are systematically different from those with longer durations of preceding discharges. These special strokes with extremely short preceding discharges frequently occur at high mountain areas. It is estimated that their channel lengths are only hundreds of meters, an order of magnitude shorter than those of normal negative RSs.

Keywords: Return stroke, Winter lightning, Negative cloud-to-ground lightning

©2021. Japan Geoscience Union. All Right Reserved.

Simultaneous Observations of a Winter Lightning Flash in Japan

*Haitao Huang[1], Daohong Wang[1], Ting Wu[1], Nobuyuki Takagi[1]

1. Gifu University

A winter lightning flash in Japan was simultaneously recorded with multiple instruments, including a high-speed video camera, an optical imaging system LAPOS (Lightning Attachment Process Observation System), a lightning mapping system FALMA (Fast Antenna Lightning Mapping Array), and a current measuring system. This flash lasted for about 0.34 seconds with a large horizontal extent of about 40 ×40 km. It started with a multiple-stroke positive cloud-to-ground flash that consists of two positive return strokes (RSs). The first RS was located about 3.2 km from the lightning initial location. The second RS was located about 13.2 km from the first RS with an interval of 55 ms. About 1.5 ms after the second RS, an upward positive leader (UPL) was triggered from the tip of a lightning protection tower. The UPL extended straight upward without clear branches. During the initial stage, the UPL propagated in stepped mode with an average speed of about 0.8×10^5 m/s. As it propagated to the higher altitude, the UPL became more continuous with a faster velocity of about 3.6×10^5 m/s. After the UPL propagated into the thunder cloud, a nearby leader connected to the UPL channel at about 620 m above the tower tip and initiated a strong discharge process. Further analysis indicates that this connection process is similar to the lightning large bipolar event (LBE), a special type of return stroke in winter thunderstorms. About 0.22 s after the initiation of the UPL, four negative RSs struck the same termination 5.2 km from the tower with an average interval of about 5.4 ms. The negative RS lightning channel was much curved from the view of the high-speed video camera. It seems that the occurrence of the first negative RS has little connection with the UPL but is associated with discharge processes near the lightning initiation area.

Keywords: winter lightning, multiple-stroke lightning flash, upward lightning, large bipolar event (LBE)

©2021. Japan Geoscience Union. All Right Reserved.

Spatio-temporal characteristics of lightning energy in Southeast Asia deduced from ELF observations

*Shunsuke Akama[1], Shu Hirai[1], Yasuhide Hobara[1], Hiroshi Kikuchi[1], Amir Izzani Mohamed[2], Chandima Gomes[3], Kazuo Shiokawa[4], Michael Stock[5]

1. The University of Electro-Communications, 2. University of Malaysia, Pahang, 3. University of the Witwatersrand, Johannesburg, 4. Institute for Space–Earth Environmental Research, 5. Earth Networks

In the Southeast Asian region, cloud-to-ground discharges cause several million dollars of damage per year. Detailed information on electrical characteristics and spatio-temporal distributions including lightning stroke energy in the relevant region is essential for lightning disaster mitigation. In this study, we investigate the spatio-temporal characteristics of cloud-to-ground discharges in the Southeast Asian region, including the charge moment change, by using the lightning locating system in combination with the ELF magnetic field observation installed at the University of Pahang, Malaysia. Specifically, we identify the sferic waveforms in ELF band corresponding to the lightning strokes ddetected by EarthNetworks's total lightning detection network. Then we calcurate the lightning charge moment Qds, lightning peak current, and polarity for each stroke. In this presentation, initial results on spatio-temporal characteristics including Qds for lightning strikes around Malay peninsula for different seasons will be presented.

Keywords: Lightning strike, ELF magnetic field, Charge moment of lightning strikes, Transient luminous event, Atmospheric electricity, Southeast Asia

©2021. Japan Geoscience Union. All Right Reserved.

Sprites observed from the summit of Mt. Fuji and their parent thunderstorm

*Suzuki Tomoyuki[1], Masashi Kamogawa[1], Syugo Hayashi[2]

1. University of Shizuoka, 2. Meteorological Research Institute

Transient Luminous Events (TLEs) are the flash phenomena observed from the top of and above thunderstorms accompanied with active strikes. To detect the family of TLEs (e.g. sprites, jets, ELVEs), since 2012, we have installed and operated high-sensitivity charge coupled device (CCD) camera at the summit of Mt Fuji in summer season. We have succeeded in observing various TLEs from the first operation. It was found that some sprites were associated with the positive cloud-to-ground strikes (+CGSs) in the stratiform region of mesoscale convective system (MCS) but one sprite was associated with the +CGS in the leading convective line of MCS. Both region of MCS were analyzed using C-band weather radar operated by Japan meteorological agency. In this study, we present the samples of TLEs family observed from the summit of Mt Fuji, radar echo structures of stratiform and convective region, the differences of relative displacement and duration time between sprites, sprite-producing +CGSs and their optical cloud flash, which was detected by CCD camera, in the convective and stratiform region.

Keywords: Transient Luminous Events , Sprites, Thunderstorm, Mesoscale convective system, Positive cloud to ground strikes, Mt. Fuji

©2021. Japan Geoscience Union. All Right Reserved.

Coupling process of large-scale atmospheric disturbances to the ionosphere through typhoon

*Shu Hirai[1], Yasuhide Hobara[1], Hiroshi Kikuchi[1], Michael Stock[2]

1. The University of Electro-Communications, 2. Earth Networks

In recent years, tropical cyclones (TCs) have caused serious damage in the world. However, few studies have comprehensively taken into account the TC effects on the ionosphere in addition to meteorological conditions and lightning discharge characteristics of thunderstorms from TCs in the atmosphere. In this study, we investigated the coupling process of meteorological disturbances to the ionosphere from simultaneous observations of thunderstorms and ionosphere during the entire period of Typhoon 15 and Typhoon 19 in 2019. The spatial and temporal characteristics of lightning activity, meteorological characteristics (visible and infrared observations by the geostationary satellite), and lower ionospheric response (VLF/LF transmitter electric amplitude) associated with these typhoons were analyzed in detail. Distinctive features were found between parameters such as the frequency of lightning strikes, discharge polarity, development of thunderclouds, and ionospheric disturbances in different typhoon stages.

Keywords: Typhoon, Ionosphere, Atmospheric electricity, Extreme weather, Thunderstorm, meteorological disturbances

©2021. Japan Geoscience Union. All Right Reserved.

[J] Oral | M (Multidisciplinary and Interdisciplinary)：M-IS Intersection

Sun. Jun 6, 2021 1:45 PM - 3:15 PM JST | Sun. Jun 6, 2021 4:45 AM - 6:15 AM UTC | Ch.12 Zoom Room 12

[M-IS26] Gas hydrates in environmental-resource sciences

convener:Hitoshi Tomaru(Department of Earth Sciences, Chiba University), Akihiro Hachikubo(Kitami Institute of Technology), Atsushi Tani(Department of Human Environmental Science, Graduate School of Human Development and Environment, Kobe University), Shusaku Goto(Institute for Geo-Resources and Environment National Institute of Advanced Industrial Science and Technology), Chairperson:Hitoshi Tomaru(Department of Earth Sciences, Chiba University), Shusaku Goto(Institute for Geo-Resources and Environment National Institute of Advanced Industrial Science and Technology)

An increasing number of researches focusing on natural gas hydrates has recently been conducted from the environmental, material, and resource scientific viewpoints. This session aims to share and discuss the latest research results associated with natural/experimental gas hydrates to understand and examine the nature and potential of gas hydrates in the past-present-future of the Earth and the development/application for our life. Because the researches on gas hydrates are interdisciplinary, broad topics from field and experimental researches, modeling, etc. will be presented in this session.

1:45 PM - 2:05 PM JST | 4:45 AM - 5:05 AM UTC

[MIS26-01] Massive seafloor methane release near the edge of the gas hydrate stability zone in southern Brazil

★Invited Papers

*Marcelo Ketzer[1], Daniel Praeg[2], Luiz F. Rodrigues[3], Adolpho Augustin[3], Maria A. G. Pivel[4], Mahboubeh Rahmati-Abkenar[1], Dennis J. Miller[5], Adriano R. Viana[5], José A. Cupertino[3] (1.Department of Biology and Environmental Science, Faculty of Health and Life Sciences, Linnaeus University, 2.Géoazur, 3.Petroleum and Natural Resources Institute, Pontificia Universidade Catolica do Rio Grande do Sul, 4.Instituto de Geociências, Universidade Federal do Rio Grande do Sul, 5.Petrobras)

2:05 PM - 2:25 PM JST | 5:05 AM - 5:25 AM UTC

[MIS26-02] **Experimental Verification of CH_4-CO_2 Replacement Occurring in Natural Gas Hydrates for Energy Recovery and CO_2 Sequestration**

★Invited Papers

*Yongwon Seo[1] (1.Ulsan National Institute of Science and Technology, Republic of Korea)

2:25 PM - 2:45 PM JST | 5:25 AM - 5:45 AM UTC

[MIS26-03] **Gashydrate accumulations in the Asian Seas and perspective on comparable research in the Indo-Pacific Region**

★Invited Papers

*Renat B. Shakirov[1], Hitoshi Tomaru[2], Pawan Dewangan[3], Prakash Kumar[4], Anatoly Obzhirov[1], Ryo Matsumoto[5] (1.POI FEB RAS, 2.Chiba University, 3.CSIR-NIO, 4.CSIR-NGRI, 5.Meiji University)

2:45 PM - 3:00 PM JST | 5:45 AM - 6:00 AM UTC

[MIS26-04] High-resolution seafloor observation of a shallow methane hydrate area off Sakata, eastern margin of the Sea of Japan, using a three-dimensional pictorial mapping system

*Miho Asada[1], Mikio Satoh[1], Manabu Tanahashi[1], Toshiyuki Yokota[1], Shusaku Goto[1] (1.NATIONAL INSTITUTE OF ADVANCED INDUSTRIAL SCIENCE AND TECHNOLOGY (AIST))

3:00 PM - 3:15 PM JST | 6:00 AM - 6:15 AM UTC

[MIS26-05] Survey of methane hydrate off Tokachi, Pacific Ocean

*Satoshi Yamashita[1], Akihiro Hachikubo[1], Hirotoshi Sakagami[1], Masaaki Konishi[1], Kzutaka Tateyama[1], Hirotsugu Minami[1] (1.Kitami Institute of Technology)

Massive seafloor methane release near the edge of the gas hydrate stability zone in southern Brazil

*Marcelo Ketzer[1], Daniel Praeg[2], Luiz F. Rodrigues[3], Adolpho Augustin[3], Maria A. G. Pivel[4], Mahboubeh Rahmati-Abkenar[1], Dennis J. Miller[5], Adriano R. Viana[5], José A. Cupertino[3]

1. Department of Biology and Environmental Science, Faculty of Health and Life Sciences, Linnaeus University, 2. Géoazur, 3. Petroleum and Natural Resources Institute, Pontificia Universidade Catolica do Rio Grande do Sul, 4. Instituto de Geociências, Universidade Federal do Rio Grande do Sul, 5. Petrobras

Ocean warming is causing gas hydrate dissociation and massive seafloor methane release in several places around the world. Our multidisciplinary and multi-scale data set demonstrated this phenomenon for the first time in the southern hemisphere, in the Rio Grande Cone, southern Brazil. Acoustic imaging of the water column shows the existence of hundreds of gas flares near the edge of the calculate methane hydrate stability zone and the outcrop of the bottom simulating reflection. Stable and radiogenic carbon isotope data of methane in gas hydrates, pores, and gas bubbles venting from the seafloor, suggest that gas hydrate dissociation is the main source of gas for the flares. Our data further indicates that gas hydrate dissociation is linked to contemporary ocean warming, and that anaerobic oxidation of methane cannot consume the massive amounts of gas released from hydrate dissociation, resulting in widespread seafloor methane emissions.

Keywords: gas hydrate, climate change, gas flares, sulphate reduction

©2021. Japan Geoscience Union. All Right Reserved.

Experimental Verification of CH_4-CO_2 Replacement Occurring in Natural Gas Hydrates for Energy Recovery and CO_2 Sequestration

*Yongwon Seo[1]

1. Ulsan National Institute of Science and Technology, Republic of Korea

CH_4 recovery using CO_2 injection into natural gas hydrates is very attractive because it can perform dual functions of energy production and CO_2 sequestration. In this study, the CH_4-CO_2 replacement that occurs in various gas hydrate structures (sI, sII, and sH) was investigated with a primary focus on phase behaviors and structural transformation. To verify the influence of CO_2 injection on the thermodynamic stability of gas hydrates, phase equilibria of the initial CH_4 hydrate (sI), CH_4 + C_3H_8 hydrate (sII), and CH_4 + 2,2-dimethylbutane (neohexane, NH) hydrate (sH) were compared with those of the corresponding gas hydrates replaced with CO_2. After the replacement reaction was completed, significant shifts in the hydrate equilibrium curves of each system were observed, which indicates that the substantial extent of the replacement was achievable through CO_2 injection. The initial and replaced hydrates were analyzed via ^{13}C NMR spectroscopy and powder X-ray diffraction (PXRD) to examine cage-dependent guest distributions and possible structural transition. To identify heat generation or absorption during the replacement process and to elucidate its influence on the thermal properties of the replaced hydrates, the changes in heat flow and dissociation enthalpies (ΔH_d) were measured using a high-pressure micro-differential scanning calorimeter (HP μ-DSC). The replacement behaviors were strongly dependent on the structure of initial gas hydrates. The overall experimental results provide further insights into the cage-specific occupation of external gas molecules and thermodynamic stability for the real replacement occurring in natural gas hydrate reservoirs for CH_4 recovery and CO_2 sequestration.

Keywords: natural gas hydrates, replacement, CO2 sequestration, phase behavior, structural transformation

©2021. Japan Geoscience Union. All Right Reserved.

Gashydrate accumulations in the Asian Seas and perspective on comparable research in the Indo-Pacific Region

*Renat B. Shakirov[1], Hitoshi Tomaru[2], Pawan Dewangan[3], Prakash Kumar[4], Anatoly Obzhirov[1], Ryo Matsumoto[5]

1. POI FEB RAS, 2. Chiba University, 3. CSIR-NIO, 4. CSIR-NGRI, 5. Meiji University

Gas hydrates - green energy resource of the future and modern marine phenomena, which significance growing up from year to year but still studied poorly in marine expeditions due to the lack of international cooperative study. Gas hydrates were found in many areas of the marginal Asian seas and evidently closely interrelated to the gas geochemistry, geology, geophysics, paleo- and oceanography, micro- and macrobiology, various environment aspects of the Asian Seas (AS) both seafloor and water column. Social effect of gashydrates research field is growing nowadays. Marginal seas of the Eastern Asia is a specific region manifested by insufficient studied gas hydrates (mainly, methane hydrates of different structures, but also carbon dioxide hydrates) phenomena as a resource, climate link and geochemical drive force, methane and accompanying gases fluxes in the "seafloor-water column-atmosphere" system. Numerous unique gas hydrate accumulations nowadays are object of few focused projects studies in Bering Sea, Japan Sea, Sea of Okhotsk, East-China Sea, South-China Sea and Philippine Sea separately by the Asian countries. There for, nature and evolution of the gas hydrate system in the lithosphere and hydrosphere of the AS, which in respect to energy resources and environmental agent is one of the most uncertain and debatable problem of World Ocean. We are also represents latest results of the bilateral Russia-Japan cooperation on gashydrates study in the Japan Sea.

Authors propose to conduct gashydrate comparable research in the promising basins of Indian Ocean and Western Pacific.

The key notice of our proposing joint research is based on the next key aspects.
Exploration of gas hydrates . Ground-truthing of gas hydrate deposits. Exploitation of gas hydrate deposits . Understanding the gas hydrate system in the active and passive continental margins; Migration of methane gas; Morphology of gas hydrates. Geo-hazards associated with gas hydrates. Cold seep and climate change.
The following scientific problems we are selected based on intense discussion:
Tectonics processes governing spatial distribution of gas hydrates: The scientists agree that most of the methane hydrate form due to gas migration from deep-seated gas reservoirs through active fault/fracture system. Several examples of methane migration through active faults are reported from both active continental margin (the Pacific Gas hydrate Rim) as well as from passive continental margin (Krishna-Godavari basin). Mapping areas of neo-tectonism based on seismological/GPS study can help in locating gas hydrate deposits. ***Role of Geo-fluids in hydrate formations*****:** It is agreed that deep-seated fluids play a major role in the formation of shallow gas hydrate deposits. ***New techniques for mapping of gas hydrate deposits:*** The conventional seismic used in gas hydrate exploration is not effective and the study of BSR may not be sufficient for mapping hydrate deposits. Most The geophysical technique should be followed by drilling/coring to validate the findings. In shallow waters, vibro-coring and drilling-rig provide long cores (up to 60 m) for validation. ***Exploitation of gas hydrate deposits:*** Indian scientists showed a keen interest in exploitation of gas hydrate deposits and highlighted some of the problems they anticipate like Sand ingress in borehole, low Gas-to-Water ratio, huge water production due to shallow acquifers, seafloor subsidence and stability and Geo-hazards triggered due to uncontrolled gas migration.

©2021. Japan Geoscience Union. All Right Reserved.

There are several locations in the Arctic Seas, Sea of Okhotsk (more than 1000 methane flares offshore Sakhalin Island or single gas flares up to 2200 m height in Kurile Basin), and Japan Sea (Tatar strait) where significant methane flux is observed. The methane fluxes from the seep sites in Indian margin are not known and hydro-acoustic techniques can be developed for estimating methane fluxes. ***Cold seep and climate change***: It is important to understand how methane migrates upon dissociation and what the sinks of methane in seawater are. The understanding of processes will help in better designing the production technology for exploitation of gas hydrate deposits in Indian margin.
Taking into account the Second International Indian Ocean Expedition (IIOE-2) and United Nations Decade of Ocean Science for Sustainable development (2021-2030) we are discussing the opportunity Joint long term cooperation on gas hydrates.

Keywords: gashydrates, Western Pacific, Indian Ocean, marginal seas

©2021. Japan Geoscience Union. All Right Reserved.

High-resolution seafloor observation of a shallow methane hydrate area off Sakata, eastern margin of the Sea of Japan, using a three-dimensional pictorial mapping system

*Miho Asada[1], Mikio Satoh[1], Manabu Tanahashi[1], Toshiyuki Yokota[1], Shusaku Goto[1]

1. NATIONAL INSTITUTE OF ADVANCED INDUSTRIAL SCIENCE AND TECHNOLOGY (AIST)

Shallow methane hydrate (MH) has been reported from the top of the Sakata knoll (tentative name) along a reverse fault at the foot of the southwest side of the knoll off Sakata, along the eastern margin of the Sea of Japan (Temma and Goto, 2018). Previous observation cruises conducted in this area acquired results from acoustic mapping using research vessels and autonomous underwater vehicles, optical observations using remotely operated vehicles (ROVs), logging-while-drilling measurements, and sediment sampling (Morita, 2015; Temma and Goto, 2018; Yokota, 2020). These results reveal a depression bordered by steep slopes at the top of the knoll (~1 km×~300–400 m in diameter, ~12-m deep), two terraces on its northern and southern sides, a single hill near its center, and swells around the depression at the top of the knoll (~15 km×~5–10 km in diameter, ~120-m relative height from the southwestern foot of the knoll). The distribution of backscatter strength is largest on the steep slopes and relatively large on the terraces within the depression and the surrounding swells continuing southwestward along the knoll.

To examine the possibility of production and to assess the environmental impact, cruise 1K20 used Kaiyomaru no.1 (Kaiyo Engineering Co., Ltd.) and the ROV-*Kaiyo3000* equipped with the *SeaXerocks 1* mapping system (Kaiyo Engineering Co., Ltd.) to acquire high-resolution 3D images on the Sakata knoll. *SeaXerocks 1* was maintained at an altitude of ~4 m above the seafloor and at a speed of ~1.5 knots. Still images and topographical data by laser scanning were acquired. The resolution of the resulting 3D images was 2 mm (in the direction orthogonal to the track) ×several centimeters (along the track), which provides a detailed distribution of the chemosynthetic animals and rocks on the seafloor. *SeaXerocks 1* does not have a function that merges overlapped images on different tracks and, thus, only displays independent images along the tracks. *SeaXerocks 1* observations were conducted in and around the depression. We observed no MH on the seafloor. Seawater tends to be turbid, and relatively large animals (e.g., of squid and starfish) are abundant in the depression. A portion of the steep slope and the hill in the center of the depression has relatively rich biological heat and rock. Sediments are present at the base of depression. The two terraces on the northern and southern sides of the depression and the swells are extensively covered with sediments; however, rock outcrops and small biological mats are rarely observed. These observations suggest that fluid seepage is limited to the steep slope around the depression and a few parts of the swells and is less active in the present stage.

This study was conducted as part of the methane hydrate research project funded by the Ministry of Economy, Trade and Industry (METI).

References:
Temma and Goto (2018) 33rd investigative commission for methane hydrate development, METI (in Japanese)
Morita (2015) FY2014 AUV survey in shallow methane hydrate fields in Japan Sea, Japan Geoscience Union meeting 2015, MIS24-02, abstract (May 27, Chiba)
Yokota (2020) Results of high-resolution 3D seismic reflection survey, Research and development of

©2021. Japan Geoscience Union. All Right Reserved.

shallow methane hydrate, FY2020 Achievements Report Meeting, Research and development project for shallow methane hydrate, AIST (in Japanese)

Keywords: shallow methane hydrate, acoustic mapping, 3D pictorial mapping system

©2021. Japan Geoscience Union. All Right Reserved.

Survey of methane hydrate off Tokachi, Pacific Ocean

*Satoshi Yamashita[1], Akihiro Hachikubo[1], Hirotoshi Sakagami[1], Masaaki Konishi[1], Kzutaka Tateyama[1], Hirotsugu Minami[1]

1. Kitami Institute of Technology

In the sea area around Hokkaido, the existence of bottom simulating reflectors (BSR) has been confirmed off Abashiri, Okushiri Island, Hidaka, and Tokachi. In the Pacific Ocean off Tokachi, the National Institute of Advanced Industrial Science and Technology conducted a seismic survey (GH02) in 2002. When the sound wave cross section obtained by GH02 was examined, gas chimneys and mound topography were confirmed at about 30 points on the survey line. Therefore, we are conducting the seafloor topography and methane plume observation by the multi-beam echosounder and quantitative echo sounder, and the sampling of seafloor sediments in the Pacific Ocean off Tokachi after 2014, using the research training ship "Oshoromaru" owned by the Faculty of Fisheries, Hokkaido University. As a result, methane plumes were confirmed at more than 30 locations with characteristic seafloor topography such as faults. In the 2020 survey, methane hydrate was successfully collected at that one site. We report the relationship between the soil properties of seafloor sediments and the seafloor topography, and the methane plume and the seafloor topography, based on previous surveys off Tokachi.

Keywords: methane hydrate, Submarine topography, marine sediment

©2021. Japan Geoscience Union. All Right Reserved.



©2021. Japan Geoscience Union. All Right Reserved.

[J] Oral | M (Multidisciplinary and Interdisciplinary)：M-IS Intersection

Sun. Jun 6, 2021 3:30 PM - 5:00 PM JST | Sun. Jun 6, 2021 6:30 AM - 8:00 AM UTC | Ch.12 Zoom Room 12

[M-IS26] Gas hydrates in environmental-resource sciences

convener:Hitoshi Tomaru(Department of Earth Sciences, Chiba University), Akihiro Hachikubo(Kitami Institute of Technology), Atsushi Tani(Department of Human Environmental Science, Graduate School of Human Development and Environment, Kobe University), Shusaku Goto(Institute for Geo-Resources and Environment National Institute of Advanced Industrial Science and Technology), Chairperson:Akihiro Hachikubo(Kitami Institute of Technology), Atsushi Tani(Department of Human Environmental Science, Graduate School of Human Development and Environment, Kobe University)

An increasing number of researches focusing on natural gas hydrates has recently been conducted from the environmental, material, and resource scientific viewpoints. This session aims to share and discuss the latest research results associated with natural/experimental gas hydrates to understand and examine the nature and potential of gas hydrates in the past-present-future of the Earth and the development/application for our life. Because the researches on gas hydrates are interdisciplinary, broad topics from field and experimental researches, modeling, etc. will be presented in this session.

3:30 PM - 3:45 PM JST | 6:30 AM - 6:45 AM UTC

[MIS26-06] Geochemical processes in surface sediments in a shallow gas hydrate reserve area off Sakata, eastern margin of the Japan Sea

*Yuki Ota[1], Masahiro Suzumura[1], Ayumi Tsukasaki[1], Atsushi Suzuki[1] (1.National Institute of Advanced Industrial Science and Technology)

3:45 PM - 4:00 PM JST | 6:45 AM - 7:00 AM UTC

[MIS26-07] Vp anomalies of gas hydrate-bearing sediments inferred from BSR and BGHS

*Ryo Matsumoto[1], Shiro Ohkawa[1] (1.Meiji University)

4:00 PM - 4:15 PM JST | 7:00 AM - 7:15 AM UTC

[MIS26-08] Purity and specific surface area of methane hydrate synthesized from fine ice powder and gas

*Daisuke Yahagi[1], Akihiro Hachikubo[1], Satoshi Takeya[2] (1.Kitami Institute of Technology, 2.National Institute of Advanced Industrial Science and Technology)

4:15 PM - 4:30 PM JST | 7:15 AM - 7:30 AM UTC

[MIS26-09] Three-dimensional nondestructive observation of natural methane hydrate

*Satoshi Takeya[1], Akihiro Hachikubo[2], Satoshi Yamashita[2], Hirotsugu Minami[2], Hirotoshi Sakagami[2], Kazuyuki Hyodo[3], Akio Yoneyama[4] (1.National Institute of Advanced Industrial Science and Technology, 2.Kitami Institute of Technology, 3.High Energy Accelerator Research Organization, 4.SAGA Light Source)

4:30 PM - 4:45 PM JST | 7:30 AM - 7:45 AM UTC

[MIS26-10] Concentration of helium at the formation of methane and helium mixed-gas hydrate

*Yuki Moriya[1], Hiromi Kimura[1], Akihiro Hachikubo[1], Satoshi Takeya[2] (1.Kitami Institute of Technology, 2.National Institute of Advanced Industrial Science and Technology)

4:45 PM - 5:00 PM JST | 7:45 AM - 8:00 AM UTC

[MIS26-11] **Simulation of methane hydrate formation in coarse-/fine-grained sediments in the Nankai Trough, Japan**

*CHAO XU[1] (1.Chiba University)

Geochemical processes in surface sediments in a shallow gas hydrate reserve area off Sakata, eastern margin of the Japan Sea

*Yuki Ota[1], Masahiro Suzumura[1], Ayumi Tsukasaki[1], Atsushi Suzuki[1]

1. National Institute of Advanced Industrial Science and Technology

Seepage of subsurface methane into shallow sediments and water column has a substantial impact on geochemical and biogeochemical processes via various aerobic and anaerobic reactions. In a knoll in a shallow gas hydrate reserve area off Sakata, eastern margin of the Japan Sea, the potential areas bearing massive shallow methane hydrates have been identified by seismic exploration. During the survey cruise SS20-1 in July 2020, the ROV observation found patchy distribution of strongly anoxic areas covered with bacterial mats-like structures in the knoll caldera. Approximately 30-cm-long push core samples were collected within the anoxic area as well as just outside the area (a few meters away), which was covered with apparently oxic sediments. As a reference, a push core sample was collected outside the gas hydrate-bearing areas. The core samples from the anoxic site consisted of dark blackish sediments in the top 6 cm with strong hydrogen sulfide odor and below the depth sediments was consisted of dark gray silt. Top 10 cm sediments of the apparently oxic site had a grey color and below the depth sediments was dark in color likely under anoxic condition. The reference sample exhibited a gray color throughout the collected depth. The core samples were sliced into sections and subjected to various analyses of interstitial water sulfate, sedimentary total organic carbon, total sulfur (TS), trace elements and $\delta^{13}C$ of total inorganic carbon.

In sediments under anoxic condition including the entire core samples at the anoxic site and the sediments below 10 cm depth at the oxic site, TS contents were substantially high compared with those at the reference site, and the values of $\delta^{13}C$ of total inorganic carbon showed strongly negative values between −20‰ and −40‰ equivalent to those of subsurface methane. These results infer that via microbial anaerobic oxidation of methane (AOM) formation of sulfide minerals and authigenic carbonates occurs in the anoxic sediments. This is supported by the results of pore water sulfate distribution. While pore water sulfate concentrations were stable from the top to the bottom of the core sample collected from the reference site, a rapid and linear decrease was observed from the value equivalent to the seawater concentration to zero within the top 10 cm at the anoxic site. It is most likely that active AOM rapidly utilizes sulfate supplied from the overlying seawater through diffusion.

From the results of some geochemical analyses, the active AOM and sulfide mineral formation seems to have a considerable impact on the behaviors of some trace elements in the gas hydrate-bearing area. For example, strong enrichment of Mo and As was found in the anoxic sediments. Positive correlations of Mo and As contents with TS contents suggest that the AOM-derived sulfide favored the capture of Mo and As into sulfide minerals such as pyrite.
This study was conducted as a part of the methane hydrate research project funded by METI (the Ministry of Economy, Trade and Industry, Japan).

Keywords: Methane, Japan Sea, Anaerobic oxidation of methane, trace elements

©2021. Japan Geoscience Union. All Right Reserved.

Vp anomalies of gas hydrate-bearing sediments inferred from BSR and BGHS

*Ryo Matsumoto[1], Shiro Ohkawa[1]

1. Meiji University

High amplitude, bottom simulating reflectors with reversed polarity (BSR) have been attributed to the base of gas hydrate stability (BGHS). TWT of the BSR of hydrate bearing sediments in Nankai trough were observed to be about 0.32 sec. below seafloor at about 945m of water depth (Tesuji et al., 2004), whereas they were 0.18 to 0.20 sec. at 895m to 1000m along the eastern margin of the Sea of Japan. Assuming that the average Vp of shallow subsurface marine sediments of 1.50km/sec, the actual depth of BSRs are estimated to be 240mbsf and 135 to 150mbsf respectively, which are assumed to be the depth of BGHS, an important factor of hydrate exploration. On the other hand, the depth of BGHS is identified by coring and logging penetrating through BSR profiles. In Nankai trough, Main Hole and Post Survey Wells have clearly recognized the BGHS at 263mbsf (Tsuji et al, 2004; Matsumoto et al., 2004), implying that the Vp of hydrate-bearing sediments of Nankai trough is not 1.50km/sec but 1.64m/sec for the interval between the sea-floor to the BGHS due to high Vp (~3.8km/sec) hydrates.

In the Sea of Japan, methane hydrates occur as massive and disseminated aggregates in gas chimney structure (Matsumoto et al., 2017). The stability of methane hydrate in seawater is determined by the pressure and temperature, and the depth of BGHS is uniquely determined by the temperature of bottom water, thermal gradient, and water depth. Thermal gradients on the Umitaka Spur at about 900m (W.D.) off Joetsu are approximately 10.0 +/- 1.0 degreeC, and the temperature of bottom water of 0.20 degreeC (Tomaru et al., 2019; Matsumoto et al., 2017). Therefore, the equilibrium depth of the BGHS is calculated to be 100 +/- 10 mbsf. On the other hand, a number of coring and logging holes on the Umitaka Spur identified the BGHS at the depth of 100 to 120mbsf, which are consistent with the equilibrium depth of BGHS.

BSR on the Umitaka Spur and Joetsu Knoll off Joetsu area appears at around 0.20sec TWT, whereas it occurs at 0.12sec to 0.14secTWT within hydrate-concentrated gas chimney structures. Vp of the host sediments off gas chimneys is calculated to be 1.0km/sec while it is 1.40 to 1.70km/sec for hydrate-bearing sediments in gas chimneys (Ohkawa et al., 2017). Vp off gas chimney is much lower than the velocity of water, anomalously low for marine sediments. This anomaly strongly suggest that free gas (methane) bubbles developed over the hydrate-bearing Spur and Knoll sediments. Vp of the gas chimney sediments (1.40 to 1.70km/sec) looks similar or a bit higher than “normal” marine sediments, however, the Vp is also unexpectedly low, considering that massive gas hydrates accumulates in gas chimneys by 25 to 80% by volume (Matsumoto et al., 2017). Based on the field observation, exploration and theoretical consideration of the occurrence of BSR and BGHS, we came to the hypothesis that development of free gases in shallow subsurface marine sediments is a critical factor to accumulate massive gas hydrates within gas chimneys, and the existence of free gas is to be identified by anomalously low Vp inferred from BSR and BGHS.

Keywords: gas hydrates, BSR, velocity anomaly, free gas

©2021. Japan Geoscience Union. All Right Reserved.

Purity and specific surface area of methane hydrate synthesized from fine ice powder and gas

*Daisuke Yahagi[1], Akihiro Hachikubo[1], Satoshi Takeya[2]

1. Kitami Institute of Technology, 2. National Institute of Advanced Industrial Science and Technology

Since gas hydrates are considered for applications such as gas storage and transportation media, an efficient method of their formation has been investigated. There are two methods for generating gas hydrate: (1) agitating water and gas and (2) contacting ice and gas. In this study, we focused on the latter method, which does not require an agitation system and can be combined with storage system. The purity of gas hydrate is controlled by some factors, such as the contact area between the ice and gas, temperature, pressure, and reaction time. The effect of temperature on the purity of gas hydrate has not been investigated in detail below the ice point. We formed samples of methane hydrate by contacting fine ice powder and guest gas, and measured their specific surface area by a gas adsorption method.
Finely powdered ice was scraped with a microtome and put into a pressure cell at 253 K, and measured their specific surface area. The pressure cell was then evacuated at the temperature of liquid nitrogen and research grade methane was introduced. Temperature of the pressure cell was controlled from 225 K to 268 K in a cold room or thermostatic bath for a week. After that, the pressure cell was immersed in liquid nitrogen and the liquefied excess methane was evacuated to leave only methane hydrate and unreacted ice in the cell. The cell was weighed on an electronic balance to calculate the purity of methane hydrate. The hydration number of methane hydrate was supposed to be 6, because the effect of temperature and pressure on hydration number of methane hydrate is relatively small.
Original specific surface area of fine ice powder was around 254 [m^2 kg^{-1}], and it was almost uniform in the range of ±2%. The purity of methane hydrate formed at 225 K was low (about 70%), and showed a peak maximum (more than 95%) at around 245-255 K. At higher temperatures (higher than 255 K), the purity decreased. In the temperature range of 245-255 K, the purity was higher in the sample produced in the cold room than in the sample produced in the thermostatic bath. These differences might be due to the fluctuation of ambient temperature in the cold rooms compared to the liquid bath.

Keywords: gas hydrate, hydration number, methane, specific surface area

©2021. Japan Geoscience Union. All Right Reserved.

Three-dimensional nondestructive observation of natural methane hydrate

*Satoshi Takeya[1], Akihiro Hachikubo[2], Satoshi Yamashita[2], Hirotsugu Minami[2], Hirotoshi Sakagami[2], Kazuyuki Hyodo[3], Akio Yoneyama[4]

1. National Institute of Advanced Industrial Science and Technology, 2. Kitami Institute of Technology, 3. High Energy Accelerator Research Organization, 4. SAGA Light Source

The density of gas hydrates varies depending on the type of guest spices encapsulated in the hydrate crystal, but is generally about the same as ice or water (0.9~1.1 g/cm^3). A material with such a relatively small density has a small absorption rate of X-rays. For this reason, it is difficult to visualize the internal structure using the X-ray absorption contrast caused by the slight difference in density within the material, which is the visualization principle of medical and industrial X-ray computed tomography (CT) systems. On the other hand, the phase of X-rays shifts significantly even in materials with small density. Therefore, if we can detect the phase shift of X-rays in a material, it is possible to observe the small density difference in the material with high sensitivity 1).

In this study, we used diffraction contrast (DEI) method2) as a method to detect the phase shift; the DEI method can detect density differences of about 0.01 g/cm^3. The DEI method can detect a density difference of about 0.01 g/cm^3 and has a relatively wide dynamic range of density (density difference: ~1 g/cm^3).3) It is also effective for high-sensitivity measurement of samples with coexisting gas (voids) in addition to gas hydrate and ice (water).3) We also performed absorption-contrast X-ray CT measurements on a sample of natural sediment. The results will be reported.

Keywords: clathrate hydrate, natural gas hydarte, Hydrate sediment, X-ray CT

©2021. Japan Geoscience Union. All Right Reserved.

Concentration of helium at the formation of methane and helium mixed-gas hydrate

*Yuki Moriya[1], Hiromi Kimura[1], Akihiro Hachikubo[1], Satoshi Takeya[2]

1. Kitami Institute of Technology, 2. National Institute of Advanced Industrial Science and Technology

It is reported that helium can be enclathrated in cages composed of water molecules, i.e. gas hydrates (Londono *et al.*, 1992; Maekawa, 2003). For example, Maekawa (2003) reported that equilibrium pressure of methane and helium mixed-gas hydrate increased with composition of helium. Because helium is one of the components of natural gas, it is possible that small amount of helium molecules are enclathrated in natural gas hydrates. In the last JpGU-AGU Joint Meeting, We reported preliminary results of synthetic methane and helium mixed-gas hydrate (Kimura *et al.*, 2020). Although the composition of helium in the hydrate-bound gas was up to 6% in the last report, it must be much lower composition in natural condition. In this report, we formed methane and helium mixed-gas hydrate in the condition of lower helium concentration, and measured composition of helium in hydrate-bound and residual gases.
Experimental method is almost the same as the last report (Kimura *et al.*, 2020). Samples of mixed-gas hydrate composed of methane and helium were synthesized in a pressure cell. Gas hydrate formed at around 273 K, and residual gas in the cell was sampled and the rest of residual gas was evacuated at the temperature of liquid nitrogen. After completion of evacuation, hydrate remained in the pressure cell was dissociated at a room temperature. Samples of hydrate-bound and residual gases were stored in vials (volume: 100 mL) and their molecular composition were measured using a portable gas chromatograph (CP-4900, Varian) in the same day.
The concentration of helium in hydrate-bound gas ranged from 0.001% to 0.1%, corresponded to those in residual gas ranged from 0.1% to 10%. Therefore, concentration of helium in the hydrate-bound gas was about two orders smaller than that of residual gas, suggesting that methane preferred to be encaged in hydrate phase rather than helium. Concentration of helium in hydrate increased with the partial pressure of helium in the initial gas. We also checked a possibility that helium escaped from the hydrate phase at the vacuum process, however, concentration of helium did not change under various vacuum time.

References

Kimura H, Shirakura S, Hachikubo A, Takeya S (2020) Formation of gas hydrates composed of methane and helium. *JpGU-AGU Joint Meeting 2020*, MIS32-P11.
Londono D, Finney JL, Kuhs WF, *et al.* (1992) Formation, stability, and structure of helium hydrate at high pressure. *J Chem Phys* **97**: 547–552.
Maekawa T (2003) Gas hydrate formation for mixtures of methane + helium and ethane + helium. *J Chem Eng Data* **48**: 1283–1285, doi:10.1021/je0301592

Keywords: gas hydrate, helium, source gas

©2021. Japan Geoscience Union. All Right Reserved.

Simulation of methane hydrate formation in coarse-/fine-grained sediments in the Nankai Trough, Japan

*CHAO XU[1]

1. Chiba University

Abstract

The morphology and formation process of methane hydrate are affected significantly by the characteristics of sediments. In coarse-grained sediments, methane hydrate is formed by pore filling, while in fine-grained sediments, methane hydrate usually forms segregated lenses, veins, and nodules by replacing rock particles. At IODP Site C0002, Kumano forearc base, in the Nankai Trough, a gas bearing reservoir about 100 meters below the hydrate stability zone is discovered by logging analysis, which is used as methane source responsible for the hydrate accumulation in the numerical model. The formation of methane hydrate in coarse-grained sediments is constrained by the salt concentration in pore water, so the distribution of methane hydrate saturation is related to the distribution of salts in aqueous phase under phase equilibrium state, and the simulation results of methane hydrate distribution are consistent with the results of logging curve analysis. On the other hand, the formation mode of methane hydrate in fine-grained sediments can be determined by calculating the relative magnitude of effective stress and capillary pressure. The short-range migration theory model and patchy hydrate saturation (whereby zones with 100% pore-space hydrate saturation are embedded in hydrate-free sediments) are used to explain the profile of saturation of methane hydrate in fine-grained sediments.

Keywords: Simulation, Methane hydrate, Nankai Trough

©2021. Japan Geoscience Union. All Right Reserved.

[J] Poster | M (Multidisciplinary and Interdisciplinary)：M-IS Intersection

Sun. Jun 6, 2021 5:15 PM - 6:30 PM JST | Sun. Jun 6, 2021 8:15 AM - 9:30 AM UTC | Ch.21_1

[M-IS26] Gas hydrates in environmental-resource sciences

convener:Hitoshi Tomaru(Department of Earth Sciences, Chiba University), Akihiro Hachikubo(Kitami Institute of Technology), Atsushi Tani(Department of Human Environmental Science, Graduate School of Human Development and Environment, Kobe University), Shusaku Goto(Institute for Geo-Resources and Environment National Institute of Advanced Industrial Science and Technology)

An increasing number of researches focusing on natural gas hydrates has recently been conducted from the environmental, material, and resource scientific viewpoints. This session aims to share and discuss the latest research results associated with natural/experimental gas hydrates to understand and examine the nature and potential of gas hydrates in the past-present-future of the Earth and the development/application for our life. Because the researches on gas hydrates are interdisciplinary, broad topics from field and experimental researches, modeling, etc. will be presented in this session.

[MIS26-P01] Geochemical characteristics of headspace gas and pore water in shallow sediment from the Tatar Trough

*Musashi Yokoyama[1], Ryo Murata[1], Hitoshi Tomaru[1], Ryo Matsumoto[2], A.V. Yatsuk[3], D.A. Shvalov[3] (1.Chiba University, 2.Meiji University, 3.V.I.Ilichev Pacific Oceanological Institute)

[MIS26-P02] Gas hydrate survey at the gas seepage area off Abashiri, the Sea of Okhotsk

*Yuki Moriya[1], Hiromi Kimura[1], Akihiro Hachikubo[1], Satoshi Yamashita[1], Hirotoshi Sakagami[1], Masaaki Konishi[1], Hirotsugu Minami[1], Yasuhito Uchida[2], Hiroshi Yamaguchi[3] (1.Kitami Institute of Technology, 2. Research Institute of Energy, Environment and Geology, Hokkaido Research Organization, 3.Kushiro Fisheries Research Institute, Hokkaido Research Organization)

[MIS26-P03] Total organic carbon and its carbon isotope ratio in subsurface sediments off Hokkaido area

*Daisuke Yahagi[1], Akihiro Hachikubo[1], Masaaki Konishi[1], Hirotoshi Sakagami[1], Hirotsugu Minami[1], Satoshi Yamashita[1], Yasuhito Uchida[2], Hiroshi Yamaguchi[3] (1.Kitami Institute of Technology, 2.Research Institute of Energy, Environment and Geology, Hokkaido Research Organization, 3.Kushiro Fisheries Research Institute, Hokkaido Research Organization)

[MIS26-P04] Characteristics of gas hydrate crystals and their hydrate-bound gases retrieved at the seepage field off Tokachi (the Pacific Ocean)

*Hiromi Kimura[1], Ryoya Kamata[1], Daisuke Yahagi[1], Yuki Moriya[1], Akihiro Hachikubo[1], Masaaki Konishi[1], Hirotoshi Sakagami[1], Hirotsugu Minami[1], Satoshi Yamashita[1] (1.Kitami Institute of Technology)

[MIS26-P05] Gas hydrate survey at the gas seepage area off Hidaka, the Pacific Ocean

*Ryoya Kamata[1], Hiromi Kimura[1], Akihiro Hachikubo[1], Hirotoshi Sakagami[1], Satoshi Yamashita[1], Masaaki Konishi[1], Hirotsugu Minami[1] (1.Kitami Institute Of Technology)

[MIS26-P06] Emission of hydrated gas from seafloor to water column in the western Oki Trough

*Hitoshi Tomaru[1], Tianyou Ze[1], Sonoka Ikemoto[1], Minori Chikada[1] (1.Department of Earth Sciences, Chiba University)

[MIS26-P07] Isotope fractionation between hydrate-bound and ambient gases - case study in Lake Baikal gas hydrates -

*Hiromi Kimura[1], Akihiro Hachikubo[1], Oleg Khlystov[2], Gennadiy Kalmychkov[3], Marc De Batist[4], Hirotoshi Sakagami[1], Hirotsugu Minami[1], Satoshi Yamashita[1] (1.Kitami Institute of Technology, 2.Limnological Institute, SB RAS, 3.Vinogradov Institute of Geochemistry, SB RAS, 4.Ghent University)

[MIS26-P08] Carbon isotope fractionation of carbon monoxide hydrate between gas and hydrate phases

*Hiromi Kimura[1], Akihiro Hachikubo[1], Satoshi Takeya[2] (1.Kitami Institute of Technology, 2.National Institute of Advanced Industrial Science and Technology (AIST))

[MIS26-P09] Hydrogen isotopic fractionation of methane at the formation of synthetic structure I and II gas hydrates

*Ryoya Kamata[1], Akihiro Hachikubo[1], Satoshi Takeya[2] (1.Kitami Institute Of Technology, 2.National Institute of Advanced Industrial Science and Technology (AIST))

[MIS26-P10] Experimental study of CO2 hydrate phase equilibrium in sediments

*Tatsuki Iwamoto[1], Hitoshi Tomaru[1] (1.Chiba University)

[MIS26-P11] Effect of temperature and pressure on hydration number of methane hydrate

*Akihiro Hachikubo[1], Ryoya Kamata[1], Hiromi Kimura[1], Yuta Komagata[1], Go Fuseya[1], Satoshi Takeya[2] (1.Kitami Institute of Technology, 2.National Institute of Advanced Industrial Science and Technology (AIST))

Geochemical characteristics of headspace gas and pore water in shallow sediment from the Tatar Trough

*Musashi Yokoyama[1], Ryo Murata[1], Hitoshi Tomaru[1], Ryo Matsumoto[2], A.V. Yatsuk[3], D.A. Shvalov[3]

1. Chiba University, 2. Meiji University, 3. V.I.Ilichev Pacific Oceanological Institute

The Tatar Trough is characterized by a number of mound with gas chimney and in particular gas flare with gas hydrate accumulation in shallow sediment, reflecting active gas generation at depth and migration to the surface environment. Because the trough is located in geologically active and important region for organic matter input and seawater circulation in the northern Japan Sea, origin and migration process could be constrained by the formation and development of the marginal sea. In this study, we characterized the geochemistry of headspace gas and pore water samples collected from northern to southern Tatar Trough and and examined biogeochemical processes associated with generation, migration, oxidation, and fixation of methane in the Tatar Trough.

All the methane concentrations and C1/C2 ratios in headspace gases increase with depth due to the active upward methane flux although the methane is oxidized at the sulfate-methane interface (SMI). These values in the northern area are higher than those in the middle and southern areas. The stable carbon isotopic ratio of methane in the northern area is relatively high (δ^{13}C=-55~-30‰). This value suggests that methane was generated by thermal decomposition of organic matter at depth. The depths of SMI significantly tended to be shallower to the north; average depth of SMI in the northern area is 2.9 mbsf, middle area is 5.9 mbsf, and southern area is 12 mbsf. This indicates that the organic matter responsible for methane generation was derived from the north probably by the oxygen-depleted water and was deposited in relatively anaerobic condition, which is strongly associated with a large-scaled environmental change.

Keywords: methane, gaschimney, AOM

©2021. Japan Geoscience Union. All Right Reserved.

Gas hydrate survey at the gas seepage area off Abashiri, the Sea of Okhotsk

*Yuki Moriya[1], Hiromi Kimura[1], Akihiro Hachikubo[1], Satoshi Yamashita[1], Hirotoshi Sakagami[1], Masaaki Konishi[1], Hirotsugu Minami[1], Yasuhito Uchida[2], Hiroshi Yamaguchi[3]

1. Kitami Institute of Technology, 2. Research Institute of Energy, Environment and Geology, Hokkaido Research Organization, 3. Kushiro Fisheries Research Institute, Hokkaido Research Organization

In the framework of collaboration between Kitami Institute of Technology and Hokkaido Research Organization, we have conducted research cruises off Abashiri (the Sea of Okhotsk) to investigate near-surface gas hydrates at the sea floor where active gas seepage exists. HKS16, HKS17, HKS18, HKS19, and HKS20 cruses were conducted using RV Hokushin-Maru (255t) of the Kushiro Fisheries Research Institute. We successfully retrieved gas hydrate crystals in the HKS18 cruise (September, 2018) at the new place. Although we could not get sediment cores because of bad weather condition at the HKS19 cruise (September, 2019), we got gas-rich sediment cores at the HKS20 cruise (September 2020). In the HKS20 cruise, two study sites located about 5 km east (site A) and 8 km southeast (site B) from the gas hydrate site of HKS18, respectively.

Because the tidal current speed reached 4 km h^{-1} and made the coring operation difficult, we used a hydrostatic corer optimally tuned for a small vessel and a transponder to understand exact position of the corer in the HKS20 cruise. We obtained nine sediment cores, including two gas-rich cores. Sediment gas samples were obtained by a headspace gas method. Molecular and isotopic compositions of gas samples were measured using a gas chromatograph and an isotope ratio mass spectrometer, respectively.

The depths of sulfate-methane interface (SMI) in HC2006 (site A) and HC2010 (site B) cores were around 10 cm and 50 cm, respectively, indicating high gas flux. C_1 / (C_2 + C_3) of headspace gases in the above two cores distributed between 6,100 and 37,000 below these SMI depths, and those of other sediment cores were less than 1,000, suggesting that the size of gas seepage was small and they are in the oxidation layer above the SMI depth. Concentration of C_2 in the HC2010 core was one order larger than that of HC2006 core, although both study sites located on the same ridge. C_1 $\delta^{13}C$ and δD of these cores concentrated -70‰ and -185‰, respectively. These molecular and isotopic compositions of sediment gases suggested microbial origin via CO_2 reduction. CO_2 $\delta^{13}C$ of these cores were small (around -40‰), indicating that CO_2 is also oxidized from CH_4 simultaneously by microbial processes.

Keywords: gas hydrate, the Sea of Okhotsk, gas origin

©2021. Japan Geoscience Union. All Right Reserved.

Total organic carbon and its carbon isotope ratio in subsurface sediments off Hokkaido area

*Daisuke Yahagi[1], Akihiro Hachikubo[1], Masaaki Konishi[1], Hirotoshi Sakagami[1], Hirotsugu Minami[1], Satoshi Yamashita[1], Yasuhito Uchida[2], Hiroshi Yamaguchi[3]

1. Kitami Institute of Technology, 2. Research Institute of Energy, Environment and Geology, Hokkaido Research Organization, 3. Kushiro Fisheries Research Institute, Hokkaido Research Organization

For five years we collected hydrate-bearing and gas-rich sediments at gas plume sites off Hokkaido to understand the formation process of natural gas hydrates. The research target of this study is an organic matter deposited on the sea floor, because it is an ultimate origin of hydrate-bound hydrocarbon and its total organic carbon relates to formation of natural gas hydrates. Carbon isotopes of the organic matter provides information of their origin. Here, we report total organic carbon and its $\delta^{13}C$ in subsurface sediment retrieved off Hokkaido area (the Sea of Okhotsk, Japan Sea, and the Pacific Ocean).
Sediment samples were obtained off Abashiri (C032, 1KY17, HKS17, HKS18, and HKS20), off Monbetsu (GA18 and GA19), off Esashi (HKY17), off Rebun Is. (HKY19), off Hidaka (K2-2020), and off Tokachi (C046, C061, C080, and C095). In total 446 sediment samples were dried, homogenized, and about 5 mg of samples were put into silver foil capsules. They were decarbonized with 12N hydrochloric acid for 24 h, and then dried and wrapped in tin capsules. These samples were analyzed their TOC with a Flash 2000 Elemental Analyzer connected to a Delta V isotope ratio mass spectrometer. The system was calibrated using a standard of JCAC-01 (L-alanine, -23.43‰ in V-PDB).
The median values of TOC and its $\delta^{13}C$ for all data were 0.9% and -24.2‰, respectively. Sediment cores collected at the gas seepage sites were mainly gas-rich; however, several normal cores with little gas were also included in these data. The TOC and its $\delta^{13}C$ values show distinct regional characteristics. In particular, certain areas off Tokachi and Hidaka had higher TOC (1.5% to 2.0%) and larger $\delta^{13}C$ values (-21‰). As for hydrate-bearing sediment cores, TOC-rich (from 1% to 2%) cores had $\delta^{13}C$ around -25‰, which was similar to other sediment cores without gas hydrates. On the other hand, in the C095-2002 core retrieved off Tokachi, TOC was small (0.6-0.8%) and its $\delta^{13}C$ was extremely small (from -46‰ to -30‰). Hydrate-bearing cores of 1KY17 obtained by ROV survey off Abashiri showed such small values in TOC $\delta^{13}C$ (below -30‰). The $\delta^{13}C$ of TOC was also relatively small in the case that sediments attached to gas hydrate crystals. These results suggest that the organic matter in the sediments close to gas hydrates may be affected by oxidized methane. Although little is known about the formation age of gas hydrate and the exchange processes of gas hydrate crystals with the surrounding gas (dissolved and gas bubble), some exchange of carbon between seepage gas, gas hydrate crystals, and organic matter might occur in the subsurface sediments.

Keywords: TOC, gas hydrate, methane

©2021. Japan Geoscience Union. All Right Reserved.

Characteristics of gas hydrate crystals and their hydrate-bound gases retrieved at the seepage field off Tokachi (the Pacific Ocean)

*Hiromi Kimura[1], Ryoya Kamata[1], Daisuke Yahagi[1], Yuki Moriya[1], Akihiro Hachikubo[1], Masaaki Konishi[1], Hirotoshi Sakagami[1], Hirotsugu Minami[1], Satoshi Yamashita[1]

1. Kitami Institute of Technology

We report the first recovery of natural gas hydrate off Tokachi, the Pacific Ocean. In the framework of practical education of Kitami Institute of Technology, we conducted research cruises off Tokachi since 2014, to investigate gas hydrate fields around Hokkaido. There are many gas seeps ascend from the sea floor and their height exceeded 700 m at the study area off Tokachi.
Using TS Oshoro-maru of Hokkaido University, 17 sediment cores were retrieved by gravity and hydrostatic corers during five cruises. The last C095 cruise was conducted on November 2020, and we obtained massive gas hydrate crystals. In this report we focus on the results of crystallographic properties of gas hydrate and their gas characteristics.
In the cruise of C095, we obtained six sediment cores, including a hydrate-bound core. Gas hydrate crystals were preserved at the temperature of liquid nitrogen, and sediment gases were obtained by a headspace gas method. Raman spectroscopic analysis was conducted to know crystallographic structure, hydration number and cage occupancies. Molecular and isotopic compositions of hydrate-bound and sediment gas samples were measured using a gas chromatograph (GC2014, Shimadzu) and an CF-IRMS (Delta V, Thermo Fisher Scientific), respectively.
Crystallographic structure of gas hydrate samples belonged to the structure I, and hydration number was estimated as 6.07±0.04 from the Raman peaks of hydrate-bound methane. Hydrate-bound H_2S and N_2 molecules were also detected in the Raman spectra, however, that of CO_2 was not detected.
Hydrate-bound gas was mainly methane, and C_1 / (C_2 + C_3) distributed between 3,300 and 6,800. $\delta^{13}C$ and δD of methane were -66‰ and -188‰. These molecular and isotopic compositions of hydrate-bound hydrocarbons suggested microbial origin, and methane was derived by CO_2 reduction. $\delta^{13}C$ of ethane was -52‰, therefore such light ethane seemed to be also microbial.
The depth of sulfate-methane interface (SMI) in C095-GC2002 (hydrate-bound core) was 45 cm, and those in other C095 sediment cores were less less than 1 m, indicating high methane flux from deep layer. Concentrations of H_2S in the headspace gas samples were in the same order (around 1 mM), suggesting that the process of anaerobic oxidation of methane was active. C_1 / (C_2 + C_3) of headspace gases in the hydrate-bound and gas-rich cores distributed between 970 and 2,090 below their SMI depths.
Hydrate-bound and gas-rich sediment cores contained carbonates; their $\delta^{13}C$ ranged from -43‰ to -39‰. Since $\delta^{13}C$ of CO_2 in headspace gases in these cores ranged from -58‰ to -34‰, the site of gas hydrate is characterized as depletion in ^{13}C of carbon dioxide and light carbon dioxide was derived from oxidation of light methane.

Keywords: gas hydrate, methane, the Pacific Ocean

©2021. Japan Geoscience Union. All Right Reserved.

Gas hydrate survey at the gas seepage area off Hidaka, the Pacific Ocean

*Ryoya Kamata[1], Hiromi Kimura[1], Akihiro Hachikubo[1], Hirotoshi Sakagami[1], Satoshi Yamashita[1], Masaaki Konishi[1], Hirotsugu Minami[1]

1. Kitami Institute Of Technology

Existence of gas chimneys have been reported off Hidaka (Hokkaido) in the sub-bottom profiler data of GH06 cruise (AIST 3.5kHz SBP database, https://gbank.gsj.jp/sbp_db/pages/cover.html). To investigate near-surface gas hydrates at the sea floor, we performed K2-2020 cruise using Kaiyo-Maru No. 2 belonging to Kaiyo Engineering Co. Ltd. on September 2020. Our research fields are two areas (sites 1 and 2 locate 60 km east and 60 km southeast from Cape Erimo, respectively). At the site 1, gas plumes were discovered by a multibeam survey. The largest gas plume was about 500 m high and was accompanied by some plumes (200-300 m high). Many mounds with specific heights ranging from several meters to more than ten meters were found. On the contrary, the site 2 had no gas plume but many mounds with specific heights of 10 to 20 meters. In this cruise, we used a hydrostatic corer and gravity corer to take sub-bottom sediment cores. We obtained 16 sediment cores, including some gas-rich cores. Sediment gas samples were obtained by a headspace gas method. Molecular and isotopic compositions of gas samples were measured using a gas chromatograph and an isotope ratio mass spectrometer, respectively.
Sediment gas analysis revealed that concentrations of CH_4 and H_2S at the gas plume site of the site 1 were relatively high (more than 1 mM), and C_1 / (C_2 + C_3) ranged 2,000-5,000 because of high methane concentration. C_1 $\delta^{13}C$ and δD were about -70‰ and around -185 to -170‰, respectively, suggesting microbial methane produced via CO_2 reduction. C_2 $\delta^{13}C$ ranged from -59‰ to 43‰ and became smaller with depth, indicating that microbial ethane is also generated in the sediment. CO_2 $\delta^{13}C$ was also small as well as methane, close to -60‰. Some sediment cores at the plume site had shallow SMI depths of 0.4 to 1.2 m, suggesting an active gas supply and existence of gas hydrates below the sea floor.
On the other hand, the concentration of methane was generally in the order of 0.01 mM at the mounds in site 2. Compared to normal sediment cores (methane concentrations ranged from 0.0001 to 0.001 mM), which show no signs of methane migration, the results showed ascending methane in these mounds. However, C_1 / (C_2 + C_3) was less than 1,000, suggesting that these SMI depths were lower than the core bottoms. The values of C_1 $\delta^{13}C$ and CO_2 $\delta^{13}C$ were around -80‰ and -20‰, respectively, and their profiles were uniform along with depth.

Keywords: gas hydrate, the Pacific Ocean, gas origin

©2021. Japan Geoscience Union. All Right Reserved.

Emission of hydrated gas from seafloor to water column in the western Oki Trough

*Hitoshi Tomaru[1], Tianyou Ze[1], Sonoka Ikemoto[1], Minori Chikada[1]

1. Department of Earth Sciences, Chiba University

Gas chimneys, characterized by a chaotic-columnar structure in acoustic image, are developed well on the western slope of the Oki Trough off Tottori. A significant amount of hydrocarbon, mostly methane, is liberated from the marine sediment to overlying water column in this area, the dynamics of hydrocarbon emission in gas-rich environment is a key to understand carbon/methane migration among atmosphere-seawater-sediment. The concentrations of methane dissolved in the seawater over the gas chimney were seasonally determined, which showed significant increases at the water depth of 200~300 m. This observation strongly suggests that the methane hydrates formed at the surface of emitted methane bubble just above the seafloor and ascended, and the hydrates dissolved at the upper boundary of its stability, so that methane was released efficiently to shallow seawater. In addition, the concentrations of methane near the seafloor were relatively low but seemed to vary in response to the tidal pressure change, indicating that the pressure increase enhanced methane emission from gas pocket in shallow sediment. The behavior of gas emission is constrained by the change of physical/chemical environment between seawater and sediment, and the formation/dissolution of hydrate-coated bubble plays a key role in the migration and distribution of methane in methane-rich water column.

Keywords: gas plume, gas chimney, Oki Trough

©2021. Japan Geoscience Union. All Right Reserved.

Isotope fractionation between hydrate-bound and ambient gases - case study in Lake Baikal gas hydrates -

*Hiromi Kimura[1], Akihiro Hachikubo[1], Oleg Khlystov[2], Gennadiy Kalmychkov[3], Marc De Batist[4], Hirotoshi Sakagami[1], Hirotsugu Minami[1], Satoshi Yamashita[1]

1. Kitami Institute of Technology, 2. Limnological Institute, SB RAS, 3. Vinogradov Institute of Geochemistry, SB RAS, 4. Ghent University

Isotope fractionation of methane occurs between gas and hydrate phases (Hachikubo *et al.*, 2007). However, such fractionation is not applied to understand the formation process of natural gas hydrates in the sublacustrine sediments of Lake Baikal. In this study, we compiled data on stable isotope ratios of hydrocarbons in hydrate-bound and sediment gases, which have been collected in the framework of collaboration between Limnological Institute (Russia), Ghent University (Belgium), and Kitami Institute of Technology (Japan) for 15 years.
Hydrate-bearing sediment cores were collected by R/V *G. Yu. Vereshchagin* using a gravity corer. Hydrate-bound gas was collected in vials by a water displacement method on board, and sediment gas was obtained using the headspace gas method by collecting sediment at 40 cm intervals from the sediment core sections. The gas composition and stable isotope ratios of volatile hydrocarbons were measured for these samples by gas chromatograph (GC2014, Shimadzu) and CF-IRMS (Delta V, Thermo Fisher Scientific), respectively. Comparison of stable isotope ratios of hydrate-bound and sediment gases at the same core and depth was performed.
The methane carbon isotope ratio of the hydrate-bound gas was 0 to +3‰ smaller than the sediment gas. These isotopic difference in carbon was slightly positive overall, indicating a concentration of lighter methane ($^{12}CH_4$) in the hydrate-bound gas than in the sediment gas. The difference in hydrogen between hydrate-bound and sediment gases distributed from -3‰ to +11‰ and is also positive overall as well. The average difference in δD was 5.4‰, which agreed fairly well with the previous report that approximately 5‰ light methane in δD is preferentially enclathrated at the formation of synthetic methane hydrate (Hachikubo *et al.*, 2007). Although the positive difference in δ^{13}C cannot be explained yet, these results can be explained generally by the isotopic fractionation of methane. In contrast, some sediment cores retrieved at the Kedr mud volcano showed small or reversed differences in methane carbon isotope ratios, as well as small differences in methane hydrogen isotope ratios, suggesting that dissociation of gas hydrate is occurring at that point.

References

Hachikubo A, Kosaka T, Kida M, Krylov A, Sakagami H, Minami H, Takahashi N, Shoji H (2007) Isotopic fractionation of methane and ethane hydrates between gas and hydrate phases. *Geophys Res Lett* **34**: L21502. doi:10.1029/2007GL030557

Keywords: gas hydrate, isotope fractionation, methane

©2021. Japan Geoscience Union. All Right Reserved.

Carbon isotope fractionation of carbon monoxide hydrate between gas and hydrate phases

*Hiromi Kimura[1], Akihiro Hachikubo[1], Satoshi Takeya[2]

1. Kitami Institute of Technology, 2. National Institute of Advanced Industrial Science and Technology (AIST)

It is possible that carbon monoxide hydrates exist in the icy bodies of outer planets of the solar system (Zhu *et al.*, 2014). Isotope signatures of carbon monoxide hydrates may provide useful information to understand formation processes of gas hydrate. Kimura *et al.* (2019) reported at the past JpGU conference that the carbon isotopic difference between hydrate-bound and residual gases distributed between between 1.2‰ and 1.5‰ in the case of carbon dioxide hydrate, suggesting that the hydrate rather concentrates light molecules ($^{12}CO_2$). Besides, the equilibrium pressure of $^{13}CO_2$ hydrate is slightly higher than that of $^{12}CO_2$ hydrate (Kimura *et al.*, 2020) and agreed with the result of carbon isotopic fractionation. On the contrary, there no information about carbon monoxide hydrate. In this study, we measured carbon isotopic difference between hydrate-bound and residual gases at the formation of carbon monoxide hydrate.
Samples of carbon monoxide hydrate were synthesized in a pressure cell (volume: 42 mL). Fine ice powder was put in a pressure cell and introduced the guest gas. The temperature was controlled by a liquid bath (253-273 K) and cold rooms (223-243 K) to form hydrate crystals from gas and ice powder. After their formation, isotopic compositions of both hydrate-bound and residual gases were measured by an isotope ratio mass spectrometer (CF-IRMS, DeltaV, Thermo Fisher Scientific).
The results of PXRD pattern showed that the crystallographic structure of carbon monoxide hydrate was the cubic structure I. The carbon isotopic differences between hydrate-bound and residual gas was 0.6 ± 0.1‰ at 223-273 K. In contrast to the result of carbon dioxide hydrate, the hydrate of carbon monoxide concentrated heavier molecules (^{13}CO), indicating that the equilibrium pressure of ^{13}CO hydrate is lower than ^{12}CO hydrate.

References

Kimura H, Matsuda J, Kikuchi Y, Hachikubo A, Takeya S (2019) Carbon isotope fractionation of CO_2 during the formation of clathrate hydrate. *Japan Geoscience Union Meeting 2019*, MIS21-P07
Kimura H, Hachikubo A, Takeya S (2020) Equilibrium pressure of gas hydrate enclathrated carbon dioxide isotopologues. *JpGU-AGU Joint Meeting 2020*, MIS32-11
Zhu J, Du S, Yu X, Zhang J, Xu H, Vogel SC, Germann TC, Francisco JS, Izumi F, Momma K, Kawamura Y, Jin C, Zhao Y (2014) Encapsulation kinetics and dynamics of carbon monoxide in clathrate hydrate. *Nat Commun* **5**, 4128, doi: 10.1038/ncomms5128

Keywords: gas hydrate, stable isotope, carbon monoxide, isotopic fractionation

©2021. Japan Geoscience Union. All Right Reserved.

Hydrogen isotopic fractionation of methane at the formation of synthetic structure I and II gas hydrates

*Ryoya Kamata[1], Akihiro Hachikubo[1], Satoshi Takeya[2]

1. Kitami Institute Of Technology, 2. National Institute of Advanced Industrial Science and Technology (AIST)

Hydrogen isotopic fractionation of volatile hydrocarbons occurs during the formation of gas hydrates. For example, the hydrogen isotope ratios of the hydrate-bound methane, ethane, and propane are lower than those of the ambient gases (Hachikubo *et al.*, 2007; Nikaido *et al.*, 2018). These results are supported by the difference in equilibrium pressures of hydrates encaged guest isotopologues (Ozeki *et al.*, 2018). The crystal structure of gas hydrate depends on the size of guest gas. Methane and ethane hydrates form the structure I, composed of large ($5^{12}6^2$) and small (5^{12}) cages, whereas propane hydrate forms the structure II, composed of the different size large ($5^{12}6^4$) and small (5^{12}) cages. Ethane and propane can be encaged only in their large cages due to the large guest size. Since natural gas hydrates are mixed-gas hydrates, these guest molecules share the cages of different size. In the case of methane + ethane and methane + propane systems, methane is selectively occupied in the small cages. On the contrary, methane can be rather encaged into large cages in the system of methane + argon, because argon is smaller than methane. Therefore, we can check the effect of cage size on the hydrogen isotopic difference in methane. In this study, we investigated the hydrogen isotope fractionation of methane in the mixed-gas system of methane + ethane, methane + propane, and methane + argon systems.

A pressure cell (volume: 40 mL) was filled with 0.7 g of fine ice powder in a cold room. After vacuuming the air in the cell at the temperature of liquid nitrogen, the guest gases (methane, ethane, propane, and argon) were introduced in the cell and formed the mixed-gas hydrates. In the formation processes, the partial pressure of ethane and propane was also controlled below the liquefaction pressure of propane. After the formation of mixed-gas hydrate, residual gas that was not encaged in the hydrate phase was collected. Hydrate crystals were sampled at the temperature of liquid nitrogen. The composition of the hydrate-bound and residual gases were determined by a gas chromatograph (GC-2014, Shimadzu). The hydrogen isotope ratio of methane was determined by a stable isotope ratio mass spectrometer (CF-IRMS, DeltaV, Thermo Fisher Scientific). Stable isotope compositions are reported as δ values (‰), and δD is given with reference to the V-SMOW standards.

The difference in hydrogen isotope ratios of methane (δD of residual gas – δD of hydrate-bound gas) is defined as $\Delta\delta$D. The $\Delta\delta$D values in the system of methane + ethane and methane + propane was smaller than that of pure methane reported by the previous works (Hachikubo *et al.*, 2007). Therefore, $\Delta\delta$D became small in the case that methane was encaged into small cages. On the contrary, the $\Delta\delta$D values in the system of methane + argon was not changed with their gas composition. The crystallographic structure depended on the gas composition and methane was rather encaged into large cages. We confirmed that $\Delta\delta$D values in large cages was larger than those in small cages.

References

Hachikubo A, Kosaka T, Kida M, Krylov A, Sakagami H, Minami H, Takahashi N, Shoji H (2007) Isotopic fractionation of methane and ethane hydrates between gas and hydrate phases. *Geophys Res Lett* **34**: L21502. doi:10.1029/2007GL030557

Nikaido T, Matsuda J, Hachikubo A, Takeya S (2018) Hydrogen isotope fractionation of propane and isobutane hydrates between gas and hydrate phases. *JSSI & JSSE Joint Conference –2018 in Sapporo*, doi:10.14851/jcsir.2018.0_158

Ozeki T, Kikuchi Y, Takeya S, Hachikubo A (2018) Phase equilibrium of isotopologue methane hydrates

©2021. Japan Geoscience Union. All Right Reserved.

enclathrated CH_3D and CD_4. *J Chem Eng Data* **63**(6): 2266-2270, doi: 0.1021/acs.jced.8b00203

Keywords: gas hydrate, methane, ethane, propane, hydrogen isotope ratio

©2021. Japan Geoscience Union. All Right Reserved.

Experimental study of CO2 hydrate phase equilibrium in sediments

*Tatsuki Iwamoto[1], Hitoshi Tomaru[1]

1. Chiba University

Gas hydrate is ubiquitously formed under the seafloor where the gas (methane) concentration exceeds its solubility within the equilibrated pressure-temperature condition. The equilibrium condition, however, readily changes to reflect the surrounding environments such as compositions of water, gas, and sediment. In this study, we experimentally determined the phase equilibrium pressure-temperature condition using carbon dioxide with natural sediments to examine the physical/chemical effects of sediment particles on the CO2 hydrate stability, of which physical properties are similar to those of methane hydrate. The phase equilibrium of CO2 hydrate with 10 wt% sediment changed to lower temperature (high pressure) region compared to the pure water system. This is because the clay minerals such as kaolinite absorb efficiently water molecules and form a structure similar to the hydrate lattice, preventing the formation of hydrate. In addition, ion dissolution from clay minerals may result in the depression of freezing point of hydrate, which also reduces the hydrate stability. The properties of host sediment as well as gas and water chemistry are important factor for assessing the distribution and amount of gas hydrate in natural environment.

©2021. Japan Geoscience Union. All Right Reserved.

Effect of temperature and pressure on hydration number of methane hydrate

*Akihiro Hachikubo[1], Ryoya Kamata[1], Hiromi Kimura[1], Yuta Komagata[1], Go Fuseya[1], Satoshi Takeya[2]

1. Kitami Institute of Technology, 2. National Institute of Advanced Industrial Science and Technology (AIST)

Gas hydrates are considered to be a potential resource of energy and a gas storage medium. Hydration number of methane hydrate decides the amount of gas in crystal lattice of gas hydrate. In the case of ideal full-occupation of hydrate cages, hydration number is 5.75. However, researchers have reported that the hydration number is around 6, because small amount of empty cages decrease the free energy and stabilize the crystal. Hydration number depends on temperature and pressure at the formation process (Cady, 1981; 1983) as van der Waals & Platteeuw model predicts. It has not been investigated how the hydration number changes over a wide temperature range. In this study, we investigated the effect of temperature and pressure on the hydration number of methane hydrate.
Small amount of fine ice powder (0.1 g) was placed in a pressure cell at 253 K, and methane was introduced and pressurized under the temperatures of 245 K, 255 K, and 273 K to form hydrate samples. The samples were retrieved under the temperature of liquid nitrogen. The Raman spectra of the C-H symmetric stretching vibrational mode of the methane molecules encapsulated in the large and small cages of the structure I were observed using a Raman spectrometer. The area ratios of the Raman peaks derived from the methane molecules in the large and small cages were determined by a peak fitting using the Voigt function, and the hydration number was estimated using a statistical thermodynamic calculation.
Generally, the hydration number of methane hydrate decreased with increasing formation pressure. This trend is consistent with the results obtained for hydrates of other guests such as xenon, hydrogen sulfide, and sulfur dioxide (Kamata *et al.*, 2020; Cady, 1981; 1983). Besides, it increased slightly with temperature. However, the change of hydration number of methane hydrate was relatively small, ranged from 5.92 to 6.11 under the pressure of 2 MPa to 21 MPa.

References

Cady GH (1981) Composition of clathrate gas hydrates of $CHClF_2$, CCl_3F, Cl_2, ClO_3F, H_2S, and SF_6. *J Phys Chem* **85**: 3225-3230
Cady GH (1983) Composition of Clathrate Gas Hydrates of H_2S, Xe, SO_2, Cl_2, CH_3Cl, CH_3Br, $CHClF_2$, CCl_2F_2, and C_3H_8. *J Phys Chem* **87**: 4437-4441
Kamata R, Kimura H, Sugimori E, Hachikubo A, Takeya S (2020) Direct measurement of hydration number of gas hydrates. *JpGU-AGU Joint Meeting 2020*, MIS32-P12

Keywords: gas hydrate, hydration number, methane

©2021. Japan Geoscience Union. All Right Reserved.

[J] Oral | M (Multidisciplinary and Interdisciplinary)：M-IS Intersection

Sun. Jun 6, 2021 1:45 PM - 3:15 PM JST | Sun. Jun 6, 2021 4:45 AM - 6:15 AM UTC | Ch.16 Zoom Room 16

[M-IS27] History X Earth and Planetary Science

convener:Yasuyuki Kano(Earthquake Research Institute, The University of Tokyo), Hiroaki Isobe(Faculty of Fine Arts, Kyoto City University of Arts), Kei Yoshimura(Institute of Industrial Science, The University of Tokyo), kiyomi iwahashi(National Institute of Japanese Literature), Chairperson:Yasuyuki Kano(Earthquake Research Institute, The University of Tokyo), kiyomi iwahashi(National Institute of Japanese Literature)

The history of modern observation in earth and planetary sciences is often far shorter compared with the timescales of their interests. Investigation of the long-term variations and occurrences of extremely rare events requires effective use of information derived from historical documents observed and recorded by pre-modern people. Thus, historical documents have been referred in various fields of earth and planetary sciences such as seismology, climatology, meteorology and astronomy. Sharing their records, methods and experiences will be beneficial for each field and bring new insights. It is also essential to involve experienced historians because one needs to carefully investigate the reliability and the context of each document in order to use it as scientific data. On the other hand, analyzing the record in the historical documents with the eyes of modern science may also bring new insights to the historians. Cooperative work between historians and earth scientists will provide better knowledge on disaster mitigation, and science, technology and society through understanding of human reaction to historical disasters.

In this session we overview the studies using the historical documents in various fields of the earth and planetary sciences as well as the recent advances in related topics such as historical-data assimilation and digital humanities, such as AI character recognition. The aim is to promote the communication and dialogues among the researchers in various background, and thus foster the new ideas and collaborations in the study of "History X EPS."

1:45 PM - 2:15 PM JST | 4:45 AM - 5:15 AM UTC

[MIS27-01] Sharing historical materials: An example of multi-disciplinal examination of historical materials in Edo period

★Invited Papers

*Hirotaka Terashima[1] (1.National Archives of JAPAN)

2:15 PM - 2:30 PM JST | 5:15 AM - 5:30 AM UTC

[MIS27-02] Improvement of climate reconstruction by focusing on the degree of detailed description of historical daily weather record

*Kenjiro Sho[1], Yoshimi Ikeda[2], Mika Ichino[3], Junpei Hirano[4], Kooiti Masuda[5], Asanobu Kitamoto[3,6] (1.Nagoya Institute of Technology, 2.Ikeda Gakuen Ikeda Senior High School, 3.Center for Open Data in the Humanities, 4.Teikyo University, 5.Tokyo Metropolitan University, 6.National Institute of Informatic)

2:30 PM - 3:00 PM JST | 5:30 AM - 6:00 AM UTC

[MIS27-03] Historical atmospheric analyses by weather information assimilation using Gaussian transformation

★Invited Papers

*Xiaoxing Wang[1], Kei Yoshimura[2], Kinya Toride[2] (1.Graduate School of Frontier Sciences, The University of Tokyo, 2.Institute of Industrial Science, The University of Tokyo)

3:00 PM - 3:15 PM JST | 6:00 AM - 6:15 AM UTC

[MIS27-04] Descriptions of natural phenomena in textbooks and people's perceptions

*Harufumi Tamazawa[1,2] (1.Kyoto City University of Arts, 2.Kyoto University)

Sharing historical materials: An example of multi-disciplinal examination of historical materials in Edo period

*Hirotaka Terashima[1]

1. National Archives of JAPAN

We have made a joint research on environmental history based on collaboration with history, biology, and forest ecology regarding historical materials of disease and insect damage that occurred in the late Edo period. Records of beech fusarium oxysporum caused by Kashinonagakikuimushi, Kashinaga or Platypus quercivorus, have not been confirmed before 1934 yet, but there is a possibility of oak damage by Kashinaga from ancient documents (Shimada Hiroshi Family, 1030, April 1863) left in Sakae Village, Nagano Prefecture. The original documents were first transcribed and interpreted based on historical methods. (1) Outbreaks of moths larvae called Kususan occured in Ohayashi or public forest between 1830 and 1843 (Tenpo year) and killed chestnuts, (2) then trees felled down with snow, (3) the reduced trees were filled up by beech. From a biology perspective, however, Kususan does not kill the trees themselves even if Kususan eats up the leaves of beech trees and konara oak. For this reason, if we think of death of trees as damage by Kashinaga, we can explain the description in the historical materials. Furthermore, it was appropriate to describe that the beech was used to resist snow from the field survey conducted by forest ecologist. In this way, knowledge of biological and forest ecology was added to historical interpretation, suggesting occurrence of damage by Kashinaga in the late Edo period. Around the same time as this study, a diary was discovered in a shrine in Iiyama City, which is a neighborhood of Sakae Village, directly describing the damage caused by Kashinaga in the 1750s. It has been pointed out that this historical document showed that damages by Kashinaga repeatedly occurred in a location with many large-diameter trees such as a shrine forest from the viewpoint of forest ecology. The introduction of unexpected perspective from natural science shows the limitations of interpretation only from historical perspective. In addition, historical examination of the historical background is also essential, for example, as there is a possibility that the document was falsely written because the residents cut trees unofficially in the forest.

Keywords: Environmental history, Ecology, Fusarium oxysporum

©2021. Japan Geoscience Union. All Right Reserved.

Improvement of climate reconstruction by focusing on the degree of detailed description of historical daily weather record

*Kenjiro Sho[1], Yoshimi Ikeda[2], Mika Ichino[3], Junpei Hirano[4], Kooiti Masuda[5], Asanobu Kitamoto[3,6]

1. Nagoya Institute of Technology, 2. Ikeda Gakuen Ikeda Senior High School, 3. Center for Open Data in the Humanities, 4. Teikyo University, 5. Tokyo Metropolitan University, 6. National Institute of Informatic

Daily weather record of old diaries is very useful for climate reconstruction in historical times because of its exceptionally high temporal resolution as paleoclimatic proxy data. However, there is difficulty in estimating quantitative meteorological variables such as precipitation from their qualitative and subjective weather description. In this study, we attempt to develop a method to quantify weather record of diaries by focusing on the degree of detailed description of weather record.

Here we define "detailed description rate" as the proportion of the number of days with detailed weather description (more detailed than simple description in one word such as “fine” or “rain”) to the number of days with any weather description. It has high negative correlation with the threshold of recording precipitation phenomenon in diary (Sho *et al.*, 2017). Based on this relationship, we used the seasonal detailed description rate to correct the seasonal number of precipitation days for weather record of diaries written in the Edo era in Kagoshima and Kyoto, Japan. As a result, unrealistic secular trend seen in the time series of the seasonal number of precipitation days before correction was cancelled and the agreement with climatic reconstructions from other proxy data was improved for the corrected time series. This infers the possibility that the difference in weather classification criterion among writers of diary can be adjusted and long time series of a meteorological variable such as precipitation can be composed from weather record of diaries by different writers by using the detailed description rate. Moreover, we are comparing weather record of various diaries written in the Meiji and Taisho periods (late 19th to early 20th centuries) with four-hourly precipitation data at the neighboring meteorological station to understand the detailed relationships between weather recorded in diaries and actual meteorological phenomena at that time.

Keywords: historical daily weather record, detailed description rate, quantification

©2021. Japan Geoscience Union. All Right Reserved.

Historical atmospheric analyses by weather information assimilation using Gaussian transformation

*Xiaoxing Wang[1], Kei Yoshimura[2], Kinya Toride[2]

1. Graduate School of Frontier Sciences, The University of Tokyo, 2. Institute of Industrial Science, The University of Tokyo

Historical climate provides a reference for predicting future climate change by analyzing the past climate variability. Before the modern instrumental weather record, old descriptive sources (i.e., diaries) are important in reconstructing daily weather conditions. Data assimilation is recently widely used in climate reconstruction because it optimally combines meteorological information with a climate model. In Japan, there is a Historical Weather Database (HWDB) derived from diaries, recording daily weather information at more than 18 observation sites during the 1750s to 1870s. Cloud cover can be converted from the descriptive weather records but is difficult to assimilate because of its non-Gaussian characteristic. The objective is to reconstruct historical weather with a 6-hour temporal resolution by cloud cover data assimilation using a Gaussian transformation method. This study conducts a practical experiment in 1995 with the Global Spectral Model (GSM) and a local ensemble transform Kalman filter (LETKF) and validates the reconstruction results by reanalysis data. The observation information used in data assimilation is cloud cover categories converted from the JMA description data, keeping the consistency with the diary weather information. A control experiment without any observation assimilated (NoDA) and two experimental runs with cloud cover assimilated (NoGT and GT) are performed over Japan. Assimilation results indicate the small fluctuation amplitude in NoDA and NoGT, but GT impacts are evident in cloud cover estimation. 2-month average RMSE over the 17 observation grids are improved by 9.9% by GT, compared to NoGT. GT also contributes to RMSE reductions in three-dimensional atmospheric variables, especially in the higher troposphere. Gaussian transformation shows the great potential to improve cloud cover assimilation in actual reconstructions. This study provides a reasonable possibility to accurately reconstruct weather (for example, in the 1820s) with a higher temporal resolution.

Keywords: historical weather reconstruction, data assimilation, Gaussian transformation

©2021. Japan Geoscience Union. All Right Reserved.

Descriptions of natural phenomena in textbooks and people's perceptions

*Harufumi Tamazawa[1,2]

1. Kyoto City University of Arts, 2. Kyoto University

By unraveling the records of the past, we can learn how people perceived natural phenomena, but there may be a gap in time between the state-of-the-art knowledge gained through specialized research in the natural sciences and the perception of the general public. However, there may be a gap between the state-of-the-art knowledge gained through specialized research in the natural sciences and the general public's perceptions over time. In the modern and post-modern periods, we can learn more about the perceptions of the time by studying the descriptions in textbooks and the extent of their dissemination. Particularly for phenomena that are unfamiliar to some people in some places, the latest knowledge is brought in from the outside, which changes how we are connected to the traditional perceptions. Although auroras are rarely seen in Japan, when they are observed on a large scale, various records may be available. On the other hand, the interpretation of these records varies from one recorder to another. In the Meiji era (1868-1912), descriptions of low-latitude auroras appeared in geography and geology textbooks, while in some books from the late Edo period (1603-1868) they were translated from European technical books. The Chinese word "red chi" was changed to "polar light" in the Meiji period (1868-1912) and written in katakana as "aurora," but the literal translation "northern light" was used in some books. In this paper, we will discuss the relationship between the phenomenon and the scientific understanding of the observed low-latitude aurora.

©2021. Japan Geoscience Union. All Right Reserved.

[J] Oral | M (Multidisciplinary and Interdisciplinary)：M-IS Intersection

Sun. Jun 6, 2021 3:30 PM - 5:00 PM JST | Sun. Jun 6, 2021 6:30 AM - 8:00 AM UTC | Ch.16 Zoom Room 16

[M-IS27] History X Earth and Planetary Science

convener:Yasuyuki Kano(Earthquake Research Institute, The University of Tokyo), Hiroaki Isobe(Faculty of Fine Arts, Kyoto City University of Arts), Kei Yoshimura(Institute of Industrial Science, The University of Tokyo), kiyomi iwahashi(National Institute of Japanese Literature), Chairperson:Kei Yoshimura(Institute of Industrial Science, The University of Tokyo), Harufumi Tamazawa(Kyoto City University of Arts)

The history of modern observation in earth and planetary sciences is often far shorter compared with the timescales of their interests. Investigation of the long-term variations and occurrences of extremely rare events requires effective use of information derived from historical documents observed and recorded by pre-modern people. Thus, historical documents have been referred in various fields of earth and planetary sciences such as seismology, climatology, meteorology and astronomy. Sharing their records, methods and experiences will be beneficial for each field and bring new insights. It is also essential to involve experienced historians because one needs to carefully investigate the reliability and the context of each document in order to use it as scientific data. On the other hand, analyzing the record in the historical documents with the eyes of modern science may also bring new insights to the historians. Cooperative work between historians and earth scientists will provide better knowledge on disaster mitigation, and science, technology and society through understanding of human reaction to historical disasters.

In this session we overview the studies using the historical documents in various fields of the earth and planetary sciences as well as the recent advances in related topics such as historical-data assimilation and digital humanities, such as AI character recognition. The aim is to promote the communication and dialogues among the researchers in various background, and thus foster the new ideas and collaborations in the study of "History X EPS."

3:30 PM - 4:00 PM JST | 6:30 AM - 7:00 AM UTC

[MIS27-05] Accomplishments and Potential Applications of Historical GIS: Researching Old Maps and Contributing Locally

★Invited Papers

*Akihiro Tsukamoto[1] (1.Tokushima Univ.)

4:00 PM - 4:15 PM JST | 7:00 AM - 7:15 AM UTC

[MIS27-06] Analysis of aftershocks of the 1855 Ansei Edo Earthquake using old documents discovered around Kanto Ko-Shinetsusing old documents discovered around Kanto Ko-Shinetsu

*Baba Michito[1], Yasuyuki Kano[1] (1.Earthquake Research Institute,University of Tokyo)

4:15 PM - 4:30 PM JST | 7:15 AM - 7:30 AM UTC

[MIS27-07] A historical record of frequent felt earthquakes on 1870 May and the destructive earthquake on 1870 May 13 felt in Yokohama

*Kentaro Hattori[1], Junzo Ohmura[2] (1.Kyoto Univ., 2.Tokyo Univ.)

4:30 PM - 4:45 PM JST | 7:30 AM - 7:45 AM UTC

[MIS27-08] Integrated IDP catalog considering the continuity of historical and modern earthquake catalog

*Yasuyuki Kano[1,2], Junzo Ohmura[1,2] (1.Earthquake Research Institute, The University of Tokyo, 2.Collaborative Research Organization for Historical Materials on Earthquakes and Volcanoes, UTokyo)

4:45 PM - 5:00 PM JST | 7:45 AM - 8:00 AM UTC

[MIS27-09] Discussion

Accomplishments and Potential Applications of Historical GIS: Researching Old Maps and Contributing Locally

*Akihiro Tsukamoto[1]

1. Tokushima Univ.

1. Introduction

Research that applies the vaunted functionalities of Geographic Information Systems (GIS) in data management and spatial analysis for analyzing past spaces and historical materials is gaining traction globally as a brand-new field called "Historical GIS." This paper will provide an overview of the past accomplishments of Historical GIS that have accompanied the spread of digital archiving and GIS technology, thereby further exploring their potential applications. Specifically, it will discuss the results of GIS research involving old maps and introduce cases where such results have been utilized for studying local regions.

2. Accomplishments of Historical GIS

First, the accomplishments of Historical GIS research are cited to include the construction of platforms used for developing old maps and other digitized historical records available to the public. For example, "A Vision of Britain Through Time," which is a project combining past maps with statistical data spearheaded by England's University of Portsmouth; and Old Maps Online, an online portal for old maps built using open-source resources. These projects use online maps to overlay past statistical information with old maps, allowing users to search location names, old maps, and more. In the early 2000s, online platforms were used in this manner to link old maps with historical geographic information and pursue historical GIS projects aimed at aggregating massive amounts of documents, materials, and data.
Using the knowledge accumulated thus far, GIS is now being utilized in the scientific research on spatial information associated with the geographic distribution of all past phenomena, while comprehensively considering traditional research on map history and historical geography that takes into account historic backgrounds. As a result, we have seen an increase in the sophistication of Historical GIS research (Hirai et al., 2014).

3. Approach to local learning through Historical GIS

The old maps made available to the public by Historical GIS projects have also contributed to initiatives aimed at local learning. For example, the online map system of the Tokushima Castle Museum, "A Historical Stroll Through Castle Town Tokushima," makes it possible to switch between the old map and the current map; this system was publicly released to impart local learning.
Old maps include a wealth of historical records, particularly spatial information, and it is relatively easy to integrate this information into online maps. Therefore, they are used as tools to gain an understanding of local regions based on comparisons between the present and the past data.

4. Conclusion

This report provided an overview of the trends observed in Historical GIS research and established that the discipline has developed to the point where its results are now being applied to studies based on local communities. Although Historical GIS research is one of the many fields that uses historical datasets, the use of GIS as a primary research tool renders it a rare field that is capable of constantly updating itself with the latest science and technology. This characteristic implies that GIS can not only provide academic contributions to adjacent disciplines, but also be utilized in a wide variety of applications that facilitate

©2021. Japan Geoscience Union. All Right Reserved.

community research.

Works cited

・A Vision of Britain Through Time, https://www.visionofbritain.org.uk/. Accessed February 15, 2021.
・Old Maps Online, https://www.oldmapsonline.org/. Accessed February 15, 2021.
・Hirai, Shogo, Susumu Asato, and Makoto Watanabe, eds. "GIS Analysis of Early Modern Survey Drawings: Local Developments," *Kokon Shoin*, Tokyo, January 2014.
・Tokugawa Castle Museum, "A Historical Stroll Through Castle Town Tokushima." https://www.city.tokushima.tokushima.jp/johaku/rekishisanpo.html. Accessed February 15, 2021.

Keywords: Historical GIS, Old Maps, Potential Applications, Local Learning

©2021. Japan Geoscience Union. All Right Reserved.

Analysis of aftershocks of the 1855 Ansei Edo Earthquake using old documents discovered around Kanto Ko-Shinetsu sing old documents discovered around Kanto Ko-Shinetsu

*Baba Michito[1], Yasuyuki Kano[1]

1. Earthquake Research Institute,University of Tokyo

The 1855 Ansei Edo earthquake occurred around pm 9 of November 11 1855 and caused damage in Edo and around Kanto area by strong shaking. Usami (2001) estimated the epicenter of the mainshock in Northern part of Tokyo bay. For this earthquake, there are many historical documents which show the details of the aftershock activity as well as the main shock. We analyzed the aftershock activity of Ansei Edo earthquake by using “Ebihara-ke Document” discovered in the beginning of 2000 and “Ohya-ke Daily” introduced in Tsuji (2003) in addition to published historical collection of earthquakes.

We focused on temporal changes of aftershock activity of Ansei Edo earthquake. We compared the records of earthquake written in “Ansei Jishin Kakitome no Koto” in “Ebihara-ke Document” with those in the old document that has detailed record of aftershock activity in Edo, for example, “Yaburemado no Ki.” We also examined difference between the number of records in daytime and night. There are various possible reasons for the difference in the number of aftershocks recorded in each document, such as the differences in the temporal resolution of earthquakes in each archive or the differences in the seismic intensity due to differences in the epicenter and magnitude of each aftershock. In this study, we applied the Omori-Utsu formula to the aftershock records in "Ansei Jishin Kakitome no Koto", and found a good agreement between the curve of the Omori-Utsu formula applied to " Ansei Jishin Kakitome no Koto " and the number of aftershocks recorded by historical documents in Edo after the third day of the main earthquake.This suggests that the "Ansei Jishin Kakitome no Koto" may have recorded aftershocks that were overlooked by some historical documents in Edo such as the “Yaburemado no Ki”.

Next, we focused on the spatial distribution of aftershock activity of the Ansei Edo earthquake. We categorized the discription on the day when aftershock occurred into four categories: "no articles", "articles without earthquake records," "articles with earthquake records," and "articles with large earthquake records," and plotted them on a map to see the distribution of felt records for each aftershock. Then, using this map, we estimated the felt area of four aftershocks, including the earthquake of November 17 1855, which is considered to be the largest aftershock of the Ansei Edo Earthquake. We compared the time of occurrence and shaking characteristics of the earthquake on November 17 1855, which is regarded as the largest aftershock by Nakamura and Matsu'ura (2011). It was found two earthquakes occured, one at dusk and the other at night, and that the sensitivities may have differed. We also compared the distribution of seismic intensity between aftershocks and main shock.

There are various possibilities for the difference of felt distribution between the aftershock and the mainshock obtained in this study, such as the difference in the location and magnitude of the epicenters of the mainshock and aftershocks, the difference in the accuracy of time of the respective records, and the inclusion of earthquakes not included in the aftershock sequences of the Ansei-Edo Earthquake or earthquakes that occurred in the other region.

©2021. Japan Geoscience Union. All Right Reserved.

©2021. Japan Geoscience Union. All Right Reserved.

A historical record of frequent felt earthquakes on 1870 May and the destructive earthquake on 1870 May 13 felt in Yokohama

*Kentaro Hattori[1], Junzo Ohmura[2]

1. Kyoto Univ., 2. Tokyo Univ.

On 1870 May 13, at about 2 AM, a destructive earthquake (M 6 ~ 6.5) occurred in the western part of Kanagawa Prefecture, causing damage to the Odawara area [Usami et al. (2013)]. Matsuura et al. (2006, 2020) defined the epicenter as the eastern part of Yamanashi Prefecture and concluded that the earthquake occurred at the seismically active area at the depth of 20 -30 km. Since early May, about 2 weeks before the earthquake, felt earthquakes had frequently occurred in the surrounding areas such as Shizuoka Prefecture [Ishibashi (1993)]. They have been interpreted as the foreshocks [Usami (2020)].

In order to investigate the frequently felt earthquakes this study examines the felt earthquake record written by a foreigner (James Gordon Kidd) who lived in Yokohama in the same period and compares it with other contemporary Japanese records. Kidd recorded the date of 131 earthquakes felt in Yokohama from 1870 May 1 to 26 including the size and duration of 9 large earthquakes. Based on this record, the diurnal variation of the number of felt earthquakes in Yokohama is shown in Fig. 1. The number of felt earthquakes per day was the largest on 1870 May 13, when the destructive earthquake of Odawara occurred. In addition, a peak of the number of felt earthquakes per day was observed on May 9.

We also examine the possibility that the frequently felt earthquake described by Mr. Kidd occurred off the east coast of Izu Peninsula. Since 1978, earthquake swarms off the east coast of Izu peninsula, caused by magma intrusions, have occurred repeatedly along and off the coast of Ito City, Shizuoka Prefecture [Earthquake Research Committee, Headquarters for Earthquake Research Promotion (2010)]. The Ito earthquake swarm, which occurred in the offshore area of Ito City in 1930, is also considered to have originated from magma intrusions [Center for Earthquake Prediction and Eruption Prediction, School of Science, Tohoku University (1990)]. Koyama (1993 , 1999), who examined earthquake swarms off the east coast of Izu peninsula before 1930, estimated that the swarm earthquake occurred either in 1868 May to July or in 1870 May to June. Our study raises the possibility that this earthquake swarm occurred not in 1868 (the former) but 1870 (the latter).

Keywords: historical earthquake, the 1870 Odawara earthquake, earthquake swarms off the east coast of Izu peninsula

©2021. Japan Geoscience Union. All Right Reserved.

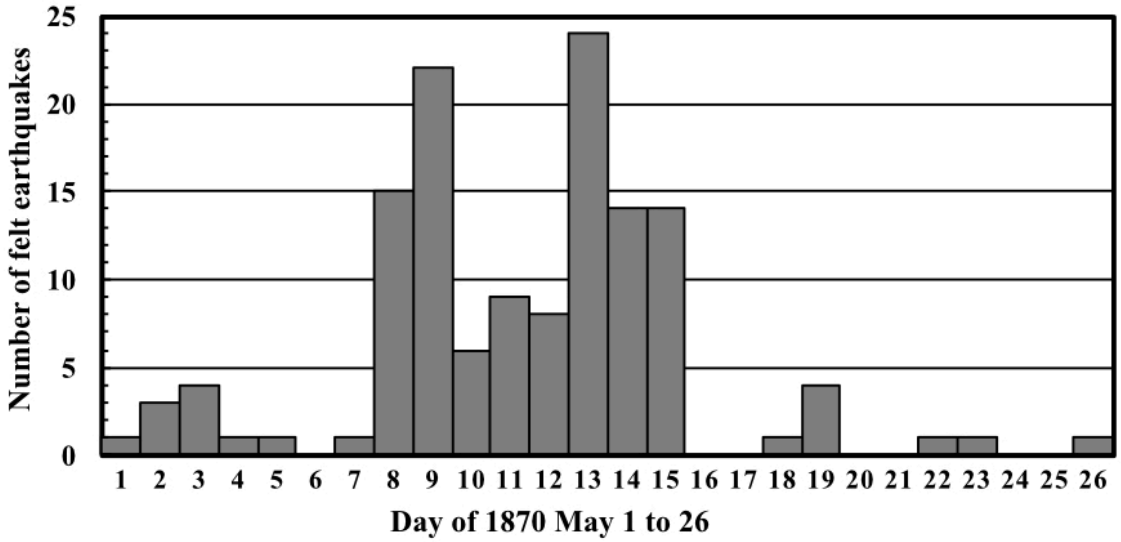


Fig. 1. Diurnal variation of the number of earthquakes felt at Yokohama from 1870 May 1 to 26.

©2021. Japan Geoscience Union. All Right Reserved.

Integrated IDP catalog considering the continuity of historical and modern earthquake catalog

*Yasuyuki Kano[1,2], Junzo Ohmura[1,2]

1. Earthquake Research Institute, The University of Tokyo, 2. Collaborative Research Organization for Historical Materials on Earthquakes and Volcanoes, UTokyo

For historical earthquakes, seismic intensities at each point is estimated based on the description of collected historical materials, and the epicenter, hypocenter, and magnitude of the earthquake are estimated. Several catalogues of the results have been published. Regarding the seismic intensity data points (IDPs), "[Intensity distribution and iso-seismal maps for historical earthquakes in Japan]" and "[comprehensive table of Japanese historical earthquake]" are compiled. For current earthquakes, Japan Meteorological Agency has been publishing JMA seismic intensity data as part of the Seismological Bulletin of Japan. It has been maintained back to 1919 and is available online.

If the IDPs can be searched and displayed through both catalogs of historical and current earthquakes, it will be useful for estimating the epicenter of the historical earthquake and for examining the validity of seismic intensity estimation. However, the differences between the two catalogues should be carefully handled for integration. The current catalog includes JMA intensity and instrumental intensity are given. For historical earthquakes, there are cases where an estimated JMA seismic intensity is given, and expressions based on historical materials such as "earthquake" and "strong earthquake" are given. Regarding the location of the observation points, the current catalog provides the location (geographic coordinates) of the observation stations. For historical earthquakes, the observation points are determined based on descriptions of historical materials, but their accuracy varies. They can be identified at the building, and in some cases only in villages, counties, or countries. In "[Intensity distribution and iso-seismal maps for historical earthquakes in Japan]" mentioned above, the observation points are provided as current municipal level. It is necessary to identify and register observation points for historical earthquakes. Also, when integrating the catalog, it is necessary to provide information on the accuracy of the seismic intensity and location of observation points, especially in the catalog of historical earthquakes.

Even if the seismic IDPs of historical and current earthquakes are integrated, the distribution of observation points is different. When comparing seismic intensity distributions of historical and current earthquakes, it is effective to create a virtual IDPs and estimate the seismic intensity of them using the attenuation relation of seismic intensity or interpolation of the seismic intensity based on site amplification zoning. We propose a system to display the integrated catalog of observed and virtual IDPs.

Keywords: Historical earthquakes, IDP, Seismic catalog

©2021. Japan Geoscience Union. All Right Reserved.

[J] Oral | M (Multidisciplinary and Interdisciplinary) | M-IS Intersection

[M-IS27] History X Earth and Planetary Science

convener:Yasuyuki Kano(Earthquake Research Institute, The University of Tokyo), Hiroaki Isobe(Faculty of Fine Arts, Kyoto City University of Arts), Kei Yoshimura(Institute of Industrial Science, The University of Tokyo), kiyomi iwahashi(National Institute of Japanese Literature), Chairperson:Kei Yoshimura(Institute of Industrial Science, The University of Tokyo), Harufumi Tamazawa(Kyoto City University of Arts)

Sun. Jun 6, 2021 3:30 PM - 5:00 PM Ch.16 (Zoom Room 16)

The history of modern observation in earth and planetary sciences is often far shorter compared with the timescales of their interests. Investigation of the long-term variations and occurrences of extremely rare events requires effective use of information derived from historical documents observed and recorded by pre-modern people. Thus, historical documents have been referred in various fields of earth and planetary sciences such as seismology, climatology, meteorology and astronomy. Sharing their records, methods and experiences will be beneficial for each field and bring new insights. It is also essential to involve experienced historians because one needs to carefully investigate the reliability and the context of each document in order to use it as scientific data. On the other hand, analyzing the record in the historical documents with the eyes of modern science may also bring new insights to the historians. Cooperative work between historians and earth scientists will provide better knowledge on disaster mitigation, and science, technology and society through understanding of human reaction to historical disasters.

In this session we overview the studies using the historical documents in various fields of the earth and planetary sciences as well as the recent advances in related topics such as historical-data assimilation and digital humanities, such as AI character recognition. The aim is to promote the communication and dialogues among the researchers in various background, and thus foster the new ideas and collaborations in the study of "History X EPS."

4:45 PM - 5:00 PM

[MIS27-09]Discussion

©Japan Geoscience Union

[J] Poster | M (Multidisciplinary and Interdisciplinary)：M-IS Intersection

Sun. Jun 6, 2021 5:15 PM - 6:30 PM JST | Sun. Jun 6, 2021 8:15 AM - 9:30 AM UTC | Ch.22_3

[M-IS27] History X Earth and Planetary Science

convener:Yasuyuki Kano(Earthquake Research Institute, The University of Tokyo), Hiroaki Isobe(Faculty of Fine Arts, Kyoto City University of Arts), Kei Yoshimura(Institute of Industrial Science, The University of Tokyo), kiyomi iwahashi(National Institute of Japanese Literature)

The history of modern observation in earth and planetary sciences is often far shorter compared with the timescales of their interests. Investigation of the long-term variations and occurrences of extremely rare events requires effective use of information derived from historical documents observed and recorded by pre-modern people. Thus, historical documents have been referred in various fields of earth and planetary sciences such as seismology, climatology, meteorology and astronomy. Sharing their records, methods and experiences will be beneficial for each field and bring new insights. It is also essential to involve experienced historians because one needs to carefully investigate the reliability and the context of each document in order to use it as scientific data. On the other hand, analyzing the record in the historical documents with the eyes of modern science may also bring new insights to the historians. Cooperative work between historians and earth scientists will provide better knowledge on disaster mitigation, and science, technology and society through understanding of human reaction to historical disasters.

In this session we overview the studies using the historical documents in various fields of the earth and planetary sciences as well as the recent advances in related topics such as historical-data assimilation and digital humanities, such as AI character recognition. The aim is to promote the communication and dialogues among the researchers in various background, and thus foster the new ideas and collaborations in the study of "History X EPS."

[MIS27-P01] An attempt to convert historical seismic data into GIS data and its challenges

*Junzo Ohmura[1,4], Miki Hamano[2], Yuta Hashimoto[3], Yasuyuki Kano[1,4] (1.Earthquake Research Institute,The University of Tokyo, 2.Graduate School of Letters, Ritsumeikan University, 3.National Museum of Japanese History, 4. Collaborative Research Organization for HistoricalMaterials on Earthquakes and Volcanoes, UTokyo)

[MIS27-P02] Historical materials of unlisted destructive earthquakes at Izu-Bonin Islands in the Meiji period: the 1873 Toshima earthquake and so on

*Kentaro Hattori[1] (1.Kyoto Univ.)

[MIS27-P03] Investigation of the stone monuments related to the hail and frost damage in the southern part of Gunma Prefecture

*Masafumi Aoyama[1] (1.Gunma University)

An attempt to convert historical seismic data into GIS data and its challenges

*Junzo Ohmura[1,4], Miki Hamano[2], Yuta Hashimoto[3], Yasuyuki Kano[1,4]

1. Earthquake Research Institute,The University of Tokyo, 2. Graduate School of Letters, Ritsumeikan University, 3. National Museum of Japanese History, 4. Collaborative Research Organization for HistoricalMaterials on Earthquakes and Volcanoes, UTokyo

Historical data on earthquakes have been collected since the Meiji era (1868-1912), and collections of historical data have been published. The collection is now being converted to electronic text. There is a plan to add location information to place names in the future.

Regarding the conversion of historical seismic data into GIS data, ohmura (2015) describes the advantages of this method. Spatial analysis is essential for the analysis of seismic phenomena. However, the identification of place names in historical documents is time-consuming and requires knowledge of history. This is one of the factors that prevent researchers outside the field from entering the field.

The Ministry of Land, Infrastructure, Transport and Tourism (MLIT) has released a number of GIS data. If the historical records of earthquakes are converted into GIS data, it will be possible to analyze them using GIS. In addition, the data can be used not only in seismology but also in other related fields.

In this study, we attempted to convert historical materials into GIS data for the 1596 Keicho-Fushimi Earthquake, for which electronic texts have already been made available.

Using GIS, we examined the relationship between the earthquake fault and the distribution of historical materials. As a result, we found that the historical materials are unevenly distributed, and it is highly possible that the epicenter cannot be estimated accurately. In analyzing historical earthquakes, it is necessary to consider the spatial bias of historical materials and to understand their limitations.

On the other hand, the tendency of the distribution of the records is different depending on the nature of the historical materials. By converting historical documents into GIS data, it is possible to examine historical documents from a spatial perspective.We plan to publish the created GIS data on the web.

In the process of converting place names into GIS data, we faced the problem of having a mixture of place names with various characteristics in the historical records. The specific problems are as follows.
1. In urban areas, there are many detailed place names, so old maps with large scales are not useful for reference.
2. There are many examples of the same place name being written differently.
3. There are place names that have disappeared in modern times.
4. We need to find out where the temples and shrines existed at the time.
5. In some cases, it is not possible to determine the location without reading before and after the historical documents.
6. Conceptual and vague place names exist.
7. There are place names that should be represented by lines and Polygon.
8. There are cases where a location is expressed as a distance from a specific point.

©2021. Japan Geoscience Union. All Right Reserved.

Keywords: historical earthquake, GIS, historical place name

©2021. Japan Geoscience Union. All Right Reserved.

Historical materials of unlisted destructive earthquakes at Izu-Bonin Islands in the Meiji period: the 1873 Toshima earthquake and so on

*Kentaro Hattori[1]

1. Kyoto Univ.

Destructive earthquakes that have occurred in the vicinity of Japan from ancient times are summarized in catalogs such as "Chronological table of earthquakes" in “Chronological scientific tables” (National Astronomical Observatory of Japan, 2020), and “Materials for a comprehensive list of Japanese destructive earthquakes 599-2012” (Usami et al., 2013). Usami et al. (2013) include earthquakes that have caused damage or changes to houses, artificial structures, or the ground. I investigate records of earthquakes that caused damage to the Izu-Bonin Islands in the Meiji period (1868 -1912) and are not listed in Usami et al. (2013).

In this study, I focus on an earthquake that occurred in 1873 (Meiji 6) and caused damage to Toshima Island (Present Toshima Village, Tokyo) in the northern Izu Islands. The earthquake caused damage to temples and shrines in Toshima Island [Toshima Village (1996a)] and caused landslides [Toshima Village (1996b)]. As for the date of the earthquake, the records in Toshima Island say "Meiji 6, 6th month, 8th day " [Toshima Village (1996a)]. These records exceptionally used the Japanese calendar system, although 1873 was the year when the Japanese calendar (lunar calendar) was switched to the Western calendar in Japan. "Meiji 6, 6th month, 8th day" on the Japanese calendar is 1873 July 2 on the Western calendar. In the study, I survey other historical records about the earthquake.

In addition, I examine the earthquake in the Izu Islands on 1885 (Meiji 18) October 26, and the earthquake in the Bonin Islands on 1885 (Meiji 18) November 4. In the former earthquake, several coastal cliffs of Niijima Island and Shikinejima Island (Present Niijima-mura, Tokyo) in the northern Izu Islands collapsed, and the channel of the water source in Shikinejima Island was blocked. In the latter earthquake, landslides occurred in the Bonin Islands such as Chichijima Island (Present Ogasawara Village, Tokyo). Neither earthquake is not listed in Utsu (1979), which compiled M6.0 or greater earthquakes and smaller destructive earthquakes in and around Japan from 1885 to 1925.

Keywords: historical earthquake, the Izu-Bonin Islands, the 1873 Toshima Island earthquake, the 1885 Niijima Island and Shikinejima Island earthquake, the 1885 Bonin Islands earthquake

©2021. Japan Geoscience Union. All Right Reserved.

Investigation of the stone monuments related to the hail and frost damage in the southern part of Gunma Prefecture

*Masafumi Aoyama[1]

1. Gunma University

We are conducting research on historical disasters in the southern part of Gunma prefecture, using disaster-related monuments. In addition to the stone monuments related to the volcanic mudflow due to the eruption of the Mt. Asama in 1783, there are many stone monuments in this area that show descriptions related to floods, debris flow and landslide disasters that occurred in 1910, 1935, and 1947. In addition to floods and landslides, there are stone monuments related to hail and frost damage, and earthquake damage. In particular, there are many stone monuments related to hail and frost damage in this area. Since this area was once a thriving area for sericulture, if mulberry leaves die due to hail and frost damage, it becomes impossible to raise silkworms that feed on mulberry leaves, causing great economic loss to sericulture farmers. When many silkworms die due to hail and frost damage, the dead bodies have buried, and created mounds on the ground, built stone monuments, and worshiped the spirits of the silkworms. The sericulture industry in this area began to flourish from the end of the Edo period and declined in the Showa period, and many stone monuments related to hail and frost damage and sericulture erected during this period are distributed. In particular, there are stone monuments with detailed descriptions of hail damage in 1887 and frost damage in 1893. These monuments are valuable records of local meteorological phenomena and meteorological disasters during the Meiji era, when meteorological observations were still vulnerable, the impact of hail and frost damage on the local community at that time, and the importance of sericulture in the local community.
Some of the stone monuments that are said to have been erected for the memorial service of silkworms caused by hail and frost damage have detailed descriptions of frost damage, but some have only the monument name and the year of construction. In this area, sericulture worship became popular with the development of sericulture, and many are said to have erected monuments in the hope of abundant cocoons. In addition, in the silkworm industry, which is the victim of silkworms, many monuments have been erected for the purpose of memorializing the silkworms that were sacrificed in the silk reeling process. These stone monuments related to sericulture have monument names such as Kokage Okami, Kokageyama Okami, and Kinugasa Myojin, but the purpose for which the monuments were erected is diverse. In this presentation, I would like to show the results of a study on the situation of hail and frost damage inferred from the inscriptions of these monuments and historical materials, which is said to be a memorial monument for silkworms caused by hail and frost damage, and the circumstance of construction of those monuments.

Keywords: hail and frost damage, silkworm industry, disaster stone monuments, historical disaster

©2021. Japan Geoscience Union. All Right Reserved.

[E] Oral | M (Multidisciplinary and Interdisciplinary)：M-AG Applied Geosciences

Sun. Jun 6, 2021 3:30 PM - 5:00 PM JST | Sun. Jun 6, 2021 6:30 AM - 8:00 AM UTC | Ch.20 Zoom Room 20

[M-AG37] CTBT IMS Technologies for Detecting Nuclear Explosion and Their Applications to Earth Science

convener:Nurcan Meral Ozel(Comprehensive Nuclear-Test-Ban Treaty Organization), Hiroyuki Matsumoto(Japan Agency for Marine-Earth Science and Technology), Dirk Metz(Japan Agency for Marine-Earth Science and Technology), Yosuke Naoi(Japan Atomic Energy Agency), Chairperson:Nurcan Meral Ozel(Comprehensive Nuclear-Test-Ban Treaty Organization), Hiroyuki Matsumoto(Japan Agency for Marine-Earth Science and Technology), Dirk Metz(Japan Agency for Marine-Earth Science and Technology)



The Comprehensive Nuclear-Test-Ban Treaty Organization (CTBTO) was founded in 1996 in response to the adaption of the Treaty in 1996 by the United Nations General Assembly, which bans nuclear explosions on the Earth's surface, in the atmosphere, underwater and underground. The Treaty has a unique and comprehensive verification regime to make sure that nuclear explosion goes detected. The regime is supported by International Monitoring System (IMS) composed of the four state-of-the-art technologies; 1) Seismic, 2) Hydroacoustic, 3) Infrasound, and 4) Radionuclide, by the International Data Centre (IDC), and by the On-Site Inspections (OSI).
IMS will, when complete, consists of 337 facilities worldwide to monitor the planet for signs of nuclear explosion. Around 90 % of the facilities are operational and sending the data to the IDC in Vienna, Austria.
The huge amount of data collected by the IMS network can be used for other purposes such as civil and scientific applications in addition to detecting nuclear explosions. For example, they can provide Tsunami Warning centers with near real-time information about an underwater earthquake. The data could also help better understand of earthquakes, volcanoes, oceans, climate change, and other issues on our planet.
This session will provide the overview of the IMS, the IMS response to the spread of COVID-19, and the scientific and engineering discussions on each technology. The session strongly welcomes young scientists and engineers who are interested in four IMS technologies.

3:30 PM - 3:45 PM JST | 6:30 AM - 6:45 AM UTC

[MAG37-01] **IMS Network Resilience and Business Continuity During Lockdown**

*Nurcan Meral Ozel[1] (1.Comprehensive Nuclear-Test-Ban Treaty Organization)

3:45 PM - 4:00 PM JST | 6:45 AM - 7:00 AM UTC

[MAG37-02] I30JP station repair following damage by typhoon “FAXAI”

*Takanari Fujii[1], Takayuki Otsu[1], Makiko Iwakuni[1], Masashi Motohashi[1] (1.Japan Weather Association)

4:00 PM - 4:15 PM JST | 7:00 AM - 7:15 AM UTC

[MAG37-03] Long-range acoustic measurements of the 2004 submarine eruption near Nightingale Island: Insights from hydrophone triplet array data recorded at IMS station H01W, Cape Leeuwin

*Dirk Metz[1], Julien Vergoz[2], Ingo Grevemeyer[3] (1.JAMSTEC, 2.CEA, 3.GEOMAR)

4:15 PM - 4:30 PM JST | 7:15 AM - 7:30 AM UTC

[MAG37-04] Operation of IMS radionuclide stations in Japan

*Yutaka Tomita[1], Yuichi Kijima[1], Akiko FURUNO[1], Yoichi Yamamoto[1] (1.Japan Atomic Energy Agency)

4:30 PM - 4:45 PM JST | 7:30 AM - 7:45 AM UTC

[MAG37-05] Atmospheric dispersion analysis for source term estimation of Xe-133 high-concentration detection events observed at the noble gas monitoring station in Takasaki regarding CTBT and two temporary experimental systems

*Akiko FURUNO[1], Yuichi Kijima[1], Yutaka Tomita[1], Yoichi Yamamoto[1] (1.Japan Atomic Energy Agency)

4:45 PM - 5:00 PM JST | 7:45 AM - 8:00 AM UTC

[MAG37-06] Discussion on how the CTBT IMS contributes to Earth and environmental sciences

Nurcan Meral Ozel[1], *Hiroyuki Matsumoto[2], Dirk Metz[2], Yosuke Naoi[3] (1.Comprehensive Nuclear-Test-Ban Treaty Organization, 2.Japan Agency for Marine-Earth Science and Technology, 3.Japan Atomic Energy Agency)

IMS Network Resilience and Business Continuity During Lockdown

*Nurcan Meral Ozel[1]

1. Comprehensive Nuclear-Test-Ban Treaty Organization

The COVID-19 pandemic has irrevocably marked the year 2020 and posed unprecedented challenges testing the resilience of the International Monitoring System (IMS) Network. In response, the Provisionary Technical Secretariat (PTS) put in place pragmatic business continuity plans and measures to mitigate the impact of COVID-19 due to travel restrictions across the globe, lockdowns and remote working.

The IMS Network has proven its operational strength and resilience with high data availability and performance throughout the first and second waves of the pandemic in spring and autumn/winter 2020. Furthermore, in the lockdown periods nothing went undetected by the IMS ranging from earthquakes, tsunami, meteorite, fireballs to a variety of seismic activities. A retrospect analysis of the success of PTS business continuity plans crystallizes a number of strategic and operational lessons.

The first lesson is strategic team play between the State Signatories, their Station Operators, National Data Centres and PTS. The IMS performance and state of health monitoring and meetings were intensified immediately prior to the first wave to coordinate preventive, planned and corrective maintenance work with key PTS staff to enhance IMS Operations & Maintenance. An even closer and continuous interaction with station operators and local contractors was sought in parallel. The immediate and seamless transfer of the whole PTS to Home Office and successful maintenance of PTS’ s large-scale IT infrastructure operations enabled this team play.

Operational measures enhanced the resilience of IMS stations to mitigate the impact of COVID-19 lockdown. An emphasis was put on remote troubleshooting and issue resolution along with increased sparing of critical spare parts and frequency of replenishment of consumables, greater use of local purchasing, shipment tracking and re-routing to alternatives.

Global travel restrictions led to delays in some PTS sustainment and station establishment activities. At the same time the right balance was struck between virtual endeavours versus essential on-site presence such as the remote certifications of RN55 Norilsk, Russian Federation in October and IS25 Guadaloupe, France in November 2020. Traditional biennial O&M Workshop an important endeavour for IMS resilience to support network of station operators was conducted virtually.

CTBTO remains vigilant in monitoring, updating and innovating business continuity plans and crisis preparedness as the world navigates the COVID-19 crisis further and carrying the lessons learned into 2021 to further strengthen IMS Network resilience.

Keywords: CTBTO, IMS, COVID-19, Business continuity, Network resilience, Lessons learned

©2021. Japan Geoscience Union. All Right Reserved.

I30JP station repair following damage by typhoon “FAXAI”

*Takanari Fujii[1], Takayuki Otsu[1], Makiko Iwakuni[1], Masashi Motohashi[1]

1. Japan Weather Association

Tremendous typhoon “FAXAI” attacked Chiba prefecture, where I30JP was installed, on 8th September 2019. It brought strong wind and heavy rainfall widely. Barometric pressure when it landed in Chiba prefecture was 960hPa. It caused tremendous damage around Chiba especially by strong wind. Power outage continued for more than 2 weeks in the vast area of Chiba prefecture.

In I30JP, IMS infrasound station in Japan, although observation data of I30H1 –I30H6 are normally transmitted to IDC miraculously, in each site so many cedar trees were fallen and observation facilities were heavily damaged, such as security fences and pipe array.

The remedial actions have been taken for the typhoon damages as the unscheduled maintenance by October 2020. The surrounding environment has been quite changed at I30H6 site before and after the typhoon. We also analyzed changes in the characteristics of the infrasound waveform data after the station repair.

Keywords: CTBT, National Data Centre, infrasound, waveform analysis, typhoon

©2021. Japan Geoscience Union. All Right Reserved.

Long-range acoustic measurements of the 2004 submarine eruption near Nightingale Island: Insights from hydrophone triplet array data recorded at IMS station H01W, Cape Leeuwin

*Dirk Metz[1], Julien Vergoz[2], Ingo Grevemeyer[3]

1. JAMSTEC, 2. CEA, 3. GEOMAR

Little is known about active volcanism in the remote regions of the global ocean. Here, we resort to long-range acoustic measurements to study the 2004 eruption at Nightingale Island, Tristan da Cunha. Underwater sound phases associated with the event were recorded at Cape Leeuwin, Western Australia, where a bottom-moored hydrophone array is operated as part of the International Monitoring System (IMS). IMS recordings in combination with local seismic observations suggest that the center of activity is located to the east of Nightingale Island, where a seafloor mapping campaign aboard R/V Maria S Merian (2012MSM20/2) revealed a previously unknown, potentially newly formed stratocone. Signal back azimuth derived from progressive-multi-channel-beamforming differ by more than two degrees from the expected geodesic value, suggesting that low-frequency sound phases may not have traveled along the direct source-receiver path, but were instead reflected off an unnamed seamount located south of Tristan da Cunha. This interpretation is supported by results from transmission loss modeling via the parabolic equation approach, which indicate significant bathymetric obstruction between the volcano and the H01W array in the Southern Ocean. Our study further highlights the potential of the IMS network for the detection and study of future eruptions both at Nightingale Island and elsewhere. Implications for test-ban treaty monitoring and volcano early warning will be discussed.

Keywords: Submarine eruption, Nightingale Island, IMS, CTBTO

©2021. Japan Geoscience Union. All Right Reserved.

Operation of IMS radionuclide stations in Japan

*Yutaka Tomita[1], Yuichi Kijima[1], Akiko FURUNO[1], Yoichi Yamamoto[1]

1. Japan Atomic Energy Agency

The Japan Atomic Energy Agency (JAEA)has operated two radionuclide stations which are Takasaki radionuclide station (RN38) and Okinawa radionuclide station (RN37) for the CTBT (Comprehensive Nuclear- Test-Ban Treaty) International Monitoring System (IMS). RN38 was built in the Takasaki Advanced Radiation Research Institute of the National Institutes for Quantum and Radiological Science and Technology (QST) in 2002. Radioactivity of particulate radionuclides and radioxenon gases are measured at RN38 by using a Radionuclide Aerosol Sampler / Analyzer (RASA) and a Swedish Automatic Unit for Noble Gas (SAUNA) respectively. It was worthy of special mention that the SAUNA of RN38 detected the radioxenons which were related to the DPRK-3 event in 2013. RN37 was installed in a renovated facility at the Okinawa Tracking and Communication Station of the Japan Aerospace Exploration Agency (JAXA) in 2006. It measures only radioactivity of particulate radionuclides by using a RASA. JAEA contributes to the CTBT international verification regime through these activities. Operation and some monitoring results of both radionuclide stations will be reported in this presentation.

Keywords: CTBT, RN38, RN37, RASA, SAUNA

©2021. Japan Geoscience Union. All Right Reserved.

Atmospheric dispersion analysis for source term estimation of Xe-133 high-concentration detection events observed at the noble gas monitoring station in Takasaki regarding CTBT and two temporary experimental systems

*Akiko FURUNO[1], Yuichi Kijima[1], Yutaka Tomita[1], Yoichi Yamamoto[1]

1. Japan Atomic Energy Agency

This research aims at source term estimations of high-concentration detection events of Xe-133, which were observed at the CTBT IMS (International Monitoring System) Takasaki radionuclide monitoring station from the viewpoint of atmospheric dispersion analysis. Japan Atomic Energy Agency operates JPX38 in the Takasaki radionuclide station for noble gas monitoring, and conducts temporary measurement project of radioxenon at Horonobe in Hokkaido (JPX81) and Mutsu in Aomori (MUX88) as a part of the noble gas joint measurement project with CTBTO. The high-concentration detection events were frequently occurred not only at the JPX38 but also at the JPX81from the end of 2020 to January 2021. In the presentation, we will describe the source term estimation analysis of these high-concentration detection events, and discuss the relationship of the events between two stations.

Keywords: CTBT, atmospheric dispersion simulation, source term estimation, high-concentration detection events

©2021. Japan Geoscience Union. All Right Reserved.

Discussion on how the CTBT IMS contributes to Earth and environmental sciences

Nurcan Meral Ozel[1], *Hiroyuki Matsumoto[2], Dirk Metz[2], Yosuke Naoi[3]

1. Comprehensive Nuclear-Test-Ban Treaty Organization, 2. Japan Agency for Marine-Earth Science and Technology, 3. Japan Atomic Energy Agency

Following the all presentations, the conveners provide a discussion time on various scopes related to the CTBT International Monitoring System from the point of view of scientific and technological aspects. We welcome multi-disciplinary discussions to deepen understanding of the Earth as well as suggestions to achieve sustainability of the IMS network from those scientists and engineers who involve four technologies; seismic, hydroacoustic, infrasound and radionuclide monitoring.

©2021. Japan Geoscience Union. All Right Reserved.

[E] Poster | M (Multidisciplinary and Interdisciplinary)：M-AG Applied Geosciences

Sun. Jun 6, 2021 5:15 PM - 6:30 PM JST | Sun. Jun 6, 2021 8:15 AM - 9:30 AM UTC | Ch.21_2

[M-AG37] CTBT IMS Technologies for Detecting Nuclear Explosion and Their Applications to Earth Science

convener:Nurcan Meral Ozel(Comprehensive Nuclear-Test-Ban Treaty Organization), Hiroyuki Matsumoto(Japan Agency for Marine-Earth Science and Technology), Dirk Metz(Japan Agency for Marine-Earth Science and Technology), Yosuke Naoi(Japan Atomic Energy Agency)

The Comprehensive Nuclear-Test-Ban Treaty Organization (CTBTO) was founded in 1996 in response to the adaption of the Treaty in 1996 by the United Nations General Assembly, which bans nuclear explosions on the Earth's surface, in the atmosphere, underwater and underground. The Treaty has a unique and comprehensive verification regime to make sure that nuclear explosion goes detected. The regime is supported by International Monitoring System (IMS) composed of the four state-of-the-art technologies; 1) Seismic, 2) Hydroacoustic, 3) Infrasound, and 4) Radionuclide, by the International Data Centre (IDC), and by the On-Site Inspections (OSI).
IMS will, when complete, consists of 337 facilities worldwide to monitor the planet for signs of nuclear explosion. Around 90 % of the facilities are operational and sending the data to the IDC in Vienna, Austria.
The huge amount of data collected by the IMS network can be used for other purposes such as civil and scientific applications in addition to detecting nuclear explosions. For example, they can provide Tsunami Warning centers with near real-time information about an underwater earthquake. The data could also help better understand of earthquakes, volcanoes, oceans, climate change, and other issues on our planet.
This session will provide the overview of the IMS, the IMS response to the spread of COVID-19, and the scientific and engineering discussions on each technology. The session strongly welcomes young scientists and engineers who are interested in four IMS technologies.

[MAG37-P01] The upgrade of the CTBT Auxiliary Seismic Stations in Japan

*RYOHEI EMURA[1], Masashi Motohashi[1], Takayuki Otsu[1], Toyomi Sakamoto[1], Mami Nogami[1], Soshi Iwata[1] (1.Japan Weather Association)

[MAG37-P02] Detections of hydrocoustic signals associated with volcanic eruptions at Kadovar Island, Papua New Guinea, using CTBT IMS hydrophones

*Hiroyuki Matsumoto[1], Mario Zampolli[2], Georgios Haralabus[2], Jerry Stanley[2], James Robertson[2], Nurcan Meral Özel[2] (1.Japan Agency for Marine-Earth Science and Technology, 2.Comprehensive Nuclear-Test-Ban Treaty Organization)

[MAG37-P03] Characteristics of seismic signals associated with the hydrothermal system beneath a giant submarine caldera

*Hiroko Sugioka[1] (1.Department of Planetology, Kobe University)

The upgrade of the CTBT Auxiliary Seismic Stations in Japan

*RYOHEI EMURA[1], Masashi Motohashi[1], Takayuki Otsu[1], Toyomi Sakamoto[1], Mami Nogami[1], Soshi Iwata[1]

1. Japan Weather Association

Japan Weather Association (JWA) is working as the Comprehensive Nuclear-Test-Ban Treaty (CTBT) National Data Centre-1 (NDC-1) of Japan. NDC-1 has two main roles. The first role is analyzing waveform data related to seismic and infrasound waves and providing advices to the Ministry of Foreign Affairs from a technical perspective. The another one is the Station Operators (SO) of the International Monitoring System (IMS) stations in Japan. There are 1 Primary Seismic (PS) station, 5 Auxiliary Seismic (AS) stations and 1 Infrasound (IS) station in Japan and NDC-1 is working for operation and maintenance of these 7 stations.
AS stations used to branch the signals of the broadband sensors owned by the Japan Meteorological Agency (JMA) and were using these signals as IMS data. But it turned out that there are some difficulties in sensor calibration from the CTBT side equipment with technical surveys conducted several times in the past. The IMS seismic observation system operation manual says that the sensor should be calibrated once a year, so in order to carry out the calibration efficiently, it is necessary to prepare the CTBT unique sensors separately from the sensors of the JMA. Therefore, over the last two years, including the construction preparation period, sensors (Guralp CMG-3T) for CTBT were installed near the existing observation sites for all five AS stations in Japan.
As a preliminary step to the installations of the sensors, 50 cm x 50 cm piers for seismic sensors were installed, which were designed according to the current situations of each site. When the installation of the seismic sensor, the sensor was placed on the pier and oriented and leveled. A metal cover was attached to prevent magnetism and a heat insulating material is wrapped around it to prevent temperature changes. The on-site calibration was performed at each site by NDC-1 after installation. After NDC-1 on-site work, the station has passed the test period by CTBTO side and it was returned to operation.
As a result of this upgrade, the new sensors for CTBT were installed at all 5 AS stations, and the annual calibration and other work related to maintenance and improvement of data quality can be performed remotely by NDC-1. In this presentation, we will introduce the details of this upgrade work.

Keywords: CTBT, International Monitoring System, National Data Centre, Seismology

©2021. Japan Geoscience Union. All Right Reserved.

Detections of hydrocoustic signals associated with volcanic eruptions at Kadovar Island, Papua New Guinea, using CTBT IMS hydrophones

*Hiroyuki Matsumoto[1], Mario Zampolli[2], Georgios Haralabus[2], Jerry Stanley[2], James Robertson[2], Nurcan Meral Özel[2]

1. Japan Agency for Marine-Earth Science and Technology, 2. Comprehensive Nuclear-Test-Ban Treaty Organization

Following an eruption series at Kadovar Island, Papua New Guinea, the hydroacoustic datasets acquired by CTBT International Monitoring System (IMS) hydroacoustic (HA) hydrophone station HA11, Wake Island, were examined. HA11 is located approximately 3500 km northeast from Kadovar. Active eruptions restarted in January 2018 after an extended quiet period that lasted approximately three centuries. Cross-correlation analysis using two months of HA11 hydrophone triplet data showed that the cumulative number of HA detections increased with time after the start of the volcanic eruption series. According to local observations of Kadovar, a first eruption at the summit of the island was followed by four additional new vent spots and two vents were created underwater near to the shoreline. Our analysis suggests that the hydroacoustic signals detected by HA11 were associated with underwater volcanic eruptions close tothe shoreline. Additionally, a lava dome collapse accompanied by some small tsunamis occurred on 09 February 2018. The present study suggests that a series of explosive bursts followed by a peculiar hiss, recorded by HA11, may constrain the time of this lava dome collapse event at Kadovar to 00:33 UTC on 09 February 2018. Given the compatibility of this observation with the computed source time of a tsunami, which was reported by eyewitnesses on the nearby island of Blup Blup, the authors interpret this particular hydroacoustic signal as being a remote observation of the tsunamigenic event. The present study demonstrates the potential contributions of the IMS HA stations data to the remote monitoring of volcanic activity over large ocean areas.

©2021. Japan Geoscience Union. All Right Reserved.

Characteristics of seismic signals associated with the hydrothermal system beneath a giant submarine caldera

*Hiroko Sugioka[1]

1. Department of Planetology, Kobe University

The submarine Kikai caldera is located approximately 50 km south from the Kyushu island and lies astride the volcanic front of the southwestern Japan. It has been recently revealed that giant rhyolite lava dome with a volume of 32 km^3 is formed after the last super eruption with an emission of more than 170 km^3 of tephra at 7.3 k.a. by multi-channel seismic reflection surveys by the Kobe University T/S Fukae Maru cruise (Tatsumi et al., 2018). We installed a seafloor seismic network composed of five ocean bottom seismometers (OBSs) on the rim of the submarine Kikai caldera from October 19, 2016 to March 14, 2017, which was the first seismic observation conducted in the vicinity of the giant submarine caldera. The seafloor seismic data observed a wide variety of signals associated with volcanic activities beneath the caldera.
In January and February of 2017, which was at around the middle of the observation period, earthquake swarm related to volcanic activity had been recorded at seismographs at Satsuma-Iwojima that is a volcanic island on the northwestern rim of the caldera (Monthly volcanic activity report by the Japan Meteorological Agency). Our OBSs clearly recorded the signals associated with those volcanic earthquakes with a dominant frequency of 6 Hz and with a duration of about 1 minute. Throughout the observation period, on the other hand, periodic signals associated with the volcanic tremors frequently observed at all stations. They had a dominant frequency of higher than 15 Hz and an interval of about 1 hour. The periodic and frequency-dependent amplitude modulation of volcanic tremors at intervals ranging from 46 to 50 minutes were observed by broadband seismic network around Satsuma-Iwojima, which are well explained by the model of a heated water pocket that pressure-controlled valve of the volcano (Ohminato, 2006). The observed signals at surrounding sites might be associated with the hydrothermal system beneath the submarine caldera.

Keywords: Volcanic activities, Caldera eruption, Seafloor observation

©2021. Japan Geoscience Union. All Right Reserved.

[J] Oral | M (Multidisciplinary and Interdisciplinary)：M-AG Applied Geosciences

Sun. Jun 6, 2021 1:45 PM - 3:15 PM JST | Sun. Jun 6, 2021 4:45 AM - 6:15 AM UTC | Ch.09 Zoom Room 09

[M-AG38] Ten years after the Fukushima Dai-ichi NPP Accident : Dynamics of radionuclides in the environment

convener:Daisuke Tsumune(Central Research Institute of Electric Power Industry), Yuichi Onda(Center for Research on Isotopes and Environmental Dynamics, University of Tsukuba), Kazuyuki Kita(Faculty of Science, Ibaraki University), Yoshio Takahashi(Department of Earth and Planetary Science, Graduate School of Science, The University of Tokyo), Chairperson:Yuichi Onda(Center for Research on Isotopes and Environmental Dynamics, University of Tsukuba), Daisuke Tsumune(Central Research Institute of Electric Power Industry)

Ten years have passed since the accident at the Tokyo Electric Power Company (TEPCO) Fukushima Daiichi Nuclear Power Station (NPP), which was triggered by the Great East Japan Earthquake and tsunami. Huge amount of radionuclides were emitted to the environment by the accident. They have been transported and diffused by atmospheric motion, depositing them to soil and vegetation. Deposited radionuclides are dynamically shifted in the earth environment; atmosphere, soil, inland water, ocean, and ecosystem. To understand this dynamic shift in the environment and for the long-term prediction of the disaster by the radionuclides, investigation and discussion based on not only the earth sciences including ecology but also on the radiochemistry and other related sciences. This session focus on various efforts to understand the dynamic behavior of radionuclides emitted from FDNPP accident in the earth system as well as to predict their influences on the environment, furthermore, to develop as global migration studies by generalization. It is expected that this session will offer a good opportunity to summarize the research activities of the past ten years and deepen the discussion on cross-disciplinary research issues for the next ten years.

1:45 PM - 2:00 PM JST | 4:45 AM - 5:00 AM UTC

[MAG38-01] New X-ray spectroscopic methods for the speciation of cesium in environment

★Invited Papers

*Yoshio Takahashi[1], Hikaru Miura[3], Daisuke Tsumune[3], Yuichi Kurihara[2] (1.Department of Earth and Planetary Science, Graduate School of Science, The University of Tokyo, 2.JAEA, 3.CRIEPI)

2:00 PM - 2:15 PM JST | 5:00 AM - 5:15 AM UTC

[MAG38-02] 10-year variation of atmospheric Cs radioactivity concentration observed at highly polluted area in Fukushima

*Kazuyuki Kita[1], Naho Hayashi[1], Peng Tang[1], Kotaro Hatanaka[1], Takeshi Kinase[2], Kouji Adachi[2], Yuji Zaizen[2], Ishizuka Masahide[5], Jun Furukawa[3], Yuko Hatano[3], Keisuke Sueki[3], Yuichi Onda[3], Kazuhiko Ninomiya[4], SHINOHARA ATSUSHI[4], Sakae Toyoda[6], Keita Yamada[6], Naohiro Yoshida[6], Yukihiko Satou[7], Yasuhito Igarashi[8] (1.Faculty of Science, Ibaraki University, 2.Meteorological Research Instutite, 3.Tsukuba University, 4.Osaka University, 5.Kagawa University, 6.Tokyo Institute of Technology, 7.JAEA, 8.University of Kyoto)

2:15 PM - 2:30 PM JST | 5:15 AM - 5:30 AM UTC

[MAG38-03] Temporal variations and future estimations of ^{90}Sr and ^{137}Cs in atmospheric depositions after the Fukushima Daiichi Nuclear Power Plant accident with long-term observations

★Invited Papers

*Takeshi Kinase[1,2], Kouji Adachi[2], Thomas Sekiyama[2], Mizuo Kajino[2], Yuji Zaizen[2], Yasuhito Igarashi[3,4] (1.Japan Agency for Marine-earth Science and Technology, 2.Meteorological Research Institute, 3.Institute for Integrated Radiation and Nuclear Science, Kyoto University, 4.Ibaraki University)

2:30 PM - 2:45 PM JST | 5:30 AM - 5:45 AM UTC

[MAG38-04] Comprehensive evaluation on wet scavenging schemes for ^{137}Cs transport modeling following the Fukushima Daiichi accident

*Shuhan Zhuang[1], sheng fang[1] (1.Tsinghua University)

2:45 PM - 3:00 PM JST | 5:45 AM - 6:00 AM UTC

[MAG38-05] Migration and distribution of radiocesium in forest 10 years after the Fukushima nuclear accident

*Hiroaki Kato[1], Yuichi Onda[1], Zul Hilmi Saidin[1], Hikaru Iida[1], Satoru Akaiwa[1], Tomoki Shinozuka[1]
(1.Center for Research in Isotopes and Environmental Dynamics, University of Tsukuba)

3:00 PM - 3:15 PM JST | 6:00 AM - 6:15 AM UTC

[MAG38-06] Discussion

New X-ray spectroscopic methods for the speciation of cesium in environment

*Yoshio Takahashi[1], Hikaru Miura[3], Daisuke Tsumune[3], Yuichi Kurihara[2]

1. Department of Earth and Planetary Science, Graduate School of Science, The University of Tokyo, 2. JAEA, 3. CRIEPI

Speciation of cesium, or radiocesium, in environment is essential for the better understanding of its behavior in environment. For this purpose, X-ray absorption fine structure spectroscopy (XAFS) in fluorescence mode is one of most effective methods, but interference of Cs signal by signals from background elements (ca. calcium (Ca) and titanium (Ti)) is a severe problem to selectively obtain the signal from Cs. To overcome the difficulties, we have employed two methods, which are using (i) high energy resolution energy dispersive detector and (ii) wavelength dispersive detection system. In this presentation, the two methods were applied to chemical state of radiocesium (RCs) using X-ray absorption near-edge structure (XANES) analysis in fluorescence mode for the RCs incorporated into cesium-bearing silica microparticles (CsMP) categorized as B-type (non-spherical, with diameter about 500 μm; RCs concentration lower than 50 μg/g) emitted by Fukushima Dai-ichi Nuclear Power Plant (FDNPP) accident in 2011. It was difficult to observe X-ray fluorescence of Cs Lα emission in this CsMP using a silicon drift detector because the Cs concentration in the particle was three orders of magnitude smaller than the concentrations of calcium and titanium, which caused severe deterioration of the signal-to-background ratio of the Cs Lα emission line. In this study, a high energy resolution (ca. 5 eV FWHM) energy-dispersive transition edge sensor (TES) spectrometer was applied to XANES spectroscopy of trace elements in environmental materials for the first time, which enabled us to measure Cs LIII-edge XANES for RCs in CsMP. It was demonstrated that TES can be a powerful tool for the speciation of trace elements in environmental samples by fluorescence XANES considering its high energy resolution coupled with wide application range and simplicity of operation as energy-dispersive type detector. The results in this study revealed that RCs was dissolved into the silicate matrix. This information is consistent with the emission process that the type-B CsMP was formed by the cooling of melted materials during the FDNPP accident suggested in previous studies. We also employed another method using crystal analyzer coupled with Pilatus detector, instead of using TES. The energy resolution is even better than TES, which finally enables us to measure high energy resolution fluorescence detection (HERFD) XANES spectroscopy, which can give more information on the chemical state of Cs. The application of HERFD-XANES will be also given in this presentation.

©2021. Japan Geoscience Union. All Right Reserved.

10-year variation of atmospheric Cs radioactivity concentration observed at highly polluted area in Fukushima

*Kazuyuki Kita[1], Naho Hayashi[1], Peng Tang[1], Kotaro Hatanaka[1], Takeshi Kinase[2], Kouji Adachi[2], Yuji Zaizen[2], Ishizuka Masahide[5], Jun Furukawa[3], Yuko Hatano[3], Keisuke Sueki[3], Yuichi Onda[3], Kazuhiko Ninomiya[4], SHINOHARA ATSUSHI[4], Sakae Toyoda[6], Keita Yamada[6], Naohiro Yoshida[6], Yukihiko Satou[7], Yasuhito Igarashi[8]

1. Faculty of Science, Ibaraki University, 2. Meteorological Research Instutite, 3. Tsukuba University, 4. Osaka University, 5. Kagawa University, 6. Tokyo Institute of Technology, 7. JAEA, 8. University of Kyoto

Contineous obeservation of atmospheric activity concentration of radiocesium has been carried out at sites in highly polluted area in Fukushima for about 10 years from 2011. Reviews on trend and sesonal variation of atmospheric activity concentration and their causes, as well as atmospheric resuspension of insoluble Cs particles (CsMP) will be presented.

Keywords: radiocesium, atmospheric radioacitity

©2021. Japan Geoscience Union. All Right Reserved.

Temporal variations and future estimations of ^{90}Sr and ^{137}Cs in atmospheric depositions after the Fukushima Daiichi Nuclear Power Plant accident with long-term observations

*Takeshi Kinase[1,2], Kouji Adachi[2], Thomas Sekiyama[2], Mizuo Kajino[2], Yuji Zaizen[2], Yasuhito Igarashi[3,4]

1. Japan Agency for Marine-earth Science and Technology, 2. Meteorological Research Institute, 3. Institute for Integrated Radiation and Nuclear Science, Kyoto University, 4. Ibaraki University

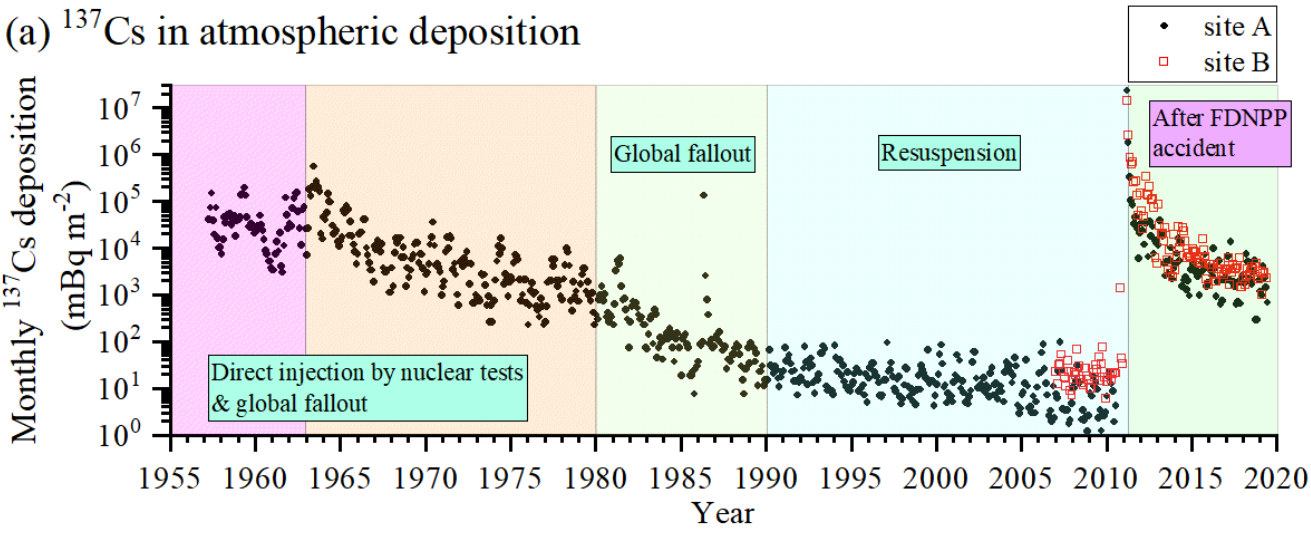
Atmospheric nuclear tests and nuclear power plant accidents have released artificial radionuclides into the atmosphere, land surface, and ocean. We have measured the artificial radionuclides, especially ^{90}Sr and ^{137}Cs, in atmospheric depositions since 1957 in the Kanto areas around Tokyo, Japan. As a result, we clarified the variations in ^{90}Sr and ^{137}Cs, which were emitted from atmospheric nuclear tests and nuclear power plant accidents, and their environmental processes due to their diffusion, deposition, and resuspension (figure). In March 2011, the Fukushima Daiichi Nuclear Power Plant (FDNPP) accident occurred in Japan, and significant increases in ^{90}Sr and ^{137}Cs were detected at our observation sites: a suburban site in the Kanto Plain (site A) and a top of the mountain in the northwestern corner of the Kanto Plain (site B), respectively. In this study, we show our long-term observation results of ^{90}Sr and ^{137}Cs in monthly atmospheric deposition samples collected at sites A and B and estimate the current environmental processes and decay periods of ^{90}Sr and ^{137}Cs with measurements of ^{134}Cs and stable elements and isotopes (Na, Mg, Al, K, Ca, Ti, Mn, Fe, Ni, Cu, Zn, Sr, Ba, ^{9}Be, ^{133}Cs, ^{232}Th, and ^{238}U).

During the period of plume arriving at site A from the FDNPP, ^{90}Sr and ^{137}Cs in monthly deposition samples increased to 2.7×10^{3} and 3.2×10^{6} times, respectively, higher than those before the accident. Our continual observations revealed that the peak of ^{137}Cs due to the FDNPP accident was much higher than those from the nuclear weapon tests and the Chernobyl accident. On the other hand, the peak of ^{90}Sr due to the FDNPP accident was lower than that from the nuclear weapon tests in the 1960s. The monthly deposition rate of ^{137}Cs in 2018 declined to ~1/8100 and ~1/4500 of the peak levels at sites A and B, respectively, but it remained more than ~400 and ~130 times higher than those before the accident. Cesium-134 was also measured at both sites until recent observations, implying that most of the radioactive Cs were originated from the FDNPP. The current ^{90}Sr deposition, on the other hand, has returned to the same radioactive level as that before the accident at both sites. The chemical analysis suggested that dust particles were the major carriers of ^{90}Sr and ^{137}Cs during the resuspension period at site A. On the other hand, at site B, ^{90}Sr was reserved and recycled in the forest, but the source of ^{137}Cs could not be identified. Presently, the effective half-lives for ^{137}Cs deposition at sites A and B due to radioactive decay and other environmental factors are estimated as 4.7 and 5.9 years, respectively. These estimations suggest that approximately 42 and 48 years from 2011 are required to reduce the atmospheric ^{137}Cs deposition to a state similar to that before the accident at sites A and B.

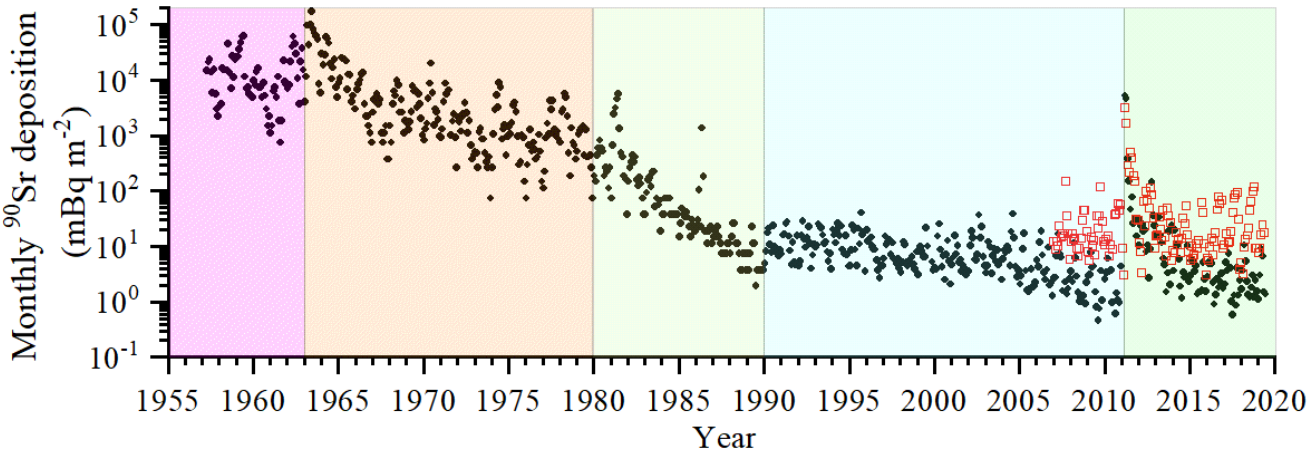
Keywords: Environmental radionuclide, Fukushima, Atmosphere, Resuspension, Deposition, Fallout

©2021. Japan Geoscience Union. All Right Reserved.

(a) ^{137}Cs in atmospheric deposition



(b) ^{90}Sr in atmospheric deposition



©2021. Japan Geoscience Union. All Right Reserved.

Comprehensive evaluation on wet scavenging schemes for ^{137}Cs transport modeling following the Fukushima Daiichi accident

*Shuhan Zhuang[1], sheng fang[1]

1. Tsinghua University

Wet deposition, including both the in-cloud and below-cloud scavenging, is critical for the atmospheric transport modeling of ^{137}Cs in the Fukushima Daiichi Nuclear power plant accident. Although intensively investigated, wet deposition simulation is still subject to uncertainties of meteorological input and wet scavenging modeling, leading to biased ^{137}Cs transmission prediction. To solve the problems, 25 different combinations of both the in- and below-cloud scavenging schemes were integrated into the Weather Research and Forecasting-Chemistry, realizing online coupled modeling of the wet scavenging processes and meteorology. With the same emission, meteorological input and WRF settings, these 25 models and their ensemble mean were systematically compared with a previous WRF-Chem model with a single below-cloud scheme on the same platform, based on both the cumulative deposition and ambient concentration of ^{137}Cs following the FDNPP accident. As far as we know, this is the first evaluation of both in- and below-cloud wet scavenging schemes based on the same online-coupled model, which may provide a clearer picture of the variation range among these schemes and the capability of WRF-Chem for ^{137}Cs transport modeling. The results demonstrate that the integration of the in-cloud scavenging scheme substantially improves the cumulative deposition simulation in light rain dominated area like Nakadori and around FDNPP, and the in-cloud schemes contribute predominately to the detailed deposition patterns, such as those in Nakadori area, which were missing in the previous below-cloud-only WRF-Chem. However, the 25 models show diverse behaviors in the presence of different meteorology for atmospheric concentration, though the ensemble mean achieves fair and stable performance for deposition and concentration under different plume events. Specifically, only the models considering cloud parameters show potential in optimizing the overall simulation, such as the Roselle-Bakla, Hertel-Bakla and Roselle-Apsimon. In comparison, the wet deposition models dependent only on the rain intensity are very sensitive to the meteorology. So, a combination of the in-cloud scheme with cloud parameters and a below-cloud scheme using a refined power function may be promising in improving the simulation of ^{137}Cs.

Keywords: wet deposition, in-cloud scavenging, below-cloud scavenging, WRF-Chem, Fukushima Daiichi Nuclear Power Plant accident

©2021. Japan Geoscience Union. All Right Reserved.

Migration and distribution of radiocesium in forest 10 years after the Fukushima nuclear accident

*Hiroaki Kato[1], Yuichi Onda[1], Zul Hilmi Saidin[1], Hikaru Iida[1], Satoru Akaiwa[1], Tomoki Shinozuka[1]

1. Center for Research in Isotopes and Environmental Dynamics, University of Tsukuba

In Japan's forests, field data on the distribution and migration of radiocesium deposited by the Fukushima Daiichi Nuclear Power Plant accident, from the initial dynamics to the distribution in the forest over ten years, have been vigorously collected. The results have been published in an IAEA technical report (IAEA-TECDOC-1927, 2020) as a database of migration parameters to be compiled by an international project (MODARIA II: Modelling and Data for Radiological Impact Assessments) promoted by the International Atomic Energy Agency (IAEA). Radiocesium's transfer mechanisms in the forest by hydrological processes and the runoff through the water system were summarized based on investigations in experimental forests and watersheds in Fukushima Prefecture. Besides, we outlined the missing links that need to be clarified by re-analysis of existing data and additional experiments based on previous studies on Fukushima and Chernobyl. Finally, we discussed the direction of future monitoring surveys.

Keywords: Fukushima nuclear accident, Forest, Radiocesium

©2021. Japan Geoscience Union. All Right Reserved.

[J] Oral | M (Multidisciplinary and Interdisciplinary) | M-AG Applied Geosciences

[M-AG38] Ten years after the Fukushima Dai-ichi NPP Accident : Dynamics of radionuclides in the environment

convener:Daisuke Tsumune(Central Research Institute of Electric Power Industry), Yuichi Onda(Center for Research on Isotopes and Environmental Dynamics, University of Tsukuba), Kazuyuki Kita(Faculty of Science, Ibaraki University), Yoshio Takahashi(Department of Earth and Planetary Science, Graduate School of Science, The University of Tokyo), Chairperson:Yuichi Onda(Center for Research on Isotopes and Environmental Dynamics, University of Tsukuba), Daisuke Tsumune(Central Research Institute of Electric Power Industry)

Sun. Jun 6, 2021 1:45 PM - 3:15 PM Ch.09 (Zoom Room 09)

Ten years have passed since the accident at the Tokyo Electric Power Company (TEPCO) Fukushima Daiichi Nuclear Power Station (NPP), which was triggered by the Great East Japan Earthquake and tsunami. Huge amount of radionuclides were emitted to the environment by the accident. They have been transported and diffused by atmospheric motion, depositing them to soil and vegetation. Deposited radionuclides are dynamically shifted in the earth environment; atmosphere, soil, inland water, ocean, and ecosystem. To understand this dynamic shift in the environment and for the long-term prediction of the disaster by the radionuclides, investigation and discussion based on not only the earth sciences including ecology but also on the radiochemistry and other related sciences. This session focus on various efforts to understand the dynamic behavior of radionuclides emitted from FDNPP accident in the earth system as well as to predict their influences on the environment, furthermore, to develop as global migration studies by generalization. It is expected that this session will offer a good opportunity to summarize the research activities of the past ten years and deepen the discussion on cross-disciplinary research issues for the next ten years.

3:00 PM - 3:15 PM

[MAG38-06]Discussion

©Japan Geoscience Union

[J] Oral | M (Multidisciplinary and Interdisciplinary)：M-AG Applied Geosciences

Sun. Jun 6, 2021 3:30 PM - 5:00 PM JST | Sun. Jun 6, 2021 6:30 AM - 8:00 AM UTC | Ch.09 Zoom Room 09

[M-AG38] Ten years after the Fukushima Dai-ichi NPP Accident : Dynamics of radionuclides in the environment

convener:Daisuke Tsumune(Central Research Institute of Electric Power Industry), Yuichi Onda(Center for Research on Isotopes and Environmental Dynamics, University of Tsukuba), Kazuyuki Kita(Faculty of Science, Ibaraki University), Yoshio Takahashi(Department of Earth and Planetary Science, Graduate School of Science, The University of Tokyo), Chairperson:Yoshio Takahashi(Department of Earth and Planetary Science, Graduate School of Science, The University of Tokyo), Kazuyuki Kita(Faculty of Science, Ibaraki University)

Ten years have passed since the accident at the Tokyo Electric Power Company (TEPCO) Fukushima Daiichi Nuclear Power Station (NPP), which was triggered by the Great East Japan Earthquake and tsunami. Huge amount of radionuclides were emitted to the environment by the accident. They have been transported and diffused by atmospheric motion, depositing them to soil and vegetation. Deposited radionuclides are dynamically shifted in the earth environment; atmosphere, soil, inland water, ocean, and ecosystem. To understand this dynamic shift in the environment and for the long-term prediction of the disaster by the radionuclides, investigation and discussion based on not only the earth sciences including ecology but also on the radiochemistry and other related sciences. This session focus on various efforts to understand the dynamic behavior of radionuclides emitted from FDNPP accident in the earth system as well as to predict their influences on the environment, furthermore, to develop as global migration studies by generalization. It is expected that this session will offer a good opportunity to summarize the research activities of the past ten years and deepen the discussion on cross-disciplinary research issues for the next ten years.

3:30 PM - 3:45 PM JST | 6:30 AM - 6:45 AM UTC

[MAG38-07] 10-year monitoring of ^{137}Cs transport in 30 river monitoring sites in 80km from the Fukushima Daiichi nuclear power plant

★Invited Papers

*Keisuke Taniguchi[1], Yuichi Onda[1], Kazuki Fujita[2], Yukio Takeuchi[2], Kazumi Katsuno[2], Hirotsugu Arai[2], Kouki Nasu[2] (1.Center for Research in Isotopes and Environmental Dynamics, University of Tsukuba, 2.Fukushima Prefectural Centre for Environmental Creation)

3:45 PM - 4:00 PM JST | 6:45 AM - 7:00 AM UTC

[MAG38-08] Impact of different land use along the Kasumigaura lake on suspended sediment delivery and particulate ^{137}Cs discharge

*Bin FENG[1], Yuichi Onda[1], Manabu Motohashi[1], Keisuke Taniguchi[1] (1.Center for research in isotopes and environmental dynamics, University of Tsukuba)

4:00 PM - 4:15 PM JST | 7:00 AM - 7:15 AM UTC

[MAG38-09] Ten years behavior of radiocaesium derived from TEPCO Fukushima Dai-ichi Nuclear Power Plant accident in surface water in the adjacent seas of the North Pacific Ocean

*Michio Aoyama[1,2], Yasunori Hamajima[3], Yayoi Inomata[3], Yuichiro Kumamoto[4], Hyoe Takata[2] (1.Center for Research in Isotopes and Environmental Dynamic, Faculty of Life and Environmental Sciences, University of Tsukuba, 2.Institute of Environmental Radioactivity, Fukushima University, 3.The Institute of Nature and Environmental Technolog, Kanazawa University, 4.Research Institute of Global Change, The Japan Agency for Marine-Earth Science and Technology)

4:15 PM - 4:30 PM JST | 7:15 AM - 7:30 AM UTC

[MAG38-10] On large-scale transport of suspended particulate matter on the continental shelf break off Fukushima, Japan.

*Kohei Kawano[1], Yusuke Uchiyama[1], Yuki - Kamidaira[2] (1.Graduate school of Engineering Faculty of Engineering, Kobe University, 2.Japan Atomic Energy Agency)

4:30 PM - 4:45 PM JST | 7:30 AM - 7:45 AM UTC

[MAG38-11] **Long-term simulation of oceanic ^{137}Cs with direct release and river discharge after the Fukushima Dai-ichi Nuclear Power Plant accident**

*Daisuke Tsumune[1], Tsubono Takaki[1], Kazuhiro Misumi[1], Hikaru Miura[1], Yutaka Tateda[1], Michio Aoyama[2]
(1.Central Research Institute of Electric Power Industry, 2.University of Tsukuba)

4:45 PM - 5:00 PM JST | 7:45 AM - 8:00 AM UTC

[MAG38-12] Discussion

10-year monitoring of ^{137}Cs transport in 30 river monitoring sites in 80km from the Fukushima Daiichi nuclear power plant

*Keisuke Taniguchi[1], Yuichi Onda[1], Kazuki Fujita[2], Yukio Takeuchi[2], Kazumi Katsuno[2], Hirotsugu Arai[2], Kouki Nasu[2]

1. Center for Research in Isotopes and Environmental Dynamics, University of Tsukuba, 2. Fukushima Prefectural Centre for Environmental Creation

Ten years have passed since the accident at TEPCO's Fukushima Daiichi Nuclear Power Plant (FDNPP). As a result of this accident, about 2.7 PBq of ^{137}Cs was deposited on the terrestrial area in eastern Japan. It is essential to clarify the transport of ^{137}Cs through rivers to ensure residents' safety living in the basin and understand the supply of ^{137}Cs to the ocean. Therefore, 30 river monitoring stations were set up in nine river basins located within 80 km of the FDNPP. We measured the radiocesium concentrations in suspended and dissolved forms and conducted a continuous observation of water level and turbidity at those stations. Monitoring began in 2011 at six stations located on the Abukuma River and its tributary. At the other 24 stations, monitoring began in 2012. Suspended sediment (SS) samplers were set up at each station to measure the suspended ^{137}Cs concentrations. SS samples were collected from the sampler every few weeks to months, dried, and the radioactivity concentration was measured with a germanium semiconductor detector. 60-100 L of river water was collected every few months to half a year. The river water was filtered through a membrane filter with a pore size of 0.45 μm, and the radiocesium dissolved in the filtrate was collected by the AMP coprecipitation method or the cation exchange resin method. Then, the radioactivity concentration was measured by a germanium semiconductor detector. The solid-liquid distribution coefficient (Kd) of ^{137}Cs was calculated by dividing the suspended ^{137}Cs concentration by the dissolved ^{137}Cs concentration. Water discharge (Q) and SS concentration (SSC) were calculated from water level and turbidity data. The SS flux (Qss) was calculated by multiplying Q by SSC, and the ^{137}Cs flux (L) was calculated by multiplying Qss by the ^{137}Cs concentration in the relevant period. During the ten years after the FDNPP accident, the concentration of ^{137}Cs in both dissolved and suspended forms decreased significantly. After a sharp decrease in concentration during the first year after the accident, a slightly slower declining trend was observed after the second year. The effective environmental half-lives (T_{eff}) of ^{137}Cs concentrations were about 0.11(4 sites) and 0.57 years (6sites) in the dissolved and suspended forms in the first year after the FDNPP accident. After the second year, the T_{eff}s were about 2.4 years in the dissolved form (29 sites) and about 3.0 years in the suspended form (29 sites). The Kd did not show any temporal change, and its geometric mean value was 2.9×10^5 L/kg (30 sites). The ^{137}Cs flux from the Abukuma River to the Pacific Ocean from August 2011 to December 2019 was about 49 TBq, which is 2.4% of the initial deposition. The ^{137} Cs discharged from August 2011 to March 2012 is 0.9%, while the flux transported in 2019 has decreased to about 0.19%. About 80 % of the 2019 flux was released in October when the heavy rains by Typhoon Hagibis occurred. After the Chernobyl nuclear power plant accident in European rivers, the decline in the ^{137}Cs concentration became more gradual around the seventh year. Similar trends may be observed in Fukushima's rivers. Also, there are still concerns that ^{137}Cs may be supplied to downstream areas via rivers from the forests located upstream. Therefore, it is necessary to continue to accumulated data and monitor the trends.

Keywords: Cesium-137, River, Fukushima Daiichi nuclear power plant accident

©2021. Japan Geoscience Union. All Right Reserved.

Impact of different land use along the Kasumigaura lake on suspended sediment delivery and particulate ^{137}Cs discharge

*Bin FENG[1], Yuichi Onda[1], Manabu Motohashi[1], Keisuke Taniguchi[1]

1. Center for research in isotopes and environmental dynamics, University of Tsukuba

Large quantities of ^{137}Cs released from the Fukushima Daiichi nuclear power plant are being continuously transported from surrounding rivers into Kasumigaura lake (Ibaraki prefecture), which may pose a potential radiation threat to millions of residents' health and the local industrial development. Given over 95% of ^{137}Cs in the river tightly combined with suspended sediment (SS), learning the dynamic variation in particulate 137Cs input/discharge and the behind mechanisms controlling their migration is essential for this region. Land use is usually viewed as a critical factor affecting sediment yield and ^{137}Cs inventory. Particularly in rain season, its difference in soil erodibility would be significantly amplified, altering fluvial sediment supply and particulate ^{137}Cs discharge. However, due to the lack of long-term river monitoring in Kasumigaura lake region, the dynamic variation in fluvial SS and particulate ^{137}Cs are still unknown, which also hamper our ability to learn the impact of land use differences on the ^{137}Cs dynamic transport.

To fill this knowledge gap, we conducted a six-year monitoring campaign in two sub-catchments (i.e., Koise river basin and Sakura river basin) where the former has a higher forest proportion, and the latter one has a higher agricultural land proportion. The river monitoring dataset shows the turbidity is significantly correlated with water discharge in Koise, whereas this relationship is not evident in Sakura. Through the hysteresis analysis, we discover that hysteresis type 3 appeared more frequently in Koise, suggesting the existence of delayed SS supply. The ^{137}Cs monitoring dataset demonstrates both sites present a significant exponential decrease trend in particulate ^{137}Cs concentration, but the activities in Koise are slightly higher. Furthermore, the estimated ^{137}Cs fluxes were also found higher in Koise. Considering the forest is usually farther from rivers and has a higher ^{137}Cs entrainment coefficient, these scenarios are thought as the result of the difference in sediment supply due to their different land use composing proportions. Additionally, combining synchronous rainfall records, we find both water discharge and sediment load in two catchments responded extremely well to rainfall, confirming the significant role of precipitation in fluvial sediment supply. Furthermore, we also utilize meteorological radar data, quantified land use, and ^{137}Cs inventory to reconstrue the spatial distribution of ^{137}Cs loss, which provides a potential tool to predict the ^{137}Cs loss with watershed characteristics.

Keywords: land use, suspended sediment dynamic, particulate 137Cs discharge, Fukushima nuclear accident

©2021. Japan Geoscience Union. All Right Reserved.

Ten years behavior of radiocaesium derived from TEPCO Fukushima Dai-ichi Nuclear Power Plant accident in surface water in the adjacent seas of the North Pacific Ocean

*Michio Aoyama[1,2], Yasunori Hamajima[3], Yayoi Inomata[3], Yuichiro Kumamoto[4], Hyoe Takata[2]

1. Center for Research in Isotopes and Environmental Dynamic, Faculty of Life and Environmental Sciences, University of Tsukuba, 2. Institute of Environmental Radioactivity, Fukushima University, 3. The Institute of Nature and Environmental Technolog, Kanazawa University, 4. Research Institute of Global Change, The Japan Agency for Marine-Earth Science and Technology

After the accident at TEPCO Fukushima Dai-ichi Nuclear Power Plant, hereafter FNPP1, the caesium-137 radioactivity concentration of caesium-137 in surface water increased sharply in a wide area in the western North Pacific Ocean, and then dropped sharply or gradually decreased according to the distance from the FNPP1. In the marginal seas of the North Pacific Ocean (Sea of Japan and East China Sea), a delay was observed in the increase in the concentration of caesium-137 radioactivity concentration, and the characteristics of time change were different from those in the North Pacific Ocean. An apparent characteristic of caesium-137 radioactivity concentration was a gradual decrease from 2012 in the Ogasawara region which locates in the subtropical gyre, and recently it is about the same as or lower than caesium-137 activity concentration in surface water in the Sea of Japan. However, in the southern part of the Sea of Japan, caesium-137 activity concentration reached its maximum in 2016 and then gradually decreased until 2020. The other situation was observed eg. the activity concentration of caesium-137 remained almost unchanged from 2017 to 2020 at around the Yonaguni Island, which is the entrance to the East China Sea from the North Pacific. The apparent half-life due to advection-diffusion after radioactive decay correction was 18.9 years for the Ogasawara region for the period 2012-2020 and 12.3 years for 2016-2020, while it is slightly longer at 22.4 years for 2016-2020 in the southern part of the Sea of Japan. On the other hand, in the vicinity of Yonaguni Island, there is no change or a slight increase in 2017-2020. Also, the 134Cs / 137Cs ratio increased in the vicinity of Yonaguni Island, reaching ca. 0.5 in 2020, which is about the same as those observed at Ogasawara and the Sea of Japan. These transports mainly follow the subtropical gyre. Regarding the transport of radioactive caesium to the northern part of the East China Sea and the Sea of Japan, a part of the radioactive cesium derived from FNPP1 in the subtropical mode water moved to the west, reached the bottom of the East China Sea, and then abducted to the surface layer and transported to the Sea of Japan. The transportation process by the main route of the subtropical gyre is considered to have taken longer than the shortcut to the Sea of Japan via the ocean interior of the North Pacific as mentioned above.

Keywords: TEPCO Fukushima Dai-ichi Nuclear Power Plant accident, radiocaesium, subtropical gyre, transport, half life

©2021. Japan Geoscience Union. All Right Reserved.

On large-scale transport of suspended particulate matter on the continental shelf break off Fukushima, Japan.

*Kohei Kawano[1], Yusuke Uchiyama[1], Yuki - Kamidaira[2]

1. Graduate school of Engineering Faculty of Engineering, Kobe University, 2. Japan Atomic Energy Agency

The Fukushima Dai-ichi Nuclear Power Plant (FNPP1) was damaged by the catastrophic tsunamis as the aftermath of the 2011 off the Pacific coast of Tohoku Earthquake occurred on March 11, 2011, leading to accidental leakages of radionuclide to the environment. Previous studies have investigated the released radionuclides to the ocean through the direct discharge at FNPP1 and the initial atmospheric deposition to monitor and quantify the amount of radioactivity in seawater, marine sediments, and marine organisms. Among others, the sediment trap data at two offshore stations, one at ~100 km east of FNPP1 (Otosaka et al., 2014) and the other at ~100 km southeast of the FNPP1 (Buesseler et al., 2015), have detected a substantial amount of suspended radiocesium absorbed into marine particles such as sediments originated from the FNPP1 accident, even in the deep ocean at depths of 500-1000 m. These results suggest that large-scale transport and dispersal of suspended radionuclides at O (100 km) could have occurred in the offshore direction to reach the continental shelf breaks. A high-resolution numerical ocean modeling study by Yamanishi et al. (2016) also reported that there might be sediment transport over the shelf break off FNPP1.

This study aims to demonstrate occurrences of such sediment transport to the deep ocean, and to identify possible mechanisms responsible for large-scale processes. To this end, a STEAMER-ROMS ocean circulation model in a double nested configuration forced by the MOVE-WNP oceanic reanalysis was developed, coupled with the multi-class sediment transport model along with a two-layer stratigraphy model of the marine bed and the SWAN spectral wave model. The inner-most ROMS-L2 model, which encompasses the coastal ocean from Ibaraki up until Iwate and stretches eastward beyond the Japan Trench, was exploited to conduct a reanalysis of 3-D oceanic sediment transport for 14 months after the FNPP1 accident at a horizontal grid resolution of 600 m. The ROMS-L2 model clarifies that large-scale sediment transport has occurred extensively. In particular, clay-class sediments have frequently extended to the offshore sediment trap sites, due primarily to eddy-induced transport. Four typical sediment transport pathways are identified: 1) entrainment in offshore migrating topographically-generated mesoscale eddies enhanced by the southward coastal currents, 2) entrainment in mesoscale pinch-off eddies detached from or on the Kuroshio and its extension jet, 3) intermittent onshore transport of deep-ocean sediments resuspended over deep seamount topography on the Japan Trench, and 4) local resuspension on the continental shelf slope under influences of internal tides.

Keywords: suspended particulate, large-scale transport

©2021. Japan Geoscience Union. All Right Reserved.

Long-term simulation of oceanic ^{137}Cs with direct release and river discharge after the Fukushima Dai-ichi Nuclear Power Plant accident

*Daisuke Tsumune[1], Tsubono Takaki[1], Kazuhiro Misumi[1], Hikaru Miura[1], Yutaka Tateda[1], Michio Aoyama[2]

1. Central Research Institute of Electric Power Industry, 2. University of Tsukuba

A series of accidents at the Fukushima Dai-ichi Nuclear Power Plant (1F NPP) following the Great East Japan Earthquake and tsunami of 11 March 2011 resulted in the release of radioactive materials to the ocean. We used the Regional Ocean Model System (ROMS) to simulate the ^{137}Cs activity in the oceanic area off Fukushima, with the sources of radioactivity being direct release, atmospheric deposition, river discharge, and inflow across the domain boundary. Note that atmospheric fallout was only considered for the first month after the accident.

Measured137 Cs activity adjacent to the 1F NPP decreased exponentially with a variation of about one order of magnitude by July 2016 and has not decreased since then. The measured ^{137}Cs activity was higher than the one before the 1F NPP accident, therefore direct release from the 1F NPP site have continued to present. One possible reason for the no decrease in measured ^{137}Cs activity since July 2016 is the impact of river discharge. In this study, measured ^{137}Cs activity adjacent to the 1F NPP was assumed to be due to direct release from the 1F NPP site, and the direct release rate was estimated by the comparison between measured data adjacent to the 1F NPP and model simulation with unit release rate.

The longer-term simulation was carried out by the estimated direct release rate until September 2020. Because the spatiotemporal variability of ^{137}Cs activity was large, the simulated results were compared with the annual averaged observed ^{137}Cs activity distribution. Simulated ^{137}Cs activity was in good agreement with measurement data in 2013. The simulated ^{137}Cs activity become smaller than the observed ones in the coastal area away from the 1F NPP site after 2014. This suggests that the impact of river discharge has become relatively larger with the decrease of direct release. Normalized annual averaged ^{137}Cs activity distributions in the regional ocean were similar for each year from 2013 to 2016. This result suggests that the annual averaged distribution is predictable. The heavy rainfall caused by the typhoon in October 2019 increased the measured ^{137}Cs activity adjacent to the 1F NPP, 2F NPP and Iwasawa coast, and the increase continued for 6 months. The simulated ^{137}Cs activity with direct release were about 7 times smaller than the measured one for 6 months after heavy rain. The increase in river flow rate due to heavy rainfall was on a scale of a few days or less, and the discharge of dissolved forms is considered to be on a much shorter time scale than six months. Since the dissolved ^{137}Cs flux from rivers was small and the impact was expected to be short-lived, it is suggested that the impact may be due to re-leaching from particle ^{137}Cs deposited in estuaries.

Keywords: Fukushima Daiichi Nuclear Power Plant accident, Radioactive cesium, Regional ocean model, Direct release, River discharge

©2021. Japan Geoscience Union. All Right Reserved.

[J] Oral | M (Multidisciplinary and Interdisciplinary) | M-AG Applied Geosciences

[M-AG38] Ten years after the Fukushima Dai-ichi NPP Accident : Dynamics of radionuclides in the environment

convener:Daisuke Tsumune(Central Research Institute of Electric Power Industry), Yuichi Onda(Center for Research on Isotopes and Environmental Dynamics, University of Tsukuba), Kazuyuki Kita(Faculty of Science, Ibaraki University), Yoshio Takahashi(Department of Earth and Planetary Science, Graduate School of Science, The University of Tokyo), Chairperson:Yoshio Takahashi(Department of Earth and Planetary Science, Graduate School of Science, The University of Tokyo), Kazuyuki Kita(Faculty of Science, Ibaraki University)

Sun. Jun 6, 2021 3:30 PM - 5:00 PM Ch.09 (Zoom Room 09)

Ten years have passed since the accident at the Tokyo Electric Power Company (TEPCO) Fukushima Daiichi Nuclear Power Station (NPP), which was triggered by the Great East Japan Earthquake and tsunami. Huge amount of radionuclides were emitted to the environment by the accident. They have been transported and diffused by atmospheric motion, depositing them to soil and vegetation. Deposited radionuclides are dynamically shifted in the earth environment; atmosphere, soil, inland water, ocean, and ecosystem. To understand this dynamic shift in the environment and for the long-term prediction of the disaster by the radionuclides, investigation and discussion based on not only the earth sciences including ecology but also on the radiochemistry and other related sciences. This session focus on various efforts to understand the dynamic behavior of radionuclides emitted from FDNPP accident in the earth system as well as to predict their influences on the environment, furthermore, to develop as global migration studies by generalization. It is expected that this session will offer a good opportunity to summarize the research activities of the past ten years and deepen the discussion on cross-disciplinary research issues for the next ten years.

4:45 PM - 5:00 PM

[MAG38-12]Discussion

©Japan Geoscience Union

[J] Poster | M (Multidisciplinary and Interdisciplinary)：M-AG Applied Geosciences

Sun. Jun 6, 2021 5:15 PM - 6:30 PM JST | Sun. Jun 6, 2021 8:15 AM - 9:30 AM UTC | Ch.21_3

[M-AG38] Ten years after the Fukushima Dai-ichi NPP Accident : Dynamics of radionuclides in the environment

convener:Daisuke Tsumune(Central Research Institute of Electric Power Industry), Yuichi Onda(Center for Research on Isotopes and Environmental Dynamics, University of Tsukuba), Kazuyuki Kita(Faculty of Science, Ibaraki University), Yoshio Takahashi(Department of Earth and Planetary Science, Graduate School of Science, The University of Tokyo)

Ten years have passed since the accident at the Tokyo Electric Power Company (TEPCO) Fukushima Daiichi Nuclear Power Station (NPP), which was triggered by the Great East Japan Earthquake and tsunami. Huge amount of radionuclides were emitted to the environment by the accident. They have been transported and diffused by atmospheric motion, depositing them to soil and vegetation. Deposited radionuclides are dynamically shifted in the earth environment; atmosphere, soil, inland water, ocean, and ecosystem. To understand this dynamic shift in the environment and for the long-term prediction of the disaster by the radionuclides, investigation and discussion based on not only the earth sciences including ecology but also on the radiochemistry and other related sciences. This session focus on various efforts to understand the dynamic behavior of radionuclides emitted from FDNPP accident in the earth system as well as to predict their influences on the environment, furthermore, to develop as global migration studies by generalization. It is expected that this session will offer a good opportunity to summarize the research activities of the past ten years and deepen the discussion on cross-disciplinary research issues for the next ten years.

[MAG38-P01] Effects of preferential flow on the spatial heterogeneity and chemical form of Cs-137 in a forest soil

*Junko Takahashi[1], Tetsuya Ono[1], Takuya Sasaki[1], Yuichi Onda[1] (1.Center for Research in Isotopes and Environmental Dynamics, University of Tsukuba)

[MAG38-P02] Contribution of fungal hyphal elongation to radiocesium transfer in deciduous broad-leaved litter

*Yoshito Sasaki[1], Tadafumi Niizato[1], Hiroki Amamiya[2], Kaori Yoshida[1] (1.Japan Atomic Energy Agency, 2.QJ science)

[MAG38-P03] The ^{137}Cs dynamics in a pond of urban area after decontamination

*Honoka Kurosawa[1], Misaki Usuki[1], Shota Moritaka[1], Kenji Nanba[2], Toshihiro Wada[2], Yoshifumi Wakiyama[2] (1.Graduate School of Symbiotic Systems Science and Technology, Fukushima University, 2.Institute of Environmental Radioactivity, Fukushima University)

[MAG38-P04] Variations in riverine ^{137}Cs concentration and its exportation to the ocean during high-flow events at three rivers in Hamadori area

Takuya Niida[1], *Yoshifumi Wakiyama[2], Hyoe Takata[2], Kazuki Fujita[3], Keisuke Taniguchi[4], Alexei Konoplev[2] (1.Graduate School of Symbiotic System and Technology, Fukushima Universiy, 2.Institute of Environmental Radioactivity, Fukushima Universiy, 3.Fukushima Prefectural Centre for Environmental Creation, 4.Center for Research in Isotope and Environmental Dynamics, University of Tsukuba)

[MAG38-P05] Comparison of cesium-bearing microparticles from marine and terrestrial sources

*Hikaru Miura[1], Atsushi Kubo[2], Takashi Ishimaru[3], Yukari Ito[3], Jota Kanda[3], Daisuke Tsumune[1], Yoshio Takahashi[4] (1.Central Research Institute of Electric Power Industry, 2.Shizuoka University, 3.Tokyo University of Marine Science and Technology, 4.The University of Tokyo)

Effects of preferential flow on the spatial heterogeneity and chemical form of Cs-137 in a forest soil

*Junko Takahashi[1], Tetsuya Ono[1], Takuya Sasaki[1], Yuichi Onda[1]

1. Center for Research in Isotopes and Environmental Dynamics, University of Tsukuba

1. Introduction

Rainfall infiltration is one of the most important mechanisms of downward migration of Cs-137 in forest soils. It has been pointed out that rainwater infiltration in soil can be divided into two types, which are relatively uniform matrix flow and non-uniform preferential flow through coarse pores and root surfaces. This preferential flow would contribute the downward migration of various substances, therefore it is possible that this preferential flow is a factor in the spatial heterogeneity of the vertical distribution of Cs-137 in soil. However, there have been few studies that have quantitatively evaluated the effects of preferential flow on the vertical distribution of Cs-137. In the presnt study, we conducted an artificial rainfall experiment using dyes in a forest and collected soil samples from dyed and un-dyed areas at different depths in order to quantify the spatial heterogeneity and chemical form of Cs-137.

2. Material and methods

The study site was a cedar forest located in Akougi district, Namie-town, Fukushima Prefecture. The estimated deposition amount by airborne monitoring was about 4700 kBq/m^2. One plot with 1 m x 1 m was set up in the forest, and 10 L of distilled water containing 2 g/L of Rhodamine B was sprayed by a simple sprinkler system as a dye, corresponding to a rainfall amount of 10 mm and the rainfall intensity of about 120 mm/h. Two days after sprinkling, a scraper plate was placed under the litter layer, and the visually dyed soil were collected little by little using a spoon, and then the un-dyed soil were collected. The sampling depths were 0-2 cm, 2-4 cm, 4-6 cm, and 6-10 cm. Although the soil was classified as a non-allophanic Andosol, these surface soil samples did not have andic properties. After air-drying and sieving, the soil samples were sequentially extracted (F1: water-soluble form, F2: exchangeable form, F3: Fe-Mn oxides form, F4: organic matter-bound form, F5: acid-soluble form, F6: residue). The concentrations of Cs-137 and several main elements in each solution were measured using a Ge semiconductor detector and atomic absorption spectrometer. In addition, several chemical properties of soil samples were determined.

3. Results

The dyed soil samples in all layers had higher root and fresh organic matter contents per unit soil weight, higher soil organic matter content, higher CEC, and higher water-soluble and exchangeable cation contents than those in the un-dyed soil samples. The ratios of Cs-137 concentrations in the dyed and un-dyed samples at the same depth were 0.98, 1.48, 1.51, and 2.64 for 0-2, 2-4, 4-6, and 6-10 cm, respectively. This suggests that the preferential flow played an important factor in the spatial heterogeneity of Cs-137 vertical distribution and the pathway of the preferential flow was relatively stable even after nearly 10 years from the accident. As a result of sequential extraction, the average percentages of Cs-137 at each depth in dyed and un-dyed samples were 0.031% and 0.022% in the F1 fraction, 1.10% and 0.97% in the F2 fraction, 0.57% and 0.50% in the F3 fraction, 3.64% and 3.12% in the F4 fraction, and 43.2% and 40.7% in the F5 fraction, showing that the dyed samples tended to be slightly higher in all fractions except the residue. This result suggested that plant-available Cs-137, especially

©2021. Japan Geoscience Union. All Right Reserved.

water soluble and exchangeable form, may be accumulated in areas where preferential flow frequently permeate, such as around the roots. Therefore, it is considered that the effects of preferential flow are important not only for the downward migration but also for the evaluation of root absorption.

Keywords: preferential flow, dye tracer, downward migration

©2021. Japan Geoscience Union. All Right Reserved.

Contribution of fungal hyphal elongation to radiocesium transfer in deciduous broad-leaved litter

*Yoshito Sasaki[1], Tadafumi Niizato[1], Hiroki Amamiya[2], Kaori Yoshida[1]

1. Japan Atomic Energy Agency, 2. QJ science

Radiocesium deposited in the forest released by the accident at the Fukushima Daiichi Nuclear Power Station would remain in the forest and part of it would circulate due to the small amount of outflow from the forest. One possible source of dissolved radiocesium that is easily taken up by organisms is the litter layer. To clarify the contribution of fungal mycelial elongation in the transfer of radiocesium in the litter layer, we investigated the effect of the presence of fungi on the transfer of radiocesium from litter Cs (H) with high radiocesium concentration to litter Cs (L) with low radiocesium concentration. Fungal growth was observed in the test plots where the fungi were present. Regardless of with or without fungi, the Cs-137 concentration of Cs (L) reached about 50 Bq / kg on the 50th day, and then gradually increased to about 100 Bq / kg on the 150th day. This result suggested that the radiocesium was transfered by a physical force other than the hyphal elongation of the fungus in the litter layer.

Keywords: radiocesium, deciduous broad-leaved tree, litter layer, Fukushima Dai-ichi Nuclear Power Plant accident

©2021. Japan Geoscience Union. All Right Reserved.

The ^{137}Cs dynamics in a pond of urban area after decontamination

*Honoka Kurosawa[1], Misaki Usuki[1], Shota Moritaka[1], Kenji Nanba[2], Toshihiro Wada[2], Yoshifumi Wakiyama[2]

1. Graduate School of Symbiotic Systems Science and Technology, Fukushima University, 2. Institute of Environmental Radioactivity, Fukushima University

More than 4,000 irrigation ponds in Fukushima Prefecture have been contaminated by radiocaesium released from the Fukushima Dai-ichi Nuclear Power Plant accident. The contaminated pond would cause problems such as increase of air dose rates around the pond by water drawdown and prevention of the restart/reconstruction of farming and agricultural activities. As a countermeasure, the decontamination has been conducted for ponds with more than 8,000 Bq/kgDW of radiocaesium (^{134}Cs+^{137}Cs) concentration in its bottom sediment. This study aims to evaluate the effect of decontamination and presents investigations on ^{137}Cs concentration in bottom sediment, pond water, inflow water, and outflow water at a decontaminated pond locate in urban area.
Study site is the Sakabuta pond located in urban area of Koriyama city. The decontamination was carried out in 2017. Bottom sediment was collected in 2015, 2018 and 2020. Bottom sediment was basically collected at 2 points around cage for commercial aquaculture of carp and additionally at 5 points in the whole pond once a year. The depth of 0-20 cm, 20-30 cm, and 30 cm or more was cut for 1 cm, 2 cm, 5 cm interval, respectively. Pond water was collected in 2015, 2018, and 2020, simultaneous to bottom sediment sampling. Inflow and outflow water was collected in 2020. The ^{137}Cs concentration in bottom sediment, pond, inflow, and outflow water were measured with the Ge semiconductor detector.
The ^{137}Cs concentrations in bottom sediment and pond water were compared between before and after decontamination. The ^{137}Cs concentrations in the top layer of bottom sediment at 2 points around cage were decreased from 36,100 and 25,500 Bq/kgDW to 15,800 and 15,300 Bq/kgDW. The ^{137}Cs concentration in pond water was decreased from 1.40 Bq/L to 0.950 Bq/L. It was said that the decontamination was effective because the ^{137}Cs concentrations in the top layer of the bottom sediment and pond water were significantly decreased by decontamination. However, the ^{137}Cs concentration in the top layer of bottom sediment was 8,000 Bq/kgDW or more even after decontamination. The ^{137}Cs concentrations in the top layer of bottom sediment at 5 points in the whole pond were 16,700-44,300 Bq/kgDW in 2015, 3,630-12,200 Bq/kgDW in 2018, and 6,800-13,500 Bq/kgDW in 2019.The layer of more than 8,000 Bq/kgDW of radiocesium concentration in the bottom sediment of 2019 was thicker than that of 2018. In 2019, Hagibis passed through about a month before the bottom sediment collection and increase of ^{137}Cs in 2019 was attributed to suspended solid input due to the typhoon. The sedimentary environments were compared between the points with more and less than 8,000 Bq/kgDW of raciocesium concentration. At the point with less than 8,000 Bq/kgDW of radiocesium concentration, it was suggested that new particle was not deposited after decontamination. However, at the point with more than 8,000 Bq/kgDW of radiocesium concentration, it was suggested that new particle was deposited after decontamination. The ^{137}Cs concentration in suspended solids of pond water was more than 8,000 Bq/kgDW even after the decontamination. Furthermore, the ^{137}Cs concentration in suspended solids of inflow water sometimes exceeded 8,000 Bq/kgDW. These results suggested that a large amount of soil particle would flow into the pond during the rainfall events, resulting in high concentration of ^{137}Cs in the top layer of bottom sediment.

Keywords: Fukushima Dai-ichi Nuclear Power Plant accident, Cs-137, Pond, decontamination

©2021. Japan Geoscience Union. All Right Reserved.

©2021. Japan Geoscience Union. All Right Reserved.

Variations in riverine ^{137}Cs concentration and its exportation to the ocean during high-flow events at three rivers in Hamadori area

Takuya Niida[1], *Yoshifumi Wakiyama[2], Hyoe Takata[2], Kazuki Fujita[3], Keisuke Taniguchi[4], Alexei Konoplev[2]

1. Graduate School of Symbiotic System and Technology, Fukushima Universiy, 2. Institute of Environmental Radioactivity, Fukushima Universiy, 3. Fukushima Prefectural Centre for Environmental Creation, 4. Center for Research in Isotope and Environmental Dynamics, University of Tsukuba

A considerable amount of ^{137}Cs deposited on terrestrial is exported to the ocean during high-flow events. Recent studies have reported increases of dissolved ^{137}Cs concentration in near-shore water after high-flow events assumedly due to desorption of ^{137}Cs from suspended solids. Existing literature on riverine ^{137}Cs dynamics during high-flow events have focused on upstream area, but little attention has been paid to downstream area. It remains uncertainties in transfer process of terrestrial ^{137}Cs to the ocean. This study aims to elucidate riverine ^{137}Cs dynamics and its influence on the ocean environment and presents analyses of river water samples taken at three rivers in the Hamadori area during high-flow events. River water samples were taken at 5 times at Haramachi site (206 km^2, 853 kBq m^{-2}) in the Niida river catchment, 3 times at Kiyobashi site (147 km^2, 2360 kBq m^{-2}) in the Ukedo river catchment, and 3 times at Takase site (262 km^2, 701 kBq m^{-2}) in the Takase river catchment during high-flow events occurred in the period of 2016-2020. Five to eight samples were taken per event and particulate and dissolved ^{137}Cs concentrations were measured. When sufficient amount of suspended solid was obtained, ^{137}Cs speciation and ^{137}Cs desorption by seawater were further analyzed. Mean ^{137}Cs concentration in suspended solid in the Niida, Ukedo, Takase rivers were 5100 Bq kg^{-1} (n = 32, CV = 40%), 23000 Bq kg^{-1} (n = 20, CV = 97%), and 4600 Bq kg^{-1} (n = 20, CV=46%), respectively. Mean dissolved ^{137}Cs concentration at the Niida, Ukedo, Takase rivers were 16 mBq L^{-1} (n = 32, CV = 53%), 73 mBq L^{-1} (n = 20, CV = 55%), and 15 mBq L^{-1} (n =20, CV = 40%), respectively. Concentration of ^{137}Cs in suspended solid was positively correlated with specific water discharge rate for three rivers. Dissolved ^{137}Cs concentration also showed positive correlation with specific water discharge rate, except for Takase river. Exportation of ^{137}Cs increased with increase of total rainfall amount and ranged from 6.6 to 60 GBq from the Niida river catchment, from 1.9 to 8.8 GBq from the Ukedo river catchment, and from 2.8 to 13 GBq from the Takase river catchment. The Ukedo river catchment showed low ratio of ^{137}Cs exportation to the total ^{137}Cs deposition in the catchment and low ratio of particulate ^{137}Cs exportation to the total ^{137}Cs exportation. They infered influences of the Ogaki dam located at midstream in the catchment. Ratio of ^{137}Cs desorbed by seawater to ^{137}Cs in suspended solid ranged from 2.8 to 6.6% and tended to be high for suspended solid with high exchangeable ^{137}Cs ratio. By assuming the ratio of desorption, potential release of ^{137}Cs from suspended solid to the ocean was estimated. The estimates for corresponded events ranged from 0.19 to 2.8 GBq. These values were 0.8-15 times higher than dissolved ^{137}Cs exportation. These results suggest that secondary release of ^{137}Cs from terrestrial suspended solid can be one of factor determining dissolved ^{137}Cs concentrations in the near-shore sea.

Keywords: River, Radiocesium, Suspended solid

©2021. Japan Geoscience Union. All Right Reserved.

Comparison of cesium-bearing microparticles from marine and terrestrial sources

*Hikaru Miura[1], Atsushi Kubo[2], Takashi Ishimaru[3], Yukari Ito[3], Jota Kanda[3], Daisuke Tsumune[1], Yoshio Takahashi[4]

1. Central Research Institute of Electric Power Industry, 2. Shizuoka University, 3. Tokyo University of Marine Science and Technology, 4. The University of Tokyo

Radionuclides including radioactive Cs were released into the environment due to the Fukushima Daiichi Nuclear Power Plant accident in 2011. Two years after the accident, glassy water-resistant particles incorporating radioactive Cs were first reported. Such glassy particles are called cesium-bearing microparticles (CsMPs). CsMPs have been studied because (i) they have information on the condition in the reactor at the time of the accident, and (ii) there is concern about the exposure to the humans and the other organisms.

Several types of CsMPs have been reported, which is assumed to reflect the difference in the accidental progress of each unit. It is also known that CsMPs were transported in the atmospheric plume at the time of emission and therefore have different deposition regions. Type-A CsMPs, are presumed to originate from Unit 2, deposited over a wide area including the Kanto region due to their small size (~0.1–10 μm). Type-B CsMPs, are presumed to originate from Unit 1, deposited in a limited area in the north direction because of their large size (50–400 μm). Matrix of Types-A and -B CsMPs is SiO_2 but Type-A CsMPs have higher concentration of volatile elements including Cs than Type-B CsMPs due to the difference in forming process. Type-A CsMPs were formed through gas condensation, whereas Type-B CsMPs were formed through melt solidification.

The presence of CsMPs emitted from Unit 3 in the ocean was confirmed by our research. The plume at the time of the emission of radionuclides from Unit 3 was in the ocean direction, which suggests that many CsMPs from Unit 3 deposited directly into the ocean. We will report the comparison of CsMPs from marine and terrestrial sources. In addition, we reported Type-A CsMPs from suspended particles in rivers and marine samples, such as plankton net and suspended particle samples. This fact suggests that Type-A CsMPs deposited on land and transported to the ocean through rivers. The presence of CsMPs may be the cause of the overestimation of solid–water distribution coefficient for marine sediments and particulate matters and apparent high concentration factor of marine biota of radioactive Cs.

Keywords: radiocesium-bearing microparticle, Fukushima Daiichi Nuclear Power Plant accident, Radioactive cesium

©2021. Japan Geoscience Union. All Right Reserved.

[J] Oral | M (Multidisciplinary and Interdisciplinary)：M-TT Technology & Techniques

Sun. Jun 6, 2021 1:45 PM - 3:15 PM JST | Sun. Jun 6, 2021 4:45 AM - 6:15 AM UTC | Ch.13 Zoom Room 13

[M-TT43] Brand-new scope of coupling geophysics being established by infrasound and associated waves

convener:Masa-yuki Yamamoto(Department of systems engineering, Kochi University of Technology), Takayuki Otsu(Japan Weather Association), Mie Ichihara(Earthquake Research Institute, University of Tokyo), Nobuo Arai(Disaster Mitigation Research Center, Nagoya University), Chairperson:Yoshihiro Kakinami(Hokkaido Information University), Masa-yuki Yamamoto(Department of systems engineering, Kochi University of Technology)

Infrasound and associated wave studies are recently focused on coupling waves with long-distant and vertical propagation characteristics. Such kinds of waves, having with coupling process between the atmosphere and the surface of ground and ocean, are linked with elastic waves in lithosphere and oceanic sphere, as well as to atmospheric regions up to the upper atmosphere, playing a role of generating many kinds of wavelike turbulence in thermosphere. Moreover, whole on the globe, these waves excited depending on the latitude regions, as well as on the environmental regions, such as snow ice, desert, rainforest, mountain, ocean, etc., have their own characteristics. These waves can be excited by large-scale geophysical events like volcanic eruptions, tsunami, thunderstorms, etc. as well as artificial explosions, propagating with long distance. In this session, we would like to discuss such "coupling geophysics" by using many new or well-known investigated data and simulations of infrasound and associated low frequency waves. It can combine multiple spheres in geophysics and bring a brand-new scope of geophysics. Your contributions from many regions are welcome!

1:45 PM - 2:00 PM JST | 4:45 AM - 5:00 AM UTC

[MTT43-01] HTV Infrasound Phase Identification in Near and Far Field Records

*I. H. HAMAMA[1,2], Masa-yuki Yamamoto[1] (1.School of Systems Engineering, Kochi University of, Japan, 2.National Research Institute of Astronomy and Geophysics, NRIAG, Egypt)

2:00 PM - 2:15 PM JST | 5:00 AM - 5:15 AM UTC

[MTT43-02] An estimation of acoustic velocity in lower thermosphere using GNSS TEC after the foreshock of the 2011 Tohoku Earthquake

*Yoshihiro Kakinami[1], Hiroaki Saito[2], Tetsuo Yamamoto[2], Chia-Hung Chen[3], Masa-yuki Yamamoto[4], Kensuke Nakajima[5], Jann-Yenq LIU[6], Shigeto Watanabe[1] (1.Hokkaido Information University, 2.Hokkaido University, 3.National Cheng Kung University, 4.Kochi University of Technology, 5.Kyushu University, 6.National Central University)

2:15 PM - 2:30 PM JST | 5:15 AM - 5:30 AM UTC

[MTT43-03] Evaluation of prototype miniature microphones for observing infrasound

*Ryouichi Nishimura[1], Taira Itoh[2], Dai Adachi[2], Yasutaka Nakajima[2], Kenichi Kidokoro[2], Toshiyuki Hasumi[2], Yôiti Suzuki[1] (1.National Institute of Information and Communications Technology, 2.RION Co., Ltd.)

2:30 PM - 2:45 PM JST | 5:30 AM - 5:45 AM UTC

[MTT43-04] A prompt report of multiple-site infrasound observation by the nation-wide infrasound observation consortium for M 7.3 Fukushima offshore earthquake on Feb. 13, 2021

*Masa-yuki Yamamoto[1], Nobuo Arai[2], Takayuki Otsu[3], Ryouichi Nishimura[4], Takuma Oi[5], Kensuke Nakajima[6], Hideki Ueda[7], Makiko Iwakuni[3], Yoshihiro Kakinami[8], Kosuke Heki[9], Islam H. HAMAMA[1] (1.Kochi University of Technology, 2.Nagoya University, 3.JWA, 4.NICT, 5.Toho Merchantile, 6.Kyushu University, 7.NIED, 8.Hokkaido Information University, 9.Hokkaido University)

2:45 PM - 3:00 PM JST | 5:45 AM - 6:00 AM UTC

[MTT43-05] Three-dimensional large-scale numerical simulation of infrasound associated with tsunami generation considering wave source and atmospheric models

*Yoshiki Saito[1], Kan Okubo[1], Kentaro Uehara[2], Hidee Tatehata[2], Hiromu Yokosu[3] (1.Tokyo Metropolitan University, 2.Japan Weather Association, 3.Chubu Electric Power Company)

3:00 PM - 3:15 PM JST | 6:00 AM - 6:15 AM UTC

[MTT43-06] Continuous excitation of atmospheric free oscillation by cumulus heating

★Invited Papers

*Kensuke Nakajima[1] (1.Department of Earth and Planetary Sciences,Flculty of Sciences,Kyushu University)

HTV Infrasound Phase Identification in Near and Far Field Records

*I. H. HAMAMA[1,2], Masa-yuki Yamamoto[1]

1. School of Systems Engineering, Kochi University of, Japan, 2. National Research Institute of Astronomy and Geophysics, NRIAG, Egypt

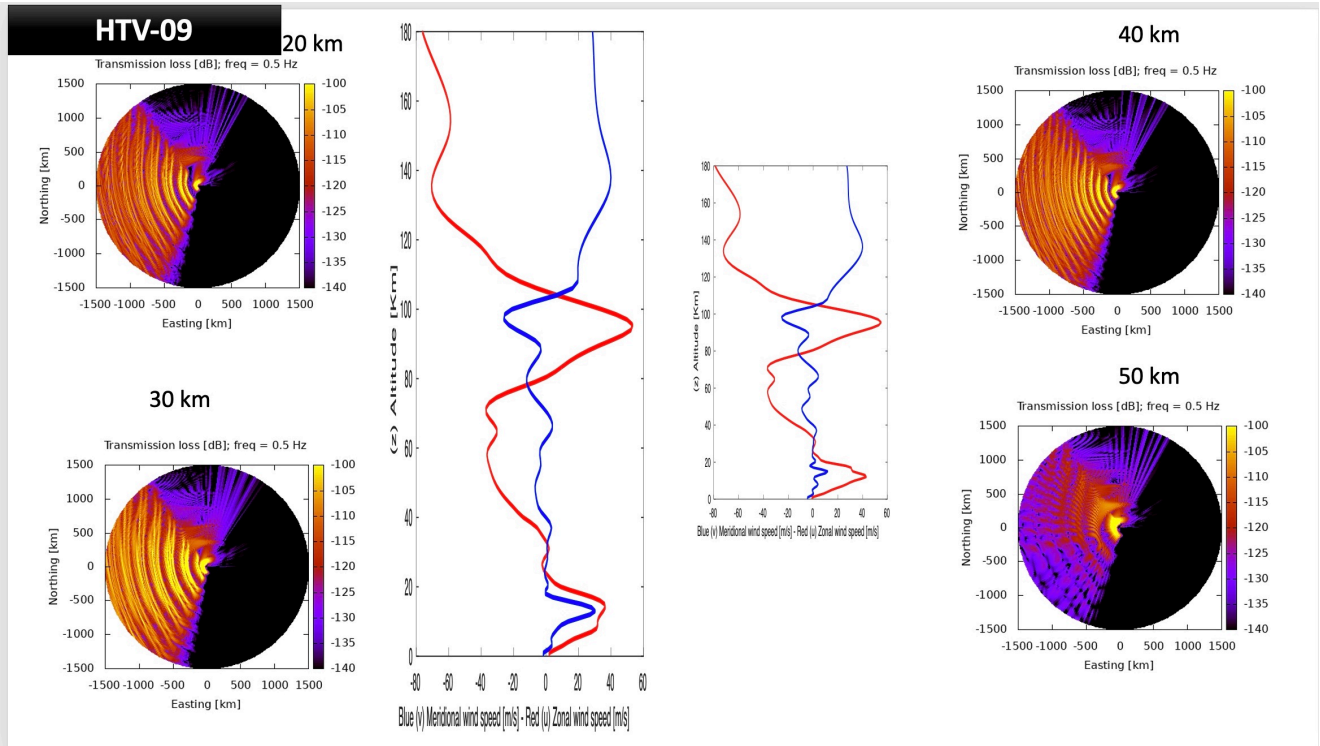
Nowadays, infrasound technology is to be involved in many applications. As the generation of shockwave in different layers in the atmosphere is a key to detect and track movable objects. Rockets can be considered one of important infrasound sources which emit acoustic signals during the launch process and the re-entry in atmosphere.

H-II Transfer Vehicle KOUNOTORI (HTV) which delivers the supplying to International Space Station (ISS) started the first mission since 2009 and operated annually until 2020, Different infrasound phases were detected at Kochi University of Technology (KUT) Infrasound Sensor Network (KUT) from HTV-06 to HTV-09. At, I30-JP infrasound observatory of the international monitoring system (IMS) recorded some phases as well. Because of the complexity of the rocket source, the assumption of point source was carried out in this study to identify the approximate height of the source in different stages which are generated infrasonic waves. Infrasound propagation modeling was applied to identify the predicted infrasound phases which could reach to the stations. Ray tracing and normal mode numerical methods were also carried out to estimate the expected celerities and the transmission loss from the source to stations from different altitudes.

In conclusion, the near and far field recordings are important in rocket induced infrasound detection to identify the different infrasound phases. In addition, the propagation modeling is a key to understand the arrivals in the stations. However, as the rocket is non-point source, additional study is still indeed to enhance the results.

Keywords: HTV, Infrasound Propagation, Ray Tracing, KUT, Rocket Launch

©2021. Japan Geoscience Union. All Right Reserved.



©2021. Japan Geoscience Union. All Right Reserved.

An estimation of acoustic velocity in lower thermosphere using GNSS TEC after the foreshock of the 2011 Tohoku Earthquake

*Yoshihiro Kakinami[1], Hiroaki Saito[2], Tetsuo Yamamoto[2], Chia-Hung Chen[3], Masa-yuki Yamamoto[4], Kensuke Nakajima[5], Jann-Yenq LIU[6], Shigeto Watanabe[1]

1. Hokkaido Information University, 2. Hokkaido University, 3. National Cheng Kung University, 4. Kochi University of Technology, 5. Kyushu University, 6. National Central University

An acoustic wave emitted by earthquake reaches thermosphere and disturb ionospheric plasma through the collision. These disturbances are often observed in GNSS total electron content (TEC) observations. However, since TEC is the integrated plasma density, it is hard to investigate the propagation of acoustic in principle when we use a single satellite data. We found that concentrically propagating disturbance retrieved by three satellites after the foreshock of the 2011 Tohoku Earthquake on 9 March 2011. When the observed altitude is fixed an altitude, the onset points did not coincide. When we relaxed the assumption of the fix altitude, we found that the onset points coincide and altitude and geographic coordinates of the onset points are determined simultaneously. The altitudes are found to be 107.8, 131.8 and 133.3 km, and the onset time at these altitudes. As a result, the vertical velocity of acoustic wave is estimated to be 448 m/s from the travel time between the altitudes of 107.8 and 131.8 km and 370 m/s between the altitude of 107.8 and 133.3 km. These velocities are comparable to those estimated from the neutral temperature given by the empirical model NRLMSISE-00. The proposed method can determine the location of ionospheric disturbance detected in TEC independently of the seismic data and gives the information of propagation of acoustic wave in the thermosphere.

Keywords: the foreshock of the 2011 Tohoku Earthquake, velocity of acoustic wave in the thermosphere, GNSS Total electron content, an estimation of altitude of total electron content

©2021. Japan Geoscience Union. All Right Reserved.

Evaluation of prototype miniature microphones for observing infrasound

*Ryouichi Nishimura[1], Taira Itoh[2], Dai Adachi[2], Yasutaka Nakajima[2], Kenichi Kidokoro[2], Toshiyuki Hasumi[2], Yôiti Suzuki[1]

1. National Institute of Information and Communications Technology, 2. RION Co., Ltd.

Experimental comparison was carried out among MEMS pressure sensors: DPS310, MBL1000-8, and prototype miniature microphones from the viewpoint of performance in observing relatively high frequency infrasound such as generated at volcanic eruptions. These sensors were put in a box set up in the Kagoshima University Research Forests, which is located approximately 12 km southeast from the Minamidake summit crater. MBL1000-8 is an infrasound measurement device on which eight BOSCH BME280 modules are mounted. It records the mean value of the eight sensor outputs, thereby suppressing internal noise signals relatively large at a high frequency region. On the other hand, DPS310 is a brand new MEMS pressure sensor. Many vendors supply modules to access it through a serial bus using I2C or SPI. We employed a module supplied by Seeed Studio Co. Ltd. in the experiment. According to the data sheets, relative accuracy is ±12 Pa for BME280 and ±6 Pa for DPS310. Other features are almost the same between the both. The miniature microphones were experimentally made by RION Co. Ltd., based on MEMS microphones initially designed for hearing aids and modified so as to measure infrasound. They can capture the sound up to 1 kHz so that outputs were preliminarily processed by an RC low-pass filter with the cut-off frequency of 15.9 Hz and then sampled at the sampling rate of 32 Hz with adafruit ADS1116 to acquire the data. In case of large level input, two microphones of different sensitivities were employed; one was −39.3 dBV/Pa and the other −67.1 dBV/Pa. Because of the different DC biases, outputs of these microphones were sampled with different input ranges. As a result, the minimum quantization resolution for the low sensitivity microphone was four times coarser than that of the high sensitivity. We compared the power spectrum density of the data obtained during the night because less influence of human activity was expected. The data length was six hours from the midnight. To determine the day with the least wind influence, we compared standard deviation of the data obtained everyday since the beginning of the experiment, January 19, 2021. Although the least variance was observed on 28 January, the data on 31 January was chosen for the analysis because it showed the second least variance and odd signals with an amplitude of 5 Pa often occurred on 28 January. The data was segmented into frames of 20 minutes with 50% overlap, and the mean power spectrum density was calculated. The results were approximately −12 [dB re 1 μPa^2/Hz] for the high sensitivity microphone and 24 [dB re 1 μPa^2/Hz] for the low sensitivity microphone at 10 Hz. According to literature, the electronic noise level of DASE MB2000, which is used IS of CTBTO, is approximately −8 [dB re 1 μPa^2/Hz]. Therefore, it suggests that one of the tested miniature microphones could capture infrasound with as the same noise level as MB2000. Besides, the results of MEMS pressure sensors were approximately 70 [dB re 1 μPa^2/Hz] for DPS310 and 81 [dB re 1 μPa^2/Hz] for MBL1000-8. The MEMS pressure sensors showed relatively large noise level at this frequency, but they are considered effective in measuring very low frequency infrasound, for example, a duration of over two minutes, such as observed when a tsunami happens, because its frequency is too low for microphones to capture. As described before, signals of approximately 5 Pa in amplitude were sometimes observed in the experiment. These signals were come not from the electronic circuit but from the air because all the tested sensors captured them. However, such signals were not observed in the data captured by other sensors located in different directions around Sakurajima. Therefore, the origin of these signals has not been determined yet. Possible reasons are an artificial noise made in a nearby factory or a wind generated by a truck passing by. This work was

©2021. Japan Geoscience Union. All Right Reserved.

partly supported by JSPS KAKENHI Grant Number 17K01351 and 19H02396.

Keywords: Infrasound, Miniature microphone, MEMS, Parallel observation

©2021. Japan Geoscience Union. All Right Reserved.

A prompt report of multiple-site infrasound observation by the nation-wide infrasound observation consortium for M 7.3 Fukushima offshore earthquake on Feb. 13, 2021

*Masa-yuki Yamamoto[1], Nobuo Arai[2], Takayuki Otsu[3], Ryouichi Nishimura[4], Takuma Oi[5], Kensuke Nakajima[6], Hideki Ueda[7], Makiko Iwakuni[3], Yoshihiro Kakinami[8], Kosuke Heki[9], Islam H. HAMAMA[1]

1. Kochi University of Technology, 2. Nagoya University, 3. JWA, 4. NICT, 5. Toho Merchantile, 6. Kyushu University, 7. NIED, 8. Hokkaido Information University, 9. Hokkaido University

Nation-wide infrasound observation consortium was established in 2019 mainly for obtaining dense collaboration when any events are rarely or occasionally happened, and rapid understanding is required. Nowadays, we have almost 100 infrasound monitoring sites in Japan to detect natural geophysical events that would make disaster level affection into the human society or as a reference sensor for another type of sensing. Members of the consortium can provide some datasets on request, but there are many types of infrasound sensors whose detectable frequency range and sensitivity is different from each other.
At 23:07 JST on Feb. 13, 2021, Fukushima Offshore M 7.3 earthquake occurred, and severe vibration made more than 100 persons injured and destructed some traffic facility, buildings, etc. in and around Fukushima pref., however no apparent tsunami was observed afterward. At Ishinomaki port, slight sea level change of 20 cm was reported. There seems to be severe vibration without tsunami was because of 60 km depth of the earthquake epicenter. For this case, there is weak affection on the bottom of the ocean thus it does not make large amplitude vertical ground motion on the ocean bottom.
On the other hand, Tohoku Offshore M 9.0 earthquake occurred on Mar. 11, 2021 brought out severe tsunami disaster. At that time, an infrasound sensor located at Mizuzawa, Oshu-city, Iwate pref. recorded huge amplitude vibration signal due to severe vertical ground motion, but followed by large scale overpressure signal of 20 Pa amplitude with a period of 24 minutes. This long period signal is considered as the Lamb waves coming from the ocean surface change above the epicenter (Arai et al., 2011).
This time, the huge amplitude vibration signals due to severe vertical ground motion were also observed by multiple infrasound sensors, simultaneously, but there is no followed signal of long-period large-scale overpressure waves. We tried to estimate the infrasound tsunami magnitude for those cases and will discuss the recorded signals in comparison with the other cases as well as possibilities of dense infrasound observation for disaster mitigation.

Keywords: Infrasound, Earthquake, Lamb waves, Consortium, Multiple-site observation, Tsunami Magnitude

©2021. Japan Geoscience Union. All Right Reserved.

Three-dimensional large-scale numerical simulation of infrasound associated with tsunami generation considering wave source and atmospheric models

*Yoshiki Saito[1], Kan Okubo[1], Kentaro Uehara[2], Hidee Tatehata[2], Hiromu Yokosu[3]

1. Tokyo Metropolitan University, 2. Japan Weather Association, 3. Chubu Electric Power Company

For several decades, pressure changes associated with tsunami generation have been observed in the case of large earthquakes, and the research on this phenomenon has been conducted. Past studies have reported that this change in atmospheric pressure (infrasound) is induced by the generation of a tsunami. Since infrasound propagates at a speed faster than that of a tsunami, it is expected to be applied to early detection of tsunamis. In other words, using infrasound as one of the observation targets for tsunami detection makes it possible to further improve the robustness and stability of tsunami detection. However, for this phenomenon, detailed numerical analysis considering the effects of wave sources and atmospheric environment based on actual physical phenomena has not been sufficiently studied. According to the frequency of tsunami occurrence, it is important to establish a highly reproducible numerical analysis method. Therefore, in this study, we implemented a three-dimensional large-scale propagation numerical analysis considering the wave source and atmospheric model, and numerically examined the infrasound induced by the tsunami. In this numerical experiment, tsunami-induced infrasound was compared and evaluated by removing the background atmospheric pressure trend from the observation results of the 2011 off the Pacific coast of Tohoku Earthquake. Through this research, it was clarified that a waveform close to the infrasound obtained in the field observation can be reproduced by numerical analysis employing the wave source and atmospheric environment models.

Keywords: infrasound, atmospheric pressure wave, large earthquake, tsunami, numerical simulation, disaster detection

©2021. Japan Geoscience Union. All Right Reserved.

Continuous excitation of atmospheric free oscillation by cumulus heating

*Kensuke Nakajima[1]

1. Department of Earth and Planetary Sciences,Flculty of Sciences,Kyushu University

Existence of Broadband Continuous Excitation of the Earth's Atmospheric Free Oscillation

A framework that linearizes the governing equations of the Earth's atmospheric motion, assumes periodicity in the direction of time and longitude, and separates variables in the vertical and latitudinal directions has been used as a framework for the consideration of atmospheric tides and other atmospheric waves (e.g., Chapman and Lindzen 1970). The eigenvalue (equivalent depth) of the vertical structure equation is about 10 km, and the horizontal velocity of the corresponding wave is the speed of sound (about 330 m/s). The horizontal structure equation is known as the Laplace Tidal Equation (LTE), and its modal solutions have been investigated in detail by Longuet-Higgins (1968), and they can be roughly classified into the slow westward propagating "Rossby mode" and the "gravity wave mode" with a large phase velocity. Corresponding to these modes, it has been known that there exist eastward propagating waves called "4-day waves" (zonal wavenumber 2), "5-day waves" and "10-day waves" (zonal wavenumber 1), which are associated with the Rossby mode, and "33-hour waves", which are associated with the global gravity wave mode (Kelvin mode with zonal wavenumber 1). Sakazaki and Hamilton (2020, J.Atmos.Sci), using global atmospheric reanalysis data, further showed that gravity wave modes with wavenumbers up to 10 or more are excited. On the other hand, Nishida et al (2014, Geophys.J.International) analyzed dense barometer data deployed in the eastern United States and found that Lamb waves are constantly excited from wavenumber 20 to about 1200. Lamb waves, which are trapped in the lower atmosphere and propagate horizontally at the speed of sound, correspond to gravity waves when considered globally with LTE, and their vertical structure is exactly the same as the eigenfunctions of the "vertical structure equation" mentioned earlier. Taken together, these results suggest that modes with an equivalent depth of 10 km are constantly excited in the Earth's atmosphere, almost continuously, from global modes with wavenumber of 1 to high wavenumber modes with wavenumber of 1000 or more.

Possibility of excitation by cumulus clouds

In this paper, we assume that cumulus convection is a possible source of excitation of the broadband atmospheric free oscillations described above. The first reason is that cumulus convection is an isolated disturbance with a spatial scale of about 1 km, so it can be a broadband wave source with a spatial range of wavenumber from 0 to 10,000. Second, since cumulus clouds have a lifetime of about one hour and there are large fluctuations in the heating structure even during their life cycle, they can be a broadband wave source with a frequency ranging from zero to several mHz in time.

Excitation of Lamb wave vertical modes by cumulus heating

When the atmosphere is heated, the direct response is the generation of sound waves, and the response after this propagates vertically contributes to the excitation of Lamb waves and the subsequent internal gravity waves Bannon (1995) showed that no surface pressure remains after the hydrostatic adjustment following heating. However, since the atmosphere above the heat source is displaced upward, positive heating results in a positive pressure anomaly as a contribution to the Lamb wave vertical mode. It can be seen that the amplitude can generally be estimated by the pressure response of the atmosphere confined to a vertical region of about scale height.

©2021. Japan Geoscience Union. All Right Reserved.

Estimation of Amplitude

Based on the above discussion, we estimated the heating response of the atmosphere in the vertical layer by referring to the current Earth observation facts about the number and lifetime of cumulus clouds. The results depend on the estimate of the Q-value of the atmospheric free oscillation, but the amplitude of the Lamb wave of Nishida et al (2013) and the global mode of Sakazaki and Hamilton (2020) can be generally explained. The details will be discussed in the day.

Keywords: atmospheric free oscillation, cumulus convection, Lamb waves, infrasound

©2021. Japan Geoscience Union. All Right Reserved.

[J] Poster | M (Multidisciplinary and Interdisciplinary)：M-TT Technology & Techniques

Sun. Jun 6, 2021 5:15 PM - 6:30 PM JST | Sun. Jun 6, 2021 8:15 AM - 9:30 AM UTC | Ch.20_2

[M-TT43] Brand-new scope of coupling geophysics being established by infrasound and associated waves

convener:Masa-yuki Yamamoto(Department of systems engineering, Kochi University of Technology), Takayuki Otsu(Japan Weather Association), Mie Ichihara(Earthquake Research Institute, University of Tokyo), Nobuo Arai(Disaster Mitigation Research Center, Nagoya University)

Infrasound and associated wave studies are recently focused on coupling waves with long-distant and vertical propagation characteristics. Such kinds of waves, having with coupling process between the atmosphere and the surface of ground and ocean, are linked with elastic waves in lithosphere and oceanic sphere, as well as to atmospheric regions up to the upper atmosphere, playing a role of generating many kinds of wavelike turbulence in thermosphere. Moreover, whole on the globe, these waves excited depending on the latitude regions, as well as on the environmental regions, such as snow ice, desert, rainforest, mountain, ocean, etc., have their own characteristics. These waves can be excited by large-scale geophysical events like volcanic eruptions, tsunami, thunderstorms, etc. as well as artificial explosions, propagating with long distance. In this session, we would like to discuss such "coupling geophysics" by using many new or well-known investigated data and simulations of infrasound and associated low frequency waves. It can combine multiple spheres in geophysics and bring a brand-new scope of geophysics. Your contributions from many regions are welcome!

[MTT43-P01] Infrasound detection of mining blasts from eastwards and westwards

*Mami Nogami[1], Takayuki Otsu[1], Makiko Iwakuni[1] (1.Japan Weather Association)

[MTT43-P02] The Infrasound signals excited by a bolide on 29th November 2020

*Makiko Iwakuni[1], Masa-yuki Yamamoto[2], Hiroaki Saito[3], Islam HAMAMA[2], Nobuo Arai[4], Takayuki Otsu[1], Mami Nogami[1], Takahiko Murayama[1] (1.Japan Weather Association, 2.Department of systems engineering, Kochi University of Technology, 3.Cosmosciences, Hokkaido University, 4.Disaster Mitigation Research Center, Nagoya University)

[MTT43-P03] Atmospheric wave energy of the 2020 August 4 explosion in Beirut, Lebanon, from ionospheric disturbances

*Ai Matsushita[1], Bhaskar Kundu[2], Batakrushna Senapati[2], Kosuke Heki[1] (1.Hokkaido University Graduate School of Science, 2.National Institute of Technology, Rourkela)

[MTT43-P04] Infrasound and seismic multiple-site observation of shock waves induced by hypersonic reentry of HAYABUSA-2 sample return capsule on Dec. 6, 2020

*Masa-yuki Yamamoto[1], Yoshihiro Hiramatsu[2], Shinsuke Abe[3], Yoshihiro Kakinami[4], Norihisa Segawa[5], Hiroshi Katao[6], Yoshiaki Ishihara[7], Taichi Kawamura[8], Satoshi Nozawa[9], Muneyoshi Furumoto[10], Phil Bland[11], Eleanor Sansom[11], Hadrien Devillepoix[11], Martin Towner[11], Yuichiro Inoue[1], Islam H. Hamama[1], Masato Yazawa[12], Kazuhisa Fujita[7], Makoto Yoshikawa[7] (1.Kochi University of Technology, 2.kanazawa University, 3.Nihon University, 4.Hokkaido Information University, 5.Kyoto Sangyo University, 6.Kyoto University, 7.JAXA, 8.Institut de Physique du Globe de Paris, 9.Ibaraki University, 10.Tono Research Institute of Earthquake Science, 11.Curtin University, 12.Mathematical Assist Design Laboratory)

Infrasound detection of mining blasts from eastwards and westwards

*Mami Nogami[1], Takayuki Otsu[1], Makiko Iwakuni[1]

1. Japan Weather Association

There are several large mines in Southwestern Siberia, Russia, blasting using explosives is carried out for the topsoiling and mining of minerals. When blasting, shock waves are generated according to the power of the explosive, including expansion of high-temperature and high-pressure gases. Even if the explosives are installed in the ground, when crushed materials and pressure waves erupt into the atmosphere with the explosion, they can be observed as infrasound. In the case of known mines, the distance to the station is known, so it is possible to estimate the propagation time depending on weather conditions. Furthermore, when seismic waves propagated through the ground are observed at several seismic stations, the seismic origin position and origin time are determined, and it is also possible to determine the location of the sound source based on the azimuth analyzed from the infrasound data and the observation time.

CTBT Infrasound station of I46RU is consisted of 4 sites installed infrasound sensor (MB2000), is also deployed at Zalesovo, Russia. Within 1,000 km of the I46RU, there are several mines in operation, and infrasound by blasting can be observed from eastward, and westward during the same time. As a feature of the signals, they have a dominant frequency between 1 Hz and 4 Hz, the duration is about 10 seconds. Since the time of mining is concentrated in the day, trace velocity of many signals are analyzed that propagate roughly straight near the ground surface due to the effect of forming a reverse fault between several height and the ground surface, after that, signals of the trace velocity which seems to have been propagated by guiding between the tropopause, or the stratopause and the ground surface can be observed.

In the poster, we would like to consider the characteristics of signals when propagated from eastward and/or westward sound sources based on the differences in seasonal atmospheric conditions.

Keywords: Infrasound, Mining blast, CTBT

©2021. Japan Geoscience Union. All Right Reserved.

The Infrasound signals excited by a bolide on 29th November 2020

*Makiko Iwakuni[1], Masa-yuki Yamamoto[2], Hiroaki Saito[3], Islam HAMAMA[2], Nobuo Arai[4], Takayuki Otsu[1], Mami Nogami[1], Takahiko Murayama[1]

1. Japan Weather Association, 2. Department of systems engineering, Kochi University of Technology, 3. Cosmosciences, Hokkaido University, 4. Disaster Mitigation Research Center, Nagoya University

An infrasound observation system has been installed in Shima region, Mie prefecture since 2015 by Japan Weather Association (JWA). Kochi University of Technology (KUT) started the operation of an infrasound sensor in 2016. Currently, many infrasound sensors are deployed over the Japanese islands (widely from Kyusyu region to Hokkaido region. JWA and KUT collect these infrasound data in real time to monitor natural disasters such as tsunami and volcanic eruption. The collection of infrasound observation system of KUT is named KISONS (Kochi university of technology InfraSound Observation data Network System).

Infrasound sensors of JWA and KUT observed infrasound signals excited by a bolide which flew over off Kii channel around 01:34 on 29th of November 2020 (JST). Many people witnessed this bolide, and optical observation data gave the information that the flying route of it. At the infrasound station closest to the bolide trajectory, Toyo town in northeastern part of Kochi prefecture, the infrasound sensor detected some signals around 01:39. Other two infrasound sensors at Cape Muroto in Kochi prefecture detected signals after 01:39. On Kii peninsula, sensors of KUT in Kumano city and Owase city and sensors of JWA in Shima also detected signals. The direct distance between the height of the vanishing point of the bolide trajectory and each infrasound station, was 86 km at the nearest Toyo town and 196 km at the farthest Shima site (Shima high school). As far as we know, this is rare case to detect signals excited by a bolide at multiple infrasound stations in Japan as close as approximately 100 km distance from the bolide trajectory. It will be a valuable case to study the changes in the signals due to propagation from the bolide trajectory.

We thank SonotaCo Network members. In this group they optically observe bolides, meteors and so on, discuss the orbit. SonotaCo Network URL: http://sonotaco.jp/

Keywords: Infrasound, Meteor, Multiple infrasound stations at short distances (100km), Microbarograph

©2021. Japan Geoscience Union. All Right Reserved.

Atmospheric wave energy of the 2020 August 4 explosion in Beirut, Lebanon, from ionospheric disturbances

*Ai Matsushita[1], Bhaskar Kundu[2], Batakrushna Senapati[2], Kosuke Heki[1]

1. Hokkaido University Graduate School of Science, 2. National Institute of Technology, Rourkela

The electron distribution in the ionosphere is often disturbed by various phenomena in the atmosphere. They are observed as changes in TEC (Total Electron Content) along line-of-sight connecting GNSS (Global Navigation Satellite System) satellites and receivers. For example, large meteorites entering the Earth’ s atmosphere often explode and are recognized as fireballs. Sound waves and internal gravity waves excited by them propagate through the atmosphere, reach the ionospheric F region, and disturb TEC. A fireball appeared near Chelyabinsk, Russia, on February 15, 2013, one of the largest fireball events in the observation history, made significant disturbance signals in TEC observed with multiple GPS satellites and ground receivers.

Here I report ionospheric disturbances following the chemical explosion that occurred in Beirut, Lebanon, on August 4, 2020 using nearby continuous GNSS stations. The scale of this explosion is 1-1.5 kt (TNT), which is about 1/100 of the fireball over the Bering Sea. Despite its small scale, N-shaped TEC changes were observed thanks to the existence of a dense continuous GNSS station network to the south of Beirut. The signals were found only at southern stations with distances >200 km from the explosion site, which is due mainly to the interaction of ionospheric electrons with the magnetic field.

Currently, we also perform a numerical simulation study of the propagation of disturbances excited by the explosion. In the simulation, we assumed the sound velocity structure in the atmosphere (US Standard Atmosphere 1976), the Chapman-type altitude dependence of electron density, and the influence of the magnetic field, and simulated the upward propagation of N-shaped sound waves. As a result, N-shaped TEC changes that match the observed waveforms could be reproduced. In the future, we plan to sort out following problems in this numerical simulation, (1) the waveform cannot be reproduced for line-of-sight penetrating the region just above the explosion, (2) propagation in the east-west direction is not sufficiently considered, and (3) objective determination of the optimum period of the disturbance.

©2021. Japan Geoscience Union. All Right Reserved.

Infrasound and seismic multiple-site observation of shock waves induced by hypersonic reentry of HAYABUSA-2 sample return capsule on Dec. 6, 2020

*Masa-yuki Yamamoto[1], Yoshihiro Hiramatsu[2], Shinsuke Abe[3], Yoshihiro Kakinami[4], Norihisa Segawa[5], Hiroshi Katao[6], Yoshiaki Ishihara[7], Taichi Kawamura[8], Satoshi Nozawa[9], Muneyoshi Furumoto[10], Phil Bland[11], Eleanor Sansom[11], Hadrien Devillepoix[11], Martin Towner[11], Yuichiro Inoue[1], Islam H. Hamama[1], Masato Yazawa[12], Kazuhisa Fujita[7], Makoto Yoshikawa[7]

1. Kochi University of Technology, 2. kanazawa University, 3. Nihon University, 4. Hokkaido Information University, 5. Kyoto Sangyo University, 6. Kyoto University, 7. JAXA, 8. Institut de Physique du Globe de Paris, 9. Ibaraki University, 10. Tono Research Institute of Earthquake Science, 11. Curtin University, 12. Mathematical Assist Design Laboratory

On Dec. 6, 2020, the JAXA HAYABUSA2 spacecraft returned to the Earth and its sample return capsule (SRC) was successfully landed on the desert area of Woomera, South Australia. At the time of hypersonic reentry of SRC in the upper and middle atmosphere, shock waves can be generated from the Mach cone along the shallow angle trajectory of SRC directly injected from the outer space. In 2010, the HAYABUSA SRC also successfully landed on the ground in the same desert area. At that time, we tried to detect the shock waves coming from the Mach cone of SRC, but little bit different condition that the mother spacecraft also reentered because of the lack of its capability to escape from the Earth's gravity due to the partial malfunction, therefore, multiple shock waves were observed at 5 sensors at that time. Over 20 seismometers simultaneously detected N-type signals with an air-to-ground coupling process at that time, as well (e.g. Yamamoto et al., 2011). After the event, we have been developed new infrasound sensors of INF01 and INF04 with data loggers by ourselves collaborating with some manufacturing companies, thus this time, we can deploy 30 sensors in a 100 km scale target area. Besides, 6 low-cost seismometers were also deployed at 4 sites.

For detecting precise trajectory and yield energy from the dataset of over-pressure amplitude at each site, we deployed 30 sensors on ground in the Woomera Prohibited Area (WPA). As for the INF04 sensors, we used 7 sites using 4 sensors per each, getting N-type waveform at every 27 sensors, except for 1 possible malfunctioned sensor. The waveform was almost the same as the HAYABUSA SRC reentry but without any complex features of the followed period just after the N type signal. The air-to-ground coupling process is also roughly investigated in comparison with previous result in 2010. By using these datasets, we will show the prompt report of the whole of the observation about the infrasound and seismic observation for HAYABUSA2 reentry. The possibility of the yield energy estimation and precise trajectory determination will be discussed in this talk.

Reference:
Yamamoto, M.-Y., Ishihara, Y., Hiramatsu, Y., Kitamura, K., Ueda, M., Shiba, Y., Furumoto, M., Fujita, K., Detection of Acoustic/Infrasonic/Seismic Waves Generated by Hypersonic Re-Entry of the HAYABUSA Capsule and Fragmented Parts of the Spacecraft, Publ. Astron. Soc. Japan, 63, 971-978, 2011.

Keywords: Infrasound, Shock wave, Multiple-site array observation, Reentry, HAYABUSA2

©2021. Japan Geoscience Union. All Right Reserved.

[J] Poster | M (Multidisciplinary and Interdisciplinary)：M-ZZ Others

Sun. Jun 6, 2021 5:15 PM - 6:30 PM JST | Sun. Jun 6, 2021 8:15 AM - 9:30 AM UTC | Ch.22_4

[M-ZZ44] Studies of Geoscience : historical, philosophical and STS studies

convener:Michiko Yajima(Tokyo Metropolitan University), Shigeyuki Aoki(Faculty of Letters, Chuo University), Toshihiro Yamada(Taisho University), Akira Yamamoto

Topics on history, philosophy and STS (science, technology and society)studies of geoscience will be discussed. Any related subject is welcome, such as history of mining, historical studies of geohazards, methodology of geoscience, sociology of natural hazards, politics of environmental issues, and risk theory.

[MZZ44-P01] The begining of lady earth scientists in Japan

*Michiko Yajima[1] (1.Tokyo Metropolitan University)

[MZZ44-P02] Finding Geoscientific Evidence in Nuclear Disaster Trials 2: Is Not "responsibility of the government" Scientific?

*Mamoru Hayashi[1] (1.University of TOYAMA)

[MZZ44-P03] Wilkins’s lunar world

*Shigeyuki Aoki[1] (1.Faculty of Letters, Chuo University)

[MZZ44-P04] The Popularization of Science and the Geo-power: Cosmic Evolution, China, and Buddhism in 1920s Shinjo Shinzo

*Toshihiro Yamada[1] (1.Taisho University)

[MZZ44-P05] Japan's first female meteorologist

*Akira Yamamoto

The begining of lady earth scientists in Japan

*Michiko Yajima[1]

1. Tokyo Metropolitan University

I continue to make research on lady earth scientists in Japan. Before the war, Marie Stopes (1880-1958) and Kono Yasui (1880-1971) studied the fossils from Japan coal field. Yasui got doctoral degree in 1927 from the University of Tokyo. This is the first doctoral degree of science that Japanese lady got.
In 1943 three ladies, Takayo Fujiwara, Tami Inoue, and Mitsu Inoue, attended the annual meeting of the Geological Society of Japan. Only Fujiwara continued the science carria. She got doctoral degree from Hokkaido University in 1961 and award from JGS in 1968.
The first lady earth scientist who got doctoral degree was Fumiko Shido. She got in 1958 from the University of Tokyo.

Keywords: lady earth scientist, Fumiko Shido, Takayo Fujiwara, Tami Inoue, Kono Yasui, Marie Stopes

©2021. Japan Geoscience Union. All Right Reserved.

Finding Geoscientific Evidence in Nuclear Disaster Trials 2: Is Not "responsibility of the government" Scientific?

*Mamoru Hayashi[1]

1. University of TOYAMA

This paper examines the way of examining geoscientific evidence in the civil trial for compensation for nuclear power plant and the criminal trial of TEPCO.

It can be said that the TEPCO criminal trial judgment (Tokyo District Court, September 19, 2019) found that the management had recognized the possibility of a tsunami (foresight). However, the Tokyo District Court acquitted the management of the case, saying that the long-term evaluation by the Earthquake Headquarters was based on weak grounds and unreliable. From the scientific point of view, "reliability" covered by the long-term evaluation of the Headquarters for Earthquake Research Promotion is not the concept of the property which can deny the probability of tsunami earthquake. From the viewpoint of the standard of IAEA which the Japanese government also joins, and from the viewpoint of the standard of severe accident prevention which makes it to be under 10,000 times or under 100,000 times/year = scientific and technological principle, it could not be "unexpected". It seems that the "reliability" came out by the logic which denies the countermeasure, closing the eye for the high probability.

In comparison with the judgment of civil suit for compensation for nuclear power plant, this paper examines the discussion on "reliability" and the judgment of existence of "responsibility of the state" which accepts the judgment which deviates from the scientific and technological principle of TEPCO from the geoscientific viewpoint.

Keywords: Tokyo Electric Power Company nuclear power plant criminal trial, civil suit for compensation for nuclear power plant, tsunami predictability, probability, Criticism of the transscience theory

©2021. Japan Geoscience Union. All Right Reserved.

東電福島原発震災裁判にかかわって

- 2019年9月19日の東電刑事裁判判決は，津波予見性を必ずしも否定していないが，刑事罰を認めるには信頼性が低いとした。
- 判決が依拠したのは，判決要旨には名前がでていない東北大学松澤暢教授（地震学）の主張（北緯38.1度より南には付加体がないので福島沖では津波地震(地震動の大きさに比べ大きな津波をもたらす地震)は生じない）らしい。
- しかし，その松澤氏も民事裁判証言意見書で，南北で差があるとは思うが，南側でも北側よりは可能性が低くとも津波地震がおこりうる，北緯38.1度より南での津波地震発生の蓋然性に関しては否定でなく，五分五分の蓋然性を考えていたと示しているが，証言を依頼された被告東電を擁護（利益相反の影響の可能性）。

原発賠償訴訟松澤意見書（被告側2016年9月28日付）から

「平成21年2月に，土木学会原子力土木委員会内の津波評価部会は，私などの地震の専門家らに対して，確率論的津波評価の重み付けアンケートを実施しました。

私はよく覚えていませんでしたが，以前，東京地検の検事から，私のアンケートの回答を見せてもらったと記憶しています。

その中に，日本海溝沿い福島沖と津波地震の発生に関する項目があり，日本海溝沿い福島沖で津波地震は発生しないという選択肢，領域を南北に分けて差異を設ける選択肢，領域を1つとして1896年明治三陸津波地震と同様のものがどこでも起きるという選択肢の3つがあり，これらの可能性に0～1の数字を振って合計が1になるように重み付けをするというものでしたが，私は，順に，0.2，0.6，0.2と付けました。」

- 日本海溝沿い福島沖で津波地震は発生しない：0.2
- 領域を南北に分けて差異を設ける選択肢：0.6
- 領域を1つとして1896年明治三陸津波地震と同様のものがどこでも起きる：0.2

- つまり，南北で差があるとは思うが，南側でも北側よりは可能性が低くとも津波地震がおこりうる，そう重みづけしていたのだから，北緯38.1度より南での津波地震発生の蓋然性に関して，松澤氏は否定でなく，五分五分に近く考えていたのだとわかる。そのような大きな蓋然性を切り捨てる判断に信頼性はあるか？

蓋然性を無効化する画策（翻訳例）「他の要因に隠れてしまうほど小さい」？

- (f) In general, increases in the incidence of health effects in populations cannot be attributed reliably to chronic exposure to radiation at levels that are typical of the global average background levels of radiation. This is because of the uncertainties associated with the assessment of risks at low doses, the current absence of radiation-specific biomarkers for health effects and the insufficient statistical power of epidemiological studies. UNSCEAR（2012）報告書
  統計的有意性で検出するには統計的パワーが足りないといった議論がされているが，バックグラウンドに付け加わる要因が「隠れて」「しまう」「小さい」というニュアンスは，ここからは読み取れない。
- 「国際的な合意では，放射線による発がんのリスクは，100mSv以下の被ばく線量では，他の要因による発がんの影響によって隠れてしまうほど小さいため，放射線による発がんリスクの明らかな増加を証明することは難しいとされる。疫学調査以外の科学的手法でも，同様に発がんリスクの解明が試みられているが，現時点では人のリスクを明らかにするには至っていない」（2011年12月22日低線量被ばくのリスク管理に関するワーキンググループ報告書）→これも「ジャパン・スタンダード」。
  ＃ここでの「しまう」は，その状態の完成を表わすor不本意？。

科学論争の裏に読み取り可能な目的意識

国土を汚染した被告が避難者に罪をなすりつけられるのか

自主的避難等対象区域からの避難者について，特別の事情を留保することなく，平成２４年１月以降について避難継続の相当性を肯定し，損害の発生を認めることは，自主的避難等対象区域での居住を継続した大多数の住民の存在という事実に照らして不当である上に，自主的避難等対象区域は，本件事故後の年間積算線量が２０ミリシーベルトを超えない区域であり，前記第２のとおり，そのような低線量被ばくは放射線による健康被害が懸念されるレベルのものではないにもかかわらず，平成２４年１月以降の時期において居住に適さない危険な区域であるというに等しく，自主的避難等対象区域に居住する住民の心情を害し，ひいては我が国の国土に対する不当な評価となるものであって，容認できない。

原発賠償群馬訴訟控訴審被告第8準備書面（2019年9月11日）から

「口頭弁論で原告側弁護人が「本当に謙虚すぎるのか」と質問し，国側は「謙虚すぎる」と答えた。原告側は敗訴に対し「避難者と残った人の分断をあおり，原発事故での国の責任を棚上げしている」と指摘した。」

上毛新聞2019年9月18日付

広島・長崎の被爆者による原爆症認定訴訟において裁判所の判断の多くは，被曝によって促進される病気であれば被爆者援護法の目的に沿って，原爆症と認定すべきだとしている。すなわち，「高度の蓋然性をもって証明を厳格に要求することは，真に救済されるべき被爆者が救済されないという事態を招きかねない」などとする（H27年行政（コ）421号原爆症認定申請却下処分取消請求控訴事件資料から）。

いっぽう，政府側は，以下のように主張する。「…放射線に起因して発症したことが証明された場合に限り，他の戦争被害者には認められない高額の特別手当を支給するものであり，…被爆者手帳の支給を受けたものであれば誰でも疾病罹患のみを要件として上記のような高額の給付を受けられるということになれば，もはや被爆者援護法の趣旨を超えるものといわざるをえない。このような事態は，大なり小なり受けた戦争の犠牲を等しく甘受することで成り立ってきた社会的コンセンサスを揺るがすことになりかねず，国民の理解を得られるものではない」。

人権のための科学なのか，それとも加害者・権威者の特権のための科学なのか？

2021年2月19日 原発賠償千葉訴訟東京高裁判決要旨　から

イ　規制権限不行使の違法性

(ｱ)　**科学的知見としての長期評価**

①　長期評価と津波評価技術

平成１４年２月に土木学会により策定，公表された**津波評価技術**は，原子力発電所の設計津波の設定について，その時点で確立しており実用として使用するのに疑点がないものを取りまとめたものである。原子力規制機関は，原子炉の設置許可処分に先立つ審査にも，津波評価技術と同様の考え方を用いて津波に対する安全性を確認していた。

平成１４年７月３１日に地震調査研究推進本部により公表された**「三陸沖から房総沖にかけての地震活動の長期評価について」（長期評価）**は，「福島沖を含む日本海溝沿いの三陸沖北部から房総沖までの海溝寄りの領域」に関しては，過去４００年にマグニチュード８クラスのプレート間大地震が３回発生しているとして，この領域全体では約１３３年に１回の割合で，このような大地震が発生すると推定されるとし，明治三陸地震（１８９６年）と同様の地震は，この領域内のどこでも発生する可能性があるとする。

津波評価技術においては，想定津波の波源設定のための基準断層モデルの領域区分に福島県沖の領域が設定されていないのに対し，長期評価においては，日本海溝沿いの三陸沖北部から房総沖までの海溝寄りの領域を一体の領域としている点で異なっている。

津波評価技術と長期評価は，いずれも，過去の地震について調査結果やそれまでの知見から整理し大地震発生に関する見解を形成しているが，用いられた調査結果や知見はほぼ同様である。上記のような相違は，これらの知見が多様であり，地震や津波発生のメカニズムが十分に解明されておらず，いずれの知見もある程度は仮説の域を出ないものであることに由来するとみることができる。

津波評価技術では，津波の波源の領域区分の設定に「地震地体構造論」の知見

5

が用いられているのに対し，長期評価はこれを取り入れたことを明示していないが，この知見にも仮説の域を出ていない部分があり，これを明示的に見解形成の基礎として用いていないことによって長期評価に示された見解の科学的信頼性が大きく減殺されるとは言い難い。

長期評価について，平成１５年３月２４日に地震本部により公表された信頼度の評価では，「発生領域の評価」「発生確率の評価」の信頼度が「やや低い（C）」とされているが，これは過去の地震データが少ないことによるものであり，長期評価の基礎となっている科学的知見の信頼性が低いことを理由とするものではない。

そして，津波評価技術と長期評価のいずれもが，専門家を含む構成員が議論を重ね，議論の結果として得られた見解を一方は学術的権威のある学会が，他方は国の機関が公表したものであり，策定に関与した専門家や議論の過程，公表した主体のいずれにおいても，科学的信頼性の観点からみて，一方が他方に比して優位であるということはできない。

これらを総合すると，**長期評価に示された見解については，相応の科学的信頼性のある知見であると評価することができ，津波評価技術と比較しても，その科学的信頼性において，優位とはいえないまでも，同等であるというべきである。**

②　**長期評価を技術基準適合性の判断の基礎としなかったことの合理性と技術基準適合性の判断について**

規制機関である経済産業大臣は，津波評価技術の知見に依拠して規制権限行使の要件具備の判断をしていたのであり，少なくともこれと同等の科学的信頼性を有する長期評価に示された見解について，これを判断の基礎としないことは，著しく合理性を欠くというべきである。

科学的知見の採否は規制機関の専門的判断に委ねられているが，原子炉施設についての規制権限の目的が，ひとたび事故等により放射性物質の大量放出という事態が発生すれば，極めて深刻な被害を広範囲かつ長期間にわたってもたらす危険性がある原子炉施設について，万全の安全対策を確保することにあることに鑑みれば，規制機関がある科学的知見を基礎として規制権限の行使の要件について判断してきたが，新たな知見が示された場合において，その新たな知見にそれまで判断の基礎としてきた知見と少なくとも同程度の科学的信頼性があると評価することができるようなときは，規制機関が，当該新たな知見を判断の基礎としないとすることは著しく合理性を欠くことになるというべきである。

6

©2021. Japan Geoscience Union. All Right Reserved.

Wilkins’ s lunar world

*Shigeyuki Aoki[1]

1. Faculty of Letters, Chuo University

The shift from the geocentric world-view to the heliocentric one, during the 16th and 17th century in the midst of the Scientific Revolution, transformed the ancient plurality worlds doctrine to more concrete theses on specific satellites and planets. This presentation deals with John Wilkins, who first argued in England that the moon is probably a habitable world.

Keywords: plurality of worlds, the Scientific Revolution in England, history of planetary science, habitable zone

©2021. Japan Geoscience Union. All Right Reserved.

The Popularization of Science and the Geo-power: Cosmic Evolution, China, and Buddhism in 1920s Shinjo Shinzo

*Toshihiro Yamada[1]

1. Taisho University

This paper presents a three-fold emergency by the cosmo-geoscientist Shinjo Shinzo (1873-1938) in his 1920s:
1) The establishment of the institute for physical astronomy at the Imperial Kyoto University;
2) The activities to popularize science, especially cosmic evolution related to Buddhist terminology;
3) The historical study of ancient Chinese astronomy with the collaboration of Orientalists in the university.
We will discuss the geocosmic consciousness cultivated in these processes as well as the international relationship in the term of geo-power.

Keywords: Shinjo Shinzo, Popularization of science, Geo-power, Chinese geoscience, Buddhist terminology

©2021. Japan Geoscience Union. All Right Reserved.

Japan's first female meteorologist

*Akira Yamamoto

Kiyoko Matsuo (1918: estimated-1997) who is considered to be Japan's first female meteorologist is described.

Keywords: history of Meteorology, female scientist, gender

©2021. Japan Geoscience Union. All Right Reserved.

[J] Oral | M (Multidisciplinary and Interdisciplinary)：M-ZZ Others

Sun. Jun 6, 2021 10:45 AM - 12:15 PM JST | Sun. Jun 6, 2021 1:45 AM - 3:15 AM UTC | Ch.16 Zoom Room 16

[M-ZZ48] Geology and culture

convener:Hisashi Suzuki(Otani University), Tohru Sakiyama(Institute of Geo History, Japan Geochronology Network), Naoki Takahashi(Natural History Museum and Institute, Chiba), Chairperson:Tohru Sakiyama(Institute of Geo History, Japan Geochronology Network), Naoki Takahashi(Natural History Museum and Institute, Chiba)

The session "geology and culture" deals with an interdisciplinary field that discusses the relationship between human and geology. We invite following research themes on the session. (1) geology as a raw material, (2) geochemical analyses of archaeological remains, (3) relationship between geology and regional cultures, (4) geoeducation with museum and geopark, (5) letters and music with geology, and (6) geology and religion. We invite presentations of research results on all geological themes concerning human being.

10:45 AM - 11:00 AM JST | 1:45 AM - 2:00 AM UTC

[MZZ48-01] A use of tuff beds in strata for natural resources at the Boso Peninsula – ‘Bosyu white clay’ or ‘Bosyu sand’

*Naoki Takahashi[1], Junichi Ohki[1] (1.Natural History Museum and Institute, Chiba)

11:00 AM - 11:15 AM JST | 2:00 AM - 2:15 AM UTC

[MZZ48-02] Change of usage patterns of Innai Tuff Member from Yuzawa City, Akita prefecture, northeast Japan: From ‘rolling stones‘ in early modern to ‘Innai Ishi’ in modern

*Norihito Kawamura[1] (1.School of Regional Resource Management, Graduate School, University of Hyogo)

11:15 AM - 11:30 AM JST | 2:15 AM - 2:30 AM UTC

[MZZ48-03] Japanese marbles used in some historic western style houses in Tokyo

*Mutsuko Inui[1], Shoji Nishimoto[2] (1.School of Science and Engineering, Kokushikan University, 2.Nagoya City Science Museum)

11:30 AM - 11:45 AM JST | 2:30 AM - 2:45 AM UTC

[MZZ48-04] Brewing culture and geology in Japan: examples of Satsuma shochu spirits and Koshu wine

*Hisashi Suzuki[1] (1.Otani University)

11:45 AM - 12:00 PM JST | 2:45 AM - 3:00 AM UTC

[MZZ48-05] The investigation of the relationship between the artificial terrain change of medieval mountain castles and the landslides in 2018

*Masami Inomata[1] (1.National University Corporation Hiroshima University)

12:00 PM - 12:15 PM JST | 3:00 AM - 3:15 AM UTC

[MZZ48-06] **Historical distribution of granitic stone materials from Setouchi area in the San-in and Hokuriku regions, Southwest Japan**

*Tohru Sakiyama[1] (1.Institute of Geo History, Japan Geochronology Network)

A use of tuff beds in strata for natural resources at the Boso Peninsula – ‘Bosyu white clay’ or ‘Bosyu sand’

*Naoki Takahashi[1], Junichi Ohki[1]

1. Natural History Museum and Institute, Chiba

From Neogene to Quaternary marine strata construct the Boso Peninsula. Their strata deposited on deep sea and rapidly uplifted, so their strata have enough degree of consolidation and are easy to dig. So, from ancient times, digging of the strata have done for various purpose on human life in the Boso Peninsula. They are majorly divided two formation. One is use of relief feature, and the other is use of components of the strata as natural resources. This time, an example of the latter case is introduced.

The strata are mainly constructed by hemi-pelagic mudstone and turbidite sandstone, and they include numerous tephra beds. Their tephra have wide variety, but especially fine glassy tephra are used as dental powder, rice polishing powder, material of roof tile and ceramics, admixture of cement from the latter part of the Edo Period, and then used on a small scale as polishing powder of glass, mold releasing agent even today (Oya, 1990; Saito, 1998). They are dug along mining gallery focus on the several 10cm to 2m thick single tuff bed, so the gallery tilt according to dip of strata, and suddenly change their height by fault. They are dug at several points and different horizons in the Boso Peninsula, so the characteristic of the strata is common in the Boso Peninsula, and show the geological history of the Peninsula. Their tuff beds are used and named as key beds for contrast of strata which distribute distant areas. For example, ‘Kd8’ tephra in the Kiwada Formation, Kazusa Grop, at Isumi City, and ‘TK-5’ and ‘Hn-8’ tephra in Higashinagata Formation, Chikura Group, at Tateyama City (Kawakami & Shishikura, 2006). These are all Pleistocene marine strata. Their origins are not specified, but ‘Kd8’ tephra is correlated to ‘Omig’ tephra in the Uonuma Group at the Niigata area (Kurokawa et al., 2002), so they are possibly from far away area. These tephra have both geological importance and usefulness as natural resources.

[References]

Kawakami, S. and Shishikura, M. ,2006, Geology of the Tateyama District. Quadrangle Series, 1:50,000, Geological Survey of Japan, AIST, 82p.

Katsuki, K., Sakai, H., Hiwatari, H., Ohashi, R. and Higuchi, Y. , 2002, Tephra beds in the Taira and Minagawa Formations in central Niitsu Hill to eastern Kamo area, Niigata Prefecture and their correlation, especially to the Kd18 and Kd8 beds in Boso Peninsula. Memoirs of the Faculty of Education and Human Sciences (Natural Sciences), Niigata University, 4(2): 65-125.

Oya, S., 1990, Consideration of ‘Boshu white clay’. Tateyama and cultural property, (24), 6-10.

Saito, N., 1998, Remained site of white clay quarry. Chiba Museum of Science and Industry (eds.), ‘Industrial and traffic heritages in the Chiba Prefecture’, 54-55, Chiba Prefectural Board of education.

Keywords: Boso Peninsula, tuff, natural resources

©2021. Japan Geoscience Union. All Right Reserved.

©2021. Japan Geoscience Union. All Right Reserved.

Change of usage patterns of Innai Tuff Member from Yuzawa City, Akita prefecture, northeast Japan: From ‘rolling stones‘ in early modern to ‘Innai Ishi’ in modern

*Norihito Kawamura[1]

1. School of Regional Resource Management, Graduate School, University of Hyogo

I'm sorry, I could't enter texts due to an error message.

Keywords: tuff breccia, Onnagawa Formation, magnetic susceptibility, shrine, stone work

©2021. Japan Geoscience Union. All Right Reserved.

Japanese marbles used in some historic western style houses in Tokyo

*Mutsuko Inui[1], Shoji Nishimoto[2]

1. School of Science and Engineering, Kokushikan University, 2. Nagoya City Science Museum

Various kinds of marble had been quarried in Japan as building stone until about the end of 1960's. Marble quarries were active in Japan from the end of the 19th century, though it is not well known nowadays. Those marbles have been used for the interior finishing of many historic buildings in Tokyo. Here we report on the domestic building stones used for the interiors (mantlepieces) in some of the historic western style houses in Tokyo, designed by Josiah Conder. The houses are: the Former Iwasaki Residence, the Former Shimazu Residence, and the Former Furukawa Residence. The construction of the houses was completed between 1896 to 1917. Provenance of the marble of the mantlepieces was identified non-destructively. Marbles from Ibaraki Prefecture, Gifu Prefecture, Iwate Prefecture, Yamaguchi Prefecture, and Tokyo Metropolis were identified. The mantlepieces are the testimonial for the fact that quarrying of those marbles was active during those years. The investigation is significant for understanding the history of the use of building stones in Japan. The hisotric aspect of the marbles is an important part of the assessment of the cultural heritage.

Keywords: building stone, marble, historic building

©2021. Japan Geoscience Union. All Right Reserved.

Brewing culture and geology in Japan: examples of Satsuma shochu spirits and Koshu wine

*Hisashi Suzuki[1]

1. Otani University

Two examples of Japanese brewing culture, Satsuma-shochu spirits in Kagoshima prefecture and Koshu wine in Yamanashi prefecture, are demonstrated in concerning with their areal geology.

Satsuma region (Kagosima prefecture): The Shirasu plateau that is composed of upper Pleistocene pyroclastic sediments is widely distributed in the Satsuma region. The plateau has water permeability due to its porous nature. This feature results in the cultivation of sweet potato on the Shirasu plateau. Soft groundwater wells out from rims of the plateau. Sweet potato and groundwater are used for brewing shochu spirits.

Katsunuma area (Koshu city, Yamanashi prefecture): Katsunuma area is a part of the Kofu basin and alluvial fans are well developed. Water permeable nature of alluvial fan is suitable for cultivation of grapevine. Although the wine brewing is not traditional in Japan, two brewers of the Katsunuma area travelled to France to learn the wine brewing in the years 1877-1879.
Both Satsuma region and Katsunuma area are characterised by the water permeability of farmlands, which are closely related with each areal geology. Whereas water is needed for brewing shochu spirits, no water is necessary to make wine. Areal geology is one of the fundamental factors to make brewing cultures in these regions.

Keywords: Shirasu plateau, alluvial fan, sweet potato, grapevine

©2021. Japan Geoscience Union. All Right Reserved.

The investigation of the relationship between the artificial terrain change of medieval mountain castles and the landslides in 2018

*Masami Inomata[1]

1. National University Corporation Hiroshima University

The purpose of this study was to investigate the relationship between the artificial terrain change of medieval mountain castles and the landslides in Higashihiroshima City 2018.

There has been few reported on the relationship between medieval castles and the landslides.Because medieval castle ruins were not damaged.

The heavy rainfall in July 2018 caused many landslides in Higashihiroshima City. There are 165 ruins of medieval castle in this city and some of them were up stream of debris flows. The number of residence of this city is increasing continuously at the foot of mountain.
Therefore, it is necessary to clarify the risks of artificial terrain change of medieval mountain castles.

This study was performed with GIS (Geo Information System) and field study. In this research, totally 124 medieval castles were studied (Fig.1).
The analysis of GIS revealed that 59 of these medieval castles were associated with landslides.

Most of medieval castles were the fortress style, and built to mountainous terrain with construction work for defense. Those medieval mountain castles had a characteristic construction.
Typically, top of the mountain and mountainside used to be artificially modified to build medieval mountain castles. Workers created a flat area known as a *Kuruwa*, cut away at the ridge to form dry moats (*Horikiri*), and used the surplus soil accumulated during these tasks to build *Dorui*. Another structural feature was the *Kirigishi*, slopes around the *Kuruwa* that were made intentionally steeper. In addition, *Unejo-tatebori*, parallel trenches dug vertically into the *Kirigishi* slopes, was developed to prevent enemies coming up the slopes diagonally (Fig.2).

In the field survey, it was confirmed that some debris flows were generated from the lower part of *Horikiri* slope. It is highly suspected that defensive features of medieval mountain castles could have affected the flow of rainwater.

Furthermore, this city is mainly composed of the Hiroshima granite, which is relatively vulnerable to the terrain modification. The analysis by GIS revealed that 85% of medieval mountain castles that were associated with landslides, were located in The Hiroshima granite.

The analysis by GIS (Geo Information System) and field study suggest that *Horikiri*, the construction of a medieval mountain castle, is one of the causal factors with landslide.
Therefore, identifying the areas of those artificial terrain change could be effective to foresee future potential of debris flow path when landslide took place in the future.

Keywords: Construction of a medieval Mountain castle, GIS, The Hiroshima Granite

©2021. Japan Geoscience Union. All Right Reserved.

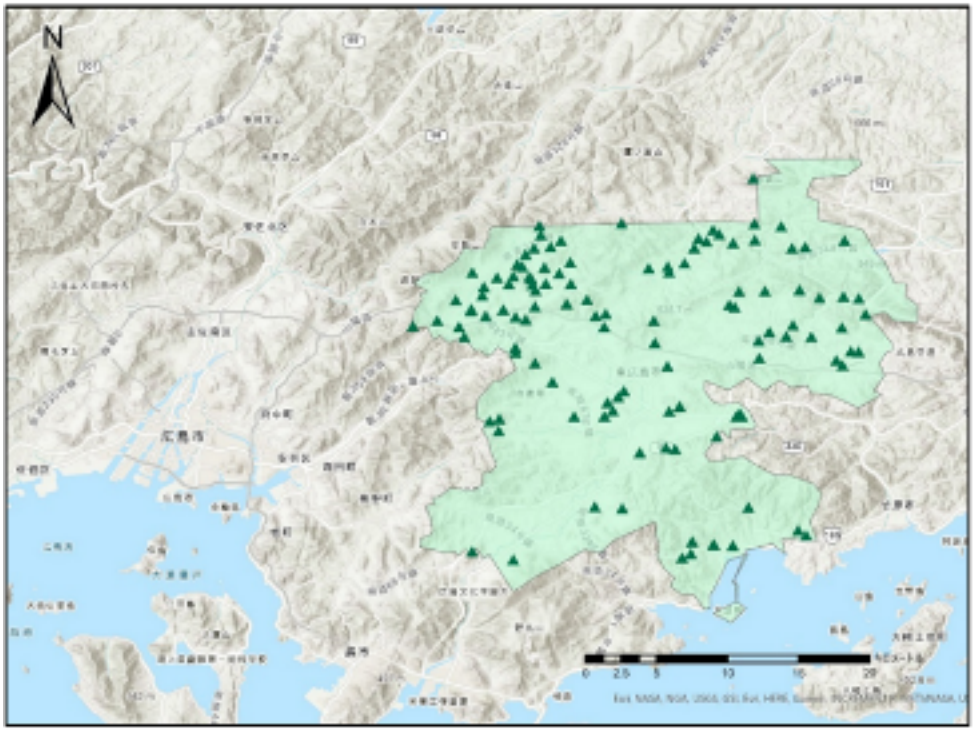


Fig1.The study area in Higashihiroshima City □ and medieval castles ▲

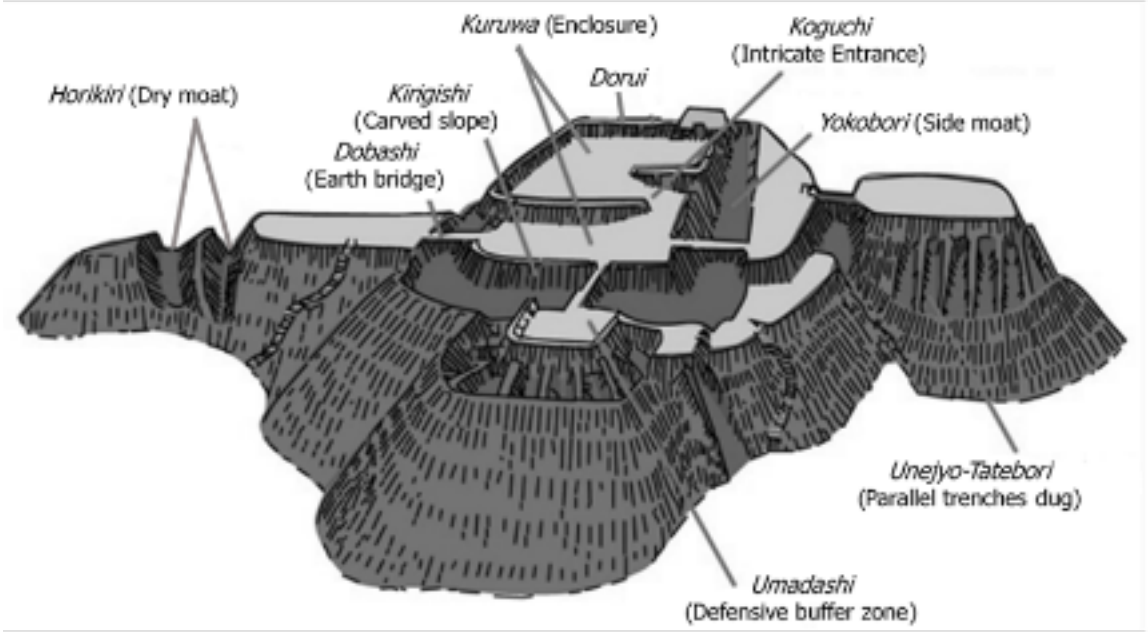


Fig2.A typical medieval mountain castle
(Created based on excavation guide: Various types of ruins[5])

©2021. Japan Geoscience Union. All Right Reserved.

Historical distribution of granitic stone materials from Setouchi area in the San-in and Hokuriku regions, Southwest Japan

*Tohru Sakiyama[1]

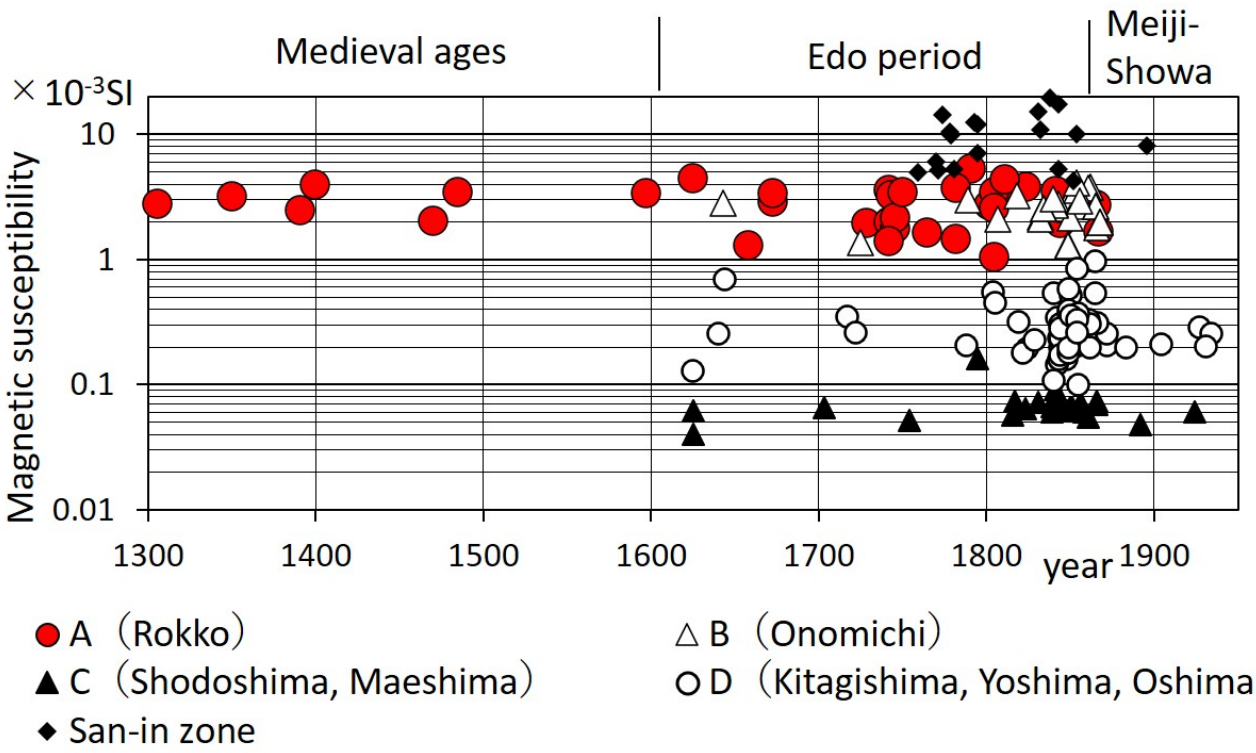
1. Institute of Geo History, Japan Geochronology Network

Many ancient quarries for granites are remained in islands and coastal area of the Seto Inland Sea. 14th to 19th century stone materials of the granites from these quarries are widely distributed in coastal area of the Sea of Japan. Identification of quarry area of the granites is one of the important issues in Japanese historical study. I reveal distribution of such granitic stone materials in San-in and Hokuriku region and discuss transition of quarried areas.

Granitic rocks of the stone materials are divided following five types resulted by magnetic susceptibility and description.
Type A (Rokko Mountains): Medium-grained biotite granite with pinkish K-feldspar interstitially, with or without hornblende. Magnetic susceptibility ranges from 1X10^{-3} to 3X10^{-3} SI.
Type B (Onomichi): Medium-grained hornblende biotite granite with white colored porphyritic K-feldspar. Magnetic susceptibility ranges from 1X10^{-3} to 3X10^{-3} SI.
Type C (Kitagishima, Yoshima or Oshima): Medium-grained biotite granite to hornblende biotite granite. Magnetic susceptibility ranges from 0.1X10^{-3} to 1X10^{-3} SI.
Type D (Shodoshima or Naoshima): Coarse-grained biotite granite. Magnetic susceptibility ranges from 0.04X10^{-3} to 0.07X10^{-3} SI.
Type E (San-in or Hokuriku area): Various granitic rocks occurred in local area. Most of them have very high magnetic susceptibility (from 5X10^{-3} to 11X10^{-3} SI), except low magnetic granites from Mihama area (from 0.03X10^{-3} to 0.05X10^{-3} SI).
Relation between age and rocks forming stone materials in San-in to Hokuriku region indicate following history. In medieval time (14th to 16th century), type A granites which have been occurred in Rokko mountains area mainly distributed to San-in area. Circulation of other granites from Setouchi area began in early 17th century and become maximum in 19th century. On the other hand, proportion of type A granites decreased from 17th to 19th century.

Keywords: granite, stone material, history, magnetic susceptibility

©2021. Japan Geoscience Union. All Right Reserved.



Types of granitic rocks forming stone materials and their magnetic susceptibility in medieval to modern ages

©2021. Japan Geoscience Union. All Right Reserved.

[J] Poster | M (Multidisciplinary and Interdisciplinary)：M-ZZ Others

Sun. Jun 6, 2021 5:15 PM - 6:30 PM JST | Sun. Jun 6, 2021 8:15 AM - 9:30 AM UTC | Ch.22_5

[M-ZZ48] Geology and culture

convener:Hisashi Suzuki(Otani University), Tohru Sakiyama(Institute of Geo History, Japan Geochronology Network), Naoki Takahashi(Natural History Museum and Institute, Chiba)

The session "geology and culture" deals with an interdisciplinary field that discusses the relationship between human and geology. We invite following research themes on the session. (1) geology as a raw material, (2) geochemical analyses of archaeological remains, (3) relationship between geology and regional cultures, (4) geoeducation with museum and geopark, (5) letters and music with geology, and (6) geology and religion. We invite presentations of research results on all geological themes concerning human being.

[MZZ48-P01] Rock species of the cornerstone of the earthen wall in the northeastern part of Ninomaru earthworks of Yamagata Castle

*Ohtomo Yukiko[1], Saito Hitoshi[2] (1.Yamagata University, 2.Yamagata City Board of Education)

Rock species of the cornerstone of the earthen wall in the northeastern part of Ninomaru earthworks of Yamagata Castle

*Ohtomo Yukiko[1], Saito Hitoshi[2]

1. Yamagata University, 2. Yamagata City Board of Education

The northeastern part of Ninomaru earthworks at Yamagata Castle encompasses the area from Higashi Otemon (Eastern Gate) to the North Gate. During an archaeological excavation conducted by the Yamagata City Board of Education from 2016 to 2018, stone walls of Ushitora Yagura and Sakanamachimukai Yagura were detected. The cornerstone of the earthen wall was successfully excavated in almost the entire area, and a geological survey was conducted on the stone walls(Ohtomo, 2020). Two periods of old and new were assigned to the cornerstone of the earthworks. It was judged that the old earthworks were updated with new construction inside because the earthworks are tilted owing to unequal subsidence(Yamagata City Board of Education, 2020). The stone materials surveyed during this project are of the new period.

Most of the cornerstones of the earthen wall are composed of andesite. In particular, 1270 of the 1383 cornerstones are andesite, accounting for 92.03%. Other major materials include dacite, granite, and rhyolite in 47, 40, and 18 cornerstones, amounting to 3.40%, 2.89%, and 1.30%, respectively . In addition, five are composed of basalt, and three are composed of tuff breccia, green tuff, and green andesite. Most occur as subcircular gravel derived from riverbeds. Most of the dacite and some of the rhyolite and granite occur as angular rock masses.

Most of the andesite is gray to black; of these, 30.39% are inclusion rocks presumed to be basalt, and 4.7% contain conspicuous volcanic gas voids. In addition, 1.89% is reddish-purple in color owing to oxidation at high temperatures.

Of the dacites, 33.33% are characterized by thin, black stripes; 31.11% have no such stripes; and 35.56% some did not distinguish between them. Both lithologies are found in the dacite bodies distributed around the Mount Sakazukiyama, although the striped lithology is limited in distribution(Ohtomo, 2016). Most of the dacite is in the form of angular rock masses having the same lithology as the rock found in the stone walls of Sakanamachimukai Yagura and Ushitora Yagura. It is believed that the dacites remaining from the stone wall construction were used in the cornerstone foundation of the earthen wall.

The granites are gravels composed of 65.00% coarse-grained biotite granite, 32.50% medium-grained biotite granite, and 2.50%, fine-grained granite originating from the granite body distributed upstream of the Mamigasakigawa River(Ohtomo et al., 2019).

The gravels assumed to be composed of basalt contain large plagioclase phenocrysts approximately l cm in diameter and numerous phenocrysts. Because this lithology is characteristic of Ryuzan basalt, the gravels of this lithology were classified as basalt.

The tuff breccia and green tuff are from the Miocene Narisawa Formation, and the green andesite is from the Houzawa Formation. The tuff breccia contains granite fragments, and the voids of the green andesite are filled with agate.

The proportion of each of these rock species is almost constant throughout the northeastern earthworks of Ninomaru; no large bias was found among the districts. In District 7, which is adjacent to Ushitora Yagura, 11 dacites having the same lithologies as those present in the stone wall are distributed.

References

Yamagata City Board of Education, 2020, Survey report on buried cultural properties in Yamagata City, Yamagata Prefecture, 39, 14-110. *

Ohtomo Y., 2016, 123rd Annu. Meet. Geol. Soc. Japan, Abstr., 190.

©2021. Japan Geoscience Union. All Right Reserved.

Ohtomo Y., 2020, IV Survey results of stone walls and cobblestone of Sumiyagura in Ninomaru. 39, 111-115. *
Ohtomo Y., et al., 2019, Applied geol. Yamagata, no.39, 89-93.
*English translation from the original written in Japanese

Keywords: cornerstone of earthen wall, rock species, Ninomaru earthworks, Yamagata Castle



©2021. Japan Geoscience Union. All Right Reserved.

[J] Oral | EVENT：EVENT

Sun. Jun 6, 2021 12:20 PM - 1:00 PM JST | Sun. Jun 6, 2021 3:20 AM - 4:00 AM UTC | Ch.01 Zoom Room 01

[EV-25] Lunchtime Special Lecture

World renowned scientists will present a series of Special Lectures in Earth and planetary sciences for students and early-career researchers across disciplines during lunch breaks (12:20-13:40) of the Meeting.

12:20 PM - 1:00 PM JST | 3:20 AM - 4:00 AM UTC

[E-11-26] Chemical constraints on the origin and early evolution of the Solar System

[J] Oral | EVENT | EVENT

[EV-25] Lunchtime Special Lecture

Sun. Jun 6, 2021 12:20 PM - 1:00 PM Ch.01 (Zoom Room 01)

World renowned scientists will present a series of Special Lectures in Earth and planetary sciences for students and early-career researchers across disciplines during lunch breaks (12:20-13:40) of the Meeting.

12:20 PM - 1:00 PM

[E-11-26]Chemical constraints on the origin and early evolution of the Solar System

This lecture will explore present and future challenges of constraining the origin and early evolution of the Solar System from the materials science point of view. Keywords: cosmochemistry, extraterrestrial materials, star and planet formation, sample return, Solar System exploration, laboratory experiments, astronomical observation.

©Japan Geoscience Union

[J] Oral | EVENT：EVENT

Sun. Jun 6, 2021 3:30 PM - 4:15 PM JST | Sun. Jun 6, 2021 6:30 AM - 7:15 AM UTC | Ch.13 Zoom Room 13

[EV-26] Exhibitors' Seminar

昨年と同じく、出展者様にセミナーを開催していただきます。
地球惑星科学関連の、有用な情報を発信してくださいますので是非ご参加ください。

3:30 PM - 4:15 PM JST | 6:30 AM - 7:15 AM UTC

[E-11-27] GRC virtual lab tour & the making of a diamond powder with Hime-diamond mortar

[J] Oral | EVENT | EVENT

[EV-26] Exhibitors' Seminar

Sun. Jun 6, 2021 3:30 PM - 4:15 PM Ch.13 (Zoom Room 13)

昨年と同じく、出展者様にセミナーを開催していただきます。
地球惑星科学関連の、有用な情報を発信してくださいますので是非ご参加ください。

3:30 PM - 4:15 PM

[E-11-27]GRC virtual lab tour &the making of a diamond powder with Hime-diamond mortar

GRC virtual lab tour &the making of a diamond powder with
Hime-diamond mortar

©Japan Geoscience Union